V International Conference on Permafrost
in Trondheim, Norway, August 1988

PERMAFROST

PROCEEDINGS VOL. 1

TAPIR

PERMAFROST

Fifth International Conference

PROCEEDINGS VOLUME 1

August 2-5, 1988

Editor:
Kaare Senneset

Organized by
The Norwegian Committee on Permafrost
The Norwegian Institute of Technology

TAPIR PUBLISHERS
Trondheim, Norway

ISBN 82-519-0863-9

Printed in Norway.

PREFACE

This International Conference on Permafrost is the fifth in a series that started in 1963 at Purdue University, Indiana, USA. The next ones were held in Yakutsk, Siberia, USSR in 1973; in Edmonton, Alberta, Canada in 1978 and in Fairbanks, Alaska, USA in 1983.

This V International Conference on Permafrost is the first one after establishing the International Permafrost Association (IPA). The Association was founded during the conference in Fairbanks in 1983 upon the initiative of Canada, China, USA and USSR.

The Norwegian Committee on Permafrost and the Norwegian Institute of Technology are honoured to be the organizers for this fifth conference. The support and guidance of the International Permafrost Association has been extremely important for us in the preparation for the conference.

These proceedings contain the majority of the papers prepared for the conference. A final volume will be published at a later date. The high quality of the papers is the result of hard work by the authors, but also the assitance given by the numerous reviewers in all the member countries.

The Norwegian Organizing Committee is indebted to all of you that have participated in the preparation for this conference. I have already mentioned the authors and the reviewers and the support from the International Permafrost Association. Important are also our sponsors who have shown a great interest in the permafrost science and engineering.

Last, but not least, I wish to thank everybody at the local level in Norway that have been working to make it a successful conference. We have our share of experience in cold regions science and engineering in Norway. The enthusiasm of everyone involved has, however, been a warming adventure.

Kaare Flaate, chairman
Norwegian Organizing Committee
Fifth International Conference on Permafrost

THE NORWEGIAN ORGANIZING COMMITTEE

Kaare Flaate (Chairman), Norwegian Road Research Laboratory
Odd Gregersen, The Norwegian Committee on Permafrost
Kaare Høeg, Norwegian Geotechnical Institute
Bjarne Instanes, Association of Consulting Engineers, Norway
Tore Jørgensen, The Norwegian Institute of Technology
William Martin, Norsk Hydro
Magne Often, The Associated General Contractors of Norway
Alv Orheim, Statoil
Ole Reistad, Store Norske Spitsbergen Kulkompani A/S
Otto Salvigsen, The Norwegian Polar Research Institute
Johan Ludvig Sollid, University of Oslo
Kaare Senneset, The Norwegian Institute of Technology/SINTEF
Reidar Sætersdal, Norsk Hydro
Jon Krokeborg (Secretary general), Sollistrand Industrier A/S

Secretariat: Norwegian Road Research Laboratory
The Norwegian Institute of Technology

CONTRIBUTING SPONSORS

The following companies and institutions contributed financial support to the Fifth International Conference on Permafrost:

A/S Nor-vei
A/S Veidekke
Barlindhaug A/S
Bjarne Instanes A/S
Civil Aviation Administration
EEG Henriksen A/S
Norsk Hydro
Norwegian Geotechnical Institute
Norwegian Ministry of Defence
Public Roads Administration
Royal Norwegian Council for Scientific and Industrial Research
Selmer-Furuholmen A/S
Statoil
The Foundation for Scientific and Industrial Research at NTH (SINTEF)
The Norwegian Institute of Technology (NTH)

CONFERENCE PUBLICATIONS

The official proceedings of the conference consist of: (1) the present volume of 288 contributed papers by authors from 19 countries, and (2) a final volume that will contain the special session presentations, additional contributed papers and a list of participants.

In response to the initial call for papers, more than 500 abstracts were submitted. The Norwegian Organizing Committee found it on this background practical and necessary to ask member countries of the International Permafrost Association to set up reviewing committees to review and recommend respective papers. This arrangement were approved by the Executive Committee of The International Permafrost Association. In the following countries such reviewing committees were organized:

Belgium:	:	A. Pissart, chairman
Canada	:	H.M. French, chairman
China	:	Cheng Goudong, chairman
France	:	J.Aquirre-Puente, chairman
Germany	:	H.L. Jessberger, chairman
Great Britain	:	C. Harris, chairman
Italy	:	F. Dramis, chairman
Japan	:	S. Kinosita, chairman
The Netherlands:		E. Koster, chairman
Norway	:	K. Senneset, chairman
Poland	:	A. Jahn, chairman
Sweden	:	R. Nyberg, chairman
Switzerland	:	W. Haeberli, chairman
USA	:	J. Brown, chairman
USSR	:	N.A. Grave, chairman

The efforts and generous cooperation of this committees and the reviewers called upon by them, are gratefully acknowledged by the Norwegian Organizing Committee.

In the following pages the reviewers involved are listed.

A publishing committee was established and given the responsibility for the cooperation with the national reviewing committees, for the final acceptance of papers and the printing of proceedings.

The members of the publishing committe were:

K.Senneset, chairman, The Norwegian Institute of Technology, The University of Trondheim.
K.Flaate, Norwegian Road Research Laboratory
O.Gregersen, The Norwegian Committee on Permafrost
R.Sætersdal, Norsk Hydro

In addition to the proceedings, guidebooks for the field trips to Svalbard and the main land are published in an official publication serie at the University of Oslo, edited by the Department of Geography.

Kaare Senneset, chairman
Publishing Committee

LIST OF REVIEWERS

REVIEWERS OF CANADIAN PAPERS

The review of Canadian papers was conducted by the Canadian National Committee for the International Permafrost Association (CNC/IPA), with the support of the Bureau of International Relations, National Research Council of Canada. A National Review Committee consisted of the following individuals:

Hugh M. French
Chairman, CNC/IPA
University of Ottawa, Ottawa, Ontario

Lorne W. Gold, National Research Council of Canada, Ottawa, Ontario
David G. Harry, Geological Survey of Canada, Ottawa, Ontario
Don W. Hayley, EBA Engineering Ltd., Edmonton, Alberta
J. Alan Heginbottom, Geological Survey of Canada, Ottawa, Ontario
G. Hank Johnston, National Research Council of Canada, Ottawa, Ontario
Alan S. Judge, Geological Survey of Canada, Ottawa, Ontario
Branko Ladanyi, Ecole Polytechnique, Montréal, Québec
J. F. (Derick) Nixon, Hardy BBT Ltd., Calgary Alberta
R. O. van Everdingen, Arctic Institute of North America, Calgary, Alberta

Reviewers

Michel Allard, Université Laval, Québec, Québec
Bea Alt, Energy, Mines and Resources, Ottawa, Ontario
T. H. W. (Harry) Baker, National Research Council of Canada, Ottawa, Ontario
D. Martin Barnett, Indian and Northern Affairs, Ottawa, Ontario
Chris R. Burn, University of British Columbia, Vancouver, British Columbia
Margo Burgess, Geological Survey of Canada, Ottawa, Ontario
Derek Cathro, EBA Engineering Consultants Ltd., Edmonton, Alberta
Ian G. W. Coms, Environment Canada, Edmonton, Alberta
Scott R. Dallimore, Geological Survey of Canada, Ottawa, Ontario
Jean-Claude Dionne, Université Laval, Québec, Québec
Len Domaschuk, The University of Manitoba, Winnipeg, Manitoba
Larry Dyke, Queen's University, Kingston, Ontario
Sylvain Dufour, International Development Research Centre, Ottawa, Ontario
Paul Egginton, Geological Survey of Canada, Ottawa, Ontario
John G. Fyles, Geological Survey of Canada, Ottawa, Ontario
Jim S. Gardner, University of Waterloo, Waterloo, Ontario
Laurel Goodrich, National Research Council of Canada, Ottawa, Ontario
Stuart A. Harris, University of Calgary, Calgary, Alberta
Peter G. Johnson, University of Ottawa, Ottawa, Ontario
Ian G. Jones, Thurber Consultants Limited, Calgary, Ontario
Jean-Marie Konrad, University of Waterloo, Waterloo, Ontario
Pavel J. Kurfurst, Geological Survey of Canada, Ottawa, Ontario
P. T. Lafleche, Geological Survey of Canada, Ottawa, Ontario
Antoni G. Lewkowicz, University of Toronto, Toronto, Ontario
Phil Marsh, National Hydrology Research Institute, Saskatoon, Saskatchewan
Fred A. Michel, Carleton University, Ottawa, Ontario
N. R. Morgenstern, University of Alberta, Edmonton, Alberta
André Paré, Geotech Engineering Limited, Calgary, Alberta
Danny Paterson, Carleton University, Ottawa, Ontario
Ed Penner, National Research Council of Canada, Ottawa, Ontario
Jean A. Pilon, Geological Survey of Canada, Ottawa, Ontario
Wayne H. Pollard, Memorial University of Newfoundland, St. John's, Newfoundland

Dennis E. Pufahl, University of Saskatchewan, Saskatoon, Saskatchewan
Vern N. Rampton, Terrain Analysis and Mapping Services Ltd., Carp, Ontario
N. W. Rutter, University of Alberta, Edmonton, Alberta
K. Wayne Savigny, University of British Columbia, Vancouver, British Columbia
W. J. (Bill) Scott, Hardy BBT Ltd., Calgary, Alberta
Dave Sego, University of Alberta, Edmonton, Alberta
Don H. Shields, University of Manitoba, Winnipeg, Manitoba
Charlie E. Sloan, Fairbanks, Alaska
Mike W. Smith, Carleton University, Ottawa, Ontario
Al Taylor, Geological Survey of Canada, Ottawa, Ontario
Charles Tarnocai, Agriculture Canada, Ottawa, Ontario
Jean J. Veillette, Geological Survey of Canada, Ottawa, Ontario
Jean-Serge Vincent, Geological Survey of Canada, Ottawa, Ontario
Ross W. Wein, University of Alberta, Edmonton, Alberta
Peter J. Williams, Carleton University, Ottawa, Ontario
M.-K. (Hok) Woo, McMaster University, Hamilton, Ontario
Steve C. Zoltai, Environment Canada, Edmonton, Alberta

The paper by

Tremblay, C.

was not available for CNC/IPA review by the deadline established to meet the Organizing Committee's publication schedule. It was, under special circumstances, submitted directly to the Norwegian Organizing Committee, reviewed and accepted for publication by this committee.

EDITING OF CHINESE PAPERS.

The Norwegian Organizing Committee wishes to thank the Canadian National Committee for the International Permafrost Association for undertaking the editing of a number of the papers submitted by China. In particular, the assistance of the following individuals is gratefully acknowledged.

T.W.W. Baker, Institute for Research in Construction, National Research Council of Canada, Ottawa, Ontario
C.R. Burn, University of British Columbia, Vancouver, British Columbia
S.R. Dallimore, Geological Survey of Canada, Ottawa, Ontario
L. Domaschuk, University of Manitoba, Winnipeg, Manitoba
S. Edlund, Geological Survey of Canada, Ottawa, Ontario
L. Goodrich, Institute for Research in Construction, National Research Council of Canada, Ottawa, Ontario
S.A. Harris, University of Calgary, Calgary, Alberta
J.A. Heginbottom, Geological Survey of Canada, Ottawa, Ontario
G.H. Johnston, Institute for Research in Construction, National Research Council of Canada, Ottawa, Ontario
A.G. Lewkowicz, University of Toronto, Toronto, Ontario
G. McCormick, Hardy BBT Limited, Edmonton, Alberta
S. Outcalt, University of Michigan, Ann Arbor, Michigan, USA
S. Parameswaran, Northwestern University, Chicago, USA
L.B. Smith Thurber Consultants Ltd., Calgary, Alberta
M.W. Smith, Carleton University, Ottawa, Ontario
R.O. van Everdingen, The Arctic Institute of North America, Calgary, Alberta
P.J. Williams, Carleton University, Ottawa, Ontario

REVIEWERS OF U.S. PAPERS

The review of U.S. papers was conducted for the Norwegian Organizing Committee by the National Research Council's U.S. Committee for the International Permafrost Association (USC/IPA). This review was made possible by a grant from the U.S. Department of Energy. The Committee gratefully acknowledges the timely efforts of the reviewers.

U.S. COMMITTEE FOR THE INTERNATIONAL PERMAFROST ASSOCIATION

Jerry Brown, Chairman, National Science Foundation, Washington, D.C.
C. William Lovell, Vice-Chairman, Purdue University, West Lafayette, Indiana
George Gryc, U.S. Geological Survey, Menlo Park, California
David M. Hopkins, University of Alaska, Fairbanks, Alaska
Virgil J. Lunardini Jr., USA Cold Regions Research & Engineering Laboratory, Hanover, New Hampshire
Rupert G. Tart Jr., Dames & Moore, Anchorage, Alaska

William L. Petrie, Staff Consultant, National Research Council, Washington, D.C.

REVIEWERS

Bernard D. Alkire, Michigan Technological University, Houghton, Michigan
Jalmer V. Alto, Alyeska Pipeline Service Company, Anchorage, Alaska
Duwayne M. Anderson, Texas A&M University, College Station, Texas
Steven A. Arcone, USA Cold Regions Research & Engineering Laboratory, Hanover, New Hampshire
C.L. Bartholomew, University of Colorado, Boulder, Colorado
Earl H. Beistline, Fairbanks, Alaska
James B. Benedict, Ward, Colorado
Richard L. Berg, USA Cold Regions Research & Engineering Laboratory, Hanover, New Hampshire
Patrick B. Black, USA Cold Regions Research & Engineering Laboratory, Hanover, New Hampshire
Jerry Brown, National Science Foundation, Washington, D.C.
Nelson Caine, University of Colorado, Boulder, Colorado
Joseph P. Callinan, Loyola Marymount University, Los Angeles, California
L. David Carter, U.S. Geological Survey, Anchorage, Alaska
Edward F. Chacho Jr., USA Cold Regions Research & Engineering Laboratory, Fairbanks, Alaska
Edwin J. Chamberlain, USA Cold Regions Research & Engineering Laboratory, Hanover, New Hampshire
J.-L. Chameau, Purdue University, West Lafayette, Indiana
K.C. Cheng, University of Alberta, Edmonton, Alberta, Canada
Barry Christopher, Purdue University, West Lafayette, Indiana
Michael G. Clark, University of Tennessee, Knoxville, Tennessee
Samuel C. Colbeck Jr., USA Cold Regions Research & Engineering Laboratory, Hanover, New Hampshire
Timothy S. Collett, U.S. Geological Survey, Menlo Park, California
John E. Cronin, Shannon and Wilson, Inc., Fairbanks, Alaska
Kenneth Dean, University of Alaska, Fairbanks, Alaska
S. Lawrence Dingman, University of New Hampshire, Durham, New Hampshire
Harvey E. Doner, University of California, Berkeley, California
Lowell A. Douglas, Rutgers University, New Brunswick, New Jersey
Philip A. Emery, U.S. Geological Survey, Anchorage, Alaska
David C. Esch, Alaska Department of Transportation & Public Facilities, Fairbanks, Alaska
K.R. Everett, Ohio State University, Columbus, Ohio
Michael L. Foster, Dames & Moore, Anchorage, Alaska
Hugh M. French, University of Ottawa, Ottawa, Ontario, Canada
David Frost, Purdue University, West Lafayette, Indiana
Leonard J. Gaydos, U.S. Geological Survey, Moffett Field, California
Kevin J. Gleason, University of Colorado, Boulder, Colorado
Richard P. Goldthwait, Anna Maria, Florida
Joan P. Gosink, University of Alaska, Fairbanks, Alaska
Anthony J. Gow, USA Cold Regions Research & Engineering Laboratory, Hanover, New Hampshire
George Gryc, U.S. Geological Survey, Menlo Park, California
Robert D. Gunn, University of Wyoming, Laramie, Wyoming
Gary L. Guymon, University of California, Irvine, California
Dorothy K. Hall, NASA Goddard Space Flight Center, Greenbelt, Maryland
Bernard Hallet, University of Washington, Seattle, Washington
Thomas D. Hamilton, U.S. Geological Survey, Anchorage, Alaska
Theodore A. Hammer, Dames & Moore, Portland, Oregon
Theodore A. Hammer, Dames & Moore, Portland, Oregon
William D. Harrison, University of Alaska, Fairbanks, Alaska
Richard K. Haugen, USA Cold Regions Research & Engineering Laboratory, Hanover, New Hampshire
F. Donald Haynes, USA Cold Regions Research & Engineering Laboratory, Hanover, New Hampshire

Beez Hazen, Northern Engineering & Scientific, Anchorage, Alaska
J. Alan Heginbottom, Geological Survey of Canada, Ottawa, Ontario, Canada
Christopher E. Heuer, Exxon Production Research Co., Houston, Texas
Ralph J. Hodek, Michigan Technological University, Houghton, Michigan
Pieter Hoekstra, Golden, Colorado
David M. Hopkins, University of Alaska, Fairbanks, Alaska
Theodore Hromadka, Mission Viejo, California
L.M. Jiji, City College of New York, New York, New York
Albert W. Johnson, San Diego State University, San Diego, California
Eric G. Johnson, Alaska Department of Transportation & Public Facilities, Fairbanks, Alaska
Koji Kawasaki, University of Alaska, Fairbanks, Alaska
William B. Krantz, University of Colorado, Boulder, Colorado
Raymond A. Kreig, Ray Kreig & Associates, Inc., Anchorage, Alaska
Thomas G. Krzewinski, Lakehead Testing Laboratory, Inc., Duluth, Minnesota
Arthur H. Lachenbruch, U.S. Geological Survey, Menlo Park, California
Daniel E. Lawson, USA Cold Regions Research & Engineering Laboratory, Hanover, New Hampshire
Y. Lee, University of Ottawa, Ottawa, Ontario, Canada
Robert M. Loesch, Texas A&M University, College Station, Texas
Erwin L. Long, Arctic Foundations, Inc., Anchorage, Alaska
Charles W. Lovell, Purdue University, West Lafayette, Indiana
Philip F. Low, Purdue University, West Lafayette, Indiana
Virgil J. Lunardini, USA Cold Regions Research & Engineering Laboratory, Hanover, New Hampshire
Robert J. Madison, U.S. Geological Survey, Anchorage, Alaska
Jerry L. Machemehl, Texas A&M University, College Station, Texas
Daniel W. Mageau, Hart Crowser, Inc., Seattle, Washington
C. James Martel, USA Cold Regions Research & Engineering Laboratory, Hanover, New Hampshire
Terry McFadden, University of Alaska, Fairbanks, Alaska
Malcolm Mellor, USA Cold Regions Research & Engineering Laboratory, Hanover, New Hampshire
Michael Metz, Geotec Services, Inc., Golden, Colorado
Scott Mills, L.R. Squire & Associates, Portland, Oregon
James A. Morrison, Woodward-Clyde Consultants, Solon, Ohio
Leslie A. Morrissey, Ames Research Center, Moffett Field, California
Yoshisuke Nakano, USA Cold Regions Research & Engineering Laboratory, Hanover, New Hampshire
Frederick L. Nelson, Rutgers University, New Brunswick, New Jersey
Gordon L. Nelson, U.S. Geological Survey, Anchorage, Alaska
Thomas E. Osterkamp, University of Alaska, Fairbanks, Alaska
Samuel I. Outcalt, University of Michigan, Ann Arbor, Michigan
Troy L. Pêwé, Arizona State University, Tempe, Arizona
Arvind Phukan, University of Alaska, Fairbanks, Alaska
Hervé Picard, Oregon State University, Corvallis, Oregon
Noel C. Potter Jr., Dickinson College, Carlisle, Pennsylvania
William F. Quinn, USA Cold Regions Research & Engineering Laboratory, Hanover, New Hampshire
Michael W. Reed, Geotechnical Resources, Inc., Portland, Oregon
Sherwood C. Reed, USA Cold Regions Research & Engineering Laboratory, Hanover, New Hampshire
William L. Ryan, Ott Water Engineers, Inc., Anchorage, Alaska
Hung Tao Shen, Clarkson University, Potsdam, New York
Robert S. Sletten, USA Cold Regions Research & Engineering Laboratory, Hanover, New Hampshire
W.E. Stewart, University of Missouri-Kansas City, Independence, Missouri
Rupert G. Tart Jr., Dames & Moore, Anchorage, Alaska
John C.F. Tedrow, Rutgers University, New Brunswick, New Jersey
Allen R. Tice, USA Cold Regions Research & Engineering Laboratory, Hanover, New Hampshire
Yau-Tang Tsao, Oregon State University, Corvallis, Oregon
Fiorenzo G. Ugolini, University of Washington, Seattle, Washington
Keith Van Cleve, University of Alaska, Fairbanks, Alaska
Ted S. Vinson, Oregon State University, Corvallis, Oregon
John D. Vitek, Oklamoma State University, Stillwater, Oklahoma
Joseph S. Walder, University of Washington, Seattle, Washington
Donald A. Walker, University of Colorado, Boulder, Colorado
James C. Walters, University of Northern Iowa, Cedar Falls, Iowa
A. Lincoln Washburn, University of Washington, Seattle, Washington
Joseph H. Westerhorstmann, Texas A&M University, College Station, Texas
Sidney E. White, Ohio State University, Columbus, Ohio
John R. Williams, U.S. Geological Survey, Menlo Park, California
John P. Zarling, University of Alaska, Fairbanks, Alaska

Papers by the following U.S. authors were not available for USC/IPA review by the deadline established to meet the Organizing Committee's publication schedule. They were, under special circumstances, submitted directly to the Norwegian Organizing Committee, reviewed and accepted for publication by this committee.

Manikian, V. and Machemehl, J.L.
Nidowicz, B., Bruggers, D. and Manikian, V.
Washburn, D.S. and Phukan, A.

REVIEWERS OF PAPERS

BELGIUM:
- D. Barsch, University of Heidelberg, Heidelberg, Germany
- B. Francou, Centre de Geomorphologie du C.N.R.S. de Caen, France
- E. Koster, University of Utrecht, Utrecht, The Netherlands
- A. Pissart, University of Liege

CHINA:
- Cheng Goudong (chairman)

FRANCE:
- J. Aguirre-Puente, Laboratoire D'Aerothermique du C.N.R.S.

GERMANY:
- H.L. Jessberger, Ruhr-Universitaet Bochum, Bochum
- J. Karte, German Research Foundation, Bonn
- L. King, Justus-Liebig Universitaet, Giessen
- H. Liedtke, Ruhr-Universitaet Bochum, Bochum

GREAT BRITAIN:
- C. Harris, University College Cardiff, Cardiff
- R. Kettle, University of Aston, Aston
- K. Richards, University of Cambridge, Cambridge
- D.E. Walling, University of Exeter, Exeter

ITALY:
- F. Dramis, Universita' de Camerino, Camerino

JAPAN:
- S. Kinosita, Hokkaido University, Sapporo
- Y. Ono, Hokkaido University, Sapporo

THE NETHERLANDS:
- H. Berendsen, University of Utrecht, Utrecht
- E. Koster, University of Utrecht, Utrecht
- J. Vandenberghe, Free University, Amsterdam

NORWAY:
- H.A. Aronsen, Statoil, Harstad
- O. Gregersen, Norwegian Geotechnical Institute, Oslo
- B. Instanes, Bjarne Instanes A/S, Consulting Engineers, Bergen
- D. Instanes, Bjarne Instanes A/S, Consulting Engineers, Bergen
- W. Martin, Norsk Hydro, Bergen
- A. Orheim, Statoil, Harstad
- O. Reistad, Store Norske Spitsbergen Kulkompani, Svalbard
- O. Salvigsen, The Norwegian Polar Research Institute, Oslo
- K. Senneset, The Norwegian Institute of Technology, Trondheim
- J.L. Sollid, University of Oslo, Oslo
- R. Sætersdal, Norsk Hydro, Oslo

POLAND:
- A. Jahn, University of Wroclaw, Wroclaw

SWEDEN:
- R. Nyberg, Naturgeografiska Institutionen, Lund
- A. Rapp, Naturgeografiska Institutionen, Lund
- H. Svensson, Geografisk Centralinstitut, København, Denmark

SWITZERLAND:
- F. Dramis, Universita' di Camerino, Camerino, Italy
- W. Haeberli, Versuchsanstalt für Wasserbau, Hydrologie und Glaziologie, ETH, Zürich
- L. King, Justus-Liebig Universitaet, Giessen, Germany
- J.P. Latridou, Centre de Gèomorphologie du C.N.R.S., Caen, France
- B.H. Luckman, The University of Western Ontario, London, UK
- A. Pancza, Universitè de Neuchatel, Neuchatel
- S. White, The Ohio State University, Colombus, Ohio, USA

USSR:
- N.A. Grave, Permafrost Institute Acad. Sc., Moscow
  Nekrassov, Institute of Northern Development Acad. Sc.
- A.I. Popov, Moscow State University, Moscow
- N.N. Romanovsky, Moscow State University, Moscow
- B.A. Saveliev, Academy of Sciences, Moscow
- K.F. Voitkovsky, Moscow State University, Moscow
- S.S. Vyalov, Moscow Engineering Construction Institute, Moscow

CONTENTS

VOLUME 1: SCIENCE

CLIMATE CHANGE AND GEOTHERMAL REGIME

REGIONAL PERMAFROST

PHYSICS AND CHEMISTRY OF FROZEN GROUND, FROST HEAVE MECHANISM

HYDROLOGY, ECOLOGY OF NATURAL AND DISTURBED AREAS

PERIGLACIAL PHENOMENA, GEOCRYOLOGY

VOLUME 2: ENGINEERING

SITE INVESTIGATIONS AND TERRAIN ANALYSES, SUBSEA PERMAFROST

GEOTECHNICAL PROPERTIES, FROST HEAVE PARAMETERS

GEOTECHNICAL ENGINEERING, PIPELINE CONSTRUCTION

ENGINEERING, -PETROLEUM, -MINING, -MUNICIPAL

PALEOCLIMATE AND PERMAFROST IN THE MACKENZIE DELTA

D. Allen[1], F. Michel[1] and A. Judge[2]

[1]Department of Earth Sciences, Carleton University, Ottawa, Canada
[2]Terrain Sciences, Geological Survey of Canada, Ottawa, Canada

SYNOPSIS Observed depths to the base of the ice-bearing permafrost (IBPF) in the Mackenzie Delta region range from over 700m to less than 100m. The wide variation in the thickness and distribution of permafrost primarily reflects trends in the Tertiary and Upper Cretaceous subsurface deltaic sediments and the complex past surface temperature history. A strong correlation with rock type, reflecting variations in thermal conductivity and the occurrence of permafrost, exists.

Paleoclimatic reconstructions for the Mackenzie Delta using numerical models of permafrost aggradation indicate that permafrost has aggraded since the end of the Sangamonian (75,000 years B.P.) when surface temperatures were approximately -1°C. An Early Wisconsinan and Late Wisconsinan surface temperature of about -18°C and a Mid-Wisconsinan rise to -8°C, similar to mean surface temperature today, are sufficient to account for the observed maximum permafrost thicknesses in the region.

INTRODUCTION

The Mackenzie Delta, N.W.T., located in the western Canadian Arctic, forms the terminus of the Mackenzie River at the Beaufort Sea coast (Figure 1). Its northern location coupled with the geomorphic characteristics of the surface and the thermal regime at depth have provided suitable conditions for the presence of permafrost which typically extends to depths of hundreds of metres.

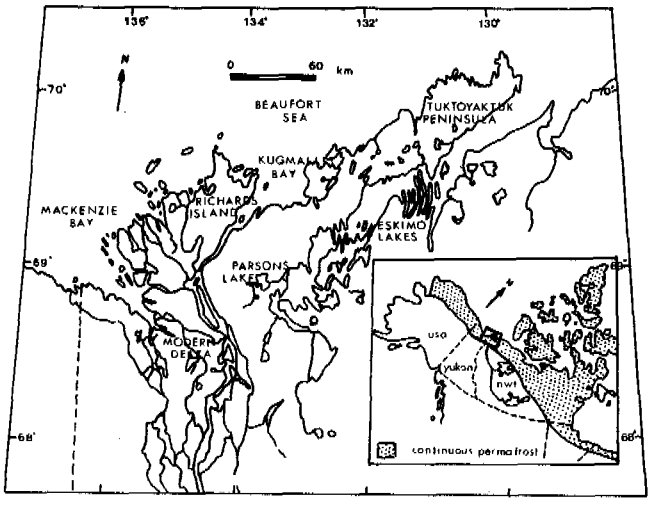

Figure 1 The Study Area

The surface topography and geomorphology of the Mackenzie Delta region, which is composed in part by modern sediments - forming the modern delta - and older deltaic and fluvial deposits - composing Richards Island and the Tuktoyaktuk Peninsula, has been described in detail by Mackay (1963). Details concerning the near-surface stratigraphy of the Beaufort Sea shelf as well as the occurrence of ice-bonded permafrost in the offshore region are reported by Hunter et al. (1976).

The Mackenzie Delta region is characterized by present ground surface temperatures which range from as low as -10°C to slightly below 0°C in the vicinity of the modern Mackenzie Delta and the offshore area (Young and Judge, 1985).

The Mackenzie Delta has in recent years been a center of northern scientific research and of hydrocarbon exploration. Increased drilling activity in both onshore and offshore regions has provided the means to map the occurrence of deep permafrost. Conventional logging surveys acquired during exploratory drilling for oil and gas have been successfully used to establish the depth to the base of the ice-bearing permafrost (IBPF) and hence permafrost thickness. This has been made possible by combining a knowledge of the physical properties of permafrost and a recognition of characteristic responses of conventional well-logging instruments to frozen ground (Osterkamp and Payne, 1981; Hatlelid and MacDonald, 1979; Hnatiuk and Randall, 1977). The measurement of subsurface temperatures in abandoned oil and gas wells - reported in the Canadian Geothermal Data

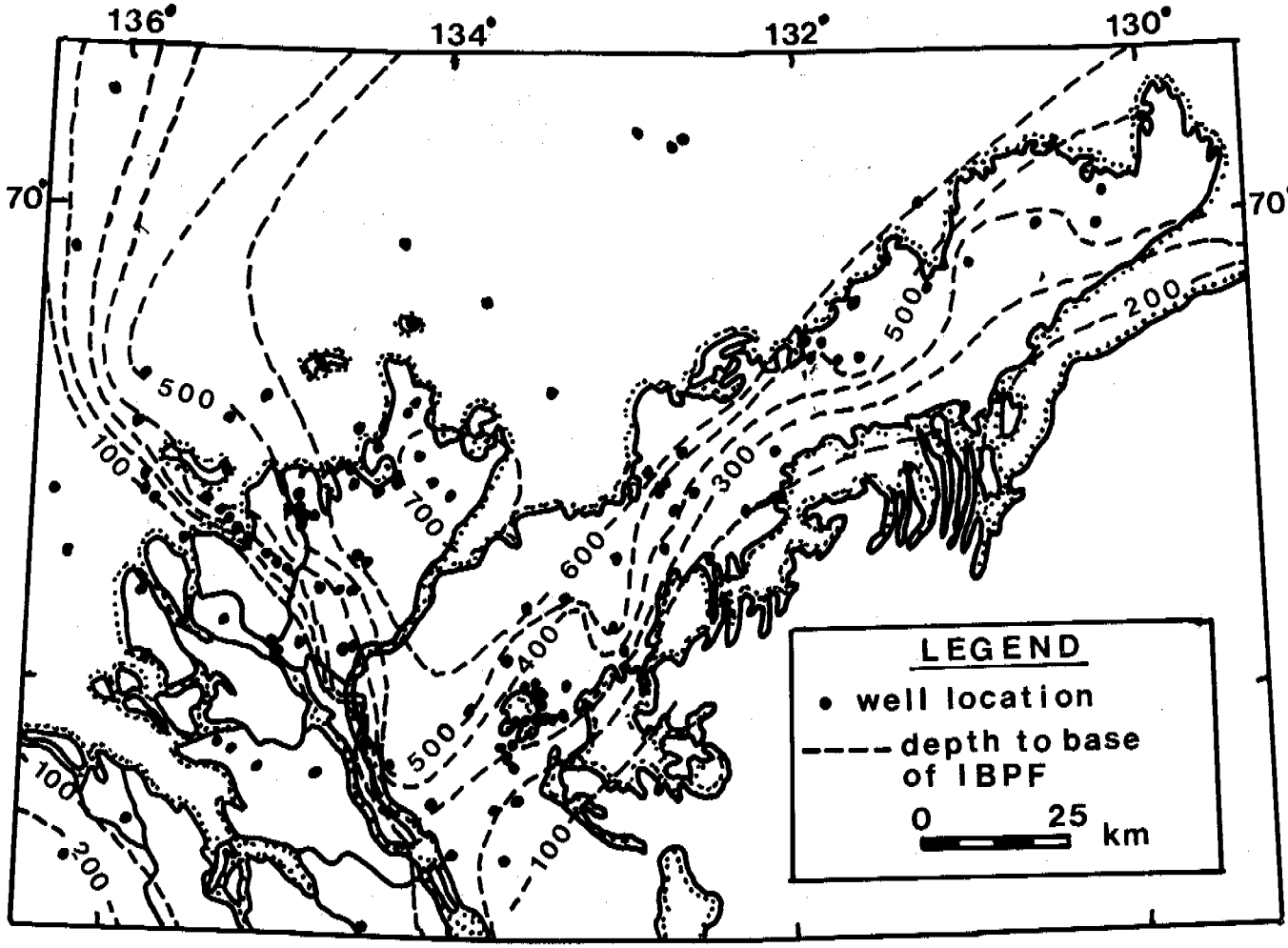

Figure 2 Depth to the Base of the Ice-Bearing Permafrost as Determined from Industry Well Logs and Government Temperature Surveys (After Judge, 1986)

Collections for Northern Wells (Taylor and Judge, 1977; Judge et al., 1979, 1981; Taylor et al., 1982) - and the measurement of sub-seabottom temperatures offshore (Weaver and Stewart, 1982) has constrained the interpretation of the log responses and given a general idea of the thermal regime at depth in the Mackenzie Delta.

The region is to a large extent underlain by thick continuous permafrost. Unfrozen sections occur in newly deposited unconsolidated sediments where the climate has just begun to impose its influence on the ground thermal regime. The ground may also be unfrozen beneath major rivers and lakes and in offshore areas which have remained submergent for a sufficient length of time. Although permafrost is absent or relatively thin beneath certain disturbed environments, it is in general very extensive and very deep - exceeding 700m in some localities.

This paper discusses the distribution of deep permafrost in the Mackenzie Delta region and details various aspects of the effects of lithology and surface temperature history on the regional permafrost regime. Through the use of relationships discussed, a paleo-climatic model is proposed to account for the observed permafrost regime.

DISTRIBUTION OF PERMAFROST

Figure 2 (after Judge, 1986) shows depths to the base of the ice-bearing permafrost in the Mackenzie Delta as determined from industry well logs and government temperature surveys for approximately 170 sites. The deepest permafrost (>700m) is observed beneath the northeastern portion of Richards Island. Permafrost thins very gradually further to the northeast but remains thick beneath much of the Beaufort Sea continental shelf. Towards the south, specifically in the Parsons Lake area, permafrost thins from over 600m to less than 200m.

Along the Tuktoyaktuk Peninsula, permafrost is generally thick but tends to thin in a southeasterly direction to depths of less than 200m in the vicinity of the Eskimo Lakes.

Beneath the western portion of Richards Island, there is a rapid decrease in the thickness of permafrost and beneath the modern Mackenzie Delta, permafrost is thin to absent. Towards the west and along the Yukon Coastal Plain, permafrost may again thicken, however, the sparcity of datapoints in this region is insufficient to confirm this. Lachenbruch et al. (1982) have reported thicknesses of up to 600m at Prudhoe Bay, Alaska.

Offshore, seismic and temperature observations in the Beaufort Sea (Neave et al., 1978; Hunter et al., 1976; Weaver and Stewart, 1982) indicate extensive ice-bonded sediments beneath much of the continental shelf. No evidence of ice-bonding has been found in offshore regions where water depths exceed 80m nor beneath most parts of Mackenzie Bay.

Where present, offshore permafrost is best described as relic degrading permafrost as its distribution is a reflection of the past emergent landscape and its present thickness has been arrived at primarily by gradual degradation due to the recent warming effect of submergence. It should be noted however, that there is evidence of aggradation at shallow depths in the seafloor - for example, pingo growth (Shearer et al., 1971).

LITHOLOGIC VARIATIONS

Late Cretaceous to Recent sedimentation was and still is dominated by deltaic processes. This resulted in a series of thick, northward prograding delta-complexes. Dixon (1986) identifies eleven sequences using reflection seismic profiles, well logs and, to a limited extent, outcrop data.

In general, the deltaic sediments are divisible into two main facies: mud-dominant and sand-dominant, corresponding to pro-delta and delta-plain depositional environments respectively. It is this variation in lithofacies which appears to be responsible for the observed regional variation in permafrost distribution. In particular, there exists a strong correlation between the upper sand-gravel unit of the Pliocene-Pleistocene Iperk sequence and the occurrence of deep permafrost (Allen et al., in press). In areas where this sequence is thick, the depth to the base of the permafrost is significantly greater than in areas where this sequence is thin to absent. In addition, where the Iperk sequence is underlain by the sand-dominant Kugmallit sequence, permafrost attains its greatest depths - in excess of 700m in some areas.

The observed correlation between lithology and the extent of permafrost is best described in terms of variations in thermal conductivity. Using all of the available temperature profiles (Canadian Geothermal Data Collections) in conjunction with the well lithologies, a number of thermal gradients were estimated for each of the various sequences. These estimates were then averaged to give a frozen and unfrozen thermal gradient for each sequence. If a constant and uniform heat flow of 60mWm^{-2} is assumed for the entire region - an assumption supported by the consistency of heat flow values calculated for various locations along the Alaskan arctic coast (Lachenbruch et al., 1982) and the uniformity of deep temperature gradients across the Mackenzie Delta region (Judge, 1986) - then estimates of the frozen and unfrozen thermal conductivities may be assigned to each sequence. The resulting thermal conductivity values are provided in Table 1.

TABLE 1

SEQUENCE	CONDUCTIVITY (W m^{-1}K^{-1})		LITHOLOGY
IPERK	mean	4.5 (f)	sand and gravel
	s.d.	1.6	
KUGMALLIT		4.6 (f)	sand and gravel
		1.8	
REINDEER		3.4 (f)	sandstone
		0.9	
		2.1 (u)	
		0.5	
RICHARDS		2.4* (u)	mudstone
		0.6	

* Conductivity for frozen material will be similar due to low ice content.
(f) frozen, (u) unfrozen

On the basis of the lithologic variations, the region was divided into five sub-regions, each having similar subsurface lithologic profiles. These include 1) the Kugmallit Bay region, which encompases the northern portion of Richards Island and Kugmallit Bay, 2) the Tuktoyaktuk Peninsula, 3) the modern Mackenzie Delta, 4) the western portion of Richards Island and 5) the offshore Beaufort shelf region. Each of these sub-regions was assigned a single value for thermal conductivity, which in most cases corresponded to the value assigned to the dominant sequence, a porosity value of either 6 or 30 percent depending on whether the sequence was mud- or sand-dominant respectively, and a diffusivity, which for all sequences was estimated at 0.015cm^{2}sec^{-1}. Variations in diffusivity were incorporated into the models and were observed to have little to no effect on the permafrost occurrence.

SURFACE TEMPERATURE HISTORY

Three major factors which affect the surface temperature history and which are incorporated into the paleoclimatic models include: surface temperature, Wisconsinan glacial cover, and the submergence-emergence history of the region.

Surface Temperature

Estimates of the surface temperatures and their fluctuation through time during the Late

Pleistocene are based on information contained in 1) oxygen isotope records for the Greenland ice cap (Dansgaard et al., 1971) and 2) amino acid surface temperature estimates for the Beaufort Sea Continental Shelf (Brigham and Miller, 1983; Smith, 1986). An average temperature of -9°C (after Young and Judge, 1985) represents current surface conditions in emergent areas of the Mackenzie Delta.

It should be stressed that there still exists considerable debate as to the duration of particular temperature intervals, however, the models presented here do not accurately distinguish variations of 2000 years or less.

Wisconsinan Glacial Cover

The glacial extent and duration in the Mackenzie Delta during the Early and Late Wisconsinan remains questionable despite efforts made by various researchers to conclusively define the limits of glaciation in the region. Those limits proposed by Rampton (1982) are utilized in the following analysis.

The majority of the Mackenzie Delta was glaciated during the Early Wisconsinan and a duration of glacial cover of 5000 years is proposed in our model. During this time, areas covered by ice would have experienced surface temperatures on the order of 0°C, as the presence of glacial striations in the region imply a temperate or wet-base glacier with basal temperatures at or around the pressure melting point.

The Late Wisconsinan ice advance appears to have affected only a small portion of the region and is therefore not included in the paleoclimatic reconstructions presented herein.

Finally, the models do not distinguish any glacial readvances which may have occurred during the latter part of the Early Wisconsinan. For example, the Sabine Phase, proposed by Rampton (1982) had minimal effect on the permafrost aggradational history, probably because it was of short duration.

Submergence-Emergence History

Fluctuations of sea level during the Late Pleistocene and Holocene have had a significant effect on mean annual ground temperature. The relative sea level curve for the Canadian Beaufort Shelf, proposed by Hill and Blasco (1986) indicates a 140m rise in sea level since the Mid-Wisconsinan (27,000 years B.P.). Paleoclimatic models for the near-offshore region incorporate a rise in temperature to 1.8°C associated with submergence over the past 10,000 years, while models for submerged areas of the modern Mackenzie Delta use an estimated bottom water temperature of 1°C (Burgess, 1977).

PALEOCLIMATIC MODELS

A paleoclimatic reconstruction for the Late Pleistocene is carried out by modelling the effect of past climatic variations on the base of the permafrost in a uniform material where phase change conditions at the frozen-unfrozen boundary are taken into consideration. Lachenbruch et al. (1982) derived the expressions used to estimate the rate of upward thinning of permafrost which are presented in their final form below. It is assumed that the unfrozen region below remains in a quasi steady-state during the process and, consequently, the heat supplied to the base of the permafrost at Z(t) remains constant and equal to the geothermal flux Q. The heat balance at the base then requires:

$$-LN(dZ/dt) = Q-K\ dT/dZ - K_f\ (Tz-T\emptyset)/Z(t) \qquad (1)$$

where L is the latent heat of fusion, N is the porosity of the material, dZ/dt is the rate of upward thinning (or equally the rate of downward aggrading), K_f is the frozen thermal conductivity, dT/dZ is the geothermal gradient, Tz is the temperature at the base of the permafrost (taken as 0°C) and T$\emptyset$ is the initial surface temperature.

For values of $t>\lambda$ where $\lambda = Z\ /4\alpha$ and α is the thermal diffusivity of the frozen material, the derivative on the right in (1) is small and may be excluded. As the base of the permafrost varies through the process, so will the value of the time constant (λ). Therefore, in order to comply with the above conditions, the time interval must vary accordingly. In the case of aggrading permafrost, an assumption is made that the transient behaviour to surface cooling results in negligible permafrost aggradation for values of $t=\lambda$. A detailed discussion of the assumptions and theory is given in Allen (in preparation).

The change in the depth of the permafrost (dZ) is calculated as a result of a step increase or decrease in surface temperature acting over a time interval (dt). The boundary conditions include an estimate of the initial steady-state permafrost depth which is determined from the initial surface temperature, the regional heat flow and the thermal conductivity. A major assumption in the modelling is that any Illinoian permafrost thawed completely during the Sangamonian, hence establishing the initial subsurface conditions.

Modelling results for three of the five sub-regions are provided in Figure 3. The first graph represents the surface temperature history applied to the sub-regions below. It should be noted that temperatures represent mean annual surface temperatures which may be of the order of 2°C warmer than mean annual air temperature (MAAT). The variations in the base of the permafrost (0°C isotherm), as a result of successive surface temperature disturbances, are shown graphically.

Onshore regions are assumed to have remained emergent from the Beaufort Sea during the Late Pleistocene. Surface temperatures in the Mackenzie Delta during the Early and Late Wisconsinan are estimated at -18°C which are sufficient to account for the observed permafrost thicknesses in the region. This estimate agrees with that proposed by Brigham

and Miller (1983) and Smith (1986) for the Alaskan Beaufort shelf. A mid-Wisconsinan rise in temperature to approximately -8°C is also proposed. Holocene temperatures are assumed to have remained relatively constant at -10°C during the past 15,000 years.

In all cases, the final calculated permafrost thickness compares well with the observed average IBPF base in the region. Again, it should be noted that the discrepancy which exists between the calculated permafrost base (0°C isotherm) and the depth to the base of the IBPF is not taken into consideration.

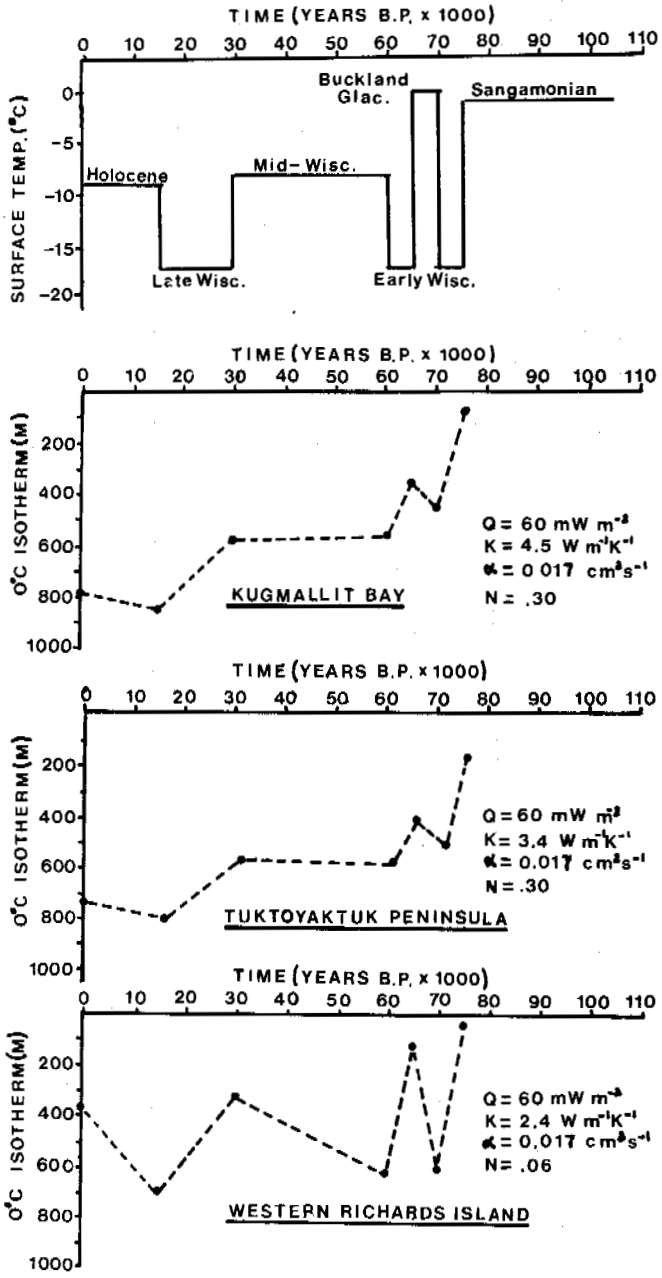

Figure 3 Surface Temperature History Applied to Onshore Regions. Modelling Results Show Variation in Permafrost Base beneath Kugmallit Bay, the Tuktoyaktuk Peninsula and Western Richards Island

CONCLUSIONS

In summary, a number of conclusions may be drawn from the analysis of the permafrost regime in the Mackenzie Delta. These include: 1) the depth to the base of the ice-bearing permafrost varies significantly throughout the region, 2) there exists a strong correlation between the Pliocene-Pleistocene Iperk sequence and the occurrence of deep permafrost, 3) Early and Late Wisconsinan surface temperatures of -18°C are required to account for the observed thicknesses of permafrost in the region, 4) a Mid-Wisconsinan rise in temperature to -8°C is proposed, 5) an Early Wisconsinan ice sheet covered the region for at least 5000 years and finally, 6) present permafrost conditions indicate that a Late Wisconsinan ice advance is unlikely to have been extensive.

ACKNOWLEDGEMENTS

This paper is based on results reported in the senior author's M.Sc. Thesis, Department of Earth Sciences, Carleton University, Ottawa, Canada. The research was originally proposed by Dr. Alan Judge, Geological Survey of Canada and the permafrost database was made available by the former Earth Physics Branch, E.M.R., Canada. A special thanks is extended to Dr. Jim Dixon at the Institute of Sedimentary and Petroleum Geology, Calgary for his assistance at obtaining information concerning well lithologies, and to Vic Allen at the Geological Survey of Canada, whose helpful suggestions with the computer programming were invaluable.

REFERENCES

Allen, D.M. (1988) The permafrost regime in the Mackenzie Delta-Beaufort Sea region, N.W.T. and its paleoclimatic implications (in preparation). M.Sc. Thesis, Department of Earth Sciences, Carleton University, Ottawa.

Allen, D., Michel, F., and Judge, A. (1988) The permafrost regime in the Mackenzie Delta-Beaufort Sea region, N.W.T. and its significance to the Paleoclimatic History (in press). Presented at the XII International Congress, International Union for Quaternary Research, Ottawa, Canada, July 1987.

Brigham, J.K. and Miller, G.H. (1983) Paleotemperature estimates of the Alaskan Arctic Coastal Plain during the last 125,000 years. In Proceedings of the Fourth International Conference on Permafrost, Fairbanks, Alaska, National Academy Press, Washington, D.C.

Burgess, M. (1977) Shallow thermal studies, Shallow Bay, Mackenzie Delta, Internal Report No. 80-10, Earth Physics Branch, E.M.R., 27 pp.

Dansgaard, W., Johnsen, S.J., Clausen, H.B. and Langway, C.C.Jr. (1971) Climatic record revealed by the Camp Century core ice. In, The Late Cenozoic Glacial Ages, Ed. Turkian, Yale University Press, p. 37-56.

Dixon, J. (1986) Cretaceous to Pleistocene Stratigraphy and Paleogeography, Northern Yukon and Northwestern District of Mackenzie. Bulletin of Canadian Petroleum Geology, 34,1, p. 49-70.

Hatlelid, W.G. and MacDonald, J.R. (1979) Permafrost determination by seismic velocity analysis. In Proceedings of Symposium on Permafrost Field Methods and Permafrost Geophysics, Assoc. Comm. Geotechnical Research, National Research Council Technical Memo 124, p. 146-147.

Hill, P.R. and Blasco, S.M. (1986) Implications of a Beaufort Sea relative sea-level curve to Arctic Mid and Late Wisconsinan Glacial Events. In, Correlation of Quaternary Deposits and Events around the Margin of the Beaufort Sea: Contributions from a Joint Canadian-American Workshop, April, 1984, J.A. Heginbottom and J-S. Vincent (Eds.), Geological Survey of Canada, Open File Report 1237, 60 pp.

Hnatiuk, J. and Randall, A.G. (1977) Determination of permafrost thickness in wells in northern Canada. Canadian Journal of Earth Sciences, 14, p.375-383.

Hunter, J.A.M., Judge, A.S., MacAulay, H.A. Good, R.L., Gagne, R.M. and Burns, R.A. (1976) Permafrost and sub-seabottom materials in the southern Beaufort Sea. Technical Report No. 22, Beaufort Sea Project, Department of the Environment, 174 pp.

Judge, A.S., Taylor, A.E. and Burgess, M. (1979) Canadian Geothermal Data Collection - Northern Wells, 1977-78. Geothermal Studies Number 11, Earth Physics Branch, E.M.R., 188 pp.

Judge, A.S., Taylor, A.E., Burgess, M. and Allen, V.S. (1981) Canadian Geothermal Data Collection - Northern Wells, 1978-80. Geothermal Series Number 12, Earth Physics Branch, E.M.R., 190 pp.

Judge, A.S. (1986) Permafrost distribution and the Quaternary history of the Mackenzie-Beaufort region: A geothermal perspective. In Correlation of Quaternary Deposits and Events Around the Margin of the Beaufort Sea: Contributions from a Joint Canadian-American Workshop, April, 1984, J.A. Heginbottom and J-S. Vincent (Eds.), Geological Survey of Canada, Open File Report 1237, 60 pp.

Lachenbruch, A.H., Sass, J.H., Marshall, B.V. and Moses, T.H. Jr. (1982) Permafrost, heat flow and the geothermal regime at Prudhoe Bay, Alaska. Journal of Geophysical Research, 87, B11, p. 9301-9316.

Mackay, J.R. (1963) The Mackenzie Delta area, Northwest Territories, Canada: Department of Mines and Technical Surveys, Geographical Branch, Memoir No. 8, 202 pp.

Neave, K.G., Judge, A.S., Hunter, J.A. and MacAulay, H.A. (1978) Offshore permafrost distribution in the Beaufort Sea as determined from temperature and seismic observations. In, Current Research, Part C, Geological Survey of Canada, Paper 78-1C, p. 13-18.

Osterkamp, T.E. and Payne, M.W. (1981) Estimates of permafrost thickness from well logs in northern Alaska. In Cold Regions Science and Technology, 5, p. 13-27.

Rampton, V.N. (1982) Quaternary geology of the Yukon Coastal Plain. Geological Survey of Canada, Bulletin 317, 49 pp.

Shearer, J.M., Macnab, R.F., Pelletier, B.R. and Smith, T.B. (1971) Submarine pingoes in the Beaufort Sea, Science, 175, p. 816-818.

Smith, P.A. (1986) The Late-Pleistocene - Holocene stratigraphic record, Canning River Delta region, Northern Alaska. In, Correlation of Quaternary Deposits and Events Around the Margin of the Beaufort Sea: Contributions from a Joint Canadian-American Workshop, April, 1984, J.A. Heginbottom and J-S. Vincent (Eds.), Geological Survey of Canada, Open File Report 1237, 60 pp.

Taylor, A.E. and Judge, A.S. (1977) Canadian Geothermal Data Collection - Northern Wells, 1976-77. Geothermal Series Number 10, Earth Physics Branch E.M.R., 194 pp.

Taylor, A.E., Burgess, M., Judge, A.S. and Allen, V.S. (1982) Canadian Geothermal Data Collection - Northern Wells, 1981. Geothermal Series Number 13, Earth Physics Branch, E.M.R., 153 pp.

Weaver, J.S. and Stewart, J.M. (1982) In situ hydrates under the Beaufort Sea shelf. In, Proceedings of Fourth Canadian Permafrost Conference, Calgary, Alberta, March 2-6, 1981. Ed. H.M. French, National Research Council of Canada, Ottawa, Ontario, p. 312-319.

Young, S.E. and Judge, A.S. (1985) A ground temperature data collection for northern Canada. Presented at the McGill Workshop on Climate and Thermal Regimes in Northern Canada, November 8, 1985, 17 pp.

METEOROLOGICAL CONDITIONS' INFLUENCE ON THE PERMAFROST GROUND IN SVEAGRUVA, SPITSBERGEN

S. Bakkehøi and C. Bandis

Norwegian Geotechnical Institute, Oslo, Norway

SYNOPSIS Recordings of meteorological data and temperatures in the ground at Sveagruva, Spitsbergen, have been taken since 1977. Based on the collected data, this paper gives a presentation of the time dependence of the isotherms in the ground. In addition, measured heat fluxes 5 cm below the surface are compared with other meteorological data, taking into account the composition of the Sveagruva clay and estimations of water content and salinity. The influence of the insulating effect of a snow cover is also described, and the snow cover's change of the albedo and the influence on the radiation conditions are investigated. Finally, thawing depths are compared with the energy exchange in the top of the soil and the snow-cover.

INTRODUCTION

In order to obtain information on the climatic conditions and the thermal effects at Svalbard, the Norwegian Committee on Permafrost has established a permafrost research station at Sveagruva, Spitsbergen (77° 54'N, 16° 41'E) which was completed in June 1978 (Gregersen, 1980, Bakkehøi, 1982), see map Fig.1.

Data collection at the permafrost station is made automatically, with measurements taken every hour on three separate Aanderaa data-loggers. Measurements are taken of air temperature, wind force and wind direction, ground temperature down to 8 m below the soil surface and down to 2.0 m below a concrete surface of 2 m x 2 m and a thickness of 5 cm, incoming and outgoing radiation, global radiation, heat flux in the ground and humidity of the air. In addition, a few manual observations are taken of snow depth and snow density, thawing depth in the summer and water content of the topsoil. Some of the observations from the permafrost station at Sveagruva have been presented by Bakkehøi and Bandis (1987), and it is intended to give a further analysis of the data in this paper. While observations have been made for a period of ten years in total, only those records for the first eight years have been analyzed.

DEVELOPMENT OF THAWING DEPTH

One of the basic concerns of foundation engineering in permafrost areas is the penetration of the thawing depth, and its influence on construction works. Typically buildings are founded in one of two ways, either on pillars or directly on the ground. If a building is constructed on pillars, the radiation balance is changed and the lack of snow cover during the winter will greatly improve the cooling of the ground; if a building is placed directly on the ground, good isolation and maybe freezing of the underground is necessary.

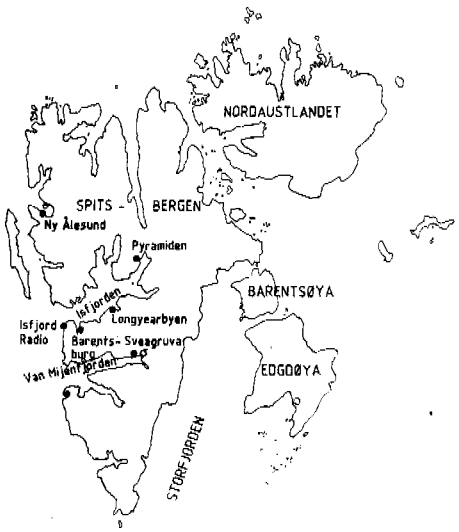

Fig. 1 Map of Svalbard showing location of Sveagruva

As a first step to solve these problems, it is of major interest to investigate what happens in an undisturbed area. Recordings of temperature data down to 8 m are available from the station at Sveagruva, and a time-depth isotherm chart has been plotted out for a tundra area, see Fig. 2 and 3. Data are presented for two periods, June 1979 to December 1980 and June 1984 to

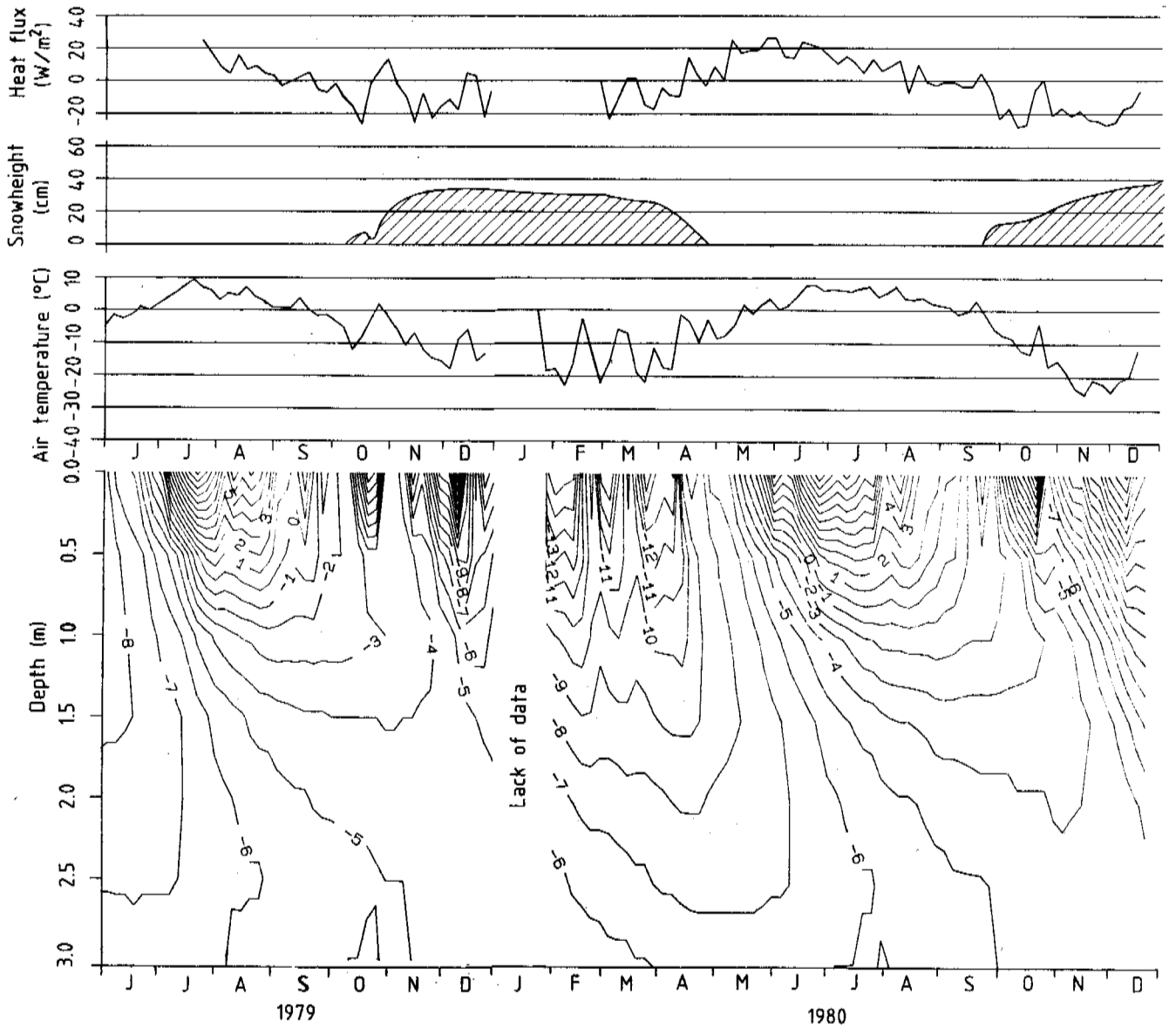

Fig. 2 Isotherm chart for the tundra area from June 1979 to December 1980. Air temperature, snow depth and heat flux through the top layer is also presented.

December 1985. From the time series of these isotherms it is easy to follow the thawing in summer and freezing in the winter period. The tundra area around the field station consists of marine clay with a mean salinity of 30 g per litre; the salinity of the pore water is as high as 60 g per litre and in the ice lences we will find fresh water. The water content below the active layer is approximately 50 percent by weight of the total dry clay content (Finborud and Berggren, 1980), which, given the salinity implies that there is no distinct freezing level, rather a continous change of hardness from 0°C to colder depths. A subjective judgement would classify the clay as frozen with a temperature below -4°C. Thawing depth is to a great extent dependent on the water content and salinity of the soil. Bakkehøi and Bandis (1987) show that the latent heat when freezing or melting is much higher than the energy needed to cool or heat the soil. Clay and sand have different thermodynamics, since in frozen sand the thermal conductivity is approximately twice as high as in clay (Ø. Johansen et al., 1976). The heat capacity for clay is therefore much higher than for sand, especially at temperatures below freezing.

As a result of this, the thawing depth in a gravel fill (a road close to the research field,

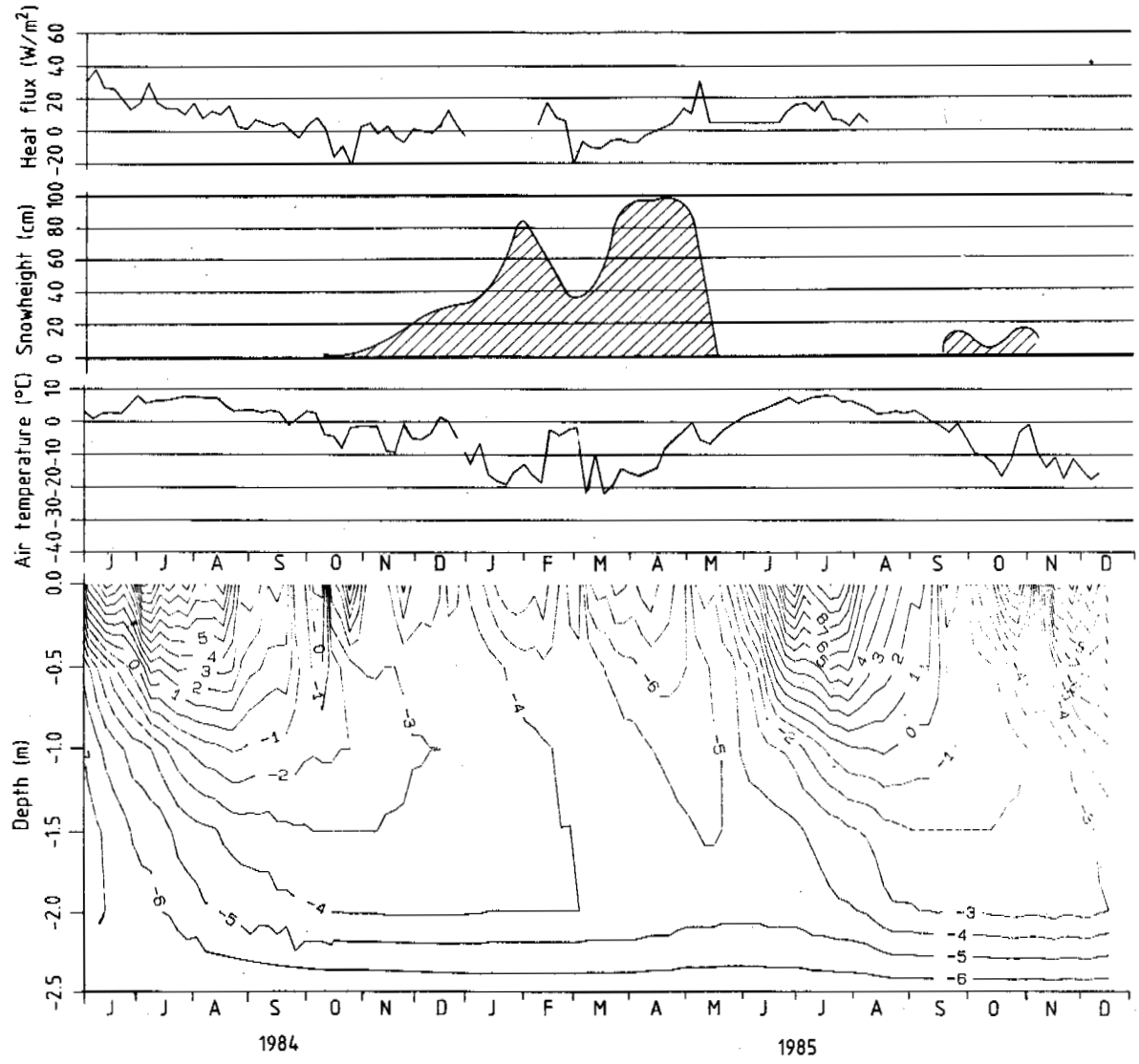

Fig. 3 Isotherm chart for the tundra area from June 1984 to December 1985. Air temperature, snow depth and heat flux through the top layer is also presented.

Table 1. Observed thawing and freezing indexes for air, soil and concrete compared with maximum depth of 0°C in soil, under concrete and in a gravel fill at Sveagruva station together with snow heights and snow covered periods.

YEAR Summer	Winter	T(air) 10^3 hK	T(soil) 10^3 hK	T(concr.) 10^3 hK	F(air) 10^3 hK	F(soil) 10^3 hK	F(concr.) 10^3 hK	Depth of 0°C in soil (cm)	Depth of 0° below concr.(cm)	Depth of 0°C in gravel fill (cm)	Max snow height (cm)	Mean snow height (cm)	Days snow covered
1978		10.6	15.8	13.7				78	75				
1979	78/79	9.3	11.3	10.7	85.5	60.2	68.4	74	71	128	65	30	275
1980	79/80	11.4	15.9	15.7	62.4	59.2	60.4	80	80	125	28	20	200
1981	80/81	9.4	14.1	13.9	90.8	69.7	77.2	80	77	134	45	30	225
1982	81/82	6.9	13.1	12.3	70.4	54.2	61.9	76	73	143	40	30	215
1983	82/83	10.7		15.8	66.6	48.6	51.2		88	196	40	30	225
1984	83/84	14.2	17.6	16.3	66.6	66.9	56.5	89		156	50	35	250
1985	84/85	12.1	16.8		47.7	30.9		104		170	78	50	200
1986	85/86									189	75	40	250
1987	86/87									210	42	25	190

T = Thawing index (hours · mean temperature above 0°C)
F = Freezing index (hours · mean temperature below 0°C)

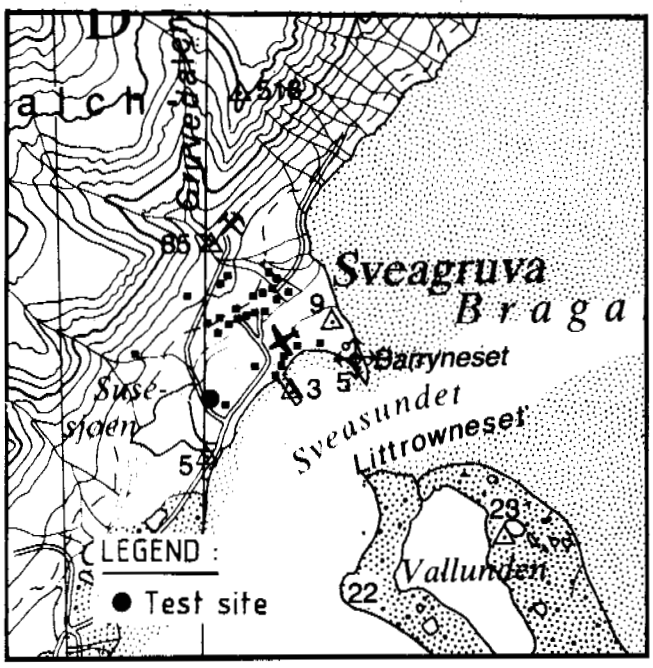

Fig. 4 Detail map showing the observation sites at Sveagruva, Spitsbergen

see Fig. 4) goes much deeper than in the tundra field. The gravel fill is placed above the groundwater level, which implies a low water content. The deepest level of the 0°C each summer is calculated from the field measurements, and is presented in Table 1 for the gravel fill, the tundra field and the ground below a concrete surface. To allow a comparison, the thawing index T is also presented for the same periods (Bakkehøi and Bandis, 1987). The freezing index for the preceding winter is also calculated and presented in the table, together with maximum and mean snow height and the length of the snow covered period.

THAWING DEPTHS RELATIVE TO SNOW COVER, AND THE FREEZING AND THAWING INDICES

A statistical treatment of the data was performed to establish any dependence among the parameters. The thawing depth has a good correlation with the thawing index, giving a correlation coefficient of approximately 0.8. Inclusion of the freezing index and snow cover increases the correlation coefficient to r=0.98, though the sample only consists of seven years of observations. The correlation between the freezing index for the preceding winter is -0.8, while the correlation coefficient between mean snow depth and thawing depth for the tundra field is 0.8. The correlation coefficient between the snow depth and the thawing depth below the concrete field is 0.7.

For the case of the gravel fill the snow is always removed. This means that observations from this place are not comparable to the tundra and concrete fields. The highest correlation of 0.7 is achieved between the freezing index and the thawing depth. Between the thawing index and the thawing depth the correlation coefficient is 0.55, while a regression equation between thawing index, freezing index and thawing depth gives no significant increase in the correlation coefficient.

For the tundra and concrete field the correlation between thawing depth and thawing index is positive, while the correlation between thawing depth and freezing index is negative as expected. Therefore, low temperatures in winter imply less thawing throughout the coming summer. The high positive correlation to the snow depth also confirms the great importance of the snow cover as an insulating layer.

As seen in Table 1, there appears to be a tendency for the thawing depth of the gravel fill to increase with time regardless of the thawing and freezing indices. The gravel fill itself is reacting quickly to the transmitted energy, yet the surrounding area might be changed in the winter period, because the road is acting as a snow fence and collecting more snow than usual on both sides. This can give a long term effect so far as heating of the surrounding area is concerned. Another explanation may of course be errors in the measurements, but compared with other readings this does not appear reasonable. The gravel fill is placed normal to the prevailing winds, which are parallel to the direction of the fiord, and for such fill placed on tundra heat exchange due to wind may be quite significant. This has not yet been investigated.

STATISTICAL PROBABILITY OF THAWING DEPTHS

With the data available it is possible to calculate a regression equation which includes snowcover, and freezing and thawing indices to determine thawing depths. This offers the possibility of extending the time series of calculated thawing depths using ordinary meteorological data from a longer observation period. The available data for thawing depths is treated statistically and plotted on Gaussion normal cumulative distribution paper, see Fig. 5. The two curves of thawing depth in the tundra and the concrete field are very well related. The seven years of observations imply that the result must be treated with care; the results show that the mean yearly depth is approximately 80 cm; the 50 year return period value seems to be approximately 1 m depth; taking the 1 in 10 year period as a mean, the 0°C isotherm will not pass 70 cm.

Thawing depths for the gravel fill are plotted on the figure and show a wider distribution of the depths, from 120 cm to 210 cm. As mentioned before, this behaviour may be a result of a time dependant increase of temperature in the gravel fill.

THAWING DEPTHS IN RELATION TO SEASONAL VARIATIONS

Fig. 3 and 4 show the time development of the thawing depths in the summers of 1980 and 1985. The thawing depths were 80 cm and 104 cm respectively in the tundra field, while the thawing indices for air were $11.4 \cdot 10^3$ h·K and $12.1 \cdot 10^3$ h·K. The thawing indexes for the top layer in the tundra field were $15.9 \cdot 10^3$ h·K and $16.8 \cdot 10^3$ hK which gives an n-factor

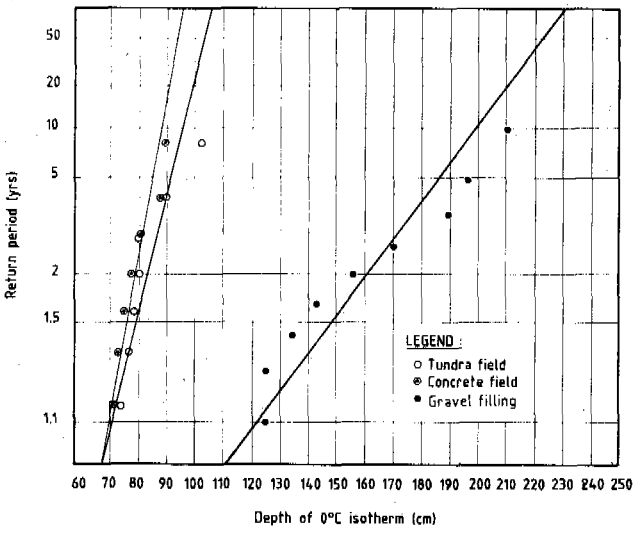

Fig. 5 Return periods for thawing depths for a tundra field, a concrete field and a gravel filling

(T(soil)/T(air)) equal to 1.4 for both summers. This implies that the radiation conditions of both summers are well correlated. The thawing index for the tundra field in 1980 can statistically be expected each third summer, while the 1985 value gives an expection to be exceeded each fourth summer (see Bakkehøi and Bandis, 1987). The position of the 0°C-isotherm in 1980 can be expected to be exceeded approximately each second year, which is in good agreement with the thawing index. However, the 104 cm reach of the 0°C-isotherm in 1985 could be expected to be exceeded only once in a twenty year period. The freezing indices, indicate that the low freezing index for the tundra field in the winter 1984/85 is most significant, since the freezing index of the air was 50% higher. This is explained by the great depth of snow during that winter; looking at the heat flux through the top layer, heating is even recorded in some periods in January and February. When the summer started, the soil was almost isothermal -5°C from the top and down to 2 m, while in 1980 the mean temperature in the soil was two to three degreees colder. The relationship between the freezing indices of air, tundra field and snow height can be expressed using a regression equation

$$F(\text{tundra}) = 0.63F(\text{air}) - 0.29S_x + 26$$

where S_x is the numerical value of maximum snow height (in cm) during the winter and the unit for the freezing index is $10^3 \cdot hK$. The correlation coefficient is 0.86; the standard deviation of the residuals is $6.2 \cdot 10^3$ h·K. This equation allows calculation of the freezing index with a high degree of accuracy when the air temperatures and snow heights are known. It also shows the importance of snow cover, since a large snow height causes a significant reduction in the freezing index. This equation should be applicable in other permafrost areas with the same type of surface.

CONCLUSIONS

Data from the permafrost station at Sveagruva have been available since 1978. The data have been used to plot time-series of isotherms in the ground, and thereby study the temperature development in a marine clay with high water content and salinity. The thawing depth, or more correctly the 0°C isotherms penetration in the soil, has been treated statistically both below a tundra field and below a concrete layer. Return periods have been given, and using the same method it has been possible to give return periods for depths of other isotherms.

Thawing depths are to a great extent dependent on the conditions of the preceeding winter, and not only the thawing indices in the summer. The importance of snow cover during the winter is shown, and a relationship between freezing index in air and in the soil, together with the snow height is given.

Data from Sveagruva clearly show that the application of meteorological data must be made with care to foundation engineering in permafrost areas, specially in areas with clays. The recording of data will continue in 1988 giving ten years of records; it is not yet decided if the recordings will continue in 1989.

ACKNOWLEDGEMENTS

The permafrost station at Sveagruva was built with financial support from The Royal Norwegian Council for Scientific and Industrial Research (NTNF) which established the Norwegian Committee on Permafrost. The Committee was responsible for the operation of the station until 1984 when NGI continued the data collection. Store Norske Spitsbergen Kulkompani A/S has also given financial support and practical assistance; the field work at Sveagruva has been carried out by engineers at the power station.

REFERENCES

Bakkehøi, S. (1982) Datainnsamling på permafroststasjonen i Svea, Svalbard. Frost i jord nr. 24, Oslo.

Bakkehøi, S. and Bandis, C. (1987) A preliminary analysis of climatic data from the permafost station at Svea, Spitsbergen. Frost i jord nr. 26, Oslo.

Finborud, L. and Berggren, A. (1980) Laboratorieundersøkelser av permafrostleire fra Svea og en kunstig frosset Trondheimsleire. Rapport til NTNF, NTH, Trondheim.

Gregersen, O.S. (1980) Permafrost Engineering Research on Spitsbergen, Frost i jord nr. 21, Oslo.

Johansen, Ø. et al. (1976) Varmetekniske egenskaper av jord og bygningsmaterialer, Frost i jord nr. 17, Oslo

THERMAL CURRENTS OF ACTIVE LAYER IN HORNSUND AREA

H. Chmal, J. Klementowski and K. Migala

Geographical Institute, University of Wroclaw, Poland

SYNOPSIS

The report contains the results of ground temperature measurements to a depth of 3 m in the vicinity of the Polish Polar Station in Hornsund, South Spitsbergen, in the period of September 1986 - June 1987, as well as the results of measurements of the thawing depth of the active permafrost layer on slopes and on the strandflat. The freezing and thawing processes of the active layer have been characterized in relation to an analysis of the temperature changes of air and snow cover. The temperature of the permafrost table has also been determined.

INTRODUCTION

Werenskiold (1922) was the first to calculate the depth of permafrost in the Hornsund region. He maintained that continuous permafrost should stretch in shallow bays some 200 m off the shoreline. Since 1957, the programme of over a dozen Polish expeditions to the Hornsund area has included geomorphological studies of periglacial processes (Fig. 1). A part of those investigations concerned the thawing rate of the ground and its thermal currents (Czeppe 1966, Baranowski 1968, Jahn 1982, Grzes 1985).

Due to those studies, the principal features of the active layer were identified, though the measurements did not exceed a depth of 160 cm. At present, at the Polish Polar Station in Hornsund a programme is being carried out which includes whole-year, systematic measurements of ground temperature to a depth of 3 m, vertical ground movements, cryogenic pressures as well as the thawing and freezing rates of the active layer along the profiles running from the mountain ridges to the shoreline. In this report the measurement results of the period from September 1986 to September 1987 are presented.

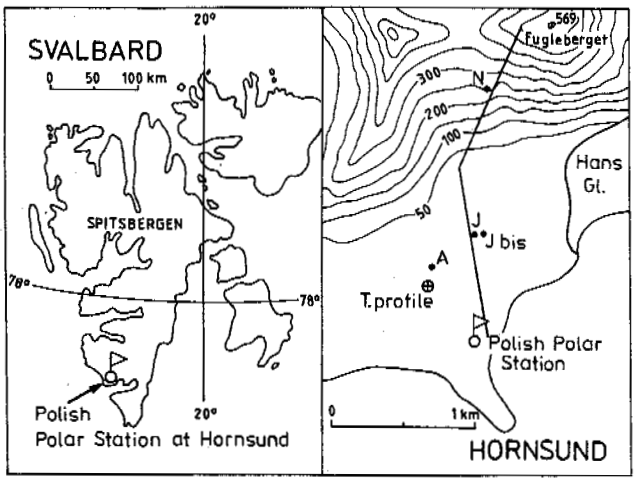

Fig. 1 Location map. The site of temerature measurements of the ground was signed as well as the line of thawing control and also the selected positions of Danilin sounders.

METHODS

The main ground temperature measurement site was located in the central part of the Fuglebergsletta strandflat. In a 3 m drillhole, resistance thermometers were placed every 25 cm in the upper part and every 50 cm in the lower part of the profile. The measurements were carried out every two days by means of the Wheatstone bridge. To control the depth of $0^{0}C$ isotherm occurrence, 16 Danilin sounders were installed on the S slope of Fugleberget and in the Fuglebergslette strandflat. In addition, during the summer months, the depth of thawing in different geomorphological positions was established by using iron rods stuck into the ground. The vertical ground movements were measured with a Bac motometer system. The rate of the movement was measured by perpendiculary moving iron rods kept by a steel frame pressed into the ground. On this frame too, dial extensometers were installed. Complete standard meteorological observations were also performed.

GEOMORPHOLOGY OF STUDIED AREA

The site of ground temperature measurements was located 500 m from the shoreline, on a 22 m raised marine terrace. The final formation of this terrace took place on the turn of the Pleistocene to the Holocene (Chmal, 1987). To

a depth of 180 cm there was fine sandy gravel (54-89% gravel), further down there was boulder clay. Down to a depth of 3 m no bedrock was reached, though about 10 m away from the site there was quartzite outcrops. 60 % of the terrace surface was covered with xerophytes (mosses and lichenes). In September the underground water level in this region occurred at a dept of 130 cm.

The investigated Fugleberget slope stretches at an altitude of 45 - 504 m a.s.l.. It is, in general, a scree slope built of metamorphic rock debris. It is only in some flat places that solifluction cover, formed into large tongues, occur. The slope is cut up by several chutes. In the subslope part, at the mouth of those chutes, there are talus mantles modelled by ablation waters and solifluction processes.

METEOROLOGICAL CONDITIONS

The mean annual air temperature measured at the Polish Polar Station in Hornsund was -3,5^{0}C in 1957-58, and -3,9 to -6,8^{0}C in the years 1978-87. The winter of 1986-87 was rather warm, with only 12 days with an air temperature lower than -20^{0}C. In all the months, with the exception of February, there were 1-3 days of thawing weather. In sum, from October to May there were 41 days with a positive mean temperature.

The very moderate snowfall of the first three months of the polar winter did not produce an even snow cover. From the beginning of winter the ground surface was glazed with ice, so that the snow was easily blown off. The snow cover did not become stabilized until the

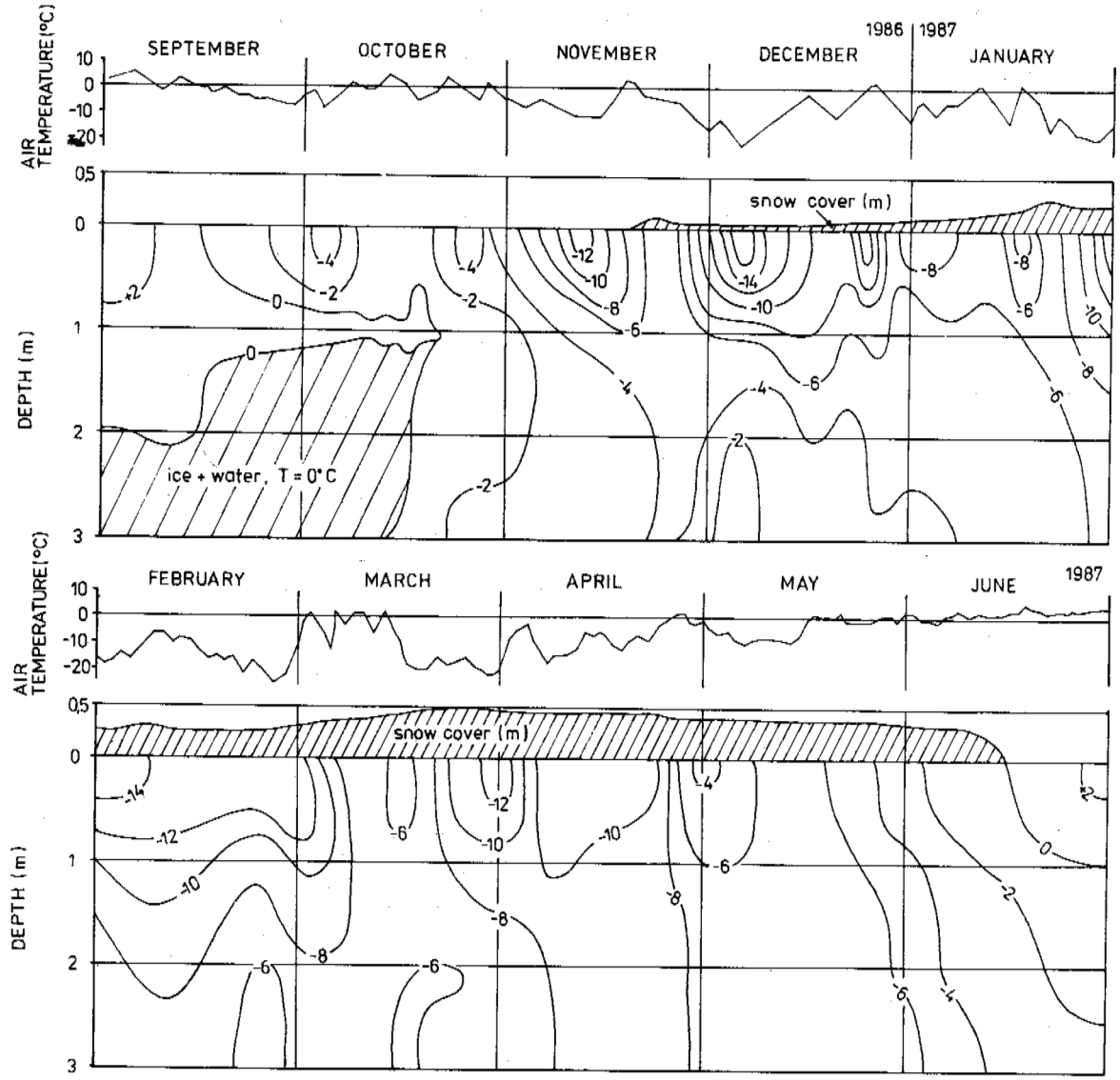

Fig. 2. Ground temperature changes dureing winter 1986/87.

middle of January. Its thickness, finally, did not exceed 50 cm in the strandflat and 90 cm in lower parts of the slopes. To the middle of March the snow density was 0,2 - 0,4 $g \cdot cm^{-3}$, and later, to the end of April 0,4 - 0,5 $g \cdot cm^{-3}$. In May, as a result of new precipitation, the snow density decreased in the upper part of the cover, but it rose again to 0,6 $g \cdot cm^{-3}$ in June after ablation had started.

The thawing weather and blowing caused a quick metamorphosis of the new-fallen snow, so that numerous icy layers formed in the snow cover.

RESULTS OF MEASUREMENTS
TEMPERATURE CHANGES IN THE VERTICAL PROFILE

The distribution of ground temperatures in the 3 m profile situated in the strandflat, in the winter 1986/87, is presented in simplified form in Fig. 2. The diagram reveals the following phenomena:

1. Toward the end of the first decade of September the thickness of the active layer reached 230 cm. Deeper in the ground there was ice of thawing temperature. Freezing advanced from above and from below, and lasted 35 days. During that time a layer of unfrozen ground, shielded from above by frozen ground, continued to exist at a depth of 80 - 120 cm. This phenomenon accounts for the development process of hydrolaccoliths which can very often be found in the Hornsund area. These forms may arise

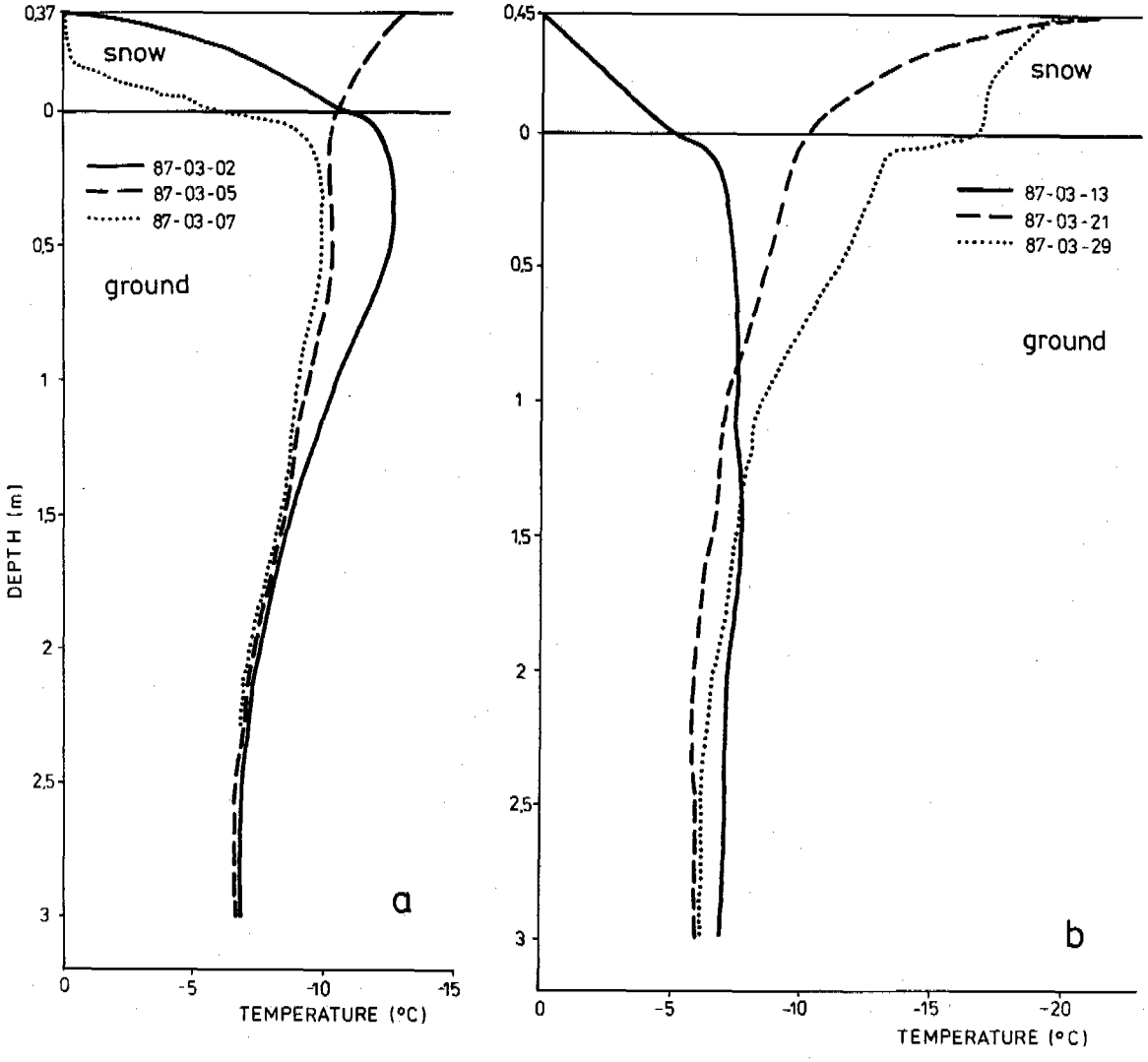

Fig. 3 Changes of thermal currents of the ground in different types of weather.

at the beginning of winter, whenever local conditions favour the occurrence of hydrostatic pressure in the unfrozen layer of the ground.

2. The two-way cooling stopped on November 21, when, at the depth of 2,5 - 3,0 m, the temperature dropped below $-4,0^0$C. At the end of April the two-way migration of heat flux, typical of spring, appeared again. After 55 days, on June 2, it stopped altogether when, at the depth of 2,5 - 3,0 m, the temperature rose above $-5,0^0$C. Later on, heat flux took place only from top to bottom. From this one may infer that the temperature at permafrost table ranges within $-4,0$ and $-5,0^0$C (approaching rather $-5,0^0$C).

3. The interruption of the two-way heat flux migration, similar to the breaking of the zero curtain, mainfested itself by a rapid change of the ground temperature in the lower part of the profile. In such cases the temperature at the depth of 2,5 - 3,0 m changed by 1,1 - 1,4^{0}C in the course of two days, which was certainly an effect of cascade type.

4. A pecularity of the temperature distribution in the first half of the winter were the several-days-long temperature rises in the lower part of the profile. This phenomenon occurred first in the period between November 29 and Desember 6. During that time the temperature at the depth of 3,0 m rose from - 4,0 to $-0,6^0$C. The same happened - with lesser intensity - four times more, always after the formation of the isothermal conditions in the profile. It may be assumed that this was the result of the emmission of heat which had accumulated during the summer in some part of the ground or bedrock (below 3,0 m) which had a greater heat capacity.

5. As long as the temperature did not drop below 0^0C in the whole profile, the changes of air temperature were reflected in those of the ground temperature only to a depth of about 80 cm (zero curtain effect). After the active layer had completely frozen, the air temperature oscillations caused ground temperature oscillations to a depth of 1,0 - 1,5 m. The lag of temperature reaction at the depth of 1,0 m amounted to 3 - 4 days. At the depth of 3,0 m the cooling of the ground advanced almost systematically over the whole winter, with the exception of the episodes described in point 4. T min. = $-8,9^0$C was recorded on April 8.

6. An air temperature rise of any duration above 0^0C (thawing weather) caused the development of isothermal condition in the profile.

7. Before the formation of a compact snow cover, the thermal gradient in the upper part of the profile reached $10^0\text{C} \cdot \text{m}^{-1}$. When the snow cover had stabilized, this gradient was about two times smaller, with air temperatures remaining the same. In general, however, the high density of the snow cover made it a good heat conductor.

Examples of the relations between the changes of snow and ground temperatures in March are shown in Fig. 3 (see also Fig. 2). These curves illustrate in detail how several cases of thawing weather result in isothermal condition (March 13), followed by heat flux from the deeper parts of permafrost to the surface (March 21). Even during the first thawing period the amount of heat reaching the upper layer of the ground was so great that the temperature in the profile continued to grow, despite a 3-day air temperature drop and freezing of the snow to about -12^0C. The subsequent days of thawing weather amplified the tendency toward isothermal condition. After March 15 there came a long period of freezing weather. Though the snow cover froze rapidly, it was only after a week the ground temperature dropped at the depth of 1,0 m and after two weeks at the depth of 2,5 m. It may thus be said that the snow cover acted as a thermal insulator in frost periods but stimulated the rise of ground temperature in thawing periods. This phenomenon also manifested itself clearly in the second half of May, i.e. at the beginning of summer in the thermal sense.

THAWING IN THE LONGITUDINAL PROFILE

In 1987 the depth of thawing of the active layer was measured lengthwise several profile lines, from mountain ridges to the shoreline. Examples of maximal depths of thawing of the ground on the slope and in the strandflat are presented in Fig. 4. This profile was running lengthwise local watershed divides and therefore illustrates the thawing of ground containing relatively less ice. It can be seen that the active layer thaws deepest in the lower part of the slope and in the subslope zone, which is a result of the privileged solar exposure of the slope. In the subslope section it is also the ablation waters running down in the debris cover and being heated up by it that play a certain role in the process.

In the mountain ridge zone (above 350 m a.s.l.) thawing began 40 days later than on the marine terraces and lasted only for 38 days. By September 16 the ground surface was frozen (to 8 cm) at the highest site. The differences in the thawing of this slope make it necessary to divide it into two distinct climatic horizons. Sounding as well as the checking of the Danilin permafrost meters on other profile lines made it possibile to determine the rate of thawing in dependence on the local physical characteristics of the ground. In morphological depressions and on the lines of ablation water flow, the thawing process was firstly twice as slow as on dry marine terraces. Next, the rate of thawing was much the same (see Fig. 5). In damp places with a compact vegetation cover (mosses, peat) thawing took place at a 2 - 3 times slower rate than on the slope. It was also found that this rate was slower near outcrops of bedrock. Commenting on those observations it should be stated that the factors decisive for the rate of thawing are first of all the ice content in the ground, further the insulating effect of vegetation, and the more

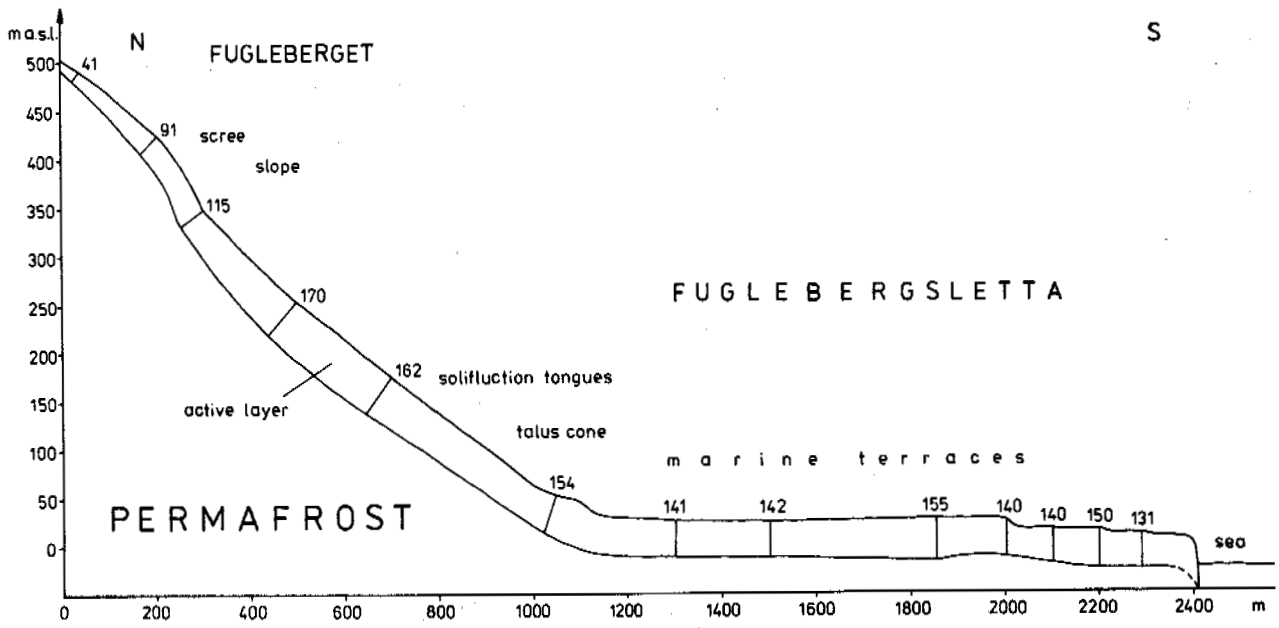

Fig. 4 Maximum thickness of the active layer recorded on September 16, 1987.

intensive cooling of solid rock outcrops in the winter and, finally, the influence of solar exposure.

FREEZING AND VERTICAL MOVEMENT OF THE GROUND

Here we intend to give only brief information about the relations between temperature changes and frost heaving of the ground. In 1987 the ground surface froze on September 17, which caused its upward movement by 1 - mm. After 6 days the ground froze down to 20 cm and in the following 5 days to 50 cm; the 5 - 10 cm surface layer reaching a temperature of $-5,5^{0}$ C. This in turn made the surface rise by 20 - 31 mm. During the whole of that period a systematic increase of cryogenic pressure, reaching at one site a value of 2040 $N \cdot cm^{-2}$ and at the other 3190 $N \cdot cm^{-2}$ was recorded. The next day thawing weather set in and the pressure dropped by 10 - 40 %. The ground surface, however, continued to rise, owing to the formation of segregated ice. In the subsequent periods of freezing the pressure again reached the above values, oscillating within $\pm$ 10 % in accordance with the temperature variations of the ground surface. Maximal vertical ground movements - coming up to 55 - 78 mm - were recorded in the centres of stone circles. On October 14 the active layer was found to be totally reduced and the period of winter stabilization of the ground surface began.

CONCLUSIONS

The freezing and thawing processes of the active layer of permafrost in the Hornsund area have been characterized in relation to an analysis of the temperature changes of air and snow cover. The thermal changes in the active layer appeared as specific by their high intensity which is rather typical of a continental climate, though the thermal currents of air and precipitation of the area should classify it among the zones of cold maritime climates. This discrepancy results from the fact that here the thin snow cover, being constantly blown and subjected to frequent thawing periods, cannot act as a thermal non-conductor.

In reference to the study by Jahn and Walker (1983) we are of the opinion that the thawing rate of the active layer in the Hornsund area indicates a microclimatic differentiation. Here a general distinction can be made between the climatic horizon of the strandflat and slopes to a height of 350 m a.s.l. and the higher horizon of mountain ridges. The temperature of the permafrost table ($-5,0^{0}$ C) permits the assumption that the 0^{0} C isotherm occurs at a depth of 100 - 250 m. In other parts of Spitsbergen the thickness of permafrost is 200 - 400 m (Stearns 1966,

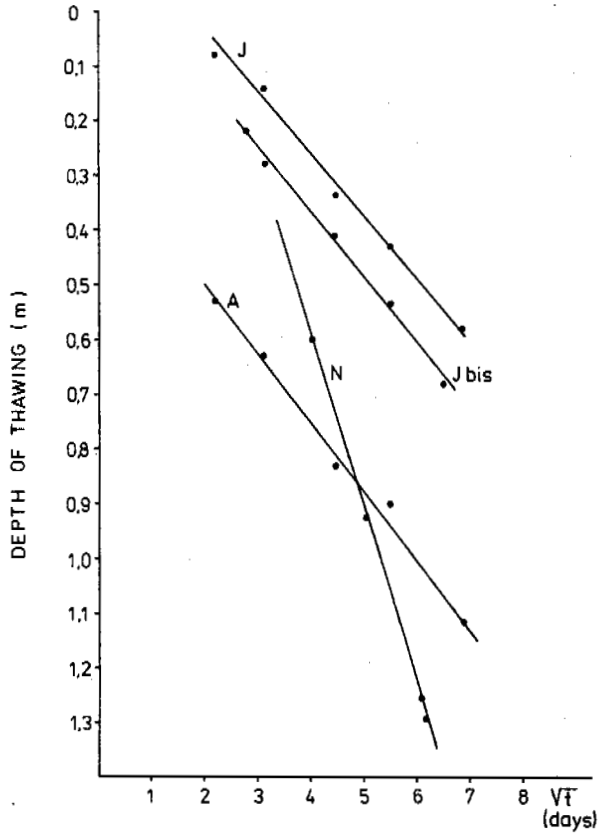

Fig. 5 Rate of ground thawing in selected sites (see location map). A - marine terrace (sandy gravel), J - dry moss tundra, Jbis - riverbed of seasonal outflow of ablation waters, N - debris slope.

Liestøl 1977). Considering the mean annual temperatures recorded in the last several dozen years in the Hornsund area it appears obvious that here the permafrost table is relatively overcooled.

ACKNOWLEDGEMENTS

We are grateful to Prof. Alfred Jahn for his tuitional guidance. Financial support for this study was provided by the Polish Academy of Sciences under CPBP 03.03. Project.

REFERENCES

Baranowski, S. (1968). Termika tundry peryglacjalnej SW Spitsbergen. Acta Univ. Wratislav., (68), pp. 1-76.

Chmal, H. (1987). Pleistocene sea-level changes and glacial history of the Hornsund area, Svalbard. Polar Res. (5), in print.

Czeppe, Z. (1966). Przebieg głównych procesów morfogenetycznych w poludniowo-zachodnim Spitsbergenie. Zeszyty Nauk. Uniw. Jagiell., (CXXVII); pp. 1-129.

Grzes, M. (1985). Warstwa czynna wieloletniej zmarzliny na zachodnich wybrzezach Spitsbergenu. Przegl. Geogr., (LVII), 671-691.

Jahn, A. (1982). Soil thawing and active layer of permafrost in Spitsbergen. Results of Invest. of the Polish Spits. Exped., (IV), Acta Univ. Wratislav., (525), 57-75.

Jahn, A., Walker, H.J. (1983). The active layer and climate. Zeit. f. Geomorph. N.F., Suppl.,m (47), 97-108.

Liestøl, O. (1977). Pingos, springs, and permafrost in Spitsbergen. Norsk Polarinstitutt Arbok 1975,, 7-29

Stearns, S.R. (1966). Permafrost (perennially frozen ground). Us Army Cold Reg. Res. and Engg Lab., Cold Reg. Sci and Engg, (I-A2), pp. 1-77.

Werenskiold, W (1922). Frozen earth in Spitsbergen. Geofysike Publikat,, (2), 1-10.

FREEZING-POINT DEPRESSION AT THE BASE OF ICE-BEARING PERMAFROST ON THE NORTH SLOPE OF ALASKA

T.S. Collett and K.J. Bird

U.S. Geological Survey, Menlo Park, California, U.S.A.

SYNOPSIS Ice-bearing sediments, common in Arctic regions, exhibit physical characteristics that can be detected with bore-hole logging devices. Properties such as anomalously high electrical resistivity and short acoustic transit-times have been used to detect qualitatively the presence of ice within sediments. Correlation of measured, near-equilibrium, formation temperatures with the log-determined base of ice-bearing sediments (ice-bearing permafrost) in North Slope wells shows temperatures lower than 0 °C at the ice/water interface, ranging generally from -1.0 °C to as low as -4.8 °C. Near Prudhoe Bay, the temperature at the base of the ice-bearing permafrost is approximately -1.0 °C, whereas 50 km or more to the west in the National Petroleum Reserve in Alaska (NPRA), the temperature ranges from -3.0 to -4.8 °C.

Temperatures at the base of ice-bearing permafrost may be influenced by pore-fluid salinity, pore-pressures, and sediment grain-size; these factors collectively depress the freezing point of water (freezing-point depression). Theoretical calculations coupled with analysis of North Slope subsurface data indicates that the maximum cumulative effect of pore-water salinity and pore-pressure accounts for only about 1.5 °C of the freezing-point depression. Freezing-point depression greater than 1.5 °C may be caused by the presence of fine-grained (clayey) moderately compacted sediments, as well as the limitations of well logs to detect relatively small or finely disseminated amounts of ice in fine-grained sediments.

INTRODUCTION

Permafrost thickness and subsurface temperatures are necessary to solve engineering and scientific problems, such as, (1) correcting seismic velocities; (2) developing safe procedures for oil-well drilling, completion, and production; (3) developing regional ground-water models; and (4) delineating the potential distribution of gas hydrates. Our interest derives from the study of natural gas hydrates on the North Slope of Alaska, a study funded by the U.S. Department of Energy (Agreement No. DE-AI21-83-MC20422). Subsurface temperature data are one component needed to calculate the depths at which gas hydrates could occur.

At the outset of this study, it was anticipated that wireline well-log responses could be utilized to identify the base of ice-bearing permafrost in some of the hundreds of wells drilled for petroleum on the North Slope, thus quickly and inexpensively enlarging the existing U.S. Geological Survey data base of 46 wells with near-equilibrium temperature profiles (Lachenbruch and others, 1982; 1987). The basis for this optimism was the general coincidence of the deepest occurrence of ice-bearing sediments with abrupt changes of resistivity and acoustic velocity in well logs and with the depth of the 0 °C isotherm observed in wells of the Prudhoe Bay Oil Field.

One-hundred and fifty-six wells with suitable log coverage were selected from available well files (Alaska Oil and Gas Conservation Commission, Anchorage, Alaska and U.S. Geological Survey, Menlo Park, California), and a map, showing depth to the base of ice-bearing permafrost was constructed from the well logs (similar to Osterkamp and Payne, 1981; Osterkamp and others, 1985). When these log-determined depths were compared to temperatures in 32 wells with both log and temperature data, it was found that the 0 °C isotherm was always deeper than the log-determined base of permafrost and the difference varied from well to well. We interpreted this observation, as others had previously, to mean that the ice-water phase boundary occurred in these wells at temperatures lower than 0 °C, a phenomenon known as freezing-point depression.

Freezing-point depression is generally ascribed to increases in salinity or pore-pressure, or to electro-chemical bonding of water to mineral particles (particle grain-size effect) (Osterkamp and Payne, 1981). From our analysis of these factors on the North Slope it was not possible to explain all of the observed freezing-point depression. We postulate that the unexplained difference in freezing-point depression is caused by (1) unevaluated particle grain-size effects or (2) by limitations of well logs in selecting the position of the base of the ice-bearing permafrost, especially when ice content is small. In this paper we document the freezing point depression phenomena on the North Slope and describe our analysis of its causes in selected wells.

ICE-BEARING PERMAFROST

In this study the term, ice-bearing permafrost refers to strata that contains or is interpreted to contain a sufficient volume of ice to be detected on geophysical well logs without the aid of temperature data. The minimum amount of ice necessary for detection by well-logging devices is unknown. Within the thick ice-bearing permafrost sequence found locally on the North Slope, multiple frozen and thawed horizons are present. In this study, the base of the ice-bearing permafrost is defined as the deepest observed frozen-to-thawed phase boundary that may exist at any particular location. The term permafrost is referred to as the thermal condition in soil or rock having temperatures below 0 °C which persists over at least two consecutive winters and the intervening summer (Brown and Kupsch, 1974). The presence or absence of water or ice is not included in the definition of permafrost, and the depth to the base of permafrost is the depth to 0 °C.

Desai and Moore (1968) were the first to report that ice-bearing sediments exhibit physical characteristics that can be detected with subsurface geophysical

devices. Others have shown that the thickness of ice-bearing permafrost can be determined from well logs (Stoneley, 1970; Howitt, 1971; Hoyer and others, 1975; Hnatiuk and Randall, 1977; Osterkamp and Payne, 1981; Osterkamp and others, 1985). Osterkamp and Payne (1981) were the first to use the term ice-bearing permafrost to describe the physical response of well logs to the presence of ice; their predecessors (cited above) used the term permafrost to describe both temperature conditions and the presence of ice within pore spaces.

Desai and Moore (1968) demonstrated that the spontaneous potential, resistivity, and acoustic logs show deflections at the base of the ice-bearing permafrost (called permafrost by these authors) in an unidentified well on the North Slope of Alaska. They observed a significant increase in electrical resistivity, a decrease in acoustic transit time, and a pronounced drift in spontaneous potential from less-negative to increased-negative values after crossing the boundary from non-ice-bearing to ice-bearing permafrost. Stoneley (1970) also observed similar log responses in the Put River-1 well in the Prudhoe Bay Oil Field, which he also attributed to the presence of ice, based on observations of cores and log responses in an unidentified Prudhoe Bay well. Later, Howitt (1971) identified that well as BP 12-10-14A and reported that ice was detected visually in cores to a well depth of 1,858 ft, 566 m below the ground surface. The log-determined base of ice-bearing permafrost is at 1,885 ft well depth (562 m from the surface). The 4 m discrepancy between depth of ice-bearing permafrost and the deepest observed ice is not considered significant because records from BP 12-10-14A show that only half of the core in which the deepest ice was observed was recovered. Howitt's (1971) identified base of ice (566 m) is therefore accurate only within plus or minus 9 m. These observations of ice-bonded cores in relation to log response for this well are summarized in figure 1 and represent the only direct evidence that verifies the accuracy of well logs as ice-detection devices. Unfortunately, no information was provided on the limits or sensitivity of well logs to ice detection.

The 156 wells used to map the (log determined) base of the ice-bearing permafrost on the North Slope (fig. 2) were selected on the basis of log coverage and quality of log data. This map shows that the depth of ice-bearing permafrost ranges from less than 200 m in NPRA to more than 600 m in the east, and that it thins to south. The electrical-resistivity and acoustic transit-time well logs were found to be the most useful in detecting the base of the ice-bearing permafrost. For a complete discussion of ice-bearing permafrost depths on the North Slope see Osterkamp and Payne (1981), Osterkamp and others (1985) and Collett and others (in press).

RELATIONS BETWEEN PERMAFROST AND ICE-BEARING PERMAFROST

Near-equilibrium subsurface temperature surveys are available for 46 North Slope wells (Lachenbruch and others, 1982; 1987). Of these 46 wells, 32 have other well logs available to determine the depth to the base of ice-bearing permafrost. In these wells the temperature profiles have been used to determine the temperature at the log-identified base of ice-bearing permafrost. This was accomplished for each well by plotting the depth of the well-log pick for the base of the ice-bearing permafrost on the recorded equilibrium temperature profiles, thus, obtaining a direct temperature measurement. The temperature at the base of the ice-bearing permafrost as determined from this data set ranges from −0.3 °C in the Prudhoe Bay area to −4.8 °C at Point Barrow. A contour map of these data (fig. 3) shows relatively small values in the Prudhoe Bay area and high values to the west, in the NPRA.

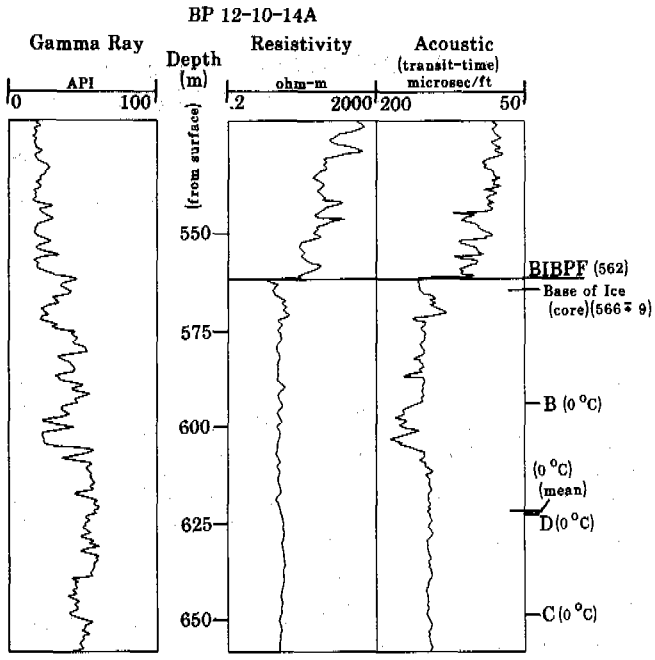

Figure 1. Selected well logs from the BP 12-10-14A well on the North Slope of Alaska. Ice-bearing permafrost base (BIBPF) is identified at 562 m, and the depth of deepest observed ice within recovered cores is reported by Howitt (1971) to be 566 m. Depth of the 0 °C isotherm in three nearby wells are shown along with the calculated mean depth (623 m) of the 0 °C isotherm in these wells. See figure 5 for location and identification of wells.

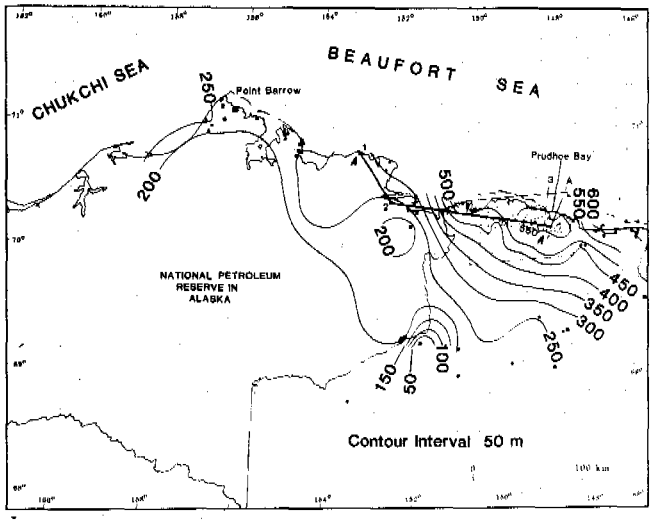

Figure 2. Depth to the base of the deepest ice-bearing permafrost on the North Slope of Alaska as determined from wireline well logs. Adapted from Collett and others (in press). Most of the wells used are within the box drawn around the Prudhoe Bay area. The location of the wells J.W. Dalton-1 (1), South Harrison Bay-1 (2), Prudhoe Bay Unit N-1 (3), and BP 12-10-14A (A) are shown. Location of geologic well-section A-A' (fig. 4) is also shown.

Three wells have been selected to demonstrate both regional and local discontinuities between permafrost and ice-bearing permafrost. These wells, shown in figure 4, include log responses, lithologies, and depths to ice-bearing permafrost and the 0 °C isotherm. The well BP 12-10-14A, which was drilled in 1969 early in the development history of the Prudhoe Bay Oil Field for the express purpose of evaluating potential permafrost engineering problems, has no temperature survey. We have used three nearby wells (fig. 5) with temperature profiles (Lachenbruch and others, 1982) to estimate the depth of the 0 °C isotherm and the temperature at the base of ice-bearing permafrost in BP 12-10-14A. The average depth of the 0 °C isotherm in the surrounding wells is 623 m, which is 61 m deeper than the log-identified base of ice-bearing permafrost in the BP 12-10-14A well (562 m; fig. 1). By using the mean depth of the 0 °C isotherm reported from the surrounding wells and the mean geothermal gradient (Lachenbruch and others, 1982), we estimate the equilibrium temperature for the base of ice-bearing permafrost in BP 12-10-14A at -1.75 °C.

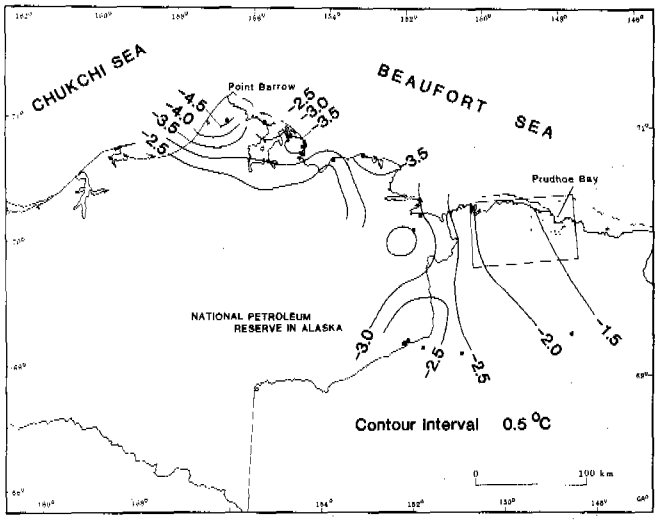

Figure 3. Temperature at the base of ice-bearing permafrost on the North Slope of Alaska. Temperature data taken from near-equilibrium temperature surveys (Lachenbruch and others, 1982; 1987). Ice-bearing permafrost depths are from Collett and others (in press). The contoured data are from 32 wells in which diagnostic well logs and equilibrated-temperature surveys are available.

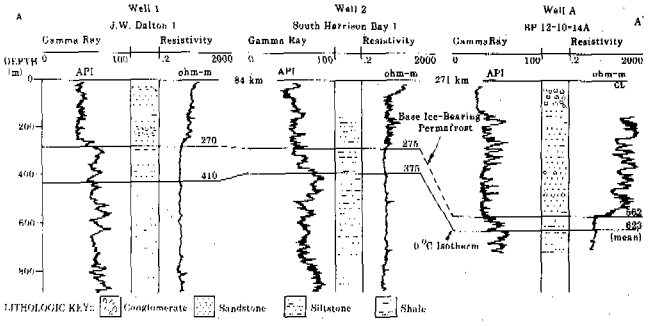

Figure 4. Selected wells from the North Slope of Alaska illustrating well log response, general lithologies, base of ice-bearing permafrost, and 0 °C isotherm. See figure 2 for location of wells.

Wells	Depth 0°C (m)	Difference Depth 0°C & BIBPF Well A (m)	G_{th} °C/100m	BIBPF Temp. Well A Calculated From Wells B-C-D
A BP12-10-14A	(BIBPF=562)	--	--	--
B BP19-10-15	595	+33	2.75	-0.91
C BP31-11-14	650	+88	2.90	-2.55
D BP27-11-14	625	+63	2.85	-1.80
Mean--	623	+61	2.83	-1.75

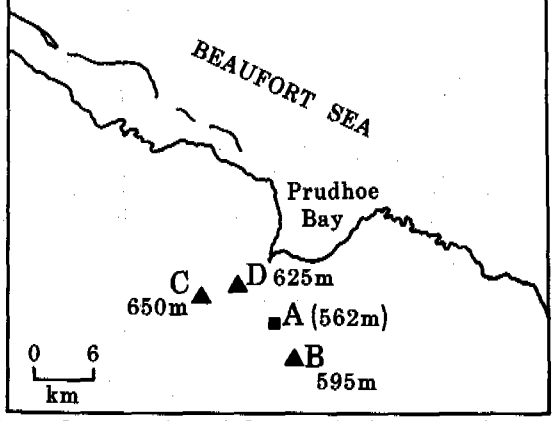

Figure 5. Location of four wells in the Prudhoe Bay Oil Field. Temperature data (Lachenbruch and others, 1982) from BP 19-10-15 (B), BP 31-11-14 (C), and BP 27-11-14 (D) were used to determine the depth of the 0 °C isotherm and calculate the temperature at the base of ice-bearing permafrost in BP 12-10-14A (A).

In South Harrison Bay-1 (fig. 4), the base of ice-bearing permafrost is tentatively placed at the resistivity deflection at 275 m. The depth of the 0 °C isotherm is at 375 m. The temperature at the base of the ice-bearing permafrost is -3.1 °C. In J.W. Dalton-1 (fig. 4), the base of the ice-bearing permafrost at 270 m appears to coincide with a distinct lithologic contact, and the depth of the 0 °C isotherm is at 410 m. The temperature at the base of the ice-bearing permafrost is -3.9 °C. The plot of the 0 °C isotherm on cross section A-A' (fig. 4) reveals a discrepancy between the well-log pick for the base of the ice-bearing permafrost and the 0 °C equilibrium isotherm. The difference in thickness between these horizons are variable. In BP 12-10-14A it is 61 m, but in J.W. Dalton-1 the difference is approximately 140 m. Temperatures at the base of the ice-bearing permafrost may be influenced by many physical parameters that collectively depress the freezing-point of water. This temperature suppression is often referred to as freezing-point depression. In the next section we have attempted to evaluate the regional variability of freezing-point depression on the North Slope.

FREEZING-POINT DEPRESSION

It is generally assumed that factors producing freezing-point depression are additive. These factors include the presence of salt-ions in solution, pore-pressure, and variations in soil or rock particle size (surface-area) and type. The cumulative effect of these factors producing freezing-point depression are expressed in the following equation, by Osterkamp and Payne (1981).

$$To = 0.0100 - Tc - Tp - Ts \quad (1)$$

The first term To represents equilibrium temperature at the base of ice-bearing permafrost, 0.0100 stands for the triple point of water and Tc, Tp, and Ts are the

temperature corrections for chemical composition (salts), pore-pressure, and soil/rock particle size effect, respectively.

Chemical Composition (Tc)

The effect of chemical composition (Tc) depends on the solute concentrations in the pore-water. The predominant salt observed in the pore-water of the North Slope is NaCl (Osterkamp and Payne, 1981; Howitt, 1971). If salt concentrations are known, the effect on freezing-point depression can be calculated from the following equation (Osterkamp and Payne, 1981),

$$Tc = 0.0137 + 0.051990\ S + 0.00007225\ S^2\ ^{\circ}C \quad (2)$$

where S is the salinity of the pore-water in parts per thousand. Equation (2) is graphically displayed for a salinity range of 0-40 ppt in figure 6. Salinity data within the near-surface sediments (0-1,500 m) of the North Slope are available from petroleum drill-stem and production tests, water samples from cores within the permafrost sequence, and spontaneous potential well-log calculations.

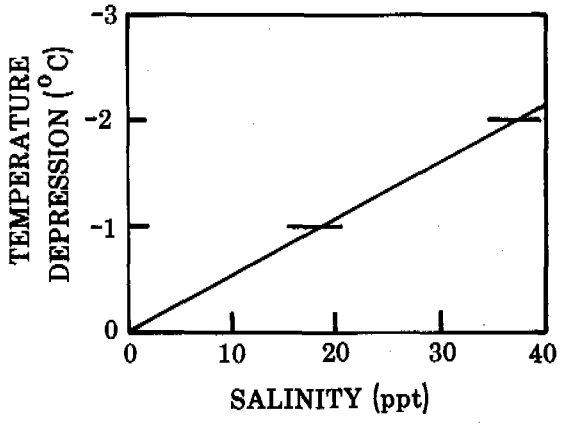

Figure 6. Freezing-point depression due to the presence of increasing volumes of salt ions in solution (Tc); not valid for salinities over 42 ppt.

Analyses of 55 water samples collected during petroleum formation testing in rock units from below the permafrost sequence are available in the North Slope well files. These analyses indicate that (bulk) pore-water salinities range from 0.5 to 19.0 ppt. Spontaneous potential well-log calculations indicate that pore-water salinities within the near-surface sediments of the North Slope are low, ranging from 2 to 19 ppt. These calculations were made by using conventional well log interpretation procedures in which the electrical resistivity of the formation-waters are calculated from the spontaneous-potential device and from which the dissolved salt content is estimated (Gondouin and others, 1957). Spontaneous potential well-log calculated pore-water salinity profiles for three wells, J.W. Dalton-1 (1), South Harrison Bay-1 (2), and Prudhoe Bay Unit N-1 (3) (located 6 km from BP 12-10-14A), are shown in figure 7. BP 12-10-14A was not evaluated because the use of oil-based drilling muds invalidated the procedure. Uncorrected log-calculated salinities from within ice-bearing permafrost and clay-rich horizons are not valid. Therefore, only sub-permafrost clean-sandstone units have been examined. All three well profiles in figure 7 are similar, with salinity values ranging from 3.0 to 19.0 ppt, and average about 9 ppt. The highest detected pore-water salinity of 19 ppt would depress the freezing-point of water about 1.0 °C.

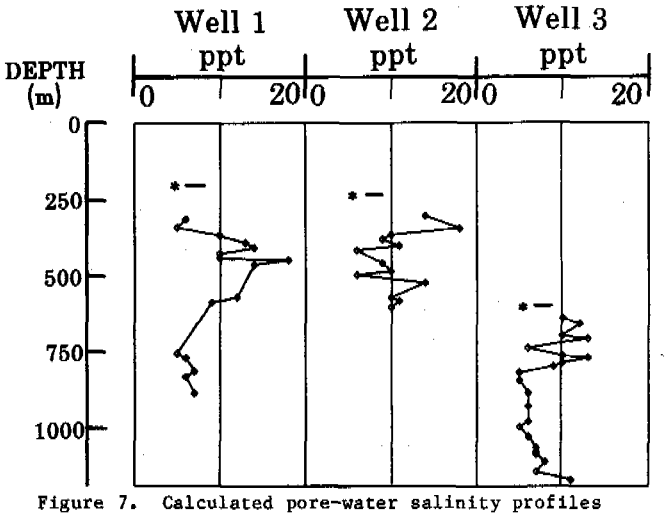

Figure 7. Calculated pore-water salinity profiles using the spontaneous-potential log method beneath the ice-bearing permafrost in selected North Slope wells (Well 1-J.W. Dalton-1; Well 2-South Harrison Bay-1; Well 3-Prudhoe Bay Unit N-1). See figure 2 for well locations. Only clean-sandstone units have been utilized in the calculations. No well log corrections have been used (* denotes base of ice-bearing permafrost).

Analysis of the BP 12-10-14A ice-bearing-cores, indicates that salinities within the sands of the ice-bearing permafrost sequence are the lowest of our data set, ranging from 0.15 to 0.50 ppt (Howitt, 1971). The low salinities in the ice-bearing horizons may be caused by connate fluvial water, meteoric recharge, salt rejection during freezing, or a combination of these factors. Salt rejection during freezing might concentrate the pore-water salts at the base of the ice-bearing permafrost. However, there is no evidence of pore-water salinities greater then 19.0 ppt at the base of ice-bearing permafrost. From the foregoing analysis, we conclude that the maximum freezing-point depression that can be attributed to the chemical composition (Tc) of the pore-waters is 1.0 °C at the reviewed sites.

Pore-Pressure (Tp)

The effect of pore-pressure on the freezing-point of water can be calculated from the following equation if P, the pore-pressure on the ice and water, is known.

$$Tp = BP \quad (3)$$

The variable B is the Clausis-Clapeyron Slope (0.00751 °C atmos^{-1}). Equation (3) is graphically displayed in figure 8 for a hydrostatic pore-pressure gradient of 0.097 atmos/m (0.433 psi/ft) and for the theoretical maximum gradient (lithostatic) of 0.223 atmos/m (1.000 psi/ft) over a depth of 0 to 800 m. Pressure data from petroleum drill-stem testing in 17 wells, and log evaluation of discontinuities in over-burden compaction profiles (pore-pressure profiles) in 22 wells have been used to evaluate pore-pressures within the near-surface sediments (0-1,500 m).

Pore-pressure gradients calculated from shut-in pressures recorded during drill-stem testing in wells from the North Slope range from 0.093 to 0.112 atmos/m, with an average gradient of 0.097 atmos/m (0.434 psi/ft), near hydrostatic (data from well files). To further evaluate pore-pressures, well logs have been used to study over-burden compaction profiles. As rocks, particularly shales, are subjected to increasing over-burden pressures they are compacted, and

subsequent transit-time velocities and gamma-ray well-log values increase with depth because of increasing formation density. If a rock interval is over-pressured, it will resist compaction and can be identified on acoustic transit-time and gamma-ray logs by a departure of the log curve from a trend line (Zoeller, 1984). Gamma-ray compaction profiles (fig. 9) from the J.W. Dalton-1 (1), South Harrison Bay-1 (2), Prudhoe Bay Unit N-1 (3), and BP 12-10-14A (A) wells are linear with depth and have no significant discontinuities, indicating hydrostatic pore-pressures. The theoretical maximum pore-pressure gradient could only be reached if the entire ice-bearing permafrost sequence, both rock and ice, acted as a solid mass, transferring its entire weight to the underlying water-bearing sequence. For this to happen, the underlying rock-pore-water system must be closed. Under large lakes and rivers permafrost may not exist (Lachenbruch and others, 1982), and these ice-free zones may act as conduits to relieve abnormal pore-pressures.

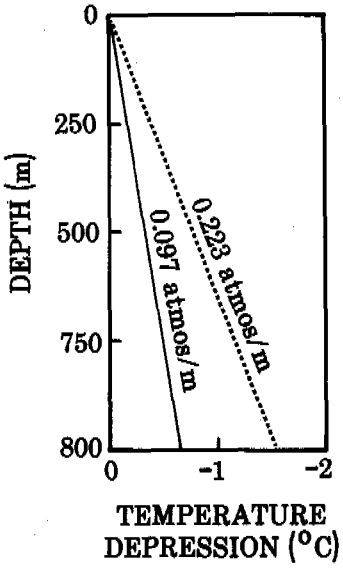

Figure 8. Freezing-point depression due to subsurface pore-pressure (Tp). The pressure effect is shown as a function of a hydrostatic pore-pressure gradient (0.097 atmos/m; 0.433 psi/ft) and the theoretical maximum pore-pressure gradient (0.223 atmos/m; 1.000 psi/ft).

Pore-pressures in the wells we have examined are a product of a hydrostatic gradient (0.097 atmos/m; 0.433 psi/ft). The pressure effect (Tp) on freezing-point depression, calculated from equation 3 for one of the deepest occurrences of ice-bearing permafrost (562 m in the BP 12-10-14A well), is only 0.5 °C. In J.W. Dalton-1, with the base of ice-bearing permafrost at 270 m, pore-pressure would depress the freezing point of water even less, 0.2 °C.

Soil/Rock Particle Size (Ts)

Particle grain-size (grain surface area) affects the freezing-point of water (Anderson and others, 1973; and Osterkamp and Payne, 1981). Anderson and others (1973) suggested that clay could suppress the freezing-point by several degrees Celsius, but for coarser material, such as silts and sands, the particle effect is negligible. However, the quantification of freezing-point depression attributed to clay is difficult. Variations in clay microstructure can affect the volume of unfrozen water, thus further complicating the freezing-point depression calculations.

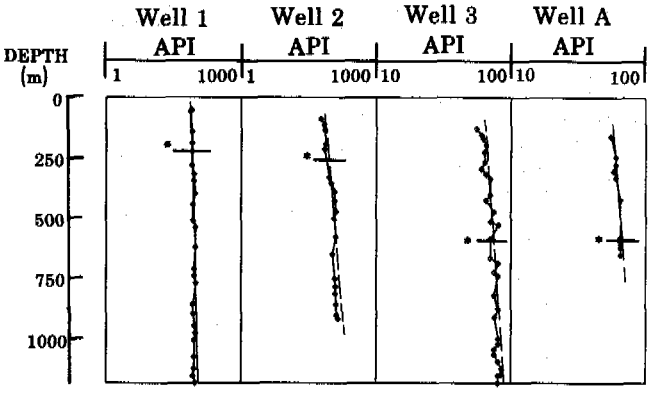

Figure 9. Profiles of gamma-ray readings of shale intervals (dotted line) and visual best-fit trend line (dashed line) for selected North Slope wells (logarithmic scale) [Well 1-J.W. Dalton-1; Well 2-South Harrison Bay-1; Well 3-Prudhoe Bay Unit N-1; Well A-BP 12-10-14A]. Increasing gamma-ray values with depth are a measure of compaction of the sediments (Zoeller, 1984). Gamma-ray values left of the trend line may indicate pore-pressures greater than normal hydrostatic or may indicate sandy or silty shales with low gamma-ray values (* denotes base of ice-bearing permafrost). See figure 2 for location of wells.

At this time it is impossible to quantify the effect of grain-size on freezing-point depression, but it is possible to identify those parts of the North Slope where the near-surface sediments are relatively rich in clay. Within the sandstones and conglomerates of the Prudhoe Bay area, grain size should not affect the freezing point of water. However, in eastern and northernmost parts of NPRA, a thick, fine-grained (shaley), moderately compacted sediment package of Cretaceous age that occurs near the surface, may significantly affect the freezing-point of water. X-ray analysis of Cretaceous shales from NPRA indicates a clay content of 40 to 60 percent.

Freezing-Point Depression Calculations Summary (To)

It is impossible to evaluate precisely the variables controlling freezing-point depression without specific data from the base of ice-bearing permafrost, such as cores and formation pressure tests. With the existing data it is possible to only estimate temperatures at the base of ice-bearing permafrost. For example, in the BP 12-10-14A well the base of ice-bearing permafrost is estimated to be at -1.75 °C. Freezing-point depression calculations show that the maximum observed temperature depression that can be attributed to chemical composition (Tc) and pore-pressure (Tp) is -1.5 °C. The equilibrated temperature survey for J.W. Dalton-1 indicates that the base of ice-bearing permafrost is at -3.9 °C. The maximum temperature depression attributed to chemical composition (Tc) and pore-pressure (Tp), as calculated from available data, is estimated to be -1.2 °C. The discrepancy between the observed and the calculated base of ice-bearing permafrost temperatures is not easily explained. The slight difference observed in wells like BP 12-10-14A may result from inconsistencies in the data. However, the discrepancy in J.W. Dalton-1 is much greater and is not easily discounted. For instance, to explain the 2.7 °C difference between the calculated and observed freezing-point depression in J.W. Dalton-1, the pore-water salinities must be increased from a maximum observed value of 19 ppt to volumes greater than 40 ppt (fig. 6). Conversely, the pore-pressure gradient would

require an increase beyond theoretical limits (fig. 8). Pore-water salinities or pore-pressure variations of this magnitude would be easily detected with the procedures used in this study. Therefore, it is assumed that an unevaluated variable is contributing to freezing-point depression in wells like the J.W. Dalton-1. It has been suggested that clays can affect freezing-point depression, and the near-surface sediment package in J.W. Dalton-1 contains a significant volume of shales. Other wells in eastern NPRA, an area underlain by near-surface shaley rocks, exhibit similar low temperatures for the base of ice-bearing permafrost (fig. 3), suggesting that grain-size (Ts) may be an important factor in explaining freezing-point depression in certain areas of the North Slope.

An additional factor not related to freezing-point depression is the sensitivity of well logs to ice in sediments. Physical factors that control the response of a well log include mineralogy, porosity, temperature, pore-fluids, and, of special concern for this study, the physical state of the pore-fluids. The ability of a well-log device to indicate the presence of ice within a rock mass is dependent on the sensitivity of the device to detect those altered physical-chemical conditions caused by the presence of ice. Well logs indicate that a substantially thick wedge of ice-bearing permafrost is present in the Prudhoe Bay area. The base of the ice-bearing permafrost in the high-porosity sandstones and conglomerates of the Prudhoe Bay region is easily detected (fig. 1). However, in many wells from the NPRA in which the shallow, potentially ice-bearing sequences are characterized by siltstone and shale lithologies, the well logs fail to indicate the presence of ice, even though the depth of the 0 °C isotherm often extends deep into the lithologic section. In these wells, either (1) ice does not exist, or (2) the volume of the pore-filling ice is small and related physical-chemical characteristics were below the detection limits of the well-logging devices. In general, shales that have not experienced deep burial have high porosity and fluid content; however, most waters associated with shales are ionically bounded to the clays, inhibiting the formation of ice. Therefore, ice may not exist within a section where clay-rich rocks are found. The thick shale sections present within the shallow substrate of parts of NPRA may affect pore-filling ice conditions, but currently there is no evidence to support this idea.

SUMMARY AND CONCLUSION

The primary purpose of this paper was to document and attempt to evaluate the discordance between the well-log identified base of ice-bearing permafrost and the depth of the 0 °C isotherm. Comparison of well-log responses to equilibrium temperature profiles in selected wells showed that the well logs were responding not to rocks with a temperature of less than 0 °C (permafrost), but to rocks with a certain content of ice (ice-bearing permafrost). Available equilibrium temperature data show that temperatures at the base of ice-bearing permafrost range from approximately -0.3 to as low as -4.8 °C. However, theoretical calculations coupled with well-log data, indicate that the maximum cumulative effect of pore-water salinity and pore-pressure accounts for only a 1.5 °C freezing-point depression. To explain the greater than 1.5 °C freezing-point depression observed, variables other then pore-water salinity and pore-pressure must be considered. Although quantitative data are lacking, we suggest that the discrepancy is caused by a combination of the presence of fine-grained clayey sediments, and the possibility that the well logs do not detect small amounts or finely disseminated ice in the sediments. Our analysis suggests that increased understanding of freezing-point depression of ice-bearing permafrost would come from new data and related laboratory experiments directed at determining (1) well-log sensitivity to ice content of sediments and (2) particle effect in a variety of typical fine-grained sedimentary rocks (siltstone, shale, mudstone) with varying clay content.

REFERENCES CITED

Anderson, D.M., Tice, A.R., and McKim, H.L., (1973). The unfrozen water and the apparent specific heat capacity of frozen soils, in Proc. of the 2nd International Conference on Permafrost, Yakutsk, U.S.S.R.: National Academy of Sciences, Washington, D.C., 257-288.

Brown, R.J.E., and Kupsch, W.O., (1974). Permafrost terminology: Canada, National Research Council, Associate Committee on Geotechnical Research, Technical Memorandum 111, 62 pp.

Collett, T.S., Bird, K.J., Kvenvolden, K.A., and Magoon, L.B., (in press). Map of the depth to the base of the deepest ice-bearing permafrost as determined from well logs, North Slope, Alaska: U.S. Geological Survey Oil and Gas Map, 1 sheet, Scale 1:1,000,000.

Desai, K.P., and Moore, E.J., (1968). Well log interpretation in permafrost: The Log Analyst (10), 1, 13-25.

Gondouin, M., Tixier, M.P., and Simard, G.L., (1957). An experimental study on the influence of the chemical composition of electrolytes on the SP curve: Petroleum Transactions, American Institute of Mineralogists, Metallurgists, and Engineers (210), 58-72.

Hnatiuk, J., and Randall, A.G., (1977). Determination of permafrost thickness in wells in northern Canada: Canadian Journal of Earth Science (14), 375-383.

Howitt, Frank, (1971). Permafrost geology at Prudhoe Bay, Alaska: World Petroleum (42), 8, 28-38.

Hoyer, W.A., Simmons, S.O., Span, M.M., and Watson, A.T., (1975). Evaluation of permafrost with logs, in Proc. of the 16th Annual Society of Petroleum Well Log Analyst Logging Symposium, June 4-7, Dallas, Texas: Transactions Society of Petroleum Well Log Analyst, 13-25.

Lachenbruch, A.H., Sass, J.H., Lawver, L.A., Brewer, M.C., Marshall, B.V., Munroe, R.J., Kennelly, J.P., Jr., Galanis, S.P., Jr., and Moses, T.H., Jr., (1987). Temperature and depth of permafrost on the Alaskan Arctic Slope, in Tailleur, Irv, and Weimer, Paul, eds., Alaskan North Slope geology: Bakersfield, California, Pacific Section Society of Economic Paleontologists and Mineralogists and the Alaska Geological Society, book 50 (2), 545-558.

Lachenbruch, A.H., Sass, J.H., Marshall, B.V., and Moses, T.H., (1982). Permafrost heat flow, and the geothermal regime at Prudhoe Bay, Alaska: Journal of Geophysical Research (87), B11, 9301-9316.

Osterkamp, T.E., and Payne, M.W., (1981). Estimates of permafrost thickness from well logs in northern Alaska: Cold Regions Science and Technology (5), 13-27.

Osterkamp, T.E., Petersen, J.K., and Collett, T.S., (1985). Permafrost thickness in the Oliktok Point, Prudhoe Bay and Mikkelsen Bay areas of Alaska: Cold Regions Science and Technology (11), 99-105.

Stoneley, Robert, (1970). Discussion, in Adkison, W.L. and Brosge, M.M., eds., Proc. of the Geological Seminar on the North Slope of Alaska: Pacific Section, American Association of Petroleum Geologists, Los Angeles, California, J2-J4.

Zoeller, W.A., (1984). Determine pore pressure from MWD gamma ray logs: World Oil, March, 97-102.

NATURAL GROUND TEMPERATURES IN UPLAND BEDROCK TERRAIN, INTERIOR ALASKA

C.M. Collins[1], R.K. Haugen[2] and R.A. Kreig[3]

[1]U.S. Army Cold Regions Research and Engineering Laboratory, Fairbanks, Alaska
[2]U.S. Army Cold Regions Research and Engineering Laboratory, Hanover, New Hampshire
[3]R.A. Kreig & Associates, Inc., Anchorage, Alaska

SYNOPSIS Surface and subsurface ground temperature measurements were made in drill holes representing a variety of permafrost/non-permafrost, slope exposure, elevation, vegetation, and soil conditions within the upland taiga of interior Alaska. Algorithms representing equivalent latitude and air temperature/elevation relationships are developed to more precisely define permafrost/non-permafrost boundaries within this complex terrain.

INTRODUCTION

In the discontinuous permafrost region of interior Alaska, the occurrence of permafrost is controlled by a complex of environmental and topographic factors. These site factors include landform, soils, vegetation community, slope, and aspect, as well as winter snow cover and the mean annual air temperature (Brown and Péwé, 1973; Brown, 1978; Lunardini, 1981; Nelson and Outcalt, 1983). Ground temperature data and related environmental information on the spatial relationships of discontinuous permafrost in the upland bedrock terrain of Alaska are scarce. Indirect methods of permafrost mapping, such as the use of remote sensing, are becoming more reliable with the development of geographic information systems modeling techniques (e.g. Morrissey et al., 1986). But this approach requires ground truth from actual drill hole measurements and/or surface and subsurface temperature measurements for accurate interpretation of terrain/vegetation associations related to permafrost distribution. To better understand the interrelationships among these factors and to provide the needed data, a series of thermistor cables were installed in drill holes on natural, undisturbed sites within the Caribou-Poker Creeks Research Watershed (Fig. 1).

The instrumentation approach employed in this study is unique because it permits comparison of non-permafrost and permafrost surface and subsurface temperature regimes in close geographic proximity, but with different slope, aspect, elevation, and vegetative cover. The resulting data and analysis provide needed documentation and algorithms for a more accurate delineation of permafrost boundaries.

SITE DESCRIPTION

Physical setting

The Caribou-Poker Creeks Research Watershed is located within the Yukon-Tanana Uplands of central Alaska, 48 km north of Fairbanks (Fig. 1). This portion of the Uplands was not glaciated during the Pleistocene and consists of rounded, even-topped ridges and hills with gentle side slopes (Wahrhaftig, 1965). Caribou and Poker creeks are in generally flat, alluvial-floored valleys that are up to 400 m wide. Elevations in the watershed range from approximately 195 m at the mouth of Poker Creek to 826 m on the ridge at the far northern edge of the watershed. Caribou Peak, at 773 m, is a prominent peak in the center of the watershed.

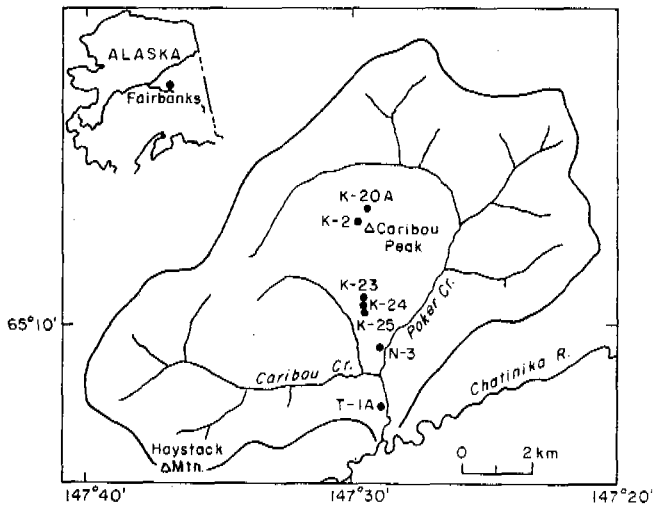

Fig. 1. Site locations in Caribou-Poker Creeks Research Watershed.

Climate

Interior Alaska is a region of pronounced continental climate characterized by large diurnal and annual temperature variations, low annual precipitation, low cloudiness, and low humidity. Primarily because of its higher elevation, most of the watershed is warmer in winter and cooler in summer than Fairbanks. Mean annual air temperatures within the watershed range from -4.9°C at the valley bottom to -2.9°C on Caribou

Peak, with the highest temperature of -1.2°C at sites on the south-facing side of Caribou Peak, at intermediate elevations between the valley bottom and the peak (Haugen et al., 1982). Within the watershed the greatest temperature contrasts are in winter, when the valley bottoms are beneath the regional air temperature inversion and are quite cold compared to the higher sites above the inversion (Bilello, 1974; Haugen and Brown, 1978).

Geology and soils

The Caribou-Poker Creeks Research Watershed is underlain by rock of the Yukon-Tanana Terrane, an igneous and metamorphic complex that extends more than 1000 km from east-central Alaska to the southern Yukon Territory (Foster et al., 1973). Within the watershed itself, the underlying rocks are quartz-mica schists, garnet-mica schists, and micaceous quartzites of the green schist facies (Forbes and Weber, 1982), with quartz-mica schist predominating. The rock is deeply weathered to >20 m.

Colluvium derived from the underlying weathered bedrock is found on the flanks of the hills and on valley slopes. The colluvium probably includes some inactive solifluction deposits. Soil creep is an important ongoing process along the north-facing valley slopes of the watershed (Wu, 1984). A thin cap of loess mantles the area, but because the loess is derived from the floodplains of streams draining areas of the same rock type, there is no sharp boundary between the loess and colluvium derived from the weathered schist below it (Rieger et al., 1972). Much of the loess that was present on the slopes has been retransported to the valley bottoms, with retransported silt fans and aprons occurring along the valley sides. These silt deposits are frozen and contain ice-rich sediments and organics (Péwé, 1982).

Soils in the watershed are generally thin, poorly developed silt loams that contain varying amounts of sand or angular gravel, which is derived from weathered bedrock within a meter or so of the surface. Rieger et al. (1972) mapped seven soil series within the watershed; they can generally be divided into permafrost-underlain soils, which are poorly drained, and permafrost-free soils. Permafrost-underlain soil series as mapped comprise 30% of the watershed. Detailed soils information based on the drill logs is available (Collins and Zenk, in prep.).

Vegetation

The vegetation of the watershed is characteristic of the interior Alaska upland boreal forest (taiga), with black spruce growing on north-facing slopes and in poorly drained valley bottoms. Aspen, birch, alder, and white spruce are found on well-drained soils, typically located on south-facing slopes. Variations in vegetation communities over short distances are caused by variations in slope, aspect, drainage, post-fire successional stage, and geomorphic processes.

A large wildfire burned over most of the watershed about 1910. The varying intensity of the fire in different areas of the watershed has apparently affected the rate of succession, the distribution of plant species, and the composition of the vegetation communities now found in the watershed (Jorgenson et al., in press).

METHODS

Instrumentation

The seven instrumented sites are located along a south-to-north transect and form an almost complete topographic profile of the watershed (Fig. 1). The profile starts on a frozen northeasterly facing low-angle slope near the valley bottom of Poker Creek. It then ascends the unfrozen south-facing slope of Caribou Peak. The profile extends over the top of Caribou Peak and ends on the frozen north-facing slope.

Instrumentation consists of cables with 10-16 thermistors spaced along the length. Cable lengths range from 4.3 to 12.3 m depending on the depth of the original borehole. Drilling was done in the winter, and great care was taken during drilling to minimize disturbance of the natural ground cover and to clean up all drill cuttings. After drilling, the multipoint thermistor cables were installed in PVC pipe filled with silicon fluid to minimize convection (Osterkamp, 1974). The cables were equipped with long readout extensions so that foot traffic was not necessary in the vicinity of the thermistor installation. Thermistor resistance measurements were made weekly using a digital multimeter.

Site descriptions

Site characteristics, including drill hole depth, setting, slope, and aspect, are listed in Table 1. Site T-1A is located in the valley of lower Poker Creek, approximately one kilometer downstream from the junction of Caribou and Poker creeks. Site T-1A is typical of a continuously frozen retransported silt fan, commonly found in valleys of interior Alaska. The vegetation varies from stands of open black spruce (Picea mariana) forest (canopy 25-60%) to a black spruce woodland complex (canopy 10-25%). The ground cover consists of a 45-cm-thick organic mat of feather mosses and lichens. The entire 10.4-m hole is in frozen silt.

Site N-3 is located near the bottom of the south-facing slope of Caribou Peak. The vegetation consists of a closed mixed forest community of black spruce, birch (Betula papyrifera), and aspen (Populus tremuloides) and a 24-cm organic mat of mosses. Seventy centimeters of silt and organic silt rests directly on bedrock.

Sites K-25, K-24, and K-23 are all located midslope on the south side of Caribou Peak. The three sites are all within 45 m elevation of each other and have similar equivalent latitudes (Table 1), but have considerably different vegetation types. All three sites have shallow silt soils over weathered bedrock. The vegetation at Site K-25 is a closed aspen forest with a thin 6-cm organic layer of forest litter. Site K-24 has a closed black spruce forest with trees to 8 m high and a 30-cm-thick mat of mosses. The vegetation at K-23 consists of a closed tall-shrub community of alder (Alnus crispa) up to 3 m high, with a 10-cm-thick organic mat.

Table 1
Caribou-Poker Creek Site Characteristics

Site	Landform	Hole Depth (m)	Elev (m)	Slope	Aspect	Equiv. Lat.	MAST (°C)
T-1A	Fs	10.8	230	3°	070°	66.24°	-1.8
N-3	Ns	4.6	250	5°	131°	61.65°	+0.7
K-25	Ns	16.2	390	12°	194°	53.42°	+1.9
K-24	Ns	12.8	410	12°	202°	53.79°	+0.4
K-23	Ns	15.9	435	10°	177°	55.71°	+2.2
K-2	Ns	4.6	770	2°	346°	67.13°	-1.0
K-20A	Ns	5.3	710	11°	004°	75.85°	-1.3

Fs - Retransported Silt (Frozen)
Ns - Schist

Site K-2 is located near the summit of Caribou Peak, which separates the drainages of Poker and Caribou creeks. It is an area of open dwarf-tree scrub consisting of scattered black spruce less than 3 m high with a 15-cm-thick organic mat over very thin rocky soil that overlies weathered bedrock. This site is a transition between non-permafrost areas on the south side of Caribou Peak and permafrost-underlain areas on the north side.

Site K-20A is located on the north side of Caribou Peak, 0.4 km north and 60 m below the summit. The vegetation consists of open black spruce forest with scattered alder and an 18-cm-thick mat of feather mosses and Sphagnum.

Equivalent latitude was calculated for each site as an index of potential insolation. The concept of equivalent latitude was applied by Dingman and Koutz (1974) to explain permafrost-topographic relationships. Any slope is parallel to a horizontal plane on the earth's surface at some latitude and receives the same potential insolation as that plane. The latitude of the horizontal plane is the equivalent latitude, θ', and depends on the inclination and azimuth of the slope:

$$\theta' = \sin^{-1}(\sin K \cos H \cos\theta + \cos K \sin\theta) \qquad (1)$$

where θ is the actual latitude of the slope, K is the inclination, and H is the azimuth. The equivalent latitude for each site is listed in Table 1.

GROUND TEMPERATURE RELATIONSHIPS

Figure 2 shows the mean ground temperature at each level for all sites within the watershed, representing averages of all the temperature readings taken between 1 June 1986 and 31 May 1987. This figure clearly shows that site T-1A was continuously frozen and was the coldest site recorded in the watershed. Ground temperatures at K-2 and K-20A were also found to be low in comparison to other sites in the watershed. The warmest sites were those located midslope on the south side of Caribou Peak. Overall, the highest surface temperatures were recorded at sites K-25 and K-23. The nearby site of K-24 showed a considerably lower average ground temperature pattern than the other two, probably because of vegetation differences at that site.

The Mean Annual Surface Temperature (MAST) for each site is listed in Table 1. We consider the surface to be the organic/mineral soil interface. Under a steady state condition, the mean annual temperature at any depth would be a linear extrapolation of the geothermal gradient. The MAST is determined by the projection of the mean ground temperature line to the surface (Lunardini, 1981). Since the mean ground temperature is markedly higher near the surface at several of the sites (Fig.1), we conclude the steady state condition no longer exists and we used the actual rather than the extrapolated

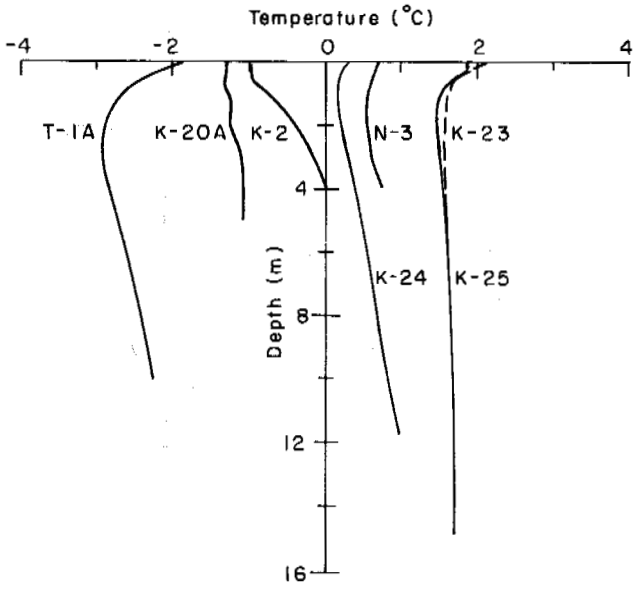

Fig. 2. Average ground and surface temperatures for all sites.

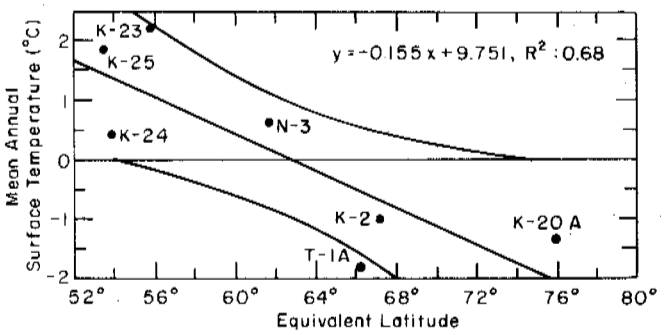

Fig. 3. Regression and correlation of mean annual surface temperature (MAST) with equivalent latitude. The curved lines show the 95% confidence interval for true mean of Y.

surface temperature for our comparison to equivalent latitude (Fig. 3). The coefficient of determination (r^2) for this relationship is 0.68. Most of the MAST differences among the sites with a similar equivalent latitude, such as K-25, K-24, and K-23, appear to be due to vegetation. The black spruce and thick moss cover of K-24 provides considerably more insulation and shading compared to the two nearby sites. The permafrost/non-permafrost boundary is represented by the intersection of the regression line with 0°C MAST (Fig. 3), which occurs at approximately 63° equivalent latitude.

The MAST at the valley bottom site, T-1A, is much lower than at any other site in the watershed. Winter inversions of the air temperature profile result in sharply lower air temperatures at the valley bottom. This site also has by far the thickest surface organic ground mat (45 cm). The moss (primarily Sphagnum spp.) tends to have a lower thermal conductivity during the summer (it is driest in June-July), which would lessen the heat flux into the ground as compared to the other sites. Site differences in depth of winter snow cover is a third major factor, but we do not have sufficient data to evaluate its effect.

The only air temperatures available for comparison are long-term annual means of -2.9°C for Caribou Peak and -4.5°C for Caribou Creek valley (Haugen et al., 1982). Applying an empirical equation developed for air and ground surface (organic/mineral soil interface) mean annual temperatures from a Fairbanks to Prudhoe Bay transect that includes the present study area, Haugen et al.(1983) found a regression relationship of

$$Y = 1.25 + 0.71X \qquad (2)$$

where X is the mean annual air temperature and Y is the MAST. The equation yields an estimated MAST of -0.8°C for the K-2 ridgetop site, and -2.2°C for the T-1A valley bottom site, close to the observed MASTs of -1.0 and -1.8°C for the two sites (Table 1).

CONCLUSIONS

The monitoring of surface and subsurface ground temperatures at seven drill hole sites in a discontinuous permafrost upland taiga environment has provided documentation of surface and subsurface temperatures for proximal permafrost/non-permafrost regimes. The measurements indicate a strong relationship between permafrost distribution and several environmental parameters; slope orientation and aspect (characterized by equivalent latitude computations), elevation and related winter air temperature inversions, and vegetation associations appear to be the most important ones. The equivalent latitude analysis yields a permafrost/non-permafrost boundary at 63°, and an empirically derived mean annual air and surface temperature equation from previous work agrees closely with the present ground surface temperature observations at the highest (Caribou Peak) and lowest (Caribou Creek valley) sites. This analysis of slope equivalent latitude, elevation-air temperature relationships, and vegetation associations has provided documentation and algorithms to permit a more accurate delineation of permafrost boundary areas in an upland taiga environment.

ACKNOWLEDGEMENTS

The authors acknowledge the contributions of Jerry Brown, formerly of USA CRREL, Hanover, N.H., who was responsible for initiating this project; Bruce Brockett, who provided technical assistance on the winter drilling work; and Anthony Zenk, who did much of the field data collection.

REFERENCES

Bilello, M A (1974).
Air masses, fronts and winter precipitation in central Alaska. U.S. Army Cold Regions Research and Engineering Laboratory, Research Report 319.

Brown, R J E (1978).
Influence of climate and terrain on ground temperature in the continuous permafrost zone of northern Manitoba. Proc. Third Int. Conf. on Perm., 15-21.

Brown, R J E & Péwé, P L (1973).
Distribution of permafrost in North America and its relation to the environment; a review. Proc. Second Int. Conf on Perm., 71-100.

Collins, C M & Zenk, A , in preparation.
Ground temperature studies in the Caribou-Poker Creeks Research Watershed, Alaska. U.S. Army Cold Regions Research and Engineering Laboratory, Special Report.

Dingman, S L & Koutz, F R (1974). Relations among vegetation, permafrost, and potential insolation in Central Alaska.
Arctic and Alpine Research, (6), 1, 37-42.

Forbes, R B & Weber, F R (1982).
Bedrock geologic map of the Fairbanks mining district, Alaska. Alaska Division of Geological and Geophysical Surveys, Open-file Report 170.

Foster, H L, Weber, F R, Forbes, R B & Graff, E E (1973).
Regional geology of Yukon-Tanana Upland, Alaska. Arctic Geology, American Association of Petroleum Geologists Memoir 19, 388-395.

Haugen, R K, & Brown, J (1978).
Climatic and dendroclimatic indices in the discontinuous permafrost zone of the central Alaskan uplands. Proc. Third Int. Conf. on Perm., 392-398.

Haugen, R K, Slaughter, C W, Howe, K E & Dingman, S L (1982).

Hydrology and climatology of the Caribou-Poker Creeks Research Watershed, Alaska. U.S. Army Cold Regions Research and Engineering Laboratory, CRREL Report 82-26.

Haugen, R K, Outcalt, S I & Harle, J C (1983). Relationships between estimated and mean annual air and permafrost temperatures in north-central Alaska. Proc. Fourth Int. Conf. on Perm., 462-467.

Jorgenson, M T, Slaughter, C W & Viereck, L A (in press). Reconnaissance survey of vegetation and terrain relationships in the Poker-Caribou Creeks Watershed, Central Alaska. Institute of Northern Forestry, U.S. Forest Service.

Jorgenson, M T (1984). Potential insolation as a topoclimatic characteristic of drainage basins. Int. Assoc. Sci. Hydrol. Bull., (9), 1, 27-41.

Lunardini, V J (1981). Heat Transfer in Cold Climates. Van Nostrand Reinhold Company, New York.

Morrissey, L A, Strong, L L, & Card, D H (1986). Mapping permafrost in the boreal forest with Thematic Mapper satellite data. Photogrametric Engineering and Remote Sensing (52), 1513-1520.

Nelson, F & Outcalt, S I (1983). A frost index number for spatial prediction of ground-frost zones. Proc. Fourth Int. Conf. on Perm., 907-911.

Osterkamp, T E (1974). Temperature measurements in permafrost. Alaska Department of Transportation and Public Facilities, Report No. TFHWA-AK-RD-85-11.

Péwé, T L (1982). Geologic hazards of the Fairbanks area, Alaska. Alaska Geological and Geophysical Surveys, Special Report 15.

Rieger, S, Furbush, C E, Schoephorster, D B, Summerfield, H & Gieger, L C (1972). Soils of the Caribou-Poker Creeks Research Watershed, Alaska. U.S. Army Cold Regions Research and Engineering Laboratory, Technical Report 236.

Wahrhaftig, C (1965). Physiographic divisions of Alaska. U.S. Geological Survey, Professional Paper 482.

Wu, T H (1984) Soil movements on permafrost slopes near Fairbanks,Alaska. Canadian Geotechnical Journal, (21), 699-709.

THAWING IN PERMAFROST – SIMULATION AND VERIFICATION

M. Yavuz Corapcioglu and S. Panday

Department of Civil and Environmental Engineering, Washington State University,
Pullman, WA 99164-3001, USA

SYNOPSIS Governing equations of thawing permafrost are developed for an unsaturated frozen porous medium, to predict the extent and rate of thawing. These are comprised of the conservation of mass equations for the unfrozen water, the melting ice, and the deforming porous medium, as well as an energy conservation equation for the entire system. Solution is achieved by discretizing these equations using the Crank-Nicolson scheme. Results are compared with laboratory experiments conducted at CRREL. Excellent match is noticed between observed and simulated temperature and pore pressure profiles, as well as settlement rates.

INTRODUCTION

Permafrost is any rock or soil material that has remained below the freezing temperature of water continuously for two or more years. Being a delicately balanced thermal phenomenon, permafrost heals very slowly when damaged, if ever. Thawing of permafrost with subsequent surface subsidence under unheated structures such as roads, air fields and railroads and ground subsidence under heated structures are two main types of permafrost related problems. The rate and extent of degradation are a few of the important considerations in geotechnical engineering in arctic and subartic regions. This can be predicted by use of a mathematical model designed to simulate the physical system under consideration in a simplified but rigorous way. The predictive ability of such methods is based on identification and quantification of the significant physical phenomena operative therein, and upon construction of mathematical representations to describe these phenomena.

The works by Tsytovich and co-workers appear to be the first studies on this subject (e.g., Tsytovich et al., 1966). A one-dimensional study of permafrost thaw and settlement was later investigated by various researchers. Some of them approached the problem from a simplistic and practical point of view (e.g., Brown and Johnston, 1970), while others preferred a more theoretical approach. Morgenstern and Nixon (1971) formulated thaw settlement in terms of the theory of consolidation. Nixon and Morgenstern (1973) later extended their study to incorporate arbitrary movements of the thaw line, including a nonlinear compressibility relation.

There are also various studies to simulate the coupled mass and heat transport in a freezing deformable soil system in addition to studies for rigid porous media. Studies on deformable media include the works of Sheppard et al., (1978), and Sykes et al., (1974). Bear and Corapcioglu (1981) developed a mathematical model for fluid pressure, temperature, and land subsidence due to temperature and pressure changes in a saturated porous medium. Conservation of mass, energy and equilibrium equations were developed and the effects of viscous dissipation and compressible work have been included in the formulation. The effects of heat transfer by forced convection as well as conduction were included in the model.

One may summarize the limitations of all current models collectively by noting that none deals with soil mechanics of any complexity, e.g., with consolidation, unsaturated medium, frozen moisture (ice) content, and none completely couple the governing equations, e.g., equilibrium equations, conservation of mass equations for frozen and unfrozen water, and heat balance equation. This study presents a mathematical model which includes coupled transport equations to obtain the governing equation of thaw of a partially frozen porous medium based on concepts developed by Corapcioglu (1983). A numerical solution scheme is applied to solve the model and comparison of these results with experimental values obtained at the CRREL (Guymon et al., 1985), is presented. A more detailed treatment of the subject is given by Corapcioglu and Panday (1988) and Panday and Corapcioglu (1988).

GOVERNING EQUATIONS

The Unfrozen Water Flow Equation

Thaw subsidence of partially frozen unsaturated soils is a complex phenomenon. At a macroscopic level, there exist four distinct phases (soil solids, ice, water, and air) within any representative elementary volume of the soil system. Due to an increase of temperature, the ice within the soil system starts melting, thus creating a two-fold effect. First, due to thawing and associated drainage, the pore water pressure decreases, leading to an increase in effective stresses on the soil grains, causing deformations. Furthermore, thaw settlement occurs due to a volume change in the melting ice. The soil air is assumed to remain at

atmospheric pressure, thus neglecting conservation of mass equation for air during the formulation. The solid phases, ice and soil grains are assumed to be incompressible individually; however, the soil matrix as a whole deforms. We assume that ice moves with the velocity of the soil particles which is the rate of deformation. Changes in the volumetric contents of the phases due to mass transfer (e.g., evaporation, sublimation, condensation) other than melting and freezing are assumed to be negligible.

A macroscopic conservation of mass equation can be written for each phase in the medium. The three-dimensional conservation of mass equation for the unfrozen water phase is given by

$$\nabla\cdot\rho_f \underset{\sim}{q} + \frac{\partial}{\partial t}(\rho_f\theta_w) - R_a = 0 \qquad (1)$$

The reader is referred to Appendix A for a definition of symbols. For a deforming porous medium, the specific discharge of water relative to the moving solid is expressed by a modified Darcy's law.

$$\underset{\sim}{q}_r = \theta_w(\underset{\sim}{V}_f - \underset{\sim}{V}_s) = \underset{\sim}{q} - \theta_w\underset{\sim}{V}_s$$
$$= -\underset{\approx}{K}\left(\frac{1}{\rho_f g}\nabla p - \nabla z\right) - \underset{\approx}{D}_{MT}\nabla T \qquad (2)$$

where the flow is induced by potential as well as thermal gradients. Assuming that the solid grains are incompressible, the equation of solid mass conservation can be expressed as

$$\nabla\cdot[(1-n)\underset{\sim}{V}_s] + \frac{\partial}{\partial t}(1-n) = 0 \qquad (3)$$

Relating the volumetric strain rate to the velocity of moving solids, and employing the concept of material derivatives with respect to moving solids the insertion of (2) and (3) into (1) yields

$$\nabla\cdot\underset{\sim}{q}_r + S_w\frac{\partial\varepsilon}{\partial t} + n\frac{\partial S_w}{\partial t} - \frac{R_a}{\rho_f} = 0 \qquad (4)$$

where the water is assumed to be incompressible under pressure and temperature conditions existing in permafrost soils and the material derivatives are replaced by partial ones by assuming a negligible convective component. Following Bear, Corapcioglu, and Balakrishna (1984) a modified relation between total stresses, effective stress, and pore pressures for an unsaturated porous medium is

$$\sigma_{ij} = \sigma'_{ij} - S_w p\,\delta_{ij} \qquad (5)$$

The strains are a function of the effective stresses, and of temperature [i.e., $\varepsilon = \varepsilon(\underset{\approx}{\sigma}', T)$] and one can write

$$\frac{\partial\varepsilon_{ij}}{\partial t} = \frac{\partial\varepsilon_{ij}}{\partial\sigma'}\bigg|_T\frac{\partial\sigma'}{\partial t} + \frac{\partial\varepsilon_{ij}}{\partial T}\bigg|_p\frac{\partial T}{\partial t} = \alpha_p\frac{\partial}{\partial t}(S_w p) + \alpha_T\frac{\partial T}{\partial t} \qquad (6)$$

with the assumption of a constant total stress, and for one-dimensional (vertical) consolidation).

The degree of unfrozen water saturation S_w is a function of the pore water pressure, p, and temperature, T. Under isothermal conditions, the relation between S_w and p, is given by the moisture retention curve [$S_w = S_w(p)$]. The phase composition of water in the frozen soil represents the variation of the volumetric content of unfrozen water remaining at a given temperature below freezing. These two curves can be plotted simultaneously in three-dimensional space (θ_w, p, and T) to obtain the surface illustrated in Figure 1. Thus, this surface can be represented as $\theta_w = \theta_w(p,T) = n[S_{w1}(p)\cdot S_{w2}(T)]$

And, we can write

$$\frac{\partial S_w}{\partial t} = \frac{\partial S_w}{\partial p}\bigg|_T\frac{\partial p}{\partial t} + \frac{\partial S_w}{\partial T}\bigg|_p\frac{\partial T}{\partial t} = \xi_p\frac{\partial p}{\partial t} + \xi_T\frac{\partial T}{\partial t} \qquad (7)$$

where the slopes ξ_p and ξ_T can be obtained from the surface generated in Fig. 1. We can also express the amount of ice mass on this surface. For example the ice mass at point D is equal to the mass of water at point A minus the mass of water at point D. Note that point A is on the θ_w vs. p plane, i.e., T = 0°C. So the volumetric ice fraction, θ_i can be calculated as $\theta_i = n(\rho_f/\rho_i)\,Sw_1(P)\,[1 - Sw_2(T)]$ where we neglect any mass transfer into the air phase from the water or the ice phase (i.e., condensation, vaporization, and sublimation). Plotting this variation of ice content with pressure and temperature, as in Figure 2, the temporal variation of ice content θ_i can be written as

$$\frac{\partial\theta_i}{\partial t} = \frac{\partial\theta_i}{\partial p}\bigg|_T\frac{\partial p}{\partial t} + \frac{\partial\theta_i}{\partial T}\bigg|_p\frac{\partial T}{\partial t} = \xi_{ip}\frac{\partial p}{\partial t} + \xi_{iT}\frac{\partial T}{\partial t} \qquad (8)$$

where the slopes ξ_{ip} and ξ_{iT} can be obtained from the surface generated in Fig. 2. The phase composition curve, like the retention curve, experiences hysteresis during the freezing and thawing cycles (Koopmans and Miller, 1966), but this effect has been neglected. These curves have been obtained at a constant porosity under equilibrium conditions. However, the use of such equilibrium curves in studies involving transient flow problems in unsaturated soils, especially in slow-varying problems like thaw-consolidation, is a valid procedure.

The Conservation of Mass Equation for Ice

The conservation of mass equation for the melting ice in a porous medium is given by

$$\frac{\partial}{\partial t}(\rho_i\vartheta_i) + \nabla\cdot(\rho_i\vartheta_i\underset{\sim}{V}_s) + R_a = 0 \qquad (9)$$

It is assumed here that ice moves with the same velocity as the solid soil particles. With the assumption that the density of ice, ρ_i, remains constant, and using the definition of strains, replacing material derivatives by partial ones, and inserting (6) and (7) for partial derivatives into (9) we obtain

$$-R_a = \{\rho_i \xi_{ip} + \rho_i \theta_i \alpha_p [p\xi_p + S_w]\} \frac{\partial p}{\partial t} + \{\rho_i \xi_{iT} + \rho_i \theta_i [p\alpha_p \xi_T + \alpha_T]\} \frac{\partial T}{\partial t} \quad (10)$$

for a one-dimensional expansion, where $\partial\theta i/\partial t$ has been expressed by (8). The unfrozen water flow equation can finally be completed by again expanding and substituting (6) and (7) in (4), to obtain

$$\frac{\partial}{\partial z}\left[-\underline{\underline{K}}\left\{\frac{1}{\rho_f g}\frac{\partial p}{\partial z} - 1\right\} - \underline{\underline{D}}_{MT}\frac{\partial T}{\partial z}\right] + \left[S_w p\alpha_p \xi_p + \alpha_p S_w^2 + n\xi_p + (\rho_i/\rho_f)\xi_{ip} + (\rho_i/\rho_f)\theta_i \alpha_p \left\{p\xi_p + S_w\right\}\right]\frac{\partial p}{\partial t} + \left[S_w p\alpha_p \xi_T + S_w \alpha_T + n\xi_T + (\rho_i/\rho_f)\xi_{iT} + (\rho_i/\rho_f)\theta_i \left\{p\alpha_p \xi_T + \alpha_T\right\}\right]\frac{\partial T}{\partial t} = 0 \quad (11)$$

for a vertical one-dimensional column, where coupling has been achieved through the R_a term to (10), and $\underline{q}_r$ is expressed by (2).

Conservation of Energy Equation

The macroscopic energy conservation equation for a saturated porous medium was developed by Bear and Corapcioglu (1981) starting from microscopic considerations and deriving the macroscopic one by averaging the former over a representative elementary volume of the porous medium. It is assumed that the thermal resistance between water and soil particles is small, hence, local water and matrix temperatures are equal. A modification of Bear and Corapcioglu's (1981) equation to incorporate the phase change due to melting in an unsaturated thawing deformable porous medium would give

$$\frac{\partial}{\partial t}[(\rho C)_m T] - L R_a + \nabla\cdot[\{\theta_w \rho_f C_{v-f} \underline{V}_{w-f} + \theta_i \rho_i C_i \underline{V}_s + (1-n)\rho_s C_{\varepsilon-s} \underline{V}_s\}T] - \nabla\cdot[\underline{\underline{\Lambda}}_m \nabla T] - p\nabla\cdot(\theta_{w-f}\underline{V}_{w-f}) + [\theta_i + (1-n)]T\gamma\frac{\partial \varepsilon}{\partial t} = 0 \quad (12)$$

The first term of (12) is the rate of change of the total heat content. The second term represents the rate of heat production due to melting. The third term represents convective heat flow, the fourth term is a Fourier heat conduction law, and the last two terms represent internal energy increase due to viscous dissipation, and compression, respectively.

Calculating the heat capacity of the total matrix, as the sum of the heat capacities times the volumetric contents of the individual phases, replacing terms involving rate of change of mass of unfrozen water and ice by (1) and (9), respectively, and using (2) for the flow rate yields, after manipulations

$$[(\rho C)_m + pn\xi_T + \{p\alpha_p \xi_T + \alpha_T\}\{(\theta_i + 1 - n)T\gamma + (1-n)pS_w\} - \{\rho_i \xi_{iT} + \rho_i \theta_i (p\alpha_p \xi_T + \alpha_T)\}\{T(C_v - C_i) - L - p/\rho_f\}]\frac{\partial T}{\partial t} + [pn\xi_p + \{p\xi_p + S_w\}\{(1-n)T\gamma\alpha_p + (1-n)S_w p\alpha_p\} - \{\rho_i \xi_{ip} + \rho_i \theta_i \alpha_p (p\xi_p + S_w)\}\{T(C_v - C_i) - L - p/\rho_f\}]\frac{\partial p}{\partial t} + C_v \rho_f \underline{q}_r \frac{\partial T}{\partial z} - \frac{\partial}{\partial z}\left(\underline{\underline{\Lambda}}_m \frac{\partial T}{\partial z}\right) = 0 \quad (13)$$

which is the energy conservation equation expressed in a vertical one-dimension where the saturation relationships of (6), and (7) have been used to express the equation in terms of the primary variables p, and T, and coupling is done to (10) through the rate of melting term R_a.

MATERIAL PARAMETERS

For solution to the system of equations developed above, one needs the hydraulic and thermal parameters of the soil system. Properties like α_p, ρ_i, ρ_f, ρ_s, C_v, C_ε, λ_i, λ_f, λs, and the latent heat of fusion, L, can be assumed to be constants within the pressure and temperature limits under consideration, while others will be pressure and temperature dependent (e.g., K, and Ao).

The hydraulic conductivity of an unsaturated, unfrozen porous medium is a function of the liquid water content [$K = K(\theta_w)$]. For the frozen zone, ice occupies part of the pore spaces, and an impedance factor is introduced to the hydraulic conductivity (Taylor and Luthin, 1978) in the freezing zone, which is a function of the ice content. Thus the hydraulic conductivity in the frozen zone is calculated as

$$K_{frozen} = K_{unfrozen}\,(\theta_w)/\,10^{10\theta_i} \quad (14)$$

The compressibility coefficient due to thermal changes, α_T, is a parameter which can be determined from the thaw settlement parameter, A_o. For complete thawing of a fully frozen, fully saturated medium, the thaw settlement parameter A_o as defined by Sykes et al. (1974) represents the thaw settlement due to the volume change of ice on melting and release of pore water. Watson et al. (1973) have performed experiments to determine the value A_o.

Assuming that for a partially frozen, partially saturated medium the strain due to melting at constant pressure, is proportional to A_o with

the proportionality constant as the ratio of change of ice content to initial porosity, n_o, (note that this ratio will equal unity when the fully saturated frozen soil totally melts), we get α_T as

$$\alpha_T = \frac{A_o}{n_o}\frac{\partial \theta_i}{\partial T} = \frac{A_o}{n_o}\xi_{iT} \qquad (15)$$

NUMERICAL RESULTS AND DISCUSSION

Equations (11) and (13) are approximated in their finite difference form, using the Crank-Nicolson scheme. An iterative successive solution scheme solves for p and T within the solution domain, until convergence is achieved at each time step. The tridiagonal matrices generated by (11) and (13) are solved using Thomas' Algorithm. At each iteration level, the values of the non-linear parameters are updated.

The initial conditions on p and T are provided throughout the length of the column. The top boundary condition for pressure is of the second kind (prescribed flux boundary condition). The bottom boundary condition is a water table, and hence, is a first kind boundary, with zero pore-pressure.

The simulation was conducted on a vertical one-meter partially frozen soil column, for a period of 12 days. The objective was to simulate results of experimental tests conducted at CRREL (Guynom et al., 1985) so initial and boundary conditions are as provided by them. A water table condition exists at a depth of 90 cm. Simulated variations of S_w, p, and T along the depth of the column are shown in Figures 3, 4, and 5, for a 1, 4, 6, and 12-day period. Figure 3 shows the saturation profile at 1, 4, 6, and 12 day periods. It portrays the increase in saturation occurring due to the melting of ice, from the first to the sixth day, within the frozen zone. Above the frozen zone, the accumulation of water increases in time due to the relative impermeability of the frozen zone. By the 12th day, all the ice has melted and the saturation starts decreasing again due to vertical drainage. Figure 6 shows how the settlement of the soil column proceeds in time. It also compares this with the settlement curve as obtained in the laboratory by Guymon et al. (1985). Most of the settlement occurring is thaw settlement due to ice melting, with very little Terzaghi consolidation due to drainage. After all the ice melts, consolidation is very slow as can be seen from the decrease in slope that occurs at the section of the graph after approximately 7.1 days (i.e., the time it takes for the ice to melt completely.) Figures 4 and 5 compare numerical results for p, and T profiles with those obtained from a laboratory soil column experiment of Guymon et al. (1985) conducted at CRREL. The agreement of the results is very good.

Summary and Conclusions

A mathematical model describing the conditions existing within a partially saturated thawing soil column has been presented. The model includes conservation of mass equations for liquid water, frozen water (ice), soil grains, conservation of energy equation, and fundamental definitions of stress and strain. The soil air is assumed to be at the atmospheric pressures. In most studies reported in the literature, the effect of air flow is neglected. In fact, as the unfrozen water migrates down, air escapes through the upper boundary. In this case, it is possible that the pressure of the air phase might differ from the atmospheric pressure due to trapped air bubbles. However, in unsaturated partially frozen soils, Fuchs et al. (1978) report that vapor phase contributes insignificantly to transport phenomena thus justifying the assumption of atmospheric air pressure. The water, soil grains, and ice have been assumed to be incompressible. Specific retention and phase composition curves, which are obtained under equilibrium conditions, have been utilized and their involvement in slow-varying problems such as this one is justified. The material coefficients of the model involved in the solution and their relation to the conditions existing within the soil are also presented briefly. During consolidation, it is assumed that there is no relative slip between the soil and ice particles, and that they compress as one, moving with the same velocity. Also, the local acceleration term of the total derivative is much larger than the convective part and so total derivatives are replaced by partial ones. In the case of thaw consolidation, we deal with small spatial gradients and/or negligibly small velocities due to the nature of the phenomenon.

The results of the simulation were encouraging. The soil column under consideration thawed completely in about seven days. the simulation, over a 12-day period produced a settlement of about 1.8 cm, most of which was produced by thaw settlement. Terzaghi consolidation continued after all the ice had melted, but this rate of settlement was extremely slow. Pore pressure and temperature profiles, as well as the settlement rate, when compared with experimental results showed close agreement.

REFERENCES

Bear, J. and M. Y. Corapcioglu, 1981, A mathematical model for consolidation in a thermoelastic aquifer due to hot water injection or pumping, Water Resources Research, v. 17, p. 723-736.

Bear, J., M. Y. Corapcioglu, and J. Balakrishna, 1984, Modeling of centrifugal filtration in unsaturated deformable porous media, Advances in Water Resources, v. 7, p. 150-167.

Brown, W. G., and G. H. Johnston, 1970, Dikes on permafrost: Predicting thaw and settlement, Canadian Geotechnical Journal, 7, p. 365-371.

Corapcioglu, M. Y., 1983, A mathematical model for the permafrost thaw consolidation, in Permafrost, 4th Int. Conference Proceedings, National Academy Press, Washington, DC, p. 180-185.

Corapcioglu, M. Y., and S. Panday, 1988, Multiphase approach to thawing of unsaturated

frozen soils: Equation development (submitted for publication).

Fuchs, M., G. S. Campbell, and R. I. Papendick, 1978, An analysis of sensible and latent heat flow in a partially frozen unsaturated soil, Soil Science Society of America Proceedings, v. 42, p. 379-385.

Guymon, G. L., R. L. Berg, and J. Ingersoll, 1985, Partial verification of a thaw settlement model, in Freezing and Thawing of Soil Water Systems, ASCE, New York, p. 18-25.

Koopmans, R. W. R., and R. D. Miller, 1966, Soil freezing and soil water characteristic curves, Soil Science Society of America Proceedings, v. 80, p. 680-685.

Morgenstern, N. R., and J. F. Nixon, 1971, One-dimensional consolidation of thawing soils, Canadian Geotechnical Journal, 8, p. 558-565.

Nixon, J. F., and N. R. Morgenstern, 1973, Practical extensions to a theory of consolidation for thawing soils, in Permafrost, The North American Contribution to the Second International Conference, Yakutsk, Washington, DC, National Academy of Sciences.

Panday, S., and M. Y. Corapcioglu, 1988, Numerical solution, experimental verification and sensitivity analysis of multiphase permafrost thaw model, (submitted for publication).

Sheppard, M. I., B. D. Kay, and J. P. G. Loch, 1978, Development and testing of a computer model for heat and mass flow in freezing soils, in Proceedings of the Third International Conference on Permafrost, v. 1, Ottawa, National Research Council of Canada, p. 76-81.

Sykes, J. F., W. C. Lennox, and T. E. Unny, 1974, Two-dimensional heated pipeline in permafrost, American Society of Civil Engineers, Journal of the Geotechnical Engineering Division, v. 100, p. 1203-1214.

Taylor, G. S., and J. N. Luthin, 1978, A model for coupled heat and moisture transfer during soil freezing, Canadian Geotechnical Journal, v. 15, p. 548-555.

Tsytovich, N. A., et al., 1966, Basic mechanics of freezing, frozen, and thawing soils, in Technical Translation 1239, Ottawa, National Research Council of Canada.

Watson, G. H., W. A. Slusarchuk, and R. K. Rowley, 1973, Determination of some frozen and thawed properties of permafrost soils, Canadian Geotechnical Journal, v. 10, p. 592-606.

ACKNOWLEDGMENTS

This research has been supported by a grant from National Science Foundation ECE-8602849.

APPENDIX A--NOTATION

A_o Thaw settlement parameter

C_ε Gravemetric heat capacity of soil solids

C_i Gravemetric heat capacity of ice

C_v Gravemetric heat capacity of water

$\underset{\approx}{D}_{MT}$ Thermal liquid diffusivity

$d_s()/dt$ Total derivative of () with respect to moving solid

$\underset{\approx}{K}$ Hydraulic conductivity

L Latent heat of fusion

n Porosity

n_o Initial porosity

p Pore water pressure

$\underset{\sim}{q}$ Specific discharge of water

$\underset{\sim}{q}_r$ Specific discharge of water relative to the moving solid

R_a Rate of melting of ice mass

S_w Degree of unfrozen water saturation

T Temperature

$\underset{\sim}{U}$ Solids displacement

$\underset{\sim}{V}_f$ Velocity of flowing water

$\underset{\sim}{V}_S$ Velocity of solid particles

α_p Compressibility of soil

α_T Thermal compressibility of soil

$\sigma'/T|_\varepsilon = T/p$

δ_{ij} Kronecker delta

ε Strain

θ_i Volumetric ice content

θ_w Volumetric unfrozen water content

$\underset{\sim}{\Lambda}_m$ Coefficient of thermal conductivity of porous medium

λ_f Coefficient of thermal conductivity of water

λ_i Coefficient of thermal conductivity of ice

λ_s Coefficient of thermal conductivity of soil

ρ_f Density of water

ρ_i Density of ice

ρ_s Density of solid particles

$(\rho C)_m$ Heat capacity of the porous medium

σ,σ' Total and effective stresses

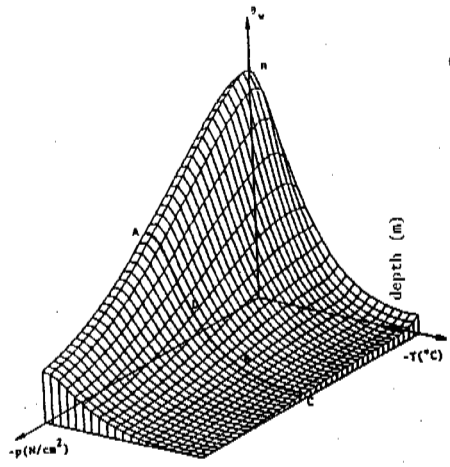

FIG. 1. Variation of liquid water content with temperature and pressure

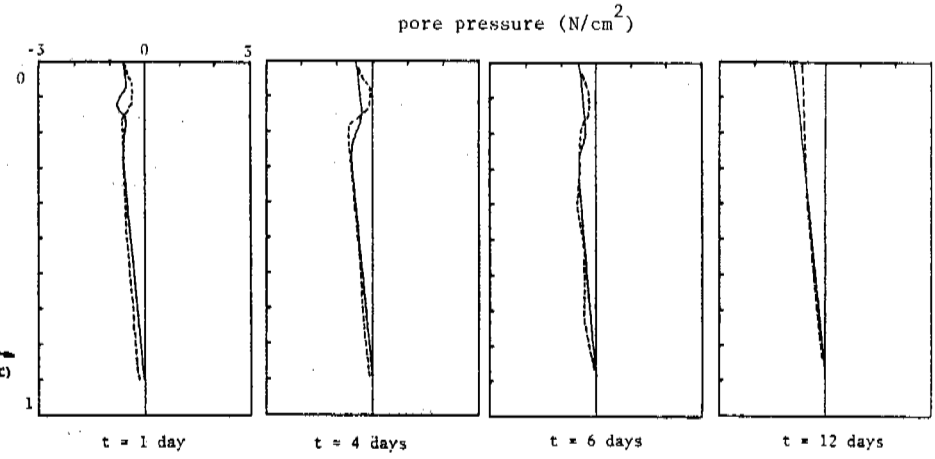

FIG. 4. Pressure profile at different times (—— numerical values, - - - experimental values)

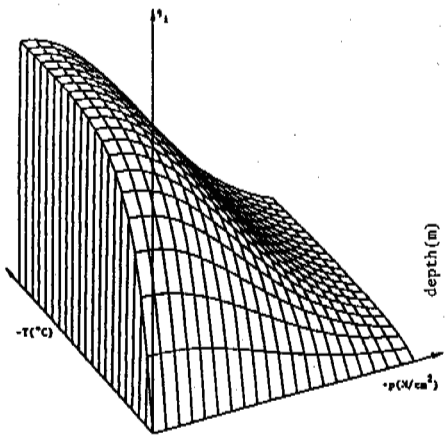

FIG. 2. Variation of ice content with temperature and pressure

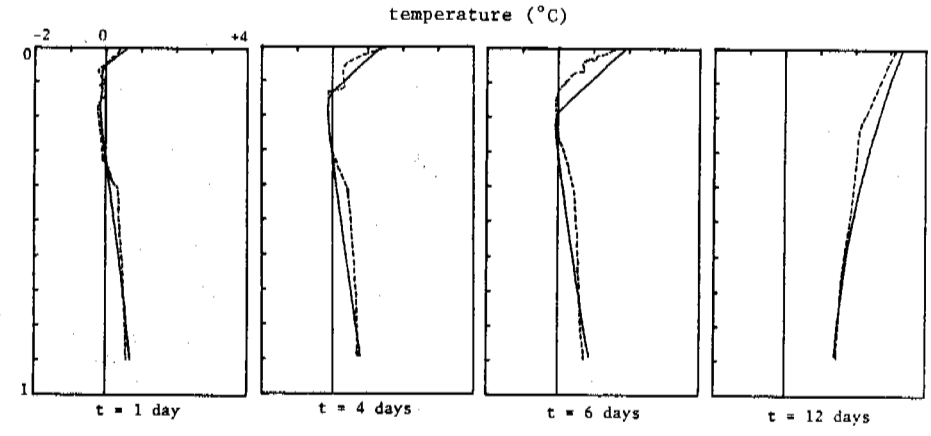

FIG. 5. Temperature profile at different times (—— numerical values, — — experimental values)

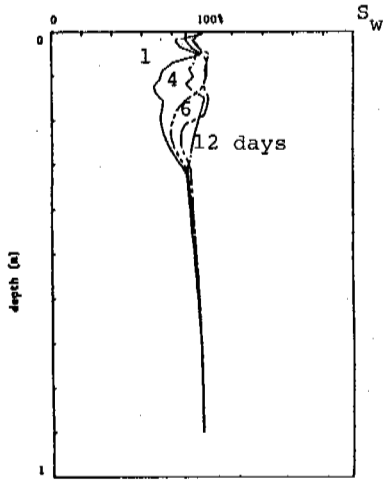

FIG. 3. Saturation profile at different times

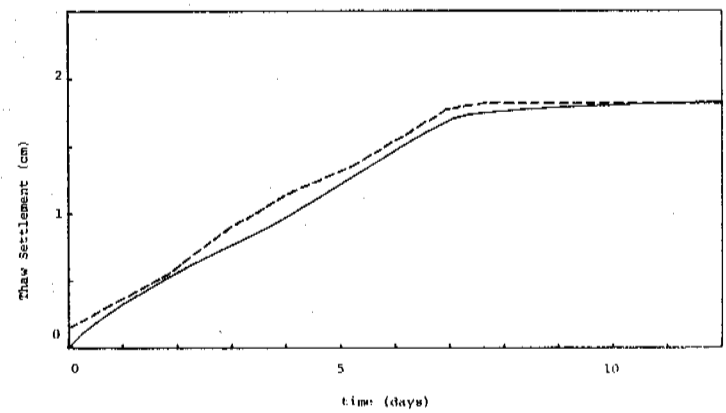

FIG. 6. Comparison of simulated(—) and experimental (- -) thaw settlement values

SCHEFFERVILLE SNOW-GROUND INTERFACE TEMPERATURES

D.T. Desrochers[1] and H.B. Granberg[2]

[1]Department of Geography, McGill University, 805 Sherbrooke Str. West, Montréal, Québec H3A 2K6
[2]Centre d'application et des recherches en télédétection (CARTEL),Université de Sherbrooke, Sherbrooke, Québec J1K 2R1

SYNOPSIS Snow-ground temperatures have been intensively monitored at an upland tundra site and an open woodland site near Schefferville, Northern Quebec. The upland site is underlain by permafrost while the woodland site is affected only by seasonal frost. The aim of the study is to develop a better understanding of the differences in thermal regime between the two sites in particular, and of regional variations in thermal regime of the Schefferville area in general. The present paper represents a preliminary analysis of the data sets. Interface temperatures beneath and between trees in the woodland are compared to similar measurements on the alpine tundra. The results indicate the great complexity of the role of the snowcover in the ground temperature regime near Schefferville.

INTRODUCTION

The snowcover has long been recognised as one of the main factors controlling the spatial distribution of permafrost in the Schefferville area (Bonnlander and Major-Marothy, 1964; Annersten, 1966; Thom, 1969; Nicholson and Granberg, 1973; Granberg, 1973; this volume; Nicholson, 1976; 1978a; 1978b). Despite many studies of the relationship between snowcover and ground temperatures (Bilello et al., 1970, 1972; Cary et al., 1978; Filion and Payette, 1978; Goodrich, 1982; Singh et al., 1984) the details of the spatial and temporal variations in temperature at the snow-ground interface remain poorly understood.

This interface is the scene of much biological activity during the winter and its thermal regime is crucial to the survival of both plant and animal life. Of particular importance in the present context is the controlling influence that spatial and temporal variations in interface temperature have on the ground temperature field. The present field study was undertaken for the purpose of developing a better understanding of the thermal regime at the snow-ground interface and also to provide baseline data for the development of ground temperature simulations routines within a Digital Geographic Permafrost Information System (GPIS) (Granberg, this volume).

STUDY AREA AND METHOD

The instrumentation for this study has been described in greater detail by Desrochers and Granberg (1986a; 1986b). Two sites were selected for this study; AT-1 in alpine tundra (54°51'N, 67°01'W 685 m a.s.l.) and SC-1 in open woodland (54°48'N, 66°49'W 514 m a.s.l.). The former site (Figure 1) was also used by Wright (1983) in a study of the hydrology of alpine tundra areas near Schefferville. Its main vegetation component is a cover of lichen with dwarf-birch (Betula glandulosa) which have been snow-abraded to heights less than the local depth of snow during the coldest part of the winter (Granberg, 1972). Stunted, procumbent spruce occur sparsely in wind-sheltered parts of the terrain while ridge-crests remain largely vegetation-free, often with a thin cover of coarse gravel and pebbles. The instrumentation for this site was installed in the summer of 1986.

The latter site (Figure 2) was instrumented in the fall of 1985. It is located in a typical lichen woodland as described by Hare (1959). The dominant tree species in this forest are black spruce (Picea mariana) and larch (Larix laricina) ranging up to 12 m in height and a crown cover density ranging from 8-20 per cent. The underbrush consists of dwarf-birch (Betula glandulosa) and labrador tea (Ledum groenlandicum) usually less than 1 m high. A 4-9 cm thick lichen mat (dominated by the species of the genus Cladina) with patches of sphagnum moss cover the surface.

The differences in snowcover regime between alpine tundra and woodlands near Schefferville have been discussed in detail by Granberg (1972; 1973). The two sites experience very different snowcovers as a result of redistribution of snow by wind. This generates a snowcover of high density which is very variable in depth both spatially and temporally. In the woodlands, the snowcover is deep and of low density as it is protected from wind erosion by the trees.

Figures 3a and 3b show the instrumentation at the two sites. Ground temperatures were measured at depths of 0.5-10 m at thirteen locations on the tundra site (AT-1), and at depths of 0.5-1.0 m at six locations on the woodland site (SC-1). Snow-ground interface temperatures were measured (at the surface of the mineral soil) at intervals of 12.5 m along the four traverses at AT-1 and at intervals of 1 m along the six traverses at SC-1. Snow tem-

Fig.1 View of the alpine tundra site (AT-1) after a mid-winter snowfall.

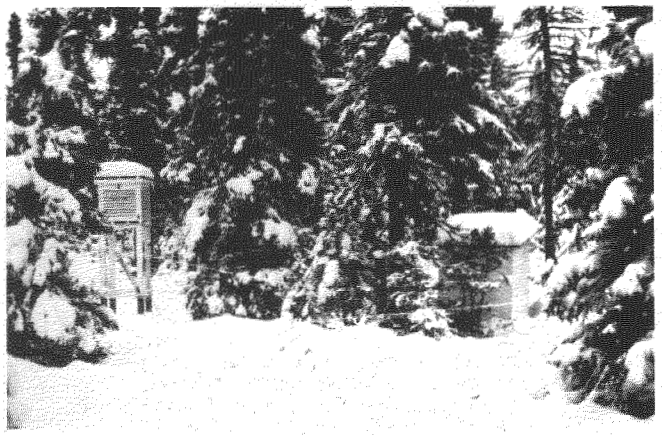

Fig.2 View of the open woodland site (SC-1) in early winter.

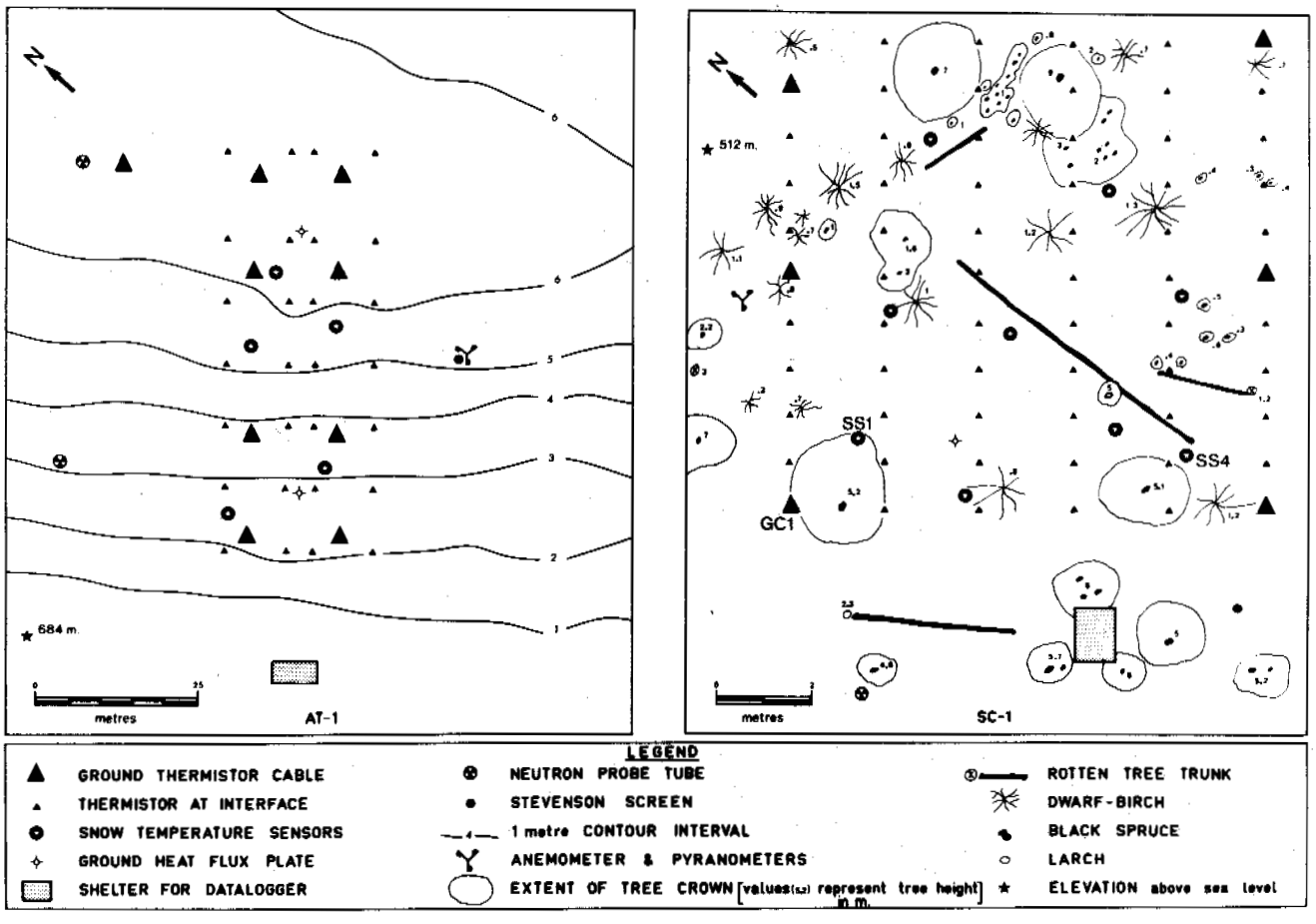

Fig.3 Maps and instrumentation of AT-1 and SC-1 near Schefferville.

peratures were monitored at levels varying from 0.5-90.0 cm above the surface at five locations at AT-1 and at nine locations at SC-1.

Air temperature, relative humidity, wind speed, global and reflected solar radiation, and ground heat flux were monitored at hourly intervals at both sites and all remaining sensors were scanned at four hour intervals using datalogging systems. Intermittently, soil moisture profiles were monitored using a neutron probe in two access holes (1.75 m) at AT-1 and one access hole (1.0 m) at SC-1.

On several occasions detailed grid surveys were made of temperature profiles through the snowcover. A set of temperature probes of low heat capacity (Granberg, 1984) were used in a portable mode to obtain 100 or more detailed temperature profiles through the snowcover on regular grids of 1 m spacing.

RESULTS

Woodland Snow Temperatures

In the forest, interception of snowfall by trees causes spatial variations in snow depth. Cavities also develop around tree branches near the ground. Free convection through these cavities may cause appreciable cooling locally. The spatial variations in ground temperature reflect spatial variations in the resistance to heat flow offered by the snowcover. They may also, to some extent, reflect microscale spatial variations in the summertime surface energy balance as a result of shading by trees, microscale variations in view factors (Reifsnyder and Lull, 1965), and local variations in turbulent fluxes.

The spatial variations in resistance to heat flow are largest in early winter when the snowcover is shallow. These variations also decrease with increasing snow depth. In general, the lowest interface temperatures occur early in the winter beneath trees while in open areas between trees, the interface temperatures are markedly warmer (Figure 4). The temperatures shown in this figure are from snow temperature sensors SS1 (beneath a tree) and SS4 (forest opening), respectively. The two sensors indicate little or no diurnal variation in the interface temperature throughout the winter. This demonstrates the excellent insulating properties of the low-density snowcover in the forest.

Figures 5a and 5b show the spatial variations in snow depth and snow-ground interface tempe-tures respectively, measured by probes on February 21, 1985. A close relationship between snow depths and temperature patterns is apparent. Extreme minimum temperatures ranged from -3.0 to -12.7°C and maximum tempe-tures were all near to 0°C.

In temperature profiles from the February survey (Figure 6) the complexity of the heat exchanges through the woodland snowcover is apparent. In the afternoon when the survey was made, the range in interface temperature was

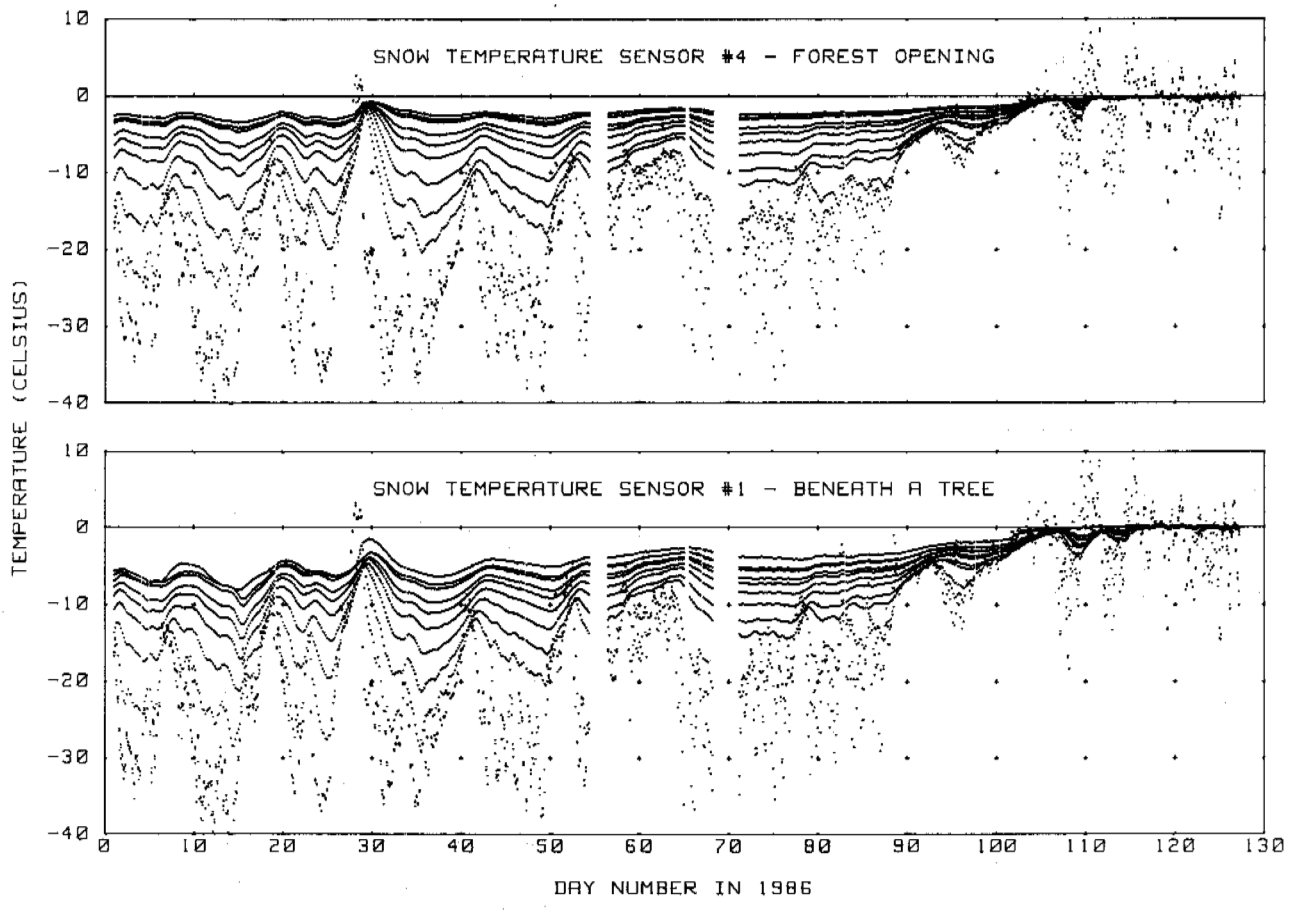

Fig.4 Snowcover temperatures in SC-1 at sensors SS4 (forest opening) and SS1 (beneath a tree) from Jan. 1 to May 10, 1986. The snow-ground interface temperatures are the warmest temperatures while snow-air interface temperatures are coldest.

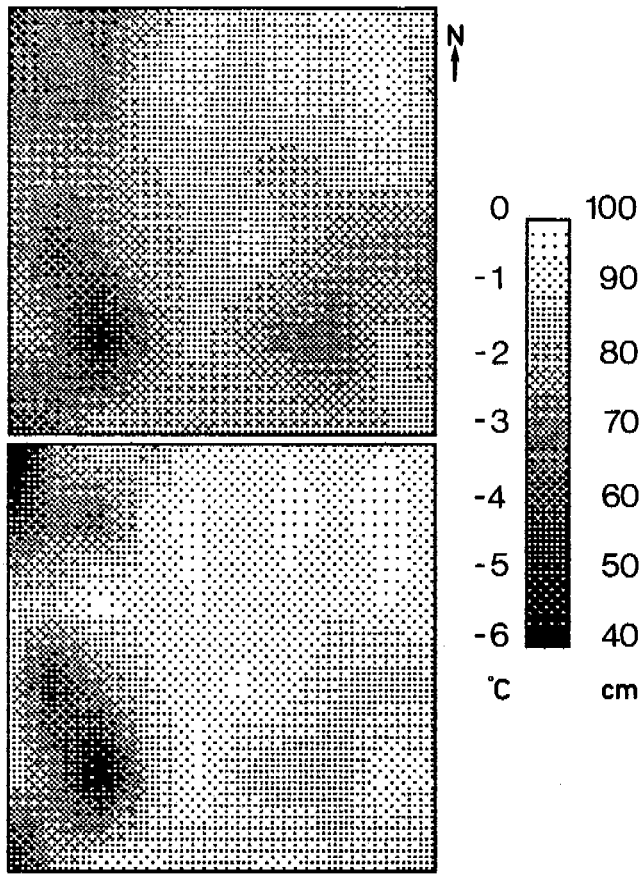

Fig.5 Spatial variations in snow depth (upper diagram) and snow-ground interface temperatures (lower diagram) near SC-1.

approximately 6°C. At the uppermost measurement level, the temperature range was approximately 3°C. While these differences arise partly from the variations in snow depth, part of the variations are probably related to effects of internal absorption of solar radiation by the snowcover itself and by vegetation in the snow. The variations may also be related to spatial variations in the effective thermal properties of the snow caused by, for example, convective heat exchanges along least-resistance paths associated with vegetation buried in the snow.

Tundra Snow Temperatures

At AT-1 the thermal regime of the snow-ground interface is entirely different from that in the woodlands. Figure 7 is a plot of temperatures measured along one snow-ground interface temperature traverse. One of the sensors is in a location of fairly deep snow (10-20 cm) while the other sensors are in shallow snow (up to 10 cm). The plot covers the period from early November to late April with some omissions due to equipment failure in very cold weather conditions.

There are large differences in snow-ground interface temperatures between areas of shallow and deep snow. In shallow snow or

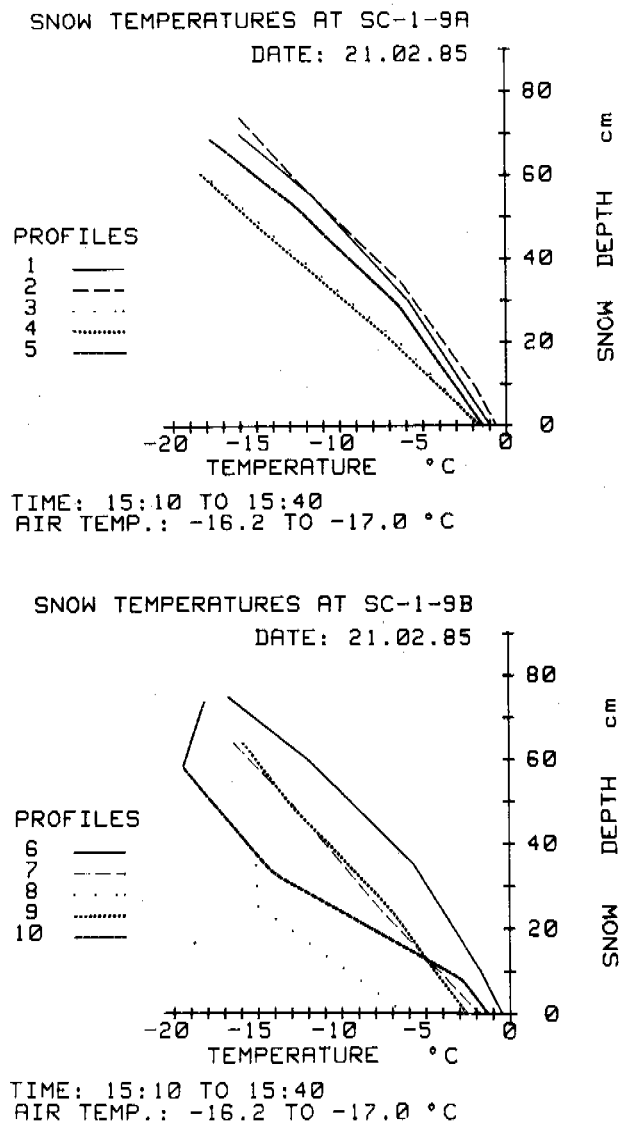

Fig.6 Snow temperature profiles near Sc-1. The snow-ground interface is taken as depth 0.

snow-free conditions, the interface temperatures tend to closely follow the air temperature fluctuations during the mid-winter period. However, as solar radiation levels increase from mid-winter on, the interface temperatures rise to several degrees above the air temperatures in the daytime. The nocturnal temperatures vary less from the air temperature and also vary less between the different shallow snow sites.

Near day 80 there is a cross-over such that the interface temperatures in shallow snow or snow-free areas become warmer than areas of deeper snow. On day 85, just at the start of a period of snowfall, the shallow snow interface temperatures reach melting temperatures. Insulation of the surface by new snow causes the interface temperatures to drop sharply,

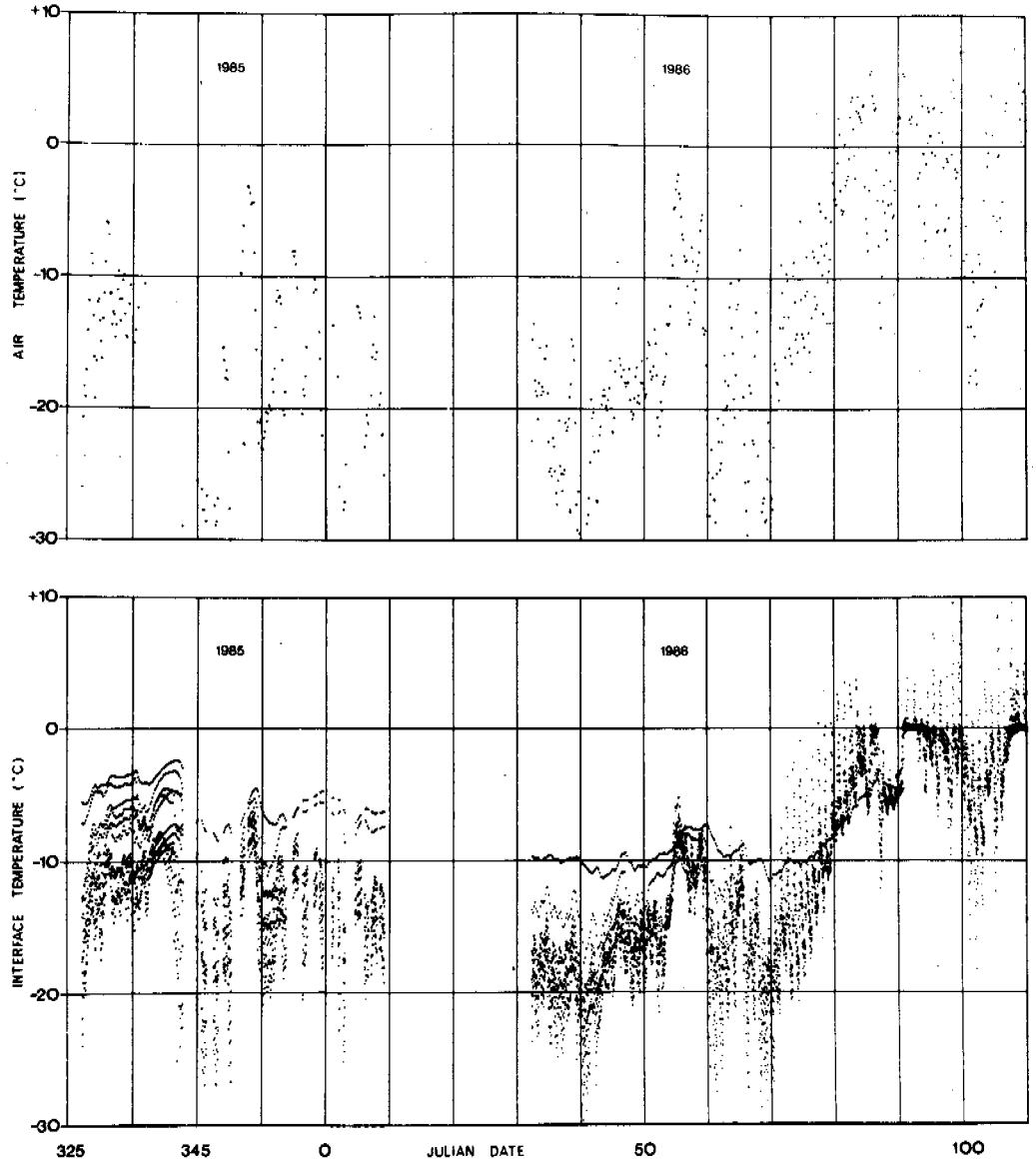

Fig.7 Plot of all snow-ground interface temperatures along a traverse at AT-1 (lower graph) and air temperature (upper graph).

indicating that the ground is still very cold closely beneath its surface.

On day 91 as warm air temperatures return, percolation of meltwater to the snow-ground interface bring all interface temperatures to the melting point, including the site with deeper snow. Effects of the cold ground below are apparent, particularly around day 100-105. By now, the snow depth at the site of deeper snow has been reduced significantly as indicated by the increased diurnal variations in interface temperature.

DISCUSSION

Comparing the data from the two sites, it is quite apparent why permafrost exists at the tundra site while not at the forested sites at Schefferville. In very general terms, the absence of the snowcover allows the ground surface temperatures to follow the air temperatures throughout the season. In an area where the average air temperature is below 0°C, permafrost may be expected to develop beneath those parts of the terrain that remain snow-free through the winter. The snow-ground interface temperatures presented in this paper also give an indication of the great complexity of heat transfers through the snowcover. The temporal variability in snow depths due to redistribution of the snowcover on the tundra complicate heat flow calculations. Similarly, cavities beneath thin parts of the tundra snowcover are important to the thermal regime of the interface. In the woodlands, the interface temperatures vary in response to snow depths but also in relation to view

factors, shading and local variations in the effective thermal properties of the snowcover as influenced by the presence of vegetation.

The present study forms a part of a comprehensive data collection program of which the aim is to obtain a different perspective on the influence of the seasonal snowcover on permafrost distribution. The snow-ground interface data will enable comparison of simulated ground temperature conditions with observed ground temperatures. We hope in this way to eventually develop the capability of spatially simulating ground temperature variations using weather and snowcover data as inputs to the GPIS.

CONCLUSION

This paper illustrates the great complexity of heat transfer through forest and tundra snowcovers at Schefferville. A wide range of factors complicates the simple relationship between snow depth and ground temperatures that has been used in permafrost prediction at Schefferville. The present findings do not necessarily render these simple relationships invalid. However, they do open a new perspective on the role of the seasonal snowcover in controlling ground temperature and the spatial distribution of permafrost at Schefferville.

ACKNOWLEDGMENT

Financial and logistical support was provided by grants from the Terrain Sciences Division, Geological Survey of Canada (TSD/GSC), the Natural Sciences and Engineering Research Council (grant A0804), and the Department of Indian Affairs and Northern Development Northern Training Grants Program. Particular thanks go to Dr. A.S. Judge and Mr. A.E. Taylor of the Permafrost Research Section (TDS/GSC) who were instrumental in obtaining funding for the project. D.R. Barr and O. Choulik of the McGill Subarctic Research Station in Schefferville provided valuable field assistance. C.A. Nadeau assisted both in the installation of the datalogging stations and in the transfer of some of the field data.

REFERENCES

Annersten, L.J. (1966). Interactions between surface cover and permafrost. Biul. Peryglacj., 15, pp. 27-33.

Bonnlander, B., and Major-Marothy, G.M. (1964). Permafrost and ground temperature observations, 1957. McGill Sub.Res.Paper 16, pp. 33-50.

Bilello, M.A., Bates, R.E. and Riley, J. (1970). Physical characteristics of the snow cover, Ft. Greely, Alaska, 1966-67. Tech.Report 230, U.S. Army CRREL, 32 pp.

Bilello, M.A., Bates, R.E. and Riley, J. (1972). Mesoscale measurement of snow cover properties. Banff's Symp. on Snow & Hydrology, pp. 624-643.

Cary, J.W., Campbell, G.S. and Papendick, R.I. (1978). Is the soil frozen or not? An algorithm using weather records, in Colbeck, S.C. & Ray, M. (eds), Proc. Modeling of Snow Cover Runoff, U.S. Army CRREL, pp. 319-327.

Desrochers, D.T. and H.B. Granberg. (1986a). Preliminary results of a study on snow and ground thermal regimes in the Schefferville area, Northern Quebec. Proc. 43rd Eastern Snow Conf., Hanover, NH, pp. 190-197.

Desrochers, D.T. and H.B. Granberg. (1986b). An investigation of woodland snow thermal regime in the Schefferville area, Northern Quebec. Proc. 43rd Eastern Snow Conf., Hanover, NH, pp. 204-211.

Filion, L. and Payette, S. (1978). Observations sur les caractéristiques physiques du couvert de neige et sur le régime thermique du sol à Poste-de-la-Baleine, Nouveau-Québec. Géogr.phys. Quat., (XXXII), 1, pp. 71-79.

Goodrich, L.E. (1982). The influence of snow cover on the ground thermal regime. Can.Geotech.J., 19, pp. 421-432.

Granberg, H.B. (1972). Snow depth variations in a forest-tundra environment near Schefferville. Unpublished M.Sc. thesis, Dept. of Geography, McGill Univ., 131p.

Granberg, H.B. (1973). Indirect mapping of the snowcover for permafrost prediction at Schefferville, Quebec. Proc. 2nd Int. Conf.Permafrost, Washington, National Academy of Sciences, pp. 113-120.

Granberg, H.B. (1984). Design and manufacture of a thermistor probe of low heat capacity for snow thermometry. Instrument Report 1, DSS Contract No.8SU81-00094,7p.

Granberg, H.B. this volume. Permafrost-snowcover relationships at Schefferville.

Hare, F.K. (1959). A photo-reconnaissance survey of Labrador Ungava. Geog.Branch Memo., 6, Dept. of Mines and Tech.Surveys (Canada), 83p.

Nicholson, F.H. (1976). Permafrost thermal amelioration tests near Schefferville. Can.J.Earth Sci., 13, pp. 1694-1705.

Nicholson, F.H. (1978a). Permafrost distribution and characteristics near Schefferville, Quebec : Recent Studies. Proc. 3rd Int.Conf.Permafrost, Edmonton, Canada, National Research Council of Canada, pp. 427-433.

Nicholson, F.H. (1978b). Permafrost modification by changing the natural energy budget. Proc. 3rd Int.Conf. Permafrost, Edmonton, Canada, National Research Council of Canada, pp. 61-67.

Nicholson, F.H. and Granberg, H.B. (1973). Permafrost and snowcover relationships near Schefferville. Proc. 2nd Int.Conf. Permafrost, Washington, National Academy of Sciences, pp. 151-158.

Reifsnyder, W.E. and Lull, H.W. (1965). Radiant energy in relation to forest canopy. U.S. Dept.Agric.Tech.Bull. No. 1344, 111p.

Singh, B., Taillefer, R. and Poitevin, J. (1984). Les échanges radiatifs et énergétiques et le bilan thermiques du sol en Jamésie. Can.Geotech.J., 21, 2, pp. 223-240.

Thom, B.G. (1969). New permafrost investigations near Schefferville, P.Q. Rev.Géog.Montréal, 23, pp. 317-327.

Wright, R.K. (1983). Relationships between runoff generation and active layer development near Schefferville, Quebec. Proc. 4th Int.Conf.Permafrost, Washington, National Academy of Sciences, pp. 1412-1417.

A LONG-TERM PERMAFROST AND CLIMATE MONITORING PROGRAM IN NORTHERN CANADA

D.A. Etkin[1], A. Headley[1] and K.J.L. Stoker[2]

[1]Canadian Climate Centre
[2]University of Toronto

1 Abstract

Four locations in Northern Canada were instrumented to monitor ground temperatures and meteorological parameters on an hourly to daily frequency. The locations chosen are shown on Fig. I. The intent is to develop a research dataset extending over a period of about 10 years for use in the analysis of climate-permafrost relationships and trend analysis. The Mayo and Churchill sites are located near representative meteorological stations, and therefore have minimal on-site instrumentation. Parameters measured include soil temperatures, precipitation, air temperature, relative humidity, wind speed and direction, soil moisture and snow depth. Despite problems such as vandalism, equipment failure and equipment noise, the data collection has been generally successful, confirming that current technology allows generation of high quality data through the use of remote systems. A preliminary analysis of data obtained from these stations is presented.

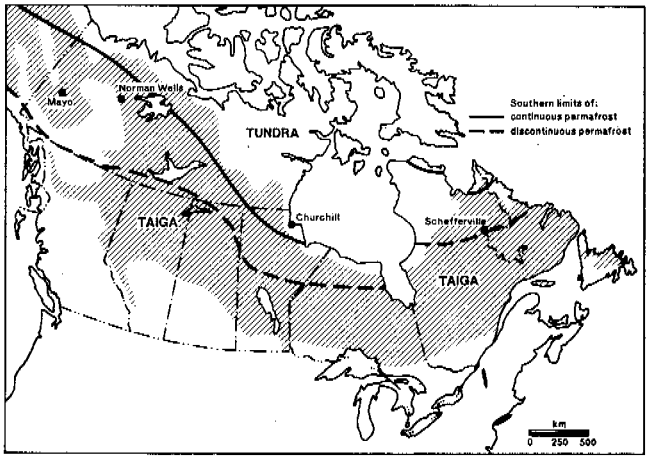

Location of monitoring stations

Fig. I

2 Introduction

The purpose of setting up this network of stations was to monitor soil temperatures in the discontinuous permafrost zone of northern Canada at locations where representative meteorological stations could be co-located, if such did not already exist. The monitoring stations were located in a variety of climatological and geological settings, with ease of access and logistical support playing a significant role with respect to the locations chosen. Sites were selected in undisturbed areas, with the exception of the one near Norman Wells, located adjacent to the Norman Wells-Zama Pipeline.

3 Station Locations and Descriptions

3.1 Mayo

Seven thermocables, of 5m depth, were installed near Mayo in July 1985, four of which appear to be in permafrost. The sites are located about 3 km south of the town of Mayo, at an elevation of about 605 m ASL. Of the seven monitoring stations, five are located in fine-grained, glacio-lacustrine deposits and two are in more recent, coarser alluvial material. Several actively expanding thermokarst lakes are found in the study area (Burn 1982), as well as two retrogressive thaw slumps (Burn et al. 1986).

The dominant tree species is white spruce, with some paper birch, alder, balsam poplar and willow. The shrub layer consists of such species as wild rose, arctic lupine, wild rhubarb and twinflower. The ground is frequently covered by a layer of peat, moss or lichen. Although the microclimate at the thermocable sites is only marginally represented by that of the climate station, the sites were not meteorologically instrumented due to lack of funds. Mayo has a mean annual temperature of -3.7°C with a snowfall of 122 cm and a rainfall of 185 mm (Etkin et al., 1987).

3.2 Normal Wells

The Norman Wells site was established as part of the Permafrost and Terrain Research and Monitoring Program (Burgess et al., 1986) of Energy, Mines and Resources Canada (EMR). The site is 74 km southeast of Norman Wells, 300 m northwest of Canyon Creek and 10 m off the pipeline clearing. Its elevation is 107 m ASL. This cable was installed in 1984 to a depth of 13 m.

The vegetation at the site is open, dwarfed, black spruce forest with some paper birch and an undergrowth of lichens. The site is underlain by warm permafrost (Fig. II). Since the climate station at Norman Wells is only marginally representative of the microclimate at Canyon Creek, the site was fully instrumented. At the climate station, the mean annual temperature is -6.2°C with an average snowfall of 141 cm and rainfall of 189 mm (Etkin et al., 1987). The Canyon Creek site tends to collect snow, due to the local vegetation, and comparisons with snow depths at the climate station support this.

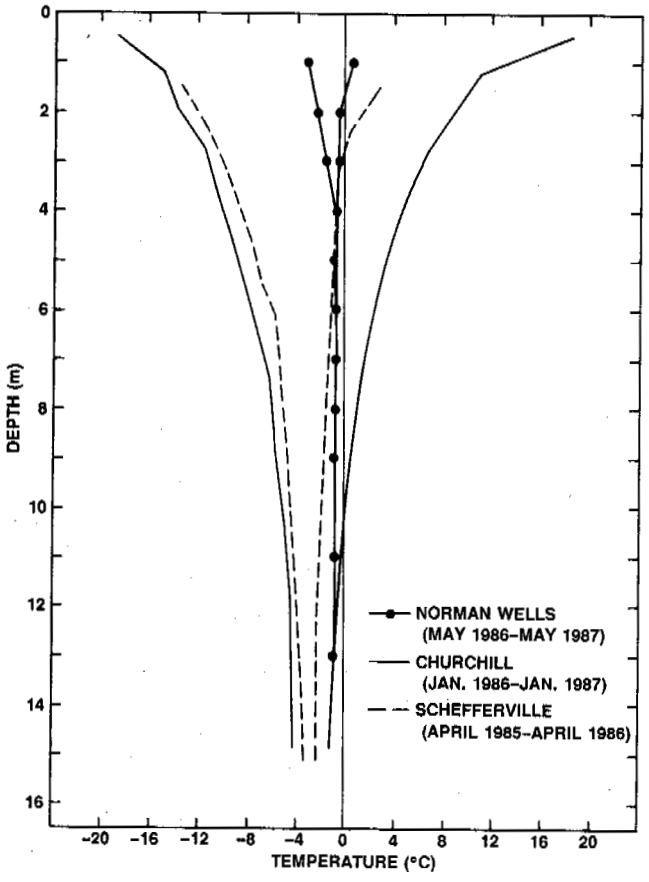

Depth graphs illustrating annual maximum and minimum observed temperatures at the sites near Norman Wells, Churchill and Schefferville.

Fig. II

3.3 Churchill

The Churchill station is located some 400 m east of the airport. This cable was installed by Dr. R.J.E. Brown of DBR/NRC in September 1973. The cable is sited in solid Ordovician sandstone with no overburden other than shallow pockets of soil in cracks and depressions on the bedrock surface. Large blocks of sandstone create a surface roughness which causes a rather uneven distribution of snow which varies with the amount of snowfall and the wind direction.

The climate of the site is well represented by the airport climate station. Only temperature and relative humidity sensors were installed. The climate is largely controlled by the presence of Hudson Bay. The mean annual temperature is -7.2°C, with winter snowfalls averaging 191 cm and annual rainfall 233 mm (Etkin et al., 1987).

3.4 Schefferville

Due to previous research conducted by the Iron Ore Company of Canada (IOC), the Schefferville thermocouple string has a data record going back to 1962. The McGill Subarctic Research Station provides excellent logistical support. A summary of the research carried out there is documented by Granberg et al. (1983).

The site is located about 8 km southwest of Schefferville, at the Ferriman permafrost experimental site. Its elevation is 593 m ASL. Details on the topographic and geological setting as well as drill records can be found in Granberg et al. (1983, 1984). The depth of permafrost is unknown, but is probably greater than 100 m. The vegetation at the site is sparse and consists of lichens with some low-grown woody plants within a general setting of alpine tundra. The site tends to be cooler, windier and more snow-free, but with greater orographically induced precipitation than the climate station located in Schefferville. Schefferville has a mean annual temperature of -4.8°C, annual rainfall of about 400 mm and snowfall of 398 cm (Etkin et al., 1987).

4 Instrumentation

The permafrost monitoring stations at Schefferville, Norman Wells, and Churchill are all equipped with Campbell Scientific 21X dataloggers, and AM32 32-channel multiplexers. At Mayo a Campbell Scientific CR21 datalogger is used at one of the sites and a CR10 at another. Campbell Scientific SM64 solid state storage modules are used to store data. The thermocables at Schefferville and Churchill are copper-constantan thermocouples while those at Norman Wells and Mayo employ thermistors.

Originally, all stations, with the exception of Mayo, were powered by 32 alkaline D-cell batteries. Although successful, this method was labour intensive and costly. A solar panel and rechargeable batteries were installed at Norman Wells, Churchill and Schefferville in August of 1987. The stations at Mayo are powered by six 12-volt lantern batteries.

Snow depth is sensed ultrasonically (Goodison et al. 1985). All sensors are off-the-shelf, except for the thermocables. The dataloggers are buried in the permafrost and covered with insulated environmental shelters to protect them and to keep them in a thermally stable environment. A full description of the instrumentation is given in Etkin et al. (1987). Data is recorded hourly or daily and collected quarterly, except at Mayo where 5 of the 7 cables are read monthly.

5 Preliminary Analysis

Temperature graphs (depth and time-series) and the calculation of 'diffusivities' from the general heat conduction equation allow for a characterization of the ground thermal regime at each site. The calculated 'diffusivities' are not precisely thermal diffusivities, but are augmented by heat transfer processes other than conduction. It is therefore possible to identify certain non-conductive heat transfers by considering the magnitude of the calculated 'diffusivity'. Details of this technique are given in Stoker (1987).

The Churchill site has the most straightforward ground thermal regime of the monitoring sites. Conduction is virtually the only mechanism of heat redistribution, as the subsurface is massive sandstone. It is therefore possible to follow surface temperature changes into the ground with the expected damping and time-lag effects (Fig. III). As a result ground temperatures exhibit great variation throughout the year as shown by the annual temperature envelope (Fig. II). Since the Churchill data is affected by minor instrument noise, use of the general heat conduction equation yielded poor results. The technique worked well for the other sites.

It was found that the soil thermal regimes at Mayo are heavily influenced by moisture. Even near-surface temperatures are remarkably constant and remain near 0°C, while evidence for strengthened conduction exists when the soil dries. The calculated 'diffusivities' indicate that freeze-thaw and perhaps evaporation/ condensation are most important in heat transfers. Deeper soil temperatures tend to be affected by a greater mobility of water.

Mass-heat flows (water) are important to the ground thermal regime at Schefferville; less so from 4 m to 6 m where the conduction component is strong (this is possibly due to a lower moisture or ice content). Near the surface rapid temperature changes can occur (Fig. IV) and cryogenic suction is probably important. Cold temperatures penetrate deeply as most of the snow is carried away by wind.

At Norman Wells conduction prevails above 4 m and below 11 m, where the subsurface is consolidated (although above 4 m latent heat effects are significant). Between 4 m and 11 m freeze-thaw latent energy exchanges dominate the thermal regime and clear seasonal patterns in the calculated values can be identified. Fig. V illustrates the 1 m soil temperature response to changes in air temperature.

The thermal regimes at Mayo and Schefferville are influenced by moving water, while latent heat effects at Norman Wells hold temperatures near freezing. Figure II shows the annual temperature envelopes for Schefferville, Churchill and Norman Wells.

6 Conclusions

Good quality, high frequency, long-term ground temperature and meteorological data can be obtained at remote sites through the use of off-the-shelf data acquisition systems. These independent systems can operate typically for 4 to 6 months without servicing. Such data sets can provide a valuable tool

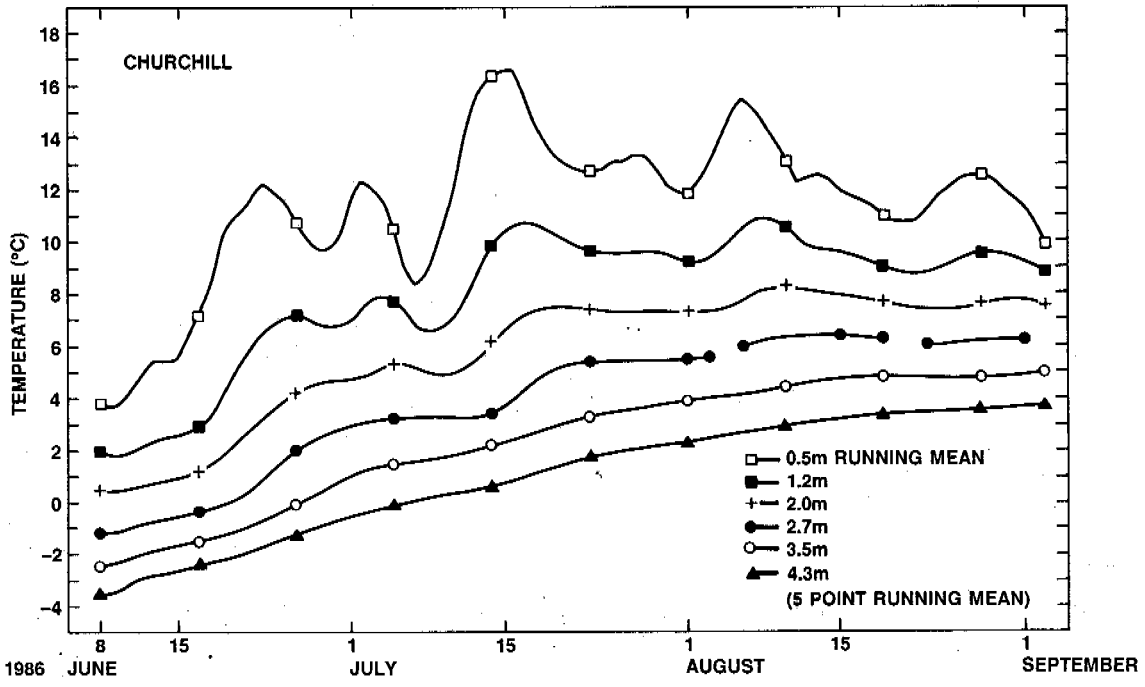

Time series of soil temperatures at Churchill. Temperatures are averaged using a 5 point running mean.

Fig. III

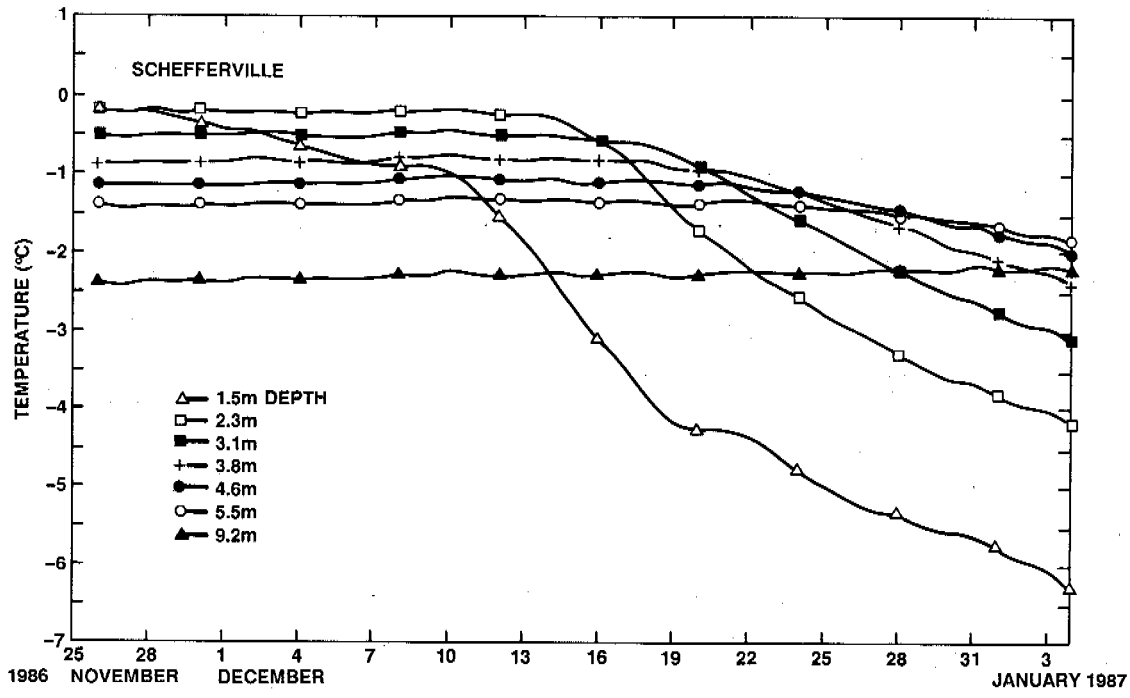

Time series of soil temperatures near Schefferville, showing the onset of winter.

Fig. IV

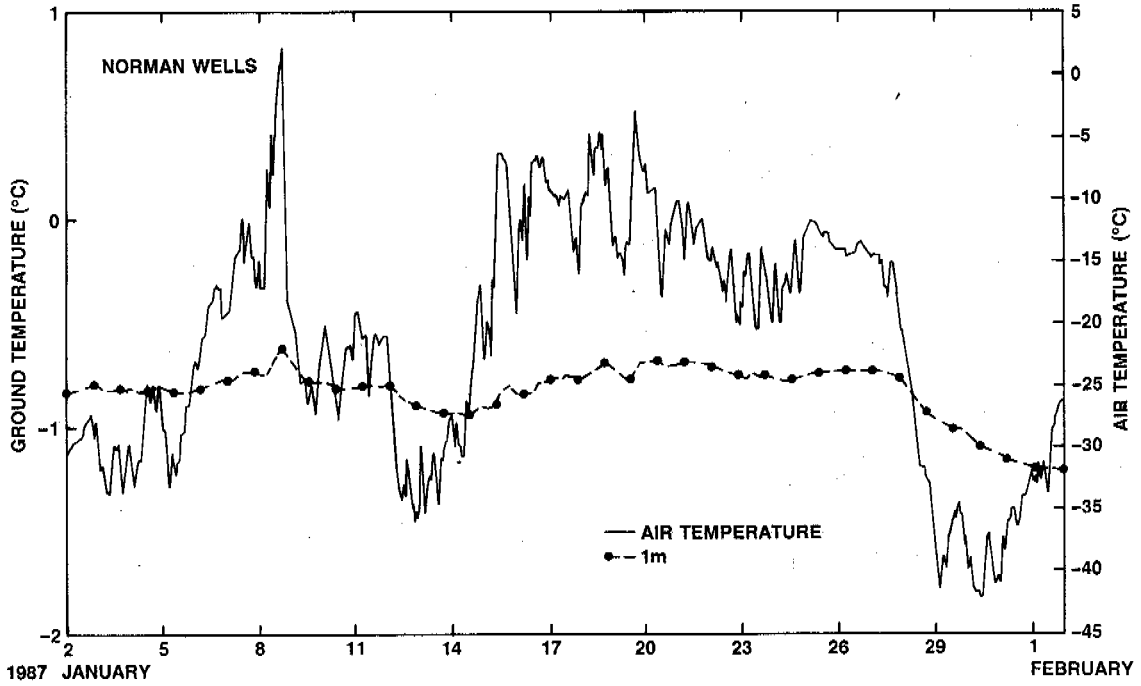

Air and 1 m soil temperatures at the site near Norman Wells.

Fig. V

for the analysis of permafrost-climate relationships and trend analysis. Preliminary analysis of the ground thermal regimes would suggest that permafrost temperatures at the Schefferville, Mayo and particularly Norman Wells sites will not respond rapidly to a climate change. Churchill would be a sensitive indicator of a changing climate.

7 Acknowledgments

I would like to thank Prof. M.W. Smith and Prof. H. Granberg for their efforts in installing the equipment at the various sites, and M. Burgess for her continual assistance. This project was mostly funded by the Panel for Energy, Research and Development (PERD).

8 References

Birdsall, S.S. and Florin, J.W. (1981). Regional landscapes of the United States and Canada, second edition. John Wiley and Sons, N.Y.

Burgess, M.M., Pilon, J.A. and MacInnes, K.L. (1986). Permafrost thermal monitoring program, Norman Wells to Zama oil pipeline. Proc. Northern Hydrocarbon Development-Environmental Problem Solving Conference. Sept. 24-26, Banff, Canada, pp. 248-257.

Burn, C.R. (1982). Investigations of thermokarst development and climatic change in central Yukon Territory. Unpub. M.A. thesis. Carleton University, Ottawa, Ontario. 142 pp.

Burn, C.R., Michel, F.A. and Smith, M.W. (1986). Stratigraphic, isotopic and mineralogical evidence for an early Holocene thaw unconformity at Mayo, Yukon Territory. Canadian Journal of Earth Sciences.

Etkin, D.A., Headley, A. and Stoker, K.J.L. (1978). Permafrost-Climate Activities within the Canadian Climate Centre. Canadian Climate Centre internal report. 130 pp.

Goodison, B.E., Wilson, B. and Metcalfe, J. (1985). An inexpensive remote snow-depth gauge. Proc. Third WMO Technical Conference on Instruments and of Observation (TECIMO-III), WMO Instruments and Observing Methods Report No. 22, Geneva, 111-116.

Granberg, H.B., Lewis, J.B., Moore, T.R., Steer, P. and Wright, R.K. (1983). Shefferville Permafrost Research Vol. 1. Summary, Review and Recommendations, and Catalogue of Available Materials. Dep't. of Geog., McGill Univ., 88 pp.

Granberg, H.B., Desrochers, D.T., Lewis, J.E., Wright, R.K. and Houston, L. (1984). Annotation, Error Analysis and Addenda to the Schefferville Permafrost Data File. Final Report, DSS Contract No. OST83-00302. 17 volumes

Stoker, K.J.L. (1987). The influence of soil moisture migration on the temperature regime of permafrost soils, Schefferville, Quebec. Unpub. B.Sc.Hons. thesis, Carleton Univ., Ottawa. 84 pp.

PERMAFROST-CLIMATIC CHARACTERISTICS OF DIFFERENT CLASSES

M.K. Gavrilowa

Permafrost Institute, Siberian Branch of the U.S.S.R. Academy of Sciences, Yakutsk, U.S.S.R.

SYNOPSIS For each class of the climate-permafrost relationship, we give generalized quantitative examples of permafrost-climatic characteristics according to the freezing and thawing seasons as well as the year. These data include the duration of each season, the sums of radiative and thermal balance components, air, ground surface and soil temperatures, the depths of seasonal freezing and thawing, the thickness of the permafrost, etc. This study has used data of stationary-based climatic, thermal-balance and geocryological observations obtained in different physico-geographic regions and situations of Eurasia and North America.

The interrelation between climate and permafrost is a composite natural phenomenon. However, the most substantial linking factors can be selected from their great variety. This author (Gavrilova, 1978; 1981) has identified several categories of relationships, each of which shows its own factors of climate formation that determine the characteristics of heat and moisture exchange and the appropriate resulting climatic and geocryological consequences. They are:

(i) cosmical relationships - solar climate.

(ii) planetary relationships - megaclimate.

(iii) regional physico-geographical relationships - macroclimate.

(iv) local physico-geographical relationships - mesoclimate.

(v) on-site physico-geographical relationships - microclimate.

(vi) subsurface-surface physico-geographical relationships - nanoclimate.

(vii) soil-ground and geological relationships - climate of soil-grounds and frozen rocks.

Let us consider the characteristics of the main regularities of the climate-permafrost relationships, except for solar climate, i.e., those relationships which are presently confirmed by available, large sets of quantitative data.

Megaclimate - the climate of superlarge regions such as continents and oceans. Thick layers of permafrost which have persisted until the present, had been forming during the course of hundred thousands or even millions of years, i.e., are associated mainly with the climate in the past. However, comparative analysis of the regional distribution of permafrost zones and the different characteristics of the megaclimate (radiation, heat balance, thermal, and others) reveals that the presence of permafrost regions on the globe is also supported by the present-day climatic characteristics. This indicates that the once produced permafrost zone is also sustained by the present-day climate, with a reniewed formation occurring in some places, because there currently are a large number of regions featuring a severe climate as well.

The figure presents a map of actual annual mean air temperature on land throughout the globe that has been constructed by the author and is, essentially, a pioneering attempt internationally (we do not consider here the sea climate and the sea permafrost zone). As is apparent from the figure, the permafrost zone coincides with the coldest regions on the globe. The lowest, currently observed, yearly air temperatures in the Northern Hemisphere are: -16° in the North-East of Yakutia, -20° on the northernmost islands of Canada, and below -20° to -25° in Greenland. Throughout most of Asia and North America the boundary of the continuous permafrost zone (90 to 100% of the area is occupied by frozen grounds) approximately coincides with the annual -8°C isotherm, that of the discontinuous permafrost zone (70 to 80%) refers to -4°, of permafrost islands (10 to 60%) corresponds to -1°, and that of sporadic permafrost (less than 10%) coincides with the 0.5-1°C isotherms.

Displacement of the regions with negative annual air temperatures, or the coldest regions on the globe, toward the polar and near-polar latitudes is attributable to the smallest solar radiation input into this part of the globe. Thus, the total radiation input per year in the region of the permafrost zone (2500 to 4200 $MJ \cdot m^{-2}$, or 60 to 100 $kcal \cdot cm^{-2}$) is by factors 2 or 3 less than that at near-equatorial latitudes (8400 $MJ \cdot m^{-2}$), while the total radiation balance (420 to 1500 $MJ \cdot m^{-2}$, or 10 to 40 $kcal \cdot cm^{-2}$) is by factors 2 to 8 less as compared to the equator (3500 $MJ \cdot m^{-2}$).

We have carried out a detailed quantitative

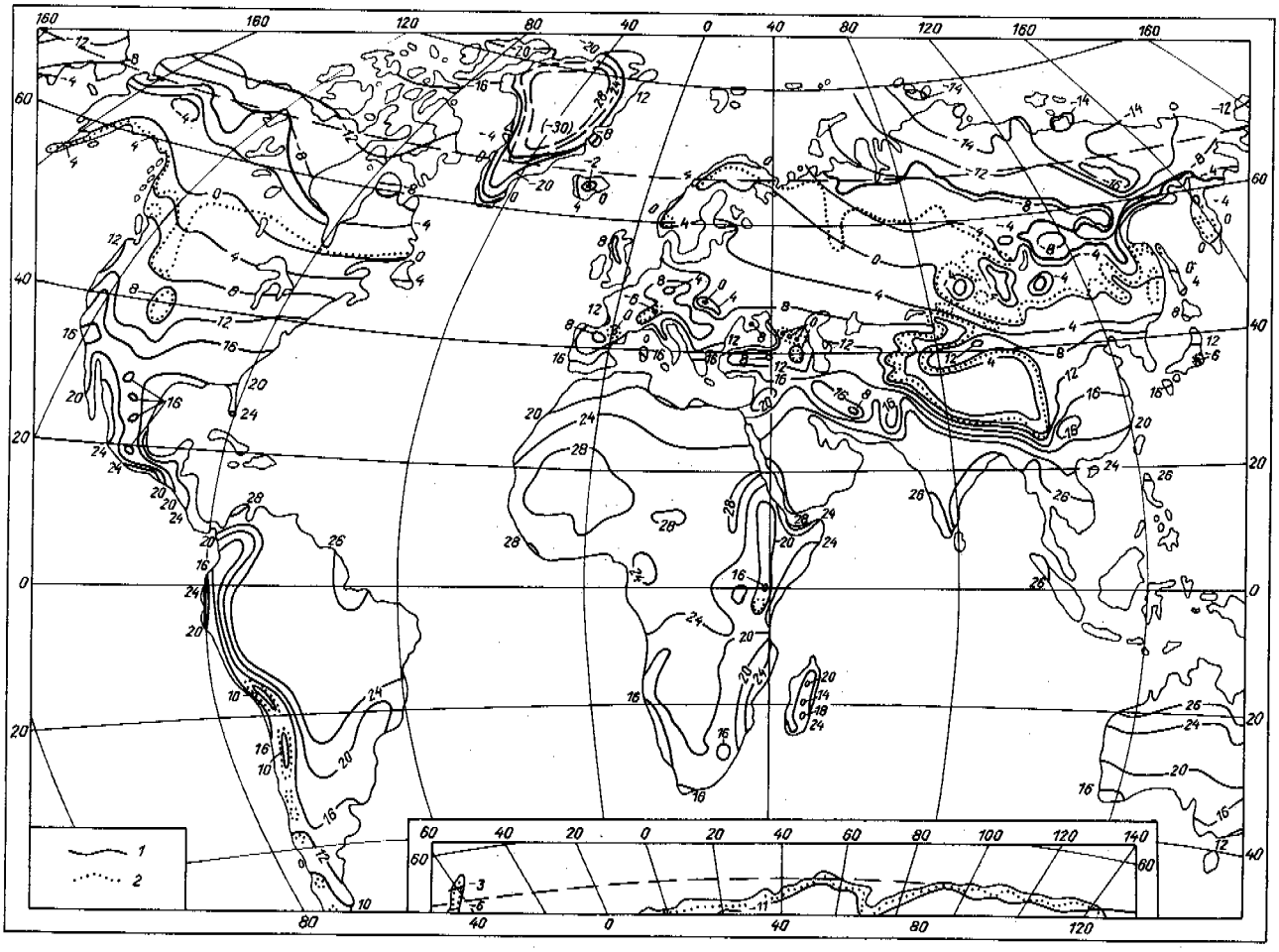

Fig. Mean Annual Air Temperature (°C) and the Permafrost Zone Boundaries.
The Permafrost Zone Boundaries: 1 - Continuous Permafrost; 2 - Permafrost Islands

analysis of the seasonal and annual characteristics of macroclimate of the permafrost zone on the Eurasian and North-American continents for 16 characteristics. Of them, the terrestrial surface temperature is the most approximate, globally measured index of climate to the object under study, or the rocks. The annual sums of temperatures reflect not only their absolute values but also the ratios of durations of the seasons with negative and positive temperatures.

The distribution of permafrost-climatic characteristics depends not only on the locality's latitude, i.e., the total solar energy input, but also on the circulation processes, or the degree of continentality of climate. As is known, the coldest regions on the continents are shifted east-north-westward. This also corresponds to the configuration of the permafrost zone boundaries. On the average, it may be assumed that the boundary of the continuous permafrost zone corresponds to the sums of annual negative temperatures of the terrestrial surface: -2800, -3000°, continuous: -2000, -2500°, and permafrost islands -1000, -1500°. Somewhat increased temperature values are observed in regions with humid maritime climate, and decreased values correspond to regions with dry, sharply continental climate.

Table I presents a number of generalized, quantitative macroclimatic and permafrost characteristics for three large physico-geographical regions of Asia and North America.

The macroclimatic regularities correspond mainly to flat country as well as large mountaneous areas, as a whole. But this pattern includes also secondary, local effects, namely the location inside mountain-masses, beneath large water reservoirs and glacier fields, etc. Mesoclimatic transformations of the original climate have their effect here.

Analysis of data from meteorological stations as well as our experimental heat-balance observations reveals that mesoclimatic factors have an exceptional influence upon the properties of perennial freezing of rocks. This does, in-

TABLE I

Permafrost-Macroclimatic Characteristics

	Western Siberia			Eastern Siberia			Canada		
	Season of freezing	Season of thawing	Year	Season of freezing	Season of thawing	Year	Season of freezing	Season of thawing	Year
	Near the continuous permafrost boundary								
Season duration (days)	235	130	365	220	145	365	225	140	365
Total radiation ($MJ \cdot m^{-2}$)	1380	1885	3265	1170	2720	3890	1425	2305	2730
Radiation balance ($MJ \cdot m^{-2}$)	-65	1050	985	-65	1255	1190	-65	795	730
Heat input into soil ($MJ \cdot m^{-2}$)	-105	105	0	-135	135	0	-95	95	0
Air temperature (degree·days)	-4000	1200	-2800	-4600	1700	-2900	-4100	1300	-2800
Freezing-thawing (m)		1-2.5			1-2		-	-	-
Ground temperature at 10 to 15 m (°C)	-2	-2	-2	-2.5	-2.5	-2.5	-	-	-
Permafrost thickness (m)	100	100	100	200	200	200	-	-	-
	Near the boundary of permafrost islands								
Season duration (days)	190	175	365	180	185	365	190	175	365
Total radiation ($MJ \cdot m^{-2}$)	1255	2260	3515	1170	3015	4185	1425	3225	4650
Radiation balance ($MJ \cdot m^{-2}$)	-65	1215	1150	-40	1550	1510	0	1465	1465
Heat input into soil ($MJ \cdot m^{-2}$)	-115	115	0	-115	115	0	-110	110	0
Air temperature (degree·days)	-3300	1600	-1700	-3000	1900	-1100	-2700	1900	-800
Freezing-thawing (m)	1.8-2	total		2-2.5	total		-	-	-
Ground temperature at 10 to 15 m (°C)	0	0	0	0	0	0	-	-	-
Permafrost thickness (m)	20	20	20	20	20	20	-	-	-

deed, explain the weakening or disappearance of permafrost beneath large rivers, seas, water reservoirs, large glaciers, etc. as well as its appearance in the mountains at moderate and southern latitudes.

Table II gives results of our investigations in mountaneous regions of South Verkhoyanie and North Zabaikalia in Siberia. A common feature shared by all mountain-masses is the altitude-dependent increase in duration of the freezing season and the reduction in the thawing season. As a result, due to large losses of heat by reflection in the case of a prolonged persistence of the snow cover, the radiation balance - in going from depressions to mountain tops - reduces greatly.

During the wintertime, mountains show an air temperature inversion, i.e., a rise in temperature with the locality's altitude. However, the summertime conditions also are important for the formation of the final temperature regime of rocks. Thus, in the mountains of Verkhoyanie at 2000 m altitude, the sum of air and ground surface temperatures for a thawing season is by a factor of 4 smaller than that for the depressions, while the sum of the radiation balance and heat input into the ground soil is twice as small. Accordingly, the depth of thawing also is twice as small. For a short summer period, earth materials are unable to warm throughout and, on the whole, they are thus colder than those in the famous Oimyakonskaya depression of the Northern Hemisphere 'cold pole'.

A great diversity in local peculiarities of perennial freezing of rocks is shown by natural complexes such as a forest, a sea, a glacier, icing, and others. We have carried out experimental field observations in about 150 areas which demonstrate that one may distinguish 'warm' and 'cold' microclimatic complexes having a constant or seasonal influence. Moreover, the combined effect of a large number of natural complexes manifests itself differently in different climatic zones. Thus, forest and icing in the northern regions have, generally, a warming effect on ground soils, whereas in the southern regions, a cooling effect is observed.

It appears that the heat-balance essence of the influence of microclimate upon the seasonal freezing-thawing of ground soils is different for each of the natural complexes. Thus, the main feature of a forest (Table III) is a reduction in input-output of all the components of the thermal balance during all periods of

TABLE II

Permafrost-Mesoclimatic Characteristics

	Season of free-of thazing	Season of thawing	Year	Season of free-of thazing	Season of thawing	Year	Season of free-of thazing	Season of thawing	Year
South Verkhoyanie	Oimyakon, 740 m (depression)			Nizhnyaya Baza, 1350 m (valley)			Suntar-Khayata, 2068 m (ridge)		
Season duration (days)	237	128	365	254	111	365	278	87	365
Total eadiation ($MJ \cdot m^{-2}$)	1591	2428	4019	2160	2102	4262	2801	1758	4559
Radiation balance ($MJ \cdot m^{-2}$)	75	1231	1306	-230	933	703	-477	603	126
Heat input into soil ($MJ \cdot m^{-2}$)	-159	159	0	-117	117	0	-75	75	0
Air temperature (degree·days)	-7669	1697	-5972	-5984	876	-5108	-5415	424	-4991
Surface temperature (degree·days)	-7590	1691	-5899	-7140	1104	-6036	-6648	436	-6212
Freezing-thawing (m)	total	1.69		total	1.35		total	0.85	
Ground temperature at 10 m (°C)	-8.5	-7.0	-7.6	-	-	-	-10.0	-8.4	-9.1
North Zabaikalia	Chara, 708 m (open depression)			Ingamakit, 1020 m (relatively closed depression)			Naminga, 1400 m (valley)		
Season duration (days)	207	158	365	221	144	365	237	128	365
Total radiation ($MJ \cdot m^{-2}$)	1616	3232	4848	1662	2449	4111	1871	1796	3667
Radiation balance ($MJ \cdot m^{-2}$)	-519	1591	1072	-389	1289	900	-172	807	636
Heat input into soil ($MJ \cdot m^{-2}$)	-167	167	0	-146	146	0	-126	126	0
Air temperature (degree·days)	-4387	1594	-2793	-3870	1298	-2572	-4144	1100	-3044
Surface temperature (degree·days)	-4562	2040	-2522	-4257	1597	-2660	-4558	1375	-3183
Freezing-thawing (m)	5.0	total		total	3.0		total	1.75	
Ground temperature at 10 m (°C)	-0.3	+0.9	+0.3	-1.8	-1.2	-1.6	-3.4	-2.6	-3.0

the year due to the overshadowing by the crowns of trees and because of the presence of a forest vegetation substrate. Depending on the predominance of winter- or summertime influences of thermal exchange, the soil grounds under the forest can be either colder or warmer than those on surrounding open terrains.

During a warm period of the year, lakes are notable for large amounts of heat that go for ice melting as well as evaporation and warming of the water and earth materials beneath the lakes. In summer in Central Yakutia the temperature under the bottom of a lake is by about 5 to 7° higher as compared with the same depth under a medow in the neighbourhoods. During a freezing season, warm earth materials under the lakes lose large amounts of heat; however, still greater amounts of heat are supplied when ice is being formed on the lake, and this subsequently prevents heat losses through the water mass. As a result, during the wintertime the earth materials beneath the lake, though becoming colder, do, however, not reach negative values. In the end, taliks commonly occur under the lakes of the permafrost zone.

We have also investigated in detail the microclimatic influence of a glacier and icing upon the freezing-thawing of soils (Table IV). Despite a certain resemblance of them that has effect on, for example, radiation regime, their heat balance characteristic is totally different. A glacier persists throughout the year, while an icing occurs mainly seasonally. The glacier mostly absorbs heat and prevents heat losses by earth materials. Icing, however, plays both a heat-protecting and warming role during the course of heat release as the water spreading through its surface freezes during the entire wintertime. As a result, against a background of severe macroclimate, earth materials under the icings show high temperatures.

The experimental investigations we have carried out indicate that the characteristic properties of seasonal freezing-thawing of soils in different areas of the same terrain also depend upon nanoclimatic effects: vegetation and soil covers, small forms of the terrain, shallow water reservoirs, natural and artificial moistening, etc. Classifying as an independent category such small-scale natural and artificial effects, amenable to control, is important for substantiating hydrothermal meliorations on frozen soils.

TABLE III

Permafrost-Microclimatic Characteristics

Central Yakutia	Season of freezing	Season of thawing	Year	Season of freezing	Season of thawing	Year	Season of freezing	Season of thawing	Year
	Waterless valley meadow			Larch forest			Small-size lake		
Season duration (days)	214	151	365	215	150	365	214	151	365
Total radiation ($MJ \cdot m^{-2}$)	1151	2755	3906	657	1411	2068	1151	2755	3906
Reflectivity (%·days)	14000	3500	17500	12000	3500	15500	15000	2000	17000
Radiation absorbed ($MJ \cdot m^{-2}$)	368	2123	2491	289	1118	1407	449	2422	2871
Effective radiation ($MJ \cdot m^{-2}$)	440	808	1248	322	498	820	524	732	1256
Radiation balance ($MJ \cdot m^{-2}$)	-72	1315	1243	-33	620	587	-75	1690	1615
Evaporation heat ($MJ \cdot m^{-2}$)	41	553	594	34	189	223	25	1038	1063
Heat exchange with the atmosphere ($MJ \cdot m^{-2}$)	-42	662	620	8	327	335	251	272	523
Snow thaw heat ($MJ \cdot m^{-2}$)	25	4	29	25	4	29	25	4	29
Heat input into soil ($MJ \cdot m^{-2}$)	-96	96	0	-100	100	0	-129	129	0
Thaw heat of ground or ice ($MJ \cdot m^{-2}$)	-59	59	0	-46	46	0	-247	247	0
Warming heat of ground or water ($MJ \cdot m^{-2}$)	-8	8	0	-4	4	0	-29	29	0
Warming heat of frozen ground or bottom ($MJ \cdot m^{-2}$)	-29	29	0	-50	50	0	-100	100	0
Air temperature (degree·days)	-5558	1774	-3784	-5332	1780	-3552	-5500	1771	-3729
Surface temperature (degree·days)	-5870	1871	-3899	-4997	1785	-3212	-4372	1888	-2484
Temperature of ground surface (degree·days)	-3112	2010	-1102	-2740	1285	-1455	400	1800	2200
Temperature of ground at 3 m (°C)	-5.6	-1.3	-3.0	-6.7	-2.5	-4.6	1.5	6.4	3.3
Freezing-thawing (m)	total	1.83		total	1.04		talik	talik	talik

TABLE IV

Permafrost-Microclimatic Characteristics

	Season of freezing	Season of thawing	Year	Season of freezing	Season of thawing	Year
	Glacier, South Verkhoyanie			Icing, Central Yakutia		
Season duration (days)	303	62	365	120	61	181
Total radiation ($MJ \cdot m^{-2}$)	3270	1009	4279	892	1185	2077
Reflectivity (%·days)	23000	3000	26000	7000	2000	9000
Radiation absorbed ($MJ \cdot m^{-2}$)	787	494	1281	389	779	1168
Effective radiation ($MJ \cdot m^{-2}$)	1088	151	1239	532	251	783
Radiation balance ($MJ \cdot m^{-2}$)	-301	343	42	-151	528	377
Evaporation heat ($MJ \cdot m^{-2}$)	0	-42	-42	42	310	352
Heat exchange with the atmosphere ($MJ \cdot m^{-2}$)	-297	-80	-377	456	-552	-96
Heat input into ice ($MJ \cdot m^{-2}$)	-4	4	0	155	8	163
Thaw heat of snow and ice ($MJ \cdot m^{-2}$)	0	460	460	-733	733	0
Thawing layer of snow and ice (m)	0	1.0+0.7	-2.14	2.14		
Heat input into ground ($MJ \cdot m^{-2}$)	0	0	0	-71	29	-42
Temperature of ice or ground at 3 m (°C)	-25	-3	-14	-0.1	0.0	0.0

An example of a nanoclimatic effect induced by sprinkler irrigation is given in Table V. Not only does irrigation make the soil temperature regime milder but is able, during the first year, to contribute to a still greater thawing of the ground as a consequence of the increase in heat conduction due to moistening. Subsequenly, however, moist soils freeze more considerably so that the thermal regime of such soils might worsen.

Heat input into rocks from the ground surface

TABLE V

Permafrost-Nanoclimatic Characteristics

Central Yakutia	For a season		Before and after irrigation			
Sprinkler irrigation	meadow	area being irrigated	meadow		area being irrigated	
	Jul-Aug	Jul-Aug	21 Jul	22 Jul	21 Jul	22 Jul
Water supply (mm)	60	166	none	none	none	35
Total radiation ($MJ \cdot m^{-2}$)	1156	1176	-	-	-	-
Reflectivity (%·days)	1054	1168	-	-	-	-
Radiation absorbed ($MJ \cdot m^{-2}$)	959	959	-	-	-	-
Effective radiation ($MJ \cdot m^{-2}$)	448	364	-	-	-	-
Radiation balance ($MJ \cdot m^{-2}$)	511	595	11.3	12.0	12.6	16.6
Evaporation heat ($MJ \cdot m^{-2}$)	297	356	-	-	6.7	14.2
Heat exchange with the atmosphere ($MJ \cdot m^{-2}$)	172	172	-	-	4.2	-0.2
Heat input into soil ($MJ \cdot m^{-2}$)	42	67	1.0	1.1	1.7	2.4
Warming heat of talik ($MJ \cdot m^{-2}$)	4	8	-	-	-	-
Thawing heat ($MJ \cdot m^{-2}$)	21	38	-	-	-	-
Warming heat of frozen ground ($MJ \cdot m^{-2}$)	17	21	-	-	-	-
Surface temperature (°C)	20.0	17.1	25.8	31.0	23.2	22.1
Soil temperature at 0.5 m (°C)	10.7	8.3	12.0	12.3	9.7	9.8
Thawing (m)	1.49	1.57	-	-	-	-

undergoes further transformations. Within the layer of seasonal temperature fluctuations during the summertime, part of heat goes for the warming of the unfrozen layer and, then, for further thawing of grounds and the rise in temperature within the layer of negative temperatures. In this case quantitative characteristics of each process depend also on the heat conduction properties of the rocks themselves which are determined by the lithological composition, density and moisture or ice content in them. During a seasonal freezing, soil grounds that have been warmed during the summer deliver their heat to the terrestrial surface.

Thus, during a thawing season in open areas of a meadow in Central Yakutia, the soil receives about 150 $MJ \cdot m^{-2}$ heat, or 11% of the amount of the radiation balance of the ground surface during that period. Of this amount of heat, about half the heat goes for thawing the soil ground of a thickness of 1.8 to 2 m. The rest goes for its warming. There also occurs a seasonal variation of thermal balance components of soil grounds. The largest amounts of heat go for thawing in the first half of the summer. During the second half of the summer, upper layers of soil grounds begin to cool down, whereas in the zone of negative temperatures the warming process goes on.

Throughout the year, under nonstationary conditions, an excess or deficit of the original heat may also affect the temperature regime of the layer of annual temperature fluctuations, i.e., in the zone of constantly negative temperatures. However, the influence of climate extends only within a certain range. The external heat input interacts with heat flows within the rocks themselves, namely the heat of underground waters, gases, chemical processes, radioactive decay, intraterrestrial flow, etc. This also accounts for anomalous manifestations of the temperature and thickness of frozen rocks in some geological, hydrogeological, tectonic, and other structures.

Thus, the quantitative permafrost-climatic characteristics indicate that a methods-based approach to identifying the particular relationships between climate and permafrost depends on the class of the coupling under consideration. Also, the smaller-scale the object under study, the more detailed investigations should be undertaken. Thus, megaclimatic indices of the annual air temperature are sufficient for a general identification of perennial freezing of rocks on the continents. In order to establish the regional regularities, it is necessary to analyze the interrelation of macroclimate according to the seasons. Local terrain peculiarities of seasonal freezing and thawing of soil grounds require a detailed monitoring of the heat and moisture regime of a micro- and nanoclimatic character. Ultimately, the temperature field of frozen rocks is determined by the combination of climatic and geological effects.

REFERENCES

Gavrilova, M.K. (1978). Klimat i mnogoletnee promerzanie gornykh porod. 214 p. Novosibirsk: Nauka.

Gavrilova, M.K. (1981). Sovremenny klimat i vechnaya merzlota na kontinentakh. 113 p. + insert. Novosibirsk: Nauka.

LATE QUATERNARY SOLIFLUCTION IN CENTRAL SPITSBERGEN

P. Klysz[1], L. Lindner[2], L. Marks[2] and L. Wysokinski[3]

[1]Quaternary Research Institute, A. Mickiewicz University, Poznan, Poland
[2]Institute of Geology, Warsaw University, Warsaw, Poland
[3]Institute of Hydrogeology and Eng. Geology, Warsaw University, Warsaw, Poland

SYNOPSIS

Slope, marine and glacial sediments on the western foot of Wordiekammen in Petuniabukta indicate ancient solifluction phenomena. Bedrock of Carboniferous limestones is overlain by lacustrine fine-grained sands and silts, thermoluminescence dated at 119 ± 17 ka. They are mantled with sands and gravels, containing marine mollusc shells that are TL dated at 66 ± 9 ka. On the top of these there is a till, TL dated at 47-53 ka. Overlying gravels with pieces of marine mollusc shells form a surface of the marine terrace 12 - 15 m a.s.l. They have been partly soliflucted together with the overlying till, TL dated at 45 ± 6 ka. The latter forms a lobate bulge on the terrace surface.

INTRODUCTION

During a scientific expedition organized in summer 1984 by the Quaternary Research Institute of A. Mickiewicz University of Poznan, we were engaged in geologic and geomorphologic mapping of the Ebbadalen-Nordenskiöldbreen Region of Petuniabukta area, Billefjorden (cf. Klysz et al. 1987, 1989). We studied a geologic profile of a ravine (up to 4 m deep and about 40 m long) cut into the slope of Wordiekammen, the eastern mountain massif of Petuniabukta (Fig. 1). The sequence of sediments seen in the walls of the ravine enabled us to distinguish a series of solifluction (gelifluction by Washburn, 1967, and Jahn, 1975) origin. The studied sequence was particularly interesting due to interfingering of slope sediments with marine shingle of the terrace at 12-15 m a.s.l..

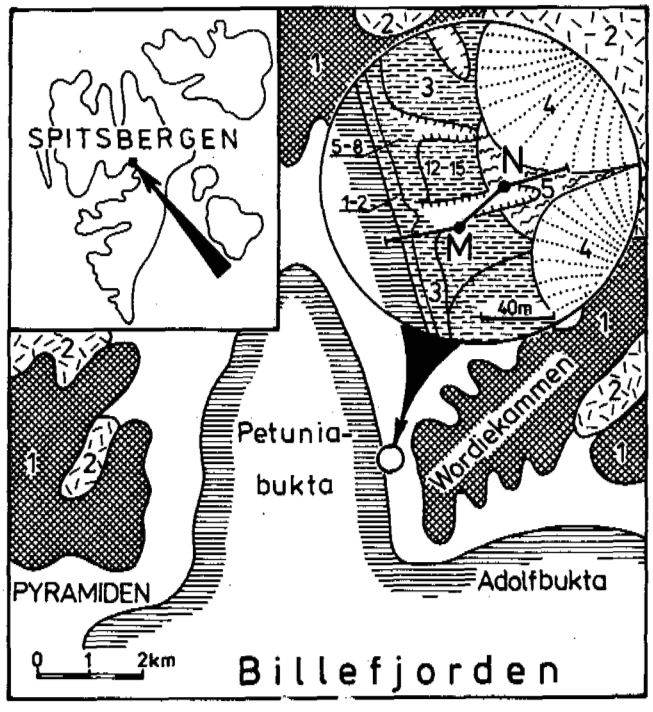

Fig. 1 Location sketch of solifluction phenomena at eastern seashore of Petuniabukta; marked are presented exposures M and N (cf. Figs. 2 and 3) and geologic section (cf. Fig. 4) 1 - mountain massifs, 2 - glaciers, 3 - marine terraces with their altitudes in m a.s.l., 4 - taluses, 5 - solifluction lobes

The age of this solifluction could be tentatively defined by thermoluminescence (TL) dating. Six samples were collected and the dating was done in the Thermoluminescence Laboratory (Institute of the Earth Sciences, M. Curie-Sklodowska University of Lublin) with application of J. Butrym's metohodics (cf. Butrym et al. 1987). However a small content of quarts grains in the sediments and their short transport could result in a tentative TL age only.

Grain size and carbon carbonate content of the studied sediments were determined with a use of 6 collected samples. On the basis of grain size analysis several typical indices were calculated, including:

(i) mean grain size (after Folk, Ward 1957)

$$M_z = \frac{\phi 16 + \phi 50 + \phi 84}{3} \qquad (1)$$

(ii) standard deviation δ (after Folk, Ward 1957)

$$\delta = \frac{\phi 84 - \phi 16}{4} + \frac{\phi 95 - \phi 5}{6,6} \qquad (2)$$

(iii) graphic curtosis K_G (after folk, Ward 1957)

$$K_G = \frac{\phi 95 - \phi 5}{2,44(\phi 75 - \phi 25)} \qquad (3)$$

(iv) graphic skewness α_s (after Friedman, 1962

$$\alpha_s = (\phi 95 + \phi 5) - 2(\phi 50) \quad (4)$$

(v) sorting belt (after Rotnicki, 1970)

$$P_s = \phi 90 - \phi 10 \quad (5)$$

(vi) index of siltiness (after Karaczewski, 1963)

$$J = \frac{< 0.002 \text{ mm}}{> 0.002 \text{ mm}} \quad (6)$$

Sediments with a supposed admixture of organic matter were subjected to a palynologic analyses but the results were negative.

GEOLOGIC-GEOMORPHOLOGIC SETTING

The mountain massif of Wordiekammen is composed of the Lower Carboniferous (Culm) clastic rocks with intercalations of hard coal. These rocks gently dip westwards whereas they pass upwards into carbonate and sandstone-conglomerate rocks of the Upper Carboniferous and permian (Hjelle, Lauritzen, 1982). Lower slope fragments of this massif that descend to Petuniabukta, are buried by marine terraces at 5-8, 12-15 and 30-35 m a.s.l.. Older marine and glacial sediments of the upper part of the slope are mantled by large taluses and a present solifluction cover (cf. Klysz et al. 1987, 1989). The plateau-like top surface of Wordiekammen at 700 m a.s.l. has numerous features and sediments that indicate past glacial activity with hanging tongues towards Petuniabukta and Adolfbukta.

A ravine cuts the terrace at 12-15 m a.s.l. and passes upslope into av chute (Fig. 1). Downslope cuts the terrace at 5-8 m a.s.l. and finally, enters the beach of Petuniabukta. The authors studied two exposures at opposite sides of the ravine (M and N in Fig. 1).

In the exposure M (Fig. 2) the ravine floor is composed of fine-bedded Carboniferous limestones (layer 1 in Fig. 2). The top of the limestone is loosened due to frost weathering processes. Limestones are covered by a 2 m thick layer of gravel (layer 2). Near the base there are minute pieces of marine mollusc shells, and sediments are cemented by permafrost. Unfrozen gravels nearer to the top of the section are more loose and have a distinct layered structure. These marine sediments were TL dated at 66 ± 9 ka (Lub-1140).

The gravels are overlain by a thin (up to 0.5 m thick) till (layer 3) with a visual graded bedding, what is also supported by its index of siltiness J (Fig. 2). The grain size distribution and morphologic setting indicate that the sediment is a basal till (cf. Boulton, Paul, 1976). It was TL dated at 47 ± 7 ka (Lub-1139). This till is overlain by gravel (layer 4), of up to 8 cm in diameter. The layer is hardly stratified and contains fine pieces of marine mollusc shells. The gravel forms the surface of the marine terrace at 12-15 m a.s.l..

In the exposure N (Fig. 3) at the opposite side of the ravine but more upslope Wordiekammen, also fine-graned Carboniferous limestones occur (layer 1) in the ravine floor. They are strongly weathered, and are overlain by a 10 cm thick layer of fine-grained sands (layer 2), covered with a 10 cm thick layer of silt with an intercalation of washed coal silt (layer 3). The layer 3 represents a sediment of a shallow pond and was TL dated at 119 ± 17 ka (Lub-1144). On the top of this there is a thin (8-10 cm) set of fine-grained sands with pieces of marine mollusc shells (layer 4).

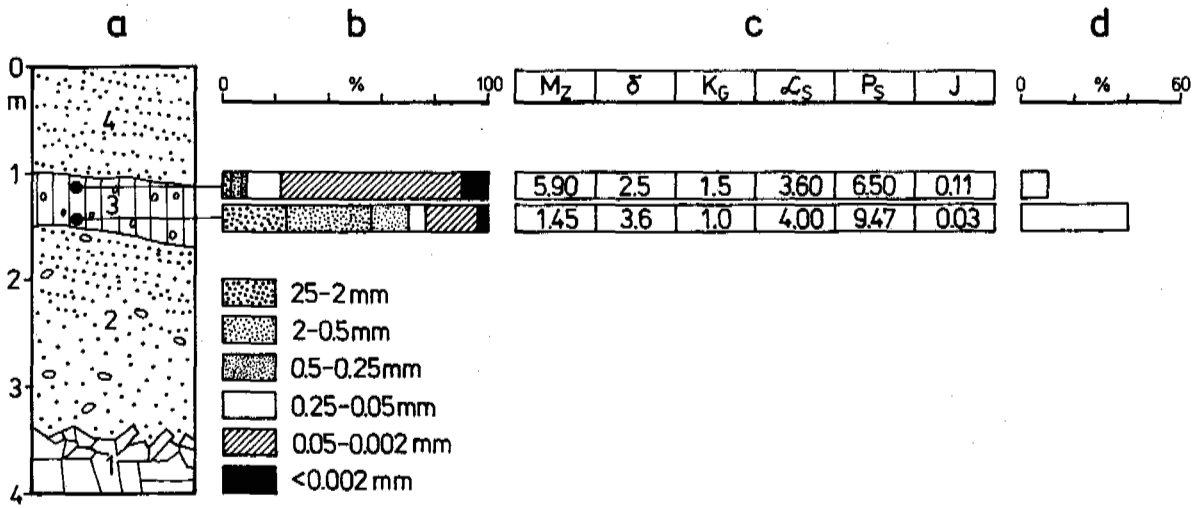

Fig. 2 Geologic profile of the exposure M (cf. Fig. 1) at eastern seashore of Petuniabukta: a - lithology, b - grain size, c - grain size indices, d - calcium carbonate content 1 - fine-beded limestones, 2 - gravels with pieces of marine mollusc shalls, 3 - till, 4 - poorly stratified gravels with pieces of marine mollusc shells

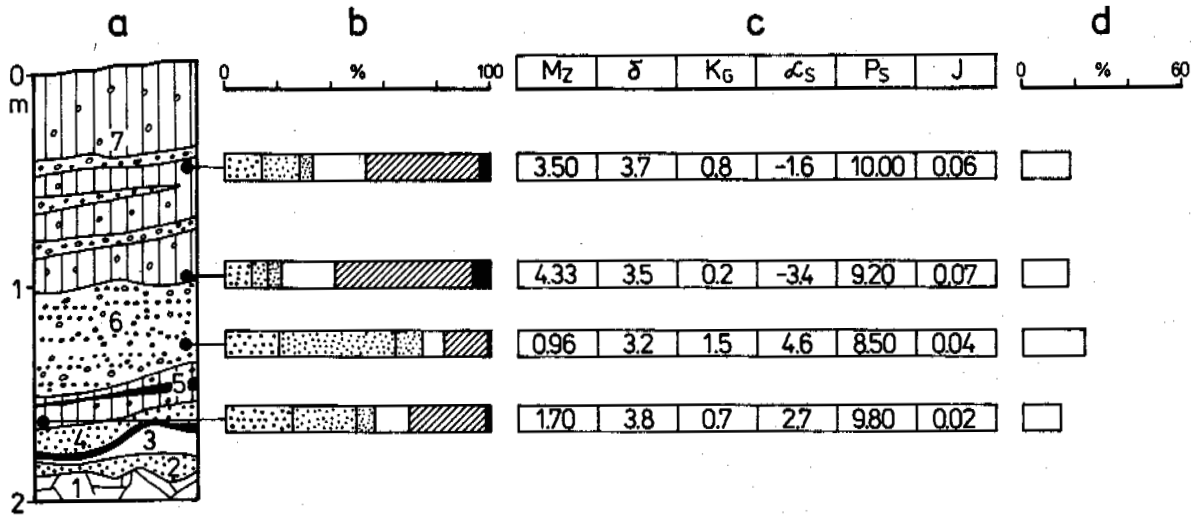

Fig. 3 Geologic profile of the exposure N (cf. Fig. 1) at eastern seashore of Petuniabukta: for a - d see Fig. 2; 1 - fine-bedded limestones, 2 - fine-grained sands, 3 - silt with washed coal intercalation, 4 - fine-grained sands with pieces of marine mollusc shells, 5 - till with insert of coal silt and pieces of marine mollusc shells, 6 - poorly stratified gravels with pieces of marine mollusc shells, 7 soliflucted till with sandy-gravel intercalations and pieces of marine mollusc shells

The above mentioned sediments are covered by a 30-50 cm thick till bed (layer 5), containing intercalations of coal silt and pieces of marine mollusc shells. Grain size characteristics and sorting of the till resemble those of the lower part of till in section M (Fig.2). Because of these characteristics, the till is interpreted as a relic of a once thicker till bed, and therefore it may also be regarded as a basal till.

The lower part of the presented till was TL dated at 53 ± 7 ka (Lub-1143). The till is

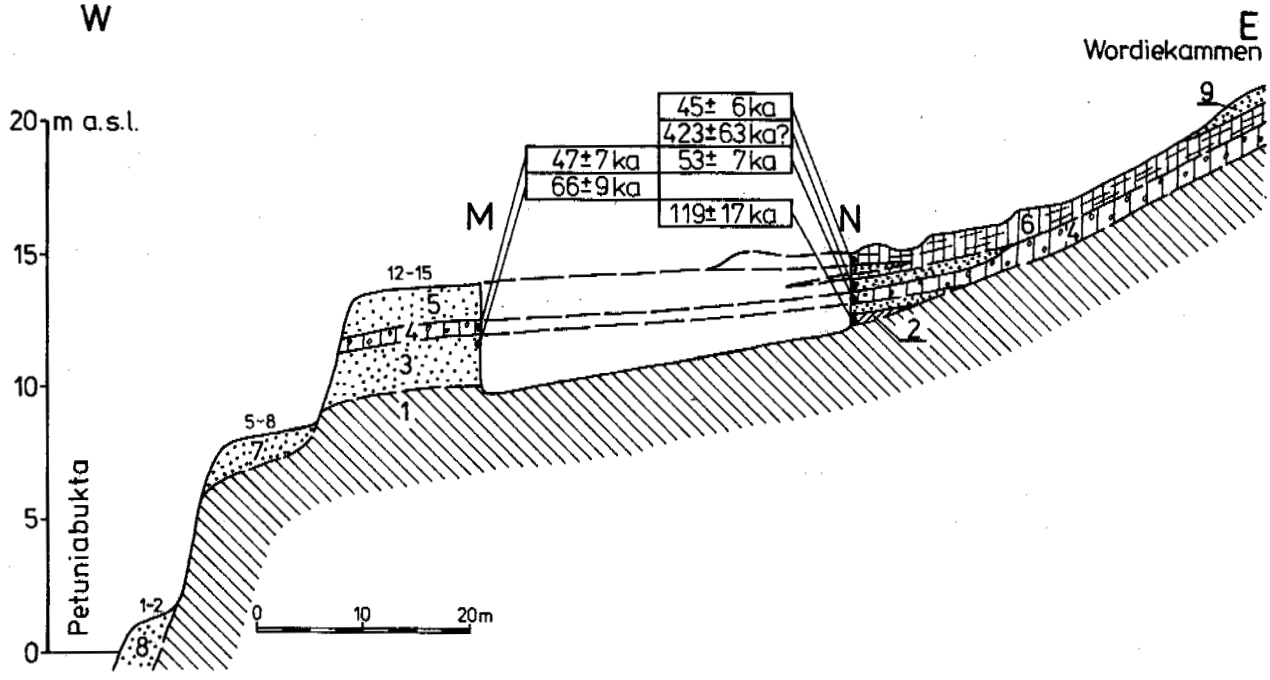

Fig. 4 Geologic section in Quaternary sediments at eastern seashore of Petuniabukta with marked exposures M and N, and thermoluminescence dates 1 - Quaternary bedrock (Carboniferous limestones), 2 - sands and silts with washed coal, 3 - marine pebbles, 4 - till, 5 - marine pebbles (terrace 12-15 m), 6 - soliflucted till, 7 - marine pebbles (terrace 5-8 m), 8 - marine pebbles (terrace 1-2 m), 9 - talus rubble

overlain by a layer of gravel (layer 6), about 0.5 m thick and with a visible stratified fabric. The gravel contains pieces of marine mollusc shells. Such grain size characteristics (cf. Fig. 3) of undoubtedly marine series resemble som features of glacial sediment. This probably reflects the influence of bedrock on which the series was deposited.

TL dating gave an age of 423 ± 63 ka (Lub-1142). This is far too old, if compared with the underlying till (layer 5). Probably the erroneous date is the result of quartz grains coming from Carboniferous-Permian rocks of Wordiekammen whereas a short transport to a marine environment has not obliterated the primary thermoluminescence.

The upper part of the section N (Fig. 3) consists of a meter thick layer of till (layer 7) with abundant streaks of sandy-gravel, and with pieces of marine mollusc shells. Index of siltiness J of this till (cf. Fig. 3) resembles the one of subglacial till of the Werenskiold Glacier (Olszewski, Szupryczynski, 1985). This till forms a distinct bulge on the terrace at 12-15 m a.s.l. close to the mountain massif slope and creates a solifluction lobe that descends a slope of Wordiekammen and interfingers with marine sediments of the mentioned terrace. TL dating of the till gave an age of 45 ± 6 ka (Lub-1141). This suggests that it is a solifluction feature of the same glacial epoch as the tills in the lower parts of both exposures.

GENETIC AND AGE INTERPRETATION

Lithology, grain size distribution and TL age of sediments of the marine terrace at 12-15 m a.s.l. at the eastern seashore of Petuniabukta reflect a complex structure of this terrace. Its sediments are represented in section M (Fig. 2) by supratill marine gravels and in section N (Fig. 3) by intertill marine gravels. In section M they are underlain by a basal till dated at 47 ± 7 ka and by marine gravels dated at 66 ± 9 ka. In section N they cover a till, dated at 53 ± 7 ka, and underlain marine sands and lake sediments dated at 119 ± 17 ka (Fig.4).

During deposition of the sediments of the marineterrace at 12 - 15 m a.s.l. on the slope of Wordiekammen, solifluction flows developed there on previosly deposited till (45 ± 6 ka). Such flows moved onto the surface of the terrace as suggested by their location and the occurrence of sandy-gravel intercalations with pieces of marine mollusc shells in the upper part of the section N (Figs. 3, 4).

Solifluction phenomena and processes develop widely in the present periglacial environment all over Spitsbergen (Klimaszewski, 1960; Dutkiewicz, 1961, 1967; Jahn, 1967, 1975; Klysz, 1986, and others). Presented fossil features suggest that they have also developed earlier and cannot be neglected in studies of geologic sections.

Acknowledgements.

The authors are indebted to Dr. J. Butrym (Institute of Earth Sciences, M. Curie-Sklodowska University of Lublin) for thermoluminescence dates. Special thanks are given to Professor A. Pissart (University of Liège) for time-wasting critical review and remarks on the first draft of the manuscript. The work was financially supported by the state project CPBP 03.03. B7.

REFERENCES

Boulton, G.S., Paul, M.A. (1976). The influence of genetic processes on some geotechnical properties of glacial tills. Quatern. J. Eng. Geol., 9, 159-194

Butrym, J., Lindner, L., Marks, L., Szczesny, R. (1987). First thermoluminescence datings of Pleistocene sediments from Sörkapp Land, Spitsbergen. Pol. Polar Res., 8, 217-229.

Dutkiewicz, J. (1961). Congelifluction lobes on the southern Hornsund coast in Spitsbergen. Biul. Perygl., 10, 285-289.

Dutkiewicz, J. (1967). The distribution of periglacial phenomena in NW Söerkapp, Spitsbergen. Biul. Perygl., 16, 37-83.

Folk, R.L., Ward, W.C. (1957). Brazos river bar: a study in the significance of grain size parameters. J. Sed. Petrol., 27, 3-26.

Friedman, G.M. (1962). On sorting, sorting coefficients, and the lognormality of the grain-size distribution of sandstones. J. Geol., 70, 737-753

Hjelle, A., Lauritzen, Ø. (1982). Geological Map of Svalbard 1:5000,000, sheet 3G, Spitsbergen northern part. Norsk Polarinsti. Skr., 154C, 1-15

Jahn, A. (1967). Some features of mass movement on Spitsbergen slopes. Geogr. Ann., A-49, 213-225.

Jahn, A. (1975). Problems of the periglacial zone, pp. 1-223, Warszawa: PWN.

Karczewski, A. (1963). Morphology, structure and texture of the ground moraine area of West Poland. Prace Komm. Geogr.-Geol. PTPN, 4, 1-112.

Klimaszewski, M. (1960). Geomorphological studies of the western part of Spitsbergen between Kongsfjord and Eidembukta. Prace Geogr., 1, 1-166.

Klysz, P. (1986). Phenomena occurring in the periglacial zone of the Ebba valley and the surrounding area of Petuniabukta region, Spitsbergen. Spraw. PTPN, 103, 11-15.

Klysz, P., Lidner, L., Marks, L., Wysckinski, L. (1987). Map of Quaternary landforms and sediments of the Ebbadalen-Nordenskiöldbreen region Olav V Land, Spitsbergen, 1:20,000. Warszawa: Wyd. Geol.

Klysz, P., Lindner, L., Marks, L., Wysokinski, L. (1989). Late Pleistocene and Holocene relief transformations in Ebbadalen-Nordenskiöldbreen region Olav V Land, Spitsbergen. Pol. Polar Res., 10, in press.

Olszewski, A., Szupryczynski, J. (1985). Texture of recent morainic deposits of the terminal zone of the Werenskiold Glacier. Przeg. Geogr., 57, 645-670.

Rotnicki, K. (1970). Main problems of inland dunes in Poland based on investigations of the dune at Weglewice. Prace Kom. Geogr.-Geol. PTPN, 11, 1-147.

Washburn, A.L. (1967). Instrumental observations of mass wasting in the Mesters Vig District, Northeast Greenland. Medd. Ann. Grønland, 166, 1-303.

GEOMORPHOLOGICAL EFFECTS AND RECENT CLIMATIC RESPONSE OF SNOWPATCHES AND GLACIERS IN THE WESTERN ABISKO MOUNTAINS, SWEDEN

L. Lindh, R. Nyberg and A. Rapp

Department of Physical Geography, University of Lund, Sweden

SYNOPSIS

A number of snowpatches and very small glaciers are studied in the Låktatjåkka area west of Abisko (800-1500 m a.s.l., mean annual temperature ranging from c. -4 to -7°C). Permafrost is present in localized frost mounds and to greater depth in the bedrock at high altitudes.
Nivation processes are studied at an instrumented snowpatch site at 1200 m altitude. The measurements include i.a. air and ground temperature, precipitation, snow depth, runoff, sediment yield and solifluction. An increased geomorphological activity at snowpatch sites is implied by the studies, especially regarding slope wash and mass movements.
Repeated aerial and field photography, snow surveys and old air photos are used to assess the present status and recent climatic response of small glaciers in the area. During the last 45 years, most of them have receded and several are probably stagnated. Variable exposure to snowdrifting seems important to explain different climatic responses.

INTRODUCTION

Research on the geomorphological effect of localized snow and ice bodies in high mountains has centered either on fairly small snowpatches (e.g. St-Onge 1969, Rudberg 1974, Thorn 1979, Hall 1985) or well developed cirque glaciers (e.g. Lewis 1960, Evans 1977, Vilborg 1977). Transitional features between snowpatches and glaciers have been little studied, concerning geomorphological importance or with respect to snow/ice dynamics and climatic response. The present paper deals with these issues. A number of snowpatches and small glaciers are being observed yearly since 1984 in the western Abisko mountains (lat. 68°) in Arctic Sweden. A mobile research hut located near an instrumented snowpatch at c. 1200 m altitude serves as a base for the field studies. The project also includes comparative studies of fossil periglacial landforms in south Sweden (lat. 56°) (cf. Rapp et al. 1986).

STUDY AREA

The western Abisko mountains (Fig.1) is a massif dominated by bedrock of mica schists, with some marble beds. It rises from the altitude of Lake Torneträsk at 341 m a.s.l. to the highest peak of Mt. Vassitjåkka at 1590 m. The morphology is characterized by glacial trough valleys, rounded mountain ridges and plateaux with gentle slopes. Most of the area is above treeline (c. 500-550 m) and is dominated by blockfields, rockwalls and talus slopes, and grass-covered solifluction slopes. A significant part of the area is occupied by perennial snow or glaciers.

The mean annual air temperature in the higher parts of the area (above 800 m) is estimated as ranging from -4 to -7° C. Precipitation varies between c. 1000 mm to the west (Katterjåkk) and c. 300-400 mm to the east (Abisko) for valley stations. Much higher amounts are obtained at high altitudes, mean values for April at Låktatjåkka (1220 m) being three times those at Katterjåkk (Eriksson 1987). A large percentage of the precipitation falls as snow. Snow drifting by predominantly westerly winds is very important.

Permafrost is present in localized mounds mainly in mires at altitudes of 800-1000 m (Åkerman & Malmström 1986), along lake shores even higher up (at 1190 m in Kuoblavagge valley, our observation), and possibly more widespread in bedrock at high altitudes (cf. King 1984).

STUDIES OF SNOWPATCHES AND NIVATION PROCESSES

Snowpatch distribution in the central W Abisko mountains

Some data on the distribution, size and shape of mainly perennial snowpatches in the western part of the area have been compiled from air photos (Table I). The classification into longitudinal, transverse and circular snowpatches follows Lewis (1939). The transverse type is the most common in the area. Large snowfields have mainly easterly aspects (leeside locations). Three snowpatches at 680, 920 and 1220 m are followed yearly in the study concerning climatic response.

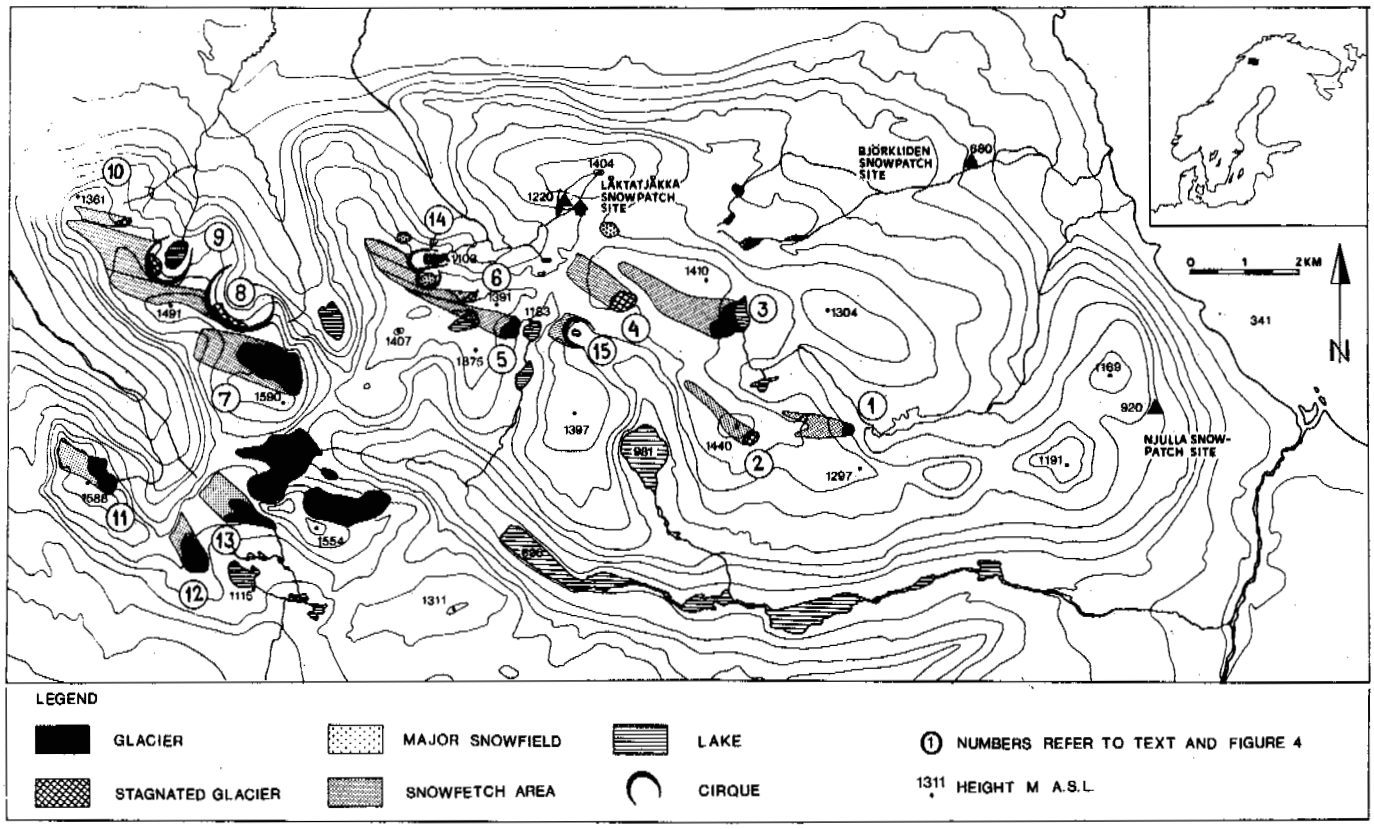

Figure 1. Distribution of glaciers and large snowfields in the western Abisko Mountains. The map also shows estimated snowfetch areas for some of the features, cf. text and Fig.4. Abisko is situated 2 km east of the map area. Contour interval 100 m.

Låktatjåkka snowpatch

This snowpatch at c. 1220 m altitude at Mt. Låktatjåkka has been selected for a study of mass balance and geomorphological activity. It is situated with a southfacing aspect 500 m west of Låktatjåkka Tourist Station. The research hut is located about midway between the Station and the snowpatch (Fig.2). Early in the summer the snowpatch is longitudinal, changing to circular as melting progresses. It occupies a shallow hollow with rock outcrops and block pavement, traversed by a small stream flowing during the early part of the melt season. The slope gradient varies between c. 15-25° along the snowbed. The drainage area at the Låktatjåkka site covers 0.212 km² at an altitude of 1150 to 1406 m. The vegetation is sparse, mainly grass and moss in the lower parts.

Field data are acquired primarily during the summer season and recorded on printers in the hut, or on datalogger at the snowpatch.

Snow depth is measured automatically near the hut with a 1 m long snow stake equipped with 5 photo resistors at 20 cm intervals from top to bottom. The snow stake is calibrated against an independent photo resistor, recording amount of cloud cover (daylight). The accuracy is sufficient to give variations in snow accumulation and melting with a resolution of about 10 cm. Fixed stakes and manual snow surveys are used to measure snow depths at the snowpatch.

Continuous measurements are made of runoff, using four water-level recorders, Fig.2 (only two were in operation during 1987). Precipitation is presently measured with a rain gauge (SMHI). PVC-pipes inserted in the slope are used to study groundwater levels. Continuous recording is made of wind speed and direction, snow drifting is monitored with an infra-red sensor. Air temperature is recorded with a THG in a screen, ground temperature with a datalogger and resistance sensors, and manually with thermistors. Creep and solifluction are studied with a line of wooden pegs. Four Gerlach traps are used to collect sediment transported by slope wash.

Njulla snowpatch

The site at Mt. Njulla 5 km W of Abisko is at an altitude of c. 920 m with an easterly aspect. This transverse snowpatch with a dimension of c. 200x50 m in early summer occupies a small terrace on the mountain slope, with a low backwall (mostly less than 5 m high). The

Table I. Some data on snowpatches in the central western Abisko mountains.

Types	transverse			circular			longitudinal			transv./long.						
number	82			30			42			17						
Altitude	<900			900-1100			1100-1300			>1300 m						
number	8			41			103			19						
Size	<5000			5000-10000			10000-50000			50000-15000			>150000 m²			
number	70			44			40			13			4			
Aspect	N	NNE	NE	ENE	E	ESE	SE	SSE	S	SSW	SW	WSW	W	WNW	NW	NNW
number	14	13	19	29	11	9	20	7	9	-	2	2	19	2	8	7
Aspect vs.	N - E			E - S			S - W			W - N						
size	<5000	>5000		<5000	>5000		<5000	>5000		<5000	>5000 m²					
number	28	47		10	36		9	4		23	13					

Data compiled from air photos (1:60000) of upper Låktajokk, Kuoblajokk and Rakasjokk basins.

gradient of the snowpatch surface is between 25-35°, that of the terrace downslope of the snowpatch 14-18°. Vegetation is absent in a zone peripheral to the snowpatch, but increases downslope with mosses and grasses. In late summer, the snowpatch melts away completely in the southern part, while the northern, steeper part is perennial. The measurements embrace slope wash and solifluction.

Björkliden snowpatch

The lowest situated snowpatch (about 50x25 m in early summer) occupies a terrace at 680 m altitude 2 km west of Björkliden. It rests against a bedrock outcrop with roche moutonnée sculpture. The terrace downslope of the snowpatch is a gentle grass-covered solifluction slope. The aspect is easterly. This transverse snowpatch normally melts away completely in August, although on September 5, 1987 it still had a size of 25x10 m. This summer was unusually cold. Measurements include snow creep and sliding, and solifluction.

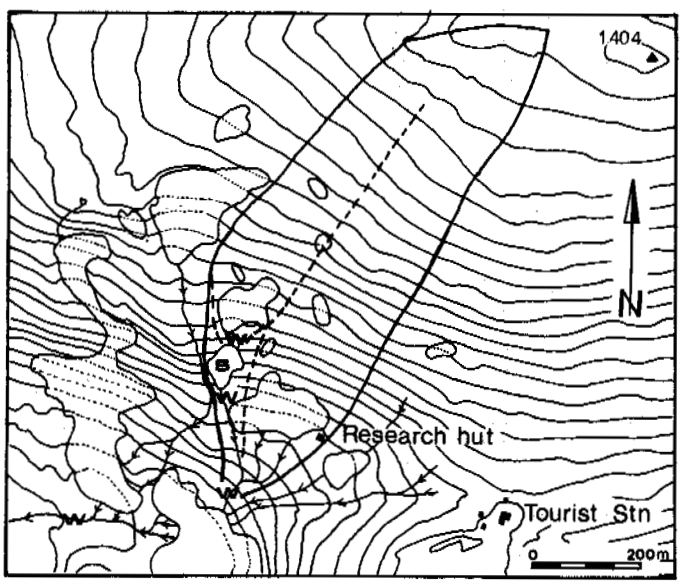

Fig 2. The drainage basin of the Låktatjåkka snowpatch (s) and the location of weirs (w) for runoff measurements. Contour interval 10m.

Snowpatch mass balance

From the observations of snowpatch size and depth during the years 1984-1987 the data of Table II have been compiled, giving the estimated maximum snow depths and volumes at the sites at the beginning and end of the summer season. Based on snow density measurements, yielding mean values of about 350 kg/m³ in early summer, estimates of runoff potential have also been made. Although some of the water will be lost by sublimation/evaporation, these estimates indicate the amount and varying duration of runoff during the summer season for the sites.

For the Låktatjåkka snowpatch drainage area, the total snow volume at the beginning of the melting season (late May) was estimated based on point sampling of snow depths to about 41000 m³ water equivalent. During the period 11 July to 26 August 1987 an estimated 27000 m³ water equivalent melted away from the area, and about 21000 m³ were added as precipitation. The measured runoff was about 51000 m³. The discrepancy may be due to inaccurate estimation of the snow volume, or to the components of sublimation/evaporation and groundwater, which have not been measured. The studied snowpatch contributed about 13 % of the total runoff from snowmelt in the basin 1987. Snowmelt was of similar importance as rainfall as a cause of runoff, although their relative significance naturally varied from time to time. Precipitation was not measured continuously, however runoff curves in July-August 1987 correlate well with air temperature, with some time lag, indicating snowmelt control of variations in runoff (Fig.3).

Yearly size variation of the snowpatches is related to prevailing summer weather and initial snow depths. E.g. in 1985, with mean temperatures during the summer months above average (At Abisko, June 8.6, July 12.5, August 10.5°C) the snowpatch at Låktatjåkka melted away completely. In 1987, a 2m deep part remained. The summer temperatures that year were below average (Abisko, June 7.9, July 9.7, August 7.6). Thus long-term trends in size

Table II. Estimated maximum snow depths, snowpatch volume and water equivalent for three snowpatch sites, western Abisko mountains. Based on repeated field measurements during 1986/1987.

site	max. depth, m		volume, m3		water equivalent
	mid-June	mid-Sept.	mid-June	mid-Sept.	m3
Låktatjåkka	4	1.5	16,000	150	5,500
Njulla	4	1.5	20,000	600	6,800
Björkliden	3	0	3,000	0	1,100

variation must be studied before the climatic response of snowpatches can be evaluated.

Geomorphological activity at snowpatch sites

Geomorphic processes at the sites are studied by qualitative observations or quantitative measurement.

Frost shattering and rockfall

Rockfall is a significant process only at the Njulla site. The Björkliden site lacks a vertical backwall. At Njulla, numerous small stones were found on the snow near the upper randkluft late in the summer of 1987 (about 1 fragment per 1-2 m). No large rockfall event has occurred at the site between 1984-1987. At the Låktatjåkka site, an attempt is made to evaluate the preconditions for freeze-thaw weathering by temperature measurements in various positions peripheral to the snowpatch or in the ground (Nyberg 1986).

Debris slides and flows

Two small debris slides/flows have recently occurred on the western backslope of the Låktatjåkka snowpatch site. Coloured lines sprayed across the slide tracks will enable further activity to be studied quantitatively. At the Njulla site, small mass movements of similar type have been observed, also on the steep backslope.

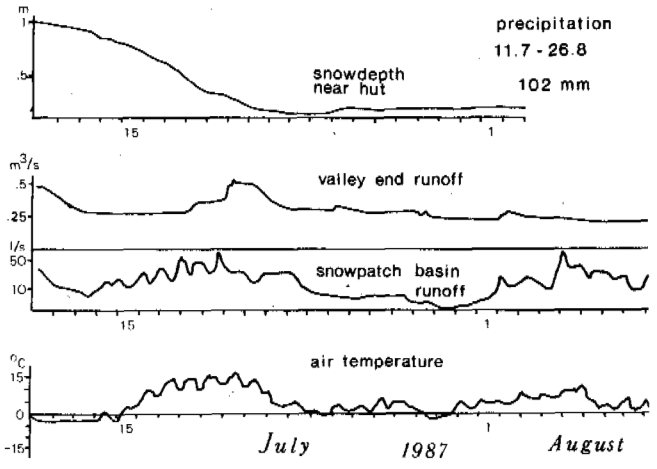

Figure 3. The relationship between air temperature, snowmelt and runoff at the Låktatjåkka snowpatch site during part of the summer 1987.

Slope wash

Slope wash is an active process in a zone downslope of the snowpatches. Sediment deposition in traps during long periods point to a highly variable transport (Table III). Traps on both sides of the Låktatjåkka snowpatch obtained lower amounts of sediment than the traps below the snowpatch. As the trap efficiency is fairly low, the results give only crude estimates of sediment transport by slope wash.

Soil creep and solifluction

Solifluction lobes at all three sites reveal slow mass movement in a zone downslope of the snowpatches. This is shown also by fabric measurements downslope of the Njulla snowpatch. Surficial rates of movement lie within 0-5 cm per year, with no clear variation between the sites.

Snow creep and sliding

Forces exerted by the snowpack have been studied at the Låktatjåkka and Björkliden sites. Two snow sliding stakes, similar to those used by Matthews & Mackay (1963), were installed at the Låktatjåkka site in early September 1984. No movement had been recorded up til July 1985, partly because a basal layer of ice was formed by repeated melting and freezing at the bed of the snowpatch, which furthermore has a fairly rough stony surface. Observations of bent snowstakes made of galvanized steel revealed the occurrence of powerful snow creep. This probably has little or no geomorphological effect.

At the Björkliden site the occurrence of snow sliding over even bedrock surfaces at an angle of 20-30° can be demonstrated (cf. Dyson 1937). In the summer of 1987 painted stones had moved 0.5-2.5 m since 1984, according to photo-

Table III. Sediment yield (g) in Gerlach traps at Låktatjåkka and Njulla sites

site	summer season 1986	1987
Njulla 1	20	<10
Njulla 2	3750	no data
Låktatjåkka 1	352	94
Låktatjåkka 2	not installed	96
Låktatjåkka 3	10	24
Låktatjåkka 4	not installed	1

Traps 3 and 4 at Låktatjåkka are control traps on either sides of the snowpatch. The traps were emptied when slope wash from snowmelt had ceased in late summer.

graphic comparisons. Many stones had striations or crush marks as a result of sliding and/or a heavy pressure against the underlying bedrock surface (cf. Costin et al.1973). This process may contribute to keeping rock outcrops free from weathered debris, or may remove till deposits. On such sites, nivation during postglacial time may cause a local redistribution of the glacial deposits.

STUDIES OF GLACIERS CONCERNING RETREAT AND GEOMORPHOLOGICAL EFFECTS

Distribution and recent retreat of glaciers in the western Abisko Mountains.

The glacierization limit in the western part of the massif is estimated to an altitude of c. 1400 m a.s.l. and rises eastwards to an altitude of c.1500 m (östrem et al.1973). Most of the glaciers are situated in the higher western and central part in an altitudinal range from 1020 to 1590m. The lower smoother eastern part lacks glaciers and the amount of major snowfields is also decreasing rapidly from the central part towards east (Fig.1). Present-day glacier distribution does not completely match the localization of cirque forms. E.g. the large cirque at Lake Ekosjön in Låktavagge is presently empty, whereas at Ekmanjaure and Käppasvagge, glaciers occur unrelated to distinct cirques. This could indicate a change in recent controls on glaciation (cf. Evans 1977) compared with earlier during the Holocene and the Pleistocene. Repeated aerial and field photography, snow depth measurements and old air photos are being used to assess the present status and recent climatic response of small glaciers in the area. During the last 45 years, some of them have receded markedly and are estimated to have lost up to 60 % of their volume, while others lost only 10 % since 1943.

Possible causes of variable response to the recent climate.

In the western Abisko Mountains most of the glaciers and large snowfields are oriented towards south to northeast (Fig.1). Especially for glaciers in southerly to easterly aspects, direct insolation plays an important role (Isard 1983). Calculations on the effect of aspects have not yet been made for the objects of this study.

Another important factor for glacier mass balance in the study area is wind transported snow. Winds from W and NW give the largest amount of winter precipitation at nearby Katterjåkk (Eriksson 1987). The annual accumulation at different sites is largely dependent upon the amount of snowfall, wind transport and the feeding area, the snowfetch. The snowfetch area has been estimated for each glacier for westerly winds (Fig.1), using air photos and detailed (1/10000) topographic maps (our own mapping from air photos) and by taking into account some factors controlling the snow drift pattern at the sites. These factors are

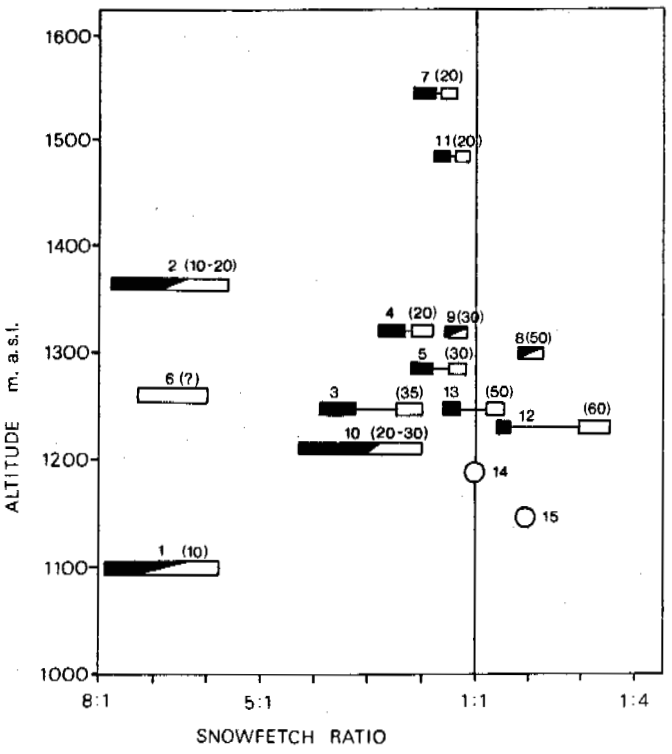

Figure 4. The relationship between altitude and ratio of snowfetch area to glacier/cirque area for features numbered in Fig.1. A snowfetch ratio of e.g. 5:1 means the snowfetch area is 5 times as large as the corresponding glacier/cirque area. Numbers within parentheses show estimated % loss in volume of glaciers since 1943. Circles=empty cirques. Length of staples indicate uncertainty in estimated snowfetch areas. Black=1943, white=present situation.

a) slope steepness, b) topographic influence on the wind flow and c) large snowfields acting as snow traps upwind (cf. Gray & Male 1981).

The relationship between estimated snowfetch area and the area of glacier cirque/hollow implies that glaciers with large retreat have a smaller snowfetch area in relation to their cirque area compared with less retreating glaciers (see Fig. 4). Thus it is inferred that snowdrifting is very important during recent decades for the mass balance of the glaciers, accounting for the small retreat of glaciers with favourable locations in this respect (large snowfetch areas). These assumptions are based on limited data and without taking aspect (insolation) fully into consideration. A slightly different wind direction will give other estimates of snowfetch areas. If the snowdrifting hypothesis is correct, the mass balance for some of the studied objects is very sensitive to changes in direction for prevailing snowbearing winds. We stress that these conclusions are preliminary.

Transitional forms between snowfields and glaciers.

It has long been suggested that the transformation of snowfields into glaciers occurs gradually (Wright 1914, Lewis 1939). However, very few field observations have been made to shed more light over this problem. As an extension of the nivation studies, transitional forms are being investigated in the western Abisko mountains (Lindh 1984, Rapp et al 1986). Out of 18 investigated features, four are suspected to be in a state more or less close to become glaciers if the climatic conditions or snow drift pattern slightly alter for their benefits, due to a rapid climatic response. Seven are glaciers of varying sizes between 0.07 km² and 0.65 km², two are recently stagnated glaciers (No. 8 and 9, Fig.1, still marked as glaciers on the glacier atlas, östrem et al.1973. Glaciers 1 and 3 are not included on the atlas map). Three are major snowfields which have been glaciers probably early in the Holocene, but are not considered to be close to glacier status presently. One of them (east of the tourist station) has a steep frontal moraine-like ridge. The remaining two features are empty glacial cirques.

The four first mentioned features (No. 2,4,6 and 10 in Fig.1) are of particular interest. They are believed to have been glaciers not very long ago. In air photos from 1943, three of them show visible ice with deformed banding structures indicating some movement. None of these features have shown visible ice during the research period because of low ablation during summer. The sizes of their ice bodies are therefore not known. The fourth feature (No.2) showed no visible ice in 1943, but on the other hand has a fresh arc-shaped ridge close to its lower margin (Lindh 1984). Whether this ridge is a terminal moraine or a protalus rampart has not yet been established.

CONCLUSIONS

For snowpatch sites in the western Abisko mountains, snow surveys, runoff measurements and monitoring of slope processes point to an increased geomorphological activity compared with snowfree slopes. Runoff in front of a near-perennial snowpatch is approx. twice that for snowfree slopes with only precipitation-generated runoff. Annual size variations of snowpatches reflect the prevailing summer weather conditions. Large snowfields and small glaciers in the area show a variable recent climatic response that may be related to their exposure to snow drifting (size of snowfetch area). Most of them have receded during the last 45 years, but some only marginally.

ACKNOWLEDGEMENTS

The study was funded by the Swedish Natural Science Research Council and the Royal Swedish Academy of Sciences (Abisko Scientific Research Station).

REFERENCES

Akerman, J & Malmström, B (1986). Permafrost mounds in the Abisko area, north Sweden. Geogr. Ann. 68A (3), 155-165.

Costin, A B, Jennings, J N, Bautovich, B C & Wimbush, D J (1973). Forces developed by snowpatch action, Mt Twynam, Snowy Mtn, Australia. Arctic and Alpine Res. Vol. 5, No. 2, 121-26.

Dyson, J L (1937). Snowslide striations. Journal of Geology, Vol. 45, No. 5, 549-57.

Eriksson, B (1987). The precipitation climate of the Swedish Fjells during the 20th century - some remarkable features. UNGI rapport Nr. 65, Uppsala.

Evans, I S (1977). World-wide variations in the direction and concentration of cirque and glacier aspects. Geogr.Ann.59A (3-4), 151-175.

Gray, D M & Male, D H (1981). Handbook of Snow Pergamon Press, Canada.

Hall, K (1985). Some observations on ground temperatures and transport processes at a nivation site in northern Norway. Norsk Geogr. Tidsskr. 39:27-37. Oslo.

Isard, S A (1983). Estimating Potential Direct Insolation to Alpine Terrain. Arctic and Alpine Res. Vol. 15, No. 1, 77-89.

King, L (1984). Permafrost in Skandinavien - Untersuchungsergebnisse aus Lappland, Jotunheimen und Dovre/Rondane. Heidelberger Geogr. Arb. 76, 125 pp.

Lewis, W V (1939). Snowpatch erosion in Iceland Geogr. Journal, Vol. 94, No 2, 153-61.

(Ed.) (1960). Investigations on Norwegian Cirque Glaciers. R.G.S. Res. Series, No 4

Lindh, L (1984). Studies of Transitional Forms between Snowpatch and Glacier in the Abisko Mountains, Swedish Lappland. Svensk Geogr. Årsbok, 60.

Matthews, W H & Mackay, J R (1963). Snowcreep studies, Mt Seymore, B.C: Preliminary field investigations. Geogr.Bull.No. 20

Nyberg, R (1986). Freeze-thaw activity at snowpatch sites. A progress report of studies in N and S Sweden. Geogr.Ann. 68A (3), 207-211.

östrem, G, Haakensen, N & Melander, O (1973). Atlas over breer i Nord-Skandinavia. Stockholms Univ. Naturgeogr. Inst. Medd. 46, 315 pp.

Rapp, A, Nyberg, R & Lindh, L (1986). Nivation and local glaciation in N and S Sweden. A progress report. Geogr.Ann. 68A (3), 197-205.

Rudberg, S (1974). Some observations concerning nivation and snowmelt in Swedish Lapland. In: Poser,H (ed) Geomorphologische Prozesse und Prozess-Kombinationen in der Gegenwart unter verschiedenen Klimabedingungen. Vandenhoeck & Ruprecht, Göttingen, 263-273.

St-Onge, D A (1969). Nivation landforms. Canada Geol.Survey Paper 69(30).

Thorn, C E (1979). Ground temperatures and surficial transport in colluvium during snowpatch meltout; Colorado Front Range. Arctic and Alpine Res. Vol. 11, No. 1 41-52.

Vilborg,L (1977). The cirque forms of Swedish Lappland. Geogr.Ann. 59A (3-4), 89-150.

Wright, W B (1914). The Quaternary Ice Age. Macmillan London (1 st ed.), 464 pp.

GAS-HYDRATE ACCUMULATIONS AND PERMAFROST DEVELOPMENT

Yu.F. Makogon

Chief of Laboratory, VNNIGas, Moscow, USSR

SYNOPSIS The existence of natural gas-hydrate accumulation is related not only to a considerable increase in hydricarbon resources but also to the necessity of serious study of "dangerous" properties of hydrates and hydrate-saturated rocks and their close control during the engineering development of HFZ both on land and in oceans.

The processes of phase transition of gas-water system under natural conditions are accompanied by a considerable change in thermoregime of section and specific volume of gas and water during hydrate formation and degradation. The value of change in phase specific volume leads, on the one hand, to a sharp increase in stresses in engineering constructions which exceed the critical stresses and, on the other hand, - to a sharp decrease in load capacity of hydrate-containing rocks. These features should be kept in mind while developing the hydrate distribution regions both on land and, especially, in ocean.

The growth of mineral raw energy consumption requires the development of oil and natural gas fields in the Arctic regions and beneath the ocean floor. The development of these fields is related to the large geotechnical and technologic difficulties because of the presence of thick permafrost sections and hydrate formation zones which are characterized by phase transition of water taking place during engineering activity.

The practice of developing the regions with large permafrost has gained tremendous experience in constructing and operating engineering structures both in the Soviet Union and abroad. The experience in developing the zones of gas-hydrate distribution is practically absent. However, the difficulties arizing while developing hydrate formation zones (HFZ) are more serious than those arizing in the permafrost.

It is well known that the majority of difficulties arizing in the permafrost zones are associated with a change of specific volume of water by 9% during its thawing and freezing. This value is enough for a sharp change of load-carring capacity of watersaturated rocks, and for arizing high stress in engineering structures.

The discovery, made by the Soviet scientists, of the existence of natural gas hydrates in the earth's crust and a complex of scientific-research and field works have allowed to reveal some reasons complicating the engineering development of HFZ.

Reserves of methane concentrated in the earth's crust in the hydrate state exceed 10^{-6} m^3. Their development and usage as power resource are very important. However it is necessary, in this case, to take into consideration the dangerous properties of gas-hydrates and hydrate-saturated rocks. The problem lies in the fact that a specific volume of water as it converts into hydrate state increases three or four times compared to its freezing. And conversely, during hydrate degradation a specific volume of water declines sharply. This fact is a basic principle and should be kept in mind while developing hydrate-formation zones.

A Short Characteristic of Gas Hydrate

Gas-hydrates are solid compound-inclusions in which molecules of gas fill, under the specific pressures and temperatures, structural voids of crystalline lattice formed by water molecules due to strong hydrogen bond. Water molecules as hydrate and voids are formed looking like to be forced apart by molecules of gas enclosed in these voids, a specific water volume increasing (depending on gas composition and the structure of hydrate lattice) up to 1.26 - 1.32 cm^3/g. Molecular pressure of gas in the hydrate lattice reaches several KBar.

In appearance hydrates resemble, depending on the condition of formation and state of hydrate formation compounds, clearly defined transparent crystals of different forms. An elementary cell of gas hydrate consists of the definite number of water and gas molecules (4-17 water molecules per one gas molecule) whose relationship depends on gas molecule size, pressure and temperature. One volume of water binds from 70 to 220 volumes of gas.

Depending on the composition and size of gas molecules crystalline hydrates of different structures are formed. Study of these hydrates has only begun. Figure I gives the structural elements of gas hydrates. Whose density varies from 0.8 - 1.2 g/cm^3.

Figures 2 and 3 present photos of some hydrates of different gases.

The hydrate formation conditions are defined - by pressure, temperature, composition and state of gas and water. The relation between pressure and temperature of hydrate formation by different gases or natural mixtures are usually presented as heterogeneous diagrams. Figures 4 and 5 illustrate such dependence for some gases and lightvolatile liquids. To the left and above the equilibrium curves hydrates are formed and are stable; to the right and under - hydrates degradate. Hydrates are formed by all known gases whose molecule size does not exceed 0.69 Mn (except hydrogen, helium and neon).

Gas hydrate can be formed and accumulated at any place having gas, water and the corresponding thermodynamic conditions, and are stable over a wide temperature and pressure range, from 100 to 400K and from $1 \cdot 10^{-6}$ MPa to 2.10^{3} MPa. Hydrates are characterized by high electric resistance. Sound velocity in hydrates is slightly below than that in ice. The velocity of seismoacoustic waves through porous rock saturated with gas hydrates by 60-100% higher than through the same rock saturated with free gas. Hydrate hardness is not well known; however, the available data show that it exceeds ice hardness about two times. Gas and water permeability through gas hydrate is very low. Gas hydrate is a perfect cover for gas and oil fields. The majority of the discovered primary gas-hydrate deposits (GHD) in oceans have no lithologic cover and are situated in the immediate vicinity to bottom.

The process of hydrate formation is accompanied by heat release and the process of degradation - by heat absorption. At t 0°C, the heat of phase conversion is about 420KJ/kg; at 0°C - about 140KJ/kg. The heat amount released under hydrate formation and absorbed under degradation depends on gas composition, pressure, temperature and water state. Figure 6 gives the dependence of heat of propane-hydrate formation (degradation).

Heat conduction of gas hydrate is considerably lower than that of ice; e.g., at 200 K methane-hydrate heat conduction 8 times lower compared to ice.

According to the works of Soviet and foriegn scientists, natural gas hydrates are found in HFZ which are spread widely both on land and in oceans.

The hydrate formation zone is a zone of sedimentary, rocks saturated with water and gas in wich the thermodynamic conditions are suitable for hydrate formation. The HFZ thickness is determiner by gas composition, reservoir water mineralization, geotherm gradient, and pressure. The present thermodynamic characteristic of the sedimentary mantle of the earth's crust corresponds to the conditions of hydrate accumulation and its stable existence on 25% of land and 90% of ocean. The HFZ thickness on land is 700-1200 (up to 1700) m, in oceans - 200-400 (up to 1100) m.

The upper boundary of HFZ on land is at depth of 100-250 m, in oceans, depending on water depth, - some cm. to sea floor. Figures 7 and 8 give the profile of a zone of the hydrate stable existence in East Siberia and in the Beaufort Sea.

The results of even the first search for gas hydrate accumulations have shown their wide distribution both on land and, especially, in oceans. Figure 9 gives the map-scheme of the explored areas of GHD distribution in the world. Figure 10 gives the scheme of the GHD distribution in the USSR.

The knowlege about the accumulation of natural gas hydrate from the viewpoint of engineering activity in the region of its distribution is extremely poor.

The process of hydrate formation in porous rocks is accompanied by the development of high stresses between the particles of rocks, these stresses passing to engineering constructions drilled into a zone of phase transition. Molecular stresses developing during hydrate crystallization exceed considerably those developing during water freezing in a closed volume.

Phase transition taking place during hydrate formation and degradation differ from phase transition of water during it's freezing and thawing not only by a value of water specific volume change but also by a considerable change of gas specific volume. If at the moment of hydrate formation hydrate-forming compound is in gaseous (vapour) state, then during hydrate formation a sharp decrease in it's specific volume takes place. For example, under methane-hydrate formation at 273K it's specific volume decreases by 693 times, i.e. high energy concentration of gas in a unite hydrate volume (one water volume bonds 181.9 volumes of methane). As hydrate degradates in a limited volume, its energy releases developing high pressure. Figure 11 shows the dependence of pressure change under hydrate degradation in the limited volume. The releasing energy of gas pressure as hydrate degradates under a heat of engineering construction may lead to failure of engineering construction itself. For example, the Soviet, as well as foriegn experts run into the facts of mud blowount due to gas liberated under hydrate degradation while drilling deep wells through hydrate-saturated beds. Such blowouts are usually of short duration, impulsive and self-regulative. To eliminate the sequence of blowout is very expensive, especially when drilling works are carried out in the Arctic ocean from drilling vessels.

When hydrates are formed by the liquid hydricarbons, the pressure increases at the moment of hydrate formation in the closed volume, the pressure increasing from 0.5-0.7 MPa to 70-80 MPa. Figure 12 gives a cut of tubing (diameter - 64 cm, wall thickness - 6 mm) collapsed by the hydrates formed by liquid gas condensate in tubing-casing annulus at the depth of 1245 m and at temperature of 7°C.

The stress in rock massif as hydrates are formed includes two components: a change of specific water volume by 26-32% and a change of specific gas volume. The studies carried out in

laboratory have shown that methane-hydrate formation in sandstones led to a complete destruction of them after degradation of hydrate formed in these sandstones. The load capacity of such sandstones after hydrate degradation is practically absent. Sandstone turns to drift sand. A deep well drilled, at temperature below equilibrium one, in rocks saturated with hydrates and operated for a long period at tempe temperature higher than equilibrium will be subjected to high pressure of gas liberating under hydrate degradation. If liberating gas outflow into the surrounding rocks is lower than it's inflow, the pressure in near-hole area may increase above the critical one and collapse casing. From this point of view, the intervals of hydrate monolith which, according to drilling of wells in oceans are widely spread and reach the thickness of 3-5 and more metres, are most dangerous.

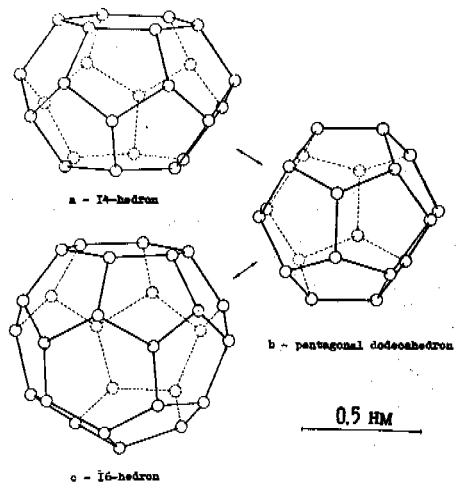

Fig. I. Structural elements of gas hydrates

Fig.I. Structural elements of gas hydrates

Fig.3. Propane hydrate

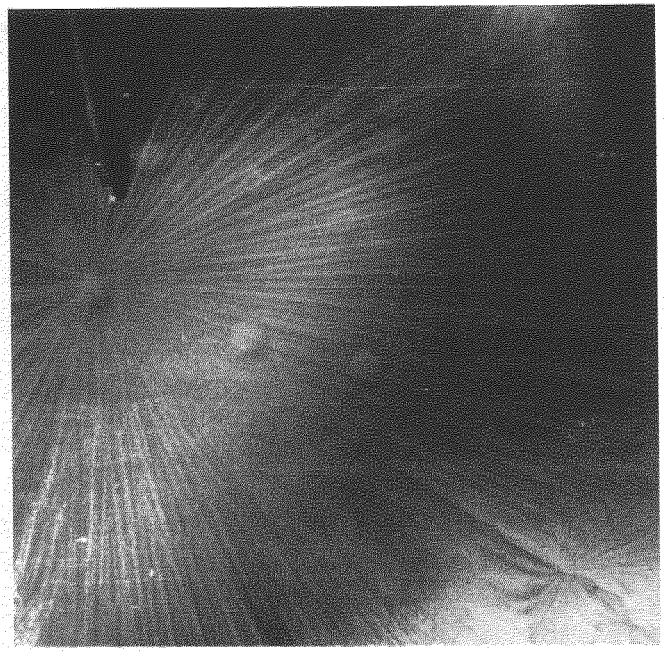

Fig.2.Methan hydrate

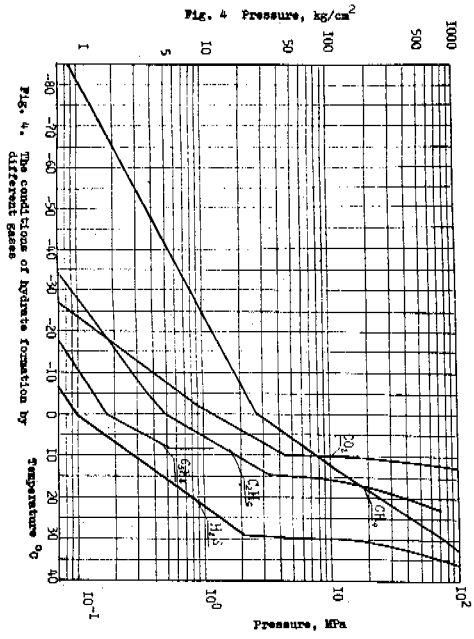

Fig.4. The conditions of hydrate formation by different gases

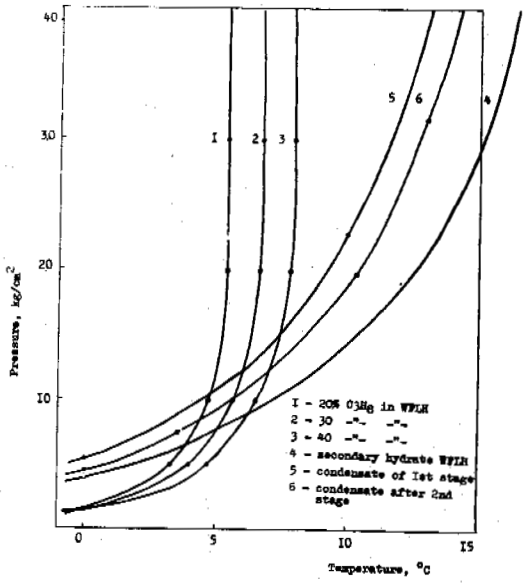

Fig. 5. The conditions of hydrate formation of wide fraction by light liquid hydricarbons

Fig.5. The conditions of hydrate formation of wide fraction by light liquid hydricarbons

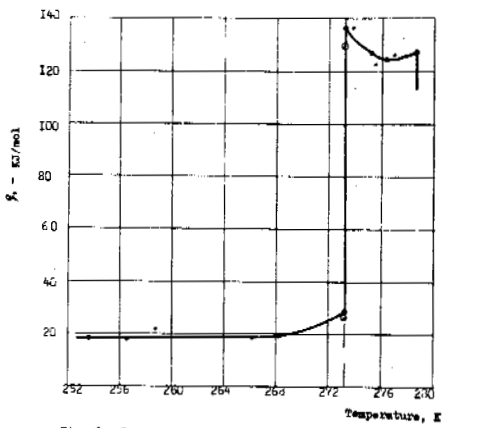

Fig. 6. Dependence of propane-hydrate formation (degradation) heat on temperature

• by W. Bulejko

o - by P. Handa

· experimental data

Fig.6. Dependens of propane-hydrate formation (degradation) heat on temperature

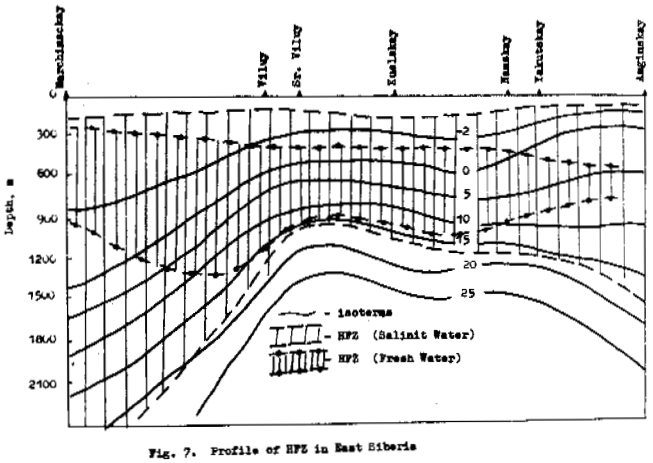

Fig. 7. Profile of HFZ in East Siberia

Fig.7.Profileof HFZ in East Siberia

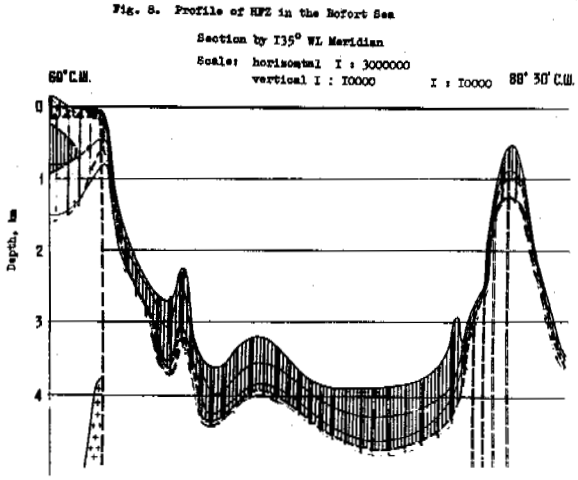

Fig.8. Profile of HFZ in the Bofort Sea

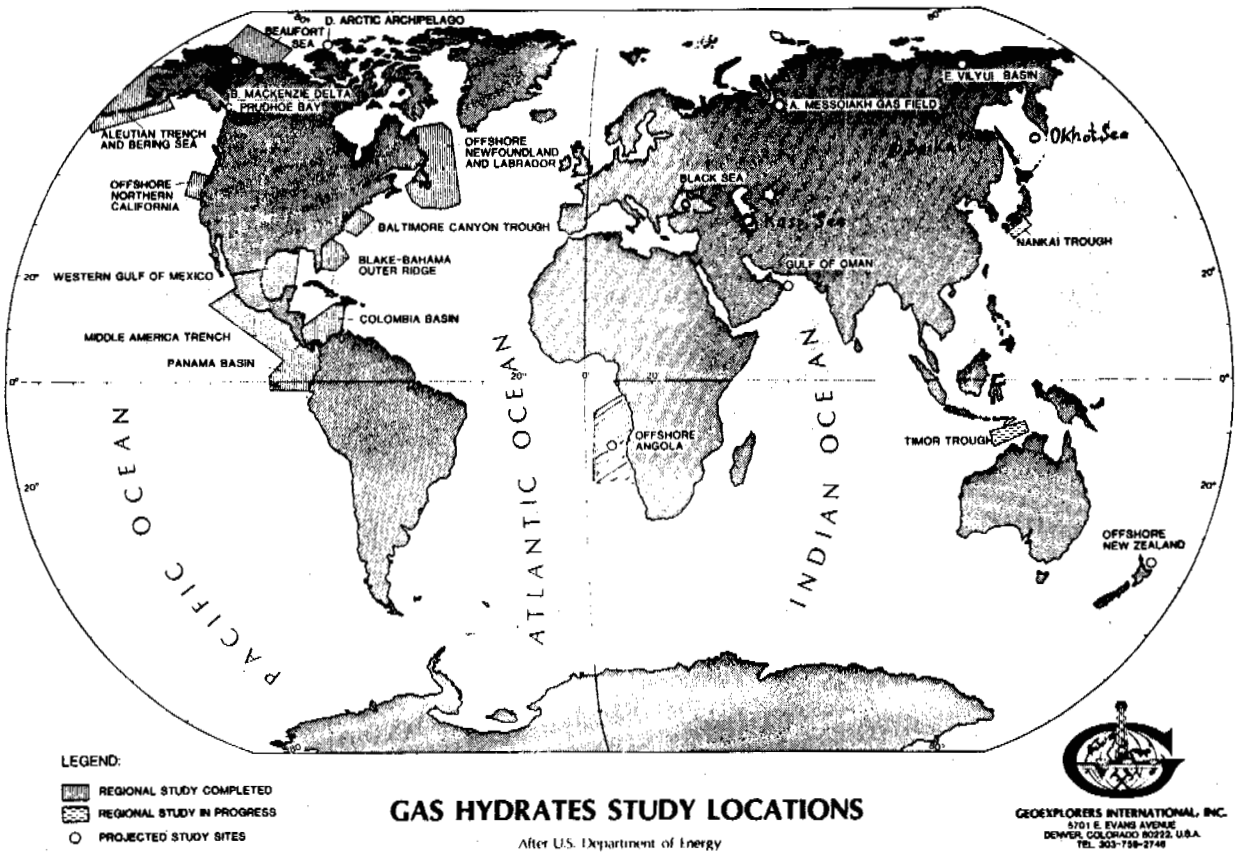

GAS HYDRATES STUDY LOCATIONS

After U.S. Department of Energy

GEOEXPLORERS INTERNATIONAL, INC.
5701 E. EVANS AVENUE
DENVER, COLORADO 80222, U.S.A.
TEL. 303-758-2748

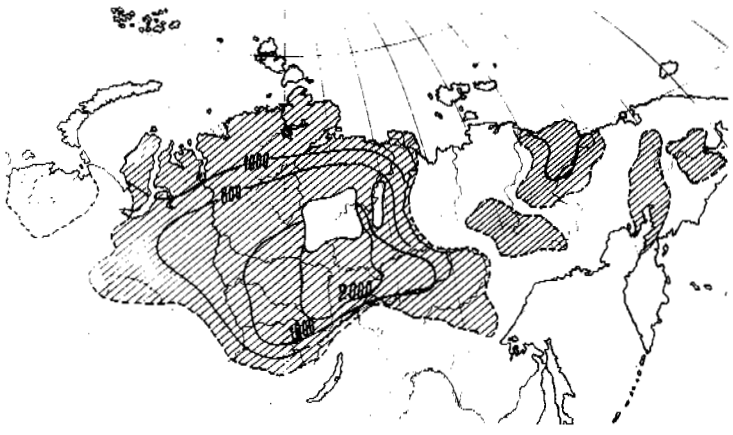

Fig.IO. Scheme of HFZ distribution in the USSR

Fig.IO. Scheme of HFZ distribution in the USSR

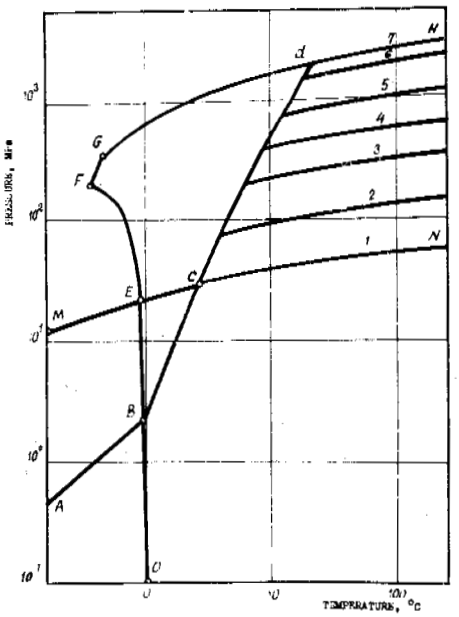

FIG.11 RELATIONSHIP BETWEEN PRESSURE AND GAS TEMPERATURE DURING METHANE HYDRATE DECOMPOSITION IN A LIMITED VOLUME

Fig.II. Relationship between pressure and gas temperature during methane hydrate decomposition in a limited volume

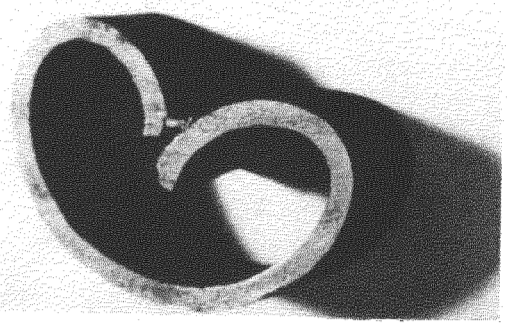

Fig.I2.

A HYPOTHESIS FOR THE HOLOCENE PERMAFROST EVOLUTION

L.N. Maximova and V.Ye. Romanovsky

Faculty of Geology, Moscow State University, Moscow, USSR

SYNOPSIS The dynamics of ground thawing and freezing in the Holocene due to climate fluctuations is discussed. The variation of summary temperature curves obtained for different regions of the USSR has been studied based on an analysis of harmonics corresponding to the climate fluctuations with periods of 41 , 21 , and 11 thousand years. The results are used to estimate the beginning of formation of the Holocene perennially frozen grounds (completely frozen after the thermal maximum). The stages of their development are related to climatic fluctuations with the period of about 1.5 thousand years. An attempt is made to explain some regional peculiarities of the Holocene permafrost. Thus, the expansion of the permafrost zone and growth of its maximum thickness (down to 150-200 m) from the west to the east in the USSR, apart from the existing regional and zonal factors, can be explained by an increase in the duration of freezing due to an earlier Holocene maximum in the eastern regions of Siberia as compared with the European North and West Siberia. The conclusions, confirmed by a series of computer calculations of perennial freezing, are in good agreement with paleogeographical reconstructions of the Late Pleistocene and Holocene.

Perennially frozen grounds of the Holocene age occupy over a third of the permafrost zone in the USSR. Their evolution is closely associater with the climatic changes in the Holocene. The climatic warming in the first half of that period, which caused an intensive permafrost degradation, and subsequent temperature decline, that resulted in permafrost development in the areas which had earlier been occupied by fully or partially thawedgrounds, are known to be the main events in the Holocene.

The paleotemperature curves (Figs.1 and 3) are proposed to investigate specific features of the Holocene permafrost evolution in the USSR. They have been calculated in accordance with the established notions (Zubakov, 1986; Maximov, 1972; Sergin, 1975; and others) based on the following assumptions: (1) climatic rhythms are characterized by a sinusoidal variation of temperatures with periods of 200(T'), 100(T''), 41(T_1), 21(T_2), and 10(T_3) thousand years; (2) the extrema of harmonics T' and T_1 occurred minimum 25-26 thousand, of T_2 minimum 22-23 thousand, and of T'' and T_3 maximum five thousand years ago; (3) extreme temperature deviations from the present-day values in the cold epoch were 9°C for high latitudes of glacier-free land in the northern hemisphere, and 5°C for moderate ones; in the warm epoch these values were 4°C and 2°C, respectively.

Based on the above-presented assumptions, a system of equations was derived yielding the amplitudes of the T_1, T_2 and T_3 harmonice and enabling construction of the summary paleotemperature curves (Maximova and Romanovsky,1986):

$$t(\tau)\Big|_{\tau=\tau_{min}} - t(\tau)\Big|_{\tau=0} = a;$$

$$t(\tau)\Big|_{\tau=\tau_{max}} - t(\tau)\Big|_{\tau=0} = b;$$

$$\frac{dt(\tau)}{d\tau}\Big|_{\tau=\tau_{max}} = 0,$$

where $t_{(\tau)}$ is a function of total temperature; τ_{min} and τ_{max} are the time periods of the last thermal maximum and minimum; τ_0 is the present time, and "a" and "b" are temperature deviations from the present-day values during the periods of minimum and maximum.

The amplitudes of T' and T'' harmonics were assumed to equal 1°C.

The climatic variations in the Late Pleistocene and Holocene obtained from the curves are in good agreement with the established notions of the paleoclimatic peculiarities of that time. The paleotemperature curve (Fig.1) illustrates principal climatic events of the Late Pleistocene - Holocene, and their time interval corresponding to the isotopic oxygen profile of ice from the boreholes at the Vostok station in Antarctica (Gordienko et al., 1983) and to its paleogeographic interpretation.

From the curve obtained for the highlands of southeastern Siberia over an interval of 160 thousand years, the following events can be identified (Zubakov, 1986): the Riss-Würmian

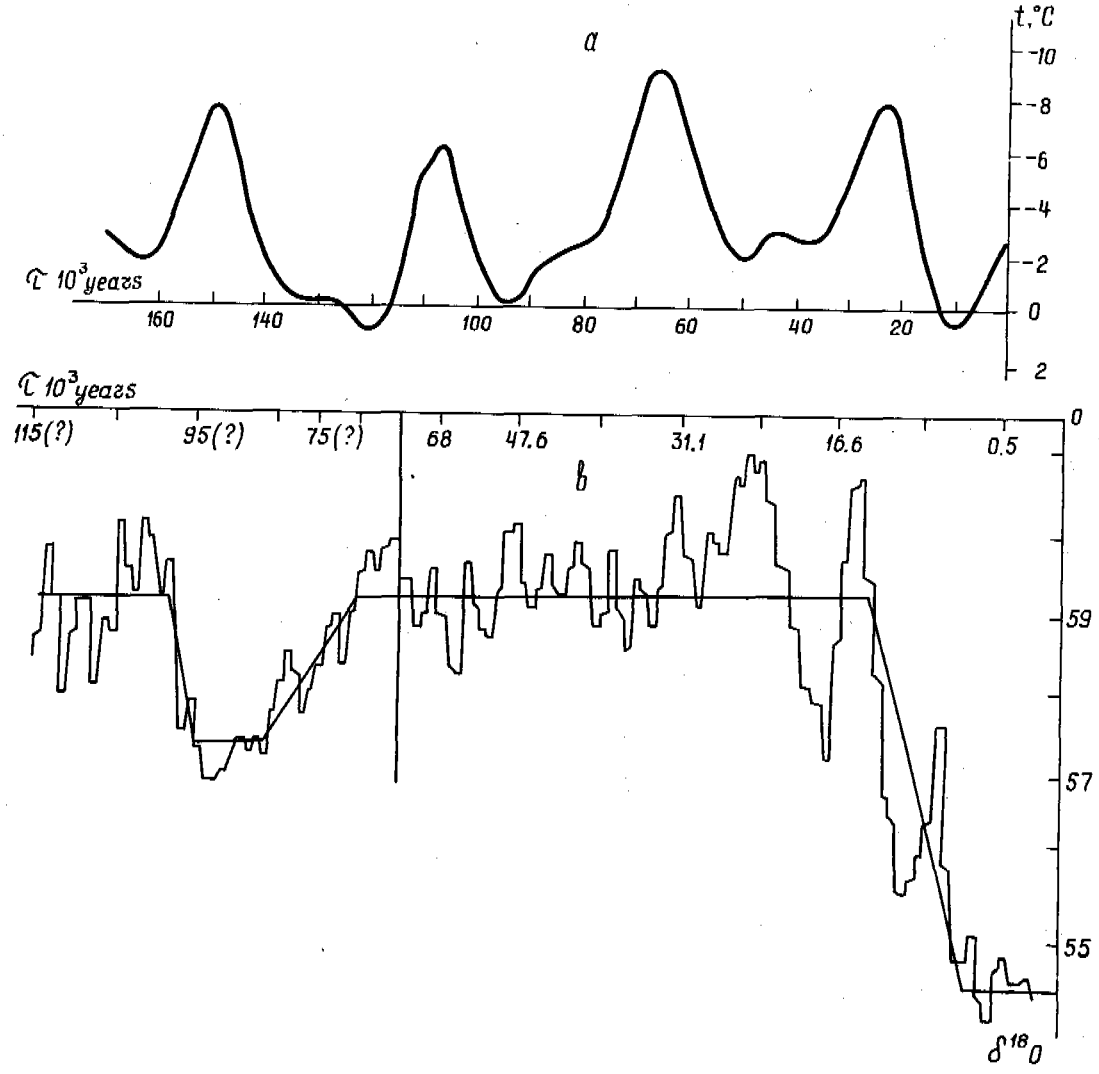

Fig.1 Theoretical paleotemperature curve for southern East Siberia (a) and isotopic oxygen profile of ice from the boreholes at the Vostok station in the Antarctica (b).

thermochron 130-117 thousand years ago with a climatic optimum 125-120 thousand years ago and the Würmian cryochron 117-15 thousand years with climatic warming about 100-90 thousand years (95-80 thousand years by the isotopic oxygen curve), a dramatic cooling about 75 thousand years (75-70 thousand years by the isotopic oxygen curve), intra-Würmian rise in temperature with a peak about 48 thousand years, and a late Würmian cooling 33-15 thousand years (with a minimum 27-24 thousand years by isotopic oxygen curve), and climatic warming in the Holocene 15 thousand years ago.

The process of ground freezing in the Late Pleistocene glacial epoch and thawing during the Holocene temperature maximum in the Baikal rift zone depressions was studied in accordance with these temperature variations. This region was chosen to implement the hypothetical temperature variations due to a number of circumstances. The position of depressions, extending latitudinally, allows us to neglect the changes in surface temperatures due to the displacement of geographical zones. The landscapes of lacustrine-alluvial plains in the depression floors over the investigated period of time (80 thousand years) changed insignificantly (Belova, 1985). This permits to suppose that the dynamics of the temperature field in the grounds was determined practically by climatic variations. Two permafrost horizons have been identified in the depressions - the Late Pleistocene and the Holocene (Zamana, 1980). They can occur independently, constitute a two-stage section (Upper-Angara and Barguzin depressions), and merge into a single frozen series (Chara depression). The appropriate cases of model are given in Fig.2. The presence of the two-stage section has made it

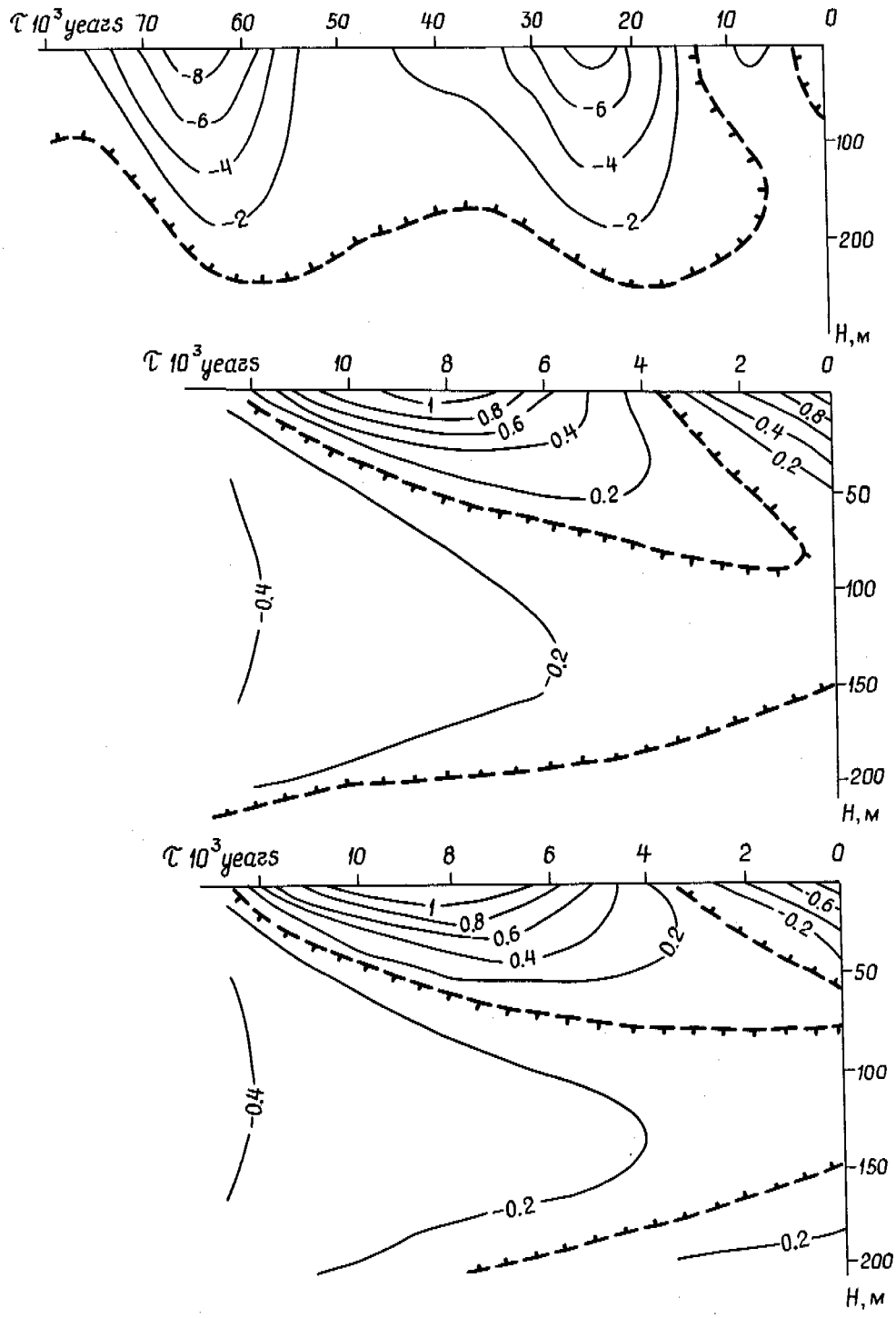

Fig.2 Variation of perennial thawing and freezing of rudaceous deposits in the mountain depressions of the Transbaikal region in the Late Pleistocene and Holocene: (a) complete thawing of the Pleistocene frozen ground strata; in the section: perennially frozen grounds of the holocenic age; (b) merging of partially thawed Pleistocene and being formed Holocene perennially frozen grounds into a single frozen stata; and (c) a two-stage section permafrost strata with the Pleistocene and Holocene horizons

possible to compare the estimated and actual depths of ground freezing and thawing at three levels: the bottom of the Holocene horizon, as well as the roof and the bottom of the Late Pleistocene frozen ground. The corresponding actual data are for the depths from 30-50 m to 80-110 m, 70-150 m, and 130-300 m; maximum thickness of the relict permafrost horizon amounts to 150-200 m, but in the regions with high present-day temperature this horizon is intensively degrading and is only several meters thick.

Ground freezing and thawing have been simulated mathematically using the programs for numerical solution of Stefan's multifront problem developed at the Department of Geocryology, Moscow State University (Seregina, in press) and realized on a BESM-6 computer.

Comparison of the computed data and factual data yields positive result. This, in the opinion of the authors, justifies the attempt of refining the paleotemperature variations in different regions of the USSR for the Late Würm - Holocene by summing up the harmonics T_1, T_2 and T_3.

The summary curves obtained (Fig.3) confirm the

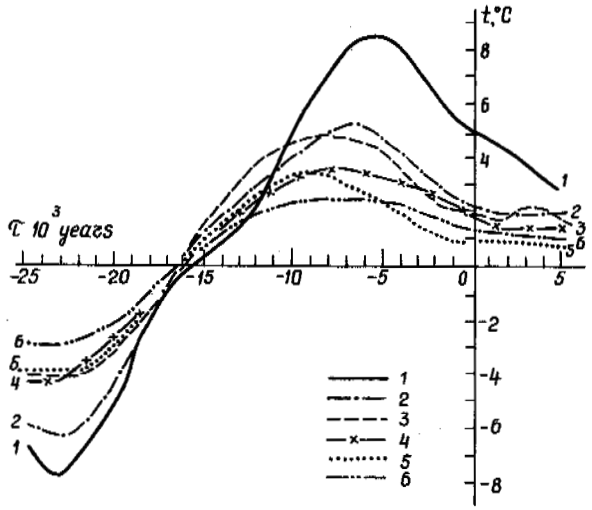

Fig.3 Relative changes of summary air temperatures with time in different regions of the permafrost zone: 1,2 - West Siberia (1 - Ob' River region; 2 - Yenisei River region); 3,4 - East Siberia (3 - north of 65°N; 4 - south of 65°N); 5 - Transbaikal region; 6 - Far East.

known facts on the rise in the amplitude of climatic changes from southeastern to northwestern USSR, as well as the Holocene thermal maximum lagging behing in the same direction (Khotinsky, 1977). The earlier terms of the thermal maximum in East Siberia, as compared with the European North and West Siberia, can be explained by the laws governing the changes in individual rhythm amplitudes in these regions. In accordance with the known Milankovic's astronomical theory of climatic fluctuations, there are significant latitudinal differences in the T_1 and T_2 rhythms: the former dominates at high latitudes and near 45°N its amplitude is approaching zero, while the amplitude of the T_2 rhythm increases toward the south.

According to the solutions obtained, the amplitude of the T_1 rhythm decreases from 8-9.5°C in the European North down to 2.5°C in the Far East. The amplitude of the T_2 rhythm increases from 1°C in northern West Siberia to 1.5-2°C in the Transbaikal region. The total range of climatic variations and the time of their maximum manifestation varies accordingly. Thus, in northern West Siberia (the Ob' River basin) where the amplitude of the T_1, T_2 and T_3 rhythms equals 7.2°, 1.2°, and 0.5°C, respectively, the total amplitude of temperature variations reaches 16°C and the Holocene thermal maximum dates around 4.5 - 6.5 thousand years ago. In the Transbaikal region, where the least difference between the T_1 and T_2 rhythms and the T_3 rhythm is practically lacking, the summary total amplitude of climatic variations is twice as small and the Holocene thermal maximum has the earliest dating from 10-11 to 8 thousand years ago. Such an early beginning of the maximum is acknowledged by the investigators of that region (Yendrikhinsky, 1982). One can refine the thermal maximum time in the Holocene by superposing the mean-period rhythm (1.5 - 1.85 thousand years) of Shnitnikov (1957) on the curves obtained.

Our studies have yielded new data for analyzing the dynamics of perennially frozen grounds in the Holocene, allowing a somewhat different interpretation of their distribution. At present, the region of the Holocene permafrost occurrence in the USSR widens from the east to the west. In the European USSR, the Holocene permafrost strata occur only in the circumpolar region. In West Siberia, their boundary extends south of the Arctic Circle, turns sharply southward east of the Yenisei River and leaves the USSR. Usually, such a pattern of permafrost distribution is, on the whole, related to the increase in severity (continentality) of present-day climate, neglecting the history of permafrost evolution in the Holocene. However, some peculiarities of permafrost distribution in the the southern part of the permafrost zone can be explained by studying its dynamics in the Holocene.

Let us discuss the location of the northern and southern boundaries of the Holocene permafrost. The northern boundary, corresponding to the boundary of thawing (full or partial, from the surface) during the Holocene thermal maximum rises from the south-east to the north-west: in East Siberia it does not run beyond 65°N and in West Siberia extends to about 68-69°N. This is in good agreement with an increase in the amplitude of climate warming in this direction. As to the southern boundary whose location is determined by the variation in ground freezing during the climatic cooling that followed the optimum, in East Siberia it moved southward much further than in West Siberia, which apparently, disagrees with the assumption of lesser dynamics of permafrost due to smaller amplitude

of climatic changes. Such a pattern can actually be explained by a delay in progressive development of the Holocene frozen grounds in West Siberia (and in the European north) due to later onset of the Holocene optimum and subsequent cooling. The delay in the Holocene permafrost development in West Siberia, as compared with East Siberia, is of the order of 2-3 thousand years as derived from the curves (Fig.3) and can be specified according to the variation of the mean-period rhythm.

Thus, a dramatic extension of the area of the Holocene frozen strata eastward to the Yenisei River is obviously associated with a longer duration of their formation and evolution in this area. Most probably, another peculiarity of the Holocene history of the permafrost zone was also important, namely, the presence of the second "center" of ground freezing in the Holocene in the highlands of the northern Transbaikal region, for which the earliest dating of the Holocene optimum has been obtained.

The most ancient Holocene frozen ground strata occur in the northern Transbaikal region and East Siberia (about 65°N). If the beginning of their formation is assigned to Novosanchugovsk cooling (7.9 - 8.3 thousand years ago), then their maximum age could reach 8 thousand years. The Holocene frozen stata of West Siberia are much younger. Their maximum age is probably about 3 thousand years (Baulin et al., 1983). Correspondingly, the thickness of the Holocene perennially frozen grounds, reaching 100-150 to 200 m near its northern boundary in East Siberia (in sedimentary rocks of the Paleozoic) and 50-60 m in West Siberia (in loose Quaternary formations), is different.

Based on the above, one may hypothesize that the Holocene frozen ground strata in the USSR are in different phases of their development relative to the variation of long-term climatic rhythms In East Siberia, the progressive development of permafrost is nearing termination (Fig.3) acquiring a pulsation pattern that corresponds to the variation of medium and short-term climatic rhythms, whereas in West Siberia (the Ob' River basin) and in the European North, permafrost agrodation will still continue during some millennia, involving areas ever further to the south, and the above-considered regional differences in permafrost distribution will gradually level off. Therefore, the present-day pattern of permafrost distribution is only an episode in the general evolution of the permafrost zone, and its dynamics in the Holocene resulted from a common global process of climatic changes with the phases component of the climatic rhythms synchronized for the entire territory of the USSR. The above-discussed regional differences in the Holocene permafrost evolution are conditioned by a specific character of the spatial variability of amplitudes of individual climatic rhythms having different physical origin.

REFERENCES

Baulin, V.V., Velichko, A.A. & Danilova, N.S. (1983). Istoriya razvitiya mnogoletnemerzlykh porod na territorii SSSR. V knige: Problemy geokriologii, pp.222-228. Moskva: Nauka.

Belova, V.A. (1985). Rastitelnost'i klimat pozdnego kainozoya yuga Vostochnoy Sibiri, 158 pp. Novosibirsk: Nauka.

Gordienko, F.G., Kotlyakov, V.M., Korotkevich, Ye.S., Barkov, N.I. & Nikolayev,S.D. (1983). Novye rezultaty izotopho-kislorodnykh issledovaniy ledyanogo kerna iz skvazhiny so stantsii Vostok do glubiny 1412 m. - Materially glyatsiol. issled. Khronika, obsuzhdeniya, vyp.46, 168-170, Moskva.

Khotinsky, N.A. (1977). Golotsen Severnoi Evrazii, 197 pp., Moskva.

Maximov, Ye.V. (1972). Problemy oledeneniya zemli i ritmy v prirode, 296 pp. Leningrad: Nauka.

Maximova, L.N. Romanovsky, V.Ye. (1986). Kolebaniya klimata i nekotorye osobennosti razvitiya mnogoletnemerzlykh porod v golotsene na territorii SSSR. - V knige: Geokriologicheskie issledovaniya,pp.45-57. Moskva: Izdatelstvo MGU.

Seregina, N.V. (in press). Programma resheniya dvukhmernoi mnogofrontovoi zadachi Stefana metodom sglazhivaniya entalpii.

Sergin, S.Ya. (1975). Temperatura poverkhosti zemli v naibolee teplye i kholodnye epokhi posdnechetvertichnogo vremeni. Izvestiya AN SSSR, ser. geogr., (3), 37-48.

Shnitnikov, A.V. (1957). Izmenchivost' obshchei uvlazhnennosti materikov severnogo polushariya, 337 pp. Zapiski BGO, v.16. Novaya seriya. Moskva-Leningrad: Izdatelstvo AN SSSR.

Yendrikhinsky, A.S.(1982). Posledovatelnost' osnovnykh geologicheskikh sobytiy na territorii Yuzhnoi Sibiri v pozdnem pleistotsene i golotsene. - V knige: Pozdniy pleistotsen i golotsen yuga Vostochnoi Sibiri,pp. 6-35. Novosibirsk: Nauka.

Zamana, L.V. (1980). Glubokozalegayushchie mnogoletnemerzlye porody vo vpadinakh Severnogo Pribaikal'ya. - V knige: Geokriologicheskie usloviya zony BAM, pp.31-37. Yakutsk: Izdatelstvo IM SO AN SSSR.

Zubakov, V.A. (1986). Globalnye klimaticheskie sobytiya pleistotsena, 286 pp. Leningrad: Gidrometeoizdat.

DIVISION AND TEMPERATURE CONDITION OF THE LAST GLACIATION IN NORTHERN CHINA

Sun, Jianzhong[1] and Li, Xinguo[2]

[1]Xi'an Geology College, China
[2]Institute of Vertebrate Paleontology and Paleoanthropology, Academia Sinica

SYNOPSIS Based on the glacial and periglacial evidences, the plant and animal fossils, the Last Glaciation in the northern China can be divided into several substages, namely the beginning stage of Dali Glaciation, 110,000 to 70,000 yr.B.P.; the early Dali substage, 70,000 to 53,000 yr. B.P.; the mid-Dali substage, 53,000 to 23,000 yr.B.P.; and the late Dali Substage, 23,000 to 10,000 yr.B.P. Each stage can be subdivided into stadials and interstadials. Also the paleoclimate in each stage is reconstructed.

INTRODUCTION

On the basis of the researches in the Northeast China (Sun, et al., 1985) and the new data obtained recently, the climate change, stages of the Last Glaciation are discussed in this paper.

EVIDENCES OF COLD CLIMATE

Glacial report

In the Taibai Shan of Shanxi Province, there is a group of cirques at the height of 3,550 to 3,610 m, below which five U-shaped valleys and two end moraines exist in an elevation of 3,000 to 3,100 m (Qi, et al., 1985). Two groups of cirques and U-shaped valleys occur at 2,400 to 2,200 m a.s.l. in the Baitou Shan, Jilin Province (Sun, 1982). These indicate that some sites of the northern China had been once glaciated during the late Pleistocene, this period can be named the Taibai Shan Ice Age or the Baitou Shan Ice Age, corresponding to the Dali Glaciation.

Permafrost

Permafrost in northeastern China is a part of the Eurasian permafrost zone. Nowadays, the predominantly continuous permafrost distributes in the northern part of the Mt.Daxinganling with a maximum thickness of 100 m. The southern limit of the island permafrost lies down to the latitude of 49°N and is coincided approximately with the 0°C isotherm of the mean annual air temperature. Alpine permafrost occurs in the Mt.Huanggangliang and Mt.Baitoushan. It is believed that the permafrost region was much larger during late Pleistocene, and the present location of the southern limit of permafrost is the result of its northward retreat during the postglaciation (Guo, et al., 1981).

The other periglacial features

Ice-wedge cast is the most important evidence to reconstruct paleoenvironment. Some of the reported ice-wedge casts are very clear in polygenal and wedge pattern and with the deformed enclosed sediment, e.g.that one found in Datong basin (Yang, et al., 1983); some, however, seem to be frost cracks filled with sand, such as those found in Dehui county, Baicheng of Jilin Province and Aohanqi of Inner Mongolia (Sun, 1981). Another important evidence, the periglacial involutions, is widely reported from the Northeast, North and Northwest China, for example, those found in Zhuolu county, Gaojiabao in Yangyuan county of the Hebei Province, salawusu of the Inner Mongolia and Huan county of Gansu Province. Thermokarsts, block fields, patterned grounds are also indicators of periglacial environment (Cui, et al., 1984). Based on the evidences mentioned above, estimation for paleoclimate can be made qualitatively and quantitatively. On the basis of stratigraphic relation, and chronometry, they can be dated. For example, the black soil filling in the ice-wedge casts in Guxiangtun of Harbin is dated 33,660± 3,270 yr.B.P. in ^{14}C age. Calcareous nodules in the involution of Hutouliang of the Yangyuan county is dated as 27,675±754 yr.B.P., sand in the wedges of Datong—26,000±2,000 yr.B.P. by means of thermoluminescence, and the involution in Zhuolu is dated as 11,030±150 yr.B.P. in ^{14}C age (Huang, 1985).

Boreal faunas

The Guxiangtun fauna of Mammuthus-coelodonta fauna is a typical one that has been recognized as the fauna living in a cold environment during late Pleistocene. The fossil sites are concentrated in the area to the north of 38°N, especially in the Northeast China. By ^{14}C dating it is known that the mammoths are 10,000 to 40,000 yr.old. The dominant species of mammoths is the M.primigenius Blumenhach. A few of M.Sungari and M.primigenius Liupanshanensis were found sometime. The finding of mammoth fossils at the bottom of Huanghai sea, or the Yellow sea, is of significance, indicating that the sea bottom had once exposed during the Last Glaciation (Zhang, 1980). A corresponding one in the northern China is the Salawusu fauna. It is questioned whether the Salawusu fauna is of

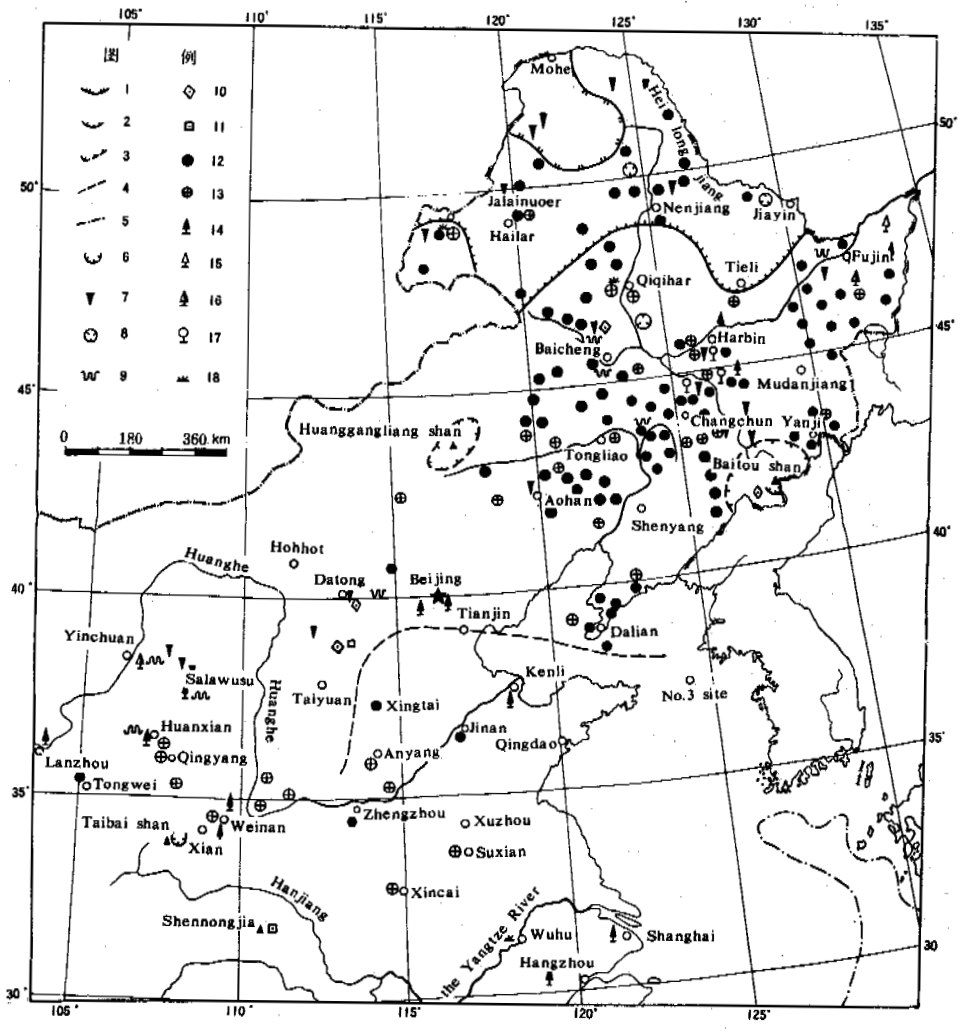

Fig.1 Paleoenvironment during Last Glaciation in Northern China

1. present southern limit of predominantly continuous permafrost; 2. present southern limit of island permafrost , observed; 3. Present lower limit of alpine permafrost; 4.southern limit of permafrost during the maximum Last Glaciation; 5. coastline at the maximum regression during Last Glaciation; 6. glacial traces; 7. ice-wedge casts and frost cracks; 8. thermokarsts; 9. involutions; 10. patterned grounds; 11. block fields; 12. fossil sites of Mammoth; 13. fossil sites of Coelodonta antiquilatis Blumenbach; 14-18 pollen sites; 14. spruce-fir dark conifer ous forest; 15. larch forest; 16. mixed forest with spruce; 17.birch forest; 18. dry steppe.

cold environment indicator, because of lacking mammoth fossil. However, a detailed comparison shows that these two faunas have similar components with a few exceptions. The Coelodonta antiquitatis Blumenbach, Equus przewalskyi poliakoff and the E.hemionus are all species living in cold environment. The Bubalus WonsjockiBoule et Teihard used to be thought as an animal living in warm period, however, being a member of the Guxiangtun fauna, it might be alao a species of cold climate. Therefore, it is believed that the Salawusu fauna also existed during the Last Glaciation, only the climate in their living area was slightly warmer than that of the Guxiangtun one. This estimation is supported by the ^{230}Th dating: in Salawusu—49,500 ±200 yr.B.P. (Yuan, et al., 1983), and in the Shuidonggou—38,000±200 yr. B.P.(Chen, et al., 1984).

be thought at about 70,000 yr. B.P. With the deepening of studies on Quaternary history, especially those in oxygen isotope of ocean sediments, it is proved that the epoch of the Last Glaciation should be lasting from 110,000 to 10,000 yr. B.P., and the period from 130,000 to 110,000 yr. B.P. should be the Last Postglaciation . The climatic evidences during 110,000 to 70,000 yr. B.P. have been found at the Xujiayao ruins in Yangyuan county of Hebei Province. This is called the Xujiayao transitional period (Table I).

RECONSTRUCTION OF PALEOTEMPERATURE CURVE

By means of the sporo-pollen diagrams of the woody plants the paleotemperature curves can be reconstructed because they are similar to each other in Shape (Fig.2). There are two peak values of pollen of woody plants during the periods of 32,000 to 23,000 yr. B.P. and 53,000 to 36,000 yr. B.P. These suggest two stages relatively warm, also, the diagrams show three arid-cold phases, i.e., from 70,000 to 53,000 yr. B.P., from 36,000 to 32,000 yr. B.P. and from 23,000 to 13,000 yr. B.P., with a peak values of grass pollen and a little of woody pollens.

It is much easier to determine the temperature depression on the decrease in mean annual air temperature during the period of from 32,000 to 23,000 yr. B.P. by comparing the elevation of the fossil site and that of the growing site of the same vegetation. For example, the spruce-fir fossil site in Huangshan, Harbin is at an elevation of 150 m, and the present spruce-fir coniferous forest distributes at 1,400 to 1,800 m a.s.l. If the temperature gradient is 0.5°C/100 m, then it could be calculated that the temperature depression should be 6°C. In the same way, it is known that the temperature depression is 7.5°C in Beijing, and 8°C in Beizhuang. Thus, it is acceptable that the temperature during the period of 32,000 to 23,000 yr. B.P. was by 7°C colder than at present.

During 53,000 to 36,000 yr. B.P., it was 4°C lower than at present according to the distribution of birch.

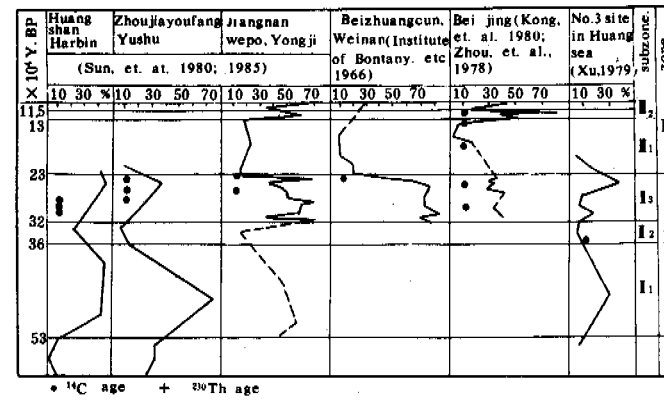

Fig.2 Comparison of Pollen Diagrams of Woody Plant in Northern China during Last Glaciation

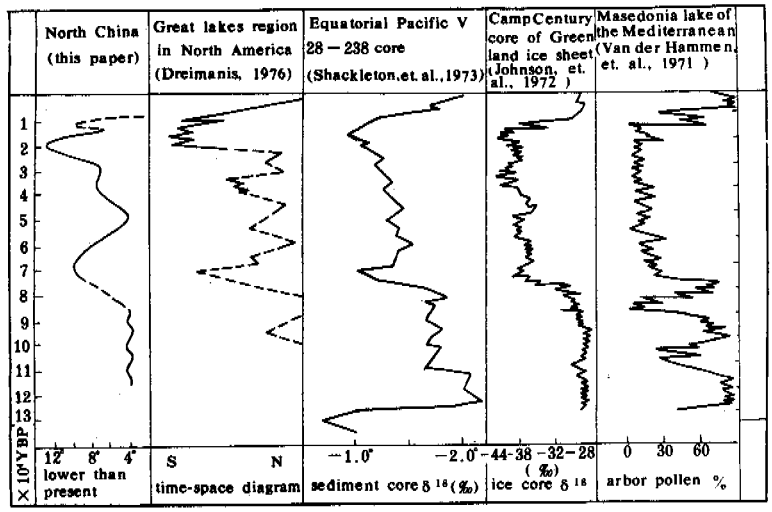

Fig.3 Paleotemperature Curves Reconstructed by Different Methods

TABLR I

Classification of Last Glaciation in North China and Other Places

North China				Yellow sea area (after Xu Jiashen, 1981)		North America (after Dreimanis, 1976)			Northern Europe		
glacial stage	sub-stage	age 10000	Stadial (S) interstadial (I)	Transgresscion (T) Regression (R)		Stadial (S) Interstadial (I)	sub-stage	Glacial stage	Stadial Intersladial	substage	Glacial stage
Dall	late	1.3	Feng zhuang (I)	Cold	Han yangdao (R)	Valders (S) Two creeks (I) Port Huron (S) Mackinnaw (I) Port Bruce (S) Erie (I) Nissauri (S)	late	Wisconsin	younger Dryas (S) Allerö̈d (I) Old Dryas (S) Bö̈lling (I) Oldest Dryas (S)		Weichsel
			Bei zhuang Cun (S)								
	Middle	2.3 3.2	Shan gen tun (I)	Marm	Guan nan (T)	Plum paint (I)	middle		weichsel B (B)	middle	
			Arshi he (S)		Wan chen shen tou (R)	Cherry tree (S)					
		3.6 5.0	Liufang tun (I)	Cold	Han zhou wan (T)	port talbat 2 (I)			weichsel A (S)		
	Early		Dayu (S)		zao chen shan						
		7.0				port talbat I (I)			Brörup (I)		
	Beijing		Xu Jiayao transction Period			Guildwood (S) St. pierre (I) Nicolet (S)	early		Early stadial (Z) Amersfoort (I) Early stadial (I)	early	
		11.0									

As to the temperature depression during the period of 23,000 to 13,000 yr. B.P., several values were suggested: i.e., 12°C (Sun, 1980), 7-12°C (Yang, 1980), 14°C (Pu, 1984) and 11°C (Cui, 1984). Such a problem can be solved by using the ice-wedge casts as the indicator. The ice-wedge cast found in Datong of Shanxi Province, where the mean annual air temperature is 6.5°C at present, implies a former mean annual air temperature of -5°C (Washburn, 1979) or -7 to -8°C (Péwé, 1974) when it was formed, or a temperature depression of 12°C or so. In addition, the mammoth fossil sites are concentrated in an area to the north of Dalian-Tianjin. Nowadays, the Tianjin is 12.2°C in mean annual air temperature, If the area with dense population of mammoth could be considered as the permafrost region, then the line of Tianjin-Dalian might have been the southern llimit of permafrost with a mean annual air temperature of 0°C. Thus,the temperature depression might be 12°C or so at Tianjin. Sone investigators suggested a 8°C temperature depression on the basis of spruce-fir fossils, however, as mentioned above, the phase, when the spruce and fir were growing,was a relatively warm period in the Last Glaciation.

Also the temperature depression is estimated as 10°C during the period from 70,000 to 53,000 yr. B.P.; 8°C — 36,000 to 32,000 yr. B.P.; 4°C in the Xujiayao transitional period.

Based on the above discussion, the paleotemperature curve is reconstruced and can be compared with those in the other places reconstructed by different methods (Fig.3).

REFERENCES

Chen Tiemei, et al., (1984). Reliability study on uranium series age of bone fossils and Uranium age order of some old stone sites in North China. Acta Anthropologic Sinica, (3), 3, 259-269.

Cui Zhijiu, et al., (1984). Discussion on the southern boundary of permafrost and periglacial environment during late Pleistocene. Acta Geologica, Sinica, (64), 2, 165-175.

Гитерман,Р.Е., Голубва, Л.В., Коренева, Е.В., Матвеева, О.В. 1965 . Перигляциальная растительность Сибири - Корреляция антропогенных отложений Северной Евразии. Наука, Москва.

Guo Dongxin, et al., (1981). Preliminary approcach to the history and age of permafrost in Northeast China. Journal of Glaciology and Geocryology, (3), 4, 1-16.

He Ruchang, (1977). Sporo-pollen composition of late Pleistocene at Loufangzi of Huan county in Gansu Province. Journal of Northwest University (Natural Science) (1),

Institute of Botany, Academia Sinica (1966). Study on paleobiology of the Cenozoic era in Lantian area of Shanxi. Proc. Cenozoic field conference in Lantian, 157-182.

Kong Zhaochen, et al., (1980). Flora and climate change during the past 30,000 to 10,000 years in Beijing area. Acta Botanica Sinica, (22), 4, 330-338.

Kong Zhaoche, et al., (1984). Floral fossil and sporo-pollen composition on the Sanjiang plain during the Last Glaciation. Scientia Geographica Sinica, (4), 1,76-80.

Li Wenyi, (1985). Characteristics of Pleistocene sporo-pollen composition on the eastern Hebei plain in China and their significance in paleogeography, Proc. Chinese national conference on Quaternary Glacier and Periglaciology, 194-197.

Péwé, T.L. (1974). Permafrost. Encyclopaedia Britannica, 15th Edition, 89-95.

Pu Qingyu, (1984). The southern boundary of permafrost and its evolution since Dali Glaciation in the eastern China. Journal of Hydrogeology and engineering Geology,4, 49-51.

Qi Chuhua, et al., (1985). Preliminary discussion of glacial geomorphy of the Mt. Taibai in East Qinling and its glacial stages. Proc. Chinese National Conference on Quaternary Glacier and Periglaciology, 51-61.

Sun Jianzhong, (1981). Division of Quaternary periglacial stages in Son-Liao plain. Scientia Geographica Sinica, (1),2,163-170.

Sun Jianzhong, (1982). Classification of Quaternary glaciation to Jilin province. Acta Geologica Sinica, (62), 2, 174-186.

Sun Jianzhong, et al., (1985). Paleoenvironment of the Last Glaciation in northeastern China. Quaternaria Sinica (6), 1, 82-89.

Washburn, A.L. (1979). Geocryology — A survey of periglacial processes and environment. 402pp, Edward Arnold, London, John Wiley, New York.

Yang Huanren, et al., (1980). Evolution of Quaternary environment in North China. Journal of Nanjing University(Natural Science), 1, 121-144.

Yang Jinchun, et al., (1983). Fossil ice wedges and environment of the late Pleistocene in Datong basin. Scientia Geographica sinica, (3), 4, 339-344.

Yuan Sixun, et al., (1983). Uraniumseries ages of Hetao Human and Salawusu culture. Acta Anthropologic Sinica, 1, 90-94.

Zhang Zhenhong, (1980). Discovery of the Lodonta antiquitatis and Mammuthus fossil in northern Huanghai. Quaternaria Sinica, (5), 1, 96-97.

Zhang Shuwei, (1983). Paleoclimate and paleovegetation since the past 20,000 years in Jiaozhou Bay of Qingdao. Acta Botanica Sinica, (25), 4, 330-338.

Zhang Shuwei, (1985). Paleovegetation and paleoclimate changes in Wuhu region in the later period of the Last Glaciation.

SHORELINE PERMAFROST IN KANGIQSUALUJJUAQ BAY, UNGAVA, QUÉBEC

M. Allard[1], M.K. Seguin[2] and Y. Pelletier[1]

[1]Geography Department, Université Laval, Ste-Foy
[2]Geology Department and conjointly Centre d'études nordiques, Université Laval, Ste-Foy

ABSTRACT Ungava Bay is a macrotidal environment with important estuaries and very large tidal flats. Discontinuous permafrost along the shoreline occurs under two sets of conditions: 1- In intertidal muds beneath the upper marsh where the total duration of tidal submersion is less than 8% of total time and, 2- As supratidal permafrost along the upper marsh edge and between tidal creeks. Polygonal cracks and small mounds are geomorphological indicators of intertidal permafrost which is in a precarious thermal state (0°C to -1°C by the end of thawing season). Ground temperature regime is controlled principally by the year to year variation of snow thickness over the ice foot. Supratidal permafrost occurs in the form of segregated ice mounds in silt. Active layer depth is 1,5 m. Permafrost temperature at the end of the thaw season is about -2°C. Negative temperatures (-0.4°C to -0.8°C) were measured below mean sea level. Basal cryopegs can be inferred from the comparison of basal thermal data and vertical electrical resistivity profiles.

INTRODUCTION

Studies of permafrost along shorelines have been more and more numerous in recent years due, principally, to the development of natural resources along the Arctic coast of the USSR, Alaska and Beaufort Sea in Canada (Are, 1983; Mackay, 1986; Smirnov, 1986) and, also, due to the damming of some reservoirs (Newbury and McCullough, 1983). Most of these studies deal with accelerated coastal erosion of cliffs in ice-rich sediments and the relative importance to coastal erosion of shoreline processes (waves, ice-foot, storm surges) vs the properties of permafrost (ice content and cryostructure, strenght of bonding, slope processes) (Harry et al, 1983; Hume et al, 1972). Coastal recession along the low arctic coastlines is linked to a transgressive sea level and storm surges; shoreline retreat results in the drowning of thick permafrost layers that have to re-equilibrate to sea bottom temperatures (Nixon, 1986; Molochuskin, 1973). Some observations of active layer thickness are also available from Arctic beaches with some inferences on the interaction of permafrost with wave erosion and sediment transport (McCann and Hannell, 1971; Owens and Harper, 1977; Taylor and McCann, 1974, 1983).

However, very few studies of permafrost in areas of tidal marshes and along the shores of estuaries have been produced. One important reason for this situation is the fact that there are very few regions along the Arctic coasts with large tidal range (Davies, 1980). Such large ranges do occur in the eastern Canadian Arctic however, particularly along Hudson Strait and around Ungava Bay. Research on shoreline permafrost has been conducted along the southeastern coastal sector of Ungava Bay, particularly along rivière George (Fig. 1). Immense tidal flats and marshes have developed in bays along this estuary. The area is still undergoing slow post-glacial emergence (Lauriol, 1982). Permafrost conditions in Kangiqsualujjuaq Bay, near the so-named Inuit settlement, have been studied in detail.

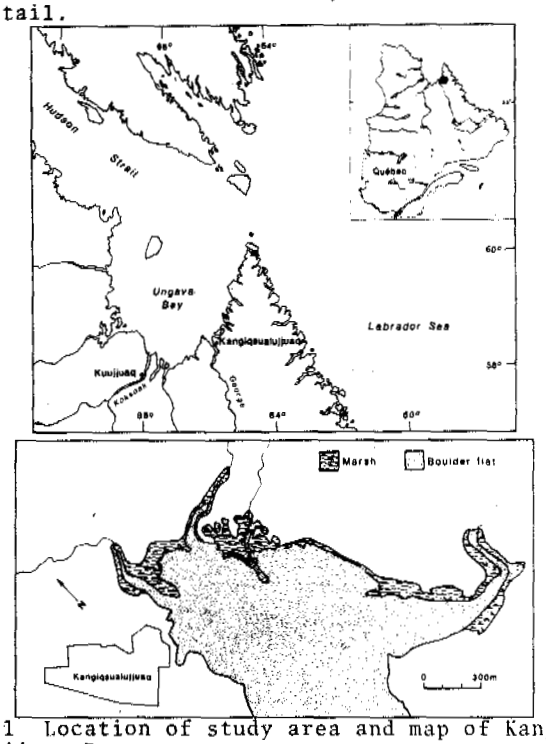

Fig. 1 Location of study area and map of Kangiqsualujjuaq Bay.

DESCRIPTION OF THE STUDY AREA

Kangiqsualujjuaq Bay is located on the eastern shore of the rivière George estuary, some 15 km from the shore of the open sea (Fig. 1). It lies right at the tree-line (Payette, 1983) and permafrost in the surrounding landscape is discontinuous. The bay occupies a deep valley bet-

ween steep rocky (mainly gneisses) hills. During the post-glacial d'Iberville Sea transgression, which started about 7400 BP, the valley was a deep and sheltered sub-basin of the sea into which marine silts were deposited. These fine sediments have emerged and presently make up a large proportion of the soils into which permafrost has aggraded (Fig. 2.).

The bay itself empties completely at low tides. The intertidal zone is 1600m wide, of which only about the upper 100 m is the tidal marsh, the rest being a mudflat strewn with ice-rafted boulders.

Mean annual air temperature at Kangiqsualujjuaq is about -5.6°C as measured by our own meteo station; it is -5.3°C in Kuujjuaq, 160 km to the southwest. Mean July temperature at both stations is between 9°C and 10°C and mean January temperature about -22°C. However, the shoreline itself is a colder environment due to wind exposure. Total precipitation is about 400 mm, of which 42% is snow (Wilson, 1971). Due to wind-drifting, snow cover is very uneven, varying from virtually nothing on wind-swept sites to over 2 m on the leeside of topographic obstacles.

Tides are semi-diurnal and range is 8.7 m for mean tides and 13.9 m for large tides at the entrance of rivière Koksoak (Canada, 1987). It is about 8 m for mean tides and 13 m for large tides in Kangiqsualujjuaq according to our own recording station that operated in the summer months of 1984 and 1985.

DEFINITIONS: INTERTIDAL PERMAFROST AND SUPRATIDAL PERMAFROST

The permafrost in the bay occurs in two different settings:

1- As intertidal permafrost, or tidal marsh permafrost. This terrain is periodically submerged by tides and has a halophytic herb cover. An ice foot forms in winter over the surface. It can therefore be assumed that the soil thermal regime is affected by tidal submersions and that intensity of freezing is dependant on the overall length of time, between spring tides, during which the marsh surface is exposed to freezing temperatures.

2- As supratidal permafrost: frozen ground with soil surface above extreme tide level but periodically in contact or surrounded by tidal water. Terrestrial tundra vegetation (shrubs and trees if below tree-line) covers the ground. Vertically, the permafrost extends to depths within tidal range elevations, sometimes as low as below mean sea level. The surface thermal regime is therefore "normally" controled by climate without interference of tidal submersions but periodic movements of saline groundwater around permafrost bodies and the base of permafrost may have an effect on permafrost characteristics at depth.

CHARACTERISTICS OF INTERTIDAL PERMAFROST

Marsh permafrost occurs in dominantly silty sediments carried by tidal currents. The sediments show a millimetre-thick layering and contain dispersed ice-rafted boulders, discontinuous sand and gravel layers and ice-rafted lumps of gravel-size debris.

Surface features

Discrete permafrost bodies are easily identifiable in tidal marshes by changes in vegetation, morphology and some patterned ground. The marsh usually spreads over two levels: a higher marsh in the upper 1,5-2 m of the intertidal zone and a lower marsh, about 1 m below, making the transition with the tidal flat. Permafrost is found only beneath the higher marsh which is only submerged for 130-140 hours per year or less than 8% of the time (Fig. 3). Figure 4 shows a topographic profile from the terrestrial environment to the mudflat in Kangiqsualujjuaq Bay; permafrost mapped under the profile with the help of electrical resistivity using the dipole-dipole array, is present beneath slight topographic humps separated from each other by tidal channels. Vegetation composition is more complex on the humps than on the flat and in channels because duration of tidal submersion is lesser on them and, inversely, air exposure is longer, allowing a larger variety of more exacting plant species to colonize the humps (see also Kershaw, 1976). The frozen patches have characteristic polygons on their surface (Fig. 5).

The polygons are on average 1,2 m accross. The cracks along the edges are open 1-2 cm immediately after spring break-up. They extend at depth to about 30 cm. In winter, the surface is covered by a 15-40 cm thick icefoot which freezes to the ground; this icefoot is formed following the November spring tides by the congelation of brash and damped snow. In normal climatic years almost no snow accumulates over this icefoot after it is formed because of important wind-drifting effects along the shore. Therefore the thin icefoot is a very poor insulating layer and frost penetration in the ground is not hindered. Temperature gradients in the surface layer of over 0.35°C cm^{-1} were measured at beginning of winter in the first 20 cm of these sediments; frost cracking therefore plays a part in polygon formation. However, as these higher marsh surfaces are not covered by sea water for weeks, particularly during summer neap tides, desiccation is probably also involved in polygon formation. Such polygons are present over intertidal permafrost exclusively and absent over just seasonnally frozen marshes and therefore, appear to be reliable indicators of the presence of permafrost. No ice wedges have been found underneath the crack system which is confined to the top of the active layer; the permafrost below is ice-poor and not cold enough to crack under frost contraction.

Small mounds are other superficial features related to intertidal permafrost: they are elevated some 20-40 cm above the marsh surface and, very often, their growth has induced dilation cracking of the turf cover (Fig. 6). Many such mounds are isolated islands of permafrost on interfluves between tidal creeks and tidal channels.

No permafrost was found beneath lower marshes and mudflats despite extensive probing with crowbars and thermistor probes. Winter observations indicate that a wedge of tidal water penetrates between the mudflat surface and the icefoot which is not frozen to the bottom; therefore the yearly frost wave is not allowed to penetrate the ground.

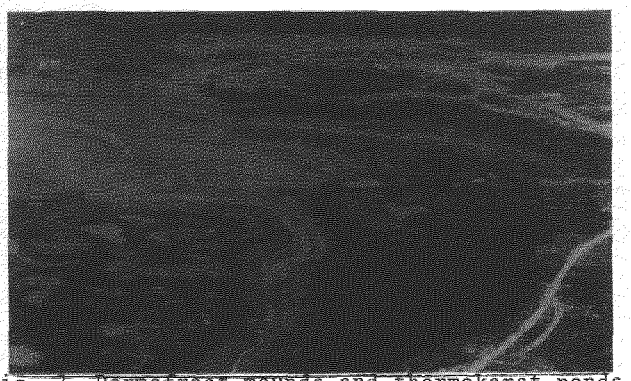

Fig. 2 Permafrost mounds and thermokarst ponds in clayey silts along the shoreline. "M" is the marsh zone profiled in Fig. 4.

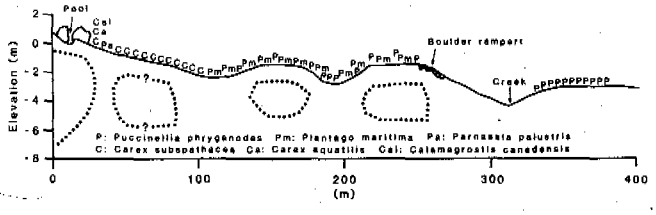

Fig. 4. Topographic profile of the marsh (see Fig. 1), permafrost distribution within dotted lines) and dominant plant species.

Interference with shoreline processes

As frost heaving locally changes the marsh topography, some erosional and depositional processes are affected. Small permafrost mounds and slopes of larger permafrost bodies are eroded by waves at high tide on windy days. Frost and extension cracks provide lines of weakness into which wave energy is locally concentrated. Some mounds get destroyed (Fig. 7). Inversely, at spring break-up thin, sediment ladden ice floes become stranded over permafrost terrain because tidal submergence is shallow; debris of silt, sand and gravel sizes are strewn over the surface, thus contributing to accretion; thicker floes that cannot float over the permafrost humps get stranded on the sides of the humps where they abandon larger clasts upon melting, thus building small boulder ramparts. (Figs. 4, 6 and 7).

Permafrost characteristics

Twenty two shallow holes 3 to 4 m deep were drilled in tidal marsh permafrost. Some core lengths were obtained with a 5 cm diameter singlewalled diamond corer. The ice appeared mostly in thin lenses and, in over 50% of the cases, as a reticulated network (Fig. 8). Contrary to supratidal permafrost (see below), there is evidently no or very little groundwater feeding for the formation of an important amount of aggradational ice; this is because the permafrost humps are some distance away from the terrestrial environment where groundwater flow usually comes from. Intertidal permafrost bodies are also often perched 5-6 m above the level of the tidal creeks at low tide. As frost penetrates from the surface in winter, only the water already present in the silt is available for cryosuction

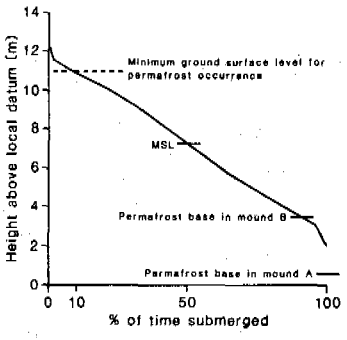

Fig. 3 Duration of submergence vs elevation within tidal range

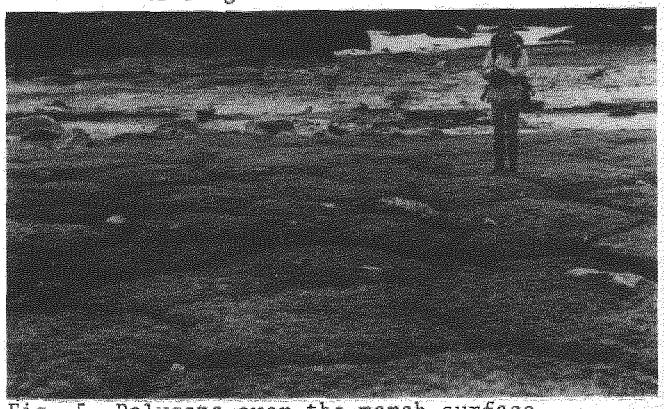

Fig. 5 Polygons over the marsh surface

and ice nucleation; it is sucked to diffuse lamination planes and small polyhedral cracks where it segregrates as thin ice lenses.

The marsh sediments have a mean clay content of 29% and contain brackish water. These two factors contribute to the freezing-point depression of the materials. The depression of ice-nucleation temperature was measured in the field in March and in June 1987, by pushing an aluminium cone (1,3 cm diameter base, 1,2 cm long) into the bottom of drill holes; a thermistor bead inside the cone measured the temperature. Readings were taken when the frozen soil was bonded just enough to barely allow cone penetration. At mid-March sediments at temperatures ranging from -2.4°C to -3°C were still penetrable; by the end of June, on the same sites, frost was not penetrable at -1°C. This suggests that salt expulsion from freezing ground had taken place during winter cooling, leaving firmer frost at the beginning of the thawing season.

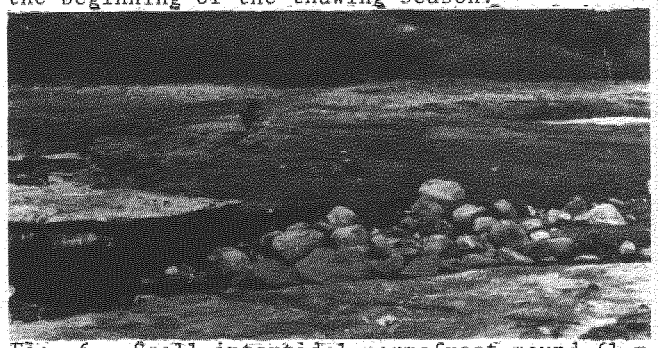

Fig. 6. Small intertidal permafrost mound (1 m high), with dilation crack on top (arrow)

Fig. 7 Intertidal permafrost mound partly eroded by waves

As measured by tive electrical resistivity soundings, intertidal permafrost lenses vary in thickness from 2,3 m to 6,0 m.

Fig. 9 shows temperature profiles in marsh sediments at different times of the year. These profiles indicate that by the end of the thaw season (mid-November) soil layers over 3 m deep are barely below 0°C. Considering the freezing point depression of the sediment, the ground can then be considered cryotic but not frozen. Considering also the precarious thermal equilibrium, some permafrost a few years old may melt in a particularly warmer summer of after a snowier winter. On the other hand, it may persist and evolve to supratidal permafrost, land uplift aiding.

CHARACTERISTICS OF SUPRATIDAL PERMAFROST

Supratidal permafrost in Kangiqsualujjuaq Bay is distributed within some 60 mounds, of which over 15 lie right along the high-tide line (Fig. 2). Some are surrounded by spring tides. Core drilling down to four meters revealed large amounts of segregation ice, reaching up to 80% of volumetric content in some 40 cm long core sections. The ratio of mound height to permafrost thickness within individual mounds, as measured with surface electrical resistivity soundings, is roughly 1:3, implying an overall ice content of 30-35% within the mounds. Ground ice however is distributed unequaly within the mounds, being concentrated in the first 2 to 4 meters below permafrost table, in the zone of coldest long-term average temperature and reversible thermal gradient within the permafrost. Permafrost base varies in depth from one mound to another but for the ones closest to the shoreline (Fig. 3) it is lower than mean sea level and, sometimes, as low as low-tide level.

Vertical electrical resistivity profiles, combined with temperature measurements were made from the top of two mounds (called A and B) with the help of thermistor and electrode cables driven in holes drilled through the permafrost by water-jet drilling. The steel pipes used for drilling were removed from the holes and replaced by the two cables; one cable has thermistors at every meter, the other has electrodes. Temperature readings are made with a multimeter; electrical resistivity readings are made by connecting the electrodes to a ABEM resistivity-meter. Both the Schlumberger array (Current electrole C1 being on top, C2 at base of hole and potential electrodes, P1 and P2, being successively displaced two at the time) and Wenner

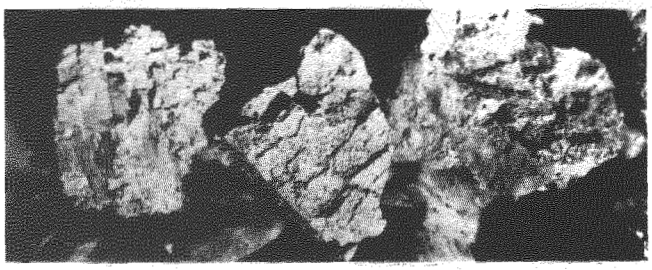

Fig. 8 Millimetre thick ice veins in intertidal permafrost

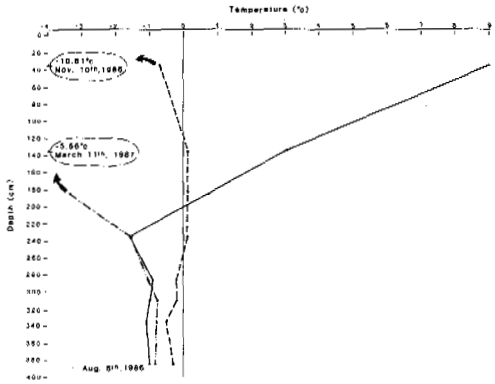

Fig. 9 Temperature profiles in intertidal permafrost

array (C1, P1, P2 and C2 being moved along the cable) were used (Fig. 10).

Permafrost mound A is located 250 m inland from the shoreline. The elevation of the summit above the high tide live is 11 m and the mound may be considered as "terrestrial" and distant from the tidal influence. Although the temperature profile is uneven, because it was still unstabilized on June 25th 1987 (disturbances from drilling and cable installation take about one year to recover), it is clear that permafrost is 22-24 m deep, reaching a depth of 13 m below high tide level.

The Schlumberger profile provides a generalized distribution of electrical resistivity values across the permafrost section. The highest values (160,000Ω·m) occur at the four meters depth and then fall off rapidly from 4 to 8 m, corresponding to the step thermal gradient in the coldest upper zone of the permafrost. From eight meters down, the resistivity is almost nil for the soil with temperature ranging between 0°C and -0,5°C. The Wenner-array resistivity profile gives a detailed view of the vertical distribution of resistivity values at one meter interval along the profile. Again high resistivities are evident in the upper permafrost zone but, also, an inverse relationship between temperature and resistivity is evident along the profile. Resistivities get definitively low from about 22 m downwards, the level of permafrost base as indicated by temperature data.

The same type of data in shoreline mound B provides a different picture. As measured on June 26th 1987, one year after installation, the permafrost base is about 9.5 m deep below mound top

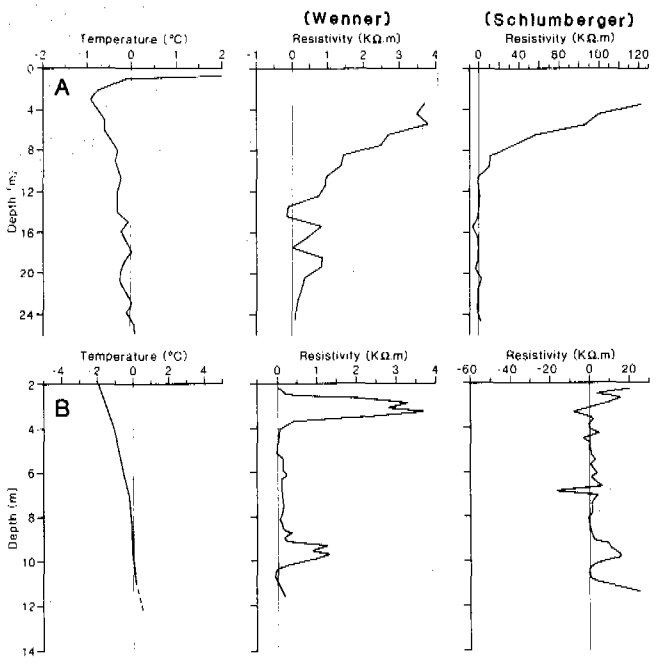

Fig. 10 Temperature and electrical resistivity profiles in mounds A and B

which is only 1 m above the high tide level. So, permafrost base is about 1-2 m below mean sea level (Fig. 3). Many very hard layers, certainly ice, were met during pipe penetration from 1,5 m to about 5 m deep and very low resistance to penetration was met further down. The Schlumberger profile does not show a clear pattern as in the case of terrestrial mound A; only two zones of high resistivity appear, one from 2 to 3 m depth, the other one from 9 to 10 m . The former corresponds approximately to the icy layers, the latter with a stratigraphic change from silt to sand, as felt during drilling. The low contrast curve with the Schlumberger array probably is due to the fact that most of the section contains only a low amount of ground ice with discontinuous bonding. Also, electrode C2, at the base of profile, was probably in soil saturated with brackish groundwater. On the other hand, resistivity data using the vertical Wenner array clearly illustrate the highly resistive icy layers in the upper zone of the permafrost. Below four meters, the resistivities are steadily low despite negative temperature, again reflecting the nonfrozen or poorly bonded nature of permafrost. These data strongly suggest that in supratidal shoreline permafrost in marine silts, formation of segregation ice can occur in the upper portion of the mound, that is above the level of tidal influence in groundwater. At depth, the cryotic ground is very probably unfrozen, forming thick basal cryopegs.

Shoreline processes

Wave erosion of the exposed supratidal permafrost mounds induces some active layer failures. In addition, the turf cover of a few mounds that are a few centimeters above the high tide level and which bears upper beach plant species such as Elymus arenarius is eroded by storm waves. These processes that change the nature of surface cover probably induce some permafrost degradation.

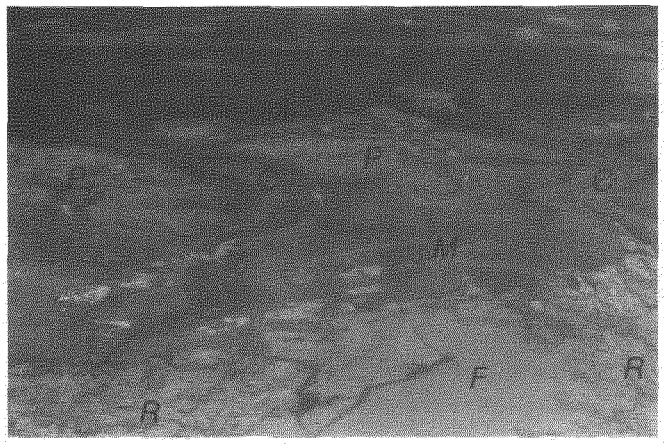

Fig. 11 Shoreline permafrost on southern shore of Ungava Bay. P, permafrost terrain; C, tidal channels; M, marsh; F, flat; R, bedrock outcrop

CONCLUSION

Permafrost in fragile thermal equilibrium forms in the wide intertidal zones beneath the upper marshes where it actually does not extend as a continuous wedge (Hansell et al, 1983) but rather as discrete bodies in between tidal channels and along the upper edge of the intertidal zone. In that respect, Kangiqsualujjuaq Bay is representative of the Ungava Bay coastline (Fig. 11). Freezing of the marsh sediments and persistance of permafrost is possible in the upper part of the tidal zone only, where submersions are few and where a thin ice-foot adheres to the substrate, allowing deep frost penetration. Such incipient permafrost is, however, in a precarious thermal state being barely below 0°C by the end of the thaw season; it can melt completely after a particularly warm and snowy winter or during a warmer than average summer.

As soon as the surface of shoreline sediments rises sufficiently high, be it by accretion, frost heave or land uplift, intertidal permafrost may establish itself. Land emergence aiding, it can then evolve to supratidal permafrost and on to terrestrial permafrost.

ACKNOWLEDGEMENTS

The authors sincerely thank the following colleages and assistants for their help in acquiring data: Robert Gauthier and Jacqueline Bouchard (botany), Jean Desbiens (tide data), Richard Fortier (thermal and electrical equipment and data), Fernando Sheriff (grain size analysis), Alain Fournier and Richard Lévesque (drilling). Research was supported from NSERC (Canada) and FCAR (Québec) grants. We also owe sincere thanks to the community of Kangiqsualujjuaq for hospitality and friendly support.

REFERENCES

Are, F.F. (1983). Thermal abrasion of coasts. Permafrost, Fourth International Conference, Proceedings, National Academy Press, Washington D.C., p. 24-28.

Canada (1987). Canadian tide & current tables. Volume 4, Arctic and Hudson Bay. Fisheries and Oceans Canada, 51 p, yearly publication.

Davies, J.L. (1980). Geographical variation in coastal development. London, Longman.

Hansell, R.I.C., Scott, P.A., Staniforth, R. and Svoboda, J. (1983). Permafrost development in the intertidal zone at Churchill, Manitoba: A possible meachanism for accelerated beach uplift. Arctic, 36:198-203.

Harry, D.G., French, H.M. and Clark, M.J. (1983). Coastal conditions and processes, Sachs Harbour, Banks Island, Western Canadian Arctic, Zeitschrift fur Geomorphology, Supp.-Bd 47:1-26.

Hume, J.D., Schalk, M. and Hume P.W. (1972). Short-term climate changes and coastal erosion, Barrow, Alaska. Arctic, 25:272-278.

Kershaw, K. (1976). The vegetational zonation of the east Pen Island salt marshes, Hudson Bay. Canadian Journal of Botany, 54:5-13.

Lauriol, B. (1982). Géomorphologie Quaternaire du sud de l'Ungava. Paleo-Québec, no 15, 174 p.

Mackay, J.R. (1986). Fifty years (1935-1985) of coastal retreat west of Tuktoyaktuk, District of Mackenzie. in Current Research, Part A, Geological Survey of Canada, Paper 86-1A, p. 727-735.

McCann, S.B. and Hannell, F.G. (1971). Depth of frost table on Arctic beaches, Cornwallis and Devon Islands, N.W.T. Canada. Journal of Glaciology, 10:155-157.

Molochuskin, L. (1973). The effect of thermal abrasion on the tenperature of the permafrost in the coastal zone of the Laptev Sea. Proceedings, 2nd International Permafrost Conference, Vol. 2, USSR Contribution, p. 90-93.

Newbury, R.W. and McCullough, G.K. (1983). Shoreline erosion and restabilization in a permafrost affected impoundment. Permafrost, Fourth International Conference, Proceedings, National Academy Press, Washington, D.C. p. 918-923.

Nixon, J.F. (1986). Thermal simulation of subsea saline permafrost. Canadian Journal of Earth Science. 23:2039-2046.

Owens, E.H. and Harper, J.R. (1977). Frost-table and thaw depth in the littoral zone near Peard Bay, Alaska. Arctic, 30:155-168.

Payette, S. (1983). The forest tundra and present tree-lines of the Northern Quebec-Labrador Peninsula. In P. Morisset and S. Payette (eds) Tree-line ecology, proceedings of the Northern Quebec tree-line conference, Collection Nordicana, Centre d'études nordiques, Université Laval, no 47:3-24.

Smirnov, V.M. (1986). Coastal processes along the west coast of Yamal. Polar Geography and Geology, 10:317-321. Translation from Izvestiya Vsesoyuznogo Geograficheskogo Obschestva, 118(5):425-428 (1986).

Taylor, R.B. and McCann, S.B. (1974). Depth of the frost table on beaches in the Canadian Arctic Archipelago, Journal of glaciology, 13:321-322.

Taylor, R.B. and McCann, S.B. (1983). Coastal depositional landforms in northern Canada. In Shorelines and isostasy D.E. Smith and A.G. Dawson (Eds), Institute of British Geographers, Special publication 16, Academic Press, p. 53-75.

Wilson, C.E. (1971). The climate of Quebec. Part one, Climatic Atlas, Canadian meteorological service, Climatological Studies II.

PERMAFROST DATA AND INFORMATION: STATUS AND NEEDS

R.G. Barry

World Data Center-A for Glaciology (Snow and Ice), University of Colorado, Boulder, CO 80309-0449, U.S.A.

SYNOPSIS Information on permafrost phenomena is collected for a wide range of purposes by many different groups of specialist. The vast extent of the published literature - 4400 entries appear in the 1978-82 bibliography compiled for the Fourth International Conference on Permafrost - is illustrative of the potential magnitude of the related data sets. Measurements range from field observations of permafrost-related features, to surface and borehole data on physical properties of frozen ground and geophysical surveys, and laboratory experiments or tests. Remote sensing is now adding new types of data on frozen ground conditions.

Up to now, there are only isolated examples of organized national programs to collect, standardize and archive permafrost-related data. The scope and content of some current data bases are illustrated.

Planning for new international activities such as the International Geosphere Biosphere Programme (IGBP) calls for monitoring global change in areas sensitive to climatic or anthropogenic disturbances. The sensitivity of permafrost conditions to such changes is well-recognized. However, the IGBP requirements imply a need to develop integrated global archives of permafrost-related variables suitable for use in multi-disciplinary research. Possible criteria for archiving permafrost data in such a system are outlined, taking into account the potential users of the data. Problems created by the variable horizontal, vertical and temporal characteristics of the measurements are discussed.

INTRODUCTION

Data on the permafrost environment are essential for energy and mineral exploration and extraction, engineering construction, water supply, waste disposal, agriculture and forestry operations in cold regions. In some countries data appropriate to meet these needs are collected primarily by government organizations while, in others, the private sector is the principal collector and user of data on a site-specific basis. There is also growing recognition of the fact that the permafrost environment is susceptible to natural and anthropogenic climate changes and that ground temperatures provide a valuable indicator of past climatic conditions (Lachenbruch and Marshall, 1986). This fact has led to the monitoring of permafrost conditions as a measure of environmental change. However, such work is severely restricted by the virtual absence of consistent regional and global data sets of permafrost - related environmental variables. This paper outlines the types of data that will be required for these and other general purposes and examines the extent to which existing archives may meet these needs. Some 1,200 papers on permafrost and related topics have been presented at the four previous international permafrost conferences and many of these report on field or laboratory data, yet inspection of the index to the conference proceedings (Heginbottom and Sinclair, 1985) reveals that none of the presentations has so far specifically treated the topic from a data management perspective.

HISTORY

Studies of frozen ground began in the mid to late nineteenth century, with research centers being established in the 1930s in the USSR and in the 1940s in North America and Japan (Harris, 1986). Comparable developments in China took place in the early 1960s following the establishment of the Division (now Institute) of Glaciology and Cryopedology in Lanzhou in 1962. This timing is an indication of the short periods over which field data have been collected, although the permafrost literature is already extensive (Heginbottom and Sinclair, 1985; Shen and Zhang, 1982). The 1978-82 bibliography compiled for the Fourth International Conference on Permafrost, for example, contains 4,400 entries (World Data Center-A for Glaciology, 1983). Specialized periodicals devoted to frozen ground phenomena are already being published in the Soviet Union (Merzlotnye Issledovaniia) and China (Journal of Glaciology and Geocryology, available in translation).

DATA TYPES AND REQUIREMENTS

Information on permafrost phenomena is collected for a wide range of purposes by many different groups of specialists, including engineers, geographers, geologists and hydrologists (Harris, 1986; Johnston, 1981; Tystovich, 1975). As recognized by the National Research Council (1983), "the need to decide on ways in which frozen ground data should be stored, retrieved and made available . . . presents a challenge."

The main variables used to characterize permafrost conditions on a global scale are summarized in Table 1. An attempt has been made to identify and rank variables that are likely to be required for programs such as the International Geosphere Biosphere Programme and for climate change monitoring. For other applied purposes these rankings could be entirely different. The spatial resolution of data required for climate modeling purposes using a General Circulation Model (GCM) is typically of the order of 1° latitude (Meehl, 1984). Currently, global maps of permafrost extent barely satisfy this first order requirement, especially in the zones of continuous and sporadic permafrost and, moreover, they

have not been prepared in digital format. More detailed information exists for particular regions (eg. a 1:500,000 scale map for a section of the Tibetan Plateau, and 1:12,000 scale maps for pipeline routes in Alaska).

Detection of changes in permafrost extent and/or thickness in response to environmental changes would require much higher degrees of horizontal and vertical resolution than are generally available at present. In the marginal areas sampling at ~100 m spatial intervals might be necessary. For relatively homogeneous terrain, such as the North Slope of Alaska, maps of permafrost thickness can be obtained from holes sited more than 100 km apart (Osterkamp, personal communication, 1987). In mountainous areas, and particularly in areas of discontinuous permafrost, holes need to be sited so as to represent terrain units having similar environmental characteristics (elevation, bedrock geology, soil properties, vegetation cover, slope aspect, hydrology, and microclimate). The vertical resolution of data on the thickness of ice-bearing permafrost, or the depth of the 0 ° C isotherm, needs to be fine if changes are to be detected on a decadal time scale. Osterkamp (1984) estimated that 25m-thick permafrost in interior Alaska might thaw within 200 years assuming a 3 ° C rise from -0.4 ° C. For monitoring such changes, vertical resolutions of a few millimetres to 1 cm at representative instrumented sites would be necessary (Osterkamp, personal communication, 1987). Alternatively, changes of temperature at 30 m depth (and other levels preferably) would need to be measured with a resolution of 0.01 ° C. Such precise measurements have been made on a daily basis to a depth of 1000 m in Arctic offshore wells in 330 m of water (Taylor and Judge , 1985). In the marginal areas where ground temperatures are approximately isothermal, thawing of permafrost patches would need to be monitored.

Data on ice content, which are needed, for example, to assess the potential effect of ice melting due to anthropogenically induced climatic warming on global sea level, are wholly inadequate at present for this purpose (Barry, 1985), although small-scale maps of ice volume have been produced in the USSR and Canada. Ice content data area also important for predicting ground disturbance resulting from thawing in climate change scenarios. Detailed ground temperature profiles are also needed to assess past environmental changes (Lachenbruch and Marshall, 1986), whereas accurate measurements at a few fixed levels will provide useful data for monitoring future trends. GCM simulations of past climates may help to 'control' calculations of past climatic changes inferred from permafrost temperature profiles and projections of future climatic changes may help permafrost researchers to design appropriate measurement networks.

For other purposes, data on many different physical, mechanical, thermal, chemical, and electrical properties of frozen ground are required. Engineering, construction, energy development, and mining activities require site-specific data on such variables as bearing capacity, compressibility, creep and frost heave and thaw settlement in the active layer, as well as on basic soil properties such as ice content, thermal conductivity, etc. Hydrogeological applications may also require basin-scale information on soil porosity and on chemical constituents in the frozen sediments.

A further category of information relates to laboratory testing of frozen materials as a basis for theoretical understanding and for engineering applications.

EXISTING DATA

The global distribution of permafrost and its mapping according to three or four extent classes is relatively well-defined in terms of small-scale (1:10 million to 1:25 million) maps of national territories and still smaller-scale global maps (Heginbottom, 1984). Such information is vital, but it needs complementing, by similar maps of the thickness of the permafrost and active layer, and ice content data in preparation for future climate modeling experiments, that will involve more detailed parameterization of ground conditions in energy budget and hydrological cycle calculations. Up to now, such studies have been limited to hypothetical calculations for selected site conditions (Smith and Riseborough, 1983; Goodwin *et al.*, 1984).

Regional and local data of the type needed to amplify the general data base are being collected by various organizations. In Canada, for example, mean annual ground temperature data are available for 305 northern sites and have been analyzed statistically in relation to mean annual air temperature and latitude (Young and Judge, 1987). Geophysical data from more than 500 well logs in northern Canada have been studied to determine the base of the ice-bearing permafrost from electric and acoustic properties of sediments (Geotech Engineering Ltd., 1983; Hardy Associates (1978) Ltd., 1984; Taylor and Judge, 1974; Judge and Taylor, 1985). A further data base compiled by the Geological Survey of Canada contains records from 11,600 boreholes drilled during road and pipeline routing studies in the Mackenzie Valley (Proudfoot and Lawrence, 1976). Well log compilations have also been made for Alaska (Osterkamp and Payne, 1981; Osterkamp *et al.*, 1985).

For the continuous permafrost zone of North America, maps of permafrost thickness with 50 m contour intervals could probably be constructed if data were available from another few hundred appropriately located holes. In fact, over 30,000 mostly shallow boreholes have probably been drilled in Alaska and northern Canada in connection with routing studies for oil and gas pipelines (R. Kreig, personal communication, 1987) and in most cases computerized data bases developed. These data remain largely proprietary but detailed summaries have been published (Kreig and Reger, 1976, Kreig, 1982). Within the discontinuous permafrost zone, a comparably dense network of boreholes would be essential for direct mapping. For the Schefferville area of Quebec-Labrador, Granberg *et al.* (1983) assembled digital data from over 200 thermo-cable sites. In addition, they developed a geographic information system in order to integrate these data with air photographs of snow cover, a digital terrain model and other information. Nelson (1986) illustrates the application of a predictive model, using air temperature and snow cover data, for mapping permafrost in the lowlands of central Canada, west of Hudson Bay. He shows that the zonal boundaries so delimited can be considerably refined by the incorporation of a 'Stefan frost number' in which soil properties are estimated. An earlier attempt by Vigdorchik (1980) to use environmental data to predict subsea permafrost occurrence on the Alaskan continental shelf also utilized a computerized synthetic approach.

DATA MANAGEMENT

The management of modern data archives involves the compilation of data sets, their quality control, storage on appropriate media, cataloging, and dissemination. Given the variety of purposes for which field data are collected, there is clearly great diversity in the types of measurement, due to differences of

instrumentation, reading and recording, as well as differences in units of measurement. Data managers need guidance on the preferred variables to be archived. Table 1 is a putative list based on literature sources and scientists' suggestions. The preceding discussion of predictive mapping using computer-based information systems suggests that, for some purposes, other environmental data maybe essential in order to provide complete spatial coverage in data-sparse areas.

The compilation of data sets involves decisions as to the level of processing that has been applied or is desirable. Table 2 illustrates the data levels conventionally recognized in geophysical science as applied to permafrost variables. Geophysical field measurements are level zero, whereas most scientific research utilises level 1 data to produce level 2 results for publication. Up to now level 3 products have been based primarily on subjective mapping compilations. Since no mechanisms for international data exchange currently exist, there also are no common formats for observational records. Guidelines for data archives need to be prepared concerning such matters as the appropriate vertical spacing of profile data, horizontal spacing of measurement sites according to spatial heterogeneity of the terrain and lithology, frequency of temporal sampling and measurement accuracy for the variables listed in Table 1. The Mackenzie Valley Geotechnical Data Bank (Proudfoot and Lawrence, 1976), for example, contains for each drill hole 27 variables describing location, topography and drill site characteristics and up to 30 geotechnical variables for each soil horizon.

The quality control of geophysical data generally involves checks for missing values and the screening of the data by comparison of individual values with a ± 3 standard deviation range about the population mean. However, this assumes that a population value can be defined. In many instances, this may not be feasible. However, other basic checks against adjacent values (in space or time), or calculations of gradients to highlight possible errors, can be made.

Storage of data may be in hard copy (tables or analog charts) or, for large data sets, electromagnetically on magnetic tapes and disks, or on optical disks. Increasingly, users also want data on floppy disks, or other media that can be used on microcomputers. Professional organizations, government agencies and university researchers could develop low cost software that could be used to create, manipulate and display such permafrost data. Efforts also need to be made to ensure preservation of digital data sets that are no longer considered to be of high priority importance for the organization which originally collected the data; tapes deteriorate if not exercised and earlier storage media (eg. 7-track tape, mass storage devices) may no longer be accessible. The United States National Research Council (1983) recommended that "the management and transfer of permafrost-related data be improved by, for example, . . . better integrating data bases with World Data Center-A for Glaciology" but, up to now, funds have not been available to permit the Center to perform such a role, beyond present bibliographic activities.

CONCLUDING REMARKS

The growth of interest in global geoscience and in the human consequences of potential changes in the global environment are leading to efforts in many fields to collect standardized consistent data on key environmental variables. In the case of permafrost research, the thickness and temperature of the permafrost and the thickness of the active layer will respond to changes in climatic conditions and ensuing changes in snow cover and vegetation. Scientists studying permafrost conditions need to assess the status of information that can contribute to interdisciplinary geoscience research. This preliminary assessment, together with recommendations from a workshop on permafrost data and information to be convened in association with the Fifth International Conference on Permafrost in Trondheim, should help to provide a framework for such an undertaking.

ACKNOWLEDGEMENTS I am grateful to Drs. J. Brown, T. Osterkamp, A. Lachenbruch and R. Kreig for their helpful comments on a first draft of this paper.

TABLE 1.

Permafrost-Related Variables Relevant to Global Change Studies

RANKING		COMMENTS
PRIMARY		
Extent		Categories of spatial continuity are used
Thickness of active layer and ice bearing permafrost, or 0°C depth		Determined by drill hole and temperature measurement, or geophysical survey (resistivity, seismic refraction, electro-magnetic)
Temperature profile		At master network sites
Ground temperature (30 m)		Special techniques are needed for subsea locations
Ice content		(%, weight of dry soil);
SECONDARY		Indirect and proxy indicators of occurrence
Air temperature (daily)		
Precipitation regime		
Snow depth		
Site location		Latitude, elevation, slope
Vegetation cover		Including disturbance history
Landform features (incl. naleds)		Indicative of permafrost; feasible to use air photography/satellite imagery
Hydrology of site		
TERTIARY		Supplementary data for global change studies, although important for most applied research
Active layer	- water content	
	- frost heave	
	- soil texture	
Frozen sediment	- grain size	
	- pore size distribution	
	- talik layers	
Ice types		Classification used
Excess ice value		(%, volume of supernatant water if sediment thawed)

TABLE 2.

Levels of Processing of Data on Permafrost Variables

LEVEL	DESCRIPTION	EXAMPLES
0	Raw data	Seismic resistivity, electromagnetic measurements
1	Primary scientific data (point, time values)	Temperature reading, ice content, thickness of ice-bearing permafrost
2	Spatial compilation of level 1 data	Gridded data on permafrost thickness; vertical temperature profile data
3	Synthesized sets of level 2 data	GIS products combining several variables.

REFERENCES

Barry, R.G. (1985). The cryosphere and climate change. In, M.C. MacCracken and F.M. Luther, eds., Detecting the Climatic Effects of Increasing Carbon Dioxide, DOE/ER-0235, U.S. Dept. of Energy, pp. 109-148, Washington, DC.

Geotech Engineering Ltd. (1983). Subsurface temperature data from Arctic wells. Earth Physics Branch, Energy, Mines and Resources, Canada, Open File 83-11, pp. 1-401, Ottawa.

Goodwin, C.W., Brown, J. and Outcalt, S.I. (1984). Potential responses of permafrost to climatic warming. J.H. McBeath, ed., The Potential Effects of Carbon Dioxide-Induced Climatic Changes in Alaska. Misc. Pub. 83-1, pp. 92-105. Fairbanks, Alaska: School of Agriculture and Land Resources Management.

Granberg, H.B., Lewis, J.E., Moore, T.R., Steer, P. and Wright, R.K. (1983). Schefferville permafrost research. Final report (DSS Contract no. 20SU 23235-2-1030, 26 volumes) to Energy, Mines and Resources, Canada, Ottawa.

Hardy Associates (1978) Ltd. (1984). A study of well logs in the western Northwest Territories and Yukon to outline permafrost thickness and/or gas hydrate occurrence. Earth Physics Branch, Energy, Mines and Resources, Canada, Open File 84-27, pp. 1-290, Ottawa.

Harris, S.A. (1986). The permafrost environment, pp. 1-276, Totowa, NJ: Barnes and Noble.

Heginbottom, J.A. (1984). The mapping of permafrost. Canad. Geographer 28: 78-83.

Heginbottom, J.A. and Sinclair, M. (1985). A cumulative index to permafrost conference proceedings, 1958-1983, Geol. Surv. Canada, Open File Rep. 1135, pp. 1-157.

Johnston, G.H., ed. (1981). Permafrost. Engineering Design and Construction, pp. 1-540, Toronto: John Wiley & Sons.

Judge, A. and Taylor, A. (1985). Permafrost distribution in northern Canada: interpretation of well logs. In: J. Brown, M.C. Metz and P. Hoekstra, eds., Workshop on Permafrost Geophysics, Special Report 85-5, U.S. Army Cold Regions Research and Engineering Laboratory, Hanover, NH, pp. 19-25.

Kreig, R.A. (1982). Airphoto analysis and summary of landform soil properties along the route of the Trans-Alaska Pipeline System: Alaska Division of Geological and Geophysical Surveys, Geologic Report 66, pp. 1-149.

Kreig, R.A. and Reger, R.D. (1976). Preconstruction terrain evaluation for the trans-Alaska pipeline project. In: Coates, D.R., ed., Geomorphology and Engineering, pp. 55-76. Stroudsburg, PA: Dowden, Hutchinson and Ross.

Lachenbruch, A.H. and Marshall, B.V. (1986). Changing climate: geothermal evidence from permafrost in the Alaskan Arctic. Science 234, 689-696.

Meehl, G.A. (1984). Modelling the earth's climate. Climatic Change 6: 259-286.

National Research Council (1983). Permafrost research: An assessment of future needs. Polar Research Board, Committee on Permafrost, pp. 103, Washington, DC: National Academy Press.

Osterkamp, T.E. (1984). Potential impact of a warmer climate on permafrost in Alaska. J.H. McBeath, ed., The Potential Effects of Carbon Dioxide-Induced Climatic Changes in Alaska. Misc. Pub. 83-1, pp. 106-113. Fairbanks, Alaska: School of Agriculture and Land Resources Management.

Osterkamp, T.E. and Payne, M.W. (1981). Estimates of permafrost thickness from well logs in northern Alaska. Cold Reg. Sci. Technol. 5: 13-27.

Osterkamp, T.E., Petersen, J.K. and Collett, T.S. (1985). Permafrost thickness in the Oliktok Point, Pruhoe Bay and Mikkelsen Bay areas of Alaska. Cold Reg. Sci. Technol., 11: 99-105.

Proudfoot, D.A. and Lawrence, D.E. (1976). Mackenzie Valley Geotechnical Data Bank Tape Description Manual. Geological Survey of Canada, Open File 350, Ottawa: Department of Energy, Mines and Resources.

Shen, J. and Zhang, X.G., editors (1982). Bibliography of literature on China's glaciers and permafrost. Part 1: 1938-1979, U.S. Army Corps of Engineers, Cold Reg. Res. Engr. Lab., Spec. Rep. 82-20, 33-41, Hanover, NH.

Smith, M.W. and Riseborough, D.W. (1983). Permafrost sensitivity to climatic change. Proceedings of the Fourth International Conference on Permafrost, pp. 1178-1183. Washington, DC: National Academy Press.

Taylor, A.E. and Judge, A.S. (1974). Canadian geothermal data collection - northern wells, 1955 to February 1974. Geothermal Series no. 1, Earth Physics Branch, Energy, Mines and Resources, Canada, pp. 1-171, Ottawa.

Taylor, A.E. and Judge, A.S. (1985). Obtaining precise measurements in abandoned offshore petroleum exploration wells. In: J. Brown, M.C. Metz and P. Hoekstra, eds, Workshop on Permafrost Geophysics, Special Report 85-5, U.S. Army Cold Regions Research and Engineering Laboratory, Hanover, NH, pp. 95-99.

Tsytovich, N.A. (1975). The mechanics of frozen ground. G.K. Swinzow and G.P. Tschebotarioff, ed., pp. 1-426, Washington, DC, Scripta Book Company. (Russian edn., 1973, Moscow.)

Vigdorchik, M.E. (1980). Submarine permafrost on the Alaskan continental shelf, pp. 1-118, Boulder, CO: Westview Press.

Young, S. and Judge, A. (1987). A ground temperature data collection for northern Canada. P. Adams, ed., Field Research on Axel Heiberg Island, N.W.T., Canada. McGill Subarctic Research Paper no. 41, pp. 195-207, McGill University, Montreal.

World Data Center-A for Glaciology (1983). Permafrost: a bibliography 1978-1982. Glaciol. Data Report GD-14, pp. 334. Boulder, CO: World Data Center-A for Glaciology.

GEOCRYOLOGICAL MAP OF MONGOLIAN PEOPLE´S REPUBLIC

V.V. Baulin[1], G.L. Dubikov[1], Yu.T. Uvarkin[1], A.L. Chekhovsky[1], A. Khishigt[2], S. Dolzhin[2] and R. Buvey-Bator[2]

[1]Research Institute of Engineering Site Investigations, Moscow, USSR
[2]Research Institute of Engineering Ulhan-Bator, MPR

SYNOPSIS Mapping technique is given and legend contents of a geocryological map at the scale of 1:1,500,000 is laid bare. The map is constructed by geologo-genetic data. Geocryological characteristics are represented by coloured shadings, point symbols and index numbers. Four highland geocryological belts are distinguished, namely, continuous and discontinuous permafrost and permafrost massive islands and islands. Within a first belt an average annual temperature of permafrost varies from zero to -4°C or below; within the rest ones it is not below -1°C. Total ice content, development of cryogenic processes, depth of seasonal freezing and thawing of permafrost and its thickness are also shown for each belt. The map is of interest for getting knowledge of regularities of forming geocryological conditions in Central Asia.

A geocryological map of MPR at a scale of 1:1,500,000 is constructed by the findings of geocryological examinations carried out in 1982-1985. A field geocryological survey at a scale of 1:100,000 assumed as the basis of the map has been conducted on 15 key sites located in different highland geocryological belts of MPR. Moreover, examination findings, publications (Melnikov,1974; Vasiliev et al., 1987; Marinov and Tolstikhin, 1963) as well as geocryological maps of MPR by N.Lonzhid and A.N.Minaev have been used.

The present map is compiled by geological data and represents functional relationship of permafrost and geologo-geographic conditions. On the map we assume separate representation of principal geocryological features which enables on the one hand to read regularities of forming the geocryological conditions on it and on the other hand to forecast a trend for change of each feature in connection with the

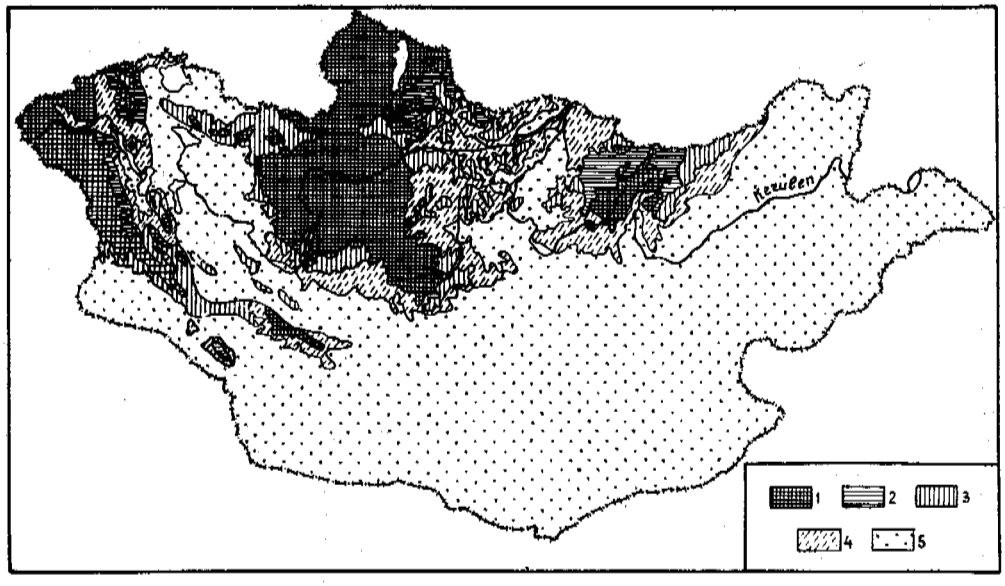

Fig. Average annual temperature and extent of permafrost at the territory of MPR:

1 - continuous permafrost,,thickness (T) = 50-100 m, average annual temperature (t) = -1 ÷ -4°C;
2 - discontinuous permafrost, T = 30÷50 m, t = up to -1°C;
3 - permafrost masses and islands, T = 5÷30 m, t = up to -1°C;
4 - permafrost islands, T = 5÷20 m, t = up to -1°C;
5 - lenses of frozen ground are possible, T = up to 2÷3 m.

territory development. Extent, thickness and average annual temperature of permafrost are shown in a reduced black and white alternative map (Fig. 1). Colour on the map represents extent, thickness and average annual temperature of permafrost. Four highland geocryological belts are distinguished, namely, continuous (more than 80%) and discontinuous (80-50%) permafrost and permafrost massive islands (50-5%) and islands (less than 5%). It is considered inexpedient to distinguish a belt of sporadic permafrost since it occur here only in overmoisted soils which occupy less than 1% of the area. Permafrost thickness does not exceed 2-3 m in such places. Due to climatic fluctuations a spatial location of permafrost lenses by both a latitude of the locality and an altitude above sea-level changes nearly every year.

According to an average annual temperature of the belt of continuous permafrost its fours levels are distinguished, namely, below -4°C, from -4°C to -2°C, from -2°C to -1°C and from -1°C to close to zero. Each temperature range of the ground is shown by tints of cold (blue) tones. In the rest highland geocryological belts the ground temperature varies between values close to 0°C and -1°C. Therefore there is no colour gradation in colouring highland geocryological belts of discontinuous permafrost and permafrost massive islands or permafrost islands.

Total ice content on the map is represented by sloping coloured (red) shading. Three levels of ice content is distinguished, namely, less than 0.2, between 0.2 and 0.4 and greater than 0.4.

Depth of seasonal freezing and thawing of the ground is shown both directly on the map and as a table of the map legend. Special point symbols indicate areas of thermokarst extent, frost heaving, formation of icing (naled) and frost cracking.

When plotting the geocryological map we have used a map of Quaternary deposits of MPR at a scale of 1:1.500.000 as a geological base. Among the Quaternary deposits there are distinguished alluvial lacustrine alluvio-lacustrine glacial glacio-lacustrine alluvial-deserptional deluvial-proluvial proluvial proluvio-lacustrine eluvial eolian and vulcanogenic sediments. Prequaternary rocks are subdivided into proterozoic paleozoic and mesozoic sedimentary metamorphic and intrusive formations. Composition genesis and age of the prequaternary deposits are shown by a special sign, that of the Quaternary ones is shown by black shading.

On the map there are used two types of boundaries, namely, geocryological (blue) and geological (black) ones. Geocryological boundaries separate highland geocryological belts (continuous line) and areas of a cryolithozone with a different average annual temperature of frozen ground within the limits of the highland belt of its continuous extent (dotted line). Geological boundaries separate rocks of different age or genesis (continuous line) and different lithological composition within uniaged quaternary deposits of similar genesis (dotted line).

Geocryological and geological boundaries are the boundaries of a first and second order respectively; if change of geocryological situation and geological conditions coincides territorially then a geocryological boundary is run out in such places.

An examination of the map content enables to reveal principal regularities of permafrost extent and quantitatively characterize its main parameters. Frozen ground in MPR occupies comparatively small area, not more than 15% of its territory, but its islands and masses are widely scattered and predominantly attributed to such mountain systems as Mongol and Gobi, Altajn Nuruu, Hövsgöl Lake region Hangayn Nuruu Hentiyn Nuruu and Orhon-Selenge Middle mountain. Permafrost extent at the territory of MPR follows highland beltness and latitudinal zonality. It resides in the fact that a hypsographical position of the highland geocryological belts distinguished rise from the North to South. A highland continuous permafrost belt in the North in Hentiyn Nuruu and Hövsgöl Lake region begins with absolute elevations of 1650-1750 m. Further south in Orhon-Selenge Middle Mountains and Buteelijn Nuruu it begins with 2000 m and in Hangayn Nuruu it begins with 2400-2500 m. In Mongol Altajn Nuruu ranging from North-West to South-East absolute elevations of a continuous permafrost belt rise from 1800-2000 m in the North-West to 2800-3000 m in the North (Ich Nuruu and Shara Nuruu), in Gobijn Altajn Nuruu a highland continuous permafrost belt is followed in upland areas of Bogdyn Nuruu and Zund Bogd beginning with absolute elevations of 2700-2900 m. At highland continuous permafrost belt begins as a whole by 150-200 m higher than at hillsides of a north arrangement.

At the map scale a highland discontinuous permafrost belt is distinguished in Hentiyn Nuruu Orhon-Selenge Middle Mountains Mongol Altajn Nuruu and Hövsgöl Lake region. In the south of Hentiyn Nuruu it begins from 1600 m, in the north it begins from 1400 m, in Buteelijn Nuruu permafrost layers discontinuous in plan occupy a height interval of 1700-2000 m. In Mongol Altajn Nuruu it is distinguished at east and north-east spurs and hillsides of a central part within a height interval between 2000-2500 and 2500-2600 m. In east and north-east Hövsgöl Lake Region it occupies heights between 1400 and 1800 m.

A highland belt of permafrost masses and islands is followed in east spurs of Hentiyn Nuruu within a height interval of 1200-1400 m. In Orhon-Selenge Middle Mountains this belt is widespread within a height interval of 1450-1600 m, within the limits of south spurs of Hangayn Nuruu (South-Hangajn high plateau) it occupies absolute elevations of 2300-2400 m; in south and south-east areas of Mongol Altajn Nuruu this permafrost belt is followed between 1900-2000 m and 2800-3000 m; in Hövsgöl Lake Region its height reference also varies over a wide range, namely, between 1800-2000 m.

A lower boundary of the belt of permafrost islands at south spurs of Hentiyn Nuruu runs at a height of 1500-1600 m lowering to the east down to 1100-1200 m; in Orhon-Selenge Middle Mountains it uses from 650-670 m in the north of the region to 900-1200 m in the south;

within the limits of Hangayn Nuruu the given geocryological belt is widespread, its lower bound running at a height of about 2000 m; in Mongol Altajn Nuruu the belt of permafrost islands includes Ureg Nur Lake basin; in east Hövsgöl Lake Region the belt of permafrost islands occupies an interfluve of the Egijn Gol and Selenge Rivers with absolute elevations of 1200-1800 m. Considerable fluctuations of an average annual temperature of rocks (between -0.1 - 0.2°C and -4°C or below) are observed only in the highland belt of their continuous extent. In the rest highland belts an average annual temperature of rocks, as a rule, does not fall below -1°C. Differentiation of average annual temperatures of the rocks in the belt of their continuous extent has been caused by the fact that frozen ground occupies here a wide (up to 800-100 m) interval of absolute elevations where a considerable variation of natural and climatic conditions is observed. The highest average annual permafrost temperatures (up to -0.1 - -0.2°C) are observed at the bottoms of wide intermontane areas and valleys in Hentiyn Nuruu and Mongol Altajn Nuruu. These areas are woodless and composed of well filtrating coarse sands. The similar temperature is also possible at the south and south-west hillsides of medium steepness located near a lower limit of the continuous permafrost belt.

An average annual temperature -1 ÷ -2°C is practically characteristic of all the forested hillsides located in Hentiyn Nuruu Hangayn Nuruu and Orhon-Selenge Middle Mountains. In woodless Mongol and Gobijn Nuruu the similar temperature is characteristic of differently oriented hillsides adjoining to a lower limit of the belt of continuous permafrost layers.

Upland woodless areas (up to 3000 m) within the limits of all the mountain systems in MPR with Hövsgöl Lake Region excluded are characterized by an average annual rock temperature of -2 ÷ -4°C. The same temperature is recorded at forested hillsides of Hövsgöl Lake Region. Above absolute elevations of 3000 m or beginning with a height of 2600 m in Hövsgöl Lake Region an average annual permafrost temperature falls below -4°C.

Total ice content of frozen ground in MPR is low. It may be attributed to the fact that coarse detrital terrigeneous rocks are widespread there and to considerable ruggedness of the relief.

In the continuous permafrost belt thickness of frozen loose deposits is low in overwhelming majority of cases, therefore a total ice content of frozen ground down to 10-15 m deep is the lowest possible there. In lower parts of hillsides and in widened parts of rivers valleys thickness of loose material increases. A total ice content of the ground in the belt of permafrost islands is the highest possible there. For Quaternary deposits a minimum total ice content is characteristic of deluvial-proluvial and deluvial deposits. Its magnitude varies between hundredth fractions of a unit in the belt of continuous extent and 0.2 in case of permafrost islands.

At upland solefluction and deserption hillsides a total ice content can increase up to 0.3, most frequently in the belt of discontinuous permafrost. A total ice content of deposits of various genesis in large river valleys and in intermountain valleys or areas varies between 0.2 and 0.4. The greatest ice content of this range of values is characteristic of lacustrine and alluvial coarse-detrital pebbled deposits. A maximum ice content of the rocks (0.5-0.55) is observed at marshed areas of little river valleys and in places of underground water discharge. Near by springs a considerable ice content is observed in rocks of any genesis and varying lithological composition.

A depth of seasonal freezing and thawing of the ground at the territory of MPR varies between 1.0 and 5.0-5.5 m. Main regional factors governing the depth of seasonal freezing and thawing of the ground are lithological composition of superficial deposits and their moisture content, zonality factors being of much lesser importance in this case.

Minimum depth of seasonal thawing is recorded at the bottoms of river valleys, intermountain areas, lake basins, flat lower parts of hillsides composed of sandy loam and loam deposits. As total moisture content of the ground varies between 20% and 40% a depth of its seasonal thawing varies between 2 and 1 m here. Maximum depth of seasonal thawing up to 5.5 m is characteristic of steep hillsides with outcrops of rocky and half-rocky ground. In gravelly-pebbled ground as its total moisture content decreases from 10 to 3-4% a depth of seasonal thawing varies between 3 and 5.5 m.

For great variety of coarse clastic ground of the most varying genesis depth of seasonal thawing at the whole territory of MPR varies between 2 and 3-3.5 m. Total moisture content of the deposits ranges between 10-20%.

Depth of seasonal freezing of the ground (Large Lakes basin, Central Gobijn peneplain, Trans-Altajn and South-East Gobi) varies between 1.5 and 5-5.5 m. Its differentiation is mainly effected by regional factors (lithological composition and total moisture content of the ground). Minimum depths of seasonal freezing (1.5-2.5 m) are characteristic of sandy loam and loam, proluvial-lacustrine, alluvial-lacustrine, proluvial deposits a total moisture content of which being 15-40%. Maximum depths of seasonal freezing (4-5.5 m) are recorded in mountain regions where Quaternary volcanogenic or prequaternary rocky or half rocky ground crops out as well as in eolian sands and deluvial-proluvial coarse-clastic soils a total moisture content of which being less than 5-7%.

In most cases depth of seasonal freezing of coarse clastic soils of the above regions varies between 2.5- and 4 m, a total moisture content being an average of 10-15%.

REFERENCES

Vasiliev, V.I., Sheshenya,N.L., Chekhovsky,A.L. (1987). Formirovaniye inzhenerno-geologicheskikh usloviy tsentral'noy Mongolii. s.s.1-144. Moskva: Nauka.

Marinov, N.A., Popov, V.I. (1963). Gidrogeologiya MNR. s.s.1-263. Moskva:Gostekhizdat.

Melnikov, P.I. (1974). Redaktor. Geokriologicheskiye usloviya Mongolskoy Narodnoy Respubliki. s. 1-267, Moskva: Nauka.

GEOTECHNICAL AND GEOTHERMAL CONDITIONS OF NEAR-SHORE SEDIMENTS, SOUTHERN BEAUFORST SEA, NORTHWEST TERRITORIES, CANADA

S.R. Dallimore, P.J. Kurfurst and J.A.M. Hunter

Geological Survey of Canada, 601 Booth Street, Ottawa, Ontario, K1A 0E8

SYNOPSIS Near-shore sediments in the southern Beaufort Sea display high spatial and temporal variability of geotechnical and geothermal conditions. This paper describes results of extensive geotechnical investigations along two diverse transects in frozen and unfrozen near-shore sediments. The geotechnical and geothermal conditions of the near-shore zone are discussed as well as the implications for the design and construction of engineering structures.

INTRODUCTION

Anticipated development of hydrocarbon resources discovered in sedimentary basins underlying the continental shelf of the Beaufort Sea has created a need for detailed knowledge of the geology of the near-shore zone. Data on the geotechnical and geothermal conditions of seabottom sediments are vital to the engineering design of structures such as pipelines and marine terminals. The near-shore zone is an unique environment which typically contains a diverse suite of geological materials undergoing constant modification by active coastal processes. In transgressive margins such as the southern coast of the Beaufort Sea, the near-shore zone can be underlain by several hundreds of metres of perennially frozen sediments which may be in a state of thermal dis-equilibrium.

This paper describes the geological, geotechnical and geothermal conditions of the near-shore sediments occurring off northern Richards Island in the southern Beaufort Sea. The results of detailed geotechnical investigations along two onshore-offshore transects (Figure 1) as well as the scope of techniques used are described in detail.

GEOLOGICAL SETTING

Richards Island is underlain by thick deposits of Quaternary sediments which are perennially frozen to several hundred metres depth. Onshore sediments consist of early Wisconsinan and older glacial, fluvial and marine sediments mantled by more recent lacustrine, colluvial and eolian materials of variable thickness (Rampton, in press). Ground ice is commonly present in terrestrial sediments in the form of discrete bodies of massive ice, ice wedges, ice lenses and pore ice (Rampton and Mackay, 1971; Dallimore and Wolfe, this volume).

Coastal areas of the Canadian Beaufort Sea have been experiencing a general marine transgression since at least late Wisconsinan times (Hill et al, 1985). This process has resulted in a typical offshore sequence of marine sediments lying unconformably over older sediments which were once sub-aerially exposed. The near-shore areas have been recently innundated by the sea and therefore represent a transitional zone between the onshore and offshore environments.

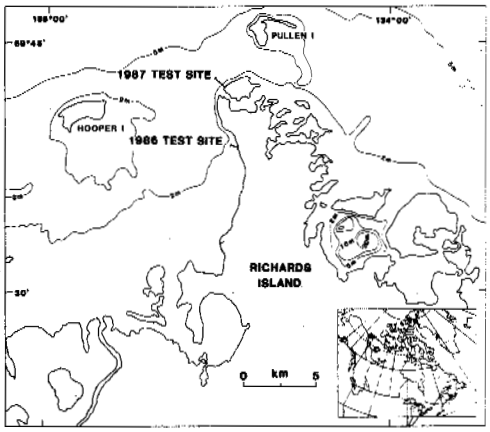

Fig. 1 Site Location Plan

The coastline of northern Richards Island exhibits a variety of erosional and accretional landforms. A summary of coastal change in the area since 1947, shown on Figure 2, indicates that retreat rates vary from a maximum of 3.2 m/a to no discernible change. In order to assess the effect of coastal retreat on geotechnical conditions of the near-shore zone, investigations were undertaken at two contrasting sites. The 1986 investigations concentrated on a stable coastal area while the 1987 study site was located in an area experiencing coastal retreat at a rate of about 3 m/a.

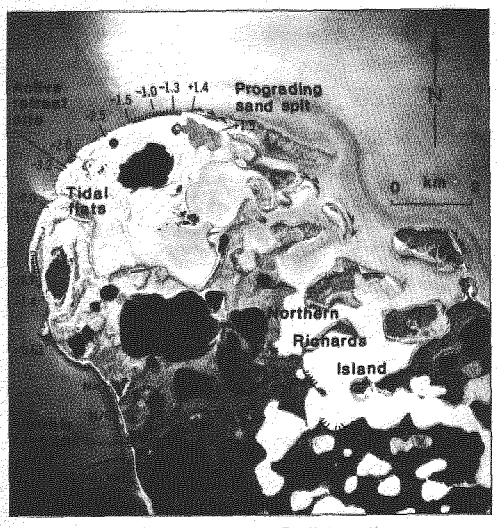

Fig. 2 Aerial Photograph of Northern Richards Island Showing Coastal Change

FIELD INVESTIGATIONS

Eighteen boreholes were drilled along two onshore-offshore transects to depths ranging from 30 m to 40 m. The locations of the drill holes and the transects are shown on Figures 3 to 6. Geotechnical drilling was carried out in the spring using a conventional rotary drill rig capable of collecting 10 cm or 7.5 cm diameter samples. Core samples were collected from all drill holes either continuously or at 1.5 m intervals. After measuring the core temperature with a needle probe, samples were photographed and logged for soil and ice type. All drill holes were cased and then used for seismic and other geophysical logging before thermistor cables were installed (Kurfurst, 1986; 1988). Thermistor cables were monitored until thermal equilibrium was reached after dissipation of disturbance caused by drilling and cable installation.

In addition to the drill holes, 13 cone penetration tests (CPT) were carried out to provide supplementary information. A standard Hogentogler electric cone penetration system and a 10-tonne compression cone were used for the testing. Soil temperatures were also monitored at the cone tip. The location and depth of the CPT soundings are shown on the cross-sections on Figures 3 to 6.

Field work conducted in the summers of 1986 and 1987 documented coastal stratigraphy, ground ice conditions and coastal retreat rates. Installations of supplemental thermistor cables to monitor temperatures at the end of the thaw season were carried out in August of 1985 and 1987 in small diameter jet-drilled holes.

RESULTS

Geological Conditions

The geological and geotechnical conditions of each site have been summarized as simplified cross-sections presented on Figures 3 through 6. Transgressive marine sequences with well defined Holocene unconformities are present at both sites (Figures 3 and 5). Sediments above the unconformity consist of re-worked sands and laminated marine silts. The predominant feature of the very near-shore areas are submerged terrestrial sequences composed of early Wisconsinan fluvial sand and marine silt.

Massive ground ice is common in the terrestrial sediments at the active coastal retreat site where an irregular-shaped ice body was encountered in four boreholes drilled near the coast (Figure 5). Its maximum thickness of more than 10 m was measured in boreholes 87-5. Examination of exposures in the cliff section carried out during the summer, indicates that ground ice in the vicinity of the drill transect has undergone glacial tectonic deformation. Several ground ice bodies exposed near the transect show recumbent folds and brecciated zones with broken ice clasts up to 1 m^2. The irregular shape of the ice body, inferred from borehole information in Figure 5, can be attributed to similar deformation. Sediments exposed in coastal sections in the vicinity of the stable coastal site and frozen terrestrial sediments in near-shore drill holes are generally ice poor (Figure 3).

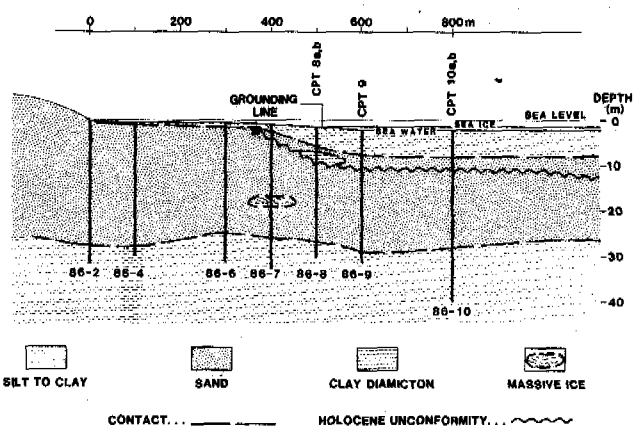

Fig. 3 Geological Cross-section of Stable Coastal Retreat Site

Geothermal Conditions

The geothermal and ground ice conditions at the two sites have been summarized in Figures 4 and 6. The permafrost table (0°C isotherm) at the stable coastal site (Figure 4) occurs close to the surface at the coast and then dips gradually offshore to a depth of more than 8 m below the sea floor at 800 m offshore. At the active coastal retreat site (Figure 6), the permafrost table dips abruptly offshore at 200 m to more than 30 m depth below the sea floor by 1 km offshore. Instrumented drill holes in onshore areas indicate that the mean annual ground surface temperature is approximately -8°C.

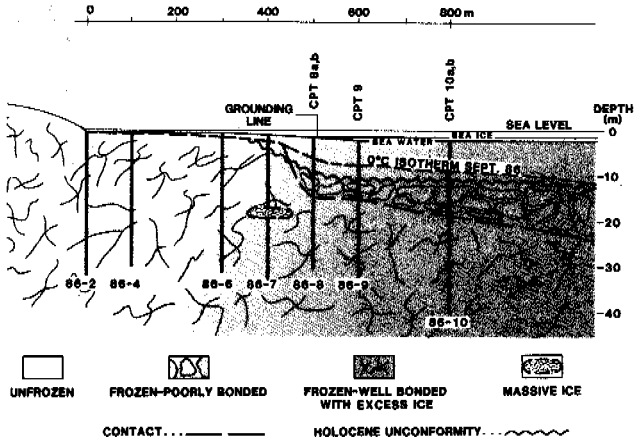

Fig. 4 Geotechnical and Permafrost Cross-section of Stable Coastal Retreat Site

It is apparent that the offshore bathymetry has an important effect on the thermal regime of seabottom sediments at each site. The sea floor at the stable coastal site has a shallow, uniform gradient with an extensive area of sand flats near the shore. During the winter sea water in this area freezes to the bottom, thus allowing cold winter temperatures to penetrate the underlying sediments, maintaining permafrost conditions (Hunter et al, this volume). The active coastal retreat site is characterized by a narrow shelf within 100 m off the coast and then by an abrupt drop in water depth farther offshore. The grounding line of the sea ice is approximately 80 m from the coastline and areas farther offshore experience relatively warm seabottom temperatures that cause deep thaw.

Seabottom temperatures were recorded during the spring 1986 and 1987 drilling programs and during a 5-week period in August and September, 1987. These data indicate that water temperatures at both sites are quite high during the summer with an average temperature range from 8°C to 11°C. However, seabottom temperatures as low as 3.6°C were recorded during short-duration storms. Seabottom temperatures measured during the spring were found to range from -0.2°C to +0.5°C.

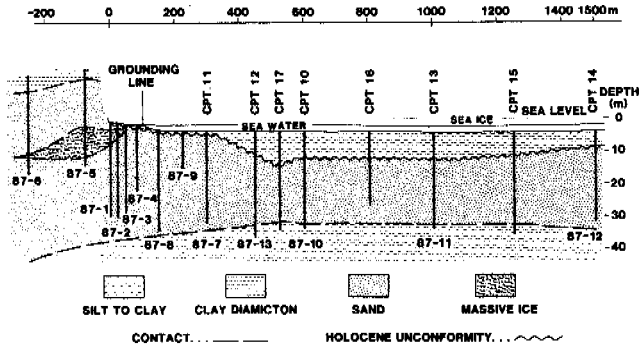

Fig. 5 Geological Cross-section of Active Coastal Retreat Site

The geothermal conditions at the sea bottom contribute to several interesting geological processes. The presence of a seasonally thawing and freezing zone in areas near the shore creates the potential for seasonal frost heave and thaw settlement. At the active coastal retreat site, thaw of buried massive ground ice will result in settlement at the sea floor creating sub-sea thermokarst conditions similar to those described by Mackay (1986). The uneven nature of the Holocene unconformity at the active coastal retreat site between boreholes 87-10 and 87-13 (Figure 5) suggests that some local settlement has occurred but that the depressions at the sea floor have been rapidly infilled by sedimentation.

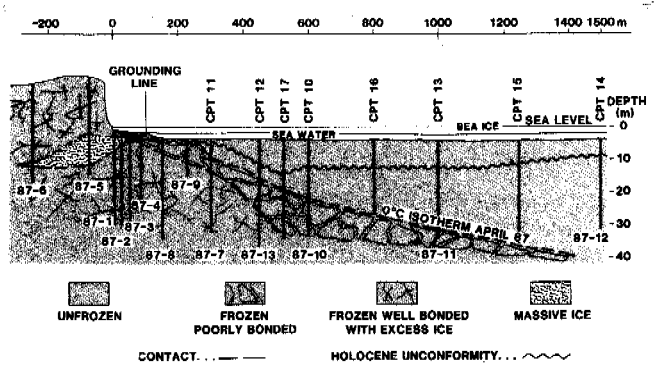

Fig.6 Geotechnical and Permafrost Cross-section of Active Coastal Retreat Site

Geotechnical Conditions

The cone penetrometer (CPT) proved to be an extremely useful complementary tool in determining the strength of unfrozen materials and their insitu geotechnical properties. Temperature data recorded by the cone penetrometer were reliable and consistent with the temperature data measured by the thermistor cables. The cone penetrometer was also useful in accurately delineating the upper limit of frozen ground. An example of typical CPT result is given on Figure 7.

The CPT results indicate a thin discontinuous zone of partially ice-bonded material at the top of the offshore Holocene sediments. As shown on Figure 7, this zone is characterized by high pore water pressure (30 m water column) and increase in sleeve friction and friction ratio just below the mudline. The presence of frozen materials is confirmed by negative temperatures (-0.11°C) recorded by both cone penetrometer and thermistor cable sensors. Both drilling and cone penetration tests indicate that the Holocene sediments present beneath this thin surface layer are relatively soft materials with low bearing capacity of less than 10 bars (Figure 7).

Core logs from drill hole 87-11 and results of CPT 13 (Figure 7) as well as data from other drill holes indicate that the lower parts of the Holocene sediments are slightly overconsolidated. The results of CPT 13 show increases in cone bearing capacity (20 bars),

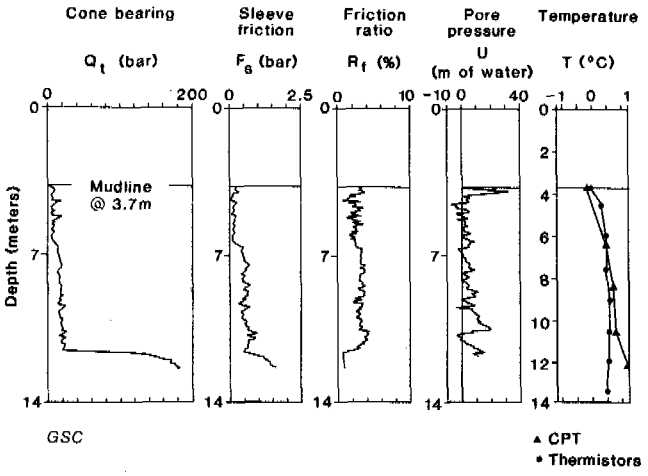

Fig. 7 Cone Penetrometer and Temperature Data for Borehole 87-11 and CPT 13

sleeve friction (0.7 bar) and friction ratio (4%), thus confirming the presence of overconsolidated sediments detected during drilling. Overconsolidation of recent Holocene sediments has also been encountered in areas further offshore (Christian and Morgenstern, 1986). This overconsolidation is likely caused by freeze-thaw effects on the Holocene sediments when they were exposed close to the sea floor. It is also possible that overconsolidation could be caused by cyclic loading by wave action.

The strength of frozen soils encountered below the Holocene sediments was found to be highly variable, especially near the 0°C isotherm. Examination of drill core and limited CPT data indicate a zone of poorly ice-bonded materials in this area. Core collected in this region was easily disturbed by sampling and handling, and varied from supersaturated sand to extremely competent, ice-bonded sand. The thickness of poorly ice-bonded sediments increases with distance from the coastline, as illustrated in Figures 4 and 6. It is assumed that migration of saline pore water affects the freezing point and geotechnical properties of the sediments in this zone. Further work is presently underway to investigate this process and its affects.

DISCUSSION AND IMPLICATIONS FOR ENGINEERING

The investigations carried out to date have indicated that the conditions of near-shore sediments are highly variable in a spatial and temporal sense. Coastal areas which are exposed can undergo high rates of retreat while nearby, more protected areas are relatively stable. The thermal regime of sediments in the near-shore area is also complex. In shallow areas where the sea ice freezes to the bottom during the winter, cold permafrost conditions can be expected. A thick layer of near-surface soil may undergo seasonal cycle of freezing and thawing, resulting in frost heave and thaw settlement. In deeper water (>2m), submerged early Wisconsinan sediments are in a condition of thermal dis-equilibrium which causes their relatively rapid thaw. When sediments are ice rich or contain massive ice, sub-sea thermokarst conditions can occur with substantial thaw settlement. Assuming an average coastal retreat rate of 3 m/a, the thick massive ice body presently exposed below sea level near the active coastal retreat site will be approximately 300 m offshore in 100 years. Assuming a similar sea floor profile as at present, the ice body would then be subjected to rapid thaw. Since this ice body contains over 95 % ice by volume, thawing of the ice will result in up to 10 m of settlement at the sea floor.

These findings have obvious implications for design of engineering structures such as pipelines located in the near-shore zone of the Beaufort Sea and in other permafrost areas with transgressive coastal margins. The highly variable geotechnical conditions of near-shore sediments require that detailed site specific geotechnical investigations are carried out prior to construction. Geotechnical drilling should investigate the properties of both recent marine sediments and of submerged terrestrial sediments. Close attention must also be paid to the present geothermal conditions of the sediments as well as the history of sea floor temperatures to determine if a condition of thermal dis-equilibrium exists. Finally, the temporal variations in coastal position, water depth and sedimentation must be considered at both a site specific and a regional scale.

Geotechnical and geophysical techniques used in the near-shore environment are often quite specialized. Although use of a standard rotary drill rig is recommended, different sampling techniques have to be applied in areas where the sea ice is frozen to the base (CRREL core barrel) then in areas where a water column is present below the sea ice (Shelby tube). The cone penetrometer was found to be a useful tool in this environment, however its penetration is limited to unfrozen and poorly ice-bonded sediments. Several surface and downhole geophysical techniques have been recently tested in the near-shore area and their results are being evaluated.

CONCLUSIONS

Two onshore-offshore transects have been investigated off the coast of Richards Island in the southern Beaufort Sea at a stable coastal retreat site and at an active coastal retreat site. Results of geotechnical drilling, cone penetration tests and thermal studies show that:

1) Near-shore geology is dominated by a wedge of Holocene silt unconformably overlying buried early Wisconsinan sand and silt.

2) Holocene silts occurring near the sea floor are relatively soft materials with low bearing capacities and shear strengths. Zones of slightly overconsolidated Holocene sediments are commonly present at depth.

3) The seabottom temperatures and geothermal regime of the near-shore zone are determined primarily by the offshore bathymetry. Permafrost is preserved in shallow areas close to the shore where the sea ice freezes to the base, thus allowing deep penetration of cold winter temperatures. Areas farther offshore, where the thicker water column maintains warm sea floor temperatures, experience rapid thaw.

4) Sediments near the sea floor are subjected to an annual cycle of freezing and thawing.

5) Thaw of ground ice present in buried early Wisconsinan sediments can result in sub-sea thermokarst conditions.

6) The thickness of poorly ice-bonded early Wisconsinan sediments, possibly resulting from migration of saline pore water, increases with distance from the shore.

ACKNOWLEDGEMENTS

The authors would like to thank members of the Terrain Dynamics Sub-Division of Terrain Sciences as well as C.Burn, L. Dyke and S. Wolfe for stimulating discussions and assistance in the field. Logistical assistance for this project was provided by Polar Continental Shelf Project and the Inuvik Research Centre. Funding was provided by the Office of Energy Research and Development and the Northern Oil and Gas Action Program.

REREERENCES

Christian, H.A. and Morgenstern, N.R. 1986. Compressibility and stress history of Holocene sediments in the Canadian Beaufort Sea. Third Canadian Conference on Marine Geotechnical Engineering, St. John's, NFld, p.275-299.

Dallimore, S.R. and Wolfe, S.A. This volume. Occurrence of massive ground ice in glacial fluvial sediments, Richards Island, N.W.T. Canada. Fifth International Conference on Permafrost, Trondheim, Norway, August 2-5.

Hill, P.R., Mudie, P.J., Moran, K.M. and Blasco, S.M. 1985. A sea-level curve for the Canadian Beaufort Shelf. Canadian Journal of Earth Sciences, Vol 22, p. 1383-1393.

Hunter, J.A.M. et al. This volume. Thermal evidence for an active layer on the seabottom on the Canadian Beaufort Sea shelf. Fifth International Conference on Permafrost, Trondheim, Norway, August 2-5.

Kurfurst, P.J. (compiler) 1986. Geotechnical investigations of the near-shore zone, North Head, Richards Island, N.W.T. Geological Survey of Canada, Open File 1376, 82 p.

Kurfurst, P.J. (compiler) 1988. Geotechnical investigations, northern Richards Island, N.W.T. -Spring 1987. Geological Survey of Canada, Open File 1707, 147 p.

Mackay, J.R. 1986. Fifty years (1935 to 1985) of coastal retreat west of Tuktoyaktuk, District of Mackenzie. Geological Survey of Canada, Paper 86-1a, p. 727-735.

Rampton, V.N. In press. Quaternary geology of the Tuktoyaktuk Coastlands, Northwest Territories. Geological Survey of Canada, Memoir 423.

Rampton, V.N. and Mackay, J.R. 1971. Massive ice and icy sediments throughout the Tuktoyaktuk Peninsula, Richards Island and nearby areas, District of Mackenzie. Geological Survey of Canada, Paper 71-21, 16p.

GSC Contribution No. 51387

MASSIVE GROUND ICE ASSOCIATED WITH GLACIOFLUVIAL SEDIMENTS, RICHARDS ISLAND, N.W.T., CANADA

S.R. Dallimore and S.A. Wolfe

Geological Survey of Canada, 601 Booth St., Ottawa, K1A 0E8

SYNOPSIS Discrete bodies of massive ground ice up to 20 m thick are commonly associated with glaciofluvial sediments on Richards Island, Northwest Territories. Drilling and ground probing radar surveys indicate that massive ice varies substantially in thickness, morphology and associated sediment. Three types of ground ice were found at the two sites investigated; these are interpreted as near surface aggradational ice, buried glacier ice and segregated ice.

The variation in massive ice type is indicative of the varied postglacial conditions which have existed in this area. During the latter stages of Early Wisconsinan glaciation, glacial ice was covered and preserved by glaciofluvial sands. In other areas, perhaps with less sediment cover over the glacial ice, substantial thaw occurred. Subsequently, ground ice has formed in these sediments during periods of permafrost aggradation.

INTRODUCTION

Massive ground ice commonly makes up a significant portion of near-surface materials in the Mackenzie Delta - Beaufort Sea region (Mackay, 1966, 1971; Rampton, 1973, 1988). Typically, massive ice is overlain by fine-grained sediment and underlain by coarse-grained sediment (Mackay, 1971). Massive ice overlain by coarse-grained materials, such as glaciofluvial sediments, is rarely reported. However, the nature and amount of massive ice in these sediments is of significant importance for exploitation of granular resources and other resource related development.

This paper describes the distribution and character of massive ground ice associated with coarse-grained, glaciofluvial sediments on Richards Island, N.W.T. (Figure 1). Field evidence from drilling and geophysical surveys is presented as well as data from laboratory analysis of ground ice samples.

SURFICIAL GEOLOGY

Richards Island is situated in the Tuktoyaktuk Coastlands of the Arctic Coastal Plain (Rampton, 1988). The area is characterized by thick deposits of unconsolidated Quaternary sediments, perennially frozen to several hundred metres depth (Taylor et al, 1982). Geotechnical borings, geophysical soundings and coastal exposures all indicate that massive ground ice is common in near-surface soils (Mackay, 1963; Rampton and Mackay, 1971; Rampton and Walcott, 1974; Pollard and French, 1980).

The central and southern portions of Richards Island are covered by variable thicknesses of glacial, fluvial and lacustrine sediments. In the vicinity of Ya Ya Lake and Lousy Point (Figure 1), glacial outwash, ice contact ridges and esker-like deposits are common. As this area is well beyond the limit of Late Wisconsinan ice, and the glaciofluvial materials are underlain by till, the sediments were probably deposited by melt water from the Early Wisconsinan Toker Point Glaciation (Rampton, 1988).

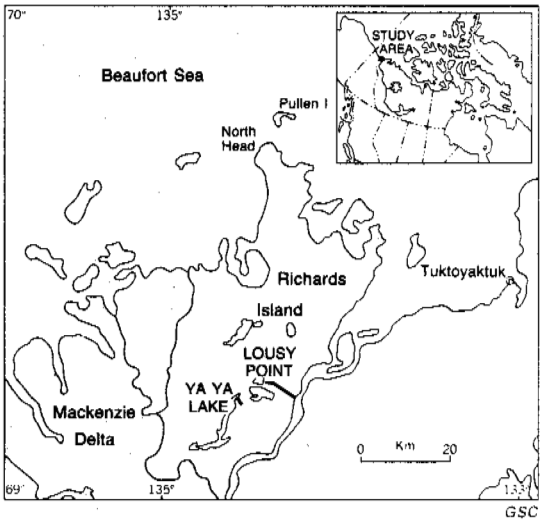

Figure 1 : Location map

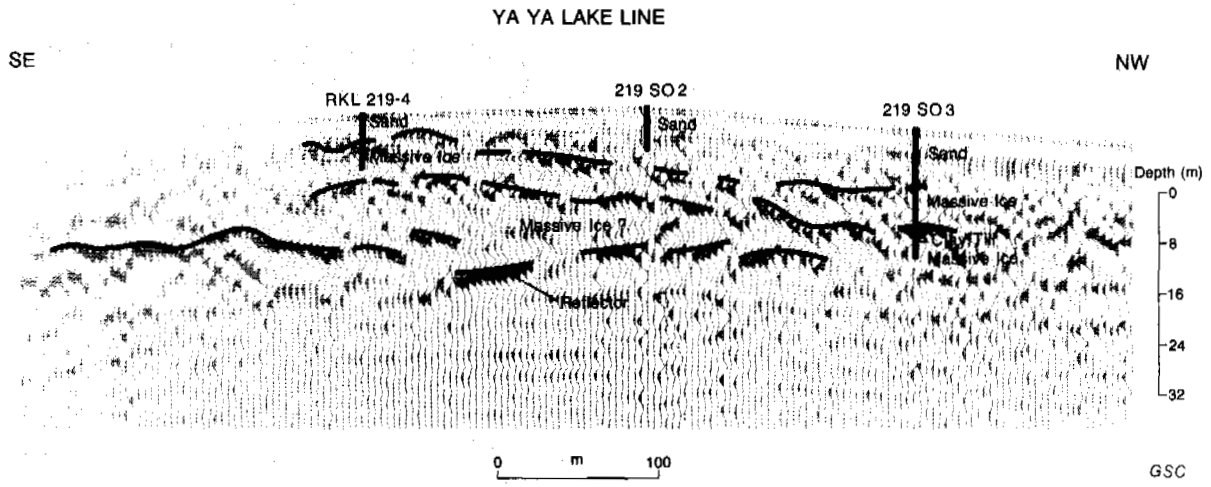

Figure 2: Radar and drilling transect, Ya Ya Lake, Richards Island, N.W.T

FIELD AND LABORATORY INVESTIGATIONS

Two areas were chosen for detailed surveys after an examination of inland and coastal exposures and a review of previous drilling data. Figure 1 shows the location of drilling and geophysical transects across an ice contact ridge near Ya Ya Lake and a glaciofluvial outwash complex near Lousy Point.

The morphology of ice bodies and associated sediments at each site was delineated with the aid of a low frequency digital ground probing radar system (Dallimore and Davis, 1987). Geotechnical drilling was undertaken using a rotary drill rig with a 10 cm diameter CRREL core barrel. Boreholes were logged and representative samples retained in the frozen state for laboratory analysis. Analyses completed on the ice samples included determination of oxygen isotope ratios ($^{18}O/^{16}O$), routine water chemistry and ice fabrics. In total, data were collected from 25 boreholes, 20 line kilometres of radar soundings and approximately 100 ground ice samples.

RESULTS

YA YA LAKE - Ice contact ridge

A discontinuous series of steep-sided, flat-topped ridges occur along the shores of Ya Ya Lake, on southern Richards Island (Figure 1). The ridges rise up to 45 m above the lake and trend northeast-southwest. Channels visible on the ridges suggest that they are composed of glaciofluvial sediments, most likely deposited in contact with glacier ice. Previous drilling in the area, carried out for the purpose of granular investigations, indicates the presence of massive ground ice beneath the ridges (Ripley et al, 1973).

Two drilling and radar transects were completed across a ridge near the north end of Ya Ya Lake. The drilling and radar data, shown on Figure 2, suggest that the stratigraphy beneath the ridge is complex with interstratified ice and sediment. Reflectors indicated on the radar records, represent changes in the velocity of propagation of electromagnetic energy. Drilling data confirm that most reflectors occur at contacts between ice and sediment.

The geology and ground ice conditions of a borehole drilled through the ridge are summarized on Figure 3. The $\delta^{18}O$ profile and natural water content values for the borehole are shown beside the stratigraphic log to aid interpretation. Two distinct ice units are recognized: a 50 cm thick layer occurs at 35 cm depth, and a 6.7 m thick layer occurs at 9 m depth.

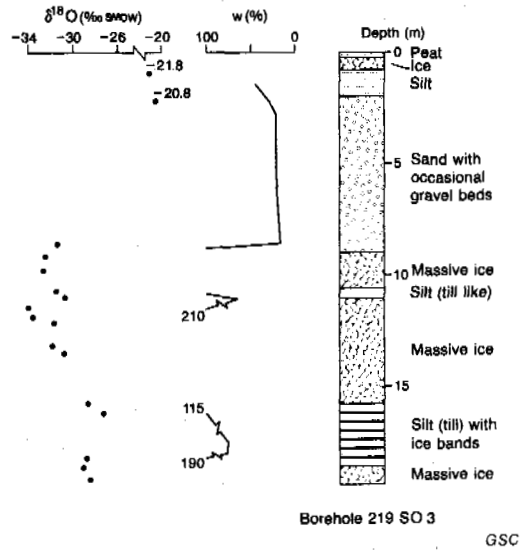

Figure 3: Borehole log of hole drilled through glacial fluvial terrace, Ya Ya Lake.

Upper ice

The 50 cm thick upper ground ice unit occurs beneath a 35 cm thick layer of peat. The ice has a horizontal structure with occasional thin bands of organic-rich silt. The depth and thickness of the ice suggests that most is situated beneath the permafrost table rather than in the active layer. Chemical analyses of the ice indicate a high conductivity and high cation content (Table 1). The Oxygen-isotope value of -21.8 ‰ for the ice (Figure 3) is similar to values reported in the Mackenzie-Beaufort area for modern ground ice (Mackay, 1983).

Table 1
Selected water-quality analyses for massive ground ice

Locality	No. Samp.	Cond. umhos/cm	+ Na	+ K	++ Ca	++ Mg
			(milligrams per l)			
Ya Ya L. 219S03						
1m	1	1573	19.0	12.7	298.6	47.8
8-12m	3	111	8.0	3.1	2.5	0.6
Lousy Pt. 216S05						
9-26m	4	197	7.6	4.1	20.8	3.8
Mackenzie River	1	150	7.8	0.9	28.2	7.2

The horizontal sediment bands, ice structure and the high conductivity and cation contents, indicate a segregated origin for this ice with a ground water source. The position at the top of permafrost suggests that the ice is probably aggradational ice which formed in the active layer and was subsequently incorporated into permafrost as the permafrost table rose (Mackay, 1977).

Other boreholes, drilled through and adjacent to the ridge indicate that the occurrence of aggradational ice is material-dependent. Of the 14 boreholes drilled on the ridge during 1986, 6 encountered a near-surface ice layer or ice-rich zone (EBA Engineering, 1986). In all six boreholes the ice-rich zone was associated with fine-grained, silty sediments while the other boreholes contained sand or gravel.

Lower ice

The upper ice and fine-grained sediments are underlain by 7 m of glaciofluvial sand with occasional gravel beds. The lower massive ice unit occurs beneath the sand (Figure 3). This ice is generally sediment free (>95% ice by volume) with occasional thin bands of disseminated grey clayey silt. Several thin layers of silty diamicton also occur within the ice and a 2.5 m thick layer of diamicton is encountered at 16 m depth. It is assumed that the diamicton and sediment contained in the ice is glacially derived since the appearance and grain size of samples collected from the borehole are similar to Toker Point Till at other sites on central Richards Island (Table 2). No borehole data are available below 20 m depth, but radar profiling suggests that the massive ice extends approximately 30 m below the surface of the ridge.

Table 2
Grain-size analyses of diamicton found in borehole 219 SO3 and Till Samples from the Ya Ya Lake area.

Sample	% > 2mm	% Sand	% Silt	% Clay
219 SO3				
10.9 m	5	24	30	41
16.0 m	4	25	33	38
17.5 m	1	37	32	30
112ROW2	2	38	29	33
113ROW3	4	28	20	52
346ROX3	3	13	43	44

Note: Samples ROW and ROX are taken from Rampton, 1988, Appendix 1.

Oxygen-18 values in the ice above the lower diamicton fluctuate between -30.6 to -34.1 ‰ (Figure 3). The lower diamicton and the ice encountered at the bottom of the borehole have more positive isotope values ranging from -27.4 to -28.8 ‰. Water quality analyses of three samples from the middle and lower ice have an average conductivity of 111 umhos with low cation contents (Table 1). Three thin sections taken from samples in the middle of the borehole show that crystal size is variable with zones of small crystals 2 to 10 mm^2 in area and coarser zones with crystals up to 8 cm^2. Determination of c-axis orientations with a universal stage suggest that the ice has a variable crystal fabric with no obvious preferred orientation but several weak maxima inclined at 30 to 60 degrees.

The likely glacially-derived sediment in the ice, the abrupt upper contact and the variable ice fabric indicate that the ice may be of glacial origin. Radar profiling and drilling indicate that the ice body has a similar morphology to the basal zones of modern ice sheets with complex interstratification of englacial debris-rich bands (Boulton, 1970). The conductivity and cation contents of the ice are similar to, but slightly higher than most data presented for modern glacial ice (Langway, 1967; Table 8), lower than modern Mackenzie River water (Table 1) and lower than data presented for massive segregated ice in the Tuktoyaktuk area by Mackay (1971). A range of 5.3 ‰ in Oxygen-18 is rather large for glacier ice but not uncommon, especially for Pleistocene ice. Hooke and Clausen (1982) for instance, report a range of up to 5 ‰ over a few metres in the basal portion of the Barnes Ice Cap on Baffin Island.

An alternative origin would be the growth of segregated ice after deposition of the till and glaciofluvial sediments. However, this seems unlikely since the configuration of the ice body is irregular, but the ridge is flat. If the ice had segregated in place between the sand and the till, the surface of the ridge would probably be hummocky and uneven, reflecting the differential thickness of the ice at depth. In addition, the oxygen isotope profile suggests fractionation did not occur.

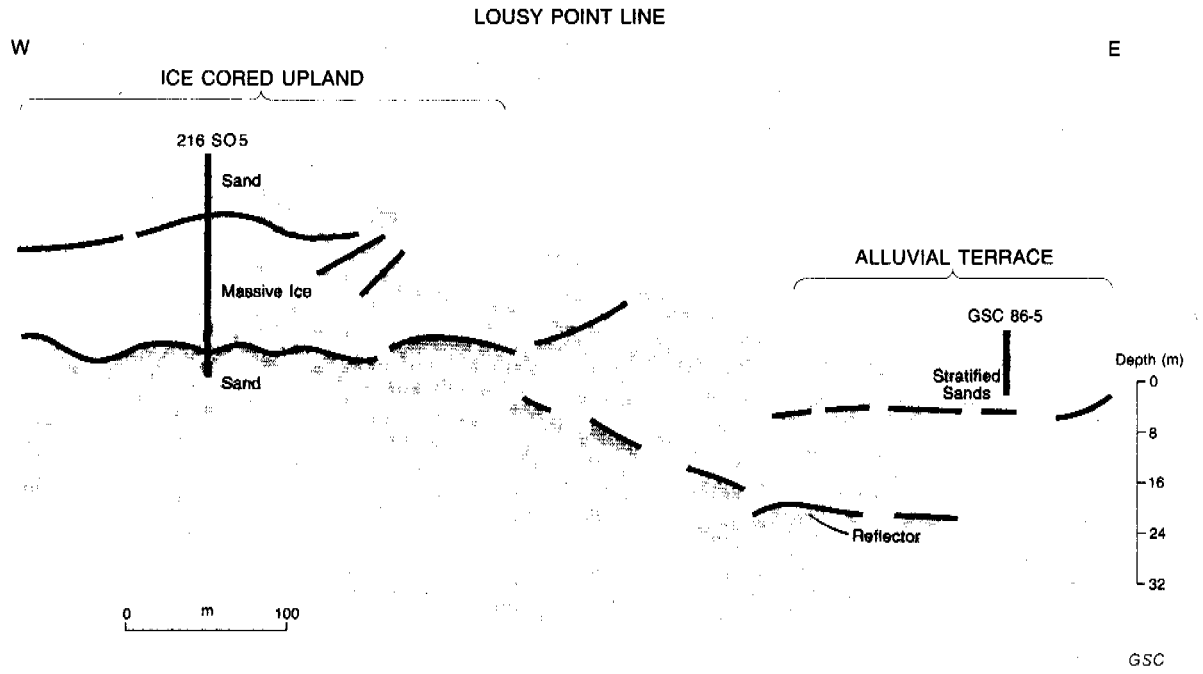

Figure 4: Radar and drilling transect, Lousy Point, Richards Island, N.W.T.

LOUSY POINT - Glaciofluvial outwash

An 11 km long drilling and radar transect was completed near Lousy Point on the east channel of the Mackenzie River. A 500 m long section of the transect adjacent to the Mackenzie River has been chosen for detailed discussion (Figure 4). It begins on a terrace of the Mackenzie River and continues over a hummocky upland area to the northwest. This upland is underlain by glaciofluvial outwash sediments deposited during retreat of Early Wisconsinan ice of the Toker Point Stade (Rampton, 1988).

The surface of the terrace is 12 m above the present level of the Mackenzie River. The fluvial sediments in the terrace are composed of ice-poor, fine-grained sand and silt with occasional organic layers. The terrace is probably related to drainage of meltwater down the East Channel of the Mackenzie River from a glacier lobe which occupied the Mackenzie Delta area for a significant period after retreat of Toker Point ice from Richards Island (Rampton, 1988).

The glacial outwash sediments in the upland areas are underlain by a thick body of massive ice. The internal structure is well defined from the radar data shown on Figure 4. The ice body appears to be relatively homogeneous with few reflectors. The base of the ice is marked by a strong reflector which is gently undulating. This probably represents an underlying sand similar to that encountered at the bottom of the borehole shown on Figure 5. The radar records and drilling suggest that the ice body pinches out towards the alluvial terrace.

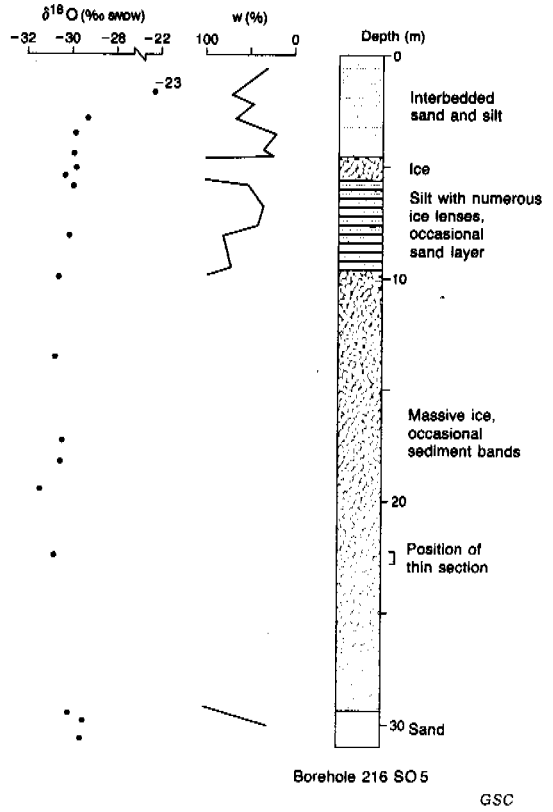

Figure 5: Borehole log of hole drilled through glacial fluvial outwash sediments, Lousy Point.

The detailed log of a borehole drilled in the glaciofluvial outwash sediments is shown on Figure 5, together with natural water contents and Oxygen isotope data. The upper 4.3 m is composed of interbedded sand and silt. The sediment immediately below is a sandy silt with alternating ice and sediment bands. A 20 m thick massive ice body occurs beneath the silt. The ice is foliated with occasional thin sediment rich zones composed primarily of disseminated fine sand and silt. Approximately 1.2 m of interbedded sand and silt with contorted bedding and ice veins occurs below the ice at the bottom of the borehole.

Thin sections were made at several locations in the massive ice, which is generally sediment poor (> 97% ice by volume) with occasional thin sediment bands of fine sand. The sediment bands dip at an angle of 10 to 15 degrees. Determination of C-axis orientations on 90 crystals indicates a preferred near vertical orientation, close to the pole of the sediment banding in the sample. The oxygen isotope data, shown on Figure 5, are relatively uniform with a range from -29.7 to -30.8 ‰. The upper silt and the upper interbedded sand and silt have similar isotope values to the massive ice, suggesting a common water origin. No fractionation pattern is readily visible. Chemical analysis of the ice, shown on Table 1, indicates it has a higher conductivity and dissolved solid content than the ice at Ya Ya Lake.

The lack of glacial sediment, and the stratified ice and sediment in the zone from 5 to 10m suggest a segregation origin for the massive ice. The preferred vertical c-axis orientation parallel to an assumed vertical heat flow direction and an apparent common water source throughout the borehole are also indicative of segregated ice. The truncation of the ice body beneath the fluvial terrace suggests that the ice pre-dates the fluvial terrace.

DISCUSSION

The occurrence of thick massive ice bodies of different origins suggests that Richards Island has experienced quite local and varied postglacial permafrost conditions. In the vicinity of the ice contact ridges at Ya Ya Lake, ground thermal and climatic conditions were such that glacial ice of the Toker Point Stade (Early Wisconsinan) has apparently been preserved to the present. At Lousy Point, glacial ice apparently melted out completely leaving a cover of glaciofluvial outwash. These sediments were subsequently frozen during permafrost aggradation forming a thick body of segregated ice. Isotope data for the ice body indicate that fractionation did not occur during ice segregation. This may indicate that an open ground water system existed.

The results of this study suggest that a major part of the present topography of Richards Island results from the presence or absence of massive ground ice at depth. Growth of segregated ground ice has raised the ground surface by as much as 20 metres. Preservation of glacial ice has probably maintained many supra-glacial features. It is quite possible for instance, that some of the high level drainage features on the island may be supra-glacial drainage patterns which have been preserved since Early Wisconsinan times.

The presence of massive ice in association with glaciofluvial materials presents obvious limitations in terms of extraction for construction materials. Borrow areas must be carefully planned to prevent thaw of buried ice bodies or plans should be made to utilize their thaw during site restoration. Geotechnical investigations for pipeline routes or other development activities should consider the distribution of massive ground ice in glaciofluvial sediments and in other surficial materials on Richards Island. Information about the origin of the ice bodies will aid in predicting their extent and characteristics.

CONCLUSIONS

Substantial volumes of massive ground ice are found in association with glaciofluvial sediments on central Richards Island. Although the two sites discussed in this paper are only 12 kilometres apart massive ground ice differs substantially in morphology, sediment association and chemistry, suggesting a different origin for the ice bodies.

A thin layer of recent ground ice was encountered near the surface of an ice contact ridge at Ya Ya Lake. This ice was most likely initially formed at the base of the active layer and has been incorporated into permafrost due to recent climatic cooling. The massive ground ice encountered at depth at Ya Ya Lake is most likely glacial ice which was covered and ultimately preserved by a mantle of glaciofluvial sediments. Since this portion of Richards Island was not glaciated during the Late Wisconsinan, it is probable that this ice is preserved Early Wisconsinan glacial ice of the Toker Point Stade. Massive ground ice in glacial outwash sediments near Lousy Point was likely formed as a result of ice segregation during local permafrost aggradation sometime after deglaciation in the area but before deposition of a fluvial terrace.

ACKNOWLEDGEMENTS

The field work upon which this paper is based has been supported by the Northern Oil and Gas Action Program and the Panel for Energy Research and Development. Logistical assistance has been provided by the Polar Continental Shelf Project and the Inuvik Resource Centre. The writers would like to thank C.R. Burn, P.A. Egginton, V.N. Rampton, J.S. Vincent, and an anonymous reviewer for comments on the manuscript. The field assistance of J.G. Bisson, F.M. Nixon, and the staff of A-Cubed Inc., EBA Engineering, and Midnight Sun Drilling is also acknowledged.

REFERENCES

Boulton, G. S. (1970). On the origin and transport of englacial debris in Svalbard glaciers. Journal of Glaciology, Vol. 9, N.56, 213-229.

Dallimore, S.R. and Davis, J.L. (1987). Ground Probing Radar Investigations of Massive Ice and Near Surface Geology in Continuous Permafrost. In: Current Research, Part A, Geological Survey of Canada, Paper 87-1A, 913-918.

EBA Engineering Consultants Ltd. (1986). Granular resource evaluation, Richards Island, N.W.T. Indian and Northern Affairs, Canada, Community Granular Inventory Series, 32p.

Hooke, R.L. and Clausen, H. (1982). Wisconsin and Holocene 18 O variations, Barnes Ice Cap, Canada. Geological Society of America Bulletin, Vol. 93, 784-789.

Langway, Jr. C.C. (1967). Stratigraphic analysis of a deep ice core from Greenland. U.S. Army, Cold Regions Res. and Engineering Lab. Res. Rept. 77, 133p.

Mackay, J.R. (1963). The Mackenzie Delta Area, N.W.T.. Canadian Department of Mines and Technical Surveys, Geographical Branch, Memoir 8, 202 p.

Mackay, J. R. (1966). Segregated Epigenetic Ice and Slumps in Permafrost Mackenzie Delta Area, N.W.T. Geographical Bulletin, Vol. 8, No. 1, pp. 59-80.

Mackay, J.R. (1971). The origin of massive icy beds in permafrost, western Arctic Coast, Canada. Canadian Journal of Earth Sciences, Vol. 8, P. 397-422.

Mackay, J. R. (1977). Ground Ice in the Active Layer and Top Portion of Permafrost. National Research Council of Canada Associate Committee on Geotechnical Research, Proceedings of a Seminar on Permafrost Active Layer, Technical Memorandum No. 103, pp. 26-30

Mackay, J.R. (1983). Oxygen Isotope Variations in Permafrost, Tuktoyaktuk Peninsula Area, N.W.T.. In: Current Research, Part B, Geological Survey of Canada, Paper 83-1B, pp.67-74.

Pollard, W.N and French, H.M. (1980). A first approximation of the volume of ground ice, Richards Island, Pleistocene Mackenzie Delta, N.W.T., Canada, Canadian Geotechnical Journal, Vol 17, 509-516.

Rampton, V.N. (1973). The influence of ground ice and thermokarst upon the geomorphology of the Mackenzie-Beaufort Region. In: Research in Polar and Alpine Geomorphology; Proceedings, 3rd Symposium on Geomorphology, Fahey, B.D. and Thompson, R.D. Eds. pp. 43-59.

Rampton, V.N. (1988). Quaternary geology of the Tuktoyaktuk coastlands, Northwest Territories. Geological Survey of Canada, Memoir 423, 103p.

Rampton, V.N. and Mackay, J.R. (1971). Massive ice and icy sediments throughout the Tuktoyaktuk Peninsula, Richards Island and nearby areas, District of Mackenzie, N.W.T. Geological Survey of Canada, Paper 71-21, 16p.

Rampton, V.N and Walcott, R.I. (1974). Gravity Profiles Across Ice-Cored Topography. Canadian Journal of Earth Sciences, Vol. 11 pp. 110-122.

Ripley, Klohn and Leonoff International Ltd. (1973). Granular Materials iventory, Zone II. Indian and Northern Affairs, Canada, Community Granular Inventory Series, 73p.

Taylor, A.E., Burgess, M., Judge, A.S. and Allen, V.S. (1981). Canadian Geothermal Data Collection-Northern Wells. Energy, Mines and Resources, Earth Phyisics Branch, Geothermal Series N. 13.

GSC Contribution No. 51187

PERMAFROST AGGRADATION ALONG AN EMERGENT COAST, CHURCHILL, MANITOBA

L. Dyke

Department of Geology, Queen's University, Kingston, Ontario, Canada K7L 3N6

ABSTRACT Permafrost along isostaticly emerging coasts must be aggrading into land as it becomes exposed in the tidal zone. The initiation of permafrost has been shown, by borehole temperature measurements, to occur in the upper half of the tidal zone at Churchill, Manitoba. A theoretical model, based on the extrapolation of a single surface temperature history, provides a prediction of permafrost extent that may be accurate enough to be of use in reconnaissance site investigations.

SIGNIFICANCE OF EMERGING COASTS

Permafrost along an isostaticly emerging coast must be aggrading as a wedge-shaped body into previously unfrozen seabottom. Mackay (1971) predicted the extent of this body with the aggradation beginning at mean sea level. Allard et al. (this volume) have examined the tidal zone of permafrost coasts in detail to determine controls on permafrost distribution in that environment. Ice bonding of coastal sediments or rock may be significant in determining foundation conditions for coastal facilities. For this reason, a detailed knowledge of permafrost distribution at the coastline may be required. This study is an attempt to predict the distribution of permafrost between high and low tide along an emerging coast where permafrost is established onshore.

As a point on the seabottom rises into the tidal zone, it begins an exposure to permafrost-forming conditions. By the time the high tide level is reached, exposuure is continuous so aggradation of permafrost must be underway. Therefore at some point in the tidal zone, permafrost must begin to form. If this point can be located and if the rate at which permafrost thickens can be determined, then the distribution of this permafrost will be known.

For a sea coast, other factors besides climate that will control the distribution of permafrost are tidal range, emergence rate, and topographic profile. Heat transfer from the seabottom to the air is aided in winter where sea ice is in contact with the seabottom. This effect has been shown to influence the extent of frozen seabottom in the Mackenzie Delta area (Mackay, 1972; MacDonald et al., 1973; Dallimore et al., this volume). Depending on the thickness of ice and the tidal range, ice may contact the seabottom at levels below low tide, therfore exerting an additional contral on seabottom temperature outside the tidal zone. Thermal properties of subsurface rock or soil are also important but will be most influential in determining the thickness of permafrost rather than its presence or absence.

APPROACH TO THE PROBLEM

The determination of the exact distribution of permafrost requires temperature measurements or borehole sampling. However permafrost thickness can be predicted as the penetration of freezing from the surface if a history of surface temperature is available. This approach is followed in this study but with a view to minimizing the data required. To do this, temperature data from one point in the tidal zone is extrapolated across the tidal zone. The extrapolation is carried out by assuming that the modification to the measured temperature can be attributed to the different times that other points across the tidal zone are submerged and to the heat taken up in melting the sea ice. The accuracy of the technique is tested by comparing the prediction to borehole temperature mesurements. The agreement is close enough that the technique may be useful for comparing coastal sites for a reconnaissance site investigation.

DESCRIPTION OF THE STUDY SITE

Churchill, Manitoba was selected as the initial site for establishing the extent of the coastal permafrost wedge and developing a technique for predicting the wedge geometry. Onshore, permafrost is well established in bedrock and is probably 50 to 100 m thick, based on comparisons with other climates where the depth of permafrost is known (Brown, 1963). Permafrost is also found in glacial deposits in the area but is no colder than $-1^{o}C$ where shrubs or standing water exist (Brown, 1978).

Several pieces of evidence suggest that isostatic adjustment to the retreat of the last glaciation is still occurring at Churchill. A discussion of this evidence by Hansell et al. (1983) favours an emergence rate of about 0.8 m per century. However, comparing the advance of distinctive bands of flora visible on both 1929 and 1978 airphotos indicates a rate of 1.0 m per century. This figure compares favourably with the prediction of Peltier (1987) and is assumed correct in this study.

Tidal variation in sea level at Churchill is commonly 4 m, occasionally reaching 5 m. In the esturary of the Churchill River and along the Hudson Bay coast, low tide exposes a tidal flat up to 2 km wide. This provides a tidal zone wide enough to ensure that the existance of permafrost in the tidal zone is in no way influenced by onshore permarost. Accordingly 8 cables equiped with thermistors were placed along a 1.2 km line extending from approximately 5 m above high tide to 2 m below high tide in the Churchill River esturary (Fig. 1). The cables extend to depths of 6 to 10 m.

The line of temperature cables begins on one of a series of raised beaches supporting forest tundra vegetation: scattered spruce with a mat of lichens, moss, sedges, and very low rhododendron. The beaches give way to a

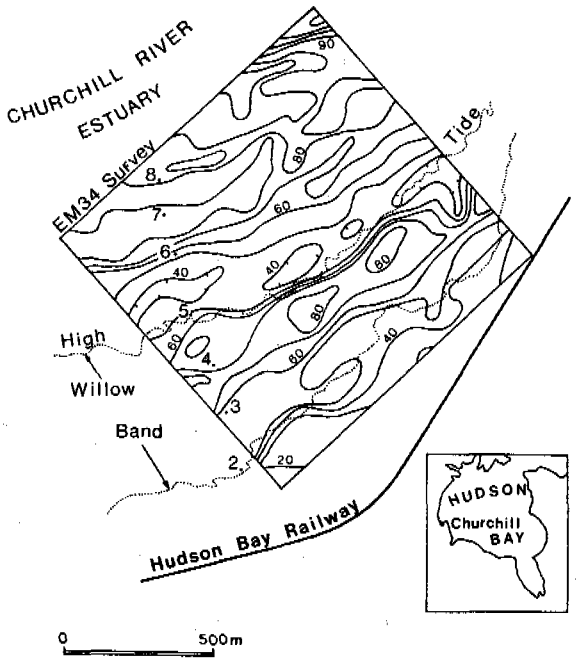

Figure 1. Location of temperature cables (2 to 8) and contours of electrical conductivity (in mmhos/m) obtained from EM34 survey

band of willows up to 2 m high. This willow band occupies hummocky terrian down to extreme high tide. A sedge-covered tidal meadow, dissected by tidal channels, then appears. Gravelly to bouldery flats replace the meadow about 1 m below extreme high tide. Subsurface materials consist primarily of silt with varying fractions of sand and clay. Pebbles and boulders are common.

This study assumes that seabottom below low tide is free of ice-bonded permafrost. While bottom temperatures down to -1.6°C have been recorded for Hudson Bay (Pelletier, 1969), this temperature is not low enough to induce ice bonding in pore water of oceanic salinity. Water of the Churchill River undoubtedly averages above this temperature and in fact may delay the initiation of permafrost relative to the open Hudson Bay coast. Test borings for the port facilities at Churchill reported no ice bonding. The estuary site was chosen in view of the protection it offered against damage to cables by ice movement.

DELINEATION OF TIDAL ZONE PERMAFROST

Temperature measurements have been carried out since the summer of 1985. Readings taken between late June and early November (1985) show that a zone remaining below 0°C exists in the upper half of the tidal zone (between cables 5 and 8) for this time interval (Figures 2, 3, and 4). Because temperatures in this zone were rising on the late June reading and falling by the early November reading, it is probable that a year-round zone remaining below 0°C does exist. This has been verified for the succeeding year and so identifies tidal zone permafrost based on the 0°C criterion.

Moving landward, a talik, coinciding with the willow band, is identified. Standing water and snow to a depth of approximately 1 m respectively take up heat and insulate during freezing. Taken in the context of an emerging coast, this talik is a dynamic feature, and it introduces a complication into an otherwise

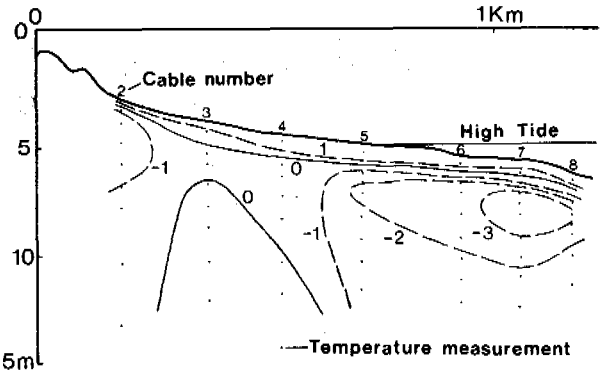

Figure 2. Contours of temperature along temperature cable transect for June 20, 1985. Dots show location of temperature measurements.

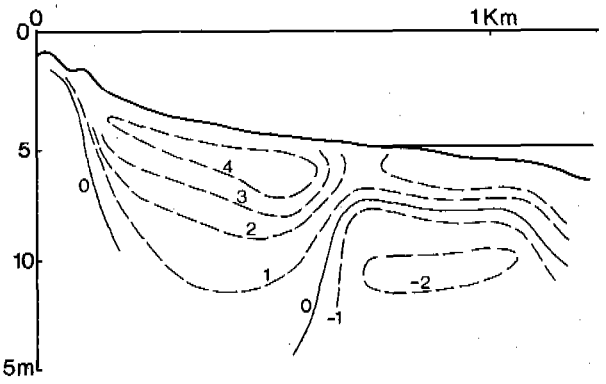

Figure 3. Contours of temperature along temperature cable transect for October 1, 1985.

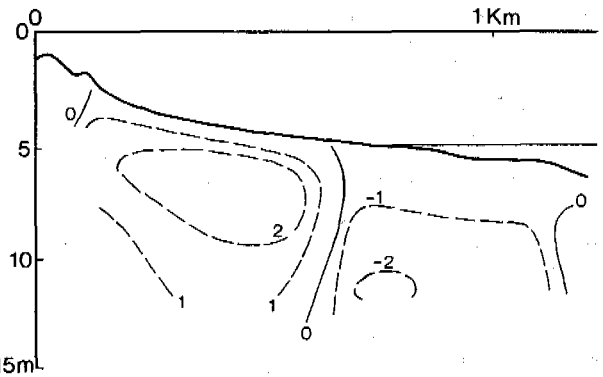

Figure 4. Contours of temperature along temperature cable transect for November 1, 1985.

progressive aggradation of permafrost. This was not anticipated and it serves to show that, for the Churchill climate, conditions immediately onshore are just as important in determining permafrost development as in the tidal zone.

The identification of ice-bonded permafrost is more difficult. Freezing point depression of sediment pore water undoubtedly occurs. It results from the salt content and small pore size associated with the clayey silt materials. Examination of any of the temperature logs for cables 5 to 8 shows that below about 3 m temperature varies little from -2°C. This is a damping

associated with uptake or production of latent heat at a temperature that probably represents the freezing point depression experienced by the pore water. It is likely that some water is always present because temperatures never rise above the narrow variation about -2°C. The existance of a steep thermal gradient within the active layer down to temperatures of -3°C (Figure 2) also suggests that considerable freezing is taking place down to temperatures that low.

The existance of the talik and tidal zone permafrost are supported by inductive electrical conductivity readings straddling about 1 km of coast and including the borehole transect. A survey in August, 1984, taken with a Geonics EM31, showed low conductivity coincident with the beach ridge zone and upper part of the tidal zone. Higher conductivities coincided with the willow band. To interpret this survey, the active layer, permafrost, and underlying frozen ground become members of a layered earth.

The EM31 receives most of the contibution to its conductivity reading from the first 6 m below the surface. The contibutions receive the greatest weighting nearest the surface. Therefore this survey essentually reflects variations in the depth to the frost table and is most suitable for interpretation as two layers. The talik appears as a very thick thawed layer which can best be interpreted as the absence of permafrost.

An EM34 survey was conducted in mid-June of 1985, effectively receiving input to a depth of 15 m. (20 m coil separation, horizontal dipole). It reproduces the general pattern of the EM31 survey but in a much smoother fashion (Figure 1). This may be the result of the lower weighting given to variations in pore water salinity associated with tidal creeks. The low conductivity band in the upper tidal zone has gained prominence, in accordance with the greater contibution the frozen zone should make to the deeper soundings. The survey shows that the tidal zone permafrost detected by the temperature measurements extends parallel to the coast and seems to be a characteristic of the tidal zone. An interpretation of permafrost thickness, assuming that the variation in conductivity relects changes in the thickness of frozen ground, is shown in Figure 5. This interpretation was

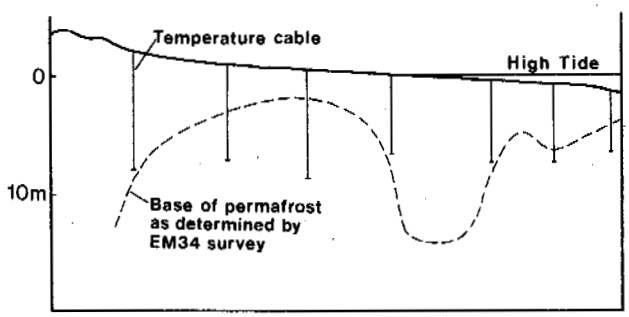

Figure 5. Base of permafrost along temperature cable transect as interpreted from EM34 survey.

made using a conductivity of 20 umho/cm for ice-bonded permafrost based on conductivity readings for sediments with little active layer development. 100 umho/cm was used for thawed ground, based on readings taken well seaward of the supposed wedge of permafrost.

PREDICTING THE EXTENT OF TIDAL ZONE PERMAFROST

At the Churchill site it is assumed that land emerges at a temperature slightly above freezing (1°C) to become impressed with freezing air temperatures of increasing severity as time below tidal waters decreases. Frost or thaw penetration can be predicted by solving a one-dimensional equation that balances heat flux on either side of a freezing or thawing boundary and latent heat produced or absorbed (Andersland and Anderson, 1978). In this case the solution used gives the depth of the 0°C temperature. The following thermal properties for a saturated clayey silt with 30% moisture content were considered to be representative of the tidal zone soil at the Churchill site:

Thermal conductivity, unfrozen	1.25 W/m°C
Thermal conductivity, frozen	2.00 W/m°C
Volumetric heat capacity, unfrozen	0.75 cal/°C cm^3
Volumetric heat capacity, frozen	0.50 cal/°C cm^3
Diffusivity, unfrozen	0.004 cm^2/s
Diffusivity, frozen	0.010 cm^2/s

Permafrost will exist for the case where the first year's freezing depth is not reached by the subsequent thaw. Freeze and thaw penetrations can then be calculated for several positions across the tidal zone to delineate the extent of permafrost.

Predicting freezing or thawing depths requires the use of an impressed freezing or thawing temperature. Freezing and thawing indices determined from meteorological records are inadequate because thermal transfer from the air to emerging seabottom is modified by the growth and decay of sea ice as well as the time that any point in the tidal zone is submerged. In this study the problem of determining thermal transfer is avoided by using temperatures from the shallowest thermistors to estimate freezing and thawing indices. These indices are then applied as an average temperature above or below freezing for the time interval for which temperatures average above or below freezing (140 and 225 days respectively for Churchill). Freeze and thaw penetration below the depth of the thermistor can then be calculated.

Because temperature measurements are not available throughout the tidal zone, a method for extrapolating those temperatures available was devised. The duration of tidal modification of an impressed temperature can be approximated as a sinusoidal function of distance from the high tide line. Therefore, if impressed temperatures are known at two points in the tidal zone, a sinusoidal curve can be used to interpolate temperatures. This was done using the temperaure record from the shallowest thermistor of cable 6 (cable position 0.5 m below high tide level) and an estimated temperature at the low tide level (Figure 6). A temperature slightly above freezing

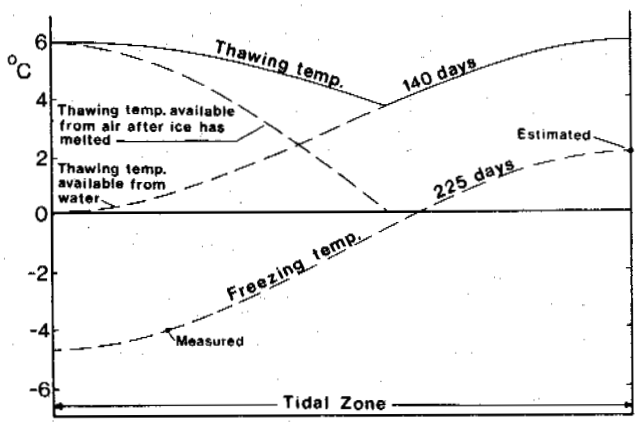

Figure 6. Freezing and thawing indices used for calculating freeze and thaw depth at any point in the tidal zone at Churchill.

(2°C) was used for the low tide point, based on the assumption that it is always in contact with water.

The thawing portion of the year was also treated by extrapolating a subsurface thawing index. However the extrapolation must take into account the heat taken up in melting the previous winter's sea ice.

The thickness of ice in the tidal zone will be controlled by the time water is available to be frozen. Using the meteorological freezing index for Churchill and the time of inundation for any point in the tidal zone, ice thicknesses were calculated (Figure 7).

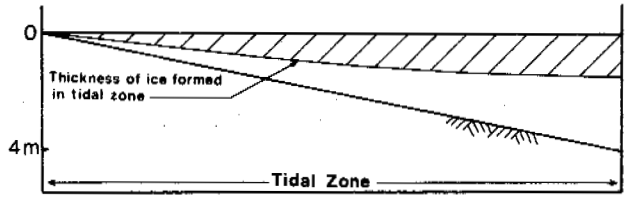

Figure 7. Maximum thickness of sea ice across the tidal zone that would develop for Churchill conditions.

thawing degree days required to thaw this ice can then be subtracted from the total available to arrive at a curve showing thaw index remaining (Figure 6). It was assumed that the thawing index available could be derived from the shallow thermistor record for the cable located at the high tide level.

Heat for thawing is also derived from the tidal waters. Based on observed values for the Mackenzie River (Mackay, 1972) and La Grande Riviere (Freeman et al., 1982), an available thawing temperature of 6°C was assumed for the low tide level. At the high tide level a thawing temperature of 0°C was assumed since no heat should be available from this source. A sine curve was again fitted to interpolate the water thawing index throughout the tidal zone (Figure 6). This curve and the curve giving the thawing index remaining after the thaw of sea ice were added to give an impressed thawing temperature across the tidal zone (Figure 6).

The curves showing freezing and thawing index can now be used to predict the location of permafrost in the tidal zone. The approach taken is to calculate the depth of freezing in an unfrozen soil suddenly subjected to a freezing temperature on emerging from Hudson Bay at 1°C. The freezing temperatures arrived at as described above, are used. The frozen soil is then subjected to a thawing temperature and any ground remaining frozen is considered to be permafrost (Figure 8).

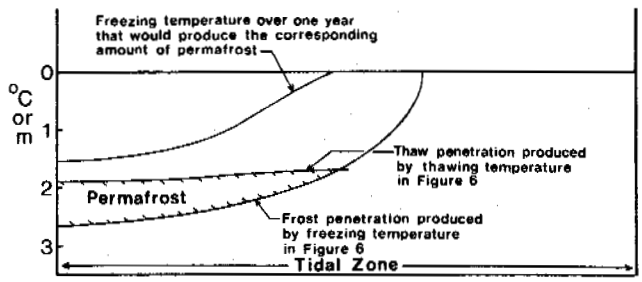

Figure 8. Extent of permafrost that would form in one year if freezing and thawing indices in Figure 6 were applied to ground initially at 1°C. The upper curve gives the equivalent constant temperature required to produuce the corresponding thickness of permafrost.

The estimate of thawing temperature in Figure 6 is characterized a minimum in the central part of the tidal zone. When applied to the determination of permafrost, this minimum is expressed as a slight decrease in the active layer thickness (Figure 8). This retardation of thaw is supported by temperatures from the late June, 1985 readings (Figure 2). The coldest ground temperatures at this time are beneath an area well into the tidal zone. These two features suggest that an area for optimum retardation of thaw exists where a relatively large ice thickness has been reached before warming by tide water has become dominant.

The thickness of permafrost produced by the hypothetical single freeze-thaw cycle provides a basis for predicting the subsequent deepening of permafrost. For any point in the tidal zone, the decrease in freezing temperature required to advance the freezing front from the top to the bottom of the permafrost body can be used to determine an equivalent temperature that would produce the corresponding thickness of permafrost. This was done for the Churchill case and the associated temperatures are shown in Figure 8. These temperatures can then be used to predict the thickness of permafrost after any time interval.

When a point in the tidal zone reaches the high tide level, a considerable time will have elapsed since that point rose to the level allowing the onset of permafrost. That time interval is determined by multiplying the elevation difference by the emergence rate. To estimate the depth of permafrost beneath the high tide point, the average temperature during this time interval can be applied. The geothermal heat flux (using a value of 0.042 W/m^2, Judge, 1973) is simultaneously applied to determine the depth at which permafrost aggradation would be matched by this heat source. This gives the depth at which aggradation would cease. Intermediate points can be similarly treated. The resulting extent of the permafrost wedge is shown in Figure 9. Other emergence

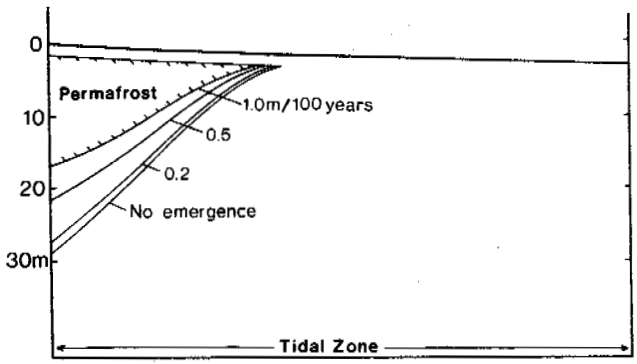

Figure 9. Extent of tidal zone permafrost for different emergence rates at Churchill.

rates are similarly treated by simply applying the corresponding time intervals that given points in the tidal zone have been above the permafrost initiation level.

CONCLUSION

The initiation of permafrost along an isostaticly emerging coast has been shown to occur in the upper half of the tidal zone at Churchill, Manitoba. The prediction of permafrost extent in the tidal zone for Churchill agrees well enough with observation to justify testing the technique at other coastal locations. The analysis is empirical in its extrapolation of measured temperatures throughout the tidal zone and lack of strict accounting

for various components of heat transfer across the ground surface. However the amount of data required to apply it is small, consisting marily of one year's record of temperature from a point at or close to the land surface. If the technique is accurate when applied to a locality with a different climate, then its use as a site investigation tool will be justified.

ACKNOWLEDGEMENTS

This work is the partial result of a contract carried out at the direction of the Geological Survey of Canada. Alan Heginbottom, as scientific authority for the contract, provided enthusiastic and helpful commentary at all stages. The success of the work would not have been possible without the supervision of borehole drilling by Mark Nixon and the field assistance of Robert Bracken, Suzanne Szojka, and Bruce Tucker.

REFERENCES

Andersland, O.B. and Anderson, D.M. (1978).Geotechnical Engineering for Cold Regions. McGraw Hill Company Limited, New York.

Brown, R.J.E. (1963). Relation between mean annual air temperature and ground temperature in the permafrost regions of Canada. Proceedings, International Conference on Permafrost, pp. 241-247.

Brown, R.J.E. (1978). Influence of climate and terrain on ground temperatures in the continuous permafrost zone of northern Manitoba and Keewatin District, Canada. Proceedings, Third International Conference on Permafrost, vol. 1, pp. 15-21.

Freeman, N.G., Roff, J.C., and Pett, R.J. (1982). Physical, chemical, and biological features of river plumes under ice cover in James and Hudson Bays. Naturaliste Canadien, vol. 109, pp. 745-764.

Hansell, R.I.C., Scott, P.A., Staniforth, R., and Svoboda, J. (1982). Permafrost development in the intertidal zone at Churchill, Manitoba. Arctic, vol. 36, pp. 198-203.

Judge, A.S. (1973). The prediction of permafrost thickness Canadian Geotechnical Journal, vol. 10, pp. 1-11.

Mackay, J.R. (1971). The origin of massive icy beds in permafrost, western Arctic Coast, Canada. Canadian Journal of Earth Sciences, vol. 8, pp. 397-422

Mackay, J.R. (1972). Offshore permafrost and ground ice, southern Beaufort Sea, Canada. Canadain Journal of Earth Sciences, vol. 9, pp. 1550-1561.

MacDonald, B.C., Edwards, R.E., and Rampton, V.N. (1973). Position of frost table in the near-shore zone, Tuktoyaktuk Peninsula, District of Mackenzie. Current Activities, Geological Survey of Canada Paper 73-1B, pp. 165-168.

Pelletier, R.B. (1969). Submarine physiography, bottom sediments, and models of sediment transport in Hudson Bay. Earth Science Symposium on Hudson Bay, Geological Survey of Canada Paper 68-54, pp. 100-135.

Peltier, W.R. (1987). Mechanism of relative sea level change and the geophysical responses to ice-water loading. R.J.N. Devoy, Ed., Sea Surface Studies, a Global View, Croom Helm, London, pp. 57-94.

CHARACTERISTICS OF THE MASSIVE GROUND ICE BODY IN THE WESTERN CANADIAN ARCTIC (11)

Fujino, Kazuo[1], Sato, Seiji[2], Matsuda, Kyou[3], Sasa, Gaichirou[3], Shimizu, Osamu[3] and Kato, Kikuo[4]

[1]Institute of Low Temperature Sci., Hokkaido University, Sapporo, Japan
[2]Faculty of Science, Hokkaido University, Sapporo, Japan
[3]Faculty of Agriculture, Hokkaido University, Sapporo, Japan
[4]Water Research Institute, Nagoya University, Nagoya, Japan

SYNOPSIS Massive ground ice bodies are one of the typical ground features in the Arctic region. However, their origin and formation processes are still arguable. In this paper, we conclude that most parts of the ice body which lies on the sand layer formed by superimposed ice. And the sediment between strata of ice was formed at an ablation stage of the ice body. Through intermittent repetitions of ablation and accumulation processes, the ice mass developed with recognizable strata which correspond to the discontinuities in ice fabrics and chemical compositions.

INTRODUCTION

Massive ground ice bodies are one of the typical periglacial ground features in the Arctic region. However, their origin and formation processes are still arguable. There are three following hypotheses as their origin(French,1976).1)snow-glacial/buried ice; 2)syngenetic ice wedges; 3)segregated ice. Among these three, the ice segregation hypothesis which has been proposed by Mackay(Mackay,1971) has been supported by many scientists in this field.

During the joint research expeditions from 1977, authors found that the mechanism of its growth is not identical to that of the growth of the pingo in which segregated ice constitutes the core(Fujino,1978),and concluded that the most parts of the massive ice body originate from superimposed ice formed by congelation of water in which it was submerged(Fujino,1983).

For obtaining more detailed information on massive ground ice bodies, the research project was carried out with geophysical, geochemical and geological conceptions in 1984, 1985(Fujino,1986),1986 and 1987.

In this paper, authors report the results obtained those for from analyses of the stratigraphic features of the ice body together with ice fabrics, pollen grains and geochemical components.

SAMPLING

The location of the massive ice body investigated is denoted by * in Fig. 1, along a seacoast about 4.5 km southwest of Tuktoyaktuk, Mackenzie Delta, N.W.T., Canada, and detailed topographic map of the massive ground ice body is shown in Fig.2.

Using a mechanical core drill, samples were collected from the till layer overlying the ice body. Observations were also carried out of the striations in the ice body,together with the sampling of the till, at the outcropping ice cliff marked by * in Fig. 2.

Observations were also made of the conformity between the till layer and the ice body along the outcropping ice cliff.

Soil samples collected were prepared for the determinations of chemical components, soil types and impurities including pollen grains.

Using an electromechanical core drill, three holes were drilled into the massive ice body. The location of each hole was shown in Fig.2. At the hole, W-3, an ice core was obtained throughout the massive ice body. The total length was 21.5 m including a 0.4 m-thick sand layer of the bed.

Cores obtained were arranged and labeled in serial order, and transported to the Institute of Low Temperature Science, Hokkaido University,where the following preparations and analyses were made.

Each piece of the cores was cut into halves along the vertical axis. One half of the core was cut perpendicular to the axis at an interval of 10 cm, from which horizontal and vertical thin sections were prepared for

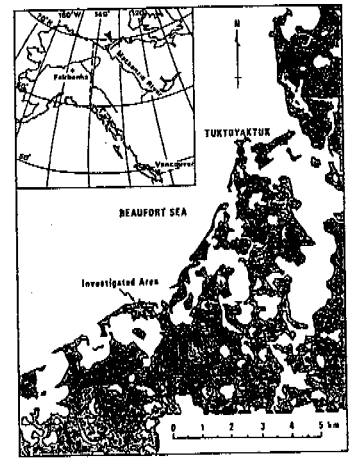

Fig. 1. Location map of Tuktoyaktuk area; *: the massive ground ice body subjected to sampling

crystal orientations and also stratigraphic features. Meanwhile, the other half was cut perpendicular to the axis at an interval of 5 cm, and were prepared for the determination of chemical components such as total numbers of ions, oxygen isotopes, etc. Moreover, soil between strata which form a boundary of the bandlike structure,as well as any impurity inclusions such as pollens and organic materials were also subjected to analyses.

ANALYSES

1) Ice core: A schematic description of the entire length of the core obtained from a hole,W-3,is shown in Fig. 3.

Ice crystals in each stratum were distinctly different in size, shape and c-axis orientation.

Distributions of air bubbles in the strata were also not uniform. Air bubbles in the strata were mostly spherical; however, many of them were deformed and had a flat face which was formed by vapor growth in the bubble. Fine Tindal figures hexagonal in shape were also observed in some strata, as shown in Fig. 4. Several strata abounded in the same elongated bubbles.

Sediment contained in layers either between adjacent ice strata or in the strata mainly consisted of sand, clay/silt or their mixtures. Configurations of the sediment had various forms as observed. Moreover, most of them abounded in pollen grains which were distinctly different from those in the till layer overlying the ice body.Three layers of sediments of them abounded in more than 3 mg of elemental carbon which is the detection limits of the tandem AMS.

2) Till layer: The soil sediment overlying the ice body consisted of two layers. The upper layer, about 50 cm in thickness, was a mixture of grass roots, peat and clay. Beneath that layer, a heavy clay layer of light gray color lay on the ice body. The clay layer was composed of clay, silt and the round pebbles which were contained sporadically. This layer is considered to be till or re-worked till.

When an ice body is exposed, it suffers thermal erosion and recession. Then, an overlying till layer collapses on the surface of the ice body losing its support and turns into fluid mud by mixing with melt water. The mud flows downslope on the ice body by solifluction and covers the eroded surface of the ice body. Thus, a newly deposited mud layer forms a secondary deposited plane on the eroded surface of the ice body.These secondary deposited layers can be observed commonly around the hill, either old or new, especially near the ice cliff and easily distinguished from the original till layer, because these layers usually lack the surface layer made of peat and grass roots.

Observations were made of the conformity between the ice body and the overlying till layer along the outcropping ice cliffs. There are many striations intercalted in the ice body, which are composed of various soil mixtures. From these striations, either conformity or unconformity is easily identified; that is, the striations in the ice body were cut by the basal plane of the sediment overlying it and the unconformity formed between them. There are some such unconformities between the ice body and the till layer which is considered to be original, as shown in Fig. 5.

3) Fossil pollen grains: Fossil pollen are found abundantly in the overlying till layer. Most of them are those of the Tertiary and pre-Tertiary Ages which had eroded out from rocks. There are a few pollen grains which were transported in the air. One sample, for instance, collected from a till layer contained a pollen assemblage with the following composition: Betula 48 %, Alnus 38 %, Picea 4 %, Pinus 1 %, Carpinus 1 %, Ericaceae 16 %, etc. (Sample No. 8408713)

Pollen grains in the ice body can be divided into two groups when observed under the microscope, that is, pollen grains of group A are transparent in color and well preserved and are mostly composed of Picea and Pinus, easily discriminated from the other group, pollen grains of group B are yellow-dark brown in color and preserved not so well in general, most of them being pre-Quatenary in age and deprived of fossils. The results obtained for pollen grains in the ice body are shown in Fig. 6.

As is clear from the Fig. 6, a large variation is found in the pollen contents of group A, which is considered to have been transported in the air;in each horizon of the ice core, the pollen contents are higher in the lower part of the core, becoming lower in the upper part generally, with an exception of Sample 6 - 2.

4) Chemical compositions: Determination of Cl^-, SO_4^{2-}, etc. in ice samples were carried out together with that of ^{18}O throughout the ice body.The results were shown in Fig. 7.

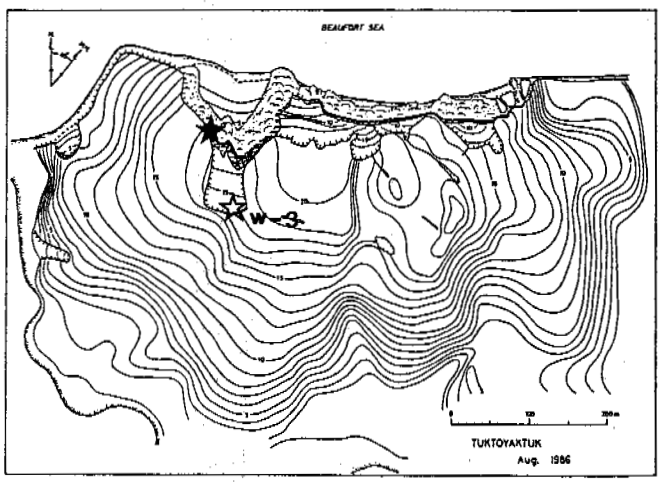

Fig. 2. Detailed topographic cap of the massive ground ice body survey in 1986

As is clear from the Fig. 7, the long-and short-term variations of ^{18}O were observed in the profile, and also distinct changes in chemical components were observed in it.
Determination of radiocabon date was carried out on organic materials contained in the layers of sediments in the ice body, and also on two wood fragments collected in the till layer overlying the ice body.
The sediments in three layers, 11.2, 21.2 and 21.5 m in depth, abounded in the elemental carbon and dated at 14270, 17000 and 17040 years B.P., respectively. Those of two wood fragments were 7520 and 9880 years B.P..

DISCUSSION

Much discussion has been made as to whether the massive ground ice body is a buried glacier, a snow bank ice body or a segregated ice body which has grown in place or an ice body frozen from bulk water injected under pressure into frozen or unfrozen sediment(Mackay,1971).
The arguments against the buried glacier or the snow bank ice body are: 1) some massive ground ice bodies are in unglaciated areas, 2) some massive ground ice bodies are found in lacustrine and marine sediment or they lie beneath topographic hights where burial would be difficult to explain, 3) salinity of most of the massive ground ice bodies is far greater than that of glacier ice, 4) the ice petrofabrics are similar to those of thin ice lenses of segregated ice, and 5) vertical profiles of the ionic contents of the ice from the ground surface to the sediment beneath the massive ground ice body tend to show a common origin of water for the ice(Ad Hoc Study Group,1984).
The present authors' findings from observations of the ice core obtained through the massive ice body are opposite to the above arguments, especially, of 3), 4) and 5), which are remarkably contradictory to their findings(Fujino,1986).
A doubt about the segregation of ice lenses as the origin of the massive ground ice can be araised as follows:
As is well known, ice segregation in sand - water system which is adaptable in the massive ground ice body, can not be readily occurred except when the migration of adsorbed water by the sand particles. If the ice lenses formed by that migration, it can be easily defined from the ice fabrics and crystal structure whether it is the migrated or not.
Trends of long-term variation in the profile of ^{18}O do not support the concept of segregated ice. Because, in equilibrium process, fractionation of isotope between ice and water takes place completely(O'Neil 1968). Then, such trend as observed in the profile is difficult to explain in the ice body of segregated origin.
Moreover, crystal structure in the core is quite different from that formed in such process as segregation.
For instance, ice crystals in each stratum of the core are distinctly different in size, shape and c-axis orientation. Strata can be divided into the three following types: 1) strata of granular ice crystals having the nearly homogeneous grain size averaging 0.5 cm; 2) strata of medium- sized ice crystals having the nearly rectangular shape averaging 2 - 3 cm on the long axis and being arranged with some orientation; 3) strata of large ice crystals more than 10

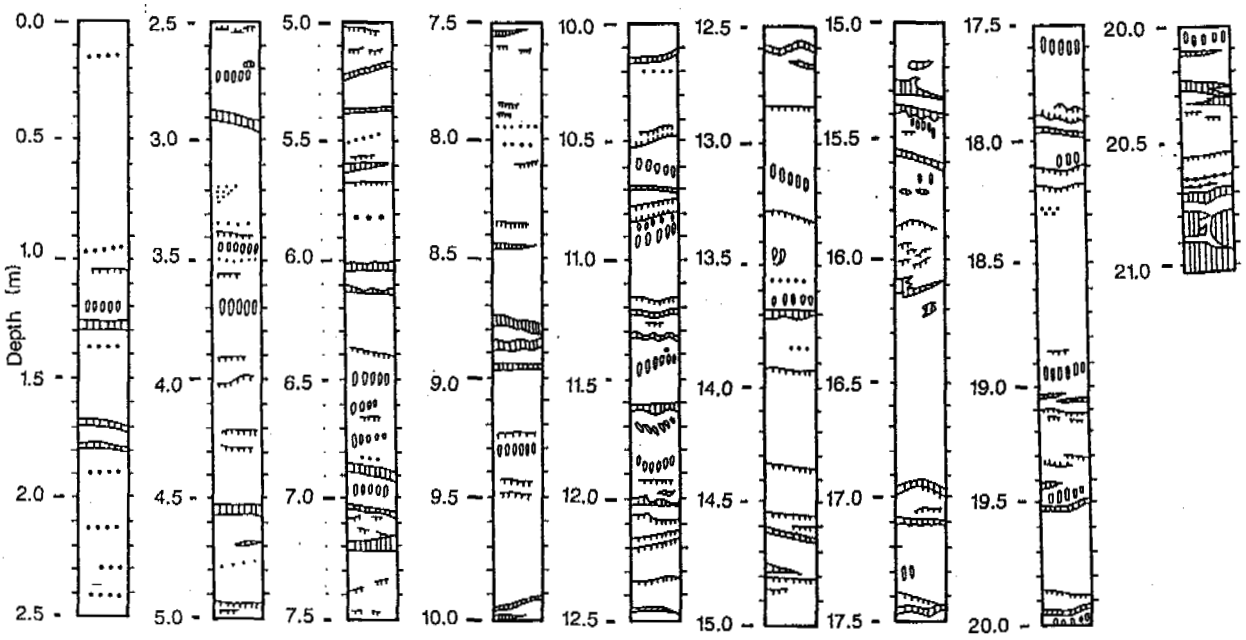

Fig. 3. Stratigraphic features of the entire length of a core

cm in diameter.
Distributions of the c-axis orientation of crystals of type 1 are comparatively random and do not have a particular concentration of orientation. Those of crystals of type 2 seem to have some tendency of arranging themselves in some particular direction. Those of crystals of type 3 seem to be arranged in the horizontal plane; however, numbers of crystals of this type are not enough for the determination of c-axis orientation.
The crystallographic feature of type 1, which constitutes more than one half of the entire core, is commonly observed in superimposed ice layers such as glacier ice, lake ice and sea ice. Ice fabrics and air bubble distributions of such ices are not uniform because of differences in the amount of water supplied to the snowpack. Ice crystals in the snowpack connect each other and form a three-dimensional network so that the c-axis of each ice crystal is oriented randomly. Thus, the pores which are formed between ice crystals also connect each other and form a three-dimensional network in the snowpack.
When the snowpack is submerged in water, the pores are isolated from each other and form air bubbles; the shape and distribution of each air bubble depend upon how much the snowpack is saturated by water in which it is submerged.
Thus, the superimposed ice layer formed by congelation of water in which the snowpack is submerged has distinctive different features of ice fabrics and air bubble distributions, compared with other ice layers which are formed by different processes.
Formation of large ice crystal layers free from bubbles may also be explained from the same concept of superimposed ice formation, that is, a snowpack which is saturated fully by submergence under water or a fairly thick layer of water which is perched upon an ice bed beneath the snowpack, freezes at a low cooling rate as commonly observed in the case of lake ice.
These facts indicate that the previous arguments that the massive ground ice body is formed by segregated ice lenses are doubtful based upon observations of the ice fabrics of the core.
Now, let us take up 3) in the arguments. It is also contradictory to our observations.
As is clear from Fig. 7, chemical compositions in the ice body are far less than those of modern natural water(Kato,1981).
The distinct changes observed in the profiles of chemical compositions and ^{18}O correspond to the distinct discontinuities of crystallographic features in the ice body.
Moreover, there are many facts other than ice fabrics, chemical components and compositions which are against the segregated ice hypothesis(Kato,1986).
Ice strata and sediment between the ice strata abound in fossil pollen grains and spores. Fossil pollen and spores are now being analyzed in quantity and quality. But, from the results obtained so far, pollen contents in the till overlying on the ice body are remarkably different from those in the ice body either in quality or quantity.

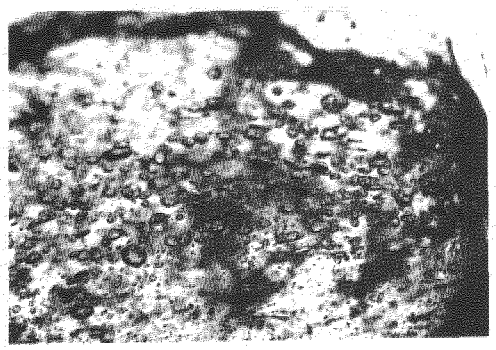

Fig. 4. Tindal figures in the ice core

Pollen grains found in large numbers seem to have been transported in the air and deposited on the ice body, from the observations of their features.
The fact that the striations in the ice body were cut by the basal plane of the overlying sediment, which are considered to be an original deposit, means that the ice body suffered erosion and then the sediment was deposited.
More detailed investigations are being made of ice fabrics and sediment including their continuities in the ice body, together with chemical analysis.
However, it may be concluded from the results obtained so far that most parts of the massive ice body except several tens of centimeters of the bottom layer which lies on the sand layer of the bed, originate from superimposed ice formed by congelation of water which was perched on the bed and the ice body was submerged in. And the sediment between strata of ice was formed at an ablation stage of the massive ice body. Thus, through intermittent repetitions of accumulation and ablation processes, the ice mass develops recognizable strata containing a sediment layer at the boundary of each stratum and also distinctive discontinuities in the ice fabrics.
Radiocarbon dates determined from the sediments in the ice body suggest that the ice body was formed from 17,000 to 10,000 years B.P.on the sand layer which was formed in 53,000-56,000 years B.P.. This age predates

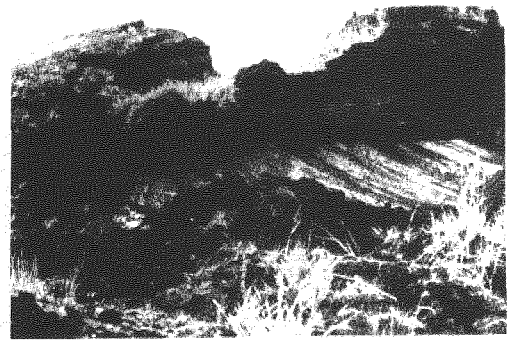

Fig. 5. Unconformity between the ice body and overlying till layer observed at the outcropping ice cliff

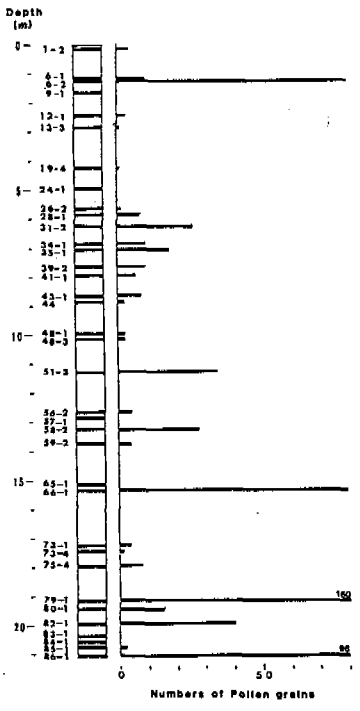

Fig.6. Pollen (group A) contents at boring site, W-3

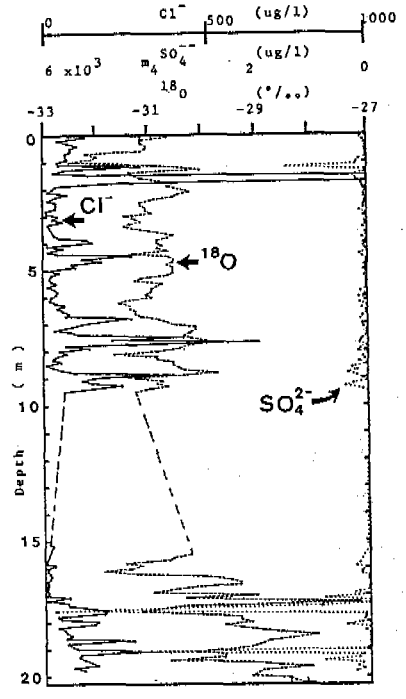

Fig. 7. Vertical profiles of chemical compositions and oxygen isotope in the ice body

the maximum of the Laurentide Ice Sheet in this region but not predate the early Wisconsin Interval. Then, after several stages of abration and deposition, the ice body covered by the overlying till layer of which dated less than 10,000 years B.P..

More detailed analyses and investigations on the massive ground ice body are being carried out for clarifying the origin and formation processes of it related to paleoclimatology.

This research project was supported by a Grant in Aid for Scientific Research, No. 61041004, from the Ministry of Education, Science and Culture of Japan and also by Polar Continental Shelf Project, Energy, Mines and Resources, Canada as project No.121-84.

REFERENCES

Ad Hoc Study Group on ice segregation and frost heaving. 1984, Ice segregation and frost heaving. Nat'l Academy Press, Washington D.C., pp 72.

Fujino, K. and Kato, K.,(1978) Determination of oxygen isotopic concentration in the ground ice of tundra area. Joint studies on physical and biological environments in the permafrost, Alaska and North Canada, July to August 1977. Inst. Low Temp. Sci., Hokkaido Univ., p.77-83

Fujino, K. et al.,(1983) Analysis and characteristics of cores from massive ice body in Mackenzie Delta, N.W.T., Canada. Proc. 4th Internat. Conf. on Permafrost, Nat. Academy Press. Washington, D. C., p.316-321

Fujino, K. and Sato, S.,(1986) Stratigraphic analyses of the massive ground ice body in Tuktoyaktuk, Mackenzie Delta, N.W.T., Canada. Characteristics of the massive ground ice body in the Western Canadian Arctic related to paleoclimatology, 1984-1985. Inst. Low Temp. Sci., Hokkaido Univ., p.9-36

French, H. M., (1976) The periglacial environment. Longman Group Ltd, London, 309pp.

Kato, K., et al. (1981) Oxygen isotopic composition of surface snow in the Arctic Canada. Observations of clouds and precipitation in the Arctic Canada. Organizing Comm. for POLEX, Tokyo, p.83-93.

Kato, K., et al.(1986) Profiles of chemical compositions in the core from a massive ground ice body in Mackenzie Delta, N.W.T., Canada: Preliminary report. Characteristics of massive ground ice in western Canadian Arctic related to paleoclimatology 1984 - 1985, Inst. Low Temp. Sci., Hokkaido Univ., p. 57-70 .

Mackay, J. R. and Black, R. F., (1971) Origin, composition and structure of perenial frozen ground and ground ice: A review. Proc. 2nd Internal. Conf. on Permafrost, North American Contrib., Yaktsk, U.S.S.R., p.185 - 192..

O'Neil, Jr. (1968) Hydrogen and oxygen isotope fractionation between ice and water. Jour. Phys. Chem., 72, p.3683-3684.

MEASUREMENTS OF ACTIVE LAYER AND PERMAFROST PARAMETERS WITH ELECTRICAL RESISTIVITY, SELF POTENTIAL AND INDUCED POLARIZATION

E. Gahe, M. Allard, M.K. Seguin and R. Fortier

Conjointly Centre d'études nordiques, Université Laval, Ste-Foy, Québec

ABSTRACT The study area is located in the southeastern part of Ungava bay, some 160 km northeast of Kuujjuaq at longitude 65°50' W and latitude 58°30' N. Electrical resistivity, induced polarization and self potential methods are used to follow the evolution of active layer and permafrost. Measurements are taken both at the surface and in drill holes in clayey and sandy soils. Three tests were also carried out in the summer 1986 to verify the effect of saline water at the base of ice-rich permafrost under a shoreline permafrost mound. The use of these methods in summer permits the delineation of four layers in the soil profiles; from surface downward these are: a dry layer, a water saturated layer, an ions exchange zone or transition layer and the permafrost upper portion. It was also pointed out along the shoreline that ice-rich permafrost is limited downward by saline water table variations.

INTRODUCTION

The purpose of this study is to compare three geophysical methods in order to follow the evolution of the active layer and the upper portion of permafrost. The saline water effect at permafrost base along the shoreline was also studied. The study area is located close to the community of Kangiqsualujjuaq along the George River estuary some 15 km south of Ungava bay, northern Québec, Canada (Fig. 1). The study area lies on Quaternary marine sediments of which some are deep-deposited clayey silts and others sandy-gravelly emergence deposits. The clayey silts outcrop on the seaboard close to the village; the aggradation of ground-ice in these silts built up permafrost mounds (Allard et al, 1988). It is at the top of one of those mounds that the active layer dynamic was observed, whereas saline water table was studied at the base of another mound located immediately on the shoreline. On the other hand, evolution of the active layer and permafrost was studied on a raised beach at the elevation of 20 m. This beach is composed of well sorted coarse sand. The comparison of three geophysical methods allows the understanding of the behaviour of measured physical parameters (electrical resistivity, chargeability and electrical potential). During a complete freezing and thawing cycle, variations in electrical properties due to displacements of the water table and temperature changes were observed. That permits identification of four layers in both the clayey silt and the sand.

METHODS

Two vertical probes (one 2 m deep, the other 3 m) were installed. The first one is on top of a clayey silt mound and the other one is in gravelly sand on a marine terrace. Along the probe in clayey silt, electrodes and thermistors are spaced at 15 cm interval from surface to 90 cm depth and at 20 cm interval from 90 cm to 190 cm depth. Thermistors and electrodes are lined up.

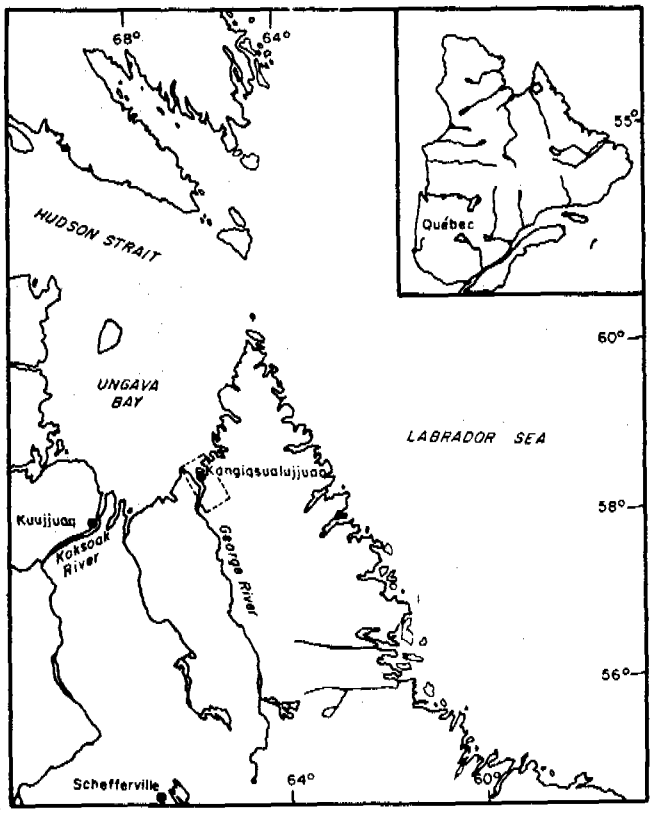

Fig. 1 Location of study area.

TABLE I: GEOPHYSICAL INSTRUMENTATION USED

ELECTRICAL RESISTIVITY		INDUCED POLARIZATION
Resistivity meter:	ABEM digital SAS 300 frequency 4Hz	The induced polarization unit is composed of a Lopo (Huntec) M-3 transmitter and a MK III Receiver. The characteristics of the transmitter are: - maximum output voltage: 1800 V - maximum current: 1.5 A - resistance range: 100 to 6200 ohms - period of current injection or turn off: 1ms - period of one cycle, 2, 4, 8, 16 s - ratio of active to passive period: 1:1, 1:28: 1, 1:67: 1, 2: 2:1 For the receiver, eleven measurement scales of the primary voltage (Vp) allow a resolution of 0.1% between 10^{-6} and 10 V. Both Vp and apparent chargeabilities ($\frac{Vs}{Vp}$ in ms or μs) are measured.
Characteristics:	the transmitter circulates a pre-selected current (0.2 to 20 mA) and the receiver coupled to a microprocessor measures the voltage (1 V to 500 V). The microprocessor controls the measurements and calculates automatically soil resistances (R V/I). The electrical resistance is read directly.	

along the probe of the marine terrace at 15 cm spacing from 0 to 165 cm and at 25 cm from 165 to 290 cm. The electrical parameters are measured along those probes. The geophysical instrumentation used is described in Table I. Periodic measurements were undertaken from July 9th 1985 to February 16th 1986 in both soils. Electrodes were set fixed on the ground surface in a preset Schlumberger array for the experiment on electrical properties of basal permafrost along the shoreline. During complete tidal cycles, electrical resistivity and induced polarization were continuously monitored at spacings corresponding to the estimated depth of permafrost base and subbase so as to detect tidally induced changes in ground water flow underneath the ice-rich permafrost.

RESULTS

A) CLAYEY SILT SITE: NEAR SURFACE MEASUREMENTS

The results covering the thawing and freezing cycle and showing the variation of electrical resistivity, chargeability and temperature with depth are plotted in Fig. 2 (A to C). Three critical dates (July 22nd 1985, December 9th 1985 and February 16th 1986) are retained to follow the thaw front on this site. According to electrical resistivity results (Fig. 2b), four layers can be distinguished: a dry layer (decreasing from 250 to 20 ohm-m) from the surface to the depth of 40 cm, a water saturated layer (20 ohm-m) situated between 40 and 90 cm, a transition layer or ions exchange layer (increasing from 20 to 150 ohm-m) from 90 to 120 cm identified between saturation level and thaw front, and the ice-rich upper permafrost zone characterized by resistivity increases from 150 to 425 ohm-m between 120 to 150 cm (Table 2). The ion exchange layer is interpreted as the zone where selective separation of ions from solid (ice) to water takes place (Yarkin, 1978). On the same day, chargeability increases from -3 μs to 3 us from soil surface down to 30 cm (Fig. 2c), corresponding to the dry layer already identified by resistivity. From 30 to 120 cm, polarity inversions of chargeabilities (positive/negative/positive) are noticed covering both saturation level and ion exchange level; in fact, the negative peak at 135 cm (-5 μs) indicated the thaw front. Electrical potential results in the same period showed that thawing potential (730 mV) is located between 80 and 160 cm placing the boundary of frozen and thawing layers of ground around 135 cm. On December 9th 1985, the ground is frozen from surface to 65 cm, whereas it is thawed from 65 to 150 cm giving the following stratigraphy: frozen layer, thawed layer, permafrost. This stratigraphy is characterized by higher resistivity for the first layer, low resistivity for the second layer and high resistivity downward from 150 cm (Fig. 2b). On February 16th 1986, the profile is completely frozen; for those dates, chargeabilities were not measured and resistivities were above the

TABLE 3: COMPARISON OF ELECTRICAL RESISTIVITY RESULTS IN TWO MEDIUMS AND RESULTING STRATIGRAPHY

CLAYEY SILT		SAND		
RESISTIVITY (ohm-m)	DEPTH (cm)	RESISTIVITY (ohm-m)	DEPTH (cm)	LAYER
250 → 20	0 - 30	12000 → 1500	0 - 50	- dry layer
20	30 - 90	500	50 -120	- saturated layer
20 → 150	90 -120	1000 → 5500	120 -210	- transition or ions exchange layer
150 → 425	120 -150	5500 → 30000	210 -240	-permafrost upper portion

reading capability of the instrumentation.

B) SAND SITE

The site is located on a raised beach composed of coarse sand with beds of gravel. The frozen ground contains interstitial ice. Three dates are also retained to illustrate the freezing and thawing cycle. Four layers are identified: a dry layer (0-50 cm), a water saturated layer (50-210 cm), the transition or ion exchange layer (120-210 cm) and the permafrost upper portion (210-240 cm) (Table 3). On December 7th 1985, only three layers are distinguished: frozen layer (0-70 cm), unfrozen layer (80-265 cm) and permafrost downward from 265 cm depth. The upper part of the profile is then freezing back whereas permafrost table is around 250 cm (Table 3). On February 16th 1986, the profile is totally frozen. The curves of electrical potentials, temperatures and chargeabilities covering the thawing and freezing cycle are shown in Figures 3 (a and b) and 4 (a and b) and 5 (a and b), respectively, whereas characteristic results of those parameters are presented in Table 3. Comparing the results obtained on the two sites, it was pointed out that the saturated zone is slightly thicker in coarse sand than in clayey silt (Table 2). This difference is best explained by the thermal properties of those materials. Indeed, sand has a higher thermal conductivity than fine-grained soil, allowing faster penetration of the thaw front and melting of interstitial ice. The saturation level is fed both by water from ground ice melting and from summer precipitations.

C) ELECTRICAL PROPERTIES OF BASAL LAYERS IN SHORELINE PERMAFROST: CRYOPEGS

Three geophysical tests were carried out in summer 1986 to verify the effect of saline water on geophysical results and also on the variation of subpermafrost groundwater flow following tidal fluctuations. The purpose of the measurements is to determine to what depth the permafrost contains ice and remains watertight. Underneath this depth, freezing point depression of soil water prevents ice formation. In watertight permafrost, chargeabilities and electrical resistivities are high while electrical potentials are around or equal to zero. According to Roy and Elliot (1980), combined resistivity and induced polarization soundings showed that simultaneous decrease of apparent resistivity and chargeability is a diagnostic of saline groundwater. It is also known that lower temperatures increase the value of chargeability (Kay and Duckworth, 1983). The preset electrodes array was installed on a shoreline permafrost mound in clayey silt. The mound top is 1 m high above spring tide level and temperature data along a thermistor cable indicates warm permafrost (between 0°C and -0.5°C) down to 9 m deep, that is below mean tide level. (see Allard et al., 1988).

Five induced polarization soundings using the Schlumberger configuration were made on July 15th 1986 (Fig. 6a to 6e). At the beginning of the rise of the tide (11h44), a progressive decrease of chargeability values from 90 to 0 ms between 4 and 7 m was noticed. Those values became negative at 8 m before becoming stable around 5 ms beyond 9 m (Fig. 6a). The results obtained at 14h52 (corresponding to the final rising time of tide) showed the same characteristics as Fig. 6a. Slack of high tide was at 15h30, whereas the tide started to ebb at 16h14 inducing a decrease in chargeability. The maximum value of the chargeability is situated at the depth of about 4 m (Fig. 6d) whereas the polarity inversion is at the depth of 6 m indicating the base of permafrost. The measurements taken at 17h30 (Fig. 6e) pointed out an increase of chargeability towards 4 m. There is a potential difference of 900 mV between 4 and 8 m (Fig. 7).

More electrical potential results were also obtained on July 22nd 1986. From results obtained during all stages of the tidal cycle, we deduce that the permafrost below 4 m, more precisely deeper than 6.5 m, is unfrozen and subject to groundwater flow variations induced by the tide. This implies that the maximum thickness of ice-rich permafrost in the mound is about 6 m. Although negative temperatures values between 0°C and -0.5°C are found down to 9 m deep. The results of electrical soundings both on the surface of this mound and in a drill hole indicated that the base of ice-rich permafrost is about 5 m deep thus corroborating these results.

CONCLUSION

Electrical potentials and resistivities measured in clayey silt were 800 mV and 20 ohm-m respectively at the thaw front and permafrost table, whereas they were 500 mV and 1000 ohm-m in coarse sand. The electrical potentials along the contact between frozen and unfrozen soils show some polarity inversions and are the same order of magnitude as these measured by Parameswaran et al (1985) and Parameswaran and Mackay (1983). Chargeabilities are negative at the thaw front because of the interface potential gradient, which probably occurs as a result of the exchange-absorption processes on the surfaces of the mineral grains of the soil. The combination of three electrical methods permits the description of the thaw front progression in two kinds of soil. This study also provides a mean to delimit, with a high degree precision, the ice-rich permafrost base and basal cryopegs in shoreline permafrost.

ACKNOWLEDGEMENTS

The authors extend their thanks to the following people: Jean Desbiens, Alain Fournier, Jacqueline Bouchard, Florence Nicolin and Yvon Pelletier for their help in the filed operations.

REFERENCES

Allard, M., Seguin, M.K. & Y. Pelletier (1987). Shoreline permafrost in Kangiqsualujjuaq Bay, Ungava, Québec. Proceedings, 5th International Conference on Permafrost.

Kay, A. & Duckworth, L. (1983). The effect of permafrost on the IP response of lead zinc ores. Journal of the Canadian Society of Exploration geophysicists, 19(1):75-83.

Roy, K.K. & Elliot, H.M. (1980). Resistivity and IP survey for delineating saline water and fresh water zones. Geoexploration, 18: 145-162.

Parameswaran, V.R., Johnston, G.H. & Mackay J.R. (1985). Electrical potentials developed during thawing of frozen ground. in S. Kinosita and M. Fukuda (editors). Proceedings of the 4th International Symposium on ground freezing, Sapporo, Japan, 5-7 August 1985, p. 9-15.

Parameswaran, V.R. & Mackay, J.R. (1983). Field measurements of electrical freezing potentials in permafrost areas. Proceedings 4th International Conference on Permafrost, Fairbanks, Alaska, National Academy Press, Washington D.C. p. 962-967.

Yarkin, I.G. (1978). Effect of natural electric potentials on water migration in freezing soils. USSR CONTRIBUTION, Permafrost Second International Conference, National Academy of Science, p. 359-361.

Table 2 - Variation of temperature, resistivity, self potential and chargeability with depth below ground surface from July 22nd 1985 to February 16th 1986.

	DATE	TEMPERATURE °C	cm	RESISTIVITY ohm	cm	SELF POTENTIAL mV	cm	CHARGEABILITY ms	cm	THAW FRONT
CLAYEY SILT	85-07-22	10.6-4.36	20-40	250-10	20-40	-66.1 - 10.3	37.5-52.5	-2.25-1	37.5-52.5	65 cm
		4.36-(-0.06)	40-90	10	40-80	10.3-(-2.43)	52.5-67.5	1-(-1.17)	52.5-67.5	
		-0.06-(-0.83)	90-130	10-420	80-160	-243-467	67.5-82.5	-0.4-2.08	100-120	
						383-(-72)	100-120	2.08-(-4.6)	120-140	
	85-12-09	-2.20-0	0-65	1400-20	0-80			-4.6-7.79	140-160	
		0-10	65-150	20-	80-120	-160-(-14)	0-100			
		0	150			-14-207	100-120	Not measured		
	86-02-16	Frozen from surface to 180 cm								
				Kohm	Cm					
MARINE TERRACE (SANDY GRAVEL)	85-02-22	9.26-5	0-60	10-1	20-60	-44.6-216	67.5-82.5	0.97-1	20-110	
		5-0.5	60-130	1	60-130	-51.2-400	112.5-127	0.79-47	110-200	150 cm
		0.30-(-15)	140-200	10	140-200	-163.8-138	157-200	47-1.12	200-250	
		-24-(-3.4)	200-400	10-40	200-400					
	85-12-07	-4.47-(-0.46)	0-75	5-20	0-50	-44.3-135.5	200-227	Not measured		
		0	90-265	20-1		97.5-250				
		0	275	1-6	250-277.5					
	86-02-16	Frozen								

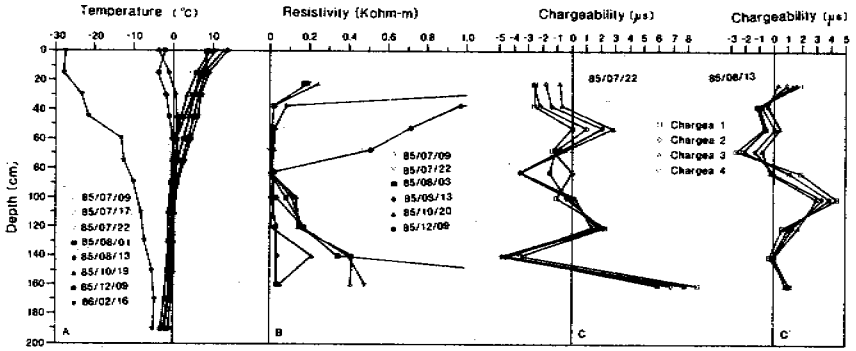

2. Temperature (A), electrical resistivity (B) and chargeability (C and C') variations in active layer and upper part of permafrost in clayey silt mound from July 1985 to February 1986.

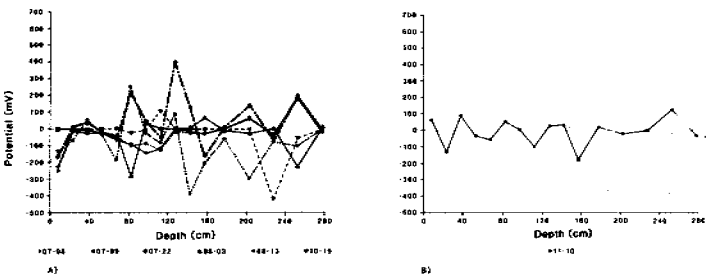

3. Electrical potential at various depths in active layer and near surface permafrost in the sandy soil. Schlumberger array results (A) and Wenner array result (B).

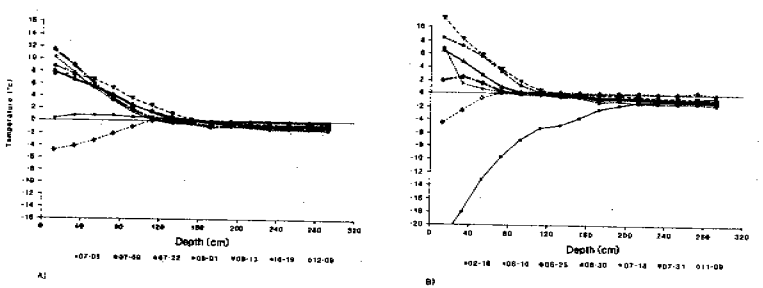

4. Temperature variations in active layer and near surface permafrost in the sandy soil.

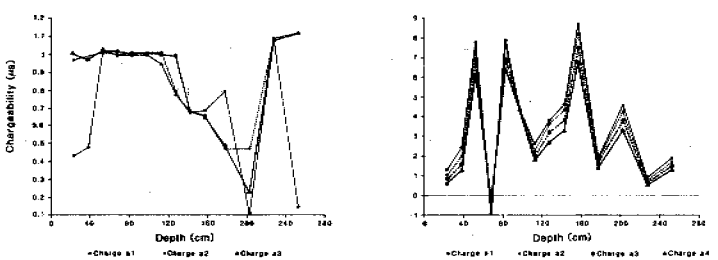

5. Vertical profiles of chargeability in the sandy soil on July 22nd 1985. Charge 9_1 to 9_4 represent different chargeabilities. A- Schlumberger array configuration, B- Wenner array.

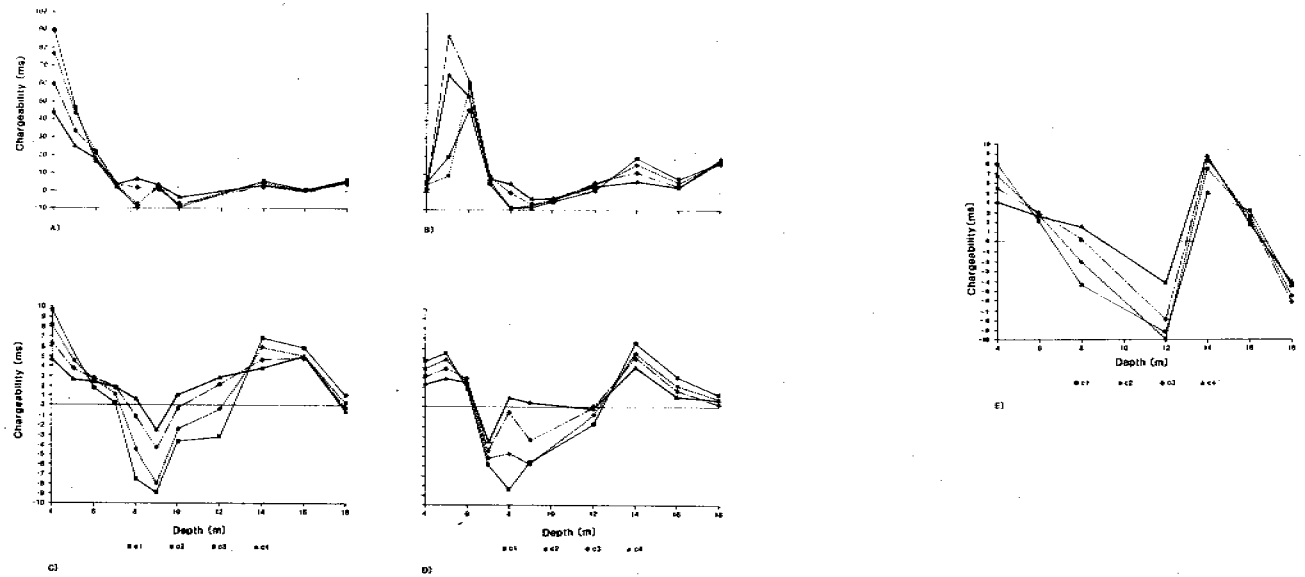

6. Chargeability vs depth from surface Schlumberger array on a shoreline permafrost mound on July 15th 1986. A- 11h44 beginning of rise of the tide, B- 14h52, tide continue to rise, C- 15h30 slack of high tide, D- 16h14 beginning of ebb, E- 17h30.

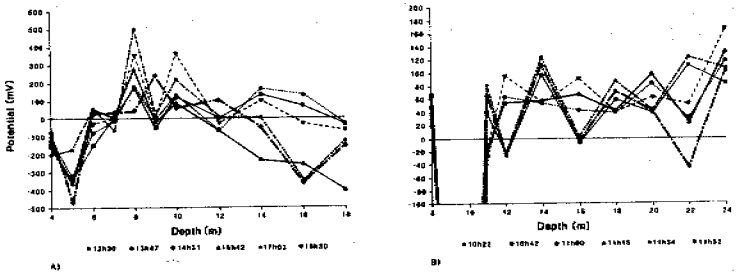

7. Variation of the electrical potential in permafrost during the rise and fall of the tide, July 15th 1986. Base of ice-rich permafrost is at about 6.5 m depth.

THE ALPINE PERMAFROST ZONE OF THE U.S.S.R.

A.P. Gorbunov

Permafrost Institute, Siberian Branch of the U.S.S.R. Academy of Sciences, Yakutsk, U.S.S.R.

SYNOPSIS This paper offers a definition of the 'Alpine permafrost zone' concept and outlines some approaches to its identification in Soviet territory. Characteristics of eight geocryological areas of the Alpine permafrost zone are given and an estimate is made of their area within the U.S.S.R.

About half the area of the U.S.S.R. is occupied by permafrost. Most of this area refers to the near-polar regions in which perennial freezing of the lithosphere had been occurring during the Pleistocene and the Holocene under the action of high-latitude climatic conditions. A smaller part of the area is occupied by permafrost that had formed on elevations under the action of severe climatic conditions predetermined by their hypsometric position. Depending on the locality's geographical latitude, these can be a low-, a middle-, or a high-mountain layer of the mountains.

The purpose of this paper is to call attention to problems of classifying the permafrost zone into a circumpolar and an Alpine one. This is dictated by two motivations. One is the need to focus attention on the factors giving rise to perennial freezing, viz. on the latitudinal position in the first case and on the hypsometric position in the second case, as regards its occurrence. The other motivation implies that data accumulated on permafrost in mountaneous regions provide ever increasing evidence for specific features of the Alpine permafrost zone. The most salient feature corresponds to the absence of absolute antagonism between the snow amount , the degree of glaciation in the mountaneous area and the height boundary of the permafrost zone. Namely, an increase in the snow content in the mountains does not cause the permafrost zone boundary to rise. However, the difference between the snow line height and the perennial freezing zone boundary increases with the increasing degree of continental climate, owing to the former's greater mobility as compared with the latter. In other words, these boundaries are both shifting in the same, rather than opposite, direction, but the amount of displacement is different.

One remark is in order here. In low (especially, subtropical and tropical) latitudes, where there is no circumpolar permafrost zone at all, the height dependence of the permafrost area boundary position on the degree of continentality of climate is the reverse as compared with high latitudes. Normally, this boundary lies substantially lower in littoral regions as compared with intercontinental regions.

The foregoing gives good grounds for identifying the Alpine permafrost zone. This was done for the first time as early as the end of the past century by L.A.Yachevsky (1889), who identified a polar and an Alpine regions of 'perennially frozen soil'. However, the terms he had coined failed to be accepted by his compatriots in their later papers. Since the 70s of this century the term 'Alpine permafrost' has again been used in a large number of publications abroad.

However, the semantic content of this term has not yet been adequately defined. I would like to illustrate this by some examples. Fujii and Higuchi (1978) and Péwé (1983) give distribution maps for the circumpolar and the Alpine permafrost zones showing that frozen ground of mountaneous elevations in the south of Siberia, as well as Kamchatka and Mongolia is not included in the region of the Alpine permafrost zone. However, Sikhote-Alin, the north of the Urals, the Rocky Mountains and the mountains of Scandinavia and Iceland lie within this region.

The map presented in Péwé's (1983) paper obviously contradicts the definition of Alpine permafrost given in the same paper. He states that "... permafrost existing on high plateaus and in high mountains of middle and low latitudes is called Alpine permafrost..." (Péwé, 1983, p. 147). In this case, however, according to Péwé's map, the North Urals, included in the region of the Alpine permafrost zone, should be classified as high mountains and the Altai and the Sayany, say, which are not included in this region, should be placed in the category of either high-latitude or low mountaneous systems, but such is not the case.

Hence, it is necessary to give concrete expression to the definition of the 'Alpine permafrost zone'. Some suggestions on this matter have been offered previously (Gorbunov, 1984), but they require some refinement. Thus, the permafrost zone, predetermined by the locality's height position, is called the Alpine perma-

frost zone. This should include only those perennially frozen soils which occur over 500 m above sea level, and they are absent below this level.

The hypsometric 500 m level has been chosen in view of a number of reasons. It is this isohypse which is usually indicated immediately following the 200 m isohypse on small-scale maps. The height range 0-500 m is sufficient in order to give a clear distinction for the zones of seasonal and perennial freezing of soils because it corresponds to the 3°C-difference of yearly mean temperatures. As far as the geomorphology is concerned, the level indicated coincides with the lower boundary of mountain valleys.

At first glance, the use of the notion 'Alpine' relative to the permafrost zone of low elevations does not appear justifiable. But this applies only to the case when it is used in the meaning such as 'Alpine belt', 'Alpine meadow' and 'Alpine terrain', i.e., when the height level is emphasized. There exist definitions, however, in which emphasis is placed on the fact that a given object or phenomenon is similar to those in the Alps, irrespective of the particular terrain belt or relief layer, 'Alpine' orogenesis, for example. Therefore, 'Alpine' may simply mean a permafrost zone that exists due to the same reasons as in the Alps, i.e., owing to the locality's hypsometric position. Moreover, the oronym 'Alps' in Celtic means 'mountains'.

The analysis of evidence concerning the U.S.S.R. area has revealed that the separation boundary between the circumpolar and the Alpine regions of the permafrost zone virtually coincides with the +3°C yearly-mean temperature isoline for rocks referenced to sea level (Osnovy geokriologii..., part 1, 1959, Fig. 32).

Indeed, for a vertical temperature gradient of 0.6°/100 m, along this line at 500 m above sea level one should expect the occurrence of mountain-masses cooled to 0°C. And this does satisfy the proposed criterion for identifying the region of the Alpine permafrost zone. The 3°C isotherm for rocks from east to west within the U.S.S.R. runs in the following fashion. On the eastern littoral of Kamchatka it begins approximately under 56° N and runs then southward - south-northward arriving at the western littoral of the peninsula under 52° N. It intersects Sakhalin under 52° N; further, along the Amur riverside, in the vicinity of and parallel to it, the boundary in the area of the cities of Birakan and Bira reaches 49° N, the southernmost location within the U.S.S.R. After that, it runs eastward - north-eastward passing through Chinese territory within the geographic latitude range 50-51° N; then, it is directed toward Lake Baikal intersecting it under 53°N and the Yenisei under 57° N. This line arrives at the Urals under 62° N and at the White Sea under 64°30 N. Then, it intersects the frontier between the U.S.S.R. and Finland under 68°30 N. It is the last point where the separation line between the two regions of the permafrost zone reaches its northernmost position. Consequently, the geographic latitude range within which, in Soviet territory, the above-mentioned boundary line varies, is nearly 20° (49° - 68°30).

Within the region of the Alpine permafrost zone in the U.S.S.R. one may identify eight areas which are characterized by certain geocryological conditions typical of them only, as well as other landscape features.

The Kamchatka-Kuril geocryological area. On the Kamchatka Peninsula there are adjacent regions of the circumpolar and the Alpine permafrost zones. The boundary between them lies approximately along the line connecting Ust-Kamchatsk (56° N) with Ust-Bolsheretsk (52° N). On Kamchatka the Alpine permafrost has been very poorly investigated (Zamolotchikova et al., 1979), while on the Kuril Islands it has not been studied at all.

This region is notable for a very complicated interaction of thermal flows of active volcanoes and hydrothermal flows with the permafrost zone. This problem is still a 'blank space'. There is fragmentary evidence showing that the lower boundary of island permafrost rises from 500 to 1000 m above sea level within the Kamchatka Alpine permafrost zone from north- north-west to south- south-east. No detailed studies have been made of the regularities of spatial distribution of permafrost masses in the Eastern ridge; it might be anticipated that the island-type of permafrost occurrence predominates there which is due to the large amount of snow as well as the geothermal characteristics of the lithosphere. According to very tentative estimates, the total area of the Alpine permafrost zone on the Kamchatka Peninsula is about 20 000 sq. km.

Within the Kamchatka permafrost zone there occur glacial-nival and mountain-tundra landscapes as well as Alpine meadows, peatland and brushwood of the sub-Alpine zone. The permafrost zone also embraces, partially, the forests consisting of stone birch.

The chain of the Kuril Islands has about 30 peaks as high as over 1000 m above sea level. Most of them are active or dead volcanoes.

Data from meteorological stations and the characteristics of the altitude landscale zoning suggest that a belt of the Alpine permafrost zone above 1000 m above sea level is present on the highest peaks of the Atlasov, Paramushir, Onekotan, Kharimkotan, Ekarma, Matua and Simushir Islands. It is possible that, to the south, small masses of permafrost occur above the 1500 m isohypse on the Urup, Iturup and Kunashir Islands. But this is merely a supposition because active volcanism, the cold current surrounding the islands on the eastern side, and stone debris in the near-summit belt of the mountains make any relevant predictions exceedingly complicated. For example, the fact that the northern islands at altitudes above, at least, 400 m are dominated by talus and stone debris which are quite favourable for perennial freezing, leads us to suppose that in some places the permafrost boundary on the North Kuril Islands occurs still lower as compared with the South Kamchatka Peninsula, i.e., at altitudes of about 500 to 600 m. On the other hand, on the slopes of active volcanoes no frozen masses may be present at the altitude level where the climatic conditions are favourable for them.

The area occupied by the Alpine permafrost zone on the Kuril Islands appears to make up tens or a few hundreds of sq. km.

As far as the diversity of landscape zones within the permafrost belt is concerned, the Kuril Islands are inferior to the Kamchatka mountains - the shrub-covered tundra predominates there as well as naked rocks and boulder screes, and debris.

The Sakhalin geocryological area. The circumpolar region of the permafrost zone there occupies the Schmidt Peninsula; possibly, it also extends farther out southward along the Sakhalin littoral as far as about 52 N.

The Alpine permafrost zone on the island occurs in the West-Sakhalin and East-Sakhalin mountains, in the geographic latitude range 51°-49° N over 1000 m above sea level.

The Sakhalin geocryological area is notable for its large amount of snow cover which does determine the island-type distribution of the Alpine permafrost zone highly characteristic for the mountains of the island. Another important feature of the climate is the decrease of the yearly mean air temperatures toward the inland depressions of Sakhalin as well as toward its eastern littoral. If there were no thick, stable snow cover, then along the eastern seaside of Sakhalin, the circumpolar region of Sakhalin would lie somewhere within the range 50-51° N.

The formation conditions for the Alpine permafrost zone are more favourable for the East-Sakhalin ridge because it is higher and more dismembered; its slopes there are steeper and rock masses and large-boulder screes occur in greater amounts; and at the same altitude levels the yearly mean air temperatures there are lower as compared with the West-Sakhalin mountains.

The permafrost zone on the Sakhalin Island includes terrains, under bald mountains, of creeping Siberian pines, and rock masses and boulder debris of the bald mountain range. The area of the Sakhalin Alpine permafrost zone seems to be less than a few hundreds of sq. km.

The Sikhote-Alin geocryological area. The valley of the lower reaches of the Amur, devoid of permafrost, separates the region of the circumpolar permafrost zone of the North-Amur area from the Alpine permafrost zone of Sikhote-Alin. It seems likely that, if there were no Amur valley, these two regions would be inseparably linked with each other. The permafrost zone in the northern part of Sikhote-Alin lies over 500 m and, on some occasions, somewhat lower, while in the southernmost part, under 43°15 N it lies above 1400 m (Korotky et al., 1981).

The past several years witnessed the emergence of very interesting lines of evidence concerning the Sikhote-Alin permafrost zone indicating that permafrost there occurs in much greater areas than thoughtof previously. Although, on the whole, the island-type permafrost occurrence predominates there, but there are reasons for anticipating the presence of fragments of subzones of its discontinuous or, even, continuous development in the middle and northern parts of Sikhote-Alin.

The permafrost in the central and northern parts of the region occurswithin the zones of mountain tundras and in birch-and-larch forests and in forests under bald mountains;in the southern part it occurs largely in the zone of mountain tundras.

The area of the Alpine permafrost zone of Sikhote-Alin may be estimated tentatively at 50 to 60 thousand sq. km.

The Baikal geocryological area. It includes the mountains of the Eastern, Central and Western Trans-Baikalia and Pre-Baikalia to the south of 51° N in the east and 53° N in the west. This area differs from the previously discussed geocryological areas by its high degree of continentality of climate, the diversity of landscapes, the extensiveness of its space, and by the relatively well-studied geocryological situation.

The region of the circumpolar permafrost zone there is inseparably linked with the Alpine one; therefore, the separation between them is a conventional one and can be established only if a definite criterion is adopted, such as one used in this paper.

The conditions favourable for perennial freezing of the zones are encountered above 550 to 800 m (Alekseev et al., 1969).

In the region within the Alpine permafrost zone there occur mountain tundras, Alpine meadows, the taiga, and forest-steppe and steppe landscapes.

The area of the region of the Alpine permafrost zone there is about 290 000 sq. km.

The Sayany-Altai geocryological area. It embraces the Sayany, the mountains of Central Tuva, the Tannu-Ola ridge, the Kuznetsk Alatau, and the Altai. In the south-eastern part it merges together with the Baikal area, but it differs from this latter by higher absolute altitudes, extensive occurrence of icing, and by a fairly clear-cut isolation from the circumpolar region of the permafrost zone. In the northern part, in the Kuznetsk Alatau, under 55° N, the altitude boundary of the permafrost zone coincides with the 500 m isohypse (Shatz, 1978), while in the southernmost part, in the South-Altai , under 48° N, it lies at the 1500-1800 m level.

In this area, the permafrost zone shows continuous occurrence within the glacial-nival and the mountain-tundra zones; at lower levels, on Alpine meadows and in the taiga and steppe zones of inland depressions of the Altai and Tuva, discontinuous or island permafrost occur.

The area of the region of this Alpine permafrost zone is estimated at 480 000 sq. km. This region of Alpine permafrost is the largest in the U.S.S.R.

The Central Asian geocryological area. It includes the Saur-Tarbagatai, the Dzhungar-Alatau, Tien Shan, and the Pamirs-Alai. This is the highest-mountain and southernmost, in the U.S.S.R., region of the Alpine permafrost zone. In the northern part of the region, under 47° N the altitude boundary of the permafrost zone lies at the 2000-2200 m level, while in the southernmost part, under 36°30 N, it is shifted upward as high as 3600 to 3800 m. A part of the area southward of 41° N lies within the subtropical geographical zone.

The area is clearly isolated from the circumpolar region of the permafrost zone and is nowhere in contact with it.

The continuous permafrost zone there occurs in the glacial-nival area, mountain tundras and, partly, in Alpine meadows; the discontinuous permafrost zone corresponds to the zone of Alpine meadows; and permafrost islands occur in sub-Alpine meadows, mountaneous meadows and deserts. Some permafrost masses in the northern half of the area occur in the zone of coniferous forests. Thus, as compared to all the other geocryological areas, the greatest landscape diversity is encountered here within the permafrost zone.

The area of the region of the Alpine permafrost zone in this case makes up 220 000 sq. km.

The Caucasian geocryological area. It includes the Great Caucasus as well as a number of separate, small masses in Transcaucasia. Most of it occurs in the moderate zone, and a smaller part is encountered in the subtropical zone. In the north of the area, the permafrost boundary lies at the 2700 m altitude, and in the south, it lies at 3200 m. The glacial-nival zone shows continuous permafrost, while discontinuous permafrost and permafrost islands occur in the zone of Alpine meadows.

Its area is 20 000 sq. km.

The Urals geocryological area. While occupying a part of the North Urals, southward of 62° N, it embraces about 1.5 to 2 tens of the highest peaks of the Central Urals, and the same number corresponds to the South Urals. In the north of the area, the permafrost boundary lies at the 500-800 m altitude, while in the south it lies at 1000 m.

The North Urals present permafrost islands as well as fragments of discontinuous permafrost; as for the Central and South Urals, only permafrost islands occur. In the first case the permafrost occupies bald mountain zones and zones below bald mountains, penetrating, partially, into the taiga zone as well. In the second case, due to the low altitude of the mountains, the bald-mountain zone does not occur and, therefore, permafrost masses may be encountered in the pre-bald-mountain zone and in the taiga zone. In the South Urals the permafrost zone is concentrated in the bald-mountain and pre-bald-mountain landscape zones. In view of the extensive occurrence of stone debris in the South Urals in which perennial freezing is known to take place even at positive yearly mean air temperatures (0° - 3°C) it should be anticipated that, down the large-debris slopes there, some permafrost masses are able to descend as low as the 500-800 m level.

The area of the Urals geocryological region is about 4 000 sq. km.

During the course of the Pleistocene the region of the Alpine permafrost zone in present-day Soviet territory underwent substantial spatial changes. These changes were twofold. A decrease in the altitude position of the permafrost zone altitude boundary led to an increase in permafrost masses in the Caucasian and Central Asian geocryological areas. At maximum falls of temperature later in the Pleistocene perennial freezing of soils was proceeding in the near-summit zone of the Carpathians, the Crimean Mountains, and the Kopetdage. However, most of the mountains of the present-day region of the Alpine permafrost zone in the late Pleistocene and, probably, in the Middle Pleistocene such as the Urals, the Saur-Tarbagatai, the Altai and the Sayany, the Pre-Baikalia and Trans-Baikalia Mountains, and the Kamchatka, Sakhalin and Kuril Mountains as well as, probably, most of the Sikhote-Alin found themselves within the region of the circumpolar permafrost zone, provided that one follows the criteria for distinguishing it from the Alpine permafrost zone as suggested previously. The 'wax' of the area of the Alpine permafrost zone in the late Pleistocene was smaller than its 'wane' because of the southward displacement of the circumpolar permafrost zone boundary. Therefore, at epochs of temperature drop the Alpine permafrost zone in U.S.S.R. territory reduced in area, whereas during periods of rise of temperature it, on the contrary, increased in area.

Let us summarize the foregoing discussion. The Alpine permafrost zone in the U.S.S.R. has an area of about 1.1 millions of sq. km, i.e., about 10 % of the entire subair region of perennially frozen rocks of the country.

The Alpine permafrost zone of the U.S.S.R. has been studied extremely nonuniformly to date. In this regard the 'state of affairs' looks better as far as large geocryological areas such as Central-Asian, Sayano-Altaic and Baikalian are concerned, and looks worse with the remaining areas; let us call them 'small'. Out of these latter, the total lack of geocryological data is typified by those in which the permafrost zone occurs at separate summits and in limited areas of the slopes. These, primarily, are the Kuril Islands and the Sakhalin and South-Urals Mountains. But it is these locations which permit a detailed study of the dependence of perennial freezing on physico-geographical microconditions.

REFERENCES

Alekseev, V.R. (1969). Vertikal'naya geokriologicheskaya poyasnost v predelakh Zabaikalya. - Zapiski Zabaikal'skogo filiala Geograficheskogo obshchestva SSSR, vyp. 37, 70-76.

Fujii, G. and Higuchi, K. (1978). Distribution of alpine permafrost in the Northern hemisphere and its relation to air temperature. - Third International Conference on Permafrost, Proceedings, 1, 366-371.

Gorbunov, A.P. (1984). Nekotorye itogi i zadachi izucheniya kriolitozony gornykh stran. - V kn.: Inzhenernaya geografiya gornykh stran, Moscow, Izdatel'stvo MGU, 160-177.

Korotky, A.M., Vysochin, V.I. and Gvozdeva, I.G. (1981). Vechnaya merzlota Sikhote-Alinya i yeyo dinamika v pozdnem vyurme-golotsene. - V kn.: Landshaftnye geograficheskie issledovaniya na Dal'nem Vostoke, Vladivostok, 45-57.

Osnovy geokriologii (merzlotovedeniya). (1959). Part 1, Izdatelstvo AN SSSR, 457 p.

Péwé Troy L. (1983). Alpine permafrost in the contiguous United States: A review. - Arctic and Alpine Research, University of Colorado, 15, 2, 145-156.

Shatz, M.M. (1978). Geokriologicheskie usloviya Altae-Sayanskoi gornoi strany, Novosibirsk, Izdatelstvo "Nauka", 102 p.

Yachevsky, L.A. (1889). O vechno merzloi pochve v Sibiri. - Izv. Russkogo geograf. obshchestva, XXV, 5, 341-355.

Zamolotchikova, S.A. and Smirnova, V.N. (1979). Temperatura porod Kamchatki. - V kn.: Merzlotnye issledovaniya, XVIII, 102-118.

ON THE SPATIAL DYNAMICS OF SNOWCOVER – PERMAFROST RELATIONSHIPS AT SCHEFFERVILLE

H.B. Granberg

Centre d'applications et de recherches en télédétection (CARTEL), Université de Sherbrooke, Sherbrooke, Québec J1K 2R1

SYNOPSIS

This paper examines the role of the seasonal snow cover as a controller of the ground temperature field at Schefferville (54°48' N, 66°49' W). The snow cover accumulation sequence in woodland and alpine tundra is described and heat transfers through the snow cover are discussed using simple spatial models.

INTRODUCTION

In cooperation with the Permafrost Research Section, Terrain Sciences Division of the Geological Survey of Canada and the Iron Ore Company of Canada two reports were produced which contain most written materials about Schefferville permafrost, ground temperature data from more than 200 thermocables, active layer/frost depth data from over 20 000 test pits and topographic and geologic information (Granberg et al, 1983; 1984). These reports form the Schefferville Permafrost Data File which is the main database for a digital Geographic Permafrost Information System (GPIS) which is now under development. The GPIS has evolved from a snowcover mapping technique which was developed to enable spatial mapping and hindcasting of snowcover and permafrost conditions over mines where permafrost was encountered but where no information on antecedent snow cover conditions was available (Granberg, 1972; 1973; Nicholson and Granberg, 1973). The main purpose of the GPIS is to facilitate the study of spatial and temporal interrelationships between the ground temperature field and terrain and climate factors. In addition to ground temperature information the main inputs are weather, snow and terrain data.

In the development of the GPIS, the initial focus is on the effects of the seasonal snow cover. The snow cover distribution has been empirically linked to the spatial distribution of permafrost at Schefferville (Annersten, 1966; Thom, 1969; Nicholson and Granberg, 1973; Jones, 1976; Nicholson, 1976; 1978a; b; 1979). Although it dominates the multiple regression equations that relate observed average annual ground temperatures to terrain factors, the snow cover is not the only factor of importance. However, in order to develop a better understanding of the effects of other factors such as spatial variations in the summertime surface energy balance (Wright, 1981; 1983) and heat transfers by moving groundwater (Nicholson and Lewis, 1976) it is important to develop a better understanding of the spatial dynamics of the seasonal snow cover and the associated thermal effects. Although heat and mass transfers through the seasonal snow cover are now relatively well understood (Palm and Tveitereid, 1979; Goodrich, 1982; Powers et al, 1985), their spatial and temporal variations are not.

This paper may be seen as a preliminary investigation of several spatial and temporal aspects of the snowcover that are of significance to the ground temperature field. Available snow data are used to illustrate the spatial dynamics of snowcover accumulation in forested terrain, where permafrost is absent, and alpine tundra, where permafrost occurrence is widespread. Spatial and temporal variations in factors which influence the net thermal effect of the snow cover are simulated using simple models within the GPIS. Among the factors simulated are thermal resistance, optical transmissivity and thermal buffering. A digital terrain model that was developed for the Timmins 4 Permafrost Experimental Site near Schefferville (Granberg, 1973) is used in the simulations. Timmins 4 has previously been described in considerable detail by Nicholson and Thom (1973) Nicholson and Granberg (1973) and Granberg (1973).

THE SNOW ACCUMULATION SEQUENCE

Time profiles of daily snow depths in 1968-1969 illustrate the accumulation sequence in the woodlands (Fig. 1a). A cover of loose snow of low density develops, usually by late October. It is even, except for interception effects. As the tree canopies are not very wide, these effects are small. The peak snow depth is reached in March and commonly exceeds 1.2 m. Commonly, the uppermost 0.10 - 0.15 m of the snow cover are of a density below .15 g/cm^3 until March, when increasing solar radiation accelerates the densification of the near surface layers. The density of the basal layers usually does not exceed .3 g/cm^3 until March (Adams et al, 1966).

Gradual changes in surface roughness and wind regime characterise the accumulation sequence in the alpine tundra areas. Vegetation-free ridge crests do not protect the snowcover from erosion and therefore exhibit the locally highest erosion rates in early winter. An outward growth of these aerodynamically smooth areas occurs as a result of accumulation at their downwind edges which act as efficient snow traps. The aerodynamic characteristics of the terrain vary with wind direction and speed, and therefore a smooth area developed by wind of one direction may be strongly eroded by wind of a different direction or speed, adding to the

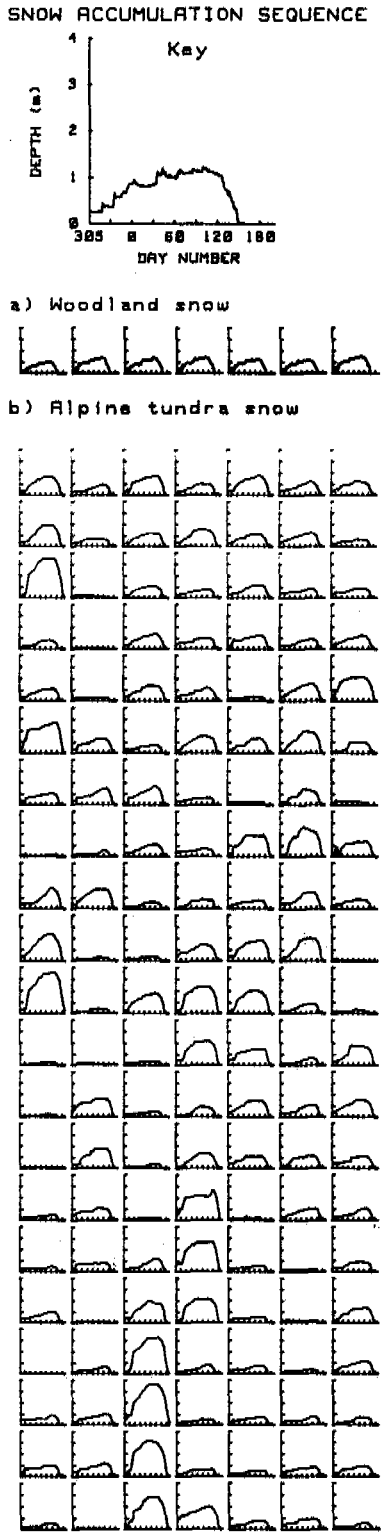

Fig. 1: Snow depth variations through the 1968-1969 winter in (a) woodland (Schefferville Snow Course and (b) alpine tundra (Timmins 4 Snow Course)

complexity of snow accumulation in open terrain. Time profiles of semi-weekly measurements in 1968-1969 (Fig. 1b) illustrate the great temporal and spatial variability in snow depth in alpine tundra as compared to woodland.

The drift transport in early winter is mainly over short distances from the smooth areas to their edges. By comparison, little drift transport occurs in aeas where dense brush still is exposed above the snow surface. Over time however, the brush vegetation is gradually buried by snowfall. This creates new source areas for dirfting snow. Later in the winter the smooth areas begin to merge, thereby eliminating the most efficient snow traps. This drastically changes the snow accumulation patterns. Snow drift transport over long distances now becomes possible, leading to a more strongly fragmented snow deposit of higher density than before (Fig. 2a). The most rapid increase in bulk density coincides with the period during which individual patches merge into a connecting surface of smooth terrain.

With continued snow accumulation the spatial variations in wind stress are gradually reduced so that the snow deposit from individual storms becomes more evenly distributed. In general, therefore, by late winter the greatest depth increase from individual storms occurs on lee slopes and in valleys while ridge crests still accumulate little or no snow. The bulk density of the snow cover depends strongly on the relative proportions of basal, low density layers and surficial high -density layers in the overall vertical snow profile. In areas of deep snow accumulation the wind-blown snow forms a larger fraction of the snow profile. In areas of very deep snow the large overburden pressure additionally compresses the basal layers. Therefore, at the time of peak snow accumulation, the bulk snow density in alpine tundra shows a general increase with depth (Fig. 2b). In shallower snow the densities are more variable. The basal layers are only covered by a thin veneer of dense snow and therefore tend to both retain their low density and form a larger, variable, fraction of the total vertical profile of the snow cover.

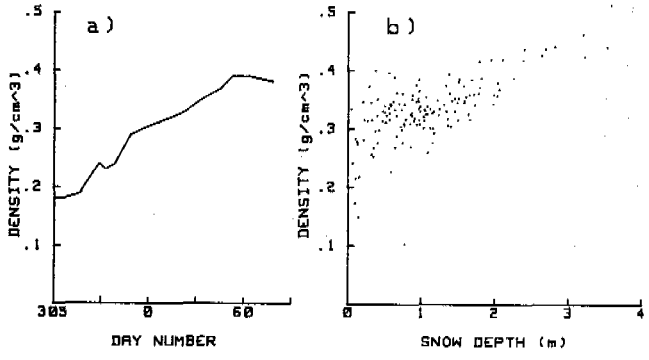

Fig. 2: Mean snow density (a) at the Timmins 4 snow course from the beginning of winter to April 21, and (b) spatial variations in bulk density on March 13, 1969.

The topographic control on snow depth is strongest in convex parts of the terrain and near ridge crests. The temporal and interannual variability in snow depth therefore tends to be smaller in areas of shallow snow, than in areas of deep snow. Figure 3 shows the spatial variations in peak snow depth on alpine tundra (March measurements) at Timmins 4 over the years 1969 to 1973. Two years of greater snow accumulation (1969 and 1970) exhibit fairly similar depth distributions which, however, are distinct from those in years of lesser snow accumulation (1971, 1972 and 1973). The depths differ proportionally more in deep than in shallow snow areas. An intermediate pattern (not shown) was observed in 1974. Particularly significant in this context, however, is the very great difference in extent of areas with very shallow snow. The area covered by snow less than .5 m deep is doubled in 1971-1973 as compared to 1969-1970. As these shallow snow areas are the main zones of heat loss, this great interannual variability adds considerable complexity to the dynamics of the ground temperature field.

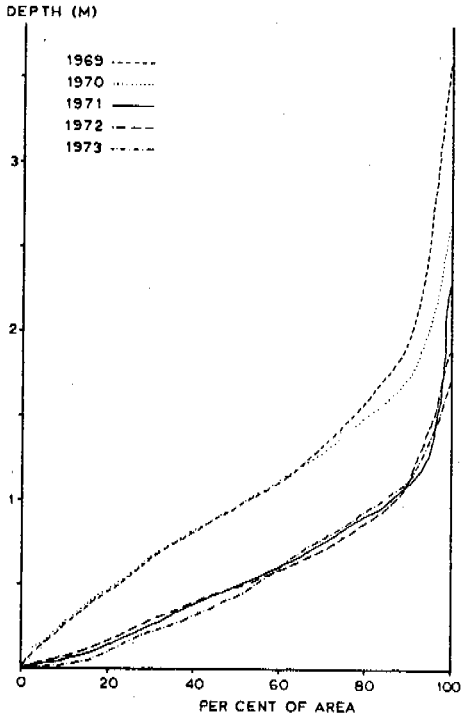

Fig. 3: Snow depth variations at Timmins 4, 1969-1973 (March surveys).

SIMULATIONS OF SNOWCOVER INFLUENCE ON THE GROUND TEMPERATURE FIELD

One of the most important aspects of the seasonal snow cover is its thermal resistance or Rsi-value which is defined as d/k where d is the depth of the snow cover (m), and k is the thermal conductivity in W/m/K. Using the densities in Figure 2, the formulation by Devaux (1933) relating thermal conductivity to snow density, and predicted snow depths (Granberg, 1973), it is possible to estimate spatial and temporal variations in thermal resistance by the snow cover at the Timmins 4 Permafrost Experimental Site (Figure 4).

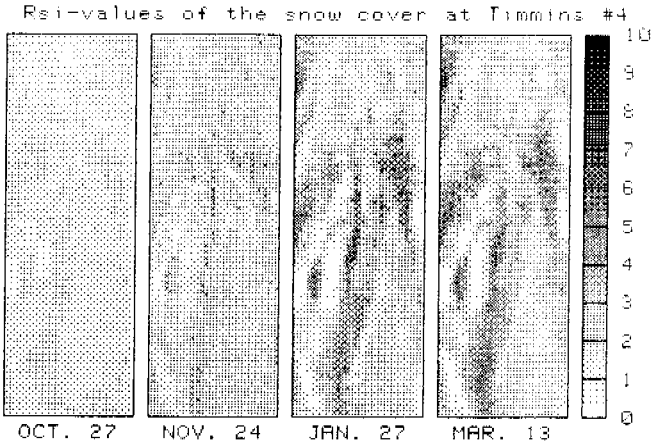

Fig.4: Spatial and temporal variations in Rsi-values at Timmins 4 in 1968-1969.

The simulations show that in early winter the Rsi-values are relatively uniform spatially. Over time they increase in some parts of the terrain while low Rsi-values remain at ridge crests and in other convex parts. By comparison, the Rsi-values computed for Stake # 7 on the Schefferville snow course (located in woodland) for the same dates were 1.4, 3.7, 3.1 and 4.1 respectively. According to the simulations, most of the alpine tundra site experiences lower Rsi-values than those at the forest site. Exceptions are several relatively narrow zones, some of which are known to be taliks or unfrozen ground (Nicholson and Thom, 1973).

Ground/snow interface temperatures are influenced by absorption of solar radiation, particularly in areas of shallow snow (Desrochers and Granberg, this volume). Figure 5, which was produced using predicted snow depths and an application of Beer's Law, shows the spatial variations in transmissivity of the snow cover at Timmins 4. The transmissivity is expressed as that percentage of solar radiation incident upon the snow surface which is available at the snow/ground interface. A spectrally integrated extinction coefficient of .15/cm was used throughout the series although values in the range from .08 to over .4/cm have been observed at Schefferville (Kulkarni, 1986).

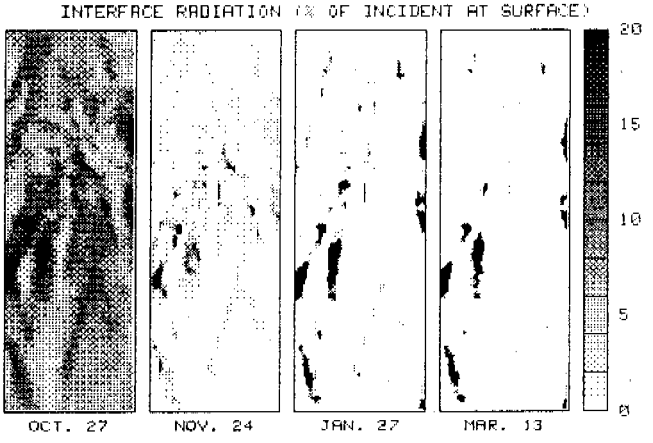

Fig. 5: Spatial and temporal variations in transmisivity of the snow cover at Timmins 4 in 1968-1969.

The map sequence shows that transmissivities are high overall in early winter because of the generally shallow snow. Later in the winter it is only in the areas adjacent to ridge crests that significant amounts of solar radiation may reach the snow/ground interface.

Meltwater percolation in spring raises the ground surface temperature to 0°C in snow covered areas (Desrochers and Granberg, this volume). The melting point is reached in April and the ground/snow interface temperature remains at this level until the snow cover disappears. The extent of ground remaining at 0°C can be mapped by applying a melt function to the late winter snowcover prediction. This melt function may be spatially uniform or spatially varied according to microclimate factors. A spatially uniform snow depth decrease was applied to the March 13 snow depth prediction in order to generate the map series of the extent of ground remaining at 0°C (Figure 6). This map sequence may be compared to Figure 5 in Granberg (1973) which is a snow depth map produced from aerial photographs taken sequentially during snowmelt in 1969.

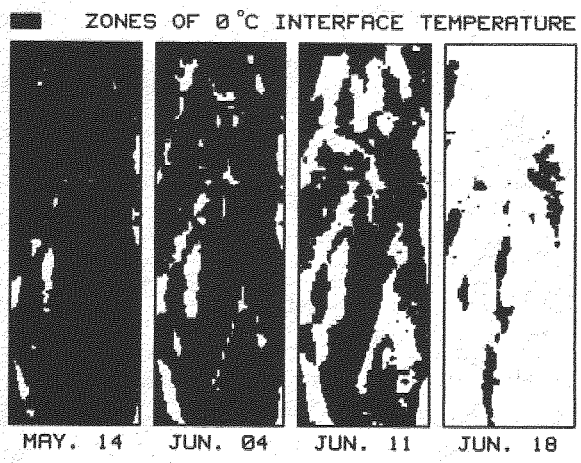

Fig. 6: Maps of ground surface temperatures of 0°C during snow melt in 1968-1969 at the Timmins 4 Permafrost Experimental Site.

RELATIONSHIPS BETWEEN SNOW AND VEGETATION

There is a close spatial correlation between the alpine tundra vegetation and several aspects of the seasonal snow cover. There is, first, a relationship between the depth of snow and the height of vegetation which is related to damage of supranivean parts by snow abrasion during winter storms. The abrasion is most severe in a "snow abrasion zone" at the snow surface where the bulk of the particle transport takes place. The abrasion is manifested by a "hedge-trimming" in those parts of the terrain where the snow cover is shallow. In areas of deeper snow, abrasion does not produce the same effect as the snow depths are more variable and the plants are protected for a longer part of the winter. Spruce trees in open terrain exhibit a "wind gap" at the height of the most commonly occuring snow depth during mid-winter. It is believed that the abrasion damage is more severe at low temperatures due to the increased brittleness of the twigs (Granberg, 1972). Dendrochronologic observations on scattered alpine spruce at Schefferville (Werren, 1981) show that it may take a tree over 140 years to penetrate the snow abrasion zone.

Secondly, there is an evident, large spatial variation in root zone temperatures which is related to spatial variations in the Rsi-values of the snow cover. In those parts of the terrain where the Rsi-value is close to 0 throughout the winter, root zone temperatures of -20°C can occur for extended periods of two to three months in most winters. Such temperatures are well below those endured by the root systems of most tree-forming species and probably, together with snow abrasion, explain the absence of trees from the ridge crests.

Third, a cover of diverse species of lichens is prominent in the alpine tundra areas near Schefferville. Observations during snowmelt indicate a grading in the species that is apparently related to snow depth. In areas of shallow snow a thin mat of dark-colored lichen species prevails while in deeper snow areas a thicker cover of light-colored species such as Cladina Alpestris occurs. Those lichens that survive on the ridge crest itself are nearly black. This color grading is probably related to the availability of solar radiation at the snow/ground interface. Several lichen species can photosynthesize at temperatures well below the freezing point, some as low as -10°C (Lange, 1965). This enables many lichens to photosynthesize beneath the snow cover. The darker colored species would have a thermal advantage over the lighter colored in those parts of the terrain where the penetration of solar radiation through the snow cover is significant. In the deeper snow areas, the lighter colored species prevail and often form a deep (.1 m or more) mat. As lichens form a highly insulating surface cover which also, outside the dark lichen areas near ridge crests, has a relatively high surface albedo, this represents an indirect thermal effect of the seasonal snow cover which probably allows a significantly greater summertime heat gain in ridge crest areas than elsewhere.

In those parts of the terrain where the snow cover remains longest in spring there is usually not much vegetation. Although the wintertime root-zone temperatures are favourable in these locations, the reduced length of the growth season, possibly paired with effects of snow-dwelling parasitic fungi and mechanical effects of snowcover settling prevents the establisment of trees.

As it is the absence of woodlands that causes the spatial variations in snowcover properties that lead to the development of permafrost, it may be assumed that the devastation by fire of woodland in the Schefferville area will lead to permafrost aggradation. Because of the interrelationships between microclimates, snow cover properties and vegetation cover, a substantial expansion of the alpine tundra areas may be expected. The nature of the microclimate modification is such that the re-establishment of a forest cover is difficult. The presence of decayed tree trunks from previous forests in alpine tundra areas near Schefferville would tend to support this conclusion. Furthermore, because of the slow regeneration, there is adequate time for substantial bodies of permafrost to be established before the forest re-invades a burned area. Many currently forested locations at Schefferville can therefore be expected to contain isolated permafrost bodies relating to earlier denudation by fire. Thermocable data in such locations should also show signs of

the amelioration in microclimate caused by the re-establishment of the forest cover.

CONCLUSIONS

Although the main conclusions from the permafrost modeling project remain to be drawn, previous research and preliminary results discussed in this paper show that it is possible not only to map and model in considerable detail the spatial distribution of snow cover and permafrost, but also to map a wide range of associated themes, using mainly weather and terrain data as inputs. While the simulations shown in this paper are at this stage only partially calibrated it is believed that they, with fairly good accuracy, indicate the spatial dynamics of the features shown.

ACKNOWLEDGEMENTS

The author would first like to acknowledge the fieldwork efforts by staff and students at the McGill Subarctic Research Station and the Iron Ore Company of Canada which generated the necessary database to make the current modeling project possible. Additional support has been provided by research contracts and grants from the Terrain Science Division, Geological Survey Sciences Division, Geological Survey of Canada (TSD GSC), the National Science and Engineering Research Council of Canada and the Department of Indian Affairs and Northern Development Northern Training Grants Program. Particular thanks go to Drs. A. Judge and A. Taylor of the Permafrost Research Section of TSD GSC who were instrumental in obtaining funding for the project.

REFERENCES

MSRP- McGill Subarctic Research Papers

Adams, W P, Cowan, W R, Findlay, B F, Gardner, J S and Rogerson, R J (1966). Snowfall and snow cover at Knob Lake, central Labrador-Ungava. MSRP (22), 114-120.

Annersten, L J (1966). Interactions between surface cover and permafrost. Biul. Peryglacj., (15), pp. 27-33.

Desrochers, D T & Granberg H B (1988). Schefferville snow/ground interface temperatures. (this volume).

Devaux, J (1933). L'économie radio-thermique des champs de neige et des glaciers. Annales de Physique (2), 2, 5-67.

Goodrich, L E (1982). The influence of snow cover on the ground thermal regime. Can. Geotechn. J. (19), 421-432.

Granberg, H B (1972). Snow depth variations in a forest-tundra environment near Schefferville. M.Sc. thesis, Geography, McGill University. 131 pp.

Granberg, H B (1973). Indirect mapping of the snow cover for permafrost prediction at Schefferville, Quebec. Proc. 2nd Int. Conf. on Permafrost, Washington, National Academy of Sciences, 113-120.

Granberg, H B, Lewis, J E, Moore, T R, Steer, P & Wright, R K (1983). Schefferville Permafrost Research. Final Report DSS Contract No 20SU-23235-Z-1030. 26 Vols.

Granberg, H B, Desrochers, D T, Lewis, J E, Wright, R K & Houston, L C (1984). Annotation, error analysis and addenda to the Schefferville Permafrost Data File. Final Report, DSS Contract No. OST83-00302, 16 Vols.

Jones, I G (1976). An attempt to quantify permafrost distribution near Schefferville, Quebec. M.Sc. thesis, Geography, McGill University, 165 p.

Kulkarni, A V (1986). A field study of the visible and near-infrared spectral reflectance and attenuation of solar radiation by snow. M.Sc. thesis, Geography, McGill University, 111 p.

Lange, O L (1965). Der CO2- Gaswechsel von Flechten bei tiefen Temperaturen. Planta (64), 1-19.

Nicholson, F H (1976). Permafrost thermal amelioration tests near Schefferville. Can. J. Earth Sci.(13),1694-1705.

Nicholson, F H (1978a). Permafrost distribution and characteristics near Schefferville, Quebec: Recent studies. Proc. 3rd Int. Conf. on Permafrost, Ottawa, National Research Council of Canada. 427-433.

Nicholson, F H (1978b). Permafrost modification by changing the natural energy budget. Proc. 3rd Int. Conf. on Permafrost, Ottawa, National Research Council of Canada. 61-67.

Nicholson, F H (1979). Permafrost spatial and temporal variations near Schefferville, Nouveau-Quebec. Geogr. Phys. et Quat. (33), 265-267.

Nicholson, F H & Granberg, H B (1973). Permafrost and snowcover relationships near Schefferville. Proc. 2nd Int. Conf. on Permafrost, Washington, National Academy of Sciences, pp. 151-158.

Nicholson, F H & Lewis, J S (1976). Active layer and suprapermafrost groundwater studies, Schefferville, Quebec. Second A.G.U. Conference on Soil Water Problems in Cold Regions, Edmonton, Alberta, Sept. 1-2, 1976.

Nicholson, F H & Thom, B G (1973). Studies at the Timmins 4 Permafrost Experimental Site. Permafrost: The North American Contribution to the Second International Conference. National Academy of Sciences, Washington, D.C., 159-166.

Palm, E & Tveitereid, M (1979). On heat and mass flux through dry snow. J. Geophy. Res. 84(C2), 745-749.

Powers, D, O'Neill, K & Colbeck, S C (1985). Theory of natural convection in snow. J. Geophys. Res., 90 (D6). pp. 10641-10649

Thom, B G (1969). New permafrost investigation near Schefferville, P.Q., Rev. Geog. Montreal, (23), pp. 317-327.

Werren, G L (1981). Dendroecology of spruce in central Labrador-Ungava. MSRP (32), 97-116.

Wright, R K (1981). The water balance of a lichen tundra underlain by permafrost. MSRP (33), 110 p.

Wright, R K (1983). Relationships between runoff generation and active layer development near Schefferville, Quebec. Proc. 4th Int. Conf. on Permafrost, Washington, National Academy of Sciences, 1412-1417.

PERENNIAL CHANGES IN NATURAL COMPLEXES OF CRYOLITHOZONE

G.F. Gravis, N.G. Moskalenko and A.V. Pavlov

All-Union Research Institute of Hydrogeology and Engineering Geology, Moscow, USSR

SYNOPSIS The paper analyzes time variability of regime parameters of geocryological conditions. A conclusion is made that perennial changes of these parameters are largely due to snow-accumulating regime and can considerably exceed depth variations in seasonal thawing. A concept of critical points in time series of evolution of cryogenous phenomena is introduced. A role of biogenous components is analyzed in dynamics of geocryological conditions after technogenous disturbances.

Among all time-dependent changes in natural complexes, the most studied in geocryology are perennial variations in thickness of seasonally thawed layer of soils (STL), which usually do not exceed 10% of average multi-annual values at temperate latitudes, reaching only in rare cases the 1/14 part of them (Epshtein, 1962; Are, Demchenko, 1972; Gavrilova, 1973; Pavlov, 1975; Vtyurina, 1976). The greatest time-dependent unstability of seasonal thawing (h_{th}) is observed at high latitudes. The variations in thickness of STL here can be more than the 1/3-1/2 part of an average multi-annual value, with the lower variations for mineral soils than for organogenous ones. As compared with an average annual air temperature and even with average temperature for summer season as well as with other thermal parameters of a natural complex, h_{th}-values appear to be in general more stable in perennial profile (Pavlov, et al., 1983). According to the results obtained in Igarka over a period of 22 years, an increase in time-dependent variability of average annual temperatures of air t_{air} and of soils t_h at the STL base, as compared with h_{th}, can be estimated by the following statistical characteristics:

Parameter	Average value ($\bar{x}$)	Maximum	Minimum	Mean square deviation σ	Normalized deviation $\sigma/\bar{x}$
t_{air}, °C	-6.2	-3.4	-10.4	2.0	0.32
t_h, °C	-5.6	-3.7	-7.3	1.0	0.18
h_{th}, m	1.58	1.85	1.40	0.17	0.11
h_f, m	1.09	1.74	0.62	0.33	0.30

Perennial changes in depth of seasonal freezing h_f as observed in Igarka, Zagorsk and other sites appear often to be, on the contrary, higher than those of determining hydrometeorological factors (Pavlov, 1984).

In Yakutsk there were carried out 6-year stationary observations of time-dependent variability of all parameters of heat transfer between soil and atmosphere (Pavlov, 1975, 1984). The observations showed that the inter-annual fluctuations of basic climatic parameters over the above period were relatively slight (e.g. total radiation - 3%, average annual air temperature - 11%, the height of snow cover - 33%) and the components of radiation-thermal balance varied in the following ranges: depth of seasonal thawing - 9%; radiation balance - 10%; heat circulation at the STL top - 14% and at the bottom - 11%; turbulent heat-transfer and heat-losses by evaporation - to 40%; average annual temperature of STL top soils - 87%. Variations of some parameters in heat-transfer between soil and atmosphere were also studied in a number of cryolithozone areas using mathematical modelling over a period of 50 years (Pavlov and et al., 1983). Annual valuates for temperature of top soils (t_s), depth of seasonal thawing (h_{th}) and time of joining (τ_f) of seasonally thawed layer with permafrost strata were determined. In the Yakutsk region the amplitudes of perennial changes of t_s, h_{th} and τ_f amounted, accordingly, to 7.3°C; 0.22 m; 1921 hr for sandy loam and 4.9°C; 0.14 m; 2214 hr - for loams. Normalized deviations of these parameters accounted for 0.37; 0.03; 0.2 for sandy loam and 0.58; 0.01; 0.2 - for loams. Real variations of modelled parameters are of a some excess of the theoretical ones because all determining factors are not possible to be taken into consideration in defining a problem. Among the geothermophysical parameters considered, the lowest variability was found also for h_{th}-values and the highest one - for t_s-values.

Changing ranges of average annual temperatures of top soils during the last 30-40 years amounted to: in the Central Yakutia - from +0.5 to -8.9°C; in the North Yenisei area - from +2 to -4.8°C and in north-east of West Siberia - from -4 to -12°C.

The studies of time-dependent tendency in changes of t_s, h_{th} and τ_f-values in Yakutsk showed that an obvious rising in height of snow cover from 1950s resulted during the subsequent 25-year period in an increase of topsoil temperature by 2.2°C and at a depth of 3 m - by 1.8°C (Fig. 1). Thus, mathematical simulation and stationary observations allowed to know that perennial changes of heat transfer, STL-freezing period and other parameters of geocryological conditions can considerably exceed the variations in the depth of seasonal thawing and depend, to a greater extent, on snow-accumulation regime than on air temperature.

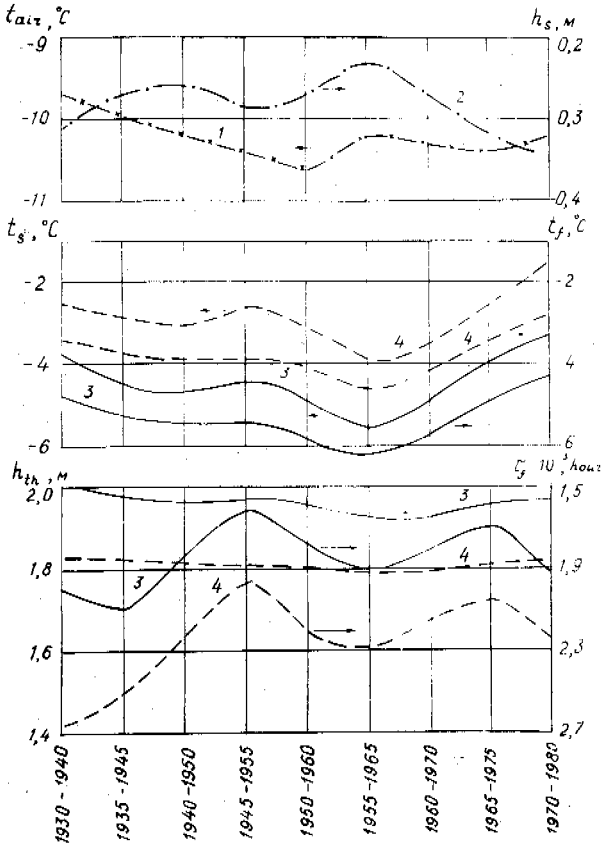

Fig. 1 Changes of: air temperature t_{air}; peak height of snow cover h_s; surface temperature t_s and at a depth of 3 m t_f; depth of seasonal thawing h_{th} and time of freezing τ_f according to average sliding values over a 10-year period in Yakutsk city and village of Syrdakh (Central Yakutia). 1,2 - both sites; 3 - Yakutsk, 4 - Syrdakh.

Man-induced impacts disturb natural evolution of natural complexes and lead to activation of geocryological processes. Possibilities to produce a directed effect on thermal regime of soils by managing external heat transfer are rather limited because an effect on one of the components of heat balance disturbs the steady natural heat equilibrium and hence changes the other components in the opposite direction. Therefore, an artificial change of any component in external heat transfer even in very broad ranges (e.g. of reflected radiation through decreasing surface albedo) results in not so significant changing of heat flux to a soil (Pavlov, Olovin, 1974). A great thermal effect can be caused by using such modes of an impulse influence as removal (disturbance) of poorly heat-conductive snow- and vegetation-covers and construction of artificial coverings and fillings. According to the observations carried out in the north of West Siberia, the removal of moss-peaty cover reduces during 2-3 years soil albedo and evaporation by a factor of 1.5-2.5, radiation balance - by 5-15%, average annual soil temperature - by 0.7-2°C, depth of seasonal thawing - by a factor of 2-4. An annual difference between a seasonal heat-flux to a soil and its heat-losses due to thawing of permafrost soils (PFS) accounts for 1/2 to 3/4 part of seasonal total heat under natural conditions. Cardinal changes in natural thermal components, after forest-cover removed, are established for the taiga zone. As a rule, these are a rise of reflectability and a decrease in radiation balance of the territory. Due to a lower evaporability of a disturbed area as compared with a forested one, moisture circulation is reduced, there is observed an increase in seasonal heat-accumulation in soils and in thickness of STL.

To perennial variations in thermo-moisture regime of soils and its thechogenous disturbances are related the changes in cryogenous processes and phenomena but these relations are complex. Time series of evolution of any cryogenous phenomenon has such critical points at which, when reached, abrupt quantitative and qualitative changes occur in the whole combination of processes forming this phenomenon. Some processes relax or come to end, other ones intensify; new processes appear or the leading process is replaced by another one.

Critical points are reached both gradually and suddenly. Gradual approach to them is associated with directed small changes of the phenomena proper (e.g. growth of ice veins and perennial frost mounds, deepening of thermokarst depressions, etc.) or of external factors of their development, in particular thermo-moisture ones. Sudden reaching of the critical points is attributed to man-induced impacts, certain combinations of components in thermo-moisture regime of soils or sharp deviations of separate components from their average multi-annual values.

A vivid example of such an irregularity is presented by stone streams. It is long become apparent that these streams of two types: slow and rapid (Solonenko, 1960; Korzhuev, 1973). Slow streams are connected with trans-

port of separate stones (cryogenous and thermogenous deserption). During rapid streams, the total stone mass darts off away. Studies carried out at the ridge of Udokan (northern Transbaikal) showed that one of the reasons for reaching a critical point, at which displacement of separate stones changes into movement of the all stone mass, lies in an increase in a depth of seasonal thawing after poor-snow winters when infiltrated or overflow-infiltrated ice is not formed within stone mass during spring snow-melting (Gravis, 1980; Konchenko, 1984).

In the mountain-taiga belt of the Udokan ridge (1250 m over sea level) the stone stream at one of the sites of the north-western 15°-slope thawed annually to a depth of 1.2 m during 1977-1980, and remained immovable. But after the poor-snowy winter of 1980-1981, the permafrost bottom of the stone steam thawed out (rock debris and stones with sandy-loamy filling to a depth of 1.45 m and soils - to a greater depth). This caused a mass movement of stones in the sites where the stream was undercut: holes and semi-hollows became partially filled.

Due to a lack of stationary observations critical points are quantified not enough yet and some of them are not established at all. For an example, investigations in the northern Transbaikal allowed to find two new critical points associated with perennial cryogenic swelling and fracturing.

The critical point in development of perennial swelling is arch formation in the lower part of frozen mass due to irregular freezing of confined aquifers. With a further increase in ground-water pressure, ice extraction begins in the apical section of the arch. Then water injections can be formed and area-regular perennial swelling changes into a differential one.

One of the critical points in development of polygonal-veined relief is the initial formation (in the top frozen mass) of cryogenic texture with subvertical elements (veins) which are inherited by frost-induced fractures. Since this moment growth of initially-soil veins in polygonal wedge structures is replaced by accumulation of wedge ice.

Generally, development of cryogenous processes comprises two types of changes in natural complexes: recurrent and unrecurrent. Recurrent changes occur when the upper horizon of frozen strata is non-icy(low-icy)and surface subsidence, thus, during thawing-out is small. Moreover, technogenous disturbances should not concentrate surface run-off. A leading factor of changes in cryogenic processes is becoming vegetation, with restoration of which cryogenic processes and their determining thermomoisture parameters return into the initial state.

Unrecurrent changes begin when the upper horizon of frozen strata is icy and (or) concentration of surface run-off takes place. In this case, sinks with an increased moisture content in their bottoms or with accumulated water initiating thermokarst-formation, or ravines appear.

In the north-taiga subzone of West Siberia sink-formation is promoted by increasing height of snow cover. Here, the subsidence of PFS (permafrost soils)-roof reaches 5 m over a period of 10-15 years. In the sinks of perennial frost mounds, small lakes are formed to a depth of 0.8-1 m.

In tundra and forest-tundra subsiding of the territory stops, if its dewatering takes place, in 5-10 years. Newly formed relief-types are fastened by turf, cryogenic processes become stable. Much slower proceeds self-recovery of biocoenoses. Some disturbed complexes are being restored extremely slowly (to 100 years) or are not restored at all.

Long-term studies of biotite components carried out in different natural zones of West Siberia (Moskalenko, Yastreba, 1980) allowed to trace the dynamics of vegetational cover under natural conditions and under influence of impulse disturbances (e.g. removal of vegetation, upper peaty layer to a thickness of 20 cm; disturbance of microrelief). The longest period (15 years) of observations over anthropogenic dynamics of vegetation was spent in the northern taiga near the town of Nadym where stationary grounds were constructed in different natural and disturbed complexes.

To obtain a quantitative evaluation of vegetation dynamics using auto-correlation method (Vasilevich, 1970), coefficients were calculated for correlation between occurrences of species in different years. Individual features of dynamics of their occurrence under natural and disturbed conditions were established for all species composing phytocoenoses.

Vasilevich V.I. (1970) reported that meadow species of the central European part of the USSR did not show oscillations (casual variations in species abundance). Studies of the West-Siberian north-taiga phytocoenoses also did not establish casual changes in species occurrence. On the testing grounds with disturbed conditions, the major species showed an continuous decrease in correlation coefficients with years, which is typical of succession changes.

Recovering succession begins always with grassy or grass-mossy coenoses. Then after 5-15-year period, a shrub-grass-mossy stage follows. In the earlier forested areas, this stage is preceded, as a rule, by grassy and grass-mossy stages with undergrowing of pioneer tree-species, usually a birch.

Observations over the areas disturbed more than 30 years ago, showed the slowest restoration of mossy cover which again begins markedly to contribute to vegetation only in 20-30 years. Thus, restoration of meadows, grassy and grass-mossy marshes can be completed during the first two tens of years whereas the restoration of tundrea- and forest coenoses with lichen cover requires about 50 years.

Leading ecological factor influencing the rate of vegetation restoration in temperate-continental regions of West Siberia lies in humidifying conditions. As soil-moisture content of disturbed natural complexes grows, the area covered by vegetation increases, number of species falling out of coenosis-composition reduces, there is observed an increase of species not occurred in the coenosis earlier, and of species common for initial and new communities. Function between covering rate of vegetation appeared in the fifth year after technogenous disturbance, and moisture content in the upper 0.5 m soil-layer is near to a linear one.

In the northern taiga the slowest restoration is undergone by disturbed mineral mounds and heaving ridges with low-moistened peat-podsol-eluvium-gley acid and poor sand soils. The mounds and ridges, before disturbed, were covered with cedar ledum-licher open woodlands. The removal of peaty horizon and vegetation cover deepened the seasonal thawing in frost mounds by more than twice (Geocryological prediction..., 1983), caused a decrease in soil moisture (by twice) and in humus content, stimulated oxidation processes. This serves a reason for slow overgrowing of mounds with vegetation. During the first years after soil disturbance, restoration of vegetation cover amounted to no more than 20% and only in 10 years it reached 50%, but the number of new plant-species even in 15 years remained almost by twice lower as compared with initial conditions. Sedge community appeared at the mounds during the first years, was replaced in 5 years by a birch-sedge one, in 10 years - by birch-sedge-mossy and in 15 years - by a birch-cowberry-sedge-mossy community.

At the mounds with poor vegetation, an activation of eolation- and thermo-erosion-processes is observed. Intermound ravines with highly wetted peat-boggy soils covered, before disturbed, by cottongrass-sedge-sphagnum marshes are being overgrown with plants several times as fast as mound-tops. Rate of grass- and moss covering of the disturbed areas where moistening conditions did not undergo considerable changes, amounted already the next year to 50%, and in 5 years increased to 70-80; species number seemed to be even higher than that under the initial conditions due to appearance of some new grass species. Fifteen-twenty years later, the marshes showed development of phytocoenoses, species composition of which slightly differed from that of initial ones. Peat-boggy soils of ravines, as soils of frost mounds, are acid, having low exchange-cation content and high hydrolytical acidity (Vasilevskaya, Ivanov, Bogatyryov, 1986), therefore revegetation rate is mainly determined, if technogenous disturbances are of the same type, by conditions of moistening and snow-accumulating, which are different in mounds and ravines.

Destruction and following restoration of vegetation cover have a considerable influence on dynamics of geocryological conditions (Tyrtikov, 1974). So, the vegetation removal from undulated areas of West Siberia with birch-pine shrub-lichen open-woodlands leads to an increase in average annual temperatures of top soils by 5-7°. In winter period due to decreased snow-cover, soil temperature drops by 1-1.5° and freezing depth rises from 1.5 m to 2 m. A technogenous site shows, with development of birch-grass-moss vegetation, a fall in average annual temperatures by 1.5-3.5° as compared with woodless areas. Differences between natural and man-induced conditions are shortened as relative to a height of snow cover and depth of seasonal freezing.

Geocryological predictions for the developing areas should take account of changes in thermo-moisture regime of soils, progress of cryogenous processes as well as restoration of turf-vegetational cover. Prediction of vegetation restoration after impulse disturbances is made for some gas deposits of cryolithozone (Moskalenko, 1983). According to a rate of vegetation restoration after technogenous disturbances, a small-scaled zoning is carried out for the northern West-Siberian territory (Fig. 2). The figure shows that a rate of vegetation covering increases from north to south and from drained uplands to flat swamped plains.

Fig. 2 Scheme of zoning of the northern West Siberia according to revegetation rate after technogenous disturbances stopped.

Rate of vegetational restoration:
A. in flat plains: 1 - rapid (80-100*); 2 - slow (60-80); 3 - very slow (40-60).
B. in high dissected plains:

at positive forms of relief	at negative forms of relief
4 - slow	rapid
5 - very slow	rapid
6 - very slow	slow

*) Degree of predicted soil covering with vegetation appeared in the 20th year after its destruction, in %.

REFERENCES

Are, A.L., Demchenko, P.Ya. (1972). Nekotorye rezul'taty mnogoletnikh nablyudenii za protaivaniem gruntov v okrestnostyakh Yakutska. V kn.: Eksperimental'nye issledovaniya protsessov teploobmena v myorzlykh gornykh porodakh. Moskva, Nauka, s.91-97.

Vasilevich, V.I. (1970). Metody avtokorrelyatsii pri izuchenii dinamiki rastitel'nosti. Trudy MOIP, t.38, s.17-23.

Vasilevskaya, V.D., Ivanov, V.V., Bogatyrev, L.G. (1986). Pochvy Zapadnoi Sibiri. Moskva: MGU, 226 s.

Vtyurina, E.A. (1976). O vremennoi izmenchivosti moshchnosti sezonnoprotaivayushchego sloya gornykh porod. V kn.: Sezonno- i mnogoletnemyorzlye gornye porody. Vladivostok, s.107-114.

Gavrilova, m.K. (1983). Klimat Tsentral'noi Yakutii. Yakutsk: Kn.izdatel'stvo, 119 s.

Grechishchev, S.E., Moskalenko, N.G., Shur, Yu.L., et al. (1983). Geokriologicheskiy prognoz dlya Zapadno-Sibirskoi gazonosnoi provintsii. Novosibirsk: Nauka, 182 s.

Gravis, G.F. (1980). Vybor ploshchadok dlya nablyudeniy za dvizheniem kurumov. V kn.: Geokriologicheskie issledovaniya. Moskva: VSEGINGEO, s.49-53.

Konchenko, L.A. (1984). Temperaturnyi rezhim kurumov i odna iz vozmozhnykh prichin ikh aktivizatsii. V kn.: Izuchenie i prognoz kriogennykh fizikogeologicheskikh protsessov. Moskva: VSEGINGEO, s.54-61.

Korzhuev, S.S. (1973). Kamennye plashchi Sibiri. Izdatel'stvo AN SSSR, seriya geograf..., No.2, s.20-33.

Moskalenko, N.G. (1983). Prognoz vosstanovleniya rastitel'nogo pokrova, narushennogo tekhnogennym vozdeistviem na severe Zapadnoi Sibiri. Izv. VGO, vypusk 2, s.113-119.

Moskalenko, N.G., Yastreba, N.V. (1980). Issledovanie dinamiki rastitel'nogo pokrova, narushennogo tekhnogennym vozdeistviem. V kn.: Biogeograficheskie aspekty prirodopol'zovaniya. Moskva: Mysl, s.144-164.

Pavlov, A.V. (1975). Teploobmen pochvy s atmosferoi v severnykh i umerennykh shirotakh territorii SSSR. Yakutsk: Kn. izdatel'stvo, 302 s.

Pavlov, A.V. (1984). Energoobmen v landshaftnoy sfere Zemli. Novosibirsk: Nauka, 256 s.

Pavlov, A.V., Votyakova, N.I., Shipitsina, L.I. (1983). Analiz mnogoletnikh izmeneniy parametrov teplovogo rezhima sezonnoprotaivayushchikh gruntov. V kn.: Inzhenernye issledovaniya myorzlykh gruntov. Svoistva gruntov i massivov, vzaimodeistvie s sooruzheniyami. Novosibirsk: Nauka, s.46-52.

Solonenko, V.P. (1960). Ocherki po inzhenernoi geologii Vostochnoi Sibiri. Irkutskoe kn. izdatel'stvo, 88 s.

Tyrtikov, A.P. (1974). Dinamika rastitel'nogo pokrova i razvitie vechnoi merzloty v Zapadnoi Sibiri. Moskva: Izdatel'stvo MGU, 196 s.

Epshtein, G.M. (1962). Merzlotnye issledovaniya. V kn.: Geologiya i inzhenernaya geologiya Verkhnego Amura. Moskva: Izdatel'stvo MGU, s.162-187.

PERMAFROST AND ITS ALTITUDINAL ZONATION IN N. LAPLAND

P.P. Jeckel

Geographisches Institut, Universität Giessen, Federal Republic of Germany

SYNOPSIS In Fennoscandia, permafrost research was concentrated on palsas for a long period. More recent reports on permafrost outside the palsa mires refer mainly to such occurrences where permafrost can be identified by other geomorphological indicators such as tundra polygons or small thermokarst ponds. In addition, permafrost occurs in Lapland at many locations where tracing by diagnostic landforms is either difficult or impossible. Two examples are given: ground temperature measurements with thermistors at Mt. Njulla, Abisko, demonstrate the existence of permafrost at 880 m a.s.l.; bottom temperatures of the winter snow cover indicate permafrost at Mt. Saana, Kilpisjärvi, at 650 m a.s.l. Based on these results, some reflections regarding the altitudinal permafrost zonation are presented.

1. INTRODUCTION

The author of this paper follows the permafrost definition given by Brown and Kupsch (1974, p. 25): "The thermal condition in soil or rock of having temperatures below 0°C persist over at least two consecutive winters and the intervening summer". With regard to the altitudinal zonation of permafrost, the terminology presented by King (e.g. 1983, 1986) has been adopted.

During a Nordqua-Symposium held at the Abisko Scientific Research Station in North Sweden in September 1987, the author established that many geoscientists, particularly from Finland, are still convinced that in Finland permafrost occurs exclusively in the palsas, even in the northernmost parts of Lapland. Indeed, permafrost research in Finland was so extensively concentrated on palsa investigations that, even in 1982, Seppälä still pointed out: "So far permafrost has been found only in the mires in the cores of palsas" (p. 232).

2. FENNOSCANDIAN PERMAFROST OCCURRENCES OUTSIDE THE PALSA MIRES

In Norway and Sweden, as early as the beginning of the century, the occurrence of permafrost outside the palsa mires had been referred to by a few authors (incl. Reusch, 1901; Hamberg, 1904; Fries, 1913). The best review of Fennoscandian permafrost discoveries known up to that time is provided by Sven Ekman (1957). He reports in detail on a drilling operation for drinking water in North Sweden in 1941. This well was situated at 1220 m a.s.l. and led to the discovery of a permafrost thickness of 70 m in bedrock (loc. cit., p. 34). Regardless of Ekman's well founded arguments, some authors maintain even years later, that permafrost in Fennoscandia is mainly restricted to the palsa mires (Vorren, 1967; Wramner, 1973). However, those researchers who consider a much wider extension of permafrost possible or even very likely are forced to conclude that in Fennoscandia very little is known on the permafrost distribution outside the palsa mires (e.g. Rapp and Rudberg, 1960, p. 152; Åhman, 1977, p. 18; Karte, 1980, p. 445; King, 1984, p. 1; Svensson, 1986, p. 123).

Since the beginning of the sixties, the number of reports on permafrost outside the palsas has increased in Norway and Sweden, most concentrating, however, on occurrences which can be traced by geomorphological indicators. These include investigations of ice-cored morains and rock glaciers (Östrem, 1959, 1964, 1971; Barsch and Treter, 1976). The reports by Rapp and Annersten (1969), Rapp and Clark (1971) and Rapp (1982, 1983), which use 'tundra polygons' and so-called 'collapsed pingos' as further permafrost indicators, must rank in the same category. The papers by Lagerbäck and Rohde (1985, 1986) and Åkerman and Malmström (1986) focus on 'small thermokarst ponds'. Moreover, some very recent papers emphasizing the wide extension of Fennoscandian permafrost are mainly based on morphological indicators (Svensson, 1986; Meier, 1987).

The extent to which permafrost mapping based exclusively on geomorphological features can provide a reliable picture must be doubted. Of course, it is accepted that the existence of certain 'diagnostic landforms' (Harris, 1986, p. 12) proves that permafrost is present at these locations, or at least was. However, the converse cannot be concluded: the lack of diagnostic landforms does not per se prove that there is no permafrost. Harris (1986, p. 12), for example, had to admit that the extension of permafrost was twice as wide as he had presumed in an area which he had mapped mainly on the basis of morphological indicators. The same risk also exists for Fennoscandia, as shown by the repeated assertion that permafrost occurs only in the palsas. Accordingly, for a satisfactory estimation of permafrost extension, diagnostic-landform mapping must be complemented by further investigations, e.g. ground temperature measurements and hammer seismic or geoelectrical soundings. In this respect, the investigations by King (1976, 1982, 1983, 1984, 1986) and King and Seppälä (1987a, 1987b) provide valuable information. These papers and his own field experience lead the present author to the conclusion that permafrost is widespread over large areas of Lapland, including locations where it cannot be identified, or at least not definitively, by geomorphological features alone.

3. PERMAFROST INVESTIGATIONS AT TWO TEST SITES IN SWEDISH AND FINNISH LAPLAND

3.1 The test sites

Mt. Njulla near Abisko in North Sweden and Mt. Saana near Kilpisjärvi in Northwest Finland were chosen as test sites (cf. fig. 1). Within each area, there is a sufficient difference in elevation (see table 1) as well as abundant examples of periglacial features. Both locations are easily accessible, but the main advantage is the fact that the Abisko Scientific Research

Station is very near to Mt. Njulla and the Kilpisjärvi Biological Station is in the immediate neighbourhood of Mt. Saana. As a result, some logistic support by the stations was possible and climatological data measured nearby were available (table 2).

FIGURE 1

Location of investigation sites and MAAT isotherms in Lapland

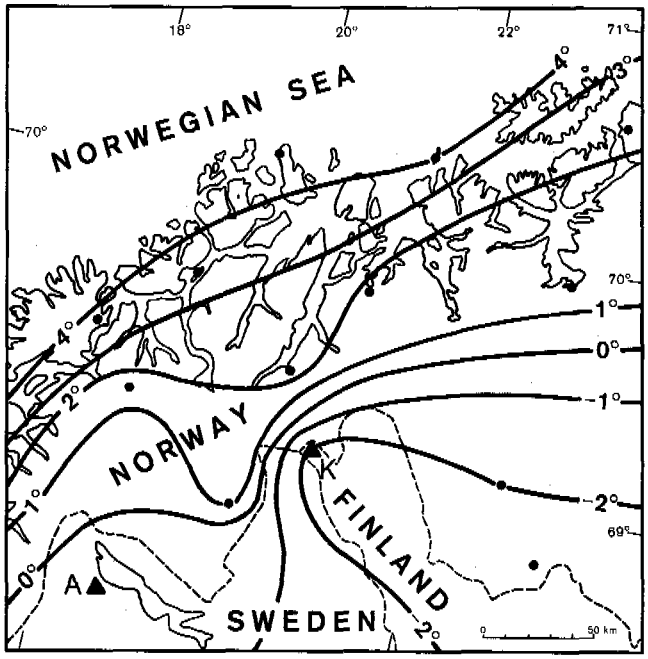

▲A investigation area Abisko/Mt. Njulla

▲K investigation area Kilpisjärvi/Mt. Saana

• Norwegian weather stations (cf. Åhman, 1977)

-1°- MAAT isotherms for the period 1931-1960

The map is partly based on figs. 26 and 28 in Åhman, 1977. The isotherms have been redrawn because they are also based on data from Swedish and Finnish stations (designed by P.P. Jeckel, drawn by S. Roth).

Abisko / Mt. Njulla

Abisko is the name of a river and a valley leading to a large lake, Torneträsk; it is also the name of a lake about 10 km upstream, a village and one of Sweden's oldest national parks. The area is one of the driest in Fennoscandia. Towards the west, the precipitation sum increases rapidly and exceeds 1000 mm per year in the western part of the mountains. While the highest positive temperature anomaly for the high sixty degrees northern latitudes is to be found in the Norwegian coastal areas, Abisko enjoys all the advantages of a foehn window behind the Scandinavian mountain chain. Further to the east, cloudiness and precipitation increase again and there the situation becomes more and more continental.

The Mt. Njulla test site is situated on the south shore of Torneträsk due west of the Abisko delta. It is the easternmost summit of the Western Abisko High Mountains, which reach 1590 m at their highest point. The surficial rocks are mainly garnet mica schists and other medium or high metamorphic rocks such as hard schists, graphite schists and calcite marbles (Kulling, 1964, plate 2). Tectonically, the massif belongs to the upper and middle allochthonous nappe system of the

TABLE I

Some topographical parameters relating to the test sites

	Njulla	Saana
latitude	68° 22'	69° 03'
longitude	18° 42'	20° 52'
elevation of mountain top	1169	1029 m a.s.l.
elevation of valley bottom	342	473 m a.s.l.
highest mt. top in a 5 km radius	1403	953 m a.s.l.
in a 25 km radius	1991	1448 m a.s.l.
closest weather station	Abisko	Kilpisjärvi
elevation of weather station	388	478 m a.s.l.
distance mt. top/weather station	5.3	3.1 km
elevation of timber line	650	600 m a.s.l.

TABLE II

Selected climatological data for Abisko and Kilpisjärvi

	Abisko	Kilpisjärvi	
MAAT	- 0.5	- 2.0	°C
MAAT February	-10.8	-13.1	°C
MAAT July	+12.3	+11.6	°C
abs. minimum temperature	-38.9	-47.2	°C
abs. maximum temperature	+31.3	+28.8	°C
precipitation	300	376	mm

All data of the weather stations Abisko and Kilpisjärvi for the period 1931-1960, partly unpublished.

Caledonides resting on the autochthonous Precambrian bedrocks (Scandinavian Caledonides, 1985).

The Mt. Njulla test site exhibits a great variety of periglacial forms which cannot be discussed here in detail, e.g. sorted polygons, unsorted stripes and steps, solifluction lobes, ploughing boulders, block fields, nivation hollows and terraces, talus cones and avalanche tracks. However, none of these features is a clear indicator of permafrost at the location concerned. The closest landforms at which permafrost is firmly established are the palsas east of the Abisko Delta (360 m a.s.l., 4 km away) and the thermokarst ponds at Rakaslako (about 1000 m a.s.l., 9 km away; see also Rapp, 1983, p. 85).

Kilpisjärvi / Mt. Saana

Kilpisjärvi is the name of both a lake and a small village on its north shore in the very northwest of Finland. Only here, near Kilpisjärvi, and in the nearby Halti area do the Caledonides extend to Finland, with elevations exceeding 1000 m. Topography and climate at Kilpisjärvi are not too different from conditions in Abisko: mean temperatures are 1 to 1.5°C lower and the entire situation is slightly more continental, as shown by the differences between mean air temperatures for July and February (23.1°C for Abisko, 24.7°C for Kilpisjärvi) and the difference between the absolute maximum and minimum temperatures (70.2°C, 76.0°C).

The Mt. Saana test site on the north shore of Kilpisjärvi consists mainly of Caledonian shales and schists. The east, south and west facing upper slopes are almost vertical cliffs ranging in height from a few dozen metres to more than 100 m. Saana is the outermost part of a Caledonian nappe overthrusted to the southeast. Compared with Njulla, bedrock outcrops are much more common and the overburden is generally thinner. Accordingly, patterned ground on Saana itself is rare; within block fields, individual stone polygons are found. Other periglacial forms present are solifluction lobes, talus cones and avalanche tracks.

3.2 Methods used

At each test site, seven ground temperature-measurement points have been installed down to a maximum depth of 2.4 m and equipped with up to eight thermistors. Temperatures of springs in late summer, as well as bottom temperatures of the snow cover (BTS) in late winter, were measured in both areas, and some electro-magnetic soundings were carried out. In addition, at Mt. Njulla, some hammer seismic soundings were conducted and air, ground and BTS temperatures have been recorded with a data logger. Complete results and procedure details will be given in another paper (Jeckel, in prep.). Here, only two examples have been selected.

3.3 Ground temperature measurements at Mt. Njulla, N. Sweden

The results given in the following were obtained at measurement points TM 6 and TM 7, both situated on the east facing slope of Mt. Njulla at 880 m a.s.l. The average gradient of this part of the slope is about 14°, or 25%. The distance between the two locations is only 21 m, but the ground temperatures are markedly different, as fig. 2 shows. The measurements were carried out with resistance thermometers with a negative temperature coefficient (NTC elements or thermistors). In the main, the same procedure was used as described by King (1984, p. 114).

FIGURE 2

Ground temperatures at test sites TM 6 and TM 7 Njulla, 880 m a.s.l.

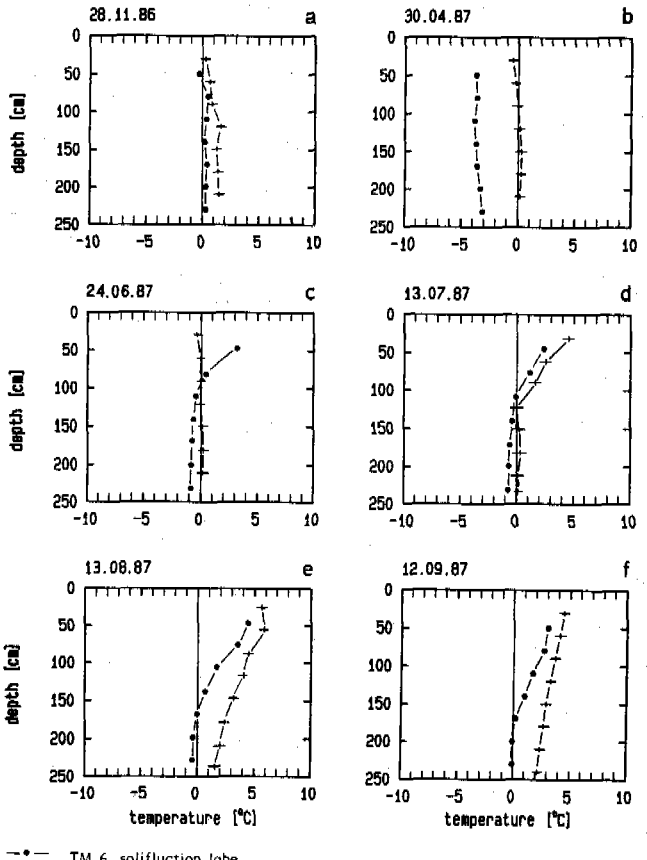

TM 6 was installed on the surface of a solifluction lobe about 10 m from its southern edge. This location is highly exposed to the wind; snow is blown away. Average thickness of the snow cover ranges between 0 and 20 cm on the surface of the solifluction lobe; within a 1 m radius of the measurement point the snow height was on no occasion found to be greater than 10 cm. TM 7 was placed in a nivation hollow between two solifluction lobes. Here, snow accumulates every winter and exceeds 3 m in the upslope part of the hollow. Directly at TM 7, snow thickness was 5 cm on 13.10.86, 51 cm on 28.11.86 and 190 cm on 30.04.87, while the surfaces of the solifluction lobes very close by were more or less free of snow. Accordingly, the cold was able to penetrate the ground deeply at locations such as TM 6; here, the late winter temperature was below -3°C, even at depth of 2.4 m. At locations such as TM 7, which at the beginning of December were already protected by a snow cover of 50 cm or more, the ground did not even freeze down to a depth of 1 m and the temperatures of the frozen layer were only slightly below 0°C (see fig. 2b). At the end of June, the upper layers were much warmer at TM 6 than at TM 7 (fig. 2c) because the latter was still covered with 25-30 cm of snow. TM 7 became free of snow on 04.07.87, and at the end of July, the snow completely disappeared in the nivation hollow. In the middle of July, ground temperatures at each depth were already higher at TM 7 than at TM 6 (fig. 2d). Subsequently, at TM 7, the ground temperatures increased continuously down to the lowest thermistor, while, from mid-July, the three lowest NTC elements at TM 6 kept almost constant temperatures: between -0.5°C and 0.0°C, which are typical for the zero curtain at the uppermost part of a frozen layer (figs. 2e, 2f). In 1986, the temperature difference between the two points was even greater than in 1987. At TM 7, the highest temperature for the lowest thermistor was recorded in September: 4.3°C. At TM 6, the maximum temperature at the lowest elements was recorded as late as 28.11.86: +0.3°C (fig. 2a). These values slightly above zero must also be regarded as typical for the zero curtain (French, 1976, p. 14).

TM 6 and TM 7 were chosen as examples because of their proximity to each other. The results prove that a perennial frozen layer exists at TM 6 and is not present at TM 7. Unfortunately, it was not possible to keep continuous records for the entire year because of the very difficult snow conditions during the winter. Nevertheless, on the basis of 12 measurements at each point from September 1986 to August 1987, mean ground temperatures for this period at a depth of 2.3 m and 2.4 m can be put at -0.8°C at TM 6 and +1.1°C at TM 7. The thickness of the active layer at TM 6 is thought to be approximately 2.5 m. Assuming that the MAGT at the permafrost table is -0.8°C and taking the average geothermal gradient to be 1°C/33 m, a permafrost thickness of about 25 m could be expected. Very probably, however, the frozen layer is much thinner here because of the higher ground temperatures in the immediate surroundings. A permafrost thickness of 5-10 m at TM 6 can be regarded as a reasonable estimation.

3.4 BTS measurements at Mt. Saana, N.W. Finland

Haeberli (1973) developed the method to prove the existence of permafrost by measuring the bottom temperature of the winter snow cover (BTS): beneath a minimum snow thickness of 1 m BTS values lower than -3°C indicate the occurrence of permafrost, while values higher than -2°C demonstrate the absence of a perennial frozen layer (loc. cit., p. 223). The method was improved by Haeberli and Patzelt (1982) and King (1984). The last-named author reduced the minimum snow thickness to 0.8 m (p. 66) and was furthermore able to detect that, at points with the same mean ground temperature, the BTS are determined by the thickness of the snow cover (p.125). Fig. 3 shows the critical values for BTS interpretation according to King: points above the horizontal line indicate a thin snow cover and should not be taken into consideration; below

this limit, low BTS values to the left of the temperature boundaries indicate the existence of permafrost, while high BTS values to the right of the two lines indicate the absence of permafrost. Temperatures between the two critical limits belong to a 'methodical uncertainty field' and do not permit definitive interpretation.

Fig. 3 shows the bottom temperatures of the winter snow cover measured within 5 profiles between 31.03.87 and 05.04.87. All 5 profiles were situated on a saddle at 720 m a.s.l. between two flat hill tops north of Mt. Saana and about 1 km northwest of Lake Saana. The two hill tops, with elevations of 750 and 760 m a.s.l., are only 30-40 m higher than the saddle and 70-80 m above the surface of Lake Saana and, on both, the snow cover was no more than 10 cm when the measurements were taken and is presumed to be very thin throughout the winter. By contrast, a maximum snow depth of 3.1 m was found in the middle of the saddle, which is to some extent in the lee of the northwestern hill top. At most points of the BTS profiles, snow depth ranged from 0.8 to 1.8 m. A distance of 10 m between the individual measuring points was chosen. Three profiles were run north to south; two were cross profiles west to east. In total, 53 values were measured; temperatures ranged between -2.4 and -6.9°C. As can be seen from fig. 3, these values indicate a perennial frozen layer underneath. This is somewhat surprising, at least for those points with a thick snow cover in the middle of the saddle, but might be accounted for as follows: permafrost patches began to develop below the permanently snow-free hill tops and increased gradually until they finally merged, even below the protective snow cover in the saddle. This would mean that the horizontal extent of this permafrost occurrence is at least 800 by 200 m, i.e. 16 ha.

FIGURE 3

Bottom temperatures of late winter snow cover
from profiles BTS K 87/4, 5, 8, 9, 10:
Saddle N.W. Saanajärvi, 720 m a.s.l.

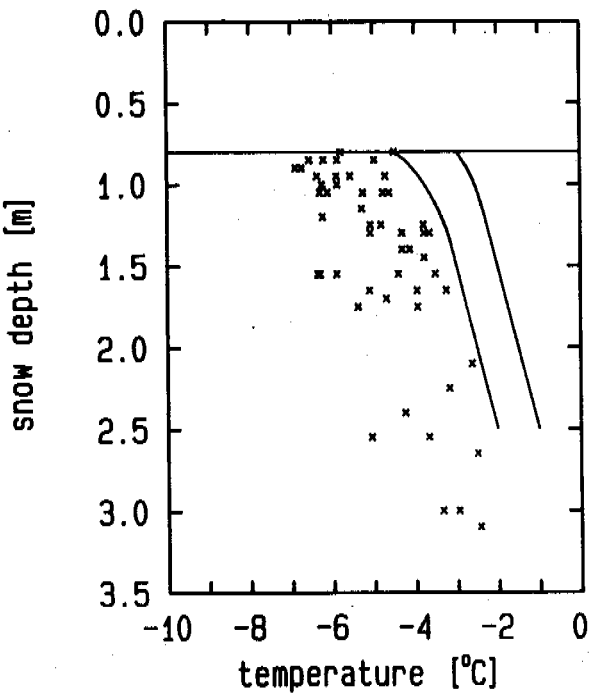

Some other profiles indicate the existence of smaller permafrost patches even at lower elevations. Almost all temperatures of a profile at 590 m a.s.l. range between the critical limits; here, definitive interpretation is not possible. However, the values of two profiles at 620 and 650 m a.s.l. provide indications of permafrost.

Harris (1986, p. 17) states that "BTS measurements do not work in continental, high latitude environments". This assertion cannot be accepted, because it is based on incorrect quoting. The fig. 2.6 presented by Harris (loc. cit.) shows BTS values between 0 and -1°C below a snow cover of about 1 m during the period February to April. According to Haeberli, these values would mean that permafrost is absent (see e.g. 1973, p. 223; 1978, p. 379) and not, as Harris quotes (1986, p. 18), "that permafrost should be present by the interpretation of Haeberli". Consequently, Harris' fig. 2.6 constitutes an argument that, even in his area of study, the BTS method works very well.

Admittedly, there is one reservation to be stated: as mentioned above, the use of BTS as permafrost indicators presupposes a snow thickness of at least 1 m according to Haeberli or 0.8 m according to King; and, of course, the more continental the investigation areas are, the more difficult it will be to find sufficient snow thicknesses. This implies that the BTS method is not universally applicable, but that does not mean that "BTS measurements do not work in continental, high latitude environments" (Harris, 1986, p. 17). The present author's investigations were carried out about 18° latitude further north than Harris' measurements and the BTS method was found to operate very well.

One more point must be stressed: first and foremost, BTS values prove the presence or absence of permafrost at the measuring point. Generalisations should be formulated very carefully. Particularly at the southern fringe of permafrost or at the lower limit of an altitudinal permafrost zone, a snow cover of about 1 m may be perfectly sufficient to protect the ground against winter cold so that there is no perennial frozen layer below the snow patch. Simultaneously, the ground at snow-free locations nearby can be cooled down so extensively that active permafrost can develop.

According to the present author's experiences in the field, the following general tendency seems to be valid for areas with a rather thin snow cover presenting only small patches suitable for application of the method: a) low BTS values below a thick snow cover demonstrate the existence of a perennial frozen layer at that location; if there are many snow-free areas nearby, permafrost is probably more widespread than can be established by means of the BTS method because of the lack of snow; b) high BTS values prove the absence of a perennial frozen layer at that location; if values are close to the critical limits and there are snow-free areas nearby, occurrences of permafrost should not be ruled out without further investigations.

4. ALTITUDINAL ZONATION OF PERMAFROST IN NORTH LAPLAND

For the latitudinal zonation of polar permafrost, both a twofold and a threefold division are in use. Regarding the altitudinal zonation of high-mountain permafrost, many authors advocate threefold classification into a continuous, a discontinuous and a sporadic permafrost belt, "as the ecological differences in alpine areas are very big" (King, 1986, p. 133; cf. also Haeberli, 1978, p. 381; Weise, 1983, p. 22) Furthermore, the threefold division of mountain permafrost is preferable because the limit between the discontinuous and the sporacid permafrost zone is thought to be not only the limit between areas with higher or lower percentages of permafrost terrain. In addition, the permafrost distribution pattern is different in both zones, as already emphasized by King (loc. cit.). Sporadic mountain permafrost occurs in areas with rather high mean annual air temperatures only slightly below 0°C or possibly, in very extreme cases, even slightly above 0°C (Haeberli, 1978, p. 381). At these temperatures, a perennial frozen layer can only develop if other local factors are highly favourable, e.g. sparse vegetation, very thin snow cover and special hydrological conditions.

Accordingly, the fact that small permafrost patches can form under these circumstances does not mean that the percentage of terrain underlain by permafrost enlarges, from the lowest individual incidences onwards, with increasing altitude. In many arctic and subarctic mountain areas, for instance, palsa situated in valley bottoms are the lowest permafrost occurrences; elsewhere in the valleys and on the lower slopes permafrost is not found, particularly if these areas are forested. Often there is a difference of several hundred metres in elevation between the palsas and the next highest permafrost occurrences. Nevertheless, there is a certain elevation above which the percentage of permafrost terrain increases fairly steadily with increasing altitude. This elevation should be considered the lower limit of the discontinuous permafrost zone. In forested parts of the mountains, this limit would normally have to be defined as being above the timber line: the trees cause snow to accumulate so that the ground is insulated against the winter cold. Below the timber line, formation of active permafrost is only possible at locations with very special conditions; if permafrost occurs here, these areas have to be characterized as parts of the sporadic permafrost zone.

In the Mt. Njulla and Mt. Saana investigation areas, permafrost was detected at locations where it could not be identified by diagnostic landforms. This is considered typical for the surrounding areas. Therefore, determination of the lower limit of the discontinuous permafrost zone in this author's investigation areas cannot be based on morphological features along the lines adopted by Barsch for the Swiss Alps (1977) or by Barsch and Treter for the Rondane area in Southern Norway (1976). By contrast, King's proposal seems to be better adapted for conditions in North Lapland. He combines the lower limit of the continuous permafrost zone with the lowest occurrence on south facing slopes and the lower limit of the discontinuous zone with the lowest occurrence on north facing slopes (1984, p. 130).

TABLE III

Air temperatures and lower limit of discontinuous permafrost zone at the investigation areas

	Abisko	Kilpisjärvi	
MAAT 1931-1960	- 0.5	- 2.0	°C
MAAT reduced to sea level [1]	+ 1.6	+ 0.5	°C
elevation of -1.5°C MAAT isotherm [1]	580	390	m a.s.l.
elevation of timber line	650	600	m a.s.l.
elevation of lowest permafrost occurrence above timber line, established by author's investigations	880	650	m a.s.l.
proposed lower limit of discontinuous permafrost zone (a)	800-850	600-650	m a.s.l.
reduced MAAT at elevation of (a) [1]	-2.7/-2.9	-2.6/-2.9	°C

[1] Gradient for all reductions 0.53°C/100 m, cf. Laaksonen, 1976

The data in table III form the basis for the following conclusions:

1. At Mt. Njulla, ground temperatures indicate a small permafrost patch at 880 m a.s.l. in a rather shaded location on the east facing slope. On the north slope, permafrost might occur somewhat lower. Therefore, the lower limit of the discontinuous permafrost zone is assumed to be 800-850 m a.s.l.
2. At Mt. Saana, BTS measurements provide evidence of an extended permafrost occurrence at 720 m a.s.l. Indications of smaller permafrost patches are to be found at 600-650 m a.s.l. on the north slope. Accordingly, this elevation is considered to be the lower limit of the discontinuous permafrost zone.
3. The mean annual air temperatures reduced to sea level show that the present author's investigation areas are appreciably colder at corresponding elevations than King's test sites, where the temperatures reduced to sea level range from 2.5 to 4.9°C (1984, p. 133). As a result, the permafrost zones extend nearer to sea level, especially at Mt. Saana.
4. In his general model of altitudinal permafrost zonation, King combines the lower limit of the discontinuous zone with the -1.5°C MAAT isotherm (e.g. 1986, p. 134). In both areas investigated, this isotherm runs well below the timber line. Therefore, any connection with the lower limit of the discontinuous permafrost zone seems unlikely.
5. At the author's test sites, reduced temperatures at the proposed lower limit of the discontinuous permafrost zone range from -2.5 to -3°C and thus do not deviate excessively from the values determined by King for his investigation areas (-2.0 to -2.5°C, cf. 1984, p. 133). Therefore, with regard to areas with conditions comparable to those at Abisko and Kilpisjärvi, it seems reasonable, for an initial approximation, to expect the lower limit of the discontinuous permafrost zone as defined above to be situated at the same elevation as the -2.5°C MAAT isotherm. It must be stressed that a modest temperature gradient of 0.53°C/100 m as proposed by Laaksonen (1976) has been deliberately applied. Using a higher gradient would have resulted in even lower reduced temperatures at the lower limit of the discontinuous permafrost zone.

Generalized assumptions on the basis of the findings presented in this paper may be premature. Of course, every permafrost occurrence is dependent on not only climate but also a number of local factors which could not be discussed here, e.g. topographic situation, vegetation, petrographical, pedological and hydrological conditions, as well as the continued existence of relic permafrost. A more detailed report will be presented in the near future (Jeckel, in prep.).

5. ACKNOWLEDGEMENTS

The results presented in this paper were obtained during investigations for a Ph.D. thesis initiated and supervised by Prof. L. King, Giessen, Federal Republic of Germany, and supported by a doctoral grant from the Konrad-Adenauer-Stiftung, St. Augustin, Federal Republic of Germany. In Lapland, accommodation and logistic support were kindly provided by the research stations in Abisko, Sweden, and Kilpisjärvi, Finland. The staff took great interest in the investigations and gave valuable help in many cases; some thermistor readings were carried out even under very difficult conditions during the winter months. Considerable encouragement was given by many visiting researchers at the stations in Lapland. Ulla Bartels and students from Giessen assisted in the field. Colleagues at the Geographical Institute in Giessen read the draft and submitted helpful comments. Stephen Atkinson checked the English text, Eva Peter typed the manuscript. To all these individuals and institutions I wish to express my sincerest thanks.

6. REFERENCES

Åhman, R. (1977).
Palsar i Nordnorge. Meddel. från Lunds Univ. Geogr. Inst. (78), 165 pp.

Åkerman, J. & Malmström, B. (1986).
Permafrost mounds in the Abisko area, north Sweden. Geogr. Ann. (68A), 3-4, 155-165.

Barsch, D. (1977).
Alpiner Permafrost - ein Beitrag zur Verbreitung, zum Charakter und zur Ökologie am Beispiel der Schweizer Alpen. In: Poser, H. (ed.): Formen, Formengesellschaften und Untergrenzen in den heutigen periglazialen Höhenstu-

fen der Hochgebirge Europas und Afrikas zwischen Arktis und Äquator. Abh.d.Akad.d.Wiss. in Göttingen, mathem.-phys. Klasse, 3. Folge, Nr. 31, 118-141.

Barsch, D. & Treter, U. (1976).
Zur Verbreitung von Periglazialphänomenen in Rondane/Norwegen. Geogr. Ann. (58A), 1-2, 83-93.

Brown, R.J.E. & Kupsch, W.O. (1974).
Permafrost terminology. Nat. Res. Council of Canada, Ass. Committee on Geotechnical Research, Technical Memorandum No. 111, 62 pp., Ottawa.

Ekman, S. (1957).
Die Gewässer des Abisko-Gebietes und ihre Bedingungen. Kungl. Svenska Vetenskapsakademiens Handlingar (6), 6, 172 pp.

French, H.M. (1976).
The Periglacial Environment. 309 pp., Longman, London & New York.

Fries, T.C.E. (1913).
Botanische Untersuchungen im nördlichsten Schweden. Vetensk. och prakt. undersökningar; Lappland, anordn. av. Luossavaara-Kiirunavaara A.B., 370 pp., Uppsala & Stockholm.

Haeberli, W. (1973).
Die Basis-Temperatur der winterlichen Schneedecke als möglicher Indikator für die Verbreitung von Permafrost in den Alpen. Zeitschrift für Gletscherkunde und Glazialgeologie (9), 1-2, 221-227.

Haeberli, W. (1978).
Special aspects of high mountain permafrost methodology and zonation in the Alps. Permafrost: Third Intern. Conf., Proceedings, 379-383, Ottawa.

Haeberli, W. & Patzelt, G. (1982).
Permafrostkartierung im Gebiet der Hochebenkar-Blockgletscher, Obergurgl, Ötztaler Alpen. Zeitschrift für Gletscherkunde und Glazialgeologie (18), 2, 127-150.

Hamberg, A. (1904).
Till frågan om förekamsten af alltid frusen mark i Sverige. Ymer (24), 1, 87-93.

Harris, S.A. (1986).
The permafrost environment. 275 pp. Croom Helm, London & Sidney.

Jeckel, P.P. (in prep.).
Untersuchungen zur Periglazialmorphologie und Permafrostverbreitung in Lappland.

Karte, J. (1980).
Rezente, subrezente und fossile Periglaziärerscheinungen im nördlichen Fennoskandien. Z. Geomorph. N.F. (24), 4, 448-467.

King, L. (1976).
Permafrostuntersuchungen in Tarfala (Schwedisch Lappland) mit Hilfe der Hammerschlagseismik. Zeitschrift für Gletscherkunde und Glazialgeologie (12), 2, 187-204.

King, L. (1982).
Qualitative und quantitative Erfassung von Permafrost in Tarfala (Schwedisch Lappland) und Jotunheimen (Norwegen) mit Hilfe geoelektrischer Sondierungen. Z. Geomorph. N.F., Suppl.Bd. 43, 139-160.

King, L. (1983).
High mountain permafrost in Scandinavia. Permafrost: Fourth Intern. Conf., Proceedings, 612-617, Washington.

King, L. (1984).
Permafrost in Skandinavien. Untersuchungsergebnisse aus Lappland, Jotunheimen und Dovre/Rondane. Heidelberger Geographische Arbeiten 76, 174 pp.

King, L. (1986).
Zonation and ecology of high mountain permafrost in Scandinavia. Geogr. Ann. (68A), 3, 131-139.

King, L. & Seppälä, M. (1987a).
Permafrost thickness and distribution in Finnish Lapland - results of geoelectrical soundings (in prep.).

King, L. & Seppälä, M. (1987b).
Permafrost Sites in Finnish Lapland and their Environment (in prep.).

Kulling, O. (1964).
Översikt över norra Norrbottensfjällens Kaledonberggrund. Sveriges geologiska undersökning, serie Ba, Nr. 19, 165 pp.

Laaksonen, K. (1976).
The dependence of mean air temperatures upon latitude and altitude in Fennoscandia (1921-1950). Ann. Academ. Scient. Fennicae A, III., Geol. Geogr. 119, 19 pp.

Lagerbäck, R. & Rohde, L. (1985).
Pingos in northernmost Sweden. Geogr. Ann. (67A), 3-4, 239-245.

Lagerbäck, R. & Rohde, L. (1986).
Pingos and Palsas in northernmost Sweden - Preliminary notes on recent investigations. Geogr. Ann. (68A), 3, 149-154.

Meier, K.D. (1987).
Studien zur periglaziären Landschaftsformung in Finnmark (Nordnorwegen). Jahrbuch der Geogr. Gesell. zu Hannover, Sonderheft 13, 298 pp.

Østrem, G. (1959).
Ice melting under a thin layer of moraine, and the existence of ice cores in moraine ridges. Geogr. Ann. (41), 4, 228-230.

Østrem, G. (1964).
Ice-cored moraines in Scandinavia. Geogr. Ann. (46), 3, 282-337.

Østrem, G. (1971).
Rock glaciers and ice-cored moraines, a reply to D. Barsch. Geogr. Ann. (53A), 3-4, 207-213.

Rapp, A. (1982).
Zonation of permafrost indicators in Swedish Lapland. Geografisk Tidsskrift (82), 37-38.

Rapp, A. (1983).
Zonation of Permafrost Indicators in Swedish Lapland. In: Poser, H. & Schunke, E. (ed.): Mesoformen des Reliefs im heutigen Periglazialraum. Abh.d.Akad.d.Wiss. in Göttingen, mathem.-phys. Klasse, 3. Folge, Nr. 35, 82-90.

Rapp, A. & Annersten, L. (1969).
Permafrost and tundra polygons in Northern Sweden. In: Péwé, T.L. (ed.): The periglacial environment - past and present, 65-91, Montreal.

Rapp, A. & Clark, M. (1971).
Large nonsorted polygons in Padjelanta National Park, Swedish Lappland. Geogr. Ann. (53A), 2, 71-85.

Rapp, A. & Rudberg, S. (1960).
Recent periglacial phenomena in Sweden. Biuletyn Periglacjalny (8), 143-154.

Reusch, H. (1901).
Evig frosen jord i Norge. Naturen, 25, Bergen.

Scandinavian Caledonides (1985).
Tectonostratigraphic map 1:2,000,000. Sveriges geologiska undersökning, serie Ba, Nr. 35.

Seppälä, M. (1982).
Present-day periglacial phenomena in northern Finland. Biuletyn Peryglacjalny (29), 231-243.

Svensson, H. (1986).
Permafrost. Some morphoclimatic aspects of periglacial features of Northern Scandinavia. Geogr. Ann. (68A), 3, 123-130.

Vorren, K.D. (1967).
Evig Tele i Norge. Ottar (51), 3-26.

Weise, O. (1983).
Das Periglazial - Geomorphologie und Klima in gletscherfreien, kalten Regionen. 199 pp., Bornträger, Berlin & Stuttgart.

Wramner, P. (1973).
Studies of Palsa Bogs in Taavavuoma and the Laiva Valley, Swedish Lapland. Akademisk avhandling. 7 pp.. Göteborg.

A MODEL FOR MAPPING PERMAFROST DISTRIBUTION BASED ON LANDSCAPE COMPONENT MAPS AND CLIMATIC VARIABLES

M.T. Jorgenson[1] and R.A. Kreig[2]

[1]Alaska Biological Research, Inc., Fairbanks, Alaska
[2]R.A. Kreig and Associates, Inc., Anchorage, Alaska

SYNOPSIS

A computer model for mapping permafrost distribution was developed that uses vegetation, terrain unit and equivalent latitude maps and regional air temperature data as the geographic data base for calculating the heat balance of the ground surface. The ratio of the amount of heat entering the soil in the summer, when the ground was seasonally thawed, and lost during the winter, when the ground was seasonally frozen, was calculated from the degree-day sums at the surface and soil thermal conductivities. Thermal parameters used in the computations were assigned to the vegetation and terrain unit types and modified by the equivalent latitude map. The simulated permafrost distribution within the Spinach Creek Watershed near Fairbanks, Alaska, agreed closely with the distribution mapped by photointerpretation. The effects of climatic warming on permafrost distribution were also assessed. Within the mapping area, permafrost covered 100% of the area below a mean annual air temperature of -7.7°C, 37.3% at -3.5°C, 21.3% at 0°C and was eliminated above 2.6°C.

INTRODUCTION

Recent efforts to develop models for predicting permafrost distribution have emphasized the relationships between permafrost and vegetation, soil, topography, air temperature and snowcover. A site-specific approach using digital terrain data, developed by Morrisey (1986), integrated vegetation, topography and thermal imagery. Nelson (1986) developed a computational method for the regional mapping of permafrost distribution based on minimal climatic data and subsurface information. The model presented in this paper uses both landscape component maps, delineating vegetation, terrain units, and equivalent latitude values, and regional climatic data for site-specific large scale mapping of permafrost. This approach allows the model to be responsive to the spatial variability of a landscape and to changes in climate.

An essential prerequisite for permafrost distribution models is the simplification of surface heat balance computations in order to reduce the number of site-specific variables needed in the geographic data base. Energy budget models (Goodwin and Outcalt 1975, Ng and Miller 1977) that utilize a large number of radiative, thermal and aerodynamic parameters of the surface, more realistically account for the pathways involved in establishing the heat balance at the surface, but are not feasible for regional mapping methodologies. More appropriate to regional mapping models are simpler approaches that relate soil temperature or soil heat flux to air temperature (Lunardini 1978, Haugen et al. 1983), net radiation (Abbey et al. 1978), and to biophysical factors of the surface (Jorgenson 1986).

Large-scale permafrost mapping models must also be able to incorporate remote sensing products that identify and classify characteristics of the landscape that have differing microclimatic and soil thermal properties. Much progress has been made in classifying and characterizing the vegetation (Viereck et al. 1983) and terrain unit (Kreig and Reger 1982) components of the landscape through the use of remotely sensed data, including satellite imagery and aerial photography. However, the weakest area for model development is the limited data base characterizing the microclimates of a broad range of vegetation types and analyses that account for the geographic variability of soil temperature.

A portion of the Spinach Creek Watershed, located 25 km NW of Fairbanks, Alaska, was selected as the test site for model development. This mountainous watershed is representative of much of the Yukon-Tanana uplands. The slopes have a shallow mantle of loess or have shallow residual soils on steeper sites. The valley bottom is generally filled with fine-grained retransported deposits removed from the hillsides. Closed stands of aspen, birch, and white spruce predominate on upland slopes, facing east, south and west. The valley bottom, ridge tops and north-facing slopes are dominated by black spruce. In valley bottoms, tussock bogs occur in small patches and low shrubs occur along small creeks and drainages.

STRUCTURE AND THEORETICAL BASIS FOR MODEL

The model uses the simple relationship offered by Carlson (1952) as the approximate criteria for permafrost formation. For any particular site, the ratio of the annual amount of heat

SYNOPSIS

A computer model for mapping permafrost distribution was developed that uses vegetation, terrain unit and equivalent latitude maps and regional air temperature data as the geographic data base for calculating the heat balance of the ground surface. The ratio of the amount of heat entering the soil in the summer, when the ground was seasonally thawed, and lost during the winter, when the ground was seasonally frozen, was calculated from the degree-day sums at the surface and soil thermal conductivities. Thermal parameters used in the computations were assigned to the vegetation and terrain unit types and modified by the equivalent latitude map.

The simulated permafrost distribution within the Spinach Creek Watershed near Fairbanks, Alaska, agreed closely with the distribution mapped by photointerpretation. The effects of climatic warming on permafrost distribution were also assessed. Within the mapping area, permafrost covered 100% of the area below a mean annual air temperature of -7.7°C, 37.3% at -3.5°C, 21.3% at 0°C and was eliminated above 2.6°C.

INTRODUCTION

Recent efforts to develop models for predicting permafrost distribution have emphasized the relationships between permafrost and vegetation, soil, topography, air temperature and snowcover. A site-specific approach using digital terrain data, developed by Morrisey (1986), integrated vegetation, topography and thermal imagery. Nelson (1986) developed a computational method for the regional mapping of permafrost distribution based on minimal climatic data and subsurface information. The model presented in this paper uses both landscape component maps, delineating vegetation, terrain units, and equivalent latitude values, and regional climatic data for site-specific large scale mapping of permafrost. This approach allows the model to be responsive to the spatial variability of a landscape and to changes in climate.

An essential prerequisite for permafrost distribution models is the simplification of surface heat balance computations in order to reduce the number of site-specific variables needed in the geographic data base. Energy budget models (Goodwin and Outcalt 1975, Ng and Miller 1977) that utilize a large number of radiative, thermal and aerodynamic parameters of the surface, more realistically account for the pathways involved in establishing the heat balance at the surface, but are not feasible for regional mapping methodologies. More appropriate to regional mapping models are simpler approaches that relate soil temperature or soil heat flux to air temperature (Lunardini 1978, Haugen et al. 1983), net radiation (Abbey et al. 1978), and to biophysical factors of the surface (Jorgenson 1986).

Large-scale permafrost mapping models must also be able to incorporate remote sensing products that identify and classify characteristics of the landscape that have differing microclimatic and soil thermal properties. Much progress has been made in classifying and characterizing the vegetation (Viereck et al. 1983) and terrain unit (Kreig and Reger 1982) components of the landscape through the use of remotely sensed data, including satellite imagery and aerial photography. However, the weakest area for model development is the limited data base characterizing the microclimates of a broad range of vegetation types and analyses that account for the geographic variability of soil temperature.

A portion of the Spinach Creek Watershed, located 25 km NW of Fairbanks, Alaska, was selected as the test site for model development. This mountainous watershed is representative of much of the Yukon-Tanana uplands. The slopes have a shallow mantle of loess or have shallow residual soils on steeper sites. The valley bottom is generally filled with fine-grained retransported deposits removed from the hillsides. Closed stands of aspen, birch, and white spruce predominate on upland slopes, facing east, south and west. The valley bottom, ridge tops and north-facing slopes are dominated by black spruce. In valley bottoms, tussock bogs occur in small patches and low shrubs occur along small creeks and drainages.

STRUCTURE AND THEORETICAL BASIS FOR MODEL

The model uses the simple relationship offered by Carlson (1952) as the approximate criteria for permafrost formation. For any particular site, the ratio of the annual amount of heat

entering the soil compared to the amount leaving (R), is dependent on the temperature degree-days sums at the surface and the thermal conductivities of the soil when it is thawed or frozen:

$$R = (DDT_s/DDF_s)/(K_f/K_t) \quad (1)$$

where DDT_s and DDF_s are surface thawing and freezing indices based on degree-day sums and K_f and K_t are the thermal conductivities of frozen and thawed soil.

The freezing and thawing degree-day sums and the frozen and unfrozen thermal conductivities of the soil are considered the most important variables. The use of n-factors (Lunardini 1978) and regional climatic data provided the simplest way to estimate surface temperature, which is a function of the total heat transfer at the surface. On the other side of the equation, the importance of the ratio of frozen to unfrozen thermal conductivities to permafrost formation has long been recognized for organic soil horizons and is of equal significance for mineral soils. The rate at which heat is lost from fine- and coarse-grained soils relative to the rate at which heat enters the profile increases rapidly with increasing moisture content of the soil (Fig. 1, Kersten 1949). This makes wet mineral soils, such as those fine-grained deposits in valley bottoms and depressions, particularly susceptible to permafrost formation. The frozen/unfrozen conductivity ratio is even higher for saturated organics approaching that of water, about 4 (Farouki 1981). However, at very low moisture contents the conductivity of frozen soil is less than that of unfrozen soil presumably because freezing reduces some of the bridge water between particles. This makes drier sites, such as well-drained soils beneath aspen stands, less susceptible to permafrost formation.

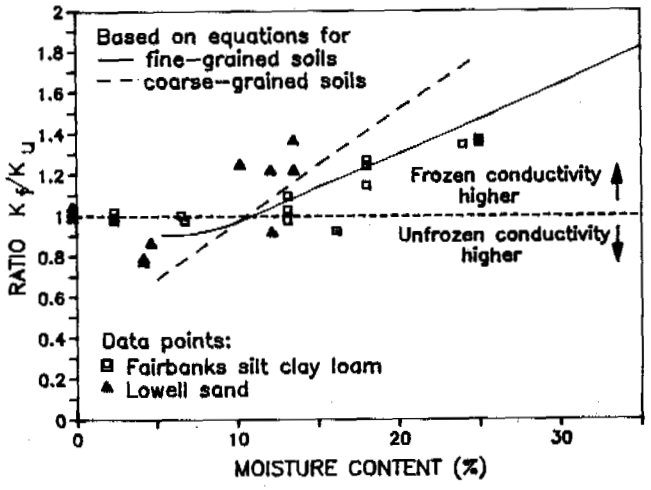

Figure 1. Effects of soil moisture on the ratio of frozen (K_f) to unfrozen (K_u) thermal conductivities. Ratios of equations (5)/(4) and (7)/(6) are plotted (see text). Data and equations are from Kersten (1949).

Surface temperatures are related to air temperatures using n-factors in the following equation:

$$R = ((DDT_a\ N_t\ P)/(DDF_a\ N_f))/(K_f/K_t) \quad (2)$$

where DDT_a is the thawing degree-days and DDF_a is the freezing degree-days of the air (above 0^oC) and N_t and N_f are thawing and freezing n-factors. P is a potential insolation index that modifies the summer n-factor according to the position on the landscape and is calculated by:

$$P = L/L_e, \quad (3)$$

where L is the latitude and L_e is the equivalent latitude of the site. The effect is to increase the n-factor on warmer sites and reduce the n-factor on colder sites.

Kersten's (1949) empirical equations were used to calculate the thermal conductivities of frozen and unfrozen soils. The equations give the thermal conductivity (K) of the soil in terms of its moisture content w (%) and its dry density γ_d. For unfrozen fine-grained soils

$$K_t = 0.1442(0.9\log w - 0.2)10^{0.6243\gamma_d} \quad (4)$$

and for frozen fine-grained soils

$$K_f = 0.00144(10)^{1.3737\gamma_d} + 0.01226(10)^{0.4994\gamma_{d_w}}. \quad (5)$$

For unfrozen coarse-grained soils

$$K_t = 0.1442(0.7\log w + 0.4)10^{0.6243\gamma_d} \quad (6)$$

and for frozen coarse-grained soils

$$K_f = 0.01096(10)^{0.8116\gamma_d} + 0.00461(10)^{0.9115\gamma_{d_w}}. \quad (7)$$

The water content of the soil was modified by the equivalent latitude of the site using:

$$w = w_m\ (L/L_e), \quad (8)$$

where w_m is the typical soil moisture for a given vegetation type. This has the effect of reducing soil moisture on south-facing sites and increasing moisture on north-facing sites.

Although the effects of snow cover on winter soil temperatures, and thus permafrost distribution, were recognized as important factors, snow depth and density were not directly incorporated into the model. Difficulties in mapping snow cover distribution precluded the use of snow effects in the model. Instead, the snow cover effects are inherent in the winter n-factors associated with each vegetation type.

MODEL INPUTS

Permafrost is mapped by calculating the heat balance at the ground surface for each pixel (picture element) of the mapping area. The FORTRAN program reads the vegetation, terrain unit and equivalent latitude map files, in raster format, and assigns landscape component classes to each pixel. Thermal parameters char-

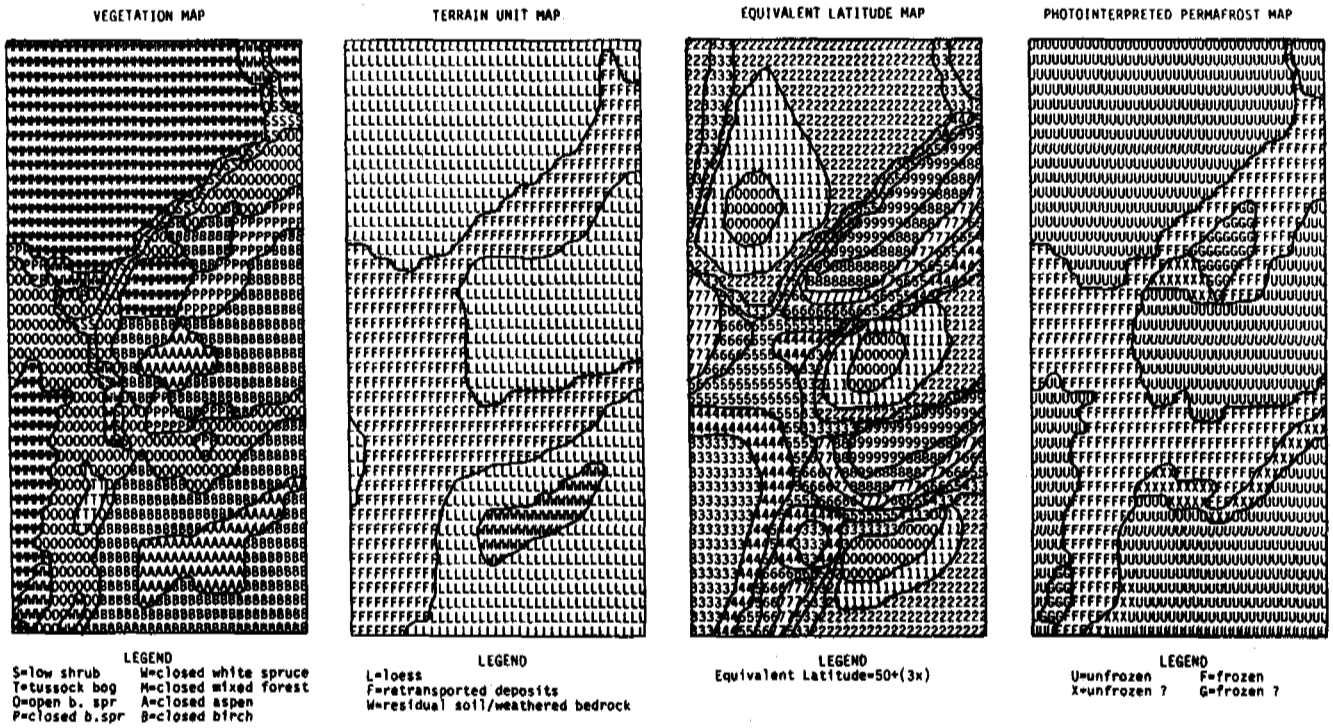

Figure 2. Landscape component maps for a portion of the Spinach Creek Watershed, Fairbanks, Alaska.

acteristic of each landscape component class were then assigned to each pixel for the heat balance computation, depending on the class assigned to each pixel. Summer and winter n-factors and soil moisture values assigned to each vegetation type are presented in Table I. The bulk densities assigned to each terrain unit were; 1.30 g/cm^3 for loess, 1.20 for retransported deposits, and 1.60 for residual soils. Thus, the frozen and unfrozen thermal conductivities of each pixel are a function of soil moisture values characteristic of each vegetation type and bulk densities characteristic of each terrain unit. A thawing degree-day value (^{o}C) of 1700 and a freezing degree-day value of 2950 were used for the Fairbanks long-term air temperature annual sums.

Table I. Thermal parameters assigned to each vegetation type.

Vegetation type	N-factor N_t	N-factor N_f	Soil Moisture (% wt.)
Closed aspen forest	1.00	0.30	15
Closed birch forest	0.90	0.35	20
Mixed birch-spruce forest	0.85	0.35	20
Closed white spruce forest	0.80	0.35	50
Open black spruce forest	0.60	0.30	50
Closed black spruce forest	0.50	0.30	45
Low shrub scrub	0.85	0.30	40
Tussock bog	0.90	0.30	55

The model was applied to a data base incorporating vegetation, terrain unit and equivalent latitude maps. The vegetation and terrain unit maps were delineated from airphotos (1:63,000 CIR) for a portion (1.6 x 3.0 km) of the Spinach Creek Watershed and then converted to raster format (Fig. 2). The equivalent latitude map was based on a 1:63,000 USGS topographic map using the approach of Dingman and Koutz (1974). Each pixel covers 43 x 74 m on the ground. To assess the validity of the model output, permafrost distribution was also delineated from the airphotos and agreement between methods was compared.

SIMULATION RESULTS

The model was initially run using n-factors developed from air and surface temperature in reports by Linnell (1973), Viereck et al. (1983), and Haugen et al. (1983). The initial run mapped 33.4% of the area as permafrost, similar to the 32.1% mapped by photo-interpretation. However, the photo-interpretation also mapped 2.6% of the area as questionably frozen and 4.4% as questionably unfrozen, thus the percentage of frozen area ranged from 25.1% to 39.1% when the uncertain areas were added or deleted. Small adjustments were then made to the thermal parameters of the vegetation types so that several of the north-facing deciduous stands and valley-bottom white spruce stands were mapped in subsequent runs as frozen instead of unfrozen. The transition zones along ridges and toes of slopes also

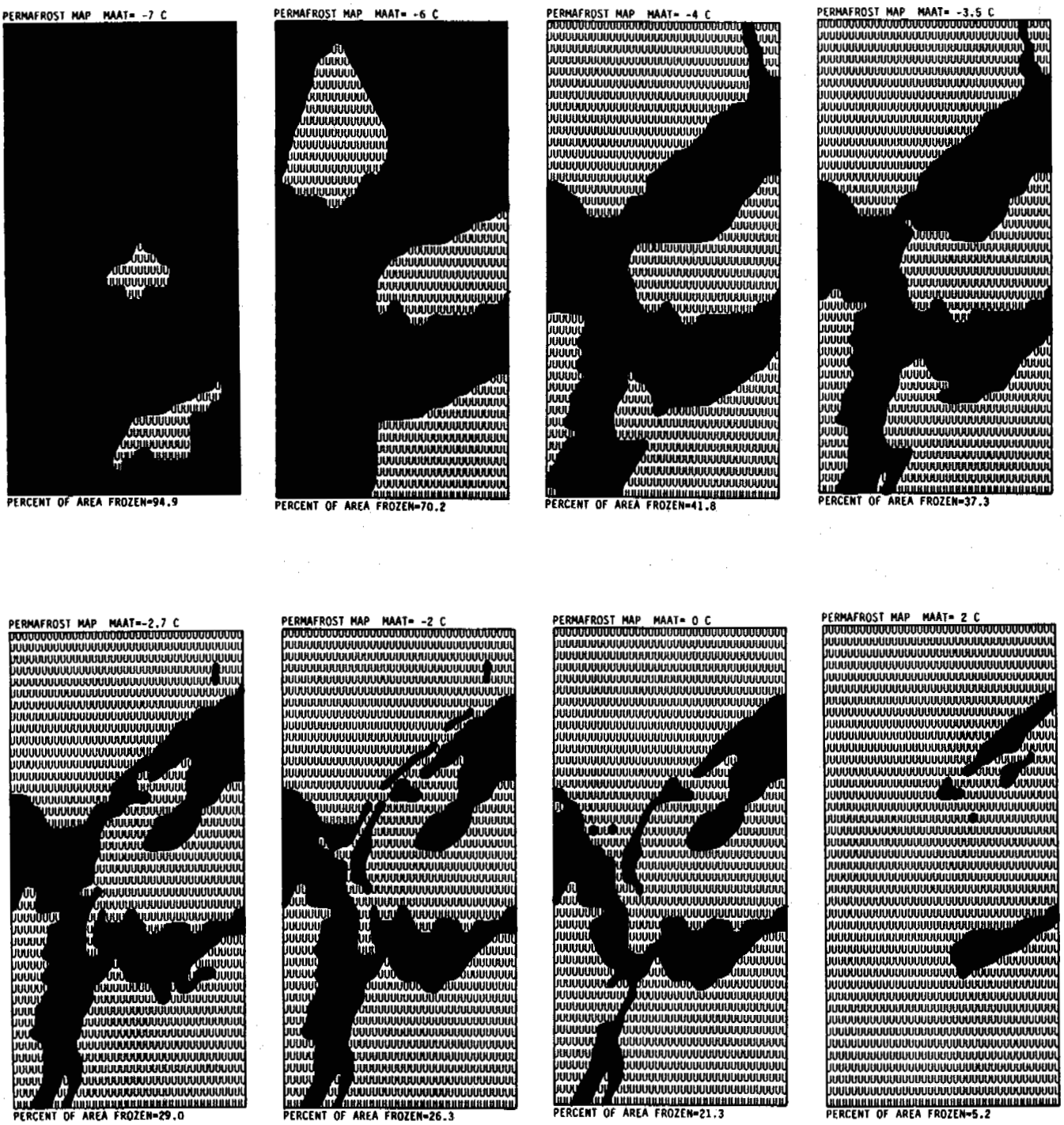

Figure 3. Simulated effects of different mean annual air temperatures on permafrost distribution.

changed slightly. In the final version used for sensitivity analysis, 37.3% of the area was mapped as frozen.

The sensitivity of permafrost distribution to changes in soil moisture and n-factors, parameters which affect the calculation of surface heat balance, were tested. When soil moisture was reduced or increased by 30%, the frozen area covered 26.4% and 45.4% respectively.

N-factors were increased and decreased by 30% in various combinations. When only the thaw n-factors (N_t) were increased and decreased, permafrost coverage varied from 26.0% to 79.2%. When only freeze n-factors (N_f) were changed, the frozen area varied from 25.6% to 53.7%. When N_t was increased and N_f was decreased, the frozen area covered 20.5%. When N_t was decreased and N_f increased, the frozen area covered 94.9%.

The analyses indicated that the model was very sensitive to n-factors but less sensitive to soil moisture variations. Therefore, some uncertainty accompanies the use of n-factors, which by their nature are quite variable from month to month and from year to year even within a given site (Lunardini 1978). However, there was only a limited range that produced a permafrost map similar to the photointerpreted permafrost map.

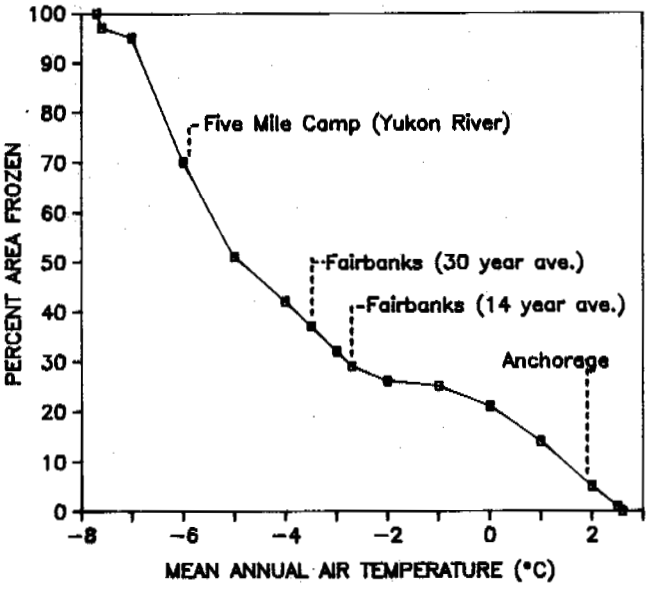

Figure 4. Simulated effects of changes in mean annual air temperatures on the percent of area frozen. Air temperatures at Five Mile Camp and Anchorage are included for comparison.

RESPONSE OF PERMAFROST TO CLIMATIC CHANGE

The model was used to assess the effects of air temperature, and thus climatic change, on permafrost distribution within the Spinach Creek test area (Fig. 3). Permafrost coverage was 100% at a mean annual air temperature (MAAT) below -7.7°C. From -7.7 to -6°C, the warmest south-facing slopes became unfrozen. From -6 to -4°C, east and west portions of midslopes, above the retransported deposits became thawed. From -3.5 to -2.7°C (the difference between the Fairbanks long-term average and 14 year average, 1968-1982), deciduous forests on NE and NW facing slopes and steep south-facing drainages became thawed. Between -2 and 0°C, change was limited to black spruce stands occurring along the lower portions of south-facing slopes. Between 0 and 2°C, all black spruce stands and tussock bogs on retransported deposits in the valley bottoms became thawed. Above 2°C, permafrost persisted only on limited portions of steep north-facing slopes. At 2.6°C, all permafrost was eliminated.

EVALUATION OF MODEL

The validity of the model can be partially evaluated by indirect means. Although no field verification was done on the permafrost map (present climatic conditions), good agreement (92.7%) was achieved between the simulated map (MAAT=-3.5°C) and the photointerpreted map.

Good agreement was also found between the results of the temperature effect simulations, in which permafrost became continuous below -7.7°C MAAT and absent above 2.6°C MAAT, and other evidence (Fig. 4). According to Haugen (1982), MAAT's on the south side of the Brooks Range, where permafrost is discontinuous, ranged from -5.9 to -6.9°C and MAAT's in the Arctic foothills, where permafrost is continuous, ranged from -6.7 to -11.1°C (years 1975 to 1979). Brown (1967) used the -8.3°C MAAT isctherm to delimit the boundary between continuous and discontinuous permafrost and -1.1°C to delimit the boundary between discontinuous and sporadic permafrost. Harris (1981) concluded that the boundary between discontinuous and sporadic permafrost lies just on the cold side of 0°C. In our model, permafrost became sporadic (<25%) in the mapping area at MAAT of -1.0°C. Harris also noted sporadic patches of ice beneath peat have been found at MAAT's as warm as 5°C but were more frequently found at MAAT's below 3°C.

The identification of north-facing slopes as the last locality for permafrost to persist is inconsistent with some observed occurrences, however, and may be due to the lack of groundwater effects in the model. Experience in south-central Alaska and other areas at the southern limit of permafrost indicates that the last pockets of permafrost would normally be expected to occur around the edges of bogs and peatlands that do not receive groundwater discharge from (warmer) higher upland slopes.

CONCLUSIONS

Several conclusions can be drawn from this preliminary effort. The approach appears to work quite well in modelling the natural distribution of permafrost in the Spinach Creek test area. The model is relatively simple and the required inputs are factors that can be mapped by skilled photointerpreters and/or derived from database analyses of soil test data and climatic data. However, it should be noted that modelling (as well as photointerpretive permafrost mapping) can be expected to be easier in hilly terrain, such as the test area, that has 1) relatively thin loess cover, and 2) strong gradients in incident solar radiation. In addition, the role of groundwater is important and cannot be neglected, especially in landscapes that are flatter, have more complex geology and vegetation, and in more maritime climates.

Although this model was run on a specific area near Fairbanks, the results of the mean annual air temperature simulations can be applied to Alaska's Interior in a general way and have implications for human development on permafrost. Relatively little change might be expected to occur from a climatic warming from -3.5 to 0°C, except at transition zones along permafrost boundaries, particularly on retransported deposits on the lower portions of south-facing slopes. Above 0°C, permafrost degradation would accelerate and all valley bottoms, where much infrastructure development occurs, would become thawed. The thawing of remnant permafrost on steep north-facing hills at MAAT's between 2 and 2.5°C would likely have little effect on human use since these sites are rarely developed.

REFERENCES

Abbey, F L, Gray, D M, Male D H, and Erickson, D E L (1978). Index models for predicting ground heat flux to permafrost during thaw conditions, in Proc. 3rd Int. Conf. on Permafrost, Vol. 1, Nat. Res. Coun. Canada. 4-9.

Brown, R J E (1967). Permafrost in Canada. Geol. Surv. of Can. Map 1246A.

Carlson, H (1952). Calculation of depth of thaw in frozen ground, in Frost action in soils. High. Res. Board Spec. Rep. No. 2, 192-223.

Dingman, S L and Koutz, F R (1974). Relations among vegetation, permafrost and potential insolation in central Alaska. Arc. Alp. Res. (6),1,37-42.

Farouki, O T (1981). Thermal properties of soils. U.S. Army Cold Reg. Res. Eng. Lab., Hanover, NH. CRREL Mono. 81-1, 136pp.

Goodwin, C W and Outcalt, S I (1974). The simulation of the geographic sensitivity of active layer modification effects in northern Canada, in Env. Soc. Comm. on North. Pipe., Task For. on Nor. Oil Dev., Rep. 74-12, 17-49.

Harris, S A (1981). Climatic relationships of permafrost zones in areas of low winter snow cover. Arctic (34),1,64-70.

Haugen, R K (1982). Climate of remote areas in north-central Alaska. U.S. Army Cold Reg. Res. Eng. Lab., Hangover, NH, CRREL Rep. 82-35, 110pp.

Jorgenson, M T (1986). Biophysical factors influencing the geographic variability of soil heat flux near Toolik Lake Alaska: implications for terrain sensitivity. Unpub. M.S. Thesis. Univ. of AK. 109pp.

Kersten, M S (1949). Thermal properties of soils, Univ. Minn. Eng. Exp. Sta., Bull. No. 28, 225pp.

Kreig, R A and Reger, R D (1982). Airphoto analysis and summary of landform soil properties along the route of the Trans-Alaska Pipeline System. Ak. Div. Geol. Geoph. Sur., Geol. Rep. 66, 149pp.

Linell, K A (1973). Long term effects of vegetation cover on permafrost stability in an area of discontinuous permafrost, in North Amer., Cont. of 2nd Int. Conf. on Permafrost, Yakutsk, Siberia., 688-693.

Lunardini, V J (1978). Theory of n-factors and correlations of data, in Proc 3rd Int. Conf. on Permafrost, Vol. 1, Nat. Res. Council of Canada, 40-46.

Morrissey, L A (1986). Mapping permafrost in the boreal forest with Thematic Mapper satellite data. Photo. Eng. Rem. Sens. (52),9,1513-1520.

Nelson, F E (1986). Permafrost distribution in central Canada: application of a climate-based predictive model. Ann. Ass. Amer. Geog. (76), 4,550-569.

Ng, E and Miller, P C (1977). Validation of a model of the effect of tundra vegetation on soil temperatures. Arc. Alp. Res. (9),2,89-104.

Viereck, L A, Dyrness, C T, Van Cleve, K, and Foote, M J (1983). Vegetation, soils, and forest productivity in selected forest types in interior Alaska. Can. Jour. For. Res. (13),5, 703-702.

Viereck, L A and Lev, D J (1983). Long-term use of frost tubes to monitor the annual freeze-thaw cycle in the active layer, in Proc. 4th Int. Conf. on Permafrost, Fairbanks, Alaska.

PERMAFROST SITES IN FINNISH LAPLAND AND THEIR ENVIRONMENT
OCCURRENCES DE PERGELISOL EN LAPPONIE FINLANDAISE

L. King[1] and M. Seppälä[2]

[1]Justus-Liebig-Universität, Giessen, West Germany
[2]University of Helsinki, Helsinki, Finland

SYNOPSIS. In the mountain of northern Finland permafrost exists in a discontinuous pattern with thicknesses between about 10 and over 50 metres. The permafrost sites are often without snow cover in winter and show deflation phenomena and a typical vegetation, then. After a short history of permafrost research in Lapland, a detailed description of the permafrost environment of northernmost Finland is given.

HISTORY OF PERMAFROST RESEARCH IN LAPLAND

Although the knowledge about permafrost distribution in Lapland is very limited and mainly concentrated on palsas, the history of permafrost research is quite long. Permafrost research started in the beginning of this century mainly in connection with the development of this northernmost part of North Europe. Permafrost findings have been done during the construction of the railway between the Swedish iron ore city Kiruna and the seaports Narvik, Norway and Luleå, Sweden, respectively (Fig. 1). At that time researchers as Andersson (1903), Hamberg (1904) or Högbom (1914) had a very good understanding of the laws that govern the distribution of permafrost. Permafrost sites were mainly discovered north of Kiruna in an area with very little precipitation and deep winter temperatures. Apart from these findings along the railway track permafrost research was concentrated on palsa studies initiated again in Swedish Lapland by Fries and Bergström (1910). A large number of palsa studies followed until today and a comprehensive description of these studies is given by Vorren (1979), Åhman (1977) and Seppälä (1987). Whereas in Finland and Norway the general opinion was, that permafrost sites are restricted to palsas, Ekman (1957) was able to report 60 meter thick permafrost in a drill hole in the Abisko Mountains. Comparable little attention was given to this sensational finding. Østrem (e.g. 1964) did extensive studies concerning the formation of ice-core moraines by an admirable multitude of methods without really realizing that the resulting inventory of ice-core moraines was at the same time a permafrost inventory (cp. Barsch, 1971; Østrem, 1971). Rapp and Annersten (1969) and Rapp and Clark (1971) reported the occurrence of large polygons in the mountains of Northern Sweden, but the role of permafrost was mentioned only marginally in these publications. King (1976) did again seismic studies on some of Østrem's ice-cored moraines and discovered that permafrost existed also regularly in exposed ridges of other origin. The regular and widespread distribution of high mountain permafrost was then summarized in King (1983, 1984, 1986). Svensson (1986) gives an inventory of periglacial forms in Swedish Lapland and puts much emphasis on relict forms (cp. Rapp, 1982). Meier (1987) gives a periglacial inventory for Norwegian Lapland and discusses the permafrost conditions.

During the construction of the road from Kiruna to Narvik (Norway) at about 1980, permafrost was again found (Knutsson, 1980). This report was received again with astonishment, although the widespread distribution of permafrost was postulated already by Högbom (1914), Åhman (1977) or King (1976, 1982). Frozen ground can regularly be found during construction work in Swedish or Finnish Lapland, but as Åhman (1977) mentions, it is often very difficult to decide whether these findings are perennially or only seasonally frozen. A climatic comparison between Finnish Lapland and the Canadian subarctic shows that large parts of Finnish Lapland belong to the subpolar forest tundra and permafrost should therefore be as widespread as in the well-studied, comparable Canadian areas (Table 1). In Norwegian Lapland, the Varanger Peninsula shows even a true polar climate, at least in its interior (Meier, 1987). This fact is missing in the mental map of most Europeans. Thorough studies of the interior parts of Varanger Peninsula will certainly bring more knowledge about permafrost features in Norwegian Lapland, similarly to those reported from Swedish Lapland by Lagerbäck and Rohde (1986) or Åkerman and Malmström (1986). It is therefore quite obvious, that permafrost exists also outside the high mountain areas of Norwegian and Swedish Lapland and then belongs to the subpolar and polar type (Karte, 1980).

DISTRIBUTION AND THICKNESS OF PERMAFROST IN LAPLAND

In a very recent paper, the authors have presented the results of 29 geoelectrical soundings for permafrost and given a detailed description of the field methods (King and Seppälä, 1987; cp. King et al., 1987). These results can be summarized as follows: In most places above timber line a permafrost thickness of 10 - 50 m was recorded. In many localities at higher altitudes, e.g. several hundred meters above the timberline, the permafrost thickness is 50 m at least, and a thickness of more than 100 m may be extrapolated for the highest mountain tops of northern Finland.

In many areas close to the timberline, permafrost appears in a discontinuous pattern, and its thickness is in the order of several meters, then (Tab. 2). The occurrences are closely related to the microtopography, and hence to the thickness of snow cover during winter. Drifting snow conditions prevail during winter storms, and a snowcover of several decimeters may isolate the ground from the cold locally and thus prevent the permafrost formation. Deflation phenomena on the other hand hint to snowfree sites and often to permafrost below. Thus, vegetation pattern is a good indicator to the winter conditions, as will be shown in the following chapter.

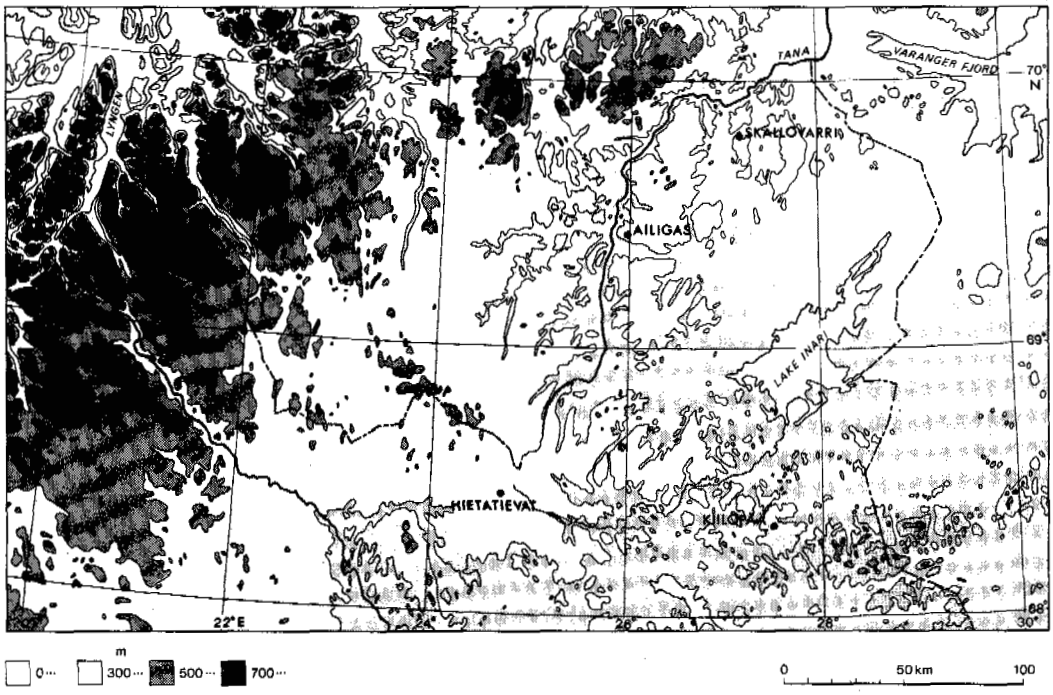

Fig. 1. Lapland and areas of research.

THE PERMAFROST ENVIRONMENT

The inlandsis of the glaciations have imprinted the topography of northern Finland. The gently rolling landscape or the rounded fjell mountains together with the vegetation cover have much similarity e.g. with the Ungava/Labrador peninsula in Canada and even the climatic values are rather similar (Tab. 1). The area belongs more to the polar/subpolar environment than to the alpine environment therefore, even in mountaineous areas.

Topography, climate and seasonal frost

Northern Finland is flatter and lower in altitudes than bordering areas in Sweden and Norway, where the Kjölen mountains in the west rise above 2000 m (Fig. 1). In Finland elevations higher than 1000 m are reached only in the NW corner of the Caledonian mountains (Kilpisjärvi and Halti). Large areas of Finnish Lapland are less than 300 m above sea level (Atlas of Finland 1986, Folio 121-122). Many fjell summits are less than 500 m high. 700 m is a rare altitude and can be found at a few summits of eastern Saariselkä south of Lake Inari, and at the Ounas-Pallas fjells about 24°E and as already mentioned, in NW Finland west of 22°E longitude. In general, the topography is smooth and the fjell slope gently. The summits are very flat and large in area as is typical of old peneplain surfaces (Seppälä and Rastas, 1980). The main part of Finland belongs to the Archaean shield area and the rather gentle mountains are the results of Tertiary uplifts as horsts and surround, arc-like, the southern and western edge of the Lake Inari basin. Typical topographic features are deep fault valleys cutting the mountains in blocks. These valleys are important for plant survival during the severe subarctic winter that dominates the fjell tops.

According to Kolkki (1965) the mean annual temperature in northernmost Finland ranges between +0.5 and -2°C (period 1931-1960). There is a pronounced moderating influence on the air temperatures along the coast. The result is that the warmest area is the NE corner close to Varanger fjord and the coldest area is the mountainous region in the NW corner (Kolkki 1965; Fig. 2 A). In the region where palsas occur, the mean annual temperature is -0.5°C or below. These temperatures represent the readings at few (about five) stations situated usually in valleys, and at a height of two metres above the ground surface. Local climatic conditions that are responsible for the permafrost formation might differ significantly (e.g. winter inversions).

The coldest months are January and February which are very similar (Fig. 2 C and D). In the long term the monthly mean temperatures range from -11°C in the NE to -14°C to the S and W. During the coldest months, the minimum temperatures often fall below -40°C (Fig. 2 B). Seasonal thaw starts in May when mean monthly temperatures rise above 0°C (Fig. 2 E) but locally much snow still remains on the ground. Snow melt in the valleys continues throughout May and lakes at higher altitudes stay frozen until mid-June. Mean June temperatures in the study areas are between +7 and +10°C (Fig. 2 F). July is the warmest month with mean monthly temperatures from +12°C to +14°C (Fig. 2 G). The duration of the thermal winter is longer in coastal areas than in the interior (Fig. 2 H).

Mean dates of first soil frost formation are between 15th and 25th of October whereas thawing takes place between 10th and 20th of June (Soveri and Varjo, 1977). In mineral soils in Utsjoki the depth of seasonal frost may reach 2 to 3.5 m (Seppälä, 1976); these measurements are made in valleys. In peatlands with normal snow cover the frost penetrates down to 40-60 cm (Seppälä, 1982 a); seldom deeper in Utsjoki. If this happens, then there is not enough time for complete thawing during the preceding summer (Seppälä, 1986). In peatlands seasonal frost may still be encountered at the end of July, but usually thaws completely before the new freezing season starts (Seppälä, 1983). The frost season in

TABLE 1. Mean air temperatures of selected weather stations in subarctic areas of Canada and Finnish Lapland.

	Lat. °N	Year °C	Jan. min.°C	July max.°C
Fort George, Quebec	54°	-2.2	-28.3	+17.8
Moosonee, Ontario	51°	-1.1	-20.0	+21.7
Nitchequon, Quebec	53°	-2.2	-28.9	+18.3
Inari, Toivoniemi, Finland	69°	-0.4	-17.4	+18.8
Sodankylä, observ., Finland	67°	-0.4	-19.0	+20.2
Pallasjärvi, Finland	68°	-0.4	-16.5	+18.9

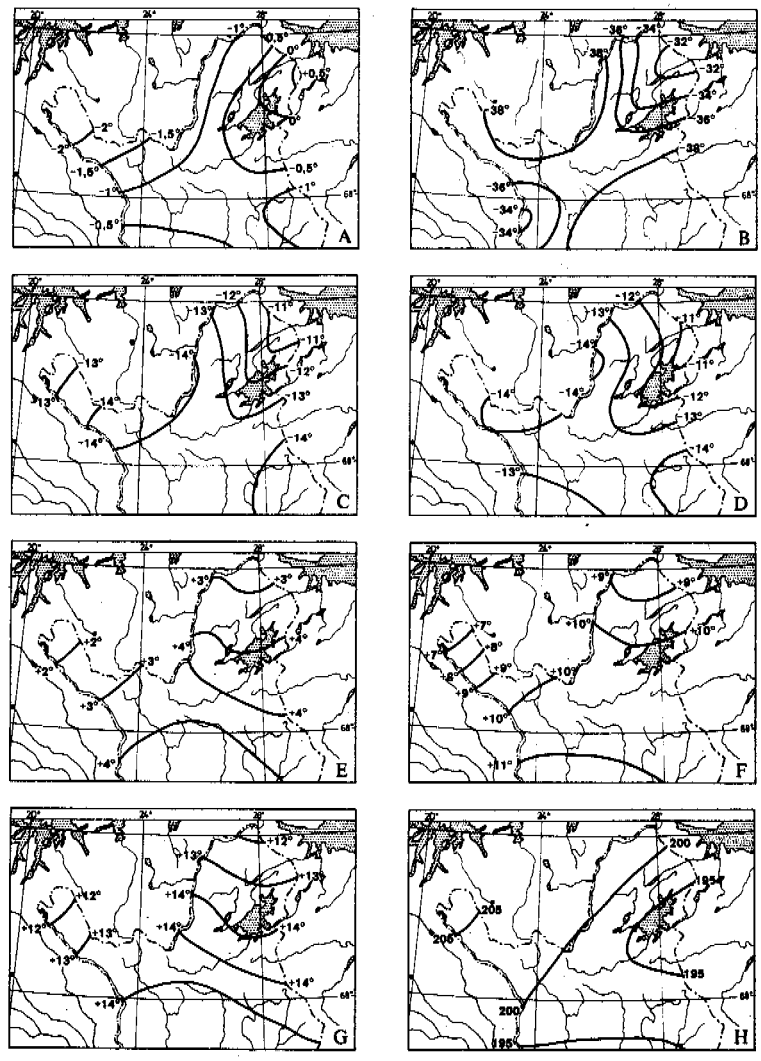

Fig. 2. The climate of northern Finland. Redrawn after Kolkki, (1965). A. Mean annual air temperature (1931-60) in northernmost Finland. B. Mean annual absolute minimum temperature. C. Mean temperature in January. D. Mean temperature in February. E. Mean temperature in May. F. Mean temperature in June. G. Mean temperature in July. H. Duration of the thermal winter (0° ... 0°) in days (1931-60).

northernmost Finland lasts up to 8 months in mineral soils and even 9 to 10 months in mires.

Lake Inari is covered with ice about 200 days a year (mean 1910-1950 according to Atlas of Finland 1960:8). The thickness of the ice cover is about 80 cm and the surface temperature during the summer time is generally less than 15°C (Kallio et al., 1969:17).

In the palsa region the annual precipitation is about 400 mm or less decreasing NW to some 320 mm at Kilpisjärvi except at the northernmost part of Utsjoki where it exceeds 380 mm a year. Precipitation maxima exist in July-August; February-May is a period of low precipitation. During June-September more than 50% of the annual total precipitation occurs (Helimäki, 1966). About 30-40% of the annual precipitation (October-May) is in the form of snow. The average maximum thickness of snow cover is 60-80 cm and normally this is reached in March or April. In the Kevo region in Utsjoki the snowfree period lasts about 5 months (Kärenlampi, 1972). In the highlands of Finnish Lapland this period is about one month shorter except on fjell-tops (Hiltunen, 1980).

In the summit areas of fjells the snow cover is very thin (5 cm or less) and it may disappear completely even at the end of February (Kallio et al., 1969). Birch forests have thicker snow cover than pine forests and by midwinter the low alpine heath possess only about 50% of the snow depth found in the birch (Kärenlampi, 1972; Clark et al., 1985). The prevailing winds are from W and SW in Finnish Lapland. The seasonal wind directions are different: During the summer time NE, W and N winds dominate, during winter winds from the W, SW and S occur (Atlas of Finland 1960:6; Seppälä, 1976). Special attention should be paid to the effects of strong winds from NW (Seppälä, 1971, 1973). The wind velocity strongly increases with higher elevations and this is of great importance for the thickness of snow cover (e.g. Solantie, 1974; King, 1986a). Snow distribution is a function of wind, interacting with microtopography and vegetation, and this changes with wind direction. At the meso scale, however, the snow distribution is a product of topography and a cause of vegetation responses (Hiltunen, 1980).

Topography has its effects on the air temperature (King, 1986b). In advective weather situations there is an adiabatic gradient of about 0.6°C/100 m altitudinal difference. On the other hand, the relief is favourable for the formation of "cold air ponds" in the valleys with stagnant cold and heavy air. Then, the fjell tops can be up to 2°C warmer than the valley bottoms for long periods (Clark et al., 1985). Occasionally it may even be 10°C warmer on the summits than in the valleys (Helimäki, 1974; Huovila, 1974). This certainly does not mean that the permafrost formation on the fjell tops would be prevented because of lack of cold. Air temperatures there are still cold enough (e.g. -30°C instead of - 40°C) and

allow, because an isolating snow cover is often missing, a cooling of the ground and much deeper penetration of frost than in the snow covered valley bottoms.

After this climatological and topographical description of typical permafrost sites, several conclusions concerning the general permafrost distribution in northern Finland can be drawn.

The relief map or the altitude as such, certainly does not tell one of the expected permafrost localities. The lower limit of discontinuous permafrost changes its altitude and drops from the more maritime to the more continental, dry climates. This has been shown clearly by King (1984, Figs. 67 and 69; Figs. 5 and 6) and a connection of the lower limit of permafrost belts with the MAAT has been postulated. The lower limit of discontinuous permafrost is at about 300 m a.s.l. in the Utsjoki area and rises to values of about 500 m a.s.l. in the NW and the S of the study area (MAAT isotherms reduced to sea level are 0°C and +1°C, respectively). But the number of weather stations in northernmost Finland is very limited and their location usually displays a rather special climate. Moreover, a maritime/continental contrast does not exist as clearly in northernmost Finland as in the Swedish and Norwegian mountains to the NW and W of our area (cf. isotherm in King, 1986, Fig. 4).

Fig. 3. A permafrost thickness of about 8 metres has been measured at this windswept spot that shows deflation. No permafrost could be found with geoelectrical soundings in the surrounding shrubby area (cp. Table 2).

Vegetation

When selecting sites for our geoelectrical soundings, our primary aim was not only to find permafrost but also to quantify the importance of snowcover and vegetation as critical factors in permafrost formation. The complex interdependence between permafrost and vegetation has been shown by many authors (e.g. Tyrtikov, 1978). In many cases vegetation is even a direct indicator for winter snow thickness (e.g. Clark et al., 1985), and snow thickness often is primarily responsible for the formation of permafrost.

A description of the vegetation at typical sites with and without permafrost is given as follows: Permafrost regularly exists in the fjell summits of northern Finland. Here, the permafrost area is in general above timberline and indicated by low and medium heath vegetation. If this hypothesis is true, then the vegetation map of northernmost Finland (Seppälä and Rastas, 1980) which indicates the distribution of barren fjell tops (*regio alpina*) can be read as a map of permafrost. Similar interpretation can be given to the vegetation classification for the Kilpisjärvi region made with Landsat MSS data (Clark et al., 1985, Fig. 5). It could be used not only as a snow depth surrogate map but also as permafrost map where parts of yellow, all orange (=light brown and grey pixels on highlands then show the existence of permafrost). Certainly, further research work has to be done in order to prove this hypothesis. But our assumption is also encouraged by the regular permafrost distribution pattern which is comparable with that obtained by a large number of geoelectric, seismic, ground and snow temperature soundings in the neighbouring Kebnekaise area (King, 1983).

In northernmost Finland, in the Tana River valley, the timberline on north facing slopes is just above 100 m a.s.l. In general, the forest limit is located between 300 and 400 m a.s.l. in the northern parts of the studied region, between 400 and 500 m a.s.l. in the western parts, and rising to 600 m a.s.l. altitude in Kilpisjärvi on the southwest facing slope of Saana mountain. Here, the timberline often corresponds to the lower limit of discontinuous permafrost.

Heaths extend above the forest line. The lower heathlands are dominated by shrubs such as *Betula nana*, *Vaccinium myrtillus* and *Empetrum hermaphroditum*, whereas in the fjell at higher elevations *Salix herbacea*, *Empetrum* and alpine grasses with lichens and mosses occur. In the mountains of the NW *Cassiope tetragona* is abundant (Clark et al., 1985). On the fjell summits blockfields and wind blown heaths with lichens and mosses as well as bare rock slabs are often found. Patterned ground (as stone polygons and stone stripes on slopes) occur regularly on fjell summits (Seppälä 1982b) signs of deflation hint to permafrost, too.

A good correlation between snow depth and type of vegetation was found in Kilpisjärvi and Kevo region by Clark et al. (1985). During the winter 1984/85 the snow depth ranged from 5 cm for medium altitude heath to 85 cm in birch forests. Plants which need a certain protection of snow cover do not survive without it, and this means that e.g. chionophilous plant communities (*Phyllodoce - Vaccinium myrtillus* heaths, meadow-like and heath like snowbeds) usually carry 80 cm snow at a maximum, while the wind swept heaths of the chionophobic communities have less than 20 cm snow (Eurola et al. 1980). Permafrost may then be expected at the latter sites. Thus, snow depth is the most critical factor for the permafrost formation (King, 1986a) and this has also been shown in experimental palsa studies (Seppälä, 1982a).

TABLE 2. Location of selected sounding sites with permafrost thickness in metres.

Nr.	Alt. in m	Permafrost base (m)	Characteristics
2.	360	45	Flat, dry low alpine heath.
3.	360	18	Deflation. Stone polygons, low alpine heath.
4.	360	11	Deflation surface. Low alpine heath.
5.	360	24	Large vegetated stone polygons with diameter 8 m. Low alpine heath.
6.	360	18	Hill with deflation patches, low heath.
7.	360	none	Flat, no deflation. Low alpine heath.
8.	320	13	Hill with big boulder, glacial till, deflation, low heath, peat on summit.
9.	315	none	Depression. Betula nana bushes.
10.	320	14	Hill. Glacial till. Some deflation.
11.	320	15	Depression, boulders, patterned ground.
12.	320	none	Large depression with wet patch.
13.	325	7	Hill with deflation. Coarse gravel, peat on summit (cp. Fig. 3).
14.	305	none	In birch forest, glacial till.
15.	335	10	Saddle between summits. Alpine heath.
16.	340	14	Summit of Skalonjuovttsa. Alpine heath.
23.	830	50	Medium altitude heath. Betula nana, Empetrum.
24.	890	50	Medium altitude heath. N slope: 13.5°.
25.	880	50	N slope, 25°. Strong solifluction. Medium altitude heath.
27.	680	12-14	Low heath. 10 m below the summit. Very fresh rock surface, few cracks.
28.	710	40	Big blocks on thin till cover, unsorted frost polygons.
29.	730	20-50	10 m below the summit. Glacial till. Frost polygons. Medium altitude heath.

Locations: (cp. Fig. 1):

Skallovarri (No. 2 to 14) Saana (No. 23 to 25)
Ailigas (No.15 and 16) Pikku Malla (No. 27 to 29)

Whether permafrost is actually forming today is both important and difficult to answer. In some places, the active layer is thick and it might be possible that some permafrost is relict. However, to assume a glacial age would certainly be too far reaching. We know that during the climatic optimum 7000-5000 years ago, the pine tree line was hundreds of kilometres north of the present stage and on many fjell summits trees were growing, then (Eronen, 1979). At other localities we are quite convinced that severe winters followed by low summer temperatures may result in the formation of new permafrost. These latter sites are at least as favourable for permafrost formation as those where Seppälä (1982a) actually proved palsa growth. But to prove the growth of permafrost, continuous temperature measurements in deep bedrock and over many years are compulsory.

ACKNOWLEDGEMENTS

Our studies would not have been successful without the help of the following persons and institutions: Mr. Peter-Paul Jeckel, Giessen, Mr. Heikki Klein, Kilpisjärvi, the Kevo Subarctic Research Station and Kilpisjärvi Biological Station and the Geophysical Institute of the University of Frankfurt. Funding came from the Academy of Finland and the Deutsche Forschungsgemeinschaft.

REFEFENCES

Aario, L. (1960). Vegetation zones of Lapland. Atlas of Finland 1960, 10:8.

Åhman, R. (1977). Palsar i Nordnorge. (Summary: Palsas in northern Norway.) Meddelanden från Lunds Universitets Geografiska Institution 78, 165 pp.

Åkerman, J. & Malmström, B. (1986). Permafrost mounds in the Abisko area, north Sweden. Geografiska Annaler 68A(3), 155-165.

Andersson, G. (1903). Tjälens djuplek i nordligaste Sverige. Ymer 23, p. 485 (Stockholm).

Barsch, D. (1971). Rockglaciers and ice-cored moraines. Geogr. Ann. 53 A, 203-206.

Clark, M.J., A.M. Gurnell, E.J. Milton, M. Seppälä & M. Kyöstilä (1985). Remotely-sensed vegetation classification as a snow depth indicator for hydrological analysis in sub-arctic Finland. Fennia 163, 195-216.

Ekman, S. (1957). Die Gewässer des Abisko-Gebietes und ihre Bedingungen. Kungl. Sv. Vetenskapsakademiens Handlingar 6:6 (Stockholm).

Eronen, M. (1979). The retreat of pine forest in Finnish Lapland since the Holocene climatic optimum: a general discussion with radiocarbon evidence from subfossil pines. Fennia 157, 93-114.

Eurola, S., H. Kyllönen & K. Laine (1980). Lumen ekologisesta merkityksestä kasvillisuudelle Kilpisjärvi alueella. (Snow conditions and some vegetation types in the Kilpisjärvi region.) Luonnon Tutkija 84, 43-48.

Fries, T. & E. Bergström (1910). Några iakttagelser öfver palsar och deras förekomst i nordligaste Sverige. Stockholm Geol. Fören. Förh. 32(1), 195-205.

Hamberg, A. (1904). Till frågan om förekomsten af alltid frusen mark i Sverige. Ymer 24, 87-93 (Stockholm).

Helimäki, U.I. (1966). Tables and maps of precipitation in Finland, 1931-60. Supplement to the Meteorological Yearbook of Finland 66,2, 22 pp.

Helimäki, U.I. (1974). Lapin ilmastosta ja tunturien ilmaston erikoisuuksista. (Summary: On the climate of Lapland, especially on the hills.) Lapin Ilmastokirja - Climate of Lapland, 23-27, Rovaniemi.

Hiltunen, R. (1980). Tuulenpieksemän ja lumenviipymän lämpötila - ja lumioloista Pikku-Mallalla. (Temperature and snow conditions on snow beds and wind-exposed places on Pikku-Malla.) Luonnon Tutkija 84, 11-14.

Högbom, B. (1914). Über die geologische Bedeutung des Frostes. Bull. Geol. Inst. Uppsala, 12, 257-389.

Huovila, S. (1974). Lämpöolojen vaihtelurajat Pohjois-Suomessa. (Summary: Temperature range in northern Finland.) Lapin Ilmastokirja - Climate of Lapland, 18-22, Rovaniemi.

Jeckel, P.P. (in prep.). Untersuchungen zur Periglazialmorphologie und Permafrostverbreitung in Lappland.

Kallio, P., U. Laine & Y. Mäkinen (1969). Vascular flora of Inari Lapland. I. Introduction and Lycopodiaceae - Polypodiaceae. Reports from the Kevo Subarctic Research Station 5, 1-108.

Kärenlampi, L. (1972). Comparisons between the microclimates of the Kevo ecosystem studysites of the Kevo meteorological station. Reports from the Kevo Subarctic Research Station 9, 50-65.

Karte, J. (1980). Rezente, subrezente und fossile Periglaziärerscheinungen im nördlichen Fennoskandien. Z. Geomorph. N.F. 24(4). 448-467.

King, L. (1976). Permafrostuntersuchungen in Tarfala (Schwedisch Lappland) mit Hilfe der Hammerschlagseismik. Zeitschr.f.Gletscherkunde und Glazialgeologie 12(2), 187-204. King, L. (1979). Palsen und Permafrost in Quebec. Trierer Geographische Studien, Sonderheft 2, Kanada und das Nordpolargebiet, 141-156.

King, L. (1982). Qualitative und quantitative Erfassung von Permafrost in Tarfala (Schwedisch Lappland) und Jotenheimen (Norwegen) mit Hilfe geoelektrischer Sondierungen. Zeitschr.f.Geomorphologie, Supplement-Band 43, 139-160.

King, L. (1983). High mountain permafrost in Scandinavia. Permafrost; Fourth International Conference, Proceedings. National Academy Press, Washington, D.C., 612-617.

King, L. (1984). Permafrost in Skandinavien. Untersuchungsergebnisse aus Lappland, Jotenheimen und Dovre/Rondane. Heidelberger Geographische Arbeiten 76, 174 pp.

King, L. (1986a). Zonation and ecology of high mountain permafrost in Scandinavia. Geografiska Annaler 68A, 3, 131-139.

King, L. (1986b). Les limites inférieures du pergélisol alpin en Scandinavie - recherches en terrain et présentation cartographique. Studia Geomorphologica Carpatho-Balcanica XX, 59-70.

King, L., W. Fisch, W. Haeberli & H.-P. Waechter (1987). Comparison of resistivity and radio-echo soundings on rock glacier permafrost. Zeitschr.f.Gletscherkunde und Glazialgeologie 23/1 (in press).

King, L. & M. Seppälä (1987). Permafrost thickness and distribution in Finnish Lapland - results of geoelectrical soundings. Polarforschung 57 (in press).

Knutsson, S. (1980). Permafrost i Norgevägen. Byggmästaren 10.

Kolkki, O. (1965). Tables and maps of temperature in Finland during 1931-60. Supplement to the Meteorological Yearbook of Finland 65, la, 42 pp.

Lagerbäck, R. & L. Rodhe (1986). Pingos and palsas in northernmost Sweden - Preliminary notes on recent investigations. Geografiska Annaler 68A, 3, pp. 149.

Meier, K.D. (1987). Studien zur periglaziären Landschaftsform in Finnmark (Nord-Norwegen). Jahrbuch der Geographischen Gesellschaft zu Hannover, Sonderheft 13, pp. 298.

Østrem, G. (1964). Ice-cored moraines in Scandinavia. Geogr. Ann. 46, 282-337.

Østrem, G. (1971). Rock glaciers and ice-cored moraines, a reply to D. Barsch. Geogr. Ann. 53A(3-4), 207-213.

Rapp, A. (1982). Zonation of permafrost indicators in Swedish Lapland. Geografisk Tidsskrift 82, 37-38.

Rapp, A. & L. Annersten, L. (1969). Permafrost and Tundra polygons in Northern Sweden. In: Péwé, T.L. (ed.): The Periglacial National Park, Swedish Lapland. Geogr. Ann. 53A(2), 71-85.

Rapp, A. & G.M. Clark (1971). Large nonsorted polygons in Padjelanta National Park, Swedish Lapland. Geogr. Ann. 53A(2), 71-85.

Seppälä, M. (1971). Evolution of eolian relief of the Kaamasjoki - Kiellajoki river basin in Finnish Lapland. Fennia 104, 88 pp.

Seppälä, M. (1973). On the formation of periglacial sand dunes in northern Fennoscandia. Ninth Congress INQUA (Christchurch) Abstract, 318-319.

Seppälä, M. (1974). Some quantitative measurements of the present-day deflation on Hietatievat, Finnish Lapland. Abhandlungen der Akademie der Wissenschaften in Göttningen, Mathematisch-Physikalische Klasse, III. Folge 29, 208-220.

Seppälä, M. (1976). Periglacial character of the climate of the Kevo region (Finnish Lapland) on the basis of meteorological observations 1962-71. Reports from the Kevo Subarctic Research Station 13, 1-11.

Seppälä, M. (1982a). An experimental study of the formation of palsas. Proceedings Fourth Canadian Permafrost Conference, Calgary. National Research Council of Canada, Ottawa, 36-42.

Seppälä, M. (1982b). Present-day periglacial phenomena in Northern Finland. Biuletyn Peryglacjalny 29, 231-243.

Seppälä, M. (1983). Seasonal thawing of palsas in Finnish Lapland. Permafrost. Fourth International Conference, Proceedings. National Academy Press, Washington, D.C., 1127-1132.

Seppälä, M. (1984). Deflation measurements on Hietatievat, Finnish Lapland, 1974-77. In: Rod Olson; Frank Geddes & Ross Hastings (eds.), Northern Ecology and Resource Management. University of Alberta Press, Edmonton, 39-49.

Seppälä, M. (1986). The origin of palsas. Geografiska Annaler 68A, 3, 141-147.

Seppälä, M. (1987). Palsas and related forms. In: M.J. Clark (ed.). Advances in periglacial geomorphology. John Wiley, Chichester (in press).

Seppälä, M. & J. Rastas (1980). Vegetation map of northernmost Finland with special reference to subarctic forest limits and natural hazards. Fennia 158, 41-61.

Solantie, R. (1974). Pohjois-Suomen lumipeitteestä. (Summary: On the snow cover in northern Finland). In: Lapin Ilmastokirja - Climate of Lapland, 74-89, Rovaniemi.

Soveri, J. & M. Varjo (1977). Roudan muodostumisesta ja esiintymisestä Suomessa vuosina 1955-1975. (Summary: On the formation and occurrence of soil frost in Finland 1955 to 1975.) Publications Water Research Institute, National Board of Waters, Finland 20, 66 pp.

Tyrtikov, A.P. (1978). Permafrost and vegetation. Permafrost Second International Conference - USSR Contribution. National Academy of Sciences. Washington, D.C., 100-104.

Vorren, K.D. (1979). Vegetational investigations of a palsa bog in Northern Norway. TROMURA, Naturvitenskap. Nr. 5. University of Troms , Institute of Biology and Geology, pp. 182.

CRYOGENIC COMPLEXES AS THE BASIS FOR PREDICTION MAPS

I.V. Klimovsky[1] and S.P. Gotovtsev

[1]Permafrost Institute, Siberian Branch of the U.S.S.R. Academy of Sciences, Yakutsk, U.S.S.R.

SYNOPSIS We consider criteria for and methods of identifying cryolithogenic complexes (CLC) on the basis of morphometric and cryolithogenic analysis. An attempt is made to associate cryolithogenic complexes with landscape conditions and, on this basis, determine the susceptibility of the surface to man-induced effects as well as predict the occurrence of permafrost-geological processes.

Economic development of permafrost rock regions is always accompanied by a vast interaction of the permafrost with a whole variety of natural conditions. In this case any man-induced effect on the natural environment, including the permafrost situation, introduces a disturbance into the heat balance of frozen rocks (Brown and Grave, 1981). Therefore, every economic development of some or other region should rely on elements of a prediction-based estimation of the possible change in the natural permafrost conditions as a result of man activity. The extent to which man's activity has effect on biogeocenoses and landscapes produced by them, is generally defined by terms 'susceptibility' and 'stability', the term 'susceptibility' being regarded as the back reaction of a natural environment to some disturbance and the term 'stability' being defined as the ability of natural-territorial complexes to resist the production or activation of cryogenic processes (Grave, 1979). Intercomparing these two terms leads us to conclude that the notion 'susceptibility' is more abstract. It involves not only the variations of engineering-geological properties of soils but also the entire natural system with its complicated ecological relationships. This term should, perhaps, be applied for small-scale mapping as the index of relative vulnerability of the landscape environment. The term 'stability' is more appropriate for characterizing the engineering-geological conditions of the areas when these are being mapped on a large scale.

Thus, in the case of permafrost mapping on different scales, when the areas are identified, depending on the aims of geocryological survey, according to the degree of their susceptibility or stability to man-induced disturbances, mapping material in itself contains an element of a preliminary qualitative prediction of the occurrence of cryogenic processes.

There is general consensus (Grave, 1978) that the response of a surface to its disturbances is determined largely by variations in characteristics of its elements such as soil covers, composition and ice content of soils, inclination, and others. The response itself most commonly manifests itself in the development of a number of permafrost-geological processes (thermokarst, solifluction, thermal abrasion, etc.) whose potential activity is always present in the natural-geological environment and in order to identify them in their manifestation requires merely a small impulse, i.e., an artificial creation of the most favourable conditions, which is often the case when the surface is subjected to man-induced action. The development of all permafrost-geological processes fits in rather well with cryolithogenic (cryolithologic) complexes (CLC). By each of them (Melnikov et al., 1985), we understand loose permafrost sediments that had formed under certain facial-geological conditions, within not only intrinsically homogeneous types of terrain but also on rocks of the same lithogenic base. Under conditions of a structure-denudation terrain which is common to platform regions, cryolithologic complexes form a cryolithogenic cover.

Using the above considerations as well as a number of techniques reported in an earlier paper (Klimovsky et al., 1986), on the basis of identifying and mapping cryolithologic complexes we have compiled medium-scale maps which make it possible to estimate the susceptibility of permafrost terrains and, to a certain extent, predict the manifestation of cryogenic processes when a given territory is developed by man. The areas being mapped have been chosen within the central part of the Mid-Siberian plateau.

The map of landscape microzoning according to susceptibility to man-induced effects of the Vilyuy-Ochchuguy-Botuobinskoe mezhdurechie (country between two rivers) has been compiled on the principle of identifying the types and subtypes of terrain taking into account certain morphometric parameters of the geomorphological structure (Fig. 1). In this case by the type of terrain, we understand the combination of a certain geomorphological element of the relief with the relevant typical vegetation associations which had been formed on a given geological-and-lithological basis. For the region under study,

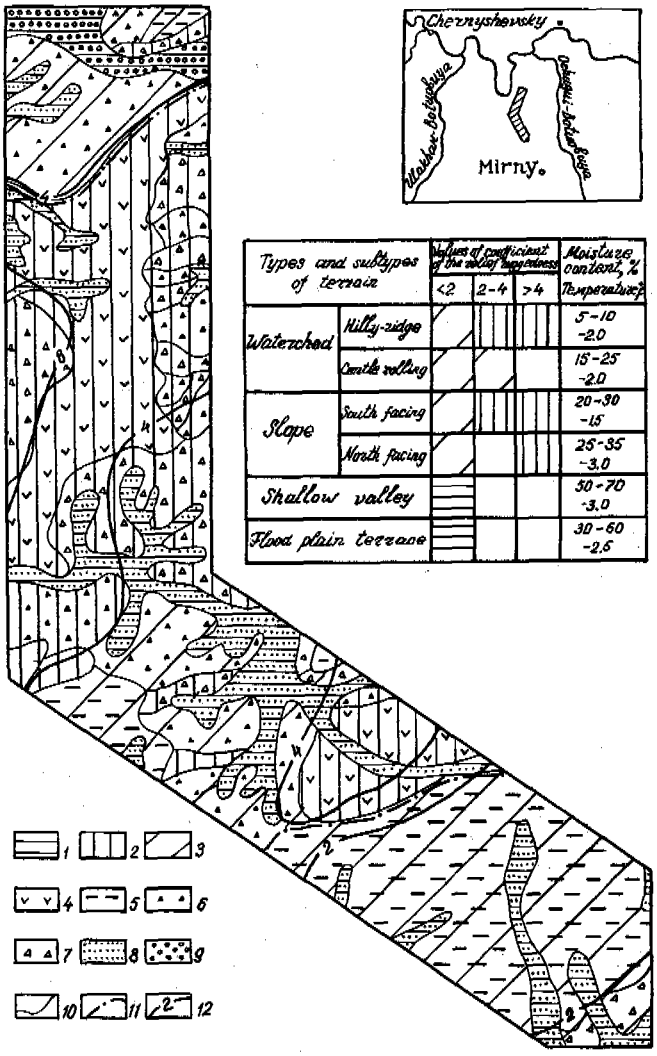

Fig.1 A Fragment of the Schematic Map of Landscape Microzoning According to Susceptibility to Man-Induced Effects for the Vilyuy-Ochchuguy-Botuobinskoe Mezhdurechie (Country between Two Rivers) (the Region Appears Shaded).

Susceptibility of the areas to man-induced effects: 1 - susceptible; 2 - moderately susceptible; 3 - weakly susceptible (stable). Types and subtypes of terrain: 4 - watershed, hill-hillock; 5 - watershed, gentle-wavy; 6 - slope of northward exposure; 7 - slope of southward exposure; 8 - shallow-valley; 9 - floodland-terrace. Other legend: 10 - boundary of terrain types and subtypes; 11 - boundary of landscape microareas; and 12 - isolines for the values of the coefficient of relief distribution.

using a topographic basis on a scale of 1:100000, four types of terrain were identified, namely watershed, slope, shallow-valley, and floodland-terrace. Besides, two subtypes are marked within the watersheds: hill-hillock and gentle-wavy, and within the slopes those of south- and northward exposure.

The geomorphological structure of the area under investigation that is generally typical of the entire Siberian Plateau, is predetermined by the geological structure. It is notable for a vast occurrence of trap-formation rocks emerging into the daylit surface in the form of subhorizontal bodies of a complex configuration. This enhances significantly contrast and roughness of the surfaces of geomorphological levels. Areas with occurrences of clayey-carbonate ground and continental ground of the Lower and Upper Paleozoic, respectively, which do not show great stability to agents of physical weathering, form a more uniform relief.

Thus, there is a considerable difference in natural conditions of watershed, slope types of terrain composed by traps and of areas with clayey-carbonate ground which determines the parameters of the permafrost situation.

When mapping permafrost landscapes according to their susceptibility, it is important to take into account the ice content of the cover of loose sediments, especially their upper horizons. For the region considered, a criterion for estimating the ice content is the facial belonging and thickness of sediments within a CLC.

As for Quarternary sediments, deluvial suglinoks and supes, with rare inclusions of gruss covering the entire surface with a continuous 'jacket' of 2-4 m thickness are most common occurrence. Alluvial sediments occur exceedingly scarcily because the river network in that region is characterized by a multitude of shallow stream flows with broad, weakly cut-in valleys. Only two major water flows have a floodland and two terraces above the floodland. Therefore, there exist differences in both the composition and ice content of mellow valleys of shallow and large water flows. Lithological cross-sections of the former are notable for the predominance of deluvial material which is accumulated due largely to flat-type wash-off. The composition of sediments which are of little thickness is diversiform, although the ice content of soils in the active layer of the shallow valleys, on some occasions, takes on typical values of sediments of major water flow valleys. Within major water flows, the deluvial coat occurs on the slopes and partly covers the terraces comparing unfavourably, in percentage, only with alluvial sediments. However, alluvial sediments proper from the surface show a two-three meter thick, very fine-grained sediments of floodland facies having an ice content between 50 and 60%. At higher levels, they contain wedge ice, owing to which the total ice content may increase substantially. Thus, the differences in lithology of shallow and major water flows are responsible for the considerable inhomogeneities in landscape conditions, and this gives grounds for recognizing them as independent types of terrain.

For a general characterization of the diversity of relief, it was subjected to a morphometric analysis following a technique suggested in a previous paper (Gotovtsev and Dorofeev, 1980).

The essence of this technique is to count the number of isohypses on the topographic map within an elementary square cell, whose size is chosen according to the map's scale, roughness of the relief and contrast of amplitudes of absolute marks. The number of isohypses inside a square on a 1:100 000 scale map is chosen arbitrarily as the coefficient of relief roughness (K_p) whose value is directly proportional to the general inclination of the terrestrial surface corresponding to a square. By connecting the isolines of the values of equal coefficients we obtain a morphometric map of relief roughness that reflects areas with different inclinations of the terrestrial surface.

Upon comparison following such a technique, the map revealed that there is a fairly well-defined association of morphological elements of the surface with the composition of their relevant bed ground and loose sediments, i.e., with cryolithologic complexes. Areas having the coefficient 1-4 are, generally, composed of carbonate-series materials, and the coefficient 4-6 is characteristic of the areas showing the emergence of trap bodies. The surface inclination determines largely the intensity of cryogenic processes. Note, for example, that the presence of appropriate inclinations contributes to the development of solifluction and thermal erosion, while favourable pre-conditions for activation of thermokarst are created on placors, due to a disturbance of the soil cover in areas composed of ice-containing sediments. It becomes, therefore, quite clear that it is necessary to take into account natural inclinations when substantiating the degree of susceptibility of cryogenic lansdcapes to man-induced disturbances.

Analysis and intercomparison of maps for terrain types and relief roughness have made it possible to construct a schematic estimating map of susceptibility to man-induced effects. According to the character of the back reaction of a natural surface to diverse disturbances, we have classified the areas into three categories: weakly-, moderately- and susceptible.

We consider the shallow-valley and floodland-terrace types of terrain to be the most susceptible to man-induced effects because they are composed of ice-rich ground and frequently contain wedge ice and occur on subhorizontal surfaces. Progressively growing thermokarst and thermal erosion are possible to evolve in such areas whenever the natural vegetation and moss covers are disturbed and inclinations changed.

When engineering activities are undertaken in slope areas, one may expect the development or regeneration of slope processes, whose intensity will depend mainly on the surface inclination and the lithogenic base of the constituent materials. Most intense development of slope processes will be observed on steep slopes (the roughness coefficient 4-6) which, according to their degree of susceptibility, pertain to the category of moderate processes. In areas composed by trap materials, in the case of a disturbance of the vegetation cover with such values of the coefficient, a selective manifestation of a rock-stream forming process is possible, which gives grounds for regarding them as regions of a moderate degree of susceptibility. More stable areas are only vast expanses with a gentle-wavy relief on watersheds (the roughness coefficient being as large as 2).

Thus, combining the types of terrain and morphometric indices provides a fairly good basis for recognizing areas of natural complexes on a cryolithogenic basis according to their back reaction to man-induced effects. The areas we have identified were estimated mainly according to two criteria. First, this was the ice content of sediments covering the chief elements of the terrain. In this case we mapped the types of terrain occurring within cryolithologic complexes with the largest value of this index. And second, we employed the degree of relief roughness, which permits us, to some extent, to identify areas showing different potential possibilities for development of cryogenic slope processes.

A morphometric approach for purposes of identifying and mapping was also used when compiling a map of cryolithologic complexes of one of the areas of the Morkoka River basin (the Vilyuy River tributary).

Owing to the use of the cartographical basis of a large scale (1:100 000), we have calculated the roughness coefficient. Its mean background index was found equal to 4. The largest values of the coefficient are observed in the upper reaches of the Morkoka River. This is due to the fact that extensive areas there are occupied by districts of trap plateaux; river and stream valleys often represent typical canyons. As one moves down the valley, the relatively high values of the roughness coefficient are shifted from the bottom to the watersheds where trap-formation ground are shielding the Paleozoic thickness. The hypsometric position of trap areas in the area between two rivers in the upper reaches of small water flows does not contribute to their erosion-denudation dismembering. Analysis of morphometric data revealed eleven cryolithological complexes showing that the coefficient 1 isoline delimits the horizontal surfaces of the watersheds and areas of the valley bottoms, thus delineating the riverside alluvial valleys (Fig. 2). The inclination angle of these surfaces does not exceed 2 or 3°. They may be considered - following A.I.Popov et al.'s (1963) terminology - to be local areas of accumulation, with a relevant gamut of cryogenic processes, phenomena and formations encountered within four cryolithological complexes (1, 2, 6, and 10). It should also be noted that the cryolithological complex of alluvial plains (2) displays a very fragmentary occurrence. The main characteristics of cryolithological complexes (CLC) identified are listed in Table I.

Using the cryolithogenic basis, together with data of morphometric analysis of a 1:30 000 scale map we have constructed a scheme for predicting shore (including cryogenic) processes in the area of the planned water reservoir on the Vilyuy River (Fig. 3) on which three regions are identified according to the character and degree of activity of the manifestation of permafrost-geological processes.

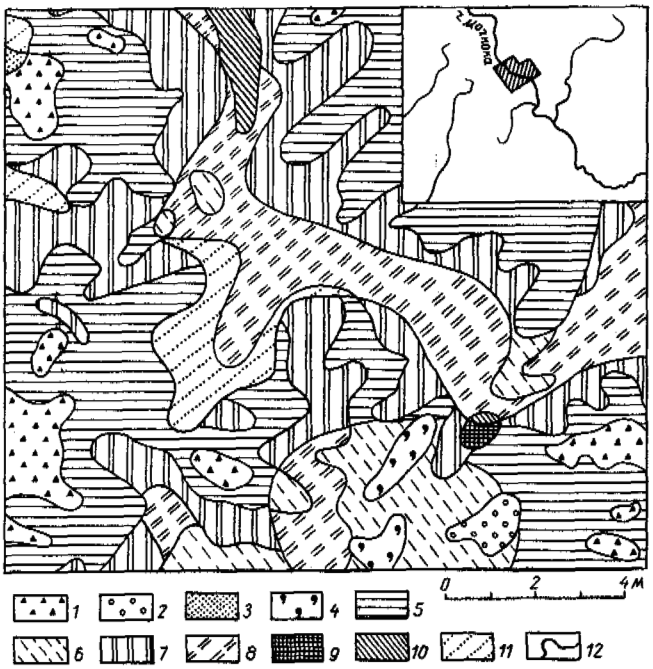

Fig.2 Cryolithological Complexes in the Morkoka River Basin. LEGEND: 1 - trap watershed plateaux; 2 - riverside alluvial plains; 3 - deluvial-decerption slopes; 4 - deluvial solifluction slopes; 5 - steep slopes of subsurface wash-off; 6 - structure-denudation plateaux; 7 - slopes of plane deluvial wash-off; 8 - slopes of linear surface wash-off; 9 - steep slopes of surface pull-down; 10 - bottoms of relic depressions; 11 - sandy masses; and 12 - boundaries of cryolithological complexes.

One is identified as being a region of prolonged and nonuniform thermal denudation. As for another region, a different processing of the shores, depending on the lithogenic basis of the slopes, is expected in areas limited by the coefficient 2. And the third region, in the character of development of working processes of the shores, is similar to the second one. However, because of the extensive development of the ground of trap composition and due to the closeness of hydrostatic upthrust (a relatively small lift of the water level), processes of alteration of the shores here will be somewhat oppressed; only the alteration of ice-containing sediments of the first and second terraces of the Vilyuy River (localized washings-off and creeps) seems to occur.

Thus, the above examples lead us to conclude thatmorphometric maps of relief roughness constructed on a cryolithogenic basis are useful for predicting not only cryodenudation processes and estimate the susceptibility of a permafrost environment to man-induced effects but also for successful planning of some or other engineering activities, in close co-ordination with issues of ecological concern.

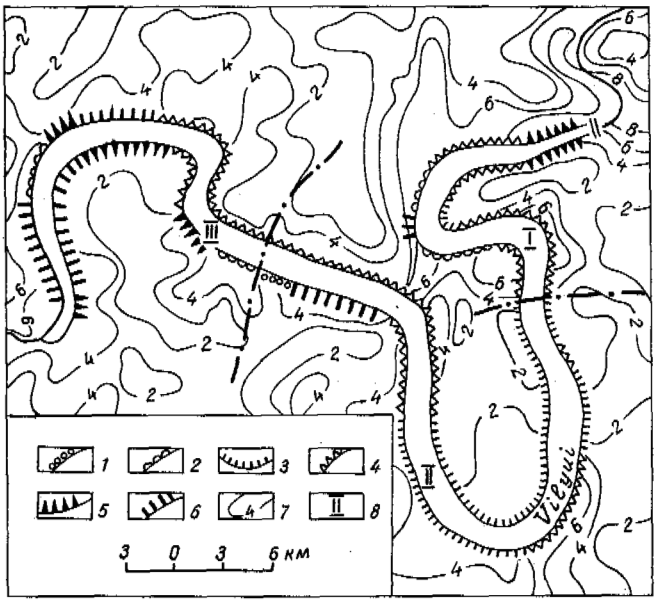

Fig.3 Prediction Scheme for Exogenic Processes in the Area of the Vilyuy River Water Reservoir. LEGEND: 1 - thermal abrasion; 2 - predominantly solifluction; 3 - thermokarst; thermal abrasion; 4 - rock falls; 5 - rock-stream formation; 6 - thermokarst cave-ins; 7 - isolines of the roughness coefficient; and 8 - area number.

REFERENCES

Brown, J. and Grave, N.A. (1981). Narushenie poverkhnosti i yeyo zashchita pri osvoenii Severa, 88 p., Novosibirsk: Nauka.

Gotovtsev, S.P. and Dorofeev, I.V. (1980). Morfologiya merzloi tolshchi Charo-Tokkinskogo mezhdurechya. - V kn.: Geokriologicheskie usloviya zony Baikalo-Amurskoi magistrali, 89-95, Yakutsk.

Grave, N.A. (1978). Chuvstvitelnost poverkhnosti k tekhnogennomu vozdeistviyu v oblasti vechnoi merzloty, priyomy i metody otrazheniya yeyo na karte. - V kn.: Metodika inzhenerno-geologicheskikh issledovaniy i kartirovaniya v oblasti vechnoi merzloty, 16-33, Yakutsk.

Grave, N.A. (1979). Printsypy otsenki chuvstvitelnosti poverkhnosti k tekhnogennym vozdeistviyam (na primere territorii Yakutii). - V kn.: Okhrana prirody Yakutii, 91-94, Yakutsk, YaF SO AN SSSR.

Klimovsky, I.V., Gotovtsev, S.P., and Konstantinov, P.Ya. (1986). Svyaz chuvstvitelnosti merzlotnykh landshaftov s raschlenyonnostyu reliefa. - V kn.: Voprosy geokriologicheskogo kartirovaniya, 113-121, Yakutsk.

Melnikov, P.I., Klimovsky, I.V., and Gotovtsev, S.P. (1985). Platformenny kriolitogenny pokrov i rossypi. - V kn.: Regionalnye i inzhenernye geokriologicheskie issledovania, 3-21, Yakutsk.

Popov, A.I., Kuznetsova, T.P., and Rozenbaum, G.E. (1983). Kriogennye formy reliefa, 40, Izd. MGU, Moscow.

TABLE I

Some Characteristics in Sediments of Cryolithological Complexes

CLC number		Genetic type and composition of loose sediments	Cryogenic structures	Ice content, % (volume)			Thawing, m	
				Ground ice	Massive ice	Total	From	To
2, 10	Riverbed	Gravel-pebble, gravel-sand	Ice-cement, crusted, basalt	50	5	55	-	-
	Floodland	Sand	Ice-cement, massive	45	5	50	0.8	1.3
		Supes-suglinok	Massive, lens, lattice	55	10	65	0.5	1.1
		Same, peaty	Pockets	80	10	90	0.15	0.9
	Lake-bog	Silty-clayey	Layered, lattice, lens	55	10	65		0.7
		Same, peaty, peat	Pockets	85	10	95	0.2	0.5
	Eluvium (bottom)	Clays and crushed rock suglinoks (in the near-'raft' area)	Basalt, crusted, layered-fissured, lens, lattice	55	7	62	0.3	1.2
3,4,5,7,8,9,11	Slope	Supes-clayey	Lens-shaped	68	5	73	0.2	1.0
		Crushed-rock supes	Lens-shaped, massive, crusted	61	5	66	-	-
		Crushed-rock suglinok	Same	70	5	75	0.4	1.0
		Sands	Contact	10	-	10	-	-
		Clod-crushed rock	Basalt, crusted	40	-	40	-	-
		Gruss-crushed rock	Crusted, pocket, ice-cement	42	-	42	0.7	1.5
		Sand, supes, suglinok	Massive, lens-shaped	40	10	50	0.4	2.0
		Crushed-rock - gruss supes	Crusted, lens-shaped	40	10	50	0.9	2.0
1, 6	Eluvium	Gruss-suglinok	Crusted, lens-shaped, pocket	62	10	72	0.5	1.9
		Clod-crushed rock	Crusted, pocket, fissured, basalt	40	-	40	0.5	1.0

GLACIAL HISTORY AND PERMAFROST IN THE SVALBARD AREA

J.Y. Landvik[1], J. Mangerud[1] and O. Salvigsen[2]

[1]University of Bergen, Department of Geology, Section B, Allégt. 41, N-5007 Bergen, Norway
[2]Norsk Polarinstitutt, Rolfstangveien 12, N-1330 Oslo Lufthavn, Norway

SYNOPSIS Glacial and sea level history play an important role as preconditions for the development and distribution of permafrost in arctic areas. Based on reconstruction of the Weichselian and Holocene history of Svalbard and the Barents Sea, we propose seven zones each of which has been subject to widely different conditions pertaining to permafrost development. The main distinguishing characteristics are whether areas have been: subject to subaerial periglacial conditions during the last glaciation; subaerially exposed due to eustatic lowering of sea level; recently raised from sea due to glacio-isostatic rebound; or, remained as nunataks.

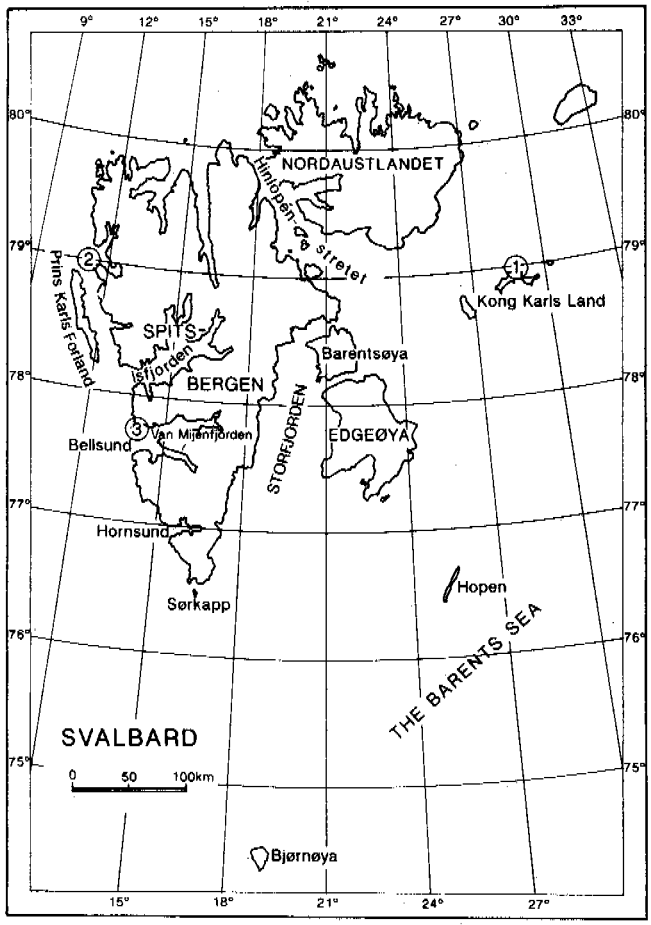

Fig. 1 Map of the Svalbard archipelago and the Barents Sea. Locations of the sea-level curves in Fig. 3 are shown.

INTRODUCTION

Permafrost covers the entire land area of Svalbard with known depths varying between 100 and 460 m (Liestøl, 1977). Thawed zones occur underneath glaciers and major lakes, and sometimes also in connection with warm ground water (Salvigsen & Elgersma, 1985).

For several years we have studied the geological history of Svalbard, with special emphasis on glacial history and sea level changes. In this paper we discuss the consequences this history has for the distribution and thickness of permafrost in the area.

We do not delve into the physics of frozen ground, but deal with the change of the physical environment through time. Permafrost needs long time spans to adjust to equilibrium with surface temperatures, and thus permafrost thicknesses and temperatures often reflect past climatic conditions. We have focused on the most prominent effects of climatic change the last 100,000 years, namely the growth and decay of ice sheets and related sea-level changes. Based on these studies and other available data from Svalbard, we use the geological history to outline some boundary conditions for permafrost development and distribution within the region.

The Svalbard archipelago is situated at latitude 74° to 81° north between the cold Barents Sea (Fig. 1) and warm Atlantic water in the Norwegian and Greenland Seas. Present mean annual temperature along the west coast is about -5°C, while to the east it is somewhat lower. The northern coast of Nordaustlandet has a probable mean annual temperature below -10°C.

Temperatures during the Late Weichselian glaciation in Svalbard are suggested to have been considerably lower than today. In contrast, climate during long periods of the Holocene has been so much warmer than the present that it must have caused significant reduction in permafrost.

GLACIAL HISTORY

The glacial history of Svalbard and the Barents Sea during the last glacial cycle has been disputed, and quite conflicting models have been proposed. Boulton (1979) suggested a very limited glaciation peaking around 11,000 years ago, while Denton & Hughes (1981) assumed that both the Svalbard archipelago and the Barents Sea were covered by a large ice sheet 18,000 years ago. Later investigations by Elverhøi & Solheim (1983) indicate that an ice sheet covered at least the northern parts of the Barents Sea. Based on field investigations in central and western Svalbard, Mangerud et al. (1987) proposed a model with a Barents ice-sheet to the east, separate ice domes over western Svalbard, and ice free margins along the western and northern coasts. They propose that an ice stream filled Van Mijenfjorden, while most of Isfjorden was probably ice free during the Late Weichselian (Fig. 2).

The most important implication of this model is that during the Late Weichselian, there were ice free areas along the coast that were exposed to severe arctic conditions. Reconstructed ice surface profiles from that period demonstrate that several mountains must have been nunataks, and thus experienced quite another temperature history than the glacier-covered lowlands around them.

Due to the warmer climate during parts of the Holocene, there was probably less glacier ice in Svalbard than today. Minimum limits for glaciers in the Holocene are not known, and many of the small glaciers were probably non-existent for long periods.

Fig. 2 Reconstructed Late Weichselian ice front positions in the Isfjorden and Van Mijenfjorden area of central Svalbard. Glaciers are shaded. From Mangerud et al. (1987).

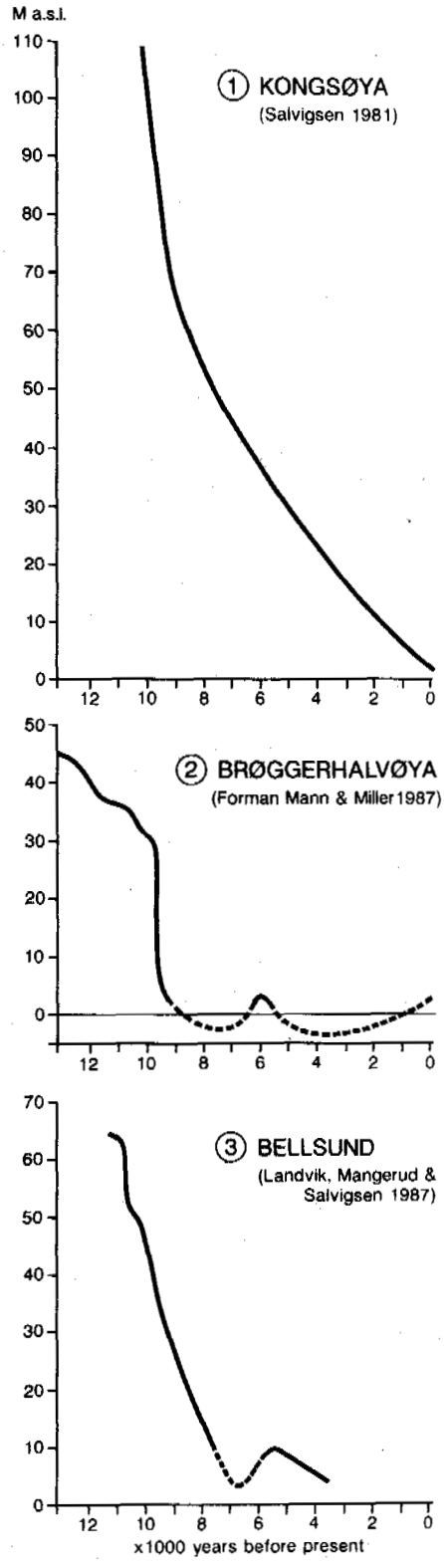

Fig. 3 Sea-level curves from the Svalbard archipelago. Locations of the curves are shown in Fig. 1.

SEA-LEVEL HISTORY

The late glacial and Holocene sea-level history for Svalbard is now well known. As demonstrated by Schytt et al. (1968), the Holocene sea-level changes in the area were governed by a glacio-isostatic rebound centered over the Barents Sea. Sea level curves from Kong Karls Land in the northern Barents Sea (Fig. 3) show a rebound of some 100 m during the last 10,000 years, and the land is still rising today at 0.3 m /100 years (Salvigsen, 1981). On the west coast, there was a very rapid initial uplift (Fig. 3) and most of the land areas emerged within some few thousand years as a response to the deglaciation of the Barents Ice Sheet (Mangerud et al., 1987). The emergence was interrupted by a Mid-Holocene transgression (Forman et al., 1987; Landvik et al., 1987), and there are indications that a transgression is in progress today (Rudberg, 1986; Forman et al., 1987; Sandahl, 1986).

ZONATION OF PERMAFROST DISTRIBUTION BASED ON THE GEOLOGICAL HISTORY

On the map in Figure 4, we have outlined 7 zones each with a different geological history that would have given rise to different pre-conditions critical for permafrost development.

1. The Barents Sea zone

This zone comprise the previously glaciated areas and shallow banks in the Barents Sea.

As demonstrated by Salvigsen (1981) and Elverhøi & Solheim (1983), at least the northern parts of the Barents Sea were glaciated during the Late Weichselian. As inferred from sea-level curves on Svalbard, this ice load disappeared some 12,000 to 10,000 years ago. The deglaciation was probably forced by the rising eustatic sea-level that caused a rapid calving of the ice front.

We thus expect that temperatures close to 0°C beneath the glaciers were replaced by sea temperatures that were also close to 0°C. Thus there was no time for subaerial exposure and permafrost development on the present sea bed. This is in contrast to parts of the Alaskan and Siberian continental shelves where permafrost is widespread.

2. The western and northern shelf zone

This zone includes former ice free areas that were transgressed by the sea during the end of the Late Weichselian and areas that were transgressed in periods of the Holocene.

If the reconstruction of the last glaciation by Mangerud et al. (1987) is correct, the present beach zone and continental shelf off parts of the west and north coast down to a depth of 50 to 150 m below sea level, were subaerially exposed during the Late Weichselian maximum. Thus, if there indeed exists any permafrost on the continental shelf around Svalbard, this is the most probable area. At present we have

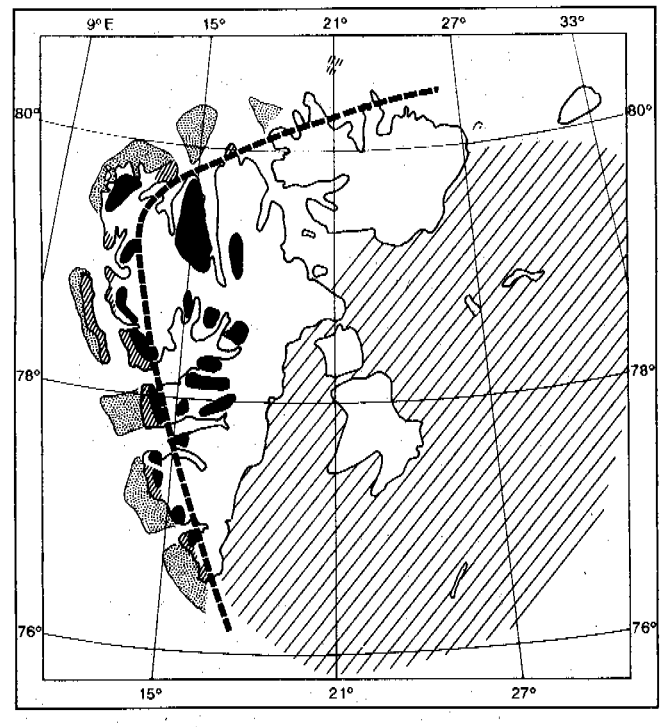

Fig. 4 A schematic presentation of the different zones discussed in the text.

little knowledge about the magnitude of isostatic depression of the crust during the Weichselian, but at least the shallower parts of the shelf should have been exposed for several tens of thousands of years. The warm Atlantic waters that reach the west coast of Svalbard today would cause rapid thawing of possible permafrost as compared to e.g. the Alaskan shelf. However, some time during the last 10,000 years relict permafrost must have existed at some depths below the present sea floor.

3. The emerging coast zone

This is a narrow zone along the coast line in areas where land is still emerging from sea, i.e. mostly in the eastern parts of the archipelago.

In this zone no permafrost is expected below present sea level. In those areas that have risen above sea level, the relatively short time of subaerial exposure poses a limiting

factor for the thickness of permafrost. The present rate of emergence at Kongsøya is around 0.3 m /100 years (Fig. 4), and areas at 10 m a.s.l. at Kongsøya have been above sea level for 2000 years. Permafrost is probably in near equilibrium with present surface temperature.

4. The transgressive coast zone

This zone comprises the coast line along the west and north coast of Svalbard. This zone is mainly a transition zone between zone 2 and zone 5, or between zones 2 and 7.

The possible ongoing transgression combined with coastal erosion, leads to capture of small areas along the coast by the encroaching sea. Thus permafrost can be expected beneath the present beach in such areas.

5. The central lowland zone

This zone comprises the land areas that were covered by the Weichselian glaciers and subsequently deglaciated at ca. 10,000 years B.P. We exclude the area covered by present day glaciers situated within this zone.

The zone was covered by warm based glaciers during the Late Weichselian, and the permafrost must have developed after the deglaciation about 10,000 years ago.

6. The central mountains zone

All mountains that penetrated the surface of the Late Weichselian ice sheet as nunataks are included in this zone. The upper parts of the ice sheet certainly also had temperatures well below zero; thus the zone includes the upper parts of the mountains, even if they were ice covered.

As shown by the reconstructed margins of the Late Weichselian ice sheet (Fig. 2) and profiles of valley and fjord glaciers, parts of the mountains in central Spitsbergen, i.e. within the central lowland zone, must have been nunataks during the last glaciation. We assume that the last extensive glaciation that covered these mountains occurred during the Early Weichselian (Salvigsen & Nydal, 1981; Miller, 1982), or even earlier.

Thus the summit areas have been exposed to severe arctic conditions for some 80,000 to 100,000 years. Immediately after deglaciation, 10,000 years ago, the permafrost temperature and thickness in these mountains was probably in equilibrium with the glacial time temperatures. Yet as this time the air temperature rose to the vicinity of present day temperatures. Thus the temperature in the permafrost must have increased, and these mountains must have experienced a net thawing of the permafrost.

7. The western and northern non-glaciated zone

This zone includes all areas above present sea level that were outside the limits of the Late Weichselian ice sheet.

Several studies have shown that the western and northern margins of Svalbard were not subject to glaciation during the Late Weichselian (Salvigsen & Nydal, 1981; Miller, 1982; Mangerud et al., 1987; Forman, in press). If we consider the eustaticly low sea-level during the Weichselian, both the present land area outside the Late Weichselian maximum and parts of the continental shelf were subaerially exposed.

The general climatic history for this zone has been parallel to the history for the nunataks (zone 6), but topographical differences between the zones likely caused large local differences in permafrost development.

ACKNOWLEDGEMENTS

This paper is a result of a co-operative research project between the University of Bergen and the Norwegian Polar Research Institute. The work has been financially supported by the Norwegian Council for Science and Humanities (NAVF) and Statoil. The staff of our two institutions and Statoil's representative Alv Orheim have been most helpful for accomplishment of the project. Olav Liestøl critically read the manuscript, and Edward King improved the English text. Jane Ellingsen, Ellen Irgens and Else Lier drafted the figures. To all these persons and institutions we proffer our sincere thanks.

REFERENCES

Boulton, G.S. (1979). Glacial history of the Spitsbergen archipelago and the problem of a Barents Shelf ice sheet. Boreas (8), 31-57.

Denton, G.H. & Hughes, T.J. (eds.) (1981). The last great ice sheets, 484 pp. John Wiley & Sons, New York.

Elverhøi, A. & Solheim, A. (1983). The Barents Sea ice sheet - a sedimentological discussion. Polar Research (1 n.s.), 23-42.

Forman, S.L. (in press). Late Weichselian glaciation and deglaciation of the Forlandsund area, west Spitsbergen, Svalbard Archipelago. Boreas.

Forman, S.L., Mann, D. & Miller, G.H. (1987). Late Weichselian and Holocene relative sea-level history of Bröggerhalvöya, Spitsbergen. Quaternary Research (27), 41-50.

Landvik, J.Y., Mangerud, J. & Salvigsen, O. (1987). The Late Weichselian and Holocene shoreline displacement on the west-central coast of Svalbard. Polar Research (5 n.s.), 29-44.

Liestøl, O. (1977). Pingos, springs and permafrost in Spitsbergen. Norsk Polarinstitutt Årbok 1975, 7-29.

Mangerud, J., Bolstad, M., Elgersma, A., Helliksen, D., Landvik, J.Y., Lycke, A.K., Lønne, I., Salvigsen, O., Sandahl, T. & Sejrup, H.-P. (1987). The Late Weichselian glacial maximum in western Svalbard. Polar Research (5 n.s.).

Miller, G.H. (1982). Quaternary depositional episodes, western Spitsbergen, Norway: aminostratigraphy and glacial history. Arctic and Alpine Research (14), 321-340.

Rudberg, S. (1986). Present-day geomorphological processes on Prins Oscars land, Svalbard - with appendix: Recent transgression in Svalbard. Geografiska Annaler (68A), 283-291.

Salvigsen, O. (1981). Radiocarbon dated raised beaches in Kong Karls Land, Svalbard, and their consequences for the glacial history of the Barents Sea. Geografiska Annaler (63A), 28-291.

Salvigsen, O. & Nydal, R. (1981). The Weichselian glaciation in Svalbard before 15,000 B.P. Boreas (10), 433-446.

Salvigsen O. & Elgersma, A. (1985). Large scale karst features and open talliks at Vardeborgsletta, outer Isfjorden, Svalbard. Polar Research (3 n.s.), 145-153.

Sandahl, T.J. (1986). Kvartærgeologiske undersøkelser i området Lewinodden - Kapp Starostin - Linnévannet Ytre Isfjorden, Svalbard. I + II, 196 + 112 pp. Unpublished thesis. University of Bergen.

Schytt, V., Hoppe, G., Blake Jr., W. & Grosswald, M.G. (1968). The extent of the Würm glaciation in the European Arctic. A preliminary report about the Stockholm University Svalbard Expedition 1966. International Society of Scientific Hydrology, General Assembly in Bern 1967, Publ. no. 79, 207-216.

REGIONAL FACTORS OF PERMAFROST DISTRIBUTION AND THICKNESS, HUDSON BAY COAST, QUÉBEC, CANADA

R. Lévesque[1], M. Allard[1] and M.K. Seguin[2]

[1]Department of Geography, Université Laval, Ste-Foy, Québec G1K 7P4
[2]Department of Geology conjointly Centre d'études nordiques, Université Laval, Ste-Foy, Québec G1K 7P4

SYNOPSIS A land systems approach was used for the study of a 3,700 km^2 area traversed by the tree line and the marine limit. Some 1,900 land systems in Quaternary deposits were identified and mapped. For each of these, the area underlain by permafrost was evaluated by means of geomorphological indicators (cryogenic morphology, vegetation structure, snow cover thickness...). Mean thickness of permafrost was then estimated according to calculated statistical relationships between morphometry of permafrost mounds and thickness of permafrost, measured at 215 sites by electrical resistivity soundings. Due to maritime climatic influence, permafrost is widespread and thicker (20 m) within a 15-20 km wide strip along the Hudson Bay coast. Further east, below the tree line, permafrost in marine sediments is sporadic and thin (< 10 m). It is observed mainly in peatlands as palsas. Permafrost is also widespread and thick (20 m) in drumlins inside the forest tundra because they have virtually no snow cover due to wind drifting. It is always absent under forest or shrubs with deep snow (> 80 cm) and beneath deep snowpatches on the leeside of hills.

INTRODUCTION

In Québec, permafrost underlies more than a third of the province (Allard and Seguin, 1987 a). Despite recent progress, the permafrost zones in northern Québec have not been mapped completely. The only available maps on permafrost distribution cover small areas and are usually restricted to palsas bogs or to the bottom of a short valley (Laprise, 1986; Couillard and Payette, 1985; Payette and Seguin, 1979; Seguin, 1976; Samson, 1975). It is difficult to interpret the regional factors affecting the distribution of permafrost by using these scattered and not very comparable maps.

A medium-scale (1:50,000) mapping project was initiated in 1982 to depict the distribution and thickness of permafrost in Quaternary sediments in the discontinuous permafrost zone. Medium-scale mapping, unlike small-scale mapping, allows identification of regional factors which characterize permafrost. This information is useful for engineering works or for assessment of the environmental impact of engineering projects such as dams and reservoirs.

STUDY AREA

Located on the Québec side of Hudson Bay, the study area stretches on both sides of the Nastapoca and Sheldrake rivers and covers 3,700 km^2 (Fig. 1). The mean annual air temperature is about -5.5°C and the amount of precipitation is about 530 mm, including 200 cm of snow (Wilson, 1971). Hudson Bay plays a major role on the coastal climate. During summer and fall, the climate is maritime; the temperature is cool, precipitation is abundant and fog often covers the area. During winter and spring, sea ice cover and the large anticyclones maintain a continental climate characterized by a dry weather and cold temperatures (mean temperature of -24°C in January). The snowcover thickness varies very much because the snow is redistributed by the wind. Sheltered areas, topographic depressions, tree stands and shrub land are covered by an average of 1 metre of snow (the extreme values may reach 3 metres) while the top of palsas, drumlins, deltas, eskers and rocky hills remains almost devoid of snowcover. This uneven snow cover plays an important role on permafrost distribution; in the Schefferville area, Nicholson and Grandberg (1973) have shown that 70 cm of snow were enough to prevent the development of permafrost.

After the retreat of the last Laurentide ice sheet (7,300 BP at Nastapoca river and 7,600 BP at Sheldrake river; Allard and Seguin, 1985), the Tyrrell Sea flooded the western half of the study area (Fig. 1) (Vincent et al., 1987; Seguin and Allard, 1984; Hillaire-Marcel and Vincent, 1980; Hillaire-Marcel, 1976), leaving fine deposits in the valleys (clayey silts) and coarser sediments (raised beaches, block fields) overlying the finer ones or located on the slopes of rocky hills. East of this zone, the area is covered by glacial (mainly drumlins) and glacio-fluvial deposits (eskers, deltas, flood-plains).
Like the marine limit, the tree line crosses the study area from north to south, some fifteen kilometres away from the coastline (Payette, 1983, 1976) (Fig. 1). This is due to the proximity of Hudson Bay which keeps the temperature cooler on the littoral fringe. Located west of this limit, the shrub tundra is basically made up of mosses, lichens and bushes (willows and

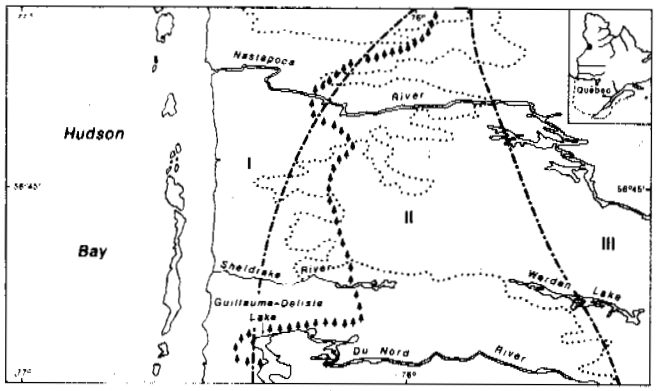

FIGURE 1 Map of the study area: ***** , tree line; ..... , marine limit; ——·——·—— limits of permafrost zones.

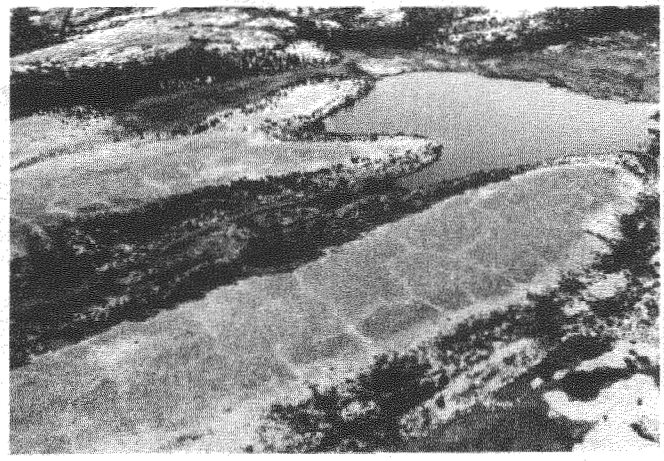

FIGURE 2 Soil wedge polygons on the top of drumlins (Zone III).

(birches). In the forest tundra, in addition to shrub tundra species, the vegetation also includes black spruces and larches in the valleys.

CRYOGENIC MORPHOLOGY

The study area shows different cryogenic landforms which characterize the discountinuous permafrost zone. Several mineral permafrost mounds and palsas occur in the bottom of the valleys covered by fine sediments (Allard and Seguin, 1987a; Seguin and Allard, 1984; Lagarec, 1982, 1980). From west to east, we observe a morphological gradient (Lagarec, 1982). In the shrub tundra zone, mineral permafrost mounds, covered by frostboils, are the main component of the landscape and the lack of palsas is explained by the very small proportion of peatlands. Below the tree line, there are a few palsas and their relative abundance versus that of mineral permafrost mounds tends to increase toward the east. By fifty kilometres from the coast, palsas are the main component of the landscape. This change is partly due to a milder climate inland than on the coast.

Because of their coarser grain-size distribution, glacial and fluvioglacial materials heave very little when they freeze; therefore, their cryogenic morphology is not well developed. Frost cracks and soil wedge polygons (Fig. 2) are the only elements which allow assessment of the presence of permafrost under drumlins, eskers or deltas. The soil-wedges are still active and correspond to the "primordial soil wedges" described by Romanovskij (1985) in similar climatic areas in the USSR.

The variety of deposits, their morphology, vegetation cover and climate effects are very suitable for the setting up of a methodology which would allow mapping the distribution and the thickness of permafrost using geomorphological characteristics.

METHODS

In order to simplify the mapping and to make sure it applies to different discontinuous permafrost zones, the approach used was that of the "land system" (Jurdant et al., 1977; Mabbutt, 1968; Mabbutt and Stewart, 1965; Christian and Stewart, 1968). This method consists of delimiting homogeneous geomorphological systems on the basis of visual observation: each of them is characterized by one type of soil material, cryogenic morphology (density of mounds, pattern), recurrent vegetation structure and a density of thermokarst pounds. This first estimation allows to set up a sampling plan which takes into account all geomorphological and ecological contexts in the area.

In total, 1,963 geomorphological systems were identified. Each of them has been described in detail; fifteen parameters were evaluated for each of them and compiled in a data base which was later used to map and analyse the factors related to permafrost.

In addition to the acquisition of various geomorphological data, 215 electrical resistivity soundings were made in all ecological contexts. Electrical resistivity sounding, a geophysical method previously used in the area (Seguin and Allard, 1984; Seguin, 1976) allows assessment of the presence of permafrost and and an estimate of thickness. This is possible because ice-rich soils have much higher electrical resistivities than unfrozen soils (Fig. 3). However, frozen sands and gravel sometimes have a resistivity similar to that of unfrozen finer sediments because of very low ice content. This method has also some restrictions when the soil temperatures, though lower than 0°C, are in the range of freezing point depression of the sediments.

The compiling of the results brings out two essential criteria for mapping:

i) There is no permafrost under continuous tree and shrub covers, mainly because of the importance of the accumulation of snow in these environments. In 90% of the cases, areas of bare ground or areas covered by herbs and mosses are associated with permafrost. Peat bogs (except palsas) and fens have no permafrost because of waterlogged soil (or peat) and snow cover thickness. Permafrost is also absent under the sides of drumlins where deep snowpatch accumulate.

ii) Statistical analyses (non-linear simple regression) have shown an obvious relation between the morphology of mineral permafrost mounds and palsas, and the thickness (Th) of permafrost. In the case of mineral permafrost mounds (1), the width (W) of the mounds gives the best correlation with a coefficient of 0.81 (Allard et al., 1987; Lévesque, 1986).

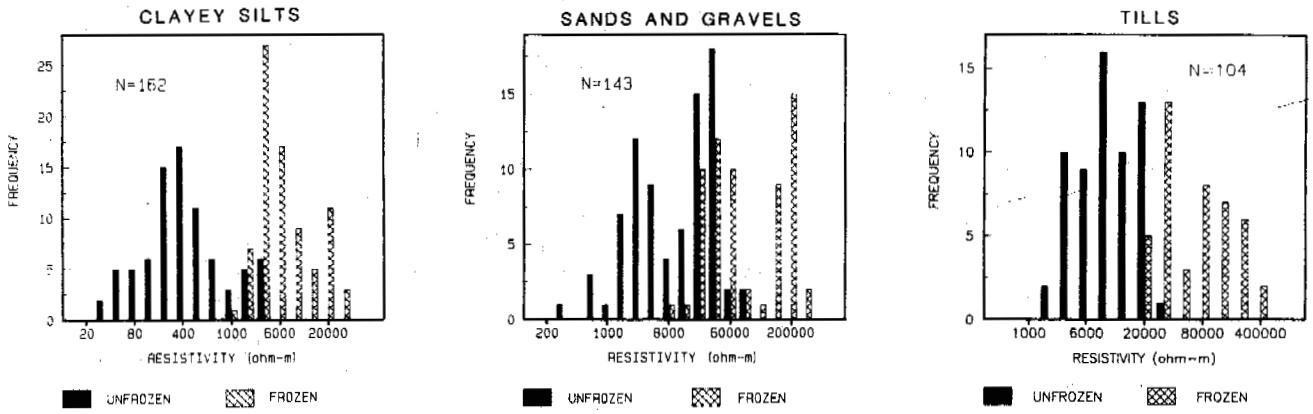

FIGURE 3 Resistivity in three types of Quaternary deposits. These values are taken directly on resistivity curves.

(1) Th $2.457252\ (W^{0.443468})\ (0.999794^{W})$

For palsas (2), it is the length (L) which gives

(2) Th $0.602319\ (L^{0.685771})\ (0.997738^{L})$

the best correlation (0,83) (Blais et al., 1985; Allard et al., 1987). In both cases, the volume may have given useful results, but it was impossible to measure the height of the mounds on the aerial photographs which were available (1:40,000).

Using these observations, it was possible to complete the mapping of the distribution and of the thickness of permafrost using aerial photographs. For the sediments which do not present particular geographic features related to permafrost (drumlins, eskers, deltas...), the average of the measures obtained by electrical resistivity is used. The limited number of eskers and deltas enable sounding of all of them to get "real" values.

For mapping, the data on the distribution and on the thickness of permafrost were sorted in class intervals in order to make the maps* easier to consult and to have a better perception of the regional disparities.

PERMAFROST DISTRIBUTION AND THICKNESS

Of the 3,700 km^2 of the study area, only 869.7 km^2 (24%) are made up of Quaternary deposits, 488.7 km^2 (56.2%) of which are permantly frozen (Table I) (Lévesque et al., 1987). The remaining (75.8%) is made up of outcrops and lakes.

TABLE I

Permafrost distribution in Quaternary Sediments

TYPES OF QUATERNARY DEPOSITS	AREAS COVERED BY QUATERNARY DEPOSITS (km^2)	AREAS UNDERLAIN BY PERMAFROST (km^2)	AREA PERCENTAGE OF PERMAFROST (%)
MARINE DEPOSITS	360.0	211.1	58.6
EOLIAN DEPOSITS	15.3	8.9	58.2
GLACIO-FLUVIAL DEPOSITS	124.3	68.9	55.4
GLACIAL DEPOSITS	244.0	161.1	66.0
ORGANIC DEPOSITS	126.1	38.7	30.7
TOTAL	869.7	488.7	56.2

Important disparities in the distribution and thickness of permafrost are obvious in the study area. The numerous micro-climates which explain these disparities are closely related to the presence of Hudson Bay and to the distribution of the sedimentary materials.

The permafrost can be sorted in three zones (I, II, III) according to its spatial density and thickness (Fig. 1).

Zone I corresponds to the shrub tundra area; the permanently frozen soils are abundant (> 80% of the area) and their mean thickness is 20 metres (min=9 m, max=29 m). The main cryogenic forms in the area are mineral permafrost mounds developed in clayey silts. The depressions between the mounds which are occupied by thermokarst pounds and shrubs, are taliks (Fig. 4).

The proximity of Hudson Bay creates conditions which favour the development of permafrost; during the summer, cool temperatures and numerous foggy days bring a more rigorous climate. The absence of trees and the scarcity of shrub vegetation along the littoral fringe in addition

* See "Posters" (V^{e} International Permafrost Conference) or Nordicana no 51 (Lévesque et al., 1987) for three series of six maps (Quaternary deposits, permafrost distribution and permafrost thickness).

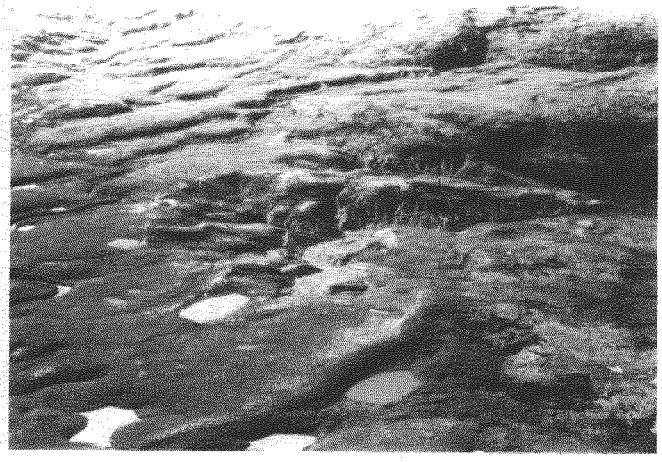

FIGURE 4 Widespread permafrost (> 80%) in clayey silts (Zone 1). Near Nastapoca river (12 km from Hudson Bay).

to strong westerly winds channelled in the structural valleys perpendicular to the coast, do not make the landscape favourable for the accumulation of snow. Only the valley sides and the shrubby depressions sheltered from the wind have a sufficient depth of snow (> 80 cm) to stop the expansion of permafrost or to form taliks. The tops of the mineral permafrost mounds which occupy the widest part of the area remain uncovered by the snow and exposed to the coldest air temperatures.

Zone II, located to the east, corresponds to the forest tundra below the marine limit. The effects of Hudson Bay on the regional climate are less pronounced (there are less foggy days). Trees take advantage of these milder conditions and colonize some areas in the valleys (Fig. 5). The more numerous tree and shrub areas provide a favourable environment for the sedimentation of drifted snow, thus for the formation of taliks. Permafrost is scattered (< 40%) and thin (average of less than 10 metres; min=2 m, max= 23 m) in fine grained marine sediments. These values progressively decrease from the northwest to the southeast, so that, there is almost no permafrost at the southeastern end of the study area. (Fig. 6).

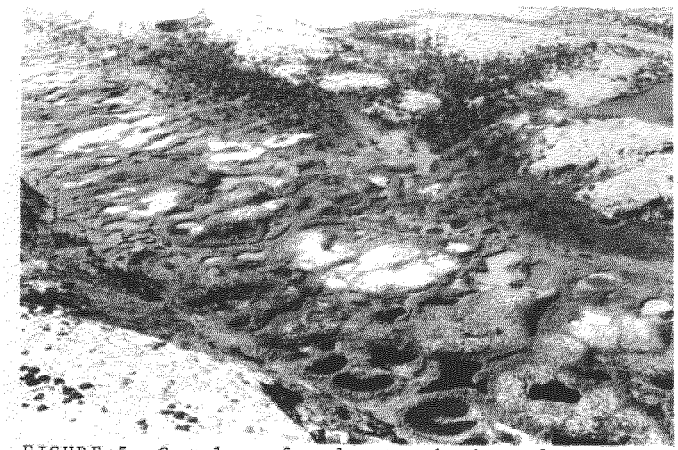

FIGURE 5 Complex of palsas and mineral permafrost mounds (white one). South of Nastapoca river, 45 km from Hudson Bay (Zone II).

FIGURE 6 Thermokarst pounds and decaying palsas. Sporadic permafrost, southeast part of Zone II.

The type of deposits does not seem to play an important role in the distribution and thickness of permafrost since great differences in the density of permafrost occured in the clayey silts found in zones I and II.

The only deposit which has some effect on permafrost is peat. It is a good thermal conductor when it is damp and a good insulating material when it is dry (Sollid and Sorbel, 1974; Brown, 1966); these peculiarities allow permafrost to develop in different underlying materials where it would be impossible without a peat cover. This is why permafrost encountered in the bottom of the valleys of the forest tundra almost exclusively occurs in the form of palsas (Fig. 7). However, their advanced state of degradation suggests that they were formed during a colder climatic period than at present; they are currently affected by erosion (Allard and Seguin, 1987b; Laprise, 1986).

Zone (III) seems to go against the established order because it has identical densities (> 80%) and thickness (average 20 metres; min = 3 m, max= 32 m) to Zone I even though Zone III is located in the forest tundra away from the sea influence.

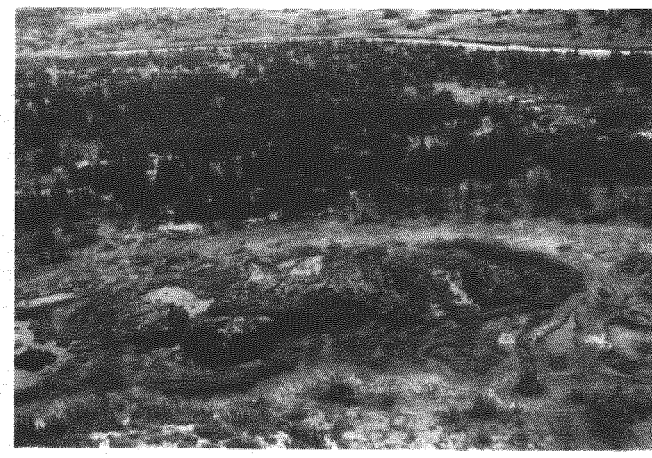

FIGURE 7 Peat plateau in forest tundra (Zone II).

This is explained by the topography of the deposits in this Zone (Fig. 2). The glacial and fluvioglacial sediments (unlike the sea deposits which are mainly located in the bottom of the valleys) form drumlins fields and sandur-deltas that are very exposed to the wind. Snow is constantly drifted off the top of these forms accumulating in the depressions located in the peripherial areas. These depressions, which constitute taliks, account for a smaller proportion than in the case of Zones I and II because the deposits are not confined only to the valleys.

CONCLUSION

This kind of mapping has allowed to specify the main factors related to the distribution and the thickness of regional permafrost. The depth of snow plays a very important role; however, this role depends largely on the particular conditions created by the proximity of Hudson Bay and on the distribution of the surficial deposits.

The application of such a cartographical method, to larger areas in discontinuous permafrost zones (widespread and scattered) in Québec can be easily realized with only minor methodological adjustments. For instance, the measurement of the thickness of permafrost could be improved if we would take into account the height of cryogenic mounds in the correlation coefficients. However, a new approach, with critical planning of geophysical surveys, will have to be considered for soils types which do not have a particular morphology related to the presence of permafrost such as drumlins, moraines, till sheets, deltas and eskers.

ACKNOWLEDGEMENTS

The authors gratefully acknowledge the support of the Centre d'études nordiques, the National Sciences and Engineering Research Council of Canada and the Québec's Fonds F.C.A.R. for providing logistical support and funding for this project. Thanks are due to Mrs. J. Bouchard, D. Couture, E. Jetchick and to Messrs R. Blais and F. Guimond for their help in the field study. The valuable comments of two anonymous reviewers are gratefully acknowledged.

REFERENCES

Allard, M. & Seguin, M.K.(1985). La déglaciation d'une partie du versant hudsonien québécois: bassin des rivières Nastapoca, Sheldrake et à l'Eau Claire. Géogr. phys. Quat., 39(1):13-24.

Allard, M. & Seguin, M.K. (1987a). Le pergélisol au Québec nordique: bilan et perspectives. Géogr. phys. Quat., 41(1):141-152.

Allard, M. & Seguin, M.K. (1987b). The Holocene evolution of permafrost near the tree-line on the eastern coast of Hudson Bay (northern Québec). Can. J. Earth Sci., 24:2206-2222.

Allard, M., Seguin, M.K. & Lévesque, R. (1987). Palsas and mineral permafrost mounds in northern Québec. Pages 285-309, in International Geomorphology 1986 Part II, Edited by V. Gardiner, John Wiley & Sons Ltd.

Blais, R., Allard, M. & Seguin, M.K. (1985). L'épaisseur du pergélisol sous les palses de la région de la rivière Sheldrake, Québec nordique. Annales de l'ACFAS 52-53(1):178.

Brown, R.J.E. (1966). Influence of vegetation on permafrost. Proceedings Permafrost International Conference, November 1963, Research Paper no 298, Division of building research, National Research Council Canada, Ottawa, 20-25.

Christian, C.S. & Stewart, G.A. (1968). Methodology of integrated surveys. Pages 233-280 in Aerial surveys and integrated studies, Proc. Toulouse Conf. 1964, UNESCO, Paris.

Couillard, L. & Payette, S. (1985). Evolution holocène d'une tourbière à pergélisol (Québec nordique). J. Can. Bot., 63(6): 1104-1121.

Hillaire-Marcel, C. (1976). La déglaciation et le relèvement isostatique sur la côte est de la Baie d'Hudson. Cah. Géogr. Québec, 20(50):185-220.

Hillaire-Marcel, C. & Vincent, J.-S. (1980). Stratigraphie de l'Holocène et évolution des lignes de rivages au sud-est de la Baie d'Hudson, Canada. Paléo-Québec, 11:165 p.

Jurdant, M., Belair, J.-L., Gerardin, V. & Ducruc, J.-P. (1977). L'inventaire du Capital-Nature, Service des études écologiques régionales, Direction des Terres. Environnement Canada, 202 p.

Lagarec, D. (1980). Etude géomorphologique de palses et autres buttes cryogènes en Hudsonie, Nouveau-Québec. Université Laval, Québec, Ph.D. thesis, 290 p.

Lagarec, D. (1982). Cryogenic mounds as indicators of permafrost conditions, northern Québec. Pages 43-48 in Proceedings 4th Canadian Permafrost Conference, the R.J.E. Brown Memorial Volume, Ottawa, National Research Council of Canada.

Laprise, D. (1986). Evolution récente du pergélisol dans une tourbière à palses du golfe de Richmond (Québec nordique). Université Laval, Québec, Master thesis, 35 p.

Lévesque, R. (1986). Géomorphologie périglaciaire et cartographie, assistée par ordinateur, du pergélisol, aux rivières Nastapoca et Sheldrake, Hudsonie. Université Laval, Master thesis, 144 p.

Lévesque, R., Allard, M. & Seguin, M.K. (1987). Distribution et épaisseur du pergélisol aux rivières Nastapoca et Sheldrake, Hudsonie, en relation avec les dépôts quaternaires. Centre d'études nordiques, Université Laval, Nordicana no 51.

Mabbutt, J.A. (1968). Review of concepts of land classification. Pages 11-28 in Land evaluation (G.A. Stewart, ed.), Macmillan, Melbourne.

Mabbutt, J.A. & Stewart, G.A. (1965). Application of geomorphology in integrated ressources surveys in Australia. Rev. de Géomorph. Dyn., 6:1-13.

Nicholson, F.H. & Granberg, H.B. (1973). Permafrost and snowcover relationships near Schefferville. Pages 151-158 in North American Contribution 2nd International Permafrost Conference, National Academy of Sciences, Washington, D.C.

Payette, S. (1976). Les limites écologiques de la zone hémiarctique entre la mer d'Hudson et la baie d'Ungava, Nouveau-Québec. Cah. Géogr. Québ., 20(50):347-364.

Payette, S. (1983). The forest tundra and present tree-line of the Northern Québec-Labrador peninsula. Pages 3-23 in Tree-line Ecology (P. Morisset & S. Payette, eds), Proceedings of the Northern Québec Tree-line Conference, Centre d'études nordiques, Université Laval, Nordicana no 47.

Payette, S. & Seguin, M.K. (1979). Les buttes minérales cryogènes dans les basses terres de la rivière aux Feuilles, Nouveau-Québec. Géogr. phys. Quat., 33(3-4):339-358.

Romanovskij, N.N. (1985). Distribution of recently active ice and soil wedges in the U.S.S.R. Pages 154-165 in Field and Theory, Lectures in Geocryology, (M. Church & O. Slaymaker, eds), Univ. of British Columbia Press, Vancouver.

Samson, H. (1975). Evolution du pergélisol en milieux tourbeux en relation avec le dynamisme de la végétation, Golfe de Richmond, Nouveau-Québec. Université Laval, Québec, Master thesis, 158 p.

Seguin, M.K. (1976). Observations géophysiques sur le pergélisol des environs du lac Minto, Nouveau-Québec. Cah. Géogr. Qué., 20(50): 327-346.

Seguin, M.K. & Allard, M. (1984). Le pergélisol et les processus thermokarstiques de la région de la rivière Nastapoca, Nouveau-Québec. Géogr. phys. Quat., 38(1):11-27.

Sollid, J.L. & Sorbel, L. (1974). Palsa bogs at Haugtjormin, Doverfjell, South Norway. Norsk Geografisk Tidsskrift, vol. 28:53-60.

Vincent, J.-S., Veillette, J.J., Allard, M., Richard, P.J.H., Hardy, L. & Hillaire-Marcel, C. (1987). Dernier cycle glaciaire et retrait des glaces de la vallée supérieure de l'Outaouais jusqu'au sud-est de la Baie d'Hudson. XIIth Congrès de l'INQUA, excursion C-10, 87 p.

Wilson, C. (1971). Atlas climatologique du Québec. Service de l'Environnement Atmosphérique du Canada, Toronto, 180 p.

PINUS HINGGANENSIS AND PERMAFROST ENVIRONMENT IN THE MT.DA-HINGANLING, NORTHEAST CHINA

Lu, Guowei

Yakeshi Institute of Forestry Survey and Design, Inner Mongolia, China

SYNOPSIS Pinus hingganensis, a new species of pine in the permafrost region of Mt. Da-Hinganling, Northeast China, grows in relatively high, shady and damp districts. This species is morphologically similar to the P.siberica and P.pumila.
The regional climate has been warming since Late Pleistocene, especially during the recent century, resulting in the northward retreat of the southern limits of permafrost and forest zones. The effects of climate and deforestation make it necessary to protect, and regenerate the forest and the ecosystem. P.hingganensis may be a good species in accomplishing this.

DEITY TREE: PINUS HINGGANENSIS

Mt. Da-Hinganling is now covered by Da-uli flora, which commonly includes Larix gmelini,Picea Koraiensis, Chosenia macrolepis. Another species, however, is worthy of notice.Pinus hingganensis, once esteemed as "deity tree" by the Owenk people and recently distinguished as a new species of pine (Zhang, 1985), also occurs there. P.hingganensis occurs in the predominantly continuous permafrost zone and is able to grow well in shade, in a relatively high, cold and damp environment, and even in an inferitile soil or the exposed weathered bed rock. The oldest living P.hingganensis is about 180 years old. P.hingganensis is morphologically similar to the p.pumila and P.siberica (Table I). They may have some successional relationship to each other.

RELATIONSHIP BETWEEN P.HINGGANENSIS AND PERMAFROST

In Northeast China, permafrost occurs mainly in the Mt.Da-Hinganling and Mt.Xiao-Hinganling regions; besides, and in the Changbaishan and Huanggongliang Mountains (Lu and Guo, 1983).The distribution of permafrost in the Da-Hinganling and Xiao-Hinganling Mountains shows latitudinal zonation. Three zones are distinguished from north to south: predominantly continuous permafrost zone, discontinuous permafrost zone with talik islands, and the island permafrost zone (Fig.1),(Zhou et al., 1983). Similarly the mean annual ground temperature of permafrost increases while it decreases in thickness and continuity from north to south. The northern part of the Da-Hinganling forest region is located in the predominantly continuous permafrost zone,

TABLE I

Morphological Characteristics of P.hingganensis,P.siberica and P.pumila

Species / Character		P.siberica	P.hingganensis	P.pumila
leaf	diameter (mm)	1.5-1.7	1.0-1.2 (1.4)	0.6-1.0
	edge	sparse sawtooth-like	sparse sawtooth-like	smooth or unclear sawtooth-like
	resin passage	3 in number, internal at corners	2 or 3 in number, most internal, seldom lateral	mostly 2 in number seldom 1, lateral
cone	size (cm)	length:5-8 diameter:3-3.5	length:5-8 diameter:3-4.5	length:3-6 diameter:2.5-3.5
	scale shield	purple-brown, with dense fine long down	purple-brown, with sparse short down	chestnut-brown, without down

where permafrost is well-developed at the shady slopes and valley bottom rather than on sunny slopes or hill tops (Table II).

TABLE II

Distribution of Permafrost in Baimakan, Manqui,Inner Mongolia

Position	east-west valley			north-south valley		
Character	south-facing slope	valley bottom	north-facing slope	east-facing slope	valley bottom	west-facing slope
mean annual ground temperature (°C)	0 to -1.0	-2 to -4.0	-1.0 to -2.0	0 to -0.5	-2.0 to -4.2	0 to -1.0
thickness of permafrost (m)	0 to 20	50 to 150	20 to 50	0 to 20	50 to >100	10 to 30
depth of seasonal thawing (m)	2.0 to 4.0	0.5 to 1.0	1.0 to 1.5	1.0 to 3.0	0.5 to 1.0	1.0 to 2.0

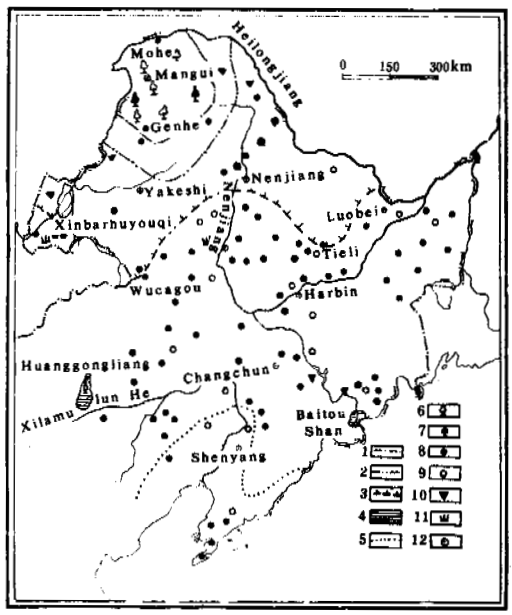

Fig.1 Distribution of P.hingganensis and changes in permafrost southern limit since the Last Glaciation
1. present southern limit of predominantly continuous permafrost; 2.present southern limit of discontinuous permafrost zone with talik islands; 3. present southern limit of island permafrost zone; 4. present alpine permafrost regions; 5. southern permafrost limit during Late Pleistocene; 6. present P. hingganensis vegetation; 7. present Picea koraiensis vegetation; 8. fossil sites of mammoth; 9. fossil sites of Coelodonta antiquitatis; 10. ice-wedge casts; 11. arid steppe; 12. city or town

Today P.hingganensis grows mainly within the predominantly permafrost zone and sporadically on the hill tops of Mt.Huangangliang. Generally, it grows in restricted areas above 900 m a.s.l. (Table III).

TABLE III

Growing Sites of P.hingganensis

site	latitude	elevation (m)
Qiqian	52°30'N	-
Angelin	51°22'N	1300
Alongshan	51°35'N	900,950
Mangui	52°13'N	900
Tuqiang	52°25'N	840
Mordaoga	51°10'N	1300

P.hingganensis is seldom found in valley bottoms, where the temperature is too low, the active layer is too thin, and the permafrost, with well-developed ground, ice is too thick.In such areas roots of P.hingganensis have difficulty growing and absorbing moisture and nutrient from the ground. In addition young seedling would probably be killed by the frost heave of the soil.

P.hingganensis vegetation occurs rarely on precipitous south-facing slopes because of severe soil erosion.

Forests are confined to areas with relatively gentle relief, such as shady slope, the middle-lower part of sunny slopes and on gentle hill tops. In these locations the active layer is relatively thick, and the soil is damp. Such conditions are favour plant growth, although the ground is still rather cold. Larix gmelini-Rhododendron dahuricum forest and Larix gmelini-P.pumili forest grow well there. Within these

forest-types, the P.hingganensis also grows very well with its twisted roots surviving in the active layer above permafrost. For example, in the Alongshan Forestry-Service, P.hingganensis grows in groups within the Larix gmeline-R. dahuricum forest at 1200 m a.s.l., and in Angelin, P.hingganensis grows within the Larix gmelini-P.pumila forest on hill tops. The forest understory is mainly composed of the Vaccinium vitis-idaes, Ledum palustre and moss. These forest-types are thought to be closely linked to the periglacial environment. P.hingganensis may be an indicator of permafrost.

FOREST AND ENVIRONMENT

The forest region of northern Hinganling is currently located in the predominantly continuous permafrost zone, where the mean annual air temperature is as low as -5 °C, the annual precipitation is about 500 mm, and the water content of soil above permafrost table is relatively high. These conditions favour forest development.

During the last glaciation of the Late Pleistocene, the southern forest limit advanced down to 42°N, and the predominantly continuous permafrost zone, to 47°N (Guo, et al., 1981). The southern limit of forest also advanced down to the hills of southern Liaoning. During a Holocene warming the southern limit of permafrost retreated (Fig. 1). As the southern limit of permafrost moved northwards, the forest requiring a periglacial environment retreated northwards also. Such forests now develop only in periglacial environments; the existence of forest, protects the frozen ground from thawing.

In the 20th century, changes in the distribution of natural forest and permafrost are closely related to the warming climate and human activity. Under the influence of these two factors, the permafrost degrades, and has disappear in some places (for example, the Yakeshi, Jiagedaqi). As a result of such changes the southern limit of natural forest is moving northwards or there are changes in vegetation associations. During the past 200 years, from 1732 to 1945, the primeval forest in Da-Hinganling and Xiao-Hinganling Mountains was destroyed to a large extent. This had a deep effect on plant-composition, soil, climate and hydrology. In 1840, deforestation occurred only from Qiqihar to Nenjiang. However, up to 1945, the forest line had retreated by 2 degrees of latitude. As are result of major forest fires and deforestation there has been an invasion of wind blow sand eastwards from the Inner Mongolian Plateau, a decrease of precipitation in the Hulunbeir Grassland, and grealter aridity of the regional climate. This resulted in the enlargement of a xerophytic flora, and the substitution of secondary forest composed of Betuta ptalyphylla, Quercus mongolica and bush fallow of Populus davidiana for the destroyed coniferous trees.

It is necessary to take effective measures to renew, regenerate and to protect the forest and environment. The P.hingganensis, a cold-resistant species that is able to grow in the inferitile soil, is a species suitable for planting in such a periglacial environment, even though its current distribution is sporadic. Such planting, together with other measures, such as controled-cutting, rodent control and seeding programs may enable P.hingganensis to become a dominant species in this region.

REFERENCES

Guo Dongxin and Li Zuofu, (1981). Preliminary approach to the history and age of permafrost in Northeast China. Journal of Glaciology and Cryopedology, (3), 4, 1-16.

Luo Guowei, Guo Dongxin and Dai Jingbo, (1983). Basic characteristics of permafrost in Northeast China. Pro.4th International Conference on Permafrost, (I), 740-743.

Zhang Hanjie,(1985). A new species of pine in China. Plant Research, (5), 1.

Zhou Youwu and Guo Dongxin, (1983). Some features of permafrost in China. Pro.4th International Conference on Permafrost,(I), 1496-1501.

NATURAL GEOSYSTEMS OF THE PLAIN CRYOLITHOZONE

E.S. Melnikov

All-Union Research Institute of Hydrogeology and Engineering Geology, Moscow, USSR

SYNOPSIS The object of regional geocryological studies for the purposes of mapping, forecasting and nature-preserve zoning is the geocryological subsystem of natural or natural technogenic geosystem. Such an approach gives an integral picture of an interaction between natural bodies in cryolithozone, their structure in space and time, functioning and matter- and energy exchange. Hierarchy of natural geosystems in plain cryolithozone is developed. A brief description is given for each of eight ranks of geosystems. Functioning and homeostasis of natural and natural-technical geosystems are studied in stationary geocryological observations; and their spatial-morphological structure - in regional investigations. Geosystem approach is the basis for geocryological prediction and nature-preserve zoning of the cryolithozone geoenvironment.

In the recent decades a great economic, ecological and social importance was gained by regional geocryological investigations due to carrying out a number of large projects on development of oil- and gas fields and on construction of long-distance line structures (e.g. pipelines, railroads, electric power transmission lines). Basing on these investigations, a prediction is being made of changes in engineering-geocryological conditions (EGC) due to economic activities, and maps of nature-preservation zoning are being compiled.

A subject for geocryological study and prediction are rocks and ground water of cryolithozone, their composition, properties and processes occurring within them. What should be an object of inquiry, what natural material bodies should be examined? This question is a debatable one. It is obvious that in choosing the main study object, various criteria can be used: geological, geocryological, engineering-geological and landscape ones. Geological criteria - establishment of geological bodies and their natural parageneses (strata and layers of rocks, lithologic-facies and stratigraphic-genetic complexes, geological formations and subformations) - cannot satisfy the aims and purposes of regional geocryological investigations, because they do not take into account a change of rock states and their role in mass-energy exchange being the basis for dynamics of exogenous geological processes.

Geocryological criteria proper (types of permafrost strata (PFS), types of seasonally thawing layer-seasonally freezing layer (STL-SFL), temperature fields, etc.) do not involve geological differentiation and summary effect of an interaction between external media (hydro-, bio- and atmosphere) and lithosphere.

Engineering-geological (geologic-engineering) criteria in assessment of rocks as being applied for ground bases and foundations, in assessment of a possibility and peculiarities of construction and exploitation of structures are short-term and momentary. This is explained by a rapid-changing level of technical development of society and a level of civil-engineering.

Therefore, most preferable is the geosystem approach to regional geocryological investigations and predictions, which proceeds from the theory of the Earth's natural complexes (Dokuchaev, Berg, Polynov, et al.) as natural bodies (after Vernadsky), within which an interaction of lithosphere with hydro-, atmo-, biospheres takes place. Natural complexes or natural geosystems are considered as a product of an interaction of lithosphere (i.e. geological bodies in a rank of formations, stratigraphic-genetic and lithologic-facies complexes of rocks) with other Earth's spheres (atmo- and hydrosphere, biota) for the up-to-date stage of territory development.

Natural boundaries of natural complexes, their materiality, full-complexity, hierarchy in space and time enable objectification of their establishment and use of system analysis allowing for an influence of any natural phenomena on state of rocks and processes within them. Natural complexes represent complicated open self-managed and self-restored material systems of interconnected elements (rocks, ground and surface waters, biota) and components (natural complexes of lower ranks) between which mass-energy exchange occurs under influence of ones or other leading factors. A depth of active mass-energy exchange is different for different ranks of complexes (Table I). Natural complexes are characterized by integrity and emergencibility. Geocryological conditions - structural element of such a system - are considered as a subsystem. Such

TABLE I

Predominant sizes of natural geosystems of the plain cryolithozone and possible cartographic scales

Rank of geosystem		Sizes			Scales of cartography
		Linear, km	Areal, km^2	Depth of active mass-energy exchange, m	
I	(land)	10^3	10^5-10^6	10^3	1:1,000,000 and smaller
II	(province)	10^1-10^2	10^3-10^4	10^2	- " -
III	(subprovince)	-"-	-"-	10^1-10^2	- " -
IV	(region)	10^1	10^2-10^3	10^1	1:2,500,000-1:500,000
V	(landscape)	1-10^1	10^1-10^2	10^1	1:1,000,000-1:200,000
VI	(tract)	1-10	1-10^1	10	1:500,000-1:25,000
VII	(stow)	10^{-1}-1	10^{-2}-1	1-10	1:100,000-1:10,000
VIII	(site)	10^{-2}-10^{-1}	10^{-4}-10^{-2}	1	1:10,000-1:1,000

an approach gives an integral idea of an interaction between elements and components of natural bodies, an idea of their structure in space and time, functioning and mass-energy exchange. Landscape principle of mapping has been applied in geocryology from the beginning of the existence of this science (Yachevsky, Abolin, Sumgin, Tumel). During recent years the principle has received its further advance due to increased regional geocryological investigations for predicting purposes. Hierarchical structure of plain natural territorial complexes (NTC) is established for the purposes of engineering-geocryological studies; sizes of NTC of different ranks and their diagnostic features are determined (Landshafty..., 1983). Below, successive descriptions are given for eight ranks of natural geosystems and their geocryological conditions.

Geosystem of rank I (landscape land) is a part of continent that is characterized by an uniform geological structure (e.g. shields, plates of platforms; orogens), common topographic features, peculiar latitude or altitude zonalities. The West-Siberian landscape land is distinguished as being belonged to the greatest geological structure - West-Siberian plate - composed of rocks of platform formations and characterized by a plain relief, general low drainability, distinct nature-climatic zonality and by strongly pronounced continental climate.

Geosystem of rank II (landscape province) is a part of landscape land that is isolated by boundaries of nature-climatic zones and geologic-geomorphological areas. A certain combination of genetic topographic types and their composing Quarternary sediments being in a certain state (frozen, overmoistened, etc.) is typical for geosystems of this rank. The examples for landscape provinces can be a tundra province of sea (initial) plains, a taiga province of glacial plains and so on. Their sizes are given in Table I.

Geosystems of rank II are subdivided into landscape subprovinces (geosystems of rank III) according to their position in nature-climatic subzone and hence, to heat and moisture content. Boundaries of landscape subprovinces agree with those of geocryological subzones within geologic-geomorphological areas (Landshafty..., 1983). Examples for subprovinces can be southern tundra subprovinces of sea plains, northern taiga subprovinces of alluvial plains and so on.

Geosystems of rank IV - landscape regions - are distinguished within landscape provinces according to topographic character corresponding to neotectonic structures (movements) of ranks II-III or to geomorphological areas. Examples for such regions can be: (i) plains-low, flat highly bogged and lake-studded or (ii) plains - high, gently ridge and hillock-ridge. Landscape regions represent natural complexes with peculiar relief and genesis of surface sediments, peculiar heat- and moisture conditions and character of soil-, vegetation- and snow covers. A difference in a thickness of surface sediments in different regions can reach tens, rarely hundreds of meters. General character of relief together with heat- and moisture regime determine a combination of PFS-types for each region. Landscape regions and all NTCs of lower ranks are indivisible in zonal concern.

A depth of intralandscape relations in a landscape region is determined by intensivity and nature of neotectonic movements manifesting, first of all, in thickness and character of Quarternary sediments. Thus, in areas of intensive latest uplifts Quarternary sediments show a considerable decrease in thickness.

All the above-mentioned taxons belong to geosystems of regional generalization level and

are represented in small-scaled maps and schemes. Their boundaries are used mainly for extrapolating constructions and general zoning.

Geosystems of rank V-VIII refer to local level of generalization and are studied in national engineering-geocryological mapping and engineering explorations.

Geosystems of rank V are landscapes as a part of landscape regions, which are characterized by common age, relief genesis and relief-forming sediments (genetic complex).

Under an age of accumulative landscape a time is meant for water removal from surface and vegetation origination in aqueous (marine, alluvial, lacustrine-alluvial) landscapes and a time of mesorelief formation (ridges, hills) and vegetation origination in terral (glacial, eolian) landscapes. Under an age of erosion (abrasion) landscapes a time is meant when activity of denudating agents is stopped. The older is landscape, more complicated and diverser is its morphological structure (i.e. composition and relationship of its NTCs of the lower ranks).

Except the geological structure, all other geoenvironmental components (geocryological and hydrogeological conditions, exogenous geological processes, aqueophysical properties of soils) have no individual features for each landform. Peculiar to them is a great scattering in characteristic values. And the more complicated is morphological composition of landscapes, the greater is this scattering. Among the most landscapes two or three PFS-types are distinguished having sharply different features.

Geosystems of rank VI (tracts) are the largest morphological section of landscape being exceptional in a rate and character of rugged topography, and in predetermined local neotectonic movements. Main characteristic features of geocryological conditions of tracts lie in a geological profile type, distribution character and variability degree of PFS temperature field, in a rate of surface drainability and paragenesis of current geological processes. PFS-type with its peculiar distribution, temperature range and predominant nature of cryogenesis has an obvious agreement with geosystem type of this rank. Thus, in the Pur-Nadym area the southern forest-tundra landscape of Middle Pleistocene initial plain consists of tracts of two types: lacusrine-boggy (A) and gentle-ridgy planohollow near-river ones (B). The former are characterized by a continuous (with only interrupting under lakes) occurrence of perennial frozen grounds (PFG) with $t = -1 \div -5°C$ and a broad development of peat bogs and marches. Typical of the latters are abundant taliks in river valleys and ravines, PFG with $t \geq 2°C$, broad development of hydrolaccoliths, lateral erosion and solifluction.

Geosystems of rank VII (stows) represent a compound natural geosystem consisting of sites (facies) and covering completely or partially topographic mesoform with typical microrelief and a certain combination of biocoenoses and soil combination. Different stows within a single tract of the same landscape differ in morphological structure and in components (one or several) of geocryological conditions, i.e. lithologic-facies complex and soil composition; PFG-temperature or its peculiar distribution; a type of STL-SFL; a character of manifesting an exogenous geological process. A depth of mass-energy exchange is determined by a layer of annual heat transfers. Thus, in near-river tracts B (see above) co-dominant stows are spotted tundras (1), small-hummocky deciduous sporadic trees (2), flat birch-deciduous light forests on ridge slopes (3). Stows of types 1 and 2 are characterized by PFG of mixed composition (sand, sandy loam, peat) with $t \geq -1°C$ and by seasonal ground heaving. Stows of type 3 are composed of sands to 5 m thick with loams underlain; PFG top here is lowered to over 5-10 m. Stows of ridges and frost mounds occur often in these tracts, which are composed of highly icy loams with ice interbeds and $t \geq -2°C$.

Geosystems of rank VIII (sites) represent the smallest natural-territorial complex. They differ in their position in topographic mesoform, a character of micro- and nannorelief, vegetation association, moistening regime and soil. Within a tract the sites differ in structure of STL-SFL and in their thickness, ground-water level, morphological features (stage) of an exogenous geological process (EGP). A depth of mass-energy exchange is determined by a depth of seasonal thawing or ground-water level. Examples for sites in forest-tundra may be peat mounds of 5-10 m in height and 50-100 m in diameter, consisted of highly icy peat to a depth of 1-2 m and having seasonal thawing to 0.5 m deep or interridge sinks in flood plain covered by meadow vegetation and composed of silty sandy loams which, due to a seasonal thawing level, can be water-saturated to 1 m deep.

Also, natural geosystems with aquatic surface are distinguished - natural-aquatic complexes, e.g. lakes, rivers, lagoons.

Typological classifications are suggested for geosystems of local level of generalization which take into account their peculiar external outlook and hence, their aerophotoimages. Such classifications are developed for Bolshezemelskaya tundra (Metody..., 1986), north of West Siberia (Landshafty..., 1983), Central Yakutia and for some areas of near-sea lowlands in North Yakutia (Metody..., 1986).

Depending on study purposes, natural geosystems can be considered as combinations of:

(1) elements of interacted spheres (litho-, hydro-, bio-, atmosphere);

(2) elements of space structure (natural complexes of lower ranks);

(3) elements of time structure (successive change of state of natural complexes in time).

In the first case a basic attention is paid to analysis of direct and reverse vertical relations - determination of conditions for

mass-energy exchange, i.e. examination of functional relations (Landshafty..., 1983). The second case concerns the studying of horizontal relations: morphological structure of natural complexes, features of their composing complexes of a lower rank, mass-energy exchange between complexes. Changes in properties of natural complexes are studied in the third case, which are caused both in the course of natural development (genetic series of natural complexes) and under influence of man's activity (Geokriologicheskiy prognoz..., 1983; Grechishchev, Melnikov,1986).

All the above three approaches are useful in geocryological investigations. In all cases geological environment ("geocryological conditions") is considered as a subsystem of the system "natural complex".

Components of EGC in different natural complexes have a different character of interrelations with other elements and differ in values of elements. These relations (direct and reverse) are studied in stationary observations. Their space variability is closely connected with variations in morphological structure of natural complexes. Qualitative analysis of this structure enables to solve problems of space variability of EGC. Such an analysis lies in establishing a composition of morphological elements of lower-rank natural complexes, calculating their quantitative (areal, linear) proportions and neighbourship contrast, determining types of topographic pattern, studying of quantitative characteristics of EGC-components of lower-rank natural complexes and their space variations and, finally, in constructing, on this basis, models of variability of EGC-components for natural complexes being mapped on a given scale (Landshafty..., 1983; Metody ..., 1986).

Starting point in dynamic aspect is a certain time - current geocryological conditions of the given natural geosystem. Historic-geological analysis, paleogeographical reconstructions allow to establish retrospections of geocryological conditions in the given territory and their dynamic potential. Prediction of dynamics and rhythm system of spheres external to EGC (atmo-, bio-, hydrosphere) and taking into account for dynamic potential enable to forecast a natural course of EGC-changes in time. Homeostasis of natural geosystems (a threshold of resistance to external impacts) is determined by a rank of geosystem. The smaller is a natural geosystem, the lower is its resistance. Most sensitive to external loads are geosystems of rank VIII-sites (Geokriologicheskii prognoz..., 1983). Studies on consequences of man's impact on the geoenvironment as a lithogenic basis of natural complexes and use of the method of natural analogues enable to forecast EGC-changes due to economic development of the territory (Braun, Grave, 1981; Vremennoe rukovodstvo..., 1980; Geokriologicheskii prognoz..., 1983; Kritsuk, Melnikov, Moskalenko, 1986) and to examine natural-technogenic systems. Geosystem principle is widely used in regional geocryological investigations, engineering-geocryological explorations, in arrangement and organization of stationary geocryological observations, prediction of changes in geocryological conditions under an influence of economic activity, in nature-preserve zoning of the geoenvironment.

Regional geocryological studies (and surveys) for the purposes of preliminary dividing of a study territory into homogeneous types are carried out using complex and individual landscape indicators - external outlook of natural geosystems and their aerocosmophotoimages. According to this dividing, key areas are selected where a complex of mine-drilling and geophysical works is accomplished. The studied natural geosystems (with surveying on a scale of 1:100,000 for ranks VI-VII and 1:25,000 - for ranks VII-VIII) are grouped then according to uniformity in quantitative characteristics of individual components of geocryological conditions (soil composition, ice content, temperature, a depth of seasonal thawing, exogeneous geological processes, etc.). Such a grouping allows compilation of both by-component (analytical) and general-purpose (synthetical) engineering-geocryological maps (Metody ..., 1986). On the basis of maps for geosystems of rank VI (tracts), the maps for types of PFS are compiled (Geokriologicheskie usloviya..., 1983; Kritsuk, Melnikov, Moskalenko, 1986). A procedure of computer-based compilation of one-, two- and three-component engineering-geocryological maps on the geosystem basis is developed.

Geosystem principle is used also in arranging points of stationary observations over PFG-temperatures, seasonal thawing and freezing, EGP. These points are located in representative typical natural complexes of rank VIII and VII.

The results of stationary observations together with data of analogue method for studying natural geosystems in natural and disturbed states and of calculating methods are used to forecast changes in geocryological conditions of natural geosystems of ranks VIII and VII due to an impact of economic development (Geokriologicheskii prognoz..., 1983; Grechishchev, Melnikov,1986 ; Metody..., 1986).

And, finally, geosystem principle is widely used in assessment of resistance of geocryological conditions to technogenic impacts on natural complexes, in assessment of restorability of disturbed geosystems (Braun, Grave, 1981; Vremennoye rukovodstvo..., 1980) and in nature-preservation zoning of geological environment in cryolithozone.

By today a great experience is gained in compiling maps of nature-preservation zoning of geoenvironment in cryolithozone on different scales (from 1:5,000 to 1:1,000,000) for different regions of the USSR. All these maps are constructed on geosystem basis.

REFERENCES

Braun, J., Grave, N.A. (1981). Narushenie

poverkhnosti i eyo zashchita pri osvoyenii Severa. Novosibirsk: Nauka, 88 s.

Vremennoye rukovodstvo po zashchite landshaftov pri prokladke gazoprovodov na Krainem Severe. Pod red. A.V. Pavlova - Yakutsk: In-t merzlotovedeniya SO AN SSSR, 1980, 48 s.

Geologicheskiye uslovia Zapadno-Sibirskoi gazonosnoi provintsii. Pod red. E.S. Melnikova. - Novosibirsk: Nauka, 1983, 193 s.

Geokriologicheskii prognoz dlya Zapadno-Sibirskoi gazonosnoi provintsii. Pod red. S.E. Grechishcheva. - Novosibirsk: Nauka, 1983, 180 s.

Grechishchev, S.E., Melnikov, E.S. (1986). Problemy regionalnogo geokriologicheskogo izucheniya i prognoza. Sovetskaya Geologiya, No.19, s. 112-116.

Kritsuk, L.N., Melnikov, E.S., Moskalenko, N.G. (1986). Sostavlenie regionalnogo geokriologicheskogo prognoza na osnove melkomasshtabnoi karty prirodnykh kompleksov kriolitozony Zapadnoi Sibiri. V kn: Voprosy geokriologicheskogo kartirovaniya. Yakutsk, s. 53-67.

Landshafty kriolitozony Zapadno-Zibirskoi gazonosnoi provintsii. Pod red. E.S. Melnikova. Novosibirsk: Nauka, 1983, 165 s.

Metody regionalnykh inzhenerno-geokriologicheskikh issledovanii dlya ravninnykh territorii. Pod red. E.S. Melnikova, G.I.Dubikova. - M.: Nedra, 1986, 207 s.

PREDICTING THE OCCURRENCE OF PERMAFROST IN THE ALASKAN DISCONTINUOUS ZONE WITH SATELLITE DATA

L.A. Morrissey

TGS Technology, Inc., Ames Research Center, Moffett Field, California, USA

SYNOPSIS A predictive permafrost model developed for the Caribou-Poker Creeks Research Watershed was extended to a portion of the surrounding Yukon-Tanana Upland and evaluated by comparison with borehole data from the trans Alaska pipeline. The logistic regression model incorporated a Thematic Mapper satellite-derived vegetation classification and a thermal band used as a surrogate for potential incoming solar radiation. The satellite-derived environmental variables predicted the spatial distribution of three permafrost mapping categories (frozen, discontinuously frozen, and unfrozen) with 75 percent accuracy.

INTRODUCTION

The presence of permafrost, or perennially frozen ground, is one of the major factors that determines the suitability or capability of the terrain for development. However, existing maps of permafrost distribution are general, given the lack of more extensive and detailed information (Péwé, 1966). Mapping permafrost directly from ground temperature measurement and borehole logs can be expensive and time-consuming. For these reasons such mapping is frequently limited to small areas. For inventories of larger areas, indirect methods of analysis must be used which rely on the interpretation of various environmental variables that are correlated with permafrost (Kreig and Reger, 1982; Ferrians and Hobson, 1973; Brown and Péwé, 1973).

Environmental variables derived from Thematic Mapper (TM) satellite data were used to develop and evaluate logistic discriminant functions for predicting the distribution of near-surface permafrost in a boreal forest watershed in the interior of Alaska. The combination of TM thermal data (used as a surrogate for a solar irradiance index) and a TM-derived vegetation map provided an overall permafrost classification accuracy of 78 percent for the Caribou-Poker Creeks Research Watershed (106 square kilometers). A number of environmental variables were initially examined for incorporation into the CPCRW model. The combination of vegetation and solar irradiance index provided the strongest relationship with permafrost and were, thus, subsequently selected for the CPCRW model. A complete description of this research can be found in Morrissey, et al. (1986). To further test this technique, the logistic coefficients developed at the initial test site were extended to classify permafrost in the surrounding Yukon-Tanana Upland Province. The permafrost classification for the extended region was evaluated with Alyeska Pipeline Service Company (APSC) inhouse data that were originally acquired for the design of the trans Alaska pipeline. These data consisted primarily of geotechnical borehole logs for 95 sites along the pipeline route segments which generally parallels the Elliot Highway between Fairbanks and Livengood, Alaska.

STUDY AREA

The study area is in the Yukon-Tanana Upland of central Alaska which is an east-trending upland located between the Yukon and Tanana rivers in central Alaska. It is characterized by schists, typically Precambrian, with shallow to thick eolian silts (loess) over bedrock on rounded ridges. Topographic elevations range from 500 to 2,000 meters. Boreal forests, alpine tundra, and bogs grow on a discontinuously frozen terrain. Because the Caribou-Poker Creeks Research Watershed study area has only a thin cover of loess, this study area was also restricted for the most part, to an area that also has a thin loess cover. Factors that control the distribution of permafrost in the Yukon-Tanana Uplands with thick loess cover are significantly different than terrain covered with thin loess. The section of Yukon-Tanana Uplands from Murphy Dome Road to Lost Creek utilized in this study has predominantly thin loess cover.

The vegetation of the study area is characteristic of the taiga or boreal forest and generally corresponds to variations in topography, drainage, fire history, and successional stage. Paper birch and aspen forests tend to occur on south-facing slopes, while stunted black spruce forests tend to occupy cold and wet north-facing slopes. Mixed coniferous and deciduous forests occur

on older sites which tend to have intermediate soil temperature and moisture. Birch (Betula glandulosa) shrub communities are found along the ridges and tall shrubs (Alnus and Salix ssp.) grow along the creeks.

The boundary between slopes underlain by permafrost and slopes that are permafrost-free is usually marked by a noticeable change in vegetation (Péwé, 1982). Stunted black spruce forests usually grow on poorly drained, gentle slopes underlain by shallow permafrost, while white spruce, birch, aspen and alder are found on better drained slopes where permafrost is absent or present only at greater depths. The boundary between black spruce and birch-aspen forest is distinct and often readily recognizable on remotely sensed imagery.

ENVIRONMENTAL DATA BASE AND ANALYSIS

The environmental data base consists of a TM-derived vegetation classification and a TM thermal band used as a surrogate for equivalent latitude (an index of long-term potential direct beam solar radiation). These data sets provided the basis for an extrapolation of the logistic regression model to the Yukon-Tanana Uplands. The model was then assessed using Alyeska Pipeline Service Company borehole data. Each of these data sets will be described in sequence.

A TM-derived classification of vegetative cover was developed using supervised clustering and maximum likelihood classification techniques for an area covering approximately 30,000 square kilometers. Training sites, delineated from ground surveys and aerial photographs, were located, and the multispectral data were extracted for six TM bands (excluding the thermal band) of a September 22, 1984 scene. For each training site, a mean vector and covariance matrix was calculated. Following image classification, individual spectral classes were verified through photointerpretation of aerial photography. The spectral classes were grouped into cover classes: closed conifer forest, open conifer forest, conifer woodland, closed deciduous forest, mixed conifer and deciduous forest, tall alder shrubland, low birch shrubland, barren land, water, snow, clouds, and shadow.

The thermal band (10.4 to 12.6 μm) was selected due to its correlation (r =.83) with equivalent latitude (Morrissey and Card, 1985). Equivalent latitude is an index of long-term potential direct beam solar radiation incident on a surface and has been found to correspond to the presence or absence of permafrost (Koutz and Slaughter, 1973; Dingman and Koutz, 1974). Like the Caribou-Poker Creeks study, TM thermal data was used as a surrogate for equivalent latitude for the Yukon-Tanana Upland. Figure 1 shows a comparison of the thermal data with equivalent latitude (generated from elevation and slope information derived from digital terrain data). Topographic features, especially aspect, are emphasized on TM thermal imagery acquired during daylight hours as a result of differential solar slope heating, and appear very similar to the image of equivalent latitude. This is significant because equivalent latitude calculations from contour maps are laborious and dependent on the contour interval for accuracy. An image or satellite-based method to measure solar potential radiation differences over a landscape would greatly assist in the study of frozen ground distribution. Therefore, the availability and large area coverage of TM satellite data make the use of thermal data a potentially viable tool for regional assessments of equivalent latitude.

A logistic discriminant function, developed for the Caribou-Poker Creeks site, was used to predict the probability of frozen ground and classify the Yukon-Tanana Uplands study area into three classes: frozen (95 to 100 percent frozen), unfrozen (0 to 5 percent frozen), and discontinuous (6 to 98 percent frozen). Logistic discrimination is based on expressing the probability of class membership for a pixel as multivariate logistic functions. Logistic discriminant functions predicting the distribution of permafrost as a function of environmental variables were developed following the method of Anderson (1972). Logistic discrimination is based on expressing the probability of class membership for a pixel as multivariate logistic functions. $P(Ci/x)$ is the probability of the pixel whose independent variables are $x=(x1,x2,\ldots,xp)$ being a member of Class Ci, for $i=1,\ldots,k$. One advantage of this formulation is that the independent variables can be either continuous or discrete, thereby allowing the use of ancillary data such as soils and vegetation in the discrimination process. Another advantage is that the procedure is nonparametric in the sense that coefficient estimates do not depend

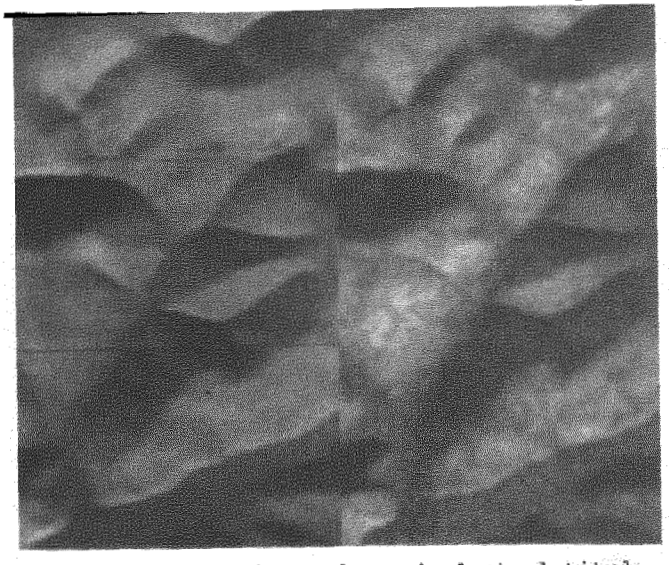

Figure 1. Comparison of equivalent latitude (left) and TM thermal data (right) for a portion of Caribou-Poker Creeks watershed.

$$P_r(C_i|x_1,\ldots,x_p) = \text{EXP}\,[\beta_{i0} + \beta_{i1}x_1 + \ldots + \beta_{ip}x_p]\; P_r\,(C_k|x_1,\ldots,x_p)$$

$$P_r(C_k|x_1,\ldots,x_p) = 1/(1 + \sum_{s=1}^{k-1} \text{EXP}\,[\beta_{s0} + \beta_{s1}x_1 + \ldots + \beta_{sp}x_p])$$

where C_i = class i, $i = 1,\ldots k$;

x_j = independent variable j, $j = 1,\ldots,p$;

k = number of classes (Permafrost classes in the present context); and

β_{sj} = regression coefficient for class s, independent variable j.

on the assumption of multivariate normality of the underlying distributions for each class.

APSC borehole logs provided the basis for an assessment of the permafrost classification accuracy. Borehole data logs for 129 drill sites along the trans Alaska pipeline were analyzed and synthesized to determine permafrost status. Each drill hole was edited according to selection criteria to eliminate holes where soil frozen state was questionable because of disturbance from drilling, cover type homogeneity, 5-acre minimum mapping unit, or inability to determine permafrost status. In addition, each hole was located on 1:24,000 aerial photographs, and identified by terrain unit, vegetation type and density, active layer depth, and permafrost status. All frozen and unfrozen soils were logged by depth in the soil. Questionably frozen intervals were also indicated. The holes varied in depth from 7 to 70 feet. Of the 129 sites, 95 sites were located within the area encompassed by the TM scene, and these sites were utilized in the subsequent evaluation of the predictive permafrost map. Of the 95 sites, 66 were frozen throughout the entire borehole and 29 were unfrozen to terminal depth.

RESULTS

Overall classification accuracy for all classes combined was 75 percent, while individual class (omission) accuracy was 74 percent for the frozen class and 76 percent for unfrozen class, respectively (Table 1). Although classification accuracy is referred to throughout this section, a more accurate description is the assessment of the degree of association between the borehole data and the permafrost classification.

Errors in the prediction of permafrost status using the satellite data occurred in two main areas: thick loess covered slopes and fire scars. Thick deposits of ice-rich, retransported silts, supporting deciduous forests (which are more commonly associated with unfrozen substrates) were not present in the Caribou-Poker Creeks Watershed where the predictive model was initially developed. Thus, a number of deciduous forest sites on south-facing slopes were misclassified as unfrozen (even though an attempt was made to eliminate most of these sites from the borehole data). Therefore, to more accurately predict permafrost status in the Tanana-Yukon Upland, logistic coefficients derived from a supplementary data layer indicating the distribution and thickness of loess-covered hills may well improve classification accuracy. Similarly, areas in the early phases of succession due to fire were also misclassified because generalized relationships among permafrost, vegetation, and topography are altered by secondary successional processes. A fire can dramatically alter substrate conditions destroying the insulating ground mat of organic material resulting in increased thaw of the underlying permafrost (Dyrness, 1982). Therefore, many burned areas on north-facing slopes, which would typically be frozen in a

Table 1

Classification Accuracy for Permafrost Model

		Classified Satellite Data			
		Frozen	Discontinuous	Unfrozen	Class Accuracy
Alyeska Borehole Data	Frozen	49	10	7	74%
	Unfrozen	3	4	22	76%

Overall classification accuracy is 75%

fire-free environment, were misclassified as unfrozen. The classified permafrost map and probability of frozen ground for a subsection of the Yukon-Tanana Upland is shown in Figure 2.

The ability to predict permafrost distribution through the analysis of environmental variables derived from satellite data requires an understanding of the relationships among permafrost, terrain, and vegetation unique to each region. Successful extrapolation of a predictive model developed from information of one watershed to the surrounding region is dependent upon the similarity of the watershed to the region. If the area used to develop the model coefficients is representative of the larger region, then the chances for success of the extrapolation of the model to the region is greater. Application of this technique to other regions requires the development of logistic coefficients based on the incorporation of appropriate environmental data.

CONCLUSIONS

The use of satellite-derived environmental factors for predicting and mapping permafrost status over large regions has been documented. The use of logistic regression for predicting the occurrence of near-surface frozen ground in hilly or mountainous terrain is a reliable and an effective technique when the relationships between permafrost and other environmental variables are known. The success of the technique is based on the degree of knowledge concerning those relationships.

Figure 2. Logistic regression classification map and associated probabilities for the frozen class for an area within the Yukon-Tanana Uplands. For the classified map (left), black is frozen, white is unfrozen, and grey is discontinuous permafrost. For the probability image (right), the grey scale ranges from zero probability of being frozen (shown in white) up to 1.0 probability (shown in black).

ACKNOWLEDGEMENTS

The author wishes to thank Alyeska Pipeline Service Company for access to their extensive borehole data base, Mr. Raymond Kreig (R.A. Kreig & Associates, Inc.) for synthesizing the Alyeska borehole data and providing valuable comments to the manuscript, Mr. Don Card for development the LOGIT software, and Mr. Laurence Strong for his participation in the development of the initial model. This research was supported by the NASA Terrestrial Ecosystems Program.

References

Anderson, J.A. (1972). Separate Sample Logistic Discrimination, Biometrika, (59), 1, 19-35.

Brown, R.J.E., and Péwé, T.L. (1973). Distribution of Permafrost in North America and its Relationship to the Environment; 1963-1973 -- A review, in Permafrost, the North American Contribution to the Second International Conference, Washington, D.C., National Academy of Science, 71-100.

Dingman, S.L., and Koutz, F.R. (1974). Relations among vegetation, permafrost, and potential insolation in Central alaska, Arctic and Alpine Research, (6), 1, 37-42.

Dyrness, C.T. (1982). Control of Depth to Permafrost and Soil Temperature by the Forest Floor in Black Spruce/Feathermoss Communities, Pacific Northwest Forest and Range Experiment station, Research Note PNW 396, 19 pp.

Ferrians, O.J. Jr., and Hobson, G.D. (1973). Mapping and Predicting Permafrost in North America: A review, 1963-73, in Permafrost, the North American Contribution to the Second International Conference, Washington, National Academy of Science, 479-497.

Koutz, F.R., and Slaughter, C.W. (1973). Equivalent Latitude (Potential Insolation) and a Permafrost Environment: Caribou-Poker Creeks Research watershed, Interior Alaska, unpublished report, 31 pp.

Kreig, R.A., and Reger, R.D. (1982). Air-Photo analysis and Summary of Landform Soil Properties along the Route of the Trans-Alaska Pipeline System, Division of Geological and Geophysical Surveys, Report 66, Department of Natural Resources, State of Alaska, 149 pp.

Morrissey, L.A., and Card, D.H. (1985). Utility of Thematic Mapper Thermal Data for Discriminating Boreal Forest Communities, Fourteenth Arctic Workshop: Arctic Land-Sea Interaction, Dartmouth, Nova Scotia, Canada, 200-202.

Morrissey, L.A., Strong, L.L. and Card, D.H. (1986). Mapping Permafrost in the Boreal Forest with Thematic Mapper Satellite Data, Photogrammetric Engineering and Remote Sensing, (52), 9, 1513-1520.

Péwé, T.L. (1966). Permafrost and its Effect on Life in the North, in Arctic Biology, Hansen, H.P., editor, Oregon State University Press, Corvallis, Oregon, 27-66.

Péwé, T.L. (1982). Geological Hazards of the Fairbanks area, Alaska. Alaska Division of Geological and Geophysical Surveys Special Report 15, 109 pp.

MODERN METHODS OF STATIONARY ENGINEERING – GEOLOGIC INVESTIGATIONS OF CRYOLITIC ZONE

A.V. Pavlov[1] and V.R. Tsibulsky[2]

[1]All-Union Institute of Hydrogeology and Engineering Geology, Moscow, USSR
[2]Industrial Institute, Tyumen, USSR

SYNOPSIS The principles of locating the experimental objects of cryolitic zone stationary study are given in the paper. Recommendations on observation conditions and automation of stationary investigations are proposed.

The founder of the Soviet geocryology M.I.Sumgin paid great attention to stationary methods of investigations of Cryolitic Zone and promoted their developing. By the 1950-s original information about heat conditions of the soil-solid complexes and dynamics of cryogenic physicogeological processes have been obtained at the stations created at the initiative of the elder geocryologists (V.P.Bakakin, I.Ya.Baranov, N.A.Grave, P.I.Melnikov, P.F.Shvetsov, N.I.Bykov, P.N.Kapterov, S.WShimanovsky). These stations were set up in a number of main places of the region of seasonal and perennial rock freezing (Igarka, Yakutsk, Škovorodino, Zagorsk, Vorkuta). The essential difference between cryogenic processes proceeding and normal engineering-geocryological processes was discovered as early as the initial stage of the stationary work development. It consists in close dependence of the cryogenic processes on the temperature factor or, broadly speaking, on heat-transfer processes between the upper horizons of the lithosphere and the surface layer of the atmosphere. Radiation and temperature conditions in the North also characterize the existence of biogeocenosises and their stability to technogenic loads. This fact predetermined priority in organizing thermal balance investigations at the geocryological stations. Stationary investigations of Cryolitic Zone were widely developed in the 50's and especially in the 60's when organizing thermal balance stations. At first stationary work was carried out mainly by the Institute of Geocryology named after V.A.Obruchev of the USSR Academy of Sciences and then continued by the Institute of Geocryology of the Siberian Branch of the USSR Academy of Sciences, the All-Union Institute of Hydrogeology and Engineering Geology, the Design Scientific Research Institute of Engineering Investigations in Construction, the Industrial Geological Union of the Ministry of Geology of the Russian Soviet Federative Socialist Republic (RSFSR).

The results of thermal balance investigations were used for solution both of scientific problems of geocryology, physical geography, micrometeorology and glaciology (Freezing of the Earth surface...,1964;Pavlov,1965,1975, 1979,1984;Gavrilova,1973,1978;Are,1974;Moskalenko et al.,1978;Geocryological forecast..., 1983) and of applied ones, i.e. optimization of the sun thawing methods of soils in the alluvial mineral deposits (Bakakin,1955; Balobaev,1961;Pavlov, Olovin,1982; Pel'shtein,1979), revealing changes of geocryological conditions on the developed territory (Khrustalev,1971; Pavlov, Prokop'ev,1982; Chernyad'ev et al.,1984), effectiveness evaluation of engineering and biological reculitivation methods of soils, destructed as a result of the North gas pipelines construction (Pavlov et al.,1979; Temporary manual..., 1984; Geocryological forecast...,1983) improving methods of irrigating agricultural areas (Pavlov,1980; Gavril'ev, Mandarov, Ugarov, 1984).

In the course of carrying out stationary work principles of locating experimental objects of stationary study (sites, profiles, separate observation borenoles or fixed points) were formed and rational methods (mainly in non-automatic variant) of condition observations of cryogenic processes and heat conditions of soils in the layer of annual heat circulation and factors defining it, temperature of perennially frozen thick layer (Golubev,1964;Pavlov,1964,1975;Balobaev et al.,1977;Methodological recommendations..., 1981) were developed and tested in field conditions.

Places of stations and proving grounds are chosen on the basis of the materials of average-scale engineering-geological or complex survey, rout or air-visual study of the

territory taking into consideration dimensions and accessibility of the area studied, locating meteorological stations, nearness of populated areas, power supply. On the chosen stable sections it is necessary to make large-scale survey for locating experimental objects. These objects must reflect the most characteristic types of the natural complex including the main (dominant) one, and maximum display of cryogenic processes. Several main experimental sites with natural (non-destructed) landscape conditions and with different technogenic influence, imitating landscape development (a kind of general technogenic influence, i.e. destruction or removal of surface and snow covers) are usually placed at one station. Stable (standard or background) site characterizing a dominant type of natural complex should be expediently located at the flat section and removed sufficiently (1km) from slopes, terrace ledges, large reservoir shores. When choosing the places for technogenic sites location it is necessary to take into consideration that their initial (i.e. before destructing) geocryological conditions should be most identical to one of the natural sites.

On the sections chosen for the experimental objects during large-scale survey or in the preparatory period of their equipping the complex of geobotanical, thermophysical, physicomechanical and geophysical tests are conducted to study in detail the covers and geocryological cut (up to the lower border of the layer of annual heat circulation). Carrying out the principle of maximum combination of observations of different elements of geocryological processes makes it possible to decrease labour expenditures for their performing and makes measuring equipment commutation easier. The determining dimension of the sites with natural (non-destructed) conditions is not less than some dozens of meters. The dimension of the technogenic sites is usually 20x20 (10x10)m^2, such dimensions permit getting rid of errors beyond the possible limits in measuring actinometric parameters of freezing-thawing layer because of the environmental influence.

The characteristic feature of stationary investigations is duration of the continuous experiment (more than 3 years), this often causes increasing of measurement errors. That is why the equipment used, including the primary (sensors) one, must be characterized by increased stability of time readings, i.e. it must have good metrological characteristics. Wide application of the electronic sensors as sensitive elements made it possible to create portable primary apparatus, which is simply manufactured. Application of the developed constructions of the primary instruments in combination with application of serial hydrometeorological, thermophysical and other measuring methods allowed to carry out in time the remote observations of the components of the external heat-transfer of soil (inflow and reflection of radiation, radiation balance, evaporation, etc.); of the surface and snow covers (heat conductivity, mass transfer, altitude, density); of hydrothermal conditions of soil in the layer of annual heat circulations (temperature, moisture, thermophysical characteristics and heat flows); of heat conditions of reservoirs and bottom sediments; of the development of cryogenic processes (seasonal and perennial heaving, thermal setlings, rock dislocation on the slopes, thermal denudation, thermoabrasion destruction of the shores, cryogenic solid cracking, ice formation). Both separate components of the natural complexes (snow, soil, vegetability, etc.) and natural complexes on the whole are studied at the stations (fig.1).

All the stationary observations or the most part of them are carried out all year round. Such study of geocryological conditions is necessary because of the fact that a long winter period in the North regions is the determining factor in the formation of hydrothermal conditions of high horizons of rock and development of a number of main cryogenic processes (cryogenic cracking, ice formation, heaving). Daily observations of the elements of heat-moisture transfer of rock and atmosphere (temperature of rock surface and up to 0,5m depth, heat flows, etc.) are carried out not more than 4 times a day. Other conditions observations depending on time changing (inconstancy) of geocryological parameters are usually conducted once a day, 5 days, 10 days or a month. The spectral analysis of time series of the main geocryological parameters (Tsibul'sky,1985) allowed to make statistical foundation of rational conditions of their stationary measurings (table 1).

TABLE I

Recommended Frequency of Sensor Inquiry (on observation materials in the North of Tyumen region)

Cycles of parameter changing	Parameters 1)				
	t	w	q	h_c	l
Daily	24	2	12	1	-
Annual	12	4	4	12	24
Perennial (11 years)	44	44	-	-	-

1)t-temperature; w-moisture; q-heat flow in the surface layer of rock (0-0,2m); h_c-height of snow cover; l-width of crack opening.

The depth increasing, high-frequent fluctuations of geocryological parameters in rock sharply decrease in amplitude and it is necessary to reduce the frequency of sensor inquiry The calculation on Furier theory made it possible to determine heat inertia to surface confusion and thereby maximum frequency and periodicity of temperature sensor inquiry in the boreholes (fig.2).

The developed constructions of primary devices (calorimeters and -meters, thermometric installations based on thermocouples,thermo-

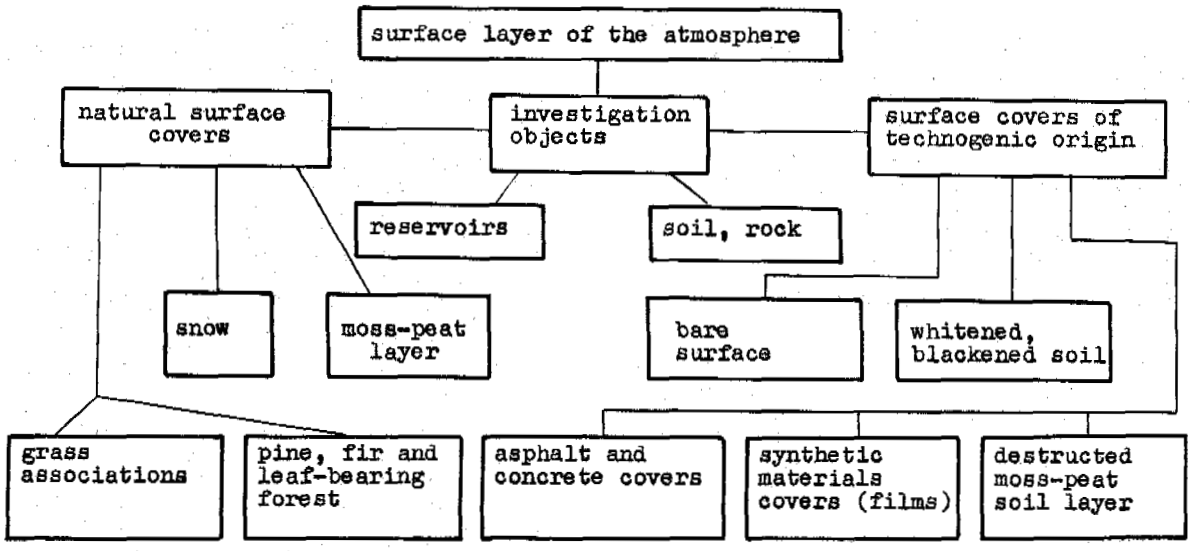

Fig.1 Components of Natural Complexes (natural and technogenic) Studied at Heat-Balance Stations

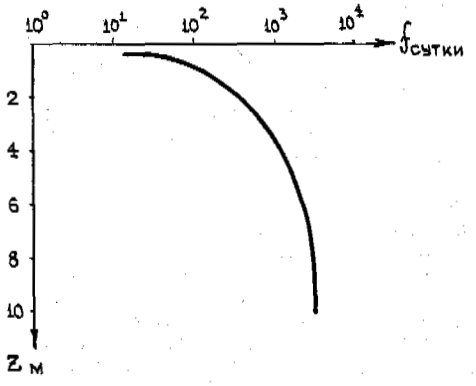

Fig.2 Frequency (f) of Depth Inquiry of Temperature Sensors

resistors and resistance thermometers for temperature measurings of litter surfaces and solids, surface and snow covers) proved to be reliable and convenient when used in any cryological-climatic conditions (Golubev, 1964; Pavlov, 1975; Balobaev et al., 1977; Chernyadiev et al.,1984).

When lowering the thermometric installation into the shallow borehole noticeable distortion of the sensor readings may happen because of convection, additional heat-transfer along casing tube and others. So at the Yakutsk station temperature distortion in the air-dry 50mm diameter borehole, lined with a metal pipe, reached 5,3°C at 1m depth; in the whole 10m thickness of solid it exceeded necessary measuring accuracy 0,1°C (table2). So during thermometric measurings arrangements excluding convection influence were taken (Pavlov,1975).

The problems of rational apparatus locating at the objects of stationary study (Pavlov, 1975; Methodological recommendations...,1981) have been solved. The example of locating experimental sites and equipment at the Sirdakh station of Gecryological Institute of the Siberian Branch of the USSR Academy of Sciences is given in fig.3.

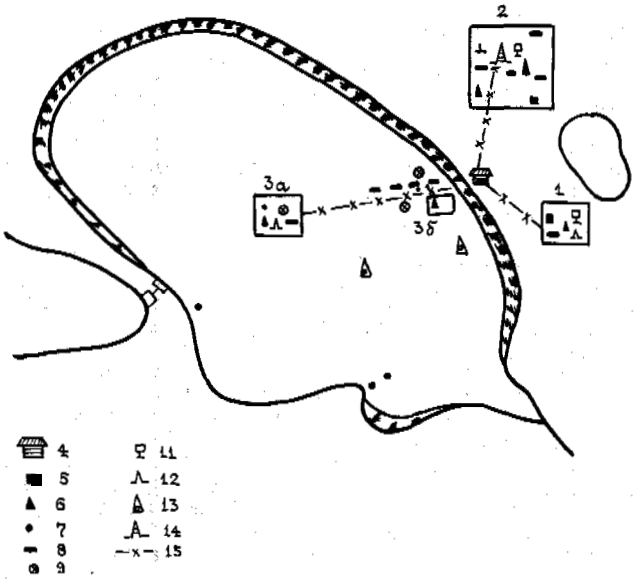

Fig.3 Schematic Plan of Syrdakh Heat-Balance Stationary and Installation

of Measuring Equipment. Sites: 1-natural non-forest; 2-in the larch forest; 3a-in the centre of the lake; 3b-in the shoal near shores; 4-heat-balance pavilion; 5-soil evaporators and rain measuring devices; 6-actinometric devices; 7-temperature installation in water and soil; 8-heat measuring devices; 9-temperature gradient measuring device in the lake; 10-the device for measuring frozen soil; 11-psychrometric box(cabin); 12-the air gradient installation; 13-the evaporator on the floating frame; 14-heat-balance tower in the forest; 15-the lines of connection.

TABLE 2

Extreme and Average Annual Values of Temperature Differences t between the Natural Solid Temperature and the Temperature Measured in the 50mm Borehole

Depth,m	t, °C		
	winter	summer	annual average
1	-5,3	0,9	-1,2
2	-2,6	0,3	-1,0
3	-1,2	0,2	-0,7
10	-0,2	0,0	-0,1

Conducting stationary geocryological observations is connected with a great number of parameters measurings which change daily, seasonally and annually[2], that is why their carrying out is extremely difficult without automation introduction into all processes of collection, storage and processing data. In the 70-s general introduction of electric measuring methods into geocryological investigations and appearance of compact and reliable computing facilities caused automation of stationary geocryological work. Automation makes it possible to intensify essentially investigations (to increase volume, regularity and reliability of information), to make the analysis of observations results quickly and accelerates adopting scientifically-based decisions when developing the territory, which is most important in extreme situations.

At the Geocryological Institute of Siberian Branch of the USSR Academy of Sciences highly productive automated installation for thermistors calibration was developed to meet the needs of scientific and industrial organizations in temperature sensors. At the Design Scientific Research Institute of Engineering Investigations in Construction their hermetization methods were improved, automatic complexes for stationary all year round observations for solid temperature, snow and vegetable covers permitting to carry out computer data output were worked out; a number of secondary instruments were improved, i.e. measuring became more simple andrequirements for maintainance conditions became less strict.

The analusis of automation trends was made at the end of the 70-s and the beginning of the 80-s (Tsibulsky,1982).; the leading geocryological institutions of the country were invited as experts; the analysis showed the paramount significance of creating new highly productive facilities for geocryological experiment, first of all field semi-automatic and automatic off-line instruments (45%) and measuring-calculating complexes for automation of stationary and laboratory works(34%). The experts determined the parameters (temperature, moisture, thermophysical properties, salt content, heat flow and others which are most important for automation and defined necessary ranges of their measurings more precisely (table 3).

In the 80's at the Tyumen Industrial Institute together with the All-Union Institute of Hydrogeology and Engineering Geology experiments were made and expert evaluations were taken into consideration; these experiments resulted in creating the complex of modern remote apparatus of equipping geocryological stations (Tsibulsky,1985).

Providing maximum level of automation necessary accuracy and dynamic measuring range of geocryological parameters, reliability and convenience in maintainance were achieved in a number of "Penguin" devices.

"Penguin T-02" device is a portable temperature register, which includes: a commutator, an analog-digital converter, a numerical printer, a microprocessor-based arithmetic-logic element performing best measuring method and plug-in (removable) programm assembly (block) which makes it possible to use industrial platinum and copper resistance thermoconverters. Inquiry of 19 sensors mounted into a thermochain is performed automatically; the range of measured temperatures is from - 30 up to +30°C; accuracy is 0,1°C.

Four-wire connecting of given current and test method of measuring allowed to exclude influence of current instability, zero drift and all manual operations. Microprocessor operation program incorporates temperature calculation of each sensor including characteristic linearization, result normalization, correction of additive error and control of measuring cycle. The device is introduced into production.

By analogy the "Penguin T-05" temperature device was designed for multichannel temperature measurings with the given periodicity and for its storage for a long time. The device works automatically without operator servicing during all off-line period (3 months when having 2 hours for inquiry periodicity) which is de-

2) General number of measured values of geocryological logical parameters at the stations reaches some hundred thousand a year; during manual data collecting each value consists of several intermediate ones. Bulk information requires that some average or general parameters and their statistical evaluation should be chosen for solving concrete problems.

TABLE 3

The List of Geocryological Parameters Which Need Immediate Automation of Measurings, the Range of Their Changes and Errors

Parameter	Range	Error of measuring checking devices	Error of measuring checking means
Temperature, °C	-60 - +50	0,1	0,02
Soil moisture in frozen	-10 - 0	0,05	0,01
and thawed state,	0 - 10	1	0,2
Thermophysical properties:			
thermal conductivity, W/(mK)	0 - 5	5	1
temperature conductivity, m^2/s	$(0 - 4)\cdot10^6$	10	2
thermal capacity, volumetric, $j/(m^3K)$	$(0,1 - 4)\cdot10^6$	10	2
Salt content, %	0,01 - 40	0,5	0,1
Heat flow, W/m^2	$(0 - 10)\cdot10^4$	5	1
Mechanical strains in the mass of frozen soil, Pa	$(2 - 100)\cdot10^4$	10	2
Freezing-cracking, m			
depth	0 - 10	1	0,2
width	0 - 1	1	0,2
Resistance to dislocation at the surface of freezing	$(0,2 - 15)\cdot10^4$	1	0,2
Normal forces of heaving,	$(0 - 100)\cdot10^4$	1	0,2
Thickness of snow cover, m	0,05 - 3	0,5	0,1
Snow density, kg/m^2	0 - 600	2	0,5

termined with the supply capacitance. After lapse of calculated time accumulator batteries and energy independable memory with stored data are replaced. Storage content printing is performed by electronic computing machine or special data output device.

Moreover, "Penguin TP-II" heat measuring device (calorimeter combined with the secondary device), "Penguin C-10" snow measuring automatic device, the device for measuring crack openings were designed. To investigate "new" cracks increase dynamics the capacitor sensor with cross-section transfer compensation was suggested; its sensitivity is $8,5\cdot10^{-12}$ F/m, inertia is not less than 2s and error is less than 1%. For long distance transfer (±5cm) a transfer sensor combined with a temperature sensor was designed; it simplifies secondary circuit maintaining given temperature error. Transfer sensitivity is $50\cdot10^{-3}$ V/m, temperature sensitivity is $4\cdot10^{-2}$ om/K. It was suggested to use alternating current density change property depending on the crack width for large dynamic ranges and closed cracks. Under certain conditions and using commutation-modulation measuring this method gives sensitivity of 50 mV/mm and possibility of measuring crack depth.

The experiments carried out at the geocryological stations are considered to be rapid enough and can be equipped (provided) with standard model complex based on the standard CAMAC of "Mera 60/45" type. Using this standard a new "ASNI -geocryology" series was developed; it includes temperature measuring (500 points), heat-flux measuring (50 sensors), heat- and electrophysical researches. To cover large territories four-wire main line with sensor removal for up to 5km and off-line automatic measuring devices, loggers for 5 thousand measurings for any distance ("Penguin-05") were developed. ASNI software includes numeral experiment.

Application of new methods and technical facilities at the stations of engineering-geocryological work gives more reliable and complete geocryological information, makes it possible to carry out its processing rapidly to evaluate the effectiveness of rock mass control methods. It is extremely necessary to proceed from stationary observations to carrying out controlled geocryological real-space-time range experiment.

REFERENCES

Are, F.E. (1974). Teplovoi Redzim Melkikh Ozer Taezhnoi Zony Vostochnoi Sibiri, Ozer Kriolitozony Sibiri, Novosibirsk, Nauka.

Bakakin, V.P. (1955). Opyt Upravleniya Teploobmenom Deyatel'nogo Sloya Merzlykh Gornykh Porod v Tselyakh Povysheniya Effektivnosti Ikh Razrabotki, Moskva, Izdatel'stvo AN SSSR.

Balobaev, V.T. (1963). Protaivaniye Merzlykh Gornykh Porod Pri Vzaimodeistvii S Atmosferoi, Teplo-i Massoobmen v Merzlykh Tolshchakh Zemnoi Kory, Moskva, Izdatel'stvo AN SSSR.

Balobaev, V.T., Volod'ko, B.V., Devyatkin, V.N., Levchenko, A.I. (1977). Rukovodstvo Po Graduirovke Termorezistorov I Ispol'zovaniyu Ikh Pri Geotermicheskikh Izmereniyakh, Yakutsk, Izdatel'stvo Im CO AN SSSR.

Chernyadiev, V.P., Chekhovsky, A.J., Stremyakov, A.Ya., Pakulin, V.A. (1984). Prognoz Teplovogo Sostoyaniya Gruntov Pri Osvoyenii Severnykh Regionov, Moskva, Nauka, str.137.

Gavrilova, M.K. (1978). Klimat I Mnogoletneye Promerzaniye Gornykh Porod, Novosibirsk, Nauka.

Gavril'yev, P.P., Mandarov, A.A., Ugarov, I.S. (1984). Gidrotermicheskaya Melioratsiya Sel'skokhozyastvennykh Ugodii V Yakutii, Novosibirsk, Nauka.

Geocriologicheski Prognoz Dlya Zapadno-Sibirskoi Gazonosnoi Provintsii (Grechishchev, S.E., Moskalenko, N.G., Shchur, Ju.L., Novosibirsk, Nauka, 1983, str.182.

Golubev, A.V. (1964). Izmereniye I Registratsiya Temperatury V Gruntakh S Pomoshch'yu Termoelementov, Moskva, Nauka, str.147.

Khrustalev, L.N. (1971). Temperaturnyi Rezhim Vechnomerzlykh Gruntov Na Zastroyennoi Territorii, Moskva, Nauka, str.167.

Metodicheskiye Recomendatsii Po Statsionarnomu Izucheniyu Kriogennukh Fisico-Geologicheskikh Protsessov, Moskva, Izdatel'stvo VSEGINGEO, 1981, str.72.

Moskalenko, N.L., Slavin-Borovski, V.B., Shchur, Yu.L., Lazareva, N.A., Malevski-Malevich, S.P. (1978). Vliyaniye Osvoeniya Territorii Na Teplovoi Balans I Termovlazhnostnyi Rezhim Gruntov Na Severe Zapadnoi Sibiri Trudy III Mezhdunarodnoi Konferentsii Po Merzlotovedeniyu. T.I., Kanada, str.55-60.

Pavlov, A.V. (1975). Teploobmen Pochvi S Atmosferoi V Severnykh I Umerennykh Shirotakh Territorii SSSR, -Heat transfer of the Soil and Atmosphere At Northern and Temperate Latitude of the USSR Territory, str.302.

Pavlov, A.V., Olovin, B.A. (1974). Iskusstvennoye Ottaivaniye Merzlykh Porod Teplom Solnechnoi Radiatsii Pri Razrabotke Rossypei, Novosibirsk, Nauka, str.182.

Pavlov, A.V. (1979). Teplofizica Landshaftov, Novosibirsk, Nauka, str.285.

Pavlov, A.V., Sergeev, B.P., Skryabin, P.N. (1976). Rezyl'taty Rezhimnykh Issledovanii Teploobmena Pochvi S Atmosferoi V Raione g. Igarki, Region. I Teplofiz. Issled. Merzlykh Porod V Sibiri, Yakutsk, str.132-143.

Perl'shtein, L.Z. (1979). Vodno-Teplovaya Melioratsiya Merzlykh Porod Na Severo-Vostoke SSSR. Novosibirsk, Nauka, str.304.

Promerzaniye Zemnoi Poverkhnosti I Oledeneniye Khrebta Suntar-Khayata (Grave, N.A., Gavrilova, M.K., Gravis, J.F. I Dr., Moskva, Nauka, 1964, str.143.

Tsibul'sky, V.R. (1982). Kompleks Priborov Dlya Issledovaniya Merzlykh Porod, Termika Pochv I Gornykh Porod V Kholodnykh Regionakh, Yakutsk, IM CO AN SSSR, str.151-160.

Tsibulsky, V.R. (1985). Avtomatizatsiya Geokriologicheskikh Issledovanii, Novosibirsk, Nauka, str.145.

Vremennoe Rukovodstvo Po Zashchite Landshaftov Pri Prokladke Gazoprovodov Na Krainem Severe, Yakutsk, IM CO AN SSSR, 1978.

PETROGRAPHIC CHARACTERISTICS OF MASSIVE GROUND ICE, YUKON COASTAL PLAIN, CANADA

W.H. Pollard[1] and S.R. Dallimore[2]

[1]Memorial University of Newfoundland
[2]Geological Survey of Canada

SYNOPSIS Massive ground ice and icy soils are widely reported in the surficial sediments beneath the Yukon Coastal Plain. At King Point and Kay Point three forms of massive ice are distinguished on the basis of their cryostratigraphic setting and petrographic characteristics. Massive foliated ground ice is composed of irregular bands of clear and sediment-rich ice. The large crystal size, blocky to puzzle-like nature of sediment bands, and fabrics with c-axes normal to foliation suggest that this ice is deformed, horizontally-bedded, segregated ice. Buried snow-bank ice is milky white to light brown, with horizontal foliation. Its structure and texture reflect compaction and transformation of snow grains to massive ice. Ice-wedge ice is also milky white to light brown but displays vertical foliation. Its fabric and texture reflect the repeated infilling and freezing of thermal contraction cracks. These petrographic signatures, together with others described in the literature, could form the basis of a petrographic classification.

INTRODUCTION

Occurrences of massive ground ice are widely reported in the Yukon Coastal Plain and Mackenzie Delta areas of the western Canadian Arctic (e.g. Harry et al., 1988; Mackay 1966, 1971; Rampton, 1982). Massive ice is a highly variable material which often show gradations from nearly pure ice to dirty sediment-rich ice. In this paper, massive ground ice is considered to have a minimum ice content of 250% by dry weight (Mackay, 1971) and exceed one meter in thickness. Massive ground ice is frequently variable in thickness and extent, reflecting the complex events and environments involved in its origin and evolution.

The aim of this paper is to demonstrate that various forms of massive ground ice found on the Yukon Coastal Plain have characteristic petrographic and stratigraphic relationships that can be used as the basis for interpreting their origin and evolution. The results of this study will contribute to the development of a petrographic classification of ground ice types, and an improved understanding of the different forms of ground ice common along the Yukon Coastal Plain.

STUDY AREA

During 1986-1987, several ice-rich permafrost sections were investigated along the Yukon Coastal Plain between Shingle Point and Herschel Island. This paper focuses on three sections in the vicinity of Kay Point and King Point (Figure 1). Glacial features in this area originated during the Buckland advance thought to be of Early Wisconsinan age (Rampton, 1982). The three sites are near a moraine-outwash complex which originated along, and adjacent to the ice margin during the Sabine Phase of the Buckland glaciation.

Massive ground ice is a major constituent of near surface materials in this area, occurring as ice-wedge ice and thick bodies of massive ice which are variable in both ice content and configuration. In some cases the larger bodies of massive ice are foliated with flat or gently undulating upper contacts and extend over many hundreds of metres.

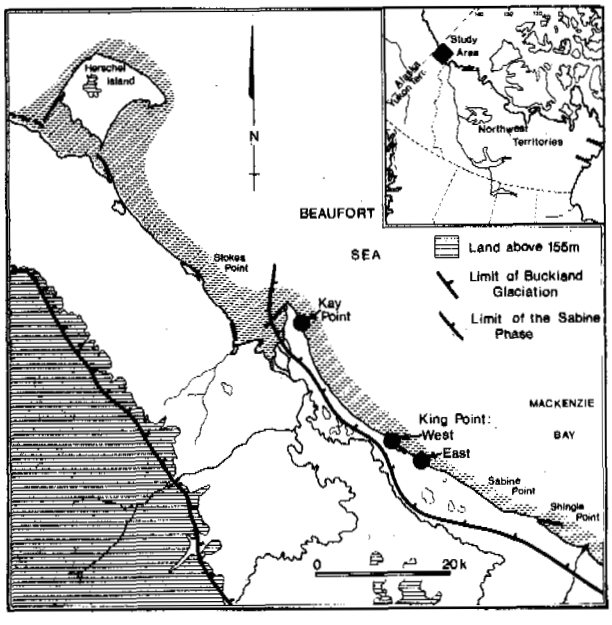

Figure 1: Location map of the Yukon Coastal Plain, showing the King Point and Kay Point study sites and the limits of Buckland Glaciation (Source ; Rampton 1982).

CRYOSTRATIGRAPHY

Kay Point:

The Kay Point site is located 3.5 km southeast of the tip of Kay Point (Figure 1) within a retrogressive thaw slump at an elevation of approximately 30 m asl (Figure 2a). Four stratigraphic units are exposed at this site. The lowest unit (Unit A), found in the floor of the thaw slump, consists of clear, sediment-free massive ice. Unit A is at least 1 m thick, however, its lower contact could not be determined. Unit A is overlain by 2.5-3.5 m of foliated, ice-rich, silty-clay diamicton (Unit B). The foliated appearance is the result of alternating layers of ice-rich silty-clay and pure to dirty ice which dip 50-70° toward the southeast. The diamicton is overlain by 3.0-4.0 m of folliated massive ice (Unit C). The contact between Unit B and Unit C is abrupt and dips at 10-25° toward the southeast. Foliation in Unit C results from thin, undulating, discontinuous silty-clay layers within the ice which dip 55-80° toward the southeast. Unit C is unconformably overlain by 2.0-2.5 m of organic-rich diamicton (Unit D). The contact between Unit C and Unit D is flat-lying and abrupt, representing a thaw unconformity associated with previous thaw slump activity. The lower part of Unit D contains horizontally-bedded layers and lenses of segregated ice.

King Point East:

The King Point East site is situated within a 1.25 km long retrogressive thaw slump (Figure 2b) located approximately 2.5 km southeast of King Point. The stratigraphic sequence at this site has a 3.0-6.0 m basal unit of foliated massive ice (Unit A). The foliated appearance results from alternating bands of pure and sediment-rich (silty-clay) ice which dip 40-60° toward the northeast. Sediment-rich layers are made up of a silty-clay diamicton with numerous pebble and cobble-sized clasts. The massive ice is unconformably overlain by 5.0-7.0 m of ice-rich diamicton (Unit B) of similar composition to the sediment-rich layers. The contact between Units A and B is abrupt and can be traced across the entire slump face (Figure 2b). The lower 1.0-1.2 m of Unit B is characterized by a laminated to reticulated structure of ice veins 2-5 mm thick. Unit B is overlain by 20-50 cm of ice-rich clay and a thin cover of organic silt and clay (Unit C). These sediments contain thin, evenly spaced segregated ice lenses up to 2 mm thick. Ice wedges penetrate the upper two units to depths of 5-6 m. An oriented block sample of ice-wedge ice was taken from a depth of 2.5 m.

King Point West:

The King Point West site is located at the west end of the King Point lagoon. The stratigraphic sequence exposed in the eastern face of this retrogressive thaw slump contains three units (Figure 2c). The lowest (Unit A), consists of 2.7-4.1 m of steeply-dipping, foliated massive ice composed of deformed layers of pure ice up to 30 cm thick and layers of sediment-rich ice up to 40 cm thick. The folia dip 70-80° toward the southeast. Unit A is unconformably overlain by up to 2 m of ice-rich diamicton (Unit B) composed of organic-rich silt with pebble and cobble-sized clasts. The irregular, undulating nature of the contact between the massive ice and the diamicton reflects a thaw unconformity associated with a previous slump event. The diamicton is highly variable in thickness, and in places two or three diamicton layers can be identified. At the east end of the exposure a milky white massive ice layer (Unit C) up to 1.4 m thick and 10 m long, occurs between two diamicton units. The white colour is produced by high concentrations of gas inclusions which form

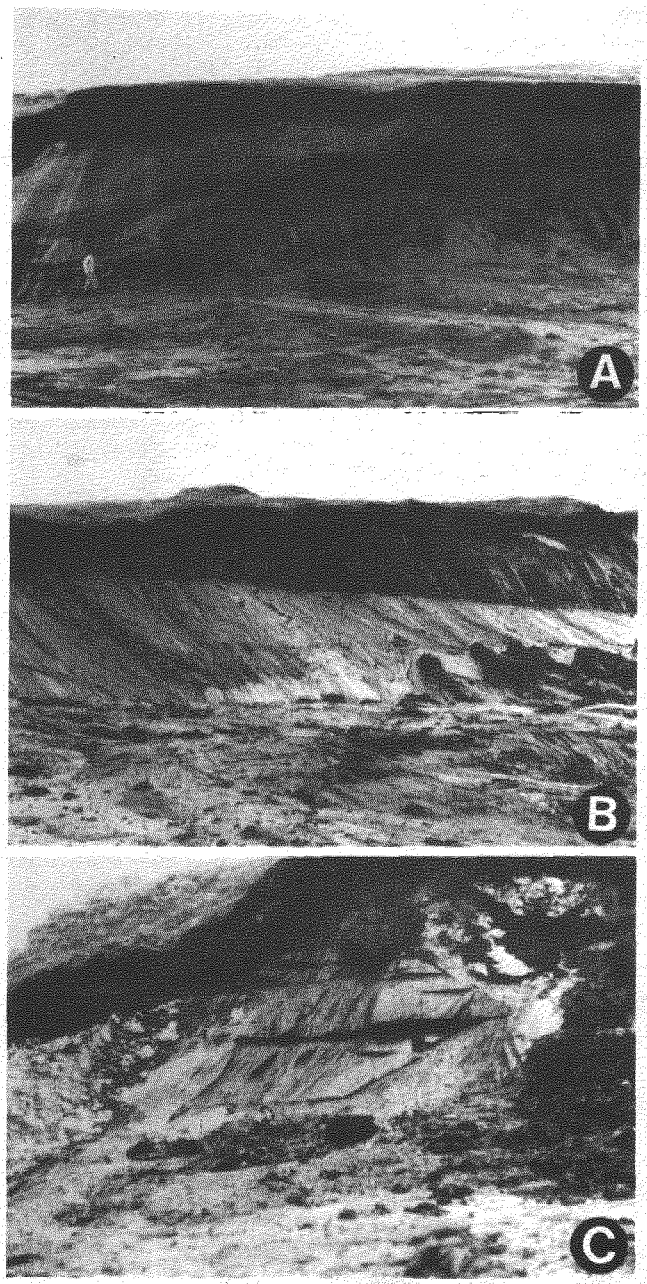

Figure 2: Permafrost sections and massive ground ice at; (A) King Point West (face height 8m), (B) King Point East (face height 8-10m), and (C) Kay Point (face height 9 m).

faint near-horizontal layers. The presence of leaf fragments and fine sediment in the ice, together with its stratigraphic position and morphology, suggest that the white massive ice layer is part of a buried snowbank.

PETROGRAPHY OF MASSIVE GROUND ICE

Petrographic analyses (following Langway, 1958) were carried out on thin sections from eight oriented block samples. Horizontal and vertical thin sections were prepared from each block sample and examined under cross-polarized light to determine crystal size, shape, c-axis orientation and inclusion characteristics.

Foliated Massive Ice:

Kay Point: Unit A and Unit C

The massive ice exposed in the floor of the thaw slump at Kay Point (Unit A) has a milky, translucent appearance resulting from a high gas inclusion content. The absence of included sediment, the random distribution of gas bubbles and lack of structure creates a massive texture. Gas inclusions display a variety of size and shapes, ranging from small spherical bubbles less than 1 mm in diameter to irregularly shaped bubbles 7-8 mm in length.

The massive ice from Unit C is clear and transparent containing small amounts of sediment. Gas inclusions have three distinct shapes: 1) irregular shapes up to 27mm long and elongated in a near-vertical direction; 2) disks up to 6 mm in diameter and less than 1 mm thick, flattened parallel to the plane of foliation; and 3) thread-like stringers that occur randomly throughout the sample. Sediment inclusions occur as small (1-3 mm diameter) clumps of silty clay forming discontinuous steeply dipping (55-80° to the southeast) bands. In some places, sediment fragments can be matched across ice layers.

The Kay Point ice is composed of medium to small subhedral to euhedral crystals (Figure 3a). Crystal size varies from 0.25 to 2 cm^2, with fine-grained textures occurring adjacent to sediment bands. Average crystal size in Unit A is 1 cm^2, and 1-2 cm^2 for Unit C. Unit A displays a more regular crystal shape and equigranular size distribution. In both units the crystals are characterized by straight boundaries and triple point junctions.

Gas and sediment inclusions are predominantly intergranular. Fine discontinuous fractures marked by planes of small flat bubbles (strain shadows) are mostly intergranular, but where they do pass through larger ice grains there is a slight dislocation of the grain boundary. Variable extinction angles within large grains indicate internal dislocation. The fabric of both samples is marked by a preferred orientation of c-axes dipping 5-20°, roughly normal to the foliation (Figure 4).

King Point East: Unit A

The massive foliated ice at King Point East contains steeply dipping layers of clear ice 15-20 cm thick that grade into bands of dirty ice. The clear ice contains randomly distributed blocks of silty clay. In some cases, larger sediment fragments can be connected across ice-rich bands. Gas inclusions are concentrated near sediment bands as small spherical to oval bubbles up to 3 mm in diameter. A vertical fracture striking approximately 270°, and a series of strain shadows also occur. Sediment and small gas inclusions are concentrated near the fracture.

This ice contains medium to large, anhedral crystals averaging 8-9 cm^2 with an average length of about 5 cm (Figure 3b). Crystal size and shape are variable with a tendency for small ice crystals to occur near sediment contacts and inclusions. Grain boundaries range from irregular and jagged to long and curving. Gas inclusions are both intercrystalline and intracrystalline, but sediment inclusions tend to occur along grain boundaries. Ice fabrics are characterized by a preferred pattern of c-axis orientations inclined 20-45° to the horizontal and roughly normal to the foliation within the block, a secondary maximum has a near-vertical orientation.

King Point West: Unit A

Block samples taken from massive foliated ice at King Point West consist mainly of clear ice in which thin (3-5 cm) discontinuous silty-clay bands dip 55-65° toward the

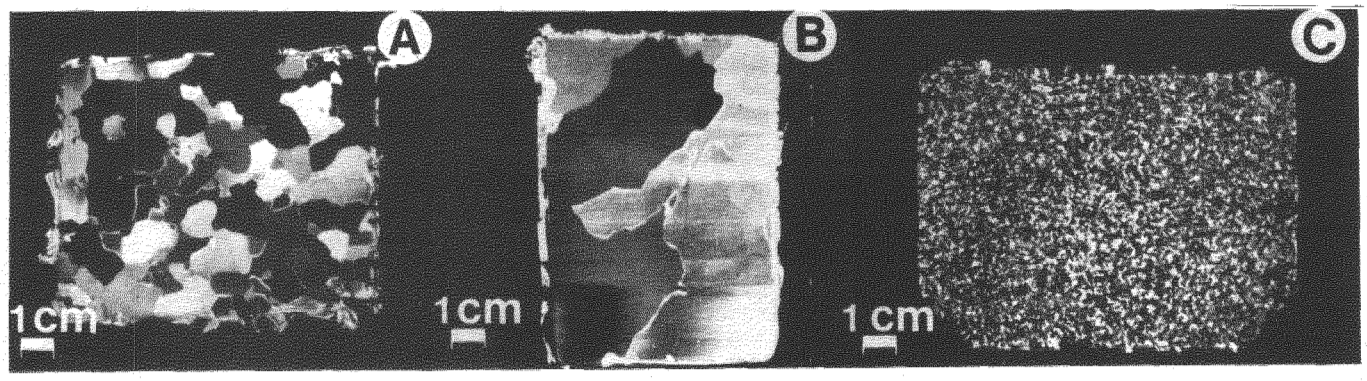

Figure 3. Thin sections of massive ice under crossed polarizers: (A) foliated massive ice, Kay Point (B) foliated massive ice, King Point West, (C) massive snowbank ice, King Point East.

southeast. Sediment bands are composed of clumps of silty clay ranging from small rounded balls to large elongated angular blocks. Gas inclusions are associated with the sediment bands and contribute to the foliated appearance. They range from small spherical and flattened shapes to large (6-8mm) oval and tear drop shapes elongated vertically. Disk-shaped gas inclusions occur in groups with long axes oriented parallel to the sediment banding. In some places gas inclusions surround sediment grains.

This ice is composed of medium to very large anhedral ice crystals from 2 to > 25 cm^2 , averaging 5-7 cm^2 . Grains are variable in size and shape with crystal lengths from 1 to > 14 cm. Grain boundaries are irregular ranging from jagged and uneven to long and curved. The ice contained in thin layers and adjacent to sediment bands is characterized by smaller more regularly-shaped ice crystals. In addition, ice grains tend to be elongated with their long axes parallel to the plane of foliation. The sediment and gas inclusions in the clear ice are intracrystalline, but toward the sediment layers the inclusions are intercrystalline. Variable extinction angles within a single crystal reflect internal dislocation produced by either the annealing of several crystals or stress. Fabric diagrams (Figure 4d) are characterized by a dispersed primary fabric upon which secondary maxima are superimposed. The dispersed pattern forms a loose girdle of c-axis orientations roughly normal to the foliation.

Wedge Ice:

Ice-wedge ice from King Point East is characterized by a white to brownish colour with vertical to steeply inclined layers of clear, bubble-rich and sediment-rich ice. Gas inclusions range from small spherical bubbles less than 1 mm in diameter to tabular bubbles 8-10 mm long. Sediment inclusions consist of fine mineral grains and organic fragments. Larger clumps of organic material and sediment are also found incorporated in the ice. The gas and sediment inclusions form vertically oriented bands.

The petrographic characteristics of wedge ice are well documented in the literature (e.g. Black, 1951; Corte, 1962; Gell 1978a, 1978b) and will be described only briefly for comparison with the other ice types. The average crystal size varies from 7-15 mm^2 , with average lengths of 5-6 mm. The middle of the wedge is characterized by crystals oriented with their long axes roughly perpendicular to the wedge axis. Crystals are generally euhedral to subhedral with short straight boundaries commonly forming triple point junctions. Gas inclusions are both intercrystalline and intracrystalline depending on their size and orientation. The c-axis directions have a strong preferred horizontal to subhorizontal orientation normal to the plane of wedge cracking (Figure 4a).

Buried Snowbank Ice:

Buried snowbank ice exposed at King Point West is translucent and milky white to pale brown in colour with a faint horizontal to gently dipping foliation. The foliated appearance is the result of alternating bands of vertically-oriented gas inclusions and clear ice. The brown colour results from fine (clay sized) sediment inclusions that are suspended throughout the sample and in places are concentrated into thin discontinuous horizontal layers. Twig and leaf fragments are also present. Gas inclusions range from small spherical and flat bubbles (<1 mm in diameter) , to thin elongated tubular bubbles up to 25 mm long. The long axes of the tubular bubbles are aligned normal to the layering and terminate at layer boundaries.

The snowbank ice is fine grained, with crystals averaging 1-3 mm^2 in size, and maximum lengths of 3-5 mm (Figure 3c). Crystals tend to be slightly elongated with preferred vertical to steeply dipping long-axis orientations (corresponding to the direction of heat flow). Crystals are euhedral to subhedral with short straight boundaries. Grain size and shape are constant through the sample with no marked change at sediment contacts. Gas and sediment inclusions are predominantly intercrystalline. The primary ice fabric is characterized by a random pattern of c-axes with weak secondary maxima (6-7%) oriented roughly normal to the plane of foliation (Figure 4b).

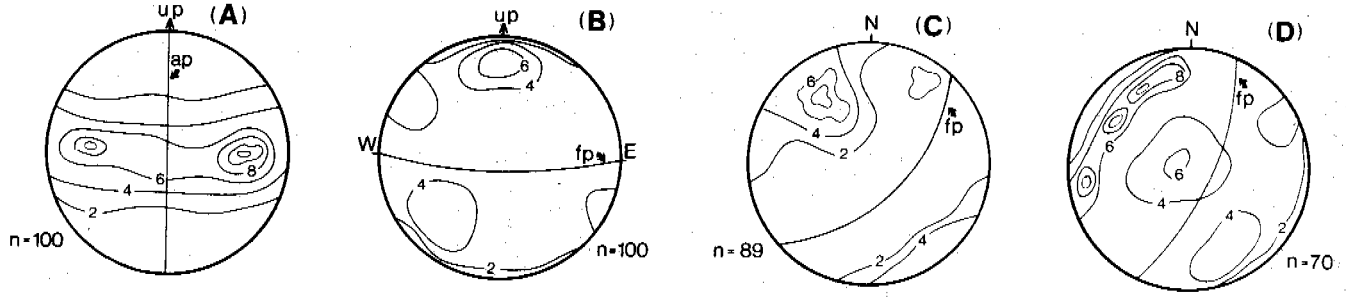

Figure 4. Fabric diagrams of crystal c-axis distributions for: (A) ice-wedge ice (vertical plane normal to wedge axis), (B) buried snowbank ice (vertical plane) (C) massive ice from Kay Point (horizontal plane), (D) massive ice from King Point (horizontal plane). (Fabric diagrams are plotted as lower hemisphere projections on a Schmidt equal area net with a contour interval of 2%. (ap - axial plane, fp - foliation plane)

DISCUSSION AND CONCLUSIONS

Massive Foliated Ice

The massive foliated ice units found at each site display many similar petrographic and cryostratigraphic characteristics, including: a well developed foliation resulting from inclined ice-rich and sediment-rich bands, c-axis maxima clustered normal to folia, matching of fractured sediment fragments across ice-rich zones, and the development of fine grained ice textures in sediment-rich zones. In addition, the sediment contained within the ice, and in adjacent sediment-rich zones, is composed mainly of a silty clay with occasional pebbles.

In the opinion of the authors, these characteristics are best explained by ice segregation resulting from penetration of a freezing plane into unfrozen, saturated, silty-clay diamicton. Fractured sediment fragments displaced across ice bands indicate ice growth possibly during a temporary stabilization of the freezing front. Alternating sediment-rich and ice-rich layers may represent subtle variations in the rate of penetration of the freezing front and/or water supply. Zones of small crystals mixed or interlayered with fine sediment develop during periods of rapid freezing. The layers of pure ice composed primarily of large crystals are characteristic of slow freezing with a constant water supply to the freezing front. Since the diamicton associated with the massive ice is most likely derived from glacial till and since the sites are within a major moraine system, then an association with glacier ice must also be considered. Although some of the petrographic characteristics documented could be attributed to glacier ice, the geometry of displaced soil fragments strongly suggest ice growth normal to the foliation rather than shearing, which is more likely in the basal area of a glacier. However, the possiblility of ice segregation in unfrozen sediments beneath a glacier or at the base of a glacier cannot be ruled out on the basis of the existing data.

It is difficult to infer the original orientation of the folia in the massive ice. However, there is strong evidence that post-depositional modifications have taken place. Vertically-oriented gas inclusions, fractures, internal dislocation of ice crystals and vertical secondary c-axis maxima are probably related to thermal and mechanical stresses resulting from local thaw or secondary crystal growth parallel to the present heat flow direction and not permafrost aggradation. The stratigraphic evidence also suggests that several of the massive ice bodies have been truncated by a deep thaw event.

Wedge Ice

The ice wedge origin of some ice sampled at King Point East was recognized implicitly by the wedge structure and cryostratigraphic relationships. However, it is useful to document the ice-wedge ice petrography as a function of its growth mechanisms. The small crystal size and the crystal fabric orientation normal to the wedge axis, are characteristic of rapid freezing of thin water-filled veins. Alternating bubble bands and thin layers of sediment rich ice produce a vertically foliated appearance which indicates the incremental growth pattern of the wedge. Occasional inclusion of organic material originating from the ground surface confirms the surface origin of the water. These observations are consistent with the growth mechanisms of most ice wedges described in the literature (e.g. Mackay, 1986).

Snowbank Ice

The texture of the snowbank ice observed at King Point West reflects the crystalline characteristics of the original snowbank with small crystal size and a random c-axis orientation. The horizontal layering, suspended sediment and occasional twigs and leaf fragments show the depositional character of the snowbank and the accumulation of wind blown detritus. The vertically oriented bubbles and secondary c-axis maxima suggest post depositional modification probably resulting from compaction and recrystallization of the snowbank.

In conclusion, three distinct types of massive ground ice have been recognized in surficial sediments of the Kay Point and King Point areas. Each type is characterized by a series of diagnostic petrographic and cryostratigraphic relationships which can be used to aid in the interpretation of the origin of the massive ice. Petrographic data are also useful in examining possible post-depositional processes and deformation.

Based on these analyses, ice segregation is concluded to be the dominant process responsible for the formation of large foliated massive ground ice bodies at the sites studied. However, the identification of buried snowbank ice at the King Point West study site and its recognition in several other permafrost sections along the Yukon Coast suggest that more consideration should be given to buried surface ice as a source of massive ground ice. At this point in our research we feel that additional work is required to document the range of petrographic characteristics of different buried forms of ground ice.

ACKNOWLEDGEMENTS

Fieldwork was supported by the Geological Survey of Canada, the Polar Continental Shelf Project (Department of Energy Mines and Resources, Canada) and the Inuvik Research Laboratory. During 1987, W.H. Pollard was supported by Natural Sciences and Engineering Research Council Grant A-1919, and Northern Supplement Grant 267. S.R. Dallimore is funded by the Northern Oil and Gas Action Program. The authors wish to thank Dr. J. B. Macpherson, Dr. D.G. Harry and two anonymous reviewers for their constructive comments on the manuscript.

REFERENCES

Black, R.F. (1951). Structures in ice wedges of Northern Alaska. Bulletin, Geological Society of America, 62. 1423-1424.

Corte, A.E., (1962). Relationship between four ground patterns, structure of the active layer and type and distribution of ice in permafrost. U.S. Cold Regions Rersearch and Engineering Laboratory, Research Report 88. 75 pp.

French, H.M. and W.H. Pollard, (1986). Ground ice investigations, Klondike District, Yukon Territory. Canadian Journal of Earth Sciences, 23, 550-560.

Gell, A.W., (1978a). Ice-wedge ice, Mackenzie Delta-Tuktoyaktuk Peninsula area, N.W.T., Canada. Journal of Glaciology, (20), 84, 554-562.

Gell, A.W., (1978b). Thermal contraction cracks in massive segregated ice, Tuktoyaktuk Peninsula, N.W.T., Canada. In: Proceedings ;Third International Conference on Permafrost. Edmonton, Alberta. Vol.1 National Research Council of Canada. 278-281.

Harry, D.G., H.M. French and W.H. Pollard, (1985). Ice wedges and permafrost conditions near King Point, Beaufort Sea Coast, Yukon Territory. In : Current Research, Part A, Geological Survey of Canada, Paper 85-1A ,111-116.

Harry, D.G., H.M. French, and W.H. Pollard, (in press). Massive ground ice and ice-cored terrain near Sabine Point, Yukon Coastal Plain. Canadian Journal of Earth Science.

Langway, C.C., (1958). Ice fabric and the universal stage. U.S. Army Snow and Ice Research Establishment Technical Report 62, 15 pp.

Mackay, J.R., (1966). Segregated epigenetic ice and slumps in permafrost, Mackenzie Delta area, N.W.T. Geographical Bulletin , 8, 59-80.

Mackay, J.R., (1971). The origin of massive icy beds in permafrost, Western Arctic Coast, Canada. Canadian Journal of Earth Sciences, 8, 397-422.

Mackay, J.R., (1972). The world of underground ice. Annals, Association of American Geographers, 62, 1-22.

Mackay, J.R., (1986). The first 7 years (1978-1985) of ice wedge growth, Illisarvik drained lake experiment, western Arctic coast. Canadian Journal of Earth Sciences, 23, 1782-96.

Rampton, V.N., (1982). Quaternary geology of the Yukon Coastal Plain. Geological Survey of Canada, Bulletin 317, 49 pp.

CONTENT OF NORTH AMERICAN CRYOLITHOLOGICAL MAP

A.I. Popov and G.E. Rosenbaum

Faculty of Geography, Moscow State University, Moscow

SYNOPSIS Principles of the map making legend and spatial regularities of spreading of cryolithogenesis types and different cryogenic rocks are stated

The elaboration of the theoretical bases of cryolithology, the cryogenic rock classification, data accumulation on the structure and spreading of these rocks in the Earth's northern hemisphere enables to compile cryolithological maps the first (the USSR cryolithological map on the scale of 1:4 000 000) being published in 1985. After that the scientists of the Moscow State University Department of Cryolithology and Glaciology of the Geography Faculty compiled the cryolithological map of North America at the scale of 1:6 000 000. Such map of North American continent was drawn for the first time, there being no analogues in the world practice.

The account of the cryolithological map making principles are considered to be necessary to be preceded by certain initial statements from the field of cryolithology, representing the basis of these very principles.

Cryolithogenesis is the generation of specific zonal conditions enherent in the Earth's cold zones, the most fully developed during Pleistocene - Holocene. It represents a complex of processes in the cryolithosphere stipulating the formation of cryogenic rocks. Cryolithogenesis occurs during the upper layer freezing of the lithosphere which may spread at different depth and be of different duration: from several hours to many millenia.

Cryolithogenesis as a specific process of lithogenesis manifests in nature in two qualities: cryodiagenesis and cryohypergenesis. Cryodiagenesis - is the process of durable irreversible ice-formation as well as the transformation of the very mineral substratum (thickening, dehydration, aggregation, cementation) without essential changing of dispersion in fresh deposits as well as in sediments having undergone different degree of lithification earlier. Ice is an authigenic mineral, a component of cryogenic rock of long existence. Cryohypergenesis is a process of cryogenic weathering of different rocks. Cryohypergenesis manifests during freezing (with transition into permafrost) of dense rocks and semirocks promoting their destruction. Multiple (mainly seasonal) freezing - thawing of any rock, including dispersive, is always cryogenic weathering process. This is a process of reversible, systematic, i.e. brocken ice-formation resulting in essential change of dispersion. There exists two intercomplimentary and interconnected mechanisms of cryogenic rock destruction: frost weathering as a consequence of wedging frost action and cryohydrational weathering caused by the oscillation of wedging pressure of thin films of unfrozen water in microcracks connected with the change of phase state of water in larger cracks and pores during the formation - thawing of ice. In this case ice is a temporary, active authigenic mineral.

As a process of cryogenic diagenesis, cryolithogenesis occurs only in the permafrost region and as a process of cryohypergenesis - both in the permafrost region and in the region of seasonal frozen grounds. The products of cryodiagenesis are two types of cryogenic rocks: cryolites and cryolitites. Cryolites are ice monomineral rocks proper; cryolitites - polymineral icy rocks, ice being one of the mineral components. The product of cryohypergenesis is cryogenic eluvium, formed as a result of cryogenic rock weathering. The following two types of cryogenic eluvium are distinguished: rocks of cryogenic predestruction (permafrost rocks and semirocks containing cracked ice), cryoclastites, cryoclastopelites, cryopelites, their varieties being loess-like rocks, loesses, nival silts, regelated moraine). Different types of cryogenic eluvium may occur both in permafrost, seasonally frozen and even in a melted state. Thus it is not only rocks of cryogenic predestruction that are in a permafrost state, but also dislocated cryoclastites, cryoclastopelites and cryopelites, their thickness essentially exceeding the depth of seasonal thawing. Permafrost cryogenic eluvium is a cryolitite as well as products of cryodiagenesis containing ice as a component of a polymineral icy rock. There are products of cryogenic weathering of Pleistocene severe epochs in the region of seasonal frozen rocks, their thickness often exceeds the depth of contemporary seasonal freezing, wherefore the considerable part of their section is sometimes in a perennially melting state. This is especially typical of loesses often attaining considerable thickness and representing the products of season syngenetic process inherent in the section of accumulation in ancient cryolithosons.

According to the a bovementioned, the map legend consists of two parts: the first part is devoted to permafrost (perennially frozen) cryogenic rocks - products of cryodiagenesis and cryohypergenesis, the second - to seasonal frozen products of cryohypergenesis.

The complexity and multistaginess of cryogenic structure of permafrost compel the authors to limit by mapping its upper relief-forming part, their thickness not exceeding 20 metres.

The main principles of the construction of the first part of the map legend is the isolation of cryogenic rock types and their combinations as occurring in nature and cryolithogenesis types inherent in them. Based on that, the map legend distinguishes the following groups in the graph "cryogenic rock types": cryolitites, cryolites with enclosing cryolitites and cryolites. The second group includes icy rocks with cryolites represented by different genetic types of underground ice: polygonalveined (relict and growing) forming with cryolitites enclosing it regularly built compexes, layered ice of different genesis and injection ice, composing the nuclei of hydrolaccoliths. The third group (cryolites) includes only surfacial glacier ices. Icings are not accounted of in the map legend due to the absence of their distribution data within the mapped territory.

Ice of two genetic types: segregation and ice cement, participates in the structure of cryolitites. It is the combination of two genetic types of underground ice that is widerspread, this being reflected in the legend. The presence of only ice-cement of frozen rocks is characteristic, its physical state excludes the presence of loosely connected water and its migration, as well as coarsely clastic and sandy sediments and peat.

The ice distribution in the rock determines the formation of various cryogenic textures. The legend uses a simple classification of cryogenic textures. There are distinguished schlieren cryotextures formed by segregation ice - stratified, latticed, and their different modifications and cryotextures formed by ice-cement: massive, basal, crustal - in loose rocks, fractured - in rocks and semirocks. Cryogenic texture character is in direct dependence on the lithology of ice enclosing rocks. This is accounted of in the map legend by introduction of the corresponding graph, characterizing enclosing rock lithology. The greater lithological changeability along the section and the strike, observed in nature, as a rule, forms definite difficulties in cryogenic texture mapping. These circumstances are taken into account by the introduction of different cryogenic texture combinations. Cryotextural and lithological changeability along the strike is shown by the fraction in which the upper horizon cryotextures are shown above the fractional line, underlying horizon cryotextures are under it, the graph of "enclosing rock lithology" shows the upper horizon lithology above the fractional line, the underlying horizon lithology is under it.

The cryogenic texture character the distribution peculiarities along the section, the participation of different genetic types of underground ice to a considerable extent are determined by the freezing type - the type of cryolithogenesis. The character of cryolithogenesis manifestation may be different depending on the conditions under which this process occurs: physical-geographical, thermal, facies-genetic, etc. But all the variety of cryolithogenesis in the Earth's crust comes down to two types - epigenetic and syngenetic.

Under epigenetic type cryolithogenesis occurs in rocks having undergone lithification previously to a certain extent. Therefore all rocks and semirocks, as well as Prepleistocene loose rocks froze epigenetically. Under syngenetic type, cryolithogenesis acts as the main process of lithogenesis, i.e. freezing is the main lithification factor accompanying sedimentation.

Pleistocene and Holocene subaqueous deposits accumulating in comparatively deep sections of water bodies (seas, lakes, rivers) freeze epigenetically. The secondary freezing of any rocks results also in the formation of epicryogenic permafrost. As seen from the map the syngenetic type of cryolithogenesis is developed in the northern lowest-terminal regions of permafrost development, predominantly in the region of its uninterrupted spreading. Epigenetic type of cryolithogenesis is solely developed in the island permafrost region. There permafrost formation began only in the very end of Upper Pleistocene after Visconsin mantle glacier degradation. But during Holocene maximum permafrost degraded and it was only in Holocene end that the development of new formations of contemporary island permafrost began.

Both cryolithogenesis types influence cryogenic rock structure, ice distribution, cryogenic texture character differently. Epigenetic permafrost is characterized by the ice-content decrease along the section, syngenetic permafrost is characrerized, on the contrary, by the proportional ice distribution along the section and often by polygonal-veined syngenetic ice presence piercing syncryogenic series through all its thickness. They are characterized by specific combination of thick layered cryotexture with fine net-like, lenticular and high ice saturation both with segregation and polygonal-veined ice. The combinations of two types of cryolithogenesis, when a thin syncryogenic horizon overlies epicryogenic (polygenetic permafrost), are very frequent in the section of mapped subsurface permafrost.
The features of cryolithogenesis zonal manifestation, subjugated to thermal permafrost zonality to a considerable extent distinctly appear on the map. It was already mentioned that syncryogenic series are predominantly developed in the northern low thermal regions in the uninterrupted permafrost region. There is most distinctly traced the connection between cryolithogenesis type and facies-genetic appertaining of deposits.

Cryolithogenesis syngenetic type is represented by glacial, fluvio-glacial and eolian deposits. The latter are developed in northern Alaska and represent the Edomian analogue of the USSR North-West which was in terpreted in a different genetic way in the Soviet literature. In the North of the continent cryolitho-

genesis epigenetic type includes Pleistocene marine deposits, composing Alaska offshore Arctic plain and Neogene-Pleistocene alluvial lacustrine deposits, as well as rocks of large greatly dissected mountain structures. Polycryogenic series are widely developed there. They are developed in mountainous Alaska, Cordillera, Canadian shield where the thin permafrost loose cover ovelies permafrost rocks. Besides that the combination in the section of syncryogenic (upper) and epicryogenic series (lower) is typical of coastal-marine deposits composing low marine terraces, alluvium and lacustrine-palustrine deposits. Here the upper syncryogenic stage of polygenetic series contains growing polygonal-veined ices. Layered ice and injection ice nuclei of hydrolaccolites are widely developed in the uninterrupted permafrost region. Thus it is in the northern regions that the greatest variety of cryolithogenesis types, high ice saturation and the greatest variaty of the underground ice genetic types are observed.

In epicryogenic series structure, zonality also manifests distinctly connected 1)with the decrease of the thermal gradient value from north to south, taking place at present having occured in the Upper Pleistocene during these series formation and 2)with the younger (post maximum) permafrost age the southern region of its spreading. Thus in the regions of the uninterrupted epigenetic permafrost are charactezed by the change along the section of fine net-like, fine stratified cryotextures by coarse stratified, coarse net-like and then by massive. The interrupted permafrost region with higher temperatures and lower gradient value is characterised by the change along the section of epigenetic permafrost of coarse net-like, coarse stratified cryotexture by massive one. Thin epicryogenic frozen groundsin the island permafrost region assigned to lacustrine-glacial deposits bear the same cryogenic structural character. Holocene peats overlying them have massive or basal cryotexture.

The relative dehydration and due to this their little ice saturation is connected with the secondary freezing of glacial deposits in the island permafrost region. Lenticular and massive cryotextures are develoved in them. The small scale of the map does not allow to contour separate permafrost islands in its island spreading area on the plains. Therefore cryotextures inherent in permafrost islands, developed within large lithogenetic countours, are plotted on the map. For example in the south of the Canadian shield the glacial Upper Pleistocene complex occupies large area, but within it small lake depressions are widely developed, filled by lacustrine-glacial deposits overlain by Holocene peats. It is impossible to plot them on the map scale, but it is to them that small permafrost islands are assigned. Besides that parmafrost islands are developed on the river valley slopes of the northern exposition. Therefore the map distinguishes large contours indicated by the index of the glacial complex, including lacustrine-glacial deposit index; this contour is rendered by the colour reflecting the array of cryotextures inherent in frozen grounds composing permafrost islands developed within this contour.

The elaboration of the principles of decorative aspects and choice of presentation methods is essential in mapping. The main depiction method - colour background is adopted for the plotting of cryogenic rocks (permafrost) and inherent in the cryolithogenesis types. Cryolithogenesis types are outlined by sharp tint differences, different tint gamut is rendered to various cryogenic rock groups outlined in the legend.

The second group (cryolite combination with enclosing cryolitites) possesses higher ice content and therefore is delineated with colder tint gamut. Cryolites represented by layered ices,ice hydrolaccolite nuclei and glacier ices are presented on the map by symbols of dark bluetints. The guarantee of the map expressiveness, its graphic visibility and readibility from the distance is achieved by the use of intense tints. Tint shade presents differences in cryogenic structure caused by cryogenic texture. The rock genesis and age are denoted by indeces. Permafrost area southern boundary, plotted on the map bears a schematic character and was lent from the 1967 Canada permafrost map compiled by Roger Brown on the scale of 1:7 603 200. The necessary cartographic data for its detailization on plain territories were not available. Seasonal frozen cryogenic rocks - cryohypergenesis products are delineated on the map by black and white shading.

Seasonal frozen rocks represented by different types of cryogenic eluvium (cryoclastites, cryoclastopelites, cryopelites, undeveloped cryoeluvium and loesses as one of the varieties of cryopelites) are shown both in the regions of permafrost and seasonal frozen grounds. Here if in the permafrost region these are only rocks of the active layer, in the seasonal freezing areas they include not only active layer rocks (seasonal freezing layers), but also underlying thawing rocks, representing relict products of cryogenic weathering, manifesting during the Pleistocene cold ages in ancient glaciation periglacial zones. In connection with this the portrayal of the boundary of Visconsin glaciation and southern boundary of permafrost expansion during Upper Visconsin is essential for the map content. In order to substantiate this boundary delineation on the map, special symbols denote sections of mass development of pseudomorphs along icy veins in Visconsin deposits as the most reliable indicators of the former permafrost development.

These are the most important principles of complication and main content of North American cryolithological map. This work is the first attempt to represent on the map North American cryogenic rocks as a unified complex of heterogenetic formations of this Kind. The map presents only such characteristics reflecting first of all causative connections between cryogenic structure, lithology, facies-genetic assignment and enclosing formation age. The map illustrates spatial distribution of cryolithogenesis types and cryogenic rocks; zonal and regional regularities of cryolithogenesis manifestation within cryolitic zones of North America are apparent.

NEW DATA ON PERMAFROST OF KODAR-CHARA-UDOKAN REGION

N.N. Romanovsky, V.N. Zaitsev, S.Yu. Volchenkoc, V.P. Volkova and O.M. Lisitsina

Faculty of Geology, Moscow State University, Moscow, USSR

SYNOPSIS The region under consideration belongs to the northern Transbaikal area and is characterized by diverse and contrast geocryologic conditions. The maximum permafrost thickness (1000-1200 m) and the lowest rock temperatures (-8, -10°C) are typical of high mountains. Temperatures rise and premafrost thickness decreases in the medium- and low-mountain belts. An active air exchange in strongly fissured solid rock massifs as well as their specific cryogenic texture have been established. The geocryologic conditions of the Verkhnyaya Chara depression of the Baikal type with its numerous open taliks, shallow modern (50-100 m) and thick(450-500 m) frozen rock strata at -2 -5°C are considered. The dependence of geocryologic conditions on climate, topography, geological-structural and hydrogeologic conditions and paleogeographic events is analyzed.

The Kodar-Chara-Udokan region is part of the Baikal rift zone. This is the first order morphostructure, the second order morphostructures are the rift zones proper: the Chara depression and the rift-adjacent zone of uplifts - the Kodar and Udokan Ranges (Noveishaya tektonika... 1975) which represent minor uplands with complex structure formed by a combination of alpinotype ridges and plateau-like massifs divided by intermontane depressions (Lopatin, 1972). Within uplands, axial strips of the highest uplifts (over 2000-2500 m above sea level) with extremely broken relief are distinguished as well as peripheral strips (1500-2000 m) that grade into low-mountain (1000-1200 m) spurs in the Udokan Range. Planation planes of the Cretaceous-Paleogene and Neogene age have remained locally in the ranges with relevant areal and linear weathering crusts elevated by block movements to different levels up to 2000 m. Minor depressions (Nizhny-Ingamakit, Verkhny-Kalar, etc.) are closed by mountain chains steeply sloping to the wide flat bottoms of depressions at 800-1400 m. Narrow deep upstream valleys in the medium-high parts of ranges are confined to grabens and are located at the heights of 1300-1500 m and more. The Chara depression, located lower at 600-700 m, served as a collector of unconsolidated material which resulted in the formation of accumulative plain relief in its bottom.

The Precambrian basement of the rift zone is composed of highly metamorphosed sedimentary rocks of the Archaean and Early Proterozoic saturated with magmatic intrusions. Since the Late Neogene this region has undergone an intensive restructuring: the stage of tectonic quiescence was replaced by a multi-stage rift formation that proceeded during the entire Pleistocene. It was accompanied by intensive vulcanicity, elevation of ranges with an amplitude of up to 2000 m, and by simultaneous deep downwarping of depressions. The Chara depression - an asymmetrical graben-syncline with steep north-western and more gently sloping south-eastern flanks and a blocky structure of the basement surface - has been formed since the Late Neogene. It is filled with loose, more than 1000 m-thick Cenozoic deposits. The time of minor intermontane depressions formation is estimated as the Middle Pleistocene. Coarser unconsolidated up to 200-500 m-thick sediments were accumulated in them. The Baikal rift structure was actively developing in the Holocene: certain parts of depressions subsided, splits and displacements occurred in the ranges.

Permafrost (PF) in the northern part of the Transbaikal region formed in extremely variable paleogeographic conditions. As regards the time when rocks started freezing, it still remains disputable. However, it can be claimed that perennially frozen rocks were existing here, at least, since the Middle Pleistocene, even though it is likely that freezing of some sites began due to the global climatic cooling as far back as the Lower Pleistocene. Substantial influence on permafrost formation was exerted by mountain-valley glaciations being the powerful factors that either protected rocks from freezing or promoted degradation of the frozen strata in the bottoms of glaciated valleys that had formed by the moment of glaciation. The number of glaciations in this region has not yet been determined. The authors assume that there were three glaciations whose traces are distinctly observed in the relief: one of them occurred in the Middle and the other two - in the Upper Pleistocene. During the first (maximum) glaciation, the glaciers, originating in the highest parts of the ranges, filled the trough valleys and minor intermontane depressions and reached the Chara depression. The other two glaciations were less intensive: during the Zyryansk time glaciers occupied valleys in the medium-high parts of ranges and some minor intermontane depressions, whereas during the Sartan time they covered only cirques and upper parts of valleys in the medium and high mountains. It is unlikely that complete thawing of frozen rocks in the region occurred during the Middle and Upper Pleistocene climatic warming. During this time only slight alleviation of freezing conditions, probably, took place (Noveishaya tektonika...,1975). The same is valid for the

Holocene climatic optimum which is evidenced by buried wedge ice found by the authors in the northern foothills of the Udokan Range at the height of 900-1000 m, whose age is dated back at least to the Upper Pleistocene.

On the background of paleographical setting and the history of permafrost development during the Anthropogene (Nekrasov et al., 1967) six regions can be distinguished differring by the duration of freezing:

(1) Watersheds at more than 2000 m that have never been covered by glaciers. The frozen strata there have been persisting from the Middle and, probably, Lower Pleistocene which resulted in the formation of the thickest (up to 1200 m and more) PF.

(2) The lower part of medium high mountains at 1200-1500 m. Glaciers were absent here either. However, the lower hypsometric position, Upper Pleistocene history of relief development, and the fact that maximum climatic cooling occurred in the Upper Pleistocene, permit to suggest that PF here formed durint that period. Its thickness (H_p) does not exceed 300-400 m.

(3) Trough valleys of the first glaciation. The beginning of steady rock freezing was likely here after degradation of glacier, i.e. at the end of the Middle Pleistocene.

(4) Trough valleys of the second glaciation and small intermontane depressions which had completely been filled with ice in the Middle Pleistocene and Zyryansk time. Continuous freezing of rocks started, probably, in the second half of the Upper Pleistocene (H_p up to 100-300 m).

(5) Cirques and trough valleys of the Sartan glaciation. Continuous freezing started at the end of the Upper Pleistocene (H_p=300-500 m).

(6) The Chara depression of the Baikal type. Major portion of the depression was ice-free both in the Upper and, probably, much of the Middle Pleistocene. On the background of downwarping and sediment accumulation during the entire Anthropogene and severe climatic conditions, the strata with H_p up to 500 m and more formed here as a result of long-term freezing (probably, from the Middle Pleistocene). Such thick PF strata in the center of the depression disprove the existence of a lacustrine water body within the limits of the depression in the Upper, and, probably, in the Middle Pleistocene.

The above time intervals of rock freezing in different regions are not indisputable, they are based mainly on the history of glaciations whose duration has not yet been finalized. However, they are in good agreement with the H_p distribution as the most inertial characteristic of frozen strata, and, consequently, can be accepted as the first approximation.

The permafrost in the Chara depression is continuous. The data on Hp were extremely limited till the present time. In 1984-85, a borehole more than 1000 m deep was drilled in the center of the depression which remained in the strata of unconsolidated deposits. As has been shown by the geothermal observations in this borehole, H_p reaches 470 m, while t_m at a depth of 20 m is -3.0°C. Down to a depth of 140-150 m the temperature curve has a negative vertical gradient, and only from a depth of 180 m there is a rise in temperature. A sophisticated pattern of the curve is suggested to reflect modern climatic fluctuations. Hence, extrapolations aimed at determining H_p by t_m of perennially frozen rocks at a depth of zero annual amplitudes are not always valid for the region described. Such a great H_p gives evidence of the long-term freezing in rather severe climatic conditions corresponding to modern ones. The maximum permafrost is characteristic of the lower blocks of the basement in the axial part of the depression filled by thick loose deposits; the upper part of their section being composed of fine-grained, highly saturated grounds. H_p decreases in the zone where the depression is conjugated with mountain structures and the thickness of loose deposits decreases to 50-100 m. It varies from 90 to 180 m in that part of the depression which adjoins the Udokan Range on the Nirungnakan and Namingnakan interfluve, as shown by geophysical investigations, drilling, and thermal logging of ten boreholes 35 to 50 m deep, at predominant t_m values of -3 to -5.5°C. As compared to the central part of the depression, the geothermal gradient, that has been calculated for the intervals of 20-40 and 20-50 m has an increased value from 2.1° to 4.8°/100 m. On the background of the above-indicated thicknesses, sites having considerably shallower permafrost were encountered. On a small granite outlier H_p was about 60 m at t_m -2.1°C. Two boreholes with lower H_p values (32.6 and 16.5 m) tapped the confined aquifers that contacted frozen strata. Continental deltas in the foothills of the Udokan Range evidently serve as the transit sites of groundwater discharging via open taliks with head-water circulation in the Chara depression. Considerable variations of H_p within short distances at similar levels of heat exchange on the surface give, in the authors' opinion, evidence of highly differentiated abyssal heat flows value increases with the distance from the center to the peripheral parts of the depressions as well as of the non-uniformity of heating action of groundwater confined to different lithologic horizons of loose deposits. A decrease in the particle-size of the loose cover deposits towards the center of the depression, that causes worsening of the seepage properties of rocks, as well as greater depth of the basement, lead to a greater cross-section of groundwater flow and reduced velocities of discharge. Accordingly, resistance of groundwater to long-term freezing is decreasing, and H_p values, as shown above, tend to increase towards the central parts of the depression.

Within the limits of the depression there are taliks whose existence is conditioned by a peculiar heat exchange between rocks and the atmosphere, and those formed under the impact of groundwater. The largest talik is the massif of deflated sand in the depression's center. Its existence is conditioned by the heating ac-

tion of summer rainfall infiltration and discharge of subpermafrost flow within the boundaries of the massif. Open taliks have been identified in a forested sand massif on the interfluve of the Namingnakan and Unkur Rivers. They are formed within the terminal moraine lines under certain lakes where ice subsidence is observed in winter which is indicative of lacustrine water percolation via the open talik zones. On some stretches of the Chara River valley and its largest tributaries there are subriver bed taliks with ground and head-water circulation.

In the north-eastern part of the depression in the foothills of the Kodar Range there is an open talik whose existance is associated with the discharge of thermal (50°C) water of deep circulation. The influence of this water source on permafrost is rather local and the talik's area does not exceed 0.5 sq km (Geokriologicheskie usloviya Zabaikal'skogo Severa, 1966). It is confined to a large fault extending along the north-eastern flank of the depression with which the existence of open taliks beneath the lakes "boiling" during the whole winter (Geokriologicheskie usloviya Zabaikal'ya i Pribaikal'ya, 1967) is also associated. Thermal springs are also encountered in that part of the depression which adjoins the Udokan Range, as, for instance, the Luktur thermal spring on the right bank of the Unkur River. The occurrence of an open talik in the downstream part of the Verkhny-Sakukan River valley, where icing with an area of about 6 sq km is formed in winter, is associated with subpermafrost water discharge.

The peculiar features of permafrost distribution within the boundaries of younger intermontane depressions will be exemplified by the Nizhny-Ingamakit basin. Even though the t_m values here are practically the same as in the Chara depression and vary from -1.2 to -4.9°, H_p does not exceed 50-100 m. This reduction H_p in thickness can be explained by a shorter period of freezing, an active resistance of vigorous groundwater flows to perennial freezing or, probably, by a higher abyssal heat flux. In general, a regular increase of permafrost from the axial part towards the basin's slopes is observed. In the Nizhny-Ingamakit River valley (right in the depression center upstream with respect to icing) there is an open, about 90 m-wide flood-plan talik whose existence is conditioned by a strong heating action of groundwater flow in the thick loose deposits and by the discharge of deep-aquifer groundwater. The latter is confirmed by the hydrochemical analysis of the talik water and ice comprising the icing. The anomalously high geothermal gradient values (from 18 to 7.3°/100 m in the basin's bottom down to a depth of 30-60 m are explained by Nekrasov and Semenov to occur due to an active efflux of heat to the surface with deep groundwater flow (Geocriologicheskie usloviya..., 1966). By extrapolating, they obtained the following pattern of H_p variation in the Nizhny-Ingamakit basin. Over the major part of the basin's bottom, H_p is less than 50 m. On the waterlogged sites with lower temperatures the permafrost thickness increases to 80 m reaching 100 m on the third above-floodplain terrace under the left slope of the basin. Within the terminal moraine line H_p is estimated at 50 to 100 m.

In the northern low foothills of the Udokan Range continuous permafrost has been established to occur within the limits of wide interfluves with rather gentle slopes at 1000-1250 m and in the bottoms of wide trough valleys of the first glaciation with elevations of 800-1000 m. Narrow, subriver bed, closed taliks with groundwater circulation occur only in some sites of the Nirungnakan, Emegachi, Sangiyakh and other River valleys. Maximum H_p values (up to 150-200 m) have been established by geophysical methods in the slopes of northern exposure at t_m ranging from -2.6° to -3.2°C. Within wide watersheds H_p varies from 120 to 160 m at a wide range of t_m (from -1.3 to -4.5°C). On the slopes of southern exposure H_p values reach 100-150 m, decreasing to 30-50 m on some sites at t_m -0.7 to -3.6°C. Of special importance is the following regularity ascertained in the foothills of the Udokan Range: irrespective of the exposure there are rather low values of t_m (-4 to -5.5°C) on the hillsides covered by coarse blocky deposits having no fill and characterized by complex conditions of heat exchange. A drastic reduction in H_p (to 50-70 m) was revealed in the zones of ancient crusts of weathering occurring on slightly waterlogged saddles, flat watersheds, and hillsides of southern exposure. In the bottoms of trough valleys of the first glaciation, where frozen strata are continuously interacting thermally with subpermafrost water, the H_p thickness, determined geophysically, does not exceed 120-150 m.

In the central medium to high mountains of the Udokan and Kodar Ranges, PF is continuous both in area and section reaching, at t_m from -8 to -10°C, 800-900 m on the sites located 2000-2200 m above sea level. According to Yu.G.Shastkevich, in the highest massifs of these ranges (2500-3000 m) H_p reaches 1200 m and more, while the t_m values decrease to -10 - -12°C and less. Among natural factors responsible for the formation of such a great PF thickness are: the longest duration of freezing of the axial parts of ranges and three-dimensional pattern of their cooling; high degree of rock drainage; high thermal conductivity and low heat capacity of solid rocks; poor heating action of snow on steep, top-adjacent sites of hillsides and crest-like watersheds; and air temperature lowering with hight. Certain role is played by air flows freely penetrating through shallow coarse deposits into the fractures of the solid rock masses whose tectonic disturbance in the rift zone is very great. The mechanism of this process has not yet been clarified, but even now a number of possible reasons of air flows origination in fractures of hard rock massifs can be indicated, viz. a permanently existing gradient of atmospheric and air pressures in fractures, gradient of air temperature and, linked to it, gradient of air densities. Some influence is, probably, exerted by a permanent change in the volumes of fractures in the up-

per part of a rock mass as a result of temperature fluctuations. The availability of air flows not only in the near-surface part of a solid rock mass, but also at the depths of 300 to 500 m can be proved by ablimation ice formation in the adits cut in the axial parts of the Udokan Range. Ablimation ice is extremely unevenly distributed in the shaft: there are sites where ice is absent and those with large amounts of ice. The latter are confined to highly fractured zones. It is characteristic that fractures in such zones remain open, while walls of the adit around them are covered by a continuous layer of ablimation ice crystals. Measurement of temperatures in the adits showed that rocks of the sites with large amounts of ice were by 0.8-0.9°C colder than those of ice-free sites.

The cryogenic structure of solid rocks in mountain ranges is inherited, therefore, their total ice saturation is determined by fracturing and moisture content prior to freezing. Fractures in a rock mass have different origin and areal extent: weathering joints, fractures in valley slopes, tectonic and lithogenetic fractures, and fractures in the zones of cryogenic disintegration. For solid rocks in the cryomassifs of ranges the following regularities of the cryogenic texture were revealed: the presence of a horizon with inherited and expanded cryostructures that is filled with overflow-infiltrational and ablimation ice and confined to the crust of weathering; completely or incompletely developed fractured cryostructures and open fracturing in the main part of a massif with congelation and ablimation ice, corresponding to the former zones of aeration and periodic flooding; and horizons with fully developed expanded fissured cryostructures controlled by groundwater tables in the valley taliks. Depending on the depth of erosional ruggedness, H_p and its evolution, neotectonics and hydrogeological conditions, some parts of mountain ranges are characterized by the presence and extensive development of certain ice-accumulation horizons or poor development or even absence of others.

In the central, medium to high-mountain part of ranges, characterized by an active neotectonic regime and intensive denudation, the upper relatively shallow horizon of ice accumulation is confined to the crust of weathering. The major part of the solid rock massif is highly dissected with zones of vertical and subvertical orientation representing glacial breccias with expanded fissure-vein cryostructures. The width of such zones reaches 3-5 m, while some monomineral ice lenses are 0.2-0.3 m wide and volumetric ice content of rocks is up to 30%. They are encountered inside solid rock massifs, in the near-surface horizons, and at a depth of 300-500 m. There exists a third zone of ice accumulation associated with cryogenic disintegration of rocks in the course of secular variations of the PF base.

In the low-mountain peripheral part of ranges within the limits of vast poorly dissected interfluves with a relatively quiescent neotectonic regime, the zone of ice accumulation in weathering crusts has been developed. Apart from the modern crust of weathering which is several meters thick, more ancient crusts are widespread that are represented by feld spar and quartz-feld spar sandstones which have a bedrock texture when frozen and become sand when thawed. Kaolinite may be also encountered. The thickness of these crusts is not less than 20 m according to the data obtained in shallow small boreholes; according to geophysical data, it is 80-90 m. The cryogenic structure is massive; and up to 5 mm-thick ice lenses occur less frequently. The ice content of these deposits reaches 30-35%. Fracturing of the major part of the massif is less intensive than in the axial part of the range. Incompletely developed fissure cryostructures with ablimation ice are widespread.

The PF distribution in the bottoms of deep trough valleys of the Zyryansk glaciation situated above 1200-1400 m is rather complicated; H_p varies from 100 to 300 m in the areas unaffected by talik zones. A decrease in permafrost thickness, along with higher t_m, is supposed to be associated with the distortion of thermal field due to topography.

Open taliks form on the sites of valleys confined to small grabens (Namingin, etc.) with highly permeable alluvial and glacial deposits up to 100 m thick. These taliks serve as collectors of considerable groundwater reserves. Fissure and fissure-vein water of subpermafrost circulation play certain role in the existence of these taliks, which is confirmed by a higher helium content in low-water period (March-April) in the spring contributing to the formation of an icing in the Naminga River valley as compared with summer period. Such grabens are characterized by an active resistance of groundwater flows to long-term freezing and, probably, by higher values of abyssal heat flux. In the cirques and trough valleys of the Sartan glaciation more homogeneous freezing conditions are observed. The t_m are higher due to snow accumulation and H_p is reduced by 1.5-2 times as compared with interfluves. Similar situation is observed in the bottoms of trough valleys covered by modern glaciers. Thus, at a height of 2160 m beneath the Nina Azarova glacier, H_p amounts to 580 m at t_m = 6.9°C (Geokriologicheskie usloviya..., 1966). However, open water-absorbing talik zones can occur on the sites of valleys with thick unconsolidated deposits in the zones of dislocations with a break in continuity even at the altitudes of 1800-2000 m.

REFERENCES

Geokriologicheskie usloviya Zabaikal'skogo Severa. (1966). 216 pp., Moskva: Nauka.

Geokriologicheskie usloviya Zabaikal'ya i Pribaikal'ya. (1967). 224 pp. Moskva: Nauka.

Lopatin, D.V. (1972). Geomorfologiya vostochnoi chasti Baikal'skoi riftovoi zony, 115 pp. Novosibirsk: Nauka.

Nekrasov, I.A., Zabolotnik, S.I., Klimovsky I.V. & Shastkevich, Yu.G. (1967). Mnogoletnemerzlye porody Stanovogo Nagor'ya i Vitimskogo ploskogor'ya, 168 pp. Moskva: Nauka.

Nekrasov, I.A. & Klimovsky, I.V. (1978). Vechnaya merzlota zony BAM, 120 pp. Novosibirsk: Nauka.

Noveishaya tektonika i formirovanie mnogoletnemerzlykh porod i podzemnykh vod. (1975). 124 pp. Moskva: Nauka.

MEAN ANNUAL TEMPERATURE OF GROUNDS IN EAST SIBERIA

S.A. Zamolotchikova

Faculty of Geology, Moscow State University, Moscow, USSR

SYNOPSIS The paper presents a brief characteristic of the mean annual temperature of grounds in East Siberia and quantitative assessment of natural factors affecting it. The ressons of the mean annual temperature inversion of grounds in eastern USSR are also revealed. Ground temperature inversion is caused by (1) heat exchange on the soil surface (parameters of the radiation-heat balance and temperature on the soil surface) that depends on natural factors; and (2) a pattern of redistribution of heat generated on the earth surface by the air masses migrating in the vertical and other directions. Examples of inversion variation of ground temperature with altitude are given and the reasons of this phenomenon are discussed.

MEAN ANNUAL TEMPERATURE OF GROUNDS

The author's participation in the compilation of the "Geocryological Map of the USSR" at a scale of 1:2,500,000 and in writing of the monograph "Geocryology of the USSR", v.4 served as a basis for the present paper.

The mean annual temperature of grounds (t_m) in the region under consideration varies at a depth of annual zero amplitudes (5-7 to 20-30 m) from +7° to -15°C with the maximum values recorded in the south of the Primorye Territory and the minimum ones - on the Cherskiy Range summits. This region displays zonal and high-altitude variations of t_m. The temperature here is greatly affected by the Pacific and the Arctic Oceans as well as regional specifics of natural conditions.

Zonal variation of ground temperature

Distinct zonal variations of t_m are associated mainly with a decrease of the radiation balance (R) from the south to the north, from 188.5 to 20.9 kJ/cm^2 a year. They are mostly pronounced on plains and low plateaus in the continental regions where t_m diminishes by 0.3 to 1.5°C per every grade of the north latitude. Thus, the typical temperature on the Khankai Plain (45°N) ranges from +3°C to +5°C, while on the Zeya Plateau (51°N) from +1°C to -2°C. On the Kolyma Plain, the mean annual temperature tends to decrease northwards from -3 to -5°C (67°N) to -5, -7°C (69°N) and -9 to -11°C (71°N). In the mountains of the continental area (at an altitude of 1 km), the same tendency as on the plains is observed: t_m decreases from the south to the north per 1°N latitude, from the Baidzhal to Stanovoy Ranges by 0.3-0.6°C, from the Stanovoy to Verkhoyansk Ranges (68°N) by 0.3°C, and in the northern part of this range (from 68° to 70°N) by 1.5-2.0°C. Farther to the east in the mountain regions (upper reaches of the Kolyma River) Nekrasov (1976) reported a difference of t_m per 1°N latitude equal to 0.7°C. In the maritime regions of the Pacific the temperature difference per 1°N latitude at an altitude of 0.5-1 km rarely exceeds 0.5°C.

Oceans essentially affect the mean annual temperature. Intrusion of air masses from the Pacific increases the temperature of air (t_a) and grounds. Within a wide coastal belt, the increased values of the warming effect of snow (Δt_{an}), infiltration of precipitation (Δt_p), etc are observed. At the same time the warming effect of the Pacific is somewhat slackened by the monsoon climate which is especially pronounced in the south of the region, as well as by a great ice cover on the nearby seas that tends to increase northwards. Intrusion of cold air masses from the Arctic regions causes the decline of t_a and t_m, and brings precipitation but in an essentially smaller amount than from the Pacific. Relatively small amplitudes of temperature fluctuation on the soil surface (A_o), typical of maritime regions, moderate the effect of many natural factors.

The impact of natural factors on ground temperature

The mean annual temperature of grounds is affected by a specific radiation regime determining t_a and temperature of the soil surface (t_s) and by a number of natural factors, such as snow, vegetation, ground composition, etc. The effect of these factors was evaluated through calculations by the methods developed at the Department of Geocryology, Moscow State University (Osnovy merzlotnogo prognoza..., 1974).

Correction for radiation (Δt_R) was made by the formula $t_R = t_s - t_a = \frac{R \frac{R}{K} LE - B}{K}$, where, R is the radiation balance of the earth surface;

LE is the loss of heat on evaporation; B denotes heat rotations through the soil surface, and K is the coefficient of turbulent exchange of heat. The correction for radiation is great in continental areas, especially in the southwest of the region where in open spaces it may reach +1.7°C, while in forested areas it may vary from +0.2 to +1.2°C. A tendency of Δt_R to decrease to 0.2-1°C is observed in maritime regions and in mountains where it decreases with altitude, and in the North at an altitude of mountain snow caps it may sometimes acquire a negative value (-0.5 to -1.5°C) (Garagulya et al., 1970).

Snow in the region produces a warming effect on t_m. By the value of Δt_{sn}, it is possible to distinguish three zones. The first zone runs as a narrow strip along coasts of seas and oceans. In open spaces, Δt_{sn} does not exceed 4°C, while in forested areas and in lowlands it sometimes rises to 6°C and more. In the second zone, extending as a wide coastal strip along the Pacific, Δt_{sn} reaches 10°C. Minimum values of Δt_{sn} up to 3°C are typical of the mountain tops and steep slopes from where snow is blown away by wind, whereas its maximum values, ranging from 5 to 10°C, are observed on the lee slopes of mountains, in depressions, particularly in the head of valleys, and in the areas covered with forests and shrubs. The third zone covers the inner continental regions where Δt_{sn} does not exceed 8°C.

The effect of vegetation (Δt_v). The cooling effect of vegetation prevails in the south, where forests, meadow vegetation and moss cover decrease t_m by 0.1-1.5°C, 0.1-0.8°C and 2°C and more, respectively. In forests with well-developed undergrowth the snow cover becomes thicker and its density decreases. Thus, t_m in such forests is often higher than in the open spaces. In maritime regions Δt_v diminishes to some extent. For instance, in coastal regions of Kamchatka Δt_v rarely rises above 1°C. In the north in forest-tundra and tundra the effect of vegetation is insignificant (0-1°C) even though its warming effect prevails. On the mountain tops nearly devoid of vegetation, on steep slopes, in some parts of plains and in alasses Δt_v does not often exceed 0.5°C.

The effect of ground composition was determined by taking into account the warming effect associated with infiltration of precipitation, moisture condensation and the so-called "temperature shift". The latter results from periodic fluctuations of t_s due to the change of heat conductivity coefficient of grounds when they transfer from the thawed to frozen state during seasonal freezing (thawing). Since frozen ground has higher heat conductivity than the thawed one, t_s usually exceeds the temperature at the base of seasonally thawing (freezing) layer.

A temperature shift (Δt_λ) in the south of the region ranges from 1 to 3°C in peat, from 0.3 to 2.1°C in moist clays, and at low moisture content equals 0.5°C. Values from 0.3 to 1.2°C are very typical. In the north of the region in Δt_λ does not exceed 2°C in peat, it varies from 0.4 to 1.2°C in sands and clays and in grounds with a low moisture content drops to 0.5°C. In mountains on wide flat intefluves and gentle slopes Δt_λ often amounts to 0.5-1°C, and on steep slopes it is less than 0.5°C.

The warming effect of precipitation percolation into well permeable grounds on plains, in depressions, and on flat influves in the region under consideration varies from 0 to 2.5°C. The maximum values of Δt_p (up to 1-2.5°C) are typical of the southern part of the region, but they are seldom observed here due to a wide occurrence of clays. In the south-east of Kamchatka the values of Δt_p are somewhat lower (0.3-1°C), and on the Kolyma upland they do not exceed 0.6°C. Still farther north in the Yano-Indigirka and Kolyma lowlands and on Chukot Peninsula as well as on highlands Δt_p seldom exceeds 0.3-0.5°C. Some researchers (Garagulya et al., 1970) have observed the warming effect (up to 1-4°C) of moisture condensation on the mountain slopes devoid of vegetation and composed of coarse-fragmental rocks.

In the southern continental areas of the region t_m on the slopes of southern exposure is higher than on the slopes of northern exposure by 1.3°C, while in the north (the Adycha River) - by 1.2°C. In the southern part of maritime regions it equals 1-2.5°C, and 0.5-1.5°C on Chukot Peninsula. In the conditions of maximum snow accumulation on the slopes of northern exposure, t_m on the slopes of southern exposure may be even lower than on those of northern exposure.

Surface and ground waters produce, as a rule a warming effect. In taliks below a river bed or a lake, t_m is higher than on the above flood-plain terraces amounting to 3-5°C in the south and 7-13°C in the north of the region, although V.A.Kudryavtzev has shown that under small surface streams in the south of the region t_m may be lower than in the surrounding parts of the valleys. The effect of groundwater on t_m is frequently observed in faults in which uprising high-temperature waters circulate, their warming effect, for example, on Kamchatka Peninsula, may be very great. But even values from 1 to 10°C, observed in some localities, may contribute much to the formation of taliks and to the rise of t_m.

Altitudinal-zonal variation of ground temperature

Altitudinal-zonal variations of t_m are observed in mountains. In the southernmost part of the region (Primorye Territory, southern Sakhalin and Kamchatka) where unfrozen grounds are widespread on plains, in depressions and valleys, and on mountain slopes, the t_m values range from +1 to +7°C. Permafrost occurs on the tops

of medium-high mountains (t_m up to -1°C) and in high mountains where t_m tends to decrease with height to -3°C on the Sikhote-Alin Range and to -5°C and lower on the tops of the Kamchatka volcanoes. The zone of insular and discontinuous permafrost, south of the Stanovoy Range, in the northern Sikhote-Alin Range, Sakhalin and Kamchatka is characterized by the occurrence of frozen grounds on waterlogged plains, in depressions and valleys (t_m from +3 to -3°C), and on the mountain tops where t_m diminishes with altitude to -7°C and more seldom to -9°C (at an altitude of 2,000 m). Unfrozen grounds (t_m from -1 to +3°C) dominate on low plateaus, ouvals, low mountain slopes and floodplains.

In the zone of continuous permafrost, covering considerable part of the region (north of the Stanovoy Range), in depressions, valleys and on the slopes of southern exposure t_m varies from +1 to -3°C, while in the northernmost areas it drops to -11, -13°C. In the mountainous regions, the decrease of ground temperature with altitude to -7, -11°C on the tops of medium-high mountains and to -15°C on the tops of high mountains is quite typical.

THE CAUSES OF GROUND TEMPERATURE INVERSION

In continental regions in the south of the Far East and Central Siberia many researchers (Lugovoi, 1970; Vtyurina, 1970; and others) have observed the inversion of air and ground temperature when t_a and t_m in the bottoms of depressions and valleys are lower than on the adjacent plateaus and low-mountain slopes, while on the tops of medium and high mountains the temperatures tend to decrease with altitude.

It has been assumed for a long time that t_a inversion was caused by the flow of cold air in winter down into closed depressions. But the actual causes of t_a and t_m inversion still remain obscure (Nekrasov, 1976). The ground temperature inversion results from: (1) specific nature of warming and cooling of air, earth surface and grounds with an increase in altitude, depending on the complex of natural conditions; and (2) redistribution of heat generated on the earth surface by the air masses moving in vertical and other directions. Thus, the causes of inversional change of the mean ground temperature are, actually similar to those responsible for the t_m variation in other conditions whose favorable combination gives rise to t_m inversion. To assess the causes of inversion one should know the t_s value variation with altitude on various features of topography and determine the effect of natural factors (ground composition, etc.) on t_m.

The causes of temperature inversion in the continental area of East Siberia

In the continental area of East Siberia the t_m inversion is sufficiently pronounced. It results primarily from the variation of the radiation heat balance, t_a and t_s. Let us consider the differences in the elements of the radiation-heat balance in the valley bottoms and on the low plateaus south of the Stanovoy Range. It has been established that the amount of incoming shortwave radiation to the shadowed bottoms of narrow and deep valleys is smaller (Nesmelova, 1970) than on the plateaus which is one of the main and sometimes the only cause of t_m inversion. For instance, in the valleys and on the plateau (400-450 m above sea level) of the Lena-Amgin watershed, t_m ranges from -2 to -4°C and -1 to -2°C, respectively. It has been estimated that there was no difference between the total warming effect on natural factors (snow, vegetation, etc.) in one of the valleys and on the interfluve. The difference in t_m can be explained only by better illumination of the watershed as compared to the valley where the mean annual value of t_a is 1-2°C lower than on the plateau. In the wide valley, the total radiation and albedo turned out to be close to their values on the plateau (Nesmelova, 1970). However, the radiation balance in the valley was lower since the values of effective radiation were higher than on the plateau. In addition, heat expenditure on evaporation is usually higher in valleys. The above conditions are responsible for lower mean annual temperatures of the soil surface in the bottoms of wide waterlogged valleys as compared to the surface of dry low plateaus.

In continental regions, formation or intensification of t_m and t_a inversion may also result from the heat redistribution in the course of air masses migration. In summer when there is no wind or when it is very weak the vertical air migration prevails. Warming of the earth surface in summer is accompanied by the uprise of warm air masses which contribute additionally to an increase of t_a and t_m primarily on low plateaus, ouvals, and low-mountain slopes; this effect is less felt at higher elevations. Besides, cold air in winter flows down and remains in relief depressions. In medium - and high mountains, the radiation balance decreases (Promerzanie,... 1974) and the effect of natural conditions diminishes with altitude. For example, as a result of the above-mentioned conditions, in some areas north of the Stanovoy Range permafrost forms in valleys and on mountain tops and is frequently lacking on plateaus and low-mountain slopes. Vital differences in natural conditions (show, vegetation, ground composition, etc.) may give rise to the formation, intensification or disappearance of the t_m inversion. Thus, when a plateau becomes covered with a thick larch forest without undergrowth decreasing the radiation balance by 30 to 40% (Nesmelova, 1970) and when it is affected by waterlogging and a valley has a thick, tall shrub vegetation, increasing Δt_{sn}, there may be no soil temperature inversion. The comparison of t_s and t_m in a valley and on a low-mountain slope of lowlands of northern exposure has shown that inversion is usually nonexistent, while the comparison of t_m in a valley bottom and on a slope of southern exposure has indicated that the t_m inversion is observed nearly always. The cause of t_m inversion is, as a

rule, a favorable combination of natural conditions. Thus, in the Turan Range area, frozen soils with t_m down to -2°C are developed in the valleys. On the slopes, t_m has often positive values (up to +2°C), while on the mountain tops it has negative values (down to -5°C). Low t_m values in valleys result from their shading, low Δt_{sn} and considerable Δt_λ, whereas its positive values on slopes result from large values of Δt_{sn} and insignificant Δt_λ. Apart from this, the slopes of western and especially southern exposure have greater radiation balance than the valley bottoms.

The causes of temperature inversion in the maritime area

The causes of inversion of the mean annual temperature of grounds in the maritime area that is influenced by the ocean differ from those in the continental regions mostly by their intensity. The radiation balance in the oceanic sector is lower than that in the continental one due to greater cloudiness, especially in summer. As a result, the values of t_m for various features of topography differ but slightly. Strong winds level the air temperature off and almost no inversion is observed. The effect of natural factors (snow, etc.) in maritime regions is weaker due to smaller annual amplitude of the soil surface temperature variation. In spite of unfavorable conditions, the t_m inversion in the lower part of the Amur River area, in the Okhotsk region, on Sakhalin, Kamchatka, and Chukotka is not observed eveywhere, but only in some localities. The t_m inversion is caused by the difference in the values of the radiation-heat balance parameters controlling t_a and t_s and the effect of natural factors on them. For example, in northen Sakhalin perennially frozen grounds (t_m varies from 0 to -0.7°C) form in the waterlogged areas of maritime plains where strong winds are common and no t_a inversion is observed. Permafrost forms here as a result of snow removal by wind, and great Δt_λ in the sites composed of peat. On the elevated sites composed of loamy sand and sand, t_m is positive (up to +3°C and more) due to high values of Δt_{sn} and Δt_R and low values of Δt_λ. The highest t_m values are observed here on well illuminated slopes of southern exposure. On Chukot Peninsula, within the above-floodplain terrace of the Ponneurgen stream, t_m equals -5 or -6°C, while on the low-mountain slope of northern exposure it is -4 or -5°C. On the mountain top t_m ranges from -6 to -8°C. An increase in t_m on the slope may only be attributed to a sparse forest with shrubs whose warming effect is greater here than in the valley and on the watershed.

Goldman and Sezonenko (1961), Nekrasov (1976), and other researchers reported a gradual decrease of T_m with altitude in mountainous regions of the North in the zone of continuous permafrost. The causes of t_m inversion there are similar to those in other regions. Comparatively high t_m values in the valleys of this zone are conditioned by extensive occurrence of coarse-fragmental material and by the warming effect of t_p as well as surface and subsurface water. The Δt_{sn} values are often increased by the forest-tundra vegetation in the valleys. The radiation balance and the effect of many natural factors decrease with the hight of mountains to such a great extent that the differences in t_m due to t_a inversion, moisture condensation, slope exposure, etc.are mainly characteristic of the continental regions up to relative altitudes of 1 km and seldom more. The t_m inversions on the summits of medium-high and high mountains become, evidently, even smaller than, for instance, in the zone of oceanic influence but at the level of the bottoms of depressions.

Hence, t_m values in the mountains decrease, increase or do not vary at all up to a relative hight of 0.5-1 km due to a considerable value of the radiation balance, more pronounced t_a inversion, and significant influence of natural factors. On higher elevations t_m, as a rule, decraeses.

REFERENCES

Garagulya, L.S., Kudryavtsev, V.A., Kondratyeva, K.A. & Maximova, L.N.(1970). Vliyanie geologo-geograficheskikh faktorov na temperaturu porod v severnoi chasti Yano-Indigirskogo mezhdurech'ya. V knige: Merzlotnye issledovaniya, vyp.10: 59-80.

Goldman, V.G. & Sezonenko, Ye.V. (1961). Temperatura i moshchnost' mnogoletnemerzloi tolshchi litosfery v gornykh raionakh Severo-Vostoka. - Trudy VNII-I, (19): 139-194. Magadan.

Lugovoi, P.N. (1970). Osobennosti geokriologicheskikh usloviy gornykh stran, 135 pp. Moskva: Nauka.

Nekrasov, I.A. (1976). Kriolitozona Severo-Vostoka i yuga Sibiri i zakonomernosti eye razvitiya, 226 pp. Yakutsk.

Nesmelova, Ye.N. (1970). Struktura teplovogo balansa nizkogornykh raionov Vostochnoi Sibiri. V sb.: Merzlotnye issledovaniya, vyp.10: 227-237.

Osnovy merzlotnogo prognoza pri inzhenernogeologicheskikh issledovaniyakh,(1974), 431 pp. Moskva: Izdat. Moskovskogo Universiteta.

Promerzanie zemnoi poverkhosti i oledenenie khrebta Suntar-Khayata. (1964), 143 pp. Moskva: Nedra.

Vtyurina, Ye.A. (1970). Vysotnaya geocriologicheskaya poyasnost' v predelakh SSSR. V knige: Geokriologicheskie issledovaniya pri inzhenernykh izyskaniyakh, 247-267. Moskva.

ALPINE PERMAFROST IN EASTERN NORTH AMERICA: A REVIEW

T.W. Schmidlin

Geography Department, Kent State University, Kent, Ohio 44242 USA

SYNOPSIS Review of the scant literature on eastern alpine permafrost indicates that permafrost exists on Mt. Washington, Mont Jacques-Cartier, and is probable on Sugarloaf Mountain. Field reports provide no evidence of permafrost elsewhere. Climatic data were used to estimate the elevation of air temperature isotherms which, along with consideration of vegetation and snowcover, provide a preliminary guide to the extent of alpine permafrost in this region. The lower limit of sporadic permafrost is estimated to occur near 1500 m in New York and New Hampshire, 1200 m in central Maine, 600 m in Gaspé, Québec, and 200-600 m in Newfoundland. This corresponds to the 0°C air temperature isotherm and is below the alpine treeline. Alpine permafrost may occur, at least sporadically, over 3780 km^2 of eastern North America with continuous permafrost on 46 km^2 of alpine summit area where mean air temperature is below -2°C.

INTRODUCTION

Much has been studied and written concerning arctic permafrost worldwide but the subject of alpine permafrost has received relatively little attention (Harris and Brown, 1978; Péwé, 1983; King, 1986). Alpine permafrost is estimated to exist over 100,000 km^2 in North America, mostly in the Rocky Mountains from Colorado northward (Péwé, 1983). The pattern of permafrost in alpine regions is a mosaic phenomenon due to extreme local variability of climate, vegetation, relief, and geologic formations (Gorbunov, 1978).

Alpine tundra and timberline vegetation exist above 1450 m elevation in the Adirondack Mountains of New York and above 1500 m in the Presidential Range of New Hampshire and on Mt. Katahdin, Maine (Fig. 1). Timberline is near 1100 m in the Chic-Chocs Mountains of Gaspé, Québec, and 300-600 m on the Long Range of Newfoundland. The Torngat Mountains of northern Labrador are an arctic region and will not be considered in this paper. Alpine tundra does not exist south of 44° latitude in eastern North America. The Presidential Range, with Mt. Washington as the highest peak, has a crest with 19.5 km^2 of alpine tundra (Bliss, 1963).

The question of the existence of permafrost in the mountains of eastern North America has received even less attention than permafrost in the western Cordilleras, in spite of the longer history of mountaineering, closer population centers, and lower elevations in the east. Ives (1974) suggested that the lack of permafrost mapping for eastern summits is due to the relatively small areas involved and lack of a continuous alpine region typical of the western Cordilleras. Speculation on the existence of eastern alpine permafrost has occurred for over 50 years. The Ad Hoc Study Group on Permafrost and Committee on Polar Research of the National Research Council (1975) recommended, "there is an urgent requirement for rapid and accurate mapping of the distribution of permafrost...and of factors that influence the occurrence...and extent of permafrost." They further noted that ground temperature data is especially important in alpine regions of discontinuous permafrost. The purpose of this paper is to review the knowledge of eastern alpine permafrost in North America and propose a climate-based distribution of permafrost for the region.

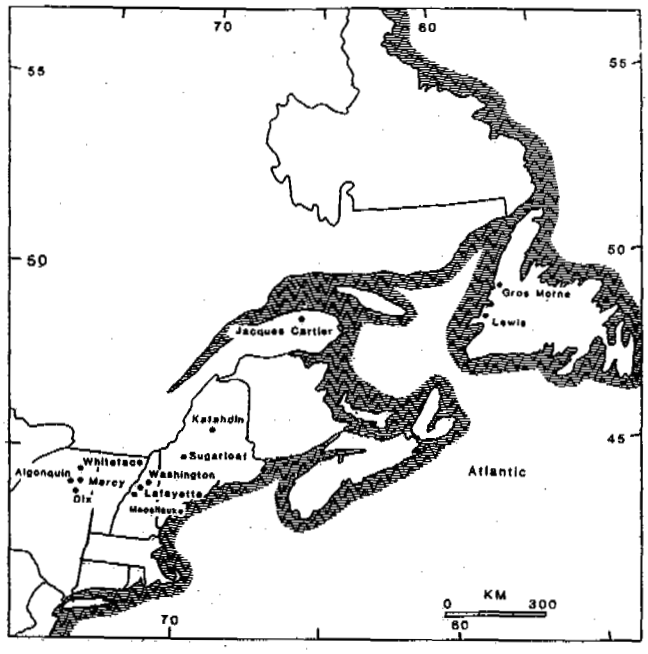

Figure 1. Selected peaks in the alpine region of eastern North America.

REVIEW OF LITERATURE

Antevs (1932, p. 34) stated,

> "The temperature of the ground in the alpine zone of the New England mountains is a subject of great interest. Is the ground now permanently frozen or has it been permanently frozen at any time since the release from the last ice sheet?"

Antevs (1932) related information provided by Joe Dodge, of the Appalachian Mountain Club, after construction excavations in New Hampshire. Dodge reported the ground at 1470 m elevation during July to be frozen at 0.6 m depth and was frozen to below 1.2 m depth. Excavations during August showed frozen ground at 1525 m elevation from 0.9 m to a depth below 1.8 m. Frozen ground was also found near the surface at 1250 m elevation in July. Antevs (1932, p. 36) concluded that, "permanent ground frost seems to persist in the White Mountains on shaded spots and on places with a poorly conductive surface layer."

Bent (1942) reported on a well drilled at the summit of Mt. Washington. Water was found 333 m below the surface and it rose to 73 m below the surface. After sitting for some time, ice was encountered in the well below 80 m depth in October 1941. Steam was used to melt 18 m of ice and water flowed again. This observation led Bent to the conclusion that permafrost existed beneath the summit.

Thompson (1961a) wrote that permafrost existed throughout the alpine zone and much of the subalpine zone in New England, with continuous permafrost on the higher peaks. Well records showed permafrost 90 m deep on Mt. Washington. Thompson (1961b) also observed that Balch ventilation through the felsenmeer and the violent winter winds contributed to permafrost on exposed sites of the Presidential Range and that permafrost existed in favorable sites even far down in the subalpine zone.

Harries (1965) reviewed this literature up to 1965 and concluded that more research was needed before definite conclusions could be drawn about permafrost in the Presidential Range. He concluded that if permafrost exists, then the active layer is at least 1.5 m thick and the permafrost has little influence on the development of soils and vegetation in the region. The soils of Whiteface Mountain, New York, were studied by Witty (1968). He found ice in alpine histosols near 1460 m elevation in July but believed that the ground did not remain frozen through the year on the mountain. Brown (1969) wrote, "permafrost should occur in the high mountains of Gaspé and New England, which rise above the tree line south of the St. Lawrence River." Howe (1971) reported on one season of temperature measurement in an 8.2 m deep hole at the summit of Mt. Washington. Frozen ground existed below 6 m depth on 23 October. The ground had refrozen to 2 m depth on 19 January and the entire profile was frozen on 12 April. Temperature at 8 m depth converged near -1°C on all three dates.

Ives (1974) suggested that alpine permafrost existed on Mt. Katahdin and the other New England summits that rise above treeline.

Goldthwait (1976) studied well records from Mt. Washington and concluded that permafrost existed above 1800 m elevation, in spite of the fact that he found no frozen ground in excavations below patterned ground near the summit.

Moyer (1978) provided data from Wayne Tobiasson of the U.S. Army Cold Regions Research Lab that showed ground temperature near the summit of Mt. Washington to a depth of 10 m over one year. The thawed period was from early July to late December at 2 m depth, from October to March at 5 m, from December to March at 8 m, and the ground was frozen through the year at 10 m. Thus, the active layer at that site was about 10 m deep.

Gray and Brown (1979) reported on temperature in a 30 m hole at the summit of Mont Jacques Cartier (1268 m). They estimated the level of zero amplitude for ground temperature to be at 11 m, the geothermal gradient was 26°C/km, the mean annual ground surface temperature was -1.2°C, the active layer was about 6 m deep, permafrost thickness was 60 m, and the permafrost was contemporary. Gray and Brown acknowledged permafrost existence on Mt. Washington but doubted whether permafrost existed on Mt. Katahdin or the other peaks of the Appalachians.

Péwé (1983), in a review of alpine permafrost in the contiguous United States, wrote that permafrost existed on Mt. Washington and, "also probably occurs nearby in Mount Katahdin, Maine, and beneath the other New England summits that rise above treeline." The U.S. Army Cold Regions Research and Engineering Laboratory reports that frozen ground was encountered in August in holes drilled at the summit (1291 m) of Sugarloaf Mountain, Maine, and water remained frozen year-around in pits at the summit (Merry, 1985).

Thus, a consensus exists in the literature that permafrost exists on Mt. Washington, probably to a depth of about 100 m in bedrock, with an active layer of 8-10 m, and a mean surface temperature near -2.5°C. Permafrost is also verified on Mont Jacques-Cartier. The existence elsewhere on the summits of eastern North America is uncertain but will be considered in the rest of this paper.

MAPPING ALPINE PERMAFROST

Harris (1986) mapped the distribution of alpine permafrost for the eastern ranges of North America's western Cordilleras and provides guidelines for this type of mapping. In general, data from previous field studies are reviewed and incorporated into the new map, with extrapolation horizontally and vertically to estimate the extent and the lower limit of permafrost. Data on the occurrence of permafrost are generally sparse in alpine regions so ground temperature must be estimated from climatic and geophysical data.

Harris (1986) showed that lapse rates of ground temperature with elevation vary among different mountain ranges and even locally within the same range. In the alpine region of eastern North America, air and ground temperature data are

rare so the best approach available is through climatic estimation. Figure 2 shows the proposed distribution of alpine permafrost in eastern North America, based on the climatic variables discussed below. This is the first estimate of its kind for the region and should be considered preliminary, to be modified as additional data become available.

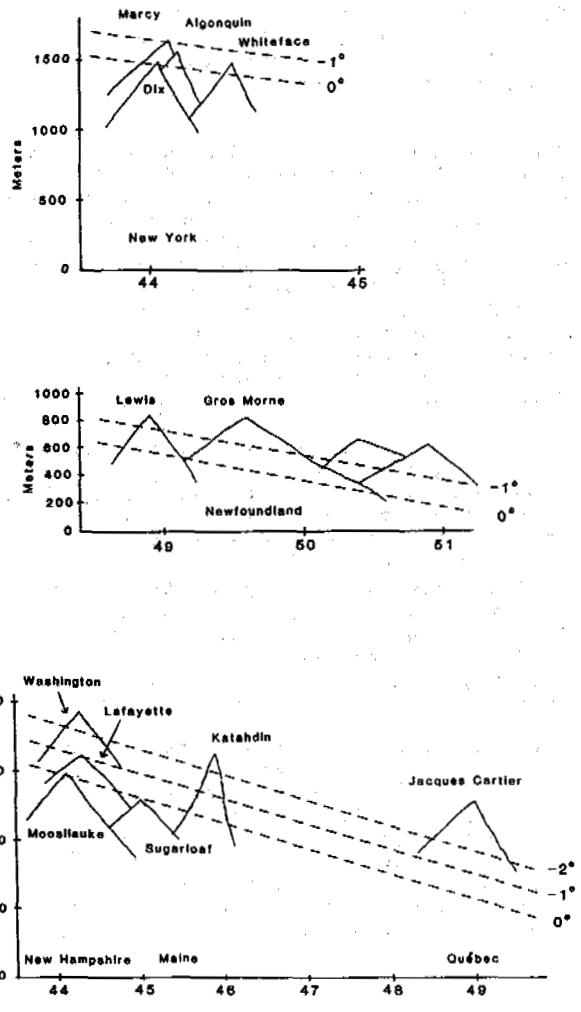

Figure 2. Summits of eastern North America and mean annual temperature isotherms. Sporadic permafrost may exist above the 0°C isotherm. Continuous permafrost is likely above the -2°C isotherm. Several other unnamed peaks in Newfoundland are not shown.

CLIMATIC DESCRIPTION AND ESTIMATION

Climate is the primary factor in permafrost formation. The alpine region of eastern North America has a harsh continental climate. Winters are cold and snowy. Summers are short, cool, and wet. Fog and strong winds are common all year. The only weather recording station in the alpine zone is at the summit of Mt. Washington, the highest peak in the region, so most statements on the alpine climate are inferences from Mt. Washington. A summary of the climate of Mt. Washington is given in Table I. Prevailing winds are from the west though they are variable depending on the daily weather situation. Clouds envelope the summit approximately 55% of the time and wind gusts exceed 120 km/hr on one-third of the days. The mean daily temperature range is 7.4°C. Fog with visibility less than 0.4 km occurs on 313 days per year and temperature falls below 0°C 243 days per year (NOAA, 1983).

The climate of the alpine zone becomes more maritime northward in North America due to the proximity to Atlantic Ocean waters. Gaspé and the Long Range of Newfoundland are bordered on two sides by water. These waters are frozen in winter, thaw during April or May and remain cold through summer, freezing again in late autumn. Thus, while the climate of the New York and New England summits is continental with a large seasonal range of temperature, the summits of Canada experience smaller seasonal variations, milder winters and cooler summers, than expected for their latitude and elevation. Of the Long Range, Hare (1952) wrote, "Nowhere else on Earth does the arctic verge drive so far south into the middle latitudes." Compared to the climate of alpine areas (>3750 m) in the Rocky Mountains of Colorado (Barry, 1973), the climate of Mt. Washington is much windier and wetter with colder winters and slightly warmer summers.

Leffler (1981) proposed equations for estimating mean monthly and annual air temperatures of Appalachians summits, based on known lapse rates. Leffler estimated that mean annual air temperature decreases 1.08°C/°latitude northward and 5.8°C/km increase in elevation. These were later verified for a larger region by Schmidlin (1982). The mean annual air temperature of Appalachian summits, based on Leffler's equations, are shown in Figure 2. The mean annual temperature is likely to be well-estimated by the equations but the maritime mountains north of 47° are likely to have a smaller annual temperature range than predicted here. The temperature gradient with elevation used here is close to the gradient of 6.1°C/km from southern Norway (Green and Harding, 1980) but smaller than the 7.8°C/km reported for the Front Range of the Rocky Mountains in Colorado (Ives and Fahey, 1971, Fig. 2).

Mean annual air temperature provides a widely used first approximation to limits of permafrost occurrence. The lower altitudinal limit for alpine permafrost coincides roughly with the 0°C to -1°C mean annual air temperature (Péwé, 1983). Brown (1969) noted that permafrost exists in favorable areas of eastern Canada where the mean annual air temperature is near 0°C due, in part, to the low values of summer solar radiation in the maritime climate. The evidence of permanently frozen water in pits on Sugarloaf Mountain (Merry, 1985) indicates that some alpine permafrost is likely to occur with a mean annual air temperature near 0°C. Leffler's (1981) equations indicated that the elevation of the lower limit of permafrost decreased by about 185 m/°latitude. This is more than estimates of

Table I. Climatic summary for Mt. Washington (1909 m) for the period 1951-80 (NOAA, 1983)

	Jan	Feb	Mar	Apr	May	Jun	Jul	Aug	Sep	Oct	Nov	Dec	Year
Mean Temp (°C)	-14.9	-15.1	-11.1	-5.3	1.3	7.0	9.3	8.4	4.8	-0.8	-6.5	-12.7	-3.0
Precip (mm)	186	203	208	179	164	179	175	193	182	171	217	227	2284
Snow (cm)	96	101	104	73	26	3	0	0	4	29	78	107	621
Wind (km/h)	74	71	67	59	48	44	41	40	46	54	63	71	57
Days over 0.25 mm precip	19	18	19	18	17	16	17	16	15	15	19	20	209

80 m/°latitude for the western United States (Péwé, 1983) and 90-100 m/°latitude in Asia (Fujii and Higuchi, 1978). The "frost number" described by Nelson and Outcault (1987) incorporated snow physical properties with climatic data but is useful only over large regions with many weather stations. These requirements are not met in the alpine zone under study.

Radiation is often cited as an important factor in determining the existence of alpine permafrost. The alpine region of eastern North America is so cloudy, wet, and windy that heat transferred to the ground is likely to be nearly the same for all aspects, except perhaps for the steepest slopes.

Snowfall and vegetation have a large impact on ground temperature, insulating the ground from temperature changes in the air. A deep early season snowfall prevents heat loss from the ground and reduces frost penetration. A snowcover late into spring or summer presents a high albedo surface, insulates the ground from warmer air, and consumes energy in melting (Ives and Fahey, 1971; Achuff and Coen, 1980). These factors prevent the ground from warming and maintain frost in the ground until the snow melts. The net effect of snowcover on mean annual ground temperature is not well documented in alpine regions. The numerical models of snowcover and ground temperature used by Goodrich (1982) are instructive, though snowcover is assumed to begin accumulating in early September and to melt in early May, both of which are earlier than reality in much of the alpine and subalpine zone. The later start to the snowcover and later melt will lead to lower ground temperatures than predicted in the Goodrich (1982) models.

The heavy snowfall of the alpine zone in eastern North America is redistributed by violent winter winds so that accumulation is generally less than 1 m above treeline and often over 2 m below treeline or in east-facing depressions. In addition to holding snow cover, vegetation shades the surface from solar radiation, reduces evaporation, and insulates the ground through contribution of surface organic material. Gray and Brown (1979) proposed that the lower limit of permafrost on Mont Jacques-Cartier is at treeline due to the winter insulative effects of the deeper snow accumulation below treeline. While frost penetration is less under deep snow, field work on Mont Jacques-Cartier in June 1985 and 1986 showed the extent of delay in thaw caused by late-lying snow below treeline. Frozen ground remained within 0.1 m of the surface under subalpine trees, while 0.1 m ground temperature was 4°C on the summit tundra. In general, a surface with substantial vegetation and moist soil will thaw slowly, while a bare, drier surface warms quickly in spring and summer (Price, 1971; Ballard, 1972). Zoltai and Tarnocai (1971) found that snow cover was less under a dense spruce forest than in clearings but the thawed active layer was thinner under the trees. Sporadic permafrost occurs throughout the boreal forest of the northern hemisphere so might also be expected in the subalpine forests where air temperature is sufficiently low. Deep snow may preserve permafrost if it exists in the subalpine zone. Perennial snow does not exist in these mountains, except for small snow patches following winters with heavy snow or during cool summers. The net effect of snowcover on ground temperature is difficult to assess in these alpine regions and needs further study, but the deeper accumulation of snow in the subalpine forest does not seem to eliminate the possibility of permafrost below treeline.

CONCLUSIONS

Previously published field work shows that permafrost exists on Mt. Washington and Mont Jacques-Cartier. Extrapolation of climatic data and supportive evidence from Sugarloaf Mountain indicate that permafrost is likely throughout the alpine zone of eastern North America and occurs sporadically down into the subalpine forests wherever the mean annual air temperature is below 0°C.

The lower limit of sporadic alpine permafrost is near 1500 m in New York and New Hampshire, 1200 m in central Maine, 700 m in Gaspé, Québec, and between 200 and 600 m in the Long Range of Newfoundland. Alpine permafrost is forecast to occur sporadically on Mt. Marcy, Algonquin, and Whiteface in New York, Mt. Lafayette and throughout the Presidential Range of New Hampshire, Mt. Katahdin, Maine, Mont Jacques Cartier and adjacent peaks in Gaspé, Québec, and through much of the Long Range of Newfoundland. The total area with at least sporadic permafrost is estimated at 1.1 km^2 in New York, 20 km^2 in New Hampshire, 8.6 km^2 in Maine, 1050 km^2 in Gaspé, and 2700 km^2 on the Long Range of Newfoundland.

Continuous permafrost is likely only on alpine summits where the mean annual temperature is below -2°C. This is estimated to occur above 1770 m on Mt. Washington, above 1470 m on Mt. Katahdin, above 890 m on Gaspé, above 780 m in the southern portion of the Long Range of Newfoundland, and above 540 m in the northern portion of the Long Range. The area covered by continuous alpine permafrost is estimated at 1.2 km^2 on Mt. Washington, 0.8 km^2 on Mt. Katahdin, 34 km^2 on Gaspé, and 10 km^2 on the Long Range of Newfoundland. This proposed permafrost distribution will be modified as new data on alpine climate and ground temperature become available for the region.

ACKNOWLEDGEMENTS

Appreciation is extended to the Kent State University Research Council and Beck Memorial Fund of the Geography Department for funding winter research at the Mt. Washington Observatory. Assistance from Kenneth Rancourt and the rest of the Observatory staff is gratefully acknowledged. A research grant from the Association of American Geographers supported summer research in Gaspé, Québec, where assistance was provided by the staff of Parc de la Gaspésie. The College of Arts and Sciences at Kent State University provided partial funding to the Fifth International Conference on Permafrost. Assistance with field work on Mont Jacques-Cartier was provided by Jeanne Schmidlin. Paul and Sherri King provided an instructive and memorable introduction to Mt. Katahdin.

REFERENCES

Achuff, P.L. and G.M. Coen (1980). Subalpine cryosolic soils in Banff and Jasper National Parks.
Canadian Journal of Soil Science (60), 579-581.

Antevs, E. (1932).
Alpine Zone of Mt. Washington Range, 118 pp. Merrill and Webber Company, Auburn, Maine.

Ballard, T.M. (1972). Subalpine soil temperature regimes in southwestern British Columbia.
Arctic and Alpine Research (4), 139-146.

Barry, R.G. (1973). A climatological transect of the east slope of the Front Range, Colorado.
Arctic and Alpine Research (5), 89-110.

Bent, A.E. (1942). The well.
Mt. Washington Observatory News Bulletin (10), 8-9.

Bliss, L.C. (1963).
Alpine Zone of the Presidential Range, 68 pp. L.C. Bliss, Edmonton, Alberta.

Brown, R.J.E. (1969).
Factors affecting discontinuous permafrost in Canada. In The Periglacial Environment: Past and Present, T.L. Péwé, ed., p. 11-53, Queen's University Press, Montreal, Québec

Fujii, Y. and K. Higuchi (1978).
Distribution of alpine permafrost in the northern hemisphere and its relation to air temperature. Proceedings of the Third International Conference on Permafrost, 367-371, National Research Council of Canada, Ottawa, Canada.

Goldthwait, R.P. (1976). Past climate on "The Hill"; Part 2, Permafrost fluctuations.
Mt. Washington Observatory News Bulletin (17), 38-41.

Goodrich, L.E. (1982). The influence of snow cover on ground thermal regime.
Canadian Geotechnical Journal (19), 421-432.

Gorbunov, A.P. (1978). Permafrost investigations in high-mountain regions.
Arctic and Alpine Research (10), 283-294.

Gray, J.T. and R.J.E. Brown (1979). Permafrost existence and distribution in the Chic-Chocs Mountains, Gaspésie, Québec.
Geographie physique et Quaternaire (33), 299-316.

Green, F.H.W. and R.J. Harding (1980). Altitudinal gradients of soil temperatures in Europe.
Transactions of the Institute of British Geographers (5), 243-254.

Hare, F.K. (1952). The climate of the island of Newfoundland: A geographical analysis.
Geographical Bulletin (2), 36-88.

Harries, H. (1965).
Soils and Vegetation in the Alpine and the Subalpine Belt of the Presidential Range, 116 pp., Ph.D. thesis, Rutgers - The State University, New Brunswick, New Jersey.

Harris, S.A. and R.J.E. Brown (1978)
Plateau Mountain: A case study of alpine permafrost in the Canadian Rocky Mountains. Proceedings of the Third International Conference on Permafrost, 386-391, National Research Council of Canada, Ottawa, Ontario.

Harris, S.A. (1986). Permafrost distribution, zonation and stability along the eastern ranges of the cordillera of North America.
Arctic (39), 29-38.

Howe, J. (1971). Temperature readings in test bore holes.
Mt. Washington Observatory News Bulletin (12), 37-40.

Ives, J.D. and B.D. Fahey (1971). Permafrost occurrence in the Front Range, Colorado Rocky Mountains, U.S.A.
Journal of Glaciology (10), 105-111.

Ives, J.D. (1974). Permafrost. In Arctic and Alpine Environments, edited by J.D. Ives and R. G. Barry, 999 pp. Methuen, London.

King, L. (1986). Zonation and ecology of high mountain permafrost in Scandanavia.
Geografiska Annaler (68A), 131-139.

Leffler, R.J. (1981). Estimating average temperatures on Appalachian summits.
Journal of Applied Meteorology (20), 637-642.

Merry, C.J. (1985). Personal communication, U.S. Army Corps of Engineers, Cold Regions Research Lab, Hanover, New Hampshire.

Moyer, M. (1978). Design for the unknown.
Mt. Washington Observatory News Bulletin (19), 66-68.

Nelson, F.E. and S.I. Outcault (1987). A computational method for prediction and regionalization of permafrost.
Arctic and Alpine Research (19), 279-288.

NOAA (1983).
Local Climatological Data - Mt. Washington Observatory, Gorham, New Hampshire, Annual Summary with Comparative Data -1983, 4 pp., NOAA, National Climatic Data Center, Asheville, North Carolina.

NRC, Ad hoc study group on permafrost and committee on polar research, National Research Council (1975). Priorities for basic research on permafrost.
Quaternary Research (5), 125-150.

Péwé, T.L. (1983). Alpine permafrost in the contiguous United States: A review.
Arctic and Alpine Research (15), 145-156.

Price, L.W. (1971). Vegetation, microtopography, and depth of active layer on different exposures in subarctic alpine tundra.
Ecology (52), 638-647.

Schmidlin, T.W. (1982). Leffler's method of estimating average temperatures of Appalachian summits: Evaluation in New York.
Journal of Applied Meteorology (21), 745-747.

Thompson, W.F. (1961a). The shape of New England mountains: Part II.
Appalachia (33), 316-335.

Thompson, W.F. (1961b). The shape of New England mountains: Part III.
Appalachia (33), 458-478.

Witty, J.E. (1968).
Classification and distribution of soils on Whiteface Mountain, Essex County, New York, 155 pp., Ph.D. Thesis, Cornell University, Ithaca, New York.

Zoltai, S.C. and C. Tarnocai (1971).
Properties of a wooded palsa in northern Manitoba.
Arctic and Alpine Research (3), 115-129.

SEASONAL FREEZING OF SOILS IN CENTRAL ASIA MOUNTAINS

I.V. Seversky[1] and E.V. Seversky[2]

[1]Institute of Geography, Kazakh SSR Academy of Sciences
[2]Permafrost Institute, Siberian Branch of the U.S.S.R. Academy of Sciences, Yakutsk, U.S.S.R.

As development of mountainous areas is being carried on, it becomes increasingly important to study the seasonal variations of natural processes occurring in mountains, including the regime of freezing and thawing of earth materials.

Since as early as the beginning of the 70s investigations of regular variations of the seasonal freezing in the mountains of the south-eastern part of Kazakhstan have been carried on by researchers from the Permafrost Institute of the Siberian Branch of the U.S.S.R. Academy of Sciences and the Institute of Geography of the Kazakh SSR Academy of Sciences. The main scope of experimental work was done on the northward slope of the Zailiisk Alatau which - as regards its natural and climatic conditions - is typical of the North Tien Shan, on the whole. As far as other mountainous areas of the region (Dzhungar Alatau, Altai, the Pamirs, Gissaro-Alai, and Central and West Tien Shan) are concerned, many years' field investigations have been under way aimed at the study of the characteristic properties of the occurrence of cryogenesis manifestations, in conjunction with mapping and description of cryogenic forms of the terrain, and incidental determinations of the depth of seasonal freezing and thawing of motley sediments, with proper account of the height difference, exposure of the slopes and the character of surface activity. The results obtained allow us to quantify the main features of the area-time variations in seasonal freezing of motley sediments in the mountains of Central Asia and Kazakhstan.

Two zones are identifiable in the structure of geocryological zonal composition of the region, namely one of seasonal freezing and another of perennial freezing. As an example, Fig. 1 illustrates the structure of geocryological zonal composition typical of the North Tien Shan, in comparison with the vertical distribution of the types of slope surfaces. The lower boundary of the permafrost zone which is traceable along the occurrence limit of small (hundreds or a few thousands of square meters) permafrost islands lies at the altitude of 1800 m. Below, as down as 1400 m, a sublayer of seasonally frozen soils (SFS) extends there, with a stable freezing of soils and earth materials as deep as 1 m on the meadow slopes, as deep as 2 m along the edge of wood stand, and as deep as 4 m on the screes. Below 1400 m, as low as a near-mountain plain, there is a sub-

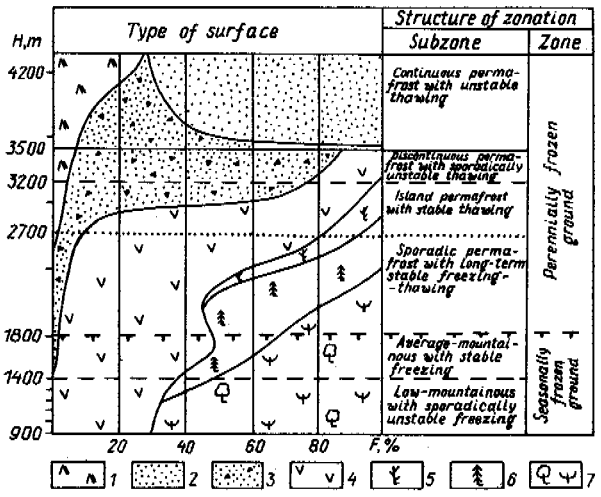

Fig.1 Geocryological Zonation and Types of Surface of Zailiisk Alatau (North Tien Shan). 1 - Rocks; 2 - Glaciers; 3 - Screes; 4 - Meadows and Steppes; 5 - Juniper Shrubs; 6 - Spruce Forest; and 7 - Deciduous Forests and Shrubs.

layer of unstable, shallowly occurring seasonal freezing notable for the smallest depth of freezing (normally less than 50 cm on the meadow slopes) as well as for the unstable character of soil freezing on the southward slopes.

A very common typical feature is the increase in depth of seasonal freezing of soils and of the degree of their ice cementation with an increase in absolute altitude. Under the North Tien Shan conditions and with a usual snow-meteorological regime, the depth of seasonal freezing of soils on the turf-covered meadow slopes as high as 2600 to 2700 m increases linearly with a mean vertical gradient of about 6 cm/100 m (Fig. 2). A stable snow cover here overlies a comparatively warm soil. The substantially greater snow accumulation, combined with a negligible wind redistribution of snow and the evolution of the snow thickness according to the type of loosening (Seversky and Blagoveshchensky, 1983) are responsible for the persistence of high heat insulation properties of the snow cover. As a result, on snow-covered meadow

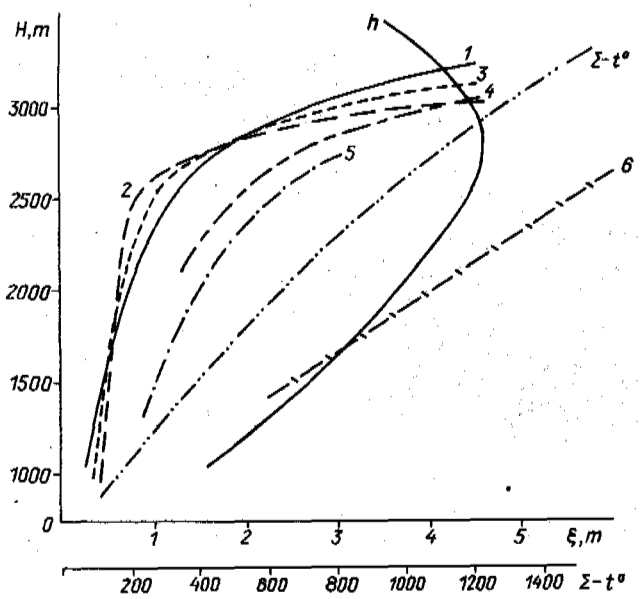

Fig.2 Snow Cover Height (h), Sums of Subzero Air Temperatures (Σ - t°) and Depth of Seasonal Thawing of Soils (ξ) as a Function of Absolute Altitude (H) and Terrain Conditions on the Northward Slope of Zailiisk Alatau.
1 - Meadow-Steppes on Southward Slopes;
2 - Meadows on Northward Slopes;
3 - Meadows on East- and Westward Slopes;
4 - Juniper Shrubs;
5 - Areas below Crowns of a Spruce Forest;
6 - Exposed Large-Sized Debris Sediments.

slopes as high as the altitudes of 2500 to 2600 m, the depth of freezing of soils generally is small (30 - 100 cm) and the soils are able to thaw out during warm, snow-abundant winters by the end of a cold period.

Above 2700 m the above-mentioned vertical gradient increases abruptly (more than twice) (Fig. 2), with an attendat, substantial increase of the degree of ice cementation of frozen ground. Such changes are attributable, first, to the fact that, as the high-altitude zone is approached, the mechanical composition of motley sediments sharply increases in its content of coarse components (Fig. 1) and there is, therefore,an increase of the degree of their autumn-wintertime cooling. Moreover, due to the decrease of the condensation level in winter, high altitudes - as late as the spring activation of the cyclones - experience a substantially smaller amount of downfall as compared with mid-altitudes; at the same time, there is a sharp increase in activity of the wind-induced redistribution of snow, which gives rise to an increase in spatial inhomogeneity of the snow cover and its evolution according to the type of solidification, with an appropriate decrease in the heat insulation properties of the snow. Taken together this results in an abrupt increase of vertical gradients of the depth of seasonal freezing of soils at high altitudes, with a simultaneous increase of the degree of ice cementation of frozen soils.

The differences in the degree of grouting of seasonally frozen soils are so significant that the structure of the high-altitude geocryological zonation in the Central Asia and Kazakhstan mountains clearly shows a sublayer of deep, intense seasonal freezing, with permafrost islands occurring there (Fig. 1). Depending on the orientation of the slopes, the mechanical composition of motley cover formations, and on the character of the vegetation, the depth of seasonal freezing here varies from 0.1-1.5 m to 3-4 m and merges within coarse-debris layers together with the permafrost roof. The degree of grouting of frozen soils here is so high that they persist in a frozen, water-impermeable state as late as the thawing-away of the seasonal snow cover, thus giving rise to the formation of water-snow flows and springtime flash floods closely associated with the temperature regime and the well-defined diurnal run-off corresponding to the variations of air temperature and cloudiness (Sosedov, 1967, and others). Determining the boundary above which soils during an intensive snow thawing remain in the frozen, water-impermeable state, has important practical implications, in particular when scientific and applied problems of hydrology and glaciology are being addressed.

The overwhelming majority of mountain basins lacks observational data, in order to determine this boundary. Nevertheless, it has become possible to do this on the basis of conjugate analysis of a run-off hydrograph for mountainous rivers and curves for the distribution of failure periods of a stable snow cover as a function of absolute altitude (I.V.Seversky and E.V.Seversky, 1986) - the abrupt increase in water flow of the rivers at the beginning of the springtime flash flood and the appearance of typical contrasts on the diurnal run-off hydrograph coincide in time with the onset of an intensive snow thawing in the part of the basin where the soils are water-impermeable as a result of a deep, intensive freezing and, therefore, most of melt snow water and atmospheric precipitation of that period run off over a frozen surface and enters into the mouth network with minimum regulation. Appropriate determinations were made for typical river basins of Central Asia and Kazakhstan. The results obtained formed the basis for constructing a schematic map for the area distribution of deep seasonal freezing of soils (Fig. 3).

According to these results, areas of deep seasonal freezing most commonly occur on the Pamirs and Central Tien Shan. The altitude position of the lower boundary of the subzone of deep seasonal freezing clearly shows the differences in snow content for different areas - with other conditions being equal (geographic latitude, relative constancy of the geological substrate), in regions with smaller amounts of snow this boundary lies at a lower hypsometric level.

The foregoing features of the vertical distribution of the depth and degree of seasonal freezing of soils characterize the main regular variation of the spatial distribution of SFS in the mountains of Central Asia and Kazakhstan, as is the case with other intracontinental moun-

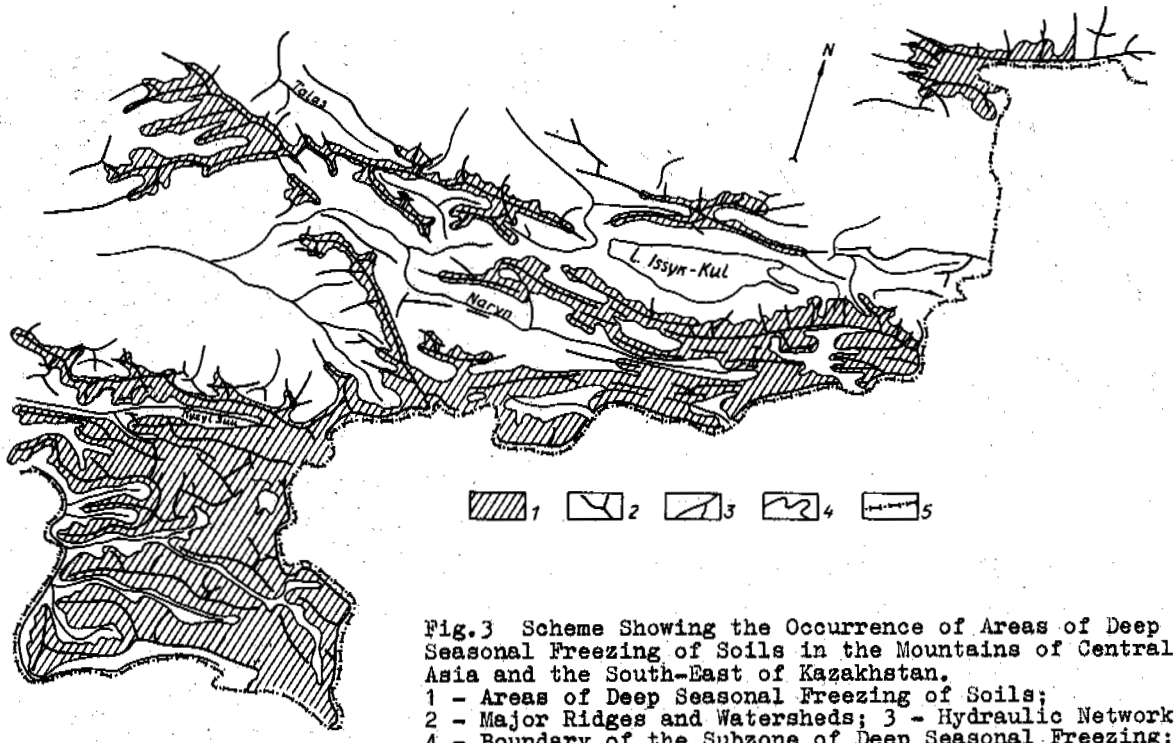

Fig.3 Scheme Showing the Occurrence of Areas of Deep Seasonal Freezing of Soils in the Mountains of Central Asia and the South-East of Kazakhstan.
1 - Areas of Deep Seasonal Freezing of Soils;
2 - Major Ridges and Watersheds; 3 - Hydraulic Network;
4 - Boundary of the Subzone of Deep Seasonal Freezing;
5 - Frontier of the U.S.S.R.

tanous regions of Eurasia. In each particular region this regularity is overlapped by the influence of regional and zonal factors. The most significant of them are the orientation of macroslopes of the ridges with respect to the winter-dominating direction of atmospheric moisture transport and the region's position with respect to the periphery of a mountainous country. The factors are both manifested in (typical of mountains) contrasts of snow abundance which ultimately determine the inter-regional differences in the depth of seasonal freezing.

A most common feature of the area variations in snow abundance is the increase of total snow accumulation in going from intra-mountainous regions to the periphery. On the periphery of mountainous regions, however, maximum snow abundance is characteristic for river basins situated on macro-slopes of weatward and southwestward exposure, namely the southward slope of the Gissarsky ridge, the basins of the Pskem, Akhangaran and Boldybrek rivers (West Tien Shan), Mailisu, Kugart and Yassy (Fergansky ridge), Chizhe, Kora and Koksu (Dzhungar Alatau) and Uba and Ul'ba (Altai). As a result of the increased snow abundance, the soils here freeze to a smaller depth and generally get unfrozen reaching the water-permeable state before the beginning of the springtime snow thawing. Macro-slopes of northward ridges on the periphery of mountainous countries, however, present a significantly smaller amount of snow as compared with the above-mentioned regions on the western periphery of the mountains, though they differ from intra-mountainous regions by a substantially larger snow accumulation. The smallest amounts of snow are encountered in intra-mountainous areas (Central Tien Shan and the Eastern Pamirs) as well as basins of rivers on macro-slopes of peripheral ridges of eastward exposure (Rgaity in Dzhungar Alatau, and Chilik, Khasan and Sumbe in the North Tien Shan Mountains). It is these regions which are notable for the maximum depth of seasonal freezing and for the largest diversity of cryogenesis (Gorbunov, 1974; 1978; Gorbunov and Seversky, 1979).

The foregoing main regular features of the spatial distribution of the depth and degree of seasonal freezing in the mountains in each particular basin are complicated by the well-defined contrasts caused by the influence of local factors, the main of which are the exposure of the slopes, the composition and water-physical properties of soils, the character of the vegetation and the associated differences in altitude and thermal properties of the snow cover.

With other conditions being equal, the coarser the mechanical composition of motley formations, the deeper and stronger cooling they are subjected to. Thus, in the mid-altitude zone of Zailiisk Alatau on snow-covered meadow slopes with a well-developed soil cover, the maximum depth of seasonal penetration of the zero isotherm does normally not exceed 1.0 m. Even within the turf horizon a relatively high temperature (from -1 to -3°) is maintained through-

out the entire winter period, while abrupt, interdiurnal air temperature fluctuations, in the absence of snow cover, have effect on the thermal regime of the upper layer of soil only (40 to 50 cm). Under the same conditions within large-sized debris scree and collapse layers, interdiurnal air temperature fluctuations penetrate as deep as 2.0 m. Due to low heat capacity of crushed-stone sediments, the surface temperature of a scree, even below a snow cover as thick as 20 to 30 cm, is able to drop as low as minus 15 to 20° and, throughout the winter, remains several times as low as compared with the temperature on a turf-covered slope. As a result of this, the depth of freezing of coarse-debris layers here reaches 5 m or more, while above 1800 m these sediments produce short-term permafrost and permafrost islands.

Exposure contrasts of snow abundance depend on the total snow accumulated, and on the average for the mountains of Central Asia and Kazakhstan are characterized by relationships presented in Table I.

The vegetation has its effect on the regime and distribution of the snow cover in (typical of mountains) sharp contrasts of the depth of frozen soils on slopes with a different character of the vegetation. According to results of many years of special-purpose investigations in the North Tien Shan Mountains, the influence of the kind of vegetation upon the distribution of accumulated snow is characterized by relationships presented in Table 2.

Such a nonuniform distribution of snow cover results in sharp contrasts of the depth and degree of freezing of soils on the slopes with a different character of the vegetation (Fig. 2, Table 3).

As is apparent in Fig. 2, with a general increase with altitude of the depth of freezing, the intensity of this process is substantially different on the slopes with a different character of the vegetation and is a maximum within coarse-debris layers of scree and collapse sediments.

TABLE I

Coordinates of the Dependences of the Exposure Coefficient of Snow Abundance (K) on the Amount of Water Accumulated in the Snow Cover on Northward Slopes (W_c)

Orientation of slopes	Value of K for snow accumulation (W_c, mm)							
	100	200	300	400	500	550	600	650
Southward	0.10	0.26	0.43	0.60	0.75	0.92	0.90	0.98
East- and westward	0.55	0.63	0.71	0.80	0.87	0.91	0.95	0.99

According to these results (Table I), with an increase in snow abundance, the above-mentioned contrasts get rapidly smoothed out and when $W_c \geq$ 600 to 650 mm the influence of the orientation becomes smaller than the errors in measuring the snow accumulated.

It is the differences in snow abundance which determine the exposure contrasts of the depth and degree of seasonal freezing of soils. Under the conditions of the medium-altitude zone of North Tien Shan, with a small difference in the height of the snow cover, the differences in the depth and degree of freezing of soils on the meadow slopes and soils similar in steepness and mechanical composition but diametrically opposite in orientation, are not significant.

Under normal conditions, however, the height and the duration of persistence of the snow cover on northward slopes are significantly larger as compared with southward slopes (Table I); the temperature regime of their soils and the depth of freezing are substantially different.

Let us summarize the foregoing discussion.

While reflecting the (typical of mountains) altitude-exposure zonation of natural factors, the depth and degree of seasonal freezing of soils in the mountains of Central Asia and Kazakhstan undergo regular variations over the area. A gradual increase in the depth of freezing, with an increase of the absolute altitude under conditions of a medium-altitude zone, is replaced by an abrupt increase in the intensity of the process as well as the degree of grouting of frozen soils with ice as the high-altitude zone is approached. The structure of geocryological altitude zonation clearly shows a subzone of deep seasonal freezing in which the soils are water-impermeable as late as the thawing-away of the seasonal cover as a consequence of strong ice grouting. This predetermines the formation of destructive water-and-snow flows as well as high floods in spring, with abrupt differences during 24 hours.

The altitude zonation of the depth and character of seasonal freezing is everywhere complicated by effects of regional, zonal and local

TABLE 2

Coordinates of the Dependence of the Coefficient of Snow Abundance K_p on the Amount of Water Accumulated in the Snow Cover on a Meadow Slope (W, mm)

Closeness of crowns	Water abundance of snow cover (W, mm)									
	50	100	150	200	250	300	350	400	450	500
					Coniferous forest					
0.2-0.4	0.16	0.33	0.45	0.53	0.60	0.65	0.70	0.75		
0.4-0.6	0.07	0.20	0.27	0.35	0.40	0.45	0.48	0.53	0.57	0.59
0.6-0.8	0.00	0.08	0.15	0.20	0.24	0.27	0.31	0.34	0.36	0.40
					Deciduous forest					
0.2-0.4	0.10	0.52	0.77	0.93	1.00	1.00	1.00	1.00	1,00	1.00
0.4-0.6	0.00	0.38	0.51	0.67	0.78	0.88	0.98	1.00	1.00	1.00
0.6-0.8	0.00	0.18	0.37	0.51	0.61	0.70	0.77	0.83	0.90	0.96
					Brushwood					
0.2-0.4	0.55	0.78	0.92	1.00	1.00	1.00	1.00	1.00	1.00	1.00
0.4-0.6	0.28	0.50	0.63	0.69	0.78	0.85	0.90	0.95	0.98	1.00
0.6-0.8	0.12	0.26	0.37	0.43	0.50	0.54	0.60	0.63	0.67	0.72

Note: K_p represents the ratio of the water accumulated in the snow cover on a slope with a given type of vegetation to that in the snow cover on a meadow slope, with the absolute altitude and slopes' exposure being the same.

TABLE 3

Characteristics of Seasonal Freezing of Soils on Slopes with a Different Character of the Vegetation (as Deduced from Observations of the Slopes Slose in Orientation and Absolute Altitude in the B. Almatinka River Basin in 1974-1975)

Type of vegetation	Closeness of crowns	Mean intensity of freezing, cm/day	Depth of penetration of the zero isotherm	Length of frost period, days	Number of days with frozen ground after thawing of soil on a meadow slope
Subalpine meadow		0.9-0.8	110	190	
High-fullness coniferous forest	1.0	1.8-1.9	300	220	45
Archevniks	1.0	1.5-1.6	240	240	60

factors, whose influence upon the processes considered is, ultimately, manifested through contrasts in the amounts of snow accumulated. These amounts are determined largely by the orientation of macro-slopes, the position of a region with respect to the periphery of a mountainous country, exposure of the slopes, and by the type of vegetation. The coefficients of snow abundance determined here permit these differences to be taken into account with high confidence.

The foregoing territorial differentiation of snow abundance, in conjunction with the (typical of mountains) contrast of the thickness and mechanical composition of soils, fragmentary distribution of the types of vegetation and terrains, on the whole, are responsible for the extremely nonuniform character of the depth and degree of seasonal freezing of motley cover formations.

The relationships determined here have been used to estimate the territorial differentiation of the degree and depth of seasonal freezing in areas not studied previously as well as for compiling geocryological maps of different scales and purposes.

REFERENCES

Gorbunov, A.P. (1974). Poyas vechnoi merzloty Tyan'-Shanya. Avtoref.dissert. doktora geograf. nauk, 33 p., Moscow.

Gorbunov, A.P. (1978). Kriogennye yavleniya Pamiro-Altaya. - V kn.: Kriogennye yavleniya vysokogoriy, 5-25, Novosibirsk.

Gorbunov, A.P. and Seversky, E.V. (1979). Geokriologicheskaya vysotnaya poyasnost' Severnogo Tyan'-Shanya. - V kn.: Kriogennye yavleniya Kazakhstana i Srednei Azii, 67-83, Yakutsk.

Seversky, I.V. and Blagoveshchensky, V.P. (1983). Otsenka lavinnoi opasnosti gornoi territorii, 218 p., Alma Ata: Nauka.

Seversky, I.V. and Seversky, E.V. (1986). Glubokoe sezonnoe promerzanie pochvogruntov v gorakh Srednei Azii i Kazakhstana. - V kn.: Voprosy geokriologicheskogo kartirovaniya, 29-38, Yakutsk.

Sosedov, I.S. (1967). Issledovanie balansa snegovoi vlagi na gornykh sklonakh, 197 p., Alma Ata: Nauka.

ALPINE PERMAFROST OCCURRENCE AT MT. TAISETSU, CENTRAL HOKKAIDO, IN NORTHERN JAPAN

Sone, Toshio[1], Takahashi, Nobuyuki[2] and Fukuda, Masami[3]

[1]Graduate School of Environmental Science, Hokkaido University, Sapporo, Japan
[2]Fellowships for Japanese Junior Scientist of JSPS, Environmental Science, Hokkaido University, Sapporo, Japan
[3]Institute of Low Temperature Science, Hokkaido University, Sapporo, Japan

SYNOPSIS Authors report the existence of alpine permafrost at Mt. Taisetsu, central Hokkaido in northern Japan. The locations of permafrost occurrence are flat summits above timber line (1500m above sea level). Continuous monitoring of ground temperature profiles gives the mean annual temperature gradients in soil layers. The extra-polation of temperature gradient to the frozen layers indicates that the permafrost table is located at 550cm depth. Active frost cracks on the ground surface were observed on the flat summits. The increase of the width of frost cracks were recorded as 1cm in one winter. No ice remained in the cracks. The palsas were formed at the area where considerable depth of peat was deposited. Freeze-thaw cycles in active layers resulted in formations of sorted circles and other sorted features on the ground surface.

INTRODUCTION

Many researchers studied the periglacial phenomena on Mt. Taisetsu, the highest peak in Hokkaido northern Japan. Especially occurrence of sorted circles with diameter of 2m or larger were reported at many locations with other sorted features and earth hummocks. Koaze (1965) reported some network patterns on the ground surface of the flat summit area. These patterns are similar in shape and size to the tundra polygon which is generally observed in continuous Permafrost regions with formations of ice-wedges. Suzuki and Fukuda(1968) investigated the sorted circles and noted these periglacial features indicated the existence of permafrost on Mt. Taisetsu. Fukuda and Kinosita(1974) first reported the existence of permafrost at the flat summit area. They found the permafrost by boring test and other geophysical investigations. The annual mean temperature was estimated as -3.2°C at the altitude of 2000m. They also estimated the permafrost table as about 6m deep or more. However, bore hore did not reach the bottom of permafrost layers. Fukuda(1976) reported the cross-sectional structure of cracks with polygonal patterns which previously were reported by Koaze(1965). He suggested that these cracks were fossil ice-wedge or ice-wedge cast.

Previous reports on permafrost on Mt. Taisetsu were mostly descriptive and no continuous observations of temperature profiles of permafrost were attempted because of severe climatic conditions in winter. Present authors have carried out the field investigations intensively even in mid-winter and monitored continuously the air and ground temperatures since 1984. Necessary attempts were made to estimate the climatic conditions of permafrost by means of newly developed devices which was enable to obtain data under severe climatic conditions for a long duration.

LOCATION AND PHYSICAL ENVIRONMENT OF MT. TAISETSU

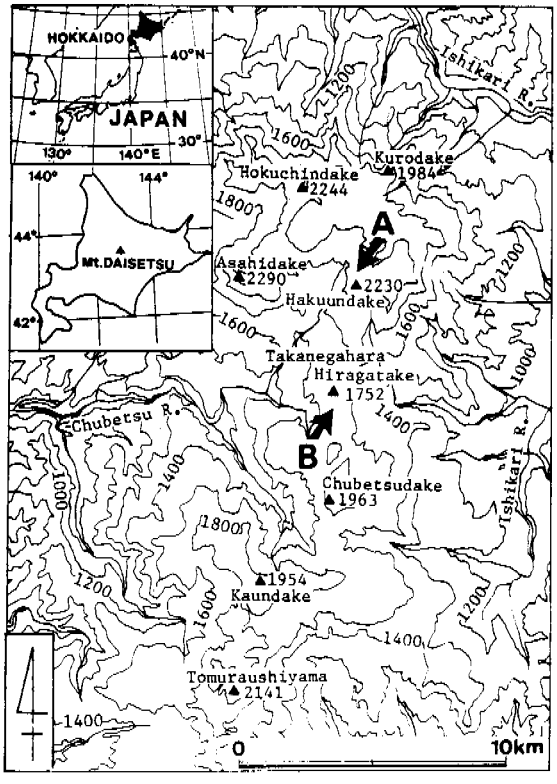

Fig. 1. Location Map of Mt. Taisetsu, Northern Japan

Mt. Taisetsu located in the central part of Hokkaido (Fig.1). Mt. Taisetsu is composed of various volcanos with different geological age of activities. The highest peak is Mt. Asahidake with elevation of 2290m above sea level. The overall shape of composed volcanos is a lava plateau with scattered cones, of which bedrocks are propilite and shale of upper Tertiary deposits. These bedrocks are covered with lava and welded tuff in age of Pleistocene and Holocene. These volcanic flow deposits formed flat table shape of central mountain abatting the bedrocks and the altitude is ranging from 1700 to 2100m. Rivers eroded lava plateau and developed deep valleys and steep cliffs with height of 300m or more. On these steep cliffs, cooling joints of Andesite were well developed. The large scale land slides and rock falls frequently occurred and formed characteristic land forms of telus deposits.

The present timber line is located below 1500m. The most of flat summits are above the timber line and are partially covered with creeping pine and meadow plants. Widely distributed flat summits areas are subjected to severe prevailing winter westerly wind and no vegetations are covered there. Flat summits are mostly snow free during winter wind. Under these physical conditions, various periglacial phenomena are well developed overall on the flat summit areas. The average height of flat summits is about 2000m. The flat summits laying between Mt. Chubetudake (1963m) and Mt. Hakuundake (2230m) have a direction of south to north. A typical crack pattern on the ground surface was reported between Mt. Hakuundake and Mt. Kurodake there lay flat summits and marked as point A in Fig.1. Many palsas are observed in mires on the flat summits (point B in Fig.1).

As no weather station was installed on Mt. Taisetsu, climatic conditions such as mean air temperature and ground temperature were not available. Fukuda(1976) estimated the mean annual air temperature at the elevation of 2000m as -3.2°C by limited number of obtained data during summer and fall based on extrapolation from the nearest weather station. The authors installed newly developed devices for data collection with battery power supply. By these measuring instruments, air temperature data were collected all through year at every

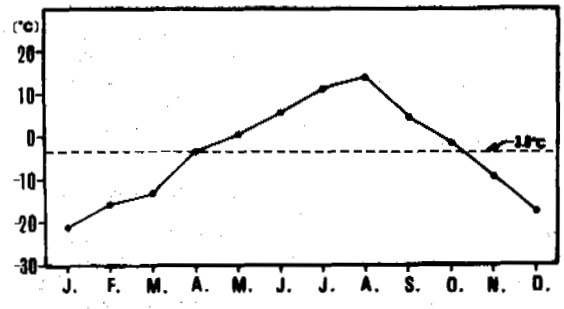

Fig. 2. Measured Mean Monthly Air Temperature at Mt. Taisetsu

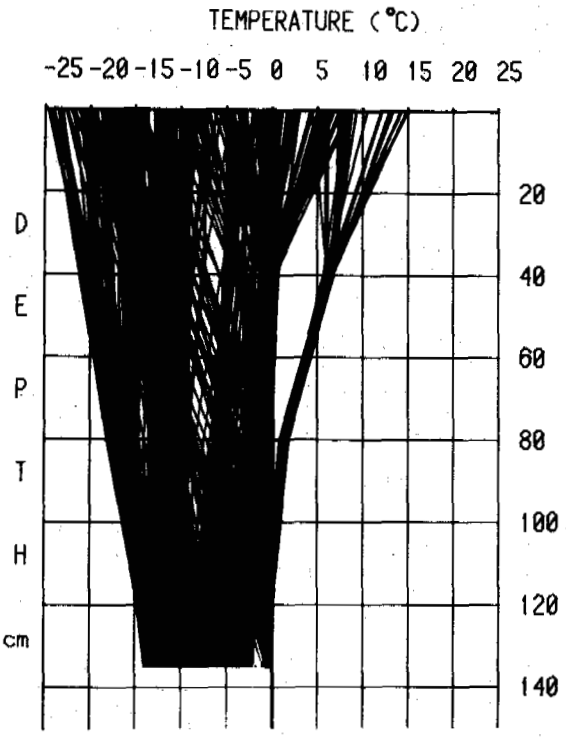

Fig. 3. Ground Temperature Profiles for A Whole Year (Mean daily temperatures of every 5 days plots)

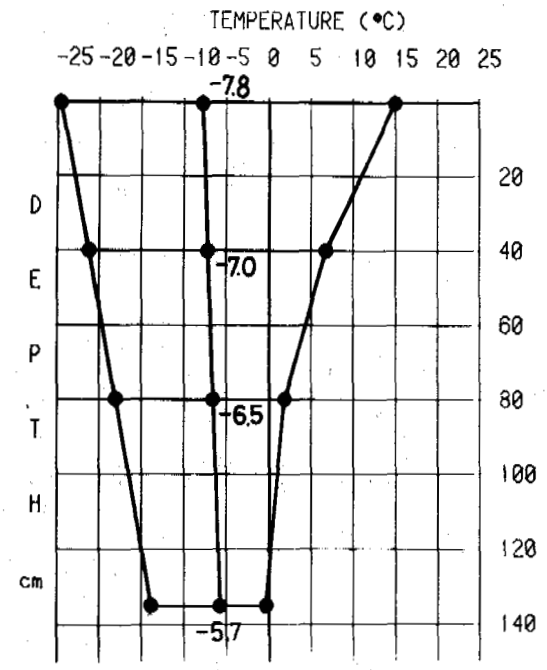

Fig. 4. Mean Annual Temperature Gradient and Temperature at Mt. Taisetsu

one hour interval on 1984 and 1985. Using these data, mean daily air temperatures were obtained (Fig.2). The calculated mean annual air temperature is -3.8°C and slightly lower than previously estimated value.

According to these data, August is the warmest month with mean monthly temperature of +13.9°C and January is the coldest month with mean monthly temperature of -21.3°C. The calculated freezing index is 2588 degree-days and the thawing index is 1191 degree-days. According to Harris(1982), no active ice-wedge might not exist under these climatic conditions. However frost cracks and palsas might be active.

Another important factor for occurrence of permafrost is snow accumulation on the ground surface. In the central part of Hokkaido, the maximum snow accumulation depth in low land is about 90cm deep or more. At higher regions more amount of snow accumulation is expected. According to Yamada(1982), the maximum snow depth at Mt. Asahidake was 200cm at the altitude of 1070m. However at lower than this altitude, snow accumulation became less. Above timber line, the maximum snow depth on the windward slope of Mt. Asahidake is 120cm deep. On the flat summit, the ground surface is subjected to prevailing winter westerly wind and each snow fall is swept away to the leeward side slope. The snow accumulated along the cliffs located under flat summits forming snow cornice. As flat summit area between Mt. Kurodake and Mt. Chuubetudake run from north to south, snow is swept to the leeward east slope which is ansymmetrically steep. Most of snow accumulates along these steep slopes during winter. The accumulated snow develops perennial snow patches at various places on the slopes. As the estimated snow line is above 3000m at this area, no glacier were formed under present climatic condition.

Authors observed no snow accumulation on the flat summit in most of winter season. It means that the ground surface is subjected to a severe cold temperature during in winter and favors to develop permafrost underneath.

GROUND TEMPERATURE PROFILE AND PERMAFROST TABLE ESTIMATION

As previous studies did not investigate the depth of permafrost table, present authors attempted to estimate the depth of permafrost by field observations. Temperature sensors (Pt100Ω) were installed on the flat summit area near Mt. Hakuundake. The location at the elevation of 2020m is indicated as A in Fig.1. No vegetations covered on the ground surface. Before starting measurement at the site, each sensor was calibrated with an accuracy of 0.05°C in the laboratory. Once data were collected at every one hour interval, then these data were stored in battery powered memory IC. At the end of measurement, collected and stored data were transferred into a portable computer. The data logging system was fabricated with special intergrated IC (so called C-MOS IC) so that it is enable to operate under a very low temperature. In cold chamber of the Institute, the performance of the instruments were tested at the temperature of -30°C or below.

Using every one hour read-out data for a whole year long, mean daily temperatures were calculated at each point, then mean daily temperature profiles were obtained. Every 5 day profiles for whole year except 20 days in July were shown in Fig.3. Temperature ranges and mean values at each position were indicated in Fig.4. The annual mean surface temperature stands at -7.8°C. The annual mean ground temperatures are -7.0°C at 40cm deep, -6.5°C at 80cm and -5.7°C at 135cm. Using these values, the annual mean temperature gradient is calculated between two different depth. A gradient ($\alpha 1$) between 40cm and 80cm is calculated as 0.01325°C/cm. Another gradient ($\alpha 2$) between 80 and 135cm is obtained as 0.0143 °C/cm. The permafrost table is estimated by extra-polation of the gradient line down below 135cm, then this gradient line crosses 0°C line at certain depth. This crossing depth of two lines indicates the permafrost table. Applying two gradient values, the permafrost table is estimated as 535cm or 550cm deep. The lower depth of active layer is indicated as 120cm by the far right temperature profile in Fig.3 and Fig.4.

COMPARISON BETWEEN MEASURED AND COMPUTED TEMPERATURE PROFILES

As there is no field station for measuring temperatures of ground and weather conditions, present authors developed the computer simulation method in order to estimate time variable temperature profiles based upon available weather data from adjacent meteorological weather station. The algorithm of numerical analysis is developed using the concept of equilibrium surface temperature (Oultcult 1972). The basic equation of energy-transfer climatology is energy conservation low written as follows;

$$R+LE+H+S=0 \quad \text{----------} \quad (1)$$

This equation expresses that the sum of net radiation, evaporation-condensation, heat flux to air and heat flux to soil is zero. Each component of equation is given by obtained data from adjacent weather stations. The main structural elements of the simulation model are follows.

STEP 1) Necessary input data of weather.
Solar radiation, cloud cover and type of cloud which are adopted from weather station of Obihiro 80km away from Mt. Taisetsu. Daily air temperature read-outs are obtained at Mt. Kauundake by present authors. Wind velocity and atmospheric pressure are calculated from data of Obihiro based upon the difference of the altitudes between two points.

STEP 2) Necessary input of ground surface and thermal properties.
Albedo (0.6) and aerodynamic roughness (2mm) are given according to type of sediments and moisture condition of the ground. The sediments at Mt. Taisetsu were collected in advance. Thermal conductivities of sediments in both frozen and unfrozen conditions are obtained by the line heat methods in the laboratory. The results are summarized that two empirical equations of thermal conductivity for frozen and

unfrozen sediments are expressed as the function of water contents.

STEP 3) The iterative solution of energy balance equation.
All data are input and each component of equation (1) is set according to the estimation method. Then iterative solution is completed resulting the sum of values sets zero.

STEP 4) The surface equilibrium temperature as upper boundary condition.
The ground surface temperature is estimated as the result of iterative solution of (1). Then the obtained surface temperature gives as the upper boundary condition of the heat conduction equation with the phase change. A differential equation of heat conduction of the ground is accomplished by the numerical analysis. Lower boundary is assumed that the temperature at the depth of 10m is equal to an annual mean temperature. The solutions are obtained as setting each 2cm interval of ground matrix and 10 minute increments of time for a whole year period.
The results of the simulation are summarized in Fig.5 indicated as time variable temperature profiles. If one compared it with Fig.3, it is rather clear that these two time variable temperature profiles are identical. The present authors pointed out that the simulation method mentioned above has the advantage for the study of permafrost area where no weather station is established. The reasonable agreements of estimated with measurement are accomplished upon the appropriate input data of weather and thermal properties of sediments. The most right temperature profiles in Fig.5 indicates that the active layer may stand at 110cm deep in the ground. This value coinsides with the measured one in Fig.3.

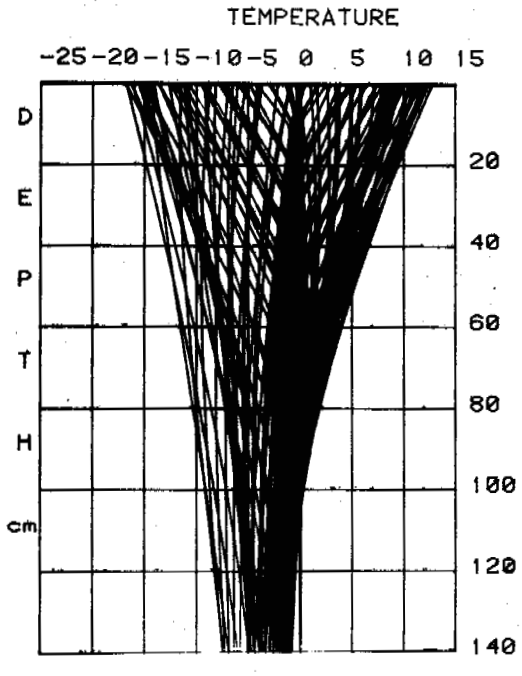

Fig. 5 Estimated Ground Temperature Profiles by Computer Simulation

FROST CRACK FORMATIONS ON THE GROUND SURFACE

One of the characteristic features related with permafrost occurrence in Mt. Taisetsu is frost cracks on the ground and their surface patterns. The area is characterized by a very flat summit running north to south between Mt. Kauundake and Mt. Kokkaidake. The average height of this flat summit is 2100m. On the surface of flat summit area, cracks, of the ground surface were formed. The width of crack gaps is about 1 or 2cm wide, and the depth of cracks is about 40cm deep. The cracks form rectangular patterns. The geomorphological map of that area is shown in Fig.6 with crack patterns and 20cm interval contour lines. The typical rectangular pattern has a size of 10m long each. The edges of cracks were covered with some kind of lichen indicating rather high moisture content of sediment.

The on-the-spot investigations were conducted to monitor the seasonal changes of crack width. The method of observations were previously reported by Mackay(1974) and Fukuda(1981). Occurrences of cracking in ice-wedge were detected by a fine wire stretched between two poles installed across a trough of a polygon, if it was broken off after the lapsed of time. The numbers appeared in Fig.6 indicate the positions of crack width observation. Crossing the crack, two iron structural angles were inserted into the ground with the depth of 85cm. Inserted depth of angle is expected to be enough for the preservation to jacking-up force due to frost heaving acting to the angle. Two angles were set about 20cm apart together in early fall. At six points, 11 pairs of observation angles were installed. The ground surface temperatures were also monitored at the same spots using thermistor sensors.

In mid winter (on 18th of February in 1984), the authors visited the observation points, and measured the distances between a pair of iron angles. The surface of the ground was covered with crusted hard snow packs of a few cm thickness. The cracks were formed on that hard snow packs under which the soil cracks were previously formed. New cracks on snow packs

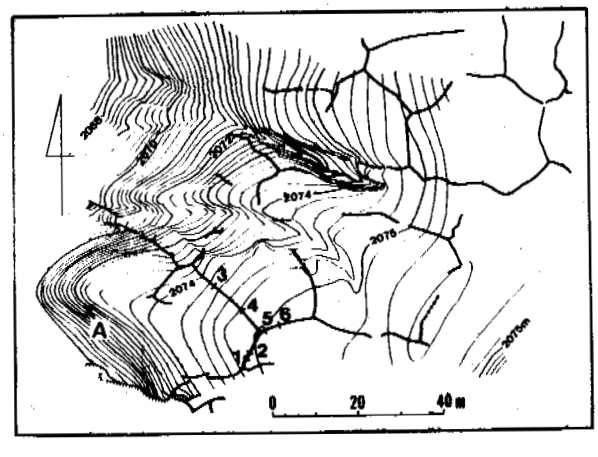

Fig. 6 Detail Geomorphologic Map and Pattern of Soil-Wedge Polygons

covering on the ground surface developed with the width of 1cm. The one of new cracks on snow packs was traced 4m long. By the frequent visits and measurements of crack width, the seasonal changes of crack gaps were obtained.

The results were summarized in Table 1. During fall and succeedingwinter indicated as duration A, all widths of cracks increased with the values ranging from 0.55cm to 2.15cm. The mean value of increased width is 1.14cm. During spring indicated as duration B, all width of cracks decreased with the values ranging from 0.18 to 1.95cm. The mean decreased width is 0.55cm. Fukuda(1981) measured the increase of distances crossing over ice-wedge polygons at Tuktoyaktuk, N.W.T., Canada by the similar method. The mean increased width was 1cm. Similar values were also reported by Mackay (1974). In early spring, authors made cross-sectional observations of cracks, and found no ice filled in the gaps of cracks. The surface sediments consist of coarse grained sand and gravel produced by the weathering of andesite bedrocks. The sediments are, therefore very permeable. Once ice filled in winter melts in spring, melt water easily percolated into sediments. As the bottom depth of cracks is within an active layer, no ice-wedge was formed. These cross-sectional features of cracks indicate that patterns and cracks at that flat summit area might be defined as active soil-wedge polygons (Karte, 1983).

PALSAS FORMATIONS AND CHARACTERISTICS

Palsas are typical features developed in discontinuous permafrost regions (Seppala 1981). In Mt. Taisetsu, the authors found them in the peat bog area on the flat summit area. The general location of the formation of palsas is indicated as point B in Fig.1. The flat summit between Mt. Chubetudake(1963m) and Mt. Hakuun-dake(2230m) has an average altitude ranging from 1710m to 1800m, where peat bogs and small ponds develop. The micro relief of peat bogs is characterized by "kermis hummocks" and "schlenkes hollows".

The formations of the peat bogs on the flat summits are originated by low evaporation in summer due to prevailing esterly wind which causes dense cloud covers over there. In winter prevailing westerly wind sweeps away snow deposits from the ground. The authors surveyed the peat bogs area and found more than 20 palsas there. The shape of palsas varies from round or oval-shaped ones to peat plateau. The size of palsas also varies from elognated plateau with mayjor axis of 50m and the height of 1m to the cone with diameter of a few meters and less than 1m high.

At the end of September, the cross-sectional structure of palsas was examined by boring core sampling. The results are summarized in Fig.7 as the cross-section of the palsas. The uppermost layer is consisted of peat with the thickness of 40cm to 90cm. Lower layer of peat is sandy gravel and gradually changes to silty sand layer. The central part of palsas forms frozen core with ice-rich silty layer. The ice-lenses indicate that the silt layer in the frozen core was very frost susceptible. The depth of the boundary of the upper peat layer and frozen core is about 60cm deep from the surface. As already mentioned before, the active layer in these area is 120cm thick. Thus the maximum depth of thaw layer in palsas is less than half of active layer with gravel and sand sediments adjacent to peat bogs. This difference of active layer thickness is mainly due to low thermal conductivity of peat layer. The lowest boundary of frozen core was not enable to determine in this study.

The air-photos covering the area where authors studied palsas were taken for a couple times on different dates. If one examines and compares with these different air photos, the time series changes palsa forms are detectable. Careful examinations by the authors imply that the

Duration		A	B
Site	1	+0.95cm	-0.18cm
		+0.80cm	-0.30cm
	2	+0.97cm	-0.20cm
	3	+2.15cm	-1.95cm
		+1.42cm	-1.28cm
	4	+0.55cm	-0.30cm
		+0.62cm	-0.22cm
	5	+1.08cm	-0.18cm
		+1.17cm	-0.31cm
	6	+1.05cm	-
		+1.77cm	-
Mean		+1.14cm	-0.55cm
S.D.		0.46	0.59

A : Sep.21,1984～Feb.18,1985
B : Feb.18,1985～Apr.12,1985

Table. 1 Changes of Distances Between Two Iron Angles Crossing Active Cracks on Frozen Ground Surface

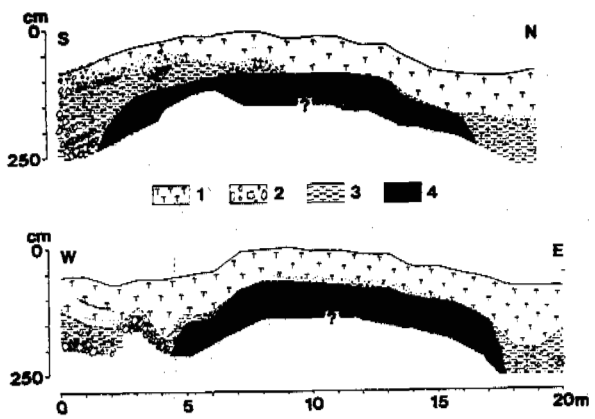

Fig. 7 Cross-Sectional Structure of Palsas (a:peat 2:gravel and sand 3:silty sediment 4:frozen core)

palsas are very active in these 30 years and thermokarst depressions are expanding. The analysis is under way and will be expected to obtain more detail tendency of palsas formations.

CONCLUSIONS

The present authors conducted the intensive field studies on permafrost occurrence in Mt. Taisetsu where the typical alpine permafrost distributes under the present climatic condition. Permafrost associates with the characteristic features such as soil wedge polygons and palsas. The physical environments for the occurrence of alpine permafrost are discussed based upon the climatic data such as temperature in both air and ground, snow accumulation and so on. The key for success of the collection of data is newly developed devices which are enable to obtain continuous data for long duration even under severe cold weather. These devices were installed at various locations in Mt. Taisetsu. Thus present authors made the first report of the occurrence of alpine permafrost in northern Japan with quantitative data. The alpine permafrost in Mt. Taisetsu is termed as discontinuous according its distribution and is characterized as followings:

(1) The permafrost distributes on the flat summit area above timber line with the altitude ranging from 1800m to 2100m.

(2) The mean annual air temperature stands -3.8°C and no snow accumulates on the ground surface due to prevailing westerly wind in winter season.

(3) The permafrost table is estimated as 550cm deep and an active layer has a thickness of 120cm.

(4) The related morphological features of discontinuous permafrost were examined such as soil-wedge polygons on the flat summits and palsas in the peat bogs area.

(5) The active cracking of the ground surface in winter was observed. The frozen ground crack opens due to the thermal contraction under the present severe winter environment. Patterns of cracking are similar to tundra-polygons in shape and size. No ice was filled the cracks.

(6) Cross-sectional structure of palsas indicates that palsas have distinct frozen cores with ice-rich silty layers. The uppermost palsas are mantled by peat layers with considerable thickness. The comparison of the successive air photos taken in different years for these 30 years implies the palsas are active in present condition.

REFERENCES

Fukuda, M. and Kinosita, S. (1974) Permafrost at Mt. Taisetsu, Hokkaido and its climatic environment. The Quaternary Research, 12, 192-202. (in Japanese with English summary)

Fukuda, M. (1976) Some observation about the fossil ice-wedge polygons at Mt. Taisetsu. Low Temperature Science, 34, 257-260. (in Japanese)

Fukuda, M. (1981) Field observation of ice-wedge cracking in the permafrost area near Tuktoyaktuk, N.W.T., Canada. Reports of Joint Studies on Physical and Biological Environments in the Permafrost, North Canada, Institute of Low Temperature Science, 45-60. Sapporo.

Harris, S.A. (1981) Identification of permafrost zones using selected permafrost landforms. Proc. Fourth Canadian Permafrost Conference, 49-58.

Karte, J. (1983) Periglacial phenomena and their significance as climatic and edaphic indicators. GeoJournal, 7, 329-340.

Koaze, T. (1965) Patterned grounds in Mt. Taisetsu. Geographycal Review of Japan, 38, 179-199. (in Japanese with English summary)

Mackay, J.R. (1974) Ice-wedge cracks, Garry Island, Northwest Territories. Canadian Jour. Earth Sci., 11, 1366-1383.

Oulcult, S.A. (1972) The development and application of a simple digital surface-climate simulator. Jour. Applied Meteorology, 11, 629-636.

Sappäla, M. (1981) An experimental study of the formation of palsas. Proc. Fourth Canadian Permafrost Conference, 36-42.

Suzuki, I. and Fukuda, M. (1968) A preliminary study of patterned ground on some mountainous regions of central and northern Japan. Geographical Review of Japan, 44, 729-739. (in Japanese with English summary)

Yamada, T. (1982) Studies on accumulation-ablation processes and distribution of snow in mountain regions, Hokkaido. Contributions from Institute of Low Temperature Science, 31, 1-33. Sapporo.

ROCK GLACIERS AND GLACIATION OF THE CENTRAL ASIA MOUNTAINS

S.N.Titkov

Permafrost Institute, Siberian Branch of the U.S.S.R. Academy, Yakutsk, U.S.S.R.

SYNOPSIS In the system of the North Tien Shan ridges, explorations revealed the existence of 871 rock glaciers of a total area of 90.28 sq. km as well as 183 inactive rock glaciers of a total area of 28 675 sq. m. Rock glaciers evolve asynchronously with the development of mountainous glaciation, during dry and cold periods following the glacial retreat. Most advantageous conditions for the existence of rock glaciers are observed in regions where the degree of glaciation leads to suppression of activity of rock glaciers. The origin of the majority of rock glaciers dates back to the Holocene epoch. The age of the ancient active generation is about 3000 years and that of the active generation is 1500 years.

Formation and development of rock glaciers is proceeding in the presence of the overall evolution of the natural environment in alpine areas, including the glaciation evolution. Interaction between glaciers and rock glaciers leads to the formation of a variety of forms, which, in addition to provide discrepant physical data on the internal structure, results in distinctly different interpretations of the genesis of these formations.

Genesis of rock glaciers is treated in terms of the origin of its main components, viz. debris material and ice enclosed beneath its cover. Currently there exist three main ideas of their formation. Advocates of glacial theory contend that rock glaciers are brought about by glacial ice conservation below a moraine cover (Iveronova, 1950; Suslov, 1967; Krasnoslobodtsev, 1971; Gobedzhishvili, 1978; Pillewizer, 1957; Carrara, 1973; Lliboutry, 1977; Griffey and Whalley, 1979) or by burying of glaciers and snowfields by landslides (Ageev and Ditmar, 1964; Benedict, 1973). The permafrost role in this case is merely to preserve the buried ice (Whalley, 1974; 1983).

Another group of investigators regard rock glaciers as purely permafrost formations which are composed of talus material and are grouted by the ice of a non-glacier origin, primarily by flow-infiltration ice (Kozhevnikov et al., 1980; Barsch, 1977; Haeberli, 1985).

The third group considers the two forms described above to be the extreme members of a unified series with transitional formations which reflect certain conditions for precipitation storage (Matveev, 1938; Grosvald, 1959; Gorbunov, 1970; 1978; 1979; Corte, 1976; Madole, 1972; Potter, 1972; White, 1976). This point of view is also shared by the author of the present paper. In the series of glacial-cryogenic formations, including rock glaciers, one of the extreme members is represented by a glacier buried below the crees, and the other extreme member is represented by large-sized materials of landslips and screes grouted by ice. Upon simplifying this scheme, one may distinguish two main types of rock glaciers which differ in the character of feed and location on the terrain: (a) those originating from final moraines and covering the valley beds; and (b) those which are unassociated with glaciation and side with talus slopes. The first type, according to I.S. Krasnoslobodtsev (1971), is called the near-glacier type, and the second one is referred to as the near-slope type. In addition, it is customary to identify rock glaciers of mixed feed which are produced due to sharp bendings of the substrate surface when a rock glacier transforms into a scree and vice versa. These formations have limited occurrence.

In order to determine the overall regularities of the geographical distribution of rock glaciers in regions with different natural and climatic conditions, reveal the complex of natural factors that are responsible for the development of rock glaciers, and to understand the way in which changes in the natural environment influence their state, an inventory of rock glaciers was drawn up, followed by statistical treatment of the results obtained. The results have been used for compiling a schematic map for active rock glaciers in the North Tien Shan (Fig. 1).

The system of the North Tien Shan includes the Zailiisk Alatau and Kyungei-Ala-Too ridges which extend in the sublatitude direction in the form of two giant arches connected in their central, protuberant part by the Chiliko-Keminsky mountainous 'knot'. The mean absolute altitudes in central parts of the ridges exceed 4000 m reaching 4973 m in the Talgarsky massif. In the west- and eastward direction there is a decrease in absolute altitudes, with a stage-like disposition of the levelling surfaces which in some places are as high as 3500 m. The twp ridges show up powerful glaciation, with

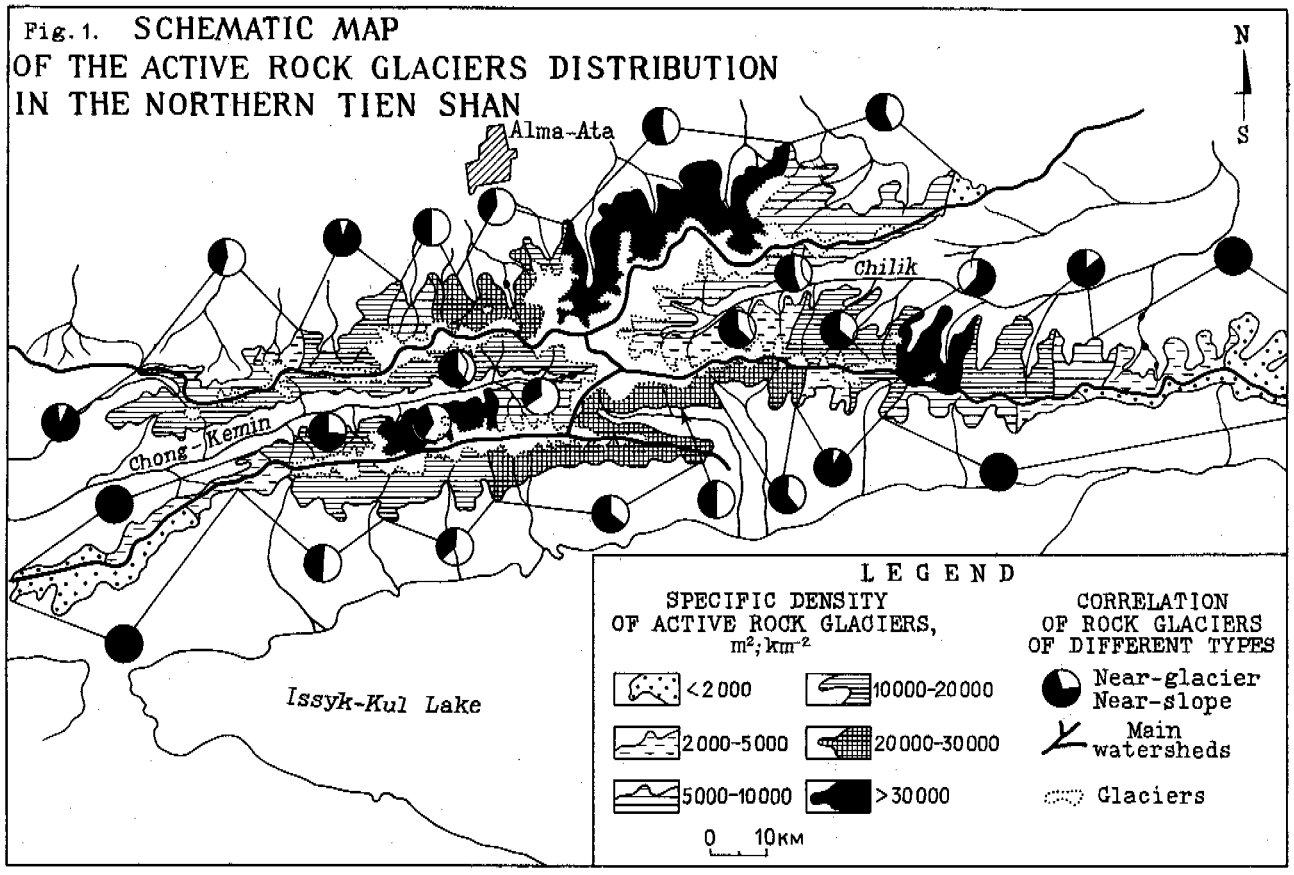

Fig.1 Schematic Map for Active Rock Glaciers in the North Tien Shan

open parts of the glaciers totaling 759 reaching 781.6 sq. km in area (Katalog lednikov SSSR, 1967; 1968; 1969; 1976).

871 rock glaciers totaling 90.28 sq. km in the area were found to exist in the North Tien Shan system (Table 1).

The ratio of the number of near-glacier to near-slope forms is 36.9%:63.1%, and that of their areas is 60.1%:39.9%, respectively. The point here is that near-glacier rock glaciers are far larger in size as compared with near-slope rock glaciers - the area of a mean-sized rock glacier of the first type is 0.171 sq. m, while that of the second one is 0.066 sq. m. In addition to detecting this number of glaciers, 183 inactive rock glaciers totaling 28 675 sq. m in their area were found to exist in the North Tien Shan. On most occasions, these are fragments of old forms partially buried by advancing active rock glaciers; however, large-sized formations are also encountered, indicating the favourable conditions for the formation of rock glaciers that had existed in the early Holocene.

Many years of observations in Zailiisk Alatau have established that the movement of some rock glaciers is pulsating in character, which is associated with accumulation and off-loading of stresses throughout their thickness.

TABLE 1

Active Rock Glaciers of the North Tien Shan (According to this author and A.P.Gurbunov's (1979) data

Ridge	Number		Area, sq. km	
	near-glacier	near-slope	near-glacier	near-slope
Zailiisk Alatau	172	257	32.63	17.14
Kyungei-Ala-Too	149	273	22.194	18.316
TOTAL	321	530	54.824	35.456
TOTAL for North Tien Shan	871		90.28	

Thus, the mean advance velocity of rock glacier Morenny for the period 1973-1977 is 64 cm per year, for 1977-1978 - 52 cm per year, and during 1978-1982 - 78 cm per year. The velocity varies not only from year to year but also undergoes a seasonal variation. For the period from June to September and from

October to May the frontal bench of rock glacier Gorodetskogo advances 51 cm and 18 cm, respectively (or about 65% of the distance covered during one year). These variations are caused by a change in plastic properties of ice inclusions in the layer of annual amplitudes of the permafrost of a rock glacier.

The lowest position of rock glaciers is observed on the northward slopes of the ridges. Thus, on the northward macroslope of Kyungei-Ala-Too the lower limit of occurrence of rock glaciers lies at the absolute altitude of 3300 m (some forms descending as low as 2700 m), and that on the southward macroslope is at 3500 m. A significant influence upon the occurrence of rock glaciers is also exerted by changes of the indices of continentality of climate, viz. the annual amplitudes of air temperatures and the amount of precipitation. Within two basins of the central part of Zailiisk Alatau notable for minimum continentality of climate (the Bolshaya and Malaya Almatinka rivers) the lower terminations of the rock glaciers are located by 200 higher as compared with the ridge, on the average.

In order to establish the quantitative indices of interrelation between rock glaciers and contemporary glaciation, use was made of the criterion for specific density of rock glaciers as introduced by A.P.Gorbunov (1979), i.e., the ratio of the total area of rock glaciers in the individual basin (sq. m) to the area of the basin above the isohypse of the lower limit of occurrence of rock glaciers (sq. km). The specific density of rock glaciers was compared with the degree of glaciation reduced to the same area of the basin. It has been found that the greatest specific density of active rock glaciers, varying from 20 to $40 \times 10^3 m^2 \cdot km^{-2}$ is observed where the degree of glaciation is in the range from 10 to 20%. A decrease of the degree of glaciation means the decrease in absolute altitudes of the ridge or the increase in aridity of climate and, hence, the decrease of the number of active rock glaciers. An increase of the degree of glaciation to 25-30%, as is observable in the region of the Chiliko-Keminsky mountain knot, has also an unfavourable effect on the existence of rock glaciers - they become devoid of sources of talus material and are buried or destroyed by advancing glaciers.

Such typical features are also observed in other mountainous countries of Central Asia. For example, in the Ak-Shiyrak massif (Inner Tien Shan), the greatest specific density of rock glaciers (23.28×10^3 $m^2 \cdot km^{-2}$) is observed in the southern framing where the degree of glaciation is 13%, while in the northern framing of the massif where the degree of glaciation exceeds 50%, no rock glaciers are present (Titkov, 1985).

The greatest contrasts in the distribution of rock glaciers are observed in the Pamirs. The West Pamirs, in the region of ridge Akademii nauk, is notable for a very diversiform terrain, severe climatic conditions and a large ($\sim$ 2000 mm) annual amount of precipitation, which leads to the development of powerful glaciation extending over significant areas of the slopes. Debris materials that formed on open rock slopes, penetrates to the surface of the glaciers which transport them away from the confines of the permafrost zone, as high as 3200-3300 m, where moraine sediments are washed out rapidly by the melt water.

Thus, this region presents unfavourable conditions for the formation of rock glaciers, with only separate rudimentary forms which receive no further development.

The natural conditions described above differ greatly from those provided by the mountainous framing of Lake Karakul - this region is only 120-150 km eastward of the Akademii Nauk Ridge. Here, on a very much elevated plateau, the character of the relief diversity is more reminiscent of mid-lands, with the annual amount of precipitation being about 70 mm. Such exceptional aridity, despite the existence in the Karakul depression of a permafrost at the annual mean air temperature of -3.8°C, prevents the formation of rock glaciers. Optimum conditions for the existence and development of rock glaciers are observed in a narrow transient zone between the abpve-mentioned regions, in ridges Kaindy and Zulumat, on the southward slope of the Zaalaisky ridge. A distinctive feature of the occurrence of rock glaciers in the ridges mentioned above is the absolute predominance of near-glacier forms which occur within the altitude range from 4200 to 3700 m. The large number of near-slope formations is accounted for by the fact that valleys which recently got rid of the glaciers, have not yet accumulated a sufficient amount of debris materials from the slopes so that the only source of feed for active rock glaciers is provided by moraine accumulations.

The development of rock glaciers is intimately coupled to surface and subsurface glaciation of the mountains. For the first time, conditions for the origination and development of rock glaciers in the region under consideration emerged at the end of the Pliocene and periodically recurred during the Pleistocene. However, pre-holoceneous rock glaciers have not persisted till the present, with few exceptions. This is accounted for by periodical advances of glaciers, eroding and seismic phenomena, and the duration of mudflows. One of the few forms of Pleistocene age is encountered on the westward slope of the Sarykolsky ridge in the East Pamirs and has persisted there in the inactive state, owing to the exceptional aridity of climate which suppresses denudation processes.

Because of lack of absolute datings, one has to determine the age of rock glaciers from their spatial correlation with stadial moraines. The present-day active near-glacier rock glaciers had evolved into a regressive stage of glaciation which preceded the so called 'minor glacial epoch' of the XVII-XIX centuries (the Fernau stage according to A.V.Shnitnikov). Then, glaciers started to advance in the wake of rock glaciers and, while having higher advance velocities, began to weigh upon them or overlap them. Most of the active rock glaciers retain traces of such movements in the form of large depressions which remained after the glacier retreat.

A different scheme for the evolution applies to near-slope rock glaciers which had formed at rock slope footings in upper-Pleistocene troughs. In the lower parts of the troughs, these rock glaciers started to form already during the early Holocene, with their activity remaining unchanged throughout that period. In the upper parts of the troughs, Holocenic glaciers, while advancing, introduced recurring disturbances into the development of rock glaciers, thereby deforming or destroying them. And each time the glaciers were retreating, new generations were originating.

Transition of rock glaciers to the inactive state results from the warming of climate, or from their displacing into a lower hypsometric level. This is accompanied by partial or total failure of permafrost, the production of a rigid frame within the rock glacier structure, and by cessation of the advance movement. A loss of activity may also be caused by a decrease of the thickness of the permafrost, which accompanies the 'spreading' of the rock glacier as it exits into broader areas of the valley. This results in the decrease in deformation stresses of the rock glacier so that its movement slows down.

The beginning of the formation of the ancient, currently inactive, generation of rock glaciers dates back to the down-egezen interstadial (about 3000 years ago) when glaciers underwent a significant reduction, with a large number of them having had disappeared. All of the preceding Holocenic regressions were, seemingly, less significant in their sizes as compared with the last two or were equal to the last two, which is evidenced by the absence of older generations of near-glacier rock glaciers.

REFERENCES

Ageev, K.S. and Ditmar, A.V. (1964). Nekotorye osobennosti reliefa vysokogornykh rayonov Koryakskogo nagorya. Uch. zap. NII geologii Arktiki. Regional'naya geologiya, vyp. 4, 137-149, Leningrad.

Barsch, D. (1977). Blockgletscher-Studien, Zusammenfassung und offene Probleme. Abh. Akad. Wiss. Göttingen. Math.-Phys. Kl., H.35, S. 133-150.

Benedict, J.B. (1973). Origin of rock glaciers. J.Glaciol., 12, 66, 520-522.

Carrara, P.E. (1976). Transition from the shear moraines to rock glacier. J. Glaciol., 12, 64, 149.

Corte, A.E. (1976). Rock glacier. Bull. perygl. LTN, Sec. 3, 26, 175-197.

Gobedishvili, R.G. (1978). Kamennye gletchery Gruzii. Soobshch. AN GSSR, t.90, N 1, 93-96.

Gorbunov, A.P. (1970). Merzlotnye yavleniya Tyan'-Shanya. Trudy KazNIGMI, vyp. 39, 265 p., Moscow: Gidrometeoizdat.

Gorbunov, A.P. (1978). Kriogennye yavleniya Pamiro-Altaya. - V kn.: Kriogennye yavleniya vysokogoriy, 5-25, Novosibirsk:Nauka.

Gorbunov, A.P. (1979). Kamennye gletchery Zailiiskogo Alatau. - V kn.: Kriogennye yavleniya Kazakhstana i Srednei Azii, 5-34, Yakutsk: In-t merzlotovedeniya SO AN SSSR.

Griffey, N.J. and Whaley, W.B. (1979). A rock glacier and moraine-ridge complex, Lyngen Peninsula, North Norway. Norsk Geogr. Tiddskr., 33, 3, 117-124.

Grosvald, M.G. (1959). Kamennye gletchery Vostochnogo Sayana.Priroda, 2, 89-91.

Haeberli, W. (1985). Creep of mountain permafrost: internal structure and flow of alpine rock glaciers, 142 p., Zürich.

Iveronova, M.I. (1950). Kamennye gletchery Severnogo Tyan'-Shanya. Tr. In-ta geogr. AN SSSR (Raboty Tyan'-Shan'skoi fiz.-geogr. stantsii, vyp. I), 45, 69-80, Moscow-Leningrad.

Katalog Lednikov SSSR. (1967). 13, 2, 1, 79 p., Leningrad: Gidrometeoizdat.

Katalog lednikov SSSR. (1968). 13, 2, 2, 52 p., Leningrad: Gidrometeoizdat.

Katalog lednikov SSSR. (1969). 14, 2, 4, 59 p., Leningrad: Gidrometeoizdat.

Katalog lednikov SSSR. (1976). 14, 2, 5, 90 p., Leningrad: Gidrometeoizdat.

Kozhevnikov, A.V., Nikitin, M.Yu. and Lyan, R.N. (1980). Kamennye gletchery gornogo Dagestana (Vostochny Kavkaz). Vestnik MGU. Ser.geol., 2, 14-26.

Krasnoslobodtsev, I.S. (1971). O kamennykh gletcherakh Bol'shogo Kavkaza. Vestnik MGU. Ser.geogr., 1, 95-97.

Llibontry, L. (1977). Glaciological problems set by control of dangerous lakes in Cordillera Blanca, Peru. II. Movement of a covered glacier embedded within a rock glacier. J.Glaciol., 18, 79, 255-273.

Madole, R.F. (1972). Neoglacial facies in the Colorado Front Range. Arct.Alp.Res., 4, 2, 119-130.

Matveev, S.N. Kamennye potoki. - V kn.: Problemy fizicheskoi geografii.

Pillewizer, W. (1957). Untersuchungen am Blockströmen der Ötztaler Alpen. Abhandl. Geogr. Inst. Freien Univ. Berlin, 5, 37-50.

Potter, N. (1972). Ice-cored glacier, Galena Creek, Northern Absaroka Mountains, Wyoming. Geol.Soc.Amer.Bull., 83, 10, 3025-3058.

Suslov, V.F. (1966). Kamennye gletchery Kichik-Alaya. - V kn.: Voprosy glyatsiologii Srednei Azii (Tr. SARNIGMI, vyp. 27 (42)), 13-17, Leningrad.

Titkov, S.N. (1985). Kamennye gletchery massiva Ak-Shiyrak. - V kn.: Regional'nye i inzhenernye geokriologicheskie issledovaniya, 80-88, Yakutsk: In-t merzlotovedeniya SO AN SSSR.

Whalley, W.B. (1974). Origin of rock glaciers. J.Glaciol., 13, 68, 323-324.

Whalley, W.B. (1983). Rock glaciers - permafrost features or glacial relics? - In: Permafrost Fourth International Conference Proceedings, National Academy Press, Washington, D.C., 1396-1401.

White, S.E. (1976). Rock glaciers and block fields: review and new data. Quatern.Res., 6, 1, 77-97.

GEOCRYOGENIC GEOMORPHOLOGY, EAST FLANK OF THE ANDES OF MENDOZA, AT 33° S.L.

D. Trombotto

Department of Geography, Heidelberg University, Federal Republic of Germany

SYNOPSIS Micro and meso geocryogenic forms and processes are reported above 4.000 m. The mean annual air temperature is about - 3 °C. Discontinuos mountain permafrost has been determined based on thermal measurements and considerations. Sorted circles up to 6 m diameter, solifluction lobes and steps, boulder fields and detritic slopes, cryoplanation surfaces, thermal contraction cracks and rock glaciers occur. The degree of activity of such forms is analysed. It is observed that most geocryogenic forms are polygenetic and that the effect of rock type on the development of either micro and meso forms is extremely important. Several kilometers of detritic slopes are underlain by ground ice on south facing slopes. Talus production is at present very high, it seems that it was still more important in the past, which is demonstrated by debris filled valleys. One of these is filled with gelifluction debris of two rock types (granite and metamorphites), which are in a remarkable white and black contact at the valley floor.

INTRODUCTION

This is a brief report which precedes my thesis at the University of Heidelberg under the supervision of Prof. Dr. Dietrich Barsch. The topic " Andean Geocryology " was initiated when the autor enjoyed a scholarship granted by the " Consejo Nacional de Investigaciones Científicas y Técnicas " (CONICET = Argentine Investigation Council) and under the supervision of Dr. Arturo Corte (Instituto Argentino de Nivología y Glaciología, Mendoza). Geocryology (periglacial geomorphology) is at present underdeveloped in Argentina, despite the fact, that cryogenic (periglacial) processes are linked with man's present activities in the Andean and Patagonian area. Also in the past, over one third of the country was subject to cryogenic conditions during the Pleistocene.

LOCATION AND CLIMATIC FEATURES OF THE STUDIED AREA

The studied area surrounds an Andean lake, " Lagunita del Plata ", Cordón del Plata, Cordillera Frontal, Mendoza, Argentina (photo nr.1, photo nr.2: aerial photograph: 6904/5 - 112-59, 1: 50.000, IGM, 1963). The studies have been carried out in an altitude between 4.000 m and 4.500 m, the already mentioned lake is situated approximately at 33° S. and 69° E. The research area has been selected, since it revealed many periglacial forms which even can be observed in satellite and aerial photographs (Corte and Trombotto,1982). Thus a clear solifluidal contact between 2 different rock types (greywacke, formation "El Plata" of dark colour and a white granite which represents the "Batolito Compuesto"of "Cuchilla de las Minas") forms a prominent line in every air photograph. This contact is generated by solifluction moving dawn from the valley sides.
There have been no previous studies on this region, except some investigations on Regional Geology, which exclude periglacial geomorphology. At the same time Wayne (1984 a, Wayne et al, 1983) started his work on the Quaternary of the Cordón del Plata applying different methods in order to display his complex and disputable theory on glaciation in the studied area. The same author(1983, 1984 b) presented a report at meetings of the "Grupo Periglacial Argentino (attached to the "Sub-Comisión Latinoamericana sobre la Importancia de los Estudios Periglaciales), which works on periglacial forms as paleoclimatic indicators. There exists no meteorologic record from the research area. Therefore data of nearby **meteorologic** stations have to be extrapolated. Accepting a temperature gradient of 0,6 °C/ 100 m, the mean annual temperature of the "Lagunita del Plata" is estimated at -2° to -3°C.

Photo nr. 1. Lagunita del Plata , further explanation in the text

The precipitation is around 600 mm. Precipitation occurs mainly during winter in solid form, but in summer there are frenquently sleet storms. The belt of maximum precipitation lies at approximately 4.000 m (Minetti, 1986, oral com.) The region belongs therefore to level "B" of Minetti (1984), i.e. permafrost ocurrs. According to empiric models the region has approx. 250 days of temperature below 0 °C. The wind is very strong and owing to the geomorphology it blows in direction NE/SW, which prevents a large quantity of snow from accumulating on the slopes. As far as altitude and vegetation are concerned, the region can be classified into the level "altoandino (Garleff,1977, Ambrosetti et al, 1986).

THE CRYOGENIC PROCESSES OF AN ANDEAN PERIGLACIAL ENVIRONMENT

The geomorphological analysis of the Lagunita del Plata was started with the study of geo-cryogenic processes, which created the peri-glacial forms.
The following cryogenic processes can be registrated in the Lagunita del Plata: 1) Congelifraction (frost shattering or frost splitting), 2) Vertical and/or horizontal sorting, 3) Cryo-turbation, 4) Solifluction, 5) Nivation, 6) Cryoplanation, 7) Creep of permafrost forming embryonal and large rock glaciers. In addition different transports exists (e.g. rock fall, avalanches,etc)

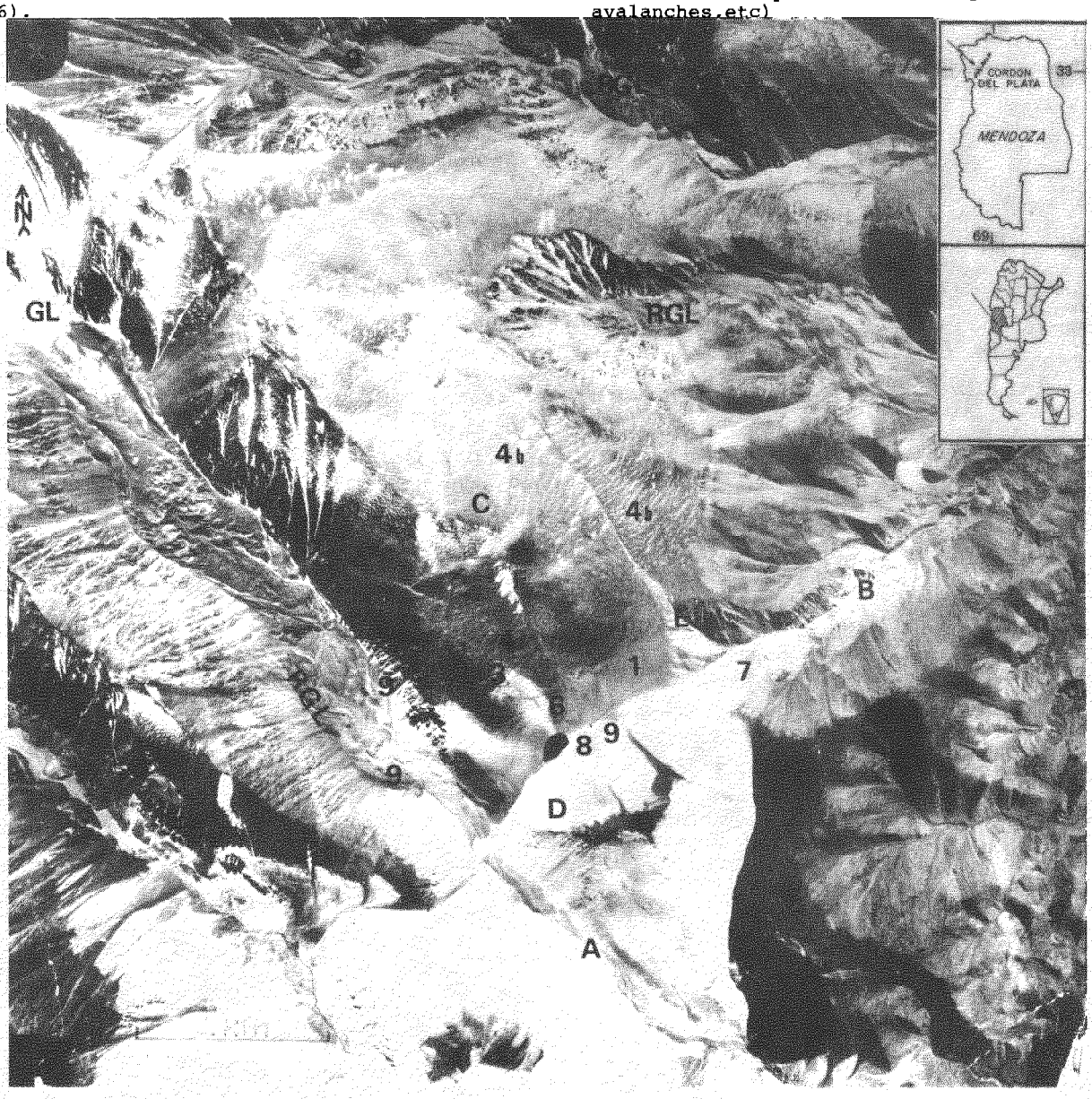

Photo nr. 2: Lagunita del Plata, aerial photograph, IGM,1963, 1: 50.000. Gl: complex of Strelkov Glacier, RGl: Rock Glacier, A: Arroyo Casas, B: Quebrada de las Mulas, C: Formation El Plata, D: Granito, E: Arroyo Criogênico, F: Snow Patch Gran Malvina, G: Sombrero Metamórfico of Cerro El Platita

Frost shattering is an elementary phenomenon in a cryogenic environment, it is essential in the Lagunita del Plata. In the Lagunita del Plata all rock types are subject to heavy frost weathering, though owing to metamorphism the greywacke is more resistant and leaves more relicts or tors.
Vertical sorting is a very active process in this region, it can be observed in cuts of patterned grounds, in lobes or solifluction terraces as well as in detritic slopes.
Cryoturbation is of frequent occurrence on all slopes or on the cryoplanation surfaces.

THE CRYOGENIC FORMS OF LAGUNITA DEL PLATA

The forms that have been registered in Lagunita del Plata and surroundings are the following: 1) Patterned ground: nets, circles, polygons, stripes and steps (generally sorted, terminology according to Washburn, 1979), 2) Mud boils or Tundra craters (extrusion forms, product of cryoturbation, which are linked with the already mentioned forms), 3) Tors, 4) Solifluction lobes and terraces, 5) Nivation hollows and terraces, 6) Detritic slopes and boulder fields, 7) Richter denudation slopes, 8) Cryoplanation surfaces, 9) Embryonal rock glaciers and rock glaciers, 10) Asymmetric valleys.
In photo nr. 2, the number corresponds to the above numbered forms.
There are various sorted forms of patterned ground. It is possible to observe nets with diameters varying between centimeters and 6 m. The Amundsen circles vary between 1,6 m and 4,4 m in diameter, while the most frequent polygons register ca. 20 cm diameter. At some places large polygons of thermal contraction seem to exist, which form today large stripes (photo nr.3). A large range of transitional forms between stripes, nets and circles exists. Almost the whole surface at the region seems to be moved by micro or macrosolifluction according to Troll (1944). At a number of localities (4a) terracettes exist. They have different sizes and surface slopes of 12° and 30°, their steps are blocky, even steeper. In other parts (4b) there are very large terraces. They are partly several decameter to over 100 m long, their relative height is up to 10 m. They display slopes of approx. 20° on the surfaces and of more than 30° at the front slope, they are best developed in the dark rocks of the formation El Plata. They are difficult to explain. Partly, they are influenced by nivation, partly they seem to be separated from each other by linear collapse structure, which form long rills parallel to the contour lines and in which during winter snow accumulates.
As relicts of frost shattering the tors have to be named. They form mainly towers on the arrete, i.e. they belong to the slope-type of French (1976). They are primarily situated in the formation El Plata on the south facing slopes. The slopes surrounding the Lagunita display slope angles between 20° and 30°. The slopes are intensively controlled by the prevailing cryogenic forms. The cryogenic slopes differ a great deal. On the one side they can be covered with debris (debris slopes) and on the other without (above 30°). To the North-East slopes with not much debris, richter denudation slopes (Glatthänge) occur. The slopes surrounding the Lagunita are asymmetric, the South-East facing slopes are steeper and it is there where there is a large snow patch of longitudinal type (Lewis,1939), surrounded by detritic slopes with an inclination varying between 28° and 29°. Asymmetric valleys can also be observed (cf. "Arroyo Casas"). Nivation is active and is manifested through the mentioned snow patch, also named "Gran Malvina" owing to its form, and through seasonally snow patches in the North-West exposed section. These snow patches are transversal and last more than a year leaving interesting samples of nivation hollows.
Hints of glaciation have been found neither in the Lagunita nor in the "Quebrada de las Mulas". Upon the Arroyo Casas, the glacier situated in the Southern front of El Plata , which has left moraines down to 3.400 m altitude, blocked the South-Western section of the Lagunita.
Rock Glaciers are very common in the region. They are found at the foot of talus slopes as well as mid slopes, often they are small or well development or juxtaposed. Some examples can be seen in the valley of "Casas". In the same valley that begins with uncovered glaciers, the Strelkov glaciers, it ends as covered glacier with thermocarst features (see "secondary rock glaciers", Corte, 1980)

PERMAFROST AND SEASONALLY FROST

In accordance with Karte's classification (1981) the mentioned forms are geomorphological indicators (type II) for a very important seasonal freezing and possible sporadic permafrost. According to other classifications (Gorbunov, 1978), the studied area belongs to the permafrost type of the Central Andes and is characterized by a region free of ice and by other 3 regions where frost occurs daily, seasonally or permanently. On the other hand, the presence of active rock glaciers suggests, in accordance to Barsch (1977) discontinuous alpine permafrost. Applying the formula that has been corrected by Barsch (1977), the presence of permafrost can also be assumed theoretically (see tables) on the basis of data provided by meteorologic stations.

a- Data provided by the meteorologic station "Las Aguaditas" and extrapolated data (°C)

(m)	J	F	M	A	M	J	J	A	S	O	N	D	Ø	Depth of Penetr Frost/Thaw I z_F (cm)	z_T (cm)	z_F (cm)
2.225	13,4	12,4	10,7	8,4	6,2	3,3	2,3	3,2	4,3	7,1	9,4	12,4	7,7	--	--	--
3.200	7,6	6,6	4,9	2,6	0,4	-2,5	-3,5	-2,6	-1,5	1,3	3,6	6,6	1,9	113	308	-19
4.000	2,8	1,8	0,1	-2,2	-4,2	-7,3	-8,3	-7,4	-6,3	-3,4	-1,2	1,8	-2,9	219	145	+ 7

b - Data provided by the meteorologic station "Cristo Redentor" (Temperaturen in °C)

(m)	J	F	M	A	M	J	J	A	S	O	N	D	Ø	Depth of Penetr Frost/ Thaw D z_F (cm)	z_T (cm)	z_F (cm)
3.832	3,9	3,6	2,0	-0,3	-3,3	-6,6	-6,8	-6,5	-5,0	-3,3	-0,4	2,5	-1,7	199	190	+

Tables"a"and"b": Calculation of the depth of penetration of frost and thaw for two stations in the Cordillera at Mendoza

Parallely to that, temperature measurements at more than 4.400 m altitude revealed 0° C at approx. 90 cm depth in the South-exposed slope. The temperature measurements carried out allow the conclusion that the permafrost table may be in about 5 m depth.

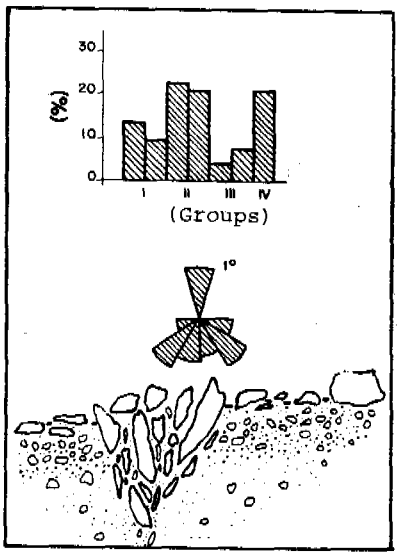

Diagram nr. 1.: Patterns of collapse,situmetric analysis

Photo nr. 3. : Stripe with the structure pf collapse

The well developed stripes are often interpreted as permafrost indicators. By situmetric analysis they display patterns of collapse (photo nr. 3, diagram nr. 1). Probably these patterns suggest a strong thermal contraction due to a strong cryogenic activity during winter.

CONCLUSIONS AND DISCUSSION

Lagunita del Plata forms a good example of an Andine cryogenic environment. As cryogenic mesoforms the talus slopes with an enormous quantity of cryoregolith and active rock glaciers have to be named. It is assumed that these forms have already been formed during the older and middle Holocene. At the moment their activity is very reduced. Thus today these periglacial forms are conserved, and the cryogenic activity is concentrated on frost shattering, sorting, cryoturbation, micro-solifluction, etc. The present day cryogenic activity is therefore, accepted as small in relation to former periods of the Holocene. This is proven by the fact that according to Barsch and King (oral comm.) the lower unit of the neighbouring rock glacier "EL Salto" is nearly inactive today.

NOTE OF THANKS

I would like to thank for many suggestions Prof. Dr. D. Barsch (Heidelberg) and Dr. A. Corte (Mendoza). I would further like to thank Karin Lundberg for helping to translate the original text.

REFERENCES

Ambrosetti, J., Del Vito, L. y Roig, F. (1986). La vegetación del Paso de Uspallata, Provincia de Mendoza, Argentina. Geobot. Inst. ETH, Stiftung Rübel, Zürich, 91 141-180

Barsch, D. (1977). Alpiner Permafrost- ein Beitrag zur Verbreitung, zum Charakter und zur Ökologie am Beispiel der Schweizer Alpen. Formen, Formengesellschaften und Untergrenzen in den heutigen periglazialen Höhenstufen der Hochgebirge Europas und Afrikas zwischen Arktis und Äquator, Göttingen, 118-141

Corte, A. (1980). Glaciers and Glaciolithic systems of the Central Andes. World Glacier Inventory, IAHS-AISH, nr. 126, 11-24

Corte, A. & Trombotto, D. (1982). Andean geocryogenic features in satellite imagery and accidents warning. Sixteenth International Symposium on Remote Sensing Environment. Buenos Aires.

French, H.M. (1976). The Periglacial Environment Longman London and New York. 309 pp.

Garleff, K. (1977). Höhenstufen der argentinischen Anden in Cuyo, Patagonien und Feuerland. Göttinger Geographische Abhandlungen. Heft nr. 68, Göttingen.

Gorbunov, A. (1978). Permafrost investigations in high mountain regions. Arctic and Alpine Research. Vol. 10 (2), 283-294.

Karte, J. & Liedtke, H. (1981). The theoretical and practical definition of the term "Periglacial" in its geographical and geological meaning. Biul. Peryglacjalny nr. 28, 123-135.

Lewis,W . (1939). Snow-Patch Erosion in Iceland Geog. Jour. Vol. 94, 153-161.

Minetti, J. y Corte, A. (1984). Zonificación altitudinal del clima en la zona andina y su relación con el límite inferior del hielo perenne (LIHP) y del límite inferior geocriogénico (LIG). Segunda Reunión Grupo Periglacial Argentino, San Juan. Acta Geocriogénica nr. 2, 129-143, Mendoza.

Troll, C. (1944). Strukturböden, Solifluktion und Frostklimate der Erde. Geol. Rdsch. , 34, 545-694. Stuttgart.

Washburn, A.L. (1979). Geocryology. A Survey of Periglacial Processes and Environments. 406 pp.,London.

Wayne, W. (1983). Geologic setting and patterned ground, Lagunita del Plata, Mendoza. Primera Reunión Grupo Periglacial Argentino, Mendoza. Acta Geocriogénica nr. 1, 157-158, Mendoza.

--- (1984 a). The Quaternary Sucession in the Río Blanco Basin, Cordón del Plata, Mendoza Province, Argentina : an application of multiple relative dating techniques. Quaternary Dating Methods. Elsevier, 389-406, Amsterdam.

--- (1984 b). Geologic controls on distribution of patterned ground, Cordón del Plata, Mendoza - Pleistocene paleo-temperatures, headwater slopes of Arroyo Negro and Río Blanco, Cordón del Plata, Mendoza, Argentina. Segunda Reunión Grupo Periglacial Argentino, San Juan. Acta Geocriogénica nr. 2, 246-249. Mendoza.

--- & Corte, A. (1983). Multiple Glaciations of the Cordón del Plata, Mendoza, Argentina. Palaeogeography, Palaeoclimatology, Palaeoecology, (42), 185-209.

OUTER LIMIT OF PERMAFROST DURING THE LAST GLACIATION IN EAST CHINA

Xu, Shuying[1], Xu, Defu[1] and Pan, Baotian[2]

[1]Department of Geography, Suzhou Railway Normal College, Suzhou, China
[2]Department of Geography, Lanzhou University, Lanzhou, China

SYNOPSIS Up to now there is no agreement in the location of the southern limit of permafrost and the lower limit of alpine permafrost during the Last Glaciation in east China. Through a comprehensive analysis for the remnants of periglacial phenomena (pingo, ice wedge and block fields), boreal forest zones (latitudinal and altitudinal zones) and periglacial fauna (Mammuthus primigenius and Coelodonta antiquitatis), the authors propose new boundaries.

INTRODUCTION

The last glaciation of Late Pleistocene, an extremely cold period in the Quaternary, had an important bearing on the changes of the sea level, the movement of climatic zones, the expansion of loess and the development of the fauna and flora in the northern part of China. With the accumulation of new information, it is clear that the southern limit of permafrost had moved southwards during the last glaciation, however, the location and altitude of these limits are still under discussion (Guo Dongxin et al., 1981; Cui Zhijiu et al., 1985; Pu Qingyu, 1985; Yang Huairen et al., 1980) (Fig.1). Opinions also vary concerning the lower limit of the permafrost zone in the mountains south of the southern limit of the main permafrost area (Zhu Jinghu and Cui Zhijiu, 1984; Yang Huairen et al., 1958; Pu Qingyu, 1984).

The various opinions concerning the location of the southern limit and the lower limit of permafrost during the last glaciation were suggested based on the periglacial traces, the composite of Abies and Picea pollen, or the fossils of Mammuthus primigenius and Coelodonta antiquitatis, indicating a cold climate. It is our contention that, though the cold climate during the last glaciation did find its expression in these phenomena, their individual of distribution, each with its own particular way of development, does not show the true outer limit of the permafrost belt. As regards this evidence of a cold climate, the present authors are in favour of the principle of a comprehensive analysis with cross-reference, that is, to find out the pattern of the relationship between these phenomen through an analysis of their development, their limits of distribution and their relations to the permafrost belt, so as to determine the limit with improved accuracy.

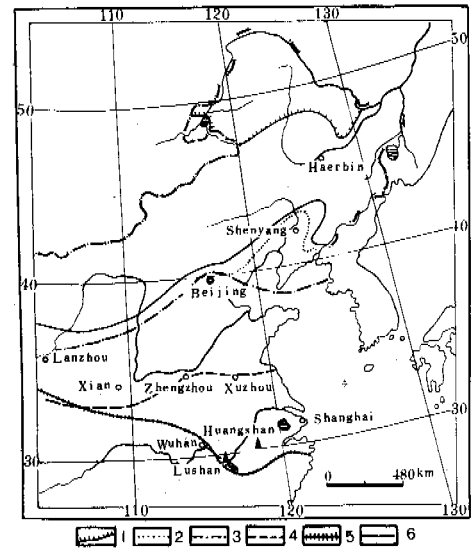

Fig.1 Comparison Among the Several Opinions about the Southern Limit of Permafrost Belt During the Last Glaciation in East China

1. Southern limit of modern permafrost;
2. Southern limit of ancient permafrost (Guo Dongxin et al., 1981);
3. Southern limit of ancient permafrost (Cui Zhijiu et al., 1985);
4. Southern limit of ancient permafrost (Pu Qingyu, 1985);
5. Southern limit of ancient permafrost (Yang Huairen et al., 1980);
6. Southern limit of ancient permafrost of this paper.

PERIGLACIAL CONSTRUCTIONS

The periglacial processes may take place in both the perennially and seasonally frozen zones. Especially in the monsoon climate zones of East China, a high amplitude in air temperature and a cold and dry winter favor frost action and the production of certain periglacial phenomena such as frost weathering and solifluction in an

area with deep seasonal freezing. French (1976) suggested that the periglacial zone might include parts of the area with a mean annual air temperature of 3°C, so that the limit of periglacial zone might differ from that of permafrost region. The reconstruction of the border of past permafrost should be on the basis of the features which can indicate the permafrost environment, such as pingo scars and ice-widge casts, block fields, flat-bottom valleys,cryoplanation terraces, thermokarst depressions; whereas the frost weatherings, frost crackings, solifluctions, nivation depressions might not be the exclusive indicator of permafrost. The distribution of flat-bottom valleys, cryoplanation terraces and thermokarst depressions is too limmited, so it is hard to use these features to reconstruct the boundary of ancient permafrost. The present authors suggest that the pingo scars, ice-wedge casts and block fields should be the key features to be used (Fig.2).

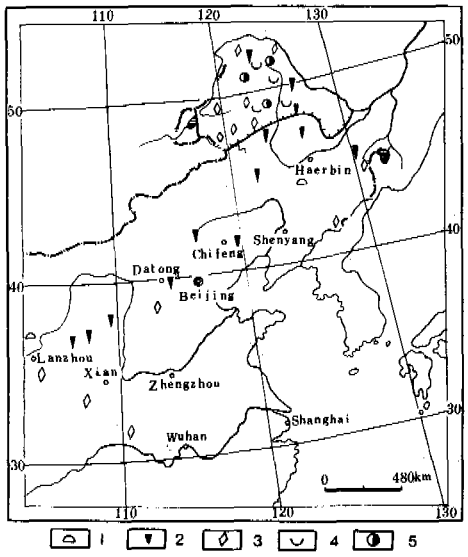

Fig.2 The Distribution of Periglacial Remnants Indicating Permafrost During the Last Glaciation in East China

1. pingo scars; 2. ice-wedge casts;
3. block fields; 4. flat-bottom valleys;
5. thermokarst depressions.

1. Pingo scars. Some traces of ancient pingo lakes were found in the upper Guxiangtuen series (30,000 to 23,000 years in ^{14}C age) in the Qianan, Nongan, etc. of the Songnen Plain, about 45°N in latitude (Pu Qingyu, 1985).

The occurrence of pingo scars was first regarded as showing that the Songhua-Liao watershed was in the central part of permafrost zone during the Last Glaciation (Study group on frozen ground in the Northeast China, 1983). However, as widely recognized, the distribution of pingo remnants is not confined in the central zone of permafrost region. Open-system pingoes develop in the discontinuous permafrost zone with a mean annual air temperature of -1 to -6°C (Washburn, 1973). Pollen analysis showed that the mean annual air temperature in Harbin was -3.6°C, 30,000 years ago (Zhou Kunshu, 1984),indicating that the Songhua-Liao watershed might be in a peripheral area of the permafrost zone at that time, and the pingos were probably formed in an open-system.

2. Ice-wedge casts and inactive sand wedges. Apart from those small wedges that may have developed in the seasonal frost zone, most ice-wedges (especially ice-wedge nets) are marks of the existence of a permafrost zone. The size of an ice wedge shows the degree of coldness, and so the nearer to the southern and lower limit, the smaller the ice-wedges will be. It is reported that the ice-wedge casts in east China are mainly distributed in the areas north to 45°N, where the wedges are approximately 1 metre in width at the top and over 2.5 metre in depth. The wedges south to 40°N tend to become progressively smaller with decreasing latitude. Sand wedges in Dehui penetrated down to the permafrost layer, while those in Aohanqi, Datong (Yang Jingchun et al., 1983) and Salawusu (Dong Guangrong et al., 1985) penetrated no more than the active layer. This suggests the possibility that the above three areas are located near the southern limit of the ancient permafrost belt.

3. Block fields. The stratigraphic and geomorphic correlations show that the block fields in the mountains to the south of the southern limit may all have appeared during the Last Glaciation. It seems that regardless of the climate in the mountains, the block fields are 200-500 m below the snow line, whereas the height difference between the block fields and the frost line varies considerably from place to place according to the aridity, e.g. it may be 600 to 700 m lower in some areas with a dry climate, but only about a hundred metres lower in a humid area.

The present limit of permafrost in the alpine regions in West China can be used for the estimation of the Late Pleistocene permafrost limit in the mountains of East China where the inactive block fields are found. Generally speaking, the mountainous areas in the east have a humid climate in modern times, but were cold and dry during the last glaciation. The difference in altitude between the block fields and the permafrost lower limit in these area is estimated to be 700 m, as occurrs today in the dry mountainous areas in the west (Table I).

It is clear from Table I that the lower limit of the ancient permafrost belt on Mt. Changbai Shan was below 1,000 m a.s.l., so it was within the latitudinal permafrost belt. However, the Mt. Wutai Shan and mountains to its south, where the permafrost lower limit was above 1,500 m, were outside the latitudinal belt during the last glaciation.

VEGETATION OF COLD ENVIRONMENT

1. The boreal forest zone and the southern limit of the ancient permafrost belt.

There have been a variety of opinions concerning the location of the coniferous forest in east China during the last glaciation (Fig.3). Based

TABLE I

The Lower Limit of the Ancient Alpine Permafrost Belt Estimated on the Basis of Heights of the Inactive Block Fields

Mountains	The height of inactive block field (m a.s.l.)	The lower limit of ancient permafrost belt (m a.s.l.)
Changbai Shan	1500-1800	700-1000
Wutai Shan	2500-2700	1700-2200
Taibai Shan	3000-3100	2300-2800
Mahan Shan	3500-3600	2700-2800
Wu Shan	2300-3100	2100-2300

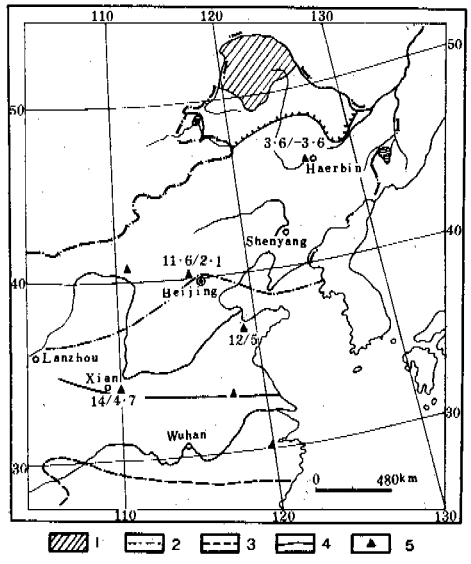

Fig.3 The Southern Limit of Boreal Forest Belt and Sites of Sporo-pollen Assemblage of Spruce and Fir During the Last Glaciation in East China

1. Modern boreal forest belt;
2. Southern limit of ancient boreal forest belt (Cui Zhijiu et al., 1985);
3. Southern limit of ancient boreal forest belt (Yang Huairen et al., 1980);
4. Southern limit of ancient boreal forest belt of this paper;
5. Sites of the sporo-pollen assemblage of spruce and fir, modern mean annual air temperature/ancient mean annual air temperature

on the distribution of Abies and Picea pollen of that period, the authors suggest that it is extended from the plains to the north of the Huai River to the central Shaanxi Plains, i.e. about 34-35°N. Southwards, the plains at the lower reaches of the Yangtze River were in a forest-steppe environment or steppe environment of the temperate zone during the Last Glaciation.

The Abies and Picea pollen in the sediment, 23,000±850 years in ^{14}C age, of Weinan County (34°31'N) indicates a mean annual air temperature of 4.7°C, while in the Salawusu layer (27,940±600 years in ^{14}C age and 37° to 38°N), it indicates -0.2°C. If the mean annual air temperature was 4-5°C at the southern limit of the coniferous forest belt and -1 to -2°C at the southern limit of permafrost belt, then it could be estimated that the distance between these two limits should be 6° to 7° in latitude during the Last Glaciation.

The coniferous forest belt in the boreal temperate zone in the eastern part of the modern Eurasian continent is wide, covering 20° in latitude (70-50°N). Based on the discussion above, it is believed that, if the southern limit of the coniferous forest during the last glaciation had moved 15° in latitude, all or most of the latitudinal permafrost belt in east China would still have been within the coniferous forest, and west China possibly had become a forest-steppe or dry steppe environment because of the dry climate. In general, from a macrogeographic view, the eastern part of China has never been a tundra area, even during the Last Glaciation.

2. The coniferous forest belt and the ancient lower limit of alpine permafrost.

The lower limit of alpine permafrost is usually lies 300-800 m above the tree line in West China. However in East China, they within 500 m of each other, or even reversed. This is due to the dry climate and the strong thermal effect of the mountain body resulting in raising of the snowline and widening of distance between the snowline and tree line. In the east, it was much more humid and the thermal effect of the smaller mountain bodies was small. As a result the tree line was ligher and the lower limit of permafrost was lower.

The lowering of the tree line during the Last Glaciation was 1,000 m in Hokkaido in Japan, 1,100 m in the Alps, 1,100-1,300 m in the mountains in North America, 1,500 m in Mt. Daxinganling and 1,200-1,500 m in the mountains at the lower reaches of the Yangtze River in China. Assuming a 300 m difference in height between the lower limit of modern alpine permafrost and the tree line, the lower limit of the ancient permafrost belt during the Last Glaciation can be calculated with reference to the ancient tree line as shown in Table II.

PERIGLACIAL FAUNA

With the movement of the climatic zone towards the south in the Last Glaciation, such cold climate species as Mammuthus primigenius and Coelodonta antiquitatis were once widely distributed over the middle-latitudes (Chow Benshun, 1978), their fossils having been found in as many as 217 places in the northeastern part of China. The distribution of Mammuthus primigenius was concentrated north to 42°N, though in north, northeast, and even central and east China the discovery is not rare (Fig.4). Judged by ^{14}C

TABLE II

The Height of the Former Tree Line and the Lower Limit of the Ancient Permafrost Belt During the Last Glaciation in East China (m a.s.l.)

Mountains	The modern tree line	The tree line during the last glaciation	The lower limit of ancient permafrost belt calculated on the basis of ancient tree line
Changbai Shan	1800	300-800	600-1100
Wutai Shan	2600	1100-1600	1400-1700
Taibai Shan	3500	2000-2500	2300-2800
Wu Shan	3100	1600-2100	1900-2400
Lu Shan	3000*	1500-2000	*1800-2300
Tianmu Shan	2700*	1200-1700	*1500-2000
Yu Shan	3600	2100-2600	2400-2700

* Exceeding the height of Mountains.

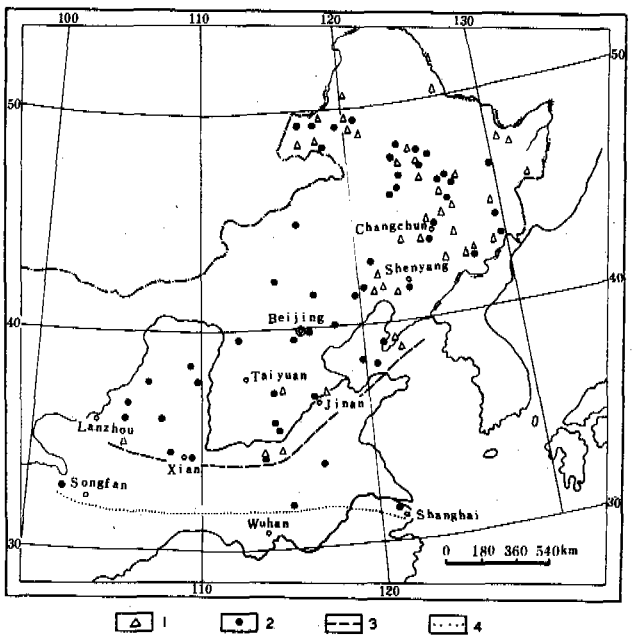

Fig.4 Fossil Sites of Mammuthus Primigenius and Coelodonta Antiquitatis During the Last Glaciation in East China (After Chow Minchen et al, 1959)

1. Mammuthus Primigenius;
2. Coelodonta Antiquitatis;
3. Southern Limit of Mammuthus Primigenius;
4. Southern Limit of Coelodonta Antiquitatis.

dates, most of these animals lived 35000-20000 years ago. The fact that the fossils of Mammuthus premigenius and Coelodonta antiquitatis were found in lower latitudes of East China indicates a colder climate during the Last Glaciation. However, the southern limit of these fossils cannot represent the southern limit of the ancient permafrost belt. Reference can be made to other areas outside China e.g. the distribution of Mammuthus premigenius near 40°N in Europe and North America; that of Coelodonta antiquitatis as far south as 36°N in Europe. The southern limit of the ancient permafrost belt in Europe during the Last Glaciation is 43-44°N, which is 3-4° and 6-7° in latitude further north than the southern limit of Mammuthus primigenius and Coelodonta antiquitatis respectively. The western section of the southern limit of the ancient permafrost belt in the Late Wisconsinan Glaciation was at 42°N, and was 2° in latitude further north than the southern limit of Mammuthus primigenius.

Mammuthus primigenius and Coelodonta antiquitatis are both species characteristic of a cold climate environment of tundra, loess steppe, plateau meadow, etc. Different environments produce different population associated with different species of animals. According to Chow Minchen (1959), there were no Rangifer tanrandus or Vulpes Arctos, which are typical periglacial animals in the Mammuthus-Coelodonta fauna in the northeastern part of China, but there were Bubalus, and Struthios that flourished in the dry environment, with other temperate zone animals. He observes that, in view of the fossils of Mammuthus-Coelodonda fauna found in Guxiangtun in Harbin, the climate there during the Last Glaciation was very much like the modern climate in the northern part of northeast China and in the southern part of Siberia, and the same is true of the associated vegetation cover. This also reflect the southward migration of the southern permafrost limit through no more than 10° in latitude.

Coelodonta antiquitatis were more adaptable to the natural environment than Mammuthus primigenius. The fact that no Mammuthus primigenius, were found with Coelodonta antiquitatis, Bubalus, and Struthios in Salawusu in the Great Bend of the Yellow River indicates a dry, cool loess steppe environment. In Late Pleistocene deposits as well as in earlier ones in China's north, etc., there have been discoveries of Coelodonta antiquitatis and associated animals that were adaptable to the warmer climate. This phenomenon was close related to the geographical position of east China and its climate during that period. The eastern part of China, strongly hit by the cold current from the north polar region during the Last Glaciation, had a low temperature at that time. Nevertheless, the area was still influenced by the monsoon, though relatively weak, from the Pacific in summer. This resulted in frequent seasonal movements of the animals, even down to lower latitudes. The development of permafrost requires a consistently cool climatic regime with low temperatures. The southern limit of its distribution lies 3-4° further north than the southern limits of Mammuthus primigenius, and 6-7° further north than the Coelodonta antiquitatis based on evidence from other continants. This suggests that the location of the southern permafrost limit

TABLE III

The Lower Limit of Alpine Permafrost Belt to the South of the Southern Limit of Ancient Permafrost Belt During the Last Glaciation

Mountains	Geographic position		The height of the highest peak (m a.s.l.)	The lower limit of permafrost belt calculated on the basis of heights of inactive block fields (m a.s.l.)	The lower limit of permafrost belt calculated on the basis of ancient tree line (m a.s.l.)	The lower limit of permafrost belt determined through a comprehensive-comparative study (m a.s.l.)
	Latitude (N)	Longitude (E)				
Changbai Shan	41°-44°	126°-130°	2029	700-1000	600-1100	800
Wutai Shan	38°33'-39°6'	113°28'-113°40'	3058	1700-2200	1400-1700	1700
Taibai Shan	34°	107°-108°	3767	2300-2800	2300-2800	2500
Wu Shan	31°20'-31°30'	110°10'-110°20'	3105	2100-2300	1900-2400	2200
Tianmu Shan	30°20'	119°30'	1507	-	1800-2300	1800*
Lu Shan	29°30'	115°50'	1426	-	1800-2300	2000*
Yu Shan	22°30'	121°	3997	-	2400-2700	2600

* Exceeding the height of mountains.

probable lay around 37-40°N.

THE LOCATION OF THE SOUTHERN LIMIT OF THE ANCIENT PERMAFROST BELT AND ITS SIGNIFICANCE

The above discussion leads to a tentative conclusion that the southern limit of permafrost belt during the last glaciation in China extended from the southern part of Songhua-Liao Watershed (42°N), along the southern slope of the hills of western Liaoning and Mt. Yan Shan (800 m a.s.l.), to the northern Hebei (40°N), then turned southwestwards to the northern Shaanxi (37°N), and westwards through the southern edge of Inner Monggolian Plateau (about 1000 m a.s.l.) to enter west China (Fig.5).

The southern limit of the ancient permafrost belt has a very similar boundary to that of the modern permafrost belt but lay about 6° in latitude to the south in the eastern sector, i.e. 42°N in the last glaciation compared with 48°N in the modern times; and 9° in latitude in the western sector, i.e. 37°N compared to 46°N.

The change in the southern permafrost limit is relatively small in east China, in terms of the changes experienced in Europe and in North America. The limit in Europe was at 43-44°N during the Last Glaciation compered with 66-68°N today for a difference of 23-24° in latitude. The limit in North America lay at 37-42°N during the Last Glaciation compered with 52-60°N at modern times. This is a difference of 15-18° in latitude.while in China, the difference is 7-10° in latitude. The reason for this lies in the fact that the eastern part of China to the north of the Yangtze River has been controlled by a strong continental monsoon climate ever since the Last Glaciation. Thus the small-scale change in the southern limit shows the relative stabilities of the climate there.

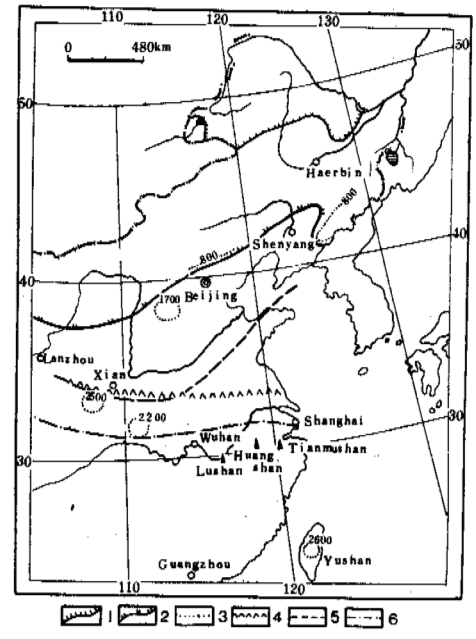

Fig.5 The Southern Limit and Lower Limit of Permafrost During the Last Glaciation in East China

1. Southern limit of modern permafrost belt;
2. Southern limit of ancient permafrost belt;
3. Lower limit of ancient permafrost belt;
4. Southern limit of ancient boreal forest belt;
5. Southern limit of mammuthus primigenius distribution;
6. Southern limit of coelodonta antiquitatis distribution.

The lower limits of permafrost on the high mountains to the south of the southern limit, whether based on the inactive block fields or the ancient tree line, are all similar in height, as is shown in Table 3. It is clear from the table that the lower limit of permafrost in the mountains near the southern limit of the ancient permafrost belt was about 800-1000 m a.s.l., while the ancient lower limit in the mountains in north China was about 1500-2000 m a.s.l. In the mountains in central China it was about 2000-2500 m a.s.l., while in the mountains in east China it was about 1800-2500 m a.s.l.. Among the mountains in the south China, only the Yushan had an altitudinal permafrost belt with a lower limit about 2600 m a.s.l.

REFERENCES

Chow Benshun, (1978). The distribution of the Woolly Rhinoceros and Woolly Mammoth. Vertebrata Palasiaica, 16(1), 47-59 (in Chinese).

Chow Minchen, (1959). Pleistocene mammalian fossils fron the Northeastern Provinces. Science Press, 9-12 (in Chinese).

Cui Zhijiu et al., (1985). On Late Pleistocence environment in the northern part of China. Quaternaria Sinica, 6(2), 115-119 (in Chinese).

Dong Guangrong et al., (1985). Ancient periglacial phenomena since the Late Pleistocene on the Eerduosi Plateau. Symposium of national conference on Quaternary glacier and periglacial. Science Press, 225-230 (in Chinese).

French, H. (1976). The periglacial environment. Longman, London, 309.

Guo Dongxin et al., (1981). Preliminary approach to the history and age of permafrost in Northeast China. Journal of glaciology and geocryology, 3(4), 1-6 (in Chinese).

Pu Qingyu, (1984). The phenomena of the Quaternary periglaciation in West Hunan and East Guichou. Marine geology and Quaternary geology, 4(1), 117-122 (in Chinese).

Pu Qingyu, (1985). South boundary of permafrost in China in Late Pleistocene. Symposium of national conference on Quaternary glacier and periglacial, Science Press, 216-220 (in Chinese).

Study group on frozen ground in the Northeast China, (1983). Distribution characteristics of permafrost in the Northeast China. Proceedings of second national conference on permafrost, Gansu people's publishing house, 36-42 (in Chinese).

Washburn, A.L., (1973). Periglacial processes and environments. Edward nrrold and sons, London, 244-257.

Yang Huairen et al., (1958). The phenomena of the Quaternary periglaciation in the lower reaches of the Yangtze River. Quaternaria Sinica, 1(2), 141-154 (in Chinese).

Yang Huairen et al., (1980). Quaternary environmental changes in eastern China. Journal of Nanjing University, No.1, 121-142 (in Chinese).

Yang Jingchun et al., (1983). Fossil ice wedges and Late Pleistocene environment in Datong basin, Shanxi Province. Scientia geographica sinica, 3(4), 339-344 (in Chinese).

Zhou Kunshu, (1984). Spruce, Fir vegetations distributed from 20,000 to 30,000 years ago in river valleys, plain regions of North China and their implications. Sporo-pollen analysis of the Quaternary and paleoenvironments, Science Press, 15-24 (in Chinese).

Zhu Jinghu et al., (1984). Basis characteristic of periglacial landforms on Wutai mountain. Journal of glaciology and geocryology, 6(1), 71-77 (in Chinese).

THE GEOCRYOLOGICAL MAP OF THE USSR OF 1:2,500,000 SCALE

E.D. Yershov, K.A. Kondratyeva, S.A. Zamolotchikova, N.I. Trush and Ye.N. Dunaeva

Faculty of Geology, Moscow State University, Moscow, USSR

SYNOPSIS The Geocryological map of the USSR gives for each feature and group of features of topography, distinguished in the map of this scale, a comprehensive characteristic of geocryological conditions according to the following parameters: distribution of frozen and unfrozen grounds and their mean annual temperatures; thickness of frozen (with/without ice), relict (beneath overlying unfrozen grounds) and chilled below 0°C saline-water containing ground strata; composition and cryogenic texture of epicryogenic formations of Pre-Quaternary rocks and genetic complexes of epi- and syncryogenic loose Neogene-Quaternary deposits with the characterization of cryogenic structures, macroinclusions of ice and ice (moisture) content; depth of seasonal freezing; under river bed and lake, open and closed taliks; cryogenic and postcryogenic phenomena, etc. The volume of information available in the map for each site allows to make engineering-geocryological assessment of the territory being developed, to predict its changes and elaborate measures aimed at protecting the geocryological environment. The map is being printed in three variants: general integrated map, map of the permafrost zone thickness, and map of mean annual temperatures of grounds.

In recent years much higher requirements are specified for showing on the maps the geocryological conditions of the territories being developed with a view to prospecting for and exploitation of oil-and-gas fields, mineral deposits, and intensive construction of dwelling houses, industrial and hydraulic structures, roads, power transmission- and pipelines. Accumulation of vast factual data and information on the USSR permafrost zone, especially, on the sites covered by integrated small-scale geocryological and engineering-geocryological surveys, made in accordance with the present-day theoretical concepts on the general and specific laws of permafrost (PF) formation and development, has enabled the Department of Geocryology, Faculty of Geology, Moscow State University, together with other organizations, to compile the Geocryological map of the USSR at a scale of 1:2,500,000.

The geocryological map of such scale, covering the entire territory of the Soviet Union, has been compiled for the first time and has no analogs in the world practice.

As regards the content and methods of compilation, this map is a complex one. It was compiled on the geologic-genetic and formation basis and reflects the relationship between PF and climatic, geobotanical, hydrogeologic, neotectonic, and abyssal geothermal conditions and topography by mapping the main permafrost characteristics classified by the types and forms of relief with their landscape-microclimatic as well as ground-moisture saturation conditions so that the geocryological setting would comprehensively be shown in the map.

The given map has been compiled in conformity with the procedure of diversified small-scale surveys with a comprehensive frozen ground investigation at key sites and extrapolation of the data obtained over the territory using the method of landscape analysis. The "key" i.e. reference sites used were those covered by small-, medium-, and large-scale geocryological surveys that resulted in compiling a number of geocryological maps. The data of deep drilling and regional geophysical investigations were also used.

This map represents:

(1) distribution of grounds and their mean annual temperatures (t_m) at the bottom level of their annual fluctuation;

(2) PF thickness and geocryological texture of frozen strata in the permafrost zone down its profile, and stages of this zone;

(3) geologic and genetic complexes of loose deposits and formations of Pre-Quaternary solid and semi-solid bedrock

(4) cryogenic and postcryogenic geologic formations and taliks.

The distribution of frozen and unfrozen grounds is shown in the map through their temperature (t_m) regime as follows:

(1) areal extent of thawed and unfrozen rocks with positive t_m;

(2) southern limit of the present-day distribution of PF;

(3) the area of noncontinuous PF distribution, i.e. the southern geocryological zone where subzones of rare islands, islands, massive islands and nonpersistent PF with massifs and islands of thawed grounds (radiation-thermal taliks) in different features of topography are distinguished;

(4) the area of continuous PF distribution, i.e. the northern geocryological zone with open and closed hydrogeogenous taliks beneath large rivers and lakes and at the sites of groundwater discharge.

Mean temperatures (t_m) of grounds are shown in detail; they reflect the level of heat exchange on the surface, i.e. resistance of PF, basically, to man-induced impacts. Thirty two gradations of t_m were distinguished within a wide range from +21 to -15°C and lower. The main temperature grade at mapping is 2°C, but on plains with a gradual change of natural conditions, it is 1°C. Thus it was possible to represent comprehensively the temperature regime over the area taking into consideration ground composition, moisture and ice content, macroinclusions of ice, and cryogenic texture.

As shown in the attached map-inset of 1:25,000,000 scale (Fig.1), that reflect the generalized temperature regime of grounds over the USSR territory, the lowest t_m values are observed in the Anabar Shield and Taimyr peninsula, on the Severnaya Zemlya Islands, and coasts of the Laptev and East Siberian Seas (in ice-saturated deposits of polygenetic Pleistocene plains) as well as on the summits of mountainous areas in southern and eastern Siberia, Chukot Peninsula and highly elevated ranges of the Pamirs and Tien-Shan. All variations of t_m of grounds are distinctly shown in the map from their highest positive values beyond the permafrost zone to the lowest ones within its most severe regions.

The permafrost zone thickness and structure were mapped based on the analysis of geologic-structural and landscape-climatic conditions of the Earth evolution in the Neogene-Quaternary period.

The permafrost zone structure has been characterized by representing the following horizons:

(a) frozen ground strata (both subaerial and submarine) that contain ice and are frozen;

(b) relict frozen strata separated from the Neo-Holocene permafrost layer or overlain by a thick layer of unfrozen ground (100-200 m more);

(c) subaerial, submarine and subpermafrost negative-temperature grounds containing saline water and brines (cryopegs).

The permafrost zone thickness is shown separately within each horizon by hatching of different color. Thus, the frozen ground thickness of the upper horizon of the permafrost zone in the southern geocryological zone is shown in the map in 0-15, 0-25, 0-50 and 0-100 m gradations which is associated with short-term climatic fluctuations and intensity of variation due to man-induced impacts. In the northern geocryological zone, the permafrost thickness on plains and mountainous regions is shown with a spacing of 100 m and 200 m, respectively. The thickness of frozen rocks is shown by red-color hatching.

The relict permafrost strata thickness is given at 100 m spacing by black-color hatching.

The thickness of grounds with subaerial, subpermafrost, and submarine cryopegs is shown by green-color hatching. The thickness values of grounds with cryopegs range from 25, 50 and 100 m to 200, 300 and 500 m. The total thickness of the permafrost zone in the map can be obtained by summing up all negative temperature horizons of the section. It is shown additionally in the map-inset of 1:25,000,000 scale.

It appears from the analysis of factual data that in the southern geocryological zone the thickness of frozen grounds is associated with their mean annual temperatures, while in the northern one, at their continuous distribution, such dependence is observed only in mountain regions, though similar t_m occur at different absolute elevations in various mountain systems in the south and north-east of the USSR.

The greatest thickness of the permafrost zone is within the limits of the most ancient geotectonic structure of the Earth - the Siberian platform where it reaches 1000-1500 m, and in the highest ranges of southern Siberia, Far East and Central Asia. The same strata are most ancient with respect to their cryogenic age, i.e. the time when ground freezing began over one million years ago.

The smallest thickness of perennially frozen grounds, naturally, occurs at the southern boundary of their present-day distribution.

Within the limits of the permafrost zone with continuous frozen ground strata, taliks are shown beneath river beds and big lakes subdivided into open and closed ones, with and without groundwater discharge. Within the boundaries of the entire territory the following cryogenic phenomena are shown in the map for genetic types of grounds: wedge ice, subsurface sheet ice deposits, groundwater icings, ground veins, frost mounds, convex and flat hillocky peatlands, thermokarst basins, hillocky (residual-polygonal) terrain, and glaciers.

Beyond the permafrost zone, in the region of thawed and unfrozen ground occurrence, depths of seasonal freezing have been mapped together with t_m. The values presented reflect the va-

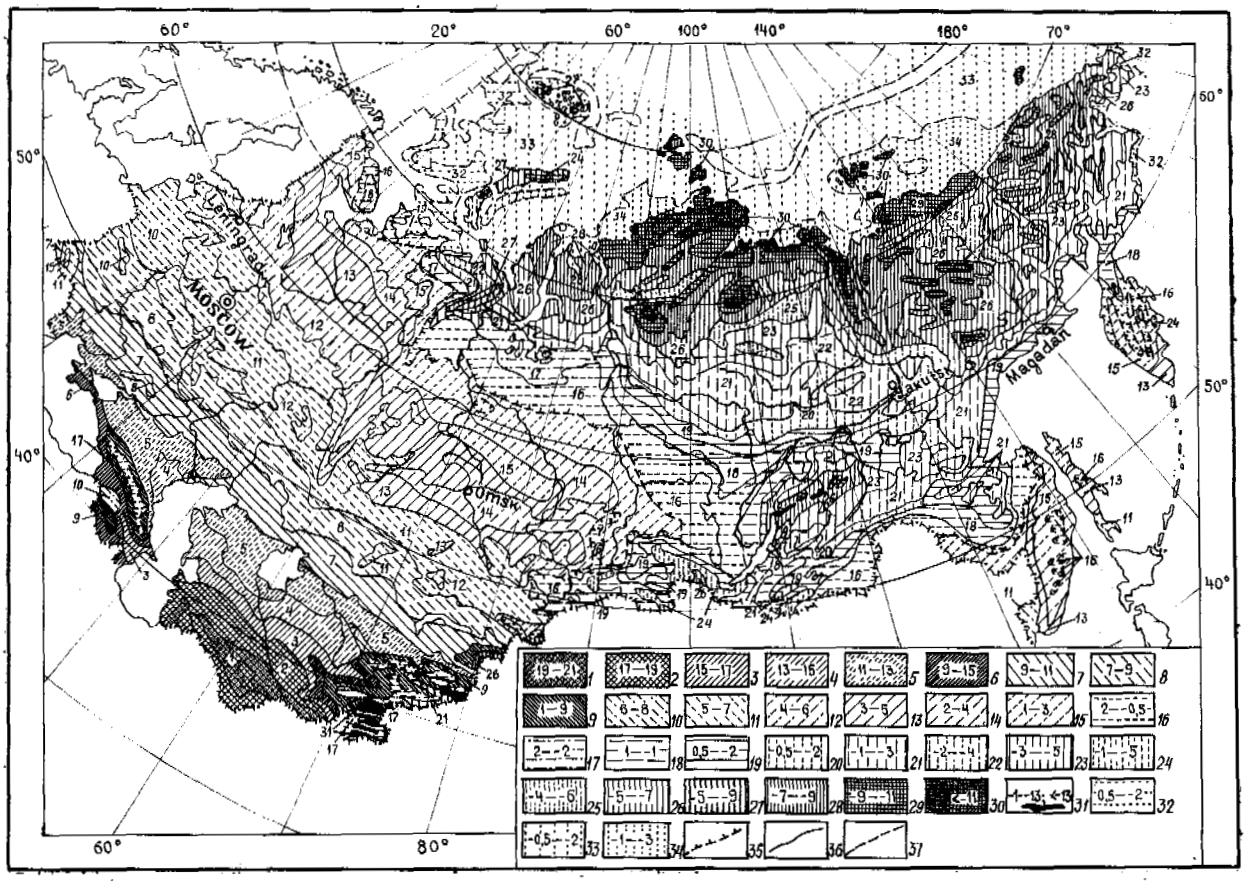

Fig.1 The map of the permafrost zone occurrence and mean annual temperatures of grounds over the USSR territory.

Distribution of seasonally and perennially frozen grounds: 1-15 - seasonally frozen grounds with positive mean annual temperatures (°C); 16-19 - southern geocryological zone of non-continuous distribution of frozen grounds with negative and positive mean annual temperatures; 20-31 - northern geocryological zone of continuous distribution of permafrost with negative mean annual temperatures; 32-34 - frozen and chilled below 0°C grounds with cryopegs in the shelf; 35 - southern limit of the permafrost zone; 36-37 - boundaries of temperature zones: within the limits of the subaerial permafrost zone (36), within the limits of the submarine permafrost zone (37).

lues presented reflect the variability of this geocryological characteristic depending on t_m of grounds, amplitude of temperature variations at the surface, composition and moisture content of seasonally freezing ground.

In the denudation areas the geologic base of the map was constructed in accordance with the formation principle of I.V.Popov which makes it possible to take into account the dependence of ground properties, composition, and fracturing pattern on conditions of sedimentation, history of tectonic development and climatic zonality. The USSR Geological map of 1:2,500,000 scale published in 1983 under the editorship of D.V.Nalivkin was used as the geologic base. The occurrence of geologic-genetic types of loose Neogene-Quaternary deposits in the accumulation areas is shown with the description in the legend of the composition, ice content, ice macroinclusions, types of cryogenic structures and type of cryogenesis (syn- or epigenetic over the area and down the profile). The greatest ice content is typical of polygenetic deposits in the accumulative northern plains (up to 0.6-0.8), erosional-accumulative thermokarst-lacustrine plains (0.4-0.7), rock streams of the bald mountain belt (0.3-0.6) of the northern geocryological zone that are characterized mainly by syncryogenic type of freezing. The epicryogenic frozen strata of solid and semi-solid types are characterized by higher (up to 0.3 ice content, largely, in rejuvenated neotectonic fracture zones of faults.

The distribution of genetic types of loose deposits and formations of Pre-Quaternary rocks is shown in the map by small grey symbols.

The information contained in the map of 1:2,500,000 scale is supplemented and generalized in six thematic map-insets of 1:25,000,000 scale, namely: (1) map of zoning by the con-

ditions of frozen and unfrozen ground occurrence; (2) map of mean annual temperatures of grounds; (3) map of the permafrost zone thickness; (4) map of zoning by the cryogenic age of grounds and type of cryogenesis; (5) map of hydrogeocryological zoning; and (6) map of engineering-geocryological zoning of the USSR territory.

Such is the structure of the USSR Geocryological map that has reflected graphically the latest concept of the permafrost zone of the country. The above-described system of presenting all the geocryological characteristics helps perceive and determine in any area the laws of spatial variability of mean annual temperatures, frozen ground thickness, depths of seasonal freezing and thawing of grounds, the development of a complex of cryogenic phenomena and the entire permafrost zone of the USSR.

A detailed presentation (by relief features) of the geocryological characteristics, especially, within the limits of the southern geocryological zone, makes it possible to use this map not only for obtaining information on the geocryological conditions of the site being investigated, but also for making regional geocryological prediction of the changes in freezing conditions under the impact of the territory development, mainly, of construction work (deforestation, removal of moss-sod layer, partial or complete removal of snow, plowing, etc). For this purpose, one can resort to the analog method, simple calculations by the express-method, etc.

The given map, owing to its comprehensiveness and information content, allows to comprehend the place of the area being studied of any scale in the general system of geocryological settings, to discern and establish the extent of variability (or extent of persistence) of its geocryological conditions.

The Geocryological map of the USSR of 1:2,500,000 scale serves as a regional geocryological background enabling to discern and to establish regional laws of freezing characteristics variation having only a small body of actual data.

An integrated analysis of the geocryological conditions of a territory that are characterized by the map, helps in making an engineering-geocryological assessment of the regions for different types of development and to determine measures aimed at controlling the freezing process and optimizing freezing conditions.

Our knowledge of the USSR geocryological conditions is generalized by the map which serves as a scientific basis for general evaluation of vast territories to be developed.

The Geocryological map of the USSR can serve as the base for compiling a series of thematic geocryological maps, such as: cryolithological, engineering-geocryological, hydrogeocryological ones and a number of prediction-estimation maps for different types of construction (roads, pipe- and transmission lines, hydraulic and industrial structures, etc.).

At present the map, is being published and, as planned by the Chief Administration of Geodesy and Cartography at the USSR Council of Ministers, its printing will be completed during the XII five-year plan period (1986-1990). With a view of making a purpose-oriented and more specific use of this map for the underground construction, additionally two maps will be produced at a scale of 1:2,500,000, namely: the map of mean annual temperatures of grounds and map of the USSR permafrost zone thickness which will be more readable and clear as they will not contain excessive information.

THE PERMAFROST ZONE EVOLUTION INDUCED BY DESTRUCTION OF SOIL OVERLYING COVER IN THE AMUR NORTH

S.I. Zabolotnik

Permafrost Institute, Siberian Branch of the U.S.S.R. Academy of Sciences, Yakutsk, U.S.S.R.

SYNOPSIS The permafrost zone of the region under study has, as a rule, a small thickness and occurs in 'mari' which dominate the terrain. The climatic conditions there are, on the one hand, unfavourable for the formation of permafrost due to a significant (up to 3-7°C) warming effect of the rather thick (0.4 - 0.6 m) snow cover and, on the other, contribute, on the contrary, to its formation due to a cooling effect (by 2°C or more) of the wide-spread moss cover 0.1 to 0.3 m thick. A quantitative assessment has been made of the influence of this kinds of cover on the basis of four years of stationary, daily observations on mari within the Upper-Zeya plain (300 m abs.) and the Turan ridge (600 m abs.). A natural and a 'technogeneous' (i.e., without some or other kind of cover) observation area was established at each station. As a result, the investigations have revealed typical features of the formation and dynamics of the seasonal thawing-freezing layer in each of the areas; conditions required by the permafrost zone to persist or degrade are determined; and specific features of the permafrost zone evolution at the beginning of a degradation process are demonstrated and relevant, tentative durations determined. A comparison is made of the observation results for the plain and an intermountain depression.

INTRODUCTION

Economic activity of man almost always entails some or other kinds of disturbances of the natural situation and frequently leads to a dramatic change in permafrost conditions of areas being developed. Hence, failure or either partial or total destruction of the soil-overlying moss-peat and snow cover are the easily accomplished and, therefore, most commonly occuring kinds of disturbances. But it is this cover that determines the main formation or degradation features of the region's permafrost. The trend and the duration length of attendant permafrost processes largely depend upon time, the character and the magnitude of technogeneous effects and can be determined, to a reasonable accuracy, by special-purpose, stationary investigations.

We have initiated such investigations in the eastern section of the Baikal-Amur Railway at two stations: one being located in the Turan ridge, and the other on the Upper-Zeya plain. The stations were both set up on mari, viz. nearly forest-free, swampy moss-peat areas. The stations' disposition was motivated by the fact that mari, on the one hand, constitute a prevailing terrain in the region and, on the other, it is these areas which offer - owing to the cooling effect of the moss-peat cover - the most favourable conditions for permafrost existence so that disturbances of the cover lead to the most pronounced changes in their conditions.

CHARACTERISTICS OF THE STATIONS

Station Eterkan was established in 1977, in an intermountain depression along the axis of the Turan ridge, at an altitude of about 600 m abs. on a relatively uniform surface of the first terrace over the flood-riverside of the Elgakan, the area typical of mari. The arboreous vegetation within its confines is oppressed greatly and exhibits only single specimens of Daurian larch. Shrubs are 0.5 to 1.2 m high consisting of Middendorf birch, ledum and swamp-bilberries. The surface presents a continuous cover composed primarily of bog-moss 0.2 to 0.3 m thick. Peat occurs everywhere beneath the moss cover overlying at 1 to 3 m depths suglinoks containing dust particles which are replaced within the range 8-14 m by streaks of clay, particle-containing supes and medium-grain sand. At the depth of the depression bottom, when exposed, the mari areas show everywhere the permafrost as thick as 50 to 60 m, with the annual temperature at the layer bottom varying from -1 to -1.5°C (Zabolotnik and Sorokina, 1981).

Station Zeisk was established in 1977-1978, at 10 km south-eastward of the Zeisk settlement near the Doeninsky bay of the Zeya River. Experimental areas were arranged on a gentle (2 or 3°), northward slope covered by hillocky mari, at an altitude of about 300 m abs. The arboreous vegetation and shrubs are similar to those described in the case of the Eterkan station. The surface is all covered by a moss cover 0.07 to 0.15 m thick. A distinctive feature of this area is that beneath the moss-turf layer there occur predominantly sandy ground with

underlying highly decayed seat bedrock consisting of granodiorites and crystal shales, as deep as 5.6 to 8.5 m. Drilling operations at the station have shown that earth materials are frozen as deep as 22 m. However, the permafrost temperature is rather high. Under natural conditions the yearly mean temperature throughout the entire thickness is above -0.5°C (Zabolotnik and Shender, 1982).

THE EXPERIMENTAL PROCEDURE

Work at both stations was accomplished according to a common program providing for an, at least, three-year series of geocryological investigations on mari in one natural area (No. 1) and three technogeneous areas. In September 1977 (Eterkan) and 1978 (Zeisk), prior to the experiment shrubs and the moss cover were removed altogether from areas Nos. 2 and 4. In addition, during the winter time when making the observations under natural conditions the snow cover of a thickness varying from 0.35 to 0.55 m was regularly removed from areas Nos 3 and 4.

The areas at each station were all arranged on experimental grounds of the size 60x60 sq. m within which the surface conditions were more or less homogeneous. The areas were 15x15 sq. m (Zeisk) and 20x20 sq. m in size and were spaced by 10 m. Because the space between the areas was maintained in natural conditions, area No. 1 was actually 35x35 sq. m in size.

In each area well were perforated as deep as 5.5 to 8.5 m (Zeisk) and to 18 m (Eterkan) in which earth temperatures were measured daily: four times a day (1, 7, 13, and 19 hr (mean solar time) as deep as 1 m (maximum penetration of diurnal variations) and once a day (19 hr) at greater depths. Four times a day at the same moments measurements were also made of air temperatures as well as surface and bottom temperatures of the snow and moss cover and surface temperatures of the naked ground. Apart from this, observations were made of the snow cover thickness and density, the amounts of precipitation and evaporation during the summer period, moisture and thermo-physical characteristics of earth materials and soil overlying cover, heat flow into the soil, and of the thermal balance components. The depth of seasonal thaw and freezing of soils was determined each day through temperature measurements within the wells and, during the summer period, was also monitored every ten days through measurements in different parts of the areas using a metalic probe.

THE MAIN RESULTS

The investigations have revealed a total analogy of the alterations occurring in the permafrost zone due to destruction of the soil overlying cover. Nevertheless, the dynamics of the accompanying processes also have their own specific features due to the different location, climatic parameters, composition and properties of earth materials.

Station Eterkan. The area of its location is notable for rather severe climatic conditions. From 1978 to 1980 the yearly mean air temperature varied within a small range around -6.5°C (Zabolotnik and Sorokina, 1988). At the same time, owing to the considerable thickness of the snow cover (as thick as 0.48 to 0.53 m) with its relatively low density (0.18 to 0.20 t. m^{-3}), the yearly mean temperature on the moss cover surface in the natural area was positive and varied from 2.1 to 3.2°C. Nonetheless, it would be premature to conclude that no permafrost is present there because beneath the thick moss-peat layer the yearly mean temperature of earth materials again becomes negative already at depths of 0.4 to 0.6 m reaching -(0.7 - 1.1)°C between 4 and 11 m.

Such a temperature distribution is favourable for permafrost formation; however, the stability of permafrost is due totally to the persistence of the moss-peat layer having a high (from 200 to 800%) moisture and possessing a large sluggishness and good heat insulation capacity, especially in the summer time. The heat conduction coefficient of this layer in the unfrozen state varies from 0.29 to 0.55 and increases in the frozen state to 1.2 W/(m·K). The heat capacity per unit volume, on the contrary, while varying within unfrozen earth materials over broad ranges $(1.76 - 3.78)\cdot10^6$ J/(m^3·K), is estimated at about $1.76\cdot10^6$ J/(m^3·K) for frozen earth materials (Gavrilyev et al., 1981).

The seasonal thaw of such earth materials proceeds very slowly, with almost no changes in its behaviour during some years, despite the rather appreciable air temperature fluctuations. As a result, the maximum thickness of the seasonally thawing layer in the natural area varied only from 0.75 to 0.8 m (Fig. 1, No. 1).

Area No. 3 (snow was removed, with the moss remaining) has shown a significant cooling of the soil already during the first year of the observation. With no snow cover present, the ground being unfrozen as deep as 0.7 m froze up completely as early as the beginning of December (Fig. 1, No. 3) or two months earlier as compared with area No. 1. Progressive, intense heat losses by the earth materials during the winter time had led to the fact that, despite the moss cover remaining in natural conditions, this area underwent a gradual decrease in the rate of seasonal thaw of earth materials and a decrease in its maximum depth which, by the end of the observing period, reduced by 0.08 m or by nearly 11.5%.

Another feature of the dynamics of the active layer in area No. 3 is the annual reduction (of up to 1 month in 1980) in the total period of its freezing which, in the natural area, is 3.5 to 4 months (Fig. 1, Nos 1 and 3).

As for area No. 4, removal of the moss cover was accompanied by annual removal of the snow. Therefore, this area has always showed an interaction of two oppositely directed processes, namely a more intense cooling of the naked ground in winter and, on the contrary, a more considerable warming in summer. As a result, the seasonally thawing layer was of almost the same thickness as that in area No. 1; however, its rate of freezing was as high as that in area No. 3 (Fig. 1, No. 4).

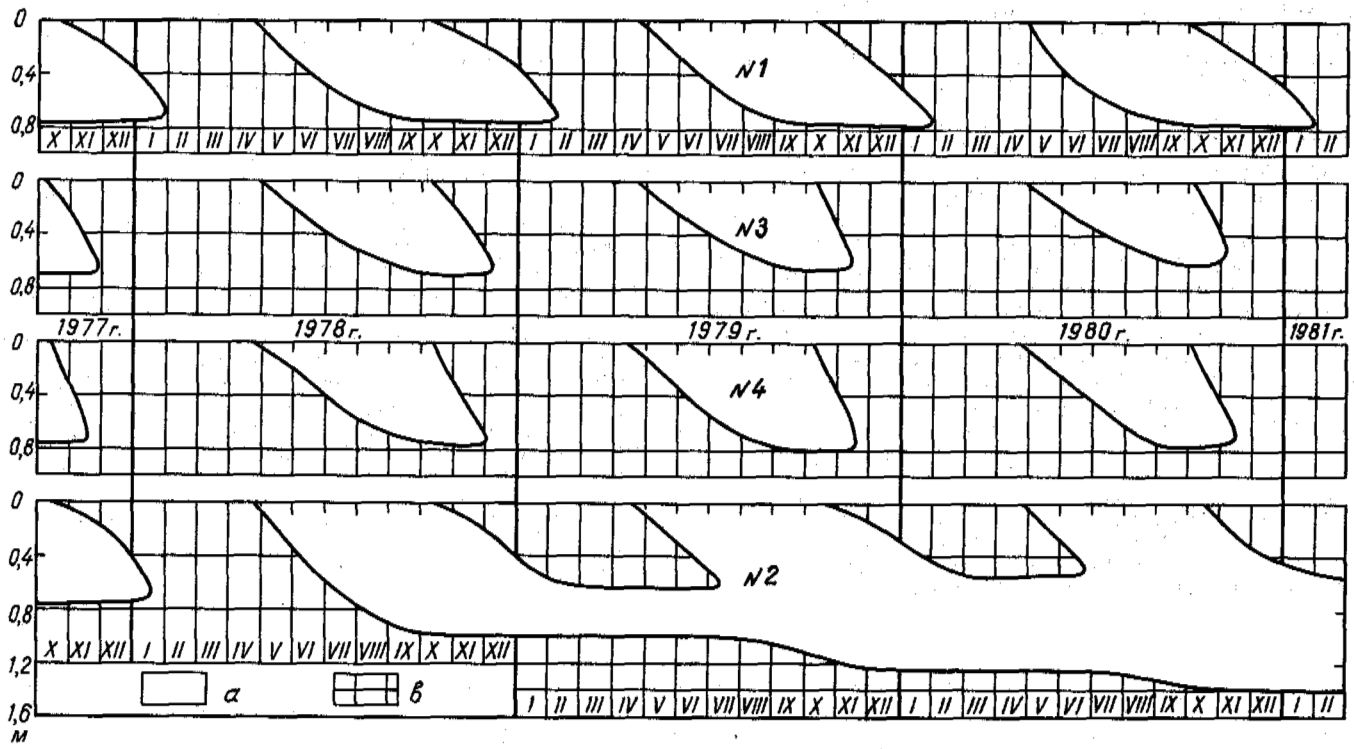

Fig. 1 The Variation of Seasonal Thawing-Freezing of Earth Materials and of Permafrost Thawing at Station Eterkan. Nos 1 to 4 - area numbers; - unfrozen ground; - seasonally- and perennially-frozen ground.

Cryogenic processes evolved in a totally different fashion in area No. 2 where only the moss cover was removed, with the snow cover remaining in its naturally occurring state. Only during the initial period (the year 1977) did the permafrost zone there undergo no substantial changes because the snow cover had been removed later in the summer. Only the seasonally thawing layer of the same thickness (0.75 m) as that in area No. 1 froze up 10 days earlier.

In 1978 the ground devoid of the significant heat insulator such as the moss, got warmed to such an extent that the seasonally thawing layer increased in thickness by more than 30%. The heat accumulated during 1978 was, thus, quite sufficient to prevent, during the next winter, a total freezing of the thus produced one-meter thick unfrozen ground. As a result, an unfrozen intermediate layer 0.35 m thick remained between the seasonally frozen layer and permafrost in the winter of 1978-1979 (Fig. 1, No. 2).

In the summer of 1979 a total thawing of the seasonally frozen layer in area No. 2 occurred as early as mid-July. During that period the upper permafrost boundary remained almost at the same level and only at the beginning of August when it was reached by a thermal wave the permafrost thickness began to further thaw up to December when it again stopped at a depth of 1.25 m. As a result, the depth of thaw, for many years in this case, in area No. 2 became by nearly 0.5 m greater than that in area No.1.

During the two summer seasons, upon removal of the moss cover, the soils accumulated an amount of heat such that in the most severe winter of 1979-1980 the depth of their seasonal freezing again decreased to 0.55 m, while the thickness of the unfrozen layer increased to 0.7 m. During the next summer such a thin, seasonally frozen layer thawed totally as early as 25 June and in August-October there occurred the further thawing of the permafrost layer, as deep as 1.4 m. In the winter of 1980-1981 the thickness of the seasonally frozen layer was estimated by us to be 0.6 m as a maximum. Therefore, the thickness of the unfrozen layer below it increased to 0.8 m.

The abrupt increase in the thickness of the seasonally thawed layer, combined with an attendant process of permafrost degradation in area No. 2, were due largely to the fact that the naked, dark peat surface favours the increase in the absorbing ability of the ground as well as heat accumulation therein. According to measurements obtained by Z.G. Sorokina (Zabolotnik and Sorokina, 1988), the amount of absorbed radiation for a warm period in area No. 2 reached 2500 mJ/m^2, or 7% greater than in the natural area. Besides, values of heat fluxes increased sharply, especially in May-June (by factors of 3 to 11). For the warm period (May-September) the heat input to earth

materials in the natural area was 85.5 and 89.9 mJ·m^{-2} in 1979 and 1980, respectively, while in area No. 2 it increased to 155.5 and 195.5 mJ·m^{-2}, respectively.

Station Zeisk features, in many respects, similar conditions, although it is located on a plain 300 m below in absolute altitude and 300 km to the north-west of Eterkan. The climatic conditions there are also rather severe. From 1978 to 1981 the annual mean air temperature varied from -5.5 to -6.7°C; however, on the moss cover surface (beneath a snow cover of a thickness between 0.35 and 0.55 m) the temperatures were above zero (from 1 to 3°C). Nonetheless, from as deep as 0.3 - 1.0 m (depending on climatic conditions of the year), the annual mean temperature again becomes negative and reaches, within 4 to 6 m, -(0.4 - 0.5)°C.

The increased permafrost temperatures at station Zeisk are attributable to the totally different composition and properties of the soil cover and underlying earth materials as well as, primarily, their much smaller degree of moistening. The moisture of the moss-turf layer of a thickness 2 or 3 times as small was only 71 to 76% there. Within the seasonally thawing layer composed largely of sandy materials, and within the permafrost it varied from 14 to 29%.

The combination of soil properties was also responsible for specific dynamical features of the permafrost zone in the station Zeisk areas. Primarily, a seasonally thawing layer nearly twice as thick was formed there, which normally freezes up later as well. In addition, there is a distinctly seen tendency for this layer's thickness to increase in the natural area for the observing interval. The reason for that was revealed by an analysis of many years' observations from weather stations located in the region, which show an abrupt (nearly by 2°C) increase in the annual mean air temperatures from the year 1972 to 1975 which recovered their previous values by the beginning of the observations at the station. Owing to great sluggishness of the moss-turf covered soils, this temperature jump at station Zeisk was observed to have a delay of 3 to 5 years, while at station Eterkan it remained hardly recognizable (see Figs 1 and 2, No. 1).

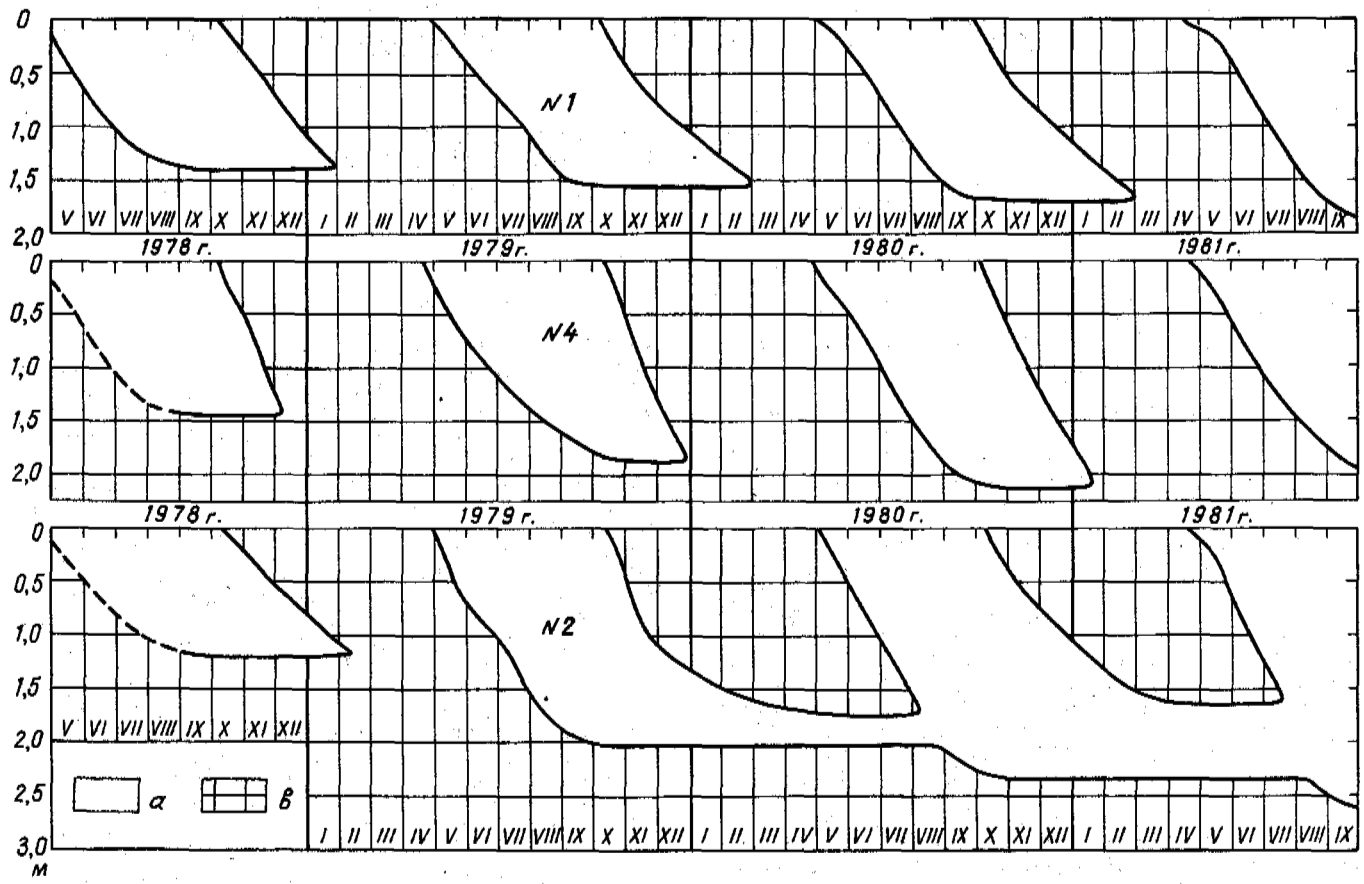

Fig.2 The Variation of Seasonal Thawing-Freezing of Earth Materials and of Permafrost Thawing at station Zeisk. Legend Same as Fig. 1.

Man-induced disturbances at the station led to an abrupt disturbance of the permafrost conditions, especially in areas No. 2 and No. 4. Removal of the snow cover only in area No. 3 had little effect on dynamics and thickness of the seasonally thawing layer but merely speeded up its freezing rate, thus enhancing the permafrost zone stability. Therefore, observation results for area No. 3 are not considered.

Most dramatic changes, as in the case of station Eterkan, occurred in area No. 2 which in September 1978 was subjected to removal of the moss cover, while the snow cover remained in natural conditions throughout the entire experiment.

The absence of the moss cover caused the thawing layer to increase significantly in thickness, namely by 0.85 m within one year and by 1.15 m (or nearly twice) within two years. In virtue of accumulation of heat reserves in the soil, there also was a simultaneous reduction in thickness of the seasonally freezing layer, from 1.75 m in the year 1980 to 1.65 m in 1981. As a result, in between seasonally freezing and permafrost earth materials there formed in 1980 a melted intermediate layer of a thickness of 0.3 m which increased to 0.7 m the next year (Fig. 2, No. 2).

The permafrost conditions were varying in a totally different manner in area No. 4 where removing the moss cover was accompanied by removal of the snow every year. The permafrost degradation process that set in within area No. 2 was stopped at once here by a significantly more intense cooling of earth materials during the wintertime. Therefore, the substantial increase in thickness of the seasonally thawing layer (by 0.4 m in the year 1979 and by 0.7 m in 1980) in this area did not lead to any undesirable consequences. Moreover, the active layer that had increased nearly by 1.5 times froze up 1.5 to 2 months more rapidly than that in the natural area.

CONCLUSIONS

Upon considering in general the geocryological situation at both stations, one is led to draw the following conclusions.

A systematic increase in thickness of the seasonally thawing layer was occurring in natural areas, with slight fluctuations of the times of the beginning of seasonal thawing and freezing of the soils (Fig. 3, No. 1). And at station Zeisk, during the observing interval, it increased so that became close to a critical one, i.e., became such which, when exceeded, will lead to the beginning of perennial thawing (degradation) of the permafrost. In our opinion, however, this will not happen in the foreseeable future. Such a supposition relies on the fact that during the period from 1975 to 1981 the air temperature in that region was generally decreasing and was largely below the many years' temperature. With a certain delay, a similar variation will also concern the soil temperature, which inevitably will lead to a decrease in thickness of the seasonally thawing layer. This is completely confirmed by the results of the investigations. Only on the surface did the annual mean soil temperature decrease at both stations during the third year of the observations, while the next year at station Zeisk when the observations at Eterkan were already stopped, the temperature decreased as deep as 1.2 m.

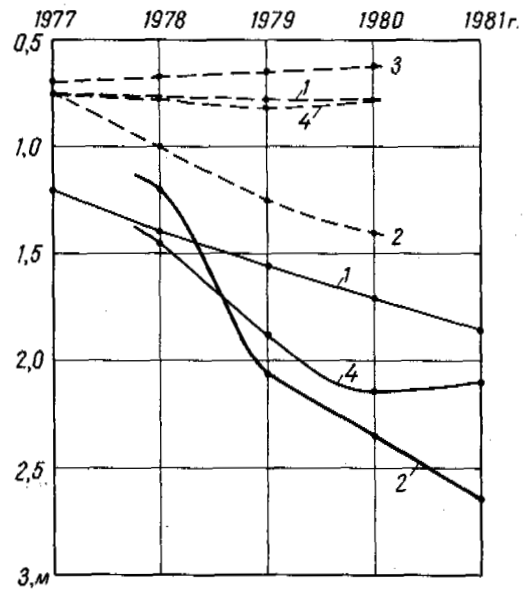

Fig.3 The Thickness Variation of the Annually Thawing Layer at Stations Eterkan (dots) and Zeisk (solid line). 1-4 - area numbers.

At the same time, the data obtained indicate unstable conditions of the region's permafrost zone. During more significant climate fluctuations, especially toward a rise in temperature, it seems quite possible that some areas may display the beginning of the permafrost degradation process without whatsoever external actions.

Removal of the snow cover in the area, with the moss cover remaining intact, causes the soils to cool down significantly, which results in a more rapid freezing and a reduction in thickness of the seasonally thawing layer (Fig.3, No.3). Therefore, such a disturbance of the naturally occurring situation should be recommendable when building - using a method of soil conservation - foundations in permafrost conditions as well as when there is a need to strengthen the freezing regime of soils of some or other area.

Even a destruction of the moss cover accompanied by complete removal of the snow does not crucially alter the geocryological situation. And during the first two years there occurs a noticeable increase in thickness of the seasonally thawing layer, although there is a decrease in the annual mean temperature of soils and a reduction in the time taken by this layer to freeze up. However, as early as the third year

upon removal of the covers, the soil cooling that dominates the annual cycle manifests itself and the seasonally thawing layer again begins to decrease in thickness (Fig. 3, No. 4).

The most unfavourable consequences occur only whenever during the summertime the moss-peat layer is disturbed, while the snow cover in the winter period remains in its natural conditions. It is such disturbances of the natural environment that have the most mass character. This is attributable to the fact that most of the organizations are carrying out their activities in newly developed regions largely during a warm period of the year, with the use of powerful, crawler-type cross-country vehicles. During the wintertime, however, almost all activities are stopped altogether.

In such a situation there occurs an annual increase in thickness of the seasonally thawing layer (Fig. 3, No. 2) and long before the building activities there sets in an irreversible process of permafrost degradation which, as a rule, escapes stoppage by economically justified methods. The calculations show that the permafrost of a thickness of 30 m, with such a kind of disturbances, would thaw during 250 years, and 14% of thawing would be from below. Also, soils with the highest ice content and greatest ground subsidence of the upper layer, of a thickness of 3 to 5 m, will be thawing during 8 to 25 years (Balobaev et al., 1979). Throughout that time interval there inevitably will be occurring nonuniform subsidences and deformations of the soils. As a result, in such areas one has to control their conservation in stable conditions already in the phase of building some or other projects or structures as well as subsequently in the process of their prolonged utilization.

REFERENCES

Balobaev, V.T., Zabolotnik, S.I., Nekrasov, I.A., Shastkevich, Yu.G. and Shender, N. I. (1979). Dinamika temperatury gruntov Severnogo Priamurya pri osvoenii ego territoriy. Tekhnogennye landshafty Severa i ikh rekultivatsiya, 74-88, Novosibirsk: Nauka.

Gavrilyev, R.I., Nikiforov, I.D. and Gulaya, O.P. (1981). Nekotorye osobennosti teplovykh svoistv gruntov vostochnoi chasti trassy Baikalo-Amurskoi magistrali. Inzhenernye issledovaniya gruntov, 5-21, Novosibirsk:Nauka.

Zabolotnik, S.I. and Sorokina, Z.G. (1981). Osobennosti evolutsii kriolitozony pri osvoenii zony Baikalo-Amurskoi magistrali v khr.Turana. Tematicheskie i regionalnye issledovaniya merzlykh tolshch Severnoi Evrazii, 137-148, Yakutsk: Institut merzlotovedeniya SO AN SSSR.

Zabolotnik, S.I. and Sorokina, Z.G. (1988). Dinamika sezonnogo protaivaniya-promerzaniya gruntov pri unichtozhenii napochvennykh pokrovov v khr.Turana. Problemy geokriologii, Moscow:Nauka.

Zabolotnik, S.I. and Shender, N.I. (1982). Nekotorye rezultaty godichnogo tsykla izmeneniya temperatury gruntov v estestvennykh usloviyakh i pri narushenii pokrovov v Verkhnezeiskoi ravnine. Termika pochv i gornykh porod v kholodnykh regionakh, 50-57, Yakutsk: Institut merzlotovedeniya SO AN SSSR.

DISTRIBUTION OF SHALLOW PERMAFROST ON MARS

A.P. Zent, F.P. Fanale, J.R. Salvail and S.E. Postawko

University of Hawaii, Honolulu, Hawaii, USA

SYNOPSIS A quantitative model of the distribution and migration of water in the shallow, high-latitude regolith of Mars is presented. All volatile migration is in the vapor phase. At latitudes > 45°, ground ice is stable near the surface. We describe the principles that govern its distribution at polar latitudes, and present results based upon the application of our model.

INTRODUCTION

The mean surface temperature of Mars is approximately 200 K and the mean atmospheric H_2O pressure is only about 3×10^{-2} Pa. These conditions are well outside the stability field of liquid H_2O, and liquid water is believed to be absent on the surface and throughout at least the uppermost kilometer of the martian crust. To the best of our knowledge, all H_2O migration on Mars today occurs either in the vapor or solid phase, both extremely inefficient relative to H_2O migration rates on Earth. The distribution of H_2O throughout the martian environment therefore reflects the average conditions over a protracted period of martian history, since it requires millions or billions of years to redistribute geologically significant amounts of ice. Ground ice is stable with respect to the meagre atmospheric inventory only at latitudes >45°; at lower latitudes, the vapor pressure of ground ice exceeds the atmospheric partial pressure of H_2O and there is diffusion of H_2O vapor out of the regolith. At latitudes >45°, the atmospheric partial pressure of H_2O exceeds the average vapor pressure of ground ice, and H_2O molecules accumulate there. A process which continues throughout the history of Mars is the withdrawal of ground ice from low latitudes and its transfer to high latitudes. The general result of this process, according to Fanale et al., (1986), is a ground ice configuration that is similar to that shown in Fig. 1. Ground ice in the top 100 to 150 m of the low latitude regolith has probably been cold-trapped to the poles, but should exist very close to the surface at latitudes >40°. At these latitudes, there is no seasonal thawing, as there is one Earth. What then determines the depth of the high-latitude ground ice on Mars? The upper limit of ground ice should occur at that depth where, over the long-term, the vapor pressure over ice is equal to the long-term average vapor pressure in the local atmosphere. That calculation must be done numerically, because the time-averaged H_2O vapor pressure over a piece of ground ice at depth Z is not equal to the vapor pressure that corresponds to the time-averaged temperature at Z. (See Fig. 2). Therefore, for example, the annual average vapor pressure over ice decreases with increasing depth, until the seasonal thermal wave is completely damped. Below, we will describe our numerical calculation of the vapor pressure over ice in the martian subsurface, the variations of P_{H_2O} in the martian atmosphere, and how the kinetics of diffusion affect the equilibration between the two. We conclude with a discussion of our estimated ground ice profile for the martian mid- and high-latitudes, and some implications for the exploitation of this resource and its potential effects on the evolution of the martian climate. Hereafter, the upper surface of ground ice will be referred to as the "permafrost table" even through that usage is not strictly correct.

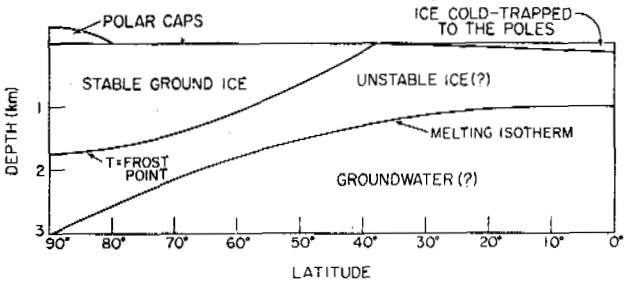

FIG. 1 - Possible configuration of ground ice on Mars. After Fanale et al., 1986.

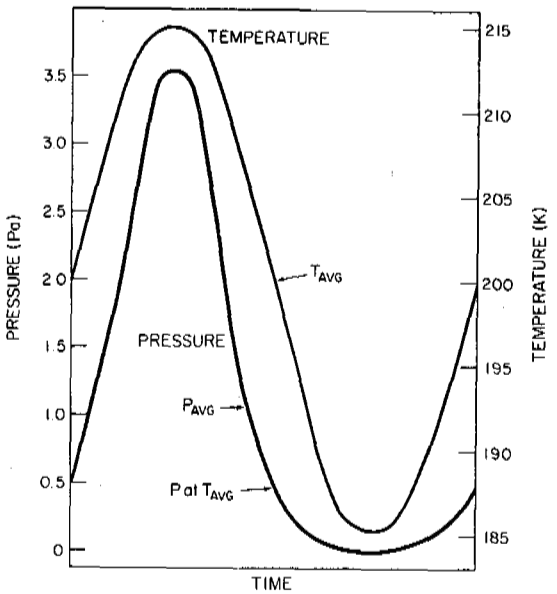

FIG. 2 - Temperature history and associated vapor pressure over H_2O ice. The average temperature is 200 K, corresponding to a pressure of ~ 0.5 Pa. The annual average vapor pressure, however, is ~ 1.0 Pa.

METHOD

The analysis of the state and distribution of water in the martian regolith is subdivided into numerical models of three conceptually separate processes. A thermal model, which treats the transport of heat through the martian regolith; an atmospheric model, which treats the transport of water through the atmosphere, and a regolith model, which treats the transport and phase partitioning of water through the regolith.

Thermal Model

Calculations of the thermal history of the Mars regolith are based on a simple energy balance model. The regolith temperatures are found from the following

$$\frac{\partial^2 T}{\partial z^2} = \frac{1}{\alpha}\frac{\partial T}{\partial t} \tag{1}$$

$$K\left.\frac{\partial T}{\partial z}\right|_{z=0} = \epsilon\,\sigma\,T^4 - I(1.0 - A) - H\frac{\partial m}{\partial t} \tag{2}$$

$$\left.\frac{\partial T}{\partial z}\right|_{z=Z} = -\frac{Q + q_s}{K} \tag{3}$$

See the list of symbols for an explanation. We calculate q_s as

$$q_s = K\frac{T_b - T_p}{\Delta Z} \tag{4}$$

Knowledge of the atmospheric pressure, as a function of obliquity, is required to describe the boundary of the seasonal CO_2 cap in time and latitude. Moreover, the flux of H_2O through CO_2, both in the atmosphere and in regolith pores, depends upon the density of the CO_2 gas. Calculation of the atmospheric pressure is performed for each modeling run via the method described in Fanale et al., (1982).

The albedo and latent heat effects due to the growth and shrinkage of the seasonal CO_2 polar caps may be taken into account once the atmospheric pressure is known. For atmospheric pressure P_v, CO_2 will condense out any time the surface temperature falls below the condensation temperature

$$T_c = \frac{-B_c}{\ln(P_v/A_c)} \tag{5}$$

Once condensation occurs, the surface temperature is buffered at T_c by latent heat effects. Thus, equation (2) may be simplified in one of two ways, according to the presence or absence of solid CO_2 at the surface. In the case of no CO_2 ice, the temperature is assumed to be above T_c, and the value of $\frac{\partial m}{\partial t}$ in (2) may be set equal to zero. Should the surface temperature fall below T_c, it is assumed that CO_2 is condensing, the temperature is fixed at T_c, and Eq. (2) is solved for $\frac{\partial m}{\partial t}$. The actual mass of CO_2 on the ground is tracked by incrementing the mass already present by the integral of $\frac{\partial m}{\partial t}$. If CO_2 is present on the ground, the albedo is 0.65. If no CO_2 is present, the albedo is 0.214, in agreement with Kieffer et al., (1977).

Atmospheric Model

The atmospheric model calculates the vapor density of H_2O at the surface as a function of latitude. It is assumed that H_2O transport is diffusive and can be approximated with simple mixing times, and that transport occurs between the summer and winter poles. This method can reproduce observed transport reasonably well (Jakosky, 1983).

Calculation of accurate atmospheric boundary conditions at the poles turns out to be complex. The polar caps subtend nearly 20° of arc on the surface of the

planet. Due to their position at the spin axis, they are never more than 20° from the terminator, and are frequently bisected by it. Insolation varies quite strongly across the polar caps, and the effective temperature at which polar atmospheric water vapor abundances are buffered is seldom clear. It is tempting to say that water vapor abundances are buffered by the coldest temperature, but this may not necessarily be so. Trial and error methods suggest that employing the temperature at latitude 85° as the effective buffering temperature provides a reasonably good fit to the observed behavior of polar water vapor abundances.

The calculation of surface temperatures at ±85° proceeds as described above. It is then assumed that water vapor in the atmosphere just above the poles is in equilibrium with the caps, and an equilibrium water vapor density may be calculated from

$$\rho_w = \frac{m_w A_w e^{\frac{-B_w}{T}}}{k T} \qquad (6)$$

A simple transport model is employed to calculate the H_2O vapor density as a function of latitude. The model assumes that the CO_2 pressure is everywhere equal and time invariant. It also assume that H_2O transport is horizontal and parallel to lines of longitude. The scale height is assumed to be 8 km and H_2O is assumed to be evenly distributed throughout the lowest scale height.

The predicted temporal and spatial variations of H_2O in the atmosphere over a seasonal cycle match Viking observations reasonably well for current orbital configurations. Our understanding of atmospheric circulation and H_2O transport at other obliquities is too poor to warrant assumption of significantly different H_2O transport patterns. Therefore, it is assumed that transport is quasi-diffusive at all orbital configurations.

Regolith Model

Applying conservation of mass to a finite element of regolith yields

$$f \frac{\partial \rho_g}{\partial t} = D_g f \frac{\partial^2 \rho_g}{\partial z^2} - \rho_s \frac{\partial \rho_a}{\partial t} - \frac{\partial \rho_i}{\partial t} \qquad (7)$$

The total water density is defined as

$$\rho_t = \rho_g + \rho_s \rho_a + \rho_i \qquad (8)$$

and is a measure of the total mass of water per cubic centimeter, summed over all phases.

The model allows the initial specification of ρ_t, and calculates the equilibrium phase partitioning based on the long term temperature profile found in the thermal model and modifies both the mass distribution and phase partitioning coefficients in a time marching manner based upon the thermal and vapor density boundary conditions previously calculated.

The calculation of the mass redistribution and phase partitioning proceeds through time and space along one of two possible algorithms, depending upon the presence or absence of ice in the regolith pores. If no ice is present in the regolith pores, then equation (7) becomes

$$f \frac{\partial \rho_g}{\partial t} = D_g f \frac{\partial^2 \rho_g}{\partial z^2} - \rho_s \frac{\partial \rho_a}{\partial t} \qquad (9)$$

The porosity, f, is assumed to be 50% and uniform with depth and latitude. The diffusion coefficient, D_g is calculated via one of two mechanisms. If the mean free path, λ of an H_2O molecule is less than the pore size, d_p, then collisions with other molecules will dominate and

$$D_g = \frac{D_a}{q} \qquad (10)$$

Where q is the tortuosity. For soils of f = 50%, q has a typical value of ~ 5 (Smoluchowski, 1968; Satterfield, 1970). If λ is greater than d_p, collisions between molecules and the pore walls will dominate, a phenomenon known as Knudson diffusion. The diffusion constant in this case is found via the method of Clifford and Hillel, (1983).

The new vapor density may be calculated directly from equation (7). Because it is assumed that transport takes place exclusively in the vapor phase, a small change in the total mass ρ_t results from diffusion of vapor into or out of the finite element The mass remaining in the adsorbed phase is calculated from conservation of mass criteria

$$\rho_a = \frac{\rho_t - \rho_g}{\rho_s} \qquad (11)$$

Partitioning into the lowest energy phase present, whether adsorbed water or ice, is always dictated by conservation of mass.

In cases where ice is present within the finite elements, it is assumed to be in equilibrium with pore vapor. The mass of adsorbed water is also assumed to be in equilibrium with the same vapor pressure. The mass of ice is likewise found from conservation of mass, and the incremental change in ρ_t. It is assumed that equilibrium is established between ice in the pores and adsorbed water instantly relative to the integration time (~ 2.0×10^6 seconds).

The upper boundary condition in ρ_g is the atmospheric vapor density found in section B. The lower boundary condition in ρ_g is found from EQ(6). The requirement that the ground ice contribute mass in

order to maintain saturation at its interface is responsible for the vertical migration of the table with time. The change in depth of the permafrost during one time step is

$$\Delta Z_i = \frac{q_\rho \, \Delta t}{\rho_i \, f} \qquad (12)$$

Where q_ρ is whatever mass flux is necessary to maintain saturation at depth Z_i.

The Mars' year is divided into 25 equal units, each 2.372×10^6 seconds in duration. For the first full day beginning each of the 25 increments, the calculation above is carried out rigorously. The results from that day are used to represent each of the remaining days in the increment. For each time step, the following calculations are performed in the order given: 1) The position of Mars in it's orbit and the mean diurnal insolation as a function of latitude are calculated. 2) The temperature gradient between the surface and the permafrost table are calculated. 3) The vapor density of H_2O at the poles is calculated. 4) The global H_2O vapor distribution is calculated. 5) The vapor density at the permafrost table is calculated. 6) The mass distribution and phase partitioning of water throughout the regolith is calculated, and 7) the incremental change in the depth of the permafrost table is calculated. The program iterates for 20 Mars' years in order to remove the effects of arbitrary initial conditions.

In order to calculate ρ_t effectively, as well as predict the position of the permafrost table, the above calculation must be performed over all obliquities. In such a case, the program iterates for five Mars years, and the predicted trends in ρ_t and Z are extrapolated through 10^3 Mars years in order to yield new values. The obliquity is re-calculated according to the expression given in Ward (1974).

RESULTS

At latitudes where the annual average atmospheric vapor density is higher than the vapor density over ice at the annual average temperature, the equilibrium position of the permafrost table is expected to occur within the annual thermal penetration depth. Based on earlier work, (e.g. Toon et al., 1980; Fanale et al., 1986), that condition holds for all altitudes $>45^\circ$. Because the atmospheric H_2O content is buffered at polar temperatures, the transport capacity of the atmosphere is extremely limited. We calculate that mass exchange is limited to $<10\,g\,cm^{-2}$ over each obliquity cycle (1.2×10^5 yr). Interesting amounts of water cannot migrate through the martian regolith in response to shorter cycles. At high latitudes however, where the permafrost table may be expected to occur within the uppermost meter of the regolith, it is necessary to combine detailed modeling of seasonal thermal drivers, finite kinetics of seasonal mass transport, adsorptive equilibria, and long term boundary conditions in order to predict the state and boundary conditions of H_2O. The questions to be considered are: What is the mean position of the permafrost table over an obliquity cycle, and do the mass fluxes which obtain in the top meter of the regolith due to seasonal thermal maxima permit the permafrost table to equilibrate with boundary conditions which are changing on the timescale of obliquity cycles?

The permafrost table will always occur at its equilibrium position provided, 1) that an equilibrium position exists at all times, and 2) that sufficient mass exchanges between the permafrost and the regolith to maintain the permafrost at its equilibrium position. For all latitudes less than 70°, criteria 1 is violated at low obliquity. Ground ice is not stable against the very strong polar cold trap at any depth. At latitudes greater than 70°, the equilibrium depth of the permafrost table varies over at least 1m from high to low obliquity. The maximum mass of H_2O which could exchange between the regolith and the permafrost may be considered equal to the total mass exchanged between the atmosphere and regolith, approximately 10 g cm^{-2}. With a nominal porosity of 50%, the exchange of 10g cm^{-2} suffices to effect only 20cm of migration in the position of the permafrost table. Therefore, the position of the permafrost table is not determined by its equilibrium position with respect to annual average conditions in P and T. Kinetics require that the average position of the permafrost table be fixed by conditions averaged over obliquity cycles.

At each latitude, the average depth to the permafrost calculated above can be checked by the following method, which is repeated at each latitude. At several obliquities the annual average atmospheric H_2O vapor density is calculated. The resulting curve of annual average atmospheric vapor density vs. obliquity is integrated over θ to yield the "astronomical" average atmospheric vapor density. In this use, the term "astronomical" is intended to imply that the average is taken over the timescale of an obliquity oscillation (1.2×10^5yr).

At every depth, the instantaneous equilibrium vapor density over ice is calculated for each season and obliquity, and averaged over season and obliquity. over season is a profile of astronomical average equilibrium vapor densities for all depths. All that remains is to choose the depth where the astronomical average of the equilibrium vapor density over ice is equal to the astronomical average atmospheric vapor density. That is the equilibrium depth of the permafrost table. The resulting profile closely matches that of the more rigorous cal-

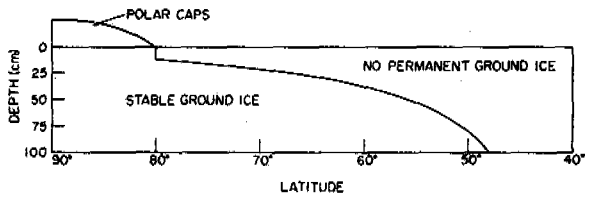

FIG. 3 - Possible ground ice configuration for top meter of regolith at latitudes >40 °.

culation and is shown in Figure 3 and Table I. Oscillations about this position are expected to occur as up to 10 g of ice cm^{-2} moves into the regolith at higher obliquities, and out of the regolith at lower obliquities.

TABLE I

Latitude (°)	Depth to ice (cm)
80.0	12
70.0	20
60.0	32
50.0	77
40.0	62000

DISCUSSION

The depths to hard-frozen permafrost presented here must be considered only an estimate of the expected distribution of ice in the martian high latitude subsurface. It is possible that the actual depth to ground ice differs from these estimates for a number of reasons. While the composition of martian surface materials remains unknown, it is possible that those materials are excellent adsorbers with a large capacity for storage of H_2O. Little mention of H_2O adsorption has been made previously, in part because we do not understand the coadsorption that would occur with both CO_2 and H_2O present in the atmosphere. Although H_2O has a higher heat of adsorption, CO_2 is present at a pressure approximately 10^4 times greater than H_2O. A very preliminary calculation of adsorptive competition in the first monolayer suggests that CO_2 will occupy a majority of the adsorption sites. However, if smectites are present in the martian soils, their high internal surface area, which can be visited by the strongly polar H_2O molecule, but not by CO_2, may provide for huge adsorptive reservoirs, and may cause changes in the estimated position of the permafrost table. Smectites swell at high relative pressures due to inclusion of interlayer H_2O molecules, and in some instances it is conceivable that all available volume in the regolith will be filled before all available adsorption sites in the particulate material. It is possible that once ice withdraws from a smectite-rich region of the regolith, it will not re-occur there.

In addition to the consideration of irreversible withdraw of ground ice, it is important to be aware that the martian surface may undergo periodic cycles of erosion and deposition at high latitudes. The permafrost table can migrate only over a range of 10 to 20cm over the course of an obliquity cycle. It may well be that the surface of the planet sporadically varies by a far greater value. It has been argued that the craters of substantial size have been filled and re-excavated (Arvidson, 1974) at high latitudes, and that a fairly deep debris mantle exists at latitudes greater than about 30 °. Therefore, it is possible that the configuration of martian ground ice is more strongly controlled by the erosional/depositional regime than by H_2O migration.

The possibility that the depth of ground ice is dependent on regolith the adsorptive capacity of the regolith material does not alter the conclusion that significant amounts of H_2O are likely to be stored in the high-latitude regolith, whether as adsorbate or as ground ice. The high latitude regolith of Mars will eventually prove to be a resource rich in H_2O.

The presence of extensive amounts of H_2O in the regolith as ground ice may have an effect on the global atmospheric CO_2 cycle. As described by Toon et al., (1980), the high-latitude regolith stores the majority of the adsorbed CO_2 by virtue of its lower temperature, As the obliquity of the planet increases, the high latitude regolith warms somewhat and the regolith desorbs enough CO_2 to raise the atmospheric pressure of Mars by several millibars. If enough ground ice is present to interfere with that cycle, by occupying the volume otherwise occupied by CO_2, or by inhibiting diffusive exchange between the atmosphere and regolith, there may be no high atmospheric pressure regime at high obliquities.

It should also be cautioned that the thermal model presented here is necessarily a "point-design", and that deviation of the thermal properties of the regolith from those assumed here will result in displacement of the permafrost table from it's calculated position.

CONCLUSIONS

1. The seasonal thermal wave reaches ground ice at latitudes >45 °. The maximum annual temperature of the ground ice strongly affects the annual average vapor pressure because of the non-linearity of the vapor pres-

sure relation.

2. Ground temperatures do not allow melting, and all transport of H_2O is in the vapor phase. Maximum annual fluxes are on the order of 10^{-4} g cm^{-2} yr^{-1}.

3. The ground ice interface should occur within the uppermost meter of the regolith at all latitudes >50°.

4. Erosion or deposition at the surface may dominate H_2O diffusion as a determinant of ground ice depth.

Symbol	Typical Value	Explanation
A	0.21-0.65	Albedo
A_c	1.22×10^{12} Pa	Empirical constant
A_w	3.56×10^{12} Pa	Empirical constant
α	7×10^{-7} m^2 s^{-1}	Thermal Diffusivity
B_c	3167.8 K	Empirical constant
B_w	6141.7 K	Empirical constant
D_a	~15	Atmospheric diffusion coefficient
D_g	~3	Soil diffusion coefficient
ϵ	0.98	Emissivity
f	~ 50%	Porosity
H	6.2×10^6 J kg^{-1}	Heat CO_2 sublimation
I	$0-2 \times 10^2$ J m^{-2} s^{-1}	Insolation
K	0.8Jm^{-1} s^{-1}	Thermal conductivity
k	1.38×10^{-23}JK^{-1}	Boltzmann's constant
m	$0-\infty$ g cm^{-2}	Column of condensed CO_2
m_w	2.98×10^{-26}kg	Mass of H_2O molecule
P_v	700 Pa	Atmospheric Pressure
Q	0.03 J m^{-2} sec^{-1}	Geothermal heat flux
q	5	Tortuosity
q_s	± 10 J m^{-2} s^{-1}	Seasonal heat flux
ρ_a	0 - 30 kg m^{-3}	H_2O Adsorbate density
ρ_g	$10^{-4} - 10^{-11}$ kg H_2O m^{-3}	H_2O vapor density
ρ_i	0 - 500 kg m^{-3}	H_2O Ice density
ρ_s	1400 kg m^{-3}	Soil density
ρ_t	0 - 500 kg m^{-3}	Total H_2O density
ρ_w	$10^{-4} - 10^{-11}$ kg H_2O m^{-3}	Equil. H_2O vapor density
σ	5.76×10^{-8} Jm^{-2} s^{-1} K^{-4}	Stephan-Boltzmann constant
T	150 - 300 K	Temperature
T_b	150-220K	T at Ground Ice
T_c	~ 150 K	Condensation T of CO_2
T_p	160-220K	Annual avg. T
t	$0 - \infty$	Time
ΔZ	0-5m	Ice - Thermal skin depth
z	0 - 1 m	Depth

REFERENCES

Arvidson, R. E., (1974). Morphologic classification of Martian craters and some implications, *Icarus,* **22,** 264-271.

Clifford, S. M., and Hillel, D., (1983). Stability of ground ice in the equatorial region of Mars. *J. Geophys. Res.* **88,** 2456 - 2474.

Fanale, F. P., J. R. Salvail, W. B. Banerdt, and R. J. Saunders, (1982). Mars: The regolith-atmosphere-cap system and climate change, *Icarus* **50,** 381-407.

Fanale, F. P., J. R. Salvail, A. P. Zent, S. E. Postawko, Global distribution and migration of subsurface ice on Mars, (1986). *Icarus* **67,** 1-18.

Jakosky, B. M., The role of seasonal reservoirs in the Mars water cycle: 2. Coupled models of the regolith, the pole caps and atmospheric transport, (1983). *Icarus,* **55,** 19-39.

Kieffer, H. H., T. Z. Martin, A. R. Peterfreund, B. M. Jakosky, E. D. Miner, F. D. Palluconi, Thermal and albedo mapping of Mars during the Viking primary mission, (1977). *J. Geophys. Res.,* **82,** 4249-4295.

Satterfield, C. N., (1970). *Mass transfer in heterogeneous catalysis,* MIT Press, Cambridge, Mass.

Smoluchowski, R., Mars: Retention of ice, (1968). *Science,* **159,** 1348 - 1350.

Toon, O. B., J. B. Pollack, W. Ward, J. A. Burns, K. Bilski, The astronomical theory of climate change on Mars, (1980). *Icarus,* **44,** 552-607.

Ward, W., Climatic variations on Mars, 1, Astronomical theory of insolation, (1974). *J. Geophys. Res.* **79,** 3375 - 3386.

ON THE METHOD OF CRYOHYDROGEOCHEMICAL INVESTIGATIONS

N.P. Anisimova

Permafrost Institute, Siberian Branch of the USSR Academy of Sciences, Yakutsk, USSR

SYNOPSIS Methodical features are examined of hydrogeochemical testing of permafrost, ice and underground water in carrying out complex geocryologic investigations. They account for specific conditions of the permafrost zone in which migration of the pore solution takes place during disturbances of the rock natural negative temperature and is accompanied by physico-chemical processes leading to re-distribution of salts between solid and liquid phases and consequently to changes in chemical composition of the rocks and ice.

Lately the hydrogeochemical methods have been enlisted more often during carrying out complex geocryological investigations. The hydrogeochemical data obtained are used as additional diagnostic indications in studying the formation and genesis conditions of frozen loose deposits, ground ice , icings, water-bearing taliks, bodies of liquid saline water below °C, in studying migration of pore solutions, etc. Experience of long-term reconnoitring and routine permafrost - hydrogeological investigations showed that trustworthiness of the hydrogeochemical materials obtained in solving the mentioned problems depends to a great extent on correct sampling of water, ice and permafrost for chemical analysis (Anisimova, 1983a, 1983b). However insufficient elucidation of this problem in methodical geocryological literature and absence of unified concrete instructions for the personnel on carrying out the work in the conditions of the permafrost zone occasionally lead to resulting materials of inferior quality. In some cases incorrect data are obtained if the samples are taken from disturbed natural environment (outcrops, pits, open cuts), in others they are determined by incorrect sampling procedure. In this case disturbances in the chemical composition of frozen rocks (permafrost), ice or water occur due to physico-chemical processes taking place during phase transitions of water, connected with environment temperature change that define either ice melting or water crystallization. Intensity of the processes may differ depending on initial salinity, composition of salts, rate of thawing or freezing, lithological composition of the rocks, ice structure, etc. (Anisimova, 1981). Unfortunately, possibility of the influence of such changes on the chemical composition of permafrost and ice is not always considered in carrying out investigations in natural permafrost zone conditions which leads to erroneous results. Below are examined the possible errors and specific methodical procedures which must be followed in carrying out hydrogeochemical testing of permafrost and ices and also during routine studies of underground waters.

In studying the history of formation and structure of permafrost and genesis of the ices contained in it, numerous information is carried by their natural outcrops in the valleys of the lower reaches of Yenisei, Lena, Yana, Indigirka and other rivers. These outcrops attract attention of wide circles of scientists and are being studied in detail. Hydrogeochemical testing is carried out occasionally. But it should be remembered in this case that data close to the natural chemical composition of permafrost can be obtained only on a condition that samples for the chemical analysis are taken from a layer not affected by the migration processes. To some extent this may be obtained on the condition that samples are taken only after deep clearing away the outcrop debris including removal of not only the thawed rocks but also of the upper (considerably warmed) layer of permafrost or ice. This is a very labour consuming and dangerous work as during the Summer period intensive caving takes place of thawed rocks which are in a floating state at the stripped outcrop.

The most reliable hydrogeochemical data may be obtained during analysis sampling in a process of dry hole sinking in permafrost, i.e., without use of a drilling fluid. In this case the sample taken from the central undisturbed and unthawed part of the core is placed into a clean, water impermeable vessel in which the thawed sample is dried.

The frequency of sampling for analysis is significant in employment of hydrogeochemical data for studying the freezing conditions of the rocks. In a vertical section of syngenetically freezing deposits (in the process of their accumulation) alternation is typical of layers with increased (or high) and lower rock salinity connected with seasonal migration and cryogenic concentration of readily soluble salts. Frequent sampling of the rock samples during borehole sinking (usually after every 0.5 m) is required to establish this feature. In case of epigenetic freezing of loose deposits salinity

distribution along their vertical section is quite uniform which permits less frequent sampling for analysis (usually after every 3-5 m).

One of the central points in modern permafrost studies is devoted to the formation problem of the deposit forming ices widely distributed in the northern regions of the permafrost zone. Analysis of the materials of detailed hydrochemical studies of underground ices - from frost mounds, sheet deposits and from ice-soil layers (Anisimova, 1963, 1981; Anisimova, Karpov, 1985; Anisimova, Kritsuk, 1983) showed the possibility of employing this data as an additional indication in studying ice genesis. Ground ices of different genesis are characterized by their distinctive changes in chemical composition along the vertical cut and by their deposit area connected with various formation conditions. Therefore ice testing must be as detailed as possible and include sampling along the vertical cut of the ice body and also of the rocks containing it. Often the studies of the deposit-forming ices are carried out in their natural outcrops along river valleys where they are represented by layers and lenses of considerable length and thickness or by wedges.

Chemical composition of ices in outcrops stripped naturally or by artificial means and of frozen rocks incorporated in them is altered as was already shown, due to migration of the readily soluble salts with melt water. Differences in the chemical composition data of ice samples taken from naturally stripped outcrops and during sinking a borehole in the same horizon are shown in Table I.

The example cited proves that the most reliable results may be obtained only during sampling of ice and permafrost that includes it in the process of borehole sinking. It is important in this case that the whole deposit is sampled, including its bottom part not stripped by the outcrop and also of its underlying rocks.

Reliability of the ice hydrogeochemical test data also depends on correct collection of the sample itself for the analysis. It is very important to collect it without thawing the ice and as far as possible without earth inclusions which may have marked influence on the chemical analysis results. This is specially important in the case of fissure - vein ices and ground ice layers.

An erroneous result may be obtained if melt water formed before the end of complete thawing of the sample is poured off for the analysis. This is explained by considerable differences in the mineralization magnitude and in the ionic composition of different ice melt fractions (Table II). The largest quantity of the readily soluble salts is carried away by the first fractions of melt water and their content diminishes in the following ones. Sometimes mineralization magnitude of ice water depends directly on the quantity of mineral suspensions contained in ice. Therefore their quantity must be taken into account by recalculating the dry residue weight in the filter for one liter of melt water.

Contents in the ice of unstable components (NH_4^+, NO_2^-, NO_3^-, Fe^{2+}, Fe^{3+}, pH) is included

TABLE I

Chemical composition of ice from "Ledyanaya gora" mountain in the valley of Yenisei river (mg/l)

Sampling location	Ca^{2+}	Mg^{2+}	$Na^+ + K^+$	HCO_3^-	SO_4^{2-}	Cl^-	Total ions
Outcrop	11.5	2.3	2.3	48.8	3.0	1	67.9
Borehole	5.6	4.5	32.2	85.4	8.2	32.5	168.4

TABLE II

Chemical composition of water formed in the process of an ice sample melt

Fraction	Ion composition, mg·eq							Total ions, g/l
	Ca^{2+}	Mg^{2+}	$Na^+ + K^+$	HCO_3^-	CO_3^{2-}	SO_4^{2-}	Cl^-	
First	0.87	5.09	26.52	5.94	0.57	10.23	15.75	1.99
Second	0.40	3.18	15.66	3.05	0.64	6.22	9.72	1.15
Third	0.33	1.80	7.15	2.39	0.22	2.47	4.22	0.64
Fourth	0.37	1.09	4.24	1.71	none	1.71	2.27	0.37
Last	0.52	0.56	2.47	1.24	none	1.92	0.40	0.18

in the interpretation of the chemical analyses data provided it is known that they were determined immediately after complete melting of ice from a given sample. However, even in this case the values obtained are only approximate since they are somewhat altered by disturbance of the natural redox conditions. Requirements stated above should be also followed in studying chemical composition of the icing. If these investigations are carried out for the purpose of determining an approximate chemical composition of water feeding the icing, then ice samples for the chemical analysis must be taken before beginning of the icing melting. Since ice chemical composition and mineralization vary considerably over its area and the vertical section, the results of the chemical analyses of single ice samples taken from the surface or over the whole section at some single point of the icing surface cannot be used for judging the chemical composition of the icing forming water. Comparatively close value of its mineralization is given by an averaged value of chemical analyses of the ice samples taken layer-by-layer of the whole icing thickness at least at three points of its area (upper, middle, lower) from one source of water discharge. To obtain a closer result, the weight of precipitated carbonates remaining in the filter must be added to the mineralization value of each sample. Data on ice tests from the samples taken after beginning of the icing melting are distorted due to migration of the soluble components with melt water.

The complex of permafrost-hydrogeological work includes both single and planned routine hydrochemical investigations of underground waters required for clarification of their formation and feeding conditions, water exchange intensity in the water-bearing layer, the nature of interaction between underground waters and perennially frozen rocks, direction of the cryogenic processes, etc. Reliability of the hydrochemical data obtained with this is determined to a considerable extent by carrying out the investigations under specific conditions of a permafrost zone that influence both the nature and the time of carrying out hydrochemical tests of underground water sources and on correctness of sampling the water for chemical analysis.

Single hydrochemical samplings of the sources usually taken in Summer or Autumn may give incorrect chemical composition characteristic of the underground water flowing out on the surface since its mixing is possible with other kinds of underground waters formed directly near the outlet of main water. The most notable influence on the source chemical composition characteristic may be made by the waters forming during thawing of ice saturated seasonally frozen rocks, during thawing of underground icing or of injected ice in frost mounds and also of water draining off during thawing of permafrost that separates a thick water-bearing layer. The share of the water varieties listed above in a mixture with water from a water-bearing horizon that is drained at different drainage locations varies and is not constant with time. This depends a lot on the specific permafrost-hydrogeological conditions. Therefore during primary survey of the sources acting the whole year round it is required to carry out obligatory sampling of water for chemical analysis from all of its functioning (permanent or temporary) heads, since water in them may differ considerably in the level of mineralization and in its ionic composition. This may be caused by mixing with melt water, as indicated above or with water being discharged from water-bearing horizons of different genesis. The degree and nature of these influences may be clarified in carrying out planned routine observations at the sources. Planned routine hydrochemical studies in Central Yakutia showed that the chemical composition of the sources acting the whole year round becomes most stable during late Autumn when atmospheric precipitations as snow and the thawing process of the grounds containing ice near the water discharge point is stopped and running-off takes place of the suprapermafrost water horizon. But even during this, the most favourable time for the composition stabilization, a mistake is possible due to incorrect sampling procedure of water. This may be easily caused by entrance into a sampler of frazil ice formed during night-freezing of water at shallow locations, or of the melt water formed during thawing of this ice at the day time. All this reduces water mineralization. Therefore the spring head must be cleaned from ice before sampling and several volumes of water must be discharged until complete clarification is obtained.

In carrying out the planned routine observation of the chemical composition of waters from underground suprapermafrost and intrapermafrost taliks and also of subpermafrost horizons opened up by the boreholes, it is necessary to account for possible errors due to cryogenic changes in water chemical composition taking place during ice formation in the borehole (formation of ice plugs). Thus it is not possible to judge the real water composition in a water-bearing earth by a sample taken from the borehole immediately after mechanical breaking of the ice plug or after its thawing. In taking a water sample from such a borehole it is necessary not only to clean it from ice but to pump away water according to the instructions.

In the pits that have opened-up underground waters the water chemical composition also changes considerably during formation or thawing of an ice cover. In these, as in the case of boreholes, replacement is required of several volumes of water by pumping it out before sampling for the chemical analysis.

In carrying out the engineering geological surveys in the permafrost areas study of the chemical composition of rocks and ground waters must not be limited by a single sample for analysis only at the moment of boring the hole or cutting the pit since the chemical analysis undergoes notable cryogenic and other changes in the course of an annual cycle, especially in the areas with high rock salinity and development of bodies of highly mineralized underground liquid saline waters with temperature below 0 °C, located near the surface.

Thus, the above description shows that successful use of the hydrogeochemical data during complex geocryological studies depends not only on correct choice of the location, the method and frequency of sampling permafrost, underground ices and waters for

the chemical analysis, but also on following a number of obligatory conditions during taking the samples themselves that will exclude cryogenic changes in the sample chemical composition. Only unified approach by all investigators may produce comparable materials.

REFERENCES

Anisimova, N.P. (1963). Khimicheskii sostav podzemnykh ldov v alluvialnykh peskakh srednego techeniya r.Leny. Ousloviya i osobennosti razvitiya merzlykh tolsch v Sibiri i na Severo-Vostoke. Moskva, Izd-vo AN SSSR, s.101-111.

Anisimova, N.P. (1981). Kriogidrogeokhimicheskie osobennosti merzloi zony. Moskva, Nauka, str. 153.

Anisimova, N.P. (1983a). Osobennosti gidrokhimicheskogo oprobovaniya istochnikov merzloi zony. Metodika gidrogeologicheskikh issledovanii kriolitozony. Novosibirsk, Nauka, str. 57-63.

Anisimova, N.P.(1983b). Osobennosti gidrokhimicheskikh issledovanii podzemnykh ldov. Regionalnye geokriologicheskie issledovaniya v Vostochnoi Asii. Yakutsk, IM SO AN SSSR, str. 12-19.

Anisimova, N.P., Kritsuk, L.N. (1985). Ispolzovanie kriokhimicheskikh dannykh pri izuchenii genezisa zalejei podzemnykh ldov. Problemy geokriologii. Tr. IV Mejdunarodnoi konferenzii po merzlotovedeniu. Moskva, Nauka, str. 230-239.

Anisimova, N.P., Karpov, E.G. (1985). Khimicheskii sostav plastovogo podzemnogo lda v nizoviyakh r.Yenisei. Rgionalnye i injenernye geokriologicheskie issledovaniya. Yakutsk, IMZ SO AN SSSR, str. 34-44.

HYDROCHEMISTRY OF RIVERS IN MOUNTAIN PERMAFROST AT 33º L.S., MENDOZA – ARGENTINA

E.M. Buk

CONICET CRICYT Mendoza, Argentina

SYNOPSIS The principal chemical characteristics of water issuing from permafrost basins with rock glaciers and debris covered glaciers, is not well known. Such characteristics are related to temperature variations and flow levels according to precipitations in different times of the year. Two basins are compared: one with metamorphic rocks (debris covered glacier) and other with volcanic rocks (rock glacier). The temperatures and conductivity of an entire year are analyzed together with discharge and precipitation.

INTRODUCTION

The permafrost limit is at approximately 3200 m asl in the Cordón del Plata, Cordillera Frontal of Mendoza (Corte et al, 1984) and the line of glacier equilibrium is at 4750 m asl. The area of uncovered ice is only 3% of the total basin area, the 97% left is a detritic cover material and rock outcrops. There are big rock glaciers which have been classified as of cryogenic, El Salto (Corte, 1987) and glacigenic origin, Vallecitos-Morenas Coloradas (Fig. 1) (Corte, 1987).

There is a series of geoforms of distinct characteristics coexisting in both basins, Morenas Coloradas and Rincón de los Vallecitos. They correspond to different stages of glacial activity (Fig. 1) and their range is from Wisconsinean moraines in the lowest part, to the large ablation Holocene moraines, limited by uncovered ice (glacier) in the highest part (Corte et al. 1981; Wayne et al 1983)

In this type of basin the discharge water is a variable mix from different sources: melt ice (glacial, interstitial),melt snow accumulated during the winter and summer precipitations in its different kinds (hail, graupel, rain, etc.). The discharge water always merges clean, without yielding sediments in suspension. The amount contributed by each one is related to the climatic situation and reflects in the chemical composition. The water provided by snow patches and glaciers is not significative because of their areal extension.

The purpose of this research is to know the chemical characteristics of the water issuing from such basins and to find the hydrochemical-climatic-geological relations in order to have a first approach to the hydrogeological model.

STUDY AREA: LOCATION AND METEOROLOGIC-CLIMATIC-ENVIRONMENTAL CONDITIONS. THE PERMAFROST.

The area under study is located NW of the province of Mendoza, between 32°55' and 32°59' S latitude, 69°21' and 69°25' W. Its height ranges from 2100 m to more than 6000 m (Fig.1). According to data registered during three years (July'78/June'81) in the meteorological station located at 2550 m, the general climatic characteristics can be summarized as follows:

- -Summer: the monthly mean summer temperature varies between 8.2°C and 11.0°C; while the relative humidity varies between 65.8% and 76.7%.
- -Winter: the monthly mean winter temperature varies between -1.5°C and 4.0°C; the relative humidity is between 30% and 52%.

Approximately half of the mean annual precipitation, which is 523 mm, falls in December, January, February and March as rain. The other half is winter snow precipitation. The mean annual air temperature is of 5.6°C and the lapse rate for this zone is 0.6°C/100 meters.

The considered basin is mainly composed of volcanic rocks of the Variscican association (Permian) represented by riolites, and sedimentary rocks from the Upper Paleozoic (Carboniferous) (Caminos 1965). The behavior of these formations varies greatly with the same weathering processes. The vegetation is very scarce and it is confined to the lower part of the basin. The environmental and climatic conditions with temperatures below 0°C, favor the existence of the andine type of permafrost. This is indicated by the active rock glacier (Corte, 1976; Barsch, 1978), by temperature profiles (Corte et al, 1984) and by geophysical prospecting (Fournier et al., 1984). Permafrost presence is implying particular chemical and hydrological conditions, as demonstrated in the Caribou-Poker Creeks, Alaska (Slaughter et al., 1983). At 2.550 m. it was recorded an average of 1.400 hours freezing temperature per year.(Regairaz,1984).

METHODS

The sample site is about 1300 m downstream from the meteorological station. There were taken 59 samples weekly on the covered glacier. Plastic containers, previously washed with the water to be sampled, were used. Five samples were taken for the rock glacier. The river water level variations were recorded with limnigraphs. The only data utilized were the temperature and river level variations corresponding to the days when the sampling was performed. The chemical analysis were done at the CRAS, San Juan.

DATA, ANALYSIS AND INTERPRETATION

The conductivity varies along the year between 308 and 240 micromhos/cm, with the highest and more stable values during the winter season for the covered glacier (Fig. 2). Analyzing the conductivity curve in relation to the water level variations, temperature and precipitations (Fig. 2), the following could be observed:

a- from July till September 21/78, the conductivity values do not show brusque variations. From here and till mid December the variations related to water level and temperature begin to be significative. Precipitations do not affect it still. The spring flow resulting from snow melt and surface ice adds itself to the winter flow (base flow), diluting therefore the first flow solutes.

b- From mid December till mid April this last relation is modified. Now the highest conductivity values correspond to water level highest values and viceversa. Temperatures cannot be clearly related to the former data because precipitations, which begin to be important, interfere with them. Precipitations also modify the conductivity adding a charge of sediments. The discharge curve goes brusquely up during the summer (January/February). This corresponds to the heavy summer precipitations which are a climatical characteristic of the location.

c- From mid April the rain precipitations become very significative, the snow and ice fusion dwindles and there is a gradual return to the initial conditions.

It can be stated than in the term of a year the total water amount is composed by the following flows:

1) Winter flow, end of June till mid September. It is characterized by a maximum of salinity and a minimum discharge, both being relatively constant. This flow is the water running off the detritus, which does not receive an important melt supply from the surface.

2) Spring flow, from mid September to mid December. This flow adds to the former winter one due to snow and ice fusion, decreasing the conductivity values as the temperature rises.

3) Summer flow, from mid december to mid April. It agregates to all the formers and originates in the different types of precipitation. The swelling curves are characteristic.

4) Autumm flow, begins in mid April and ends in mid June. It is the gradual return to the beginning situation due to the total freezing of the basin. The heavy precipitations of late summer and autumm do not appear in the discharge, thus indicating that they join the rock glacier detritus already frozen (Fig. 2)

The chemical characteristics change markedly along the year (Fig. 3) according to the climatic situation, while the relative proportions of waters from different sources also vary. There was neither a correlation between the different ions, nor between them and the total mineralization. The hydrochemical characteristics of these waters, which are in contact with sedimentary and igneous rocks, are given by the relation is: Ca> Na+K >Mg for the cations and SO_4> HCO_3> Cl for the anions.

For the neighbouring basin, El Salto (Fig. 1) which is composed exclusively by igneous rocks (andesites and riolites), the relation is: Ca> Na> Mg> K for the cations and HCO_3> SO_4> Cl for the anions. The high sulphate proportion in the first case is mainly related to the sedimentary rocks. In Table I it is shown the mean percentage of the principal ions in relation to the total amount of ions for each sample, of the Vallecitos (V) and El Salto (S) basins:

	% Ca	%Mg	%Na+K	%HCO_3	%SO_4	%Cl	Mean % total ions mg/l
(V)	18.2	2.7	5.2	30.3	37.2	1.5	203.0
(S)	18.6	2.5	6.1	41.5	26.3	4.9	71.3

TABLE I: (V) 59 samples; (S) 5 samples

El Salto basin, besides having vulcanites in its composition, does not have glacial ice and is filled with outcrops and abundant talus detritic material, plus the rock glacier in its lowest part. The discharge of this rock glacier, same as in covered glaciers, is always clear, without suspension material. The water temperature, 1.5°C, would indicate that the discharge originates in the frozen core (Michel Evin, 1984).

For the metamorphites zone, the rest of the ions are shown in the following table, with less significant amounts. It can be seen that not all the ions appear continuously throughout the year.

	mg/l	
Ion	Minimum	Maximum
B**	0.02	0.39
F**	0.80	1.50
NO_3*	-	2.00
Fe*	-	4.40
Mn*	-	0.06

** Appears throughout all year

* Appears inttermitently

TABLE II

SiO_2 appears along the entire year with values oscilating among 2.3 and 11.0 mg/l. The hardness in CO_3Ca varies between 92 and 139 mg/l. Ph fluctuates among 6.7 and 8.0. On the other hand, water samples were analized in the recharge area, at 3.100m. (samples a and a´) and in the discharge area at 2.750 m. (b samples) as well, in the Morenas Coloradas basin. The mean conductivity values corrected at standard temperatures are:

a - snow patch: 2.6 micromho/cm.

a´- water from snow patch fusion: 7.0 micromho/cm.

b - issuing water: 243.0 micromho/cm.

Obviously, the sudden increase in the amount of solutes recorded in the discharge zone (b) occurs within the detritic mass through which the water flows. This experience was performed in two days, during which samples were regularly taken in point (b) only at daylight. The flow was almost constant (190/200 l/sec.) owing to the cold and cloudy day which did not favor ablation, and consequently the conductivity variations were not significant. The water temperature oscilated between 4.9°C and 5.8°C.

CONCLUSIONS

1. The chemical quality is indicated in the composing seasonal flows: winter is the season with greater amount and smaller variations of solutes with respect to the summer season.
2. The quality is defined by the lithological nature of the detritus in which the water flows and by its freezing.
3. Rock glaciers and covered glaciers produce water without suspension material.
4. The total average of ions is higher for the metamorphic zones than for the vulcanites rocks (only 5 samples of this last zone). We need more data for this last rock type, for that reason this is a progress report.

REFERENCES

Barsch, D.(1978). Active rock glaciers as indicators for discontinuous Alpine permafrost. An example from the Swiss Alps. Proceedings Third International Conference on Permafrost, (1), 348-353.

Caminos, R. (1965). Geología de la vertiente oriental del Cordón del Plata, Cordillera Frontal de Mendoza. Revista de la A.G.A., (XX), 3, 351-392.

Corte, A.E. (1976). Rock Glaciers. Biuletyn Peryglacjalny, 26, 175-197.

Corte,A.E. & Espizúa, L.E. (1981). Inventario de los cuerpos de hielo de la cuenca del Río Mendoza, Parte 1. Memoria Anual Ianigla - Conicet, 3-34.

Corte, A.E. & Buk, E.M. (1984). El marco criogénico para la hidrología cordillerana. Programa Hidrológico Internacional - Jornadas de Hidrología de Nieves y Hielos en América del Sur, Chile, 1-15. (ROSTLAC) - UNESCO.

Corte,A.E. (1987). Geocriología. (In press). 444 pp., Eudeba, Buenos Aires.

Evin, M. (1984). Caractéristiques physico-chimiques des eaux issues des glaciers rocheux des Alpes du Sud (France). Zeitschrift fur Gletscherkunde und Glazialgeologie, (20), 27-40.

Fournier, H., Corte,A.E., Mamaní,M., Maidana,M., & Borzotta, E. (1985). Estructura interna del glaciar cubierto (escombros), Vallecitos, Cordón del Plata, Mendoza, Argentina. Acta Criogénica, 4, 53-55. (in press).

Regairaz,M.C. (1984). Suelos de montaña de Mendoza. Aspectos geocriogénicos y edafológicos. Acta Geocriogénica, 2, 162-173.

Slaughter, C.W., Hilgert, J.W. & Culp, E.H. (1983). Summer streamflow and sediment yield from discontinuous-permafrost headwater catchments. Permafrost Fourth International Conference - Proceedings, 1172-1177. Fairbanks, Alaska.

Wayne, W.J. & Corte,A.E. (1983). Multiple glaciations of the Cordón del Plata, Mendoza, Argentina. Palaeogeography, Palaeoclimatogy, Palaeoecology, 42, 185-209.

ACKNOWLEDGEMENTS

I wish to thank Dr. A.E.Corte for his discussions and recommendations. To M.E.Soler for her translation.

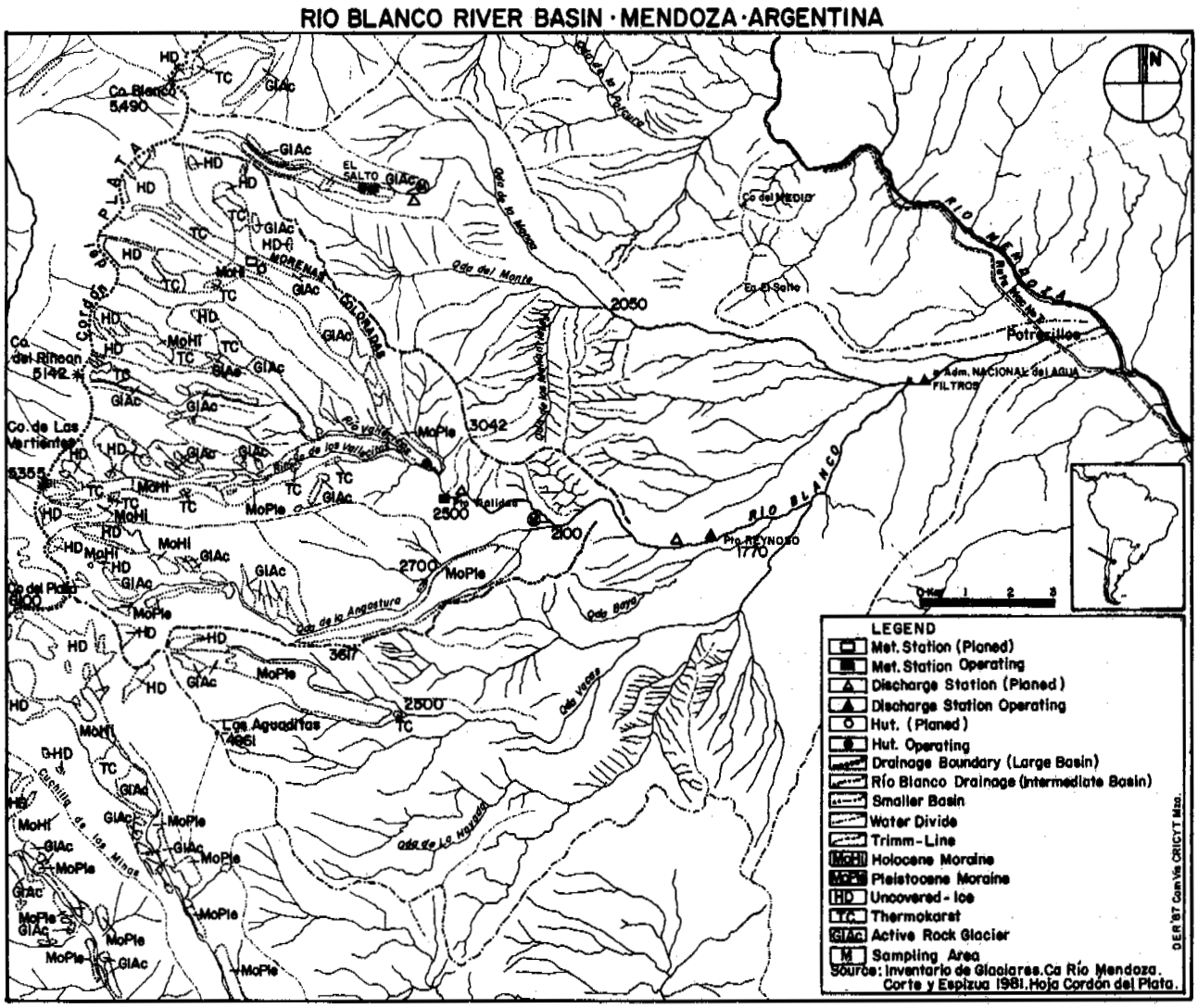

Figure 1. Studied area (N-W corner) shows debris covered glaciers and rock glaciers.

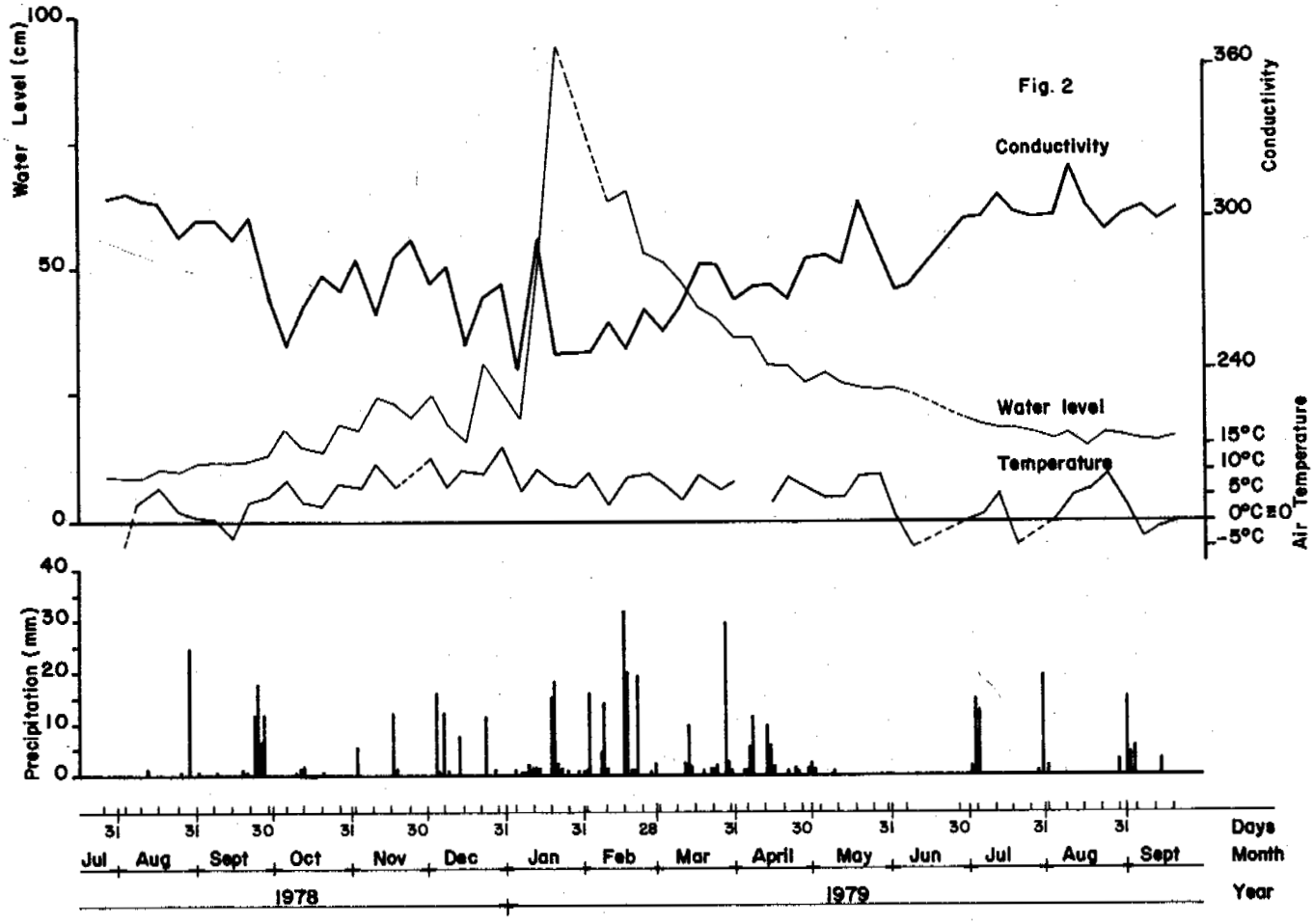
Fig. 2
Water Level (cm)
100
50
0
Conductivity
360
300
240
Conductivity
Water level
Temperature
15°C
10°C
5°C
0°C ≡ 0
-5°C
Air Temperature
Precipitation (mm)
40
30
20
10
0
31 31 30 31 30 31 31 28 31 30 31 30 31 31
Days
Jul Aug Sept Oct Nov Dec Jan Feb Mar April May Jun Jul Aug Sept
Month
1978
1979
Year

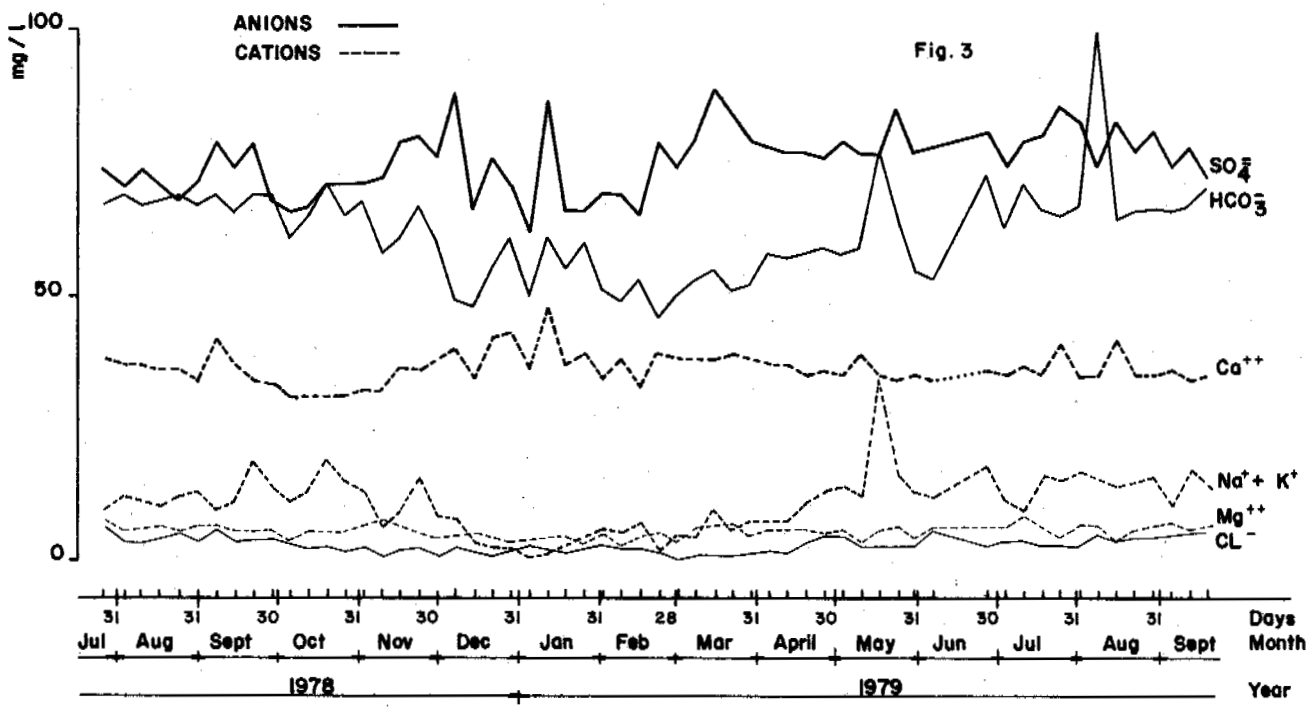
Fig. 3
ANIONS
CATIONS
mg / l
100
50
0
$SO_4^{=}$
HCO_3^{-}
Ca^{++}
$Na^{+} + K^{+}$
Mg^{++}
CL^{-}
31 31 30 31 30 31 31 28 31 30 31 30 31 31
Days
Jul Aug Sept Oct Nov Dec Jan Feb Mar April May Jun Jul Aug Sept
Month
1978
1979
Year

FROST LINE BEHAVIOUR AROUND A COOLED CAVITY

A.M. Cames-Pintaux and J. Aguirre-Puente

C.N.R.S. France

ABSTRACT The Stefan Problem and two numerical methods for its resolution are discussed. The two-dimensional problem was solved using a finite element method based on an enthalpy formulation and, on the other hand, the axisymmetrical problem was solved using the Goodrich method. Applications of these two models to geotechnical problems of cryogenic underground storage and urban gas pipelines also allowed the determination of the domain of validity of the axisymmetrical scheme. In this paper we propose a simple practical and very rapid method of estimating freezing/thawing behaviour around buried pipelines and underground cavities.

INTRODUCTION

Geotechnical problems such as underground storage of liquefied gas, urban pipelines transporting chilled gas, pipelines in Permafrost areas, etc, involve heat transfer with phase change (Stefan Problem).

To study the thermal behaviour of soils around an underground chilled cylindrical cavity, we first have proposed a finite-element enthalpy method to solve a two-dimensional problem of heat transfer with phase change considering the phase change front to be at a fixed temperature /1/. This method was used to study the thermal behaviour of a cryogenic storage pilot station and to evaluate the limit of validity of an axisymmetrical two-dimensional scheme for a realistic range of thermal conditions and burial depths of either similar possible cryogenic storage cavities /2/ or a cooled urban pipelines /3/.

In this paper, we propose an easy method for the practical exploitation of the results obtained from our different studies. The following problem is adressed :

We consider an underground cryogenic cylindrical cavity. We suppose that the thermal conditions are defined for the cavity, the surface and the initial state of the ground and that the thermo-physical characteristics of the soil are known. We would like to determine quickly and easily

- the time necessary to obtain the steady-state
- the progress of the freezing front particularly on the upward vertical axis of the cavity.

MODEL CONSIDERATIONS

Stefan Problem general equations

The very classic statement of the problem is the following /4/ : in a two-dimensional homogeneous domain Ω, one considers a solid phase or a liquid phase of a pure substance. The isothermal surface S which separates these two regions is at the liquid-solid transformation temperature Θ_f. The problem is studied in the interval $[0, t_M]$.

In the absence of sources and sinks and neglecting convection, the energy conservation conditions are written :

$$\text{in the solid, } \rho_s c_s \frac{\partial \Theta}{\partial t} - \text{div}\,(k_s \text{grad}\Theta) = 0 \ ;$$

$$\text{in the liquid, } \rho_\ell c_\ell \frac{\partial \Theta}{\partial t} - \text{div}\,(k_\ell \text{grad}\Theta) = 0 \ ;$$

At the interface $\Theta = \Theta_f$, and the energy balance gives :

$$\left(k_s \frac{\partial \Theta}{\partial \vec{n}}\right)_s - \left(k_\ell \frac{\partial \Theta}{\partial \vec{n}}\right)_\ell = L \left.\frac{ds}{dt}\right|_\varepsilon \cdot \vec{n} \qquad \text{, sur S}$$

$ds/dt|_\varepsilon$ represents the velocity of the interface and $\vec{n}$ the unit normal, positive outward from the frozen zone, at a point of this interface and L is the latent heat released or absorbed at the boundary per unit volume.

In the case of buried cavities, the boundary of Ω is divided in segments Γ_1 (the ground surface), Γ_2 (vertical and horizontal limits of the domain) and Γ_3 (the symmetry surface of the system) subjected to different boundary conditions :

$$\text{on } \Gamma_1,\ \Theta = \Theta_1^t \ ; \ \text{on } \Gamma_2,\ \Theta = \Theta_2^t \ ; \ \text{on } \Gamma_3,\ \frac{\partial \Theta}{\partial \vec{n}} = 0$$

The initial temperature distribution in Ω is written :

For $t = 0$, $\Theta(x, y, 0) = \Theta_o$

The specific heat c_s, c_ℓ, the density ρ_s, ρ_ℓ and the thermal conductivity k_s, k_ℓ are continuous functions of Θ except at the freezing interface where discontinuities may exist.

Two-dimensional enthalpy method for discrete phase change

Numerical techniques for phase change problems can be separated into two distinct groups based on the formulation of the problem. The first group deals with the energy equations written in terms of temperature as the dependent variable and includes an interface between the solid and the liquid region. The interface is a surface whose position and shape varie with time and special equations need to be written using finite difference /5/ or finite element techniques /6, 7/ to account for the interfacial energy balance.

In the second group, the interface is eliminated from consideration but enthalpy is used as the dependent variable. The enthalpy is related to temperature and includes the effects of both specific and latent heat. The problem is made equivalent to the non linear heat conduction problem without change of phase. The method is

well adapted for disperse substances that change phase over a range of temperatures /8, 9/ ; but when the phase change occurs at a fixed temperature the discontinuity of apparent specific heat leads to significant numerical difficulties /10/.

We have presented in an other paper /1/, the principle of an finite element enthalpy method for the two-dimensional problem of heat transfer which performs well whether phase change occurs at fixed temperature or is distributed over a temperature range. This mathematical formulation gives a regular solution for the temperature distribution at each time step and is obtained with the help of a Kirchhoff transformation (thermal potential) /4/ and the Heaviside function /11/.

One-dimensional axisymmetrical model

When the cavity is buried at a relatively great depth, one can assume that the horizontal ground surface influence is not significant so that the Stefan Problem can be studied by an axisymmetrical cylindrical formulation.

We solved the axisymmetrical Stefan Problem for discrete phase change by an axisymmetrical one-dimensional model developed from Goodrich's method /12, 13/. This model calculates the front position by solving the moving interface equation along with the equation for the temperature distribution.

Previous applications to practical ground freezing problems

1) Underground cryogenic pilot station

The two-dimensional mathematical model for Stefan Problems was used to study the thermal behaviour of soil around a cryogenic storage /2/. This pilot station, built at Schelle (Belgium) by Geostock (Paris) and Distrigaz (Brussels) consisted of a horizontal, 30 m long, 3 m diameter section located at the end of a 100 m concrete lined cylindrical tunnel, hollowed out of a clay soil at a depth of 23 m below the surface.

For calculation purposes we adopted the physical and thermal properties of clay estimated from Kerstern's empirical formulae based on measured values of dry density ($1.7.10^3$ kg.m^{-3}) and moisture content (35%).

The comparison of the calculated values with the experimental measurements showed that the model performed satisfactorily.

The two-dimensional model also provided the means of evaluating the range of validity of the axisymmetrical one-dimensional scheme.

2) Cooled urban gas pipe

The one-dimensional axisymmetrical model was used to study the freezing front progression in the soil surrounding an urban chilled gas pipeline. The schematic model of a transverse vertical section of the pipe is indicated in Fig. 1. The radius R* delimitating the axisymmetrical field was judiciously chosen to represent the actual physical characteristics of a pilot station built at Mitry-Mory by "Gaz de France".

Measurements obtained in situ giving the freezing front position on the upward vertical axis for the steady-state were in good agreement with that calculated using the axisymmetrical scheme when the freezing front attained equilibrium.

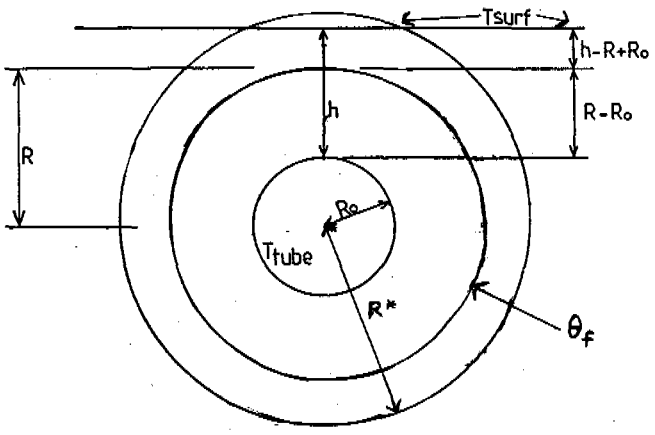

Fig. 1 Axisymmetrical buried pipe

Moreover, we have examined the influence of burial depth and of temperatures in the cavity or at the ground surface on the freezing front position.

The axi-symmetrical scheme was also used /3/ for the systematic study of the interface position when the steady-state is practically obtained. This study showed the influence of two important thermo-physical parameters : the frozen soil diffusivity "a" and the latent heat of the phase change "L".

NEW DEVELOPMENTS

In order to study the limit of validity of the axisymmetrical scheme we used as reference the numerical results of the two-dimensional model applied to the liquefied underground cryogenic storage problem. The results of the two models for different thermal conditions including the temperature program of the pilot station and different burial depths of the cavity were compared, and the domain of validity of the axisymmetrical model was defined.

To generalize the results of the first approach, we defined two dimensionless parameters, the first (P) characterizes the geometric properties (burial depth and diameter of cavity) and the constant thermal conditions imposed on the system (temperature at the soil surface and in the cavity) ; the second parameter (K_1) characterizes the geometric properties and the freezing front location :

$$P = \frac{h}{2R_o} \frac{[T_{p/s}]}{[T_{surf}]} \quad \text{and} \quad K_1 = \frac{R - R_o}{h - (R - R_o)} \cdot \frac{h}{2R_o}$$

In these equations, h is the burial depth of the cavity and $2.R_o$ its diameter, $[T_{p/s}]$ and $[T_{surf}]$ are the absolute values of the temperatures deviation from the freezing point at the cavity/soil interface and at the soil surface respectively. $(R - R_o)$ represents the freezing zone thickness on the upward vertical axis of the cavity.

In the parameter P, the coefficients T_{surf} and $T_{p/s}$ can be used only when the temperatures in the cavity and on the soil surface are constant. In the case of variable temperature, we should consider new parameters taking into account the thermal history of the system.

Instead of temperature $T_{p/s}$ at the interface cavity/soil, we propose to consider the square root of the freezing index $I_{p/s}$ defined by :

$$I_{p/s} = - \int_o^t T_{p/s}\,(t)dt$$

Indeed the integral in time of the surface temperature of a structure is an important technical parameter and even more generally useful results can be described in terms of indexes of temperature defined everywhere /14/.

For the case of the Mitry-Mory pipeline pilot station, Fig. 2 shows the evolution of the freezing front according to the square root of the freezing index. We see that during the early freezing period, before the surface boundary influence becomes important, $(R - R_o)$ is proportional to $\sqrt{I_{p/s}}$. In this case the pipe temperature was constant.

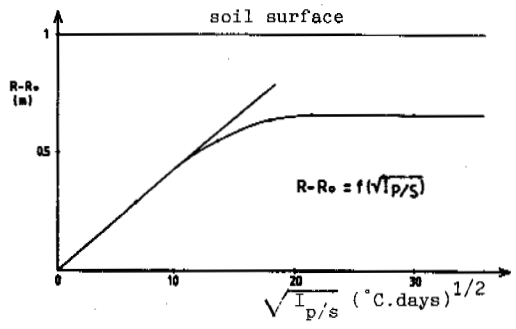

Fig. 2 $(R - R_o)$ vs $\sqrt{I_{p/s}}$ for gas pipe of Mitry-Mory

But even when $T_{p/s}$ depends on time as in the case of the underground cryogenic storage, this linearity exists. Figure 3 illustrates this conclusion for different burial depths and for the temperature history corresponding to a temperature in the cavity decreasing linearly from 0°C to -196°C over a period of 300 days. Moreover a similar presentation (not illustrated) of results for the same system subjected to a -100°C constant temperature lead to identical slopes of the straight line representing the freezing front $(R - R_o)$ as a function of the square root of the freezing index.

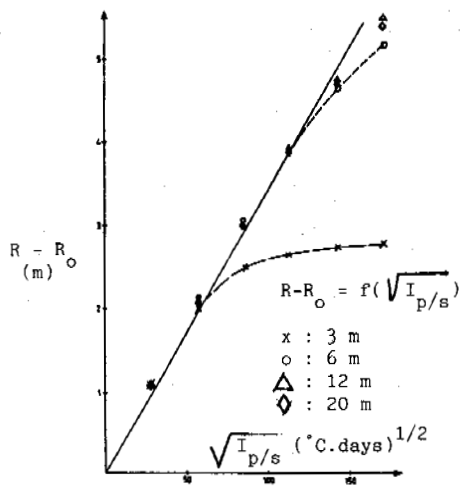

Fig. 3 $(R - R_o)$ vs $\sqrt{I_{p/s}}$ for different depths of the cryogenic pilot station cavity

In view of this, we can define a new parameter representing the slopes,

$$S_{a,L} = (R - R_o)/\sqrt{I_{p/s}}$$

and in order to also consider the influence of variable surface temperature, we define, in addition, the thermal index,

$$I_{surf} = \int_o^t T_{surf}\,(t)dt$$

These three parameters ($I_{p/s}$, I_{surf} and $S_{a,L}$) make it possible to do an easy and rapid study of the soil for any kind of thermal history in the cavity, pipes, or ground surface.

APPLICATION AND REMARKS

Sawada and Ohno /15/ give thermal characteristics for many soils found in geotechnical practice. In order to study sensitiveness of the Stefan Problem to the thermal soil properties /3/, we selected practically the two extreme values for diffusivity a and latent heat L. With the help of these values we defined four fictitious soils, characterized by the four possible ratios a/L, to make the calculations :

$$a_1/L_2 = 0{,}203.10^{-14}\ m^5.s^{-1}.J^{-1}$$

$$a_1/L_1 = 0{,}685.10^{-14}\ m^5.s^{-1}.J^{-1}$$

$$a_2/L_2 = 0{,}876.10^{-14}\ m^5.s^{-1}.J^{-1}$$

$$a_2/L_1 = 2{,}956.10^{-14}\ m^5.s^{-1}.J^{-1}$$

The couple a_2, L_1 corresponds to the case for which the time necessary to obtain the steady-state is the shortest. The other extreme case appears for a_1, L_2.

In this paper, for the four different cases defined by a/L, we exploit the results obtained by the axisymmetrical one-dimensional model for a buried pipe.

The following values were chosen for the calculation :

R_o = 0,10 m R^* = 1.15 m

pipe/soil temperature (constant) $T_{p/s}$ = -15°C

boundary temperature (constant) T_{surf} = 6.2°C

The figure 4 shows the freezing front evolution vs the square root of the freezing index for the different values of a/L. Using these curves, we can accurately determine the time when the steady-state is reached. This is show in figure 5.

In figure 4, the first part of $(R - R_o)$ vs $\sqrt{I_{p/s}}$ shows that the freezing front progression is similar to that in a semi-infinite region. The second part of the curves corresponds to a progression in an axisymmetrical region where the influence of the boundary is manifested. We can compare this part to an elliptical function. In the final part of the curves the value of $R - R_o$ is that of the steady-state regime.

The above remarks suggest a rapid and simple method to obtain useful information about the progression of the freezing front for the range of a/L values occuring in practice and for constant or variable boundary temperature conditions.

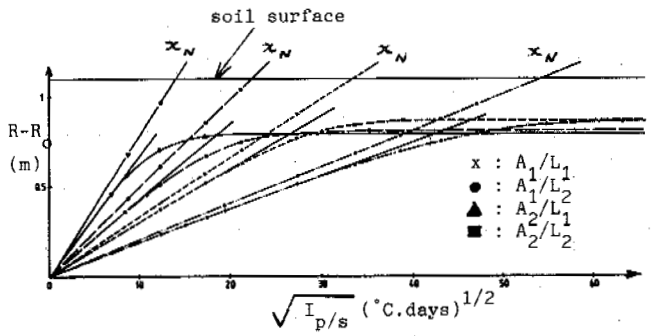

Fig. 4 $(R - R_o)$ and the Neumann frozen thickness x_N vs $\sqrt{I_{p/s}}$ for different values of a/L

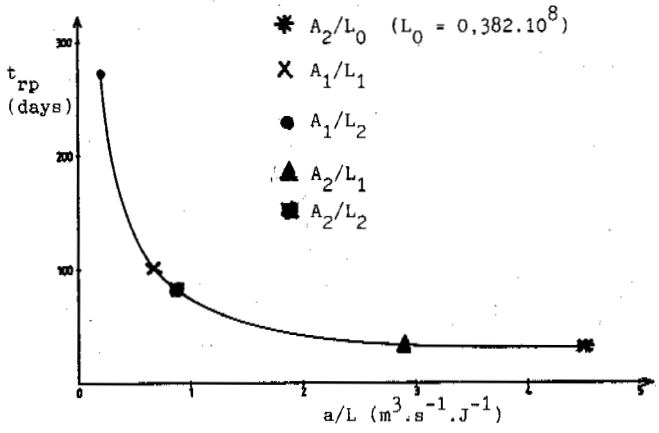

Fig. 5 Time to establishment of the steady-state vs a/L

PRACTICAL METHOD TO DETERMINE THE FREEZING FRONT EVOLUTION

The slope for the early part of the freezing front evolution can be determined from figure 4 using the appropriate value of a/L corresponding to the estimated soil thermal properties. To determine the final freezing front location corresponding to steady-state conditions analytical methods such as that of Lunardini /16/ are available, or a sample overall thermal balance calculation can be made. We recommend taking an overange of the two.

To represent the freezing curve evolution for intermediate values of freezing index and freezing distance, when the influence of the ground surface boundary begins to manifest itself, we propose using an elliptical law with parameters chosen to match both the short and long time behaviour as determined by the above methods.

The ellipse must be have its foci along a line parallel to the $\sqrt{I}$ axis and be tangential to the straight line $(R - R_o) = (R_{rp} - R_o)$ at the point RP where the steady state is reached and to the straight line $(R - R_o) = S_{a/L} \sqrt{I_{p/s}}$ at the point D where the influence of the surface boundary condition begins to manifest itself. Knowing the coordinates of the points RP and D, it is easy to calculate the equation of the elliptical curve. Using figure 5 we can find the time necessary for the establishment of the steady-state and consequently the value of I_{rp} corresponding to point R.

The remaining problem is to find the position of the point D with sufficient accurancy. As suggested in figure 6, the difference in frost penetration rate calculated for the axisymmetric early time case and that calculated for a fictional one-dimensional Neumann problem with otherwise identical parameters can be used to provide an empirical formula for the approximate determination of the point D :

$$I_D = \frac{0{,}09}{(S_N - S_{a/L}).(S_{a/L}/S_N)}$$

where $S_N = x_N / \sqrt{I_{p/s}}$ and $S_{a/L}$ as has been defined previously.

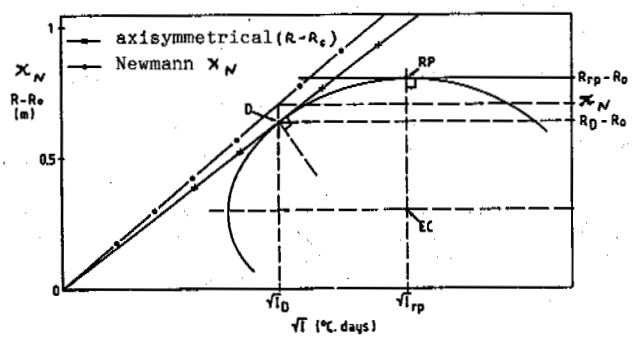

Fig. 6 Drawing of the elliptical curve

VERIFICATION

To verify this method, the following table shows values of $(R - R_o)$ evaluated with the help of elliptical relationships and values of fitted calculated curves.

a/L	DATA		COMPARISON					
	$\sqrt{I_D}$	$\sqrt{I_{rp}}$	$\sqrt{I}$		$\sqrt{I}$		$\sqrt{I}$	
($m^5.s^{-1}.J^{-1}$)	R_D-R_o	$R_{rp}-R_o$	$(R-R_o)_e$	$(R-R_o)_c$	$(R-R_o)_e$	$(R-R_o)_c$	$(R-R_o)_c$	$(R-R_o)_e$
$0{,}20.10^{-14}$	33,6	63,6	38,73		43,3		47,3	
	0,61	0,87	0,69	0,70	0,76	0,75	0,80	0,79
$0{,}69.10^{-14}$	23	39	27,4		30		33,54	
	0,66	0,87	0,77	0,77	0,81	0,81	0,85	0,84
$0{,}68.10^{-14}$	10,95	35,28	17,32		24,44		30	
	0,46	0,81	0,67	0,67	0,76	0,78	0,80	0,80
$2{,}96.10^{-14}$	8,66	21,91	12,25		15		17,32	
	0,56	0,79	0,68	0,70	0,74	0,76	0,77	0,77

($\sqrt{I}$ in $(°C.day)^{\frac{1}{2}}$ and $(R - R_o)$ in m.)

Table 1 Comparison between $(R - R_o)_e$ obtained by the elliptical relationship and $(R - R_o)_c$ calculated by the axisymmetrical model for different values of $\sqrt{I}$

CONCLUSION

TThis paper proposes a rapid and simple method estimate the upward progression of the frost line in the case of an pipeline transporting chilled gas or an underground cryogenic storage cavity.

The method is based on the linearity of the frost line progression as a function of the square root of the freezing index in the cavity during the early freezing period and on the elliptical shape of the frost line progression during the period when the influence of the ground surface thermal conditions manifestes itself. At the end, this elliptic curve joints the horizontal line representing the frost line at the thermal steady-state of the system.

These bases are supported by the examination of many calculations done with the help of an axisymmetrical model as well as with a two-dimensional finite element numerical model describing the Stefan Problem around underground cavities.

For a range of practical thermal conditions, the results of these calculations give values of the frost line propagation rates as a function of the ratio thermal diffusivity/latent heat characterizing the soil and the time of establishment of the steady-state.

In order to be able to apply this method to a wider range of problems, supplementary calculations are being carried out which will allow the determination of the time to reach the steady-state for more complicated boundary conditions.

AKNOWLEDGEMENTS

We are very thankful to Dr. L.E. Goodrich for his helpful comments and corrections on the original manuscript and the N.R.C. of Canada, Institute for Research in Construction, which received one of the authors during the period necessary to put the finishing touches to the paper.

NOTATIONS

θ	temperature
θ_f	frost line temperature
t	time
a	thermal diffusivity
k	thermal conductivity
c	specific heat
ρ	density
L	latent heat per unit volume
h	buried depth of the cavity
d	diameter of the cavity
R_o	Radius of cavity
R*	external radius of the cylindrical domain
R	frost line radius
$T_{p/s}$	temperature at interface cavity/soil
T_{surf}	temperature at the soil surface
$I_{p/s}$	freezing index in the cavity

REFERENCES

Cames-Pintaux, A.M., Nguyen-Lamba, M. (1986). Finite-element enthalpy method for discrete phase change. Numerical Heat Transfer, 9, 403-417.

Cames-Pintaux, A.M., Nguyen-Lamba, M., Aguirre-Puente, J. (1986). Numerical two dimensional study of thermal behaviour around a cylindrical cooled underground cavity. Domain of validity of an axisymmetrical scheme. Cold Regions Sciences and Technology, 12, 105-114.

Cames-Pintaux, A.M., Aguirre-Puente, J. (1987). Problème de Stefan appliqué à l'étude des cavités souterraines et conduites enterrées. C.R. XVIIème Congrès Int. du Froid, Vienne, B 241-248.

Carslaw, H.S., Jaeger, J.C. (1959). Conduction of heat in solids, 2d ed., Oxford Univer. Press, London, 11.

Hsu, C.F., Sparrow, E.M., Patankar, S.V. (1981). Numerical solution of moving boundary problems by boundary immobilization and a control-volume-based finite difference scheme. Int. J. Heat Mass Transfer, 24, 1335-1343.

Lynch, D.R., O'Neil, K. (1981). Continuous deforming finite elements for the solution of parabolic problems with and without phase change. Int. J. Numerical Eng., 17, 81-96.

Yoo, J., Rubinski, B. (1983). Numerical computation using finite elements for the moving interface in heat transfer problems with phase transformation. Num. Heat Transfer, 6, 209-222.

Voller, V., Cross, M. (1981). Accurate solutions of moving boundary problems using the enthalpy method. Int. J. Heat Mass Transfer, 24, 545-555.

Lewis, R.W., Morgan, K., Roberts, P.M. (1984). Application of an alterning-direction finite-element method to heat transfer problems involving a change of phase. Numerical Heat Transfer, 7, 471-482.

Rolph, W.D., Bathe, K.J. (1982). An efficient algorithm for analysis of non linear heat transfer with phase changes. Int. J. Num. Meth. Eng., 18, 119-134.

Damlamian, A. (1977). Some results on the multiphase Stefan Problem . Commun. Partial Differential Equations, 2, n°10, 1017-1044.

Goodrich, L.E. (1978). Efficient numerical technique for one dimensional thermal problems with phase change. Int. J. Heat Mass Transfer, 21, 615-621.

Cames-Pintaux, A.M., Giat, M., Aguirre-Puente, J. (1983). Introduction de nouvelles géométries et conditions aux limites dans la méthode de Goodrich pour le changement de phase. C.R. XVIème Congrès Int. du Froid, Paris, t. II, 595-602.

Aguirre-Puente, J., Fremond, M. (1976). Frost and water propagation in porous media. 2ème Conf. on Soil. Water Problems in Cold Regions, Edmonton, Proc. 137-154.

Sawada, S., Ohno, T. (1985). Laboratory studies of thermal conductivity of clay silt and sand in frozen and unfrozen states. IV Int. Symp. on Ground Freezing, Sapporo, t. II, 53-58/

Lunardini, V.J. (1985). Analytical methods for ground thermal regime calculations. Thermal design considerations in frozen ground engineering. Technical Council on Cold Regions Engineering Monograph ASME, 204-257.

A FROST HEAVE MODEL OF SANDY GRAVEL IN OPEN SYSTEM

Chen, X.B., Wang, Y.Q. and He, P.

Lanzhou Institute of Glaciology & Geocryology, Academia Sinica

SYNOPSIS Experimental results show that the frost heave of sandy gravel in an open system can occur and depends on not only the content of fine grained soil but also the frost penetration rate. Based on Miller's secondary frost heave theory and the theory of soil moisture energy, a frost heave model of gravel has been suggested in this paper. According to the model, ice segregation will appear while the frost penetration rate is low enough under which the suction gradient of soil moisture occurs in frozen fringe. Conversely, under relatively higher penetration rates, the extra water produced by water crystallization to form ice will be expelled from frozen fringe. For a step temperature boundary condition, the frost heave ratio, η, of gravel is related to both the penetration rate, V_f, and the content of fine grained soil, C, and can be expressed by $\eta = B_0 V_f^{B1} C^{B2}$ which might be used to evaluate the frost susceptibility of sandy gravel in an open system satisfactorily.

ICE SEGREGATION OF SANDY GRAVEL DURING FREEZING

The classical work of Tsytovich (1973) has concluded that ice segregation and frost heave can not occur in sand in an open system. The suthors arrived at the same conclusion while the frost penetration rate was relative fast (1979). However, while working on permafrost in the Qinlian Mts in 1965, Chen (1981) found gravel that contained 6.7 % by weight of less than 0.05 mm particles, surrounded with lots of ice crystals which gave rise to a thaw settlement coefficient of 12.8 %. Wang's results (1983) show that the frost heave of a coarse sand bedding cushion was 60 to 100 mm in seasonal frost area with a groundwater table of less than 50 cm from the ground surface, in Lianin province. In other words, the frost heave ratio is about 10 %. The above phenomenon gives an idea that ice segregation might taken place in a sand or gravel in an open system subject to certain favorable conditions.

In order to explore the above phenomenon, we have conducted frost susceptibility tests on sandy gravel containing different percetages of fine grained soil (see Table I) in open sysem under a step boundary temperature condition of -2 and -4 °C, with an accuracy of ±0.1 °C. The sample temperature along its depth and the heave amount were measured by a HP-3054 S Automatic Data Acqusition/Control system with a resolution of ± 1μV, and a displacement gauge with an accuracy of ±0.01 mm.

Figure 1 and Figure 2 show the curves of heave ratio vs penetration rate of sample No.1, having no fine grained soil, and sample No.2, which contained 17.74 % of less than 0.05 mm fines

TABLE I

Distribution of particle Size (mm) of Samples

Sample No.	Size (mm)	<10	<5	<2	<.5	<.1	<.05	<.01	<.005	<.002
1		100	70	40	25	0				
2		100	70	40	25	4	3.55	1.19	0.86	0.65
3		100	70	40	25	12	10.65	2.41	3.60	1.96
4		100	70	40	25	20	17.74	6.00	4.34	3.27

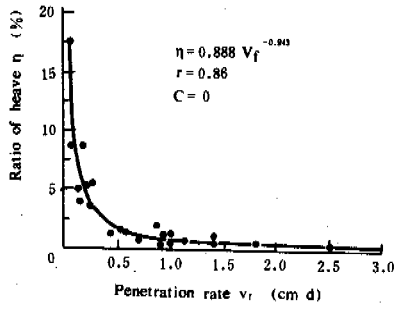

Figure 1 Frost heave ratio vs penetration rate of sandy gravel with zero content of 0.05 mm particle

respectively. It is obvious that the relation between frost heave ratio and penetration rate of sandy gravel is quite similar in form to a clayey soil, and can be expressed by a power function (Chen, 1983):

$$\eta = A\ V_f^B \qquad (1)$$

where, η--frost heave ratio, %;

V_f--frost penetration rate, cm/day;
A,B--characteristic constants that vary with soil type.

After regression, the characteristic constants A,B and correlation coefficient r of formula (1) for sample NO.1 to No.4 are listed in Table II.

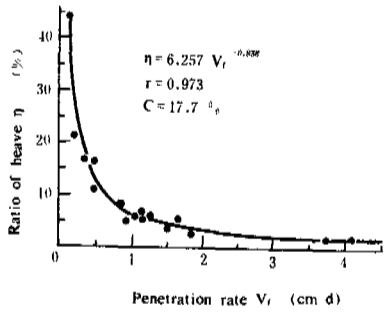

Figure 2 Frost heave ratio vs penetration rate of sandy gravel with zero content of <0.05 mm particle

TABLE II

Characteristic constants & correlation coefficient of $\eta = A\ V_f^B$ of samples

C*	0%	3.55%	10.65%	17.74%
A	0.888	3.460	4.470	6.257
B	-0.943	-1.073	-1.054	-0.938
r	0.860	0.898	0.919	0.973
N**	22	20	19	18

* C--content of <0.05 mm particles; ** N--statistic groups.

As a result, ice segregation and frost heave can occur in sandy gravel (including a pure gravel) in an open system during freezing, while the frost penetration rate is low enough. We suggest that V_{fo} is a critical frost penetration rate under which frost heave ratio will be more than 4 % so that significant ice segregation occurs. Figure 3 shows the V_{fo} will increase with the content of <0.05 mm particle nearby linearly.

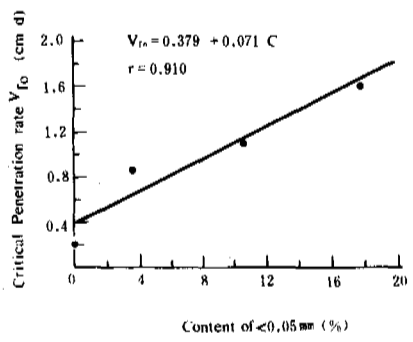

Figure 3 V_{fo} vs the 0.05 mm particle size

FROST HEAVE MODEL

With the help of Miller's secondary frost heave model (1979) and the theory of soil moisture energy, the authors would like to propose a model appropriate for sandy gravel during freezing in an open system (see Fig.4), that would explain the above phenomenon. It is assumed that only a part of the pore water surrounding each particle surface is held by absorption, and most of it is free water influenced by gravity (especially for pure sandy gravel, e.g.sample No.1). As soon as the temperature at a given level is down to its freezing point, the free water will freeze and become ice crystals surrounding sandy gravel particles forming an "ice lens-like" zone. This is the zone from the bottom surface of the lens to the frost front where the temperature is equal to its freezing point, and is called a frozen fringe. The ice vein will absorb pore water forming film water. Thus, compared with unfrozen zone, there is much more film water developed in the frozen fringe. At the warm side of the "ice lens-like", the matrix (including sandy gravel particle and ice crystals) potential is the smallest because of the lowest temperature. This is also the most developed ice crystal with the least thickness of film water in the frozen fringe. Meanwhile, there is a zero matrix potential at the frost front saturated with water. Consequently, a matrix potential gradient is present in the fringe and induces water migration from the unfrozen zone toward the bottom (warm side) of the "ice lens-like", forming ice segregation.

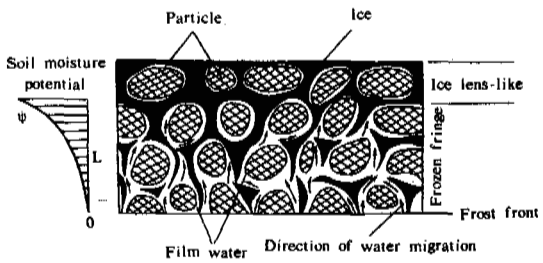

Figure 4 A model of ice segregation of sandy gravel in open system

In addition, the early work of Chen(1980) shows that pore water pressure of saturated sandy gravel will increase during freezing in closed system because of volume expansion, resulting from water-ice phase transformation, and is proportional to penetration rate, ie.

$$P_w \propto V_f \qquad (2)$$

Therefore, the total soil moisture potential at the warm side of "ice lens-like" is

$$\Psi = P_w + \Psi_m \qquad (3)$$

where, P_w—additional pore water pressure produced by growing ice crystals at the warm side of the "ice lens-like";
ψ_m—matrix potential at the warm side of the "ice lens-like".

Obviously, under the condition of higher penetration rate, when P_w is greater than $-\psi_m$, a positive pressure gradient will result in the fringe. The extra water produced by the volume expansion of water into ice at the bottom of ice lens-like will be expelled, so, the soil will not appear to be frost susceptible. Conversely, in the condition of lower penetration rate, as P_w is less than $-\psi_m$, ie. $\psi<0$, ice segregation will occur under the action of the negative pressure (suction) gradient in frozen fringe, causing frost heave.

FROST SUSCEPTIBILITY CRITERION

The frost heave ratio is used as an index of frost susceptibility of sandy gravel in China and many countries (Chamberlin, 1981). However, in current criteria for coarse granular soil, the fine grained soil fraction (for instance, <0.02 mm or <0.05 mm) is generally the only factor considered. The effect of penetration rate on frost heave has not been taken into account because of practical difficultes.

Regression analyses were carried out for 79 groups of data for frost heave ratio and penetration rate in the four samples with different particle size distribution (see Table I). The relationship between heave ratio, η, penetration rate, V_f, and the fine-grained soil fraction, C, can be expressed by an experial formula:

$$\eta = B_o V_f^{B_1} C^{B_2} \qquad (4)$$

where, B_o, B_1 and B_2 are the characteristic constants that vary with different particle size distribution, and are listed in Table III.

TABLE III

Characteristic constants and correlation coefficient r of $\eta=B_o V_f^{B_1} C^{B_2}$ as C is the content of less than given diameter d

D(mm)	B_o	B_1	B_2	r
<0.1	2.63123	-0.99881	0.24800	0.96086
<0.05	2.68700	-0.99877	0.25237	0.96093
<0.005	3.64432	-0.99670	0.31593	0.96155
<0.02	2.91197	-1.00045	0.27034	0.96124
<0.002	3.94850	-0.99612	0.33250	0.96158

As C is the content of <0.02 mm diameter particle by weight, the function of formula (4) can be plotted in Figure 5 for engineering use.

CONCLUSIONS

For sandy gravel freezing in an open system as a result of a step boundary temperature condition, the following preliminary conclusions might be obtained:

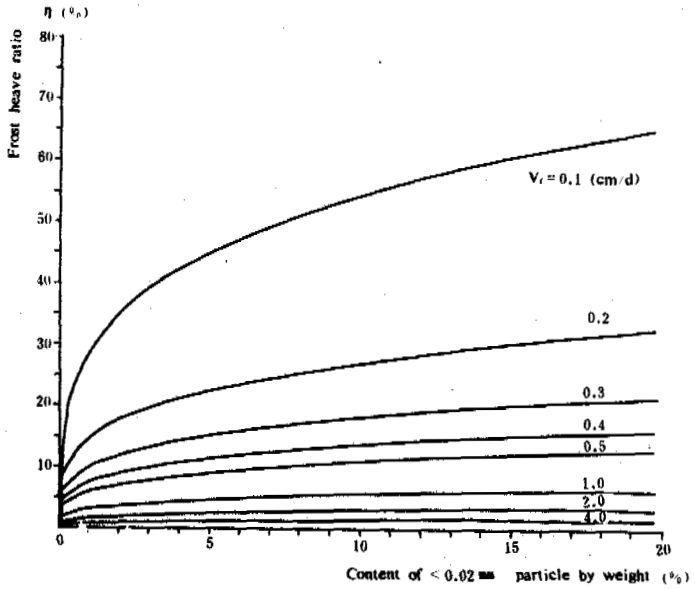

Figure 5 Frost heave ratio vs penetration rate and less than 0.02 mm particle content of sandy gravel in open system

(i) Ice segregation and frost heave of sandy gravel (including a pure gravel with no fines) will occur when the penetration rate is low enough, so that the suction gradient of soil moisture appears in frozen fringe;

(ii) The frost heave ratio, η, when used as a frost susceptibility index, is related to the penetration rate, V_f, and the content of fine grained soil less than a given diameter, C. This can be expressed by $\eta=B_o V_f^{B_1} C^{B_2}$ to a reasonble level of accuracy.

REFERENCES

Chamberlin, E.J. (1981). Frost susceptibility of soil, Review of index tests, CRREL Mongraph 81-2.

Chen, X.B. et al. (1979). On antiheave measure by replacing clayey soil with gravel. Bulletin of sciences. No.20, p.935-939.

Chen, X.B. et al. (1980). Pore water pressure of saturated gravel during freezing. J. Glaciology & Geocryology, Vol.2, No.4, p.33-37.

Chen, X.B. (1981). The characteristics of thaw consolidation of permafrost, Muli district, Qilian Mts. Memoirs of Lanzhou Inst. of Glaciology & Geocryology, Academia Sinica, No.2, p.97-103.

Chen, X.B. et al. (1983). Influence of frost penetration rate and surcharge stress on frost heave. Proc. 2nd National Conference on permafrost. p.223-228.

Miller, R.D. (1979). Frost heaving in non-colloidal soil. Proc. 3rd International Conference on Permafrost. p. 33-37.

Tsytovich, N.A. (1973). Mechanics of frozen ground. Highest school press, Moscow.

Wang, X.Y. (1983). Discussion on the destruction by frost heave in trapezoidal canal, Proc. 2nd National Conference on Permafrost. p.447-454.

OBSERVATIONS OF MOISTURE MIGRATION IN FROZEN SOILS DURING THAWING

Cheng, Guodong[1] and E.J. Chamberlain[2]

[1]Lanzhou Institute of Glaciology and Geocryology, Academia Sinica, Lanzhou, China
[2]U.S. Army Cold Regions Research and Engineering Laboratory, Hanover NH 03755, USA

SYNOPSIS Open and closed system tests on prefrozen silt and clay were conducted to investigate moisture migration in frozen soils during thawing. In all tests, an increase in water content just below the thawing front was observed. In some cases, a thawing fringe, ice lenses and frost heave were recorded. Water migration into the frozen part of thawing soil was greatly reduced after a continuous ice lens had formed across a sample. A regelation mechanism for ice formation in frozen soil during thawing is suggested.

INTRODUCTION

It is well established that temperature gradients in frozen soil are associated with gradients of free energy. Water movement is to be expected in the direction of decreasing temperature. As unfrozen water accumulates at some place in the frozen soil, its Gibbs free energy rises so that the ice and unfrozen water are no longer in equilibrium. As a result ice formation and frost heave occur. It is reasonable to expect, therefore, that water migration, ice formation and frost heave will occur in the frozen portion of thawing soil.

After Ershov (1976) documented water migration and ice formation in the frozen portion of thawing soils, downward water migration into frozen ground in summer has been confirmed by other field investigations. Parmuzina and Lagov observed that the massive cryogenic texture in the lower zone of the active layer was replaced by a streaky cryogenic texture, i.e.segregated ice lenses formed in the still-frozen part of the active layer, while thawing proceeded from the surface (Parmuzina, 1978; Lagov and Parmuzina, 1978). In 1976, measurements with a neutron probe carried out by the Department of Modern Physics, Lanzhou University and the Northwestern Institute, Chinese Academy of Railway Research revealed that as the active layer was thawing the water content of the frozen active layer and subjacent permafrost increased after downward water migration from the thawed active layer (Cheng, 1982, 1983). Mackay (1983) also showed an increase in near-surface ice volume and heave occurring in the frozen active layer during the summer. Chizhov et al.(1985) showed that as a result of diffusion of moisture from the active layer into the upper part of permafrost, tritium extends over practically the entire depth of zero annual amplitude. The concept of the downward movement of water in summer from unfrozen to frozen ground has been connected with several geocryologic phenomena, such as the formation of massive near-surface ground ice, generation of patterned ground, downslope frost creep, and the water budget of cold regions (Ershov,1976, 1979; Cheng, 1982, 1983 ; Outcalt, 1982; Mackay, 1983).

Until recently, most laboratory investigations of moisture migration have dealt with freezing and frozen soils. Laboratory investigations of moisture migration in frozen soils during thawing are surprisingly few, and in none of these does the movement of the phase boundary enter into the theory of moisture migration.

The objective of the study reported here was to reproduce moisture migration, ice formation and frost heave in the still-frozen portion of thawing soils under controlled laboratory conditions, and to investigate some details of the process.

TEST PROCEDURE

The materials used in this study were Fairbanks silt and Morin clay. For prefrozen Fairbanks silt, the average water content was 24.3% and the average dry density was 1.6 g/cm^3. For prefrozen Morin clay, the average water content was 46.4% and the average dry density was 1.17 g/cm^3.

The sample, 70 mm in diameter and 152 mm in height was confined by a latex rubber membrane and by an arrangement of acrylic plexiglass rings. A surcharge of 0.13 kg/cm^2 was placed on top of the top cold plate in order to keep good thermal contact. A direct current differential transformer (DCDT) was arranged on top to follow the deformation of the sample. 6 thermistors were placed along the sample and 5 thermocouples on either the top or the bottom to monitor thawing. Four samples were tested at the same time in a modified freezer chest. The top and base plates were connected in series in two separate circuits. Ethylene glycol-water solutions were circulated through the cold plates from two refrigerated circulating baths to control the end temperatures. The freezer chest provided an ambient temperature just above

the melting point of ice, so that radial heat flow was minimized. The thawing process data collection, except for water intake, was accomplished automatically with a data acquisition and control system.

Downward-thawing tests of frozen Fairbanks silt and Morin clay were conducted in either closed or open systems with various temperature gradients and thawing rates. Slightly different temperature regimes were observed for the 4 samples tested at the same time. Therefore the data obtained were used in qualitative analyses only.

RESULTS

A total of 20 thawing tests, 16 on frozen silt, 4 on frozen clay were conducted. An increased water content just below the thawing front was observed in all tests.

Closed system

Figure 1 presents the results from a typical closed system test on a prefrozen silt sample.

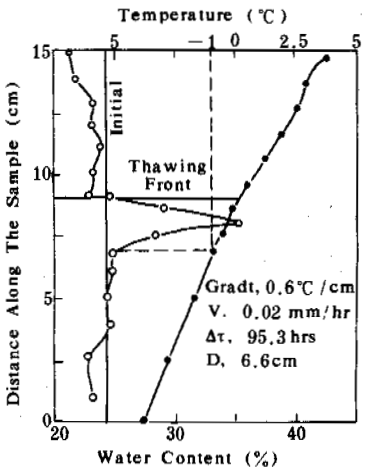

Fig.1 Results from Test B4; Closed System

A definite change in water content was observed within the upper portion of the frozen part of the sample. A few discrete small ice lenses were observed just below the thawing front. A dark color zone below the thawing front was also observed. The dark color was caused by the melting of invisible micro ice lenses. Moisture from the thawed part of sample apparently migrated into the frozen part of the sample as a result of a temperature-induced potential gradient. Note that the temperature at which moisture migration appears to be negligible is about -1°C. A slight reduction of water content near the thawing front was recorded.

As the thawing front was advancing, the temperature gradient and thawing rate gradually decreased (Table 1), and the water content just below the thawing front continuously increased. Some small discrete ice lenses had grown at about 32 hours after the start of thawing. By the end of the test, after 95.3 hours, no continuous ice lenses had formed across the sample.

Open system

In open system tests, water access was through a porous plastic drainage disk in the top of the sample. The water head was kept at the same level as the top of sample. An increase in water content in the frozen part just below the thawing front was also detected. The temperature at which moisture migration appeared to be negligible was near -1.0°C.

As the thawing front advanced, the water content just below the front increased continuously (Fig.2). After 48.4 hours, a 0.2 mm thick ice

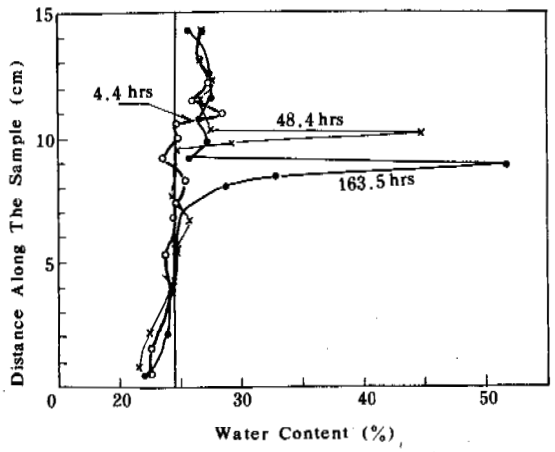

Fig.2 Moisture Migration for Fairbanks Silt, Open System

lens had formed 0.8 mm below the thawing front. After 163.5 hours, a 0.3 mm thick ice lens was observed, again 0.8 mm below the thawing front (Fig.3). It appears that after a continous ice

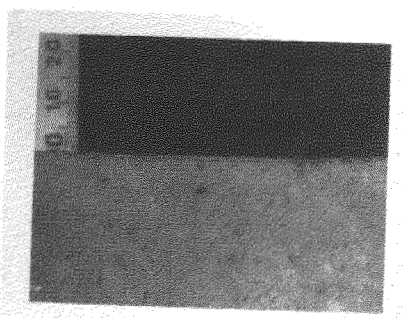

Fig.3 Ice Lens Formed during Thawing, Fairbanks Silt, Open System, Test C_4

TABLE I

Conditions for Test B (Closed System)

Test	Grad t °C/cm	Thawing rate mm/hr	Elapsed time hr	Thaw depth cm	Water content just below thawing front %	Ice lens
B_1	0.9	3.64	1.6	1.6	24.18	Invisible
B_2	0.9	1.20	8.1	2.1	26.40	Invisible
B_3	0.7	0.51	32.0	4.3	29.42	Discrete
B_4	0.6	0.02	95.3	6.6	35.23	Discrete

lens had grown across the sample, moisture migration into frozen soil was greatly reduced. The temperature at whick moisture migration was negligible increased to -2°C as a result of the longer testing time.

A prefrozen Morin clay was tested in an open system mode under nearly the same conditions as the Fairbanks silt(Table II). However, a 2 mm

TABLE II

Comparison of Testing Conditions between Clay and Silt

Material	Grad t °C/cm	Thawing rate mm/hr	Elapsed time hr	Thickness of ice lens mm
Fairbanks silt	1.0	0.02	163.5	0.3
Morin clay	1.2	0.02	155.0	2.0

ice lens formed, an order-of-magnitude thicker than that in the Fairbanks silt. Also, the width of the visible ice forming zone extended to 4.5 cm (Fig.4). Its end coincided with the -3°C isotherm. These differences are due to the higher unfrozen water content of clay at lower temperatures, indicating that frozen clay may have a relatively high hydraulic conductivity compared with frozen granular soils (Burt and Williams, 1976).

Frost heave

The deformation of frozen soil during thawing may be expressed (Ershov, 1980):

$$H = h + h_{sw} - h_{sh} - s$$

where H—Total deformation of thawing soil;
h—Frost heave;
h_{sw}—Swell caused by increase of water content;
h_{sh}—Shrinkage of thawed soil due to water migrating into the frozen zone;
s—Thaw settlement.

In this study, saturated Fairbanks silt with dry density of 1.6 g/cm³ was used. For high density granular soils s will be small. For saturated soil h_{sw} and h_{sh} are also small. Thus most deformation during thawing will be caused by frost heave.

Frost heave measured during thawing for a closed system is presented in Fig.5. After thawing was slower than a certain rate, a steady heave was

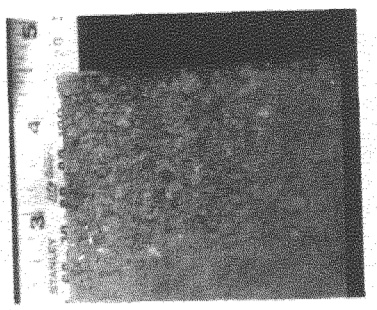

Fig.4 Ice Lens Formed during Thawing, Morin Clay Open System, Test C_1

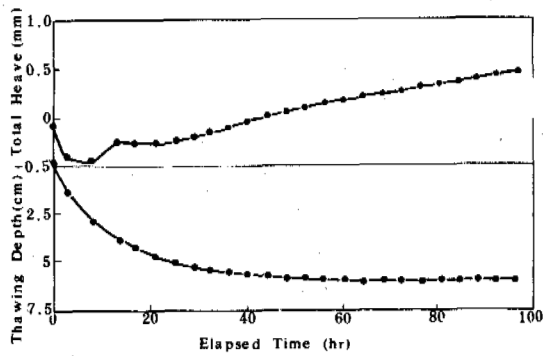

Fig.5 Frost Heave during Thawing, Fairbanks Silt, Test B_4, Closed System

observed. As shown in Fig.6, frost heave during thaw in an open system was somewhat different. After thawing was slower than certain rate, heave took place, and as soon as a continuous ice lens had grown across the sample, no more heave was detected. In Ishizaki and Nishio's (1985) experiment, the same phenomenum was recorded by x-ray photos and a dial gauge.

DISCUSSION

In thawing soils, four zones can distinguished (Fig.7): the thawed zone; the thawing fringe; the zone of intensive ice formation; and the zone of weak ice formation.

In the thawed zone, all ice has melted. The boundary between the thawed zone and the thawing fringe is the melting point isotherm. In saturated soil, the melting point is very close to 0°C.

In the thawing fringe, pore ice melts due to the rising temperature. The maximum thickness of the thawing fringe recorded in this study was 0.8 mm. It was impossible to measure the thawing fringe precisely in this study, but the thawing fringe is likely thinner than the frozen fringe. A thin thawing fringe was also recorded on the x-ray photos presented by Ishizaki and Nishio (1985).

The boundary between the intensive and weak ice-forming zones coincides with the -1° to -2°C isotherm in Fairbanks silt, and with the -3°C isotherm in Morin clay.

It is not clear what happened on the warm side of the ice lens. If ice was melting on the warm side of the ice lens, it is hard to explain how the first ice lens could form. We suggest that ice grows on the warm side of the ice lens. The liberated latent heat is conducted through the ice to cause the cold side of the ice lens to melt. The pressure induced by the ice growth on the warm side forces the first ice lens to move toward cooler soil. Concurrent melting and freezing on opposite sides of the ice lens, causes the ice to be in motion although it appears to be stationary (Miller, 1972; Ohrai, 1985). Under the influence of the temperature-induced

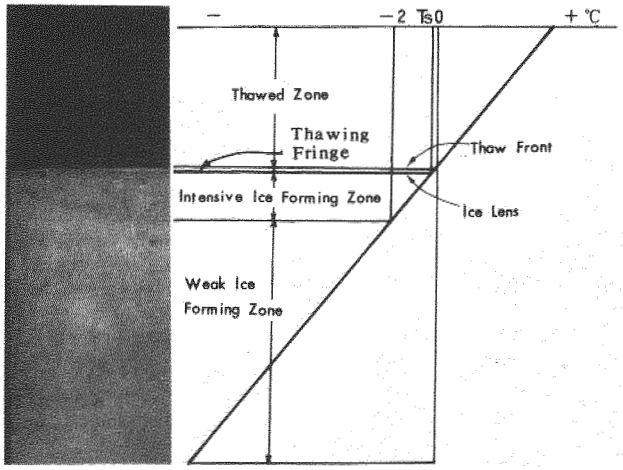

Fig.7 Cross Section of a Thawing Soil

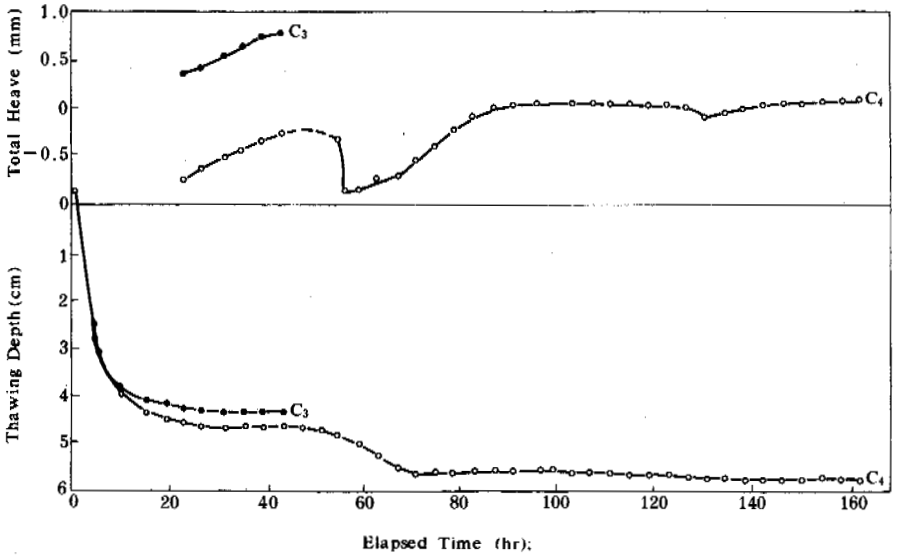

Fig.6 Frost Heave during Thawing, Fairbanks Silt, Test C_3, C_4, Open System

potential gradient, the melted water at the bottom of the ice lens migrates through the frozen soil and refreezes on the warm side of second ice lens. As a result,the dimensions of the first ice lens do not change greatly, but the second ice lens appears to grow. There is a net apparent water migration through the first ice lens.

SUMMARY

(i) Water migration, ice formation and frost heave in frozen soils during thawing have been observed;

(ii) The observed maximum thickness of the thawing fringe was 0.8 mm, considerably smaller than that in freezing soils;

(iii) The rate of water migration depends greatly on the hydraulic conductivity of frozen soil; it is larger in clay than in granular soil;

(iv) The presence of an ice lens greatly reduced total moisture migration. After a continuous ice lens had grown across the sample, the principal mechanism of moisture migration was regelation.

ACKNOWLEDGEMENTS

The authors wish to express their gratitude to the following: Dr.J.Brown for his continuous concern with this study; Messrs D.Carbee; A.Tice; J.Bayer and J.Ingersoll for their technical assistance, and in particular Mr. B.Brockett for his helpful and persistent advice and assistance.

REFERENCES

Burt, T.P. and Williams, P.J. (1976). Hydraulic conductivity in frozen soils. Earth Surface Processes, Vol.1, pp.349-360.

Cheng, G.D. (1982). The forming process of thick layered ground ice. Scientia Sinica(Series B), 25, pp.777-788.

Cheng, G.D. (1983). The mechanism of repeated-segregation for the formation of thick layered ground ice. Cold Regions Science and Technology, No.8,pp.57-66.

Chizhov, A.B., Chizhova, N.I., Romanov, V.V., Morkovkina, I.K. and Boyarskiy, O.G. (1985). Tritum analysis in geological research. International Geology Review 27(11), pp. 1370-1377.

Ershov, E.D., Chevorev, V.G. and Lebedenko, Yu. P. (1976). Experimental study of moisture migration and ice formation in the frozen zone of thawing soils (in Russian). Vestn. Mosk. Univ. Ser. Geol.Vol.31, No.1, pp.111-114.

Ershov, E.D. (1979a). Moisture transfer and cryogenic texture in fine grained soils (in Russian) . Moscow: Moscow University Press 214p.

Ershov, E.D. (1980). Method to quantitatively evaluate heave of thawing saturated soils (in Russian). Geocryology Research, Vol,XIX, pp.59-66.

Ishizaki, T. and Nishio, N.(1985). Experimental study of final ice lens growth in partially frozen saturated soil. Proceedings of the Fourth Int'l Symposium on Ground Freezing, pp.71-78, Sapporo Japan.

Lagov, P.A. and Parmuzina, O.Yu.(1978). Ice formation in the seasonally thawing layer (field observations at the Ust'-Yenisey Research Station), (in Russian). In P.I. Melnikov (ed.) General Geocryology, Novosibirsk, USSR, pp.56-59.

Mackay, J.R. (1983). Downward water movement into frozen ground, western arctic coast, Canada. Can. J.Earth Sci.20, pp.120-134.

Miller, R.D. (1972). Ice sandwich: Functional semipermeable membrane. Science, 169, pp.584-585.

Ohrai, T. and Yamamoto, H.(1985). Growth and migration of ice lenses in partially frozen soil. Proc.of the 4th Int'l Symp. on Ground Freezing, pp.79-84, Sapporo, Japan.

Outcalt, S.I. (1982). Massive near-surface ground ice in arctic Alaska: description and modeling analysis. Physical Geography, 3(2), pp.123-147.

Parmuzina, O.Yu. (1978). Cryogenic texture and some characteristics of ice formation in the active layer (in Russian). In A.I. Popov (ed.), Problems of Cryolithology, VII, pp.141-146, Moscow: Moscow University Press, Translated by William Barr, University of Saskatchewan.

GEOCRYOLOGIC STUDIES AIMED AT NATURE CONSERVATION

A.B. Chizhov, A.V. Gavrilov and Ye.I. Pizhankova

Faculty of Geology, Moscow State University, Moscow, USSR

SYNOPSIS The problems associated with nature-conservation activities in the permafrost zone are discussed and an integrated approach to environmental protection is substantiated. This necessitates comprehensive studies based on integrated geocryological survey with maximum employment of aerial-space, geophysical and other methods. The data are given on the aerial-space photographs used to evaluate the changes in the geologic environment. Zoning of an area by the types of natural and natural-man-made systems is shown to be the basis for predicting the changes in the geologic environment, identifying areas by the degree of their feasibility for economic development, distinguishing hazardous areals, and those areas that need special protection. Materials of these studies are used to select the most rational variants of locating various projects and facilities of national economy, to determine an admissible man-made load on the environment as well as the basic trends in nature-protective measures, and to plan the control (monitoring) system of the state of the environment.

INTRODUCTION

At present, about 15% of the permafrost zone, i.e. more than 30 regions, each of them up to several tens of thousands of square kilometers, experience man-induced impacts. As compared to 1926, the population in the North has increased by a factor of 5, the urban population amounting to 80%. An intensive development of industry (first and foremost of mining industry), geological prospecting surveys, civil, transport and hydrotechnical engineering predetermine a rapid growth of areals of man-induced impacts. The environmental protection under these conditions includes: (a) an ecologically optimal location of engineering structures and complexes; (b) rational use of national resources; (c) utilization of technologies and machinary designed to reduce the level of man-induced impacts; (d) measures aimed at eliminating the adverse consequences of technological development; and (e) identification of areas that have to be protected. The substantiation and planning of nature-protective measures require special studies taking into account specific features of the permafrost zone.

THE SUBJECT AND OBJECTIVES OF RESEARCH

The natural environment of the North is a complex hierarchical dynamic system consisting of ice as a specific system-forming element (cryosystem). The lithosphere (the geologic environment) is a part of this natural system comprising frozen seasonally thawed grounds, taliks, and groundwater. By interacting, they form cryosystems which constitute the subject of our studies. They are open systems whose dynamics is determined by heat and mass transfer processes, and are rather sensitive to thermal, mechanical and chemical impacts resulting in water-ice transitions that lead to the development of cryogenic processes, and to the change in geocryological, hydrogeological, engineering-geological and geochemical characteristics. This, in turn, exerts an influence on the state of landscapes, surface waters and engineering structures.

Investigation of the geologic environment should be integrated and based on the study of frozen grounds and cryogenic bonds. It should concentrate on the cryosystems both under natural conditions and within the natural-technological systems. In the latter case, the following deep man-made changes in the structure and properties of the lithospheric cryosystems are observed:

(1) Formation, due to human activities, of frozen grounds and ice which is especially intensive in mining industry regions where the volumes of freezing dumps range from 0.5 to 1 billion m^3 and the rates of their accumulation reach several tens of millions m^3 a year. The underground ice, formed in exploratory wells and mine workings, is widespread.

(2) Formation of man-made taliks and change in the heat and hydrodynamic interaction between perennially frozen grounds and groundwater that are the most typical of the sites of civil, industrial, and hydrotechnical engineering, open-cast placer development, the zone of influence of drainage systems of deep mines and quarries whose radius can reach several tens of kilometers.

(3) Formation of highly saline (up to 100 -150 g/l^{-1}) supra- and intrapermafrost waters accompanied by ice melting in frozen ground usually occurs with active participance of cryogenic concentration processes and results in a drastic increase in the content of organic matter, ferrum and other metals. This is observed in the area of some settlements, industrial sites and during freezing of tailing dumps.

(4) Development of the man-induced and intensification of natural geologic processes, and formation of technogenic relief features which is associated largely with the growth of road construction and mining industry.

Geocryological studies are directed to the prevention or elimination of the adverse effects of human activities, and to the use of favorable properties of cryosystems. They are aimed at: (a) studying the structure, dynamics and properties of concrete cryosystems of the lithosphere; (b) determining the methods for controlling the state of cryosystems; (c) predicting and evaluating the changes occurring in the latter; and (d) substantiating nature protection measures and rational use of the geologic environment.

COMPLEX GEOCRYOLOGICAL SURVEY

Ecological investigation of the permafrost zone is based on the comprehensive geocryological survey which involves studying geocryologic, topographic, hydrogeologic, geochemical and engineering-geologic conditions and man-induced impacts upon the latter. A wide spectrum of field and laboratory research is used to this end. A tendency is noted to increasing the share of geophysical and aerial-space methods, and using new procedures, such as tritium analysis of natural water and ice, allowing to obtain information on the current processes of moisture transfer in the cryosystems. The tritium analysis data are used to assess the activity of underground ice formation and moisture exchange, pollution propagation, the relationship between surface and ground water, and to determine the moisture-conductive properties of frozen grounds.

An increase in the efficient use of aerial-space photographs (ASP) is one of the most urgent tasks of geocryological surveys. An analysis of the experience gained in using ASP allows us to draw the following conclusions:

(1) The most informative are multi-zonal photographs, then spectro-zonal, infrachromatic and isopanchromatic (black and white) ASP. Man-made objects distinctly differ from the natural ones along the entire visible zone of the spectrum. To identify them, it is reasonable to use the material of the surveys made on black and white films with high geometric resolution.

(2) High information content of multizonal materials is fully realized using optic and numerical methods for their processing. For color synthesis and work with initial images, it is necessary to use photographs in near infra-red and red zones.

(3) The information content of ASP in the permafrost zone is, to a considerable degree, determined by the season of photography. The optimum time for multi-zonal, spectrazonal and infrachromatic photographing under conditions of middle and southern taiga is the beginning of summer (the greening phenophase of the larch) and the period corresponding to a phase when the larch trees have acquired autumn coloring. Multi-zonal and, to a lesser extent, spectrozonal and infrachromatic photographs obtained during these periods permit identification of surface deposits different in composition. The second period is more preferable for black and white photography. The winter ASP make it possible to identify openings in ice and non-freezing springs, the sites of dust pollution, and those of mine, industrial and domestic waste water discharge along with the associated phenomena.

(4) An effective method for evaluating changes caused by the economic activity is interpretation of the repeated ASP. It is reasonable to compare the photographs obtained: (a) before the development of the area; (b) at the moment of the termination of engineering works; and (c) in the course of exploitation. Thus, an analysis of the large-scale, threefold aerial photographic survey materials gives evidence of a considerable impact of railway construction on the state of water-logged sites where an intensive development of polygonal thermokarst topography is occurring. The age of the latter amounts to some tens of years. Also noted is the formation of icings, erosion scours, man-made reservoirs, and water-logging.

The ASP analysis permits zoning of the area by the types of natural and natural-technical systems to predict man-made changes. Forecasting and evaluation of such changes is an inherent part of the integrated geocryological survey. The search forecasting is usually carried out along with small- and medium-scale surveys. It is aimed at identifying the main trends in the development of the geologic environment and its possible states for a period up to and over 20 years. The method "by analogy", calculations and expert estimates are used to that end. The data on cryosystems obtained as a result of the survey serve a basis for the prediction.

Surveys of 1:50,000 - 1:500,000-scales permit zoning of the area by the degree of its feasibility for economic development, taking into account ecological consequences. Usually, 3-4

categories of regions (favorable, relatively favorable, unfavorable, and extremely unfavorable) are singled out. For each region a list of factors which complicate its development is compiled, prediction of the evolution of man-induced processes is made, nature-protective measures are determined, groundwater resources are assessed and recommendations on their protection and rational use are given.

In the course of survey, the objects and areas subject to special protection are identified. They include unique cryogenic phenomena, such as: giant icings and frost mounds, deposits of ancient underground ice and big thermokarst lakes. Specific hydrogeologic conditions of the permafrost zone predermine the necessity of protecting sources of thermal and mineral waters, big fresh water sources and water-bearing taliks. Of special protective value are the standard landscapes typical of a given region as well as their unique kinds (the latter are often connected with talik zones), and the landscapes of particular sensitivity to man-induced impacts.

Great attention is focused on the analysis and prediction of hazardous situations, and mapping of the man-induced impact areals. Hazardous situations usually result from: (a) development of dangerous geological processes; (b) deterioration of the quality of landscapes; (c) depletion of groundwater resources; (d) pollution of soil, surface and groundwater, and soil salinization; (e) spreading of the impacts onto the areas of special protection. The essence of a hazardous situation and its acuteness depend on the type, intensity and duration of economic development and specific features of natural conditions in a given region.

The materials of small- and medium-scale integrated geocryological survey can be used to choose the most rational and economically feasible variant of locating industrial complexes, settlements, transport communications and protected areas; to determine an admissible man-made load on the environment; to substantiate the major trends in the elaboration of nature-protective measures and requirements to the engineering structures; and to plan more detailed research and monitoring systems of the environment. They are indispensible for selecting ecologically optimal variants of the economic development of the area in the course of regional planning and elaboration of territorial comprehensive schemes of environmental protection.

GEOLOGIC MONITORING OF THE ENVIRONMENT

This monitoring envisages a combination of aerial-space and on-land observations. The latter include observations of the development of cryogenic processes, ground temperature, hydrodynamic regime, temperature and composition of groundwater, and geochemical situation. Observations are carried out both under natural and disturbed conditions, taking into account the state of air basin and surface water.

Aerial-space monitoring is effected on three levels: regional, local and detailed. The work on the regional level covers areas comparable to territorial-industrial complexes. Monitoring at this level has to: (a) reveal regional man-made changes in natural landscapes, permafrost and hydrogeologic conditions; and (b) delineate and characterize the areals of the impact and regional pollution. The first problem solution is based on comparable interpretation of the space photographs made at different time, whereas that of the second problem - on the synthesis of the aerial-space and on-land methods. The impact pollution areal is identified by the contour of an earlier snow disappearance on the television space photographs taken in the pre-spring period, the zone of the regional pollution - by the results of airborne gamma-ray surveying of the snow cover. The composition and concentration of pollutants are determined from the snow samples.

The local-level solution is applicable to such problems that require medium-scale photographs, corresponding to the characteristics of objects and areas under study. The particular natural and man-made systems happen to be the monitoring objects on the detailed level. This type of monitoring is carried out with the help of the materials obtained from a repeated large-scale aerial photographic survey and accompanied by on-land investigations.

The materials of integrated geocryological survey are used to plan and implement monitoring in the regions of intensive economic development. It plays an important role in maintaining the environmental quality. With its help, it is supposed to correct the forecasts of the changes in the geologic environment and landscapes, to ensure the control of man-induced processes and prevention of their harmful consequences.

CONCLUSIONS

The results of comprehensive geocryological studies can effectively be used for working out optimal variants of economic and ecological decisions. The analysis has shown that (a) integrated geocryological surveys must be conducted in the regions of economic development and their results should ensure a rational management of nature; (b) maximum use of aerial and space photographs and employment of new methods of studies increase the efficiency of geocryological surveys; (c) comprehensive investigation of the geologic environment, as a part of the natural and man-made systems of different types, is extremely significant; (d) it is expedient to monitor the geologic environment in the regions of intensive development by combining aerial-space and on-land methods of investigations.

IRON AND CLAY MINERALS IN PERIGLACIAL ENVIRONMENT

T. Chodak

**Institute of Soil Science and Agricultural Environment Protection,
Academy of Agriculture in Wroclaw, Poland**

SYNOPSIS

In soil and weathered rock samples the contents of total iron oxides (Fe_d), as well as oxalate-soluble iron (Fe_o) were determined. In < 2 μm fractions the quantitative composition of clay minerals was determind. It was found that the Fe_d and Fe_o contents in the active layer of permafrost increase with the depth of the profile. The content of the investigated forms of iron weathered rocks depends on their mineral composition. In the composition of < 2 μm fractions micas have an 80-95 % share, the rest being accessory minerals, chlorite, smectite and corrensite.

INTRODUCTION

In dependence on the climatological conditions the regoliths and initial soils occuring in a given area receive their specific colouring from weathering products. In the periglacial climate the prevailing colours are different shades of grey. The principal factors accounting for the colour of the rock mantle and the genetic horizons of the soil are the quantity as well as the quality of iron compounds and also the organic matter content. The colours of different rocks and minerals with varying iron contents in divalent and trivalent form depend on the mutual relationships of those forms. Minerals in which Fe^{3+} predominates are distinguished by their bright colours (red and yellow). The presence of divalent iron brings about a blue colouring. In the presence of Fe^{2+}, organic substances of a different humification degree cause the colour to change into grey. Iron content of different forms may also be an indicator of the prevailing oxidation-reduction conditions in a given environment. It is particularly the increase of numerical values in the relation Fe_o/Fe_d that will indicate a predominance of reduction conditions. On account of the high activity of iron in geochemical processes its importance becomes appearent in the course of different soil-forming processes (Konecka-Betley, 1968; Schwertmann, 1982). According to Maruszczak (1960), iron compounds in periclacial covers have accumulated in the lower part of the thawing layer of active permafrost. The course of the weathering processes in the permafrost conditions of Spitsbergen confirms the fact that iron performs and important function in the development of certain morphological features of soil profiles (Szerszen, 1974; Tedrow, 1977). It is already in the first stage of weathering that most of the minerals containing iron remove it from their crystal lattics to the outside where it oxidizes and forms oxides and hydrated oxides (hydroxides) which give the regoliths a brown colour. Dark micas are particularly rich in iron. Secondary products of weathering are most often enriched with iron compounds.

STUDIED AREA AND METHODS

The soils and weathering rocks analysed are to be found in the periglacial environment of the Hornsund area, in the south-west part of Spitsbergen (Fig. 1). Detailed investigations were made into:

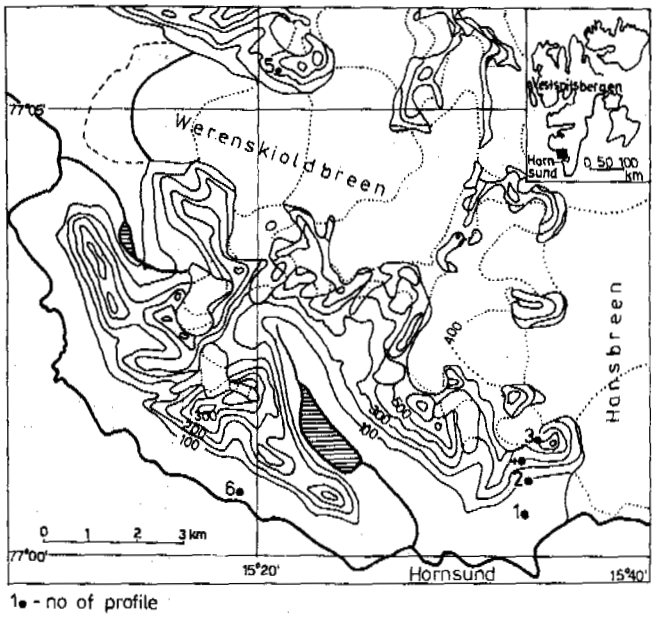

Fig. 1. Location of investigated samples

1. Accumulation soil on a coastal terrace
A soil pit was located on a coastal terrace covered with moss. The pit had the following morphology of soil profile:

	0-2 cm	- compact layer of mosses
	2-3 cm	- black layer of mineral-organic matter
A_1A_3g	3-5 cm	- light-grey, no more dry, nonstructural, loose sand
A_1B,C	5-15cm	- grey-brown, loose, dark-streaked sand
C	15-40cm	- brown-grey, loose, no more dry sand with interstitial gravel soil and bags filled up with medium sand.

2. Brown soil developed in situ from marl sandstone and quartzite-micra schists. A test sample was taken from horizon A_1 at a depth of 5-10 cm. The grey-brown sample had the granulometric composition of sandy loam.

3. Regolith of methamorphic rock origin on the Fugleberget pass, with a granulometric composition of very fine sandy soil.

4. Brown weathered rock limestone (weathered carbonate rock) on the Fugleberget slope, with a granulometric composition of sandy loam.

5. Weathered rock of pink marble (near Werenskiold glacier).

6. Regolith of biotite crystalline schist.

The above mentioned soils and regoliths were analysed for their total iron content (Fe_d) by the Mehr and Jackson method 1960 as well as for their oxalate-soluble iron content (Fe_o) by the method suggested by Schwertmann (1964), by means of the atomic absorption spectrophotometer Perkin Elmer 420.

After the < 2µm fraction had been separated from the samples, its mineralogical composition was determined by means of the Philips PW 1040 X-ray diffractometer, according to the method described by Niederbudde and Kussmaul (1978).

RESULTS

The analysed soils and regoliths reveal essential differences in the total content of iron (Fe_d) x and the oxalate-soluble iron content (Fe_o) (Table 1). The largest quantities of both of these forms of iron can be found in the accumulation soil of the terrace. In this soil the Fe_d and Fe_o content increases with the depth of the profile. There the Fe_d/Fe_o ratio reaches its highest value at a depth of 25-30 cm. It may be assumed that Fe_o iron has been displaced from the surface into the deeper parts of the profile. The highestoxalate-soluble iron content was found in weathering brown soil in situ of marly sandstone and quartzite-micre schist. In this soil the Fe_o/Fe_d ratio amounts to 0.50 (Table 1). In the ramaining regoliths analysed the total iron content is high and varies in the range of 1.0 % in regolith of biotite schist to 3.0 % in brown weathered carbonate rocks on the slope of Fugleberget. In those weathered rocks the Fe_o content is small, and therefore the Fe_o/Fe_d ratio also takes on small values. It is probably due to the chemical composition of biotite schist that this relation was not found in its regolith. The X-ray diffraction pattern of the accumulation soil sample taken from the terrace did not show any crystalline forms of iron (Fig. 2).

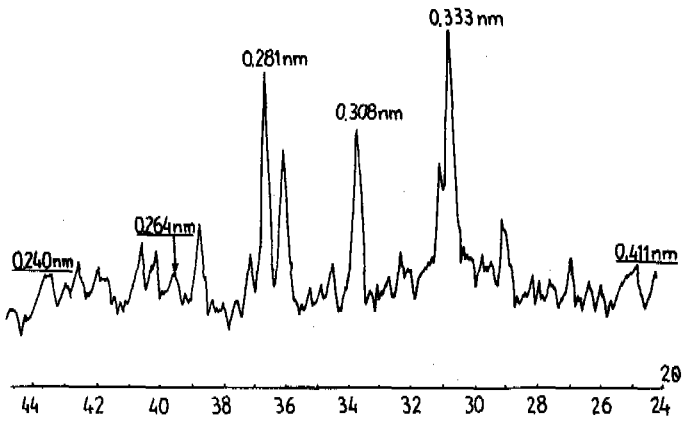

Fig. 2. X-ray diffraction pattern of < 2 µm fraction from horizons A_1 B C, A_1 B C_1 of accumulation soil of coastal terrace

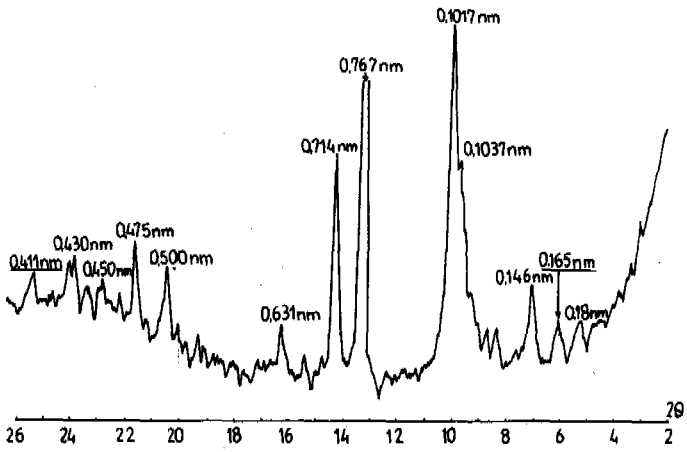

Fig. 3. X-ray diffraction pattern of < 2 µm fraction from horizons A_1 B C, A_1 B C_1 of accumulation soil of coastal terrace (Glycerol-saturated sample).

TABLE 1.

Iron content and mineralogical composition of investigated soils and weathered rocks

Genetic horizon	Depth /in cm/ of witch sample wastaken	%		Fe_o / Fe	mineralogical composition fraction of < 2 µm /in %/				
		Fe_o	Fe		mica	chlorite	smectite	corens-site	min. 0.10 - 0.14 nm
	1. Aecumulation soil of coastal terrace								
A_1	0 - 3	0.20	0.50	0.40	-	-	-	-	-
A_1 A_3 g	3 - 5	0.17	0.62	0.27	80	5	0	2	13
A_1 B_1 C_1	10 - 15	0.27	0.50	0.54	86	4	1	2	7
C_2	25 - 30	0.36	0.63	0.57	-	-	-	-	-
C_3	35 - 40	0.57	1.10	0.52	89	4	1	1	5
	2. Brown soil formed from marl sandstone and quarcite - mica schists								
A_1	5 - 10	0.85	1.70	0.50	87	2	1	0	10
	3. Regolith of methamorphie rock orgin								
(A_1)	0 - 2	0.07	1.75	0.04	95	2	1	0	2
	4. Brown weathered rock limestone								
(A_1)	0 - 2	0.16	3.00	0.05	92	2	1	0	5
	5. Weathered rock of pink marable								
(A_1)	0 - 2	0.15	2.60	0.06	93	5	2	0	0
	6. Regolith of biotite cristalline schist								
(A_1)	0 - 2	0.40	1.10	0.36	83	5	1	0	11

Within the boundaries of the peak diffraction of geothite only a slight rise of the background level was found (diffraction lines 0.411 nm, 0.236 nm and 0.240 nm). From this it may be inferred that in permafrost conditions the iron released by weathering takes on the form of mainly amorphous iron hydroxide (Fig. 2).

An analysis of the mineralogical composition of < 2 µm fractions of the investigated soils and regoliths made it possible to state x/ iron oxides and hydrated oxides that the main component of this fraction is mica with its content ranging from 95 % in weathered carbonate-mica-quartzite rocks to 80 % in the accumulation soil of the terrace. The line of the reflection plane (00 1) is characteristically split (branched) into 0.1017 nm and 0.1037 nm (Fig. 3). In permafrost conditions rock weathering involves also the presence of minerals in < 2 µm fractions, which give a diffraction line in the range of 0.10 - 0.14 nm. In this fraction the presence of chlorite was recorded on the basis of the occurrence of line 0.14 nm. The weak diffraction lines 0.18 nm in a pattern obtained from a glycerol-saturated sample permit the assumption that smectite may also occur in periglacial weathering conditions. The presence of line 0.165 nm in the diffraction pattern proves the formation of interstratified chlorite-smectite minerals called corrensite (Table 1, Fig. 3).

The first results of investigations into the forms of iron and the composition of clay minerals in the permafrost environment of S-W Spitsbergen have shown essential differences in the Fe_o and Fe_d contents. In permafrost conditions, formations from which soil develops, i.e. those in which - among other processes - organic matter accumulation takes place, contain increased amounts of oxalate soluble iron (Fe_o) in comparison with weathered rock formations where soil-forming processes do not occur. In the soils and weathered rocks analysed the content of the investigated forms of iron depends on their mineralogical composition. A quantitative analyses of the colloidal fraction has proved micas to be its main component. Transitional minerals providing diffraction lines in the range of 0.10 - 0.14 nm occur in secondary amounts. In the above mentioned fraction small amounts of chlorite, smectite and corrensite have been found as well.

ACKNOWLEDGEMENTS

The author would like to thank Professor U. Schwertmann and Professor E.A. Niederbudde of the Institute of Soil Science, T.U. Munchen Freising-Weihenstephen for making it possible for them to carry out this research and for discussing its results. Special thanks are given to Professor A. Jahn (Geografical Institute of Wroclaw University) for a possiblility to take part in the expedition and on appreciable help during field works.

REFERENCES

Konecka-Betley, K. (1968). Zagadnienia zelaza w procesie glebotwórczym. (Iron problem in soil-forming process). Roczniki Gleboznawcze. T.XIX, z. 1, 51-97.

Maruszczak, H. (1960). Peryglacjalne utwory pokrywowe na obszarze Wzgórz Szeskich. Biuletyn Peryglacjalny nr 7, 14

Mehra, O.P. and Jackson, M.L., (1960). Iron oxides removal from soils and clays by a dithionite-citrate system buffered with sodium bicarbobate. Clays Clay Miner., 317-327.

Niederbudde, E.A., and Kussmaul H., (1978). Tonmineraleigenschaften und- Umwandlungen in Parabraunerde- Profilpaaen unter Acker und Wald in Suddeutsch.-land. Geoderma 20, 239-255.

Schwertmann, U., (1964). Differenzierung der Eisenoxide des Bodens durch photochemische Extraktion mit saurer Ammoniumoxaist-Losung. Z Pflanzenernahr., Dung, Bodenkd., 105, 194-202.

Schwertmann, U., Murad, E., Schulze, D.G., (1982). Is there holocene reddening (hemetite formation) in soils of exeric temperate areas? Geoderma, 27, 209-223.

Szerszen, L., (1974). Wplyw czynników i Spitsbergenu. (Effect og bioclimatic factors on processes occuring in soils of the Sudety mountain and Spitsbergen). Roczniki Gleboznawcze. T.XXXV, z.2, 53-99.

Tedrow, I.C., (1977). Soil of the Polar Landscapes. New Brunswick, New Jersey, 1-638.

FROZEN SOIL MACRO- AND MICROTEXTURE FORMATION

Ye.M. Chuvilin and O.M. Yazynin

Faculty of Geology, Moscow State University, Moscow, USSR

SYNOPSIS The results of experimental investigations of macro- and microtexture formation and transformation in frozen soils of diverse chemical and mineral composition, fineness, textural and structural peculiarities are discussed with regard to thermophysical, physico-chemical, and mechanical processes occurring in them. The changes of frozen soil texture under the effect of compressional compaction and contraction, water injection, temperature variations, and interaction with salt solutions are examined. Significant changes in the macro- and microtexture of soils during freezing and thawing and also in the frozen state caused by external impacts, leading to the changes in the morphology and size of textural elements, their correlation and orientation, kinds of contacts and strength of textural bonds, have been identified.

The cryogenic texture of fine-grained soils is formed due to thermophysical, physico-chemical, and mechanical processes occurring during freezing. Experimental investigations, using optic and electronic microscopy, have shown that transformation of structural and textural characteristics of fine-grained soils depends greatly on the intensity of heat and mass exchange, ice formation, and deformation of mineral skeleton in freezing soils. The dynamics of these processes, in its turn, depends naturally on the fineness, mineral and chemical composition, density, and moisture saturation of soils and is also determined by heat and moisture exchange conditions in them, which is evidenced by frozen soil macro- and microtexture. Aggregation and comminution of structural elements, their reorientation, pore space rearrangement, and changes in the strength of structural bonds simultaneously occur.

The pattern of change in the cryogenic texture of frozen soil under deformation (compressional compaction, shear) and water injection show that macro- and microtexture transformation depends also on the intensity of external impact.

The most significant role in transforming initially unfrozen soil texture is played by water-to-ice phase transitions, mass exchange, and mineral skeleton deformation during freezing. With a rapid frost penetration into water-saturated soils at low temperatures (from -30°C to -60°C) and high cooling rates (tens of degrees per hour), when water is fixed in the form of ice-cement and moisture exchange is non-existant, desintegration of textural elements, caused by thermal deformations and destructive effect of the ice inclusions being formed, predominates. Microaggregate average size reduction may reach 20 percent, mostly due to destruction of microaggregates and particles of coarse aleurite and sand fractions. On the contrary, under intensive moisture exchange conditions (at higher freezing temperatures), a significant dehydration of mineral skeleton causes predominating aggregation of textural elements resulting in a possible microaggregate average size increase by more than one order of magnitude. At one-dimentional freezing, the most thorough microtexture rearrangement takes place within the horizons adjacent to the freezing boundary where the processes of moisture migration and mineral skeleton dehydration and shrinkage deformation are most intensive. As a result of microtexture transformation during freezing, the plastic strength of soils in the thawed zone may increase by one, and within the frozen zone, by two or three orders of magnitude (Fig. 1, a).

The research findings show that transformation of initial microtexture of fine-grained soils during freezing occurs both before their transition to the frozen state and in the negative temperature range, and the extent of such transformation is conditioned primarily by the intensity of processes associated with freezing: moisture migration and ice formation, mineral skeleton dehydration and deformation. This is proved by the data on microtexture transformation of freezing soils of different fineness, mineral and chemical composition, density and moisture saturation as related to heat- and moisture-exchange conditions.

An analysis of microaggragate size changes in clays of various mineral composition subjected to freezing in equal conditions (surface temperature -8°C) has shown that the maximum increase in the average size of microaggregates appeared to be 12 percent for montmorillonite and over 50 per cent for polymineral clay, whereas for kaolinite clay there was a more than twofold increase. The difference in aggregation ratio is due to a more intensive moisture exchange and mineral skeleton dehydration when passing from montmorillonite to kaolinite soils. Electronic microscopy showed

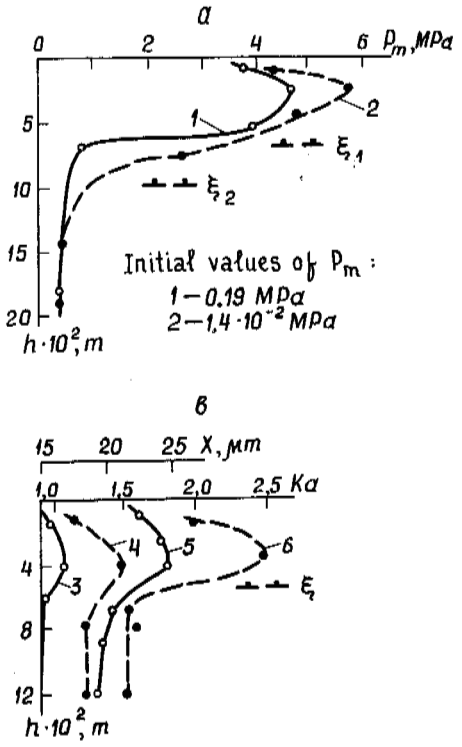

Fig. 1 Changes with depth (h) in freezing kaolinite clay (a) and loam (b) of plastic strength values (P_m), average size of microaggregates x (3, 5), and aggregation ratio K_a (4, 6) versus soil humidity (1-W=39%; 2-W=48%) and moisture exchange conditions (3, 4 - open and 5, 6 - closed system). ξ_t - freezing boundary.

that microaggregates of kaolinite particles in the ice formation zone are mostly destroyed, whereas those of montmorillonite are compacted and practically remain intact owing to their greater elasticity. While freezing, the textural elements in the unfrozen soil zone acquire subvertical orientation along the direction of moisture migration flow (more distinct in montmorillonite soils) resulting in a slit-shaped porosity formation, whereas in the freezing and frozen zones, polygonal microtexture is formed due to segregated ice formation in soil pores and their size increase.

The microstructure of frozen soils of various mineral composition is largely determined by the morphology of textural elements. In coarse-textured soils (sands) of quartz and feldspar composition with isometric particle shaps, ice-cement looks like irregular polygons. In the presence of biotite, muscovite, and other mineral particles of platy shape, a wedge-shaped ice-cement is formed. In fine-grained soils, the influence of mineral composition is evident not only in the morphology of particles and aggregates but mainly in different intensity of moisture exchange and ice formation during freezing. Frozen kaolinite clays feature friable mineral skeleton composition represented by irregularly-oriented platy microaggregates with evenly distributed isometric ice-cement inclusions in the intermicroaggregate pores. Formation of ice interlayers with a thickness of a few hundredths of millimeter and more in kaolinite clays ensures favorable conditions for moisture migration. A peculiar feature of frozen montmorillonite clays is the existance of cellular macro- and microstructure characterized by a negligible ice-cement content inside the compacted mineral blocks which is associated with a local pattern of mineral skeleton dehydration and shrinkage of such soils when water migrates to the cell-limiting ice microinterlayers.

When investigating the effect of chemical composition on texture formation in freezing clays, a more prominent aggregation was observed in the presence of univalent cations (Na^+) as compared to bivalent (Ca^{2+} and Mg^{2+}). This is because unfrozen fine-grained soils saturated with univalent cations contain significantly greater amount of fine-grained (clayey-colloidal) material capable of aggregation when the mineral skeleton is dehydrated during freezing.

The fineness of soil particles is one of the determining factors of frozen soil macro- and microtexture formation. On the one hand, the size of mineral separates characterizes the peculiar texture of the soil and determines the size of ice crystalls being formed during freezing, and on the other hand, it conditions the intensity of moisture migration and ice formation, mineral skeleton shrinkage when dehydrated, coagulation and aggregation of fine-textured material.

Investigation of the microtexture change of freezing polymineral soils of different fineness (clays, loams) has demonstrated that microtexture transformation is enhanced with an increase in the fineness of soil particles which is evidenced by a more prominent aggregation and coagulation of textural elements, greater deformation of mineral skeleton, and reorientation of microaggregates. The mineral skeleton portions adjacent to ice interlayers experience appreciable compaction. Within these portions, the reorientation of textural elements along the ice interlayers is observed which is caused by the growing pressure of ice inclusions. The thickness of such portions of mineral skeleton is different in the soils of various fineness and increases in finer soils, as measured by electronic microscopy, for example, in loams from 10 to 100 μm and more. The subvertical orientation of textural elements within mineral interlayers (before the soil transition to a frozen state during mineral skeleton dehydration and shrinkage) and their perpendicular orientation at the boundary with the segregated ice interlayers frequently determine the anisotropy of the microtexture of frozen soils which were freezing under intensive moisture exchange and dehydration conditions when lamellar cryogenic structures were formed. It has been established that freezing of coarser soils brings about an increase in the homogeneity and average size of ice-cement inclusions and decreases the degree of morphological transformation of mineral skeleton aggregates. An increase in soil fineness intensifies moisture exchange and formation of

ice macro- and microinterlayers as well as porphyraceous ice inclusions thus decreasing the share of moisture migration flow spent on ice-cement formation.

The macro- and microtexture pattern of frozen soils depends, in a certain measures, on their structure and moisture saturation prior to freezing. Lower humidity and higher density of soils determine smaller size of ice-cement inclusions and their less regular shape due to restricted growth conditions in dense soils. The strongest aggregation of the textural elements at considerable moisture exchange is observed in loose and strongly moist soils. The difference in density and moisture content has a significant bearing on soil consolidation when freezing (Fig.1,a). Aggregation of textural elements and change in the microtexture morphology during freezing are less prominent in the soils of incomplete than complete moisture saturation. Also poorly varied are strength of structural bonds and water resistance of microaggregates.

Investigation of the effect of moisture exchange conditions showed that the presence of a water-bearing horizon sharply reduces the intensity of texture formation in freezing soils due to lower dehydration of the mineral skeleton and its compaction (Fig.1,b). At the same time, the presence of a water-bearing horizon promotes an intensive ice accumulation and a more prominent increase in the mineral skeleton porosity in the frozen zone as contrasted to the absence of migration water source.

The macro- and microtexture of frozen soils formed during freezing may change under the impact of external thermodynamic fields. Temperature variation affects practically all the textural elements of frozen soils. The experiments showed that a clayey soil temperature decrease from -1°C to -10°C results in the enlargement and compaction of the separates of the mineral skeleton during its dehydration due to freezing out of water and local migration (into greater pores towards the growing ice crystals) of unfrozen water. The mineral skeleton compaction is accompanied by reduction in the number and size of air inclusions present in the soil prior to the change of temperature. Part of the pores are filled with ice forming porphyraceous and lens-like microinclusions.

As shown by electronic microscopy, a polymineral clay temperature decrease from -1°C to -15°C reduces porosity from 37.2 to 32. This is accompanied by differential porosity change (Fig.2). The average statistical pore size in this clay decreases from 11.4 to 9.96 μ m. Further cooling of frozen soil results already in intraaggregate water crystallization causing mineral skeleton loosening and microaggregate size reduction. The pore shape transforms from isometric to slit-shaped.

External pressure which causes not only deformation and destruction of the frozen soil structural elements, but also the mass-exchange processes, triggered off by the emerging strain gradients, plays an important role in frozen soil textural and structural transformations. Thus, a slow displacement of frozen clays is

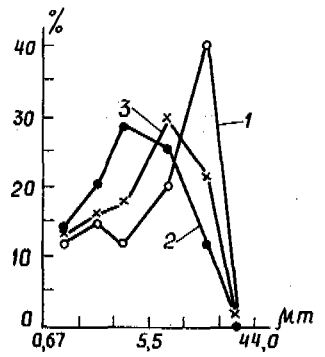

Fig.2 The change of differential porosity in frozen polymineral clay samples at a temperature (t) decrease: (a) t = -1°C, (b) t = -15°C, and (c) t = -25°C.

accompanied by moisture migration towards the plane of shear. In the region of displacement, soil structure changes significantly. Mineral aggregate compaction and deformation, as well as formation of segregated ice macro- and microinterlayers are also observed. The process of compression compaction is also accompanied by the transformation of all frozen soil components. This brings about ice melting, moisture redistribution and sqeezing out, interaggregate and intraaggregate porosity reduction, and change in the morphology and orientation of the textural elements (Fig.3).

In case of mechanical impacts, frozen soil macro- and microtexture is greatly affected by the rate of deformation. Investigation into the frozen soil texture transformation under uniaxial compression has shown that at low rates of clay deformation ($6 \cdot 10^{-7}$ m/s and lower) there occurs differentiation of mineral and ice components, compaction of mineral aggregates, formation of certain elongated ice microinterlayers due to viscous-plastic redistribution of ice into large pores and along the boundaries of mineral separates. With a deformation rate increase to $8 \cdot 10^{-5}$ m/s, the ice capability to viscous-plastic deformation is reduced, and the process of ice and mineral skeleton differentiation is practically inhibited. Microfractures originate and decrease in number but grow in size with a further increase in the deformation rate.

In case of water injection into frozen soils, the macro- and microtexture transformation involves the formation of new ice interlayers and change of the shape and size of mineral aggregates and ice inclusions and also of the type of ice-cement. For example, water injection at 0.2 MPa into a sample of loam, having massive cryogenic structure with porous ice-cement and dense mineral skeleton texture, resulted in a 15 percent moisture content increase. The microtextural studies revealed three specific zones (Fig.4,b). Within the first $5 \cdot 10^{-3}$ m-thick zone, no visible changes in soil texture were detected close to the water injection source as compared to initial state. Farther away form the source (in the second zone about

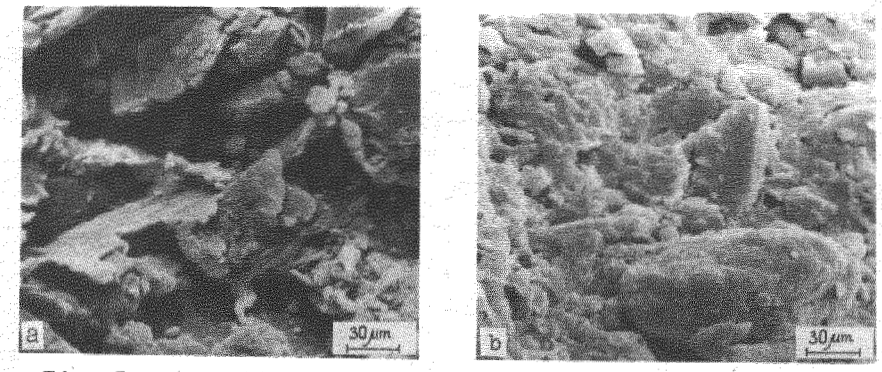

Fig. 3 Transformation of frozen loam microtexture due to compressional compaction (P_c = 0.9 MPa, t = -1.5°C) a and b - before and after the test, respectively.

3.10^{-3} m-thick), new lenticular branching ice formations were detected. The thickness of ice microinterlayers, oriented perpendicular to the direction of water injection, reached 5.10^{-5} m. They often devided ground blocks into small aggregates of irregular shape with uneven boundaries. Mineral separates had loose structure due to an increased ice-cement content; porphyraceous ice inclusions and basal ice-cement patches were detected. In the third zone (still farther from the water source), the thickness of ice microinterlayers was reduced to 2.10^{-5} m and their sparser distribution and irregular orientation were observed. The structure of mineral separates was not uniform: both loose and dense blocks and aggregates occurred.

An intensive transformation of the macro- and microtexture of frozen soils is observed when they interact with salt solutions (Fig.4,c). Initially, microtexture transformation occurs due to water migration and ice formation; later (upon sufficient soil salinization) due to melting of ice-cement and ice inclusions which results in frozen soil "soaking". When investigating the changes in a kaolinite clay with massive cryogenic structure interacting with 0.2 N sodium chloride solution at -1.5°C, the following phenomena were observed. After 3 hours of experiment, the ice content in the frozen soil increased at the contact with the solution due to basal ice-cement formation. Then, ice-lens inclusions were formed whose thickness reached 1.10^{-4} m after 7 hours of experiment. Simultaneously, individual blocks and aggregates, separated by ice interlayers, were swelling and acquiring an indistinct flocculent shape. Upon the formation of the ice-saturated zone and deformation of the lower part of the sample contacting with the solution, ice formation process in this region terminated and ice formation was observed in the middle and then, in the upper part of the sample. With the advance of the intensive ice generation zone inside the sample, pore ice melting and fusion of the earlier formed ice interlayers, acquiring porphyraceous shape, were enhanced in its lower portion due to salt diffusion.

The research findings give evidence of significant changes occurring in the texture of fine-grained soils during freezing and in the frozen state under external impacts. The data obtained show that macro- and microtexture transformations should be taken into account when assessing the deformation and strength, thermophysical and mass-exchange properties of such soils with due regard to complicated combinations of the physico-chemical processes causing changes in soil texture.

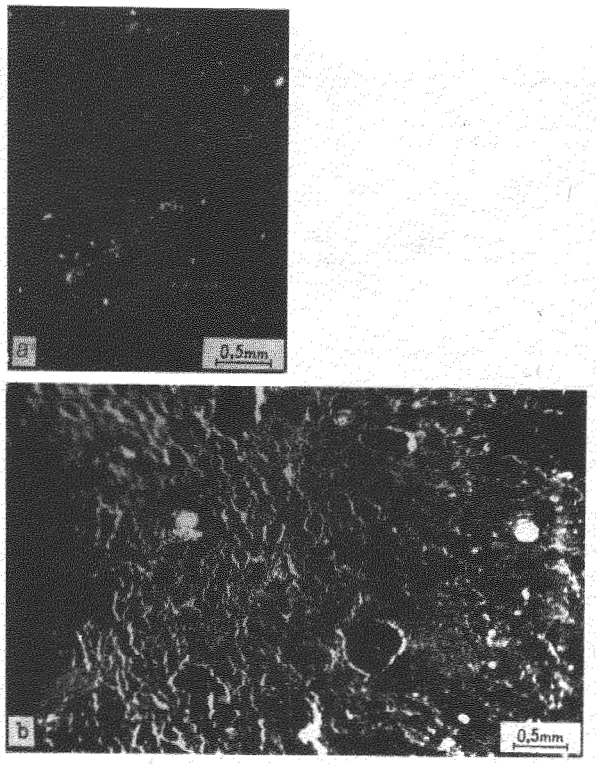

Fig.4 Micro- and macrotexture transformation pattern in frozen loam samples: a - initial state, b - during moisture injection, c - when interacting with 0.2 N NaCl solution

ACOUSTICS AND UNFROZEN WATER CONTENT DETERMINATION

M.H. Deschatres[1], F. Cohen-Tenoudji[2], J. Aguirre-Puente[1] and B. Khastou[1]

[1]Laboratoire d'Aérothermique du C.N.R.S. (Meudon)
[2]U.F.R. de Physique, Université de Paris VII

ABSTRACT The velocity and attenuation of ultrasonic waves were measured in porous samples, soaked with water, from -20°C to room temperature. The considered samples were made of glass spheres and kaolinite. The measurements were performed in transmission through the medium of compressional ultrasonic short pulses with frequencies within a band from 0.2 MHz to 1 MHz. The exploitation of results can be done by taking into account the velocity obtained from the time of arrival of the transmitted pulses or the velocity as a function of frequency obtained from the phase law of the pulse Fourier Transform which may show the dispersivity of the medium at a given temperature. The attenuation as a function of frequency, also presented in this paper, gives complementary information about the frozen medium behaviour. The results may lead to an evaluation of the proportion of unfrozen water.

INTRODUCTION

During the freezing process of a finely textured soil, the water-ice transformation front evolves in the pores of the medium. The interface so created develops differently in each pore in function of its dimensions and of particular interface thermodynamical properties.

In fact, the shape and dimension of the solid matrix create capillary effects in the ice-water-substrate system which depend on curvature, local temperature and pressures on different phases. Particularly, the molecular nature of water leads to adsorption on the solid substrate as a liquid layer, between the ice and the substrate, of which thickness depends upon the local temperature. This layer thickens continuously as temperature rises in the medium. The liquid water content is then variable with temperature under 0°C. The knowledge of this unfrozen water content at negative Celsius temperature is valuable in the theoretical study of soaked soils and in the prediction of their behaviour (cryogenic suction, ice segregation, frost heave, etc...). Moreover, this knowledge is necessary for a good use of coupled Stefan problem mathematical models which can be very performant.

Permeability measurements of frozen soils confirm the existence of unfrozen water /1, 2, 3/. Calorimetric measurements /4/ and flux measurements of slowly varying thermal systems /5/ have allowed the determination of the unfrozen water content vs temperature below 0°C. Unfortunately, these methods are tedious and difficult of use.

Ultrasonic wave propagation could be a valuable theoretical and practical way of studying the unfrozen water content. It presents the advantage of being a quick and non destructive method. Our results and those reported in the literature show, for finely textured soils and even for coarsed porous media, important velocity variations between -10°C and 0°C due to a substantial presence of unfrozen water.

An extensive survey of theoretical and experimental results of elastic wave propagation in porous media may be found in the book of Bourbié et al /6/. The first theoretical results have been obtained by Biot /7/. He has established the coupling equations between the displacements of the solid and the liquid in a two constituents medium. This model leads to a dependance of the wave velocity and attenuation on viscous characteristics of the medium as a function of frequency. Experimental verifications has been done by Plona /8/ and by Bacri and Salin /9/. The later authors proposed a simplified theory of Biot model.

Earlier work by Wyllie et al /10/ has shown the correlation of measured velocities with semi-empirical relations at constant temperature for a medium with two components. Frozen media have been studied by Timur /11/ who proposed a generalization to three components of a relation given by Wyllie. More recently, Pearson et al /12/ have made experiments to measure compressional waves in frozen grounds and discussed the Timur model. The former authors and Rong et al /13/ have presented and commented acoustical measurements.

In this paper we present our experiments and the comparison with the existing models. We use the approach of Wood /14/ and the developments of Wyllie /10/. We also propose an extension of the model based on the compressibility characteristics of the porous system components. This approach allows a consistent determination of the unfrozen water content from the experimental data.

THEORETICAL APPROACH

Velocity of sound waves

a) Wyllie et al /10/ have first proposed a model giving the velocity in a two constituents compound medium based on the average of the propagation times in the two constituents :

$$(1) \quad 1/V = \phi/V_1 + (1 - \phi)/V_2$$

Where V_1 and V_2 are the velocities within the components and ϕ and $1 - \phi$ their volume proportion. This formula has given good results in consolidated media. It has been extended to the case of three constituents by Timur /11/.

b) In 1941, Wood /14/ studied the case of the absorption of sound in turbid media, i.e. a two-fluid system (small air bubbles in water). He gave the relation

between the elasticity E of the compound and the elasticity of each component :

$$(2) \quad 1/E = \phi/E_1 + (1 - \phi)/E_2$$

In 1956, Wyllie et al /10/ in the second part of their paper gave a similar formulation for the propagation in a solid-fluid or solid-solid system in function of the bulk moduli. They took into account the relationship between the bulk modulus K, the wave velocity V and the Poisson's ratio to establish a formula for two components. ρ_k being the density of the component k :

$$(1+q^*)/V^{*2}=[(1+q_1)\phi/V_1^2\rho_1+(1+q_2)(1-\phi)/V_2^2\rho_2](\phi\rho_1+(1-\phi)\rho_2)$$

Here the asterix references the system as a whole, and q_k is related to the bulk modulus K_k by the expression : $K_k = \rho_k V_k^2/(1+q_k)$. q reflects the contribution of the shear modulus. Its value is generally between 0 et 1.2. These authors particularly comment the values of q (for example q = 0 for a liquid) and suggest empirically the use of $q^* = 0.6$ for a rock system soaked with a fluid.

The particular case of freezing medium has only been studied yet by the model considering the average time of propagation /11, 12/. The interpretation of our experimental measurements using this approach and with the help of a series-parallel approach as in the thermal Mickley's model /15/ led to incompletely satisfactory results /16/.

It has appeared that an extension of the Wood /14/ and Wyllie /10/ models to the case of freezing media could lead to better interpretation of our experimental measurements. More particularly, we have used the relationship :

$$1/V^{*2}=(\phi_s/V_s^2\rho_s+\phi_i/V_i^2\rho_i+\phi_w/V_w^2\rho_w)(\phi_s\rho_s+\phi_i\rho_i+\phi_w\rho_w) \qquad (4)$$

where s, i and w are the indices corresponding respectively to the solid particles, ice and unfrozen water.

This is an extension to three components of the Wyllie's relation. Nevertheless, we do not take into account the values of q : As stated above, q is a quantity which reflects the influence of the shear modulus. This is the reason why in a liquid media q can be considered as null. Because the unfrozen water in the thawing medium below 0°C is located around the solid particles, we believe that the propagation of the shear stresses in negligible as soon as unfrozen water appears, implying that $q^* = 0$. On the other hand, when the medium is completely frozen, all values of q and q^* are in the same order of magnitude and the factors (1 + q) disappear. Moreover, q has not been experimentally measured and by a reason of continuity, we propose not to consider the values of q_s and q_i during the thawing process. This simplification is not too excessive because in the equation giving V^*, the terms containing the values $(1 + q_s)$ and $(1 + q_i)$ become very fast small in comparison to the terms corresponding to the unfrozen water.

Sound wave attenuation

In the Biot theory /7/, the attenuation of waves is controlled by the energy transfer between the solid particles in the random medium and the fluid in the pores. Particularly, it depends on the viscous skin depth δ as pointed by Bacri and Salin /9/, $\delta=(2\eta/\rho\omega)^{1/2}$, where η is the viscosity and ω the angular frequency. Two asymptotic regimes may be met, depending on the relative size of δ and of a, the size of the pores. At low frequencies, $\delta >> a$, the wave attenuation α in Neper/m varies as ω^2, and at high frequencies $\delta << a$ and α varies as $\omega^{1/2}$. Furthermore, when the porous medium is composed of very regular particles, it is possible to observe geometric resonance phenomena which will affect the amplitude of the transmitted wave at particular frequencies.

EXPERIMENTAL

The experimental set-up has been reported in /16/. The soaked soil fills two identical cells with parallel plastics walls. The ultrasonic transmitter and receiver are pressed upon the walls of one of the cells. This cell contains a thermocouple located outside of the ultrasonic path. In order to have a thermal reference, 6 thermocouples fit out the second cell. The two cells being submitted to an identical thermal treatment, the overage temperature gradient along the direction of ultrasonic propagation varies between $0.5K.cm^{-1}$ and $0.2Kcm^{-1}$ The cells, filled with the compound, are stocked at a temperature of -20°C. During the experiment, they are put in a closed container filled of polystyrene foam beads such that the temperature increases slowly during the experiment (3K/hour in the beginning). The ultrasonic probes are highly damped and allow the generation of very short compressional pulses with a broad frequency content. By Fourier analysis of the digitized transmitted signals, the characteristics of propagation are obtained in the frequency band from 200 kHz to 1 MHz.

For the velocity determination as a function of temperature, the time of propagation of the pulse through the cell is measured with accuracy with the help of an oscilloscope and computer recordings. This may be done either in the time domain by determining the beginning of the pulse or, with a better accuracy, in the frequency domain, after the division of the phase by the angular frequency.

The attenuation as a function of frequency for different temperatures is evaluated in the Fourier domain. The transfer function of the measuring equipment being unknown, a normalization has been done in a complementary experiment with the cell filled only with distilled water where the attenuation is negligible within the frequency range of the transducer.

Corrections have been done to take into account the diffraction beam spreading in the materials along the acoustical path and the variation of sound velocity and sound attenuation with temperature in the plastic walls.

Description of constitutive media

One of the samples was constituted with 0.57 mm diameter glass spheres of density $2.7.10^3$ $kg.m^{-3}$. After addition of distilled water the compound was saturated giving a density of $2.07.10^3$ $kg.m^{-3}$. The porosity was 0.37.

The second sample was kaolinite incompletely saturated with distilled water. The degree of volumic saturation was 80%, the porosity 0.50 and the density $1.75.10^3 kg.m^{-3}$.

RESULTS

Sound velocity

Using the time of arrival of the pulse, the general variation with temperature of the velocities in the glass beads and in the kaolinite is shown in figure 1. One may note the more abrupt transition, around -4°C, of the velocity in the glass beads sample compared to that in the kaolinite sample. The absence of abrupt transition for the kaolinite suggest the presence of unfrozen water in the whole range of temperature in this medium constituated with very fine particles.

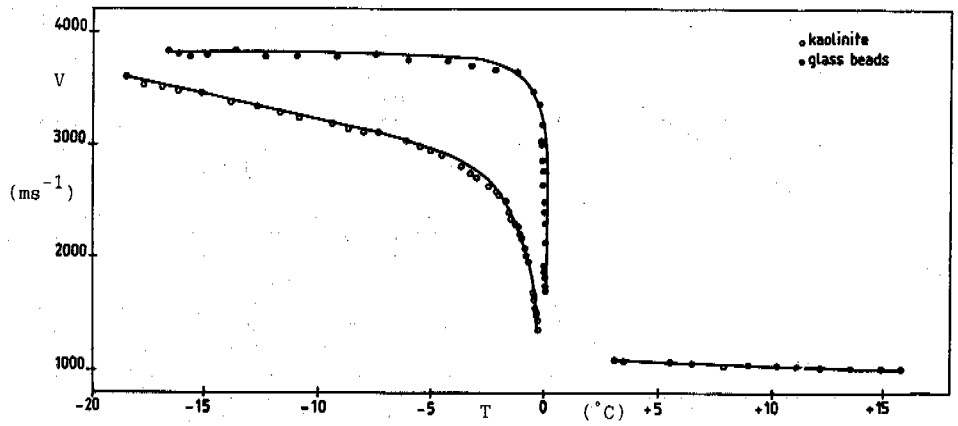

Fig. 1 Sound velocities Vs temperature for soacked glass beads and kaolinite

a) glass beads

The determination of phase velocity vs frequency for different temperatures has been performed in the case of the glass beads sample. It appears that the dispersivity of the medium is small for temperatures under -8°C and is important above -0.5°C. In figure 2 are represented the phase velocities vs temperature for different frequencies as well as the velocity determined by the time of arrival. One may note the low dispersion of experimental points determined from the phase measurements. The relatively important variation in the lower temperature range seems to be created by the experimental conditions occuring in the beginning of the warming process. Between -14°C and -8°C velocity curves present a rectilinear aspect and a dispersion effect manifested as an increase of phase velocity with frequency. The strong variation of velocity above -8°C suggests a rapid transformation from ice to water.

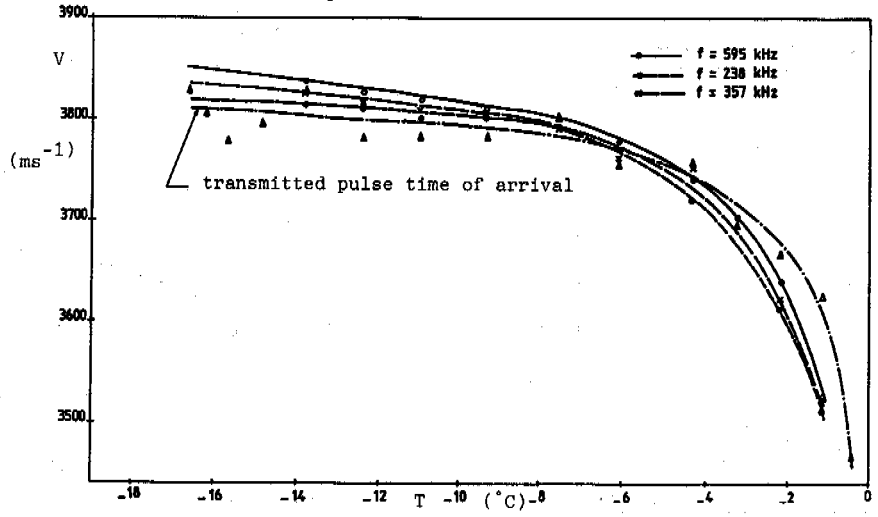

Fig. 2 Phase velocity Vs temperature for different frequencies (soaked glass beads)

With the help of the relation (4), we have evaluated the unfrozen water content as a function of temperature using the 238 kHz phase velocities which present a low spreading and are near of the values determined by using the time of arrival method. Velocity in ice at 0°C and velocity in the glass matrix at 20°C are taken respectively equal to 3800 m.s^{-1} and 5900 m.s^{-1}. One uses the same coefficient with temperature for the two velocities (-3.2 m.s^{-1}.°C^{-1}), identical to that of the experimental phase velocity of the compound medium between -14°C and -8°C. This coefficient is in good agreement with that reported by Roethlisberger /17/ for ice. The velocity in the unfrozen water below 0°C was considered constant and equal to 1410 m.s^{-1}. The densities of the constituents have been supposed constant :

$\rho_i = 0.92.10^3 kg.m^{-3}$, $\rho_s = 2.7.10^3 kg.m^{-3}$ and $\rho_w = 10^3 kg.m^{-3}$

These values reported in relation (4) lead to an estimation of the ratio of the unfrozen water volume to the total water volume. Its variation with temperature is shown in figure 3 in a linear-log graph. It appears that above -8°C the variation of the water content is the more important. The right scale represents the corresponding thickness "a" of the water film on the spherical beads taking into account the specific surface of the medium (4.10^{-3} m^2.g^{-1}).

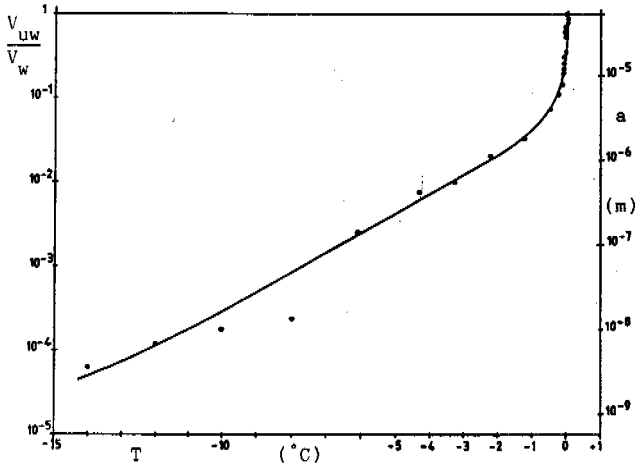

Fig. 3 Volume unfrozen water (left) and unfrozen water thickness (right) Vs temperature (glass beads)

b) Kaolinite

The variation of velocity vs temperature has been presented in figure 1. It may note a slow, quasi-linear decrease of the velocity between -19°C and -8°C with a slope of -50.8 $ms^{-1}°C^{-1}$. This value is sensibly higher than that for any of the constituents. This is interpreted by a continuous variation of the unfrozen water content. Between -8°C and 0°C, the important variation of velocity is related to a fast increase of unfrozen water when temperature rises as confirmed by other methods /4, 5/.

Sound attenuation

The normalized amplitude vs frequency of the transmitted pulse, theoretically equal to one for a non attenuating medium, is presented in figure 4 for the glass beads medium at different temperatures.

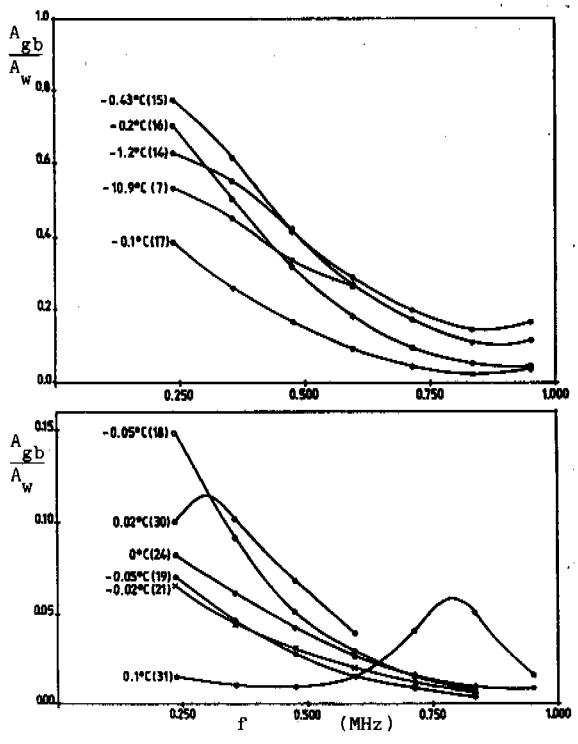

Fig. 4 Normalized amplitude Vs frequency for different temperatures (glass beads)

When the temperature increases the water content increases and it is expected that attenuation should increase. Now, from -10.9°C (curve 7) to -0.43°C (curve 15) and from -0.02°C (curve 21) to +0.02°C (curve 30) the pulse amplitude increases. Resonance effects can explain this fact. This resonance could be caused by the regular size of beads and occurs when the wavelength is in the order of magnitude of the sphere circumference or of one of its multiples.

Far of the resonance zones one may expect that the attenuation variation is dominated by the viscous process. This seems to be the case at -0.02°C where the attenuation is the highest. Indeed, in figure 5 is represented the ratio α/a_p where a_p is the wave number ω/V. The upper curve corresponds to -0.02°C and varies as $1/\omega^{1/2}$, as in the high frequency regime of viscous attenuation. For -0.02°C the unfrozen water thickness is 14 µm (figure 3), an order of magnitude higher than the viscous skin depth (1 µm at 0.5 MHz).

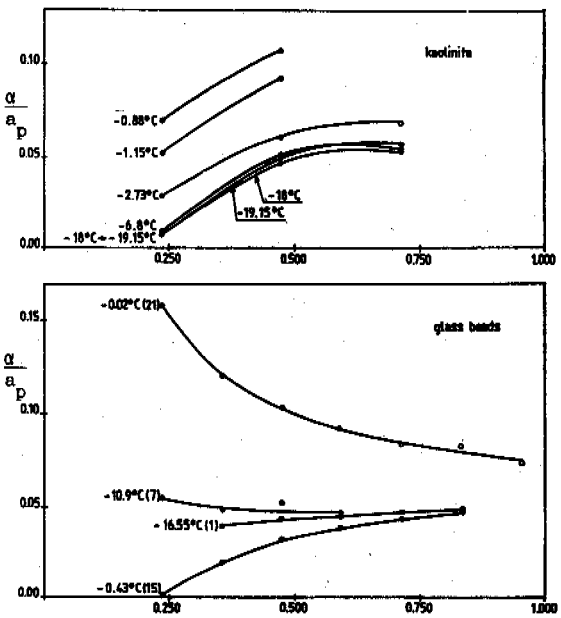

Fig. 5 α/a_p Vs frequency

In figure 5 the curve 15 corresponds to -0.43°C and seems to be dominated by the resonance phenomenon. At low temperature, -10.9°C for sample, the ratio α/a_p is constant ; the amount of water is too small to involve viscous attenuation. It is possible that this case be in the transition region between the two scattering regimes : the Rayleigh regime where α/a_p is proportional to ω^3 and the high frequency regime where α/a_p is proportional to $1/\omega$. Other causes could be the thermal losses or the elastic hysteresis losses /18 /.

For kaolinite the normalized amplitude is shown vs frequency for different temperatures in figure 6. On may remark that for the lowest temperatures between -19.15 and -14.4°C, when the unfrozen water content is the smallest, the curves superimpose at the lowest frequencies, between 0.238 and 0.714 MHz and present small differences for frequencies higher than 0.714 MHz. For temperatures higher than -8°C, the amplitude decreases when the temperature increases, the amplitude being too small to be measured at high frequencies near 0°C. The large specific surface in the kaolinite sample (4 $m^2.g^{-1}$)

implies that the film layer thickness is always smaller than the viscous skin depth (a = 0.1 µm when all water is liquid). This implies attenuation in the low frequency regime. In figure 5, one also presents α/a_p vs frequency for different temperatures, which should vary as ω in this case. This behaviour is approximately observed.

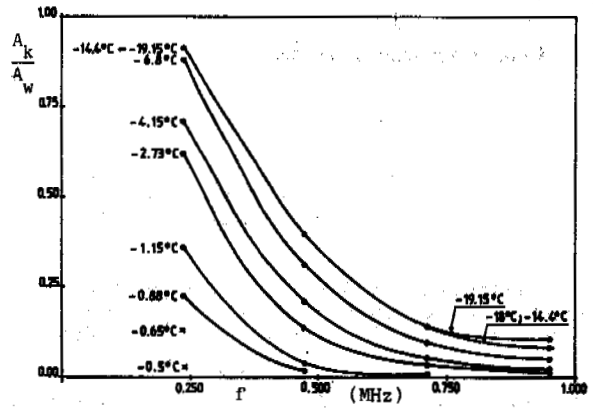

Fig. 6 Normalized amplitude Vs frequency for different temperatures (kaolinite)

CONCLUSION

This paper proposes the use of easy and non destructive acoustic measurements in order to attain a better knowledge of the porous media freezing phenomenon. From a quantitative point of view, the sound velocity is a strong parameter allowing the evaluation of the unfrozen water and ice contents. It was necessary to establish a model taking into account the acoustic theories and the texture of media used in our experiments under slowly variable thermal conditions. The obtained results seem very satisfactory. Correlations of these results with those obtained by thermal methods are desirable. From a qualitative point of view the consideration of attenuation curves lead to very interesting remarks concerning the acoustic behaviour of compound media containing ice and water. Although the results are not totally understood in the presence of resonance effects, the results are consistent with the present freezing knowledge. This encourages the systematic use of the acoustic technics in this field. Isothermal experimental set-up is presently being conceived and constructed in order to have accurate results.

ACKNOLEDGEMENTS

The authors thank the GENRAD Company for its support for the use of the data processing equipment and D. Calippe for his help in building the experimental set-up.

REFERENCES

/1/ Burt, T.P., Williams, P.J. (1976). Hydraulic conductivity in frozen soils. Earth Surface Processes, 1, 349-360.

/2/ Miller, R.D., Loch, J.P.G., Bresler, E. (1975). Transport of water and heat in a frozen permeameter. Soil Sciences Soc. Am. Proc., 39, 1029-1036.

/3/ Aguirre-Puente, J., Gruson, J. (1983). Measurement of permeabilities of frozen soils. Permafrost 4th Int. Conf. Proceed., Fairbanks, 5-9.

/4/ Williams, P.J. (1967). Properties and behaviour of freezing soils. Norvegian Geotechnical Institute, pub. n° 72, Oslo.

/5/ Szanto, I., Aguirre-Puente, J. (1971). Etude des caractéristiques thermiques des milieux fins humides lors de leur congélation. Progress in Refrigeration Science and Technology, Proceed. of the XIIIth Cong. of Refrig., Washington, 1, 751-757 (Avi. Publis. Comp. Ed.).

/6/ Bourbié, T., Coussy, O., Zinszner, B. (1987). Acoustics of porous media. Ed. Technip, Paris.

/7/ Biot, M.A. (1956). Theory of propagation of elastic waves in fluid-saturated porous solid. I-Low-frequency range. II-Higher frequency range. J. Acoust. Soc. Am., 28, 168-178 and 179-191.

/8/ Plona, T.J., Johnson, D.L. (1980). Experimental study of the bulk compressional modes in water-saturated porous structures. Ultrasonic Symp. IEEE, 868-872.

/9/ Bacri, J.C., Salin, D. (1982). Propagation du son dans les milieux poreux saturés. Rev. du Cethedec, n°76, 111-120.

/10/ Wyllie, M.R., Gregory, A.R., Gardner, L.W. (1956). Elastic wave velocities in heterogeneous and porous media. Geophysics, 21(1), 41-70.

/11/ Timur, A. (1968). Velocity of compressional waves in porous media at permafrost temperature. Geophysics, 33(4), 584-595.

/12/ Pearson, C., Murphy, J., Halleck, P., Hermes, R., Mathews, M. (1983). Sonic and resistivity measurements on Berea sandstone containing tetrahydrofuran hydrates : a possible analog to natural gas hydrate deposits. Permafrost, 4th Int. Conf. Proceed., Fairbanks, 973-978.

/13/ Rong, F., Jinsheng, Z., Zhongjie, H. (1983). Ultrasonic velocity in frozen soil. Permafrost, 4th Int. Conf. Proceed., Fairbanks, 311-315.

/14/ Wood, A.B. (1941). A textbook of sound. The Macmillan Company, New York.

/15/ Mickley, A.S. (1981). Thermal properties of soils, CRREL Monograph 81-1, O.T. Farouki Ed.

/16/ Cohen-Tenoudji, F., Deschatres, M.H., Khastou, B., Aguirre-Puente, J. (1987). Propagation des ultrasons dans les sols. Influence de l'eau non gelée en fonction de la température. 2ème Colloque Gel et Génie Civil (Ecole Polytechnique de Varsovie, CNRS, LCPC), Paris.

/17/ Roethlisberger, H. (1972). Seismic exploration in cold region. CRREL Monograph II-A2A.

/18/ Papadakis, E.P. (1968). Ultrasonic attenuation caused by scattering in polycristalline media, chapter 15 of Mason, W.P. Editor, Physical Acoustics, Vol. IV, Part B., Academic Press.

THERMODYNAMICS THEORY FORECASTING FROZEN GROUND

Ding, Dewen

Lanzhou Institute of Glaciology and Geocryology, Chinese Academy of Sciences

SYNOPSIS In this paper, the basis of present thermodynamic theory of frozen ground and the general conception in geocryological research are reviewed. The thermodynamic theory frame of frozen ground system is presented for the first time and the foundamental principle of thermodynamic parts of geocryology is also briefly introduced.

The evolution direction and limitation of frozen ground system in the isolated, close-balanced and far-balanced state, respectively, are discribed emphatically, and the thermodynamic principle used for the forecast is also been presented.

THE BRIEF INTRODUCTION OF PRESENT THERMODYNAMIC THEORY OF FROZEN GROUND

The subject of frozen ground forecasting is in forward position in present geocryological research and it marks the beginning of a new stage in geocryological research. Meanwhile, it requires the corresponding concepts or methods, especially the systematic theory or concept as its developing premise and guarantee. Kudliyavtzev has carried out the pioneer research work and has made a great contribution to the research field of frozen ground forecasting.

Kudliyavtzev is also the first scientist who tries to apply the thermological theory of frozen ground into the forecast systematically. From his monographs (Kudliyavtzev, 1974 and 1979) and other relative publications, we can find that the frame of thermological theory of frozen ground consists of three parts as follows.

Theory of radiation balance on ground surface, heat balance, water-heat balance, their spatial distribution and dynamics theory

At present, this theory is regarded as the thermodynamic conditions of the formation, the existence and the development of frozen ground.

Kudliyavtzev not only made a study on the absolute values of radiation, water and heat, and on their time-space distribution features, but also he put his main attention to the exploration of the following matters: the change of climate with the large scale climate the intensity of climate with the middle and small scale climate and the relations between the microclimate factors and the frozen ground, i.e., the features of thermal exchanging between the ground and the atmosphere, the water-heat background of frozen ground changing, and the reactions of the frozen ground on the environment and so on. Meanwhile, by using the features of temperature, and structure of frozen ground, he made the inversion of the ancient climate evolution. Besides, the effect of human activity, such as the local production development, the regional abnormality and the whole global change of 2XCO2, were thought to be more important.

Theory of energy-matter transportation and transformation in the earth's surface layer

This theory is the heart part of thermodynamic study in geocryology.

On the one hand, he tried to perfect the equations for describing heat, water (or solution), motion (or momentum) and the process of phase change, revealing the dynamic temperature, moisture field, deformation, motion process of frozen ground and other things formed under the geological and geomophological actions and the time-space features of ice formation. On the other hand, in the view point of energy (or water), he discussed the factors, such as composition, quality and structure of rocks, geological conditions (including structure and structural motion), sedimenary environment and surface water (or underground water), as well as geochemical or geophysical factors in relation to the freezing-thawing actions. By the synthetical studies of the relations, the laws and the features of the composition, structure, evolution and regional change of the geological-geomorphic products may be revealed.

Physico-chemical theory of system on the molecular-colloid level system (including surface-solution-crystal)

It is the quasi-microcosmic basis of the irreversible course in frozen ground.

By adopting the theories of thermodynamics, quantum mechanics, statistical physics and electrodynamics, he tried to solve the problems, such as, unfrozen water content (or water-film thickness), freezing point depression and thermo-rheological feature, as well as the power and the mechanism of diffusion, phase change and

dynamic course, and to establish the boundary conditions or binding eqution of macroscopical phenomena for the multiple-transportation equations.

It should be pointed out that at present, corresponding to the development of above thermodynamic theory, the basically applied theory and the thermo-technique of frozen ground are also advanced, such as the following branches or directions concerning the engineering thermodynamics, agro-eco-thermodynamics and environmental thermodynamics in frozen ground regions. These problems mentioned above are not necessary to go into details in this paper, which have been discussed by the author in other papers.

THERMODYNAMIC THEORY FRAME OF FROZEN GROUND SYSTEM

In a previous paper (Ding, 1985), the author pointed out the limitations and the deficiency of Kudliyavtzev's research sense and methods, and discribed the concepts of frozen ground system and systematic methods in details.

The present thermodynamic theory of frozen ground mentioned in last section, is not perfect and exists serious shortcomings which is far away to be a rigorous system. We can find easily that the present thermodynamic theory of frozen ground is based on the theory of classical equilibrium with microscopic and surface phase state, and the uncomplete, nonlinear and nonequilibrium transportation. In addition, for some random problems, the statistics can be made only under the presuppose of normal distribution. Therefore, even if it is under the requirment of present concept, there are many kinds of problems which can not be solved perfectly. Since the limitations of the concepts and methods, the theoretical development is restricted.

Now we simply analyse the basic chracteristics of frozen ground system. First of all, we confirm the shortcoming of the present concept and the theory, and then we try to explain the necessity of establishing a new theory (including the systematic concept) and the global frame-model.

1. Seeing that the frozen ground system is a complicated entirety, the use of simplicity-principle and restoration-method will need some additional conditions and will be strictly restricted. The equilibrium thermodynamics and uncomplete transportation theory can not discribe the interactions of feedback-coherence, coupling and self-orgnizition between frozen ground system and environment and inside of the system. The main factors simply piling up are not the real object, and the mechanical combination of partial regularities is also not a universal law.

2. The nature of the freezing (or thawing) action is the nonequilibrium phase change, ordered state and self-orgnization in frozen ground system. Therefore, it is invalid to use the Boltzmann's equilibrium phase change theory. The structure of frozen ground structure is a new kind of dissipation structure, namely, the stable and ordered structure formed under the conditions of nonlinear and far from equilibrium state. In other words, non-equilibrium state is the source of frozen ground, and the possible appearance and stability of new sequence have to be solved with the nonlinear thermodynamic theory.

3. The non-equilibrium state phase change course of frozen ground system is the evolution course of the system. The change of frozen ground system is irreversible, and its corresponding phase change products, i.e., structure, can remember its evolutionhistory. Equilibrium state in frozen ground is not existed, and the linear theory can only be used to solve the problem of evolution which is developing towards the steady state. Using the transportation theory to solve the evolution (i.e. history and forecast), the determined model will be taken, so that it can not reflect the positive actions of the random process and the fluctuations.

4. On orgnization level, the freezing soil layer is identical to all kinds of geological-geomorphological products in frozen ground system, all of which can be regarded as dissipation structure. There are common functions in diagensis and external force actions, which change the sequence levels in different frozen ground systems. The landforms in frozen ground areas are the surface configration of various frozen ground systems, and each has its corresponding evolution process. If we choose a proper frozen ground system, the frozen ground layer and the regional differentiation-features of geomorphology are a kind of dissipation structures, which depends on the regional self-orgnizing process. The statistical methods of traditional geocryology, the mechanical and regional explaination, the Quaternary and geomorphological methods all need to be remoulded on the basis of the new concept.

Now we can propose the following thermodynamic theory frame of frozen ground system:

1) Thermodynamics-dissipation structure theory (Shen, 1982).

The equilibrium thermodynamic theory of frozen ground system.

The linear non-equilibrium thermodynamic theory of frozen ground.

The nonlinear non-equilibrium thermodynamic theory of frozen ground system.

2) Transportation theory (Groot, 1981).

The linear energy-matter transportation theory in frozen ground system.

The nonlinear energy-matter synthetical transportation theory in frozen ground system.

The synthetical and irreversible course theory dealing with internal diffusion chemistry, phase change and power in frozen ground system.

3) Statistical physics and coordination theory

(Hao, 1981).

The equilibrium statistical theory and measure-geography direction.

The Marlkov's course theory.

The coordination theory.

Concerning thermodynamics theory, it can be divided into the following parts:

a) Entropy is the non-equilibrium meassurement of frozen ground system and the law of entropy-increasing is the increasing regularity of orgnizing non-sequence. Equilibrium state is corresponding to the non-sequence state, and the non-equilibrium state is the source of frozen ground sequence.

b) The non-equilibrium of frozen ground system is caused by the processes of the diffusion (including energy, water and solution), the chemistry (including phase change, adsorption and hydration) and the power (including stress and long-length force).

c) The speed and intensity of processes in frozen ground system will make the system satisfies the principle of local entropy conservation,and the process can also be considered as a continuously changing course.

d) The dissipation structure formation in frozen ground system is caused by its internal and external random fluctuations. When some characteristic values reach a certain threshold value, the fluctuation is being enlarged, and gets the guarantee of the exchanging between environment and matter-energy. Therefore, it follows the Einstein's fluctuation theory.

e) The internal description of frozen ground system in non-equilibrium state or the description of coordination equation can be sumed up as the nonlinear partial differential equation set, which may be having random terms. Therefore, its stability should obey the Liyafnov's stability theory. For the analysis of process, the relative parts of the branch-mathematics theory and the random-mathematics theory are completely suitable. The concrete content and application concerning the whole theory will be discussed, in details, in other papers. In the following section we will discuss the application of thermodynamic theory to the forecast.

THE THERMODYNAMICS NATURE OF THE EVOLUTION OF FROZEN GROUND SYSTEM

In fact, any find of frozen ground system is a open system and in non-equilibrium state. Only in the very specific situation, it can be regarded as a isolated or closed system. Furthermore, the equilibrium state is approximately tenable only under the extreme conditions. Therefore, the evolution of frozen ground system actually is the phase change process in the non-equilibrium state. Thus the following discussion is started from the non-equilibrium state.

For any system with non-equilibrium state, the change of the state quantity, entropy s in the interval dt is denoted as ds which consists of two parts, $d_e s$ and $d_i s$, where $d_e s$ is the entropy flow passing through the system boundary and dis denotes the entropy produced in the system inner in the irreversible process of the system.

$$ds = d_e s + d_i s \qquad (1)$$

and

$$d_i s >= 0 \qquad (2)$$

Thus, for the isolated system, it indicates a period of time. During this time, frozen ground is formed or retreated with zero gradiens existed at both the upper and lower interfaces, or in engineering, it indicates the earth body within the strictly insolated and water-proofed structure. In this case, $d_e s=0$ so that $ds=d_i s>=0$ ($ds=0$ means reversible). If the system is originally in non-equilibrium state, it will be developed towards the direction of entropy increasing until reaching equilibrium state where s has the maximum value. In this situation the system is homogenuous and the original structure is disappeared. So long as the isolated condition exists, the equilibrium state is keeping on.

For the open or closed system, as long as $d_e s> d_i s$, $ds<=0$, which indicates that the sufficient environmental negative- entrop current will make the system developing towards lower-entropy and sequential direction (frozen ground advancing). Even if $ds=0$, the irreversible course can also keep going on (at this time the system is in a stable state), and it is possible to form a new dissipation structure. If $ds>0$, which means that the environment supplies the positive-entropy current,or the negative-entropy current of environment is not large enough to offset the influence of entropy producing. Thus the frozen ground system will develop towards high-entropy and non-sequence state (frozen ground retreated), and the original frozen ground structure tends to be disappeared.

According to the equilibrium equation of frozen ground system (Ding, 1986), we know that entropy-change rate ds/dt is equal to the sum of both the entropy current rate $d_e s/dt$ and the entropy-producing rate $d_i s/dt$, that is

$$\frac{ds}{dt}=\frac{deS}{dt}+\frac{diS}{dt}=-\mathrm{div}\ J_s+\sum_k^4 J_k \cdot X_k \qquad (3)$$

where J_s is the sum of entropy current caused by energy and mass exchange; J_k and X_k are the generalized current and force of irreversible process (i.e. heat, water, phase change and power) respectively.

In the linear and non-equilibrium area, using thelinear relations of current and force, and Onsager's theory, we can obtain

$$\frac{dp}{dt}=\frac{d}{dt}\left(\frac{diS}{dt}\right)<=0 \text{ and } P=\frac{diS}{dt}>=0 \qquad (4)$$

(P=0 is the stable state)

The above equation may be named as inertia principle of frozen ground system, it indicates that frozen ground system always develops towards the equilibrium state in the linear or close-equal-

ibrium area. But since the environmental binding, the system is in the stable state corresponding to the minimum value dP/dt. Thus even though there is a little disturbance (or fluctuation) which makes the system being far from stable state, the system can also return to the normal stable state. Therefore, in linear and non-equilibrium area, a new structure can not be formed and its original structure also will be disappeared. In a certain thyeshold value along with the continous change of environment, the system develops continuously towards a stable state with corresponding bindance, so that ds/dt can be used as a stability standard, and dP/dt as a variable indicating the sensitivity.

In the nonlinear area far from the equilibrium state, frozen ground system is always penetrated with energy and matter currents, and also strongly binded by the environment. This situation is usually happened in the annual change layer and the lower limit of frozen ground, especially in the active-layer. When the system crosses the equilibrium state branche (the oritical threshold value), it will lose stability and dissipate energy in the interactions between system and environment, and enlarge the fluctuation. Besides, a new sequence, dissipation structure (e.g. ice filling and some other frozen ground phenomena) will appear under the action of self-orgnization. If the bindance is removed, or reduced to a value which is less than the threshold, the system tums into the close-equilibrium stable state again and the new structure will be collapsed.

According to the entropy calculation of the frozen ground system, we know that the condition of super-entropy produced is $-\frac{1}{2}\ \delta^2 s<=0$, while the value of $\frac{d}{dt}\ \frac{1}{2}\ (\delta^2 s)$ may be greater than zero, equal to zero or less than zero, the corresponding states of which are non-stable state, critical state and new stable state of the system forming dissipation structure, respectively. Therefore, in a nonlinear area, the stability of frozen ground system may be discussed as the stability of structure forming. Thus, we can know that in the evolution of frozen ground system, random fluctuation plays a imporant role, the evolution process is obviously displayed in structure change, in other words, the evolution can remember the history (Ding, 1986).

The problems of the structure forming are not the subject discussed in this paper, but we may point out that in the ice formation of frozen ground, the situation which satisfies the sequence principle of Boltzmann, is very special. Even in the close-equilibrium state, it may be only a binary-pole phase change with binding force field. In most cases, they are always a non-equilibrium (or nonlinear) phase change. The time and space sequence structures, as mentioned above, (e.g. frozen ground phenomena, regional differences and surface landform) are all the products of non-equilibrium state phase change. These problems will be discussed in other papers.

REFERENCES

B.A. Kudliyavtzev, (1974). The forecast principle of engineering geocryology: Moscow University Publishing House.

B.A. Kudliyavtzev, (1979). Survey methods of frozen ground: Moscow University Publishing House.

Ding Dewen, (1985). Frozen ground system and its research method: Journal of Engineering and Frozen Ground, 4. 124-131.

Ding Dewen, (1986). The entropy of frozen ground system and its calculations: Journal of Lanzhou University, 4. 622-632.

Ding Dewen, (1986). A discussion on the thermodynamical basis of frozen ground stability: The Collection of III Chinese National Conference on Permafrost.

Hao Bailin et al., (1981). The development of statistical physics: Science Publishing House, Chapter 8.

Shen Kenhua et al., (1982). I.Prigogine and dissipation structure: Shanxi Publishing House, China.

S.R. De Groot et al., (1981). Thermodynamics of irreversible process: North-Holland Publishing Company.

PORE SOLUTIONS OF FROZEN GROUND AND ITS PROPERTIES

G.I. Dubikov, N.V. Ivanova and V.I. Aksenov

Research Institute of Engineering Site Investigations, Moscow, USSR

SYNOPSIS Two types of frozen ground salinity are under consideration: marine and continental; spread and conditions of its formation are elucidated;natural distribution of pore solutions concentration in frozen ground is revealed. Relationship of non-freezing water content versus temperature for marine type salinity;as well as freezing point of different salt solutions and saline ground with different moisture content or composition depending on concentration of pore solutions are under consideration. It is shown that strength characteristics of sandy soils under saline conditions are decreasing more rapidly than that of clayey soils. For the first it was proved that strength characteristics of frozen ground depend on composition of salts in pore solutions: under marine chloride salinity a decrease in strength characteristics is resulted from increasing salinity and the latter is more intensive than under continental type salinity.

A major part of cryolithozone in the USSR is occupied by saline* permafrost with frequent lenses of cryopegs - highly mineralised waters with a negative temperature. Latest investigations showed that pore waters in saline cryogenic strata are heterogeneous by chemical composition at different areas. This heterogeneity is stable at big areas; it depends on formation conditions and freezing of sedimentary rocks, which predetermine two main types of salinity: marine and continental (Fig.1). A marine type (original) is character of permafrost in the North areas along the Arctic coastline of the USSR and islands; a continental type (secondary) is character of Tsentralnaja Jakutia and Zabaikalje. It can be also encountered in frozen dispersed deposits of Alpine lacustrine basins of the plateau of Thibet and intermountain areas of Mongolia.

Recent occurrence of frozen ground with a marine type of salinity is characterized by two main factors: development of Pleistocene marine transgressions resulting in accumulation of sediments with silty saline solutions of different concentration(on the northern coastal lowlands), physico-chemical diagenic changes and desalinization of the top layer of marine strata under condition of their local or regional thawing during a period of warm weather. Process of thaw-freezing in marine strata is accompanied by differentiation of salts in liquid and solid phase as well as by relative changes in concentration of pore solutions under condition of water crystallization or ice thawing. Under condition of pore water freezing the dissolved salts are partly captured by ice crystals, partly fall out and partly squeeze to underlying strata - all this lead to an increase in mineralization of a residual solution. Thawing of frozen massives is accompanied by ground desalinization due to percolating surface and ground waters and partially dissolving salts fell out in the process of a massive freezing; as a result saline permafrost forms low marine plains and a laida along the littoral plain in the north-east of the European part of the USSR and at the islands; at the area of developing Early Pleistocene transgressions the boundary of which passes further south saline permafrost is encountered at places and, as a rule, at a depth exceeding 50 m.

As for Zapadnaya Sibir, the data available permit to compile a detailed map with representation of not only areas of saline permafrost but also of the types and degree of salinity (Fig.2). Saline permafrost occure here and there in the north latitude of Novyi Port on Jamal and Ust Port on Enisei. At this area cryogenetic stratum is saline along all the cross-section and its upper part of 150-250 m thick is turned to be frozen; its lower part of 100-200 m thick is under cool condition (freezing point $\theta_{f.p.}$ is lower than its negative temperature θ_{nat}). This conclusion is illustrated by a cross-section of cryogenetic strata of Mys Kharasavei (Fig.3). Weakly saline or non-saline marine Quaternary deposits compose a top layer spread further south of the mentioned latitude. This fact can be explained by high desalinization of sediments at the accumulator basin and by intensive affect of percolation and desalinization of thawing deposits during warm periods of Pleistocene and Holocene. Frozen Paleogene highly dispersed clays are also saline at this area. The map represents areas with frozen saline Paleogene outcropping strata and areas where

*/Frozen ground saturated with readily soluble salts in amount of 0.05% for sand; 0.15% for sandy loam, 0.20% for loam and 0.25% for clays is related to saline permafrost.

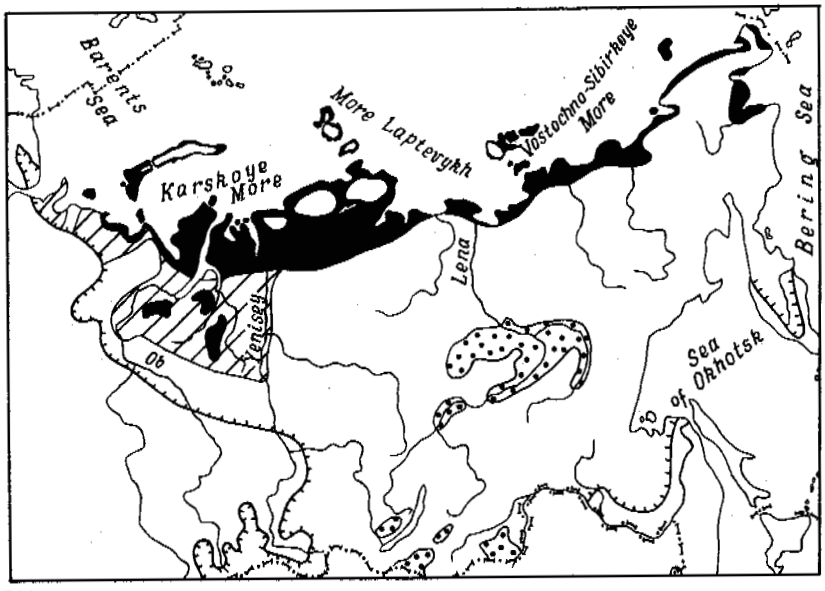

Fig.1. Spread of saline permafrost at the territory of the USSR

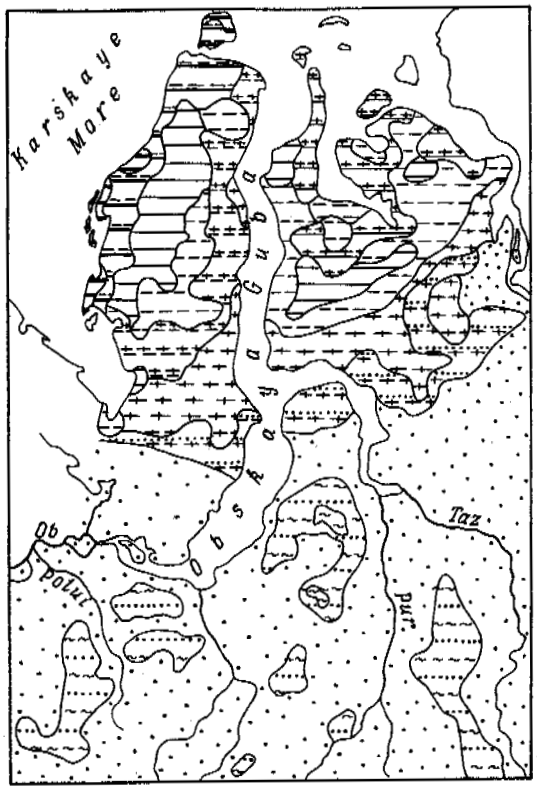

Salinity (Z), %	Salt-ion composition	Main strata
1,0 (80) / 0,5 - 2,5 *	Cl'-Na'	Saline marine Quaternary
0,7 (200) / 0,2 - 1,5		
0,5 (250) / 0,2 - 1,0		
0,25 (250) / 0,05 - 0,1	Cl'-Na', Cl'-SO_4''-Na'	Saline and desalted marine Quaternary
<0,1 (280) / 0,01 - 0,1	SO_4''-HCO_3'-Na'	Desalted marine and non-saline continental Quaternary
0,75 (70) / 0,2 - 1,6	SO_4''	Saline marine Paleogenic

Permafrost with different salinity by a cross-section: top layer upto 3-10 m deep; bottom layer

Area of saline cover upto 50 m deep

*/ mean (quantity of samples) / min - max

Fig.2. Map of saline permafrost in Zapadnaya Sibir

the strata can be found within the interval from 0 to 50 m.

Saline permafrost occurs in the strata of marine Pleistocene and Holocene deposits within the limits of Severo-Sibirskaya nizmennost, littoral Jakutia and Chukotsk as well as on the Anadyr nizmennost. The top layer 50 m thick is characterized by saline permafrost occur at places or by alternation of saline or non-saline ground.

Permafrost of marine type salinity is characterized by a persistent in area and in section

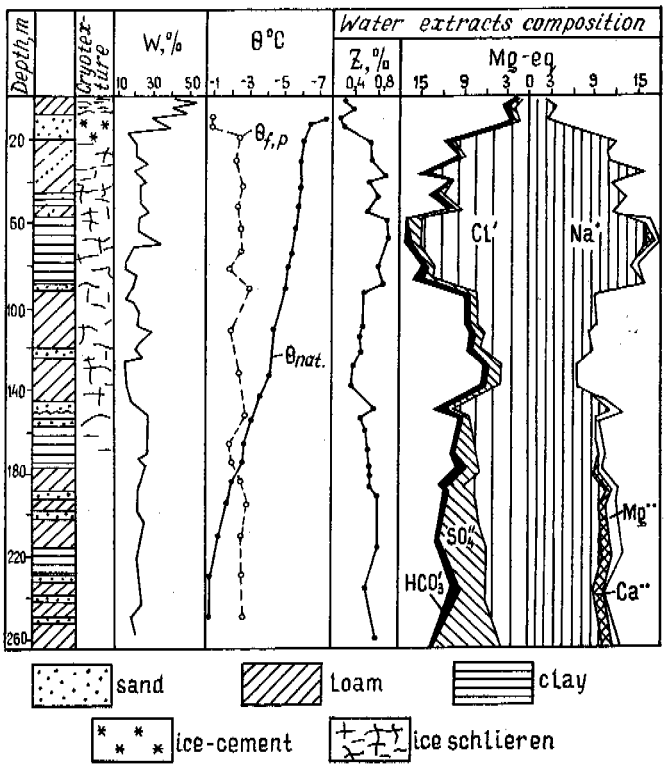

Fig.3. Cross-section of saline permafrost at Mys Kharasavey

homogene chloride-sodium composition of pore solutions resulting from the primary sedimentation salinity of marine silty waters. Salinity is character of the strata under a seasonal thawing layer or a stratum inclined to thawing desalinization and freezing anew. Salinity reaches 2.0-2.5% or 4-6% at places. Salt-ion composition of pore solutions in frozen marine Quaternary deposits is characterized by the following relations: $Cl' \gg SO_4'' > HCO_3'$ and $Na' \gg Mg'' > Ca''$, that is the same as for the recent marine silts and so for marine water. Composition of water solutions in marine non-saline silts changes to chloride-sulphate-sodium or sulphate-hydrocarbonate-sodium; amount of salts in these solutions does not exceed 0.1%.

Paleogene frozen ground in Zapadnaya Sibir is characterized by a sulphate type of pore solutions conditioned by their repeated changes in the process of diagenetic transformations of marine clays, by active oxidization of pyrite and by formation of sulphates before freezing

Distribution of salts in a permafrost depends on a number of factors the main of which are as follows: soil composition; facial conditions of soil accumulation; cryogene differentiation of salts under freezing conditions. Content of readily soluble salts in the marine Quaternary deposits depends in the first turn, on amount of clay particles. Clayey frozen soils, capable to maintain sedimentational salinity, contain salts in greater amount than the sandy frozen soils. Therefore changes in salt concentration in a cross-section of cryogene strata depend on lithological composition of deposits and do not conform to a law of equilibrium condition known for thawing ground (vertical hydrochemical zoning) when heavy brines migrate downward and the liquid ones - upward. This is a typical feature of frozen ground for which stria movement of solutions is not character at all or to a very small degree.

Frozen ground of a continental type of salinity is widely spread at the areas where high summer temperature and negative balance of moisture promotes salt accumulation at the top layer and underlying strata during long periods of sedimentation and freezing. Arid climate, gently sloping surface and slow water exchange provides annual evaporation of flood waters and saturation of soils with salts in closed cavities.

In Tsentralnaya Yakutia a salt content in the ground of different composition and genesis varies from hundredth - tenth percent to 1.5-2% or even 5-8%. Maximum salinity of ground is fixed at a depth of 1-5 m but sometimes it can be traced down to 15 m saline ground and halite interlayers in the deposits of lake basins of Thibet are traced down to 40-60 m. By chemical composition pore solutions of frozen ground with a continental type of salinity are characterized by a great difference as in area so in section depending on geological structure of an ablation area, conditions of formation and freezing of ground as well as developing differentiation of salt content in the process of dynamic freezing. Dominating salinity types are both: as sulphate-chloride and chloride-sulphate so hydrocarbonate ones.

Chemical composition and a concentration value of pore solutions produce a great influence on physico-mechanical characteristics of frozen ground. The main characteristic of saline ground is salinity (Z), which determines a salt content in a weight unity of dried soil. Saline ground is characterized by the following indices: density, dry density, salt density, total moisture content (W), concentration of pore solutions ($K_{p.s.}$) freezing point and amount of unfrozen water (W_{unf}).

Concentration of pore solutions is characterized by a degree of water mineralization in soil pores. Normal solution (N_{eq}) contains 1 gramme-equivalent of a dissolved substance in 1 litre solution. At present we lack research data to estimate unfrozen water in saline ground. Therefore the relationship of W_{unf} and a temperature of saline ground characterized by a marine type of salinity gives much information on phase composition of this ground (Fig.4). The curves are similar to each other by their nature but moved to the area of high temperature as compare to the design ones.

A freezing point of saline ground characterizes crystallization of pore water in the soil. Saline ground gets frozen at a temperature lower than that of a pure solution of the same salt which the ground is saturated with. Fig.5 shows

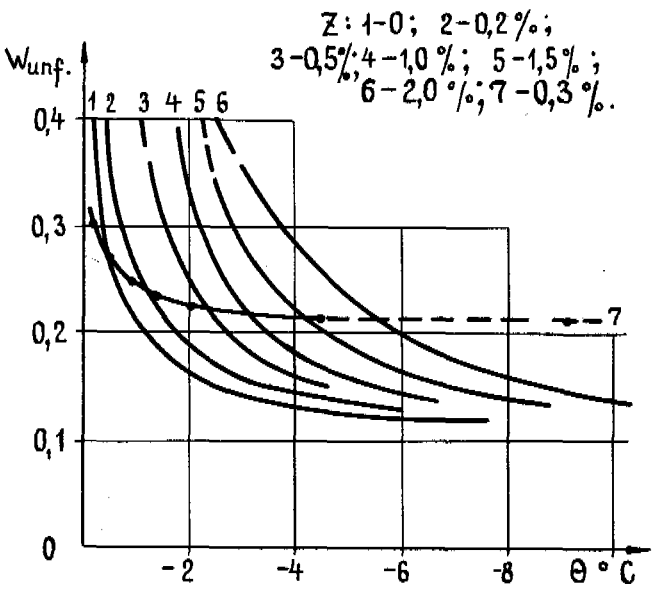

Fig.4. Content of unfrozen water in loam (1-6) and clay (7) with marine salinity (by Ju.S.Petrukhin and G.I.Dubikov)

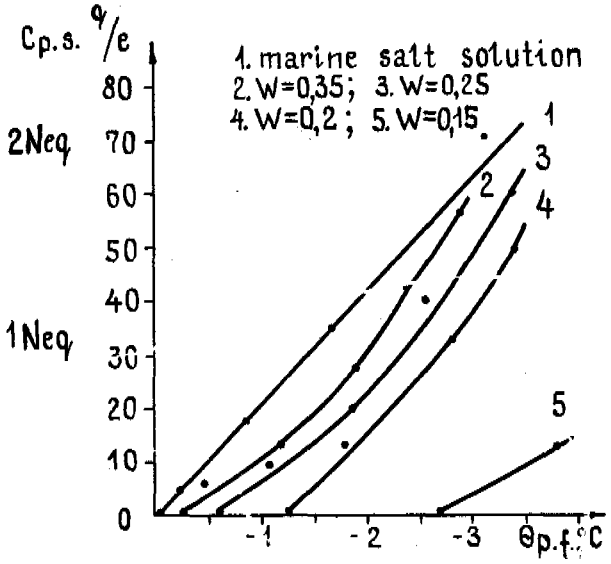

Fig.5. Freezing point of loam saturated with marine salt solution of different concentration

a relation of pore solution concentration for the loam with different moisture content (curves 2-5) and a solution of marine salt (line 1) with concentration up to 2 N_{eq} (70 g/l). If moisture content in saline loam decreases a freezing point decreases also.

A freezing point of saline ground depends on salt composition (Fig. 6). The lowest freezing point is character of the NaCl solution and

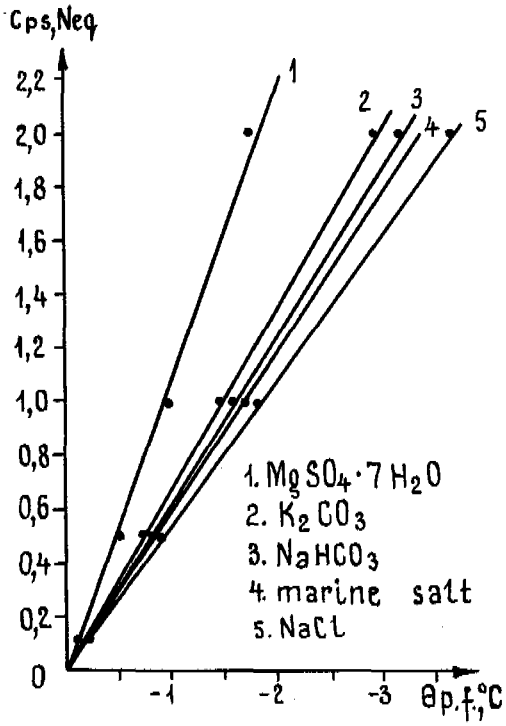

Fig.6. Freezing point of salt solutions of different composition

marine salt and the highest one - of the magnesium sulphate solution. As Raoult's law says equimolecular quantities of different solutes in equal quantities of solvents reduce a freezing point by the same value. But other salt solutions are characterized by a higher freezing point as compare to the NaCl solution (1 Neq.NaCl solution has a cryoscopic constant -1.86°C).

Freezing point of different salt solutions and saline loam (with the same salts) (Z=1%; W = 0.3) obtained as a result of experiments were compared to the design values reduced to normal salt concentration NaCl (Table). It follows from the comparison that salinity is to be taken from Raoult's presentation, it means that salinity corresponds to equivalent quantities of different salts. The Table shows that loam saturated with magnesium sulphate being reduced to a normal concentration towards NaCl is characterized by Z = 3.69% but not 1% as it was assumed in Jarkin's experiment (1986). Values of freezing point for water saturated loams, salinized with different salts, and solutions turned to be almost identical (Sheikin); it confirms law of solution freezing.

Strength properties of saline frozen ground are less studied than those of non-saline. Comparison of design values of pressure (R) and design shear strength at the lateral surface of congelation (R_f) showed that strength indices

Experimental and design values of freezing temperature of soil salt solutions depending on their concentration

N	$C_{p.s.}$		Z,%	$\theta_{f.p.}$ °C		
	g/l	$N_{eq.}$		solution	loam	Evaluation by NaCl solution
1*	123	1.0	3.69	-0.95		
	35.7	0.29	1.0	-0.3	-0.35	-0.54
2	73	1	2.19	-	-	
	35.7	0.49	1.0	-	-0.95	-0.91
3	35	1.0	1.05	-1.7	-	
	35.7	1.02	1.0	-1.72	-1.8	-1.88
4	29	1.0	0.87	-1.86		
	35.7	1.23	1.0	-2.8	-2.3	-2.28
5	104	1.0	3.12	-		
	35.7	0.34	1.0	-	-0.75	-0.68

Note: * Salt composition
1 - $MgSO_4 \cdot 7H_2O$; 2 - $CaCl_2 \cdot 6H_2O$;
3 - Marine salt (77% NaCl and others); 4-NaCl;
5 - 42% NaCl, 30% $MgCl_2$, 16% $CaSO_4$ (Jakutsk, continental salinity).

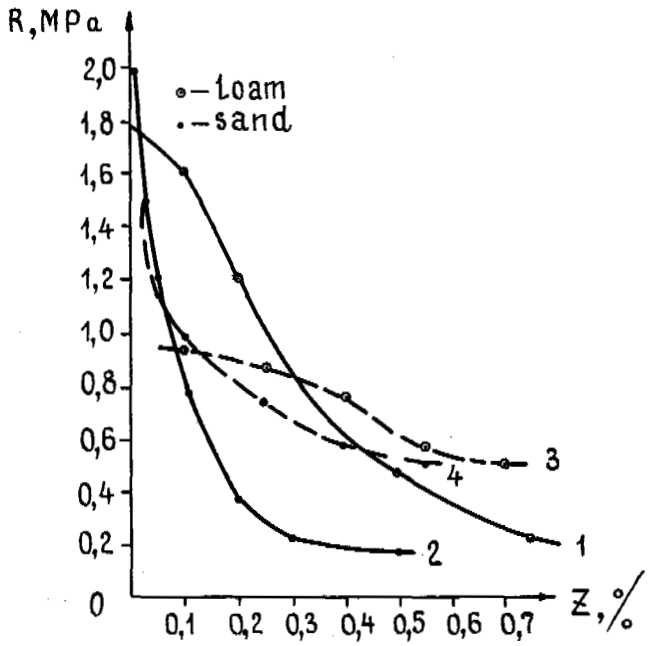

Fig.7. Ratio R=f(Z) for frozen ground with marine (1,2) and continental (3,4) type of salinity, θ = -4°C

of saline sands decrease rapidly (Fig.7). Strength of sand saturated with marine salt at a temperature -4°C and increasing salinity from 0 to 0.5% decreases by a dozen times but as for loam it decreases by 4 times only. The temperature decreases the strength properties of saline ground increase more intensively than those of non-saline. For example, the R value for loam with Z = 0.5% and temperature from -2 to -4°C increases by 3.2 and for non-saline loam - by 1.7. A salt effect is more intensive under high negative temperature. It results from the fact that under a high temperature and concentration of solutions the major part of water remains liquid but when concentration is weak great amount of water changes to ice and it leads to an increase in strength characteristics.

Attention should be paid to a character of relationship of strength and salinity depending on different granulometric composition of permafrost. If sands have a tendency to a sharp decrease in their strength characteristics almost when Z varies from 0 to 0.1% then loams are characterized by a slight decrease in strength up to Z = 0.4%.

An effect of salts chemical composition on permafrost strength can be seen from the test results presented at Figs 8,9 and Table.

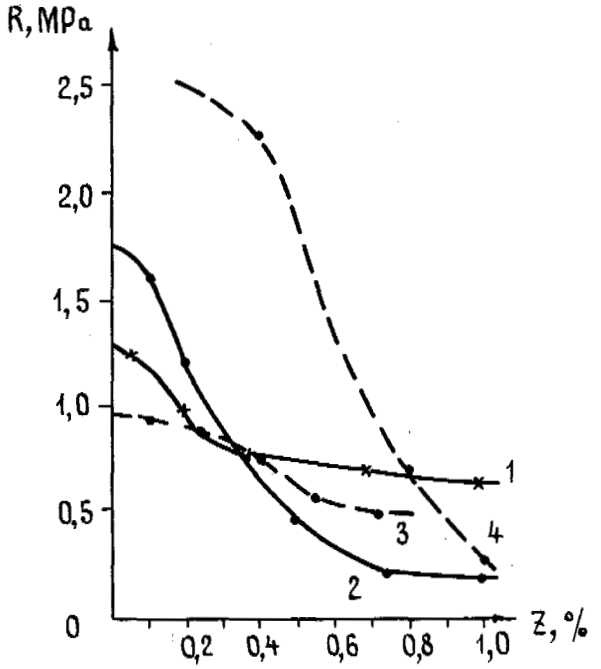

Fig.8. Ratio R=f(Z) for frozen loam of different genesis, θ = -3 ÷ -4°C

Salinity increases, the design shear strength at the foundation surface decreases, but the decrease intensity depends on a salinity type: marine type (curves 4,5 at Fig.9) is characterized by a more intensive decrease than a continental one (curves 1,2). Salinity is low (0.2% at least) a marine type salinity involves higher strength as compare to continen-

tal one. On the contrary if $Z > 0.2\%$ $R_{fr.}$ is higher for sulphate salinity than that for loam with NaCl salinity.

Interesting experimental results were obtained when comparing a relationship of R versus Z (Fig. 8) for loam samples taken in Amderma and Jakutsk (Karpunina, 1974; Jarkin, 1986). The tests showed that the samples were saturated with local salts and salts from other areas. Alluvial loam (Jakutsk) saturated with marine salt (curve 4) turned to possess the highest strength. A character of strength decrease depending on salinity for the loam of alluvial genesis (Jakutsk) and marine (Amderma) with local salinity (curves 2,3) is similar to curves 2,6 at Fig. 9. This fact indicates a predominant effect of a salt type on a character of strength decrease depending on salinity.

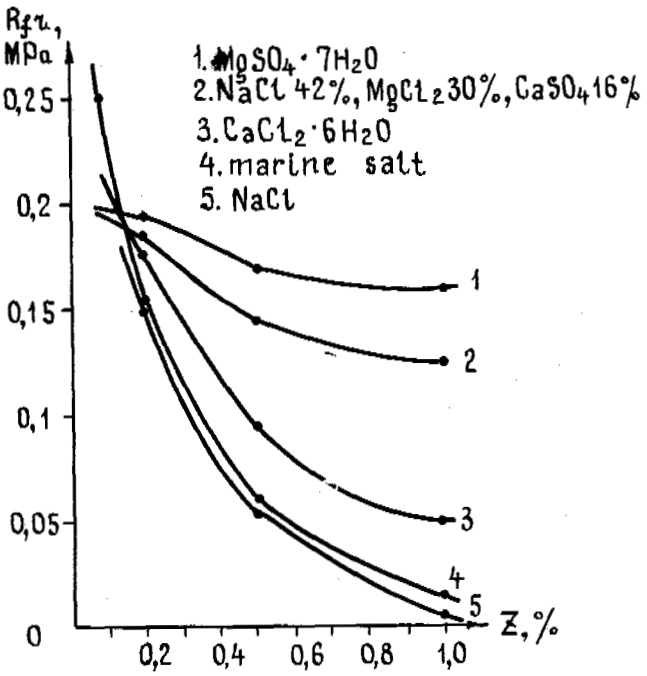

Fig.9. Ratio $R_{fr.} = f(Z)$ for loam ($\theta = -3°C$) saturated with solutions of different salts (by A.N.Jarkin's data, 1986)

All the foregoing data help to establish spread of saline frozen ground at the territory of the USSR. Dominating chemical composition of salts reveals two types of soil salinity - marine and continental. The experimental research shows that physical and mechanical characteristics of saline ground depend not only on concentration of pore solutions (temperature and soil composition being identical) but also on chemical composition of dissolved salts. Further research works in this field are planned to compile classification of saline frozen ground with account of chemical composition of pore solutions.

REFERENCES

Jarkin, A.N. (1986). Osobennosti stroitelnyh svoistv merzlyh gruntov kak osnovaniy sooruzeniy. Avtoreferat cand. dissert. 1-18, Leningrad.

Karpunina, A.A. (1974). Issledovanie physiko-mehanicheskih svoistv zasolionnyh gruntov dlia injenernyh izyskaniy. Avtoreferat cand. dissert. 1-26, Moskva.

Permafrost Institute, Siberian Branch of the USSR Academy of Sciences, Yakutsk, USSR

SYNOPSIS Potential possibilities are examined of crystalline-pellicular and vacuum-filtration mechanisms of moisture migration in a case of formation of thick (over 2-3 cm) ice streaks in permafrost. Experimental laboratory results are presented on moisture migration for both epigenetic and syngenetic freezing of earth.

Here we investigate mass transfer processes leading to formation of segregation ice only. We are interested, first of all, in potential capabilities of different mechanisms of segregation ice formation in a sense of providing unlimited growth of ice streaks leading towards formation of not only ice saturated horizons but also of sheet ice deposits. Laboratory experiments were carried out on earth samples 100 mm in diameter, 200--250 mm high at constant initial humidity and volumetric density of unfrozen earth. Initial temperature of the unfrozen earth was near 0 °C and side thermal insulation provided unidimensional process of freezing - thawing. A pilot installation permitted assigning the required, practically constant, rate of the earth freezing (thawing); phase transition boundary fluctuations at a given horizon; ground water level in modelling epigenetic type of freezing or a layer of water on a sample surface in modelling syngenetic type of freezing. In the process of experiments the magnitude heaving and amount of water entering the sample were measured; texture formation and freezing depth were observed visually. Experiments have been carried out on samples of sandy, suglinok and clayey soils with disturbed texture.

A number of mechanisms are known today that explain segregation ice formation in freezing earth - formation of vacuum on mobile freezing boundary; capillary forces; vapour transfer; "compression" pressure caused by the growing ice crystals; differentiation of the water and earth particles in the zone of thawing frozen ice-saturated earth; "cryostatic" pressure at permafrost base causing forcing out of water from underlying thixotropic melted earth; vacuum-filtration and crystalline-pellicular. Of all of these mechanisms the most recognized ones are the crystalline-pellicular and vacuum-filtration, and we shall therefore examine their potential possibilities in the sense of forming thick ice streaks.

CRYSTALLINE-PELLICULAR MECHANISM OF MOISTURE MIGRATION

Combined action of two mechanisms - crystallization and pellicule formation is usually examined in this case.

Bouyukos, Teber and Rukly have proposed a theory of "crystallization forces" explaining the capability of the growing ice crystals to attract water from underlying unfrozen earth in the process of their crystal lattice formation. Feeding of the growing ice crystal will be maintained due to high rupture resistance of thin water filaments of loosely bound water which connect the adsorbed film on the ice crystal faces with bound water of the underlying unfrozen earth. But the main point, in our opinion, is that the growing ice crystals attract the loosely bound water pellicule tearing it off the adjoining earth particles, while the mineral skeleton only creates the loosely bound moisture.

The pellicular moisture migration mechanism was proposed by Beskov probably under the influence of the work by Lebedev. Free and part of loosely bound moisture freezes in the phase transition zone leading to formation of a moisture gradient (along liquid phase) between the freezing boundary and the underlying unfrozen earth. It is surmised that under the influence of this moisture gradient migration of moisture takes place towards the front of freezing: from earth particles with thicker pellicules of bound moisture towards the particles with thin pellicules. Such pellicular mechanism of moisture migration is stipulated by adsorption forces of the earth mineral skeleton. The main point here is that due to the moisture gradient unfrozen earth transfers the bound moisture towards growing ice crystals and the fact of the moisture crystallization appears only as a cause of the moisture gradient formation.

Subsequently the crystallization and pellicule formation mechanisms were combined into one - crystalline-pellicular where each water molecule travels under joint action of adsorption forces both of the mineral skeleton and of the growing ice crystals. In the opinion of the majority of investigators, moisture migration to the freezing front takes place mainly due to the adsorption forces of the mineral skeleton, i.e., the earth moves the moisture towards the growing ice crystals. The most surprising and important property of the crystalline-pellicular mechanism is considered the possibility of an unlimited ice streak growth during very slow freezing of thinly dispersed earth or an immovable freezing front over a water-bearing horizon. This property is often cited as an explanation for genesis of not only thick streaks (over 2-3 cm), but also of sheet ice deposits. According to Beskov, loosely bound moisture travelling over the pellicules towards the freezing front can be replenished from a free water storage. Therefore, in the case of presence of a water-bearing horizon (with unlimited water storage) and practically immovable freezing boundary the thickness of an ice streak being formed in finely dispersed earth may be very large and will be limited only by time. This idea of huge potential possibilities of a pellicular mechanism of migration (in the sense of forming sheet ice deposits) was reflected and supported practically in all works dedicated to this problem.

In our opinion this idea is erroneous. It is well known that during the growth of crystals in supercooled liquids tearing off and scattering of the crystal nuclei takes place, this process being the more intensive the higher is the degree of supercooling. Shubnikov notes that often the crystals grow in the shape of needles, skeletons; this confirms that crystal growth is stipulated

not only by substance influx in a direction perpendicular to its surface, but also by molecule movement along the faces. This permits an assumption that with sufficient supercooling in the freezing zone the needle crystals of ice are capable of attracting the bound moisture to the growing streak. It is established by the experiments of Pousakov (1960) and Jestkova (1982) that the boundary zone of an ice streak is represented by needle crystals of ice which "grow into" the unfrozen earth and attract the loosely bound moisture pellicule to the growing streak. Therefore segregational ice accumulation intensity depends both on the intensity of growing into the earth of the needle crystals and on presence of loosely bound moisture. It follows from this that pellicular moisture migration is possible only in the case of spontaneous freezing of earth when there is sufficient supercooling of the earth moisture, while segregational ice accumulation only accompanies this process of earth freezing. Continuity of the loosely bound moisture pellicule in finely dispersed earth is supported only within definite range of its moisture - it is absent both in low moisture and diluted earth.

Experiments carried out by us have shown that moisture migration towards the freezing front (with presence of a ground water level) does not take place in case of an immovable freezing border or low rate of its movement - less than 0.04 mm/h. Considering that the maximum rate of the epigenetic earth freezing (approximately 0.002 mm/h) is one order lower, it may be assumed that the genesis of thick streaks and sheet ice deposits under natural conditions is not connected with segregational ice accumulation stipulated by crystalline - pellicular mechanisms.

VACUUM-FILTRATION MECHANISM OF MOISTURE MIGRATION

Comparatively recently (Borosinets, Feldman, 1981; Melnikov, Feldman and Anisimova, 1984) a new mechanism of ice accumulation in freezing earth has been proposed, connected with multiple oscillations of the freezing earth boundary in presence of a water source (water bearing horizon, vadose water, shallow water reservoir). Under such oscillations is meant thawing of a comparatively small layer of frozen soil followed by its freezing. In the zone of frozen soil (or ice) thawing vacuum is formed due to reduced volume of ice during its thawing. Under the action of this vacuum water filtration is started into the thawing zone (9 % of the thawing ice volume is filled) and the following freezing fixes the introduced water. In case of epigenetic freezing the water bearing horizon is located below the oscillating boundary of the phase division and in the case of syngenetic freezing the water source (vadose water, shallow water reservoir) is located higher. Since water flow is caused by appearance of vacuum and nature of the water flow is filtration, the mechanism is termed by us as vacuum-filtration. Multiple freezing boundary oscillations in a definite layer may lead to formation of thick ice streaks (the ice lens thickness being determined by the number and amplitude of these oscillations), while similar oscillations with gradual advance of the phase transition boundary lead to formation of ice saturated frozen deposits. Naturally, the number of horizon levels at which such multiple oscillations took place determine the number of thick ice streaks or ice saturated horizons within permafrost.

To prove wide possibilities of the vacuum - filtration mechanism a series of laboratory experiments have been carried out on growing ice streaks in suglinoks, sands and coarse fragmentary matrials (duration of one experiment being about 1.5 months). Modelling results of epigenetic type of freezing are shown on Figs. 1, 2, 3, 4. On Fig.1 is shown an ice lens 80 mm thick in suglinok; on Fig.2 - three ice lenses in fine-grain sand; on

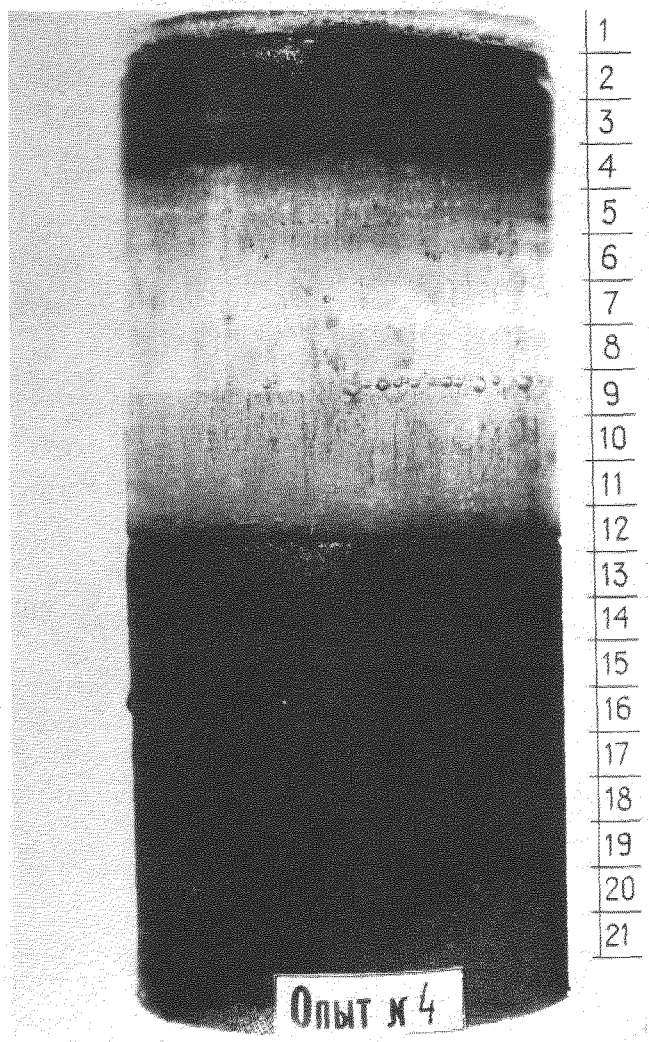

Fig.1 Ice lens in suglinok (epigenesis)

Fig.3 - two ice lenses in gravel; on Fig.4 - two ice saturated horizons in clay. Modelling results of syngenetic type of freezing are shown on Figs. 5 and 6. On Fig.5 - an ice lens 1 cm thick in medium-grain sand; on Fig.6 - an ice lens 2 cm thick in suglinok.

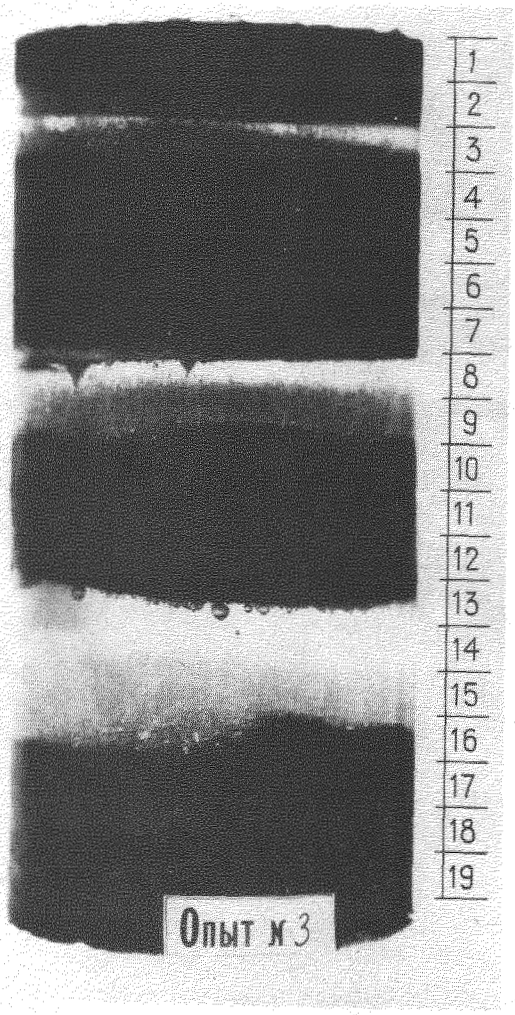

Fig.2 Three ice lenses in sand (epigenesis)

Oscillating nature of boundary movement of perennial epigenetic freezing of earth under natural conditions is stipulated by variations of climate and the depth of shallow water reservoirs (in the case of sub-aqueous permafrost) and also presence of a geothermal heat flow.

In the case of syngenetic freezing the annual variations of phase transition boundaries at the base of an active layer are caused by alternations of seasonal processes of the earth thawing and freezing. It is obvious that the rate of oscillating movement of the freezing boundary in laboratory experiments is several orders higher than the similar rate in natural conditions, but the physics of the phenomenon and the result - the possibility in principle of an unrestricted growth of an ice streak - remain without changes.

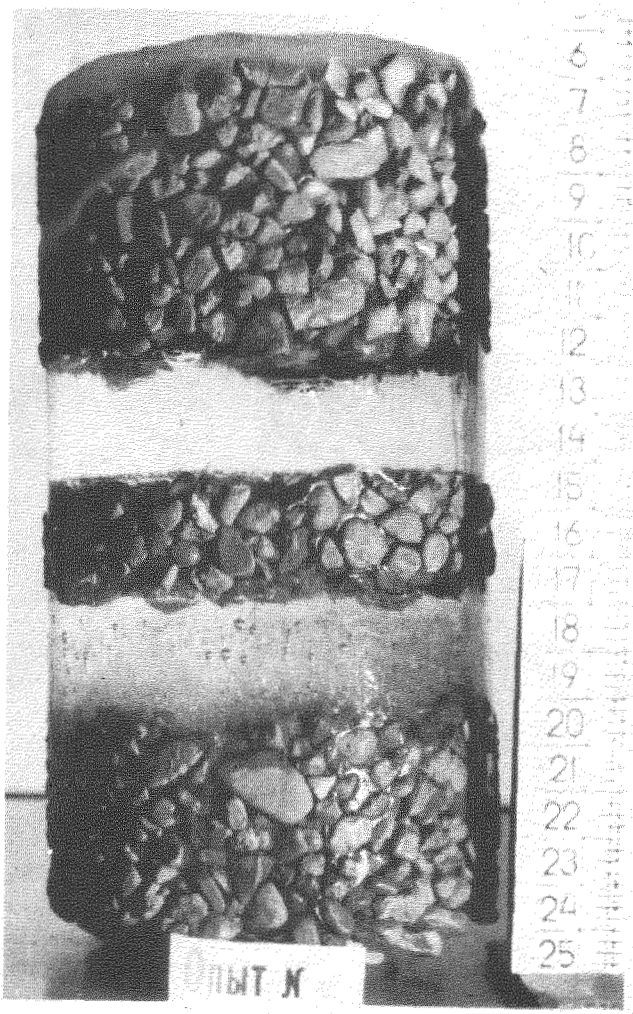

Fig.3 Two ice lenses in gravel (epigenesis)

From the position of vacuum-filtration mechanism it is possible to explain intensive roadbed heaving in the areas of seasonal earth freezing. It is known that the most intensive heaving is observed after the winters noted by frequent lengthy periods of thawing weather. During these periods of thawing weather variations in the freezing boundary take place caused by daily changes in air temperature and with presence of a water-bearing horizon these variations cause growth of ice streaks and intensive ground heaves.

CONCLUSION

Formation of thick ice streaks, ice saturated horizons within permafrost and also intensive heaves on the roadbeds in the regions of deep seasonal freezing may be explained by the

action of a vacuum-filtration mechanism of the moisture migration towards a mobile freezing boundary in presence of a water-bearing horizon.

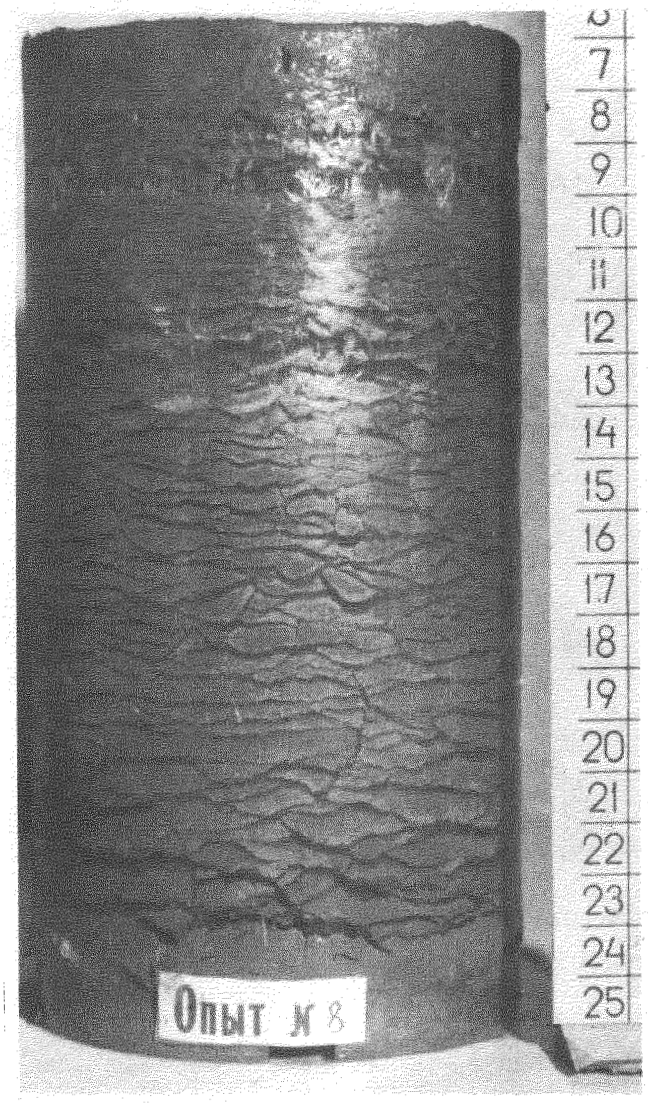

Fig.4 Two ice saturated horizons in clay (epigenesis)

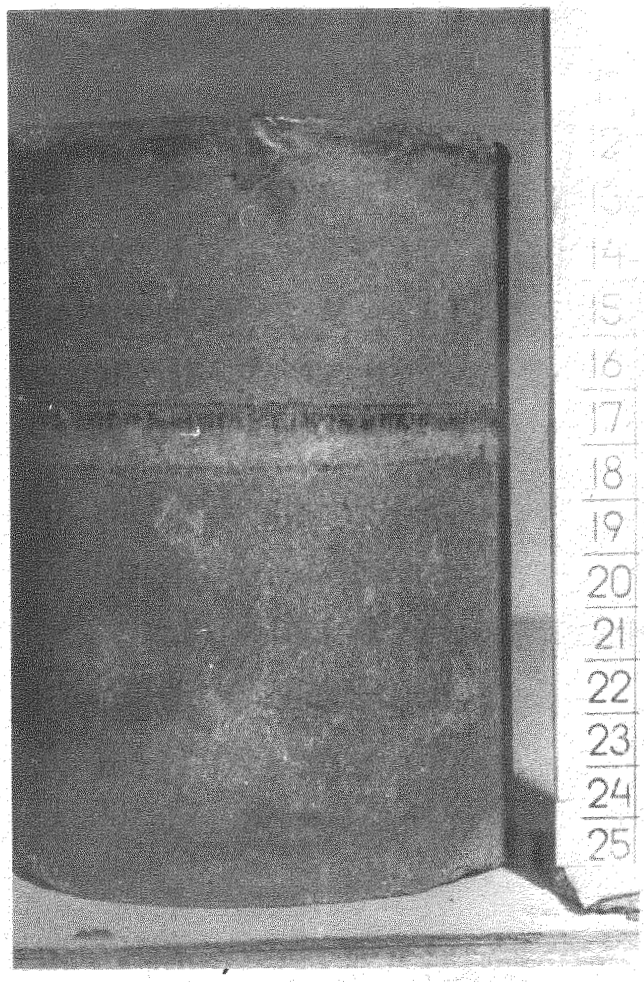

Fig.5 Ice lens in sand (syngenesis)

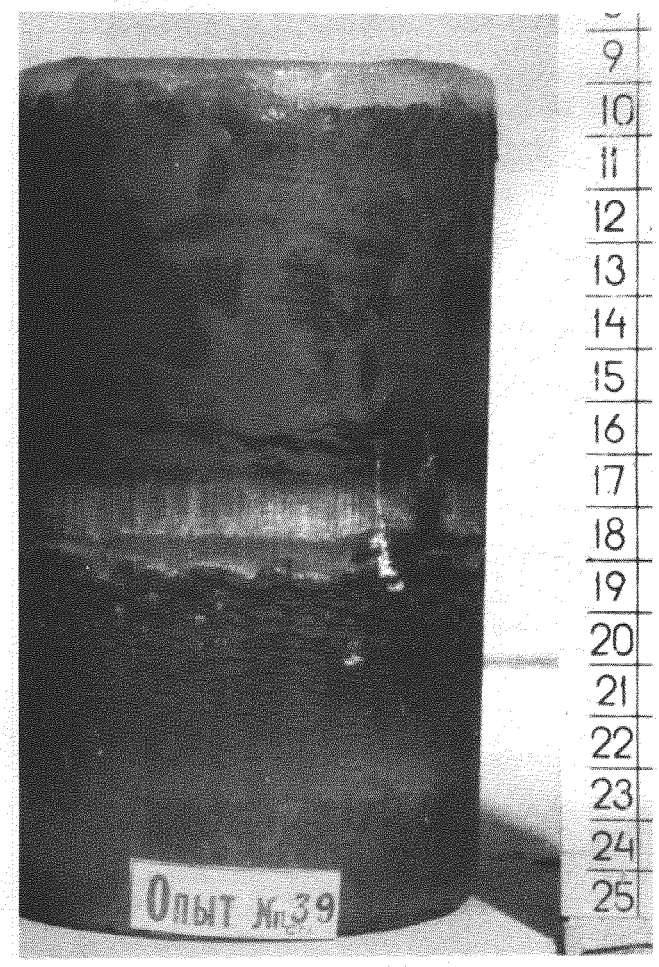

Fig.6 Ice lens in suglinok (syngenesis)

REFERENCES

Borosinets, V.E., Feldman, G.M.(1981). Vakuumno-filtrazionnyi mekhanism obrasovaniya moschnykh shlirov lda. Problemy kriolitologii. Vyp.IX, MGU, s. 165-178.

Jestkova, N.A. (1982). Formirovanie kriogennogo stroeniya gruntov. Moskva, Nauka, str. 216.

Melnikov, P.I., Feldman, G.M. and Anisimova N.P. (1984). Formirovanie shlirov lda pri kolebaniyakh granitsi promerzaniya nad ourovnem gruntovykh vod. DAN USSR, (279), 2, s. 476-480.

Pousakov, N.A. (1960). Vodno-teplovoi rejim zemliyanogo polotna avtomobilnykh dorog. Moskva, Avtotransizdat, str. 168.

FROST HEAVE

K.S. Førland[1], T. Førland[2] and S.K. Ratkje[2]

[1]Division of Inorganic Chemistry, University of Trondheim, NTH, Norway
[2]Division of Physical Chemistry, University of Trondheim, NTH, Norway

SYNOPSIS Frost heave is a non-equilibrium phenomenon which can be dealt with by means of irreversible thermodynamics. In frost heave a substantial part of the heat transport is coupled to the water transport. We shall treat frost heave as a case of thermal osmosis. Where the temperature is 0°C in the ground, ice and liquid water are in equilibrium. Under influence of the temperature difference ice melts absorbing heat, and liquid water migrates through the pores of the soil to the colder zone, where it refreezes releasing heat. Thus heat corresponding to the enthalpy of melting is transported with the water. The transport of water to the colder zone leads to a pressure increase, which counteracts the movement of water. Maximum frost heave pressure is the pressure difference that halts the flux of water. Calculated values for maximum frost heave pressure fit very well with experimental values.

INTRODUCTION

When a soil containing water freezes, its surface heaves, often unevenly, this is called frost heave. When the soil thaws again, it becomes soft and muddy. These phenomena are serious problems in construction engineering. In areas where frost heave occurs, one must take extra care with the foundation of buildings and roads.

Frost heave can be a large effect where the average temperature of the coldest month is below 0°C. The geographic region where frost heave occurs, covers large parts of Asia, North America and Europe. The extent of the frost heave also depends on the soil. There is very little frost heave in coarse sandy soils, while fine grain soils like clay, and particularly silt, are inclined to have much larger effects.

When a soil has been allowed to settle, the solid particles are packed together so that they are in contact with one another. The solid particles in contact form a framework which is able to resist pressure. There will be a distribution of pore sizes between the particles. These pores may be more or less filled with water. This water is called *bound water*. If there is more water in the soil than the space between the particles in contact permits, the framework must expand. Contact between particles is lost, and the soil loses its strength. The excess of water is called *free water*.

By frost heave the soil expands more than corresponding to the freezing of the bound water in the unfrozen soil. Excess of water forms ice lenses under the surface. When the soil thaws from the top, the excess or free water makes it soft. This excess of water was *transported* to the ice lens during freezing.

TRANSPORTS DURING FROST HEAVE

In order to study the transports more closely, we shall look at the frost heave in more detail. Figure 1 gives a schematic picture of a vertical column of soil where frost heave takes place.

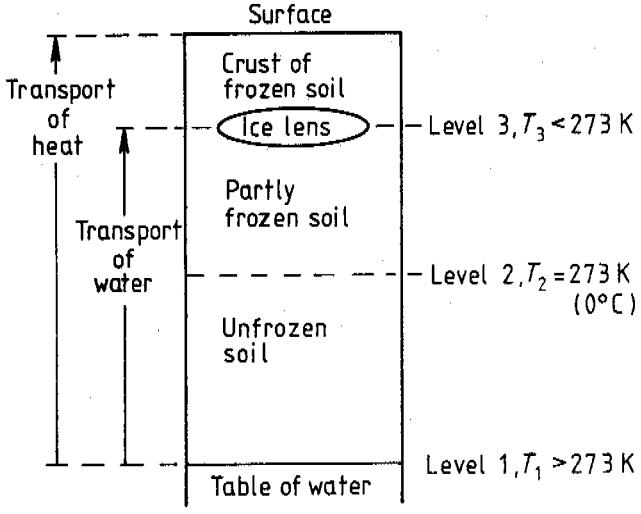

Fig.1 Schematic picture of frost heave in a section of freezing soil.

We shall consider the transports of water and heat in two steps. The capillary rise of water from the table of water, level 1, through the unfrozen soil at temperatures above freezing up to level 2 at the freezing point is the first step. The transport of heat through this region will also be considered. The second step is the transport of water and heat from level 2 through

the partly frozen soil to the ice lens at level 3. Here *thermal osmosis* takes place, in addition to capillary rise.

First Step

The pores of the fine grain soil act as a set of capillaries. These are filled by capillary rise from the table of water. As we shall see when discussing the second step, water is transported away from level 2. If there is no access to air, the void must be filled with water flowing through the soil from the table of water. The force for this flux is given by a pressure reduction at level 2. The temperature difference between levels 1 and 2 will cause a flux of heat.

At level 2 there is an equilibrium between ice in the pores and liquid water. One can change the relative amounts of the two phases without changing the Gibbs energy. We shall include in the first step freezing of all the transported water at level 2. The water is transported in liquid form in the second step, and this means that the second step will involve the remelting of the ice at level 2.

Second Step

The ice melts at level 2. Liquid water is transported through pores of the partly frozen soil in the direction of decreasing temperature. The temperature is below zero degree centigrade. Liquid water below 0°C is a well known phenomenon in capillaries. In the smallest pores the water will remain liquid at temperatures several degrees below 0°C, while ice can form at 0°C and atmospheric pressure in the largest pores. At a sufficiently low temperature even the water in the smallest pores will freeze. Below this temperature there is a solid crust of ice which does not permit any transport of water. The transport process from level 2 to level 3 can be treated as thermal osmosis.

Thermal osmosis may occur over a membrane when the transfer of mass across the phase boundaries to the membrane leads to absorption or release of heat. In frost heave ice melts at level 2 absorbing heat. The partly frozen soil between levels 2 and 3 serves as a membrane. At level 3 the water freezes and heat is released. Under a solid crust of ice the thermal osmosis leads to an increased pressure at level 3. The termal osmosis is a slow process.

The increased pressure under the crust acts on the solid framework of the soil. When an ice crystal at level 3 has grown to fill the pore, it will be subject to the same pressure. The wall of the pore breaks at a weak point, and the crystal will continue to grow. In the end a lens of ice is formed below the frozen crust. As the ice lens grows, the pressure under the frozen crust increases until the transport of water stops, or until the crust breaks. When the surface temperature decreases, the frozen crust grows in thickness. The border between the crust of frozen soil and the partly frozen soil (level 3) is pushed further down in the ground, and a new lens may form at this lower level.

FLUX EQUATIONS FOR THE TRANSPORTS

There is experimental evidence that we have little or no coupling between the flux of water and the measurable heat flux in the first step (the measurable heat flux does not include the molar enthalpy of the transported water). This will be discussed in the section about the experimental studies.

In the first step the heat flux is given by the thermal conductivity, λ, and the temperature difference, ΔT, $J_q = -\lambda\Delta T$. The flux of water, J_w, is given by a transport coefficient, $\bar{l}$, and the difference in chemical potential for water. With pure water (or no variation in concentration of impurities) the difference in chemical potential is given by $\Delta\mu_{H_2O} = V_{H_2O}\Delta p$, where V_{H_2O} is the molar volume of water and Δp, the pressure difference, is the pressure reduction created at level 2 by the thermal osmosis in the second step. Thus we have $J_w = -\bar{l}V_{H_2O}\Delta p$.

Heat is released when water freezes at level 2.

In the first step the flux of heat and the flux of water are independent of each other. Both are linear functions of the forces acting upon them.

In thermal osmosis (the second step) the fluxes of heat and material are both dependent on the two forces, temperature difference and pressure difference. For slow processes we may assume *microscopic reversibility*, that is *local equilibrium*, and *irreversible thermodynamics* may be applied. According to the theories of irreversible thermodynamics the fluxes are linear homogeneous functions of the forces in the following way,

$$J_q = -\bar{l}_{11}\Delta\ln T - \bar{l}_{12}V_{ice}\Delta p \qquad (1)$$

$$J_w = -\bar{l}_{21}\Delta\ln T - \bar{l}_{22}V_{ice}\Delta p \qquad (2)$$

The direct coefficients, $\bar{l}_{11}$ and $\bar{l}_{22}$, relate conjugate fluxes and forces. They will always be positive. According to the *Onsager Reciprocal relations*, the cross coefficients are equal, $\bar{l}_{12} = \bar{l}_{21}$.

The forces are $\Delta\ln T = \ln(T_3/T_2)$ and $V_{ice}\Delta p$, which is equal to the difference in chemical potential when we have pure ice at both levels. The V_{ice} is the molar volume of ice, and Δp is the difference between the pressure acting on the ice lense at level 3 and on an ice crystal at level 2. See Fig. 1. Ice and liquid water are in equilibrium at level 2, and the pressure on the ice is the same as the pressure on the water in the pores.

The maximum possible frost heave pressure is the pressure that completely suppresses the flux of water, $J_w = 0$. We obtain from eq (2),

$$\Delta p_{J_w=0} = -(1/V_{ice})(\bar{l}_{21}/\bar{l}_{22})\Delta\ln T \qquad (3)$$

The *heat of transfer*, q_w^*, is defined as the heat

transferred with the water when there is no temperature difference, we obtain from eqs (1,2),

$$q_w^* = (J_q/J_w)_{\Delta T=0} = \bar{l}_{12}/\bar{l}_{22} \qquad (4)$$

The transfer of *liquid* water between levels 2 and 3 gives but negligible contribution to the transfer of heat. This is in agreement with the lack of coupling between J_q and J_w in the first step. The main contribution to the heat of transfer is given by the melting of ice at level 2 with absorption of heat, and the freezing of the water at level 3 with release of heat.

In contact with a solid surface there is always a layer of water with properties different from those of bulk water. This layer stays unaltered, however, during the transport process. The phase changes are between ice and *mobile* water with bulk water properties. The heat of transfer is equal to the enthalpy of melting,

$$q_w^* = \Delta H_m \qquad (5)$$

Remembering that $\bar{l}_{12} = \bar{l}_{21}$, we obtain from eqs (3-5) the maximum frost heave pressure,

$$\Delta p_{J_w=0} = - (\Delta H_m/V_{ice}) \Delta \ln T \qquad (6)$$

The enthalpy of melting varies with pressure and temperature. The variation with pressure is negligible within the pressure ranges of frost heave, while the variation with temperature may be of importance when there is a large temperature difference between levels 2 and 3. The variation of V_{ice} with pressure and temperature is negligible.

When ΔT is much smaller than T, we have $\Delta \ln T \approx \Delta T/T$. Since $\Delta H_m/T_m = \Delta S_m$, we obtain,

$$\Delta p_{J_w=0} = - (\Delta S_m/V_{ice}) \Delta T \qquad (7)$$

At zero degree centigrade and one atmosphere pressure we have $\Delta S_m = 22.0$ J/(K mol) and $V_{ice} = 19.6 \cdot 10^{-6}$ m^3/mol. When the temperature of the ice is not too low, we thus have,

$$\Delta p_{J_w=0} = - 11.2 \Delta T \text{ bar} \qquad (8)$$

$$(\text{or } - 11.1 \Delta T \text{ atm or } - 11.4 \Delta T \text{ kg cm}^{-2})$$

If a soil permits transport of water down to a temperature of - 5°C, an ice lens will grow at this temperature. The flux of water will not be suppressed until a pressure of more than 50 atm has been built up.

In eq (2) we may substitute $\bar{l}_{22}\Delta H_m$ for $\bar{l}_{21}$, see eqs (4,5), and further $\Delta S_m \Delta T$ for $\Delta H_m \Delta \ln T$, and we obtain,

$$J_w = - \bar{l}_{22} (\Delta S_m \Delta T + V_{ice} \Delta p) \qquad (9)$$

The flux of water, J_w, is equal to the rate of growth for the ice lens, and $\bar{l}_{22}$ is the *average hydraulic permeability* for the total transport path for water. The value of $\bar{l}_{22}$ may chiefly be determined by low local values of l_{22} close to the ice lens. The value may also decrease with time as the ratio of ice to liquid water increases in the partly frozen soil.

EXPERIMENTAL STUDIES OF FROST HEAVE

Frost heave has been investigated in laboratories under controlled conditions. We shall refer to measurements carried out by Takashi, Ohrai, Yamamoto and Okamoto (1979). Their experimental arrangement is shown schematically in Fig.2. To emphasize the resemblance to frost heave in nature (Fig.1), the apparatus was rotated 180° in Fig.2. In the real experiment the cooling plate was at the bottom and the piston at the top.

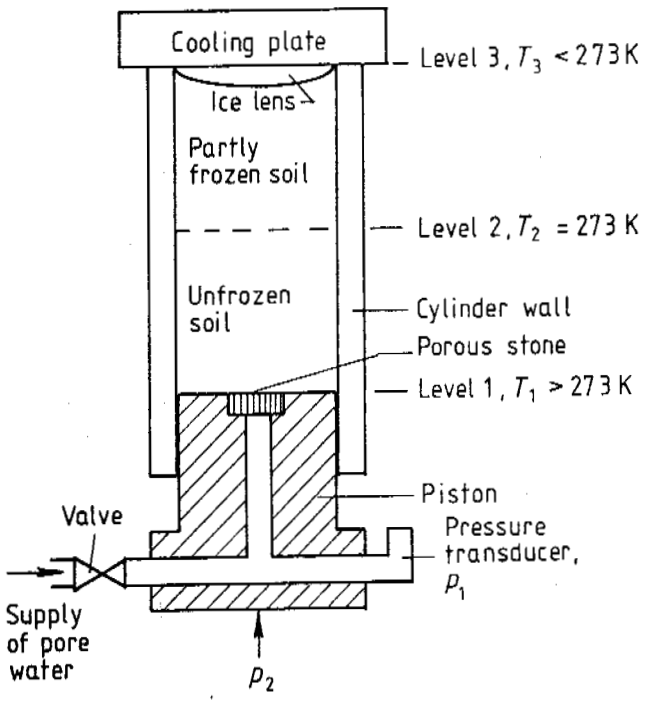

Fig.2 Schematic picture of experimental arrangement for measuring frost heave. Apparatus rotated 180°.

The soil sample is contained in a transparent, thermally insulated cylinder. In preparation for the experiment the sample is subjected to a high pressure in order to obtain a good packing of the soil particles, to form a strong framework. The pressure is released, and the pore water is de-aired. Thereafter partial freezing of the sample is achieved by keeping the temperature at both ends constant, the piston at a temperature above 0°C and the cooling plate at a temperature below 0°C. During this freezing there is free access to a reservoir of water.

When the sample has been prepared in this way,

the valve for the pore water supply is closed, and the sample is subjected to a pressure by means of the piston. The pressure is taken up by the framework of the soil. The pore water will also be under increased pressure, but lower than the pressure on the framework. Pressure on the piston, p_2, and in the pore water, p_1, are measured.

When the difference in pressure, $\Delta p = p_2 - p_1$, is less than the maximum frost heave pressure obtainable for the chosen temperature on the cooling plate, there will be a flux of water towards the cooling plate, $J_w > 0$, the ice lens will grow, and the pressure difference will increase over time. When the difference is larger than the maximum frost heave pressure, the flux of water will be in the opposite direction, $J_w < 0$, the ice lens will be melting, and the pressure difference will decrease over time. Thus one can approach the maximum frost heave pressure from both sides.

Takashi and coworkers tested two types of soil, Manaita-bridge clay and Negishi silt. The time needed to obtain maximum frost heave pressure was long, ranging from 500 to 2000 hours. They measured the upper limit of frost heave pressure, σ_u kg cm^{-2}, for different temperatures on the cooling plate, θ_c °C. The pressure σ_u corresponds to $\Delta p_{J_w=0}$. Assuming that the first ice crystals in pores form at 0°C, we have $\theta_c = T_3 - T_2 = \Delta T$. In the temperature range 0 to - 17°C for the clay, and 0 to - 4°C for the silt, the linear relation was found, $\sigma_u = - 11.4\ \theta_c$. This agrees well with the theoretical value given in eq (8). The experimental results are given in Figs. 3 and 4.

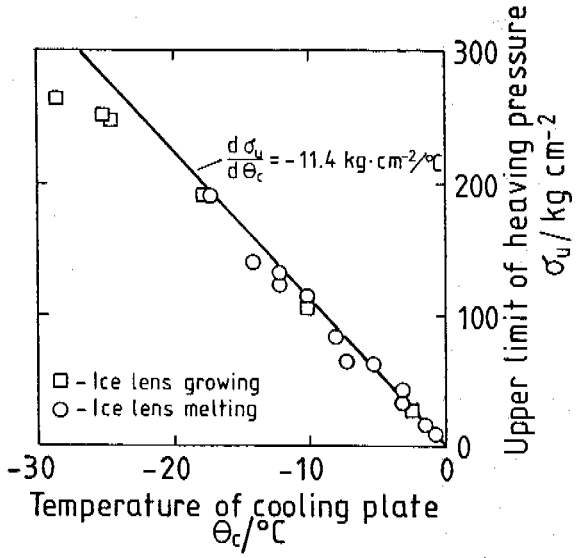

Fig.3 Frost heave in Manaita-bridge clay

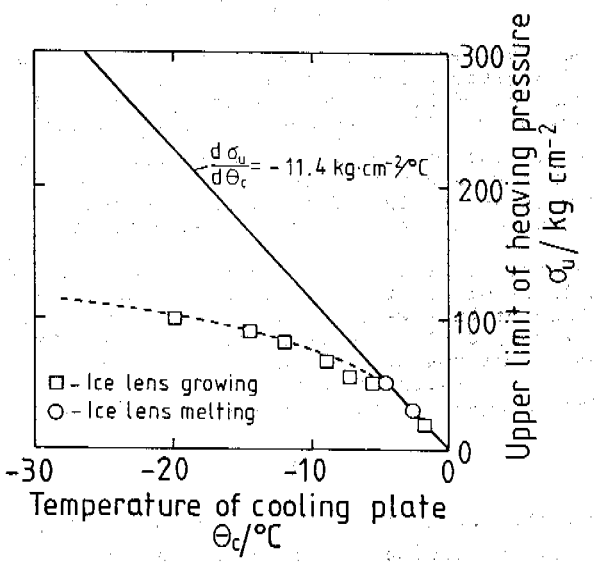

Fig. 4 Frost heave in Negishi silt

We can see from Figs. 3 and 4 that when θ_c approaches 0°C, the σ_u approaches zero pressure difference within the limits of experimental error. As we shall see below, this observation makes possible a check of eq (5), which is based on the assumption that mobile water has bulk water properties. We can also deduce that there is no coupling between transports of heat and water in the first step.

In most experiments carried out by Takashi and coworkers, the temperature of the piston was + 6°C. For θ_c = 0°C, the experimental conditions can be described by the cell,

$$H_2O(l),\ 6^{\circ}C \left| \begin{matrix}\text{Porous}\\ \text{stone}\end{matrix} \right| \begin{matrix}\text{Water}\\ \text{in soil}\end{matrix} \left| \text{Ice lens},\ 0^{\circ}C \right.$$

In this case there is no pressure difference, the temperature difference does not cause a transport of water. The ice lens is in equilibrium with liquid water at the same temperature. If the ice lens were replaced by liquid water, there would still be no transport of water. The arrangement,

$$H_2O(l),\ 6^{\circ}C \left| \begin{matrix}\text{Porous}\\ \text{stone}\end{matrix} \right| \begin{matrix}\text{Water}\\ \text{in soil}\end{matrix} \left| H_2O(l),\ 0^{\circ}C \right.$$

would have given some thermal osmosis effect and shown a pressure increase on the low temperature side, if there were a significant heat of adsorption for the mobile water in the soil. Since there is no pressure increase, the enthalpy of mobile water in the soil is approximately equal to the enthalpy of bulk water, and eq (5) is valid. With no significant heat of adsorption, there is no heat of transfer in the first step and no coupling between measurable heat flux and flux of water.

The results illustrated in Figs. 3 and 4 show deviations from straight lines at lower temperatures. The deviation is small for the clay. It may, at least partly, be explained by the change in ΔS_m with temperature. At - 20°C ΔS_m is about 13 % smaller than at 0°C. Equation (7) was derived assuming a constant value of ΔS_m over the temperature interval ΔT.

The deviation for the silt is too large to be explained by a change in ΔS_m. The authors report that in some cases an ice lens was observed about midway between the freezing front and the cooling plate. This means that the ice lens is formed at a temperature higher than the one at the cooling plate, corresponding to a lower maximum frost heave pressure. We can also see from Fig. 4 that measurements have only been done with growing ice lens at the lower temperatures, no measurements with a melting ice lens are reported. As the rate of growth is very low at the low temperatures, there is a possibility that maximum frost heave pressure was not obtained.

CONCLUSIONS

The important parameters for evaluating frost heave are given in eq (9), which expresses the rate of growth for an ice lens. The parameter $\bar{l}_{22}$, the average hydraulic permeability, depends on the type of soil, the distances between table of water, freezing front where the first crystals of ice appear, and the ice lens. As freezing proceeds, it's value may decrease.

The entropy of melting, ΔS_m, and the molar volume, V_{ice}, are essentially constant parameters. The variable parameter ΔT is mainly given by the temperature (°C) of the lowest lying ice lens. The variable parameter Δp increases with time. As the pressure difference increases, the rate of growth of the ice lens decreases. If the crust of frozen soil is not able to withstand the increased pressure, and breaks, the flux of water may continue indefinitely as long as the temperature is low enough to allow ice formation.

Frost heave can be prevented if the continuity of water between the table of water and the freezing front is broken. Empirically it is known that a layer of coarse sand or gravel deep in the soil, and ditches to drain the water, reduce frost heave.

REFERENCES

Takashi, T., Ohrai, T., Yamamoto, H. and Okamoto, J. (1980). Upper limit of heaving pressure derived by pore water pressure measurements of partially frozen soil. Proc. 2nd Int.Sym.Ground Freezing, 713 - 724, Trondheim.

PARAMETRIC EFFECTS IN THE FILTRATION FREE CONVECTION MODEL FOR PATTERNED GROUND

K.J. Gleason[1], W. B. Krantz[2] and N. Caine[3]

[1]Department of Chemical Engineering, University of Colorado, Boulder, CO 80309-0424, U.S.A.
[2]Department of Chemical Engineering and Institute of Arctic and Alpine Research, University of Colorado, Boulder, CO 80309-0424, U.S.A.
[3]Department of Geography and Institute of Arctic and Alpine Research, University of Colorado, Boulder, CO 80309-0450, U.S.A.

SYNOPSIS In previous papers the authors developed a model which explains the origin and regularity of a class of patterned ground formed in recurrently frozen soils. This model is based on Rayleigh free convection of water in porous media induced by unstable fluid density stratification occurring during the melting of frozen soils. In contrast to other models which contend that weak convection currents can directly affect sorting by moving clasts, this model recognizes that filtering free convection cells can create a corrugated underlying ice front. Subsequent frost action then can create sorted patterns on the ground surface which mirror the patterns in the ice front. The spacing of the ice front corrugations is directly related to the depth of thawing which implies that the characteristic width of the patterned ground is a predictable function of the thawing depth. This paper explores the effects of variable fluid properties (viscosity and coefficient of volume expansion) and variable soil properties (permeability and thermal conductivity) on patterned ground characteristics.

INTRODUCTION

The term "sorted-patterned ground" refers to the more-or-less symmetrical forms such as circles, polygons, and stripes occurring in areas of ground frost (past or present) which are made prominent by the segregation of stones and fines (Washburn, 1956, 1980). It includes patterns resulting from diurnal as well as annual freeze/thaw cycles. These patterns can be found at the bottom of shallow ponds or on nonsubmerged plateaus, above timberline in the high mountains of the temperate zone or at sea-level in the Arctic. In areas where both polygons and stripes exist, there tends to be a progressive transition from polygons on horizontal ground to stripes on sloped terrain. Among the many distinctive features of sorted-patterned ground the most pronounced is the striking regularity of the patterns. Regardless of their shape, location, or size (ranging from < 15 cm to 10 m in width) the patterns display a nearly constant ratio of pattern width to sorting depth.

Great strides have been made recently in developing a better understanding of the processes important in the formation of patterned ground. Of particular interest is the modeling work of Ray et al. (1983a, 1983b) and Gleason et al. (1986). They have developed a model based on Rayleigh free convection of water in porous media which explains many features of sorted patterned ground including its regularity and nearly constant ratio of pattern width to sorting depth. Also of note is the field work of Hallet and Prestrud (1986) who have studied the processes taking place in existing active patterns. Their work indicates that there is a net soil circulation within the fines that leads to a pattern refinement.

This paper examines the deficiencies of the Rayleigh free convection model in an attempt to improve our understanding of the processes occurring in frozen soils. The scope of this paper is as follows. First a brief review of the Rayleigh free convection model for patterned ground formation is given. Next the deficiencies in this model are examined and addressed. In considering the deficiencies the effects of variable fluid and soil properties on the direction of fluid circulation for polygonal patterns and on the characteristic size (W/D) of these and other patterns are explored.

THE RAYLEIGH FREE CONVECTION MODEL

Rayleigh free convection refers to the circulation of fluid driven by buoyancy forces arising as a result of unstable density stratification. When saturated frozen soil melts during the thaw season, the potential for free convection

exists on account of the density inversion in water between 0° and 4°C. That is, more dense water (at 4°C) is overlying less dense water (at 0°C). Before convection can occur, the system conditions must reach a critical value (called the critical Rayleigh number). That is, the buoyancy forces must be able to overcome the resistance to flow caused by low soil permeability or high fluid viscosity.

Once the critical Rayleigh number is reached and convection begins, it will imprint a pattern on the ice front, since in areas of downflow, the warmer water is being brought down to the ice front thus causing preferential melting. Conversely in areas of upflow the colder water is being convected away from the ice front thus retarding the melting. What results is a pattern in the ice front consisting of periodically spaced peaks and troughs. This pattern is then transformed to the ground surface through the process of sorting. Thus the repeated cycle of freezing and thawing causes the stones to be heaved upwards relative to the ice peaks and troughs, thereby leading to the pattern which is observed.

Subtleties of Model

There are several subtleties of this model which need to be emphasized. First it is a filtering convection which occurs whereby the fluid filters through the soil and stone mixture impressing the pattern on the ice front. The convection does **not** sort the stones. Also the model does **not** require the soil always to be saturated with water, but rather only during convection. Likewise the free convection is **not** assumed to occur throughout the entire thaw period. The free convection only needs to take place long enough to imprint the pattern on the ice front. Once the pattern is imprinted, subsequent freeze-thaw cycles and frost heaving determine further pattern development. It is the system conditions (permeability,thermal conductivity, etc.) at the onset of convection that determine the characteristic size of the convection cells (and by extension the ratio of pattern width to sorting depth for the subsequent patterned ground). In fact once sorting has made the patterns prominent the soil properties are known to be quite different than those at the onset of convection. Finally there is an implicit assumption here that the thaw depth at the onset of convection corresponds to the sorting depth of the observed patterns.

This Rayleigh free convection model is able to explain many of the distinctive features of patterned ground such as its striking regularity, the preference for hexagonal shapes on horizontal surfaces, the transition from polygons to stripes as one moves to sloped surfaces, and the

TABLE I Comparison between the Rayleigh free convection model and field data for three types of patterned ground (from Gleason et al., 1986).

Patterned Ground Type	Model Predictions (W/D)		Field Studies		
	flat-to-flat	peak-to-peak	n	$\overline{W/D}$	S
Nonsubmerged Polygons	3.1	3.6	23	3.8	0.13
Underwater Polygons	4.1	4.8	8	4.8	0.34
	negligible downslope flow	dominant downslope flow			
Stripes	2.7	3.8	21	3.6	0.27

nearly constant ratio of pattern width to sorting depth (W/D). This W/D ratio is a quantitative prediction which has been tested with field measurements. Table I is a summary of the comparison between the Rayleigh free convection model predictions and the field data for nonsubmerged polygons, underwater polygons, and stripes (from Gleason et al. 1986). For the polygonal patterns the two predictions represent the limits of W/D corresponding to the maximum (peak-to-peak) and minimum (flat-to-flat) widths of the hexagonal pattern. For the striped patterns the two predictions represent the limits of W/D corresponding to the effects of downslope subsurface flow (negligible versus dominant) on the convective pattern. Figure 1 is a representative plot of the comparison between the model predictions and field data for pattern width versus sorting depth for nonsubmerged polygons (from Gleason et al. 1986).

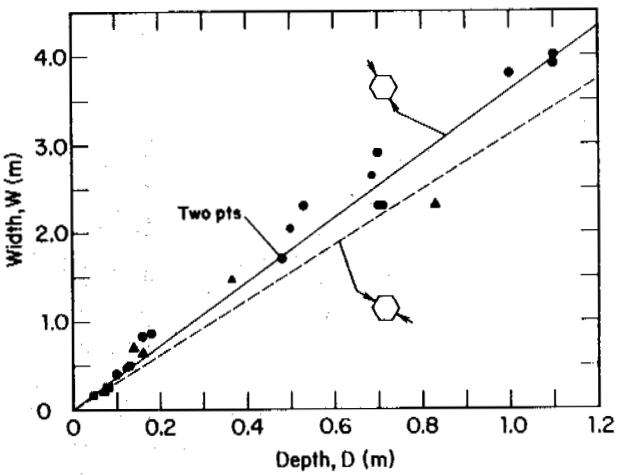

Figure 1. Characteristic width versus sorting depth for nonsubmerged polygons (from Gleason et al., 1986). The two lines represent theoretical predictions of W/D for the width measured as indicated.

Critique of Model

The most obvious criticism of the Rayleigh free convection model is that many of the field data lie somewhat above the maximum model predictions. Also, although the model seems to explain sorted polygons and sorted stripes quite well, there are other sorted features that seem to contradict the model predictions. One example is that of stone pits (Figure 2). One possible explanation for the underpredictions of the model is the previously mentioned assumption that the thaw depth at the onset of convection corresponds to the sorting depth of the patterns. In fact the sorting depth is probably a conservative estimate of the true thaw depth thus causing the measured W/D ratio to be larger than the actual one. Another possible explanation for these deficiencies is that the model was developed for constant soil properties (permeability, thermal conductivity, etc.). However, owing to freezing and thawing the soil is lofted (generally unevenly), thus increasing the permeability in certain regions. Also one would expect the horizontal permeability to be quite different from the vertical permeability. This might have an added effect on the direction of fluid circulation in the hexagonal convection cell, which could have a significant influence on whether sorting produces stone-bordered polygons or stone-centered polygons (stone pits).

DIRECTION OF FLUID CIRCULATION

Determining the direction of circulation allows one to infer the pattern geometry of the underlying ice front and as such provides insight concerning the sorting process (i.e., whether stones concentrate over the ice troughs or over the peaks).

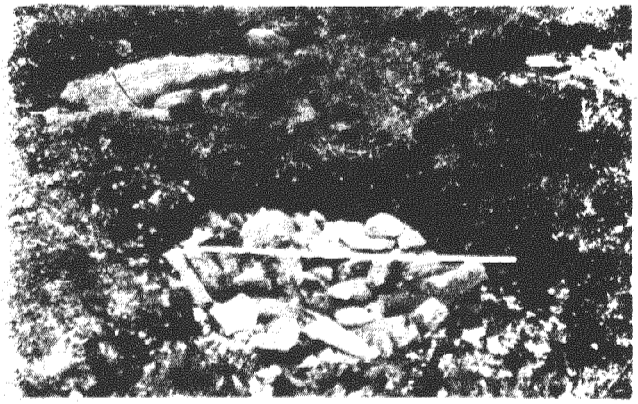

Figure 2. Nonsubmerged stone pit, Boxfjäll, S. Storfjället (from Beskow, 1930).

It was first believed that the manner in which the kinematic viscosity varies with temperature determined the direction of fluid circulation in hexagonal convection cells. This was owing to the observation that liquids and gases have opposite directions of circulation as well as contrasting behavior with respect to the temperature dependence of their kinematic viscosity. The analysis of Palm (1960) confirmed this correspondence. However subsequent analyses showed that, from the mathematical point of view, it is the existence of asymmetries in the system (e.g., temperature-dependent properties, nonuniform heating from below, etc.) which induce nonlinearities in the system of describing equations that determine the direction of circulation. It is not sufficient to include only spatial nonhomogeneities (such as a variation of permeability with depth), since they do not add any nonlinear terms to the system equations. Thus in order to determine the direction of circulation it is necessary to retain nonlinear terms and hence consider nonlinear stability theory.

Weakly nonlinear stability theory was employed in determining the direction of circulation for a water-saturated porous media near 0°C (Gleason, 1984). In this analysis the model allowed for a temperature-dependent kinematic viscosity and a temperature-dependent coefficient of volume expansion (i.e., an extremely nonlinear density profile). It was discovered that there are competing effects on the direction of fluid circulation in hexagonal convecton cells for the system of interest. When the temperature dependent kinematic viscosity dominates, the circulation is down in the cell center. When the temperature dependent coefficient of volume expansion dominates, the circulation is up in the cell center.

There is a physical interpretation that can explain both directions of circulation. Consider a single idealized hexagonal convection cell surrounded by six other cells. The circulation is such that the fluid flows one direction in the center and the opposite direction at the borders. At the borders there is less resistance since the flow is in the same direction for the adjacent cells. Thus there is more resistance to the flow of fluid through the centers than through the collective borders. One would expect the system to minimize its dissipation of energy; thus the flow will be into the cell center from the boundary where either the flow resistance is a minimum or the density driving force is a maximum.

In the case where viscosity is the determining factor, the least resistance to flow is at the upper surface where the viscosity of water is less owing to the warmer temperature. Thus there should be flow down the center. However in

the case where the coefficient of volume expansion (β) is the determining factor, a larger magnitude of β implies a larger density gradient. One would then expect the larger gradient to drive the flow through the center thus countering the maximum resistance to flow. Since the larger magnitude of β is at the lower surface (since a maximum in density at the upper surface requires that $\beta = 0$), there should be flow up the center.

It is quite clear that these are two competing effects. However viscous effects are not believed to be important in homogeneous porous media, especially considering the small changes in the viscosity of water between 0^o and 4^oC. Thus one would expect that the coefficient of volume expansion should determine the direction of circulation in most situations. This would correspond to an ice front pattern of isolated peaks and continuous troughs which would lead to stone-bordered polygons based on the sorting scheme proposed by Gleason et al. (1986).

However there is the potential for cooperative effects on the determination of the direction of fluid circulation. In the system of describing equations the viscosity (μ) and the permeability (k) appear grouped as one term. This term (k/μ) represents the mobility of the system. Thus although the viscosity of water changes little over the temperature range from 0^o to 4^oC, and spatial nonhomogeneities (such as permeability), in and of themselves, cannot determine the direction of circulation, a nonhomogeneous permeability can act as a multiplying factor on the viscosity thus enhancing its effect.

Consider the following. Owing to the continued freezing and thawing of the ground, the soil is lofted upwards such that one would expect the permeability to be greater near the ground surface than near the ice front. Thus there is less resistance to flow (i.e., a greater fluid mobility) near the ground surface owing to a higher soil permeability and a lower viscosity of the warmer water. Based on the above physical explanation for direction of circulation, this form of nonhomogeneous permeability enhances the viscosity effect and there should be flow down the cell center. In some cases this may be enough to counteract the effect of the coefficient of volume expansion. This sort of flow pattern would lead to a melt pattern in the ice front consisting of isolated troughs and a continuous ridge which in turn would lead to stone-centered polygons or stone pits (Figure 2).

EFFECT OF SOIL PROPERTIES ON PATTERNED-GROUND SIZE

Seldom are natural soils completely homogeneous and isotropic. When one considers the substantial lofting of soil due to freezing and thawing and the subsequent uneven settling, it is not difficult to imagine soil whose permeability decreases with depth (i.e., nonhomogeneous permeability). In contrast the soil may be homogeneous, but show anisotropic behavior. That is, the soil may have different (but constant) physical properties in the vertical direction than in the horizontal directions. This is particularly common in sedimentary soils where the permeability in the plane of sedimentation is usually higher than that in the direction perpendicular to it. Thus one might expect variable soil properties to have a profound effect on the predictions of the patterned ground model.

Nonhomogeneous Effects

As discussed above, nonhomogeneous permeability can affect a change in the direction of fluid circulation (and thus the type of pattern ground formed) when acting in conjuntion with a temperature dependent viscosity. In this section the effect of nonhomogeneities in permeability (k) and thermal conductivity (λ) on the characteristic aspect ratio (W/D) of the convection cells (and hence patterned ground) is explored.

Gheorghitza (1961) considered a porous layer with small, linear changes in permeability and constant thermal conductivity. Green and Freehill (1969) considered large linear variations of both the thermal conductivity and inverse permeability with depth. Their results for constant λ indicate that nonhomogeneous permeability alone has no effect on the convective cell width and has only a slight effect on the critical Rayleigh number. However the added effect of nonhomogeneous thermal conductivity causes some interesting behavior.

The thermal conductivity of porous media is a weighted average of that of the dry medium and of the saturating fluid (water in this case). If the conductivity of the dry porous medium is greater than that of the saturating fluid, the conductivity of the saturated medium will decrease with an increase in permeability. However if the conductivity of the dry medium is less than that of the saturating fluid, the conductivity of the saturated medium will increase with an increase in permeability.

For the case of thermal conductivity (λ) increasing as permeability (k) increases Green and Freehill (1969) found little change from the results for homogeneous porous me-

dia. However for the case of λ increasing as k decreases (as one would expect with water saturated soils; i.e., the patterned ground problem) they found the combined variations caused a substantial decrease in the aspect ratio.

The implications for patterned ground are as follows. For patterns that develop in soil whose permeability at the inception of convection varied with depth, the resulting ratio of pattern width to sorting depth might be expected to fall within the model predictions for homogeneous soils unless the permeability variations are substantial and are accompanied by substantial variations in thermal conductivity that increase as the permeability decreases. In that case the W/D ratio should be smaller than previously predicted.

Anisotropic Effects

The problem of free convection in anisotropic porous media has been studied by several investigators with application to problems ranging from heat transfer in insulations to groundwater movement in geothermal fields. Castinel and Combarnous (1975) derived the stability criteria (critical Rayleigh number and wave number) for porous media whose permeability in the horizontal plane was different than that in the vertical direction. Epherre (1975) extended this analysis to include anisotropy in thermal conductivity as well. In both these cases the medium was assumed to be horizontally isotropic. Kvernvold and Tyvand (1979) generalized the analysis to include anisotropy of permeability and thermal diffusivity in both horizontal directions. In all these analyses the porous medium was bounded by isothermal and impermeable surfaces.

By inference it is possible to apply the generalized results of Kvernvold and Tyvand (1979) to a system with boundary conditions appropriate to free convection in recurrently frozen soils. This is summarized in Table II where $\eta = \lambda_H/\lambda_V$ is the ratio of horizontal thermal conductivity to vertical conductivity, $\xi = k_H/k_V$ is the ratio of horizontal permeability to vertical permeability, and α_c is the critical wavenumber. The vertical permeability and the vertical thermal conductivity are used in the evaluation of the critical Rayleigh number.

Of principal interest to the patterned ground model is the effect of the property variations on the critical wave number and hence the aspect ratio (W/D). In most cases the anisotropy in permeability is more pronounced than that in thermal conductivity. Thus, for the purpose of showing the general effect on W/D we will consider isotropic thermal conductivity (η=1). The effect of anisotropic permeability on the aspect ratio predictions (W/D) of nonsubmerged polygons is summarized in Table III. We can expect similar effects for underwater polygons and sorted stripes.

TABLE II Effect of anisotropy on the critical Rayleigh number and wavenumber for Rayleigh free convection in saturated porous media.

Isothermal and impermeable boundaries	
isotropic porous media (Lapwood, 1948)	anisotropic porous media (Kvernvold and Tyvand, 1979)
$Ra_c = 4\pi^2$	$Ra_c = \pi^2 \left[\left(\frac{\eta}{\xi}\right)^{1/2} + 1 \right]^2$
$\alpha_c = \pi$	$\alpha_c = \pi(\xi\eta)^{-1/4}$
Isothermal, impermeable upper boundary and a moving, compliant, phase transition lower boundary (i.e., melting front)	
isotropic porous media (Ray et al., 1983a)	anisotropic porous media (This work)
$Ra_c = 27.1$	$Ra_c = \frac{27.1}{4} \left[\left(\frac{\eta}{\xi}\right)^{1/2} + 1 \right]^2$
$\alpha_c = 2.33$	$\alpha_c = 2.33(\xi\eta)^{-1/4}$

As can be seen from Table III, it is only necessary for the horizontal permeability to be twice that of the vertical permeability in order to affect a substantial change in W/D. However if an increase in the permeability ratio is accompanied by a proportional decrease in the thermal conductivity ratio, the net result is the same as that of isotropic porous media. But seldom are the permeability and thermal conductivity that intimately related. Thus it is quite apparent that anisotropic permeability can account for the Rayleigh free convection model underpredictions of W/D.

TABLE III Effect of anisotropy on the predicted aspect ratio of nonsubmerged polygons. A value of $\eta = 1$ and $\xi = 1$ corresponds to isotropic porous media.

conductivity ratio (η)	permeability ratio (ξ)	critical wavenumber (α_C)	Aspect Ratio (W/D)	
			flat-to-flat	peak-to-peak
1	0.5	2.77	2.62	3.02
1	1	2.33	3.11	3.60
1	2	1.96	3.70	4.27
0.5	2	2.33	3.11	3.60

Another interesting result obtained by Kvernvold and Tyvand (1979) is that if the porous medium is more permeable in one horizontal direction than in the other horizontal direction, there is a preference for two-dimensional roll cells oriented in the direction of greater permeability. This could account for the appearance of sorted stripes on shallower slopes ($\sim 5^o$ tilt angle) than determined by the laboratory experiments of Bories and Combarnous (1973) for homogeneous isotropic porous media ($\sim 15^o$ tilt angle). It could also account for the seemingly anomolous behavior of sorted stripes oriented perpendicular to the direction of steepest slope as observed by Hall (1983).

CONCLUSIONS

Variable soil properties combined with variable fluid properties can explain many seemingly anomolous results for patterned ground when compared with the filtration Rayleigh free convection model.

- Nonhomogeneous permeability in concert with the thermal effects on viscosity can reverse the fluid circulation and thereby explain stone pits.
- Antisymmetric variations of permeability and thermal conductivity with depth can explain anomolously low observed W/D values.
- A greater horizontal permeability than vertical permeability can explain anomolously high observed W/D values.
- Horizontal anisotropy in permeability can explain the occurrence of stripes at lower slope angles and their orientation perpendicular to the fall line.

When one considers this filtration free convection model together with complementary models for subsequent sorting and pattern refinement (Hallet and Prestrud, 1986) a more complete picture emerges. The model discussed here describes the initiation, regularity and characteristic size of the sorted patterns. Models such as that of Hallet and Prestrud describe the processes taking place once the stone borders, and hence the patterns have been initiated.

ACKNOWLEDGMENTS

The authors wish to acknowledge financial support provided for these studies by the National Science Foundation (grant DPP-8210156) and the Council for Research and Creative Work of the University of Colorado. One of the authors (KJG) was partially supported by a Graduate School Fellowship and a Graduate School Foundation Fund Award from the University of Colorado.

REFERENCES

Beskow, G. (1930). Erdfliessen und Strukturböden der Hochgegirge im Licht der Frosthebung. Geologiska Föreningens Stockholm, Förhandlingar, (52), 4, 622–638.

Bories, S. and Combarnous, M.A. (1973). Natural convection in an inclined porous layer. Journal of Fluid Mechanics, (57), 63–79.

Castinel, G. and Combarnous, M. (1975). Convection naturelle dans une couche poreuse anisotrope. Revue Générale de Thermique, (14), 168, 937–947. [English translation in International Chemical Engineering, (17), 4, 605–614, (1977).]

Epherre, J.F. (1975). Critère d'apparition de la convection naturelle dans une couche poreuse anisotrope. Revue Générale de Thermique, (14), 168, 949–950. [English translation in International Chemical Engineering, (17), 4, 615–616, (1977).]

Gheorghitza, St.I. (1961). The marginal stability in porous inhomogeneous media. Proc. Cambridge Phil. Soc., (57), 871–877.

Gleason, K.J. (1984). Nonlinear Boussinesq free convection in porous media: application to patterned-ground formation. M.S. Thesis, 175 pp. University of Colorado, Boulder, Colorado.

Gleason, K.J., Krantz, W.B., Caine, N., George, J.H., and Gunn, R.D. (1986). Geometrical aspects of sorted patterned ground in recurrently frozen soil. Science, (232), 216–220.

Green, T. and Freehill, R.L. (1969). Marginal stability in inhomogeneous porous media. Journal of Applied Physics, (40), 1759–1762.

Hall, K.J. (1983). Sorted stripes on sub-Antarctic Kerguellen Island. Earth Surface Processes and Landforms, (8), 115–124.

Hallet, B. and Prestrud, S. (1986). Dynamics of periglacial sorted circles in western Spitsbergen. Quaternary Research, (26), 81–99.

Kvernvold, O. and Tyvand, P.A. (1979). Nonlinear thermal convection in anisotropic porous media. Journal of Fluid Mechanics, (90), 609–624.

Lapwood, E.R. (1948). Convection of a fluid in a porous medium. Proc. Cambridge Phil. Soc. (44), 508–521.

Palm, E. (1960). On the tendency towards hexagonal cells in steady convection. Journal of Fluid Mechanics, (8), 183–192.

Ray, R.J., Krantz, W.B., Caine, T.N., and Gunn, R.D. (1983a). A model for sorted patterned-ground regularity. Journal of Glaciology, (29), 102, 317–337.

Ray, R.J., Krantz, W.B., Caine, T.N., and Gunn, R.D. (1983b). A mathematical model for patterned ground: sorted polygons and stripes, and underwater polygons. Permafrost: Proceedings of the Fourth International Conference, National Academy of Sciences, Washington, DC, 1036–1041.

Washburn, A.L. (1956). Classification of patterned ground and review of suggested origins. Geological Society of America Bulletin, (67), 823–865.

Washburn, A.L. (1980). Geocryology, 406 pp. Wiley, New York.

HEAT AND MOISTURE TRANSPORT DURING ANNUAL FREEZING AND THAWING

J.P. Gosink, K. Kawasaki, T.E. Osterkamp and J. Holty

University of Alaska, Fairbanks, Alaska, USA

SYNOPSIS Measurements of soil temperature and water content were obtained repeatedly for an annual cycle on the University of Alaska (UAF) Agricultural Station Farm. The site of the UAF farm was cleared of trees about forty years ago, and the permafrost is presently thawing slowly due to the change in surface conditions and a local decade-long warming trend. These data were analyzed to obtain information on heat and moisture transport in land cleared for agricultural use and underlain by permafrost. The data were compared to predictions of a coupled heat and moisture, finite element model, using local meteorological data for surface boundary conditions. Soil temperature, moisture and position of the freeze front are reasonably well predicted by the model. Discrepancies between measurements and predictions are related to inadequate information on soil moisture boundary conditions, and to the sensitivity of the model to constants in the empirical soil moisture-tension formulae.

INTRODUCTION

The thermal and moisture regimes of freezing soils are of concern to scientists and engineers interested in agricultural, engineering, environmental and hydrological problems. There is a need to be able to predict soil temperature, freeze front positions, ice segregation, soil dessication and frost heave in these soils. For engineering purposes, this information is essential for design and planning of highways, airfields and structures. The information can also be used in the design of strategies for enhancing soil moisture content and soil temperature regime and for evaluating the impact of anthropogenic activities on the environment.

In areas subject to annual freezing and in permafrost areas, the analysis of the soil thermal and hydrological regimes is complicated by phase change effects and by moisture migration. During freezing, mobile soil moisture is drawn toward the freezing front, increasing the available latent heat; therefore, it is critical that moisture transport and soil water phase change be correctly simulated, particularly in unsaturated soils. The moisture transport is affected by soil moisture tension gradients and hydraulic conductivity, as well as by the soil thermal regime. Moisture transport and soil temperatures in freezing soils are strongly coupled due to the freezing of water which produces high soil moisture tension. The analysis of the ground thermal regime is therefore extremely complex, involving coupled heat and moisture transport, changing surface boundary conditions, and soil thermal and hydrologic properties which vary both spatially and temporally with freezing. The most feasible method of analysis for these types of problems involves the use of computer modeling.

This paper presents the results of an experiment involving measurements of soil temperature and moisture and the comparison of these data with a computer model for the ground thermal and moisture regimes. The data included are temperature and moisture measurements obtained over a winter cycle at the University of Alaska experimental farm site. The computer model (Guymon and Hromadka, 1977) was identified in a preliminary report (Kawasaki, Osterkamp and Gosink, 1982) as being physically realistic and appropriate for freezing soil conditions in interior Alaska. The application of the model to real soil conditions over a period of several months should provide information on the sensitivity of the model over an extended period when driven by varying surface conditions.

THE GUYMON/HROMADKA MODEL

The Guymon/Hromadka model is a two-dimensional finite element simulation of the equations for heat and moisture transport in an unsaturated soil with phase change. It has been discussed in numerous reports (Guymon and Hromadka, 1977; Guymon and Luthin, 1974; Guymon et al., 1980; and Hromadka et al., 1981), and so only a brief outline of the major characteristics of the model are reported here.

Heat transport near the phase front is calculated by an "isothermal" phase change approach which involves special treatment of elements undergoing phase change via a calorimetric balance. This approach assumes a unique unfrozen water content, i.e., that the temperature of the element will remain at the freezing point until the unfrozen water content is reduced to a small prescribed value. Numerically, this feature causes an abrupt change in slope in the temperature profiles since the moisture content is not smoothly continuous, and physically, it eliminates the "freezing fringe" region in which substantial fractions of unfrozen water may be found in certain soils at temperatures below the freezing point (Anderson and Morgenstern, 1973; Anderson and Tice, 1972; O'Neill and Miller, 1985). However, state-of-the-art models (O'Neill and Miller, 1985; 1983) which include the dynamics of ice lens formation are lengthy and complex, and are more appropriately considered research tools rather than engineering techniques. The Guymon/Hromadka model should be considered an intermediate level model, containing empirical formulations which attempt to define the physics of moisture migration in unfrozen soils, and ad hoc formulations to extrapolate the theory for thawed soils to frozen soils. When the model is calibrated for known soils samples, it should be possible to use the model for engineering purposes. An objective of this study was to test the Guymon/Hromadka model against field measurements of temperature and moisture for an extended period.Thermal conductivity and specific heat are specified in the model as linear functions of moisture, ice and soil content:

$$v = \theta_i v_i + \theta_w v_w + \theta_s v_s \quad (1)$$

where v is either thermal conductivity or specific heat, v_i, v_w and v_s are the same properties for ice, water and dry soil, respectively, and θ_i, θ_w and θ_s represent their relative volume fractions. More recent formulations of thermal conductivity (e.g., Farouki, 1981) provide a more accurate calculation method for this property and may easily be incorporated into the model. This improvement was not attempted in the present study since the primary objective was to compare predictions of an existing model with field data.

In the general freezing case, total volumetric water content may vary within the calculation domain, allowing ice in excess of soil porosity to form; the excess ice results in frost heave. Moisture may enter the soil surface as precipitation, or may be drawn from the water table or wetter soils at depth. In the model, the availability of this moisture is limited by the magnitude of the hydraulic conductivity, the calculated pressure gradients, and the assumed relation between pore pressure and hydraulic conductivity, and between pore pressure and unfrozen water content as given by Gardner (1958).

VARIATION OF OTHER SOIL PARAMETERS

The Gardner formulations for hydraulic conductivity, $K(\psi)$, and unfrozen water content, $\theta(\psi)$, as functions of soil water potential, ψ, are as follows:

$$K(\psi) = K_o/(A_k|\psi|^{n_k} + 1) \quad (2)$$

and

$$\theta(\psi) = \theta_o/(A_\theta|\psi|^{n_\theta} + 1) \quad (3)$$

where K_o is the saturated hydraulic conductivity, θ_o is the saturated volumetric moisture content (porosity) and A_k, n_k, and A_θ, n_θ are the empirical constants appropriate for hydraulic conductivity and soil moisture, respectively. These formulae are applicable only when $\psi < 0$, i.e., when soil water tension exists due to drying or freezing effects. For $\psi \geq 0$, $K(\psi) = K_o$ and $\theta(\psi) = \theta_o$.

The Gardner expressions simulate the reduction of hydraulic conductivity and moisture content as soil water tension increases. Both expressions predict a reduction in the transport of moisture and associated latent heat to the freeze front as the empirical constants increase. For a given moisture gradient, any increase in the denominator in equation (2) decreases the available latent heat transported to the freeze front, and consequently, accelerates the downward motion of the freezing front. Guymon (personal communication) has compiled a table of values for the four empirical constants: A_k, n_k, A_θ and n_θ. Hydraulic conductivity is further reduced whenever ice is present, through an empirical attenuation factor E, such that:

$$K_h(\psi,\theta_i) = K(\psi) \cdot 10^{-E\theta_i} \quad (4)$$

where K_h is the actual hydraulic conductivity. Relatively little information is available regarding E (Gosink, et al., 1986); however, typical values are between about 8 for fine sands and silts to about 20-30 for coarse gravelly soils. The use of the empirical formulae given by equations 2 and 3 may be questioned (O'Neill, 1983; Miller, 1973) since these expressions do not allow for explicit temperature or ice pressure dependency. It is probably this inadequacy in the soil moisture-tension relation which necessitates the use of an additional empirical expression, given by equation 4. However, once the appropriate values of the five empirical coefficients are determined for a given soil, it should be possible to predict the thermal and moisture regimes for arbitrary surface conditions for engineering purposes.

In a typical calculation, the soil temperature equation is solved first using initial estimates of soil moisture and ice content in the calculation of the thermal conductivity and specific heat. Next, the above expression for hydraulic conductivity is used in Richard's equation (de Marsily, 1986) to solve for the pressure field, which then allows determination of the unfrozen water content through equation (3). Calculations proceed with alternating solution of the heat conduction equation and Richard's equation which are strongly coupled because of moisture migration.

TEMPERATURE AND MOISTURE MEASUREMENTS

Five sites at the University of Alaska Agricultural experimental area were selected in a study to determine the effects of introducing a solar absorptive material such as lampblack on the snow surface to accelerate springtime thawing. The sites were located on open tilled farmland. Further details regarding the sites and the experimental methods may be found in Holty et al. (1987). Each site was instrumented to a depth of 50 cm with strings of thermistors that also extended above the snow surface. Temperature measurements were obtained almost monthly between November 1981 and May 1982, although the present analysis includes only measurements from November 1981 to February 1982.

Moisture measurements to depths of about 300 cm were obtained using a neutron probe calibrated to a standard. The soil at the UAF farm located in interior Alaska is quite dry, due to the low annual precipitation rate, and it is known that the top layer of soil becomes dessicated under the snow cover during the long Alaskan winter (Trabant and Benson, 1972). The water table is generally about 4 m below the ground surface at the farm sites.

Daily air temperature maxima and minima were obtained from an existing weather station at the UAF experimental farm about 300 m from the location of our measurements. At the time of preparation of this report no wind speed data were available; therefore, a complete surface heat balance to determine surface boundary conditions was not attempted. Instead, an empirical relation based on air temperatures and surface temperature was devised. This is explained in the next section.

TEMPERATURE AND MOISTURE BOUNDARY AND INITIAL CONDITIONS

In its original form, the numerical model could accept three types of boundary conditions for either temperature or pressure: a constant value, a periodic value, or zero gradient. The latter condition implies zero heat flux when applied to the temperature equation, and zero moisture flux when applied to the pressure (Richard's) equation. For the purpose of this study, the model was modified to provide the capability of including user-defined boundary temperatures and pressures on a daily basis. In principle, the model may also be modified to utilize a prescribed surface heat or moisture flux. The surface boundary conditions drive the

model, and so it is essential that reasonable estimates of surface temperature and pressure are prescribed. In the present study, neither surface temperature nor pressure measurements were available on a daily basis. However, meteorological data from the UAF farm were available, including daily maximum and minimum air temperatures, and rainfall or snow equivalent and evaporation (NOAA, 1981, 1982). These data were used to set ground surface temperature and pressure boundary conditions by the methods described below.

Since wind velocity and cloud cover data were not available at the time of this study, a complete heat balance could not be attempted and the surface temperature condition was defined in terms of the average daily air temperature. In particular, the boundary temperature was assumed to equal 19% of the average air temperature in °C for the previous 24 hour period. This percentage represents the average value of the ratio of measured soil temperature at 1 cm depth to measured air temperature on six dates; the measured soil temperature distributions were obtained on November 24, December 9 and 12, 1981, and January 4 and 19 and February 24, 1982. The use of these temperatures as a surface boundary condition is a site-specific empirical device which permits a reasonable approximation of the actual surface temperatures to be used in the model. It is important to note that the goal of this study was to test the model rather than to test a complete surface heat balance model. Daily maximum and minimum air temperatures at the experimental farm starting from August 1, 1981 are displayed in Figure 1. Zero heat flux was assumed at the bottom of the calculation domain.

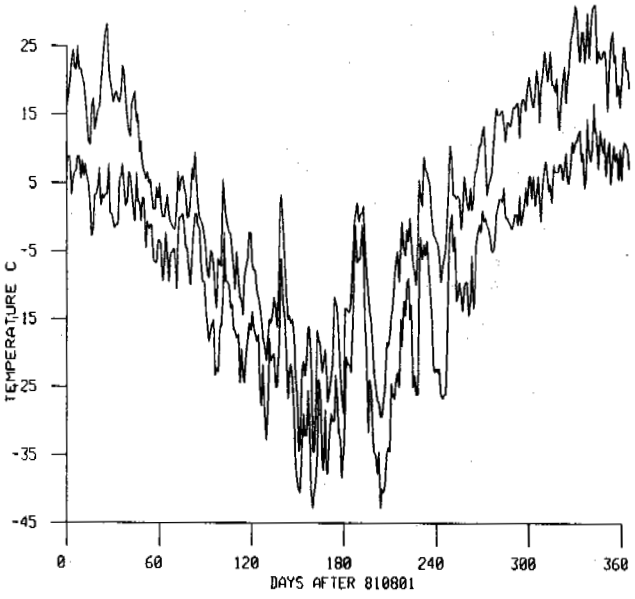

Fig. 1: Daily maximum and minimum air temperatures from the UAF experimental farm commencing August 1, 1981.

At first, initial temperature and moisture distributions were assumed for September 1, 1981 based on previous data from interior Alaska. However, early calculations indicated consistent discrepancies between measured and the first set of predicted temperatures for November 24. For this reason, another month of air temperature data was added, providing a longer initial adjustment period. The initial temperature and moisture conditions on August 1 consisted of uniform temperature equal to 1°C and uniform moisture equal to 0.24.

The water table was assumed to remain at a constant level of 4 m throughout the calculations, based on sporadic data obtained in previous years. Since we used a calculation grid extending 5 m down from the surface, the pressure boundary condition was ψ = 100 cm at y = 500 cm. Several other water table depths were used in the simulations (± 50 cm) but there was very little change in the predicted temperature and moisture profiles.

At the ground surface, a daily pressure boundary condition was defined by the following procedure. On rainy days the moisture was assumed to infiltrate the surface and the surface pressure was set equal to zero in units of hydraulic head. It was assumed that the soil at the surface would dry to a residual water content in four days. Thus, following a rainfall, the surface moisture would drop linearly from its saturated value to its residual water content in four days; the surface pressure could then be calculated from equation 3 since the soil water tension equals ψ. This method of determining surface pressures is somewhat arbitrary; however, since actual surface moisture is unknown, and since the time step for the model is one day, the method provides a rough first estimate of the actual surface moisture.

Figure 2a displays precipitation and evaporation measured at the UAF experimental farm during the study period. Note that these are referenced to the left axis. The net accumulation of moisture added to the soil in the form of rainfall minus evaporation is also depicted in Figure 2a, referenced to the right axis. The net accumulation was negative throughout the study period indicating a net loss of moisture from the soil. Positive precipitation on days with temperatures below 0°C represents snow and is not added into the net accumulation. For example, the precipitation occurring after about day 105 (November 14, 1981) is snowfall and does not add moisture to the soil. The surface moisture condition determined by the above method is shown in Figure 2b. The porosity of the soil was taken to be 0.5 and the residual water content 0.2.

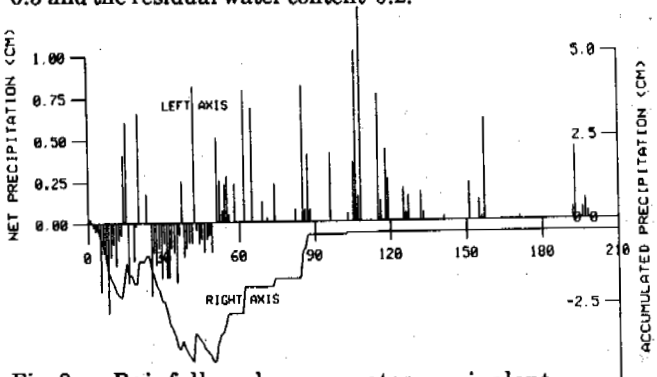

Fig. 2a: Rainfall and snow water equivalent minus evaporation at the UAF farm from August 1, 1981 (left axis). Accumulated rainfall minus evaporation at the UAF farm from August 1, 1981 (right axis).

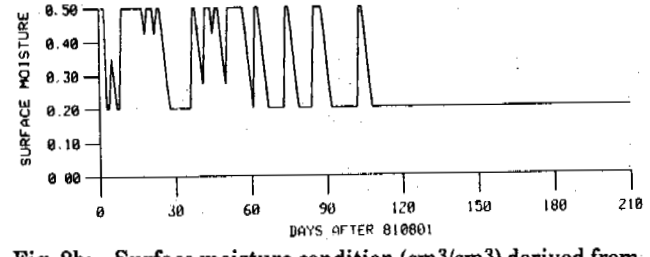

Fig. 2b: Surface moisture condition (cm^3/cm^3) derived from rainfall minus evaporation (see text).

After the snow cover was in place in mid-November, it was assumed that the soil surface received no additional moisture and dried to the residual water content. Values of the constants associated with the hydraulic conductivity and moisture formulae were obtained from the tabulation determined by Guymon (Gosink, et al., 1986):

$$A_k = 5.83\ 10^{-3};\ n_k = 1.559;\ K_o = 0.042\ \text{cm hr}^{-1};$$

$$A_\theta = 5.05 \cdot 10^{-3};\ n_\theta = 0.782.$$

PREDICTIONS

Predicted and measured temperatures for the six dates and at the five sites are displayed in Figure 3. The identification of site number with its respective symbol is given in the figure caption. Note that the range of measured temperatures for these adjacent sites is almost 2°C (see 820119 at 20 cm), a large variation for very similar plots of dry, tilled agricultural soil. The calculated temperatures agree quite well with the measured soil temperatures. Discrepancies between calculated and measured profiles occur on the dates when the imposed surface boundary temperature, equal to 0.19 times the daily air temperature, diverges from the actual soil temperature at the 1 cm depth. In an effort to test the effect of a more accurate surface temperature condition, we altered the imposed surface temperature for the day of the calculation and the previous day to match the measured surface temperature. This corresponds to changing 12 of the 208 imposed surface temperatures during the period from August 1, 1981 to February 24, 1982. The results of this calculation using the "corrected" meteorological forcing are shown in Figure 4.

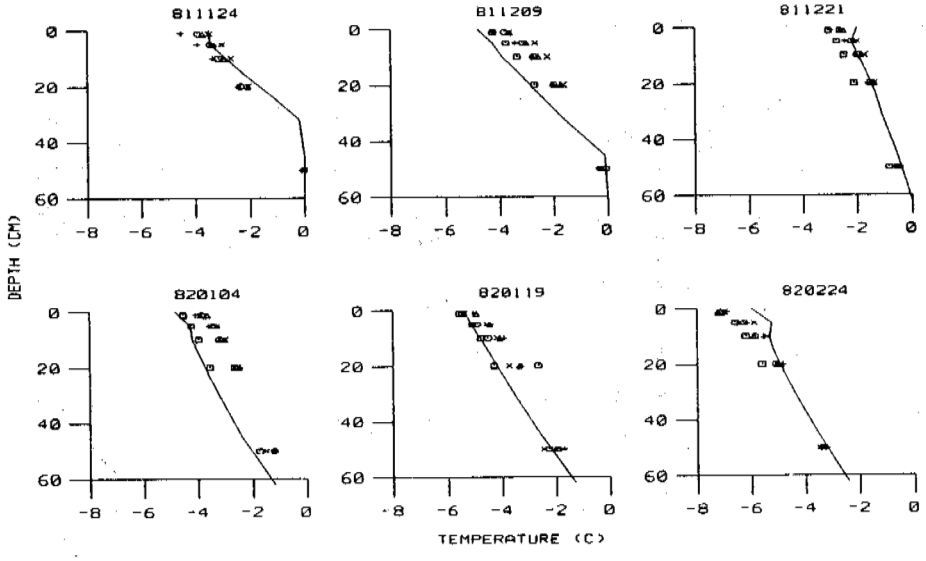

Fig. 3: Temperature measurements (□ site 2; O site 3; Δ site 4; + site 5; × site 6) and predicted temperatures (solid line) using uncorrected surface temperature.

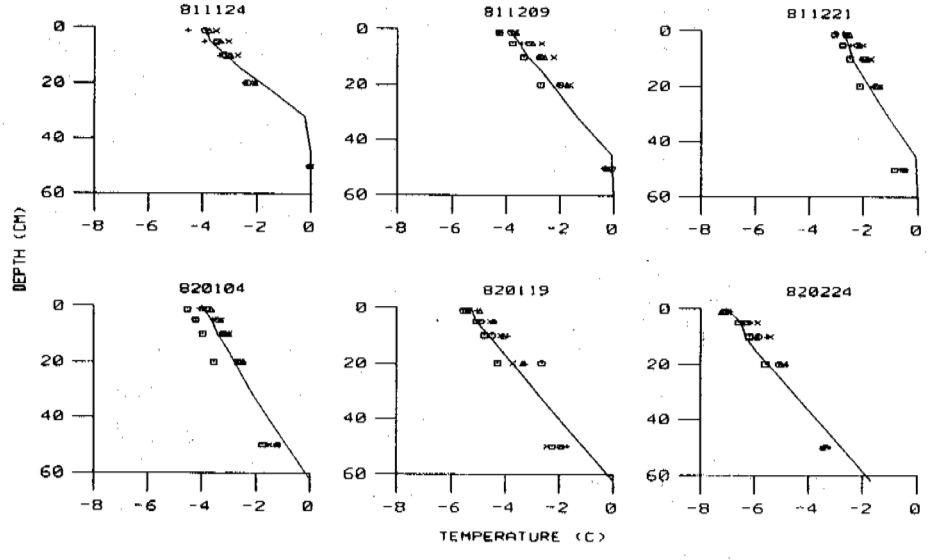

Fig. 4: Temperature measurements (□ site 2; O site 3; Δ site 4; + site 5; × site 6) and predicted temperatures (solid line) using corrected surface temperature.

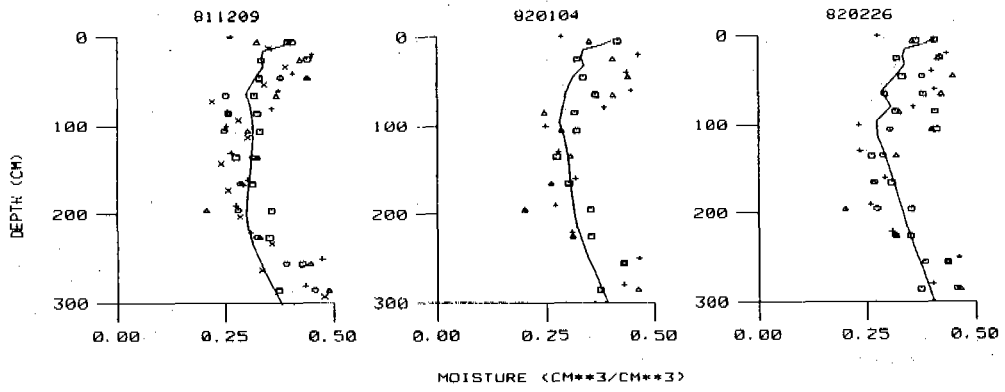

Fig. 5: Soil moisture measurements (□ site 2; O site 3; Δ site 4; + site 5; × site 6) and predicted soil moisture (solid line).

The agreement between calculated and predicted temperatures is improved over those shown in Figure 3, particularly near the surface. It is expected that the agreement would be excellent if daily measured soil surface temperatures were available to drive the model. Alternatively, a reliable heat balance method for determining surface heat flux or temperature with daily air temperature, wind speed, cloud cover and radiation measurements could be used to improve the prediction.
Calculated and measured total moisture contents (ice and water) for three dates are displayed in Figure 5. The calculated moisture profiles are in qualitative agreement with the measured values, although measured moisture profiles show a greater curvature. The discrepancies are probably due to the assumed pressure boundary conditions, including both the level of the water table and the soil tension at the surface, and to the sensitivity of the empirical constants in equations 2 and 3. For example, the sensitivity of the calculated moisture content to the constants A_θ and n_θ is:

$$d\theta = -\theta^2 \psi^{n_\theta} (dA_\theta + A_\theta \ln \psi \, dn_\theta) / \theta_o \qquad (5)$$

Since in very dry soils, soil tension may be as large as several thousand centimeters, small changes in A_θ, in particular, can strongly alter the calculated soil moisture. Note that the term $A_\theta \ln \psi$ is quite small for this case ($A_\theta = 5.05 \cdot 10^{-3}$), showing that the calculated moisture is relatively insensitive to changes in n_θ. Although the method used to define surface moisture in this study was at best a reasonable approximation, it is clear that the assumed value of the parameter A_θ may dominate the calculations for θ.

For all these calculations, the hydraulic conductivity attenuation factor, E, was set equal to 16. This value, in the mid-range of those recommended by Guymon et al. (1980), was found to provide the best agreement between measured and predicted temperature and soil moisture. The predictions are relatively sensitive to E; however, variations in E by as much as 25% (±4) generate acceptable predictions of temperature and soil moisture from an engineering viewpoint.

The calculated pressures are also sensitive to the residual water content; a value of 0.2 was used in the calculations, slightly less than the minimum water content measured in the study. Since the residual water content determines the surface soil tension (see Figure 2b), this parameter strongly controls moisture migration near the ground surface. Furthermore, there is some question regarding the reliability of soil moisture measurements near the ground surface. The neutron probe effectively integrates moisture contents over a finite region approximately 25 cm of depth, and therefore the actual minimum water content near the soil surface may be quite different from the measured value. Clearly improved estimates of soil moisture content and water table levels are required for reliable moisture prediction.

CONCLUSIONS

Measurements of shallow soil temperature and moisture content were obtained at the UAF experimental farm station during winter 1981-82. These data were compared with predictions from a coupled temperature and moisture finite element model of Guymon and Hromadka (1977). The agreement between measured and predicted soil temperatures was excellent when realistic meteorological forcing was prescribed. This forcing was incorporated into the model through a modification which permits the imposition of user-defined daily temperatures and pressures. The major area of discrepancy was in the soil moisture calculations, and this probably reflects uncertainties in the prescription of both the pressure boundary conditions and the empirical constants in the Gardner expressions. However, the general trend of the data is very well predicted using the assumed boundary contions. It is clear that reliable temperature and moisture predictions in freezing soils depend strongly upon accurate knowledge of the forcing or boundary conditions, primarily surface temperature and moisture, and that experimental programs should include frequent measurements of these parameters.

ACKNOWLEDGMENTS

This work was supported by the U. S. Department of Agriculture, Grant No. 59-2021-1-2-101-0, the U.S. Geological Survey, Award Number 14-08-0001-G1305, the National Science Foundation, Grants DPP84-03280 and DPP86-19382, and the State of Alaska. We would also like to thank Dr. James V. Drew, Director, Agriculture and Forestry Experiment Station, University of Alaska, for providing an area for conducting this research.

REFERENCES

Anderson, D. M. and N. R. Morgenstern (1973). Physics, chemistry and mechanics of frozen ground, Proceedings of the Second International Conference on Permafrost, Yakutsk, U.S.S.R., 257-288, July 13-28, 1973

Anderson, D. M. and A. R. Tice (1972). Predicting unfrozen water contents in frozen soils from surface area measurements, Highway Research Record No. 393, National Academy of Science-National Research Council, Washington, D.C., 12-18.

de Marsily, G. (1986), Quantitative Hydrogeology, Academic Press, Inc., London.

Farouki, O. T. (1981). Thermal properties of soils, CRREL Monograph 81-1, U.S. Army CRREL, Hanover, N.H.

Gardner, W. R. (1958). Some steady-state solutions of the unsaturated moisture flow equation with application to evaporation from a water table, Soil Sci., 85, 228-232.

Gosink, J. P., T. E. Osterkamp and K. Kawasaki (1986), A comparison of two finite element models for the prediction of permafrost temperatures, Final Report, Alaska Dept. of Transportation and Public Facilities, Agreement 82IP361, Univ. of Alaska, Fairbanks, Alaska.

Guymon, G. T. and T. V. Hromadka, II (1977). Finite element model of transient heat conduction with isothermal phase change (two-and three-dimensional), U.S. Army Cold Regions Research and Engineering Laboratory, Special Report 77-38.

Guymon, G. T., T. V. Hromadka II, and R. J. Berg (1980). A one-dimensional frost heave model based upon simulation of simultaneous heat and water flux, Cold Regions Sci. Technol., 3, (2+3): 253-262.

Guymon, G. T. and J. N. Luthin (1974). A coupled heat and moisture transport model for Arctic soils, Water Resources Research, 10(5), 995-1001.

Holty, J. G., K. Kawasaki and T. E. Osterkamp (1987). Observations of the effects on agricultural soils of the enhancement of snowmelt in Interior Alaska, Agroborealis, 19, 20-26.

Hromadka, T. V., G. L. Guymon and R. L. Berg (1981). Some approaches to modeling phase change in freezing soils, Cold Regions Science and Tech., 4, 137-145.

Kawasaki, K., T. E. Osterkamp and J.P. Gosink (1982). A preliminary evaluation of numerical models suitable for thermal analysis of roadways and airstrips, Report No. AK-RD-82-22, State of Alaska, Dept. of Transportation and Public Facilities.

Miller, R. D. (1973). Soil freezing in relation to pore water pressure and temperature, paper presented at 2nd International Conf. on Permafrost, National Academy of Science, Yakutsk, USSR.

O'Neill, K. (1983). The physics of mathematical frost heave models: A review, Cold Regions Sci. and Tech., 6, 275-291.

O'Neill, K. and R. D. Miller (1983). Numerical solutions for a rigid-ice model of secondary frost heave, CRREL Rep. 82-13, Cold Regions Res. and Eng. Lab., Hanover, N.H.

O'Neill, K. and J. Miller (1985). Exploration of a rigid ice model of frost heave, Water Resources Research, 21(3), 281-296.

Trabant, D. and C. Benson (1972). Field experiments on the development of depth hoar, in Studies in Mineralogy and Precambian Geology, ed. B. R. Doe and D. K.. Smith, The Geological Society of America, Inc., Boulder, Colorado., 309-322.

U.S. National Oceanic and Atmospheric Administration (NOAA) (1981). Environmental Data and Information Service, National Climatic Center. Climatological Data, Alaska. Vol. 67, Asheville, North Carolina.

U.S. National Oceanic and Atmospheric Administration (NOAA) (1982). Environmental Data and Information Service, National Climatic Center. Climatological Data, Alaska. Vol. 68, Asheville, North Carolina.

SUMMER THAWING OF DIFFERENT GROUNDS – AN EMPIRICAL MODEL FOR WESTERN SPITSBERGEN

M. Grzes

Poland Academy of Science, Institute of Geography Dept. of Geomorphology and hydrology, 87-100 Torun, Kopernika 19, Poland

SYNOPSIS

Studies of summer thaw in various kinds of ground were carried out in Spitsbergen during five summer seasons. The results of 950 measurements made on the coastal plains lying at an altitude of up to 60 m a.s.l. were subjected to analysis. Seven different environments have been recognized. They display a varying rate and depth of thaw, i.e. a varying depth of the active layer. Empirical curves have been plotted to illustrate the scheme of the operation of this process. They have been approximated by means of simple formulae. The proposed model represents the simplest solution, i.e. the operation and depth of summer thaw in the function of the duration of this process.

INTRODUCTION

One of the basic characteristics of permafrost regions is the depth of seasonal thaw in the ground layer immediately below the surface. This layer is refered to in the literature as actice the layer. It is necessary in many branches of biological and geographical sciences to acquire information pertinent to the depth, its spatial and time variations. Note should be made of the fact that most summer expeditions come to the study area when the thaw process has already become advanced and leave before it ceases. Depth of the thawed layer are expressed in centimetres in the geological-geographical field. The research is, however, of quantitative character and provides a discription of the influence of selected environmental elements on the course of the thaw process. This paper presents a tentative quantitative assessment of the seasonal thaw process from the geological-geographical viewpoint.

COURSE AND DEPTH OF SUMMER THAW: SCHEME INTERPRETATION

The depth of summer thaw in various kinds of ground has been presented as a scheme by Mackay (1970) who explored the Atctic portion of Canada. One of the subjectives to be reached by the present author is to work out a similar scheme with reference to Spitsbergen (Fig. 1). It should allow for the operation of the process with time. From the analysis of a set of estimates available, it follows that at least seven different environments which differ in the course and depth of thaw, i.e. the thickness of the active layer, may be recognized:

Ia, Ib. grounds varying in particle, size distribution, with a blanketing continuous organic layer, more than 20 cm thick (Ia) and 10 to 20 cm thick (Ib).

II. tills with high moisture contents which are colonized by luxuriant tundra vegetation,

III. gravels, sands and silts within depressions at marine terraces, which are occupied by luxuriant tundra vegetation,

IV. modelled ground (Jahn, 1970), the interior of which is built up of predominant earth particles and which is colonized by extremely luxuriant tundra vegetation,

V. Sands, gravels of which marine terraces covered with sparse tundra vegetation are built up,

VI. gravels and sands forming present-day outwash fans,

VII. mineral mantle (boulders, silts) over ice-morainic ridges.

With reference to (Ia) and (Ib), it is commonly that an organic layer in the form of either turf or peat serves as a heat insulator in the thawing of ground. There is 50-60 percent fall in the annual ground temperature amplitude beneath a peat moss layer is thick. Czeppe (1969) and Jahn (1970) have provided interesting data from Spitsbergen. From the above, it can be inferred that a layer of moss and grass less than 10 cm thick has a marked effect on a fall in the rate of thaw. Jahn (1982) carried out his observations in test field 1 m^2 in surface area. An organic-mineral layer of varying thickness was removed from them. The results of Jahns experiment and authors experiments as well as 120 measurements performed at similar sites permitted determination of the average course and depth of summer thaw beneath organic layers more than 20 cm thick (Ia) and 10-20 cm thick (Ib). In the former case the active layer

was about 40 cm in thickness in late September, whereas it approached 55 cm in the latter case. The diurnal rate of thawing beneath an over 10 cm thick organic layer was 0.25 to 0.35 cm. As concerns (II), the environment consists of tills with high moisture contents, which are colonized by luxuriant tundra vegetation occuring as a continuous cover up to 10 cm thick at some places. It is there that the ground thaws down to the depth of about 70 cm. In the initial stage of thaw down to 50 cm the rate of thawing ranges from 1.7 to 1.3 cm throughout the 24 hour period and next, drops off abruptly to 0.8 to 0.3 cm throughout the 24 hour period within a layer 50-70 cm thick. The diurnal rate of thawing was slower than 0.11 to 0.12 cm below the depth of 70 cm.

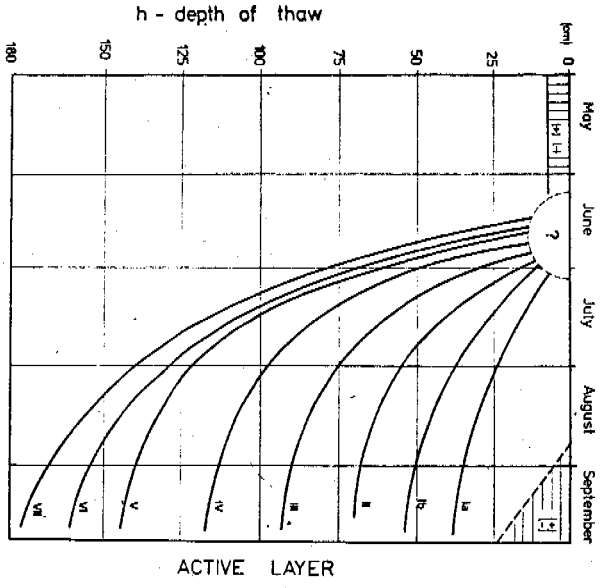

FIGURE 1

Fig. 1. Scheme of summer thaw, the western coast of Spitsbergen (see text for explanation)

With regard to (III), shallow depressions with high moisture contents within marine terraces, which frequently lie along tracks of periodic surface runoff, are covered by well-developed tundra vegetation. They are usually filled with fine silty material up to several centimetres thick. Sheets of strongly recrystallized snow showing ilusive resemblance to icings (naled) lie till late summer. These sites thaw down to the depth of 90 cm of the average. A 0-70 cm thick layer thaws at the diurnal rate of 2.5 to 1.2 cm, whereas the rate of thawing of a 70-90 cm deep layer is merely 0.5 to 0.2 throughout the 24 hour period. Such sites occupy vast areas of the Spitsbergen tundra.

As regards (IV), regular measurements of the depth of thaw were performed within a few forms near the Polish Polar Station. They are refered to by Jahn (1970, p. 116-118) as modelled grounds of type A. The base of debris likes forming garlands is in contact with the top of permafrost. The course of summer thaw was traced inside the garlands where till is the predominant constituent. Heat transfer into its interior within stone garlands alone is of considerably greater magnitude. The garlands serve as drains. Among others, this accounts for deep thawing of the ground within these forms (down to 140 cm). The permafrost surface is highly diversified. The average depth of summer thaw is 110 to 115 cm. It is rather difficult to measure it precisely since there is coarse material with particles having sharpness around their edges at the contact plane with permafrost. A 0-50 cm deep ground layer thaws at a rate of up to 4 cm throughout the 24 hour period, whereas the diurnal rate of thawing of a 50-90 cm deep layer is merely 1.8-2.0 cm. Beneath the depth of 90 cm the rate of thawing drops off to below 1 cm throughout the 24 hour period to become decreased in a 105-115 cm deep layer by 0.2 cm throughout the 24 hour period.

Refering to (V), terraces and early storm ridges are dissected by the multiplicity of large-size polygons. On the average, they thaw down to the depth of 140 cm. In winter a thin snow cover lies there; it melts away as early as in mid-June. These areas are well drained. As early as in mid-July a layer of the thawed ground is 100 cm thick. Thaw proceeds then at a rate slower than 1 cm throughout the 24 hour period.

As far as (VI) is concerned, the course and depth of thaw in outwash fans heaved up at a present time resemble those observed in environment V. In the initial stage the diurnal rate of thawing is up to 4.5 cm. There is a marked fall in the rate of thawing as deep down as 100 to 110 cm. Such operation of the process can be linked to numerous outwash streams in which discharge decreases markedly as late as at the beginning of August. The average depth of thaw is 145 cm. Deviations from this value may be ± 40-50 cm. In late August in the summer of 1979 the maximum thickness of thawed sands and gravels was even 230 cm on the outermost outwash plain of the Gås Glacier. Generally, the grounds thaws about 50-55 cm deeper close to the streams compared with the surounding area.

With reference (VII), measurements of the depth of thaw in a mineral mantle over ice morainic ridges are extremely difficult. Plotting of a curve was based on ground (a layer down to the depth of 120 cm) temperature values recorded sporadically on ice morainic ridges of the Werenskiold (at one point) and Hans (at three points) glaciers. The measurements were performed using lifting thermometers. Information was also supplied by 24 holes bored by the use of a corer, by measurements carried out in natural exposures and by data quoted in the literature. As mentioned above, the earliest thawing of the ground begins along the creats of the ice morainic ridges with no snow laying. The existing water-filled depressions are due to thermokarst activity, i.e. the melting of an ice core. The depth of summer thaw on the ice morainic ridges is closely related to their degradation. Szponar (1982) has established that the thickness of an ablation moraine over the ice morainic ridges does not exceed 1.7 m. Szupryczynski (1963) has estimated the same values while Troicki (Troicki, Singer et al, 1975) has stated that an ablation moraine may

attain 2 m in thickness in Spitsbergen. The maximum thickness of a mineral mantle over the ice morainic ridges of the Hans, Werenskiold and Gås Glaciers was 2.2 m. Kozarski (1974, 1982) has discussed in detail ablation morainic covers as heat-insulators. He has pointed out that they protect ice against progressive melting out after they have attained definite depths and under certain conditions they initiate the formation of ice morainic ridges refered to by Kozarski as ablation end moraines. It has been established that a 175 cm thick ablation layer protects the ice core against melting out under the existing climatic conditions. Ice has been detected beneath a till layer of similar thickness in 17 cases, whereas summer thaw has not reached the top of ice core in 7 cases (over slopes). There is a tendency for the basal portion of the slope to thaw at shallow depths, i.e. down to the depth of 30-40 cm. It can be linked to a prolonged period with snow lying, on the one hand, and to a higher percentage of finer fractions of particles, on the other hand.

CONCLUSIONS

The stablished pattern of seasonal thaw in various kinds of ground at an altitude of up to 60 m a.s.l. provides the bases of plotting of eight empirical curves, the approximations of which are given by the equation:

$$h = a \lg (T \pm c) - b$$

where h is the depth of a thawed layer, a and b are constant coefficients defining a thawing layer, T is the duration of thaw in days, c is allowance for earlier (+) or a later (-) disappearance of snow at a given locality. Index c is calculated in the following way: the actual number of the 24 hour periods of delay devided by 4. Definite formulae for particular environments are given below:

Ia. $h = 29 \lg (T- 6) - 20$
Ib. $h = 39 \lg (T- 6) - 20$
II. $h = 53 \lg (T- 5) - 28$
III. $h = 62 \lg (T- 3) - 25$
IV. $h = 84 \lg (T-40)$
V. $h = 96 \lg (T-37)$
VI. $h = 105 \lg (T-41)$
VII. $h = 116 \lg (T+ 7) - 57$

If the duration of thawing in a selected kind of ground environments is known, the above formulae permit determination of the thickness of the active layer with high precision. Jahn (1982) also constructed a model of summer thaw in Spitsbergen. It implies that the rate of thawing decreases with depth by means of geometrical progression. This is illustrated by curves (Fig. 1). The proposed model is based on time, a generally well-known factor, it takes for a ground layer of the same thickness to thaw. The time increases by means of geometrical progression.

REFERENCES

Czeppe, Z. (1969). Thermic differentation of the active layer and its influence upon the frost heave in periglacial region Spitsbergen. Bull. Acad. Polon. Sci., Ser. Sci. geol. et geogr., Vol. VIII, No 2, Warszawa.

Jahn, A. (1970). Zagadnienia strefy peryglacjalnej. PWN, Warzawa.

Jahn, A. (1982). Soil thawing and active layer of permafrost in Spitsbergen. Res. of invest. of the Pol. Sc. Spits. Exp., Vol. IV, Acta Univ. Wratislav., No 527, Wroclaw.

Kozarski, S. (1974). Procesy powstawania i zaniku pagórkow lodowo-morenowych ice-cored moraines w strafach brzeznych niektorych lodowcow regionu Hornsundu. Materialy z Sympozjum Spitsbergenskiego, Pol. wypr. na Spitsbergen 1970 i 1971 r., Wroclaw, 1972, Wyd. Uniw. Wroclaw., Wroclaw.

Kozarski, S. (1982). The genetic variety of ice cores in the marginal forms at some Spitsbergen glaciers. Hornsund region. Res. of invest. of the Pol. Sc. Spits. Exp., Vol IV, Acta Univ. Wratislav., No 529, Wroclaw.

Mackay, J.R. (1970). Disturbance of the tundra and forest tundra environment of the western Arctic. Canadian Geotechnical Journal, Vol. 7.

Szponar, A. (1982). Earthslides of ablation type on the ice-morain ridges. Res. of invest. of the Pol. Sc. Spits. Exp., Vol IV, Acta Univ. Wratislav., No 525, Wroclaw.

Szupryczynski, J. (1963). Rzezba strefy marginalnej i typy deglacjacji lodowcow poludniowego Spitsbergenu. Prace Geogr. IG PAN, nr. 39, Warszawa.

Troitsky, L.S., Singer, E.M. et al. (1975). Glaciation of the Spitsbergen, Svalbard. The Publishing House "Nauka", Moskow (in Russian).

OBSERVATIONS ON THE REDISTRIBUTION OF MOISTURE IN THE ACTIVE LAYER AND PERMAFROST

S.A. Harris

The University of Calgary, Alberta, Canada

SYNOPSIS Neutron probe measurements of moisture in the ground in permafrost areas of the Cordillera of Canada indicate that there is a characteristic concentration of moisture in the top layers of the permafrost table. It consists of both segregated and pore ice and distinctive movements of moisture take place as the temperature changes. Moisture moves in the direction of the lowest temperature, so that the moisture maximum is fed by moisture coming from above and below. These changes can be demonstrated as thawed profiles become permafrost, and they also take in palsas. Addition from above is dominant, but there is a specific limit for each substrate. Thereafter, additional moisture can only be added by moisture injection, but the excess moisture dissipates quickly when injection ceases.

INTRODUCTION

Permafrost is defined as a cryotic temperature condition in the ground for more than two years, but this definition disregards moisture status and phase. In this paper "moisture" refers to total H_2O content regardless of the proportions in solid, liquid and gaseous phase. In practice, the phase change from liquid to solid and vice versa is accompanied by volume changes causing heaving and settlement, respectively. These changes play a major role in the formation of most zonal permafrost landforms (Harris, 1982a, 1982b), and they are of fundamental importance in engineering design and the use of permafrost regions by Man (Andersland & Anderson, 1978; Johnston, 1981; Harris, 1986).

It is only in the last 12 years that the processes involved in producing typical moisture regimes in permafrost have begun to be studied in the field. This paper summarizes a series of observations on total moisture content with depth in several areas of the Cordillera of Canada by the author since 1980.

FIELD METHODS

Figure 1 shows the sites used by the author and his students for moisture studies of alpine permafrost in the Canadian Cordillera. Access tubes for neutron moisture probes were emplaced in holes drilled in the ground by diamond drilling (at Summit Lake A), by hot water drilling using a modification of the method of Napoleoni and Clarke (1978), or by digging a hole in the ground and placing access tubes in the corner of the pit followed by backfilling of the hole (Plateau Mountain and Slims River rock glacier). Of these methods, the hot water drilling in winter produces the least disturbance of the pre-existing moisture regime since the hole that is thawed is only just the width of the access tube. The pit method causes the greatest disturbance.

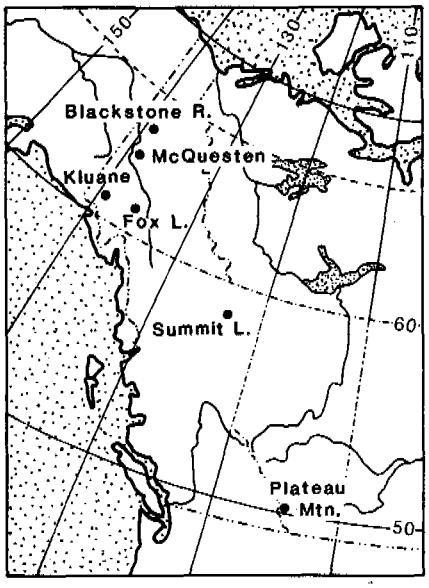

Fig. 1 Location of the Neutron Probe Studies in the Canadian Cordillera.

Steel access tubes may become unusable after two years due to conduction of cold into the ground accompanied by severe icing on their insides. This also raises the possibility of an altered moisture regime around the access tube. PVC plastic tubes proved far superior since they largely overcome the icing problem and do not corrode. They do, however, absorb some of the neutrons and each batch of plastic

tubing is tested in a standard soil plot to check on the degree of absorption. Ground temperatures were measured in adjacent access tubes containing thermistor strings.

The neutron probe is a model which averages the moisture content by volume in a sphere approximately 30 cm in diameter. The standard deviation of the count is under 1%. When the count is divided by the standard count (mean of 10 measurements), the resulting ratio is corrected for variations in electrical performance of the circuitry. The ratio can be converted to percentage by weight if the soil density is measured and the resulting values calibrated against soil samples whose moisture content is determined gravimetrically.

TYPICAL WINTER MOISTURE PROFILE

Figure 2 shows a diagram of the typical moisture profile determined in winter in homogeneous materials in permafrost ground lacking ice wedges (from Harris, 1986, Fig. 2.14). This pattern is very distinctive and is quite different from that found in non-permafrost areas. In summer, the maximum A is missing but is replaced by a maximum located immediately above the base of the thawed zone.

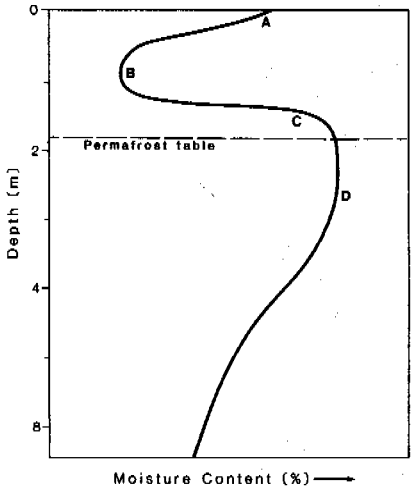

Fig. 2 Typical Winter Moisture Profile in the Upper Layers of Permafrost (from Harris, 1986, Fig. 2.14, with permission). The origin of the parts marked by letters is given in the text.

In Figure 2, maximum A is partly due to snowmelt infiltration into the surface of the soil prior to freezing of the ground, and is augmented by water moving to the freezing plane from below. Maximum C corresponds to the frozen perched water table at the base of the active layer from the previous summer, again augmented by water moving to the freezing plane from above. Both maxima are characterized by the presence of ice lenses as well as pore ice (Mackay, 1971a; French & Pollard, 1986). Minimum B corresponds to the zone of maximum water depletion in the middle of the active layer during freeze-up.

As noted by many authors (Brown & Sellmann, 1973; Washburn, 1979; Pollard & French, 1980), the upper part of the permafrost (D) usually contains the largest quantities of ice (Fig. 3).

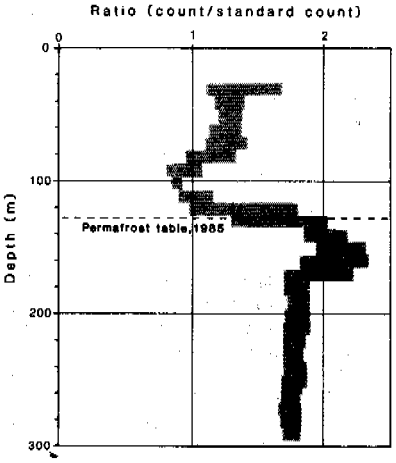

Fig. 3 Range of 14 Measurements of Moisture Content in the Surface Layers of Permafrost at NP4, Push Lobe in Front of a Rock Glacier, Slims River Valley (from Blumstengel, 1988, with permission).

This appears to be true regardless of the form of the ice, and the position of the profile, or the landscape. Ice wedges become increasingly important in the western Arctic coastal plain (Harry et al., 1985) but produce a similar ice distribution with depth. There is usually a gradual decrease in total moisture content at depth in the main mass of the permafrost body. Actual amounts of ice vary widely but may range up to 2000% by dry weight in peat (Konosita et al., 1978), and 1000% by dry weight in silts. The thick (up to 48 m) massive icy beds of the Arctic coastal plain of Yukon and Alaska (Mackay, 1956, 1959; Mackay & Stager, 1966; Rampton, 1971; Brown & Sellman, 1973) may be of similar origin, but they are much thicker than the icy beds at the top of the permafrost in southern Yukon. This may represent a difference in moisture regime, temperature regime and time for formation, unless it is due to a different cause, e.g. buried glacial ice or the injection of moisture into the upper layers of the permafrost (e.g. pingos).

ACTUAL MOISTURE PROFILES

Figure 3 shows the range of soil moisture present in a push lobe in front of the rock glacier on the Slims River valley floor (see Blumstengel & Harris, 1988). It is in well graded coarse silts and the data consist of measurements taken at 20 cm intervals with the neutron probe at different seasons of the year. The moisture minimum in the active layer and the maximum at the top of the permafrost table are clearly shown.

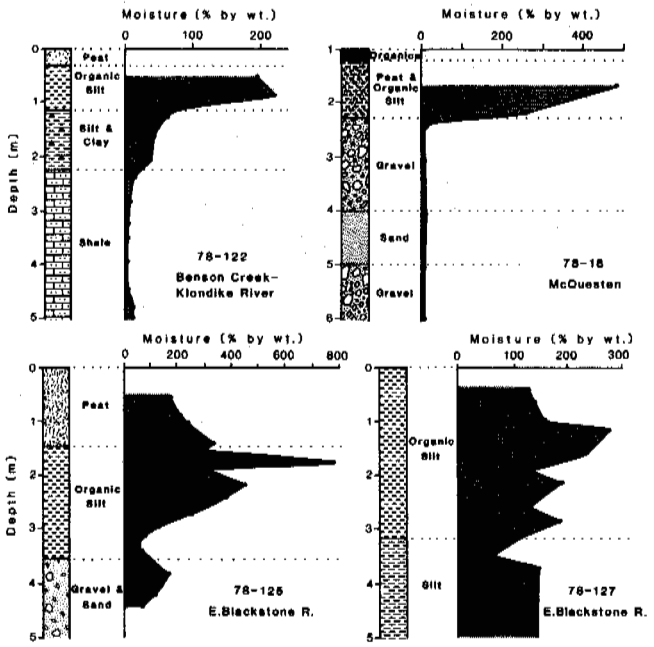

Fig. 4 Moisture Contents in 4 Drill-holes Along the Dempster Lateral Pipeline Route (redrawn from Klohn Leonoff, 1978).

Similar results are found in the published data, although the minima and maxima may be distorted considerably. Figure 4 shows selected profiles of gravimetrically determined moisture contents for drill-holes along the Dempster Lateral Pipeline route, redrawn from Klohn Leanoff (1978). The samples used were small and tended to represent extremes of moisture content, while the neutron probe averages the moisture within its 30 cm sphere of influence.

The effects of different textures, lithologies, and stratigraphy are obvious, and the pattern of moisture distribution may be grossly distorted with certain combinations of stratigraphy, grain size and history of the profile as predicted by Harlan (1974, p. 73). However, all four profiles demonstrate the existence of a moisture maximum at the base of the active layer.

DYNAMICS OF THE MOISTURE PROFILES

Figure 5 shows repeated measurements of moisture with season for profile NP4 on the push lobe in front of the rock glacier (after Blumstengel, 1987). Since it is a well drained site on a slope, there is negligible perched water table effect, and the changes with season can be clearly discerned. These occur mainly in spring and fall when the temperature gradients are greatest. The moisture appears to move to the coldest part of the ground, and this has the effect of moving moisture into the permafrost from the active layer at the end of the summer and from the permafrost table into the lower part of the active layer in spring (c.f. Burn, 1987).

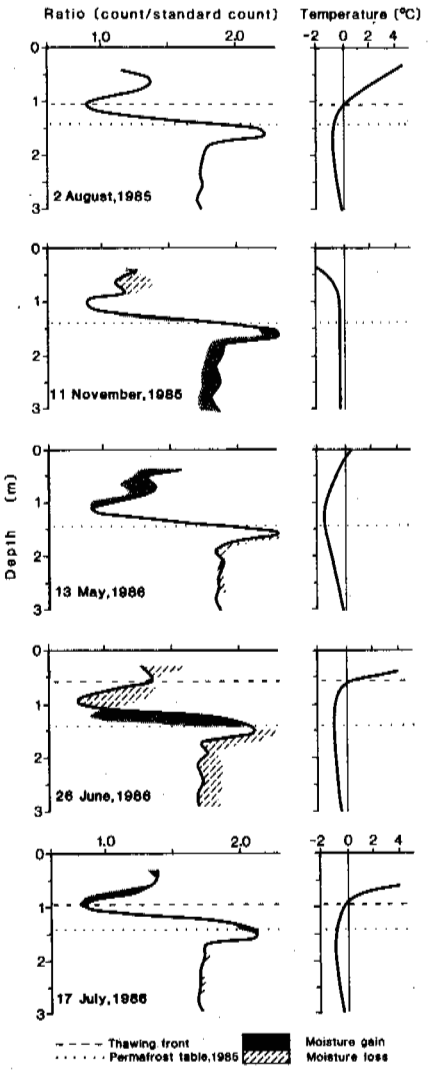

Fig. 5 Changes in Moisture and Temperature with Season for NP4 (from Blumstengel, 1988, with permission).

The latter effect is probably partly compensated for in summer as the moisture moves back down when the centre of the cold wave descends. Thus the temperature gradient appears to be the most critical force in redistributing the moisture through the profile. This is consistent with the arguments of Harlan (1974) and Burn and Smith (1985a) and would also explain the decreasing moisture content at greater depths within the permafrost table. Similar moisture accumulation in the frozen active layer is implied in the results of Mackay et al. (1979), and was demonstrated in Kane and Stein (1983), Burn and Smith (1985b) and Harris (1986). Particle surface-layer effects are also important and presumably are the cause of the unusual moisture profiles that occur where the moisture supply, grain size and stratigraphy

produce particularly favorable conditions for their operation (see Fig. 4).

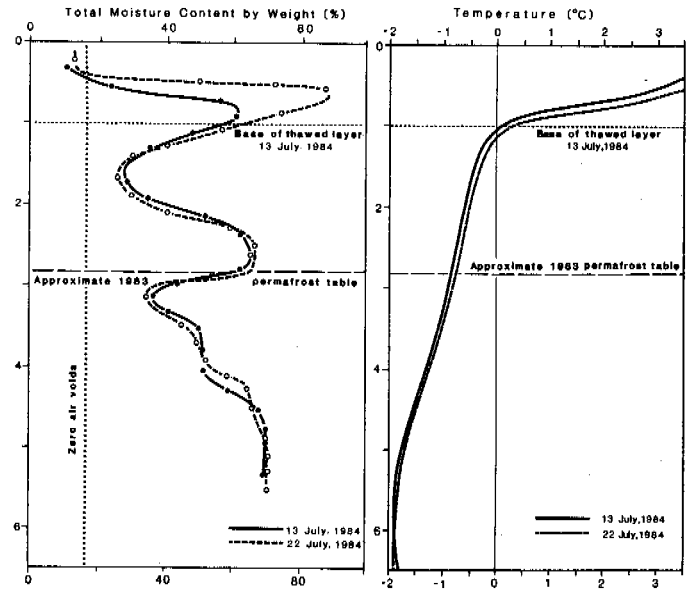

Fig. 6 Build-up in Moisture in the Permafrost Table Between 1981 and 1984 at Summit Lake, B.C. (modified from Harris, 1986, Fig. 2.16, with permission).

Figure 6 shows the effect of drilling a borehole through shallow permafrost with a diamond drill at Summit Lake A, British Columbia. The hole was drilled in November 1981, and resulted in thawing of the ground around the hole so that the water drained away. The ground quickly refroze, and in subsequent years, moisture returned to the drained zone. As the thermal equilibrium changed, the active layer became thinner and the moisture forming the perched water table in the active layer became frozen in place each fall and formed the nucleus of the zone of high moisture content at the top of the permafrost table. Once again, moisture redistribution could be detected.

Figure 6 also shows the effect of summer rains on the moisture status of the active layer. Between 13th and 24th July, 1984, 1.5 cm of rain fell. Thus, the moisture not only comes from thawing of ground ice and from throughflow over the underlying frozen layer, but from summer precipitation.

MOISTURE PROFILES IN PALSAS

Since 1984, a study has been carried out of the moisture distribution with depth in a sequence of developmental stages in wooded palsas at Fox Lake. The results (Fig. 7) indicate that in the early stages of palsa development, the total moisture content of the frozen core is greatest at depth but is still only slightly greater than the surrounding unfrozen material. However, as the palsas become older, a zone of markedly increased moisture appears at the surface of the core and gradually extends downwards with time. The maximum moisture content is fairly constant for a given material (66% by volume for lacustrine silt). Extra water can be injected in artificially under pressure and freezes in place, but rapidly diffuses away when the injection process ceases (Fig. 8). Thus, although palsas may be initiated by water moving to the freezing front under the mound from the adjacent unfrozen fen (Seppälä, 1986), subsequent growth may be due to surface water added to the permafrost core from above over time.

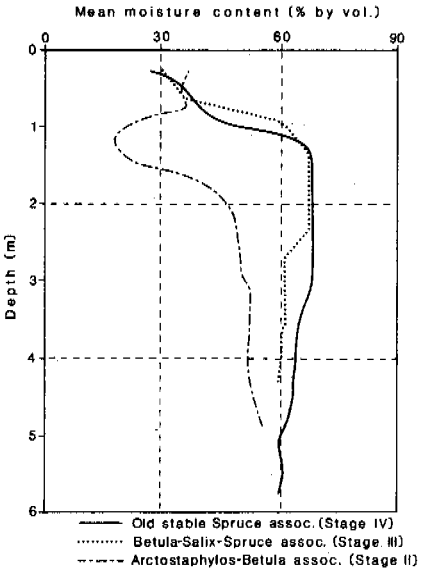

Fig. 7 Differences in Total Moisture Content of the Icy Interiors of Young (Stage II), Adolescent (Stage III) and Mature (Stage IV) Palsas (mean of 8 measurements at 20 cm intervals). Note the build-up in ice from the surface down in the later stages of palsa formation.

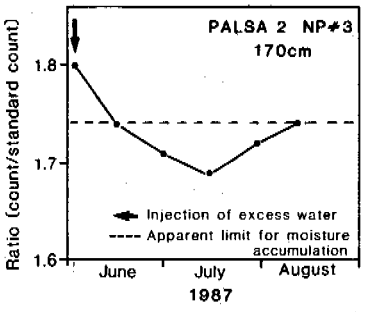

Fig. 8 Results of Injecting Excess Water into the Upper Layers of Permafrost in a Palsa.

CONCLUSIONS

Mature permafrost profiles usually show a characteristic concentration of total moisture in

the form of segregated and pore ice at the top of the permafrost table. This corresponds to the zone subjected to the greatest thermal gradients and it appears that these gradients are the reason for its development. The moisture is concentrated there from both the active layer and from lower layers in the permafrost, apparently under the influence of thermal gradients (as predicted by Harlan (1974) and Burn and Smith (1985a & b). The bulk of the moisture appears to move down from the active layer. However, there appears to be a maximum ice content that can be produced in this way in any given substrate. Higher moisture contents can only be produced by continuous injection of water; the excess water tends to be dissipated when the injection ceases. Thus, continuous injection of moisture would be necessary to form massive icy beds.

ACKNOWLEDGEMENTS

The Terrain Sciences Division, Geological Survey of Canada, funded the work at Summit Lake, while NSERC grant A-7483 supported the other studies.

REFERENCES

Andersland, O.B. & Anderson, D.M., Eds. (1978). Geotechnical engineering for cold regions. New York: McGraw-Hill. 576 pp.

Blumstengel, W. (1988). Lobate rock glacier study, east side, Slims River Valley, St. Elias Range. Unpublished M.Sc. thesis, Department of Geography, University of Calgary.

Brown, J. & Sellman, P.V. (1973). Permafrost and coastal plain history of Arctic Alaska. In: M.E. Brittan, Ed., Alaskan Arctic tundra. Arctic Inst. of N. America Technical Paper #25. 244 pp.

Burn, C.R. & Smith, M.W. (1985a). Comment on "Water movement into seasonally frozen soils" by D.L. Kane and J. Stein. Water Resources Res., (21), 1051-1052.

Burn, C.R. & Smith, M.W. (1985b). On the origin of aggradational ice in permafrost. In: D.M. Anderson & P.J. Williams, Eds. Freezing and thawing of soil-water systems. Technical Council on Cold Regions Engineering Monograph, American Society of Civil Engineers, New York, pp. 77-84.

Cheng, Guodong. (1982). The forming process of thick layered ground ice. Scientia Sinica (Series B), (25), 777-788.

French, M.M. & Pollard, W.H. (1986). Ground-ice investigations, Klondike District, Yukon Territory. Can. J. Earth Sci., (23), 550-560.

Harlan, R.L. (1974). Dynamics of water movement in permafrost: A review. In: Permafrost Hydrology. Proceedings of a workshop seminar, Ottawa. Environment Canada. pp. 67-77.

Harris, S.A. (1982a). Distribution of zonal permafrost landforms with freezing and thawing indices. Biuletyn Peryglacjalny, (29), 163-182.

Harris, S.A. (1982b). Identification of permafrost zones using selected periglacial landforms. In: "Proceedings of the Fourth Canadian Permafrost Conference", Roger J.E. Brown Memorial Volume, H.M. French, Ed. pp. 49-58.

Harris, S.A. (1986). The permafrost environment. Totowa, N.J.: Barnes & Noble. 276 pp.

Harry, D.G., French, H.M. & Pollard, W.H. (1985). Ice wedges and permafrost conditions near King Point, Beaufort Sea coast, Yukon Territory. Geol. Surv. Can. Paper 85-1A, pp. 111-116.

Johnston, G.H., Ed. (1981). Permafrost engineering design and construction. Toronto: John Wiley & Sons. 540 pp.

Kane, D.L. & Stein, J. (1983). Water movement into seasonally frozen soils. Water Resources Res., (19), 1547-1557.

Kinosita, S., Suzuki, Y, Noriguchi, K. & Fukuda, M. (1978). The comparison of frozen soil structure beneath a high center polygon, trough and center, at Barrow, Alaska. Proc. 3rd Int. Conf. on Permafrost, Edmonton, Alta. Vol. 1, National Research Council, Ottawa. 947 pp.

Klohn Leonoff Consultants, Ltd. (1978). Dempster lateral drilling program, Vol. 1 & 2. Foothills Pipe Lines (Yukon) Ltd.

Mackay, J.R. (1956). Deformation by glacier-ice at Nicholson Peninsula, N.W.T., Canada. Arctic, (9), 218-228.

Mackay, J.R. (1959). Glacier ice-thrust features of the Yukon coast. Can. Geog. Bull., (13), 5-21.

Mackay, J.R. (1971). Ground ice in the active layer and the top portion of the permafrost. Proceedings of a seminar on the permafrost active layer. National Research Council, Ottawa. Technical Memorandum #103, pp. 26-30.

Mackay, J.R., Ostrick, J., Lewis, C.P. & Mackay, D.R. (1979). Frost heave at ground temperatures below 0°C, Inuvik, Northwest Territories. Geol. Surv. Can., Paper 79-1A, pp. 403-405.

Mackay, J.R. & Stager, J.K. (1966). Thick tilted beds of segregated ice, Mackenzie Delta area, N.W.T. Biuletyn Periglacjalny, #15, pp. 39-43.

Napoléoni, J.-G. & Clarke, G.K.C. (1978). Hot water drilling in a cold glacier. Can. J. Earth Sci., (15), 316-321.

Pollard, W.H. & French, H.M. (1980). A first approximation of the volume of ground ice, Richards Island, Pleistocene Mackenzie

Delta, Canada. Canadian Geotechnical J., (17), pp. 509-516.

Rampton, V.N. (1971). Ground ice conditions, Yukon coastal plan and adjacent areas. Geol. Surv. Can., Paper 71-1B, pp. 128-130.

Seppälä, M. (1986). The origin of palsas. Geografiska Annaler, (68A), pp. 141-147.

Washburn, A.L. (1979). Geocryology - A survey of periglacial processes and environments. London: Edward Arnold, 406 pp.

A MATHEMATICAL MODEL OF FROST HEAVE IN GRANULAR MATERIALS

D. Piper[1], J.T. Holden[2] and R.H. Jones[2]

[1]W.S. Atkins Eng. Sciences, Epsom, Surrey, U.K.
[2]University of Nottingham, U.K.

SYNOPSIS A one-dimensional model for predicting frost heave in a finite column of a saturated granular soil is presented. The model is based on the theory of secondary heave due to Miller. It embodies a quasi-static approximation for the temperature and water pressure profiles and improves and extends earlier work by the authors. This improved model is applicable to the full range of overburden pressures, including zero. Although at low overburden pressures a change to a primary heaving model is necessary as the frozen fringe disappears. The results agree well with observed measurements by a number of researchers.

INTRODUCTION

Whenever a soil is frozen, whether naturally or as part of a construction project, there is always the possibility that heave and ice lensing will occur. The modelling of this phenomena has received a considerable boost since 1970 by the increasing development of Arctic regions and the use of artificial ground freezing in construction. A number of review papers (Anderson and Morgenstern, 1973, Loch, 1980, O'Neill,1983) have set out the various ideas and theories seeking to describe this phenomena. Classes of model which have proved most successful are those theories for granular materials based on a capillary theory of ice lens growth and can be traced to the work of Everett (1961). Earlier models have been termed primary heaving models because the ice lenses were assumed to grow at the freezing front whereas, in general, ice lenses form just behind the freezing front. In addition some models do not have a proper mechanism for the initiation of a new lens. The present work is based on the work of Miller (1972,1977,1978), whose theory includes the existence of a partially frozen region below a growing lens in which a new lens may form and a proper criterion for the formation of a new lens.

The model has been quantified for one-dimensional freezing by O'Neill and Miller (1980,1985). Their formulation involved the solution of two non-linear, coupled partial differential equations and required considerable computing effort. The approach used in this paper is based on quasi-static approximations for the temperature and pore water pressure profiles and leads to the solution of two ordinary differential equations. This approach was developed by Holden (1983) and Holden et al(1985) and is similar to that used by Gilpin (1980). It is much simpler in approach and does successfully describe all the phenomena of ice lensing.

In this paper the method is applied to the freezing of a soil column of finite length. Energy and mass conservation equations are written down which link the parameters introduced by the temperature and water pressure profiles. Algebraic elimination between these equations gives two ordinary differential equations to determine the total heave and position of the freezing front. In order to ensure mass conservation across the frozen fringe the profile for the water pressure contains a parameter which is calculated from the solution by simple iteration. An important development of the model is that it has been extended to include overburden pressures down to zero. At low overburdens the frozen fringe eventually disappears and then the process becomes a primary heaving model until heaving finally ceases.

Results are given for the range of overburden pressures from 0 to 200kPa using some typical values of the physical parameters. The model is sensitive to variations in the hydraulic conductivity and also in the freezing characteristic curve.

THE RIGID-ICE MODEL OF FROST HEAVE

When a column of saturated soil is frozen from one end the column is observed to heave and there are three distinct regions of soil (see Figure 1):

1. a solid frozen region of soil containing distinct ice lenses;
2. a partially frozen region of soil (known as the frozen fringe) containing soil, ice and water;

and

3. an unfrozen region of wet soil.

During freezing, water moves up through the unfrozen soil and enters the frozen fringe to feed the ice lens at the bottom of region 1. The water is sucked towards the lens in region 2 by the large suctions which accompany decreasing temperatures and increasing ice content. The

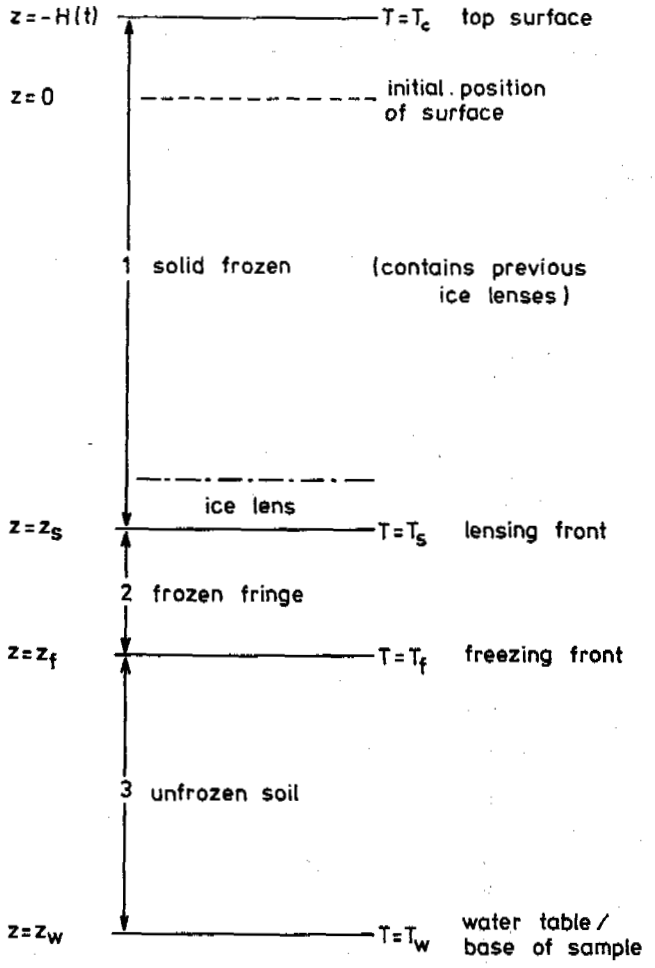

Figure 1
Schematic section through a freezing soil sample

model of this process developed by Miller (1972, 1977,1978) is termed a rigid ice-model, because the ice present in the frozen fringe is assumed to be rigidly connected to the growing ice lens. This pore ice moves through the soil by a process of microscopic regelation as heave takes place.

To describe the frost heave mechanism within the frozen fringe, a suction parameter ψ is introduced by the equation

$$\psi = (u_i - u_w)/\sigma_{iw} , \qquad (1)$$

where u_i is the ice pressure, u_w is the water pressure and σ_{iw} is the ice/water interfacial energy. ψ is a convenient parameter to use in relating ice content and hydraulic conductivity to suction in the frozen fringe and can be interpreted as a mean curvature of the ice/water interface. Using the Clapeyron equation, which relates the equilibrium values of u_i and u_w and the temperature T, the parameter ψ may be written as

$$\psi = Au_w + BT , \qquad (2)$$

where A and B are constants. The volumetric ice content θ_i is assumed to depend only on ψ (Koopmans and Miller, 1966).

Another important component of the model is the criterion for the formation of a new lens. The stresses are assumed to be isotropic. By analogy with a partially saturated soil (Bishop, 1955), the neutral stress u within the frozen fringe is calculated by the formula (Miller, 1977)

$$u = \chi u_w + (1-\chi)u_i , \qquad (3)$$

where χ is a stress partition factor. In general, u has a maximum in the frozen fringe, and it is when this maximum value reaches the overburden pressure, P, that a new lens is initiated.

APPROXIMATE PROFILES

We consider a finite column of soil that is initially at a uniform temperature of $T_i > 0$. The top surface $z = 0$ is then cooled at a given rate to a temperature of $T_c < 0$ and then held constant at this temperature. During this initial cooling period, once the surface temperature becomes negative, the freezing front moves down through the soil, ice lenses form and the soil heaves. The space coordinate, z, is measured downwards and the cumulative heave at time t is denoted by H(t) so that the surface is given by $z = -H(t)$. We denote the position of the base of the lowest lens by $z = z_s$, the position of the freezing front by $z = z_f$ and the level of the water table (which is also the bottom of the sample) by $z = z_w$. The different levels and the associated temperatures are shown in Figure 1.

Because the freezing front moves relatively slowly, the temperature profiles in both the solid frozen region and in the frozen fringe are close to linear and may be written as follows:

$$T = \begin{cases} \dfrac{z_s - z}{z_s + H} T_c + \dfrac{z + H}{z_s + H} T_s & (-H \leq z \leq z_s), \\ \dfrac{z_f - z}{z_f - z_s} T_s + \dfrac{z - z_s}{z_f - z_s} T_f & (z_s \leq z \leq z_f), \end{cases} \qquad (4)$$

where T_s and T_f are the temperatures at levels z_s and z_f respectively. The temperature ahead of the freezing front $z = z_f$ must be computed directly from the one-dimensional heat equation

$$\frac{\partial T}{\partial t} = \mu \frac{\partial^2 T}{\partial z^2} , \qquad (5)$$

where μ is the thermal diffusivity. This equation is also used to compute the temperatures during the cooling down period prior to the onset of freezing.

Profiles are also required for the water pressure in regions 2 and 3. The water pressure in region 3, the unfrozen soil, decreases linearly from zero at the water table level z_w to a small negative value u_f at the freezing front ($z = z_f$).

In the frozen fringe the water pressure decreases rapidly from u_f to a very much larger negative value u_s at $z = z_s$. An exponential curve is used which contains a parameter α which is calculated from a consideration of the mass conservation across the frozen fringe. In the previous paper (Holden et al, 1985) a quartic profile was used but it was found subsequently that this approximation was not adequate to ensure the overall mass balance across the frozen fringe.

The profiles are;

$$u_w = \begin{cases} C + D\, e^{-\alpha(z-z_s)} & (z_s \leqslant z \leqslant z_f), \\ \dfrac{z_w - z}{z_w - z_f}\, u_f & (z_f \leqslant z \leqslant z_w), \end{cases} \tag{6}$$

where $C = \dfrac{u_f - u_s \exp\{-\alpha(z_f - z_s)\}}{1 - \exp\{-\alpha(z_f - z_s)\}}$

and $D = \dfrac{u_s - u_f}{1 - \exp\{-\alpha(z_f - z_s)\}}$.

CONSERVATION EQUATIONS

The equations of the model are obtained by writing down equations of conservation of mass and energy at the lensing front and at the freezing front. The Clapeyron equation at the lensing front and Darcy's law complete the set of equations.

The energy balance equation at $z = z_s$ is

$$K_f \left.\frac{\partial T}{\partial z}\right|_{z_{s+}} - K_s \left.\frac{\partial T}{\partial z}\right|_{z_{s-}} = \rho_w L v_s, \tag{7}$$

and at $z = z_f$ is

$$K_u \left.\frac{\partial T}{\partial z}\right|_{z_{f+}} - K_f \left.\frac{\partial T}{\partial z}\right|_{z_{f-}} = -\rho_i L \theta_{if} \frac{dz_f}{dt}, \tag{8}$$

where K_f, K_s and K_u are the thermal conductivities of the frozen fringe, solid frozen region and unfrozen region respectively, ρ_w and ρ_i are the densities of water and ice respectively, L the latent heat of fusion of water, θ_{if} the volumetric ice content at $z = z_f-$ and v_s is the water flux at the top of the frozen fringe.

Substitution of the temperature profiles (4) into equations (7) and (8) gives

$$K_f \frac{T_f - T_s}{z_f - z_s} - K_s \frac{T_s - T_c}{z_s + H} = \rho_w L v_s, \tag{9}$$

$$K_u \left.\frac{\partial T}{\partial z}\right|_{z_{f+}} - K_f \frac{T_f - T_s}{z_f - z_s} = -\rho_i L \theta_{if} \frac{dz_f}{dt}. \tag{10}$$

The temperature gradient $\partial T/\partial z$ at $z = z_{f+}$ comes directly from the numerical solution of the heat equation (5). The mass balance at $z = z_s$ is

$$\rho_i (1-\theta_{is}) \frac{dH}{dt} = -\rho_w v_s, \tag{11}$$

whilst the mass balance at $z = z_f$ is given by

$$\rho_i \theta_{if} \frac{dH}{dt} = \rho_w (v_f - v_w) + (\rho_w - \rho_i)\theta_{if} \frac{dz_f}{dt}, \tag{12}$$

where θ_{is} is the volumetric ice content at $z = z_{s+}$ and v_f and v_w are the water fluxes at levels $z = z_{f-}$ and $z = z_{f+}$ respectively. Each of the water fluxes v_s, v_f and v_w is assumed to satisfy Darcy's law which has the general form

$$v = -\frac{k}{\rho_w g}\left(\frac{du_w}{dz} - \rho_w g\right), \tag{13}$$

where k is the appropriate hydraulic conductivity and the water pressure gradients, du_w/dz, come from equations (6).

The remaining equation is the Clapeyron equation applied to the top of the frozen fringe, namely

$$u_s = \frac{\rho_w}{\rho_i} P + \frac{\rho_w L}{T_0} T_s, \tag{14}$$

where P is the overburden pressure.
By direct algebraic elimination the above system of equations can be reduced to two non-linear, coupled, ordinary differential equations of the form

$$\frac{dz_f}{dt} = F(z_f, H, t; z_s, \alpha), \tag{15}$$

and

$$\frac{dH}{dt} = G_1(z_f, H, t; z_s, \alpha). \tag{16}$$

The right hand sides contain two parameters z_s and α. z_s, the position of the lensing front is constant during the growth of any one lens and α is determined by iteration from the solution itself. These ordinary differential equations for z_f and H are solved using standard numerical methods.

DETERMINATION OF α

If we consider the total mass, M, of water and ice contained in a control volume between z_0 and z_1 (where z_0 is in the ice lens and z_1 below the freezing front) the rate of change of M is equal to the difference between the rate at which mass enters and leaves the control region. We obtain the expression

$$-\rho_w v_w - \rho_i \frac{dH}{dt} = \int_{z_s}^{z_f} (\rho_i - \rho_w) \frac{d\theta_i}{dt} dz + (\rho_i - \rho_w)\theta_{if} \frac{dz_f}{dt}. \tag{17}$$

It should be noted that this equation is not the sum of the mass balance equations (11) and (12). This is because the frozen fringe is growing, the ice content is increasing, and only part of the water entering the frozen fringe at $z = z_f$ actually feeds the growth of the lens. To apply equation (17) in a straightforward manner to calculate the exponent α it is necessary to approximate the integral term. Figure 2 illustrates two ice content profiles separated by

a time interval dt and if we assume that the curves are nearly parallel then we may write

$$\int_{z_f}^{z_f} \frac{d\theta_i}{dt}\, dz \approx (\theta_{is}-\theta_{if})\frac{dz_f}{dt} . \qquad (18)$$

Using this approximation equation (17) may be expressed as

$$\alpha \approx \frac{1-\exp\{-\alpha(z_f-z_s)\}}{k_s(u_s-u_f)}\left\{k_0(1-\theta_{is})\left(\frac{u_f}{z_w-z_f}+\rho_w g\right) - \rho_w g k_s - g(\rho_w-\rho_i)(1-\theta_{is})\theta_{is}\frac{dz_f}{dt}\right\}. \qquad (19)$$

Written in this form the value of α can be obtained by simple iteration.

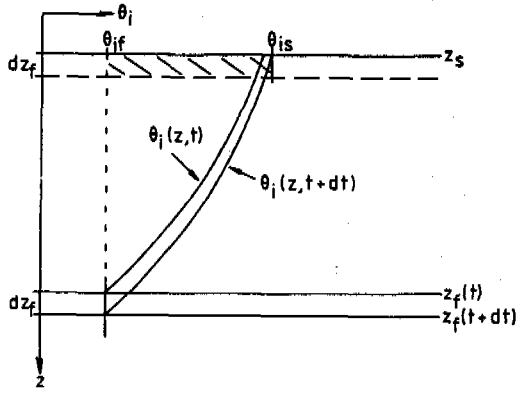

Figure 2
Ice content profiles in frozen fringe at times t and t+dt

LOW OVERBURDEN PRESSURES

The model as described above works well for overburden pressures greater than, say, 30kPa when the self-weight of the soil is negligible. The self-weight is easily included by replacing the constant overburden pressure P by the total pressure P' at the base of the lens given by

$$P' = P + \rho_i g H + \rho_s g z_s, \qquad (20)$$

where ρ_s is the density of the frozen soil between the lenses. At the lower overburden pressures where self-weight is significant the frozen fringe may disappear. This occurs after the formation of the final or terminal lens when the temperature profile below the freezing front is close to linear and, because the sample is still heaving, dz_f/dt becomes negative. Then it is possible for z_f to become equal to z_s before the growth of the terminal lens, and hence the heave, stops.

In the absence of a frozen fringe, the base of the lens is also the extent of freezing and this level is referred to using the subscripts "ss". The freezing column now contains only two distinct regions, the solid frozen and the unfrozen, the boundary between them being at level $z = z_{ss}$. Since a near steady state exists the energy balance at this level may be written

$$K_u \frac{T_w - T_{ss}}{z_w - z_{ss}} - K_f \frac{T_{ss} - T_c}{z_{ss} + H} = \rho_w L v_{ss}. \qquad (21)$$

(compare equation (9)). Without the frozen fringe there is no ice just below the lens and the mass balance equation becomes

$$\rho_i \frac{dH}{dt} = -\rho_w v_{ss}. \qquad (22)$$

The water flux towards the ice lens is described by Darcy's law

$$v_{ss} = -\frac{k_0}{\rho_w g}\left(\frac{-u_{ss}}{z_w - z_{ss}} - \rho_w g\right) . \qquad (23)$$

The Clapeyron equation has the same form as before with P replaced by P' (Equation (14)). The equations (21), (22), (23) and (14) form a system of four equations in the four unknowns T_{ss}, v_{ss}, u_{ss} and H, from which by elimination a single ordinary differential equation of the form

$$\frac{dH}{dt} = G_2(H) , \qquad (24)$$

is easily found.

NUMERICAL RESULTS

The computer simulations were performed for a soil column of height 150mm and initially at a temperature of 4°C. The top surface was cooled at a constant rate down to -6°C and then held constant. The freezing temperature, T_f, was assumed to be constant and freezing begins when the top surface reaches this temperature. The two ordinary differential equations (15) and (16) were solved using the standard Runge-Kutta formulae. The right hand sides of equations (15) and (16) require a knowledge of the temperature gradient ahead of the freezing front and this was calculated using a Crank-Nicolson finite difference method based on a convected mesh (Murray and Landis, 1959). A simple search procedure was used to find the maximum of the neutral stress u in the frozen fringe. During the formation of a lens, z_s remains fixed and the lens grows at this level until the maximum value of u reaches the overburden P when a new lens forms. At this time, z_s is set equal to the position of the maximum of u and the cycle continues with the growth of the new lens. At low overburden pressures, when the final lens has formed and the frozen fringe has disappeared, equation (24) is solved until the heave finally stops. The physical data used in the computations are given in the Appendix.

To demonstrate the overall capability of the model the heave was calculated for a range of overburden pressures up to 200kPa and these heave curves are shown in Figure 3. The shape of these curves is as expected with initially a high heave rate which decays to zero with time and also a decrease of heave with overburden.

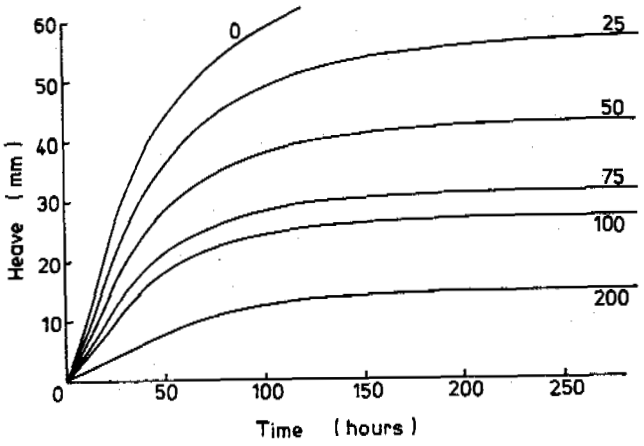

Figure 3
Heave versus time curves for different overburden pressures (values in kPa)

One aspect of the heaving mechanism which is not apparent in Figure 3 is the cyclic variation in heave rate and frost penetration rate with the formation of each lens. This is shown in Figure 4 where the heave rate is plotted against penetration rate for the last few lenses (at P = 100kPa). The plot begins at point a_1 and

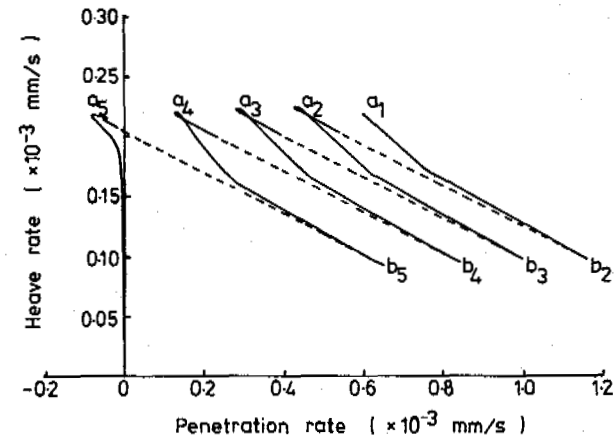

Figure 4
Heave rate versus penetration rate, for the closing stage of a simulation (P=100kPa)

between a_1 and b_2 a lens is growing and the frozen fringe extends beneath it. At b_2 a new lens is initiated and z_s jumps to a new value. As a result there is a sudden change in the heave rate and penetration rate to point a_2. Between a_2 and b_2 this new lens grows. This cycle repeats until the final lens is initiated at b_5 and the penetration rate becomes negative. Then the two rates eventually drop down to zero. This behaviour is reflected in Figure 5 where the heave curve is shown on an enlarged scale.

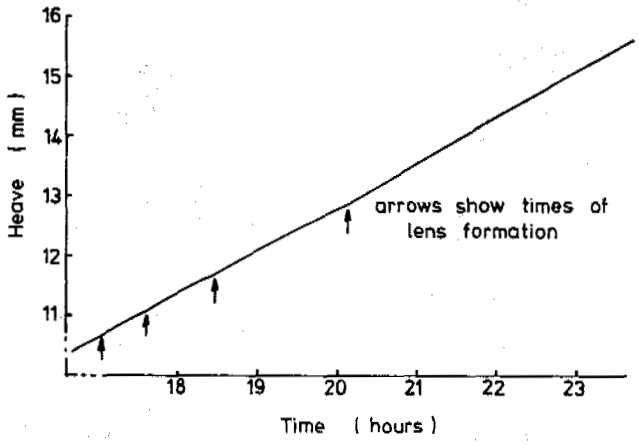

Figure 5
Heave versus time showing initiation of four ice lenses (P=100kPa)

DISCUSSION

The mathematical model of frost heave described in this paper has been found to be numerically stable and robust. Some of the earlier difficulties with this model were due to poor modelling of the soil freezing characteristic $\theta_i(\psi)$ and attention is drawn to the importance of adequate modelling of this function. Subsequent parametric studies have indicated that the predicted heave is insensitive to variations in thermal conductivity. In contrast the influence of variations in the hydraulic conductivity just below the lens is considerable. Unfortunately this parameter is very difficult to measure. The main features of the results agree with the observations of, for example, Konrad and Morgenstern (1980), McCabe and Kettle (1983) and Berg et al (1980). Several other researchers have traced only the linear portion of the heave versus time curve before terminating their experiments (e.g. Penner and Ueda, 1977, Loch and Kay, 1978). The small scale variations in heave rate depicted on Figure 5 do not appear to have been reported in the literature probably because measurements are usually taken at discrete time intervals which are too large to show these variations.

CONCLUSIONS

A robust quasi-static model of frost heave has been developed which simulates the frost heave process and is numerically efficient and stable. The general agreement of the model predictions with observed behaviour provides further support for Miller's theory of secondary heave. The model is sensitive to variations in certain critical parameters, particularly the variation of ice content and permeability with suction. Unfortunately these characters are difficult to measure experimentally.

REFERENCES

Anderson, D.M. and Morgenstern, N.R. (1973). Physics, chemistry and mechanics of frozen ground: a review. Second Int.Conf. on Permafrost, North American Contribution, Nat. Acad. Sci. 257-288.

Berg, R., Ingersoll, J. and Guymon, G.(1980). Frost heave in an instrumented soil column. Cold Regions Science and Technology,(3), 211-221.

Bishop, A.W. (1955). The principle of effective stress. Lecture delivered in Oslo, reprinted in Teknisk Ukeblad, (39),859-863, (1959).

Everett, D.H. (1961). The thermodynamics of frost damage to porous solids. Trans. of the Faraday Soc., (57), 1541-1551.

Gilpin, R.R. (1980). A model for the prediction of ice lensing and frost heave in soils. Water Resources Research, (16), 918-930.

Holden, J.T. (1983). Approximate solutions for Miller's theory of secondary heave. Proc. Fourth Int. Conf. on Permafrost, Fairbanks, Alaska, 498-503.

Holden, J.T., Piper, D. and Jones, R.H. (1985). Some developments of a rigid ice model of frost heave. Proc. Fourth Int. Symp. on Ground Freezing, Sapporo, Japan, (1),93-99.

Konrad, J.M. and Morgenstern, N.R. (1980). A mechanistic theory of ice formation in fine grained soils. Can. Geotech. J.,(17), 473-486.

Loch, J.P.G. (1980). Frost action in soils. State of the art. Second Int. Symp. on Ground Freezing, Trondheim, Norway. Preprints, 581-596. (Also Engineering Geology, (18), (1981), 213-224.)

Loch, J.P.G. and Kay, B.D. (1978). Water redistribution in partially frozen, saturated silt under several temperature gradients and overburden loads. Soil Science Society of America J., (42), 400-406.

McCabe, E.Y. and Kettle, R.J. (1983). The influence of surcharge loads on frost susceptibility. Proc. Fourth Int. Conf. on Permafrost, Fairbanks, Alaska, 816-820.

Miller, R.D. (1972). Freezing and heaving of saturated and unsaturated soils. Highway Research Record, (393), 1-11.

Miller, R.D. (1977). Lens initiation in secondary heaving. Proc. Int. Symp. on Frost Action in Soils, Lulea, Sweden, (2), 68-74.

Miller, R.D. (1978). Frost heaving in non-colloidal soils. Proc. Third Int. Conf. on Permafrost, Edmonton, National Research Council of Canada, (1), 707-713.

Murray, W.D. and Landis, F. (1959). Numerical and machine solutions of transient heat conduction problems involving melting or freezing. J. Heat Transfer, Trans.ASME(c), (81), 106-112.

O'Neill, K. (1983). The physics of mathematical frost heave models: a review. Cold Regions Science and Technology, (6), 275-291.

O'Neill, K. and Miller, R.D. (1980). Numerical solutions for a rigid ice model of secondary frost heave. Second Int. Symp. on Ground Freezing, Trondheim, Norway, Preprints, 656-669. (Also CRREL Report (82-13),(1982). Hanover, N.H.).

O'Neill, K. and Miller, R.D. Explorations of a rigid ice model of frost heave. Water Resources Research (21), 281-296.

Penner, E. and Ueda, T. (1977). The dependence of frost heaving on load application. Proc. Int. Symp. on Frost Action in Soils, Lulea, Sweden, (1), 92-101.

Thompson, J.D. (1981). Subgrade effects on the frost heave of roads. Ph.D. thesis, University of Nottingham, U.K.

APPENDIX

Following O'Neill and Miller (1980,1985) the form used for the stress partition factor χ is

$$\chi = (1 - \theta_i/\theta_0)^{1.5} \quad , \tag{25}$$

where θ_0 is the porosity, and that for the hydraulic conductivity k is

$$k = k_0(1 - \theta_i/\theta_0)^7 \quad , \tag{26}$$

where k_0 is the hydraulic conductivity of saturated unfrozen soil. It should be noted that O'Neill and Miller also use a power of 9 in this formula. The form of the ice content θ_i as a function of ψ is based on data of Thompson (1981) for Attenborough silt. The data is shown in Figure 6 together with straight line fits to the data.

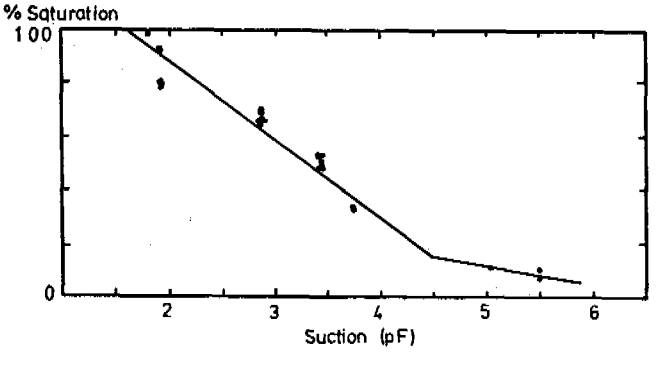

Figure 6
Soil suction data for Attenborough silt, with straight line fits

In the units of this paper the ice content is written as

$$\theta_i = \begin{cases} 0.1179(\log_{10}\psi) - 0.5583 & (\psi \leqslant 4.25 \times 10^7) \\ 0.0198(\log_{10}\psi) + 0.19, & (\psi > 4.25 \times 10^7) \end{cases} \quad (27)$$

The values for the physical constants we use are:

$K_f = 4 Wm^{-1}{}^0C^{-1}$, $K_s = 4 Wm^{-1}{}^0C^{-1}$,

$K_u = 3 Wm^{-1}{}^0C^{-1}$, $\mu = 1.07 \times 10^{-6} m^2 s^{-1}$,

$\rho_w L = 3.35 \times 10^5 kJm^{-3}$, $\rho_i L = 3.072 \times 10^5 kJm^{-3}$,

$\rho_w g = 9.81 kNm^{-3}$, $\rho_i g = 8.996 kNm^{-3}$,

ρ_w/ρ_i 1.0905 , $\sigma_{iw} = 0.0331 Nm^{-1}$,

$T_0 = 273.15^0 K$, $\theta_0 = 0.4$,

$k_0 = 5 \times 10^{-9} ms^{-1}$, $T_f = -0.02^0 C$.

ELECTRIC CONDUCTIVITY OF AN ICE CORE OBTAINED FROM MASSIVE GROUND ICE

Horiguchi, Kaoru

Institute of Low Temperature Science, Hokkaido University, Sapporo, Japan

SYNOPSIS Various kinds of ground features such as polygon, pingo and massive ground ice body are commonly observed in the arctic area, especially around Mackenzie Delta, N.W.T., Canada. As for the massive ground ice body, the origin and the mechanism of formation still remain arguable. We have observed distinctive spikelike projections in a profile of electric conductivity of an ice core against depth. In this paper, I will discuss the origin of high electric conductivity, the specific surface area and morphology of the sediment within the massive ground ice body. We suggest that some sediments come from tefra.

INTRODUCTION

Various kinds of ground features such as polygon, pingo and massive ground ice body are commonly observed in the arctic area. As for the massive ground ice body(Mackay 1971, French 1976), the origins and the mechanisms of formation still remain auguable.

From data of a massive ground ice body obtained during the research expedition(Fujino et al. 1983), we observed distinctive spikelike projections in a profile of electric conductivity of an ice core against depth. The electric conductivity is mainly determined by free ions in a specimen. Some projections of the massive ground ice body have a small amount of sediment, and other portions have a look of relatively pure ice. Massive ground ice bodies are commonly observed in the coastal region. Then if the distribution of free ions does not depend upon the existence of sediment, there is a possibility that they originated in sea water and deposition on the surface of the ground ice body when it was formed.

Therefore, in order to clarify the local portion where free ions exist, the electric conductivity of a massive ground ice body was investigated in detail. And also the specific surface area and morphology of the sediment were determined by a method using the differential scanning calorimeter(DSC)(Horiguchi 1985) and the scanning electron microscope(SEM), respectively.

SAMPLING

Samplings were made from a massive ground ice body, the location of which is shown by • in Fig.1, along the seacoast about 4.5 km southwest of Tuktoyaktuk, Mackenzie Delta, N.W.T., Canada. The detailed locations of sampling sites are shown by w-1, w-2 and w-3 in Fig.2. Ice samplings were collected between late February and early of March 1985, using a newly designed electro-mechanical core-drill. At site w-3, the depth was about 22 m including a 40-cm-thick

Fig.1 Location of massive ground ice

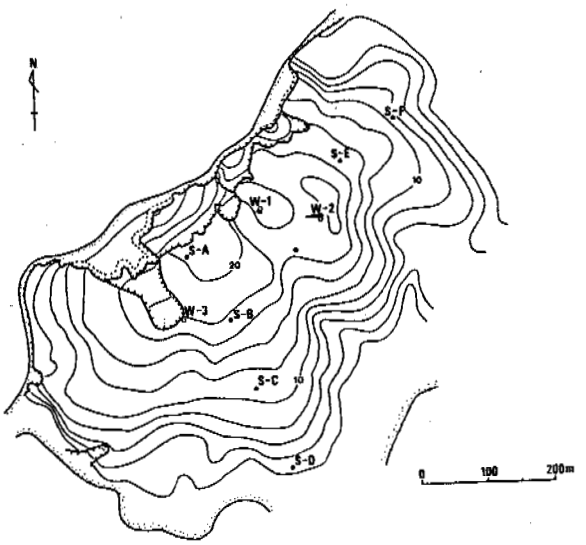

Fig.2 Sampling sites

sand layer of the bed. All of ice cores were arranged and labeled in serial order, put in refrigerated containers and transported to the cold laboratory of the Institute of Low Temperature Science, Hokkaido University.

Each piece was cut into halves along the vertical axis of the core. One half was cut perpendicular to the axis at an interval of 10 cm, from which samples were prepared for the determination of electric conductivity and so on. Sediment in an ice sample was collected to prepare for the determination of specific surface area and for the observation morphology.

MEASUREMENTS

As for the measurements of electric conductivity of the massive ground ice body, an ice sample about 50 g was put in a vinyl bag and melted. Then, the melted water, together with sediment in it, was poured into a 50 ml vial with a cap. The electric conductivity of the melt water was measured after the deposition of the sediment. A portable conductivity meter(TOA Co., Ltd., Model CM-1K) was used to measure the electric conductivity at room temperature.

According to the conventional method to measure the surface area, we need several grams of sediment in the dry state. However, each ice sample contains a little sediment, usually less than several tens of milligrams. Accordingly, we used a newly developed DSC method to measure the surface area of the sediment.

This method is based on the following principle: A soil particle carries an electric charge on its surface as a result of the breaking up of bonds at its surface, isomorphous substitution and so on; therefore, it attracts ions to the surface in order to achieve overall electrical neutrality. The ions which exist with water molecules and attract other ions to the surface are partly located in a layer more or less fixed in the proximity of the particle surface, and partly diffused in their distribution some distance away from the particle surface. Then, water near the surface of the soil particle does not freeze at 0°C, because the potential energy of the water is decreased, while water forming the diffused layer can be frozen at temperatures lower than 0°C. On the other hand, water forming a mono-molecular layer on the surface of the soil particle does not freeze at any low temperature.

When a specimen is being warmed at a constant rate, we need to add a quantity of heat to melt ice in the frozen sediment. At that time, if we can measure the quantity of heat added, it is possible to calcualte the total mass of ice, namely, the amount of freezable water in the sediment. Then, the difference between the total amount of water and the amount of freezable water correspondings to the amount of the water which constitutes a mono-molecular layer coating all the surface of the sediments. DSC Model SSC-580(Dainiseiko Co., Ltd.) with a cooling system was used to measure the quantity of heat added to melt ice. Using several kinds of specimens with a given specific surface area, we obtained the following relationship:

$$S = 3.13 \times 10^{-3} W$$

where S is the specific surface area in m^2/g and W is the amount in grams of the water constituting a mono-molecular layer per gram of the dry specimen. We used the DSC method to evaluate the value of W for each sediment; then, the specific surface area S was estimated.

DISCUSSIONS

In order to examine the effect of sediment on electric conductivity, the dry weight of the sediment was measured after it was dried in an electric oven for one day at 110°C. According to the amount in terms of the dry weight obtained, the specimens were classified into three groups A, B and C. The specimens in groups A, B and C contained the amount of sediment in the ranges less than 13.4 mg, between 13.4 and 32.9 mg and more than 32.9 mg per melted water of 50 ml, respectively.

Total numbers of specimens in groups A, B and C are 100, 56 and 47, respectively, as shown in Table 1. The last column of percentage in the table represents the ratio of the number of each group to the total number per every 10 μs/cm of electric conductivity. The ratio is also shown in Fig.3 for each group. The abscissa shows the electric conductivity(μs/cm), and the ordinate shows the percentage which is occupied by each group. Mark ○, △ and ● represent groups A, B and C, respectively. This reveals that the melt water containing a comparatively large amount of sediment has a large value of electric conductivity of the melt water mainly depends upon the amount of sediment in it. Though the absolute amount of sediment in the melt water is small, the conductivity is relatively large compared with that of suspension with the same amount of clay, such as kaoline. The electric conductivity is decided by the number of free ions which come from the

Electric conductivity (μs/cm)	Number in each group			Percentage of each group		
	A	B	C	A	B	C
0 - 10	25	0	0	100	0	0
11 - 20	49	5	0	90	10	0
21 - 30	16	19	0	32	68	0
31 - 40	4	17	7	14	61	25
41 - 50	3	6	9	17	33	50
51 - 60	1	4	3	12	50	38
61 - 70	0	0	6	0	0	100
71 - 80	0	2	5	0	29	71
81 - 90	0	0	5	0	0	100
91 - 100	0	1	3	0	25	75
101 - 120	0	1	3	0	25	75
121 - 140	1	0	2	33	0	67
141 - 160	0	0	3	0	0	100
161 - 180	0	0	1	0	0	100
181 - 200	1	0	0	100	0	0
> 201	0	1	3	0	25	75
Total number	100	56	47			

Table 1 Numbers and percentages of melted ice samples of groups, A, B and C against every 10 μs/cm of electric conductivity

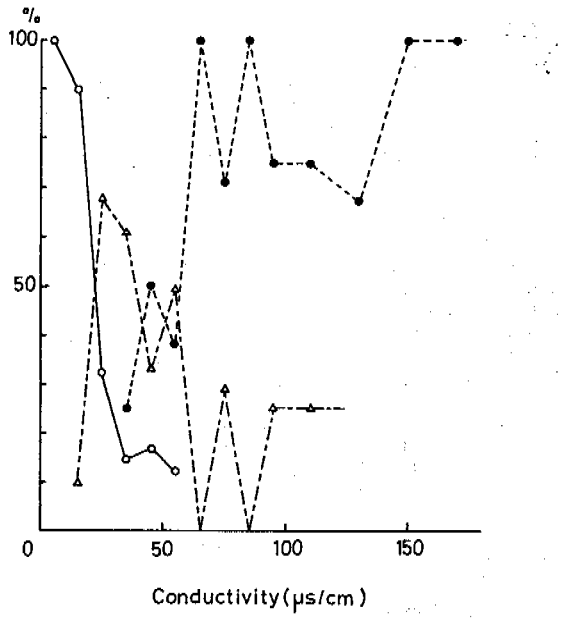

Fig.3 Distribution of electric conductivity
○ : group A, △ : group B, ● : group C

surface of sediment. Then, it is suggested that each of the sediment has a larger specific surface area than kaoline. Then, the kinds of sediment were collected from the melted water to measure their surface areas. Each one is located at a respective depth from the ground surface. The depth and specific surface area are shown in Table 2 for each sediment. The specific surface area of kaoline is about several tens of square meters per gram. When the obtained value of sediment is compared with that of kaoline, the sediment is ten times that of kaoline, except for the sediment at the depth of 19.90-20.00 m, which is near the bottom of the massive ground ice body.

Clay is defined as a particle with a diameter less than 2 μm, kaoline being a typical clay mineral. From the viewpoint of the specific surface area, it is considered that each of the sediment consists of very fine particle. Then, to confirm it the pictures of the sediment were

Depth (m)	Specific surface area (m^2/g)
0.90 - 1.00	209
1.20 - 1.30	103
2.00 - 2.10	195
5.10 - 5.20	140
5.60 - 5.70	256
6.80 - 6.90	310
8.70 - 8.80	276
8.80 - 8.90	283
15.30 - 15.40	198
19.90 - 20.00	45

Table 2 Specific surface area of sediment

taken by the scanning electron microscope. Judging from their picture, however, the sediment consists of silt with an irregular surface, and there are some differences in surface morphology depending upon the depth where each sediment is located. Two typical pictures among them are shown in Fig.4. Pictures A and B are taken from the sediment collected at the depth of 1.20-1.30 m and 8.80 -8.90 m, respectively. The sediment of picture A has the specific surface area of 103 m^2/g, which is about one-third that of the sediment of picture B. The two differ in surface morphology. Namely, the sediment in picture B has many small holes on the surface of the particles as you can see. At present, we cannot say for sure where such sediment came from and when it deposited in the massive ground ice body. However, the actual fact that pumice stone originated from a volcanic eruption and has many small holes on its surface suggests that the particles with small holes on their surface may have come from tefra in the vastly remote past.

I wish to thank Prof. K. Fujino for stimulating my interest in this field. I wish to express my thanks to PCSP at Tuktoyaktuk and Inuvik Research Center, Canada, for helpful support during the expedition. This paper is a contribution from the Institute of Low Temperature Science and is published with the approval of the Director of the Institute.

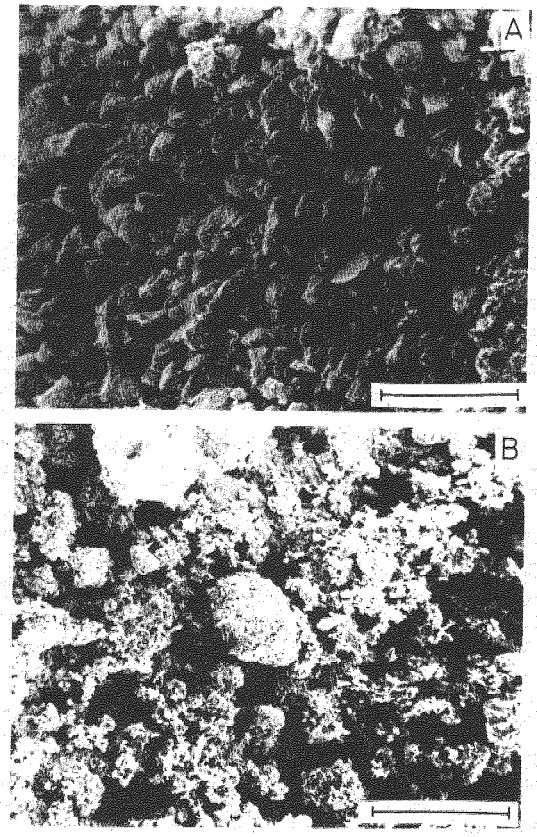

Fig.4 Surface morphology. Scale: 100 μm

REFERENCES

Mackay, J.R. (1971). The origin of massive ice body, Western Arctic, Canada. Proc. 2nd Internat. Conf. on Permafrost, North American Contrib. Yaktuk, U.S.S.R., 223-228.

French, H.M. (1976). The periglacial environment. Longman Group Ltd., London, 309pp.

Fujino, K., K. Horiguchi, K. Shinbori and K. Kato (1983). Analysis and characteristics of cores from a massive ice body in Mackenzie Delta, N.W.T., Canada. Proc. 4th Internat. Conf. on Permafrost, National Academy press, Washington, D.C., 316-321.

Horiguchi, K (1985). Determination of unfrozen water content by DSC. Proc. 4th Internat. Symposium on ground freezing, Sapporo, Japan, 33-38.

PHYSICAL-CHEMICAL TYPES OF CRYOGENESIS

V.N. Konischev, V.V. Rogov and S.A. Poklonny

Moscow State University, Permafrost Institute Academy of Science, USSR

ABSTRACT. Cryogenic weathering of principle rock-forming minerals in different physical-chemical environments is disscussed in present report.Datum are based on experiments with different fractions of quartz,albite and labradorite.The experiments showed that the lower quartz stability compared to feldspar under cryogenic condition is preserved in any pH values.But cryogenic disintegration is a little bit more active in acidic environment than in alkaline.

INTRODUCTION AND THEORY

Specificity of fine-grained sediments composition in cryolithozone is determined by the peculiarity of cryogenic stability of rockforming minerals compared to minerals stability seria in warm climatic conditions.The principle process of cryolitozone is desintegration of primary minerals during phase water-ice changes.Abroad programme of experiments gave a chance to find the limits of cryogenic disintegratiom of major rock-forming minerals.For quartz,amphibole and pyroxen it appeared to be 0,05-0,0Imm,for feldspar unchanged by chemical influence - 0,I-0,05mm,for biotite - 0,25-0,I mm,for muscovite - 0,5-0,25mm (Konischev,I98I) In contrast to the known mineral stability row in warm climatic conditions the cryogenic row has its peculiarities.The fundamental peculiarity of this row is the lower quartz stability compared to unchangable feldspar and shistous silicates.

The result of cryogenic disintegration modelling in laboratory appeared to have good correlation with mineralogical and chemical composition of sediments of various genesis,formed in different climatic condition - Central and Northen Yakutia,the Bolshezemelskaya tundra,the Russian plain,the Middle Asia and the Spitsbergen Archipelago.Differential studies of mineralogical and chemical composition according to separate granulometric fractions showed cryolitozone sediments are characterized by maximum content of debris quartz and SiO_2 (chemical analysis) in fraction 0,05mm.On contrast monotonous decreasing of quartz and SiO_2 content from coarse to fine granulometric fraction is observed.The minimum fraction Al_2O_3 and Fe_2O_3 content in cryolitozone is found in coarse aleurite (0,05-0,0Imm).In warm and moderate climatic conditions the distribution of this components is significally different - their content grows from sand to clay fraction. In order to find cryogenic phenomenom in the sediments composition using recommended approach of natural strata analysis character of distribution according to granulometric spectrum of minerals or chemical components must be considered not the values of their absolute content.The mineralogical essense of cryogenic disintegration process is to the most simple attribute forms of hypergenezis.But the nature of cryogenic disintegration process is rather complicated and attribute to physical-chemical type.The determining role in fine-grain cryogenic mineral disintegration plays their specific surface energy (SSE).The form of SSE influence on the existence of protective role of unfrozen water film.This was proved by experimental freezing and thawing of monomineral (quartz, feldspar and ect.) granulometric fractions of different size in various temperature and moist regimes of phase transformation of water into ice (Konischev,Rogov,I983).

Natural conditions of cryogenic mineral disintegration prosess are significantly heterogeous.From this point of view it is enough to consider the greatest permafrost zone of Eurasia.The broad spectrum of natural zones from polar deserts and tundra at the North to steppes and deserts at the South is represented at the territory with cryogenic disintegration phenomenon.The magnitude of natural conditions of cryogenic mineral disintegration coused vertical nature differentiation is also broad.The modelling of criogenic transformation of substances enable to find different mineral reaction to thermic conditions of freezing.The influence of grain size,moisture content and dinamic of cryogenic disintegration process were also studied (Konischev,I98I).But the significance of physical-chemical environments (pH-values) for cryogenic evolution of mineral matter needs further investigations.

EXPERIMENTS AND RESULTS

The aim of the report is the analysis of cryogenic disintegration of principle rockbuilding minerals (quartz and feldspar) in physical-chemical environment characterized by different pH-values.Formulating the task of the investigation,we considered two premises.First,it is known,that the value of the surface energy of

minerals is determined not only by their crystalline-chemical features, but by the characteristics of the physical-chemical environment (for example pH-value) in which they exist. Second, the real heterogenity of physical-chemical environment at the territory of the cryolithozone enables to detail the manifestation of cryogenic processing of minerals in different natural regions.

Seria of experiments were held to study the influens of pH-value of the pore solution on the course of cryogenic destruction. The pH-value was set by preparing of alcaline (pH 9 - IO,5), neutral (pH 6,5-7,0) and acidic (pH 3,5-4,0) solutions, composed by the mixture of phosphoric, acetic and boric asids (concentration - 0,04M) and 0,2H solution of NaOH. This mixture was chozen due to relative stability of pH-values during the experiment. The modelling of cryogenic weathering was performed by cycling conditions of freezing-thowing out (t=-20÷+20) for samples of artifical fractions of quartz, albite and labradorite (0,5-0,25 and 0,25-0,I mm) and natural sand from Lyubertzy (fraction 0,5-0,25mm). In order to make comparison similar experiments were feld simultaneously with the same fractions using distilled water as pore solution. The sample weight was 30g; the number of cycles of freezing-thowing out - 50. The influence of cryogenic processes on minerals was estimated according to granulometric changes of samples and was manifested in increasing of finer minerals fractions. We do not show the tables of granulometric composition for shot. The evaluation of dispersion changes is based on diagram analysis. The vertical line is the content in percent of the newformed (more disperse) fractions. For experiments with samples of fractions 0,5-0,25mm this is practically (97-99,5) fraction of 0,25-0,Imm, and for samples of fractions 0,25-0,Imm - 0,I-0,25 mm.

Pore solution concentration at the first experiment with mineral fraction 0,25-0,Imm was 0,I-0,I4 g/l. Due the fact, that the solution was not changed during the experiment, pH-values changed with the increasing of the namber of cycles of freezing-thowing out turning progressively to neutral. The analysis of the granulometric composition of samples before and after the experiment (fig.IA) showed that in any pH-values quartz remains to have lower stability than feldspar; it desintegrate neavly two times more intensively than feldspar. Among the latter labradorite appears to be a little but more stable than albite. If there is need to consider stability of each mineral in connection with pH-values then quartz has lower stability in acidic environment than in neutral or alkaline and albite - on the contrary is more stable. Labradorite appeared to be more stable in neutral environment than in acidic or alkaline.

The difference of the second experiment from the first one was that the pore solution concentration was greater - 0,5 g/l and the fraction of 0,5-0,25 mm was processed. It is clealy seen (fig.IB) that mineral disintegration became lower at the same correlation between quartz and feldspar. The quartz correlation with different pH-values remained the same. Disintegration albite appeared to be greater in acidic environment as for labradorite it was greater in alkaline environment.

The difference of the third experiment was that the pH-value was preserned during the experiment by changing the used solution after several cycles by a fresh one. The solution concentration was similar to that of in the first experiment. This experiment showed that even in such conditions quartz appears to a less stable mineral than feldspar, though quartz disintegration appeared to be significantly (nearly 4 times) lower than in the first experiment and even more low than in samples, where distilled water has been used as pore solution. The same is true for feldspar, though the difference of disintegration of these minerals under the conditions of distilled water and solutions mixture was only two times lower. Correlation within the pH-values in this experiment was similar for all minerals - they are more quickly destroyed in acidic than in alkaline environment. Only quartz reveals higher disintegration in neutral environment compared to other (fig.IC).

The fourth experiment was similar to the third, but fraction of 0,5-0,25mm was processed as a sample and compared to natural sand of the same fraction from Lyubertzy. The granulometric analysis showed (fig.ID) the maximum for all experiments disintegration degree for minerals, but the structure of values of the newformed fractions was practically the same as in the third experiment, excluding labradorite, which appeared to be more stable in a alkaline environment compared to acidic. It must be mentioned that the natural sand from Lyubertzy proved to have much lower stability than the artifically prepared fractions. The peculiarity of this experiment is also the following: as in the third experiment the process of disintegration of sand and quartz was more intensive with distilled water than solution, but the difference was about several percents.

One of the authors conductered similar experiments with different quartz and feldspar fractions using KOH and HCL as pore solution with a broad range of pH-values. It was found out that maximum destraction of quarts as well as feldspar is observed in the intervall of pH-value 5,5 and 8, the minimum - at pH - 7, that the influence of the pH-value on the course of cryogenic disintegration is not connected with the pore solution composition.

CONCLUSION.

These experiment give new data, supporting the previously received fact (Konishev, Rogov, Scshurina, I977; Konishev, I98I) of the lower quartz stability compared to feldspar in cryogenic processes. This regularity is preserved in any case of presence of ions in pore solution up to the concentration 0,5 g/l. Alongside with this the experiments show that the increase of the ions content in pore solution due to concentration increase or change of the used solutions by fresh ones significantly retard the process of cryogenic disintegration.

The received data support the idea of protective role of unfrozen water in the course of mineral disintegration during phase water - ice transformations (Konishev, I98I), because

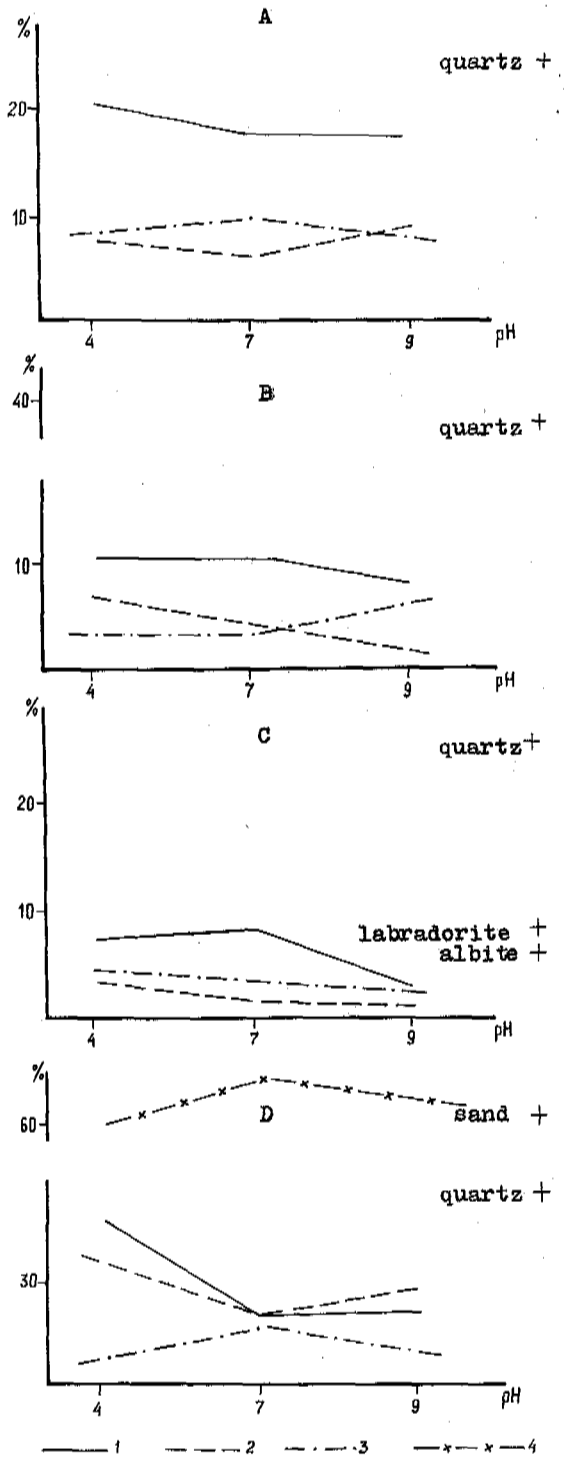

Fig.I Distribution of the newformed fractions during freezing-thowing out decording to pH-values.
A,C - for fraction of 0,25-0,Imm.
B,D - for fraction of 0,5-0,25mm.

I - quartz, 2 - albite, 3 - labradorite, 4 - the sand from Lyubertzy.

it is known that their thickness increases with the value growth of the electrolyte concentration. This is particulary true for quartz and is explain by the fact that it has the lowest thickness of the unfrozen water film among the discussed minerals and that is reason why even small change of its size is reflected in the process of cryogenic weathering more than in other minerals.
As far as regularities of minerals destruction connected with pH-values changes are conserned it must be mentioned that higer degree of disintegration for quartz occurs in acidic environment that in alkaline. Alongside with this disintegration in neutral environment may be lower as well as higher than in acidic or alkaline. Due to the fact that the intensity of mineral disintegration is in proportion to the thickness of the unfrozen water film of the corresponding fraction. In accord data of the 3 and 4 experiments it is to suggest that with the increase of quartz disintegration the difference in destruction at various pH-values would approximate the parabolic relationship of distribution of boundary water films thickness in fine quartz fraction according to pH-values as it has been described by Tchernoberezsky Yu.N., etc. (I979), with the minimum for neutral pH-values. But there is still a problem with the limits of mineral disintegration at different pH-values. Apparently further investigation of more fine fractions behaviour of the minerals mentioned are needed.

REFERENCES

Konischev V.N.,Rogov V.V.,Scshurina G.N. Vliyanie criogennih factorov na pervichnie minerali. (I976). Sb. Problemi criolytologii. (5), 50-60, Moscva.

Konischev V.N. (I98I). Formirovanie sostava dispersnih porod v criolytosfere. Nauka, Moscva.

Tchernoberezsky Yu.M. (I979). Otsenka tolschini granichnih sloev po dannim ustoichevosti i agregatsii chastits v vodnom zole kvartsa. Sb. Poverhnostnie sili v tonkih plenkah. 67-7I, Moscva.

TEMPERATURE OF ICE LENS FORMATION IN FREEZING SOILS

J.-M. Konrad

Department of Earth Sciences, University of Waterloo, Waterloo, Ontario N2L 3G1

SYNOPSIS The computer-controlled "ramped freezing" mode associated with the X-ray photography technique developed at the National Research Council of Canada by Penner was used to study the changes of the temperature at the face of a growing ice lens during transient freezing. The temperature at ice lens initiation is not a constant for a given soil, but is dependent upon the rate of cooling of the current frozen fringe. For Devon silt, freezing under an applied pressure of 50 kPa, the temperature at ice lens formation changed from -0.28 to -0.20°C when the rate of cooling decreased from 0.54 to 0.11°C/day. The experimental data also suggest that the difference between the maximum and minimum ice lens temperature increased from -0.022 to -0.064°C for the same variation of the rate of cooling.

INTRODUCTION

Konrad and Morgenstern (1980, 81, 82) proposed a comprehensive engineering theory of frost heave based on the concept of the segregation potential, SP. Excellent agreement was found between the prediction of frost heave of a buried chilled pipeline and that observed in long-term full-scale experiments at a test site in Calgary, Canada. The proposed model is based on average properties of the current frozen fringe and cannot therefore predict the actual ice structure in the field, although it can provide the average ice content with depth. It was established that SP is dependent upon applied load, rate of cooling and suction at the frost front. Since SP is directly related to the temperature of the growing ice lens, it is expected that the latter should also be dependent upon these factors.

This paper is directed towards demonstrating that the temperature at the base of a growing ice lens is not a constant during freezing associated with steady frost penetration into unfrozen soil.

THE MECHANISM OF ICE LENS FORMATION

Figure 1 represents schematically the process of initiation and growth of a single ice lens and the formation of the subsequent ice lens during transient freezing. Let us consider the time t at which a new ice lens is initiated at a given location defined by its particular segregation-freezing temperature T_{sf}. Because there is thermal imbalance, the frost front advances at some rate dX/dt. This, in turn, produces changes in the temperature profile across the sample and more specifically across the frozen fringe. During a time interval t the base of the ice lens cools below T_{sf} and the extent of the frozen fringe increases by X. Consequently, the overall permeability of the fringe decreases, the flow path increases, and the suction potential developed at the base of the ice lens becomes greater. For temperatures close to 0°C, the suction at the base of the ice lens varies linearly with temperature below 0°C. In contrast, the unfrozen water content and hence the frozen soil permeability decay more or less exponentially with decreasing temperature (Johansen, 1977). As long as the relation between suction and frozen fringe permeability is such that the water flow entering the fringe is able to traverse it, water will be drawn to the base of the ice lens and thus contribute to its growth. Therefore, during the time interval t the ice lens grows to a thickness equal to 1.09v t where v is the average water intake flux. Because the hydraulic conductivity of the frozen fringe decreases more rapidly than the suction increases with decreasing temperature, it follows that the average water flux decreases continually with time during the growth of a single ice lens. Further penetration of the frost front results in further cooling of the frozen fringe. After a while, the temperature at the base of the growing ice lens reaches a value T_{sm} at which the permeability of the upper part of the fringe is so small that water flow is essentially stopped in the zone of extremely low permeability. Water now accumulates somewhere below the base of the former ice lens. The new level of accumulation is governed by the local permeability of the

current frozen fringe, which can be associated with a segregation-freezing temperature of ice lens formation, T_{sf}. Because T_{sf} is warmer than T_{sm}, the average permeability of the new current frozen fringe is larger than the one associated with the former ice lens. The rate of ice lens growth is therefore higher at the initiation of a new ice lens but steadily decreases during its growth. Experimental data reported by Penner (1986) support the above described mechanism.

Recent experimental developments at the National Research Council of Canada using X-ray photography have been used to locate the position of a growing ice lens in order to determine its temperature by means of its position in the thermal gradient field (Penner and Goodrich, 1981). If the temperature distribution is linear in the frozen soil near the frost front, which is often the case, the temperature of the actively growing face can be calculated as:

$$T_{sm}(t) = d(t).\text{grad } T_f(t) \qquad (1)$$

where d(t) is the thickness of the frozen fringe and grad $T_f(t)$ is the temperature gradient in the frozen zone near 0°C at time t.

It should be noted that this estimated temperature lies between T_{sf} and T_{sm}. However, as shown in fig. 1, the spacing, s, between two consecutive ice lenses provides additional information because:

$$T_{sm} - T_{sf} = s.\text{grad } T_f \qquad (2)$$

It is assumed that the conditions controlling the initiation of a new ice lens are not significantly different for consecutive ice lenses unless there is a marked change in the rate of cooling and/or the suction at the frost front.

The temperature of ice lens initiation, T_{sf}, can also be estimated from the temperature of the active ice lens if it is possible to establish the time of its initiation which allows us then to obtain the relevant temperature distribution. The position of the ice lens, which is too small to be visible, is back-calculated from the position of the fully grown ice lens by accounting for heave that occurred between its initiation and the X-ray photograph.

EXPERIMENTAL PROCEDURE

Due to the fact that step-freezing is characterized by drastic changes of rate of cooling of the current frozen fringe (e.g. going from 70°C/day to almost 0°C/day in less than a day), temperature changes at the growing ice lens have been studied using the "ramped-freezing" technique introduced by Myrick et al. (1982). In these tests a linear reduction with time of the top and bottom plate temperatures is used to impose a constant rate of frost penetration. The rate of cooling of the frozen fringe, $\dot{T}_f$, is related to the frost penetration rate, $\dot{X}$, and the temperature gradient as: (Konrad and Morgenstern, 1982, 1983)

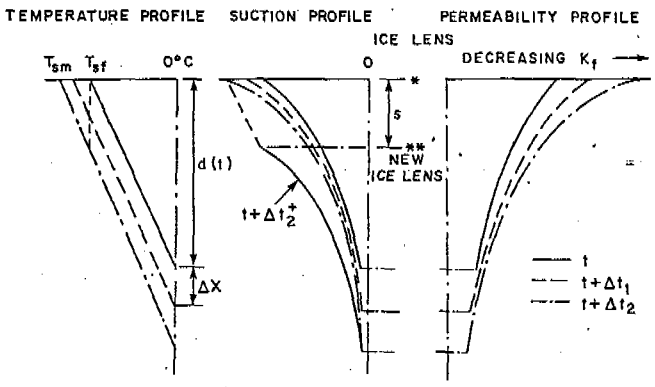

FIGURE 1. Changes in the frozen fringe during transient freezing

$$\dot{T}_f = \text{grad } T_f . \dot{X} \qquad (3)$$

Thus, if the temperature gradient across the sample is maintained constant, eq. (3) indicates that this freezing mode results in tests with a constant rate of cooling of the fringe. However, as the frost front advances into the unfrozen soil, the flow path decreases and it is expected that the suction at the frost front does not remain constant during freezing. Penner (1986) introduced improvements in temperature control as well as in computer-control in order to change the temperature at each end of the sample to within ±0.004°C. The thermistors used in the freezing cell were calibrated to within ±0.001°C. The freezing cell used in this investigation has been fully described by Penner (Op. Cit.)

Rather than conducting several freezing tests on different samples at different rates of ramping, it was decided to run only one freezing test in which the rate of cooling was changed in stages. The advantage of this procedure is to minimize sample variability. As shown by eq. (3) the rate of cooling is directly related to the rate of frost advance if the temperature gradient is given, and is therefore controlled by the ramp rate. If the temperature gradient is maintained constant during freezing, the observed spacing between consecutive ice lenses is directly related to the difference between the minimum and maximum ice lens temperatures at a given rate of cooling.

In order to minimize the effect of wall friction, the sample was frozen from bottom upwards. The temperature control was set at the bottom plate and at the warm side using the output of thermistor #10 located in the cell wall at a distance of 101.6 mm.

The properties of Devon silt are as follows: liquid limit=46.1%; plastic limit=19.8%; passing #200=95%; % clay size=28%. The sample was consolidated in the freezing cell from a slurry to a pressure of 210 kPa and was frozen from bottom upwards after rebound under an applied pressure of 50 kPa.

EXPERIMENTAL RESULTS

Fig. 2 gives the thermal conditions used during freezing leading to different frost penetration rates as shown in fig. 3. During the first 69 hours the end temperatures were lowered at a constant rate of 0.67°C/day, followed by a rate of temperature decrease of 0.36°C/day for about 30 hours, then for a period of 100 hours the ramp rate was less than 0.05°C/day . Finally, the rate was increased to 0.22°C/day for approximately 40 hours. At the end of stage IV the temperature of thermistor #10 was very close to 0°C and was maintained constant for the remaining freezing period while the bottom plate temperature was lowered at 0.22°C/day. It is noted that the position of the frost line is given with respect to the fixed bottom plate and that the actual rate of frost penetration into unfrozen soil must account for total heave since the unfrozen soil is steadily pushed upwards as frost heaving occurs. Eq. (3) with the corrected frost penetration rate yields the rate of cooling of the current frozen fringe for stage I to V as illustrated in fig. 4. The actual values of $\dot{T}_f$ are 0.53 (0.0224), 0.25 (0.0102), 0, 0.11 (0.0047), and 0°C/day (°C/hour) for stage I, II, III, IV, and V respectively. In general, the rate of cooling of the fringe stayed fairly constant during each stage, but showed some variation in stage IV with respect to the average value.

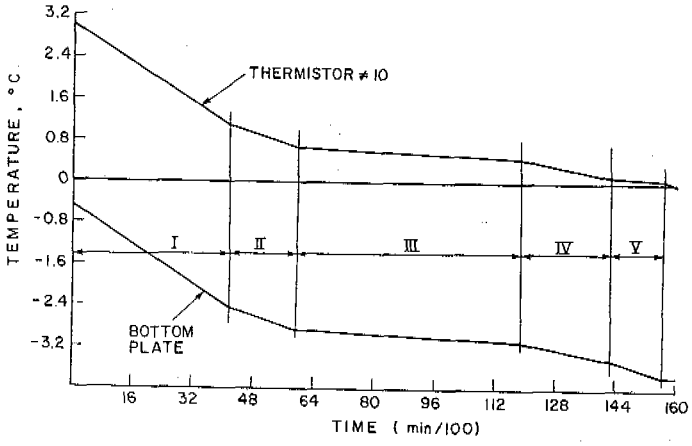

FIGURE 2. Temperature boundary conditions during freezing

Seven X-ray photographs were taken while freezing was in progress at different elapsed times as indicated on fig. 3 and 4. Temperature measurements were taken at the same time as the X-ray pictures to determine the corresponding temperature distribution within the sample as shown in fig. 5. As noted by Penner and Goodrich (1981), the thermistor points and wires show on the X-rays which helps to locate the position of the growing face of the ice lens very accurately. No discontinuities were noted in the temperature profiles and the ice lenses were essentially horizontal. As a result, linear interpolation of temperatures between measured points, or the use of grad T_f is adequate for the present study.

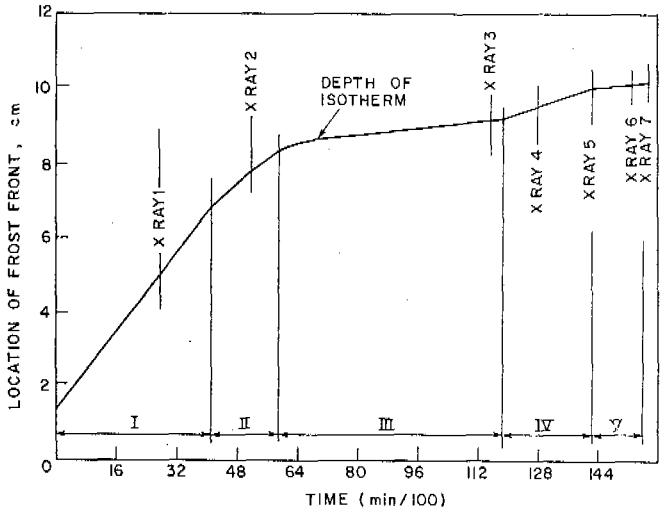

FIGURE 3. Frost penetration during freezing.

Each X-ray photograph was taken from the same distance from the freezing cell with a film installed at the same location behind the cell in order to keep the same scale. The X-ray beam was centered with respect to the actual position of the frost front to minimize distortion in the area of interest. Fig. 6 presents the X-rays indicating the position of the growing ice lens with respect to the thermistors placed at ten different distances from the bottom plate: 0, 8.4, 16.8, 25.4, 38.1, 50.8, 63.5, 76.2, 88.9,and 101.6 mm.

The soil between ice lenses appears as a dark tone. Thin ice lenses are lighter whereas thicker ice lenses appear white.

The results of the experiment are summarized on table I. According to the proposed mechanism of ice lens formation, the inferred temperature of the growing face of the active ice lens depends upon the time elapsed since the initiation but it will always be between T_{sf} and T_{sm}. It is possible to estimate the relative stage of growth of a single ice lens using X-ray photographs obtained for longer freezing periods. T_s is then closer to T_{sf} if the current ice lens is near its beginning while it is closer to T_{sm} near its termination.

The interpretation of the first 4 X-rays in terms of T_s indicates that the temperature of ice lens formation depends upon the rate of cooling. The temperature of the ice lens increased from -0.283 to -0.204°C as the rate of cooling decreased from 0.54 to 0°C/day in support of the proposed mechanism .

In stage I, the imposed rate of cooling of about 0.54°C/day produced a regular ice-soil structure composed of thin ice lenses separated by soil lenses of about 0.6 mm. Using eq. 2 , the difference between the temperature of the current ice lens at its formation and at its

termination is of the order of -0.022°C. Since X-ray 1 was obtained near the termination of the ice lens, it is argued that T_{im} is slightly below T_s and that the temperature of ice lens initiation is slightly below -0.26°C.

In stage II, the imposed rate of cooling of 0.24°C/day also resulted in a regular ice structure but with increased spacing between ice lenses as shown in fig. 6. The temperature of the current ice lens was estimated as -0.239°C and was near its beginning. The average spacing between ice lenses was about 1.2 mm indicating that the difference between T_{im} and T_{ir} was -0.042°C.

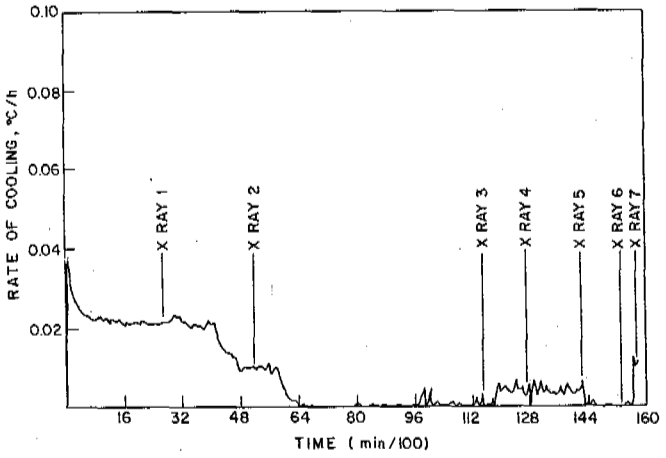

FIGURE 4. Rate of cooling of the frozen fringe during freezing

In stage III, the rate of cooling was zero which permitted a large ice lens to grow. The estimated T_s after 11327 minutes of freezing was -0.204°C. The time of formation was estimated from the measured thickness of the ice lens to be about 6622 minutes after the beginning of freezing and the corresponding temperature profile indicated that the temperature of formation of the current ice lens was also -0.204°C. Freezing from the bottom upwards pushes the unfrozen soil upwards as heaving progresses and the position of the 0°C isotherm is moving even if there is no additional frost penetration into the unfrozen soil. This is illustrated in fig. 7 which compares the same freezing situation for upward and downward freezing. If, for the case of upward freezing, the increment in frost penetration, $\triangle X$, is equal to the increment of ice lens thickness, $\triangle h_s$, then there is no net increase in frost penetration. If $\triangle X$ is larger than $\triangle h_s$, then there is cooling of the frozen fringe while warming and subsequent melting is obtained if $\triangle X$ is less than $\triangle h_s$.

For the ice lens under consideration, $\triangle X$ was 5.59 mm for elapsed times of 6622 and 13327 minutes and $\triangle h_s$ was 5.64 mm indicating in turn that the net frost penetration in stage III was essentially zero. Thus, the temperature at the growing face of the ice lens did not change since the temperature gradient remained constant during this stage. The fact that the rate of cooling was also zero points out that the actual frost penetration rate was also zero according to eq. 3. The temperature of ice lens formation for an extremely small cooling rate was thus about -0.20°C.

X-ray 4 was taken during stage IV where the frost front penetrated again into unfrozen soil and the estimated temperature at the face of the same ice lens was -0.25°C. Furthermore, the ice lens was near its maximum thickness indicating that the measured T_s should be close to T_{im}.

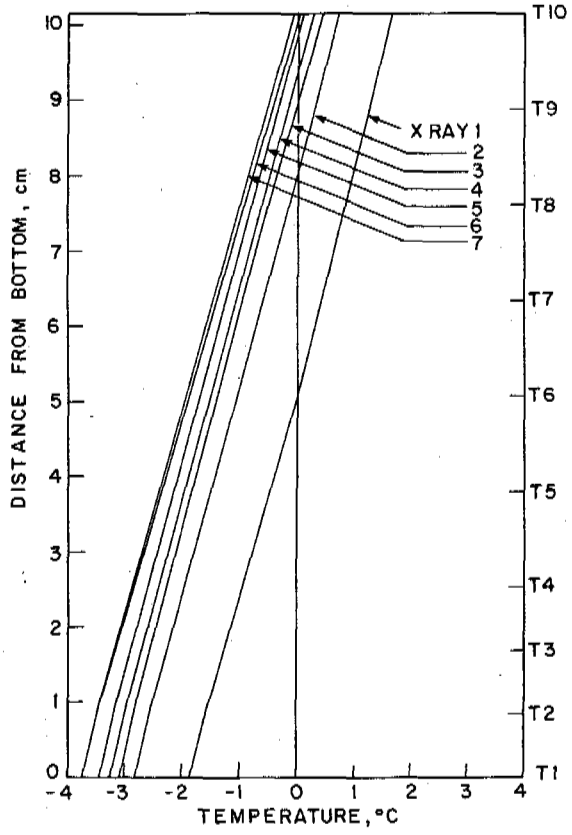

FIGURE 5. Temperature profiles in sample for each X-ray

X-ray 5, which corresponds to the end of stage IV, shows that the spacing between ice lenses increased to about 1.8 mm when the rate of cooling was 0.11°C/day. This, in turn, means that the difference between T_{im} and T_{ir} was about -0.064°C. Furthermore, the temperature at the growing face of the warmest ice lens was -0.206°C. It should be noted that this ice lens was barely visible indicating that it had just formed. X-rays 6 and 7 show that the growing ice is the same as that detected in X-ray 5. Therefore, it should be expected that T_s becomes colder with time provided the frost front steadily penetrates into the unfrozen

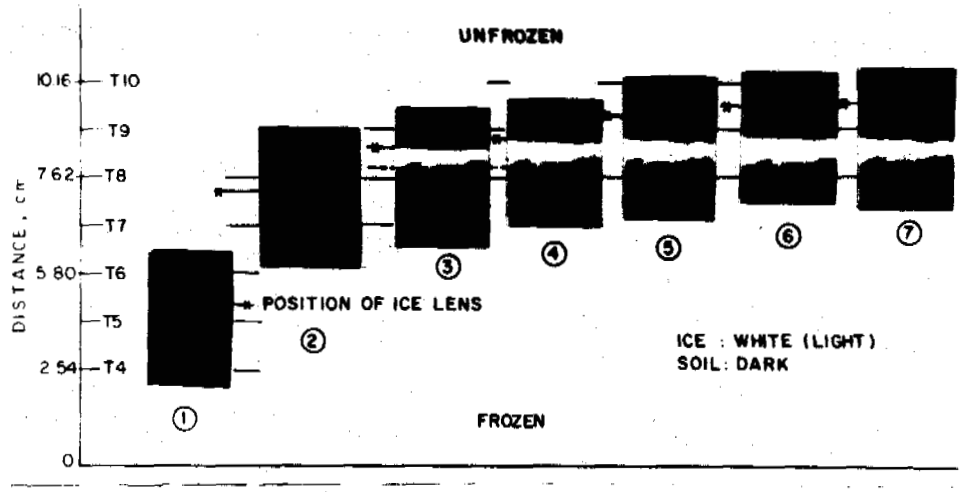

FIGURE 6. Location of growing ice lens using X-ray prints

soil resulting in further cooling of the frozen fringe. However, as shown on fig. 4 , the calculated rate of cooling is zero and even negative (not plotted) which means that the current frozen fringe was actually warming and thus thawing . The estimated temperatures at the growing ice lens are given in Table I and are consistent with the above discussion.

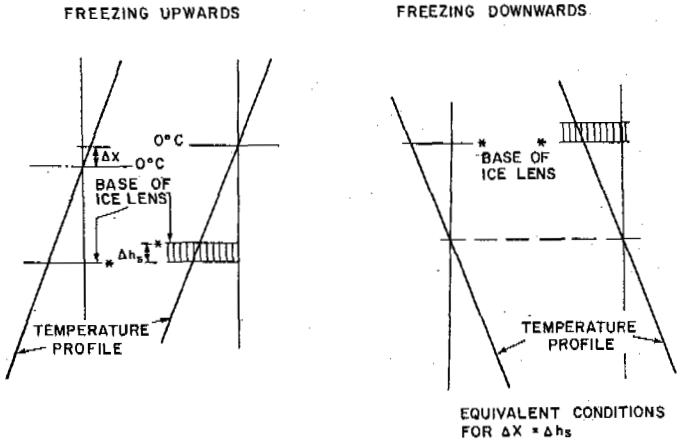

FIGURE 7 Location ice lens in downward and upward freezing tests

Table II summarizes the main results obtained in the present study. The suction at the frost front was different for each stage but to date no systematic study of its effect on T_{sr} and T_{sm} has been undertaken. Nevertheless, it is clearly shown that the temperature of ice lens formation in Devon silt with steady frost penetration is dependent upon the rate of cooling . T_{sr} was respectively -0.26, -0.23 and -0.20°C for cooling rates of about 0.54, 0.24 and 0.11°C/day. The study also revealed that the difference between the maximum and minimum temperature of a growing ice lens is also dependent upon the rate of cooling and increases with decreasing rates of cooling. For Devon silt, T_{sm}-T_{sr} is respectively -0.022, -0.042, and -0.064°C for $\dot{T}_s$ of 0.54, 0.24 and 0.11°C/day. This, in turn, indicates that the variation of T_{sm} with rate of cooling is not as important as it is for T_{sr}.

SUMMARY

The development of computer-controlled, ramped-temperature freezing and computer-aided measurements of moisture migration, frost heave, and thermistor output by Penner (1986), associated with the X-ray technique made it possible to study the effect of rate of cooling on the temperature of ice lens initiation and on the difference between the maximum and minimum temperature of the same ice lens.

The results of the present investigation indicated that the temperature of ice lens initiation was not a constant for Devon silt, but increased when the rate of cooling decreased from 0.54 to 0.11°C/day. Furthermore, it was noted that the difference between the maximum and the minimum temperature of a given ice lens increased when the rate of cooling decreased from 0.54 to 0.11°C/day.

ACKNOWLEDGEMENTS

The author wishes to thank Mr. D. Eldred for his conscientious efforts in conducting the freezing tests. This experimental program was conducted while the author was a research officer at the National Research Council of Canada. The cooperation of Mr. E. Penner, former head of the geotechnical section, is greatly appreciated.

REFERENCES

Johansen, O., 1977. Frost penetration and ice accumulation in soils. International Symposium on Frost Action in Soils, University of Lulea (Sweden), Feb. 16-18, Proceedings, Vol. 1, pp. 102-111.

Konrad, J.-M. and N.R. Morgenstern, 1982. Prediction of frost heave in the laboratory during transient freezing. Canadian Geotechnical Journal, 19, pp. 250-259.

Konrad, J.-M. and N.R. Morgenstern, 1981. The segregation potential of a freezing soil. Canadian Geotechnical Journal, 18, pp. 482-491.

Konrad, J.-M. and N.R. Morgenstern, 1980. A mechanistic theory of ice lens formation in fine grained soils. Canadian Geotechnical Journal, 17, pp. 473-486.

Myrick, J.E., Isaacs, R.M., Liu, C.Y., and Luce, R.G., 1982 . The frost heave program of the Alaskan Natural Gas Transportation System. Presented ASME Conf., Phoenix, Arizona.

Penner, E., 1986. Aspects of ice lens growth in soils. Cold Regions Science and Technology, Vol. 13, pp. 91-100.

Penner, E. and L.E. Goodrich, 1981. Location of segregated ice in frost susceptible soil. Engineering Geology, Vol. 18, pp. 231-244.

TABLE I: Estimated Ice Lens Temperature From X-Ray Photographs in Devon Silt.

X-ray	Time (min)	Distance of ice lens (mm)	0°C (mm)	grad T_s °C/mm	T_m (measured) °C	Comments
1	2867	42.64	50.40	0.0365	-0.283	near termination of ice lens
2	5588	72.91	79.75	0.0350	-0.239	near beginning of ice lens
3	11327	84.20	89.80	0.0364	-0.204	
4	12768	86.45	93.28	0.0366	-0.250	near termination of ice lens
5	14205	92.66	98.42	0.0358	-0.206	near beginning of ice lens
6	15643	95.96	100.12	0.0393	-0.163	same ice lens as #5 but warming of base of ice lens
7	16084	96.71	100.96	0.0362	-0.154	

TABLE II: Estimated Temperatures at the Formation and Termination of a Growing Ice Lens in Devon Silt.

Rate of Cooling °C/h (°C/day)	Suction at 0°C kPa	Average Spacing mm	Grad T_s °C/mm	$T_{sm}-T_{sf}$ °C	Measured T_s °C	Estimated T_{sm} °C	Estimated T_{sf} °C
0.0224 (0.54)	-22	0.6	0.0365	-0.022	-0.283	slightly below T_s	-0.26
0.0102 (0.24)	-16	1.2	0.0350	-0.042	-0.239	-0.27	-0.23
0.0047 (0.11)	-8	1.8	0.0358	-0.064	-0.206	-0.26	-0.20

MICROSTRUCTURE OF FROZEN SOILS EXAMINED BY SEM

Kumai, Motov

U.S. Army Cold Regions Research and Engineering Laboratory, Hanover, New Hampshire, U.S.A.

SYNOPSIS Physical properties of bentonite, dickite and sand samples for freezing experiments were examined with a scanning electron microscope (SEM), and elemental compositions were measured with an energy dispersive x-ray (EDX) analyzer. Bentonite from Umiat, Alaska, is a typical cold-regions swelling clay with thin, crumpled and folded structures. The soil samples with relatively high water contents were frozen, and the frozen characteristics were examined with the SEM equipped with a cold stage. SEM images of frozen bentonite and dickite showed characteristic segregated ice and coagulated soil patterns formed during freezing processes and porous structures formed during the sublimation stage of ice in frozen soils. However, frozen sand showed no typical ice segregation and sand grain coagulation because of the large grain size. The freeze sublimation process of frozen clay and silt increases the permeability to water vapor because of the porous structure formation.

INTRODUCTION

In a laboratory experiment of frozen soils, polygonal ice patterns were found in horizontal thin sections of frozen Morin and Ellsworth clays (Chamberlain and Gow, 1979). The development of ice lenses in Morin and Ellsworth clays was greater than that in CRREL clay and Hanover silt at low applied stress. The freezing and thawing caused an increase in vertical permeability due to the formation of polygonal shrinkage cracks, especially for the soil of high plasticity.

The object of this work on frozen soils is to provide fundamental information on freeze-drying effects, morphology, size distributions, and elemental compostion of soil grains. This paper presents the results of physical and chemical properties of bentonite from Umiat, Alaska, dickite from San Juanito, Mexico, and sand from Hyannis, Massachusetts. Characteristics of the microstructure of frozen soils and ice sublimation in frozen soil samples during freeze-dry processes are described to assist in understanding the mechanism of void formation leading to increased permeability.

MATERIALS AND METHODS

A swelling clay, a non-swelling clay and a sand were selected to examine the characteristic structure of soils during the freeze-drying processes. Bentonite from Alaska was used as the swelling clay. The bentonite beds are 25 to 30 cm thick and are conveniently accessible at Umiat Mountain, 6.5 km northeast of the village of Umiat (Detterman et al., 1963). Dickite, a non-swelling clay, from San Juanito, Mexico and a sand from Hyannis Beach, Massachusetts, were also used in these experiments. The bentonite, dickite and sand samples were coated with Au and Pd (60:40) to a thickness of about 100Å in a vacuum chamber for the determination of the elemental composition and morphology.

The processes of freezing these soil samples were examined under an optical microscope in a cold room at -10°C. Then, the details of the characteristic structure were examined with a scanning electron microscope (SEM) equipped with a cold stage. The morphology and size distribution of soil grains were examined with the SEM. Elemental compositions of these soil grains were determined by an energy dispersive x-ray (EDX) analysis.

A schematic illustration of the SEM equipped with a cold stage is shown in Fig. 1. A soil sample with a known water content was placed in a hole 3 mm in diameter on the specimen holder and rapidly frozen by immersing it in liquid nitrogen. The specimen holder and frozen sample were then fixed to the specimen exchange rod and inserted into a pre-evacuation chamber, which was quickly evacuated to a pressure of 1×10^{-5} torr. The frozen specimen was then immediately transferred onto the cold stage, which had previously been cooled to around -100°C with liquid nitrogen. The temperature of the frozen soil sample in the SEM was thermostatically controlled with a built-in heater.

The ultimate vacuum for the SEM observation of frozen soil samples is about 5×10^{-5} torr. The ice temperature at a water vapor pressure of 5×10^{-5} torr is about -92°C in the SEM. SEM images of frozen soils were taken at temperatures -92°C or lower. SEM images of ice sublimation from frozen soil samples were obtained at temperatures higher than -92°C. The

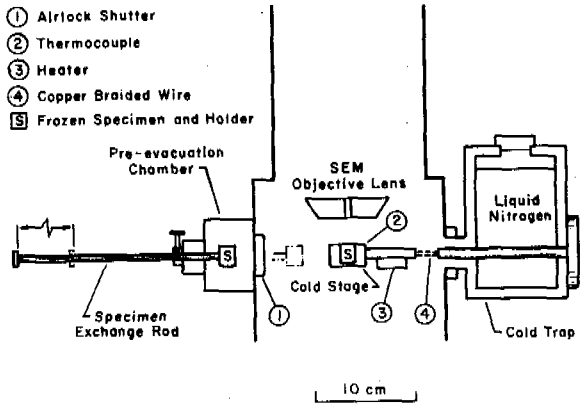

Fig. 1. Schematic illustration of a scanning electron microscope (SEM) equipped with a cold stage for frozen soil studies.

temperature of the frozen soil samples was measured continuously using a built-in copper-constantan thermocouple. The temperature range of the soil samples was from -100°C to -40°C in this experiment. The working distance of the frozen soil samples was 15 mm, the tilt angle 0°, and the accelerating voltage 5, 10 or 20 kV.

RESULTS

Chemical composition and morphology

A typical SEM image of unfrozen Umiat bentonite is shown in Fig. 2a, which shows that bentonite grains have crumpled and folded structures. The elemental spectral image of the bentonite obtained by EDX analyzer is shown in Fig. 2b, which shows that the major elements are Si, Al, Fe, Mg, Ca, Na, K, and Ti. The major chemical composition of the bentonite as oxides is shown in Table 1 and compared with those of Anderson et al. (1966). The molecular ratio of silica (SiO_2) to alumina (Al_2O_3) for the bentonite was calculated to be 492:100 for the terrestrial bulk sample and 503:100 for the <2 μm fraction sample.

Table 1. Major element analysis (wt. %) of Umiat bentonite, San Juanito dickite, and Hyannis sand.

Oxides	Umiat bentonite **	Umiat bentonite *	San Juanito dickite ***	San Juanito dickite *	Hyannis sand •
SiO_2	55.99	52.90	44.85	45.49	95.91
Al_2O	18.92	18.28	40.05	39.04	3.20
Fe_2O	3.38	3.56			
FeO			0.01	0.01	
MgO	3.08	2.61	Trace	Trace	0.89
CaO	1.61	1.63	0.51	0.55	
Na_2O		1.19	0.12	0.12	
K_2O	0.08	1.26	0.15	0.16	
TiO_2	0.16	0.65	0.02	0.02	

• This paper.
** Anderson et al. (1966).
*** Kerr et al. (1950).

The dickite grain from San Juanito (Fig. 3a) consisted of both well-developed and partly developed hexagonal crystals. The elemental spectral image of the dickite is shown in Fig. 3b, which shows that the major elements are Si, Al, Fe, Ca, Na, K, and Ti. The major chemical composition of dickite is shown in Table 1 and compared with those obtained by Kerr et al. (1950).

The SEM image of Hyannis sand (Fig. 4a) shows that the grains are irregular in shape. The main chemical composition of the sand is Si, Al, and Mg as shown in Fig. 4b and Table 1. The sand consists mainly of quartz grains.

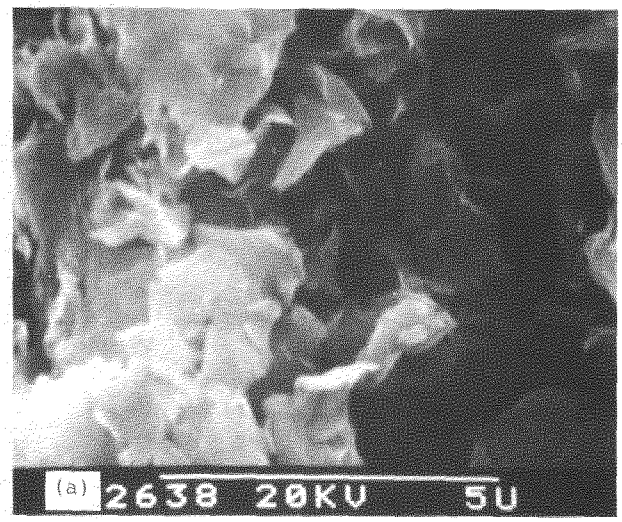

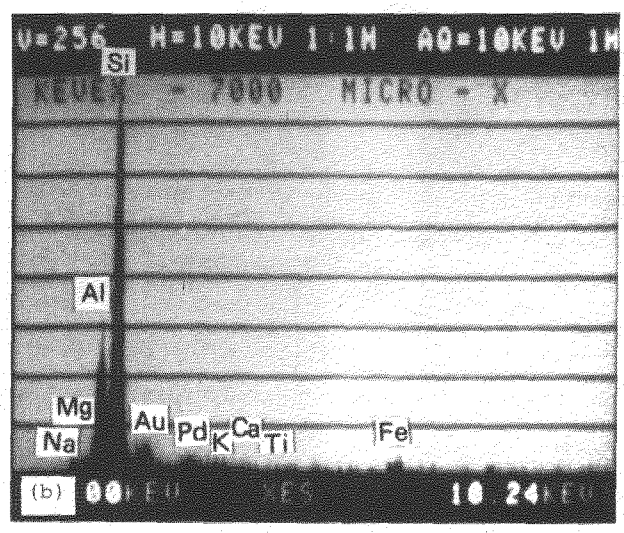

Fig. 2. SEM image (a) and EDX analysis (b) of unfrozen Umiat bentonite.

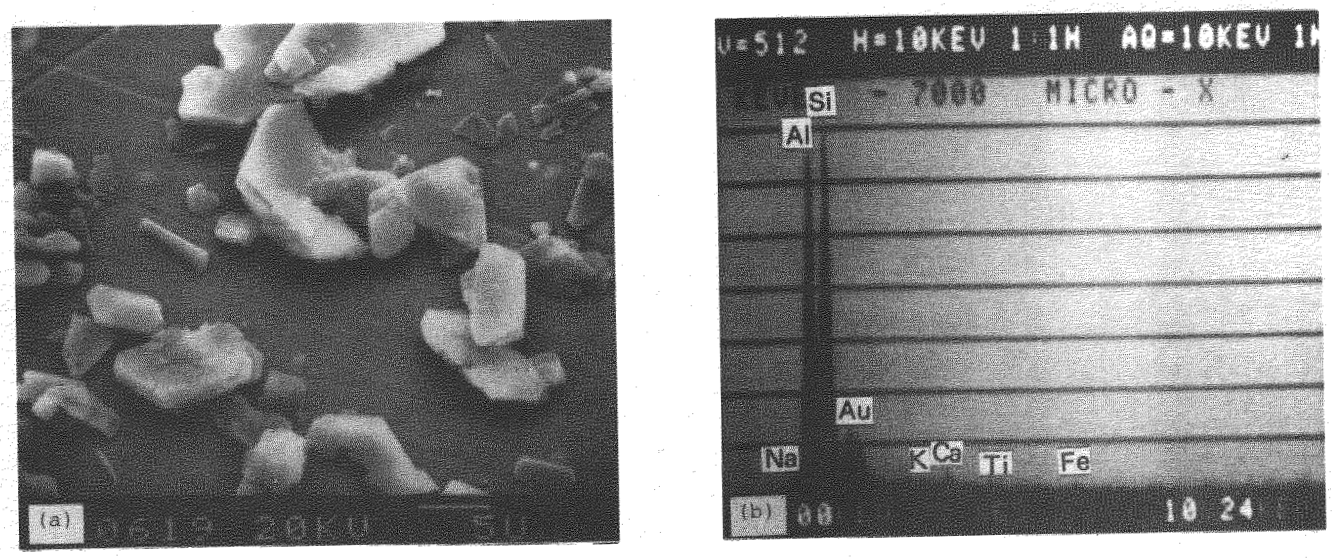

Fig. 3. SEM image (a) and EDX analysis (b) of dickite from San Juanito, Mexico.

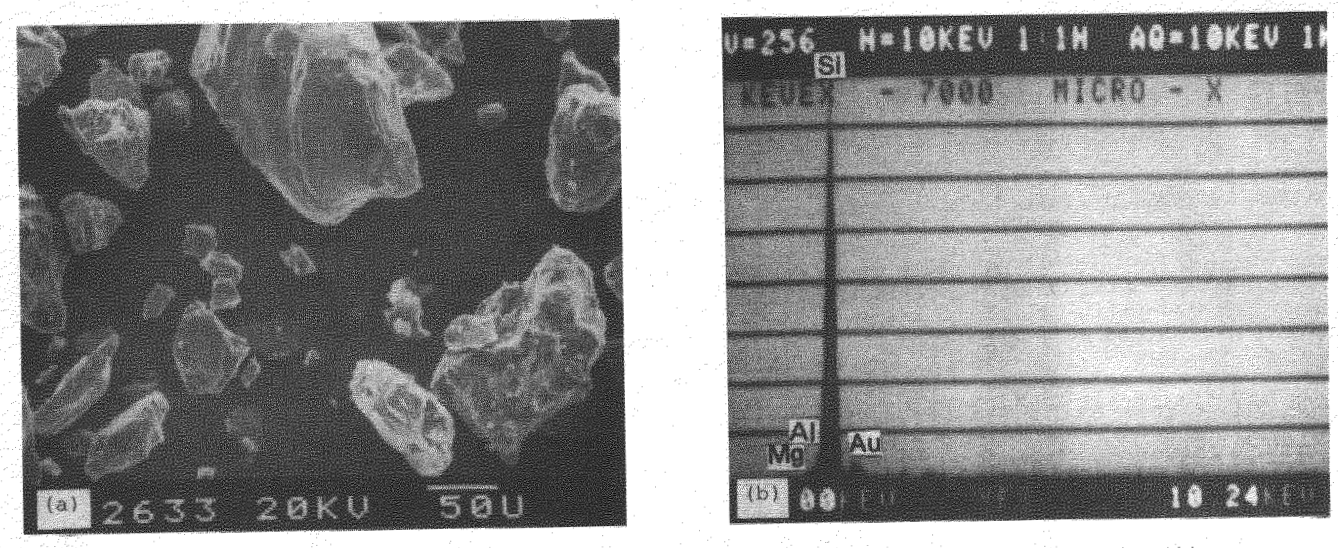

Fig. 4. SEM image (a) and EDX analysis (b) of sand from Hyannis, Massachusetts.

Size distribution

Mean diameters of about 500 soil grains were measured from SEM images of each soil sample. Grain size distributions of bentonite, dickite, and sand samples are shown with a semilogarithmic scale in Fig. 5. The size range of the bentonite sample was 0.2 to 6 μm in diameter, 90% of the grains were smaller than 2 μm, and the number of grains exponentially decreased with size. The mean diameter of Umiat bentonite was calculated to be 1.9 μm. The thickness of the grains was measured to be 2 to 200 nm by electron microscopy (Kumai, 1979). The d-spacings of the bentonite, measured from the electron diffraction patterns, were determined to be a = 5.18 Å and b = 8.97 Å for ortho-hexagonal indexes. The particle size of dickite ranged from 0.5 to 25 μm with a mean diameter 4.0 μm, and 50% of the

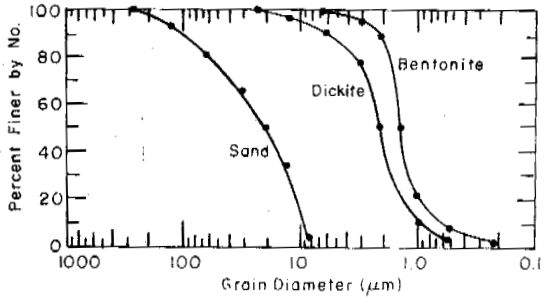

Fig. 5. Grain size distributions of bentonite, dickite, and sand samples.

grains were smaller than 2 μm in diameter. The sand grains ranged from 8 to 260 μm in diameter with a mean diameter 53.3 μm, and 50% of the grains were larger than 20 μm in diameter.

Structure of the frozen soils

The maximum water content of bentonite, a swelling clay, is higher than that of non-swelling clays. An Umiat bentonite sample with 900% water content by weight was frozen with liquid nitrogen, and the structure was examined by SEM. A typical SEM image of the frozen bentonite at -100°C (Fig. 6a) shows segregated ice (dark areas) and coagulated bentonite grains (light areas) formed in the freezing process. The temperature of frozen bentonite was raised from -100° to -60°C using the built-in heater to allow the observation of the change in structure during the process of sublimation of ice. The ice in the frozen bentonite was observed to sublime slowly. Cavities were formed at locations where the ice sublimed (Fig. 6b). In this freeze-drying process, micron-sized bentonite grains were coagulated to form a sheet structure as seen in Fig. 6b.

Bentonite samples with 230% water content by weight were also frozen. The SEM image of frozen bentonite at -80°C is shown in Fig. 6c, in which the crumpled and folded structure of bentonite grains is shown. When the coagulated bentonite lost moisture during the freeze-drying process, the structure of the

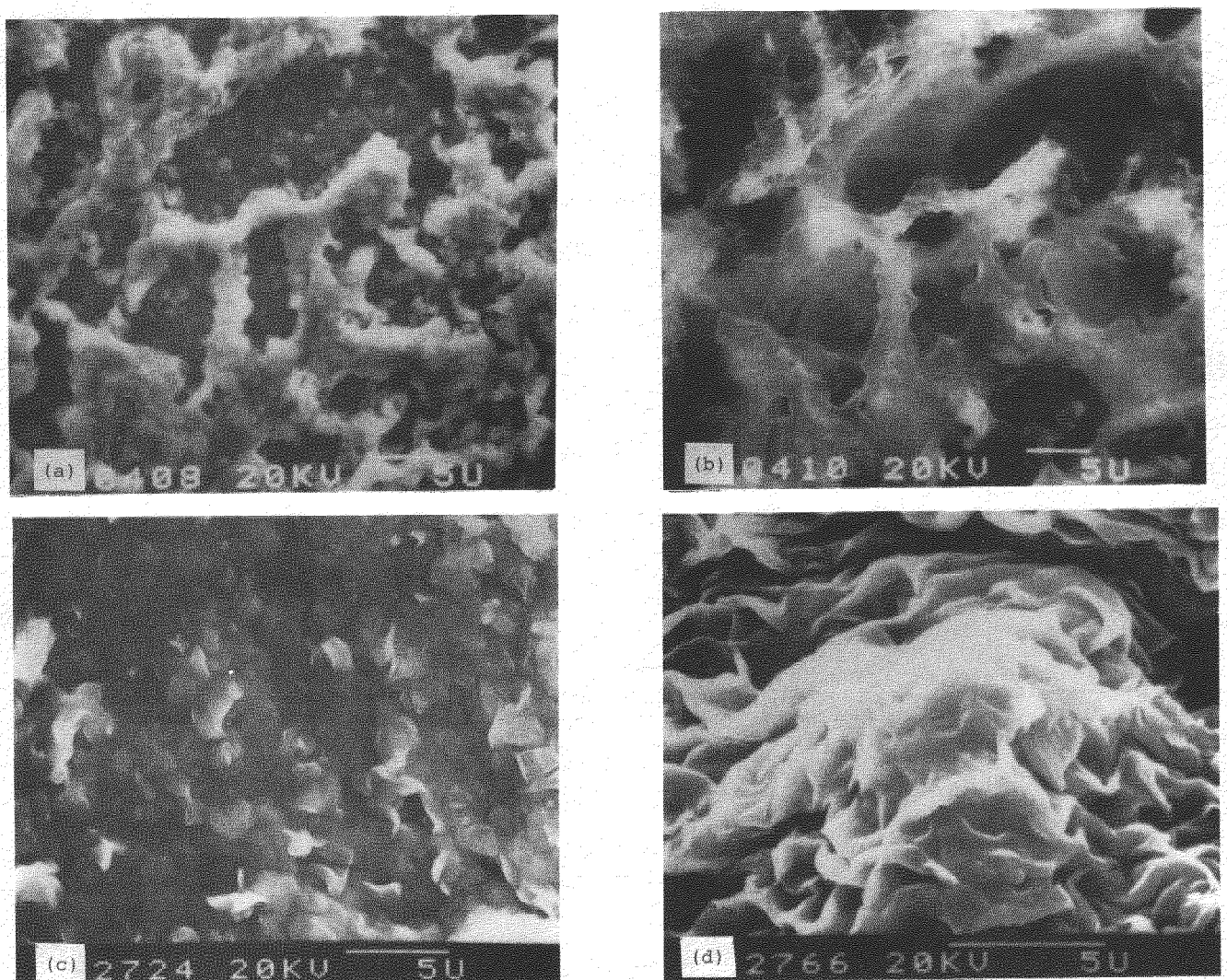

Fig. 6. (a) SEM images of frozen Umiat bentonite with 900% water content at -100°C with 10^{-5} torr. The ice (dark areas) is segregated, and the bentonite grains (light areas) coagulate during freezing process. (b) The ice was allowed to sublime at -60°C, and cavities formed at the locations of the sublimed ice. (c) Bentonite grains in frozen bentonite with 230% water content at -80°C. (d) Folded sheet-like structures of coagulated bentonite after freeze-drying processes at -50°C.

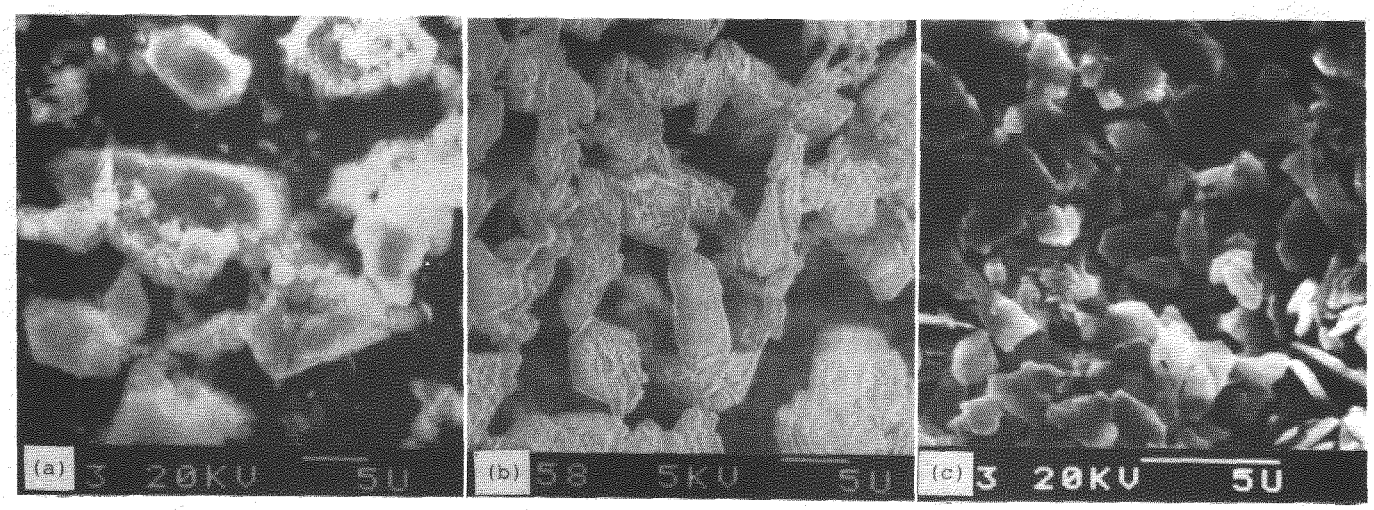

Fig. 7. (a) SEM images of frozen dickite with 100% water content at -100°C. The ice (dark areas) is segregated, and the dickite grains (light areas) coagulate during freezing process. (b) The porous structure of frozen dickite after sublimation of ice at -40°C. (c) The dense structure of dickite grains with 19.5% water content at -40°C.

micron-sized bentonite grains changed to a folded sheet-like structure as seen in Fig. 6d.

A specimen of the dickite with 100% water content by weight was prepared and cooled by liquid nitrogen. A typical SEM image of the frozen dickite at -100°C is shown in Fig. 7a, in which the segregated ice and the coagulated dickite grains formed during the freezing process are shown. The temperature of the frozen dickite was raised from -100° to -40°C using the built-in heater to examine the change of texture due to ice sublimation. The ice in the frozen dickite was observed to sublime gradually and form a porous structure as shown in Fig. 7b. During the ice sublimation process, the dickite grains moved slightly, but the morphology and size of the grains were not changed.

A dickite sample with 19.5% water content by weight was prepared and frozen with liquid nitrogen. The texture of the frozen dickite after ice sublimation at -40°C is shown in Fig. 7c, where the dense structure of dickite grains is shown. Ice segregation during the rapid freezing process was not distinguished at this water content.

A Hyannis sand sample with 20.9% water content by weight was frozen with liquid nitrogen. A typical SEM image of the frozen sand at -85°C is shown in Figure 8a, in which sand grains with ice are shown. The temperature of the frozen sand sample was raised to -55°C, and

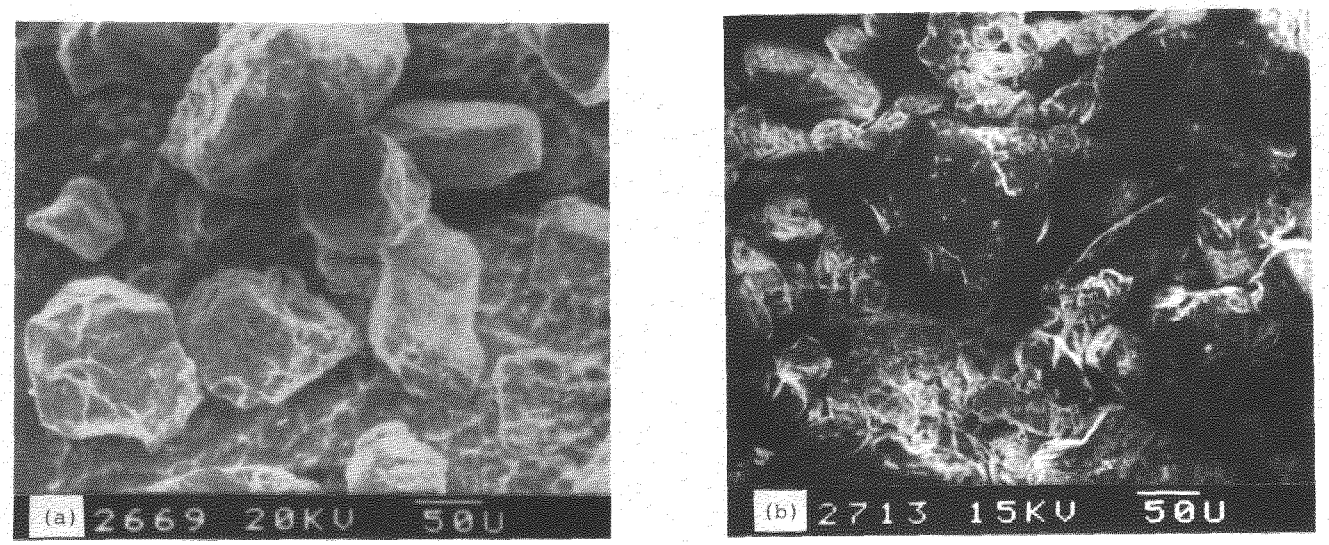

Fig. 8. (a) SEM image of frozen sand with 20.9% water content at -85°C. (b) The dense structure of sand grains after sublimation of ice at -55°C.

ice sublimation in the sample was observed. The frozen aggregated sand grains at -55°C are shown in Fig. 8b. Ice segregation and sand coagulation during the freezing process were not observed for the sand sample.

DISCUSSION

Clay minerals are hexagonal structures with lattice spacings about 10% greater than those of hexagonal ice. Ice nucleation by clay minerals occurs at threshold temperatures from -5° to -15°C (Anderson 1974, Kumai 1976, 1987). The freezing processes of clay samples with relatively high water contents are considered as follows: 1) Water in clay samples is supercooled during cooling. When the temperature reaches the threshold temperature, ice nucleation occurs heterogeneously. 2) The ice grows from the supply of water and the ice segregates from soil grains. The soil grains coagulate by losing bound film water separating particles to the growing ice grains.

The SEM images of bentonite or dickite samples, for given water contents, when frozen at -10°C showed the same structure as frozen with liquid nitrogen (-190°C). However, the sizes of the segregated ice features increased with the freezing temperature and water content.

The frozen bentonite and dickite samples mounted on the cold stage were broken to examine the fractured surface. The SEM image of the fractured surfaces were similar to those of the unfractured surface structure.

The amount of segregated ice in the frozen bentonite samples increased with the water content in the sample. Frozen bentonite samples with high water contents had three-dimensional honeycomb structures (Fig. 6b), which formed by coagulation of bentonite grains during ice segregation. However, the frozen bentonite at lower water contents (<230%) showed no honeycomb structure when cooled with liquid nitrogen (Fig. 6c). The honeycomb structure, however, did occur at the low rate of cooling in the -10°C environment.

The bentonite and dickite samples were frozen by liquid nitrogen and thawed at room temperature. After 50 freeze-thaw cycles, the grain size distributions were examined. No change in the particle size distribution was observed.

CONCLUSIONS

Ice segregation and soil grain coagulation during freezing were observed directly on the bentonite and dickite samples with an SEM equipped with a cold stage. Cavity formation at segregated ice locations were observed during the sublimation process. Frozen bentonite and dickite with high water contents developed honeycomb structures due to the three-dimensional structure of coagulated clays formed during freeze-drying processes. The freeze-drying processes of frozen clay and silts such as bentonite and dickite increase the permeability to water vapor due to the cavity formation. Ice segregation and soil grain coagulation were not observed in the frozen sand where the particle sizes were much larger in comparison with those of the clay and the silt.

ACKNOWLEDGEMENTS

This work was supported by DA project 4A161102AT24/SOA at the U.S. Army Cold Regions Research and Engineering Laboratory, Hanover, NH. The author wishes to acknowledge Mr. E. Chamberlain and Mr. A. Tice of CRREL for their comments on the manuscript.

REFERENCES

Anderson, D.M. and R.C. Reynolds (1966) Umiat bentonite: An unusual montmorillonite from Umiat, Alaska. The American Mineralogist (51), 1443-1456.

Anderson, D.M., A.R. Tice and A. Banin (1974) The water-ice phase composition of clay/water systems. 1. The kaolinite/water system. CRREL Research Report 322, 1-8.

Chamberlain, E.J. and A.J. Gow (1979) Effect of freezing and thawing on the permeability and structure of soils. Engineering Geology (13), 73-92.

Detterman, R.L., R.S. Bickel and G. Gryc (1963) Geology of the Chandler River Region, Alaska. U.S. Geological Survey Professional Paper 303-E, p. 223-324.

Kerr, P.R. et al. (1950) Analytical data on reference clay minerals. Petroleum Institute Project 49. Preliminary Report No. 7. 1-160.

Kumai, M. (1976) Identification of nuclei and concentrations of chemical species in snow crystals sampled at the South Pole. J. Atmos. Sci. (33), 833-841.

Kumai, M. (1979) Electron microscope investigation of frozen and unfrozen bentonite. CRREL Report 79-28. 1-14.

Kumai, M. (1987) Scanning electron microscope examination of growing ice needles on freezing bentonite. Proceedings of the Conference on Snow, Ice and Frozen Soils, 4-7 October 1987, Kushiro, Japan. p. 426, Japanese Society of Snow and Ice.

CRYOGENIC DEFORMATIONS IN FINE-GRAINED SOILS

Yu.P. Lebedenko and L.V. Shevchenko

Faculty of Geology, Moscow State University, Moscow, USSR

SYNOPSIS Results of investigations into the nature, mechanism, dynamics, specific and general patterns of cryogenic deformation of freezing, thawing, and frozen moisture-saturated soils are discussed. Comprehensive methods of experimental simulation of heat and mass exchange, physico-chemical, mechanical, texture- and structure-forming processes were used to study heaving, shrinkage, swelling, volumetric heaving, and other processes responsible for the cryogenic deformation of soils. It has been established that heaving deformations occur not only in freezing, but also in thawing moisture-saturated fine-grained soils at increasing negative temperatures, and also in frozen soils under salinization. Frozen soil experiences heaving when salinized in a stationary temperature field. Quantitative data on water migration flow, intensity of segregated ice formation, soil heaving, settlement, shrinkage, and swelling have been obtained. Deformation patterns have been found for freezing, thawing and frozen soils as a function of their fineness, chemico-mineral and chemical composition of the external water solution, moisture content and density, as well as regimes of freezing, thawing, external pressure and salinization.

Deformation of freezing soils is caused by complex physico-chemical, heat- and mass-exchange processes (water migration, water-to-ice phase transition, ice interlayer formation, dehydration, coagulation and communition of mineral particles and aggregates). The resulting deformations may have opposite directions and varying values. In the frozen and primarily in freezing soil zones, deformations prevail that are associated with volume increase (heaving and volumetric heaving) and volume decrease (shrinkage) in thawed zones. Volume increase (positive) deformations in the freezing soil result from the crystallization of water contained in it prior to freezing (volumetric heaving) and of the water coming to the freezing front from the thawed zone (deformations caused by migration ice formation). A thawed zone shrinkage occurs as a result of dehydration of mineral particles and aggregates when moisture migrates into the frozen zone.

It has been found experimentally and supported by field investigations that an increase in soil fineness boosts the share of positive deformations due to segregated ice accumulation (in accordance with moisture migration flow density increase in the loamy sand - loam - clay series) and reduces the share of volumetric heaving deformations. The share of volumetric heaving in loamy sands may reach 70 to 80 percent, while it is not higher than 12 to 20 percent in clays (Fig.1). Soil fineness increase brings about an increase in negative deformation (shrinkage) which may partially and sometimes completely compensate for positive deformation.

The investigation of heat and mass transfer, segregated ice accumulation and heaving processes in freezing soils of various mineral

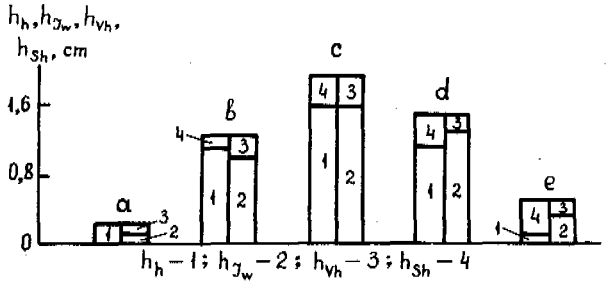

Fig.1 Correlation of heaving (h_h), caused by migration ice accumulation (h_{Iw}) and volumetric heaving (h_{vh}) (shrinkage deformation (h_{sh}) is taken into account) in freezing samples under open system conditions: a - loamy sand, b - loam, c, d, e - kaolinite, polymineral, and montmorillonite clays, respectively.

composition was conducted on kaolinite (W_i=0.50; ρ_d = 1.25 g/cm^3), polymineral (W_i=0.53; ρ_d = 1.21 g/cm^3), and montmorillonite (W_i=0.78; ρ_d = 0.72 g/cm^3) clay samples. Freezing was modeled under the same boundary temperature conditions as in the above-mentioned experiments with soil humidities equal to complete water saturation. The results show that the maximum value of moisture migration flow density, 36.10^{-6} g/cm^2 . s, is found in kaolinite and

the minimum in montmorillonite clay (I_w = 22 . 10^{-6} g/cm^2 . s). Moisture migration flow density in polymineral clay was 28.10^{-6} g/cm^2.s. The curve of moisture migration flow density as a function of time shows a smooth downward trend (Fig.2). Whereas in clays of kaolinite and hydromicaceous composition.

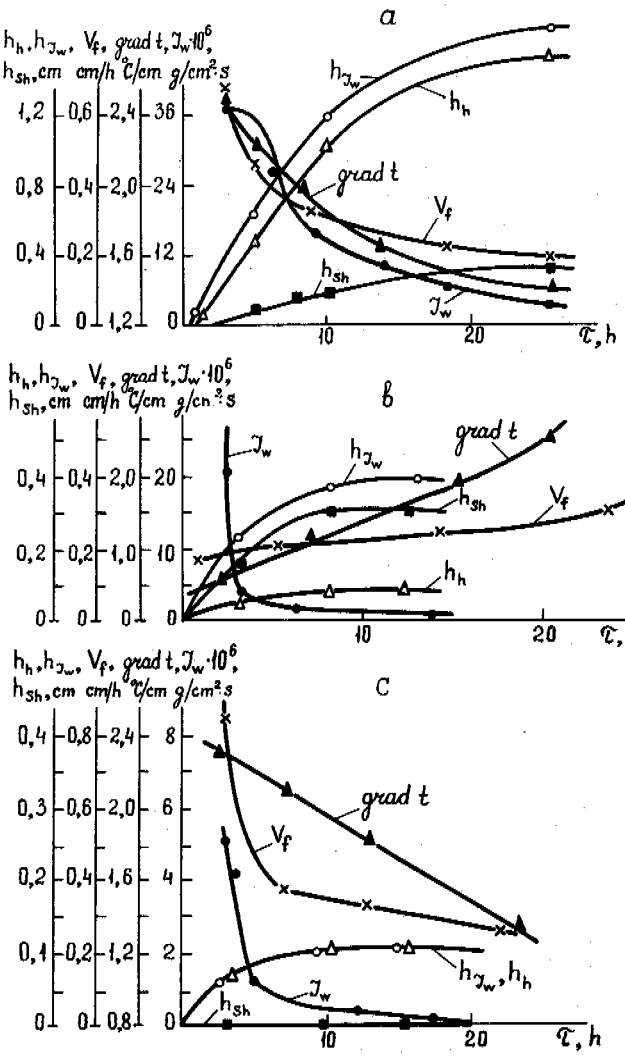

Fig.2 Dynamics of heaving (h_h), shrinkage (h_{sh}), and segregated ice accumulation (h_{I_w}) deformations; freezing rate (V_f); temperature gradient in the intensive phase transition zone (grad t); and moisture migration flow density (I_w) in kaolinite (a) and montmorillonite (b) clays freezing under open system conditions and in kaolinite clay (c) freezing under closed system conditions.

the external migration flow (due to inflow from without) plays the basic role in moisture redistribution, in montmorillonite clay the dominant factor is in montmorillonite clay the dominant factor is internal migration flow (resulting from soil moisture redistribution). The share of migration ice accumulation in the heaving of soils of different mineral composition is practically the same and equals, respectively, 84, 86, and 80 percent (Fig.1). However, heaving is different in them. Such different values of heaving in the soils of different mineral composition at similar values of moisture migration flow density are attributed primarily to shrinkage. Thus, shrinkage deformation in freezing kaolinite clay compensated for about 16 percent of the total positive deformation, and for 27 percent in polymineral clay. The maximum effect of shrinkage deformation in leveling off soil heaving is found in montmorillonite clay where its value exceeds 80 percent. When the external conditions vary, the correlation of positive and negative deformations changes too. Thus, an increased temperature gradient results in an increased moisture migration flow density; however, the net ice accumulation may decrease as a result of a rapid advance of the freezing front. With increasing freezing rate most of the water crystallizes in situ which enhances volumetric heaving deformation and decreases shrinkage. The correlation of positive and negative deformations is also influenced by the moisture content, density, groundwater table, and other factors.

Studies of the effect of initial moisture content of soil and its skeleton density on the extent of heaving, when freezing occurs under "closed" system conditions, have shown that an increase in the skeleton density of soil and a simultaneous decrease in the moisture content bring about a decrease in heaving deformation owing to both migration ice accumulation and volumetric heaving deformation; shrinkage is also reduced. With lower initial moisture content, rapid and intensive dehydration of the thawed zone (beneath the phase boundary) takes place whose further freezing forms massive cryogenic structure. In a wetter and less denser soil sample, maximum moisture migration flow density was found to be 30.10^{-6} g/cm^2. s, while in a dense soil sample the value was smaller by a factor of 6 (Fig.3,c).

In a freezing kaolinite clay of high initial moisture content a smoother decrease of moisture migration flow is observed as compared to its sharp drop in a dense soil, and heaving deformation dynamics due to migration ice accumulation is completely controlled by the pattern of moisture migration flow density distribution with time. A considerable moisture migration flow in a wetter and less denser soil caused an intensive thaw zone dehydration, whereas in a dense soil sample no visible shrinkage deformation sensor displacement was detected. A higher initial soil skeleton density combined with a lower initial moisture content result in reduced heaving due to volumetric heaving which is associated with a decrease in the amount of pore moisture at lower porosity (higher density) of soil.

A completely different pattern of heaving deformation in freezing soils of various initial humidity and density is observed when freezing

occurs under "open" system conditions.

It has been shown experimentally that at free moisture inflow from the outside, a higher initial soil density results in a stronger heaving deformation. This is associated primarily with increasing migration flow

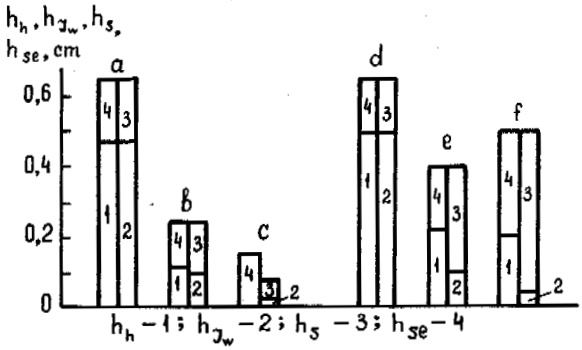

Fig.3 Correlation of heaving (h_h) caused by migration ice accumulation (h_{I_w}) and swelling (h_s) (shrinkage (h_{sh}) and settlement (h_{se}) are taken into account) in unilaterally thawing under open system conditions, soils of different composition: a, d - kaolinite clay; b - loam; c - loamy sand; e, f - polymineral and montmorllonite clays, respectively.

density at a simultaneous shrinkage decrease, i.e. with a lesser compensation for the positive deformation caused by segregated ice formation and volumetric heaving. In the kaolinite samples studied, an initial density increase (skeleton density increased from 1.25 to 1.36 g/cm^3) caused a more than 15 percent reduction of shrinkage deformation.

In the process of frozen soil thawing and soil freezing, the following three zones are formed: thawed, thawing, and frozen. In these zones, deformations of opposite orientation, such as thermal settlement and shrinkage (negative deformation), and heaving and swelling (positive deformation) occur. The laboratory tests were conducted on unidirectional thawing of frozen samples (4x4x12 cm) of fine-grained soil of massive cryogenic structure with +2°C at the top and -4°C at the bottom assigned as boundary values. The tests envisaged free water inflow (open system) at +2°C to the top of the samples. The external migration flow under open system conditions is spent to produce segregated ice in the frozen zone and to swell the thawed soil. Under these conditions, shrinkage deformations in the thawing zone are negligible. In a thawing kaolinite clay thermal settlement was recorded caused by pore ice melting equal to 2 percent, and a swelling deformation of 4 percent. The most interesting are the processes occurring in the frozen zone of thawing grounds. The temperature gradient causes water migration from the thawing to the frozen zone, which upon freezing, forms new segregated ice interlayers.

Analysis of mass-exchange patterns showed that migration ice accumulation increases in the loamy sand - loam - clay sequence, and moisture migration flow (I_w) is close to the flow values recorded during freezing. Thus, our tests yielded 40.1 . 10^{-6} g/cm^2 . s migration flow in kaolinite clay (W_i = 0.51 and ρ_d = = 1.25 g/cm^3) and four times smaller flow in loam (W_i = 0.36 and ρ_d = 1.70 g/cm^3). The share of deformations, caused by segregated ice formation, amounted in thawing clay, loam and loamy sand to 73, 41.6 and 33.3 percent of the total positive deformations, respectively (Fig.3). Investigation of deformations of clayey soils has shown that these processes depend on their mineral composition. Thawing was studied (at the same temperature conditions) in kaolinite (W_i = 0.51 and ρ_d = 1.25 g/cm^3), polymineral (W_i = 0.52 and ρ_d = 1.28 g/cm^3), and montmorillonite (W_i = 0.68 and ρ_d=0.81g/cm^3) clay samples. Analysis of moisture migration flow density as a function of time showed that moisture migration flow diminishes with increasing proportion of the montmorillonite group minerals. Thus, migration flow in montmorillonite clay is one order of magnitude smaller than that in kaolinite and polymineral clays. This resulted in lesser segregated ice formation in them. The maximum value of deformation due to segregated ice formation was found in kaolinite clay and a significantly lower one in polymineral clay. No visible ice interlayers formed in montmorillonite clay under our experimental conditions. The clays studied can be arranged, according to their thermal settlement, in the sequence: kaolinite polymineral clay montmorillonite. Since the samples were thawing in free moisture inflow conditions, their moisture content increased and corresponding swelling deformations increased either. The resulting value of opposite deformations was positive in our experiments, i.e. instead of the expected (in 8 hours) subsidence of the sample top, its rise was observed. Similar resulting positive deformation values in kaolinite and montmorillonite clay samples are determined by the differences in swelling deformations. Swelling deformations in kaolinite, polymineral, and montmorillonite clays accounted for 27, 75, and 96 percent of the total positive deformations, respectively.

The deformation process in thawing frozen soils is greatly affected by their initial compactness, since this determines the dynamics of heat and mass exchange, physico-chemical, and physico-mechanical processes. The increasing density of thawing kaolinite samples (from 1.25 to 1.36 to 1.41 g/cm^3) brings about a decrease in migration flow from the thawed to frozen zone by more than one order of magnitude. The largest heaving deformation occurred in the sample of lesser density (Fig.4).

The change of thawing conditions (temperature and absense of water inflow) significantly affects the deformation. The greatest factor of thawing ground deformation is the advance rate of the phase boundary. It was found that at a thawing rate exceeding 1.5 cm/h, ice interlayers

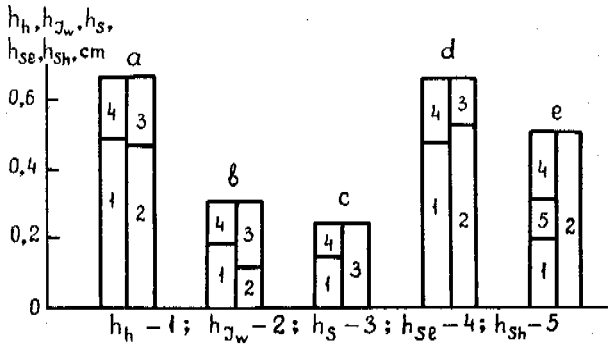

Fig.4 Correlation of heaving (h_h) caused by migration ice accumulation (h_{I_w}) and swelling (h_s) (shrinkage (h_{sh}) and settlement (h_{se}) were taken into account) in unidirectionally thawing kaolinite clay samples, initially compacted at 0.1 MPa (a,d) and 0.4 MPs (c), in open system conditions; and at 0.1 MPa (b) in closed system conditions.

in our tests were not formed. In this case, deformation of the samples is determined by the sum total of swelling and shrinkage deformations. Slower thawing rates result in an intensive development of all types of deformation, especially, of heaving due to segregated ice formation.

Comparison of thawing results for identical samples (W_i = 0.51 and ρ_d = 1.25 g/cm^3) with and without moisture inflow enables the following conclusions to be drawn. In undirectionally thawing samples, in both cases, segregated ice accumulation involves a certain amount of water which migrates to the frozen zone forming ice interlayers. Then, these ice interlayers are thawing with the approach of the thawing front, and the melt water again migrates to the region of lower negative temperatures. However, under closed system conditions, segregated ice accumulation is based on internal water redistribution. In this case, dehydration and shrinkage but not swelling of the thawed zone were observed.

In a closed system, shrinkage deformation compensated for over 20 percent of the total positive deformation.

Of special interest are experimental observations of deformation of frozen fine-grained soils interacting with cooled solutions of water-soluble salts of various concentration at different values of external pressure. All tests did not allow lateral deformation of samples. Hence, the change in the hight of samples corresponds exactly to the change in their volume. As shown by laboratory tests, deformation of samples contacting with cooled salt solutions and experiencing constant external load (P = 0.2 MPa) occurs in different ways. At a low concentration of NaCl solution, the volume of samples increases up to a certain constant value, i.e. deformation stabilizes (Fig.5).

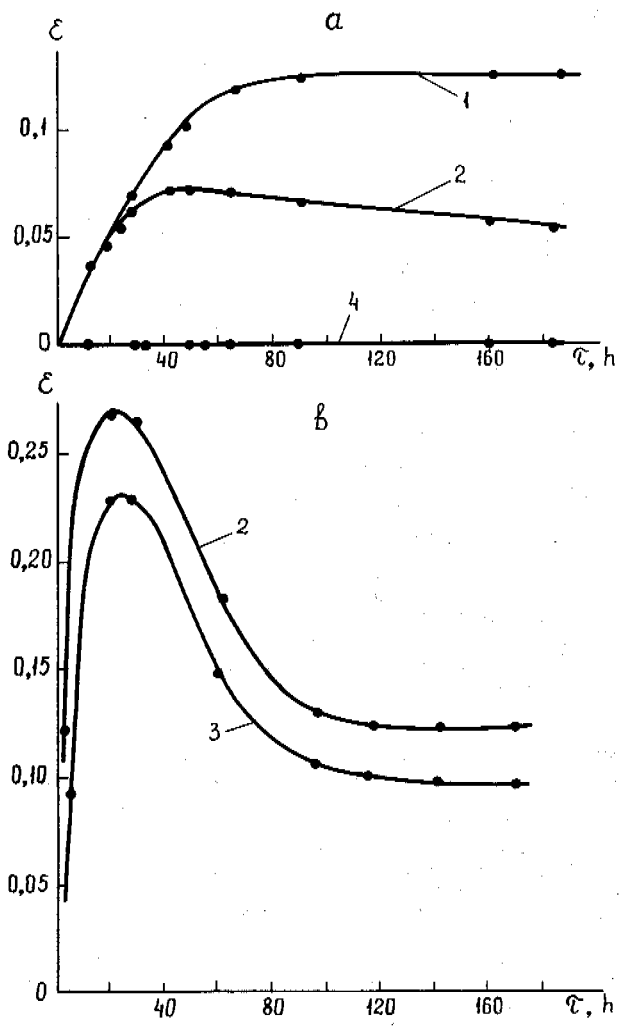

Fig.5 Dynamics of relative heaving deformation of frozen kaolinite semples interacting with NaCl solution; -2°C constant temperature of the experiment; a and b - with and without 0.2 MPa external pressure; 1, 2, 3, and 4 - external solution concentrations of 1.5, 2.0, 3.0, and 4.0 N, respectively.

At a more than 3-fold increase in NaCl solution concentration, positive deformations are followed by negative ones that reduce the volume of samples (Fig.5). This pattern of deformation shows that accumulation of moisture is replaced by its squeezing. The experimental proof of this is moisture distribution along the height of samples. Without external load, the curve $\varepsilon = f(\tau)$ is of more sharply expressed extreme character (Fig.6). This proves that at higher concentrations of an external water solution, interacting with a "fresh" (non-saline)

frozen soil, there occurs its intensive salinization, and the soil passes from frozen to frost-affected state; compaction and settlement of soil also develop. Analysis of relative heaving deformations of salinized frozen soils showed an extreme character of their maximum values dependence on an external salt solution temperature and concentration*/ (Fig.6).

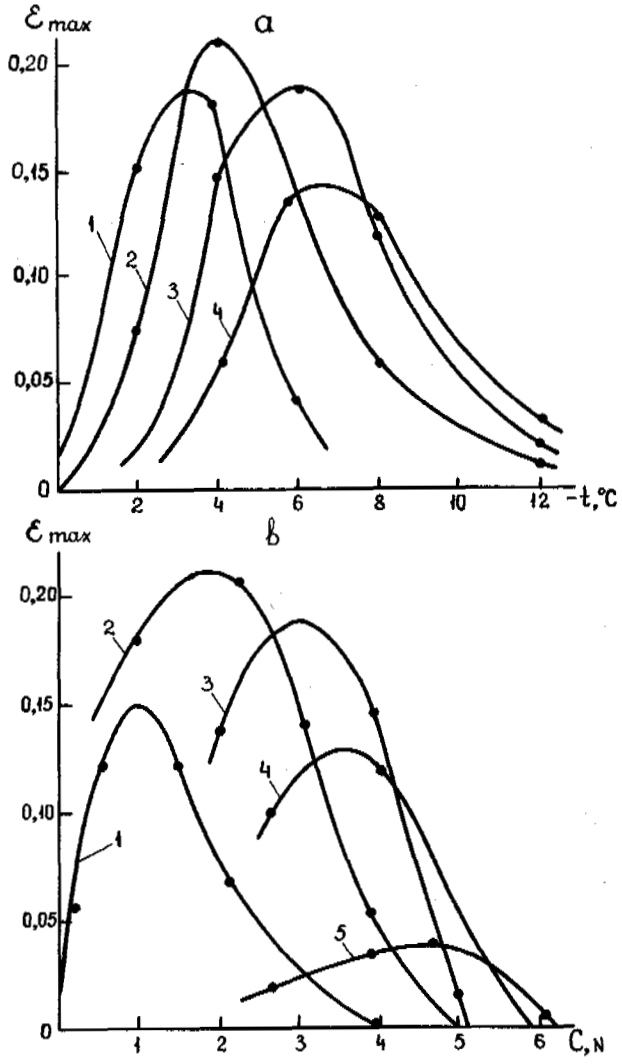

Fig.6 Dynamics of relative heaving maximum deformation of frozen kaolinite clay samples, at 0.2 MPa external pressure, as a function of: (a) temperature at different external solution concentrations (1, 2, 3, and 4 N); and (b) external solution concentration at different temperatures: 1, 2, 3, 4, and 5 correspond to -2, -4, -6, -8, and -12°C, respectively.

This shape of sample deformation curves results primarily from the nature of unfrozen moisture migration from external solutions to frozen samples. Moisture migration intensity variation as a function of external solution temperature and concentration were of similar extreme character.

Deformation of frozen soils in contact with NaCl solutions and brines is very strongly dependent on the externally applied load. Thus, when external pressure increases from 0 to 0.2 MPa, maximum deformation decreases by a factor of 3, and when the external pressure increases to 1 MPa, positive deformations are not observed.

*/ At temperatures below the freezing point of solutions, frozen nonsaline soils interacted with salinized ice.

PROPERTIES OF GEOCHEMICAL FIELDS IN THE PERMAFROST ZONE

V.N. Makarov

Permafrost Institute, Siberian Branch of the U.S.S.R. Academy of Sciences, Yakutsk, U.S.S.R.

SYNOPSIS This paper examines some properties of geochemical fields in the permafrost zone in relation to mineral deposits and 'technogenesis'. Currently, cryogeochemical fields of mineral deposits form in both residual and cover formations. Within the low-temperature permafrost overlying buried deposits, there arise superposed cryogenic areas having a significant vertical range of migration. During the course of the formation of technogenic geochemical fields there occur seasonal variations in intensity of geochemical fields caused by migration of chemical elements deep into a seasonally thawed layer under the action of a freezing front. Most of contamination products are concentrated in suprapermafrost waters, thus forming bodies of liquid saline water below 0°C saturated with heavy metals, and partly penetrate into the permafrost roof.

Over the past several years the study of specific features of geochemical fields in the permafrost zone has increasingly gained in significance, owing to active development of the northern regions, the need to tackle tasks associated with prospecting and exploitation of a mineral deposit as well as questions of construction and environment control in the permafrost zone. This determines the need for special-purpose investigations aimed at the study of characteristic properties of physico-chemical processes, migration and concentration of chemical elements at subzero temperatures.

Let us consider geochemical fields arising during the course of diversiform processes occurring actively in the permafrost zone which are associated, first, with the formation of cryogeochemical fields of mineral deposits and, second, technogenic areas produced as a result of man-induced processes.

Most authors who have addressed hypergenic processes in the permafrost zone that determine the formation of geochemical fields, limited the thickness of physico-chemical changes of the permafrost to its upper part as deep as 15 to 20 m, with the most probable depth being thought of 3 to 6 m, i.e., the layer of annual temperature fluctuations. However, recent natural-scale and experimental investigations on rock weathering and migration of chemical elements and their compounds at subzero temperatures, have revealed the existence of hypergenic processes occurring in the range of subzero temperatures.

A possibility of formation of geochemical fields in the permafrost zone was first pointed out by N.I. Safronov (1957), who noted two factors lending support to the formation of saline areas in the permafrost, namely (1) development of fibroferrite and melanterite on pirrotine in the permafrost, and (2) the existence of natural electric fields in conjunction with sulphide formations.

Hypergenic changes in ores of permafrost deposits are known to occur at considerable depths (Pitul'ko, 1977; Smirnov et al., 1941; Brown, 1942; Saksela, 1953; and others). There exists a hypothesis of contemporary origin of sulphate oxidized ores developed by Ivanov (1966; 1967), Kravtsov (1970) and Chaikovsky (1960). Ivanov explained the development of oxidizing processes by migration of combined water through the permafrost. Criticism of this view implied the impossibility of formation of deep sulphate areas of oxidation in such a fashion because of the limitation imposed on combined water migration by the layer of annual temperature fluctuations, i.e., by the temperature gradient.

Pitul'ko (1977), who has given a most thorough consideration to hypercryogenesis questions, notes that under the present-day conditions the main transformations of ore material are occurring within a seasonally thawed layer and through upper horizons of frozen ground, as high as the layer of annual temperature fluctuations. Incidental influence is exerted by penetrating surface waters, but the principal mineral-forming role pertains to pellicular waters migrating within the 'upper layer' (Shvetsov, 1961) of the permafrost, and to electrochemical processes.

The character of rock weathering in the cryogenesis zone at subzero temperatures is poorly studied. It is noted that in this case elements which under normal conditions are classified as sluggish - A^1, Ti, V, and Cr - are mobile (Tyutyunov, 1961). Pitul'ko (1961) found that Ca, Mg, Fe, Mn, Ti, Si, K, and Na are carried away from the cryogenesis zone. Inhibited water exchange, combined with carrying-away of chemical elements in frozen ground, lead to formation of mineral features rich in mobile elements, including mentmorillonite, various car-

bonates, hydromicas, and, sometimes, sulphates. Formation of salts on the bedrock surface occurs during a cold period of time as well (Kokin, 1985; Shwartsev, 1979). Cryogenic salts were observed by this author to occur in the form of leak-ins and thin crusts on outcrops of sand-clay shales of Permian age in the northern part of Ulakhan-Sis. Salts of white colour consisted of tenardite with admixture of astrakhanite ($Na_2Mg\ SO_4\ _2 4H_2O$) and vanthoffite ($Na_6Mg\ SO_4\ _4$) and contained (in %): silicon (1.0), aluminum (0.7), iron and cadmium (0.1), titanium (0.03), lead (0.005), silver (0.002), vanadium (0.001), manganese (0.0005), and copper (0.0002).

Investigations made by Kokin in the South Verkhoyanie showed evidence that this process was occurring on a considerable scale. Thus, about 200 mg of iron alum were released over the area of 1 sq. m on the surface of fissured terrigenous ores for two winter months (at the air temperature of -40°C).

Most dramatically, processes of scattering and concentration of chemical elements manifest themselves in the hypercryogenesis zone of a mineral deposit that has been comparatively well studied by exploration geochemists. It has been found that contemporary, secondary areas of scattering form in both seasonally thawed and frozen covers. In the frozen part of eluvial-deluvial deposits the mechanical constituent of the areas is formed as a result of frost cracking and the filling of cracks thus produced. The salt constituent in this case is formed due to vertical migration of the components within thin pellicles of unfrozen water. Lateral migration of material is usually hindered, but with considerable amounts of concentration, it occurs as well (Fig. 1).

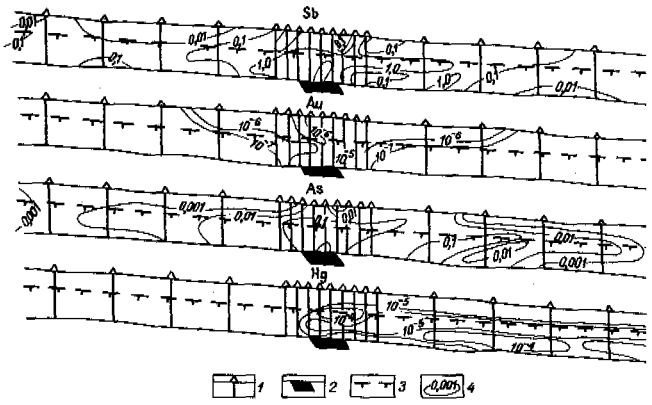

Fig.1 The Secondary Lithochemical Area of Scattering. 1 - Sampling Intervals; 2 - Ore Body; 3 - Upper Boundary of Permafrost; 4 - Isoconcentrations of Indicator-Elements, %.

The permafrost is dominated by salt scattering, and below buried deposits there arise superposed cryogenic areas. Mechanical displacement of material is possible only as a result of a manifestation of a number of cryogenic phenomena such as the formation of ice veins. With syngenetic freezing of the permafrost, a progressive increase of the seasonally thawed layer boundaries contributes to the drift of the area zone upwards along the overburden section, with a gradual increase in its breadth. A geochemical area formed due to syngenetic freezing of sediments, is normally mushroom-shaped and widely occurs at moderate latitudes.

During the course of epigenetic freezing of a friable uverburden, depending on the mechanism of formation of the superposed cryogenic area, there arise fan-shaped or post-shaped areas.

Fig. 2 shows an example of an epigenetic (with respect to the permafrost) superposed cryogenic area. The geochemical field above the ore

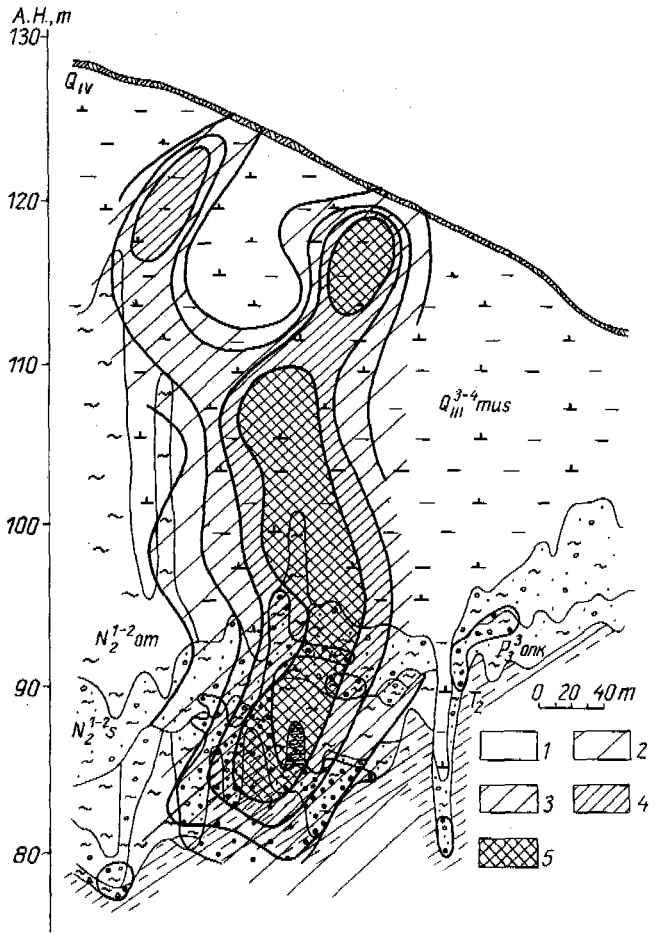

Fig.2 The Epigenetic, Superposed, Cryogenic Area of SO_4 in Allochtonic Sediments above the Ore Zone. Content of SO_4, mg.equiv.: 1 - less than 0.1; 2 - 0.1-0.2; 3 - 0.2-0.3; 4 - 0.3-0.4; 5 - more than 0.4.

body has a complex structure and is divided into a pre-cryogenic and cryogenic parts. The sulphate-ion distribution in permafrost sediments has a typical form of a geochemical area centered on the upper part of the ore body and with a gradual decrease in concentration. The area had formed due to oxidation of sulphides, whose increased concentrations are associated with the zone of ore mineralization occurring near sand-clay shales of Trias age and at overlying gravel-clay sediments. This is the pre-cryogenic part of the geochemical field and had formed under conditions of warm, wet climate. The sulphate-ion anomaly occurring in overlying Pliocene-Pleistocene sediments could have been produced only due to increased sulphidization of Paleogene sediments existing within the contour of the pre-cryogenic area. According to the current understanding, the beginning of formation of the permafrost zone in the North-East of the U.S.S.R. dates back to the first half of Pleistocene and has been persisted continuously since then.

Thus, areas occurring in Pleistocene sediments could have formed only under conditions of cryogenesis. It is beyond all shadow of doubt that the sulphate-ion anomaly is formed due to upward migration from the source in Trias and Paleogene sediments. In this regard, it is fundamentally important that cryogenic areas also occur within the permafrost occurring below the horizon of annual temperature fluctuations, whose depth in the region involved is 10 to 12 m (Makarov and Vinokurov, 1985).

Another example of migration of chemical elements through perennially frozen sediments may be hydrogeochemical anomalies occurring in Arctic lowlands of the North-East of the U.S.S.R. The permafrost zone thickness varies, according to drilling data, from 158 to 470 m and more. Open taliks are rare and are possible only below large rivers and deep eroding lakes.

Water flows are notable for lakes and rivers with increased mineralization. Hydrogeochemical fields are associate (with respect to mineralized waters and anomalies of a number of heavy metals) with tearing disturbances and ring structures identified on air- and satellite photo interpretation. Although the chemical composition of alochtonic sediments is uniform, it is evident that sources of hydrogeochemical anomalies associated with tectonic elements, occur in bedrocks and are covered by a thick layer of Cainozoic permafrost sediments (Makarov and Kondratyev,1986).

In the absence of gravitational moisture, geochemical fields are produced as a result of ion diffusion within liquid pellicles of an unfrozen solution under the action of the concentration gradient and electrochemical fields. The established vertical range of occurrence of geochemical fields through the permafrost sediments, with temperatures of -6.6... -10.2°C at the base of the yearly fluctuation horizon, constitutes the first hundreds of meters for anomalies associated with mineral deposits.

Geochemical fields in the permafrost zone associated with manifestations of man-induced processes, show some characteristic properties.

For technogenous landscapes of cities and urbanized areas, the epigenetic component of soils is formed largely due to pollutions precipitating from the atmosphere. It is known that, outside of the permafrost zone, the greatest soil pollution by technogenesis products occurs on the soil surface (Nezhdanova et al., 1984). Primarily, it is due to aerotechnogenous flows of material and occurs as deep as 20 to 40 cm. Under cryogenesis conditions there occurs an intense transfer of technogenous pollution products (mainly, the mobile component composed of easily solvable constituents) with subsoil waters and soil solutions deep into the seasonally thawed layer (STL). As freezing is progressing, soil and suprapermafrost waters saturated with technogenous components, are pushed down into lower horizons of the STL where there occurs their cryogenic concentration as well as the formation of bodies of liquid saline water below 0°C and their localization in the form of lenses at the bottom of the STL and in the permafrost roof. Cryogenic transfer of technogenesis products accumulated in soils that occurs during the freezing and thawing of the STL, leads to seasonal intensity variations of the geochemical field. For purposes of carrying out observations of this process in the area of Yakutsk situated in the permafrost zone (a continuous permafrost zone of 250-350 m thickness with localized taliks below rivers), a study was made of the chemical composition of bank soils and soil extracts from them prior to the beginning and after the end of a cold period (28-30 September and 15-18 May, respectively). The study revealed noticeable changes in composition of the components within the contours of technogenous anomalies and their productivity (the amount of material and chemical element over the city's area with a soil layer 1 m thick), depending on the season.

From the difference in the magnitudes of productivity of technogenous geochemical anomalies in territory of the city during different seasons, an estimate was made of the absolute amount of substance displaced as a result of cryogenesis into the STL bottom. Geochemical fields of SO_4, Cl, Na, Ca, Mg, HCO_3, Cu, V, Cr, Pb, Mo, Ga, Sn, and Ag show greatest contrast prior to onset of a cold period when the upper horizons of the STL accumulate technogenesis products. During the winter period, however, during the cryogenic redistribution of dissoluted substances and their migration deep into the STL under the action of the freezing front, there occurs depletion of the upper horizons of soils, thus giving rise to a decrease in the content of most components and in their productivity by the beginning of a warm period. Most of mobile pollution products, however, are concentrated in gravitational waters forming bodies of saline water below 0°C, while a certain amount of them are able to penetrate into the permafrost roof. The main mechanism for ion migration is the concentration gradient in this case.

Let us consider an example of a technogenous geochemical field that has formed in unfrozen and frozen ground in the area of a thermal power station situated in the same city. Earth materials at the base of the station include

overcast sandy-aleurite materials subdividing into two: perennially frozen ground that froze immediately after being overcast and have virtually not been affected by technogenous processes, and unfrozen ground that has frozen during the last two or three years and had been subjected - before freezing - to the influence of many years (about 50) of technogenous pollution.

The main source for formation of a geochemical field is provided by atmospheric discharges and escapes of the thermal power station so that heavy metals should be concentrated in the subsurface layer of soils. Indeed, in frozen and unfrozen ground (or taliks persisting below the thermal power station building), an accumulation of microelements is observed in the upper layers showing maximum concentrations of Mn, V, and Cu; other metals such as Cd, Zn, and Sn are also present. Down along the section the composition of chemical elements decreases.

A most dramatic decrease in the content of contaminating substances in the unfrozen and newly frozen ground is observed within the 5-8 m range of depths. However, also at a depth of 10 or 11 m the concentration of pollution components reaches background values, i.e., compositions in the permafrost. It is obvious that migration of chemical elements within soils of a technogenous talik has reached a considerable depth, owing to an intense washout regime associated with the closeness of a drainage system.

Interestingly, pollution substances are observed to accumulate in the permafrost as well (Figs 3 and 4). In the permafrost, however, anomalous concentrations of chlorine, zink, cadmium and chromium are markedly lower as compared with frozen ground and occur at smaller depths, as small as 5 to 9 m. Since the greatest depth of seasonal thaw at the base of the thermal power station is 2.4 m, therefore it should be assumed that migration of substance does, indeed, occur into the permafrost roof at subzero temperatures (-3.5...-5 at 5 m depth, and -2.5...-4.5°C at 10 m depth).

The results presented in this paper may be summarized as follows. The knowledge of the properties of geochemical fields arising in the permafrost zone under the influence of natural and man-induced factors is of major importance in connection with intense development of northern regions. A study of cryogeochemical fields produced below concealed mineral deposits would be useful for easing the search for such objects, especially in closed regions. The knowledge of geochemistry of technogenous processes gains particular importance because, according to demographers' estimations, over 80% of the population of Arctic and subArctic regions will be concentrated in towns and settlements by the year 2000.

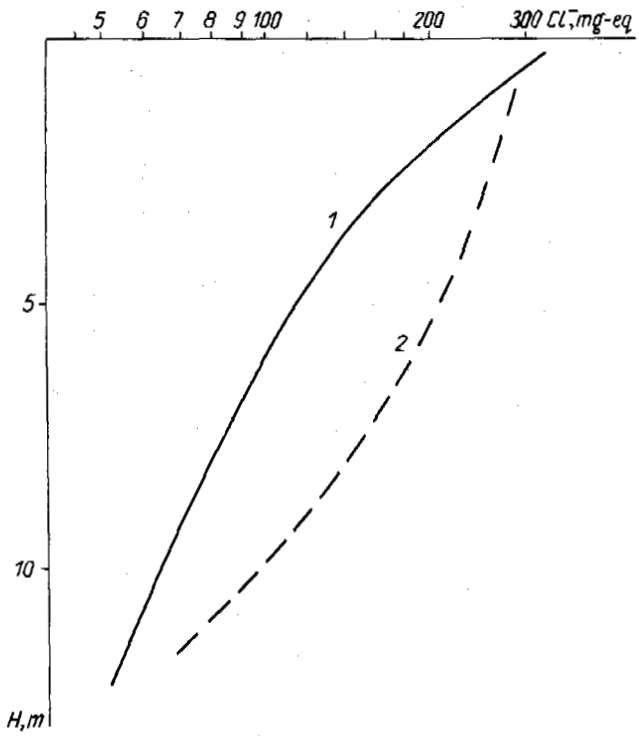

Fig.3 Cl^- Concentration in Water Extracts from Soils at the Base of a Thermal Power Station. 1 - in the Permafrost; 2 - in Frozen Ground.

REFERENCES

Brown, J.S. (1942). Differential density of ground water as a factor in circulation, oxidation and deposition. Econ. Geol., v. 37, No. 4, 124-129.

Chaikovsky, V.K. (1960). Geologiya olovonosnykh mestorozhdeniy Severo-Vostoka SSSR, 334 p., Moscow: Gosgeoltekhizdat.

Ivanov, O.P. (1966). Osnovnye faktory razvitiya zon okisleniya sulfidnykh mestorozhdeniy v usloviyakh mnogoletnei merzloty. Geokhimiya, No. 9, 1095-1105.

Ivanov, O.P. (1967). O kriogennykh solevykh oreolakh rasseyaniya rudnykh komponentov. Uchen.zap. TsNIIOlovo, No. 1, 3-12, Novosibirsk.

Kokin, A.V. (1984). Prirodnye solevye vytyazhki i ikh poiskovoye znachenie v zone razvitiya mnogoletnei merzloty. Geologiya i geofizika, No.6, 37-44.

Kravtsev, E.D. (1970). Morfologiya, mineraly i usloviya obrazovaniya zony okisleniya Dyakhtardakhskogo mestorozhdeniya. - V kn.: Geokhimicheskie poiski v oblastyakh kriogeneza, 30-35, Leningrad.

Makarov, V.N. and Vinokurov, I.P. (1985). Kriogeokhimicheskie polya mestorozhdeniy poleznykh iskopaemykh. - V kn.: Migratsiya khimicheskikh elementov v kriolitozone, 4-13, Novosibirsk: Nauka.

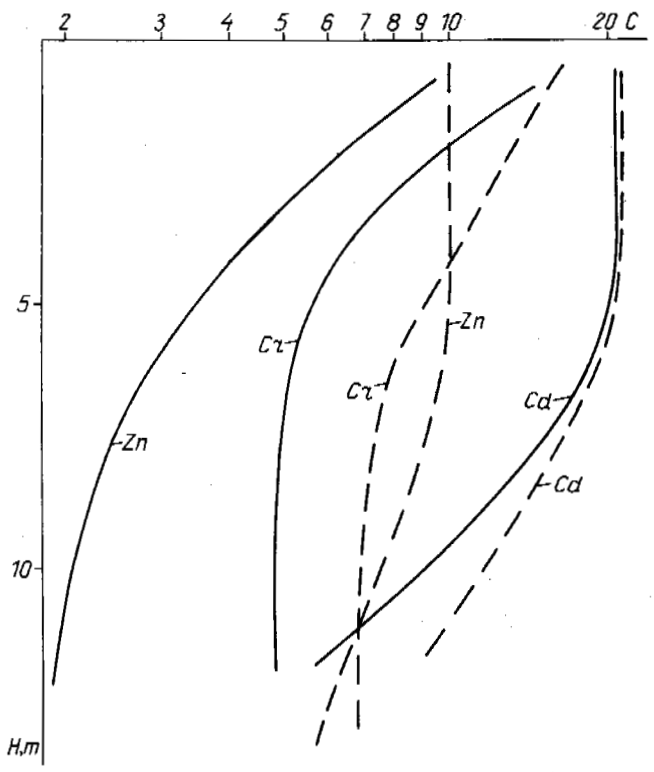

Fig.4 Zn, Cr and Cd Concentrations in Water Extracts from Soils at the Base of a Thermal Power Station. 1 - in the Permafrost; 2 - in Frozen Ground.

Makarov, V.N. and Kondratyev, P.S. (1986). Distantsionnoe zondirovanie i rasshifrovka prirody kriogidrogeokhimicheskikh anomaliy. - V kn.: Voprosy geokriologicheskogo kartirovaniya, 133-144, Yakutsk: Institut merzlotovedeniya.

Nezhdanova, I.K., Suentin, Yu.P. and Veselago, A.D. (1984). Ob izuchenii zagryaznennosti gorodskikh pochv v svyazi s okhranoi okruzhayushchei sredy. Vestnik LGU, No. 12, 89-93.

Pitul'ko, V.M. (1977). Vtorichnye oreoly rasseyaniya v kriolitozone, 197 p., Leningrad: Nedra.

Safronov, N.I. (1957). Opyt geokhimicheskikh poiskov na Krainem Severo-Vostoke SSSR. - V kn.: Geokhimicheskie poiski rudnykh mestorozhdeniy, 236-241, Moscow: Gosgeoltekhizdat.

Saksela, M. (1953). Über die Verwitterung einiger finnischer Kieserze. Bull. Com. Geol. Finlande, No. 157, 221-238.

Smirnov, S.S., Dubovik, M.M. and Epifanov, P. P. (1941). Mineralogicheskiy ocherk Yana-Adychanskogo rayona. Trudy In-ta geol. nauk AN SSSR. Ser.mineral., v.46, 1-62.

Shvetsov, P.F. (1961). Kriogennye geokhimicheskie polya na territorii kriolitozony. Izv. AN SSSR, Ser.geol., No.1, 46-51.

Shvartsev, S.L. (1979). Usloviya formirovaniya vtorichnykh oreolov rasseyaniya i osobennosti primeneniya geokhimicheskikh metodov poiskov v oblasti kriogeneza. - V kn.: Osobennosti geokhimicheskikh oreolov v oblasti kriogeneza. Gazo-solevye oreoly, 5-7, Yakutsk: Izd. Instituta merzlotovedeniya SO AN SSSR.

Tyutyunov, I.A. (1961). Vvedenie v teoriyu formirovaniya merzlykh porod. 102 p., Moscow: Izd. AN SSSR.

Ugolini, F.C. and Anderson, D.M. (1972). Ionic migration in frozen Antarctic soil. Antarctic J.U.S., 7, No. 4, 112-113.

THE DYNAMICS OF SUMMER GROUND THAWING IN THE KAFFIÖYRA PLAIN (NW SPITSBERGEN)

K. Marciniak, R. Przybylak, W. Szczepanik

Institute of Geography, Nicholas Copernicus University, Toruń, Poland

SYNOPSIS The dynamics of ground thawing on the beach ridge situated at the coastal Kaffiöyra Plain is presented on the base investigations carried out during three summer seasons (1979, 1980 and 1982). The influence of meteorological factors upon the course, rate and maximum depth of summer ground thawing is analyzed.

INTRODUCTION

The research carried out by the authors of the present paper was aimed at the study of the depth and rate of summer ground thawing in relation to meteorological conditions. Measurements of the thickness of the active layer were made during three Toruń Polar Expeditions in 1979, 1980 and 1982. The seasons differed considerably from each other in respect of weather conditions in Spitsbergen, which made achievement of set research objectives possible. The summer season of 1979 was characterized by higher than normally values of air temperature, longer sunshine duration and less precipitation. However, in the summer of 1980 there was exceptionally much precipitation and very little sunshine duration at the temperature approximating normal. The summer of 1982 was different from both listed above, first of all, because of air temperature which was much lower.

THE AREA AND METHOD OF RESEARCH

Measurements of the depth of ground thawing were made every day at the same plot situated at the Scientific Station of Nicholas Copernicus University (Toruń, Poland) in the northern part of Kaffiöyra coastal plain (Oscar II Land, NW Spitsbergen), on a coastal bank (1.5 m above sea level) which was not covered by vegetation at a distance of about 150 m from Forlandsundet coastline (Fig.1). In the summer seasons of 1979 and 1980 the duration of measurements was practically identical (6th July - 5th September 1979 and 6th July - 7th September 1980) while the measurement period in the summer of 1982 was slightly shorter (14th July - 5th September 1982).

The depth of ground thawing was measured by means of percussive method with the use a hand operated auger 1.5 m long and 10 mm in diameter made of hardened steel. In order for the measurements to be more representative sounding was made three times and a mean value was calculated from the obtained results. The distance between the points of sounding forming the shape of a triangle was ca 10 m. In the profile of

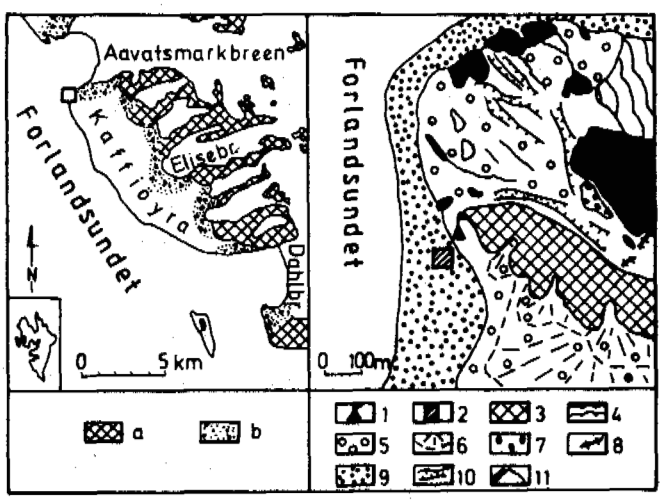

Fig.1 Location sketch of the area with systematic measurements of the ground thawing by the Scientific Station Nicholas Copernicus University, Kaffiöyra (morphological features by W. Niewiarowski map - 1982)

a - mountain ridges, b - morainic zones
1 - Scientific Station Nicholas Copernicus University, 2 - measurement field, 3 - end and lateral moraines, 4 - undulat morainic plain, 5 - outwash plains, 6 - outwash cones, 7 - kames, 8 - eskers, 9 - beaches and beach ridges, 10 - scarps, 11 - lakes and streams

these points there appears gravel and sand material down to the floor of maximum thawing depth.

Ground temperature was measured four times a day (00, 06, 12, 18 GMT) at depths: 1 cm, 5 cm, 10 cm, 20 cm, 50 cm. The measurements were made at the sounding plot, i.e. at the same lithological and moisture conditions. Meteorological observations were carried out at the station, about 30 m away from the points of ground sounding. Obtained in this way measurement results are suitable for an analysis of the dynamics of ground thawing dependent on weather conditions.

TABLE I

Mean decade depths and ground thawing rate as well as values of some meteorological elements in summer seasons of 1979, 1980 and 1982

Observation period	Maximal thawing depth cm	Thickness increase of an active layer		Ground thawing rate cm/day	Relative sunshine duration %	Mean daily air temperature 2 m above a ground °C	Mean daily ground temperature, °C		Atmospheric precipitation mm
		cm	%				-1 cm	-50 cm	
1979									
6.07 - 15.07	57	27	29.3	2.7	19.0	4.4	6.0	-	-
16.07 - 25.07	75	18	19.6	1.8	59.5	6.9	11.3	2.7	.
26.07 - 5.08	87	12	13.0	1.1	16.8	3.0	5.4	2.2	2.8
6.08 - 15.08	90	3	3.2	0.3	19.4	5.0	6.2	2.1	7.1
16.08 - 25.08	92	2	2.2	0.2	22.7	5.3	6.2	2.6	7.8
26.08 - 5.09	91	-1	-	-0.1	22.5	2.8	3.1	1.4	0.8
26.07 - 5.09	92	17	18.5	0.4	20.3	4.0	5.2	2.1	18.5
6.07 - 5.09	92	62	67.4	1.0	26.4	4.5	6.3	2.1	-
1980									
6.07 - 15.07	66	12	12.5	1.2	30.7	3.4	8.2	1.9	0.2
16.07 - 25.07	78	12	12.5	1.2	5.8	4.2	8.1	2.3	6.0
26.07 - 5.08	88	10	10.4	0.9	7.1	5.0	6.9	2.6	10.3
6.08 - 15.08	91	3	3.1	0.3	11.9	4.1	5.0	2.0	45.9
16.08 - 25.08	94	3	3.1	0.3	15.2	3.8	4.9	2.3	42.7
26.08 - 5.09	96	2	2.1	0.2	3.8	2.9	3.3	1.5	4.4
26.07 - 5.09	96	18	18.8	0.4	9.1	4.0	5.0	2.1	103.3
6.07 - 5.09	96	42	43.8	0.7	12.0	3.9	6.0	2.1	109.5
1982									
6.07 - 15.07	-	-	-	-	-	-	-	-	-
16.07 - 25.07	70	5	5.7	0.5	0.9	3.3	5.8	1.4	18.6
26.07 - 5.08	75	5	5.7	0.5	7.8	3.9	5.8	1.7	12.1
6.08 - 15.08	84	9	10.2	0.9	20.0	5.6	7.3	2.3	15.3
16.08 - 25.08	88	4	4.5	0.4	6.9	3.0	4.7	1.9	5.4
26.08 - 5.09	87	-1	-	-0.1	31.7	-0.3	0.1	0.2	9.4
26.07 - 5.09	88	18	20.5	0.4	15.9	3.0	4.4	1.5	42.2
6.07 - 5.09	-	-	-	-	-	-	-	-	-

THE INFLUENCE OF METEOROLOGICAL CONDITIONS ON THE COURSE AND RATE OF SUMMER GROUND THAWING

Our measurements of the depth of ground thawing were made during each of the three summer seasons by means of the same methods and at the same plot, i.e. at the same topographic and geological conditions. Therefore the differences in the course and depth of ground thawing between the seasons were caused exclusively by meteorological conditions.

Table I and figures 2 - 4 show the course and rate of ground thawing against the background of meteorological conditions. Unfortunately, they do not include the beginning of the thawing period for the reason of the duration of the expeditions. Of all Polish stations appropriate data for the whole thawing period are in the possession of the station Hornsund (SW Spitsbergen).

Ground thawing in Spitsbergen begins several days after (the delay resulting from the time necessary for complete snow melting) mean daily temperatures 0°C prevail (the beginning of the warm season of the year). On the base of the meteorological data from the period 1946 - 1965 for Isfjord Radio it has been ascertained that the season begins on 5th June on the average. Hence ground thawing on the western coast of Spitsbergen begins in mid June on the average, which corresponds to the data obtained by Grześ (1984, 1985).

The calculation of the data of the beginning of ground thawing in particular years encounters difficulties caused by fluctuations of the value of heat balance around 0 W/cm^2 on the top of permafrost. Therefore, short periods with thawed and frozen ground may directly follow each other.

The authors of the present paper calculated the beginning of ground thawing in Kaffiöyra in each of the listed summer seasons on the base of the data from the stations in Barentsburg and Ny Alesund (situated similarly to our research area on the western coast of Spitsbergen). It was the earliest in the summer of 1982 (the second decade of June) and the latest in 1979 (the first pentade of July). It follows from this that the beginning of ground thawing in Kaffiöyra in the three analyzed summer seasons was delayed (5 - 15 days) in comparison with many-years data for the western coast of Spitsbergen.

The rate of ground thawing is not constant during the summer season (Table I, Figures 2 - 4). As follows from the diagrams showing this process, published among others by Grześ (1984,

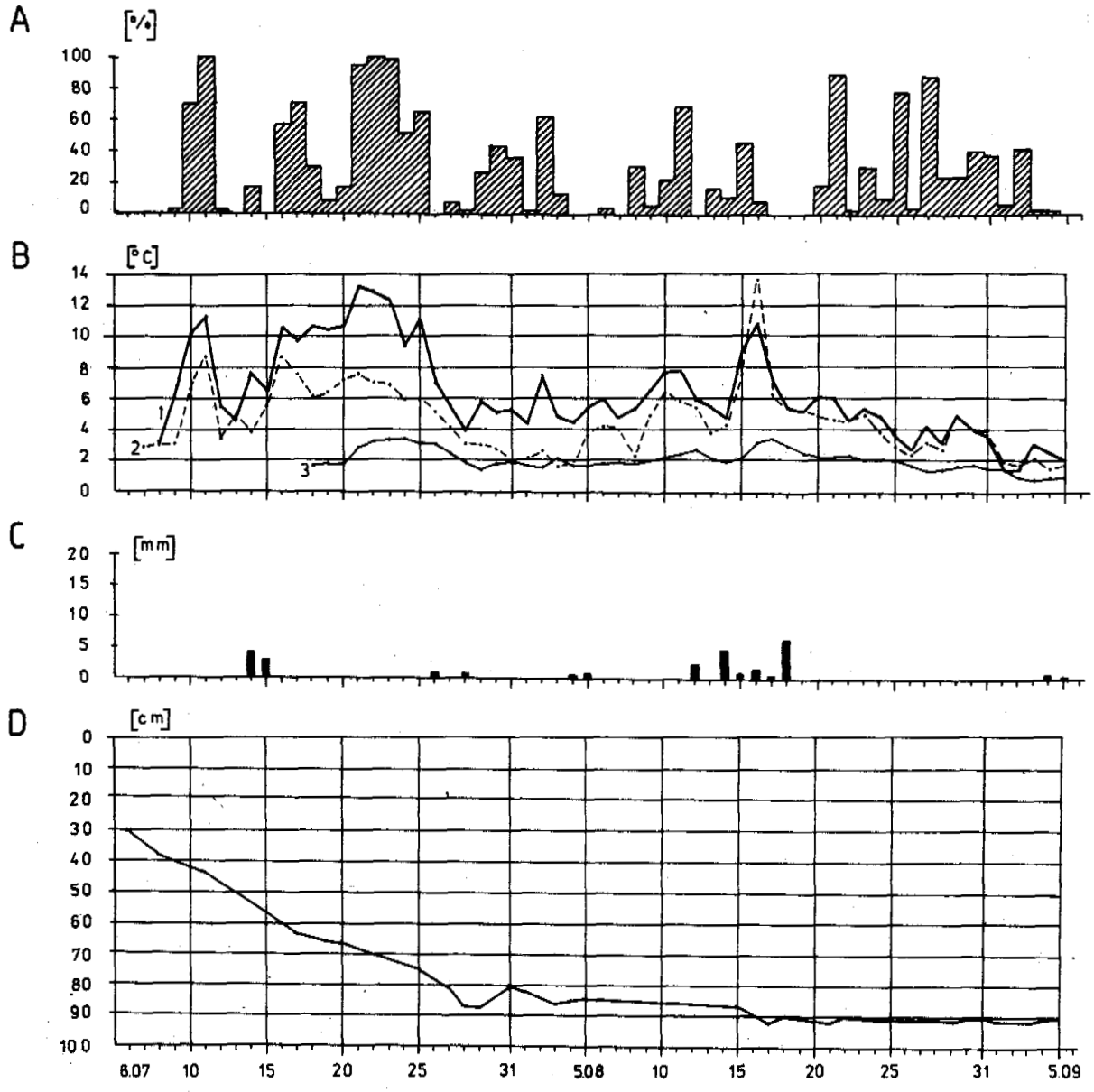

Fig.2 A course of a ground thawing and values of some meteorological elements in summer 1979

A - relative sunshine duration; B - temperature changes: 1 - ground surface temperature, 2 - air temperature 2 m above the ground, 3 - ground temperature at depth of 50 cm ; C - precipitation; D - ground thawing depth

1985), Jahn (1982), Jahn and Walker (1983), Mackay (1970), Marciniak and Szczepanik (1983), ground thawing is most intense in the initial period right after snow cover has melted. This is caused by the strongest influence of meteorological factors on permafrost degradation in this time resulting from the smallest thickness of isolating active layer. Moreover, due to the melting of still present snow patches and permafrost it is highly moisturized, which favours a quick flow of heat from the ground surface to the top of permafrost.

Our research results in Kaffiöyra for the initial period of ground thawing are in accordance with the results obtained by Jahn (1982). For example it was estimated that in the beginning of July 1979 the thawing rate of ground with no vegetation was 5 - 6 cm/day , and when the thickness of the active layer exceeded 30 cm, the rate dropped to below 3 cm/day to reach 0.2 - 0.3 cm/day in the end of the summer.

As has already been mentioned, the influence of meteorological conditions on the rate of thawing is most apparent in the early part of the summer, i.e. approximately to the end of July. For example, the ground thawing rate in the decade 16th - 25th July was 1.8 cm/day in the warmest summer season of 1979, 1.2 cm/day

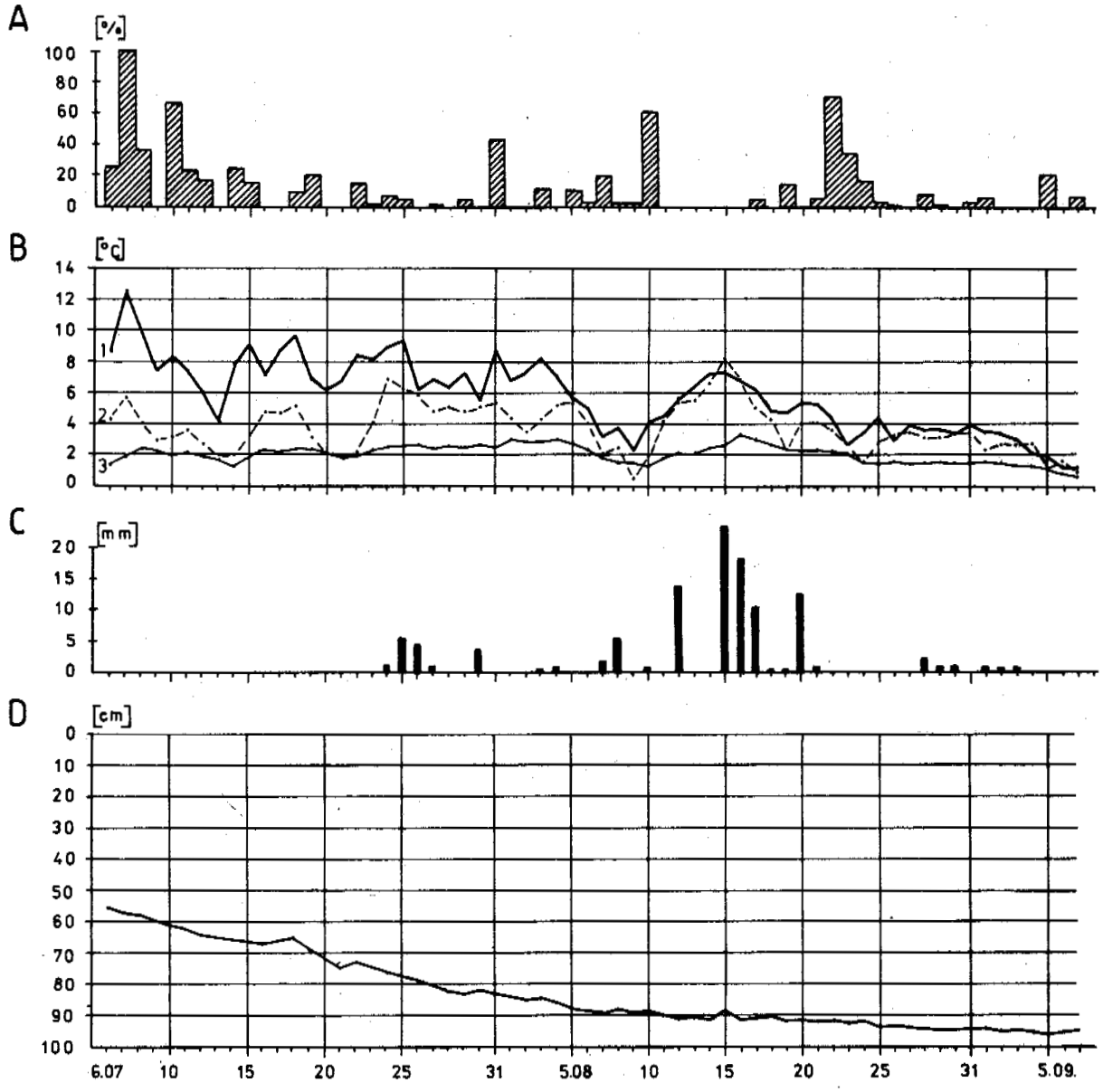

Fig.3 A course of a ground thawing and values of some meteorological elements in summer 1980. Description as to Fig.2

in the moderate one of 1980 and 0.5 cm/day in the coolest one of 1982 (Table I). It should be added that on 16th July in all the years the depth of permafrost deposition was similar, therefore the intensity of thawing in the particular years depended exclusively on the meteorological conditions existing in the analyzed decade. In the latter part of the summer (August and the beginning of September), due to a considerable thickness of the active layer, the rate of ground thawing was almost equal in each of the three summer seasons (0.4 cm/day) in spite of different mean temperatures of the ground surface (from 5.2°C in 1979 to 4.4°C in 1982 - Table I). A similar scheme of summer ground thawing occurs in Northern Alaska (Walker, Harris 1976). In this time only considerable and long-lasting weather anomalies may cause changes in the rate of ground thawing.

During the summer, especially in the latter part, not only stagnation in the increase of thawed layer can be observed but also a periodical decrease in its thickness (Table I, Figs 2 - 4) due to the renewed ground freezing above the top of permafrost (freezing from the bottom). The process takes place when the mean daily temperature of air drops below 2°C (e.g. the end of July 1979, the middle of August, the second decade of August 1982). Formation of snow cover in the end of August 1982 slowed down ground freezing from the bottom of the active layer. The process of ground freezing began on 24th August when the mean daily tempera-

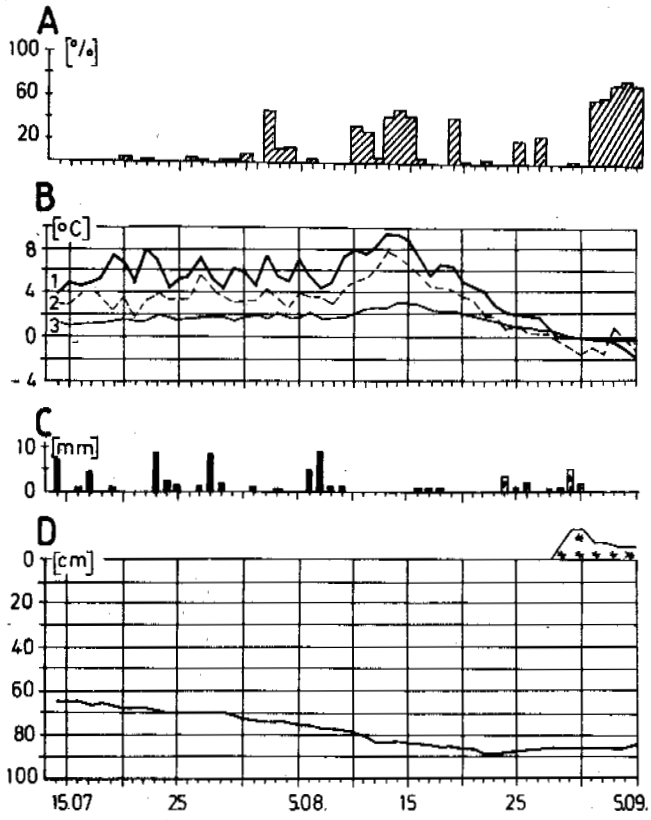

Fig.4 A course of a ground thawing and values of some meteorological elements in summer 1982. Description as to Fig.2

ture of air dropped below 1°C. A further drop of air temperature below 0°C lasting to the end of the research period as well as intense night heat radiation from snow resulted in the drop of the ground temperature under snow below 0°C to the depth of 50 cm. Thus freezing of the active layer from the surface began, followed by freezing from the bottom - since 4th September (Fig.4).

The end of summer ground thawing in Kaffiöyra takes place when the daily mean air temperature drops below 2°C. This happens predominantly in the first decade of September (Figs 2 and 3), and exceptionally it happens earlier when the summer is cooler than normal. The period of ground thawing in Kaffiöyra lasts on the average from the turn of the second and third decade of June to the first decade of September. This notion is conceived as a period from the beginning of constant presence of thawed layer to end of its increase. Before the beginning and after the end of the period conceived in this way there occurs a phenomenon of repeated thawing and freezing of the most subsurfacial layer of ground without snow cover (the so-called multigelational cycles). This is a result of frequent fluctuaction of air temperature - characteristic of the oceanic variant of arctic climate. For this reason short periods of ground freezing and thawing may occur in Spitsbergen during the whole year. It should be marked that spring and autumn temperature fluctuation on the ground surface with frequent passing 0°C are prolonged in comparison to respective air temperature fluctuation at the height of 2 m above ground level (Czeppe 1961, 1966).

THE INFLUENCE OF METEOROLOGICAL CONDITIONS ON MAXIMUM DEPTH OF SUMMER GROUND THAWING

Grześ (1984, 1985) distinguishes between seven „environments" in Spitsbergen differing in the course and depth of thawing. He gives a simplified scheme of thawing to each of them. Our measurement plot belongs to the fifth „environment" which he describes as follows: „sand, gravel, ..., building sea terrace levels with scanty tundra vegetation." It should be added that at our place there was no vegetation at all. According to Grześ's scheme (1984, 1985) in about mid July the depth of thawed ground should be 100 cm and its maximum depth in the beginning of September - 140 cm. The values should be greater at our measurement plot as it is devoid of vegetation but, as is shown in Tables I and II, Figures 2 - 4, the values of ground thawing obtained in our study are smaller than in Grześ's scheme. This is caused, among other things, by a considerable moisturization of ground at our plot situated in the coastal zone. One should be careful in extending research results concerning ground thawing because, as Jahn and Walker showed (1983), the maximum depth of the active layer varies in relation to the location and climatic conditions both in the macro- and mesoclimatic scale.

Of the three seasons analyzed in the present paper the highest maximum thickness of the active layer was measured in 1980 (99 cm) in spite of lower ground and air temperatures in the period compared to 1979. This was probably caused by high atmospheric precipitation which occured in the summer of 1980 (e.g. 78.8 mm in the second decade of August). The precipitation considerably increased ground moisturization and contributed to an increase in heat conductivity. Ryden and Kostov (1980) also stress the importance of precipitation in the process of ground thawing in the northern part of the Scandinavian Peninsula.

In the summer season of 1979 a slightly lower maximum value of the depth of ground thawing (96 cm) in spite of remarkably more favourable, in comparison with 1980, solar and thermic conditions but little sum of precipitation (Table I, Figure 2). In the coolest of the analyzed summer seasons, 1982, the maximum depth of the thawed layer was the smallest (88 cm) although the beginning of thawing was the earliest in the season. This is confirmed by Jahn and Walker (1983) who noticed that the length of the summer is relatively unimportant in the light of the fact that the thickness of the active layer begins to stabilize in midsummer. For comparison, the maximum depth of thawing in the summer of 1985 was 106 cm (Table II). The period was still warmer than in 1979.

The role of atmospheric precipitation occuring in the summer season as a factor affecting the depth of ground thawing is complex (Svecov, Zaporozceva, 1963). While examining this prob-

TABLE II

Maximum thickness of an active layer and mean values of some meteorological elements in summer seasons of 1979, 1980, 1982 and 1985

Observation period		1979		1980		1982		1985[1]	
		21-31.07	1-31.08	21-31.07	1-31.08	21-31.07	1-31.08	21-31.07	1-31.08
Ground temperature, °C	-1 cm	8.3	5.6	7.6	5.0	5.8	5.0	11.2	5.9
	-50 cm	2.6	2.1	2.4	2.1	1.6	1.7	4.5	2.8
Air temp. 2m a.g.l., °C		4.9	4.4	4.8	3.9	3.5	3.2	8.1	4.5
Atmosph. precipit., mm		1.9	15.8	15.2	92.8	23.6	30.9	6.4	15.1
Rel. sunshine dur., %		47.4	21.9	7.0	10.1	1.7	11.0	35.4	30.0
Max. measured thickness of an active layer, cm		96		99		88		106	

[1] After M. Kejna and M. Dzieniszewski (personal communication, 1987)

lem one should take into consideration the influence of precipitation on: 1) ground moisturizing, infiltration of precipitation water and heat transfer into frozen ground in the process of ground thawing, 2) degree of ground moisturization directly before its freezing in the autumn which determines the amount of ice in the ground which, in turn, affects the rate and depth of ground thawing in the following summer season. The present paper analyze the problem over four summer seasons (1979, 1980, 1982, 1985) for which we have comparable measurement results (Table II).

The thermic conditions of the compared summer seasons are remarkably less differentiated than the quantity and distribution in time of atmospheric precipitation. It can be concluded from this that the differences in maximum thawing depths between the particular years are to greater degree a result of the influence of precipitation rather than thermic conditions. It turns out that the highest maximum depths of ground thawing occured in the seasons following summer seasons with little precipitation in the end of the summer.

We have neglected here a closer analysis of meteorological conditions of the cool season of the year. However, it follows from our observations that in the first place they influence the length of the thawing period, especially its beginning, but they do not remarkably affect maximum values of ground thawing in the end of a summer season.

CONCLUSIONS

1. On the average, the beginning of ground thawing in Kaffiöyra falls at the turn of the second and third decade of June. Thus the mean time of its duration from the beginning of uninterrupted occurence of the active layer to the end of its increase is about 2.5 months.

2. One can distinguish between two periods in the process of ground thawing in Kaffiöyra: a - the period of a quick increase in the thawed layer at a rate of about 3 cm/day in the early part of the summer (on the average to the end of July), b - the period of a very slow increase in the thawed layer and even periodical stagnation or regression at a mean rate of 0.3 - 0.4 cm/day in the latter part of the summer (August and the beginning of September). During the first two weeks from the beginning of the process at least half the maximum thickness of the active layer thaws in the given summer season. In August the thawed layer increases only by 20 % of the whole active layer.

3. Varying year to year meteorological conditions result in different dates of the beginning, course (rate) and duration of the thawing process in particular summer seasons. The most significant influence of thermic and precipitation conditions take place in the early part of the polar summer. In the latter part of the summer the influence of the conditions occurs mainly at considerable weather anomalies.

4. In the process of summer ground thawing the increase in the thickness of the thawed layer appears sometimes side by side with its decrease. It occurs as a sequence of periodical coolness especially in the latter part of summer.

5. There are differences in the maximum thickness of the thawed layer between particular summer seasons dependent mainly on varying meteorological conditions in each year.

REFERENCES

Czeppe, Z. (1966). Przebieg głównych procesów morfogenetycznych w południowo-zachodnim Spitsbergenie. ZN UJ, Pr. Geogr. 13, 1-129

Grześ, M. (1985), Warstwa czynna wieloletniej zmarzliny na zachodnich wybrzeżach Spitsbergenu. Prz. Geogr. (57), z. 4, 671-697

Jahn, A., Walker, H. J. (1983). The active layer and climate. Z. Geomorph. Suppl. - Bd 47, 97-108, Berlin - Stuttgart

Mackay, J. R. (1970). Disturbances of the tundra environment of the western Arctic. Canad. Geotech. J. (7), No 4, 420-432

Walker, H. J., Harris, M. K. (1976). Perched ponds: An arctic variety. Arctic 29, 223 -238

A METHOD FOR MEASURING THE RATE OF WATER TRANSPORT DUE TO TEMPERATURE GRADIENTS IN UNSATURATED FROZEN SOILS

Nakano, Yoshisuke and A.R. Tice

U.S. Army Cold Regions Research and Engineering Laboratory

SYNOPSIS A new experimental method is introduced to determine the rate of water movement caused by temperature gradients in unsaturated frozen soils. When a linear temperature distribution is imposed on a closed soil column with initially a uniform water content, a redistribution of water occurs in the column. As time increases, the profile of water is stabilized to approach a stationary profile, which is used to calculate the rate of water movement due to temperature gradients. The theoretical justification of the method is presented and the feasibility of the method is demonstrated by experiments with a marine-deposited clay.

INTRODUCTION

Water in unsaturated frozen soils generally exists in three phases: vapor, unfrozen (liquid) water and ice. An accurate description of physical laws governing the water movement in frozen soils is needed for various engineering practices in cold regions.

We will consider a closed horizontal soil column with a length x_o [cm]. Assuming that all physical variables under consideration are uniform at any given cross section of the column, we will introduce a coordinate $x(x_o \geq x \geq 0)$ directed horizontally. We will then consider a special case in which the content of water in three phases $w(x)$ [g/g soil] and the dry density $\rho(x)$ [g/cm^3] in the column are initially given constants. In such a case it is known that the migration of water does not occur as long as the temperature of the column $T(x)$ is kept constant. However, if a temperature gradient is imposed on the column, the movement of water may take place.

In a part of the column where $T(x) > 0°C$, the soil is obviously unfrozen. The flux of water f[g/(cm^2·day)] in this unfrozen part may be written in a general form (Philip and deVries, 1957):

$$f = - \rho D_1(w,T) \frac{\partial w}{\partial x} - \rho D_2(w,T) \frac{\partial T}{\partial x} \quad \text{if } T > 0 \qquad (1)$$

where functions D_1 [cm^2/day] and D_2 [cm^2/(°C·day)] are the properties of a given soil and generally are continuous functions of w and T. Since the dependence of f on T and $\partial T/\partial x$ is generally believed to be not as significant as that on w and $\partial w/\partial x$, thermal effects on f are often tacitly ignored in many studies of water movement in unfrozen soils.

In a part of the column where $T(x) < 0$, ice may appear if $w(x)$ is greater than the equilibrium unfrozen water content $w^*(x)$ at $T(x)$. Nakano and Tice (1987) studied a special case in which $T(x)$ is constant. Using a marine-deposited clay, they have found that f is given as

$$f = - \rho D_1(w,T) \frac{\partial w}{\partial x} \quad \text{if } \frac{\partial T}{\partial x} = 0 \text{ and } T < 0 \qquad (2)$$

It is easy to see that Eq. 1 is reduced to Eq. 2 when $\partial T/\partial x$ vanishes.

Hadley and Eisenstadt (1955) studied thermal effects on f by using a column of granular media initially with uniform ρ and w. The column, which was thermally insulated around its circumference, was subjected on one end ($x = 0$) to a positive temperature T_w and on the other end ($x = x_o$) to a negative temperature T_c. Their experiments confirmed by means of radioactive tracers that there was a pronounced movement of water in the liquid phase toward the cold end.

Similar experiments to those of Handley and Eisenstadt (1955) were conducted by Dirksen and Miller (1966), and Hoekstra (1966) by using columns of soils. In the more recent experiments from our laboratory (Oliphant et al., 1983) a nearly constant temperature gradient was imposed on a column of soil, and approximate rates of water transport due to a temperature gradient were determined. According to these reported experimental data, it appears certain that a temperature gradient is an important driving force for the transport of water.

The transport coefficient D_2 due to a temperature gradient is believed to be the property of a given soil that must be determined experimentally. Assuming that gradients of w and T (and nothing else) are driving forces for the water movement in frozen and unsaturated soil with a uniform dry density, we will introduce an experimental method for the measurement of D_2. The theoretical justification of the method will be presented under the assumption that Eq. 1 holds true in frozen and unsaturated soil with a uniform dry density. Using a marine-deposited Morin clay, we will demonstrate the feasibility of the method.

THEORY

Assuming that Eq. 1 holds true also for $T \leq 0$, we will write the flux of water f as

$$f = f_1 + f_2 \tag{3}$$

$$f_1 = - \rho D_1(w,T) \frac{\partial w}{\partial x} \tag{4a}$$

$$f_2 = - \rho D_2(w,T) \frac{\partial T}{\partial x} \tag{4b}$$

where f_1 and f_2 are the flux of water due to a gradient of w and that of T, respectively.

We will consider a problem in which a closed soil column initially with given uniform ρ and w is subjected on one end $x = 0$ to a temperature T_w and on the other end $x = x_o$ to a temperature $T_c < T_w$ at time $t > 0$. We assume that the temperature distribution T(x) is strictly linear, namely

$$\frac{\partial T}{\partial x} = - a = (T_c - T_w)/x_o \tag{5}$$

where a is a positive number. We will describe the problem in mathematical terms as follows.

The equation of mass balance for water is given as

$$\rho \frac{\partial}{\partial t} w(x,t) = - \frac{\partial}{\partial x} f \qquad \text{for } x_o > x > 0 \ , \ t > 0 \tag{6}$$

The initial condition is given as

$$w(x, 0) = w_o \tag{7}$$

where w_o is a positive number. The boundary condition is given as

$$f(0, t) = f(x_o, t) = 0 \tag{8}$$

It follows from Eq. 5 that there is a one-to-one correspondence between x and T. Substituting T by x in Eqs. 4a and 4b and using Eq. 5, we rewrite f as

$$f = - \rho [D_1(w,x) \frac{\partial w}{\partial x} - a \, D_2(w, x)] \tag{9}$$

We will introduce a new function $\phi(w,x)$ defined as

$$\phi(w,x) = \int_0^w D_1(w,x)dw - a \int_0^x D_2(w,x)dx \tag{10}$$

Using ϕ, we reduce the problem of Eqs. 6, 7 and 8 to a commonly used form given as

$$\frac{\partial w}{\partial t} = \frac{\partial^2}{\partial x^2} \phi(w,x) \qquad \text{for } x_o > x > 0 \ , \ t > 0 \tag{11}$$

$$w(x,0) = w_o \tag{12}$$

$$\frac{\partial}{\partial x} \phi(w,0) = \frac{\partial}{\partial x} \phi(w, x_o) = 0 \tag{13}$$

Oleinik et al. (1958) have studied the problem of Eqs. 11, 12 and 13. They prove the existence of a unique solution to this problem if ϕ satisfies certain conditions of regularity. The problem of Eqs. 11, 12 and 13 has a particular solution $w^+(x)$ that is independent of time t. It is easy to see that such a stationary solution must satisfy the following equation if it exists:

$$D_1(w^+,x) \frac{dw^+}{dx} = a \, D_2(w^+,x) \tag{14}$$

It follows from Eq. 14 that the stationary solution $w^+(x)$ is a non-decreasing function in a part where D_1 is positive because D_1 and D_2 are believed to be nonnegative.

The solution w^+ corresponds to a stationary state of the soil column in which f vanishes everywhere in the column while the dry density is kept at the initial value. When the soil column initially with uniform ρ and w is subjected to the temperature gradient given by Eq. 5, the transport of water is expected to occur in the positive direction of x because of Eq. 4b. As water moves toward the cold end, the initial uniformity of w breaks down and a driving force of water toward the warmer end starts to build up because of Eq. 4a. Sooner or later two driving forces of water, one due to a temperature gradient and the other to a gradient of water content, tend to balance each other while the profile of water content w(x,t) asymptotically approaches the stationary profile $w^+(x)$ with increasing time. If we are able to measure $w^+(x)$ experimentally, then D_2 can be determined by Eq. 14 for a given soil with known D_1.

It is not certain that the anticipated event described above actually takes place. For instance, the transport of water may cause a significant change in the dry density of the column that is initially uniform. Also the time required for the column to reach a stationary state may turn out to be too long for the method to be practical. These problems must be examined by experimentations.

EXPERIMENT

In order to examine the feasibility of our proposed method, we conducted experiments in which closed soil columns initially with uniform ρ and w were subjected to a constant and linear temperature gradient. We designed the apparatus shown in Figure 1 for this purpose.

The apparatus consists of four parts made of aluminum: an upper plate, a lower plate and two end plates. The upper and lower plates are approximately 23 cm long by 20 cm wide by 5 cm thick. Four grooves with a rectangular cross section, 20.32 cm long by 1.27 cm wide by 0.625 cm deep, were machined on the upper surface of the lower plate. The center lines of these grooves, which are parallel to the longer side of the plate, are spaced 3.8 cm apart. Grooves for O-ring seals were also machined around each rectangular groove in the upper plate so that when the upper and lower

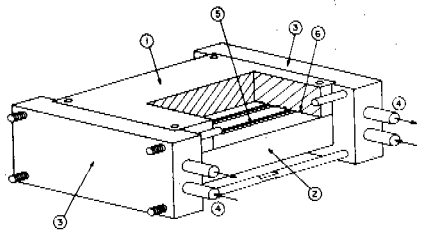

Figure 1 Apparatus. (1) Upper plate, (2) Lower plate, (3) End plates, (4) Inlet and outlet of an antifreeze mixture, (5) Groove, (6) O-ring.

plates are bolted together, four closed empty spaces of rectangular column shape are formed to be used as containers of soil.

Each of the two end plates has a 2.54-cm hole drilled into it, through which an anti-freeze mixture from a temperature-controlled bath is circulated. The two end plates are positioned by four bolts. Two sides of the upper and lower plates bolted together have a small taper that matches the taper of the end plates so that the bolted upper and lower plates smoothly slide into the spaces created by the two end plates with assured close contact. The four aluminum parts, when assembled together, are thermally insulated by foam plastic. A row of 10 copper-constantan thermocouples is placed with equal spacing through the upper plate along the center line of each groove to measure and record temperatures in a soil sample.

The soil selected for the experiment, called Morin clay, was a marine-deposited clay obtained from the Morin brickyard, Auburn, Maine. Morin clay is a non-swelling clay with a specific surface area of 60 m^2/g and a specific gravity of 2.75 g/cm^3. This clay was used in the experiments reported by Nakano and Tice (1987). For given dry density ρ and initial water content w_o, the exact amounts of oven-dry Morin clay and distilled water were weighed to be packed into a groove. Mixing thoroughly the weighed soil and water, we allowed the mixture to set for a few days to attain moisture equilibration. After all four grooves were packed with soil samples, we bolted together the upper and lower plates to seal each of four soil columns with a rectangular cross section and kept it at a temperature that was several degrees lower than the temperature of the cold end T_c.

An experiment began by placing the bolted upper and lower plates into the space between the two end plates. A stable and linear temperature field was usually established within 1 hour by adjusting the temperatures of two baths. After a specified time passed, the bolted upper and lower plates were brought into a coldroom with its temperature being set at -10°C. The two plates were separated and each sample was quickly sectioned into a total of 25 equal segments. Each segment was placed in a glass weighing bottle and oven-dried. The water content and the dry density of each segment were determined gravimetrically.

RESULTS AND DISCUSSION

The test conditions of experiments are presented in Table 1. For all these experiments we aimed to maintain the average dry density of the soil columns at 1.42 g/cm^3, although the uniform packing of soil in each column was quite difficult. We examined the uniformity of the soil columns by using the measured dry density of all segments after each experiment. The mean ρ_a and the standard deviation σ of dry density ρ are given in Table 1. Although these values are affected by errors involved in rapidly sectioning a soil column into 25 segments with ideally equal lengths, they serve as an indicator of uniformity in packing and accuracy in sectioning. The maximum water content measured among all experiments listed in Table 1 was about 25%, which is less than

Table 1. Experimental Conditions.

Exp. No.	Experimental Conditions w_o [%]	ρ_a [g/cm³]	σ [-]	T_w [°C]	T_c [°C]	a [°C/cm]	Time Duration [day]
1	15	1.42	0.13	1.40	-4.95	0.31	7
2	15	1.41	0.10	1.40	-4.95	0.31	14
3	15	1.43	0.14	1.40	-4.95	0.31	22
4	15	1.46	0.14	1.40	-4.95	0.31	34
5	20	1.43	0.13	1.40	-4.95	0.31	7
6	20	1.41	0.14	1.40	-4.95	0.31	14
7	20	1.40	0.10	1.40	-4.95	0.31	22
8	20	1.46	0.12	1.40	-4.95	0.31	34
9	5	1.40	0.13	1.40	-4.95	0.31	22
10	10	1.47	0.10	1.40	-4.95	0.31	22
11	5	1.38	0.14	1.35	-8.06	0.45	21
12	10	1.39	0.14	1.35	-8.06	0.45	21
13	15	1.41	0.11	1.35	-8.06	0.45	21
14	20	1.40	0.13	1.35	-8.06	0.45	21
15	5	1.38	0.12	0.35	-8.83	0.45	21
16	10	1.48	0.13	0.35	-8.83	0.45	21
17	15	1.51	0.12	0.35	-8.83	0.45	21
18	20	1.47	0.14	0.35	-8.83	0.45	21

the estimated saturated water content about 31%. The variation of ρ in each sample was examined to find any particular pattern. The values of ρ were found to vary more or less at random and the redistribution of water does not appear to have caused any significant change in the dry density.

Experiments 1 through 8 were conducted to find the change of the water content profile w(x,t) with time under the same thermal condition. In Exp. 1 through 4 the initial water content w_o was kept at 15% while in Exp. 5 through 8 w_o was at 20%. The measured w of Exp. 1 through 4 are presented in Figure 2. It is clear from Figure 2 that water moves in the direction of negative temperature gradient and that w tends to converge to a stationary profile as time increases. The profiles at t = 22 days and at t = 34 days differ little. This implies that the flux of water f(x) almost diminishes everwhere after t = 22 days. An interesting feature of the profiles w is

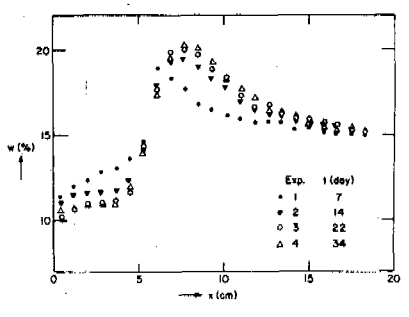

Figure 2. The water content w[%] vs. x[cm] for Exp. 1, 2, 3 and 4 with w_o = 15%.

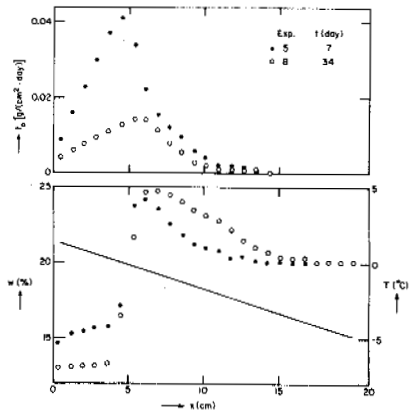

Figure 3. The water content w[%] and the average flux f_a[g/(cm^2·day)] vs. x[cm] for Exp. 5 and 8 with w_o = 20%.

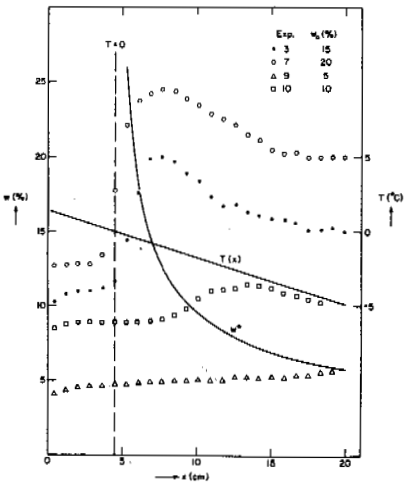

Figure 4. The water content w[%], the temperature T[°C] and the unfrozen water content w*[g/g soil] vs. x[cm] for Exp. 3, 7, 9 and 10 with w_o = 15, 20, 5 and 10%, respectively.

the appearance of a maximum. At the left of the maximum, w is monotonically increasing while at the right w is monotonically decreasing.

The measured w of Exp. 5 and 8 are presented in Figure 3. The profile of Exp. 8 with t = 34 days differs little from the profile of Exp. 7 with t = 22 days that is presented in Figure 4. For this case of w_o = 20%, the flux of water almost vanishes everywhere after t = 22 days. The general features of profiles presented in Figure 3 resemble those in Figure 2. In Figure 3 the linear temperature distribution T(x) imposed on soil columns is also drawn. It is easy to see from Figure 3 that water was taken away from the part where T(x) > 0 and was added to the part where T(x) < 0 as time increased.

From a measured profile $w(x,t_o)$ we can calculate the average flux of water $f_a(x)$ at x during the time period $t_o \geq t \geq 0$ as

$$f_a(x) = (\rho/t_o) \int_x^{x_o} [w(x,t_o) - w_o]dx \qquad (15)$$

In our experiments each sample was sectioned into 25 equal segments. Starting with the coldest segment, we will assign each segment with numbers 1 through 25 and denote the location of the center of the ith segment by x_i (i = 1,2,....,25). Then the average flux of water $f_a(x_i)$ at the ith segment during $t_o \geq t \geq 0$ is given as

$$f_a(x_i) = (\rho/t_o)\Delta x \sum_{k=i+1}^{25} [w(x_k, t_o) - w_o] \qquad (16)$$

The calculated values of f_a by Eq. 16 for Exp. 5 and 8 are plotted in Figure 3. The average flux f_a increases with increasing x, attain its maximum near the point where T = 0[°C], and then decreases. The vanishing f_a in the part where T is less than -4°C obviously implies that water hardly moves in this part. The behavior of f_a indicates the strong dependence of the flux of water on the temperature.

The measured profiles w of Exp. 3, 7, 9 and 10 are presented in Figure 4. These four experiments were conducted under the same thermal conditions to find the effect of the initial water content w_o. The initial water contents of Exp. 3, 7, 9 and 10 were 15, 20, 5, and 10%, respectively. The temperature distribution T(x) and the equilibrium unfrozen water content w* were determined by the nuclear magnetic resonance technique on a separate sample of Morin clay and are also shown in Figure 4. The time duration of these four experiments was 22 days and the measured profiles w are considered to be nearly stationary. We may expect that the phase equilibrium holds true under such a stationary condition. Therefore, in the part of measured profiles where w(x) is greater than w*(x), the presence of ice is anticipated.

Among the four profiles in Figure 4, the measured profile for the case of w_o = 5% (Exp. 9) is monotonically increasing, and the maximum appears in the profiles for other three cases at a point where ice is presumably present. In the cases of w_o = 15 and w_o = 20%, the gradient of w is small near the warmer end, but it increases suddenly near the freezing point T = 0 and decreases again near the point where w = w*. In three cases (except the case of w_o = 5%), the content of liquid phase water increases with x up to the point where w = w*, but it decreases sharply beyond this point.

The values of average flux f_a calculated from each of four profiles in Figure 4 are plotted in Figure 5. Since the time duration of these four experiments was the same, f_a is obviously proportional to the total flux during the time period of 22 days. From Figure 5 we find that f_a is greater when w is greater near the warmer end, while f_a is greater when w is smaller near the cold end. This behavior of f_a indicates that the mobility of water tends to increase with increasing w in a part where no ice is present, while the mobility of water tends to decrease with increasing w in a part where ice

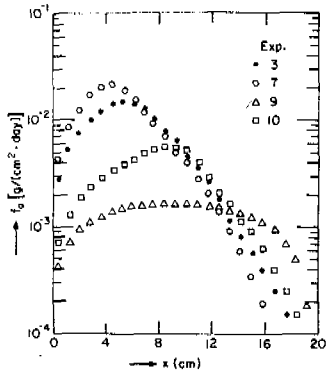

Figure 5. The average flux f_a[g/(cm^2·day)] vs. x[cm] for Exp. 3, 7, 9 and 10.

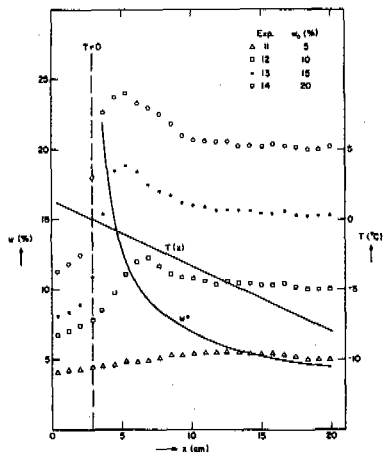

Figure 6. The water content w[%], the temperature T[°C] and the unfrozen water content w*[g/g soil] vs. x[cm] for Exp. 11, 12, 13 and 14 with w_o = 5, 10, 15 and 20%, respectively.

is present. In other words the presence of ice may decrease the mobility of water caused by temperature gradients.

Exp. 11 through 14 were conducted to find the effect of a temperature gradient by lowering T_c by about 3.0°C. The measured profiles w of these experiments are presented in Figure 6. The general features of these profiles resemble those in Figure 4 except for the noticeable increase of the part where the gradient of w is very small, particularly for the cases with a greater initial water content w_o. In the cases with w_o = 15 and 20%, the gradient of w near the point where T = 0°C is greater than that of the corresponding cases in Figure 4. Such behavior is expected because the gradient of w must increase to counteract the increased driving force of water due to the greater negative temperature gradient.

In all the experiments presented above, water in the warmer part was redistributed in the colder part. It is apparent that water in the unfrozen part (T > 0°C) of the column is a source of movable water. Hence, the ratio of an unfrozen part to a frozen part in the column is expected to affect the stationary profiles. In order to examine such an effect we conducted Exp. 15 through 18 in which the unfrozen part was reduced. The measured profiles w of these experiments are presented in Figure 7.

It is clear from Figure 7 that the reduced unfrozen part affected the case with w_o = 20% by flattening the profile as a whole in comparison with those of corresponding cases in Figures 4 and 6. However, the effect of the reduced unfrozen part is not pronounced in the other three cases. Maxima appear in the profiles of the three cases except the one with w_o = 5%, but the temperature of the point where the maximum appears is lower that those in Figures 4 and 6.

When a soil column with uniform ρ and w is subjected to a linear temperature gradient, we have found that the transport of water indeed occurs in the direction of negative temperature gradient in accordance with Eq. 4b. As water moves toward the cold end, the initial uniformity of w breaks down and a driving force of water starts to build up toward the warmer end . After three weeks or so, two driving forces of water, one due to a temperature gradient and the other due to a gradient of water content, tend to balance each other so that the flux of water tends to diminish. We have found that the profile of water content w(x,t) indeed asymptotically approaches the stationary profile $w^+(x)$ with time.

From the results of experiments described above, we have found that the stationary profile $w^+(x)$ generally consists of two parts, depending upon the value of $w_x^+ = dw^+/dx$. If we denote the point where w^+ attains its maximum by x_m, one part where $w_x^+ > 0$ is located in the region $0 < x < x_m$. The other part where $w_x^+ \leq 0$ is located in the region $x_m < x < x_o$. Since the flux of water must vanish everywhere in the stationary profile, $w^+(x)$ should satisfy Eq. 14. Using the part of $w^+(x)$ where $w_x^+ > 0$, we can determine $D_2(w^+, T)$ as

$$D_2(w^+, T) = \frac{1}{a} D_1(w^+, T) \frac{dw^+}{dx} \qquad (17)$$

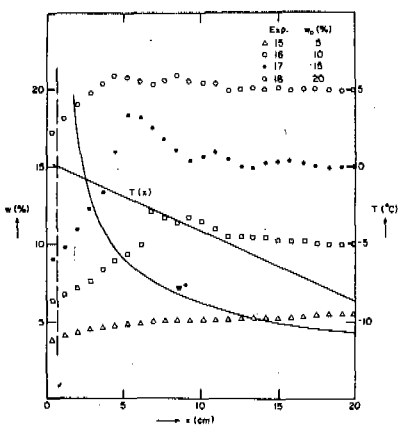

Figure 7. The water content w[%], the temperature T[°C] and the unfrozen water content w*[g/g soil] vs. x[cm] for Exp. 15, 16, 17 and 18 with w_o = 5, 10, 15 and 20%, respectively.

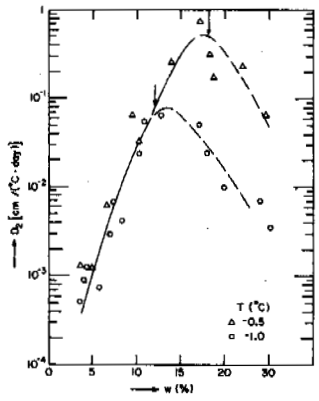

Figure 8. The values of D_2[$cm^2/°C \cdot day$)] vs. the water content w[%] at temperatures T = -0.5 and -1.0°C.

Assuming that the measured profiles of w with the time duration of more than 3 weeks are approximately stationary and using the reported values of D_1 (Nakano and Tice, 1987), we calculated the values of D_2 by Eq. 17. The calculated values of D_2 at t = -0.5 and -1.0°C versus w are presented in Figure 8. From Figure 8 we find that D_2 increases with increasing w, attains its maximum, and then decreases. Arrows in Figure 8 indicate points where w is equal to the equilibrium unfrozen water content w*. The appearance of the maximum near the point w = w* implies that the presence of ice decreases the mobility of water due to temperature gradients. The behavior of D_1 similar to this was reported by Nakano and Tice (1987).

CONCLUSION

A new experimental method is introduced to determine the rate of water movement caused by temperature gradients in unsaturated frozen soils. When a linear temperature distribution is imposed on a closed soil column with initially a uniform water content, a redistribution of water occurs. The profile of water content has been found to approach a stationary profile after three weeks or so.

Assuming that the gradients of water content and temperature were driving forces for the water movement, we calculated the transport coefficient function D_2 by using the measured stationary profiles of water and the measured values of the transport coefficient function D_1. The function D_2 was found to depend not only the temperature but also on the water content.

REFERENCES

Dirksen, C and Miller, RD (1966). Closed-system freezing of unsaturated soil. Soil Sci Soc Amer Proc, (30), 168-173.

Hadley, WA and Eisenstadt, R (1955). Thermally actuated moisture migration in granular media. Trans Am Geophysical Union, (36), 615-623.

Hoekstra, P (1966). Moisture movement in soils under temperature gradients with the cold-side temperature below freezing. Water Resources Research, (2), 241-250.

Nakano, Y and Tice, AR (1987). Transport of water in frozen soil: VI. Effects of temperature. Advances in Water Resources, (10), 44-50.

Oleinik, OA, Kalashnikov, AS and Yui-Lin, Chzhu (1958). The Cauchy and boundary problems for equations of the type of non-stationary infiltration. Izv Akad Nauk USSR Ser Mat, (2), 667-704.

Oliphant, JL, Tice, AR and Nakano, Y (1983). Water migration due to a temperature gradient in frozen soil. Proc 4th Permafrost Conference, 951-956, Fairbanks.

Philip, JR and de Vries, DA (1957). Moisture movement in porous materials under temperature gradients. Trans Am Geophysical Union, (38), 2, 222-232.

FILTRATION PROPERTIES OF FROZEN GROUND

B.A. Olovin

Permafrost Institute, Siberian Branch of the U.S.S.R. Academy of Sciences, Yakutsk, U.S.S.R.

SYNOPSIS Large-debris and fissured permafrost often have very high permeability, therefore it becomes possible to investigate the structure of a frozen mass by gas-dynamic methods. This paper presents some results of an investigation of permafrost gas permeability for a mass excited due to oscillations of thermodyncamical parameters of the air (temperature and pressure) within the ground layer of the atmosphere; the results were derived through stationary-scale investigations at the dam plugging the Vilyuy river and field investigations in a watershed area in Western Yakutia.

INTRODUCTION

The relatively high permeability of permafrost is evidenced by observations of gases moving through shallow mine workings and bore holes in the Soviet Far East and Middle and Western Siberia (Sumgin, 1927; Velmina and Uzemblo, 1959; Lazarenkov, 1959; Olovin, 1983; 1986; et al.) as well as results of laboratory-scale experiments (Ananian et al., 1972; Chamberlain and Gow, 1978). The air moving through a ground mass has a substantial influence upon the factors that largely determine the static and filtration stability of engineering structures, namely the annual mean values and the amplitude of yearly temperature fluctuations of soils, and the character and intensity of the secondary intraground ice formation within a mass. The knowledge of the permafrost filtration properties is necessary when designing underground reservoirs for storage of liquids and gases, water-development projects and when prospecting for hydrocarbon deposits.

LABORATORY EXPERIMENTS

The experiments have been conducted with artificial earth materials, viz. dolerite gruss, with the grain size averaging 1.5 to 5.5 mm in samples 100 mm in diameter and 100 mm high, at negative air temperatures and with diverse soil moisture. The samples were moistened through the upper boundary surface, without disturbing the original ground. This is the most commonly occurring moistening of frozen soils under natural conditions, in particular the formation of ice-cement caused by the infiltration of atmospheric precipitation in artificial deposits.

The investigations have been carried out in the region of viscous flow and transitory to inertial flow which is described by the equation:

$$\frac{\Delta P^2}{L} = \frac{\mu v}{K_\mu} + \frac{\rho v^2}{K_\rho} \qquad (1)$$

where ΔP is the pressure difference at the sample's boundaries; v is filtration rate; L is the sample length; μ and ρ are the viscosity and density of the gas; and K_μ and K_ρ are permeabilities of the ground at very low and very high filtration rates, respectively, Under experimental conditions the pressure gradient $\Delta P/L$ coincides, to an accuracy of 2% with the value of $\Delta P^2/L$; therefore, it was assumed that $\Delta P \approx \Delta P^2$.

The results were handled by the method of least squares in the coordinates $(\Delta P/L \cdot v,\ v)$, in order to determine the coefficients A and B of the linear equation

$$\frac{\Delta P}{Lv} = A + Bv, \qquad (2)$$

and these coefficients were used to determine, based on ρ and μ inferred experimentally, the coefficients of viscous, K_μ, and turbulent, K_ρ, permeability. The degree of saturation of the porous space with ice, S_w, was determined by a weighing method. Most of the experiments showed very high, over 0.90, correlation coefficients between the parameters $\Delta P/L \cdot v$ and v.

The character of variation of relative viscous $K_{\mu w}/K_{\mu o}$ and relative turbulent $K_{\rho w}/K_{\rho o}$ permeability was substantially different, depending upon the ice content S_w of the porous space of the frozen ground under investigation (Figs 1 and 2), in which case the differences in the magnitude of the coefficients $K_{\rho w}/K_{\rho o}$ not infrequently reached two orders of magnitudes or more as observed in experiments with

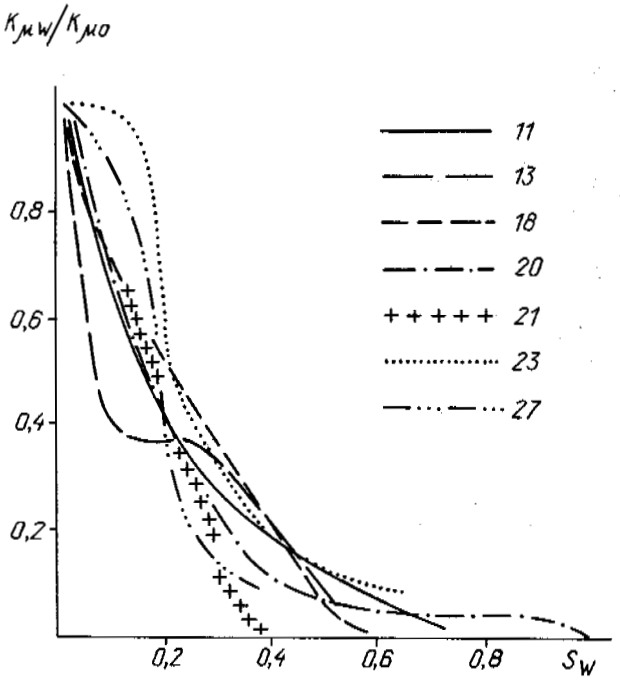

Fig.1 Relative Viscous Permeability $K_{\mu w}/K_{\mu o}$ of Grained Ground in Experiments Nos 11-27, Depending on the Degree of Ice Saturation of the Porous Space S_w (Fractions of Unity). The Particle Size of the Ground Investigated Averages 1.5 to 5.5 mm

different samples. For $S_w < 0.2$, two samples showed anomalously high (in excess of unity) values of relative turbulent permeability. With the degree of ice saturation $S_w = 0.6$ to 0.8, the gas permeability of the frozen ground normally decreases by 100 to 1000 times as compared with dry ground. A total cessation of the air movement through the samples was most frequently observed at $S_w = 0.90$ to 0.95.

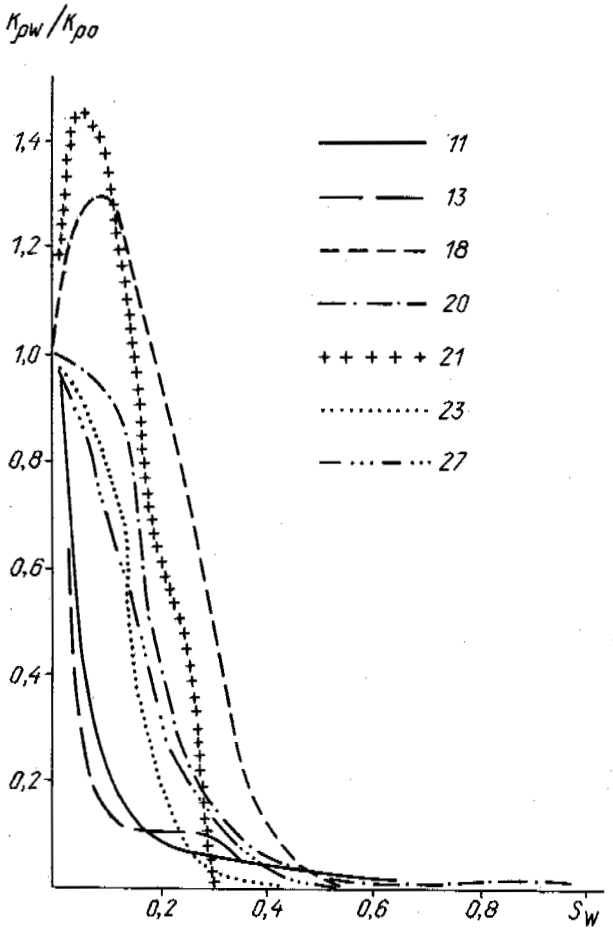

Fig.2 Relative Turbulent Permeability $K_{\rho w}/K_{\rho o}$ of Grained Ground in Experiments Nos 11-27, Depending on the Mean Degree of Ice Saturation of the Porous Space

FIELD EXPERIMENTS

The field experiments have been conducted in Western Yakutia in a watershed area near a small-size, shallow lake about 300 m in diameter. The geological structure of the area is the following: at the base of a stripping opened by means of bore holes Nos 308-318 (Fig.3) there occur dense, largely carbonate grounds (chalky clays, limestones, dolomites, and aleurolites) of Cambrian age covered by a thick (up to 100 m thickness) layer of sandstones of Permian age which, in some places, emerge on the ground surface. Throughout most of the stripping the sandstones are covered by a layer of dolerites of Trias age, of a thickness of up to 40 m. These are fine-grained, very dense, weakly fissured dolerites, with veins of fine-crystalline calcite. The sandstones are fine- and medium-grained, quartz-feldspar formations, with a well-defined horizontal stratification, and are, in some places, carbonized; toward the layer bottom the size of sand particles increases, with occurrence of gravel interlayers. The ground at the stripping base includes chalky clays, with interlayers of highly dense dolomites; stratification is horizontal. In the area of contacts between the layers, as deep as 1.5 to 2 m from the boundary, dolerites are severely fissured, while sandstones at the boundary with dolerites are very dense as deep as 2 m and, as a result of metamorphism processes, have turned into cornei. The crust of weathering of chalky clays is about 1 to 1.2 m thick. The ponderable moisture content - within the layer of seasonal thawing - approaches 20 to 40% for the grounds, 1 to 5% for dolerites, 10 to 20% for sandstones, with a tendency for the moisture content to somewhat increase with depth, and 14 to 16% in the vicinity of the layer top; at greater depths it decreases down to 8 to 10%.

The temperature of frozen ground at depths of up to 120 m from the surface remains almost unchanged and is minus 1.8 to 2.4°C. The zone

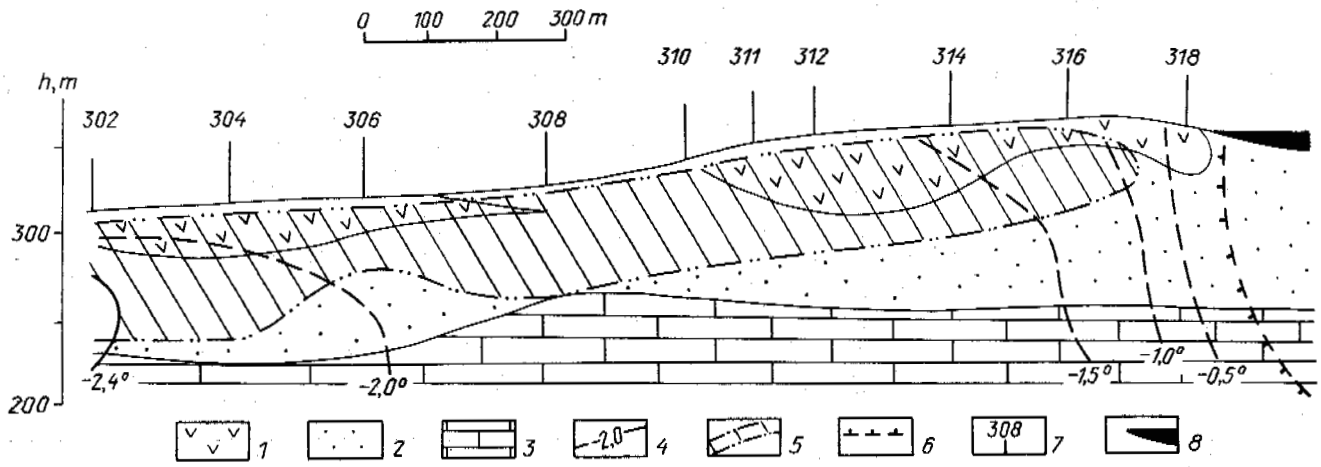

Fig.3 The Position of the Gas-Permeable Layer within the Permafrost in the Experimental Area: 1 - Dolerites ($\gamma_\beta T_1$); 2- Sandstones (P + C); 3 - Limestones ($\epsilon_3 il$); 4 - Isotherms, °C; 5 - Region of Occurrence of Gas-Permeable Ground; 6 - Boundary between Frozen and Unfrozen Grounds (Calculated); 8 - Lake

of the thermal influence of the reservoir is traceable at a distance of at least 300 m from the boundaries of the talik below the lake, whose position is marked on the basis of modelling results on a stationary temperature field in terms of a three-dimensional electrical model. The thickness of the cryogenic layer is about 700 m and that of the permafrost is about 250 m.

The following items were measured in the area: air flows through bore holes Nos 302-318 in the upper part of which casing pipes were installed at depths from 0 to 4-6 m (stage 1); air pressure in the ground layer as well as in all bore holes stopped with plugs in the vicinity of the outlet; air flow in the open bore hole No. 311 that has been used as an exciting one, and air pressure in the remaining bore holes which were closed and were used as piezometric ones (stage 3); air pressures in all bore holes following a fast stoppage of the exciting bore hole No. 311 (stage 4); and air pressures and flows in some sections of the bore holes in depth which were isolated from other horizons by means of inflatable plugs (stage 5).

When conducting the stage No. 1 experiments, which can be called 'flow rate grammetry', the bore holes had all a free communication with the atmosphere. Air flows through the bore holes were measured on a continuous basis at a frequency of 6 to 8 times per day during several months, by means of an impeller flowmeter. As a result of the experiments it has been established that air flows through the mouth of any bore hole are directly proportional to the magnitude of atmospheric pressure P_a , i.e.,

$$q_i = \eta_i (P_a - P_{oi}) \qquad (3)$$

and the productivity coefficients η_i remained almost unaltered for each bore hole during a very long period of time. The range of variation of $\eta_i = 10^{-3}(7.3 - 47.5)$ m^3/hr Pa. Very stable is also the value of P_{oi} which varies with time significantly less as compared with P_a. The correlation coefficient of the dependence $q_i(P_a)$ varied within 0.92 to 0.98.

During the stage No. 2 experiments (barogrammetry) the mouths of all the bore holes were plugged and air pressure measurements were made at 3 hr intervals during the course of two days. It has been established that already within several hours after plugging the pressure in the bore holes stabilized, the subsequent variations of P_i in time did not exceed 10 to 20 Pa, and the difference of P_i -values in some bore holes was proportional to absolute marks of the bore hole mouths. This indicates, on the one hand, the presence of a hydraulic coupling within the mass between individual bore holes and, on the other, either a total absense or presence of a very weak association of the underground atmosphere with the surface air layer.

A treatment of the results of the stage No. 3 experiments have revealed that the intensity of air movement through the walls of the exciting bore hole corresponds to the predicted intensity on the basis of the previous solution of the equation for an axisymmetric stationary flow of an incompressible fluid, with a constant flow and with the radius of the supply circuit of 100 m and pressures at the boundaries of the region equal to the mean atmospheric and mean stratum pressures. A very simple empirical formula has been obtained for calculating the mean permeability of ground within the mass:

$$K_M = \frac{5{,}61 \cdot 10^9 \cdot \eta}{h_s} \qquad (4)$$

The productivity coefficient can be determined from flowmeter investigations, and the

total thickness h_s of the permeable layer is obtainable from log surveys.

The stage No. 4 experiments involved studying the intra-bore pressures during 60 days after plugging the exciting bore hole No. 311. The experimental results are: during the first 12 hours the pressure in bore hole No. 312 was decreasing similar to that observed in bore holes operated with a constant flow rate, i.e., is directly proportional to $\ell n \tau$. At $\tau > 12$ hr, the rate of pressure decrease $\partial P / \partial(\ell n \tau)$ decreased substantially, at $\tau = 400$ hr the pressure in the bore hole was a minimum; afterwards, it began to increase reaching a maximum value in $\tau = 1\,000$ hr and, then, again began to decrease to values smaller than those observed at $\tau = 400$ hr. Such a character of the variation may be accounted for by periodic variations of the mean values of atmospheric pressure during the period preceding the plugging of the bore hole as well as the presence in the mass of weakly permeable soils. The stripping under study, as has already been mentioned, includes sandstones containing considerable amounts of intraground ice which may well be responsible for such a response of the mass. Rather high permeability may be shown by cavernous limestones as well as chalky clays and aleurites within the crust of weathering. If it is assumed that the character of the pressure recovery curve has been influenced by the layer of weakly permeable, porous soils of a thickness of about 40 m and 0.1 porosity, then the phase shift of the pressure wave can be used to estimate the permeability of this layer at: $K_\mu \approx (2 - 5) \cdot 10^{-15}$ m^2.

An estimate of the soil permeability at different depths (stage No. 5) can be made on the basis of data derived from a study of the vertical distribution of inputs q_j into the bore hole or redundant values of pressures ΔP_j of air for individual horizons Δz_j . Experimentally it has been established that measurement of inputs q_j or redundant pressures P_j is of quite equal importance in connection with the presence between them of a relationship of the form

$$q_j = c \cdot \Delta P_j \qquad (5)$$

The coefficient c involved in formula (5) depends only on additional hydraulic resistance produced by packers. Under conditions of our experiments $c = 1.67 \times 10^{-5}$ m^3/hr·Pa.

On the other hand, taking into consideration that, at a certain distance from the bore hole, the pressure, to an accuracy of the gravitational component $\rho g z$, is a constant, it may be concluded that the amount of input for any horizon depends mainly on permeability of soils at this horizon; therefore, in order to make a rough estimate of permeability $K_{\mu,j}$ at depth z , one can employ the relationship

$$K_{\mu,j} = \bar{K}_\mu \cdot \frac{\Delta P_j}{\overline{\Delta P_j}} , \qquad (6)$$

where $\bar{K}_\mu$ is mean permeability of the mass opened by means of a bore hole; and ΔP_j is the mean redundant air pressure in the bore hole.

Calculations performed using the formula obtained (table) indicate that the greatest permeability applies for soils occurring at depths of 20 to 40 m corresponding to the zone of contact of a trap intrusion with sandstones.

The investigations discussed above provide evidence that the permafrost can include quite large-sized areas with non-water-saturated grounds which are prptected against inflitration of atmospheric precipitation by a layer of ice-saturated, moisture-impermeable soils occurring at the base of the layer of seasonal thawing. The integrity of the intermediate ice-saturated layer remains unchanged during very severe variations of climate. The thickness of the gas-permeable, non-water-saturated layer decreases near lowerings of the water-containing layer surface, as is the case in the area of bore hole No. 306 (Fig. 3) and near water reservoirs. Of 15 bore holes investigated, the only bore hole in which no interlayers permeable to gas were detected, was No. 318 situated near the shore of the lake. The thickness of the ice-saturated permafrost contiguous with the talik below the lake appears to be in the range 50-100 m.

TABLE

Permeability $K_\mu \cdot 10^{12}$, m^2, of Permafrost at Different Depths z , m, from the Surface in Bore Holes 308, 311, and 312

z, m	$K_\mu \cdot 10^{12}$, m^2		
	Bore hole No.		
	308	311	312
10 - 20	1.4	1.8	0.4
21 - 30	1.1	2.8	0.9
31 - 40	1.1	3.7	1.2
41 - 50	0.6	1.4	0.6
51 - 60	1.0	1.1	0.4
61 - 70	0.8	0.7	0.2
71 - 80	0.1	0.5	0.1

PERMEABILITY OF LARGE-DEBRIS MAN-MADE DEPOSITS

In regions with severe climatic conditions it is customary to utilize, for building purposes, fragmented rocks which are characterized by very high permeability to gas and, therefore, high intensity of mass exchange processes, accompanied by the formation within the mass of secondary intra-ground ice due to sublimation of water vapour from the air that moves within the porous space as well as infiltration of atmospheric precipitation into the cooled-down mass. For practical purposes, it is often important to know the magnitude of permeability of large-debris rocks within the mass, in order to have a possibility of estimating the mean values and the magnitude of the temperature fluctuations of rocks within the mass or at its boundaries with structure elements made of other materials, whose properties are able to depend substantially on the structure's temperature regime.

We have investigated the permeability of large-debris rocks on one of the large stone-fill dams of a hydroelectric station. The dam is 75 m high and is made of dolomite clods, with an inclined shield (a core in the upper part) of suglinok serving as the filtration-counter-acting element. The permeability of suglinok approaches $1 \cdot 10^{-12}$ m^2, and that of overcast stones is several orders of magnitude as high. A continuous movement of the air is observed within the body of the stop prism which is caused by the difference in air densities of the intraporous space and the surface layer. Air movement at depths over 30 m from the dry slope surface is characterized by a relative stability, namely in winter the air moves from below upwards, viz. from the base of the bottom wedge to the crest, and in summer the reverse is the case. At depths less than 20 m the air movement is more complicated in character; the direction of movement is often reversed during 24 hr, although, on the average, it obeys a periodic law with a period of 1 hr. An absolute maximum of air filtration rates is observed in December. These inferences were obtained on the basis of flowmeter observations of the air movement through the surface of the dry slope as well as the behaviour of the surface temperature variation within the structure as reported in previous papers (Olovin, 1981; 1986).

The rate of temperature fluctuations of the earth materials at any point of the mass depends, with other conditions being equal, upon permeability of soils; therefore, geothermal observations are useful for determining the mean values of filtration rates or permeability of the medium. In particular, a suitable formula for calculating the values of K_M is derivable in terms of a piston model of fluid transfer inside the intraporous space. The derivation of this formula is presented below.

Let us consider the heat balance of an element of a current tube of a cross-section S and a length $\Delta \ell$ having a temperature t, through which an air flow is moving whose temperature at the element inlet is $t + \Delta t$ and at the outlet is t, under the following simplifying assumptions: conductive transfer of heat in the grain phase in the direction ℓ is absent, and heat conductivity of the porous medium in a direction normal to ℓ is infinitely large.

Air flow q inside a volume $S \cdot \Delta \ell$ corresponds to the amount of heat released in time $\Delta \tau$ $q \cdot c_a \cdot \Delta t_a \cdot \Delta \tau$ (c_a and t_a being the heat capacity and temperature of the air, respectively) which will be absorbed by the grain phase. Its heat content will increase by an amount $C_s (1 - \xi) \times \Delta t_s \cdot S \cdot \Delta \ell$ (C_s being the heat capacity of a mineral skeleton, ξ porosity, and t_s the skeleton's temperature). Upon setting the expressions obtained equal, taking into consideration that for any cross-section $t_a = t_s = t$ and, therefore, $\Delta t_s \approx \Delta t_a$ we obtain:

$$q \cdot c_a \cdot \Delta t \cdot \Delta \tau = c_s (1 - \xi) \cdot \Delta t \cdot S \cdot \Delta \ell \qquad (7)$$

Bearing in mind that the filtration rate $v = q/S$ following a limiting transition $\Delta \ell \to \partial \ell$, $\Delta \tau \to \partial \tau$, and $\Delta t \to \partial t$, we get

$$v = \frac{C_s}{C_a} (1 - \xi) \frac{\frac{\partial t}{\partial \tau}}{\frac{\partial t}{\partial \ell}} \qquad (8)$$

We, then, substitute the expression obtained into the Darci equation

$$v = - \frac{K_M}{\mu} \cdot \frac{\partial p}{\partial \ell},$$

by representing preliminarily the air pressure in terms of the equation of state of gas as a function of its density ρ_0 at °C and temperature t

$$p = \frac{R \cdot \rho_0}{M} \cdot \frac{t}{1 + \beta t}, \qquad (9)$$

where R is a gas constant; β is the coefficient of volume expansion of the air; and M is the molecular weight of the gas.

It follows from (9) that

$$\frac{\partial p}{\partial \ell} = \frac{\partial t}{\partial \ell} \cdot \frac{R \cdot \rho_0}{M} \cdot \frac{1}{(1 + \beta t)^2} \qquad (10)$$

Because $\beta t \ll 1$, the final formula to be used in the calculation may be represented as

$$K_M = \frac{\mu \, C_s (1 - \xi) \cdot M}{C_a \cdot \rho_0 \cdot R} \frac{\frac{\partial t}{\partial \tau}}{\left(\frac{\partial t}{\partial \ell}\right)^2} \qquad (11)$$

From the plot $K_M(x, y)$ constructed (Fig. 4) on the basis of geothermal observations in the stop prism of the dam obtained in different years, it is possible to make assessments of the main tendencies of the variation in permeability of large-debris soils during the period of exploitation of the dam. These are: a substantial decline of permeability of overcast stones at depths over 10 to 15 m from the surface of the bottom slope at the stop prism contiguous to the lower reach, and an appreciable increase in permeability of the central part of the dam. These results lead us to suppose that the moisture content of frozen ground along the axis of the dam's crest remains at the original level or decreases with time, especially at depths of 30 m and more from the surface and only in the area of the dam to the right of the vertical axis through the " ∇ 55 m" berm toward the lower reach does the moisture content of soils increase appreciably with time.

Indirect evidence for the conclusion about the predominant influence of the moisture content increase rather than density increase of the mineral skeleton of soils which was also observed under service conditions, upon the amount of permeability of soils is provided by the following factors:

(i) infiltration moisture flow through unit surface of a dry slope per year increases toward the lower reach (Olovin, 1981).

(ii) soil consolidation caused by vertical subsidence is greatest in the central part, near the dam's crest where no increase in permeability of soils occured.

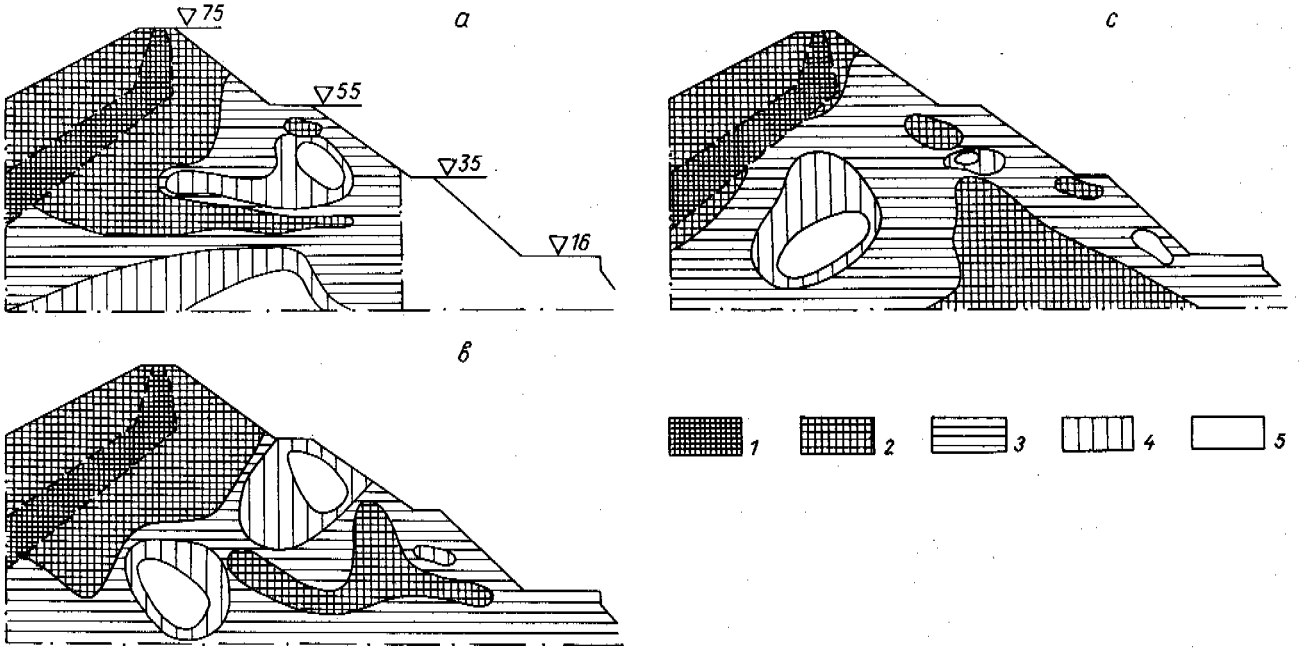

Fig.4 Permeability to Gas of Soils of the Shield and Stop Prism in 1969 (a), 1977 (b) and 1981 (c): 1 - Suglinok of Permeability $K_м = (1-10)\cdot10^{-12}$ m^2; 2 - Large-Debris Ground (Clods, Detritus) with Permeability $K_м = (0.01-0.1)\cdot10^{-9}$ m^2; 3 - the Same, $K_м = (0.1-1.0)\cdot10^{-9}$ m^2; 4 - the Same, $K_м = (1-3)\cdot10^{-9}$m^2; 5 - the Same, $K_м = (3-10)\cdot10^{-9}$ m^2.

The proposed method of analysis of the structure of a mass, which can be called 'thermogrammetry', makes it possible to estimate the ice content of a porous space of the frozen ground, with a mineral skeleton of high solidity, which is impossible when coring a bore hole - the process of drilling is accompanied by a release of large amounts of heat which contributes to melting and evaporating the intraground ice.

CONCLUSIONS

The experiments reported in this paper have established a very high permeability of frozen grained and fissured soils and the formation of intraground ice there is due to infiltration of drop-shaped moisture through the upper boundary surface. Under natural conditions, during a very long (10^4 - 10^5 years) period there persist thick (up to 70-80 m) layers of non-water-saturated, highly permeable ($K_м = 10^{-15}$ - 10^{-12} m^2) soils covered by a comparatively thin (not more than 2 or 3 m) layer of impermeable, ice-containing soils occurring at the bottom of the layer of seasonal thawing. Soils permeable to gas may be absent at a distance of less than 50 m from the thaw basin limits below water reservoirs; the layer of permeable soils reduces in areas of waterflow roof decline. As for fill-type engineering structures, along with the formation of intraground ice due to atmospheric precipitation infiltration and water vapour condensation, in some areas intraground moisture can emerge from below due to convective air flows. In order to study the structure of a permafrost mass, it is possible to invoke gas dynamical methods of investigations, including modifications of these methods such as described in this paper.

REFERENCES

Ananian, A.A., Arutyunian, N.A., Mazurov, V.A. and Silverstov, L.K. (1972). O pronitsaemosti merzlykh porod. - V kn.: Merzlotnye issledovaniya, v. 12, 205-208, Izd. Mosk. un-ta, Moscow.

Chamberlain, E. and Gow, A.J. (1979). Effect of freezing and thawing on the permeability and structure of soils. Engineering Geology, v. 13, 73-92.

Lazarenkov, G.V. (1959). Dvukhstoronnyaya tsirkulyatsiya vozdukha cherez burovuyu skvazhinu. - Materialy po obshchemu merzlotovedeniyu. VII Mezhduved. soveshch. po merzlotovedeniyu, 362-368, Izd. AN SSSR, Moscow.

Olovin, B.A. (1981). Dinamika fizicheskikh svoistv krupnoblomochnykh vechnomerzlykh gruntov. - V kn.: Inzhenernye issledovaniya merzlykh gruntov. 96-116, Novosibirsk: Nauka.

Olovin, B.A. (1983). Gazoobmen mnogoletnemerzlykh porod s atmosferoi. - V kn.: Teplofizicheskie issledovaniya kriolitozony Sibiri. 86-213, Novosibirsk: Nauka.

Olovin, B.A. (1986). Temperaturny rezhim plotiny Vilyuiskoi GES. - V kn.: Problemy inzhenernogo merzlotovedeniya v gidrotekhnicheskom stroitelstve, 151-161, Moscow: Nauka.

Sumgin, M.I. (1927). Vechnaya merzlota pochvy v predelakh SSSR, Vladivostok.

Velmina, N.A. and Uzemblo, V.V. (1959). Gidrogeologiya Tsentralnoi chasti Yuzhnoi Yakutii, 179 p., Moscow-Leningrad: Izd. AN SSSR.

THERMODIFFUSE ION TRANSFER IN GROUNDS

V.E. Ostroumov

Institute of Soil Science and Photosynthesis, Academy of Sciences of the USSR, Pushchino, USSR

SYNOPSIS Ion transfer in the grounds under conditions of heterogeneous temperature field is related with moisture migration and is described as a thermodiffuse process. The thermodiffusion coeffecients of ions in the frozen and thawed grounds vary from 0 to 10^{-8} m^2/s degree and be both positive and negative. It has been found that the ion transfer in the frozen grounds is directed towards the temperature decrease whereas in the thawed ones it has the opposite direction. The model of the three layer structure suggested for the mobile liquid in the disperse grounds is in a good agreement with the experimental results.

INTRODUCTION

Thermodiffuse ion transfer in grounds is an important and insufficiently known component of mass transfer. Together with the other processes of the ion transport it participates in the liquid phase content changes, in creating conditions favourable for dissolving and forming the secondary minerals and determines the content and properties of frozen and thawed grounds. Thermodiffusion of ions plays an important role in the processes of salinization (desalinization) of soils and grounds.

The main regularities of moisture transfer in grounds affected by the temperature gradients are known from the works of G.-J.Bouyoucos, A.V.Lykov, D. de-Vries and J.-R.Philip, R.-D.Jackson, D.Rose and H.Penman, N.V.Churaev et al. (Globus, 1983). Accordingly, moisture migration in the grounds under the temperature gradient effect:

i) is directed, as a rule, towards the temperature decrease;

ii) is carried out due to the effect of some mechanisms:thermal vapour diffusion, change in the volume of jammed gas, liquid thermocapillary and thermoosmotic transfer (in the integral form all the flows corresponding to them are described as diffusional ones and are directed towards the temperature decrease, except thermocapillary ion-electrostatic and thermoosmotic flows;

iii) reaches the greatest intensity at a comparatively low moisture content, that is accounted for by a sli ght dependence of free moisture mobility on temperature;

iy) is decreased with the increase of pore solution concentration;

y) results in moisture circulation in the grounds.

The main regularities of ion transfer in the grounds have been also studied (Krákov, Lebedev, Polynov, Ershler, Bolt and Camper, Pakshina, 1980 et al.). In the disperse grounds the ions are transferred by the following flows:

i) with gravitational moisture during filtration;

ii) with capillary moisture flow during water rising along ground capilaries;

iii) with osmotic moisture flow;

iy) with film moisture that is of particular importance at incomplete moisture saturation;

y) with diffusional flow.

As it was stated by A.F.Lebedev in 1937, no anion diffusion occurs in the moisture film (undissolving moisture volume) within the moisture content range from zero to the maximal hygroscopy.

The experiments carried out by A.M.Globus with the thawed saline soils (1983) showed that under the temperature gradient effect the dissociated salts are transferred towards the temperature increase. The author explaines this phenomenon by the fact that the moisture vapour transfer creates an additional gradient of moisture content resulting in the corresponding liquid flow together with a salt one. Thus, the ion transfer in the grounds under the effect of the temperature gradient was experimentally found. Its nature is insufficiently studied.

The complexity of the mechanisms of substance transfer in the grounds did not allow to describe them in detail. Therefore, in case with ion transport as well as during investigations of moisture transfer it is expedient to use phenomenological approach.

THEORY

In evenly moistured frozen and unsaturated thawed grounds with heterogeneous distribution of low concentrations and contents of salts there appears a gradient of ion chemical potential under the effect of the temperature gradient. Besides, in the horizontal samples due to the thermodiffuse ion transfer (I_{td}) there appears an opposite diffusional (concentration) flow (I_d). A resultant flow of ions in the ground (I_o)

is presented by the following equation:

$$I_o = I_d + I_{td}$$

Temperature and pressure are usually taken as independable variables for thermodynamic description of the upper ground layers. The external gas pressure for similar systems is slightly changed and close to the atmospheric one. Isobar-isothermic potential (Gibb's energy) plays the role of the characteristical function: $G = f(T, P, C_1, C_2 \ldots C_n)$ where G, Gibb's energy, J; T, temperature, °K; P, pressure, P; C_i, mole fraction of i-mobile component (ion) in the system. Gibb's energy partial values the ions, i.e. their chemical potentials ($\mu = \frac{dG}{dC_i}$, J/kg), present their ability of chemical interaction, whereas the spatial gradient μ (J/kg m = = N/kg) is the motive power of their migration flow.

The resultant flow is determined by the chemical potential gradient and mobile conductivity of ground:

$$I_o = -\lambda grad \mu \qquad (1)$$

or taking into account diffusion and thermodiffusion components:

$$I_o = -\lambda \left(\frac{\partial \Psi_d}{\partial x} + \frac{\partial \Psi_{td}}{\partial x} \right)$$

where λ – coefficient of the ground conductivity vs. the ion flow, kg s/m^3; μ – their chemical potential, J/kg; Ψ_d – diffusion component of the chemical potential, J/kg; Ψ_{td} – thermodiffusion component of the chemical, potential, J/kg.

The coefficient of ion conductivity in the ground is correlated with the coefficient of ion diffusion as:

$$\lambda = \mathcal{D} Q \qquad (2)$$

where $Q = \frac{dc}{d\mu}$ – isothermic differential ground capasity vs. the ions of the given form, kg s^2/m^5. Physically, the isothermic differential ground capacity is the amount of the ions of the given form which should be added to (extracted from) the ground to change the chemical potential by unit.

Placing (2) in (1) we can get the intensity of ion flow, expressed through the diffusion coefficient:

$$I_o = -\mathcal{D} \left(\frac{dc}{dx} + \delta \gamma \frac{dt}{dx} \right)$$

or

$$I_o = -D \frac{dc}{dx} - \mathcal{D}_t \gamma \frac{dc}{dx} \qquad (3)$$

where D – diffusion coefficient, m^2/s; C – ion content in the ground, kg/m^3; γ – volumetric ground mass, kg/m^3; δ – thermodiffusion ratio, degree^{-1}; D_t – thermodiffusion coefficient, m^2/s degree.

Physically, the diffusion coefficient is the amount of ions penetrating through the cross-section of the unit area for the time unit under the effect of the unit gradient of the concentration. Under steady-state conditions $I_o = 0$, and $D_t = \left| \mathcal{D} \left(\frac{dc}{dx} \right) / \left(\frac{dt}{dx} \right) \right|$.

Hence, the thermodifussion coefficient is the amount of ions which have to pass through the crossection of the unit area for the time unit at the unit gradient of temperature to balance the opposite diffusion flow at the unit gradient of the concentration under steady-state conditions. D_t sign shows the flow direction: at $D_t < 0$ and $D_t > 0$ the ions are transferred towards the decrease and increase of temperature, respectively.

MATERIALS AND METHODS

D and D_t as phenomenological coefficients are obtained on the basis of ion distributions experimentally found in the grounds. Man-made ground mixtures (pastes) were placed in hermetic sample-holders with heat bearing lids at the butt-ends. The sample holders were of cyllindrical shape with a 40 mm inner diameter and 110 mm long. The grounds under study contained the fraction of quartz sand with 0.25...0.5 mm diameter as well as medium loam sampled from AI horizon of grey forest soil. The initial volumetric moistures were within the range of 0 to 20% for the sand and up to 30% for the loam (that was higher than the capilary moisture capacity). 10% solution of potassium chloride was used for moistening.

The samples evenly moistened and kept under isothermic conditions were placed in the device maintaining constant ($\pm 0.3°$) but different temperatures at the opposite ends. In predetermined time periods the samples were taken from the device and each was quickly divided into three parts. Every part was analyzed for the moisture content by the weighing technique, for the potassium content by the flame photometry and for the chlorine content by the titrimetry with argentum in water extracts.

As a result, the ion and moisture distributions along the samples were obtained for various time and temperature conditions in the device as well as for the frozen and thawed samples of different mechanical and moisture contents. Balance approach was used for determining the diffusion and thermodiffusion coefficients, accordingly:

$$I_o^{\ell} = \frac{\left(\int_0^{\ell} C dx \right)_{\tau_2} - \left(\int_0^{\ell} C dx \right)_{\tau_1}}{\Delta \tau}$$

where I_o^{ℓ} is the resultant ion flow (kg/m^2·s) through the cross-section situated at a distance l (m) from the beginning of coordinates; C is the ion content in the grounds, kg/m^3; t is time, s. Hence, basing on (3)

$$\frac{\left(\int_0^{\ell} C dx \right)_{\tau_2} - \left(\int_0^{\ell} C dx \right)_{\tau_1}}{\tau_2 - \tau_1} = -\mathcal{D} \frac{dc}{dx} - \mathcal{D}_t \gamma \frac{dt}{dx} \qquad (4)$$

Having a system of two equations of type (4) and C = f(x) graphs describing various periods of time, one can calculate D and D_t coefficients being

present in (4). The initial (without gradient) distribution of moisture and ion should be presented by one curve ($\tau_0 = 0$, C(1) = const). Two other curves belong to the stages when $\tau > 0$. This system is presented in the following way:

$$\begin{cases} I_1 = -D g_{c1} - D_t \gamma g_{t1} \\ I_2 = -D g_{c2} - D_t \gamma g_{t2} \end{cases}$$

hence

$$\begin{cases} D = \dfrac{I_2 g_{t2} - I_1 g_{t2}}{g_{c1} g_{t2} - g_{c2} g_{t1}} \\ D_t = \dfrac{I_2 - D g_{c2}}{\gamma g_{t2}} \end{cases}$$

where g_{c1}, g_{c2}, g_{t1}, g_{t2} - gradients of ion content and temperature of the ground for the first and second periods of observations (τ_1 and τ_2); I_1 and I_2 - corresponding ion flows.

Special computer programs on the basis of (5) and the experimental data on the distributions of temperature, ion content and moisture were used to calculate these coefficients. The obtained data are well reproduced.

RESULTS

Fig.1 shows the dynamics of the distributions of moisture and ions in the samples affected by the constant temperature gradient. Stationary distributions of ions were carried out for about 70 hours. A.M.Globus (1983) observed the same periods of establisment of the moisture stationary distributions. They exceed the periods of observations used for determining the mass exchange properties of the unsaline grounds (Vasiliev, Chistotinov, 1983).

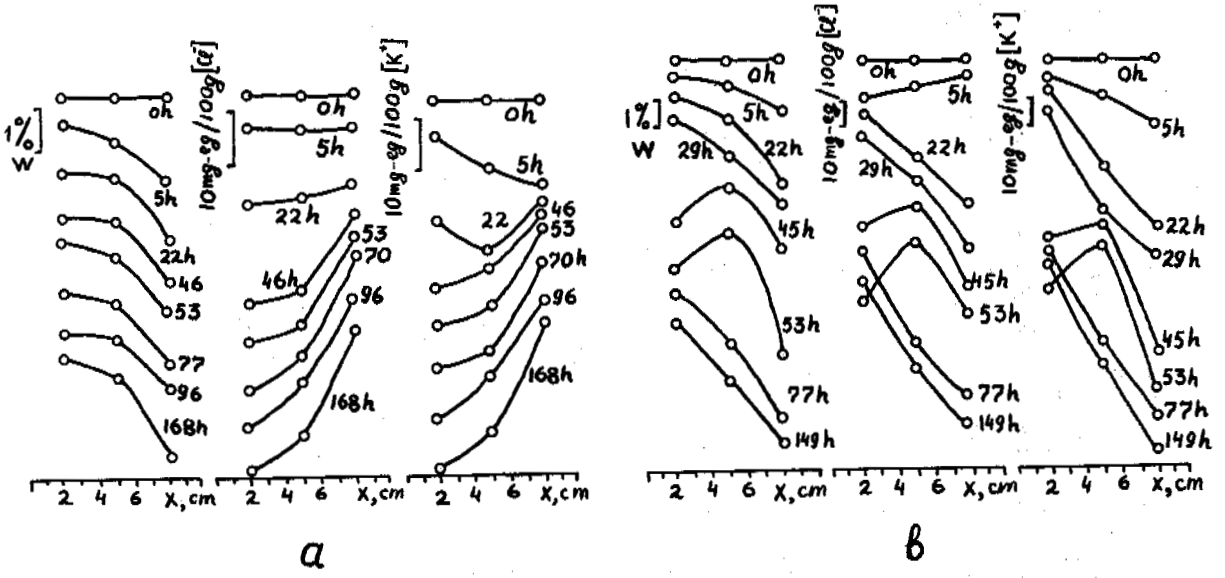

Fig.1. Dynamics of Distributions of Moisture, Chlorine and Potassium Ions in the Thawed (a) and Frozen (b) Sand

Each curve shows the way the volumetric moisture or ion content is distributed along the sample at the time moment indicated to the right of it. The middle point of each curve corresponds to the initial value of moisture (about 7.5%) or to the content of chlorine (about 6 mg-equiv/100 g) and potassium (about 6 mg-equiv/100 g). The vertical scale for each series of the curves is given to the left of the graphs. Quartz sand fraction, o.25...0.5 mm; initial moisture, 7.5%; potassium chloride moistening solution concentration, 10%; temperature gradient, approximately I degree/cm; mean temperature of the frozen ground samples, $-7.5^{\circ}C$, of the thawed ones, $+12.0^{\circ}C$.

The distributions of moisture and ions (Fig.1) are generally of a monotonous character, however, within the range of 48-57 and 22-77 hours for the frozen and thawed grounds, respectively, their graphs are of the extreme form. The intensity of the extremums as well as the rate of their appearance (disapearance) turn out to be higher in the frozen than in the thawed samples. The analogous distributions of salts - with the extremum in the columns- were obtained by A.M.Globus (1983). According to his data the extreme contents of the salts resulted from the increased gas pressure which suppressed the gaseous component of moisture transfer, thus enhancing the intensity of the film migration. No extremums were observed by us during the balance distributions of the ions and moisture.

The values of the moisture and ion diffusion coefficient obtained by the technique described above agree with the data published by various authors (Globus, 1983; Pakshina, 1980 et al.). The magnitudes of the coefficient of the ion thermodiffusion in the grounds vary, as a rule, from 0 to

10^{-9} m^2/s degree, and sometimes this range can be greater including both negative and positive values. The greatest module values D_t found for the potassium ion are 57×10^{-7} and 0.56×10^{-7} m^2/s degree in sand and loam, respectively, at the moisture content somewhat lower than the capilary moisture capacity and at about 15% concentration of the solution. The corresponding extreme values for the chlorine ion are 7.2×10^{-9} and 0.7×10^{-9} m^2/s degree. The values of the thermodiffusion coefficient are determined by the content and composition of the ground, its moisture content, state (frozen-thawed), by the type and concentration of the ions. They depend on the efficient cross-section of the flow, ion mobility and its interaction with moisture and solid phase.

The direction of the resultant moisture transfer is the same in the thawed and frozen grounds: the moisture moves towards the regions with the decreased temperatures (Fig. 1, 2). This fact is stated by the majority of investigators (Globus, 1983; Ershov, 1986 et al.). The direction of the ion transfer in the thawed ground is opposite to that of moisture, i.e. the ions move towards the regions with the increased temperatures. So the experimental data of A.M.Globus are shown to be reproduced. Our observations of the ion transfer in the samples with various moisture saturation indicate that at very low moisture content (for sands about 2% of the ground volume) the ions are transferred to the regions with the decreased temperature.

In the frozen ground the ion transfer is directed in the same way as the moisture one, i.e. towards the regions with the decreased temperature (Fig.1).

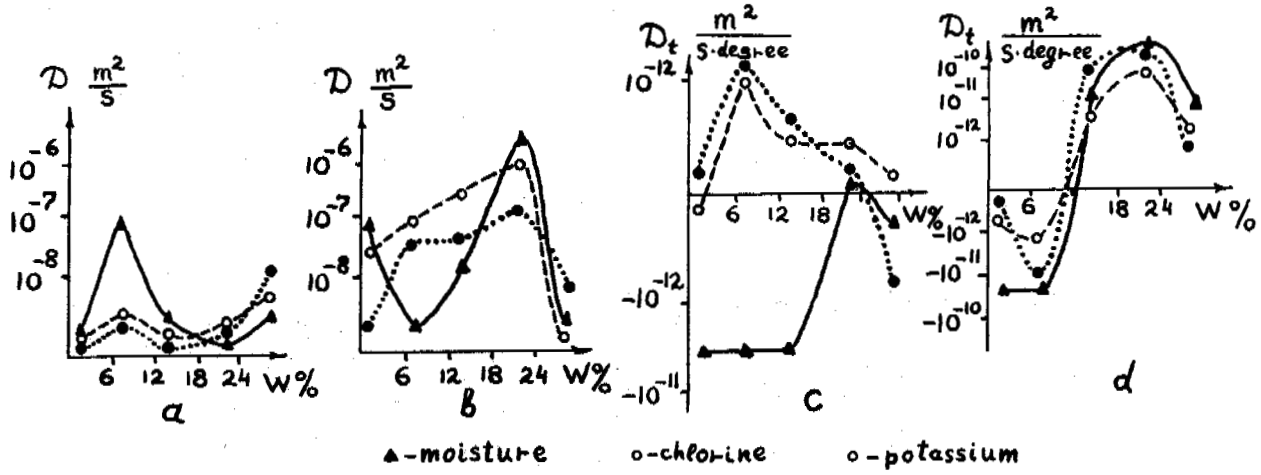

Fig.2. Dependence of Mass Exchange Parameters of the Thawed and Frozen Sand on the Volumetric Moisture Content

a) on the diffusion coefficient of moisture and ions in the thawed sand, b) on the diffusion coefficient of moisture and ions in the frozen sand, c) on the thermodiffusion coefficient of moisture and ions in the thawed sand, d) on the thermodiffusion coefficient of moisture and ions in the frozen sand. Quartz sand fraction, 0.25...0.5 mm; initial volumetric moisture, 10%; exposure periods, 0, 72 and 120 h; temperature gradient, ca. I degree/cm; average temperature of the thawed and frozen sand samples, +12.5°C and -7.5°C, respectively.

Fig.2 shows the moisture dependences of the moisture and ion diffusion and thermodiffusion coefficients in the frozen and thawed sand ground. The moisture diffusion coefficients in the thawed ground at about 6% moisture have their maximums found by E.D.Ershov (1983 et al.). The same maximum, though less exhibited, exists on the corresponding curves for the ions (Fig.2a). The moisture dependence D in the frozen grounds as well as the graphs $D_t = f(w)$ (Fig.2 b,c,d) are of more complicated character.

Fig.3 presents the diagram which allows to evaluate the values of the moisture and ion diffusion and thermodiffusion coefficients in the loam grounds and to observe their changes during transition from the frozen state into the thawed one at a moisture content of about capilary moisture capacity. Under these conditions the values of the D and D_t coefficients of the frozen ground are higher than those for the thawed one.

DISCUSSION

The obtained D and D_t values of the ions in the frozen and thawed grounds can be used in the corresponding models to predict the content of the ground liquid phase, underground water and ice, for paleogeographic reconstructions and for determining the age of deposits.

The complex character of the following dependences $D = f(w)$, $C = f(x, \tau)$, $C = f(w)$, $D_t = f(w)$ for the ions proves the complex form structure of the mobile liquid in the frozen and thawed grounds. To explain this fact it is suggested that the mobile liquid ion-containing moisture in the ground (expect

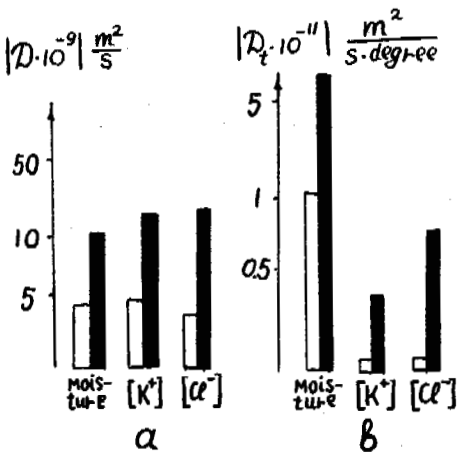

Fig.3. Diffusion and Thermodiffusion Coefficients of the Medium Loam in the Thawed (white columns) and Frozen (black columns) State

Initial volumetric moisture, 28%; potassium chloride moistening solution concentration, 10%; exposure periods, 0, 120, 288 h; temperature gradient, ca. I degree/cm; average temperature of the thawed and frozen ground samples, $+12^{\circ}C$ and $-7^{\circ}C$, respectively.

undissolving volume) has a three layer structure. The inner layer is in the field of strenghs of the solid phase active surface, the intermediate one interacts with it, the external one is in the volumetric state. The moisture and ions in these layers are transferred in various directions: in the inner layer - towards the temperature decrease, in the intermediate one - towards the temperature increase, no moisture and ion transfer observed in the outer one (Fig.4).

Thermodynamically this suggestion is valid. The chemical potential of the ion interracting with the immobile surface of the liquid phase in the inner layer is increased with the increase in temperature. The potential gradient induces the ion transfer towards the temperature decrease. In the intermediate layer the ion interacts mainly with the moisture but not with the surface. The influence of the chemical potential increasing with the temperature increase is due to the thermocapilary ion electrostatic effect resulting in the solution transfer towards the temperature increase (Globus, 1983). No thermodiffuse ion and moisture transfer occurs in the outer layer due to slight dependence of the mobility of the volumetric moisture on temperature.

Let us consider the facts given above using the basis of the three-layer model.

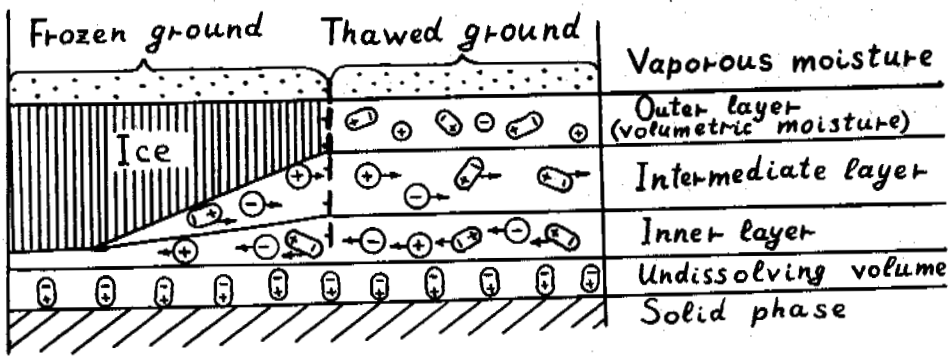

Fig.4. Structural scheme of the liquid phase flow appearing in the disperse ground under the the temperature gradient effect.

Positive and negative particles designated by the circles are ions, dipoles designated by the ellipses are water molecules, the arrows show the particle transfer direction. In the left part of the schematic column the temperature is negative, in the right - positive. No effects specific for the frozen and thawed ground boundary zone are shown.

The direction of the resultant ion transfer can be due to the ratio of the conductances of the inner and intermediate layers. At small moisture contents the inner layer prevailing in the transfer provides the movement towards the temperature decrease. With the increase of moisture content the intermediate layer begins to prevail. It is likely to have higher conductance. The resultant flow direction becomes opposite. In the thawed ground the inner layer has very low ion conductance. Small values of D_t at a moisture content of about 2% prove this fact (Fig. 2c). In the frozen ground obviously due to the solution concentration in the inner and intermediate layers during ice formation in the volumetric liquid the conductance of these layers for the ions is increased (Fig. 2d).

The effect of the transfer in the intermediate layer directed towards the flow in the inner layer accounts for the decrease of D within the range of moisture content from 10 to 25% in the thawed ground (fig. 2a). As it was shown the extreme character of this curve in case with moisture transfer was emphasized by E.D.Ershov (1983, 1986). Obviously, the effect of the transfer in the

two layers with the opposite direction at various dynamics of the flows accounts for the extremums on the curves in Fig.1.

It is also probable that the greatest values found concern the D cases when the flow in one of the layers is supressed and these values characterize the transfer in a particular layer. Thus, the model of the three-layer structure of the mobile liquid in the ground satisfactorily describes the complex character of the direction and dynamics of the ion and moisture flows affected by the temperature gradient and does not contradict to the existing assumptions on nonisothermic moisture transfer in the grounds.

REFERENCES

Globus, A.M. (1983). Fisika neizotermicheskogo vnutripochvennogo vlagoobmena. Leningrad, Gidrometeoizdat, 279 s.

Ershov, E.D. (1986). Fiziko-chimia i mechanika mjorzlykh porod. Moskva, 333 s.

Pakshina, S.M. (1980). Peredvischenie soley v pochve. Moskva, Nauka, 120 s.

Vasiliev, AA. and Chistotinov, L.V. (1983). Metody opredelenja massoobmennykh characteristik peschanykh i poluskalnykh porod. Novye metody issledovania sostava, stroenija i svojstv miorzlykh porod. Moskva, Nedra, s. 79-88.

ELECTROACOUSTIC EFFECT IN FROZEN SOILS

A.S. Pavlov[1] and A.D. Frolov[2]

[1]Research Institute of Engineering Site Investigations, Moscow, USSR
[2]Moscow Geological Prospecting Institute, USSR

SYNOPSIS An electroacoustic effect (EAE) which is an onset of elastic waves exciting by an alternative electric field has been examined. The authors established two EAE differ from each other by a dependence on intensity E and frequency of the exciting electric field: a) linear $A_1(E)$ arising at an exciting frequency and b) non-linear $A_2(E)$ - at a double frequency. Experimentally relations of the both EAE to moisture, ion composition and concentration of pore solutions, temperature within the interval 0 - -40°C obtained on model samples of frozen quartzy sand are under consideration. It is shown that a non-linear effect is highly sensitive to ion composition and concentration of pore solutions.

INTRODUCTION

Development of physics and chemistry of permafrost with different composition and structure is one of the fundamental scientific problems of top priority in the field of geocryology. Studying of physical and chemical phenomena and processes in frozen earth materials reveal of character features of a mechanism of energy transformations in this medium serve a base for creation of new rather sensitive and reliable methods of obtaining information on a nature of formation and interrelation of its physical properties, kinetics of freezing and thawing, composition, state and content of a liquid phase, etc.

An important problem in this field close to dynamic relaxation spectroscopy (Frolov,1978) is an investigations and analysis of mechano-electrical processes of an energy transformation in frozen soils. There are many papers devoted to a direct seismoelectric effect in moist sandy-clayey soils under positive temperatures (Parkhomenko, 1968; Chermak, 1975 et al.). But a reverse seismoelectric effect and other electromechanical phenomena in moist soil lacks information even at positive temperature whereas their use for examination of ion composition and energetic condition of pore solutions is undoubtedly preferable. Some scientists displayed an interest to seismoelectric phenomena in permafrost (Migunov et al., 1976; Frolov, 1976b, Kokarev et al.,1978, 1981),but it was only a fragmental information.

Last years the authors carried out for the first time a detailed laboratory analysis of an electroacoustic effect (EAE) in frozen sandy-clayey soils. The experimental research was devoted to estimating a number of character features of EAE depending on many factors. Main data of the first stage investigations are given below.

Samples and Methods

A subject of our inquiry is a sandy-clayey soil characterized by a variable composition, content, space distribution and state (degree of bound state) of pore moisture. For the first experiment stage a model samples of disperse soil were prepared from pure quartzy sand, size of fractions is about 0,1 - 0.05mm weight moisture was assumed from ~ 0% (air-dry) to ~ 20%. The samples were saturated with distilled water or with solutions of salts widely spread in natural waters: HCl, NaCl, $CaCl_2$, K_2CO_3, Na_2CO_3 with a concentration of 10^{-3}, 10^{-2}, 10^{-1}, 10°N, which envisages a rather wide interval for modelling of natural conditions. The test samples were prepared in cylindric forms made of dielectric 40 mm in diameter and 20 mm high, where sand of any moisture content was compacted to approximately adequate porosity. Then the forms were scaled and kept dozen hours to reach an uniform distribution of moisture in a sample volume. A moisture content was controlled before and after each experimental cycle. In order to creation a massive cryotexture the samples were frozen in the refrigerator at a temperature of -60°C. Before each of experiment the samples were kept at a prescribed temperature during 24-48 hours providing a quazistationary condition of frozen soil. All the experiments were performed at an increasing temperature from -(50+60)°C by step of 2 - 5°C. A cylindric form with a sample (bottom and cap of the form were electrodes) represented a measuring cell. One of electrodes of a measuring cell without an electric contact was attached to a calibrated piezoelectric transducer with a self-frequency of about 100 KHz. A sample was excited through electrodes by a harmonic electric signal from the audio-generator with a power amplifier, output voltage- up to 500 V. A signal from piezotransducer characterizing EAE in the

sample under examination was measured with an aid of a selective microvoltmeter. Frequency, amplitude and a form of exciting and measuring signals were controlled by special devices and visually with an aid of an electronic oscillograph (Pavlov, 1984). Measurements were taken as a rule within an interval of frequences 3-12 KHz of the exciting field where the highest intensity and the best reproduction of the effect under examination were observed. A number of EAE measurements were taken within a rather wide range of frequences. A special attention was paid to elimination of volume and phase distortions and providing a good reproducibility of measurement results. Values of two signals were registered for each chosen temperature: A - at a frequency of the exciting field and A_2 - at a double frequency. Signals of other multiple harmonics were measured sometimes but their values were usually so small that could be hardly reproduced. Registration of signals A_1 and A_2 was accurate and reliable.

Results and Discussions

The exciting field intensity changes within a wide range of voltage applied to the samples permit to determine two EAE (Fig.1): linear (A_1) and non-linear (A_2) available in moist sand and clay under thawing and frozen condition. A non-linear effect is always observed

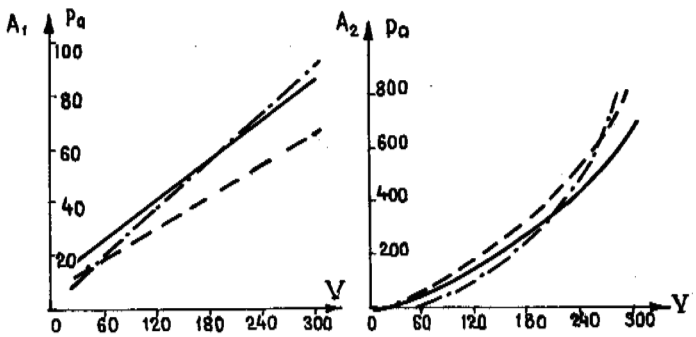

Fig.1 Intensity of EAE vs applied voltage.

at a double frequency as compare to the frequency of the exciting electric field.

Unlike the previous data (Cherniak, 1975) a non-linear electroacoustic transformation in the moist disperse soil cannot be considered "quadratic" towards to the electric field intensity and therefore cannot be identify with electrostriction. A law of non-linear relation $A_2(E)$ requires an additional precision but all the obtained experimental data testify to the fact that it is far from parabolic. The established two EAE shows the different processes of displacement of mobile charge carriers in the pore solution which can be related to two states of a liquid phase: quasifree and quasibound. It is confirmed by experimentally obtained variable relations of A_1 and A_2 and parameters of their dependence on intensity of the exciting field (curve slopes at Fig.1) with account of different degree of filling up the pores, concentration and ion composition of pore solutions, frequency of an exciting electric field, degree of freezing of a soil, dispersity and mineral composition of grains.

In accord with the methods specified a relation between EAE and moisture content of fine quartzy sand was found (Fig.2). As it is

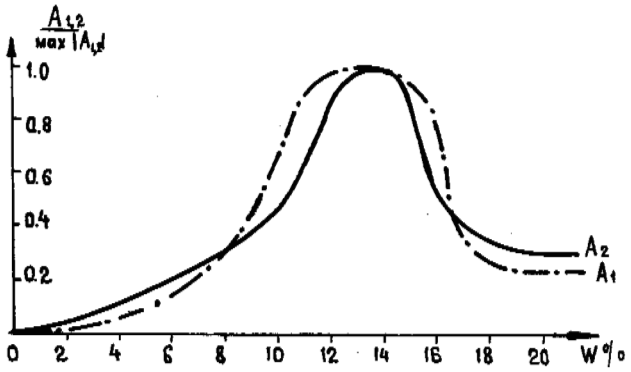

Fig.2 EAE Intensity vs Moisture of Sandy Samples

shown at Fig. 2 the relation is of an extreme character with maximum at 12-14% moisture content, but as for a linear effect the maximum area is wider and an amplitude slope of the effect curve is more distinctly expressed. The slope to small moisture content is rather slow for a non-linear effect. It should be mentioned that amplitude values of the linear effect for thawing sand are always higher than those for a non-linear effect. Still, a difference in A_1 and A_2 at high moisture content increases by an order as compare to the low moisture (1-3%) i.e. a specific contribution of the electroacoustic transformation in quasibound water decreases at increasing moisture of sand and intensity of electroosmosis as well.

When moist non-saline sand pass to frozen state an amplitude of linear effect A_1 decreases sharply due to ice segregation, formation of a cryotexture and freezing out of "free water". In this case, an amplitude of non-linear effect A_2 (unlike A_1) increases highly and then quickly decreases practically to zero (Fig. 3a). For sands saturated with salt solutions (Fig. 3b,c) this character feature of two EAE can be expressed rather distinct due to extended phase transition within the domain of negative temperatures. Two areas with an increase in A_2 are registered for concentration of saturating solutions 10^{-1}N (Fig.3c): a) about 0°C when segregation of pore ice begins; b) at a temperature of intensive formation of crystallohydrates and freezing out of associated solutions of salts. It is evident that the above mentioned processes are related to sharp variation of distribution of a liquid phase in frozen soil, when a contribution of EAE to "quasicohesive water" increases. If concentration of a saturated solution is about 10^{-2}N the second area can be

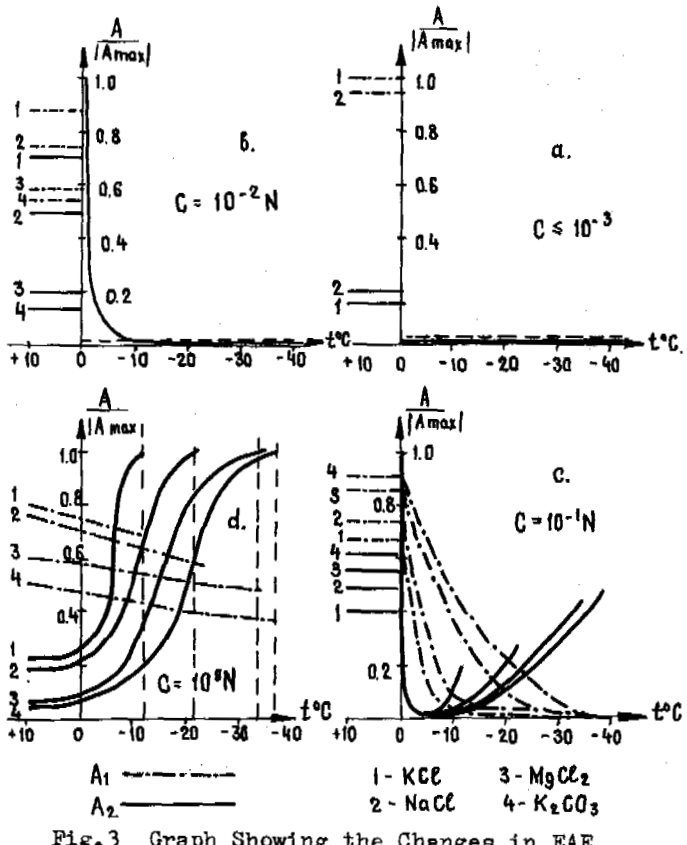

Fig.3 Graph Showing the Changes in EAE vs Temperature for Different Saturated Solutions

hardly observed (Fig. 3) and if concentration is high i.e. 1 N (Fig. 3d) there is no first area of A_2 increase at a temperature about 0°C. A linear effect, A_1 is characterized by monotonous diminution in EAE at a decreasing of temperature (Fig. 3b-d) with a sharp drop at about eutectic temperatures that can be rather distinctly registered at high concentration of solutions (Fig. 3d).

Studying the effect of concentration of saturated solutions permits to establish relationships especially of a non-linear effect, the example of which is shown at Fig.4.

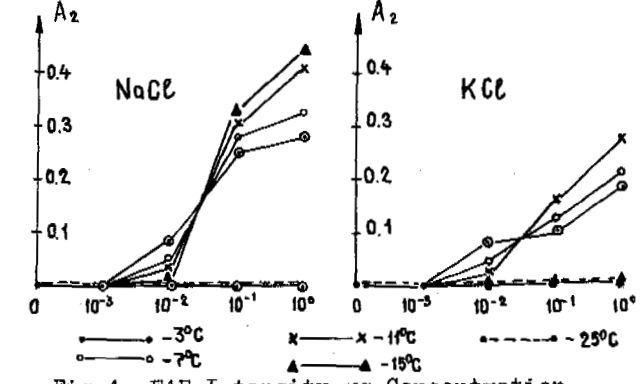

Fig.4 EAE Intensity vs Concentration of Porous Solutions

If concentration of pore solutions increases the A_2 is also increases and concentration 10^{-2} is assumed a boundary to a certain extent. If concentration is high (Fig. 4) an inversion temperature influence is observed, that is to say that high values of A_2 are at lower temperature. Besides that an increase in A_2 becomes more intensive and reaches an eutectic temperature. These peculiarities characterize of the solutions of all the salts used in experiments.

Electromechanical transformations of energy in moist sandy-clayey soils are estimated, as a rule, by composition, state and distribution of pore moisture. It was considered for a long time that a direct seismoacoustic effect is conditioned by dynamic (in an alternative field) variant of filtration potentials originated from charges displacement of diffusion parts of double-electric layers at a contacts of a liquid and solid phases of the moisture-carrying porous media. And a reverse effect is conditioned by an electroosmosis (Parkhomenko, 1968). The further experiments showed that a reverse seismoelectric effect can be related to frequency and amplitude of an exciting field in the most complicated manner (Chermak, 1975, 1976). But an explanation of the obtained peculiarities was not reasonable enough and arouse valid objections (Migunov et al., 1976). Nevertheless it becomes clear from the present paper that a reverse seismoelectric effect can be observed in a little moist soils and its development is much variable as compare to the direct effect. Thus the reverse effect is a good tool for studying of a liquid phase states in porous media.

Our observations of EAE in frozen soils permit to establish new characteristic features of this phenomenon and to give it an uncontradictory explication. The experimental data obtained on available two EAE: a linear effect at a frequency of the exciting field and a non-linear effect - at a double frequency can be explained in the following way.

Apparently, the first one is a reverse seismoelectric effect conditioned by the electroosmosis in a relatively permeable medium. This statement is verified by a temperature relation A_1 (Fig.3) as the A_1 value decreases monotonously as far as segregation of pore ice and decreasing permeability of a frozen soil takes place.

A non-linear effect due another mechanism. Its characteristic features can be explained by migrational displacement of ions within the limits of discontinuous cells of pore solutions in the electric field. Availability of such cells is related to heterogeneity and goffering of absorbed layers of "bound water" which formation and space distribution in a disperse moist soil depend on characteristics of grains' surface of a solid phase (distribution of non-compensated charges), cryotexture of soil and composition of pore solutions. Relate to a model of migrating macrodipole polarization (Frolov, 1976, Frolov, Fedjukin, 1983) when a degree of discontinuous space distribution of a pore solution increases a non-linear effect at a double frequency must increase too, but a linear effect, on the contrary,

decreases. That was proved by the results of our experiments on frozen saline sand (Fig.3) and on frozen clay also. A non-linear electroacoustic transformation - A_2 in frozen clay of different dispersity and mineral composition (kaolin, bentonite, Gzhel) can be registered at a temperature up to -50 - -70°C; at the same time a linear effect decreases practically to zero at rather high temperatures.

A non-linear effect is characterized by an optimal condition of the frozen medium when a degree of discontinuity of a liquid phase is high but a size of cells permits to migrating ions to acquire necessary kinetic energy and impulse to transfer the latter to the walls of cell and create a tensile deformation. In this case a concentration of pore solutions should not be very high. So, Fig. 3 c,d show that in frozen sand saturated with salt solutions of concentration 10^{-1} - 10°N the mentioned state of frozen ground comes for example at a temperature near to eutectic, when a degree of discontinuity of the liquid phase increases sharply and concentration of solutions decreases due to formation of salt crystalohydrates. Such a condition related to a maximum of non-linear effect in frozen non-saline water saturated clays is character of a stage of forming a massive cryotexture and sharp increasing of discontinuity of a liquid phase. A migrational model permits to explain also a double frequency character of a non-linear effect. Pore solution ions of different signs will displace to the walls of the cell giving them a part of impulse obtained during every half-period of an exciting harmonic electric field. It means that every half-period the cell walls experience impulses of increasing of dilatation and then its decrease. In such a way a double frequency is formed in an acoustic signal of a non-linear effect as well as a slight dependence of mechanic deformations on changing of sign of an electric field. But this is not electrostriction due to the fact that the dependence on the intensity of the electric field is far from being quadratic. Besides that when ions migrate within the limits of cells there appear gradients of on concentration of different signs. The higher is a temperature the stronger these gradients "put on the brakes" the ion migration, therefore value A_2 is less at positive temperatures and at high concentration.

The obtained relations between A_2 and concentration (Figs.3,4) permit to consider value 10^{-2}N to be a "boundary value" with different development of a non-linear effect when concentration of the saturated solution is less or higher than the boundary value. The same concentration turned to be specific when studying dielectrical permeability of saline moist frozen sand (Frolov, Fedjukin, 1983). It is related also to "isoconductivity" of similar media if their electric conductivity turns to be practically independent on volumetric fraction of a solid disperse soil phase. So, we proved again an opportunity to get information in detail on specific features and kinetics of freezing out of a liquid phase on the basis of studying electrodynamic and electrokinetic phenomena in earth frozen material use of EAE in these purposes is especially perspective for clay and saline sand. A non-linear EAE highly sensitive to ion composition and to concentration of pore solutions that makes its use rather perspective in elaboration of a method to estimate condition and development of kinetics of freezing (thawing) of saline soil at the coastal areas of north seas as well as at the areas of cryopegs occurrence.

Conclusions

1. Two electroacoustic effects are established in moist disperse soils under thawing and freezing conditions: a) linear and b) non-linear (towards intensity of an exciting electric field). The first one is a reverse seismoelectric effect E originates on exciting frequency is conditioned by electroosmosis. The second one originates on a double frequency; its nature is different, it can be explained by a mechanism of migrational displacement of ions in discontinuous accumulations (cells) of the liquid phase under effect of an external electric field.
2. Non-linear electromechanical transformation is far from quadratic dependence on intensity of the exciting electric field and cannot be considered analogous to electrostriction.
3. The obtained ratio of the both electroacoustic transformations versus soil moisture content with a maximum related to weight moisture of quartzy sand approximates 12-14%.
4. For the first time an electroacoustic transformation of energy in frozen soils was investigated by experiment and temperature relations of the both effects to changes in content, space distribution and state of a liquid phase (kinetics of freezing of soil) were established.
5. Characteristics of an electroacoustic effect in frozen saline sand are examined at different concentration and ion composition (5 salts) of pore solutions. The established relations show high sensitivity of non-linear electroacoustic transformation to composition and concentration of pore solutions.

So, the first stage investigations of new physical phenomenon in permafrost has been completed and the perspectives of using the electroacoustic effect in geocryology is elucidated.

REFERENCES

Cherniak, G.J. (1975) O priamom i obratnom seismoelectricheskikh effectah v osadochnikh porodah pri garmonicheskom vozbuzhdenii. Izv. AN SSSR, Ser.Phys.Zemli, N 7.

Cherniak, G.J. (1976). O phizicheskoi prirode seismoelectricheskogo effecta gornykh porod. Izv. AN SSSR, Ser.Phys.Zemli,N 2.

Frolov, A.D. (1976a). Electricheskie i uprugie svoistva kriogennykh porod, Nedra, Moskva.

Frolov, A.D. (1976b).Nekotorye resultaty izuchenia seismoelectricheskogo effecta v merzlykh porodakh. Sb. Merzlotnye issledovaniia, vyp. 16, MGU.

Frolov, A.D. (1978). Problems and Possibilities of studying the processes of Dynamic Relaxation in Frozen Earth Materials. Proc. of III Int. Conf. on Permafrost,

vol.1, Edmonton, Alberta, Canada.

Frolov, A.D., Fedjukin, I.V. (1983). O poliarizatsii v merzlykh dispersnykh porodakh v peremennykh elektricheskikh polish. Izv. VUZov Ser. Geologia i Razvedka N 6.

Kokarev, A.A., Migounov, N.I., Frolov, A.D. (1978). Seismoelectricheskii effect kimberlitov pri ponizhennykh temperaturakh. Sb. Izuchenie gornykh porod acusticheskimi metodami. VNIIJGG, Moscow.

Kokarev, A.A., Migounov,N.I., Frolov, A.D. (1981). Seismicheskie i acusticheskie issledovaniia kimberlitov Sibirskoi platformy. Depon. VINITI, N 1548-81.

Migounov, N.I., Sobolev, G.A., Frolov, A.D. (1976a) Perspectiva primeneniia seismoelectricheskogo i piezoelectricheskogo metodov pri inzhenerno-geologicheskikh izyskaniiakh. Respubl. soveschanie po vnedreniiu geofizicheskikh metodov pri izyskaniiakh dlia stroitelstva.

Migounov, N.I., Sobolev, G.A., Frolov, A.D. (1976b). Po povodu usileniia seismoelectricheskogo effecta postojannym electricheskim polem. Izvestiia AN SSSR, Ser. Fizika Zemli N 10.

Parhomenko, E.I. (1968). Yavleniia electrizatsii v gornykh porodakh, Nauka, Moskva.

Pavlov, A.S. (1984). Nekotorye voprosy metodiki issledovaniia electroakusticheskikh javlenij v merzlykh porodakh. Deponir. VINITI N 2171-84.

SPATIAL VARIATION IN SEASONAL FROST HEAVE CYCLES

E. Perfect†, R.D. Miller and B. Burton

†Department of Land Resource Science, University of Guelph, Guelph, Ontario, Canada N1G 2W1

SYNOPSIS Our knowledge of frost heave is based upon laboratory and theoretical studies which give little indication of the spatial variability of soil displacements. We present a preliminary geostatistical analysis of frost heaving in a cultivated silt loam soil near Ithaca, NY, USA. Weekly measurements were made over an area of ~1500 m^2 using conventional surveying equipment. One hundred point locations, clustered within individual forage stands, were monitored throughout the winters of 1982/83 and 1983/84. Maximum heave cycles of 23 ± 1 mm and 39 ± 1 mm were recorded, respectively. Autocorrelation within each stand showed the soil displacements to be spatially dependent over relatively small distances up to ~3.5 m. Semivariograms at the whole-field scale were unbounded; a "linear model" appeared to best fit this structure during frost penetration and at a maximum heave. "Nugget effects" predominated upon thaw consolidation. Further soils frost research employing a geostatistical approach is warranted, including "kriging" and spatial cross-correlation.

INTRODUCTION

The spatial variability of soil displacements caused by ice segregation and subsequent thaw consolidation is of interest to agronomists, geomorphologists and hydrologists. An understanding of the effects of differential frost heaving is also important for engineers working on foundations and pipelines in areas of seasonally frozen soil (Williams, 1986). However, most of our knowledge about this process comes from laboratory tests (Chamberlin, 1981) and theoretical models (O'Neill, 1983) which give little indication of the scale of variation. Comparatively few field data are available. For the most part, these come from early descriptive studies of cryopedoturbation (eg. Troll, 1944). With the development of automated measurement techniques, the emphasis of field workers has shifted from extensive, non-continuous observations to intensive, continuous monitoring of heave at one or two locations (Matthews, 1967; Fahey, 1979). Notable exceptions include a quantitative spatial analysis of frost heaving by Andrews (1963), and data used by Guymon et al. (1981) in the development of a probabilistic model for ice segregation.

Variation is often treated stochastically using classical statistical approaches such as sampling theory and analysis of variance. These procedures assume independence of samples. However, a given set of observations may be autocorrelated in space and/or time. Spatial autocorrelation requires the use of a relatively new methodology known as "geostatistics." This approach evolved out of empirical research on the estimation of gold ore reserves (Krige, 1951). Subsequently, the theory was formalized by Matheron (1971). It is based upon the idea that values of a parameter over small distances are likely to be similar, while those over greater distances are not. Geostatistical techniques are now used extensively in hydrology (Delhomme, 1979), soil science (Vieira et al., 1983; Trangmar et al., 1985), and by the mining industry (Journel and Huijbregts, 1978). Their application to soil frost phenomena is a logical, but unexplored extension.

We present measurements of soil heaving associated with seasonal frost penetration in an agricultural field. The data were collected as part of a larger study investigating the effects of freeze-thaw cycles on forage crops (Perfect, 1986). Soil displacements were monitored at numerous points, instead of one or two locations as reported in recent field studies. This permitted a preliminary geostatistical analysis of the heaving process. Our objectives were to describe the spatial structure of soil displacements caused by ice segregation and thaw consolidation, introduce the methods of geostatistics into the soil freezing literature, and encourage further research in this direction.

MATERIALS AND METHODS

Fieldwork was conducted near Ithaca, NY, USA, over the course of two winters: 1982/83 and 1983/84. The experimental plots covered an area of ~1500 m^2 on a complex 2 - 3% slope. Classified as moderately well drained, Collamer (fine-silty, mixed, mesic Glossoboric Hapludalf) intergrading to somewhat poorly drained Niagara (fine-silty, mixed, mesic Aeric Ochraqualf) both soil types at this location were highly frost susceptible. Their profiles are described in detail by Cline and Bloom

(1965). The 2 x 7 m forage stands had been established in a randomized block design and were managed for other purposes. All plots were cut in October to remove dead growth, reduce snow capture and improve access to the soil surface in winter. Plot selection was determined by the forage varieties monitored, resulting in a non-ideal sampling strategy from a geostatistical perspective (Fig. 1).

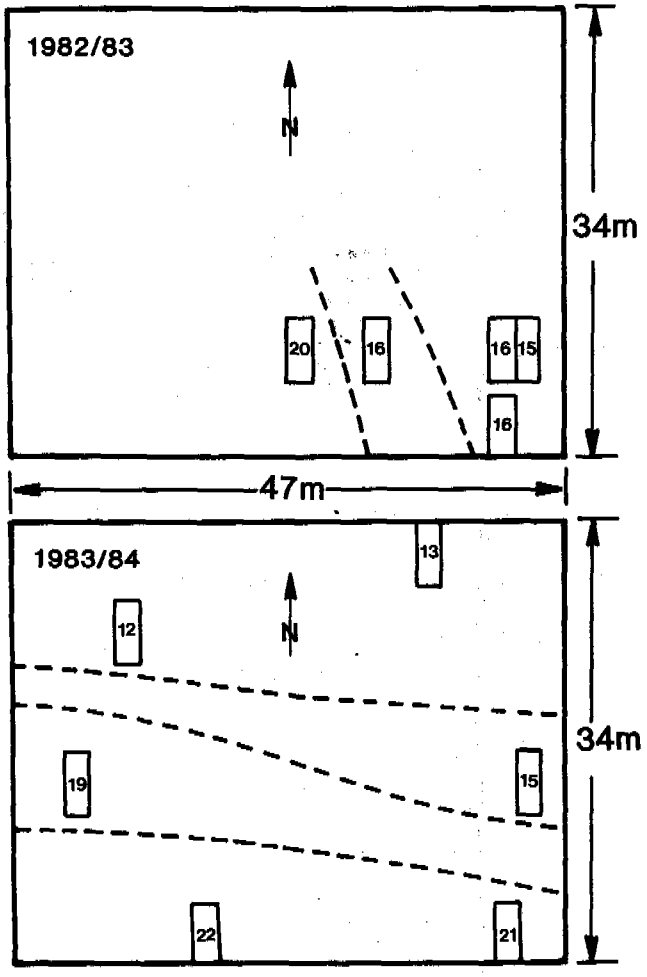

Fig. 1 Location of individual forage stands showing mean soil displacements in mm during frost penetration (FP): 12-11-82 and 12-22-83, respectively. Plot means which are significantly different at $p < 0.05$ are separated by two or more dashed lines.

Point locations on the soil surface were identified by stakes clustered within individual stands. Altogether, we monitored 100 points (in 5 plots) throughout the winter of 1982/83 and 108 points (in 6 plots) during 1983/84. The soil displacements were measured with reference to 3 stable benchmarks, isolated from the effects of frost action, using conventional surveying equipment (James, 1971). A lightweight stadia rod was used, to preserve fragile ice forms such as needle ice. This was placed next to each stake on the side facing the level. Constant use of this placement procedure ensured repeated measurement of essentially the same point on the soil surface over time. Readings were accurate to ± 1.6 mm. Measurements were made at approximately weekly intervals throughout both winters, unless snow cover was excessive; small accumulations (<10 cm) were removed from the soil surface with a brush. In the spring, the X-Y coordinates of the stakes were determined for geostatistical analysis of the heave data.

Supplementary data collection included soil water profile determinations using the neutron thermalization method (Dickey et al., 1964) and depth of freezing (in the second winter only) as indicated by frost gauges (Rickard and Brown, 1972). Following thaw consolidation in the spring of 1984, the forage stands were sampled for soil physical properties. Saturated hydraulic conductivity was measured in the field (Klute, 1986). Undisturbed soil cores were obtained from the plough layer. In the laboratory, standard methods were used to determine bulk density, particle size distribution, air intrusion and soil moisture retention (Klute, 1986). The soil physical properties are summarized in Table I.

TABLE I Soil Physical Properties of the Plough Layer†

Measurement	n	Mean ± Standard Error
Hydraulic conductivity ($x10^{-5}$, $m.s^{-1}$)	12	2.3±0.49
Mechanical analysis (%)	6	Sand: 4±0.3, Silt: 76±0.7 Clay: 20±0.6
Bulk density (Mg. m^{-3})	18	1.4±0.02
Water content ($x10^2$, $m^3.m^{-3}$, %)	12	0.3 bar:37±1.0 15 bar: 12±0.6
Air entry value (kPa)	3	13.2±1.28

†Ap horizon, 0-15 cm depth

Fractile diagrams were constructed for each set of weekly heave measurements. These showed the soil displacements to be normally distributed, and no transformations were made before taking a geostatistical approach. Since all data followed a normal frequency distribution, we calculated the number of samples (N) required to estimate the mean of each population at a specified level of precision using the following equation (Klute, 1986, p.8):

$$N = t_{\alpha}^2 \cdot S^2/d^2 \qquad [1]$$

where t_{α} is the two-tailed student's t value at risk level α, S is the standard deviation of the sample, and d is the half-width of the chosen confidence interval.

Autocorrelograms and semivariograms (Journal and Huijbregts, 1978) were constructed using an algorithm suggested by Wagenet (personal communication, 1983). Because sample locations were irregularly spaced an averaging technique was employed. Separation distances were determined for all possible pairs of observations

including zero lag. These were grouped into classes of $h \pm \Delta h/2$; classes with fewer than 10 pairs were omitted. A mean autocorrelation coefficient and semivariance, associated with an average lag distance, $\bar{h}$ were then computed for each class. Directional searching (Trangmar et al., 1985) proved impractical because of the clustered experimental design (see Fig. 1). Therefore, all results reported are isotropic. Appropriate functions (McBratney and Webster, 1986) were fitted to the experimental semivariograms using least squares approximation procedures. The temporal persistence of spatial heave patterns was evaluated by correlating subsequent soil displacements with those produced during initial frost penetration.

RESULTS AND DISCUSSION

Frost gauges indicated the soil was frozen for a total of 58 days during the second winter. The maximum rate of freezing was 2.2 cm.day^{-1} and maximum depth of frost penetration was 37 cm. The neutron probe data showed increases in the volumetric soil water/ice content of between 4 and 9% in 1982/83, and between 8 and 15% in 1983/84. These increases occurred in the upper 35 cm (i.e. above the frost line) during midwinter and were accompanied by concommitant decreases within the subsoil, indicating freezing-induced redistribution of soil water.

The frost heave cycles for both winters are presented in Fig. 2. Maximum rates of heave were 1.0 ± 0.07 mm.day^{-1} in 1982/83, and 2.1 ± 0.08 mm.day^{-1} in 1983/84; these occurred during mid-December as frost first entered the ground. In 1982/83, the heave cycle reached a maximum amplitude of 22.6 ± 0.94 mm on 19 Feb. The following winter the cycle was bi-modal, with two major peaks occurring on 4 Jan. and 16 Mar. Maximum heave was 38.8 ± 0.67 mm; in situ freezing of soil water could only account for one third of this displacement.

Coefficients of variation (CV) for soil displacements over the whole-field ranged from 12.0% to 89.6% (Table II). The CV values for MH were considerably lower than those reported by Guymon et al. (1981), and those which can be calculated from Andrews' (1963) data. Variability was more pronounced during rapid FP than at MH. The moderately high CV values for TC in both winters indicate uneven thawing. Sample numbers, calculated to give an estimate of MH within 10% of the true mean at $p < 0.05$, were 27 and 6 in 1982/83 and 1983/84, respectively. Thus, relatively few measurements were needed to obtain an accurate estimate of mean displacement at MH in this case.

Autocorrelograms for the soil displacements during FP are shown in Fig. 3. These are ensemble averages for the individual forage stands. Both functions decrease with increasing lag distance; the curves are similar in shape, although r_a decreases more gradually in the second winter. The heaving process appears to be spatially dependent over relatively small distances, up to ~3.5 m. Analysis of variance procedures (ANOVA) indicated significant differences in mean displacements between the forage stands during FP (Fig. 1). Consequently, non-stationarity was expected at the whole-field scale and semivariograms were computed instead of the autocorrelation function.

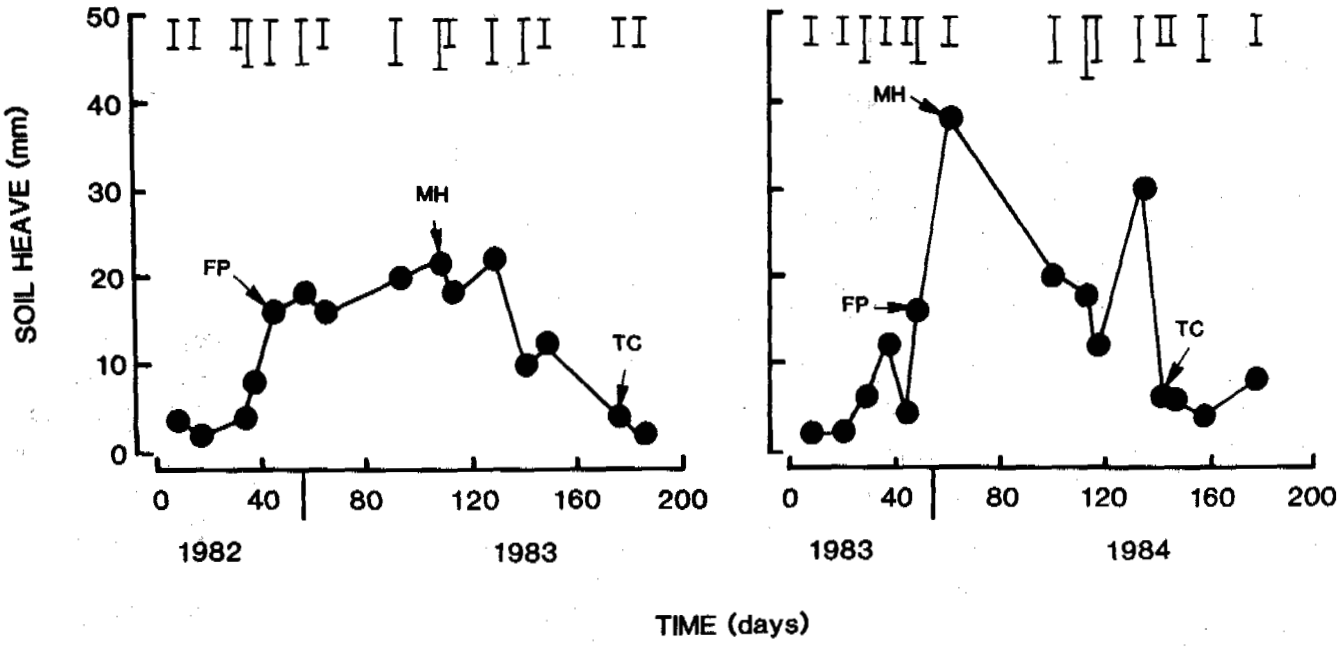

Fig. 2 Mean frost heave cycles. Upper bars indicate the standard deviation for each date. FP, MH and TC denote the maximum rate of heave during frost penetration, maximum displacement and complete thaw consolidation, respectively.

TABLE II Sample Number Determinations for Soil Displacements During Frost Penetration, Maximum Heave and Thaw Consolidation[†]

	Frost Penetration[‡]			Maximum Heave[§]			Thaw Consolidation[¶]		
Winter	n	CV	N	n	CV	N	n	CV	N
		-%-			-%-			-%-	
1982/83	100	31.6	38	41	26.7	27	96	89.6	308
1983/84	108	35.4	48	49	12.0	6	107	64.3	109

[†] Sample number (N) calculated to give an estimate of the sample mean which will be within 10% of the true mean at $p < 0.05$.
[‡] FP: 12-19-82 and 12-22-83, respectively.
[§] MH: 2-19-83 and 1-4-84, respectively.
[¶] TC: 4-30-83 and 3-22-84, respectively.

Examples of these during FP, MH and TC are shown in Fig. 4. The soil displacements varied increasingly without limit as frost first entered the ground and at MH in each winter. A "linear model" appeared to best fit this structure, signifying the presence of trend or "drift." In contrast, linear models fitted to the semivariograms for TC approximated a pure "nugget effect" (i.e. random variation).

It is unlikely that the periodicity apparent in the second winter (Fig. 4) is related to any kind of previous tillage or traffic pattern. The "holes" in the variance structure are probably due to our use of an isotopic calculation procedure with the non-ideal sampling pattern. There was no relationship between semivariances and number of sample pairs used in their estimation. However, the whole question of how many samples are needed to derive an acceptable semivariogram deserves more attention (McBratney and Webster, 1986). Currently, there is no theoretical basis for calculating confidence limits.

It is clear from Fig. 4 that the spatial dependence of soil displacements caused by frost heaving changes over time. No spatial structure was apparent until the onset of freezing. The semivariogram functions are steepest during FP. This structure is preserved at MH and throughout the major heave cycle. However, it collapses upon TC when the semivariograms can be interpreted as mainly "nugget effect." The pattern of soil displacements produced during FP explained up to 50% of the subsequent spatial variation in heave in 1982/83, and up to 41% in 1983/84.

The temporal pattern of change can best be understood in terms of active and passive processes. Frost heaving is an active thermomechanical process. Variability is probably due to differences in soil physical properties, drainage and microclimatic conditions. The resultant spatial structure appears to be produced during a relatively short period of time, as frost first enters the ground and heaving is most rapid. Andrews (1963) arrived at a similar conclusion. In contrast, subsidence is a passive thawing process, related to the pattern of snow melt. The spatial variation in soil displacements produced by frost action is transient. At this location, no residual structure was carried over into the growing season.

It is useful to compare the spatial variability of soil displacements in the forage stands (Fig. 3) with that over the whole-field (Fig. 4). Differences are probably due to the fact that heaving operates at two or more nested scales of variation or "domains." The correlation structure for the individual stands is indicative of its range of influence within a single soil type (~3.5 m). In contrast, the variance structure obtained over the entire field incorporates differential heaving between soil types. Thus, we are begining to describe variation at the landform scale. Since the experimental area only included two soil types, this unbounded increase in variance may represent the initial near-linear portion of a "spherical model" (Webster and Burgess, 1984). According to this scenario, heave will vary increasingly, as the area and number of soil types sampled increase, until it asymptotically approaches the sill for that particular domain.

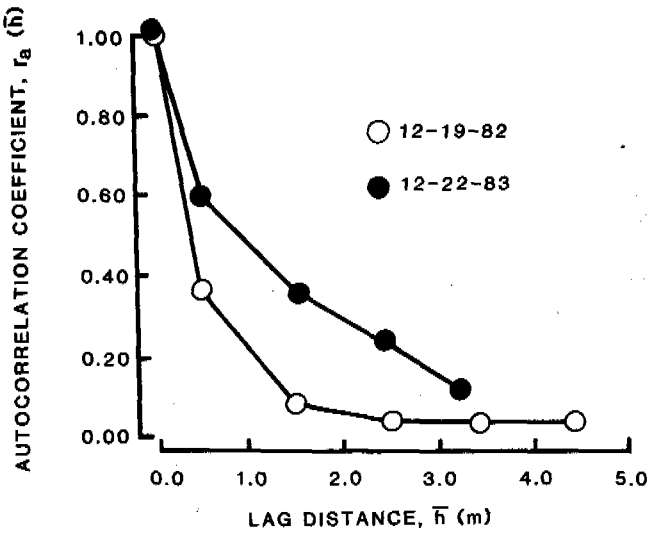

Fig. 3 Autocorrelograms for pooled soil displacements within the forage stands during frost penetration (FP).

Further research employing a geostatistical approach is warranted. This should include alternative sampling strategies, designed specifically for estimation and mapping of regionalized variables (Webster and Burgess, 1984). Our sample number determinations (Table

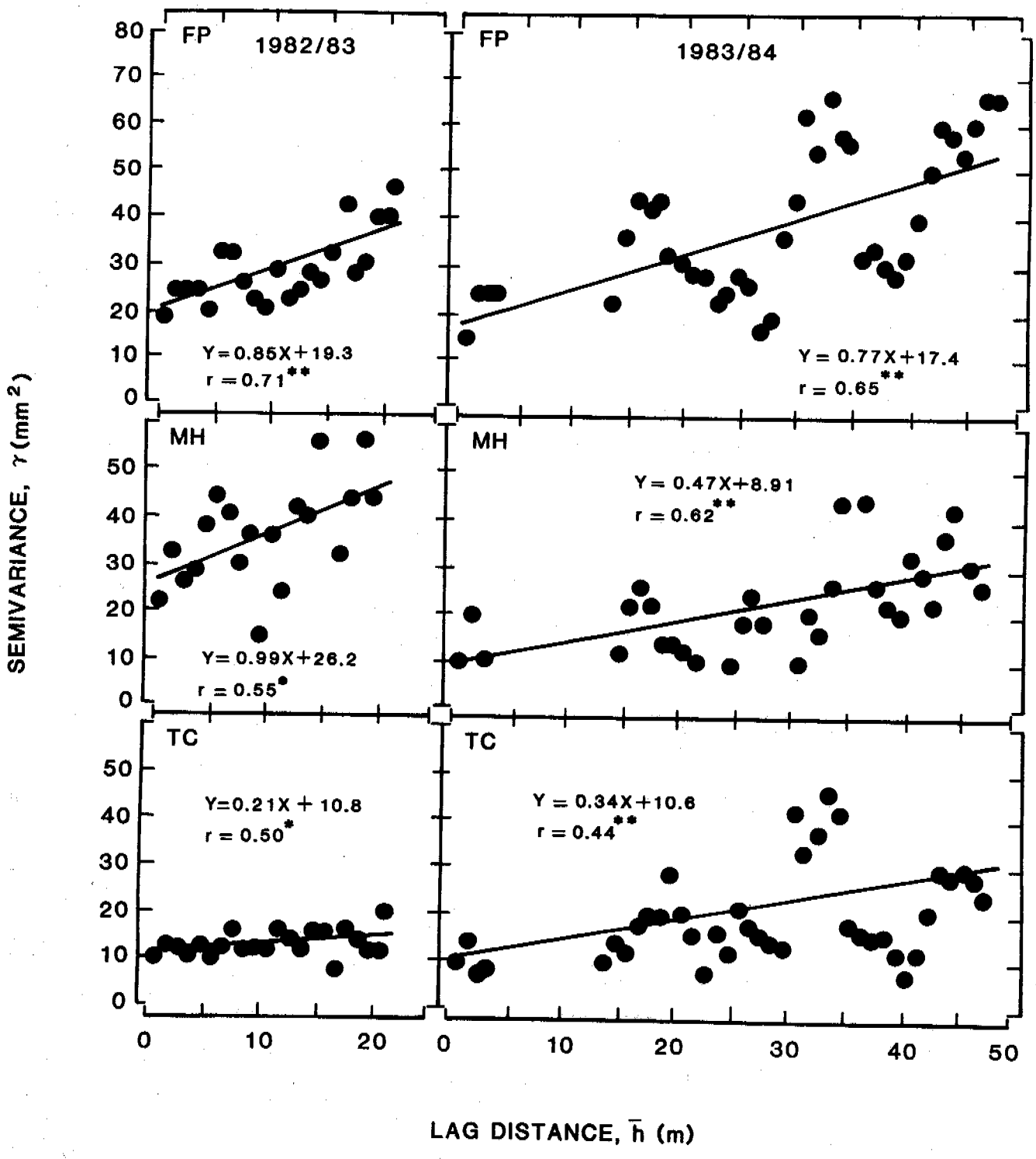

Fig. 4 Semivariograms at the whole-field scale for soil displacements during frost penetration (FP), maximum heave (MH) and thaw consolidation (TC) in both winters. Note: * and ** indicate significance at the $p < 0.05$ and $p < 0.01$ levels, respectively.

II) may be used as a guide for future measurements of frost heave in the field. With improved sampling, it should be possible to investigate anisotropic variation using semivariograms calculated for a fixed direction. Fitted functions can be used to estimate values at locations for which measurements are unavailable. The interpolative mapping procedure for doing this is known as "kriging" (Journal and Huijbregts, 1978). The scope of future studies might be widened to include simultaneous analyses of selected soil physical properties, frost penetration and snow depth. This could lead to the estimation of frost heave from knowledge of the spatial structure of cross-correlated, and easier to measure parameters by "cokriging" (Trangmar et al., 1986).

CONCLUSIONS

The purpose of this research was to analyze the spatial variation in soil displacements caused by seasonal frost action. We have shown that geostatistics is a useful approach for doing this. Autocorrelation indicated that soil displacements within a pedon were spatially variable over relatively small distances up to ~3.5 m. As additional soil types were sampled at the whole-field scale, the semivariogram functions became unbounded; a "linear model" appeared to best fit this structure. Trend was most pronounced as frost first entered the ground, suggesting that differences in maximum displacement are produced over a limited period of time when heave rates are high. The resultant spatial structure collapsed upon thaw consolidation and "nugget effects" predominated. Future research might include "kriging" of soil displacements and cross-correlation with other spatially dependent parameters. Such techniques should prove invaluable for engineers and scientists studying soil freezing phenomena in the field. We hope this preliminary analysis serves to introduce geostatistics to those investigators and encourages additional research.

ACKNOWLEDGEMENTS

This research was funded by Cornell University, Dept. of Agronomy. Dr. D.R. Viands of the Dept. of Plant Breeding and Biometry allowed us to use his forage plots. Thanks also to Drs. J.L. Hutson, J.W. Biggar and R.J. Wagenet for many helpful suggestions regarding the analysis.

REFERENCES

Andrews, J.T. (1963). The analysis of frost-heave data collected by B.H.J. Haywood from Schefferville, Labrador-Ungava. The Can. Geogr. (7), 163-173.

Chamberlin, E.J. (1981). Frost susceptibility of soil: Review of index tests. CRREL Monograph 81-2, 110 pp.

Cline, M.G. & Bloom, A.L. (1965). Soil survey of Cornell University and adjacent areas. Cornell, Misc. Bull (68), 31 pp. NYS Coll. Agric., Ithaca, NY, USA.

Delhomme, J.P. (1979). Spatial variability and uncertainty in groundwater flow parameters: A geostatistical approach. Water Resour. Res. (15), 269-280.

Dickey, D.D., Ferguson, H. & Brown, P.L. (1964). Influence of neutron meter access tubes on soil temperature and water under winter conditions. Soil Sci. Soc. Am. Proc. (30), 168-173.

Fahey, B.D. (1979). Frost heaving of soils at two locations in Southern Ontario, Canada. Geoderma (22), 119-126.

Guymon, G.L., Harr, M.E., Berg, R.L. & Hromadka II, T.V. (1981). A probabilistic - deterministic analysis of one-dimensional ice segregation in a freezing soil column. Cold Regions Sci. and Tech. (5), 127-140.

James, P.A. (1971). The measurement of frost heave in the field. Brit. Geomorph. Res. Group Tech. Bull. (8) 43 pp. Geo Abstracts, Norwich, UK.

Journel, A.G. & Huijbregts, C.J. (1978). Mining geostatistics. Academic Press, London, UK.

Klute, A. (ed.) (1986). Methods of Soil Analysis. Agronomy (9), pt. 1, 1188 pp.

Krige, D.G. (1951). A statistical approach to some basic mine valuation problems on the Witwatersrand. J. Chem. Metal. and Min. Soc. South Africa (52), 119-139.

Matheron, G. (1971). The theory of regionalized variables and its applications. Cahier No. 5, Centre de Morphologie Mathématique de Fontainbleau, 211 pp.

Mathews, B. (1967). Automatic measurement of frost heave: results from Malham and Rodley (Yorkshire). Geoderma (1), 107-115.

McBratney, A.B. & Webster, R. (1986). Choosing functions for semivariograms of soil properties and fitting them to sampling estimates. J. Soil Sci. (37), 617-639.

O'Neill, K. (1983). The physics of mathematical frost heave models: A review. Cold Regions Sci. and Tech. (6), 275-292.

Perfect, E. (1986). Frost heave of established alfalfa plants (Medicago sativa) at Ithaca, NY. 470 pp. Ph.D. Thesis, Cornell U., Ithaca, NY, USA.

Rickard, W. & Brown, J. (1972). The performance of a frost tube for the determination of soil freezing and thawing depths. Soil Sci. (113), 149-154.

Troll, C. (1944). Strukturböden, solifluction und frost klimate der erde. Geol. Rundschau (34), 545-694. (English Transl. Wright, H.E. (1958). US Army SIPRE Transl. No. 43, Wilmette, IL, USA, 120 pp.)

Trangmar, B.B., Yost, R.S. & Uehara, G. (1985). Application of geostatisics to spatial studies of soil properties. Advances in Agron. (38), 45-94.

Vieira, S.R., Hatfield, J.L., Biggar, J.W. & Nielsen, D.R. (1983). Geostatistical theory and applications to variability of some agronomical properties. Hilgardia (51), 1-75.

Webster, R. & Burgess, T.M. (1984). Sampling and bulking strategies for estimating soil properties of small regions. J. Soil Sci. (35), 127-140.

Williams, P.J. (1986). Pipelines and Permafrost. 137 pp. Carleton University Press, Ottawa, Canada.

DIRECTION OF ION MIGRATION DURING COOLING AND FREEZING PROCESSES

Qiu, Guoqing, Sheng, Wenkun, Huang, Cuilan and Zheng, Kaiwen

Lanzhou Institute of Glaciology and Geocryology, Academia Sinica

SYNOPSIS Experiments have shown that in freezing pure solution and moist sand the solutes would migrate towards the unfrozen zone. In cases of silt and clay, however, the ions would migrate towards the freezing zone of the soil column. Direction of ion migration in the freezing medium depends on the combined effect of four factors, namely temperature gradient; concentration gradient; moisture flow, and pressure gradient.

INTRODUCTION

It is important to understand the direction of ion migration during freezing of aqueous solutions and moist soils. If the solutes migrate mainly towards the unfrozen zone of the soil column, then the freezing zone would tend to dilute, so that the freezing technique could be practically applied to the desalination of water and soils. However, the soils or water in the unfrozen zone nearby should be concentrated, this might lead to a deterioration in quality of ground water or soil under the active layer. On the contrary, if ions migrate mainly towards the freezing zone, then the freezing zone would increase in salinity. During the repeated freeze-thaw cycles, the interlaced effect of freezing and evaporation would lead to a salination of active layer.

Some researches on this problem have been done. Osterkamp et al., (1970) conducted a freezing test using the dilute KCl solution and demonstrated that there was a concentration gradient and solute diffusion from the surface of the growing single ice crystal to the rest part of unfrozen solution. Hallet's (1978) freezing tests in gravels saturated with $CaCO_3$ solution showed a similar result that solutes concentrated in the unfrozen zone. Hanley and Rao (1980) proposed other idea that salts in a soil column might migrate together with the moisture towards the freezing fringe. Field observation and laboratory studies and theoretical analysis by Kay and Groenevelt (1983) led to the conclusion that exclusion of solute by an advancing freezing front may not be a particularly significant mechanism for solute redistribution, but substantial redistribution was found to occur due to convective transport during the process of ice lens formation.

Results of experiments to study the effects of the medium and the freezing conditions on the direction of ion migration during freezing process are presented and discussed in this paper.

EXPERIMENTAL DATA

Lanzhou tap water

An unidirectional downward freezing test was conducted by using the Lanzhou tap water (Qiu and Huang, 1983). Before the freezing test, the concentration of Lanzhou tap water was 0.71 g/l. After the freezing test, the average concentration of ice layers at the upper part of the specimen was 0.27 g/l, while the unfrozen solution at the bottom was 1.74 g/l in concentration.

The ion distribution is shown in Fig.1.

This experimental result confirms that ions do migrate towards the unfrozen part of the pure solution.

Wyoming sand

Before freezing test the Wyoming sand was saturated with NaCl solution, 39.67 me./l in concentration, the average water content of the column was 23.07%. After freezing test carried out in a close system, the average water content of the frozen part was 22.35%, about 3.1% lower than the initial value. As the frozen sand rethawed, the pore solution was 36.03 me./l in average concentration, by 9.18% lower than the initial value. The average water content of the unfrozen sand was 26.04% and had increased by 12.8% as compared with that before freezing test. The average concentration of pore water in the unfrozen sand was 53.59 me./l and was by 34.59% higher than the initial value. It is obvious that the direction of ions and moisture migration during freezing process was toward the unfrozen part of the sand column (Fig.2). The fact that the variation in ion content is higher than in water content shows that the ions not only migrate together with the moisture, but also move independently.

Althouth the general direction of ion migration during freezing of sand is similar to that in solution case, there are some differences. First, the ratio of desalination in sand case is lower;

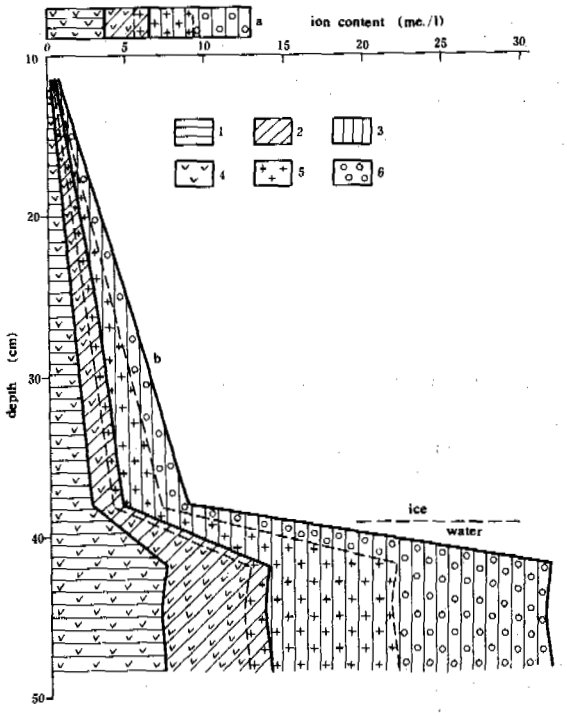

Fig.1 Ion Distribution in Lanzhou Tap Water Before and After Freezing Test

a. before freezing test;
b. after freezing test;
1. HCO_3^-; 2. $SO_4^=$; 3. Cl^-;
4. Ca^{++}; 5. Mg^{++}; 6. $Na^+ + K^+$.

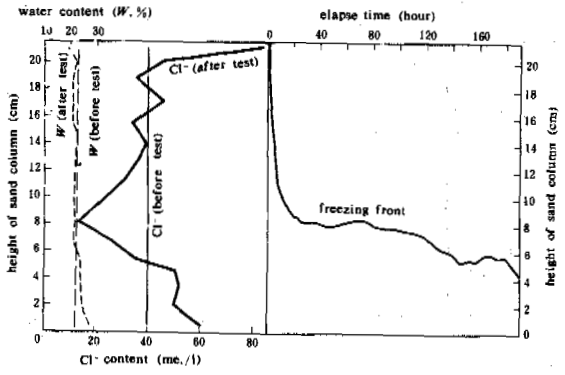

Fig.2 Distribution of Cl^- and Water Content in Wyoming Sand Before and After Freezing Test

second, the redistribution curves of water and ion in solution case are much smoother (Fig.1), however they reveal a fluctuation in sand case (Fig.2). The uppermost part of sand column is 19.6% in water content and 83.28 me./l in Cl^- content. This could be due to the formation of the pure ice at the top of sand column, which rejected salts to the first sand layer. From the second to sixth layers, Cl^- content fluctuates around the mean value of 39.29 me./l.This could be explained by the fast frost penetration, under which ions can migrate only to a short distances, for example, from the third to the 4th and from the fifth to the sixth layer. The NaCl can migrate more thoroughly when frost penetration is slower. Thus, the ion content becomes lower from the seventh to the tenth layer. In particular, the freezing front stayed at the tenth one for 60 hours, under such a condition of slow freezing, solutes could diffuse sufficiently downwards to the unfrozen zone. Because of the obvious downward migration of solutes, the layers beneath reveal a gradual increase in Cl^- content.

Fairbanks silt

The tested soil column was composed of two parts: the 8 cm Fairbanks silt at the upper, and the 2 cm gravels at the bottom. The specimen, presaturated by 0.04 mole NaCl solution, was freezing downward with a temperature condition of -5°C at the top and 0°C at the bottom. The concentration of ions and moisture contents before and after freezing test are shown in Table I.

The experimental results showed that the moisture, Cl^-, Na^+ and Mg^{++} migrated from the lower gravel layer towards the upper freezing silt. This is quite different from what happened in the tests with Wyoming sand and Lanzhou tap water.

Morin clay

It was reported that the dominant ions and moisture were migrating towards the freezing zone of Morin clay in an open freezing system (Qiu, et al., 1986). Now, two cases can be taken as examples for further discussion (Fig.3).

When the sample was fed by 0.01 N NaCl solution, the water content in frozen part of the clay column increased by 70 to 140% (or 89.7% in average), and the Cl^- content in frozen part increased by 88 to 194% (or 129.3% in average), as compared with the initial values before the freezing test (Fig.3 a).

When the sample was fed by 0.01 N Na_2SO_4 solution, the water content in the frozen clay was by 71 to 105% (or 89.5% in average) higher than the initial value, and the increase of dominant anion $SO_4^=$ was by 47 to 100.3% (or 79.0% in average), as compared with the initial values before freezing test (Fig.3 b).

This also shows a tendency that the moisture and dominant anions migrate towards the freezing zone of the clay column.

TABLE I

Change in Ion and Water Content of the Fairbanks Silt Before and After Freezing Test

	Water content %	Ion content (me./100g soil)								
		F^-	Cl^-	NO_3^-	$SO_4^=$	HCO_3^-	Na^+	Ca^{++}	Mg^{++}	K^+
Before freezing test	41.10	0.019	1.94	0.032	0.07	0.28	1.49	0.065	0.19	0.02
After freezing test	46.84	0.020	2.30	0.032	0.08	0.27	1.73	0.064	0.27	0.02
Relative increase %	14.0	-	4.0	-	-	-	1.7	-	24.7	-

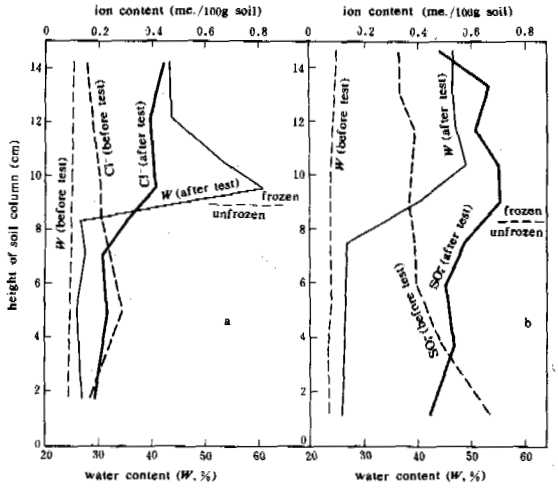

Fig.3 Distribution of Water and Dominant Anion in Morin Clay Before and After Freezing Test

a. fed by NaCl solution;
b. fed by Na_2SO_4 solution.

Fenghuo Shan silty clay

After an unidirectional freezing test in a close system, the tested column composed of Fenghuo Shan silty clay can be divided into four zones downwards, i.e.: 1. the solidified frozen zone at the uppermost part with obvious segregated ice layers and ice veins, where the Na^+ and Cl^- ions and water content increased to some extent; 2. the dehydrated and contracted-cracked zone, where the water content, Cl^- and Na^+ concentrations revealed some decrease; the Ca^{++}, $SO_4^=$ concentrations, however, showed some increase; 3. the super-cooling region, where the temperature was down to subzero, but the salinity and behavior of soil was not significantly different from that before the freezing test; 4. the unfrozen zone, in which the ion content and moisture content were as the same as that before the test. As the rate of penetration of freezing front tend to decrease, the migration of active ions and water tend to increase also (Table II).

It could be concluded that the active ions and moisture were migrating from the unfrozen zone to the freezing zone as observed in the freezing tests with the Fairbanks silt and Morin clay.

Dunhuang saline soils

The tested saline soils were obtained from the Sule River basin north of the Dunhuang county and were of the type $Cl\text{-}SO_4\text{-}Na\text{-}Ca$ with salinity of 15.78% (loam) and 7.57% (clay) respectively. As the water content was 16%, the freezing point of loam was -25.3°C; and, in clay case, as the water content was 22%, it did not freeze until the temperature fell down to -16.7°C. Field observation showed that the minimum temperature in natural soil profile was no less than -10°C, which was much higher than the freezing points, so that these soils in general would not be frozen in field condition during winter time. The specimens for cooling test were compacted in layers with a water content of 15.7% (loam) and 19.5% (clay), and with a dry density of 1.22 g/cm³ (loam) and 1.48 g/cm³ (clay) respectively. Then, the unidirectional downward cooling tests of specimens were conducted under a condition of lateral insulation. As the temperature was down to -15°C, the soils did not freeze, however, salt redistribution and volumatic-expansion did occur (Fig.4,5). The direction of ion migration pointed to the colder end, with the solutes NaCl and $MgCl_2$ moved rapidly.

DISCUSSION

It is believed that the ion migration might be

TABLE II

Distribution of Solutes and Moisture in Soil Column Made of the Fenghuo Shan Silty Clay Before and After Freezing Test

Number of test	Freezing rate cm/hour	Sampling time	Region	Water content		Cl^-		$SO_4^{=}$		Ca^{++}		Mg^{++}		Na^+	
				W	η	C	η	C	η	C	η	C	η	C	η
IV	0.68	a	1	25.6	+3.2	2.29	+4.1	11.72	-3.2	8.19	-3.9	0.94	-2.1	4.93	+0.6
			1+3	22.5	-9.3	1.99	-9.5	12.81	+5.9	9.16	+7.5	0.99	+3.1	4.86	-0.8
			4	24.9	+0.4	2.22	0	12.31	+1.7	8.56	+1.5	0.96	0	4.87	-0.6
		b		24.8	-	2.20	-	12.11	-	8.52	-	0.96	-	4.90	
III	0.31	a	1	27.7	+7.8	2.38	+9.2	10.9	-0.5	7.58	+0.1	0.91	+5.8	4.79	+5.5
			2+3	22.5	-12.5	1.81	-1.7	11.01	+0.5	7.77	+2.6	0.82	-4.7	4.12	-9.3
			4	25.1	-2.3	2.13	-2.3	11.02	+0.6	7.36	-2.8	0.78	-9.3	4.44	-2.2
		b		25.7	-	2.18	-	10.95	-	7.57	-	0.86	-	4.54	-

Note: 1. W — value of water content (%); C — value of ion content (me./100g soil);

a — after freezing; b — before freezing.

$$\eta \text{ — relative increase} = \frac{\text{(Value measured after freezing test - Value measured before freezing test)}}{\text{Value measured before freezing test}} \times 100\%$$

2. Data from the unpublished manuscript by Qiu Guoqing and Huang Cuilan: Test on ion migration and the origin of chemical profile of No.9 Bore hole in Fenghuo Shan, Qinghai-Xizang Plateau (1982).

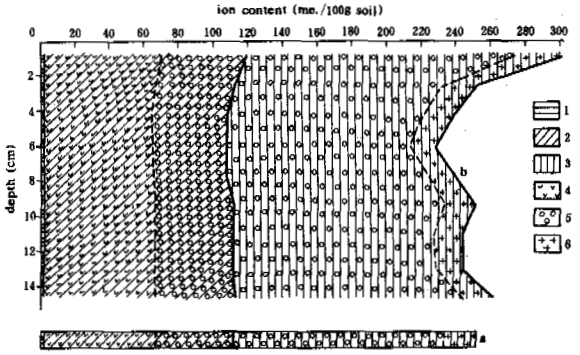

Fig.4 Ion Distribution in Dunhuang Saline Loam Before and After Cooling Test

a. before cooling test;
b. after cooling test;
1. HCO_3^- + $CO_3^{=}$; 2. $SO_4^{=}$; 3. Cl^-;
4. Ca^{++}; 5. Na^+ + K^+; 6. Mg^{++}.

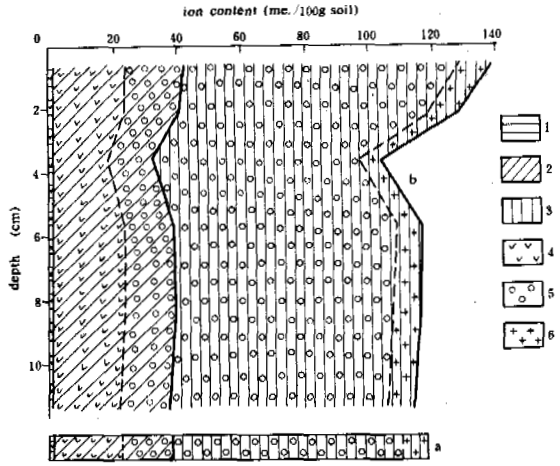

Fig.5 Ion Distribution in Dunhuang Saline Clay Before and After Cooling Test

a. before cooling test;
b. after cooling test;
1. HCO_3^- + $CO_3^{=}$; 2. $SO_4^{=}$; 3. Cl^-;
4. Ca^{++}; 5. Na^+ + K^+; 6. Mg^{++}.

caused by diffusion, filtration and their combined effect (Shen, et al., 1985). During cooling and freezing the processes of diffusion-filtration do occur and the migration flux might include four parts, i.e., I_T — ion migration due to temperature gradient; I_C — that due to concentration gradient; I_W —that due the water mivement; and, I_P — that due to pressure gradient.

The mechanism of ion migration due to temperature gradient can be explained as follows. First, the ions in the warmer part are leaping faster than in the colder part of the soil column. According to the Einstein-Brown Movement Equation, the square of mean displacement of microparticles in a certain period of time

is directly proportional to the absolute temperature (Huang, 1962). Therefore, in a certain period of time, the number of ions leaping from the warmer part to the colder part will be larger than that moving in an opposite direction. As a result, the salinity in the colder end would become higher. Second, the colder part of soil column might reach the crystallizing point first. The crystallization of solutes might lead to a decrease in concentration of soil solution, or a concentration gradient develops under which solutes might diffuse from the warmer part to the colder part. In a unidimensional case, the concentration change due to temperature gradient can be expressed by the following temperature-diffusion equation:

$$\frac{\partial C_1}{\partial t} = - \frac{\partial}{\partial X} \left(n \, D_T \frac{\partial T}{\partial X} \right)$$

where, n is the porosity coefficient of the medium;
D_T is coefficient of temperature-diffusion;
t is time; and
$\frac{\partial T}{\partial X}$ is temperature gradient.

The Dunhuang saline soils,for example, showed temperature-diffusion. The soils were premixed and had no gradient in both moisture and concentration before cooling tests. During cooling tests, there was no evaporation occuring on the top of the spiciments since they were covered. After tests, the speciments were still homogeneous in moisture content. Thus, the salination of the colder end could only be caused by temperature-diffusion.

The mechanism of ion diffusion due to concentration gradient during the freezing process can be explained as follows. In the freezing zone, the solutes were rejected from the growing ice crystals, causing the concentration at the ice-liquid interface to rise much higher. Under such a gradient, material can diffuse from a region of high concentration to the unfrozen part of the freezing zone, and from the unfrozen part in the freezing zone to the unfrozen zone of the soil column. This can be expressed by the concentration diffusion equation:

$$\frac{\partial C_2}{\partial t} = - \frac{\partial}{\partial X} \left(n \quad D_C \frac{\partial C}{\partial X} \right)$$

where, D_C is coefficient of concentration diffusion;
$\frac{\partial C_2}{\partial t}$ is the concentration gradient.

The diffusion flux, for a certain kind of ion and under a certain concentration gradient, depens on the porosity of medium. The flux is largest in pure solution, then, the sand; and, least in silt and clay. Besides,the growth of ice crystals not only result in a concentration gradient but also impedes ion migration, there by diminishing the intensity of ion diffusion will become weakened. In saline soils, under rapid freezing, the highly concentrated unfrozen solution in the region behind the freezing front can not sufficiently diffuse to the unfrozen zone ahead the freezing front.

During the process of freezing, moisture moves to the freezing zone, there-by taking the solutes with it,

$$\frac{\partial C_3}{\partial t} = - \frac{\partial}{\partial X} \left(C_{(X)} \; V_{(X)} \right)$$

where, $V_{(X)}$ is the filtration velocity of water flow and is dependant upon the permeability of soil and soil-water potential.

Under a condition of restricted frost heave, the ice crystallization pressure would exclude the unfrozen solution in freezing zone to the unfrozen zone.

$$\frac{\partial C_4}{\partial t} = - \frac{\partial}{\partial X} \left(C \, D_P \frac{\partial P}{\partial X} \right)$$

where D_P is the coefficient of pressure diffusion.
$\frac{\partial P}{\partial X}$ is pressure gradient.

Ion migration is the result of the combined effect of the above processes. The effect of each factor on ion migration varies in different media.

In the Dunhuang saline soils only occurs temperature-diffusion, which makes solutes migrate towards the colder end.

In pure solution and in Wyoming sand with a high permeability, the amount of solutes transported out by concentration gradient are much more than that brought by water migration towards the freezing zone and that moved to the colder end by temperature-diffusion. As a final result, one can see the phenomenon that the solutes move to the unfrozen zone.

In the cases of clay or silt, ion migration due to temperature-diffusion during cooling, the ion migration together with water make the solutes migrate towards the freezing zone much sufficiently. However, the concentration-diffusion that makes the solutes migrate towards the unfrozen zone will be more and more weakened because of the diffusion path being blocked by the growing ice crystals. Therefore, the solutes moved to the freezing zone are much more than that moved to the unfrozen zone. As a result, the total effect reveals an ion migration towards the freezing zone.

ACKNOWLEDGEMENTS

The experiments on Wyoming sand, Fairbanks silt and Morin clay were conducted by Qiu Guoqing at the Periglacial Laboratory of Quaternary Research Center of the University of Washington, and the U.S.Army Cold Regions Research and engineering Laboratory, Hanove, N.H. respectively. The help and advice rendered by Prof. B. Hallet, Prof. A.L. Washburn, Dr. E. Chamberlain, Dr. T.

Iskandar and other colleagues in these two laboratories are much appreciated. Prof. T.Osterkamp of the University of Alaska, Fairbanks also provided valuable suggestions to this research work. The authors would like to expressed their thanks to all of them.

REFERENCES

Hallet, B., 1979, Solute redistribution in freezing ground. in: Proceedings of the 3rd International Conference on Permafrost, Edmonton, Alta., 10-13 July, 1978. Canada Natl. Research Council. Vol.1, pp.86-91.

Hanley, T. and Rao, S., 1982, Electrical freezing potential and the migration of moisture and ions in freezing soils. in: Proceedings of the 4th Canadian Permafrost Conference,Calgary, Alta., March 2-6, 1981. Natl. Research Council of Canada. pp.453-458.

Huang Ziqing, 1962, Physico-chemistry. Education Pressing House. p.438.

Kay, B.D., Groenevelt, P.H., 1983, The redistribution of solutes in freezings: exclusion of solutes. in: Proceedings of the 4th International Conference on Permafrost, Fairbanks, Alaska, 17-22 July, 1983. Natl. Academy Press. Vol.1, pp.584-588.

Osterkamp, T.and Weber, A., 1970, Electrical Phenomena accompanying the phase change of dilute KCl solutions into single crytals of ice. Journal of Glaciology, Vol.9, No.56. pp.269-277.

Qiu Guoqing and Huang Cuilan, 1983, Ion migration in freezing solution. in: Proceedings of the 3rd Chinese National Conference on Permafrost, Lanzhou, 12-18, Oct., 1981, Gansu People's Publishing House. pp.314-320.

Qiu Guoqing, Chemberlain, E. and Iskandar, I., 1986, Ion and moisture migration and frost heave in freezing Morin clay. in: Journal of Glaciology and Geocryology, Vol.8, No.1, pp.1-14.

Shen Zhaoli, et al., 1985, Hydrogeology. Science Press. p.863.

DYNAMICS OF PERMAFROST ACTIVE LAYER – SPITSBERGEN

J. Repelewska-Pekalowa and A. Gluza

Institute of the Earth Sciences, Maria Curie-Sklodowska University, Akademicka 19, 20-033 Lublin, Poland

SYNOPSIS

The investigations carried out on Calypsostranda allowed to determine the size and the rate of summer thawing within the permafrost active layer.

Assuming that the meteorological conditions over the whole area investigated were the same, the attempt was made to determine the influence of the factors differentiated locally such as: exposition, water conditions and vegetation.

Especially remarkable is the role of water - a factor which may accelerate as well as retart the process of ground thawing.

INTRODUCTION

The investigations of the active layer of permafrost were carried out in the summer seasons of 1986 and 1987 during the geographical Expeditions of the Maria Curie-Sklodowska University in Lublin. The subject of the investigations was the area in NW part of Wedel-Jarlsberg Land on the Calypsostranda coastal plain, being in western margin of the Recherche Fiord. The particular attention was paid to the rate and size of the summer thawing of the ground within the area of the occurence of the many-year permafrost, according to the local conditions of the natural environment.

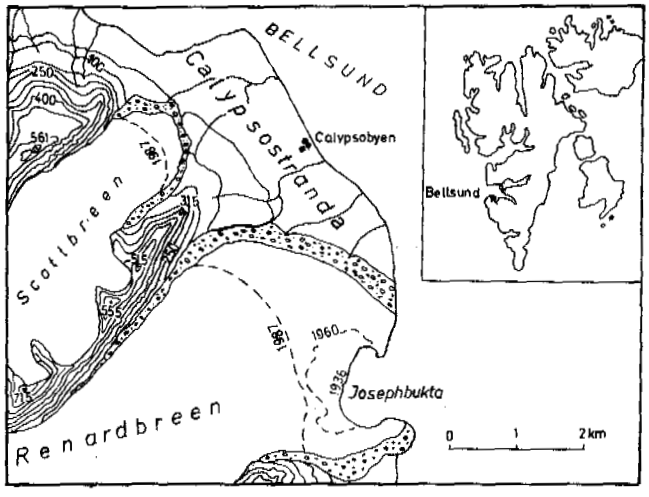

Fig. 1. Localization of the area investigated

THE AREA AND THE METHOD OF INVESTIGATIONS

Calypsostranda is a coastal plain, on the forefield of the Scott and Renard Glaciers (Fig. 1). It is built of a system of uplifted marine terraces, from 4 m up to 150 m a.s.l. at height of 20-25 m a.s.l. cut up by the erosion of glacier rivers, built by the Quaternary deposits of sands with gravels, sea silts and boulder clays. Within this form the investigations of the active permafrost layer were carried out, a free movement of the air masses and a considerable differentiation of the geocomplexes, being a favourable circumstance.

Within the period of investigations (27.06 - 20.08.1987) the cyclonal weather prevailed, i.e. very windy, with frequent recipitations and a considerable cloudiness. Mean 24-hour air temperatures ranged from 0.8 to 8.7°C. The precipitation sum reached 31.8 mm, where 23 days had the precipitation more than 0.1 mm. The sum of evaporation was 121.6 mm. Mean wind velocities ranged from 0.5 to 14.2 m/s. Total cloudiness reached 83 %. The decade occurences of the most important meteorological elements are shown in Table I.

The measurements of the thickness the permafrost layer were carried out at more than 300 points, located in different geocomplexes. The thickness of the active layer was determined with the method of sounding and by constant measurements with the Danilin's soil frostmeter. In the summer season of 1987 five series of soundings were made within the geocomplexes differing in water conditions, vegetation and exposition.

The characteristic of the active layer of permafrost is based of the data taken from representative stands, in which the thermal conditions of the ground were carried out.

Month	June	July			August	
Decade	3	1	2	3	1	2
Air temperature 2 m above ground level, in°C	2.4	3.7	5.4	4.1	5.5	3.0
Maximal temperature 5 cm above ground level, in°C	6.4	8.6	11.3	8.6	10.0	6.9
Radiation intensity cal/cm²/min	0.20	0.17	0.18	0.12	0.13	0.11
Precipitation, in mm	2.7	1.5	2.6	11.6	0.6	12.7

Table I. The decade occurences of the most important meteorological elements. Calypsobyen, summer season of 1987

The geocomplexes are as follows:

Point 1 - a flat sea terrace of 20-30 m a.s.l. (Fig. 2) built with sea sands and gravels, modelled by washing-out and also by niveo-eoloc processes, covered with scarce tundra vegetation (saxifrages, lichens)

Point 2 - patterned grounds periodically wet with moving water within the sandy-gravelly covers. Mosses on the peat layer thick up to 20 cm (Fig.3)

Point 3 - active patterned grounds. Moving water in the covers built with sands and coarse gravels. Lack of compact vegetation (Fig.3)

Point 3a - small stream flowing in the vicinity of stations 2 and 3. Gravelly sandy cover, lack of vegetation (Fig.3)

Point 4 - a 50 m^2 peat ait within a shallow lake

Point 5 - a plain at the foot of a fossil cliff, in the vicinity of the beach. Height - 4 m a.s.l. Lack of the compact vegetation connected with active accumulation. Variable level of the ground waters, fed with permafrost waters. Sandy-gravelly cover

Additionaly, four profiles were selected in the slopes with N,S,W and E exposition. All slopes were built with sandy-gravelly material and covered with scarce tundra vegetation. Their inclination reached 10-15°. As it was already mentioned, all measurements stations were connected with the 20-30 m a.s.l. terrace.

In each series of measurements a few soundings were made at points 1 - 5 and on the slopes at every one meter along the profile line. The results of the soundings allowed to determine the mean thickness and the rate of the thawing of the active permafrost layer on Calypsostranda.

THE INFLUENCE OF VARIOUS FACTORS ON THE THICKNESS OF THE ACTIVE LAYER OF THE PERMAFROST

It is commonly known that the thawing of ground begins with the vanishing of the snow cover and lasts the whole period of the polar summer. Thus, it is a function of time and may be presented as a linear dependence (Jahn 1982, Jahn and Walker 1983). The intensity of that process was distincly differentiated in the summer time of 1987, which is presented on the figures 4 and 5 (points 1 - 5) and figures 6 and 7 (slopes of differend exposition).

The influence of the exposition on the intensity of thawing is presented by mean extreme values (Table II). The slope of S exposition shows to be privileged with insulation. On the other slopes the thickness of the active layer was smaller by ca. 30 cm on an average. Within the whole observation period the differences oscillated between 20 to 40 cm. Such a distribution of the thickness of the active layer on the slopes with W,N and E exposition is influenced by snow patches lasting up to the second decade of July. The exposition of the slopes with snow patches as well without them has a deciding influence on the thickness of the active layer, in spite of the fact that the snow patches reduce its thickness by 20 cm on the average.

In order to observe the influence of water and vegetation on the development of the active layer of the permafrost, the measurements were taken in six stations, situated in different geocomplexes. The thickness of the active permafrost layer shows table III. The deepest thawing was started at points 2, 3 and 3a, and it was, on the average, by 40 - 80 cm larger that at the remaining points. The reason for it was the presence of moving water in the covers, being a good heat conductor. Prior observation confirm that fact (Repelewska-Pekalowa et al. 1987). The problem was discussed more widely (Gluza et al. 1988).

Stagnant water exerted a different influence. It fullfilled a function of an insulator, and the effect of insulation was intensified by the presence of peat and vegetation. Because of these facts, the thickness of the active layer in such an environment was relatively small. It was stated in point 4 (peatbog on the tundra pool) where the smallest value among all investigated geocomplexes was noted.

The mean thickness of the active layer under the tundra pool was 70 cm, and only 45 cm under the watered peat. The distinct lowering of the roof of the permafrost was started in the zone of the contact of the water and the land, which corresponds to the observation made in NW part of Spitsbergen (Pietrucien and Skowron, 1987). Within the active layer wet and dry parts of the ground were distinguished The wet part amounted to 12 - 91 % of the whole active layer. It may be supposed that it was fed with waters to different origin, i.e. coming not only from the permafrost but also from waters occuring in the ground and infiltrating from the surface. In the case of feeding exclusively by permafrost water the thickness of the wet layer amounted to 10 - 20 % of the whole active layer, while at the supply of waters of different origin, even to 60 - 91 % of the active layer.

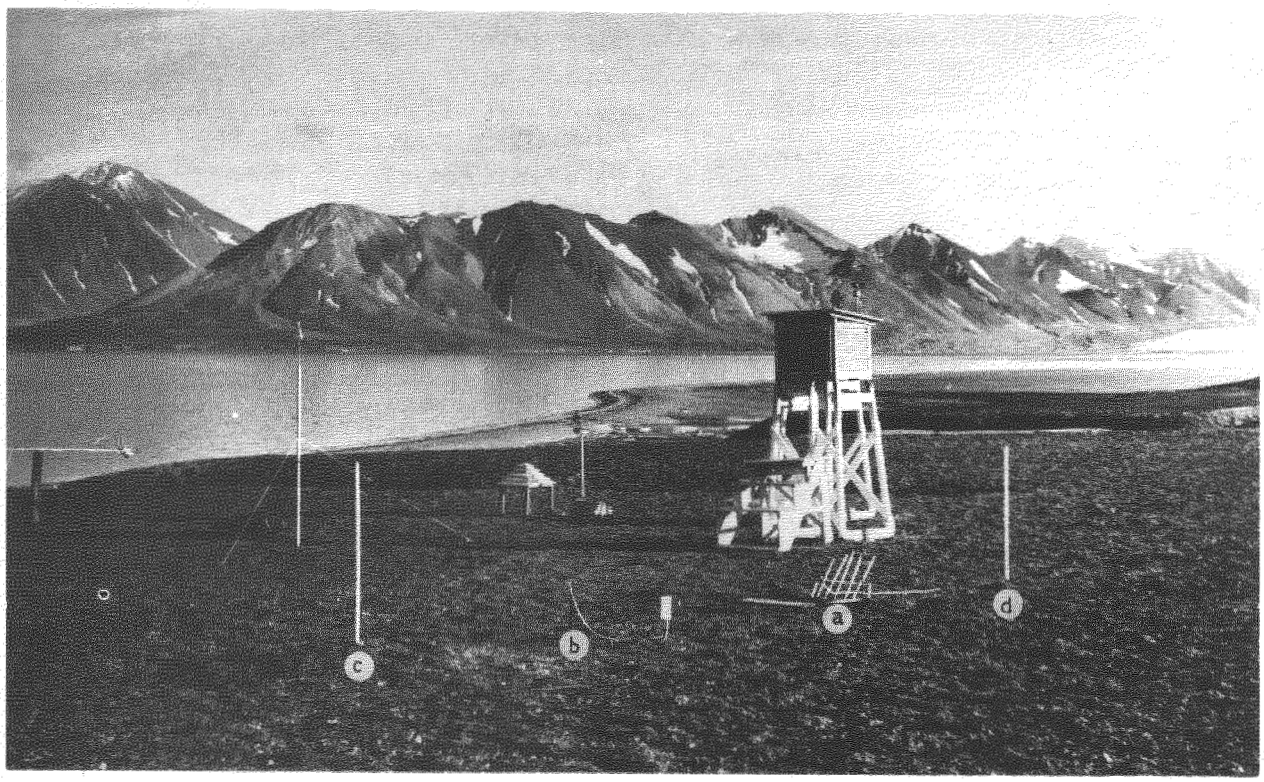

Fig. 2. Meteorological station in Calypsobyen (point 1)
a,b, - thermometers
c,d, - Danilin's soil frostmeter

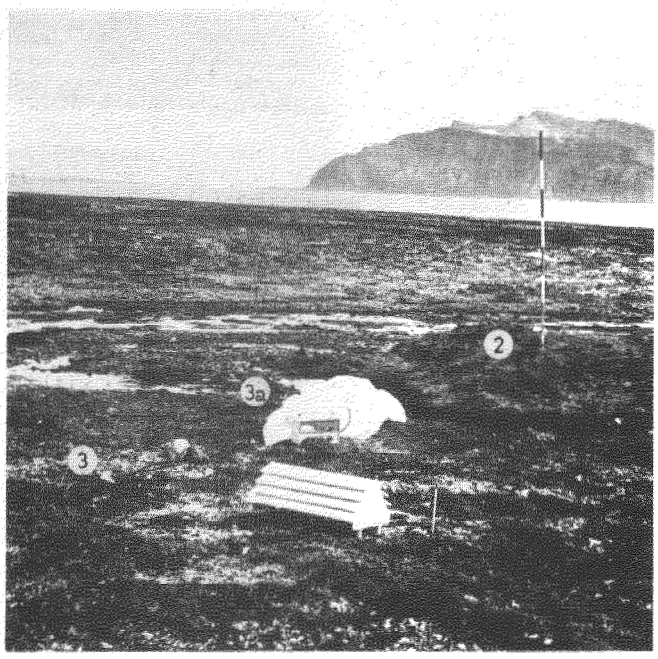

Fig. 3. Observation points: 2,3 and 3a

The rain precipitation registered in the area investigated in the summer season of 1987 were too little intensity to influence the size and rate of soil thawing in an essential way. However even very small presipitation may cause some change of the colour of dry surface of the ground for a darker one, and as a result of this the decrease of the albedo takes plase, which in turn influences the increase the thickness of the active layer (Heginbottom 1973).

The vegetation is considered to be a factor restraining the thawing (Czeppe 1966, Stäblein 1970, Jahn 1982, Vasiliew 1982, Jahn and Walker 1983). However it depends on the character of the water connected with it: in the case of the moving water vegetation does not play any important role as an insulator (Fig. 6, station 2).

RATE OF THAWING OF THE PERMAFROST ACTIVE LAYER

The measurements of the permafrost active layer allowed to observed the changes in the rate of thawing (Table IV).

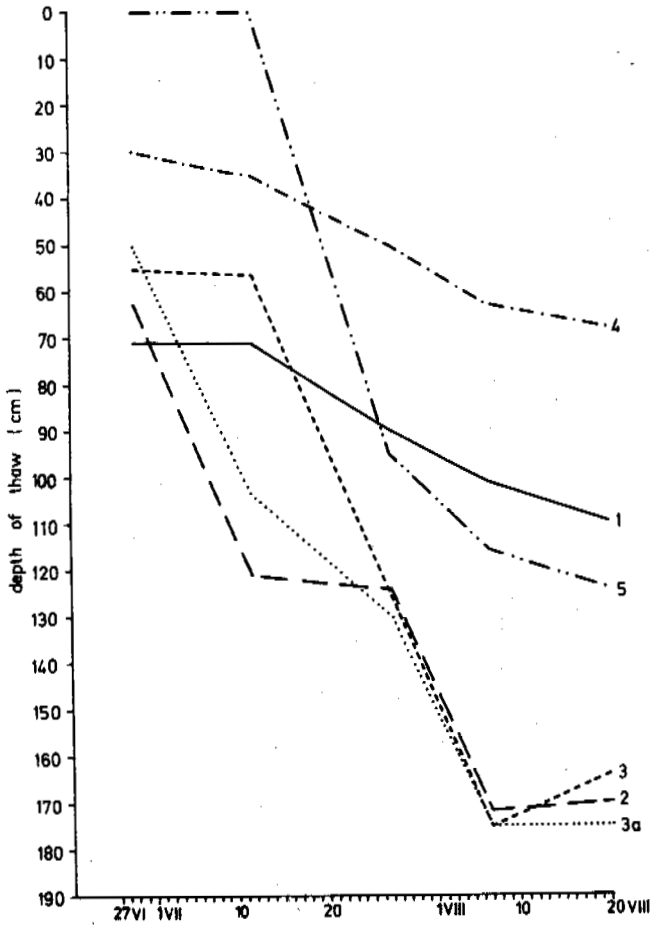

Fig. 4. Permafrost active layer thickness in the summer season of 1987 in Calypsostranda (points: 1 - 5)

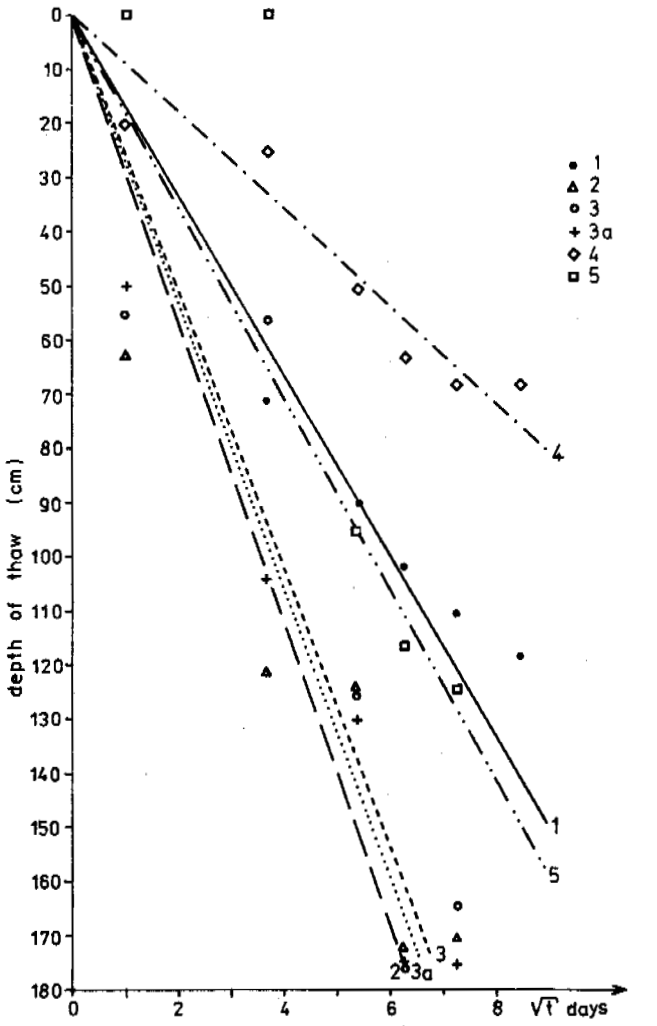

Fig. 5. Summer thawing of the ground in relation to the square root of time (Calypsostranda, points 1 - 5)

The increase in thickness of the active layer occured with a differentioned velocity. Two types of thawing were distinguished:

1. Thawing with a velocity gradually increasing and then decreasing.

2. Thawing with a velocity changing stepwise.

Among the stations investigated the first type of thawing prevailed, implied by the vanishing of the compact snow cover and snow patches. It was noted that the violent thawing of the ice- and snow cover was accompanied by a very quick process of soil thawing (Table IV, point 5). Thawing occuring at the stepwise changing rate was noted on the stations marked with the presence of the moving waters on the surface as well as in the covers (station 2 and 3a, slope of W exposition). Such a situation was due to the quick reaction of the ground to the change of the meteorological elements, mainly air temperature (see Table I).

Taking under consideration the mean values characterizing the whole period of the investigations, it can be stated that the thawing occured quickest (with a velocity more than 2 cm) 24 hour in the grounds remaining within the reach of the moving waters, both superficial and inter-covers ones. The process occured twice as slow where the isolating influence of stagnant water as well as of vegetation took place (Table IV, point 4).

Distincly marked is a great variability of the rate of the development of the permafrost active layer, which is closely connected with local conditions. Jahn (1982) and Stäblein (1970, 1971) also stressed the very correlation.

Recorded thawing rates are similar to those reported by Herz and Andreas (1966) for the Blomstranda (Kongs Fiord) and much greater than published by Stäblein (1970) for the Akselöya (Bellsund region).

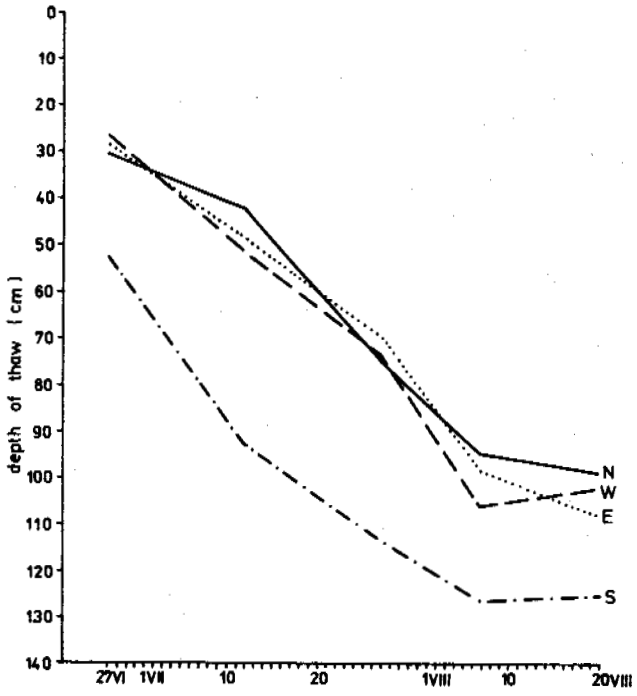

Fig. 6. Permafrost active layer thickness in the summer season of 1987 in Calypsostranda (slopes with different exposition)

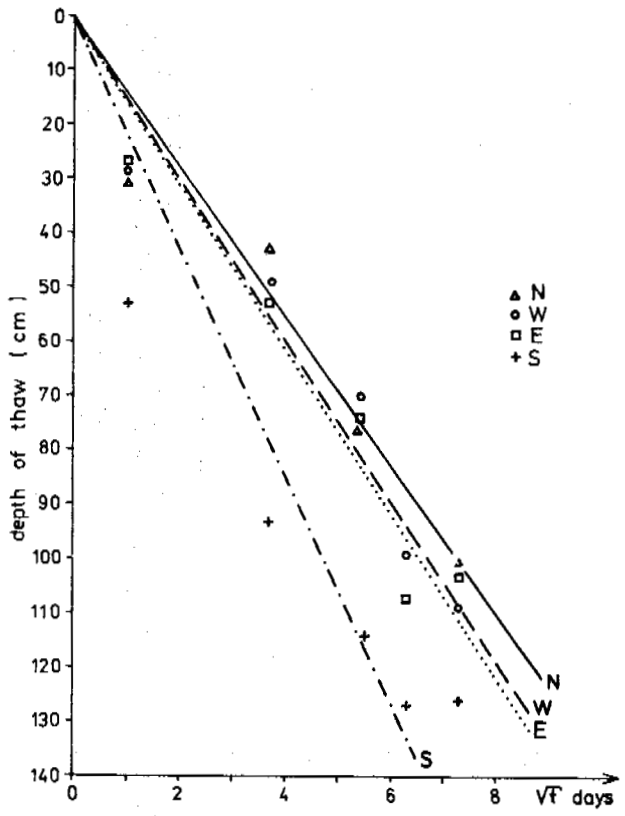

Fig. 7. Summer thawing of the ground in relation to the square root of time (Calypsostranda, slopes with different exposition)

Slope of the exposition	Mean values in cm		
	minimal	maximal	total period
S	52.7	126.6	102.3
N	30.6	99.6	68.7
W	26.8	106.5	72.2
E	28.9	108.4	71.0

Table II. Thickness of the active layer of the permafrost on the slopes with the inclination 10 - 15° and of the different exposition. Calypsostranda, summer season of 1987

Station	Mean values in cm		
	minimal	maximal	total period
1	71.0	110.0	88.7
2	62.5	172.0	129.9
3	55.0	175.0	115.0
3a	50.0	175.0	126.8
4	20.0	68.0	45.2
5	0.0	124.0	67.0

Table III. Thickness of the active layer of the permafrost in the chosen stations on Calypsostranda, in the summer season of 1987

Period / Place		29.06-12.07	12.07-27.07	27.07-7.08	7.08.-20.08	total period
		mean values cm/24-hour				
Station	1	0.0	1.3	1.1	0.7	0.7
"	2	4.5	0.2	4.4	0.2	2.2
"	3	0.1	4.6	4.5	0.9	2.1
"	3a	4.2	1.7	4.1	0.0	2.5
"	4	0.4	1.7	1.2	0.4	0.9
"	5	0.0	5.9	5.9	0.7	3.2
Slopes of the exposition	S	2.7	1.7	1.1	0.1	1.5
"	N	0.8	2.7	1.3	0.4	1.3
"	W	1.9	2.6	2.5	0.3	1.3
"	E	1.5	2.5	2.2	0.7	1.6

Table IV. Rate of thawing of the permafrost active layer. Calypsostranda, summer season of 1987

REFERENCES:

Czeppe, Z /1966/
Przebieg głównych procesów morfogenetycznych w poludniowozachodnim Spitsbergenie. Zesz. nauk. UJ, 127, Prace geogr. 13, 124 pp. Kraków.

Gluza, A, Repelewska-Pekalowa, J, Dabrowski, K /1988/Thermic of permafrost active layer - Spitsbergen V International Conference on Permafrost, Trondheim.

Heginbottom, J A /1973/
Some effects of surface disturbance on the permafrost active layer at Inuvik. N.W.T. Canada, North american Contribution Permafrost, Second International Conference, Yakutsk, 649-657.

Herz, K, Andreas, G /1966/
Untersuchungen zur Ökologie der periglazialen Auftauschicht im Kongsfjordgebiet /Westspitzbergen/. Petermanns Geogr. Mitt. 110, 45-57.

Jahn, A /1982/
Soil thawing and active layer of permafrost in Spitsbergen. Results of investigations of the Polish Scientific Spitsbergen Expeditions, /IV/, Acta Univ. Wratisl. 525, 55-75.

Jahn, A, Walker, H J /1983/
The active layer and climate. Zeitschr. f. Geomorph. N.F. Suppl. 47, 97-108.

Pietrucien, Cz, Skowron, R /1987/
Wplyw zjawisk wodnych na glebokosc rozmarzania gruntu na Ziemi Oscara II /NW Spitsbergen/, XIV Sympozjum Polarne, 119-127, Lublin.

Stäblein, G /1970/
Untersuchung der Auftauschicht über Dauerfrost in Spitsbergen. Eiszeitalter u.Gegenwart, 21, 47-57, Obringen

Stäblein, G /1971/
Der polare permafrost in die Auftauschicht in Svalbard. Polarforschung 1/2, 112-120.

Wasiliev, I C /1982/
Zakonomernosti sezonnogo protaivanya gruntov v Vostochnoy Yakutyi.izdat. "Nauka",pp.132,Novosibirsk

INVESTIGATION OF ELECTRIC POTENTIALS IN FREEZING DISPERSE SYSTEMS

V.P. Romanov

Permafrost Institute of the Siberian Branch of the USSR Academy of Sciences, Yakutsk, USSR

SYNOPSIS Employment of geophysical prospecting by electric means, studies of moisture migration in freezing earth require knowledge of the nature of an electric potential jump at the boundary between unfrozen rocks and permafrost. Possibilities and initiation conditions for Workman-Reynolds potentials in the freezing disperse systems are examined in this work on a basis of experimental investigations of the freezing potentials of moisture-saturated SiO_2 powders and polystyrene of various degree of dispersion. Peculiarities of the ice crystallization in the earth pore spaces, accounting for the thermophysical characteristics of the heterogenous medium components are reviewed to explain the results obtained.

It is established that freezing of diluted aqueous solutions causes a jump of electric potentials between the ice and the solution. The cause of the freezing potential initiation is preferential inclusion of the ions of one sign into the growing ice lattice: the Workman -Reynolds effect (WR). The WR potential magnitude (φ_{WR}) depends on the composition of dissolved salts and may reach tens and hundreds of volts (Workman, Reynolds, 1950).
In the course of freezing of the soils and the earth appearance is also noted of a potential jump at the interphase boundary between the frozen and unfrozen parts of the deposits (Jumikis, 1958; Borovitsky, 1969; Yarkin, 1973; Lagov, 1978; Parameswaran, Mackey, 1983).
Majority of the authors presume that freezing potentials of the disperse systems are of the same nature as WR potentials. The results of the experimental investigations by Korkina (1965) are cited as a proof of this assumption. She has obtained in the case of freezing suspensions of clayey minerals electric potentials over 6 volts which undoubtedly shows their close connection with WR potentials. But in the use of these results the sight is lost that the investigation object used by the author can be referred with greater reasons to the aqueous solutions than to the natural disperse deposits (solid phase content in a litre of suspension did not exceed 1-2 g).
Summated results of the experimental and field investigations (Parameswaran, Mackey, 1983) show that potentials of the freezing earth, as a rule, are below 0.2 V and rarely exceed this magnitude. Values of the same order are noted for the permafrost lower boundary in the state of its static position, i.e. during absence of the freezing processes (Lagov, 1978; Volodjko, 1981). Comparison of these data does not allow a reliable conclusion to be made on any contribution of WR potentials to the magnitude of a general interphase jump of potentials at the boundary between unfrozen and frozen rocks.
At the same time knowledge of the electrical phenomenae peculiarities at this boundary may assist more successful application of the natural electrical field method for determining the thickness and development dynamics of permafrost and of the freezing deposits (Lagov, 1978; Pitulko, Sedov and Musin, 1978). Knowledge of the freezing potentials nature is also necessary for evaluation of the existing notions on the electroosmotic transfer of moisture to the freezing front (Borovitsky, 1969; Korkina, 1965; Yarkin, 1973; Parameswaran, Mackey, 1983).
It was of interest in connection with this to reveal the possibilities and to attempt determination of the conditions for initiation of WR potentials in disperse media.
Washed powders of SiO_2 and of different dispersion grade polystyrene were used as an investigation object. Samples of SiO_2 are glass balls 4.5 to 1 mm in diameter and also quartz sand of 0.5 - 0.25 mm and 0.25 - 0.16 mm fractions. Dimensions of the polystyrene particles were varied in different samples from 3.5 to 0.5 mm. Measurements of the freezing potentials were carried out in a glass cylindrical cell of 21 mm inner diameter and 50 mm high. The sample was cooled from the cell bottom through a stainless steel plate serving simultaneously as one of the electrodes. The other electrode - a platinum wire in a shape of a helix was placed in the solution above the sample surface. An eutectic mixture of NaCl and snow was used for cooling. The solution for saturation of the samples was KCl of 10^{-3} mol/l concentration.
The potential difference between electrodes was determined with the aid of an electrometric amplifier with input resistance of 10^{14} ohms. Freezing potential readins were taken relative to the top electrode. Each experiment was repeated at least three times and the deviations from the mean value did not exceed 20 %.
On Fig.1 (curve 1) an example is given of the records of potentials resulting during freezing

of the solution being investigated in the absence of a disperse phase. It is seen from the drawing that the initial ice crystallization moment is noted by sharp jumpy potential change.

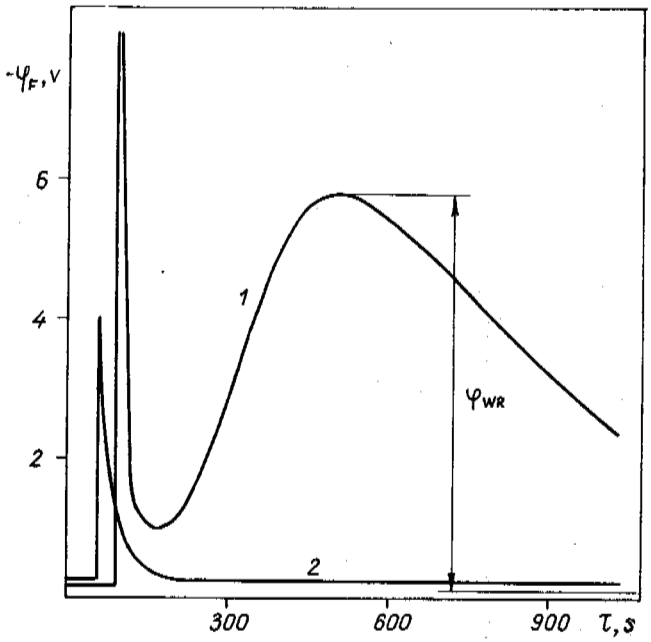

Fig.1 Changes in freezing potentials (φ_F) with time (τ) for a KCl solution (1) and quartz sand of 0.5 - 0.25 mm fraction (2). Solution concentration 10^{-3} mol/l; pH = 6.0.

Smooth potential increase is observed after this until the maximum is reached after 2 - 3 minutes followed by its gradual reduction. Nature of the potential change shown is typical for the experiments carried out with the use of cooling substrate (Gross, 1967). As in the classic work (Workman, Reynolds, 1950), the value φ_{WR} was determined from a difference between the maximum value of the potential and the value corresponding to the condition for termination of the ice crystallization. Thus, one of the basic appearance signs of WR potentials in a freezing system may be considered the presence of a maximum on the curve of the freezing potential relation with time. In the case of absence of φ_{WR} either monotonous change in the recorded φ_{WR} potential or its constant magnitude during the whole experiment period is observed after the initial jump (Fig.1, curve 2).

On Fig.2 (curve 1) are given the results of WR potential measurements depending on the particle size of SiO_2 powders. It is seen that in a given system φ_{WR} appear only with particle sizes exceeding 10^{-3} m. For the powders with particle size equal to or less than 10^{-3} m appearance of WR potentials was not observed. It can be noted that the particles which form majority of the loose deposits are included within this range.

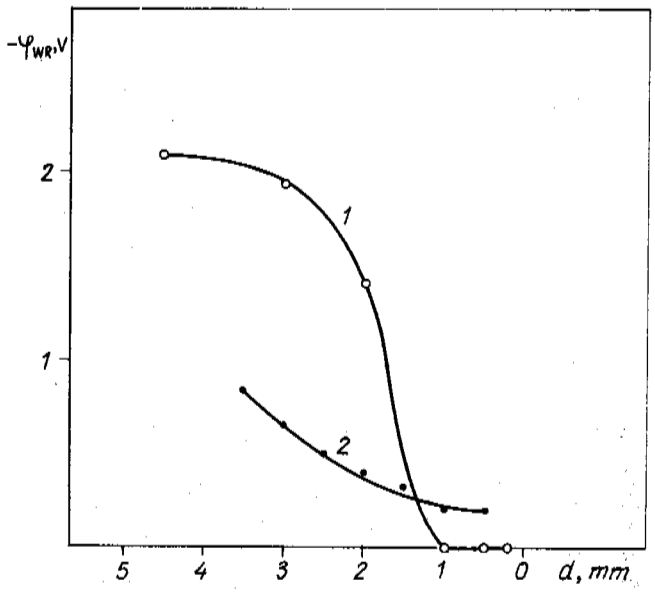

Fig.2 Relation between WR potential (φ_{WR}) and the particle size (d) of SiO_2 (1) and polystyrene (2) powders. Solution concentration of KCl 10^{-3} mol/l; pH = 6.0

For explanation of the results obtained we suggest that the discovered cause of φ_{WR} dependence on the size of SiO_2 particle dimensions is connected with the peculiarities of ice crystallization in the powder system pores. In studying the crystallization process in a micro scale it may be assumed that water freezing in the pore spaces begins with formation of ice branches or pellicles that grow over the mineral particle surface in the direction of unfrozen zone. Causes of the advanced ice growth in the shape of branches (pellicles) may be conditioned by the following circumstances:

(I) It is well known that surface of the particles shows definite activity relative to formation of ice nuclei that facilitates the crystallization process that follows.

(II) Particles of the earth mineral skeleton possess higher values of thermal conductivity in comparison with ice. Therefore temperature fall within their body and over the surface is faster than within the pore solution.

(III) Due to this difference in thermal conductivity the particles promote more effective abstraction of heat liberated during ice crystallization.

Then, if the length of ice branches (pellicles) is smaller than the effective pore size, the crystallization front surface will retain its directed travel (in our case - from the bottom - upwards). The possibility of WR potentials appearance is retained. With increase of the pore size or of the relative contents of the

liquid phase, the particle walls introduce less disturbance into planar distribution of the crystallization front which results, in conformity with the well-known conceptions (Eyerer, 1972), to growth of φ_{WR}. From this point of view may also be explained high values of freezing potentials discovered for the diluted clayey suspensions (Korkina, 1965). A situation arises with reduction in the particle size when the pore surface is covered completely with ice pellicle. Unidimensional character of the crystallization surface travel is replaced in a given case by multi-dimensional, directed from the walls towards the pore centre. Therefore the origin of WR potentials, even if possible, must be localized within the pore limits and cannot be registered by the electrodes separated by a large distance. It follows from here that with small pore dimensions the hopes of determining φ_{WR} may be connected with the powders whose particles have lower thermal conductivity than water.

Studies of the freezing potentials carried out with polystyrene powders have confirmed the correctness of this assumption. As seen from Fig.2 (curve 2) φ_{WR} relation does not change sharply over the whole range of the particle dimensions tested, which confirms constant ice crystallization conditions. Starting from the known conceptions, the lower φ_{WR} values in comparison with SiO_2 samples may be explained by lower freezing rate of the powders composed of particles with thermoinsulating properties. For polystyrene particles less than 10^{-3} m φ_{WR} values are 0.2-0.25 V.

Thus, investigations carried out indicate close connection between WR potentials in disperse systems with morphology changes in the ice - solution partition surface. Such a connection was also studied as a cause of φ_{WR} reduction and disappearance for the freezing aqueous solutions (Jindal, Tiller, 1972). At the same time, if the change in the morphology of crystallizing surface for the solutions is caused by appearance of constitutional supercooling, then the basic influence in the freezing disperse system is due to the presence of mineral particles and the difference in thermo-physical characteristics of the heterogenous medium components. It can be noted that in a number of works the notions of constitutional supercooling were used in conformity with the description of the ice crystallization process in the porous spaces of earth (Hallet, 1978; Kay, Groenevelt, 1983). But in the case of diluted solutions slight supercooling cannot lead to a picture discussed by these authors.

For the natural disperse objects there is also a number of circumstances that reduce the occurence probability of WR potentials. It is well known that maximum values of the solutions freezing potentials correspond to concentrations of 10^{-5} - 10^{-4} mol/l. With concentration increase φ_{WR} reduce rapidly and at salt content of 10^{-2} mol/l and higher are practically not observed (Lodge, Baker and Pierrard, 1956). The liquid phase in the soils and earth also represents a solution with different chemical components. Their average content for permafrost may be taken as equal to 10^{-2} - $5 \cdot 10^{-2}$ mol/l recalculated for unfrozen earth conditions (Anisimova, 1981). It follows that freezing of rocks containing a given quantity of salts cannot cause appearance of noticeable φ_{WR}. In addition, ice formation in the pores is accompanied by an increase in salt concentrations in a liquid phase distributed as thin pellicles of unfrozen solution. Such pellicles may be considered as electrical conductors that shunt the transition space between unfrozen and frozen rocks. Possessing comparatively low electrical resistance they promote fast charge redistribution in a crystallizing system which also reduces the probability of φ_{WR} initiation.

Thus, the investigations carried out show that WR potentials in the freezing natural disperse media occur, apparently, only in exceptional cases.

There is no sense in expounding in this work all the diversities of phenomenae able to lead to a jump of potentials between unfrozen and frozen grounds. As one of the causes that have the most common character is given an inequality in the solution concentrations in unfrozen and frozen parts of the sample able to cause appearance of a diffusion potential (Lagov, 1978). Since each particle of the mineral skeleton and ice is surrounded by a double electrical layer, a relation of the ion concentrations that possess the same or opposite charge sign relative to the particle charge may be reviewed in addition to this. As is well-known, inequality in concentrations of ions of one type in adjacent phases stipulates coming into existence of Donnan's potential φ_d :

$$\varphi_d = \frac{RT}{zF} \ln \frac{a_+^1}{a_+^2} = \frac{RT}{zF} \ln \frac{a_-^2}{a_-^1}$$

where a_+^1, a_+^2, a_-^1, a_-^2 are ion activity in phases 1 and 2.

It follows from qualitative representations for φ_d (Fridrichsberg, 1984) that in the conditions of a negative surface charge, peculiar to the particles of soils, earth and also ice (Romanov, Nechaev and Zvonareva, 1976) frozen rocks must be charged negatively relatively to the unfrozen ones. Given relationship of the charge signs agrees well with the results of the experimental and field investigations of electrical potentials (Borovitsky, 1969; Yarkin, 1973; Lagov, 1978). More complicated is a qualitative evaluation of an interphase potential jump. Thus, application of φ_d representations requires knowledge of the exchange volume (quantity of adsorbed ions) which is yet an insoluble problem for permafrost. But by making definite assumptions, value of φ_d on the boundary between unfrozen and frozen rocks must not exceed 0.15 - 0.2 V. It is important to note here that φ_d does not depend much on whether the interphase boundary travels or is in a stable balanced state. The latter condition allows an assumption to be made that presence of a potential jump

cannot be viewed as a cause of moisture migration towards the freezing front. Otherwise moisture transfer to the interphase boundary had to be recorded in the conditions of its stable state.

Of the existing investigations of freezing potentials the work by (Parameswaran, Mackey, 1983) merits attention, the results of which can be explained at first sight only on the basis of representations on WR potentials. In this work potential values discovered for the freezing earth reached 1 V and over. In studying this data it should be remembered that measurement of the electrical potentials (natural or induced) in permafrost and freezing rocks demand special specifications for measuring equipment and electrode construction. It is important that the instrument input resistance was not below 10^8-10^9 ohms and, generally exceeded many times the electrode contact resistance. Non-observance of this condition may lead to registration of potentials that differ from the true values by an order or more. Authors of the work discussed do not give specifications of the equipment used, but indicate the necessity of its improvement. Therefore it may be conjectured that anomalous potential values are a result of methodical errors during measurements.

CONCLUSIONS

Results of the investigations carried out demonstrate an error in existing notions on a connection between the freezing potentials of natural disperse deposits and the Workman - Reynolds (WR) potentials that occur during freezing of diluted solutions. Cause of WR potentials absence in the freezing earth is explained by the complicated nature of the ice crystallization process in the disperse system pores. Possibility is shown of employing notions on membrane equilibrium potentials (Donnan's potentials) for explaining the nature of an electrical jump on the boundary between unfrozen and frozen rocks. An assumption is made that anomally high values of freezing potentials (over 0.15-0.2 V) obtained in a number of works may be connected with methodical errors of measurements. This circumstance must be taken into account in the following experimental and field investigations connected with measurements of electrical potentials in permafrost and freezing deposits.

REFERENCES

Anisimova, N.P. (1981). Kriogidrogeokhimicheskie osobennosti merzloi zony. Novosibirsk, 152 s.

Borovitsky, V.P. (1969). O vliyanii estestvennykh elektricheskikh potenzialov na migraziu vlagi i soderjaschikhsia v nei komponentov v dejatelnom sloe. Materiyaly komissii po izucheniu podzemnykh vod Sibiri i Dalnego Vostoka. Irkutsk, 180-185.

Eyerer, P. (1972). Electric charge separation and charge storage during phase changes in the absence of external electric fields: thermodielectric effect (Costa Ribeiro effect and Workman-Reynolds effect). Adv. Colloid Interface Sci., (3), 223-273.

Fridrikhsberg, D.A. (1984). Kurs kolloidnoi khimii, 368 s., Leningrad.

Gross, G.W. (1967). Ion distribution and phase boundary potentials during the freezing of very dilute solutions at uniform rates. J. Colloid Interface Sc., (25), 2, 270-279.

Hallet, B. (1978). Solute redistribution in freezing ground. Proc. 3-rd Intern. Conf. on Permafrost, (1), 86-91, Ottawa.

Jindal, B.K., Tiller, W.A. (1972). Freezing potential - effect of substrate on potential during the freezing of aqueous solution at uniform rates. J. Colloid Interface Sci., (39), 2, 339-348.

Jumikis, A.R. (1958). Some concept pertaining to the freezing soil systems. Highway Res. Board. Spec. Rep., 40, 178-190, Washington D.C.

Kay, B.D., Groenevelt, P.H. (1983). The redistribution of solutes in freezing soil: exclusion of solutes. Proc. 4-th Intern. Conf. on Permafrost, 584-588, Washington D.C.

Korkina, R.I. (1965). Elektricheskie potenzialy v zamerzayuschikh rastvorakh i ikh vliyanie na migraziu. Prozessy teplo- i massoobmena v merzlykh gornykh porodakh, s. 56-65, Moskva.

Lagov, P.A. (1978). Elektricheskie polia sezonno-talogo sloya kak pokazatel proiskhodiaschikh v nem prozessov. Problemy kriolitologii, (7), 199-205, Moskva.

Lodge, J.P., Baker, M.L. and Pierrard, J.M. (1956). Observation on ion separation in dilute solution by freezing. J.Chem. Phys., (24), 4, 716-719.

Parameswaran, V.P., Mackey, J.R. (1983). Field measurement of freezing potentials in permafrost areas. Proc. 4-th Intern. Conf. on Permafrost, 962-965, Washington D.C.

Pitulko, V.M., Sedov, B.P. and Musin P.M.(1978) Ispolzovanie polei estestvennykh potenzialov dlja opredeleniya moschnosti mnogoletnemerzlykh ldystykh porod. Materialy po geologii i poleznym iskopaemym Severo-Vostoka SSSR, 238-241, Magadan.

Romanov, V.P., Nechaev, E.A. and Zvonareva G.V. (1976). Izmerenie elektrokineticheskikh potenzialov na granize rasdela lied-rastvor elektrolita. Kolloidn. J., (38), 5, 1009-1012.

Volodko, B.V. (1981). O nekotorykh osobennostiakh povedeniya temperaturnogo i elektricheskogo polya PS vblisi nijnei granizy merzloty v terrigennykh tolschakh. Stroenie i teplovoi rejim merzlykh porod, 70-76, Novosibirsk.

Workman, E.J., Reynolds, S.E. (1950). Electrical phenomen occuring during the freezing of dilute aqueous solution and their possible relationship to

thunderstorm electricity. Phys. Rev., (78), 3, 254-259.

Yarkin, I.G. (1973). Vliyanie estestvennykh elektricheskikh potenzialov na migraziu vody v promerzayuschikh gruntakh. Dokl. 2-oi Mejdunar. konf. po merzlotovedeniyu, (4), 230-234, Yakutsk.

PHYSICO-CHEMICAL NATURE OF CONGELATION STRENGTH

B.A. Saveliev[1], V.V. Razumov and V.E. Gagarin

[1]Research Institute of Engineering Site Investigations, Moscow, USSR

SYNOPSIS Problems of congelation are of prime importance in an engineering practice. In some cases it is necessary to increase the congelation strength or to decrease it in the other ones. To soundly and rationally control a congelation process one should evaluate the effect of different factors on formation of the congelation strength. In the present paper complex laboratory analyses of the congelation strength of ice which crystallizes from distilled or sea water and salt solutions at the surface of frozen ground or building materials are examined.

The present knowledge on the nature of the congelation strength of frozen ground or ice with different materials relies on a model proposed by B.A.Saveliev. In accord with the model at the boundary of congealing bodies there developes a multilayer system consisting of material of a base, a strongly bound layer of water, diffusion envelope, floating superficial layer of ice, contact layer of ice and volumetric phase of ice. The congelation strength is governed by a particular kind of a structural bond due to a variety of intermediate layers. The model of a multilayer system enables to soundly determine under which conditions adhesive bonds will be stronger than cohesive strength of ice and under which thermodynamic conditions they will be weaker. A main factor governing congelation is ice crystals which are formed near the congelation zone. Ice formed on different solid bodies differs in its texture. Occurrence of mineral salts in water crystallizing near the surface of a solid body affects in a certain way the texture of the contact ice as well.

With a view to bringing to light the nature of the congelation strength we have carried out complex laboratory analyses of ice crystallizing from distilled water or univalent bivalent and trivalent salt solutions at the surface of frozen ground concrete or metal and field study of contact ice which is formed of sea water at the surface of cooling pipes. As a result of the studies the following has been established.

The texture of contact ice due to a crystallochemical composition of the base differs from that of volumetric ice. Structural characteristics of contact ice produced of distilled water on bases from different materials are shown in Table 1. It is seen from Table 1 that sizes of contact ice crystals developing on identical bases decrease with depression of the freezing point. On materials differing in their physico-chemical properties the crystal sizes change differently depending on the temperature of the base its heat conduction and concentration of the active centers of crystallization along it, the number of the active centers per unit mass apparently being a major governing factor of forming the contact ice on montmorillonite whereas temperature and heat conduction being of determining importance for other materials.

Table 1

Structural Characteristics of Contact Ice Produced of Distilled Water on the Bases from Different Materials

Material of the base	freezing point, θ,°C	Cross-section area of averaged crystal, Sa, cm^2	Surface of crystals per unit volume, P, cm^2	Height of an averaged crystal Ha, cm	Coefficient of bending, C
Loam	-10	0.00601	72.06	0.0832	1.87
	-20	0.00311	100.32	0.05989	1.98
Montmorillonite	-10	0.00137	149.82	0.0398	1.65
	-20	0.00103	175.72	0.03439	1.93
Caolinite	-10	0.01702	42.83	0.1401	1.69
Sand	-10	0.00510	78.44	0.0767	1.87
	-20	0.00391	89.47	0.06713	1.93
Concrete	-10	0.02824	33.22	0.1804	1.50
	-20	0.00561	74.70	0.08047	1.93
Metal	-10	0.00812	61.77	0.0970	1.81
	-20	0.00403	87.85	0.06815	1.90

Occurrence of salts in a crystallizing solution leads to formation of the contact ice of a finer texture than under formation of ice of distilled water. Ice which is produced of salt solutions at the surface of montmorillonite is an exception which confirms an assump-

tion that the ice texture on it is formed under an action of the active centers of its surface.

Sizes of the contact ice crystals at the surface of one and the same base depend on the valency of salt cations of an initial solution. At a freezing point, T = -10°C at the surface of metal concrete and loam or at a freezing point, T = -20°C at the surface of sand an averaged volume of the ice crystals (Va) increases in the following series:

$$\text{cation}^{3+} < \text{cation}^{+} < \text{cation}^{2+}$$

At the surface of sand and montmorillonite at a freezing point, T = -10°C, and at the surface of metal concrete and loam at a freezing point, T = -20°C, with an increase in the cations' valency of an initial solution an averaged volume of the crystals (V_a) decreases.

Transition from contact ice to volumetric one is followed by an increase in the number of captured mineral salts which is verified by field experiments.

Ice of a peculiar texture formed at the surfaces of solid bodies has been obtained by us in the process of full-scale experiments on volumetric freezing of sea water mass. The main point of the experiments has consisted in producing the artificial ice massives of sea water using sources of cold (cooling pipes) placed inside water mass. Coolant (kerosene, cold free air) to ensure a continuous heat removal from the front of freezing the ice has circulated along the pipes. In the given case formation of crystals occurs under conditions of an open thermodynamic system, that is, in a general case processes of mass transfer accompanying the crystallization follow without difficulty.

It gives a possibility for free growth of a polycrystal ice containing a low amount of admixtures.

Ice which is formed at the surface of the cooling pipes is clearly differentiated into two zones. A first zone formed at a great heat loss rate has been poor in salts (the salinity of an initial solution being 33‰ salt content of ice has ranged between 0.5-2.0‰). The ice of this zone has been composed of fine (up to 3 mm in diameter) randomly oriented crystals. A second zone has been formed at a lesser rate of ice formation. The salinity of this layer has gradually increased towards a periphery reaching 9‰. A growth of large crystal aggregates which radially branch off of the pipe and consist of polelike ice plates between which there are salt or gaseous inclusions is characteristic of the ice of the zone. The crystal orientation is beltwise. These crystals include admixtures in the form of capillary tubes or cells oriented in a certain way.

Thus, for conditions of volumetric freezing the admixture content of ice is not only a function of its growth rate but of the crystals size and orientation as well and the more is the crystal the more admixtures it includes. Moreover, a beltwise orientation of the crystals which branch off radially and their predominant growth along basal planes produce favourable conditions for inclusion of admixtures inside the crystal itself into intrabasal spaces.

Changes in the texture and composition of the contact ice affect the strength of ice congelation with different materials. As a result of the tests performed (congelation tests of frozen ground metal or concrete with ice) a highly complex nature of the strength of their congelation has been brought to light. It is seem from Table II that shearing congelation strength is due to the following types of strains; namely, cohesive shear (along ice, along frozen ground); adhesive shear (along ice-base interface) and adhesive-cohesive shear (along ice and along interface; along frozen ground and along interface; along frozen ground, along ice and along interface). In case of congelation of a particular base and ice produced of distilled water the temperature fall causes an increase in the congelation strength which is due to gradual frost injury of a diffusive layer. Simultaneously an area of cohesive shear along the contact ice increases. Occurrence of salts in an initial solution complicates a multilayer congelation bond. In certain cases as the temperature falls the congelation strength increases since the brine from the diffusive layer is eighter absorbed by the base or precipitates as solids, in the other ones it decreases due to the fact that the brine acts as a lubricant. Moreover when the contact ice of a finer texture is produced of salt solutions there can also occur a sharp change in cohesive strength along ice as the congelation temperature falls since as a result of this the ice loses its strength due to a larger salt concentration in it.

More detailed examination of Table II enables to draw a conclusion that congelation forces of the multilayer system elements exhibit a specific character depending on quality and salt content of a crystallizing fluid which determines in the long run the surfaces along which main strains will occur.

Table II

Magnitude of Instantaneous Strength ($\tau_{inst.}$) Along the Surface of Congelation Between Ice and Frozen Ground or Cooled Bases of Metal or Concrete

Material of a base	Congelation point, θ°C	Congelation strength τ_{inst}, MPa	Crystal area per unit volume, P, cm²	Characteristic of a shear surface
1	2	3	4	5
Contact ice layer of distilled water				
Sand	-10	1.56	78.44	88% along ice
	-20	2.81	89.47	87% along ice
Loam	-10	1.26	72.06	along loam
	-20	1.33	100.32	along loam
Montmorillonite	-10	1.77	149.82	66% along ice, 2% along clay, 32% along interface

Table II cont.

1	2	3	4	5
Mont-morillo-nite	-20	1.79	174.72	71.7% along ice-ground interface, 28.3% along ice
Metal	-10	1.13	61.77	along metal-ice interface
	-20	0.98	87.85	along metal-ice interface
Concrete	-10	1.01	33.22	95% along concrete-ice interface, 5% along ice
	-20	0.97	74.70	98.5% along concrete-ice interface, 1.5% along ice
Contact ice layer of pore solution containing NaCl				
Sand	-10	1.41	54.96	87% along ice
	-20	2.28	94.71	85% along ice
Loam	-10	0.85	107.90	along loam
	-20	1.40	96.04	72% along ice, 28% along loam
Mont-morillo-nite	-10	1.51	57.41	74% along ice, 26% along interface
	-20	1.44	115.49	69% along ice, 31% along interface
Metal	-10	-	89.60	Liquid phase over metal
	-20	0.08	155.87	along interface
Concrete	-10	0.85	45.44	2-3% along ice, the rest along interface
	-20	1.02	77.02	38% along ice, 62% along interface
Contact ice layer of pore solution containing $MgSO_4$				
Sand	-10	1.66	86.86	83% along ice, 17% along interface
	-20	1.90	93.73	100% along ice
Loam	-10	1.28	90.92	along loam
	-20	1.44	103.53	87% along loam, 13% along ice
Mont-morillo-nite	-10	2.11	97.14	16% along clay, 31% along ice, 53% along interface
	-20	1.78	89.24	8% along clay, 29% along ice, 63% along interface
Metal	-10	1.13	78.10	100% along interface
	-20	1.25	171.20	36% along ice, 64% along interface
Concrete	-10	1.08	34.98	100% along interface
	-20	1.44	84.51	51% along ice, 49% along interface
Contact ice layer of pore solution containing $FeCl_3$				
Sand	-10	1.79	88.85	92% along ice, 8% along interface
	-20	1.54	141.45	87% along ice, 13% along interface
Loam	-10	1.47	121.20	90% along loam, 10% along ice
	-20	1.12	152.07	69% along loam, 31% along ice
Mont-morillo-nite	-10	2.03	125.42	23% along clay, 43% along ice, 34% along interface
	-20	2.05	126.01	2% along clay, 23% along ice, 75% along interface
Metal	-10	0.02	156.21	liquid phase above metal
	-20	0.04	217.91	liquid phase above metal
Concrete	-10	0.27	64.14	liquid phase above concrete
	-20	0.60	104.97	liquid phase above concrete

Thus, structural and crystallographic analysis of the contact ice layer and morphometric analysis of the shear surfaces enable to determine a degree of the action of different factors upon the congelation strength.

HYDROGEOCHEMISTRY OF KRYOLITHOZONE OF SIBERIAN PLATFORM

S.L. Schwartsev, V.A. Zuev and M.B. Bukaty

Politechnical Institute, Tomsk, USSR

SYNOPSIS The study of geochemical phenomena in the permafrost districts has a considerable scientific and practical significance. Underground waters are the most interesting in this aspect. Different geochemical processes are tied with water as the most mobile and chemically active agent. Together with this in the conditions of kryolithozone water itself suffers deep structural and property transformations under the influence of low temperatures and phase inversions "water-ice". In this report the hydrogeochemical features of the Siberian Platform conditioned by permafrost and the severe modern climate are considered.

INTRODUCTION

The Siberian Platform distinquishes among the other platform regions of the world by a range of peculiarities. One of them is the existance of kryolithozone unique both for its thickness and spreading area. As a result of various hydrogeological investigations connected with the ore and petroleum deposit search, decision of the problems of water supply and sites, mineral deposit exploitations and other problems of natural-economic mastering of this huge territory it is more and more obvious that 0.5-1.5 million years of the kryolithozone existance and evolution essentially defined the modern geochemistry of underground waters of hypergenesis zone and to a certain degree influenced on all studied waters of the many-kilometred sedimentory cover and even on the foundation. At the same time the theoretical questions of the formation of hydrogeochemical zonation, the water migration of chemical elements, the physico-chemical interaction of underground waters with rocks and alive substance in the districts of wide spreading of permafrost rocks have been still very little.

STRUCTURE OF KRYOLITHOZONE

The most important peculiarities of the modern kryolithozone spreading and structure are shown in Fig. 1. Practically the whole northern and central part of the Siberian Platform is occupied by the field of mainly continuous spreading of the permafrost rocks. In western Yakutia, on the slopes of the Anabar Anteclise, in the south of the Plateau Putorana and near the coasts of the Arctic Ocean they are underlied by the powerful thickness of the cold rocks containing kryohaline waters. The area of interrupted spreading of the permafrost rocks extends along the south-west outlying districts of the Tungus Artesian Basin and the south districts of the Yakut one as a zone of 100-300 km wide. The rest of the platform territory including the most part of the Angaro-Lena Artesian Basin can be regarded as a district of the island, sometimes rare-island permafrost development.

The thickness of the permafrost rocks increases from the north-east and reaches 700-900 m under the highest parts of the Plateau Putorana and the Anabar Crystal Shield. Maximum thickness of the cold rocks (to 1000 m) in its upper part with a partial ice-educing and with full saturation by kryohaline waters in its lower part is fixed in the west of the Yakut Basin in the district of the river Marha. Minimum rock temperatures in the zone of absence their season fluctuations are (-7)÷(-11) and in the upper part of the season thaw zone they fall to (-20)÷(-40) °C in winter. The clear straight dependance of the thickness of the permafrost rocks on the absolute relief marks is observed in the area of the Plateau Putorana. To the south and east of the region an ocean type of altitudinal zonation is replaced with the continental one which has the widest development in the Central and Western Yakutia.

Northward of the Plateau Putorana and the river Viluyi valley the continuous cover of the frozen rocks is very seldom broken by the through thaw zones under the largest water reservoirs and courses. Southward of these districts there are rather many springs of underground waters whose higher mineralization (very often it is of brine one) and specific composition say about underpermafrost feeding.

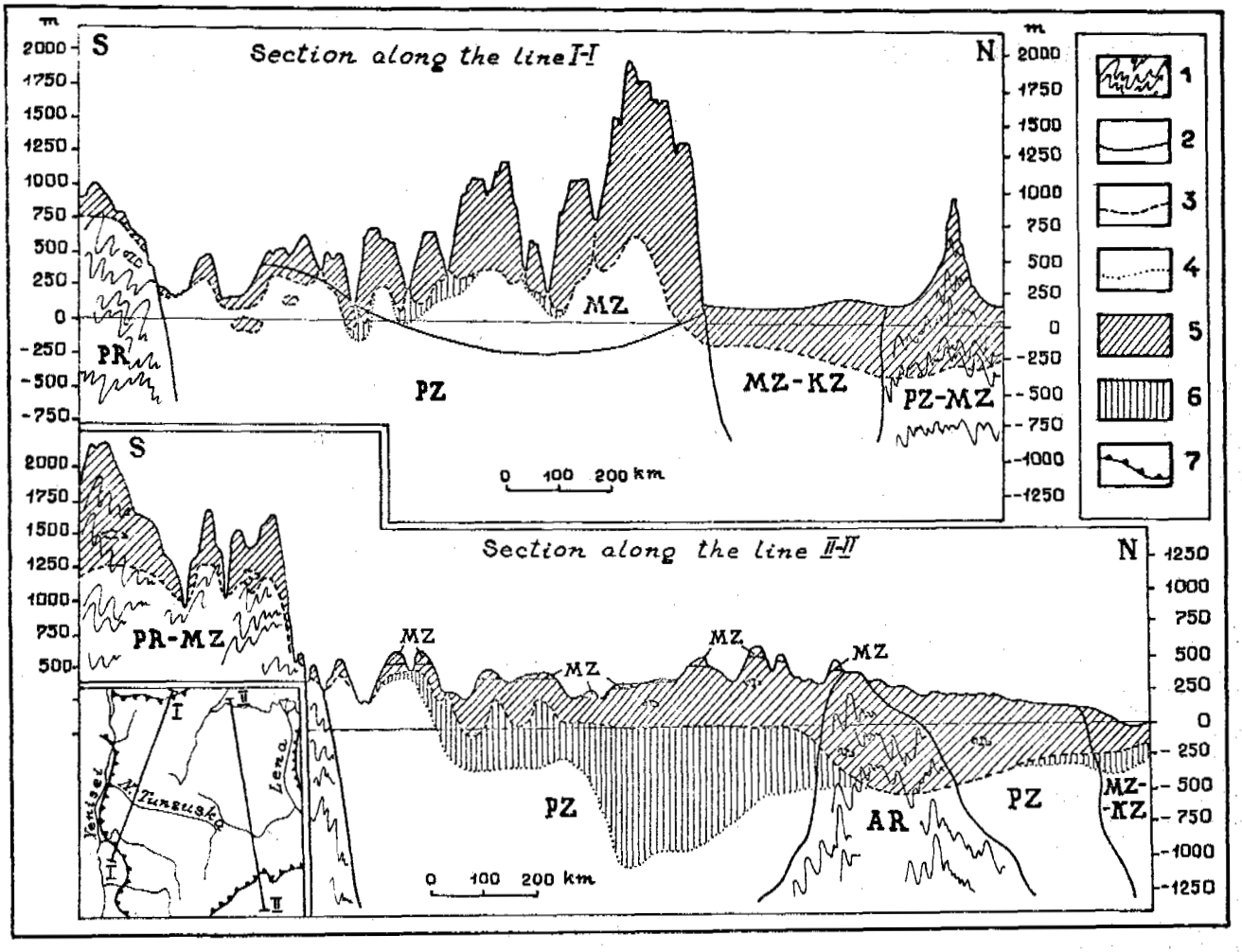

Fig.1 Schematic Geokryologic Sections of the Siberian Platform

1 - plicated systems, 2 - platform depositions and age boundaries, 3 - foot of permafrost rocks, 4 - foot of kryolithozone, 5 - permafrost rocks, 6 - kryohaline waters and frost rocks, 7 - boundary of platform

The rising unloading of underground waters run through the powerful thickness of the permafrost rocks especially intensively appears in the Tungus Basin. In contrast to the other districts of the Siberian Platform where now discending tectonic movements dominate and the distraction of the permafrost foot is observed, for this territory, as a result of neotectonic rising and erosion of the upper parts of geological section, inculcation of permafrost for new deeper lithologo-stratigraphic levels is typical. As a result of such geokryologic situation is, from one side, overhydrostatic character of the pressure of the underpermafrost waters and, from the other side, their intensive rising unloading. The most favourable spots for the realization of this rising unloading are the numerous zones of intrusive and tectonic deformations of considerably lithificated sedimentory cover mainly in negative the least frozen landforms. In this connection the presence of the through thaw zones under the lake and river valleys is not only the condition for the rising unloading realization in kryolithozone, but the consequence of kryohydrodynamic regime of entrails and endothermic influence of the underpermafrost waters on the permafrost rocks in the unloading hearths. The narrow thaw zones of mainly continuous permafrost spreading in the west of the Siberian Platform are highly streched - to 100 km and more. One can mark the concentration of the thaw zones along the periphery of the Plateau Putorana and the sharp decrease of them in its inner

districts where the water-proof basalt covers are developed everywhere and the thickness of the permafrost rocks is the most powerful.

GEOCHEMISTRY OF NATURAL WATERS

The main features of hydrogeochemical zonation of the upper underpermafrost horizons of the Siberian Platform are shown in Fig. 2. The

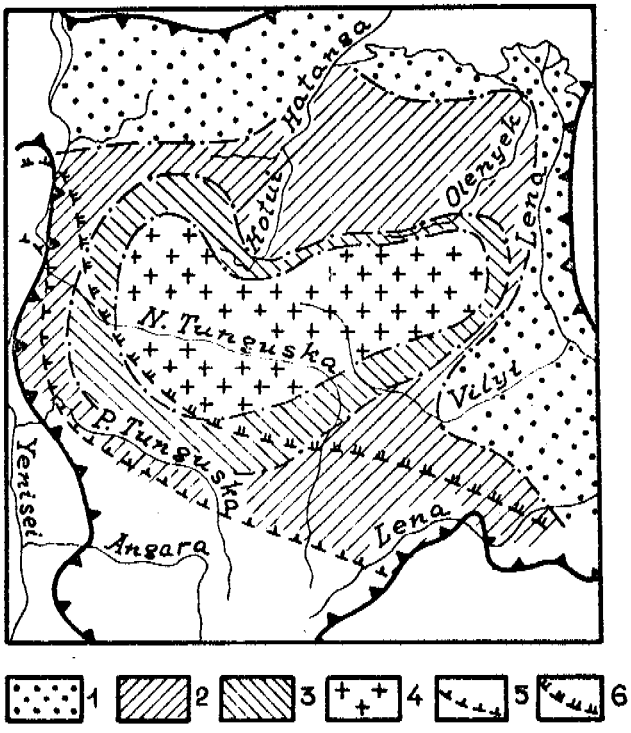

Fig.2 Scheme of Hydrogeochemical Zonation of the Upper Part of Underpermafrost Horizons

and chloride-hydrocarbonate calcium-sodium and sodium composition, 2 - fresh and saline waters, sometimes brines of hydrocarbonate-sulfate and sulfate calcium and hydrocarbonate-chloride and chloride sodium composition, 3 - saline waters and brines of chloride, sometimes sulfate-chloride calcium-sodium and sodium-calcium composition, 4 - brines of chloride magnesium-calcium, calcium-magnesium and calcium composition. South boundaries: 5 - broken and 6 - mainly continuous spreading of permafrost rocks

geochemical peculiarities of the underpermafrost waters are mainly conditioned by such causes as the composition of the initial waters buried during sedimentogenesis, the intensity of water exchange directly depended upon the geokryological conditions, the rising migration of underground waters out of the deeper horizons. To less degree the geochemical peculiarities of the underpermafrost waters are depended on the lithology of water-bearing rocks.

Wide spreading of the saline and brine waters being directly under the foot of permafrost is very typical for the Siberian Platform. This fact is considered by some investigators as a result of the kryogene methamorphism of underground waters in the course of their many-yeared freezing. It has been confirmed by the experimental and individual natural observations. At the same time the absence of the straight connection between the frozen zone thickness and the concentration degree of the underpermafrost waters does not permit to exaggerate the importance of this factor. For example, on the vast areas of the Tungus Basin where the thickness of permafrost is not the most powerful, the salinity of the underpermafrost waters is especially great. Moreover, it is known that the greatest mineralization (up to the high-concentrated chloride calcium brines) is observed not in the north deeply frozened districts of the basin and not in the periphery terrigenous-carbonate and saliferous ones, but in the central districts formed with the coal and volcanogenic-sedimentory deposits. Such a situation can be well explaned by the rising unloading out of deep horizons of the sedimentory cover. This unloading is one of the most typical features of the Siberian Platform and it shows itself the most intensively in favourable geologo-tectonical conditions of the Tungus Syneclise. The development of the kryogene screne favoured the single-directed (rising) fluid migration at the expense of increasing of energy of the initial hydrostatic system and simultaneously secured the effective isolation of the entrails from rainfall infiltration.

Fresh and slightly mineralizated underground waters are mainly developed: 1) in the west and south-west outlying districts of the platform kryolithozone where the permafrost has a broken structure and a small thickness and the intensity of the underground water exchange is maximum, 2) in the district of the Anabar Krystal Massif, 3) on the territories of the deep meso-cenozoic depressions for which the presence under the foot of frozen rocks of "freshening" zone is typical. This zone reaches by its thickness a few hundred metres below which the mineralization of the underground waters sharply increases. The formation of the "freshening" zones can be well explaned by the degradation of the permafrost foot at the expense of increasing of the endogeneous heat influence during neotectonical sinking of the territory which is in accordance with the belonging of such kryolithozone areas to the districts suffering absolute or relative bending in the newest epoch.

In the contrast of the waters lying under the foot of the permafrost general background appearance of the overpermafrost waters is rather common and does not show any contrast alterations in the regional plan. They are fresh hydrocarbonate mainly calcium waters whose insignificant variations of the ionic composition are depended generally on the

composition of the water-bearing deposits. At the same time both the dinamics and the existance of the overpermafrost waters are wholly influenced on by kryogenesis and this also forms their geochemical peculiarities. The existance of the frozen ground screen in immediate proximity (up to 0.5 m) to the day surface prevents from the deep penetration of the rainfall the year sum of which is highly considerable and changes along the region territiry from 400 to 1700 mm. Under these conditions practically all the infiltration loading falls to the share of the thin active layer. The results of this are: the high degree of the washing out of the well-dissolved salines, organic compounds and thin-dispersed mineral substance from the overpermafrost part of the section; lack of colour and smell, unique transparency and ultrafresh mineralization of the overpermafrost waters; the close connection of the underground waters composition with the rainfall composition.

The rainfall of the region is acid (pH = 4.8 - 6.4), non-sulfate, with the low content of chlorine (0.8 - 1.4 mg/l), episodical meeting of calcium, practically absolute lack of magnesium and total mineralization 4-8 mg/l. Nitrates, nitrites, twice and third-valenced iron were not discovered in the rainfall. Sometimes there is ammonium in little quantities (0.1-0.4 mg/l) and there is always organic substance (1-6 mg/l). Even within the first minutes the interaction of the rainfall with the soil-grounds, which mainly consist of carbonate, sand-clay and magmatic (basic) rocks, the rough alkalization (up to pH = 6.8-7.8, in carbonate districts up to 8.2-8.4), uneven increasing of the total mineralization (up to 30-60 mg/l) and the deep cooling (up to 4-2 ^{o}C) of the infiltrate rainfall take place. The increasing of the total mineralization and alkalinity mainly takes place at the expense of the dissolution out of the carbonate minerals and hydrolysis of the silicate and aluminosilicate minerals together with the active participation of CO_2 containing in the atmosphere and forming in soils. These processes are the cause of the predominance of the ions HCO_3^-, Ca^{2+}, Mg^{2+} and Na^+ in the chemical composition of the overpermafrost waters; the contence of the ions Cl^- and SO_4^{2-} keeps the level of the atmospheric consentrations.

The thickness of the seasonal thawing zone which defines, from one side, the degree of the infiltration loading on the overpermafrost part of the section and, from the other side, the nearness of the ground waters to the soil-vegetable layer is the function of the radiant-climatic conditions. In this connection the latitude and altitude hydrogeochemical zonation consisting in decreasing of the total mineralization (from 200-300 to 20-30 mg/l) and the quantity of pH (from 7.5-7.8 to 6.5-6.8) with simultaneously increasing of the organic substances and biophilous elements (Na, K) from the south districts towards the north ones and from valleys towards the watersheds is especially typical for the kryolithozone.

The most important feature of the hydrogeochemistry of the Siberian Platform is the high-amplitude change of the mineralization and the composition of the natural waters in a year cycle which is in mutual connection with the unique scale of the kryogene mineral formation and is closely connected with the processes of the season freezing-thawing, underground chemical carrying out and rising unloading of the underpermafrost waters. Regime observations on the springs with mixed feeding show that during a year their chemical appearance changes from ultrafresh hydrocarbonate calcium in the time of spring floods and freshets to saline and salt-brine chloride calcium (natrium) in winter time. Side by side with the season change of the mixture degree of genotypes of different natural waters the most important cause of this phenomenon is their straight kryogene methamorphism which reaches even the stage of sedimentation of well-dissolved salines.

The quantative calculations based on studying of the dinamics and regional changeability of the underground chemical carrying out as well as the natural mineralogical observations show that kryogene mineral formation is highly considerable in its scale, various in spectrum of the second minerals and regularly intensifies towards the north as far as frost-climatic situation becomes more and more severe. So, the part of SO_4, that goes into the solid phase in the river Norilka Basin in winter time, reaches 80-120 t/day and evaluated in $CaSO_4\ 2H_2O$ it reaches 140-210 t/day. On an average during winter about 1 g of gyps forms on each square metre.

The predominance of the calcium and magnesium carbonate precipitation is typical for the whole region. In the periphery of the Tungus Basin especially in northern districts is widely developed the sulfate precipitation including the natrium sulfates. In the spots of the outlets of the saline and salt-brine waters the crystallization of the halite is possible. There are unique finds such as nickelhexahydrite - six-aqueous nickel sulfate. The morphology of the kryogene mineral formations is very diverse: from the trivial veins, thin coatings and crusts to exotic (gyps "roses") accumulations.

With the beginning of snow and frost zone thawing and rain coming the mineral salines formated during winter intensively dissolve in the superfresh and acid rainfalls. One part of them is included into the biological circle, but the main quantity is taken away by thawed and rain streams. It is quite probable that modern kryogene saline formation plays not the last role in such lush animation of the northern vegetation in spring and total realization there of all phenological phases during the short vegetative period.

Another important side of the season kryogenesis on the Siberian Platform is the

annual tying of huge moisture mass in the frost zone, underground ices, icings and snow patches whose thawing during the whole warm year period secures a considerable water abundance of the rocks, ground-soils and a lake-river system even during dry periods.

The comparative analysis of the waters of the frozen ground thawing and the infiltration waters which did not pass the stage of kryogene methamorphism showed that their differences were not limited by the known and experimentaly grounded difference between their total ionic-saline composition. It is determined that thawed waters together with the low temperature and minimum content of well-dissolved salines are characterized by the essential differences in the content of the microcomponents, water-soluble gases and bacteria. In these waters the higher concentrations of such metals as Pb, Cu, Zn, Ag, Ni, Co, Sb, Sn, etc. are systematically discovered. As compared with the ordinary ground-rain waters the background level of these microelements is higher 2-3 times as much in thawed waters.

The higher content of the hydrocarbon gases and helium is typical for the thawed waters. Besides that the higher total gaseous saturation, the lower pH values and the higher CO_2 content are noted. The importance of principle has the discovery of the active and the most various microflora. Especially remarcable is the higher development of the bacteria oxidizing the liquid hydrocarbons. of the methane range.

The discovered geochemical specificity of kryogene waters is confirmed by the results of comparison of the gas content and microbial inhabitants of the rocks sampled out of the frozen ground and outside it: in frozen rocks the content of the hydrocarbon oxidizing bacteria is considerable higher.

To the number of causes determining the geochemical peculiarities of the kryolithozone natural waters may be taken the structural particulars of the ice and thawed waters, the higher gas solubility in the conditions of low temperatures, the formation of the gas hydrates, the accumulation of the migrating components in the frozen ground during the long winter period (the effect of "molecular sieve"), the kryophilic character of the microorganisms adopted to the low temperatures by the corresponding frozen-climatic contemporary conditions and those of the last hundreds of thousands years, high micropore pressures appearing in the rocks in time of their freezing, different electrochemical reactions being initiated by the phenomenon of the ice crystal polarization during phase converisons "water-ice" and etc.

The ability of the frozen ground and kryogene waters to accumulate the metals and hydrocarbon gases in the conditions of abundance of the thawed waters on the Siberian Platform in a warm time of a year permits to consider these objects as highly informative for sampling during ore and oil-gas hydrogeochemical search.

While touching the questions of the petroleum and gas geochemical search in the districts of wide development of kryolithozone we must especially underline that side by side with the rising migration of the naphthidogene components proved by practical results and sufficiently intensive development of the processes of their biological oxidition the biochemical synthesis of the whole range of aliphatic saturated and unsaturated hydrocarbons takes place on the kryolithozone territory. It is on principle importance that the quantitative correlation between individual varieties of hydrocarbons of hypergenno-biochemical (modern) and lithogenno -epigenetic (migratory) origin in the overpermafrost horizons and in the zone of intensive water exchange regulary changes in the first ones favour as far as hydrocarbon molecular mass increases. Thus, if the lightest compounds - methane and ethane - have mainly migratory origin even out of obvious tie with the unloading spots then for their heavier homologues the domination of the hypergenno-biochemical component is typical. The biological synthesis of the hydrocarbons in the kryolithozone, the peculiarities of their migration and distribution in various types of natural waters permit to see the new decision of some problems of geochemical petroleum and gas search.

CONCLUSION

All these facts show that the kryolithozone essentially influences on the dinamics and geochemistry of the natural waters of the Siberian Platform. In spite of severe frozen-climatic conditions many phenomena typical for the out-of-permafrost districts are realized there. And there are own especially specific processes which secure an active migration of various elements and compounds. The determined regularities open new possibilities for the effective interpretation of the results of the geochemical search of mineral deposits and can be regarded as a foundation for a wider practical application of these methods in the kryolithozone conditions.

THE FORMATION OF PEDOGENIC CARBONATES ON SVALBARD: THE INFLUENCE OF COLD TEMPERATURES AND FREEZING

R.S. Sletten

University of Washington, Seattle, WA 98195, USA

SYNOPSIS Soils of Kongsfjord, Spitsbergen that have formed on dolomitic limestone contain calcite and aragonite as secondary minerals. Aragonite is uncommon in soils of temperate regions, but little is known about its occurrence in arctic regions. This study reports the results of several experiments on low temperature carbonate formation in order to develop a model of natural carbonate diagenesis in Spitsbergen soils. In experiments designed to precipitate $CaCO_3$ at 0°C, it was determined that when Mg was present in a Mg/Ca molar ratio of 8, aragonite would precipitate. At a Mg/Ca ratio of 1.7 only calcite formed. Since Mg/Ca ratios in natural soil solutions were 0.6 to 0.7, I propose that this molar ratio increases as Ca is preferentially removed by calcite precipitation, thereby leading to aragonite formation. In experiments to assess the influence of freezing on the soil solution Mg/Ca ratio, it was determined that the equilibrium distribution coefficients (concentration in ice/concentration in water) for Ca and Mg are $10^{-3.3}$ and $10^{-4.3}$, respectively.

INTRODUCTION

Many of the soils of Spitsbergen have developed on limestone and dolomite, or receive eolian input of carbonates. In these soils, secondary carbonate minerals (also called pedogenic carbonates here) may have formed through dissolution-precipitation of primary carbonates. Pedogenic carbonates are common in soils of arid regions existing in temperature regimes from hot to frigid, and the terms hot and cold desert are used (Claridge and Campbell 1982). The area of Svalbard is a cold semi-arid region and it is of intrest since aragonite is common as a pedogenic carbonate (Sletten 1987).

Calcium carbonate occurs in three polymorphs at normal surface conditions: calcite, aragonite, and vaterite (Lippmann 1973). The Gibb's free energies of formation at 0°C are -10.40, -10.27, and -9.68 kcal mol^{-1} for calcite, aragonite, and vaterite, respectively (Plummer and Busenberg 1982). Vaterite is the most soluble and has not been reported in soils. Calcite is thermodynamically more stable than aragonite, however, it was established early this century that aragonite could form when Mg is present in solutions precipitating $CaCO_3$ (Lettmeier 1910). Secondary aragonite has been found in soils on dolomite (Quigley and Dreimanis 1966, Sticher and Bach 1971); in antarctic soils that have salt accumulations (Ugolini 1964, MacNamara and Usselman 1972); in basaltic bedrock overlying a limestone deposit (Veen and Arndt 1973); in carbonate stalactites and stalagmites in caverns (Cabrol *et al.* 1978); in littoral zone carbonate deposits (Callame and Dupuis 1972); and as subglacial deposits (Hallet personal communication).

In each case, the availability of magnesium was documented. This is also the case for the Spitsbergen soils; most aragonite here occurs in soils formed on dolomitic bedrock. Despite these examples, aragonite is rare in soils. In temperate climates, calcite appears to be the usual secondary carbonate mineral in soils, although, pedogenic Mg-calcites are widespread (Doner and Lynn 1977). In the soils discussed here, aragonite and calcite commonly occur as secondary minerals and Mg-calcites are rare.

The most obvious differences between the soils examined at Spitsbergen and temperate soils are the cryic temperature regimes and the presence of permafrost. In order to assess the effects of these factors in the formation of aragonite, two sets of experiments were performed. The first set was done to determine distribution coefficients for Mg and Ca during freezing of salt solutions. From these results, the effect of freezing on the soil solution Mg/Ca ratio was assessed. In the second set of experiments, conducted near 0°C to reflect soil temperatures, $CaCO_3$ was precipitated from solutions with various concentrations of Mg. Based on these results, a mechanism for precipitation of pedogenic aragonite is proposed.

STUDY SITE DESCRIPTION

Svalbard is an archipelago located approximately 600 miles north of Norway (Figure 1). The study site was located in the Kongsfjord region of Spitsbergen, where climatic information is available from the Ny-Ålesund station. The mean annual precipitation, primarily snow, is 385 mm and the mean annual air temperature is -5.8°C,

with a July mean air temperature of +5.2°C (Steffensen, 1982).

Two soil profiles at the Carrington site on the Brøgger peninsula were studied. The site is located at 35 to 40 m above sea level on a reworked beach deposit consisting primarily of dolomite with a minor amount of quartz (Hjelle and Lauritzen 1982). Vegetation is classified as Barren Zone (Brattbakk 1981) with less than 10% vascular plant cover, dominated by *Saxifraga oppositifolia* (Purple saxifrage) and several crustose lichens. Detailed soil descriptions have been published for a similar neighboring site (Cannes site, Mann *et al.* 1986). A brief soil description is given in Table I. The soils here have developed in stratified layers of beach gravel and sand and are about 9,000 to 12,000 years old. Secondary carbonates occur on the undersides of clasts throughout the soil, especially on open gravel in the BC/C horizon. The carbonate coatings range from white to brown in color and vary from thin skins to pendants several mm in thickness. An example of a well developed coating is shown in Figure 2. Silt caps are common and consist primarily of silt size dolomite particles. In the U.S. Soil Taxonomy, these soils would be classified as Pergelic Cryopsamments (Reiger 1983).

TABLE I Brøggerhalvøya soil descriptions. DP refers to desert pavement.

Horizon	Depth	Texture
Carrington 1		
DP	0-5 cm	very gravelly sand
A	5-8	gravelly loamy sand
Bw	8-24	gravelly loam
BC/Ck	24-115	gravelly sand
Cf	115	(ice cemented permafrost, 26 Aug. 84)
Carrington 2		
DP	0-4 cm	very gravelly sand
A	4-6	gravelly loamy sand
Bw	6-29	gravelly loam
BC/Ck	29-130	gravelly sand
Cf	130	(ice cemented permafrost, 26 Aug. 84)

METHODS

Procedures and equipment are presented in detail in Sletten (1987) and only a brief summary is given here. Carbonate coatings were carefully chipped from the host rock to minimize contamination; when possible, coatings were isolated from non-calcareous host rock. X-ray diffraction patterns were made of random powder mounts with a Picker unit x-ray diffractometer with CuK_{α} radiation and a Ni filter. Samples of soil solutions were collected by tension lysimeters placed at depth intervals and maintained at 10 kPa vacuum. The soil solutions were filtered in the field at 0.22 µm. Alkalinity and pH were measured in the field, generally after the sample had warmed to 10 to 15°C. Dissolved inorganic carbon (DIC) and dissolved organic carbon (DOC) were determined with an OI 700 carbon analyzer (OI Corp., College Station, TX). A subsample was acidified to pH 2 with nitric acid for analysis of the cations with a Jarrel-Ash Model 96-955 inductively coupled plasma spectrophotometer (ICP). A second sample was preserved with methyl cyanide for subsequent analysis of inorganic anions with a Dionex Model 2010 ion chromatograph.

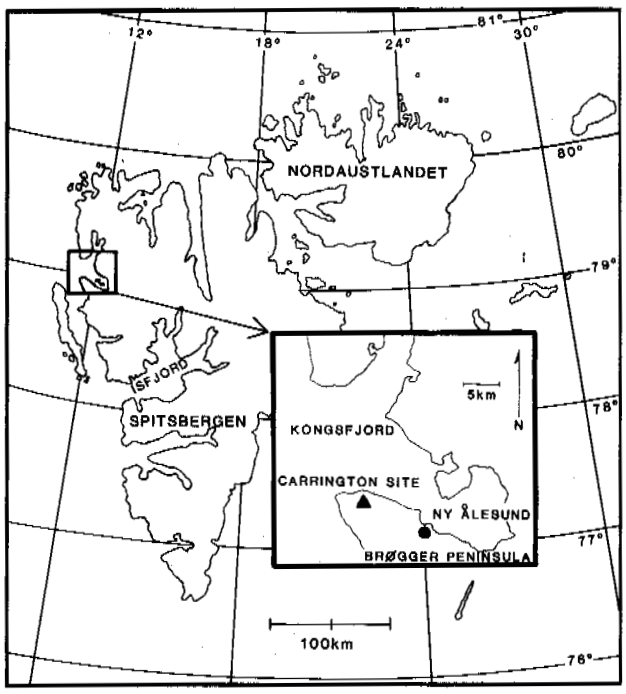

FIGURE 1 Location of field site at Svalbard archipelago.

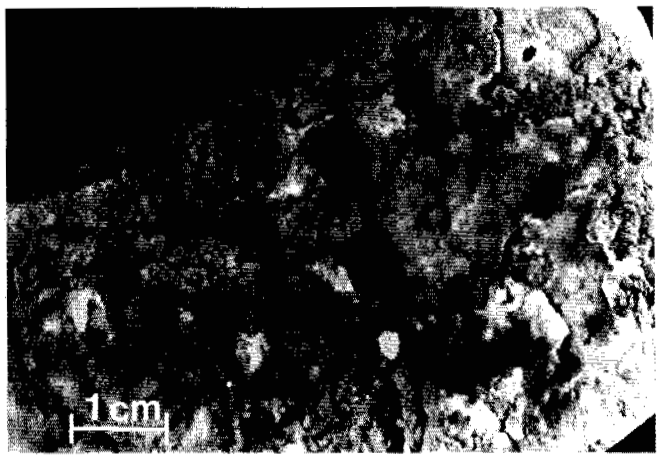

FIGURE 2 Pedogenic carbonate coating on the underside of a stone from the study site.

Freezing experiments were performed utilizing an apparatus similar to one used by Hallet (1976) consisting of a 9 cm diameter acrylic tube with an aluminum plate fastened on top. The bottom acrylic plate was connected via tubing to a buret, thereby allowing volumetric changes to measure the amount of ice which had formed. The solutions to be frozen were prepared by adding high purity $CaCl_2$ or $MgCl_2$ to distilled-deionized water which had been boiled for 1/2 hour to remove CO_2 and other gases, in order to minimize gas bubble formation during freezing. The experiments were performed in a 1°C cold room and a freezing front was developed by placing an aluminum block, through which an ethylene glycol/water mixture at -10 to -20°C was pumped, on top of the cylinder. The freezing progressed from the top of the cylinder downward and the unfrozen water was kept well mixed with a Teflon coated stirring bar actuated by a magnetic stirrer. At given time intervals, a syringe was inserted into the cylinder through a silicon septum and a 3 to 5 ml sample of water was removed and analyzed on the ICP for Ca and Mg. The experiment was terminated when the entire cylinder had frozen. The ice core was removed by gentle warming; cut into sections; rinsed with distilled-deionized water; allowed to thaw; and analyzed on the ICP for Ca and Mg.

Laboratory precipitation of $CaCO_3$ in the presence of Mg was conducted in a 1 L glass jacketed reaction vessel. The temperature was maintained at 0.15 ± 0.1°C. The pH was maintained at a preset value with a Radiometer Model PHM 62 pH meter fitted with a Radiometer Model ABU11 autoburette, TTA60 titration assembly, and pH-Stat interface. The pH was adjusted with the addition of 0.05 M NaOH/0.025 M $CaCl_2$. The partial pressure of CO_2 was maintained at the atmospheric value by bubbling excess air at 1.5 L min^{-1}. Ten mg of calcite or aragonite were added as seeds for crystal growth. At the completion of a pH-stat run the precipitate was isolated on a 0.22 µm Nucleopore filter mounted in a Buchner funnel. Precipitation runs were done at Mg/Ca molar ratios varying from 0 to 8.

RESULTS AND DISCUSSION

Soil Secondary Carbonates

X-ray diffraction results from analyses of carbonate coated clasts collected by depth are given in Table II. Aragonite is present at all depths. The silt and clay size fraction in the soil was shown (Mann *et al.* 1986) to consist almost exclusively of dolomite and quartz, therefore the presence of dolomite and quartz in the coatings is likely due to incorporation of detrital silt and clay. This detrital material may impart the light to dark brown color seen in some samples.

Soil Solution

The charge balance for the soil solutions collected at various depths is given in Fig. 3. The solutions at 5, 20, and 60 cm depths were collected on 6-21-85, while the 120 cm sample is from 8-17-85. This sampling schedule is imposed by the fact that this soil does not thaw at 120 cm until late in the summer, while all the upper horizons are too dry to collect soil solutions at this time. In the soil solution, Mg^{2+} and Ca^{2+} are the major cations while HCO_3^- is the major anion. The deficit between the summation of cations and anions reflects excess anions and is believed to represent organic anions. DOC is correlated with organic anion concentration and follows the same trend as the charge deficit (DOC values vary from 15 to <1 ppm C from the upper to the lower lysimeter). The Mg/Ca molar ratios of the soil solutions are consistently at 0.6 to 0.7 for all horizons at all times and probably reflect the dolomitic bedrock. As time progresses over a few days, the concentrations of the anions and cations increase, but the Mg/Ca ratio remains constant. The soil solutions may become supersaturated by 2 to 3 times with respect to calcite. This is similar to calcareous soils in temperate regions

TABLE II Mineralogy of pedogenic carbonates by XRD. o = no peak, + to ++++ indicate minor to major abundance.

Depth	aragonite	calcite	dolomite	quartz
Carrington Profile 1				
20 cm	++	++++	++	+
20	+++	++++	++	+
60	+	+++	+	o
100	+++	++++	++	++
Carrington Profile 2				
20 cm	+++	++++	++	++
20	+	++++	+	+
35	++++	++++	++	++
35	++++	++++	++	++
50	+++	++++	+++	+
50	+++	++++	o	+
75	+	++++	o	+

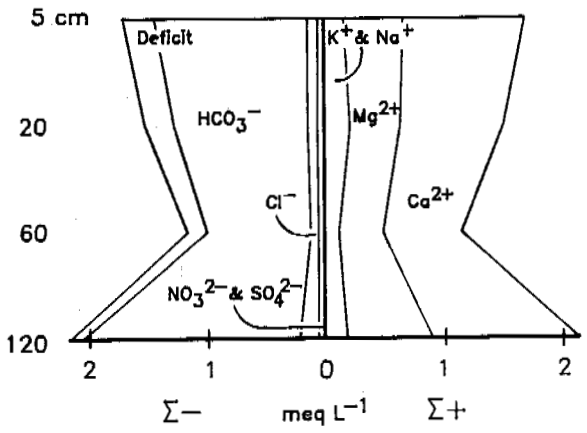

FIGURE 3 Detailed charge balance of soil solution from the Carrington study site.

where supersaturation with respect to calcite is common (Suarez and Rhoades 1982).

Freezing Experiments

To assess how freezing affects the Mg/Ca ratios in the soil solution, laboratory experiments were performed to determine the ionic exclusion of Mg and Ca salts in pure solutions. In these experiments, an effective distribution coefficient was determined (the concentrations of Mg or Ca in ice divided by the concentration in the unfrozen water). The initial solution concentrations were 0.079 mM $CaCl_2$ and 0.237 mM $MgCl_2$, values similar to those in the soil solutions. Figure 4 shows the concentration of Mg and Ca in the ice and water phases as the cylinder froze. The effective distribution coefficient was calculated by measuring the Ca and Mg concentration in each of 5 sections of ice and dividing this by the concentration in water subsamples collected when a given section of ice was forming (Table III).

At the beginning of the freezing run, there were no ice crystals in the solution, and supercooling probably occurred. As a result of this, the first 5% of the ice was cloudy due to polycrystalline growth. After this, the ice crystal was clear with a planar front until the final 5 to 10% of the water was frozen, at which time the freezing front became distorted due to gas bubble formation. The higher distribution coefficients at the beginning and end of the run reflect these irregularities.

The data presented in Table III and Figure 4 indicate that Mg is excluded from ice to a greater degree than Ca. A better comparison can be made by comparing the equilibrium distribution coefficient ($K_{(0)}$), determined by extrapolating to a zero freezing rate. Using the model of Burton, Prim, and Slicher (cited in Pfann 1966), it was determined that $K_{(0)}^{Ca} = 4.52 \times 10^{-4}$ and $K_{(0)}^{Mg} = 5.02 \times 10^{-5}$ for these experiments. These values reveal that Mg is excluded more effectively by one order of magnitude. Data in the literature for $K_{(0)}^{Ca}$ and $K_{(0)}^{Mg}$ are scarce. Leung and Carmichael (1984) found $K_{(0)}^{Ca}$ to be 0.69, and Hallet (1976) using a similar apparatus, but without stirring, obtained a $K_{(0)}^{Ca}$ of 0.01 to 0.02.

In summary, Mg is excluded to a greater degree than Ca, although both ions are excluded very

TABLE III Effective distribution coefficients determined from the freezing experiment.

Ice Sections	K_{Ca} X 1000	K_{Mg} X 1000
0 - 1.8 cm	100.6	108.9
1.8 - 3.6	5.81	0.779
3.6 - 5.4	3.79	0.481
5.4 - 7.2	2.29	0.296
7.2 - 9.0	1.71	0.661

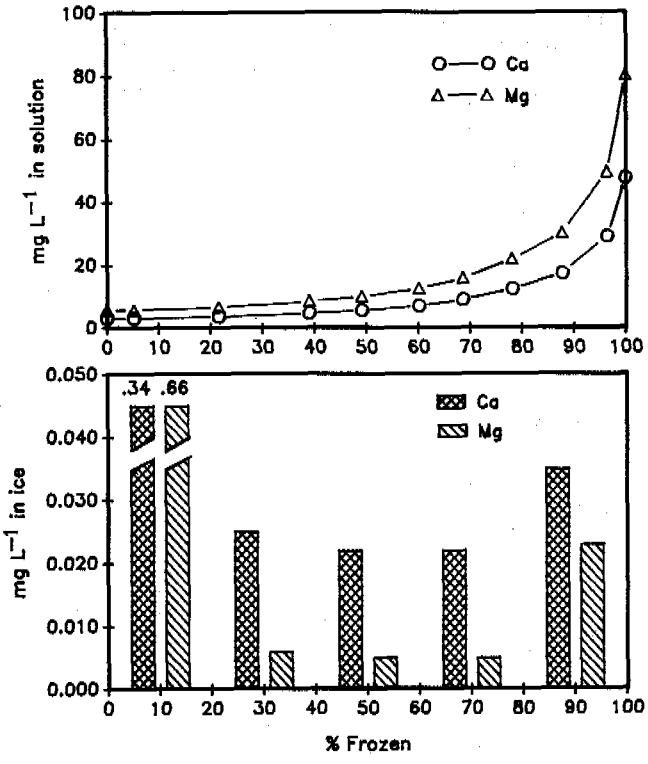

FIGURE 4. Results of experiments on ionic exclusion during freezing of Ca and Mg salt solutions.

efficiently. Therefore, in freezing solutions, most of the Mg and Ca remains in the water and the Mg/Ca ratio is not be significantly altered. Freezing does concentrate the ions and this may be important in producing supersaturated conditions. Data on studies of stable O isotopes in the carbonate coatings suggest both freezing and evaporation to be important in generating supersaturation (Sletten and Ugolini 1987).

Carbonates Synthesized in the Laboratory

In the experiments designed to precipitate $CaCO_3$ at various Mg/Ca ratios, with Mg present, aragonite was used as the seed crystal since calcite and aragonite will nucleate on aragonite surfaces, whereas aragonite will not nucleate easily on calcite (deBoer 1977, Berner 1975). To induce precipitation, titrant was added until the saturation index exceeded unity. As precipitation occurred and the pH decreased, additional titrant was automatically added. When no Mg was present, the only product formed was calcite (Table IV) displaying typical rhombohedral morphology as viewed in the SEM. At a solution Mg/Ca molar ratio of 1.7, according to XRD data, calcite precipitated and SEM revealed a rhombohedral form that appeared distorted due to partial inhibition of crystal growth along the C-axis. At a Mg/Ca molar ratio of 8, both calcite and aragonite were detected. The calcite d-spacing was 3.025 to 3.030 Å which corresponded to a 0.9 ± 0.02% Mg-calcite. SEM micrographs revealed a massive growth with

TABLE IV. Steady state precipitation rates and major products from precipitation experiments.

Mg/Ca	pH	Sat. Index		Rate	Product
		Cal.	Arag.	mgCa hr^{-1}	
0	8.30	1.1	0.7	0.32	calcite
0	8.70	10.1	7.0	0.70	calcite
1.7	8.85	13.9	9.6	0.23	calcite
1.7	8.70	6.3	4.4	1.26	calcite
8	8.70	4.8	2.3	0.26	1% Mg-calcite and aragonite

rhombohedral crystals occurring in pockets (Fig. 5). In order to determine which morphology represented the aragonite and which the Mg-calcite, the chemical composition of the precipitates was analyzed by energy dispersive x-ray analysis (EDXRA). According to the EDXRA, low levels of Mg were present in the rhombohedral crystals, but no Mg was detected in the massive matrix. Therefore, the massive growth must be aragonite and the rhombohedral crystals are the Mg-calcite. It appears that aragonite initially precipitated and later partially dissolved forming pockets in which a 0.9% Mg-calcite precipitated.

These results suggest that at a Mg/Ca ratio of 8, aragonite formation is faster than formation of Mg-calcite, but the Mg-calcite is ultimately more stable. Therefore aragonite formation is kinetically controlled, whereas Mg-calcite is the thermodynamically more stable phase. In contrast, Glover and Sippel (1967) and Cabrol *et al.* (1978), reported the transformation of high Mg-calcites to aragonite at room temperature. In cold water sediments, Dean (1981) noted that Mg-calcites are the predominant form, over aragonite and calcite. The data of Thorstenson and Plummer (1977), Chave *et al.* (1962), and Walter and Morse (1984) at 25°C, indicate that high Mg-calcites (>7 - 10%) are less stable than aragonite, but that low Mg-calcites (<7 - 10%) are more stable. There has been little experimental work considering the stability of Mg-calcites at low temperatures, although it has been shown that the distribution coefficient of Mg in calcite decreases with decreasing temperature (Katz, 1973). The work presented here suggests that aragonite is less stable than 0.9% Mg-calcite at near 0°C, in a solution with Mg/Ca = 8. Since the soil solution had a Mg/Ca ratio of 0.6 to 0.7, it is expected that the ratio must be increased to above 1.7 for aragonite to from. Furthermore, since no Mg-calcite was detected in the samples collected in the field, the Mg/Ca was probably lower than 8, possibly forming very low Mg-calcites which are difficult to differentiate from calcite with XRD.

CONCLUSIONS

It was determined that the equilibrium distribution coefficient of Mg in ice/water is greater than that for Ca by a factor of 10. However, both Mg and Ca are excluded so efficiently during freezing that the solution ratios of Mg and Ca do not change significantly. The major effect of freezing may be to induce supersaturation, as has been suggested to occur in other natural systems (Cailleux 1964, Hallet 1976). The distribution coefficients determined here are the lowest found in the literature for Ca and Mg and they approach the equilibrium distribution coefficient.

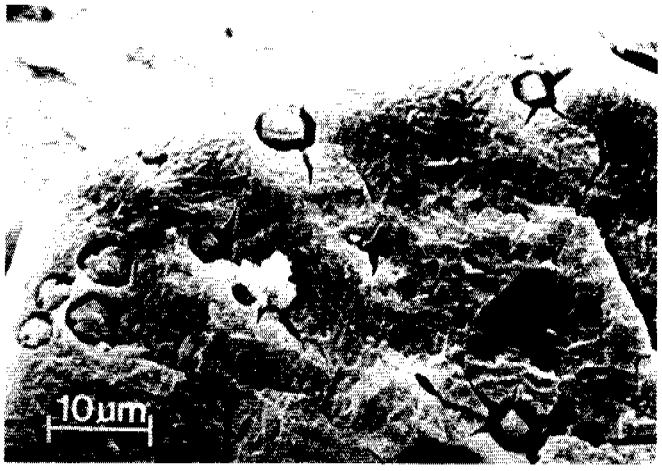

FIGURE 5 SEM Micrograph of precipitate formed in the laboratory from a solution with Mg/Ca ratio of 8. The massive growth is aragonite and the rhombohedral crystals are 0.9 % Mg-calcite.

Aragonite formation in the Spitsbergen soils may be explained by the presence of Mg if the Mg/Ca soil solution ratio is increased. Since the secondary carbonates form on the undersides of clasts, I suggest that soil solutions become stranded and precipitation occurs here. As these soil solutions become supersaturated, either by freezing or by evaporation, $CaCO_3$ precipitates and Ca is preferentially removed over Mg from the solution. Doner and Lynn (1977) have suggested a similar mechanism for Mg-calcite formation in soils. Lower temperatures will enhance this effect, since less Mg goes into calcite at lower temperatures. As the Mg/Ca ratios increase, calcite growth will be inhibited and aragonite may form. Experiments presented here suggest the threshold Mg/Ca ratio for aragonite formation lies between 1.7 and 8. The actual ratio may be mediated by the degree of supersaturation and the sites of crystal growth. Over time the aragonite may dissolve and form calcite, or very low Mg-calcite virtually indistinguishable from pure calcite by XRD. Alternatively, aragonite may remain as a metastable phase as these soils become dry.

ACKNOWLEDGEMENTS

I would like to acknowledge and thank F. Ugolini, J. Ferguson, and B. Hallet for their generous input and suggestions. Kings Bay Coal Company on Svalbard and the Norwegian Polar Institute were helpful with logistics. This work was supported by National Science Foundation Grant DPP-8303624.

REFERENCES

Berner, R. A. (1975) The role of magnesium in the crystal growth of calcite and aragonite from seawater. *Geochemica et Cosmochimica Acta* 39; 489-504.

Brattbakk, I. (1981) Brøggerhalvøya, Svalbard, Vegetasjonskart 1:10,000. *Kongelige Norske Videnskabers Selskabs Museum, Botanisk avd.*, Trondheim, Norway.

Cabrol, P., Coudray, J., Danurnad, J. L., and Schott, J. (1978) Sur la possibililité de transformation naturelle calcite "to" aragonite dans les conditions ordinaires de température et de pression: reproduction expérimentale du phénoméne. *Comptes Rendus des Séances de L' Académie des Sciences, Paris* 287; 411-414.

Cailleux, A. (1964) Genése possible de dépôts chimiques par congélation. *Comptes Rendus Soc. Géol. France Compte Rendu* 1; 11-12.

Callame, B. and Dupuis, J. (1972) Sur la précipitation d'aragonite à partir des eaux interstitielles des sols littoraux et des formations sableuses intertidales de la Pointe d'Arcay (Vendée). *Comptes Rendus des Séances de L' Académie des Sciences, Paris* 274; 675-677.

Chave, K. E., Deffeyes, K. S., Weyl, P. K., Garrels, R. M., and Thompson, M. E. (1962) Observation on the solubility of skeletal carbonates in aqueous solutions. *Science* 137; 33-34.

Claridge, G. C. G. and Campbell, I. B. (1982) A comparison between hot and cold desert soils and soil processes. In: *Aridic soils and geomorphic processes*, D.H. Yalon, ed. Catena supplement 1, Braunschweig, p. 1-28.

de Boer, R. B. (1977) Influence of seed crystals on the precipitation of calcite and aragonite. *American Journal of Science* 277; 38-60.

Dean, W. E. (1981) Carbonate minerals and organic matter in sediments of modern north temperate hard-water lakes. *The Society of Economic Paleontologists and Mineralogists, Special Publication No.* 31; 213-231.

Doner, H. E. and Lynn, W. C. (1977) Carbonate, halide, sulfate, and sulfide minerals. In: *Minerals in Soil Environments*, J.B. Dixon and S.B. Weed, ed. Soil Science Society of America. Madison, WI, p 75-98.

Glover, E. D. and Sippel, R. F. (1967) Synthesis of magnesium calcites. *Geochemica et Cosmochimica Acta* 31; 603-613.

Hallet, B. (1976) Deposits formed by subglacial precipitation of $CaCO_3$. *Geological Society of America Bulletin* 87; 1003-1015.

Hjelle, A. and Lauritzen, Ø. (1982) Geological map of Svalbard (1:500,000), Spitsbergen, northern part. *Norsk Polarinstitutt Skrifter* 154C, 15 pp. and map.

Katz, A. (1973) The interaction of magnesium with calcite during crystal growth at 25 - 90°C and one atmosphere. *Geochemica et Cosmochimica Acta* 37; 1563-1586.

Lettmeier, H. (1910) Zur kenntnis der carbonate; Die dimorphie des kohlensauren kalkes. *Neues Jahrbuch für mineralogie, geologie und paläontologie* (Jahrgang 1910), p. 49-75.

Leung, W. K. S. and Carmichael, G. R. (1984) Solute redistribution during normal freezing. *Water, Air, and Soil Pollution* 21; 141-150.

Lippmann, F. (1973) *Sedimentary carbonate minerals*. Springer- Verlag, New York. 228 pp.

MacNamara, E. E. and Usselman, T. (1972) Salt minerals in soil profiles and as surficial crusts and efflorescences, coastal Enderby Land, Antarctic. *Geological Society of America Bulletin* 83; 3145-3150.

Mann, D. H., Sletten, R. S., and Ugolini, F. C. (1986) Soil development at Kongsfjord, Spitsbergen. *Polar Research* 4; 1-16.

Pfann, W. G. (1966) *Zone Melting, 2nd Edition*. John Wiley and Sons, Inc., NY. 310 pp.

Plummer, L. N. and Busenberg, E. (1982) The solubilities of calcite, aragonite and vaterite in CO_2 - H_2O solutions between 0 and 90°C, and an evaluation of the aqueous model for the system $CaCO_3$-CO_2-H_2O. *Geochemica et Cosmochimica Acta* 46; 1011-1040.

Quigley, R. M. and Dreimanis, A. (1966) Secondary Aragonite in a Soil Profile. *Earth and Planetary Science Letters* 1; 348-350.

Rieger, S. (1983) *The Genesis and Classification of Cold Soils*. Academic Press, NY. 230 pp.

Sletten, R. S. (1987) *Aragonite Formation in Polar Soils*. Master's thesis, University of Washington, Seattle. 88 pp.

Sletten, R. S. and Ugolini, F. C. (1987) Stable carbon and oxygen isotopes of pedogenic carbonates in arctic soils. *1987 Agronomy Abstracts*, American Society of Agronomy, Madison, WI, p. 231.

Steffensen, E. L. (1982) The climate at Norwegian arctic stations. *Klima* 5, 44 pp.

Sticher, H. and Bach, R. (1971) Aragonit-Konkretionen in Dolomit- Rendzinen. *Geoderma* 6; 61-67.

Suarez, D. L. and Rhoades, J. D. (1982) The apparent solubility of calcium carbonate in soils. *Soil Science Society of America Journal* 46; 716-722.

Thorstenson, D. C. and Plummer, L. N. (1977) Equilibrium criteria for two-component solids reacting with fixed composition in an aqueous phase - example: The magnesian calcites. *American Journal of Science* 277; 1203-1223.

Ugolini, F. C. (1964) *A Study of Pedologic Processes in Antarctic*. (Final report to the National Science Foundation Grants G-17212, G-23787, and GA-74). Rutgers University, NJ. 81 pp.

Veen, A. W. L. and Arndt, W. (1973) Huntite and aragonite nodules in a vertisol near Katherine, Northern Territory, Australia. *Nature Physical Science* 241; 37-40.

Walter, L. M. and Morse, J. W. (1984) Magnesian calcite stability: A reevaluation. *Geochemica et Cosmochimica Acta* 48; 1059-1069.

MEASUREMENT OF THE UNFROZEN WATER CONTENT OF SOILS: A COMPARISON OF NMR AND TDR METHODS

M.W. Smith[1] and A.R. Tice[2]

[1]Geotechnical Science Laboratories, Carleton University, Ottawa K1S 5B6, Canada
[2]U.S. Cold Regions Research and Engineering Laboratory Hanover, NH 03755, U.S.A.

SYNOPSIS A laboratory testing program was carried out to compare two independent methods for determining the unfrozen water content of soils. With the TDR method, the unfrozen water content is inferred from a calibration curve of apparent dielectric constant versus volumetric water content, determined by experiment. Previously, precise calibration of the TDR technique was hindered by the lack of a reference comparison method, which NMR now offers. This has provided a much greater scope for calibration, including a wide range of soil types and temperature (unfrozen water content). The results of the testing program yielded a relationship between dielectric constant and volumetric unfrozen water content that is largely unaffected by soil type, although a subtle but apparent dependency on the texture of the soil was noted. It is suggested that this effect originates from the lower valued dielectric constant for adsorbed soil water. In spite of this, the general equation presented may be considered adequate for most practical purposes. The standard error of estimate is 0.015 cm^3 cm^{-3}, although, if desirable, this may be reduced by calibrating for individual soils. Brief guidelines on system and probe design are offered to help ensure that use of the TDR method will give results consistent with the relationship presented.

INTRODUCTION

The two methods which are the subject of this paper - pulsed Nuclear Magnetic Resonance (NMR) and Time Domain Reflectometry (TDR) - offer complementary attributes in the measurement of soil water content: NMR provides a fast and accurate method for use with laboratory samples, whilst TDR can be used for this in addition to in situ measurements in field or laboratory experiments.

Time domain reflectometry (TDR) is used to measure the travel time of a MHz pulse through the soil, from which an apparent dielectric constant is determined. The unfrozen water content is inferred from a calibration curve of the apparent dielectric constant versus volumetric water content, determined by experiment. Previously, precise calibration of the technique for determining water content was hindered by the lack of a reference comparison method, which NMR now offers. The calibration procedure involved simultaneous measurements of unfrozen water content (NMR) and dielectric constant (TDR) for a variety of soil specimens. Before describing the experiment, a very brief review of the two methods is provided.

Nuclear Magnetic Resonance (NMR)

All atomic nuclei have magnetic moments and the quantum energy levels are characteristic of the particular nuclear species. When radio frequencies are applied, atoms absorb a certain amount of energy to realign to another stable position within the magnetic field. If a soil-water mixture is placed in a pulsed NMR analyser and a single radio frequency pulse is applied, a voltage (which corresponds to the number of atoms absorbing energy) is induced in a receiver coil that surrounds the specimen. This voltage is detected by the NMR analyser; its magnitude (minus the background) is directly proportional to the amount of water (hydrogen) in the mixture. Therefore, the NMR can be used as a soil water detector (subject to certain considerations - e.g. see Tice et al. 1984).

A drop in signal intensity is observed as soil water freezes, since the NMR used (Praxis model PR-103) was tuned to the hydrogen proton associated with liquid water (10.72 MHz). The signal associated with the protons of the solid ice and soil constituents is not recorded. Tice et al. (1982) describe the NMR technique for determining the unfrozen water content of soils, and demonstrated the accuracy of the technique by the agreement of NMR results with physical desorption data.

Time Domain Reflectometry (TDR)

TDR is a common method for obtaining frequency-dependent permittivity (dielectric constant) values in the VHF through microwave frequency range, utilising Fourier transformations of picosecond duration pulses incident and reflected from a test material contained in a suitable waveguide (e.g. Delaney and Arcone 1984). In a different application, Topp et al. (1980) proposed obtaining single (frequency-independent) permittivity values for soils using a non-Fourier approach, in which the travel time of an electromagnetic pulse, launched along a coaxial line of known length (L) containing a soil specimen, is measured. (Alternatively, a pair of parallel metallic rods may be embedded in a soil specimen.) The reflections originating at the front and back (beginning and end) of a sample (or in situ sample volume) are recorded and the time delay (t) between these reflections is measured (Figure 1).

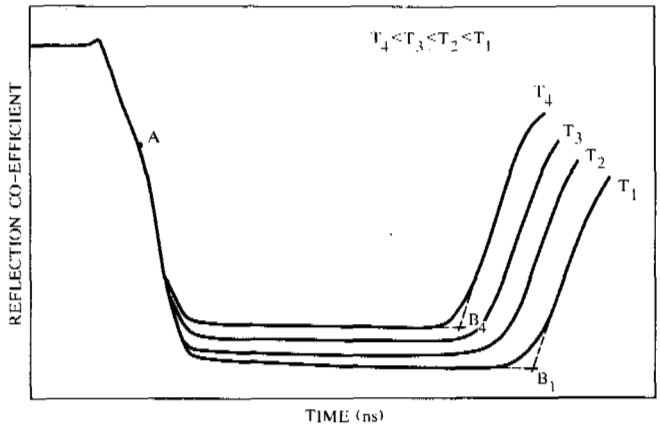

Figure 1. Typical TDR traces at a variety of freezing temperatures.

Electromagnetic theory shows that the velocity of propagation, v, can be expressed in terms of an "apparent dielectric constant", Ka for the test medium and the velocity of electromagnetic radiation in free space, c ($3x10^8$ m s^{-1}):

$$v = c/\sqrt{Ka} \quad (1)$$

since $$v = L/t \quad (2)$$

then $$Ka = (ct/L)^2 \quad (3)$$

However, since wet soils are generally dispersive at frequencies in the low GHz range (Hoekstra and Delaney 1974, Delaney and Arcone 1984), the value of Ka determined by the travel time method will approach the true value of K only if the TDR pulse contains no such high frequencies by the time it returns from the end of the transmission line (see also Arcone and Wills 1986). Two features of the TDR measurement system used in our experiments contribute to this condition:

(i) the TDR model used (Tektronix 1502) has a relatively slow rise time (about 140 ps), and thus the incident pulse has virtually no frequency content above about 800 MHz.

(ii) When transmission lines of about 20 cm or longer are used, most of the high frequency content of the signal is dispersed along the line and the reflection at the end of the line is dominated by the lower frequencies in the launched signal.

EXPERIMENTAL RATIONALE

Topp et al. (1980) determined an empirical relationship between Ka and the volumetric water content (θv) which is nearly independent of soil type, density, temperature and salinity. As the water content increases, t increases (i.e. Ka increases); thus a relationship exists as follows:

$$\theta u = f(Ka)$$

Patterson and Smith (1981) argued that Topp's relationship could be applied as a first approximation to the determination of the volumetric unfrozen water content, θ_u, of frozen soils, since the low frequency dielectric constant of ice (3.2) is close to the value for soil minerals (3 to 4). This hypothesis was confirmed by combined TDR and dilatometer measurements (Patterson and Smith 1981, Smith and Patterson 1984), although results were restricted to temperatures above -3 or -4°C, because dilatometer errors are cumulative with cooling. These authors expected, however, that the relationship for frozen soils would depart from the Topp curve at lower temperatures (lower unfrozen water contents and higher ice contents), as ice is "substituted" for air (K=1) in the soil. In addition, Topp et al. (1980) passed their calibration curve through a value of 80 for bulk water, although their maximum soil water contents were below about 50%. Our measurment system yielded a value for the apparent dielectric constant of water which was consistently lower than 80 (about 72). Thus a departure from the Topp curve is also to be expected at high soil water contents.

These considerations pointed to the need for a calibration dedicated to frozen soils, and the NMR technique provides a suitable reference method for this. The TDR/NMR approach offers considerable scope for comparison, accomodating a wide range of soil types and temperature (unfrozen water content).

Further details concerning the NMR and TDR methods can be found in Tice et al. (1978, 1982, 1984), Topp et al. (1980) and Patterson and Smith (1981).

EXPERIMENTAL METHODS

Separate specimens, from the same prepared soil sample, were subjected to NMR and TDR measurements. All the samples were saturated with distilled water to the point of dilatancy, to facilitate filling of the TDR coaxial specimen container. The containers were from 12 to 20 cm long, and 1.35 cm in diameter. The specimen volume was from 16 to 25 cm^3, and the specimen mass was typically 25 to 40 g. The NMR specimens were compacted in test tubes to the same density as in the TDR tests; the specimen was typically 12 to 15 g.

The two sets of specimens were placed in precision temperature baths containing an ethylene glycol-water mixture. They were cooled to between -10°C to -15°C and progressively warmed to 0°C. NMR and TDR readings were taken at predetermined temperatures on the warming cycle. Readings were also taken for the completely thawed specimens. The TDR traces were recorded on a Hewlett-Packard 7045B X-Y recorder; this allowed the travel time to be determined to within ± 1%.

Anderson and Tice (1972) demonstrated that the unfrozen water content of frozen soils depends not only on the temperature but also the specific surface area (SSA, m^2 g^{-1}) of the soil. Thus for the present experiments, a variety of

soils (16 in number) was selected which covered a representative range in specific surface area (Table 1). An additional 8 soils (Table 1), which were not part of the calibration set, were also tested as a means of verifying the relationship determined for Ka versus θu.

TABLE 1

Soil	SSA	w	θv	ρ_d
West Lebanon gravel	15	.240	.375	1.563
Castor sandy loam	-	.261	.385	1.475
Manchester silt	18	.303	.432	1.425
Kaolinite (KGa-1)	23	.396	.500	1.262
Chena Hot Springs silt	40	.284	.414	1.456
Leda clay	58	.333	.470	1.412
Mayo silty clay	-	.378	.495	1.311
Morin clay	60	.362	.472	1.305
O'Brien clay	61	.381	.515	1.352
Goodrich clay	68	.362	.467	1.289
Tuto clay	78	.733	.674	0.920
Sweden VFB 478 clay	113	.491	.548	1.116
Suffield silty clay	148	.340	.455	1.339
Frederick clay	159	.426	.492	1.209
Ellsworth clay	184	.372	.450	1.210
Regina clay	291	.595	.572	0.961
Lanzhou silt	34	.220	.364	1.655
Niagara silt	37	.222	.365	1.645
Norway LE-1 clay	52	.337	.477	1.415
Kaolinite #7	72	.570	.587	1.029
Athena silt loam	83	.352	.456	1.296
Sweden CTH 201 clay	106	.508	.573	1.128
Hectorite	419	1.023	.722	0.706
Volcanic ash	474	.668	.602	0.901

RESULTS

With the dielectric constant at each temperature determined by the pulse reflection method (TDR), and the unfrozen water content determined by the NMR technique, a typical set of results is shown in Figure 2. Correlation of the dielectric constant with the amount of unfrozen water present was achieved by matching the two curves on the basis of temperature. Since the NMR values are on a gravimetric basis (wu), the volumetric unfrozen water content in the TDR specimen at any temperature was obtained by multiplying the NMR value by the dry soil density, ρ_d, of the TDR specimen:

$$\theta u = \rho_d . wu / \rho_w$$

where ρ_w is the density of water. The gravimetric moisture content and soil density were determined at the completion of each test.

The comparison procedure resulted in a plot of Ka versus θu (Figure 2c), providing a calibration of the TDR technique for unfrozen water content determination. In this case, a cubic polynomial fits the data with a standard error (S.E.) of 0.5% in θu, which is indicative of the accuracy possible with the TDR technique when it is calibrated for a single soil. However, the real purpose of the experiment was to examine the dependence or otherwise of the TDR technique on soil type.

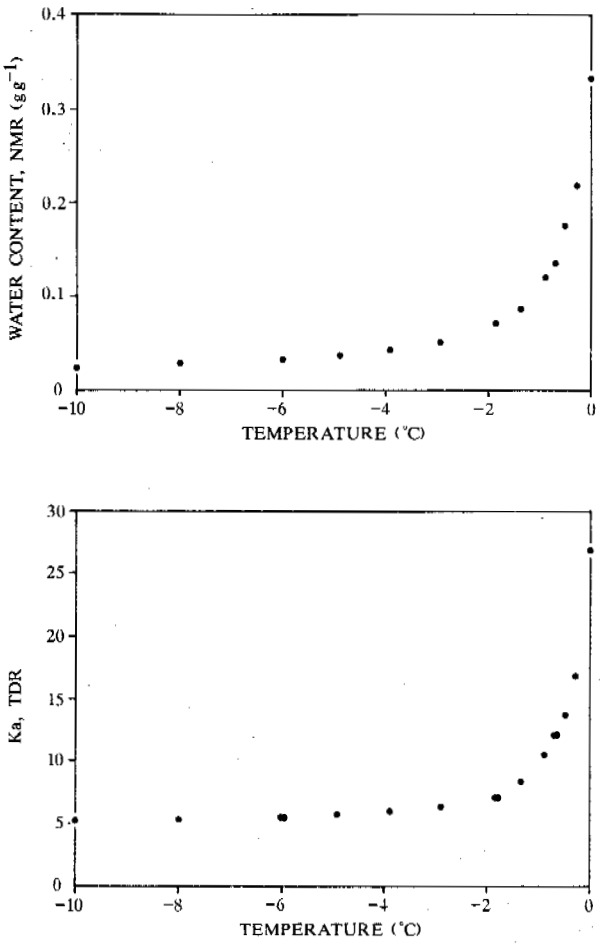

Figure 2. Water content, NMR and TDR relationships for Leda clay.

To this end, the comparison procedure was repeated for all 16 test soils, yielding over 220 points for Ka versus θu (Figure 3). A third-degree polynomial fitted to these data gives the following general relationship:

$$\theta u = -1.458E\text{-}1 + 3.868E\text{-}2Ka - 8.502E\text{-}4Ka^2 + 9.920E\text{-}6Ka^3 \quad (4)$$

with a standard error of estimate of ± 1.55% in θu.

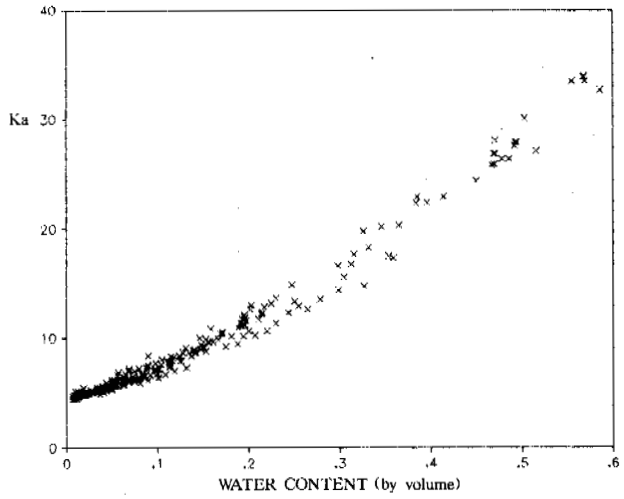

Figure 3. Water content versus Ka (data for all soils).

The main reason for the scatter in Figure 3 is a subtle but apparent dependency on the texture (specific surface area?) of the soil. This is demonstrated in Figure 4, where data for three soils are illustrated; it is evident, that for a given water content, the apparent dielectric constant is lower the finer the soil. It is suggested that, since the dielectric constant of adsorbed water must be (much) lower than bulk water, the large proportion of adsorbed water in materials with high SSA lowers the overall dielectric constant (travel time) of the soil system at a given water content.

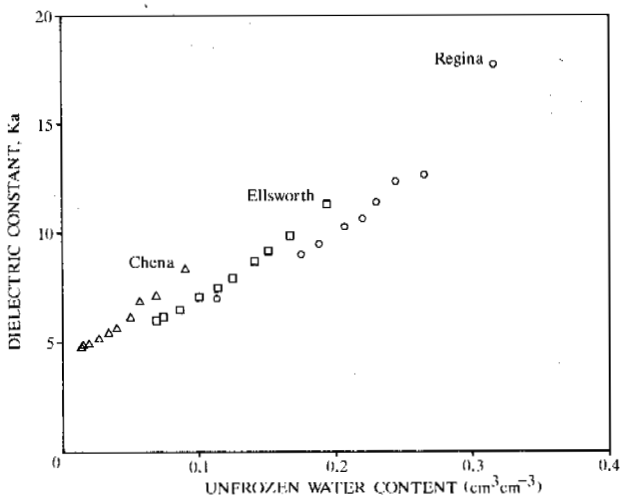

Figure 4. Water content versus Ka (data for three soils).

For most practical purposes, however, equation (4), which does not distinguish between soil types, may be used to determine θu from the measurement of Ka, to within ± 0.03 $m^3\ m^{-3}$ (2 S.E.'s) with a 95% level of confidence. As a verification of this relationship, a further 8 soils, which did not form part of the calibration set, were tested. These results form an independent assessment of equation (4) for determining the unfrozen water content of soils. The comparison, which is shown in Figure 5, indicates that the relationship given by (4) is generally satisfactory, and that the TDR method could be used without regard to soil type. The slight bias noticeable in Figure 5 is probably due to the phenomenon illustrated in Figure 4.

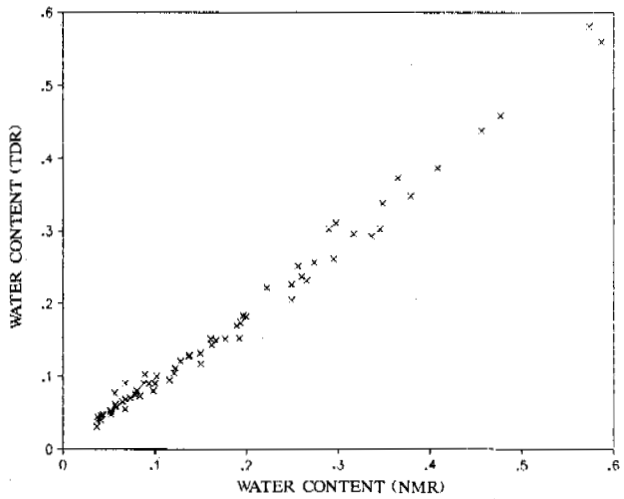

Figure 5. Results of verification tests of equation (4).

The most notable departure from the general relationship described in equation (4) was observed in the results for two colloidal soils - Hectorite (SSA = 419) and volcanic ash (SSA = 474). In both cases, the unfrozen water contents determined via equation (4) were consistently lower than the NMR data, except very near 0°C (Figure 6). These soils presumably represent an extreme case of the phenomenon discussed above. Further investigations of this are warranted since it appears at present that a separate calibration would be necessary when using the TDR with such materials.

Errors

In light of the comments in the introductory section of the paper about Ka and K, it appears that use of a measurement system which is distinctly different from that used in the calibration experiments - such as TDR equipment with faster rise times, or the use of very short transmission lines - could lead to a larger error than suggested by equation (4).

Finally, one other possible source of error derives from observed variations in the time-base calibration of different 1502 TDR units. Using different machines, we have measured Ka values for distilled water ranging from 69 to 77. The unit which was used in determining

equation (4) gave a value of 72 for water at 20°C, in a 20 cm coaxial line (50Ω in air). If one were to obtain a value of 75, say, on another unit, then all measurements using that unit should be reduced by 4% in order to use equation (4) without additional error.

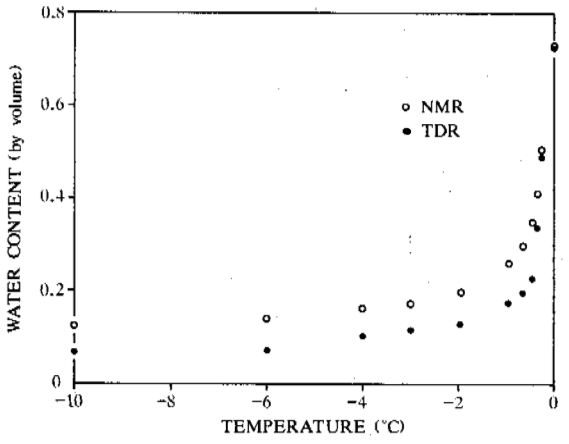

Figure 6. Comparison of NMR and TDR data for Hectorite.

CONCLUSIONS

It appears that the TDR technique, which is appropriate for use in undisturbed soil conditions (in the field or laboratory), does not require special calibration for most practical purposes. Overall, the results obtained from the combined NMR and TDR experiments, based on 22 soils covering a wide range of SSA's likely to be normally encountered in the field, yield a relationship between apparent dielectric constant and unfrozen water content that is only very slightly dependent on soil type. Use of this relationship implies a likely error of about ± 0.03 cm^3 cm^{-3} in water content with the TDR method. The only notable exceptions observed so far are the results for two soils with very high SSA's, for which the predicted water contents were markedly lower than the corresponding NMR values.

ACKNOWLEDGEMENTS

The research was carried out while the senior author was on sabbatical leave at the Cold Regions Research and Engineering Laboratory. He wishes to thank colleagues and staff there for their help and hospitality and he is especially grateful to Mr.Bill Quinn who was instrumental in arranging his stay. The authors also wish to thank D.E.Patterson and an anonymous reviewer for their constructive comments on the paper.

REFERENCES

Anderson, D.M. and A.R.Tice. 1972. Predicting unfrozen water contents in frozen soils from surface area measurements. Highway Research Record, 393:12-18.

Arcone, S.A. and R.Wills. 1986. A numerical study of dielectric measurements using single reflection time-domain reflectometry. J.Phys.E:Sci.Instrumen. 19: 448-454.

Delaney, A.J. and S.A.Arcone. 1984. Dielectric measurements of frozen silt using time-domain reflectometry. Cold Reg.Sci. Technol. 9: 39-46.

Hoekstra, P. and A.Delaney. 1974. Dielectric properties of soils at UHF and microwave frequencies. J.Geophys.Res. 79(11): 1699-1708.

Patterson, D.E. and M.W.Smith. 1981. The measurement of unfrozen water content by time domain reflectometry: Results from laboratory tests. Can.Geotech.J. 18: 131-144.

Smith, M.W. and D.E.Patterson. 1984. Determining the unfrozen water content in soils by time domain reflectometry. Atmosphere-Ocean 22(2): 261-263.

Tice, A.R., C.M.Burrous and D.M.Anderson. 1978. Determination of unfrozen water in frozen soil by pulsed nuclear magnetic resonance. Third Inter.Conf.Permafrost, Edmonton, Alberta, Volume 1: 149-155.

Tice, A.R., J.L.Oliphant, Y.Nakano and T.F.Jenkins. 1982. Relationship between the ice and unfrozen water phases in frozen soil as determined by pulsed nuclear magnetic resonance and physical desorption data. U.S.Cold Regions Research and Engineering Laboratory, Report 82-15, 8p.

Tice, A.R. and J.L.Oliphant. 1984. Effects of magnetic particles on the unfrozen water content of frozen soil determined by nuclear magnetic resonance. Soil Science, 138(1): 63-73.

Topp, G.C., J.L.Davis and A.P.Annan. 1980. Electromagnetic determination of soil water content: Measurements in coaxial transmission lines. Water Resources Res. 16: 574-582.

GENESIS OF ARCTIC BROWN SOILS (PERGELIC CRYOCHREPT) IN SVALBARD

F.C. Ugolini and R.S. Sletten

College of Forest Resources, University of Washington, Seattle, WA 98195, USA

SYNOPSIS Soil solution studies were undertaken to understand the mechanism responsible for formation of the Bw horizon in Arctic Brown soils of Svalbard. It was assumed that the Bw horizon forms either (1) by illuviation of Fe, Al, and organics or, (2) by *in situ* weathering of iron bearing minerals. Field collections of soil solutions were made at Kongsfjord and Wijdefjord, Spitsbergen and on Nordaustlandet. Coarse textured soils generally younger than 12,000 years were investigated since soils with finer texture are subjected to cryoturbation and horizonation is perturbed. Solution data show only low levels of metal illuviation, occurring primarily as Al-organic complexes. Illuviation does not account for the B horizon formation, therefore weathering *in situ* appears to be the most important mechanism. Factors such as eolian input of carbonates, soil pH, and precipitation mediate the formation of these soils.

INTRODUCTION

Pedogenic gradients following an idealized northern transect from the tundra zone into the polar desert have been described by Tedrow *et al.* (1958), Tedrow (1977), and Ugolini (1986). The weakening of soil-forming processes involving chemical reactions parallels the decrease in precipitation, temperature, and biological activity. In contrast, soil-forming processes leading to an accumulation of soluble salts and carbonates increase. Pedogenic differences along an idealized northern transect are better expressed in the well-drained soils than in poorly drained ones (Tedrow 1977). Of concern in this presentation is the Arctic Brown (Pergelic Cryochrept), a well-drained soil of circumpolar distribution (Ugolini 1965) that coexists with Podzols (Spodosols) in the low Arctic and with Polar Desert soils (Entisols) in the high Arctic.

The prominent feature of Arctic Brown soils is a brown Bw horizon, not containing illuvial clay, but hypothesized to contain illuvial Fe, Al, and organics (Tedrow 1977). An important question in arctic pedology today is whether the Bw horizon is a vestigial remnant of previous milder climates or a manifestation of the present environment. Furthermore, if it represents a modern process, is the Bw horizon formed by metals illuviated from the upper horizons or is it formed by *in situ* weathering? Illuviation requires a percolative moisture regimen and either the presence of soluble organics capable of chelating and mobilizing the iron and aluminum, or strong acid conditions. Current research in Svalbard has shown that while percolative events are rare because of the low precipitation, percolation does occur during spring thaw. Production of proton donors including organic acids, however, is not sufficient to acidify the soil and to cause solubilization of Fe and Al. But while the soil pH approaches neutrality, significant levels of dissolved organic carbon (DOC) occur in the soil solution. These soluble organics are not evidently effective chelators for Fe and Al and it is believed that *in situ* weathering involving oxidation and hydrolytic reactions dominate the formation of the Bw horizons.

There have been relatively few studies of the soils of Svalbard, and most of these have focused on descriptive aspects (Szerszeń 1965, Fedoroff 1966, Forman and Miller 1984, Mann *et al.* 1986). Other studies have emphasized cryogenic aspects of soil development (Smith 1956, van Vliet-Lanoe 1983). In addition, most of these investigations have been limited to more accessible areas and therefore represent only a small portion of Svalbard. In view of these considerations, we have elected to examine B horizon formation on northwest and northcentral Spitsbergen and Nordaustlandet. In this inquiry we have used a dual approach: the traditional analysis of soil samples, and the dynamic pedological approach where soil solutions are collected *in situ* and analyzed (Ugolini *et al.* 1982).

STUDY AREA DESCRIPTION

Soils in three locations on the Svalbard Archipelago were studied in detail (Fig. 1). The Arrigetch site (79°01'N, 12°01'E) and the Ryper site (79°07'N, 16°15'E) are located on the island of Spitsbergen in Kongsfjord and Wijdefjord, respectively. The Brånevatnet site (79°48'N, 22°03'E) is located on the island of Nordaustlandet near Brånevatnet Lake.

Soils at the Arrigetch site, 14 m above sea level (asl), have developed in reworked beach deposits consisting primarily of limestone, marble, mica schist, and quartzite (Hjelle and

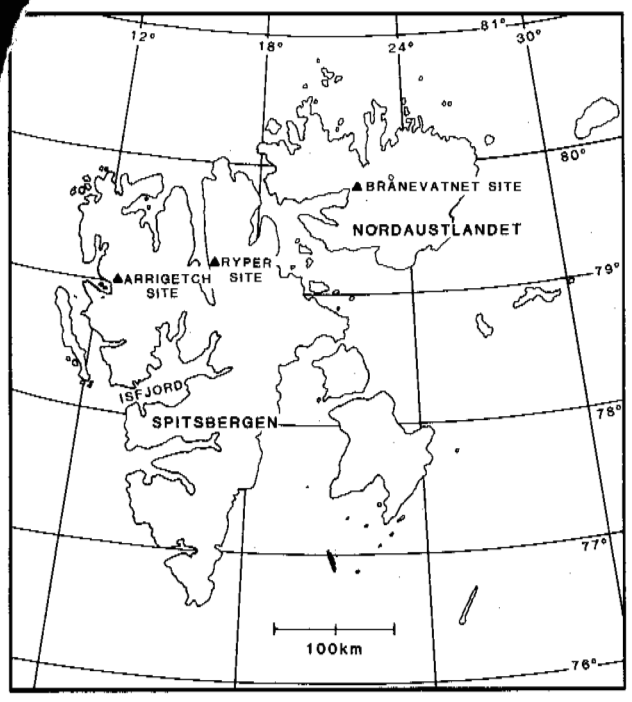

FIGURE 1 Location of study sites on Svalbard.

Lauritzen 1982). Plants cover 60-90% of the surface with 25% *Cassiope tetragona* and 30% lichen-*Cetraria delisei*, being the major species. Other common plants include *Salix polaris*, *Polygonum viviparum*, *Dryas octopetala*, and *Cetraria islandica* (Mann *et al.* 1986). Periglacial features are manifested as large scale polygons. The site was selected inside the perimeter of an apparently inactive polygon. Climatic information for the Kongsfjord area is available from the Ny-Ålesund station where the mean annual air temperature is -5.8°C, with a July mean air temperature of +5.2°C, and the mean annual precipitation is 385 mm, primarily as snow (Steffensen 1982).

The Ryper site is located on a stable bench at 75 m asl with primary bedrock lithology consisting of gneiss and amphibolite (Hjelle and Lauritzen 1982). Plant cover is continuous with 50% moss/lichen, 20% *Carex* species, 20% *Dryas octopetala*, and 10% *Salix polaris* and *Saxifraga oppositifolia*. Little climatic information is available for this area, but late spring snow cover, prior to the 1979 thaw, reveals snowfall to be about 1/3 of that in Ny-Ålesund, or about 120 mm water equivalent (Khodakov 1985). Field observation and temperature comparisons during the summers of 1984, 1985, and 1986 suggest temperatures similar to Ny-Ålesund.

The Brånevatnet site is located on a stable delta deposit above Brånevatnet Lake at 50 m asl. Granite and shale clasts are the major lithologies (Lauritzen and Ohta 1984) and comprise the predominant parent material for the soils. The plant cover is continuous and consists of 50% *Carex* species, 40% white and black crustose and foliose lichens, 10% *Polygonum viviparum*, with less abundant *Salix polaris*, *Saxifraga oppositifolia*, and *Papaver dahlianum*. Climatic information is also scant for this area. Published isotherms (Vowinckel and Orvig 1970) suggest a temperature several degrees cooler than Ny-Ålesund, which agrees with summer field observation during 1985 and 1986. Precipitation at Brånevatnet is probably less than at Ny-Ålesund, but higher than Ryper.

METHODS

Soil solutions were collected during the spring and summers of 1983 through 1986. Lysimeters were emplaced in the soil under the genetic horizons, usually the year before the collections of soil solutions were made. They consist of mullite discs, with 12-15 µm pores, mounted in a nylon base and connected to polyethylene collection bottles with Teflon tubing. The portable vacuum system (Ugolini *et al.* 1982) was maintained at 10 kPa (0.1 atmospheres) vacuum. The soil solutions were filtered in the field with 0.22 µm disposable filters, and pH and alkalinity were measured. Subsamples were acidified to pH 2 and later analyzed for Fe, Al, and the major cations with a Jarrel-Ash model 96-955 (Fisher Scientific Co., Waltham, MA) inductively coupled argon plasma spectrophotometer (ICP). Another subsample was preserved with CH_3CN for subsequent analysis of the inorganic anions, Cl^-, NO_3^-, HPO_4^{2-}, and SO_4^{2-}, with a Dionex model 2010 (Dionex Corp., Sunnyvale, CA) ion chromatograph. Total inorganic carbon (TIC) and dissolved organic carbon (DOC) was determined with an OI 700 (OI Corp., College Station, TX) carbon analyzer.

All soil samples were air dried and sieved at 2 mm. Organic carbon was estimated by the modified Walkley-Black procedure (Allison 1965). Total N and P were extracted by Li_2SO_4 digest (Parkinson and Allen 1975). Iron and Al were extracted with citrate-buffered dithionite (Jackson 1969) and with 0.1 N sodium-pyrophosphate (McKeague 1978), and assayed on the ICP. Soil pH was determined on a 1:2 soil:H_2O suspension. Particle size was determined by sieving of the sand and silt fractions. The silt and clay fractions in the <50 µm fraction were dispersed in 0.5% sodium hexametaphosphate and measured with a SediGraph 5000D (Micromeritics Instrument Co., Norcross, GA) particle size analyzer.

RESULTS AND DISCUSSION

The three selected profiles are approximately arranged along a climatic transect, Arrigetch being wetter and milder than Brånevatnet, whereas Ryper is the driest with similar temperatures to Arrigetch. Descriptions of a representative profile from each of the three sites are given in Table I. All of these soils display O, A, B, C horizonation and are morphologically similar. According to Soil Taxonomy

TABLE I Soil description of Arrigetch, Ryper, and Brånevatnet sites.

Site/ Horizon	Depth	Color	Texture	Structure	Consistence
ARRIGETCH					
Oi/Oe	2-0 cm				
A	0-7	5YR3/1	lsa	2tpl	fr,np,ns
Bw1	7-27	10YR4/3	lsa	1thpl	fr,np,ns
Bw2	27-44	10YR4/3-4	sa	1thpl	fr,np,ns
Ck	44-60+	V	sa	0	lo,np,ns
RYPER					
Oi/Oe	5-0 cm				
A	0-12	7.5YR3/2	sil	2pl	fr,ss,sp
Bw1	12-30	10YR4/2-3V	gr lsa	1cr	fr,np,ns
Bw2	30-57	10YR5/2-3V	gr lsa	1cr	fr,np,ns
BC	57-69+	V	gr sa	0	lo,np,ns
BRÅNEVATNET					
Oi/Oe	4-0 cm				
A	0-7	5YR3/2	sil	1tpl	lo,ss,sp
Bw1	7-20	10YR4/2	gr sa	1thpl	lo,ss,sp
Bw2	20-38	10YR4/2V	sa	0	lo,np,ns
C	38-70+	10YR4/1V	gr sa	0	lo,np,ns

Key: Color: V-variegated
Texture: si-silty,sa-sand or sandy, gr-gravelly, l-loam or loamy
Consistance: fr-friable, lo-loose, s-slightly, n-non, p-plastic, s-sticky
Structure: 0-none, 1-weak, 2-medium, t-thin, th-thick, pl-platy, cr-crumb

(Soil Survey Staff 1975), these soils would be classified as Pergelic Cryochrepts. The coarse texture in the B and C horizon of these soils allows periodic percolation to occur and the development of stable profiles. Each of these soils is 9,000 to 12,000 years old (Mann *et al.* 1986, Sletten (unpublished data)). In older soils, with a greater accumulation of fine particles, cryoturbation typically occurs and the horizonation is disrupted. Common to all three sites, although less prominent at Arrigetch, is the presence of a surficial accumulation of fines (<0.05mm, Fig. 2). These fines are believed to be eolian deposits and to be an important source of detrital carbonates. This input is probably crucial to the overall genesis of these soils.

Soil reaction is slightly acid at the surface to mildly alkaline in the lower horizons (Fig. 3) indicating a low leaching potential and a low level of acidification. Carbon, nitrogen and phosphorus are restricted to the O and A horizons where most of the biological activity occurs (Table II). Weathering is most intense in surficial mineral horizons and the highest levels of extractable Fe_d and Al_d occur in the A horizon of the Ryper and Brånevatnet profiles. The Arrigetch profile displays the highest Fe_d and Al_d in the Bw1 horizon suggesting that illuviation may have occurred. The actual levels of extractable Fe and Al are low and only a fraction of these metals is organically complexed as determined by pyrophosphate extraction (Fig. 3). Organically bound metals tend to prevail at the surface. The apparent

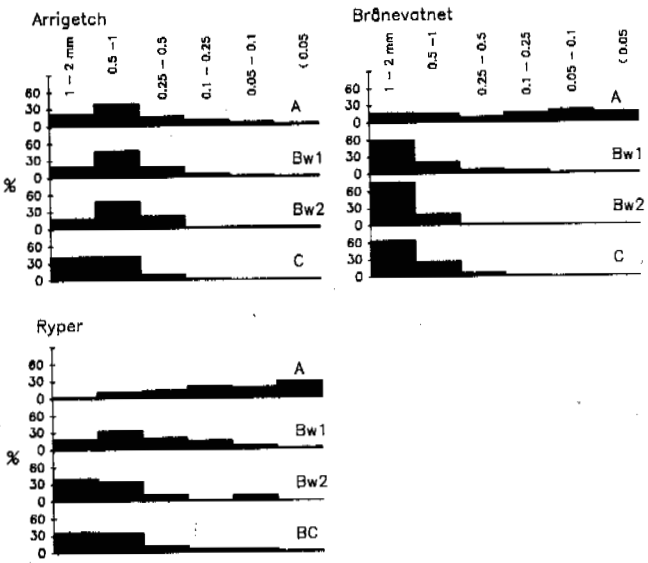

FIGURE 2 Particle size distribution in the three profiles.

increase in the B at Arrigetch, especially Fe_d, may reflect the wetter and milder conditions

TABLE II Soil Carbon, Nitrogen, and Phosphorous.

Site/ Horizon	%C	%N	%P
ARRIGETCH			
O	-	0.87	0.13
A	7.4	0.14	0.04
Bw1	1.0	0.06	0.04
Bw2	0.5	0.03	0.04
C	<0.1	0.01	0.03
RYPER			
A	11.1	0.67	0.17
Bw1	1.1	0.07	0.08
Bw2	0.3	0.02	0.11
BC	0.3	0.03	0.10
BRÅNEVATNET			
A	28.4	0.70	0.14
Bw1	0.5	0.11	0.02
Bw2	0.3	0.08	0.04
C	0.1	0.05	0.04

than at the other sites. Low eolian input of carbonates may also favor weathering of the minerals in the B horizon.

Solution composition for all three profiles shows that Fe and Al are only slightly soluble and are migrating minimally through the profile (Fig. 4). A factor unfavorable for solubilization of Fe and Al is the near neutrality of pH at the surface (Fig. 4). Calcium is the prevailing cation and is expected to stabilize the organics decreasing their chelating capacity. The input of calcareous loess will continue to maintain high pH and Ca levels. Nevertheless, Al in solution does show a high correlation with DOC in spite of the low Al concentrations (r^2 = 0.98 for Arrigetch, 0.87 for Ryper, and 0.92 for Brånevatnet). From the solution data, it appears that illuviation is minimal, but some movement of Al and DOC is taking place.

Support for the *in situ* weathering mechanism may be obtained by estimating the rate of Fe illuviated into the B horizon. The Arrigetch site is used as an example. Iron flux into the B horizon is estimated from the Fe concentration in soil solutions entering and leaving the Bw horizons. It is assumed that present day values have existed since the beginning of soil formation 10,000 BP and also it is assumed that only half of the precipitation percolates through the soil. This calculation suggests that 0.025 Kg of Fe has been illuviated into 1 m^2 of B horizon. Actual values of Fe accumulated in the Bw1 and Bw2 horizons, estimated from Fe_d and corrected for C horizon levels, is 1.4 Kg. While admittedly this is an approximate calculation, the 50 times difference between these values does suggest that *in situ* weathering is primarily responsible for these Bw horizons. It

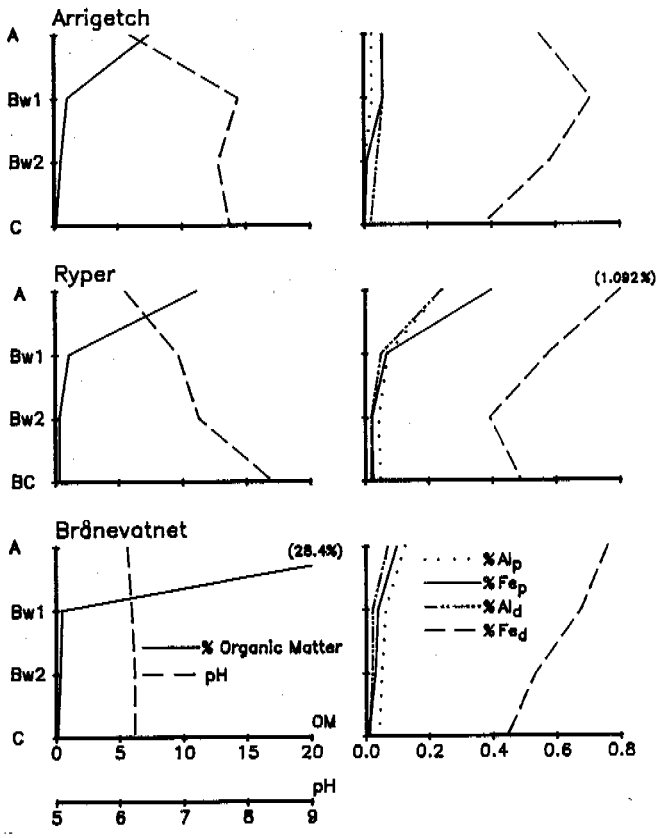

FIGURE 3 Soil chemistry. Distribution of pH, organic matter, and pyrophosphate and dithionite extractable Fe and Al for each profile.

is not expected that past climate variations could account for these differences.

While the nature of the DOC is not known, it appears to be mobile through all the profiles and to progressively decreases with depth in the mineral soil (Fig. 4). An approximate assessment of the nature of the organic carbon can be obtained assuming that the charge deficit displayed by the soil solutions is entirely due to the organics (Fig. 5). This deficit, obtained by subtracting the summation of anions from the cations, provides an estimate in ueq L^{-1} per mg of DOC. The O horizon at Arrigetch contributes 4.3 ueq L^{-1} mgC^{-1} of negative charge, whereas the A horizon provides 10 ueq L^{-1} mgC^{-1}. These values correspond to 19 atoms of carbon for each dissociated functional group in the O horizon, and 8 C atoms in the A horizon. The high carbon to functional group ratio in the O horizon indicates low charged compounds, assumed to be undecomposed plant remains. On the other hand, the same ratio for the A horizon is 8, indicating a similarity to high molecular weight compounds such as fulvic acid that contain approximately 7 carbon atoms

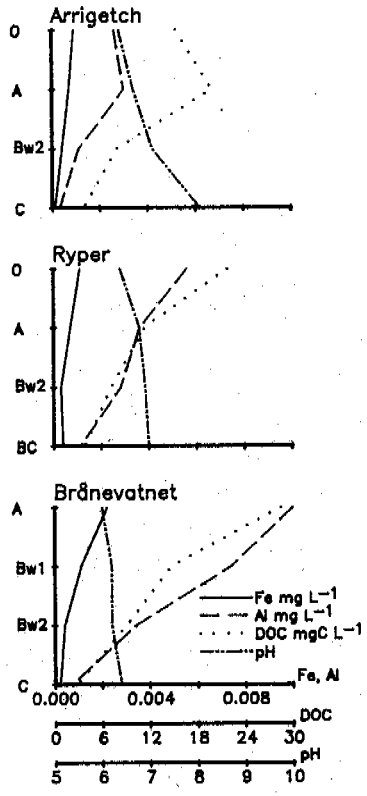

FIGURE 4 Soil solution chemistry. Concentrations of Al, Fe, DOC, and pH values are shown for soil solutions collected via tension lysimeters.

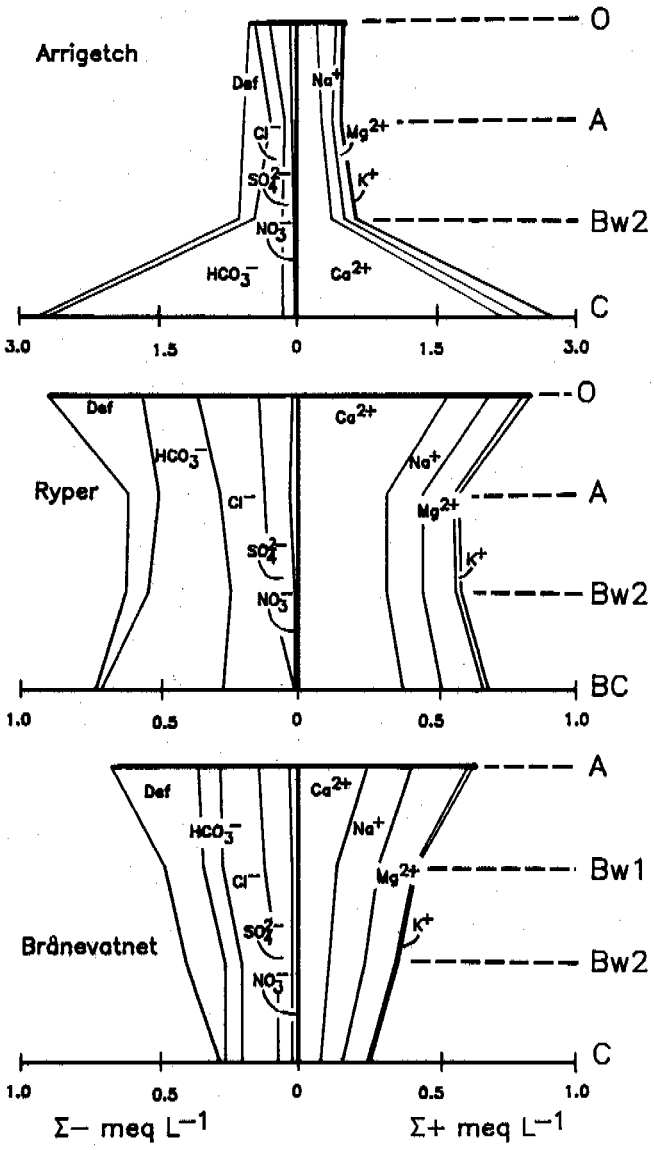

FIGURE 5 Detailed charge balance of soil solutions.

for each carboxylic group (Thurman 1986). The same calculations for the Ryper and Brånevatnet soils show that more highly charged compounds in the leachates from the O horizon, similar to the Arrigetch A horizon.

With respect to other ions in solution (Fig. 5), the following order exists for the cations at Arrigetch and Ryper: Ca > Mg = Na > K; at Brånevatnet the sequence shows: Ca = Mg = Na > K. Among the anions, dissociated organic acids prevail in the A of Brånevatnet, and in the O of Ryper. Bicarbonate dominates the anions of the Ryper and Arrigetch sites, while chloride is the second most abundant in all the three profiles. Marine air masses and loess input are considered responsible for Cl^- and HCO_3^- inputs, the same explanation is offered for the $SO4^{2-}$. Nitrate is present only at low levels.

The charge balances in Fig. 5 appear to be related to eolian input. At Ryper and Brånevatnet the accumulation of surficial fines is a source of salts and detrital carbonates. Low leaching prevents the dissolution of these components through the soil. At Arrigetch the influx of eolian fines is low (Fig. 2) and no detrital CO_3^{2-} are added. Consequently the soil solution is less concentrated. A milder and wetter climate at Arrigetch than at the other sites may also be responsible for more intense weathering and leaching at the surface. Textural differences and the presence or absence of an ice-cemented frost table may account for differences in the solution concentration at the three sites. At Brånevatnet the gravelly texture of the B and C horizons reduces the residence time of the solutions and therefore dissolution of carbonates may be less.

Consequently, the concentrations of HCO_3^- and Ca^{2+} are low (Fig. 5).

CONCLUSIONS

In summary, the solid and soil solution analyses of the three Arctic Brown soils (Pergelic Cryochrepts) from Svalbard tend to depict a situation dominated by *in situ* weathering rather than illuviation for the formation of the Bw horizon. The Arrigetch profile shows, nevertheless, some evidence of metal illuviation in the Bw. Evidence for illuviation in the other profiles is less clear. The chemical behavior of Fe and Al provide some insight into the illuvial process. While Fe only shows a monotonous decrease with depth in all the profiles, Al at the Arrigetch site shows a weak eluvial-illuvial trend. The coincidence of the curves depicting the Al and the organic carbon in solution suggests that the Al is organically complexed. Thus, it appears that Al may be useful for indicating pedological trends at high latitudes. Leaching potential is low but percolation does occur during the spring thaw period.

A factor of great importance in the genesis of these soils is the influence of calcareous loess. In addition to providing fines at the surface, the introduction of detrital carbonates will maintain an alkaline pH. Acidification of the soil is thus attenuated. Relating the pedogenesis of the Arctic Brown soils of Svalbard to the soils of northern Alaska, the former appear less developed (Ugolini 1986). Furthermore, whereas in northern Alaska at 69° latitude N, the Arctic Browns coexist with Podzols (Brown and Tedrow 1964), such association was not found at 79°N in Svalbard.

ACKNOWLEDGEMENTS

This research was conducted under National Science Foundation Grant DPP-8303624. We acknowledge discussions with Dr. D. Mann. We are grateful for logistical assistance from K. Sneltvedt of Kings Bay Coal Company, and O. Rogne and T. Siggerud of the Norwegian Polar Institute. We thank M. Lahde for skillfully typing the manuscript.

REFERENCES

Allison, L.E. (1965) Organic Carbon, In: *Methods of Soil Analysis*. C.A. Black, ed. Publication number 9 in the series: Agronomy, American Society of Agronomy, Inc., Madison, Wisconsin, 1572 pp.

Brown, J. and Tedrow, J.C.F. (1964) Soils of the Northern Brooks Range, Alaska: 4. Well-drained soils of the glaciated valleys. *Soil Science* 95:187-195.

Fedoroff, N. (1966) Les sols du Spitsberg occidental. *Spitsberg, 1964 et premieres observations 1965*, Centre National de Recherche Scientifique, R.C.P. 42, Audin-Editeur, Lyon, p. 111-228.

Forman, S.L. and Miller, G.H. (1984) Time-dependent soil morphologies and pedogenic processes on raised beaches, Brøggerhalvøya, Spitsbergen, Svalbard Archipelago. *Arctic and Alpine Research* 16; 381-394.

Hjelle, A. and Lauritzen, Ø. (1982) Geological map of Svalbard (1:500,000), Spitsbergen, northern part. *Norsk Polarinstitutt Skrifter* 154C, 15 pp. and map.

Jackson, M.L. (1969) *Soil Chemical Analysis - Advanced Course*. Department of Soil Science, University of Wisconsin, Madison, Wisconsin, 895 pp.

Khodakov, V.G. (1985) Snow Cover. In: *Glaciology of Spitsbergen*, V.M. Kotljakov, editor, USSR Academy of Sciences, p. 35-46.

Lauritzen, Ø. and Ohta, Y. (1984) Geological map of Svalbard (1:500,000), Nordaustlandet. *Norsk Polarinstitutt Skrifter* 154D, 15 pp. and map.

Mann, D.H., Sletten, R.S., and Ugolini, F.C. (1986) Soil development at Kongsfjord, Spitsbergen. *Polar Research* 4; 1-16.

McKeague, J.A. (1978) *Manual on Soil Sampling and Methods of Analysis, 2nd Edition*, J.A. McKeague, editor, Canadian Society of Soil Sciences, 212 pp.

Parkinson, J.A. and Allen, S.E. (1975) A wet oxidation procedure suitable for the determination of nitrogen and mineral nutrients in biological material. *Communications in Soil Science and Plant Analysis* 6; 1-11.

Smith, J. (1956) Some moving soils in Spitsbergen. *Journal of Soil Science* 7; 10-21.

Soil Survey Staff (1975) *Soil Taxonomy, Agricultural Handbook 436*. Soil Conservation Service, USDA, Washington, D.C., 754 pp.

Steffensen, E.L. (1982) The climate at Norwegian arctic stations. *Klima* 5, 44 pp.

Szerszeń, L. (1965) Studia nad glebami strefy klimatu arktycznego na przykładzie południowo-zachodniego Spitsbergenu, *Zeszyty Naukowe Wyższej Szkoły Rolniczej We Wrocławiu Rolnictwo* 19; 39-82.

Tedrow, J.C.F. (1977) *Soils of the Polar Landscapes*. Rutgers University Press, New Brunswick, New Jersey, 638 pp.

Tedrow, J.C.F., Drew, J.V., Hill, D.E., and Douglas, L.A. (1958) Major genetic soils of the arctic slope of Alaska. *Journal of Soil Science* 9; 35-45.

Thurman, E.M. (1986) *Organic Geochemistry of Natural Waters*. Martinus Nijhoff/Dr. W. Junk Publishers, Dordrecht, Netherlands, 497 pp.

Ugolini, F.C. (1965) The recognition of Arctic Brown soils in northeast Greenland. *Arctic* 18; 49-51.

Ugolini, F.C., Zachara, J.M., and Reanier, R.E. (1982) Dynamics of soil-forming processes in the Arctic. *Proceeding of the Fourth Canadian Permafrost Conference*, Calgary, Alberta, p. 103-115.

Ugolini, F.C. (1986) Pedogenic zonation in the well-drained soils of arctic regions. *Quaternary Research* 26; 100-120.

van Vliet-Lanoe, B. (1983) *Etudes cryopedologiques au sud du Kongsfjord, Svalbard*. Publication Interne du Centre de Geomorphologie du Centre National de la Recherche Scientifique, 39 pp.

Vowinckel, E. and Orvig, S. (1970) The climate of the north polar basin, In: *Climate of the Polar Regions, World Survey of Climatology Volume 14*, S. Orvig, editor, Elsevier Publishing Co., Amsterdam, 370 pp.

OXYGEN ISOTOPIC COMPOSITION OF SOME MASSIVE GROUND ICE LAYERS IN THE NORTH OF WEST SIBERIA

R.A. Vaikmäe[1], V.I. Solomatin[2] and Y.G. Karpov[3]

[1]Institute of Geology ESSR Academy of Sciences, Tallinn, USSR
[2]Moscow State University, Moscow, USSR
[3]Igarka Scientific Research Permafrost Station, Igarka, USSR

SYNOPSIS Massive ground ice layers are widely spread in the north of West Siberia, in the southeastern part of Chuckotka, on Alaska and in Arctic Canada. Their genesis is still a disputable question. In the given study massive ground ice was investigated using the oxygen-isotope method. $\delta^{18}O$ variations together with data on the structure of ice and the interbedded sediments showed that some of the studied layers may have burried glacier origin.

INTRODUCTION

Formations with signs of burried glacier ice are of special interest among the massive ground ice widely spread in the north of West Siberia, in the southeastern part of Chuckotka, on Alaska and in Arctic Canada (Karpov, 1986; Kaplyanskaya, Tarnogradskiy, 1976; Solomatin, 1986; Mackay, 1983). Study of the conditions of their formation and distribution may result in unique information on the palaeoclimatic and palaeocryological conditions of the investigated area. However, the occurrence of burried glacier ice in the permafrost zone was not commonly acknowledged till lately.

Attempts have recently been made to apply isotopic and geochemical methods to the study of ice and interbedded sediments alongside with complex lithological-phacial, stratigraphic, textural and structural approaches (Mackay, 1983; Vaikmäe, Karpov, 1985; Lorrain, Demeur, 1985; Kritsuk et al., 1986). It should at once be pointed out that conclusions about the genesis and palaeo-climatic formation condition of ice layers based merely on isotopic data, are not well grounded in most cases and may lead to erroneous interpretations. For this reason isotopic analysis should be combined with traditional investigation methods.

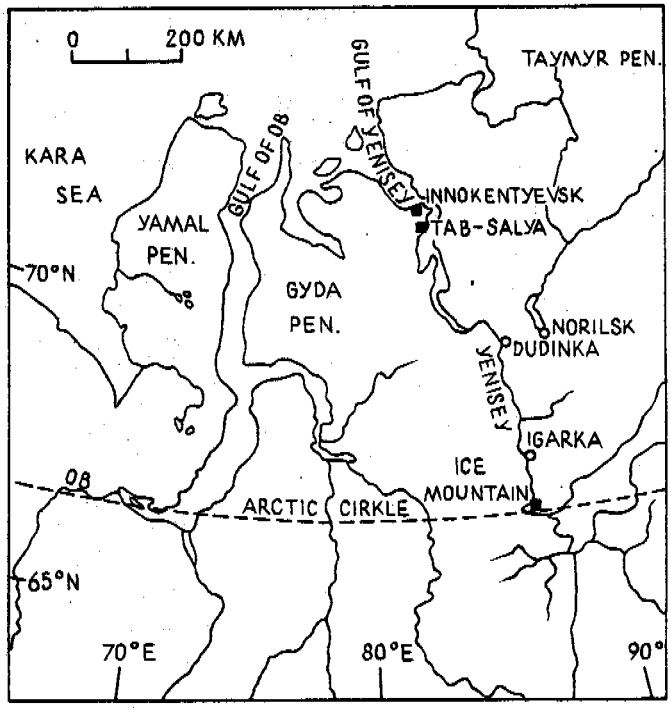

Fig.1 Location Map of the Study Area

LEDYANAYA GORA (ICE MOUNTAIN) SECTION

We first attempted to use the oxygen-isotope method in the study of massive ground ice layers in 1981. One of the most well-known and thoroughly studied ground ice layers - the Ledyanaya Gora (Ice Mountain) on the right bank of the Yenisey river near the Polar Circle served as the study object (Fig. 1). This section was disclosed in 1972 and has constantly been examined by the workers of the Igarka Scientific Research Permafrost Station since 1973. As thorough descriptions of the section have repeatedly been published (Karpov, 1986; Astakhov, 1986; Vtyurin, Glazovskiy, 1986; Solomatin, 1986) we will here only point out its most characteristic features.

The walls of the huge thermocarstic cirque with quickly growing area comprise sediments of a ridge-knob morainic plain (Troitskiy, 1975). In the natural sections of the thermocirque as well as in drill-holes (Karpov, 1986) the thickness of massive ice reaches 40 m. The ice massif is exposed over a

distance of several hundred meters. The roof of the massif in the section is not even, smooth declines and rises extend 10 to 15 meters. The massive ice is covered by a layer of varied composition and facial structure. A one meter thick layer of coarse alluvial sands and shingle beds forms lenses in the immediate contact zone of the massif. Higher up a layer of clayey silty loams with high but variable contents of boulders and shingle is observable. Stratification can be noticed in some intervals. The loams have, in general, an inconstant composition and a complicated structure characteristic of glacial formations. The layer of clayey loams contains local lenses of lacustrine loams with patches of peat. Underneath there is a sharp decline of the roof and the covering deposits, indicating thermocarstic subsidences under the lakes that had formed and later grown over again.

Though the views of investigators as to the genesis of the massive ice in the Ledyanaya Gora section differed greatly at the initial stage of studies, the majority of authors has by now arrived at the conclusion about its burried glacier origin (Karpov, 1986; Grosswald et al., 1985; Solomatin, 1986; Vtyurin, Glazovskiy, 1986). The main argument in favour of the glacial genesis of the ice massif are the following (Solomatin, 1986):

(1) The ice of the massif is intensely dislocated. Folds, shifts varying in extent are clearly observable. At the same time no corresponding disturbances occur in the covering deposits. This contradicts the theory of interground development of the massive ice.

(2) Facial changes in the covering deposits are observable directly above the ice roof, depending upon the relief of the latter. This refers to the accumulation of sediments on an already existing surface of ice body and excludes the possibility of interground ice genesis.

(3) Abundance in ice of fragmental material up to great boulders (1.5 m in diameter), shingles, the layered distribution of sandy and clayey elements are characteristic of morainic glacier ice.

(4) The structure of ice characterizes its dynamic-metamorphistic petrogenesis typical of glacier ice.

(5) The interground origin of the massif is also contradicted by the absence of such forms in the relief which would correspond to the growth of an ice massif in permafrost.

First samples for oxygen-isotope analysis from this layer were taken from the cores of drill-holes 12 and 13. The oxygen isotopic composition of these cores varied from -17,9‰ to -22,1‰ with the mean $\delta^{18}O$ value being -21,2‰ (Vaikmäe, Karpov, 1985). Later the scientists of the Institute of Geography USSR Academy of Sciences carried out isotopic analysis of separate samples from the massive ice and arrived at the mean value $\delta^{18}O$ = = -20,4‰ (Vtjurin, Glazovskiy, 1986). To get a better idea of the limits and distribution of $\delta^{18}O$ values in the massive ice layer of Ledyanaya Gora we determined the isotopic composition of ice in the cores drilled in the last years in various parts of the ice massif. In some cases the drill-holes reached the basic icesaturated layers which were also sampled. Table 1 gives a short survey of the obtained results. The mean $\delta^{18}O$ of all drill-holes is -20,4‰, at which the means of separate drill-holes vary in rather small limits (see Table 1). At the same time, the vertical profiles display comparatively big and irregular $\delta^{18}O$ variations, which is a strong argument against the hypothesis about the segregational formation mechanism of Ledyanaya Gora. Laboratory and natural experiments (Michel, 1982; Youzel, Souches, 1982; Lorrain, Demeur, 1985) have shown that segregational ice

TABLE 1

Isotopic Composition of the Ledyanaya Gora Massive Ice Layer

No. of drill - hole	Depth of drill-hole in ice m	Range of $\delta^{18}O$ variations ‰	Mean $\delta^{18}O$ value ‰	$\delta^{18}O$ in ice of underlying ice - saturated soil ‰
12	7.9	-17.9 to -22.1	-20.8	-
13	3.3	-19.1 to -21.9	-21.1	-
15	6.9	-12.4 to -21.8	-18.7	-
16	5.8	-19.6 to -21.3	-20.4	-
17	9.8	-18.9 to -22.5	-20.7	-18.6
18	5.3	-15.2 to -23.5	-19.7	-19.3
24	12.0	-20.6 to -21.8	-21.0	-20.0
25	9.5	-20.1 to -21.6	-20.7	-20.1

formation under equilibrium conditions is accompanied by isotopic fractionation. As a result, the ice formed is isotopically by about 3‰ heavier than the initial water. Isotopic section profiles of segregated ice display gradual changes in either direction. Sharp leaps with a value higher than 3‰, characteristic of the isotopic profiles of the Ledyanaya Gora section, are absent as a rule (Michel, 1982).

As known, seasonal isotopic variations in ice are smoothed in the course of time due to diffusion (Johnson, 1977). In view of this the limits of $\delta^{18}O$ variations indicated in the Table 1 may at first seem too big even for glacier ice. However, it should be born in mind that judging by the structure of the ice massif we here deal with the bottom part of the glacier in which separate layers from various parts of the glacier are mixed. In addition to this, processes of melting-freezing often take place in bottom ice, influencing the initial isotopic composition. So there is no reason to expect any strict regularities in the isotopic profiles of such ice bodies.

It should be stressed, that the character and range of $\delta^{18}O$ variations in the massive ice of Ledyanaya Gora are rather similar to the analogous parameters of massive ice detected on the Canadian Arctic Archipelago by Lorrain and Demeur, which they consider having glacier origin (Lorrain, Demeur, 1985).

TAB-SALYA SECTION

A section with low 20-25-meter surface (the Tab-Salya section) covering a massive layer of ground ice with visible thickness of about 5 m is located some 25 km south the Dorofeyevskiy cape on the left bank of the Yenisey bay.

The main part of the layer goes under the water boundary and drilling data indicate that the thickness of ice at places exceeds 15 m (Karpov, 1986). A peculiarity of this massive layer of ground ice is its paragenesis with the covering lake-glacial varved clays with a thickness of up to 10 m. The formation conditions of varved clays make it questionable whether any kind of burried ice may have preserved under them. However, in some current areas of glaciation aufeis lakes occur in fields of dead ice. Formation of small lake basins in the course of deglaciation and quick freezing of accumulated precipitations after soil drainage is possible in closed depressions on the glacier surface under high-arctic conditions. Studies of interbedded sediments and the structure of the ice massif itself led one of the authors of this article to the conclusion about its injectional origin (Karpov, 1986). We carried out isotopic analysis of ice samples obtained from two drill-holes in different parts of the studied layer. The amplitude of $\delta^{18}O$ variations in the vertical profiles of both drill-holes do not exceed 2,4‰, the mean $\delta^{18}O$ value of the ice is -17,7‰. Though the range of $\delta^{18}O$ variations in the massive ice of Tab-Salya is a bit smaller than in the ice of Ledyanaya Gora, it is still bigger than is typical of injected ice (Michel, 1982; Mackay, 1983). Isotopic profiles of injected ice have a smoothed character, i.e. no sharp leaps occur in the isotopic composition. Variations in the isotopic composition of Tab-Salya may be explained by the segregational mechanism of ice formation. As the segregation process is accompanied by fractionation, the isotopic composition of segregated ice, as a rule, differs from that of the initial water by 1-3‰ depending on the rate of freezing. So the massive ice of Tab-Salya may be assumed to have formed from water with an isotopic composition of about -14,5 to -16,5‰. However, neither the peculiarities of the isotopic composition nor the structure of the layer in Tab-Salya exclude the possibility of burried glacier genesis. The somewhat heavier isotopic composition with a smaller range of fluctuation in Tab-Salya as compared to the Ledyanaya Gora may be explained by more intensive recristallization processes in ice. As a lake basin was forming above the ice, the temperature of recristallization must have increased up to valued near 0°C. Interground growth of the layer is contradicted by the absence of corresponding forms of ground heave in the relief. Deformations by heaving have neither been found in varved clays. Massive ice streaks wedging from the sheet into the covering deposits have a different nature and most likely result from the injection of water from the melted roof of the ice massif into the covering lake sediments, followed by freezing after the drying up of the basin.

INNOKENTYEVSKOYE SECTIONS

In the summer of 1986 the authors used isotopic sampling methods in the study of numerous, though relatively small fragments of massive ice outlets and ice-soil bodies concealed in the thermocirques of the Gyda bank of the Yenisey bay near the village of Innokentyevsk. Here a ridgelike upland with heights of more than 100 meters approaches the bank. The bank is in general not steep and is formed of numerous thermoterraces, thermocirques of various generations, actively developing and already stable, fresh and overgrown mud slides and taluses. A few ridgelike remains of the initial surface have preserved in the almost incessant field of intensive thermodenudational processes. The upper part contains a one-meter horizon, clearly reduced in thickness, of unsorted cobbleshingle material with variegated filler material, under which lies a layer almost totally formed by well-preserved shells. Such layer evidently reflects the glacier-marine environment of sedimentation. Some thermocirques were disclosed on a 20 to 25 kilometer stretch of this bank and studied by isotopic methods.

Ice massifs and deformations in ice-soil here were first described by V.I.Vtyurin (1966). In 1986 Y.G.Karpov came to the conclusion about the burried glacier origin of the massive ice

studied by him in this region.

The authors of this article obtained unexpected results in the study of the south-most outlet of massive ice. The wall of the thermocirque is in this case situated at the height of 15 meters above the beach. The ice massif is exposed to a stretch of 40 meters. Its thickness fluctuates from 1 to 2 meters. The ice is transparent, containing subhorizontal interlayers enriched in gaseous inclusions. The covering deposits represent lake-bog loams with inclusions of organics. The visible thickness of loams is 6 meters. The contact with the overlying massif is uneven, with pockets and tongues. The ice massif is cut by wedges of vein ice with peaks located at the height of 2 meters above the upper contact of the massif. The multitude of ice wedges cutting the massif leaves no doubt about the burried origin of the latter. In this connection the unusual isotopic composition of ice is of special interest: it appeared to vary from -0,8‰ to -4,8‰ (-7,2‰ in case of one sample). Only marine ice has isotopic characteristics similar to the indicated ones. However, the chemical composition of ice was fresh, with insignificant contents of Cl^- (from 4,6 to 7,3 mg/l). Such association of the isotopic and chemical compositions of ice is unique in the whole study practice known to the authors. Just now only a preliminary conclusion can be drawn that we here deal with a preserved ice raft of freshed marine basin. Metamorphism and recristallization of burried ice may have led to even greater dilution.

The next of the studied thermocirques is situated some kilometers north from the described one. Its escarp is located at the height of 10 meters above the beach. The massif is covered by multicoloured boulder loams with a thickness of about 2 m. Ice-soil with interlayers of pure ice exposed at the height of 3 m from the talus can be observed lower. The ice-soil has a schistose structure and abounds in slightly rounded boulders with maximum diameter of 40 cm. Glacial striation is clearly seen on the boulders. The isotopic composition of the ice-soil as well as of the interlayers of pure ice varies in the small interval from -21,8 to -22,1‰, i.e. it is comparable to the composition of ice in Ledyanaya Gora and even slightly lighter than the latter.

In another thermocirque ice-soil of analogous structure was drilled and three measurings of the isotopic composition were carried out on the core. The obtained values from upwards down run as follows: -20,1‰ ; -17,3‰ ; -11,7‰ .

Ice-soil with interlayers of pure ice pressed in sloping deformations was sampled 4 km north from the village of Innokentyevsk. The ice-soil abounds in unevenly distributed boulders. The isotopic composition ranges from -20,1‰ to -22,1‰ .

Thus, all the sections in the region of the Innokentyevsk village, with the exception of the first described one, are of similar structure and have an isotopic composition of ice-soil ranging in narrow limits, which in general confirms the burried glacier origin. As to the conclusion about the occurrence of freshed marine ice in burried state in one of the sections, this one and only discovery of the authors may only be confirmed by new examples of the kind.

CONCLUCIONS

The performed studies of the oxygen isotope contents and the structure of massive ground ice layers, as well as the composition of interbedded sediments indicated that some of the layers (the Ledyanaya Gora, a part of the Innokentyevsk layers) are evidently of glacier origin. At the same time the isotopic data on the Tab-Salya section and on another part of the Innokentyevsk layers allow to make no definite conclusion about their genesis as yet. More detailed investigations are needed using a wide variety of isotope-geochemical methods together with the study of the geological structure of the entire ice complex.

REFERENCES

Astakhov, V.P. (1986). Geologicheskiye usloviya zahoroneniya pleistotsenovogo lednikovogo lda na Yeniseye. Materialy glyatsiologicheskikh issledovaniy, (55), 72-78, Moskva.

Grosswald, M.G., Vtyurin, B.I., Suhodrovsky, V.A., Shishorina, Zh.G. (1985). Podzemniye ldy Zapadnoy Sibiri: proishozhdeniye i geoekologicheskoye znacheniye. Materialy glyatsiologicheskikh issledovaniy, (54), 145-152, Moskva.

Johnson, S.J. (1977). Stable isotope homogenization of polar firn and ice. In: Isotope and impurities in snow and ice. IAHS publ. (118), 210-219.

Jouzel, J., Souchez, R.A. (1982). Melting--refreezing at the glacier sole and the isotopic composition of the ice. J. of the Glaciology, (98), 28, 35-42.

Kaplyanskaya, F.A., Tarnogradskiy, V.D. (1976). Reliktoviye glecherniye ldy na severe Zapadnoy Sibiri i ih rol v stroyeny raionov pleistotsenovogo oledeneniya kryolitozony. Doklady Ak. Nauk SSSR, (231), 5, 1185-1187.

Karpov, Y.G. (1986). Podzemniye ldy Yeniseyskogo Severa, 134 pp. Nauka, Novosibirsk.

Kritsuk, L.N., Dubikov, G.I., Polyakov, V.A. (1986). Issledovaniye stabilnykh isotopov pri izucheny podzemnykh ldov. Materialy glyatsiologicheskikh issledovaniy, (55), 92-97, Moskva.

Lorrain, R.D., Demeur, P. (1985). Isotopic evidence for relict pleistocene glacier ice on Victoria Island, Canadian Arctic Archipelago. Arctic and Alpine Res., (17), 1, 89-98.

Mackay, J.R. (1983). Oxygen isotope variation in permafrost, Toktoyaktuk Peninsula area, Northwest Territories. Current Res.,

part B, Geol. Survey of Canada paper, 83-1B, 67-74.

Michel, F.A. (1982). Isotope investigations of permafrost waters in Northern Canada. Ph.D. thesis, 424 pp. Waterloo.

Solomatin, V.I. (1986). Petrogenez podzemnykh ldov, 216 pp. Nauka, Novosibirsk.

Troitskiy, S.L. (1975). Sovremenniy antiglyatsializm, 161 pp. Nauka, Novosibirsk.

Vaikmäe, R.A., Karpov, Y.G. (1985). Izucheniye plastovykh zalezhey podzemnogo lda iz razreza "Ledyanaya Gora" v doline Yeniseya izotopno-kislorodnym metodom. Materialy glyatsiologicheskikh issledovaniy, (52), 209-214, Moskva.

Vtyurin, B.I. (1966). Kryogennoye stroeniye chetvertichnykh otlozheniy v nizovyakh Yeniseya. Materialy k nauchno-tekhnicheskoy konferentsy PNIIS, 177-180, Moskva.

Vtyurin, B.I., Glazovskiy, A.F. (1986). Sostav i stroyeniye plastovoy zalezhi podzemnogo lda "Ledyanaya Gora" na Yeniseye. Materialy glyatsiologicheskikh issledovaniy, (55), 35-43, Moskva.

OXYGEN ISOTOPE VARIATIONS IN ICE-WEDGES AND MASSIVE ICE

Yu.K. Vasilchuk[1] and V.T. Trofimov[2]

[1]Research Institute of Engineering Site Investigations, Moscow, USSR
[2]Moscow State University, USSR

SYNOPSIS Results of accurate measurements of content of stable oxygen isotopes in more than 600 samples taken by the authors and in hundreds of samples taken by other explorers from the ice deposits of Western Siberia, Jakutia and Chukotka. The $\delta^{18}O$ content in syngenetic repeated ice-wedges permits to reconstruct permafrost temperatures within a time period of its formation and in an massive ice the mentioned value serves, as a rule, a cryogenetic indicator. In Late Pleistocene and Holocene 14 cold and warm cycles can be distinguished and plotted at isotope diagrams by syngenetic ice wedges of different regions.

Oxygen isotope composition was examined on repeated ice-wedges, texture-forming ice and massive ice at all the territory of a cryolithozone in Northern Asia. The data obtained are interpreted in different manner for different types of ice. Therefore the results and their analysis are given separately.

Sampling of all the ice-wedges was conducted in similar way-mainly vertically near the vein apis. At the first stage of investigations the authors compared the data obtained with the results of horizontal sampling at a proper depth within the veins of different age and established a close proximity of spread in values. This made it possible to estimate representation of vertical sampling. Based on ice age the authors concluded that vertical sampling is much preferable with account of the fact that as a rule, an ice age increases from top to bottom. An available total statistical representation of the results (over 600 analyses by 35 cross-sections) serves a basis to assume that the main characteristics of $\delta^{18}O$ distribution within the repeated ice wedges of different age and different areas of cryolithozone have been already established. The $\delta^{18}O$ variations in the Late Pleistocene ice-wedges by 6-10‰ less, as a rule, than in the Holocene or recent veins. It is proved by the fact that a moment comes quickly enough when the authors can predict an expected spread in $\delta^{18}O$ values for a massif studied anew in the process of investigations in the new regions. So, in Northern Yakutia two thick Late Pleistocene polygonal systems in Zelenyi Mys and outcroppings of Duvannyi Jar were examined by the authors (Vasilchuk, Esikov et al., 1985, Vasilchuk, Vaikmjae et al.,1987). For the ice veins at Zelenyi Mys formed as back as from 37 to 16-18 Kyr (thousand years) B.P. the $\delta^{18}O$ content varied from -34.1 to -25.2‰ and at the strata of Duvannyi Jar dated by a shorter time interval the $\delta^{18}O$ varied from -32.7 to 28.7‰. A range narrow enough of $\delta^{18}O$ variation which is character of the second example, results from a more conservative facial structure dominating during a period of forming strata in Duvannyi Jar. In the process of later investigations of repeated ice veins similar to the strata mentioned above the authors of the present paper assume that the $\delta^{18}O$ variations will be similar to those established before and the values variation will be more intensive in the massives with more variegated facial characteristics. This supposition was corroborated by the research works on a number of regions of Severnaya Yakutia. At a cross-section of massive veins in the Omolon R. mouth the $\delta^{18}O$ varies from -33.8 to -33.1‰; at the middle River - from -32.3 to -28.1‰; in heterogeneous massives at Plakhinskyi Jar - from -34.7 to -29.9‰ and at the edoma of Bykovskyi peninsula - from -34.9 to -29.4‰ (Vasilchuk, 1988). A narrow range from -34.0 to 28.4‰ is also character of repeated ice-wedges of Ayon, which is near Chukotka but from the point of view of Paleocryogenic structure it is "a relative" to the edomas of Northern Yakutia.

Spread in $\delta^{18}O$ values for the inland complex of repeated ice-wedges at Kular is estimated from -32.6 to -30.0‰. As for Anadyr, formation of Late Pleistocene veins is affected as it was expected by the Pacific ocean: at this area the $\delta^{18}O$ varies from -23.4 to -18.6‰ an Atlantic "breath" is felt in composition of ice of Western Siberia. Thick syngenetic repeated ice-wedges of Late Pleistocene in Western Siberia is characterized by $\delta^{18}O$ variation from -24.8 to -21.4‰ in veins 27-20 Kyr B.P. old and from -22.6 to -19.9‰ in veins formed 14-11 Kyr B.P. (Vasilchuk, Trofimov, 1984, 1985; Vasilchuk, Esikov, 1986). Thus, a regular tendency of changes in isotope composition in the direction from west to east: it becomes light in the direction from polygonal vein complexes of Western Siberia to those of Northern Yakutia and then becomes heavy from vein massives of Northern Yakutia to those of Chukotka. The same tendency is character of Holocene vein massives the main

character feature of which is much heavy isotope composition as compare to the Late Pleistocene veins. Such a characteristic can be related to the cryolithozone as a whole. The $\delta^{18}O$ varies from -20.1 to -14.1‰ in Holocene veins of Zapadnaya Sibir. The Holocene ice-wedges of Northern Yakutia were formed under natural conditions of rather steady climate. At this region the $\delta^{18}O$ varies from -27.9 to -23.7‰ (authors' data); in Central Yakutia (Mamontova Gora) - from -29.2 to -22.9‰ and in Chukotka - from -17.0 to -15.8‰. The same tendency and a range of $\delta^{18}O$ variation similar to the Holocene one are also character of the recent elementary syngenetic ice-wedges (not older 100 years) forming at the floodplains and laidas in North Eurasia. In the north Western Sibir the $\delta^{18}O$ varies from -19.5 to -18.3‰ ; in Severnaya Yakutia - from -27.1 to-23.0‰; in Central Yakutia - from -26.3 to -25.1‰ and in Chukotka - from -16.7 to -15.8‰ . Pleistocene ice-wedges within the area under investigation are different in size but their similarity was also established: vertical spread of the biggest veins makes up 10-15 m and more (i.e. it exceeds maximum depth of probable percolation of water along the frost fissures). Identical is a structure of veins bearing rocks which are as a rule, presented by sandy loam abound in organic matters. This particular fact gives a good chance to date strata by residual detritus, roots, wood, bones and as a result to compile reliable oxygen-isotope diagrams of strata dated by syngenetic ice veins.

Just at present some paleocryogenic problems are solved with an aid of an oxygen-isotope analysis. For example, separation of Pleistocene and Holocene repeated ice vein complexes and resulting from this separation the problems on syngenesis of ice veins and depth of vein penetration under conditions of epigenetic ice formation. Thick ice-wedges occurring at the upper cross-section of the third marine terrace of Northern Javsi turned to be isotopically very heavy (from -17.8 to -16.8‰), that is character of Holocene epigenetic veins only; the thick ice-wedges mentioned above were referred by the authors to syngenetic by a number of direct cryolithological character features. A more complicated situation others we faced with was studying of ice veins of Aleshkin terrace (Northern Yakutia) and Mamontova Gora (Central Yakutia). Ice veins (over 5 m thick) character of the first cross-section are considered to be syngenetic and are dated as back as the end of Late Pleistocene based on the ages of vein bearing deposits. It follows from the present research that it is not quite true (Vasilchuk, 1988). Isotope composition of a number of veins in a cross-section of Aleshkin terrace varies from -27.5 to -23.9‰ by $\delta^{18}O$; it varies within the same limits as the $\delta^{18}O$ value for recent and Holocene veins in the strata of floodplains and alassies Kolyma River regions (Vasilchuk, Esikov et al., 1985). Later there were described veins with $\delta^{18}O$ content below -31.0‰ . This fact indicates that vein paragenesis of Aleshkin terrace is a heterochronic formation comprising as Holocene so Late Pleistocene veins. Ice-wedges heavy by $\delta^{18}O$ were formed under permafrost conditions similar to the recent ones and dated as Holocene confirmed by radiocarbone dating - about 6.7 Kyr B.P. by peat hummocks of the upper vein bearing deposits (Vasilchuk, 1988).

A rather difficult problem is to estimate age and genesis of veins occurring within the Mamontova Gora a cross-section of the upper 60-metre terrace of the Aldan River. At this area ice veins reaching 5 m high by vertical occur in the deposits with character features of syngenetic freezing. Datings established by the authors by wood are related to 35-38 Kyr B.P. (Vasilchuk, 1988). But dating by pure autochthonic peat of the ground vein adjacent to the underlying ice vein probably synchronic to the ground vein approximates 4.8 Kyr B.P.; that makes it possible to assume an epigenetic origin of encountered repeated ice-wedges. Oxygen-isotope composition of ice at the area in question is highly heterogeneous. The $\delta^{18}O$ content at the main part of the ice wedge varies from -29.2 to -25.9‰. The $\delta^{18}O$ content varies from -22.7 to-16.5‰ in"tail" veins, which are composed of segregational and ice-wedges formed of swampy water at the first stages of a massive cracking. The "tail" ice is by 2-10‰ heavier than the recent elementary ribs in the syngenetic veins at the flood plain of R. Aldan and overlying Holocene ice is in the main by 1.5-3‰ lighter than the recent ice. A problem of the vein ice nature with $\delta^{18}O$ content below -28‰ is not quite clear. However the only fact that an analysis of oxygen-isotope composition provokes a doubt in syngenetic vein complex on a high terrace of Mamontova Gora is considered to be an impressive argument in favour of wide use of oxygen-isotope analyses when solving Paleocryogenic problems (however isotope composition of textural ice testifies to Holocene age of freezing vein bearing rocks: in this case the $\delta^{18}O$ varies from -17.3 to -15.8‰). Wide spread in $\delta^{18}O$ values of veins in Mamontova Gora makes to think of great variations of isotope composition of Holocene sediments just on the inland areas. The Holocene veins of the coastal areas are very often characterized by the $\delta^{18}O$ values by 3-4‰ exceeding the recent ones and the $\delta^{18}O$ values tend to recent minimum even in the veins of an "optimal" age. The authors have already pointed out that ice-wedges are growing in the Holocene "optimum" not only in the extreme north regions of the low temperature cryolithozone but also in the central parts of Yakutia.

Not all the extreme climatic oscillations can be expressed by an oxygen curve specially it is related to the periods of rather warm climate and permafrost conditions, where the repeated ice veins do not grow at all or they do grow in the most favourable facies. But it should be mentioned that not all the vein systems are affected by abnormally cold weather. Under such conditions a number of veins cannot be formed not only because of reaching their critical dimensions but also under conditions almost unfavourable for facies fissuring (for example, veins can be covered with a layer of water) and if a thick snow cover

be accumulated above the veins in winter.

The authors point out that a comparatively homogeneous geocryological situation can be considered such a situation when variation of $\delta^{18}O$ in ice-wedges do not exceed 2‰ (Vasilchuk, 1987). It relates to a difference in winter mean air temperature by 3°C at least and permits to distinguish accurately oxygen-isotope zones on diagrams (Fig. 1). The most considerable variations of $\delta^{18}O$ are registered at the boundary of Holocene and Pleistocene, that is about 10 thousand years ago. This period is characterized by a range of $\delta^{18}O$ variations reach 10-12‰ at some regions. The isotopically lightest ice has been practically formed in all regions of Subarctic 36-38 Kyr B.P.; almost the same light ice - 38-40 Kyr B.P. Variable conditions character of a period between the dates mentioned we have already said (Vasilchuk, Trofimov, 1984; Vasilchuk, Esikov, 1986; Vasilchuk, 1988). Besides two minimums mentioned,

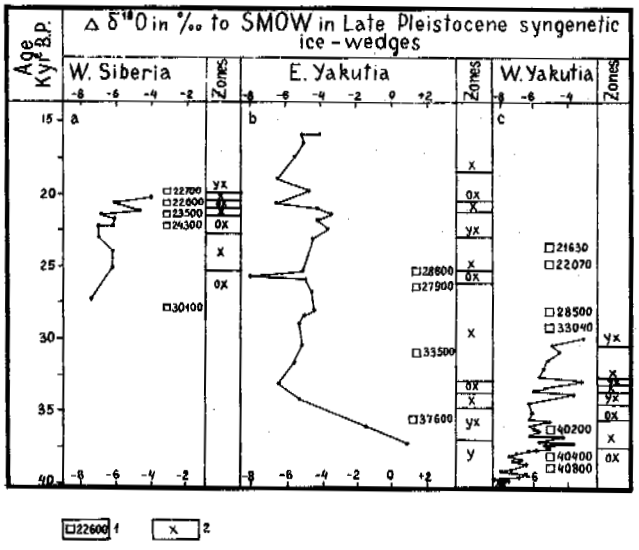

Fig.1. Oxygen-isotope diagrams of repeated ice-wedges of large regions of Pleistocene accumulations in Northern Asia:
a-cross-section at Sejakha;
b-cross-section at Zelenyi Mys;
c-cross-section of Bykovskyi Peninsula
1- ^{14}C-datings of organic matters from ice-wedges bearing strata synchronic to ice;
2-indexing of oxygen-isotope zones;
YT-moderately warm,
Y - moderate (similar to modern),
YX - moderately cold,
X - cold,
OX - very cold.
An ordinate axis shows an ice age obtained by interpolation of radiocarbonic dates; an abscissa axis shows a difference in values of $\delta^{18}O$ in vein samples from mean recent values of $\delta^{18}O$ in elementary ribs in syngenetic ice-wedges on floodplains, laidas and peat beds of the same regions, where a Pleistocene vein is encountered.

dated almost for sure chronologically there are some more extremes, the age relation of which is rather approximate so far. They are first of all, minimums of oxygen -18 content in veins samples approximately dated 19 and 35 Kyr B.P. are less distinctly expressed. Relative maximums are defined as relative due to the fact that the Pleistocene ice-wedges is always lighter than the recent and Holocene ice, they are dated approximately 13,21,31 and 37 Kyr B.P, when $\delta^{18}O$ was by 2-4‰ less the recent average. Differentiated four minimums and four maximums serve a base just at present to distinguish 14 at least isotopic phases (beside the mentioned phases as independent are considered zones with intermediate variances between the extreme values) in Late Pleistocene within a period from 40 to 10 Kyr B.P.

The authors consider an interpretation of $\delta^{18}O$ content to be presently a very difficult and unsynonymous problem in studying a cryogenetic nature of vast massive ice (ice sheet) deposits. This is mainly explained by different genesis of waters which freezing results in formation of deposit forming ice. Total number of samples of massive ice to determine the $\delta^{18}O$ content accounts for about 100 pcs. Oxygen - 18 in ice sheet deposits of Western Siberia varies from -34.3 to -4‰ ; in massive ice of Severnaya Yakutia - from -31.2 to -13.7 ‰ and those of Chukotka - from -22.7 to -13.2‰ . Cryogenetic interpretation comprises as mean values of all the isotope measurements so all the variances. Segregational massive ice sheet deposits are most isotopically heterogeneous: under segregation conditions an isotope fractioning may reach 20‰ ; buried sea ice is heaviest (from -13 to -4‰) and isotopically homogeneous (variances account for 10‰ at least for all the massive ice and 2‰ at least for a massive taken separately). The problem is to find a standard ice sheet, the genesis of which is self-evident. Besides that not all the types of massive ice can be related to recent analogues therefore a method of actualism can be hardly used in practice. Isotopic data should be considered by different types of ice with account of all the existing concepts of massive ice formation as well as its variety. The authors mention that even heavy (from the point of view of isotope composition) sea blocks of ice can be hardly related to ice deposits by a content of heavy isotopes only. This can be explained by the fact that a heavy isotope composition may also originate from active evaporation of small ponds water which percolates downward to the bottom of a season-thawing layer and as a result can form segregated ice comparatively heavy by isotope composition, heavier than synchronic atmospheric precipitation. This can be proved also by oxygen -18 content in mezotexture-forming ice of an edoma of Duvannyi Jar: here the $\delta^{18}O$ averages -24.2 - 22.2‰ (in the same horizons, where $\delta^{18}O$ in ice-wedges averages -32 - 30‰). Enrichment with heavy isotopes is character of all the types of segregated ice formation. Thus, an interlayer of segregated ice formed in the erosion cavity by means of congelation of water of the Kolyma River is characterized by $\delta^{18}O$ equal to -27.0‰, which is lighter than the river

water ($\delta^{18}O$ equals -20.4‰ in September) by over 7‰. Anomalously low content of oxygen heavy isotopes is character of an ice lens (probably of infiltration-segregation genesis) of Late Pleistocene (13-14 Kyr B.P.) occurring in the organic-mineral strata of the first terrace in the mouth of R.Gyda. Here the $\delta^{18}O$ in three samples makes up -30.1; -34.3 and -30.7‰ (Vasilchuk, Esikov, 1986). It should be mentioned that in the same outcrop some more analogous lenses (0.3-0.4 m high, 15-20m long, of a lentile-like form in a cross-section) were discovered near the lens in question, stratigraphically up and down; isotope composition of the lenses turned to be rather heavy and highly variable from -24.3 to -16.2‰. Syngenetic repeated ice-wedges of the cross-section under investigation are characterized by the $\delta^{18}O$ variances in 16 samples be 2.7‰ in the interval -22.6 + -19.9‰ (Vasilchuk, Esikov, 1986). Consequently, atmospheric precipitation during a period of strata formation were stable enough by the content of oxygen heavy isotopes (the climate was rather severe as compare to the modern). It should be noted that a number of explorers and first of all the Canadian colleagues are quite optimistic from our point of view (sometimes even too much) when estimating a role of massive ice and mezotexture-forming ice as paleoindicators (Mackay, 1983; Michel, 1983). The authors suppose that an approach to the massive ice as a paleoclimatic indicator should be very careful.

Massive ice can be considered an indicator of climatic situation within a time period of accumulation of water feeding an ice sheet only in case if the latter differs from the recent ice by an isotope composition keeping a rather great distance as by vertical so by horizontal.

At present a problem of paleotemperature reconstructions to estimate stable isotopes in syngenetic repeated ice-wedges can be solved in a unique and positive manner. Cryogenic research in deposit-forming ice requires a whole complex of analytical investigations in parallel with isotope estimation but this does not eliminate an importance of revealing the distribution of isotope composition in the mentioned ice. Expansion of research works in the both directions permit to interpret in the nearest future a great number of cryolithological problems insoluble in the past.

REFERENCES

Mackay, J.R. (1983). Oxygen isotope variations in permafrost. Tuktoyaktuk Peninsula area, Northwest Territories. Geological Survey of Canada. Paper 83-1B. 67-74.

Michel, F.A. (1983). Isotope variations in permafrost waters along the dempster Highway pipeline corridor. Proceedings Fourth International Conference. National Academy Press. Washington. D.C. 843-848.

Vasilchuk, Yu.K. (1987). Problemy correlyacii paleoclimatitcheskikh sobytii po isotopno-kislorodnym diagrammam povtorno-zhilnykh ldov (The problems of correlation in case of palaeoclimatic events on the basis of oxygen isotope diagrams of reformed ice wedges). Novye dannye po geohronologii chetvertichnogo perioda. (New Data in Quaternary Geochronology). Moscow, Nauka. P.136-143.

Vasilchuk, Yu.K. (1988). Paleomerzlotnaja interpretatsiia izotopno-kislorodnogo sostawa pozdnepleistocenovykh i holocenovykh povtorno-zhilnykh ldov Yakutii (Paleogeocryological interpretation oxygen isotope composition of Late Pleistocene and Holocene reformed ice-wedges of Yakutia). Doklady AN SSSR. T.298. N 2. 425-429.

Vasilchuk, Yu.K., Esikov,A.D. (1986). Izotopno-kislorodnyi sostav syngeneticheskikh povtorno-zhilnykh ldov (Oxygen isotope composition of syngenetic secondary ice veins (analytical data, problems of paleoclimatic reconstructions). Bull. Moskovskogo Obshchestva ispytateley prirody. Otdel Geol. T.61. N 5. 107-119.

Vasilchuk,Yu.K., Esikov,A.D. et al. (1985). Novye dannye po soderzhaniyu stabilnykh isotopov kisloroda v syngeneticheskikh povtorno-zhilnykh ldach pozdnepleistocenovogo vozrasta Husoviy r. Kolymy (New data on stable oxygen isotope content in Late Pleistocene syngenetic reformed ice-wedges in lower reaches of the Kolyma River). Doklady AN SSSR. T.281. N 4. 904-907.

Vasilchuk, Yu.K., Trofimov, V.T. (1984). Izotopno-kislorodnaya diagramma povtorno-zhilnykh ldov Zapadnoi Sibiri eyo radiologicheskiy vozrast i paleogeokryologicheskaya interpretatsiia (Isotopic-oxygen diagram of reformed ice wedges of West Siberia, its radiological age and paleogeocryological interpretation). Doklady AN SSSR. T.275. N 2. 425-428.

Vasilchuk, Yu.K., Trofimov, V.T. (1985). Osobennosti formirovaniya mnogoletnemyorzlykh tolshch severa Zapadnoy Sibiri v Karginskuyu i Sartanskyu epochi pozdnego pleistozena (Formations features of permafrost sediments of North of Western Siberia during Karginskyi and Sartanskyi interval of Late Pleistocene.) Razvitie cryolitozony Evrazii v verchnem Caynozoe. Moscow. Nauka. P.67-81.

Vasilchuk, Yu.K., Vaikmjae,R.A. et al. (1987). Izotopiya, palinologiya i godrochimiya povtornozhilnykh ldov organo-mineralnogo kompleksa Duvanniy Yar. (Isotopic, palynological and hydrochemical data on organic and mineral ice-wedge complex of Duvanny Yar). Doklady AN SSSR. T.292. N 5. 1207-1211.

THERMODYNAMIC AND MECHANICAL CONDITIONS WITHIN FROZEN SOILS AND THEIR EFFECTS

P.J. Williams

Geotechnical Science Laboratories, Carleton University, Ottawa, K1S 5B6, Canada

SYNOPSIS Recent theoretical and experimental studies of the stress states and movements of the ice and water in soil pores help to explain the microstructural characteristics of soils that have been frozen. Such studies also help explain the unique creep and deformation characteristics of freezing soils, and the origin of certain solifluction phenomena.

INTRODUCTION

This paper analyses recent theoretical and experimental studies of frost heave and examines their significance in various natural situations. In addition to the heave effect, the thermodynamic and mechanical processes occurring in freezing soils are important for the strength and long-term deformation behaviour (on slopes, for example) and to the understanding of micromorphological and pedological characteristics.

In the simplest view, frost heave is the expansion of the soil due to ice which forms by accumulation of water drawn to the freezing zone from adjacent unfrozen material. Exactly where most of the accumulation occurs is debated (e.g. O'Neill and Miller 1985), but it is highly significant that water coexists with ice in the frozen soil (fig. 1). Thus freezing and thawing occur within frozen soil.

The dependence of the unfrozen water content on temperature and soil type is well-established. There is also general agreement (even though still argument about detail) that the appropriate form of the Clausius-Clapeyron relation accounts for the presence of the water at 'below-freezing' temperatures. The relation implies the existence of stresses which must influence the behaviour of the frozen soil.

Clausius-Clapeyron relation

The Clausius-Clapeyron relation is fundamental and has many applications in natural science. From it is derived the equation for the well-known change of freezing point of water as a function of pressure:

$$\frac{dT}{dP} = \frac{(V_w - V_i)T}{L} \qquad (1)$$

where T = temperature, K, P = pressure, V_w, V_i are the specific volumes of water and ice respectively, and L the latent heat of fusion.

Equation 1 does not, however, explain the existence of the unfrozen water in soils. But if we assume the ice in the soil has a different, higher, pressure than the water, a different form of the Clausius-Clapeyron relation applies (Edlefsen and Anderson 1943):

$$dT = \frac{(dP_w V_w - dP_i V_i)T}{L} \qquad (2)$$

The relevance of this equation has been confirmed by experimental and theoretical studies. Water is pulled towards the freezing zone, while the accumulating ice

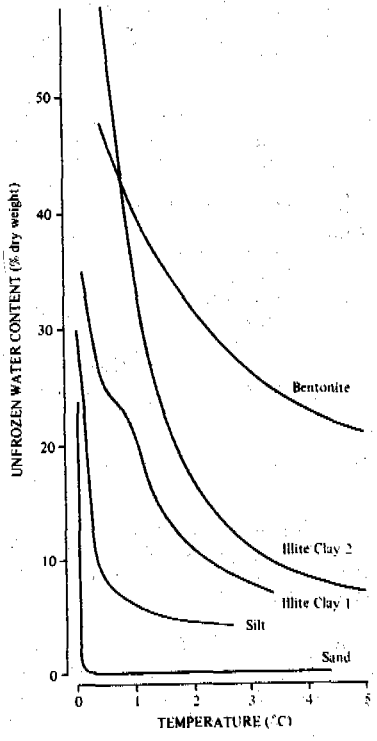

Fig. 1 Amount of water remaining unfrozen at temperatures below 0°C, various soils.

expands the soil and heaves it, so that, obviously, the pressure of the water must be lowered while that of the ice is elevated. The magnitude of the difference in pressure, $P_i - P_w$, is greater the lower the temperature (Koopmans and Miller 1966, Williams 1967). As water is progressively changed to ice, the pressure difference increases because of the physical circumstances of the water. Initially the unfrozen water partially fills the soil capillaries but when the amount is less it is tightly adsorbed onto soil particles. Capillarity and adsorption are responsible for the presence of the unfrozen water. Strictly speaking, the 'pressure' of such water may not be exactly similar to 'pressure' as ordinarily understood, but the water behaves as though it is.

The dependence of the difference $P_i - P_w$ on temperature suggests the likelihood of a gradient of water pressure within the frozen soil in association with a temperature gradient. Equation 2 can also be satisfied by a gradient (in the opposite direction) in the ice pressure.

Continuing frost heave

For many years it was tacitly assumed that the ice layers or lenses formed as the ground froze initially. One lens at the boundary between the frozen and unfrozen soil (the frost line) would form, to be followed by another as the boundary moved down with the penetration of the frost. But if there is a continuity in the water right into the frozen layer, it becomes probable that some formation of lenses takes place within the frozen layer. The heave that results is often called secondary frost heave, although Smith and Patterson, 1988 have proposed 'initial' and 'continuing' (for secondary) frost heave - and this terminology will be followed.

There is difference of opinion over the extent of this heave. Some authors (Konrad and Morgenstern, 1980) believe an ice lens form exclusively in a narrow frozen fringe, between the frost line and the immediately previously formed lens. Others believe continuing frost heave occurs even at temperatures as low as -4°C or -5°C with significant migration of water (Parmuzina 1980). There is experimental evidence of growth of ice lenses one behind another (Ohrai and Yamamoto 1985) and field measurements by Mackay (1983) show continuing heave to occur over quite thick layers of soil.

The uncertainty over this important matter is largely due to the inherent difficulties of measurement. Mackay (1983) developed a telescopic tube device for field studies. A development of this procedure (Mackay and Leslie 1987), used by the Geotechnical Science Laboratories, involves magnetic rings buried at specified intervals around a vertical access tube in the ground (Geotechnical Science Laboratories 1986). The position of each ring is precisely located with a special probe (fig. 2). An increasing distance between successive rings (e.g. between 2 and 3, or 1 and 2) when frozen in represents strains due to continuing frost heave.

Observations of this kind, made in a controlled environment facility, where conditions resemble those in nature (particularly with regard to temperature gradients), show continuing heave occurring over layers of more than 40 cm, which is clearly due to migration of water into and within the layers. (Geotechnical Science Laboratories, 1988).

Ice pressures in frozen soil

Usually some part of the difference $P_i - P_w$ is due to an increase in the ice pressure, as must be the case if frost heave occurs and overburden or other resistance is overcome.

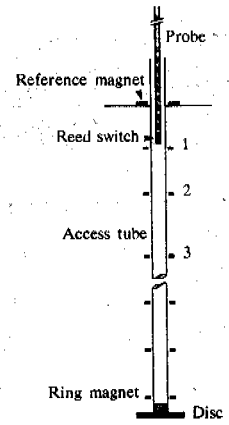

Fig. 2 Device for observation of displacement of magnetic rings ('ring magnets') in frozen soil (from Geotechnical Science Laboratories, 1988).

If ice lenses enlarge within frozen ground they must develop considerable pressure to pry apart the frozen soil. There are a number of reports in the literature of what appear to be such pressures (Mackay 1980, Pissart 1972, Tsytovich 1975), although experimental measurement is, again, difficult. In the vicinity of the measurements of continuing frost heave described above, pressure cells of two types have been used, Glotzl cells roughly the size of a hand, and modified Petur cells about the size of a finger. Both work on a hydraulic principle with an internal valve opening when a controlled pressure balances the pressure of the surroundings. These cells have shown large, sharp pressure increases to 100 kPa or more, as the frost line passes (Geotechnical Science Laboratories 1986). The pressures rise to a maximum fairly soon after the cell has become frozen in, and then fall slowly (fig. 3).

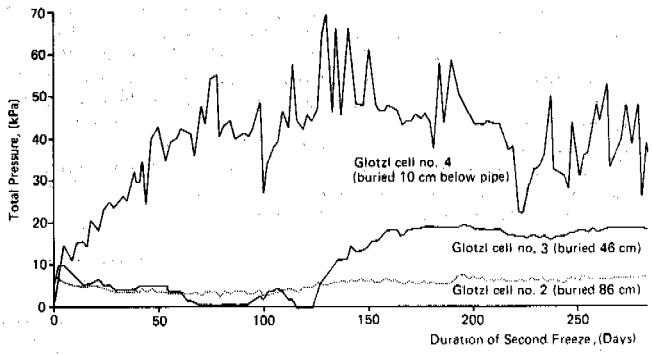

Fig. 3 Pressures below a chilled pipeline. Freezing of the silt occurred after a few days at cell 4 and after approximately 125 days at cell 3. The ground remained unfrozen around the deepest cell (2). The overburden pressures acting on each cell would be 1 kPa approx. (cell 4), 1.6 kPa (cell 3) and 2.4 kPa (cell 2). The high pressures observed must be due to freezing and the resistance of the frozen ground.

An experiment on a much smaller scale has been developed which allows measurement of pressures within small samples. The principle is shown in fig. 4 and further details are given in Williams and Wood (1985) and Wood and Williams (1985). Two pressure microtransducers, each covered by a small bulb of grease in a rubber bladder, are located a short distance apart in a sample whose temperature conditions are controlled by thermo- electric cooling modules at each end. An additional

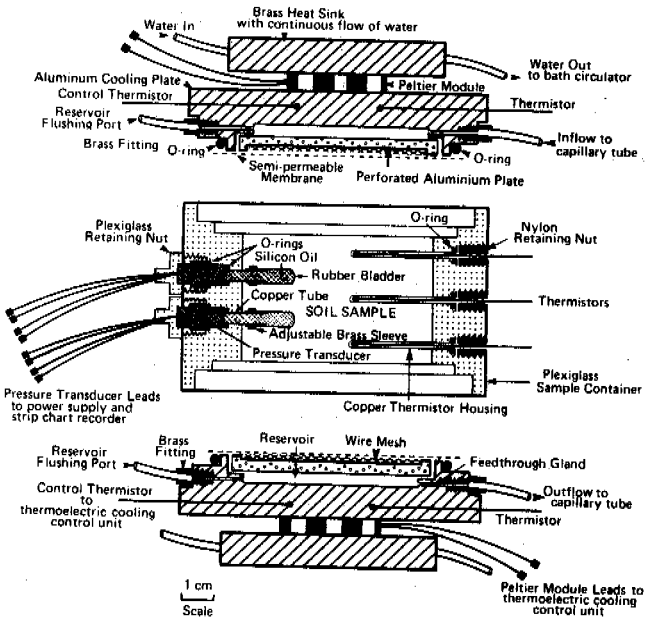

Fig. 4 Cell for frozen soil sample, with provision for access of water and for measurement of pressures at two points in the sample ('exploded' cross-section) - from Wood and Williams, 1985.

feature is a reservoir at each end separated from the sample by a fine-pored dialysis membrane. The reservoirs can be filled with an osmotic solution or supercooled water and give a source or sink for water leaving or entering the sample.

Somewhat compressible silty soils containing some clay and sand, show large pressure gradients in association with temperature gradients. A typical result is shown in fig. 5. A uniform temperature gradient was established in the first 36 hours. During this period there was a sharp rise in pressure associated with expansion as much of the water in the sample froze rapidly. Subsequently the pressure at the colder position remained fairly constant while that at the warmer slowly fell. Water flowing out of the sample (as, initially, at the warm end) is represented by a positive value, that flowing into the sample by a negative value.

The temperature gradient in these tests is precisely controlled, and is an order of magnitude steeper than generally occurs in the ground. The pressures in the ice at the two measuring points in these soils become approximately equal to those predicted by the Clausius-Clapeyron equation (2) for the temperature at each point, if it is assumed the water pressure is atmospheric. Because the two reservoirs contain water, at atmospheric pressure, continuous with that in contact with the ice, this is reasonable. The experiment draws attention to the importance of the resistance of frozen soil to the growth of an ice lens within it. The pressure of the growing ice is dictated by the mechanical properties and eventual creep and stress relaxation of the frozen soil around it. If, as a result of creep, the ice pressure falls, so must the water pressure (to satisfy equation 2). A hydraulic gradient is established in the water, and the movement of water along this gradient will nurture the lens. Thus one arrives at the conclusion that the rate of continuing frost heave (ice lens growth) is controlled by rheological properties, that is, the yielding of surrounding material.

The experiment just described is quite reproducible although the pattern of pressure development varies with type of soil and with the temperature gradient. Using similar soils, three operators working independently and at different times in our laboratories have obtained similar results. More than twenty experiments using compressible soils, and extending over thousands of hours have been carried out. If the temperature is changed there is an initial sharp change of pressure. If the temperature gradient is reversed, the pressure differential eventually reverses to match the new direction (fig. 6).

An important element in the experiment is the grease-filled bladder associated with the transducer. The metal diaphragm of the microtransducer, if exposed to the soil directly, might respond to the stress of a single pointed particle pressed against it, or the microtransducer's rigidity might affect the readings. The bladder is believed to provide an effective sensor activated by the accumulation of minute amounts of ice adjacent to it.

Frozen sands give different results to silts. The maximum pressures observed are smaller (L-K. Lundin, personal communication) and the pressure gradients less. There is some increase in pressure observed as the frost line moves through the sample. But only a few hours after the steady-state temperature gradient is estab-

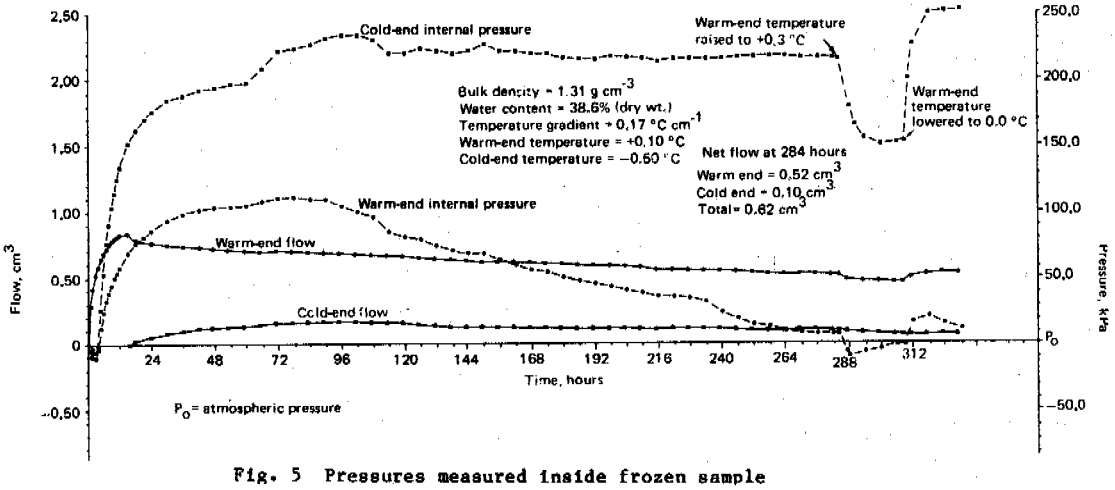

Fig. 5 Pressures measured inside frozen sample and flows of water into and out of sample (from Wood and Williams, 1985).

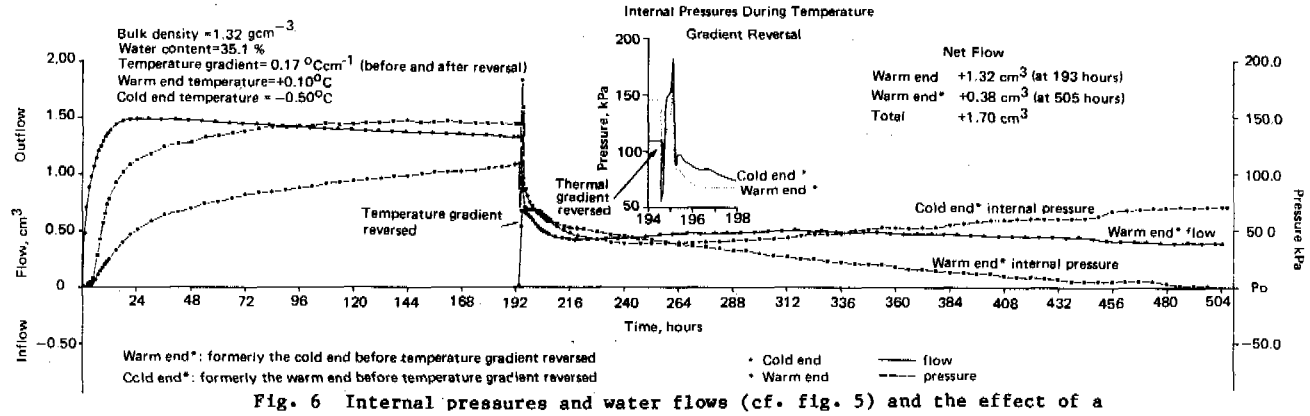

Fig. 6 Internal pressures and water flows (cf. fig. 5) and the effect of a reversal of temperature gradient.

lished, the pressure of the colder transducer may fall, even to below atmospheric. The warmer transducer, especially if very near to the frost line, then often shows a higher pressure with these soils. Soils which have been packed to a very high density, show somewhat similar behaviour even though they may in fact contain significant amounts of fine-grained material (Wood, 1985). Frozen slurries, which are necessarily ice-rich, also show relatively small pressure gradients (fig.7). The explanation of these differences in behaviour probably lies in the different ability of water to move in each case.

Movements of water and ice, and particle displacements

The existence of the unfrozen water suggests that frozen soils are permeable and there is general agreement that the movement of water in the frozen material, along freezing-induced gradients of suction (pressure) is an essential element of the continuing frost heave. The situation is complicated by the ice which Miller (1970) first showed could also be mobile because of regelation. This occurs under isothermal conditions if the water pressure is higher on the one face (the upstream side) of the ice, and is easily understood from equation 2. The higher pressure of the water raises the equilibrium freezing temperature and freezing occurs on this face. In due course, the ice pressure rises at the downstream face, and thawing occurs there. The effect was also apparent in Williams and Burt's (1976) permeability experiment when using a soil sample with an ice lens completely occupying the transverse section. The flow through the sample continued.

Usually however, we are concerned with movement occurring under a thermal gradient. Miller (1980) believed that a gradient in the water pressure following from equation 2, will cause regelation and an effective movement of the ice in the same direction as the temperature gradient. However if there is a substantial pressure gradient in the ice, as in our experiments, the ice might be expected to undergo creep - moving in the opposite direction to the temperature gradient (Wood 1985). Miller, Loch and Bresler (1975) also mention this possibility. It is not yet possible to assess the relative importance of these opposing tendencies.

Romkens and Miller (1973) demonstrated how particles of soil minerals are displaced in ice, in a direction counter to the temperature gradient. This occurs by regelation in which ice on the warmer side of the particle melts, with the adsorbed water moving round the particle to freeze where it is colder. If there is a dependence on particle size, the effect may be a sorting of particles.

The conditions of the experiment, fig. 4, the sources of water (in the reservoirs, at atmospheric pressure) and the confinement of the sample (in its perspex container), are not likely to be duplicated in nature. Nevertheless the experiment shows the various considerations necessary in the comprehensive interpretation of frost heave and its effects.

The observation that, in the coarse-grained soils and in highly compacted fine-grained material, there are only

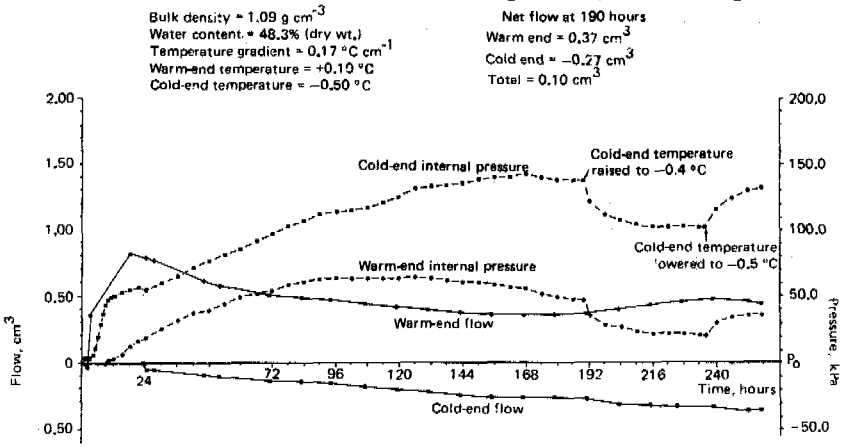

Fig. 7 Internal pressures and water flows, sample of same material as in Fig. 5, but prepared as a slurry. The temperature gradient was also the same in the two tests (except during final periods).

small rises in ice pressure which are limited to the region of the boundary of the frozen layer may be explained as follows. As the soil cools further, the amount of unfrozen water is so small and the permeability to the water correspondingly so small that there is no water flux for continued growth of the enclosed lens. On the contrary there will be stress relaxation, with microscopic deformation, of the frozen soil around lenses, and of the lenses themselves, and perhaps flow of the ice in the direction counter to the temperature gradient. In contrast to the fine-grained compressible soil, the movement of water along the temperature gradient is insufficient to maintain or restore the pressure in the ice, which is observed to fall. This implies that there is no continuing heave. For sands, where the ice pressures are particularly low, this is in accordance with the well-known lack of frost heave in such materials generally. The observation that ice pressure rose somewhat and then fell again, in a narrow zone as it initially froze and then cooled further, can be compared to field observations by Mackay (1983), which also showed transient pressure rises of warm frozen ground. He ascribed these to phase changes in response to a temperature change.

The observations showing only small pressure gradients in extremely ice-rich slurries may be the result of creep of the ice relatively unencumbered by soil structure or strength.

Significance for soil micromorphology, solifluction and patterned ground

In the traditional view the characteristic soil features associated with cold climates have been ascribed to conditions associated with the abrupt transition from a frozen to unfrozen condition (or the reverse). Excess pore pressures at thaw (giving slope instability) and heaving on initial freezing (for example of boulders) are examples. However the thermodynamic phenomena analysed above show that frozen soil undergoes a series of continuing effects that are likely to promote, and in some cases are essential to the development of various terrain features. For example, the large frost heave forces necessary to move boulders have their origin within the frozen soil at temperatures in accordance with eqn. 2. Freezing of the contained water at 0°C would not produce the forces required.

Freezing of a soil produces changes observable at the microscopic or near microscopic levels. The most common effect, in soils which are cohesive, is the formation of aggregates. This is easily understandable as the result of the effective stress (in the soil mechanics sense) following from the difference in pressure between the ice and the water predicted by eqn. 2. Each aggregate is composed of consolidated material and was probably surrrounded by segregated ice, even though this might also have been very small. In some soils, where ice lenses are larger and more widely spaced, the aggregates also may be centimeters across. The aggregates persist from year to year. The density of the aggregates increases as the temperature is decreased although the effect is limited to within a degree or so of 0°C.

There are other, cumulative micromorphological effects of freezing cycles. The sorting of particles and in particular the development of cappings of silt over larger particles or aggregates, and the development of cavities or vesicles have been reported by several authors (Harris 1981, Van Vliet Lanoe 1985). Van Vliet Lanoe has shown the existence of numerous small shear planes which she believes develop during thaw. These effects may have several causes. The translocations of the ice and water and displacements of particles, arising because of the stresses developed in the ice, water and consequently, on the particles and aggregates, are important. The translocations occur in frozen soil (although at temperatures near to 0°C), and are thus independent of the completion of a freeze-thaw cycle.

The strength and deformation properties of frozen soils, in the geotechnical sense, are of course, highly temperature dependent. The thermodynamic conditions discussed above, associated with transitions of water and ice, are responsible to a large degree for this temperature dependence. Externally applied pressures enhance the effect of these transitions. These effects, as characterised by the geotechnical properties, will also find expression in nature.

There are certain forms of solifluction, apparently slow creep movements of millimetres per year, which give rise to widespread terraces or lobes, on slopes of very low angle - sometimes only a few degrees. Often vegetation-covered, there is no obvious instability in the spring thaw (fig. 8). Such a creep movement, involving a surface layer of 0.5 to 1.5 m, may, however, be expected as a consequence of the cumulative effects of the ice and water displacements occurring in the frozen soil in connection with temperature gradients. Soil particles will be disturbed by forces acting in various directions but each of the continuing, multitudinous microscopic displacements is likely to have a component of movement downslope because of the ubiquitous stress in that direction.

Fig. 8 Front of solifluction terrace. The slow advance of such features down very slight slopes may be explained by a creep resulting from the thermodynamic-rheologic processes in frozen soil.

Although the evidence from our observations supports the view that, at least for some soils, there is only a limited temperature range of a few tenths of a degree near to 0°C where the continuing heave processes occur with effects easily measurable over periods of months, or perhaps years, natural temperature gradients are themselves small and such temperatures widespread. Furthermore in the near-surface layers of the ground the gradients change with the passage of the seasons (and the upper part, even diurnally), and reverse annually. These changes and the reversals of stress gradients (cf. fig. 6) and of directions of displacement will augment the downslope creep effect.

Related effects are involved in the development of patterned ground features, particlarly where sorting of fine particles is important. Differential frost heave

within frozen soils, especially those of varying textures, will produce narrow zones of shear, and particularly where the effect is enhanced by irregular rates of frost penetration or the presence of cracks or other discontinuities, will result in substantially irreversible displacements. These may subsequently be recognized as cryoturbates and find expression on the ground surface as hummocks and other surface disturbances.

CONCLUSION

The thermodynamic conditions within frozen ground, particularly at temperatures just below 0°C, are such that there are continuing translocations of water and ice and displacement of particles. The dynamic nature of the frozen ground is expressed in micromorphological changes and in larger-scale effects apparent in certain solifluction and patterned ground features. Research into such features should therefore consider conditions while the ground is frozen as much as those applying during freeze-up or thaw.

ACKNOWLEDGEMENTS

Many people have contributed to the results reported in this paper, and I am especially indebted to Dr. J.A. Wood, who has helped greatly in the development of the ideas and whose thesis research provided some of the observations illustrated.

REFERENCES

Edlefsen, N.E. and A.B.C. Anderson (1943). Thermodynamics of soil moisture. Hilgardia, 15, 2, 298 pp.

Geotechnical Science Laboratories (1986). Investigations of Frost Heave as a Cause of Pipeline Deformation. Report to Earth Physics Branch, Energy Mines and Resources, Canada. 71 pp.

Geotechnical Science Laboratories (1988). The Third Freeze Cycle of the Canada-France Ground Freezing Experiment. Report for Permafrost Res. Section, Geol. Surv., Canada. 76 pp.

Harris, C. (1981). Periglacial mass-wasting a review of research. 204 p. Geobooks, Norwich.

Konrad J-M and Morgenstern N.R. (1980). A mechanistic theory of ice lens formation in fine-grained soils. Can. Geot. Jour. 17, 473-486.

Koopmans, R.W.R. and R.D. Miller (1966). Soil freezing and soil water characteristic curves. Soil Sci. Soc. Amer. Proc. 30, 680-685.

Mackay, J.R. (1983). Downward water movement into frozen ground, western arctic coast, Canada. Can. Journ. Earth Sci. 20, 1. 120-134.

Macksy, J.R. and R.V. Leslie (1987). A simple probe for the measurement of frost heave within frozen ground in a permafrost environment. in Current Research, Part A, Geol. Surv. Can., Paper 87-1A, 37-41.

Miller R.D. (1970). Ice sandwich: functional semi-permeable membrane. Science, 169, 584-585.

Miller, R.D., J.P.G. Loch and E. Bresler (1975). Transport of water and heat in a frozen permeameter. Soil Sci. Soc. Amer. Proc. 39, (6): 1029-1036.

Miller, R.D. (1980). Freezing phenomena in soils. in Hillel: Applications of Soil Physics, Academic Press.

Ohrai, Takahiro and Hideo Yamamoto (1985). Growth of ice lenses in partially frozen soil. Proc. Fourth Intern. Symp. Ground Freezing. 1, 79-84.

Parmuzina, O. Yu. (1980). Cryogenic texture and some characteristics of ice formation in the active layer. Polar Geogr. & Geol. IV, 3, 131-151. (transld. from: Problemy kriolitologii, 7, 1978, 141-164).

Pissart, A. (1972). Resultats d'experiences sur l'action du gel. Biul. Peryglac. 23, 101-113.

O'Neill, K. and R.D. Miller (1985). Exploration of a rigid ice model of frost heave. Water Res. Res. 21, (3), 281-296.

Romkens, M.J.M. and R.D. Miller (1973). Migration of mineral particles in ice with a temperature gradient. Jour. Colloid Interface Sci. 42, 103-111.

Smith, M.W. and D.E. Patterson (1988) - in preparation.

Tsytovich, N.A. (1975). The Mechanics of Frozen Ground. McGraw-Hill. 426 pp.

Van Vliet Lanoe, B. (1985). Frost effects in soils. pp. 117-158 in Soils and Quaternary Landscape Evolution (Ed. J. Boardman), Wiley.

Williams, P.J. (1967). Properties and Behaviour of Freezing Soils. Norw. Geotech. Inst., Publn. 72, 120 pp.

Williams, P.J. and T.P. Burt (1976). Hydraulic conductivity in frozen soils. Earth Surface Processes 1, 349-360.

Williams, P.J. and J.A. Wood (1985). Internal stresses in frozen ground. Can. Geot. Jour. 22, 3, 413-416.

Wood, J.A. (1985). Internal Pressures of Freezing Soils. Ph.D. thesis, Carleton Univ. 261 pp.

Wood, J.A. and P.J. Williams (1985). Stress distribution in frost heaving soils. Fourth Intern. Symp. Ground Freezing. 165-171.

TIME AND SPATIAL VARIATION OF TEMPERATURE OF ACTIVE LAYER IN SUMMER ON THE KAFFIÖYRA PLAIN (NW SPITSBERGEN)

G. Wójcik, K. Marciniak and R. Przybylak

Department of Climatology, N. Copernicus University, Toruń, Poland

SYNOPSIS Ground temperature measurement results in main ecotopes of the Kaffiöyra coastal plain (Oscar II Land, northwestern Spitsbergen): sea beach, tundra and morainic plateau from six summer seasons (1975-1982), are presented and discussed in the paper. The change from year to year and the spatial distribution of the ground temperature is discussed with particular regard to temperature of the active surface and vertical gradients of temperature dependent on daytime and weather conditions.

INTRODUCTION

This paper is based upon fieldworks in 1975 - 1982 during 6 polar expeditions to Spitsbergen, organized by the Institute of Geography, N. Copernicus University of Toruń. Investigations were carried through on the Kaffiöyra Plain in northwestern Spitsbergen (Oscar II Land). Their results were already presented in successive post-expedition reports and papers (Leszkiewicz, 1977; Wójcik, 1982; Wójcik, Marciniak, 1983; Marciniak, Przybylak, 1983).

In Spitsbergen studies of ground temperature are carried regularly in meteorologic stations (e.g. at Barentsburg, in Hornsund). Observations are also collected in various areas, usually in summer, by scientific expeditions (Baranowski 1963, 1968; Czeppe 1961; Jahn 1961; Grześ 1984; Kamiński 1982; Wójcik, Marciniak 1987). Some papers deal with depth of thawing, that is with thickness of active layer. In a broader, i.e. spatial-geographic approach, this problem is presented by Jahn and Walker (1983), and for Kaffiöyra by Marciniak and Szczepanik (1983). The first Polish paper on ground temperature in a polar zone was written by Jahn (1948) and based on studies of 1937, carried through in Greenland during the Polish Polar Expedition supervised by A. Kosiba.

Thermic regime of a ground depends from absorbed heat but also from thermic characteristics of a ground, i.e. its heat capacity and conductivity that correlate with lithology and water content. In Spitsbergen these factors are so varying that result in distinct spatial temperature variation of a ground. Degree of such variation remains strictly connected with climatic and weather conditions.

In this paper the collected material allows to present spatial (horizontal and vertical) variability of ground temperature in a diurnal cycle and from year to year during a regressive phase of the summer season and related to weather conditions. Presented problems are illustrated by chosen temperatures from several depths and by mean temperatures of the whole layer of 1-50 cm (Tables I and II, Figs. 2-3). The latter are arithmetic means of temperatures from 5 standard depths.

METHODS AND MATERIAL

Measurements of ground temperatures were done with a use of mercury ground thermometers at depths 1, 5, 10, 20 and 50 cm, and every day at 01, 07, 13 and 19 LMT. Measuring periods have not been always the same. This presentation is generally based on comparable data for the interval starting from July 21 untill August 31, but in case of need the data beyond this period have been also used.

Spatial variation of ground temperature was studied, taking three characteristic for Kaffiöyra ecotopes as examples: sandy beach, moraine and tundra. Location and morphologic descriptions of measuring sites near the expedition base ($\varphi = 78^{\circ}41'$ N, $\lambda = 11^{\circ}51'$ E, h = 1.5 m a.s.l.) are presented in figure 1.

a). A beach (B) is composed of medium-grained sand which is over 1 meter thick. Depth of summer thawing is about a meter. The whole layer is quite wet, partly due to capillary water rising from a surface of permafrost and partly due to inflow of sea water during high tide and precipitation.

During wet weather with precipitation the whole layer over the permafrost possesses a high water content. On the other hand during dry weather, particularly during high insolation, a thin outer layer 1-2 cm thick gets dry. This layer with a lower heat capacity and conductivity influences much heat circulation in the whole vertical section. Thermal regime of a beach is modelled similarly as of other ecotopes, in connection with a shallow occurence of permafrost.

b). The site „tundra" (T) occurs on a flat outwash fan in forefield of end moraine of the Aavatsmark Glacier. The fan is composed of coarse gravels with admixtu-

re of sands and silts. Ground surface is covered with tundra vegetation with predominating cup-moss (Cladonia rangiferina). Vegetation cover although thin and discontinuous (70% of the land), influences to a certain degree a modelling of ground temperature. Water content is here lower than at a beach.

c). The third ecotope is constituted by end moraine (M). Measuring site was located on flat surface of outer oldest morainic rampart composed of rock pieces of varying diameter and shape, mixed with fine gravels and loamy material. A moraine core is still composed of buried ice. Water content is the lowest in the active layer here.

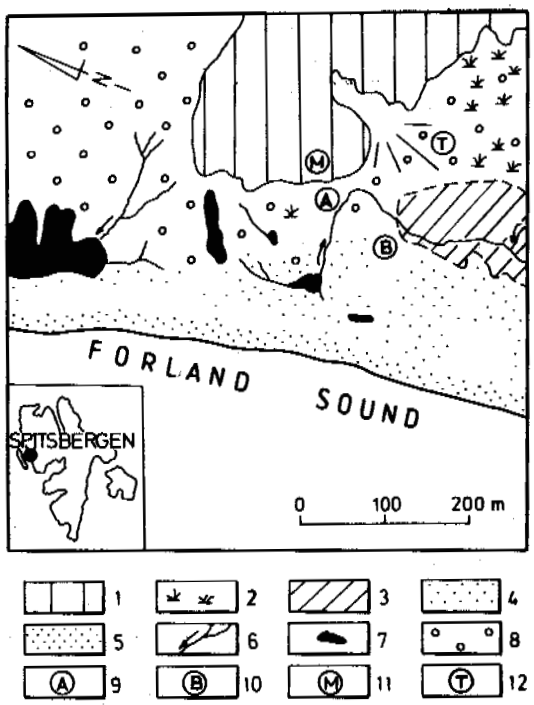

Fig. 1 Morphologic sketch of the area of the Research Station of the N. Copernicus University, Toruń, and location of measurement stands

1 - moraine, 2 - tundra, 3 - area periodically flooded during tides, 4 - storm ridges, 5 - area of the beach flooded during tides, 6 - streams, 7 - lakes, 8 - outwash plain, 9 - Research Station, 10 - ground temperature measuring stand „Beach" (B), 11 - ground temperature measuring stand „Moraine" (M), 12 - ground temperature measuring stand „Tundra" (T)

VARIATION OF GROUND TEMPERATURE FROM YEAR TO YEAR

Thermic indices of ground during summer develop under influence of current weather conditions, but in connection with the preceding winter (its duration and severity). Mean values of some meteorological elements from six analyzed summer seasons are presented in table I.

Variations of mean ground temperature from year to year are presented on the basis of investigations at a beach. These variations are changed what depends on depth and diurnal cycle. Mean variation is equal 0.6°C at active surface, increases with depth to 0.8°C at depth of 10 cm and then gets lower, reaching 0.4°C at depth of 50 cm. In a diurnal cycle mean variations of ground temperature from year to year are the lowest at night (from 0.3°C to 0.5°C at 01 o'clock) and the greatest at noon (to 1.0°C at depth of 10 cm).

Difference between temperature of the warmest year (1977) and the coolest one (1982) changes also with the depth, preserving a poorly indicated diurnal rhythm (Fig. 2). Greatest difference occured at depth of 10 cm where it varied from 1.5°C at 01 and 07 to 1.8°C at 19, with mean of 1.6°C. Therefore, they decrease (more weakly) upwards to the active surface where they changed from 1.3°C at 19 to 1.7°C at 07 and 13, with a diurnal mean of 1.5°C, and (more distinctly) downwards to larger depths and varied at 50 cm from 0.8°C at 01 to 1.0°C at 07 and 19, with a diurnal mean of 1.0°C.

Vertical gradients of temperature have also changed from year to year. At a beach in the layer 1-50 cm at 01 they varied from -0.28°C/10 cm in 1980 to -0.49°C/10 cm in 1978, with a mean of six years equal -0.37°C/10 cm. At 13 they varied from -1.12°C in 1980 to -1.39°C in 1979, with a mean of six years equal -1.22°C/10 cm. Mean diurnal gradients varied from -0.71°C in 1975, 1980 and 1982 to -0.84°C in 1979, with a mean of all the years equal -0.78°C/10 cm. Changes due to weather conditions seem to disappear quickly towards a permafrost surface.

Change of ground temperature from year to year is well illustrated by mean temperature of the whole layer 1-50 cm (Table II).

SPATIAL VARIATION OF GROUND TEMPERATURE

A problem of spatial variation of ground temperature is presented on the basis of measurements at three chosen ecotopes (beach, tundra, moraine) in summer seasons of 1978 and 1979 (Table II).

Vertical distribution of ground temperature enables to distinquish in all three ecotopes the three layers (Fig. 3), described in the previous paper on the basis of data from a single year, i.e. from 1978 (Wójcik, Marciniak 1987).

a). Outer layer of varying thickness, thermic differences in which between particular ecotopes are significant at the surface, but quickly decrease with depth and sometimes disappear. Such smoothed or almost smoothed temperature at a horizon is named a monothermy, whereas a depth at which it occurs - a monothermy horizon or depth. Described outer layer is lo-

TABLE I

Mean values of the chosen meteorological elements from the summer season 21st July - 31st August on the Kaffiöyra Plain (NW Spitsbergen)

Year	Cloudiness 0 - 10	Sunshine duration		Wind velocity m/s	Air temperature			Humidity		Precipitation mm
		hours	%		m	min	max	%	hPa	
1975	8,7	112,9	11,5	4,3	4,9	3,3	6,7	90	7,8	66,5
1977*	8,7	146,6	15,9	3,2	5,0	3,5	7,0	89	7,8	44,4
1978	8,8	119,9	12,2	4,6	4,7	3,1	6,3	90	7,7	44,2
1979	7,3	281,9	29,7	5,0	4,5	2,5	6,6	90	7,6	17,7
1980	9,1	90,9	9,3	5,5	4,1	2,6	5,6	89	7,3	108,0
1982	8,8	91,3	9,3	4,2	3,3	1,8	4,8	88	6,8	54,5
mean	8,6	140,6	14,5	4,5	4,4	2,8	6,2	89	7,5	55,9

* 21.07 - 28.08

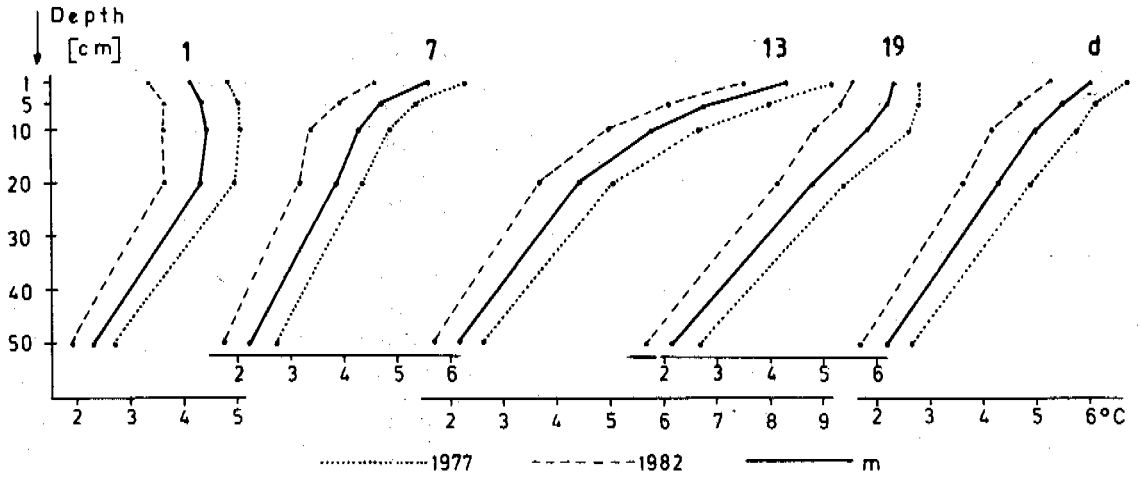

Fig. 2 Mean vertical distribution of the ground temperature in the beach (B) from the period 21st July - 31st August, from the wormest year (1977), the coolest year (1982) and mean from the 1975 - 1982 for the particular observation terms (01, 07, 13, 19) and daily means (d)

cated between the active layer, the temperature of which is considerably varying, and the monothermy horizon. Its thickness depends on depth of occurrence of the monothermy and depending on weather as well as part of the day, changes from 0 cm at cloudy day (e.g. 78.08.15 at 01) to about 15-17 cm at cloudless day (e.g. 78.08. 13 at 19) and mean thickness is equal about 5 cm (Fig. 3).

Curves of figure 3 indicate that this upper part of the studied section has been almost every time the warmest at a beach and the coolest at a moraine; it occupied an intermediate position at a tundra. Only in the diurnal cycle at night a tundra was the warmest, a beach was the coolest whereas a moraine occupied an intermediate position.

The greatest thermic differences in the outer layer between particular ecotopes occurred at an active surface, correlating with weather conditions as usual. At a cloudless sky as e.g. on 1978.07.24 the mean diurnal value at a beach was equal 11.2°C, 9.6°C at a moraine and 8.7°C at a tundra. During cloudy and rainy weather the thermic differences disappear and e.g. on 1978.07.30 mean diurnal values for particular ecotopes were equal 6.6-6.7°C.

Thermic spottiness of an active surface change in a diurnal cycle and their greatest intensity is noted at a largest insolation i.e. at noon during cloudless weather. Therefore e. g. on 1978.07.24 at 13 the temperature at a depth of 1 cm at a beach was equal 17.0°C, at a moraine 14.0°C and at a tundra 12.8°C. Spatial differentiation of temperature is then considerable over 4°C. Night cooling of the active surface depends slightly on its characteristics

TABLE II

Term (01, 07, 13, 19) and daily (d) means of ground temperature (1, 5, 10, 20, 50 cm) from the summer season 21st July - 31st August on the Kaffiöyra Plain (NW Spitsbergen)

Ecotope	Year	1 cm					5 cm					10 cm				
		01	07	13	19	d	01	07	13	19	d	01	07	13	19	d
Beach	1975	4,4	6,0	8,5	6,4	6,3	4,7	5,0	6,9	6,3	5,7	4,9	4,6	6,0	6,1	5,4
	1977*	4,8	6,2	9,1	6,8	6,7	5,0	5,3	7,4	6,8	6,1	5,1	4,8	6,6	6,6	5,8
	1978	4,4	5,4	7,8	6,3	6,0	4,5	4,6	6,3	6,0	5,4	4,4	3,9	5,0	5,3	4,6
	1979	3,9	5,9	8,7	6,9	6,3	4,3	4,8	7,4	6,8	5,8	4,6	4,3	6,3	6,3	5,4
	1980	3,7	5,2	7,6	6,1	5,7	3,9	4,3	6,3	5,7	5,1	4,1	4,0	5,5	5,4	4,8
	1982	3,3	4,5	7,4	5,5	5,2	3,6	3,8	6,0	5,3	4,7	3,6	3,3	4,9	4,8	4,2
	m	4,1	5,5	8,2	6,3	6,0	4,3	4,6	6,7	6,2	5,5	4,4	4,2	5,7	5,8	5,0
Moraine	1978	4,5	5,2	7,0	5,9	5,7	4,9	5,0	6,6	6,1	5,7	5,1	4,8	6,0	6,1	5,5
	1979	4,1	5,3	8,2	6,4	6,0	4,5	4,9	7,4	6,5	5,8	5,0	4,7	6,5	6,5	5,7
	1980	4,0	4,9	6,7	5,7	5,3	4,2	4,4	6,2	5,7	5,1	4,5	4,4	5,8	5,7	5,1
Tundra	1978	4,7	5,3	7,2	6,4	5,9	5,0	5,0	6,6	6,3	5,7	5,0	4,6	6,0	6,1	5,4

Ecotope	Year	20 cm					50 cm					1 - 50 cm				
		01	07	13	19	d	01	07	13	19	d	01	07	13	19	d
Beach	1975	4,6	4,1	4,6	5,0	4,6	2,8	2,8	2,7	2,8	2,8	4,3	4,5	5,6	5,3	5,0
	1977*	4,9	4,3	5,0	5,4	4,9	2,7	2,7	2,6	2,7	2,7	4,5	4,7	6,1	5,7	5,2
	1978	4,3	3,8	4,3	4,7	4,3	2,0	2,1	2,0	2,0	2,0	3,9	4,0	5,1	4,9	4,5
	1979	4,5	3,8	4,7	5,1	4,5	2,0	2,0	1,9	1,9	2,0	3,9	4,2	5,8	5,4	4,8
	1980	3,9	3,5	4,1	4,5	4,0	2,3	2,2	2,1	2,2	2,2	3,6	3,8	5,1	4,8	4,4
	1982	3,6	3,1	3,6	4,1	3,6	1,8	1,7	1,7	1,7	1,7	3,2	3,3	4,7	4,3	3,9
	m	4,3	3,8	4,4	4,8	4,3	2,3	2,2	2,2	2,2	2,2	3,9	4,1	5,4	5,1	4,6
Moraine	1978	5,2	4,8	5,4	5,8	5,3	4,6	4,6	4,5	4,6	4,6	4,9	4,9	5,9	5,7	5,4
	1979	5,4	4,7	5,6	6,1	5,4	4,9	4,7	4,6	4,7	4,6	4,8	4,9	6,5	6,0	5,5
	1980	4,9	4,5	5,0	5,4	4,9	4,4	4,2	4,2	4,3	4,3	4,4	4,5	5,6	5,4	4,9
Tundra	1978	4,8	4,3	4,9	5,4	4,8	3,6	3,6	3,4	3,5	3,6	4,6	4,6	5,6	5,5	5,1

* 21.07 - 28.08

and for this reason, thermic spottiness disappear at night, especially when clouds are present.

b). Lower layer that occurs beneath the monothermy. In it the increasing depth is accompanied by thermic differentiation between particular ecotopes (curves in Fig. 3), therewith that a beach is always the coolest and a moraine is the warmest (thus otherwise than in the outer layer). At depth of 50 cm means for the whole summer season of 1978 were equal 2.0°C at a beach, 3.6°C at a tundra and 4.6°C at a moraine. It is remarkable that differentiation of temperature at depth of 50 cm between the ecotopes is quite stabile and changes slightly if referred to weather and diurnal cycle.

c). Both described layers are separated by an intermediate one that comprises fragments of the lower part of layer (a) and of the upper one (b). A monothermy occurs there and so, this

layer indicates the lowest difference of temperature at the horizon between the particular ecotopes.

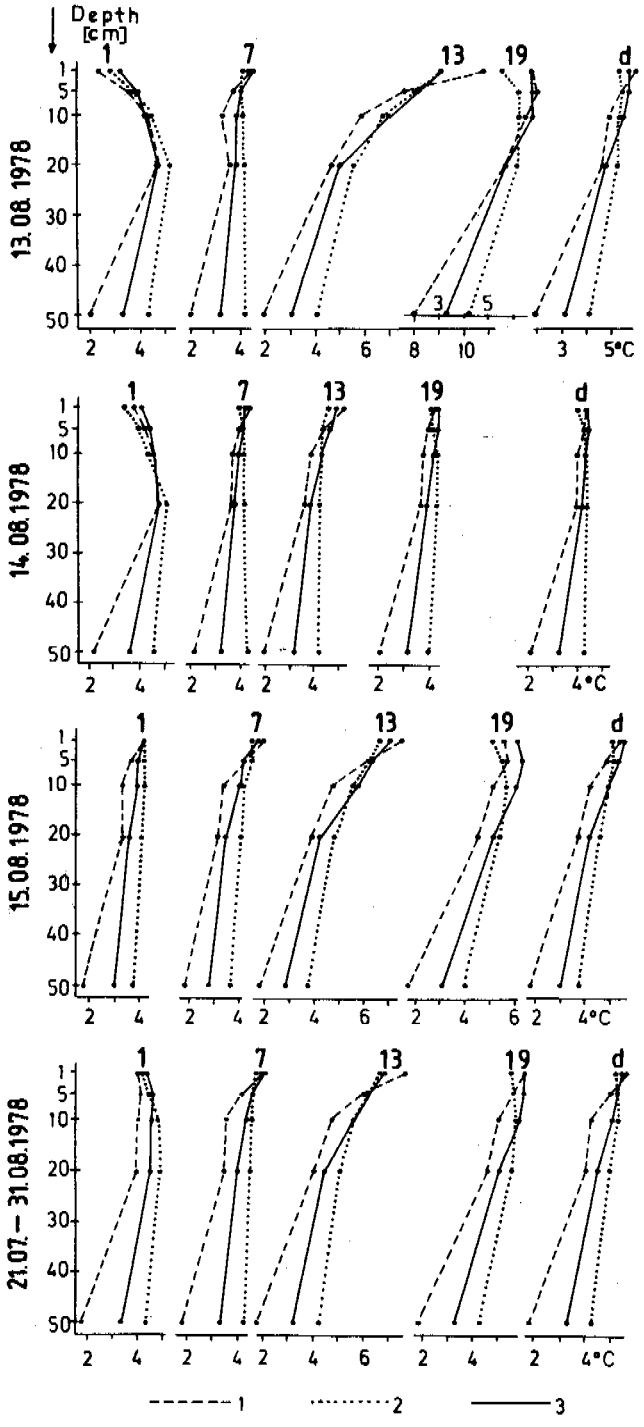

Fig. 3 Vertical ground temperature distribution for the particular observation terms (01, 07, 13, 19) and daily means (d) during a sunny weather (August 13), at a partial cloudiness (August 15) and at full cloudiness (August 14), and means for the period 21st July - 31st August 1978 on the beach (1), the moraine (2) and the tundra (3)

Spatial differentiation of ground temperature is noted in the mean from the layer 1-50 cm (Table II). The lowest values of this index occur at a beach, intermediate at a tundra and the highest at a moraine. Diurnal means from 1978 are equal 4.5°C, 5.1°C and 5.4°C respectively. Such relations between the ecotopes are also preserved from day to day, therewith the same difference between them changes in relation to the weather. They are larger at a cloudless weather e.g. on 1978.07.24 diurnal means were equal 6.9°C at a beach, 7.0°C at a tundra and 8.3°C at a moraine. A difference between the warmest moraine and the coolest beach reached 1.4°C, whereas during a cloudy weather, e. g. on 08.19 it was equal 0.3°C.

Described studies were carried through in three neighboring ecotopes. Influx of heat to them from the outside was then uniform. Due to a similar albedo, radiation absorbed by every ecotope is almost the same. Therefore heat properties of ground, i.e. heat capacity and conductivity, seem to be the main factor that makes spatial variation (horizontal and vertical) of thermic relations.

VERTICAL DISTRIBUTION OF TEMPERATURE

Carried investigations indicate that in Spitsbergen during polar summer, i.e. when a snow cover is absent, there are in the outer part of the active layer three types of vertical temperature stratification (Fig. 3).

a). Summer - insolation type predominates (temperature decreases with depth). It is marked by diurnal means for the whole period and occurs during a day in the diurnal cycle (Fig. 3). It is created early in the morning and is already noted at 07, is best expressed at noon and disappears towards the evening, being still indicated at 19 at a beach and tundra. This type occurs essentially during all the days from early morning untill afternoon, and is especially distinct at cloudless or slightly cloudy weather (Fig. 3).

b). Radiation-insolation type (in upper part of the section temperature rises whereas drops in the lower one with depth) that occurs „at night" in a diurnal cycle due to georadiation. Generally it appears although at a moraine only, already at 19 and is already well developed at 01 (Fig. 3). The night cooling is not very deep as reaches 20-25 cm only.

The radiation-insolation pattern of temperature divides the analyzed ground section into three varying thermic layers, two cool ones (upper and lower) are separated by a warm layer (Fig. 3).

c). Insolation-radiation type (in upper part of the section temperature drops and in lower one rises with depth). It does not comprise the whole analyzed section but is limited to its outer part, about 20 cm thick and usually occurs on single days in the morning at cloudless sky or with some clouds only. This layer is subdivided into three thermic layers: two warmer ones (upper and lower) separated by a cooler layer. Beneath, a temperature decreases with

depth due to obviously near occurrence of permafrost.

Carried investigations prove that in Spitsbergen the outer ground layer is subjected to active temperature changes in a diurnal cycle, modified by weather conditions, and their quantitative characteristics are different what depends on ecotope. In a vertical section temperatures at a beach are most varying; they are less varied at a tundra and least at a moraine. Mean vertical gradients from the interval of 1978.07.21 - 08.31 in the layer 1-50 cm were equal -0.82°C/10 cm at a beach, -0.47°C/10 cm at a tundra and 0.33°C/10 cm at a moraine.

Vertical gradients change in a diurnal cycle (Fig. 3). They are the largest by noon at 13, equal -1.22°C/10 cm at a beach, -0.73°C/10 cm at a tundra and -0.51°C/10 cm at a moraine. They are the lowest at night, being at 01: -0.49°C, -0.22°C and 0.01°C/10 cm respectively. Therefore, a radiation type of vertical temperature pattern (although at very low gradient) occurred at a moraine only.

Vertical gradients depend on weather conditions. The largest occur during a day at sunny weather (Fig. 3) and e.g. on 08.13 at 13 at a beach in the layer 1-50 cm it was equal -1.80 °C/10 cm. Respective values at a tundra were equal -1.22°C and -2.20°C whereas -1.02°C and 2.30°C/10 cm at a moraine. During cloudy and rainy weather the temperature in a vertical section is smoothed and gradients in all terms are small. Thus e.g. on 1978.08.14 at 13 (Fig. 3) the gradient at a beach was equal -0.66°C, at a tundra -0.34°C and at a moraine -0.06°C/10 cm, while in the evening at 19 due to further smoothing of temperature, vertical gradients were equal respectively -0.44°C, -0.24°C and 0.01°C/10 cm.

FINAL REMARKS

A theory of molecular heat conductivity of J. B. B. Fourier presents a model of annual and diurnal thermic pattern of a ground. In natural conditions the quantitative indices of this model are disturbed by clouds and precipitation, and in Spitsbergen also due to presence of permafrost, occurring beneath the active layer.

A more complete discussion of thermic regime of active layer in polar regions against weather conditions demands further investigations of ground density and dynamics of water content as well as of heat capacity and conductivity.

REFERENCES

Baranowski, S. (1963). Some results of investigations of ground temperature on Spitsbergen. Biul. Inf. Komit. MGW 2, 56-67

Baranowski, S. (1968). Thermal conditions of periglacial tundra SW Spitsbergen. Acta Univ. Wratislav. 68, 1-17

Czeppe, Z. (1961). Annual cycle of frosts and ground movements in Hornsund (Spitsbergen) 1957-1958. Zesz. Nauk. UJ 42, 1-74

Grześ, M. (1984). Characteristics of the active layer of permafrost on Spitsbergen. 11th Polar Symposium. Papers and reports. Poznań, May 4-5, 1984, 65-67

Jahn, A. (1948). Badania nad strukturą i temperaturą gleb w Zachodniej Grenlandii. Rozpr. Wydz. Mat.-Przyr. PAU, (72), 63-184

Jahn, A. (1961). Quantitative analysis of some periglacial processes in Spitsbergen. Zesz. Nauk. Uniw. Wrocław., Ser. B 5, 1-34

Jahn, A., Walker, H. J. (1983). The active layer and climate. Z. Geomorph. N. F., Suppl. Bd. 47, 97-108

Kamiński, A. (1982). Meteorological investigations in southern Spitsbergen in summer 1978. Dokumentacja Wyprawy Polarnej Uniw. Śl., 1977-1980, t. I, 135-150

Leszkiewicz, J. (1977). Meteorological conditions on the northern part of Kaffiöyra Plain during the period from July 1 to August 31, 1975. AUNC, Geografia 13, 97--111

Marciniak, K., Przybylak, R. (1983). Meteorological conditions in the Kaffiöyra (NW Spitsbergen) since 7th July to 5th September 1979. AUNC, Geografia 18, 113-123

Marciniak, K., Szczepanik, W. (1983). Results of investigations over the summer ground thawing in the Kaffiöyra (NW Spitsbergen). AUNC, Geografia 18, 69-97

Wójcik, G. (1982). Meteorological conditions at the Kaffiöyra Plain - Spitsbergen, from 21st July to 28th August 1977. AUNC, Geografia 16, 151-166

Wójcik, G., Marciniak, K. (1983). Meteorological conditions in the Kaffiöyra Plain (NW Spitsbergen) since 21st July to 7th September 1978. AUNC, Geografia 18, 99--111

Wójcik, G., Marciniak, K. (1987). Ground temperature of main ecotopes of Kaffiöyra, Spitsbergen, summer 1978. Polish Polar Research 8, 1, 25-46

TEMPERATURE OF ACTIVE LAYER AT BUNGER OASIS IN ANTARCTICA IN SUMMER 1978-79

G. Wójcik

Department of Climatology, N. Copernicus University, Torun, Poland

SYNOPSIS The results of the ground temperature measurements in the Bunger Oasis from the summer season 1978-79 are presented and discussed in the paper with particular regards to temperature of active surface, vertical distribution and vertical gradients of temperature dependent on daytime and weather conditions.

INTRODUCTION

At the beginning of regressive phase of Antarctic summer from 1979.01.23 to 1979.02.20 measurements of ground temperatures at depths: 0 (active surface), 5, 10, 20 and 50 cm were collected in Bunger Oasis at the Polish A. B. Dobrowolski's Station ($\varphi = 66^{\circ}18'$ S, $\lambda = 100^{\circ}43'$ E, h = 28 m a.s.l.) The data were collected at climatologic observation time of 07, 13 and 19 LMT with a use of mercury thermometers. Minimum and maximum temperatures were also measured at a ground surface with a use of extremal mercury thermometers. Measurements were done at a meteorologic station, located in the area composed of fine glacial debris.

Figure 3 presents general weather conditions prevailling in the Oasis during the observations. Table I compiles data on maximum and minimum temperatures at active surface and 2 m above a ground, set in order of decades. Table II indicates decade values of ground temperature. Figure 4 presents examples of vertical patterns of temperature at some weather situations.

GENERAL DESCRIPTIONS OF BUNGER OASIS

The Bunger Oasis is located in a marginal part of West Antarctica between $65^{\circ}58'$ and $66^{\circ}20'$ φ S, and between $100^{\circ}28'$ and $101^{\circ}20'$ λ E. It is surrounded from all the sides by ice. It contacts with ice sheet in the east. Dynamic glaciers flow around it in the south (the Apfel

Fig.1 Typical landscape of Bunger Oasis - Antarctica, near the Polish A. B. Dobrowolski's Station. Phot. G. Wójcik, February 1979

Glacier), west (the Edisto Glacier) and north-east (the Remenchus Glacier). In the north the Oasis is closed by the vast shelf Shackleton Glacier, that separates the Oasis from the Mawson Sea. The area of the Oasis is equal 952 km^2, 395 km^2 of which is occupied by a land, 470 km^2 by epishelf lagoons, 36 km^2 by lakes of various sizes and at last, 51 km^2 is occupied by snow fields and glaciers (Korotkievič 1972; Simonov 1971; Wiśniewski 1983).

The Oasis was deglaciated about 12-15 ka ago due to general Holocene warming, with a participation of glacioisostatic rebound of its margins, suitable bedrock-influenced distribution of ice masses flowing from a thinning ice sheet and local climatic conditions (Shumsky 1969; Simonov 1971; Korotkievič 1972). The latter started to be modelled when dark rocks appeared above the ice surface, and increased absorption of sun radiation.

are almost devoid of them and thoroughly polished. Roche moutonnées indicate distinct glacial striae that mark a direction of ice mass movement. Deposits are composed of rock debris which is angular with only slight traces of roundness. A size of rock pieces is varying, the fraction of several to a dozen or so centimeters in diameter predominates, with an admixture of blocks over 1 m. Depressions are filled with fine patches of glaciofluvial deposits composed of finer gravels. Such patches, fed with water from higher-located snow fields and glaciers, are subjected to frost segregation of material and polygons with 1-2 m in diameter are created (Fig.2).

Climatic conditions of the **Oasis** and particularly considerable diurnal amplitudes of temperature connected with a frequent pass over 0^oC (freezing point), favor development of physical weathering and so, slopes and their feet are covered with mantles and heaps of blocks. Dryness of the climate and high wind velocity

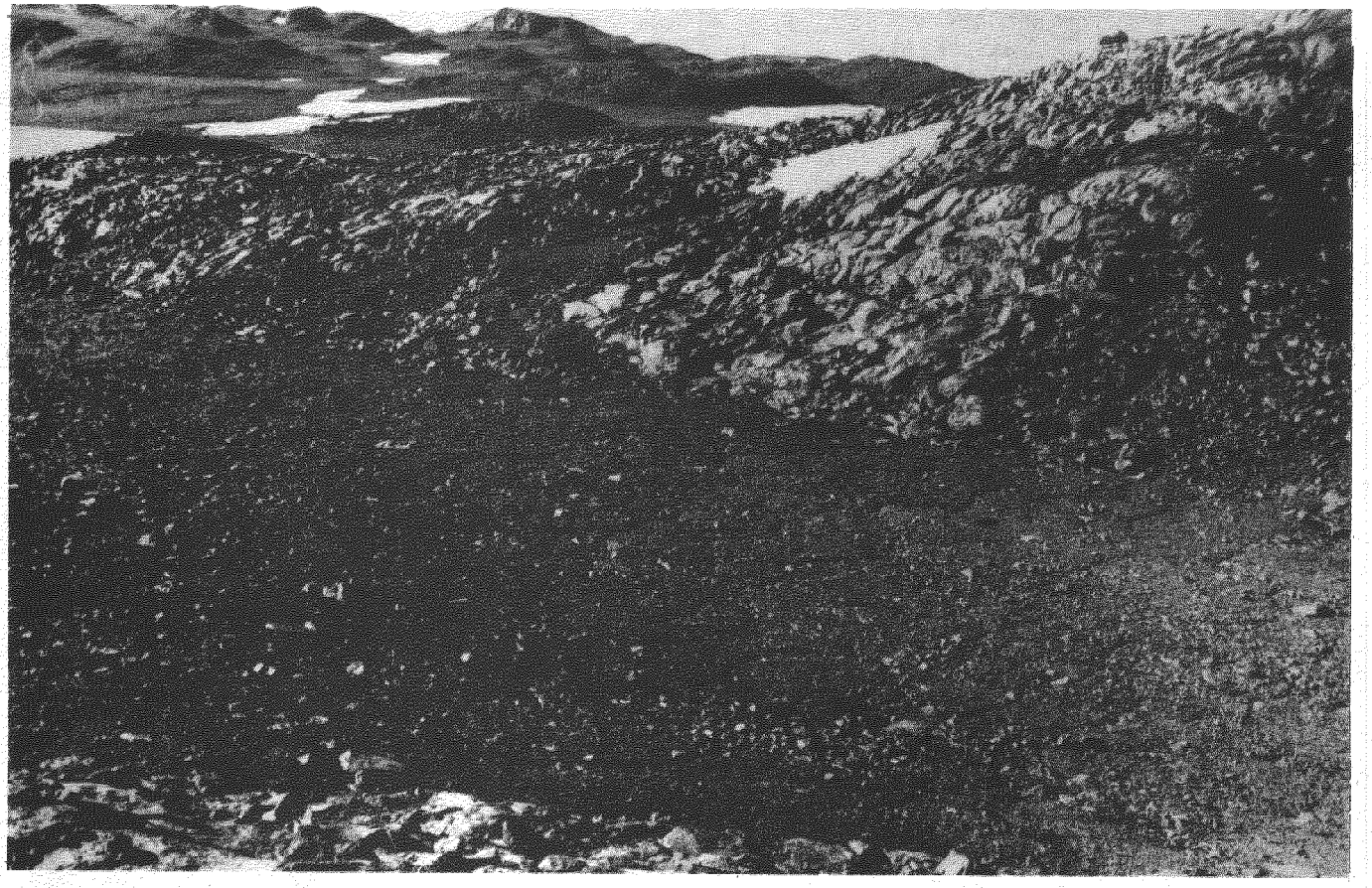

Fig.2 An example of frost segregation and of polygons with 1-2 m diameter in Bunger Oasis - Antarctica. Phot. G. Wójcik, February 1979

Relief of the Oasis reflects its geologic structure, glacial history and climate. In general it represents a hummocky area (Fig.1), in which individual hills are not over 200 m high, with the highest hill Piramidalne at 172 m a.s.l. The whole Oasis is covered by glacial deposits of varied thickness. Deposits in depressions are the thickest whereas convex features enable intensive aeolian weathering (corrasion). This phenomen is noted in summer with a participation of sand grains carried by wind, but in winter also with application of ice crystals that are very hard and sharp at low temperatures.

TABLE I

The lowest (L), highest (H) and mean (m) values of the daily minimal (t_{min}), maximal (t_{max}) temperatures and of the daily temperature amplitudes in A. B. Dobrowolski Station (Bunger Oasis - Antarctica) from the period 23.01 - 20.02.1979

Height	Decade	t_{min}			t_{max}			Amplitude		
		L	H	m	L	H	m	L	H	m
Ground surface	III	-10.0	-4.7	-7.1	12.0	28.5	20.7	20.6	38.5	27.8
	I	-12.4	-3.5	-8.4	2.3	29.5	16.3	9.0	37.7	24.8
	II	-12.7	-4.4	-7.6	-0.5	23.5	12.4	6.5	35.5	19.9
	III-II	-12.7	-3.5	-7.7	-0.5	29.5	16.5	6.5	38.5	24.2
Air 2m	III	-6.0	-2.5	-4.1	0.9	3.4	2.0	4.4	7.5	6.2
	I	-8.7	-1.6	-5.5	-1.8	5.6	0.7	4.1	10.0	6.2
	II	-7.9	-4.6	-5.9	-3.3	2.2	-0.5	2.6	10.0	5.4
	III-II	-8.7	-1.6	-5.2	-3.3	5.6	0.7	2.6	10.0	5.9

Decades as in the Table II

WEATHER CONDITIONS DURING STUDIES

They are illustrated by curves in figure 3. A cloudiness was in general temperate, the lowest at the beginning of the measuring period, i.e. during the last decade of January (4.9). In February it was equal 5.2 during the first decade and 8.3 during the second one. A mean for the whole period reached 6.1 in a scale 0-10. The whole period had 8 sunny days (with mean diurnal cloudiness $C_i < 2.0$), with 4 cloudless days ($C_i = 0$) inclusive. There were 12 cloudy days ($C_i > 8.0$) with 10 days with a complete cloudiness ($C_i = 10.0$).

Due to a temperate cloudiness a sunshine duration was quite large, greater than could be expected from cloudiness, because of relatively considerable participation of thin clouds of a high stage that were shone through. A total number of hours with sun was equal 249 what corresponds with 48% of possible ones. In compliance with cloudiness distribution, the sunshine duration gradually decreased from decade to decade and was equal 71%, 52% and 23% respectively, during the successive decades.

Mean daily air temperatures varied from -5.3 °C (February 20) to 1.4°C (January 30), with a mean for the whole period equal -1.9°C. During the whole period there were only 4 days with mean daily temperatures above 0°C. Mean of the whole period for each observations terms were also below freezing point and equal: -2.9°C at 07, -0.9°C at 13 and -1.9°C at 19, with a mean daily value equal as already presented, also -1.9°C. Minimum diurnal temperatures varied from -8.7°C (February 7) to -1.6°C (February 2), with a mean equal -5.2°C. Maximum diurnal temperatures changed from -3.3°C (February 20) to 5.6°C (February 1), with a mean value equal 0.7 °C.

During the studies temperate wind velocities predominated. Mean daily values varied from 1.5 m/s (February 20) to 8.9 m/s (February 2), with a mean for the whole period equal 3.8 m/s. The largest velocity was measured on February 2 at 07 and equal 15.4 m/s. Calms were absent during the observation period.

Air is dry in the Oasis. Mean diurnal values of water vapour pressure varied from 1.7 hPa (February 15) to 4.8 hPa (January 29), with a mean for the whole period equal 2.9 hPa. During the studies 6 times trace precipitation and 2 time larger ones were noted, giving in total 21.8 mm.

The atmosphere in the Oasis, similarly as in the whole Antarctica, is considerably transparent due to absence of pollution and small content of water vapour. The transparency is close to the ideal one and according to the author's investigations, e.g. on February 4, integral coefficient of transparency p, was equal $p_2 = 0.841$ at optical thickness of atmosphere m = 2. Due to such great transparency, there is intensive sun radiation during a day and earth radiation at night, when the weather is cloudless or with some clouds only. In consequence there are considerable diurnal temperature amplitudes especially of the active surface.

GROUND TEMPERATURE

Temperature at two extremal measurement levels will be described more broadly. They include

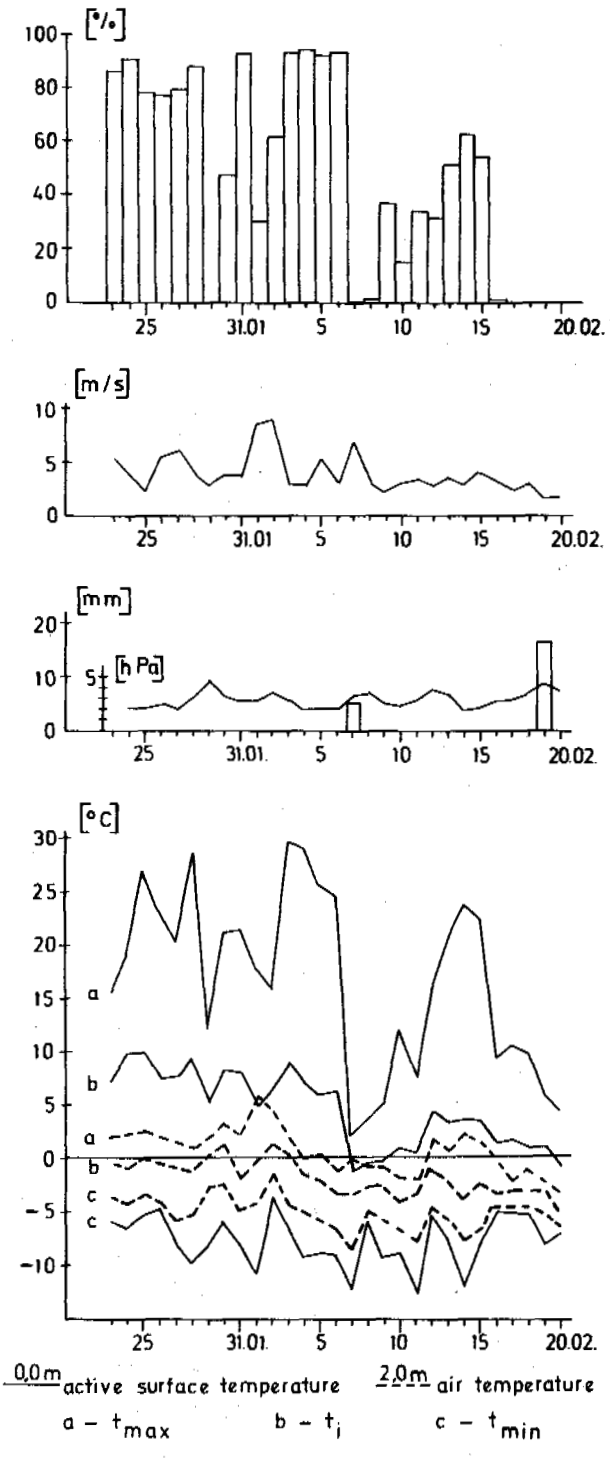

Fig.3 Courses of daily values of relative sunshine duration (%), wind velocity (m/s), water vapour pressure (hPa), precipitation (mm) and temperature (°C) of active surface (0.0 m) and of the air (2.0 m) in A. B. Dobrowolski Station (Bunger Oasis - Antarctica) in the period 23.01 - 20.02.1979

a depth of 0 cm (active surface) and 50 cm. All the other depths represented an intermediate distribution of temperature.

Mean daily temperatures of the active surface (Fig.3) varied during the described period from -1.5°C (February 7) to 9.9°C (January 25), with a mean for the whole interval of 4.4°C. The active surface got gradually and quickly cooler: means for successive decades are equal 7.9°C, 3.7°C and 1.9°C (Table II). Means for the whole period at 07, 13 and 19 are equal 1.1 °C, 9.0°C and 3.1°C respectively.

Diurnal oscillations of temperature at the active surface are fully presented by extremal temperatures (Table I). Minimum temperatures were always during the observation period below the freezing point and varied from -12.7°C (February 11) to -3.5°C (February 2), with a mean of -7.7°C (Fig.3). Decade means are respectively equal -7.1°C, -8.4°C and -7.5°C. The last value is relatively high. It refers to the period with predominant advection weathers and considerable cloudiness (8.3), that stopped night drops of temperature and influenced a rise of minimum temperatures.

Maximum temperatures at the active surface during the observation period were generally over 0°C, the only value below this point occured on the last day of measurements. Daily maxima varied from -0.5°C (February 20) to 29.5°C (February 3), with a mean for the whole period equal 16.5°C (Fig.3). Decade means gradually got lower and were respectively equal: 20.7°C, 16.3°C and 12.4°C (Table I). Daily warming of a ground surface in the Oasis is great and dark rock surfaces inclined towards the sun reach the temperatures considerably over 30°C.

Daily temperature amplitudes of active surface are very high and varied from 6.5°C (February 20) to 38.5°C (January 28), with a mean of 24.2°C (Table I); they gradually decreased and were equal during successive decades 27.8°C, 24.8°C and 19.9°C. Daily temperature amplitudes of rocky walls are considerably larger and reach about 50°C.

In the light of the above mentioned numbers, the temperature of active surface during the summer seems to pass twice a day the freezing point, resulting in freezing (in the evening) and thawing (in the morning). This frequently repeated phenomenon is, in connection with high temperature amplitudes, the reason of intensive physical weathering. It results in a common occurrence of thick covers of block rocks at the foot of slopes.

The data enclosed in the tables and also curves enable to see mutual relations between a temperature of the active surface and of the air at 2 m above the ground. As obvious from figure 4, mean daily temperatures (t_i) of active surface (0.0 m) are higher than of air ones (2.0 m) and mean difference is equal 6.3°C. It changes in a diurnal cycle and is equal 4.4°C

at 07, 9.9°C at 13 and 5.0°C at 19 (suitable data in Table I and II). At active surface there are also higher (15.8°C on the average) maximum temperatures. On the other hand minimum temperatures are lower, generally about 2.4°C. To compare I would like to add, that according to the investigations of 1956 - 1958 the temperature of active surface in the Bunger Oasis is higher in summer about 5-6°C and lower in winter about 4-5°C than the air temperature (Rusin 1961).

In the whole analyzed vertical section the lowest temperatures, and in the same time the smallest variation either in a diurnal cycle or from day to day, occurred at depth of 50 cm. Diurnal means gradually got lower from 2.8°C on the first day (January 23) to -0.1°C on the last observation day (February 20), with a mean for the whole period equal 1.1°C. Means for successive decades were equal 2.1°C, 1.0°C and 0.3°C. Diurnal amplitudes at this depth are insignificant and are approximately illustrated by data from three terms at 07, 13 and 19. Means for the whole period are equal 1.2°C, 1.1°C and 1.0°C respectively (Table II). A variation is therefore small and even disappears on some days, but e.g. on February 1 reached 0.6°C.

Slightly deeper, approximately at depth of about 70 cm, diurnal amplitudes of temperature disappear in the Oasis.

As mentioned before, course of temperature at other measurement levels, i.e. at depths of 5, 10 and 20 cm, indicated intermediate characteristics if referred to the above mentioned ones. Daily means for the whole period are equal 2.8°C, 2.4°C and 1.9°C respectively.

Table II presents mean temperatures of the whole layer 0 - 50 cm; it was calculated as arithmetic mean of all 5 depths. This simple index, not precise from a physical point of view, describes however changes of temperature of the whole analyzed layer quite well. Daily means vary from -0.4°C (February 20) to 5.6°C (January 25), with a mean for the whole period equal 2.5°C. Means of successive decades are equal 4.6°C, 2.1°C and 1.0°C.

In the active layer of the Oasis all types of vertical stratification of temperature are formed. Curves in figure 4 present examples of characteristic vertical distribution of temperature in some weather situations, i.e. during cloudless weather (February 4), with partial cloudiness (February 14), with full cloudiness (February 8) as well as with full cloudiness and snow cover (February 29), compared with mean distributions for the whole period (m). Individual curves represent observations terms (at 07, 13 and 19) and daily means (d). An additional curve for 05 was only drawn for February 4.

In summer during a sunny day, as e.g. on February 4, all possible types of vertical temperature distribution are well developed. Carried every-hour observations indicate, that insolation type (temperature drops with depth) occurs during a day approximately at 11 - 18; it is represented by curve for the 13. Radiation type (temperature rises with depth) is preserved at 03 - 06 and represented by curve for the 05. Transitional radiation-insolation type (in upper part of the section temperature rises with depth but then drops) occurs at 19 - 02, and the other transitional insolation-radiation type (temperature at first drops but then rises with depth) occurs at 07 - 10. Both the last types are represented by suitable curves from 19 and 07.

During a cloudless weather or with a small cloudiness, vertical gradients of temperature reach their largest values. So e.g. on February

TABLE II

Mean decade ground temperature in A. B. Dobrowolski Station (Bunger Oasis - Antarctica) from the period 23.01 - 20.02.1979

Depth cm	Decade	07	13	19	m
0	23.01-31.01	4.4	13.0	6.4	7.9
	01.02-10.02	0.6	8.0	2.5	3.7
	11.02-20.02	-1.5	6.4	0.8	1.9
	23.01-20.02	1.1	9.0	3.1	4.4
5	23.01-31.01	0.9	7.7	6.9	5.2
	01.02-10.02	-1.0	4.4	3.6	2.4
	11.02-20.02	-1.8	3.3	2.1	1.2
	23.01-20.02	-0.7	5.1	4.1	2.8
10	23.01-31.01	0.9	5.6	6.4	4.3
	01.02-10.02	-0.5	2.9	3.6	2.0
	11.02-20.02	-0.9	1.6	2.3	1.0
	23.01-20.02	-0.2	3.3	4.0	2.4
20	23.01-31.01	2.3	3.4	5.0	3.6
	01.02-10.02	0.8	1.4	2.7	1.6
	11.02-20.02	0.1	0.4	1.5	0.7
	23.01-20.02	1.0	1.7	3.0	1.9
50	23.01-31.01	2.2	2.1	1.9	2.1
	01.02-10.02	1.1	1.0	0.8	1.0
	11.02-20.02	0.4	0.3	0.2	0.3
	23.01-20.02	1.2	1.1	1.0	1.1
0 - 50	23.01-31.01	2.1	6.4	5.3	4.6
	01.02-10.02	0.2	3.5	2.6	2.1
	11.02-20.02	-0.7	2.4	1.4	1.0
	23.01-20.02	0.5	4.0	3.0	2.5

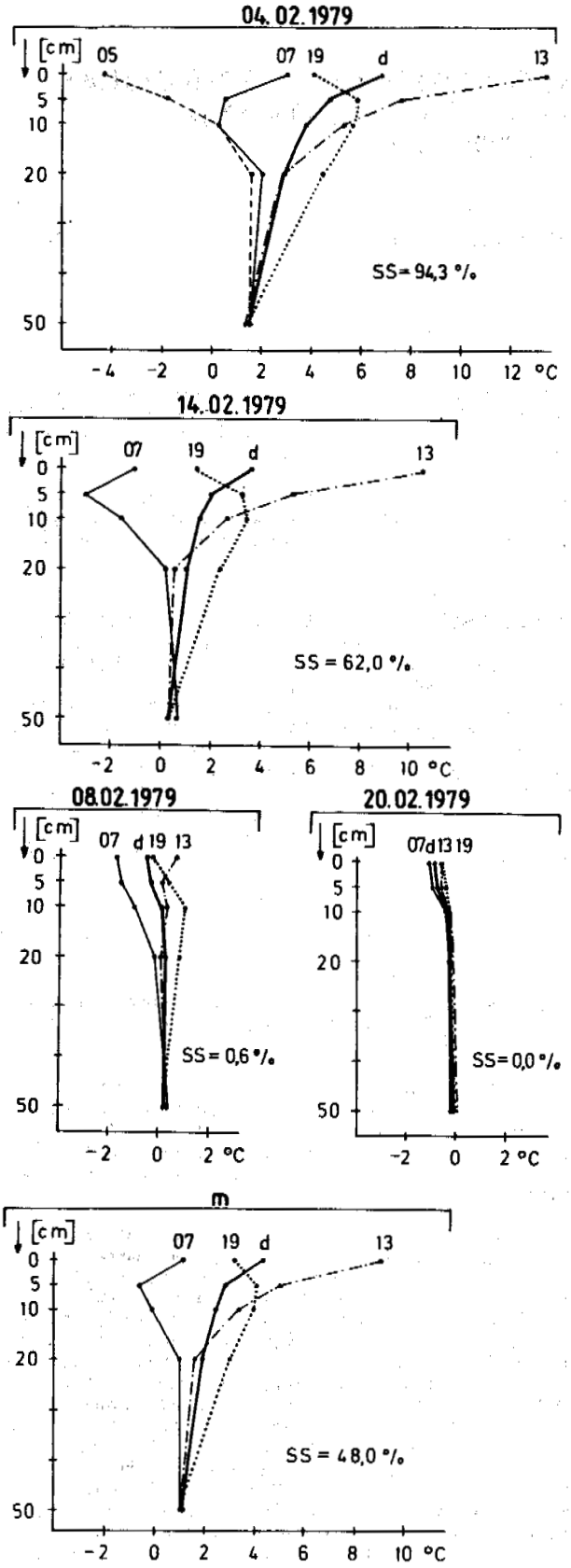

Fig.4 Vertical ground temperature distributions in the diurnal cycle (07, 13, 19 h and mean daily d) at a cloudless weather (February 4), at a partial cloudiness (February 14), at a full cloudiness (February 8), at a full cloudiness with snow cover (February 20) and mean in the period 23.01 - 20.02.1979 in A. B. Dobrowolski Station (Bunger Oasis - Antarctica)

4 at sunshine duration equal 94.3%, a vertical gradient at 13 in the layer 0 - 50 cm was equal -2.36°C/10 cm, and was -11.60°C/10 cm in the outer layer 0 - 5 cm. On the other hand at 05 at radiation type, mean gradient was equal +1.20°C /10 cm in the layer 0 - 50 cm and +5.20°C/10 cm in the layer 0 - 5 cm.

The largest measured gradients were noted on January 28 at 13 and equal -2.82°C/10 cm in the layer 0 - 50 cm and -15.4°C/10 cm in the outer layer 0 - 5 cm.

During weather with partial (e.g. February 14) or even full cloudiness (e.g. February 8) in summer there are also all types of vertical stratification, on condition that all gradients get considerably lower.

Vertical gradients decrease also as antarctic autumn comes nearer. Vertical distributions of temperature at this time and at full cloudiness are illustrated by curves from February 20. Snow cover that developed the previous day and was 12 cm thick, first cooled the outer layer of ground, resulting in radiation distribution of temperature with poorly marked gradients. So e.g. at 07 it was equal +0.22°C/10 cm in the layer 0 - 50 cm, whereas was larger in the outer layer 0 - 10 cm, +0.60°C/10 cm, and +0.12°C/10 cm in the remaining part of the section, during the same time.

CONCLUSIONS

Presented results of field works prove that in bedrock of antarctic oases there are temperature oscillations with a very significant diurnal amplitudes and frequent passing through the freezing point. They are of primary importance for development of physical weathering and frost phenomena in wetter locations.

REFERENCES

Korotkievič, E. S. (1972). Polarnyje pustyni. 1-420, Leningrad

Simonov, I. M. (1971). Oasisy Vostocnoj Antarktidy. 1-176, Leningrad

Rusin, N. P. (1961). Meteorologiceskij i radiacionnyj rezim Antarktidy. 1-446, Leningrad

Shumsky, P. A. (1969). Oledjenienije /in:/ Atlas Antarktiki. Moskwa - Leningrad

Wiśniewski, E. (1983). Oaza Bungera - polski skrawek Antarktydy. Czasopismo Geograficzne, V. 54, No 1

CHEMICAL WEATHERING IN PERMAFROST REGIONS OF ANTARCTICA: GREAT WALL STATION OF CHINA, CASEY STATION AND DAVIS STATION OF AUSTRALIA

Xie, Youyu

Institute of Geography, Academia Sinica, Beijing, China

SYNOPSIS Although it is cold and dry in permafrost region of Antarctica, chemical weathering and ion migration do occur. Some elements move upwards, and some — downwards. $CaCO_3$ is leached downwards and deposited at a depth of about 1 m in Great Wall Station area. Chemical weathering is stonger in the Great Wall Station of China than in the Casey and Divis Stations.

This paper deals with the chemical weathering process of bed rock in some regions of the Antarctica. The samples were collected from the Great Wall Station of China by Xie Youyu and Zhang Qingsong in 1984 to 1986, Casey Station by Xie Zichu in 1984 and the Davis Station by Zhang Qingsong in 1980.

THE BACKGROUND OF NATURE ENVIRONMENT FOR WEATHERING ACTION

Great Wall Station of China (62°12'S, 58°57'W) is located in Feldes penisula of King George island. The Feldes penisula, a hilly area lower than 200 m a.s.l., is -1.1°C in mean annual air temperature, 656.3 mm/yr. in precipitation, and is underlain by a 0.35 to 1.2 m active layer and a 30 to 50 m thick permafrost (Zhang, 1985). This is available for weathering process.

Casey Station (110°34'E, 66°17'S) is situated in the margin of Low Dome ice cap, Wilkes Land, East Antarctica. The samples were collected from some bedrock hilly penisulas, such as Clark, Bailey and Robunson penisulas, having emerged during the retreat period of the ice sheet in Quaternary. The samples include bed rocks, young and old moraines.

The Casey Station is -9.3°C in mean annual air temperature. All months but January are in a subzero temperature. The warmest mean temperature is 0.02°C in January, and the coldest — -15.4°C in August. The amplitude of daily variation is less than 5°C, and the mean amplitude of annual variation is 15.8°C. The minimum temperature is -41°C and the maximum — 8°C.The dalily variation amplitude can be more than 20°C on the surface of bedrock under or without the direct sunshining. The annual precipitation is 388.1 mm/yr, almost all in solid state. This climate is favorable for physical weathering, especially for frost weathering.

The Davis Station of Australia is set up in the Vestfold Hills area (77°30'E, 68°22' to 68°40'S) in the southeast of the Princes Elizabeth Land on the eastern side of Prydz Bay. The mean annual temperature of the area is -10.2°C, with a minimum temperature of -40°C in winter and the maximum one of 13°C in summer. The daily mean temperature variation is 4°C in summer and 2°C in winter. The precipitation is 70 to 130 mm/yr (Zhang, 1985). The intense frost action in this area results in a great amount of frost weathering debris and a specific weathered crust. Advance and retreat of ice sheets in this area caused the bedrocks sometimes to be under weathering condition and sometimes to be covered with ice bodies, thus limiting the duration of the growth of the weathering crust and making it become weathered along the fractures instead of forming a weathering belt. The fractures penetrate only about 2 m deep, in the bedrocks of schistose actinolite hyperothenits.

BEHAVIOR OF THE ELIMENTS IN CHEMICAL WEATHERING PROCESS

1. Correlation analysis of the chemical elements in "GW" and "TW" weathering crusts in Great Wall Station of China

The correlation coefficient of elements in colloid (<0.001 mm) and silt (<0.076 mm) of the two weathering crusts developed on andesite-basaltic volcanic agglomerate lava and tuff were computed by means of the REM cluster analysis (Table I).

For petrogenic element series, in "GW" weathering crust developed on volcanic agglomerate lava, only the couples of Al and K is 0.940 in correlation coefficient; but in the "TW" weathering crust developed on volcanic tuff, there are four couples of elements; Ca-Mg, Ti-Na, Al-Fe and Si-K, have close correlativity with correlation coefficients ranging from 0.938 to 0.904 (Table I) due to the exogenic geologic process. These phenomena are also reflected on the rare and dispersed elements. For example, there are 11 couples of elements with correlation coefficients above 0.9 in "TW" weathering crust, and 8 couples in "GW" weathering crust, and the lowest correlation coefficients also appeared in the "GW" weathering crust. It seems

TABLE I

Correlation Coefficient of Elements in "TW" and "GW" Weathering Crusts

"TW" weathering crust (Tw 01-05)		"GW" (2,3,4,5,6,7)		"GW" weathering crust (Gw 2-07)	
Ca — Mg	0.938	Ti — Fe	0.982	Al — K	0.940
Ti — Na	0.931	Mg — K	0.958	Ca — Mg	0.783
Al — Fe	0.913	Al — Ti	0.847	Si — Al	0.698
Si — K	0.904	Al — Si	0.768	Si — Ti	0.678
Al — Ti	0.653	Ca — Na	0.705	Si — Ca	0.630
Si — Ca	0.626	Al — Mg	0.534	Fe — Na	0.580
Si — Al	0.496	Al — Ca	0.515	Si — Fe	0.533
				Se — Br	0.996
				Cu — Sb	0.986
				V — Sc	0.966
				Ba — Rb	0.951
		Ta — Hf	0.988	V — Co	0.943
Mn — Co	0.987	Sc — Co	0.982	Mn — Se	0.938
Se — Br	0.986	Cs — Zn	0.980	As — Cs	0.935
Cu — Rb	0.977	As — Ca	0.964	V — Mn	0.911
V — As	0.971	U — Ta	0.951	Cu — As	0.895
Mn — Sb	0.967	U — Ta	0.939	V — Ba	0.879
V — Se	0.958	Mn — Sc	0.911	Cu — V	0.878
Mn — Sc	0.955	Cs — Rb	0.900	Cu — Zn	0.844
Zn — Ba	0.935	U — Tb	0.899	Cu — Cr	0.836
V — Cr	0.934	U — Sb	0.889	Cu — Hf	0.662
Zn — Mn	0.918	U — Cs	0.878	Cu — Sr	0.595
Cu — Cs	0.905	AS — U	0.863		
V — Hf	0.890	V — As	0.862		
Cu — Zn	0.884	V — Ba	0.836		
Cu — Sr	0.751	Cu — Br	0.822	Ce — La	0.991
Cu — V	0.750	Mn — Cr	0.810	Sm — Yb	0.984
		V — Sr	0.788	Lu — Sm	0.982
(Particle size <0.076 mm)		V — Se	0.771	Ce — Lu	0.982
		V — Mn	0.710	Ce — Eu	0.953
				Th — Ce	0.952
				Th — Tb	0.942
				Th — Nd	0.927
				U — Th	0.914
				Ta — U	0.896
				Ta — W	0.667
		(Particle size <0.001 mm)		(Particle size <0.076 mm)	

that after a long-termed exogenic geologic process, some couples of elements, Ca-Mg, Ti-Na, Al-Fe, Si-K, Mn-Co, Se-Br, Cu-Rb, V-As, Mn-Sb, V-Se, Mn-Sc, Zn-Ba, V-Cr, Zn-Mg and Cu-Sc, all have correlation coefficient above 0.9. The rare-earth elements(REE) in weathering crusts developed on volcanic agglomerate lava and tuff all have close correlation because of their congreicty and stability.

Different correlation properties exist in the elements in colloid and silt are different. For example, Ti and Fe, Mg and K have close correlation (correlation coefficient 0.982 to 0.958) in the colloid fraction but only Al and K has 0.94 in silt fraction.

2. The characteristics of enrichment and migration of the elements in chemical weathering process

In order to examine chemical weathering process under cold environment in Casey Station area the bedrocks are cut in slices from different depth for chemical analysis. The surface of bedrock is the one on which lichen grows. Furthermore, the silt and clay are analysized by means of the neutron activation and plasma spectrum.

Based on the comparison between different slices, the characteristics of the variation of ordinary, micro- and rare element contents in different layers of bedrock in Casey Station area is known as follows.

SiO_2 content decreases from interior upwards, this shows that SiO_2 was depleted in weathering process. But the amplitude of variation is about 1 only.

There is no any significant variation in Al_2O_3 content from surface downwards, this implies that the weathering does not cause Al migration.

Iron content varies between 5.11 to 0.46%, and tends to concentrate to the surface of weathered layer. The ratio of SiO_2 to Al_2O_3 has no an obvious variation in ten layers. This shows that the weathering action is very weak.

From the surface to interior, the CaO content obviously increases with an increment of about 1%. It shows that Ca migration has happened in weathering process. MgO tends to concentrate toward the surface, but TiO_2 content remains constant. The behavior of Sr and Ba tends to be opposite, Sr content decreases towavd the surface, while Ba content increases. K, Cs and Rb all tend to concentrate to the surface. The contents of Th and other rare elements vary greatly from rock to rock, but the general tendence of the variation from surface downwards are similar for all kinds of rock. Based on the analysis of Casey 1 and Casey 3 samples, it is known that the chemical weathering have not yet worked to the full extent, but element migration does reveal in different size particles.

Chemical weathering is also reflected in the migration and enrichment of elements in the "DTRW" weathering crust of Davis Station area. For instance, SiO_2 and Al_2O_3, MnO_2 and TiO_2 generally tend to decrease from the bottom upwards, MgO, K_2O and Na_2O migrate upwards, CaO becomes enriched in the middle part, usually 1 m from the ground surface, due to the leaching and accumulating of the CaO from the surface to the permafrost table. In addition, the enrichment of the active elements in the surface layer is probably due to capillary — evaporation. The sublimation of snow in summer may also be one of the reasons for the soluble salts concentrated on the ground surface.

Cation exchange capacity of the clay fraction in four weathering crusts of the Great Wall Station area are obviously reduced from the bottom upward, for example, in "SWT" section, the cation exchange capacity (CEC) in 100 g soil reduces from 38.13 at a depth of 120 cm to 26.85 on the top of the profile; in the "We" weathering crust it is from 69.04 to 51.91 in a same direction. This indicates a stronger weathering at the surface layer. In "GW" weathering crust, the content of Fe is about 4% in the lower part of the profile and increases to 6.35% at the surface; and in the "TW" weathering crust, it is 5.80% to 6.54% in a same direction. The Mg content obviously increases upwards in clay fractions. The toxicity elements As and Br enriches in both the silt and clay fraction at surface layer, the As element might come from the other place because its content is very low in the bedrock.

At surface layer of the Great Wall Station, the Br content is as high as 70 ppm, while the Se element is only 14.88 ppm at the surface of "GW" weathering crust and 3 to 6 ppm in sediments of beach terraces and fluvioglacial deposits in contrast of its Clark value of 80 ppm.

$CaCO_3$ content in weathering crust in the Great Wall Station is considerably high, for example, it is 12.85% in total soil profile of the "GW" weathering crust, 10.60% in "TW", 17.73% at the bottom of "CW" weathering crust, and 9.13% at the bottom of "SWT". In all these 4 weathering crusts, the $CaCO_3$ content is lower at the surface layer and is higher at a certain depth due to the leaching process by the plentiful precipitation. The total content of soluble salts is dispersed at the surface, while the humus content is enriched at the top of profile, for example, in the "SWT" weathering crust, the humus content is 0.48% at the bottom, 1.08% in the middle part and 4.29% at the top of the profile, this might result from the biological action.

Also, in the Davis Station area, the variation in the contents of Ca^{++}, Mg^{++} and K^{+} and $CaCO_3$ reflect the features of the migration of cations. The content of $CaCO_3$ increases from 25.5 to 29.67% from the bottom upwards, and the total salt content of the soluble salts also increases to some extent. A.D. Hoc pointed out that in both the seasonally and perennially frozen grounds, the movement and redistribution of water and easily soluble substances are the common and fundamental phenomena. They are temperature-dependent and have many practical effects. He considered that in the dry permafrost of Antarctics, the migration of ions is very rapid due to the daily and seasonal changes of heat (Hoc, 1975). The leaching is one of the chemical processes in active layer of cold regions.

In summer, it is relatively warm, the water and oxygen are relatively sufficient to the chemical weathering. It seems that the weathering action in Great Wall Station area is stronger than in Davis and Casey Station areas.

The abundance of rare-earth elements (REE) varies for different types of bedrock in Casey Station area. In the sample Polar 1, granodiorite composed of quartz, biotite, andesine, brown mica, magnetite, agustite etc., the contents of three light rare-earth elements, Ce, La and Nd, are most abundant (Fig.1). The sample Casey 1 is garnet-granite, abundant in aluminium, iron,with some acanthconite, chlorite, feldspar, quartz, mica etc. Its REE are mainly Yb, and then, Ca. This means that in Casey 1 the heavy REE are more abundant than light ones completely different from the case of Polar 1.

In clay soils, no matter what kind of parent rock they come from, the REE distribution patterns are similar to each other (Fig.2). Based on 11 diagrams of REE distribution patterns, in all sample of silt and clay, it can be seen that the main REE element here is Ce, the second one is Sm. Ce content is about 60% in all REE, Ce and the other elements,La and Sm after Ce form three peaks in the distribution diagrams. The lacking of Nd shows that Nd is completely migrated in weathering process, no matter what kind of parent rock is processed. On the contrary, Yb, Cu and Tb are stable in content in silt or in clay and form a triangle peak.

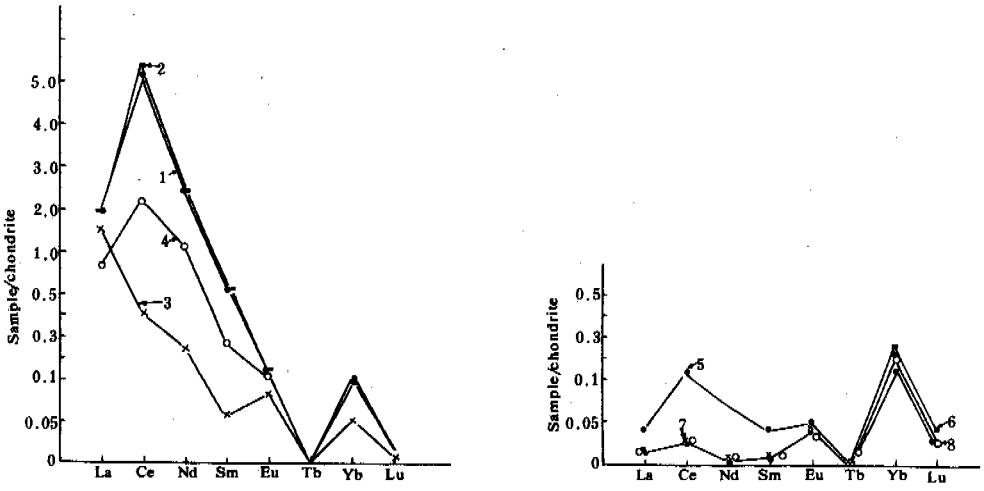

Fig.1 Relative Abundance of REE in Different Weathering Bedrocks

1. Polar 1-(4) weratering crust;
2. Polar 1-(3) lower part of the weathering crust;
3. Polar 1-(2) 11 the 1st weathering layer;
4. Polar 1-(1) 11 the 2nd weathering layer;
5. Casey 1-(4) weathering layer;
6. Casey 1-(3) the 2nd weathering layer;
7. Casey 1-(2) 1 cm from surface;
8. Casey 1-(1) 2 cm from surface.

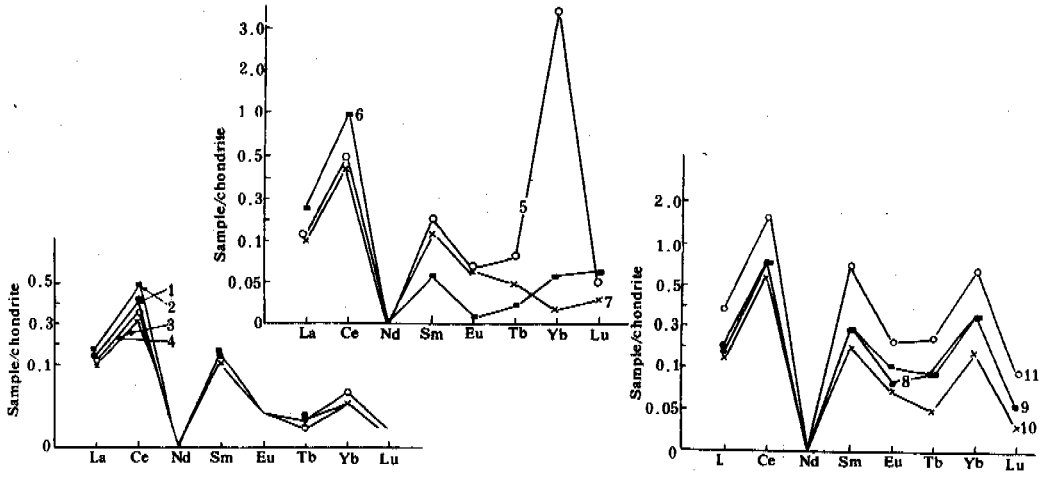

Fig.2 Relative Abundance of REE in Samples of <0.001 mm and <0.076 mm

1. Casey 3 (clay);
2. Casey 4 (clay);
3. Casey 2 (clay);
4. Casey Station (clay);
5. Casey 11 (silt);
6. Casey 10 (silt);
7. Casey 4 (silt);
8. Casey 13 (sily);
9. Casey 7 (silt);
10. Casey 2 (silt);
11. Casey 9 (silt).

It is hardly found any Tb in unweathered bed rock but Tb always exists in all kinds of weathering products. So Tb must be the migration product from other place. In short, all light REEs are active in weathering process of bed rock, while Ce and La concentrates, Nd depletes.

Ce, La and Nb concentrate to the weathering curst. Yet on the whole LREE is influenced more easity by the weathering process than HREE. This phenomena may be caused by the fact that the three- valence cations of REE have a bigger radius and lower chemical bonding.

3. The influence of grain size on elements' migration

Because the duration of chemical weathering process is different, almost no clay particle has been formed in the moraine of Neoglacial period (2,000 to 3,000 yr. B.P.). Many clay grains exist in the older moraine; for example, Casey 4 contains 46.5% of grains smaller than 0.102 mm, but the young moraine Casey 14 contains 90% of grains larger than 0.25 mm. The ratio of SiO_2/Al_2O_3, the most distinct index for weathering process, is 4 to 5 in clay fraction, 6 in the silt fraction and 6 to 7 in the bed rock. Similarly, the Fe_2O_3+FeO content obviously increases in moraine rather than in bed rock. Calcium is depleted from clay fraction but is enriched in silt fraction. The behavior of Ca here is similar to that in loess.

TiO_2 and MgO are enriched in clay. Na is depleted from clay fraction, but K, Cs and Rb are enriched in clay fraction.

4. Clay minerals and the absorption of rare elements

X-ray diffraction analysis show that the main component of clay minerals is illite hydromica and a few kaolinite in Casey Station, where the weathering action appears rather weak. Clay minerals can absorb the Ti, K, Cs, Sc, Sb, As, etc. The content of these elements is lower in bed rock and debris, but increased in clay. Among all the ordinary elements, only Fe increases in clay.

There are all complex clay minerals in weathering crust in Great Wall Station area, and the main components are illite hydromica, chlorite, kaolinite and montmorillonite. These clay minerals are different in content, for example, illite content is 69% in "GW" weathering crust, the montmorillonite content is very low, of which highest value is only 5.34%. But in the "TW" weathering crust, the montmorillonite content is relatively high, of which the highest value is 63.6% and the lowest — 56.3%. Contents of kaolinite and chlorite are higher in "TW" weathering crust than in the "GW" one, the kaolinite content is as high as 69% and does not change from bottom to surface. This shows that the clay mineral composition mainly depends on the kind of bedrock but not the weathering degree.

5. Types of weathering crust in different region

(1) Great Wall Station area

According to the analysis of aggregation and dissemination of elements, it is known that some elements change from bottom upwards, such as the cation exchange capacity content, which is the best indicator reflecting weathering intensity; contents of K,Na,Ca and Mg all had dispersed during the weathering process, but contents of Co, Ti, Fe and Mn all concentrated upward. The content of $CaCO_3$ is high at a certain depth. As mentioned above, an obvious differentiation of element occurred in the weathering crust of volcanic andesite-basaltic agglomerate and tuff in this area. It appears that there is a stratified weathering crust type and can be named the carbonate-stratified weathering crust.

(2) Davis Station area

Based on the distribution and migration of elements, it is evident that the chemical weathering process does occur in such a polar area, although it is rather weak and in an initial stage. There is a tendency that the debris weathering crust is changing to the silica-alminium-chloride type. The weathering crust there can be termed the debris-carbonate type weakly weathering crust.

(3)Casey Station area

There is no any secondary $CaCO_3$ in sediments and the weathering crusts in Casey Station area.The content of soluble salt is also very low, 0.03 to 0.11% in salinity. It can be concluded that this area is still in an initial stage of weathering with a debris type of weathering crust.

REFERENCES

Hoc, A.D., (1975). Quaternary Research, (5),1, 125.

Zhang Qingsong, (1985). Geomorphology of the Vestfold Hills, East Antarctica. Collecting papers on Antarctic Scientific Research Studies of late Quaternary Geology and Geomorphology in the Vestfold Hills, East Amtarctica. Science Press, 1-18.

WATER MIGRATION IN SATURATED FREEZING SOIL

Xu, Xiaozu, Deng, Youseng, Wang, Jiacheng and Liu, Jiming

Lanzhou Institute of Glaciology and Geocryology, Academia Sinica, Lanzhou

SYNOPSIS Using Lanzhou loess as a test material, tests of water migration in saturated freezing soil in a open system under low overburden pressure (less than 30 KPa) were conducted in the laboratory. It was found that the intake flux of water in the saturated freezing soil was in relation to the elapsed time in power form and had a maximum. Based on Darcy's law, a concept of the permeable capacity is proposed. It depends on the water content and the dry density of the soil, and the overburden pressure at the cold end of the soil column. Using data for the permeable capacity, frost depth and the underground water table, a simple method for predicting the intake flux in the field conditions is proposed and compared with Konrad and Morgenstern's method (1982).

INTRODUCTION

A large number of papers has been published on studies of water migration in saturated freezing soils. Among them the following points of view are of great significance: Miller, R.D. (1972) pointed out that there is a frozen fringe between the freezing front and the bottom of the ice lens when fine-grained soil is freezing. Konrad, M.J. & Morgenstern, N.R. (1980) presented the concept of the segregation potential which is the ratio of the intake flux of water migration to the temperature gradient adjacent to the frozen fringe when the heat regime in the freezing soils has become stable. Both of the statements mentioned above have been widely noted by scientists and engineers studying water migration and frost heaving in freezing soils. But studies of water migration under different testing conditions and of the methods for predicting the intake flux in the field conditions are still undertaken because of the complexity of the factors influencing the intake flux, especially in field conditions.

The purpose of this paper is to describe water migration in saturated freezing soils in an open system under low overburden pressure (less than 30 KPa) and to present a simple method for predicting the intake flux in natural conditions.

EXPERIMENTATION

The test material is the Lanzhou loess. Its physical properties are shown in Table I. To obtain uniform samples with respect to the water content, the dry density and the temperature distribution, the procedure of sample preparation is as follows: First, the air dried Lanzhou loess is mixed with distilled water to obtain a slurry with initial water content of 35% and placed in a sealed container for one or two days to allow moisture equilibration. Then, it is packed into the soil box with a plastic film surrounding it to prevent water seepage at the wall of the soil box, and consolidated under the same overburden pressure as used during testing, for three days. Afterwards, the soil column is cut down to 12 cm in height. The sample is placed in the constant temperature chamber. The thermocouples are fixed at the wall of the soil box every 2 cm. Insulated material with a thickness of 10 cm surrounds the outside of the soil box. A gauge is set up at the top plate. The temperatures in both the top and the bottom plates and in the chamber are controlled at +1°C for one or two days to allow uniform temperature distribution in the sample. Finally the test is started. The temperatures at both plates are controlled constantly to meet the needs of the tests after temperature at the bottom plate is suddenly dropped down to -12°C for a few minutes to allow the sample to freeze quickly at the bottom. The soil temperature, the amount of the soil deformation and the amount of the intake flow of water are determined during testing. The soil column is cut into two sections (unfrozen and frozen section, respectively), and the water content and the density of soils are determined every centimeter, after testing.

RESULTS AND ANALYSIS

Common behavior of water migration during freezing

When a negative temperature is suddenly applied to the bottom of the soil column, the freezing front moves up gradually (Fig.1). For the given initial and boundary conditions, the change of the freezing front with the elapsed time could be divided into four sections as follows: the fast freezing, the transitional, the quasi-stable and the stable section, respectively.The moisture characteristic in each section will be described later.

TABLE I

The Physical Properties of Lanzhou Loess

grained size composition (%)				specific gravity g/cm³	liquid limit %	plastic limit %
0.1	0.1-0.05	0.05-0.005	<0.005			
0.3	11.0	59.5	29.2	2.73	28.6	20.1

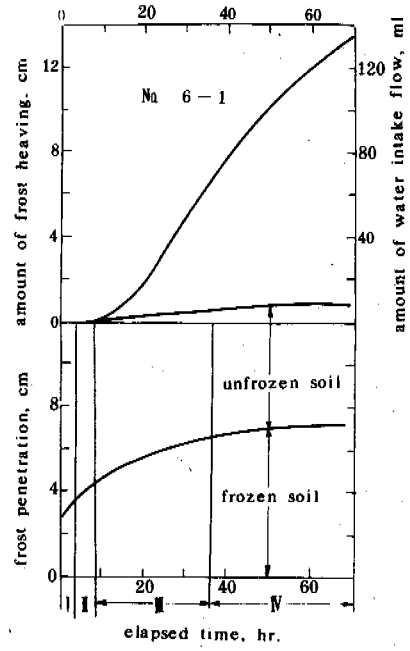

Fig.1 The Curves of the Frost Penetration, the Frost Heaving and the Water Intake Flow

The change of the freezing depth with the elapsed time could be expressed by

$$H_f = A\sqrt{T} + B \qquad (1)$$

Where H_f—the freezing depth, cm; T—the elapsed time, hr; A and B—coefficients depending on the soil properties and the boundary conditions.

During freezing, the frost heaving occurs because of both the phase change of the pore water and the ice segregation. From Fig.1 it can be seen that the amount of the frost heaving is different in the different sections. It is quite small in the fast freezing section, slightly increasing in the transitional section, increasing with a certain rate in the quasi-stable section and increasing at a declining rate in the stable sections.

The two physical processes of the frost penetration and the frost heaving result in the change of the length of the unfrozen portion in the soil column. The length of the unfrozen portion in any moment could be calculated by the following equation:

$$L_u(T) = H - H_f(T) + H_v(T) \qquad (2)$$

Where L_u—the length of the unfrozen portion, cm; H—the initial height of the soil column, cm, H_v—the amount of the frost heaving, cm.

The change of the length of the unfrozen portion with the elapsed time could be expressed as follows:

$$L_u = \frac{A}{\sqrt{T}} + B \qquad (3)$$

From the curve of the intake flow in Fig.1, it can be seen that the water intake does not occur immediately at the beginning of the test, but occurs at the start moment of the quasi-stable section, depending on the water pressure in the pores. The water pressure changes from zero to a positive value in the fast freezing section and drops down to zero again in the transitionsl section.

Fig.2 shows the profiles of the water content and the dry density in the soil column after testing. It can be seen that the water content is increased, but the dry density is decreased in the frozen portion, vice versa in the unfrozen portion, by the actions of water migration, frost heaving and densifying. Taking No. 6-2 as an example, by calculation we have the total amount of water in the unfrozen portion before and after testing equal to 515.1 and 514.64 g, respectively. It shows that the total amount of water is almost the same, although the water content and the dry density in the unfrozen portion are changed during freezing.

Therefore, it could be concluded that in the freezing test within the open system, the amount of water migrating to the freezing front is equal to the amount of the water intake during freezing. Thus, on the one hand, the water migration could be directly evaluated by the amount of the water intake. There is no water migration caused by the water redistribution in the soil column. On the other hand, the permeability and the soil-water potential could be influenced by the soil densifying in the unfrozen portion although the total amount of water in this por-

TABLE II

The Values of Both the Maximal Intake Flux and the Maximal Permeable Capacity*

No	W_o %	ρ_d g/cm³	θ_w °C	θ_c °C	P_e KPa	θ_f °C	$V_{max}\cdot10^6$ cm/s	$KP_{max}\cdot10^5$ cm²/s
21-2	36.8	1.54	1.0	-3.0	8.86	-0.1	7.035	2.909
10-1	28.3	1.39	0.8	-1.9	9.03	-0.13	4.557	2.563
6-1	28.8	1.43	1.0	-1.8	13.79	-0.13	2.439	2.165
9	28.4	1.44	1.1	-1.8	13.84	-0.13	3.796	2.287
21-2	29.5	1.50	1.0	-3.5	18.59	-0.1	7.10	2.157
11	29.8	1.42	1.0	-1.9	18.84	-0.1	3.627	2.108
8-2	28.1	1.46	1.0	-1.6	18.89	-0.13	3.449	1.970
10-2	29.1	1.45	0.8	-1.9	23.36	-0.1	3.322	1.829
24-2	30.0	1.57	1.0	-3.0	23.78	-0.13	5.113	1.974
6-2	27.7	1.53	1.0	-1.5	28.57	-0.15	3.91	2.202
23-2	24.7	1.56	1.0	-3.5	29.71	-0.2	4.908	1.87

* W_o—the initial water content; ρ_d—the initial dry density; θ_w—the temperature at the warm end; θ_c—the temperature at the cold end; P_e—the overburden pressure; θ_f—the freezing point depression; V_{max}—the maximal intake flux; KP_{max}—the maximal permeable capacity.

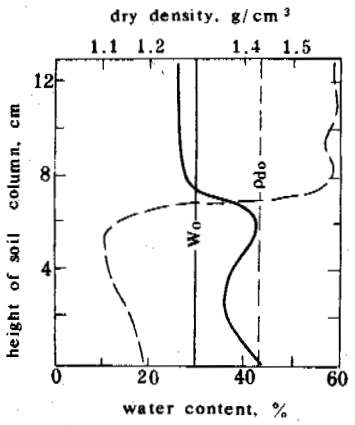

Fig.2 The Profiles of the Water Content and the Dry Density before and after Testing

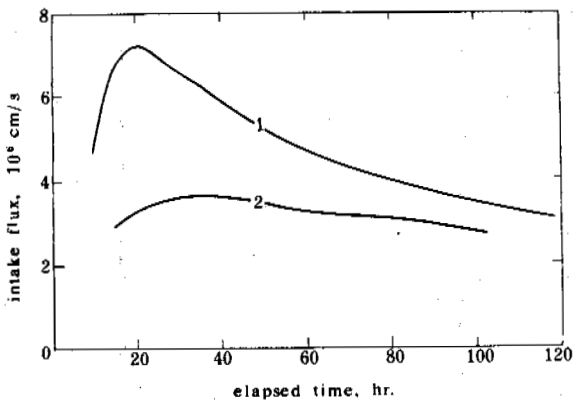

Fig.3 The Curves of the Intake Flux vs. the Elapsed Time

1—No.21-2: W_o=29.51%, ρ_d=1.50g/cm³, θ_w=1.0°C, θ_c=-3.5°C, P_e=18.6 KPa

2—No.11: W_o=29.78%, ρ_d=1.42 g/cm³, θ_w=1.0°C, θ_c=-1.9°C, P_e=18.8 KPa

tion is not changed.

Changing behavior of the intake flux of water migration

Fig.3 shows the curves of the intake flux (V) vs. the elapsed time (T) for two samples. There is the instable flow, i.e., the intake flux is always changing with the elapsed time and has a maximum. The relationship between them could be expressed by

$$V(T)=A(T-D)^{(B-1)}\exp[-C(T-D)] \qquad (4)$$

where A,B and C are the empirical coefficients; D—The elapsed time when water intake flow occurs.

Table II shows the testing results for the maximum of the intake flux and the maximum of the

permeable capacity for the Lanzhou loess with the different initial and the boundary conditions.

From Table II it can be seen that the maximum of the intake flux is increasing with the decrease in the temperature at the cold end because the length of the unfrozen portion is shorter and the suction at the freezing front is higher, and decreasing with the increase in the overburden pressure because both the permeability of the unfrozen soil and the suction at the freezing front are lower.

Simple method for predicting the intake flux in field

One of the essential purposes of the freezing tests in the lab is to find out the method or the dominant factors for predicting or evaluating the intake flux during freezing in the natural conditions.

Suppose that the Darcy's law is still valid for the unstable flow, the intake flux through the unfrozen portion of the soil column could be expressed by

$$V(T)=K_u(T)\ P(T)/L_u(T) \qquad (5)$$

where K_u—the permeability of unfrozen soils; P—the pressure difference between the top of the soil column and the freezing front. In the tests the water supply is at the top of the soil column, where the soil-water potertial equal zero so that P could be considered as the suction at the freezing front (P_u).

Here, we propose a concept called the permeable capacity KP, which is defined as the product of the permeability and the pressure differences, namely, the product of the intake flux and the permeable length, cm^2/s.

From equation (5) it can be seen that if we only consider the water intake flow in the unfrozen portion of the soil column, the permeable capacity will be the product of the permeability of the unfrozen soil and the suction at the freezing front. Numerically, it equals the product of the length of the unfrozen soil and the intake flux.

To evaluate or predict the intake flux by using the parameter of the permeable capacity, let us first look at the relation of the permeable capacity to its influencing factors . From its definition we know that the term of the permeability contains the influences of the initial conditions (for instance, the influences of the water content and the dry density). In the following we lay emphasis on discussing the permeable capacity in relation to the boundary conditions (the temperature at the cold end and the overburden pressure).

From Table II it can be seen that in the samples of No.21-2,11 and 8-2, the initial water conent, the initial dry density and the overburden pressure are almost the same, but the temperature at the cold end is quite different. Although the maximal intake flux is quite different among the three samples, the maximum of the permeable capacity is close to each other. It implies that the maximal permeable capacity has nothing to do with the temperature at the cold end. To verify this point of view, here we cite the data published by Konrad and Morgenstern (1980) and calculate the parameter of the permeable capacity (Table III).

From Table III it can be seen that the calculated permeable capacities are very close to each other even though the initial height of the soil column changes from 7.6 to 28 cm and the temperature at the cold end changes from -2.5 to -6.2°C. Therefore, that the maximal permeable capacity has nothing to do with the temperature at the cold end has beed proved again.

By using the data shown in Table II, the following relationship between the maximal permeable capacity and the overburden pressure could be obtained by the statistical analysis:

$$(KP)_{max}=2.872\times10^{-5}\exp(-0.01494P_e) \qquad (6)$$

where P_e—the overburden pressure.

To predict the intake flux in the natural conditions the following procedures are suggested: 1) taking the soil samples from the different layers in the field; 2) preparing samples in the lab according to the data of the water content, the dry density and the overburden pressure before freezing,taken from the field; 3) conducting controlled freezing tests in the lab, preferably using the same temperature gradient as that in the field to obtain the peameable capacity; 4) predicting the intake flux in the natural conditions by the following equation:

$$V(T)=KP(P_e)/[H-H_f(T)] \qquad (7)$$

where H—the underground water table, cm.

The permeable capacity is a function of the elapsed time because of the suction at the freezing front changing with time. The relationship between them could be expressed as follows:

$$KP=AT^B\exp(-CT) \qquad (8)$$

For the value of KP, the maximum or the equation (8) could be used in the prediction. It is more accurate to use equation (8), but it is necessary to use the data for the temperature gradient and the underground water table in the test.

Konrad and Morgenstern have proposed a method for forecasting the intake flux in field conditions (1982) according to the segregation potential and the temperature gradient in frozen soils as follows:

$$V(T)=SP_o\ \mathrm{grad}\,\theta_f(T) \qquad (9)$$

where SP_o—the segregation potential at the beginning of the final ice lens formed; $\mathrm{grad}\,\theta_f$—the temperature gradient of frozen soils.

TABLE III

The Values of the Maximal Permeable Capacity Calculated by the Data from Konrad and Morgenstern (1980)*

No	θ_w °C	θ_c °C	L_o cm	$K \cdot 10^7$ cm/s	L_t cm	gradT C/cm	$V \cdot 10^7$ mm/s	$KP \cdot 10^5$ cm^2/s
NS-1	+1.1	-3.4	10.4	1.0	3.20	0.37	31.5	1.008
NS-2	+1.1	-4.8	10.4	0.9	2.35	0.51	41.5	1.009
NS-4	+1.1	-2.5	7.6	1.1	3.00	0.40	40.0	1.200
NS-5	+1.1	-6.2	10.0		1.80	0.67	60.0	1.08
NS-6	+1.1	-3.4	6.4	0.95	1.80	0.67	59.0	1.06
NS-7	+1.1	-3.5	12.0		3.25	0.37	36.0	1.17
NS-8	+1.1	-4.2	8.3		2.80	0.43	40.7	1.12
NS-9	+1.0	-6.0	28.0		10.6	0.10	9.0	0.954
NS-10	+1.0	-1.0	18.0		4.50	0.24	18.5	0.833

* L_o—the initial height of the sample; K—the permeability of the unfrozen soil; L_t—the total permeable length equal to the length of the unfrozen soil plus the thickness of the frozen fringe; V—the intake flux; KP—the permeable capacity.

Fig.4 shows the results of the intake flux predicted by the two methods. It can be seen that for the method proposed by Konrad and Morgenstern, the predicted value is much greater than that determined before the intake flux reaches the maximum, but very close to the determined value after reaching to the maximum. For our method by using the maximal permeable capacity, the predicted value is close to the determined. Both of the methods result in higher valuse of the predicted intake flux, which is safe for evaluating the frost heaving in engineering construction.

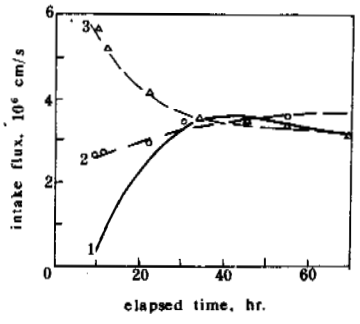

Fig.4 A Comparison of Two Methods for Predicting the Intake Flux in the Field Conditions

1—determined;
2—predicted by our method;
3—predicted by Konrad's method.

CONCLUSIONS

(i) The water migration in the saturated freezing soils in the open system could be directly analyzed by the data of the water intake flow observed in the tests because the total amount of water in the unfrozen portion is the same before and after freezing although the unfrozen soil is densified during freezing by the action of the frost heaving.

(ii) The advancing of the freezing front and the developing of the frozen fringe result in the unstable water flow during freezing. The intake flux is changing with the elapsed time in the power form and shows a peak.

(iii) Based on Darcy's law, the concept of the permeable capacity is proposed, which is the parameter depending on the soil properties and the overburden pressure and changing with the elapsed time. Its maximum has nothing to do with the temperature at the cold end of the soil column. The intake flux in the natural conditions could be predicted by the permeable capacity taken from the freezing test in the lab and the data for the freezing depth, the elapsed time and the underground water table taken from the field. The predicted value is higher than the determined value so that it is safe for evaluating frost heaving in the engineering construction. The precision of the proposed method should be verified in practice.

ACKNOWLEDGEMENTS

The authors wish to express their gratitude to the Division of Engineering Geocryology for their support in the equipment and the instruments and to give special thanks to Shen Zhonyan and Zhang Chanqing for their helpful discussion.

REFERENCES

Chen Xiaobai (1984). Current developments in China on frost heave processes in soil. Final Proc 4th ICP, 55-60.

Fukuda, M. (1984). Profiles of pore water pressure in porous rocks during freezing. Proc. 4th ICP, 322-327.

Ishizaki, T. & Nishio, N. (1984). Experimental study of final ice lens growth in partially frozen saturated soil. Proc. 4th ISGF, 71-78.

Kinosita, S. (1984). Physics of frozen ground. Publishing House of Science and Technology in Jiling province, 119-160.

Konrad, J.M. & Morgenstern, N.R. (1980). A mechanistic theory of ice lens formation in fine-grained soils. Can Geotech, J., (117),473-486.

Konrad, J. M. & Morgenstern,N.R. (1981). The segregation potential of a freezing soil. Can. Geotech. J., (18), 482-491.

Konrad, J.M. & Morgenstern, N.R. (1982). Prediction of frost heave in the laboratory during transient freezing. Can. Geotech. J., (19), 250-259.

Konrad, J. M. & Morgenstern, N.R. (1982).Effect of applied pressure on freezing soils. Can. Geotech. J., (19), 494-505.

Miller, R.D. (1984). Thermally induced regelation: A qualitative discussion. Final Proc. 4th ICP, 61-63.

Knutsson, S., Domaschuk, L. & Chandler, N.(1984). Analysis of large scale laboratory and in situ frost heave test. Proc. 4th ISGF, 65-70.

Williams, P.J. (1984). Moisture migration in frozen soils. Final Proc. 4th ICP, 64-66.

Xu Xiaozu, (1982). Research in the question of water migration in frozen soils abroad. J. of Glaciology and Geocryology, (3), 100-103.

Xu Xiaozu, Oliphant, J.L. & Tice, A.R. (1984). Experimental study on factors affecting water migration in frozen Morin clay. Proc. 4th ISGF, 123-128.

EFFECT OF OVER CONSOLIDATION RATIO OF SATURATED SOIL ON FROST HEAVE AND THAW SUBSIDENCE

Yamamoto, H., Ohrai, T. and Izuta, H.

Seiken Co., Ltd., 2-11-16, Kawarayamachi, Minamiku, Osaka, Japan

SYNOPSIS This paper describes the result of experiments concerning frost heave and thaw subsidence using specimens of consolidated and water-saturated clay, followed by a discussion. The specimens were frozen in an open system unidirectionally under various confining stresses. The frost heave ratio, ξ, defined as the ratio of a volume increment to the initial volume of a specimen, takes its maximum for a given value of the over consolidation ratio OCR. Upon thawing, the volume of the thawed specimen shrinks or expands in comparison with the volume before freezing. The subsidence ratio, ξ_s, defined as the ratio of a volume change to the initial volume of the specimen (ξ_s is taken as negative, when the thawed soil shrinks), decreases with decreasing OCR. This tendency of ξ and ξ_s can be explained theoretically by resistance to the movement of soil-water through the unfrozen part of the specimen and by the consolidation of unfrozen soil during the freezing.

INTRODUCTION

It has been well known that when wet soil freezes, frost heaving occurs and when the soil thaws, subsidence occurs. Factors influencing the frost heaving can be classified into two groups: external and internal factors. External factors are confining stress, penetration rate and pore water pressure before freezing. Takashi et al. (1972; 1978) have shown a relation between frost heaving and external factors. As for the internal factors, there are physical and chemical properties of soil particles and pore water; fundamental physical properties, e.g., water content, porosity and unit weight of soil; texture and structure. If the soil is saturated with water and its property is known, then the other properties can be calculated functionally. There is a logarithmic relation between void ratio and consolidation stress of soil; so, if the history of consolidation stress is sought, we can find out the functional properties. Therefore, when we investigate a relation between frost heave and functional physical properties, it is good enough to conduct an experiment as to a property among them.

Since subsidence should occur as a result of the reaction during the freezing of soil, it is considered that the subsidence is affected by the external and internal factors of frost heaving.

This paper shows the experimental results and discussions concerning the frost heaving and thaw subsidence of saturated soil, taking notice of the stress history of the soil.

EXPERIMENTAL PROCEDURE

Material and preparation of specimens

The soil used is Fujinomori yellow clay, which is obtained in Kyoto, crushed and air-dried.

Table I Physical properties and constants concerning frost heave

specific gravity		2.656
Liquid limit		55.8 %
Plastic limit		28.1 %
fraction	sand	2.3 %
	silt	57.6 %
	clay	40.1 %
water content		$w=29.2-4.21\ln\sigma_c$ %
coefficient of volume change		$m_v=0.192\sigma_c^{-1.01}$ MPa
permeability		$k=2.5*10^{-9}\sigma_c^{-1.25}$ cm/s
ξ_0		0.002
σ_0		0.0028 MPa
U_0		17.65 cm/h
n_f		0.255

Table I shows properties of the soil and specimens.

The specimens were made as follows: water was added to the soil, the particles of which could pass through the sieve (the opening=420 μm); and its state became slurry. The slurry was then consolidated under the objective consolidation stress σ_c for two days. After consolidation, the shape of the soil was 11 cm in diameter and 6 cm in height; and after it was trimmed to 10 cm in diameter and 4 cm in height it was used for a freeze-thaw test. A relation between the water content of the specimens and σ_c is shown in Table I. Saturation was approximately 100 %. The permeability k and the coefficient of volume change m_v were obtained by a consolidation test as shown in Table I.

Apparatus and procedure

The apparatus shown in Figure 1 was used in a freeze-thaw experiment under confining stress in an open system for water movement.

The confining stress σ_1 is applied by a spring and is maintained at a constant value during the freeze-thaw cycle. The access

material via the porous plate to the water supply container, which serves as a measuring system of water migration, is filled with de-aired and distilled water. Since the water supply container is open to the atmosphere, the pore water pressure of the top end of the specimen is always equal to the atmospheric pressure.

The specimen in the acrylite cylinder is frozen at the constant penetration rate U from the bottom to the top. From the following U can be obtained: The specimen is precooled at 0 C. The temperature θ_1 of the cooling plate and the temperature θ_2 of the piston are controlled, according to the following equations (Takashi et al., 1978):

$$\theta_1 = -L\gamma_1 U^2 t/\lambda_1 \quad (1)$$

$$\theta_2 = 0 \quad (2)$$

Where L is the quantity of latent heat, γ_1 the unit weight , λ_1 the thermal conductivity of the frozen soil and t the time.

The specimen is thawed from both ends by keeping both temperatures θ_1 and θ_2 at 10 C.

Freeze-thaw tests were carried out under various values of σ_c, σ_1 and U.

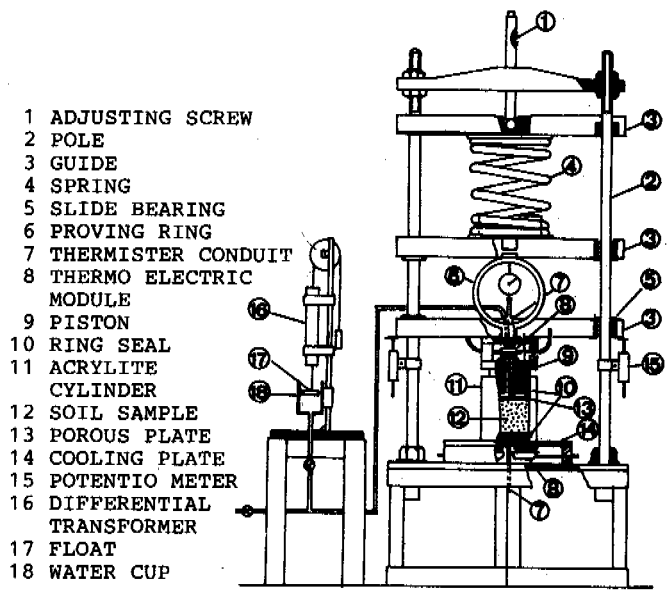

Fig. 1 Apparatus

EXPERIMENTAL RESULT CONCERNING FROST HEAVE RATIO

Frost heave ratio vs. consolidation stress

Frost heave occurs accompanied by intake or discharge of water as the freezing front penetrates into the unfrozen part. The frost heave ratio ξ and the water intake or discharge ratio ξ_w are defined as follows from the total heave amount h and the total water intake or discharge amount w when the specimen is frozen completely:

$$\xi = h/H_0 \quad (3)$$

$$\xi_w = w/A/H_0 \quad (4)$$

Where the height and the cross sectional area of the specimen before freezing are H_0 and A,respectively. In each figure, ξ and ξ_w are shown by percentage. Figure 2 shows a relation between ξ, ξ_w and consolidation stress σ_c. Both ξ and ξ_w have a maximum value at a certain value σ_{ccrit} of σ_c under constant σ_1. The value of σ_{ccrit} increases with increasing σ_1. Since the specimens are saturated, physical properties can be calculated, if σ_c is determined. Therefore, as the relations between ξ, ξ_w and σ_c are obtained, the relations can be obtained between ξ, ξ_w and physical properties as shown schematically in Figure 3.

Figure 4 shows the relation between ξ and over consolidation ratio OCR($=\sigma_c/\sigma_1$). The soil is normally consolidated when OCR=1 and over

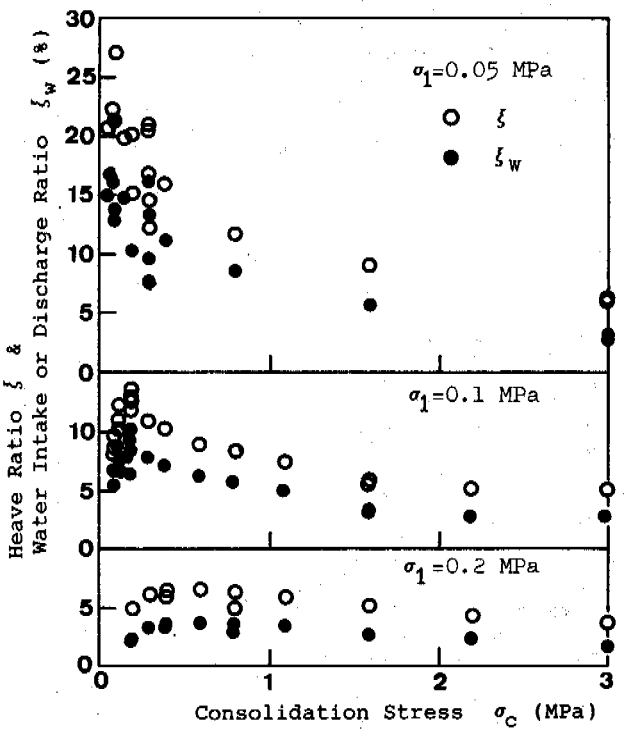

Fig. 2 ξ and ξ_w vs. σ_c

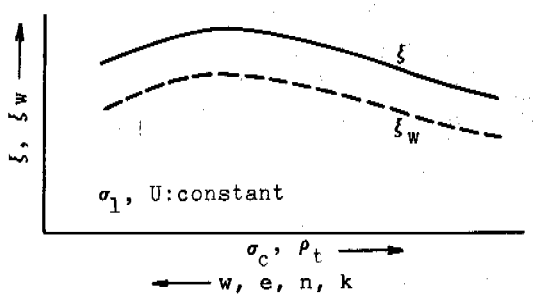

Fig. 3 ξ and ξ_w as function of fundamental properties. Arrows show the direction that the value of each parameter increases when σ_c increases.

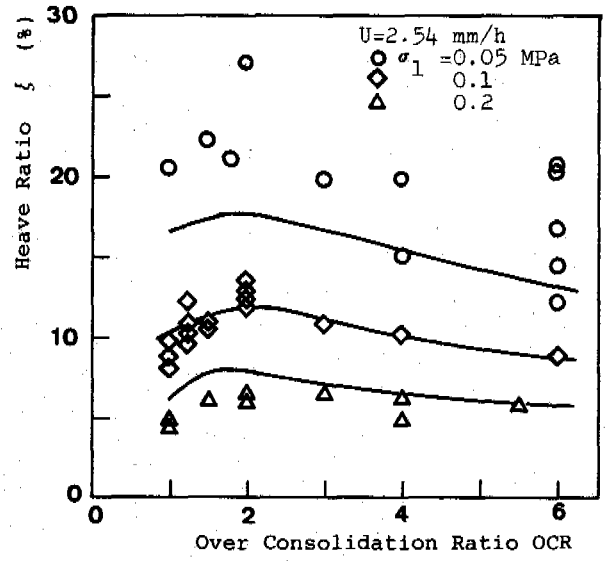

Fig. 4 ζ vs. OCR

consolidated when OCR>1. Figure 2 shows σ_{ccrit} varies with σ_1. Figure 4 shows, however, that ζ has a maximum when OCR=2.

ζ vs. σ_1

The relation between ζ and σ_1 as functions of OCR is shown in Figures 5. The value of ζ decreases with increasing σ_1. However, ζ differs when OCR differs even if σ_1 remains the same. Takashi et al. (1978) have obtained the following equation using hard clay and silt (maximum past stress is ca. 4 MPa) in the experiment.

$$\zeta = \zeta_0 + \frac{\sigma_0}{\sigma}\left(1+\sqrt{\frac{U_0}{U}}\right) \qquad (5)$$

where ζ_0, σ_0 and U_0 are constants. The value of ζ as a function of σ_1 coincides with equation 5. However, ζ_0, σ_0 and U_0 are determined for each OCR and for a given soil. From the analysis (See Discussion), it was revealed that equation

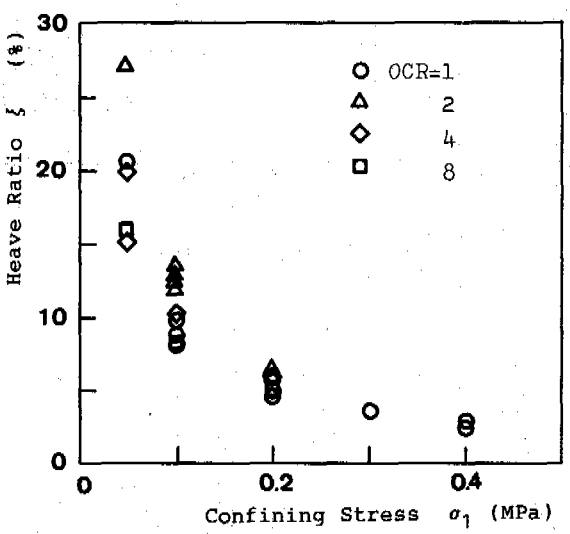

Fig. 5 ζ vs. σ_1

5 can be adopted for the soft soil, i.e., normal consolidated soil (OCR=1), assuming that ζ_0, σ_0 and U_0 are constants for a given soil.

EXPERIMENTAL RESULT OF THAW SUBSIDENCE RATIO

Thaw subsidence ratio vs. consolidation stress

Upon thawing, the height of the specimen decreases and at the final stage the volume of the thawed specimen shrinks or expands in comparison with the volume before freezing. The ratio of the displacement s to the initial height H_0 is defined as the subsidence ratio ζ_s as follows:

$$\zeta_s = s/H_0 \qquad (6)$$

When the thawed soil shrinks ζ_s is taken as negative; and when it expands ζ_s is taken as positive. In each figure, ζ_s is shown by percentage. Figure 6 shows the relation between consolidation stress σ_c and subsidence ratio ζ_s. The value of ζ_s increases, i.e., the volume of thawed soil changes from shrinking to expanding, with increasing σ_c. This tendency is the same when σ_1 is different. The value of ζ_s has a minimum value when the soil is normally consolidated. The consolidation stress, when ζ_s=0, increases with increasing σ_1.

The following explanation is given concerning thaw subsidence (Nixon and Morgenstern, 1973). The effective stress σ of the unfrozen part of the specimen during the freezing is given as follows:

$$\sigma = \sigma_1 - u \qquad (7)$$

where u is the pore water pressure. When the specimen freezes accompanied by water intake, u is negative and causes an increase in σ. When σ becomes larger than σ_c, the unfrozen part of the specimen can consolidate during the freezing, even if confining stress is always constant. Upon thawing, the specimen subsides due to consolidation during the freezing. However, subsidence occurs, even though the soil freezes accompanied by water discharge on account of large σ_1, i.e., u>0, and then σ is always smaller than σ_c (See Figure 8). Therefore, it is

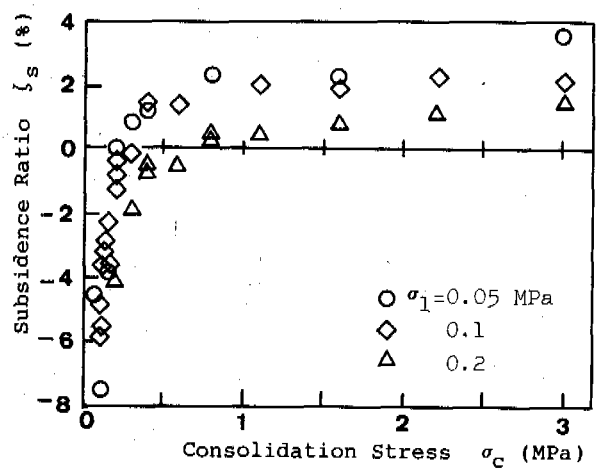

Fig. 6 ζ_s vs. σ_c

considered that the consolidation in the unfrozen part before freezing is a part of the origin of the thaw subsidence.

In order to understand the thaw expansion, the following explanation may be considered: The specimen is broken down into blocks by the ice lenses due to intake of water. Upon thawing, if the blocks does not always turn back to the initial position, the degree of biting each other increases and then the volume of the thawed specimen can increase apparently.

Only either σ_1 and σ_c cannot determine whether the specimen subsides or not upon thawing. We obtain Figure 7, readjusting ζ_s as a function of the over consolidation ratio OCR in Figure 6. The value of ζ_s increases with

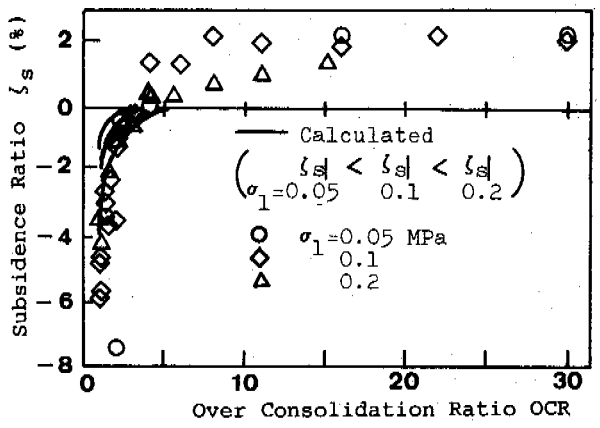

Fig. 7 ζ_s vs. OCR

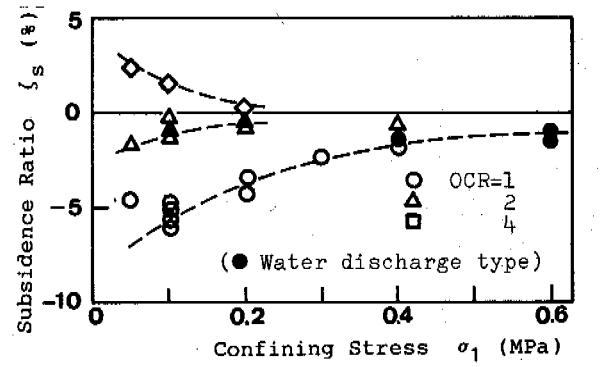

Fig. 8 ζ_s vs. σ_1 as function of OCR

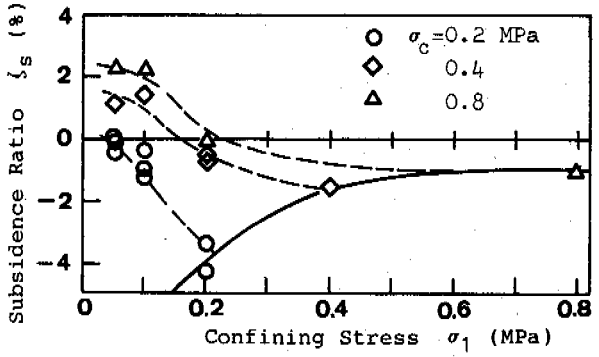

Fig. 9 ζ_s vs. σ_1 as function of σ_c

increasing OCR. The tendency agrees with the relation between ζ_s and σ_c, but OCR when ζ_s=0 is approximately the same, i.e., OCR=4, for the soil used in this experiment. It seems that OCR is an important index to determine whether thawed ground subsides or not in the field.

ζ_s vs. σ_1

The curves of the relation between ζ_s and σ_1 are different depending on whether ζ_s is adjusted as a function of σ_c=constant or OCR=constant.

The relation between ζ_s and σ_1 when OCR=constant is shown in Figure 8. There is an inversely proportional relation between ζ_s and σ_1. On the other hand, ζ_s decreases with increasing σ_1 in case σ_c=constant as shown in Figure 9. When σ_c is constant, OCR decreases with increasing σ_1 and the soil becomes normally consolidated soil. Therefore, in other words, the relation as shown in Figure 9 is that ζ_s decreases with decreasing OCR and then agrees with the results as shown in Figure 7.

ζ_s vs. ξ

It is considered that thaw subsidence is relative to frost heaving, since the subsidence should occur due to any reactions during the freezing of soil. Figure 10 shows the relation between ζ_s and ξ. The values of ζ_s scatter in this figure and there is not a correlation between ζ_s and ξ. When all data are divided into two groups by OCR=4, the sign of ζ_s is determined by OCR.

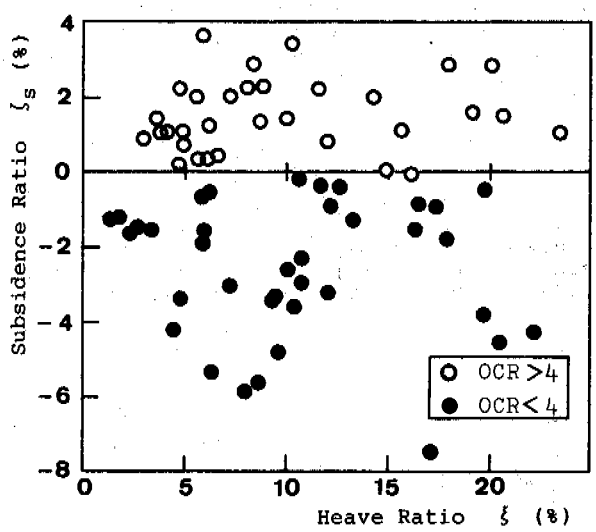

Fig. 10 Correlation between ζ_s and ξ

DISCUSSION

Factors affecting frost heaving and thaw subsidence concerning OCR

The following are the factors of frost heaving when OCR differs.

(a) Consolidation of unfrozen soil during the freezing: When the soil freezes accompanied by intake of water, pore water pressure decreases toward the freezing front in the unfrozen part and then effective stress increases. It is

possible for the soil to consolidate. Since we observe the amount of frost heave through the unfrozen part, the real amount of frost heave (in the frozen part) is canceled by consolidation and then the observed amount apparently decreases (Takashi et al., 1977).
(b) Resistance of water movement: The effective stress changes at the freezing front because resistance in unfrozen soil is different, when permeability is different according to OCR. Frost heaving is governed by the effective stress at the freezing front and consequently affected by OCR (Takashi et al., 1976).
(c) The number of soil particles in a unit volume: If the water intake pressure is generated in the frozen part consisting of soil particles, ice and unfrozen water (Dirksen and Miller, 1966; Takashi, 1982), it is possible to change the number of water intake pumps because of an increasing the number of soil particles in a unit volume.
(d) Tensile and/or shear strength of unfrozen soil: When the soil heaves during the freezing, the distance between soil particles must expand. It is considered that with an increase in strength, the resistance to this expansion increases.

The following are the factors of thaw subsidence when OCR differs:
(e) Consolidation during freezing (Logsdon et al., 1971; Nixon and Morgenstern, 1973; Chamberlain and Blouin, 1978).
(f) Compression and/or consolidation in frozen soil: When the temperature of frozen soil lowers, the soil can be compressed due to the expansion of freezing of unfrozen water. Since frost heaving occurs in the frozen part, it is supposed that the pore water pressure is lower than that in the unfrozen part and then the soil can consolidate .
(g) Changing of water retention capacity of soil due to the freeze-thaw cycle.
(h) Changing of structure of soil aggregates due to the freeze-thaw cycle.

It is difficult to analyze all factors mentioned above. In this section, the effect of OCR on frost heaving is analyzed as to consolidation and resistance of water movement in the unfrozen part. Concerning thaw subsidence, only the consolidation of unfrozen part is considered.

Analytical model and differential equation

Analysis was made under the following assumptions:
(a) The soil is uniform and saturated by water.
(b) The soil freezes unidirectionally and under the constant penetration rate U macroscopically (Holden et al., 1985).
(c) Terzaghi's consolidation equation can be applied to consolidation, when the effective stress of the unfrozen soil exceeds the maximum past consolidation stress σ_c.
(d) Water intake rate at the freezing front is given by the experimental equation shown by Takashi et al. (1978).
(e) Thaw subsidence occurs due to consolidation in the unfrozen part during freezing.

An analytical model is shown in Figure 11.
The differential equation is as follows:

$$m_v \gamma_w \frac{\partial u}{\partial t} = \frac{\partial}{\partial z}(k\frac{\partial u}{\partial z}) \qquad (8)$$

where u is the pore water pressure, z the distance from the cooling plate, t the time, m_v the coefficient of volume change, k the permeability, and γ_w the unit weight of water.

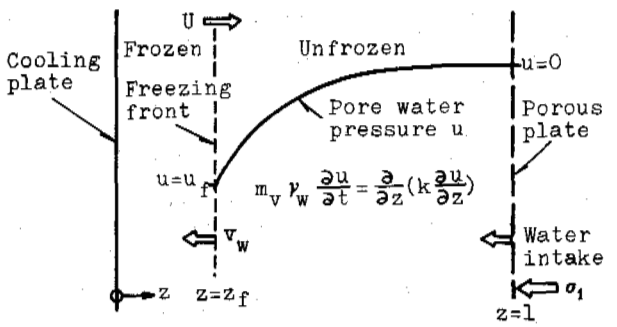

Fig. 11 Calculation model

Initial condition: u=0 (9)
Boundary condition: u=0 at z=l (10)

If the pore water pressure u is u_f at the freezing front $z=z_f$, the second boundary condition concerning the water intake rate v_w from the unfrozen part into the frozen part is as follows (Takashi et al., 1978):

$$v_w = \frac{U}{1+\Gamma}\frac{\sigma_0}{\sigma_1-u_f}\left(1+\sqrt{\frac{U_0}{U}}\right)-n_f\frac{\Gamma}{1+\Gamma}U \qquad (11)$$

where σ_0, U_0 and n_f are the constants concerning frost heaving and Γ is the freezing expansion ratio of water (Γ=0.09).

Then calculation was made using the explicit difference calculus (Fujii et al., 1976). The amount of frost heave was calculated as the sum of the total amount of water intake from the end cup into the specimen, its freezing expansion and freezing expansion of soil water. The amount of subsidence is calculated as the sum of the amount of consolidation obtained from the maximum effective stress $\sigma_{max}(=\sigma_1-u_f)$ of each element.

Frost heave ratio

The calculating results shown by pore water pressure profiles are given in Figure 12. When

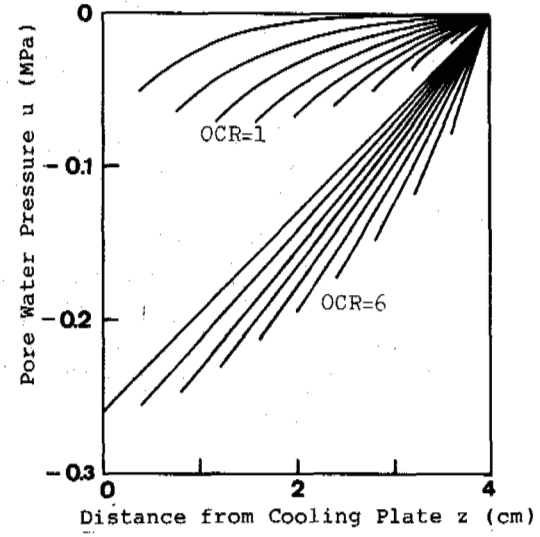

Fig. 12 Pore water pressure profile during freezing

OCR is large and then consolidation does not occur, the profile is linear and the pressure has a minimum value at the cooling plate. On the other hand, when the soil is normally consolidated soil, consolidation occurs in the unfrozen part due to an increase in σ and the profile is nonlinear. The minimum value of u occurs when the soil freezes to some extent. When both soils are compared, pore water pressure depression is smaller in normally consolidated soil than in over consolidated soil.

Calculating results concerning a relation between frost heave ratio ζ and over consolidation ratio OCR is shown by solid lines in Figure 4. When OCR is larger than that at which ζ takes its maximum, ζ decreases mainly due to the resistance in soil water movement through the unfrozen part of specimen. Meanwhile, ζ decreases with decreasing OCR, when OCR is small, which can be explained by the consolidation of unfrozen part. As for k and m_v measured values were used. However, the constants of ζ_0, σ_0, U_0 and n_f were determined so as to agree with the calculating results using the data under σ_1=0.1 MPa and OCR=2. Though the agreement is a matter of course at this point, the result of calculation agrees with the result of the experiment over a wide range of OCR. The same tendency is observed in calculation that ζ has a maximum as a function of OCR in the experiment. Thus, it is considered that the theory can describe well the actual phenomenon. In this analysis, calculation is carried out as frost susceptibility does not change even if OCR of the specimen differs. The constants of σ_0, U_0 and n_f in equation 11 are related to the frost susceptibility and do not depend on OCR. It is considered that the degree of effect of other factors is smaller than resistance to water migration and consolidation in the unfrozen part, because the result of this analysis agrees with the result of the experiment.

Subsidence ratio

Figure 7 shows the calculating results concerning ζ_s. The tendency, in which the amount of subsidence decreases with increasing OCR, agrees with the result of the experiment. However, when OCR increases, the result, in which $\zeta_s>0$, cannot be obtained because calculation was made under one condition, in which subsidence originates in consolidation of the unfrozen part. Furthermore, the result of calculation shows the value larger than that of the experiment. The volume of consolidated soil cannot come back to the volume before consolidation, even if the overburden pressure is removed. Therefore, consolidation during the freezing should appear as thaw subsidence. It is considered that the cause of differences in values occurring between the calculation and the experiment is that thaw subsidence occurs due to other factors (e.g., consolidation and/or compression in frozen soil) added to consolidation of unfrozen soil.

CONCLUSIONS

The experiment was carried out to investigate frost heaving and thaw subsidence for different value of the over consolidation ratio OCR of soil. The following are the conclusions:

(1) Frost heave ratio ζ has a maximum as a function of OCR. The relations between ζ and physical properties of unfrozen soil, e.g., water content, porosity, unit weight, are the same as the relation between ζ and OCR.

(2) The equation (Takashi et al.,1978) can be applied to the relation between ζ and the confining stress σ_1, when OCR of soil differs.

(3) Upon thawing, two cases are observed in volume change of soil; i.e., the soil does not always shrink but expands compared to the volume before freezing.

(4) Thaw subsidence ratio ζ_s increases with increasing consolidation stress σ_c of the specimen, where $\zeta_s>0$ shows expanding and $\zeta_s<0$ shows shrinking. For a given soil $\zeta_s=0$, when OCR=4.

(5) The relation between ζ_s and σ_1 is approximately hyperbolic, when OCR is constant. On the other hand, when σ_c=constant, ζ_s decreases with increasing σ_1.

(6) There is little correlation between ζ and ζ_s.

(7) Theory is presented concerning the relation between ζ and OCR and the relation between ζ_s and OCR.

REFERENCES

Chamberlain, E.J. and S.E. Blouin (1987). Densificasion by freezing and thawing of fine material dredged from waterways. Proc. 3rd Int'l. Conf. Permafrost, Edmonton, Alberta, Canada, 31-44.

Dirksen, C. and R.D. Miller (1966). Closed-system freezing of unsaturated soils. Soil Sci. Soc. Am. Proc. (30) 168-173.

Fujii, T., K. Katayama, A. Saito, H. Hattori and S. Toda (1976). Dennetsu kougaku no sinten 3. 2nd Ed., 330pp. Youkendo, Tokyo.

Holden, J.T., D. Piper and R.H. Jones (1985). Some developments of a rigid-ice model of frost heave. Proc. 4th Int'l Symposium on Ground Freezing, 93-99.

Logsdon, Gary and Edgerley, J. (1971). Sludge dewatering by freezing. J. AWWA, Nov. 1971, 734-740.

Nixon, J.F. and N.R. Morgenstern (1973). The residual stress in thawing soils. Can. Geotech. J., (10) 571-580.

Takashi, T. and M. Masuda (1972). Effect of pore water pressure of soil on frost heave ratio. Proc. 27 Annual Conf. of JSCE (3) 297-300.

Takashi, T., M. Masuda and H. Yamamoto (1976). Influence of permeability of unfrozen soil on frost heave. Journal of the Japanese Society of Snow and Ice, (38) 1, 1-10.

Takashi, T., T. Ohrai and H. Yamamoto (1977) Pore water pressure and consolidation in unfrozen soil near the freezing front. SEPPYO, J. Japanese Soc. Snow and Ice, (39), 2, 53-64.

Takashi, T., H. Yamamoto, T. Ohrai and M. Masuda (1978). Effect of penetration rate of freezing and confining stress on the frost heave ratio of soil, Permafrost, 3rd Int. Conf., (1), 737-742.

Takashi, T. (1982). Analysis of frost heave mechanism (in Japanese)

MASS TRANSFER IN FROZEN SOILS

E.D. Yershov, Yu.P. Lebedenko, V.D. Yershov and Ye.M. Chuvilin

Faculty of Geology, Moscow State University, Moscow, USSR

SYNOPSIS The results of investigation into the processes of mass transfer in frozen soils under the effect of different driving forces are reported. The data presented explain the mechanism and relationships between moisture transfer and segregated ice formation in frozen soils in a gradient temperature field under the effect of salt solution concentration gradient, mechanical loads, compression, and injection. The data available today on moisture transfer in the field of electric stresses have also been generalized and presented. A quantitative evaluation of migration flow density values and other thermodynamic parameters was made. Changes in the texture and structure of frozen soils due to unfrozen moisture migration are discussed. Based on the experimental data and other materials, a comprehensive analysis has been carried out to identify common features and differences in the processes of mass transfer in frozen soils under the impact of various driving forces. The results obtained are of great significance both for general and engineering geocryology.

Moisture transfer and ice accumulation in frozen soils constitute one of the most important problems of general and engineering geocryology, physico-chemistry and mechanics of frozen soils. Successful solution of both the scientific problems concerned with the transformation of the composition, cryogenic texture and properties of frozen soils and those of engineering geocryology responsible for the stability of buildings and structures erected on them depends on the extent of cognition of the above-outlined processes. This necessitates studying a great number of complicated chemical, physical and physico-mechanical processes occurring in frozen soils under the impact of different thermodynamic fields. Insufficient knowledge of the problem, its great scientific and practical importance predetermine the actuality of the present studies.

The authors have conducted experimental studies to identify the mechanism and laws of moisture transfer and ice accumulation in frozen soils under the influence of different driving forces. To solve the tasks, the procedures of experimental studies of the processes of moisture transfer and ice formation in frozen soils under the impact of mechanical stresses and osmotic forces have been worked out.

In the course of the experiments, frozen soils of disturbed structure were used: monomineral clays of the Paleogene: kaolinite (eF_2) and montmorillonite ($ef_1$0 gl) of eluvial genesis; and polymineral clay (mF_2kv) of marine genesis to investigate the influence of mineral composition. The effect of particle-size distribution was studied on loam (aIII) and loamy sand (gmII) from the Quaternary and glacial-marine sediments of West Siberia, and the sands of marine genesis (mI_3).

It is known that unfrozen water films in frozen soils are located in the field of action of the adsorption forces of the surface of mineral particles. Their properties and, first and foremost, mobility are determined by the surface energy of these particles, as well as chemical and mineral composition, fineness and temperature of soils. Therefore, studies of the processes of physico-chemical interaction between mineral particles and soil moisture, phase transfer of water and conditions of its thermodynamic equilibrium are deemed to be important. The perturbation of general thermodynamic equilibrium is possible when frozen soils are affected by temperature, electric, magnetic and gravitational fields, mechanical forces and hydrostatic pressure, and due to chemical interaction between the soil and chemically active environment. Such effects on frozen soils lead to the changes in temperature, pressure, concentration, and mobility of water films, and to the formation of moisture potential gradients.

The experimental studies (Yershov, 1979) showed that the presence of temperature and electric fields in frozen soils results in moisture migration and segregated ice formation. The migration of moisture in the gradient temperature field is conditioned primarily by the processes of diffusion and thermodiffusion. The diffusional transfer of water results from its non-uniform freezing in the gradient temperature field, and formation of unfrozen water-content gradients. A decrease in ground temperature disturbs the thermodynamic equilibrium between the unfrozen water films and ice. The freezing out of a part of water and the attainment of a new equilibrium bring about thinning of water films and reduction of the unfrozen water thermodynamic potential in the region of lower negative temperatures. In the region of higher negative temperatures, the water films are

thicker, they are more mobile, and, naturally, the thermodynamic potential values are higher. A difference in water mobility causes its migration from the regions of higher mobility to the ones of lesser mobility, i.e. from high to low temperatures.

When studying the laws of moisture migration in the soils of different composition, texture and properties, it has been shown that the greatest redistribution of moisture is observed in clays, the first place among which belongs to the clay of kaolinite composition. It is associated with great values of moisture diffusion coefficients in kaolinite clays having thicker unfrozen water films. In montmorillonite clays, the unfrozen water films are less mobile. The clays of polymineral hydromicaceous-montmorillonite composition take an intermediate position between the kaolinite and montmorillonite ones. The densities of moisture migration fluxes decrease when transferring from clays to loams and loamy sands because the amount of unfrozen water decreases in coarser soils. In addition, the pore space structure in coarser moisture-saturated frozen soils is such that continuous water films are not formed in them on fairly long ways of moisture transfer. The moisture migration flux density in frozen loams decreases by two-three times, as compared to clays, that reduces segregated ice accumulation in the former. The region of segregated ice interlayer formation in finer soils is shifted to the side of higher negative temperatures. With the temperature gradient build-up there occurs an increase in the density of the moisture migration flux, and in the intensity of moisture redistribution and segregated ice formation.

The studies of the process of moisture migration and segregated ice formation in frozen soils under the effect of temperature gradient have shown that its presence causes water films flow from the region of high to the region of lower negative temperatures; the moisture migration flux density being of the order of 10^{-7} gr/cm^2 . s.

Moisture migration in frozen soils under the impact of the electric field gradient has been studied less thouroughly. Contrary to moisture migration under the effect of the temperature gradient, its transfer in the field of electrical forces is conditioned by the electric potential gradient changing the total thermodynamic potential of soil moisture. The electric tension gradient in frozen soils causes migration of the unfrozen water films from the positively charged electrode - anode to the negative one - cathode. Creation of the electric field disturbs the equilibrium. The external electric field affects primarily the electric double layer in water films and changes the total thermodynamic potential of film moisture and ions of the dissolved salts. The formation of the thermodynamic potential gradient of moisture between the anode and cathode causes moisture migration in that direction and increases the total moisture content of soil in the region of the cathode. Moisture migration from the anode results in the thinning of water films there and in disturbing the thermodynamic equilibrium between the unfrozen water and ice. It leads to melting of the pore ice and recuperation of the thickness of water films. Nearby the cathode, on the contrary, the inflowing moisture increases the thickness of water films and disturbs the thermodynamic equilibrium, A surplus moisture freezes up while changing to pore and segregated ice.

It is obvious, that water migration in frozen soils in the gradient electric field depends on their composition and properties. Besides, in coarser soils the coefficient of moisture diffusion diminishes thus conditioning a decrease in density of the moisture migration fluxes from the anode to the cathode. Therefore, the smallest migration fluxes in the field of electric forces are in frozen sands and loamy sands which, practically, do not contain the most mobile loosely-bound water, whereas the biggest moisture fluxes are in kaolinite clays wherein unfrozen water films are very thick. In frozen montmorillonite clays characterized by small values of moisture diffusion coefficients, the moisture flux in the field of electric forces is also insignificant.

The studies of moisture migration in frozen soils interacting with water solutions of salt have shown that simultaneously with ion diffusion from the water solution (or salted ice) a liquid phase is also transferred to a sample. The main reason of such a transfer of salts lies in the presence of ion concentration gradient in the water solution and nonsaline soil. This gradient is directed from the water solution deep down the frozen soil causing transfer of ions in the same direction. The liquid phase migration in the same direction is conditioned by both the transfer of water films hydrated by ions, and, perhaps, by the difference in the total thermodynamic potential of moisture between the water solution and bound groundwater. Thus, when frozen soils in the process of slinization, contact water solutions or salted ice, there occurs an undirectional transfer of the salt ions and unfrozen water films.

Investigations into specific features of moisture migration in frozen soils under the effect of osmotic forces have shown that maximum densities of moisture migration fluxes are observed on the contact of saline soils with fresh ice (10^{-7} gr/cm^2. s) (or nonsaline soils with water solutions of salts) due to the presence of strong driving forces of moisture migration. A decrease in the moisture migration flux density with the distance from the contact cross-section is conditioned by a corresponding decrease in the gradients of the dissolved ions concentration and driving forces. The interaction of frozen soils with water solutions of salts results in a considerable moisture accumulation due to an intensive transfer of the liquid phase. The freezing of a portion of migrating moisture gives rise to the formation of segregated ice interlayers and streaky cryogenic structure, which causes strong volumetric heaving of frozen soils in the process of their salinization.

In has been shown that moisture transfer

process also occurs when the liquid phase is influenced by the hydrostatic pressure. The main parameters which influence the process of injected ice formation are: pressure in soil moisture, ultimate shear strength of the unfrozen water films, and ultimately-long and instantaneous strength of the frozen soils. The injected moisture flow density, the seepage coefficient and the amount of ice accumulation increase with an increase in the fineness of soil particles and in the content of the kaolinite group minerals: the former reaches the values $6\ 10^{-5}$ gr/cm^2 · s to $3\ 10^{-4}$ gr/cm^2 · s. The value of initial hydrostatic pressure, under which the process of moisture injection begins, decreases with an increase in the fineness of soil particles and the growth of content of the kaolinite group minerals. Soil temperature decline increases the initial hydrostatic pressure needed for moisture injection and decreases the density of moisture injection flow and ice formation.

As has been demonstrated experimentally, soil deformation at the stage of long-term creep causes the flow of water films into the region of shear thus increasing the moisture and ice content therein and forming segregation micro- and macrointerlayers. It is known that due to the shear of thawed rocks, a change in the pore pressure and the moisture migration to the shear zone occur in the region of displacement. In contrast to the unfrozen soils, the pore space of frozen ones is filled with ice, therefore, only thin water films of bound moisture can be found in the field of mineral particle action. A decrease in the potential of bound water when it is influenced by shearing forces is caused by the tensile stresses between soil particles in the plane of shear. The action of shearing forces in frozen sois results in the formation of the total thermodynamic moisture potential gradient causing the transfer of the unfrozen water films into the region of shear. An increase in the water film thickness disturbs the thermodynamic equilibrium between the liquid phase and ice and leads to the freezing out of the excess unfrozen water. As a result, the total moisture and ice content increases and segregated ice interlayers are formed in the zone of shear. In the regions remote from the shear zone, the thinning of unfrozen water films also disturbs the thermodynamic equilibrium and causes pore ice melting. The total moisture content in these regions decreases.

It has been shown that the development of the migration process is significantly determined by the acting load and velocity of deformation, which is, probably, associated with different values of stress gradients.

A predominantly mixed migration-seepage mechanism is in operation when frozen soils are acted upon by press tools of different size and shape, because alongside with the formation of the microshear regions at an angle to a press tool plane, the compaction regions are also formed directly beneath the press tool. As a result, the moisture transfer in the shear zones occurs mainly due to the above-described mechanism, whereas the unfrozen water films are transferred to the regions of the compacted nucleus due to pressure, i.e. moisture is suezed out from the nucleus being compacted. The experiments proved that configuration of the zones of ice accumulation and dehydration depends on a press tool shape.

The maximum moisture accumulation in the shear region is observed in clay as compared to loam and loamy sand. The determination of the density of moisture migration flows to the shear zone in frozen soils of different fineness of particles has shown that their values considerably increase on the transition from sands to clays and reach $1\ 3\ 10^{-7}$ gr/cm^2 · s. This is conditioned primarily by a high content of the liquid phase in clays and their high water conductivity in the frozen state. The influence of mineral composition on the processes of moisture transfer and ice accumulation is especially great in clays. Maximum values of moisture accumulation in the shear zone and dehydration of remote sections are observed in kaolinite clays and minimum values - in montmorillonite ones, the polymineral clay occupies an intermediate position.

The impact of soil density on the processes of moisture transfer and ice accumulation has been studied on the samples of kaolinite clay. As a result, it was established that an increase in soil density, other things being equal, entails a decrease in the density of moisture migration flows to the shear zone, and moisture accumulation therein (Fig.1), which is associated

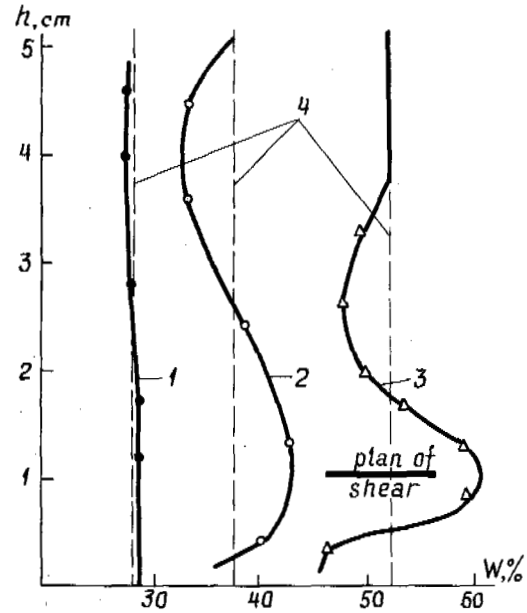

Fig.1 Redistribution of moisture in the samples of frozen kaolinite clay with various initial moisture content due to shear

1 - W_{in} = 29% ρ_d = 1.47 g/cm^3
2 - W_{in} = 39% ρ_d = 1.23 g/cm^3
3 - W_{in} = 52.2% ρ_d = 1.08 g/cm^3
4 - average moisture content

with smaller velocities of deformation of compacted clays. The intensity of moisture trans-

fer and ice accumulation in the shear zone was shown to decrease with a negative temperature decline. This happens due to a decrease in the content of the unfrozen water capable of micrating, and owing to a simultaneous decrease of the moisture transfer coefficients.

The main reason of moisture transfer under the effect of frozen soil compression lies in the presence of pressure gradients in the unfrozen water films. The pressure difference is responsible for the moisture movement to the periphery of samples under compression. At the same time, application of load to the frozen soil results in the thermodynamic equilibrium disturbance and melting of pore ice. The maximum unfrozen water seepage has been established in the clays with a high content of liquid phase. The intensity of seepage decreases with an increase in the size of soil particles from clays to sands, and maximum values of dessication of the frozen grounds under compression have been recorded in frozen clay samples. A decrease in the intensity of the unfrozen water seepage in the row from clay to loamy sands is associated, in considerable measure, with worsening of their moisture-conducting properties in this series. As has been established earlier, moisture diffusion coefficients decrease with an increase in the size of soil particles. It is due to this phenomenon that the intensity of unfrozen water seepage drops in coarser-grained soils. It has also been established experimentally, that the intensity of unfrozen water seepage depends on the load applied. With increasing load the seepage intensity increases as well. Thus, an increase of the load applied to a frozen clay from $3\frac{kg}{cm^2}$ to $12\frac{kg}{cm^2}$ caused a decrease in its moisture content by 20-25% on the average.

The impact of temperature on moisture seepage under compressional compaction is, as described above, analogous to that of temperature gradient in frozen soils. The intensity of water seepage in frozen soils drops with a decrease in temperature.

The studies conducted and the data available on the moisture transfer in frozen soils permitted a camparative analysis of this process occurrence under the effect of different driving forces with the aim of identifying its common and distinguishing features. The comparison showed that irrespective of different character and nature of impacts upon the frozen soil, common features of moisture transfer and ice formation process were revealed, namely: disturbance of thermodynamic equilibrium between liquid and solid phases of water and formation of gradients of driving forces. The redistribution of moisture and ice, i.e. dehydration of some of the soil zones and ice accumulation in the other have been noted. This leads to the transformation of the cryogenic texture of soils (Fig.2).

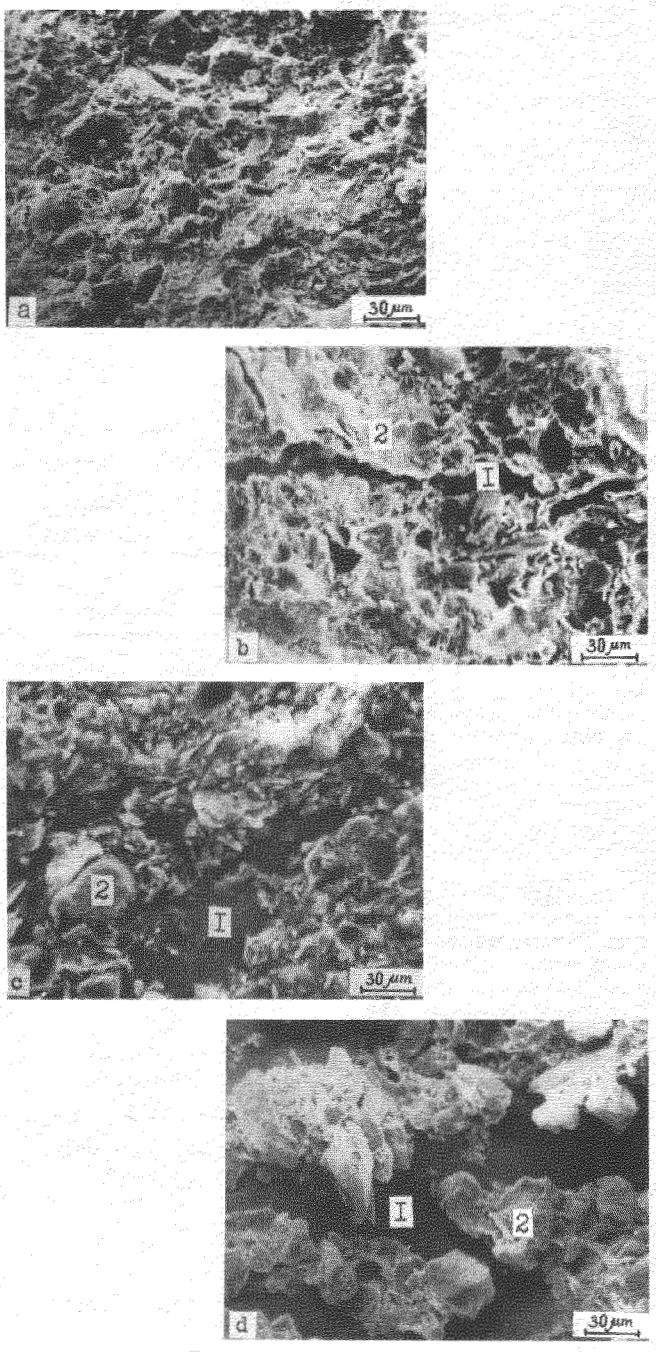

Fig.2 The patterns of ice formation in frozen soils under the impact of different driving forces of moisture transfer: a - original state of soil; b,c, and d - under the impact of gradients of hydrostatic pressure, temperature and osmotic forces, respectively; 1 - ice; 2 - mineral skeleton.

However, depending on the kind of impact on frozen soils, the moisture transfer and ice formation are characterized by their specific features. External effects, depending on the mechanism caused by them, can be subdivided into three groups. The first group comprises such effects on frozen soils which lead mainly to the migration of the unfrozen water films. The second group includes external effects on frozen soils that cause seepage of the unfrozen water films. And, finally, the third group includes external effects trigger-

ing off a combined migration-seepage mechanism of moisture transfer (Table 1). According to

TABLE 1

The Main Mechanisms and Driving Forces of Moisture Transfer in Frozen Soils

Mechanism of moisture transfer and ice formation	Main driving forces of moisture transfer	Main kinds of external effects on frozen soils
Migration - segregation	Gradient of osmotic forces	Interaction of soils with water solutions of salts; and saline frozen soils with fresh ice
	Temperature gradient	Temperature field
	Gradient of electric potential	Electric field
Seepage-injection	Gradient of hydrostatic pressure	Hydrostatic pressure
Combined migration-seepage mechanism of moisture transfer and segregated-injected ice formation	Gradient (driving forces of migration and seepage)	Different kinds of external mechanical impacts on frozen soils (shear, compaction, extention, compression).

the different moisture transfer mechanisms, the processes of ice formation can be grouped into segregated, injected, and combined segregated-injected ice-forming ones. An analysis of moisture accumulation, depending on the mechanism of moisture migration and ice formation, has shown that maximum moisture accumulation is associated with the seepage-injection mechanism (average values of water flows I_w reach $10^{-4} - 10^{-5}$ gr/cm^2· s), and the smallest - with the migration-seepage mechanism ($I_w = 10^{-7} - 10^{-8}$ gr/cm^2· s).

REFERENCES

Yershov, E.D. (1979). Vlagoperenos i kriogennye textury v dispersnykh porodakh, 213 pp., Moskva: Izdat. Moskovskogo Universiteta.

STRESS-STRAIN PREDICTION OF FROZEN RETAINING STRUCTURES REGARDING THE FROZEN SOIL CREEP PRÉDICTION DE L'ETAT CONTRAINTE-DÉFORMATION DES OUVRAGES DE SOUTÈMENT CONGÉLES COMPTE TENUE DU GLISSEMENT DU SOL GLACÉ

Yu.K. Zaretsky[1], Z.G. Ter-Martirosyan[2] and A.G. Shchobolev[2]

[1]Scientific Research Centre of the "Hydroproject" Institute, Moscow, USSR
[2]Civil Engineering Institute, Moscow, USSR

SYNOPSIS A procedure is suggested for the stress-strain state prediction of frozen retaining structures at great depths, which accounts for basic mechanisms of frozen soil creep and provides the actual structure geometry and its 3D performance in the computation scheme. A rheological model based on the viscoplastic flow theory was applied in the evaluation of the frozen soil strain history in the pre-limiting and limiting states. An investigation was performed of the frozen retaining structures stress-strain state for two technological schemes.

The artificial soil freezing method being applied in deep rock excavations (500-800 m) under difficult engineering and geological conditions creates the temporary frozen retaining structure (Vjalov, 1981). This one undergoes the pressure of the surrounding soil and prevents groundwater from entering an excavation pit.

The efficiency of the method is dependent, to a great extent, on the proper correlation between the depth of a frozen retaining structure and the height of stope. With the specified depth, the value of the radial displacement of a frozen retaining structure is influenced by the height of stope and the time of the shaft section being unsupported (from driving to lining). The deformation of a frozen retaining structure results in deflection of freezing core barrels causing them to break, which in turn creates an emergency situation - the defrosting of the whole system.

The design of frozen retaining structures regarding two limiting states (strength and strain) and rheological properties of frozen soil is suggested (Vjalov, 1981). However the problem of the stress-strain state prediction of frozen retaining structures cannot be fully solved by the analytical methods. This is the reason for developing a frozen soil creep model and adopting a procedure for the stress-strain state history prediction of the said structures by the finite element method (FEM), (Zaretsky, 1986).

Frozen soils possess the definite rheological properties showing a nonlinear relation between stresses and strains which being mainly viscoplastic are developing with time. One cannot predict the performance of a real structure, if the frozen soil creep behaviour is not considered in the engineering computations. Frozen retaining structures serve until the shaft section is supported. For this reason the ultimate stress is assumed at some points of a structure, if only, without causing it to break or to undergo too large strains by the time of lining. In this connection the stress-strain prediction of frozen retaining structures should account for the frozen soil creep both in the pre-limiting and limiting states.

The defining relations, a modified version of Zaretsky's model (Zaretsky, 1980), are proposed to describe the basic frozen soil creep behaviour (Zaretsky, 1986).

The rheological model presented in the viscoplastic flow theory is based on the following assumptions:

(1) the tensor of complete strain is presented as the sum of elastic and viscoplastic components,

$$E_{ij} = E^{e}_{ij} + E^{p}_{ij} \qquad (1)$$

where E^{e}_{ij} is the elastic component of the strain tensor, E^{p}_{ij} the viscoplastic component of the strain tensor. The elastic strains are associated with stresses by Hooke law.

(2) The concept of the instantaneous loading surface f_o is introduced, in which the material shows elastic behaviour.

(3) The viscoplastic strains velocity is defined by the associated flow law expressed as

$$\dot{E}^{p}_{ij} = \dot{h}\,\frac{\partial f_o}{\partial \sigma_{ij}} \qquad (2)$$

where h is some scalar parameter.

The conditions of loading, unloading and neutral loading are formulated within the theory of viscoplastic flow (as it is in the case of the plastic flow theory).

A partially smooth instantaneous loading surface was suggested for description of the Kellovej sand loam creep in the isothermic conditions (Zaretsky, 1983). The analytical express-

ion of regular sections of the instantaneous surface is

$$\text{section 1} \quad f_o^{(1)} = \sigma_i - \sigma_i^* \qquad (3)$$

$$\text{section 2} \quad f_o^{(2)} = \sigma_i - \sigma_i^{*}(t)\Phi(e_i^{\nu p}) - \eta_i \ln\left(1 + \frac{e_i^{\nu p}}{e_i^*}\right)$$

$$\text{section 3} \quad f_o^{(3)} = \sigma_i - p^*$$

where σ_i is the intensity of tangential stresses, σ the average stress, $\sigma_{i(t)}^* = C_t + \sigma \operatorname{tg}\varphi_t$ the long-term strength of soil, C_t and $\operatorname{tg}\varphi_t$ are introduced into the computation program in the tabulation form directly by the experimental data in relation to σ, t, $\Phi(e_i^{\nu p})$ the functions of strengthening, e^* the minimum intensity of the strains velocity, η_i the viscoplastic coefficient, and σ^* the tensile strength of soil.

The parameters of the frozen soil model are defined on a stabilometer in triaxial compression tests.

The developed model of a frozen soil describes its creep both in the pre-limiting and limiting states, reflects the non-linear relation between stresses and strains, considers the effect of the average stress upon the soil deformability, and predicts dilatancy (Zaretsky, 1986).

The developed prediction procedure of the stress-strain state of frozen retaining structures is based on the most common FEM version, the displacement method using tetragonal square elements for the axially symmetric formulation of the problem (Zaretsky, 1986, Shchobolev, 1984).

The system of the FEM defining equations is numerically implemented by the method of direct integration using the time step procedure (Zienkiewicz, 1977). The increment of viscoplastic strains in time step is determined using the algorithm suggested by Zaretsky and Lombardo (Zaretsky, 1986).

For better accuracy of the solution, the computation process incorporates a correcting operation proposed by Stricklin. The variable time step is employed in the solution of any problem, and its value is controlled automatically provided that the counting is accurate and permanent (Zienkiewicz, 1977, Zaretsky, 1986).

The stress-strain state prediction of frozen retaining structures according to the proposed procedure was initiated using a computation scheme with an axial symmetry, Fig.1. The boundary conditions on displacements: neither vertical displacements on the faces of frozen retaining structures, nor horizontal displacements on the bottom in the axis of symmetry. The elastic yielding of the supports was included in the computation. The design load of the surrounding thawed ground on the frozen retaining structure was assumed to be distributed according to the linear law, and the dead load of the frozen soil was taken into account. The design studies were undertaken with the average integral temperature 10°C below zero.

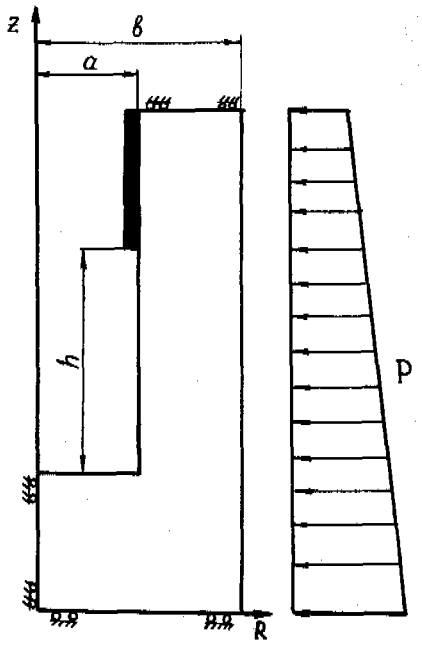

Fig.1 Computation scheme for a frozen retaining structure

When selecting a computation scheme, the real working conditions of frozen retaining structures dictated by the construction procedure were considered. Two design cases of small and big stopes driving were analysed. The first case is $h \gg a$, $a = 5.0$ m, $b = 10.0$ m, $h = 20.0$ m, $p = 2.0$ MPa, and the second case is $h < a$, $a = 5.0$ m, $h = 2.5$ m, $p = 5.0$ MPa.

The analysis of the sress-strain state with $h \gg a$ permits selection of three zones with a typical distribution of stresses, i.e. the zones of the support and bottom effects with a high concentration of stresses, and the zone in the middle of the section exposed, Fig.2a. From the character of the stress state of the middle section of the frozen retaining structure (the stress τ_{RZ} is closer to zero, and the isolines σ_R, σ_Z, σ_θ are parallel to the vertical axis) it is inferred that it works under a plane strain, however the sizes of the plane strain region diminish with time.

With $h < a$ the distribution of stresses is characterized by a high concentration on the edge and the bottom of support, Fig.2b.

The results of the stress-strain prediction of a frozen retaining structure, obtained by the aforesaid procedure, make it possible to evaluate the performance of the structure by the limiting states.

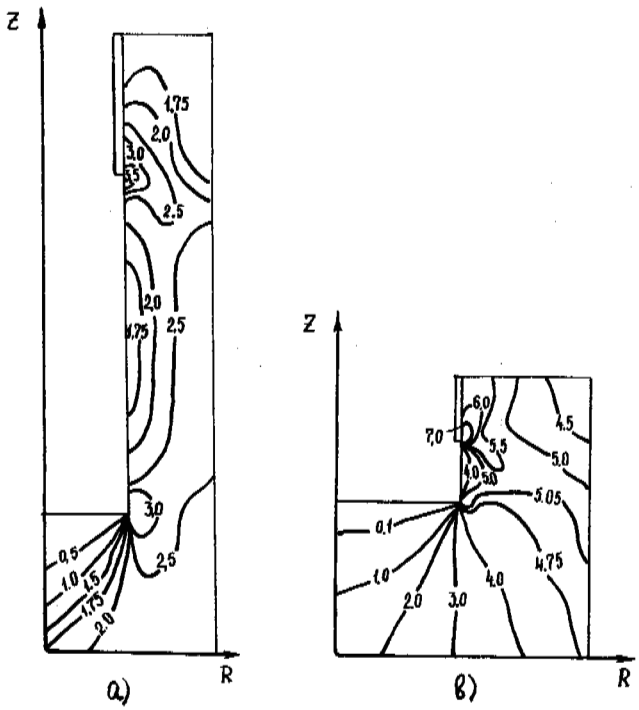

Fig.2 Stress distribution, , for a frozen retaining structure. a) with h>>a,p = 2.0 MPa; b) with h<a,p = 5.0 MPa, t=24h

The computation permits of constructing a line of radial displacements of the interior wall of a frozen retaining structure, Fig.3a,b, for any given moment of time, and consequently the performance testing with the admissible strains.

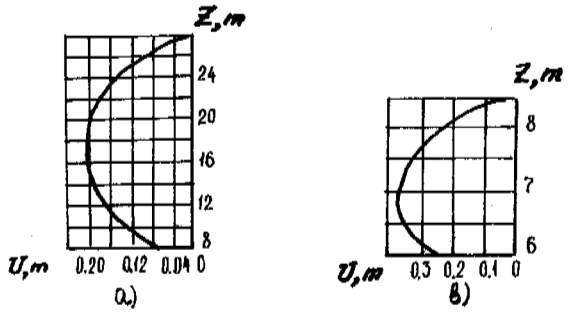

Fig.3 Radial displacements of the interior wall of a frozen retaining structure. a) with h>>a,p = 2.0 MPa; b) with h<a,p = 5.0 MPa,t=24h

Since the calculated model of a frozen soil describes the relation between stresses and strains both in the pre-limiting and limiting states, the obtained displacement history curve of the interior wall of a frozen soil cylinder, Fig.4, enables the state of developing displacements to be followed (damped, steady or undamped).

The destruction of a frozen retaining structure appears as a progressive time increment of radial displacements of the interior wall of the frozen retaining cylinder.

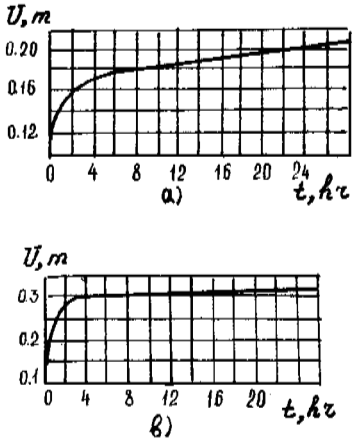

Fig.4 Time variation in radial displacement of the interior wall of a frozen retaining structre in the middle of an exposed section a) with h>>a,p = 2.0 MPa; b) with h<a,p = 5.0 MPa

The important factor effecting the safe state of a frozen retaining structure is the strength of freezing core barrels which work under a transverse-longitudinal bending, being displaced jointly with a frozen soil cylinder. In this connection control is suggested over the growth of frozen retaining structures on the basis of strength of freezing core barrels (Nasonov, 1976).

The line of radial displacements of the freezing core barrel, Fig.5, is constructed on the basis of the numerical solution, which adds a lot to verification of strength of freezing core barrels restricting the limiting value of deflection,

$$\alpha \leq \alpha^* \qquad (4)$$

where α is the relative deflection of a core barrel, equal to the relation of the difference between its maximum and minimum radial displacements within the exposed section, to the height of deflection; α^* the ultimate tolerable value of the relative deflection, 0.01, which is preset depending on the flexibility of the core barrel, and the specifications.

As seen from Fig.5a, the relative bending is α = 0.0059 with h >> a, p = 2.0 MPa, and α = 0.04 with h < a, p = 5.0 MPa, Fig.5b. Consequently for the second case the condition of freezing core barrels strength is not fulfilled (although considering the strength the retaining structure is in the pre-limiting state).

The strength of freezing core barrels can be estimated from their stress state, the value of which should not exceed the bearing capacity of the core barrels material.

The stress in a freezing core barrel is

$$\sigma = \sigma_b + \sigma_{ten} + \sigma_t + \sigma_a \qquad (5)$$

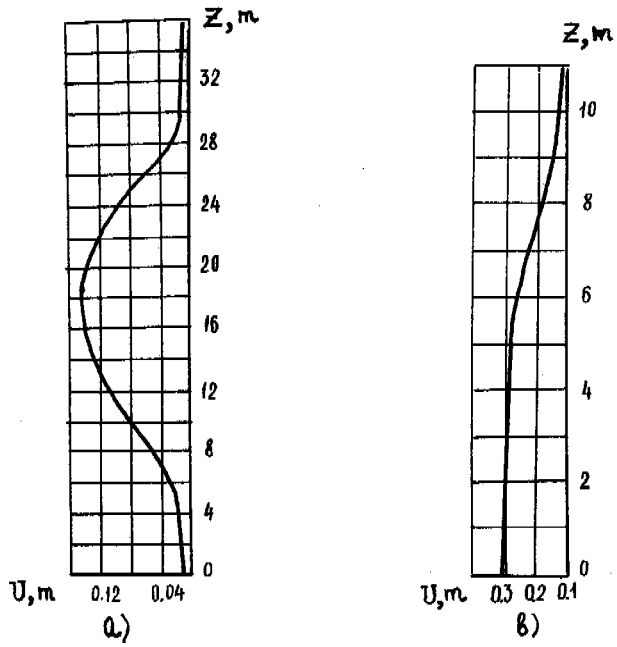

Fig.5 Radial displacements of a freezing core barrel, situated at a distance of R = 8.2 m a) with h>>a, p = 2.0 MPa, b) with h<a, p = 5.0 MPa

where σ_b is the stress from the transverse bending of the core barrel, σ_{ten} the stress from the longitudinal tension (the longitudinal force also results in the bending moment, which has no value of stress exceeding 5% from σ_b, and is not included in the computations); σ_t the temperature stress; σ_a the assembly stress. Consequently the stress of the transverse bending σ_b and of the longitudinal tension σ_{ten} must be obtained for evaluation of the stress state of a core barrel, and σ_t, σ_a can be easily found (Nasonov, 1976).

The curves of the bending moment M and of the stresses σ_b and σ_{ten} including the curve of the total stress $\sigma = \sigma_{ten} + \sigma_b$ are plotted on the line of radial displacements of the core barrel (Zaretsky, 1986).

Fig.6 shows the results of the analysis of the stressed state of the freezing core barrel for the second case. From the total stress curve of bending and tension it follows that the maximum stress exceeds 500 MPa that is more than the bearing capacity of the core barrel material, 400 MPa.

The following conclusions can be drawn:

(1) the developed procedure and the model permit of predicting the stress-strain state of frozen retaining structures considering basic regularities of frozen soil creep and incorporating structural features in the computation scheme.

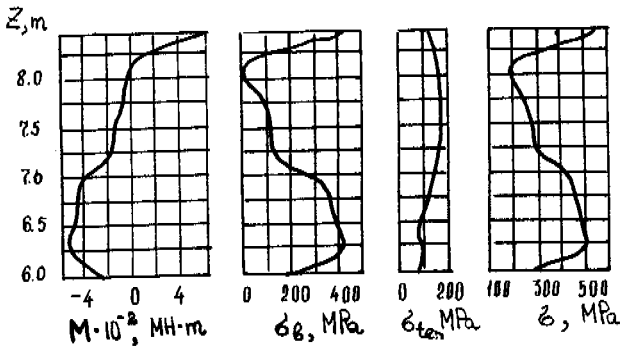

Fig.6 The analysis of the stress state of a freezing core barrel with h<a, p = 5.0 MPa a) the bending moment curve; b) the bending stress curve; c) the longitudinal tensile stress curve; d) the total stress of bending and longitudinal tension

(2) The developed procedure permits of evaluating the performance of frozen retaining structures in the two limiting states (strength and strain) with regard to the strength of freezing core barrels.

(3) The studies revealed that when frozen soils can develop considerable viscoplastic strains without destruction, satisfaction of the strength conditions of freezing core barrels is the deciding factor in the computation of frozen retaining structures.

REFERENCES

Vjalov, S.S., Zaretsky, Yu.K., Gorodetsky, S.E. (1981). Raschety na prochnost' i polzuchest' pri iskustvennom zamorazhivanii gruntov. Strojizdat, pp.220, Moskva.

Zaretsky, Yu.K., Choumichev, B.D., Shchobolev, A.G. (1986). Vjazkoplastichnost' l'da i merzlych gruntov. Nauka, pp. 184, Novosibirs

Zaretsky, Yu.K. (1980). Novaja kontseptsija vjazkoplasticheskogo techenija gruntov. In: Trudy tretjego vsesojuznogo simpoziuma po reologii gruntov. Universitet Erevana, 58-73. Erevan.

Zaretsky, Yu.K., Shchobolev, A.G. (1983). A mathematical model for the viscoplastic deformation of frozen soils. In: proc. 4th Intern. Conf. on Permofrost, vol.1, 1457-1462. Fairbanks.

Zienkiewicz, O.C. (1977). The finite element method. McGraw-Hill Book Comp., pp. 787.

Nasonov, N.D.; Shchouplik, M.N. (1976). Zakonomernost' formirovanija ledoporodnych ograzhdenij pri sooruzhenii stvolov shacht. Nedra, pp. 237, Moskva.

Shchobolev, A.G. (1984). Prognoz deformatsyj polzuchesti v merzlych gruntach. In: Materialy konferentsij i soveshchanij po gidrotechnike inzhenernoje merzlotovedenie v gidrotechnicheskom stroitel'stve. Energoatomizdat, 153-158, Leningrad.

STUDY OF FROZEN SOILS BY GEOPHYSICAL METHODS

Yu.D. Zykov, N.Yu. Rozhdestvensky and O.P. Chervinskaya

The Industrial and Scientific-Research Institute on Engineering Investigations in Construction, the USSR

SYNOPSIS Complex of geophysical methods to define composition, structure and properties of frozen soils in the massif is represented. The complex is make of radioisotopic, seismoacoustical methods and methods of geophysical prospecting by electrical means. The complex is used in engineering investigations in construction. The following characteristics of frozen soil are determined: compaction, contents of ice, cryogene texture, physico-mechanical properties. The example of application of this complex approach is given.

Investigations of frozen series by means of geophysical methods are make to solve two problems:

- definition of massif structure,
- estimate of composition, structure and physico-mechanical properties of frozen rocks.

The first problem is quite traditional. To dismember a section a great deal of geophysical methods of necessary physical pre-conditions are in use. Those are rocks contrasts due to properties, taken by one or the other method. As a rule, in order to define the depth of boundaries occurrence by means of geophysical methods, knowledge of rocks properties is necessary. They are estimated either way: a priori, or are calculated synchronously with the depth in the process of interpretation of materials. Peculiarity of the first problem lies in the fact, that meanings of properties are used but only indirectly. In a number of cases quantitative properties are never estimated. This is the most typical way concerning the study of peculiarities of square structure of areas. Of late the second problem is more and more recognized owing to the successes attained. They are conditioned by information accumulation on connections among the above-mentioned parameters on the one hand and properties, due to results of geophysical investigations - on the other hand.

Radio-isotopic methods, geophysical prospecting by electric means by direct or low-frequency alternating current, seismoacoustical methods are basical methods, which permit to obtain the quantitative meanings of geophysical properties of soils.

The other methods in the majority of cases do not provide such possibilities. Radio-isotopic measurements result in the definition of moisture and density of soils. It is realized by means of calibration curves representing by themselves the functional connections of counting speed of thermalized neutrons with moisture and counting speed of gamma-quanta with density, being established by experimentary method and suitable for just this apparatus in use.

While performing the works of geophysical prospecting by electrical means and seismoacoustical investigations by specially-elaborated methodics with observations both from surface and in the inner spots of surroundings, electric resistivity (ER) and propagation speeds of elastic waves are correspondingly defined. In both methods simultaneously to these parameters the position of boundaries of rocks is defined, which are characterized by their close meanings. To obtain the ER meanings resistivity logging of dry holes, which are unplanted, and vertical electrical sounding (VES) are used. Typical peculiarities of frozen series are the availability of non-horizontal boundaries of rocks, according to changeability of their composition, ice content and temperature, and also anisotropy, conditioned by cryogene textures. To study the inclined boundaries of rocks, VES is recommended to be used in modification of two components, fulfilled by two-way three-electrode units AMN$^{\infty}$ and $^{\infty}$MNB. (Bogolyubov and others, 1984 b). In horizontally anisotropic sections ER, defined by means of VES, corresponds to root-mean-square ρ_m, and the one, defined under logging - to longitudinal ρ_t. They are interconnected by ratio $\lambda = \frac{\rho_m}{\rho_t}$, where λ - anisotropy coefficient. ρ_t is defined due to the data, obtained by means of potential - sonde AMN$\to\infty$ B$\to\infty$. Gradient-sonde AMNB$\to\infty$ or A$\to\infty$ MNB is used to specify the position of boundaries. Transition from the ER meanings to parameters of composition and structure of frozen soils realized by means of nomogrammes (Figure Ia and Ib). The first nomogramme (Figure Ia) had been obtained empirically and it shows the connection of rock ER (ρ_{mp}) to temperature and lithological composition. The rest nomogrammes (Figure Ib),

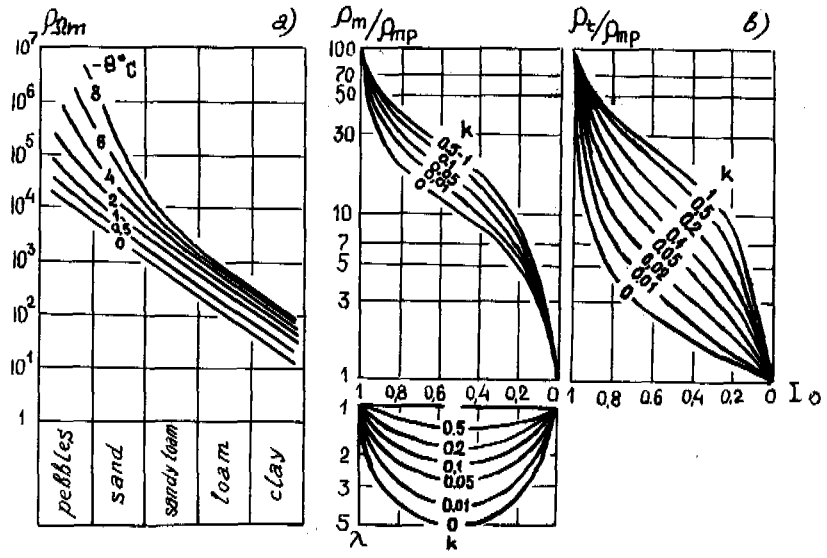

Fig. 1 Electrical properties of frozen soils:
a) dependency of ER from lithological composition of the mineral part and temperature,
b) connection of ER and anisotropy coefficient - λ with ice contents I_o of frozen loams: k - ratio of summary thickness of schlieren of subordinate system to the basical one (due to Bogolyubov).

connecting ER with ice content - I_o , are calculated theoretically on the basis of model conceptions concerning rock, as bicomponent surroundings-grid, composed of conductive elements - mineral cells and non-conductive ones -ice (Bogolyubov and others, 1984a).

To define the parameters of composition, structure and physico-mechanical properties of frozen soils by means of data of seismo-acoustical investigations the meanings are used of speeds of longitudinal waves in two interperpendicular directions $V_p^x = V_p^{\parallel}$ and $V_p^z = V_p^{\perp}$, anisotropy coefficient $\varkappa = V_p^{\parallel}/V_p^{\perp}$, speeds of shear ($V_s$) or Relay ($V_R$)waves. The most exact meanings of these values are defined as the result of observations in holes. The foundation of transition from speeds of elastic waves to parameters of composition and structure of frozen soils makes the theoretical conceptions and quantitative ratios, having been investigated in laboratory conditions. By this time a sufficiently vast material has been accumulated on dependencies V_p in frozen soils from the temperature (Baulin and others, 1979; Votyakov, 1975; Djurik and others, 1972; Zykov and others, 1975; Frolov, 1976; Khazin and others, 1974; Kaplar, 1965; Kurfurst, 1975; Nakano, Froula, 1973; Müller, 1962, and others). In spite of its relation as to concrete soils, different regions and discreet meanings of moisture (W), being different from each other, by way of analysis, generalization and statistical treatment of information we had been lucky to make summary dependencies $V_p(W_s,\Theta)$ for continuous number of meanings of argument for continuous number of meanings of arguments in the wide range of change of lithological composition (from coarsely-grained washed-off sands to highly-plastical clays). On the basis of these dependencies the dependencies had also been made of speeds of longitudinal waves from a number of soils plasticity to compose the fixed meanings of temperature (picture 2a). Mistake of obtained moisture meanings for coherent soils does not exceed 10%, it makes average 5-6%.

To estimate cryogene structure, ratios are used, found out as a result of theoretical consideration of model of quasianisotropic surroundings and laboratory experiments, fulfilled specially (Zykov, 1984). The experiments resulted in establishment of basical regularities, connecting speeds of longitudinal waves in different directions to properties of layers and their relative thickness. And it had been proved there, that dependency of speeds of elastic waves from ice contents in frozen rocks is submitted to the law of the average time, if rock is quasianisotropic one or propagation of waves coincides with direction, perpendicular to the surface of predominant system of ice schlieren. On the basis of exposed regularities and meanings of speeds of elastic waves and anisotropy coefficient ($\varkappa$), obtained as a result of experiments, there had been worked out grid nomogrammes, which permit to estimate the elements of ice

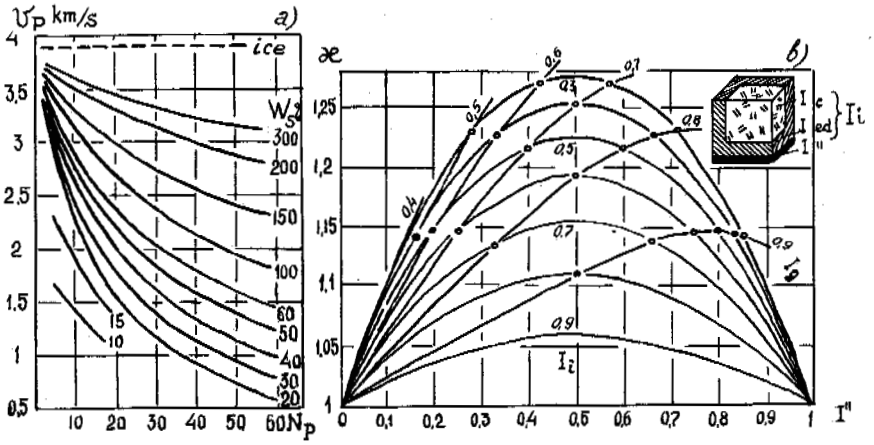

Fig. 2 Acoustical properties of frozen soils:

a) dependency of speeds of longitudinal waves - V_p from the number of plasticity - N_p under the temperature -I°C; W_S - summary moisture of soil,

b) connection between anisotropy coefficient of speeds of longitudinal waves - $\partial\varepsilon$ and elements of ice contents: I_g - general ice contents; I_c - ice-cement, I_{ed} - ice, evenly distributed; I'' - ice of schlieren, mainly orientated towards one of the directions.

contents of frozen soils: contents of ice, evenly distributed at the volume (I_{ed}) and ice schlieren, orientated mainly towards one direction (I'') (picture 2b). For that purpose meanings of ε and moisture are used, found out either due to acoustical (as it had been abovementioned) or due to some other data.

The definition of dynamical moduli (Poisson's ratio, Young's modulus, shear, compression), statical moduli of deformation and elasticity, strength limit to uni-axial compression is made either analytically according to formulae of elasticity, theoretically-known, with application of the data concerning compaction, or due to correlational connections among speeds of longitudinal waves or dynamical moduli and the parameters of definition, which are found out by now, but are not investigated completely so far (Baulin and others, 1979; Goryainov and others, 1975; Khazin and others, 1979). Temperature must be often known as to the last occasion (Baulin and others, 1979). General scheme of usage of geophysical information of electrometrical, acoustical, radioisotopic and thermometric investigations of holes to define composition, structure and properties of rocks is given in the picture 3. In the occasions, when results may have been obtained independently (for instance, due to data of geophysical prospecting by electrical means and acoustical measurements), their comparison serves as a criterion of the truth of definitions.

At the final stage of joint interpretation of geophysical data the mutual correlation is done of obtained physico-mechanical characteristics, singling out the most true meanings and dismembering of all the section in the hole location into intervals, being characterized by them. Permanency of meanings of parameters inside the intervals serves as criterion of singling out the interval. Results may be presented numerically or in the form of diagrammes of proper characteristics on depth. Distribution of information about physico-mechanical properties, characterizing rocks at the location of drilling, on by-hole area is done due to the data of ground and ground-hole geophysical investigations: seismoprospecting by method of refracted waves, vertical seismical profiling, vertical electrical soundings, made in diverse removal from the hole. Criterion of such a transfer is coincidence and relative permanency of geophysical parameters of rocks, obtained in the hole and outside of it. As an example, the results of investigations, which had been done during engineering investigations in the North of the West Siberia, may be considered. Geological section of the area is represented by soil of sand loams and loams, frozen from 0.5 m, cryogene structure along all the section is stratificationally-gridded with different by thickness ice schlieren: from 2-4mm to 25 mm at the depth lower than 2,5 m. Soils temperature -0 - -1°C. Results of field investigations are represented in the form of corresponding diagrammes (picture 4), results of definition of composition, structure and rocks properties due to geophysical data - in the table (table I). In a brief contribution all the succession of operations on interpretation of geophysical data, peculiarities, hindrances could not be given quite completely as it is. A whole number of moments in

demand of special investigations is still not taken into consideration. But it could be set forth, that the efficient complex of geophysical methods, directed upon increase of quality and economical indicators of investigations, practically-stable, had been created.

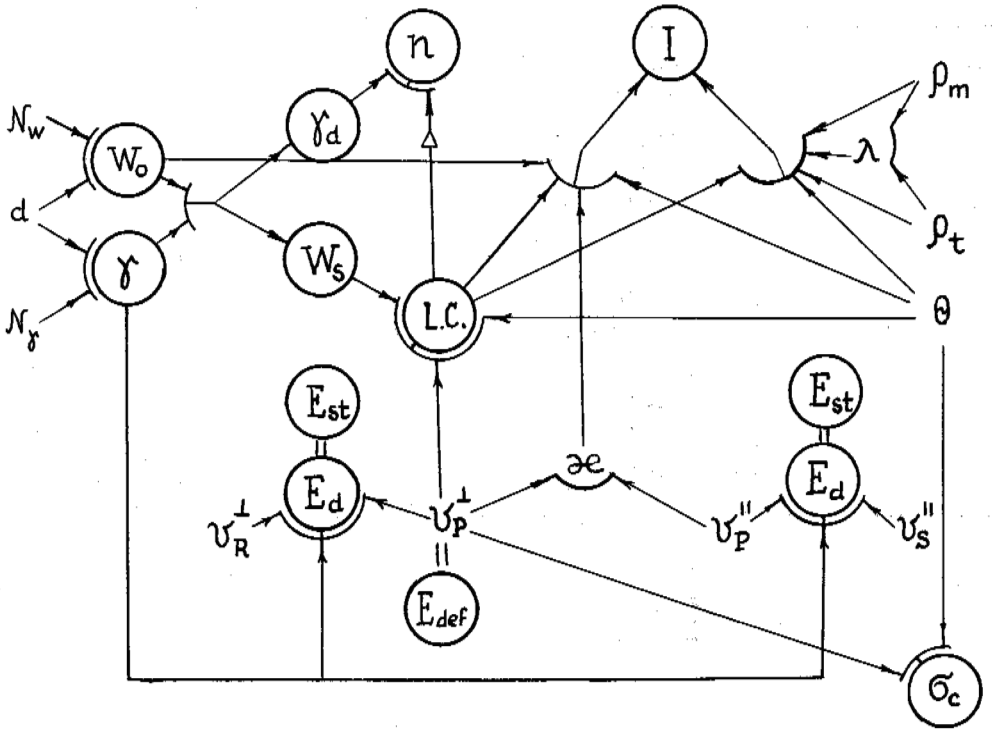

Fig. 3 Scheme of application of geophysical parameters to define composition, structure and properties of frozen soils:
N_W - speed of counting of impulses of thermalized neutronic radiation, N_γ - speed of counting of impulses of attenuated gamma-radiation; speeds of propagation of elastic waves: $V_p^{\parallel}$ - of longitudinal one towards horizontal direction, $V_p^{\perp}$ - of longitudinal one towards vertical direction, $V_R^{\perp}$ - of Relay wave one towards vertical direction, $V_S^{\parallel}$ - of shear one towards horizontal direction;
electrical resistivity: ρ_m - root-mean-square, ρ_t - longitudinal, d - diameter of hole; θ - temperature; Δ - specific gravity of soil skeleton; L.C. - lithological composition; W_o - volume moisture; I - ice contents and its parameters, γ - soil density; γ_d - dry density; n - porosity ; E_d - dynamical modulus of elasticity; E_{st} - statical elasticity modulus; E_{def} - deformation modulus; σ_c - temporary resistance to uni-axial compression; $\mathcal{E}$ - anisotropy coefficient of speed of propagation of longitudinal waves; λ - anisotropy coefficient of electrical resistivity; = - estimate on correlational connection.

TABLE I

Results of Defining Composition and Properties of Frozen Soils Due to the Data of Complex of Geophysical Investigations of Prospecting holes

Depth of interval, M	μ	E_d, GPa	E_{st} GPa	E_{def} GPa	σ_c MPa	N_p	n %	Ice contents, fractions of the unit		
								I_g	I_c	I^x
1,0-1,2	0,36	5,9	1,5	0,042	1,15	-	47	-	-	-
1,2-1,5	0,35	7	1,8	0,045	1,22	8,9	47	-	-	-
1,5-1,8	0,32	7,8	2,1	0,047	1,28	8,9	47	0,40	0,23	0,13
1,8-2,2	0,36	6,5	1,65	0,046	1,25	11,6	45	0,44	0,22	0,18
2,2-2,4	0,36	6,6	1,65	0,047	1,27	8,6	45	0,32	0,07	0,26
2,4-2,6	0,30	8,2	2,20	0,047	1,27	8,6	46	0,32	0,12	0,26
2,6-2,8	0,38	5,4	1,35	0,044	1,20	8,6	46	0,28	0,03	0,25
2,8-3,0	0,33	6,7	1,70	0,044	1,20	8,6	43	0,28	0,05	0,24
3,0-3,3	0,37	6,2	1,6	0,050	1,37	8,6	43	0,40	0,13	0,27
3,3-3,5	0,35	6,5	1,65	0,045	1,22	8,1	55	0,26	0,15	0,21
3,5-3,75	0,33	6,5	1,65	0,042	1,15	8,1	55	0,18	0,14	0,03
3,75-4,05	0,34	7,1	1,8	0,046	1,25	-	51	0,31	0,11	0,20
4,05-4,5	0,34	7,6	2,0	0,049	1,32	6,9	51	0,31	0,11	0,24

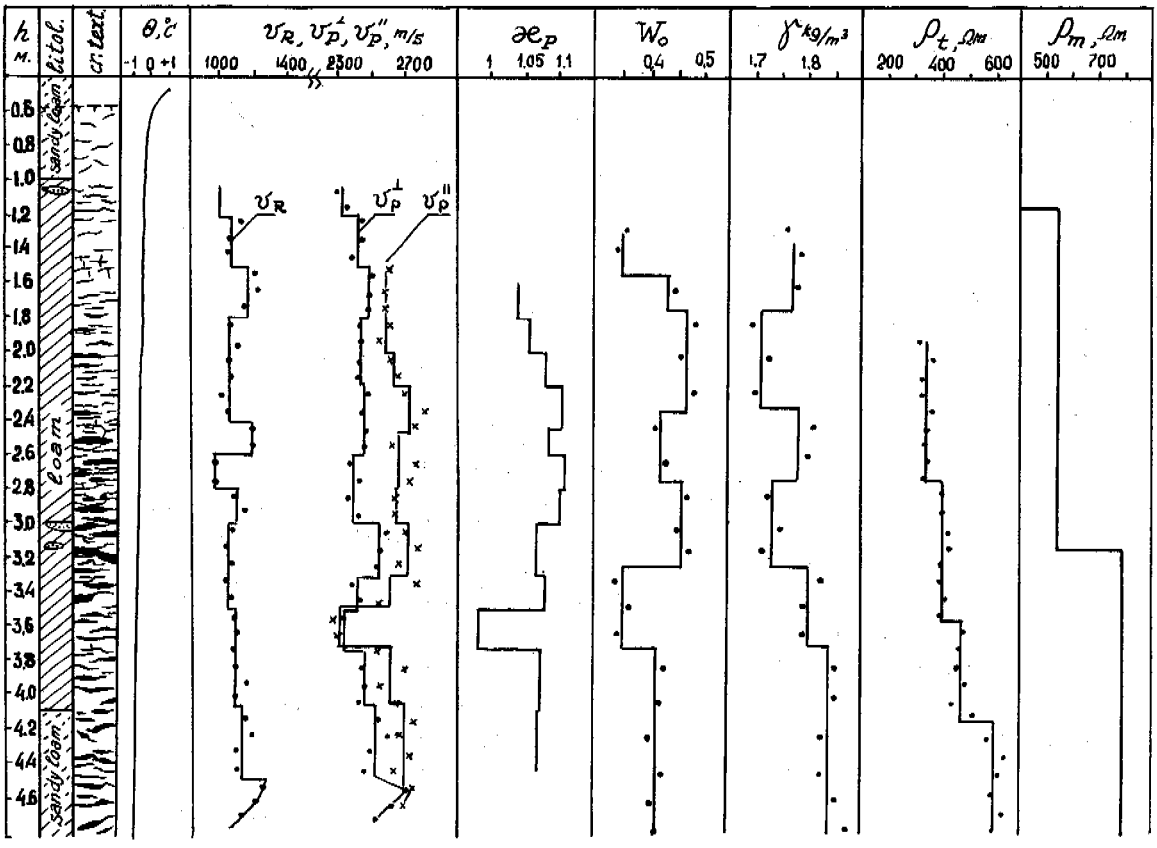

Fig. 4 Results of complex geophysical investigations.

REFERENCES

Baulin, Y.I., Zykov, Y.D. (1979). Svyaz mezhdu sostavom, prochnost'ju i uprugimi svoistvami dispersnykh myorzlykh gruntov. Inzhenernoye merzlotovedeniye. (Materialy k III Mezhdunarodnoi Konferentzii po merzlotovedeniyu). Novosibirsk: Nauka, str.257-261.

Bogolyubov, A.N., Bogolyubova, N.P., Kurandin, N.P., Lisitzin, V.V. (1984). Rekomendatzii po geofizicheskim rabotam pri inzhenernykh iziskaniyakh dlya stroitelstva (elektrorazvedka). Moskva: Stroizdat, str.1-104.

Bogolyubov, A.N., Bogolyubova, N.P., Mozganova, E.Ja. (1984). Rukovodstvo po interpretatzii krivykh VEZ MDS. Moskva: Stroizdat, str.1-200.

Dj'urik, V.I., Leshchikov, F.N. (1972). Eksperimental'niye issledovaniya seismicheskikh svoistv myorzlykh gruntov. II Mezhdunarodnaya Konferentziya po myorzlotovedeniyu. Doklady i soobshcheniya, vyp.6, Jakutsk, str.63-64.

Frolov, A.D. (1978). Elektricheskiye i uprugiye svoistva kriogennykh porod. Moskva: Nedra, str.1-254.

Goryainov, I.N., Skvortzov, A.G., Kiryunin, A.V. (1975). Opyt primeneniya seismicheskikh metodov pri inzhenerno-geokriologicheskikh issledovaniyakh rykhlykh porod. Trudy VSEGINGEO. Ispol'zovaniye geofizicheskikh metodov pri gidrogeologicheskikh i inzhenerno-geologicheskikh issledovaniyakh, Vyp.97, Moskva, str.26-39.

Khazin, B.G., Goncharov, B.V., Nizamutdinov, D.H. (1974). Ob otzenke prochnosti i klassifikatzii myorzlykh gruntov po akusticheskim kharakteristikam. Trudy nauchno-issledovatelskogo instituta promyshlennogo stroitelstva, Vyp.15, Moskva, str.209-214.

Kaplar, C.W. (1965). Laboratory determination of dinamic moduli of frozen soils and of use. Proceeding Permafrost International Conference, Washington, pp.1025-1056.

Kurfurst, P.I. (1977). Acoustic properties of frozen soils Report of Activities, Part B; Geol. Surv. Can., pp.277-280.

Müller, G. (1962). Ultraschallmessungen zur Uberwachung des Frostkorper an Gefrierschuchten. Gluckauf. H.7, pp.23-30.

Nakano, Y., Froula, N.H. (1973). Sound and shook transmission in frozen soils. In Permafrost North American Contribution to the 2-nd International Conference. Washington, pp.359-369. Jakutsk, USSR. Nat. Acad.

Votyakov, I.N. (1975). Phiziko-mekhanicheskiye svoistva myorzlykh i ottaiwayushchikh gruntov Jakutii. Moskva: Nauka, str.1-176.

Zykov, Y.D., Korkina, R.I. (1975). Izucheniye skorostei uprugikh voln v obraztzakh myorzlykh gruntov dlya otzenki ikh stroitel'nykh kharakteristik. Trudy proizv. i nauchno-issledovatelskogo instituta po inzhenernym izyskaniyam v stroitel'stve Gosstroya SSSR, Vyp.35, str.26-33, Moskva.

Zykov, Y.D., Chervinskaja, O.P., Lyahovitsky, F.M. (1984). Experimental investigation of transverse isotropy in ise/clay thin layered periodic models. Geophys. J.R. astr. Soc., v.76, pp.269-272.

THE OUTFLOW OF WATER IN PERMAFROST ENVIRONMENT – SPITSBERGEN

S. Bartoszewski, J. Rodzik and K. Wojciechowski

Institute of Earth Sciences, Maria Curie – Sklodowska University, Akademicka 19, 20-033 Lublin, Poland

SYNOPSIS:

The paper deals with the results of the investigations carried out within the forefield of the Renard and Scott Glaciers by the members of the Geographical Expedition of the M.C. Sklodowska University. The research took place during the two hydrological seasons of the year 1987 - spring and summer. The thawing of the snow cover on the coastal plain was the source of the superficial runoff dominating in the springtime. The occurence of the thaw flood attests to a strong dynamics of both meteorological and hydrological processes. As the hydrological calculations showed the inconsiderable extent of the outflow of permafrost origin results from a small retention ability of the active permafrost layer.

INTRODUCTION

Waters coming from the thawing of the many years permafrost are the main source of supplying the periglacial streams during the polar summer. The aim of the research carried out since 1986 by the Geographical Expeditions of the UMCS in Lublin was the recognition of the process of the outflow and making an attempt at the quantitative estimation of the phenomenon within the chosen basins situated in the area of the southern frame of Bellsund.

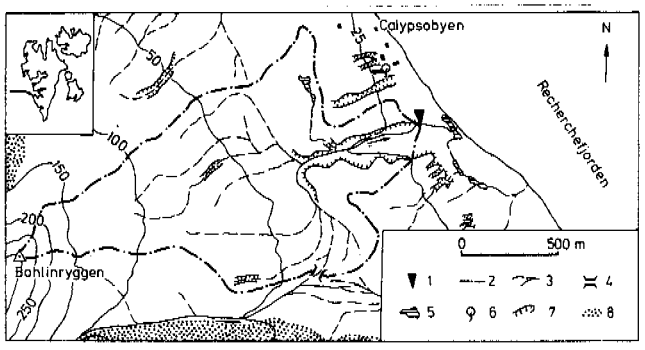

Fig. 1. Situation of the investigated area 1-limnigraph, 2-watershed, 3-constant and periodical streams, 4-place of bifurcation, 5-reservoir of stagnant waters, 6-spring, 7-margin, 8-moraine.

THE AREA OF INVESTIGATIONS

The spring as well as the stream mouthing to the Recherche Fiord at Calypsobyen were the subject of systematic observations (Bartoszewski 1986). The efflux is situated at the outlet of a small valley, cutting a gravelly-sandy coastal terrace 20 - 25 m a.s.l. (Fig. 1). The floor of the terrace is built of sea silts and boulder clays deposited on the Tertiary sandstones (Flood, Nagy, Winsnes 1971). The yield measurements were carried out every day, within the period 11 July - 17 August 1987 with the method of gathering water into a container, held beneath the effluence. The periglacial stream under study enters to the fiord in close vincinity to the base camp of the UMCS Expedition. Its catchment area includes a fragment of the Bohlinryggen massif, a system of uplifted coastal terraces and a marginal part of the Renard Glacier outwash. The gorgelike valleys, cutting the 20 - 25 m a.s.l. terrace down to its bottom witness the former direc tions of the outflow of fluvioglacial waters. The ravine, the nearst to Calypsobyen is exploited by the stream investigated. The hydrometric profile has been localized at the mouth of the ravine. The water levels observations were taken with the limnigraph B-2 recording weekly within the period 14 June - 17 August 1987. Mean water levels over 24-hour periods were calculated on the basis of the limnigrams. The conversion of the water levels into discharge flows was based on the discharge curve equation, taking under consideration periodical discharge measurements and adequate water levels.

OUTFLOW

The active hydrological seasons within the area Western Spitsbergen begins on average in June and lasts to October (Baranowski 1977, Pulina 1984). In 1987 the field investigations were inaugurated at the time when the tundra was still covered with a compact layer of snow and the phenomen of the river outflow was about to begin. In the period of the hydrological spring the superficial runoff dominated on the frozen substratum, in the conditions of the underdeveloped outflow

system. In period 14 June - 1 July 1987 the waters flowing through the gauge profile did not come exclusively from the reserve of the catchment investigated. Owing to the bifurcation the inflow of the waters from the stream draining the SE slope of Bohlinryggen took place. The cause of the temporary bifurcation was an enormous ice bank in the bed of that stream, preventing the outflowing of water directly to the fiord. Periodical measurements of discharge performed up- and downstream of the bifurcation allowed to estimate the quantity of water coming additionally to the catchment area. The total volume of the inflow reached 58 320 m^3. The values set in the table I show the total outflow "A" in the gauge profile, an outflow from the reserve "B" and, additionaly, the outflow in the period 11 July - 17 August 1987. These numbers allow to compare directly the respective values for both the periglacial river and spring.

Tab. I. The Outflow of the periglacial river and the yield of the spring in 1987

		River			Spring
		14 June - 17 August		11 July-17 August	
		A	B		
total outflow	m^3	536458	478138	105840	232
mean flow	dm^3/s	95,5	85,1	32,2	0,071
max flow	dm^3/s	538	474	92	0,18
min flow	dm^3/s	6	6	6	0,031
Q max : Q min		89,7	79	15,3	5,8
mean unitary flow	$dm^3/s\ km^2$		66	25	11,8
max unitary flow	$dm^3/s\ km^2$		367,4	71,3	30
min unitary flow	$dm^3/s\ km^2$		4,7	4,7	5,2
runoff index	mm		370,7	82,1	38,7

The outflow from the reserve amounted to 478.138 m^3, it means that the layer of the runoff was 370,7 mm and the unitary outflow 66 $dm^3/s\ km^2$. The values were much lower than those in the nearby Scott's glacial catchment. The curve of the daily discharges enables to differentiate the thaw flood on 14 - 23 June 1987, and some secondary floods of different origin (Fig. 2). During 10 days the runoff of the reserves in the catchment was 211.248 m^3, which was 44,2 % of the water flowed out in the period discussed. The occurrence of the flood depended on air temperature distribution and especially on the maximum of the 24 - hour temperature, measured at a height of 5 cm over the ground. The culmination occurred on 16 June at the temperature of 7,1°C, the secondary maximum on 19 June at the temperature of 8,1°C. Thawing waters had relatively low mineralization the minimum 71 mg/dm^3 on 18 June 1987.

Spring flood ended at the moment of the disappearance of the compact snow cover on the coastal plain. The periglacial streams, however continued to have the ablation rhythm of the changes of water levels, with a minimum at about 8 and maximum at 17 of the zonal time.

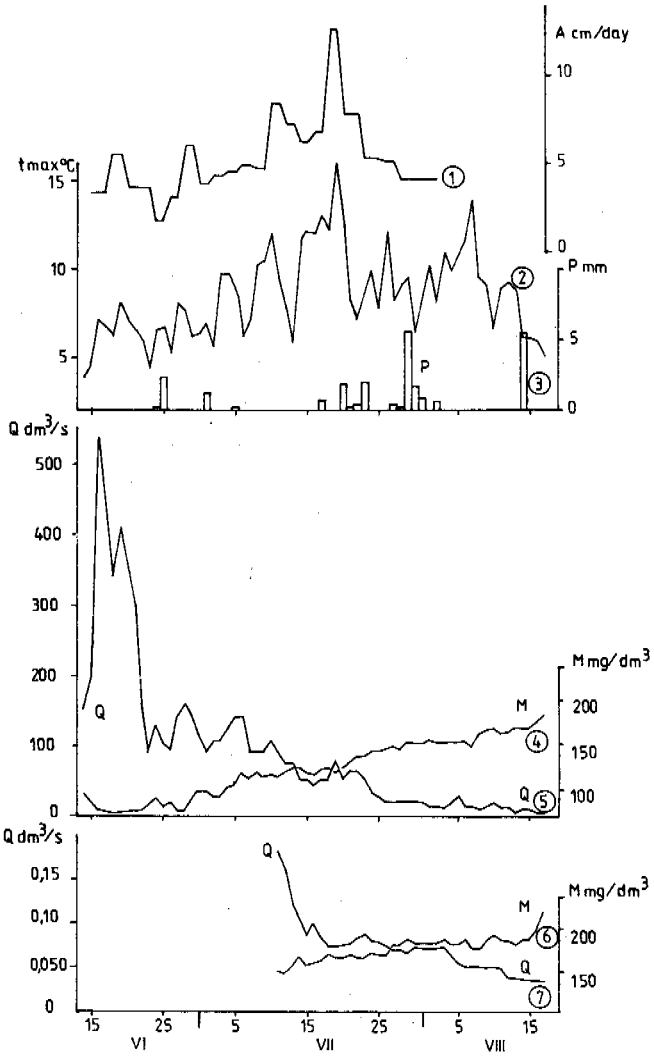

Fig. 2. Curves for total mineralization, mean 24-hour flows and yield of the spring at Calypsobyen in 1987
1-intensity of snow ablation A, 2-maximum 24-hour air temperature 5 cm over ground t max, 3-24-hour total precipitation P, 4-total mineralization of periglacial river waters M, 5-mean 24- hour flow of the periglacial river Q, 6-total mineralization of spring waters M, 7-24-hour yield of the spring Q

The secondary floods in the last decade of June and the first of July were connected with the increase of the ablation intensity of the snow patches within the upper part of the catchment basin, as well as in the depressions of the terrain.

Gradually, with a raise in air temperature, the thickness of the active permafrost layer was growing. A subsurface runoff increased, taking plase on its roof. The increase in total mineralization in the last decade of June, attests to the greater share of permafrost waters in the whole of the runoff. The 24 - hour rhythm of the outflow was becomming less and less distinct, to cease since 12 July 1987.

The spring in Calypsobyen started its activity on 11 July 1987. At the beginning, most of the outflow proceeded from the thawed snow patch filling the bottom of the valley. The diminution tendency of the yield stopped on 19 July, and on turn, the increase began to take place, up to the value 0,085 dm^3/s on 23 July 1987 (Fig. 2). The maximum in the yield showed a 4 - day delay in relation to the maximum in air temperature. At the next stage, the yield of the spring gradually decreased down to the minimum 0,031 dm^3/s on 17 August 1987. The decreasing tendency stopped temporarily at the end of July when the air temperature increased and a small precipitation took place.

The quantity of the water retentioned within the active layer of permafrost was determined on the basis of the chosen curves of falling and drying up. The calculations were taken with the Maillet method (Debski 1970) :

$$V = 86400 \cdot Q \cdot \alpha^{-1}$$

where:
V = volume of the retentioned water in m^3,
Q = yield or discharge intensity in m^3/s,
α = regression coefficient.

The highest states of retention (after exchanging m^3 into the water layer in mm) occurred in the river catchment on 19 July : 35,2 mm, in the spring catchment 23 July : 27,8 mm and the lowest ones on 17 August 2,3 mm and 11,2 mm respectively. The much lower final state of retention in the river catchment basin indicates some better conditions of the drainage of ground waters and also the faster consumption of supplies.

The supplying of the spring exclusively with permafrost waters was the cause of a total mineralization index higher than that in river waters. In the period 11 July - 17 August 1987 the mean value of the total mineralization of spring waters amounted to 164 mg/dm^3, while that of river waters to 136 mg/dm^3.

REFERENCES

Baranowski, S / 1977 /
Subpolarne lodowce Spitsbergenu na tle klimatu regionu Acta Univ. Wratisl., 393, 157 pp, Wroclaw

Bartoszewski, S / 1986 /
Obserwacje nad odplywem wód zmarzlinowych w okolicy Calypsobyen w lecie 1986 r. Przewodnik XIV Sympozjum Polarnego, 157-161, Lublin

Debski, K / 1970 /
Hydrologia
Arkady, 368 pp, Warszawa

Flood, B, Nagy, J, Winsnes, T S / 1971 /
Geological map of Svalbard 1:500000, Sheet 1G, Spitsbergen southern part
Norsk Polarinst.

Paulina, M / 1984 /
Water balance and chemical denudation in the unglaciated Fugleberget basin /SW Spitsbergen/
Pol. Polar Res., v. 5, no 3-4, 183-205, Warsaw

Paulina, M / 1986 /
Problematyka geomorfologiczna i hydroglacjologiczna polskich wypraw na Spitsbergen w latach 1979 i 1980
Czas., Geogr., LVII, 3; 367-392, Wroclaw

MODELLING OF AVERAGE MONTHLY STREAMFLOWS FROM GLACIERIZED BASINS IN ALASKA

D. Bjerkelie[1,2] and R.F. Carlson[1]

[1]Water Research Center, University of Alaska Fairbanks, Fairbanks, AK 99775 U.S.A.
[2]Dames and Moore, P.O. Box 75981, Seattle, WA, 98125 U.S.A.

SYNOPSIS Many streams in the mountain regions of central Alaska are dominated by glacier runoff. The presence of glaciers results in a highly periodic flow which is caused by temperature and radiation inputs and is modified by total precipitation and basin elevation. A Fourier and regression analysis of 17 basins revealed the deterministic nature of the flow and its dependence on physiographic and climatic characteristics. The resulting equations allow simulation of the average monthly flow hydrograph with good results on seven out of 12 test basins, however, additional calibration and data analysis is necessary to provide statistical confidence in the simulation results.

INTRODUCTION

Hydrographs with a significant melt flow component tend to be highly periodic for many regions in Alaska. This periodic nature is readily observed by inspection of mean daily flow hydrographs from glacierized basins throughout the state (Chapman, 1982). The periodicity can be surmised to be related to the periodic nature of the solar inputs, which drive the melt process (Mayo and Pewe, 1963) as well as other basin variables which may influence the timing of streamflows, such as basin elevation and precipitation. In basins where rainfall runoff dominates the hydrograph, the local storm patterns dominate the hydrograph characteristics such as the timing and periodicity of the streamflows. In basins dominated by melt flows, the hydrograph characteristics are dominated by the thermal and radiation regime and the amount of ice and snow available for melt. Recent studies have shown that the presence of glaciers within a basin can be related to a general delay of peak monthly runoff as compared to less glacierized and nonglacierized basins in southeast Alaska and Washington State (Fountain and Tangborn, 1985).

As many streams and rivers in Alaska emanate from glacial areas, a need exists to understand and predict hydrograph characteristics from glacierized basins. Also, there is often a lack of streamflow and other hydrologic data for many of these same basins. This paper presents a method to estimate the mean monthly flow hydrographs from glacierized basins in Alaska based on available published information using Fourier analysis and multiple regression techniques. The moderating effects of glaciers in glacierized basins tends to reduce monthly streamflow variability (Fountain and Tangborn, 1985) which enabled the development of a Fourier prediction model of mean monthly streamflows. The intent of this paper is to illustrate the use of these techniques and to show that general climatic and physiographic variables can potentially be used to predict average monthly streamflows from glacierized basins. A previous study analyzed mean daily hydrographs (Bjerklie and Carlson, 1986).

METHODS

Five years of mean monthly streamflows from 17 glacierized basins were analyzed. Streamflow data was obtained from the USGS Water Resources Data for Alaska, 1973 to 1977. This period of time was chosen because physiographic and climatic data was available for this period. The data set was manageable for a small computer, and the data sequence was long enough to develop comparative statistics over more than one year. The basins studied were chosen in order to provide representative data from regions throughout the state.

Basic statistics, multiple regression and Fourier analysis programs were available and adapted for use with an HP 9845 computer. Description of the statistical techniques used can be found in Davis (1985). Climatic and physiographic data were obtained from Lamke (1979) and Hartman and Johnson (1978).

FOURIER ANALYSIS

Fourier analysis was used to investigate the periodic nature of streamflow from the glacierized basins shown in Table 1. The results of the analysis produced a statistical best fit model for each monthly streamflow sequence made of 30 (N/2) distinct harmonics (Davis, 1985), where N is the total length of the time series (months, in this analysis). Each harmonic is represented by an equation of

TABLE 1

Climatic and physiographic data for glacierized stream basins used to calibrate and test the simulation method.

Stream	Percent Glacier Cover (%)	Average Basin Elevation (m)	Average Annual Precipitation (cm)	Average Annual Air Temperature (degrees C)	Freezing Index (degree-days)	Thawing Index (degree-days)	Basin Area (km)	Average Annual Streamflow (m /s)
Harding River	9	732	381	4.4	139	2222	175	20.6
Gold Creek	8	732	305	4.4	139	2222	25.3	3.1
Mendenhall River	66	994	305	4.4	139	2222	221	32.6
Copper River	17	1104	94	-2.2	1944	1667	53397	1116
Wolverine Creek	72	1138	406	2.2	833	1667	24.7	2.6
Bradley River	36	854	305	2.8	556	1667	140	13.1
Eagle River	13	952	127	-0.6	1111	1667	498	14.2
Knik River	54	1220	254	-1.7	1111	1667	3059	192
Little Susitna River	5	1129	127	0.6	1389	1667	160	5.6
Susitna River near Denali	25	1376	152	-3.9	2500	1667	2462	78.5
McClaren River	19	1379	140	-2.2	2222	1667	726	28.0
Susitna River near Gold Creek	5	1043	74	-2.8	2222	1667	15967	246
Talkeetna River	7	1107	178	-2.2	1944	1667	5200	109
Kuskokwim River	1	451	56	-3.3	2222	1389	80614	1064
Tanana River at Tanacross	7	1177	46	-4.4	3333	1667	22162	219
Phelan Creek	69	1769	203	-4.4	2778	1667	31.6	2.0
Tanana River at Nenana	6	1196	43	-4.4	3055	1667	66368	657
Non-calibration Basins Used to Test the Model								
Skwentna River	16	857	109	-2.8	1500	1500	5832	183
Taiya River	37	1037	203	1.7	278	1667	464	31.4
Spruce Creek	8	607	203	3.3	389	1667	24.0	2.3
Power Creek	27	610	406	0.0	833	1667	53.1	7.1
Nenana River	4	1068	102	-5.0	2778	1667	4951	84.6
Tonsina River	11	1098	64	-2.2	1944	1667	1089	22.6

TABLE 2

Comparative statistics of actual flows versus simulated flows.

Stream	Average Annual Streamflow (m /s)		Standard Deviation of Streamflows (m /s)		Standard Error of the Mean (m /s)		Correlation Coefficient Actual vs Simulated
	Actual	Simulated	Actual	Simulated	Actual	Simulated	
Harding River	20.0	21.0	14.7	14.3	1.9	1.9	0.77
Copper River	1064	1505	1168	1704	151	220	0.76
Wolverine Creek	2.5	2.7	3.7	3.3	0.5	0.4	0.74
Kuskokwim River	1048	461	801	704	103	91	-0.04
Knik River	188	187	222	242	29	31	0.80
Susitna River near Denali	76.8	68.4	99.0	82.0	13	11	0.65
Non-calibration Basins Used to Test the Model							
Skwentna River	183	88.6	202	112	26	15	0.72
Taiya River	31.4	28.4	36.9	35.2	4.8	4.5	0.77
Spruce Creek	2.3	1.5	2.6	1.4	0.3	0.2	0.72
Power Creek	7.1	4.1	6.0	2.9	0.8	0.4	0.58
Nenana River	84.6	56.8	90.4	63.4	12	8.2	-0.42
Tonsina River	22.6	23.1	28.3	27.0	3.7	3.5	0.69

the form

$$Y_k = A_k(\cos(kP)) + B_k(\sin(kP)) \quad (1)$$

where

k = the harmonic number between 0 and N/2
A_k = the alpha coefficient associated with each harmonic
B_k = the beta coefficient associated with each harmonic
P = an angle between 0 and 360 degrees representing the entire time series

Y_k represents the predicted flow associated with each harmonic, k, and the time series is sequenced according to P. Each harmonic series is a sine/cosine function with an associated amplitude and phase angle. The alpha and beta coefficients represent both the phase angle shift and amplitude of each harmonic series. The summation of all 30 harmonics represents the best fit Fourier model of the entire time series, with each harmonic series accounting for a percentage of the total time series variance.

For the glacierized basins studied here, the 5th, 10th and 15th harmonics were found to account for an average of 87 percent of the total variance of the modeled hydrographs, with a range from 74 to 96 percent. The 5th harmonic represents the annual periodic variability, the 10th harmonic represents the semiannual periodic variability and the 15th harmonic represents the 1/3-annual periodic variability. The largest contributor to the time series variance in all the glacial streams was the annual period, indicating that the annual melt event dominates the hydrograph shape. The semiannual and 1/3 annual harmonics may represent the variance associated with the period from September to May, during which streamflow is predictably low for most of the basins studied. Because most of the variance could be explained by these three primary harmonics, we attempted to relate the values of the alpha and beta coefficients to the climatic and physiographic variables listed in Table 1 for the glacierized basins.

MULTIPLE REGRESSION ANALYSIS

The coefficients from the Fourier model described by the 5th, 10th and 15th harmonics, were normalized by dividing each by the watershed area of the associated glacier stream and then were regressed against basin variables using stepwise multiple linear regression (Davis, 1985). The stepwise multiple regression analysis produce an optimum, best-fit regression equation of the form

$$y = B_o + B_1(X_1) + B_2(X_2) \ldots B_n(X_n) + e \quad (2)$$

where B_o, B_1, B_2 ... B_n are regression coefficients, y is the dependent variable, X_o, X_1, X_2 ... X_n are independent (basin) variables and e is the residual. The following regression equations resulted: (Q')

$$Q' = 0.00074(\text{PERCENT}) - 0.00002(\text{ELEV}) + 0.00001(\text{FI}) + 0.00007(\text{TI}) + 0.00009(\text{AAP}) + 0.00634(\text{AAAT}) - 0.089 \quad (4)$$

where

Q' = the average annual streamflow per unit area of watershed (cubic meters/second/km^2)
PERCENT = the percent area of glacier cover
ELEV = the average basin elevation (meters)
FI = the freezing index (degree-days)
TI = the thawing index (degree- days
AAP = average annual precipitation (cm)
AAAT = average annual air temperature (degrees C)

and

$R^2 = 0.98$
standard error = 0.008 (cubic meters/second/km^2)

(A_5)

$$A_5 = 0.00276(\text{PERCENT}) - 0.00009(\text{ELEV}) + 0.00004(\text{FI}) + 0.00009(\text{TI}) - 0.0002(\text{AAP}) + 0.01991(\text{AAAT}) - 0.079 \quad (4)$$

where

A_5 = the alpha Fourier coefficient associated with the annual or 5th harmonic (cubic meters/second/km^2)

and

$R^2 = 0.96$
standard error = 0.017 (cubic meters/second/km^2)

(B_5)

$$B_5 = 0.00358(\text{PERCENT}) - 0.00003(\text{FI}) - 0.0001(\text{TI}) - 0.03047(\text{AAAT}) + 0.125 \quad (5)$$

where

B_5 = the beta Fourier coeffic
B_5 = the beta Fourier coefficient associated with the annual or 5th harmonic (cubic meters/second/km^2)

and

$R^2 = 0.97$
standard error = 0.0256 (cubic meters/second/km^2)

(A_{10})

$$A_{10} = 0.00202(\text{PERCENT}) - 0.00009(\text{AAP}) + 0.001 \quad (6)$$

where

A_{10} = the alpha Fourier coefficient associated with the semiannual or 10th harmonic (cubic meters/second/km^2)

and

$R^2 = 0.86$
standard error = 0.024 (cubic meters/second/km^2)

(B_{10})

$$B_{10} = -0.00265(\text{PERCENT}) + 0.00007(\text{ELEV}) - 0.042 \quad (7)$$

where

B_{10} = the beta Fourier coefficient associated with the semiannual or 10th harmonic (cubic meters/second/km^2)

and

$R^2 = 0.85$
standard error = 0.026 (cubic meters/second/km^2)

(A_{15})

$$A_{15} = 0.00135(\text{PERCENT}) + 0.00006(\text{TI}) - 0.08 \quad (8)$$

where

A_{15} = the alpha Fourier coefficient associated with the 1/3-annual or 15th harmonic (cubic meters/second/km^2)

and

$R^2 = 0.81$
standard error = 0.018 (cubic meters/second/km^2)

(B_{15})

$$B_{15} = 0.00006(\text{ELEV}) - 0.00005(\text{TI}) + 0.00012\ (\text{AAP}) + 0.005 \quad (9)$$

where

B_{15} = the beta Fourier coefficient associated with the 1/3-annual or 15th harmonic (cubic meters/second/km^2)

and

$R^2 = 0.77$
standard error = 0.0135 (cubic meters/second/km^2)

The above regression equations can be used to predict the Fourier coefficients necessary to reconstruct a Fourier model of an average monthly flow hydrograph. The predicted Fourier model will incorporate the errors inherent in the statistics as well as the error associated with using only three harmonics (up to 26 percent). The model can be constructed for any glacierized basin where the appropriate climatic and physiographic information is available or can be reasonably approximated. The model is represented by the following equation

$$Q = Q' + \sum_{k=5,10,15} A_k(\cos(kP)) + B_k(\sin(kP)) \quad (10)$$

The hydrograph prediction method was tested by simulating the average monthly flow hydrograph for six basins within the calibration data set and six basins not used in the calibration. The basins were chosen to represent the range of regions used in the original calibration data set. The results of the simulated hydrographs as they compare to the actual hydrographs are illustrated in Figures 1 and 2 and the statistics of the comparisons are in Table 2. Negative flows were predicted by the model and were incorporated into the comparative statistics, however, since negative flows do not exist they were not shown on the figures. The negative flows are a result of using only three harmonics to develop the hydrographs, and errors in the regression models. The poor prediction of monthly streamflows for those basins with less than 5 percent glacier cover (Nenana and Kuskokwim rivers), indicates that the dominant processes that contribute to streamflow in these basins is significantly different than the dominant processes that contribute to streamflow in basins with greater than 5 percent glacier cover.

CONCLUSIONS

The highly periodic nature and lower monthly flow variability of hydrographs emanating from glacierized basins allows the modeling procedures presented here based on Fourier analysis to be potentially successful. However, in basins where the percent glacier cover is less than 5 percent, the Fourier model developed from the regression equations, does not seem to simulate the actual hydrograph with very much accuracy (Kuskokwim and Nenana rivers). In basins with percent glacier cover greater than 5 percent the accuracy was much better, although considerable error was still exhibited in some cases. The modeling procedure yields results that would be valuable in cases where streamflow data are not available and possibly in studies to characterize climatic and hydrographic regions.

The calibration data set can be enlarged and regionalized in order to yield more accurate prediction equations, thus rendering the resulting Fourier model useful in more situations. In addition, daily flow hydrographs may also lend themselves to this type of modeling procedure and should be investigated in the future.

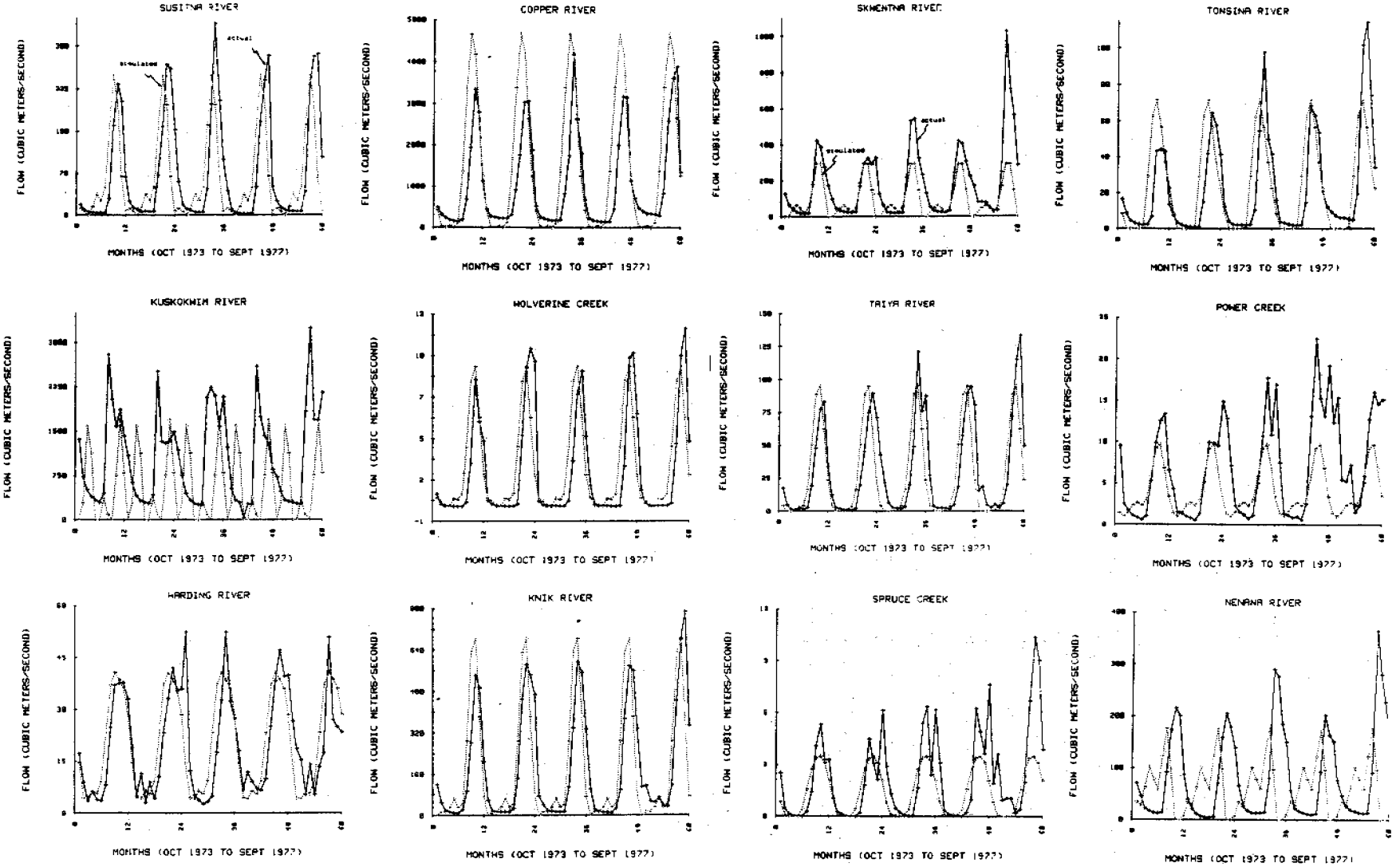

Fig.1 Actual and simulated average monthly streamflow hydrographs for representative calibration basins

Fig.2 Actual and simulated average monthly streamflow hydrographs for representative basins outside of the calibration data set.

REFERENCES

Bjerklie, D., and R.F. Carlson, 1986. Estimation of Glacier Meltwater Hydrographs. Cold Regions Hydrology Symposium. Amer. Water Resources Assoc., p. 345-352.

Chapman, D.L., 1982. Daily Flow Statistics of Alaskan Streams. NOAA, National Weather Service, Anchorage, AK.

Davis, J.C., 1985. Statistics and Data Analysis in Geology. 2nd Edition, John Wiley and Sons, New York.

Fountain, A.G., and W.V. Tangborn, 1985. The Effect of Glaciers on Streamflow Variations. Water Resources Research, Vol. 21, No. 4, pp. 579-586.

Hartman, C.W., and P.R. Johnson, 1978. Environmental Atlas of Alaska. 2nd Edition, Institute of Water Resources, University of Alaska Fairbanks.

Lamke, R.D., 1978. Flood Characteristics of Alaskan Streams. USGS Water Resources Investigations, publication No. WRI 78-0129.

Mayo, L., and T.L. Pewe, 1963. Ablation and Net Total Radiation, Gulkana Glacier, Alaska. In: Ice and Snow Properties, Processes and Applications, W.D. Kingery (ed.). MIT Press, Cambridge, MA, pp. 633-643.

U.S. Geological Survey, Water Resources Division, 1973-1977. Water Resources Data for Alaska. Report AK-73-1 through AK-77-1.

PROTECTION OF THE ENVIRONMENT IN JAMESON LAND

C. Bæk-Madsen

Danish Geotechnical Institute, Denmark

SYNOPSIS The Danish Geotechnical Institute (DGI) has conducted a number of geotechnical investigations in Jameson Land as part of a program for baseline studies of the physical environment. Jameson Land is situated on the east coast of Greenland and the region encompasses a potential oilfield. Together with baseline studies of geomorphology, soil temperatures and climate the geotechnical investigations are used by Greenland Technical Organization (GTO) to assess the impact of exploration and construction in the region. Through assesments the operations are regulated in order to protect environmentally sensitive permafrost terrain. This article summarizes the main investigations undertaken by DGI during the period from 1980 to 1986 for GTO. In situ surveys have been correlated for single points and thereafter integrated on air photo map base. This has allowed the subdivision of Jameson Land on the basis of degree of environmental sensitivity as well as mapping of possible low impact traffic corridors and estimation of geotechnical parameters.

INTRODUCTION

Human activity in regions of permafrost terrain is known to have serious negative environmental consequences. This knowledge has led to a combined environmental and geotechnical investigation on the desolate Jameson Land prior to potential oil exploration. The task of conducting geotechnical investigations was given to the Danish Geotechnical Institute and was carried out over a period of six years for Greenland Technical Organization. Denmark, however, has neither tradition for nor experience in environmental investigations related to permafrost. With quite a different landscape in Greenland compared with those described in foreign literature, GTO had decided to provide a basic knowledge of factors involved in evaluation of environmental controls and techniques to minimize negative impacts.

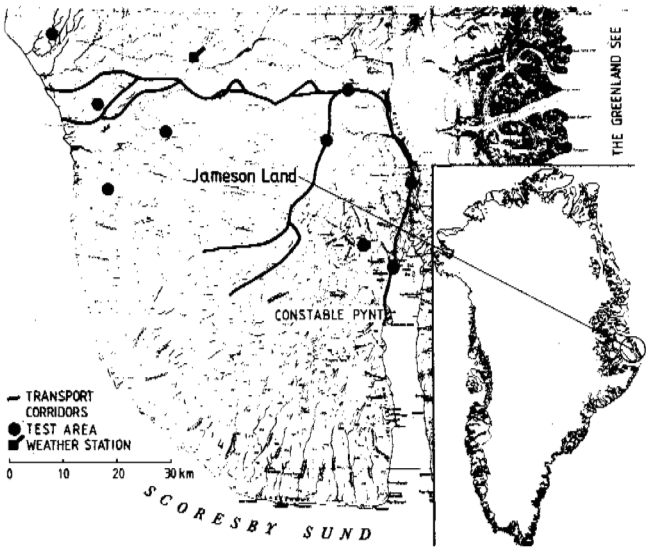

Figure 1. Location and map for Jameson Land on the east coast of Greenland.

The task was prepared in 1980-81 and field investigations were carried out during the short summers in 1982-85 with a provisional final working up in 1986.

Jameson Land occupies almost 8,000 km² on the eastern coast of Greenland between latitudes 70°30' and 71°35'N and longitudes 22°30' and 24°30'W. One of the world's largest inlet systems - Scoresby Sound - forms the border to the south and to the west; northwards rise higher mountains and towards east lies the ice-filled Greenland Sea, cf. Figure 1. The area had been mapped at a scale of 1:250,000. In 1982 one of GTO's other contractors covered the area with aerial photographs at a scale of 1:30,000.

GEOLOGY

Jameson Land is underlain by a major structural belt, the East Greenland Caledonian fold belt, which occurs on both sides of the North Atlantic Ocean (Henriksen, et al, 1976).This metamorphic crystalline complex is overlain by mainly marine sediments of Jurassic age, consisting of sandstones and shales with an almost horizontal bedding attitude (Funder, 1972) upon which the present geomorphology has been developed.

To the north, and in a stretch parallel to the eastern border the jurassic layers form gorged extensive plateaus at altitudes up to 500 m, cf. Figure 2.

These plateaus are in places overlain with quaternary ground moraine of pre-Weichselian age.

Towards west and south, a smoothly sloping plain forms the landscape to Scoresby Sound. In comparison, the eastern slope is more steep, characterized by a branched complex of valleys. The near-shore areas, with altitudes up to 100 m, are characterized by glacial deposits and marine sediments connected with isostatic response to the Weichselian deglaciation. The remainder of the sloping plain is predominantly overlain by fluviatile materials and local eolian deposits of silt and sand. Landslides and talus are common in steeper slope terrains.

Jameson Land is situated north of the continuous permafrost border, and the geomorphology is dominated by landforms related to permafrost processes. The frost extends to an unknown depth, whereas the seasonally thawed active layer can be fixed to 0.5 to 1 m.

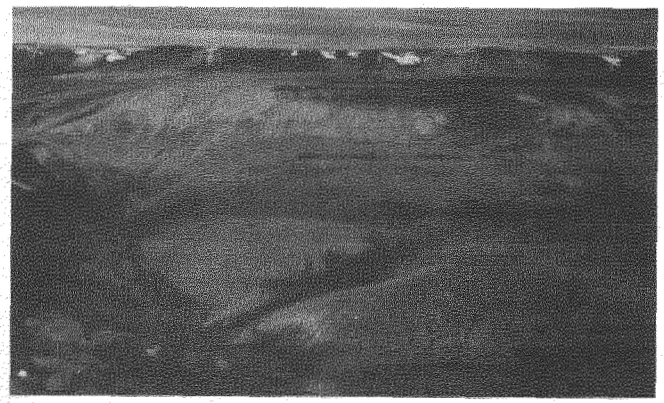

Figure 2. Typical landscape with higher mountains, plateaus and gorges.

CLIMATE

Jameson Land is situated in the extreme arctic area. According to measurement of climatic conditions conducted by GTO in central Jameson Land, the mean temperature in the warmest month is just below 5°C; the annual mean temperature is approx. -7°C (Thingvad, et al, 1985). The sun is above the horizon for about 95 consecutive days and below the horizon for about 70 consecutive days in midwinter. The land is normally free from snow from the middle of July to the end of August.

It may be stated generally that the eastern and high altitudes are highly affected by wind during winter, whereas the lower level western areas are less affected by wind. The dominant winter wind direction is northerly, in the summer wind directions are more variable.

ACCESS

Due to a very great quantity of drifting ice, navigation through Scoresby Sound is only possible from the end of July to the beginning of September.

Air transport was possible to Mestersvig approx. 100 km north of Jameson Land until 1985, afterwards the new airfacilities at Constable Pynt in Harry Inlet are used, cf. Figure 1.

INVESTIGATIONS

During the period 1982-1985, geotechnical investigations were undertaken, involving several types of field investigations and transport studies, in order to ascertain appropriate methods and equipment suited to the unique terrain characteristics of Jameson Land. Personnel, materials and equipment were largely carriaged by air to Mestersvig; transport from Mestersvig to the test sites shown on Figure 1 was accomplished by helicopter. Within the test area, walking was the only permitted mode of transportation in 1982. A special motorcycle with trailer and fitted with low pressure wheels was provided by GTO in 1983 to 85, and an off-road vehicle was added in 1985. The period from 1980 to 86 has included the following activities:

- 1980 to 81: Air reconnaissance by the GTO followed by planning and study of relevant literature.
- 1982: Digging of test pits, diamond core drilling with a two man portable rig. Geophysical investigations consisting of electrical soundings, electrical resistivity surveying, seismic surveying and electromagnetic terrain conductivity measurements. Assistance in foundation of a weather station and off-road vehicle experiment.
- 1983 to 84: Digging of test pits and boring using ice auger equipment, cf. Figure 3. Electrical and electromagnetic surveying. In Denmark, development, construction and testing of a mobil drilling unit consisting of an off-road vehicle with hydraulic boring equipment.
- 1985: Continuation of the above-mentioned research, including testing of the new boring rig.
- 1986: Evaluation of test results, air photo studies and preparation of concluding reports.

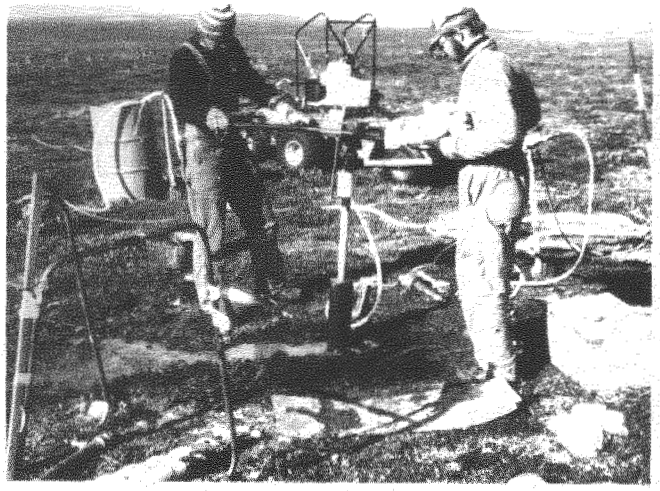

Figure 3. Boring with ice auger equipment in frozen soil.

The accumulated investigations on Jameson Land have included approx. 130 test pits in the active permafrost layer, 145 borings in permafrozen strata and 40 kilometres of geophysical profiling.

Test pits and borings

Test pits were dug down to the frost level, permitting detailed examination of materials in situ. Temperature per 0.1 m and vane test per 0.2 m were measured. Rotary power drilling was used to obtain borings in the underlying frozen strata. Disturbed samples were taken in the test pits whereas augered boreholes provided both disturbed and undisturbed samples with nearly 100 % recovery in the frozen materials.

Geophysical investigations

As geophysical surveys are considered very important for establishing the thickness of the active layer, ice inclusions in the permafrost and characteristic composition properties of the frozen ground, such methods as geoelectrical, electromagnetic and seismic surveys have been used. Comparison of these methods, correlated with results given from the test pits and borings, shows that the electromagnetic surveys using a Geonics 31 and 38 and geoelectrical survey with an ABEM equipment using frequences below 100 kHz have been found most useful under the actual conditions, whereas the seismic results have been ambiguous.

As the geophysical techniques require knowledge of electrical properties of frozen ground, laboratory tests have been carried out to determine the specific resistance, ρ, for sediments under frozen and thawed conditions. The results, given in Table I, show a significant increase in resistivity with decrease in temperature as also reported by Johnston (1981).

TABLE I

Soil resistivity

Soil type	Moisture Content	Dry Density	Resistivity ohm m Thawed	Frozen
Sandstone	3.6	25.1	2,700-5,300	>12,400
Sandstone, silty	8.6	22.0	300-2,000	>14,000
Sandstone, fissured	10.4	22.5	200-6,300	>16,000
Clay	22.3	20.0	90- 250	> 400
Sandstone, micascious	0.7	27.0	1,500-2,000	> 3,000

Due to a very high resistivity for pure ice, it is often possible to register great differences in resistivity between frozen and thawed materials. The relationship between resistivities for fully and partially saturated soil in a thawed condition can be illustrated by the equation relating resistivity to the degree of saturation (Keller, et al 1966):

$$\rho : \rho_{100} = a\, S_w^{-n_2} \; ; \; S_w < S_{wc}$$

(a and n_2 are parameters determined experimentally, ρ and ρ_{100} are the resistivity of a partially or completely saturated sediment, S_w is the fraction of the total pore volume filled with electrolyte and S_{wc} is a critical value). Due to this it has been possible to evaluate depth to the frost table as well as to estimate the general conditions as shown by results given in Figure 4.

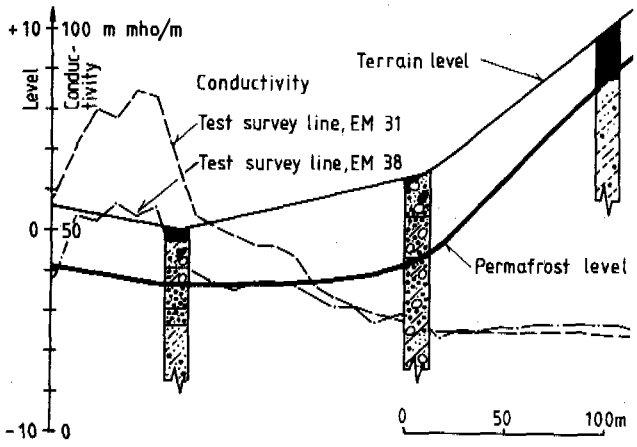

Figure 4. Part of test line with results from borings and electromagnetic surveys with Geonics EM 31 and EM 38.

Off-road vehicle experiments

DGI has assisted GTO with the evaluation of the impact of motorized vehicles on typical Jameson Land soils and landform units. Initially, an all-terrain vehicle from Geophysical Service Inc. with a ground pressure of 11 kN/m² was tested with 1, 5 and 10 passes in straight as well as in curved lines. The degree of impact was examined with photos and measurement and the areas were inspected the following year, cf. Figure 5.

Judging from these tests the disturbance of the active layer was limited in drained areas and the most essential parameter for traffic over the terrain appeared to be degree of soil moisture. Traffic with no negative impact would accordingly be possible over dry or slightly saturated surfaces, or in well drained areas. The above tests included the motorcycle and the mobile drilling unit; all DGI-transports have consequently been carried out through non-sensitive areas.

The risk for serious damage to the terrain has further been examined through execution of plate load tests directly on the ground. These tests have given further knowledge about the

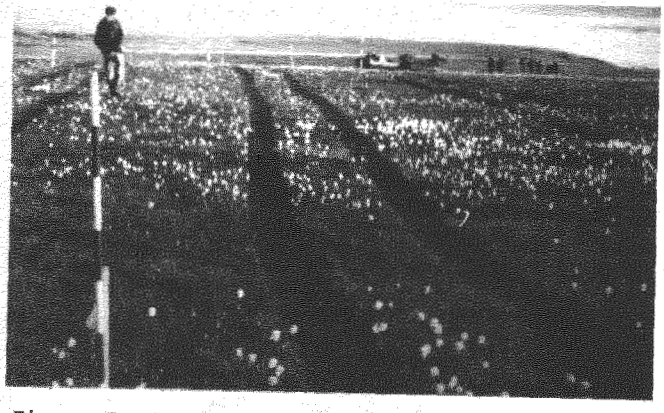

Figure 5. Tracks after the All Terrain Vehicle tested in 1982.

bearing capacity of the top soil. Permanent deformations derived from dynamic loads have been determined for an increasing number of loads as shown in Figure 6 and the results have given the modulus $E = 1.5 \times r \times \Delta\sigma/s$, where r is the radius of the plate, $\Delta\sigma$ the change in loads and s the reversible deformation on the third unloading curve.

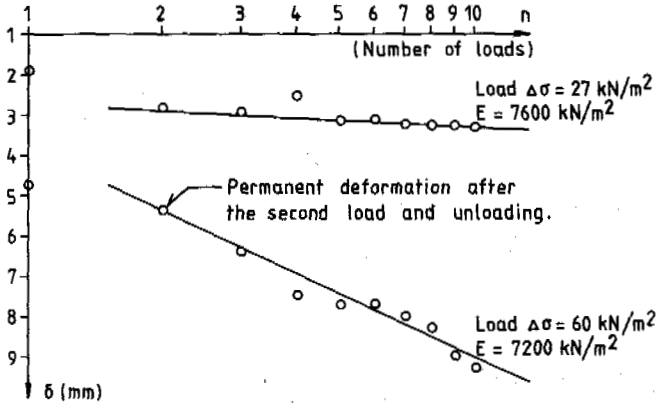

Figure 6. Plate load test, d=0.15 m. Measured permanent deformation after every load and unloading.

Weather station

An automatic weather station supplemented with registration of ground temperatures was established and put into operation by GTO in July 1982. The station's position is shown in Figure 1 (Langager, 1982). Data for wind, barometric pressure, precipitation, snow height, air temperature, humidity, short wave radiation and temperatures 0, 1/2, 1, 1 1/2, 2, 3, 4, 5, 6, and 7 meter below ground level are stored on tape at 3 hour intervals in a datalogger. The tape is replaced and brought to GTO, Copenhagen once a year. In addition, a satellite transmission system was installed, allowing actual values to be monitored in Copenhagen with a delay of 3 to 10 hours.

MOBILE DRILLING UNIT

As vehicular activities on the more sensitive parts of the landscape in the summer period could damage the vegetation and land surface, a very low pressure wheeled vehicle is desirable for transporting personnel and equipment. Based on a transporter (Seiga, manufactured by Harvester Co., Ltd.), the DGI has been assisting in manufacturing a special cabin allowing stays of approx. one week plus special auger equipment for boring. All functions are driven hydraulically with power from a diesel engine and the total pressure with full load amounts to less than 10 kN/m².

After transport by ship to Jameson Land, the vehicle was assembled and tested in 1985 over a route of approx. 60 km. The vehicle was capable of driving - with detours - over the very rough and impassable landscape; only very soft areas or regular water were severe obstructions. Slopes with an inclination up to 13 % were passable parallelwise. One day routes of up to 20 km seemed to be possible with previous reconnaisance, and up to 30 km in well-known terrain, cf. Figure 7. The hydraulic boring equipment has worked without difficulties. After mounting of pontoons, the vehicle can cross minor lakes with propulsion from the rotating wheels. As no rutted tracks have been observed and no vegetation has been torn up, this vehicle seems to be suitable for use under controlled conditions and responsible treatment.

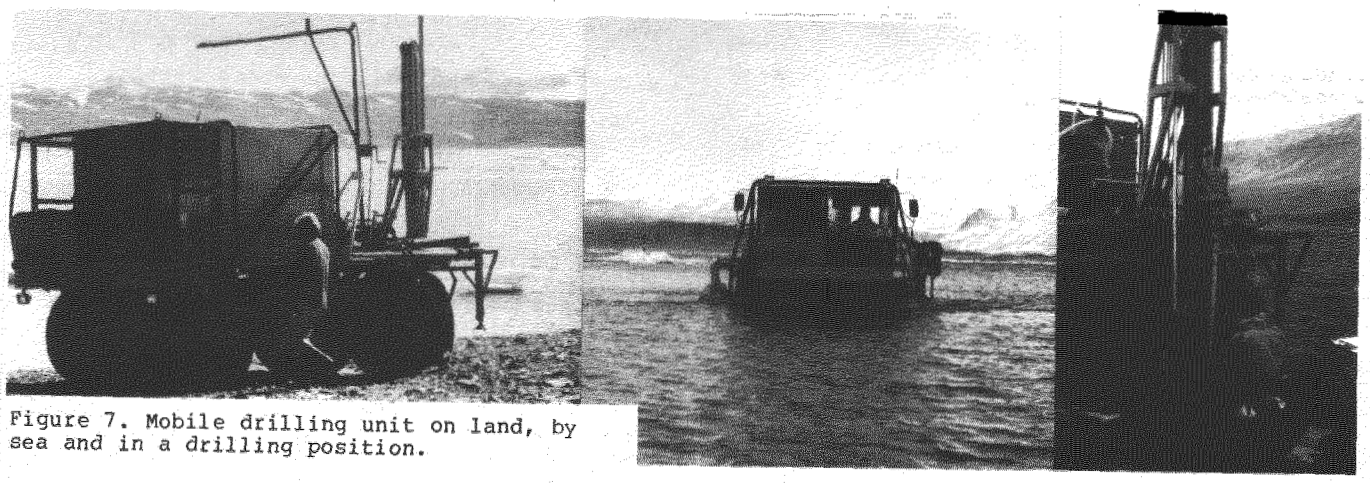

Figure 7. Mobile drilling unit on land, by sea and in a drilling position.

CALCULATIONS

Thermal properties are important parameters, indeed fundamental to all ground heat transfer problems as is strength of the cohesive soil layers fundamentally related to mechanical impacts. Thus, laboratory tests were carried out concerning the above-mentioned and computer calculations were made to estimate the time for freezing of the active layer after the summer season.

The computer program TODIM - developed at the Technical High School in Norway by Thue, (1971) and modified by DGI - was the fundamental tool used in estimating the latent heat necessary to freeze soil to a given depth. The computer system calculates a two-dimensional temperature field dependent on time, and the calculations are based on a known initial distribution of temperatures and thermal parameters. Thermal conductivity and heat capacity may be given different values over and under a temperature of 0 degree Celsius in that part of the computer program where soil materials are involved.

The program in this instance was used to calculate temperature in the ground as a function of time for a given fall in temperature, in this case air temperature. Soil properties were estimated from the general regional geology, calculated with both no and 0.2 m snowcover.

The results of the calculations for a single station are shown in Figure 8, supplemented with the temperature measured 0.5 m under ground level. The idealized temperature field and profile for the soils may give some instabilities in the calculations. However, they seem to give a fairly good indication of freezing time of the active permafrost layer. This was used to evaluate the required frost thickness of the active layer to support vehicles with a static pressure of 75 kN/m².

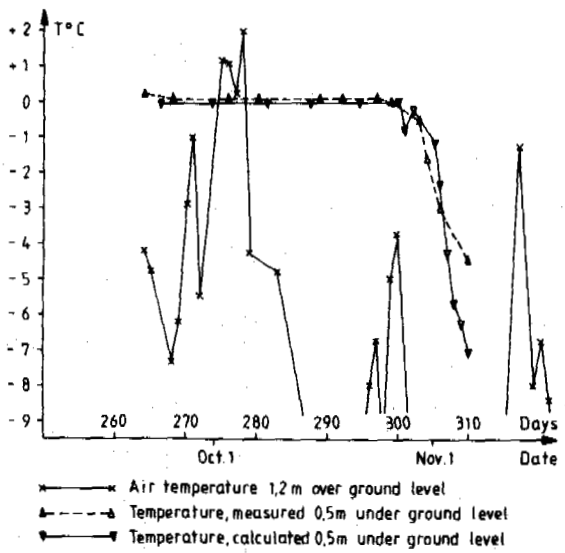

Figure 8. Frost penetration, measured and calculated. Temperature-day graph with days after jan. 1.

TERRAIN ANALYSIS

With the enormous area a scematic presentation of the results would be necessary to complete the task. Thus, with inspiration from Walker, et al (1980) it was decided to present the information on aerial photos. With a terrain typing modified to the landscape in question a great deal of information has been presented as shown in Figure 9. Registration of the physical parameters of the overburden soil has been essential at the mapping site in order to create a necessary background for appropriate further work.

Breakage and resulting environmental damage in frozen soils occur under conditions of too large deformation in the underlying thawed zone. The ability of frozen soils to bear loads is therefore based on a deformation condition where the consolidation module, K, of the soil horizon under consideration is based on an empirically determined relationship between geology and water content. Initial deformations were calculated for various thicknesses of the thawed portion of the active zone. It was estimated that deformations greater than 2 cm would be unacceptable, where in these instances there should be a reasonable frost cover to support vehicles.

Depth of the required frost layer was estimated according to the method outlined in Johnston, (1981), thickness calculation is based on ground temperature of -0.5°C. The amount of time necessary to freeze ground to a particular depth was calculated to be approx. 20 days longer for clay profiles than for those composed of relatively dry, sandy peat. A snowcover of 0.2 m will further delay freezing by approx. 10 days. Using this method of calculation, where all of the input variables can be adjusted to particular site conditions, the essential frost depth necessary to sustain required loads can be established at any time using known parameters. By use of the satellite connection to the Jameson Land weather station and four small stations measuring soil and air temperatures, the time periods during which vehicular traffic can operate with minimum environmental damage can be monitored from Copenhagen and used for evaluation of the earliest start-up and latest stop for the operations.

USE

On the basis of field survey results, air photo evaluation and the compiled weather station data, a portion of Jameson Land has been divided into different terrain units. The purposes of this subdivision were to delineate environmentally sensitive regions and to determine optimal traffic corridors. In addition, computer calculations were used to estimate necessary seasonal frost thicknesses for minimal environmental disturbance resulting from vehicular movement over the permafrost terrain. Interpretation of the air photos incorporated the detailed data from field test-areas, and led to a determination of sensitive areas where transport by heavily loaded vehicles (static loads of 80-90 kN/m²) would be environmentally destructive. Effects

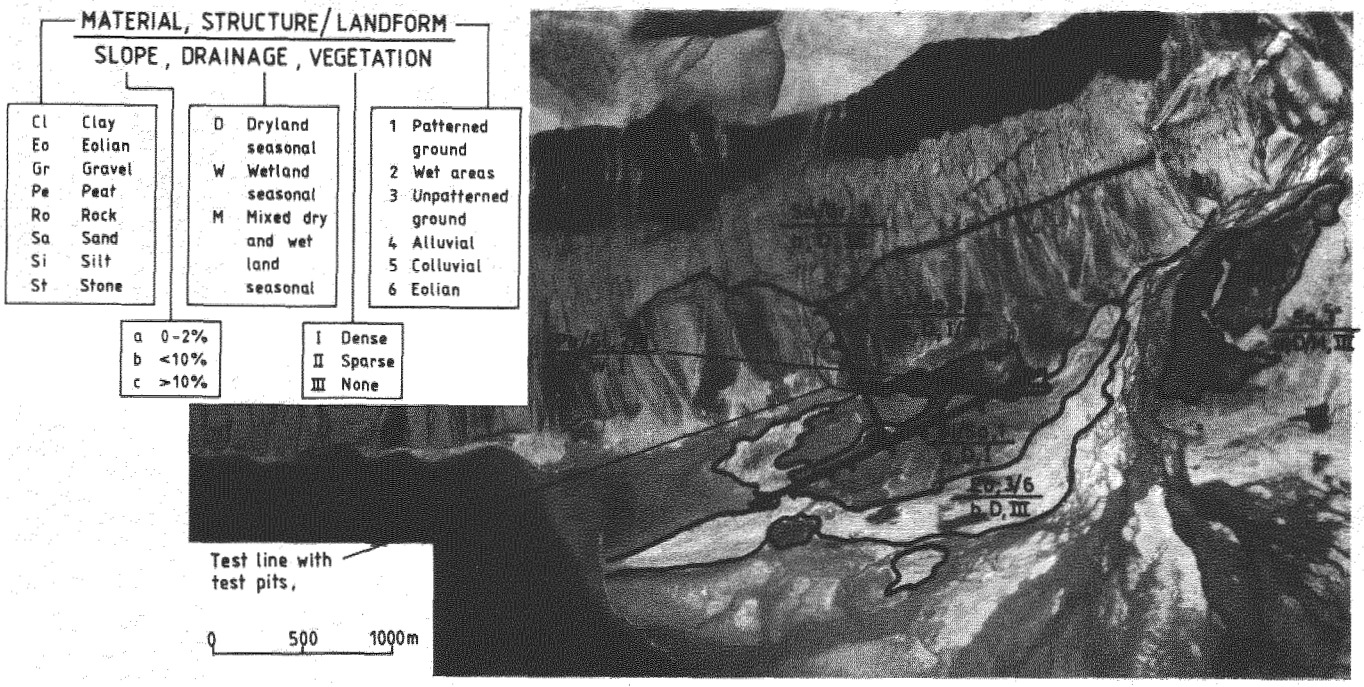

Figure 9. Delta with test lines, test pits and terrain classification.

were predicted for terrains with no snowcover in connection with winter seismic surveying. Damages could include:

- destruction of vegetation root systems and formation of deeply rutted tracks
- erosion and/or landslides affecting areas of at least 10,000 m²
- disruption of drainage systems affecting areas of at least 50-100,000 m²
- destruction of vegetation with consequent eolian and/or water erosion.

For the areas in question, sensitive regions have been outlined on the air photos.

In a similar manner, possible traffic corridors have been determined from Constable Pynt towards north and thereafter west and southwest. Passage directly west from Constable Pynt is not feasible due to the mountainous terrain. Traffic corridors have been mapped in detail on airphotos, and GTO has verified the corridors by helicopter survey and field check, cf. Figure 1. The Owl River delta (Figure No.9) is the test-area first crossed after Constable Pynt.

CONCLUSIONS

Preliminary conclusions from the environmental surveying of Jameson Land show the importance of evaluating the ground's physical properties so that permanent deformation and possible erosion can be assessed.

Regarding specialized investigations, it is felt that plate load studies are of particular interest. In a systematic survey, plate load studies can be carried out in connection with the mobile drilling unit's other activities.

From information presently available, it is believed to be possible to base a large proportion of environmental impact studies on air photo interpretations in conjunction with measurements and calculations derived from field instruments and surveying.

REFERENCES

Henriksen, N & Higgins, A K (1976)
Geology of Greenland, Geological Survey of Greenland, Copenhagen.

Funder, S (1971)
Report on the 1971 geological expedition to Scoresby Sound, East Greenland. Geological Survey of Greenland, Report No 48

Thingvad, N, Andersen, E I, & Thomsen, T (1985)
Pre-investigations, Jameson Land, Climate, Greenland technical Organization (GTO).

Langager, H C, (1982)
Pre-investigation, Jameson Land, Station 133 (Weather Station), GTO.

Keller, G V & Frischknecht, F C (1966)
Electrical Methods in Geophysical Prospecting. Pergamon Press. New York.

Johnston, G H ed. (1981).
Permafrost. Engineering, Design and Construction. National Research Council of Canada.

Walker, D A, Everett, K R, Webber, P J & Brown, J. (1980).
Geobotanical Atlas of the Prudhoe Bay Region, Alaska, CRREL Report 80-14.

Thue, J.V.(1971).
Frost i Jord. (unpublished).

SUSPENDED SEDIMENT TRANSPORT IN ARCTIC RIVERS

M.J. Clark, A.M. Gurnell and J.L. Threlfall

Department of Geography, The University, Southampton, United Kingdom

SYNOPSIS: Within the permafrost and seasonal freezing zones, hydrological studies face methodological problems which have counterparts in other environments. In particular, investigative design may mask the patterns of water quality and quantity that are the target of the study both in spatial terms (as with specification of catchment sediment sources) and in a temporal context (as in lags and leads between peak discharge and peak sediment transfer). Published studies indicate the complexity and the spatial and temporal scale dependence of the interactions between snow and ice melt, ground thaw, discharge and fluvial sediment transport. These interactions are investigated further using field data from a small instrumented upland catchment in arctic Finland. Three subperiods exhibiting different relationships between suspended sediment concentration and discharge are identified from two-hourly observations over the snowmelt and ground thaw period, and their process significance is discussed.

INTRODUCTION

Reviews of the development of arctic hydrology such as those included in Williams and van Everdingen (1973), Chaco and Bredthauer (1983) and Slaughter et al. (1983) agree that the serious study of basin hydrology within the permafrost zone commenced around the beginning of the 1960s. Despite this relatively short history, it is apparent that description, analysis and modelling are all dependent upon data quality which itself reflects standards of sampling design and instrumentation. Problems relating to the adequacy of the sampling interval and of sample timing have been manifest at many scales, with perhaps the most extreme problem of sampling being the under-representation of winter conditions. Problematic in a different sense are studies which give almost no information on these points. For example, Corte (1978) states merely that in order to compare discharge from glacier-covered and glacier-free parts of a river basin 'measurements of the run-off were made up to 4 times a day depending on the weather conditions.' Detailed comparisons between studies are impossible on the basis of such ill-defined techniques.

It seems likely that investigative design may mask the patterns of water quality and quantity that are the target of a study both in spatial terms (e.g. in the specification of catchment sediment sources) and in a temporal context (e.g. in lags and leads between discharge and sediment transfer). This paper focuses on the temporal implications, and explores this theme by reviewing the sparse published record before presenting data from a small upland catchment in arctic Finnish Lapland.

HYDROLOGICAL IMPLICATIONS OF TEMPORAL SAMPLING DESIGN

An early northern attempt to address the problems of sampling design is represented by James and Vieira-Ribeiro (1975) in a study of snowmelt discharge modelling near Pangnirtung, Baffin Island. They recognized the need to disaggregate the information both seasonally and spatially, but concluded that a daily timeframe and fourfold spatial division of the basin was the highest resolution warranted by their data. Even so, the significance of the sampling frame is apparent, and using serial cross correlation of hourly temperature and streamflow they demonstrated a steady growth in lag through the ablation period and showed that the temporal sampling design is of importance in the context of, firstly, sampling resolution and, secondly, the synchroneity between sampling frame and physical events.

Sampling resolution influences the physical processes that can be determined. For example, Clark et al. (1988) show that a progressive degradation of a data set through 2-hourly, 6-hourly, 12-hourly and 24-hourly intervals substantially alters both the apparent nature and magnitude of the trends recorded. In particular, an increase in sampling interval causes underestimation of both mean and total discharge and suspended sediment yield in a regime dominated by short-duration peaks.

In addition to the significance of sampling resolution or interval, observations are often fixed to clock units rather than attempting synchroneity with physical attributes. For example, if the sampling interval does not allow full representation of diurnal temporal

patterns, then the coarser timing of observations may fail to resonate with processes exhibiting a near-diurnal rhythm. For example, Röthlisberger and Lang (1987) demonstrate that the peak of the Alpine proglacial daily hydrograph shifts substantially through the ablation season from close to 18.00 h in May and June to around 14.00 or 15.00 in August and September. A fixed daily sampling time would thus exhibit a progressive shift in its timing relative to position on the diurnal hydrograph and particularly to the hydrograph peak, and would thereby produce an entirely artificial trend in the data.

STUDIES OF TEMPORAL PATTERNING IN ARCTIC HYDROLOGIC SYSTEMS

The form and timing of the stream hydrograph in response to snowmelt is dependent upon a series of components (snowpack energy balance; water movement through snowpack; water movement over or through the ground surface; transient storage in depressions at the surface or in the frost table; water movement within the channel network), each of which is subject to complex variations through time. It follows that the interaction of these variables will also change significantly through time and will provide complex patterns of both discharge and sediment transfer. Temporal patterning and its sampling implications can usefully be considered at the scale of both individual diurnal thaw cycles and storms and also at the scale of the complete thaw season.

Detailed hydrologic studies are less frequent for northern basins than for their temperate counterparts but they have become increasingly available and detailed over the past decade (for example, Dingman (1973) and Chaco and Bredthauer (1983) for Glenn Creek, Central Alaska; Cogley and McCann (1975) for Mecham River, Cornwallis Island), whereas detailed studies relating discharge to fluvial sediment transfer are far less common.

One of the first quantitative specifications of the diurnal variability of suspended sediment concentration was McCann et al.'s (1972) study of the River Mecham (Cornwallis Island). In addition, several studies have investigated the changing relationship between suspended sediment concentration and discharge through the thaw season. In proglacial streams, detailed observations of suspended sediment concentration and discharge show that there is a general tendency for suspended sediment to reach a maximum concentration prior to peak discharge at a range of temporal scales (Gurnell, 1987). On the basis of the less detailed data available for northern nonglacial rivers, relationships between suspended sediment concentration and discharge appear to be more complex. Arnborg et al. (1967) recognised that 'accuracy depends partly on frequency and spacing of the samples collected' and demonstrated that for the Colville River, Alaska, there were complex relationships between suspended sediment concentration and discharge at both the seasonal and event scales. Within each of the first three floods recorded in 1962, suspended sediment concentration was higher on the rising limb of the discharge hydrograph and peaked in advance of discharge, thus providing a clockwise looped relationship between the two variables, which is the norm for more temperate basins.

The influence of ice and ground freezing conditions may explain some of the complexity of observed suspended sediment transfer. For example, Forbes (1975) tabulated the results of periodic sediment surveys for the Babbage River in the early melt season and inferred that bottomfast ice inhibited bed scour in the pre-breakup period, although 'the extent to which scour may be inhibited by a frozen channel perimeter remains an important unanswered question.' Scott (1978) noted considerable disagreement in the literature concerning the extent to which permafrost encouraged or inhibited lateral erosion rates in river channels. He found similar controversy concerning the timing of erosion, with authors split between those according greatest significance to the breakup flood and those stressing summer storms. Scott's (1978) study of streams in the Brooks Range, Alaska, recognized that general relationships may be elusive, due in particular to the varied nature of bank and bed material together with variations in catchment size. Bank erosion often proceeded more slowly than thaw, implying that thaw is not a general constraint on erosion, though in all the streams that were sampled there were occurrences of frozen material in direct contact with channel flow. However, the interaction between snow and ice melt, discharge variations, bank thaw and erosion is probably related to catchment size. In large basins a lengthy delay between breakup and flood peak may allow bed/bank thaw (and thus sediment availability) to precede the flood peak over much of the basin. In contrast, in smaller basins (and in the headwater areas of larger basins) the reverse may be true so that the potential for erosional activity may not be significant until after the main breakup flood.

In part, these relationships hinge on the thermal mechanisms linking the river to its perimeter materials (McDonald and Lewis, 1973). Miles (1976) elaborated on the timing of erosion in relation to discharge, and noted that whilst several factors inhibited erosion during breakup, sediment is contributed to the channel prior to breakup, and may also be significant several weeks later in relation to higher water temperatures. A number of studies of the thermal effect of a river on the surrounding bed and bank materials are available (for example, Corbin and Benson, 1983), but the temporal resolution of these thermal surveys is not ideally suited to examining the interaction between the discharge hydrograph of a single thaw-period flood event (perhaps an individual diurnal cycle) and the bed or bank temperature changes that result, and that possibly contribute to sediment release.

Although the literature is sparse, it is clear that the relationship between sediment and discharge in arctic rivers is complex and varied. It is also apparent that the thermal mechanisms linking the river to its perimeter

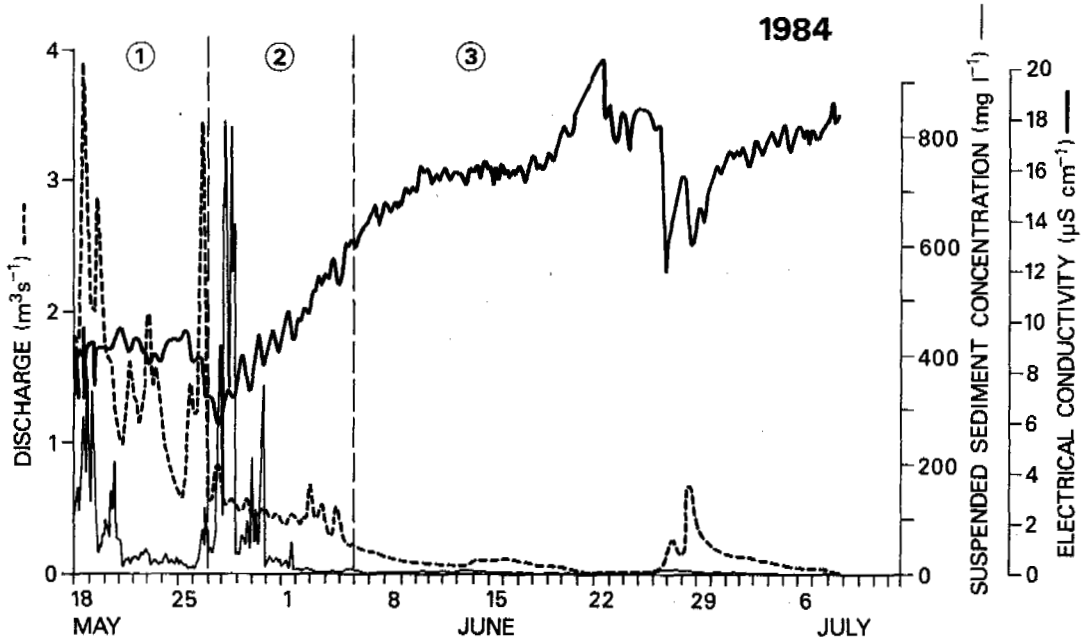

Figure 1: Two-hourly observation of discharge, suspended sediment concentration and electrical conductivity (corrected to 25°C) at the main gauging site, Skirhasjohka, Finland 1984. 1, 2 and 3 refer to time periods used in data separation in Figure 2.

and the inter-relationships between snow and ice melt, ground thaw, discharge variation and erosion are critical in controlling sediment transfer patterns and can most easily be identified if the variables are sampled sufficiently frequently. Detailed temporal observations of discharge, suspended sediment concentration and electrical conductivity of a river draining a small catchment in northern Finland will now be used to illustrate and discuss some of these relationships further.

FLUVIAL SUSPENDED SEDIMENT TRANSFER IN A SMALL UPLAND CATCHMENT IN FINNISH LAPLAND

The value of a short and systematic temporal sampling interval can be demonstrated with reference to data collected from the Skirhasjohka catchment near Kilpisjarvi in Finnish Lapland at 69° 04′ N, 20° 46′ E. The catchment, which is fully described in Clark et al. (1985) and Threlfall (1987), has an area of 8.9 km^2, and is bounded by fjells rising to a little over 1000 m. The heavily glaciated rolling till-covered topography is underlain by Palaeozoic schists, and carries subalpine birch forest up to 550-600 m, above which lies treeless subarctic heath and bare fjell surfaces. Mean annual temperature is -2.0°C, with annual precipitation of 419 mm (representing 50-100 cm snow between mid-October and early-June). The catchment is thus one of seasonal ground freezing, and the Skirhasjohka represents the small Subarctic nival regime of the classification developed by Church (1974). Continuous discharge data were derived from continuous stage records at a rated section 500 m upstream from the Skirhasjohka's lake outlet for the periods 20 May to 11 July 1983 and 18 May to 16 July 1984. These observation periods include the entire snowmelt period in both years with the exception of the first five and two days of flow in 1983 and 1984 respectively, when snow jamming prevented data collection at the gauging site. For the purpose of illustrating the utility of high temporal frequency observations, only the 1984 data will be considered here. Two-hourly observations of suspended sediment concentration at the same site and for the same periods were derived from filtration of water samples obtained using an automatic pumping sampler with fixed intake nozzle located 1.2 m from the bank and 0.15 m from the bed on a 4m wide section. Samples were filtered through Whatman 42 papers with a 2.5µm pore size in 1983 and through Whatman cellulose nitrate membrane papers with a .45 µm pore size in 1984.

Figure 1 illustrates the temporal pattern of discharge and suspended sediment concentration at the main gauging site during the 1984 observation period. The high flows early in the period are accompanied by variable but often relatively high concentrations of suspended sediment, whereas the subsequent low flows are accompanied by extremely low suspended sediment concentrations. However, close examination of these detailed time series of suspended sediment concentration and discharge observations reveal that the relationship between them is far from a simple positive one.

A scatter plot (Figure 2B) reveals enormous variability rather than a simple positive relationship between the two variables. At least three zones with some clustering are evident within the scatter of data points, and these correspond to three separate time periods within the full data set. Zone 1 contains observations from the period 18 May to 26 May,

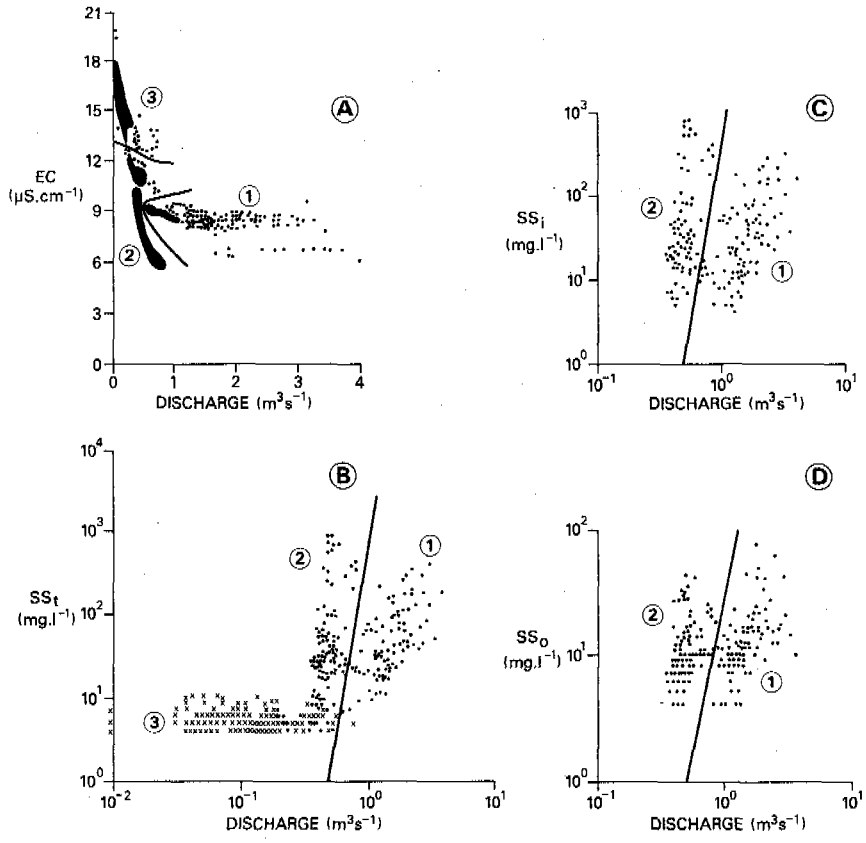

Figure 2: A: Electrical conductivity (EC) - discharge scatter plot. Areas of very dense data are shaded solid black). B: Total suspended sediment concentration (SS_t) - discharge scatter plot. Data plotted as crosses for period 3 to distinguish them from the dots used for periods 1 and 2 in areas where there is overlap in the data. C: Inorganic suspended sediment concentration (SS_i) - discharge scatter plot for periods 1 and 2. D: Organic suspended sediment concentration (SS_o) - discharge scatter plot for periods 1 and 2. 1: Data for 18-26 May 1984. 2: Data for 27 May - 5 June 1984. 3: Data for 6 June - 9 July 1984. Linear separation of low suspended sediment concentrations in B,C and D result from logarithmic scale, minimum concentration plotted, 4mg.l^{-1}.

zone 2 represents the period 27 May to 5 June and zone 3 represents the period 6 June to 9 July (after which flow became too low for further observations at the main gauging site). From Figure 1 it can be seen that during period 1 there are three major flood hydrographs, each extending over more than one day, but only the first of these is accompanied by a major increase in suspended sediment concentration. During period 2 there are clear diurnal discharge hydrographs, all of which have relatively low peak discharges in comparison with the hydrographs of period 1, but suspended sediment concentration is relatively very high, particularly during the first four days of the period. Period 3 is characterised by generally low discharge, although there is a period of higher flows from 27 to 30 June, and extremely low suspended sediment concentration. A further interesting property of Figure 1 is that where it is possible to link a peak in the discharge records to a peak in suspended sediment concentration, the latter appears to lag behind the former, a clear contrast to results from studies in more temperate areas where the reverse is usually observed. The identification of grouping, lags and leads within the data would be impossible without the high temporal resolution of the series.

Although it is possible to speculate about the causes of the observed patterns in the discharge and suspended sediment time series, such speculation can be greatly refined by a consideration of the electrical conductivity of the river water (which is related to its dissolved solids concentration). Electrical conductivity was continuously monitored at the main gauging site and was then corrected to a standard temperature of 25°C using continuous records of water temperature and both field- and laboratory-derived temperature correction curves. Figure 1 shows that the electrical conductivity of the water fluctuated within the range 6 to 9 μS.cm^{-1} during period 1, exhibited diurnal cycles around a sharply increasing trend during period 2, and experienced a less sharp increase followed by wide variation within the range 12 to 19 μS.cm^{-1} during period 3. A scatter plot of the electrical conductivity and discharge data (Figure 2A) reveals a negative relationship between the two

variables but it is also possible to identify zones within the data which relate to the same three time periods already identified from the suspended sediment concentration and discharge scatter plot.

The three time zones that have been identified in Figures 2A and 2B indicate that there are changes in the relationships between the three variables during the observation period. Spatial surveys of electrical conductivity of water in the Skirhasjohka catchment throughout the observation period showed that the lowest conductivity, 4 $\mu S.cm^{-1}$, was for pure melted snow which had not been in contact with the soil and vegetation, whereas the highest conductivity, 37 $\mu S.cm^{-1}$, was for groundwater seepage at the end of the observation period. The electrical conductivity of water monitored in the spatial surveys increased with the degree of contact of the water with soil and underlying till. These results and a sub-division of the suspended sediment into its organic and inorganic components for periods 1 and 2 (Figures 2C and 2D) permit interpretation of the process significance of Figure 1.

The relatively low electrical conductivity of the water throughout period 1 suggests that the flow is derived almost entirely from snowmelt draining rapidly into the river system whilst the catchment is still frozen. The relatively low suspended sediment transport and the greater importance of organic material in the suspended sediment in period 1 (in comparison with period 2) suggests limited exposure of the flow to the frozen suspended sediment source areas and the greater importance of vegetated areas (e.g. hillslopes and flood plain) than unvegetated areas (e.g. river banks and bed) as sediment sources.

The increasing electrical conductivity of period 2 indicates the mixing of decreasing amounts of snowmelt water (released in diurnal floods) with increasing quantities of soil and groundwater, which may themselves experience an increasing electrical conductivity during this period depending upon their residence time in their storage area. The increased routing of water through soil and groundwater storage is related to ground thawing. Thawing of sediment source areas (particularly the stream banks) makes sediment available for transport by the stream and so explains the higher suspended sediment concentrations during period 2. Of particular interest is the very high suspended sediment transport by the small diurnal discharge hydrograph during the first day of period 2. A possible explanation for this event is that the last and highest discharge hydrograph during period 1 provided a prolonged and high flood stage which warmed the banks of the river channel sufficiently for thawed sediment to become available for transport by the next (small) discharge event.

Finally, the relatively high electrical conductivity and low discharge of period 3 presumably results from drainage of the catchment after snowmelt and ground thawing are complete. Thus the fluvial processes in period 1 are dominated by snowmelt whilst the ground remains frozen, period 2 is dominated by ground thawing with small diurnal discharge cycles resulting from snowmelt, and period 3 represents conditions once the snow has cleared and the ground has thawed, when discharge hydrographs are a direct response to precipitation. High suspended sediment transport can occur only when sediment is available and this is strongly affected by ground thaw and particularly by the thawing of the banks of the river channel network.

This brief examination of the hydrological attributes of a small subarctic catchment demonstrates a number of ways in which the short-interval regular sampling design has aided analysis and interpretation. The near-continuous record makes it possible to identify the fine detail of patterning and reveals physically-significant relationships between variables. In particular, within the short duration of the snowmelt period (which accounts for about 95% of annual sediment transport and 65% of annual discharge), a short temporal sampling interval is essential. By adopting a design which gives equal weight to night as well as daytime conditions and avoids measurement related solely to high-flow events, the study provides a greatly enhanced ability to estimate both total sediment and discharge yield and daily average conditions (particularly during periods of strong diurnal rhythm).

IMPLICATIONS

The studies discussed above yield conclusions in two contexts: the substantive hydrology of the arctic and subarctic zones, and the methodology appropriate to the investigation of these attributes. There are substantial variations in the measurement standards applied in published studies which make comparison and identification of trends difficult. Data from a small instrumented upland catchment in arctic Finland demonstrate considerable variability in suspended sediment transport, and show how the identification of trends within such data is dependent upon frequent sampling.

It is increasingly obvious that sediment transfer within the arctic is a complex and variable response to the interaction of a range of processes. There are many different arctic hydrological regimes as a result of differing snow depth conditions, ground freezing and the extent to which within-pack processes are significant. There are also major differences between permafrost and seasonal freezing, and the hydrological system of these areas may be scale-dependent. Scale dependence in this context may take several forms. Basin spatial scale is significant, but so too is time (seasonal v. diurnal/event). Scott (1978) identified scale-dependent relationships between catchment size and erosion timing, and on the basis of the present study this link might be extended to suspended sediment transport also. Large rivers, particularly if there is a long period between breakup and flood peak, could well experience sediment exhaustion and thus a suspended sediment concentration peak ahead of the main seasonal flood peak. Smaller catchments, particularly with very rapid rise to flood peak, are more

likely to experience ice/freezing armouring of bed and banks until after flood peak, giving a sediment transport lag. This would be exacerbated if water temperature did not rise to the point where it was thermally effective on the channel perimeter until after the flood peak. If such important aspects of regional variability are to be specified rigorously, then it will be necessary for a range of studies to adopt the sampling levels here discussed in order to provide the robustness, detail and comparability necessary.

REFERENCES

Arnborg, L., Walker, H.J. and Peippo, J. (1967). Suspended load in the Colville River, Alaska, 1962. Geogr. Ann., 49A, 131-144.

Chaco, E.F. and Bredthauer, S. (1983). Runoff from a small subarctic watershed, Alaska. Proc. 4th Intl. Permafrost Conf., July 17-22 1983, Fairbanks, Alaska, Natl. Acad. Press, Washington D.C., 115-120.

Church, M. (1974). Hydrology and permafrost with reference to northern North America. In Permafrost Hydrology: Proc. Wkshp. Sem. 1974, Can. Natl. Com., I.H.D., Environment Canada, Ottawa, 7-20.

Clark, M.J., Gurnell, A.M., Milton, E.J., Seppälä, M. and Kyostilä, M. (1985). Remotely sensed vegetation classification as a snow depth indicator for hydrological analysis in sub-arctic Finland. Fennia, 163, 195-225.

Clark, M.J., Gurnell, A.M. and Threlfall, J.L. (1988) Investigative design for fluvial sediment transfer in Arctic and Subarctic regions: implications for comparisons in time and space. Zeit. für Geomorph. (in press).

Cogley, J.G. and McCann, S.B. (1975) Surface runoff characteristics of an arctic nival catchment: Mecham River, Cornwallis Island. Proc. Can. Hydrol. Sem. 75, Natl. Res. Council of Canada, 282-288.

Corbin, S.W. and Benson, C.S. (1983). Thermal regime of a small Alaskan stream in permafrost terrain. Proc. 4th Intl. Permafrost Conf., July 17-22 1983, Fairbanks, Alaska, Natl. Acad. Press, Washington D.C., 186-191.

Corte, A.E. (1978). Rock glaciers as permafrost bodies with a debris cover as an active layer. A hydrological approach. Andes of Mendoza, Argentine. Proc. 3rd Intl. Conf. on Permafrost, July 10-13 1978, Edmonton, Alberta, Canada. Ottawa, (1), 263-269..

Dingman, S.L. (1973). Effects of permafrost on streamflow characterstics in the discontinuous permafrost zone of central Alaska. Proc. 2nd Intl. Permafrost Conf., Yakutsk, USSR. Natl. Acad. Sci., Washington D.C., 447-453.

Forbes, D.L. (1975). Sedimentary processes and sediments, Babbage River delta, Yukon Coast. Geol. Surv. Canada Paper 75-1, B, 157-160.

Gurnell, A.M. (1987). Suspended sediment. In Gurnell, A.M. and Clark, M.J. (eds) Glacio-fluvial Sediment Transfer, 305-354, John Wiley, Chichester.

James, W. and Vieira-Ribeiro, A.R. (1975). Effect of spatially disaggregated snowmelt on seasonal degree-day-factor variations in the High Arctic. Can. Hydrol. Sem. 75, Natl. Res. Council of Canada, 291-295.

McCann, S.B., Howarth, P.J. and Cogley, J.G. (1972). Fluvial processes in a periglacial environment, Queen Elizabeth Islands, N.W.T., Canada. Trans. Inst. Brit. Geogr., 55, 69-82.

McDonald, B.C. and Lewis, C.P. (1973). Geomorphological and sedimentologic processes of rivers and coast, Yukon coastal plain. Env.-Soc. Comm. N. Pipelines (Canada), Taskforce on N. Oil Devt. Report 73-39.

Miles, M. (1976). An investigation of riverbank and coastal erosion, Banks Island, District of Franklin. Geol. Surv. Canada Paper 76-1A, 195-200.

Röthlisberger, H. and Lang, H. (1987). Glacial hydrology. In Gurnell, A.M. and Clark, M.J. (eds) Glacio-fluvial sediment transfer, 207-284, John Wiley, Chichester.

Scott, K.M. (1978). Effects of permafrost on stream channel behavior in arctic Alaska. U.S. Geol. Surv. Prof. Paper 1068, 19 pp.

Slaughter, C.W., Hilgert, J.W. and Culp, E.H. (1983). Summer streamflow and sediment yield from discontinuous-permafrost headwaters catchments. Proc. 4th Intl. Permafrost Conf., July 17-22 1983, Fairbanks, Alaska, Natl. Acad. Press, Washington D.C., 1172-1177.

Threlfall, J.L. (1987). The relationship between discharge and suspended sediment in a small nival subarctic catchment. In Gardiner, V. (ed) International Geomorphology 1986, I, 823-41.

Williams, J.R. and van Everdingen, R.O. (1973). Groundwater investigations in permafrost regions of North America: a Review. Proc 2nd Intl. Permafrost Conf., July 13-28 1973, Yakutsk, USSR. North American Contribution, Part 2, Natl. Acad. Sci., Washington D.C., 435-446.

ACKNOWLEDGEMENTS

Data collection by J. L. Threlfall was funded by the Natural Environment Research Council, and support to the authors was also forthcoming from the University of Southampton Research Fund. The field co-operation of Matti Seppälä is gratefully acknowledged.

THE BUFFERING POTENTIAL OF CARBONATE SOILS IN DISCONTINUOUS PERMAFROST TERRAIN, AGAINST NATURAL AND MAN-INDUCED ACIDIFICATION

L.A. Dredge

Geological Survey of Canada, Ottawa, Canada, K1A 0E8

SYNOPSIS In boreal Manitoba, dispersal of fine-grained carbonate till westwards beyond the limit of carbonate bedrock increases the buffering potential of soils underlain by Shield rocks. At non-permafrost sites these soils have been partially leached progressively from the surface to a depth of about 2½ m; large quantities of carbonate are still available for further buffering. Carbonate soils at permafrost sites have been leached less, and the depth of carbonate depletion corresponds to the average depth of the active layer. It appears that groundwater circulation, hence leaching, is severely restricted in icy frozen terrain. In these areas, the buffering potential is probably very low, even though the soils have high carbonate contents. In permafrost areas with mudboils, this trend is counteracted to some degree by the upward transport of fresh carbonate into the active layer from greater depths.

INTRODUCTION

Studies dealing with the buffering potential of soils against the effects of acid rain have been increasingly emphasized over the last decade. Calcareous soils, particularly fine-textured soils, are considered to be good buffers because they tend to neutralize acid solutions and increase the pH of hydrologic systems. This paper addresses one aspect of the problem by determining how much material is available for buffering the effects of natural and man-induced acidification in an area of discontinuous permafrost. The problem is approached by examining the extent and manner in which naturally calcareous soils, in permafrost and non-permafrost terrain, are being leached. The results presented here are based on a number of soil profiles from one part of northern

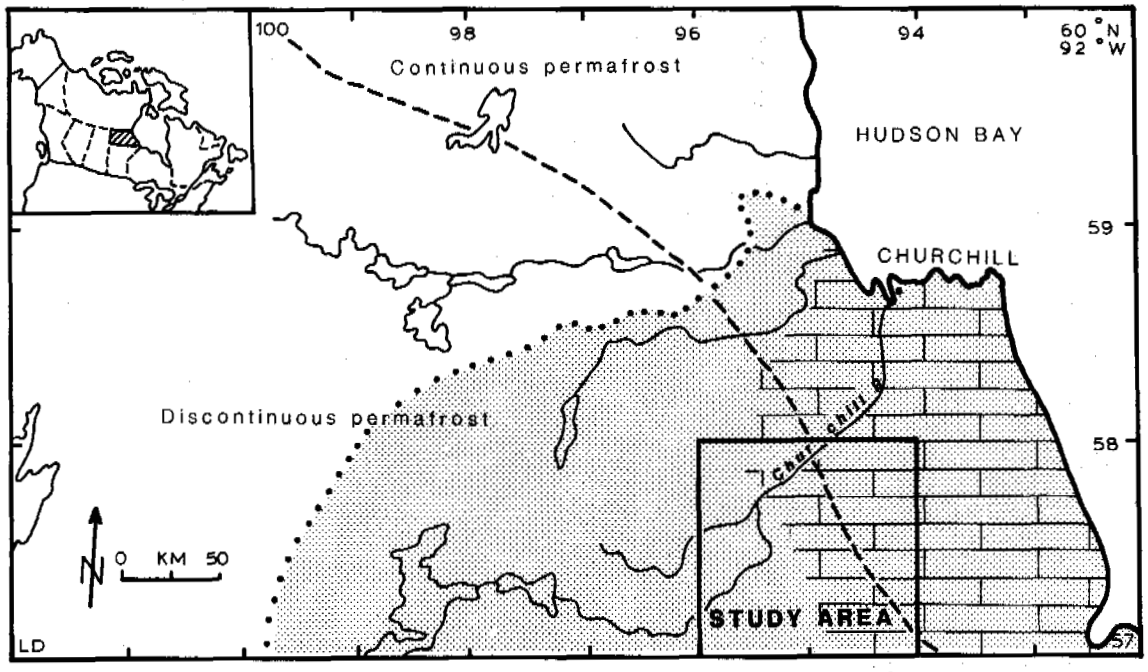

Figure 1 Location of the study area, distribution of calcareous soils in northern Manitoba (stipple), and areas underlain by carbonate bedrock, chiefly dolomitic limestone (brick pattern). Dashed line delineates areas of continuous and discontinuous permafrost

Manitoba; however terrain and environmental conditions at the study sites are typical of extensive areas of boreal Canada, and the conclusions drawn from this study may be widely applicable.

Leaching of calcareous soils occurs when calcium and magnesium carbonates are dissolved by percolating meteoric water charged with carbon dioxide. The process begins at the surface and gradually progresses downwards. The thickness of the leached zone and intensity of leaching depend on the hydrological and biochemical environment, the ground thermal regime, the texture and original carbonate content of the substrate, and the time available for the leaching process to occur.

The area studied lies in Manitoba between 57° and 58°N and between 94° and 96°W, near the west coast of Hudson Bay, above the area covered by postglacial marine deposits (Fig. 1). The land rises gently from an elevation of 120 m ASL in the east to 250 m in the west; the surface drainage network is poorly developed. There is little variation in the terrain apart from the Churchill River valley, which is deeply incised into till and bedrock. The region is vegetated by spruce forest, interspersed with fens and shallow thermokarst pools. In many places the forest is developed on an organic stratum which varies in thickness from a few centimetres to 4 m. The peaty vegetation creates a strongly acidic environment; the pH of shallow thermokarst pools in peat terrain ranges from 3 to 5, while the pH in lakes which extend into mineral soil is commonly 5 to 6. The port of Churchill lies to the north of the study area and the mining communities of Thompson, Lynn Lake and Leaf Rapids lie to the south and west.

Annual precipitation is 40 cm; mean annual air temperature is -7.3°C, but temperatures reach 12°C in July. The area lies at the northern limit of the zone of discontinuous permafrost. Areas with peat cover are more prone to permafrost than those without peat. In areas of permafrost which are relatively dry, the depth of thaw rarely exceeds 60 cm; below that depth the soil remains frozen all year, but ground temperatures do not fall below -5°C (Brown, 1978; Dredge et al., 1986). Thaw depths are greater in wetland terrain (Dredge and Nixon, 1979). In both permafrost and non-permafrost terrain seasonal frost sorting and cryoturbation of materials are manifested by mudboils.

Although the bedrock underlying the study area is of granitic shield lithology, the soils are calcareous. They consist of silty till and related glaciolacustrine sediment. These materials were emplaced by glaciers moving out of or across Hudson Bay, and were first exposed to subaerial processes between 7700 and 8000 years ago, following the draining of Glacial Lake Agassiz, the major waterbody which covered the region during deglaciation (Dredge et al., 1986). The parent material and leached soil are uniformly fine textured. The carbonate content of the parent materials is homogeneous areally, and makes up between 32% and 38% of the dry soil weight.

SOURCES AND AVAILABILITY OF CARBONATE MATERIALS IN SOILS

Carbonate bedrock, mainly Ordovician and Silurian limestone and dolomite, underlies the eastern part of the study area shown in Fig. 1, as well as the Hudson Bay basin. These rocks are the source of more than 98% of the carbonate in the soils (Dredge, 1988). Shield rocks of granitic and gneissic lithology underlie the rest of the area; marbles and soluble feldspars from the Shield account for minor amounts of carbonate. Shilts (1981) constructed maps showing areas sensitive to acid precipitation which are based on the limits of major bedrock types. While these limits provide a good first approximation for delimiting areas with soils of high buffering capability, carbonate soils in boreal Manitoba and other parts of central Canada are much more widespread than bedrock maps indicate (Fig. 2). Extensive areas were glaciated by ice flowing out of, or across Hudson Bay. This ice eroded and entrained carbonate rock and deposited calcareous till sheets over both the carbonate bedrock and adjoining areas of Shield terrain. Carbonate-rich tills extend for more than 250 km beyond the limit of carbonate bedrock in northern Manitoba (Fig. 1). This till has a silty-clay matrix, being roughly 35% sand, 43% silt and 22% clay. It forms a blanket which is 2 to 8

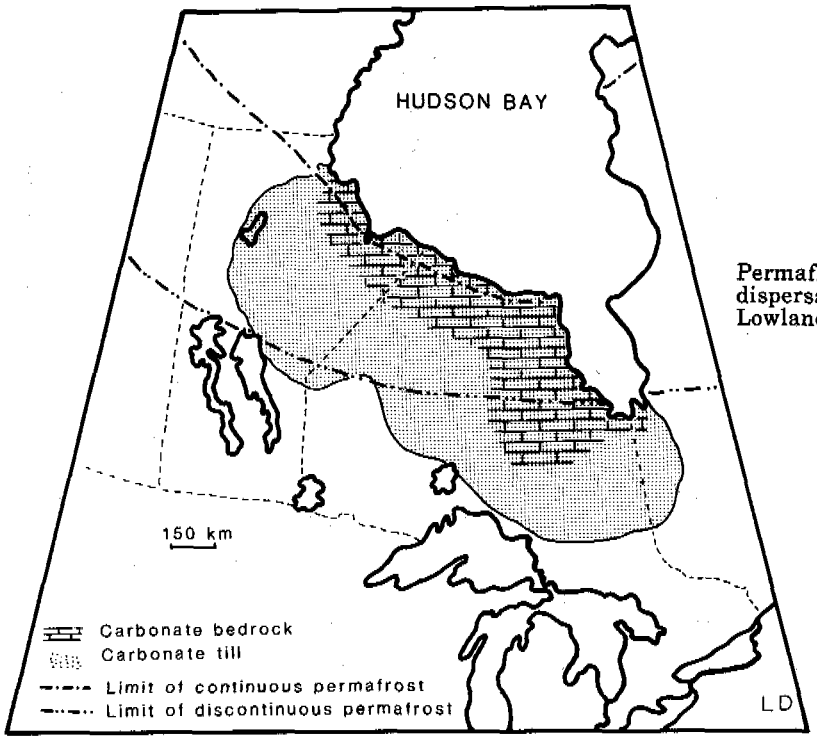

Figure 2

Permafrost conditions, carbonate bedrock, and dispersal of carbonate till in the Hudson Bay Lowlands.

m thick over much of the region and as deep as 30 m in some places. Overlying the carbonate till and extending beyond the till limit are related silty calcareous glaciolacustrine deposits, also derived from the Hudsonian ice sheet.

The carbonate content of surficial materials is relatively homogeneous across the study area, being between 32 and 38% of the total soil weight. The presence of calcareous till over Shield terrain greatly increases the buffering potential of the soil over what would otherwise be expected in Shield areas. The glacial crushing of carbonate rock into silt-clay sized till particles has further enhanced the buffering capability of soils overlying areas of carbonate bedrock areas as well. The buffering potential of fine particles is considerably higher than uncrushed bedrock because of the relatively large particle surface areas exposed.

	Site No.	Depth (cm)	c%[1]	% sand	% silt	% clay
Permafrost terrain						
	1A	20	9	31	40	29
	1B	60	34	35	43	22
	1C	120	34	32	44	24
	2A	20	10	34	43	23
	2B	50	24	36	42	22
	2C	80	34	35	45	20
	3	30	15	37	44	19
	4	15	10	35	41	24
	5	15	6	36	42	22
	6	30	24	38	43	19
	7	15	9	28	40	32
	8	200	35	36	44	20
	9	250	32	32	46	22
Mudboils						
	10	30	26	37	44	19
	11	48	28	30	41	29
	12	50	26	35	42	23
	13	70	25	33	45	22
Nonpermafrost terrain						
	14A	50	17	29	45	26
	14B	75	20	33	40	27
	14C	100	33	36	44	20
	14D	200	30	36	40	24
	15A	20	5	32	42	26
	15B	50	15	38	47	15
	15C	500	32	32	41	27
	16	40	11	36	43	21
	17	20	8	35	41	24
	18	20	5	33	43	24
	19	25	6	37	42	21
	20	20	4	33	40	27
	21	40	11	34	46	20
	22	90	20	32	46	22
	23	120	24	35	41	24
	24	200	29	34	40	26
	25	218	33	34	42	24
	26	250	36	38	45	17
	27	400	36	35	43	22
	28	900	35			

[1] c is carbonate content

On the basis of 96 samples, the carbonate content of the parent material is 35% (standard deviation 3.2).

Table 1 Carbonate content (by percent dry weight) and grain size of soil samples used in construction of the leaching profiles.

CARBONATE DEPLETION IN SOIL PROFILES, RESULTING FROM NATURAL LEACHING

Procedures

Near-surface and subsurface samples used to construct the leaching profiles were collected at 28 sites. The sites chosen each have similar geological, vegetational, topographical, and drainage characteristics. Because sampling was conducted primarily for surficial geological mapping purposes, most samples were obtained from a variety of depths, but at four sites soil samples were taken at regular intervals throughout vertical profiles (Table 1). Carbonate contents from widespread spot samples are consistent with the pattern determined from sites where samples were taken at a number of depths. This suggests that the depths and degrees of carbonate depletion are consistent over a broad area. Figure 3 is a composite of the results and shows the typical relationship between carbonate content and depth.

In areas of unfrozen terrain, samples were taken from hand-dug soil pits. A Hoffer coring probe and Stihl power corer were used to obtain near-surface samples in frozen terrain and all subsurface samples to a depth of 3 m. Samples from greater depths (3-20 m) were obtained by excavating in from riverbanks.

Carbonate contents of the <2 mm fraction were determined by digesting the samples in hydrochloric acid. Minor amounts of other minerals may also have been dissolved.

Degree and depth of leaching in a boreal forest environment at sites without permafrost

The profile (Fig. 3) shows that carbonates have been removed from the soil to a depth of 2.5 to 3 m. The greatest leaching has occurred near the surface, and about half of the carbonates originally present have been leached from the upper 0.5 m. The degree of leaching decreases gradually with depth. Below about 3 m carbonate values approach 35 per cent (the amount of carbonate in unweathered parent material) and are relatively constant to depths of at least 20 m.

Soil and climatic conditions in this area favour relatively extensive leaching. The soil parent material is carbonate-rich, and its silty texture enables a large surface area to come into contact with meteoric water and groundwater despite its relatively low permeability. Because low soil temperatures (5°C in summer) promote solution of carbonates, solubility may be 50 per cent greater at the temperatures prevailing in this boreal environment than in warm temperate climates (Arkley, 1963). The acidity of the environment also promotes dissolution of the carbonate fraction. The ubiquitous bogs and fens, which are the principal groundwater reservoirs, have pH values between 3 and 5, and consequently a greater rate of carbonate solution might be expected here than in areas where the groundwater is neutral (Arkley, 1963). Depth of leaching in this region, therefore, may be expected to exceed that in warmer climates, provided that sufficient time has elapsed for the weathering process to reach equilibrium conditions.

Data from dated sites below the limit of postglacial marine submergence in the nearby Hudson Bay Lowland indicate that the leaching profile shown here could have developed in about 5500 years. Since this area has been exposed to soil development for 7700 to 8000 years, Figure 3 may represent an equilibrium profile for the northern boreal forest environment.

In the northern environment, the depth of leaching may be more closely controlled by depth limitations in the flow of the meteoric component of groundwater than by factors related to chemical equilibrium. A zone of carbonate accumulation, typically present in the lower part of leaching profiles at sites from warmer and drier climates, is not present in the profile

shown here. Its absence suggests that groundwater may be leaving the soil system (and entering rivers) before it is saturated with bicarbonate ions.

Effect of permafrost

A substantial difference exists in both depth and amount of leaching between substrates with permafrost and those without. Under perennially frozen conditions, carbonate depletion is considerably less than for unfrozen terrain, and the rate of depletion declines sharply below a depth of about 60 cm. This depth corresponds closely to the regional thickness of the active layer. Because groundwaters at permafrost sites, which tend to have some peaty cover, are at least as acidic as those flowing through non-permafrost sites, which tend to have less peat, the difference in leaching is attributed to restricted groundwater movement in permafrost terrain. However, the fact that even small amounts of carbonate depletion have occurred below that level suggests either (1) that a minor degree of circulation of unfrozen water occurs through soil capillaries in this relatively warm permafrost environment (soil temperatures reach -2°C in summer), or (2) that thaw depths may have been slightly deeper in the past..

The Effect of Frost Churning

Mudboils are prevalent in northern Manitoba both in permafrost and non-permafrost terrain. Near-surface and surface samples taken from mudboils have carbonate values similar to those in frozen terrain or to those in unfrozen terrain at greater depths. The higher percentage of carbonate in mudboils than at other unfrozen sites suggests the incorporation and mixing of material from depths of 2 m or more.

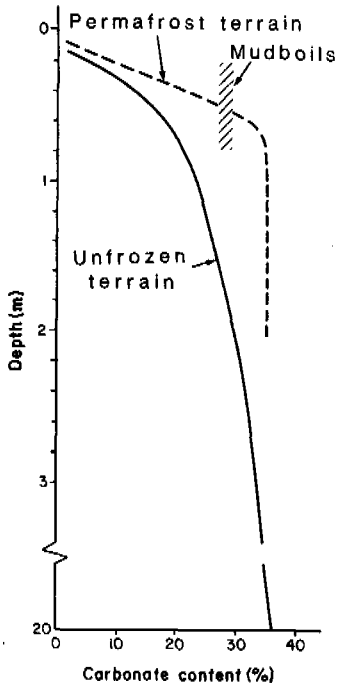

Figure 3 The leaching of calcareous soils in discontinuous permafrost in northern Manitoba as shown by systematic changes in carbonate content below the ground surface at permafrost sites, sites without permafrost, and mudboils. Carbonate depletion has resulted from the infiltration of acidic meteoric and shallow ground water.

CARBONATE SOILS AS BUFFERS OF ACID RAIN

The results of this study have several implications pertaining to the effects of acid rain in areas of discontinuous permafrost.

1. Where glaciers have dispersed a calcareous till westward beyond the limit of carbonate rocks onto shield terrain, the soils over granitic shield rocks may potentially serve as buffers against natural or man-induced lake acidification. Materials capable of buffering are spread more widely than bedrock maps would indicate.

2. The glacial crushing of carbonate rock into silt and clay sized particles increases the "short term" buffering potential over that of carbonate bedrock by providing greater surface areas for chemical reactions. The "short term" effect operates over a period of thousands to millions of years: the ultimate buffering capacity of carbonate bedrock and its derived soil is the same.

3. In areas without permafrost, the leaching process is active. Soils have been partially leached, indicating that carbonate ions have operated as buffers against acidic groundwaters. Partial leaching to a depth of about 2½ m has already occurred but large amounts of calcareous material are still available for buffering.

4. The leaching profiles for permafrost terrain, however, suggest that groundwater circulation and leaching may be restricted primarily to the active layer. The high amount of carbonate in the frozen subsoil appears to be unavailable for buffering. If this is the case, then perhaps soils in permafrost should not be considered as good potential buffers even though they may have high carbonate contents. The problem of restricted groundwater circulation may be partially counteracted in areas where mudboils are prevalent because fresh carbonate is continually brought up into the active layer; this carbonate can then act as a buffering agent.

REFERENCES

Arkley, R.J. (1963). Calculation of carbonate and water movement in soil from climatic data; Soil Science, v. 96, p. 239-248.

Brown, R.J.E. (1978). Influence of climate and terrain on ground temperatures in the continuous permafrost zone of northern Manitoba and Keewatin District, Canada; in Proceedings, 3rd International Conference on Permafrost (Edmonton), p. 19-21.

Dredge, L.A. (1988). Drift carbonate on the Canadian Shield II: Carbonate dispersal and ice flow patterns in northern Manitoba; Canadian Journal of Earth Sciences, in press.

Dredge, L.A. and Nixon, F.M. (1979). Thaw depths and permafrost in polygonal peat terrain, Hudson Bay Lowland, Manitoba; Geological Survey of Canada, Paper 79-1C, pp. 27-30.

Dredge, L.A., Nixon, F.M. and Richardson, R.J. (1986). Quaternary geology and geomorphology of northwestern Manitoba; Geological Survey of Canada, Memoir 418, 38 p.

Shilts, W.W. (1981). Sensitivity of bedrock to acid precipitation: modification by glacial processes; Geological Survey of Canada Paper 81-14, 7 p.

PHYSICAL AND CHEMICAL CHARACTERISTICS OF THE ACTIVE LAYER AND NEAR-SURFACE PERMAFROST IN A DISTURBED HOMOGENEOUS *PICEA MARIANA* STAND, FORT NORMAN, N.W.T., CANADA

K.E. Evans, G.P. Kershaw and B.J. Gallinger

Department of Geography, University of Alberta, Edmonton, Alberta, T6G 2H4

SYNOPSIS Characteristics of the soil and near-surface permafrost included: moisture content; pH; cation exchange capacity; and concentrations of calcium, magnesium and potassium. Probing of the active layer to determine the depth to permafrost indicated a mean increase of 17% after one full growing season following tree canopy removal. Results confirm that variability among soil and near-surface permafrost characteristics is high both areally and with depth.

INTRODUCTION

During the early 1970's a number of studies were initiated in the Mackenzie Valley in response to the proposed Arctic Gas Pipeline. Permafrost and soil investigations were included in these studies (Tarnocai, 1973; Reid, 1974; Reid and Janz, 1974; Brewer and Pawluk, 1975; Pawluk and Brewer, 1975; Pettapiece, 1975; Zoltai, 1975; Tarnocai and Zoltai, 1978). In a relatively short time a large portion of the western Subarctic and Arctic was surveyed, with the result that few detailed sampling programmes were possible. In Alaska a number of soil/nutrient cycling studies have been conducted on a more concentrated basis than the Canadian investigations (Weber and Van Cleve, 1981; Chapin, 1983; Fox and Van Cleve, 1983; Van Cleve, et al., 1983; Van Cleve and Dryness; 1983a; Weber and Van Cleve, 1984). Within the Mackenzie Valley there remains a paucity of indepth, process-oriented information on the productivity and nutrient cycling in Picea mariana Subarctic forest ecosystems.

OBJECTIVES

The purpose of this study was to quantitatively describe the wide variations in both physical and chemical characteristics of the soil, active layer and near-surface permafrost. These large scale variations among soil characteristics were the object of study within a Subarctic Picea mariana (Mill) B.S.P. stand near Fort Norman, N.W.T. (Fig. 1). The study area was a relatively small portion of the 4.6 ha SEEDS (Studies of the Environmental Effects of Disturbances in the Subarctic) study site. These data form the basis of this study and provide a baseline description for further studies of the changes that may occur in the soils, active layer and near-surface permafrost as a result of a simulated transport corridor (Kershaw, 1987).

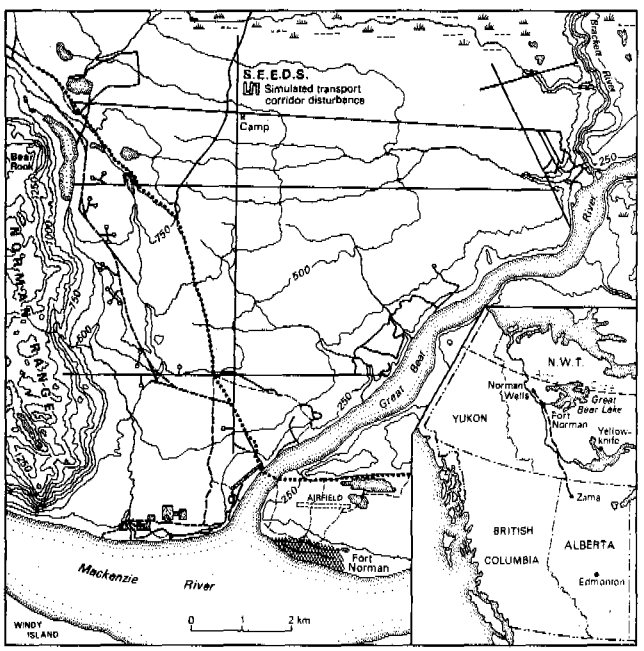

Fig. 1. Location of the simulated transport corridor disturbance installed for the project - Studies of the Environmental Effects of Disturbances in the Surbarctic (SEEDS), Fort Norman N.W.T.

STUDY AREA

The study area has been mapped as a flat to sloping lacustrine and moraine plain (Reid, 1974; Interprovincial Pipeline (NW) Ltd., 1980). The study site is within the discontinuous permafrost zone (Brown, 1978) with a permafrost-influenced soil, classified as

Gleysolic Turbic Cryosol (Canada Soil Survey Committee, 1978; Kershaw and Evans, 1987). Climatic records from the two nearest meteorological stations at Fort Norman (10 km) and Norman Wells (80km), have identical mean annual temperatures of -6.3°C (Crowe, 1970; Anon., 1982).

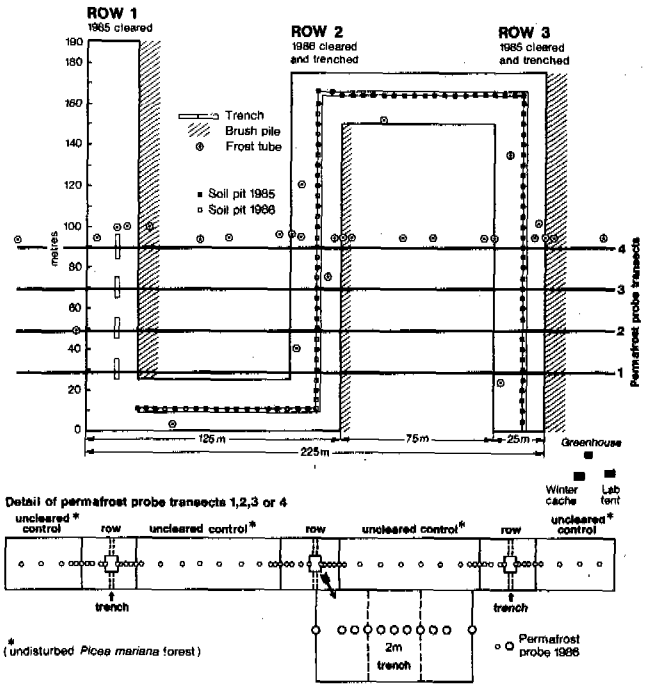

Fig. 2. Survey and sampling locations on the SEEDS study site, Fort Norman, N.W.T.

METHODS

Field Methods

Soil pits (n=100) were dug to the frost table, at 5m intervals along a hand-excavated simulated pipeline trench (Fig. 2). Soil sampling was conducted over 2 seasons - 19 July to 5 August 1985 (n=49) and 17 June to 5 July 1986 (n=51). Horizon thickness and sequence was described for each soil pit prior to sampling. Field pH was determined immediately following sampling, using the soil paste method (McKeague, 1978; Sheldrick, 1984).

Permafrost coring was conducted at 29 locations at various times in 1985 and 1986 (Fig. 2). Cores samples were extracted, at 15 cm intervals, to depths of 225cm unless prevented by a subsurface gravel layer. Thaw depth was monitored weekly during the 1986 thaw season along four transects consisting of 84 sample sites in each line (Fig. 2). The frost probe method of Mackay (1977) was used.

Laboratory Analyses

Unfortunately, due to logistical delays in 1985, many samples remained moist for an extended period before reaching the lab. Consequently it was not possible to determine nutrient content for these samples. However, in 1986 this problem was avoided by air drying samples prior to leaving the field.

Air-dried soil samples were passed through a No. 10 sieve (2mm opening) in preparation for soil nutrient extractions. Concentrations of calcium, magnesium, potassium and sodium were then determined using an ammonium acetate (NH_4OAc) extraction (Atkinson, et al. 1958; Kalra, 1971; McKeague, 1978). This extraction was passed through an Inductively Coupled Argon Plasma Autoanalyzer (Plad Research Laboratories, Model 34000). Cation exchange capacity was determined using standard leaching methods (Atkinson, et al., 1958; Kalra, 1971; McKeague, 1978) with the leachate subjected to a Kjeltec Auto Analyzer (Tecator, Model 1030).

Moisture content for the 1985 and 1986 soil pit samples was expressed as a per cent of the dry weight (Sheldrick, 1984). Moisture content of the permafrost core samples was expressed on a similar basis after oven drying at 105°C (Gardner, 1965).

RESULTS AND DISCUSSION

At the time of soil sampling in 1985, the thaw depth averaged 47.5cm (n=49 S.D.=12.8) and in 1986 it was 46.1cm (n=51 S.D.=9.0). The typical soil on the site consisted of 5 horizons: a fibric Of, a slightly decomposed Om, a discontinuous Bm, a gleyed-cryoturbated Cgy and a perennially frozen Cz. Soil moisture content from each of the soil horizons was highly variable (Table I). Soil moisture values, coupled with thaw layer thickness were assumed to be influenced by the hummocky microrelief. Moisture content decreased with depth and proximity to the premafrost table (Fig. 3). The high moisture content in the Of and Om horizons is possible due to the low bulk density of organic layers.

The pH of each horizon increased with depth (Table I) as anticipated in this region of the Subarctic where the litter is acidic as a result of the vegetation which is dominated by evergreen and ericaceous trees and shrubs. Equally important is the calcareous bedrock (Yorath and Cook, 1981) from which local glaciolacustrine deposits have been derived. It is this parent material that has buffered the effects of the otherwise acidic Of and Om horizons.

Within the permafrost, moisture content increased to a maximum of 120.4% in the 60-75cm sample (Fig. 3). However, upon passing below the permafrost table, moisture content decreased to 29.23% at the 195-210cm depth. Moisture content of the active layer and near-surface permafrost was highly variable with depth, as reflected by the standard deviation values (Fig. 3).

Cation exchange capacity (C.E.C.) and macronutrient levels declined with depth in the

TABLE 1

Soil horizon moisture content and pH values with 95% and 99% confidence level n-sizes derived from soil pit samples: SEEDS site, Fort Norman, N.W.T.

Horizon	N	Mean	Std. Dev.	n	Mean	Std. Dev.	Confidence Limit n-size 95%	99%
Of	100	260.6	94.5	97	6.5	0.55	98	102
Om	100	242.8	143.1	97	6.8	0.31	98	102
Bm	15	140.0	62.4	15	7.2	0.71	13	12
Cgy	94	52.0	56.6	95	7.1	0.31	96	100
			Permafrost Table					
Cz	95	185.9	238.5	96	7.1	0.28	95	101
Bmz	1	117.5	NA	1	7.2	NA		

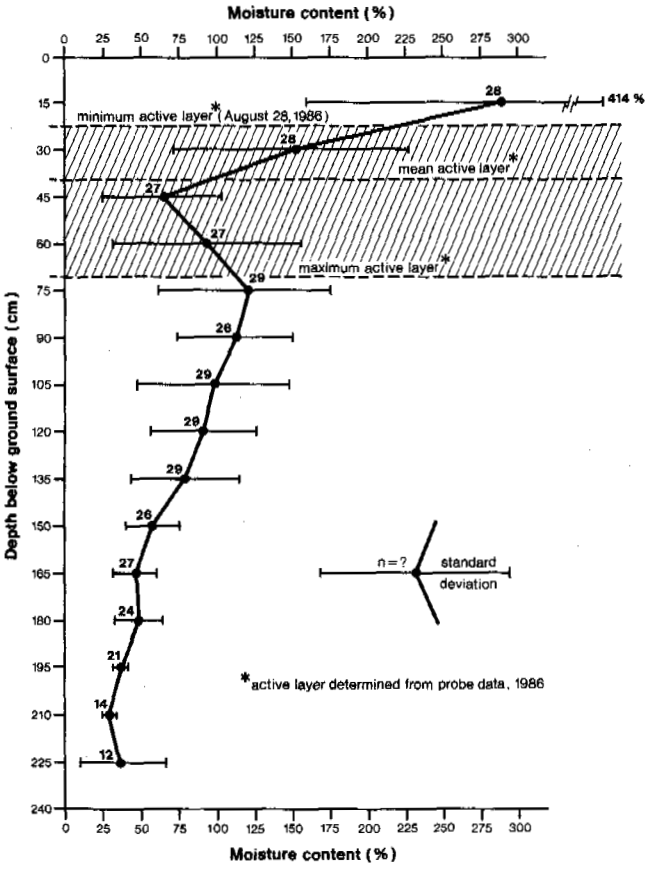

Fig. 3. Active layer thickness (n=123) and moisture content of the active layer and near-surface permafrost at the SEEDS site, Fort Norman, N.W.T.

active layer (Table II). C.E.C. is important in soil nutrient status since it is an indicator of the ability of the soil to hold cations, such as calcium, magnesium, potassium and sodium (Pritchett, 1979). Further analyses should therefore confirm a reduction in nutrient concentrations with depth. C.E.C. and a majority of the macro-nutrient concentrations were higher at the SEEDS site than nearby sites surveyed by Reid (1974)(Table II). Potassium, which is essential to many physiological functions of forest plants, is rarely deficient in most forest ecosystems. Pritchett (1979) suggested that 20 to 100 mg/kg of potassium was sufficient for adequate growth. The SEEDS site is rich in this nutrient ranging from 37.8 to 633.2 km/kg. Fifty to 1000 mg/kg of calcium can be found in most forest soils (Pritchett, 1979), although 12230 mg/kg was the average concentration at the study site. Magnesium, the only mineral constituent of the chlorophyll molecule and therefore, essential to photosynthesis (Pritchett, 1979; Tisdale et al., 1985), was not found to be deficient.

The degree of alteration to the vegetation and soil surface will determine the increase in active layer thickness. At the end of the field season (28 August, 1986) the mean thaw depth of the control (undisturbed) was 48.5cm (n=123 S.D.=10.67), whereas in the cleared rights-of-way it was 56.96cm (n=156 S.D.=12.09) (Fig. 4). The rights-of-way sustained minimal surface disturbance involving removal, by hand, of the tree canopy. The greatest increase in thaw depth occurred in a simulated pipeline trench where it was 80.86cm (n=59 S.D.=14.46). Trench thaw depths were much greater than the adjacent rights-of-way reflecting the higher degree of surface disturbance. Removal of the insulative organic cover and the complete mixing of all soil horizons resulted in an exposed mineral soil surface, thereby allowing greater heat penetration. Variation in mean maximum thaw depths was high, regardless of whether one considers the control, right-of-way or trench data. Increases in the thaw depth values are expected in the future, however, based on first and second year results spatial variability should persist.

With detailed soil sampling programmes it is desirable to have an indication of the number of samples required to maintain high levels of confidence in the data collected. Under conditions similar to those found at the

TABLE II

Cation Exchange Capacity (C.E.C.) and macro-nutrient status of soils, with 95% and 99% confidence level n-sizes* derived from soil pit samples SEEDS site, Fort Norman, N.W.T.

	Of	Om	Bm	Cgy	Cz	Reid 1974
n	23	24	8	23	23	
C.E.C. (meg/100g)						
mean	108.6	123.9	97.1	41.0	50.2	36.7
S.D.	31.8	24.6	26.5	30.1	25.6	
n*	21,20	22,21	5,4	20,20	20,20	
Ca (mg/kg)						
mean	14567.9	19488.5	14856.6	6000.4	8051.6	9160.0
S.D.	3713.2	3935.3	4280.7	2016.1	2994.0	
n*	21,20	21,21	5,4	20,20	20,20	
Mg (mg/kg)						
mean	2074.7	2453.7	1854.9	726.5	897.6	1219.0
S.D.	505.0	521.8	541.9	236.1	355.6	
n*	21,20	22,21	5,4	20,20	20,20	
K (mg/kg)						
mean	633.2	115.9	37.8	38.2	45.8	42.9
S.D.	145.7	134.9	34.6	7.8	37.4	
n*	21,20	22,21	5,4	20,20	20,20	
Na (mg/kg)						
mean	14.1	8.6	7.5	4.8	6.7	18.4
S.D.	9.4	7.4	0.7	1.0	2.3	
n*	20,20	21,21	5,4	18,18	21,21	

* sample sizes required at the 95% and 99% confidence level respectively.

SEEDS site, comparable results for soil nutrient analyses would be expected using a similar sample size. When calculating the sample size required for certain levels of confidence, the formula (Khazanie, 1979) is limited if standard deviations are high. Predicted sample sizes for pH at 95% and 99% confidence levels were similar to the actual sample sizes of this study (Table I). However, the high number of samples required to obtain reliable results for soil pH is related to the variability within this soil characteristic. Findings for C.E.C. and macro-nutrient concentrations were similar to pH (Table II). High standard deviations among C.E.C. and macro-nutrients result in a smaller sample size necessary to obtain results with high confidence levels. However, in practice, the number of samples required is such that detailed sampling may be restricted by the availability of laboratory resources.

CONCLUSIONS

The variability that exists both areally and with depth necessitates detailed and large-scale soil sampling in Subarctic ecosystems. Moisture content of the soil and near-surface permafrost averaged 287.9% in the surface sample. The moisture content decreased to a low of 63.4% in the active layer and then increased to 120.4% immediately below the permafrost table. Below the permafrost table the moisture content dropped to 29.2% at 210cm below the ground surface. The variability in moisture content with depth in the core samples was also expressed in the variation in moisture in Of and Om soil horizons. Standard deviations for these horizons were, respectively, 94.5 and 143.1%.

When attempting to reestablish plant cover on disturbed northern soils, knowledge of the nutrient characteristics within the soil is vital. Great variability in basic soil and near-surface permafrost characteristics exist within Subarctic *Picea mariana* forests and is confirmed by detailed and large-scale soil sampling. All factors of soil nutrient status must be carefully analyzed in order to ensure that decisions regarding fertilizer application, species selection for revegetation, and other recovery methods are appropriate to the site conditions.

ACKNOWLEDGMENTS

We wish to acknowledge the financial support from Northern Oil and Gas Action Program, (NOGAP), Boreal Institute for Northern Studies, Royal Canadian Geographic Society and Student Temporary Employment Program (STEP) that made this work possible. Additional assistance is gratefully acknowledged from the Northern Forest Research Centre and in particular Steve Zoltai. The Department of Geography and the Reprographics Section were responsible for the illustrations. We also thank all those people involved with SEEDS that contributed time and effort during field sampling.

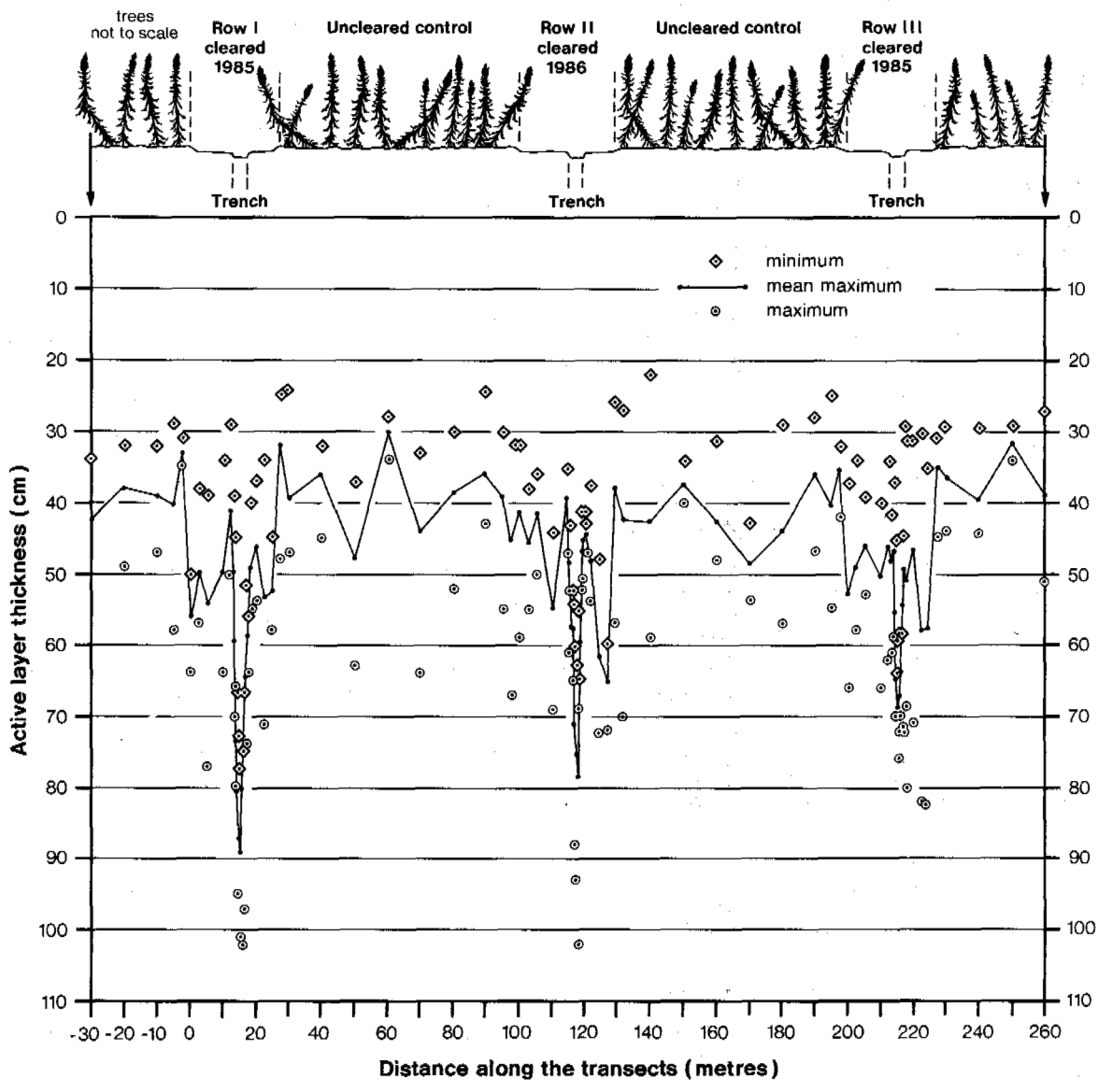

Fig. 4. Variation in active layer thicknesses across a simulated transportation corridor. SEEDS site, Fort Norman N.W.T.

BIBLIOGRAPHY

Atkinson, H J, Giles, G R , MacLean, A J and Wright, J R (1958). Chemical methods of soil analyses, 90pp. Chemical Division, Science Service, Canada Department of Agriculture, Contribution No. 169. Ottawa.

Anonymous (1982). Canadian Climate Normals, Temperature and Precipitation 1951-1980, The North - Y.T. and N.W.T. 55 pp. Environment Service, Toronto.

Brewer, R and Paluk, S (1975). Investigations of some soils developed on hummocks of the Canadian Sub-Arctic and southern Arctic Regions. 2. Analytical characteristics, genesis and classification. Can. J. Soil Sci. (55), 301-319.

Brown, R J E (1978). Permafrost, Hydrological Atlas of Canada, Plate 32, Fisheries and Environment Canada, Ottawa.

Canadian Soil Survey Committee (1978). The Canadian System of Soil Classification, 164 pp. Research Branch, Canada Department of Agriculture Publication No. 1646, Ottawa.

Chapin, F S III (1983). Nitrogen and phosphorus nutrition and nutrient cycling by evergreen and deciduous understory shrubs in an Alaskan black spruce forest. Can. J. For. Res. (13), 773-781.

Crow, R B (1970). A Climate Classification of the Northwest Territories for Recreation and Tourism, Volume Five, Appendix Three, 96 pp. Department of Transport, Canadian Meteorological Service, Toronto.

Fox, J F and Van Cleve, K (1983). Relationships between celluose decomposition, Jenny's k, forest-floor nitrogen, and soil temperature in Alaskan taiga forests. Can. J. For. Res. (13), 789-794.

Inter-provincial Pipeline (NW) Ltd. (1980). Geotechnical maps. In Norman Wells Pipeline Project Environmental Impact Statement, (NW). Esso Resources Canada Ltd.; Interprovincial Pipeline (NW) Ltd. Calgary.

Kalra, Y P (1971). Methods used for soil, plant, and water analysis at the soils laboratory of the Manitoba-Saskatchewan region, 1967-1970. Northern Forest Research Centre Information Report. NOR-X-11, 87 pp. Canadian Forestry Service, Department of the Environment, Ottawa.

Kershaw, G P (1986). Year-End Report:1985-1986, Studies of the Environmental Effects of Disturbances in the Subarctic (S.E.E.D.S.), 45 pp. Department of Geography, University of Alberta, Edmonton.

Kershaw, G P and Evans, K E (1987). Soil and Near-surface permafrost characteristics in a decadent black spruce stand near Fort Norman, N.W.T. B.C. Geographical Series (44), 151-166.

Khazanie, R (1979). "Confidence intervals (A single population)". In Elementary Statistics in a World of Applications. Goodyear Pub. Co., Inc., Santa Monica. p. 247-266.

Mackay, J R (1977). Probing for the bottom of the active layer. Geological Survey of Canada Paper, 77-1A:327-328.

McKeague, J A (ed.) (1978). Manual on Soil Sampling and Methods of Analysis, 212 pp. Canadian Soil Survey Committee, Canada Department of Agriculture, Ottawa.

Pawluk, S and Brewer, R (1975). Investigations of some soils developed in hummocks of the Canadian Subarctic and Southern-Arctic. 1. Morphology and Micromorphology. Can. J. Soil Sci. (55), 301-319.

Pettapiece, W W (1975). Soils of the Subarctic in the Lower Mackenzie Basin. Arctic (28), 35-53.

Pritchett, W L (1979). Properties and Management of Forest Soils, 500 pp. John Wiley and Sons, Inc. New York.

Reid, D E (1974). Vegetation of the Mackenzie Valley - Part One. Arctic Gas Biological Report Series, (3), 148 pp.

Reid, D E and Janz, A (1974). Vegetation of the Mackenzie Valley - Part Two. Arctic Gas Biological Report Series, (3), 166 pp.

Sheldrick, B H (1984). Analytical methods manual 1984. Research Branch, Agriculture Canada, Land Resource Research Institute Contribution No. 84-30.

Tarnocai, C (1973). Soils of the Mackenzie River Area. Environmental-Social Committee Northern Pipelines, Task Force on Northern Oil Development. Report No. 73-26, 136 pp. Information Canada, Ottawa.

Tarnocai, C and Zoltai, S C (1978). Earth hummocks of the Canadian Arctic and Sub-Arctic. Arctic and Alpine Research (10), 581-594.

Tisdale, S L, Nelson, W L and Beaton, J D (1985). Soil Fertility and Fertilizers, 4th Edition, 754 pp. Macmillan Publishing Company. New York.

Van Cleve, K and Dryness, C T (1983a). Conclusions and directions for future research in taiga forest ecosystems. Can. J. For. Res. (13), 914-916.

Van Cleve, K and Dryness, C T (1983b). Effects of forest-floor disturbance on soil-solution nutrient composition in a black spruce ecosystem. Can. J. For. Res. (13), 894-902.

Van Cleve, K, Oliver, L, Schlentner, R., Viereck, L A and Dryness, C T (1983). Productivity and nutrient cycling in taiga forest ecosystems. Can. J. For. Res. (13), 747-766.

Weber, M G and Van Cleve, K (1981). Nitrogen dynamics in the forest floor of interior Alaska black spruce ecosystems. Can. J. For. Res. (11), 743-751.

Weber, M G and Van Cleve, K (1984). Nitrogen transformations in feather moss and forest floor layers of interior Alaska black spruce ecosystems. Can. J. For. Res. (14), 278-290.

Yorath, C J and Cook, D G (1981). Cretaceous and Tertiary Stratigraphy and paleogeography, Northern Interior Plains, District of Mackenzie. 76 pp. Geological Survey of Canada, Memoir 398, Ottawa.

Zoltai, S C (1975). Structure of Subarctic forests on hummocky permafrost terrain in Northwestern Canada. Can. J. For. Res. (5), 1-9.

HYDROLOGY AND GEOCHEMISTRY OF A SMALL DRAINAGE BASIN IN UPLAND TUNDRA, NORTHERN ALASKA

K.R. Everett[1] and B. Ostendorf[2]

[1]Byrd Polar Research Center, The Ohio State University, Columbus, OH 43210 USA
[2]Systems Ecology Research Group, San Diego State University, San Diego, CA 92182 USA

SYNOPSIS In a 210 ha watertight drainage basin, typical of the upland tundra of northern Alaska the most significant hydrological and geochemical event in a year is snow-melt runoff. The 1986 peak discharge was 515 l/s. In the early phase of this event pH was at its seasonal minimum (5.0) while most recorded ions reached their maximum at concentrations, 3.5 - 9 x that of the snow pack in which they ranked Cl>>Ca>F>K,N>Mg. The only anion at measurable (mg/l^{-1}) concentration in melt-off was Cl. Three significant storm events occurred over the summer with discharge peaks between 85 and 312 l/s^{-1}, to which in channel precipitation contributed <1% and overland flow 30%. The remaining 70% was near surface interflow and water-track discharge. Ion concentration in summer precipitation was NO_3>SO_4Cl>K>Ca, Na>NH_4>F>Mg and was of continental origin. Post melt-off stream concentrations for most elements were low (<2 mg/l^{-1}) with Ca>>Mg >Na. Potassium and chloride were below mg/l^{-1} levels after melt-off. Other ions displayed a broad, low level peak during the protracted mid-summer low flow. Precipitation constitutes the principal source of chemical imput to the basin. Magnesium was the only measured ion lost from the basin in 1986.

INTRODUCTION

Hydrological and geochemical studies were begun at Imnavait Creek in 1985 and continue to the present. They are conducted on scales ranging from the entire (210 ha) basin to individual slope components (<5 ha) and are part of a large multidisciplinary study focused on arctic ecosystem response to disturbance. The data, results and conclusions that follow reflect primarily the 1985/86 hydrologic year.

Site Characteristics

The headwater basin of Imnavait Creek is approximately 207 km south of Deadhorse (Prudhoe Bay) Alaska (Fig. 1) at an elevation of 900 m. It is near the southern limit of the northern foothills of the Brooks Range. The Continental Divide is 40 km south at approximately 1500 m elevation.

The headwater drainage basin of Imnavait Creek includes 210 ha and is well defined except for a short stretch in the strangmoor area, where, during meltoff, a small amount of water may enter from outside the basin. Groundwater is not a factor since the underlying acidic, clay-rich till is perennially frozen. Imnavait Creek is regarded as a perennial stream even though measurable flow may cease for short periods in some years. The stream begins in a sedge-dominated string-bog that comprises five percent of the total basin. Beyond the bog and for most of its length within the basin, the stream is nearly straight. It is characterized as beaded consisting of relatively short, narrow, channelized segments separated by relatively deep, subrounded pools. The channel and flood plain comprise three percent of the basin. In its lower reaches the creek flows through both beaded reaches and those in which it flows over and/or between boulders. The average gradient is 0.015 m/m. To study the stream, a 1-meter "H" flume was placed 100 meters upstream of the point where the stream channel flows through a bedrock restriction (Fig. 1).

The basin is asymmetrical. The northeast-facing slope is shorter and less steep than its opposing slope and has mineral soil exposed in slope parallel stripes. The opposing slope is dominated by dwarf shrub-sedge tussock tundra in which active (mineral soil exposed) and inactive frost medallions may comprise 25 percent or more of the surface. Numerous subparallel drainage lines (water-tracks) traverse the slopes. Some have well-defined, commonly multiple channels at least through their mid-slope reach. Divides are spaced from a few tens to several hundred meters and circumscribe drainage basins that range in size from 2 to 7 ha. In most cases the water-tracks and their drainage basins loose definition as they approach the ridge line and likewise the flood plain or channel of Imnavait Creek. It is common for willow and birch to make up a substantial component of water-track vegetation. Discharge from these small drainages is measured daily with compound weirs.

The Snow Melt Regime

In the foothills region probably all streams have what Woo (in Carter et al. 1987) describes as a nival regime in which the snow-melt flood dominates the seasonal runoff.

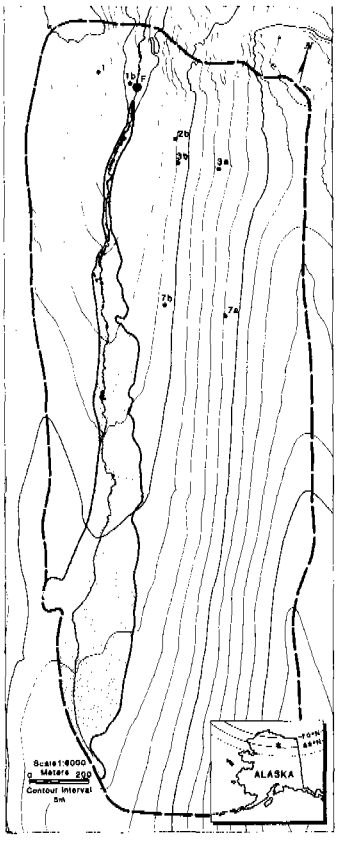

Fig. 1 Contour map of Imnavait Creek drainage basin with location (inset at star). Numbered circles are weir and water sample sites. F indicates flume site. Shaded area defines flood plain; major stream beads are in black.

In 1986, with the snow pack saturated, overland flow (mostly subnival) and probably very shallow interflow, together with channelized (water-track) flow, began on the southwest-facing slope (once the detention storage had been filled) some 24 hours before it began (again as subnival flow) in Imnavait Creek (1 June). The melt-off discharge curve (Fig. 2) for Imnavait Creek was developed by Kane and Hinzman, 1985).

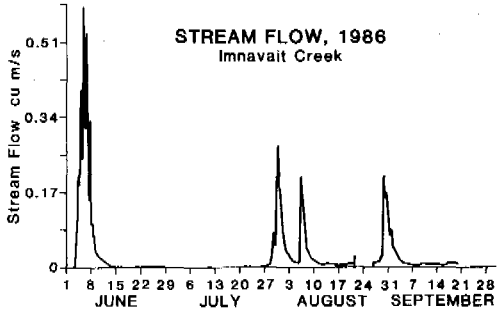

Fig. 2 Streamflow hydrograph for Imnavait Creek (1986).

The sharpness and symmetry of the discharge trace indicate that all or nearly all storage in the form of near surface voids was filled as the snow pack became saturated (D. Kane and Hinzman, 1988). The entire melt-off event probably represents overland flow.

The contrast in melt-off between the two valley slopes is apparent (Fig. 3) with the average peak occurring on the southwest-facing slope on 4 June (a day that also shows significant changes in such associated climatic parameters as reflected solar radiation, albedo and net radiation for that slope). The peak for the opposing slope occurred 72 hours later. The very steep rising limb in all cases indicates the intensity of the melt. The protracted response time for the northeast-facing slope is related to the very much thicker snow cover in the basin of water-track 1.

The curve for water-track 2 on the southwest-facing slope is representative of discharge from a small drainage basin where snow-melt is the only significant flow event.

Summer Regime

During the period of record 2 May 1986 through 2 September 1986, 176 mm of precipitation was recorded. The rainfall was generally of low intensity (0.1 - 0.5 mm/hr^{-1}), but one or two high intensity (37 mm in 1/2 hr) storms are common in most summers. The total precipitation between September 1, 1985 and September 1, 1986 is 344 mm; 51% as rain, 49% as snow.

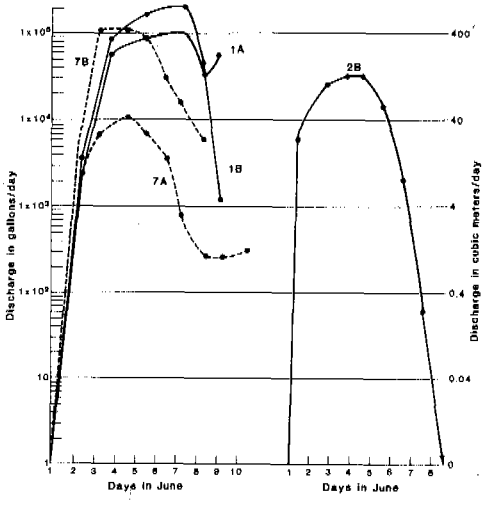

Fig. 3 Snow-melt discharge (1986) curves for three water-tracks in Imnavait Creek basin. Water-tracks 7 and 2 face southwest, water-track 1 faces northeast.

The thaw period stream flow of 1986 consisted of three significant rainfall/snow events following the melt-off peak after which discharge remained less than 28 l/s^{-1}

and ceased altogether on 9 July. Flow returned on 10 July in response to the second rainfall event with discharge less than 14 l/s^{-1} until 24 July when the first major rainfall event occurred during which discharge reached 312 l/s^{-1}. This was followed on 6 August by the second event of only slightly less peak discharge. The third peak was snow induced and took place on 29 August with a discharge of 153 l/s^{-1} (Fig. 2).

It is instructive from the standpoint of understanding the hydrological and hydrogeochemical response within small basins to examine in detail one or more morphologically simple events as hydrographs portray them. To this end the events of 27 July - 2 August and 5-9 August have been selected. It is desirable in these analyses to choose discharge events that are free of antecedent flow. In practice, however, this is seldom possible.

Composite hydrographs for the July/August event pair are shown for Imnavait Creek and three water-track basins each of different areas (Fig. 4). Part A of the runoff hydrograph shown in Figure 4 represents a protracted storm event (actually composed of 164 separate periods of generally low intensity precipitation) between 24 July and the 5th of August, 1986, and a total rainfall of 31.0 mm. Antecedent runoff constitutes less than 2% of the primary peak discharge of 314 l/s^{-1}. Event B (Fig. 4) differs significantly from A in two important ways. First, the response time is 87% faster (14 hrs vs 111 hrs). Second, the antecedent runoff constitutes 15% of the peak discharge but does not directly influence the response time (Dingman 1971). Two things are involved here: the available storage capacity of the basin was satisfied by event A and the precipitation was more intense. The close hydrologic relationship among the water-tracks and Imnavait Creek suggest that the larger water-tracks are good models for larger basins.

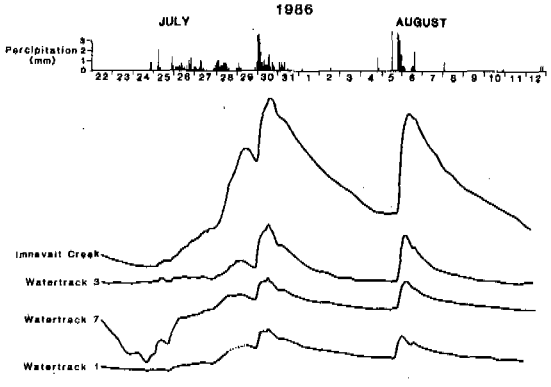

Fig. 4 Comparison of storm hydrographs for Imnavait Creek watershed (210 ha) and tributory water-tracks 3 (6.5 ha) and 1 (3.7 ha). Hourly rainfall is shown above.

Source of Stream Flow

In the Imnavait basin, as well as the individual water-track basins, stream flow results from a combination of in-channel precipitation, overland flow, and active layer interflow. The presence of permafrost precludes deep groundwater flow which is not considered to be a source in this sealed basin. Each of these sources will be considered separately with regard to (Fig. 4).

Channel flow:

The flood plain of Imnavait Creek consists of about 24 ha or 11% of the basin. Within this area the channel is defined as the area covered with water at melt-off and during significant summer storms and includes about 0.8 ha (or 0.4% of the basin). Calculations using parameters of basin geometry and storm characteristics show in-channel precipitation contributes about 1% to peak discharge.

Overland flow:

Dingman et al. (1966) have demonstrated that response time (steepness of the rising limb) is not related to antecedent flow conditions and this is amply demonstrated in Fig. 4 and water-tracks 1 and 3, and especially by an event on 19 July, which had a rise time of only 8 hrs from a dry channel. Overland flow may be evoked to explain the stream response from dry bed conditions or zero antecedent discharge. Overland flow occurs in the Imnavait basin only rarely after soil thaw begins and is not thought to contribute to the rising limb especially if antecedent moisture is low on the slopes.

If the total valley bottom is considered to contribute as overland flow - that contribution plus the in-channel precipitation, comprises 31% of the hydrograph peak. The remainder of the flow is at this time considered to be due to interflow and water-track runoff.

Interflow:

Adequate direct measurement of interflow is yet to be made for the active layer. It is probable, however, that the lower slopes (lower back slope and toe slope) are the principal contributing areas to interflow since they have the thickest moss and organic soil horizons whereas overland flow and shallow interflow are more important on the upper back slope and near crest areas. Since the stream hydrographs require a rapid response for the interflow component, it is the fibrous organic horizons (0-10 to 20 cm) with their high hydraulic conductivity (average 0.02 - 0.1 cm/sec^{-1}) (Kane and Hinzman, 1987) that are important. Mass flow occurs rapidly through the large pores and is concentrated at the boundary with the mineral organic and mineral soil (hydraulic conductivities between 0.004 and 0.009 cm/sec^{-1}).

GEOCHEMISTRY

When estimating the natural state of the watershed(s) or evaluating response to disturbance it is essential to know the degree to which the basin approaches equilibrium in terms of chemical inputs and outputs. To this end the chemistry of Imnavait Creek flow and that of three of the water-tracks has been monitored over the summer seasons 1985, 1986 and 1987, together with winter snow, and in 1986 and 1987, atmospheric inputs. The data reported in the following section is for 1986.

Methods

Approximately 1 liter of water was taken daily from Imnavait Creek at a point 1 meter upstream from the gaging station and at the spill point of each water-track weir site. A sample of 250 ml was placed in a rinsed polyethylene bottle and frozen. A second 250 ml aliquot was passed through a 0.45 m filter under vacuum, acidified to pH 2.0 with 6N HNO_3, stored at 4°C and shipped as soon as possible in a cooler along with the unfiltered aliquot to Ohio State. Upon receipt, or as soon there after as practical, the unfiltered sample was thawed and passed through a washed, dried, dessicated and weighed prefilter for determination of suspended solids. A 20 ml aliquot of the filtrate was allowed to equilibrate for one hour at 22°C, then used for determination of pH and electrical conductivity. A 2 ml aliquot was passed through a Dionex 2000i ion chromotograph and analyzed for Cl, F, PO_4, NO_3 and SO_4.

A 25 ml aliquot of the acidified sample was analyzed for Ca, Mg, Na, K with a Varian AA6 Atomic Absorption Spectrophotometer. Each value represents the average of three readings.

Hydrologic event timed, automatically collected samples from Imnavait Creek and the water-track weir site were analyzed as above. All data are reported in mg/l^{-1}.

Snow

In early May 1986 prior to snow-melt the snow pack was sampled at 17 sites in the lower half of Imnavait Creek watershed (Fig. 1). Channel samples from two or three snow pits from each site were melted and the water combined, filtered and analysed. The data summarized in Table 1 indicate substantial site to site variability. Ionic ratios taken in total, support a continental origin for ions in the frozen precipitation.

Liquid Precipitation (Wetfall)

Wetfall was collected with a standard National Atmospheric Deposition Program (NADP) collector at seven day intervals. The samples were analyzed by Global Geochemistry, Inc., in accordance with EPA requirements. The data (Fig. 5) show considerable temporal variability which cannot be attributed to air masses of different geographic origin since all originate in the southwest quadrant, and possess both maritime and continental components.

Solid Precipitation (Dryfall)

Dry deposition was collected from a bucket open only during no-rain periods over eight weeks. The bucket was washed with 250 ml of

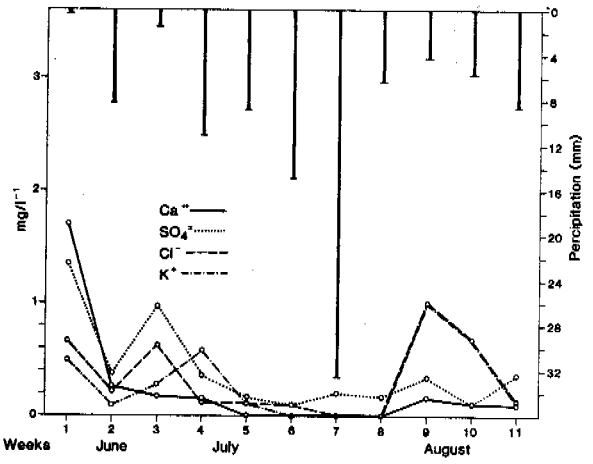

Fig. 5 Trends in some selected ions in wetfall during the summer of 1986.

deionized water. The wash was allowed to equilibrate in the bucket at 22°C for 24 hours, transferred to a clean, rinsed polyethylene bottle and sent to Global Geochemistry, Inc., for analyses. There is nothing in the data in Table 2 to suggest that solid precipitation is in any way more important than liquid precipitation in contributing to anions to the valley. It does, however, point to the importance of wind-blown particulate matter in the addition of the principal cations (except sodium) to the Imnavait Creek basin. The Na/Cl value is similar to sea water.

Table 1
Average analysis (mg/l^{-1}) with ranges of snow from 17 sites in the Imnavait Creek drainage basin. (May 17-20, 1986)

	pH	Ec	Na	K	Ca	Mg	Pb	Cl	F	PO_4	NO_3	SO_4
$\bar{X}$	5.4	65	0.15	0.15	0.33	0.06	<0.5	0.56	0.21	0.0	0.0	0.0
Range	5.1-5.5	45-155	0-.46	0-.39	.2-.5	0-.1	<0.5	.34-.83	0-.24	0-T	0-T	0-T

Partitioning of ions with respect to precipitation type indicates that nitrate, and sulfate are almost exclusively associated with rainfall, while chloride and fluorine are dominant in snow. The cations with the exception of sodium are spread across the three precipitation categories with dryfall at least as important as rain and snow in contributing potassium and magnesium.

Imnavait Creek Water Analyses

Ion concentrations (mg/l^{-1}) commonly fluctuate, sometimes considerably, from day to day. There is no relationship to discharge at this scale, however, on an event basis such as that between 25 July and 5 August (Fig. 4), synoptic sampling showed a minimum in pH and maximum of dissolved solids corresponding to peak discharge. Data of Oswood and Flanagan (1987) indicate a peak in DOC and POC at peak event discharge.

At melt-off stream pH begins to increase rapidly even before the discharge peak is reached and continues a general upward trend through June. Seasonal maximum values are reached in July. At least some of the variability in the pH curve appears to be related to stream flow (i.e., the storm events already described (Fig. 4) following periods of low flow.

Electrical conductivity shows a peak value with the inception of snowmelt runoff and summer events, especially those not preceded by high antecedent drainage conditions. The mean monthly values of 100 or more are high compared to more temperate watersheds (generally <50 s) probably reflecting the concentration of organic acids at a particular time in Imnavait Creek. Seasonally the conductivities reach a mean high in July.

Calcium and magnesium are the dominant cations but even so are in low concentrations in the stream-water (seasonal mean of ca. 1.22 mg/l^{-1}). It is likely that most, if not all of these ions is supplied by precipitation.

The potassium ion is easily leached from plant tissue but because of its high turnover rate during the growing season in tundra areas is seldom seen in stream water. The rapid disappearance of potassium after snowmelt reflects the almost immediate demand for the element by vegetation. It is probable that most of the K that cycles through the basin is the product of cell lysis or of atmospheric origin associated with dissolved organics.

Subsequent to melt-off sodium concentrations like those of calcium decrease rapidly to a sporadic presence until mid-July with a mean concentration of 0.20 mg/l^{-1} which is approximately the seasonal mean concentration in precipitation. Thereafter it is below detectable limits except very infrequently. Unlike potassium, sodium is not considered to be a biologically important element in tundra plants but is taken-up by many and thus removed from the system. The atmospheric input (0.31 mg/l^{-1} through the period of Na presence to 15 July) can account for all found in the stream. After that date atmospheric sodium decreases by a third.

Table 2

Solid Precipitation (mg/l^{-1})

1986 Sampling Period	Ca	Mg	K	Na	NH_4	NO_2	NO_3	SO_4	PO_4	F	Br	Cl	A/C	pH	Ec
6/3-9/1	2.76	0.54	4.15	0.16	0.03	0.00	0.07	0.13	0.03	0.008	0.00	0.10	0.45	7.62	116.1

Chloride is the only important anion found in Imnavait Creek water and its seasonal distribution follows closely that of potassium. Sulfate appears only in trace amounts during melt-off but appears again late in the season possibly reflecting the oxidation of sulfur as the active layer reaches its maximum depth soils warm and the potential for biological oxidation is high. Both ions together with fluoride are sporadic components of precipitation mostly at levels below 0.02 mg/l^{-1}. The seasonal trends in concentration in Imnavait Creek are summarized in (Fig. 6).

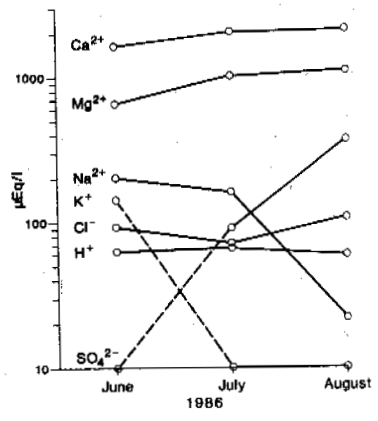

Fig. 6 Seasonal trends in ionic composition of Imnavait Creek water in 1986. Dashed line indicates the ion rises from or declines to 0 in the June-July interval.

It is apparent in Fig. 6, that a considerable imbalance exists in charge, favoring the positive charge. It is probable that much of this missing negative charge is associated with organic acids. The very low alkalinity of the water (mean of 2.1 mg/l^{-1}, as $CaCO_3$, M. Oswood personal communication) precludes it from contributing to a balance.

SUMMARY

The hydrologic year for the Imnavait Creek watershed begins sometime within the last week of May or the first week in June. The year ends, for surface flow, in mid-September. Total yearly precipitation is 344 mm; 51% rain and 49% snow. Discharge of Imnavait Creek began in June 1986, 4.5 days after mean air temperatures rose above 0°C. Peak discharge of 515 l/s occurred 84 hours later when 80% of the southwest-facing slope was snow-free. Water-track flow from the southwest-facing slope preceded flow in the main channel by about 36 hours, with peak discharges ranging between 6 l/s and 14 l/s depending on basin area. Peak discharge from the opposing slope water-track lagged 48 hours and most probably does not exceed 9 l/s. Hydrograph analyses indicate the snowmelt runoff can be likened to a major storm event occurring when all detention storage filled. Surface flow in all drainages ceased within two weeks of the discharge maximum and at several other times during the year. Three significant storm events occurred, one of which had a peak discharge of 320 l/s. In-channel precipitation contributes less than 1% to the total event discharge. Overland flow in most events is restricted to the total valley bottom of Imnavait Creek and contributes 30%. The remaining 70% of the flow is contributed by interflow and water-track discharge.

Snow chemistry represents a total accumulation of specific ions over the winter, essentially mid-September through May 1986. Data indicate considerable site to site variability and suggest a continental origin for the ions except Cl, Na and Mg. During the summer liquid precipitation (rain) was analyzed weekly. The data indicate seasonal peaks for most ions occurred in the early, post melt-off rains. Potassium and calcium were the principal cations supporting the dominance of a continental source (e.g., loess). Dry precipitation (eight week accumulation) again indicates a continental source with anion/cation ratios dominated by cations. Under natural conditions the most significant geochemical event in the Imnavait Creek watershed (including individual water-tracks) is the melt-off discharge. All measured parameters, except pH, show elevated values during the early phase of this event; pH is at a seasonal minimum during the event. Potassium is present in surface waters at detectable limits (mg/l^{-1}) during melt-off and for a short time after. Sodium follows a similar pattern but persists until mid-July. Calcium, magnesium, suspended solids and electrical conductivity all reach broad, poorly defined peaks in July. Chloride is the only measurable anion (mg/l^{-1}) and follows a trend similar to K and Na. Precipitation constitutes the principal source for chemical input to the watershed. The substantial imbalance in the anion/ cation ratio can probably be accounted for by organic acids that constitute the bulk of the DOC. Hydrologically and geochemically Imnavait Creek appears similar to other northern and mountain basins.

ACKNOWLEDGMENTS

The authors wish to thank the U.S. Department of Energy Ecological Research Division, office of Health and Environmental Research, office of Energy Research for support of the forgoing research over the past three years.

REFERENCES

Carter, L.D., Heginbottom, J.A., and Woo, M. (1987). Arctic Lowlands, in Graf, W.L., ed., Geomorphic Systems of North America: Boulder, Colorado, Geol. Soc. of Am., Centennial Special Vol. 3, pp. 583-628.

Dingman, S.L. (1966). Hydrologic studies of the Glenn Creek watershed near Fairbanks, Alaska. U.S. Army Cold Regions Research and Engineering Laboratory Special Report 86, 30 pgs.

Dingman, S.L. (1971). Hydrology of the Glenn Creek watershed Tanana River Basin, Central Alaska. U.S. Army Cold Regions Res. and Eng. Laboratory, Res. Rept. 297, 111 pgs.

Hinzman, L.D. and Kane, D.L. (1987). Active layer hydrology for Imnavait Creek, Toolik, Alaska. Prelim-data rept. for Dept. of Energy, April 1987, 47 pgs.

Kane, D. L. and Hinzman, L. O. (1988). Permafrost hydrology of a small arctic watershed in: Proceedings of the V International Conference on Permafrost, Trondheim, Norway.

Oswood, N.W. and Flanagan, P. (1987). Stream ecology, Imnavait Creek. Prog. Dept. for Dept. of Energy, April 1987, 25 pgs.

ENVIRONMENT PROTECTION STUDIES IN PERMAFROST ZONE OF THE USSR

N.A. Grave

Permafrost Institute, Siberian Branch Academy of Sciences, Yakutsk, U.S.S.R.

SYNOPSIS General state of the environment protection problem in the permafrost zone of the USSR. Development of the scientific studies, their progress and shortcomings. Basic directions of further studies (permafrost zone monitoring).

Wide distribution of permafrost and increased sensitivity of the northern landscapes to the human impact impel to treat the problem of the environment protection and that of the rational land use in the polar and circumpolar regions as a specific part of the global ecological problem.

Great attention is paid in the USSR to the environment protection problem as reflected in the State document on the basic directions of the economic and social development in the USSR for the period up to the year 2000. The USSR Supreme Soviet in conformity with clause 18 of the Constitution of the USSR has ratified the principles of the land, water and forest legislation and the legislation on the minaral resources.

Standards on the environment protection that define the relations between the man and the environment are being woked out.

The Government of the USSR has approved additional measures on the improvement of the protection of the environment and exploitation of the natural resources as well as has enacted complex legislation on environment protection of the tundra and the Baikal-Amur railway zone. The control over the state of the environment in these areas and implementation of the protection measures is entrusted to the USSR State Committee on Hydrometeorology and Environment Control, the USSR Ministry of Land Reclamation and Water Economy and on the Committe on Safe Conduct of Work in Industry and on the Mining Inspection under the USSR Council of Ministers. Environment protection departments have been set up in the Ministries concerned with implementation of the environment protection measures in industry and transport and control their effectiveness. The environment protection societies have been founded in the republics, territories and regions, including the North of the country and in some places - the environment protection universities which popularize the principles of the rational use of the natural resources.

However, the measures listed above turned out to be insufficient. Large capital investments allocated in the country's budget for environment protection measures are not always used for the direct purposes and nature is unrecoverably damaged both in the already developed and in the areas under development in Siberia and in the Far East. Examples of this are frequently published in the press and are discussed in the scientific conferences.

The main reason of such situation is a narrow bureaucratic approach to the solution of the environment protection problem. So far there are no united requirements on environment protection and use of natural resources, equally binding for all. All this has affected to some extent the organization and effectiveness of the research work in this field.

The scientific studies in the environment protection sphere are coordinated by different scientific councils of the USSR Academy of Sciences and are not unified by a common State programme. It is true that several complex regional programs do exist. Permafrost area studies are integrated into a program of "Ecology, environment protection in Siberia" which is a part of a complex program "Siberia" coordinated by Scientific Council on the Siberia environment problems, Siberian Branch of the USSR Academy of Sciences.

The program structure meets the problems of the biosphere monitoring and includes sections on the assessment of the state and prediction of environment changes, rational use of natural resources, working out the methods and means of environment protection against injurious technogenic impact. At the same time, individual sections of the program, worked out by different institutes, are insufficiently interconnected.

The geocryological studies are concentrated on defining the soil and landscape stability against man-induced impact upon the terrain under development. Such research is being conducted by the Institutes of the Siberian Branch of the USSR Academy of Sciences, the USSR Ministry of Geology, the USSR Ministry of Gas Industry, the USSR State Construction Committee "Gosstroy", the geologic and geographic de-

partments of the Moscow State University and certain other organizations. The results of the geocryological studies made in the USSR over a period between 1979 and 1984 have been summarized earlier (Grave, 1984).

By the present time the information on geocryological and physico-geographical conditions has been collected in the USSR on large areas under development and attemts have been made to predict the changes in these conditions due to different human activity for separate regions. Various estimate and forecast maps have been compiled. The principle of allowance for the permafrost thermal inertia and cryogenic processes characteristics both under natural and disturbed conditions in the course of the terrain development was taken for the basis of geocryologic evaluation mapping.

For the purposes of the industrial and civil construction on permafrost procedure has been worked out for the engineering-geocryologic survey preceeding the design (the USSR Gosstroy). A method of physico-geographic analogues merits an interest. It consists in comparison of the territory landscapes allocated for development with a landscape of a territory analogous in conditions that has already been developed, altered by human activities (the USSR Ministry of Geology). Recommendations are given on the choice of the construction sites, the requirements for their engineering preparation, recommendations on the use of thermal insulation coatings, on biological recultivation of the damaged sites, on the use of thermal piles on gas lines, suggestions on the construction control and operation.

Measures have been worked out on prevention of the dangerous cryogenic processes in the course of mining work, borehole drilling, agricultural work, hydraulic engineering in permafrost areas.

The recommendations listed above can not be considered as sufficient: no sections refer to wildlife, air and partially to waters and vegetation. It is known that industrial air and water pollution, non-regulated animal grazing destroy vegetatation cover and affect the thermal insulating properties of the snow cover causing changes in permafrost heat balance.

Insufficiently studied are the problems of the chemical pollution of permafrost by mineralized waters in the mining workings and by the household effluents of the settlements and towns. The technique and methods of the ground protection against salinization are still not developed.

For the present, fundamental developments of a geocryologic forecast are few.

Long-term investigations at the field stations permitted revealing the physical-mathematical dependence of the ground seasonal freezing and thawing depths on the main factors of the natural environment, i.e. radiation balance, air temperature, thermal resistance of the soil surface covers. A methodical manual supplied with an atlas of the geocryological forecast cartograms of West Siberia north has been compiled permitting determination of the permafrost temperature changes and depths of its summer thawing depending on a degree of vegetation and snow cover disturbances (Feldman, 1983, 1984). Similar atlas has been compiled for Yakutia territory, and it will soon be published.

The given method is already employed for thermokarst forecast in Central Yakutia and in the eastern Baikal-Amur railway zone. Forest stubbing for agricultural land use causes thermokarst in Yakutia without considerable permafrost degradation, but peat-moss cover removal on larch peatmass bog forests ("mari") in the BAM zone causes not only thermokarst but also complete thawing of frozen layer. Therefore, environment protection measures in Yakutia are directed against permafrost thawing and thermokarst formation along the BAM route - towards preliminary thawing of permafrost prior to terrain development.

Geocryological data obtained in Siberia, European North and North America show that far from all regions in permafrost area are being intensively destroyed under the effect of human activity. Certain landscapes, for example thermokarst ones, become converted to new, more productive natural complexes. This observation requires thorogh verification.

In the far north of Siberia, in the Arctic desert with underlying thick ground ice, due to a very cold and short summer, the ground seasonal thawing is not deep and the ground ice practically does not thaw. Only thermal erosion and thermal abrasion, becoming especially active under the human activity, promote in this case thermokarst and cause destruction of the coastal sections of water bodies.

In the taiga zone of Central Yakutia, where post-Pliocene ground ice is widely spread, forest felling and soil ploughing limit thermokarst, as a rule, to hillocky deformations of surface and, due to climate dryness, it disappears rapidly, except for cases of water accumulation in thermokarst depressions. A large number of alasses in Yakutia are the results of periodic air temperature and precipitation fluctuations, the majority of alasses being formed during the Holocene warming. At present, alas development is limited there and is mainly associated with human activity.

In geocryological forecast for many years, the tendencies of natural cryolithozone changes should be considered with rapid changes resulting from human activity on this background.

The tendency in the cryolithozone development may be marked by permafrost temperature gradient change that reflects the value and direction of thermal flows in cryogenic structure. Meanwhile, today we have information on the thermal field of the Earth's crust in the permafrost zone of Siberia. On the basis of temperature measurements in deep boreholes drilled for industrial purposes in various

geostructures of North Asia, a map of the Siberian platform and the Verkhoyansk-Kolymsk folded mountain area has been compiled at a scale of 1 : 5 000 000. The map shows regions with dissimilar intensity of thermal flows and deep freezing of the Earth's crust. A wide zone of anomalous deep freezing of rocks in Yakutia and on Chukotka was discovered with this, being related to peculiarities of deep terrestrial processes. All this indicates considerable difficulty in using deep temperature profiles for forecasting evaluations of the cryolithozone evolution (Touchkov, Lysak, Balobaev, 1987; Balobaev, Volodjko, Goloubev et al., 1985).

Unfortunately, long-term continuous precise instrumental observations are still not carried out on permafrost evolution caused by the environmental changes.

An attempt to compare the temperature measured by A.F.Middendorf almost one hundred and fifty years ago in the walls of a deep pit excavated in Yakutsk, with the temperature measured in deep boreholes drilled adjacent to the pit almost 100 years later, turned out to be unsuccessful: the pit walls during many years of its deepening were supercooled by very cold air flowing in from the surface that has distorted the natural rock temperature.

In order to establish evolutionary permafrost changes a network of stations is required in permafrost area in the USSR and North America for cryolithozone monitoring. Complex geocryologic studies should be carried out at these stations and in the adjoining regions, employing geophysical, geological, geomorphological and paleogeographic methods, and the results of earlier investigations should be summarized.

The results of such investigations will assist in more precise establishment of connection between cryolithozone and other environment components and in evaluation the historic parameters in the cryolithozone and environment changes in the past and future taking into account human activity.

REFERENCES

Balobaev, V.T., Volodjko B.V., Goloubev, V.A. et al., (1985). Katalog dannykh po teplovomu potoku Sibiri. Novosibirsk, s. 82.

Feldman, G.M. (1983). Metodicheskoe posobie po prognozu temperaturnogo rejima vechnomerzlykh gruntov. Yakutsk, s.

Feldman, G.M. (1984) Termokarst i vechnaya merzlota. Novosibirsk, 360 s.

Grave, N.A. (1984). Development and Environmental Protection in the Permafrost Zone of the USSR: A review; Permafrost. Fourth International Conference, Final Proceedings, Washington, D.C., pp.116-124.

Touchkov, A.D., Lysak, S.V., Balobaev, V.T. et al. (1987). Teplovoe pole Zemli. Novosibirsk, s. 195.

CLASSIFICATION OF GROUND WATER IN PERMAFROST AREAS ON THE QINGHAI-XIZANG PLATEAU, CHINA

Guo, Pengfei

906 Hydrogeological and Engineering Geologic Brigade, Ministry of Geology and Minerals, China

SYNOPSIS The Qinghai-Xizang Plateau is an area in which permafrost is broadly distributed in China, occupying a total area of about 1,591,000 square kilometres. According to a great deal of hydrogeological information obtained in recent years, ground water in the permafrost regions over the Qinghai-Xizang Plateau can be divided into three basic types which are suprapermafrost water, subpermafrost water and ground water in the talik in terms of the spatial relation between the buried conditions of ground water and permafrost distribution. If the storage conditions of ground water, the lithological character of the aquifers, and the hydrodynamic properties are considered, the ground water can further be divided into eighteen subtypes.

INTRODUCTION

The Qinghai-Xizang Plateau in China, well-known as "the roof of the world", is an area with widespread permafrost . According to incomplete statistics, the permafrost covers an area of more than 1,591,000 square kilometres. The permafrost in the Qinghai-Xizang Plateau belongs to the type of middle and low latitudes and high elevation, usually possessing the characteristics of widespread discontinuous permafrost. However, during their historical development, there also exists open taliks (unfrozen zones) in belt and island shapes in the widespread permafrost areas, influenced by the heat surficial exchanges and terrestrial heat flow. The permafrost which acts as a special regional water-resisting layer can divide a single aquifer into upper and lower ones, and cut the hydrodynamic connection between the upper and lower parts, in effect both supporting the upper part and controlling the lower one during the process of the formation and movement of ground water. Therefore the distribution and thickness as well as the structural features of the permafrost form the basis upon which we have classified the ground water in the permafrost areas on the Qinghai-Xizang Plateau. Various open taliks are either the recharge areas, or the drainage areas of the subpermafrost water in some sections, and at the same time they can be classified as containing a special type of ground water.

CLASSIFICATION OF GROUND WATER IN PERMAFROST AREAS ON THE QINGHAI-XIZANG PLATEAU

The classification of ground water in the permafrost areas was first proposed by a Soviet scholar, N.I. Tolstikhin in the early 1940s. The ground water in the permafrost areas was divided into three types, suprapermafrost water, intrapermafrost water and subpermafrost water, in his paper "Ground Water in the Frozen Zones of the Lithosphere". The Soviet hydrogeologists have universally paid attention to and accepted his classification (Ovchinnikov, 1957, 1960; Klimentov, 1959; Shepeler, 1983). The method of classification of ground water in the permafrost areas put forward by N.I. Tolstikhin has continued to be used in textbooks and related literature (Wang, 1980; Hydrologic Bureau..., 1960; Xian..., 1970) published in China since the fifties of the century. There is no doubt that the classification of N.I. Tolstikhin is of certain instructive significance in promoting the classification of ground water in the permafrost areas and in the performance of hydrogeological investigations.

The Qinghai-Xizang Plateau is a huge geological massif which has been severely uplifted since early Quarternary time , and its geological structure is complex. Permafrost of great thickness (>100 m) plays a role in controlling the hydrogeological structures and the types of ground water on the Plateau (Fig.1). On the basis of the hydrogeological information obtained in the last ten years or more and in accordance with the spatial relations between the occurrence of ground water and the distribution of permafrost, ground water in the permafrost areas on the Qinghai-Xizang Plateau may be divided into three basic types that are suprapermafrost water, subpermafrost water, and ground water in taliks. If we take into account the storage conditions of ground water and the lithological character of the aquifers as will as their hydrodynamic properties, the ground water can be further divided into eighteen subtypes (Table I).

Suprapermafrost water

Suprapermafrost water is a type of ground water which is widely distributed and commonly seen in the permafrost areas on the Qinghai-Xizang Plateau, usually possessing the characteristics of unconfined ground water or perched water. At

Classification of Ground Water in the

Ground water types			Conditions and areas of occurrence
Supra-permafrost water	Ground water in the pores of unconsolidated Quarternary sediments overlying in permafrost layer		In the active layer, occurring widely, lithological character of the aquifers is varied
	Semi-confined water and instant pressure water in unconsolidated Quarternary sediments on the permafrost layer		In the active layer, distributed along the piedmont or in low marshes
	Ground water in fractures of the weathering crusts of bedrock on the permafrost layer		In the active layer of bedrock, occurring widely
Sub-permafrost water	Ground water in the pores of Quarternary system underlying in permafrost layer	Unconfined water (watertable aquifer) in the pores below the permafrost	Beneath the permafrost, in intermontane basins (or valleys)
		Confined water in the pores underlying the permafrost	Below the permafrost, in various intermontane basins
	Water in the pores and fractures of the bedrock beneath the permafrost layer	Unconfined water in the fractures beneath the permafrost	Beneath the permafrost, in high mountains
		Confined water in the pores of the interlayer below the permafrost layer	Below the permafrost, distributed in the intermontane valleys and beneath the surface of the Plateau
		Confined water in the veined cracks of fault zones underlying the permafrost	Beneath the permafrost; occurring locally along the fault
		Confined water in fractures below the permafrost	Below the permafrost, very common occurrence

TABLE I

Permafrost Areas over Qinghai-Xizang Plateau

Main hydrogeological characteristics	Hydrodynamic properties	Relation between recharge area and distribution region
The aquifer is discontinuous, its thickness usually being 1 to 2 m, the thickest is 3 to 7 m. The lithological character is complicated. The discharge of a spring is commonly 0.2-1.5 l/sec., the maximum being 2-74 l/sec., and the salinity is 0.1-0.5 g/l. Its dynamic state changes greatly with the seasons	Commonly unconfined water; semi-confined or confined locally	identical
The aquifer is discontinuous and, controlled by seasonal freezing, its thickness varies with seasons. The rate of flow is 0.5-1 l/sec. (a single spring), the salinity is less than 0.5 g/l, its dynamic state varies greatly with the seasons	Semi-confined aquifer	identical
The aquifer is discontinuous and its lithology may consist of various pre-quarternary consolidated clastic sedimentary rocks. The thickness of the aquifer is 1 to 2 m, the flow of a spring is 0.5-3 l/sec., its salinity being 0.2-0.5 g/l. The dynamic state usually changes considerably with the seasons	Usually unconfined; may become semi-confined in early winter	identical
The aquifer is continuous. The lithological character is loose sand and gravel layers of the Quarternary system; there exisis an unsaturated zone between the aquifer and the permafrost. The discharge per unit is less than 1 l/sec., and the salinity is less than 1 g/l. The dynamic state is comparatively stable	Unconfined, watertable aquifer	inconsistent
The aquifer is continuous in loose sedimentary deposits of the Quarternary system; the apical plate is 20-90 m thick, the watertable is within minus 2.3-0.82 m. The discharge per unit is 0.23-5.17 l/sec·m and salinity 0.2-0.5 g/l	Confined and artesian aquifer	"
Pre-quarternary bedrock forms the aquifer. The aquifer belongs to the type of watertable aquifer due to poor recharge conditions and rapid discharge. The discharge per unit is 0.1-1 l/sec·m and salinity is less than 0.5 g/l.	Watertable aquifer	
Sandy slates of the Mesozoic and Cenozoic groups form the aquifer, the buried depth of apical plate is 40-129 m, watertable is 0.64-60 m below the surface, the discharge per unit is 0.01-0.2 l/sec·m, its salinity is usually 0.3-1 g/l., the highest being 3.4 g/l	Confined aquifer	"
The aquifer consists of pre-Pleistocene bedrock. It usually is confined owing to the overlying and confining permafrost; the discharge per unit is 0.1-1.0 l/sec·m and its salinity is 0.5-1 g/l	"	"
The aquifer is composed of pre-pleistocene bedrock, the buried depth of apical plate is 70-170m, the watertable is 0.7-50 m beneath the surface, the discharge per unit is 0.01-1 l/sec·m, its salinity is 0.5-3 g/l	"	"

Table I (continued)

Ground water types			Conditions and area of occurrence	
Water in taliks	Water in the pores of Quaternary system in taliks of river valleys	Ground water in the pores of Quarternary system	In sand and gravel layers of the talik, distributed in the talik of each big river valley	The aquifer is layers, 20–50 discharge per
		Confined water in the pores of Quarternary system	In each big river valley, and commonly in the strata of the early and middle Pleistocene lakes in the basin	The aquifer layers; the aquifer is 5 charge per unit
	Water in the pores and fractures of isolated taliks	Ground water in the pores of Quarternary system	In the back edge of desert zones along the margins of isolated thaw areas,distributed in each intermontane basin (valley)	The aquifer thick, watertable the discharge per
		Confined water in the pores of Quarternary system	In the central part of isolated taliks, in the middle of each large basin	The aquifer occurs watertable is 10 to 1 1/sec·m,
		Ground water in the of bedrock fractures	In taliks along the margin of each mountain area as well as the hilly country	The aquifer is the storage of components of conditions
		Confined water in the pores and fractures of clastic rock	In isolated taliks in the hilly land of bedrock overlain by Quarternary system	The rock formation groups, beneath water quality
	Water in the pores and fractures of structural thawed zones	Ground water in the pores of the Quarternary system in structural valleys	In structural valleys, distributed in the areas of Qubu and Yanshiping etc	The aquifer glacial and watertable is than 1 1/sec·m,
		Water in the veined cracks of fault zones	In the mylonitic zone of faults with relatively high pressure, pressed-torsion and tension	The lithological flows from the spring is 1 to
		Thermal mineral water in the veined cracks of fault zone	In the loosened zone of major faults, distributed widely	The lithological spring water flow of water temperature of is usually less

Main hydrogeological characteristics	Hydrodynamic properties	Relation between recharge area and distribution region
continuous, its lithological character is pebble-gravel m thick; watertable is 1 to 10 m below the surface. The unit is 1 to 10 1/sec·m, its salinity is 0.2 to 0.5 g/1	Watertable aquifer	basically identical
is composed of lacustrine sand and gravels as well as sandy buried depth of apical plate is 80-100 m. The thickness of the to 10 m, wetertable is 7 to 20 m beneath the surface the dis- is 0.1 to 0.5 1/sec·m, its salinity is less than 1 g/1	Confined aquifer	inconsistent
of mud-gravel and sand gravel layers, it is 5 to 50 m is 5 to 50 m below the surface, the lowest being 80-100 m, unit is more than 1 1/sec.m, the salinity is less the 1 g/1	Watertable aquifer	"
in the morainic mud-gravel layer which is 5 to 10 m thick, to 50 m beneath the surface, the discharge per unit is 0.1 salinity is less than 1 g/1	Confined aquifer	"
formed in the weathering crust of the pre-pleistocene bedrock; water in the rock formation is related to water quality, salts contained in the rock, as well as recharge and discharge	Watertable aquifer	basically identical
of the aquifer is sandy slate of Mesozoic and Cenozoic the permafrost. The aquifer has usually pressure head, its is comparatively bad, the storage capacity is rather small	Confined aquifer	inconsistent
exists in morainic and glacio-fluvial mud-gravel as well as in alluvial sand and gravel layers, being more than 30 m thick; 0 to 50 m below the surface. The discharge per unit is more the salinity is less than 1 g/1	Watertable aquifer	"
character of the aquifers is complex. Spring water usually upper wall in the fault zone, the flow of water of a single 3 1/sec., its salinity is less than 0.5 g/1	Confined aquifer	"
character of the aquifers is complex. The thermal mineral gushes out from the top wall of the fault zone, the rate of is 0.1 to 0.5 1/sec., the maximum being 1 to 3 1/sec., the water is 10 to 50°C, the highest being 94°C, its salinity than 1 g/1, the highest being 1 to 3 g/1	Confined aquifer	"

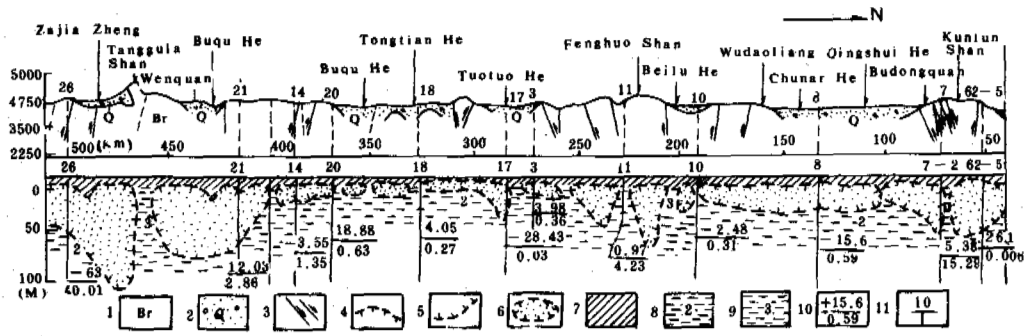

Fig.1 A Comprehensive hydrogeological Cross Section in the Permafrost Areas Over the Qinghai-Xizang Plateau

1. Pre-Quarternary strata; 2. Quarternary strata;
3. Faults; 4. Permafrost table; 5. Permafrost base;
6. Blocks of permafrost; 7. Suprapermafrost water;
8. Subpermafrost water; 9. Water in the talik;
10. Numerator: water level (m); Denominator: discharge per unit (l/sec·m); 11. Well or borehole No.

times the suprapermafrost water may be partly or truly confined, because of seasonal freezing of the soil and turf layers overlying the aquifer. The lithological character and thickness of suprapermafrost aquifers very with different regions, their rock formations have generally high storage capacity, and flow systems are short and unobstructed. The salinity of suprapermafrost water is low and the quality of it is quite good. The dynamic state of the suprapermafrost water changes greatly, frozen in winter, flowing freely in summer. Generally speaking, it is not easy for man to use it as a perennial source of water supply.

In light of the storage conditions and hydrodynamic properties suprapermafrost water can further be divided into the following types:

1. Ground water in the pores of unconsolidated sediments of the Quarternary system overlying the permafrost;

2. Semi-confined water and confined water in the unconsolidated Quarternary sediments on the permafrost;

3. Ground water in the weathering crust of the bedrock overlying the permafrost.

Subpermafrost water

Subpermafrost water also occurs widely on the Plateau, being one of the most important types of ground water and a good source of water supply as well. Verified by the available exploration information, the subpermafrost water is generally found everywhere beneath the permafrost. The subpermafrost water might be further divided into as follows:

1. Non-pressure water (watertable aquifers) in the pores of unconsolidated Quarternary sediments below the permafrost;

2. Pressure water (confined aquifers) in the pores of unconsolidated Quarternary sediments beneath the permafrost;

3. Non-pressure water in the fractures of the bedrock underlying the permafrost;

4. Pressure water in the pores of the bedrock beneath the permafrost;

5. Pressure water in the veined cracks of falt zones in the bedrock below the permafrost;

6. Pressure water in the fractures of the bedrock underlying the permafrost.

Ground water in talik zones

Ground water in talik zones on the Qinghai-Xizang Plateau is discontinuously distributed, often occurring in isolation. Besed on the type of talik, its hydrogeological texture, storage conditions, and hydrodynamic properties, ground water in talik zones can be fundamentally divided into nine different types:

1. Ground water in the pores of the Quarternary system in the talik zones of river valleys;

2. Pressure water in the pores of the Quarternary system in the talik zones of river valleys;

3. Ground water stored in the pores of unconsolidated Quarternary sediments in isolated talik areas;

4. Pressure water in the pores of unconsolidated Quarternary sediments in isolated talik zones;

5. Ground water in the fractures in bedrock in isolated talik areas;

6. Pressure water in the pores and fractures in the interlayer in clastic rocks of the Mesozoic and Cenozoic groups in isolated talik zones;

7. Ground water in the pores of Quarternary sediments in the talik areas of structural valleys;

8. Pressure water in the veined cracks of fault zones in the structural thawed areas;

9. Thermal mineral water in the fractures of fault zones in the structural thawed zones.

The basic characteristics of various types of ground water are listed in Table I.

CONCLUSION

The classification of ground water in this paper has been carried out on the basis of a great deal of available information. Based on the spatial relations between the occurrence of ground water and permafrost distribution, ground water in the permafrost regions on the Qinghai-Xizang Plateau, can be divided into three basic types which are suprapermafrost water, subpermafrost water and ground water in talik zones. Intrapermafrost water does fundamentally not exist on the Plateau. If the storage conditions of ground water and hydrodynamic properties are considered, eighteen subtypes can further be distinguished.

It should be pointed out that our classification is preliminary yet, it will be further perfected with the passage of time and continuous accumulation of exploration data.

ACKNOWLEDGEMENT

Grateful acknowledgement, is made to Interpreter Ran Longde for his help in translating this paper into English.

REFERENCES

Guo Pengfei, (1983). A Classification of Ground Water in the Permafrost Areas of Qilian Mountains, Glaciology and Cryopedology, Vol.6, No.1.

Hydrologic Burean of Geological Ministry, Institute of Hydrologic Engineering and Geology, (1960). Practical Hydrogeology, Geological Press, Beijing.

Klimentov, P.P., (1959). A General Handbood of Hydrogeology, Geological Press, Beijing (Chinese version translated from Russian).

No.4 Hydrogeological Brigade of the Geological Bureau of Hebei Province, (1978). A Handbook of Hydrogeology, Geological Press, Beijing.

Ovchinnikov, A.M., (1957). General Hydrogeology, Coal Industrial Press, Beijing (Chinese version translated from Russian).

Ovchinnikov, A.M., (1960). General Hydrogeology (second revised edition), Geological Press, Beijing (Chinese Version translated from Russian).

Shepeler, V.V., (1983). A Classification of Ground Water in the Cryolithozone, Permafrost Fourth International Conference Proceedings, p.1139-1142, July 17-22.

Wang Dachun et al., (1980). A Basis of Hydrogeology, Geological Press Beijing.

Xian Geological College, (1970). Hydrogeology (part 1), Geological Press, Bejing.

PERMAFROST HYDROLOGY OF A SMALL ARCTIC WATERSHED

D.L. Kane and L.D. Hinzman

Institute of Northern Engineering University of Alaska, Fairbanks, AK 99775-1760, U.S.A.

ABSTRACT: A small 2 km^2 watershed in an area of continuous permafrost has been monitored for three years. Measurement of precipitation, including detailed snow surveys prior to ablation, runoff leaving the basin, and the soil moisture regime in the active layer permit the determination of the basin water balance. Similar measurements were made for four bounded hillslope plots. As expected, spring snowmelt is the major hydrologic event each year, with this water being partitioned into soil storage, evaporation and runoff. Runoff dominates this portion of the annual hydrologic cycle. This is visually evident in the watershed by the large number of water tracts that convey water to the main stream channel. Moist soil conditions in the fall that produce high ice contents when frozen severely limit infiltration into the mineral soil. Summer precipitation events, although never near the volume of snowmelt, can produce peaks in the streamflow hydrograph if the intensity is high. How fast the basin responds depends upon the antecedent soil moisture conditions. Downslope movement of water is initiated when saturated conditions develop in the near-surface organic soils since the less permeable underlying mineral soils retard infiltration.

INTRODUCTION

The hydrology of an arctic watershed conforms to the accepted principles of watersheds in temperate and tropic regions. However, the predicted response can vary substantially because of environmental and physical differences. The large amount of energy lost during the winter months is responsible for maintaining permafrost quite near the ground surface. This severely limits the role of the subsurface system in the hydrologic cycle.

In this paper, we examine the water balance of an arctic watershed underlain by continuous permafrost. The hydrologic roles of the subsurface active layer, surface or near-surface runoff, and evaporation are discussed in conjunction with snow and rainfall precipitation. Water balances during the spring snowmelt and the period of surface runoff have been calculated based on numerous field measurements.

Snow plays a very important role in arctic watersheds from the viewpoint of hydrology, climatology, and ecology (Woo, 1982). Snow may accumulate for as long as 9 months in the Arctic and then ablate in a relatively short time, typically 10 days. The ability of the active layer soils to absorb and store snowmelt runoff is limited in poorly drained organic (Roulet and Woo, 1986a) and mineral (Kane and Stein, 1983a) soils by the high ice contents. Evaporation during the snowmelt period and evapotranspiration during the summer months are difficult to quantify. There have been several attempts at measuring evaporation using small lysimeters and evaporation pans (Brown et al., 1968; Dingman, 1971; Addison, 1977; Marsh et al., 1981; Ohmura, 1982; and Kane and Stein, 1983b). Alternatively, it is possible to determine evaporation from the residual term of an energy balance (Wendler, 1971; and Weller and Holmgren, 1974). Finally, there are several quasi-theoretical approaches such as the Thornthwaite method (Brown et al, 1968; Dingman, 1971; and Kane and Carlson, 1973) and Priestley and Taylor (Rouse and Stewart, 1972; Rouse et al., 1977; Wright, 1981; and Woo et al., 1983). Ohmura (1982) also used both an aerodynamic profiling method and the Bowen ratio method.

The most important factor controlling summer evapotranspiration in the Arctic for tussock tundra is the moisture level in the active layer. In very few studies has this parameter been measured continuously throughout the year; yet this measurement is critical to understanding the response of the watershed to hydrologic mass and energy inputs.

Precipitation measurements in the Arctic can be characterized as sparse, of short duration, and of very poor quality. This is particularly true for snowfall precipitation, for which the water content is typically underestimated by a factor of 2 to 3 when windy conditions prevail (Benson, 1982).

Probably the most reliable hydrologic measurements made in the Arctic are those of runoff. Again, there is the complaint that there are too few streamflow gaging stations and the quality of the data is questionable during periods of ice and high flows.

SITE DESCRIPTION

Imnavait Creek is a small, 2.2+ km^2 watershed located in the northern foothills of the Brooks Range of Alaska, U.S.A. (Figure 1). Permafrost underlies the entire watershed and the active layer thickness ranges from 25 to 60 cm. Soils with organic surface horizons of varying thickness and bulk density mantle the mineral sub-soil and are classified as Histic Pergelic Cryaquepts. The primary vegetation are sedge tussocks, mosses and low shrubs. The stream drains northward between east and west-facing slopes that dominate the basin. The stream is a typical beaded stream and no significant bodies of free-standing water exist. Numerous water tracts, flowing directly down the slopes, carry water to the base of the slope. From the base of the slope, no well-defined channel exists from the water tracts to the stream, and water takes a dispersed path across the valley bottom. Tussock tundra dominates the slopes and the valley bottom, so water moving downslope alternates from surface to subsurface flow. Near-surface flow is prevalent during snowmelt, and may exist during prolonged periods of rainfall.

WATER BALANCE

Numerous techniques can be used to determine the water balance of a watershed, hillslope or plot (Van der Beken and Herrmann, 1985). Woo (1986) presents a water balance equation to define the various hydrologic relationships for a basin underlain by permafrost:

$$P + (Q_m+Q_i)/\rho_w\gamma + Q_{in} = E+Q + \Delta S_D+\Delta S_T+\Delta S_A \qquad (1)$$

where
- P = rainfall
- $Q_m/\rho_w\gamma$ = quantity of snowmelt
- $Q_i/\rho_w\gamma$ = quantity of ice melt in active layer
- ρ_w = density
- γ = latent heat of fusion
- Q_{in} = inflow
- E = evaporation or evapotranspiration
- Q = outflow
- ΔS_D = change in depression storage
- ΔS_T = change in detention storage
- ΔS_A = change in active layer storage

Each term in Equation 1 represents a flux or a storage change with units of depth over time for a unit area.

This equation can be simplified and it can take many forms depending on the physical system and the assumptions made. In this paper, we will look at the water balance during snowmelt, over the summer period, and during individual rainfall events. In addition, we will look at the water balance at the scales of both the plot and watershed.

For the snowmelt period, we simplified Equation 1 to the following form:

$$Q_m/\rho_w\gamma = E + Q + \Delta S_A \qquad (2)$$

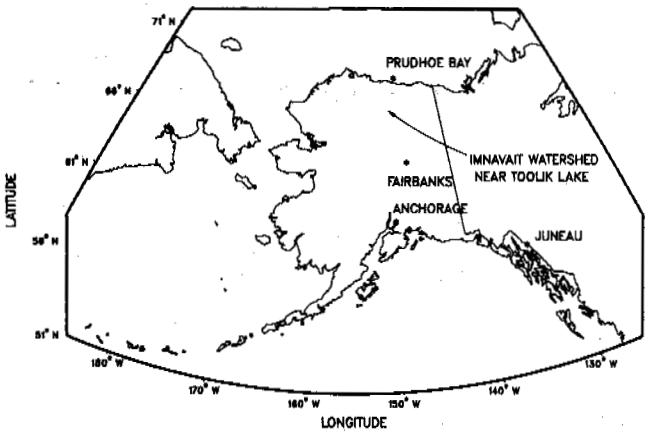

Figure 1: Map of Alaska indicating research site.

Rainfall was insignificant in our study during ablation. We also assumed that ice melt in the active layer and inflow did not exist and that there was no change in storage terms, except active layer storage. From laboratory measurements of soil properties and field measurements of moisture levels, we determined changes in storage of the active layer. Daily snowmelt and runoff were measured in the field directly. Therefore, estimates of evaporation during the snowmelt period can be made.

For the summer water balance the equation is quite similar to Equation 2:

$$P = E + Q + \Delta S_A \qquad (3)$$

From measurements of field soil moisture levels, it appears that prior to freeze-up each fall the amount of water in storage within the active layer is virtually the same each year. This means, on an annual basis, that both changes in soil storage and melting of ice in the active layer can be ignored. Simply, inflow is equated with outflow.

Very few hydrologic studies in areas of continuous permafrost have measured enough elements of the hydrologic cycle to calculate a water balance. Brown et al. (1968) studied the summer hydrology of a small drained lake basin near Barrow, Alaska. They reported the response of the watershed to individual storms and concluded that summer rainfall was offset by evapotranspiration during a normal year. Marsh and Woo (1979) reported on data from four basins near Resolute, N.W.T., Canada. They showed that 67-81% of the annual precipitation left the basin as runoff and 13-23% as evaporation. Lewkowicz and French (1982) measured the runoff from four plots on Banks Island in the Canadian archipelago during snow ablation. Three of the plots were located in areas of drifting snow. Woo (1983) completed an annual water balance for McMaster Basin near Resolute, N.W.T., Canada for a number of years. Only small changes in storage occurred; evaporation was minimal, and runoff dominated. Roulet and Woo (1986a and 1986b) determined the annual water balance for a peat wetland near Baker Lake, N.W.T. Water moving downslope from a lake was the main hydrologic activity in this basin.

For all of the above studies, it is difficult to make comparisons among the data. The soil types range from coarse grained soils to peat, and some have no surface vegetation. During snowmelt some soils in the active layer were capable of storing meltwater, while in other settings soil storage was nil. In almost all cases, the snowmelt event during breakup was the major hydrologic event of the year in terms of runoff peaks and volumes. The compelling reason is that permafrost close to the ground surface severely limits storage regardless of the soil type.

RESULTS

Measurements of snowfall and rainfall were made continuously within the Imnavait Creek watershed. A Wyoming shielded precipitation gage operates throughout the year and two standard 8 inch (20 cm) shielded gages complement the Wyoming gage during the summer (Figure 2). In addition, at winter's end, detailed surveys of snow on the ground are made using an Adirondack snow corer. Liston (1986) has shown that the Wyoming gage gives a good indication of the snow on the ground at the end of the winter. It is known that, throughout the winter moisture is lost from the snowpack due to sublimation. Sturges (1986) has shown that Wyoming gages, although shielded, under-measure the total snowfall. Therefore, it appears that the error of the Wyoming snow gage is comparable to the cumulative sublimation during the winter. For water balance computations, the water content of the snow on the ground just prior to ablation was used.

The pattern of rainfall for 1986 and 1987 (Figure 2) illustrates both low intensities and low quantities. There is a general trend of increasing rainfall during the summer months.

Four arrays of time domain reflectometry (TDR) probes were installed along the slope to measure the unfrozen water content of the active layer. TDR is an indirect method of measurement whereby the dielectric properties of the soil are measured(Stein and Kane, 1983). The annual variation in the unfrozen water content at selected depths for one of the profiles (Figure 3) indicates that the unfrozen water content increases as the active layer thaws and as the rainfall shown in Figure 2 occurs.

The soils above 15 cm depth in Figure 3 are highly organic, with mineral soils at greater depths. Once the mineral soil thaws at a given depth during the summer, the moisture content remains practically constant. This is also true when data from a number of years are compared. A plot of the unfrozen water content profile in late summer (Figure 4) shows that there is very little variation from year to year for the mineral soil, but there is some variation at the two upper depths in the organic soil. The actual values depend upon the length of time since rainfall or late summer snowmelt. The water content in the organic layer becomes constant after freeze-up. By spring this layer of organic soil is quite dry, except where it is highly decomposed and has a density approaching that of the mineral soil. So, we see virtually the same quantity of water in active layer storage each spring prior to ablation. A major assumption in our annual water balance calculation is that there is no change in storage from year to year.

Runoff was measured both in four plots constructed on the hillslope and in the Imnavait Creek basin. The plots were 89 m^2 in size and bounded with heavy (40 mil) plastic to prevent overland and subsurface flow into the plots. Runoff above the mineral soil was collected in a collection gutter and was routed to a holding tank equipped with a water level

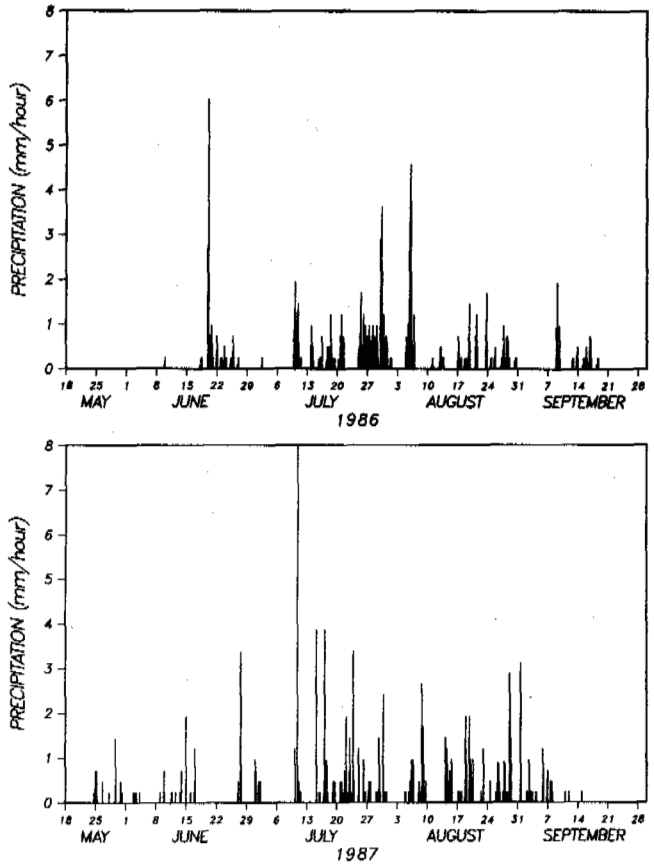

Figure 2: Pattern of summer rainfall at Imnavait Creek watershed.

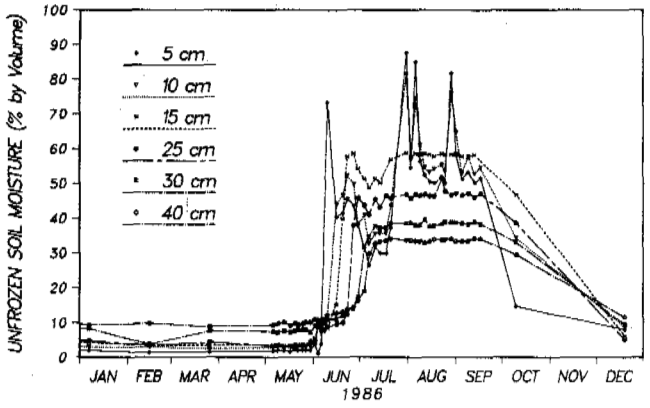

Figure 3: Soil moisture variation at selected depths, 1986.

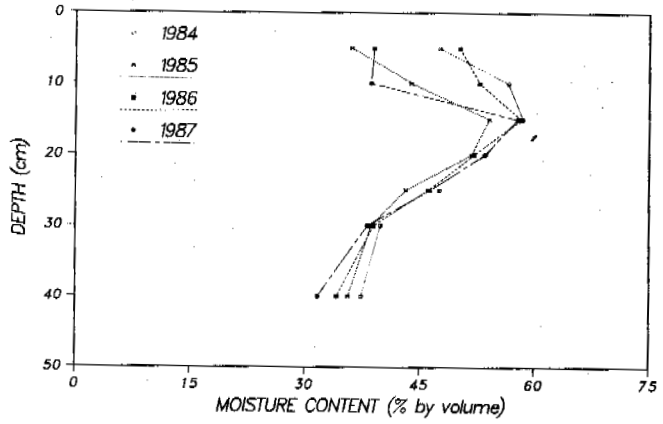

Figure 4: Typical soil moisture profiles just prior to seasonal freezing.

recorder. The plots are uniformly spaced from near the base to near the top of the west-facing slope and are continuously monitored during snowmelt. For the summer months, they have been monitored for some individual storms.

The watershed outflow was measured continuously in 1986 and 1987 (Figure 5), allowing annual water balances to be determined. A stage-discharge curve was constructed for the stream in 1986, and a flume was installed in the channel in 1987. Spring snowmelt is usually the peak annual runoff event because of both the limited storage in the active layer and the significant quantities of snow that accumulate during the winter. Runoff during the summer months is minimal, except during substantial rainfall events that produce near-surface runoff.

A comparison of pan evaporation with summer precipitation (Figure 6) shows that potential evaporative losses exceed precipitation. While there is a gradual decline in pan evaporation over the summer, precipitation increases in late July and August.

Water balances were computed for two periods, spring snowmelt and annual. For the snowmelt period, computations were made for

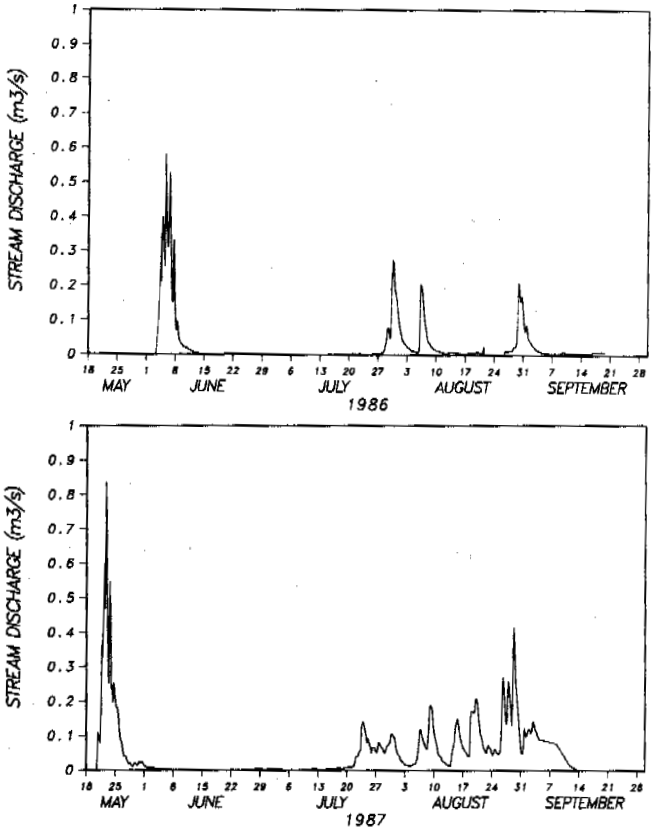

Figure 5: Snowmelt and rainfall generated runoff from Imnavait Creek.

both the plots and the basin using three years of data (Figure 7). The annual water balance was calculated for the basin only in 1986 and 1987 (Table 1). The runoff measurements for the plots are not continuous over the summer, so annual balances cannot be performed for them. During 1985, a breakdown of the water level recorder during a major rainfall event prevented similar calculations.

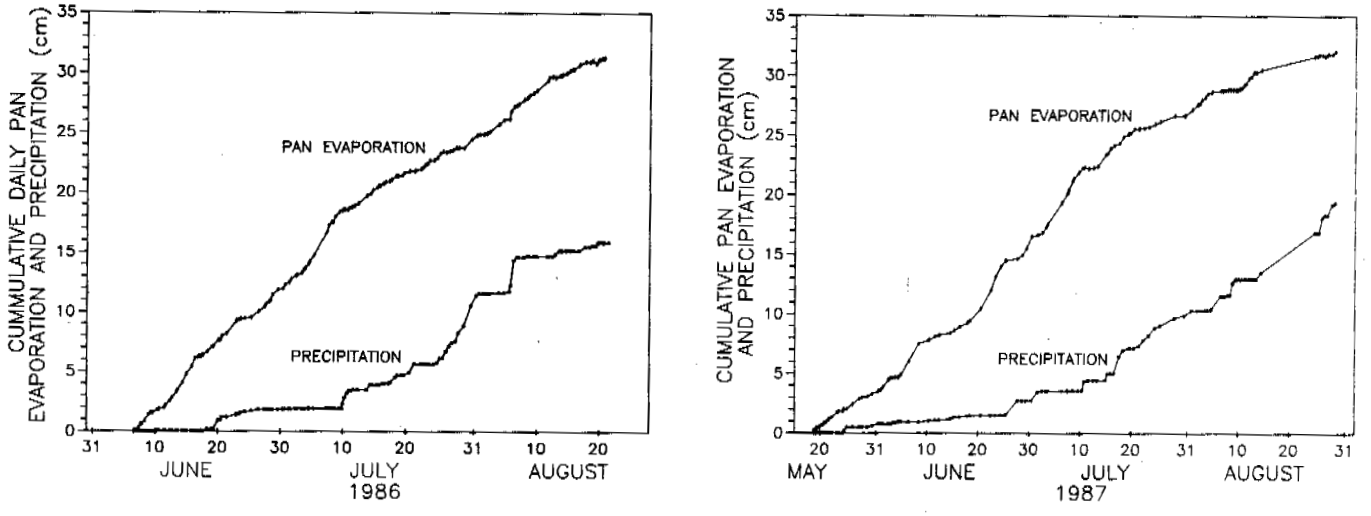

Figure 6: Cumulative pan evaporation and summer rainfall precipitation.

Table 1: Annual Water Balance

Year	Snowpack Water Content (cm)	Summer Precip (cm)	Total Precip (cm)	Snowmelt Runoff (cm)	Summer Runoff (cm)	Total Runoff (cm)	Evapo-trans piration (cm)	Pan Evap (cm)
1986	10.9	16.3	27.2	5.7	6.2	11.9	15.3	31.0
1987	10.8	27.2	38.0	7.1	17.9	25.0	13.0	32.0

CONCLUSIONS

Considerable variation exists among the four runoff plots in regards to percentages of runoff and evaporation losses during snowmelt. Although there are some differences between the plots in terms of slope and active layer soil structure, the most important factor is the distribution of snow on the ground. The plots with the highest snowpack water equivalent also have the highest percentage of runoff. Likewise, those plots with the least snow have the highest percentage of evaporation. Where snow is thin, vegetation extending through the snow and bare ground enhances radiation absorption and surface heating. This provides considerable energy to drive evaporation, whereas the surface albedo remains quite high for the thicker snowpacks. Comparison of the same plots over the three years of study shows that there is much less variation temporally than spatially.

In 1986, snowmelt runoff represented 48% of the annual runoff, while the snowpack water content represented 40% of the annual effective precipitation (snow on ground just prior to ablation plus summer precipitation). Although the water content of the 1987 spring snowpack was nearly equivalent to the 1986 spring snowpack, the snowpack water content was only 28% of the annual effective precipitation and snowmelt runoff was also only 28% of the annual runoff. Runoff is the dominant process during the snowmelt period, and evapotranspiration dominates during the dryer summers.

Summer runoff events are controlled by the antecedent moisture conditions of the organic soils in the active layer because once thawed, the mineral soils remain near saturation throughout the summer months. Runoff from the plots ceases shortly after snowmelt or rainfall events. During summer periods of little or no precipitation, runoff is virtually zero in the stream. Water from the thawing active layer which could provide runoff during the summer does not appear to be an important process in Imnavait Creek watershed. The water that is made available by the thawing active layer is probably used by plants or lost through evaporation. A comparison of the pan evaporation data and the computed evapotranspiration (Table 1) shows that insufficient water is available for evapotranspiration to proceed at its potential rate.

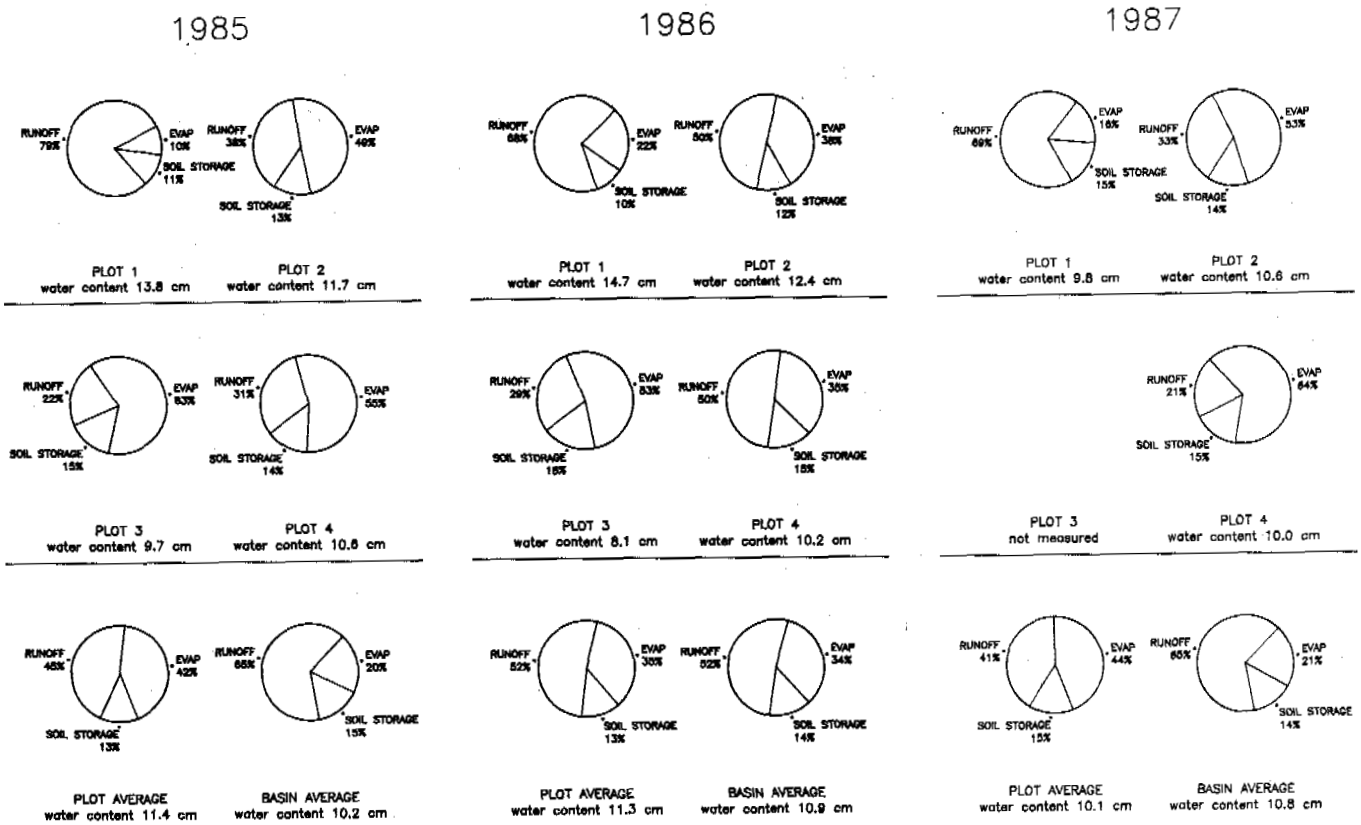

Figure 7: Charts illustrating the partitioning of snowmelt into runoff, storage and evaporation.

ACKNOWLEDGMENTS

The research reported here was supported by the U.S. Department of Energy's Office of Health and Environmental Research Ecological Research Division as part of the R4D program in Arctic Tussock Tundra. This research project was quite labor intensive and we would like to thank several individuals for their contributions: Dr. Kaye R. Everett, Dr. Carl S. Benson, Catherine G. Egan, Robert E. Gieck, Elizabeth S. Lilly, Glen E. Liston, Bertram Ostendorf, Michael R. Lilly, Steven J. Hastings, Knut Sand, and Matthew D. Zukowski.

REFERENCES

Addison, P. A.(1977) Studies on Evapotranspiration and Energy Budgets on Truelove Lowland. In: Truelove Lowland, Devon Island, Canada; A High Arctic Ecosystem, L. C. Bliss(Ed.). University of Alberta Press, 281-300.

Benson, C. S.(1982) Reassessment of Winter Precipitation on Alaska's Arctic Slope and Measurements on the Flux of Wind Blown Snow. University of Alaska, Geophysical Institute, UAG R-288.

Brown, J., S. L. Dingman, and R. I. Lewellen(1968) Hydrology of a Drainage Basin on the Alaska Coastal Plain. U. S. Army, Cold Regions Research and Engineering Laboratory, Research Report 240.

Dingman, S. L.(1971) Hydrology of Glenn Creek Watershed Tanana River Basin, Central Alaska. U. S. Army, Cold Regions Research and Engineering Laboratory, Research Report 297.

Kane, D. L. and R. F. Carlson(1973) Hydrology of the Central Arctic River Basins of Alaska. University of Alaska, Institute of Water Resources, Report No. IWR 41.

Kane, D. L. and J. Stein(1983a) Water Movement into Seasonally Frozen Soils. Water Resources Research, 19, 1547-1557.

Kane, D. L. and J. Stein(1983b) Field Evidence of Groundwater Recharge in Interior Alaska. Proc. Fourth International Conference on Permafrost. National Academy Press, 572-577.

Lewkowicz, A. G. and H. M. French(1982) The Hydrology of Small Runoff Plots in an Area of Continuous Permafrost, Banks Island, N.W.T. Proc. Fourth Canadian Permafrost Conference, 151-162.

Liston, G. E.(1986) Seasonal Snowcover of the Foothills Region of Alaska's Arctic Slope: A Survey of Properties and Processes. University of Alaska, MS Thesis.

Marsh, P. and M. K. Woo(1979) Annual Water Balance of Small High Arctic Basins. Proc. Canadian Hydrology Symposium: 79-Cold Climate Hydrology, National Research Council of Canada, 536-546.

Marsh, P., W. R. Rouse and M. K. Woo(1981) Evaporation at a High Arctic Site. Journal of Applied Meteorology, 20, 714-716.

Ohmura, A.(1982) Evaporation from the surface of the Arctic Tundra on Axel Heiberg Island. Water Resources Research, 18(2), 291-300.

Roulet, N. T. and M. K. Woo(1986a) Hydrology of a Wetland in the Continuous Permafrost Region. Journal of Hydrology, 89, 73-91.

Roulet, N. T. and M. K. Woo(1986b) Low Arctic Wetland Hydrology. Canadian Water Resources Journal, 11(1), 69-75.

Rouse, W. R., P. F. Milles, and R. B. Stewart(1977) Evaporation in High Latitudes. Water Resources Research, 13, 909-914.

Rouse, W. R. and R. B. Stewart(1972) A Simple Model for Determining Evaporation for High Latitude Upland Sites. Journal Applied Meteorology, 11, 1063-1070.

Stein, J. and D. L. Kane(1983) Monitoring the Unfrozen Water Content of Soil and Snow Using Time Domain Reflectometry. Water Resources Research, 19(6), 1573-1584.

Sturges, D. L.(1986) Precipitation Measured by Dual Gages, Wyoming Shielded Gages, and in a Forest Opening. Proc. Cold Regions Hydrology, American Water Resources Association, 387-396.

Van der Beken, A. and A. Herrmann(1985) New Approaches in Water Balance Computations. International Association of Hydrological Sciences, Pub. No. 148.

Weller, G. and B. Holmgren(1974) The Microclimates of the Arctic Tundra. Journal Applied Meteorology, 13, 854-862.

Wendler, G.(1971) An Estimate of a Heat Balance of a Valley and Hill Station in Central Alaska. Journal Applied Meteorology, 10, 684-693.

Woo, M. K.(1982) Snow Hydrology of the High Arctic. Proc. of Joint Western/Eastern Snow Conference, April 20-23, Reno, NV, pp 63-74.

Woo, M. K.(1983) Hydrology of a Drainage Basin in the Canadian High Arctic. Annals of the Association of American Geographers, 73(4), 577-596.

Woo, M. K.(1986) Permafrost Hydrology in North America. Atmosphere-Ocean, 24, 201-234.

Woo, M. K., P. Marsh, and P. Steer(1983) Basin Water Balance in a Continuous Permafrost Environment. Proc. Fourth International Conference on Permafrost, National Academy Press, 1407-1411.

Wright, R. K.(1981) The Water Balance of a Lichen Tundra Underlain by Permafrost. McGill University, Subarctic Research Paper No. 33, Climatological Research Serial No. 11.

FLOWING WATER EFFECT ON TEMPERATURE IN OUTWASH DEPOSITS

A. Karczewski

Quaternary Research Institute, Adam Mickiewicz University, Poznan, Poland

SYNOPSIS Study was made of the influence of air and water temperature on the thermal properties of outwash deposits. Statistical analysis of thermistor thermometer readings indicates that water temperature has a definitely greater effect on thermal properties of the ground, night temperatures reach much higher values of determinants than afternoon temperatures do, water affects significantly thermal properties of the ground as far as the distance of 1.5 m from the channel. This is of principal importance in thermoerosive processes whereby proglacial waters act on a presently forming outwash plain.

INTRODUCTION

The thermal action of flowing water on channel banks is one of morphogenetic factors affecting areas of permafrost occurrence. This process is referred to in the literature as thermal erosion. Publications by French, Egginton /1973/ and French /1974/ are concerned with the Canadian Arctic or those by Walker, Arnborg /1963/, Mackay /1963/ deal with the Alaska area. These authors point out chiefly the effect of ice veins approaching the terrace edge on the scale of thermoerosion, as is the case for Siberia /e.g. Soloviov 1973/. Throughout this process there is heat exchange between water and the frozen bedrock since water has greater thermal capacity than air. Therefore, wetter ground has higher thermal conductivity.

Studies concerning thermoerosion may fall under two groups. One is concerned with the thermal action of waters in rivers flowing from the south northward, i.e. in Siberia, Canada or Alaska. In summer their water is much warmer than the ambient temperature since it flows from areas at lower latitudes. The other group deals with areas belonging to the Arctic zone, mostly those glaciated at the present time. Proglacial runoff comprises most streams there. Jahn /1975/ gave attention to these problems in his monograph on the periglacial zone. For instance, he has stated that "limited thermal erosion may also be linked to streams which originate in glaciers".

As a distance between proglacial waters and glaciers becomes longer, the water increases its temperature by flowing through either shallow proglacial lakes or a heated outwash area in the whole system of shallow channels.

Members of the Polish expeditions to Spitsbergen conducted research into the thermal properties of tundra mostly in respect of their vertical variations. Among others, Baranowski /1968/, Grześ, Babiński /1979/, Marciniak, Szczepaniak and Przybylak /1981/ observed deeper-reaching thawing of outwash surface /114 cm/ rather than tundra surface /99 cm/ in the Kaffiöyra coastal plain in summer. Grześ /1984/ has established that the ground thaws by 50-55 cm deeper inward near the streams than in the adjoining terrain but he attempts no generalizations because of such complicated hydrological conditions existing in outwash plains.

METHODS

In view of the above remarks about the effect of flowing water on the distribution of ground temperatures, the present author carried out studies of an extramarginal outwash plain of the Hörbye Glacier closing the area around the Petunia Bay /Billefjorden/ to the north in the summer of 1986 /Fig. 1/.

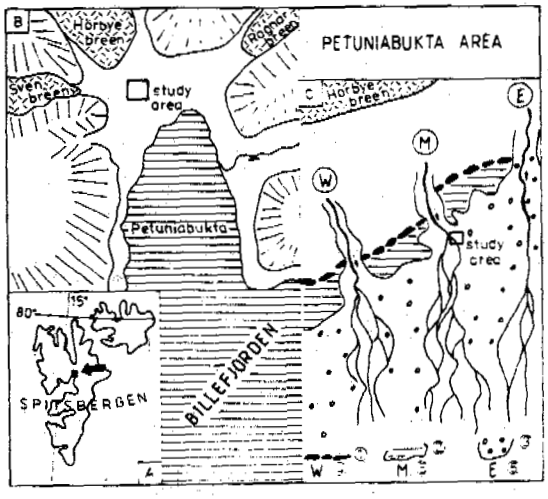

1-outer belt of ice-cored moraines
2-flat ground moraine
3-outwash plain
4,5,6,-gaps:W-western. M-middle. E-eastern

Fig. 1. Study area.

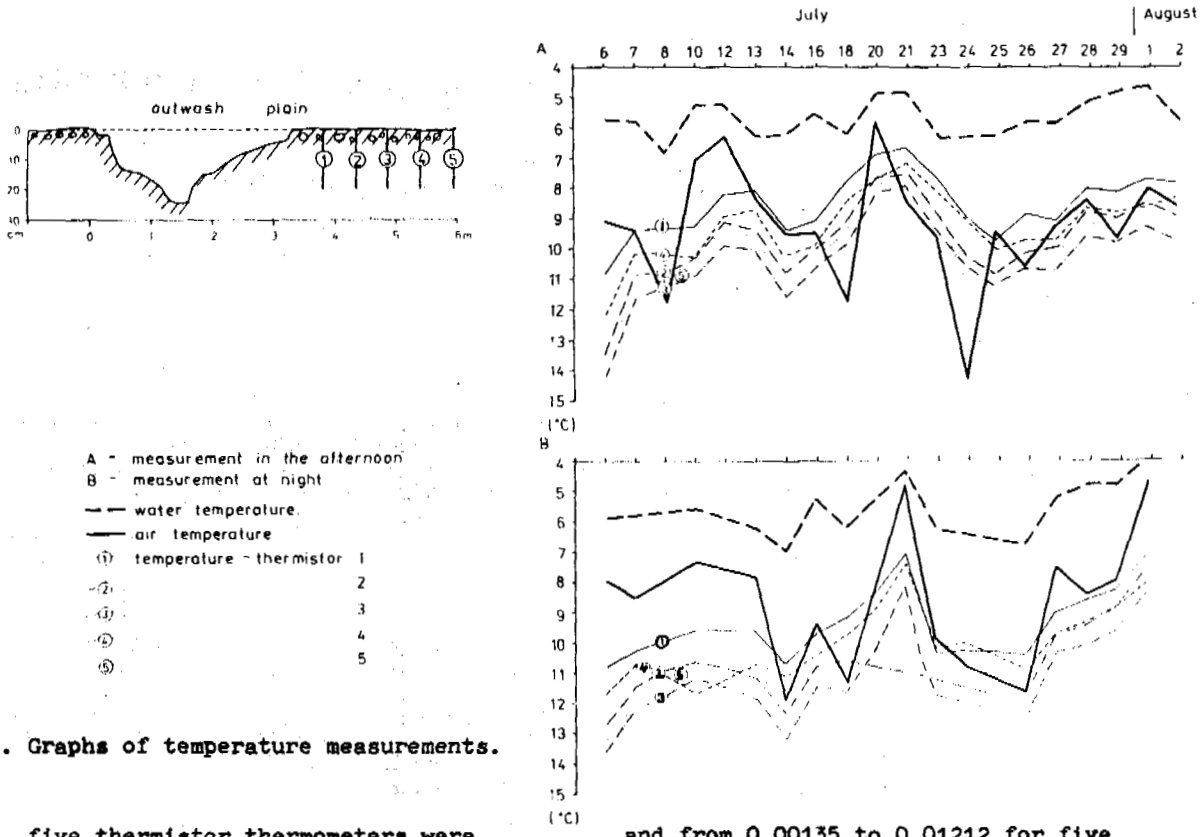

Fig. 2. Graphs of temperature measurements.

Thus, five thermistor thermometers were installed near one of outwash channels 3.25 m wide and 25 cm deep at the maximum, at the depth of 20 cm and at a distance of 0.5, 1.0, 1.5, 2.0 and 2.5 m from the bank. In addition to ground /gravelly-stony and sandy series/ temperature readings, water and air temperatures were also measured twice throughout the 24-hour period, i.e. during the afternoon and night hours. The afternoon measurements were made between 12.30 pm and 2.00 pm, while the night figures were read off from 6.00 pm to 10.00 pm because of technical constraints.

RESULTS

Throughout the period of measurement, i.e. from 6 July till 2 August, air temperatures fluctuated between 5.8 and 14.4°C and between 4.8 and 12.0°C during the afternoon and night hours, respectively. The temperature of water in an outwash stream ranged from 4.6 to 6.4°C and from 4.0 to 7.0°C during the afternoon and night hours, respectively /Fig. 2/. The temperature of water in a supraglacial stream fluctuated between 0.3 and 0.4°C by comparison.

When a comparison has been made between variations of air and water temperature and those of temperature readings on thermistor thermometers by the use of regression coefficient, it has been established that water temperature x_2 has a more marked effect on temperature distribution in outwash deposits than air temperature x_1 /Table 1/. Values of this coefficient ranged from 0.13841 to 0.286114 and from 0.00135 to 0.01212 for five thermometers during the afternoon and night measurements, respectively.

Thus, the preliminary procedure of measurement involved establishing a principal relationship of water temperature effect to outwash deposit temperature by calculating the coefficient of determination. Its diurnal values vary in an interesting way. In case water temperature is measured during the afternoon hours, they are much higher since they are 59.00 to 81.00 /Table I/.

Analysis of ground temperature plots for particular thermistors /Fig. 2/ reveals a marked heating effect on outwash deposits. It attains its maximum over a distance of 1.5 m from the outwash channel bank during both the afternoon /A/ and night /B/ measurements. The influence of water observable as far as this distance is characterized by high coefficients of determination /Table I/. Thus, its thermal action occurs over the distance of 1.5 m from the stream. Throughout the period of observation, maximum ground temperatures were recorded from early July till the end of its second ten-day period. In late July and early August there was a decreasing tendency, especially during the night measurement. This was undoubtedly due to a decreasing angle of the Sun's ray incidence and to prolonged shade over the proglacial runoff area.

The above remarks are pertinent to merely one incomplete summer season. However, they suggest a marked effect of water as a heat carrier on the potential of thermoerosive processes operating on the surface of a forming outwash plain.

TABLE I

	Regression coefficients				Coefficients of determination	
	Afternoon measurement		Night measurement		Afternoon measurement	Night measurement
	air x_1	water x_2	air x_1	water x_2		
1	0.89536	0.16977	0.93253	0.00483	18.48	78.00
2	0.88643	0.13841	0.60205	0.00135	21.06	81.00
3	0.96657	0.15081	0.75293	0.00258	18.75	79.44
4	0.80734	0.28614	0.33260	0.01212	8.51	59.00
5	0.75454	0.20629	0.62891	0.01193	18.64	66.97

REFERENCES

Baranowski, S. /1968/. Termika tundry peryglacjalnej SW Spitsbergenu. Acta Univ. Wratislawiensis /68/, 74 pp.

French, H.M. and Egginton, P. /1973/. Thermokarst development, Banks Island, Western Arctic. Permafrost, North American Contribution, 2nd Int. Conf. Permafrost, Yakutsk, USSR, Nat. Acad. Sci. Publ. /215/, 203-212, Washington D.C.

French, H.M. /1974/. Active thermokarst processes, Eastern Banks Island, Western Canadian Arctic. Can. J. Earth Sci. /11/, 785-794.

Grześ, M. and Babiński, Z. /1979/. Z badań nad letnim odmarzaniem gruntu na Spitsbergenie i w Mongolii. VI Sympozjum Polarne, 45-47, Burzenin.

Grześ, M. /1984/. Charakterystyka warstwy czynnej wieloletniej zmarzliny na Spitsbergenie. XI Sympozjum Polarne, Referaty i sprawozdania, 65-83, Poznań.

Jahn, A. /1975/. Problems of the periglacial zone. 223 pp, Warszawa.

Mackay, J.R. /1963/. The Mackenzie Delta Area. N.W.T. Dep. of Mines and Techn. Survey Geogr. Branch Memoir /8.1/, 202 pp.

Marciniak, K., Szczepaniak, W. and Przybylak, R. /1981/. Letnie odmarzanie gruntu na Kaffiöyrze /SW Spitsbergen/. VIII Sympozjum Polarne, Materiały, 163-168, Sosnowiec.

Soloviov, P.A. /1973/. Atlas thermokarst of Central Yakutia. Guidebook, 2nd Int. Conf. Permafrost, Yakutsk, USSR, July 1973, 48 pp.

Walker, H.J. and Arnborg, L. /1963/. Permafrost and ice-wedge effect on river bank erosion. Permafrost Inter. Conference 1983 /Lafayette, Ind./, Proc. Nat. Acad. Sci. Nat. Research Council Publ. 1987, 164-171.

SALIX ARBUSCULOIDES ANDERSS. RESPONSE TO DENUDING AND IMPLICATIONS FOR NORTHERN RIGHTS-OF-WAY

G.P. Kershaw[1], B.J. Gallinger[1] and L.J. Kershaw[2]

[1]Department of Geography, University of Alberta, Edmonton, Alberta
[2]Arctic and Alpine Environmental Consultants, Tofield, Alberta

SYNOPSIS The Subarctic zone is characterized by a wide variety of natural and human-induced perturbations which may disrupt or destroy the existing vegetation. During an experimental study of the effects of terrain disturbances on a decadent black spruce (Picea mariana (Mill.) B.S.P.) stand (Fort Norman, N.W.T.), Salix arbusculoides, the dominant understory deciduous shrub, was denuded to the ground. This was conducted in an effort to simulate the result of corridor activities in the North. The willow shrubs were able to compensate for the loss of above ground biomass through prolific resprouting from intact root crowns and by increasing the annual production and growth rates. The rapid and prolific regrowth has important implications for northern rights-of-way rehabilitation following disturbance.

INTRODUCTION

Subarctic ecosystems cover 7.6% of Canada (Zoltai et al., 1987) and in the Northwest much of this area has been affected by both natural and human-induced disturbances, which disrupt or destroy the existing vegetation. Natural disturbances are considered an essential component of the system. Wildfires in particular, have an pre-eminent role in the evolution and function of Subarctic ecosystems. Human induced disturbances such as seismic exploration, winter road, pipeline, powerline, and communication line corridors, crisscross much of the landscape. In many respects the impacts of clearing operations are similar to those resulting from wildfires since the soil and rooting zone are usually left intact (Zasada, 1986). Buried roots may provide an important source for revegetation as many plant species can regenerate by resprouting following damage to the above ground portion of the plant (Berg and Plumb, 1972; Zasada, 1986). Considerable interest has been shown in those plant species that show a strong recovery following disturbances as these species help to produce stability in the ecosystem (Hernandez, 1973; Younkin, 1976). Resprouting after partial or complete denudation by fire, chemicals or mechanical means has been the subject of many investigations. These studies have had various objectives; the regeneration of forest stands following clear-cutting operations (Marks and Bormann, 1972), increasing vegetative reproduction (Tew, 1970), increasing browse (Leege and Hickey, 1971; Wolff, 1978), or reducing the vigor of regrowth or eliminating regrowth (Jones and Laude, 1960). Shrub species serve an important role in the stability of Boreal and Subarctic forest ecosystems as they help to: minimize or prevent thermokarst and fluvial thermal erosion, reestablish soil thermal regimes, provide wildlife habitat and forage, and serve as a reservoir for nutrients (Zasada and Epps, 1976; Cargill and Chapin, 1987).

Members of the genus Salix often dominate disturbances. This is due to an interrelated complex of ecological, reproductive and evolutionary characteristics (Argus, 1973; Chmelar, 1974). Salix arbusculoides is perhaps the most common erect deciduous shrub in upland Boreal and Subarctic ecosystems throughout North America, west of Hudson Bay (Porsild and Cody, 1980). Although currently considered to be endemic to North America, Argus (1973) maintains that further study will likely confirm it to be conspecific with the Siberian S. boganidensis Trautv. This combination of factors provided the impetus for detailed, post-disturbance studies on the recovery of this species. The objective of this study is to monitor the regrowth of S. arbusculoides following total above ground harvesting in order to quantitatively describe the response of specific individuals over a 5-year period and to determine the effectiveness of regrowth from rootstock for the rehabilitation of northern disturbances. Results from the first year are presented in this paper.

STUDY SITE

The study area is 10 km north of Fort Norman, N.W.T. which is at the confluence of the Mackenzie and Great Bear Rivers (Fig. 1) (Evans et al., this volume). This site is within a 200-year-old Picea mariana-dominated Subarctic forest, underlain by permafrost-affected Gleysolic Turbic Cryosolic soil (Kershaw and Evans, 1987). This is also the site of a broader, ecosystematic study of the ecological effects of human-induced disturbances and the response to various rehabilitation/reclamation treatments. The nature of the site disturbance involved the creation of a cleared right-of-way and a simulated buried pipeline.

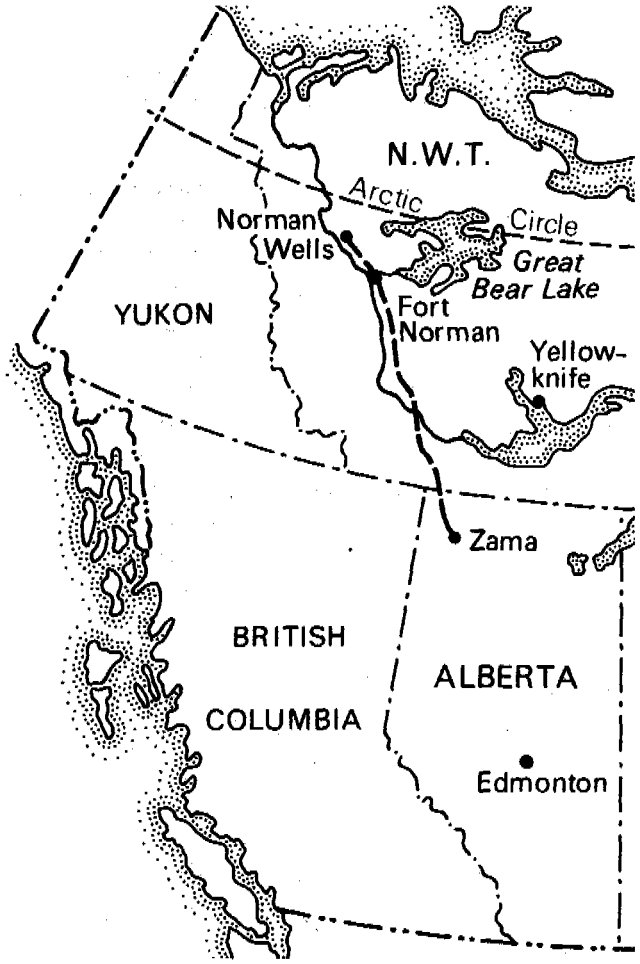

Fig. 1 Site location map, with existing pipeline corridor.

METHODS

Prior to clearing of the simulated transport corridor in May 1986, 149 randomly-selected shrubs were clipped at the ground surface. This denuding occurred prior to bud-break to ensure that no new growth was present. The following measurements were made prior to denuding of the above ground portion of the plant: live crown diameter (two measurements taken perpendicularly to each other), maximum live-crown height and the number of basal sprouts. Each shrub was then separated into its component parts; pre-1985 production, 1985 production, and dead shoots. Measurements of shoot lengths, basal diameters, and weights were recorded. At the end of the first growing season (80-85 days after clipping) a randomly selected subsample (n=30) of the original 149 shrubs was resampled. The resprouted canopy was measured and harvested along with the root crown. From these collections, current growing season woody and herbaceous production, leaf and shoot dimensions, and green and dry weights were measured and recorded. As suggested by the high standard deviations (Table I) these samples were not normally distributed, therefore the non-parametric Spearman rank correlation test was used to describe the relationships between the pre- versus post-harvest values. The significance level selected was 0.005 (one-tailed test) unless otherwise stated.

RESULTS

In general, the willows in this disturbance-simulation experiment responded to the removal of their aerial portions by increasing production. The post-harvest canopy volumes were only 48% of the pre-harvest values. While the mean canopy radii reached three-quarters of their original size in just one growing season, the mean post-harvest canopy height was reduced by 51%. The reduced shrub height is largely responsible for the lower post-harvest canopy volumes. The pre-harvest canopy volumes were significantly correlated (r_S=0.82) with the post-harvest volumes.

The denudation of the above ground portions of the shrubs promoted prolific resprouting and generally stimulated twig production. The number of shoots resprouting from intact root crowns increased from a mean of 7 per shrub prior to clipping, to 47 shoots per shrub at the end of the first growing season: an average increase of 673%. The high rank correlation value (r_S=0.79) suggests that the greater the number of basal shoots that a shrub has, the greater degree of resprouting from the root crown following disturbance. In addition to the prolific resprouting, the mean cumulative shoot lengths per shrub increased by 212% (pre-:post-harvest r_s=0.68). This increase in annual shoot production, however, was not reflected in the basal shoot diameters. Following denuding, the mean basal shoot diameter decreased by 57% (from an average of 6.7 mm to 2.9 mm), with very little correlation (r_s=0.18) between the pre-: and post-harvest values. The increase in shoot diameter tends to be secondary production, occurring as an annual increase to the stem width (Shaver, 1986). Pre-harvest number of shoots and cumulative shoot length proved good indicators of the production, based on these parameters, after disturbance (r_s=0.79 and r_s=0.68 respectively). Large, densely branched shrubs resprouted most vigorously.

Prior to clipping, the standing woody crop averaged 93.1g/shrub representing the accumulation of woody tissue over a number of decades. Following harvesting, these shrubs produced an average of 20% (18.4 g dry weight/shrub) of the pre-harvest standing crop in the 1986 growing season. Current annual stem growth (1985 production) prior to denuding was, on average, 1.6 g dry weight/shrub. The harvested shrubs produced 11.5 times as much annual growth in only one season following manipulation. This value does not include the average 15.9 g dry weight foliage per shrub. The post-harvest production was strongly correlated (r_s=0.81) with

TABLE 1

Performance of Salix arbusculoides in the first growing season (1986) following total above ground harvesting (values rounded off) and Spearman rank correlation coefficients for pre-:post-harvest relationships

CHARACTERISTICS	PRE HARVEST		POST-HARVEST	PRE:-POST-HARVEST
	Total Sample MEAN (n=149)	Subsample MEAN (n=30)	Subsample MEAN (n=30)	Spearman rank correlation r_s (n=30)
Canopy height (cm)	96 ± 43	96 ± 37	47 ± 47	0.60*
Canopy radius (cm)	33 ± 19	34 ± 26	25 ± 16	0.82*
Canopy volume (cc)	4431 ±5622	5791 ±9672	2774 ±3893	0.82*
No. of basal shoots	5 ± 5	7 ± 9	47 ± 72	0.79*
Cumulative length of shoots (mm)	1193 ±4186	4730 ±8574	10,043 ±18,055	0.68*
Basal shoot diameters (mm)	7 ± 3	7 ± 3	3 ± 1	0.18
Standing woody crop (g)	67 ± 253	93 ± 126	18 ± 41	0.81*
Current annual growth (g)	2 ± 4	2 ± 3	18 ± 41	0.71*

* significant correlation $p<0.005$ level (one-tailed test).

the pre-harvest standing crop.

A comparison of the mean pre-:post-harvest ratios (Fig. 2) demonstrates the higher rates of production in terms of post-harvest cumulative stem length and the number of basal shoots, while the mean ratios for the other characteristics indicate that the pre-harvest values were greater. Mean ratios greater than 1 can probably be attributed to multiple growing seasons. High standard deviations for some of the shrub characteristics (Table 1) suggests that there is a high degree of variability in the age/size class distribution within the population. Resprouting from below ground root stock or crowns, in the first growing season, resulted in generally shorter, denser shrubs comprised of longer but smaller diameter shoots.

DISCUSSION

It is apparent from the ratios of pre-:post-harvest values (Fig. 2) that resprouting from root stock is an effective mechanism in early revegetation of rights-of-way. The rapid response of these shrubs to clipping is demonstrated in the mean accumulation of 20% of the pre-harvest phytomass and 50% of the pre-harvest canopy height and volume in just one growing season. Rapid initial growth is essential as arctic/subarctic plants have approximately 70-90 days to initiate growth, expand and develop, reproduce and translocate nutrients below ground prior to dieback (Archer and Tieszen, 1980). Carbohydrate reserves in below ground storage organs (e.g. roots, rhizomes and crowns), are the primary source of energy governing plant regrowth following defoliation (Trlica, 1977; Archer and Tieszen, 1986). Many subarctic species have a high ratio of below ground to above ground biomass (e.g. 5:1) (Dennis and Johnson, 1970) and therefore retain large storage reserves that can be mobilized to re-establish foliage. In response to a stimulus such as thinning, defoliation or fire, supressed lateral and/or adventitious buds are activated giving rise to new sprouts (Berg and Plumb, 1972; Archer

and Tiezen, 1980). The hormonal imbalance activating bud development (McNaughton, 1983), may be caused by a change in the root to shoot ratio (Doorebos, 1953) or a suppression of apical dominance (Ferguson and Basile, 1966; Garrison, 1972). Several studies have revealed a direct relationship between regrowth and carbohydrate content of the storage reserves (Tew, 1970; Donart and Cook, 1970; Willard and McKell, 1973; Trlica, 1977). The seasonal effects of clipping on the resprouting ability of most shrubs parallels the carbohydrate flux in the storage reservoirs (Miyanishi and Kellman, 1986). The extent and vigor of regrowth probably depends not only on the carbohydrate reserves but also on the age and vigor of the plant and the environmental conditions prior to and following the disturbance.

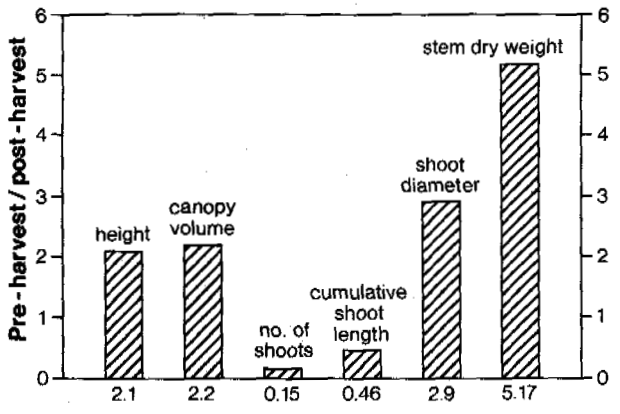

Fig. 2. A comparison of the mean ratios of pre- vs post-harvest characteristics of Salix arbusculoides by the end of the first growing season (1=no change, >1=post-harvest is greater than pre-harvest, <1=pre-harvest is greater than post-harvest.

In the two years since disturbance (canopy removal) the active layer has increased by 17% (Kershaw and Evans, 1987). Increased soil temperatures and thaw depths following disturbance generally result in a short-term increase in nutrient availability (Haag and Bliss, 1974; Chapin and Shaver, 1981; Cargill and Chapin, 1987), a greater soil volume for plant root activity (Hernandez, 1973; Younkin, 1976), higher organic mineralization rates (Chapin, 1983), increased bulk density and a higher volumetric concentration of nutrients (Gersper and Challinor, 1975). This improved nutrient status also promotes higher productivity (Chapin and Shaver, 1981).

The general conclusions from various clipping, browsing, and burning experiments is that manipulations to the above ground portions of shrubs promoted prolific resprouting and stimulated twig production (Ferguson and Basile 1966; Leege and Hickey, 1971; Wolff, 1978). Although most shrubs can survive a single top kill/removal (Krefting et al., 1966; Willard and McKell, 1973) repeated removal can exhaust the plants' nutrient reserves, resulting in depressed vigor and productivity and even mortality (Miyanishi and Kellman, 1986). Further studies at this site will determine the effects of repeated harvesting of S. arbusculoides.

CONCLUSION

Resprouting from intact root stock following total above ground harvesting is an effective, short-term means of revegetating cleared rights-of-way where root stocks remain intact. Within one growing season S. arbusculoides achieved canopy production that was almost 50% of the volume and height of pre-harvest values. The number of shoots and their cumulative length exceed pre-harvest values. If this rapid growth continues, the shrubs could reach their pre-harvest size in only a few years. From a management point of view, shrub resprouting may be viewed as desirable. It enhances wildlife habitat, and helps to stabilize slopes by retarding runoff and reducing soil heat flux in ice-rich soils. The preservation of rootstocks could prove to be an important planning step in areas that may be susceptible to thermal degradation and slumping such as ice-rich slopes. However, in other circumstances where shrub cover is undesirable (e.g. when a visible soil surface is necessary for aerial surveilance of pipeline, powerline or transportation corridors), rapid regrowth may prove to be a costly problem.

The study of natural recolonization can help to determine the rate and effectiveness of this process and, consequently, the importance of assistance in ensuring the successful rehabilitation of northern disturbances. Salix arbusculoides has a highly developed ability for resprouting and appears to be well adapted to producing and sustaining a plant cover on natural or human-induced surface disturbances, especially those resulting in the denudation of surface vegetation.

ACKNOWLEDGMENTS

Financial and logistical support for this research was provided by the following agencies; the Northern Oil and Gas Action Programme (NOGAP), the Boreal Institute for Northern Studies, and the Geography Department of the University of Alberta.

The authors would also like to express their thanks and appreciation to our fellow SEEDS'ters who participated in the data collection, and the Reprographics section of the Geography Department for drafting the illustrations.

REFERENCES

Argus, G W (1973). The genus Salix in Alaska and the Yukon. Publications in Botany, (2) National Museums of Canada., 279 pp. Ottawa.

Archer, S R and Tieszen, L L (1980). Growth and physiological responses of tundra plants to defoliation. Arctic and Alpine Research (12), 531-552.

Archer, S R and Tieszen, L L (1986). Plant response to defoliation: hierarchical considerations. In Grazing research at Northern latitudes. Gudmundsson, O (ed.) NATO ASI Series, 45-99.

Berg, A R and Plumb, T R (1972). Bud activation for regrowth. In Wildland shrubs: their biology and utilization. McKell, C M Blaisdell, J P and Goodwin J R (eds.). U.S. Dept. of Agriculture, Forest Service, General Technical Report INT-1, 279-286.

Cargill, S and Chapin, F S (1987). Application of successional theory to tundra restoration. Institute of Arctic biology, University of Alaska. In press.

Chapin, F S and Shaver, G R (1981). Changes in soil properties and vegetation following disturbance of Alaska arctic tundra. J. Applied Ecology (18), 605-617.

Chapin, F S (1983). Patterns of nutrient absorption and use by plants from natural and man-modified environments. In Disturbance and Ecosystems: Components of response. Mooney, H A and Gordon, M (eds.). Ecological Studies (44), 175-187.

Chmelar, J (1974). Propagation of willows by cuttings. New Zealand J. For. Sci. (4), 185-190.

Dennis, J G and Johnson, P L (1970). Shoot and rhizome-root standing crops of tundra vegetation at Barrow, Alaska. Arctic and Alpine Research (2), 253-266.

Donart, G B and Cook, W C (1970). Carbohydrate reserve content of mountain range plants following defoliation and regrowth. J. Range Manage. (23), 15-19.

Doorebos, J (1953). Review of literature on dormancy in buds of woody plants. Mededelingen Landbouwhogeschool, Wageningen (53), 1-24.

Evans, K E, Kershaw, G P, and Gallinger, B J (1988). Physical and chemical characteristics of the active layer and near-surface permafrost in a disturbed homogeneous Picea mariana stand, Fort Norman, N.W.T., Canada. (this volume)

Ferguson, R B and Basile, J V (1966). Topping stimulates Bitterbrush twig growth. J. Wildl. Manage. (30), 839-841.

Garrison, G A (1972). Carbohydrate reserve levels and response to use. In Wildlife shrubs: their biology and utilization. McKell, C M, Blaisdell, J P, and Goodwin, J R (eds.). U.S. Dept. of Agriculture, Forest Service. General Technical Report INT-1, 271-278.

Gersper, P L, and Challinor, J L (1975). Vehicle perturbation effects upon a tundra soil-plant system: I - Effects on morphological and physical environmental properties of the soils. Soil Sci. Soc. Am. Proc. (39), 737-744.

Haag, R and Bliss, L C (1974). Functional effects of vegetation on the radiant energy budget of the Boreal forest. Can. Geotech. J. (11), 374-379.

Hernandez, H (1973). Natural plant recolonization on surficial disturbances, Tuktoyaktuk Peninsula region, N.W.T. Can. J. Bot. (51), 2177-2196.

Jones, M and Laude, H (1960). Relationships between sprouting in Chamise and the physiological condition of the plant. J. Range Manage. (13) 210-214.

Kershaw, G P and Evans, K E (1987). Soil and near-surface permafrost characteristics in a decadent black spruce stand near Fort Norman, N.W.T.. B.C. Geographical Series (44), 151-166.

Krefting, L W, Stenlund, M H, and Seemel, R K (1966). Effect of simulated and natural deer browsing on mountain maple. J. Wildl. Manage. (30), 481-488.

Leege, T A and Hickey, W O (1971). Sprouting of Northern Idaho shrubs after prescribed burning. J. Wildl. Manage. (35), 508-515.

Marks, P L and Bormann, F H (1972). Revegetation following forest cutting: Mechanisms for return to steady state nutrient cycling. Science (176), 914-915.

McNaughton, J S (1983). Compensatory plant growth as a response to herbivory. Oikos (40), 329-336.

Miyanishi, K and Kellman, M (1986). The role of nutrient reserves in regrowth in two savanna shrubs. Can. J. Bot. (64), 1244-1248.

Porsild, A E and Cody, W J (1980). Vascular plants of continental Northwest Territories, Canada. National Museums of Canada, Ottawa.

Shaver, G R (1986). Woody stem production in Alaskan tundra shrubs. Ecology (67), 660-669.

Tew, R J (1970). Root carbohydrate reserves in vegetative reproduction of Aspen. For. Sci. (16), 318-320.

Trlica, M J (1977). Distribution and utilization of carbohydrate reserves in range plants. In Rangeland plant physiology. Sosebee, R E et al. (eds.). Range Science Series (4), 74-93.

Willard, E E and McKell, C M (1973). Simulated grazing management systems in relation to shrub growth responses. J. Range Manage. (26), 171-174.

Wolff, J (1978). Burning and browsing effects on willow growth in interior Alaska. J. Range Manage. (42), 135-140.

Younkin, W E (1976). Revegetation studies in the Northern Mackenzie Valley region. Northern Engineering Services Company Ltd. Canadian Arctic Gas Study - Biological Report Series. (38).

Zasada, J (1986). Natural regeneration of trees and tall shrubs on forest sites in interior Alaska. In Forest Ecosystems in the Alaskan Taiga. Van Cleve, K, Chapin, F S III, Flanagan, P W, Viereck, L A and Dryness, C T (eds.). Springer-Verlag, New York. 44-73.

Zasada, J C and Epps, A C (1976). Use of woody plant material in soil and site stabilization and rehabilitation. In Proceedings of the surface protection seminar. Evans, M N (ed.) U.S. Bureau of Land Management, Anchorage, 284-295.

Zoltai, S C, Tarnocai, C Mills, G F, and Veldhuis, H (1987). Wetlands of the Subarctic regions of Canada, Wetlands of Canada. In press.

ABLATION OF MASSIVE GROUND ICE, MACKENZIE DELTA

A.G. Lewkowicz

Department of Geography, University of Toronto, Canada

SYNOPSIS Short-term rates of ablation and components of the energy fluxes causing melt are described for massive ground ice exposed near Tuktoyaktuk, Northwest Territories, Canada. Ice face orientation affects both the timing and total amount of ablation recorded under clear skies. Little variation is present when the incoming short-wave radiation is mainly diffuse. A trend in ablation rates downslope is not evident, indicating that the ice face undergoes essentially parallel retreat. A regression equation using net radiation and a turbulent energy term as independent variables successfully explains 73% of the variation in the ablation flux. Net radiation provides approximately half of the energy used for ablation, and is less important here than at sites on southern Banks Island.

INTRODUCTION AND LOCATION

Ground ice constitutes a significant percentage of the upper few metres of permafrost in many parts of the western Canadian Arctic (e.g. Pollard and French, 1980). When erosional processes expose the ice to summer heat inputs, the permafrost thaws and a ground-ice slump (Mackay, 1966; French and Egginton, 1973) may be initiated. Headwall retreat in a ground-ice slump is determined by the rate of ice ablation and the slope geometry (Lewkowicz, 1987). Ablation rates in turn are related to the energy exchanged between the atmosphere and the ice surface.

There is a paucity of measurements in the literature on short-term rates of ablation of ground ice. Values have been obtained only from Mayo, Yukon Territory (Burn, unpublished), from Garry Island in the Mackenzie Delta (Kerfoot, unpublished), and from south-west Banks Island (Lewkowicz, 1985; 1986). Measurements of components of the energy exchange affecting ablation are limited to results from Fort Simpson, N.W.T. (Pufahl and Morgenstern, 1980) and Banks Island (Lewkowicz, 1986). Both studies showed radiation to be the most important source of energy for ablation but it is not known if this conclusion is valid for all ice face locations and orientations.

This paper describes short-term rates of ablation and associated energy exchange in massive ice at a ground-ice slump near Peninsula Point, Mackenzie Delta, N.W.T. (lat. 69°24'N, long. 133°8'W). This site is located 5 km south-west of Tuktoyaktuk and is well-known because an extensive section of mainly segregated ice (Mackay, 1971) up to 10 m in in thickness is exposed. The ice has been ablating for at least 50 years resulting in a mean rate of slump headwall retreat of 7 m/a (Mackay, 1986). The site was chosen because the exposure permitted experiments to be carried out down the ice and across the ice at orientations varying from west through north to east (Figure 1). Field measurements of ablation and associated meteorological factors were carried out over 16 days from July 12-28, 1985.

METHODS

Direct measurements of the rate of surface ablation were made using up to 6 pairs of ablatometers simultaneously. A full description of the instruments and their use

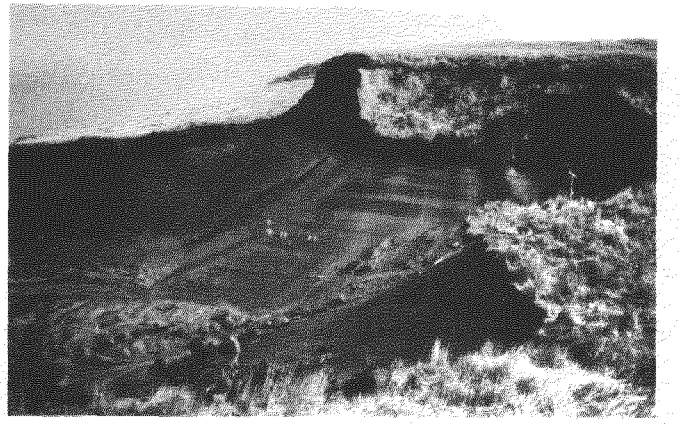

Fig. 1 The ground-ice slump studied near Peninsula Point. Note the variable overburden thickness resulting from previous episodes of slumping, stratified sediment bands within the ice, meteorological equipment on the right and ablatometers in the middle distance.

is given in Lewkowicz (1985). Ablatometer readings were recorded at 30-minute intervals on a Campbell Scientific CR21X data-logger. Mounting each ablatometer required that two cores of ice be collected using an ice screw and these samples were employed together with the ablatometer records to evaluate the ablation flux (Q_m) in W/m^2 using (Lewkowicz, 1986):

$$Q_m = d \cdot L \cdot M_w / [(M_w/\rho_i) + (M_s/\rho_s)] \quad ...(1)$$

where d is the surface ablation rate (m/s), L is the latent heat of fusion of ice (334×10^6 J/Mg), M_w is the mass of water from a sample of the ice (Mg), ρ_i is the density of ice (0.91 Mg/m^3), M_s is the mass of dried soil from a sample of the ice (Mg), and ρ_s is the specific gravity of the soil solids (assumed to be the 2.65 Mg/m^3). This method may overestimate volumetric latent heat and hence Q_m since it neglects the unfrozen moisture content of the sediment (Lewkowicz, 1985). However, the sediment content of the Peninsula Point ice face was so low that this is considered to be a minor inaccuracy.

Values of Q_m from equation (1) were compared with half-hourly meteorological data collected at the site (Table I) on a Campbell Scientific CR21 data-logger, or with hourly weather information from the Atmospheric Environment Service weather station at Tuktoyaktuk. Net short-wave fluxes (K^*) were derived for each ablatometer position (orientation and ice angle) using the method described in Lewkowicz (1986). However, the average albedo of the Peninsula Point ice face was higher than that of the Banks Island site (0.21 and 0.15 respectively) and the proportion of diffuse radiation reaching the ice was greater (0.75 and 0.65 respectively) due to differing headwall geometries. The net long-wave radiation flux (L^*) was obtained by subtracting K^* values measured parallel to the ice from measured net all-wave flux values (Q^*). This L^* value was added to K^* calculated for each ablatometer to obtain an individual Q^* value. After derivation of all Q_m and Q^* fluxes, the ablation data were screened to eliminate records where one or both of a pair of ablatometers were hit by falls, were covered by debris, or were not operating correctly. This was done by subtracting Q^* from Q_m to obtain the residual flux. If the calculated residual fluxes for a pair of ablatometers differed by more than 80 W/m^2 then it was assumed that a problem existed and the data were excluded from further analysis. Following screening, the 30-minute Q_m fluxes for each pair of ablatometers were averaged and this value could then be compared with the mean of the corresponding Q^* fluxes.

RESULTS

Spatial variation in ablation

Experiments were carried out to examine the spatial variability of ablation within the slump. In one set of experiments, pairs of ablatometers were set up around corners within the slump to monitor various orientations of the ice face (Figure 2). On sunny days, orientation affected the diurnal cycle of ablation. For example, peak ablation occurred

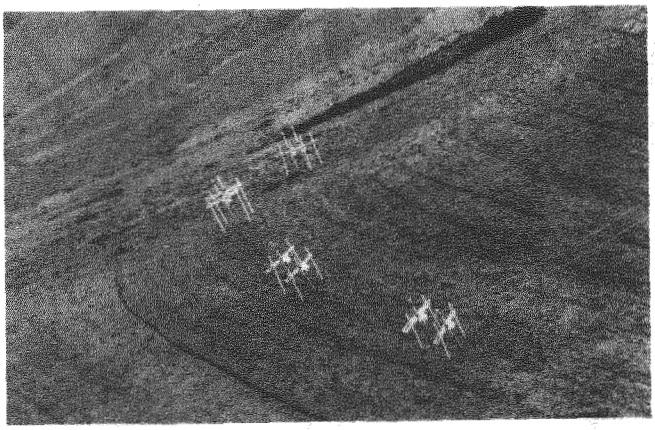

Fig. 2 Four pairs of ablatometers set up around a corner in the slump. Instruments were mounted orthogonally to the ice and 10 m downslope of the contact between ice and overburden.

TABLE I

Meteorological Equipment at Study Site

Meteorological Factor	Instrument
Global radiation (horizontal)	Pyranometer (Kipp and Zonen CM-10)
Diffuse radiation (horizontal)	Pyranometer (Kipp and Zonen CM-6 with shadow band)
Global radiation (over slump face)	Pyranometer (Kipp and Zonen CM-6)
Net all-wave radiation (over slump face)	Net radiometer (Middleton CN-2)
Net short-wave radiation (over slump face)	Net radiometer (Middleton CN-2)
Air temperature (1.5 m level)	Shielded thermistor (Campbell Scientific 101)
Wind speed (2 m level)	Cup anemometer (Met One Inc.)
Wind direction (2 m level)	Wind vane (Met One Inc.)
Precipitation	Tipping bucket rain-gauge (Weathermeasure P501-I)

at 12.30 h solar time (15.30 h local time) for ice with an orientation of 30°, but did not occur for a further 5.5 h for ice facing 290° (Figure 3). This pattern resulted from differences in the timing of maximum direct beam radiation onto each face and illustrates the potential importance of this component of the energy balance. On overcast days, however, incoming solar radiation became essentially isotropic. Consequently, variability in ablation across the ice was low and rates were greatly reduced (Figure 4). It is interesting to note that peak ablation occurred within a few hours of solar noon on all days despite the northerly orientation of the ice face.

Weather conditions affected not only the timing of ablation cycles but also daily totals for

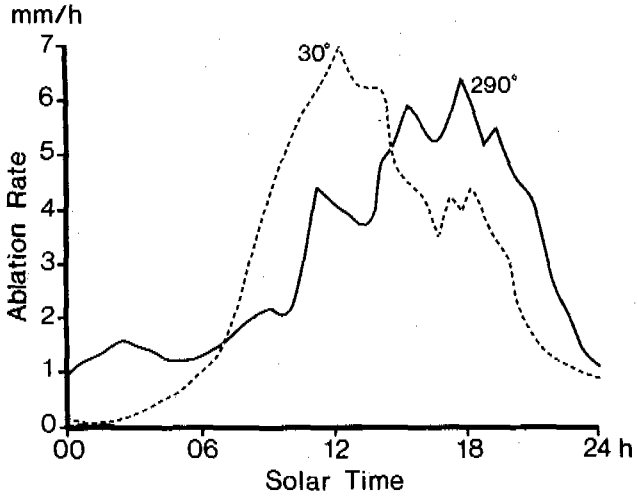

Fig. 3 Variation of ablation with orientation on clear days. Note: lines represent average readings from two ablatometers on July 15, 1985 (30° orientation at 30° slope) and July 22, 1985 (290° orientation at 35° slope).

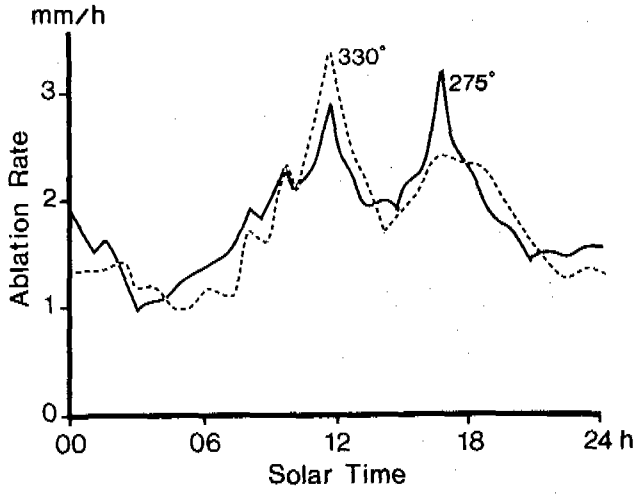

Fig. 4 Variation of ablation with orientation on overcast days. Note: lines represent average readings from two ablatometers on July 19, 1985 (275° orientation at 35° slope and 330° orientation at 33° slope).

different orientations (Table II). On clear days, the lowest amounts of ablation were recorded on ice facing due north, with increasing amounts on ice oriented towards the west and the east (e.g. July 22-23 and July 15-16). Lower rates for north-facing ice were partly the result of shading by the overburden for several hours around solar noon. The degree of variability in ablation decreased on clear days with higher air temperatures although rates could double (e.g. July 26-27). This indicates an increase in the importance of turbulent heat transfer relative to direct beam radiation. As noted above, ablation was slow and practically uniform around the slump on overcast days (e.g. July 19-20).

TABLE II

Effect of Orientation on Ablation

Date	Sky Condition	Air Temperature (°C)		Orientation (°)	Beginning of 24 h period (Solar Time)[a]	Daily Ablation (mm)
		Minimum	Maximum			
July 22-23	Mainly clear, occasional scattered clouds	1.0	9.0	270	0030	66
				290	0030	71
				340	0100	59
				360	0100	41
July 15-16	Clear	-1.0	9.0	355	0200	43
				30	0230	69
				55	0300	64
July 26-27	Clear	3.5	16.5	355	0030	96
				45	0030	103
				75	0230	117
July 19-20	Mainly overcast, occasional broken clouds	1.0	3.0	330	0430	43
				290	0430	41
				275	0430	39

[a] taken from time of rise in ablation rate.

The maximum 30-minute ablation rate recorded was 10.0 mm/h, corresponding to an ablation flux of 835 W/m^2. This was about 10% less than the highest rate measured at a site on Banks Island (Lewkowicz, 1986). The maximum 24-hour ablation was 117 mm on east-facing ice over July 26-27, a slightly greater value than that recorded on Banks Island, but less than previous measurements made in the Mackenzie Delta area (150 mm on Garry Island (Kerfoot, unpublished)) and near Mayo, Y.T. (155 mm (Burn, unpublished)).

A second set of experiments examined whether a trend existed in ablation rates down the ice face. The surface temperatures of water films on thawing ground ice can be above 0°C, and tend to increase downslope as a result of greater film thickness and the incorporation of soil particles (Mackay, 1978). Air to surface temperature gradients might therefore be reduced, causing diminishing sensible heat inputs and melt rates downslope. Greater melt near the top of the ice might also be caused by heat derived from the collapse of warm headwall material onto the face. Conversely, deepening water films downslope might convert greater amounts of kinetic energy into heat, leading to increasing ablation rates downslope. To examine the net effect of these influences, five ablatometers, with an orientation of 30° and a spacing of 2 m, were positioned in a row down the ice. The results of three days of measurements made under both clear and cloudy conditions are shown in Figure 5.

Although some differences in cumulative ablation did result from shading effects and variations in ice angle, no trend was present either towards increasing or decreasing ablation downslope. A further experiment on July 23-24, with ablatometers sited within rills in the ice and alongside them, gave the same result for the latter group. The importance of flowing water within the rills could not be assessed because ablatometers sited in them were hit frequently by large

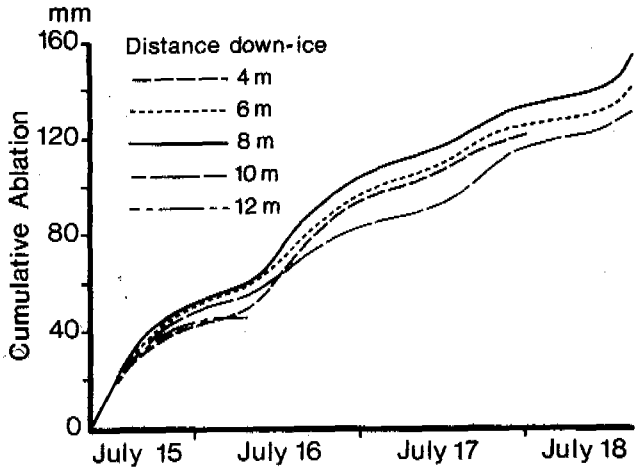

Fig. 5 Cumulative ablation in a downslope direction, July 15-18, 1985. Note: lines represent readings from single ablatometers oriented at 30° on ice slopes of 29° (4 m), 33° (6 m), 24° (8 m), 22° (10 m) and 18° (12 m).

tussocks moving downslope over the ice. These data suggest that while flowing water may affect ablation rates within drainage channels on the ice (e.g. Kerfoot, unpublished; Mackay, 1966), neither water films in general nor heated debris cause a significant downslope trend in ablation rates to develop.

Energy balance of the ice face

Ablation flux values were compared with a number of meteorological variables representing components of the energy balance in an effort to develop a predictive equation. A scatter diagram of Q_m versus Q^* values shows the expected strong positive relationship between the two variables but with more than 70% of the points lying above the 1:1 line (Figure 6). During most measurement periods, therefore, a substantial part of the energy used for ablation came from non-radiative sources. The size of the residual fluxes varied from a loss of 200 W/m^2 to a gain of 450 W/m^2 with a mean value of 87 W/m^2. The range is similar to that recorded previously on Banks Island (Lewkowicz, 1986), but both mean and modal values are about 50 W/m^2 higher at Peninsula Point, indicating that turbulent heat inputs are greater at this location.

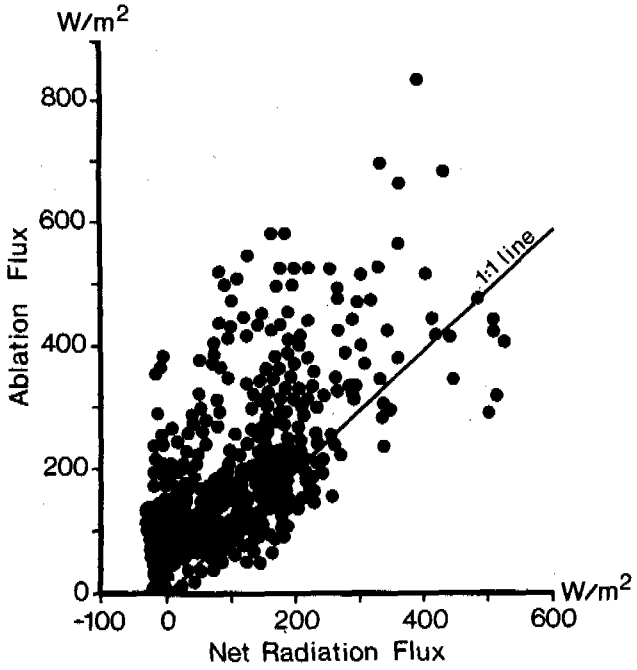

Fig. 6 Comparison of net radiation and ablation flux values. Note: data screened to remove points when simultaneous residual flux values differed by >80 W/m^2 (see text).

Figure 6 indicates that prediction of Q_m using only Q^* would result in a fairly high standard error. In order to reduce this error, the bulk transfer approach (e.g. Male and Grey, 1981) can be taken and factors representing air to surface temperature (T_a-T_s) and humidity gradients (e_a-e_s) together with wind speed (U_z), can be introduced into a multiple regression equation. Multiple regression is used rather than physically-based modelling,

because of the importance of horizontal advection of heat which results in an absence of well-developed vertical temperature and humidity profiles above melting ground ice (Pufahl, unpublished).

The results of a number of regression analyses performed on the complete data set (n=1057) of 30-minute ablation flux measurements are given in Table III. Q^* alone (Eq. 1) explains less than half of the variance in the ablation flux and as a single variable is less successful than T_a (Eq. 2). The linkage of U_z to T_a (Eq. 3) improves the explanation to 57%, and a still higher value of 72% is achieved if Q^* is re-introduced (Eq. 4). However, the further inclusion of the vapour pressure gradient (assuming that the vapour pressure over the ice was the saturation value at 0°C) did not result in a higher r^2 value (Eq. 5). This was surprising because field experiments with small ice lysimeters (100 mm diameter) produced an excellent correlation between their hourly latent heat flux and (e_a-e_s) multiplied by U_z (n=42, r^2=0.89). This apparent contradiction seems related to the small size of the lysimeters, which permitted only thin films of water to develop. Their temperature of interaction with the atmosphere must have been at or very close to 0°C. On the melting ice face as a whole, however, 0°C is the minimum boundary temperature and Mackay's (1978) results suggest that generally it will be higher than this. Thus the saturation vapour pressure will also be higher than 6.11 mbar, changing the calculated gradient between the air and the ice. It appears, therefore, that the ice lysimeters were not fully representative of the face and that this technique was not suitable for assessing the latent heat flux.

Since the minimum ice face temperature was 0°C, the mean temperature lay above this value. Step-wise multiple regressions were run with surface temperatures up to 5°C and corresponding saturation vapour pressures. The optimum r^2 value of 0.728 was achieved at a boundary temperature of 1.2°C (Eq. 6, Table III). An additional analysis of the 1984 Banks Island data (Lewkowicz, 1986) showed that a slight (<1%) improvement in statistical explanation could be achieved by assuming an average boundary condition of 1.5°C. Regression Eq. 6 (Table III) produces a relatively even scatter about the 1:1 line of observed versus predicted values of Q_m, with a slight tendency to underpredict in the high range (Figure 7). Compared to a similar equation developed for a site on Banks Island (Lewkowicz, 1986), the statistical explanation of Q_m achieved is about 7% less, the Q^* coefficient is lower and the turbulent energy transfer coefficient is higher. The lower r^2 value may be the result of making ablation measurements at a number of ice orientations and distances down-ice at Peninsula Point, while assuming L^* recorded at the top of the

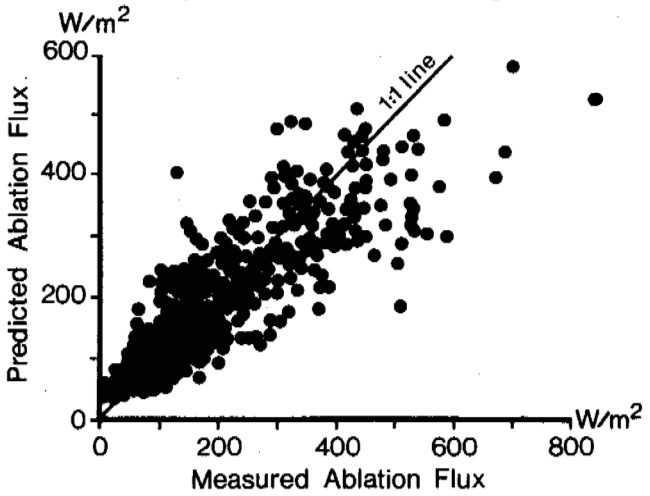

Fig. 7 Measured ablation flux versus predicted ablation flux. Note: predicted values obtained from multiple-regression equation No. 6 (Table III) using a surface boundary temperature of 1.2°C.

TABLE III

Regression Coefficients: Ablation Flux (Q_m) vs. Meteorological Factors

Regression Equation No.	r^2	Standard Error of Estimate	Regression Coefficients[a]				
			Q^* (W/m^2)	T_a (°C)	$U_z \cdot T_a$ (m°C/s)	$U_z(T_a - T_s + (e_a - e_s)/\gamma)$[b] (m°C/s)	Constant
1	0.448	80.87	0.80	n.u.[c]	n.u.	n.u.	102.63
2	0.488	77.87	n.u.	23.96	n.u.	n.u.	72.96
3	0.573	71.15	n.u.	n.u.	6.71	n.u.	47.90
4	0.719	57.67	0.51	n.u.	5.11	n.u.	36.32
5	0.688	60.81	0.59	n.u.	n.u.	3.30[d]	33.81
6	0.728	56.75	0.57	n.u.	n.u.	3.57[e]	44.29

Note: [a] all coefficients are significant at the 0.001 level (n=1057); [b] e_a values from Atmospheric Environment Service Weather Station, Tuktoyaktuk; γ is the psychrometer constant introduced to render the temperature and vapour pressure gradients dimensionally equivalent; [c] n.u. not used in regression; [d] surface boundary of 0°C; [e] surface boundary of 1.2°C.

face at a single location to be representative of all of the ice. Locations with warmer water films would likely experience elevated long-wave losses. In contrast, only minor variation was present in the orientation of the ice exposed in the slump studied on Banks Island and the maximum length of ice slope was about 4 m compared to >15 m at Peninsula Point.

The overall importance of net radiation as an energy source for ablation of the ground ice can be assessed by comparing the values of Q_m and Q^* used in the regression. Over the study period, net radiation on average contributed 47% of the energy necessary for ice ablation. Although the fieldwork was of short duration, it included a wide range of weather conditions, so that this figure is probably representative of the bulk of the summer thaw period. It can be compared with the estimate of at least 60% of the energy for melt being derived from net radiation, obtained using the same methodology in the Sand Hills moraine of Banks Island (Lewkowicz, 1986). The difference in results from the two sites is attributed partly to higher air temperatures and humidities at Peninsula Point which increase the magnitude of the turbulent heat inputs. In addition, the northward orientation of the ice combined with a higher albedo lead to a decrease in the magnitude of the net short-wave radiation. Overall, net radiation assumes lesser importance and turbulent energy transfer greater significance at Peninsula Point than on Banks Island.

CONCLUSIONS

Three main conclusions can be drawn from this study at Peninsula Point. First, orientation affected both the timing and total amount of ground ice ablation during periods with clear skies, but was not significant during overcast conditions. Second, a short-term trend in ablation rates downslope could not be detected. Third, in contrast to results obtained previously from southern Banks Island, turbulent energy exchange with the ablating ground ice was as important as radiative exchange. Consequently, both energy sources must be considered when developing methods to stabilise ground-ice slumps initiated in road or railway cuts.

ACKNOWLEDGMENTS

This study was supported by funds from the Natural Sciences and Engineering Research Council of Canada and a University of Toronto grant. Generous logistical support was provided by the Polar Continental Shelf Project, Energy, Mines and Resources, Canada, and by the staff of the Inuvik Scientific Research Laboratory. The author is grateful for the excellent field assistance of J.M.C. Lalonde. Comments from M.-K. Woo and an anonymous reviewer helped improve the original manuscript. The camera-ready copy was skilfully prepared by L. White.

REFERENCES

Burn, C.R. (unpublished). Investigations of thermokarst development and climatic change in the Yukon Territory. M.A. thesis, Carleton University, Ottawa, 142 pp.

French, H.M. & Egginton, P.A. (1973). Thermokarst development, Banks Island, western Canadian Arctic. Permafrost: the North American Contribution, 2nd International Conference, Yakutsk, U.S.S.R., 203-212, National Academy of Sciences, Washington, DC.

Kerfoot, D.E. (unpublished). The geomorphology and permafrost conditions of Garry Island, N.W.T.. Ph.D. thesis, University of British Columbia, Vancouver, 308 pp.

Lewkowicz, A.G. (1985). Use of an ablatometer to measure short-term ablation of exposed ground ice. Canadian Journal of Earth Sciences (22), 1767-1773.

Lewkowicz, A.G. (1986). Rate of short-term ablation of exposed ground ice, Banks Island, Northwest Territories, Canada. Journal of Glaciology (32), 511-519.

Lewkowicz, A.G. (1987). Headwall retreat of ground-ice slumps, Banks Island, Northwest Territories. Canadian Journal of Earth Sciences (24), 1077-1085.

Mackay, J.R. (1966). Segregated epigenetic ice and slumps in permafrost, Mackenzie Delta area, N.W.T. Geographical Bulletin (8), 59-80.

Mackay, J.R. (1971). The origin of massive icy beds in permafrost, western Arctic coast, Canada. Canadian Journal of Earth Sciences (8), 397-422.

Mackay, J.R. (1978). The surface temperature of an ice-rich melting permafrost exposure Garry Island, Northwest Territories. Current Research, Part A, Geological Survey of Canada Paper (78-1A), 521-522.

Mackay, J.R. (1986). Fifty years (1935-1985) of coastal retreat west of Tuktoyaktuk, District of Mackenzie. Current Research, Part A, Geological Survey of Canada Paper (86-1A), 727-735.

Male, D.H. & Gray, D.M. (1981). Snowcover ablation and runoff. Gray, D.M. & Male, D.H. (eds.), Handbook of snow: principles, processes, management and use, pp. 360-436, Pergamon Press, Toronto.

Pollard, W.H. & French, H.M. (1980). A first approximation of the volume of ground ice, Richards Island, Pleistocene Mackenzie delta, Northwest Territories, Canada. Canadian Geotechnical Journal (17), 509-516.

Pufahl, D.E. (unpublished). The behaviour of thawing slopes in permafrost. Ph.D. thesis, University of Alberta, Edmonton, 323 pp.

Pufahl, D.E. & Morgenstern, N.R. (1980). The energetics of an ablating headscarp in permafrost. Canadian Geotechnical Journal (17), 487-497.

HYDROGEOLOGICAL FEATURES IN HUOLAHE BASIN OF NORTH DAXINGANLING, NORTHEAST CHINA

Lin, Fengton and Tu, Guangzhong

The Forestry Design and Research Institute of Heilongjiang Province, China

SYNOPSIS Hydrogeologically, the Huolahe basin is characterized by that the whole basin is underlain by subpermafrost water while the water rich zone is just concentrated along the geologic-structurally shattered zone. Geological structure controls the quantity of groundwater and permafrost functions as a modifier to the recharge, runoff and discharge of the subpermafrost water.

Huolahe basin is located in permafrost region of the northern Daxinganling. The mean annual air temperature in this area is -4.9°C, and the minimum temperature in winter is as low as -52.3°C. Cracks in clastic rocks spread locally due to the geological structure.

FORMATION AND FEATURES OF THE ARTESIAN BASIN

Groundwater in permafrost region, its distribution, recharge, runoff, and discharge, differing from that in non-permafrost region, is strictly restricted by permafrost. The anthors try to discuss the hydrogeological characteristics of the basin as follows.

Talik-geological structure recharge system

It has been well known for several decades that the higher the continuity of permafrost, the less the recharge of the groundwater. Subpermafrost water can not directly get vertical recharge from precipitation because of the widespread cover of permafrost. Within this basin, only through taliks and geologic—structurally shattered zone surrounding the basin can rainfall and surface water soak downwards untill it reaches the subpermafrost water table, and then the penetrated water stores in pores and cracks in sedimentary rocks (Fig.1).

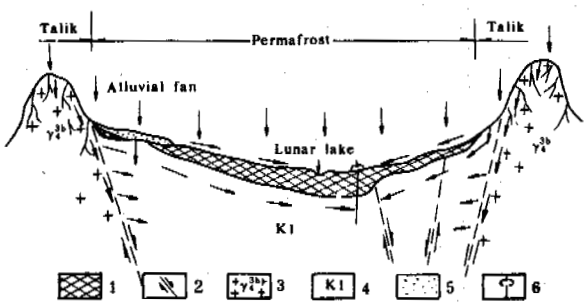

Fig.1 Recharge Mechanism of Subpermafrost Water in Huolahe Basin
1—Permafrost; 2— Fault; 3—Granite; 4—Cretaceous strata; 5—Quaternary sand; 6—Artesian borehole.

Store-runoff system of Subpermafrost water

The geological structure, pores and cracks, especially structure cracks, are widespread in coal-bearing strata. These pores and cracks provide spaces for the distribution of groundwater. Quaternary ice age brought frost climatic environment to the basin, and permafrost was formed. With the increase of permafrost thickness, water-bearing conditions has changed. As a result, the aquifer descented, and this gave rise to the artesian characteristics to subpermafrost water. The movement and runoff of groundwater in pores and cracks under permafrost base form the pore-crack store and runoff system. As mentioned above, permafrost as a frost aquifuge, is an important factor for the changes of ground water movement pattern, while geological structure is a basic factor in providing the spaces for the store and migration of groundwater.

Structure-talik discharge system

The distribution of permafrost not only controls the recharge and movement of groundwater but also hinders the discharge of subpermafrost water within the basin. The isopiestic lines of subpermafrost water (Fig.2) show that subpermafrost water finally accumulates in the southern part of the basin, near the Luner lake, flows through geological structurally shattered zone to the talik area outside the basin.

HYDROGEOLOGICAL FEATURES OF THE BASIN

Huolahe basin has its own particular systems of recharge, runoff and discharge, compared with non-permafrost areas (Lin, 1985).

Effects of permafrost on the depth of aquifer

Groundwater in the basin exists in pores and cracks in conglomerate, sandstone and shale of Cretaceous system under permafrost base, belong-

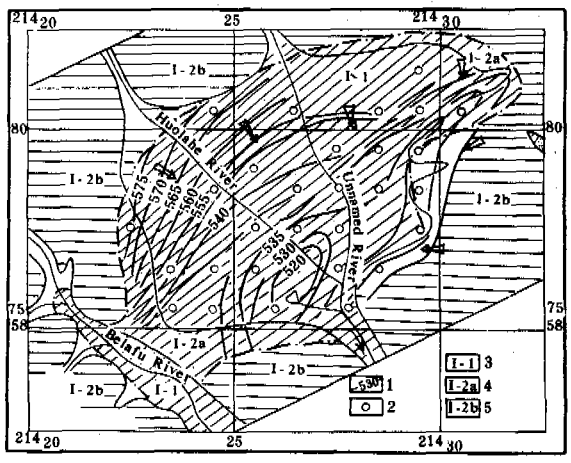

Fig.2 Isopiestic Line of Subpermafrost Water in Huolahe Basin

1. Isopiestic line and its altitude;
2. Suprapermafrost water;
3. Subpermafrost water;
4. Subpermafrost water.

ing to pore-crack type. In other words, permafrost layer increases the buried depth of ground water. Thus, with the increase of permafrost thickness from the fringe to the center of the basin, the depth of subpermafrost aquifer increases accordingly, ranging from 15 to 55 m in the fringe area, and 70 to 130 m in the center.

Artesian characteristics of subpermafrost water

The thickness of permafrost within the basin ranges from 70 to 130 m. So thick an impermeable layer confines the spaces for the ground water, and results in the high piezometric head of groundwater in artesian well. The highest piezometric head is 10.58 m above ground surface. Large artesian flow and high pressure are the main hydrogeological features of the artesian basin (Table I).

Distribution and accumulation of subpermafrost water

That the subpermafrost water exists everywhere and accumulates along the fault shattered zone is one of the obvious features of the basin. Generally, subpermafrost water was incountered in every borehole, with a different hydraulic discharge. For example, the artesian discharge in some boreholes reaches 2000-3000 tons per day, while pump discharge of some other boreholes is less than 10 ton per day. Table II shows boreholes with abundant discharge (1000-3000 ton per day), small drawdown (less than 10 m), and large specitic capacity (from 1.0 to 10 1/s·m) as well as stable water level. Boreholes in Table II are near or within structurally shattered zone with linear accumulation of subpermafrost water. This is a special kind of water-bearing strata, in which groundwater exists in the cracks, especially in tectonic cracks. Boreholes often influence on each other in some way hydraulically, for example, borehole HZ-14 is about one kilometer away from HZ-15, and both of them are artesian boreholes with large artesian discharge. When the water began to errupt from HZ-14, the piezometric head of HZ-15 decreased obviously, and so did S_5 and HZ-15. The distribution of subpermafrost water is controlled by the geological structures. The boreholes with pump discharge ranging from 100 to 1000 tons per day, generally from 300 to 400 tons per day are listed in Table III. These boreholes are characterized by their large drawdown of from 20 to 50 m, and small specific capacity with not too large pump discharge indicates the characteristic of pore-water filling in the pore spaces of sandstone and conglomerate. Table IV lists boreholes with small pump discharge less than 10 tons per day, large drawdown, more than 50 m, and small specific capacity, less than 0.005 1/s·m. This might result from two reasons, first, these boreholes exist within the structurally squeezed zone with relatively closed cracks, therefore there is not enough crack spaces for the groundwater, secondly, the boreholes are in thick shale with little cracks and pores.

Zonation of subpermafrost water in hydrogeochemistry

Water within the basin is of HCO_3-Na type, with minerlization of less than 0.3 g/l and PH value from 7 to 9. It belongs to low mineralized fresh groundwater. Around the fringe of the basin, subpermafrost water is HCO_3-Ca.Mg type, with a mineralization of from 0.1 to 0.2 g/l and PH value of about seven. This type of subpermafrost water is similar to suprapermafrost water or surficial water chemically, this suggests that the subpermafrost water is supplied by the latter. The trend of mineralization increase from the fringe to the center of the basin also indicates that the subpermafrost water gets its recharge from the talik surrounding the basin and accumulates within the basin, and finally discharges through the south mouth of the basin.

The bicarbonate types of subpermafrost water reflect the hydrogeological characteristics of abundant recharge, good runoff and cycle conditions as well as good water quality for water supply.

CONCLUSIONS

The Huolahe basin has large subpermafrost resources. The activity of groundwater favors the degradation of permafrost, and in return , the degradation provides more spaces for the movement and store of subpermafrost water.

Subpermafrost water existing throughout the basin and accumulating linearly along geological structurally shattered zone are the main hydrogeological features of the frost basin.

Geological structure controls the movement and accumulation of subpermafrost water, meanwhile, permafrost functions as a modifier to the pattern of recharge, runoff and discharge of sub-

TABLE I

Hydrogeological Features of Artesian Boreholes in the Basin

Borehole No.	HZ-15	HZ-27	HZ-14	HZ-8	HZ-13	HZ-16	HZ-12-1	HS7	HS1
Groundwater level above the surface (M)	10.85	2.45	3.25	1.34	5.77	0.19	8.67	4.51	7.84
Potential head (M)	116.58	85.35	127.25		142.27	>70	75.34	167.31	117.26
Artesian flow (T/D)	2706.7		1651.0		432.0	<10	1846	668.3	256.61
Permafrost and groundwater	Contacted			Uncontacted		Contacted		Uncontacted	
Permafrost base (M)	106	77.9	110	72	122.6	≥70		112	109

TABLE II

Pump Discharge of Some Boreholes

Borehole No.	HZ-1	HZ-2	HZ-6	HZ-7	HZ-10	HZ-11	Hz-14	HZ-15	HZ-20	HZ-27	HZ-23
Pump discharge (T/D)	1002.2	911.1	1229	1845	985.2	1627	1651	2706	1229	2768	1054
Drwndown (m)	2.5	1.64	4.54	4.56	13.14	0.26	1.51	5.75	5.73	8.67	22.0
Specific capacity (1/s·m)	4.64	6.43	3.13	4.68	0.87	72.5	12.66	5.45	2.48	3.7	0.56

TABLE III

Boreholes with Pump Discharge of 100-1000 T/D

Borehole No.	HZ-8	HZ-9	HZ-12	HZ-13	HZ-18	HZ-19	HZ-21	HZ-25	HZ-28
Pump discharge (T/D)	330.1	668.2	256.6	432.2	107.4	453	392.2	217.9	401.9
Drwndown (m)	45.56	24.84	48.97	4.67	50.04	44.51	41.3	46.35	46.96
Specific capacity (1/s·m)	0.084	0.311	0.061	1.07	0.025	0.118	0.110	0.054	0.099

TABLE IV

Boreholes with Pump Discharge of Less Than 10 T/D

Borehole No.	HZ-3	HZ-4	HZ-16	HZ-17	HZ-24	HZ-26
Pump discharge (T/D)	5.36	19.87	6.99	<10	<10	6.91
Drwndown (m)	50.57	>66	>52	>65	>65	41.37
Specific capacity (l/s·m)	0.0012	0.0035	0.0016	0.0018	0.0018	0.0019

permafrost water.

REFERENCE

Lin Fengtong, (1985). Evaluation method and features of crack-water in bedrocks of Daxinganling Continuous permafrost region. Journal of Glaciology and Geocryology, (7), 3, 221.

SHALLOW OCCURRENCE OF WEDGE ICE: IRRIGATION FEATURES

A.A. Mandarov[1] and I.S. Ugarov

[1]Permafrost Institute, Siberian Branch of the U.S.S.R. Academy of Sciences, Yakutsk, U.S.S.R.

SYNOPSIS Many years of investigations have established that sprinkler irrigation, with judicious irrigation rates, does not lead to thawing of wedge ice residing at a little depth which occurs, in particular, in the valley of the Amga River in Central Yakutia, the area that has received extensive development over the past several years. Increased irrigation rates can cause deformations of the arable land surface due to ground subsidence above melted ice veins and wedges. Irrigation canals present the greatest hazards in this regard because they contribute to increasing the rate of thaw for such ice; therefore, in such a situation, preference should be given to closed distributors (pipelines).

The need for development of new areas for the arable land designed to satisfy the demand of the population for agricultural products is dictated by the constantly-increasing development of newly-discovered deposits of valuable minerals, construction of industrial and transportation projects, and by the associated intense growth rate of the population in northern and eastern regions of the country. Yakutia is one such region of the country, with its central areas being the main granary. Because of the severe continentality of climate here the arable land suffers droughts and is in need of improvement through irrigation. In this situation attention is focused on development of new areas in valleys of major and medium-sized rivers which are reliable water sources for irrigation meliorations. In recent years much work has been done in Central Yakutia on developing the Amga River valley where sown parcels for haymaking, pastures and arable fields for cereal and forage crops are being created. In the years to come, it is planned to develop here as many as 30 thousand of hectares of the virgin lands.

From the standpoint of geocryology the main feature of this territory is that wedge ice occurs close to the sunlit surface.

Results of engineering-geological surveys obtained by "Yakutgiprovodkhoz" for 20 districts totaling more than 5 thousand ha in area as well as the aerial photo interpretation for the entire valley of the Amga River have indicated that ground ice occupies 20 to 90% of the area of vast (both existent and being developed) tracks of arable land (Gavril'ev et al., 1984). In the area of Khospokh , for example, ground ice occurs throughout 200 to 220 ha (50%); 80 ha (80%) refer to the Kenide-Terde locality, 280 to 300 ha (70%) refer to the Batyuntsy locality, and 250 ha (80%) are occupied by ground ice in the Noyan locality.

Besides, predominant occurrence applies to wedge ice residing at a depth of 1.2 to 2 m, having a width of 0.8 to 2 m on the top and a thickness between 2 and 5 m. The density of the ice polygonal lattice is, on the average, 5 or 6 longitudinal and 6 to 8 transverse rows per ha. Such a kind of ice is well developed on elevated flood-lands and on terraces above flood-lands which are the most valuable arable tracts for State farms.

Whenever the thawing depth, at the time melioration activities are being carried out, exceeds the occurrence depth of ground ice, formation and development of thermokarst processes should be expected to take place in the areas being meliorated; as a result, within the first 5 to 10 years of development of the locality ground surface subsidence is able to occur, in the form of ditches over the polygonal lattice of wedge ice. If, then, the amount of precipitation does not exceed 0.2 or 0.3 m, this will be not hazardous, provided that the ground surface is ploughed and leveled every year. As the thawing depth increases by 0.5 m and more, deep ditches are produced above ground ice as a result of melioration so that in order to restore the field, it is necessary to add soil brought from other localities to subsidence-produced ditches as well as plane the surface smooth, but this may turn out economically unprofitable.

In 1983, in an effort to develop irrigation regimes for applications where wedge ice occurs at small depths, the Permafrost Institute embarked upon investigations of the water-thermal regime of soils in the valley of the Amga River, in areas allotted for forage crops.

The experimental field is situated on the elevated flood-lands along the Amga River that is flooded by high waters of the river once every 8 to 10 years. The total area of the field is 80 ha, including 46 ha occupied by experimental plots of land (of the size 20x25 square meters) in which studies have been made of ir-

rigation regimes of forage crops, which occupied an area of about 10 ha. The irrigation regime for three forage crops was studied, namely oats Yakutsky, sunflower and colza from the Canadian selection, Candle (rape). The influence of irrigation regimes upon crop capacity was studied for mineral fertilizers $(NPK)_{90}$, and comparisons were made with the variant without irrigation, but with the same amount of fertilizers applied.

A field group from the Permafrost Institute of the Siberian Branch of the U.S.S.R. Academy of Sciences made observations of the water-thermal regime of soils in 7 lots: lot 1 - virgin-land area of a miscellaneous-grass meadow; lot 2 - oats without irrigation; lot 3 - oats with irrigation in the case where the soil moisture has decreased to 70% of the minimum moisture capacity (MC); lot 4 - rape without irrigation (for 1985, sunflower without irrigation); lot 5 - rape with irrigation in the case where the soil moisture has decreased to 70% of MC (for 1985, sunflower with irrigation in the case where the soil moisture has decreased to 70% of MC); lot 5a - same as 5 but for the ice wedge; and lot 6 - bare fallow.

The soils of the stationary, experimental field refer to permafrost, meadow-black-earth, weakly saline (up to 0.15%) soils of the sulphate-carbonate type, with a weakly-alkaline reaction of a lightly- and moderately-suglinok-like composition, and with the predominance of coarse dust. Such soils provide high crop yields, without desalination and pH control, and are favourable for growing forage crops, provided that mineral fertilizers and irrigation are applied.

The soils throughout the area of the stationary field show a small volumetric mass, which is attributable to the great content of organic material in the soil. Only in the virgin-land plot as deep as 0.5 m does the volumetric mass reach 1160 to 1260 kg m^{-3}; in all plots of the arable land, however, it does not exceed 900 to 1000 kg m^{-3}, and below 0.5 m in all of the plots it varies within 1000 - 1100 kg m^{-3}. Owing to the diversity of the mechanical composition, combined with the different content of organic material in the soil, the value of the maximum moisture capacity is characterized by broad variations, in both the area of the stationary field and depth.

Below 2 m the flood-lands are composed of stratified sands and suglinoks, while aleurites containing as much as 20 to 28% of clay particles are predominant as deep as 5 m. Earth materials show a comparatively high ice content, up to 30-40% against dry weight, and a lens-shaped structure, but a massive structure in sands. Wedge ice occurs throughout the area at depths between 1.55 and 1.65 m, having a width of 0.8 to 1.2 m on the top and a thickness as great as 2 to 4 m; the size of polygons is 5 or 6 m in width and 6 to 8 m in length.

With low initial moisture of the soil, irrigation causes a small reduction in the temperature of the upper 0.2 to 0.4 m layer of the soil and a temperature increase in the lower part of the seasonally thawing layer, and is even capable of increasing the thawing depth by 0.1 or 0.2 m. With initial moisture in excess of the minimum moisture capacity, there, on the contrary, is a slight temperature decrease within the lower part of the unfrozen layer. Besides, the thermal effect of irrigation also depends on its amount (rate) - the larger the amount of water supplied to the soil, the greater is the effect because during the summer time water temperature generally is above the soil temperature at depths below 0.3 or 0.4 m.

Shadowing of the soil surface is of major importance for the temperature regime of soils. Typically, within the first 10 to 15 days after sowing forage crops, the soil surface temperature on the arable land, averaged over many days, is by 2 to 4°C higher as compared to a meadow. As the crops in the field evolve into the bushing-out phase, the degree of shadowing of the surface approaches that of the meadow, and this causes their temperatures to equalize as well. As the forage crops grow further, the field surface decreases in temperature and becomes lower as compared with the meadow, due to the increasing degree of shadowing.

In the second half of vegetation the daily mean surface temperature under non-irrigated crops is by 2 or 3° lower than that for the meadow and is 3 to 5° as low under irrigated crops. On fair days at noon the surface temperature for forage crops in that period is 5 to 7° lower as compared to the meadow, while following irrigation this difference reaches 12 to 15°.

Such a decrease in surface temperature due to irrigation contributes to slower thawing of the soil in the second half of vegetation. Therefore, the greatest depth of thawing on a field (1.65 to 1.75 m) does not exceed its value on a virgin-land plot (1.74 to 1.76 m). The thawing depth beneath a wedge of ice does not increase either (lot 5a). According to observations for the period 1984-1985 it is between 1.48 and 1.54 and does not reach the upper edge of the wedge ice. Such a small amount of thawing is accounted for by the fact that ice-rich soils (up to 40-60% of the weight of dry soil) occur above the ice wedge near its upper surface, and the thawing rate decreases abruptly as early as mid-July - early August. As a rule, throughout the entire summer period the soil moisture above the ice wedge is higher as compared with the center of the polygon.

Thus, three years of investigations have shown that sprinkler irrigation, with judiciously applied irrigation rates, does not lead to thawing of the ground ice under conditions of the valley of the Amga River. A most appropriate irrigation rate implies such amounts of water which are necessary to achieve the minimum moisture capacity (MC) of a soil layer of a maximum thickness of 0.5 m where roots of annuals mostly occur. Under conditions of the Amga River valley, for the most commonly occurring kinds of soil during sprinkler irrigations which are carried out when the soil moisture within the upper 0.5 m layer has decreased to 70-80% of MC, this rate varies in the range from 250 to 300 m^3 per ha.

Irrigations with smaller rates fail to provide soil moisture optimum for the growth and development of crops or more frequent waterings are required, in order that the soil moisture should not decrease below optimum moisture, equal to the capillary rupture moisture (CRM), or 70% MC. Irrigations with far greater rates, however, lead to moistening (and, accordingly, to a temperature increase) of deeper layers accompanied by an increase in the thawing depth. This, in turn, may cause the near-lying wedge ice to thaw out. As the infiltration water reaches the surface of this ice and begins to filter through it, the thawing-out rate can be intensified because ice veins overlie intensively filtering, humus-rich veins of the soil.

The thawing-out of ground ice is often, to a great measure, accompanied by deformations of the arable land surface caused by soil subsidence over the thawed ice veins. Thus, high rates of irrigation are fraught with major hazardous consequences and should be avoided.

Wedge ice presents particularly serious hazards, while occurring close to the surface, in the case where open irrigation canals are being utilized. When such a canal has a depth of 0.8 to 1 m, there remains only 0.5 to 0.7 m of soil from the surface of this ice to the bottom of the canal. Moreover, this soil is often composed of very mellow earth materials, because these are formed by humus-rich soils washed away from the surface layers which fill frost cracks appearing every year. As the water fills the canal, it infiltrates very rapidly through such formations upward to the surface of ice veins, giving rise to intense filtration along them through loose, humus-rich veins, which, in turn, causes fast thawing of the upper terminations of wedge ice. This can entail its precipitous thawing-out, not only under the canals but also beneath the arable land, ultimately leading to deformations of the cultivated field surface and, on some occasions, to complete deterioration of the field due to deformations not amenable to subsequent improvement by levelling.

In order to avoid such detrimental processes, it is necessary to apply special-purpose methods of building such canals which would rule out the possibility of water losses in the canal as well as its penetration to the surface of ground ice. As far as this kind of arable land, with near occurrence of ground ice, is concerned, the most advantageous method of water supply to sprinkler irrigation facilities is to utilize enclosed-type distributors and main conduits composed of metal and plastic pipes.

As regards the arable land with close occurrence of ground ice, a major hazard is associated with the filling and prolonged retention of water within enclosed, inclined sections of the pipeline, which also causes this kind of ice to thaw out. This may be brought about by water leakage from pipelines as well as during surface drainage from the fields being irrigated due to great rates of sprinkler irrigation. Therefore, it is necessary to carry out preliminary levelling operations in such low areas by adding the soil brought from other localities; moreover, strict attention is mandatory to avoid water leakage from conduits, sprinklers and sprinkling installations.

Thus, the present investigations have demonstrated that, even with a very close occurrence of wedge ice, sprinkler irrigation of forage crops, provided that optimum irrigation rates are maintained, does not create conditions for such ice to thaw out, which, otherwise, cause detrimental processes to evolve.

REFERENCES

Gavrilyev, P.P., Mandarov, A.A. and Ugarov, I.S. (1984). Gidrotermicheskie melioratsii selskokhozyastvennykh ugodiy v Yakutii, Novosibirsk, Nauka, 201 p.

SOIL INFILTRATION AND SNOW-MELT RUN-OFF IN THE MACKENZIE DELTA, N.W.T.

P. Marsh

National Hydrology Research Institute, Canada

SYNOPSIS A field study of snow-melt run-off was carried out in a lake basin in the Mackenzie Delta, N.W.T. The strong negative soil heat flux delayed the arrival of melt water at the snowcover base by refreezing water as ice layers and columns in the snow. Once melt water reached the snowcover base, most infiltrated the soil. However, even though the soil was below 0°C, only a small portion of the melt water which infiltrated the active layer refroze. As a result, the soil warming, due to the release of latent heat of fusion, was not as large as would be expected if all the melt water had refrozen. The large soil infiltration also limits snow-melt run-off, which has important implications to the hydrology of lakes in the Mackenzie Delta.

INTRODUCTION

Run-off from seasonal snowcovers is an important source of water in many alpine and northern environments (Church 1974, Marsh and Woo 1981, Woo et al 1983). Studies of snow-melt run-off in temperate regions have concentrated on warm snowcovers underlain by unfrozen soil (eg. Anderson 1976, U.S. Army 1956, Colbeck 1976), where the influence of the soil is minimal and soil heat flux is small. Under these conditions, snow-melt run-off begins when the irreducible liquid water content of the snowcover is filled, and the snow is warmed to 0°C. This is not the case for snowcovers underlain by soils with temperatures below 0°C.

Until recently, frozen soil was considered to be an impermeable barrier which had little influence on the metamorphism of the overlying snowcover. Recent studies, however, have demonstrated that infiltration into seasonally frozen soils (Kane 1980, Gray et al. 1985, Granger et al. 1984), and soil heat flux may be important (Marsh and Woo 1987). Since the ground in permafrost environments is below 0°C at the beginning of the snow-melt period, soil heat flux removes a significant amount of energy from the snowcover throughout the melt period (Marsh and Woo 1984, 1987). This increases the freezing of melt water into ice layers and ice columns in the snow, ensures that much of the soil infiltration freezes, and may result in the formation of basal ice. As a result of these processes, it is necessary to consider the combined snow-soil system in order to predict the initiation and volume of snow-melt run-off. In permafrost regions, snow-melt run-off may not occur until after the liquid and thermal capacity of the snow and soil are filled (Marsh and Woo 1984).

The purpose of this paper is to demonstrate the importance of the cold, underlying soil in delaying and limiting snow-melt run-off in permafrost environments.

STUDY AREA AND METHODOLOGY

Field work was carried out at a small (0.069 km^2) lake (unofficial name NRC Lake) approximately 5 km southwest of Inuvik (Marsh 1986). NRC Lake is perched above the surrounding Mackenzie River distributary channels. The basin surrounding this lake is 0.43 km^2 in area, and is covered by an open, mature spruce forest. The zone beneath the lake is unfrozen, while the permafrost is in excess of 80 m in thickness beneath the land areas surrounding the lake (Johnston and Brown 1964), and the active layer is up to 0.5 m deep by late summer. The soils are silts with an organic content of between 15 and 30%.

In the Inuvik area, mean annual precipitation is 266 mm, of which 57% occurs as snow. Snow-melt is initiated in mid May when air temperatures rise above 0°C. Spring flood water from the Mackenzie River is the primary source of water for NRC Lake. Higher-elevation delta lakes which do not flood annually experience declining water levels between flooding events (Marsh 1986).

Daily changes in the soil moisture profile were determined at 3 sites at NRC Lake using a twin probe gamma density meter. Individual measurements at 5 cm increments are accurate to ± 2 mm of water. In addition, snow and soil temperatures were measured at each of these sites. Snow depth and density measurements were taken to determine mean snowcover water equivalent, and changes in snowcover properties were monitored daily at two snow-pits using the method described by Marsh and Woo (1987). Measurement of NRC Lake stage provided estimates of melt run-off from the surrounding basin.

Micrometeorological measurements were made at a height of 1 m above the snow surface. A Campbell CR21 data

logger recorded air temperature, relative humidity, wind, net radiation, and precipitation. Hourly averages of these parameters were obtained from measurements taken at 60-second intervals. Surface snow-melt was calculated using the bulk transfer approach (Price and Dunne 1976, Heron and Woo 1978, Moore 1983).

SNOW-MELT RUN-OFF

The snow-melt period may be divided into two well-defined intervals. The first begins at the start of melt and continues until the entire snowcover has been warmed to 0°C, and has been wetted (Figure 1). The second continues until the snowcover has been depleted. It is during this second period when snow-melt run-off may occur. In 1986, the initial warming and wetting of the snow-pack covered the period May 28 to May 31, and the snowcover was depleted by June 4. The remainder of this paper will deal primarily with the 1987 melt season, when the two periods were May 22 to 26 and 27 to 31 respectively.

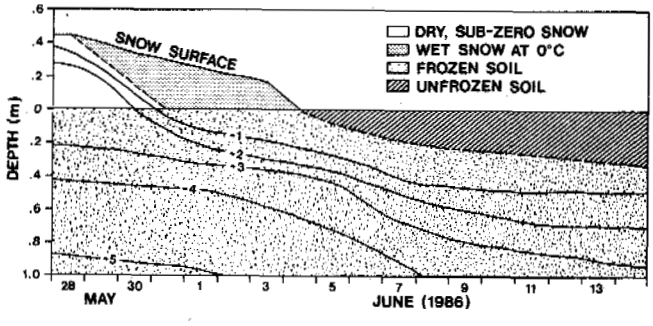

Figure 1. Changes in snow and soil temperatures during the snow-melt period in 1986. Note that the melt period can be divided into two intervals, the first from May 28 to May 31 when the snowcover is warming to 0°C and is being wetted, and the second continuing to June 4 when the snowcover is depleted.

Initial metamorphism of the snow cover

During this phase of the snow-melt period, warming of the snow and soil plays an important role in delaying the arrival of melt water at the snow base. Between May 22 and May 26 conduction through the isothermal surface snow layer (Figure 2) was negligible, and therefore the only source of energy available to warm the snowcover was from the release of latent heat of fusion due to the freezing of water as ice layers and ice columns within the snowcover. The freezing of 3 mm of water supplied the 0.9 MJ/m^2 of energy that was required to warm the snowcover to 0°C (Figure 2 and Table 1).

Of much greater importance in delaying the snow metamorphism between May 22 and May 26, however, was the large soil heat flux. Calculation of the change in heat storage in the top metre of the soil (Figure 2), and the heat conduction below 1 m, show that there was a soil heat flux of 7.2 MJ/m^2 (Table 1) during this period. This soil heat flux was driven by the freezing of 21 mm of water within the snowcover and the conduction downward into the soil of the released latent heat.

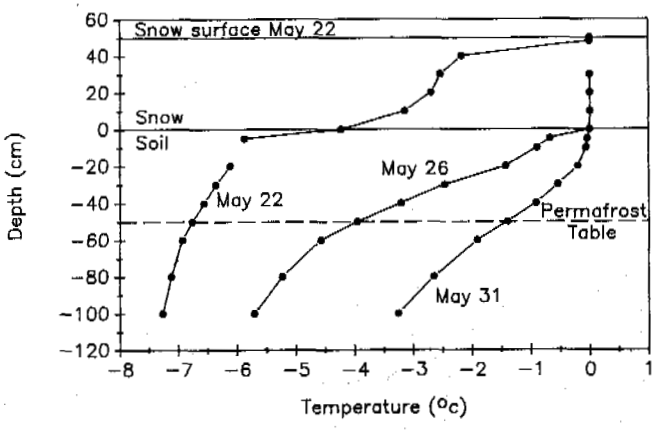

Figure 2. Snow and soil temperatures at the start of snow-melt (May 22), when melt-water first reached the snow pack base (May 26), and at the end of snow-melt (May 31) in 1987.

Date	Snow-melt		Snow cold content		Soil heat flux		Snow liquid water storage	Total
	MJ/m^2	mm	MJ/m^2	mm	MJ/m^2	mm	mm	mm
22-26 May	15.0	45	0.9	3	7.2	21	26	50
27-31 May	26.3	79	0	0	7.7	23	0	23
TOTAL	41.3	124	0.9	3	14.9	44	26	73

Table I. Surface snow-melt, and the energy required to account for the observed warming of the snow and soil in 1987.

In addition to the 24 mm of water which froze within the snowcover, an additional 26 mm of melt water filled liquid storages in the snow-pack. The combination of refreezing and filling of liquid storages delayed the arrival of melt water to the snowpack base by 4 days. Approximately half of this delay was due to the soil heat flux alone.

Soil infiltration

Once melt water reaches the snow-pack base, it may either run off laterally or infiltrate the soil. Field observations in both 1986 and 1987 suggest that the majority of the melt water at the Mackenzie Delta study sites infiltrates into the soil and there is a minimal amount of surface run-off. For example, liquid water was not observed draining from any late lying snow patches, and ponded surface water occurred only in a few larger depressions. A small rill draining into

NRC lake had no surface flow in 1986 and only a small volume of flow in 1987. In addition, no basal ice was observed in 1986 and only small isolated patches in 1987. These observations suggest that the infiltration capacity of the soils was not exceeded in 1986 and was exceeded only in a few locations in 1987. The mean infiltration capacity of these frozen soils is probably between the mean pre-melt snow-pack water equivalent of 51 mm in 1986 and 139 mm in 1987. The gamma soil density measurements, which were carried out in 1987, substantiate these visual observations. At each measurement location, water infiltrated throughout the total thickness of the active layer (Figure 3) and total infiltration was 52, 61, and 111 mm with a mean value of 75 mm. At the gamma measurement sites, the mean premelt snow water equivalent in 1987 was 92 mm. However, surface energy balance calculations indicate a total sublimation of 8 mm. Therefore, only 84 mm of water was available for infiltration. Considering the errors involved with measuring soil water storage for a profile 40 cm in thickness, the measured mean soil infiltration of 75 $\pm$ 16 mm is essentially equal to the available snow water equivalent of 84 mm. Since the soil was always below 0°C during this period (Figure 2), little of the water was available for run-off to the lake. This is supported by the small volume of visible run-off to the lake and by the nearly constant lake level over the melt period.

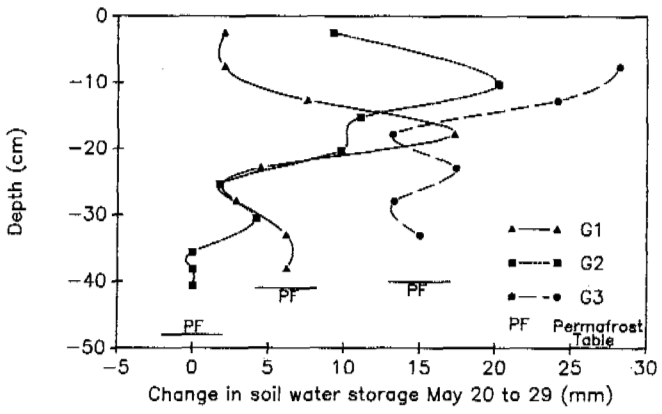

Figure 3. Changes in soil moisture between May 20 and May 29, 1987.

The soil infiltration also played an important role in the warming of the active layer and underlying permafrost during the May 26 to 31 period. Since the snowcover was isothermal at 0°C during this period (Figure 2), heat conduction downward from the snow surface to the underlying soil was impossible. The only source of energy was the movement of water downward into the soil, and its resultant refreezing and release of latent heat. Since the water infiltrated deeply into the soil (Figure 3), it provided an efficient mechanism for energy transfer. However, the change in soil heat storage indicates that not all the infiltrated water refroze. The calculated change in heat storage of 7.7 MJ/m^2 (Table 1) required the freezing of only 23 mm of water within the soil. The remainder of the infiltrating water (52 mm of the 75 mm which infiltrated the soil) did not freeze. As shown by other studies (eg. Scott 1969, Akimov et al. 1984), silts with a temperature between 0 and -2°C contain unfrozen water of between 5 and 30% by dry soil weight. Assuming that 10% by dry soil weight of the infiltrated water at the study sites did not freeze, this would represent approximately 20 mm of unfrozen water in the 40 cm thick frozen active layer. As Tice et al. (1978) suggested, this may be a lower limit. In fact a higher percentage of unfrozen water may occur with increasing ice content in the soil.

DISCUSSION AND CONCLUSIONS

These results have general implications for snow-melt run-off and active layer warming, and specific implications to the hydrology of lakes in the Mackenzie Delta. First, the cold substrate is responsible for removing considerable energy from the snow-pack during the melt period. The primary effect is to extend the snow-melt period. Second, soil infiltration may consume a large proportion of the initial snowcover water equivalent and therefore limit direct snow-melt run-off. The freezing of this infiltration is an important source of heat which can warm the active layer prior to the removal of the snowcover. However, in fine-grained soils, a significant portion of this infiltrating water may not refreeze, even if the soil is below 0°C. This effectively limits the energy available to warm the active layer, and must be taken into account when modelling active layer warming and the increase in the thaw depth once the snowcover is removed.

Lakes which are perched at a sufficiently high elevation, do not receive flood water from the Mackenzie River at annual intervals. As a result, they are dependent on run-off from the surrounding basin to sustain water levels between flooding events. However, snowmelt run-off to these lakes in negligible and Marsh (1986) found that summer run-off is also near zero. In addition, Marsh and Bigras (1988) showed that summer evaporation (230 mm) from the lakes is greater than summer precipitation (101 mm) onto the lake surface. As a result, these high perched lakes experience a negative water balance and declining water levels between flooding events (Marsh 1986). These lakes are therefore very sensitive to reduced spring flood levels due to flow regulation. Flow regulation could result in decreased flood frequency and declining lake levels for high sill elevation lakes. The number of lakes and the total lake area would decline with serious consequences to the ecology of the Mackenzie Delta.

ACKNOWLEDGEMENTS

The generous logistical support of The Polar Continental Shelf Project, Department of Energy, Mines, and Resources, and the Inuvik Scientific Resource Centre, Department of Indian and Northern Affairs is gratefully acknowledged. I would like to thank M. Ferguson for her assistance in the field.

REFERENCES

Akimov, Y.P., E.D. Yershov, and V.G. Cheveryov. 1984. The physicochemical nature of the formation of unfrozen water in frozen soils. Permafrost, Fourth International Conference, Final Proceedings. Fairbanks, Alaska, 195-199.

Anderson, E.A. 1976. A point energy and mass balance model of a snowcover. N.O.A.A. Tech. Report NWS 19, 150 pp.

Church, M. 1974. Hydrology and permafrost with reference to northern North America. Proc. Workshop Seminar on Permafrost Hydrology, Can. Nat. Comm., IHD, Ottawa, 7-20.

Colbeck, S.C. 1976. An analysis of water flow in dry snow. Water Resour. Res., 12, 523-527.

Granger, R.J., D.M. Gray, and G.E. Dyck. 1984. Snowmelt infiltration to frozen prairie soils. Can. J. Earth Sci., 21, 669-677.

Gray, D.M., P.G. Landine, and R.J. Granger. 1985. Simulating infiltration into frozen prairie soils in streamflow models. Can. J. Earth Sci., 22, 464-472.

Heron, R. and M.K. Woo. 1978. Snow-melt computations for a high arctic site. Proc. 35th Eastern Snow Conf., 162-172.

Johnston, G.H. and R.J.E. Brown. 1964. Some observations on permafrost distribution at a lake in the Mackenzie Delta, N.W.T., Canada. Arctic, 17, 163-175.

Kane, D.L. 1980. Snowmelt infiltration into seasonally frozen soils. Cold Regions Sci. Technol., 3, 153-161.

Marsh, P. and S. Bigras. 1988. Evaporation from Mackenzie Delta Lakes, N.W.T., Canada. Arctic and Alpine Res., 20(2). In press.

Marsh, P. and M.K. Woo. 1981. Snowmelt, glacier melt, and high arctic streamflow regimes. Can. J. Earth Sci., 18, 1380-1384.

Marsh, P. and M.K. Woo. 1984. Wetting front advance and freezing of meltwater within a snow cover 1. Observations in the Canadian Arctic. Water Resour. Res., 20, 1853-1864.

Marsh, P. and M.K. Woo. 1987. Soil heat flux, wetting front advance and ice layer growth in cold, dry snow covers. Snow Property Measurement Workshop, Lake Louise, Alta., April 1-3, 1985, NRC Technical Memorandum 140, 497-524.

Marsh, P. 1986. Modelling water levels for a lake in the Mackenzie Delta. Cold Regions Hydrology Symposium, American Water Resources Association, Fairbanks, Alaska, 23-29.

Marsh, P. 1988. Hydrology of Mackenzie Delta Lakes. Northern Rivers and Lakes Workshop, Knowing the North: Integrating Tradition, Technology and Science. Boreal Institute for Northern Studies, University of Alberta, in press.

Moore, R.D. 1983. On the use of bulk aerodynamic formulae over melting snow. Nordic Hydrology, 14, 193-206.

Price, A.J. and T. Dunne. 1976. Energy balance computations on snowmelt in a subarctic area. Water Resour. Res., 12, 686-694.

Scott, R.F. 1969. The freezing process and mechanics of frozen ground. U.S. Army, Cold Regions Research and Engineering Laboratory, Monograph II-D1, 65 pp.

Tice, A.R., C.M. Burrous, and D.M. Anderson. 1978. Determination of unfrozen water in frozen soil by pulsed nuclear magnetic resonance. Third International Conference on Permafrost, Edmonton, Canada, 150-155.

Woo, M.K., P. Marsh, and P. Steer. 1983. Basin water balance in a continuous permafrost environment. Proc. Fourth International Conference on Permafrost, Fairbanks, Alaska, 1407-1411.

U.S. Army. 1956. Snow hydrology, Summary report of the snow investigations, Corps of Enging., North Pac. Div., Portland, Oreg., 437 pp.

LATE PLEISTOCENE DISCHARGE OF THE YUKON RIVER

O.K. Mason and J.E. Beget

University of Alaska, Fairbanks 99775

SYNOPSIS Geologic and paleoecologic evidence suggests that during the late Pleistocene much of unglaciated interior and northern Alaska was arid tundra or polar desert. We estimate the extent of aridity during the late Pleistocene in Alaska by a paleohydrologic reconstruction of discharge in the Yukon River. Using infrared, radar, and landsat imagery, we compare stream morphology in abandoned portions of the Pleistocene Yukon River delta with the modern Yukon River channel. If variations in sediment flux are damped by large upstream basins and other hydrologic parameters were relatively invariant, then changes in stream morphology across the Yukon Delta have been primarily a function of discharge. First order changes in river morphology can be examined by empirical hydrologic equations which relate river discharge to meander wavelength. The data suggest that during the late Pleistocene the Yukon River had approximately 45% of the modern discharge, implying that average annual precipitation integrated over the entire Yukon drainage basin was approximately half of modern values.

INTRODUCTION

During the late Pleistocene, lower sea levels exposed an enormous area of continental shelf between Siberia and Alaska. This area, known as the Beringian subcontinent, helped produce hypercontinental conditions in Interior Alaska and the Yukon, which resulted in increased aridity and fostered a unique biota (Hopkins et.al., 1982). In isolated places, the landscape may have resembled a polar desert (Ritchie and Cwynar, 1982). Extensive "sand seas" dominated lowland regions in the Tanana valley (Collins, 1985), the North Slope (Carter, 1981) and northwest Alaska (Fernald, 1964). The prevalence of arid northeasterly winds, reconstructed from dune orientation (Hopkins, 1982), implies that the Alaskan Interior was largely cut off by the Cordilleran ice mass from the storm-generating area in the Gulf of Alaska.

We compare morphometric characteristics of modern and late Pleistocene channels of the Yukon River (Figure 1), the dominant drainage system of eastern Beringia (Alaska and the Yukon Terr.), in order to gain a quantitative sense of the average aridity of the late Pleistocene Beringian landmass. River morphology and deposits may contain direct climatic records (Knox, 1983) because changes in climatic conditions and vegetation cover of the landscape should be reflected in the amount of water flowing in the channel.

Channel measurements from false-color infrared imagery were analyzed using mathematical relationships equating river morphology to discharge. Comparison of the resultant paleo-discharge estimates with the short historical hydrological record suggests that the late Pleistocene discharge of the Yukon River was significantly lower than the present discharge.

LATE PLEISTOCENE HISTORY OF THE YUKON RIVER

The late Quaternary history of the Yukon River valley is known only in outline because access to much of the region is difficult. Part of its history is recorded in a core from beneath the Bering Sea collected offshore from Cape Romanzof together with seismic profiling data collected by Knebel and Creager (1973), and from cores from beneath Norton Sound (MacDougal, 1982). Prior to 16,000 B.P. the principal deltaic distributaries of the Yukon River lay to the east of Nunivak Island through Etolin Strait, as evidenced by (1) a buried channel the width of the modern river and (2) discernible sediment progradation off the northwest shore of Nunivak Island. After 16,000 B.P., the Yukon shifted course northward to debouch into the eustatically rising waters of the Bering Sea at a point south of St. Lawrence Island. The Yukon continued to migrate northeasterly throughout the late Pleistocene and the early Holocene. Cores in Norton Sound reflect an influx of Yukon water around 2500 years ago based on biofacies changes (MacDougal, 1982).

On land, a similar pattern is apparent. Two substantial sedimentary accumulations occur at the Manokinak and Kashunuk river deltas, which enter the Bering Sea just north of Etolin Strait (Shepard and Wanless, 1971, Dupre, 1977). In the late Pleistocene,

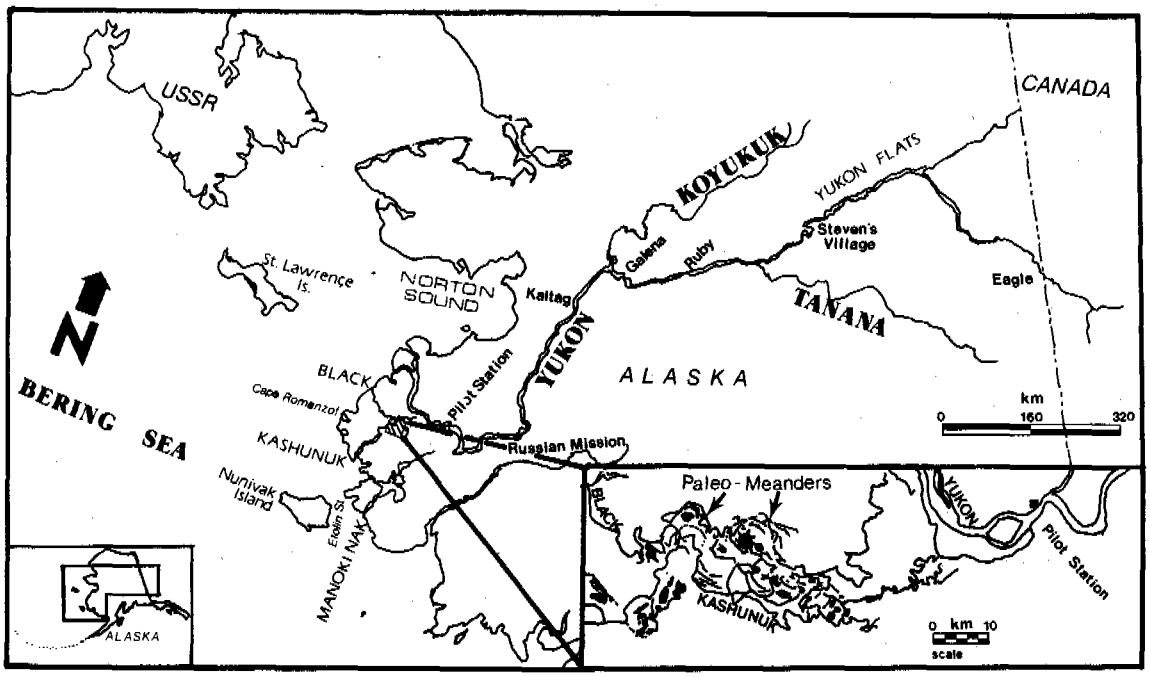

Figure 1. Map of central Alaska. Study area highlighted. Yukon Delta tributaries formerly active: Manokinak from 16-11,000 B.P., Kashunuk & Black until 2500 B.P.

16,000-11,000 B.P., the Yukon constructed a delta sublobe through both the southerly Kashunuk and the northerly Black River. About 2450 yr. B.P., the Yukon River abandoned the Black River sublobe, based on radiocarbon dates from chenier deposits developed seaward as the modern delta discharged sediment southward and in cutbanks (Robinson and Trimble, 1983). The Yukon occasionally re-occupied the Black River lobe, with its last outflow through the region at about 1300 years ago (W.R. Dupre, written comm., 1984). The transition from late Pleistocene to the present fluvial system is recorded in a series of abandoned terraces along the now underfit course of the Black and Kashunuk Rivers, southeast of the Kusilvak Mountains and west of the present great northerly inflection in the Yukon River (Figure 1).

Farther upstream, the late Pleistocene stratigraphic and alluvial history of the Yukon River is known only in outline. Important geological studies describe the sedimentology of cutbank exposures (Eardley, 1938) or interpret alluvial history using a relative chronology in lieu of radiometric dates (Williams, 1962). More recent research in the Galena region, in the middle course of the Yukon, provides some radiocarbon control on alluvial history (Weber and Pewe, 1970). Many late nineteenth century village sites have eroded in only 50 to 60 years (de Laguna, 1947). Shifts in position of the Yukon channel are rapid (Williams, 1952). Most or all of the floodplain is covered by very thick alluvium but permafrost is very restricted in the active floodplain (Pewe, 1975, Williams, 1970).

Our morphometric analysis was restricted to the lower and middle reaches of the Yukon River, where bedrock control over channel morphology was absent (Figure 1).

THE MORPHOMETRY OF MEANDERING STREAMS

Meandering streams show regularities in channel configuration in response to the amount of water flowing within their banks. The tendency to meander can be empirically related to the combined effects of slope and size of particles in transit, as well as to discharge (Richards, 1982). Meandering streams are favored by gentler gradients and finer, more cohesive sediments, whereas braided streams are more common in steeper reaches and with coarser materials.

The meandering habit of rivers appear to be a stable part of alluvial morphology although rapid shifts from meandering to braided form

may result from sudden overwhelming fluxes of sediment (Coleman, 1969). The shape of meanders is defined by the parameters of amplitude, wavelength, mean angle of curvature and point of inflection (Leopold et.al., 1964). The meanders of a river can be described by a mathematical function relating various states of discharge (Q) to meander wavelength (L_m) following an exponential of the following general form (Jefferson, 1902):

$$L_m = c \quad Qx^b \qquad (1)$$

where b and c are constants. Various workers, especially Carlston (1965) and Dury (1965) refined this general equation. The principal influence on meander wavelength is generally thought to be water level during falling stages of floods (sub-bankfull discharge) because so much erosion may occur at this time (Carlston, 1965).

We used the following empirical equations relating discharge to meander wavelength in our calculations (where q_m = mean discharge, q_{ma} = mean annual discharge, q_{mm} = mean monthly discharge, q_b = bankfull discharge and q_d = dominant discharge):

$L_m = 46\ q_m^{0.5}$ (Jefferson, 1902) (2)

$L_m = 106.1\ q_{ma}^{0.46}$ (Carlston, 1965) (3)

$L_m = 80\ q_{mm}^{0.46}$ (Carlston, 1965) (4)

$L_m = 166\ q_m^{0.46}$ (Carlston, 1965) (5)

$L_m = 32.86\ q_b^{0.55}$ (Dury, 1976) (6)

$L_m = 62\ q_d^{0.47}$ (Dury & Charlton, 1970) (7)

$L_m = 54.3\ q_b^{0.5}$ (Dury, 1965) (8)

The grain size of sediment along a river's banks can also affect the development of meanders (Schumm, 1963). Banks composed mainly of sand are more erodible, forming shallow wide channels, as compared to silt and clay banks which are more cohesive and resistant to failure. The composition of terraces (Eardley, 1938; Weber and Pewe, 1970; Williams, 1962) along the Yukon and evidence from boreholes (Pewe, 1975) indicate that the Pleistocene load of the river included predominantly silt and very fine sands, and thus was similar to modern Yukon alluvium. For the purposes of this study, we assume that sediment flux and grain size were more or less constant through time in the lower Yukon drainage, though temporal variations in deposition certainly did occur. Thus, we use the general form of the meander wavelength to discharge equations as discussed above.

METHODOLOGY

Delta and channels of the modern and Pleistocene Yukon River are easily seen on small scale radar and Landsat images of central Alaska. To compare the morphometry of these features, we examined 1978 and 1980 flightlines of false color infrared photography of the Yukon drainage system (approximate scales 1:30,000 and 1:60,000) archived by the Geophysical Institute in Fairbanks. False-color imagery allows one to perceive subtle differences in vegetation cover and presumably lithology and thereby to easily identify old oxbow lakes and paleomeanders.

Our studies concentrated on relict channels in unconfined alluvial plains. Two portions of the Yukon drainage possess terraces with well-defined sequences of relict pointbar deposits: the middle Yukon reaches around Galena, just upriver from the tributary junction of the Koyukuk River, and along the Pleistocene Yukon River channel now filled with the underfit Kashunuk River west of Mountain Village. Within the two areas, point bar complexes of differing ages are recognizable, marked by the development of thaw lakes. Following Weber and Pewe (1970), the older, higher terrace, characterized by pervasive thaw lakes is thought to be late Pleistocene in age, based on a 8000 yr. ^{14}C date from a pointbar complex closer to the modern Yukon River.

Working solely from aerial photos, we can only estimate the age of the pointbar complexes within broad limits. Pointbar deposits in the Kashunuk River, within the Black River subdelta lobe, are only roughly dated to ca. 16-11,000 B.P. If this late Pleistocene age assignment is correct, it is possible that a significant time span and several differing climatic regimes may be represented by these pointbars. Modern meanders were studied along reaches of the Yukon River near Pilot Station, Galena and Stevens Village.

Ancient pointbar sequences are distinguished by several topographical criteria: (1) a semi-circular boundary occasionally marked by incision of the river into a scarp distant from the active channel of the river or the outline of a relict or re-occupying stream; (2) the extent of irregular thaw lakes, integrating several swale deposits within the sediment package; (3) the development of local drainage systems within the pointbar complex; (4) photographic textural differences due to variations in sediment grain size, surface relief, or vegetation breaks evident in hue changes; (5) cross cutting relationships with younger deposits and (6) rare oxbow lakes.

Measurements of meander wavelength for each pointbar complex were based on the geometry of the pointbar complexes. After channel abandonment, pointbar complexes should

reflect former channel morphology. Efforts were made to select pointbar complexes not truncated by subsequent alluvial activity. Measurements of the pointbar sequences were derived from 1:63,360 (1 inch=1 mile) USGS topographic series maps. Due to the infrequent preservation of entire pointbar wavelengths along the river, half meander wavelengths were measured and doubled to estimate the original meander wavelengths.

RESULTS

The presumed late Pleistocene (N=10) include eight from the abandoned Yukon channels occupied by the Kashunuk River in the Delta region and two from the middle course Galena vicinity (Table I). The mean meander wavelength value of all late Pleistocene sites is about 10069 m, with a standard deviation of 1494 m (Table I). Meander wavelength values just for the abandoned delta are between 8850 and 12675 m (Table I).

Table I
Measurements of Paleomeanders and modern meanders

Localities	Meander Wavelength (M)	Relative Age
Paleo-meanders (n=10)		
Galena vicinity		
1) Squirrel Creek A	7590	Late Pleistocene
2) Squirrel Creek B	8613	Late Pleistocene
Lower Yukon River:		
Kashunuk Sublobe--abandoned Yukon channels		
3) Owl Village NW	12674	Late Pleistocene
4) Owl Village SW	10461	Late Pleistocene
5) Nungatak	9455	Late Pleistocene
6) Meninglik	8851	Late Pleistocene
7) Nantak	11265	Late Pleistocene
8) Kashunuk A	10461	Late Pleistocene
9) Kipungdak	11265	Late Pleistocene
10) Kashunuk B	10058	Late Pleistocene
	Late Pleistocene Meander Wavelength (N=10):	
	Mean:	10069
	Standard Deviation:	1494
Modern Yukon Meander Wavelengths (N-5)		
1) Galena	14667	
2) Galena	13943	
3) Galena	16956	Modern Meander Wavelength (N=5):
4) Pilot Station	11259	Mean: 14586
5) Pilot Station	16106	Standard Deviation: 2203

The sample (N=5) of modern Yukon River meanders includes locations near the paleo-meanders examined, as at Galena, and from regions outside those considered, as at Pilot Station (Table I). The two meanders from near Pilot Station show widely differing wavelengths though they are in a serial relationship to one another: 11,259 m in the downstream meander and 16,106 m in the one immediately upstream. The mean value for all measurements (n=5) of the modern meander wavelength is 14586 m with a standard deviation of 2203 m (Table I). Using this value and equations (6) and (8), estimates of modern bankfull discharge (q_b) range from 16170 m^3/s to 21969 m^3/s (Table II). Again, using equations (2) and (5), estimates of mean discharge (q_m) are widely disparate, ranging from 6298 to 30611 m^3/s (Table II). Again, using equations (2) and (5), estimates of mean discharge (q_m) are widely disparate, ranging from 6298 to 30611 m^3/s (Table II). Mean monthly discharge (q_{mm}) is estimated by equation (4) to be about 30788 m^3/s (Table II).

Table II also shows discharge estimates using equations (2)-(8) for the late Pleistocene Yukon. Calculated values for late Pleistocene Yukon River discharge are generally lower than those for the modern Yukon (Table II). Estimates of late Pleistocene bankfull discharge (Q_b) range between 8236 to 10470 m^3/s. The various equations yield divergent values for mean discharge (Q_m), with a range between 2814 to 14589 m^3/s. Mean monthly discharge (Q_{mm}) values lie at 13756 m^3/s. This discharge level, reflecting the influence of falling water stages, was thought by Carlston (1965) to be the most significant factor in determining meander wavelength. Although all calculations using equations (2)-(8) agree that late Pleistocene discharge was lower than modern discharge, the range of discharge estimates in Table II is large. Clearly, some of the equations are more realistic than others--a problem possibly resolvable by considering empirical data from gauging station records along the Yukon (see below).

DISCUSSION

It is apparent that late Pleistocene meanders preserved along the now-abandoned Pleistocene course of the Yukon River within the Black River subdelta are smaller than modern

Table II
Estimates of Yukon River Discharge (m3/s)
during Late Pleistocene and Holocene

	(a) $L_m=45\ q_m^{0.5}$	(b) $L_m=106.1\ q_{mb}^{0.46}$	(c) $L_m=80\ q_{mm}^{0.46}$	(d) $L_m=166\ q_m^{0.46}$	(e) $L_m=32.86\ q_b^{0.55}$	(f) $L_m=62\ q_b^{0.47}$	(g) $L_m=54.3\ q_b^{0.5}$
Late Pleistocene	14589	7445	13756	2814	8236	17936	10470
Modern	30611	16664	30788	6298	16170	39464	21969

Equations shown as originally derived, ie. in English units (cubic feet per second), calculations were converted to metric.

meanders, suggesting that Pleistocene discharge was lower than modern discharge. All discharge calculations suggest that the Pleistocene flow in the Yukon was significantly less than present, assuming that the entire discharge of the Yukon River flowed through the Kashunuk channel. While the two sets of meanders can be statistically distinguished (i.e., late Pleistocene = 10069±1494m vs. modern = 14586±2203m), one of the abandoned meanders in the Black subdelta is larger and two are about the same size as the smallest of the modern meanders at Pilot Station. The range in size of pointbar complexes probably reflects natural hydrologic variability, but may also be due to other causes (idiosyncratic avulsions, etc.).

The several theoretical discharge estimates presented here may be calibrated by comparing the estimates with modern data on discharge from gauging stations at widely scattered locations along the Yukon (Table III). Water records are relatively scanty for the Yukon, with the period of record generally less than twenty years for most of the river (USGS 1961, USGS 1964, Bigelow et.al., 1984). Records generally date from 1956 at the earliest, with occasional records from 1911-1913 at Eagle, far upstream. Since the mid-1970's gauges have monitored water levels at Pilot Station, Ruby, Stevens Village, and Eagle. Sporadic records from the late 1950's to early 1960's are also available from Kaltag and Rampart.

Mean discharge averaged over the entire available historical record for the Yukon increases downstream and is 2335 m^3/s at Eagle, 3350 m^3/s at Stevens Village, 3650 m^3/s at Rampart, at 4720 m^3/s at Ruby, 5635 m^3/s at Kaltag, and 6250 m^3/s at Pilot Station (Table III).

Table III
Water Gauge Data on Yukon Discharge (m3/s)

STATION	MAXIMUM	MEAN	YEARLY EXTREMES
Eagle	15424 (6/12/64)	2335 (36yrs)	396-7160 (1964)
Stevens Village	18961 (6/9/77)	3348 (8 yrs)	536-11943 (1964)
Rampart	26885 (6/15/64)	3654 (9 yrs)	425-14376 (1961)
Ruby	27451 (6/20/64)	5001 (9 yrs)	594-15678 (1961)
Kaltag	29149 (6/22/64)	6215 (9 yrs)	708-17263 (1961)
Pilot Station	21253 (5/27/82)	6252 (10 yrs)	991-18169 (1964)

Quite consistent values of extreme events occur longitudinally down the river. The maximal flood event of June, 1964, registered 15420 m^3/s upstream at Eagle, with increases in the middle reaches: 26885 m^3/s at the Rampart station, 27450 m^3/s at Ruby and 29150 m^3/s at Kaltag. Similarly, the 1957 flood had a discharge of 28820 m^3/s at Kaltag while upriver at Ruby only a 21310 m^3/s discharge was recorded.

When the estimates of discharge based on meander wavelength are compared with modern gauge data, it is apparent that four equations are more realistic than others. The best estimates come from equation (4) for mean monthly discharge: $L_m = 80\ Q_{mm}^{0.46}$, generating an estimate of about 30788 m^3/s; equation (5) for mean discharge: $L_m = 166\ Q_m^{0.46}$, gives an estimate of about 6298 m^3/s. Equation (8) ($L_m = 54.3\ Q_b^{0.5}$) and equation (6) ($L_m = 32.86\ Q_b^{0.55}$) yield estimates of about 16170-21969 m^3/s for bankfull discharge.

If only the most realistic equations from Table II are used, it is possible to make an estimate of late Pleistocene discharge in comparison to modern discharge. These data suggest late Pleistocene discharge levels were only 45% of modern discharge (Table II). We cannot resolve precisely how late Pleistocene discharge was distributed through the hydrologic year. The figures for bankfull discharge imply that the magnitude of channel-forming events was substantially less, translating perhaps into smaller winter snowpacks and spring floods, or less frequent and smaller rainstorms resulting in smaller floods or a lower average discharge.

If discharge is a reliable reflection of overall climatic conditions, then late Pleistocene Alaska and Beringia were profoundly different than at present. Rainfall in the Alaskan Interior at present rarely exceeds 150-360 mm yr^{-1} (Streten, 1974), with the existence of permafrost and relatively low evaporation supporting the taiga biome.

The water balance of the Yukon watershed can be expressed in terms of the hydrologic continuity equation (Alford, 1985):

$$P - Q - E - S = 0 \qquad (9)$$

where P is precipitation, E is net evapotranspiration and condensation, S is water storage and Q is river drainage. It can be generally assumed that, averaged over several

years, S is zero. During the late Pleistocene, the extent of permafrost should have been greater and seasonal thaw less than at present, reducing groundwater flow and increasing overland flow and runoff. A decrease in the total amount of surface vegetation, as suggested by paleoecologists, should also have acted to increase runoff by reducing evapotranspiration. Similarly, evaporation should have been minimized by lower temperatures during the late Pleistocene. Because this suggests that processes which operate to increase runoff and discharge (Q) should have been facilitated during the late Pleistocene, it seems likely that average annual Pleistocene precipitation (P) must have been even less than half of modern values, as suggested by the paleodischarge calculations presented here.

REFERENCES

Ackers, P & Charlton, F G (1970). Meander geometry arising from varying flows. Journal of Hydrology (11), 230-252.

Alford, D (1985). Mountain hydrologic systems. Mountain Research and Development (5), 349-363.

Bigelow, B B, Lamke, R D, Still, P J, van Maanen, J L & Vail, J E (1984). Water Resources Data, Alaska, U.S. Geol. Survey Water Data Report AK-84-1.

Carlston, C W (1965). The relation of free-meander geometry to stream discharge and its geomorphic implications. Amer. Jour. Science (263), 864-885.

Carter, L D (1981). A Pleistocene sand sea on the Alaskan arctic coastal plain. Science (211), 381-383.

Coleman, J M (1969). Brahmaputra River: Channel processes and sedimentation. Sedimentary Geol. (3), 129-239).

Collins, F R (1985). Map showing a vegetated dune field in central Alaska. U.S. Geol. Surv. Misc. Field Studies Map MF-1708.

de Laguna, F (1947). The Prehistory of North America as seen from the Yukon. Memoirs, Soc. for Amer. Archaeo., (3), Menasha, WI.

Dupre, W R (1977). Yukon Delta Coastal Processes Study. Report to U.S. Dept. of Commerce, NOAA, Boulder, CO.

Dury, G H (1965). Theoretical Implications of Underfit Streams. U.S. Geol. Surv. Prof. Paper 452-C.

Dury, G H (1976). Discharge prediction, present and former, from channel dimensions. Journal of Hydrology (30), 219-245.

Eardley, A J (1938). Unconsolidated sediments and topographic features of the lower Yukon Valley. Bull. Geol. Soc. Amer. (49), 303-342.

Fernald, A T (1964). Surficial geology of the central Kobuk River, northwestern Alaska. U.S. Geol. Surv. Bull. 1181-K.

Hopkins, D M (1982). Aspects of the paleogeography of Beringia during the late Pleistocene. IN Paleoecology of Beringia, edited by D M Hopkins et.al., 425-444, Academic Press, New York.

Hopkins, D M, Matthews, Jr. J V, Schweger, C E & Young, S B (1982). Paleoecology of Beringia. 489 pp. Academic Press, New York.

Jefferson, M S W (1902). Limiting width of meander belts. National Geographic (13), 373-384.

Knebel, H J & Creager, J S (1973). Yukon River: Evidence for extensive migration during the Holocene transgression. Science (179), 1230-32.

Knox, J C (1983). Responses of river systems to Holocene climates. IN Late Quaternary Environments of the United States, Vol. 2: Holocene, pp. 26-41, University of Minnesota Press, Minneapolis.

Leeder, M R & Bridges, P H (1975). Flow separation in meander bends. Nature (253), 338-9.

Leopold, L B, Wolman, M G & Miller, J P (1964). Fluvial Processes in Geomorphology. 522 pp. W.H. Freeman & Co., San Francisco.

MacDougal, K (1982). Microfaunal analysis of late Quaternary deposits of the northern Bering Sea. Geologie en Mijnbouw (61), 19-27.

Pewe, T L (1975). Quaternary Geology of Alaska. U.S. Geol. Surv. Prof. Paper 835.

Richards, K (1982). Rivers: Form and Process in Alluvial Channels. 358 pp. Metheun, London.

Ritchie, J C & Cwynar, L C (1982). Late Quaternary vegetation of the north Yukon. IN Paleoecology of Beringia, edited by D M Hopkins et.al., pp. 113-126, Academic Press, New York.

Robinson, S W & Trimble, D A (1983). U.S. Geological Survey, Menlo Park, CA. Radiocarbon measurements III., Radiocarbon (25), 1, 143-151.

Schumm, S A (1963). Sinuosity of rivers on the Great Plains. Bull. Geol. Soc. Amer. (74), 1089-1100.

Shepard, F P & Wanless, H R (1971). Our Changing Coastlines. 579 pp., McGraw-Hill, New York.

Streten, N A (1974). Some features of the summer climate of Interior Alaska. Arctic (27), 273-286.

U.S. Geological Survey (1961). Water Data Report AK-61-1.

U.S. Geological Survey (1964). Water Data Report AK-64-1.

Weber, F R & Pewe, T L (1970). Surficial and engineering geology of the central part of the Yukon-Koyukuk lowland. USGS Misc. Geol. Invest. Map I-590, Scale 1:125,000.

Williams, J R (1952). Effect of wind-generated waves on migration of the Yukon River in the Yukon Flats. Science (115) 519-520.

Williams, J R (1962). Geologic reconnaissance of the Yukon Flats district, USGS Geol. Surv. Bull. 1111-H.

INFLUENCE OF WATER PHENOMENA ON DEPTH OF SOIL THAWING IN OSCAR II LAND, NORTHWESTERN SPITSBERGEN

C. Pietrucień and R. Skowron

Institute of Geography, Dept. of Hydrology, University of Nicolas Copernicus, Torun, Poland

INTRODUCTION

During successive Toruń Polar Expeditions to Oscar II Land /northwestern Spitsbergen/ in 1982 and 1985, the authors carried through observations on depth and rate of soil thawing under influence of water phenomena. Investigations were carried through either for depressions of shallow tundra lakes as well as for river beds and adjoining tundra clusters or bank ridges. Arrangement of investigated objcts is presented in Fig. 1. Their altitudes were different. The observation site of the Waldemar River occurred at about 1-3 m a.s.l. whereas measuring sites in lake basins were located at considerable altitudes. The lake defined by the letter "A" /1700 m^2/ occurs in northern part of Kaffiöyra at 10,2 m a.s.l. whereas the lake "B" /6700 m^2/ in southern Sarsöyra on a high terrace at about 40 m a.s.l. Both depressions form small basins amidst ancient storm ridges and are permanently filled with water coming from melting ice and degradation of permafrost. Considerable changes in water levels /10-45 cm/ were noted in these lakes. They resulted in a decrease of their volumes of 40-80 % at the end of summer. Varying altitudes at which these lakes occur are connected with location and rate of uplifting of the western seashore of Spitsbergen during the Holocene /Klimaszewski, 1960/.

Investigations, some results of which are to be presented below, were supposed to find relations betwen rate and depth of soil thawing and wetness of the area, expressed in extreme case by occurrence of surface waters. Rate and degree of vegetation covering of the area as well as lithology of substrate were also taken into account.

A phenomenon of influence of soil water content on rate of thawing does not create a new idea in literature. There is a well known opinion that increased water content results in greater thermic conductivity of soil and therefore, in quicker thawing rate /Kossowski and Sikora, 1978, Monteith, 1977/.

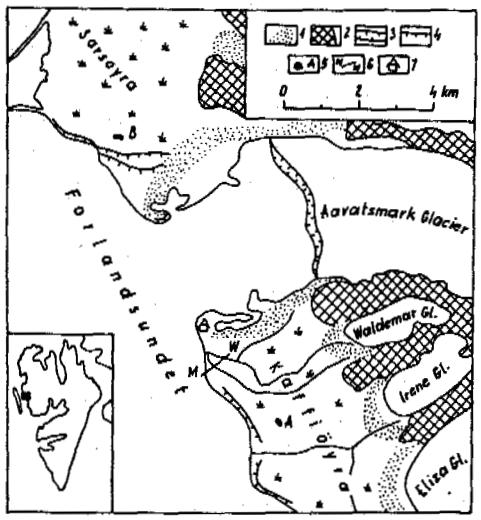

Fig. 1 Location of observation sites: 1 - end moraines, 2 - mountain massifs, 3 - observation section "Waldemar River - sea", 4 - dead and active cliffs, 5 - lake basins under investigation, 6 - base of Toruń Polar Expeditions

Closer information on development and thickness of active layer and particularly, influence of climate and altitude on depth of soil thawing are presented by Stäblein /1970/ and Washburn /1976/. Lithologic conditions and influence of vegetation covering on development of active layer are also underlined by Jahn and Walker /1983/.

Polish investigations on soil thawing have been mainly carried through in the Hornsund Region /Cze-

ppe, 1960, 1961 and 1966, Baranowski, 1968, Jahn, 1961, 1982, Grześ and Babiński, 1979/. Since 1977 members of Toruń Polar Expeditions have been studing degradation of permafrost in Kaffiøyra and Sarsøyra /Marciniak et al., 1981, Marciniak and Szczepanik, 1983/. An attempt of spatial variation of active layer thickness along the whole western seashore of Spitsbergen is presented by Grześ /1985/. He presented the scheme of thawing and analyzed rate of growing of the active layer as dependent on the type of substrate /environment/.

Observations carried through during field works by Toruń Polar Expeditions proved that thickness of active layer reached maximum values at the end of August: 101,2 cm in tundra-covered area and about 116 cm in vegetation-less outwash /Marciniak and Szczepanik, 1983/. Investigations of this subject were particularly focused on lithology and structure of soil as well as on vegetation cover. Neither water content nor occurrence of surface water reservoirs were taken into account.

Present authors decided to discuss this problem as referred to areas of varying water content, in substrate of several water reservoirs as well.

ANALYSIS OF RESULTS OF INVESTIGATIONS

Investigations were carried through during two summer seasons: in 1982 and 1985, in the same measuring sections. Observations were done every two weeks by hammer method with accuracy of 1 cm. Due to a time of the expedition /usually July and August/, observations of thawing were initiated already during a considerable development of this process. Juny 1 is commonly accepted for the beginning of the thawing period /initiation of ablation/ although in some cases there are possible deviations from this term /Troitsky et al., 1975/. Last measurements were done at the turn of August and September. Collected data indicate that in that time a thawing was stopped and even a renewed growth of permafrost occurred. Thus it seems possible that every time the maximum thickness of active layer was received for every season. It forms therefore the basis for evaluation of rate and varying depth of soil thawing, dependet on water content, lithology and vegetation.

This subject is perfectly illustrated by Fig. 2. It presents thickness of active layer at the begin-

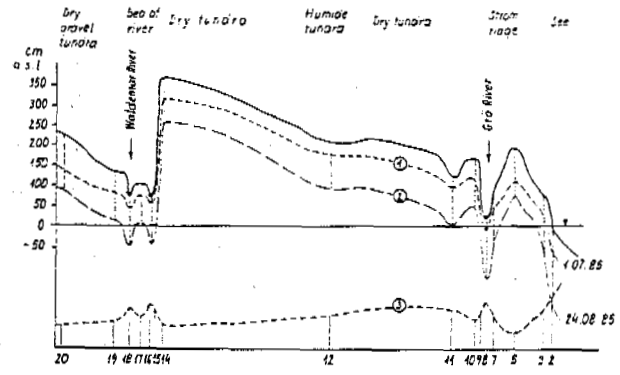

Fig. 2 Depth of soil thawing in observation section "Waldemar River - sea": 1-2 - thickness of active layer at some terms, 3 - growth of thickness of active layer /thawed layer/ between extreme observation terms.

ning and end of observation period in the section from the bed of the Waldemar River through tundra areas of varying water contents, sandy storm ridges to the sea. The upper line corresponds with measurements on July 1 and describes the beginning of thawing. A thickness of active layer was rather small in that time. At the site 15 it was equal 0 m and largest depth of thawed soil was noted at storm ridge /60 cm/ and in a dry tundra /sites 14 and 20/.

Maximum depth of active layer was noted on August 24. Later measurements noted growth of permafrost and so, the final term of August 24 was accepted for discussions on thawing rate. The greatest thickness of active layer occurred in that time at mean sea level /site 2/, under river beds /sites 8 and 18/ and in other areas /site 12/. The lowest thawing occurred at storm ridge and in dry raised tundra /sites 5, 12 and 20/. It is expressed by the line that presents difference in thicknesses of active layer between July 1 and August 24, 1985. Its location is opposite to the both previous ones and indicated values enable to define a mean rate of soil thawing /Table 1/.

An analysis of the table 1 proves that the greatest thawing occurred at sites 2, 8, 11 and 18, where it was equal from 1.7 to 2.5 cm a day. All these values correspond with water objects or areas with high water content. During shorter time intervals a thawing rate reached even 3.4 cm a day /site 2/ and considerably exceeded the values cited by Jahn and Walker /1983/ for Alaska, Greenland and Spitsbergen.

TABLE I

Rate of soil thawing in some sites of the section "Waldemar River-sea"

/in cm a day/ in different observation intervals.

Period	Site number							
	2	5	8	10	11	14	18	20
1.07-17.07.1985	2.8	1.6	1.5	1.8	2.2	1.7	2.4	1.4
1.07-29.07.1985	1.7	1.4	2.5	2.2	2.7	1.8	2.8	1.5
30.07-24.08.1985	3.4	0.0	1.6	0.4	0.7	0.3	0.6	0.4
1.07-24.08.1985	2.5	0.7	2.1	1.4	1.7	1.1	1.8	1.0

The lowest degradation rate of permafrost was noted on sandy storm ridge /site 5/, equal 0.7 cm a day only, and at dry tundra clusters /sites 14 and 20/.This fact made the authors to list the rate of growth of active layer with mean air temperatures for the periods between the measurements /Table II/. In this way a distinct correlation was received for measuring

TABLE II

Mean rate of active layer growth in some sites of the section "Waldemar River - sea".

Observation period	Mean air temperature	Sandy storm ridge /site 5/	Bed of Waldemar River /site 18/	Dry gravel tundra /site 20/	Bed of Grø River /site 9/	Dry mossy tundra /site 14/
1.07 - 5.07.1985	3.9	0.7	1.3	1.0	1.9	1.1
5.07 -17.07.1985	6.1	2.2	3.2	1.8	1.2	2.1
17.07 -29.07.1985	8.3	1.1	3.3	1.5	3.9	2.0
29.07 -10.08.1985	5.6	0.2	0.4	0.7	2.2	0.3
10.08 -24.08.1985	4.4	-0.1	0.9	0.2	1.1	0.4
24.08 -29.08.1985	2.7	0.0	-3.4	-2.2	-8.4	-1.8
1.07 -29.08.1985	5.2	0.7	1.8	1.0	1.4	1.0

sites under river beds whereas it did not occurred for dry, sandy areas.

Investigations of soil thawing under and around two lake basins with various volumes of water were carried simultaneosly with observations in a section across the areas with varying water contents.

The lake "A" is a typical, small and shallow tundra reservoir /Table III/. Basin of the lake "B" is considerably larger and deeper what is also reflected in Fig. 3. Dates that describe section lines in both cases indicate a soil thawing at the beginning of observation and during the maximum thickness of active layer. We can speak in both cases about similar dependencies but their degree is different. Around the lake "A" a soil thawing was more significant during the first of July /July 3, 1985/ than in its substrate. The difference reached 32 cm. With time and water

TABLE III

Main parameters of studied lakes

Lake.	Area in m^2	Volume in m^3	Depth max.	Depth mean
A	1737.5	239.3	0.26	0.14
B	6766.5	2816.0	0.92	0.42

warming in the resevoir, there was a quick growth of active layer under the lake. Thus at the end of the summer, its total thickness as well as difference of values coming from the first and last measurements, was the greatest here. This problem is connected with rate of permafrost degradation as illustrated by the tabeleIV which presents a rate of soil thawing under and around the described lake. The rate in growth of

TABLE IV

Rate of soil thawing /in cm a day/ under and around tundra lake /A/ in Kaffiøyra /Oscar II Land/ in 1985.

Period	W	Distance from the shore in m						E
	+20	+5	0.0	-5	-10	-5	0.0	+5	+20
3.07-16.07.	2.4	2.5	2.4	2.7	2.9	3.3	3.3	2.7	2.5
3.07-29.07.	2.2	2.6	2.7	2.6	2.7	3.1	3.0	2.8	2.5
30.07-24.08.	0.7	0.8	0.9	0.8	0.8	0.9	0.8	0.7	0.6
3.07-24.08.	1.5	1.7	1.8	1.6	1.6	2.0	1.9	1.7	1.6

active layer is varying in time and in space. It reached greatest values in July, particularly during its first half, and considerably smaller in August when it gradually ceased. Spatial variation is best illustrated by mean values for the whole research period. Highest values of thawing rate are noted to occur within the lake shoreline. Still more striking variation in soil thawing was noted around the lake "B". This reservoir is considerably larger than the lake "A" in its area as well as its volume. This fact is reflected in rate of development as well as thickness of active layer /Fig. 3/. Difference in depth of soil thawing between July 4 and August 17, 1985, under this lake is particularly significant and reaches in extreme case three times a growth of

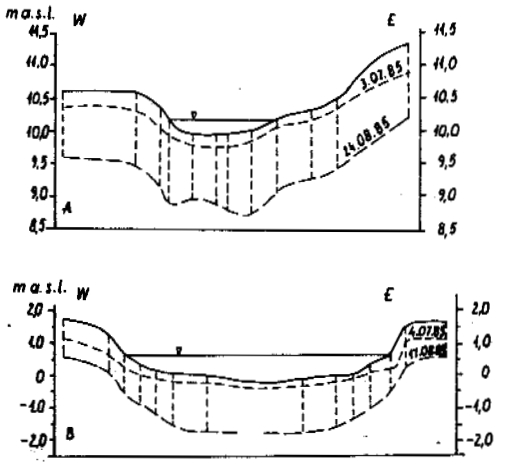

Fig. 3 Depth of soil thawing in basins of lake "A" and "B" during some terms.

active layer in adjacent area. Absolute values of thawing depth are also found to be very high, many a time over 150 cm what has not been noted during investigations of the lake "A".

TABLE V

Rate of soil thawing /in cm a day/ under and around tundra lakes in Oscar II Land /northwestern Spitsbergen/.

Lake /period/	/W/ +20	Distance from the shore /in m/ +5	0.0	-5	-10	-15	-15	-10	-5	0.0	+5	/E/ +20
A /3.07-24.08.85/	1.6	1.7	1.7	1.8	1.9	-	-	2.0	1.9	1.9	1.8	1.6
B /4.07-17.08.85/	1.27	1.25	2.0	2.09	2.64	3.59	3.11	2.77	2.43	1.54	1.95	1.16

Analysis of the figure 3 enables to compare a thawing process around two reservoirs with different parameters. Besides the mentioned differences, an influence of water mass on thawing process is illustrated by a list of rate of permafrost degradation for these reservoirs /Table V/. It is considerably larger for the lake "B" but also more diversified. Under the lake it reaches the highest values to 3.59 cm a day whereas only slightly over 1 cm a day around the lake. The rate of soil thawing around around the smaller reservoir is distinctly lower and its mean velues does not exceed 2 cm a day. It is also less differentiated and equal from 1.6 to 2.0 cm a day.

CONCLUSIONS

Above remarks and calculations lead to the following conclusions:

- investigations of 1982 and 1985 in Kaffiöyra and Sarsöyra confirmed the influence of water content of soil on depth and rate of thawing,
- it is particularly distinct around surface water reservoirs,
- extents of surface water influence of degradation of permafrost depends on size of reservoir and collected heat,
- at the beginning of thawing /June, beginning of July/ cool surface waters conserve permafrost and decrease rate of its degradation,
- highest thawing rate occurs in July when water and air temperatures reach their maxima,
- mean rate of permafrost degradation under water reservoirs and in areas with higher water content is greater than intensity of this process in adjacent areas,
- absolute values of thickness of active layer under water reservoirs are the greatest.

REFERENCES

Baranowski, S. /1968/. Termika tundry peryglacjalnej, SW Spitsbergen. Acta Univ. Wratisl, Bd 68, Wrocław.

Czeppe, Z. /1960/. Thermic differentiation of the active layer and its influence upon the frost heave in periglacial region /Spitsbergen/. Bull. Acad. Polon. Sci. Ser. Sci. Geol. et Geogr., Bd 8, 2.

Czeppe, Z. /1961/. Roczny przebieg mrozowych ruchów gruntu w Hornsundzie /Spitsbergen/ 1957/58. Zesz. Nauk. UJ, Prace Geogr., Ser. 3, Kraków.

Czeppe, Z. /1966/. Przebieg głównych procesów morfogenetycznych w południowo-zachodnim Spitsbergenie. Zesz. Nauk. UJ, Prace Geogr., Bd 13, Kraków.

Grześ, M. and Babiński, Z. /1979/. Z badań nad letnim odmarzaniem gruntu na Spitsbergenie i w Mongolii. Mater. VI Sympozjum Polarnego.

Grześ, M. /1985/. Warstwa czynna wieloletniej zmarzliny na zachodnim wybrzeżu Spitsbergenu. Przegl. Geogr., Bd 57, Warszawa.

Jahn, A. /1961/. Quantitative analysis of some periglacial processes in Spitsbergen. Zesz. Nauk. UJ, ser. B, No 5, Kraków.

Jahn, A. /1982/. Soil thawing and active layer of permafrost in Spitsbergen. Res. of invest. of the Pol. Sci. Spits. Exp., Bd 4, Acta Univ. Wratisl., No 525, Wrocław.

Jahn, A. and Walker, H.J. /1983/. The active layer and climate. Z. Geomorph. N. F., Bd 47.

Klimaszewski, M. /1960/. Geomorphological studies of the western part of Spitsbergen between Kongsfjorden and Eidembukta. Zesz. Nauk. UJ, Bd 32, Prace Geogr., No 1, Kraków.

Kossowski, J. and Sikora, E. /1978/. Cieplne właściwości gleb i metody ich wyznaczania. Probl. Agrofiz., No 27.

Marciniak, K., Szczepanik, W. and Przybylak, R. /1981/. Letnie odmarzanie gruntu na Kaffiøyrze /NW Spitsbergen/. Materiały VIII Sympoz. Polar. No 1.

Marciniak, K. and Szczepanik, W. /1983/. Results of investigations over the summer ground thawing in the Kaffiøyra /NW Spitsbergen/. Acta Univ. Nicholai Coper., Geografia XVIII, No 56, Toruń.

Monteith, J.R.L. /1977/. Fizyka środowiska biologicznego. Biblioteka Problemów, No 232.

Stäblein, G. /1970/. Untersuchung der Auftauschicht über Dauerforst in Spitsbergen. Eiszeitalter u. Gegenwart, Bd 21.

Troicki, L.S., Singer, E.M. et al. /1975/. Oliedienienije Szpitsbiergiena /Svalbarda/. Rez. Issl. po miezd. geofiz. proj..

Washburn, A.L. /1976/. Geocryology. A survey of periglacial processe and environments. E. Arnold, London.

INFLUENCE OF AN ORGANIC MAT ON THE ACTIVE LAYER

D.W. Riseborough and C.R. Burn[1]

Geotechnical Science Laboratories, Department of Geography, Carleton University,
Ottawa, Canada K1S 5B6

SYNOPSIS Field investigations of the thermal and hydrological regime of the active layer were carried out in summer at sites in the boreal forest near Mayo, Yukon Territory, Canada. The ground surface at these sites was covered by Hypnum spp. mosses. Active layer recharge occurred only when the mosses were saturated. The surficial 5 cm of the moss did not retain water readily, but precipitation from rainshowers throughout the summer was stored in the peat below the surface. Little net evaporative transfer occurred between mineral and organic horizons. Instead, the mineral soil in the active layer lost water either by temperature-induced downward migration or evapotranspiration through the root systems of vascular plants. The apparent thermal diffusivity of the surficial 5 cm of the organic layer was inversely related to a drying index. Below the surface, the diffusivity of the organic material remained constant. Hence the organic horizon buffered the ground thermal regime from the higher surface temperatures commonly associated with dry conditions.

INTRODUCTION

The atmosphere's influence on the active-layer regime may be moderated by the buffering effect of processes in the surface vegetation layer (Luthin and Guymon 1974). At many sites in the northern boreal forest, the active layer may be divided into 2 units: the surface organic horizon and the underlying mineral soil. There are commonly three soil interfaces across which exchanges of energy and moisture occur: (1) at the ground surface between the atmosphere and the organic horizon; (2) between the organic horizon and the mineral soil; and (3) between frozen and unfrozen mineral layers. These exchanges depend on many site-specific variables, such as local forest canopy closure, and soil properties such as thermal conductivity, moisture content and density. This paper reports field measurements and subsequent analyses made during the summers of 1983-85 at sites near Mayo, central Yukon Territory (Figure 1), in order to isolate the particular influence of the organic horizon on the active layer thermal and hydrologic regimes.

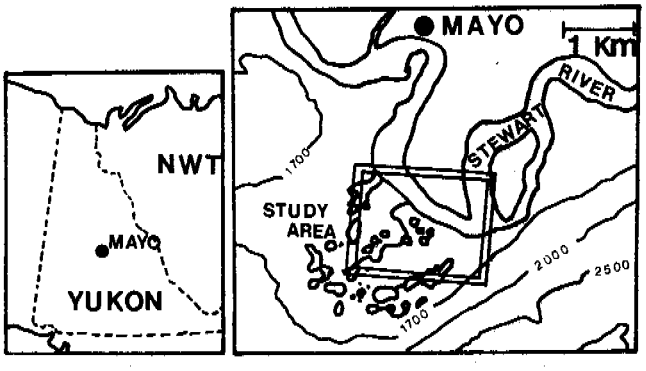

Fig. 1 The Study Site

BACKGROUND

Several authors have noted the particular influence of organic soils (especially peat) on the ground thermal regime, which leads to the association of these soils with permafrost at the southern margin of the discontinuous permafrost zone (e.g. Nakano and Brown 1972; Brown and Pewe 1973). This has been attributed to:

(1) the low conductivity of organic soils relative to mineral soil (Nakano and Brown 1972, FitzGibbon 1981);

(2) the effect of seasonal variations in the water content of organic soil on its thermal conductivity;

(3) the seasonal evaporative regime of the surface as controlled by climatic and surface factors (Ng and Miller,1977).

In hydrologic terms, the significance of the organic layer is principally due to the effects of its moisture retention properties on throughflow, storage and evaporation. Santeford (1979, cited by Chacho and Bredthauer, 1983) reported that drainage through the organic horizon only occurs after it is saturated. At other times, precipitation is absorbed by mosses and utilized for respiration. Furthermore, as will be demonstrated in this paper, evaporation from a moss surface is limited after initial drying, and vapour flow may then be dominantly downward along the saturation vapour pressure gradient.

These effects have been modelled descriptively by Luthin and Guymon (1974) Atmospheric mass and energy flows and the geothermal heat flux are boundary conditions, with the vegetation canopy, snow cover and surface organic layer acting as buffers between the atmosphere and mineral soil. In the present case, the "vegetation canopy" is a forest (predominantly white and black spruce) with associated understorey. The living ground cover combined with the dead organic substrate is the organic layer. In this paper some of the processes occurring within Luthin and Guymon's (1974) "buffer layer" are described for the Mayo sites.

FIELD MEASUREMENTS

Field studies were conducted at sites in a study area 3 km southeast of Mayo (mean annual temperature -4 C)(Figure 1). The mineral soil at the sites is ice-rich and predominantly of a silt loam or silt clay loam texture. The organic horizon is generally 10 to 20 cm thick, but may reach 40 cm.

Several sites were chosen in order to accommodate the variety of thermal and hydrologic regimes which may be found in a small area. The majority of these are in mature Picea glauca forest (sites 2,4,5,6). All sites but 3 and 7 have an organic horizon as described in the following section. Site 1 is situated on a hummock adjacent to a Picea/Salix thicket; site 3 is in agrading permafrost (in the emergent sediments of a thermokarst lake) and is covered by grasses; site 7 is in a grove of Betula and Picea, and has a leaf litter ground cover. The interaction between atmospheric demand, evaporation, and the thermal diffusivity of the the surface layer was studied at a separate Picea glauca forest site, having an organic layer approximately 15 cm thick.

The Organic Layer

At all sites, the organic layer is predominantly Hypnum spp. bryophytes, with scattered Ledum, Vaccinium and other herbaceous plants. The bryophytes cover the mineral soil completely. Hypnum spp. can be classified as "ectohydric", i.e. they function on water stored after the rhizomes are moistened by rain or dew (Proctor 1982). These species absorb and lose water over their entire surface area and operate in effective hydrologic isolation from the mineral soil. Attachment to the ground is to procure stability rather than moisture, and often a 5 to 10 cm gap between bryophytes and mineral soil can be found around the edges of soil hummocks. The moisture retention capacity of this organic material is 4 to 5 g g^{-1}; the bulk density of the organic soil varies from 0.04 g cm^{-1} at the surface to 0.11 g cm^{-1} 15 cm below the surface.

From June 20 to August 9 1983, soil and air temperatures and net radiation were recorded at five minute intervals, in order to investigate climate-surface interaction. Soil temperatures were measured with thermistors at 1, 5, 10, 25, 50, 100 cm depths; air temperatures were monitored at 1 and 15 m above ground with naturally ventilated, shielded thermistors; and net radiation was measured with Swissteco net pyradiometers. Because of variations in canopy closure, net radiation was measured at a lower height than normal (60 cm) in order to tie the measurement as closely as possible to the site where evaporation was monitored.

Evaporative Demand

Atmospheric evaporative demand was evaluated using the "Equilibrium" evaporation model (Priestley and Taylor 1972):

$$LE = (Q^* - G).\ s/(s + \gamma) \qquad (1)$$

where:

L	=	latent heat of evaporation
E	=	evaporated water
Q*	=	net radiation
G	=	ground heat flux
s	=	slope of saturation vapour pressure curve
γ	=	psycrometric constant.

Notwithstanding its potential significance, the ground heat flux was ignored in the present study. Radiation measurements were taken within 1.5 m of the lysimeter.

Lysimeters

Evaporation was monitored with lysimeters 9.8 cm in diameter and 20 cm deep. Lysimeter mass (~800 g) was measured on an approximately daily basis with a portable balance to $\pm$ 0.1 g (= 0.02 mm water). The lysimeters, which were sealed at the bottom, were weighed as soon as possible after rainshowers, and were drained manually when water accumulated at the bottom. Precipitation values obtained by the lysimeters are measurements of "net precipitation", since evaporation occurred during and after rainfall, but before measurement. Similarly, rainfall at night and early morning dew were compounded in some measurements of evaporation.

Neutron Probe

Soil moisture content profiles were measured with a Pacific Nuclear neutron probe (model CPN-503). Soil specimens were recovered at the time of access tube installation for calibration of probe counts against soil moisture content.

Apparent Thermal Diffusivity

The apparent thermal diffusivity of the soil was determined from the amplitude of the daily temperature wave at two depths. Assuming that the daily wave is approximately sinusoidal, k can be determined using:

$$k = \frac{\omega(z_2 - z_1)}{2\ \ln^2(A_2/A_1)} \qquad (2)$$

where ω = angular frequency
z_1, z_2 = depths below the surface
A_1, A_2 = temperature amplitude at depth z
k = apparent thermal diffusivity.

Equation 2 was used to determine the apparent diffusivity of two layers within the organic mat: between 1 and 5 cm, and between 5 and 10 cm below the surface.

RESULTS AND DISCUSSION

1. The atmosphere-organic interface.

The net radiation and temperature data were used to determine the evaporative demand ($Q^* \cdot s/(s+\gamma)$) over lysimeter measurement intervals of 4 to 28 hours duration. The relationship between demand and evaporation is shown in Figure 2. The symbols show the number of intervals which have elapsed since the last rainfall rewetted the moss surface. The data show that a fairly consistent relationship exists between evaporation and demand during the initial period. However, as drying proceeds, the evaporation rate declines.

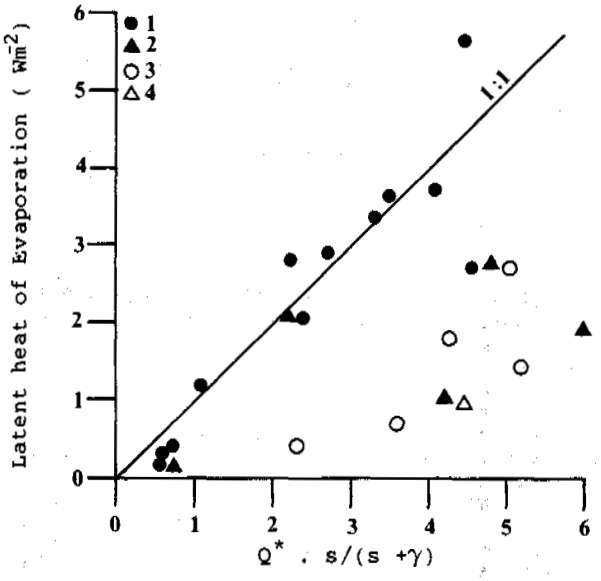

Fig. 2 Evaporation vs. Evaporative Demand (numbers refer to evaporation periods elapsed since rain)

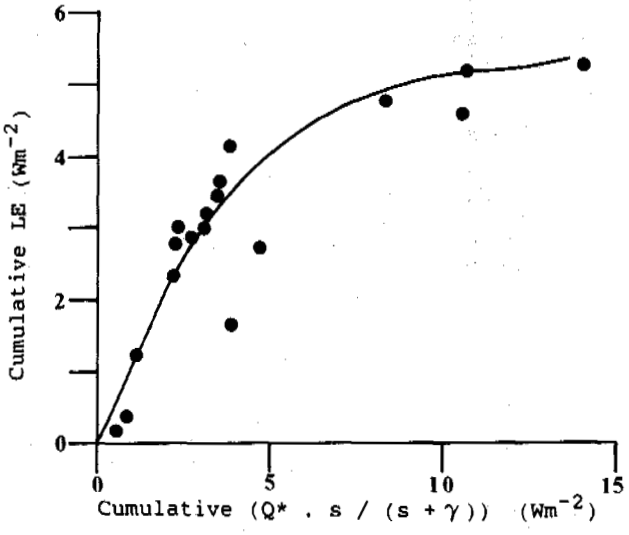

Fig. 3 Cumulative Evaporation vs. Cumulative Demand

To examine the effect of progressive drying on the surface response to evaporative demand, the two variables were accumulated: Cumulative values were obtained by summing values from the individual measurement intervals between rainfall events (starting from zero after each rain). Data for all of the individual cumulation periods are plotted together in Figure 3. The curve shown was generated by polynomial regression. Two points fall significantly below the line. These represent periods when the preceeding rainfall was insufficient to replenish surface water completely.

The evaporation rate becomes limited after a loss of about 1 mm. This may be attributed to: (1) the properties of the organic layer; and (2) the presence of permafrost. The density of the moss surface is very low, limiting uptake of water from below: hence the availability of water for evaporation is restricted. As the desiccated surface layer becomes thicker, the level from which water evaporates becomes deeper, and therefore cooler. The lower temperature at depth implies a lower saturation vapour pressure. Evaporation is curtailed when the vapour pressure gradient is dominated by the soil temperature gradient, forcing vapour flow toward the frost table.

2. Recharge.

Lysimeter measurements of precipitation and evaporation at seven sites in the study area are summarized in Table I. The lysimeters provide an index of the relative amounts of precipitation received at the various sites. The "net evaporation" at each site is also indicated in the table. The results suggest that when precipitation is inadequate to saturate the surface (e.g. in July 1985 no water

TABLE I

Net Lysimeter Precipitation and Evaporation July 1984, and June and July 1985.

Net precipitation (cm).

	Site						
MONTH	1	2	3	4	5	6	7
7-84	1.47	2.24	2.29	0.69	1.16	2.76	2.19
6-85	2.69	3.44	3.80	2.33	3.44	3.41	3.40
7-85	2.40	1.19	1.72	-	2.95	0.78	1.42

Net evaporation (cm).

	Site						
MONTH	1	2	3	4	5	6	7
7-84	1.45	1.73	1.21	1.15	2.81	1.21	2.14
6-85	2.05	1.60	1.64	2.23	2.03	1.31	1.62
7-85	1.56	1.40	1.29	-	2.00	0.84	1.55

Net change (cm).

	Site						
	1	2	3	4	5	6	7
7-84	+0.02	+0.51	+1.08	-0.46	-1.65	+1.55	+0.05
6-85	+0.65	+1.84	+2.16	+0.09	+1.41	+2.10	+1.78
7-85	+0.84	-0.21	+0.43	-	+0.95	-0.06	-0.13

was drained from the lysimeters), net evaporation is approximately equal to net precipitation. This implies that recharge is not affected by rainfall events which do not saturate the organic layer, as suggested by Santeford (1979).

Further evidence supporting Santeford's hypothesis can be obtained from a comparison of net moisture content changes in the surface layer (measured by lysimeters), and soil moisture changes in mineral soil (detected by the neutron probe) (see Table II). The water content of the mineral soil did not increase over any of the measurement intervals due to evapotranspiration by trees, shrubs and herbs (cf. Wright 1981; Rouse 1984). In contrast, the water content of the surface layer either increased, or declined by a relatively small amount.

TABLE II

Net Change in Water Content (cm) of Organic and Mineral Horizons, July 1984 and June and July 1985.

	Site 1		Site 2		Site 3		Site 4	
MONTH	L[a]	NP[a]	L	NP	L	NP	L	NP
7-84	+0.02	-1.6	+0.51	-7.6	+1.08	-2.9	-0.46	-4.3
6-85	+0.65	-3.2	+1.84	-8.9	+2.16	-5.5	+0.09	-1.5
7-85	-0.84	-3.0	-0.21	-0.8	+0.43	-1.8	-	-

	Site 5		Site 6		Site 7	
MONTH	L	NP	L	NP	L	NP
7-84	-1.65	-10.4	+1.55	-0.5	+0.05	-4.9
6-85	+1.41	-0.7	+2.10	-4.2	+1.78	-4.0
7-85	+0.95	-2.0	-0.06	-2.2	-0.13	-1.4

Several papers reviewed by Rutter (1975) indicate that the ground surface accounts for only 10 to 12 percent of total evaporation from coniferous forests. The data in Table II are not directly comparable with these figures, since they do not account for the evaporation of precipitation intercepted by vegetation. In addition, it is difficult to isolate inflow and outflow (evapotranspiration) from the mineral soil, when the rate of infiltration is small as a result of low soil permeability. Therefore, changes in the water content of mineral soil measured by the neutron probe are underestimates of evapotranspiration. However, Table II does indicate that the two layers function independently.

Neutron probe measurements of mineral layer desiccation may be compared with the net evaporation determined with the lysimeters through inspection of Tables I and II. Given that the neutron probe observations under-estimate evapotranspiration, these data compare favourably with those presented by Rutter (1975).

The lysimeter data support the physiological concept of the surface moss forming a unit hydrologically separated from the mineral soil. Flow into mineral soil occurs only when the organic layer is saturated. Flow out of mineral soil continues throughout the summer through transpiration via trees and shrubs.

TABLE III

Net Lysimeter Evaporation and Mineral Soil Desiccation (cm), July 1984 and June and July 1985.

	Site 1		Site 2		Site 3		Site 4	
MONTH	L[a]	NP[a]	L	NP	L	NP	L	NP
7-84	1.45	1.6	1.73	7.6	1.21	2.9	1.15	4.3
6-85	2.05	3.2	1.60	8.9	1.64	5.5	2.23	1.5
7-85	1.56	3.0	1.40	0.8	1.29	1.8	-	-

	Site 5		Site 6		Site 7	
MONTH	L	NP	L	NP	L	NP
7-84	2.81	10.4	1.21	0.5	2.14	4.9
6-85	2.03	0.7	1.31	4.2	1.62	4.0
7-85	2.00	2.0	0.84	2.2	1.55	1.4

a.: L = Lysimeter measurement.
NP = Neutron probe measurement

These results imply that changes in the moisture content of mineral soil during the summer at these sites may be analysed without reference to the hydrodynamics of the organic layer.

The decrease in moisture content of the active layer implies that discharge continues throughout the summer. Hence the importance of snowmelt as a major recharge period in the soil hydrologic cycle, as determined by Kane and Stein (1983) for much of Alaska, should be recognised.

3. Thermal diffusivity and surface drying.

While the apparent thermal diffusivity (k) of the organic surface layer could be estimated (from the record of temperature measurements), changes in the moisture content of the upper surface of the organic layer as drying proceeded could not. In order to establish the relationship bewteen these variables, an index of soil dryness was extracted from the lysimeter data.

Surface Water Deficit

From the lysimeter data, an index of surface dryness ("Surface Water Deficit") was calculated as follows:

- the initial deficit was assumed to be zero.
- evaporation (i.e. falling lysimeter water content) increased the deficit, while rain (increasing lysimeter water content) decreased the deficit (to a minimum of zero).
- changes in the deficit were assumed to occur at a constant rate between measurements.
- the deficit was assumed to be zero during periods of rain for which rainfall exceeded cumulative evaporation.

Using these rules, the raw lysimeter data (Figure 4.) were transformed into the Surface Water Deficit (Figure 5.), and subsequently converted to daily average values.

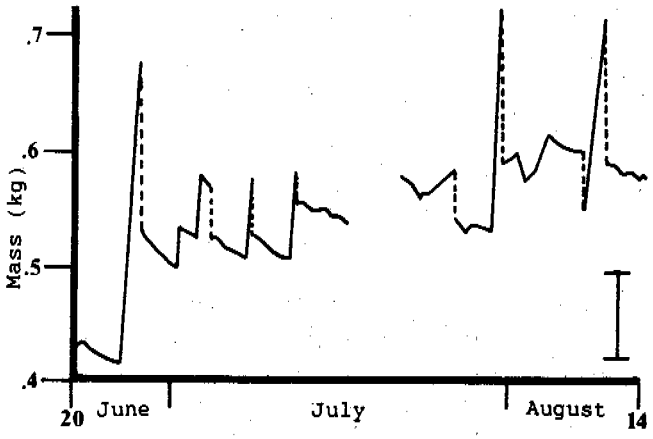

Fig. 4 Seasonal Variation in Lysimeter Mass

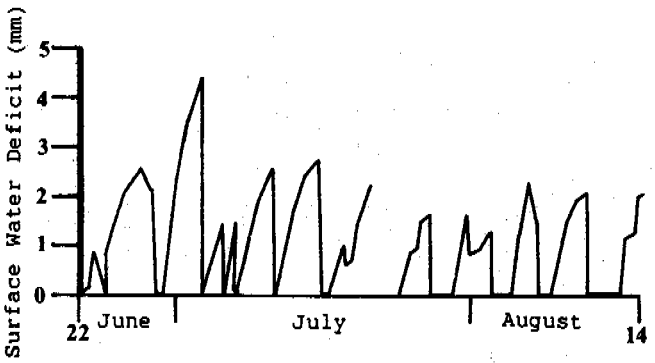

Fig. 5 Seasonal Variation in Surface Water Deficit

The relationship between the surface water deficit and the apparent diffusivity at two depths is shown in Figures 6 and 7. The results for the 5-10 cm layer show a few very high values for k over the range of water deficits. These may be due to the influence of lower frequency surface temperature variations (such as those associated with synoptic weather patterns), which become relativly more important at depth. These are assumed to be artifacts of the method of analysis, and are not considered further.

The diffusivity of the 1-5 cm layer shows an approximately inverse relationship with the water deficit. When the deficit is near zero, the diffusivity is approximately similar to that for mineral soils, falling to the value for the lower layer after the deficit has reached two mm.

The high diffusivity of the 1-5 cm layer at water deficits below 2 mm indicates that conduction and thermally driven vapour diffusion are not the only heat transfer processes functioning in this layer. Nakano and Brown (1972) noted a similar effect in the validation of their model of the ground thermal regime, which they ascribed to "intensive evaporative heat transfer". The effect measured here is much greater than that observed by Nakano and Brown (1972); however, their results apply to the entire organic layer, so that an effect limited

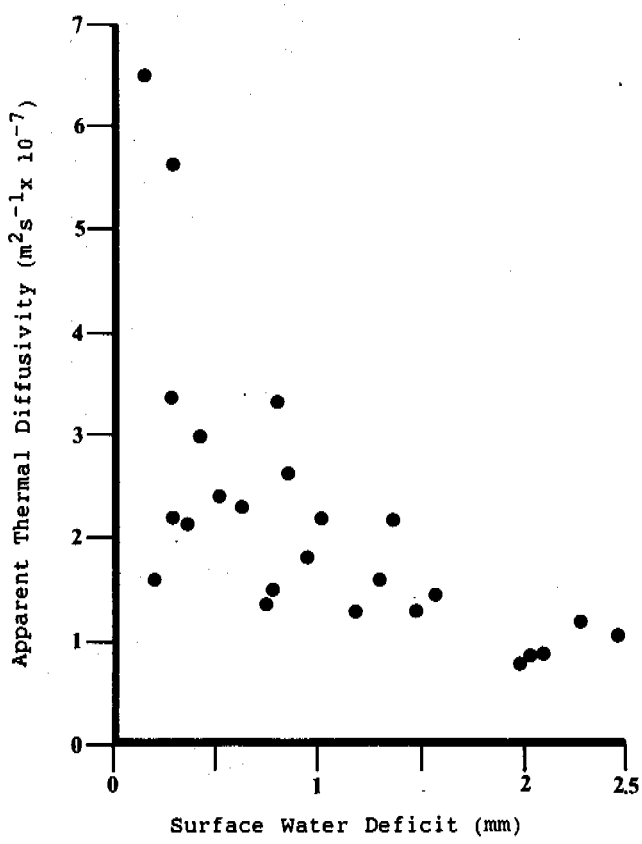

Fig. 6 Apparent Diffusivity vs. Surface Water Deficit : 1—5 cm Layer

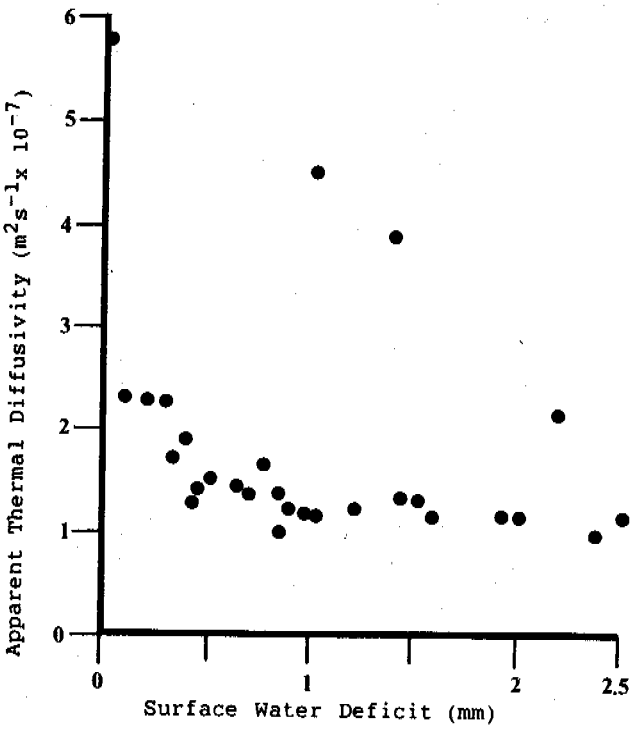

Fig. 7 Apparent Diffusivity vs. Surface Water Deficit : 5—10 cm Layer

to the surface would be averaged over the entire layer.

When the deficit is higher than 0.5 mm, the diffusivity of the deeper layer is consistently in the range 1.0 - 1.4 x 10^{-7} $m^2 s^{-1}$. At lower deficits, diffusivity shows a slight dependence on the deficit, which may be due to heat transfer by percolating rain water. The stable diffusivity value at higher deficits indicate either that the water content of this layer is not affected by surface drying, or that the diffusivity of the organic material is not significantly affected by such variations.

CONCLUSIONS

We conclude:

(1) The reduced evaporation rate after a loss of only 1 mm of water, and the consistently low apparent thermal diffusivity of the lower part of the organic layer indicates that evaporative moisture loss does not reach this layer. If it did, one would expect the apparent diffusivity of this layer to increase as the drying layer extended into it.

(2) The moisture regime of the surface organic layer is not linked closely to that of the mineral soil. Evaporation from the organic layer is retarded as drying proceeds, indicating that little uptake from mineral soil occurs: indeed, vapour flow may be downward along the soil temperature gradient. In turn, the mineral soil is not recharged during summer precipitation unless the organic layer is saturated.

(3) The moisture-dependent thermal diffusivity of the upper part of the organic layer , combined with the consistently low thermal diffusivity of the lower part, is primarily responsible for the maintenance of cool conditions in the mineral horizon of the active layer. When the organic material is moist and has a high k value, evaporation lowers the ground surface temperature. As the organic material dries and the surface temperature rises, k declines, inhibiting propagation of the surface temperature wave. Thus, the mechanism described by Brown and Pewe as operating at a seasonal time scale also operates on a synoptic time scale.

ACKNOWLEDGEMENTS

Field studies were supported by Earth Physics Branch, Energy, Mines and Resources Canada; Atmospheric Environment Service, Environment Canada; Department of Indian and Northern Affairs Canada; Arctic Institute of North America; and the Canadian Commonwealth Scholarship Committee.

1. C.R. Burn's present address:
Department of Geography, University of British Columbia, Vancouver, Canada V6T 1W5.

REFERENCES

Brown, R.J.E. and T.L Pewe (1973). Distribution of permafrost in North America and its relationship to the environment: a review, 1963-1973. Proc. 2nd Int. Conf. on Permafrost, North American Contr., pp. 71-100.

Chacho, E.F., Jr. and S. Bredthauer (1983). Runoff from a small sub-arctic watershed, Alaska. Proc. 4th Int. Conf. on Permafrost. pp. 121-126.

FitzGibbon, J.E. (1981). Thawing of seasonally frozen ground in organic terrain in central Saskachewan. Can. J. Earth Sci. 18, pp. 1492- 1496.

Kane, D.L. and J. Stein (1983). Field evidence of groundwater recharge in interior Alaska. Proc. 4th Int. Conf. on Permafrost. pp. 572-577.

Luthin, J.N. and G.L. Guymon (1974). Soil moisture-vegetation-temperature relationships in central Alaska. J. Hydrology 23, pp.233246.

Nakano, Y. and J. Brown (1972). Mathematical modelling and validation of the thermal regimes in tundra soils, Barrow Alaska. Arct. Alpine Res. 4, pp 19-38.

Ng, E. and P.C. Miller, (1973). Validation of a model of tundravegetation on soil temperatures. Arct. Alpine Res. 9, pp. 89-104.

Priestley, C.H.B. and R.J. Taylor (1972). On the assessment of surface heat flux and evaporation using large scale weather parameters. Mon. Weath. Rev. pp.81-92.

Proctor, M.C.F. (1982). Physiological ecology: Water relations, light and temperature responses, carbon balance. Ch. 10,pp. 333-381, in Smith, A.J.E. (ed.) Bryophyte ecology.Chapman and Hall, London.

Rouse, W.R. (1984). Microclimate of arctic tree line 2. Soil microclimate of tundra and forest. Water Res. Res. 20, pp. 67-73.

Rutter, A.J. (1975). The hydrological cycle. in Monteith, J.L.,(ed) Vegetation and the atmosphere, Vol. 1. Priciples. Academic Press. 278 p.

Santeford, H.S. (1979). Toward hydrological modelling of the black spruce/permafrost ecosystems of interior Alaska. Presented at the Third Northern Research Basin Symposium Workshop, The State-of-the-Art in Transposable Watershed Models: Quebec, Canada, Laval University.

Wright, R.K. (1981). The water balance of a lichen tundra underlain by permafrost. McGill U. Sub-arctic Res. Paper 33, Climatological Res. Series 11. 110 p.

PERENNIAL DISCHARGE OF SUBPERMAFROST GROUNDWATER IN TWO SMALL DRAINAGE BASINS, YUKON, CANADA

R.O. van Everdingen

The Arctic Institute of North America, Calgary, Canada T2N 1N4

SYNOPSIS The discharge of groundwater by perennial springs feeding Snag Creek and Mirror Creek in the Yukon indicates that subpermafrost water in alluvial and glacio-fluvial fans can provide high-quality water supplies in the zone of widespread discontinuous permafrost.

INTRODUCTION

Snag Creek, originating in the Wellesley Mountain - Carden Hills area in Alaska, is a tributary of the White River in Canada; Mirror Creek, originating in Canada, is a tributary of the Chisana River in Alaska. Both receive discharge of groundwater from springs in an extensive area of peatland situated between the Alaska Highway and the Yukon - Alaska border. The Alaska Highway crosses Snag Creek near latitude 62°28'33"N and longitude 140°51'52"W, about 11 km north of the settlement of Beaver Creek, Yukon (Fig. 1).

Information on the spring area was obtained from a variety of sources, including airphotos taken in May 1964, August 1976, and April 1978; maps of the surficial geology of the area (Rampton, 1978a, 1978b); shallow testholes drilled between 1976 and 1980 along two routes selected for the proposed Alaska Highway Gas Pipeline; part-time discharge records from a gauging station on Snag Creek for the period 1978-1983; and chemical and isotope analyses on water samples from the two creeks and several springs, collected between September 1979 and October 1983. This paper presents an interpretation of the available information.

TESTHOLE DATA

Shallow (3.0 to 12.0 m) test drilling was carried out in the study area along two routes selected for the proposed Alaska Highway Gas Pipeline. Testhole data from several drilling projects completed during the period 1976-1980 were made available by Foothills Pipe Lines Ltd., Calgary. Locations of the testholes are indicated in Figure 1.

The testhole logs indicated that the spring area is underlain by a sequence consisting of: gravelly glacio-fluvial deposits, ranging in thickness from 2.5 m to more than 11.4 m; sandy/silty alluvium, ranging in thickness from 0 m to more than 10.0 m; and an extensive cover of peat up to 1.1 m thick.

Perennially frozen ground, ranging in thickness from 1.5 m to more than 10 m, was found in 24 of the 43 testholes for which data are available (Fig.1). No frozen ground was found in the testholes at Mirror Creek, Snag Creek and Beaver Creek, or in those near spring sites. Visible, segregated-ice content in core samples collected from the permafrost ranged from 0 to nearly 100 percent by volume. Moisture contents ranged from 2 to 220 percent of dry weight in the clastic sediments, and up to 670 percent in the peat cover.

Groundwater was encountered below permafrost in several of the testholes, at depths ranging from 2.5 to 7.0 m. Waterlevels in testholes equipped with standpipes ranged from groundlevel to 6.5 m below ground.

SPRING LOCATIONS

A total of 34 springs and their discharge channels (Figure 1) were identified, primarily on false-color infrared airphotos taken in August 1976 (National Air Photo Library No. A37365IR/7-91). Flow directions in Beaver Creek, Snag Creek, and Mirror Creek are indicated by arrows near the borders of Figure 1.

The water discharged by the springs is clear and cold (see columns D, H, and I in Table I), and the discharge channels show little of the brown coloring common in peatland discharge elsewhere. The April 1978 airphotos revealed that the discharge from the springs maintains long reaches of open water in both Mirror Creek and Snag Creek during the winter. Icings up to 1.3 m thick can extend several kilometres downstream from the open-water reaches.

DISCHARGE DATA

A gauging station was operated on Snag Creek just downstream from the highway crossing

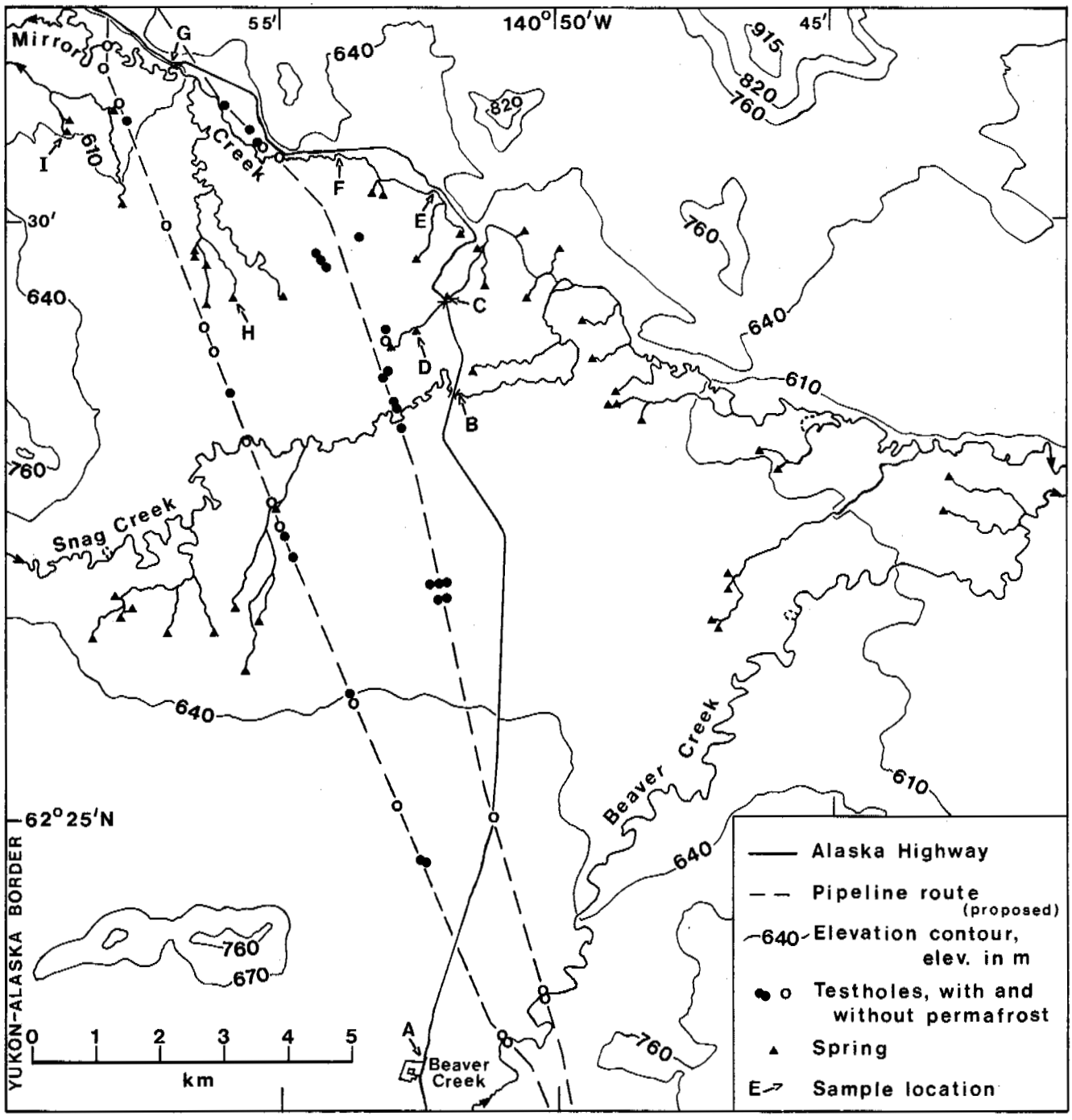

Fig. 1 Location map of the Snag Creek - Mirror Creek spring area, Yukon.

during the period from early-May to mid-October in each of the years 1978 to 1983. Daily discharge data for this station were made available by the Water Resources Division, Department of Northern Affairs, Whitehorse, Yukon (Anon., 1984).

A plot of the discharge data for the period 1978 to 1983 is shown in Figure 2. The plot indicates a baseflow rate of about 4 m^3/s in Snag Creek. Minimum measured discharge rates for the years 1978 to 1983 ranged from 4.0 to 4.8 m^3/s. Unfortunately, streamflow data are not available for any year for the period between mid-October and early-May to confirm that these are indeed the annual minima. The baseflow values represent primarily the flow from the 11 springs that discharge into Snag

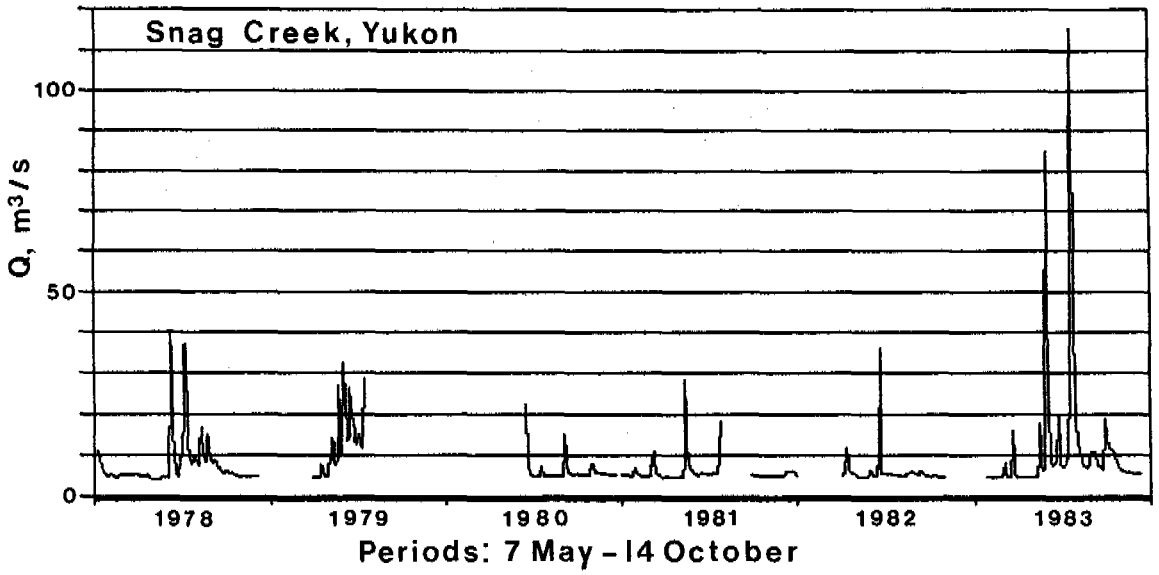

Fig. 2 Daily discharge data for the period from 7 May to 14 October in the years 1978 1983 for the Snag Creek gauging station.

Creek above the gauging station. This suggests that the total discharge from the spring area as a whole could be as high as 12 m^3/s. Seepage from the active layer in the area surrounding the springs probably makes only a minor contribution to the baseflow in Snag Creek, because the creek water does not show the brownish colour characteristic for seepage from peatlands.

The only discharge measurement available for Mirror Creek, made at site G (Fig.1), representing discharge from 8 spring sites, indicated a discharge rate of 2.8 m^3/s.

WATER CHEMISTRY

Water samples were collected from a number of locations in the area on several occasions between late-September 1979 and early-October 1983. The sample locations are indicated in Figure 1. Major-ion analyses were performed by the Water Quality Laboratory of Environment Canada in Calgary. Table I lists sampling dates, results of field measurements, and results of selected chemical analyses. The analyses are illustrated by Figure 3, showing graphs representing the major-ion composition of the three springs sampled in the area, and

TABLE I

Physical and Chemical Data Sum

Location	A Shallow well	B Snag Creek	C Channel from D	D Spring	E Mirror Creek	F Mirror Creek	G Mirror Creek	H Spring	I Spring
Sample Date	25-3-80	25-3-80	25-3-80	29-4-82	23-7-82	5-10-83	5-10-83	29-4-82	29-4-82
Temp., °C	0.5	0.0	0.5	1.0	12.9	0.8	1.1	1.0	1.0
pH, units	7.9	8.0	7.5	7.6	7.4	7.5	7.8	7.6	7.5
Cond., µS/cm	305	360	295	283	310	305	335	315	311
CONC., mg/l (1)									
Calcium	47.7	54.9	47.2	46.1	45.2	43.3	50.9	50.7	50.7
Magnesium	7.3	10.1	7.5	7.8	8.1	6.9	7.4	9.0	9.5
Sodium	3.1	3.0	3.9	4.4	3.7	4.2	3.1	2.8	3.0
Potassium	1.2	1.3	1.3	1.4	1.0	1.5	1.3	1.2	1.2
Bicarbonate	158.6	183.0	146.0	140.3	146.4	146.3	164.6	152.5	170.7
Sulfate	20.0	39.0	31.0	32.0	26.0	28.0	34.0	30.0	26.0
Chloride	2.0	0.7	0.8	0.8	1.8	1.3	0.8	0.3	0.4
Fluoride	0.05	0.06	0.06	0.13	0.08	0.06	0.07	0.09	0.11
Silica	14	14	14	15	7	15	14	12	13
SUM	254.0	306.1	251.8	247.9	239.3	246.6	276.2	258.6	274.6

(1) Analyses: Water Quality Branch, Environment Canada.

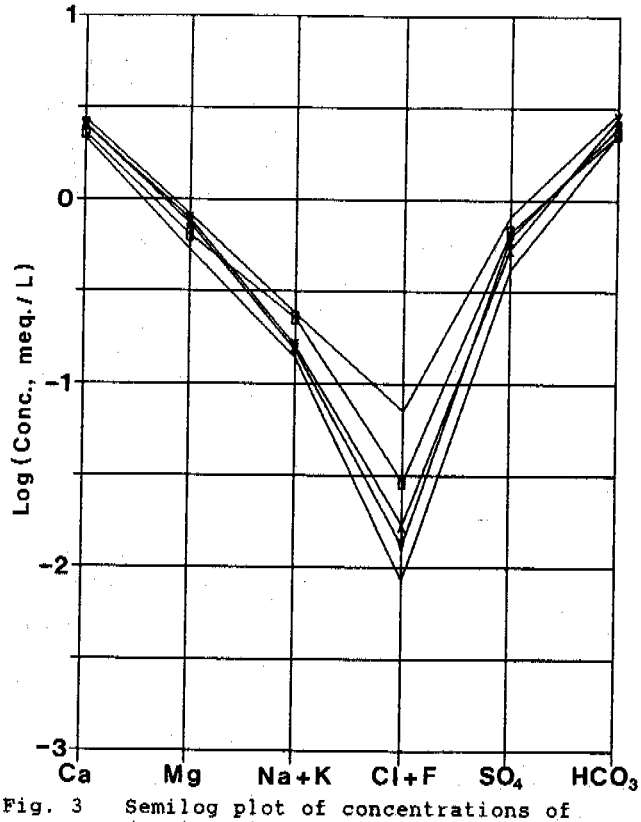

Fig. 3 Semilog plot of concentrations of major ions in water samples from 3 springs (□ - D, ▽ - H, and X - I), compared with the maximum and minimum concentrations for the whole sample set from the spring area.

graphs for the maximumn and minimum concentrations for the whole sample set.

The results of the analyses show relatively narrow concentration ranges both for total dissolved solids and for individual ions. Concentrations of silica were relatively high in all the samples, reflecting the high silicate content of both bedrock and unconsolidated sediments in the two drainage basins. Seasonal variations for individual sample locations were small.

The analytical results suggest that the spring area could provide a high-quality water supply with a relative constant chemical composition.

ISOTOPE DATA

Isotope analyses for deuterium (^2H), oxygen-18 (^{18}O), and radioactive tritium (^3H) were carried out on a number of the water samples by the Environmental Isotope Laboratory, Department of Earth Sciences, University of Waterloo, Waterloo, Ontario. The resulting δ^2H and $\delta^{18}O$ values are expressed as per-mil deviations from the usual standard, Standard Mean Ocean Water (SMOW); the results of the

TABLE II

Isotope Data (1)

Location (Fig. 1)	Date	δ^2H ‰ SMOW	$\delta^{18}O$ ‰ SMOW	^3H T.U.
A	25-3-80		-22.4	200
B	27-9-79		-22.1	150
B	25-3-80		-23.1	200
B	17-5-80		-22.2	201
B	1-5-82		-22.5	246
B	5-10-83	-173	-22.5	205
C	27-9-79		-22.1	100
C	25-3-80		-22.9	146
C	17-5-80		-22.5	108
C	23-7-82			174
C	16-7-83	-181	-22.3	183
C	5-10-83	-176	-22.5	179
D	29-4-82		-22.8	157
E	23-7-82			62
F	17-5-80		-22.5	47
F	23-7-82			102
F	16-7-83	-178	-21.7	100
F	5-10-83	-175	-22.5	99
G	27-9-79		-22.2	63
G	1-5-82		-22.6	134
G	23-7-82		-22.8	131
G	16-7-83	-177	-22.5	140
G	5-10-83	-173	-22.3	134
H	29-4-82		-22.6	183
I	29-4-82		-22.5	72

(1) Analyses: Environmental Isotope Lab., University of Waterloo

tritium analyses are expressed in tritium units (1 T.U.= 1 tritium atom per 10^{18} hydrogen atoms). They are listed in Table II and illustrated by Figures 4 and 5.

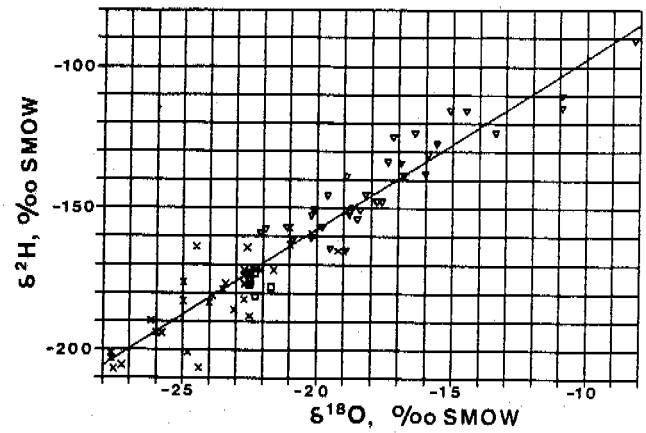

Fig. 4 Comparison of δ^2H and $\delta^{18}O$ values for samples of discharge from the spring area (□), with similar data for rain (▽) and snow (X) at Whitehorse (1961-1965) and other places in the S.W. Yukon (1979-1983).

In Figure 4, the δ^2H and $\delta^{18}O$ values for the samples from the study area are compared with data for precipitation samples collected during the period 1961-1965 at Whitehorse, Yukon, the nearest station for which such data are available (I.A.E.A., 1962-1969), and between 1979 and 1984 at various other places in the S.W. Yukon. The position of the points for the spring-water samples in Figure 4 suggests that the spring water represents recharge from precipitation, with a significant contribution from snowmelt.

The tritium values for the samples from the study area are plotted in Figure 5, which also shows the tritium values for precipitation collected at Whitehorse during the period 1961-1967 (I.A.E.A., 1962-1969), and at other places in the S.W. Yukon during the study period. Back-extrapolation of the sample values, along lines representing the tritium half-life of 12.35 years, indicates that the water discharged from the springs represents precipitation that fell some 15 to 20 years earlier. The actual residence time of the water in the aquifer could be somewhat longer than that, because the tritium values are likely depressed by dilution of the spring water with more recent precipitation draining from the peatlands in the spring area.

The recharge area for the spring system is presumed to be located in the hills and low mountains just west of the Yukon-Alaska border, from 5 to 8 km distant. The approximate distance between the recharge and discharge areas, in combination with the derived residence time of 15 to 20 years suggests average flow velocities of about 1 m/day, not unreasonable for the gravelly glaciofluvial deposits.

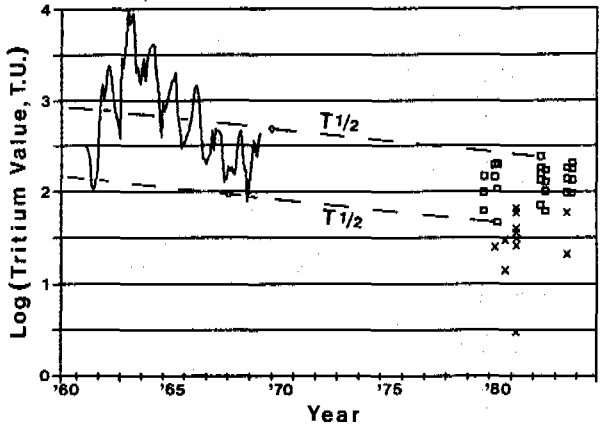

Fig. 5 Comparison of ^3H concentrations for samples of discharge from the spring area (□) with similar data for precipitation at Whitehorse (1961-1967, line graph) and at other locations in the S.W. Yukon (1979-1983, x). The slope of the lines labelled $T^1/_2$ represents the tritium half-life of 12.35 years.

CONCLUSIONS

The baseflow rates measured at the Snag Creek gauging station indicate that the 11 spring sites feeding the creek year-round have average discharge rates of 360 l/s or about 31,000 m^3/day, of water with total-dissolved-solids concentrations varying form 235 to 310 mg/l. The available isotope data indicate that the water discharged by the springs represents snowmelt and rainfall that entered the groundwater system as recharge some 15 to 20 years earlier.

The Snag Creek - Mirror Creek spring area thus provides an example of the significant water-supply potential of subpermafrost aquifers in alluvial and glacio-fluvial fan deposits in the area of widespread discontinuous permafrost.

ACKNOWLEDGEMENT

Field work in the study area was carried out when the author was employed by the National Hydrology Research Institute, Environment Canada, in Calgary. Assistance in the field was provided by J.A.Banner.

REFERENCES

Anonymous. (1984). Yukon Water Resources Hydrometric Program - Historical Summary 1975-1983. Water Resources Division, Department of Indian and Northern Affairs, Whitehorse, Yukon, 214 pp.

I.A.E.A. (1962-1969). Environmental Isotope Data Series. International Atomic Energy Agency, Vienna, Austria.

Rampton, V.N. (1978). Mirror Creek, Yukon Territory. Geological Survey of Canada, Ottawa, Map 4-1978.

Rampton, V.N. (1978). Koidern Mountain, Yukon Territory. Geological Survey of Canada, Ottawa, Map 5-1978.

WETLAND RUNOFF REGIME IN NORTHERN CANADA

Woo, M.K.

McMaster University, Hamilton, Ontario, Canada

SYNOPSIS Large areas in northern Canada are occupied by wetlands. The runoff regime of these areas is governed by the prolonged seasonal frost, rapid and considerable release of snowmelt water, limited groundwater storage capacity, and the prevalence of surface flow on the wetlands. The regimes of two wetland streams, one in the arctic and the other in subarctic Canada were analysed in conjunction with hydrological process studies. Winter is a period with little runoff because of intense coldness; but spring snowmelt, couple with frozen ground conditions, generates freshets that may be intensified by snow dams and ice jams in the channels. As the ground thaws, subsurface and depression storage capacities increase. Although runoff responds readily to rainstorms, the recession flow is extended by water released from storage. The seasonal flow pattern as described above is typical of most wetlands rivers in the cold region.

INTRODUCTION

Wetlands, defined as areas where the water table is at or near the ground surface for most parts of the thaw season, cover extensive territories in permafrost regions. The seasonal runoff pattern of those rivers that drain the wetlands of northern North America has been designated as muskeg regime by Church (1974). According to Church, flood flows in wetlands are greatly attenuated "because of the large water-retaining capacity of muskeg vegetation, as well as the high resistance to runoff presented by it and the frequently irregular surface". The basin response "to individual input events is also affected by the presence of permafrost", with "the recession time (being) very great in relation to comparative data in temperate regions".

Church quoted two examples to illustrate muskeg regime, but they are probably not typical of most northern wetland rivers. Flow data for Kakisa River in the Northwest Territories of Canada (area 14,900 km^2) were collected below a large lake and the lake storage effect overwhelms any wetland influence. In fact, the regime of a river next to the Kakisa, but not immediately affected by a large lake, reveals a different runoff regime. Figure 1 contrasts the seasonal flow patterns of Kakisa and its neighbouring Little Buffallo River (area 3,600 km^2), both located in the subarctic. It is evident that in the absence of a large lake, the wetland influence is not strong enough to smooth out the flashiness of snowmelt and rainstorm generated peak flows. This negates Church's (1974) claim that the hydrological effect of extensive wetlands "is similar to that of the presence of a relatively large lake". The other example quoted by Church, the Ogotoruk basin in Arctic Alaska (area 98 km^2, 68° 07'N, 165° 45'W) has a very low winter precipitation (Allen and Weedfall 1966) so that the absence of a spring freshet is due to water limitation instead of wetland storage. This example contrasts sharply with the Barrow basin, also in Arctic Alaska, with an area of 1.6 km^2, at 71°10'N, 156°15'W, (Brown et al. 1968). Church mentioned the Barrow basin but did not explain why it has a pronounced spring freshet (Fig. 1).

In the decade since Church proposed the muskeg regime, more data have become available and further research has added to an understanding of the hydrological processes which govern wetland runoff. This paper proposes to relate the wetland runoff regime to the processes occurring in the Arctic and the subarctic and then generalize upon the flow characteristics typical of the northern wetland regime.

ARCTIC WETLAND

Arctic wetlands are often limited in areal extent and may exist alongside non-wetland zones within the same drainage basin. In many instances, their presence is due to the abundant water supply from lakes, late-lying snowbanks or river discharge upslope of the wetlands (Roulet and Woo 1986a), or they occupy narrow coastal plains with low gradient and poor drainage (Brown et al. 1968). A small basin located in the District of Keewatin in northern Canada (64°27'N, 97°47'W) provides an example of a stream influenced by arctic wetland runoff.

Study site

The study basin is located in a continuous permafrost area with an active layer thickness of 0.5-1.3 m. The 12 km2 basin has a series of lakes connected by wetlands and streams (Fig. 2). Tundra vegetation covers most of the land surface and the wetlands are vegetated by sedges, grasses and mosses. Peat development is limited, reaching only

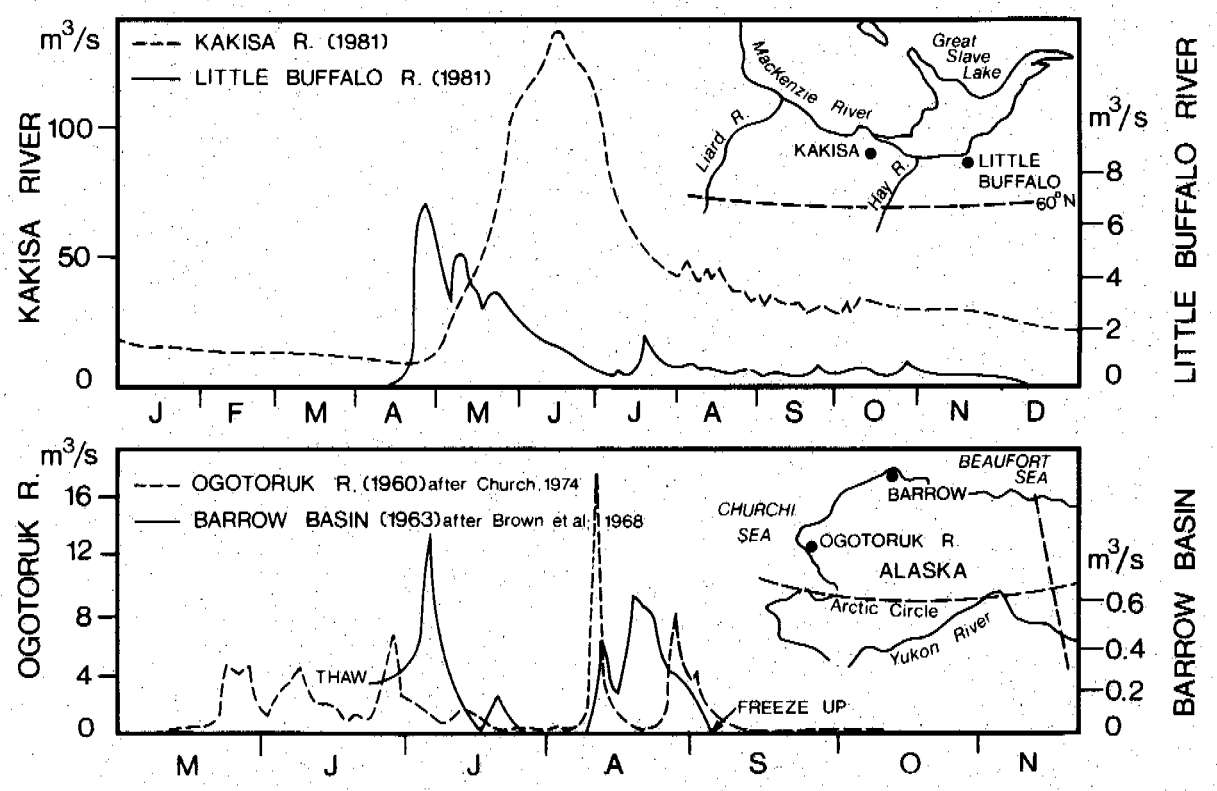

Figure 1. Streamflow regime of typical wetland rivers (Little Buffalo River and the stream from Barrow basin) compared with Kakisa Rivr below a large lake and Ogotoruk River where winter snow accumulation is limited.

0.25 m in the wetlands. The peat is highly compacted, with a large specific retention, and a specific yield of only 6±3%. Thus, the organic layer can absorb a lot of moisture without yielding much to runoff. The hydraulic conductivity is 3.2±1.4 m/d. The wetland surface is uneven, and this provides a depression storage of 0.024 m which is twice that of the non-wetland sites (Woo 1986).

Roulet and Woo (1986b) has reported on the hydrological behaviour of the wetlands in this basin. The present paper will compare the streamflow regime of the basin with the wetland storage and runoff processes as described by Roulet and Woo (1986b).

Spring period

Owing to intense coldness (mean January air temperature -34o C) and a shallow active layer, winter runoff ceases completely. Snow accumulates without melting until late May while the lakes acquire an ice cover that exceeds 2 m. At Baker Lake, 80 km east of the study basin, over 40% of the 235 mm annual precipitation comes as snow, but this may be an underestimate given the frequent blowing snow conditions in the tundra (Woo and Marsh 1978).

In the spring melt period, the stream often experiences its annual peak flow. It is unlikely that the wetland can regulate the meltwater runoff through storage in its sodmats because: (1) there is a large amount of meltwater released rapidly, with the bulk of the entire winter snow cover (about 200 mm in 1982-83) melting within two to three weeks; (2) the ground remains frozen and despite the possibility of meltwater infiltration into frozen soil (Kane and Stein 1983, Granger et al. 1984), there is insufficient storage capacity to accommodate the large meltwater supply. On the other hand, a time lag exists between the melt event and the arrival of peak wetland runoff (Fig. 3). While the frozen wetland could not retain the meltwater, the snow cover itself and the lakes could store this water temporarily (cf. Woo et al., 1983). Indeed, the small lakes were observed to expand in size as the meltwater flooded the shoreline until the lake ice blockage was cleared (Fig. 2).

Further insight into the streamflow generating processes can be gained by examining in detail the sequence of melt, storage and flow events on the wetland and non-wetland slopes (Fig. 3). Surface flow on the non-wetland slopes started several days after the commencement of snowmelt, but overland flow in the wetland area was delayed for a few more days. The difference in timing cannot be due to groundwater storage because the ground was frozen everywhere, but may be attributed to the deeper snow cover on

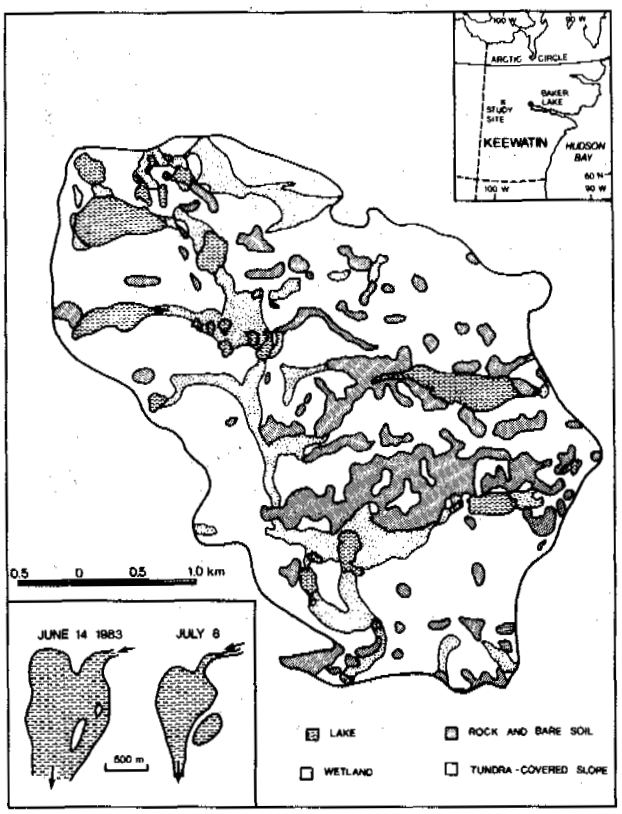

Figure 2. Distribution of wetlands and lakes in a study basin in central Keewatin, Canada. Also shown is the areal expansion of a small lake due to spring flooding.

the wetlands which enabled water retention for a longer duration. Surface flow then rose sharply as the remaining snow was ablated. When the ground began to thaw, the subsurface storage capacity increased and the suprapermafrost water table dropped. Streamflow declined because it was deprived of much of the overland flow. Thus, it is the meltwater storage in the snow, the lake storage, and depression storage of the wetlands that regulate the lag response of streamflow in spring. The magnitude of the streamflow freshet is controlled by overland flow rather than by subsurface flow from the wetlands.

Summer period

Wetland streamflow declines after the spring, partly because the receding frost table enlarges the storage capacity of the soil, but mainly because of increased evaporation. A comparison of the wetland and non-wetland plots shows that the wetlands have a shallower frost table because of (1) the insulating properties of the thawed, wet peat; (2) the higher ice content in the frozen peat which consumes more ground heat as it thaws; and (3) the lesser amount of evaporation from the non-wetland, making more energy available to ground heat flux. With a deeper frost table, the suprapermafrost water table in the non-wetland is considerably lower, and consequently a larger storage capacity is available for any rainfall input.

The streamflow hydrograph shows low flow conditions in non-rainy periods, suggesting that there is little baseflow from the groundwater source. This is expected because of the low hydraulic conductivity of the soils. After a prolonged dry spell, a small amount of rain will not raise the water table above the ground and streamflow response remains insignificant. When sufficient rain causes the water table to rise above the ground, overland flow follows and streamflow response becomes considerable. These features demonstrate that summer streamflow is sustained by surface rather than subsurface flow in the wetlands.

SUBARCTIC WETLAND

In contrast to the Arctic, wetlands are continuous over vast areas of the subarctic, and these wetlands are clad by woodlands in a discontinuous permafrost setting. A basin located at the southern border of subarctic Canada, (51o 08'N, 79°55'W) in the coastal lowland of James Bay, offers an example of a subarctic wetland study site.

Study site

The Washkugaw basin, draining an area of 175 km2, has a regional gradient of about 1 m/km. It experiences continental subarctic climate, with mean January and July temperatures of -20°C and 15°C respectively. Annual precipitation is 727 mm, 30% of which comes as snowfall. Vegetation cover includes spruce woodland with alder, willow and Labrador tea bushes on the higher ground, and sedges, grasses, mosses and stands of tamarack on the wetter bogs and fens.

Peat depth ranges from 0 at the coast, to 1.5 m at the headwater region of the basin. Owing to compaction, the peat has a much lower porosity at depth. Typically, within the hydrologically more active surface zone (the acrotelm, according to Ingram 1983), the hydraulic conductivity is 2-3 m/d, in contrast to the hydrologically inert bottom peat layer (the catotelm) where the value drops to 0.016 m/d. Thus, most of the subsurface flow and water storage takes place within the top 0.5-1.0 m of the peat.

Washkugaw River was gauged at its lower course. Near to the gauging site, groundwater wells and overland flow measurement sites were deployed. Tipping-bucket gauges and a pre-melt snow survey provided rainfall and snow storage information. Evaporation was computed using Priestley and Taylor (1972) approach and the requisite instrumentation included net radiometers, thermometers and ground heat flux plates.

Breakup period

In winter, seasonal frost underlies the entire basin but groundwater seepage maintains a minimal amount of flow (about 0.001 m^3/s for Washkugaw River). Spring breakup comes in April. This is preceded by snowmelt and wetland runoff. The rivers then

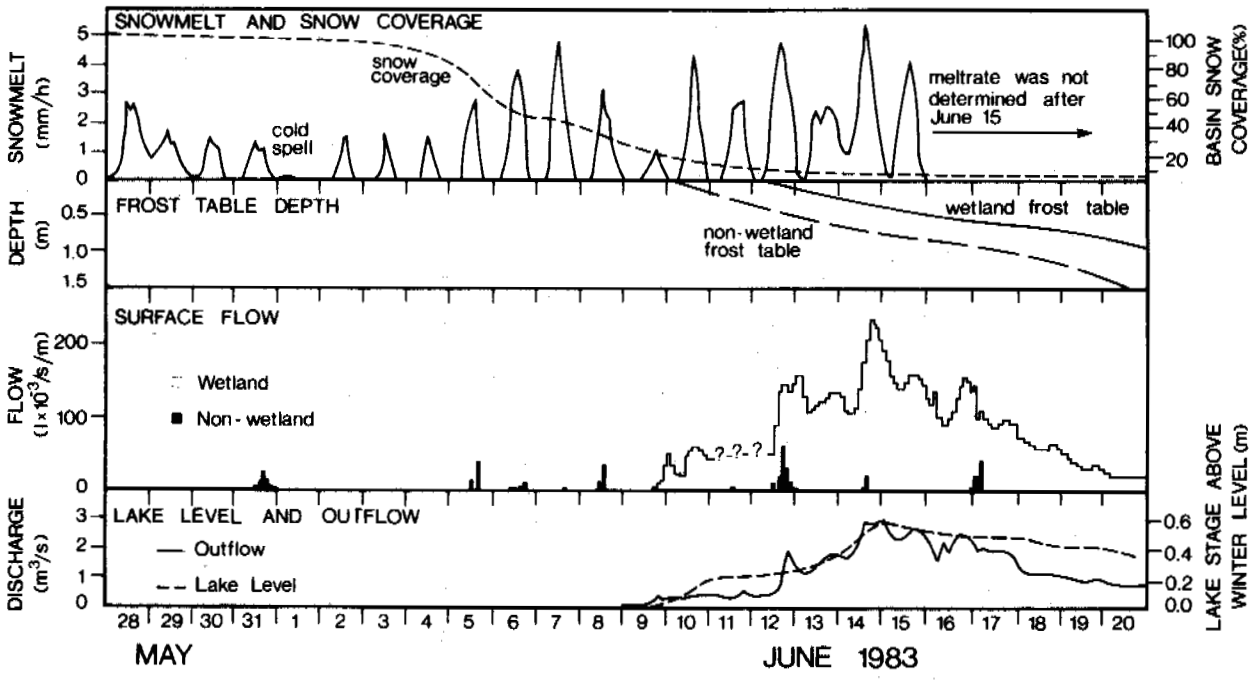

Figure 3. Snowmelt, active layer thaw, overland flow on wetland and non-wetland slopes, and streamflow during the 1983 melt season at central Keewatin study site.

rise to a peak, with floods accentuated by snow and ice in the channels. At the study basin, daily melt began first in the open wetland, followed by the shrubs and then the wooded areas. The prevalence of frozen ground inhibited infiltration and most of the water released became surface flow. Woo and Heron (1987) have described the complex flow pattern during the breakup of 1984. The abundance of meltwater released over a short time ensures that the spring period is the time of peak flow in subarctic wetland rivers.

Summer period

The ground thaws soon after the disappearance of snow, but the low gradient and the restricted thickness of the acrotelm, limit the amount of groundwater discharge.

Field observation shows that surface flow in wetland occurs as sheet flow during the wet period, and as miniature rills that thread from puddles to puddles on the drier days. In the study area, many depressions are constantly saturated, if not overflowing, and this water maintains surface flow which discharges into the streams. Figure 4 shows the water table fluctuation at wetland sites, as well as the daily rainfall and evaporation. The water table remained at or near the surfce most of the time, permitting surface flow to continue throughout most of the summer.

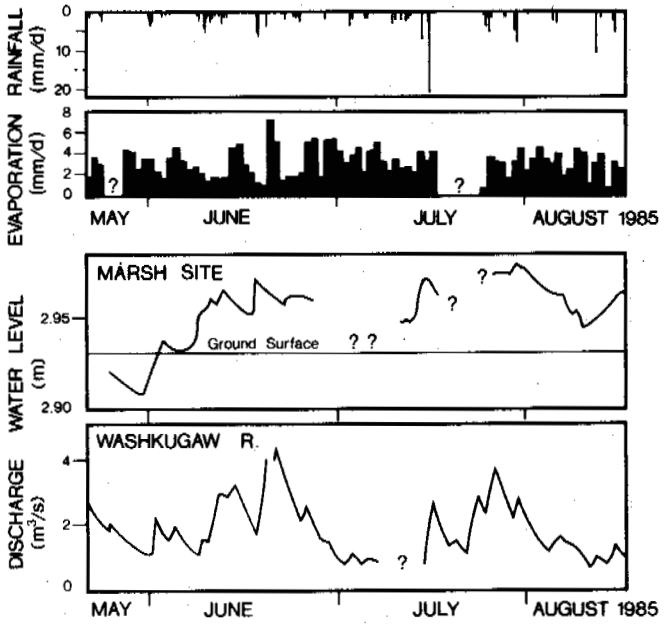

Figure 4. Rainfall, evaporation, water table in the wetland, and discharge of Washkugaw River, 1985.

When rain falls, the puddles coalesce rapidly and surface flow rises quickly. Since streamflow is mainly fed by surface runoff, the hydrograph lag time is governed only by the time needed to satisfy depression storage and by the transit time of surface flow. Thus, hydrograph rises tend to be steep. After a rain event, the puddles drain slowly and surface flow does not cease abruptly. Streamflow therefore tends to have a long recession. Computation of groundwater discharge based on Darcian flow shows that groundwater alone cannot sustian baseflow at the rate measured at Washkugaw River. It is the gradual drainage of the wetland depressions by surface runoff which support streamflow long after a storm has passed.

DISCUSSION

This paper has related the regimes of two wetland rivers to the hydrological activities observed in the wetlands. Although there are climatic and site differences between the Arctic and the subarctic basins, they both exhibit common traits that reflect the controlling influence of northern wetlands. It is therefore possible to distinguish such streamflow regime as the wetland regime, equivalent to Church's (1974) muskeg regime.

Based on this study and the result from other research in northern wetlands, several distinguishing features of the wetland streamflow regime can be identified.

(1) The annual runoff ratio, Q/P, where Q is runoff and P is precipitation, is relatively small for wetland basins. For comparison, annual P and Q from Intensive Watershed, a wetland basin of 0.12 km2 located in Devon Island, Canada (75° 33'N, 84° 40'W) yielded a runoff ratio of 0.45 (Ryden 1977). This contrasts against such nival regime basins as the McMaster basin of Cornwallis Island, Canada (area 33 km2, 74° 45'N, 94° 50'W) where the ratio was 0.83 (Woo et al. 1983).

(2) Another feature is the small quantity or absence of winter flow because (a) intense cold freezes the soil and (b) there is little suprapermafrost groundwater reserve in the Arctic, and the rate of seepage is quite slow in the subarctic. This contrasts with the spring-fed rivers found in some discontinuous permafrost areas of northern Alaska and Yukon, referred to by Craig and McCart (1975).

(3) During the snowmelt period, wetland basins discharge the bulk of their winter precipitation within a short time, often generating high flows in spring. The magnitude of the peaks depends upon winter snow accumulation and the rate of melt. Where there is little winter snowfall, the spring freshet is absent. An example is Ogotoruk basin where winter snowfall of under 60 mm, representing about 20% of annual precipitation, yielded insignificant snowmelt runoff (Likes 1966). Low snow melt rates during a cool spring also prohibit high flow, as is demonstrated by the 1973 hydrograph of the Intensive Watershed (Ryden 1977). In the other years (1972 and 1974), however, high peaks were generated by snowmelt.

(4) Response to summer rainfall is often rapid because it takes little rain to produce surface flow that feeds the streams. Barrow basin in Alaska, for instance, showed a mean response time of 8±4.7h between the centroids of rainstorms and the time of runoff peak (Brown et al. 1968). These response times are also comparable to that of the nival regime rivers. The Mecham River in Cornwallis Island (87 km2, 74° 41'N, 94° 47'W) had an average response time of 9 h (Cogley 1975) but there, the fast response is due to the shallow active layer which hinders percolation and favours rapid runoff from the basin slopes.

It is proposed that a wetland streamflow regime in the Arctic and subarctic regions consists of negligible or low flow during the long, cold winters. This is followed by spring freshet when surface flow is produced by abundant snowmelt and enhanced by low infiltration into the frozen ground. The exception is where winter snowfall is so low that the spring snowmelt is insufficient to generate overland flow. In summer, poor drainage leads to considerable water retention in ponds and the organic soils and flow attenuation is the most effective during this time. Unlike lakes which can sustain a moderate level of baseflow, wetlands do not yield much groundwater discharge because the shallow acrotelm or the proximity of the frost table to the ground surface limits baseflow in the dry seasons.

ACKNOWLEDGEMENTS

Financial support was provided by the Natural Sciences and Engineering Research Council of Canada. I wish to thank Drs. Richard Heron and Nigel Roulet, and Mr. Peter diCenzo for their help, and Dr. Antoni Lewkowicz for commenting on this manuscript.

REFERENCES

Allen, P.W. and Weedfall, R.O., (1966). Weather and climate. In Wilimovsky, N.J. (ed.) Environment of the Cape Thompson Region, Alaska. U.S. Atomic Energy Commission, 9-44.

Brown, J., Dingman, S.L., and Lewellen, R.I., (1968). Hydrology of a drainage basin on the Alaska coastal plain. U.S. Army Corps of Engineers CRREL Res. Rep., 240. 18 pp.

Church, M. (1974). Hydrology and permafrost with reference to northern North America. Proc. Workshop Seminar on Permafrost Hydrology, Can. Nat. Comm., IHD, Ottawa, 7-20.

Cogley, J.G. (1975). Properties of surface runoff in the High Arctic. Ph.D. Thesis, McMaster University, 358 pp.

Craig, P.C. and McCart, P.J. (1975). Classification of stream types in Beaufort Sea drainage between Prudhoe Bay, Alaska, and the Mackenzie delta, N.W.T., Canada. Arctic and Alpine Research, 7, 183-198.

Granger, R.J., Gray, D.M. and Dyck, G.E. (1984). Snowmelt infiltration to frozen prairie soils. Canadian Journal of Earth Sciences, 21, 669-677.

Holecek, G.R., and Vosahlo, V.M. (1975). Water balance of three High Arctic nival regimes. Proceedings Canadian Hydrology Symposium, Winnipeg, 75: 448-461.

Ingram, H.A.P. (1983). Hydrology. In Gore, A.J.P. (ed.), Ecosystems of the World 4A: Mires, Swamp, Bog, Fen, and Moor, Amsterdam: Elsevier, 67-158.

Kane, D.L. and Stein, J. (1983). Water movement into seasonally frozen soils. Water Resources Research, 19, 1547-1557.

Likes, E.H. (1966). Surface-water discharge of Ogotoruk Creek. In Wilimovsky, N.J. (ed.) Environment of the Cape Thompson Region, Alaska, U.S. Atomic Energy Commission, 115-124.

Priestley, C.H.B.and Taylor, R.J. (1972). On the assessment of surface heat flux and evaporation using large-scale parameters. Monthly Weather Review, 100, 81-92.

Roulet, N.T. and Woo, M.K. (1986a). Low arctic wetland hydrology. Canadian Water Resources Journal 11, 69-75.

Roulet, N.T. and Woo, M.K. (1986b). Hydrology of a wetland in the continuous permafrost region. Journal of Hydrology 89, 73-91.

Ryden, B.E. (1977). Hydrology of Truelove Lowland. In Bliss, L.C. (Ed.) Truelove Lowland, Devon Island, Canada: A High Arctic Ecosystem. University of Alberta Press, 107-136.

Woo, M.K. (1986). Permafrost hydrology in North America. Atmosphere-Ocean 24, 201-234.

Woo, M.K. and Heron, R. (1987). Breakup of small rivers in the subarctic. Canadian Journal of Earth Sciences 24, 784-795.

Woo, M.K. and Marsh, P. (1978). Analysis of error in the determination of snow storage for small High Arctic basins. Journal of Applied Meteorology, 17, 1537-1541.

Woo, M.K., Marsh, P. and Steer, P. (1983). Basin water balance in a continuous permafrost environment. Proceedings, Fourth International Conference on Permafrost, Fairbanks, Alaska, 1407-1411.

STREAMFLOW CHARACTERISTICS OF THE QINGHAI (NORTHERN TIBETAN) PLATEAU

Yang, Zhengniang and Woo, Ming-ko

Lanzhou Institute of Glaciology & Geocryology, Academia Sinica Lanzhou, Gansu 730000 China

SYNOPSIS The Qinghai (northern Tibetan) Plateau is the headwater area for many large Asiatic rivers. Permafrost occurs above 4200 m and glaciers occupy the summits and high valleys of the east-west trending mountain chains. Annual runoff generally increases with precipitation which is augmented southward by the rise in topography. Rainfall, snowmelt, glacier melt and groundwater are the primary runoff responses to rainfall and snowmelt events.

Peak flows are concentrated between June and September and winter is the low flow season. Three types of runoff patterns may be distinguished according to their primary sources of water: snowmelt and rainfall, glacier melt and snowmelt, and groundwater. Large rivers generally drain more than one environment and their runoff regime reflects an integration of the various flow patterns found on the plateau.

INTRODUCTION

A study of the characteristics of streamflow in a region is useful, if not essential, to most hydrological investigations for scientific or engineering purposes. Church (1974) proposed several types of streamflow regimes for rivers in the permafrost region of northern North America based on his and other works (e.g. McCann and Cogley, 1972). Craig and McCart (1975) have similarly summarized the runoff patterns for northern Alaska and the Yukon coast. These results were synthesized by Woo (1986) to identify regimes that are influenced by snowmelt, glacier melt, rainfall, spring-water and the presence of wetland in the arctic and subarctic belts of North America. In the glacierized mountainous areas of northwestern China, Yang (1981) classified regimes according to the extent that runoff is controlled by snowmelt, glacier melt and rainfall.

The Qinghai-Xizang (Tibetan) Plateau covers an area of 1.5 million km^2, most of which is underlain by permafrost. Many large rivers of continental Asia originate from this plateau, including the Chang Jiang (Yangtze), the Mekong and the Brahmaputra. The scarcity of data has long prevented a systematic study of the runoff characteristics of the rivers that are either internally drained or that ultimately unite with other eastward or southeastward flowing rivers. The Chinese Physical Geography Editorial Committee (1981) provided an incomplete summary of the runoff characteristics of the northern Tibetan rivers. Runoff is considered to be maintained largely by snow and glacier ice melt, and is concentrated in the summer and autumn periods. Low precipitation often results in intermittent flows. This monograph did not provide any illustrative examples of the typical flow patterns and no mention was made of the influences of other sources of runoff such as rainfall or groundwater supplies.

The purpose of this paper is to analyze hydrometric data for the Qinghai (Northern Tibetan) Plateau that are avaiable from along the Qinghai-Xizang Highway between the drainage divide of Tanggula Mountains and the northern flank of the Tibetan Plateau. Results from this study should have applications beyond the Tibetan Plateau because these permafrost regions of Qinghai Province are the source areas of some of the largest Asiatic rivers.

STUDY AREA

The Qinghai Plateau lies between 33° and 36° N. The general elevation of this plateau is above 3500 m, but several east-west trending mountain chains rise above 5000 m, attaining heights in excess of 7000 m at their summits. This low latitude but high altitude region is underlain by alpine permafrost extensively (Fig. 1a). The lower limit of permafrost lies at 4150-4200 m where the mean annual temperature is -2 to -3° C. Above 4600 m the air temperature remains below 0°c for over 8 months in each year. Even between June and September, temperatures as low as -3°C have been known to occur.

Precipitation increases southward. In the arid northern zone, annual precipitation averages only 100 mm, but exceeding 600 mm in the south (Fig. 1b). The bulk of the precipitation arrives between May and September, and solid precipitation in the forms of snow and hail may fall at the higher elevations throughout the year. A semi-permanent snow cover exists on the high mountains, and glaciers are found on the summits and high valleys. Annual evaporation

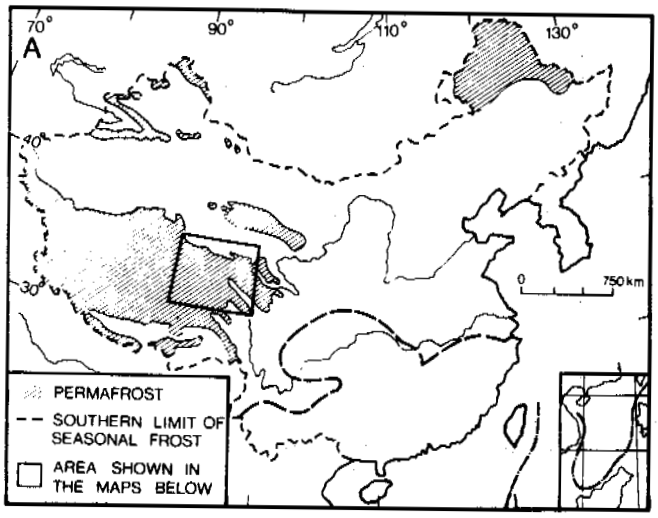

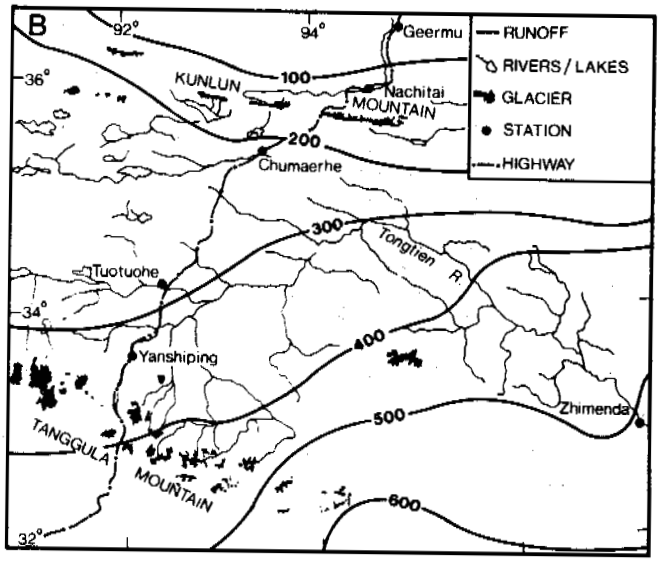

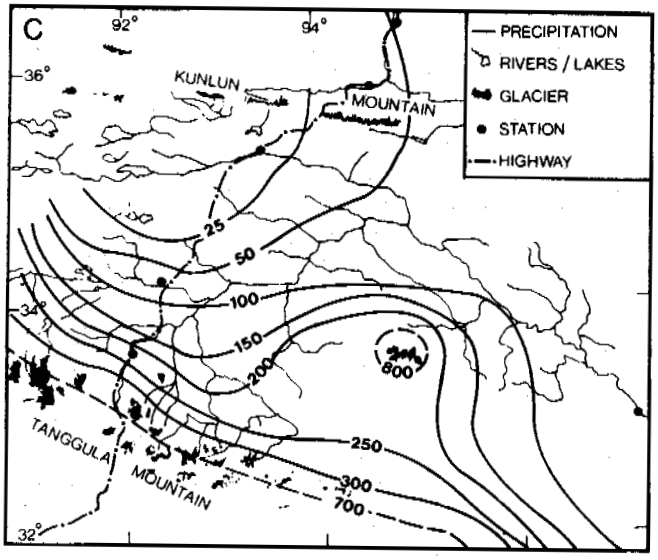

increases from about 50 mm in the north to 350 mm in the south, as more radiation energy becomes available to evaporate the higher precipitation supply (Fig. 1c). On the whole, the plateau has low precipitation but high evaporation, and may therefore be considered as a cold arid region. Under such conditions, the plateau is devoid of trees.

The Qinghai Plateau has numerous lakes, many of which have no outlet. Rivers on the western and northern sides of the plateau flow into and disappear in internally drained depressions. Rivers on the eastern half are tributaries of the Chang Jiang. The Qinghai-Xizang Highway traverses the plateau longitudinally and encounters both groups of rivers. It is these rivers that provide the hydrometric data for the present study.

FACTORS AFFECTING STREAMFLOW

Precipitation

The spatial distribution of mean annual runoff (Q) is governed by the long term water balance $Q = P - E$ where P and E are mean annual precipitation and evaporation. There are very few weather stations in the headwater regions of the basins and neither precipitation nor evaporation can be determined accurately, although their general trends can be established with some confidence. Precipitation increases southward, as does evaporation. In the northern part of the plateau, much of the low annual precipitation is consumed by evaporation and runoff is very low, particularly for such rivers as the Chumaer which flows across predominantly arid lands. Runoff increases sharply towards the Tanggula Mountains and the annual discharge of such rivers as the Baidu reaches 300 mm or more. However, since extensive tracts of the plateau are arid, large rivers leaving the plateau eastward tend to have only moderate runoff. For example, the Tongtien River which is a tributary of the Chang Jiang, receives only 88 mm of annual runoff from the plateau.

Precipitation exhibits pronounced seasonality. The low period is in winter when precipitation arrives mainly as snowfall. This is likely to be underestimated by the weather stations because of blowing snow conditions in the exposed terrain (c.f. Goodison 1978). Because of the limited amount of winter precipitation, the snowmelt contribution to runoff can be small compared with rainfall. A comparison of precipitation with the runoff regime of rivers demonstrates that summer precipitation is responsible for the seasonal high flows (Fig. 2). The greatest monthly discharge for many rivers is in August while monthly precipitation peaks in July. One exception is the Chumaer River whose peak

Fig. 1 Distribution of (a) permafrost (b) annual precipitation in mm and (c) annual runoff in mm.

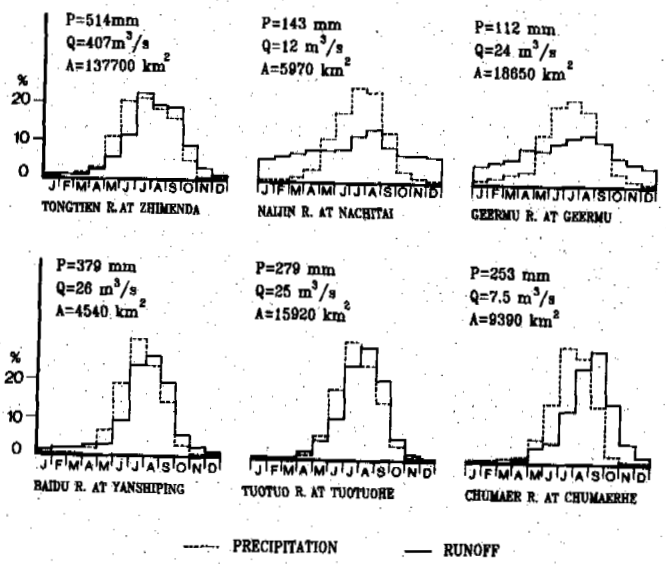

Fig. 2 Monthly distribution of runoff (full line) and precipitation (dashed line) as recorded at selected hydrometric stations. Also given are mean annual precipitaiton (P in mm) runoff (Q in mm) and basin area (A in km^2).

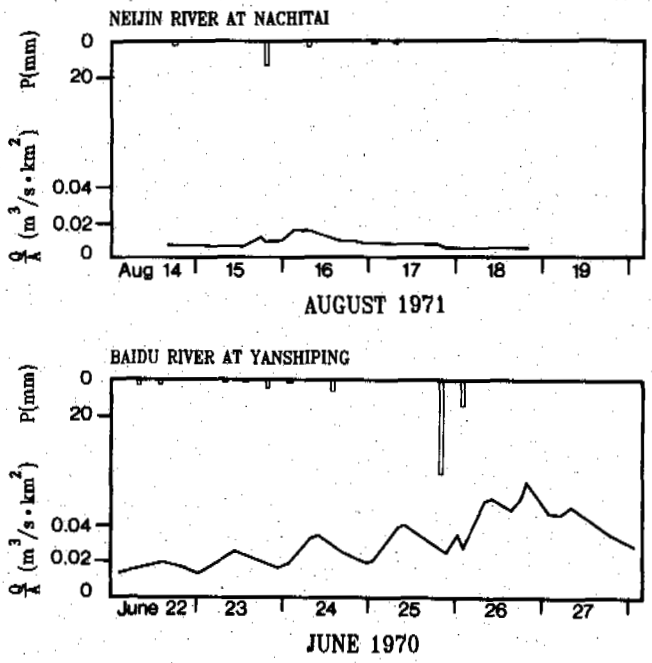

Fig. 3 Streamflow response to rainfall in basins underlain sporadically (Neijin River) and continuously (Baidu River) by permafrost.

monthly flow is delayed to September, possibly because by then, evaporation has declined sufficiently that more of the precipitation becomes available for streamflow.

Glacier melt

Most mountains on the plateau are clad by glaciers. Yang (1982) compared the contribution of glacier melt to runoff from various mountain chains of northwestern China. She found that given similar percentages of glacierized area, basins of northern Tibetan plateau yield the least amount of runoff. For instance, glacier meltwater runoff exceeds 0.1 $m^3/s.km^2$ in southern Tibet while it is only 0.03-0.04 $m^3/s.km^2$ in northern Tibet. The former area has maritime glaciers with a long melt season (Apr.-Oct.) while the latter area has continent-type glaciers, with a melt season between May and September. Glacier meltwater runoff peaks in July and August, but the effects of glacier melt on streamflow cannot be distinguished readily from those of summer precipitation because both of them peak in similar months. Between July and August, the more glacierized Baidu basin (5.2% glacierized) yields 25-30% of its annual flow, but the less glacierized (1.8%) Geermu River produces 10-15% of its annual discharge.

Permafrost effects

Permafrost is absent at the lower elevations on the plateau fringe. This rapidly changes with height, giving rise to a transitional zone with sporadic permafrost and finally to the continuous alpine permafrost that underlies most of the high plateau. Being relatively impermeable (c.f. Newbury 1973), permafrost encourages flashy basin runoff responses to rainfall in summer (Slaughter et al. 1983) and sheds much of the melt water as surface flow in spring (Woo et al. 1983). One consequence is that given a rainstorm of similar magnitude, a basin in the permafrost area will generate a higher runoff ratio (Q/P). An example is provided in Figure 3 to contrast the streamflow responses to rainfall events in a basin underlain continuously by permafrost (Yanshiping) and one where the occurrence of permafrost is sporadic (Nachitai).

Groundwater discharge

Basins fed by subterranean springs along major fault zones or in carbonate terrain receive significant amounts of groundwater throughout the year. Large base flows are maintained in the winter low flow period and the seasonal contrast in flow is reduced. For most of the winter, spring-fed rivers along the northern fringe of the plateau are kept open by groundwater discharge (e.g. Neijin River at the gauging site) while most others are ice-covered for about six months. On the plateau, river segments fed by groundwater flow are prone to extensive icing formation in the channels (c.f. some of the Alaskan rivers described by Kane and Slaughter, 1972).

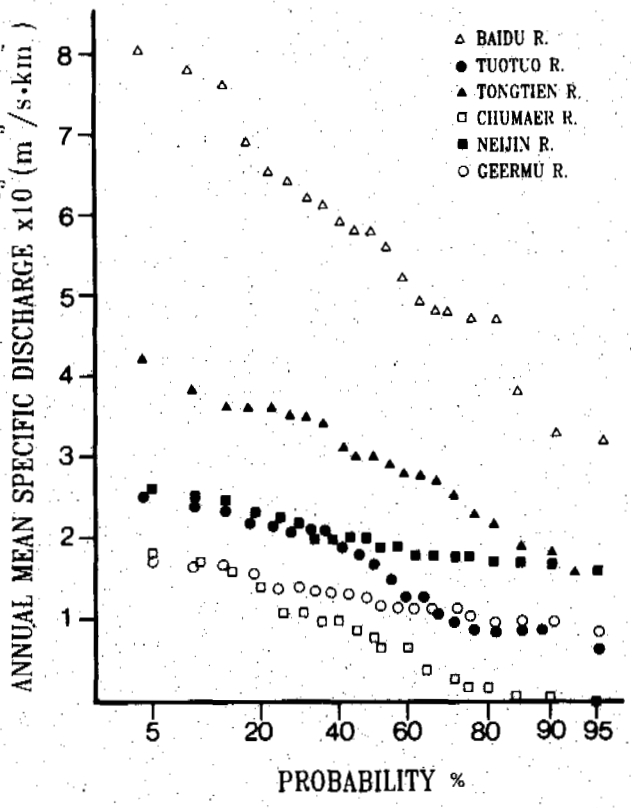

Fig. 4 Distribution of mean annual flows of selected rivers on the Qinghai Plateau plotted on probability graph paper.

RUNOFF CHARACTERISTICS

Hydrometric data from five rivers for the period 1962-82 provide the basis upon which runoff characteristics of the Qinghai Plateau rivers may be generalized. The three streamflow characteristics to be examined are mean annual runoff, annual peak flow and annual low flow. All flow values are reduced to specific discharge ($m^3/s.km^2$) to permit comparisons without the interference of basin size.

Mean annual runoff

Mean annual flows of the selected rivers follow a normal distribution (Fig. 4). The long term mean for Baidu River which lies in the Tanggula mountains far exceeds that for the rivers in the more arid zones of the plateau. In addition, its year to year variation is low as showed by a small coefficient of variation (C_v = 0.244). In contrast, the Chumaer River experiences the lowest annual flow (mean = 7.95 x 10^{-4} $m^3/s.km^2$) but its year-to-year variation is high (C_v = 0.728). This is attributed to the low precipitation and regularly high evaporation at the northern portion of the plateau. The remaining rivers (Tuotuo, Neijin and Geermu) reveal mean annual discharge values that are intermediate between those of the mountainous and the very arid zones.

Annual peak flow

Annual peak flow, defined as max[Q_i], i = 1, .. 365 days of the year, often occurs in summer (July and August) for the rivers of The Qinghai Plateau (Fig. 5). These peaks are usually related to intense storm events. The pattern of annual peak flows is similar to that of mean annual flows, with the highest for such mountainous rivers as the Baidu, the least for Chumaer River, and with the remaining rivers taking up intermediate positions. The year to year variation is largest for Baidu River, indicating that rivers in the mountains are prone to a wide range of flood conditions. Other rivers reach lower annual peaks and they generally exhibit lesser year to year differences.

Annual low flow

November to March are the low flow months, but the annual low flow, defined as min[Q_i],i = 1, .. 365 days of the year, can occur at any time between October and April. The occurrence of annual low flows during this period is due to low precipitation as well as low temperatures which inhibit melting and induce ground freezing to retard groundwater discharge. Rivers such as the Chumaer usually have zero flow in the winter. Other rivers maintain a positive flow (Fig. 6) fed by groundwater from non-permafrost zones (e.g. Geermu River) or from taliks (e.g. Baidu River).

TYPES OF RIVER

Although handicapped by the paucity of streamflow data, an attempt can be made to classify the runoff pattern of medium-sized rivers (basin area 2000-20,000 km^2) based on a knowledge of the streamflow generating processes.

(1) Rivers fed by rainfall and snowmelt

Winter is the low flow season for these rivers because of the small amount of winter precipitation which arrives almost entirely as snowfall. Spring snowmelt runoff is not as important as in the rivers of other alpine or polar environments (c.f. the nival regime rivers described by Church, 1974), partly because of the low winter precipitation and partly because of delayed melting at higher altitudes. Summer precipitation can occur as rainfall, hail or snowfall, and it is rainstorms at the lower elevations and snowmelt at the higher altitudes that produce large summer discharges. In their study of several arctic Alaskan rivers, Carlson and Kane (1973) raised the possibility that in drainage basins with large elevation ranges, snowmelt is spread out over the summer rather than concentrated within the spring season. A similar situation may exist on the Qinghai Plateau.

The presence of permafrost prevents deep percolation of rain or meltwater, and a sizable portion of the water input is shed as runoff. This accentuates the contrast between summer high flow and the winter lows so that the annual variation of runoff is higher for the rivers in the permafrost region (e.g. Tuotuo River). Rivers along the

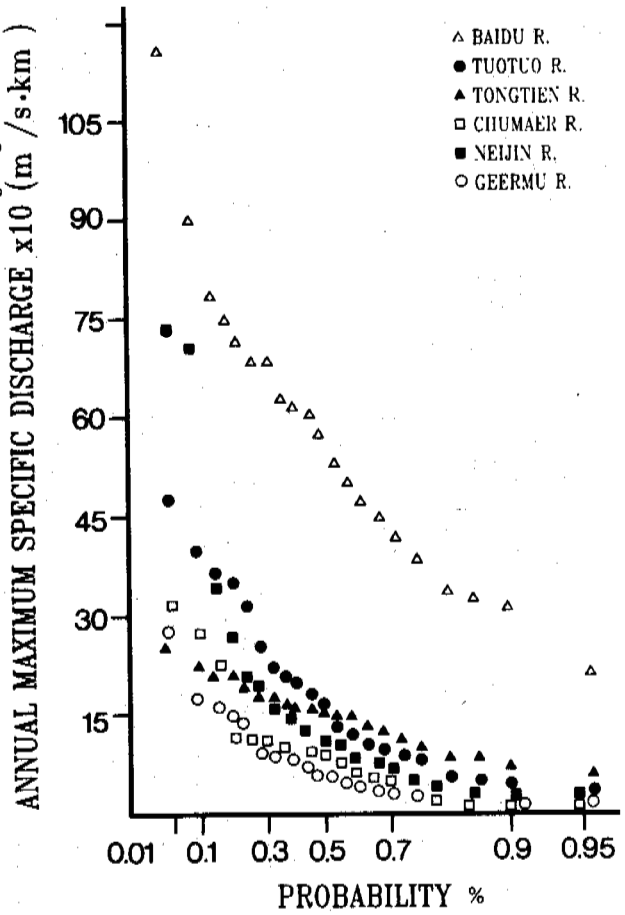

Fig. 5 Distribution of annual peak flow of selected rivers on the Qinghai Plateau plotted on Gumbel paper.

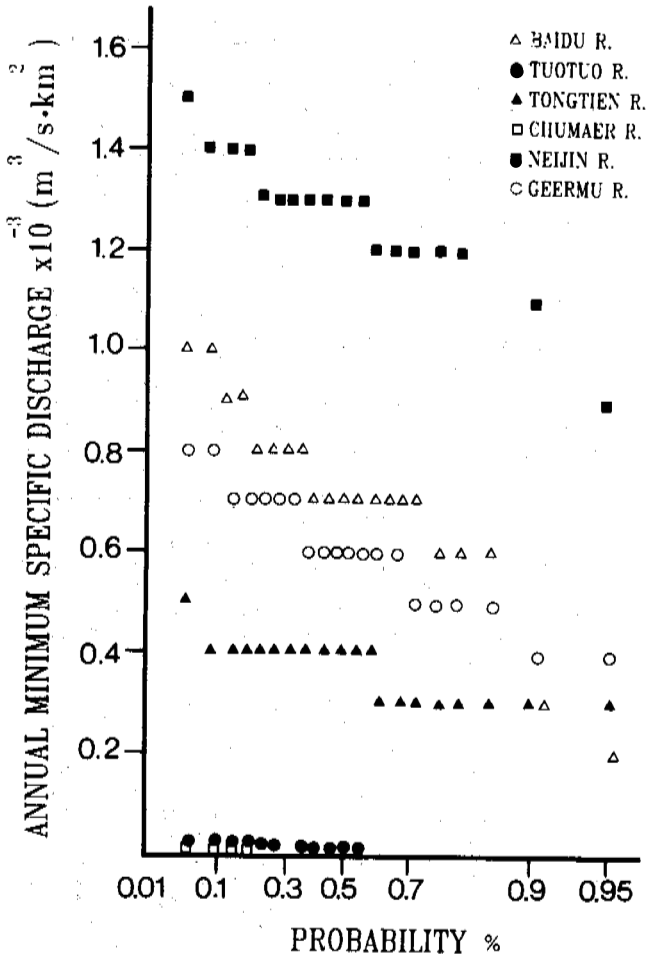

Fig. 6 Distribution of annual low flow of selected rivers on the Qinghai Plateau plotted on Gumbel paper.

non-permafrost fringe of the plateau also receive less precipitation but more uniform rain from May to September (e.g. Geermu River) thus reducing the seasonal variations in streamflow.

(2) Rivers nourished by glaciers

Many basins are partially occupied by glaciers. Where the percentage of glacierization is large, the influence of glacier meltwater upon runoff becomes noticeable (e.g. Baidu River which is 5.2% glacierized). These proglacial rivers have headwaters in high mountains which usually receive more precipitation and therefore generate higher annual runoff. Annual peak flows are concentrated in July and August when both glacier melt and precipitation are high. Winter is a period of low flow because of low precipitation and low temperatures.

(3) Rivers maintained by groundwater

Rivers along fault zones or in carbonate terrain receive a significant amount of water from groundwater sources. These spring-fed rivers therefore drain across non-permafrost areas or traverse talik zones. The effects of groundwater discharge include a reduction in year-to-year flow variation, and a more uniform seasonal flow distribution.

Like most other rivers on the plateau, groundwater-fed streams have summer as their high flow season because of high rainfall. Unlike the other rivers, winter low flows are increased by groundwater discharges. The augmented low flows are able to maintain ice-free open channels at low elevations and produce thick icings along channels at higher altitudes.

DISCUSSION AND CONCLUSION

Despite the scarcity of hydrometric data, this study has identified the significance of several runoff generating processes in the Qinghai Plateau, including rainfall, snowmelt, glacier melt and groundwater discharge. Both annual and seasonal distributions of streamflow reflect the spatial and temporal changes in precipitation, and the influence of rainfall in this region appears to be more pronounced than has been reported in other permafrost

areas. The presence of permafrost amplifies the runoff responses to rainfall and snowmelt while the contribution of groundwater flow tends to even out the annual changes in streamflow. Many medium-sized basins are partly occupied by glaciers and the extent to which glacier meltwater influences the streamflow regime is dependent upon the percentage of glacier cover.

Many basins on Qinghai Plateau receive more than one source of water for runoff production. For instance, the Baidu River has a strong component of runoff sustained by glacier melt, but is fed by spring-water as well to maintain a moderate base flow throughout winter (Fig. 6). The Neijin River exhibits a strong spring-fed runoff regime but is located in a basin that is 3% glacierized. Thus it is difficult to classify a river as one with solely, say, a proglacial regime or a rain-nourished (pluvial) regime. This is analogous to the finding of Marsh and Woo (1981) in the permafrost area of Canada that an arctic nival regime (snowmelt dominant) can at times be indistinguishable from a proglacial regime (mainly glacier-fed).

Large rivers of the plateau always rise in a set of tributary basins with different hydrological environments. The runoff regime of each of these rivers necessarily reflects an integration of various flow patterns found on the plateau. The basin of the Tongtein River (area 142,780 km^2), for example, is 10.5% glacierized and it spans a large latitudinal range. Being fed by snowmelt, rainfall, glacier melt and groundwater flow, the runoff characteristics take on intermediate positions in comparison to the rivers examined earlier (Figs. 4-6). Thus, the annual peak flow and annual low flows are less extreme than those rivers sustained by rainfall, snow and glacier melt, but more variable than those rivers with an overwhelming spring-fed component. It is not possible to attribute specific features of runoff for the Tongtien River to individual flow-generating processes. However, its discharge characteristics are generated by an integration of the flow regimes of its tributaries, and this principle can be used to explain the general flow pattern of other large rivers draining the Qinghai Plateau.

REFERENCES

Carlson, R.F. and Kane, D.L. 1973. Hydrology of Alaska's Arctic. In Weller, G. and Bowling, S.A. (eds.) Climate of the Arctic, Geophysical Institute, University of Alaska, 367-373.

Chinese Physical Geography Editorial Commitee 1981. Surface Water. Scientific Pub., Beijing (in Chinese).

Church, M. 1974. Hydrology and permafrost with reference to northern North America. Proceedings Workshop Seminar on Permafrost Hydrology. Can. Nat. Comm., IHD, Ottawa, 7-20.

Craig, P.C. and McCart, P.J. 1975. Classification of stream types in Beaufort Sea drainages between Prudhoe Bay, Alaska, and the MacKenzie delta, N.W.T., Canada. Arctic and Alpine Research, 7, 193-198.

Goodison, B.E. 1978. Accuracy of Canadian snow gage measurements. Journal of Applied Meteorology, 17, 1541-1548.

Kane, D.L. and Slaughter, C.W. 1972. Seasonal regime and hydrological significance of stream icings in Central Alaska. In: The Role of Snow and Ice in Hydrology. Proceedings Banff Symposium, IAHS. Publication 107, 528-540.

Marsh, P. and Woo, M.K. 1981. Snowmelt, glacier melt, and High Arctic streamflow regimes. Canadian Journal of Earth Sciences 18, 1380-1384.

McCann, S.B. and Cogley, J.G. 1972. Hydrologic observations on a small Arctic catchment, Devon Island. Canadian Journal of Earth Sciences 9, 361-365.

Newbury, R.W 1974. River hydrology in permafrost area. Proceedings Workshop Seminar on Permafrost Hydrology. Can. Nat. Comm. IHD, Ottawa, 32-37.

Slaughter, C.W., Hilgert, J.W. and Culp, E.H. 1983. Summer streamflow and sediment yield from discontinuous-permafrost headwaters catchments. Proceedings Fourth Internation Conference on Permafrost, Fairbanks, Alaska, 1172-1177.

Woo, M.K. 1986. Permafrost hydrology in North America. Atmosphere-Ocean 244, 201-234.

Woo, M.K., Marsh, P. and Steer, P. 1983. Basin water balance in a continuous permafrost environment. Proceedings Fourth International Conference on Permafrost, Fairbanks, Alaska, 1407-1411.

Yang, Z.N. 1981. Types of rivers in the mountainous areas of northwestern China. Journal of Glaciology and Cryopedology, 3, 24-31 (in Chinese).

Yang, Z.N. 1982. Basic characteristics of runoff in glacierized areas in China. Hydrological Aspects of Alpine and High Mountain Areas, IAHS Publ. 138, 295-307.

RATIONAL EXPLOITATION AND UTILIZATION OF GROUND WATER IN PERMAFROST REGION OF THE MT.DA-XINGANLING AND MT.XIAO-XINGANLING, NORTHEAST CHINA

Zheng, Qipu

The Third Survey and Design Institute, Ministry of Railways, People's Republic of China

SYNOPSIS Ground water in permafrost regions of the Mt.Da-Xinganling and Mt.Xiao-Xinganling varies in buried condition. Based on exploration data, it is known that the ground water in taliks under river bed or lake and those in cracks of bedrocks are of significance in water supply.Because of the seasonal variation of ground water, it is necessary to promote and maintain the yield and regenerating ability of ground water resource by means of the artificial techniques. Pollution abatement is also necessary.

NATURAL CONDITION AND ITS RELATION TO GROUND WATER

The permafrost region in the Mt.Da-Xinganling and Mt.Xiao-Xinganling, with a mean altitude of 600 to 800 m, crosses 6.5 degrees in latitude (47°N to 53°30'N), ranging from Mohe by the Heilongjiang River in the north to Mt. Alshan in the south. The climate there has typical continental characters with a long and frigid winter and a short warm summer. Its mean annual air temperature is from -2° to -6.2°C, and the minimum temperature can be as low as -50°C. The period with an average monthly subzero temperature lasts 6 to 7 months. The annual precipitation is from 450 to 500 mm, with rain as the main form. Such a condition is favorable to the growth of forest. On the other hand,the dense vegetation on hills and swampy lowlands is helpful to the storage of ground water.

The hydrogeologic condition is complicated by frozen ground and the cold climate (Zhang,1959, 1980). First, the existence of permafrost restricts the reservation and supply of ground water. Second, the recharge and movement of ground water reveal a seasonal behavior, for example, an aquifer, which would be continuous and with a phreatic water table in warm season, might be separated into several parts with a confined water head by frozen ground during cold winter; the quantity of available and exploitable ground water varies periodically in accordance with seasonal variation of water balance. During a warm period the ground water may recharged by surface water; in cold period, however, since the surface water is frozen and the supply is blocked by frozen ground as aquifuge, the water intake might reduce considerably. Also, ground water changes in quality because it is protected by frozen ground during the cold season, however, in warm period, without the protection of frozen ground on the surface, it would be polluted in some extent.

Finally, the repeated frost weathering creates and increases the cracks in bed rock, this is favorable to the infiltration of rainfall and the recharge of ground water.

TYPES AND CHARACTERISTICS OF GROUND WATER

Based on the spatial relationship between permafrost and aquifer, N.I. Tolstikkin suggested that the ground water in permafrost region is categorized into three main classes: the suprapermafrost water, the intrapermafrost water and the subpermafrost water. In the Mt.Da-Xinganling and Xiao-Xinganling area, all these kinds were found and have their local names 'Fu Shui', 'Yao Shui' and 'Di Shui' correspondingly. It was also widely found the ground water in taliks.

Based on survey data, it is believed that the following two kinds of ground water are of great economical value and widely distributed in this area, i.e.the ground water in talik under or along river or lake; ground water in cracks of bedrocks.

The gound water being stored in shallow-buried aquifer in taliks under or along river or lake and easy to exploitate is the major water supply in this area. Tens of the water supply stations along the railroad are mainly utilizing this kind of ground water. The larger the river and the talik, the thicker the effective aquifer will be. Commonly, the yield of a well can be 250 to 600 T/day. Chemically the water belongs to HCO_3-Ca or SO_4-HCO_3-Ca-Mg types.

Ground water in cracks of bedrocks, mainly the andesite, granite, basalt and volcanic agglomerate, is another major water resource, which is deposited at a depth of 30 to 100 m beneath the permafrost base. Yield of a well can be 150 to 300 T/day. Usually the water belongs to HCO_3-Ca type. In most of the wells with an insufficient head to raise water above land surface, water will be frozen , even causes the well abandoned.

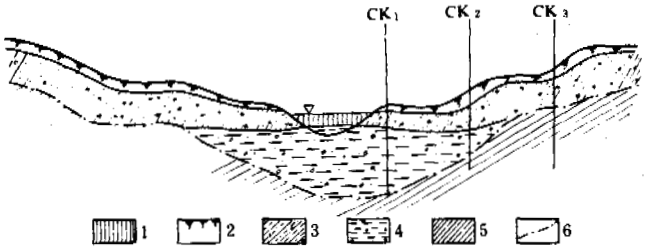

Fig.1 Sketch Map of Ground Water in Talik beneath and along the Mujigong River in the Cuifeng Water Station of Nenlin Railroad

1. ice; 2. peat; 3. silty clay with gravel and pebble; 4. aquifer; 5. permafrost; 6. permafrost table.

EXPLORATION OF GROUND WATER RESOURCE

Seasons for exploration

The exploration of ground water in deep bedrock fissures and voids is generally not affected by seasons, however, water pumping tests must be made in dry season so as to find out the exploitable quantity in the driest period. The ground water in shallow layers bed better be explored in both the warm and dry seasons. In the warm season (from May to September), hydrogeological survey is usually performed in accordince with the characteristics of terrain, landform and vegetation in the survey region. If a small amount of drilling and dugging is added, then the seasonal thawing depth, the range of talik can be known. A hydrogeological survey during the dry seanon (from February to April), when it is unfavorable to the recharge of ground water because the surface earth is completely frozen, can provide the reliable data in the extent and thickness of aquifer and the water yield, permeability for a water supply design.

Exploration of shallow ground water

The following phenomena are useful for permafrost-hydrogeological survey.

1. The growth of marsh-grass and other hydrophilic plants on swampy lowland and bog with poor drainage indicates the permafrost table is not far from ground surface; while the growth of willows,poplars and other hydrophilic plants on alluvial deposits indicates an existence of talik.

2. Ground water might be more active in those places, where,
- the snow cover in winter is relatively thin or comparatively easy to melt;
- ground surface doesn't crack even in the dry and cold season;
- icings or frost heaving mounds occur;
- springs occur;
- earth thaws earlier and freezez later.

3. If a section of river or lake doesn't freeze or freezes rather thin or has a temperature higher than the other section, then there might be a ground water supplying.

4. In the frigid winter when the surface water has been frozen completely, if there is a place, where birds or beats haunt frequently, trees nearby are always covered with thin frost, and, it is often foggy in the morning, then it coule be assumed that the ground water is still unfrozen and active there.

5. 'Drunken trees' may indicate a frost heaving mound or an icing field; 'Trees uprooted by wind' may indicate a shallow-buried permafrost table.

Exploration of ground water in deep bedrock fissures and voids

The distribution of this kind of ground water is close-related to the geological condition, therefore, a hydrogeological survey must be proceeded on the basis of an understanding in geology and geomorphology. It was found in many wells that the water level was lowering and the water yield was reducing year by year. Thus, during exploration, one should pay a special attention to the reliability of water resource. A reasonable proposal for extraction can only by put forward after an observation no less than one-year period.

RATIONAL EXTRACTION AND UTILIZATION OF GROUND WATER

In the past 30 years, about 200 water supply stations were established along the railroad and in the forest regions of this area, and some experience and lessons were obtained.

1. The ground water resource of economic value and being able to extract all year round are those in taliks under or around the river or lake and those in fissures, cracks and voids of bedrock. The perched water in active layer and the intrapermafrost water can only be used temporarily because the former is unstable and the latter is limited in quantity.

2.The hydrogeological parameters, such as the radius of influence and permeability, should be determined in situ, because those in permafrost regions are quite different from that suggested in hand book or calculated by empirical equations (Zheng, 1959).

3.The water yield would reduce with elapsed time due to the insufficient supply of aquifer, thus the designed allowable long-termed extractable yield should be no more than 20% of that by pumping test in dry season. Wells should be close to the intake area as possible to guarantee the water yield. A well far from the intake area of the Jinlin Water Supply Station provided a good lesson: at the beginning the well yield was as high as 325 T/day, several months later, it became 93 T/day only, and finally, the well became dry and abandoned.

4. The well for extracting water from a shallow

aquifer should be 4.0 to 6.0 m in diameter and 5 to 10 m in depth to guarantee the water yield. If it is by a river, a horizontal water-collecting pipe can be designed at the bottom of river to obtain more water supply. In this way, the water supply stations in Jintao and in Derbur obtain a good result.

5. The well for exploitating subpermafrost water would be frozen if the water head is insufficient to raise the water table above ground surface. Experiments have proved that the electric heating is helpful to prevent the well or pipe from freezing (He and Zheng, 1982).

6. Some artificial methods were proved to be successful to increase the water yield. Deepening the seasonal thawing depth and reducign the freezing depth can thicken the effective aquifer and increase the groundwater resource. For example, in the Cuifeng Water Supply Station of t the Nenlin Railroad, the well increases in water yield from 350 T/day to 600 T/day by filling the slag on the surface around the well and on the terrace of Mujigong River to control the thawing and freezing depths. Besides, it is possible to recharge the ground water during the warm season artificially.

7. The protection of water resource should be taken into accout. For instance, at the water supply stations in Mangui and Derbur, wells and intake area were surrounded by residential area and near the toilelts, the ground water there has been polluted. Besides, the wells are close and influenced to each other, some of which have been abandonded. Therefore, a planning in water utilization and protection is necessary.

8. The ground water is lacking in iodine, thus, it is also necessary to develop a technique to improve the water quality.

REFERENCES

He Jie and Zheng Qipu, (1982). Experiments and application of electric heating for the prevention of water pipes from frozen damages in the Da-Xinganling District. Journal of Glaciology and Geocryology, (4) 1, 55-59.

Heilongjiang Comprehensive Investigation Team, Academic Sinica (1963). Geology of Heilongjiang basin and its adjacent region, Vol.2, Science Press.

Zheng Qipu, (1959). Experience from hydrogeological and engineering geological investigation in permafrost region. Journal of Hydrogeology and Engineering-geology, (11), 13-15.

Zheng Qipu, (1980). Hydrogeological characteristics of permafrost and cold regions in Da-Xinganling Journal of Glaciology and Geocryology, (2) 4,44-51.

GROUNDWATER PROTECTION IN THE PERMAFROST ZONE

V.Ye. Afanasenko and V.P. Volkova

Faculty of Geology, Moscow State University, Moscow, USSR

SYNOPSIS An intensive development of the permafrost zone makes it imperative to protect groundwater in hydrogeologic structures from depletion and pollution. A new approach to the solution of this problem is based on two principles: (1) classification of hydrogeologic structures by the degree of their protection by cryogenic water-impermeable beds; and (2) assessment of underground drainage basins in cryogenic hydrogeologic structures. As a result, the analysis of the pollution sources location in an area allows to plan measures of groundwater protection from depletion and pollution and to create the water-protection zones of different categories and for various geocryologic zones.

Intensive development of the platform and mountain-folded regions of the permafrost zone in recent years demands more and more fresh water to provide for reliable sources of drinking, municipal and domestic water supply as well as to satisfy the needs of industry, power stations and agriculture. Development is accompanied by prospecting, exploration and construction work leading to intensive man-made loading involving an inevitable pollution of groundwater and interference in the existing water exchange conditions. Water consumption is known to entail a complete loss of a portion of water, while most of it, already polluted, returns to the environment. The polluted water is discharged into rivers, and then through the sites of groundwater recharge gets into groundwater, thus endangering further use of the aquifer or a set of aquifers.

The water exchange conditions vary in perennially frozen grounds of different continuity and thickness. In the hydrogeologic structures of the open type, water exchange is intensive, the pathways of groundwater flow are distinctly localized, as a rule, they are well scoured and have high permeability resulting in a fast expansion of pollution areals. The groundwater pollution can vary in a considerable degree, the self-purification process being slow under natural conditions. Therefore, the need of groundwater protection should already be emphisized at the early stages of the permafrost zone development and the relevant measures elaborated.

The objects of development (settlements, industrial enterprizes, construction sites, etc.) should be treated as probable sources of groundwater pollution, which can occur at any place of groundwater recharge. Hence, special evaluation should be carried out of the susceptibility of hydrogeologic structures to probable man-induced impacts, i.e. determination of natural protection of groundwater in each type of hydrogeologic structures, resulting in recommendations on the creation of special water-protection zones wherein measures aimed at protecting surface and ground waters from depletion and pollution must purposefully be implemented.

It is only upon evaluation of the main peculiarities of the recharge, flow and discharge of groundwater within the entire region under study, one can foresee and forestall the consequence of its probable pollution. Hence, the location and character of engineering and industrial-economic facilities, both existing and planned, have to be taken into account from the standpoint of a potential hazard for groundwater pollution. To solve this problem, it is necessary to adhere to two basic principles at the early stage of development:

(1) To carry out the study and classification of hydrogeologic structures, according to the degree of their protection by cryogenic and lithological confining layers with subsequent mapping of cryogenic hydrogeologic structures and indication of the extent of their freezing.

(2) To identify specific features of hydrogeologic structures, as several cryogenic hydrogeologic structures belong frequently to a single drainage basin where groundwater recharge occurs within one structure, whereas its transit in another, and discharge - in the third one. Other combinations are possible. As a result, a map of underground drainage system, as complicated and modified by the presence of perennially frozen grounds, is compiled for the hydrogeologic and cryogenic hydrogeologic structures under consideration.

The main condition in substantiating the first principle is the specific nature of hydrogeo-

logic structures in the permafrost zone, namely the fact that perennially frozen grounds serve as the upper impermeable bed protecting the deep subpermafrost water flow from areal pollution. Recharge and discharge of this water occur locally through open taliks with head-water circulation. Therefore, the hydrogeologic structures of the permafrost zone have to be evaluated according to the character of their transformation by perennial freezing, taking into account general patterns of groundwater flow formation in each structure separately and jointly with neighboring structures. Such an analysis should result in classifying hydrogeologic structures by the degree of their protection by cryogenic and lithological confining beds from possible pollution. Using this classification, special maps of cryogenic hydrogeologic structures have been compiled indicating the degree of their freezing and potential susceptibility to man-induced impacts. Based on the assessment of factors of natural protection of groundwater (Rogovskaya, 1976), it seems reasonable to distinguish the following three groups of cryogenic hydrogeologic structures:

(A) Cryogenic hydrogeologic structures of continuous freezing (shallow, deep and superdeep) that are closed and partially open. Groundwater recharge in these occurs only through the subriver bed and sublacustrine open taliks. They include cryogenic hydrogeologic massifs, artesian and adartesian basins, and cryogenic head-water basins. The deep recharge within the last three structures is absent. It occurs exclusively due to the overflow and inflow of groundwater from neighboring structures beneath the cryogenic impermeable beds.

(B) Cryogenic hydrogeologic structures of intermittent and insular freezing, open and partially open ones with groundwater recharge in valleys by surface water through open taliks, and in the unfrozen ground interfluves, due to percolation of precipitation water through open pluvial-insolation taliks. These structures include cryogenic hydrogeologic massifs, artesian and adartesian basins and massifs, and cryogenic basins of head- and subhead fracture waters.

(C) A number of hydrogeologic structures (hydrogeologic massifs, artesian, adartesian, and cryogenic basins) of noncontinuous insular freezing that are closed or partially open, and are frequently overlapped from the surface by lithological impermeable beds (crusts of weathering) preventing the percolation of atmospheric and surface waters. The deep-flowing groundwater is recharged in these structures due to overflow of water from the neighboring hydrogeologic structures.

To clarify specific features of hydrogeologic structures from the viewpoint of their hydraulic connection, subordination and openness, and the role of each structure in the water exchange, a "Map of groundwater flow" has been compiled representing the conditions of groundwater flow formation by a number of important factors:

(1) Sources of the infrastructural groundwater recharge through open, subriver bed, sublacustrine and pluvial-insolation infiltration taliks are distinguished.

(2) Sites are indicated of interstractural recharge due to groundwater overflow from rocks of the crystalline basement to the rocks of the sedimentary cover and vice versa.

(3) Sites of deep groundwater flow discharge are indicated by openings in ice, icings, thermal and mineral springs.

(4) The directions of deep groundwater flow are shown by different symbols in the zones of active and slowed-down water exchange, and also in those of groundwater flow in subriver bed and flood-plain taliks with groundwater circulation.

This map reflects distinctly the specific features of and differences in groundwater flow, weakened and modified by the presence of frozen grounds in various hydrogeologic and cryohydrogeologic structures. In a number of structures, the direction of groundwater flow in the active zone of water exchange does not coincide with that in the deep part of the hydrogeologic section. It should be noted that groundwater recharge occurs within the limits of one structure, transit in another, and discharge - in the third, i.e., all three types of different hydrogeologic structures occur in a single drainage basin. More complicated combinations are possible.

On the basis of the analysis of existing drainage basins, a "Map of natural protection of groundwater in cryogenic hydrogeologic structures" has been compiled containing information on groundwater protection from pollution. The map is based on the principal assumptions: (1) groundwater pollution can occur in any place of recharge; (2) the response of the identified types of hydrogeologic structures to engineering-economic activity in the course of territorial development is different. In this respect, hydrogeologic structures of continuous as well as non-continuous insular freezing, overlapped by lithological impermeable beds where groundwater pollution can occur only through valley drainage, are least susceptible to man-induced impacts. More susceptible to human economic activities are open hydrogeologic structures of discontinuous and insular freezing, because the places of concentration of pluvial-insolation taliks in the interfluves, as practical development shows, are extremely convenient for erecting various facilities, but they are most susceptible to any pollution.

The authors have worked out recommendations on the establishment of special water-protection zones at early stages of development. Economic activity within the prospective water-protection zones should be regulated as follows:

(1) certain kinds of land use (removal of vegetation, construction of roads, etc.) are prohibited; and (2) a system of measures is introduced to exclude or reduce natural water pollution to the maximum permissible level. The "Map of natural protection of groundwater" shows the areas of water-protection zones for each type of cryogenic hydrogeologic structures. These zones are subdivided into categories according to the area which they have to cover. The water-protection zones of the first category occupy from 30 to 60% of the area of a hydrogeologic structure including areas of pluvial -insolation infiltration taliks; river valleys with surface runoff and near-surface flow through closed and open subriver bed, floodplain and sublacustrine taliks with groundwater circulation. Groundwater pollution occurs within a hydrogeologic structure. The water-protection zones of the second category cover up to 20-30% of the area of a hydrogeologic structure. These are valleys with surface runoff and near-surface water flow through closed and open subriver bed and sublacustrine taliks with groundwater circulation. The pollution of groundwater occurs also within a structure. The water-protection zones of the third category cover only 10-15% of the area of a hydrogeologic structure. They include valleys whose surface runoff and sub-surface water flow through closed and subriver bed and sublacustrine taliks with groundwater circulation. Groundwater pollution within a hydrogeologic structure is impossible, but it will quickly affect groundwater flow in neighboring hydrogeologic structures. The water-protection zones of the third category are, as a rule, recommended for hydrogeologic structures in the first and third groups (A and C), whereas water-protection zones of the first and second categories should be created for hydrogeologic structures of the second group (B).

The combination of maps of cryogenic hydrogeologic structures, of drainage basins and natural protection of groundwater together with a "Map of location of pollution sources" that was being compiled simultaneously made it possible to compile a "Map of pollution spreading by groundwater" for the investigated hydrogeologic structures (Volkova and Afanasenko, 1986).

While compiling such a map, the following factors should be taken into consideration: specific features of the location of groundwater recharge sources; the season when pollutants can get into the aquifer; the area of a hydrogeologic structure that falls into the region of undesirable influence; and the depth of hydrogeologic section accessible to pollution.

The pollution sources on the above-mentioned map of their location should be classified according to the kind of territorial development: open-cast and underground mining; industrial and power-engineering facilities; civil engineering construction; towns and cities, settlements; industrial forest utilization; agricultural work etc. In addition, the sources of pollution have to be subdivided according to the duration of operation (permanent, periodic and occasional) and by the character of their impact on the chemical composition of natural waters. With a set of such maps one can plan measures for groundwater protection. As a first version, the proposed approach has been described in the book "Natural protection of groundwater in the cryohydrogeologic structures" (Romanovsky et al., 1985). At present, all these principles are being further developed with respect to hydrogeologic and cryohydrogeologic structures of the entire South of the permafrost zone and the north-eastern USSR.

REFERENCES

Volkova, V.P. (1986). Printsipy sostavleniya karty zagryazneniya podzemnykh vod v kriogennykh gidrogeologicheskikh strukturakh. V knige: Geokriologicheskie issledovaniya. Moskva: Izdatel'stvo Moskovskogo universiteta, pp.95-99.

Osnovy gidrogeologii. Ispol'zovanie i orhrana podzemnykh vod. (1983). 231 pp. Novosibirsk: Nauka.

Rogovskaya, N.V. (1976). Karta estestvennoi zashchishchennosti podzemnykh vod ot zagryazneniya. Priroda, 3, 57-61.

Romanovsky, N.N. (1983). Otsenka kriogidrogeologicheskikh struktur gorno-skladchatykh oblastei s pozitsii okhrany podzemnykh vod. Vestnik Moskovskogo universiteta. Geol. 6, 65-79.

Romanovsky, N.N., Afanasenko, B.Ye. & Volkova, V.P. (1985). Estestvennaya zashchishchennost podzemnykh vod v kriogidrologicheskikh strukturakh. 118 pp. Yakutsk.

MINERO-CRYOGENIC PROCESSES

A. L. Ahumada

**Universidad de Catamarca IANIGLA,
C.C. 330, 5500 Mendoza, Argentina**

SYNOPSIS We understand as minero-cryogenic processes an increase in concentration of heavy ores at the bottom of the active layer or top of the permafrost. This heavy ore selection occurs in the fine granulometry (sands and silt) as a consequence of vertical sorting or inverted gradation, a typical texture of geocryogenic regions caused by freeze-thaw processes. Sampling, further analyses and evaluations let us know that in the study area, Central Cordillera of the Andes in Mendoza, heavy ores concentration increases in depth down to the bottom of the active layer or top of the permafrost. (It is impossible to distinguish increase rates according to morphology, where the sample profile is made). Morphogenesis and morphodynamic are reflected in the concentration results.

INTRODUCTION

The Andes is under the effects of various geocryogenic processes (Corte, 1982).

In this case, the study of what is called Minecryogeny is a contribution to the knowledge, evaluation and interpretation of either colluvial or heavy mineral deposits, located in high mountain geocryogenic environments. This research project aims at getting further information to detect deposits that could be interesting from an economical scope point of view.

Freezing and thawing of rock materials produces (apart from physical cryoweathering), a selection of particles, in the presence of water, rearranging the layer undergoing a cyclic process. In this way, coarse material stands in an upper layer while the fine one migrates to the bottom. The structure obtained by this method is called vertical selection (Corte, 1969). When these systems have heavy minerals (whether economically interesting or not) fine particles become concentrated at the bottom of the affected layer.

The study area, Nacientes del río Cuevas, is at 32°10' and 32°50' south latitude and at aproximately 70°2' to 70°10' west latitude in Mendoza province, Central Andes, Argentina. This paper is part of a Ph.D. degree thesis at the University of Tucumán.

BACKGROUND

Prokopchuk (1978) synthesizes cryogenic processes contributing to the formation of the Lena river diamond placers (USSR). Diamond distribution is characteristic in either colluvial or residual placers: the upper layer is the most enriched due to frost heaving.

Grigoriev (1978) analyzes the genesis of placer deposits in the Laptev sea where continuous permafrost, whether marine or coastal is fundamental.

Pitul'ko and Shilo (1969) state that geochemical studies in the USSR get to the conclusion that negative temperatures tend to increase mineral concentration in soils, under conditions of underground water because of partial freezing processes.

Horsnail and Fox (1973) in their field work in Yukon find out that the geocryogenic environment introduces other criteria as far as geochemical research is concerned: samples should be taken at the profoundest depth as possible of the active layer.

Shumilov (1983), as a summary of all the knowledge acquired in USSR about placer formation in permafrost regions, has proved and confirmed that up to 30 to 50% of the ore components in the form of free primary minerals are concentrated in the minor fraction of cryogenic alluvium.

CLIMATE

Annual mean temperature at the Cajón del Rubio is of -4,7°C (permafrost conditions). Monthly maximum temperatures are below 0°C from April to October and above 0°C from November to March (only 5 months a year). Annual thermic range is -9,4°C. Daily records of temperatures at Nacientes del Cuevas confirm that every day freezing cycles take place from December to April, with a daily thermic range between 6,4°C and 4°C. During the rest of the year, mean temperature remains below 0°(-5°C to -2°C).

The study area is located in a mountain perma-

frost system, with daily freezing and thawing cycles in summer, with an average active layer depth of 1.0 meter.

Annual precipitation values for this area (Minetti, 1985) are above 500 mm, with snow precipitation from May to September and sometimes with graupel precipitations in the summer. A more thourough analysis of the climate of this region is made by Ahumada (1986).

GEOCRYOGENIC ENVIRONMENT

The study area is situated between 3500 and 4500 m asl. This area was defined as upper or geocryogenic zone (Ahumada, 1985) according to Corte's classification (1983) due to the association of geoforms and processes acting at this altitudinal level.(Fig. 1)

Active rock glaciers can be observed at 3500 m asl. The landscape turns to an environment with generalized cryofragmentation. In the profiles of the different geoforms, there can be noticed cyclic freezing activity at the level of the active layer (1 m deep, average) where vertical selection, cryoturbation and the typical "open work" can be seen (Corte, 1985a; Washburn, 1980).

The superficial cover is constituted by angular blocks. All summits have an abrupt aspect, with distinct traits produced by cryofragmentation, nivation, avalanche channel-like corridors, snow patches, etc.

Morphological associations of the geocryogenic zone are shown in the map of Fig. 1: soligelifluction, talus, patterned groups and primary and secondary rock glaciers (Ahumada, 1985, 1986; Corte, 1976). The latter indicate the lower limit of high mountain discontinuous permafrost (Barsch, 1978; Haeberli, 1978, 1976; Cui Zhijui, 1982; Cheng, 1983; Corte, 1983) in an environment of annual mean temperature below -1°C (Ives et al., 1971; Fujii et al., 1978; Ives, 1973; Trombotto, 1983; Ahumada et al., 1984).

MATERIALS AND METHODS

Once the geocryogenic inventory was made, the sampling sites were chosen:

There were made trial pits in geoforms with smooth slopes in the surface, 6 to 16°gradient, block cover and vertical selection. The samples were constituted by the fine material of the profile. Three samples were taken in each trial pit:

a. sample 1 was taken at the point of contact between fine and coarse materials of the vertical selection profile.

b. Sample 2 was extracted at almost half way from the site from where the first sample was taken and the level where 0°/-0°C temperature was recorded.

c. Sample 3 was obtained at the same depth where the 0°/-0°C temperatures were recorded (base of the seasonal active layer).

Trial pits for excavations were made using spade and manually, with frequent temperature measurements recorded with Weston thermometers.

Field samples were granulometrically analyzed, then fine fractions were separated from heavy minerals by means of heavy liquids.

Granulometric analysis was made by means of dry sieving up to the particles of 0.074 mm diameter. The sieves used were ASTM system. The fraction of less than 0,074 mm diameter was evaluated in its weight percentage.

Samples were taken in the surfaces of rock glaciers and moraines, which receive debris and minerals from a mineralized outcrop of a vulcanite with the following minerals: magnetite, hematite, rutilo, pyrite, chalcopyrite, goethite, ilmenite, etc.

PROFILE DESCRIPTION

Profiles were made on the moraine which shows geocryogenic activity on the surface as there can be observed boulder areas and sorted nets as well as stripe patterned ground. Excavations were made at the end of the summer after full development of the active layer.

Profiles P_1 and P_7 were made in sectors of the moraine with boulders on its surface. Only two samples were taken from P_1, and three samples could be extracted from P_7 according to the above mentioned methodology. Depth of negative temperature in P_1 is at 1 m deep (-0,5° C) and in P_7 at 1,02 m (-1°C). In P_1, the general gradient is of 10°and in P_7 of 12°. Vertical selection or inverted gradation is the most characteristic trait of these profiles. There was observed "open work" which is an expresion of segregation or needle ice activity: very freezing holes or vesicles of a quite heterogeneous size. It was also found fine material accumulation on the top of the boulders, displaying the same alveolar structure.

At the front of the secondary rock glacier, there were made three profiles: P_2, P_4 and P_6. In all the cases we came across superficial extrusion. The ground where the trial pits were done has from 14°to 17°gradient. In "frost soils", vesicles formation in the surface is outstanding at first sight. In these pits, it is evident the fine material migration to the surface, with pseudo lineament at the border indicating, in turn, the fall of coarse material in the lateral sectors of the patterns. In these cases, depth of negative temperatures does not exceed 90 cm with -1°C average.

Profiles P_3 and P_6 were made in forms with low gradients, these are fields of small boulders. The general gradient of the field is 6°. Macroscopically, the vertical selection is the

structure most clearly seen.

Profiles P_8 and P_9 were made in primary rock glaciers or talus. In these cases, the surface gradient is of 6° and vertical selection is observable at first sight with some cryoturbation manifestations. Depth of negative temperatures is at 1,20.

EVALUATION OF HEAVY MATERIAL CONCENTRATION IN FIELD SAMPLES

Proportional distribution of heavy material was analyzed according to form and processes involved.

Obtained concentrations are displayed in Table I.

a. Moraine: in P_1, samples of heavy mineral concentration in the whole show an increase of 10% depth. Concentration is permanent in fine sand granulometry and increased in very fine sand and silt fractions.

   In P_7, total heavy material concentration increases 11% in the two lower sampling levels. Silt and fine sand fractions correspond to the increase produced by vertical selection.

b. Boulder field: heavy minerals analyses in P_3 does not show heavy minerals in total concentration at depth, nevertheless, it does display increase in fine and very fine sand fractions concentration. The silt fraction does not show an increase with depth probably due to aeolian and/or cryofragmentation contribution in the upper layers (Birkeland, 1973; Mahaney, 1981).

   In P_5, total heavy mineral increase is of 50% in depth. Heavy mineral migration is more noticeable in fine and very fine sand fractions, and not so clearly seen in silt fractions.

c. Primary rock glacier or talus glacier: in P_8, total heavy minerals concentration has an increase of 60% in depth. In distinctive fraction analysis it shows an increment in fine and very fine sands in the silt fraction; migration takes place in the first two levels of the profile.

d. Extrusion: each profile made in extrusion areas show a different behaviour in relation to heavy mineral selection.

   In P_2, it is observed fine heavy mineral migrations to the surface in total percentages, 60% increase, as well as in percentages corresponding to finer fractions.

   In P_4, heavy material migrates toward the bottom of the seasonal thawing layer and the increase percentage is of 75%. Fine differentiated fractions fit with this situation.

In P_6, heavy mineral percentages are homogeneous in all levels, except for the silt fraction where there is an increase towards the bottom of the profile.

These differences could be related to the existence or lack of extrusion activity, with the quantity of water, with the speed of freezing penetration in the respective places, etc. This study will not be undergone in this paper.

CONCLUSIONS

Most of the profiles show an increase in heavy mineral concentration toward the bottom of the active layer.

In the case of extrusion, there is no homogeneous results. Evidently, it is a more complex formation phenomenon to be studied thoroughly in the future.

Even though there have been obtained clear evidences to state that there is heavy mineral concentration at the bottom of the active layer, it is considered that, in order to use these data as a research guide in the feasibility of colluvial and placer deposits in the high mountain, it is necessary to increase the number of studied zones and to improve the geochemical aspect of the sample analysis.

ACKNOWLEDGEMENTS

Thanks are due to doctor A.E.Corte for his guide and advice in this work, which was supported by IANIGLA-CONICET. To my colleagues: geologist Darío Trombotto, technician Alberto Ripalta; to Susana Bottero for drawing the maps and tables and to Adriana Buglio for the translation of the paper into English.

REFERENCES

Ahumada, A.L. (1985). Zonación altitudinal Geocriogénica en Qda. Matienzo. IX Jornadas de Investigación de la Universidad Nacional de Cuyo: 258.

Ahumada, A.L. (1986). Procesos Criogénicos y mineralógicos. Tesis doctoral. U.N. Tucumán. Inédita.

Ahumada, A.L. & Trombotto, D. (1984) Estudios periglaciales en la Lagunita del Plata, Provincia de Mendoza. IX Congreso Geológico Argentino, Actas IV: 22-34.

Barsch, D. (1978). Active rock glaciers as indicators for discontinuous alpine permafrost. An example from the Swiss Alps. Permafrost Third International Conference in Permafrost. Otawa, Canadá, Natl. Research Council, I: 348-355.

Birkeland, P.W. (1973). Use of relative age-dating methods in a stratigraphic study of rock glaciers deposits. Mt. Sopris, Colorado. Arctic and Alpine Research V, 4: 401-416.

Geoform	Sample	Depth (cm)	Heavy minerals concentration Total (%)	Heavy minerals per fraction (%)			Increase (%)
				Fine sandstone	Very fine sandstone	Silt	
Moraine	P_1M3 P_2M4	80 100	10 11	8 8	11 12	12 14	10
Moraine	P_7M16 P_7M17 P_7M18	20 50 102	9 9 10	8 8 9	10 10 9	9 8 12	11
Boulder Field	P_3M7 P_3M8 P_3M9	70 100 130	4.5 4 4	2 3.5 4	4 2.5 4	7 5 4	–
Boulder Field	P_5M10 P_5M11 P_5M12	60 90 100	2 3 3	1 2 2	2 3 3	5 3 4	50
Primary Rock Glacier	P_8M37 P_8M38 P_8M39	30 70 120	5 7 8	5 7 9	6 7 9	4.5 8 6	60
Extrusion	P_2M5 P_2M6	20 65	5 2	3 3	4 1	7 3	Process Inversion
Extrusion	P_4M19 P_4M20 P_4M21	10 60 85	4 6 7	5 6 8	4 6 9	4 5 5	75
Extrusion	P_6M13 P_6M14 P_6M15	24 70 90	4 4 4	3 3 3	4 4 4	4 4 6	–

TABLE I

Evaluation of heavy mineral concentration in the different granulometric fractions of cryogenic profiles

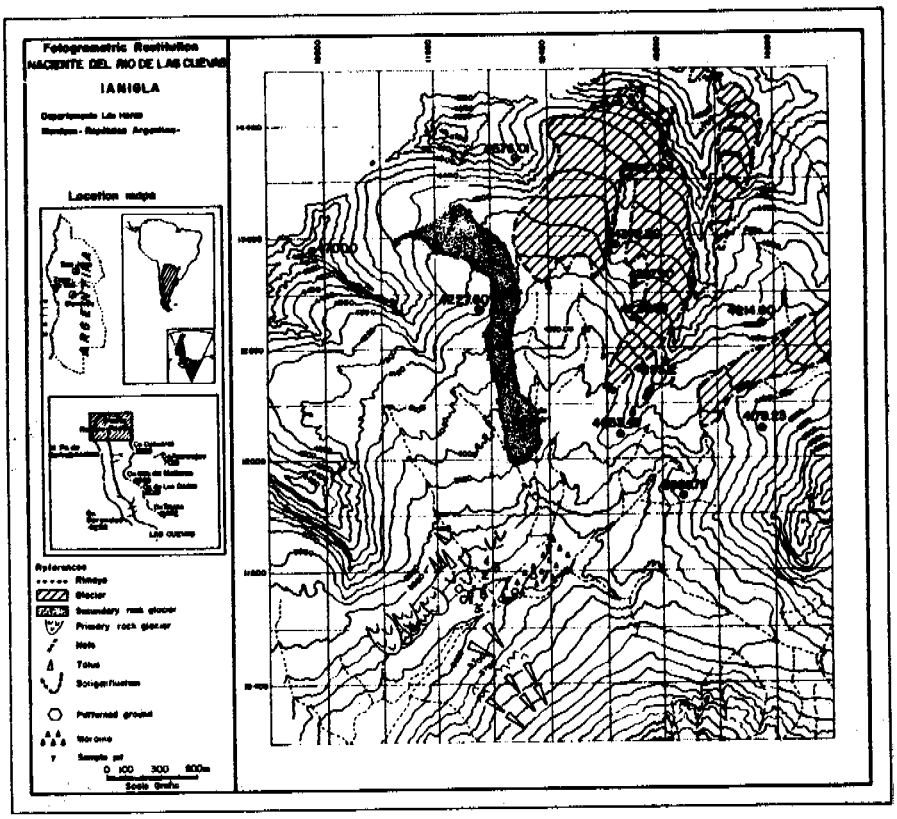

Fig. 1- Sample locations. (1-Moraine, 2- Extrusion, 3- Boulder Field, 4- Extrusion, 5- Boulder Field, 6- Extrusion, 8- Primary Rock Glacier.).-

Corte, A. (1976). The hidrologyc significance of rock glaciers. Journ. of Glaciology, V 17, N°75: 157-158.
Corte, A. (1982). Geocriología General y Aplicada, Revista del Instituto de Ciencias Geológicas, Univ.Nac. de Jujuy, V.5, 33 p.
Corte, A. (1983). Los conceptos: geocriogénico y glacial-paraglacial en los Andes Centrales de Argentina, latitud 30°. IANIGLA. Anales 83. Primera Reunión del Grupo Periglacial Argentino: 43-63. Mendoza.
Corte, A. (1985). Geocriología General y Aplicada. Argentina. En prensa, Eudeba, 450 p.
Cui Zhijui (1982). Periglacial landforms and their regional characteristics on Quinghai-Xizang Plateau. Proceedings of Symposium on Qinghai-Xizang (Tibet) Plateau (Beijing, China). Gordon and Breach, Science Publishing, Inc. V. II; 1777-1788. New York.
Cheng, G. (1983). Vertical and horizontal zonation of high altitude permafrost. Permafrost Fourth International Conference, Proceedings National Academy Press: 136-141. Washington D.C.
Fujii, Y. & Higuchi, K. (1978). Distribution of alpine permafrost in the northern hemisphere and its relation to air temperature. Permafrost-Third International Conference on Permafrost I: 366-371. Ottawa, Canada.
Grigoriev, N.F. (1978). The role of cryogeneous factors in the formation of placers along the shelf coastal zone of the Laptev Sea. Permafrost-Second International Conference on Permafrost. National Academy of Sciences: 165-167. Washington D.C.
Horsnail, R. & Fox, P. (1973). Geochemical exploration in permafrost terrains with particular reference to the Yukon Territory. Papers at the Yukon Territory. Papers at the 75th Annual General Meeting of the CIM, Vancouver.
Haeberli, W. (1978). Special aspects of high mountain permafrost methodology and zonation in the Alps. Third International Conference on Permafrost: 378-384. National Research Council, Ottawa, Canada.
Haeberli, W. (1985). Creep of mountain permafrost: Internal structure and flow of alpine rock glaciers. Mitteilungen der Versushsanstalt fur Wasserbau, Hydrologie und Glaziologie Eidgenossische Technische Hoschschule Zurich, 142 p.
Ives, J. (1973). Permafrost and its relationship to other environmental parameters in a midlatitude, high altitude setting, Front Range, Colorado Rocky Mountains. North American Contribution, Second International Conference on Permafrost. Natl.Acad.Sci.: 121-125, Washington D.C.
Ives, J. & Fahey, B.D. (1971). Permafrost ocurrence in the Front Range Colorado Rocky Mountains, USA, J. of Glaciology, V. 10:105-111.
Mahaney, W.C. (1981). Palaeoclimate reconstructed from paleosols: evidence from Rocky Mountains and East Africa. Quaternary Palaeoclimate. Norwich, U.K. Geoabstracts: 227-247.
Pitul'ko, V. & Shilo, N.A. (1968) Geochemistry of cryogenic landscapes and prospecting of ore deposits. C.A. 72-81379. (Traducciones internas de Amax Explorations, Inc. Colorado).
Prokopchuk, B.I. (1978). Formation of diamond placers under conditions of arctic climate and permafrost. 2nd International Conference on Permafrost. USSR. Contribution. Natl. Acad. Sci.: 206-207.
Shumilov, Y.V. (1983). An Experimental Study of Criogenic Factors Affecting Geological Processes in Placer Formation. Fourth International Conference on Permafrost: 1157-1159. Alaska
Trombotto, D. (1983). Geocriología de la Lagunita del Plata. Anales 83 IANIGLA. Primera Reunión del Grupo Periglacial Argentino: 149-156.
Washburn, A.L. (1979). Geocryology: A survey of periglacial processes and environments. 2nd. ed. Edward Arnold (Publishers) Ltd. London, 406 p.

UPFREEZING IN SORTED CIRCLES, WESTERN SPITSBERGEN

S. Prestrud Anderson

Quaternary Research Center, University of Washington, Seattle, Washington, 98195 USA

SYNOPSIS In sorted circles at Kvadehuksletta, Spitsbergen, the rate of upfreezing of single stones predicted from measured frost heave strain and freeze/thaw frequency in the soil decreases exponentially with depth. These predicted upfreezing rates are insufficient to produce the deep sorting observed in excavations of Kvadehuksletta sorted circles over time scales of 10^3-10^4 years, the estimated age of these patterns. The calculated horizontal component of clast movement caused by realistically inclined freezing fronts is small compared to the radius of the fine domains. Hence, upfreezing alone cannot account for the observed depth or pattern of sorting in Kvadehuksletta sorted circles. However, upfreezing operating in conjunction with buoyancy-driven convection of the fine-grained soil in the active layer is capable of producing both the deep sorting and other aspects noted in the three-dimensional morphology and structure of sorted circles.

INTRODUCTION

Sorted circles are impressive soil patterns defined by frost-induced segregation of stones from fine material in Arctic and alpine areas (Fig. 1). Upfreezing is frequently cited as a mechanism for development of the distinctive sorting within these features (Huxley and Odell, 1924; Paterson, 1940; Sharp, 1942; Washburn, 1956; Czeppe, 1961; Corte, 1963; Goldthwait, 1976; Ballantyne and Matthews, 1982; Muir, 1983; Ray et al., 1983; Gleason et al., 1986). Despite this wide acceptance, the precise function of upfreezing in the dynamics of sorted circles has not been documented. Recent experiments on upfreezing (Anderson, in press) provide the basis for a rigorous assessment of the role of upfreezing in producing the pattern and sorting of sorted circles.

Little field data exist on the rate at which segregation of a homogeneous mixture occurs. Estimates of a few years to a few decades for the development of "significant" vertical sorting have been put forth by Jahn (1961) for sediments in Spitsbergen and by Corte (1962a) for deposits near Fairbanks, Alaska. Sorted circles 1-4 m in diameter have been documented on surfaces ranging in age from 50 to 200 years (Sharp, 1942; Schmertmann and Taylor, 1965; Ballantyne and Matthews, 1982), implying relatively rapid segregation and pattern development.

The rate of upfreezing of a single clast depends primarily upon its length, the magnitude of the strain in the soil caused by ice lensing during freezing, and the number of freeze/thaw cycles it experiences per year. Non-horizontal freezing fronts impart a horizontal component to clast displacements that depends on the inclination of the freezing front (Muir, 1983; Hallet, unpub. manuscript). Thus, upfreezing rates can be calculated if the frost-heaving strain in the soil and clast size are known; furthermore, the direction of clast movement can be deduced from the freezing front geometry. Such data exist for well-developed sorted circles at Kvadehuksletta, western Spitsbergen (Fig. 2), the site of a comprehensive field study (Hallet et al., 1988) aimed at elucidating the processes active in well-developed sorted circles. Using data from that study and the model of upfreezing developed in Anderson (in press), I calculate the movement of clasts expected due to upfreezing in the Kvadehuksletta sorted circles. I then evaluate the influence of upfreezing on the rate and pattern of sorting.

Sorted circle morphology

Sorted circles form coalescing nets in the swales between emergent beach ridges at Kvadehuksletta, and are abundant and well-developed adjacent to lakes and meltwater channels. The surficial morphology of these features has been described by Hallet and Prestrud (1986). The sorted circles studied are located on a surface dated at 60-160 ka (Forman and Miller, 1984), and have probably been active for millennia (Hallet and Prestrud, 1986).

Three sorted circles excavated at Kvadehuksletta revealed that the distinctive sorting observed at the surface continues to at least a

Figure 1. Sorted circles at Kvadehuksletta, Spitsbergen. The fine domains range up to 2-3 m in diameter, and the coarse borders are typically 1 m wide. The term "sorted circle" is used, in agreement with the literature, though these features only occasionally approach circular form. (Photo by B. Hallet).

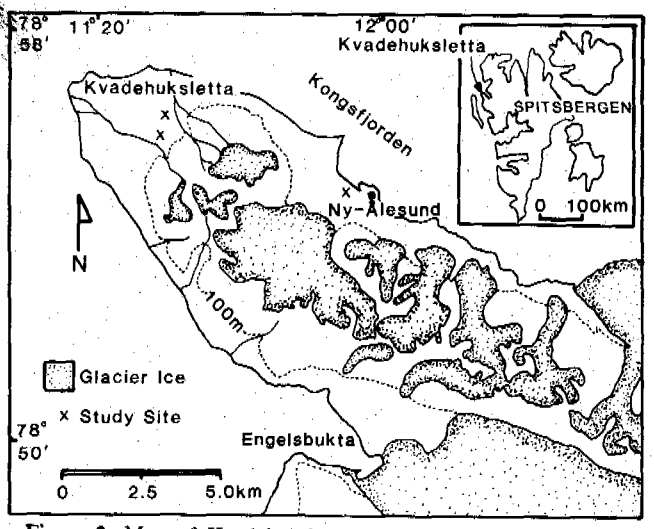

Figure 2. Map of Kvadehuksletta, western Spitsbergen.

depth of 0.9m (Prestrud, 1987). In each excavation, the contact between the fine material of the circle center and the gravel in the border steepened from about 20° near the surface to vertical at a depth of 0.2 to 0.3m. The contact remained sharp over the entire depth excavated (0.5-0.9m). This sorting probably continues throughout the 1.5-1.8m deep active layer, as metal probes easily penetrated to these depths in the fine centers.

Number of freeze/thaw cycles

In Spitsbergen, fluctuations of the air temperature around the freezing point are common at all times of year. Van Vliet-Lanöe (1983) reports an average of 60 days per year when the temperature crosses 0 °C in Ny Ålesund. Only July is free of freezing days, and the most frequent fluctuations occur in June and September. Czeppe (1961) measured 120 freeze/thaw cycles at the ground surface in Hornsund, 250 km south of Kvadehuksletta, during 1957-58. The number and amplitude of the fluctuations, however, drop off considerably with depth in the soil. Czeppe's (1961, Fig. VI) measurements, taken every 6 hours, show only three freeze/thaw cycles before the fall freeze-up at a depth of 0.05 m, and only one freeze/thaw cycle in addition to the annual cycle at 0.2 m.

Data gathered daily during the fall and winter of 1985 from 36 thermistors buried between 0.1 and 1.0 m in two instrumented sorted circles at Kvadehuksletta show only the fall freeze-up, without oscillation about the freezing point, below 0.2 m depth. Above 0.2 m depth, only one fall freeze/thaw cycle occurred, despite three episodes of sub- freezing air temperatures.

Freeze/thaw cycles occur during the spring as well as the fall. However, the sorted circles at Kvadehuksletta are covered by a blanket of snow ranging from 0.5-1.0 m in depth for much of the year. The insulating effect of the snow damps out the springtime air temperature oscillations, making numerous freeze/thaw episodes unlikely. In two years of observation at Kvadehuksletta, no refreezing of the ground was noted in the early summer after melting of the snow pack.

In general, the number of freeze/thaw cycles decreases with depth. During the three years represented in the Kvadehuksletta and Hornsund data, only the annual freeze/thaw cycle occurred below 0.3 m in the soil. A total of three freeze/thaw episodes occurred in the top decimeters of the soil. Both the number of autumn freezing episodes at the surface of the soil, and the depth of their penetration vary from year to year. Hence, for this analysis, I will assume a maximum of seven freeze/thaw cycles occur at the surface, damping to only the annual cycle at 0.5 m depth (see Eq. 7). This range encompasses the observations from Kvadehuksletta and Hornsund.

Geometry of freeze and thaw fronts

Thawing proceeds downward from the surface during the summer. The rate of thaw differs between the borders and fine domains of the sorted circles at Kvadehuksletta, giving rise to non-horizontal thaw fronts. Although the coarse borders emerge earliest from the snow, and, hence, begin thawing before the fines, the thaw front lies deepest within the fine domains throughout most of the summer. Measurements of thaw depth, made by probing with a steel rod, show that the difference in thaw penetration in the two materials increases through late July (Fig. 3), forming deep thaw basins beneath the fine domains. By the end of the summer, thaw rates beneath the borders appear to exceed those in the fines, and the thaw front flattens. This pattern is apparently common, as it was observed by Schmertmann and Taylor (1965) in sorted circles near Thule, Greenland; frozen ridges beneath the coarse borders were observed by Sharp (1942) in the St. Elias Range, Alaska; and thaw basins formed under the centers of non-sorted circles in western Arctic Canada (Mackay, 1980).

During winter, the downward progression of the freeze front also proceeds non-uniformly through a sorted circle. Working in Thule, Greenland, Schmertmann and Taylor (1965) demonstrated with 2-dimensional arrays of thermocouples that the 0 °C isotherm propagates more quickly through the coarse borders than through the fines in sorted circles. Their measurements show that the freezing front progressing down from the surface has convex upward geometry within the fine domains, and concave upward geometry within the borders– the opposite of the thaw basin developed during the summer. Chambers (1966) found a similar pattern in a sorted circle at Signy Island in the South Orkney Islands. He also noted that the difference in freezing front penetration rate between the fines and the coarse border decreased below 0.2 m, the vertical extent of the sorting at the site. At Kvadehuksletta, the geometry of the freezing front propagating downward from the suface was not well documented, as only 3 of 36 thermistors were installed in the gravel borders. However, the available data is consistent with the freezing front geometry observed by Schmertmann and Taylor, with freezing progressing most rapidly through the borders.

In an excavation of a Kvadehuksletta sorted circle in late September 1984, the visible 0.1 m deep freezing front followed the contour of the surface in the fines. Beneath the border, it dipped away from the circle center about 15°, reaching a depth of 0.3 m below the surface. The dip of the freezing front beneath the border in Schmertmann and Taylor's (1965) study ranged up to 25°, in good agreement with the freezing front observed in this excavation.

Relatively low moisture content in the gravel borders is probably the primary reason for more rapid freezing in the borders. Above the water table the coarse borders are well-drained. In contrast, fine material tends to retain water; hence release of latent heat slows progression of the freezing front in the circle centers. Water drawn from the border to growing ice lenses in the fines, a phenomenon demonstrated experimentally by Taber (1929), both increases the difference in moisture content and advects heat out of the borders. The borders may also have greater exposure to cold air temperatures due to lesser snow cover, and to wind- or buoyancy-driven air circulation through the large pores.

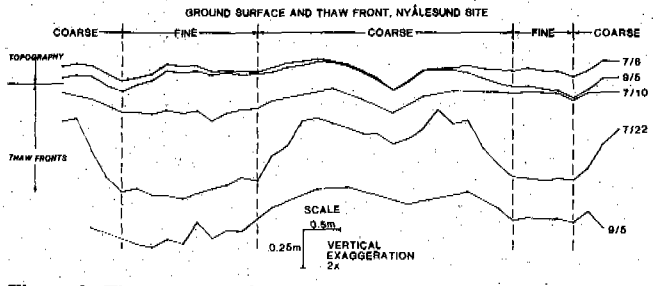

Figure 3. The evolution of the surface topography and the thaw front geometry beneath two sorted circles near Ny-Ålesund, Spitsbergen, in 1984. Thaw proceeds more quickly through the fines than through the coarse borders, producing deep thaw basins in mid-summer. The two upper profiles show the topography of the surface near the beginning and the end of the thaw season.

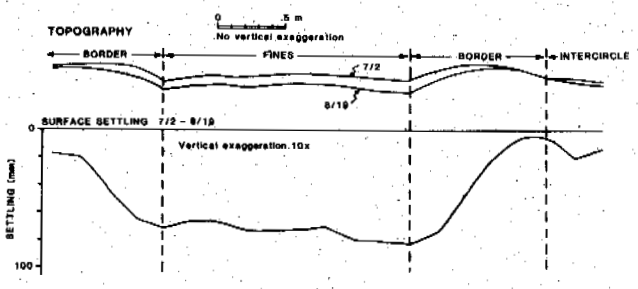

Figure 4. Thaw settling of the surface of a sorted circle at Kvadehuksletta during summer, 1985. Maximum settling occurred in the fine domains, reflecting the greater frost heave strain there in the winter. Two upper curves show surface topography on 2 July and 19 August.

The line of reasoning outlined above for rapid freezing front propagation in the coarse borders during the winter does not explain their slower thaw during summer. Other factors, such as an increase in the effective thermal diffusivity due to a decrease in moisture content with depth in the fine domains, or the free convection of pore water modeled by Ray et al., (1983) and Gleason et al., (1986), may be important during thaw. However, it is the inclination of the *freezing front* that proves most important in determining the differential lateral movement of clasts by upfreezing (Corte, 1963; Muir, 1983; Hallet, unpub. manuscript). In the Kvadehuksletta sorted circles, the freezing front appears to advance downward parallel to the contour of the surface of the fines, steepening to a dip of 15-25° away from the fines beneath the borders.

Magnitude of frost heave

If one assumes that the surface of a sorted circle is not changing in height from year to year, then the amount of surface settling during the thaw is identical to the frost heave during the winter. Field measurements from heave frames firmly anchored in the permafrost, with dowels free to slide in the vertical direction, show 80-120 mm of settling (e.g. Fig. 4) in the fine domains during the thaw season at Kvadehuksletta. Total thaw settling drops off considerably in the coarse borders (Fig. 4), reaching a minimum at the outer edge of the border. Most settling within the border occurs close to the fine/coarse contact, where the coarse material is limited to a thin layer above the fines. The minimal settling at the outer edges of the border and in the intercircle area presumably reflects lesser amounts of segregation ice in gravelly material.

Direct field measurements of frost heave at Kvadehuksletta were made with heave meters consisting of linear potentiometers read daily by a microprocessor-based datalogger. During 1985-1986 fall and winter, two transducers recorded 90 and 96 mm of frost heave at the surface of the fine center, and 50 mm was measured by a third transducer at the top of the border of a sorted circle. These measurements represent minimum values, as the extension limits of the potentiometers were reached.

The magnitude of vertical frost-induced strain in the soil and its variation with depth are of particular interest with regard to upfreezing. At the time the extension limits of the two surface heave meters over the fine domains were met, the freezing front was 0.2-0.3 m below the surface. As shown in the first two entries of Table I, these measurements imply average vertical soil strains of 0.45 and 0.32 in the top decimeters of the active layer. Heave strain was also measured directly with heave meters modified to measure small changes in distance between two pvc (polyvinyl chloride) plates originally spaced about 0.2 m apart. The data from the heave strain meters (Table I) show a marked drop in heave strain with depth to negligible values at 0.6-0.8 m depth.

The decrease in heave and strain (differential heave) with depth in the fines implies a decrease in ice content in the soil. Another way to estimate the ice content of a soil, as outlined by Hallet et al. (1987), is through analysis of temperature profiles. In the absence of phase changes or heat advection, the heat conduction equation describes the rate of change of temperature, T, at a point in the soil. The one-dimensional diffusion equation is:

$$\frac{\partial T}{\partial t} = \frac{\partial}{\partial z}(\kappa \frac{\partial T}{\partial z}) \qquad (1)$$

where t is time, z is depth, and κ is thermal diffusivity. A phase change causes an additional source or sink of heat, which can be expressed by the addition of a latent heat term, yielding:

$$\frac{\partial T}{\partial t} - (\frac{\partial W_i}{\partial t})(\frac{L\rho_i}{C_s\rho_s}) = \frac{\partial}{\partial z}(\kappa \frac{\partial T}{\partial z}) \qquad (2)$$

where W_i is the volume fraction of ice, L is the mass specific latent heat of fusion for ice, ρ_i is the ice density, ρ_s is the soil density, and C_s is the mass specific heat of the soil. Eq. 2 was rearranged to yield an expression for $\frac{\partial W_i}{\partial t}$. This quantity, and subsequently W_i, the ice content, was calculated for six different depths in a sorted circle at Kvadehuksletta. The data set used in this calculation consisted of temperatures measured daily at 0.1 m intervals to a depth of 1.1 m in the soil over most of one year. Finite difference approximations allowed calculation of the derivatives. The heat capacity, soil density and thermal diffusivity were treated as constants, but different values were assigned for frozen and unfrozen soil. Field measurements yielded an average bulk density of $2.2 \times 10^3\ kg/m^3$ for thawed soil. Using reasonable values for dry soil density, moisture content, and mineral content, C_s and κ were estimated from Johnston (1981) to be $1.7\ kJ/kg°K$ and $0.8\ mm^2/s$ for unfrozen soil, and $1.1\ kJ/kg°K$ and $1.2\ mm^2/s$ for frozen soil, respectively. Over the course of the year of measurements, two estimates of W_i are possible. In the fall, $\frac{\partial W_i}{\partial t}$ becomes positive, reflecting the growth of ice lenses in the soil. In the summer, $\frac{\partial W_i}{\partial t}$ becomes negative when thawing occurs. Summing $\frac{\partial W_i}{\partial t}$ over the fall freeze-up and over the summer thaw yielded two independant estimates of ice content, shown in Table II. The ice content decreases markedly below the 0.4 m level in the soil. Presumably ice contents in the soil above 0.4 m were equivalent to or greater than at 0.4 m, though it was not possible to calculate ice content from Eq. 2 for higher levels, as the noise arising from rapid temperature fluctuations and steep temperature gradients rendered the finite difference approximations inaccurate.

Table I. Strain measured with heave strain meters.

Depth m	Year	Measurement	Extension mm	Strain
0-.20	1985-86	Surface Heave	90.0	.45
0-.30	1985-86	Surface Heave	96.0	.32
.15-.35	1984-85	Strain Meter	34.0	.17
	1985-86		39.0	.19
.30-.54	1984-85	Strain Meter	35.0	.15
	1985-86		45.0	.19
.62-.80	1984-85	Strain Meter	1.7	.01
	1985-86		1.8	.01

Table II. Ice content as a function of depth.

Depth m	Volumetric Ice Content* %	Excess Ice Content† %
.4	.33-.43	.20 to -.02
.5	.24-.26	.03 to -.11
.6	.26-.17	.03 to -.18
.7	.21-.17	-.02 to -.18
.8	.21-.17	-.02 to -.18
.9	.17	-.06 to -.18
1.0	.13-.15	-.08 to -.22
1.1	.13-.24	.01 to -.11

*Volumetric ice content calculated using eq.2.
†Excess ice content denotes the difference between the ranges of the volumetric ice content and the soil porosity.

An ice content in excess of the soil porosity can be attributed to segregation ice and equated with frost heave. The porosity, p, of a saturated soil can be estimated from

$$p = \frac{\rho_s - \rho_m}{\rho_w - \rho_m} \quad (3)$$

where ρ_s, ρ_m, and ρ_w are the densities of the bulk soil, the mineral constituents of the soil particles, and water, respectively. Bulk density of the fine material in Kvadehuksletta sorted circles ranges from 2.1-2.3x10^3 kg/m^3 (Hallet and Prestrud, 1986), and the primary mineral constituent is calcium carbonate, with a density of 2.7x10^3 kg/m^3. Thus, the porosity of these soils ranges from .23 to .35. The difference between the ice content and the porosity yields the excess ice contents shown in Table II. The plausible range of positive excess ice content at 0.4 m depth overlaps with the heave strain measured at this depth (Table I). The negative excess ice contents below 0.4 m suggest that the soil was unsaturated when freezing occurred. Ice segregation may occur in unsaturated soils, and this may be occurring at Kvadehuksletta, as very small heave strains were measured at 0.6-0.8 m depth in the soil (Table I).

Evidence from the surface heave meters, the heave strain meters, and the ice content calculations point to a decrease in frost heave strain with depth in the soil. All of the positive strains calculated from these data are shown in Fig. 5. The very low strains measured below about 0.6 m are consistent with observations by others. In a cross-section dug in a frozen non-sorted circle, Mackay (1980) found that no ice was visible between about 0.5 m and the bottom of the active layer (roughly 1.0 m). Schmertmann and Taylor (1965, Fig. 28) measured no heave in the bottom half (lower 0.9 m) of the active layer in their study of sorted circles. Chambers (1967) concluded from his surface frost heave measurements that there was no ice segregation between 0.4 m and the base of the 1.2-1.5 m deep active layer in sorted circles at Signy Island, South Orkney Islands.

Upward freezing from the top of the permafrost may cause frost heave at the base of the active layer (Mackay, 1983). The results of an upfreezing experiment (Anderson, in press) simulating conditions at the base of the active layer were equivocal, but suggest that motion of clasts would be smaller than, and may be in the opposite direction of, the downward freezing case.

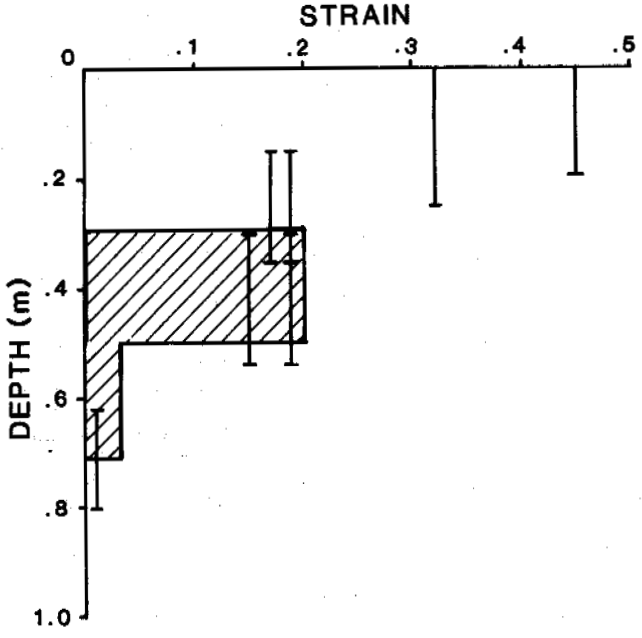

Figure 5. Frost heave strain as a function of depth. Compiled data from 1) surface heave and depth of frost penetration, 2) heave strain meters, and 3) ice content calculations. Hachures delineate the range of strain from the ice content calculations.

ANALYSIS

Rate of sorting

A clast moves up during freezing and settles downward during thaw in a regime of downward propagating freeze and thaw fronts. The upward clast displacement expected due to upfreezing at completion of a freeze/thaw cycle is (Anderson, in press):

$$D_{net} = \alpha f H \epsilon \quad (4)$$

where ϵ is the vertical frost heave strain in the soil caused by growth of ice lenses, H is the length of the clast measured parallel to heat flow, f is the fraction of the clast length not adfrozen to the soil at the onset of its heave during freezing, and $0 < \alpha < 1$ gives the portion of the upward heave that persists after thaw.

Both the strain, ϵ, and the number of freeze/thaw cycles per year, n, decrease with depth in the soil, so the relative speed of a clast through the soil is a function of its depth, z:

$$\frac{dz}{dt} = \alpha f H \epsilon(z) n(z) \quad (5)$$

It is convenient and reasonable to approximate the available data on strain (Fig. 5) and number of freeze/thaw cycles in the active layer from Kvadehuksletta by simple exponential functions:

$$\epsilon(z) = \epsilon_0 e^{-az} \quad (6)$$

$$n(z) = 1 + n_0 e^{-bz} \quad (7)$$

where a and b are empirical constants, ϵ_0 is the heave strain at the soil surface, and n_0 is the number of freeze/thaw cycles per year at the surface, exclusive of the annual freeze/thaw cycle. The exponential approximation of $n(z)$ is physically justified, since the amplitude of periodic temperature disturbances at the soil surface decay exponentially with depth in the soil (Gold and Lachenbruch, 1973). Substitution of Eq. 6 and 7 into Eq. 5 now shows explicitly the exponential increase in the rate of upfreezing of a clast as it nears the surface:

$$\frac{dz}{dt} = \alpha f H \epsilon_0 \left[e^{-az} + n e^{-(a+b)z}\right] \quad (8)$$

Solving Eq. 8 for the time required for a clast to reach the surface from some depth, z_0, yields:

$$t = \frac{1}{\alpha f H \epsilon_0} \int_{z_0}^{0} \frac{dz}{e^{-az} + n_0 e^{(a+b)z}} \quad (9)$$

which can be integrated numerically.

The range of empirical constants from the Kvadehuksletta data on strain and number of freeze/thaw cycles per year are: $\epsilon_0 = 0.7 - 1.0$, $a = 4.6 - 9.2\ m^{-1}$, $n_0 = 0 - 6\ yr^{-1}$, and $b = 0 - 2\ m^{-1}$. In the upfreezing experiments described in Anderson (in press) values of f ranged from 0.5-0.6, and values of α ranged from 0.2-0.7. The times required for a representative 20 mm clast (Prestrud, 1987) to reach the surface along with the clast velocity at a variety of depths, using these ranges of constants are shown in Table III. The number of freeze/thaw cycles per year, $n(z)$, and the fraction of the clast heave retained after thaw, α, had the largest effects on the range of calculated surfacing times and velocities. This suggests that the amount of upfreezing occurring in any given year will strongly depend on the weather: alteration of the number and

Table III. Surfacing time and initial velocity for a 20 mm clast due to upfreezing.

Depth, z_0 m	Time to Surface yr	Velocity at z_0 mm/yr
.1	4-90	.8-18
.3	26-810	.1-5
.5	.1-5.4x10^3	.02-2
1.0	.02-5.4x10^5	.02-.09
1.5	.003-5.4x10^7	.002-.006

penetration depth of short duration freeze/thaw cycle events will substantially affect upfreezing rates. However, the importance of short freeze/thaw cycles may be modulated by the magnitude of frost-heaving strain in the soil, which for this simple analysis was assumed to be identical during both the short freezing episodes in the fall, and the annual winter freeze.

The surfacing time for a representative clast increases dramatically with depth (Table III), which clearly presents a dilemma. In excavations, the segregation of fines and stones extended to at least 0.9 m depth, and probing with steel rods suggest that segregation continues throughout the 1.5-1.8 m thick active layer at Kvadehuksletta. However, the vertical upfreezing velocities of clasts in the lower portion of the active layer are far too slow to produce significant deep sorting in the few thousand years Hallet and Prestrud (1986) estimate they have been active. The data in Table III indicate that upfreezing is important and vigorous in the upper levels of the active layer, but other processes must be invoked to produce the deep sorting in these features over time scales of 10^3 years.

Pattern of sorting

Inclined freezing fronts impart a horizontal component to clast movement (Corte, 1962b, 1963; Muir, 1983; Hallet, unpub. manuscript) that can be easily parametrized. Assuming that the clast moves parallel to the heat flow direction during freezing, Equation 4 can be modified to yield a vertical component (Hallet, unpub. manuscript)

$$D_{(z-net)} = \alpha f H \epsilon \sin\theta \qquad (10a)$$

and a horizontal component

$$D_{(x-net)} = \beta f H \epsilon \cos\theta \qquad (10b)$$

of clast movement, where θ is the angle between the heat flow vector and a horizontal plane, and β is the fraction of horizontal freezing displacement that persists after thaw. The fraction of the clast displacement that persists after thaw is expected to be greater for the horizontal component than for the vertical component since the restoring force during thaw is primarily due to gravity. Hence, the value of β is probably of order 1, while α ranged between 0.2 and 0.7 in the downward freezing experiment of Anderson (in press). Assuming that α does not vary with inclination of the freezing front, the clast velocity and time required to surface from a given depth differ from the horizontal freezing front case by only a factor in the numerator of $\sin\theta$ and $1/\sin\theta$ respectively. Rearranging Eq. 10a and 10b yields the magnitude of lateral displacement expected for a clast for any given upward movement, $D_{(z-net)}$:

$$D_{(x-net)} = \left(\frac{\beta}{\alpha}\right) \frac{D_{(z-net)}}{\tan\theta} \qquad (11)$$

Note that Eq. 11 implies that the net horizontal displacement is proportional to the original depth and is independent of clast size, number of freeze/thaw cycles, or heaving strain in the soil. The horizontal displacement of a 20 mm clast as it moves toward the surface is shown in Table IV for several depths and values of θ.

The magnitude of lateral displacements possible from upfreezing (Table IV) are small relative to the size of the fine domains of sorted circles at Kvadehuksletta. The fine centers are typically 2-3 m in diameter, implying lateral displacements of up to 1-1.5 m. Deeply buried stones can move this lateral distance by upfreezing, but they can do so only over unreasonably long periods.

The freezing front was shown by Schmertmann and Taylor (1965) to be broadly convex upward in the fine domains of sorted circles. This geometry does yield a generally diverging radial pattern of clast displacement by upfreezing; however, in detail it does not produce the observed pattern of sorting in circles. In the center of the fine domains freezing fronts are nearly horizontal; hence, clasts there will tend to move nearly vertically. Close to the border, the freezing front is more likely to be inclined and lateral movement of clasts should be greater. However, this effect should decrease with depth in the soil, as the freezing front flattens with depth. Hence, the overall radial divergence of clasts due to upfreezing will be greatest near the surface. Whereas this does concentrate clasts near the borders, it does not explain the distinct and nearly vertical textural boundary of the fines/coarse contact, nor does it provide a mechanism for moving clasts from the center of a circle to the borders. Since upfreezing moves clasts primarily vertically, the gross features of the sorting requires other processes acting in addition to upfreezing.

Table IV. Cumulative lateral displacement of a 20 mm clast, initially at depth z_0, due to upfreezing with an inclined freezing front.

	Lateral movement, m		
z_0, m	theta=80°	theta=70°	theta=60°
.1	.03-.07	.05-.15	.08-.23
.3	.08-.21	.16-.44	.26-.69
.5	.12-.44	.26-.91	.41-1.4
1.0	.27-.70	.55-1.5	.87-2.3

Many authors (Poser, 1933; Taber, 1943; Goldthwait, 1976) assert that clasts move laterally toward the border through surface processes after upfreezing has brought them to the surface. Significant solifluction occurs only on slopes greater than 3-4° (Jahn, 1961), and hence, is unimportant in the center of the fine domains of sorted circles, which are usually flat at Kvadehuksletta. Solifluction may be important close to the borders where the surface slope increases. I did not observe needle ice formation in the fine domains of the sorted circles at Kvadehuksletta during fall of 1984, suggesting that frost creep does not occur on these surfaces. Thus, surface processes are slow and ineffective in the central portion of these sorted circles. Moreover, the sharp contact between fine domains and coarse borders seen at the surface, and continuing into the subsurface, imply that horizontal segregation does not occur by surface processes.

Hallet et al. (1988) presented an intriguing mechanism that accounts for lateral motion of clasts, involving convective circulation of fine material, driven by unstable density stratification of the soil. The pattern of soil motion expected is upwelling in the center of the fine domains and downwelling at the fine/coarse contact. Assuming that clasts are entrained by and move with the soil, the motion of clasts would be the resultant of net soil motion and net upfreezing-induced displacement. Clasts in the center of a convecting cell, then, can be expected to rise to the surface more rapidly than predicted by upfreezing alone. As they approach the surface, an increasing horizontal component arising from soil motion will move them toward the borders, adding to the horizontal component due to upfreezing. Clasts near the bottom of the convecting cell may actually move away from the border because of the return circulation at depth in the soil. Downwelling of the soil near the border competes with upfreezing, diminishing the rate of vertical ascent of the clast. Together, the motion of clasts due to both upfreezing and soil motion can account for the depth of sorting (as the entire active layer presumably convects), and the lateral segregation of fines and clasts.

CONCLUSION

The upfreezing process alone cannot explain the depth of sorting, the geometry of the fine/coarse contact, or the size of the sorted circles at Kvadehuksletta. The present day number of freeze/thaw cycles per year and soil frost-heaving strain are insufficient to move an average size clast from deep in the active layer to the surface within reasonable time constraints. The amount of lateral motion predicted, which is a function only of the freezing front inclination and the fraction of the movement retained after thaw (α and β) for a given depth, is small compared to the radius of the fine domains. Furthermore, the pattern of clast migration arising from the convex-upward freezing fronts in the fine domains does not concentrate clasts at the border strongly enough to explain the sharp and nearly vertical textural boundary at the border.

The depth to which upfreezing is a significant process would increase if the heave strain and the number of freeze/thaw cycles per year were greater deep in the active layer. During the Holocene climatic optimum, warmer annual temperatures may have increased the occurrence of autumn freeze/thaw episodes. However, these events would need to have been of greater duration or severity than they are at present to increase the upfreezing rates in the lower half of the active layer. In addition, lateral displacements of clasts by upfreezing are independent of the heaving strain in the

soil or the number of freeze/thaw cycles per year, and hence, remain insufficient to produce the broad clast-depleted fine domains even under a climatic regime different from the modern one.

Convective circulation of the fines in the active layer working in conjunction with upfreezing does explain many of the features of sorted circles. The distinct fine/coarse contact forms the outer boundary of the downwelling limb of the convection cell. Clasts may be entrained by soil circulation from deep in the active layer, and moved into regions where upfreezing rates are significant. Hence, the movement of clasts by upfreezing in the large, well-developed sorted circles at Kvadehuksletta appears to highlight the soil convection pattern.

ACKNOWLEDGMENTS

Field work in Spitsbergen was conducted under the auspices of the Norsk Polarinstitutt via collaboration with J.L. Sollid. I thank J. Fortun, P. Aaseröd, M. Bentzen, and especially K. Johansen for help in Spitsbergen. E.C. Gregory, C.W. Stubbs, and R.S. Anderson each provided invaluable assistance in Seattle and Pasadena. Finally, I thank B. Hallet for his consistent support and guidance. This research was funded by the National Science Foundation (DPP-8303630).

REFERENCES

Anderson, S.P. (1988). The upfreezing process: Experiments with a single clast. GSA Bull. (in press).

Ballantyne, C.K., and Matthews, J.A. (1982). The development of sorted circles on recently deglaciated terrain, Jotunheimen, Norway. Arc. Alp. Res. (14), 4, 341-354.

Chambers, M.J.G. (1966). Investigations of patterned ground at Signy Island, South Orkney Islands: II. Temperature regimes in the active layer. Brit. Antarc. Sur. Bull. (10), 71-83.

_____ (1967). Investigations of patterned ground at Signy Island, South Orkney Islands: III. Miniature patterns, frost heaving, and general conclusions. Brit. Antarc. Sur. Bull. (12), 1-22.

Corte, A.E. (1962a). The frost behavior of soils: Laboratory and field data for a new concept, Part I: Vertical sorting. U.S. Army CRREL Research Report (85),1, 1-22.

_____ (1962b). The frost behavior of soils: Laboratory and field data for a new concept, Part II: Horizontal sorting. U.S. Army CRREL Research Report (85),2, 1-20.

_____ (1963). Particle sorting by repeated freezing and thawing. Science (142), 499-501.

Czeppe, Z. (1960). Annual course and the morphological effect of the vertical frost movements of soil at Hornsund, Vestspitsbergen. Bull. De L'Acad. Pol. des Sci., Série des Sci. Géol. et Géogr. (8),2, 145-148.

_____ (1961). Roczny Przebieg Mrozowych Ruchów Gruntu, W Hornsundzie (Spitsbergen) 1957-1958. (English summary: "Annual course of frost ground movements at Hornsund"). Zeszyly Naukowe Uniwersytetu Jagiellońskiego, Prace Geograficzne- Seria Nowa Zeszyt 3, 50-63.

Forman S.L., and Miller, G.H. (1984). Time- dependent soil morphologies and pedogenic processes on raised beaches, Brøggerhalvøya, Spitsbergen, Svalbard Archipelago. Arc. Alp. Res. (16), 4, 381-394.

Gleason, K.J., Krantz, W.B., Caine, N., George, J.H., and Gunn, R.D. (1986). Geometrical as- pects of sorted patterned ground in recurrently frozen soil. Science (232), 216- 220.

Gold, L.W., and Lachenbruch, A.H. (1973). Thermal conditions in permafrost--A review of North American literature. N. Am. Cont., Permafrost Sec. Intl. Conf., 3-23, Washington, D.C.

Goldthwait, R.P. (1976). Frost sorted patterned ground: A review. Quat. Res. (6), 27-35.

Hallet, B., Anderson, S.P., Gregory, E.C., and Stubbs, C.W. (1987). Active layer temperature and ice content, western Spitsbergen. (abs.) EOS (68) 44,1264.

_____(1988). Surface soil displacement in sorted circles, western Spitsbergen. Proc. 5th Intl. Conf. on Permafrost.

Hallet, B., and Prestrud, S. (1986). Dynamics of periglacial sorted circles in Western Spitsbergen. Quat. Res. (26), 81-99.

Huxley, J.S., and Odell, N.E. (1924). Notes on surface markings in Spitsbergen. Geog. J. (63), 207-229.

Jahn, A. (1961). Quantitative analysis of some periglacial processes in Spitsbergen. Uniw. Wroclawski, Zeszyty Naukowe, Ser. B, No. 5. 34 pp.

_____(1963). Origin and development of patterned ground in Spitsbergen. Proc. Intl. Conf. Permafrost, 140-145, Washington, D.C.

Johnston, G.H., ed. (1981). Permafrost: Engineering Design and Construction, 540 pp. John Wiley and Sons, Toronto.

Mackay, J.R. (1980). The origin of hummocks, western Arctic coast, Canada. Can. J. Earth Sci. (17), 996-1006.

_____(1983). Downward water movement into frozen ground, Western Arctic Coast, Canada. Can. J. Earth Sci. (20), 120-132.

Muir, M.P. (1983). The role of pre-existing, corrugated topography in the development of stone stripes. Permafrost: Fourth Intl. Conf. Proc., 877-882, Washington, D.C.

Paterson, T.T. (1940). The effects of frost action and solifluxion around Baffin Bay and in the Cambridge District. Quart. J. Geo. Soc. London (46), 381, 99-130.

Poser, H. (1933). Das problem des strukturbodens. Geol. Rundsch. (24), 105-121.

Prestrud, S. (1987). The Upfreezing Process and its Role in Sorted Circles, [M.S. Thesis] 122 pp., University of Washington, Seattle.

Ray, R.J., Krantz, W.B., Caine, T.N., and Gunn, R.D. (1983). A model for sorted patterned ground regularity. J. Glac. (29), 317-337.

Schmertmann, J.H., and Taylor, R.S. (1965). Quantitative data from a patterned ground site over permafrost. U.S. Army CRREL Research Report (96), 76 pp.

Sharp, R.P. (1942). Soil structures in the St. Elias Range, Yukon Territory. J. Geomorph. (5), 274-301.

Taber, S. (1929). Frost heaving. J. Geol. (37), 428-461.

_____ (1943). Perenially frozen ground in Alaska: its origin and history. GSA Bull. (54), 1433-1548.

Van Vliet-Lanöe, B. (1983). Études cryopédologiques au sud du Kongsfjord -Svalbard, 39 pp. Centre de Géomorphologie du CNRS, Caen, France.

Washburn, A.L. (1956). Classification of patterned ground and a review of suggested origins. GSA Bull. (67), 823-866.

TEPHRAS AND SEDIMENTOLOGY OF FROZEN ALASKAN LOESS

J.E. Beget

University of Alaska, Fairbanks, AK 99775

SYNOPSIS Tephras are preserved as thin, discrete layers in loess in interior Alaska. Large structures in the loess, such as faults, slumps, sand wedges, and ice wedge casts, which are difficult to discern in massive loess, are quite evident where tephras or paleosols are incorporated in the disrupted section. Tephras and paleosols mark multiple former ground surfaces in the loess. The sedimentology of the tephras and loess suggests that much of the silt in low-lying valleys in the Fairbanks area, previously attributed to reworking of loess from adjacent hillslopes, records eolian deposition subject to only minor local retransport. The mechanics of eolian dust entrainment, transportation, and deposition are consistent with the preferential accumulation of thick airfall loess deposits in "loess traps" on valley floors at low elevations, probably in areas of vegetation cover.

INTRODUCTION

Although long and continuous geologic records in terrestrial localities are rare (Kukla and Aharon, 1984), several types of long records of Pleistocene sedimentation and climate change are now available. Isotopic studies of precipitation preserved in long ice cores from high latitude ice sheets provide a record of Pleistocene climate change which is remarkably similar to the climatic record inferred from isotopic variations in foraminifera preserved in deep-sea sediment cores. Similar patterns of climate change are inferred from some long pollen records (Hooghiemstra, 1984; Molfino and others, 1984; Woillard, 1978). Kukla (1975) first attempted to correlate loess records in central Europe with the marine isotope record. Recently, thick sequences of loess and paleosols have been described in China which appear to closely resemble other climatic records of the Pleistocene, with massive loess deposits formed during glaciations being separated by paleosols formed during interglacial and interstadial times (Tungsheng and others, 1985; Kukla, 1987). This paper re-examines the thick, frozen valley-bottom loess deposits in the Fairbanks area of central Alaska to determine their potential for depositional continuity through the late Quaternary (Fig. 1). Thick loess deposits in Alaska may potentially contain long proxy records of high-latitude climate change and permafrost history (Beget and others, 1987).

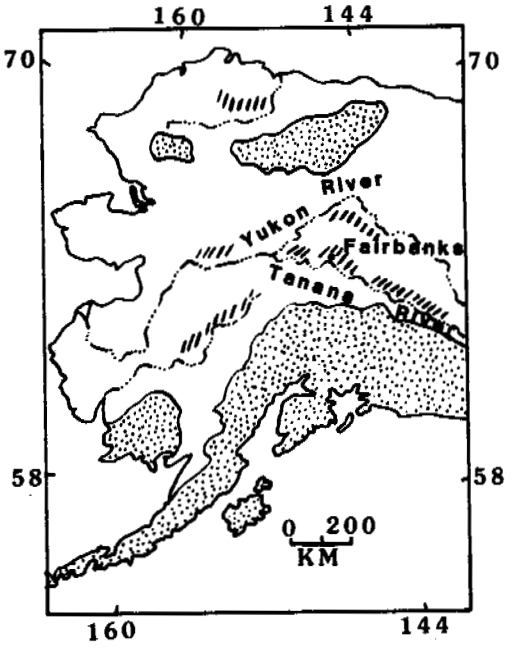

Figure 1. Limits of late Wisconsin glaciation (stipled pattern), location of thick, frozen loess deposits in unglaciated central Alaska (slash pattern). Modified from Pewe (1975).

Much controversy has been attached to the loess deposits in the Fairbanks area. The earliest workers, such as Spurr (1898), Prindle (1913), Eakin (1916), and Harrington (1918), maintained that the widespread silt deposits were waterlaid, either in fluvial, lacustrine, or estuarine environments. Spurr named these deposits the "Yukon silts". Taber (1953) suggested the silts were a residual or weathering product. Tuck (1938; 1940) and Fardley (1938) first suggested that the loess was of eolian origin.

The work of Pewe (1955) finally demonstrated, in a scientific and convincing approach, that the loess deposits on upland areas were wind-transported. Pewe also developed a stratigraphy and nomenclature which can be locally applied to loess in lowland basins, but argued that all loess in low valleys "represent deposits reworked from adjoining slopes" (Pewe, 1975, p. 40). Two very prominent forest beds, designated the Dawson Cut and the Fva, locally divide the loess in valleys into two assemblages of roughly equal thickness (Fig. 2). Pewe (1975) suggested these forest beds may correspond to the Sangamon and Yarmouth interglacials of the mid-continental United States, and the two intercalated loess beds, each approximately 30 m thick, to the Wisconsin and Illinoian glaciations.

Pewe also identified numerous volcanic ash beds within the Fairbanks loess. His recognition in the 1950s of the potential significance of these tephras as chronological markers within the loess was farsighted. Recent fission track dating of the Ester Ash, for instance, indicates the basal part of the Gold Hill loess is at least 450,000 years old (Westgate, pers. comm., 1987). This date alone suggests that loess as old as marine isotope stage 12 is present in cuts near Fairbanks.

SEDIMENTOLOGICAL SIGNIFICANCE OF TEPHRA DEPOSITS: IS ALL VALLEY-BOTTOM LOESS REWORKED?

The tephra layers found in the interior of Alaska provide important information on the local sedimentology of the loess deposits. The loess itself commonly consists of massive buff to yellow silt, and contains relatively few horizons which can be used to infer its stratigraphy or structure. Tephra beds are an important exception.

It has been proposed that the loess deposits found in valley bottoms in unglaciated central Alaska accumulated as a result of the retransport of loess from hillsides at higher elevation (Pewe, 1975). This is suggested by the much greater thickness of loess at low elevations than on uplands (Pewe, 1955). Small mudflows, slumps, and landslides clearly are present in some places in the valley bottom loess facies, locally called "muck" by miners. However, I argue here that the presence of multiple, discrete, continuous layers of undisrupted airfall tephras within the valley bottom loess indicates that some of these deposits, locally as much as 50 m thick, actually consist largely of airfall loess which has been subject to only minimal retransport, principally by additional wind reworking after deposition. Similar conclusions about the lowland loess have been reached independently by Hamilton and others (in press).

In many cases tephras can be traced across several meters of outcrop, and in a few cases single airfall units can be followed for tens of meters. At least 10 such tephras, some only a few centimeters thick and some more than 15 cm thick, are found within the thickest loess sections (Pewe, 1975; Beget, unpubl. mapping). The tephras commonly have sharp bases but are mixed with loess at their tops. Some tephras show crossbeds, and small dune-like ripples can be identified at their tops. The lack of channelling and the ubiquitous appearance of these ripples across many meters of outcrop suggest they reflect wind action on the ash beds, and are not due to flowing water.

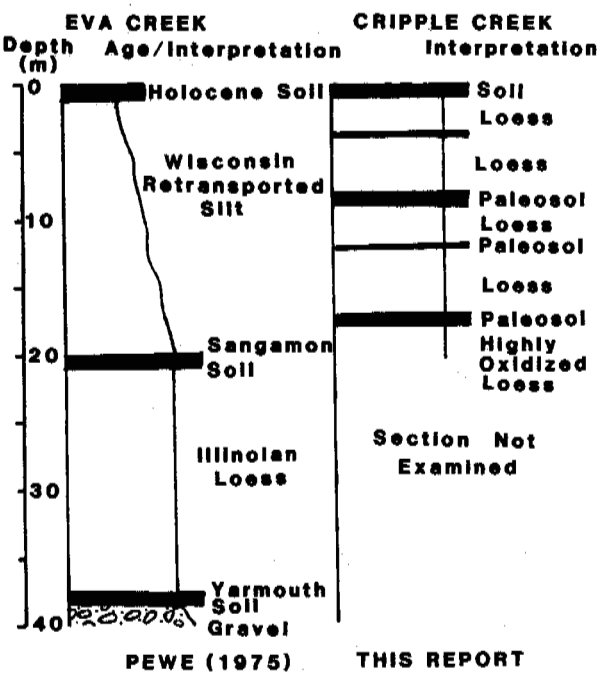

Figure 2. Simplified stratigraphy of thick loess sections near Fairbanks, Alaska, from Pewe (1975), and this paper.

The unmixed character of the fine-grained ash beds within the loess deposits is good evidence for airfall deposition of that ash. Clearly it would be impossible to produce a horizontal, clean, segregated ash layer as a result of creep, slopewash, solifluction, or some combination of mass-wasting processes moving mixed ash and loess downslope. The multiple tephras can be found at many points within the extensive, nearly horizontal loessial valley fills, at distances as far as several kilometers from adjacent hills. The sharp bases of the tephra layers presumably mark former ground surfaces at the times of ash deposition. The common occurrence of apparently wind-reworked ash mixed with loess at the top of the thickest ash beds must reflect a continuation of eolian deposition of loess following the tephra fall, suggesting that at least the immediate loess deposits in which tephras are intercalated are also eolian deposits. This hypothesis is strongly supported by the observation in some areas of local and gradual lateral thinning by mixing of ash beds and loess. Changes in thickness of tephras appear to occur where clean ash grades into ash-loess mixtures and then into loess, a feature here interpreted as reflecting wind-reworking of ash and loess. If a tephra disappears altogether when traced across an exposure, it is generally possible to excavate laterally in the loess and find additional occurrences, more or less mixed with loess, at the same stratigraphic position across section. This is also consistent with the tephras marking a former ground surface and being intermittently reworked by wind.

Multiple massive loess deposits through the thickest exposures of the valley bottom loess closely resemble the apparent airfall loess found overlying the tephras. Massive loess beds, like the upper parts of the ash beds, sometimes show very subtle and fine partings 1-5 cm in length with gentle dips which are present across many meters of outcrop. Because several centimeters of loess can be deposited in one storm (Pye, 1987), these features may be primary eolian depositional structures, or may reflect aeolian reworking of thick, fresh loess deposits.

The horizontality of the tephra deposits is also consistent with an airfall origin for the underlying loess. If the massive loess underlying the tephras has been reworked and redeposited by streams or solifluction lobes, there should be considerable relief of the ground surface buried by the ashfall. Instead, the sub-horizontal surfaces buried by tephras resemble the flat top of the modern loessial valley fill, where dust is deposited today during summer wind storms.

If much of the valley bottom loess in central Alaska actually consists of well sorted, occasionally laminated massive airfall or minimally retransported loess, then these loess deposits contain a record of eolian sedimentation and climate. Thick eolian loess deposits in China and other areas of the world are interrupted by paleosols, interpreted as forming during insolation peaks corresponding to interglaciations during the Pleistocene (Tungsheng and others, 1985; Kukla, 1987; Pye, 1987). Pewe (1975) identified only a single prominent buried forest bed within the valley bottom facies, but I suggest here that there are at least 4 laterally continuous paleosols within the upper 20 m of several 60-m-thick loess sections (Fig. 2). While the correlation between the forest bed of Pewe (1975) and the multiple paleosols is not yet clear, it is certain that more organic-rich paleosols are found within the loess than was previously thought.

Horizons of retransported organic-rich silts are often closely associated with the organic-rich soil zones in Alaskan loess, and probably reflect regional thawing during times of soil formation. In a few places it has been possible to identify ice wedge casts in paleosol zones, by tracing the collapse of tephras and organic-rich soil horizons, supporting an interpretation of increased thawing or active layer thickness in the frozen loess during times of soil formation.

The tephras associated with paleosols are sometimes abruptly truncated by erosion or incorporated in slopewash or solifluction deposits in zones associated with the paleosols. These disturbed horizons, from 10-50 cm thick, form laterally continuous marker units between the massive eolian loess deposits and constitute widespread, laterally continuous breaks in depositional sequences of airfall loess beds. This suggests that the localized disruptions, discontinuities, unconformities, and small slumps found in many areas of the valley bottom loess need not reflect mass-transport of loess from upland areas into the basins, but may instead record multiple episodes of loess deposition and ice-wedge growth followed by melting and collapse of ground ice within the loess during cycles of loess accretion and soil development. The identification of several new sub-horizontal paleosols in the upper parts of thick loess sections is consistent with the model presented here of accumulation of the Fairbanks loess due to episodic eolian sedimentation.

LOESS TRAPS AND EOLIAN LOESS DEPOSITION IN CENTRAL ALASKA

If, as is proposed here, the thick valley-filling loess in central Alaska records episodic eolian sedimentation, then a new model must be presented which can explain preferential loess accumulation in the valley bottoms. Why are the thickest airfall loess deposits restricted to lowland basins in interior Alaska, while loess is thin or absent in adjacent upland areas?

Several factors are probably involved. First, loess in the Fairbanks area is relatively coarse-grained, with as much as 20% of samples as coarse as 50 μm in diameter (Pewe, 1975). Tsoar and Pye (1987) have shown that the distance such particles can be transported in eolian suspension (L) is given by:

$$L = U_m t = 2U_m \beta / K^2 D^4 \qquad (1)$$

where U_m is mean wind velocity, t is time the particle remains in turbulent suspension, β is the Taylor coefficient of turbulent exchange, K is a constant, taken as 8.1 x $10^5 cm^{-1}s^{-1}$ for air, and D is grain diameter. Values of $\beta > 10^5 cm^2 s^{-1}$, present only during intense cyclonic storms, are required to carry particles <20 μm to heights of 100 m (Tsoar and Pye, 1987). Windstorms with wind shear velocities more than six times greater are necessary to transport particles > 50 μm, such as are found in typical Alaskan loess. For realistic values of U_m = 15 m s^{-1}, and $\beta < 10^5 cm^{-1}s^{-1}$, equation (1) predicts that transport distances of less than 5 km are to be expected for loess as coarse as that found in the Fairbanks deposits. The thickest valley fills of loess, at Goldhill and Ester in the Fairbanks area, are very close to the Tanana floodplain, while surrounding hillslopes are typically several kilometers farther away. This probably accounts in part for the observed steep altitudinal gradient in thickness.

While thin loess deposits are found at elevations as much as several hundred meters above the Tanana River, the top of the thick loessial fills found in basins at Ester and Goldhill lies at most only 10-20 meters above the modern floodplain of the Tanana River. The relative concentration of loess particles of a particular size in eolian suspension during transport (C/C_a) at any elevation (a) is given by:

$$C/C_a = \exp[2.5(KD^2/u^*)\ln(a/y)] \qquad (2)$$

where u* is the threshold shear velocity, and y is total height of transport (Tsoar and Pye, 1987). From (2) it is apparent that particles larger than 20-50 μm will be transported almost exclusively at heights no more than a few meters above the ground, even in the most severe windstorms. From (1) and (2) it is apparent that the valley-filling loess deposits probably were not largely reworked from higher elevation slope deposits, as is generally thought, because eolian transport would inevitably result in the thickest and coarsest loess deposits being formed on and near valley bottoms.

Relatively low velocities of 0.2-1.0 m s^{-1} are reported as sufficient to entrain loess-sized dust from smooth, unvegetated surfaces (Iversen and others, 1976; Gillette and others, 1980; Iversen and White, 1982). This suggests that loess will be readily re-mobilized from bare rock and soil surfaces, and that loess cannot accumulate unless some factor, such as surface vegetation, inhibits wind shear. When dust in suspension encounters a surface roughness element, deposition of loess will occur from the lower portion of the dust cloud, where wind shear and velocity are reduced. Typical roughness heights for forests are as much as 30 m, while for grasslands or tundra they are only 0.5 m or less. Roughness heights for clean loess or sand are 0.0003 m (Thom, 1976; Oke, 1978).

This suggests that the thick loess deposits found in low basins in central Alaska, such as Goldstream Valley and the Ester area in Fairbanks, reflect long-term eolian deposition in a region where some type of vegetation was generally present. Differential vegetation cover could result in substantial differences in loess accumulation rates. Guthrie (1968) and Ager (1975) have suggested that treeline was greatly depressed in central Alaska during much of the Pleistocene, and altitudinal vegetation gradients were steep. The most effective "loess traps" were therefore probably at low elevations.

It is interesting to note that the tephras found in the loess which are more than 1-2 cm thick, such as the well-known 10-15 cm thick Old Crow ash (Westgate and others, 1983; 1985), are commonly associated with organic-rich silts or paleosols. Fine-grained tephras, like loess, are readily re-entrained from vegetation-free areas by moderate winds, as has been observed following modern tephra eruptions (Schuster, 1981). This suggests that thick ash layers, like loess, will be most readily preserved where substantive surface vegetation exists. The observations of wind-reworked tephra layers and apparent eolian mixing of loess and tephra discussed above are entirely consistent with preferential deposition and preservation of loess and ash on a vegetated surface. Indeed, since it would be difficult to preserve a discrete fine ash layer on an unvegetated surface, it seems likely that the upper portions of ash falls which completely bury vegetation would be readily eroded by wind. This suggests that the tephra thicknesses observed in the loess must be somewhat less than the roughness height of plant cover at the time of the ash fall. Therefore, extensive tephras in valley bottom loess in central Alaska constitute evidence for the presence of vegetation which presumably also entrapped eolian loess through the Pleistocene.

The thick loess found in valley bottoms is therefore attributed to (1) the low elevation of the valleys, subject to deposition from the lower portions of dust clouds, where loess concentration and grain size are greatest; (2) the proximity of the valley bottom to streams which were sources of loess; and (3) the probable existence of vegetation in valley bottoms, which

constitute "loess traps." These conditions are also conducive to preservation of airfall tephras. The thickest valley bottom loess deposits presumably reflect areas with the highest eolian sedimentation rates, and may contain a high resolution, nearly continuous record of mid- to late Pleistocene sedimentation, climatic change, and permafrost history in central Alaska.

ACKNOWLEDGEMENTS

Reviewed by Dr. David M. Hopkins and Dr. Mary Keskinen of the University of Alaska. Discussion in the field with Dr. Troy Pewe of Arizona State University were most enlightening. Support from the Archeometry Program of the National Science Foundation and the American Chemical Society is gratefully acknowledged.

REFERENCES

Ager, T.A. (1975). Late Quaternary environmental history of the Tanana Valley, Alaska. Ohio State University Institute of Polar Studies Report 54.

Beget, J., Stone, D., Hopkins, D. (1987). A continuous record of the influence of orbital parameters on local climate change in late Pleistocene loess deposits from central Alaska: Geol. Soc. America Abst. Prog. 19, 584.

Eakin, H.M. (1916). The Yukon-Koyukuk region, Alaska: U.S. Geol. Survey Bull. 631, 88 p.

Eardley, A. (1938). Unconsolidated sediments and topographic features of the lower Yukon valley (Alaska). Geol. Soc. America Bull. 49, 303-341.

Gillette, D., Adams, J., Endo, A., and Smith, D. (1980). Threshold velocities for input of soil particles into the air by desert soils. Journal Geophysical Research 85, 5621-5630.

Guthrie, R. (1968). Paleoecology of a late Pleistocene small mammal community from interior Alaska. Arctic 21, 223-244.

Hamilton, T., Craig, J., and Sellman, P. (1988). The Fox Permafrost Tunnel: A Late Quaternary Geologic Record in Central Alaska. Geol. Soc. America Bull. (in press).

Harrington, G.L. (1918). The Anvik-Andreafski region, Alaska (including the Marshall district). U.S. Geol. Survey Bull. 683, 70 p.

Hooghiemstra, H. (1984). A palynological registration of climatic change of the last 3.5 million years, in Milankovitch and Climate, Pt. 1 (A.L. Berger and others, eds.), 371-378, Dordrecht, Boston.

Iversen, J.D., Greeley, R. and Pollack, J.B. (1976). Windblown dust on Earth, Mars, and Venus: Journal of Atmospheric Science (33), 2425-2429.

Iversen, J.D., and White, B. (1982). Saltation threshold on Earth, Mars, and Venus: Sedimentology (29), 111-119.

Kukla, G. (1975). Loess stratigraphy of central Europe, in After the Australopithecines, K.W. Butzer and G.L. Isaac, (eds.) 99-108, 911 pp. Mouton, Chicago.

_____ (1987). Loess Stratigraphy in Central China. Quaternary Science Reviews (6), 191-219.

Kukla, G. and Aharon, P. (1984). Plio-Pleistocene land records: summary and conclusions and recommendations, in Milankovitch and Climate, Pt. 1 (A.L. Berger and others, eds.), 835-838, Dordrecht, Boston.

Molfino, B., Heusser, L.H., and Woillard, G.M. (1984). Frequency components of a Grande Pille pollen record: evidence of precessional orbital forcing, in Milankovitch and Climate, Pt. 1 (A.L. Berger and others, eds.), 391-404, Dordrecht, Boston.

Oke, T.R. (1978). Boundary Layer Climates, 372 pp. Metheun, London.

Pewe, T. (1955). Origin of the upland silt near Fairbanks, Alaska. Geol. Soc. America Bull. (66), 699-724.

_____ (1975). Quaternary Geology of Alaska. U.S. Geological Survey Professional Paper 835, 145 pp.

Prindle, L.M. (1913). A geological reconnaissance of the Fairbanks quadrangle, Alaska; with a detailed description of the Fairbanks district, by L.M. Prindle and F.J. Katz, and an account of the lode mining near Fairbanks, by P.S. Smith. U.S. Geological Survey Bulletin 525, 220 pp.

Pye, K. (1987). Aeolian Dust and Dust Deposits, 334 pp. Academic Press, London.

Schuster, R.L. (1981). Effects of the eruptions on civil works and operations in the Pacific Northwest, U.S. Geological Survey Professional Paper 1250, 701-718.

Spurr, J.E. (1898). Geology of the Yukon gold district, Alaska. U.S. Geol. Survey 18th Ann. Rept., pt. 3, 87-392.

Taber, S. (1953). Origin of Alaskan silts. Am. Jour. Sci. (251), 3211-336.

Thom, A. (1976). Momentum, mass and heat exchange of plant communities, in Vegetation and the Atmosphere--1: Principles (ed. by J. Monteith), 57-109. Academic Press, London.

Tsoar, H., and Pye, K. (1987). Dust transport and question of desert loess formation. Sedimentology (34), 139-153.

Tuck, R. (1938). The loess of the Matanuska Valley, Alaska. Journal of Geology (46), 647-53.

_____ (1940). Origin of muck-silt deposits at Fairbanks, Alaska. Geol. Soc. America Bull. (46), 1295-1310.

Tungsheng, L., Zhisheng, A., Baoyin, Y. and H. Jiamao (1985). The loess-paleosol sequence in China and Climatic History: Episodes (8), 21-28.

Westgate, J., Walter, R., Pearce, G. and Gordon, M. (1983). Old Crow tephra: A new late Pleistocene stratigraphic marker across north-central Alaska and the Yukon territory. Quaternary Research (19), p. 38-54.

Westgate, J., Walter, R., Pearce, G., and Gordon, M. (1985). Distribution, stratigraphy, petrochemistry and paleomagnetism of the late Pleistocene Old Crow tephra in Alaska and the Yukon. Canadian Journal of Earth Sciences, v. (22), 893-906.

Wilkerson, A.S. (1932). Some frozen deposits in the gold fields of interior Alaska. Am. Mus. Novitates (525), 22 p.

Woillard, G.M. (1978). Grande Pile Peat Bog: a continuous pollen record for the last 140,000 years. Quaternary Research (9), p. 1-21.

MORPHOLOGICAL FEATURES OF THE ACTIVE ROCK GLACIERS IN THE ITALIAN ALPS AND CLIMATIC CORRELATIONS

S. Belloni[1], M. Pelfini[1] and C. Smiraglia[2]

[1]Dipartimento di Scienze della Terra, Università di Milano
[2]Istituto di Geografia, Università Cattolica di Milano

SYNOPSIS Rock glaciers on the Italian side of the Alps have been mapped through the use of aerial photographs. We believe that many of these forms are active at present and this interpretation has been confirmed by field observations taken in the most important mountain groups and above all in the Cevedale Group. Minimum altitude ranges between 2050 and 3150 m, depending upon the mountain group (for example, the minimum average altitude descends to 2640 m on Monte Rosa, whereas the minimum altitude is 2770 m on the Cevedale massif). Maximum altitudes have been found to exceed 3000 m.

A statistical analysis of morphological features was performed for approximately one hundred rock glaciers and the characteristics of the "average" active rock glacier in the Italian Alps were deduced. Climatic parameters were also examined. Records from six different meteorological stations in the Italian Alps were analyzed, covering a period of 16 years. The stations are situated between 1236 and 2340 m. We used mean annual temperature with a vertical gradient derived from previous authors as the principal criterion. A highly significant correlation was found between the altitude of the annual isotherm of -2°C and the lowest altitude of the active rock glaciers.

INTRODUCTION

The distribution of rock glaciers is for the most part determined by morphology and climatic conditions (Haeberli, 1985). Active rock glaciers may in fact be defined as patches of discontinuous permafrost. The study presented here is intended as a preliminary contribution concerning the active rock glaciers in the Italian Alps. The recent studies on this side of the Alpine chain promoted by the CNR Group on Physical Geography and Geomorphology have demonstrated how numerous and varied these forms are from a typological point of view and probably from a genetic point of view as well. A special research unit appointed within the group mentioned above has identified and mapped numerous rock glaciers situated in several mountain groups in the Italian Alps (Carton, Dramis, Smiraglia, in press). Many of these rock glaciers are considered to be active on the basis of various criteria such as the absence or almost complete absence of vegetation, the steepness of the front and lateral slopes, and the generally convex profile.

Field surveys were also carried out in almost all of the mountain sectors in order to confirm hypotheses made after the study of the aerial photographs. In this manner, further evidence of the presumed activity of the rock glaciers was observed. Such evidence includes the lack or limited presence of lichen and the absence of particular forms (i.e., hollows, sinkholes) deriving from collapse phenomena. Moreover, it was observed that the above-mentioned rock glaciers are situated in altimetric zones where periglacial forms abound (patterned ground, solifluction lobes, etc.). Ice lenses and frozen sediments were also identified at a depth of 2-3 m through natural sections, below the surficial layer of large blocks, in two rock glaciers, in the Gran Paradiso and in the Cevedale Group.

The rock glaciers taken into consideration number slightly over one hundred. Proceeding from west to east, the rock glaciers are distributed in the Gran Paradiso and the Monte Rosa Groups (Piedmont - Val d'Aosta sector), the Bernina Group, the Cevedale Group, the Adamello Group, and the Orobie Group (Lombard sector), in the Brenta Group, the Venoste Alps, and the Noric Alps (Venetian sector). As far as the other regions situated at the borders of the Alpine chain are concerned, namely the Maritime Alps, the Dolomites, and the Carnic Alps, rock glaciers that could be considered active proved to be quite infrequent.

It was possible to obtain a series of morphological data for each rock glacier identified, in addition to a series of observations on morphology, lithology and location.

The data from the six meterological stations (2 in the Piedmont - Val d'Aosta sector, 2 in the Lombard sector, and 2 in the Venetian sector) were corrected with suitable vertical gradients and utilized for the purpose of identifying correlations with climatic parameters and above all, to verify observations recorded by numerous authors (among others, Barsch, 1978, Evin 1983, Cheng, 1983, Haeberli 1985) on the required conditions for the existence of active rock glaciers.

THE CHARACTERISTICS OF ACTIVE ROCK GLACIERS

One hundred thirty-one rock glaciers held to be active were identified in the mountain groups taken into consideration. Their distribution is shown below in Table I.

As may be observed in the table and in

TABLE I

The Active Rock Glaciers in the Italian Alps

Group	Number of forms
Gran Paradiso	24
Monte Rosa	16
Stella-Bernina	20
Piazzi-Cevedale	27
Adamello	3
Orobie	3
Brenta	6
Venoste Alps	12
Noric Alps	20

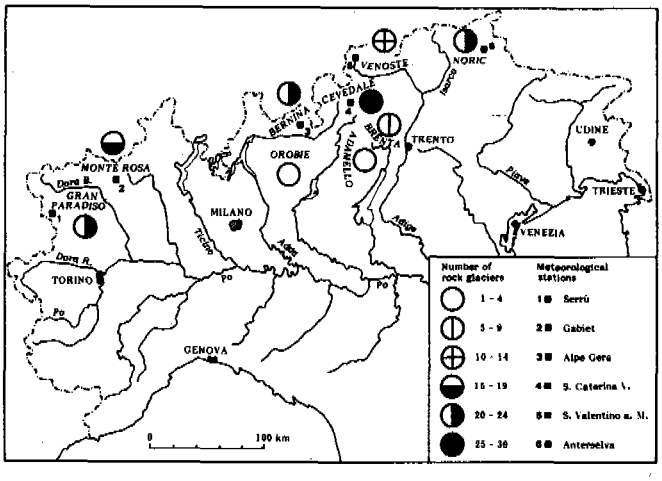

Fig. 1 Location of the active rock glaciers and the meteorological stations in the Italian Alps

in Figure 1, the greatest concentrations of active rock glaciers are found in the central sector of the chain. The great crystalline massifs of the Gran Paradiso Group, the Monte Rosa Group, the Bernina Group, the Cevedale Group, the Venoste and the Noric Alps are situated in the central sector. In the outermost sectors, on the other hand, where carbonate rocks prevail, these forms are quite infrequent.

The overall surface of the rock glaciers identified is approximately 10 km^2. These are forms that are mainly located inside cirques and, to a lesser extent, on slopes. Rock glaciers situated in narrow valleys and gorges are less common.

The majority of the forms observed presents a complex lobe morphology, which is often very distinct and developed. The frontal margin is sometimes rendered complex and multilobed by the convergence of more than one flow.

Moreover, the relations existing, at least from a topographical point of view, with glaciers and moraines should also be noted. More than half of the rock glaciers (55%) are in fact characterized by the presence of semipermanent snow above, but the proximity of glaciers (27%) and glacierets (20%) has also been reported. Forms for which there exist connections with moraines are less frequent.

There are two main parameters which are important to discuss in more detail because they offer interesting data on the genesis and the existence of rock glaciers, that is, the lithology of the surrounding rock walls and aspect. As far as the former is concerned, the obvious predominance of metamorphic rocks (87%) may be observed. They are mainly gneiss, micaschists, phyllites, calc-schists, and green stones - all of which are rock types characterized by intense fracturing and schistosity in the majority of cases. Therefore, they are rocks that are extremely sensitive to frost processes. In terms of frequency, carbonate rocks, such as the dolomites in the Brenta Group, follow (8%), then plutonites (5%), such as the granodiorites in the Adamello Group, the cryoclastic detrition of which yields fragments that are coarser and less tabular.

As regards aspect, there is a distinct prevalence of northern directions, as may be seen in Figure 2. The northern aspect alone in fact, is evident in 28% of the rock glaciers. When the north-west, north, and north-east sectors are considered together, the number of rock glaciers exceeds 52%. The percentage of rock glaciers facing other directions falls sharply below the previous one (with a maximum of 14% facing west).

The data collected on the various morphometric parameters were analyzed statistically. The results of the analysis are shown in Table II and in the graphs shown in Figure 2.

TABLE II

Morphometric Features of the Rock Glaciers in the Italian Alps

	A	B	C	D	E	F	G
mean	2603	2736	3020	72815	221.6	342.3	32.3
standard deviation	240.2	215.5	192.3	123572.6	213.4	199.6	14.2
coeff. of variation	9.2	7.9	6.4	169.71	96.3	58.3	43.8
min.	2050	2200	2643	2500	40	50	8
max.	3150	3200	3433	1203125	1750	1140	71
interval scale	1100	1000	790	1200625	1710	1090	63
skewness	-0.1	-0.1	-0.1	6.5	4.9	1.2	0.8
kurtosis	2.8	2.6	2.1	55.3	32.9	4.6	3.2

(A = minimum altitude of the front in meters; B = maximum altitude of the rock glaciers in meters; C = maximum altitude of the basin en- closing the rock glaciers; D = area in square meters; E = maximum width in meters; F = length in meters; G = slope in percentages.)

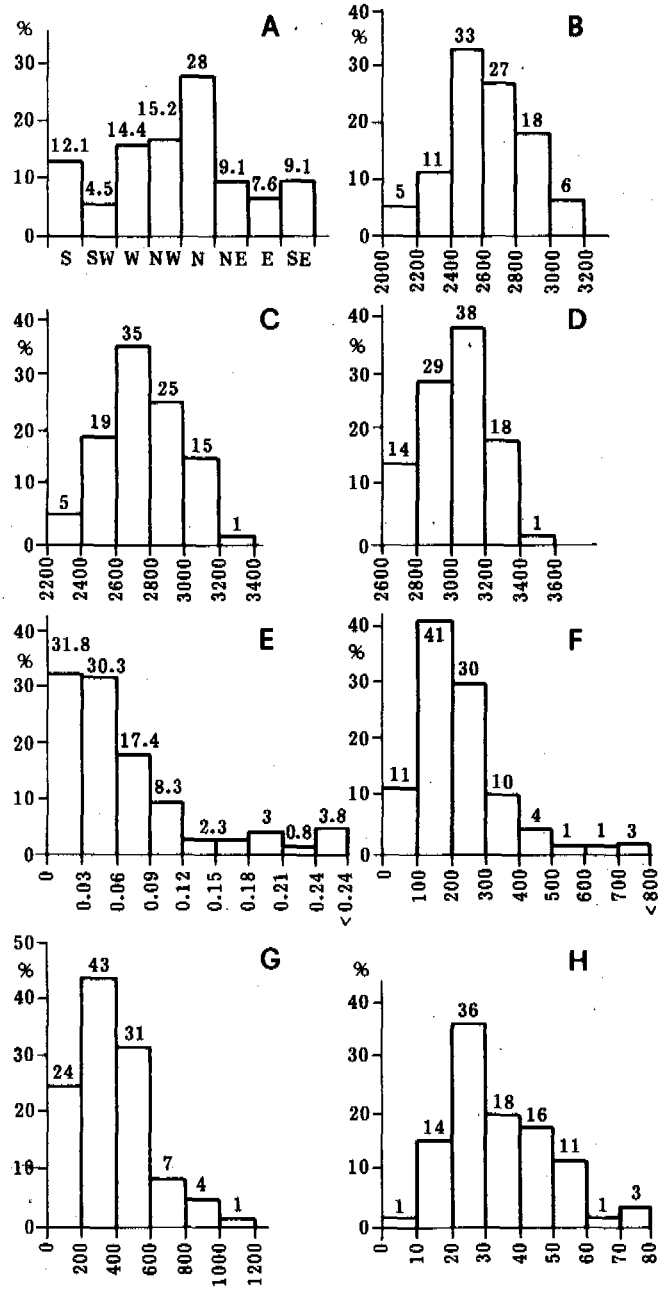

Fig. 2 Histograms of the Parameters Examined for the Active Rock Glaciers. A: aspect; B: minimum altitude of the front (in meters); C: maximum altitude of the rock glaciers (in meters); D: maximum altitude of the basin enclosing the rock glaciers (in meters); E: area (in square kilometers); F: maximum width (in meters); G: length (in meters); H: slope (in percentages).

As may be noted in the table, the altitude of the fronts of the active rock glaciers in the Italian Alps ranges between 2050 and 3150 m, with a mean altitude of 2603 m. The related histogram shows that rock glaciers with fronts at fairly high altitudes prevail. In fact, 60% of the forms show a minimum altitude ranging between 2400 and 2800 m.

The maximum altitude of rock glaciers is somewhat difficult to determine, especially when there are transitions with glacerets or moraines. The upper limit of the rock glaciers, however, is generally situated at an altitude slightly higher than 2700 m, with a maximum of 3200 m. The modal class ranges between 2600 and 2800 m. The dispersion of the data is very limited, as is demonstrated by the fairly low coefficient of variation (7.9%).

The distribution of the data regarding the highest altitude of the basin enclosing rock glaciers also appears to be homogeneous (coefficient of variation: 6.4%). The height of the peaks varies from a minimum of 2643 m to a maximum of 3433 m, with a mean of 3020 m.

The mean of the area of the rock glaciers (72815 m^2) appears to be of little significance. The area of the rock glaciers is, in fact, extremely varied. The rock glacers vary from those with a surface greater than 0.3 - 0.5 km^2, with the maximum reaching 1.2 km^2, to those with surfaces less than 0.01 km^2 (the minimum surface area was 0.002 km^2). The statistical parameters also highlight this remarkable dispersion in the data regarding area. In fact, the standard deviation is very high and the coefficient of variation is just as high. However, it may be observed from the relative histogram that there is a prevalence of forms with limited areas. In fact, the modal class has a range between 0 and 0.03 km^2 with 32% of the total (if one also considers the class from 0.03 to 0.06, the result is 62%).

The data regarding length and width also appear rather varied. The data on width are extremely variable with a minimum of 40 m and a maximum of 1750 m. The mean value is slightly over 200 m, whereas the coefficient of variation indicates that the standard deviation represents more than 96% of the mathematical mean of the seriation. The greatest number of rock glaciers is concentrated within the modal class from 100-300, which includes over 70% of all the rock glaciers. On the other hand, rock glaciers with a maximum width greater than one kilometer are quite infrequent.

As for length, it may be observed from the histogram in Figure 2 that there is a prevalence of rock glaciers in which this parameter is clearly less than one kilometer (74% of the forms is included in the class from 200 to 600 m. Dispersion remains quite marked (coefficient of variation: 58%).

The analysis of the last parameter taken into consideration, that is, slope, yielded a mean value of 32% with values ranging between 8% and 71%.

From the examination of Table II it may be noted that as far as the morphometric features are concerned, there is great heterogeneity in the data within some of the parameters. Examples of such parameters include area, maximum width, and length, which all stands to confirm the existence of various types in so far as the general form of the active rock glaciers in the Italian Alps is concerned. Altitudinal parameters, on the other hand, appear to be more

homogeneous. Data concerning the minimum altitude of the front, the maximum altitude of the rock glaciers, and the highest altitude of the basin above are examples.

The following characteristics of the "average" active rock glacier in the Italian Alps emerge from the considerations and the data reported above. Its surface is somewhat limited (forms with surfaces less than 0.06 km^2 prevail). The altimetric zone for the location of rock glaciers lies between 2400 and 2800 m for the altitude of the front and 2800 -3000 for the higher altitudes. The basin enclosing it, on the other hand, reaches heights between 2700 and 3200 m. Length and maximum width are limited (with a prevalence of classes from 200 to 600 m and from 200 to 300 m respectively). It must also be added that generally speaking, the forms with a transversal axis greater than the longitudinal axis are more widespread. This is also shown by the correlation coefficient between area and width (r = 0.72). The predominant aspect is northern. It is interesting to note that the rock glaciers with the greatest lengths (over 500 m), are, for the most part, characterized by a northern aspect (65%). The same holds true, though to an even greater extent (89%), for the greatest widths, that is, over 300 m.

Moreover, it must be noted that fronts facing south are generally situated at higher altitudes with respect to those facing north. In addition, the largest forms (with areas over 0.09 km^2) for the most part (77%) have a northern aspect.

CLIMATIC LIMITS

As Haeberli (1985) observes, from the point of view of climate, the required conditions for the existence of active rock glaciers consist in a mean annual temperature of the air between -1°C to -2°C. This temperature should represent the lower limit of the distribution of discontinuous permafrost. Another condition is annual precipitation lower than 2500 mm. Consequently, our objective was also to verify the validity of these parameters in the case of the active rock glaciers on the southern side of the Alps.

The difficulty of calculating temperature at high altitudes when metereological stations do not exist at particularly high altitudes, is well known. In this case, several stations were chosen at the highest possibile altitudes and as close as possibile to the mountain groups in which the rock glaciers are situated. The Alpine sectors considered were limited to those in which these forms are more numerous and that is, from the west (the meterological station is indicated between parentheses): Gran Paradiso (Serrù), Monte Rosa (Gabiet), Bernina (Alpe Gera), Cevedale (S. Caterina Valfurva), Venoste Alps (S. Valentino alla Muta), Noric Alps (Anterselva). The altitude of these stations varies from 2340 m (Gabiet in the Monte Rosa Group) to 1236 m (Anterselva in the Noric Alps). They are listed below in Table III. Records from each station were used. They covered a fifteen-year period (1970-1984 for the first four, 1966-1980 for the last two). The mean annual temperature for each one was calculated first. It varied from 0° C at the Gabiet station to 6.1° C at the Anterselva station. Then the altitude of the isotherm of -2° C was calculated. With reference to the research that has been done on the entire Po Valley basin (Belloni, 1982) or on more limited sectors (Belloni and Pelfini, 1987), the mean annual thermal gradient of 0.53° C was used. As may be observed in Table III, the isotherm of -2° C is located at an altitude that varies from 2764 m at the Anterselva station in the Noric Alps to 2538 m at S. Valentino in the Venoste Alps. The mean is 2662 m. If the Anterselva station is excluded, a fairly uniform decrease in values may be observed from west to east.

TABLE III

Meterological Stations

Name	Altitude	Mean Annual Temperature	-2° C Isotherm Altitude
Serrù	2 275	+ 0.4° C	2 728
Gabiet	2 340	0.0° C	2 717
Alpe Gera	2 090	+ 0.9° C	2 637
S. Caterina	1 738	+ 2.5° C	2 587
S. Valentino	1 500	+ 3.5° C	2 538
Anterselva	1 236	+ 6.1° C	2 764
		mean	2 662

TABLE IV

Rock Glaciers and Temperature

Mountain Group	Mean Altitude Rock Glacier Fronts	Mean Annual Temperature
Gran Paradiso	2760	- 2.2° C
Monte Rosa	2640	- 1.6° C
Bernina	2414	- 0.8° C
Cevedale	2770	- 2.9° C
Venoste	2570	- 2.2° C
Noric Alps	2588	- 1.1° C
mean	2624	mean - 1.8° C

Table IV, on the other hand, shows the mean values for the altitude of the fronts of the rock glaciers for each mountain group. These values are sufficiently indicative when we consider, as was noted previously, the reduced dispersion in the data. In addition, the table shows the mean annual temperature as calculated for the altitude in question through the vertical gradient mentioned above.

It can be noted that the mean altitude of the fronts (2624 m) is slightly lower than the mean altitude of the isotherm of -2°C (2662 m). Moreover, the mean annual temperature (-1.8°C) is not very far removed from that value. When the individual mountain groups are examined in detail, somewhat different findings emerge. In fact, from -2.9°C in the Cevedale Group, we find -0.8°C in the Bernina Group, with variations that remain within acceptable limits and that place the rock glacier fronts just slightly above or slightly below the lower thermal limit of the distribution of the discontinuous permafrost.

The same methods were used to calculate the approximate altitude at which the annual isotherm of - 6°C is located, which, in turn, should determine the lower limit of the continous permafrost (Evin, 1983). The values obtained vary from 3519 m in Anterselva in the Noric Alps to 3292 m in S. Valentino in the Venoste Alps. The mean is 3416 m. The limit indicated lies above the highest peaks enclosing the basins where the rock glaciers examined are situated. Even when only the maximum altitude of the highest peaks is considered, a mean value of 3351 m is the result.

In order to identify more precisely the climatic characteristics of this periglacial zone, some data on the presence and duration of the frost should be supplied. Using the mean annual temperatures calculated previously for the altitude of the fronts of the rock glaciers in the various mountain groups, the evaluation of the number of days without thaw (days with maximum temperature equal to or less than 0°C) and days with frost (in which the minimum temperature is equal to or less than 0°C and the maximum temperature is greater than 0°C) was carried out following the method indicated by Belloni (1982). As for the first parameter, the number of days varies from 187 for the Cevedale massif to 147 for the Noric Alps, with a mean of 163. It should be kept in mind that these findings refer to the altitude of the fronts of active rock glaciers. The number of days with frost varies from 101 for the Bernina Group to 73 for the Cevedale Group, with a mean of 88 days. On the whole, it may be noted that the effect of the frost (days without thaw and days with frost) is evident for 250 days on the average. Naturally, the duration may be longer in the cases in which the fronts of the rock glaciers are found at higher altitudes (260 days in the Cevedale Group, 254 days in the Gran Paradiso Group). However, it is necessary to stress that the effect of the frost is twofold and that the inter-relations between the two resulting conditions vary with altitude. In fact, days without thaw, which permit the conservation (and the formation) of the discontinuous permafrost predominate at the higher elevations. On the other hand, days with frost (in the sense indicated above) are much less frequent. In the Cevedale Group, for example, the days without thawing represent 71% of the total. With the decrease in altitude, days without thawing become less frequent and their number tends to approach that of the days with frost. The latter favor congelifraction and the supply of rocky material for the rock glaciers through the alternation of the temperature above and below 0°C. In the Bernina Group, days in which the maximum temperature is equal to or less than 0°C, represent 58% of the total number of days without thaw and with frost.

As far as precipitation is concerned, it is well known that the application of vertical gradients may yield unreliable results. Therefore, we will limit ourselves to several data regarding the mean annual values for precipitation in the fifteen-year period at the stations considered. The amount of precipitation varies from a maximum of 1414 mm annually for the station located in the Alpe Gera (Bernina) to a minimum of 505 mm at S. Valentino (Venoste Alps). However, it was not possible to identify a correlation with altitudinal variations. The average for the six stations was slightly below 1000 mm.

CONCLUSIONS

The main morphological characteristics of the rock glaciers considered to be active in the Italian Alps emerging from the data reported in the above, should be sufficiently reliable. However, it should be kept in mind that given that this is a preliminary study of a sample type some caution is in order. These are forms that are very widespread on the southern side of the Alps too, and particularly in the central sector. In fact, it could be said that they make up an essential part of the landscape in the high mountain areas.

As far as correlations with climatic conditions are concerned, it was found that the rock glaciers studied are located in an altitudinal and climatic zone below the permanent snow line. This surely permits the conservation (and probably the formation as well) of patches of discontinuous permafrost. Thus, the forms examined may very well be considered within the framework of the set of environmental conditions outlined previously by other authors (for example, Barsch, 1969; Haeberli, 1975; Hollerman, 1983; Haeberli, 1985), who consider rock glaciers to be a phenomenon that is typical of the periglacial morphology of cold and relatively dry mountain regions.

ACKNOWLEDGEMENTS

This study has been carried out with the financial help of the CNR (850089705, Dir: G.B. Castiglioni).

The authors wish to thank their colleagues in the CNR Group on Physical Geography and Geomorphology, who contributed to the collection of data on active rock glaciers. They are G.B. Castiglioni, C. Catasta, U. Mattana, C. Ottone, G. Palmentola, B. Parisi, and P. Petruzzelli.

In addition, the authors would like to thank Professor G. Orombelli for having edited the English translations of the papers presented by Italian researchers in this conference.

REFERENCES

Barsch, D. (1969). Permafrost in der oberen subnivalen Stufe der Alpen. Geogr. Helvetica, 24, 10-12.

Barsch, D. (1978). Rock glaciers as indicators for discontinuous permafrost. An example from the Swiss Alps. Third Int. Conf. on Permafrost, Ottawa, NRC, I, 394-352.

Belloni, S. (1982). Temperature medie annue e mensili nel Bacino Padano e parametri fisici derivati. Geogr. Fis. Dinam. Quat., 5, 46-54.

Belloni, S. and Pelfini, M. (1987). Il gradiente termico in Lombardia. Acqua Aria, 4, 441-447.

Carton, A., Dramis, F., and Smiraglia C. (in press). A first approach to the systematic study of the rock glaciers in the Italian Alps. Fifth Int. Conf. on Permafrost, Trondheim, Norway, 1988.

Cheng, G. (1983). Vertical and horizontal zonation of high-altitude permafrost. Fourth Int. Conf. on Permafrost, 136-141.

Evin, M. (1983). Structure et mouvement des glaciers rocheux des Alpes du Sud. These 3 cycle, Grenoble, Institut de Géographie Alpine.

Haeberli, W. (1975). Untersuchungen zur Verbreitung von Permafrost zwischen Fluelapass und Piz Grialetsch (Graubunden). Mitteil. Versuch. Wasserbau, Hydrol. Glaz., 17, 1-221.

Haeberli, W. (1985). Creep of mountain permafrost. Internal structure and flow of Alpine rock glaciers. Mitteil. Versuch. Wasserbau, Hydrol. Glaz., 77, 1-142.

Hollerman, P. (1983). Blockgletscherstudien in europaischen und nordamerikanischen Gebirgen. Ak. Wiss. Gottingen Abh., Math. Phys. Kl., 35, 116-119.

OBSERVATIONS ON NEAR-SURFACE CREEP IN PERMAFROST, EASTERN MELVILLE ISLAND, ARCTIC CANADA

L.P. Bennett[1] and H.M. French[2]

[1]Department of Geology, University of Ottawa, Ottawa-Carleton Centre for Geoscience Studies, Ottawa, Ontario K1N 6N5
[2]Departments of Geography and Geology, University of Ottawa, Ottawa-Carleton Centre for Geoscience Studies, Ottawa, Ontario K1N 6N5

SYNOPSIS Rates of near-surface frozen soil creep of between 0.03-0.05 cm/yr are typical of four sites on a low angle (5°) west-facing slope near Rea Point, Melville Island. Highest movements are concentrated in a 0.5 m thick ice-rich zone lying immediately below the active layer. At depths greater than 1.2 m, where ground temperatures rarely rise above -3.0°C, no measureable deformation was noted. These rates are of the same order of magnitude, although approximately two-thirds less, than those reported from relatively warm permafrost in the Mackenzie Valley. Variability of movement between sites may be related to differences in snow cover and resulting ground thermal conditions. An upslope movement component observed in winter is probably related to thermal contraction.

INTRODUCTION

Perennially cryotic ground is subject to a variety of time dependent stresses and strains (e.g., Vyalov, 1959; 1986; Ladanyi, 1981). According to Vyalov (1986, 147) the stresses induce deformation which leads to attenuating creep, steady state flow and/or progressive creep and failure. A recent study in the Mackenzie Valley, Canada by Savigny (1980; Savigny and Morgenstern, 1986a; 1986b; 1986c) represents one of the few attempts to measure the magnitude of in situ frozen soil creep.

The deformation of frozen ground has relevance not only to geotechnical engineering design and construction in permafrost regions today (e.g., Johnston, 1981, 80-101), but also to the interpretation of certain non-diastrophic Pleistocene structures observed in temperate regions (e.g., Hollingsworth et al, 1944; Kellaway, 1972). In this paper, we add to the understanding of the data of Savigny (1980) by presenting observations upon near-surface in situ frozen soil deformation from a locality on Eastern Melville Island, Arctic Canada.

FROZEN SOIL CREEP

In relatively warm permafrost, Savigny (1980) found the rate of creep to vary according to the scale and spacing of ground ice structures at depth (e.g., Savigny and Morgenstern, 1986b, 512-513). Relatively uniform velocities occur over depth intervals that are several metres thick and which are ice-rich (e.g., borehole GBIA at depth of 24-29 m; Savigny and Morgenstern, 1986b). A second type of deformation, similar to shearing, occurs where large ice lenses are more widely spaced. All the movements measured by Savigny (1980) took place in unconsolidated sediments, notably glaciolacustrine clays and silty clays.

If one excludes complex Quaternary stratigraphies and massive bodies of ice occurring at depth within permafrost (e.g., see Mackay, 1973), ground ice volumes are generally highest in the top 1-5 m of permafrost, being concentrated at or just below the base of the active layer (e.g., Pollard and French, 1980; Lawson, 1983). Such a concentration reflects the seasonal migration of water within frozen ground in response to a temperature gradient (e.g., Parmuzina, 1978; Cheng, 1983; Mackay, 1983). Accordingly, some of the highest rates of in situ frozen soil creep should occur within the upper 1-2 m of permafrost. In all probability, these movements should represent a more widespread process than the relatively deep-seated deformation described by Savigny (1980). On the other hand, the deformations occurring in areas underlain by cold permafrost might reasonably be expected to occur at a much slower rate than the 0.15-0.30 cm/yr^{-1} reported by Savigny (Savigny and Morgenstern, 1986b, 513). Studies of polycrystalline ice suggest that ice creeps readily in response to applied stress when temperatures exceed the threshold values of -3°C (Hobbs, 1974, 326). Clearly, as ice temperatures decrease, creep strength is enhanced.

The creep strength of frozen soils is also strongly dependent on temperature (e.g., Johnston, 1981, 92). Tsytovich (1975) notes that as the temperature of a medium sand changes from -1.0°C to -2.0°C, the compressive strength of this material increases by 15%. Under the same conditions, he suggests that the compressive strength of clay would increase by 50%. As the creep strength of a material increases, the creep rate decreases where all other factors are equal. It is expected that measureable deformations be virtually non-existent at depths greater than 10.0 m or wherever average ground temperatures remain below -5°C throughout the year.

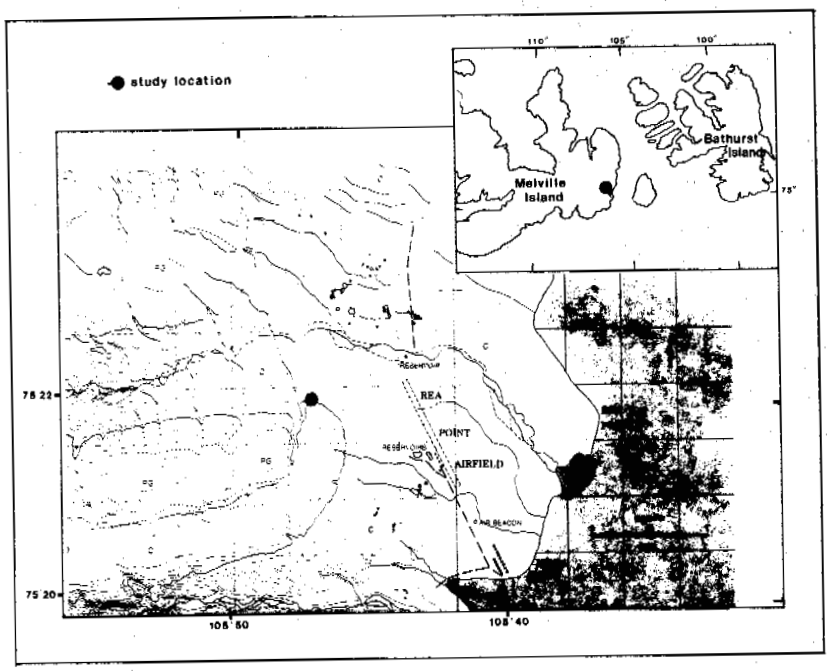

Fig.1 Location Map of Rea Point Vicinity, Eastern Melville Island, Showing Study Location.

STUDY AREA

The data presented in this paper were measured on a west-facing, dominantly convex slope, approximately 1.5 km west of Rea Point, eastern Melville Island (Figures 1, 2), between August 1985 and August 1987.

Permafrost conditions

The area is underlain by permafrost over 500 m thick (Taylor et al., 1982). Maximum depth of seasonal thaw usually does not exceed 0.6 m, and at many localities it extends only 0.2 m below the surface. The mean annual ground temperature (MAGT) is approximately -17°C and

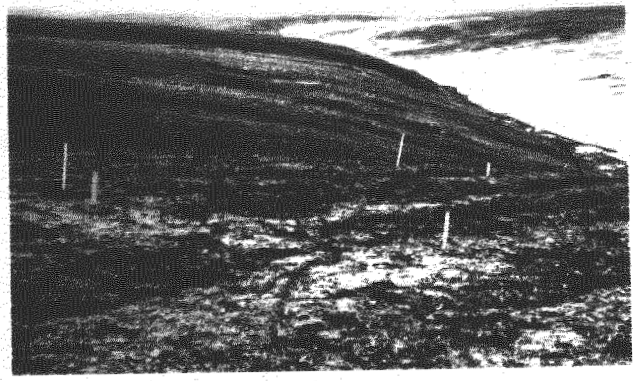

Fig.2A General View of Sites 2 and 3 Showing Instrumentation in Place, August 1985

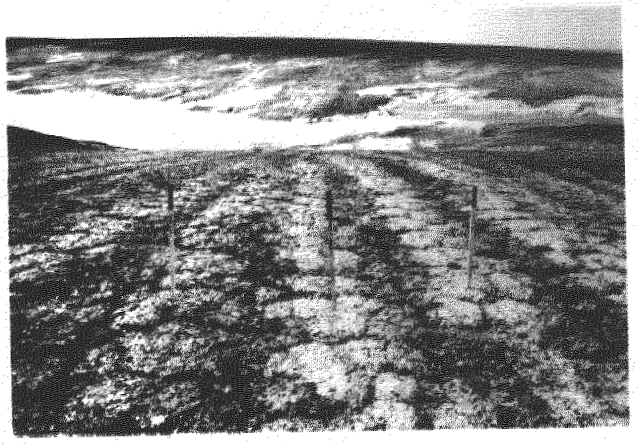

Fig.2B Non Sorted Stripes Adjacent to Sites 2 and 4, August 1985

the depth of zero annual amplitude ranges between 15 to 18 m. Given the typical ground temperature envelope that is implied (e.g., Stangl et al., 1982, Figure 2), any seasonally-induced creep deformations within permafrost are probably restricted to the upper 3.0 m or so.

Soil conditions

Cold, ice-rich permafrost soils are typical of Melville Island. These are derived from the cryogenic weathering of weakly lithified sandstones, siltstones and shales (e.g., Stangl et al., 1982; Hodgson et al, 1984). This leads to the development of considerable quantities of fine sand and silt. A generalized cross-section may be divided, therefore, into three units to reflect their derivation from the cryogenic weathering of bedrock. Normally, relatively intact bedrock is overlain by fractured bedrock which then grades into a residuum or surface regolith of cobbles, gravels and fines.

Ground ice conditions

A detailed description of the ground ice conditions in the vicinity of Rea Point has already been given (French, Bennett and Hayley, 1986). Consequently, they are only briefly summarised here. During the winter of 1981-82 a trench, approximately 530 m long and 2.0 m deep, was excavated adjacent to the study location as part of a field ditching trial (EBA, 1983; Hayley et al., 1984). The wall log, compiled from this trench, provides an excellent approximation of ground ice conditions at the site (Figure 3). In general, the near-surface soils must be regarded as ice-rich.

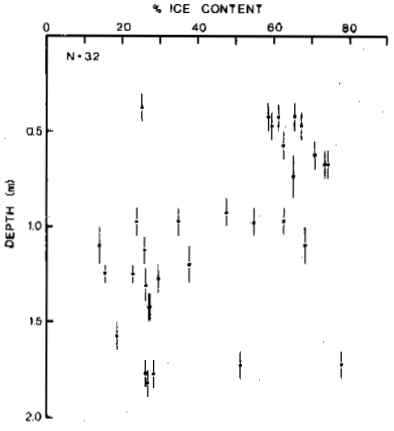

Fig.3 Ground Ice Conditions Associated With Weatherall Formation Sandstones and Siltstones Near Rea Point. (From French, Bennett and Hayley, 1986, Figure 3.)

Ground ice volumes appear to be influenced by the distribution of colluvium, residuum and the depth to weathered bedrock. The latter consists of thin beds of Late Devonian age Weatherall Formation sandstones and siltstones with occasional shale and coal seams (Thorsteinsson and Tozer, 1976). These weather to silt or gravelly silt. The distribution of ice content values with depth (Figure 3) shows that the colluvium, consisting primarily of silts and silty gravels, contains 60-75% ice by volume. Maximum amounts occur between 0.4-0.9 m depth (i.e., just below the active layer). Then, ice content decreases with depth in the residuum, only to rise again at the residuum-bedrock contact. Temperature gradients within the predominantly silty materials induce high negative pore pressures which are thought responsible for this concentration of ground ice within the colluvium. The residuum-colluvium boundary, ranging from 0.6-1.8 m in depth, is also characterised by a concentration of excess ice. In the residuum, the concentration of ground ice decreases with depth from 50% by volume at the surface contact to 10% by volume at the bedrock contact.

INSTRUMENTATION

Four sites were each instrumented with multistring YSI thermistors, 4-tube telescoping heavemeters, and 3 m long bottom-sealed inclinometer casing designed to accommodate a Terra Technology MP-20 inclinometer torpedo. Accuracy of the inclinometer system, as measured in field tests, is demonstrated by a maximum variability of 0.0061 cm. Drilling was undertaken in May 1985 using a seismic drill mounted on a FN60 Nodwell. The plastic inclinometer casing (O.D. 70.9 mm) was surrounded by a slurry of grout mixed in situ and damped in place by a long thin metal rod. The grout was developed by Haliburton Services Ltd. of Edmonton and intended for use in filling all void space between casing and soils in a permafrost environment. Sold under the trade name "Permafrost Cement", it is designed to set rapidly at sub-zero temperatures with minimum expansion. This Permafrost Cement was used successfully by Savigny and Morgenstern (1986b) in similar circumstances.

The grout was left to set for 60 days before readings commenced. The thermistor strings extend to 2.5 m depth, with individual thermistors spaced at 12.5 cm apart between depths of 20-95 cm, in order to present an accurate picture of the ground thermal regime at the critical interface between perennially and seasonally cryotic ground. At greater depths, thermistors are 25 cm apart. Two 5 m cables and one 15 m cable installed at the location provide additional temperature data.

Reference measurements were made on August 1, 1985, with follow-up measurements taken three times a year during the following two years. In this paper, space limitations allow only a discussion of the inclinometer data.

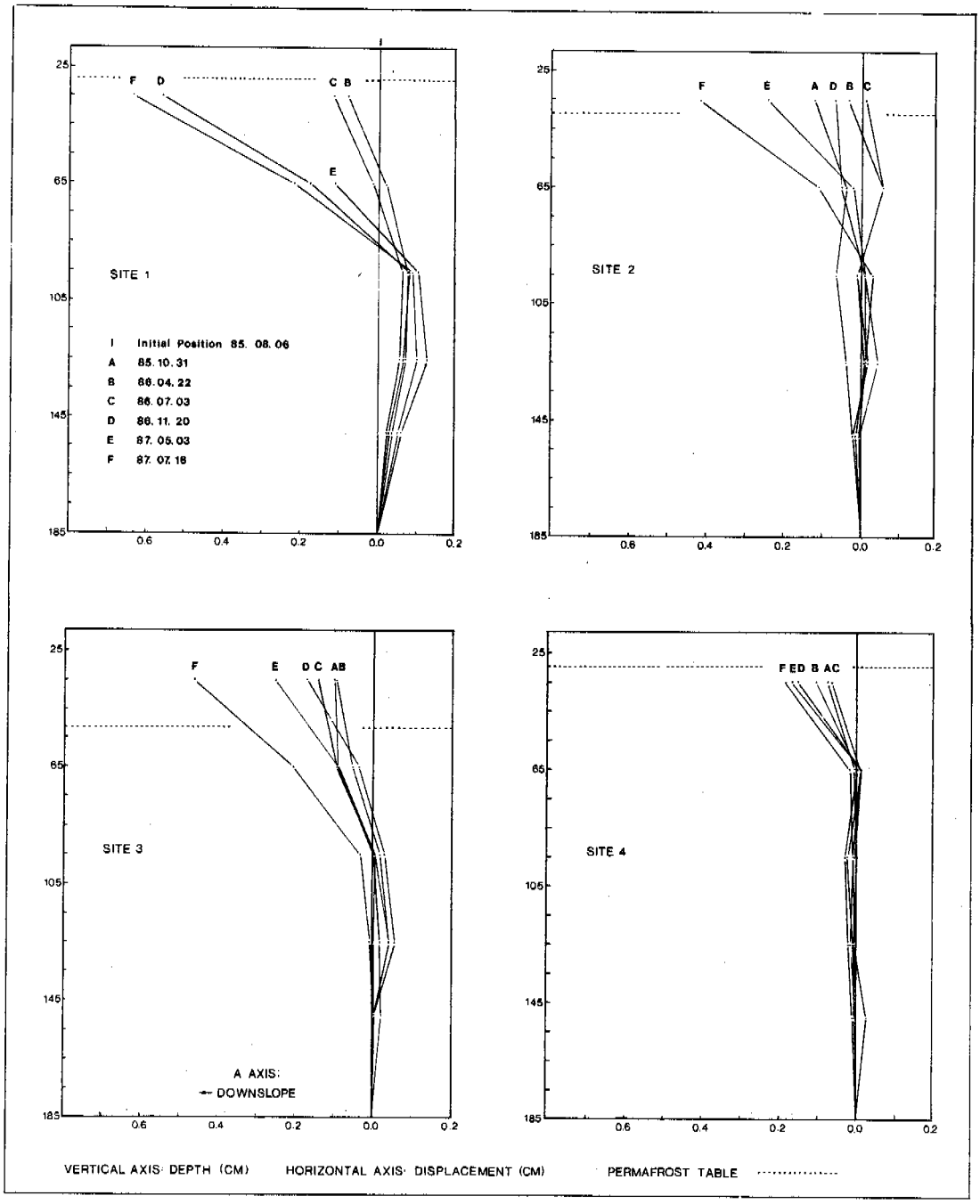

Fig.4 Diagram Showing A-Direction (Parallel-To-Slope) Inclinometer Data for All Four Sites

RESULTS

The inclinometer tubes record movement at all times of the year and therefore the values recorded include not only frozen soil creep, which occurs in both perennially and seasonally cryotic ground, but also gelifluction, which occurs in seasonally cryotic ground when it is in its thawed (i.e., non-frozen) state.

Our concern in this paper is with frozen soil creep rather than with gelifluction. Since the maximum thickness of the active layer varies between only 20-45 cm, any net downslope movement observed at depths greater than 45 cm must unequivocably be related to frozen soil creep. Figure 4 indicates that significant movement does occur in the upper 0.5 m of

permafrost. This is also the zone of highest ground ice volumes (see Figure 3). However, movements are not continuous and seasonal reversals are recorded. The typical pattern of deformation consists of a recognisable downslope component during summer and early autumn, followed by a weaker upslope component during the winter and early spring. For example, at the 65 cm depth (i.e., at least 20-45 cm below the permafrost table), downslope creep at three of the four sites averages 0.08 cm/yr^{-1}. The greatest frozen soil creep occurs at site 2 and also is clearly associated with the zone of ice-rich permafrost (see Figure 3). Maximum rates of approximately 0.10 cm/yr^{-1} appear typical of the 20 cm thick ice-rich permafrost layer occurring immediately below the active layer.

At depths greater than 1.2 m below the surface, where ground temperatures rarely rise above -3.0°C and ice contents are lower, no measureable net downslope creep occurs.

The amount of frozen soil creep varies not only from site to site, but also seasonally. The greatest downslope movement occurs in the summer and autumn when permafrost temperatures are warmest. During the winter, upslope movement is measured at most sites (see Figure 4). We hypothesize that the predominantly downslope creep observed in summer is related to the higher rate of deformation which occurs when the temperature of ice-rich frozen soil rises to the pressure melting zone of ice (see Hobbs, 1974, 326). This would occur in combination with the effects of thermal expansion. The upslope creep observed in winter is probably related to ice segregation (frost heave) and thermal contraction cracking.

Occasionally, these trends are obscured by seemingly random movements within the permafrost which defy traditional creep theory. For example, at site 1, movement at the 65 cm depth is upsloped from time E to F while points above it and below it are displaced downslope (Figure 4). A model accounting for such random movements of soil particles is discussed by Culling (1983a, b). Since a frozen soil will creep in response to the sum of all applied stresses, it cannot necessarily be assumed that gravity is the dominant stress, especially over the short term. In the case of permafrost regions, thermal contraction and expansion, and ice segregation processes are considerations.

DISCUSSION AND CONCLUSIONS

The data presented above confirm that frozen soil creep does occur in permafrost terrain. Total annual deformation at Rea Point is approximately one-third of that at the Mackenzie Valley site. We believe the lower values reflect predominantly the colder ambient air and ground temperatures at Rea Point which limit the potential for frozen soil creep to 90 days per year and to the upper 1-3 m of permafrost. Collectively, the data highlight the well known relationship which exists between frozen soil deformation, ground ice amounts and ground thermal conditions. It may be that deformations at greater depths in frozen strata occur only when ground temperatures are significantly warmer, as in the lower Mackenzie Valley, or during the degradation of permafrost, as happened on several occasions during the Pleistocene. The occurrence of certain non-diastrophic structures in sedimentary rocks in temperate areas which experienced periglacial conditions during the Pleistocene are probably related to the in situ creep of frozen ground.

ACKNOWLEDGEMENTS

Fieldwork on Melville Island has been supported by the Natural Sciences and Engineering Research Council of Canada (Grant A8367 - H. M. French), the University of Ottawa Northern Research Group, and the Polar Continental Shelf Project of the Federal Department of Energy, Mines and Resources, Ottawa. We also express our appreciation of A. R. Rossiter, Panarctic Oils Ltd., Calgary, who kindly provided logistics and transportation north of Edmonton, accommodation at Rea Point, and field drilling support.

REFERENCES

Culling, W. E. H., (1983a). Slow particulate flow in condensed media as an escape mechanism: mean translation distance. In: Rainfall Simulation, Runoff and Soil Erosion, Catena, Supplement 4 (Jan de Ploey, Ed.), 161-190.

Culling, W. E. H., (1983b). Rate process theory in geomorphic soil creep. In: Rainfall Simulation, Runoff and Soil Erosion, Catena, Supplement 4 (Jan de Ploey, Ed.), 191-214.

EBA Engineering Consultants Ltd., (1983). Geotechnical evaluation of ditching trials, Rea Point, N.W.T. Report submitted to Novacorp Engineering Services Ltd., April 1983.

French, H. M., Bennett, L., and D. W. Hayley, (1986). Ground ice conditions near Rea Point and on Sabine Peninsula, eastern Melville Island. Canadian Journal of Earth Sciences, 23, 1389-1400.

Hayley, D. W., Inman, D. V., and R. J. Gowan, (1984). Pipeline trench excavation in continuous permafrost using a mechanical wheel ditcher. Proceedings, 3rd International Specialty Conference on Cold Regions Engineering, 1, 103-107.

Hobbs, P. V., (1974). Ice Physics. Clarendon Press, Oxford, 720 p.

Hodgson, D., Vincent, J-S., and J. G. Fyles, (1984). Quaternary geology of central Melville Island, Northwest Territories. Geological Survey of Canada, Paper 83-16, 25 p.

Hollingsworth, S. E., Taylor, J. H., and G. A. Kellaway, (1944). Large scale superficial structures in the Northampton Ironstone Field. Quarterly Journal of the Geological Society of London, 100, 1-44.

Johnston, G. H. (Ed.), (1981). Permafrost: Engineering design and construction. J. Wiley and Sons, Toronto & New York, 540 p.

Kellaway, G. A., (1972). Development of non-diastrophic Pleistocene structures in relation to climate and physical relief in Britain. Reports, International Geological Congress, 24th Session, Montreal, 12, 120-146.

Ladanyi, B. (1981). Mechanical behaviour of frozen soils. In: Mechanics of Structured Media, Proceedings International Symposium on the Mechanical Behaviour of Structured Media, Ottawa, Canada, May 1981. (Selvadurai, A.P.S., Ed.), Part B, Elsevier, Amsterdam, 205-245.

Lawson, D., (1983). Ground ice in perennially frozen sediments, northern Alaska. Proceedings, Permafrost, Fourth International Conference, Fairbanks, Alaska. National Academy Press, Washington, D.C., 695-700.

Mackay, J. R., (1973). Problems in the origin of massive icy beds, western Arctic. In: North American Contribution, Permafrost, Second International Conference (Yakutsk, U.S.S.R.). National Academy of Sciences, Washington, D.C., 223-228.

Mackay, J. R., (1983). Downward water movement into frozen ground, western Arctic coast, Canada. Canadian Journal of Earth Sciences, 20, 120-134.

Parmuzina, O., (1978). The cryogenic structure and certain features of ice separation in a seasonally thawed layer. In: Problems of cryolithology (Popov, A. I., Ed.). Moscow University Press, Moscow, 141-164.

Pollard, W. H. and H. M. French, (1980). A first approximation of the volume of ground ice, Richards Island, Pleistocene Mackenzie Delta, Northwest Territories. Canadian Geotechnical Journal, 17, 509-516.

Savigny, W., (1980). In-situ analysis of naturally occurring creep in ice-rich permafrost soil. Ph.D. Thesis, Department of Civil Engineering, University of Alberta, Edmonton, 449 p.

Savigny, W. and N. R. Morgenstern, (1986a). Geotechnical condition of slopes at a proposed pipeline crossing, Great Bear River valley, Northwest Territories. Canadian Geotechnical Journal, 23, 490-503.

Savigny, W. and N. R. Morgenstern, (1986b). In situ creep properties of ice-rich permafrost soil. Canadian Geotechnical Journal, 23, 504-514.

Savigny, W. and N. R. Morgenstern, (1986c). Creep behaviour of undisturbed clay permafrost. Canadian Geotechnical Journal, 23, 515-527.

Stangl, K., Roggensack, W. D., and D. W. Hayley, (1982). Engineering geology of surficial soils, eastern Melville Island. In: The R.J.E. Brown Memorial Volume, Proceedings of the 4th Canadian Permafrost Conference, Calgary, Alberta. National Research Council of Canada, Ottawa, 136-147.

Taylor, A., Burgess, M., Judge, A. S., and V. S. Allen, (1982). Canadian geothermal data collection--northern wells, 1981. Earth Physics Branch, Geothermal Series, 13, 153 p.

Thorsteinsson, R. and E. T. Tozer, (1976). Geology of the Arctic Archaepelago. In: Geology and economic minerals of Canada, Part B (Douglas, R. J. W., Ed.). Geological Survey of Canada, Economic Geology Report, 1, 548-590.

Tsytovich, N. A., (1975). The Mechanics of Frozen Ground. McGraw-Hill Book Co., New York, 426 p.

Vyalov, S. S., (1959). Rheological properties and bearing capacity of frozen soils. U.S. Army, Cold Regions Research and Engineering Laboratories, Translation 74 (1965), Hanover, New Hampshire, 237 p.

Vyalov, S. S., (1986). Rheological fundamentals of soil mechanics. Elsevier, New York, 564 p. (Translated by O. K. Sapimov).

OBSERVATIONS ON AN ACTIVE LOBATE ROCK GLACIER, SLIMS RIVER VALLEY, ST. ELIAS RANGE, CANADA

W. Blumstengel & S.A. Harris

Department of Geography, University of Calgary, Calgary, Alberta, Canada

SYNOPSIS A forested, active lobate rock glacier 1.7 km long occurs on the east side of the Slims River Valley, 7.3 km south of Kluane Lake, Yukon Territory. It is developed in a diamicton with a loess cover over the lower one-third of its surface. The lower two-thirds is forested and the trees at the front move with the ground at up to 20 cm/a. Split trunks of trees, open crevasses and pressure ridges are common on the rock glacier, while tilted trees occur on the push-lobe developed in the silts in front of it. The rate of movement is consistent with creep of ice.

Springs around the front show no diurnal fluctuations, but discharge increases with increasing mean air temperature. ^{18}O composition of the spring water and interstitial ice within the rock glacier approximates the average of the present-day snow and rain. Tritium distribution in the interstitial ice indicates a decrease of 15-20 cm in the thickness of the active layer on the rock glacier since 1953. Available measurements of moisture distribution into and within the permafrost suggest present-day moisture movement and accumulation of ice under the influence of near-surface temperature gradients. The interstitial ice is probably modern, and when the ice content reaches a critical value, movement commences.

INTRODUCTION

Active rock glaciers are accumulations of loose, unsorted material (diamictons) with an icy core that usually has a covering of coarse clasts. They move downslope to produce an oversteepened front (Wahrhaftig & Cox, 1959; Vernon & Hughes, 1966; Washburn, 1979). They can even form in piles of mine waste (Gorbunov, 1983).

Despite numerous studies (see Benedict, 1973; Washburn, 1979; Höllerman, 1983; Haeberli, 1985, etc.), the nature and origin of rock glaciers is still in dispute. Suggested sources of ice include buried snow avalanches (Howe, 1909; Outcalt & Benedict, 1965), former glacial ice (Cross et al., 1905; Capps, 1910; Kesseli, 1941) and accumulations of ice in permafrost from various (usually unspecified) near-surface sources such as snow sifting into cavities between large stones on the surface, meltwater from snow, springs, etc.

Rock glaciers are normally classified into two main groups, viz.: lobate rock glaciers formed without glacial ice and tongue-shaped rock glaciers that originate in former cirques in glaciated terrain (e.g. Barsch, 1977; P. G. Johnson, 1978, 1980). The lobate rock glaciers are zonal permafrost landforms, whereas the tongue-shaped rock glaciers are not (Harris, 1981). In active rock glaciers, the main body of the landform moves at a rate between 0.003 and 5.000 m/a (Washburn, 1979, p. 230), with 0.2 to 0.7 m/a being typical. Whalley (1985) has suggested that the rate of movement of the main body of the rock glacier may be used to differentiate movement by downslope creep of icy permafrost (Haeberli, 1985) from glacier flow. Giardino (1983) has argued that the movement can be due to basal sliding over an unfrozen water body. Unfortunately, velocity profiles are rarely available to differentiate the various different potential modes of movement (Wahrhaftig & Cox, 1959). Inactive rock glaciers without an icy core may still exhibit collapse of the oversteepened front when the main mass is stationary.

The St. Elias Range, Yukon Territory, is an area with abundant rock glaciers. In 1984, the authors commenced a long term study of a forested, active lobate rock glacier situated 7.3 km south of Kluane Lake on the east side of the Slims River valley. The rock glacier lies across the proposed route of an access road to the Kaskawulsh glacier in Kluane World Heritage park (Fig. 1) and Parks Canada wanted to know its cause and speed of movement. This paper discusses the preliminary results of this study.

STUDY AREA

The active lobate rock glacier on the east side of the Slims River valley in Figure 1 is 1.7 km long and 0.6 km wide where it spreads out onto the valley floor (Figs. 2 & 3). It is developed in a diamicton with greenstone clasts up to 20 cm long that originate at about 1230 m elevation below a cliff on the valley side. The valley was deglaciated about 12,500 ± 200 years B.P. (Y-1386 - Denton & Stuiver, 1966).

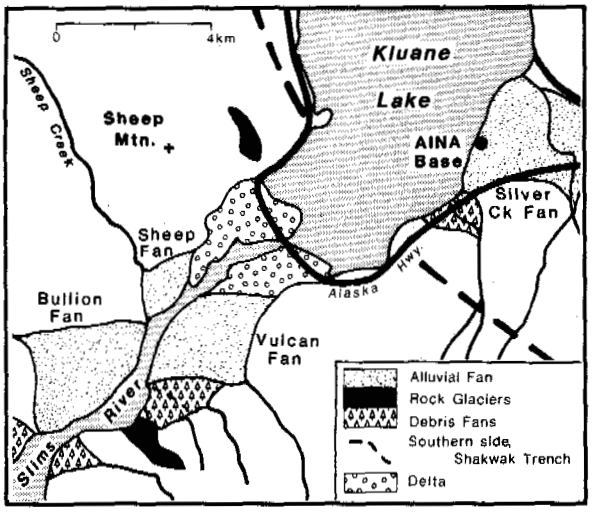

Fig. 1 Location of the Active Rock Glacier, East Side, Slims River Valley, Yukon Territory.

The lower two-thirds of the rock glacier is forested with a spruce-lichen woodland, while the lower third is mantled in a silty loess cover that reaches 60 cm in thickness close to the river. This is probably being added to by silt blown off the Slims River delta by northerly winds in winter. Nickling (1978) discusses this process in more detail.

At the front of the rock glacier, the steep front has ploughed into silty alluvium, and these deposits form a push-lobe banked against the front of the rock glacier (Fig. 3). Permafrost has developed in this push lobe. Four springs occur along the front or sides of the rock glacier (Fig. 2), while small ponds occur in some of the depressions between the main ridges on its surface.

Evidence of movement consists of split trunks of live trees (Fig. 4), the presence of fresh collapse structures along the front of the rock glacier, the steep rock glacier front, and trees being pushed over (Fig. 3). The area experiences an estimated mean annual freezing index of about 2200 degree days and a mean annual thawing index of about 1300 degree days.

METHODS USED

A series of ground temperature cables, using YSI 44033 thermistors, were emplaced in access tubes drilled or dug into the push lobes and rock glacier (Fig. 2). Similar access tubes were used for moisture determinations with a neutron probe. The tubes in the push-lobe were up to 2.9 m deep, while those in the rock glacier were dug 0.60-2.10 m into the ground using pits. The thickness of the thawed layer was noted and samples of the interstitial ice at various depths were obtained for tritium and ^{18}O analysis. Samples of both rain and snow were collected at different times during the year for comparison with these ice samples.

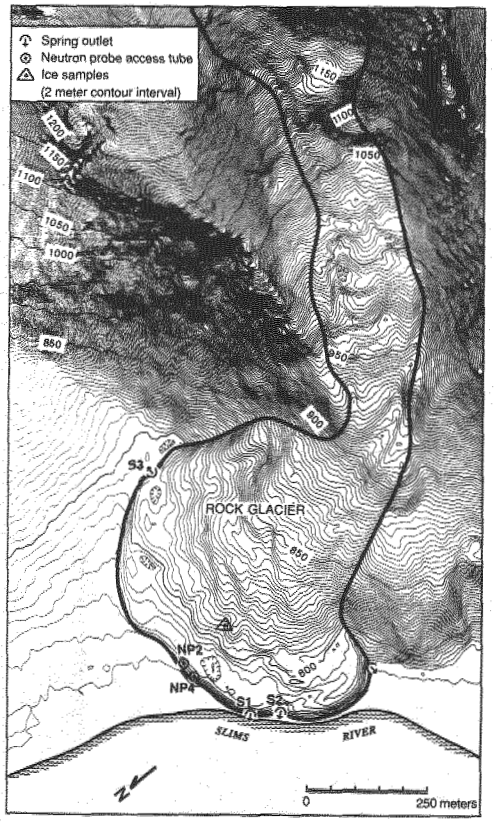

Fig. 2 Contour Map (2 m Intervals) of the Rock Glacier Showing the Location of Springs and Access Tubes on and Around the Rock Glacier Front.

Regular water sampling of the springs was carried out throughout the summer, while detailed sampling studies were made of individual springs for 24 hours. V-notch weirs were used for determining the rate of flow both diurnally and seasonally. Standard precipitation gauges permitted the measurement of rainfall, while a hygrothermograph was installed in a Stevenson screen on site to determine the air temperature between May and August (inclusive).

Finally, a detailed survey grid was laid out around the front of the rock glacier and in a band up the middle of the lobe, and tied in to bench marks located outside the rock glacier. This was resurveyed at yearly intervals. In addition, a levelling survey was run up the length of the rock glacier to establish the elevation of control points that could be identified on the aerial photographs. The latter were then used with a Wild AC-1 Analytical Plotter (1 μ precision) to produce the requisite grid matrix of elevation data. The contour map of the rock glacier with contours at 2 m intervals (Fig. 2) was then

generated using the computer graphics software available on DISSPLA V.10.

Fig. 3 Push-Lobe in Silts Containing Permafrost in Front of the Rock Glacier (Photograph by S. A. Harris).

RESULTS

1. Topography

Figure 2 shows the topography of the rock glacier based on photogrammetric contouring. The depressions and ridges show up clearly on its surface, as does the fan-shaped form of the rock glacier as it spreads across the valley floor. The appearance of the rock glacier from its source is shown in Figure 5.

2. Movement

Figure 6 shows the amount of movement of the rock glacier based on the surveys of the network points from 1984 to 1986. Movement of the front varies from almost 20 cm/a to almost 0 cm/a and clearly it moves in a series of lobes. Far greater rates of movement are found in the central portion of the lower rock glacier with maximum rates exceeding 200 cm/a. This difference presumably explains the formation of the oversteepened front of the rock glacier.

The vectors of movement show that overall movement is much more complicated than would be predicted on the basis of a few isolated observations. The survival of the loess as a discrete layer on the surface of the rock

Fig. 4 Split Trunk of a Tree on Rock Glacier Surface (Photograph by S. A. Harris).

Fig. 5 View Down the Length of the Rock Glacier (Photograph by W. Blumstengel).

glacier, together with the presence of straight, mature spruce trees, appears to indicate that the surfaces of the lower lobes are moving as a sheet without turbulence.

3. Thermal Regime

In front of the rock glacier, the push-lobe exhibits permafrost below 1.25 m with the active layer reaching equilibrium with its environment within a year after drilling. The snow tends to blow off the push-lobe in winter, hence the development of permafrost. On the surface of the rock glacier, ice was encountered at 0.6 - 2.0m in August during the original pit-digging. Although the access tubes were dug into slots in the side of the pits and care was taken to replace the moss cover, the permafrost was only returning slowly into the lower layers of the pits three years later.

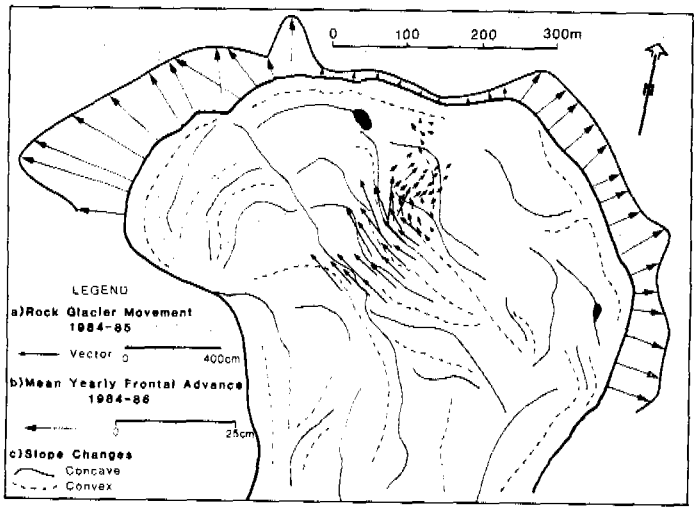

Fig. 6 Rates of Movement of Different Parts of the Lower Portion of the Rock Glacier (length of arrows being proportional to distance moved).

4. Moisture Regime

Ice was encountered in all the pits dug in the rock glacier, and was of sufficient quantity to hold the individual clasts apart. The grain size of the ice crystals was up to 5 mm diameter, and the size of the mineral clasts decreased with depth. Although ponds occasionally occurred in the closed depressions on the rock glacier surface, perched water tables over ice were not usually encountered in the pits, which were always located on the ridges.

Detailed studies show that there is a movement of moisture within the permafrost of the push-lobe (Blumstengel, 1988; Harris, 1988), and there are signs that moisture is returning to the lower levels of the refilled pits in the surface of the rock glacier, and is being added to as refreezing and seasonal temperature changes occur. However, the evidence for this is still being accumulated.

5. Hydrology of the Springs

Figure 2 shows the location of springs 1-3. Figure 7 shows the discharge for springs 1 and 2, which is also representative of spring 3. The temperature of the spring water was consistently below 1°C and the discharge showed no diurnal fluctuations.

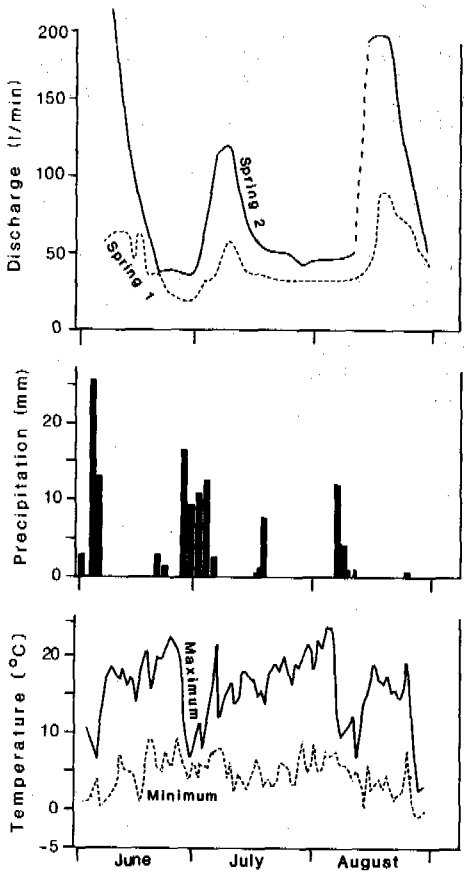

Fig. 7 Discharge of Springs 1 and 2 in Summer 1984, as Related to Air Temperature and Precipitation.

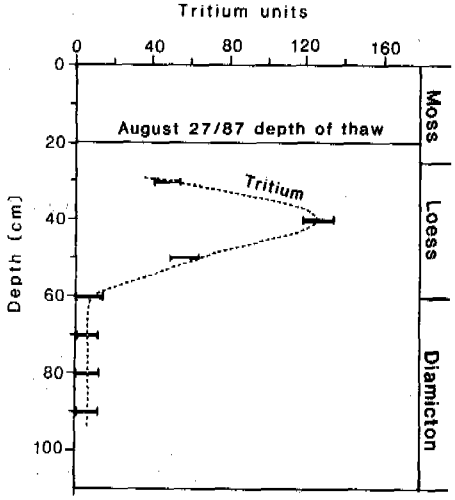

Fig. 8 Tritium Distribution in the Upper Layer of the Permafrost in 1985.

Springs 1 and 2 at the front of the rock glacier also exhibited increased discharge about 10 days after a major precipitation event. This suggests that the water comes from ice melting in the active layer, augmented by precipitation, i.e. it is coming from above the permafrost table, not underneath (cf. Haeberli, 1985). The delay represents the through-flow velocity.

6. Tritium Distribution

Figure 8 shows the changes in tritium content within the ice in the permafrost within the upper layers of the rock glacier. A pronounced peak occurs about 15-20 cm below the thawing front in August, which approximates the base of the active layer. This suggests that the permafrost table has moved upwards 15-20 cm since 1953, i.e., there has been a cooling of the area since then. There is no reason to think that this is due either to loess accumulation or to growth of moss.

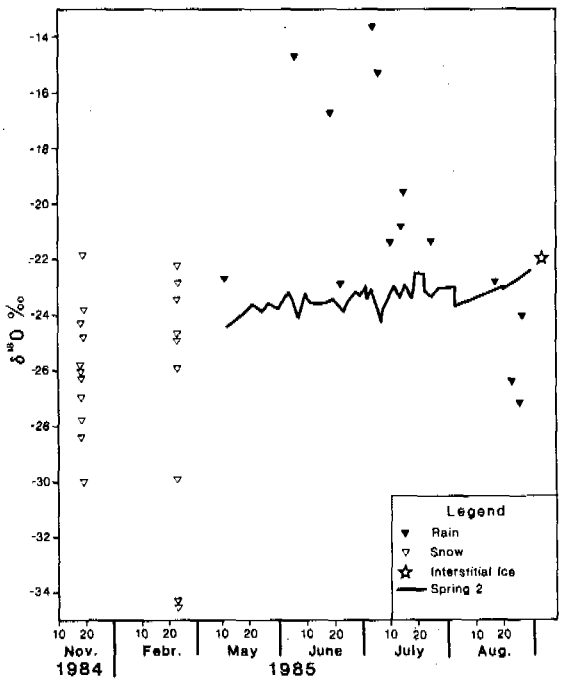

Fig. 9 ^{18}O in Precipitation and in Spring Water in Summer and Winter Compared With Interstitial Ice from the Rock Glacier. N.B.: The interstitial ice value was the average of 7 samples from 4 sites.

7. ^{18}O Distribution

Figure 9 shows the ^{18}O distribution in precipitation, in interstitial ice at the base of 4 pits in the permafrost on the rock glacier, and in spring #2. The ice from the rock glacier gave an average δ value of -21.9 0/00 and the isotopic composition of spring 2 tends to change to this value as the summer progresses. Similar trends were seen in springs 1 and 3. This suggests that the interstitial ice is modern.

DISCUSSION AND CONCLUSIONS

The front of the rock glacier is advancing at different rates ranging up to 20 cm/a. On the rock glacier surface, the direction and amount of movement vary considerably but may be >200 cm/a.

The tritium composition of the ice suggests 15-20 cm upward movement of the permafrost table into the active layer since 1953, resulting in a tritium peak preserved in the interstitial ice. The ^{18}O results for the interstitial ice approximate the mean of the ^{18}O values for winter snow and summer rains, i.e., the ice appears to be modern. The spring water is consistently cold and appears to result from thawing of the ice in the active layer during the summer, augmented by summer rains. It comes from the surface of the rock glacier and shows no signs of ^{18}O depletion that would indicate colder conditions, i.e. old glacial ice.

The modern composition of the interstitial ice suggests continued input into the permafrost from present-day precipitation via the active layer under the influence of temperature gradients (Harlan, 1974; Burn, 1986; Harris, 1986, p. 28), as is occurring today in the push-lobe (Harris, 1988). When the build-up is sufficient to prevent contact of individual clastic grains, the mass commences to flow by creep of the interstitial ice.

ACKNOWLEDGEMENTS

Parks Canada are thanked for logistical and financial help. The field work was funded by NSERC grant #A7483 and by Northern Scientific Training grants.

REFERENCES

Barsch, D. (1977). Nature and importance of mass-wasting by rock glaciers in alpine permafrost environments. Earth Surface Processes, vol. 2, pp. 231-245.

Benedict, J.B. (1973). Origin of rock glaciers. Jour. Glaciology 12(66):520-522.

Blumstengel, W. (1988). Lobate rock glacier study, east side, Slims River valley, St. Elias Range. Unpublished M.Sc. thesis, Department of Geography, University of Calgary.

Burn, C.R. (1986). The origin of aggradational ice. Unpublished Ph.D. thesis, Ottawa-Carleton Centre for Geoscience Study, Carleton University, Ottawa, Ontario.

Capps, S.R. (1910). Rock glaciers in Alaska. Journal of Geology 18:359-375.

Cross, C.W., Howe, E. & Ransome, F.L. (1905). Description of the Silverton Quadrangle. U.S. Geol. Surv., Geological Atlas of the United States, Silverton Folio, 120, 34 p.

Denton, G.H. & Stuiver, M. (1966). Late Pleistocene glacial stratigraphy and chronology, northeastern St. Elias Mountains, Yukon Territory, Canada. Geol. Soc. Amer. Bull. 78:485-510.

Giardino, J.R. (1983). Movement of ice-cemented rock glaciers by hydrostatic pressure: an example from Mount Mestas, Colorado. Zeitschrift für Geomorphologie, N.F. 27:297-310.

Gorbunov, A.P. (1983). Rock glaciers of the mountains of Middle Asia. In: Permafrost: Fourth International Conference, Proceedings, National Academy Press, Washington. 1524 p., pp. 359-362.

Haeberli, W. (1985). Creep of mountain permafrost: Internal structure and flow of alpine rock glaciers. Mitteilungen der Versuchsanstalt für Wasserbau, Hydrologie und Glaciologie, #77, Zürich. 142 p.

Harlan, R.L. (1974). Dynamics of water movement in permafrost: A review. In: Permafrost Hydrology. Proceedings of a workshop seminar, Ottawa. Environment Canada, pp. 67-77.

Harris, S.A. (1981c). Distribution of active glaciers and rock glaciers compared to the distribution of permafrost landforms, based on freezing and thawing indices. Can. J. Earth Sci. 18:376-381.

Harris, S.A. (1986). The permafrost environment. Totowa, N.J.: Barnes & Noble. 276 p.

Harris, S.A. (1988). Observations on the redistribution of moisture in the active layer and permafrost. Proc. 5th Int. Permafrost Conf., Trondheim.

Höllerman, P. (1983). Blockgletscher als Mesoformen der periglazialstufe. Bonner Geographische Abhandlungen, vol. 67. 73 p. Fred. Dümmlers Verlag, Bonn.

Johnson, P.G. (1978b). Rock glacier types and their draimage systems, Grizzly Creek, Yukon Territory. Can. J. Earth Sci. 15: 1496-1507.

Johnson, P.G. (1980). Glacier-rock glacier transition in the southwest Yukon Territory, Canada. Arctic and Alpine Research, 12:195-204.

Kesseli, J.E. (1941). Rock streams in the Sierra Nevada, California. Geog. Review 31:203-227.

Nickling, W.G. (1978). Eolian sediment transport during dust storms: Slims River Valley-Yukon Territory. Can. J. Earth Sci. 15: 1069-1084.

Outcalt, S.I. & Benedict, J.B. (1965). Photo interpretation of two types of rock glaciers in the Colorado Front Range. Jour. Glaciology 5(42):849-856.

Vernon, P. & Hughes, O.L. (1966). Surficial geology, Dawson, Larsen Creek, and Nash Creek map-areas, Yukon Territory. Geol. Surv. of Canada Bull. 136. 25 p.

Wahrhaftig, C. & Cox, A. (1959). Rock glaciers in the Alaska Range. Bull. Geol. Soc. Amer. 70:383-436.

Washburn, A.L. (1979). Geocryology. E. Arnold, London. 406 p.

Whalley, W.B. (1985). Models of rock glacier formation and movement. In: 1na Acta Geocriogenica, Instituto Argentino de Nivologia y Glaciologia, pp. 122-123.

GENERAL MOISTENING OF THE AREA AND INTENSITY OF CRYOGENIC PROCESSES

N.P. Bosikov

Permafrost Institute, Siberian Branch of the U.S.S.R.
Academy of Science, Yakutsk, U.S.S.R.

SYNOPSIS Based on an integrated approach to the study of alas landscapes the dependence of the intensity of cryogenic processes on general moistening of the area is demonstrated. It is found that an intensification of thermal abrasion on the shores of alas lakes as well as thermokarst processes within inter-alas areas occurs in the years with increased moistening. In dry years cryogenic processes decrease in intensity.

One of the challenging problems of dynamical geography is that of studying present-day relief-forming exogenic processes. When investigating these processes, it is important to establish the cyclicity of their manifestations. Data of this kind provide the basis for developing protection measures against destruction phenomena and for their prediction.

The expanses between rivers of Central Yakutia are notable for wide-scale occurrence of alas depressions, whose bottoms show drying or totally dried lakes. These depressions evolve through a number of stages, from the elementary form of a dyuyodya to a mature alas depression with a drying lake. The development of alas depressions is not restricted to a simple transition from one form to another but is of a more complicated cyclic character.

Natural field observations have shown that the development of some or other cryogenic processes on alas terrains is determined by the water content of an alas depression (Bosikov, 1976) which can be represented as the ratio of the water volume to the volume of the entire alas depression. Alas lakes with decaying shores over the area under study generally has a water content of 0.6 and higher. It is such water-rich alasses that merge together forming huge alasses of a composite shape as a result of the washing-out of dams separating them. As alas lakes are drying out, the talik below the alas is freezing. This process is not infrequently accompanied by a growth of pingo, and other cryogenic processes (Solovyev, 1952).

Following A.V. Shnitnikov's (1957) views of the role of the fluctuation of climate in the variability of the state of a lake, the present author examines evidence concerning the present state of alas lakes and their time variations.

In an attempt to gain insights into the intensity of development of cryogenic processes in disturbed and undisturbed areas of the terrain between alasses, we have carried out semi-permanent observations of the development of thermokarst lakes on the terrain between the Lena and the Amga in the vicinity of the Yukechi alas.

As far as geomorphology is concerned, according to a schematic map compiled by M.S. Ivanov (1984), the region of interest is situated within the confines of the erosive-accumulative Abalakhskaya plain. Areas between alasses have small inclination angles toward the lower-lying geomorphological level.

The upper horizon of a thickness of up to 40--60 m presents brownish-grey loessial suglinoks involving cryogenic structures in the form of ice lenses and small ice layers as well as very old syngenetic wedge ice. According to the depth of the alas depression (11 m), the thickness of wedge ice is about 12 to 15 m and, according to calculations from the volume of the alas depression, about 2.6 m^3 of ice corresponds to 1 m^2 of the area (Tolstikov and Bosikov, 1976). The occurrence depth of the ice vein surface varies in the range 1.5 to 2.0 m. On abandoned arable land the upper end of wedge ice frequently coincides with the depth of seasonal thawing.

As regards the degree of surface susceptibility to technogenic effects, the Yukechi testing area pertains to high-susceptibility regions (Bosikov et al., 1985). Such complexes are notable for quiet substantial changes in their structure, including the formation of new natural-territorial complexes. Processes caused by the thawing-out of ice-containing soils, once disturbed, are distinguished by activity, and are progressing and sometimes disastrous in their character of development. On the terrain between the alasses, there is a continuous cover of larch forest with motley grass and cowberries distinguished by good growth and dense stand. The height of the upper layer is about 20 m; however, trees are also encountered as tall as 25 to 27 m. At 2 m height mature trees are as thick as 30 to 40 cm in diameter. The closeness of the crowns fluctuates between

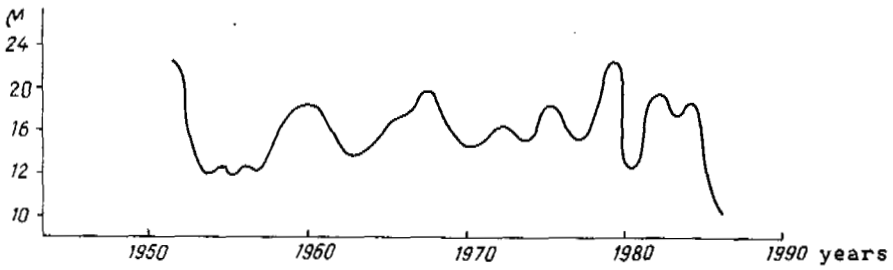

Fig.2 Plot of General Moistening Variation of the Area for the Yakutsk Station. The Plot is Constructed Following A.V.Shnitnikov's (1957) technique.

formation and growth of thermokarst lakes. On many occasions, the lakes undergo a reduction in size. During the years indicated, there, probably, occurred a reduction in the size of dyuyordya situated in the forest.

Earlier and later in the 1960's, there were years with increased moistening, while in the year 1967 the alas lakes of the area between the Lena and Amga rivers showed an abrupt increase of the water level (Bosikov, 1977). These years witnessed an increase in size of the dyuyordya indicated above on the Yukechi testing ground.

According to information received from local inhabitants, dyuyodya on ploughed fields "K" and " Ж " originated in the 60s, which also coincides with the years of increased moistening of the area.

In 1975, places of origination of dyuyodya "Д", "Т", " У " and " Ф " were complicated by a hillocky terrain, with the subsidence of the area by about 0.5 to 0.7 m from the surface of the terrain between the alasses. During the first years of the observation, melt water on these depressions remained stagnant as late as mid-July. From 1981 on, the melt water accumulated on undrained-off areas was leading to the appearance of small lakes.

It is known that the appearance of water on low-lying terrains leads to an increase in temperature of the soil surface of the water reservoir bottom. Below small polygonal lakes and small trenches filled with water, the depth of seasonal thawing increases abruptly. In this case, as the water layer in such shallow reservoirs increases, there also is an increase of the depth of seasonal thawing below it. The thawing below shallow water reservoirs is one and a half to two times that in dry polygonal features (Vasilyev, 1982).

The increase in general moistening of the area in 1981 led to the formation of small interpolygonal lakes on ploughed fields as well as an increase of the water level in pre-existing dyuyordya on the Yukechi testing ground. As has already been mentioned previously, on ploughed fields the depth of seasonal thawing almost coincides with the depth of ground ice (1.7 m). Therefore, in the case of an abrupt increase of the depth of seasonal thawing the thawing-out of ground ice leads to an increase in depth of the small lake. This all is responsible for the progressive development of thermokarst (Obshchee merzlotovedenie, 1978).

The further evolution of thermokarst lakes depends on the lake's depth. If before the winter freezing-over the depth of water in the lake is more than 1 m, then the progressive development of thermokarst goes on. In the case where ice freezes to the bottom, the further development of thermokarst depends on the weather conditions of the next year, i.e., on moistening. Under conditions of Central Yakutia, with an increase in the depth of seasonal thawing due to the rise in air temperature, no thermokarst lakes are produced because the water produced owing to the thawing-out of upper parts of ground ice dries up due to the moisture deficit. An increase in thickness of unfrozen deposits leads to an increase of the protecting layer below ground ice. Hence, it is evident that the increase in moistening of the area is the most important condition for the development of thermokarst.

The results of natural-scale observations of the development of thermokarst processes on the Yukechin testing ground are presented in the table. From the table it is apparent that origination and development of small thermokarst lakes on ploughed fields are proceeding much more intensive as compared with undisturbed terrains between the alasses. Thus, no new small thermokarst lakes originated on undisturbed terrains during the observing period, whereas seven small lakes appeared on ploughed fields (see Figs 1 and 3). The natural-scale observations have shown that the depression cuts in the forest and on the ploughed fields exhibit an almost the same growth. The deepest cut of lakes "A"and "X" is accounted for by their long lifetimes. The mean amount of expansion which characterizes the increase of the small lakes in plan, is several times greater as compared with undisturbed areas between the alasses. The relatively small expansion of dyuyodya "K" (9.6 m) is attributable to the limited size of the ploughed field itself. Where the size of the ploughed field and the drainage conditions are favourable, the rate of ex-

0.5 and 0.8 and sometimes reaches 0.9. The soil cover consists of cowberries. The association involves birch-trees, with pine-trees growing along the alas edge. On the area under investigation no traces of fires are observed. Cleared spaces are encountered which are produced by felling of some groups of trees.

Regular observations of the development and growth of thermokarsk subsidences were made during the period 1975-1985 using as well verbal communications of local inhabitants and an aerial photograph taken in 1952.

Fig. 1 is a schematic map of the Yukechi tes-

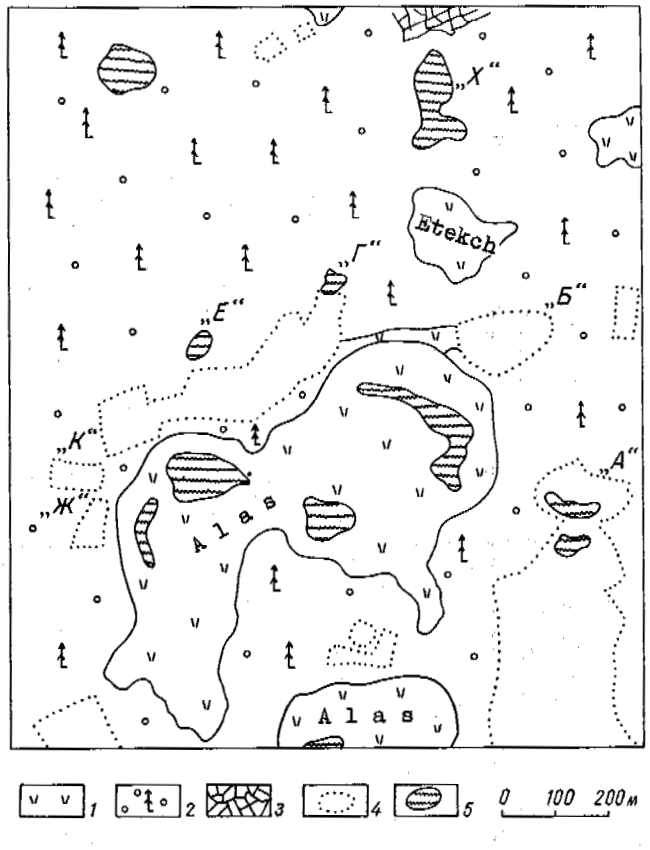

Fig. 1 Schematic Map for the Relative Position of Arable Lands and Permafrost Terrain Forms on the Yukechi Testing Ground in 1952.
1 - Waterless Valley-Meadows; 2 - Motley Grass - Cowberries Larch Forest; 3 - Hillocky Terrain; 4 - Arable Lands; 5 - Water Reservoirs.

ting ground as compiled using an aerial photograph. The schematic map shows that the arable lands are all not affected by thermokarst. According to information received from local inhabitants, the grubbing-out of the forest for estate "A" was accomplished during about 1870-1880. In 1935, the undrained area of the estate produced a small lake of the size about 20x30 m. According to the aerial photograph of the year 1952, the forest exhibits two cave-in lakes, which indicates a progressive growth of small thermokarst lakes on the terrain between the alasses.

According to information received from local inhabitants, the lake denoted on the map by letter "X" formed by about 1922 as a "dyuyodya" (the local name of the early stage of development of a thermokarst lake with a stable water regime, below which ground ice still persists). In 1975, the lake already was in a stage of "tyympa" (a thermokarst lake below which ground ice has thawed out completely, with the formation of a stable talik below the lake. The depression's water content is 0.6). Small lakes "Е" and "Г" situated in the forest near the northern arable land, evolved into a "dyuyodya" in 1933.

In 1939, the arable lands depicted on the schematic map consisted of separate, small ploughed fields, with forest stripes remaining in between. In order to obtain two large ploughed fields, these stripes were grubbed out in 1950. The ploughed fields were sown with grain-crops as late as 1960. As a result of amalgamation of collective farms into bigger units, the ploughed fields were abandoned. The fields are slowly overgrown with forest - over the past 30 years only separate specimens of trees have appeared.

According to information received from local inhabitants, intense surface failure began on the ploughed fields in 1960. During the second year after the fields had been abandoned, a well-defined hillocky terrain already made appearance. Approximately in the late sixties, a thermokarst lake was produced in an undrained area on ploughed field "Б". By the beginning of regular observations (the year 1975), the lake increased to 20x40 m in size, and the water depth was between 0.6 and 1.2 m. In 1975, the size of "tyympa" "Х" did not differ substantially from those obtained from the aerial photograph of 1952. In 1975, the maximum depth of the depression cut was about 6.0 m (see Fig. 1). Dyuyodya "Г" and "Е" also remained unaltered during the period 1952-1975.

During 1952 to 1957, the area between the Lena and the Amga rivers underwent a decrease in its general moistening (Fig. 2), while the preceding period included years with increased moistening. Because the original size and growth of thermokarst lakes are most closely associated with general moistening of the area (Bosikov, 1986), it might be supposed that the lakes observed originated and slightly expanded in the years with increased moistening. Subsequently, in the years of decreased moistening of the area (1952-1957) there seems to have occurred a reduction in size of the dyuyodya because at this stage of development the thermokarst had not yet reached the degree of self-evolution due to an intense thawing of ground ice. In the years with decreased moistening, i.e., in dry years, the amount of water evaporated from Central Yakutia lakes is two to four times the amount of precipitation (Gavrilova, 1973). Therefore, during dry years melt water evaporates rapidly, with the cessation of the

TABLE

The Amount of Expansion of Water Reservoirs as Deduced from Natural Observation Data, m

Dyuyodya symbol	1976	1978	YEARS 1980	1981	1982	1985	Total depth of the cut	Averaged value of expansion for 10 years
"A"	0.59	1.3	4.25	3.84	1.85	1.18	5.6	13.0
"Б"	2.0	4.5	10.0	12.25	9.25	10.0	3.04	48.0
"Х"	0.4	0	0.73	0.15	0	1.3	6.3	2.6
"Г"	1.64	0.65	3.56	6.58	0.83	1.61	3.46	14.8
"Е"	0.56	0.62	1.36	1.35	1.65	2.5	3.24	8.0
"К"	1.2	0.5	2.56	2.6	1.5	1.2	3.6	9.6

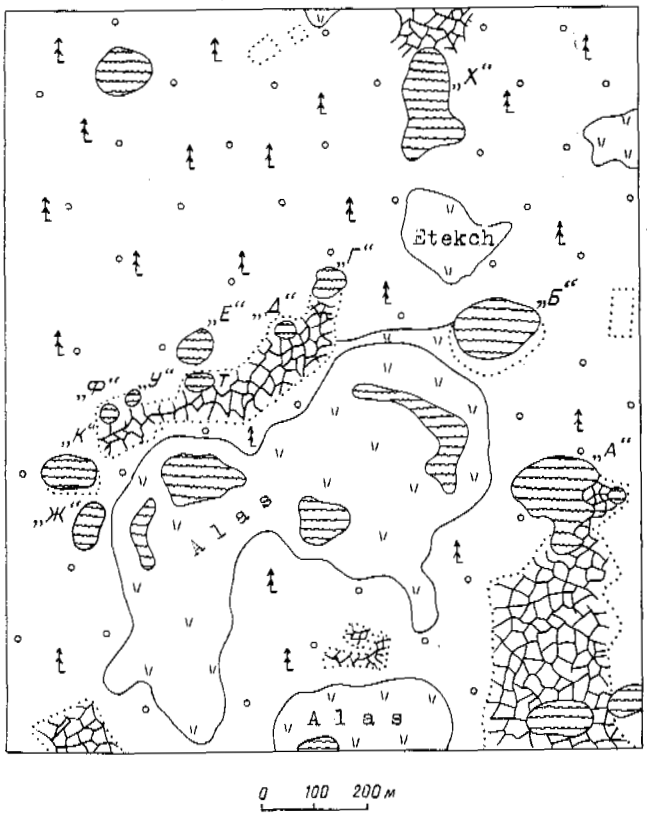

Fig.3 Schematic Map for the Relative Position of Ploughed Fields and Permafrost Terrain Forms on the Yukechi Testing Ground in 1985. For Legend See Fig. 1.

pansion of the small thermokarst lake is very high (dyuyodya "Б" - 48 m).

Comparison of the plot of general moistening of the area with the table giving the expansion values for water reservoirs as deduced from natural observations reveals that both the origination and the most intensive expansion of thermokarst lakes coincide with the years of increased moistening of the area.

Based on the statement that fluctuations of the level of alas lakes depend on the degree of moistening, we attempted - through a reconstruction of these fluctuations - to obtain the course of development of moistening of the area. The analysis of archives, literature and verbal evidence has permitted us to identify - from the end of the 17th century on - several periods in the level fluctuation of the lakes within Central Yakutia: the end of the 17th century - low water-level; mid-18th century - high water-level; beginning of the 19th century - low water-level; mid-19th and beginning of the 20th century - high water-level; and mid-20th century - low water-level (Bosikov, 1977).

Using dendrological determinations we have examined typical features of the water-content fluctuations of alas lakes in Central Yakutia for a period of 160 years (from 1813 to 1973) (Bosikov and Lovelius, 1979). The analysis of data obtained showed that the fluctuations of the level of alas lakes obey secular tendencies and intrasecular cycles. We identified cycles of an increase of the level of lakes, of a duration of 10 to 12 years, on the average.

A comprehensive study of bottom deposits of alas lakes, including radiocarbon datings, permitted us to construct plots of moistening variation of the area between the Lena and the Amga rivers for the last three millenia (Bosikov, 1986) (Fig. 4).

The results of continuous and one-time observations of the formation of the beds of thermokarst lakes and alas water reservoirs have indicated that bottom sediments are composed by products of shore failure (Bosikov, 1983). In high-water depressions the shores are being destroyed very intensively. It has also been established that the rate of intensity of sediment accumulation depends on the composition and ice content of the soils forming the shore as well as the water level in the depression, i.e., on the state of general moistening of the area.

Thus, the character of moistening of the area is responsible for the decay or the development

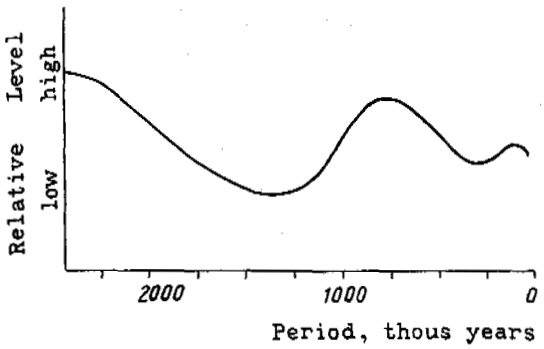

Fig.4 The General Moistening Variation of the Area between the Lena and the Amga Rivers during the Last Three Millenia.

of the thermokarst process in Central Yakutia.

REFERENCES

Bosikov, N.P. (1976). Primer morfometricheskoi kharakteristiki alasnykh obrazovaniy Tsentralnoi Yakutii. - V kn.: Voprosy geografii v trudakh molodykh uchenykh i spetsialistov, 44-49, Yakutsk: In-t merzlotovedeniya SO AN SSSR.

Bosikov, N.P. (1977). Dinamika urovnei i razvitie alasnykh ozyor Tsentralnoi Yakutii, t. 109, vyp. 4, 357-362, Izv. VGO.

Bosikov, N.P. and Lovelius, N.V. (1979). O dendroindikatsii kolebaniy urovnya alasnykh ozyor Tsentralnoi Yakutii. Izv. VGO, t. III, vyp. 1, 64-66.

Bosikov, N.P. (1983). Stratifikatsiya donnykh otlozheniy alasnykh ozyor Tsentralnoi Yakutii, 3-12, Yakutsk: YaF SO AN SSSR.

Bosikov, N.P., Vasilyev, I.S and Fedorov, A.N. (1985). Merzlotnye landshafty zony osvoeniya Leno-Aldanskogo mezhaurechya, 124 p., Yakutsk: In-t merzlotovedeniya SO AN SSSR.

Bosikov, N.P. (1986). Alasy kak indikatory uvlazhnyonnosti territorii. - V kn.: Gidrologicheskie issledovaniya landshaftov, 80-85, Novosibirsk: Nauka.

Vasilyev, I.S. (1982). Zakonomernosti sezonnogo protaivaniya gruntov v Vostochnoi Yakutii, 133 p., Novosibirsk: Nauka.

Gavrilova, M.K. (1973). Klimat Tsentralnoi Yakutii, 120 p., Yakutsk: Kn. izd.

Ivanov, M.S. (1984). Kriogennoe stroenie chetvertichnykh otlozheniy Leno-Aldanskoi vpadiny, 125 p., Novosibirsk: Nauka.

Obshchee merzlotovedenie (ed. by V.A.Kudryavtsev). (1978). 463 p., Moscow: Izd. MGU.

Shnitnikov, A.V. (1957). Izmenchivost obshchei uvlazhnyonnosti materikov severnogo polushariya. Zap. GO SSSR, nov.ser., t. 16, 347 p.

Solovyev, P.A. (1952). Bulgunnyakhi Tsentralnoi Yakutii. - V kn.: Issledovaniya vechnoi merzloty v Yakutskoi respublike, vyp. 3, 226-258, Moscow: Izd. AN SSSR.

Tolstyakov, D.N. and Bosikov, N.P. (1976). K voprosu rascheta kolichestva podzemnogo l'da v rayonakh rasprostraneniya termokarstovykh kotlovin. - V kn.: Voprosy geokriologii v trudakh molodykh uchenykh i spetsialistov, 126-141, Yakutsk: In-t merzlotovedeniya SO AN SSSR.

THERMOKARST LAKES AT MAYO, YUKON TERRITORY, CANADA

C.R. Burn and M.W. Smith

Geotechnical Science Laboratories, Carleton University, Ottawa, K1S 5B6, Canada

SYNOPSIS The evolution of thermokarst lakes in ice-rich glaciolacustrine sediments near Mayo, Yukon Territory, has been documented through examination of aerial photographs, field surveys and analysis of the annual growth rings of submerged trees. In addition, the thermal regime of a typical lake has been studied, and a geothermal simulation analysis of lake development carried out. The tree-ring analysis indicates that the lakes were initiated around 1880. The geothermal simulation analysis of talik development also indicates that the lakes are about 100 years old. It is suggested that the lakes were initiated by forest fire. The growth of three lakes has been relatively constant since 1949, and shows little correlation with climatic variations. Careful observation of lake development over the next 10 to 20 years could yield information on growth patterns as a function of climatic changes.

IN MEMORIAM

Michael J. Hare
17 May 1960 - 16 January 1988
Field companion, colleague and friend.

INTRODUCTION

Investigations have been made of the evolution of thermokarst lakes in the Stewart River valley, near Mayo, Yukon Territory (Figure 1). Mayo (63° 35'N, 135° 35'W), which has a mean annual air temperature of -4°C, lies in the northern boreal forest and the zone of widespread permafrost. Within the study area there are 28 thermokarst lakes and two major thaw slumps. These features are confined to ice-rich glaciolacustrine silty clay, deposited beneath a proglacial lake which filled Stewart Valley eastwards for 48 km from an ice dam just west of Mayo (Green, 1971). Throughout the valley, much of this material has been eroded to depth and replaced with river alluvium.

Exposures in the headwalls of the thaw slides reveal large bodies of segregated and reticulate vein ice, which extend to a depth of at least 12 metres. In addition, truncated, inactive ice wedges are exposed along a thaw unconformity (see Burn et al., 1986). Numerous boreholes, 5 m deep, have been drilled around the thaw lakes, and have all revealed ice-rich material (Burn, 1982a).

Thermokarst and climatic change

Thermokarst develops where an increase in the depth of thaw results in the melting of shallow ground ice and the formation of a depression. Once created, the depression establishes a new thermal regime which further promotes its

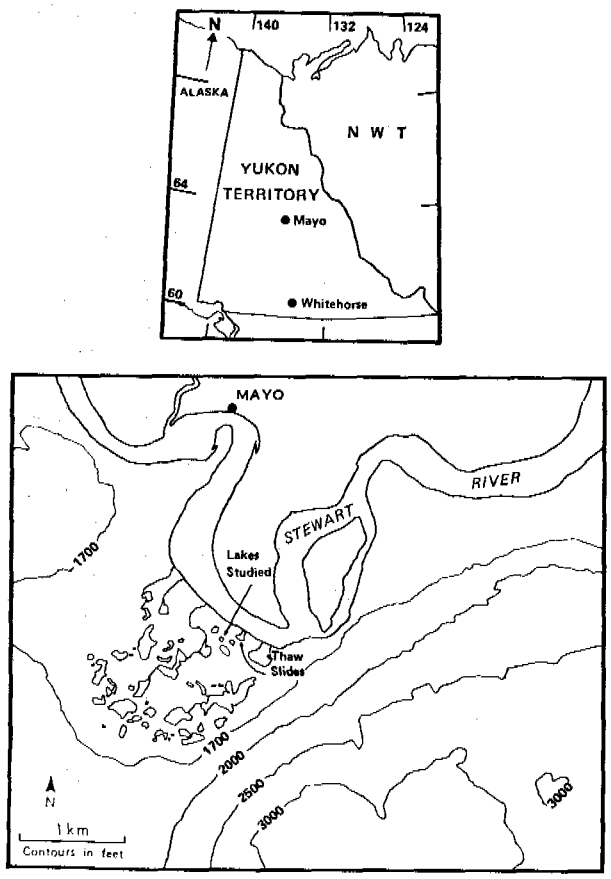

Fig. 1. Location of study sites.

development (Mackay, 1970). Either a change in climate or of surface conditions (microclimate) is responsible for thermokarst initiation. Regional climatic change includes amelioration, resulting in a rise in mean annual surface temperature, or an increase in the seasonal amplitude of temperature. The northern hemisphere experienced a warming in 1850-1950, which has been suggested as the principal cause of permafrost degradation in some areas (e.g. Thie, 1974; Mackay, 1975; Chatwin, 1981). Throughout much of the 100,000 km^2 of northernmost Alaska, the temperature in the upper two metres of permafrost has generally increased by 2°C or more during the last several decades to a century (Lachenbruch and Marshall, 1986).

Carson (1968) and Rampton (1973) have hypothesised that thaw lakes in the western North American Arctic have expanded during periods of warmer climate. However, the short-term sensitivity of thaw lakes to climate change is not well understood. Careful observations of lakes over a 10 to 20-year period could yield important information on growth patterns as a function of climatic variation.

While the effects of climatic variations evolve over many years, changes in microclimate can be sudden and dramatic. Forest fires, for instance, are frequent and widespread in the north, and lead to fundamental alterations in the surface energy regime. As a result, Rouse (1976), for example, found that soil temperatures were as much as 5°C warmer in recently burned-over areas.

THERMOKARST LAKE DEVELOPMENT

The evolution of three particular thermokarst lakes near Mayo has been studied in detail from the aerial photographic record (1949-1976) and by field surveys (1982-1987). These lakes are of similar size, and were of approximately 100 m diameter in 1987. No surface channels connect with these lakes. As is typical of thermokarst lakes in the boreal forest, the collapsing shorelines support "drunken" trees, and the lakes contain many submerged trees which are well preserved. The annual growth rings of a number of these trees were analysed for dates of submergence.

The surface area of each lake at various times since 1949 was obtained from the aerial photographs. The development of individual lakes is somewhat idiosyncratic (Figure 2), due to ground ice distribution in the surrounding sediments, for instance. Therefore, index radii (r) were computed to describe the development of each lake, assuming the lake surface to be circular (Table 1). The rate of change in mean radius ($\Delta\bar{r}/t$) varies between 0.9 m yr^{-1} and 0.2 m yr^{-1} between successive dates, with a mean value of 0.41 m yr^{-1}. The mean rates of radial expansion for lakes 1, 2 and 3 between 1949 and 1987 are 0.36, 0.47 and 0.41 m yr^{-1} respectively.

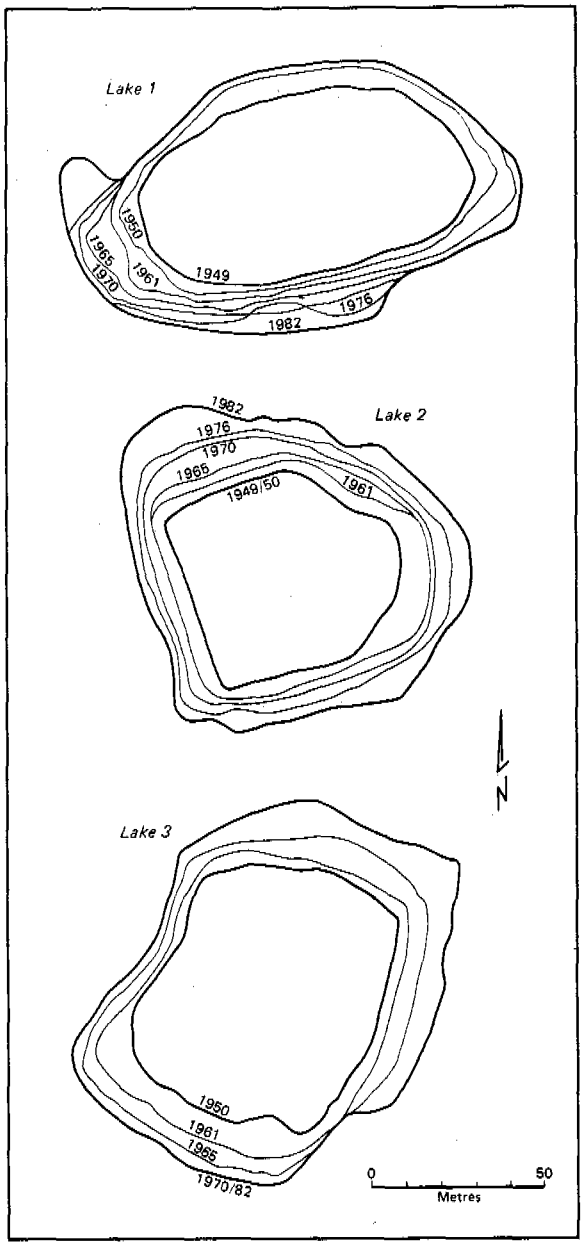

Fig. 2. Thermokarst lake expansion, 1949-1987.

During the period since 1949, mean annual and summer air temperatures in central Yukon declined until the early 1970s, which were the coolest years this century. Subsequently, a sharp recovery from these low temperatures has occurred, at a rate similar to the pre-1940s warming (see Burn, 1982b). The relatively rapid growth of the lakes in the 1960s, when climatic conditions were deteriorating, indicates that no simple relationship between lake development and climate exists. Apparently, the thermal buffering effect of the lake mitigates the influence of annual climatic variation.

TABLE 1

Index radii (m) 1949-1987 of three thermokarst lakes near Mayo.

Lake	1	2	3	Mean radius (m)	Rate of growth ($m\ yr^{-1}$)
Year	r	r	r	$\bar{r}$	$\Delta\bar{r}/t$
1949	36.4	30.7	36.8	34.6	-
1950	38.1	30.7	36.8	35.2	0.60
1961	40.0	35.7	41.6	39.1	0.35
1965	45.0	36.8	46.2	42.7	0.90
1970	46.1	39.9	51.2	45.7	0.60
1976	46.8	42.5	51.2	46.8	0.20
1982	48.4	47.2	51.2	48.9	0.35
1987	49.9	48.6	52.4	50.3	0.30
Mean rate of radial increment 1949-1987 ($m\ yr^{-1}$):					
	0.36	0.47	0.41		0.41

Simple backward extrapolation of the mean growth rate for each lake on the radius in 1949 gives dates of initiation for lakes 1, 2 and 3 of 1848, 1884 and 1859 respectively. To examine this further, the annual growth ring patterns of submerged trees were analysed.

Tree-ring analysis

In order to reconstruct lake development from the annnual ring records of submerged trees, it is assumed that the trees stopped growing when their roots became immersed, and that the last annual ring represents the date at which the lake expanded past that location. Trees whose roots were submerged during the summers between 1982 and 1986 did not bear green leaves the following year. Additionally, the roots provide an anchor, and no trees appear to have been displaced during and after submergence.

In order to fix the date of submergence, the unknown tree-ring chronologies had to be matched to a chronology with known fixed dates. Cross sections of trees were sawn off underwater and the locations of stumps were surveyed onto a base map. Six sections were obtained from lake 2 and three each from lakes 1 and 3 (Figure 3). The sections were each mounted on a travelling stage and the ring widths measured by microscope. Index series were developed using standardised methods (see Fritts, 1976).

Initially, samples were taken from some living trees on land, with which the submerged series could be cross-correlated and hence dated. However, suitably old trees contained too much reaction wood to be useful, as a result of unstable ground conditions due to shallow, ice-rich permafrost. Thus, instead, the ring-width series were cross-correlated with two trees which were known from aerial photographs to have been immersed between 1970 and 1976. This introduces a minor uncertainty of 6 years into the dating. The ring records of these trees date from 1824 and 1846.

In the cross-correlation procedure, the index series of each submerged tree was repeatedly lagged with respect to the stationary (reference) series. The Pearson product-moment correlation coefficients (r) obtained by this method may increase after several lags, since the number of values being correlated decreases as the lag increases. Three criteria were used to assess the significance of the coefficients:

(i) only the highest four values of any series were considered;

(ii) if any of these were less than 0.5, they were rejected;

(iii) any correlation involving less than ten pairs of observations was ignored.

The highest r values from cross-correlations with lag, and the inferred date of tree submergence are presented in Table 2. Of the trees dated by this procedure, there is only one clear anomaly, L1C. This tree may have fallen into the lake from a small thaw slide on the south side of the lake. The other results in Table 1 point to a date of initiation of shortly before 1880 for lakes 2 and 3 and 1900 for lake 1, since the trees were not taken precisely from

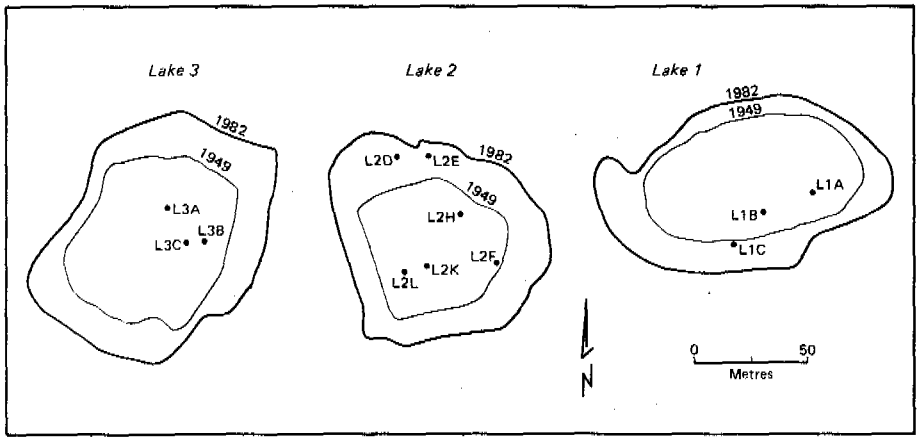

Fig. 3. Location of submerged trees collected for cross-dating.

TABLE 2

Submergence dates of trees in Mayo thermokarst lakes

Tree	Date	r*
L1A	1902	.71
L1B	1918	.81
L1C	1967	.84
L2F	1894	.53
L2H	1908	.75
L2K	1933	.70
L2L	1880	.86
L3A	1889	.90
L3B	1902	.74
L3C	1888	.77

* Correlation coefficient with reference series.

the centre of each lake. This is in reasonable agreement with the results from the previous section.

GEOTHERMAL ANALYSIS

Lake thermal regime

Temperatures in the thermokarst ponds were obtained using calibrated thermistor cables of various lengths at a number of locations. The cables were anchored to the bottom and suspended from floats. In addition, we were able to drive a thermistor cable 2m into the bottom of lake 2.

The monitoring of lake temperatures indicates that the ponds have similar thermal regimes and that they display some features that are common to many lakes. The lakes freeze over in mid-October and the ice melts again by mid-May. The ice thickness reaches about 1.25 m by late-March. As surface temperatures increase during the spring and summer months, a stratification develops between the colder, denser water at depth and warmer, lighter water near the surface. The thermocline is found near the lake bottom in spring, but rises to about 2 m below the surface or so by mid-summer. Below the thermocline, the bottom of the profile is characterised by a relatively steady decline of temperature with depth. This part of the lake is not directly affected by daily weather conditions.

The thermal regime of lake 2 was monitored on a monthly basis over the 12-month period beginning in April 1984, with bi-weekly observations in summer. The annual temperature envelope is shown in Figure 4. While the near-surface temperature varied between -1.4 and 20°C, the lake bottom (4.25 m) temperature varied between only about 2 and 5°C, with a mean value of 3.3C.

Heat conduction model

A simple heat conduction model was used to obtain a first approximation of talik development beneath an expanding circular pond assumed to have been initiated in 1880. Using lake 2 as a model, a constant rate of radial growth of 0.5 m yr^{-1} was assumed for the period 1880 to 1985, by which time the lake was actually just under 100 m in diameter.

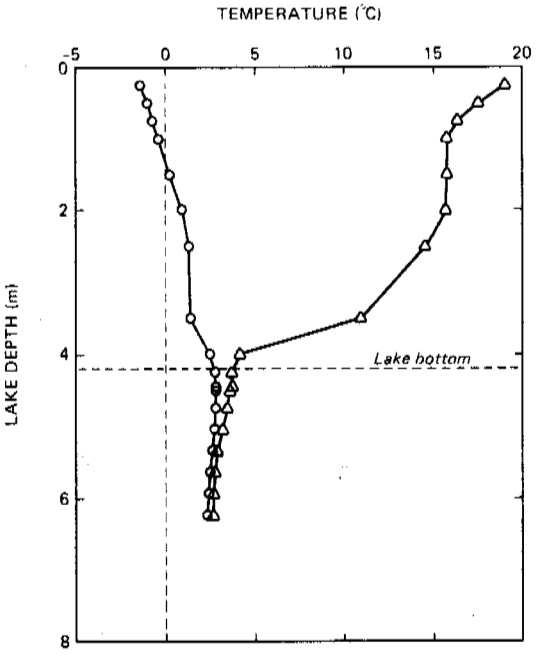

Fig. 4. Annual temperature envelope of lake 2.

With reference to mean annual conditions, the temperature profile in the vicinity of a lake is modified as follows:

$$T(x,y,z) = (To+Gg.z) + (Tw-To).\ f(x,y,z) \quad (1)$$

where the first term on the right-hand side represents the undisturbed temperature profile for the area, and the second term is the thermal disturbance due to the water body. To is the mean annual ground surface temperature, Tw the mean annual lake-bottom temperature, and z is depth. The geothermal gradient was taken as 0.02 K m^{-1} in the present case, although its effect is negligible for the small values of z in question here (see below).

The magnitude of the second term in (1) depends on the time, t, since the lake was initiated. In the case of a circular lake, of radius R, the thermal disturbance beneath the centre can be calculated from (Lachenbruch, 1957):

$$f(z,t) = (Tw - To)\ \{\ (1/\sqrt{(1+(R/z)^2)})\ \mathrm{erfc}(\sqrt{(z^2+R^2)}/2\sqrt{Kt})\ \} \quad (2)$$

where K is the thermal diffusivity of the ground. In order to account for the predominant effects of latent heat on the penetration of the thawing front, an apparent thermal diffusivity value (8.8×10^{-9} m^2 s^{-1}) was used (see Smith and Riseborough, 1985). The mean annual lake-bottom temperature of 3.3°C recorded in lake 2 was used. The mean annual surface temperature of the land surrounding the lakes was estimated from shallow borehole data to be about -1°C (Burn, 1986).

In geothermal terms, the growth of a lake can be represented by a sequence of annular-shaped disturbances, whose age decreases with distance

from the centre. By summing the contribution from all the annular rings, the evolving thermal effect of an expanding lake can be simulated (Lachenbruch, 1957; Smith, 1976). No allowance was made in the analysis for ground settlement.

Figure 5 shows the temperature profile predicted from the simulation; the depth of the talik is estimated at about 9 m. The extremely close agreement with the measured lake-bottom temperatures supports the interpretation of lake evolution represented by the simulation. The conclusion of the simplified thermal analysis is that the thermokarst ponds at Mayo were initiated sometime in the late-19th century.

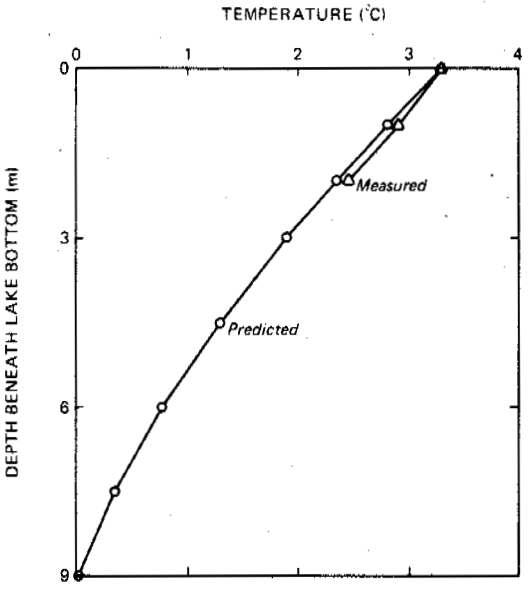

Fig. 5. Results of geothermal simulation.

DISCUSSION

The results of this study, specifically the tree-ring analysis and the geothermal simulation, indicate that the thermokarst ponds near Mayo were initiated around 1880, and are in a relatively early stage of development. It is tempting to relate the initiation of the lakes to the post-Little Ice Age climatic warming since 1850, but we suggest a more probable cause is forest fire. Historically, fires have been common in Stewart Valley, and charred remnants are present in the vicinity of the thermokarst lakes. In addition, observations of thermokarst ponds in the Takhini Valley near Whitehorse, Y.T., indicate that recent expansion is related to a forest fire in 1958 (Burn, 1982a).

The pattern of lake growth since 1949 shows no obvious relationship to climatic conditions; it is suggested that the thermal buffering of the lake modulates the effect of annual climatic variations. Moreover, a borehole transect drilled across a recently-drained pond revealed aggrading permafrost; the presence of both aggrading and degrading permafrost in the study area under the same climatic conditions, further implies that the thermokarst development near Mayo is not simply climatically-driven.

ACKNOWLEDGEMENTS

This paper is dedicated to the memory of our colleague and friend Michael J. Hare, who was a field companion at Mayo in 1982 and 1983. Field studies have been supported by the Earth Physics Branch, Energy, Mines and Resources, Canada; Northern Scientific Training Programme grants from Indian and Northern Affairs, Canada; the National Scientific and Engineering Research Council; and the Canadian Commonwealth Scholarship Committee. We are also grateful to Alan Dufour, David MacLeod, Peter Bissett and Pierre Friele for assistance in the field. Valuable comments on the manuscript were received from Drs J.R. Mackay and A.G. Lewkowicz.

REFERENCES

Burn, C.R. (1982a) Investigations of thermokarst development and climatic change in the Yukon Territory. Unpublished M.A. thesis, Dept. of Geography, Carleton University, Ottawa, Canada. 142 p.

Burn, C.R. (1982b) Yukon temperature cycles: An application of simple techniques to reveal a comprehensible order. The Albertan Geographer, 18, 11-27.

Burn, C.R. (1986) On the origin of aggradational ice in permafrost. Unpublished Ph.D. thesis, Department of Geology, Carleton University, Ottawa, Canada. 222 p.

Burn, C.R., Michel, F.A. and Smith, M.W. (1986) Stratigraphic, isotopic and mineralogical evidence for an early Holocene thaw unconformity at Mayo, Yukon Territory. Canadian Journal of Earth Sciences 23(6), 794-803.

Carson, C.E. (1968) Radiocarbon dating of lacustrine strands in arctic Alaska. Arctic 21(1), 12-26.

Chatwin, S.C. (1981) Permafrost aggradation and degradation in a sub-arctic peatland. Unpublished M.Sc. thesis, Dept. of Geology, University of Alberta, Edmonton, Canada. 163 p.

Fritts, H.C. (1976) Tree rings and climate. Academic Press, New York. 567 p.

Green, L.H. (1971) Geology of Mayo Lake, Scougale Creek and McQuesten Lake Area, Yukon Territory. Geological Survey of Canada Memoir 357, 72 p.

Lachenbruch, A.H. (1957) Three dimensional heat conduction in permafrost beneath heated buildings. United States Geological Survey Bulletin 1052-B, 19 p.

Lachenbruch, A.H. and Marshall, B.V. (1986) Changing climate: Geothermal evidence from permafrost in the Alaskan arctic. Science 234, 689-696.

Mackay, J.R. (1970) Disturbances to the tundra and forest tundra environments of the western Arctic. Canadian Geotechnical Journal 7(4), 420-432.

Mackay, J.R. (1975) The stability of permafrost and recent climatic change in the Mackenzie Valley. In Current Research, Part A, Geological Survey of Canada Paper 75-1A, 173-176.

Rampton, V.N. (1973) The influence of ground ice and thermokarst upon the geomorphology of the Mackenzie-Beaufort region. In Research in Polar and Alpine Geomorphology, Proceedings, 3rd Guelph Symposium on Geomorphology, Guelph, Ontario, 43-60.

Rouse, W.R. (1976) Microclimatic changes accompanying burning in subarctic woodland. Arctic and Alpine Research 8(4), 291-304.

Smith, M.W. (1976) Permafrost in the Mackenzie Delta, Northwest Territories. Geological Survey of Canada Paper 75-28. 34 p.

Smith, M.W. and Riseborough, D.W. (1985) The sensitivity of thermal predictions to assumptions in soil properties. Proceedings, Fourth International Symposium on Ground Freezing, Vol. 1, 17-23. Balkema, Rotterdam.

Thie, J. (1974) Distribution and thawing of permafrost in the southern part of the discontinuous permafrost zone in Manitoba. Arctic 27(2), 189-200.

LOESS AND DEEP THERMOKARST BASINS IN ARCTIC ALASKA

L.D. Carter

U.S. Geological Survey, 4200 University Drive, Anchorage, AK 99508-4667 U.S.A.

SYNOPSIS Silt, locally more than 30 m thick, forms a discontinuous east-west trending belt 5 to 70 km wide across northern Alaska. In the central part of this belt, stratigraphic details and geologic relations indicate that much of the silt was deposited as loess during the last glacial cycle. Syngenetic ice wedges as much as 26 m deep and 3 m wide occur within the loess and in places penetrate the entire deposit. Because ground ice formed as the loess accumulated, ice content does not decrease with depth as it does in sediments that primarily contain epigenetic ice. This ice distribution within the loess has allowed thermokarst basins as deep as 20 m to form during the Holocene, whereas outside the area of loess, thermokarst basins commonly are only a few meters deep. Ice-rich loess may characterize much of the northern Alaska silt belt, which in the east extends across the coastal plain of the Arctic National Wildlife Refuge (ANWR). Research should be undertaken to determine the extent of ice-rich loess in ANWR, because it is a possible future site of oil exploration activity, and such sediments are especially sensitive to modern anthropogenic disturbance of the ground surface.

INTRODUCTION

Silt, locally more than 30 m thick, forms a discontinuous, east-west trending belt 5 to 70 km wide across northern Alaska (Fig.1). The silt has been studied only in reconnaissance, except in the central part of the belt that is the focus of this report (Fig.2). In this area, the silt was initially interpreted to have a fluvial-marine origin (O'Sullivan, 1961), but parts of it have been recently interpreted as loess (Williams and others, 1978; Lawson, 1986). Thermokarst basins as much as 20 m deep that contain weakly oriented to unoriented lakes are common in the silt (Williams and Yeend, 1979), in sharp contrast to the thermokarst basins only a few meters deep that contain oriented lakes and characterize much of the coastal plain north of the silt belt (Carson and Hussey, 1962; Sellmann and others, 1975). Williams and Yeend (1979) pointed out that the formation of such deep thermokarst basins

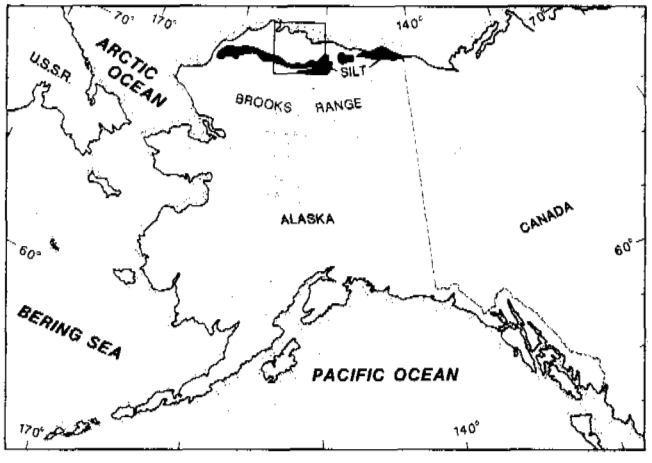

Fig.1. Distribution of thick silt deposits north of the Brooks Range. Generalized from U.S. Geological Survey engineering geologic maps of northern Alaska (e.g., Carter and others, 1986, and maps cited therein). Rectangle shows location of Fig.2.

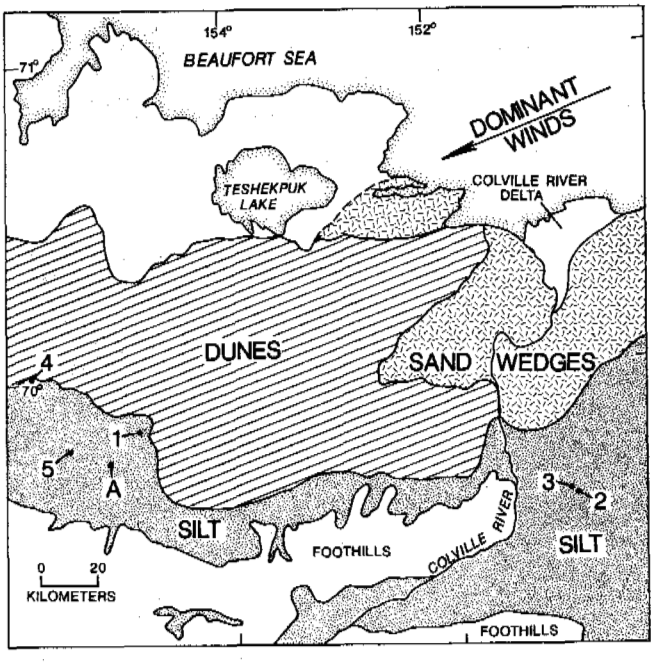

Fig.2. Distribution of silt, dunes, and sand wedges, and location of sites mentioned in text. "A" shows location of Fig.6.

requires that excess ice (the volume of ice in excess of the volume of natural voids in the sediment) be present to much greater depths than is common north of the silt belt, where excess ice may be absent below 6 m (Sellmann and others, 1975). This greater vertical extent of excess ice was confirmed by drilling (Lawson, 1982, 1983), but the character of the excess ice has not been well defined.

Several exposures described here provide evidence that silt in the areas containing deep thermokarst basins initially was deposited as loess, and show that much of the excess ice occurs as deep, syngenetic ice wedges. Thermoluminescence (TL) dating of the loess and radiocarbon dating of organic materials collected from it demonstrate that at the dated localities the loess was deposited during the last glacial cycle.

DESCRIPTION OF THE SILT

The silt was called the foothill silt by O'Sullivan (1961) and was in part included in the Meade River unit of the Gubik Formation by Black (1964). More recently, it was included within map units called "upland silt" by several authors (e.g., Williams and others, 1978; Carter and others, 1986, and maps cited therein). The silt mantles fluvial sediments and irregular bedrock surfaces of sandstone, siltstone, and conglomerate along the northern edge of the Arctic Foothills, extends up valleys into the foothills, and occupies lowlands within them. The silt underlies a surface of low relief that is dissected by modern streams and thermokarst basins, and it occurs south of an extensive area of stabilized Pleistocene dunes and inactive sand wedges (Fig.2; Carter, 1981, 1983).

Natural exposures that exhibit stratigraphic details of the silt are rare, but the few that occur have similar characteristics. Three exposures for which radiocarbon and TL age control are available are described below.

Site 1 (Fig.2) is a river cutbank 51 m high that exposes, from the base upwards, 24 m of sand and silty sand, 24 m of silt, 2 to 3 m of sand and silty sand, and 0.3 to 1.0 m of peat, peaty silt, sand, and turf (Figs.3, 4). The contacts between the silt and sand are sharp, and where active thawing and erosion are occurring the lower contact is marked by a 1 to 2 m overhang, above which ice-rich silt forms a vertical bluff. The sand beneath the silt is predominantly current-bedded fluvial sand, with detrital organic debris common in the lower 10 m but absent above. A fossil tundra mat with ice wedges is locally present 9 m above the base of the bluff. Above the zone containing common organic debris, three beds of eolian sand occur, and at least one sand wedge is at the base of the second of these eolian units.

The silt, in contast to the underlying sand, contains no current bedforms, but rather is horizontally stratified as evidenced by horizontal partings in thawing silt, and by differential erosion that appears to be controlled by vertical variations in the concentration of rootlets. Visible organic

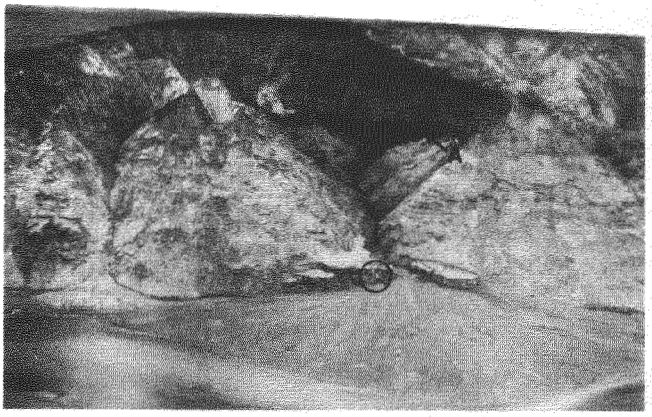

Fig.3. Aerial photograph of site 1. Letter "A" denotes base of silt. Letter "B" indicates ice wedge that penetrates entire thickness of silt. Man in circle at base of bluff indicates scale.

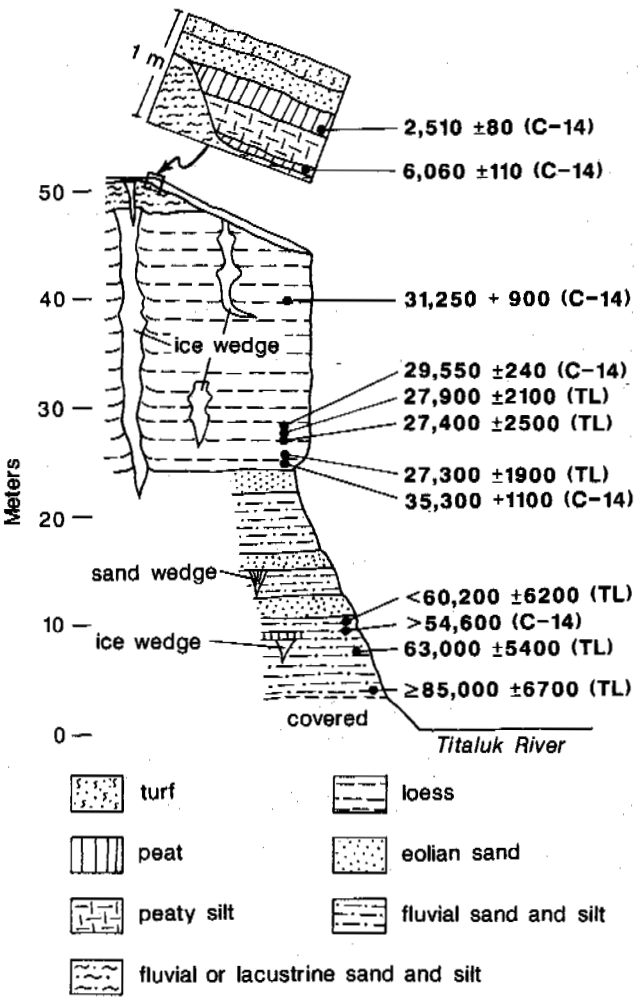

Fig.4. Stratigraphic section at site 1 showing position of radiocarbon (C-14) and thermoluminescence (TL) dates.

matter is sparse, but is present throughout the unit as rootlets and in the lower 6 m as rare woody stems and roots less than 1 cm in diameter that are in growth position. Ground ice in the silt consists primarily of pore ice and ice wedges, which are described in detail below.

Current bedforms, principally climbing ripples, are present in the sand that overlies the silt, and this deposit is interpreted as having formed in a small stream or pond. The sand could have been supplied by eolian bluff-top accretion, which is occurring today at this locality.

TL ages on silt separated from the lower fluvial sand shows that deposition began at or before 85 ka (Table I). Sometime after 60 ka, organic debris became rare and eolian sand became a significant part of the accumulating sediment. Radiocarbon analysis of rootlets and fine-grained organic matter near the base of the silt suggests that silt deposition began about 35.3 ka, and wood in growth position 4 m above the base is dated as 29.5 ka. Three TL ages on silt in this interval are consistent with the radiocarbon results. Radiocarbon ages that would date the end of silt deposition are not available, but deposition ceased well before 6 ka, which is the age of the paleosol that truncates the sand that overlies the silt.

Site 2 (Fig.2) is a large, active thermokarst amphitheater (Fig.5). The face of the amphitheater is formed by the longitudinal section of an enormous ice wedge, transverse sections of truncated intersecting wedges, and silt pinnacles or baydjarakhs (Czudek and Demek, 1970) that were enclosed by the ice wedges. The face of the amphitheater was estimated as about 15 m high, and the ice wedges extend to some unknown depth. Horizontal stratification is visible in the silt pinnacles, which are permeated by rootlets. Two radiocarbon analyses of rootlets collected near the base of the face are 32.3 and 28.6 ka (Table I), showing that silt deposition here was contemporaneous with silt deposition at site 1.

Site 3 (Fig.2) is an inactive thermokarst area in which the baydjarakhs are well preserved and silt is exposed to a depth of 20 m. The silt is very thinly bedded to laminated and contains abundant rootlets. Sparse herbaceous plants are preserved in growth position, and a radiocarbon date on one of these collected 17.2 m below the top of the loess is 21.6 ka (Table I). Three TL ages on the silt are 12.6 ka at a depth of 7.4 m, 21.8 ka at a depth of 17.4 m, and 34.7 ka at a depth of 20 m. Although they are considered minimum limiting ages because of anomalous fading, the concordance of the TL and radiocarbon ages for samples at about the same depth suggests that the TL ages may closely approximate the time of loess deposition.

Some exposures of the silt, especially in valleys within the foothills, differ from those at the sites described above in that current bedforms, principally climbing ripples, are present. The percentage of current bedforms relative to thinly bedded to laminated stratification is highest near valley axes. Where exposures begin at or near modern stream levels, a common stratigraphic sequence is trough cross-stratified sand and pebbly sand,

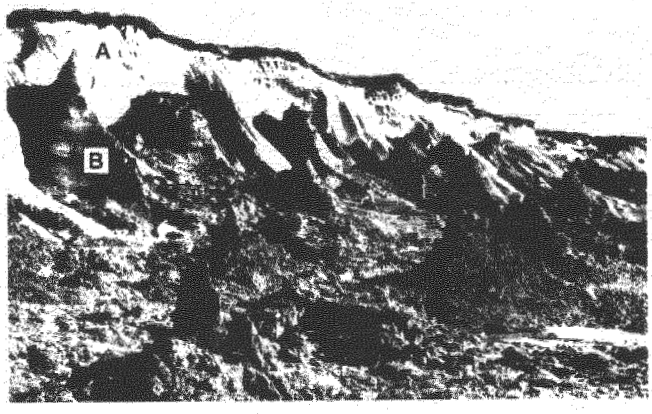

Fig.5. Large ice wedges (A) and silt pinnacles (B) at site 2. Height of ice face about 15 m.

grading upwards into ripple-bedded silt, which is overlain by thinly bedded to laminated silt. Ice wedges generally are present only in the thinly bedded to laminated silt.

ENVIRONMENT OF DEPOSITION AND REGIONAL RELATIONS

The silt has a grain-size distribution like that of loess (O'Sullivan, 1961; Black, 1964), and its occurrence as a mantle over bedrock and unconsolidated deposits of a variety of lithologic types and across a surface of irregular relief supports an interpretation of the silt as loess. Although an absence of clearly discernable stratification is sometimes cited as a characteristic of loess, and has been used as a criterion for its identification (Péwé and Journaux, 1983), the deposits of horizontally stratified, thinly bedded to laminated silt with common rootlets and terrestrial herbaceous and woody plants in growth position described here are clearly of eolian origin. In places within the foothills and near modern stream courses, however, part of the silt is waterlaid, as shown by current-formed sedimentary structures, such as climbing ripples. The most likely depositional model is eolian deposition of the silt, with local redeposition by fluvial and possibly lacustrine processes within the foothills and on floodplains beyond them. The flat to gently rolling surfaces between the floodplains and in lowlands within the foothills are areas where loess accumulated and was preserved.

This model is supported by the relation of the silt to Pleistocene sand wedges and dunes to the north (Fig.2). The radiocarbon and TL ages presented here show that silt was accumulating during middle and late Wisconsin time, which was coincident with dune activity and the growth of sand wedges (Carter, 1983). The sand was moved by northeasterly winds (Carter, 1981, 1983), and the loess evidently was the downwind part of this system of eolian sediment transport, and marks the zone in which waning winds were no longer able to move sand. TL analyses of the sediments beneath the loess at site 1 (Table I, Fig.4) and other field evidence and TL analyses

Table I. Radiocarbon (^{14}C) and thermoluminescence (TL)[1] ages. Site locations shown on Fig. 2.

Material	Occurrence	Type of Analysis	Age (yr B.P.) and Laboratory Number	Significance
		Site 1 (69° 51.25'N, 154° 51.5'W)		
Peat	See Fig. 4 for stratigraphic details	^{14}C	2510 ± 80 (I - 14,861)	Dates inception of paleosol
Peat		^{14}C	6060 ± 110 (I - 14,860)	Minimum limiting age for sand overlying loess
Fine-grained organics		^{14}C	31,250 ± 900 (Beta - 23458)	Dates loess deposition[2]
Wood		^{14}C	29,550 ± 240 (USGS - 2441)	Dates loess deposition
Loess		TL	27,900 ± 2100 (Alpha - 3097)	Dates loess deposition
Loess		TL	27,400 ± 2500 (Alpha - 3150)	Dates loess deposition
Loess		TL	27,300 ± 1900 (Alpha - 3096)	Dates loess deposition
Fine-grained organics		^{14}C	35,300 ± 1100 (USGS - 2529)	Dates loess deposition
Fluvial silt		TL	<60,200 ± 6200 (Alpha - 3093)	Maximum limiting age for this horizon
Wood		^{14}C	>54,600 (USGS - 1031)	Minimum limiting age for paleosol
Fluvial silt		TL	63,000 ± 5400 (Alpha - 3297)	Dates fluvial sediments and gives maximum limiting age for overlying paleosol
Fluvial silt		TL	≥85,000 ± 6700 (Alpha - 3092)	Minimum limiting age for lowest exposed fluvial sediments
		Site 2 (69° 34.45'N, 150° 5 4.6'W)		
Fine-grained organics	15 m below top of loess	^{14}C	28,610 ± 270 (USGS - 1151)	Dates loess deposition
Fine-grained organics	15 m below top of loess	^{14}C	32,300 ± 1500 (I-11,530)	Dates loess deposition
		Site 3 (69° 35.2'N, 150° 56.4'W)		
Loess	7.4 m below top of loess	TL	≥12,600 ± 700 (Alpha - 3292)	Minimum limiting age for this horizon
Herbaceous plant	17.2 m below top of loess	^{14}C	21,580 ± 310 (AA - 2361)	Dates loess deposition
Loess	17.4 m below top of loess	TL	≥21,800 ± 1200 (Alpha - 3291)	Minimum limiting age for this horizon
Loess	20.0 m below top of loess	TL	≥34,700 ± 2200 (Alpha - 3290)	Minimum limiting age for this

[1]TL ages are presented without details of the analyses because the results are supported by radiocarbon ages. A discussion of the TL analyses will be published elsewhere.

[2]Fine-grained organic material in this region sometimes includes redeposited organic carbon (Nelson and others, 1988), and thus may yield a radiocarbon age that is older than the true age of deposition.

(L.D. Carter, unpublished data) suggest that eolian sand movement occurred either episodically or continuously throughout much of the last glacial cycle. It seems likely that each episode of eolian sand movement was accompanied by loess deposition, and that the age of the base of the loess at site 1 indicates only the time at which local conditions became suitable for loess accumulation.

THERMOKARST AND GROUND ICE

The loess plains are characterized by thermokarst basins 15 to 20 m deep (Fig.6). Radiocarbon analyses of organic materials from basal lake beds in three basin fills show that the basins developed during the Holocene (Williams and Yeend, 1979; Nelson, 1982; L.D. Carter, unpublished data). Williams and Yeend (1979) pointed out that these basins are analogous to those in the loess deposits south and east of the Yukon flats (Williams, 1962), and to the alass thermokarst relief of central Yakutia, USSR, which forms when extremely ice-rich permafrost thaws (Czudek and Demek, 1970; Are, 1973; Tomirdiaro, 1982). During the thaw process, individual basins develop that expand and eventually coalesce to produce large, flat-floored depressions containing residual knolls of ice-rich sediment. The silt containing the alass basins has been interpreted in recent studies as loess (Tomirdiaro, 1982; Péwé and Journaux, 1983), although virtually every environment of deposition also has been proposed (e.g., see Péwé and Journaux, 1983).

Large volumes of excess ice to depths of at least 20 m are clearly necessary to form the Alaskan thermokarst basins. Williams and Yeend (1979) calculated a total ice volume of about 78% for one locality (site 4, Fig.2), based upon consideration of the depth of the lake basin and the thickness of thaw lake deposits. They noted that this is in general agreement with an estimate by Livingstone and others (1958) of 68 % by volume for a nearby area based on similar reasoning. Lawson (1982) measured similar ice volumes in samples obtained by drilling at East Oumalik (site 5, Fig. 2), and he described the ground ice there as including large ice wedges (5 to 10 m wide and 7 to 14 m deep), an ice sill up to 10 m thick of probable segregation origin, and other forms of segregated ice (Lawson (1983, 1986).

Ground ice in the loess is well exposed at site 1 (Figs.3, 7), and is representative of the conditions observed at other exposures of thick, unconsolidated deposits. The ground ice consists of pore ice and vertically foliated wedge ice. Ice wedges have estimated maximum widths of 2 to 3 m, and are spaced up to 10 m apart. They have diverse trends (strikes), and a few ice-wedge intersections are exposed, showing that the wedges form a three-dimensional network. Bedding is commonly upturned at ice-wedge margins. Some ice wedges start at the top of the loess and penetrate the entire unit, extending 1 to 2 m into the underlying sand. Other ice wedges that start at the top of the loess terminate within it, and still others have their bases and tops entirely within the loess. Ice-wedge tops within the loess are at various levels, but multiple tops were not observed at any horizon. The tips of a few ice wedges curve and become horizontal to subhorizontal, in some cases joining the top of a lower ice wedge a few meters away. These horizontal to subhorizontal ice bodies were the only large ice masses observed that are possibly segregation ice, but it seem most likely that they are related to ice wedge growth. Many ice wedges have shoulders or flarings at multiple horizons, which is characteristic of ice wedges that grow upwards as deposition occurs, and are thus syngenetic (Jahn, 1975). These characteristics show that ice wedge growth was occurring throughout the period of loess deposition. Some ice wedges became inactive during loess deposition, some were initiated during this interval, and some grew upward as the permafrost table rose concommittant with loess deposition.

These conditions differ from those described by Lawson for East Oumalik (1983, 1986), perhaps because bedrock is at or near the level of modern streams there, and hydrologic or other conditions during silt deposition and ground-ice genesis may have been much different. Other

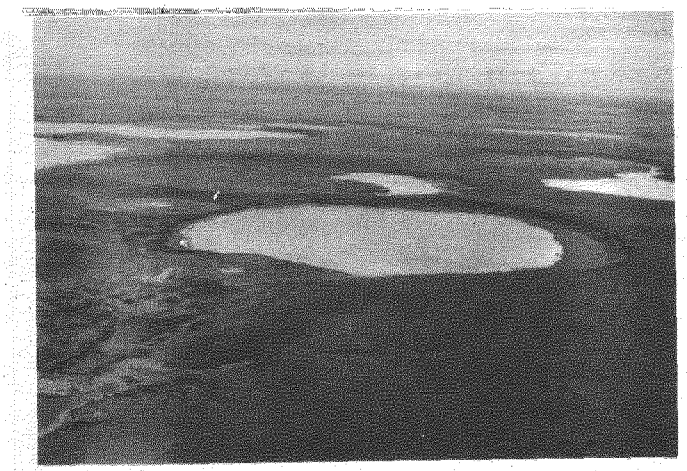

Fig.6. Deep basins developed by melting of ground ice in loess. Bluffs bordering basins are 15 to 20 m high.

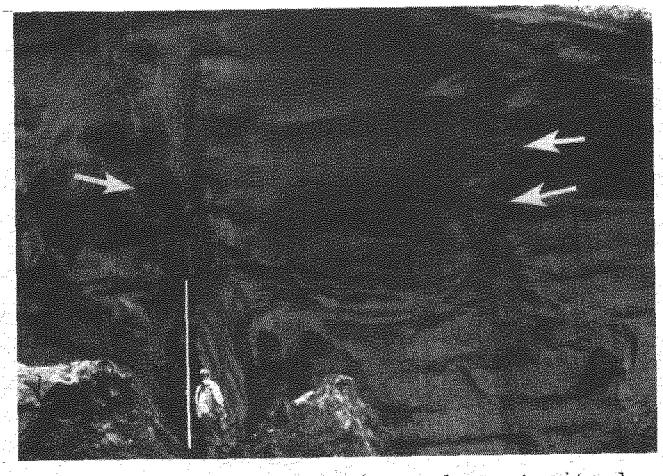

Fig.7. Large syngenetic ice wedges at site 1. Arrows point to flarings typical of syngenetic ice wedges. Man is about 1.7 m tall.

localities may contain both syngenetic ice wedges and large ice masses of other forms such as those described by Lawson.

REGIONAL SIGNIFICANCE

The loess and ground ice described above may be representative of the conditions over a large part of the northern Alaska silt belt. Ice-rich loess is especially sensitive to modern anthropogenic disturbance of the ground surface (Ferrians and others, 1969; Lawson, 1986; Walker and others, 1987), and the silt thus deserves more than the reconnaissance study it has so far received. Research should especially be concentrated in the eastern part of the belt in and adjacent to the Arctic National Wildlife Refuge because this area may be the site of future oil exploration activities.

REFERENCES

Are, F.E. (1973). Development of thermokarst lakes in central Yakutia. International Conference on Permafrost, 2nd, Yakutsk, USSR, Guidbook, 29 pp.

Black, R.F. (1964). Gubik Formation of Quaternary age in northern Alaska. U.S. Geol. Survey Prof. Pap. 302-C, 91 pp.

Carson, C.E., and Hussey, K. M. (1962). The oriented lakes of arctic Alaska. Journal of Geology (70), 417-439.

Carter, L.D. (1981). A Pleistocene sand sea on the Alaskan Arctic Coastal Plain. Science (211), 381-383.

Carter, L.D. (1983). Fossil sand wedges on the Alaskan Arctic Coastal Plain and their paleoenvironmental significance. Permafrost: Fourth Int. Conf., Proc. Washington, D.C., National Academy Press, 109-114.

Carter, L.D., Ferrians, O.J., Jr., and Galloway, J.P. (1986). Engineering geologic maps of northern Alaska, coastal plain and foothills of the Arctic National Wildlife Refuge. U.S. Geol. Survey Open-File Report 86-334, 10 pp., scale 1:250,000, 2 sheets.

Czudek, T., and Demek, J. (1970). Thermokarst in Siberia and its influence on the development of lowland relief. Quaternary Research (1), 103-120.

Ferrians, O.J., Jr., Kachadoorian, Reuben, and Greene, G.W. (1969). Permafrost and related engineering problems in Alaska. U.S. Geol. Survey Prof. Pap. 678, 37 pp.

Jahn, A. (1975). Problems of the periglacial zone. Warsaw, Poland, Panstwowe Wydawnictwo Naukowe, 212 pp. Available from National Tecn. Inf. Serv., Springfield, Virginia.

Lawson, D.E. (1982). Long-term modifications of perennially frozen sediment and terrain at East Oumalik, northern Alaska. Hanover, New Hampshire, U.S. Army Cold Regions Res. and Eng. Lab., CRREL Report 82-36, 33 pp.

Lawson, D.E. (1983). Ground ice in perennially frozen sediments, northern Alaska. Permafrost: Fourth Int. Conf. Proc. Washington, D.C., National Academy Press, 695-700.

Lawson, D.E. (1986). Response of permafrost terrain to disturbance: A synthesis of observations from northern Alaska, U.S.A.. Arctic and Alpine Research (18), 1-17.

Livingstone, D.A., Bryan, K., Jr., and Leahy, R.G. (1958). Effects of an Arctic environment on the origin and development of fresh water lakes. Limnology and Oceanography (3), 192-214.

Nelson, R.E. (1982). Late Quaternary environments of the western Arctic Slope, Alaska. Seattle, Washington, University of Washington, Ph.D. Dissertation, 146 pp.

Nelson, R.E., Carter, L.D., and Robinson, S.W. (1988). Anomalous radiocarbon ages from a Holocene detrital organic lens in Alaska and their implications for radiocarbon dating and paleoenvironmental reconstructions in the Arctic. Quaternary Research (29), (in press).

O'Sullivan, J.B. (1961). Quaternary geology of the Arctic coastal plain, northern Alaska. Ames, Iowa, Iowa State University of Science and Technology, Ph.D. Dissertation, 191 pp.

Péwé, T.L., and Journaux, A. (1983). Origin and character of loesslike silt in unglaciated south-central Yakutia, Siberia, U.S.S.R.. U.S. Geol. Survey Prof. Pap. 1262, 46 pp.

Sellmann, P.V., Brown, J., Lewellen, R.I., McKim, H., and Merry, C. (1975). The classification and geomorphic implications of thaw lakes on the arctic coastal plain, Alaska. Hanover, New Hampshire, U.S. Army Cold Regions Res. and Eng. Lab., CRREL Research Report 344, 21 pp.

Tormirdiaro, S.V. (1982). Evolution of lowland landscapes in northeastern Asia during late Quaternary time, in Hopkins, D.M., Matthews, J.V., Jr., Schweger, C.E., and Young, S.B., eds., Paleoecology of Beringia. New York, N.Y., Academic Press, 29-37.

Walker, D.A., Cate, D., Brown, J., and Racine, C. (1987). Disturbance and recovery of arctic Alaskan tundra terrain. Hanover, New Hampshire, U.S. Army Cold Regions Res. and Eng. Lab., CRREL Report 87-11, 63 pp.

Williams, J.R. (1962). Geologic reconnaissance of the Yukon Flats district, Alaska. U.S. Geol. Survey Bull. 1111-H, 289-331.

Williams, J.R., Carter, L.D., and Yeend, W.E. (1978). Coastal plain deposits of NPRA. U.S. Geol. Survey Circular 772-B, B20-B22.

Williams, J.R., and Yeend, W.E. (1979). Deep thaw lake basins of the inner Arctic Coastal Plain, Alaska. U.S. Geol. Survey Circular 804-B, B35-B37.

A FIRST APPROACH TO THE SYSTEMATIC STUDY OF THE ROCK GLACIERS IN THE ITALIAN ALPS

A. Carton[1], F. Dramis[2], and C. Smiraglia[3]

[1]Instituto di Geologia, Università di Modena
[2]Dipartimento di Scienze della Terra, Università di Camerino
[3]Istituto di Geografia, Università Cattolica di Miano

In collaboration with
G.B Castiglioni, C. Catasta, U. Mattana, M. Meneghel, A. Onorati, C. Ottone, G. Palmentola, B. Parisi, G.B. Pellegrini, M. Pelfini, P. Petruzzelli, U. Sauro, C. Tellini, V. Toniello, C. Voltolini

SYNOPSIS This article is a preliminary review of the existence, distribution, and number of rock glaciers in the Italian Alps. The data analyzed, refer to several mountain groups chosen over the entire Alpine chain, and were obtained from the analysis of large-scale aerial photographs and field surveys. The rock glaciers are clearly very numerous in the areas with large crystalline massifs and appear to face prevalently northern directions. The consistent decrease in altitude in several parameters W to E seems to indicate a link between rock glaciers and general climatic characteristics of the southern flank of the Alps. The consistently different altimetric distribution of some of the parameters relating to active and inactive rock glaciers can be explained by the rise in altitude of the average annual isotherm of -2°C from the past to the present.

INTRODUCTION

According to the now classic definition by Wahrhaftig and Cox (1959), rock glaciers are tongue-shaped or lobate masses of poorly sorted angular debris lying at the base of cliffs or talus slopes or extending down-valley from the lower end of small glaciers. They are a characteristic form of permafrost and represent one of the most widespread and characteristic phenomena of the periglacial morphology found in mountainous regions where the climate tends to take on continental aspects. According to many researchers (Barsch, 1978; Evin, 1983; Haeberli, 1985; Belloni, Pelfini, and Smiraglia, in press) in the case of active rock glaciers, the mean annual isotherm of -2°C should represent the climatic requirement for their formation and maintenance as it represents the lower limit of discontinuous permafrost. It follows then that rock glaciers have been observed and described in all of the mountain chains on the Earth with climatic features suited to their formation, and that the scientific literature dedicated to them is extremely vast, as may be seen from several ample bibliographies (Barsch, 1983; Evin, 1983; Dramis and Smiraglia, 1986).

As concerns the Italian side of the Alps, several reports and descriptions regarding these forms were published in the 1950's and 1960's (Hermann, 1929; Nangeroni, 1929; Capello, 1947, 1959). They did not, however, approach complete detailed studies on their distribution and/or their morphological features.

Only recently have more systematic studies been planned within the "Glaciology" section of the CNR National Group on Physical Geography and Geomorphology. The preliminary results of these studies have already been published (Smiraglia, 1985; Dramis and Smiraglia, 1986; GNGFG, 1987). This paper has been written as part of this research program and is intended as a preliminary factual investigation into the existence, the distribution, and diffusion of rock glaciers in the Italian Alps. We shall also provide the most significant data collected on the morphological parameters which characterize rock glaciers, by distinguishing between the most frequent types and pointing out the principal differentiations appearing in the various mountain groups of the southern side of the Alps. This collection of data could thus represent a preliminary body of indispensable knowledge for future studies in the field of dynamic geomorphology, which investigates correlations between rock glaciers and climatic and litho-structural parameters.

The data on rock glaciers in the Italian Alps are given below in a preliminary summary. They were collected by numerous researchers participating in the National Group on Physical Geography and Geomorphology, who strove for as much homogeneity as possible in terms of the methodologies utilized. In the first stage of this study, the researchers carried out a selection of the mountain groups and sectors of the Italian Alps (listed below). The criteria adopted focused on selecting groups and sectors that would be as widely representative as possible of the different climatic, lithologic, and morphological situations characterizing the southern slope of the chain. Large-scale aerial photographs were then examined in order to identify forms that could be classified as rock glaciers. The rock glaciers were then reproduced on official large-scale maps (1:10.000 to 1:25.000), which made it possible to obtain numerous morphological and topographical parameters with good approximation. In the cases of areas of particular interest, field surveys were carried out with the purpose of identifying in a more detailed manner the most characteristic and widespread types of rock glaciers. A data sheet was compiled for each form and all the numerical and non-numerical elements were supplied, permitting a complete description.

CHARACTERISTICS OF THE ROCK GLACIERS IN THE ITALIAN ALPS

An area of approximately 20,000 square km

was examined using the methodology mentioned above. The area was subdivided into the various mountain sectors W to E as follows (fig. 1): Maritime Alps (1000km^2), Cottian Alps (800 km^2), Gran Paradiso (300 km^2), Monte Rosa (1400 km^2), Masino-Bernina (580 km^2), Piazzi-Cevedale (780 km^2), Brenta (180 km^2), Venoste Alps (1680 km^2), Noric Alps (1300 km^2), Dolomites (8100 km^2), Carnic Alps (3680 km^2). A total of approximately one thousand forms (987) was identified. A preliminary typological classification was carried out, distinguishing between active and inactive rock glaciers, those with uncertain activity, questionable forms and complex forms (that is, characterized by both active and inactive parts). This subdivision was carried out on the basis of some indirect signs of activity or inactivity which could be verified on the aerial photographs and compared with field observations recorded above all in the cases of the Gran Paradiso Group, the Cevedale Group, and the Dolomites. Forms held to be active are those with an absence of or almost completely lacking vegetation and which on the whole present a convex morphology with well-defined and steep margins, especially on the terminal area.

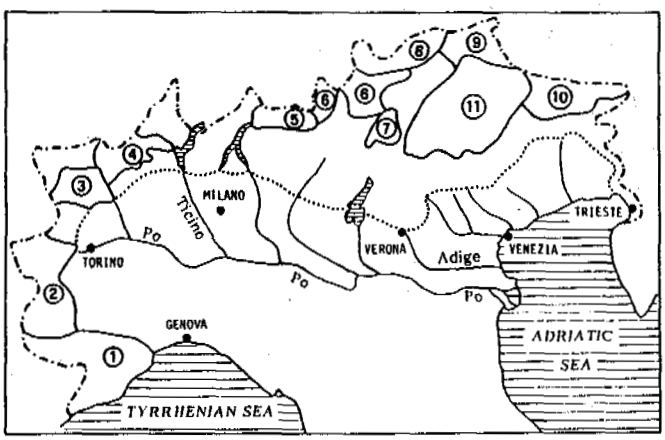

Fig. 1 Location of the mountain sectors. (Names of researchers and their respective Institutes between parentheses). 1) MARITIME ALPS (Tellini C. - Istituto di Geologia e Geografia, Università di Parma); 2) COTTIAN ALPS (Onorati M. - Dipartimento di Scienze della Terra, Università di Camerino); 3) GRAN PARADISO (Smiraglia C. - Istituto di Geografia, Università Cattolica di Milano); 4) MONTE ROSA (Ottone C. - Dipartimento di Scienze della Terra, Università di Pavia); 5) MASINO-BERNINA (Catasta C. - Dipartimento di Scienze della Terra, Università di Milano); 6) PIAZZI-CEVEDALE (Catasta C., Pelfini M. - Dipartimento di Scienze della Terra, Università di Milano); 7) BRENTA Group (Parisi G. - Istituto di Geografia, Università Cattolica di Milano); 8) VENOSTE ALPS (Palmentola G., Petruzzelli M. - Dipartimento di Geologia e Geofisica, Università di Bari); 9) NORIC ALPS (Castiglioni G.B., Mattana U. - Dipartimento di Geografia "G. Morandini", Università di Padova); 10) CARNIC ALPS (Meneghel M. - Dipartimento di Geografia "G. Morandini", Università di Padova); 11) DOLOMITES (Carton, A., Voltolini C. - Istituto di Geologia, Università di Modena; Castiglioni G.B., Pellegrini G.B. - Dipartimento di Geografia "G. Morandini", Università di Padova).

On the whole, 131 active forms were identified (13%), 449 inactive forms (45%), 215 with uncertain activity (21%). The remaining 21% is made up of complex forms, which clearly represent a minority, and questionable forms. Although the latter cannot be defined as rock glaciers in the usual sense of the term, they do show some morphological affinities with them. Distribution is very differentiated in the various mountain sectors and groups. The greatest number of forms was observed in the Noric Alps (218, that is 22%, taking all types into account), followed by the Cevedale massif (183) and the Venoste Alps (172). In contrast, the number of forms identified in the Carnic Alps (15) and in the Brenta Group (8) was very limited (fig 2). The highest density of forms

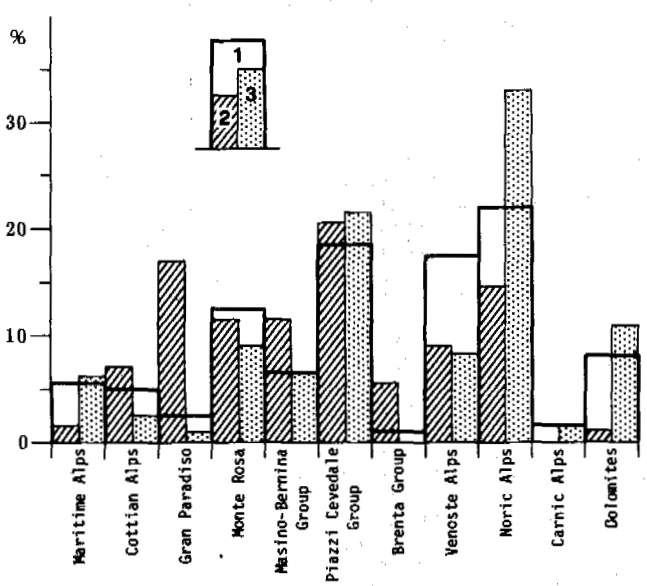

Fig. 2 Distribution of the rock glaciers in the various mountain groups in the Italian Alps. 1) all of the rock glaciers; 2) active rock glaciers; 3) inactive rock glaciers. (The percentages refer to each individual category.)

may be noted in the Piazzi-Cevedale Group (0.234 R.G./km^2), followed by the Noric Alps (0.167 R.G./km^2), and the Masino-Bernina Massif (0.106 R.G./km^2). The lowest density may be noted at the outermost borders of the chain in the Maritime Alps and in the Carnic Alps respectively. The majority of active rock glaciers can be observed in the Piazzi-Cevedale Group (21% approximately), followed by the Gran Paradiso and Monte Rosa Groups (approximately 17% for both) (fig. 2).

At any rate, a greater number of active forms is observable in the mid-western sector (70% of the total number of active rock glaciers). As far as the vertical distribution of the rock glaciers in the Italian Alps is con-

cerned, taking into account all the forms examined and all the data collected, it was found that the altitude of the fronts varies from a maximum of 3150 m (in the Gran Paradiso Group) to 1550 m (in the Carnic Alps) (fig. 3). The mean altitude of the fronts evidently tends to decrease from the westernmost groups to the eastern ones (fig. 3). Another interesting finding concerns the altitudes of the fronts of

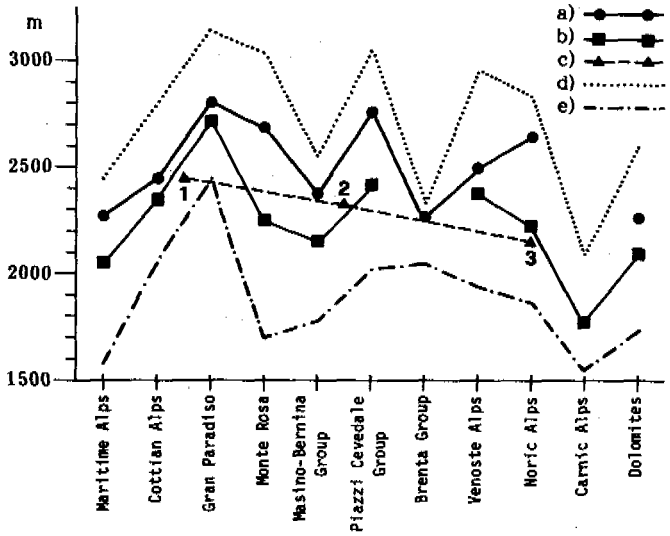

Fig. 3 Patterns of the mean maximum and minimum altitudes of the rock glacier fronts in the various mountain groups. a) mean altitudes: active forms; b) mean altitudes: inactive forms; c) mean altitudes of the active forms, inactive forms and forms with uncertain activity in the western (1); central (2); and eastern (3) sectors; d) maximum altitudes amongst all the rock glaciers; e) minimum altitudes amongst all the rock glaciers.

the active rock glaciers, which range from 3150 m in the Gran Paradiso Group to 2150 m in the Brenta Group. They are consistently higher than those of the inactive rock glaciers (which range from 2900 m in the Gran Paradiso Group to 1550 m in the Carnic Alps) (fig. 3). The forms identified are situated in basins circumscribed by ridges, the altitudes of which range between 3600 m (Monte Rosa) and 1750 m (Maritime Alps). In the case of this parameter as well, it may be noted that both the maximum and minimum altitudes of the highest peaks of the basin are almost always higher in correspondence with the active forms with respect to the inactive forms. With regard to the area of the rock glaciers, a marked variability was observed in the data collected. Taking into account all of the forms identified, one finds rock glaciers, in fact, ranging from those of very limited size (2500 m^2 in the Gran Paradiso Group) to those over one-half km^2 in area (for example, 843000 m^2 in the Cottian Alps, 690000 m^2 in the Dolomites, 600000 m^2 in the Masino-Bernina Group). In this case as well, it is possible to point out a considerable difference between active and inactive forms. The areas of the inactive forms are on the average, greater than those of the active forms. The last two parameters taken into consideration were length and longitudinal slope. As was observed in the case of area, there is considerable variability in the data concerning length. The greater lengths were identified in the Cottian Alps (2200 m) and in the Dolomites (2125), whereas minimum lengths (50m) were reported in the Gran Paradiso and Monte Rosa Groups. This variability seems to be less marked in forms of the same typology from a dynamic point of view: inactive rock glaciers prove to be longer than active ones in most of the mountain groups. Longitudinal slope, ranging between 10 and 110 %, also appears to be extremely variable, although no particular correlations with different types of rock glaciers were revealed.

The findings on aspect supplied some precise indications. Forms facing northern quadrants predominate. As may be observed in fig. 4, 46% of all the forms is concentrated in the NW-NE sector. The remaining 54% is distributed in the other sectors with a maximum of 15% facing S. The same distribution is rigorously maintained in the analysis of both active and inactive forms.

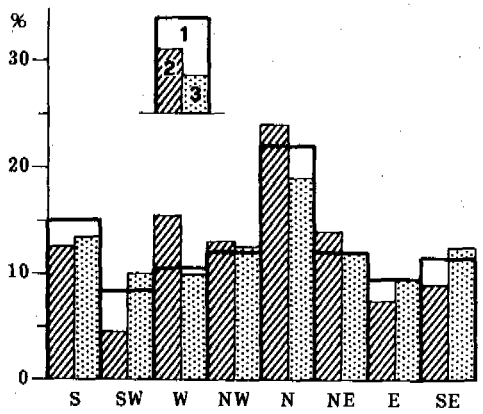

Fig. 4 Distribution of the aspect of the rock glaciers. 1) all of the rock glaciers; 2) active forms; 3) inactive forms. (Percentages refer to each individual category).

The rock glaciers are located prevalently in cirques (43%) and on slopes (42%). The percentages are markedly lower for those located in the bottoms of valleys and in gorges. When the forms were analyzed separately according to the different types of activity, it was found that the active forms are prevalently located in cirques (50%) and only to a lesser extent on slopes (30%). The percentages for forms with uncertain activity (49% in cirques and 36% on slopes) approach the same levels as those for the above-mentioned active forms. There is a clear difference, however, with respect to the inactive forms (which yield percentages of 41% and 44% respectively) (fig. 5).

The rock type from which almost all rock glaciers originate is represented by metamorphites (82%) (fig. 6). They are principally calc-schists, micaschists, green stones, phyllites, and gneiss which make up some of the most impressive crystalline massifs in the

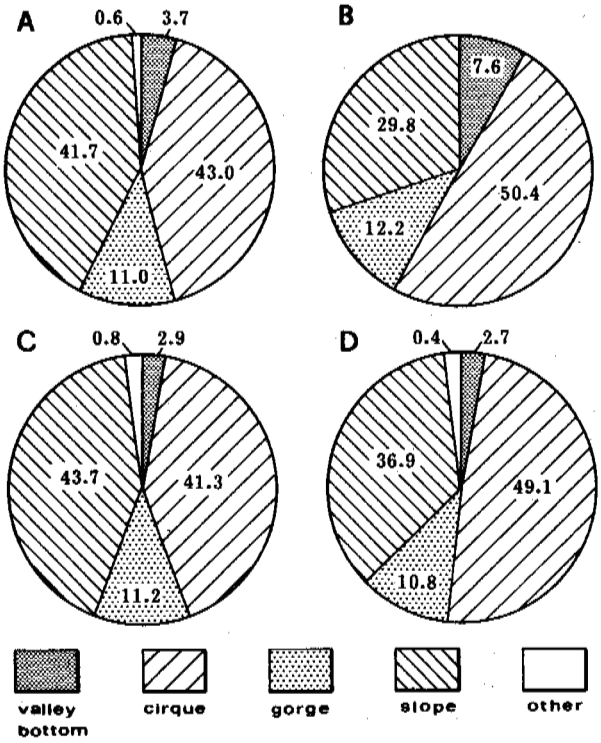

Fig. 5. Location of the rock glaciers (in percentages). A) all of the rock glaciers; B) active forms; C) inactive forms; D) forms whose activity is uncertain.

Alps, such as the Gran Paradiso, Monte Rosa, the Bernina, the Cevedale, and the Venoste and Noric Groups. Forms originating from other rock types are clearly less common (such as the carbonate rocks in the Dolomites and the plutonites in the Masino Group).

From the point of view of geomorphological lineaments, some of the more evident features are the presence of a steep front, curved furrows, and a well developed tongue. The latter is more frequent in the inactive forms.

The proximity of rock glaciers to various types of glacial forms and moraines appears to be significant. Taking into account all the various forms observed, it may in fact be noted that almost half are situated near end moraines (46%) and another large percentage (38%) present semi-permanent snow banks in the upper part (fig.7). Considering the forms by activity, the percentages change remarkably. Active forms are connected with semi-permanent snow banks (53%), glacierets (20%), and moraines (19%). Inactive forms, on the other hand, prove to be linked prevalently to moraines (82%).

As regards relationships between the position of the front and local vegetation limits, it was observed that the active rock glaciers are above the vegetation (85%). In contrast, the inactive forms descend within the zones of grassy vegetation (51%) and tree-growth also (21%)(fig. 7). In those types of rock glaciers with uncertain activity, the front is located above and below the upper limit of the grassy vegetation with the same percentage.

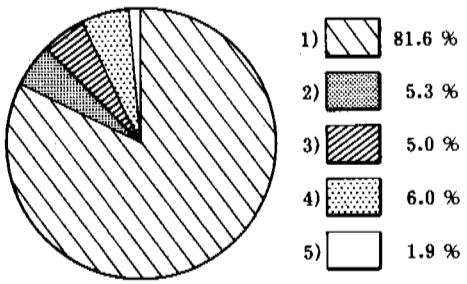

Fig. 6 Distribution of the rock glaciers according to rock type. 1) metamorphites; 2) plutonites; 3) vulcanites; 4) carbonate rocks; 5) other sedimentary rocks.

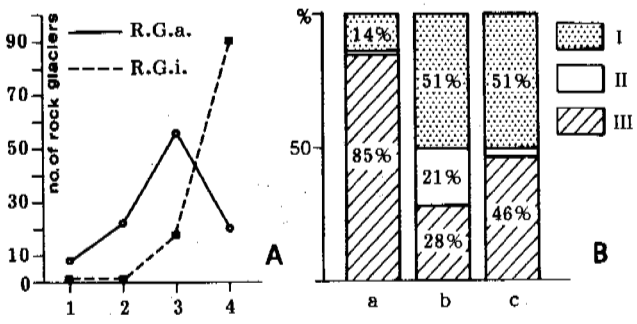

Fig. 7 A: Relation between active rock glaciers, inactive rock glaciers, glacial forms and moraines located above them. R.G.a.) active rock glaciers; R.G.i.) inactive rock glaciers; 1) glaciers; 2) glacierets; 3) semi-permanent snow banks; 4) morainic deposits; (the number of forms identified is indicated on the y-ordinate axis).
B: Relations between the position of the rock glacier fronts and the local vegetation limits; (The percentages refer to each category). a) active forms; b) inactive forms; c) forms whose activity is uncertain; I) front below upper limit of the continuous grassy vegetation; II) front below the upper limit of tree-growth; III) front above all vegetation zones.

REGIONAL DIFFERENTIATIONS

The principal typological differences between rock glaciers in the various mountain sectors examined, can be generally summarized in the following manner. The first significant finding is the limited number of forms and above all, their limited density in the outermost zones of the Alpine chain. For example, in the Maritime Alps, where, from the lithological point of view, the gneiss of the Argentera alternate with permocarboniferous porphyrites and Triassic and Jurassic limestones of the Marguareis, over the area examined which is over 1000 sq. km, only fifty forms (approximately) were identified. Of those forms, at least eighteen can be included amongst rock glaciers only with some reservations. The remaining are

almost all covered with discontinuous vegetation and present a morphology with curved furrowed tongues and distinct collapse phenomena (funnel-shaped hollows); the fronts descend even below 2000 m with a minimum of 1575 m. On the other extremity of the chain to the east, in the Carnic Alps, rock glaciers are an even rarer phenomenon (in over 3500 sq. km in fact, approximately fifteen forms were identified and they are of limited size, usually situated on the bottom of the cirques). This is a region that is characterized by abundant precipitation (i.e., the highest rate of rainfall in all of Italy), with a snow line that is rather low, and where even the lithological and morphological elements are not favorable for the diffusion of rock glaciers. The limited height of the reliefs (the peaks, which are prevalently made up of carbonate rocks, do not exceed 2800 m) is accompanied by sharp crests and very steep slopes, which reduce still further the areas suited to rock glaciers.

The situation in the great crystalline massifs is quite different. Their summits exceed 4000 m in altitude in the western and central sectors (Monte Rosa, Gran Paradiso, Bernina). In the eastern sector, on the other hand, the main peaks rarely descend below 3700 m (Cevedale) and 3500 (Venoste and Noric Alps). In these areas, the rock glaciers truly become an essential element of the mountain landscape, situated immediately between the zone occupied by the glaciers and that occupied by the tree-growth. In the Gran Paradiso Group, for example, where from a lithological point of view, gneiss, calc-schists, and green stones dominate, about thirty rock glaciers have been identified in an area of over 300 sq. km. Medium- to large-sized forms prevail and they have very regular tongues. Their surfaces are characterized by dozens of large concentric arches with a distinct scarp border. Metamorphic schistose rocks, such as gneiss, micaschists, and prasinites, feed the numerous rock glaciers in the Monte Rosa Group as well and are prevalently situated somewhat distant from the amply glaciated nucleus of the massif, especially in the case of the inactive forms.

In the regions of the Bernina and the Cevedale Groups, where 62 and 183 rock glaciers were identified respectively, (in the case of the Cevedale Group, the second largest number of rock glaciers after the Noric Alps was identified, but their density is highest there), further confirmations of the influence that lithology has on the distribution of these forms are provided. These forms are in fact quite rare in the Masino area, slightly west of Bernina Group, where intrusive rocks (granodiorites) prevail. On the contrary, they are quite numerous in those areas (Antognasco Valley, Grosina Valley, Rezzalo Valley) where schistose rocks (gneiss and micaschists) outcrop. In addition, the complex typology of the rock glaciers in this sector should be emphasized. Along with the classic tongue or lobe forms with steep fronts and curved or folded surface furrows, other types may be observed. For example, there are very extensive forms in a transversal direction, located in terminal cirques at the base of steep rocky walls, with only slightly inclined surfaces covered with large boulders and funnel-shaped hollows and inactive forms with steep fronts and internal depressed areas, but abundant in isolated blocks. In addition, rock glaciers with overlying lobes of different ages may be observed and also forms consisting in rejuvenated lobes with regular curved furrows at the base of the moraines dating from the Little Ice Age.

Research on some of the rock glaciers in the Cevedale Group has been done on the part of the National Group of Physical Geography and Geomorphology (GNGFG, 1987). This research has dealt with the examination of the dynamics, genesis, and structure of these forms. The eastern rock glacier in the Val Pisella has been studied in detail. It presents a classic tongue form with a length of 400 m approximately. The front, the inclination of which reaches 37 degrees, stops at 2830 m and is made up for the most part of fine material (small stones and sand). Above the front the visible part of the rock glacier is completely made up of large blocks that are distributed chaotically. However, regular longitudinal and transversal structures may be distinguished on the surface. The transversal structures are principally made up of arches with the hollow facing up valley, which demonstrates the compressive flow of that part and the differential velocity. The longitudinal structures are visible on the borders, in the form of elongated narrow ridges, and in the central part, in the form of fractures and trenches, which extend for dozens of meters. The arrangement of the clasts on the surface of the accumulation seems to suggest the existence of processes of solifluction in the distal portion of the rock glacier and of a block stream that is rather rapid in the proximity of the lateral margins and in the more elevated part. The presence of fractures and steps on the surface may be retraced to the overall movement of the mass and to local collapse phenomena due to melting of the buried ice.

The overlapping of many protruding lobes with steep fronts was observed in the Noric Alps and in the Venoste Alps where the highest number of forms identified is concentrated (22% in the Noric Alps, and, together with the rock glaciers in the Venoste Alps, approximately 40% of the total in the Italian Alps). Both regions are made up of metamorphic rocks (principally gneiss, micaschists, phyllites, calc-schists). The forms considered to be active are clearly a minority (6% of the total in the Venoste Alps and 10% in the Noric Alps). In this second area, they are located in places where glaciers are also present. Sometimes, however, the rock glaciers are found in marginal positions or in locations little suited to glaciers; the highest altitude of the surrounding peaks often exceeds 3000 m, whereas the lowest altitude of the frontal margins ranges between 2800 m and 2400 m. The inactive rock glaciers, on the other hand, are found in very extensive areas where mountain peaks rarely exceed 2800 m and usually reach 2500 m (approximately). One of the factors favoring the notable diffusion of rock glaciers in this area seems to be the existence, within limited distances from the crests which supply deposits, of surfaces that are not too inclined and which are capable of receiving such deposits, which could have resettled with the typically slow movement of these forms.

The Dolomite sector is characterized by the almost complete absence of active forms (only 2 out of the 55 definite forms identified) and by an equally low density of forms per sq. km. The altitudes of the frontal margins of the active rock glaciers descend to

2225 m, whereas the inactive ones reach 1750 m. Forms deriving from sedimentary rocks are quite rare. In fact, although the latter outcrop abundantly in the Dolomite sector, of all the forms identified, only 12 are related to those rock types. Porphyries, on the other hand, appear to be quite suited to the formation of rock glaciers, as is observable in the Lagorai Group. The rock glaciers in the Dolomite sector prove to be prevalently located on slopes and, to a lesser degree, in cirques and in valleys respectively. They present tongues that are fairly developed but not very long, prevalently lowered, and with the presence of curved furrows and frontal margins that are almost always distinct. The presence of an inactive form in this sector should also be noted. It is one of the largest in the entire Italian Alpine chain and is just slightly smaller than the largest rock glacier of uncertain activity in the Cottian Alps. The tongue is 1250 m long, with several funnel-shaped hollows and numerous curved and irregularly bending furrows which are separated by ridges 10-12 meters high. Three different phases of activity are evident, one inside the other. The oldest part of the rock glacier appears to be almost entirely covered with tree-growth and presents several hollows that are dozens of meters in diameter. However, the general morphology of the three overlapping forms appears to be very much lowered.

CONCLUSIONS

Above all, this preliminary and general analysis of the morphological features of the rock glaciers in the Italian Alps permits the identification of the regions in which active forms are clearly prevalent. They are the great crystalline massifs, in which the lithological factor must evidently play a fundamental role. Another determining factor in the distribution of the active rock glaciers may undoubtedly be seen in their aspect. The northern sectors, in fact, appear to be markedly privileged when the number and size of the rock glaciers are considered. The uniform lowering of the altitude of the frontal margins from the west to the east may be an indication of a link between the distribution of the rock glaciers and the general climatic characteristics of the southern side of the Alps, where there is a parallel decrease in the climatic snow line. The influence of climate and particularly of its variations in time, may find further confirmation in the different altitudinal distribution of several parameters, such as the altitude of frontal margins and the maximum altitude of the basins that contain both active and inactive rock glaciers. In fact, besides being characterized by frontal altitudes that are higher than those of inactive rock glaciers, active rock glaciers are situated in basins that are enclosed by peaks that are higher than those which enclose basins where inactive rock glaciers are found. More specifically, the rise in altitude of the mean annual isotherm of -2° C, caused by the changes in climatic conditions, no longer permitted the formation and conservation of discontinuous permafrost in areas below this altitude limit. This determined the fossilization of the rock glaciers existing there and caused the rise of the vegetation line, as is amply demonstrated by the greater part of the inactive forms. The latter, in fact, very often prove to be located below the upper limit of the continuous grassy vegetation and sometimes below that of the tree-growth line, and are in most cases connected with morainic deposits.

ACKNOWLEDGEMENTS

This study has been carried out with the financial help of the CNR (850089705, Dir.: G.B. Castiglioni).

REFERENCES

Barsch, D. (1983). Blockgletscherstudien, Zusammenfassungen und offene Probleme. Akad. Wiss. Göttingen, Abh. Math., Phys. K l., 35, 133-150.

Belloni, S., Pelfini, M., and Smiraglia C. (in press). Morphological features of the active rock glaciers in the Italian Alps and climatic correlations. Atti V Int. Conf. on Permafrost, Trondheim, Norway 1988.

Capello, C.F. (1947). Le pietraie semoventi (rock glaciers) delle Alpi Occidentali. Natura, 38, 17-23.

Capello, C.F. (1959). Prime ricerche sulle pietraie semoventi del settore montuoso del Gran Paradiso. Riv. Mens. Club Alpino It., 78, 294-300; 371-376.

Dramis, F. and Smiraglia, C. (1986). I rock glaciers, problemi e metodi di studio. Rassegna bibliografica. Riv. Geogr. It., XCIII, 2, 209-228.

Evin, M. (1983). Structure et mouvement des glaciers rocheux des Alpes du Sud. These 3 cycle, Grenoble, Institut de Géographie Alpine.

Gruppo Nazionale Geografia Fisica Geomorfologia. (in press). Nuovi dati per lo studio dei rock glaciers del gruppo Ortles Cevedale (Alpi). Riv. Geogr. It.

Haeberli, W. (1985). Creep of mountain permafrost. Internal structure and flow of Alpine rock glaciers. Zurich: E.T.H.

Hermann, F. (1929). I rock glaciers della Valsavaranche. Natura, 16.

Nangeroni, G. (1929). Grotte e laghi subglaciali, colate e mari di pietra. Natura, 20, 152-161.

Smiraglia, C. (1985). Contributo alla conoscenza dei rock glaciers delle Alpi Italiane. Riv. Geogr. It., XCII, 2, 117-140.

Wahrhaftig, C. and Cox, A. (1959). Rock glaciers in the Alaska Range. Bull. of the Geol. Soc. of America, 70, 383-436.

GEOCRYOLOGY OF THE CENTRAL ANDES AND ROCK GLACIERS

A.E. Corte

CONICET, CRICYT, Mendoza, Argentina

SYNOPSIS The cryogenic characteristics of the Central Andes between 22-25° SL and at 33°SL are indicated. The internal structure of a debris covered glacier is presented. Geocryogenic marks between the Pacific slopes and the Atlantic are observed. The permafrost lower limit for the Andes is compared with northern hemisphere. The applied aspects are dealing with hydrology, concentration of heavy minerals and road constructions.

INTRODUCTION

The Andes extending from 10°NL till 55°SL, offer a unique laboratorium for the study of cold geosphere and biosphere processes, in which altitude and latitude are the main static variables affecting permafrost conditions, freeze-thaw and vegetation distribution.

1. GENERAL GEOCRYOGENIC CONDITIONS OF THE ANDES

Permafrost lower appearance along the cordillera from 10°NL till 55°SL, is indicated (Fig. 1 a-b) , according to Table 1 data. The permafrost along the Andes is below the average for the northern hemisphere (Chen Guodong, 1983). The lowest distributions for permafrost along the Andes as compared to the northern hemisphere (Cheng Guodong 1983) is adscribed to the large land masses of the northern hemisphere, shifting the thermal equator 5 degrees to the north of the geographical equator. In the case of the central and southern Andes moisture is supplied from cold Antarctic waters flowing north along western South America and also in the south eastern coast.

In the east-west section of the Andes at lat. 33°using 18 cryogenic elements (Corte et al., 1985) are indicating that permafrost lower limit is dipping from the Pacific slopes to the Atlantic side.

Permafrost lower limit in Chile at 33°S1 is at 3500-3700 m (Lliboutry, 1986; Marangunic, 1976). In the eastern Atlantic side of Mendoza is at 3200 meters (Corte et al., 1985). The greater elevation of the permafrost lower limit in Pacific side is considered a consequence of heavier snow precipitations which are insulating the ground from freezing and also as result of greater cloudiness. In the Argentinian eastern side on the contrary, the less precipitation are permiting a deeper ground freezing and permafrost development.

2. PERMAFROST CONDITIONS IN THE DRY PUNA (22°-25°SL)

Under the dry conditions of the Puna (Fig. 2) permafrost is observed in: a) in salt lakes, above 3670 m, as big domes of ice 1,5 km long and up to 7 m high (Hurlbert et al., 1984), such ice segregation of the palsa or pingo types are considered a product of the Little Ice Age (1490-1880) (Thompson et al., 1986). They are observed from 22° till 25°SL. b)Rock glaciers of glacigenous origin above 4500 m (Corte, 1987). c) Segregated ice in peat bogs at 4500 m (Igarzabal, 1983). If such permafrost was generated during the Holocene cold stages, needs further evaluation.

3. PERMAFROST GEOCRYOGENIC CONDITIONS - EASTERN SECTOR OF THE ANDES AT 33°SL

According to figure 3 the following geocryogenic regions can be differenciated: Y- the geocryogenic or permafrost region: its lowest limit is indicated by the lowest terminus of rock glaciers at 3200 m with a mean annual temperature of about 0°C(Fig.3).This region is separated into two subregions: the W subregion is the permafrost with active layer region which in rock glaciers is decreasing continuously upwards till 4800 m where it tends to become small under a mean year temperature of -10°C. The X sub-region of intense freezing. This is the least known geocryogenic region. The tops of the mountains at 7000 m are at about -20°C. Z- the parageocryogenic or paraperiglacial region: this is the seasonal ground freezing region. Its lowest terminus cannot be determined with precision but it can be set at the level where needle-ice ceases to up-root vegetation. For the Mendoza region it is at 850 m or the 13°or 14°C mean year temperature

The geomorphic implications of cryogenic belts.

The W sub-region. It is characterized by the following geocryogenic features:

1. Active rock glaciers are located in the range of 3200 m till 4700 m. The debris thickness on the surface of rock glaciers decreases upwards (Fig. 3). Values of the active layer above 4800 m are not available.
2. Large gelifluction lobes, steps and benches.
3. Vertical sorting on the debris cover of rock glaciers, taluses are well developed in layers up to two meters thickness.
4. Large sorted features of 1-4 m diameter.
5. Thermal contraction cracking.
6. Planation surfaces. It is not possible to say if this planation figures, within this sub-region, are active at the present time or they are product of a past colder climate.
7. Asymmetry.
8. Stratified debris in slopes.
9. Thermokarst features.

The X sub-region. This the intense freezing region: permafrost widespread. Because of its elevation this region is little known. Values of the active layer above 4800 m are not available. The following geocryomorphic features characterize this sub-region:

1. Large cryoplanation surfaces: these planation surfaces are present over the range of 5000 m.
2. Debris slopes "acarreos": the largest are indicated for the Aconcagua region.

The Z region. This is the mild cryogenic or parageocryogenic region with a mean annual air temperature higher than 0°C. In this sector of the Andes it is located below the lowest terminus of the active rock glaciers at 3200 m. This is also the seasonal ground freezing (Fig. 3). This term, parageocryogenic is used as an equivalent of Kowalkowski's paraperiglacial. The following features of processes characterize this region:

1. Gelifluction and solifluction.
2. Needle-ice growth.
3. Cryoweathering in rocks forming pits and hollows with vertical sorting.
4. Stratified debris in slopes.
5. Up-rooted vegetation by needle-ice (mainly grasses).
6. Small sorted features, 10-20 cm in diameter, by freeze-thaw action and also by dessication.

4. ROCK GLACIERS AND DEBRIS COVERED GLACIERS

Central Andes rock glaciers were systematized into two broad groups: (Corte 1976 a-b; Corte et al.,1981) 1. those produced by cryogenic activity: cryofraction, gelifluction, snow and debris activity and avalanches are called"cryogenic rock glaciers" (Corte, 1986) (Photo 1). 2. Those debris bodies related to glaciers ice or glaciers activity in cirques; which still contain a nucleus of glaciers ice should be called:debris covered glaciers or glacigenic rock glaciers (Photo 2).

Thermokarst activity is a negative feature resulting from ground-ice melting under the thermal effects of the debris cover, it is remarkable over debris covered glaciers (Photo 2) and less evident over cryogenic rock glaciers (Photo 1).

The internal structure of a debris covered glacier (Photo 2) is known from thermal interpretations (Fig. 4) upper right corner, indicating an active layer of 2.50 meters and a permafrost depth of 68 meters. Geoelectric and audiomagnetoteluric soundings by Fournier et al. (1986) are indicating an active layer 2.0 meters and a permafrost depth of 70 meters. There is a subpermafrost aquifer of 63 meters (Fig. 4 transversal and longitudinal profile). The debris cover was subjected to relative dating by Wayne et al. (1983). In the lower parts of this debris covered glacier there was Wisconsin activity, while the whole debris cover is Holocene. It is of interest to note that the first geophysical sounding revealed a permafrost core of ice and debris and not glacier massive ice. This would indicate that after the Wisconsin advances the glaciers melted completely and during the Holocene cold fases mixture of ice and debris was incorporated. Future soundings are underway.

Besides the two rock glaciers described, there are rock glaciers-like features which are produced under special conditions of precipitations, rock types and debris accumulation (Corte 1976a; Lliboutry,1986).

5. APPLIED ASPECTS

Hydrology: in the Central Andes at latitude 33°the inventory of debris covered glaciers, rock glaciers and uncovered glaciers is given areas of: 5.0% and 5.5% respectively (Corte et al., 1981). Geophysical soundings are indicating a subpermafrost aquifer below debris covered glaciers in their lower tongues (Fournier et al., 1986).

The hydrological significance of debris covered glaciers, rock glaciers and all cryogenic debris covers, is observed when comparing the run-off from snow surveys: the larger the area of rock glaciers and debris covered glaciers the greater the error (Corte, 1986). This is indicating that a substantial amount of the fall and winter precipitations is melted and refrozen in the boulderly covers. This water may appear years later in times with poorer precipitations giving unexpected discharges. Consequently future glaciers inventory for dry cryogenic regions, should not only contain information on the clean glaciers, the debris covered glaciers, rock glaciers but also on the debris covers including talus. Their hydrological characteristics should be determined.

Heavy minerals concentration: the cryofraction

of rocks, the ejection of coarse particles to the surface and fines migrating down to the bottom of the freeze-thaw layer (active layer)produces the well known cryogenic texture of vertical sorting. With the fines migrating down are also concentrated the heavy minerals (Corte, 1987; Ahumada's article in this volume). Under laboratory experiments magnetite mixed uniformly with saturated sands migrated down to the bottom of the probe after 35 cycles of freeze-thaw.

Road construction in cryogenic regions: the whole patagonian region is subjected to seasonal freezing and road constructors are using cryogenic criteria for roads design (Angelini, 1986).

In the Central Andes (at latitude 33°) road constructors are using cryogenic criteria for projects above 2500 meters (depending on exposure). For latitude 22°and according to information here indicated, besides seasonal freezing there is sporadic permafrost, above 4500 meters.

CONCLUSIONS

1. At 33°SL in the Pacific slopes of the Andes, permafrost is at a higher elevation than in the Atlantic side. This is due to greater snow precipitations and cloudiness in the Pacific or Chilean side.
2. Lower permafrost along the Andes is about 1000 meters below the average for the northern hemisphere. This is adscribed to the large land masses in the northern hemisphere shifting the thermal equator 5 degrees to the north. Besides, Central and southern Andes are under the influence of cold Antarctic waters.
3. Large geocryogenic features of the Central Andes are: rock glaciers, debris covered glaciers, segregated ice bodies (pingo or palsa types), cryoplanations and extrusion.
4. At latitude 33°, east side of the Andes geocryogenic regions are subdivided: a- the region of seasonal freezing below the lower permafrost limit at 3200 m; b- the region of permafrost with active layer between 3200-5000 m; c- the region of permafrost with negligeable or unknown thawing above 5000 m; 5- past Holocene cold stages are responsible for some of these processes. Cryoplanation has been working for a much longer time.

TABLE I

PERMAFROST LOWEST APPEARANCE ALONG THE ANDES

Place	Lat.	Altitude			Feature	Source
		Act.	Past	Dif.		
Venezuela	10°N	4765	2600	2065	Temperature data	Schubert 1979
Ecuador	1°S	5000	-	-	Temp., vegetation	Lauer 1979
Ecuador	2°S	5000	-	-	Temp., vegetation	Lauer 1979
Bolivia	22°S	4500	-	-	Segregated ice	Hurlbert et al. 1984
Argentina	23°S	4500	3000	1500	Permafrost, peat bogs	Igarzabal 1985
Chile	25°S	3670	-	-	Segregated ice	Hurlbert et al. 1984
Argentina	27°S	3750	2600	1150	Rock gl. fossil	Czajka 1955
Argentina	31°S	3150	-	-	Rock glacier	Simon 1984
Argentina	33°S	3200	1200	2000	Rock glacier	Corte 1976a
Chile	33°S	3500	-	-	Rock glacier	Lliboutry 1961, 1986
Chile	33°S	3700	-	-	Rock glacier	Marangunic 1976
Argentina	35°S	2800	-	-	Rock glacier	Grosso, oral com.1987
Argentina	52°S	1000	-	-	Active layer bottom	Roig, oral com.1987

REFERENCES

Angelini, U. (1986). Comportamiento de pavimentos en servicio,bajo los efectos del congelamiento: Chubut, Patagonia. Acta Geocryogenica No. 4, p.17-22.

Corte, A.E.,(1976a). Rock Glaciers. Biul. Peryglacjalny, No. 26, p. 175-198.

Corte, A.E. (1976b). The hydrological significance of rock glaciers. Journ. of Glaciology, 17 No. 75, p.157-158.

Corte, A.E. & Espizua, L.E. (1981). Inventario de Glaciares de la Cuenca del río Mendoza. Text, 64 p. Atlas with 18 color maps at the scale 1:30.000.

Corte, A..E. & Buk, E. (1984). El marco criogénico para la hidrología cordillerana. Programa Hidrológico Internacional, Santiago, Chile. 16 p.

Corte, A.E. & Cui, Z. (1985) Comparative study of geocryogenic (periglacial) conditiond features and processes in the Andes and Himalayas. Acta Geocryogenica No.3, p.6-63.

Corte, A.E. (1986). Andean Geocryology and Rock Glaciers, in: Rock Glaciers, edit. by Giardino et al., Texas A. and M. University, 15 p.

Corte, A.E. (1987). Geocriología, con especial énfasis en los Andes y Antártica. In press, by Eudeba, Buenos Aires, 444 p.

Cazjka, W. (1955). Rezente und Pleistozane Verbreitung und typen des periglazialen Denudationszyklus in Argentinien. Acta Geographica No. 14, Soc. Geog. Fenniae, p. 121-140.

Cheng Guodong (1983). Vertical and horizontal zonation of high altitude permafrost. Proc. Fourth Internat. Permafrost Conf., Fairbanks, pp.136-141.

Fournier, H.G., Corte, A.E., Mamaní, M.J., Maidana, A. & Borzotta, E. (1986). Ensayos de confirmación de la estructura de un glaciar cubierto en Vallecitos (Andes, Cordón del Plata, Argentina) por medio de sondajes eléctricos y magnetotelúricos. Acta Geocriogénica No.4, pp.53-54.

Igarzabal, A. (1983). Aspecto geocriogénico de la Puna y Cordillera Principal. Acta Geocriogénica, No. 1, pp.133-140.

Lliboutry, L. (1986). Rock glaciers in the dry Andes, Materiali Glaziologicheskii Isledovanii, No. 58, Russian text pp.18-35; English pp. 139-144.

Lliboutry, L. (1961).Phenomenes cryoniveaux dans les Andes de Santiago, Chile. Biul. Peryglacjal., No. 10, pp.209-224.

Hurlbert, S.H. & Chang, C.C.Y. (1984). Ancient ice islands in salt lakes of the Central Andes. Science (224), No. 4646, pp.299-302.

Lauer, W. (1979). La posición de los páramos en la estructura del paisaje de los Andes tropicales. Actas del Seminario El Medio Ambiente Páramo, pp.29-46.

Marangunic, C. (1976). El glaciar de rocas Pedregoso, Río Colorado, V Región, Chile. Primer Congreso Geológico Chileno, pp.71-80.

Schubert, C. (1979). La zona del Páramo. Morfología glacial y periglacial de los Andes de Venezuela. Actas del Seminario El Medio Ambiente Páramo, pp.11-28.

Thompson, L.G., Mosley-Thompson, E., Dansgaard, W. & Grootes, P.M. (1986). The Little Ice Age as recorded in the stratigraphy of the tropical Quelccaya ice cap. Science(234) No. 4774, pp.361-364.

Simon, W. (1984). Observaciones sobre procesos geocriogénicos en la cordillera del límite SO de la Pcia. de San Juan, Acta Geocriogénica No.2, pp.197-203.

Wayne, W.J. & Corte, A.E. (1983). Multiple glaciations of the Cordón del Plata, Mendoza, Argentina. Palaeogeography, Palaeoclimatology, Palaeoecology, (42), pp.185-209.

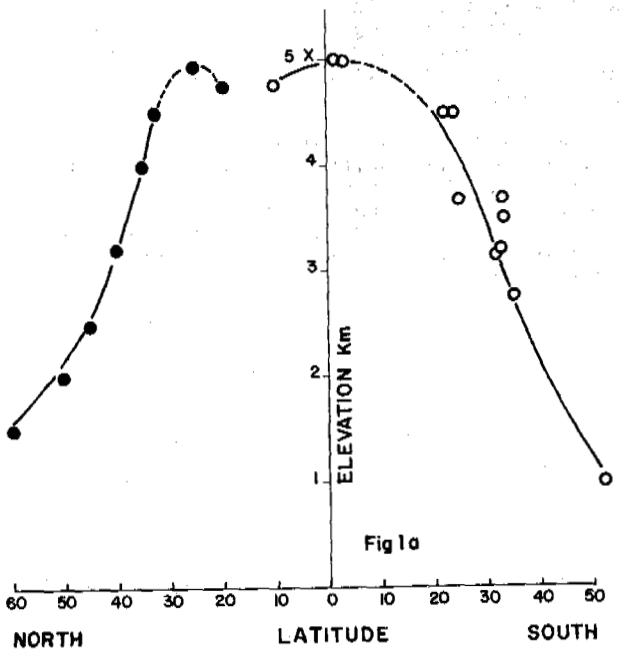

Fig.1 a-b:Andes permafrost lowest limit compared with the average for the northern hemisphere (Cheng Guodong 1983).

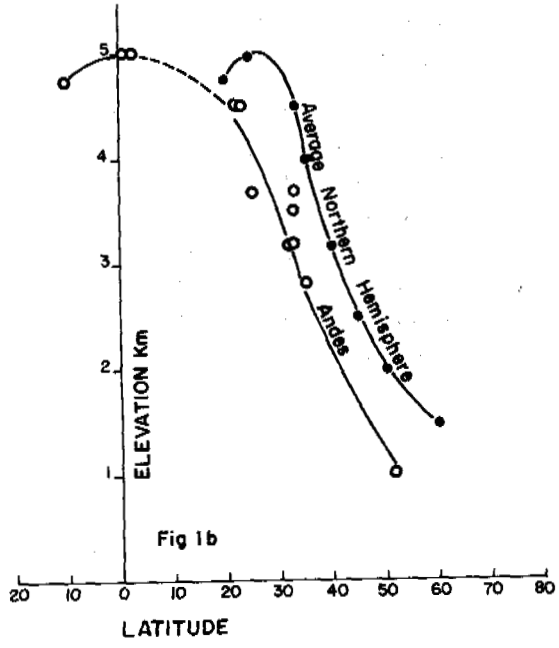

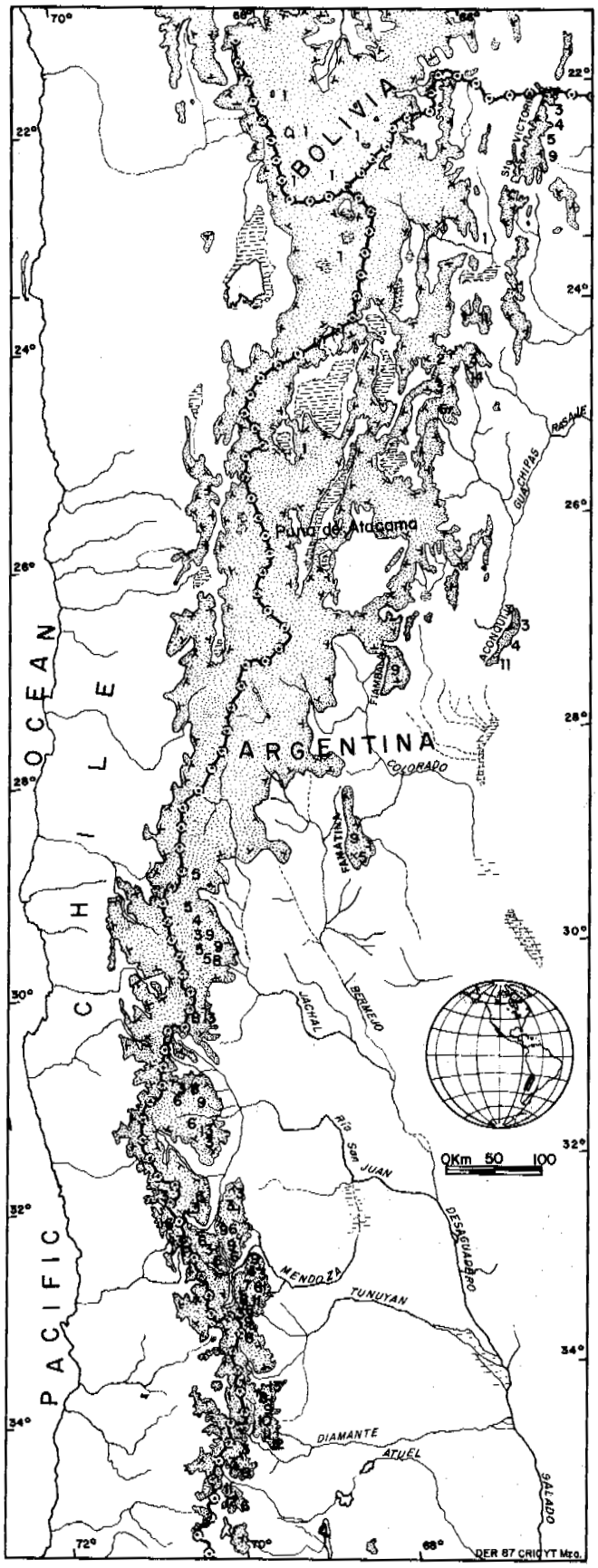

Fig.2. Permafrost associated processes Central Andes:1-Segregation ice(Palsas-pingos); 2-Segregation ice in peat bogs; 3-rock glaciers;4-gelifluction;5-debris slopes;6-debris covered glaciers; 7-thermalcontraction;8-thermokarst; 9-cryoplanation; 10-extrusion;11-sorting larger than 1 m.;12-sorting smaller; 13- asymetry;14-peat bogs.Permafrost region with dots, broken line.

Fig.3. Central Andes geocryogenic regions; depth of the active layer on rock glaciers(southern exposures)and precipitations in differents altitudes.

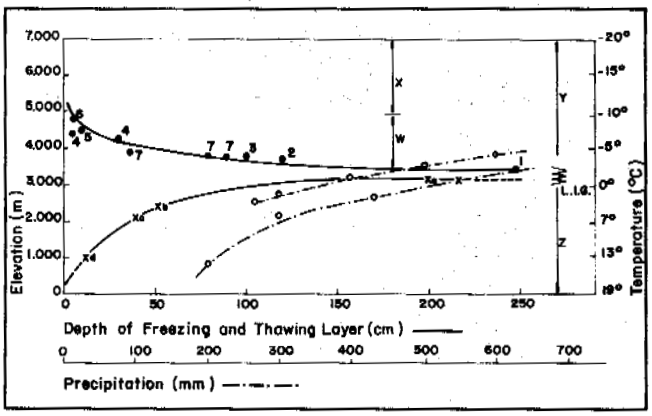

Photo 1: Cryogenic rock glacier "Los Blancos"

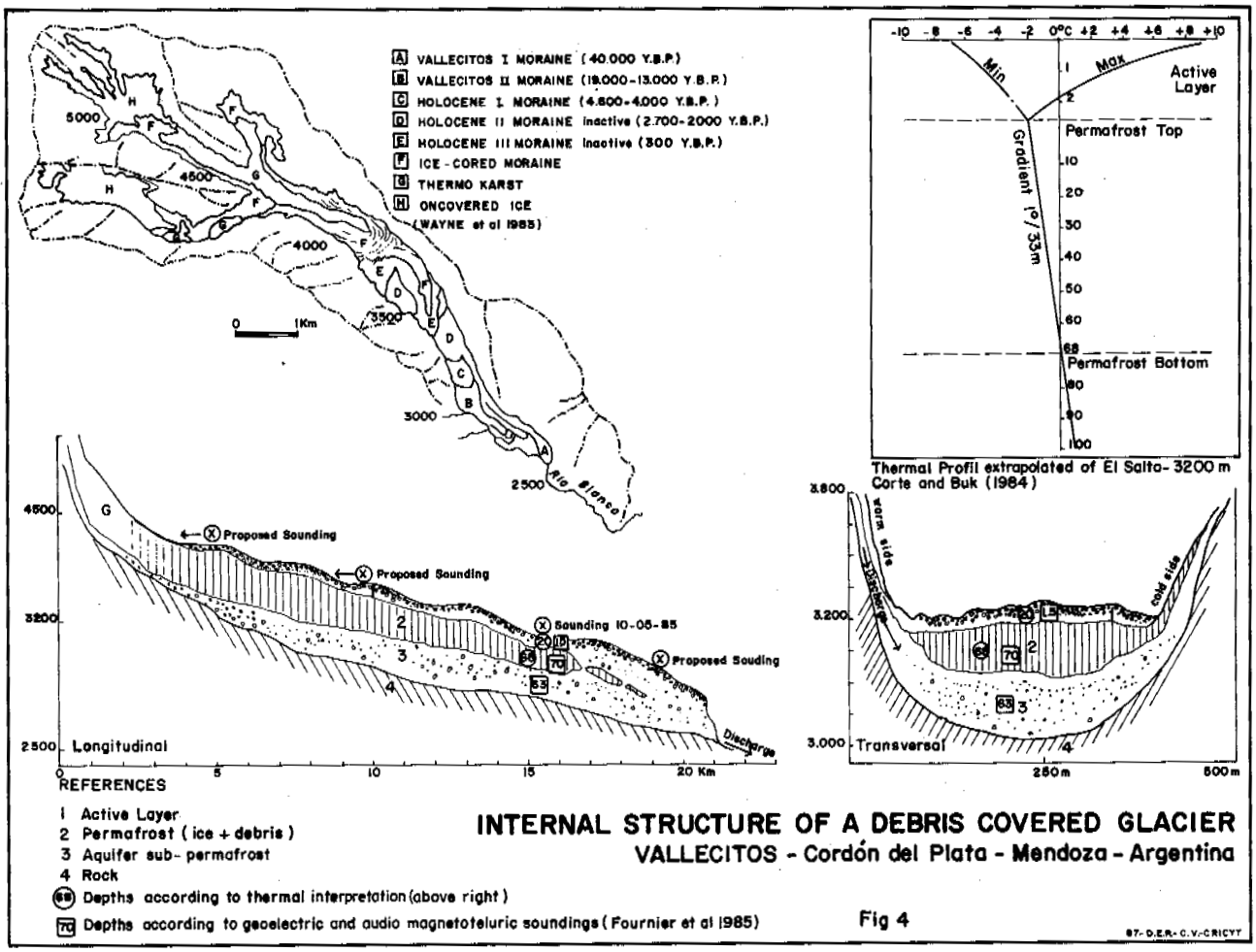

INTERNAL STRUCTURE OF A DEBRIS COVERED GLACIER
VALLECITOS - Cordón del Plata - Mendoza - Argentina

Fig 4

87- D.E.R.- C.V.-CRICYT

Photo 2: Vallecitos Debris-covered glacier

ROCK GLACIERS IN THE SOURCE REGION OF URUMQI RIVER, MIDDLE TIAN SHAN, CHINA

Cui, Zhijiu[1] and Zhu, Cheng[2]

[1]Department of Geography, Beijing University
[2]Lanzhou Institute of Glaciology and Geocryology, Academia Sinica

SYNOPSIS More than 15 rock glaciers of talus type or Colorado type occur in groups or apart from each other above the lower limit of alpine permafrost (3,200 m a.s.l.), within the area of the Tian Shan Glaciological Station. They might be formed during the Little Ice Age.

Based on geoelectrical prospectings, it became known that the rock glaciers are composed of 3 layers, i.e., the active layer with a resistivity of $10^3\Omega m$, the perennially frozen body with a resistivity ranging from 10^4 to $10^5\Omega m$, and the perennially frozen bed rock.

Observations show that the middle part of the front moves much faster than the other parts of the rock glacier, and its main body undergoes the partial shear stress.

INTRODUCTION

The source region of Urumqi River, lying on the Northern slope of Mt. Kelaucheng, a branch of Middle Tian Shan, is in a typical glacial and periglacial environment, where most of the crests are at an elevation ranging from 4,100 to 4,300 m, the snowline — at 4,000 to 4,100 m, while the lower limit of apline permafrost is at 3,200 to 3,300 m a.s.l. The mean annual air temperature ranges from -5.4°C at the Daxigou Meteorological Station (3,539 m) to about -8° to -12°C on hilltops. The Urumqi River is mainly fed be seven modern glaciers, of which the ice tongues terminate at an elevation of about 3,700 m. Bed rocks in this region are of granite and gneiss.

Many kinds of periglacial phenomena, including frost weatherings, mass wastings and frost sortings, were reported from this region (Ji, 1980; Li et al., 1981; Qiu et al., 1981; Qiu et al., 1983). However, reports of rock glacier are very few.

In this paper, the authors intend to describe the basic characteristics of rock glaciers in their morphology, constitution and movement based on the field observations during the period of 1985 to 1986.

CLASSIFICATION, MORPHOLOGY AND DISTRIBUTION OF ROCK GLACIERS

There are different ideas in rock glacier classification (Wahrhafting and Cox, 1959; Barsch, 1971 ; ϕstrem, 1971; White, 1976, 1981). Based on the position, material source, morphology, ground ice and regional characteristics, Cui (1982, 1985) suggested that the rock glaciers can be classified into 4 types, namely the Alaska-Yukon type, Alps type, Colorado type and the Kunlunshan type. Since the rock glaciers in this working area, more than 15 in number, are developed from talus and protalus rampart, they should be of colorado type.

Most of them are lobate-shaped with a proportion of width to length greater than 1, except the tongue-shaped RG 1.

Haeberli (1985) pointed out that rock glacier generally occurs between the equilibrium line and the lower limit of alpine permafrost. In the Middle Tianshan, it was found that the higher limit of rock glacier is at about 3,900 m a.s.l., and is about 150 m lower than the equilibrium line. They occur in groups or apart from each other at hill feet. For example, a group of rock glaciers occurs within a restrict, 300 to 400 m in width and 30 to 50 m in length, at the foot of the southeast headwall of an empty cirque. The separate ones are commonly 30 to 60 m in length and 100 to 150 m in width with a front ridge 30 to 40 m in height and 30° to 60° in slope. The tongue-shaped RG 1 is about 100 m in length and 60 m in width with a front 40 m in height.

From the top down to the front, the rock glacier changes in slope, and ahead an obvious turning point the slope becomes antidip. Some rock glacier reveals a platform (Photo 1) or troughs and ridges on its surface (Photo 2), caused by compression.

CONSTITUTION OF ROCK GLACIER

By geoelectrical prospectings it becomes known that rock glaciers in this region are composed of three layers, i.e. the active layer at the uppermost with a resistivity of 2,500 Ωm, commonly less than 2 m in thickness; the perennially frozen sediment body, $3.7X10^4$ Ωm, in resis-

Photo 1 Compressive Platform at the Front of RG 3

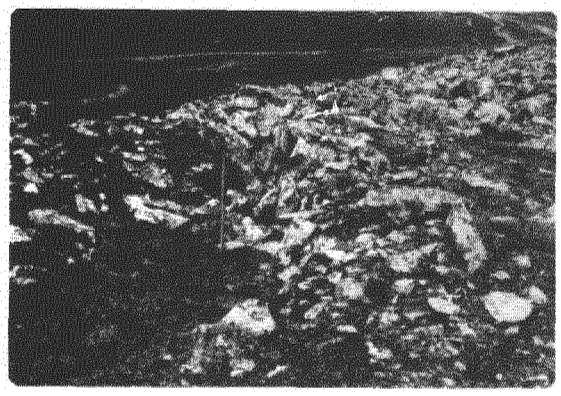

Photo 2 Troughs and Ridges on RG 3

tivity, about 110 m in thickness; and the frozen bed rock with a resistivity of 3.2×10^4 Ωm (Fig. 1a). Haeberli (1985) suggested a 4-layer model for rock glacier in Alps that the main body composed of perennially frozen gravel and sand is separate from the bed rock by an unfrozen sediment layer (Fig.1b).

The absence of unfrozen subpermafrost sediment might be a character of the rock glacier in a continental periglacial region like the Middle Tianshan.

By pit observations it is known that the rock glaciers are ice-cemented. Ice lenses of $20 \times 15 \times 8$ cm^3 and $20 \times 14 \times 6$ cm^3 in size were found at a depth of 1.3 to 1.43 m of RG 3 during June 26 and July 26, 1986.

MOVEMENT OF ROCK GLACIERS

Rock glacier varies in moving velocity. Some measurement data are listed as follows.

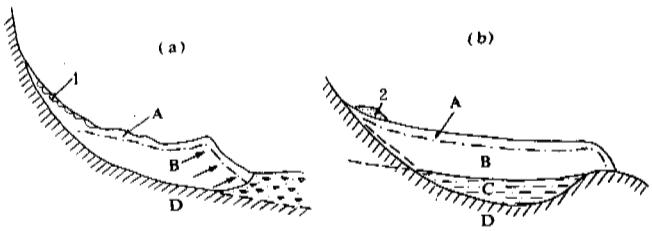

Fig.1 Constitution of Rock Glaciers in Tianshan and in Alps

a. in Tianshan;
b. in Alps (after W.Haeberli, 1985).

A. active layer;
B. perennially frozen body;
C. unfrozen sediment;
D. bed rock.
1. modern talus;
2. perennial snow patch or small glacier.

RG 1 It is the lowest rock glacier in this region, at an elevation of 3,350 m, near the lower limit of alpine permafrost. Fourteen blocks on the surface of this rock glacier had a downward movement of only 1 cm per year in average, while 22 blocks did not move at all.

RG 2 This rock glacier is located on a north-facing slope at 3,600 m a.s.l., and is 70 m in length, 119.5 m in width (Photo 3). On the top of the front region with an antidip slope of 8°, among the 37 measured blocks, 13 had moved forwards for 11.2 m per year in average, and 2 had backward moved for 4.5 cm and 1 cm, respectively. On the front slope, the results of measurement of 100 blocks are as follows. On the upper part with a slope of 60° (Photo 4), 20 blocks were

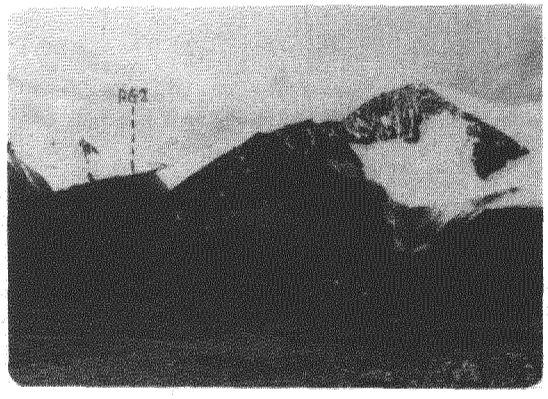

Photo 3 RG 2 and Little Ice Age of Glacier 2 at Its Right Side

Photo 4 Front Slope of RG 2

a. upper part;
b. middle part;
c. lowest part

observed no movement at all; on the middle part with a 43° slope, among the 50 blocks, 28 had moved 2-4 m vertically and 1.5 m horizontally in average; and on the lowest part with a 34° slope, only 2 of the 30 blocks moved in a short distance. Therefore, the RG 2 is much active than the RG 1.

It is believed that a rock glacier is in initiative and passive movement (Haeberli, 1985;White, 1971). The initiative movement of the perennially frozen body along the shearing plane would cause the pebbles and blocks on the surface moving passivelly. The faster movement of the middle part of the front slope, the occurrence of finer debris on the middle and lower part of the front slope indicates an initiative movement of the main body of the rock glacier, while the generally forwards, downwards movement and local reverse movement of the pebbles and blocks on the surface indicates a passive movement. This is clearly shown in RG 1, RG 2, etc.

RG 3 It is located at an elevation of 3,500 m and is 60 m in length, 150 m in width with a front 30 m in height. Thirty-two targets and 20 blocks were measured during the period of 1985-1986 (Fig.2). The mean value of moving velocity was known as 75 cm/year horizontally and 14 cm/year vertically.

RG 4 It is located on a north-facing slope by an abandoned highway, 3,550 m a.s.l., and is 100 m in width, 35 m in length with a front slope of 35°. Observations of 5 targets during 1985 to 1986 showed that 9 targets had a forward movement, 3 targets had a backward movement, 11 targets had a downward movement, and 2 — upwards.

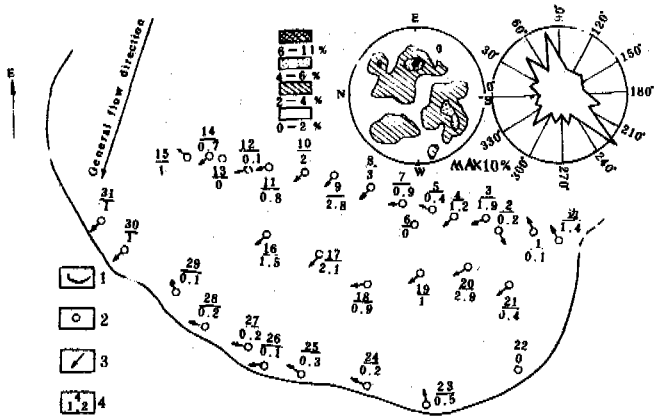

Fig.2 Target Movements Within the Depth of 0 to 1.4 m of RG 3 and the Rose Diagram of AB Face of RG 3

1. boundary of rock glacier;
2. targets;
3. moving direction;
4. number of target (upper) and moving speed, in m/year (lower).

The distance of forward movement was 49 cm per year in average, and the mean value of downward movement was 38 cm/year. The abandoned highway was 5.5 m in width in 1969, however, up to 1985, 1.5 m of this rod road had been covered by the RG 4. In other words, the RG 4 advanced 6 cm per year in average. Based on the following formula, the discharge V from the rock glacier to the road could be calculated.

$$V = L \cdot a \cdot b \cdot \sin\alpha$$

where, L — width of the RG 4, 100 m;
a — length of the front slope of RG 4, 25 m;
b — horizontall advance of the rock glacier, 1.5 m;
α — slope of the front, 35°.

Thus, the total amount of discharge of RG 4 on the road was 1760 m^3 during the past 25 years or 70.6 m^3/year in average. It was reported from Colorado that the discharge of Arapho and other two rock glaciers were 215 to 771 m^3/year in average during 1961 to 1966 and the mean annual advancing velocity were 5 to 9.7 cm (White, 1976). Therefore the discharge and advancing speed were higher in Colorado than in the Middle Tianshan. Also, the mean creeping velocity of rock glacier in Alps (Haeberli, 1985) and Central Alaska (White, 1971) can be as high as 0.5-1 m/year, which in the working area of Middle Tianshan it was 0.3 m/year in average. This might be due to the drought climate, high elevation, low temperature, less ice content and absence of bace-slide of rock glaciers in Tianshan.

CONCLUSION

Rock glaciers in the Middle Tianshan are of Colorado type developing from talus or protalus ramparts. Most of them are of lobate-shaped. They are of cold-based rock glaciers. It seems that the rock glaciers are less possible to slide at the base. There occurs an initiative movement with the perennially frozen body and a passive movement on the surface. In comparison with the results from Colorado, it could be concluded that rock glaciers in Middle Tianshan are much stable.

ACKNOWLEDGEMENTS

This work was conducted in the Tianshan Glaciological Station. The authors would like to express their cordial thanks to the leaders, colleagues of the Lanzhou Institute of Glaciology and Geocryology, Academia Sinica for their effective support. Also the authors would express thanks to Dr. W. Haeberli, who offered good suggestions and some of his books related to this work.

REFERENCES

Barsch, D. (1971). Rock glaciers and ice-cored moraines. Geografiska Annaler 53 A, 203-206.

Barsch, D. (1978). Active rock glaciers as indicators for discontinuous alpine permafrost. An example from the Swiss Alps. Proc. 3rd International Conference on Permafrost, Edmonton, Albt. Canada, 348-353.

Cui Zhijiu, (1982). Characteristics of periglacial landforms in the Qinghai-Xizang Plateau. Scientia Sinica (Series B), (25) 1, 79-91.

Cui Zhijiu, (1985). Discovery of Kunlunshan-type rock glaciers and the clossification of rock glaciers. Kexue Tongbao (30) 3. 365-369.

Haeberli, W. (1985). Creep of mountain permafrost: internal structure and flow of alpine rock glaciers. 24-105, Nr. Mitteilmnger.

Li Shude, Cui Zhijiu and Zhang Zhenshuan, (1981). Preliminary study on weathering rate of rock in Shengli Daban at the head of Urumqi River, Tianshan. Journal of Glaciology and Cryopedology, Vol.3, Special Issue, 114-119.

Ji Zixiu, (1980). The modern periglacial process in the central part of Tianshan. Journal of Glaciology and Cryopedology,(2) 3, 1-10.

Qiu Guoqing, et al., (1981). Some new data on periglacial phenomena and alpine permafrost at Tianshan Glaciological Station. Annual Report of the Tianshan Glaciological Station (1), 113-124.

Qiu Guoqing, Huang Yizhi, Li Zuofu, (1983a). Basic characteristics of permafrost in Tianshan, China. Proc. 2nd Chinese Natl. Conference on Permafrost, 21-29, Lanzhou.

ϕstrem, G. (1971). Rock glaciers and ice-cored moraines: a reply to Barsh, Geogratiska Annaler 53A, 207-213.

Wahrhaftig, C., Cox, A. (1959). Rock glaciers in the Alaska Range. Geological Society of Amer. Bull., 3, 383-436.

White, S. (1971). Rock glacier studies in the Colorado Front Range, 1961 to 1968. Arctic and Alpine Research, (3) 1, 43-64.

White, S. (1976). Rock glaciers block fields, review and new data. Quaternary Research, (6), 77-97.

White, S. (1981). Alpine mass movement forms (noncatastrophic), classification, description and significance. Arctic and Alpine Research, (13) 2, 127-137 .

SEASONAL FROST MOUNDS IN AN EOLIAN SAND SHEET NEAR SØNDRE STRØMFJORD, W. GREENLAND

J.W.A. Dijkmans

**Department of Geography, University of Utrecht,
Heidelberglaan 2, 3584 CS Utrecht, The Netherlands**

SYNOPSIS An eolian sand sheet of about 1 km² lies along a broad fluvioglacial valley that connects the inland ice with the fjord in the Søndre Strømfjord area, in W. Greenland. Permafrost is found in the sand sheet. Several small ice-cored hummocks have been encountered in a relatively low, wet part of the sand sheet near a spring. They developed in less than one year and were in a decaying stage during the summer of 1987. They are interpreted as seasonal frost mounds, most likely of the frost blister type. They occur in an arid climate and are not dependent on perennial groundwater discharge for their formation. Decay may lead to specific sedimentological structures in the eolian stratification.

INTRODUCTION

Ice-cored hummocks have not yet been described from eolian sand sheets, although these environments have been studied in several parts of the arctic region. In the summer of 1987 ice-cored hummocks have been encountered on a sand sheet during a geomorphological study of periglacial eolian sand deposits in the Søndre Strømfjord area. Because of its unusual occurrence in an eolian environment and the possible role that remnants of these forms could play in case of preservation in the eolian strata, the hummocks are described and compared with similar features known from the literature.

THE STUDY AREA

Environmental setting

The Søndre Strømfjord air force base is located at 67°N - 50°40'W at the head of an approximately 150km long WSW-ENE trending fjord of the same name in W. Greenland (fig. 1A). The edge of the inland ice sheet, approximately 25km East of the base, is connected to the fjord by two East - West oriented valleys, Sandflugtdalen (Driftsand Valley) and Ørkendalen (Desert Valley) (fig. 1B). The valleys are bordered by mountain ridges, mainly consisting of gneiss of Precambrian age (Escher, 1971), locally covered by morainic ridges (Ten Brink, 1975).

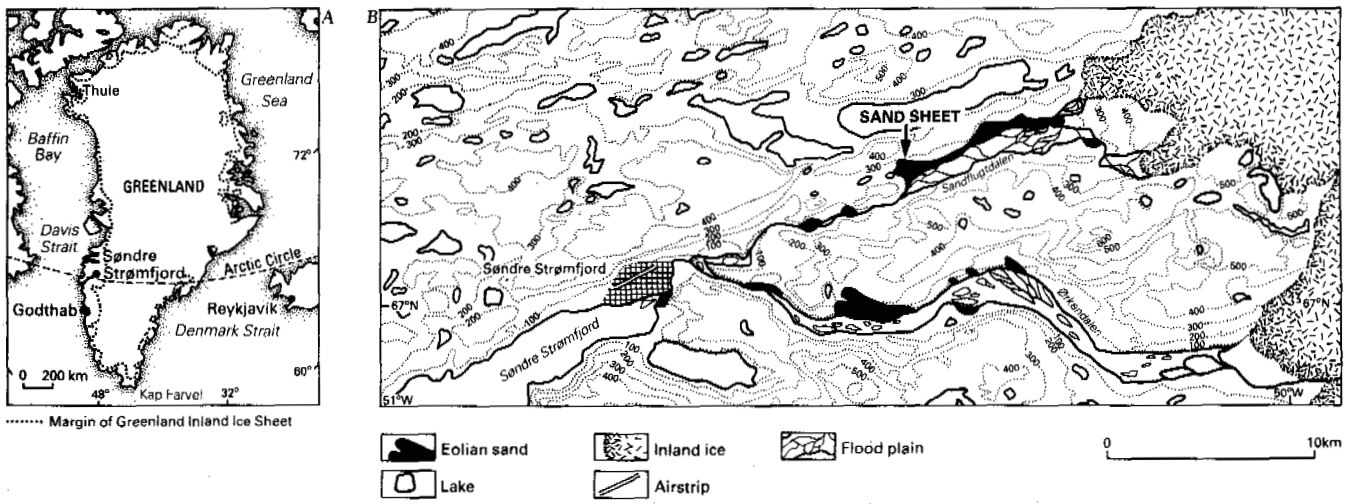

Fig. 1A Location of Søndre Strømfjord, W. Greenland and B. Map of the Søndre Strømfjord area. The occurrence of eolian sand along fluvioglacial river valleys that drain outlet glaciers of the inland ice cap is indicated.

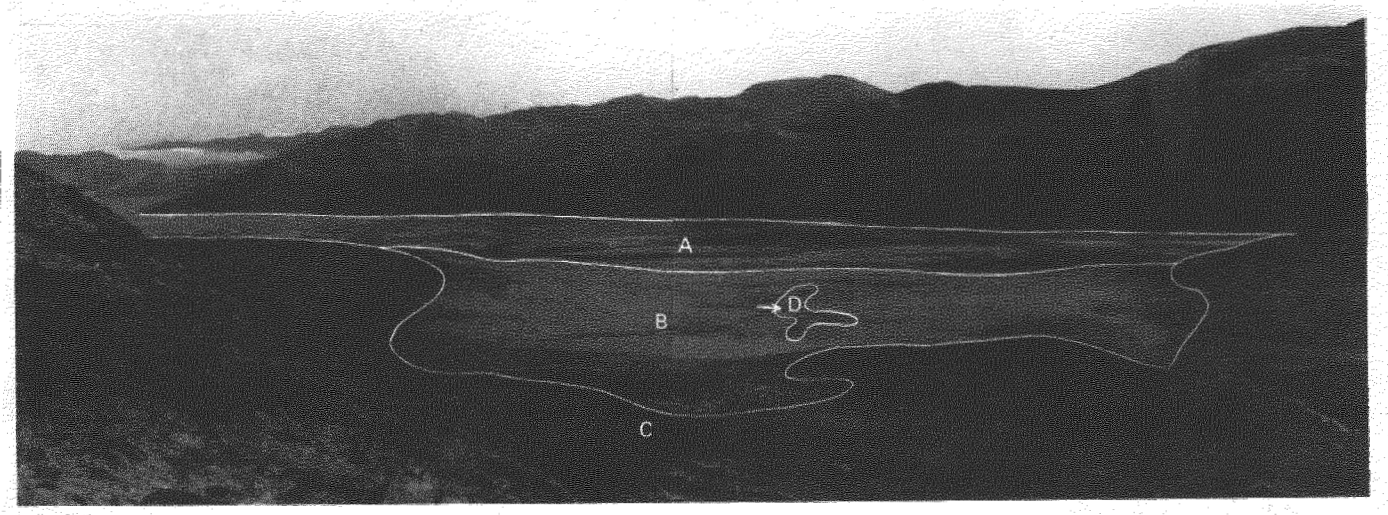

Fig. 2 Overview of the sand sheet in the central part of Sandflugtdalen looking to the southeast. A: broad flood plain, B: sand sheet with partly stabilized edges, C: bedrock, completely stabilized eolian sand, morainic ridges, D: seepage zone in the central part of the sand sheet. The location of the ice-cored hummocks is indicated by an arrow. The distance from the middle of the flood plain to the mountain ridge where the photograph has been taken is about 2km. One of the outlet glaciers that drains into Sandflugtdalen can be seen to the left.

In summer braided rivers carry meltwater from the glaciers through the broad valleys to the fjord. Part of the sediment load is redeposited by wind, hence the names of the valleys. Eolian sand lies on the northern fringes of the valleys (fig. 1B). The morphology and sediments of Sandflugtdalen have first been described by Hansen (1970).

The area has an arid, continental polar tundra climate. Yearly precipitation is less than 200mm. About half of this falls as snow from September to May. Temperatures are relatively mild during the short subarctic summer. The mean July temperature is about 11°C, whereas mean January temperature is about -18°C (Hasholt & Søgaard, 1978).

Morphology of the Sandflugtdalen sand sheet

Only the eastern part of Sandflugtdalen has an approximately 1km wide flood plain. In the western part the river has cut itself through a narrow valley. North of this lies a former valley at a higher level, separated from the present river valley by a bedrock ridge. The entrance to the northern valley forms a wide area where a partly vegetated sand sheet of about 1km² has developed at an elevation of ±200-250m a.s.l. (fig. 1B). The shape of the sand sheet as well as the small dune forms on it suggest a main direction of eolian transportation to the northwest.

Active eolian sand was found to a height of about 65m and stabilized eolian sand, on the footslope of a bedrock ridge, to a height of 85m above the flood plain. The sand sheet forms a bowl shape (fig. 2) with a low central area dipping 2-3° towards the flood plain, where groundwater seepage occurs during the summer months. An intermittent creek, that carried very little water during field observations in the summers of 1986 and 1987, drains the sand sheet and redeposits some sand. Downslope the water infiltrates into the sandy soil.

Sediments of the Sandflugtdalen sand sheet

The sediments of the sand sheet consist characteristically of (sub)horizontally parallel bedded, fine to medium grained, moderately well-sorted sand (fig. 3) alternating with a minor occurrence of 1-2cm thick medium to coarse-grained, poorly sorted sand layers (fig. 4). A thickness of at least 250cm of sand has locally been established. Fluvial sand and gravel underlies the eolian sand close to the flood plain; locally morainic material underlies the sand or even lies at the surface.

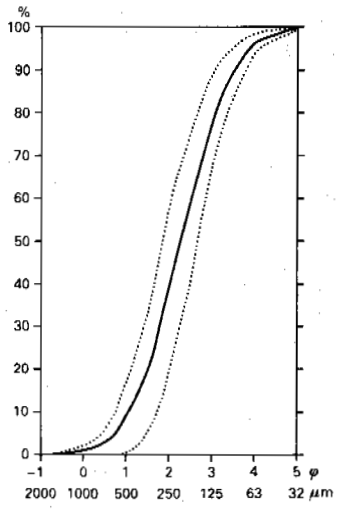

Fig. 3 Mean cumulative frequency curve ± standard deviation (dotted lines) of 20 eolian sand samples from Sandflugtdalen.

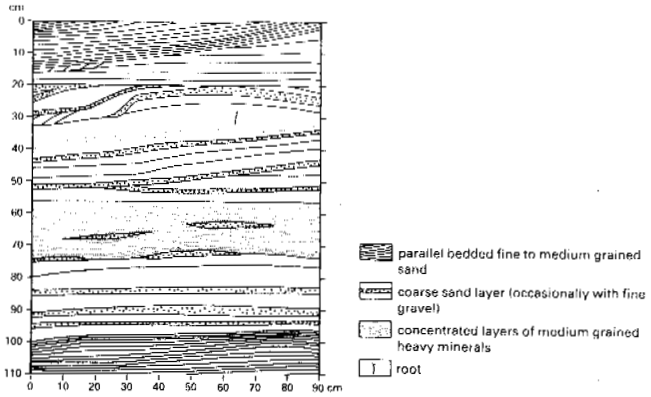

Fig. 4 Sketch of small trench in vegetation-free part of the Sandflugtdalen sand sheet. Groundwater defined the maximum depth of the trench. Permafrost was established at a depth of 175cm.

Permafrost

The Søndre Strømfjord area lies at the boundary of continuous and discontinuous permafrost (Weidick, 1968). Permafrost is found throughout the sand sheet. It is uncertain whether permafrost occurs in the flood plain in front of the sand sheet. In other parts of the valley an active layer of less than 50cm was found in peaty soil. The permafrost depth increases irregularly from 125cm near the flood plain to 170cm in the higher part of the sand sheet. In the wet central zone it is locally found to be about 50cm. The permafrost table rises somewhat under isolated dunes, as isotherms follow the topography (fig. 5). The dunes on the sand sheet apparently have only little influence on the depth of the permafrost table.

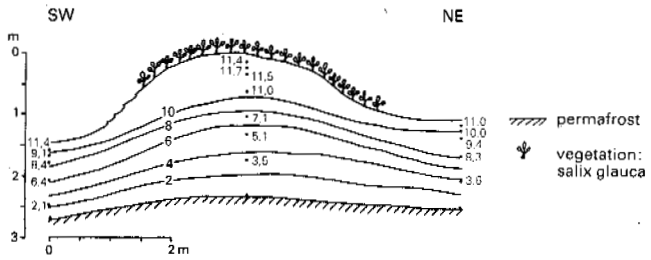

Fig. 5 Soil temperature profile through a relatively high, isolated dune on the sand sheet covered by Salix glauca. Temperatures in °C as measured around noon, 26 July 1987.

DESCRIPTION OF THE ICE-CORED HUMMOCKS

During the summer of 1987 several ice-cored hummocks were observed in the wet central part of the sand sheet (fig. 2) that were not present one year before.

The largest ice-cored hummock is shown in fig. 6. It is 12m long and 4m wide. The top is 50cm higher than the relatively flat surroundings. More or less parallel open cracks are conspicuous. They tend to be perpendicular to the slope of the hummock. At the surface they have a width of 1-3cm. On the

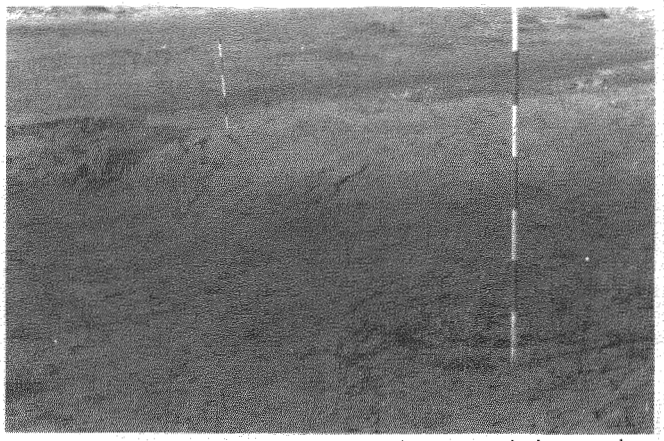

Fig. 6 Overview of large ice-cored hummock. Intermittent creek is visible in the background. Note a second small hummock in the foreground that is also shown in the sketch of fig. 7. Poles, with markings of 20cm, indicate the position of the trench.

western side cracks can be as wide as 10cm due to slumping. Small blocks of wet sand are redeposited by the creek. This undercutting indicates that the hummock has probably been larger. Compared with the dry part of the sand sheet the surface is covered by a relatively dense vegetation of Carex bigelowii, Juncus arcticus and Salix glauca with a degree of cover of less than 5%. The small ice-cored hummock (fig. 6, foreground) is more or less circular in shape and has a diameter of about 1.5m. At the surface it shows radial cracks.

A section through the above described hummocks (fig. 7) shows an unfrozen sand layer of 35-50cm thickness. Several cracks penetrate the whole unfrozen sand layer. Except for a thin surficial layer on top of the large hummock the unfrozen sand is wet, obscuring the sedimentary structures. Wavy parallel (to the surface of the ice) bedded sand with a grain size of 150-300µm could be distinguished, alternating with thin layers of

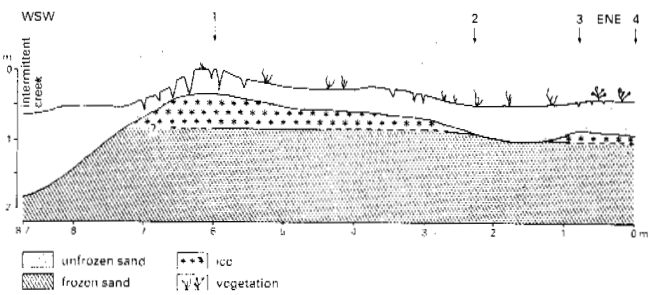

Fig. 7 Sketch of trench through ice-cored hummocks shown in fig. 6. Note the absence of air or water-filled chamber underneath the ice. High moisture content in the unfrozen sand prevented observation of stratification of these sediments. The nature of the permafrost boundary near the creek could not be established for the same reason. Full line means boundary is proven, broken line if boundary is assumed. Numbers indicate measuring locations of soil temperature as shown in fig. 10.

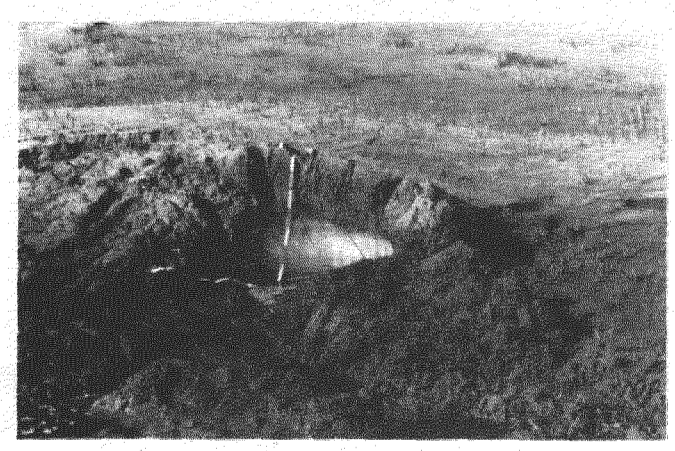

Fig.8 Section in large ice-cored hummock shown in fig.6 on the side where it is eroded by the creek. A clear solid ice core is visible underneath a surface layer of 35cm sand. Water in the foreground derived from creek.

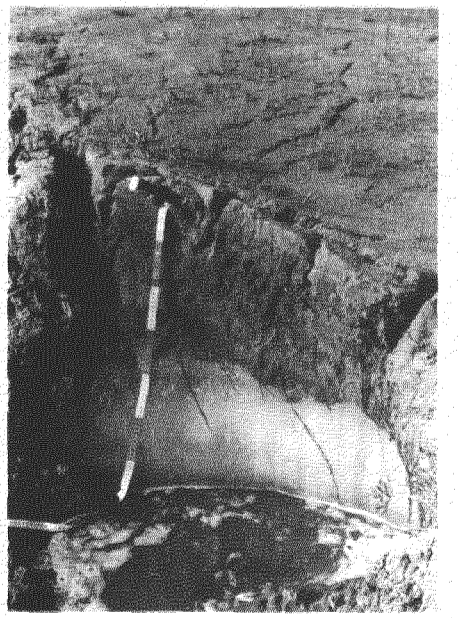

Fig.9 Detail of fig.8 showing vertical growth of ice crystals.

coarser sand (150-420µm) characteristic for the sand sheet (figs.3 and 4). Individual laminae could vaguely be followed for 1-2m.

Solid ice underlies the unfrozen sand in the hummocks. It forms lenses with a maximum thickness of 50cm corresponding in shape with the surface expression of the hummocks (fig.7 and 8). The ice is clean. Long vertical crystals (fig.9) and air bubbles (1mm in diameter) are recognized. The lower boundary of the ice is horizontal and as sharp as the upper boundary. The hummocks are underlain by frozen sand which is similar to the sand overlying the ice with regard to grain size and sedimentary structures.

Soil temperatures of the unfrozen sand have been measured at 4 localities along the

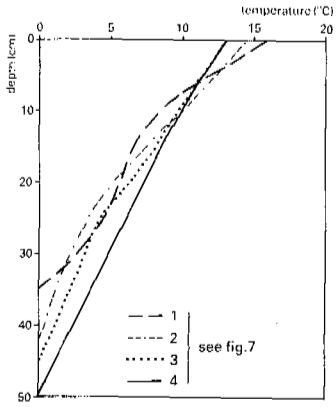

Fig.10 Soil temperature profiles in unfrozen sand overlying the ice core in trench shown in fig.7 (2 August 1987, around noon).

Fig.11 Some of the small hummocks (dunes) on the sand sheet outside the wet zone show cracks at the surface. These must not be confused with dilation cracks due to uplifting of ice cores.

section (fig.10). There is no major difference in temperature curves in these localities, although location 1 has a greater temperature gradient in the upper part. Due to dryer conditions near the surface greater thermal conductivity leads to higher temperature at the top of the hummock. Surface temperatures on the sand sheet during midday range from 13 to 30°C (!) depending on weather and moisture conditions and degree of vegetation cover. The steep temperature gradient and the occurrence of deep open cracks in the ice-cored hummocks combined with the undercutting by the creek will cause a rapid decay of these features.

Several more 15-30cm high ice-cored hummocks occur near the creek. Morphologically they resemble small dunes found both in the same area and in dryer parts of the sand sheet. These dunes often have a cracked surface, probably caused by small frost cracks, that are more randomly distributed however (fig.11). The permafrost table in these dunes was about 1m deep during the fieldwork period and appeared to be almost horizontal, comparable with the permafrost table shown in fig.5.

SEASONAL FROST MOUNDS - A REVIEW

Seasonal frost mounds as defined by Pollard & French (1983, 1984, 1985) are a suprapermafrost groundwater discharge phenomenon. They form when the hydraulic potential increases in the active layer during winter freezeback and uplifting of surface layers takes place. They differ from other types of frost mounds (such as morphologically similar palsas) by their ephemeral nature, a relatively short period of rapid growth, their genesis i.e. injection of groundwater under pressure and their association with springs, rivers etc. A variety of seasonal frost mounds have been described in many cold climate regions (e.g. Åkerman, 1987; Åkerman & Malmström, 1986; Froehlich & Slupik, 1978; Malmström, 1987; Pollard & French, 1983, 1984, 1985; van Everdingen, 1978, 1982 and van Everdingen & Banner, 1979). The process of development and decay of these ephemeral forms has been well-documented in the papers by van Everdingen, whereas Pollard & French focussed on the groundwater hydraulics and ice crystal structure to differentiate between these and other frost mound types. The origin of seasonal frost mounds has not yet been related to a purely sandy eolian environment.

Three types of seasonal frost mounds are distinguished by van Everdingen (1978, 1982). In a frost blister a surficial icing is overlain by frozen ground, ice, a water-filled or empty cavity and frozen ground respectively. An icing blister consists of an icing overlying a water-filled or empty cavity. The substratum can be either river ice, icing or frozen ground. An icing mound lacks the cavity.

INTERPRETATION OF THE ICE-CORED HUMMOCKS

The ice-cored hummocks in the Sandflugtdalen sand sheet have been developed in less than 1 year, indicating a relatively rapid growth. The groundwater on top of the permafrost and the morphological position of the hummocks in a low part of the sand sheet in a seepage zone indicate that the hummocks are a groundwater phenomenon with injection ice. This is in agreement with the vertical elongation of air bubbles and ice crystals indicating a vertical freezing direction. Moreover subsurface segregation ice is not envisaged in moderately well-sorted medium grained sand. Therefore it is assumed that these ice-cored hummocks are seasonal frost mounds.

At first glance it seems that the mounds under discussion do not correspond with one of the types of seasonal frost mounds distinguished by van Everdingen (1987, 1982). This might be caused by local processes during the decay. As mentioned by van Everdingen (1978, p. 273) differences in the observed character of mounds at different times of the year may lead to confusion in terminology.

One can argue that the Sandflugtdalen frost mounds are of the icing type being buried by eolian deposition or by redeposition of sand by the creek flowing over the ice. Subsequent partial melting of the icing will lead to the morphology of separate mounds with tension cracks. This sequence of events is comparable with ephemeral denivation forms in similar active eolian sand where the melting of snow causes a similar relief (Koster & Dijkmans, 1988). However field observations indicate that eolian transportation during one year is minimal and it is hard to envisage that the small creek is able to deposit a considerable layer of 35-50cm on the icing during one spring season, even if its discharge is larger than in summer. The drainage of the creek will be limited due to the dry climate and the small drainage area.

It is more likely that the frost mounds in Sandflugtdalen are of the frost blister type of which the cracks are interpreted as a dilation phenomenon. The requirements for the formation of this type of seasonal frost mounds (van Everdingen, 1978, 1982) are mainly fulfilled: A. there is a groundwater discharge with low temperature, although it is doubtful whether it is perennial. B. permafrost occurs in the shallow subsurface to serve as a very low permeability layer and C. there is a long period with daily subzero temperatures to ensure seasonal freezing of the ground. Moreover van Everdingen argues that grain size has no limiting influence on the occurrence of frost blisters. The mounds differ from the stratigraphy of frost blisters described above. Any surface ice would be melted in July. Possibly the mounds are in the decay stage where the cavity has disappeared by subsidence and/or collapse of the mound (compare van Everdingen, 1982, fig. 18, stage 6a), but sedimentary structures in the unfrozen sand show no evidence of this.

Small solid frost blisters less than 1m high that are similar to the mounds in Sandflugtdalen have also been described by Pollard & French (1983). These also have vertically oriented elongate bubbles and consist of a single clear ice core. Only larger forms showed a water-filled chamber and indicate repeated growth by a sequence of sediment-rich and clear ice. The occurrence of a single clear ice core in the Sandflugtdalen mounds corresponds with the observation that they are less than one year old.

DISCUSSION

It is uncertain whether the frost mounds in Sandflugtdalen disappear completely during one summer. Open cracks in sand overlying the ice core, a steep temperature gradient in this sand and erosion by the small creek cause rapid melting of the ice. Decay of the mound is obvious in July and August. On the other hand temperatures drop rapidly after that time (Hasholt & Søgaard, 1978), so that these forms possibly survive the subarctic summer. Seasonal frost mounds can be destroyed only partly during the summer following their formation (van Everdingen, 1978, 1982). No terminological distinction is made between annual and short-living perennial frost mounds; only more permanent

forms with a different genesis such as palsas and pingos are differentiated from them.

Little precipitation and snow drift in Sandflugtdalen lead to a limited snow cover in winter, causing a high frost penetration on the sand sheet. It seems likely that a water-filled chamber, caused by a high hydraulic potential, freezes completely sometime during winter in these relatively small mounds and groundwater discharge ceases, leaving autumn and early winter for the formation of the frost mounds.

The mounds are small compared to most of the forms described from the Canadian Arctic. Moreover they do not form every year. The small drainage area and the arid climate in the sand sheet obviously form relatively small hydraulic potentials, indicating a limiting factor for the growth of seasonal frost mounds. This arid environment is marginally suitable for the development of seasonal frost mounds. Only small mounds can develop depending on the hydrological conditions during a specific year. Contrary to large frost blisters (van Everdingen, 1978, 1982) these small mounds do not require a perennial groundwater discharge.

Degradation of frost mounds could lead to relict forms of depressions, possibly with ramparts, although it must be mentioned that no such features were recognized on the sand sheet. Although these forms are not stable in an eolian environment, a (rapid) burial, either by eolian or any other material, can theoretically preserve these scars if the conditions are right. The frost mound scars described by de Groot et al. (1987) from Late Dryas time are comparable in size and morphological position to the mounds in Sandflugtdalen. They were developed in eolian sands and covered by gyttja. Although frost mound scars are usually interpreted as pingo remnants, these Late Dryas scars were interpreted as seasonal forms. The observation of present day seasonal frost mounds in a periglacial eolian sand sheet supports the possible occurrence of frost mound scars in Pleistocene sediments.

ACKNOWLEDGEMENTS

The commission for Scientific Research in Greenland granted permission for expeditions to the Søndre Strømfjord area in 1986 and 1987 instigated by Prof. Dr. E.A. Koster (University of Utrecht). The Geological Survey of Greenland (GGU) provided some equipment. P. Frich (University of Copenhagen) and T. E. Törnqvist (University of Utrecht) assisted in the field. O. Thomsen and P. Kjeldsen (Søndre Strømfjord) offered logistical support.

REFERENCES

Åkerman, J (1987). Periglacial forms of Svalbard: a review. In: Boardman, J (ed). Periglacial processes and landforms in Britain and Ireland, 9-25.

Åkerman, H J & Malmström, B (1986). Permafrost mounds in the Abisko area, Northern Sweden. Geografiska Annaler (68A), 155-165.

Escher, A (1971). Geological Map of Greenland 1:500,000, Sheet Søndre Strømfjord-Nûgssuaq.

Froehlich, W & Slupik, J (1978). Frost mounds as indicators of water transmission zones in the active layer of permafrost during the winter season (Khangay Mts., Mongolia). Proc Third Intern Conf on Permafrost, National Research Council of Canada, (1), 189-193.

Groot, Th de, Cleveringa, P & Klijnstra B (1987). Frost-mound scars and the evolution of a Late Dryas environment (northern Netherlands). Geologie en Mijnbouw (66), 239-250.

Hansen, K (1970). Geological and geographical investigations in Kong Frederik IX's Land, morphology, sediments, periglacial processes and salt lakes. Meddelelser om Grønland (188), Nr. 4, 77pp.

Hasholt, B & Søgaard, H (1978). Et forsøg pa en klimatisk-hydrologisk regionsinddeling af Holsteinsborg kommune (Sisimut). Geografisk Tidsskrift (77), 72-92.

Koster, E A & Dijkmans, J W A (1988). Niveo-aeolian deposits and denivation forms, with special reference to the Great Kobuk Sand Dunes, northwestern Alaska. Earth Surface Processes and Landforms (13),

Malmström, B (1987). Frost mounds in the marginal zone of permafrost, northern Sweden. In: Pecsi, M & French, H M (eds). Loess and Periglacial phenomena, 191-201.

Pollard, W H & French, H M (1983). Seasonal frost mound occurrence, North Fork Pass, Ogilvie Mountains, Northern Yukon, Canada. Proc 4th Intern Conf. on Permafrost, 1000-1004, Fairbanks.

Pollard, W H & French, H M (1984). The groundwater hydraulics of seasonal frost mounds, North Fork Pass, Yukon Territory. Canadian Journal of Earth Sciences (21), 1073-1081.

Pollard, W H & French, H M (1985). The internal structure and ice crystallography of seasonal frost mounds. Journal of Glaciology (31), 157-162.

Ten Brink, N W (1975). Holocene history of the Greenland ice sheet based on radiocarbon-dated moraines in West Greenland. Meddelelser om Grønland (201), Nr. 4, 44pp.

van Everdingen, R O (1978). Frost mounds at Bear Rock, near Fort Norman, Northwest Territories, 1975-1976. Canadian Journal of Earth Sciences (15), 263-276.

van Everdingen, R O (1982). Frost Blisters of the Bear Rock Spring Area near Fort Norman, N.W.T. Arctic (35), 243-265.

van Everdingen, R O & Banner, J A (1979). Use of long-term automatic time-lapse photography to measure the growth of frost blisters. Canadian Journal of Earth Sciences (16), 1632-1635.

Weidick, A (1968). Observations on some holocene glacier fluctuations in West Greenland. Meddelelser om Grønland (165), Nr. 6, 200 pp.

PINGOS IN ALASKA: A REVIEW

O.J. Ferrians, Jr.

**U.S. Geological Survey, 4200 University Drive,
Anchorage, Alaska 99508-4667, USA**

SYNOPSIS More than 1,000 pingos and pingo-like mounds have been identified on the Arctic Coastal Plain in the continuous permafrost zone in northernmost Alaska; about 70 pingos have been located within valleys of the central Brooks Range in northern Alaska; and nearly 300 pingos and pingo-like mounds have been found in the forested discontinuous permafrost zone in central Alaska. Additional pingos have been reported on Seward Peninsula. However, many areas in Alaska have not yet been searched for pingos. Almost all of the pingos on the Arctic Coastal Plain and the northern part of Seward Peninsula are closed-system pingos. Those in the central Brooks Range, the southern part of Seward Peninsula, and central Alaska are predominantly open-system pingos. The climatic conditions, along with the geologic and topographic setting, determine the type of pingo that forms.

INTRODUCTION

Pingos are large ice-cored mounds, typically conical in shape, which can form and persist only in areas of permafrost (Figs.1, and 2). They generally range from 3 to 70 m in height and from 30 to 1,000 m in basal diameter. Pingos are formed by heaving or doming from below caused by hydrostatic and cryostatic pressure. A closed-system pingo derives its hydrostatic or artesian pressure from pore-water expulsion caused by aggrading permfrost, whereas, an open-system pingo derives its hydrostatic or artesian pressure from a distant hydraulic head. Review papers that describe pingos and, in some cases, additional forms of frost mounds, have been prepared by Maarleveld (1965), Müller (1968), Washburn (1973, p. 153-162; 1980, p. 180-191), Jahn (1975, p. 90-103), Flemal (1976), French (1977, p. 93-104), Mackay (1978), and Pissart (1985).

EARLY STUDIES

The first significant work on pingos in Alaska was by done Leffingwell (1919, p. 150-155), who described them as "gravel mounds" (pingos) (Fig.3) of Pleistocene and Holocene age on the extensive, relatively flat-lying, Arctic Coastal Plain of northern Alaska. One of these mounds (Fig.4), about 40 km southeast of Prudhoe Bay, was measured by Leffingwell, who used an aneroid altimeter, as being 230 ft (70 m) above the surrounding plain. According to recent 1:63,360-scale topographic maps, the mound is approximately 60 m high and 1,000 m in diameter. Even if one assumes that the smaller figure is correct, this pingo is still one of the largest, if not the largest, feature of its kind in the world. Leffingwell also made a thorough review of the existing literature concerning similar mounds. He reported that in Alaska, Schrader (1904, p. 94) observed occasional low mounds on the flats east of the Colville River on the Arctic Coastal Plain and above the delta; Smith (1913, p. 28) described mounds on the Mission lowland (Fig.2, locality 1) of the Noatak River in northwestern Alaska, and Mendenhall (1901, p. 207) reported numerous sand and gravel mounds rising 10 to 13 m above the general level of the Fish River lowland (Fig.2, locality 2) in the southeastern part of Seward Peninsula. George L. Harrington of the U.S. Geological Survey investigated several mounds in the Ruby mining district in west-central Alaska. He provided Leffingwell with descriptions of mounds and a photograph of one in the valley of Main Creek near Ruby (Leffingwell, 1919, p. 153, Plate XVII,B). Several years later, Mertie and Harrington (1924, p. 8-9, Plate V,A) described these mounds in more detail and suggested several ways in which they might have originated.

RECENT STUDIES

During the past 25 years, most studies of pingos in Alaska have been limited to inventorying and describing them and to studying their geologic and topographic setting. Wahrhaftig (1965) mentioned the presence of pingos in several different physiographic provinces in the interior and northern part of the state. Péwé (1975, p. 56-59) described what was known about pingos in Alaska at that time and reviewed the literature. Brown and Péwé (1973, p. 80-81) reviewed the status of pingo research in North America.

Northern Alaska

Galloway and Carter (1978) and Carter and Galloway (1979) mapped 732 closed-system pingos and pingo-like features on the Arctic Coastal Plain in northwestern Alaska. These pingos, which generally form in drained or partially drained shallow lake basins, were located by using aerial photographs. A few were visited to corroborate the interpretations made from the aerial photographs. Most of the pingos are

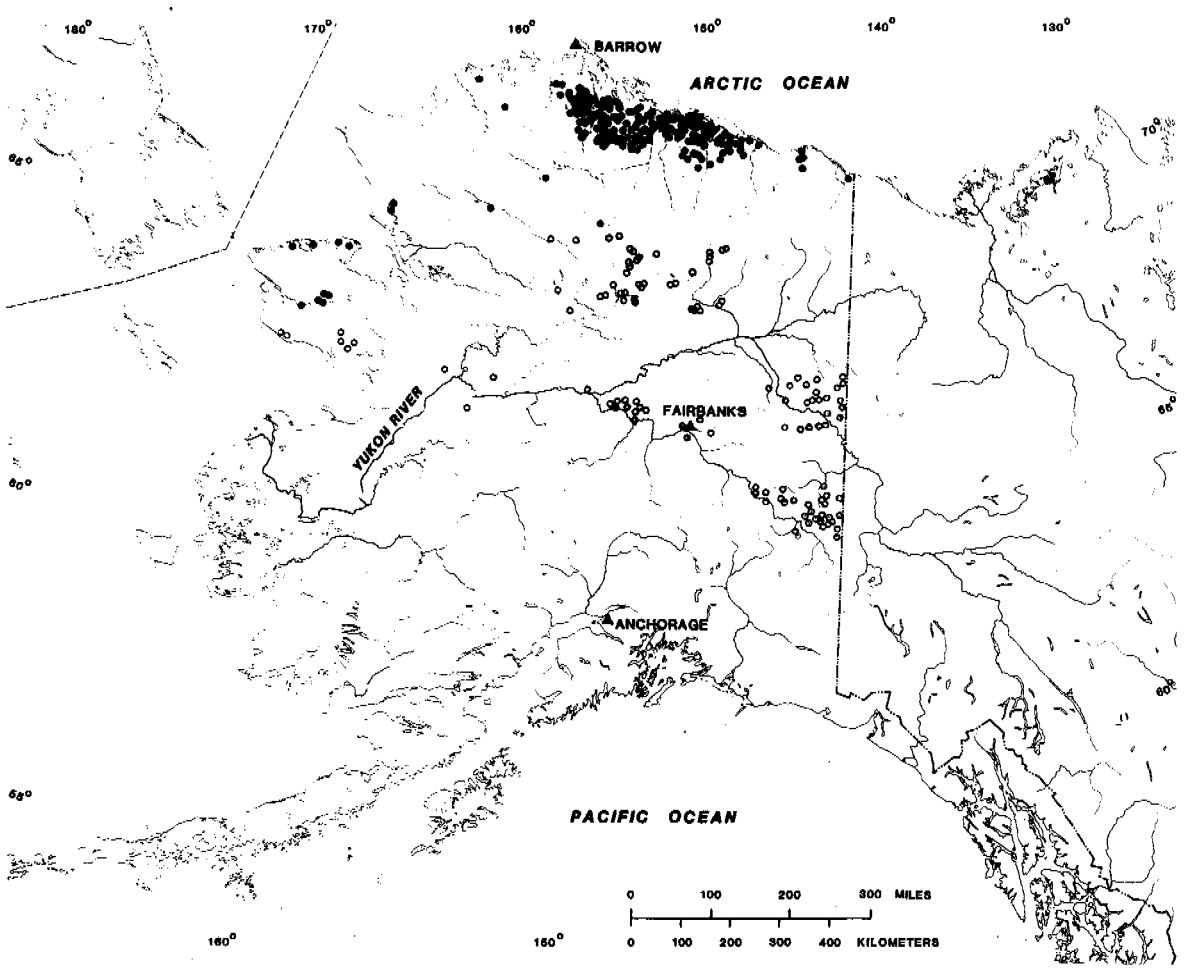

Fig.1 Generalized distribution of known closed-system (solid circle) and open-system (open circle) pingos in Alaska (Principal sources of data: Holmes, Hopkins, and Foster, 1968; Brown and Péwé, 1973; Galloway and Carter, 1978; Hamilton and Obi, 1982; Kaufman, 1986; and Ferrians, unpublished compilations).

conical in shape and range from 6 to 10 m in height; a few are low broad mounds as wide as 200 m and as long as 600 m. The highest pingo measured is 21 m. More than 97 percent of the mapped pingos occur in areas underlain by sandy unconsolidated deposits.

More than 300 additional closed-system pingos have been identified on the Arctic Coastal Plain between the Colville River and the Canadian border (Ferrians, 1983). The typical pingo in this region (Fig.3) is 10-15 m high and 65-100 m in diameter at its base, and virtually all occur on the floors of drained or partially drained shallow lake basins. The region is generally underlain by sandy gravel and has a thin mantle of fine-grained sediments.

Walker and others (1985) described two distinct types of pingos in the Prudhoe Bay region in the central part of the Arctic Coastal Plain. One is the typical closed-system pingo with a relatively small basal diameter and steep side slopes; these pingos occur primarily in drained thaw-lake basins. The other type consists of relatively low mounds with large diameters. These so-called broad-based pingos commonly occur outside the drained thaw-lake basins on older surfaces and, therefore, are considered to be older than the typical pingos. The origin of these broad-based mounds is unknown. One of the mounds, drilled and logged by the U.S. Army Cold Regions Research and Engineering Laboratory (Brockett, 1982), was found to have an ice core. A description of the materials encountered in the drilling together with the stratigraphy was reported by Rawlinson (1983, p. 138, 139), Walker and others (1985, p. 324), as well as by Brockett (1982).

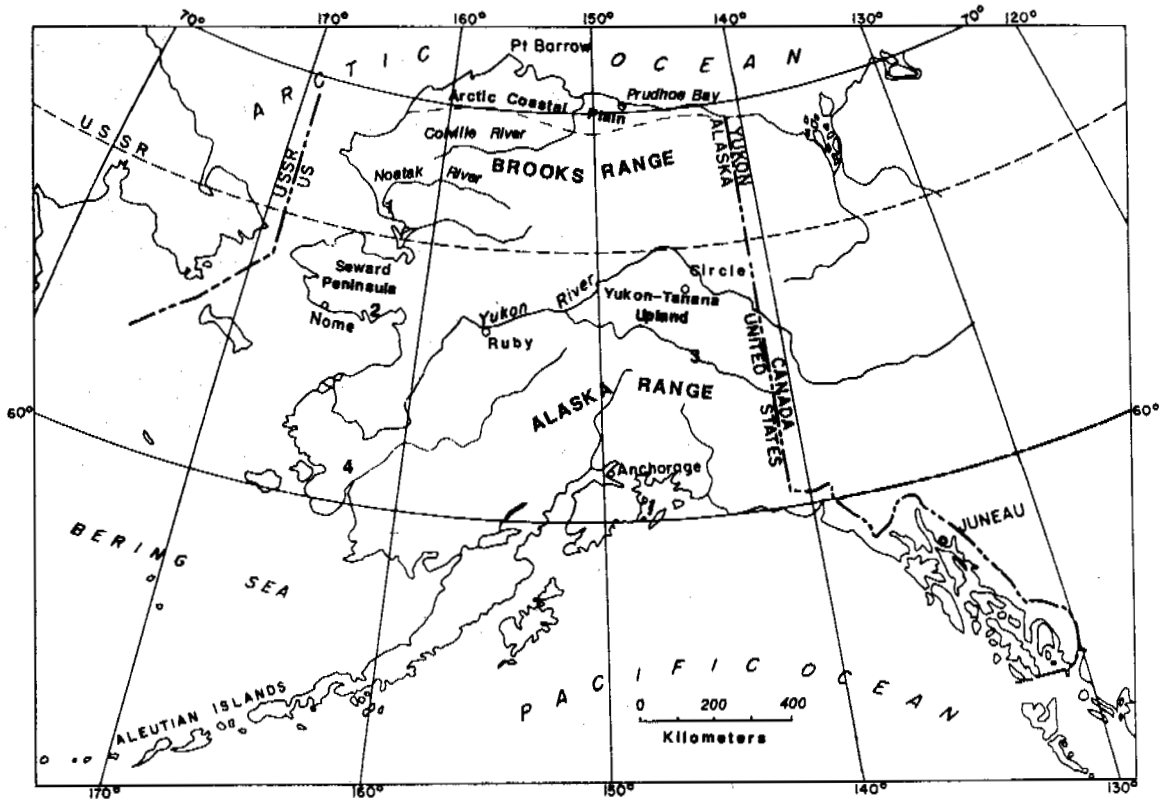

Fig.2 Index map showing Alaskan place names used in text and the location of: Mission Lowland, 1; Fish Creek Lowland, 2; Johnson River area, 3; and the area of frost mounds in the Yukon-Kuskokwim Delta area, 4.

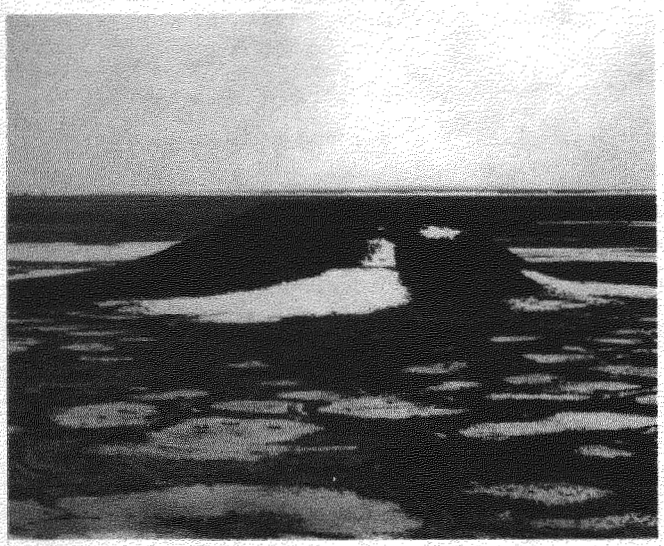

Fig.3 A typical well-developed closed-system pingo formed on the floor of a drained, shallow lake basin on the Arctic Coastal Plain. The pingo is about 15 m high and 75 m in diameter at its base. Photograph by O. J. Ferrians, Jr., June 1973.

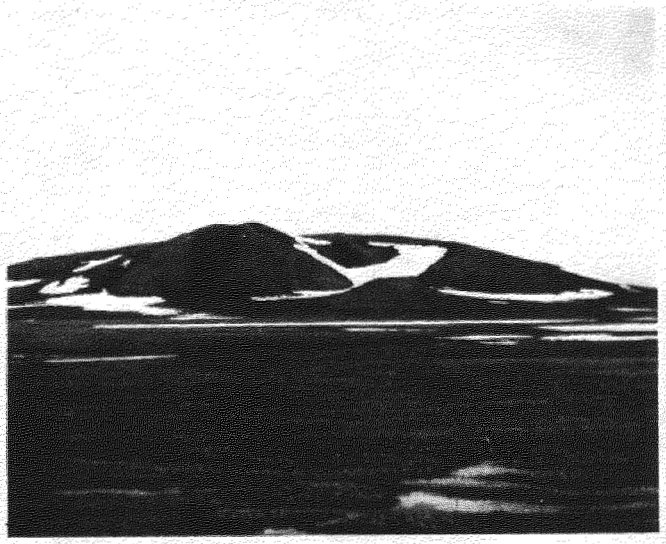

Fig.4 A large closed-system pingo, about 60 m high and 1,000 m in diameter at its base, on the Arctic Coastal Plain about 40 km southeast of Prudhoe Bay. Photograph by O. J. Ferrians, Jr., June 1973.

Burned bone from a hearth at a prehistoric hunting site on top of a small pingo near the coast of northern Alaska gave a radiocarbon age of 5,915±295 yr B.P. (Lobdell, 1986). Because the pingo was probably the highest point within an area of some 30 km and was used as an observation site, Lobdell (1986) concluded that the pingo is probably more than 6,000 yr old. The pingo currently is being degraded rapidly by wave action and thermal erosion from an adjacent lake.

Brooks Range

About 70 pingos within and near the central Brooks Range in northern Alaska were identified by Hamilton and Obi (1982), and additional pingos farther west in the Brooks Range have subsequently been mapped by Hamilton (1984a). These pingos, which are mostly the open-system type, occur in mountain valleys at altitudes as high as 725 m and in terrain glaciated as recently as late Wisconsin. Many of the pingos appear to be localized in areas where bedrock is near the surface and possibly are related to fracture systems in the bedrock. The water for the growth of the pingos probably is ground water emanating from the fracture systems. Elliptical pingo-like mounds have been reported by Hamilton (1984b) along the Kobuk fault zone parallel to the southern flank of the Brooks Range.

Central Alaska

Nearly 300 open-system pingos or pingo-like mounds were found in the forested discontinuous permafrost zone in central Alaska between the Brooks Range to the north and the Alaska Range to the south (Holmes, Foster, and Hopkins, 1966; Holmes, Hopkins, and Foster, 1968). These pingos tend to form on south- and southeast-facing slopes, near the base of slopes, and near the transition between valley fill and the slope mantle. They are commonly clustered along a contour and are primarily composed of colluvium and valley-fill material. The pingos are generally circular or elliptical, but a few are irregular in plan and probably were formed by several coalescing mounds. They range in basal diameter from 15 to 442 m and in height from 3 to 30 m. Commonly their summits are cratered and occupied by springs or ponds (Fig.5). Similar open-system pingos are found in Canada, and Hughes (1969) has studied them in the central Yukon Territory.

Krinsley (1965) made a detailed study of the Birch Creek open-system pingo, which is near Circle in interior Alaska. The pingo is forested and elliptical. It is approximately 400 m in diameter at its base and 15 m in height. The top of the pingo is cratered and is occupied by a shallow pond. A radiocarbon age determination indicates that the pingo started to grow after 5,720±65 yr B.P. This maximum age is similar to the 5,500±250 yr B.P. maximum age determined for a pingo in Thelon Valley, N.W.T., Canada (Craig, 1959, p. 509); and to the 6,800±200 yr B.P. maximum age determined for the Sitiyak pingo in the Mackenzie Delta area (Müller, 1962, p. 284). These age determinations suggest that the pingos started to grow after the climatic optimum.

Fig.5 Open-system pingo in Yukon-Tanana Upland, east-central Alaska. Light birch trees on pingo contrast with dark spruce trees and shrubs surrounding it. Pingo is about 15 m high and 90 m in diameter at its base; water-filled crater on its summit makes it "donut shaped." Photograph by H. L. Foster, August 1960.

As part of the study of the geology of the Johnson River area (Fig.2, locality 3) in central Alaska, Holmes and Foster (1968, p. 40-43) identified two open-system pingos and two pingo-like mounds. The larger of the two pingos is located near the break in slope between the loess-covered bedrock valley side and the silt-filled valley floor. The pingo is about 46 ft (14 m) high and 310 ft (94.5 m) in diameter at its base and is nearly symmetrical in plan. Its crater holds a circular pond. A fragment of a spruce tree from a depth of 2.5 ft (0.8 m) on the north rim of the crater yielded a radiocarbon age of 7,010±150 yr B.P.; however, according to the Holmes and Foster, the presence of a weakly developed Brown forest soil profile indicates that the age of the pingo is probably no more than a few thousand years. The smaller pingo is on the edge of a silt-filled, unglaciated valley at the foot of a loess-covered bedrock slope. It is about 25 ft (7.6 m) high and 100 ft (30.5 m) in diameter at its base. In a collapsed depression at the summit of the pingo, a subarctic Brown forest soil is exposed; its development suggests that this pingo is older than the other one. The two pingo-like mounds, which were not visited on the ground, are about 30 ft (9 m) high and 300 ft (90 m) in basal diameter.

Several hundred so-called closed-system pingos were reported in the Yukon-Kuskokwim Delta area (Fig.2, locality 4) by Burns (1964); however, the descriptions and photographs of examples of these mounds suggest that they are not pingos, but are palsas. Péwé (1975, p. 57) also came to this conclusion.

CONCLUSIONS

Many areas in Alaska have not been studied carefully enough to determine whether or not pingos are present; however, more than a thousand of them have been observed on the Arctic Coastal Plain in northern Alaska, and a lesser number in the central Brooks Range, Seward Peninsula, and central Alaska. Almost all of the pingos on the Arctic Coastal Plain and the northern Seward Peninsula are of the closed-system type, and most of the pingos in the central Brooks Range, southern Seward Peninsula, and central Alaska are of the open-system type. The permafrost-climatic conditions, along with the geologic and topographic setting, determine the type of pingo that forms. Studies of pingos in Alaska have been mostly limited to inventorying them and determining their geologic and topographic setting. Few detailed studies have been carried out.

REFERENCES

Brockett, B.E. (1982). Modification of and experience with a portable drill, Prudhoe Bay, Alaska, spring 1982. U.S. Army Cold Regions Research and Engineering Lab. Unpublished memorandum, 14 p.

Brown, R.J.E., & Péwé, T.L. (1973). Distribution of permafrost in North America and its relationship to the environment--A review, 1963-1973, in Permafrost, the North American contribution to the Second International Conference, Yakutsk, U.S.S.R., July 13-28, 1973. Washington, D.C., Nat'l. Acad. Sci., 71-100.

Burns, J.J. (1964). Pingos in the Yukon-Kuskokwim delta, Alaska; their plant succession and use by mink. Arctic (17), 3, 203-210.

Carter, L.D., & Galloway, J.P. (1979). Arctic Coastal Plain pingos in National Petroleum Reserve in Alaska, in Johnson, K.M., & Williams, J.R., eds., The United States Geological Survey in Alaska--Accomplishments during 1978. U.S. Geol. Survey Circ. 804-B, B33-B35.

Craig, G.B. (1959). Pingo in the Thelon Valley, Northwest Territories. Geol. Soc. America Bull. (70), 4, 509-510.

Ferrians, O.J., Jr. (1983). Pingos on the Arctic Coastal Plain, northeastern Alaska, in Permafrost, Fourth International Conference, Fairbanks, Alaska, July 18-22, 1983, Abstracts and program: Univ. of Alaska, 105-106.

Flemal, R.C. (1976). Pingos and pingo scars: Their characteristics, distribution, and utility in reconstructing former permafrost environments: Quat. Research (6), 1, 37-53.

French, H.M. (1976). The periglacial environment. London and New York, Longman, 309 p.

Galloway, J.P., & Carter, L.D. (1978). Preliminary map of pingos in National Petroleum Reserve in Alaska. U.S. Geol. Survey Open-File Rept. 78-795, scale 1:500,000, 1 sheet.

Hamilton, T.D. (1984a). Surficial geologic map, Ambler River quadrangle, Alaska. U.S. Geol. Survey, Misc. Field Studies Map MF-1678, 1 sheet, scale 1:250,000.

Hamilton, T.D. (1984b). Late Quaternary offsets along the Kobuk and related fault zones, northwestern Alaska. Geol. Soc. America Abstracts with Programs (16), 5, 288.

Hamilton, T.D., & Obi, C.M.. (1982). Pingos in the Brooks Range, northern Alaska. Arctic and Alpine Research (14), 1, 13-20.

Holmes, G.W., & Foster, H.L. (1968). Geology of the Johnson River area, Alaska. U.S. Geol. Survey Bull. 1249, 49 p.

Holmes, G.W., Foster, H.L., & Hopkins, D.M. (1966). Distribution and age of pingos of interior Alaska, in Permafrost, International Conference, Lafayette, Indiana, November 11-15, 1963, Proceedings. Washington, D.C., Nat'l. Acad. Sci., 88-98.

Holmes, G.W., Hopkins, D.M., & Foster, H.L. (1968). Pingos in central Alaska. U.S. Geol. Survey Bull. 1241-H, 40 p.

Hughes, O.L. (1969). Distribution of open-system pingos in central Yukon Territory with respect to glacial limits. Canada Geol. Survey Paper 69-34, 8 p.

Jahn, Alfred (1975). Problems of the periglacial zone (Zagadnienia strefy perglackalnej). Warsaw, Państwowe Wydawnictwo Naukowe, 223 p. (Translated from Polish for the National Science Foundation, Washington, D.C.).

Kaufman, D.S. (1986). Surficial geologic map of the Solomon, Bendeleben, and southern part of the Kotzebue quadrangles, western Alaska. U.S. Geol. Survey Misc. Field Studies Map MF 1838-A, 1 sheet, scale 1:250,000.

Krinsley, D.B. (1965). Birch Creek pingo, Alaska, in Geological Survey research 1965: U.S. Geol. Survey Prof. Paper 525-C, C133-C136.

Leffingwell, E. de K. (1919). The Canning River region, northern Alaska. U.S. Geol. Survey Prof, Paper 109, 251 p.

Lobdell, J.E. (1986). The Kuparuk Pingo site: A northern archaic hunting camp of the Arctic Coastal Plain, north Alaska. Arctic (39), 1, 47-51.

Maarleveld, G.C. (1965). Frost mounds: A summary of the literature of the past decade. Mededelingen van de Geologische Stichting, Nieuwe Serie 17, 3-17.

Mackay, J.R. (1978). Contemporary pingos: A discussion. Biuletyn Peryglacjalny (27), 133-154.

Mendenhall, W.C. (1901). A reconnaissance in the Norton Bay region, Alaska, in 1900, in Brooks, A.H., Richardson, G.B., Collier, A.J., & Mendenhall, W.C., Reconnaissances in the Cape Nome and Norton Bay regions, Alaska, in 1900. U.S. Geol. Survey Spec. Pub., 181-222.

Mertie, J.B., Jr., & Harrington, G.L. (1924). The Ruby-Kuskokwim region, Alaska. U.S. Geol. Survey Bull. 754, 129 p.

Müller, Fritz (1962). Analysis of some stratigraphic observations and radiocarbon dates from two pingos in the Mackenzie Delta area, N.W.T. Arctic (15), 4, 278-288.

___(1968). Pingos, modern, in Fairbridge, R.W., ed., The encyclopedia of geomorphology. New York, Reinhold, 845-847.

Péwé, T.L. (1975). Quaternary geology of Alaska. U.S. Geol. Survey Prof. Paper 835, 145 p.

Pissart, Albert (1985). Pingos and palsas: A review of the present state of knowledge. Polar Geog. and Geol. (9), 3, 171-195.

Rawlinson, S.E. (1983). Prudhoe Bay, Alaska, guidebook to permafrost and related features. Alaska Div. Geol. and Geophys. Surveys Guidebook 5, 177 p.

Schrader, F.C. (1904), A reconnaissance in northern Alaska, across the Rocky Mountains, along Koyukuk, John, Anaktuvuk, and Colville Rivers, and the arctic coast to Cape Lisburne, in 1901. U.S. Geol. Survey Prof. Paper 20, 139 p.

Smith, P.S. (1913). The Noatak-Kobuk region, Alaska. U.S. Geol. Survey Bull. 536, 160 p.

Wahrhaftig, Clyde (1965). Physiographic divisions of Alaska. U.S. Geol. Survey Prof. Paper 482, 52 p.

Walker, D.A., Walker, M.D., Everett, M.D., Everett, K.R., and Webber, P.J. (1985). Pingos of the Prudhoe Bay region, Alaska. Arctic and Alpine Research (17), 3, 321-336.

Washburn, A.L. (1973). Periglacial processes and environments. New York, St. Martin's Press, 320 p.

___(1980). Geocryology: A survey of periglacial processes and environments. New York, Halsted Press, 406 p.

REGULARITIES IN FORMING THE DISCONTINUITY OF A CRYOGENIC SERIES

S.M. Fotiev

Research Institute of Engineering Site Investigations, Moscow, USSR

SYNOPSIS A foundation of contemporary zonation differences in a degree of the discontinuity of a Cryogenic Series (CS) is shown to be laid at the beginning of the Holocene. It was determined by a latitude - zonation influence of exogenetic factors and conditions on both thawing the Pleistocene frozen ground in the Lower Holocene and freezing the thawed ground in the Upper Holocene. By conditions of developing the CS and taliks in the Pleistocene and Holocene zones of the continuous and discontinuous CS are rather clearly distinguished. Zonation non-uniformity of a degree of the CS discontinuity is shown to be determined by conditions of developing the open, infiltration and radiogenic taliks. Due to the conditions of forming the above taliks on the territory of the USSR regions and provinces are distinguished where these or those taliks play main role in forming the CS discontinuity.

Soil temperature, thickness and discontinuity of a CS have often and materially changed during the Pleistocene and Holocene Periods. A contemporary geocryological situation in any area of a cryogenic region (CR) is a result of a complex and highly differential evolution history of the CS during three last geocryological periods, namely: 1. a period of maximum extent of the Pleistocene low-temperature CS (from 37-35 to 10 thousand years ago), 2. a period of maximum thawing of the Pleistocene Permafrost (from 10 to 4.5 thousand years ago) and 3. a period of a new formation of the Holocene high-temperature CS (from 4.5 thousand years) up to now.

As it is known during the first period in the conditions of a time-independed and most rigorous sharply continental climate the most low-temperature and thickest CS has been formed at a vast circumpolar area. According to V.T. Balobaev's opinion (1978) a ground temperature has been by 8-10° below a contemporary one. The CS area has reached its maximum at the expense of a perennial and deep ground freezing both in South latitudes(right up to 48°N) and in North ones - at a dried part of the Shelf (up to 82°N). Climatic and geocryological conditions of the period has been extremely unfavourable for conservation or evolution of open taliks. At vast areas a continuous CS has been formed which discontinuity has been insignificantly small since only local ground areas near water-absorbing or water-withdrawing tectonic fractures with a constant and significant heat and water transfer could withstand a perennial freezing.

During the second period due to a sharp uneven heat and moisture increment there have occured rise in a rock temperature, degradation of the Pleistocene CS thickness and decrease in an area offits extent. Climatic conditions of the period have been highly favourable for forming the radiagenic and gidrogenic taliks (Fotiev, 1978). Absence of forest tracks and thick peat-moss covers (especially at the beginning of the period) has contributed to an active thawing of the upper horizons of frozen ground under the influence of a solar radiation and rain waters. Depth of thawing obeying the law of a latitudinal zonation has decreased to a north direction. An increase in the thickness of a seasonally thawing layer has caused a rapid progress of a thermokarst process. At accumulation plains there have formed numerous large thermokarst lakes. As a result of higher accumulation of the sun heat by lake waters numerous taliks below a lake have been formed under their bottoms: open - in south areas of the CS and closed ones - in north areas. By the end of the period in north areas of the CR a rock temperature of the Pleistocene CS has reached positive values within the whole profile and at the whole area at the expense of an internal and external heat exchange. Further northward a rock temperature has reached positive values only in lower and upper horizons of the CS at the expense of a heat flow from an interior part of the earth and accumulation of the sun heat respectively whereas in middle horizons of the CS there remained rocks with a negative temperature. At last, in north subaerial areas of the CS average annual rock temperatures have remained negative despite the softenning of the climatic conditions and increase in the rock and air temperature: the CS discontinuity has remained negligible even in this warmest period.

During the third period a perennial freezing of the ground thawed in the Lower Holocene has begun again: high-temperature cryogenic beds small in thickness and discontinuous have been formed. The CS boundary has again moved down to the South.

By conditions of the CS evolution in the Pleistocene and Holocene at the territory of the USSR as well as at the whole area of a North hemisphere two geocryological zones can be rather clearly distinguished, namely north and

south ones.

A north zone territorially coincides with a zone of the continuous low-temperature (from -2 to -10°) thick (from 150 to 1500 m) CS of the Pleistocene Age continuously occurring at all the relief features during tens and hundreds of thousands years. In such a severe time-independent geocryological situation conditions for the formation and conservation of the open taliks have been extremely unfavourable. Owing to the fact only local areas of the ground with an active heat and moisture transfer have remained from a perennial freezing within the limits of the open taliks of an underwater class. An area of the open taliks shaped as a pipe or slot is incommensurably small (between 0 and 5%) as compared to that occupied by the CS. At platforms they are associated with eigther large transit river valleys at the areas of a non-migrating river-bed or with the bottoms of large (a diameter being in the order of 1000 m) deep lakes. In mountain - folded areas the open taliks have remained only in the vicinity of large water absorbing and water withdrawing fractures. A south boundary of a north zone in all the regions coincides with a conjugation boundary (in section) of the Holocene and Pleistocene CS. At the territory of the USSR the boundary when running west to east moves down to the south owing to continentalization of the climate. It passes at 67°N, 66°N and 60-61°N respectively at the territory of a Timan-Ural region, in West Siberia and in Middle and East Siberia.

Similar rigorous and extremely rigorous geocryological conditions are also characteristic of highland structures of the South of Siberia and Zabaikalie. These structures are located further south than the north zone within which limits rigor of climatic and geocryological conditions has been mainly governed by latitude-zonation peculiarities of heat exchange between the rocks and atmosphere. In highland structures stability of rigorous climatic and geocryological conditions during tens and hundreds of thousands years has been exceptionally governed by altitude-belt peculiarities of heat exchange. Only due to a significant (1500-3000 m) absolute altitude of alpine-type mountain structures in such lower latitudes (up to 53-54°) could be formed and never cease to occur during three last geocryological periods such low-temperature (from -2 to -11°) thick (300-1000 and more metres) continuous CS of the Pleistocene Age. The CS discontinuity in mountain structures is rather small since the area of the open water absorbing and water withdrawing taliks associated with fractures is negligibly small.

Within the USSR a zone of the continuous CS occupies the most part (61%) of the area of a contemporary subaerial CR.

A south zone coincides territorially with that of the high-temperature (between 0 and -2°) and thin (from 0 to 100-150 m) CS of the Late Holocene Age. The CS discontinuity is considerable there but irregular. It is governed by the conditions of forming the open taliks of hidrogenic, radiagenic, hemogenic and volcanogenic classes. The author has ascertained that the radiogenic and infiltration taliks are primary in forming the CS discontinuity (Fotiev, 1978). The conditions of their formation are ruled in the first instance by the law of latitudinal zonation, since a magnitude of an accumulated solar radiation (Q_r) and amount of heat carried into the ground with infiltrating rain waters in a warm period of a year ($Q_{inf.}$) are regularly decreased in a direction from the South to the North. Values of Q_r and Q_{inf} are known to be small by an absolute value but equidimensional for a considerable area. Just therefore both the radiogenic and infiltration taliks are most widely extended in south areas of the CR and just they govern the character of the CS discontinuity within the whole south zone. An area of the mentioned taliks may be considerably less than that of the CS in a zone of the slightly discontinuous CS (5-25%), commensurable with it in zones of the discontinuous (25-50%) and massively sporadic (50-75%) CS or considerably exceed it in zones of the sporadic (75-95%) and occasionally sporadic (95-100%) CS Table No.1.

On the territory of the accumulation plains the taliks below a lake which areas in particular provinces are commensurable with or considerably exceed that of the CS are primary in forming the CS discontinuity. It is accounted for by an abundance of thermokarst lakes their large water area and small depth contributing

TABLE 1

Degree of Cryogenic Series Discontinuity

Degree of CS discontinuity	Area of frozen ground, %	Area of open taliks, %	Type of CS by extent	Subtype of CS by extent
Rather insignificant	95-100	0-5	continuous	continuous
Insignificant	75-95	5-25	discontinuous	slightly discontinuous
Significant	50-75	25-50		highly discontinuous
	25-50	50-75	sporadic	massively sporadic
Highly significant	5-25	75-95		sporadic
	0-5	95-100		occasionally sporadic

to a considerable warming up of the bottom sediments during a warm period. Formation of the taliks below a lake depends upon a considerable degree on the conditions of forming of the thermokarst lakes and to a lesser degree on a magnitude of a solar radiation.

An area of hemogenic and volcanogenic taliks as well as of the rest 13 types of the gidrogenic taliks is usually small: they govern a degree of the CS discontinuity only on a level of geocryological provinces (Fotiev,1978). For example, taliks below a lake, hemogenic and volcanogenic ones are primary respectively within alluvial-lacustrine plains, at the areas of sulphur and coal fields and at the areas of a contemporary volcanicity.

By the length of an existence period the infiltration taliks, the radiagenic taliks and that below a lake can be subdivided into 2 types: primary and secondary ones. Primary taliks were formed in the Low Holocene as far back as a period of a maximum thawing of the frozen ground of the Pleistocene age owing to a warming effect of a solar radiation and rain, river and lacustrine waters. They have never ceased to occur during the whole period of forming the Upper Holocene CS areas of the primary taliks are most considerable and their role in forming the discontinuity of the Upper Holocene CS is great. Secondary taliks have been also formed under a heat action of a solar radiation and natural waters. But they have been formed only in the Upper Holocene as a result of thawing the frozen ground of the Upper Holocene Age. The secondary taliks occupy evidently lesser areas and their role in forming the CS discontinuity is less significant particularly in the north areas of the south zone where the CS thickness reaches 100 and more metres.

At the territory of the south zone both presently and during the Pleistocene Age a zonal and intrazonal non-uniformity of forming the varying types and subtypes of the CS by extent was governed by either a considerable non-uniformity of conditions of a rain water infiltration or by a snow cover depth and conditions of its transfer with a snow storm along the area.

Optimal conditions for forming the infiltration taliks are considered to be as follows: 1. a considerable amount of heat (Q_{inf}) carried to a ground surface with rain waters; 2. wide and flat interfluvial spaces which absolute elevations do not exceed the ceiling of an air temperature inversion; 3. a considerable porosity or fracturing of a rock mass and its good drainability. Such natural situation is most characteristic to the south regions of Middle Siberia and Zabaikalie. Just in these very regions a slightly discontinuous, highly discontinuous, massively-sporadic, sporadic or occasionally sporadic CS has been formed depending on conditions of a rain water infiltration. At the plains of West Siberia and European North-East a wide extent of clayey deposits and peat bogs coupled with a small depth of an erosional dissection of the territory limits the possibility of forming the infiltration taliks notwithstanding a considerable value of Q_{inf} and a great width of flat interfluvial spaces. Unfavourable are the conditions of forming the infiltration taliks in mountain-folded structures as well. In upland structures they can not be formed due to the rigor of geocryological conditions. In middle-mountain and lower-mountain structures located below the ceiling of an air temperature inversion a quots of rain waters infiltrating inside a massif is small since their most part quickly streams down along the slopes surface. Therefore, at the accumulation plains and in mountain-folded regions a role of the infiltration taliks in forming the CS discontinuity is small.

Optimal conditions for forming the radiagenic taliks are considered to be as follows: 1. an abundance of heat due to a solar radiation under its small losses by a turbulent heat exchange, evaporation, etc. and 2. a considerable depth of a snow cover being small in density. Conditions of formation of the radiagenic taliks of an insolation type forming under a natural snow cover depth and that of an isolation type forming as a result of a higher snow accumulation owing to a snow storm transfer differ.

The radiagenic taliks of an insolation type are most typical for south areas of the CR since an amount of a solar radiation is known to increase in a south direction and rigor of a geocryological situation increases in a north one. In south areas of the CR at the areas composed of clayey soild or pit bogs conditions of forming the sporadic and occasionally sporadic CS are governed by a degree of a surface shadowing (thick forests, bottoms and sides of narrow deeply incised valleys, ravins etc.). Should a depth of erosional dissection be considerable (50-150 and more metres) which is characteristic of plateaux and high plateaux of Middle Siberia and Zabaikalie a maximum amount of a solar radiation, as it is known, is carried to the surface of southly arranged slopes. Owing to this only in these very areas are the taliks of an insolation type formed far from a south boundary of the CS and equally with the infiltration taliks take part in forming the discontinuous and massively-sporadic CS.

The radiagenic taliks of an isolation type are most characteristic of plains in West Siberia and European North-East. Owing to heavy winter precipitations (100-150 mm) and a considerable snow storm transfer a snow cover depth often reaches 1-2 m in depressions. This contributes to a wide development of the open radiagenic taliks of an isolation type. That is why, areas of the massively sporadic and sporadic CS in West Siberia are located near the Polar Circle! A role of these taliks in forming the sporadic and occasionally sporadic CS in areas of a Siberian anticyclone is limited.

Depending on conditions of developing the infiltration and radiogenic taliks at the territory of a south zone there can be distinguished areas of extension of 5 subtypes of the CS (see table), namely, slightly discontinuous, highly discontinuous, massively sporadic, sporadic and occasionally sporadic. Depending on geologo-geomorphological and climatic conditions in various regions of the USSR they can be classified in the form of subzones or change each other in mosaic. Subzones or provinces

distinguished according to extent of these or those subtypes of the CS differ not only in composition and sizes of the open taliks area but in a rock temperature, the CS thickness and length of its existing period as well.

The proposed classification of the CS according to an extent (see table) can and must be used in geocryological mapping on any scale. An introduction of the above classification of the CS in geocryological investigations will save the researchers from unnecessary confusion in existence at present.

In conclusion let us touch upon the problem of a contemporary south boundary of the CR. The boundary as it is known runs through a territory with positive average annual rock temperatures. In fact it separates an area of the open taliks at the territory of the CR from that composed by non-frozen rocks outside the CR. In our opinion a possibility of a new formation of the CS under disturbance of natural conditions of heat exchange between the rocks and the atmosphere (disturbance of rain water infiltration conditions, removal or compaction of a snow cover, etc.) should serve as a criterion for drawing a boundary line. At the territory of the CR that is within the limits of the open taliks a technogenic or natural disturbance or change in heat exchange conditions will inevitably lead to a rock temperature fall below a zero and a new formation of the CS. Southward of the CR boundary a new formation of the CS does not take place under any changes in a natural heat exchange.

REFERENCES

Balobaev,V.T. (1978). Rekonstruktsiya paleoklimata po sovremennym geotermicheskim dannym. Trudy III Mezhdunarodnoi konferentsii po merzlotovedeniyu. T.1, pp.10-14. Canada.

Fotiev, S.M. (1978). Gidrogeotermicheskie osobennosti kriogennoi oblasti SSSR. Nauka, p. 1-236, Moskva.

ROCK GLACIER RHEOLOGY: A PRELIMINARY ASSESSMENT

J.R. Giardino[1] and J.D. Vitek[2]

[1]Texas A & M University, College Station, Texas 77843, U.S.A.
[2]Oklahoma State University, Stillwater, Oklahoma 74078, U.S.A.

SYNOPSIS Explaining the development of rock glaciers requires knowledge of the movement of an ice-rock mixture. Without detailed internal evidence of stresses and strain rates, temperatures, ice-rock mixtures, and bedrock characteristics, discussion of the process or processes that form rock glaciers is premature. Improved collection of internal evidence and the development of a mathematical model to describe dynamics will generate the most acceptable explanation of the process or processes of formation.

Surficial movement rates derived from both strain nets and dendrogeomorphology must be correlated with internal characteristics (i.e.,to reveal the process(es)). Evidence of surficial movement only provides initial data for the development and assessment of a rheological model. Interrelationships among variables indicate that movement may be attributed to plastic flow or stratified flow in which viscosity changes with depth. This paper summarizes previous work on rheology from glaciology that may be applicable to rock glaciers. Data from internal characteristics and surficial measurements will contribute to a simplistic mathematical model to describe the movement mechanics of a rock glacier.

INTRODUCTION

The past one hundred years have seen a large amount of rock glacier research being undertaken since the work by Steenstrup (1883). Although Wahrhaftig and Cox's (1959) landmark paper stated that knowledge of rock glacier formation and movement was related to movement mechanics, few researchers followed their suggestion. Because rock glacier data (both internal and external) are difficult to obtain, explanation, for the most part, has been based upon speculation. Fortunately, some researchers have followed Wahrhaftig and Cox's suggestion and have attempted to develop movement models (Whalley 1974; Barsch et al. 1979; Thompson 1981; Giardino 1983; Olyphant 1983; Johnson (1984); Haeberli 1985; Giardino et al. 1985).

Our purpose is to provide an overview of the status of rheological work on rock glaciers. Because of the scarcity of basic information necessary to establish the rheology of rock glaciers this paper should be viewed as a first-order approximation. In developing our rheological perspective we have relied upon the works of Wahrhaftig and Cox (1959), Anderson and Morgenstern (1973), Barsch et al. (1979), Thompson (1981), Olyphant (1983), Haeberli (1985), and Ranalli (1986). In addition we have borrowed from the research and techniques used in glacial studies, and we have been guided specifically by the works of Paterson 1981 and Kamb and Echelmeyer (1986).

BACKGROUND TO ROCK GLACIER MODEL DEVELOPMENT

The movement of a rock glacier involves the interaction between the stress field within the rock glacier and the changing stress-strain relationships of the upper surface (active layer), which changes seasonally from unfrozen, supersaturated sediments to a frozen sediment mixture. The active layer responds to the yearly climatic cycle, including energy and moisture inputs. Climatic input into the upper surface will extend into the rock glacier as far as the interface of the permanently frozen subsurface. At present little information exists with regard to the active layer or the frozen subsurface layer because stresses occurring within a rock glacier are difficult and complex to assess and study. Determination of the unfrozen-frozen interface is problematic at best, and whereas Nickling and Bennett (1984) have carried out laboratory experiments on ice-sediment mixtures, their work provides only short-term estimates of stress-strain relationships for limited mixtures of ice/rock percentages. A complete understanding of the evolution and flow of rock glaciers will be possible only with improved knowledge of the vertical and horizontal movement mechanics. Haeberli (1985) provides a very compelling case for the necessity of improved knowledge of rock glacier rheology.

Essentially rock glacier models have ranged from a generalized flow model through specific models that consider rock glaciers from a materials-

flow point of view (e.g., viscous, pseudoplastic, etc.) to models that suggest specific process-response relationships. Apparently much of the work done on rock glacier flow modeling has been carried out independently of work that was related to glacier flow. Limited cross-fertilization of ideas has occurred from either field of study. Although rock glacier researchers acknowledge the existence of ice-cored rock glaciers, they view rock glacier movement as an inhomogeneous mass rather than flow and deformation of an ice mass. Another point of view is expressed by both Barsch (1977) and Haeberli (1985) who consider movement of the rock glaciers to be a function of creep and sliding of masses of perennially frozen sediments. They attribute movement to permafrost creep.

Olyphant (1983) summarized Wahrhaftig and Cox's (1959) and Barsch's (1977) considerations of rock glacier flow. Wahrhaftig and Cox (1959) indicated that a one-parameter viscous model could be used to represent rock glacier flow as:

$$2d\varepsilon/dt = dV/dz = \tau/\eta \qquad (1)$$

where $d\varepsilon/dt$ is the rate of shear strain and dV/dz is the vertical velocity gradient of flowing material, τ is the gravitational shearing stress, and η represents the rock glacier flow viscosity.

Barsch et al. (1979) considered rock glacier flow to be similar to normal glacier flow which can be expressed as:

$$d\varepsilon/dt = dV/dz = ((\rho g(H \sin \alpha)/B)^n \qquad (2)$$

where ρ is the density of the rock glacier mass, g is the acceleration resulting from gravity, H is the total flow thickness, α is the slope of the rock glacier surface, B is the resistance term and n is the exponent of the power flow law.

Non-linear ice flow is complicated by several factors: the form of the flow law and the rate of deformation are temperature dependent; ice crystal size and orientation and/or the occurrence of impurities change the properties of the ice body. Paterson (1981) discussed how experiments conducted to determine strain rates, using the application of constant stress (50-200 kPa), usually produced a creep curve showing initial elastic deformation followed by decreasing strain which is then followed by a period of constant strain. From the last point, strain rates begin to increase. From this curve glaciologists identify three types of creep: primary, secondary and tertiary. Of these three types of creep, secondary and tertiary creep are the most important in rock glacier studies. Haeberli (1985) reported that tertiary creep has occurred when flow induced thickening of the mass occurs. The flow law can be expressed as:

$$\varepsilon = A\tau^m \qquad (3)$$

where ε is the shear strain rate, τ is the shear stress, m is a constant, and A is the flow law coefficient. The flow law coefficient (A) is a function of the variables ice temperature, crystal size and orientation, and impurity type and volume. In this form the rate of secondary creep is related to the amount of applied stress. Whereas size and orientation of ice crystals are important in glaciers, the internal characteristics of rock glaciers suggests that the variables of ice temperature and impurities may be more critical in movement mechanics. Research on glacial ice has demonstrated that a temperature value can be obtained.

The flow law coefficient (A) is a function of several factors, most of which cannot be quantitatively assessed. However, the influence of temperature (T) values on A can be isolated and can be assessed quantitatively as:

$$A = A_o\, e^{(-Q_R/RT)} \qquad (4)$$

where A_o is the component of A that is not temperature dependent; Q_R is the energy required for the initiation of creep and R is the gas constant. Equation 4 produces satisfactory results for calculating ice deformation (Paterson 1981).

ROCK GLACIER MODELS

The complexity of rock glacier movement can be related to variation in topographic, lithologic, and climatic variables. General characteristics have not been established as representative of all rock glaciers. Obvious differences in surficial characteristics have contributed to several hypotheses of movement. Movement processes range from short-term catastrophic events to long-term, slow creep. We view rock glacier movement from a rheological point of view as two processes: deformation and sliding. Whereas these two processes may operate in concert, we will discuss each process independently.

Deformation Model

Rock glacier movement by deformation is the most widely described movement process. Barsch (1977) and Haeberli (1985) view deformation of the ice in the rock glacier as the primary means of rock glacier movement. Haeberli (1985) specifically considers rock glaciers as long-term creep phenomena. If one considers the frozen mass of the rock glacier to flow by deformation as expressed with equation 2, then one must be able to determine the internal deformation.

glaciological research (Paterson 1981) has shown that surface velocity (V_s) can be used to interpret the internal deformation component through the use of:

$$V_s = V_i + V_b \qquad (5)$$

where V_s is surface velocity, V_i is the internal deformation velocity and V_b is the velocity at the base. Because rock glaciers occur in valleys, their width and depth are controlled by the shape of the valley. Paterson (1981) has shown that the base stress equation can be modified in order to consider the influence of valley shape as:

$$\tau_{xy} = -F\rho gH \sin \alpha \qquad (6)$$

where τ_{xy} is the basal shear stress; F is the shape factor for the valley; ρ is the density; g is the acceleration resulting from gravity; y is the thickness of the body; and α is the surface slope. Using digital elevation data, topographic models of regions with rock glaciers could be constructed in an effort to extract estimates of the thickness of the rock glaciers. Moreover, such a model could be used to derive other estimates of the physical characteristics.

With the exception of the Camp Byrd rock glacier in the San Juan Mountains of Colorado, U.S.A. (Griffiths, 1977, personal communication), no active rock glaciers have been tunneled. Whereas many authors cite Siebenthal (1907) as a source for a rock glacier that has been tunneled Haeberli (1987, personal communication) points out that careful reading of the description shows that Siebenthal was discussing a glacier and not a rock glacier. With the exception of initial investigations carried out by Haeberli and other researchers in Switzerland (Haeberli, 1987, personal communication), we do not have data either on the relationship between surface velocity (Vs) and basal velocity (Vb) nor data in order to adequately assess internal and basal shear stresses. Because internal rock glacier stresses are almost impossible to measure over a short-time interval, a model must be used that permits them to be calculated. But a rock glacier is not a homogeneous body, which complicates mathematical modelling.

Sliding Model

Wahrhaftig and Cox (1959) theoretically considered the movement of a rock glacier by basal sliding, but little attention has been directed toward this movement mechanism. The movement of a rock glacier by sliding can occur along a discontinuity interface between the dynamic rock glacier mass and the static bedrock. Haeberli (1985) suggests three areas where sliding can occur in the rock glacier: (1) between the frozen mass and bedrock with a negative temperature; (2) between the frozen mass and bedrock with a positive temperature, and (3) between frozen and non-frozen sediments within the rock glacier. Thus, sliding is not restricted to the discontinuity interface at the base of the rock glacier. Sliding can occur along shear planes developed within the rock glacier mass. White (1976, 1987) suggested this mechanism of movement from work on rock glaciers in the Colorado Front Range. These zones can be associated with temperature differentials developed between frozen and unfrozen material. Giardino and Vitek (in press) observed and measured the internal fabric of a rock glacier. An excavation to a depth of 15 m in a rock glacier in the Sangre de Cristo Mountains of southern Colorado, U.S.A. provided the opportunity to identify the existence of several shear planes within the rock glacier. The platy felsite clasts and lack of fines contribute to the well defined fabric and recognition of planes. An observed cyclic pattern in the fabric appears related to movement of the rock debris. The idea of differential sliding or deformation occurring within the rock glacier complicates the problem of modeling the rheology of a rock glacier.

Although Haeberli (1985) cites the occurrence of talus aprons adjacent to the frontal slopes of rock glaciers as suggesting that movement by sliding plays a minor role, Giardino (1983) describes "push lobes" present in front of many rock glaciers as evidence of the important role basal sliding plays in rock glacier movement. The presence of push lobes reflects that movement has not ceased, although the actual rate of movement may be minor.

Sliding along either the basal contact and/or along internal shear planes created by temperature differentials occurring between frozen/unfrozen material will produce notable changes in material properties. The above situation is further complicated by the differential movement within a rock glacier. If we assume that the amount of deformation increases with depth because of increasing shear stresses, and velocity decreases with depth, we accept a "power-type" creep law. Movement contributes to frictional heat, the amount being a function of depth. Paterson (1981) discusses the application of heat flow in ice glaciers. However, none of his assumptions are appropriate for rock glaciers. Haeberli (1985) has shown that the frictional heat (ζ_f) in a rock glacier can be calculated as:

$$\zeta_f = \tau V_s \ (Jk)^{-1} \qquad (7)$$

where τ is the basal shear stress; V_s is the surface velocity; k is the thermal conductivity of the rock glacier mass, and J is the mechanical equivalent of heat. The frictional heat in rock glaciers has the potential for producing unfrozen water at basal contact and/or along internal shear zones. Unfrozen water is an important variable in hypotheses of movement proposed by Giardino (1983) and Haeberli (1985).

Boulton and Jones (1979) demonstrated that the shear strength (σ) of beds of glacial ice can be obtained as:

$$\sigma = C + (\rho_p \, g \, h_p - p_s) \tan \theta \qquad (8)$$

where C is cohesion; ρ_p is density of the thickness of the ice; p_s is pore water pressure, and θ is the angle of internal friction. This equation can be modified to calculate shear strengths in rock glaciers by establishing ρ_p as the density of the material that composes the rock glacier and hp as the thickness of the frozen material.

Enhancement of the Sliding Model

Giardino (1979,1983) suggested a model to explain the development of hydrostatic pressure within a rock glacier. He assumed that as surface and frontal freezing occurs, fluid water is trapped between the upper freezing plane and a lower freezing plane which marks the upper limit of the permafrost. As the freezing planes approach each other, confining water pressure increases. When force (f), which is the mass of the talus, is applied to an area (A), the resulting pressure is f/A which is exerted upward on an area (B). Thus, the total upward force on the area (B) is:

$$F = (f \, a^{-1}) \, B = f \, (B \, A^{-1}) \qquad (9)$$

Concurrent with compaction of the talus which results from settling and load from additional talus on the surface, the area of talus moves downslope a distance x. Because in theory the volume of the fluid remains constant, the area (B) must then move upward a given distance (y). Therefore, one can demonstrate that:

$$By = Ax \qquad (10)$$

Further, if one assumes no loss from friction, then the work done by f must equal that done against F. Therefore:

$$Fy = fx \qquad (11)$$

and it follows that:

$$F/B = f/A \text{ and } f \, (B/A) \qquad (12)$$

In addition to the upward force generated by the confined fluid, there is an additional movement force present at the face of a lobe which results from hydrostatic pressure. If one considers the face of a lobe as (AB), and the width of the face is (w), and the height of the meltwater trapped behind the toe as (H) then the average pressure Q_a is:

$$Q_a = 1/2Hd_w \qquad (13)$$

where d_w is the density of water as the pressure increases from zero at the top of the liquid water surface to Hd_w at the base of the liquid water. The total force (f) against the interior of the lobe of given width (w) is:

$$F = Q_a \, wh = wH^2 \, d_w/2 \qquad (14)$$

where h is the area.

Building upon this model, we suggest that maximum movement along the discontinuity interface will occur in the late Fall when the freezing planes are at minimum distance and hydrostatic pressure is at maximum. Development of a rheological explanation of rock glacier movement that employs the hydrostatic pressure concept requires documentation of hydrostatic pressure in the field. One of the major aspects that must be examined is the relationship among hydrostatic pressure, internal movement, and surface movement.

The relationship of surface movement to internal movement is being investigated with geophysical techniques to document the location of freezing planes and subsequent estimates of hydrostatic pressure. To date two years of monitoring have been completed. Whereas preliminary results appear to indicate that movement of the freezing plane can be documented, any conclusions are premature. Once sufficient data have been collected, we will add a temporal framework for surface movement. Giardino et al. (1984) demonstrated that surface movement on a rock glacier could be interpreted temporally during 500 years using dendrogeomorphological techniques. Their study linked increased movement of the rock glacier with climatic fluctuations. With internal and surficial data, a model can be formulated.

Giardino et al. (1985) developed two preliminary models to explain the interrelationships among variables in the development of a rock glacier. Model one was based upon perfect plastic flow and model two on stratified fluid movement with viscosity changing with depth. Built upon this initial model and based on our field work we believe that rock glacier movement is a combination of deformation of the frozen material and sliding along both the base and internal shear planes. To meet data needs, we have established a series of strain networks on three rock glaciers. To aid in the formulation of a complex rheological model, we have developed a shear box apparatus that allows simulation of differential stresses. From these activities we will formulate a rheological model that considers rock glacier movement as the sum of internal deformation of the frozen material (i.e., the permafrost), basal sliding, and internal movement along shear planes.

SUMMARY

The foregoing discussion demonstrates that rock glacier movement is complex. Researchers have literally spent a hundred years climbing, mapping, measuring, and digging into rock glaciers, producing, quite frankly, more questions about rock glaciers than answers. That rock glaciers move by deformation of the frozen mass is apparent. The important role that sliding and water pressure play in movement is slowly gaining research interest. Unfortunately, only limited field and laboratory data exist today. Where, then, should our energies be directed in the future? Rock glacier research in the future should involve: rheology and numerical modeling. The importance of different temperatures, stresses and strain rates on the ice-rock matrix are some of the problems that require evaluation. The manner in which deformation occurs is critical to the development and movement of rock glaciers. The ability to develop mathematical models to explain the multitude of differences reflected in rock glaciers represents the major challenge in the future.

REFERENCES

Anderson, D M and Morgenstern, N R (1973). Physics, chemistry, and mechanics of frozen ground: a review. Permafrost Second International Conference, North American Contribution NAS, 257-288, Washington D.C.

Barsch, D (1977). Nature and importance of mass-wasting by rock glaciers in Alpine permafrost environments. Earth Surface Proc. 2, 231-245.

Barsch, D, Fierz, H, & Haeberli, W (1979). Shallow core drilling and bore-hole measurements in permafrost of an active rock glacier near the Grubengletscher, Wallis, Swiss Alps. Arctic and Alpine Res. (11), 2, 215-228.

Boulton, G S & Jones, A S (1979). Stability of temperate ice caps and ice sheets resting on beds of deformable sediments. J. of Glaciology (23), 89, 247-256.

Giardino, J R (1979). Rock glacier mechanics and chronologies: Mount Mestas, Colorado; Ph.D. Dissertation, 228 pp., Univ. Nebraska.

Giardino, J R (1983). Movement of ice-cemented rock glaciers by hydrostatic pressure: an example from Mt. Mestas, Colorado: Zeit.fur Geomorph. (27), 297-310.

Giardino, J R, Shroder, J F, Jr., & Lawson, M P (1984). Tree-ring analysis of movement of a rock glacier complex on Mt. Mestas, Colorado, U. S. A. Arctic Alpine Res. (16), 299-309.

Giardino, J R, Vitek, J D, & Hoskins, E R (1985). Rheology of rock glaciers: A preliminary assessment. Abs. with Prog. Geol. Soc. Am.(17), 591.

Giardino, J R & Vitek, J D (1985). A statistical study of the fabric of a rock glacier. Arctic Alpine Res. (17), 165-177.

Giardino, J R & Vitek, J D (in press). Interpreting the internal fabric of a rock glacier. Geog. Annaler.

Griffiths, T (1977). Personal Communication.

Haeberli, W (1985). Creep of mountain permafrost: internal structure and flow of alpine rock glaciers: Mitt. der Versuch. fur Wasserbau, Hydrol. und Glaziol., nr. 77, 142 pp.

Haeberli, W (1987). Personal communication.

Hooke, R L, Dahlin, B B, & Kauper, M T (1972). Creep of ice containing dispersed fine sand. J. of Glaciology (11), 63, 327-336.

Kamb, B, & Echelmeyer, K A (1986). Stress-gradient coupling in glacier flow: I. Longitudinal averaging of the influence of ice thickness and surface slope. J. of Glaciology (32), 111, 267-284.

Nickling, W G & Bennett L (1984). The shear strength characteristics of frozen coarse granular debris. J. of Glaciology (30), 348-357.

Olyphant, G (1983). Computer simulation of rock-glacier development under viscous and pseudo-plastic flow. Geol. Soc. Am. Bull. (94), 499-505.

Paterson, W S B (1981). The Physics of Glaciers, 380 pp Pergamon Press, Oxford.

Ranalli, G.(1987). Rheology of the Earth, 384 pp. Allen & Unwin, London.

Siebenthal, C E (1907). Notes on glaciation in the Sangre de Cristo Range, Colorado. J. of Geology (15), 15-22.

Steenstrup, K J V (1883). Bidrag til Kjendskab til Braeerne og Brae-isen i Nord-Grønland. Meddelelser øm Grønland (4), 69-112.

Thompson, D E (1981). Mechanics of flow and erosion potential of rock glaciers and glaciers in compression flow. In Holt, H E & Kosters, E C (eds), Reports of Planetary Geology Program, NASA Tech. Memorandum 82385, 384-385.

Wahrhaftig, C & Cox, A (1959). Rock glaciers in the Alaska Range. Geol. Soc. Am. Bull. (70), 383-436.

Whalley, B (1974). Rock glaciers and their formation as part of a glacier debris-transport system. Geographical paper 24, 60 pp. Department of Geography, University of Reading.

White, S E (1976). Rock glaciers and block fields, review and new data. Quaternary Res. (6), 77-97.

White, S E (1987). Differential movement across transverse ridges on Arapaho rock glacier, Colorado Front Range, U.S.A. in Giardino, J R , Shroder, J F , & Vitek, J D Rock Glaciers, Allen & Unwin, 145-149.

THE USE OF MICROBIOLOGICAL CHARACTERISTICS OF ROCKS IN GEOCRYOLOGY

D.A. Gilichinsky[1], G.M. Khlebnikova[2], D.C. Zvyagintsev[2], D.C. Fedorov-Davydov[2] and N.N. Kudryavtseva[2]

[1]Institute of Soil Science and Photosynthesis, USSR Academy of Sciences, Puschino
[2]Moscow State University, Moscow, USSR

SYNOPSIS The reliable amount (10^3-10^8 cells per 1 g of soil) of viable organisms of the Pliocene--Pleistocene age has been isolated from frozen rock sequences by sowing them on thick nutrient medis. These microorganisms found in 87% of 220 samples are the only living ones that can remain in anabiosis or in a similar state for such a long time. The analysis of both morphological and functional characteristics of these organisms allows to establish paleoecologic environmental differences of ancient epochs. Using microbiological investigations (undoubtedly, their resolving capacity and application are limited together with the traditional methods, a number of important geological problems can be solved for the regions where permafrost rocks are wiledy spread. In particular, this approach allows to characterize syncryogenic and epicryogenic rocks, sedimentary facies accumulated during syngenetic freezing and their diagenetic changes during epigenetic process. It also permits to determine the stratigraphic layers of thawing during Cargin, Kazan and other Pleistocene thermochrones.

Unlike sedimentary coner of any other regions, the geological potentiality of that of the cryolithozone is difficult to evaluate because cryometamorphosed rocks differ from the original ones in granulometria, mineralogic and geochemical parameters. Investigation of their genetic and stratigraphic origin by means of conventional geological methods do not always yield inambignous results particularly so for "covered" plains. It is also difficult to do paleoclimatic and paleolandscape reconstructions after the buried soils which are broken and deformed as a result of cryogenic processes. Finally, except for palynologic diagnostics, these are practically no data that would allow to model the paleofrost dinamics in a vertical cross-section (ancient levels and cups of melting, frozen talic zones, ets.) and consider the age of the frozen rock sequences.

Therefore, new criteria are necessary to distinguish between paleoecological regimes of different geological epochs within areas of development of permafrost rocks. Microbiological investigations of frozen sediments based on the established fact of the presence of numerous and various viable microflora in the Pleistocene - Pliocene frozen rock sequences might be highly prowising in that they can yeield the sought for criteria. That microflora had been reported from the frozen sediments of the North--Eastern Eurasia (Zvyagintsev et al., 1985) and the Antarctic Continent (Cameron, Morelly, 1974). The microflora preservation seem to occur together the sediments freezing. Therefore, it can characterize both the with depositional environment under the regime of syngenetic freezing of the Cenozoic sediments and those corresponding to the beginning of cryolithogenesis under the regime of epigenetic freezing of older rock sequences that had undergone the stage of diagenesis. It should be noted here that hard surfaces of rocks and buried soils are more favourable media for the preservation of microorganisms as compared with ice, snow, firn from where only single cells were reported.

In the cryolithozone, especially in the areas of continuous horizontal and vertical development of low-temperature frozen rocks laching in waterbearing horizons, the effect of outer environmental factors is greatly limited by the depth of seasonal melting, while matter migration due to infiltration and thermodiffusion is hampered. Therefore, there is practically no inflow of the outside microflora. The main factor controlling the natural selection of microorganisms is the formation and presence of permafrost which accounts for the peculiarity of a microbial complex of a frozen rock as compared with fresh sediments, melted and unfrozen deposits. The same is valid for the Quarternary time when natural selection implies preservation of a viability of microorganisms under negative temperatures. In the permafrost rocks that selection had undoubtedly been stimulated by regular melting under the effect of climatic changes and geological events: the revived microorganisms became active and reproduced themselves anow. It appearsfrom the above said that the permafrost rocks provide a unique possibility to solve a number of geological and microbiological problems. It especially concerns those of anabiosis and duration of microorganisms preservation which can't be tacled under the laboratory conditions.

A great quantity and morphological variaty of separated autochthonous microflora that had formed together with sediments accumulation and preserved during their freezing seem to give and opportunity to reconstruct paleoenvironments using microbiological characteristics of permafrost deposits and buried soils. It should be noted here that while all the known methods of bioindication use fainal remains, microbiological interpretation is based on living organisms using not only their morphological features but physiological ones as well.

Microbiological samples had been collected during the period from 1982 to 1985 in the Kolyma tundra region. Core drilling was applied without washing and adding any chemical reagents. Sampling technique as well as samples storage and transportation

technique excludes any possibility of melting and contamination by any alien microorganisms (Zvyagintsev et al., 1985). Registration of the microflora number and its separation from a rock sample was done using various nutrient media: wort-agar, storch-and-ammonia agar, soil agar, starvation agar, the Arystovskaya medium, ets (Zvyagyntsev, 1980). Sandy-loam deposits of different age (from Middle Plyocene to Holocene) and of different genesis lying at the depths up to 70 m from the surface at average annual temperatures from (-7) to (-12°C) and buried soils were studied.

Maximum number of viable microorganisms have been reported from organogenic horizons endependent of the burial depth and age of deposits. 10^8 cells per 1 g of soil were revealed in buried peats that mark the bottom of the Oloer Suite (N_2^3-Q_1) at the depth of 60-65 m from the surface (Fig.1.1). Less number of viable cells (10^5-10^6) have been reported from buried soils of the cover from the middle part of a glacial complex (Q_3^{2-4}) (Fig.1.2) as well as from the near-surface Holocene peats (Fig.1.6, 1.8) and from modern tundra soils (Fig. 1.3). In the absence of peats and paleosoils, the quantity of microorganisms in sediments is independent of a burial depth of rocks but decreases with their age (Fig. 1.10)

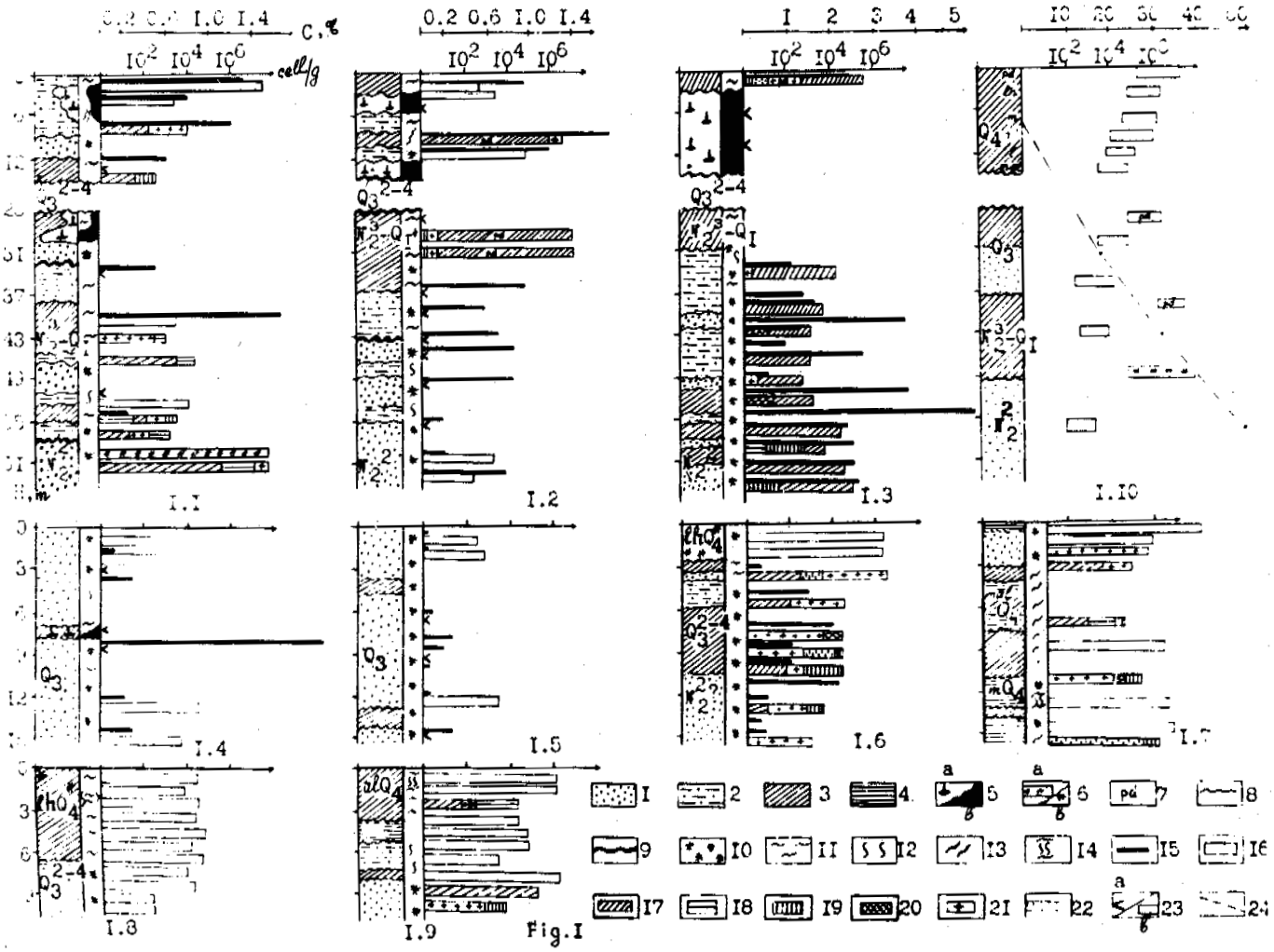

FIG.1. Quantity and morphological variety of microorganisms in the Late Cenozoic permafrost deposits of the Noth-Eastern Eurasia.

Sedimentary complex: 1 - sand, 2 - loamy sand, 3 - loam, 4 - clay, 5 - ice, 6 - peat (a - buried, b - modern), 7 - modern and buried soils. Boundaries: 8 - lithological boundary. 9 - age boundary. Cryogenic textures: 10 - massive, 11 - horizontally layered thin schlieren, 12 - single vertical ice schlieren, 13 - tilted, 14 - reticular or wettled. Content in %, 15 - C_{org}, 16-22 - microorganisms of various morphologic content, 16 - yeast, 17 - corine bacteria, 18 - gram-positive nonsporogenous bacilli, 19 - actinomyces, 20 - sporogenous bacteria, 21 - cocci, 22 - gram-negative bacilli, Quantity of microorganisms: 23^a- microflora in reliable amounts was not observed, 23^b- number of the revealed cells, 24^c- percentage of the sterile samples.

Microorganic content in the Holocene sediments that reflect climatic and landscape environments of the last 7–10 thousand years was evaluated by means of the technique and varied from $6 \cdot 10^3$ to $5 \cdot 10^6$ (Fig. 1.10), the majority being registered in marine silts of lagoons ($2–9 \cdot 10^5$ cells/g; Fig. 1.7). A considerable amount of cells ($6 \cdot 10^3–2 \cdot 10^6$) was reported from loamy deposits of different facies confined to floodlands alluvium which is characterized by a great range of values (Fig. 1.9). Sands of alluvial delta and coastal lacustri sands contain less microorganisms: $7 \cdot 10^3 – 2 \cdot 10^5$ cells/g and $1 \cdot 10^4 – 4 \cdot 10^5$ cells/g, respectively (Fig. 1.7; 1.10).

Late Pleistocene sediments of the Edom Suite (glacial complex), the established radiocarbon age of which is 15–40 thousand years (Lozgkin, 1977), are characterized by the samples collected at five bore holes (Fig. 1.1–1.3; 1.6; 1.8). This singenetically frozen rook sequence of dusty loamy sands and loams includes thick polygonal veins of ice and had formed in more severe environments than the modern ones (Scher et al., 1979). Microorganisms are less abundant here than in the Holocene sediments, i.e. a sample of a suite 30–40 m thick contains $5 \cdot 10^3 – 8 \cdot 10^4$ cells/g regardless depth of burial.

The Oloer loams 0.6–1.8 mln years age (Vyryna et al., 1984; Mynyuk, 1986) that had accumulated under the forest-tundra and contained from $9 \cdot 10^2$ to $1 \cdot 10^4$ viable cells per gramme (Fig. 1.1–1.3).

Peatted Plyocene sands are the most ancient studied sediments 3–5 Ma. They have formed under the conditions of northern taiga landscape and are recognized as the Tomus-Jar Suite. These sediments countain less viable cells compared with the Oloer deposits by an order of 1 (Fig. 1.2). Together with the Plyocene sediments of the Antarctic Continent (Cameron, Morelly, 1974), the Tomus-Jar sands are the most ancient known rocks that contain preserved viable microflora.

It has been established flat the quantity of the separated microorganisms depends on the lithological composition of a rock. Loams contains more microorganisms than sands by an order of 1–2 which is well exemplified by the Holocene deposits. The same pattern has been observed while comparing the microorganic composition of the Khalarcha tundra sands ($10^3 – 10^4$ cells/g, Fig. 1.4; 1.5) with that of glacial loams of the same age (Fig. 1.1–1.3; 1.6; 1.8).

It has been shown that average, maximum and minimum number of the separated viable cells would decrease with the deposits age (Fig. 1.10). The percent variations of the samples lacking viable microflora showed the same tendency (Fig. 1.10) whereas all the studied Holocene samples contain microorganisms, 19% of the Late Pleistocene samples, 33% of the Late Plyocene–Early Pleistocene samples and 50% of the Plyocene samples are sterile.

The quantity of microorganisms can be served as an indicater of levels of melting of frozen rock sequences. Seasonal melting depth depends on the landscape and climatic environments . It has been established that microorganisms are carried out of soil with thawed snow , accumulated in a horizon overlying the frozen one and increase in number as compared with the overlying layers (Lysak , Dobrovolskyay, 1982). It's possible that regular melting of frozen rocks brings about getting down of microorganisms accumulated at the base of a layer of seasonal melting together with lowering of the melting depth being carried out thawed snow. The lower the quantitative peak is in the cross-section, the older is the melting depth and the lower is the temperature maximum of the considered climatic cycle.

To reveal the Holocene melting levels, boreholes were bored in the Holocene alas (Fig. 1.6; 1.8), in the cover horizons of the Edom Suite and in the Khalarcha sands. There are four quantitative peaks amounting to $10^4–10^5$ cells/g and one minimum estimated as $10^2–10^3$ cells/g (Fig. 2.1). The first peak

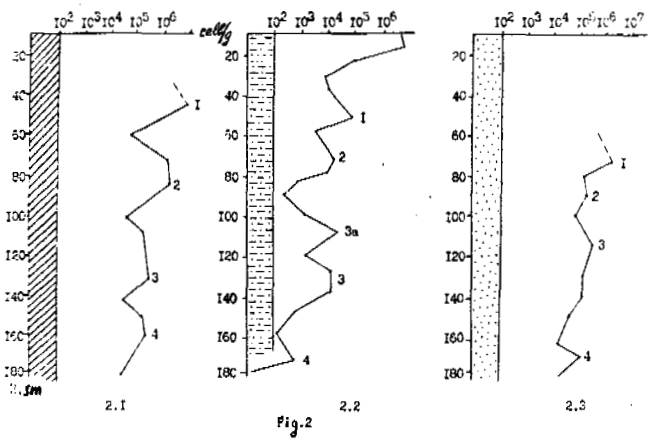

Fig. 2. Quantitative peaks marking levels (depths) of melting for the last 7–8 thousand years (from the Holocene optimum to the present day). Fig. 2.1 and 2.2 – in the loams of the cover and loamy sands of the glacial complex (Q_3^{2-4}); Fig. 2.3 – in the eolian Holocenic sands. Symbols 1, 2, 3 are the same as in Fig. 1.

corresponds to the bottom of a layer of modern seasonal melting at the depth of 0.55 m which has been evidenced by visual observations. The second peak corresponds to the depth of 0.75 m and marks maximum melting durring secular rise in temperature registered in the Arctic in 1930-1940. The third peak corresponds to the depth of 1.1 m and is likely to reflact the subatlantic rise in temperature. The fourth peak corresponds to the depth of 1.35m and characterizes the Holocene rise in temperature as confirmed by the cryolithological data. Similar results have been obtained from another bore hole in the cover horison (Fig. 2.2). The correspounding peaks for sands were registered lower in the cross-section by 30-40 cm due to a greater melting depth (Fig. 2.3).

The microbial content in syngenetically frozen deposits that in the horizons that had melted during interglacial periods or during other climatic optima and refrozen. Microorganisms distribution pattern along the profiles of the bore-holes 6 and 8 (Fig. 1.6; 1.8) is in evidence of this difference. The upper 4-5 m of the cross-section are represented by the alas deposits melted during the Holocene optimum and refrozen up to the present. Microorganisms in these deposits varies in member from 2 to $8 \cdot 10^6$ cells/g, the peak being registered at the boundary between the taber epigenetic frozen alas deposits and the underlying unmelted Edom sediments containing only $2-4 \cdot 10^4$ cells/g, or less by an order of 2. The authenticity of the said boundary is also supported by field observations.

Difference in the background quantity of microorganisms and its peak corresponding to the top of both modern and ancient permafrost water impermisible horizons allow to registed depths of maximum welting during comparatively short periods of the Holocene climatic optima ($T = n \cdot 10^2 - 10^3$ years) and to establish a boundary between the alas and the underlying unmelted Late Pleistocene deposits. New data being available, it will be possible to establish the boundary of regional melting during the Holocene optimum and in the future, during other Pleistocene thermochrones microbial content in a rock can serve as a means to establish the thickness of the refrozen pseudotalics in dried out basins of migrating lakes. Hence, it is justifiable to use this approach to recognize paleotalic zones under meandering paleoriver beds and levels of deformation frost rocks during the periods of marine transgression.

The growth of microorganisms under different temperature regimes is an informative feature of frozen rocks. The microorganisms separated from the Edom and Oloer samples are characterized by a narrow range of growth temperatures from -4°C to 20°C and from -4°C to 30°C, respectively (Fig. 3.1).

A higher Oloer limit is most likely due to higher average annual and summer accumulation temperatures. That conclusion is supported by palynologic data (Scher et al., 1979). The microbial complex of the Edom and Oloer suites may be characterized as psychrophilic and psychrotrophic (Lyakh, 1976; Zhizn' mikrobov..., Reichard, Morita, 1982). At the temperatures higher than +30°C, microorganisms from the above said suites were unable either to grow or exhibit viability. The taber alas deposits formed during the Holocene optimum demonstrate a wide range of possible growth temperatures (from - 4°C to +68°C). In this case, the greatest number of microorganisms tends to be revealed at higher

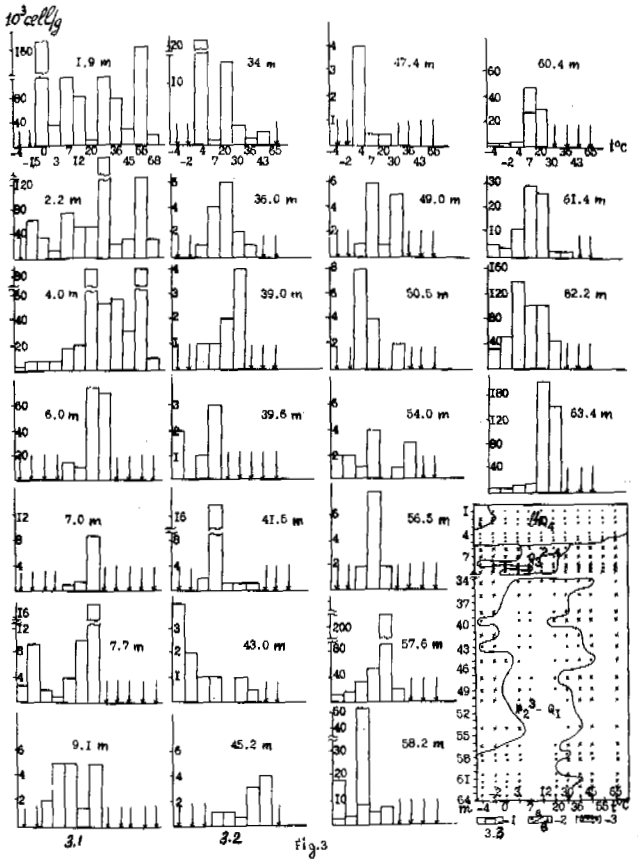

Fig.3. The effect of the growth temperatures on the quanting of microorganisms separated from the Late Pliocene-Pleistocene sediments. 1 - quantity of microorganisms; 2 - reliable amount of microflora was not observed; 3 - vital activity temperature spectra of the microflora of different age.

temperatures (Fig. 3.1).
Morphological variety of the separated microorganisms can be used to characterize sedimentary facies and consequently, to serve as auxiliary criterion for stratigraphic differentiation of rocks. For example, the Holocene sediments contain both eucariotes and procariotes, whereas older Plyocene and Pleistocene deposits are poorer in microorganisms. They contain only procariotes whose variety decreases with the age of a rock untill cocci and corine bacteria prevail.

It follows from the above said that it is quite reasonable to distinguish between Holocene and Pleistocene on the basis of certain microbiological characteristics. That approach is most effective as ap - plied to modern shelf and continental environment where the boundary is lower than the upper level of the modern drainage system It also seem to be useful while establishing older stratigraphic boundaries within cryolithozone, or age intervals. The decrease in the number of cells, increase of a morphological spectrum due to the frozen rock sequences age increase implies falling out of separate groups of microorganisms. Having revealed these groups and established their absence from the samp-

les under study it is possible to suggest a time scale for the rocks that are or had been frozen.

Taking into account the already established facts that microbial communities form together with sedimentation and there is no inflow of the outside microflora into the frozen rock sequences, it is reasonable to consider these microbial communites as indicative of the enclosing sediments. Few facial specifications of microorganisms has been recognized as yet. However, it has been convincingly established that gram-negative bacily are confined to marine deposits, while yeast, fungi and actynomyces belong to the alas ones. Therefore it is necessary to reveal prevailing microbiological spectra in sediments of different composition and genesis and, in the future, to obtain indicative strains.

Other microbiological characteristics are being studied at present that can be used to solve geological problems within areas of development of permafrost rocks. It has been established that the enzyme activity data available for all the deposits under study are indicative of climatic, geobotanical and other environment controlling the present-day or ancient biogeocenosis. Up to now, catalase, amilase, urease, invertase and protease, but not dehydrogenase, activity has been observed. The same problem can be solved while recognizing the type of soilforming processes by microbial spectra preserved in destroyed buried soils horizons.

Cryolithozone up to 1000 m thick provides an opportunity to study the evolution of the groups in sediments of different age. Microflora preserved in epigenetically frozen sediments that had formed under the conditions of warm climate are of most interest as unusual or new form can be met with. The latter suggests the possibility to create paleomicroflora data bank to develop ideas on the problem of microbial cenosis of the past.

CONCLUSION

The available data allow to distinguish between the Holocene sediments and older rocks. They are also promising in that they might used to establish age differentiation of the latter by means of microbiological scale for the permafrost rocks.

The above mentioned problems require further experimental talking treatment. Together with the approved criteria and on the basis of the available geological information, microbiological methods of study of frozen rocks can appear to be an effective approach to the study of temporal and spacial boundaries of the biosphere.

REFERENCES

1. Virina E.N., Zazhigin V.S., Sher A.V. (1984). Paleomagnitnaya kharacteristika tipovykh mestopologenii olerskogo faunisticheskogo kompleksa. - Izvestiya Akademii Nauk SSSR, Seria geologicheskaya, N 1, str. 61-71.
2. Zhizn' mikrobov v ekstremal'nykh usloviyakh (1981) Moskva, Mir, str. 519.
3. Zvyagintsev D.G., Gilichinsky D.A., Blagodatsky S.A., Vorobieva E.A., Khlebnikova G.M., Arkhangelova A.A., Kudryavtseva N.N. (1985). Dlitel'nost' sokhraneniya microorganismov v postoyanno merzlykh osadochnykn porodakh i pogrebennykh pochvakh. Microbiologiya, tom 54, vypusk 1, str. 435.
4. Lozhkin A.V. (1977). Radiouglerognye datirovki verkhnepleistotsenovykh otlozhenii Novosibirskikh ostrovov i vozrast edomnoi svity Severo-Vostoka SSSR. Doklady Academii Nauk SSSR, tom 235, N 2, str. 435.
5. Lysak L.V., Dobrovol'skaya T.G. (1982). Bacterii v pochvakh tundry Zapadnogo Taimyra. - Pochvovedeniye, N 9, str. 74-78.
6. Lyakh S.P. (1976). Adaptatsiya microorganismov k nizkim temperaturam. Moskva, Nauka, 160 str.
7. Metody pochvennoi microbiologii i biokhimii (1980) Pod redaktsiei D.A. Zvyagintseva, Moskva, Izdatel'stvo Moskovskogo Universiteta, 224 str.
8. Minjuk P.S. (1986). Paleomagnitnoye obosnovanie stratigrafii pliosenovykh i chetvertichnykh otlozhenii tsentral'noi severnoi Yakutii. Avtoreferat dissertatsii, Leninfgrad, 24 str.
9. Sher A.V., Kaplina T.N., Giterman D.E., Lozhkin A.V., Arkhangelov A.A., Virina E.N., Zazhigin V.S. Kisselev I.E., Kuznetsov Yu.V. (1979). Tikhookeanskii naychnyi kongress. Putevoditel' nauchnoi ekscursii "Posdnekainozoiskie otlozheniya Kolymskoi nizmennosti". Tur XI. Moskva, Nauka, 116 str.
10. Cameron R.E., Morelli F.A., 1974. Viable microorganisms from ancient Ross Island and Taylar Valley drill core. - Antarctic J.U.S., v.9, N 4, pp. 113-116.
11. Reicharct W., Morita R.J., 1982. Temperature characteristics of psychrotropic and psychrophilic - J. Gen. Microbiol., v.128, N 3, p. 565.

THERMIC OF PERMAFROST ACTIVE LAYER – SPITSBERGEN

A. Gluza, J. Repelewska-Pekalowa and K. Dabrowski

Institute of Earth Sciences, Maria Curie-Sklodowska University,
Akademicka 19, 20-033 Lublin, Poland

SYNOPSIS

The temperature of the active layer of permafrost within the area of the coastal plain of the southern margin of Bellsund (Western Spitsbergen) was investigated. The measurements were taken i 5 points representing main geocomplexes of the polar environment of Calypsostranda. The geocomplexes were characterized by different water conditions, vegetation and the dynamics of contemporaneous morphogenetic processes. The analysis was made of the distribution and occurence of the ground temperature in connection with meteorological conditions and the features of the tundra environment (vegetation, water conditions, contemporaneous geomorphological processes). The influence of the individual features of the particular geocomplexes on the development and distribution of the ground temperature was shown.

INTRODUCTION

The distribution of the ground temperature in the vertical profile as well as its occurence in time depends on the features of the natural environment. Uppermost are climatic factors, soil- and vegetation conditions along with hydrological and morphological ones. The result is the regional differentiation of the thermic of ground. This problem was the chief aim of investigations in the area of Spitsbergen carried out by Czeppe (1961), Jahn (1961), Baranowski (1968), Jahn and Walker (1983), Glowicki (1985), Grzes (1985), Kaminski (1985), Repelewska-Pekalowa et al. (1987), Wójcik and Marciniak (1987).

The investigations of the thermic conditions of the permafrost active layer in the Western Spitsbergen were started in 1986 within the programme of the Geographical Expedition of Maria Curie-Sklodowska University (Repelewska-Pekalowa et al. 1987). The investigated were localized in NW part of Wedel-Jarlsberg Land, on the Calypsostranda coastal plain (Fig. 1).

Taking under consideration the climatic conditions, the area belongs to the transitional zone between a warmer part of Spitsbergen in the region of Isfiord and a colder one around Hornsund (Pereyma 1983, Rodzik et al.1985). In this paper the materials gathered in the summer season of 1987 were exploited. During the investigations (14.06. - 20.08.1987) the cyclonal weather prevailed i.e. windy with frequent precipitations and great cloudiness. The elements of the weather at that time were as follows:

mean daily air temperature at a height of 2 m:	3.8°C
oscillations of the mean daily air temp.:	0.8°C-8.7°C
mean maximal temperature at a height of 2 m:	5.9°C
mean maximal temperature at a height of 5 cm:	8.4°C
mean minimal temperature at a height of 2 m:	2.3°C
mean minimal temperature at a height of 5 cm:	2.1°C
precipitation sum:	31.8 mm
number of days with precipitation: $\geq$ 0.1 mm:	23
evaporation sum:	121.6 mm
mean wind velocity:	4.8 m/s
oscillations of the mean daily wind vel.:	0.5-14.2 m/s
general cloudiness (scale 1-10):	83 %
cloudiness by low clouds:	62 %

In comparison with the similar period of 1986, the summer of 1987 was about 1° cooler and more windy.

The thermic of the active layer of permafrost was investigated at five points on Calypsostranda (Fig. 1-C). They represented the following main geocomplexes of the tundra environment:

Point 1: Dry tundra covering the maritime terrace of the height 20-30 m a.s.l. with a brown, arctic soil. The vegetation cover consists of species of saxifrages, lichnes and mosses. The surface of this geocomplexes is flat, modelled to-day by niveo-eolic processes and washing out.

Point 2: Patterned grounds, periodically wet, with water flowing in covers, fed with waters from the shallow lake. The vegetation cover consists of mosses developing on a peat layer up to 20 cm thick. The vertical movements of the ground caused by the action of frost prevail among morphogenetic processes.

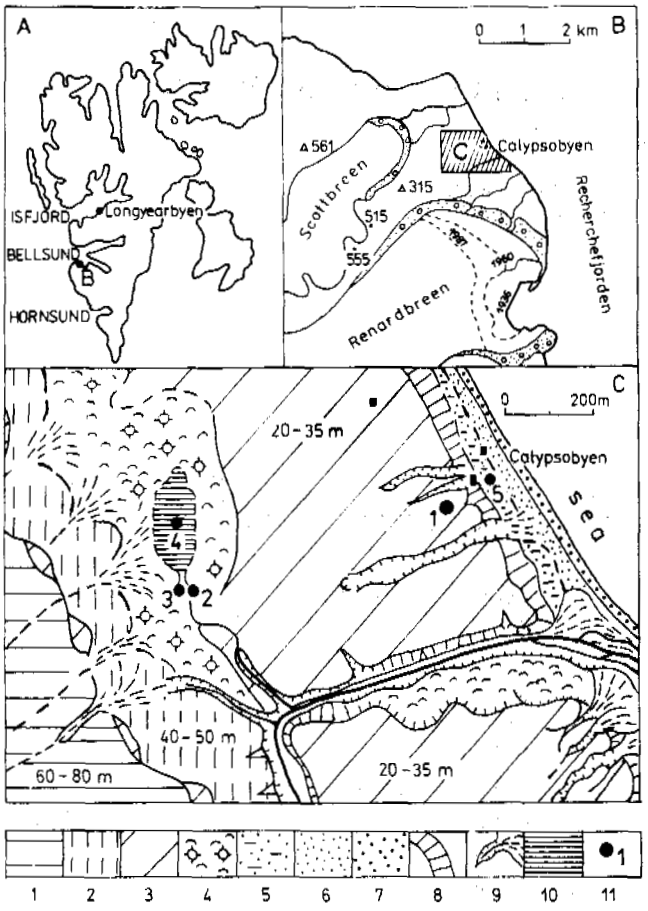

Fig. 1. Localization of the investigation area (A,B) and a geomorphological outline (C) 1,2,3 - marine terraces, 4 - zones of the occurence of patterned grounds, 5 - glacis, 6 - beach, 7 - stormbank, 8 - fossil cliff, 9 - erosive forms, 10 - tundra pool, 11 - measurements points (1-5)

Point 3: Patterned grounds, active with moving water in the covers, fed like in point 2. Lack of compact vegetation, due to the strong dynamics of frost process.

Point 4: Watered peatbog 50 m^2, within a shallow lake. Thickness of the peat reaches 25 cm. Active frost processes.

Point 5: Plain at the foot of a fossil cliff in the vicinity of a beach. Lack of compact vegetation (only tufts of mosses, grass and lichens) is connected with active proluvial accumulation and with the development of flat taluses (Repelewska-Pekalowa 1987). Variable level of ground waters supplied with permafrost waters from the fossil cliff.

A common feature of all geocomplexes investigated is a similar formation of the covers (sand with gravels), relief (flat terrains) and general climatic conditions. Thus, the differentiation of the thermic of the ground is connected with water conditions and vegetation.

METHODOLOGY OF INVESTIGATIONS

Ground temperature measurements within the chosen geocomplexes were initiated in different periods (14.06, 17.06, 22.06, 10.07.1987) according to the moment of the vanishing of the compact snow and ice-cover.

The temperature was observed at a depth of 2 to 200 cm, four times daily (00,06,12,18 GMT), during the standard meteorological observations, by means of both mercuric and electric thermometers.

Station \ Depth cm	2	5	10	20	50	70	80	100	150	170	200
1	54	53	48	38	16	–	–	00	-07	–	-10
2	–	55	56	48	42	–	35	32	–	33	–
3	–	55	51	43	25	–	20	18	–	15	–
4	–	48	40	16	06	-02	–	–	–	–	–
5	–	–	–	–	22	–	–	07	-04	–	-08

Table I. Distribution of mean ground temperatures in the summer season of 1987 (in the period investigated).

On the basis of the obtained data the mean daily temperature at the particular depth were calculated (Table I). It allowed to present the vertical and spatial distribution of the ground temperature, day by day as well as in the 24-hour cycle (Fig. 2-5).

ANALYSIS OF RESULTS

Vertical distribution of the ground temperatures

In all geocomplexes investigated the uneven rate of the lowering of the ground temperature along with depth was observed (Fig. 2). In the layer to 50 cm a fast decrease took place, on the average 1^0C/10 cm, then the temperature lowered by 0.3^0C/10 cm to a depth of 100 cm. Within the layer below 100 cm the decrease in temperature amounted on the average to 0.1^0C/10 cm. The warmest were the structural grounds (point 3) and a dry peatbog with moving water in the covers (point 2). The insulation role of the peat was marked here, which was reflected by temperatures higher at a depth of 10 cm, than at a depth of 5 cm. On the other hand, the low temperatures were noted on the peatbog saturated with stagnant water (point 4). A similar verticular distribution in these geocomplexes was registered in the summer season of 1986 (Repelewska-Pekalowa et al.1987).

The daily course of the ground temperature

The daily amplitudes grew smaller together with an increase in depth, the biggest being noted to a depth of 20 cm. At a depth of 50-80

cm the isothermic of temperature dominated (Fig. 3). The essential daily changes of temperatures appeared in the geocomplexes devoid of compact mossy vegetation (points 1 and 3). The daily amplitude of temperatures in these points, in the layer near the surface, oscillated between 2 and 3°C, while in the geocom-

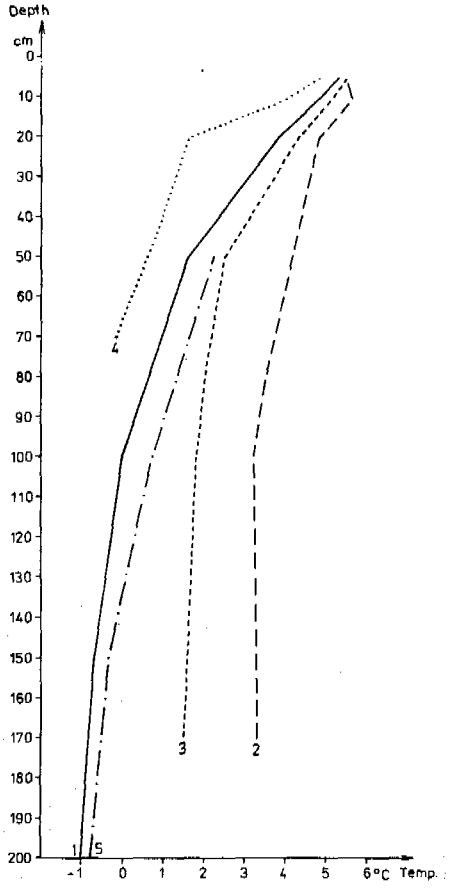

Fig. 2. Course of the ground temperature according to depth (tautochrons)

plexes with compact vegetation (points 2 and 4), the values ranged from 1.0°C to 1.5°C.

Two groups of geocomplexes may be isolated in which the daily course of the temperature of the ground is different (Fig. 3):

1. In the geocomplexes without a compact vegetation the increase in temperature was marked from the morning hours up to noon (12 GMT), with a quick decrease in the afternoon hours (points 1 and 3).

2. The geocomplexes with a vegetation (points 2 and 4) were characterized by a period of warming of the ground longer by ca. 6 hrs. Maximum temperatures occured between 18 and 06 hours GMT. At night (00 GMT) peat

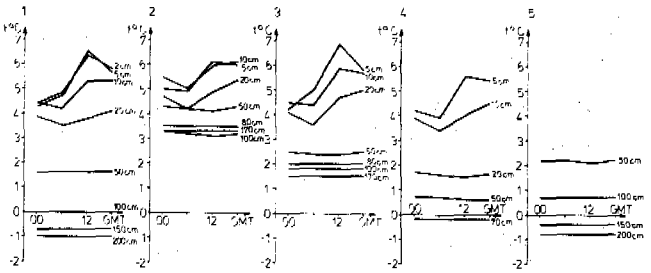

Fig. 3. Daily course of the ground temperatures (points 1-5)

grounds were warmer than the others by ca. 1°C. Similar regularity was observed on the wet peatbog, the temperatures being lower due to the loss of warmth for water evaporation.

Distribution of the day by day ground temperature

The spatial disturbation of the temperature of the ground in the summer season of 1987 was presented in connection with basic weather elements as well as with the thermic of superficial waters (Fig. 4). A distinct influence of the weather elements was marked especially of the maximum air temperature at a height of 2 m and 5 cm above the ground, as well as on influence of the insolation factors, mainly of the intensity of the radiation absorbed. Other weather elements, such as insolation and wind play less important role. The air temperatures at a height of 5 cm and 2 m above the ground had the strongest influence. Correlation coefficients of the air temperature at a height of 5 cm and those of the ground temperature at a depth of 5 cm are shown in particular stations respectively:

point 1 r = 0.83
point 2 r = 0.83
point 3 r = 0.77
point 4 r = 0.86

Correlation coefficients of the air temperature at a height of 2 m and those of the ground temperature at a depth of 5 cm, amounts to 0.79. It follows that the changes of the ground temperature at a depth of 5 cm in 70 % depend on the changes in air temperature. It results from the determination coefficient (r^2) and the linear dependence between these two elements is expressed by the following equation:

$y = 0.5163x + 10$ (Fig. 5)

The distribution of thermoisopleths in the geocomplexes with moving water in the covers (point 2) and with stagnant water (point 4) was different from that in the dry tundra (point 1). The moving water being warmed on the surface, and in the layer near the sur-

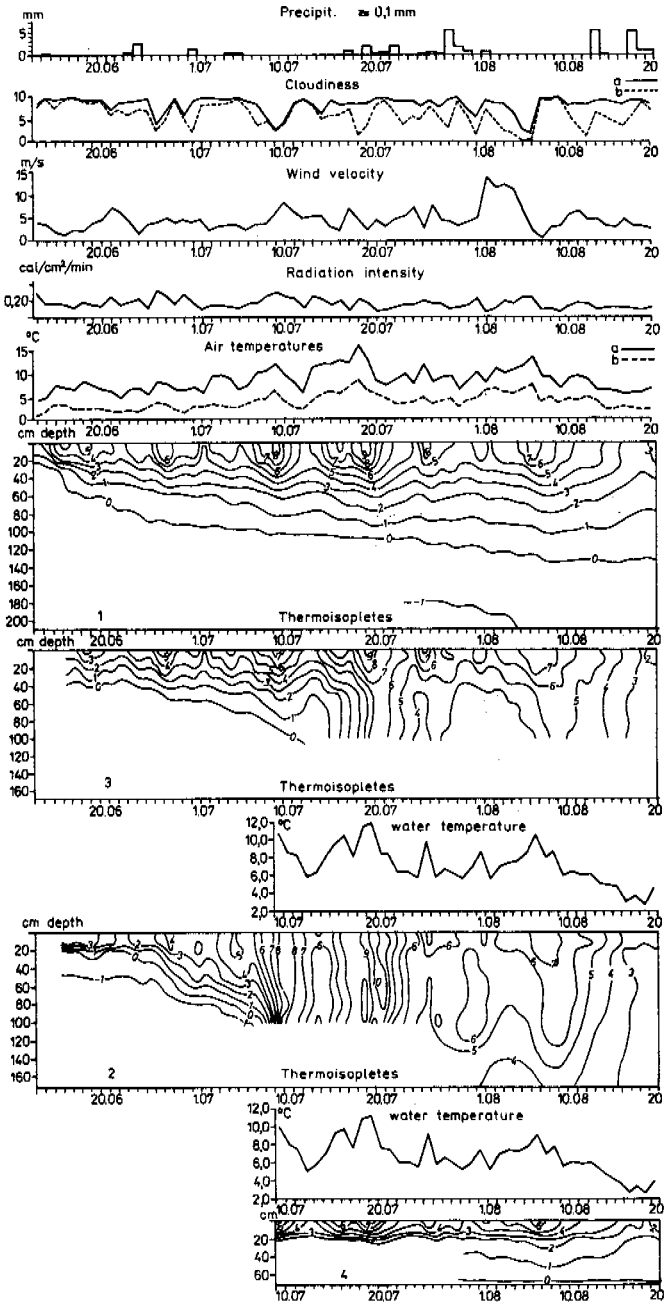

Fig. 4. Thermoisopleths of the ground at the particular points and daily course of chosen meteorological elements: precipitation 0.1 mm, cloudiness (a - cloudiness, b - lower clouds, in the scale 1-10), wind velocity, radiation intensity, air temperature (a - maximum at a height of 5 cm, b - mean temperature at the height of 2 m).

face, was a heat carrier and was giving warmth to the deeper layers. The mean water temperature was about 7°C and was higher than the ground temperature by ca. 1.5°C to 2°C. The influence of water as a heat carrier was smaller in the near surface layers, where the tem-

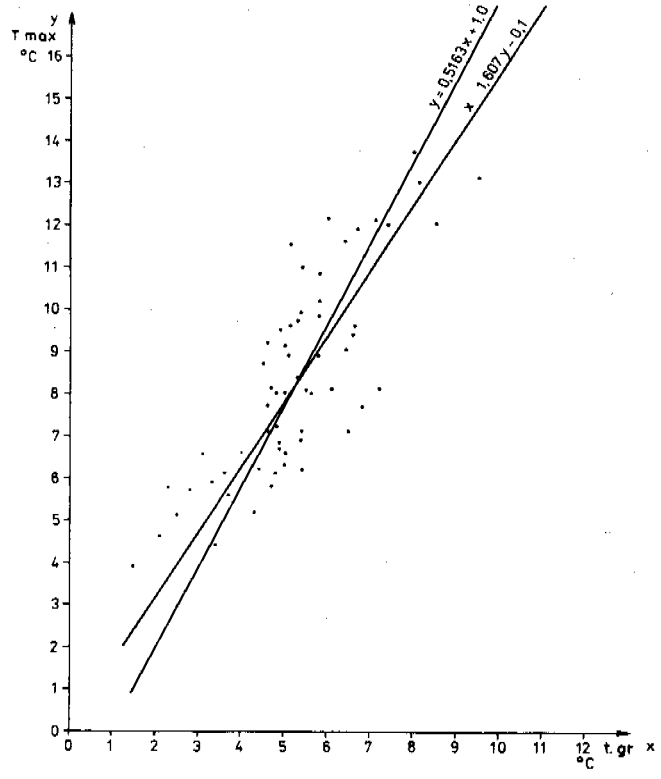

Fig. 5. Functional dependence of the maximum air temperatures at a height of 5 cm (y) and mean daily ground temperatures at a height of 5 cm (x) during the summer season of 1987

peratures were relatively high as a result of warming. On the other hand, its influence was stronger in deeper layers, and therefore the isopleths were drawn vertically. Within the peatbog with the stagnant water (station 4) of the same temperature as in station 2 and station 3 (6.7°C), water did not play the role of a heat carrier but of an insulator. The parallel scheme of the isopleths (Fig. 4) shows that the heat did not reach the deeper layers. Another cause of such a scheme was also a waste of the warmth for evaporation of the water infiltrating upward in the peat (mosses).

All mentioned above elements and factors influence the variability of the ground temperature and its occurence. However, they generally do not explain the local differences in temperatures. In order to recognize them and to choose the factor deciding about the very differentiation; a decision was made to analyse the distribution of the temperature of the ground at a depth of 5 cm on a chosen day (Fig. 6). General meteorological conditions on the terrain investigated were the same (the distance between the extreme stations being quite small) and the main element, influencing the ground temperature at a depth of 5 cm, i.e. the maximum air temperature at a height of 5 m above the surface - was almost identi-

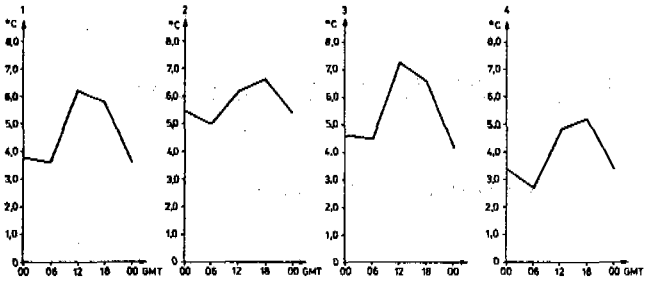

Fig. 6. Daily ground temperature course at a depth of 5 cm on 13th/14th of August 1987 at the particular points

cal and oscillated between 8.4°C and 8.7°C, while ground temperatures were as follows: point 1 - 4.8°C, point 2 - 5.8°C, point 3 - 5.8°C, point 4 - 4.0°C.

The picture obtained of the distribution of the temperatures corroborates earlier statements of a general nature about the prevailing influence of the local conditions, except insolation, i.e. of the moisture and a vegetation of the particular geocomplexes upon the differentiation of temperatures within the active layer.

CONCLUSIONS

The investigation carried out within the coastal plain, in the area of Calypsostranda during the arctic summer (Fig. 4) confirmed the known schemes of changes temerature of the active layer as well as the quantitative estimation of the thermic of the ground in the tundra area. The thermic differentiation of the ground in particular weather conditions was observed. The differentiation was connected with individual features of particular geocomplexes and above all with the occurence and a type of vegetation and also with water conditions. The thermal conductivity and caloric capacity depended on these features. Although the problem of the water in the grounds was discussed many times, the data obtained now allow us to postulate that water and its dynamics is one of important factors modelling the thermic of the ground. According to the way of its supplying, exchange, and movement in the covers, it can play the role of an insulator or of a heat carrier. This is an important feature when analysing the problems connected with the development and dynamics of the active layer of the permafrost (compare - Repelewska - Pekalowa et al. 1988).

REFERENCES

Baranowski, S (1968)
Thermal conditions of periglacial tundra SW Spitsbergen. Acta Univ. Wratisl.,68,

Czeppe, Z (1961)
Roczny przebieg mrozowych ruchow gruntu w Hornsundzie (Spitsbergen) 1957-1958. Zesz. Nauk. UJ,42 Prace geograficzne III, 74 pp, Kraków

Grzes, M (1985).
Warstwa czynna wieloletniej zmarzliny na zachodnich wybrzezach Spitsbergenu. Przegl, Geogr. (57),4, 671-691.

Glowicki, B (1985).
radiation conditions in the Hornsund area (Spitsbergen) Polish Polar Research (6),3, 310-318

Jahn, A (1961)
Quantitative analysis of some periglacial processes in Spitsbergen Zesz. nauk. Univ. Wratisl. B,(5), 34 pp, Wroclaw

Jahn, A, Walker, H J (1983)
The active layer and climate. Zeitschr. f.Geomorph. NF.Suppl. (47), 97-108.

Kaminski, A (1985)
Investigations of the extreme temperatures of the ground surface in the Gåshamnöyra region (Spitsbergen).
Polish Polar Research (6),3, 319-329.

Pereyma, J (1983)
Climatological problems of the Hornsund area Spitsbergen
Acta Univ.Wratisl. 714, 134 pp, Wroclaw

Repelewska-Pekalowa, J, Gluza, A, and Dabrowski, K (1987)
Termika tundry i dynamika czynnej warstwy zmarzliny na przedpolu lodowców Scotta i Renarda (rejon Bellsundu, Zachodni Spitsbergen). XIV Sympozjum Polarne, Lublin, 108-115

Repelewska-Pekalowa, J (1987)
Rozwój równiny nadmorskiej pod wplywem procesów erozji (na przykladzie Calypsostrandy, rejon Bellsundu, Zachodni Spitsbergen) XIV Sympozjum Polarne, Lublin, 103-107

Repelewska-pekalowa, J, Gluza A (1988)
Dynamics of the permafrost active layer-Spitsbergen. V International Conference on Permafrost, Trondheim

Rodzik, J, Stepko, W (1985)
Climatic conditions in Hornsund (1978-1983). Polish Polar Research (6)4, 561-576

Wójcik, G, Marciniak K (1987)
Ground temperature of main ecotopes of Kaffiöyra, Spitsbergen, summer 1978. Polish Polar Researche (8), 1,25-46

Gluza A., Repelewska-Pekalowa J., Dabrowski K.
Thermic of permafrost active layer - Spitsbergen

SOIL FORMATION PALEOGEOGRAPHIC ASPECTS IN YAKUTIYA

S.V. Gubin

Institute of Soil Science and Photosynthesis USSR Academy of Sciences, Puschino, USSR

SYNOPSIS The formation of modern soils in the tundra zone of the Primorskaya lowland of the Northern Yakutiya during Holocene and manifestation of some properties of the Pleistocenic singenetic soil formation in them are discussed in the present paper.

The Kolymskaya lowland occupies the eastern part of the vast Primorskaya lowland and is characterized by the most severe and continental climatic conditions on the territory of all the Europe-Asia tundra. Air average yearly temperatures are $-14.2 \div -15.2^{\circ}C$, the amount of annual precipitation – 147 mm. The thickness of the frozen rocks is 300-600 m and their average yearly temperature – $-10 \div -12^{\circ}C$. The depth of the seasonal thawing does not exceed 40-55 cm on elevated flat sites.

The formation of the modern landscape environment on the territory of the Primorskaya lowland began from the late Pleistocene -early Holocene. In the upper Pleistocene the processes of active sediment accumulation took place under conditions of low yearly temperatures. It results in the formation of a great thickness of coldgenic dusty deposits with thick veins of polygonal syngenetic ice, i.e. edomic sediments. The width of the veins is 1-3.5 meters, ice can make up 30-40% of the rock volume.

The sediment accumulation was accompanied by the soil-forming process, as a result the deposit material had a number of properties characteristic of soils, namely, high content of plant residues, the presence of humus forms of organic matter, biogenic elements, etc.

Hitherto no common conception of the origin of these deposits has been recognized. According to one of them the deposits of the loessial glacial complex were accumulated under conditions of lake-floodplain bogged tundra landscape periodically flooded with spring waters (Popov, 1953; Sher et al.,1979). The subaerial hypothesis (Tomirdiaro, 1980) suggests that these thicknesses are formed under conditions of dry periglacial arctic tundra-steppe or steppe with active eolian processes. The differences found in the properties and structure of the upper Pleistocene deposits on the territory of the Primorskaya lowland and rather profound conceptions obtained on the effect of physical and chemical weathering agents on the material being for a long time within the limits of the seasonal thawing layer allow to consider edomic deposits as genetically heterogenous formations. The thicknesses similar in many properties were formed by different ways of accumulation.According to T.N.Zhestkova et al. (1986) they lose their properties obtained during sediment accumulation and become similar due to the same development during diagenesis. The way of sediment freezing is of particular importance.

It should be noted that the processes of singenetic soil formation occurred during the Pleistocene period mainly under similar bioclimatic conditions contributed, to a certain extent, to the formation of the thicknesses with similar final properties.

Thus, the Holocenic soil was formed on the rocks having a number of properties characteristic of soil material. The detailed analysis of the upper parts of the walls of the two base Pleistocenic cuts on the Kolymskaya lowland – Duvannyi yar outrops on the Malyi Chukochii cape showed that there was no indication of material differentiation according to genetic horizons. The profile organization of the material of separate layers was weakly manifested only on the Duvanyi yar outcrops at a depth of 4-6 m. The thickness of these profiles did not exceed 0.2-0.25 m (Gubin, 1984).

In the upper parts of the Pleistocenic thickness there are no indications of aggregation and microaggregation of the material but there are a lot of small fresh and semidecomposed crop residues. The presence of dark humus coagulates and evolution of one and a half oxides in the form of small brown scalles was observed on the surfaces of mineral grains in the rock sections. Relatively high content of C_{org} is characteristic of the upper Pleistocene deposits. It varies from 0.6 to 2.5%, moreover the humic substance contains the greatest amount of it. Humus is of fulvatic composition with high content of nonhydrolizable residue. The deposits are inriched with nitrogen, phosphorus, potassium. Ca dominates in the composition of the bases adsorbed. The values of pH, carbonate content, absorption capacity and a number of some other indexes are different in the deposits of various regions of the Kolymskaya lowland.

These thicknesses with a set of features and properties of the Pleistocenic soil formation gave origin to modern soils of watersheds.

As it was known there was a temperature increase in the Arctic during the period of late Pleistocene--early Holocene (Khaotinsky, 1977). Basing on the

mass paleobotanic data and the results of the radiocarbon datings T.N.Kaplina and A.V.Lozhkin (1982) give the following temporal boundaries of the main Holocenic periods.

Pre-boreal period (10.500-9.500 years ago). It has rather significant temperature decrease. Pollen spectra characterize the vegetation of tundra-steppe type. Wood and dwarf shrub vegetation practically disappears even in those regions where there are thin larch forests.

Boreal period (9.500-8.000 years ago). It is characterized by considerable temperature increase and shift of vegetation zones to the north. In the spectra of the modern arctic tundra territory the shrub pollen dominates. The peak of alder shrub pollen is observed. In the northern outlying districts of the Primorskaya lowland and the arctic islands there are a lot of microresidues of alder shrubs and big birch. It results from a considerable increase in temperatures of the vegetation period.

Atlantic period (8.000-5.000 years ago). The analysis of the sporepollen diagrams indicated that the beginning of the Atlantic period was considerably warmer than the modern one. During its second part the wood vegetation steps back towards the south and the landscape zonality on the territory of the Northern Yakutiya is similar to a modern one. The authors assume that about 6.000 years ago the vegetation of the arctic tundra was already of modern type.

Subboreal period (5.000-2500 years ago) . The tundra vegetation cover corresponded to a modern one and there were no considerable differences in the landscape if this period was compared with nowdays. There is a number of data indicating that during that time the conditions of the vegetation period were probably improved and the thickness of the snow cover in the mountain systems adjacent to the lowland was increased. Subatlantic period (the last 2.500 years). The vegetation cover and the landscape zonality are analogous to modern ones.

The data given above allow to attribute the Boreal and the first half of the Atlantic period to the Holocene climatic optimum. The last 3.200 years are considered by N.A.Khaotinsky (1982) as more or less single stage in the development of the natural conditions of the Northern Europe-Asia with a general tendency of the climate towards temperature fall and, in particular, with temperature decrease about 2.200 years ago as well as during the small glacial epoch (the second half of the XVI-XIX centuries).

The Holocenic temperature rise accompanied by the humidity increase led to the reconstruction of the landscape environment on the Primorskaya lowland (Kaplina et al., 1980; Romanovsky, 1961). During this process thermokarst lakes were formed and downthrown and alas depressions appeared. The thermokarst processes resulted in active destruction of edomic elevations, flattening of their slopes and formation of lake-thermokarst plains.

The process of bogging and peat accumulation was the main one during the Holocene in the alas kettles. Peatbogs of a 3-4 m thickness were formed in the alas kettles, the majority of which should be attributed to the Holocene (Tormidiaro, 1980). They lay on the taberal sediments which as well as the edomic deposits are inriched with organic substance and nutrients. Sometimes the wood residues of the Holocenic optimum epoch are found in the alas deposits of the typical and arctic tundra. The wood trunks and branches are slightly decomposed. In the peatbog thickness no changes in the peat accumulation rate during the Holocene or in the degree of its decomposition have not been observed yet.

The development of soils in the floodplain -bog landscapes on the territory of the lowland is determined both by the regime of the flowing rivers and by the regional bioclimatic environment. The dynamics of the development of the floodplain landscapes as well as the degree of their structural differentiation also affect these soils. The modern floodplains probably appeared at the beginning of the subboreal period when the modern landscape was formed. Their deposits consist of alternating layers of slightly-decomposed peat and thin river sediments Low heat provision of the zone leads to a slow increase of the peat horizon as a result its thickness seldom exceeds 30-50 cm in modern peat-bog soils.

On the above floodplain terraces and high floodplains the thickness of the peat horizon can reach one meter or more. The radiocarbon datings of the beginning of the horizon formation are still absent.

In the lake-thermokarst kettles the general tendency of the Holocene soil formation is preserved for the landscapes additionally moistened or slightly drained and the process of bog formation with accumulation of slightly decomposed peat absolutely prevails. The thickness of the peat layer can be compared with its thickness on the above floodplain terraces.

Modern tundra soil formation is different under automorphic or similar conditions. The soils with a thin organogenic horizon and a mineral part slightly differentiated by genetic horizons are formed here. The processes of gleying play a key role in this differentiation. On the surfaces of flat slopes - edoms, in the typical tundra zone there are frozen tundra gley (according to N.A.Karavaeva (1969), frozen tundra gley humus) soils, and in the arctic tundra zone - frozen arctic tundra slightly gley humus soils.

The tundra soils of the USSR North-East are characterized by the presence of loose organogenic horizons well aerated and slight indications of profile gleying. The above frozen horizons are the most gleyed due to small amount of precipitation and specific conditions of the soil profile thawing at the beginning of the summer period when there are favourable conditions for moisture evaporation (Karaeva, 1969). Specific properties and structure of the organogenic horizon consisting of well-decomposed organomineral mass are related with the peculiarities of the thermal regime and moistening of these soils. The depth of the soil seasonal thawing is 40-45 cm.

A change in the climatic environment during the Holocene led, first of all, to a change in the depths of seasonal thawing of the frozen thicknesses. In the upper parts of the Pleistocene deposits there is a layer of a 1-2.5 m thickness, it is called a cover one. Generally, it is similar to the edomic deposits (granulometric composition, colour, presence of small roots and organic residues) but there

are no thick veins of syngenetic ices in it. The layer differs from the edomic material by ice content and other cryogenic indexes. The origin of the layer is connected with the epoch of the Holocene optimum and the maximal thawing of the edomic thicknesses.

In the bottom part of the cover there is a 20–30cm intercalation of slightly light and gleyed material, being a horizon of the above frozen gleying.

Analitically, the gleying is very poorly observed but the study of the material in the rock sections shows that in the intercalation the amount of the brown scales evolved by the one and a half oxides on the surface of the mineral grains is considerably decreased. At the same time the amount of small dark coagulations of the humic substances remains unchanged.

The lower parts of the cover layer are similar to the edomic deposits by their chemical properties. Only the upper layers (Fig. 1) were affected by the soil forming process but these changes were not great and clearly manifested.

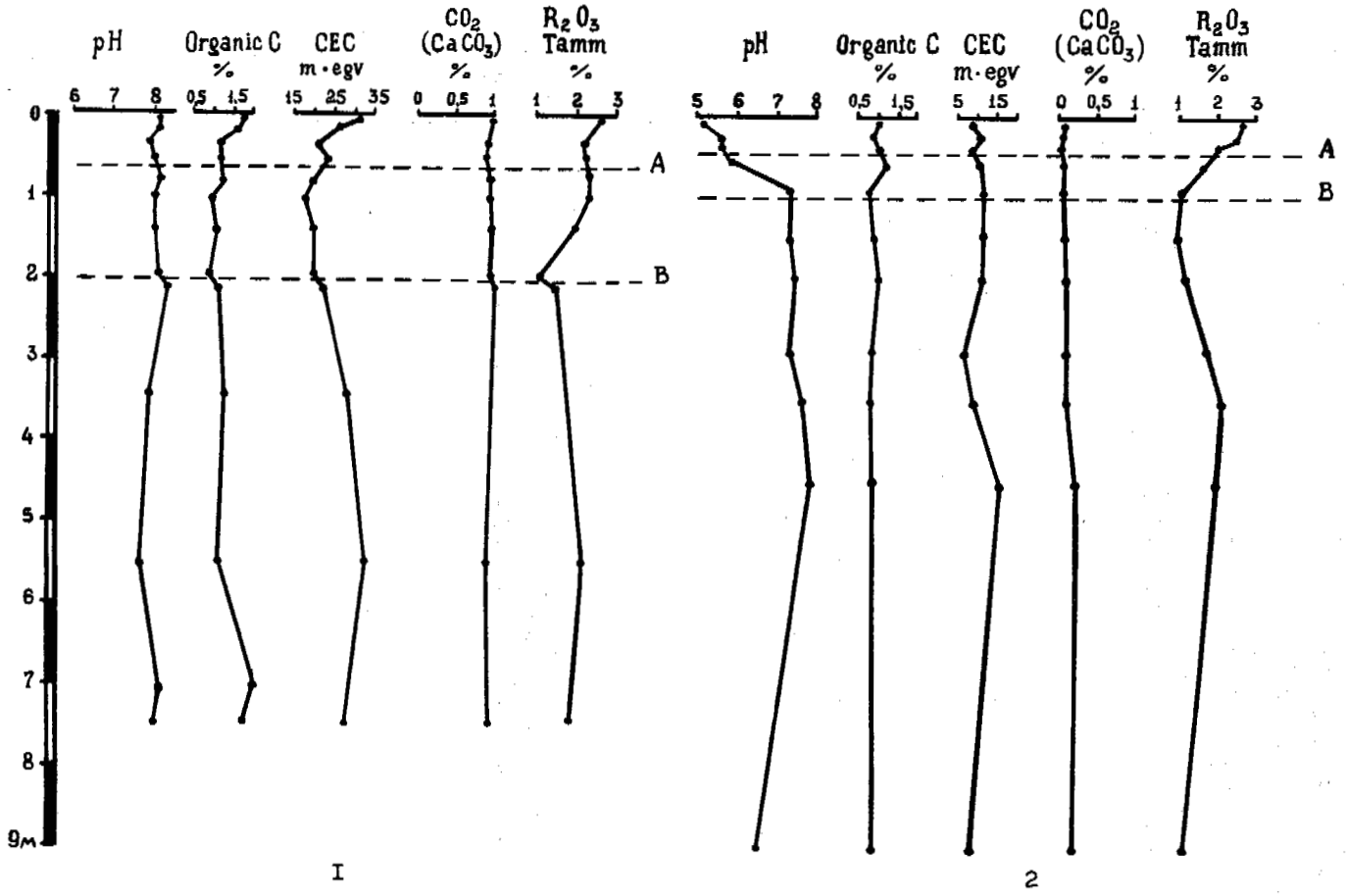

Fig. 1. Properties of the edomic deposits, cover layer and modern soils of the Kolymskaya lowland.
1 – Outcrop Duvanyi yar
2 – Outcrop Malyi Chukochii cape.
A – lower boundary of modern soils
B – lower boundary of the cover layer

The thickness of the cover layer on the territory of the Kolymskaya lowland is increased towards the south from 1 m on the ocean coast to 2–2.5 m in the north of the forest tundra. The thickness of the intercolation of the above frozen gleying and morphological manifestation of the process are also increased in the same direction. It should be noted that no other layers and intercolations having similar properties were found in the thickness of the seasonal thawing layer of the Holocenic optimum inspite of the fact that a great number of pits and outcrops on the Kolymskaya lowland had been

studied.
As it has been shown above the upper parts of the cover layer being now in a constantly frozen state are more similar to modern soils by a number of properties than to the edomic deposits. The presence of changes in the pH-values, content of the bases absorbed, organic substance and a number of some other indexes at the depths of 30-50 cm lower the boundary of the modern seasonal thawing layer can be regarded, on the one hand, as an indication of more active soil formation penetrating deeper during the period of the Holocene optimum. On the other hand, as a fact of frequent involvement of these depths of the cover layer in the soil formation process during the epoches of less significant temperature rises or during extreamly warm years. However, no relict features indicating more active character of the soil forming processes were found either in the structure of the material of the cover layer upper parts or in the profiles of the modern soils. The existing processes were characterized by low activity of chemical weathering, mobilization and redistribution of soil formation products. The humic compounds due to regular and deep freezing of the profiles coagulated and were sedimented on the surface of the mineral particles. It prevented their migration to the lower parts of the profiles and above frozen retinization of humus.

It is important to consider the problem of the intensity of soil profile gleying processes during the Holocene. This process results in the uptake of the ion compounds from the gley horizons and destroying of the ion-containing minerals (Yarilova et al.,1985). The manifestation of the gley processes in the tundra soils is poorly registered by the analytical methods. It can be accounted for not only by low activity of this process but also by poor withdrawal of substances due to a close deposit of a frozen aquiclude as well as by the cryoturbation phenomena which contributing to material mixing in the profile give much informational noise in the evaluation of this process. Micromorphologically the process of gleying in the soils of the region under study is determined by a considerable decrease in the amount of the brown scale forms of iron hydroxides on the surfaces of the mineral grains. As it has been already shown, a similar picture is observed by us in the lower part of the cover layer. The above frozen horizon of the modern soils and the 10-25 cm layer of the upper part of the cover thickness have a microstructure similar to that of the cover layer. We are inclined to consider this gleying zone to be affected both by the modern above frozen gleying processes and by those occurred during moderate temperature rise in the Holocene. As for the main part of the thicknesses of the cover layer it has neither morphological nor micromorphological, nor chemical features of this process. It also has no indications of eluviation of the one and a half oxides from the material lying above. Basing on these results there is much certainty about the fact that the gleying processes during the Holocene were not considerably developed in the soil profiles of the territory under study.

It is also important that neither modern soil formation nor the Holocenic optimum processes have considerable effect on the organic material of the Pleistocene deposits, namely, small organic residues and coagulated humus forms. It allows to consider that the part of the organic substance of the modern tundra soils and those of larch thin forests formed on the edomic deposits is of relict origin. The gleying process has a little effect on this organic material and so the latter masks its exhibition in the soil profiles.

Since there are no chronological series of the Holocenic fossils or buried soil, the data on paleoclimatic, paleobotanic reconstructions, properties and composition of the cover layer and modern soils allow us to present the following ways and stages of the lowland soil evolution during the Holocene.

1. Soil formation under automorphic conditions and on the drained sites considerably differs from that occurring on the areas having additional moistening or without drainage and stagnation of atmospheric moisture. During the Holocene the processes of bogging, progressive peat accumulation with the formation of tundra peat bog gley soils and peats took place on these areas.

2. On the drained territories the soil formation was characterized by low intensity, poor mobilization and migration of the products in the profiles. The biomass increase during various stages of the Holocene was in such a dynamic equilibrium with the processes of its transformation that prevented the the accumulation of considerably thick organogenic horizons. The above frozen but not the innerprofile gleying was mainly developed.

3. In the Kolymskaya lowland in the zone of the modern typical tundra during the Holocene the soil formation was within the limits of the tundra slightly gleying and frozen taiga slightly gleying (continental) processes during temperature falls and rizes, respectively. The soils of these subzones have similar morphological and chemical properties. The frozen taiga soils considerably differ from the tundra ones by slight surface gleying.

4. Weak intensity of soil forming processes during the Holocene contributed to the preservation in the profiles of the modern soils a number of relict properties and features of the Pleistocenic formation inherited from the soil forming rocks having passed the stages of the syngenetic soil formation. They include qualitative composition of humus and morphological forms of its accumulation, granulometric composition, content and distribution of the majority of the elements and compounds and even of such mobile ones as carbonates.

REFERENCES

Gubin S.V. (1984). Paleopedologicheskii analiz verkhnepleistotsenovykh (edomnykh) otlozhenii obnazheniya Duvanyi yar. Bulleten' Komissii po izucheniyu chetvertichnogo perioda, N 53, 125-128.

Zhestkova T.N., Shvetsov P.F., Shur Yu.L. (1986). K voprosu o proiskhozhdenii edomy. V sbornike: Geokriologicheskie issledovaniya, Moskovskii Gosudarstvennyi Universitet, 108-113.

Kaplina T.N., Lozhkin A.V. (1982). Istoriya razvitiya rastitel'nosti Primorskikh nizmennostei Yakutii v golocene. V sbornike: Razvitie prirody territorii SSSR v pozdnem pleistocene i golocene, Moskva: Nauka, 207-219.

Karavaeva N.A. (1969). Tundrovye pochvy Severnoi Yakutii. Moskva: Nauka, pp. 1-205.

Khaotinsky N.A. (1977). Golocen Severnoi Evrazii. Moskva: Nauka, pp. 1-186.

Khaotinsky N.A. (1982). Golocenovye chronosrezy: diskussionnye problemy paleogeografii golocena. Moskva: Nauka, 207-219.

Yarilova E.A., Zeidel'man F.R., Narokova R.P. (1985). Izmeneniye micromorfologicheskogo stroeniya i pervichnykh pochvoobrazuyushchikh porod pod vliyaniem ogleeniya. Pochvovedenie, N 7.

AEROPHOTOGRAMMETRICAL MONITORING OF ROCK GLACIERS

W. Haeberli and W. Schmid

Versuchsanstalt für Wasserbau Hydrologie und Glaziologie, ETH Zürich, Switzerland

SYNOPSIS: In order to aerophotogrammetrically monitor the behaviour of permafrost within active rock glaciers, an observational network has been established in the Swiss Alps. Five rock glaciers were selected which all exist in a periglacial environment of discontinous permafrost and a moderately continental climate. Results from measurements on the rock glacier Gruben are presented to illustrate the observational programme. Altitudes and displacement vectors at the rock glacier surface were determined within a regular 50m-grid by comparison of aerial photographs taken in 1970, 1975 and 1979. Information on surface topography, flowline patterns, velocity distributions and principal strain rates is deduced, as well as changes in these parameters with time. The geometry and creep of the roughly 100m-thick permafrost change slowly. Melting of thin dead ice buried on top of the rock glacier permafrost seems to occur in the marginal zone of former contact with glacier ice.

INTRODUCTION

Creep of rock glaciers is mainly influenced by the temperature, ice content and geometry of their saturated to supersaturated permafrost. Due to the thermal inertia of ice-rich permafrost, these boundary conditions change little with time. In contrast to the drastic changes which have affected mountain glaciers all over the world during the past century, significant thinning or thickening of rock glaciers has been hardly detectable so far (Messerli and Zurbuchen 1968, Barsch and Hell 1976, Haeberli 1985 a,b). In order to monitor long-term developments, and especially possible reactions to recent warming, an observational network has been established in the Swiss Alps. It includes five active rock glaciers which exhibit either predominantly compressing flow (Muragl and Murtèl in the upper Engadin, Réchy in the Wallis) or mainly extending flow (Gufer/Aletsch and Gruben in the Wallis). All these rock glaciers are found in the altitudinal belt of discontinous permafrost and within the relatively dry interior parts of the Alps (Haeberli 1978, 1983). The first survey net for analysing large-scale aerial photographs was installed at GRUBEN ROCK GLACIER. This rock glacier is known to have been in direct contact with GRUBEN GLACIER, a partially cold glacier, in the past. Results of a 9-year observation period are now available for this complex rock glacier. They are presented to illustrate the chosen procedure and its potential applications.

SITE DESCRIPTION

The region under study is a cirque in which the tongues of GRUBEN GLACIER and GRUBEN ROCK GLACIER lie side by side (Haeberli et al. 1979). Following two outburst floods of the ice-dammed lake 3 in 1968 and 1970 (Fig.1), an access road was constructed to help flood-protection work (Röthlisberger 1979); the presence of the access road encouraged a number of measurements and soundings to be carried out (cf. Haeberli 1985a and King et al. 1987, for references). 10m-temperatures of the Gruben glacier tongue are -0.5 to -2.5°C and the ice is known to be frozen to its bed at the margins. Non-frozen sands and silts with a thickness of up to 100m and more exist beneath the glacier. Permafrost of the adjacent rock glacier contains supersaturated sands and silts with ice lenses, and carries remains of buried glacier ice on the top in the area of former contact with the glacier. It is more than 100m thick in places. Mean annual surface temperature is about -1°C and may have been 1 or 2°C colder during the Little Ice Age. Pronounced seasonal variations of flow velocity and of water levels in surrounding lakes indicate that the rock glacier's flow probably includes some sliding on wet and deformable subpermafrost sediments. Drastic glacier shrinkage in the early 20th century must have considerably changed the stress and flow field in the former contact zone between the glacier and the rock glacier. In fact, this zone can possibly be considered to be a push moraine s.str. ("Stauchmoräne" = glacitectonically deformed perennially frozen sediments) formed upslope during past glacier advances and which is now slowly creeping back into the depression left by the vanished glacier ice (cf. Evin and Assier 1982). Unpublished results of seismic refraction soundings point to the existence of a marked transverse bedrock riegel underlying the tongue of Gruben rock glacier immediately above its steepest and narrowest part. A thermokarst lake has been continously growing in massive ice near the rock glacier head since the mid 60's. Recently, two large and often water-filled crevasses formed in buried glacier ice in the former contact zone between the glacier and the rock glacier.

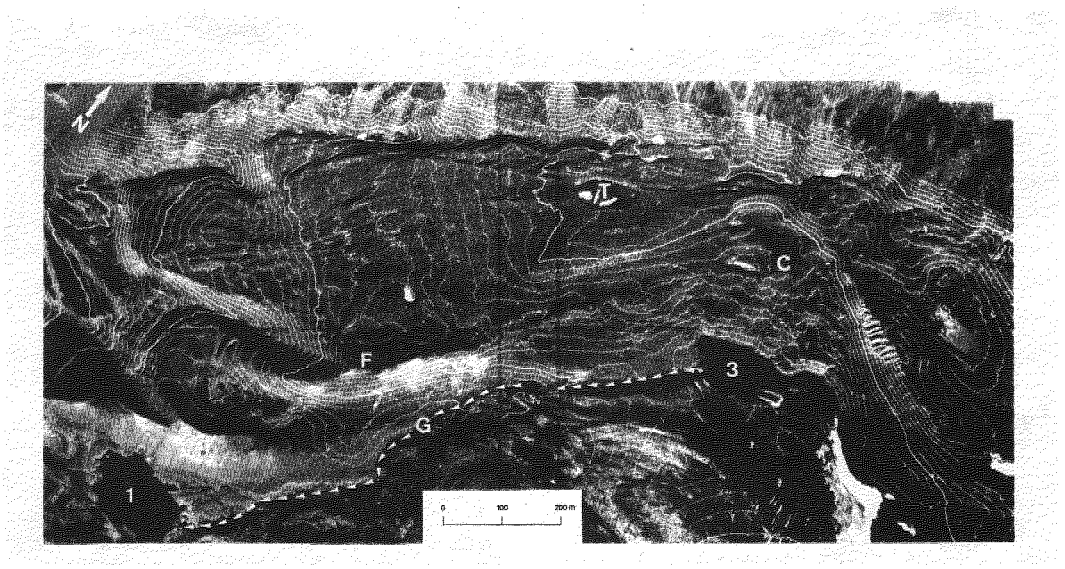

Fig.1: Orthophoto of Gruben rock glacier with 5m-contour lines. 1, 3 = lakes 1 and 3 (lake 2 between them recently disappeared because of the continuing advance of the glacier margin), C = water-filled crevasse in buried glacier ice, F = fixed point (ground-survey station) where the orographic right lateral 19th-century moraine of Gruben glacier and the orographic left margin of the active Gruben rock glacier converge, G = marginal part of partially cold and debris-covered Gruben glacier, T = thermokarst lake on rock glacier surface. Aerial photo taken by the Eidgenössische Vermessungsdirektion, Bern, on 2 September 1985. Preparation of Orthophoto by Swissair Foto- und Vermessungs AG; Zürich.

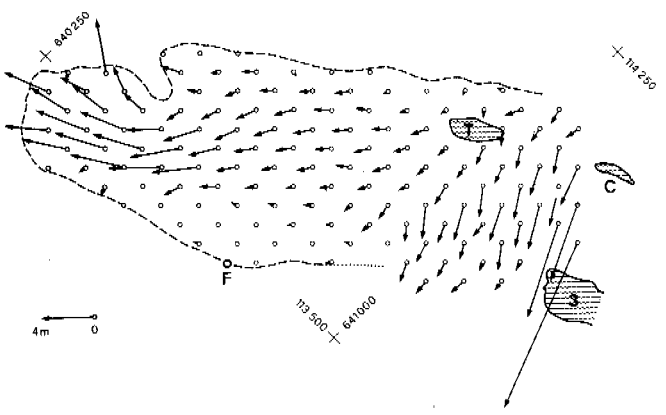

Fig. 2: Measurement grid and displacement vectors 1970 to 1975.

APPLIED METHOD

Surface altitudes and displacement vectors (Figures 1 and 2) were photogrammetrically determined within a fixed, regular 50m-grid using aerial photographs taken on 24 September 1970, 2 October 1975 and 5 September 1979. The scale of the model was about 1 : 6,000 and reference points on the ground could be matched within less than a decimeter in horizontal and slightly more than a decimeter in vertical position. Movement patterns were mapped by directly comparing two photographs taken at different times (cf. Flotron 1979, Haeberli et al. 1979) using a computer-based first-order analog plotter. Data processing and the plotting of the various derived quantities were done with a desk-top computer. Annual velocity values are estimated to be correct within a few centimeters per year. Altitudes, however, are strongly influenced by the extreme roughness of the slowly moving surface. Altitudinal changes within the average boulder size of about 1m can be due to the shift of the surface with respect to the fixed grid points and are thought to be significant only if averaged over large areas.

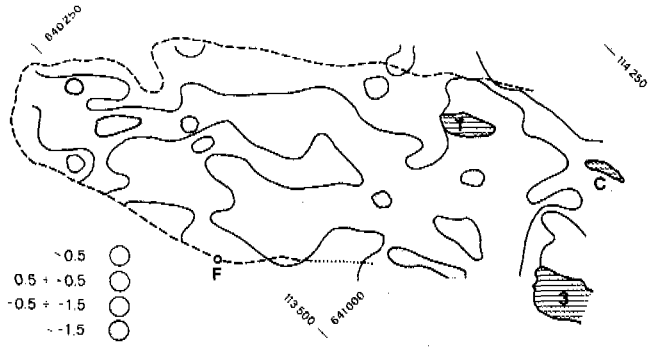

Fig. 3: Changes in surface altitude between 1970 and 1975 (m).

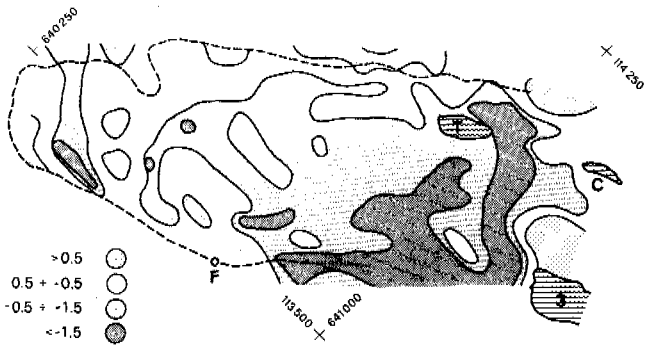

Fig. 5: Changes in surface altitude between 1970 and 1979 (m).

DISCUSSION OF RESULTS

Surface topography of the rock glacier is displayed on the orthophoto of Fig. 1. Figures 3, 4 and 5 show the changes in its surface altitude. Between 1970 and 1975, surface lowering generally predominated with an average total value of a few decimeters. From 1975 to 1979, surface lowering of about 1m continued in the formerly ice-covered zone, whereas the remaining surface rose slightly. It is interesting to note that (ice) glaciers of the Swiss Alps suffered predominantly negative mass balances during the first period, whereas mass gain occurred during the second period mainly due to extremely positive mass balances in 1977 and 1978 (cumulative balances of Gries glacier: -1.62m and +1.0m, Müller 1977, Haeberli 1985b). The periglacial part of the rock glacier seems to follow the same, if somewhat attenuated pattern. This may indicate that freezing and thawing processes at the permafrost table have played an important role here in contrast to the situation in the zone of buried glacier ice which is obviously far out of equilibrium. Over the whole 9-year period (1970 to 1979), changes of surface altitude clearly remained within the uncertainty range due to surface roughness, with the exception of the former glacier-contact zone where buried ice appears to melt at a rate of a few decimeters per year.

Based on the interpolation of measured vectors (Fig. 2), flow trajectories were constructed (Fig. 6) and isolines of surface velocities were drawn (Fig. 7). Movement was away from the scree slopes at the foot of the cirque wall and velocity generally increased towards the margins (extending flow). Exceptions to this picture can be recognised along the now-readvancing glacier margin and where the lateral moraine of the 19th-century glacier forms the orographic left margin of the rock glacier; compressing flow and near stagnation occurred in both cases. Surface velocities were in the order of decimeters per

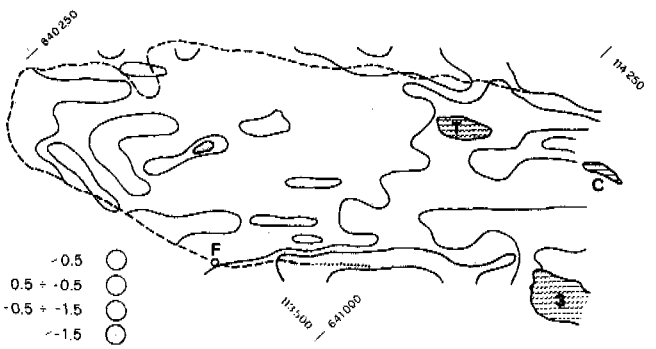

Fig. 4: Changes in surface altitude between 1975 and 1979 (m).

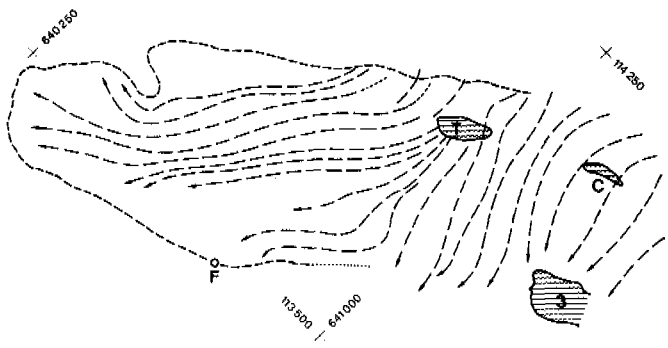

Fig. 6: Selected flowlines (average for 1970 to 1979) interpolated from measured vectors.

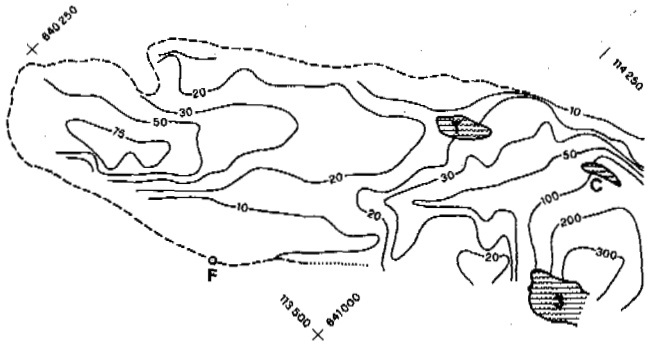

Fig. 7: Distribution of surface velocities (average for 1970 to 1979) interpolated from measured vectors. Note nonlinear sequence of isolines (cm/year).

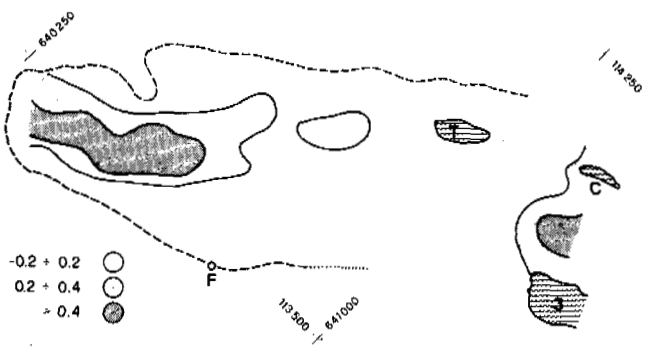

Fig. 9: Changes in vector azimuths 1970/75 to 1975/79 (degrees).

year, but reached extreme values of several meters per year in the buried glacier ice close to the border of lake 3. Annual velocity changes (Fig. 8) between 1970/75 and 1975/79 amounted to a few centimeters per year and, hence, remained close to the estimated uncertainty range. It is, however, noteworthy that a consistent pattern of decreasing velocities seems to exist in the zone of former contact with the glacier. Vector azimuths (Fig. 9) changed by far less than one degree, confirming the pronounced stability of the flow process. The slight tendency of deflection towards the orographic left could possibly indicate that the rock glacier is still adjusting its flow to the stress changes caused by the disappearance of glacier ice at its left side.

Fig. 10 shows the horizontal deformation represented by the principal strain rates which were calculated from the measured displacement vectors. The zone of minimum horizontal deformation around and south of the thermokarst lake represents the flow divide between (a) the part of the rock glacier which moves under strong longitudinal extension into the now glacier-free area of lake 3, and (b) the part which advances more or less parallel to the glacier towards the south-west. The frontal section of the latter part shows a complex pattern of compression (orographic left) and extension (orographic right), both patterns showing a strikingly predominant east-west direction which is oblique to the main flow direction. The huge 19th-century lateral moraine of Gruben glacier as well as an older topographic ridge emerging from it at the orographic left end of the rock-glacier front both lie in the same direction and may therefore have some influence. The general pattern of horizontal strain rates was reproducible in 1975 to 1979, but for details the differences were considerable, especially in the marginal parts of the rock glacier. These differences are assumed

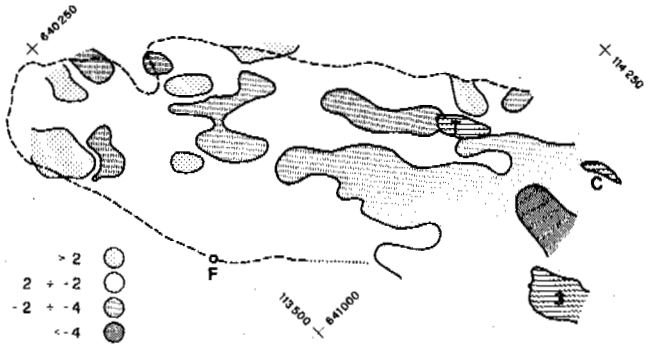

Fig. 8: Changes in surface velocity 1970/75 to 1975/79 (cm/year^2).

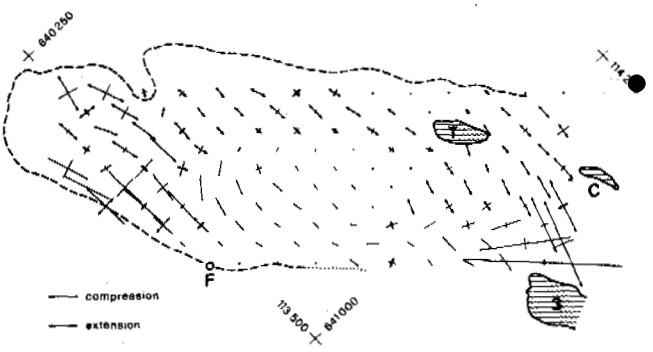

Fig.10: Horizontal principal strain rates 1970 to 1975. Unit length: 10^{-3} per year.

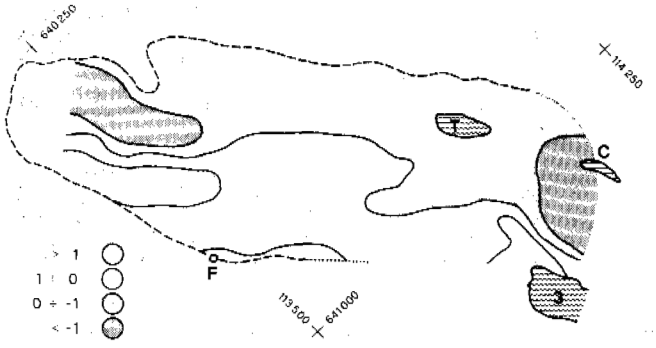

Fig.11: Vertical principal strain rate 1970 to 1979, (positive values = extension, negative values = compression, 10^{-3} per year).

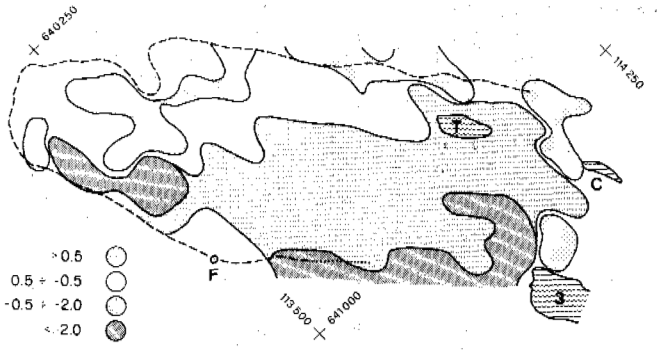

Fig.12: Difference between changes in surface altitude and total vertical strain 1970 to 1979 (m).

to be mainly due to errors in vector determination. Vertical strain rates (Fig. 11) were calculated from horizontal strain-rates averaged for 1970 to 1979 assuming rock-glacier permafrost to be incompressible; mean absolute values are between 10^{-3} and 10^{-4} per year. The corresponding change in permafrost thickness due to deformation alone is within the centimeter range. This is the same order of magnitude as the estimated rate of freezing or thawing at the permafrost base (Osterkamp 1984). In areas of strong shear, strain-induced annual thickness changes may even be in the decimeter range. Vertical strain therefore has to be subtracted from measured changes in surface altitude to enable investigation of geothermal effects (formation or melt of underground ice). Fig. 12 shows the corresponding differences based on an assumed uniform permafrost thickness (100m) and a pure sliding condition (vertical strain rate remains constant with depth). Because of the possible cumulation of surface roughness effects and errors in strain estimation, only spatial means exceeding ∓0.5m may be assumed to be significant. Positive values indicating permafrost aggradation mainly appear where the surface is highest or exposed to the west, i.e. in climatically favoured places. Strong melting obviously takes place at lower altitudes, in slopes exposed to the south and in the zone of buried glacier ice; the average over a total of 165 grid points is -0.55m or -6cm/year. When considering the western part only - this was not in direct contact with the glacier in the last century - the average value is -0.28m or -3cm/year (92 grid points). The rock-glacier permafrost as a whole seems to be out of equilibrium and slowly melting, as one would expect with the 20th-century warming (Haeberli 1985a, UNEP 1987). In the formerly glacier-covered part (73 grid points), melting of buried ice is estimated to be -0.89m or 10cm/year with local maxima reaching 50cm/year.

CONCLUSIONS

Aerophotogrammetrical monitoring of Gruben rock glacier from 1970 to 1979 confirmed that

- the flow pattern of creeping rock glacier permafrost changes very slowly with time,
- permafrost deformation can contribute as much or even more than thermal effects to changes in thickness of the creeping perennially frozen sediments,
- growth and degradation of permafrost can take place simultaneously at different places within the same rock glacier,
- an overall tendency exists for rock glacier permafrost to thin at a rate of a few centimeters per year, probably as a consequence of 20th-century warming.

As a next step in analysing the data, the application of overlay and correlation techniques is planned; extrapolation of long-term trends will be tried on the basis of special large-scale aerial photography repeated after suitable time intervals (5 - 10 years).

ACKNOWLEDGEMENTS

Thanks are due to Dr. Almut Iken and Jürg Schweizer for critically reading the manuscript, to Werner Nobs for preparing the drawings as well as the printed text and to Pamela Alean for editing the English of the present contribution.

REFERENCES

Barsch, D and Hell,G (1976). Photogrammmetrische Bewegungsmessungen am Blockgletscher Murtèl I, Oberengadin, Schweizer Alpen. Zeitschrift für Gletscherkunde und Glazialgeologie (11), 2, 111 - 142.

Evin, M and Assier, A (1982). Mise en évidence du mouvement sur le glacier rocheux du Pic d'Asti (Queyras, Alpes du Sud, France). Revue de Géomorphologie Dynamique (31), 4, 127 - 136.

Flotron, A (1979). Verschiebungsmessungen aus Luftbildern. Mitteilungen der Versuchsanstalt für Wasserbau, Hydrologie und Glaziologie der ETH Zürich (41),39 - 44.

Haeberli, W (1978). Special aspects of high mountain permafrost methodology and zonation in the Alps. Third International Conference on Permafrost, NRC-Ottawa, (1), 378 - 384.

Haeberli, W (1983). Permafrost-glacier relationships in the Swiss Alps - today and in the past. Fourth International Conference on Permafrost, NAP-Washington, Proc., 415 -420.

Haeberli, W (1985a). Creep of mountain permafrost: internal structure and flow of Alpine rock glaciers. Mitteilungen der Versuchsanstalt für Wasserbau, Hydrologie und Glaziologie der ETH Zürich (77) 142pp.

Haeberli, W (1985b). Fluctuation of Glaciers 1975 to 1980. IAHS and UNESCO, Paris.

Haeberli, W, King, L and Flotron, A (1979). Surface movement and lichen-cover studies at the active rock glacier near the Grubengletscher, Wallis, Swiss Alps. Arctic and Alpine Research (11), 4, 421 - 441.

King, L, Fisch, W, Haeberli, W and Waechter, HP (1987). Comparison of resistivity and radio-echo soundings on rock glacier permafrost. Zeitschrift für Gletscherkunde und Glazialgeologie (23), 1, 77 - 97.

Messerli, B and Zurbuchen, M (1968). Blockgletscher im Weissmies und Aletsch und ihre photogrammetrische Kartierung. Die Alpen, SAC (3), 139 - 152.

Müller, F (1977). Fluctuations of Glaciers 1970 to 1975. IAHS and UNESCO, Paris.

Osterkamp, TE (1984). Response of Alaskan permafrost to climate. Permafrost Fourth International Conference, NAP-Washington, Final Proc., 145 -152.

Röthlisberger, H (1979). Glaziologische Arbeiten im Zusammenhang mit den Seeausbrüchen am Grubengletscher, Gemeinde Saas Balen (Wallis). Mitteilungen der Versuchsanstalt für Wasserbau, Hydrologie und Glaziologie der ETH Zürich (41), 233 - 256.

UNEP (1987). United Nations environmental data report. Monitoring and Assessment Research Center, London, 352pp.

SURFACE SOIL DISPLACEMENTS IN SORTED CIRCLES, WESTERN SPITSBERGEN

B. Hallet[1], S. Prestrud Anderson, C.W. Stubbs and E. Carrington Gregory

[1]Quaternary Research Center and Department of Geological Sciences,
University of Washington, Seattle, U.S.A.

SYNOPSIS Considerable data have been gathered in several well-developed sorted circles to elucidate processes active in these enigmatic features, which comprise domains of fine-grained soil encircled by gravel ridges. A three year record of horizontal soil displacements at the ground surface reveals a coherent pattern strongly suggestive of intermittent soil convection in the active layer, with maximum long-term displacement rates of about 10 mm a^{-1} and a characteristic cycling time on the order of 500 a. Several driving mechanisms for this convection appear plausible, including buoyancy forces resulting from a vertical gradient in soil moisture that arises naturally in thawing ice-rich soil. Alternatively a "border forcing" mechanism may operate, in which the summer settling of gravel ridges previously elevated by frost-heaving induces convection.

INTRODUCTION

Distinct patterns in periglacial soils have been recognized for well over a century, and despite the obvious curiosity and interest they have instilled, little is known definitively about how they form and function. A number of scenarios, many rather ingenious, have been developed to explain the development of such features; for example, an extensive review by Washburn (1956) includes nineteen dominant processes. None has been clearly verified, however, through direct field measurement and observation. Furthermore, with the possible exception of ice-wedge polygons, no consensus currently exists about the genesis of any type of patterned ground (Washburn, 1980).

The lack of systematic measurements of principal physical parameters, and of their year-round variation in space and time has hampered precise understanding of the phenomena. To improve this situation, we initiated a long-term study of active and exceptionally well developed sorted circles in Kvadehuksletta, a plain in western Spitsbergen that consists of a series of elevated beach ridges. The study focuses on the underlying processes; it involves tightly coordinated field, laboratory and theoretical work. Much of our effort has been directed at the development and installation of automated data acquisition systems. They are capable of periodically monitoring throughout the seasons numerous sensors imbedded in sorted circles to define the spatial and temporal variation of temperature, moisture content, soil displacement and tilt, pore pressure and total soil pressure in the active layer. In addition to this instrumentation effort, we have established extensive marker arrays that permit precise definition of complex displacement patterns at the soil surface.

Results of our initial field work, together with detailed descriptions of the sorted circles in our study area and preliminary interpretations have been presented (Hallet and Prestrud, 1986; Hallet, 1987; Prestrud, 1987). A related laboratory study of the sorting process and its implications are described by Prestrud (1987) and Anderson (in press). In this paper, we focus attention on a three year record of surface soil displacements, and discuss plausible driving mechanisms for the observed soil motion. Our results further strengthen the soil convection hypothesis developed by Hallet and Prestrud (1986), a paper that we will refer to as HP.

DESCRIPTION

As described in HP, the most distinctive soil patterns in our study area generally comprise equidimensional and slightly domed domains of essentially unvegetated, fine-grained soil bordered by broad curvilinear ridges of gravel. Although they only rarely approach a true circular form, we follow existing usage and refer to these as sorted circles. Whereas certain areas are completely covered with polygonal arrays of adjoining stone circles that share common borders, adjacent circles in our study sites are generally separated by lower areas lacking the textural contrasts characteristic of sorted circles (Figure 1). In extreme cases individual sorted circles may be isolated from all others. The size of stone circles varies considerably from one area to another. Within a single network, however, they tend to be rather uniform in size with diameters between 3 and 5 m.

Fig. 1 Overview of sorted circles on Kvadehuksletta, western Spitsbergen. The circle diameter ranges from 3 to 5 m, including the gravel border that generally rises 0.1 to 0.3 m above the unsorted and relatively low inter-circle areas. Concentrations of rock fragments can be seen in the center of several circles.

HORIZONTAL SURFACE SOIL DISPLACEMENTS

To study surface displacements of soil in several sorted circles, we have installed and monitored extensive arrays of markers, consisting of both marked stones and pegs vertically implanted within the upper decimeter of soil (Figure 2). The measurement technique and analysis of errors, which largely reflect the instability of reference points, are discussed by HP; relative displacements can be defined within about 2 mm. At a site of coalescing circles, K7, we observed systematic horizontal displacements up to 20 mm over week-long intervals in 1985 (Figure 3). The displacements formed coherent patterns generally showing a reversal in direction at the center of both fine domains and coarse borders. Moreover, most displacements switched direction in mid-July 1985. Similar surface displacement patterns and temporal variations in soil motion in 1985 were observed at an isolated circle, K1, for which displacement data are available starting in 1984. Displacement rates range up to millimeters per day during the early phase of the thaw period, and vary considerably in magnitude and direction through time. Remarkably coherent patterns of displacements have emerged by combining horizontal and vertical displacements measured during the 1985 thaw season (HP, Figure 6). A marked reduction in the settling rate of the fines and a pervasive reversal in the direction of horizontal displacements in the coarse material are evident in mid-July.

The reversal in displacement patterns in mid-July 1985 was also evident in high resolution (10^{-6}) measurements of horizontal surface strains using linear motion transducers, and in automated readings from a tilt sensor 0.4 m below the ground surface. These reversals are most intriguing because they appear widespread and reflect coherent subsurface motion extending to a depth of at least 0.4 m. They occur while thawing is proceeding monotonically with time (thaw depth on July 15 was about 0.5 m). Furthermore, they do not seem to correspond to significant metereological events that could, for example, have changed the soil moisture.

Multiple year data from K7 (Figure 4) illustrate the cumulative nature of the horizontal displacements in a network of adjoining sorted figures. Two surface markers on either side of a fine-coarse contact, which were initially 0.75 m apart, moved somewhat erratically through time but after three years had converged by 0.1 m. Relative motions of comparable magnitude were also observed in other parts of these sorted figures; distinct net divergence was measured across both the fine domain and coarse borders. More spatially complete net displacements are presented in Figure 5. This yearlong record is representative of three full seasonal freeze-thaw cycles starting in 1984, and hence appears to be a reliable indicator of the net annual displacement pattern. The lateral variations in displacement reflect the pronounced convergence and divergence of markers at the surface already illustrated in Figure 4. Net yearly displacements are on the order of 10 mm and tend to peak in border areas.

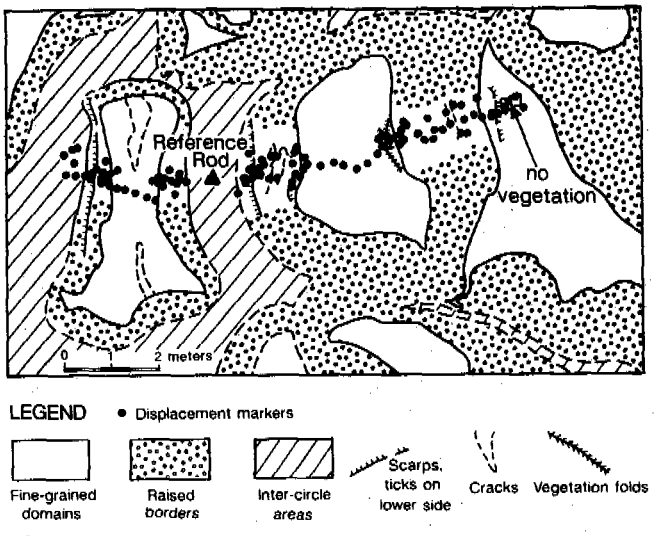

Fig. 2 Map of site K7, showing array of displacement markers and the rather irregular form typical of most sorted "circles". Data from markers to the right of reference rod are shown in Figures 3, 4 and 5.

INTERPRETATION

Considerable residual motion is apparent after three full-year cycles. Most notable are the systematic divergence of surface markers across borders, as well as across fine-grained domains, and the net convergence across fine-coarse

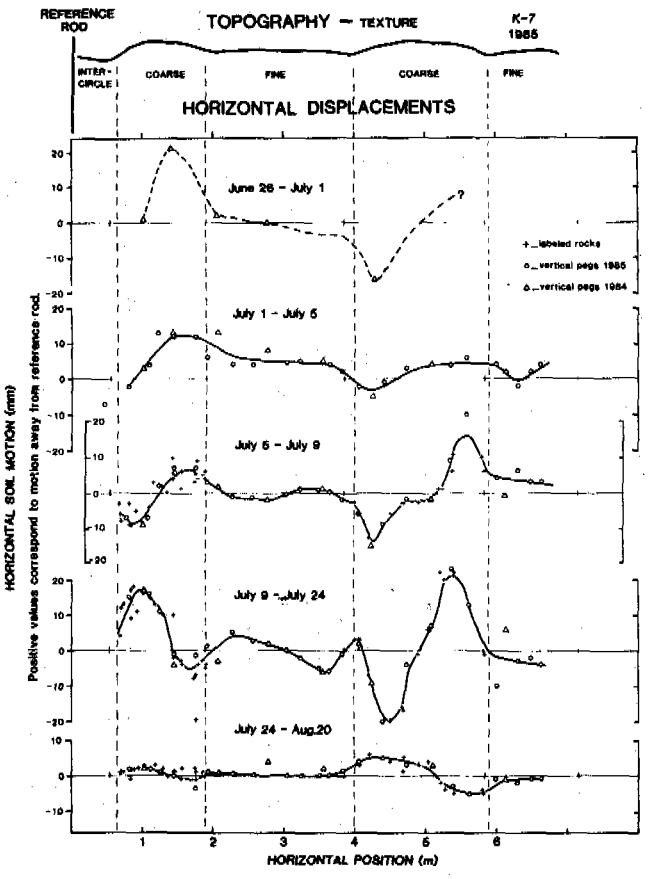

Fig. 3 Horizontal surface soil displacements during summer 1985 at site K7. Topography and texture are shown at the top. Sequential displacements of labeled rocks (x) and vertical pegs (o,Δ) are measured relative to the vertical reference rod hammered into permafrost in the intercircle area during the 1985 thaw season. Note systematic anti-symmetric displacements across fine domain (from 2 to 4 m) and coarse border (from 4 to 6 m), which reach 15 mm in several days. Line segments with a positive slope reflect radial divergence of soil, and those with a negative slope reflect radial convergence.

boundaries. If maintained in the long-term, these relative horizontal displacements can only be sustained by considerable subsurface soil motion. For example, in areas where the upper 0.25 m of soil is extending at a high average rate of 4% per year, the soil must be rising about 10 mm a^{-1}, otherwise these areas would subside at that rate. Such rapid changes in microrelief are inconsistent with observations that the microrelief of several circles in our study area has not changed appreciably during the four year duration of our study. That little if any geometric difference exists among circles developed on different beach terraces at Kvadehuksletta that vary in age by thousands or tens of thousands of years (HP) also suggests that the circles are essentially in a steady state.

Assuming the microrelief is effectively steady, measurements of horizontal displacements can be used to calculate rates of vertical soil displacement. If subsurface soil movements are largely restricted to vertical planes cross-cutting pattern centers, the rate of upward soil motion required to maintain the microrelief is simply the product of the average horizontal tensile strain rate and the depth of soil undergoing that motion. The depth can be inferred to be a fraction of the active layer thickness; notably if the motion resembles fluid convection, as we have proposed (HP), the horizontal velocity at the top of a convecting roll diminishes to zero near the center of the convecting layer and reverses sign below that. Using a characteristic depth of 0.25 m, the measured relative horizontal displacements spanning a full year yield a clear pattern of widespread upwelling and divergence in both the fine domains and coarse borders (Figure 5). Marked subsidence and convergence are localized close to the periphery of the fine domains. Deep-seated return flows are required to maintain the observed long-term surface displacements. The simplest overall pattern of soil motion compatible with the net surface displacements is illustrated in Figure 6. We stress that actual soil motions are likely to be much more complicated as they reflect large fluctuating displacements associated with freezing and thawing, separated by long periods of quiescence particularly when the active layer is frozen. Nevertheless, the pattern of net motion over a number of years is expected to resemble the circulation in both fine and coarse domains shown in Figure 6. The characteristic cycling time is about 500 years, which corresponds to maximum displacement rates of 10 mm a^{-1}, a 1 m-thick active layer, and a sorted circle radius of 1.5 m.

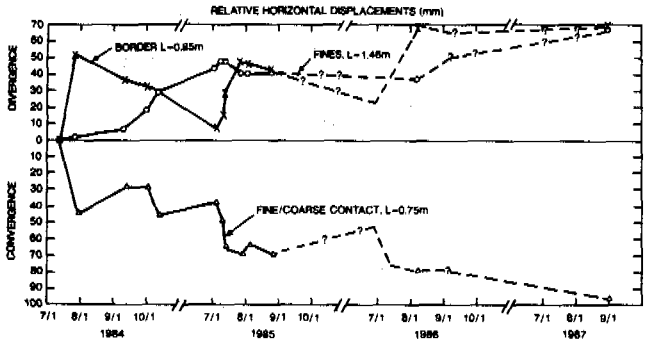

Fig. 4 Three year record of relative horizontal soil surface displacements in a radial direction at K7 using three pairs of markers. L is the initial separation between markers. The total convergence of about 0.1 m across the fine-coarse contact amounts to more than 4% convergence annually. Position of this pair of markers can be seen in Figure 5D; it was centered at 4.1 m. Distinct divergence is evident between markers placed both across the fine-grained soil domain and across the border, the latter being interrupted by extended periods of convergence.

These results are supported by work of other researchers. Mackay (1980) obtained a similar cycling time for soil in earth hummocks. Radial motion and tilt of dowels initially inserted vertically in the fine domain of sorted circles have also been measured by other workers, notably by Jahn (1967) in the Hornsund area of Spitsbergen, and by Washburn (personal communication, 1988) at Resolute, N.W.T., Canada. That markers move and tilt outward is generally in accord with the inferred convective motion of the fine-grained soil. Maximal rates of long-term lateral motion in the fine-grained soil are on the order of 10 mm a^{-1}. The data from Resolute do, however, suggest that outward motion is largely confined to the upper decimeter of soil. No previous measurements have pointed to the circle border as the locus of maximal displacement activity.

EVIDENCE REFLECTING LONG-TERM MOTION

Dynamic Maintenance of the Microrelief

The bulbous ridges of coarse material, and the sharp troughs that separate them from the subtly domed fine domains, are prominent sorted circle characteristics (HP). This microrelief is striking in view of the numerous processes that tend to reduce relief. These include gelifluction, pluvial erosion, and biotic surface disturbances, all of which result in downslope transfer of material. Because relatively steep slopes converge to form a trough at the fine-coarse contact, the troughs would tend to fill particularly quickly; yet they persist (Hallet, 1987, Figure 3). A simple diffusional model of overall relief relaxation, using the range of plausible effective topographic diffusivities 10^{-2} to 10^{-3} m^2 a^{-1}

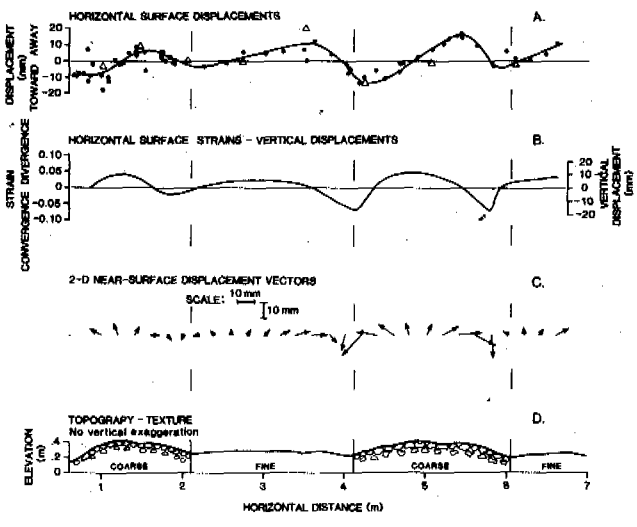

Fig. 5 Annual net near-surface motion at site K7. A) Measured horizontal displacements relative to reference rod between 8/20/85 and 8/3/86; solid line is drawn manually to delineate the trend; 1984-1985 data, shown as triangles, are compatible with 1985-1986 trend; B) measured horizontal strains at the ground surface, and corresponding vertical displacements assuming the microrelief is essentially steady (see text); C) combination of measured horizontal soil displacements and inferred vertical displacements clearly delineate near-surface soil motion; and D) microrelief and texture of sorted circles.

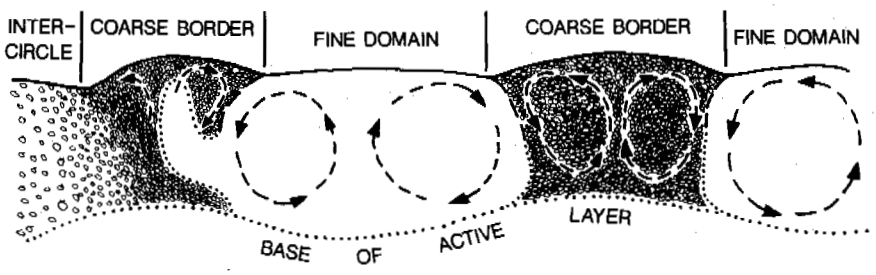

Fig. 6 Convection of both the fine-grained soil and the gravel-rich border material is the simplest pattern of soil motion that is compatible with the measured surface displacements, persistence of microrelief, subduction of surface organics, and indications of occasional diapirism under circle borders. Geometry of sorted circles and of soil motion in the lower part of the active layer are poorly constrained. Fine-grained soil extends under the borders in some circles.

(Kenyon and Turcotte, 1985) that includes conservative values representing low gelifluction rates (Jahn, 1967), suggests that troughs at fine-coarse contacts would essentially disappear in decades or, at most, centuries. Thus for this conspicuous microrelief to persist for periods on the order of 10^3 to 10^4 years, degrading processes must be compensated by subsurface motions; in other words, the microrelief must be dynamically maintained.

Both the domed fine center and the high coarse border reflect long-term upwelling of soil in these areas. Conversely the trough at fine-coarse contacts reflects relative downward soil motion there. The simplest overall pattern of motion compatible with these constraints is identical to that deduced from surface displacements (Figure 6).

Folding and Subduction of Surface Vegetation Mat

A sparse cover of mosses is generally found at the periphery of the fine-grained soil domains along with occasional bunch grasses and clusters of dicotyledonous plants (family: Saxifragaceae). This thin vegetation mat and the underlying soil commonly form small folds with axes paralleling the fine-coarse contact (Huxley and Odell, 1924; Jahn, 1967). The folds indicate that at least a portion of the convergence recorded near fine-coarse contacts (Figures 4 and 5) persists in the long-term (HP).

A diversity of related observations all support the inferred pattern of soil motion. Distinct wedges of dark organic-rich soil generally dip beneath the coarser border material (Prestrud, 1987); these are suggestive of the subduction of organic material. Throughout the active layer, the organic carbon content of the soil at the periphery of fine domains is considerably higher than in the center (HP). The vegetation cover is often discontinuous or absent in the center of the fines, whereas it is thickest at the periphery of the fines; although this may reflect micro-environmental differences, it may also reflect the expected radial increase in time available for plant colonization and growth. Along the axis of coarse borders, progressive upwelling and lateral divergence may help explain the occurrence of plant roots up to 150 mm long fully exposed on the gravel surface, where "frost-jacking" is likely to be minimal.

^{14}C dates of organic material below a gravel border provide independent constraints on rates of long-term soil motion. Three samples were collected along the subsurface extension of a fine-coarse contact where "subducted" organic material forms a distinct wedge of organic-rich soil. Samples centered at distances of 0.05, 0.15 and 0.25 m along this "subduction" zone yielded dates of 315±10, 505±30 and 860±70 years before present, respectively. These dates were corrected for past variations in ^{14}C, as recommended by Stuiver and Pearson (1986). The systematic increase in age with depth provides strong support for the inferred subduction and associated soil convection. The ages suggest that the long-term subduction rate for this circle is only about 0.3 mm a^{-1}, nearly thirty times slower than our measurements suggest. That our measurements overestimate long-term rates receives support from our observations of sorted circles near our study sites that were thoroughly disrupted by bulldozers before 1970; their reestablishment has been minimal. However, actual long-term rates are likely to be considerably higher than the 0.3 mm a^{-1} value based on ^{14}C dates because old carbon is likely to be recycled either chemically through the vegetation, or mechanically through overturn of the border material. More extensive ^{14}C studies of organic material, including the existing vegetation, are needed to define long-term rates, particularly because past rates may have varied considerably in concert with climatic variations.

Other Geologic Evidence

Additional geologic data gathered by a number of researchers further support elements of long-term convective soil motion in other types of patterned ground (e.g. Nicholson, 1976; Mackay, 1980). Upward flow of material and vanishing radial displacement rates in circle centers are compatible with the recognized upward migration of stones and fossils to the surface (e.g., Gripp, 1926, 1927), in places forming islands of coarse material near the centers of fine domains as can be seen in Figure 1. Furthermore, the radial flow pattern characteristic of hexagonal convection cells is in accord with the preferred alignment in a radial direction of elongated rock fragments in sorted patterns reported by Schmertmann and Taylor (1965).

DISCUSSION

Similarity Between Sorted Circles and Convection Cells

A wealth of evidence suggests that soil in active sorted circles undergoes a circulatory motion intermittently. This notion is not new; comparisons have long been made between patterned ground and Benard cells, the convection cells known to form in layers of fluid heated from below. It is primarily the regular geometry of sorted patterns that has invited comparison with convection cells, starting with Nordenskjold (1907) shortly after Benard's (1901) original free-convection experiments. Other geometric aspects of sorted circles are strikingly similar to convection cells. In plan view, sorted circles closely resemble the cell form found in numerical simulations of buoyancy-driven free

convection (Hallet, 1987), as well as in experiments. In our study area, diameters of sorted circles range from 3 to 5 m, and active layer depths range from 1 to 1.5 m. Assuming that the entire active layer convects, the diameter-to-depth ratio of sorted circles is in agreement with the theoretical aspect ratio of about 3 for convection cells in a fluid layer heated uniformly from within and cooled from above along a free surface (e.g. Turcotte and Schubert, 1982). The central domain of sorted circles is invariably convex upward, in accord with theoretical analysis (Jeffreys, 1951) and experimental study (Cerisier et al., 1984) of the form of the free surface deflected by buoyancy-driven convection. Stones accumulate at the periphery of circles much like various inclusions gather to form distinct patterns in convecting fluids (Benard, 1901; Romanovsky, 1939). Stones remain at the surface to form borders because the rate of stone upfreezing near the ground surface is likely to exceed the rate of downward soil motion there (Prestrud, 1987). Thus the upfreezing process "may be considered as a substitute for buoyancy, and the stones behave as if floating on the mud" (Wasiutynski, 1946).

Driving Mechanism for Soil Convection

In sorted circles long-term convection is interrupted by periods during which the soil is frozen, or unable to convect for other reasons. Our reference to this motion as soil convection may be questioned because the term "convection" generally refers to motion that is maintained through time. As inertial forces are not important for this slow motion of very viscous soil, imposed interruptions would cause hiatuses in soil motion but are not likely to alter the physics of soil convection in other ways. Hence, the soil motion we discern (Figure 6) can be conveniently referred to as soil convection.

In view of the initial work on free convection, which dealt with thermally-driven fluid motion, it is natural that early considerations of soil convection focused on temperature gradients for a mechanism to drive such motion (e.g. Romanovsky, 1939). It was recognized early that the density of water could be expected to decrease with depth during the thaw season. Simple calculations showed, however, that the maximum variation in bulk density of the soil that could result from variations in the density of pore water between 0°C and 4°C is insufficient to induce soil convection (Gripp, 1926; Wasiutynski, 1946). Moreover, such small bulk density differences, less than one part in 10^4, are likely to be completely overshadowed by differences in bulk density arising from realistic variations in soil moisture or texture (Mortensen, 1932, Dzulynski, 1966). The fact that temperature-induced buoyancy forces are incapable of driving soil convection, and that other driving mechanisms are not widely accepted, appears largely responsible for the current general skepticism about soil convection in sorted circles. Soil convection is commonly dismissed outright, as echoed in recent work by Ray et al. (1983) and Gleason et al. (1986). The difficulty with thermally-induced free convection does not, however, indicate that soil cannot convect in sorted circles; rather it highlights the need to identify the actual mechanism driving the well-documented circulatory motion.

It has long been recognized that differences in soil moisture may provide the required driving mechanism (Mortensen, 1932; Gripp and Simon, 1934; and Sorensen, 1935). A compelling case for soil convection caused by a vertical gradient in water content was presented by Wasiutynski (1946, p. 202) who clearly recognized that "...if we substitute water content for temperature, the equations of motion in the mud layer will be the same as those of the problem of thermally maintained instability." Such convection, which is also supported by Palm and Tveitereid's (1977) theoretical considerations, could be maintained by a supply of water produced by melting ice that is in excess of the pore space in the thawed soil.

The well known settling of thawing soil, which can exceed 10% of the active layer depth, reflects considerable compaction. Starting near the surface, where soil thaws first, compaction progresses downward at a rate determined by the upward water percolation above the thaw front. Near-surface consolidation may naturally give rise to denser material near the surface than at depth because the time available for consolidation decreases with depth along with the duration of the thaw period. This density distribution is conducive to convection as denser soil tends to sink while lighter soil tends to rise. The few measurements of soil bulk density in sorted circles that are available show that density does decrease with depth under parts of a sorted circle (HP). Moreover, our calculations of the evolution of bulk density profiles in thawing soils show that density can be expected to decrease with depth through much of the active layer.

The viability of the postulated convective motion of periglacial soils can be assessed by calculating the effective Rayleigh number, which defines a threshold for the onset of convection. Although it can only be estimated roughly because of the wide range of soil physical properties and the highly idealized treatment of soil reheology, fine-grained soils appear capable of convecting because of their relatively low effective viscosity and hydraulic diffusivity (Hallet, 1987). Convection would be strongly favored in fine-grained materials with low viscosity and hydraulic diffusivity. Moreover, moist fine-grained soils are likely to contain considerable ice, leading to large initial gradients in bulk density during the thaw period. This may account for the observed abundance of sorted circles in our study areas in wet swales rich in fine material and their absence from adjacent gravelly beach ridges.

Although buoyancy forces arising from vertical gradients in moisture content in thawing soils appear capable of inducing soil convection, they do not necessarily constitute the primary driving mechanism. Significant buoyancy forces are most likely to develop in the fine-grained soil domains because the potential for heaving and subsequent settling is greatest there. It follows that rates of soil displacements ought to be relatively high in the fine domains. This is not, however, supported by the lateral motion and surface heave data nor by related field observations and measurements that point to a focus of activity along the coarse-grained ridges. It is becoming evident from considerable data, which will be presented in a subsequent publication, that a "border forcing" mechanism could provide an alternative means of driving long-term convection in stone circles. Convection of the fine-grained material could be "forced" by the settling of borders previously elevated by frost heaving, and would contrast with the "free convection" that arises strictly from buoyancy forces.

Free Convection of Water in the Active Layer?

Although the expected thermally-induced decrease in water density with depth in the active layer is incapable of causing soil convection, Ray et al. (1983) and Gleason et al. (1986) recognized that it could induce percolative convection of water through soil. Moreover, they proposed that such water convection could affect the thaw pattern at the base of the active layer, and that the resulting scalloped geometry of the thaw front dictates the development of certain patterned ground. Much as is the case for soil convection, pore water convection appears to be an attractive mechanism because it is in accord with the regularity, shape and size of stone circles. However, at best, this water convection mechanism could influence only the geometry of the incipient patterns; the conspicuous size sorting, distinct microrelief, and observed surface displacements of the soil cannot be accounted for directly. Moreover, whether percolative convection of water can occur, or can be sufficiently vigorous to affect heat transport significantly in fine-

grained soil typical of sorted circles is questionable. For example, Palm and Tveitereid (1977) have suggested that free convection of water in the active layer would not be possible through material finer than gravel.

CONCLUSIONS

Our three year record of surface soil displacements is interpreted to reflect systematic soil circulation with net annual displacements reaching 10 mm. These data provide a measure of the temporal and spatial pattern of long-term soil convection we have inferred previously on the basis of the size, geometry, microrelief, vegetation cover, and subsurface distribution of organic carbon of sorted circles. Theoretical considerations suggest that intermittent free convection is plausible in thawed fine-grained soil, and that the requisite bulk density decrease with depth arises naturally during the thawing and consolidation of ice-rich soil. However, the actual driving mechanism remains to be established. Our ongoing automated monitoring of sorted circles promises to yield considerable additional data about their dynamics, and about more general active layer processes. This should permit us to assess further the ideas discussed here, and to improve our understanding of these and similar patterns.

ACKNOWLEDGEMENTS

This research was rendered possible by funding from the National Science Foundation (NSF-DPP-8303630) and the Army Research Office (DAALO3-87-K-0058). Our field studies involve fruitful collaboration with J.L. Sollid of the University of Oslo and several of his students and co-workers. We rely heavily on logistical support from the Norsk Polarinstitutt and Kings Bay Kull Company. Norsk Polarinstitutt engineers E. Knudsen, P. Aaserod, J. Fortun, M. Bentzen and B. Fjeld have provided considerable technical assistance under field conditions that are often difficult; it is due to their efforts that our instrumentation program has been implemented successfully since 1983. M. Stuiver provided the ^{14}C dates on "subducted" organic material. We have benefitted greatly from stimulating discussions with or assistance from R. Anderson, N. Caine, A. Heyneman, D. Mann, R. Sletten, J. Sollid, E. Waddington, J. Walder and, alphabetically last, but far from least, A.L. Washburn. The manuscript was typed by G. Hunter, L. Carothers, and S. Rasmussen, and the figures were drawn by F. Bardsley. We sincerely thank these organizations and individuals for their significant contributions.

REFERENCES

Anderson, S.P. (in press). The upfreezing process: experiments with a single clast. Geol. Soc. Am. Bull.

Benard, H. (1901). Les tourbillons cellulaires dans une nappe liquide. Rev. Gen des Sci. (11), 1261-1271, 1309-1328.

Cerisier, P., Jamond, C., Pantaloni, J., and Charmet, J.C. (1984). Deformation de la surface libre en convection de Benard - Marangoni. J. Physique (45), 405-411.

Dzulynski, S. (1966). Sedimentary structures resulting from convection-like pattern of motion. Rocz. Pol. Tow. Geol. (36), 3-21.

Gleason, K.J., Krantz, W.B., Caine, N., George, J.H., and Gunn, R.D. (1986). Geometrical aspects of sorted patterned ground in recurrently frozen soil. Science (232), 216.

Gripp, K. (1926). Uber Frost und Strukturboden auf Spitzbergen. Ztschr. d. Ges. F. Erdkunde zu Berlin, 351-354.

_____(1927). Beitrage zur Geologie von Spitzbergen. Naturwiss. Ver. Hamburg, Abh. (21), 1-38.

Gripp, K. and Simon, W. (1934). Die experimentelle Darstellung des Brodelbodens. Naturwiss. (22), 8-10.

Hallet, B. (1987). On geomorphic patterns with a focus on stone circles viewed as a free-convection phenomenon. C. Nicolis and G. Nicolis (eds.), Irreversible Phenomena and Dynamical Systems Analysis in Geosciences, 533-553. D. Reidel Publishing.

Hallet, B. and Prestrud, S. (1986). Dynamics of periglacial sorted circles in Western Spitsbergen. Quat. Res. (New York) (26), 81-99.

Huxley, J.S. and Odell, N.E. (1924). Notes on surface markings in Spitzbergen. Geog. J. 63, 207-229.

Jahn, A. (1961). Quantitative analysis of some periglacial processes in Spitsbergen. Univ. Wrocklawski im. Boleslawa Bieruta, Zeszyty Naukowe, Nauki Przyrodmicze, ser. B (5), 1-34.

_____(1967). Origin and development of patterned ground in Spitsbergen. Proc. 1st Int. Conf. Permafrost, 140-145, Lafayette, Indiana.

Jeffreys, H. (1951). The surface elevation in cellular convection. Quart. J. Mech. Appl. Math (4), 283-288.

Kenyon, P.M. and Turcotte, D.C. (1985). Morphology of a delta prograding by bulk sediment transport. Geol. Soc. Am. Bull. (96), 1457-1467.

Mackay, J.R. (1980). The origin of hummocks, western Arctic coast, Canada. Can. J. Earth Sci. (17), 996-1006.

Mortensen, H. (1932). Uber die physikalische Moglichkeit der "Brodel"-Hypothese. Centralblatt f. Min., Geol. u. Palaont., Abt. B, 417-422.

Nicholson, F.H. (1976). Patterned ground formation and description as suggested by Low Arctic and Subarctic examples. Arctic and Alpine Res. (8), 329-342.

Nordenskjold, O.L. (1907). Uber die Natur der Polarlander. Geog. Ztschr. Jhg. 13, 563-566.

Palm, E. and Tveitereid, M. (1977). On patterned ground and free convection. Norsk Geog. Tidsskr. (31), 145-148.

Pissart, A. (1966). Experiences et observations a propos de la genese des sols polygonaux tries. Rev. Belge de Geog. (90), 55-73.

Prestrud, S. (1987). The upfreezing process and its role in sorted circles, M.S. Thesis, Univ. Washington, 122 pp.

Ray, R.J., Krantz, W.B., Caine, T.N., and Gunn, R.D. (1983). A model for sorted patterned ground regularity. J. Glaciology (29), 317-337.

Romanovsky, V. (1939). Application de la theorie convective aux terrains polygonaux. Rev. Geog. Phys. et Geol. Dynamique (12), 315-325.

Schmertmann, J.H. and Taylor, R.S. (1965). Quantitative data from a patterned ground site over permafrost. U.S. Army cold Regions Res. and Engr. Lab. Res. Rep. 96, 76 pp.

Sorensen, T. (1935). Bodenformen und Pflanzendecke in Nordostgronland. Medd. om Gronland 93, 69 pp.

Stuiver, M. and Pearson, G.W. (1986). High-precision calibration of the radiocarbon time scale, AD 1950-500 B.C. Radiocarbon (28), 805-838.

Turcotte, D.L. and Schubert, G. (1982). Geodynamics, 450 pp. New York: Wiley.

Washburn, A.L. (1956). Classification of patterned ground and review of suggested origins. Geol. Soc. Am. Bull. (67), 832-865.

_____(1980). Geocryology, 406 pp. New York: Wiley.

Wasiutynski, J. (1946). Studies in hydrodynamics and structure of stars and planets. Astrophysica Norvegica (4), 1-497.

MICROMORPHOLOGY AND MICROFABRICS OF SORTED CIRCLES, JOTUNHEIMEN, SOUTHERN NORWAY

C. Harris and J.D. Cook

Department of Geology, University College Cardiff, P.O. Box 78, Cardiff CF1 1XL, U.K.

SYNOPSIS Two active sorted circles were excavated and their fine grained centres systematically sampled for granulometric, micromorphological and microfabric analyses. Steeply inclined zones of silt/clay-rich and gravel-rich sediment extending upwards from close to the base of the active layer are described. Micromorphological phenomena consistent with ice segregation during freezing and thixotropic conditions during thaw-consolidation are illustrated, together with microfabrics indicating upward or downward mass displacement of sediment. It is concluded that small-scale upward injection of over-saturated sediment occurs in circle centres during thaw, producing the complex granulometric patterns observed.

INTRODUCTION

Sorted patterned ground in Jotunheimen includes circles and nets, which give way to stripes as gradients increase. This report relates to sorted circles at Glittertind (1810 m a.s.l.) and below the terminal moraine of the glacier Gråsubreen (1890 m a.s.l.) in Veodalen, eastern Jotunheimen (Fig. 1). At these sites circles consist of fine grained centres, generally around 2 m in diameter, surrounded by borders approximately 1 m wide comprising pebbles and boulders. The borders are commonly integrated to form networks (Fig. 2). At these high altitude sites circle centres are largely free of vegetation other than mosses and lichens, and are apparently active, but below about 1700 m sorted circles and stripes become increasingly vegetated and appear to be less active.

Theories relating to the formation of sorted patterned ground were reviewed by Washburn (1956, 1970). Frost sorting has been adequately explained (e.g. Corte, 1962, Kaplar 1965, Bowley and Burghardt 1971), but the problem of the development of relatively regularly spaced, repeated patterns has remained the subject of debate. Recently Hallet and Prestrud (1986) re-emphasized the role of convectional circulation of fines, by mass displacement upwards beneath circle centres and downwards close to the margins. Similar circulatory sediment movements within sorted nets and circles have been suggested by a number of earlier workers (e.g. Romanovsky 1939, Tröll 1944, Dżułyński 1963, Chambers 1967, Nicholson 1969, 1976, Palm and Tveitereid 1977).

According to the convection theory, free Rayleigh convection within a thawing active layer may be driven by moisture induced density differences. A potentially unstable density gradient results from thawing at depth releasing low density over-saturated sediment beneath higher density near-surface sediments which have already undergone thaw consolidation (Palm and Tveitereid 1977, Hallet and Prestrud 1986). The size of convection cells and hence of associated sorted circles is related to the thickness of the active layer whereby cell width is approximately 3.3 times cell depth (Hallet and Prestrud 1986). The initiation of regular cells has also been attributed to thermally induced Rayleigh convection of soil water (Ray et al. 1983a, b), creating an undulatory permafrost table, which in turn controls sorted circle size.

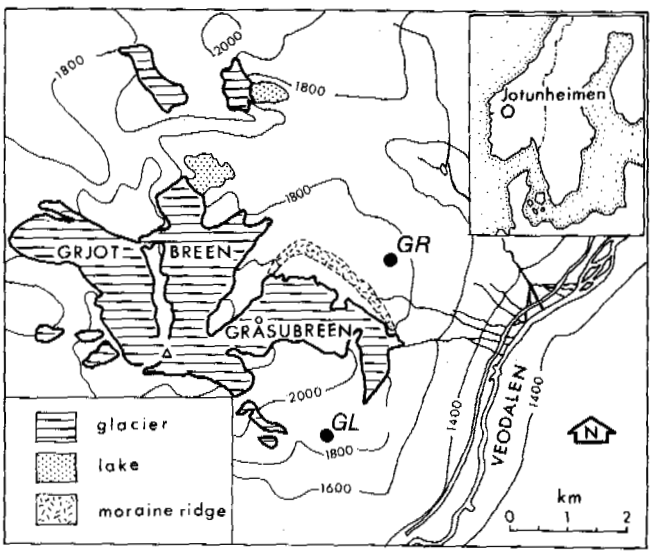

Figure 1 Location Map, Veodalen. GL Glittertind; GR Gråsubreen.

In this study two sorted circles, one at Glittertind and one at Gråsubreen, were trenched and sampled for granulometric and micromorphological analyses. The results show complex microfabrics and granulometric patterns within fine-grained circle centres, and indicate that upward and downward movements of sediment probably take place during thawing of the active layer.

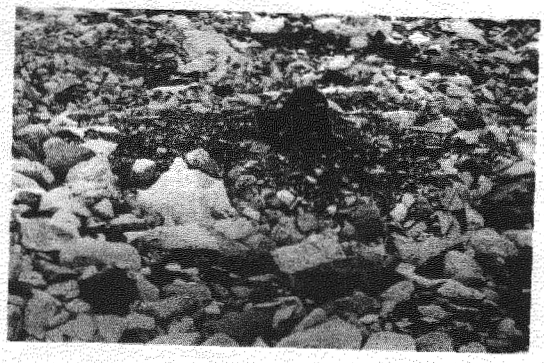

Figure 2 Sorted circles, up to 2 m diameter, Gråsubreen site.

SITE DESCRIPTION

At both study sites gradients are less than 4° and the substrate comprises poorly sorted diamicton, probably representing till deposited during the last regional glaciation of the Jotunheim. Bedrock consists of pyroxene-gneiss (Battey and McRitchie 1975).

Mean January and July temperatures at the nearest Norwegian meteorological station at Fannaraken (2062 m a.s.l.) are -12.3°C and +2.6°C respectively (1931-1960, Bruun 1967). Grant automatic temperature recorders installed within circle centres at both study sites have provided six hourly records of 1-50 cm ground temperatures for up to 3 years (Cook in prep.). Mean ground surface temperatures (1 cm below surface) are given in Table 1. Unusually warm surface temperatures at both sites in 1984-5 are attributed to above average snowfall during that winter.

Seismic surveys (Harris and Cook 1986) have proved the presence of permafrost at both sites. At the end of August 1984, the active layer at Gråsubreen was 0.79 to 1.06 m deep and at Glittertind, 1.13 to 1.62 m deep. Excavation to the permafrost table was not however possible, due to trench wall collapse below approximately 0.75 m, caused by excessive inflow of ground water. On the basis of soil temperature records, Cook (in prep.) has estimated the lower altitudinal limits of discontinuous and continuous permafrost to lie at approximately 1640 m and 1840 m respectively.

If Raleigh convection, either of saturated sediment or of groundwater, is important in circle initiation and development, circle diameters should be approximately 3.3 times the depth of sorting (Hallet & Prestrud 1986, Ray et al. 1983a, b). At Glittertind the average circle diameter was 3.8 m, with maximum and minimum dimensions 5.0 m and 3.1 m respectively, and at Gråsubreen the average diameter was 4.7 m, with maximum and minimum values of 7.8 m and 2.7 m. Based on average circle diameters, depths of sorting (equivalent to active layer thickness) of 1.15 m at Glittertind and 1.4 m at Gråsubreen are anticipated. Although the Gråsubreen value is greater than the active layer depth measured at the end of August 1984, the predicted depth of sorting at Glittertind is consistent with the measured depth of the active layer at that site. Excavation of circles at each site failed to reach the base of the coarse margins, but borders appeared to narrow with depth (Fig. 3). Excavation of the margins of smaller-scale circles approximately 1.8 m in diameter at Glittertind, clearly indicated wedge-shaped margins extending to a depth of around 0.65 m.

FIELD AND LABORATORY TECHNIQUES

A trench was dug across a typical sorted circle at each of the study sites. A 25 cm square sampling grid was utilized (Fig. 3) for both undisturbed and subsequent disturbed sediment sampling. Undisturbed samples were obtained by carefully pushing 6 cm square, 4 cm deep, open plastic boxes with chamfered leading edges into a cleaned vertical section of the trench face. Samples were retained in their boxes, air dried, then placed in an oven at 50°C for 48 hours prior to impregnation with low viscosity resin. Oriented thin sections were then cut in the vertical plane.

Disturbed bulk samples were analysed for granulometry using standard wet sieving procedures. To facilitate discussion of the two excavated sections, the coordinate system employed in the sampling design (Fig. 3) is adopted to locate samples.

GRANULOMETRY

Grain size distributions for the fine grained circle centres are shown in Figure 4. Due to the problem of obtaining representative samples from sediments containing large clasts (Head 1980), the largest material included in granulometric determinations was 20 mm, corresponding to the upper limit of medium gravel. At both the Gråsubreen and the Glittertind sites circle centres comprise silty and gravelly sand, and are frost susceptible.

Isolines of % silt and clay (% finer than 63 μm) and the % fine and medium gravel (% coarser than 2 mm) are plotted in Figure 3. Both circles contain zones rich in fines which, at depth, resemble diapiric upward intrusions. At the Glittertind site a gravel-rich tongue extends vertically upwards through part of the circle centre, while at Gråsubreen a horizontal tongue of gravel-rich sediment extends from one

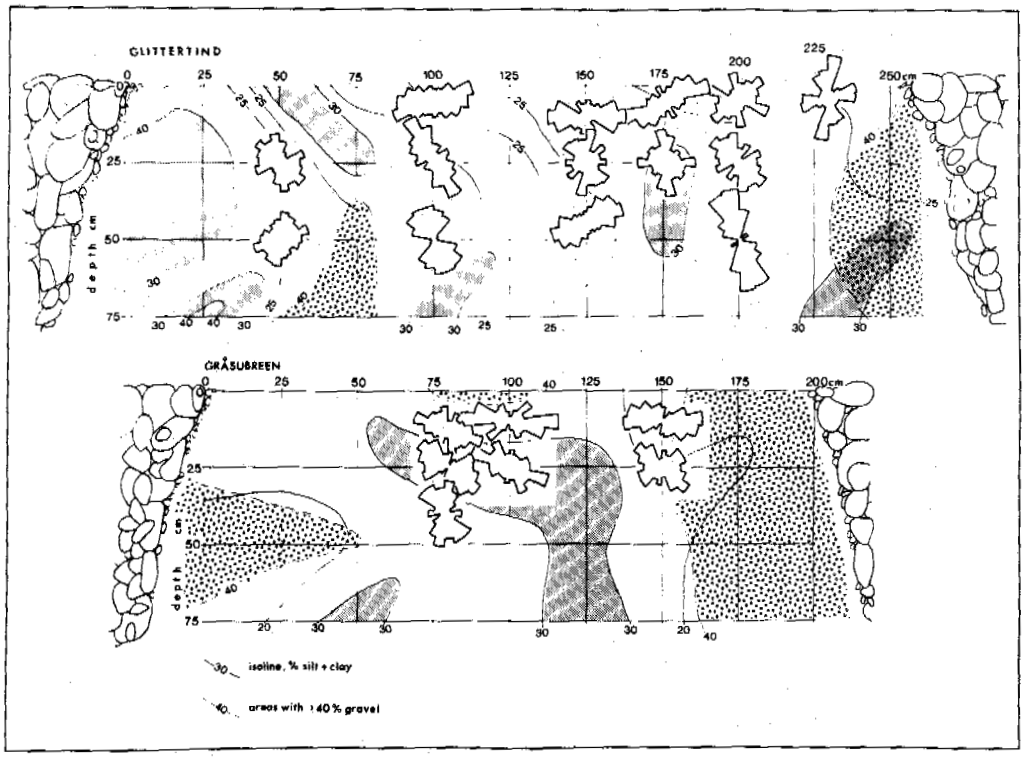

Figure 3 Granulometry and microfabrics of excavated circles, Glittertind and Gråsubreen. Dots show areas with greater than 30% silt plus clay, circles show areas with greater than 40% gravel.

coarse margin into the adjacent finer sediments at a depth of 50 cm. These complex granulometric patterns point to both lateral and vertical movements of fines and gravel within the circle centres, and illustrate the necessity for caution in interpreting granulometric data derived from single vertical profiles within sorted patterned ground.

MICROFABRICS

The apparent dips (Harris & Ellis 1980) of elongate sand grains of long axis length between approximately 200 μm and 1500 μm were determined from thin sections cut in the vertical plane. The sand grain fabrics presented in Figure 3 represent 200 readings where large thin sections were available, and 100 readings where less material was available in thin section. In addition, the apparent dips of elongate grains with long axes greater than 5 mm were measured by tracing the grain outline over a light table (Fig. 5).

At the Glittertind site steeply-dipping fabrics are apparent at depth. Near-surface samples adjacent to the circle margin also dip steeply, but otherwise display sub-horizontal dips. Sand grain dips tend to be oriented parallel to the adjacent isolines of percent silt/clay content. Gravel sized grains (>5 mm) generally exhibit a range of dips close to the surface, although in one sample (230/3) the three grains observed were all oriented close to vertical. A strong vertical component is evident in all samples from 25 cm depth, but at 50 cm considerable scatter occurs.

At Gråsubreen relatively gravel-rich sediments prevented undisturbed sampling over parts of the trench face. However, sufficient samples were obtained to indicate fabrics parallel to the isolines of percent silt/clay content, with grains in the central zone displaying low angled preferred dips (Fig. 3). Gravel-sized clasts (>5 mm) dip steeply in all samples (Fig. 5).

MICROMORPHOLOGY

(a) Granulometry of the matrix

The sampling framework for granulometric analysis allowed only the broad pattern of grain size variation to be determined. Smaller scale variations in texture were however observed in certain of the 6 cm x 6 cm thin sections. At both Glittertind and Gråsubreen the silt/clay content of the matrix was highly variable both between and within thin

sections. Abrupt steeply-dipping granulometric boundaries separating silt-rich sediments from sandy sediments were frequently observed (Fig. 6a, b, c). For example, a silt-rich zone 6-9 mm wide was detected extending vertically up through sample 80/40 from Gråsubreen. In addition, near-surface sample 230/3 from Glittertind revealed diapir-like areas of fines apparently intruded upwards into a wedge of relatively clean sand which displayued a severely contorted upper boundary (Fig. 6b).

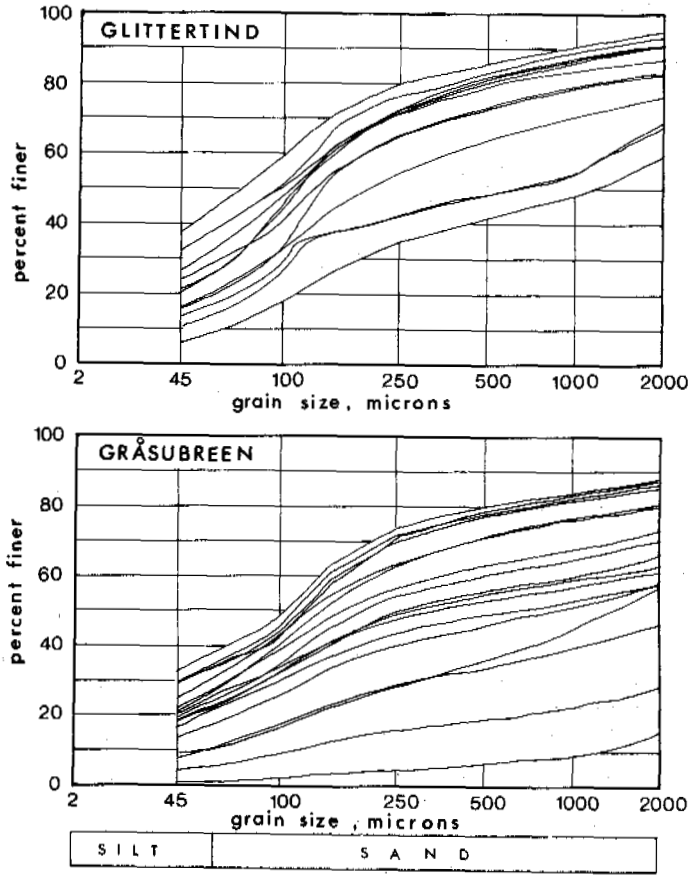

Figure 4 Examples of granulometric curves.

(b) Vesicles

Rounded bubble-like voids were widespread in thin sections from both sorted circles. Although not present in all samples, vesicles up to 1800 μm diameter were noted in most thin sections from 10 cm, 25 cm and 50 cm depths at both Gråsubreen and Glittertind (Fig. 6i, j). In near surface samples (e.g. Glittertind 230/3, 200/5) bubbly voids linked into linear channels, extending upwards to the surface (Fig. 6d). These are interpreted as routes of air escape during thaw consolidation (Van Vliet-Lanöe 1985).

(c) Lenticular and banded structures

At both sites lens-shaped silt rich aggregates up to 5000 μm in length and 350 μm in thickness often with smooth upper surfaces, frequently occurred in the upper 25 cm samples. They were often roughly parallel to the surface, and appeared to be draped over clean compact lenses of sand (Fig. 6f, g). They resembled closely the 'silt droplet' structures described by Harris and Ellis (1980) and Harris (1981, 1985), and the freeze-thaw structures described by Van Vliet-Lanöe (1982, 1985) and Van Vliet-Lanöe et al. (1984). There was however a marked absence of these structures within zones of apparent sediment displacement, such as diapir-like zones, and where abrupt granulometric boundaries brought sandy material into contact with silty sediment (Fig. 7b, c).

(d) Skeletal grain coatings

Coatings of silt and clay were observed on the upper surfaces of skeletal grains. Coatings showed a flecked extinction pattern parallel to the grain surface, and generally smooth streamlined surfaces (Fig. 6g, h). In many thin sections coatings were observed on the sides, underneath and occasionally completely surrounding some sand grains, suggesting that grain rotation had occurred (Fig. 6h).

Both banded structures and silt coatings on skeletal grains were best developed where the granulometry consisted of mixed silt and sand. They were largely absent where the matrix was either predominantly sand (Glittertind 230/3, Gråsubreen 50/50, 150/25) or predominantly silt (Glittertind 175/10, 175/25, 150/25, Gråsubreen 150/25).

(e) Flow structures

In two samples from Glittertind (200/20, 200/50), streaks of silt up to 30 mm in length and 1.5 mm thick were observed forming a fibrous wavy fabric (Fig. 6k). The streaks dipped at about 50° to the horizontal, towards the adjacent border and parallel to the preferred dips of elongate sand grains. The matrix of silt and fine to medium sand had apparently been subjected to shearing or flowage, creating flow structures.

DISCUSSION

The secregation of openwork marginal clasts from fine-grained circle centres is clearly defined. However, within the fine centres granulometric variability is considerable. Thin sections show abrupt changes from relatively clean sand to silt-dominated matrix, with boundaries often vertical or steeply dipping. On a larger scale, granulometric determinations across the two excavated circle centres revealed similar variability. Upward and downward movement of sediment within circles is strongly suggested.

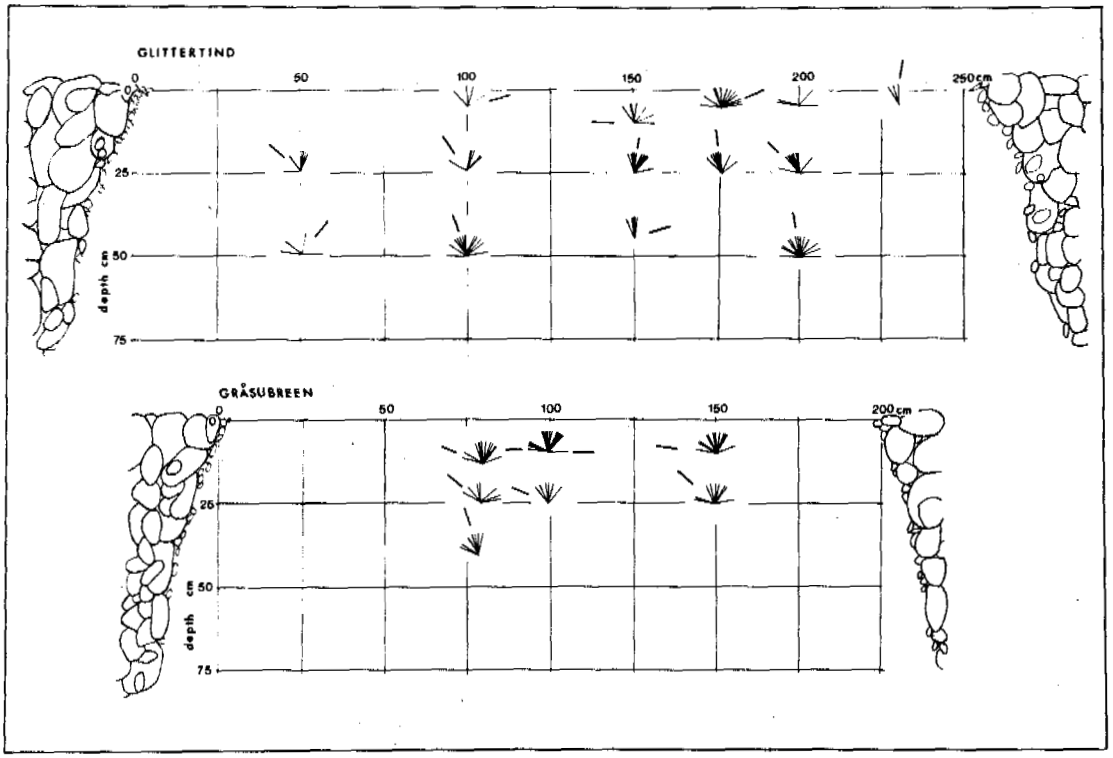

Figure 5 Dips of elongate grains > 5 mm in length.

In laboratory freezing experiments on layered fine sediments, Corte (1971) described upward diapir-like intrusions and the formation of irregular mounds on the horizontal surface. Corte emphasized the significance of high segregated ice content in the frozen sediments and the subsequent release of excess water during rapid thawing, although he offered no explicit explanation of the process of sediment deformation.

Upward intrusion of semi-fluid sediment into the centres of unsorted hummocks has been reported to occur during thaw consolidation of the active layer (Mackay 1979, 1980). Chambers (1966) also described diapir-like injection beneath large sorted circles on Signy Island. Bunting and Jackson (1970) have proposed that the downwards movement of coarse material in polygon borders in Arctic Canada is responsible for the formation of slip planes in the fine grained soil close to the steep junction with the coarse margins. In Spitsbergen, Hallet and Prestrud (1986) reported upward injection of fluidized sediments beneath the centres of sorted circles with compensatory downward movement of fines close to the margins.

In the sorted circles discussed here, the presence of silt banding and silt droplet structures indicates significant ice segregation during freezing, and this is confirmed by frost heave measurement at nearby sorted circles (Cook in prep.) where maximum winter heave equivalent to 6.6% of the active layer thickness and 7.5% of the active layer thickness was recorded at Glittertind and Gråsubreen respectively. Micromorphological evidence in the form of vesicular voids indicated that on thawing the fine grained circle centres became thixotropic. It is suggested that thaw consolidation resulted in the liquefaction of formerly ice rich sediments, allowing trapped air to form bubbles (Harris 1983, Van Vliet-Lanöe 1985). Rotation of skeletal grains and the presence of flow-induced fabrics, in addition to the juxtaposition of sediments of contrasting grain size, provide further evidence for the mass displacement of liquidized sediment within circle centres during thaw. Such movement often apparently involved injection of sediment upwards through overlying material, on a scale ranging from a few millimetres to several centimetres.

Clear evidence for near surface upward displacement of fine grained sediment was provided by the observed extrusion of small mounds of fines at the surface of sorted circle centres during the summer thaw period (Fig. 7). These fines were apparently forced upwards in a fluidized state through the patina of small stones covering the circle centres.

Although Warburton (1985) reported mainly horizontal microfabrics in sorted circles in the Colorado Front Range, Fahey (1975) noted

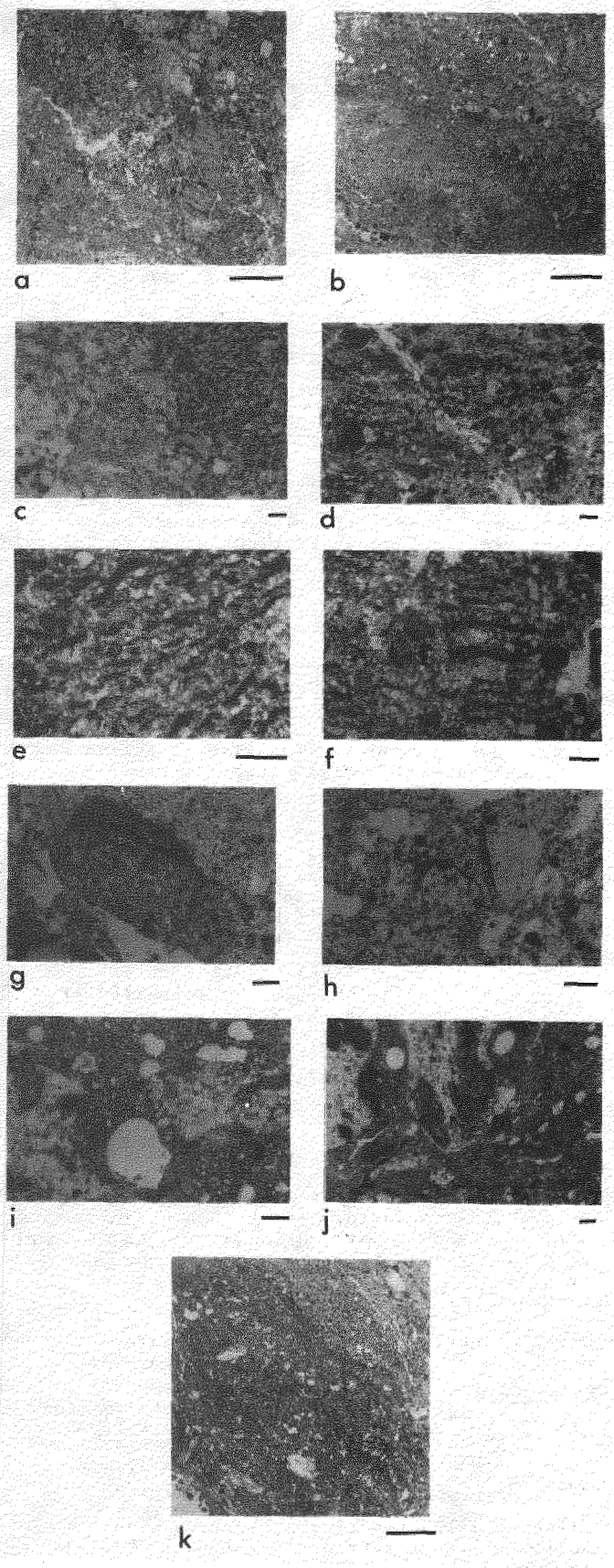

Figure 6

a) Glittertind sample 200/25, showing boundary between silty sediment on right and sandy sediment on left. Scale bar 10 mm.

b) Glittertind sample 230/3, showing irregular wedge of well sorted sand, centre left, thinning to right. Note air escape channel, top right. Scale bar 10 mm.

c) Glittertind sample 200/25, showing sharp, steeply dipping boundary between silty sand with abundant silt droplet structures (left) and medium to fine sand with no silt droplets (right). Scale bar 1 mm.

d) Glittertind sample 230/3. Air escape channel which extends up to the soil surface. Scale bar 1 mm.

e) Silt droplet structures. Glittertind sample 200/25. Scale bar 1 mm.

f) Silt banding draped over dense sand layers and forming cappings over larger skeletal grains. Glittertind sample 100/5. Scale bar 1 mm.

g) Silt capping on skeletal grain, Gråsubreen sample 80/40. Scale bar 1 mm.

h) Silt coating on upper surface and sides of skeletal grains, suggesting grain rotation. Gråsubreen sample 80/10. Scale bar 1 mm.

i) Vesicles, Glittertind sample 150/10. Scale bar 1 mm.

j) Vesicles, Glittertind sample 150/45. Scale bar 1 mm.

k) Glittertind sample 50/50, showing silt streaks and oriented sand grains aligned from top left to bottom right, due to shearing during flow. Scale bar 10 mm.

vertical preferred orientations of sand grains produced by freezing and thawing in nonsorted circles. Likewise, in the Colorado Front Range, Benedict (1969) observed strong vertical orientation amongst sand grains close to the surface of a degraded hummock, where frost action was intense. Sand grain orientations approximately parallel to sedimentary and pedological boundaries beneath other earth hummocks were attributed to soil movement which deformed these boundaries, doming them upwards beneath the hummocks.

Reference to Figure 3 shows sand grain orientations apparently related to the pattern of grain size variation within both the Glittertind and Gråsubreen circles. It may be argued, therefore, that sediment displacement within the circle centres, which was largely responsible for the observed pattern of granulometric variation, also orientated elongate sand grains, by shearing within the mobile fluidized sediments. However, micromorphological investigations revealed sharp sedimentary boundaries within individual

thin sections and bimodal or multimodal fabrics may indicate at least two dominant stress fields in close proximity. Where sediment displacement has not occurred recently, compression due to ice segregation may generate sub-horizontal sand grain orientations together with silt banding and lenses. In contrast an adjacent zone of recent saturated flow may exhibit a steeply dipping fabric related to the direction of sediment movement.

The generally steep dips of > 5 mm grains (Fig. 5) indicate that frost sorting of such clasts (and presumably larger clasts) towards the surface is also active at both sites. These larger clasts are frequently aligned almost perpendicular to the preferred orientation of medium to fine sand grains, especially in near surface samples.

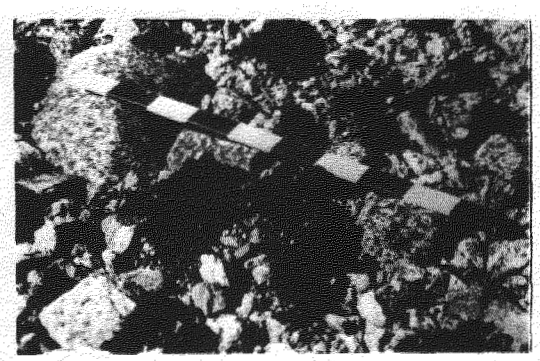

Figure 7 Fine grained sediment extruded through the surface of sorted circles, Glittertind. Scale divisions 5 cm.

CONCLUSION

This study has shown that the granulometry of the fine grained centres of two sorted circles in Jotunheimen, Norway is complex and often includes steeply dipping silt-rich and sand-rich zones. Micromorphological evidence is presented which indicates ice segregation during active layer freezing, and thixotropic behaviour of the soil during thaw consolidation. It is concluded that sediment within the central zones of sorted circles is injected upwards as thawing proceeds downwards. A compensatory downward displacement of fines close to the margins is also considered to be likely. However, the present study indicates that such sediment displacements are complex, and individually much smaller in scale than suggested by the model of Hallet and Prestrud (1986). The cumulative effect of small (mm to cm scale) sediment displacements as thaw progresses downwards through the fine circle centres, probably generates the complex pattern of granulometric variation described here, dominated by steeply inclined zones of finer and coarser sediment at depth, and sub-horizontal zones immediately below the surface.

REFERENCES

Battey, M.H. & McRitchie, W.D. (1975). The petrology of the pyroxene-granulite facies rocks of Jotunheimen, Norway. Norsk Geologisk Tidsskrift 55, 1-49.

Benedict, J.B. (1969). Microfabric of patterned ground. Arctic & Alpine Res. 1, 45-48.

Bowley, W.W. & Burghardt, M.D. (1971). Thermodynamics and stones. Am. Geophys. Union Trans. 52, 4-7.

Bruun, I. (1967). Standard Normals 1931-1960 of the air temperature in Norway. Oslo: Det Norske Meterologisk Institut. 270pp.

Bunting, B.T. & Jackson, R.H. (1970). Studies of patterned ground on S.W. Devon Island, N.W.T. Geogr. Annlr. 52A, 194-208.

Chambers, M.J.G. (1966). Investigations of patterned ground at Signy Island, South Orkney Islands: II. Temperature regimes in the active layer. British Antarctic Survey Bulletin 10, 71-83.

Chambers, M.J.G. (1967). Investigations of patterned ground at Signy Island, South Orkney Islands: III. Miniature patterns, frost heaving and general conclusions. British Antarctive Survey Bulletin 12, 1-22.

Cook, J.D. (in prep.). Zonation of active and inactive periglacial sorted circles, eastern Jotunheimen. Unpubl. Ph.D. Thesis, Univ. of Wales.

Corte, A.E. (1962). The frost behaviour of soils: laboratory and field data for a new concept, II. Horizontal Sorting. U.S. Army Corps of Engineers, C.R.R.E.L. Research Report 85(2), 20pp. (also H.R.B. Bull. 331, 46-66).

Corte, A.E. (1971). Laboratory formation of extrusion features by multicyclic freeze-thaw in soils. Etude des phénomenès périglaciaires en laboratoire, Colloque International de Géomorphologie, Liège-Caen, 1971, Centre de Geomorphologie à Caen, Bulletin no. 13-14-15, 157-182.

Crampton, C.B. (1977). A study of the dynamics of hummocky microrelief in the Canadian North. Can. J. of Earth Sci. 14, 639-649

Dżułyński, S. (1963). Polygonal structures in experiments and their bearing upon some periglacial phenomena. Bulletin de L'academie polonaise des sciences, Serie des sci. geol. et geogr. V. XI no. 3, 145-150.

Fahey, B.D. (1975). Nonsorted circle development in a Colorado Alpine location. Geogr. Annalr. 57A 3-4, 153-164.

Hallet, B. & Prestrud, S. (1986). Dynamics of periglacial sorted circles in western Spitsbergen. Quaternary Research 26, 81-99.

Harris, C. (1981). Periglacial Mass-Wasting: A Review of Research. B.G.R.G. Research Monograph 4, 204pp. Norwich: Geo Abstracts (Geo Books).

Harris, C. (1983). Vesicles in thin sections of periglacial soils from north and south Norway. Proc. 4th International Permafrost Conf., Fairbanks, Alaska. University of Alaska & Nat. Acad. of Sci., 445-449.

Harris, C. (1985). Geomorphological applications of soil micromorphology with particular reference to periglacial sediments and processes. Ch. 11 in Geomorphology and Soils, ed. K.S. Richards, R.R. Arnett & S. Ellis. 219-232. London: Allen & Unwin.

Harris, C. & Ellis, S. (1980). Micromorphology of soils in solifluted materials, Okstindan, Northern Norway. Geoderma 23, 11-29.

Kaplar, C.W. (1965). Stone migration by freezing of soil. Science 149, 1520-1521.

Mackay, J.R. (1979). An equilibrium model for hummocks (non-sorted circles), Garry Island, Northwest Territories. Current Research, Part A. Geol. Surv. Can. Paper 79-1A, 165-167.

Mackay, J.R. (1980). The origin of hummocks, West Arctic Coast, Canada. Can. J. Earth Sci. 17, 996-1006.

Nicholson, F.H. (1969). An investigation of patterned ground. Unpubl. Ph.D. Thesis, University of Bristol, 238pp.

Nicholson, F.H. (1976). Patterned ground formation and description as suggested by low Arctic and Subarctic examples. Arctic & Alpine Res. 8, 329-342.

Palm, E. & Tveitereid, M. (1977). On patterned ground and free convection. Norsk Geogr. Tidsskr. 31, 145-148.

Ray, R.J., Krantz, W.B., Caine, T.N. & Gunn, R.D. (1983a). A model for sorted patterned ground regularity. J. Glaciol. 29, 317-337.

Ray, R.J., Krantz, W.B., Caine, T.N. & Gunn, R.D. (1983b). A mathematical model for patterned ground: sorted polygons and stripes, and underwater polygons. Proc. 4th Int. Permafrost Conf., Fairbanks, Alaska. University of Alaska & Nat. Acad. of Sci., 1036-1041.

Romanovsky, V. (1939). Application de la théorie convective aux terrains polygonaux. Rev. géogr. phys. et géol. dyn. 12, 315-327.

Rydquist, F. (1960). Studier inom olandska polygonmarker. Stockholm Hogskola, Geografiska Inst. Medd. 125, 50-74.

Tröll, C. (1944). Strukturböden, Solifluktion und Frostclimate der Erde. (Structure soils, solifluction and frost climates of the earth; translated by H.E. Wright, translation no. 43, U.S. Army SIPRE, 1958, pp. 121). Geol. Rundschau 34, 545-694.

Van Vliet-Lanöe, B. (1982). Structures et microstructures associées à la formation de glace de ségrégation: leurs consequences. R.J.E. Brown Memorial Volume, Proc. 4th Canadian Permafrost Conference, Calgary, 116-122.

Van Vliet-Lanöe, B. (1985). Frost effects in soils. Ch. 6 in Soils and Quaternary Landscape Evolution, ed. J. Boardman, 117-158. Chichester: Wiley & Sons.

Van Vliet-Lanöe, B., Coutard, J.P. & Pissart, A. (1984). Structures caused by repeated freezing and thawing in various loamy sediments. A comparison of active, fossil and experimental data. Earth Surface processes and Landforms 9, 553-565.

Warburton, J. (1985). Rayleigh convection and the initiation of sorted patterned ground: three field investigations. Unpubl. M.A., Dept. Geog., Univ. Colorado.

Washburn, A.L. (1956). Classification of patterned ground and review of suggested origins. Geol. Soc. Am. Bull. 67, 823-865.

Washburn, A.L. (1970). An approach to a genetic classification of patterned ground. Acta Geographica Lodziensia 24, 437-446.

TABLE 1

Ground surface temperatures, Glittertind and Gråsubreen, °C

	Glittertind			Gråsubreen
	1983-84	1984-85	1985-86	1984-85
Mean Annual Ground Surface Temperature (1 cm)	-2.29	+0.98	-3.58	-0.33

CRYOSTRATIGRAPHIC STUDIES OF PERMAFROST, NORTHWESTERN CANADA

D.G. Harry[1] and H.M. French[2]

[1]Geological Survey of Canada, 601 Booth Street, Ottawa, K1A 0E8, Canada
[2]Departments of Geology and Geography, University of Ottawa, Ottawa, K1N 6N5, Canada

SYNOPSIS The cryostratigraphic approach to permafrost geology emphasizes ground ice, and the dynamics of its aggradation and degradation, as an integral component of the geological record. In particular, stratigraphic evidence of paleothermal and paleohydrological conditions may be used to infer both local and regional permafrost history. Cycles of environmental change may be marked by the presence of thaw unconformities. These frequently form sharp boundaries between stratigraphic zones posessing contrasting cryotextures and may also truncate pre-existing ice structures providing evidence of partial permafrost degradation followed by the regrowth of frozen ground. Studies undertaken at four sites in northwestern Canada illustrate the principles of cryostratigraphy in relation to specific problems in permafrost geology.

INTRODUCTION

Cryostratigraphy is the science of perennially frozen sequences of earth materials. The cryostratigraphic approach emphasizes ground ice, and the dynamics of its aggradation and degradation, as an integral component of the geological record. In the Soviet Union, cryostratigraphy is a well-established branch of permafrost science (e.g. Katasonov, 1978; Kudryavtsev, 1978, pp. 300-316; Popov et al., 1985, pp. 90-103) and is especially relevant to the extensive permafrost record of unglaciated central and eastern Siberia (e.g. Katasonov, 1975; Katasonov and Ivanov, 1973; Sher and Kaplina, 1979). In arctic North America, relatively few stratigraphic studies of permafrost have been undertaken, for example in Alaska (e.g. Sellman and Brown, 1973) and the Western Canadian Arctic (e.g French et al., 1982; Mackay, 1975, 1976; Mackay and Matthews, 1983).

This paper adds to the North American literature by decribing the principles of cryostratigraphy and, with reference to four case studies, demonstrates its application to permafrost investigation in northwestern Canada. By characterizing ground ice occurrence with respect to lithologic and hydrologic factors, the cryostratigraphic approach facilitates the reconstruction of Quaternary environmental history. It provides a framework within which detailed studies of ice crystallography, water chemistry and stable isotopes may be interpreted in order to determine ground ice origin.

CRYOSTRATIGRAPHY

Cryostratigraphic analysis focuses upon the identification of discontinuities within frozen ground. These are often marked by the development of distinctive cryogenic textures, reflecting changes in the quantity or form of occurrence of ground ice. Cryotexture is determined by the thermal, hydrological and depositional history of permafrost. In many cases, therefore, the existence of distinct vertical or lateral sequences of cryotextures may be used as a framework for paleoenvironmental reconstruction.

Soviet researchers generally distinguish between cryotextures formed within epigenetic and syngenetic freezing systems (e.g. Kudryavtsev, 1978; Popov et al., 1985). During epigenetic freezing, most ground ice forms within existing earth materials either in situ, by the freezing of pore water, or as a result of upward moisture migration to the freezing front. Depending upon the balance between pore water pressure and overburden pressure, a range of ice types may be developed from pore ice through segregation ice to intrusion ice. Mackay (1973a) has demonstrated the existence of this sequence of cryotextures, associated with pingo growth during epigenetic freezing of a sub-lake talik. In syngenetic systems, ground ice forms more or less simultaneously with the deposition of earth materials in which it occurs. Most moisture originates near the ground surface and migrates downwards to the freezing front. A range of cryotextures may develop, which can be classified according to the depositional environment and moisture content of initial sediments, and the morphology of aggradational ice bodies (Melnikov and Tolstikhin, 1974).

Thermokarst events may also be recorded within the cryostratigraphic sequence, in the form of thaw unconformities. These are horizons within permafrost which mark the level to which thawing temperatures once extended. They frequently separate two zones of contrasting cryotextures, and may truncate ground ice

structures. In cases where the thawing front passed downwards through permafrost, materials above the unconformity were thawed and then refrozen, while underlying cryostructures and textures may predate the thaw event. Thaw unconformities may represent the effects of local thaw caused, for example, by the development of tundra ponds. They may also indicate cycles of climatic change, resulting in regional permafrost degradation, followed by the regrowth of frozen ground. For example, a well-developed thaw unconformity occurs at depths of 1.5-1.7 m below surface in the Mackenzie Delta area of the Northwest Territories (e.g. Mackay, 1975), and at about 2.0 m below surface in central Yukon (Burn et al., 1986). This is believed to represent the maximum depth of thaw attained during the Holocene climatic optimum.

CASE STUDIES, NORTHWESTERN CANADA

Four case studies, selected from northwestern and arctic Canada (Fig. 1) illustrate the application of cryostratigraphy to three problems in permafrost geology. The origin of massive ice, the occurrence of ground ice in bedrock, and the paleoenvironmental significance of multiple ice-wedge systems are recurrent themes in the North American permafrost literature. The four study locations illustrate ground ice development in a range of Quaternary environments from the unglaciated interior Yukon, through the marginal zone of Laurentide glaciation, to an area possibly affected by thin, local ice caps. They also provide a transect across the permafrost zone of northwestern Canada, from the discontinuous fringe to areas of thick continuous permafrost.

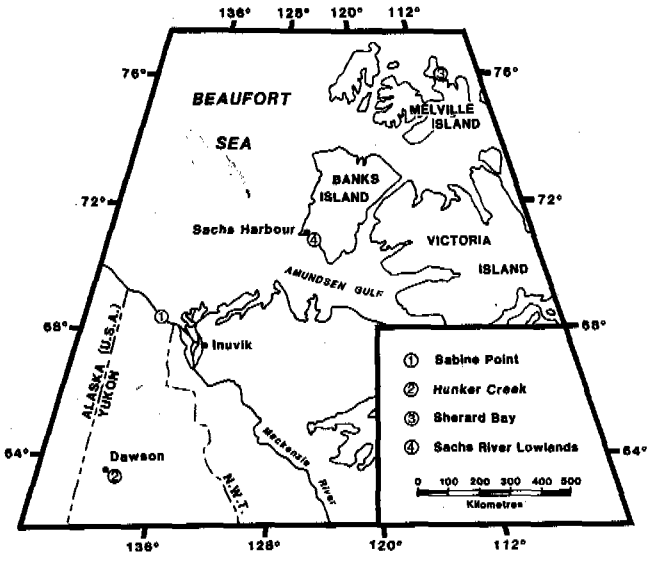

Fig. 1 Case study locations, northwestern Canada.

Case Study 1: The origin of massive ice, Sabine Point, Yukon Coastal Plain

The occurrence of large layers of massive ground ice in the Pleistocene Mackenzie Delta and on the Yukon Coastal Plain is well known (e.g. Mackay, 1966; Rampton, 1982; Rampton and Mackay, 1971); however, the origin of this ice remains problematical. Mackay (1971, 1973b) has suggested that massive ice may originate by processes of segregation or segregation-intrusion during closed system freezing. At the same time, the possibility exists that some massive ice may represent buried surface ice, preserved by permafrost aggradation (e.g. Lorrain and Demeur, 1985).

Cryostratigraphic analysis provides one method of resolving the problem of massive ice origin, since it links ice characteristics to the nature and depositional history of enclosing sediments. For example, Harry et al. (in press) describe the cryostratigraphy associated with massive ice occurrence at a site approximately two kilometres northwest of Sabine Point, on the Yukon Coastal Plain. At this locality, massive ice is exposed within the headwall of a retrogressive thaw-flow slide (ground ice slump), developed in an isolated area of rolling moraine, related to a major stillstand or readvance of the pre-Late Wisconsinan Buckland Glaciation (Rampton, 1982).

Several distinct cryotextural zones may be recognized within this section (Fig. 2). Materials beneath the massive ice consist of ice-rich silty-clay diamicton, containing thin inclined and undulating ice lenses and layers, together with horizontal ice lenses up to 10 cm in thickness. Immediately below the contact with massive ice, the diamicton is characterized by a well-developed network of reticulate ice veins, aligned horizontally and vertically in the exposure. The lower part of the massive ice body comprises a tabular unit of dirty ice, possessing a sediment content of 13-15% by volume. Alternating bands of dirty ice and cleaner, bubble-rich ice, give the unit a layered appearance. This sediment-rich ice grades into an upper unit of clear, structureless ice. The upper surface of the ice body is truncated by at least two thaw unconformities, which separate it from overlying mudflow deposits and organic material.

This cryostratigraphic sequence suggests that the massive ice originated as permafrost aggraded epigenetically at some time following Buckland deglaciation. The transition from clear ice, through sediment-rich ice, to reticulate ice veins, is indicative of a progressive change in freezing rate and water supply experienced as a freezing front moved downwards through unfrozen sediments. The thaw unconformities above the massive ice mark multiple episodes of thermokarst, which resulted in thaw settlement and slumping of Buckland and post-Buckland sediments into adjacent lacustrine basins.

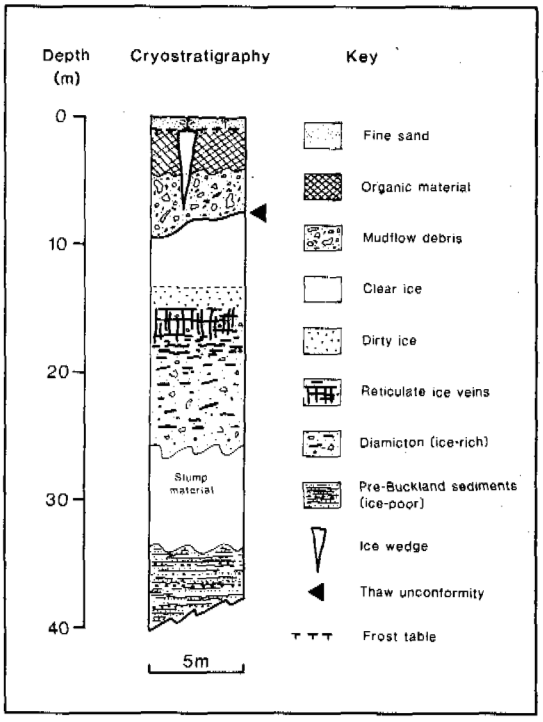

Fig. 2 Cryostratigraphic section near Sabine Point, Yukon Coastal Plain

Case Study 2: The origin of massive ice, Hunker Creek, Klondike District, central Yukon

A different interpretation of massive ice origin is provided by cryostratigraphic studies in the Klondike District of central Yukon. This area remained unglaciated throughout the Quaternary, and therefore a buried glacier origin for massive ice may be eliminated. During the Late Pleistocene, many Klondike valleys were partially infilled by paraglacial clastic sediments, and by muck deposits representing a melange of windblown silt and mass-wasted, organic-rich colluvium (French et al., 1983, p. 38). Within this stratigraphic context, French and Pollard (1986) describe permafrost and ground ice exposed on the west side of Hunker Creek approximately 15 km east of Dawson City. At this site, hydraulic mining of auriferous gravels has exposed both ice wedges and bodies of massive ice in overlying organic 'muck' deposits (Figure 3).

As at Sabine Point, the massive ice body comprises a lower sediment-rich unit and an upper clear ice unit. However, major contrasts are provided by the small crystal size and presence of large organic inclusions within the ice at Hunker Creek. The lower unit is characterized by bands of almost pure ice, (10-27 cm thick) and organic silt (10-20 cm thick), together with discontinuous layers and pods of peat. The ice content of the unit as a whole varies between 60% and 80% by volume. The contact with underlying gravels is irregular and transitional. The upper, clear ice unit is translucent and grey or pale brown in colour, as a result of the large number of gas and fine sediment inclusions which in places form foliations within the ice. The ice also contains a number of larger inclusions of organic material and angular cobbles. The contact between the massive ice and overlying muck deposits is abrupt. Large, inactive ice wedges within the muck deposits are truncated by a thaw unconformity at a depth of 2.0-2.5 m below surface.

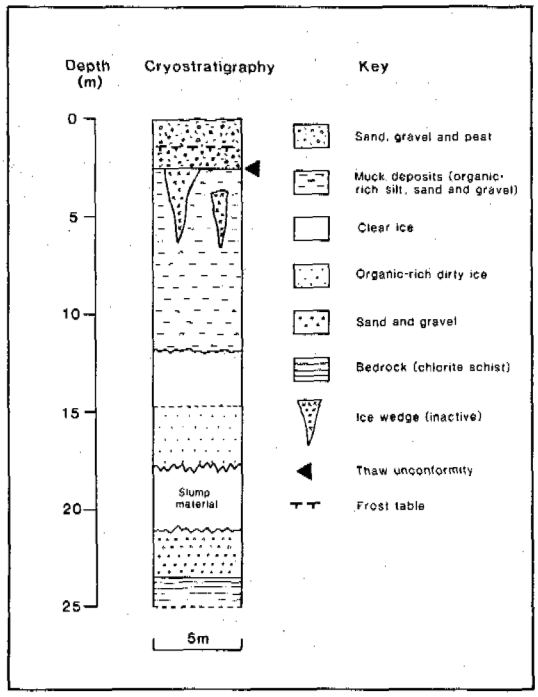

Fig. 3 Cryostratigraphic section, Hunker Creek, central Yukon

Two possible hypotheses may be considered for the origin of the massive ice at Hunker Creek. First, the ice may be of segregational origin. According to this model, as permafrost aggraded, possibly syngenetically, into the Late Pleistocene valley fill, pore water moved upwards through the permeable gravel to form bodies of segregated massive ice. However, certain characteristics of the massive ice, particularly the inclined orientation of gas inclusions, wide dissemination and organic nature of enclosed sediment particles and uniform small crystal size, argue against the slow growth of a large segregated ice layer. Instead, a buried ice origin must be considered. Given the ice characteristics and the nonglacial environmental history of the area, the most likely origin of the ice appears to be as a snowbank. Rapid muck sedimentation under cold, periglacial conditions could have resulted in the burial of a valley-side perennial snowbank, which would then be preserved within aggrading permafrost.

Case Study 3: Ground ice in bedrock, Sabine Peninsula, eastern Melville Island

Where clearly recognizable ground ice

structures and ice bodies are absent from the stratigraphic sequence, subtle differences in ground ice conditions, revealed in the form of contrasting cryotextures, may offer the only means to reconstruct permafrost history. For example, the Sabine Peninsula of eastern Melville Island lies beyond the limits of Laurentide glaciation and near-surface materials generally comprise shattered and/or poorly lithified bedrock, overlain by colluvium on slopes (Hodgson et al., 1984). Since natural permafrost exposures are rare, relatively few data are available regarding ground ice conditions. French et al. (1986) describe permafrost conditions exposed during sump excavation at the Panarctic Oils Limited Sherard Bay F-34 wellsite in the winter of 1982-83.

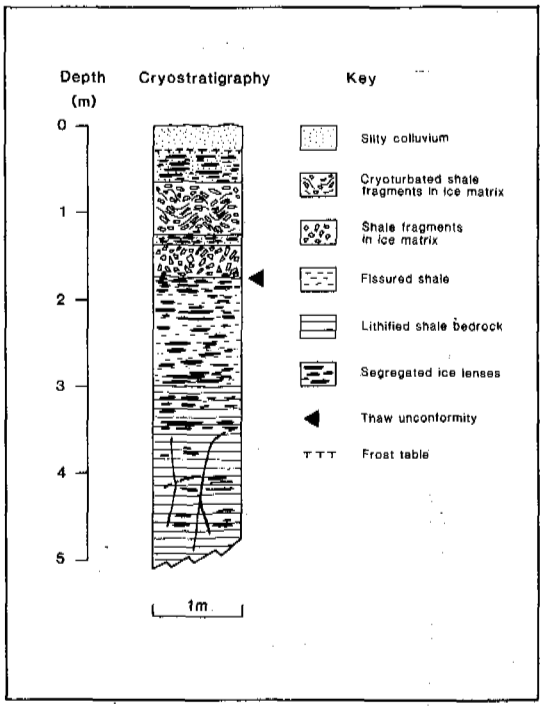

Fig. 4 Cryostratigraphic section, Sherard Bay wellsite, eastern Melville Island

The site is located in an area underlain by poorly lithified, deeply weathered and frequently ice-rich sediments of Mesozoic age. Several cryostratigraphic units may be identified in this section (Fig. 4). The basal material seen in the sump wall consists of lithified shale bedrock, containing pore ice and occasional ice lenses. Overlying this material is 3.0-4.0 m of ice-rich weathered bedrock and/or colluvium. A clear cryogenic discontinuity occurs at a depth of 1.7 m. Below the discontinuity, visible ice is limited to voids along bedding planes, and to bedrock joints and fractures. Horizontal and near-horizontal ice lenses up to 2.5 cm in thickness occur, particularly within zones of fractured bedrock. Above the 1.7 m level ice contents are higher, typically 30-60% by volume. In addition to lenses, ice also occurs at two levels as a matrix, enclosing angular, displaced and reoriented shale fragments. Within the upper level, the ice content is greater than 70% by volume, and the shale fragments display a distinctive cryoturbation texture.

The cryogenic discontinuity 1.7 m below surface probably represents a thaw unconformity, marking the greatest depth of seasonal thaw experienced in these materials. It is not possible to date this event, however the depth of the unconformity in a region of extremely cold contemporary climate suggests that it may represent a period of interglacial warm climate, rather than the more recent Holocene climatic optimum. The cryoturbation structures observed above the discontinuity support the interpretation that this zone was at one time subject to seasonal freezing and thawing. The concentration of segregated ground ice lenses and layers above the thaw unconformity may in part reflect the growth of aggradational ice (Mackay, 1972; Cheng, 1983). This forms at or near the base of the active layer, and is incorporated into permafrost if the permafrost table rises.

Case Study 4: Multiple ice wedge systems, southwestern Banks Island

A final example of the usefulness of the cryostratigraphic approach is provided by its application to the study of ice wedges. The identification of ice wedge structures provides an important indicator of environmental conditions in regions of both contemporary and former permafrost occurrence (e.g. Black, 1976). Moreover, the recognition of multiple systems of wedges, sometimes including both epigenetic and syngenetic structures of different ages, may provide evidence of sequential environmental change (e.g. Black, 1983; Harry et al., 1985). This is the case on southwest Banks Island, where French et al. (1982) describe several ice wedge systems, developed in the aggrading deltaic and alluvial permafrost environment of the Sachs River Lowlands outwash plain (Vincent, 1983).

Four systems of ice wedges of different ages may be recognized in a section located approximately 2.5 km southeast of Sachs Harbour (Fig. 5). They are developed in a sequence of grey silty sand and yellow-brown medium sand, overlain by a discontinuous organic unit and a surface layer of eolian sand. The oldest set of wedges, 3-5 m high and 0.5-1.0 m wide, occur only within the grey silty sand and are truncated at or near a horizon containing detrital willow roots and stems, which marks the contact with overlying yellow-brown sand. Since they contain inclusions of grey silt with in the well-developed foliations, they may be partially syngenetic in origin. A second system of wedges consists of small multiple syngenetic ice veins, 1-2 m in length and of variable width, which occur at various levels within the yellow-brown sand. The third system comprises epigenetic wedges, 1-3 m high and up to 0.5 m wide. They occur primarily within the yellow-brown sand and are probably related to a former surface, now buried by the overlying organic deposit. The fourth system consists of large epigenetic wedges, 4-5 m high and up to

2 m wide, which relate to the present ground surface.

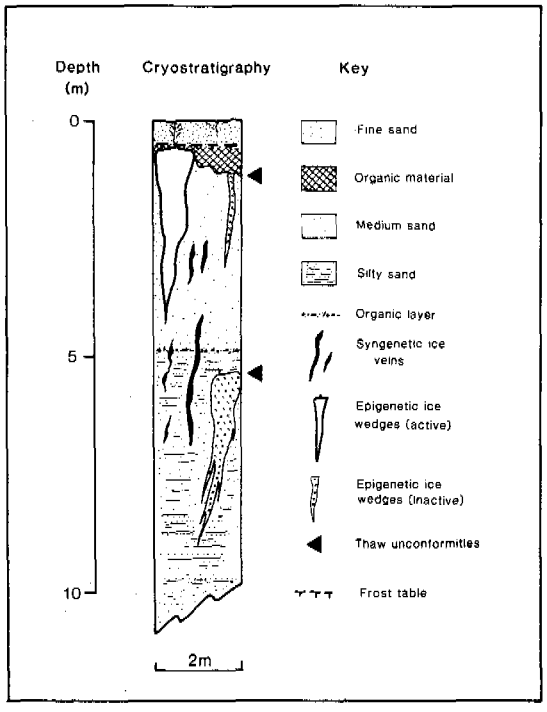

Fig. 5 Cryostratigraphic section, Sachs River Lowlands, southwest Banks Island

The recognition of four distinct ice wedge systems, and their relationship to enclosing sediments, forms the basis for a cryostratigraphic interpretation of Late Quaternary history in this area. The earliest set of wedges appear to have developed in relation to a ground surface marked approximately by the detrital organic horizon. Radiocarbon dating provides a minimum age of 10,600 ± 130 years B.P. (GSC-3229) for this surface. Subsequent rapid deposition of the overlying sand unit resulted in the erosion and/or burial of these ice wedges. At the same time, small syngenetic veins developed within the sand as permafrost aggraded. The third set of wedges grew epigenetically, in relation to an Early Holocene surface, a minimum age for which is provided by a 14C date of 6490 ± 60 years B.P. (GSC-3216) on overlying peat. During the Holocene climatic optimum, these wedges were truncated by deeper seasonal thaw and are now inactive. The fourth set of wedges have also grown epigenetically and are currently active, reflecting current cold climate conditions.

CONCLUSION

Several problems remain in the application of the cryostratigraphic approach to permafrost studies in northwestern Canada. First, the region has experienced a complex and sometimes poorly understood sequence of Quaternary environmental change. In some areas, therefore, permafrost conditions may be interpreted with respect to two or more models of glacial history. Second, a lack of natural exposures in some areas, particularly the Arctic Islands, limits cryostratigraphic analysis to the study of borehole records. More generally, the absence of a method for directly dating ground ice bodies restricts the precision of age control in the reconstruction of permafrost history. However, as the examples presented above demonstrate, cryostratigraphy provides a useful framework for studies of permafrost history. Stratigraphic analysis has traditionally formed a basic research methodology in investigations of Quaternary geology and geomorphology in nonpermafrost regions. Within the permafrost zone, cryostratigraphic analysis of ground ice and cryotextures provides supplemental information regarding the thermal and hydrological history of frozen ground.

REFERENCES

Black, R.F. (1976). `Periglacial features indicative of permafrost: Ice and soil wedges', Quaternary Research, v.6, pp. 3-26.

Black, R.F. (1983). `Three superposed systems of ice wedges at McLeod Point, Northern Alaska, may span most of the Wisconsin stage and Holocene', in Proceedings, Fourth International Conference on Permafrost, Fairbanks, Alaska, Volume 1. National Academy Press, Washington D.C., pp. 68-73.

Burn, C.R., Michel, F.A., and Smith, M.W. (1986). `Stratigraphic, isotopic, and mineralogical evidence for an early Holocene thaw unconformity at Mayo, Yukon Territory', Canadian Journal of Earth Sciences, 23, pp. 794-803.

Cheng, G. (1983). 'The mechanism of repeated-segregation for the formation of thick layered ground ice. Cold Regions Science and Technology, 8, pp. 57-66.

French, H.M. and Pollard, W.H. (1986). `Ground ice investigations, Klondike District, Yukon Territory', Canadian Journal of Earth Sciences, 23, pp. 550-560.

French, H.M., Harry, D.G. and Clark, M.J. (1982). `Ground ice stratigraphy and late-Quaternary events, south-west Banks Island, Canadian Arctic', in Proceedings, Fourth Canadian Permafrost Conference. National Research Council of Canada, Ottawa, pp. 81-90.

French, H.M., Bennett, L. and Hayley, D.W. 1986). `Ground ice conditions near Rea Point and on Sabine Peninsula, eastern Melville Island', Canadian Journal of Earth Sciences, 23, pp. 1389-1400.

French, H.M., Harris, S.A. and van Everdingen, R.O. (1983). `The Klondike and Dawson', in French, H.M. and Heginbottom, J.A. (eds.), Guidebook to permafrost and related features, Northern Yukon Territory and Mackenzie Delta, Canada. Fourth International Conference on Permafrost, Fairbanks, Alaska. State of Alaska, Division of Geological and Geophysical Surveys, College, Alaska, pp. 35-63.

Harry, D.G. French, H.M. and Pollard, W.H. (1985). `Ice wedges and permafrost conditions near King Point, Beaufort Sea coast, Yukon Territory', Geological Survey of Canada, Paper 85-1A, pp. 111-116.

Harry, D.G., French, H.M. and Pollard, W.H. (in press). `Massive ground ice and ice-cored terrain near Sabine Point, Yukon Coastal Plain' (Canadian Journal of Earth Sciences).

Hodgson, D.A., Vincent, J.S. and Fyles, J.G. (1984). `Quaternary geology of central Melville Island, Northwest Territories', Geological Survey of Canada, Paper 83-16, 25 p.

Katasonov, E.M. (1975). `Frozen ground and facial analysis of Pleistocene deposits and paleogeography of central Yakutia', Biuletyn Peryglacjalny, 24, pp. 33-40.

Katasonov, E.M. (1978). `Permafrost-facies analysis as the main method of cryolithology', in Permafrost: U.S.S.R. Contribution to the Second International Conference, Yakutsk, U.S.S.R. Washington: N.A.S., pp. 171-176.

Katasonov, E.M. and Ivanov, M.S. (1973). `Cryolithology of central Yakutia', Guidebook, Second International Conference on Permafrost, Yakutsk, U.S.S.R., 38 p.

Kudryavtsev, V.A. (1978). `General Permafrost Science -Geocryology', 2nd edition. Izdalielstova Moskovskogo Universitieta, 464 p. (in Russian).

Lorrain, R.D. and Demeur, P. (1985). `Isotopic evidence for relic Pleistocene glacier ice on Victoria Island, Canadian Arctic Archipelago', Arctic and Alpine Research, v.17, pp. 89-98.

Mackay, J.R. (1966). `Segregated epigenetic ice and slumps in permafrost, Mackenzie Delta area, N.W.T.', Geographical Bulletin, 8, pp. 59-80.

Mackay, J.R. (1971). `The origin of massive icy beds in permafrost, western Arctic coast, Canada', Canadian Journal of Earth Sciences, v.8, pp.397-422.

Mackay, J.R. (1972). 'The world of underground ice, Annals of the Association of American Geographers, 62, p. 1-22.

Mackay, J.R. (1973a). `The growth of pingos, Western Arctic Coast, Canada', Canadian Journal of Earth Sciences, 10, pp. 979-1004.

Mackay, J.R. (1973b). `Problems in the origin of massive icy beds, Western Arctic, Canada', in Permafrost: North American Contribution to the Second International Conference, Yakutsk, U.S.S.R. National Academy of Sciences, Washington, D.C., pp. 223-228.

Mackay, J.R. (1975). `Relict ice wedges, Pelly Island, N.W.T.', Geological Survey of Canada, Paper 75-1A, pp. 469-470.

Mackay, J.R. (1976). `Pleistocene permafrost, Hooper Island, Northwest Territories', Geological Survey of Canada, Paper 76-1A, pp. 17-18.

Mackay, J.R. and Matthews, J.V. (1983). `Pleistocene ice and sand wedges, Hooper Island, Northwest Territories', Canadian Journal of Earth Sciences, v.20, pp. 1087-1097.

Melnikov, P.I. and Tolstikhin, N.I. (1974). `Permafrost Studies', Nauka, Novosibirsk, 291 p. (in Russian).

Popov, A.I., Rozenbaum, G.E. and Tumel, N.V. (1985). `Cryolithology', Izdalielstova Moskovskogo Universitieta, 238 p. (in Russian).

Rampton, V.N. (1982). `Quaternary geology of the Yukon coastal plain, Canada', Geological Survey of Canada, Bulletin 317, 49 p.

Rampton, V.N. and Mackay, J.R. (1971). `Massive ice and icy sediments throughout the Tuktoyaktuk Peninsula, Richards Island, and nearby areas, District of Mackenzie', Geological Survey of Canada, Paper 71-21, 16p.

Sellmann, P.V. and Brown, J. (1973). `Stratigraphy and diagenesis of perennially frozen sediments in the Barrow, Alaska, region', in Permafrost: North American Contribution to the Second International Conference, Yakutsk, U.S.S.R. National Academy Press, Washington D.C., pp. 171-181.

Sher, A.V. and Kaplina, T.N. (1979). `Late Cenozoic of the Kolyma Lowland', Tour XI Guidebook, XIV Pacific Science Conference, Khabarovsk, U.S.S.R. Moscow, Academy of Sciences, 115 p.

Vincent, J-S. (1983). `La geologie du Quaternaire et la geomorphologie de l'Ile Banks, Arctique Canadien', Geological Survey of Canada, Memoire 405, 118p.

CSC Contribution No. 49287

THAW LAKE SEDIMENTS AND SEDIMENTARY ENVIRONMENTS

D.M. Hopkins and J.G. Kidd

Alaska Quaternary Center, University of Alaska, Fairbanks, AK 99775

SYNOPSIS The thaw-lake sediment sequence, seen in cross section, consists of (1) a basal, coarse, time-transgressive sequence consisting largely of sand and organic detritus, often cross-bedded, which accumulates near the migrating basin margin, and (2) an overlying sequence of thin- and flat-bedded silt, peaty silt, or detrital peat which accumulates in the quiet water of the central basin. Thick accumulations of detrital peat, representing lee-shore accumulations of organic detritus, appear at the margins of some thaw-lake sediment sequences. Analyses of organic remains preserved in thaw-lake sediment suites can contribute to reconstruction of ancient vegetation mosaics.

INTRODUCTION

Thaw lakes--lakes that result from surface collapse caused by the thawing of ice-rich permafrost (Hopkins, 1949)--are important and conspicuous features of Arctic and subarctic lowland landscapes in both tundra and taiga regions. Organic remains from diverse parts of the modern landscape become incorporated in the bottom sediments of thaw lakes along with older organic detritus derived from the substrate in which the lake develops. Although account must be taken of the potential presence of redeposited material, the organic remains preserved in sediments of ancient thaw lakes can provide a valuable record of ancient vegetation mosiacs.

The major purpose of this paper is to facilitate recognition of thaw-lake sediments in the field. Cross-sectional exposures of thaw-lake sediment sequences are widespread in subarctic and low-arctic regions but are commonly misinterpreted or go unrecognized in spite of the useful descriptions of Livingstone and others (1958), McCulloch and others (1965), McCulloch and Hopkins (1966), Carson (1968), Tedrow (1969), and Nelson (1982). Our discussion is based mostly upon unpublished geochronological, sedimentological, and paleontological studies and observations of Pliocene, Pleistocene, and Holocene thaw lake sediments in Alaska, Canada, and Siberia by Hopkins (1961-1987) and upon a study of sediments and sedimentary environments in two active thaw lakes near Cape Espenberg, Seward Peninsula, Alaska (fig. 1) by Kidd in 1987. We have also examined sediments and sedimentary environments in two thaw lakes in Goldstream Valley near Fairbanks, Alaska.

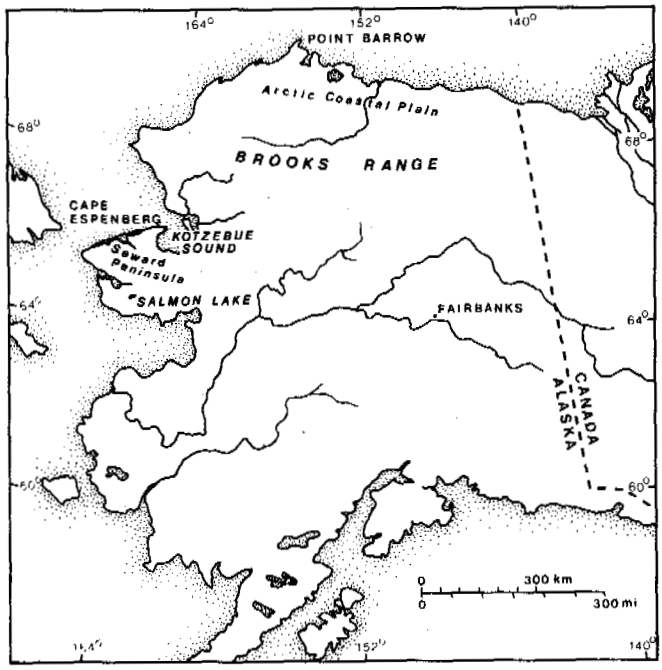

Figure 1. Map showing location of places named in text.

ORIGIN AND EVOLUTION OF THAW LAKES

Ponding of surface water to some critical depth is required to initiate the thawing of ice-rich permafrost that produces a thaw lake. We have seen two incipient thaw lakes developing over ice-wedge intersections on

hilltops near Cape Espenberg. In lowland landscapes, disruption of drainage by growth of palsas may be a common cause of initial ponding. Harry and French (1983, p. 456) suggest that thaw lakes originate in lowland landscapes "by basin coalescence following breaching of [low-center ice wedge] polygon ramparts", and a similar suggestion is made by Rex (1961, p. 1022). Surface disturbance by heavy equipment and drainage obstruction by construction activities are also well-known causes of thaw lake development (e.g. Walker and others, 1987).

Once formed, a tundra pool tends to warm and thaw the ground beneath its bed and beyond its banks, because water has a low albedo (especially if, as is common, it is darkened by dissolved organics) and a high heat capacity compared to surrounding vegetation and to most soil materials. As ground-ice melts, the pond deepens. Meanwhile, undercutting by wind-generated waves causes banks to slump and collapse. When and if the basin deepens sufficiently to allow liquid water to persist below winter pond ice, the heat anomaly intensifies, and a basin of thawed ground develops beneath the lake bottom[1]. Thus the lake continues to enlarge, often radially, until growth is terminated by a drainage event.

The essential requirement for thaw lake development is the presence of substantial quantities of ground ice. Ice wedges and segregation ice generally comprises 40% to 80% of the volume of perennially frozen silt and peat (Sellman and others, 1975; Williams and Yeend, 1979; Harry and French, 1983). Ground ice in the form of ice wedges and buried snow can also form a considerable part of the volume of frozen eolian sand. Ice wedges may also be present in gravel. Melting of buried glacial ice is responsible for development of thaw lakes in ancient drift near Salmon Lake on the Seward Peninsula (D.M. Hopkins, field notes, 1973) and in valleys in the Brooks Range (Hamilton, 1986), but these are more properly regarded as a special type of glacial kettle and are not discussed further here.

The depth to which a thaw-lake basin will subside depends upon the amount and distribution of ground ice in the substrate, and this, in turn, depends upon local depositional and thermal history. In areas subjected to repeated cycles of thaw-lake development, epigenetic wedges extend no deeper than six or eight meters, and only minimal segregation ice is present (Sellman and others, 1975; French and Harry, 1983; D.M. Hopkins, field notes, 1978-1987). Potential thaw-subsidence is limited to a few meters. At the other extreme, syngenetic ice wedges in loess can extend from the surface to depths as great as 60 m (Kaplina and Lozhkin, 1984), and segregation ice is distributed to equal depths (Are, 1973). Thaw-lake basins as deep as 25 m are known in areas of syngenetic wedges (Williams and Yeend, 1979; Carter, 1987; J.G. Kidd, unpublished field notes, 1987).

Climatic change can affect the presence or absence, abundance, depth, and hydrology of thaw lakes. Numerous radiocarbon dates establish that thaw lakes were present on the coastal lowlands around Kotzebue Sound throughout the past 35 kybp (thousand years before present) and probably throughout the past 100 kybp (McCulloch and others, 1965; Kaufman and Hopkins, 1985). In northern Alaska, on the other hand, thaw lakes seem to have been lacking during the cold, dry Duvanny Yar interval (30 to 14 kybp), of Hopkins (1982), although numerous thaw-lake sediment sequences older and younger than the Duvanny Yar interval are known (Hopkins and Robinson, 1979; L.D. Carter, written comm., 1988).

Historical records show that water levels have diminished and that many lakes disappeared during the past century in the alassy (themokarst basins with or without thaw lakes) of central Yakutia (Are, 1973). Carson (1960) argues that concentric shorelines around thaw lakes on the Alaskan Arctic coastal plain also record generally higher lake levels several thousand years ago, but all three of the lakes that he illustrates have well-defined outlets that seem likely to be responsible for the episodic lowerings of lake level indicated by the shorelines. Nevertheless, appreciable but unmeasured year-to-year fluctuations in lake levels have been noted on the Arctic coastal plain (D.M. Hopkins and L.D. Carter, field notes, 1976-1982).

Thaw lakes drain, generally catastrophically, when some part of the perimeter expands into a nearby stream valley or lower lying lake basin or when a retreating coastline intersects the lake basin. Thaw-back along an ice wedge is probably the most frequent proximal cause of thaw-lake drainage. Partial drainage events are common, leaving one or more small lakes persisting in the central basin, or, not uncommonly, at the basin margin.

The life span of a thaw lake is relatively short. Radiocarbon dates on samples from cores and exposed sediment sequences indicate that thaw lakes typically persist 2.5 to 3.0 ky, but several large lakes on the flat terrain near Point Barrow appear to have been in existence for 4.0 to 5.0 ky (Carson, 1968; D.M. Hopkins, unpublished data). Local relief and spacing of incised streams appear to govern the potential size and life span of thaw lakes in a particular region.

[1]In northern Alaska, however, some moderately large thaw lakes never deepen enough to permit unfrozen water to persist beneath winter ice. Ice wedges in perennially frozen ground may then persist beneath the lake bottom, covered by less than half a meter of lake sediment (Billings and Peterson, 1980; D.M. Hopkins and L.D. Carter, field notes, 1978).

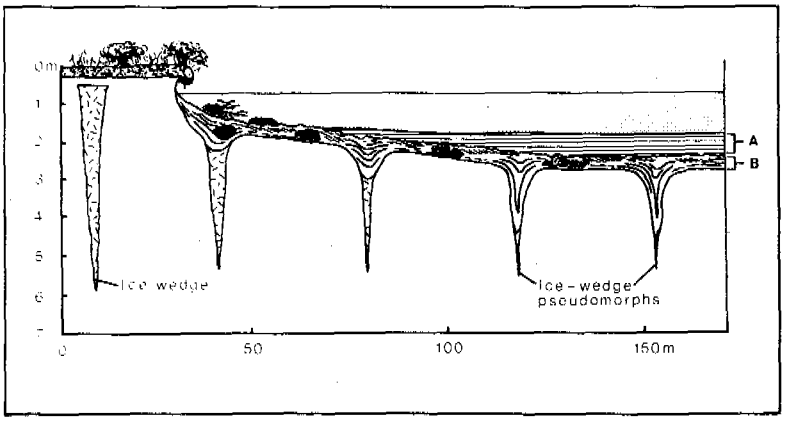

Figure 2. Diagramatic cross section through a thaw lake developed in silt with epigenetic ice wedges showing sediment suites, including (A) basal transgressive sequence and (B) central-basin sequence.

Over a long period, thaw lakes can form repeatedly on the same site. Superposed sets of as many as three thaw-lake sediment sequences resting on Pelukian (last interglacial) marine deposits are exposed in some places on the north coast of the Seward Peninsula (D.M. Hopkins, unpublished field notes, 1970).

SEDIMENTARY ENVIRONMENTS

The floor of a typical thaw lake is divisible into a nearshore zone shallow enough to be affected by waves and strong currents and a central basin at least slightly below wave base. Evidence of active wave erosion or thaw-collapse can be seen throughout the perimeter of some thaw lakes, but others have stable shores in places. In treeless regions of low relief, winds affect the distribution of stable and actively eroding shore, as well as lake orientation (Rex, 1961; Carson and Hussey, 1962). Downwind shores are subject to rapid erosion, while protected shores are more or less stable and may even prograde.

Thaw lake basins formed in peat or silt mantled by turf-forming tundra vegetation and containing epigenetic ice wedges generally are saucer-shaped: a nearshore zone several tens of meters wide slopes gently to a central basin lying about a meter lower. In these lakes, shoreline retreat is chiefly a consequence of undercutting by wave erosion[2]. Actively eroding or collapsing shorelines retreat so rapidly that aquatic plants are unable to establish. Instead, the lake is likely to be expanding into sedge marsh or mesic low-shrub tundra.

Beaches are lacking at the actively caving banks of shallow thaw-lake basins developing in areas of epigenetic ice wedges. Large, undercut chunks of root-bound turf, commonly with woody shrubs attached, tumble into the water, and abrade by rubbing against the bank or one another. The peat chunks are somewhat buoyant and may drift some distance along the nearshore bottom and aggregate in protected down-wind waters before burial in sandy or silty nearshore sediment. Twigs, stems, leaves, seeds, sclerotized insect remains, bones of small-mammals, and comminuted detritus derived from abrasion of the turf and peat balls form a finer component of ultimately water-logged organic sediment. Thawing ice wedges persist beneath the nearshore area (fig. 2), causing the bottom to subside. Organic detritus trapped in the subsiding trenches forms dark bands, visible from the air, which extend normal to the shore.

Much of the coarse and fine organic detritus drifts to small embayments and protected shores, where it may form beach-like accumulations more than a meter thick. Protected shorelines prograde, and in-situ peat forms when aquatic plants colonize the silty or peaty substrate.

Wave- and current-winnowing in the nearshore zone separates sand, which moves by traction and becomes concentrated in the nearshore zone, from silt, which moves in suspension and becomes concentrated in the central basin. If sand is abundant and currents strong, current ripples form on the shallow nearshore bottom. The central basin of a newly drained saucer-shaped thaw lake on the Seward Peninsula was a featureless, nearly flat surface floored by organic mud (D.M. Hopkins, unpublished field notes, 1947).

---

[2]Not by passive subsidence of the banks, as Carson (1968) suggests, except in the case of small, incipient thaw ponds and in some thaw lakes in spruce forest, discussed below.

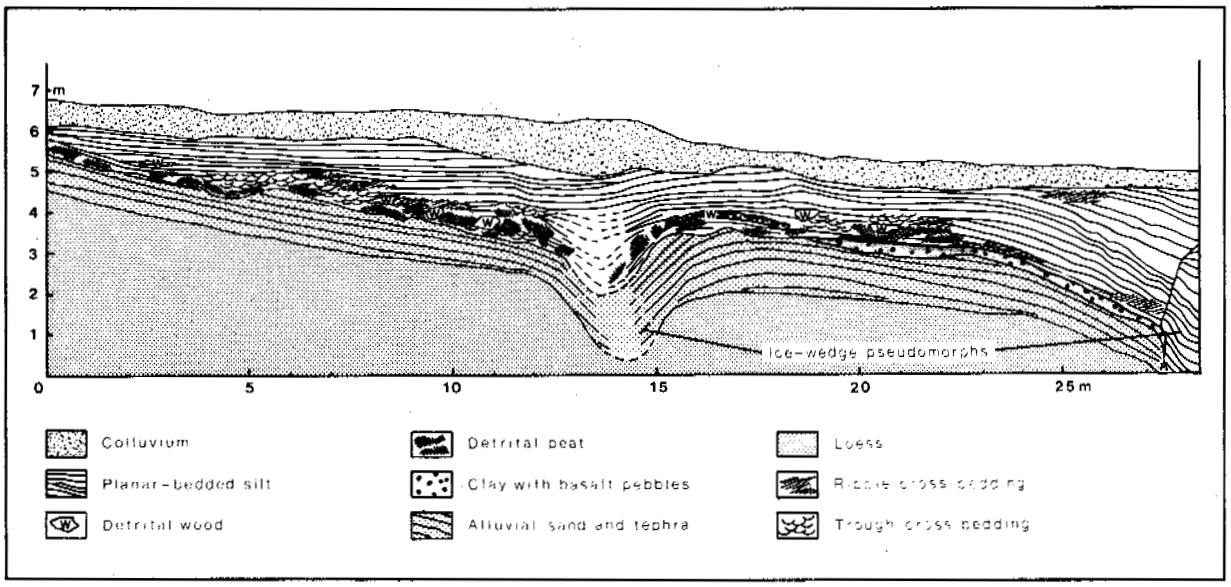

Figure 3. Detailed sketch extending obliquely from shore toward central basin through sediments in a thaw-lake basin that was drained about 7 kybp. Basal transgressive sequence consists of wood and chunks of peat embedded in a mixture of redeposited eolian sand and tephra, in places including a basal layer of basalt pebbles and silt or clay pellets. Central basin sequence onlaps on basal transgressive sequence and consists of planar-bedded silt.

Shallow thaw lakes in the forest zone, appear to develop more passively. The root mat beneath mature spruce forest is too coherent and strongly bound to fragment when deep thawing causes surface subsidence. Instead, the subsiding, root-bound forest floor tilts into the lake, protecting underlying silt from wave erosion. A belt of drowned, more-or-less upright trees may then extend several tens of meters from the shore.

Thaw lake basins developed in eolian sand consist of a broad lacustrine shelf subjected to waves and strong currents and a quiet central basin that may be only decimeters deeper and that may occupy less than half the area of the lake. Excellent examples are illustrated by Black (1951, figs. 3 and 4) and Sellman and others (1975, fig. 4). In detail, the lacustrine shelf is floored by prograded sand. Fine organic detritus accumulates in ripple troughs and on prograded slopes, and the central basin is floored by loose plant detritus with little or no admixed inorganic sediment (D.M. Hopkins and L.D. Carter, unpublished field notes, 1978).

Thaw lake basins formed in silt or sand containing syngenetic ice wedges are characterized by steeply sloping, actively slumping banks as much as 10 m high and a steep sublacustrine slope that may descend to depths of 10 m. The lakes that we investigated near Cape Espenberg had steep subaerial banks that were a mosaic of bare mudflows and patches of early successional vegetation including such pioneers as Calamagrostis sp., Artemisia tilesii, Aconitum delphinifolium, and Senecio congestus, interspersed with slumping blocks of turf that bore mesic upland tundra and large Salix alaxensis shrubs. Strand lines consisted of an alternation of short, narrow sandy beaches interspersed with semi-submerged blocks of turf with half-drowned willow shrubs. On the steep sublacustrine slope, block-sliding and gliding processes probably predominate over wave and current effects. Turbidity currents generated on the steep marginal sublacustrine slopes, though as yet undetected, may dominate sediment deposition processes in the central basin.

THAW LAKE SEDIMENTS

Thaw lakes are host to distinctive suites of sediments, readily distinguishable from other lacustrine sediment suites as well as from sediment suites deposited in other arctic and subarctic environments. Seen in cross-section, thaw-lake sediment suites may range in total thickness from as little as one to as much as ten meters and consists of

(1) a sandy, organic-rich basal detrital unit between 0.1 and 1.0 m thick which thickens at lateral intervals of a few meters to fill ice-wedge pseudomorphs extending several meters downward into older sediments, and

(2) an overlying unit of fine-grained, thin-bedded central-basin deposits between one and ten m thick (fig. 2).

The row of ice-wedge pseudomorphs at the base of a thaw-lake suite, the sandy, organic-rich character of the basal detrital unit with its mixture of remains of terrestrial upland and freshwater aquatic organisms, and the thin- and even-bedded character of the overlying central-basin unit collectively distinguish the thaw-lake sediment suite from any other lacustrine or non-lacustrine sediment suite.

The basal detrital unit consists of material deposited at or near the shore of an actively enlarging thaw lake. Consequently, this unit is time-transgressive; it is oldest at the site where the lake originated and youngest at sites which were at the basin margin when sedimentation was terminated by a drainage event (Carson, 1968). In most Holocene thaw-lake sediment sequences, this unit consists of well-bedded fine sand, silt, organic silt, and detrital peat interspersed with flattened masses of peat in which woody shrubs may be rooted (fig. 3). Current and trough cross-bedding are common sedimentary structures in this unit. The peat masses are the compacted remains of turf blocks; if abundant, they may be mistaken for a continuous layer of buried turf (**vide** Carson, 1968). This unit is generally rich in twigs, bark, berries, graminoid stems, moss shreds, and sclerotized remains of both aquatic and upland insects. Well preserved leaves are common, as are rodent teeth and bones, fish scales, bones, and otoliths, and fresh-water ostracode tests. The basal detrital sequences of thaw-lake sediment suites dating from colder intervals of the Pleistocene differ in having much less detrital organic material and much sparser mollusk shells and aquatic microfossils.

Redeposited eolian sand and tephra are prominent constitutents of the basal transgressive unit in areas where these are present in the sediments in which the thaw-lake basin formed. Holocene thaw lake basins developed entirely in eolian sand have a basal transgressive sequence that consists of a thin, organic-rich layer overlain by a zone generally less than 1.5 m thick of foreset-bedded sand with organic laminae, representing material deposited on the sub-lacustrine shelf.

Compact, thick-bedded or unbedded accumulations up to five m thick of graminoid stems and moss fibers, through which are scattered many twigs and sticks, evidently represent lee-shore peat accumulations. The twigs and sticks are typically short and blunt and lack attached roots and are generally in strong alignment, imparting a pronounced inclined fabric or parting to the peat matrix. Fresh-water mollusk shells and sclerotized insect parts are scarce in these deposits, perhaps because diluted in the enormous volume of detrital plant material that drifts into protected embayments. Lee-shore peat deposits rarely extend for more than a few tens of meters in cross-sectional exposures. One might easily mistake these bodies for in-situ peat filling ancient swales, but the broken condition of the wood fragments clearly indicates that these are detrital deposits.

Central-basin sequences generally consist of thin- and flat-bedded silt or organic silt which in some exposures can be seen to on-lap the underlying basal transgressive sequences (fig. 3). Central basin sequences of Holocene thaw lakes developed in fine-grained sediments typically consist of organic silt layers separated by laminae of detrital organics. Holocene central-basin deposits in eolian sand consist of detrital organics with little or no admixture of silt or sand. Central-basin deposits developed in loess during the colder parts of the Pleistocene consist of well-bedded inorganic silt. Fresh-water mollusk shells are rare in central-basin sequences, but ostracodes and other microfossils have been recovered (L.D. Carter, written comm., 1988).

In a series of measured sections from northern Seward Peninsula, thaw-lake sediment suites of latest Pleistocene and Holocene age are 1.3 to 4.0 m thick (median 2.0 m, n=5), while older thaw-lake sediment suites are 2.3 to 5.0 m thick (median 3.5 m, n=8). The thicker thaw-lake sediment sequences were probably deposited in basins developed in loess with syngenetic ice wedges. Most of the generally thinner Holocene thaw-lake sediment sequences were deposited in second- or third-cycle thaw lakes in which only epigenetic wedges had developed. The latest Pleistocene and Holocene sediment suites have thicker basal transgressive sequences (median 1.0 vs 0.3 m) and thinner basinal sequences (median 2.0 vs. 3.5 m) than do older Pleistocene sediment suites. The greater abundance of organic remains in the latest Pleistocene and Holocene thaw lakes accounts for their generally thicker basal transgressive sequences.

CONCLUSIONS

A distinctive sediment suite is deposited in thaw lakes, and ancient thaw-lake sediment suites are easily recognized on the basis of the underlying series of ice-wedge pseudomorphs and the presence of mixtures of fossils of terrestrial upland and fresh-water aquatic organisms. Study of the taphonomy of organic remains in modern thaw lakes and of the character of organic remains in ancient thaw-lake deposits provides an opportunity for detailed reconstructions of the vegetation at different times during the Pleistocene.

ACKNOWLEDGEMENTS

We gratefully acknowledge the financial and logistic support of the United States Geological Survey and the United States National Park Service. The interest and support of Ms. Jeanne Schaaf of the National Park Service was especially helpful. We benefited from thoughtful critical reviews by L.D. Carter, A.L. Washburn, and R.E. Nelson.

REFERENCES

Are, F.E. (1973). Development of thermokarst lakes in Central Yakutia: International Conference on Permafrost, 2nd., Yakutsk, USSR, Guidebook, 29 p.

Billings, W.D. and Peterson, K.M. (1981). Vegetational change and ice-wedge polygons through the thaw-lake cycle in Arctic Alaska: Arctic and Alpine Research, v. 12, p. 413-432.

Black, R.F. (1951). Eolian deposits of Alaska: Arctic, v. 4, p. 80-111.

Carson, C.E. (1968). Radiocarbon dating of lacustrine strands in Arctic Alaska: Arctic, v. 21, p. 12-26.

Carson, C.E. and Hussey, K.M. (1962). The oriented lakes of Arctic Alaska: Journal of Geology, v. 68, p. 417-439.

Carter, L.D. (1987). Loess, syngenetic ice wedges, and deep thermokarst basins on the Alaskan north slope (this volume).

Hamilton, T.D. (1986). Late Cenozoic glaciation of the central Brooks Range: in Hamilton, T.D., Reed, K.M., and Thorson, R.M., Glaciation in Alaska: the Geologic Record: Alaska Geological Society, p. 9-49.

Harry, D.G. and French, H.M. (1983). The orientation and evolution of thaw lakes, southwest Banks Island, Canadian Arctic: in Permafrost, Fourth International Conference, National Academy of Science Press, p. 456-461.

Hopkins, D.M. (1982). Aspects of the Paleogeography of Beringia: in Hopkins, D.M., Mathews, J.V., Jr., Schweger, C.E., and Young, S.B., 1982, Paleoecology of Beringia, Academic Press, p. 3-28.

Hopkins, D.M. (1949). Thaw lakes and thaw sinks in the Imuruk Lake area, Seward Peninsula, Alaska: Journal of Geology, v. 57, p. 119-131.

Hopkins, D.M. and Robinson, S.W. (1979). Radiocarbon dates from the Beaufort and Chukchi Sea coasts: U.S. Geological Survey CIrcular 804-B, p. 44-47.

Kaplina, T.N. and Lozhkin, A.V. (1984). Age and history of accumulation of the "ice complex" of the maritime lowlands of Yakutiya: in A.A. Velichko, ed., Late Quaternary environments of the Soviet Union, University of Minnesota Press, p. 147-151.

Kaufman, D.S. and Hopkins, D.M. (1985). Late Cenozoic radiometric dates, Seward and Baldwin Peninsulas, and adjacent continental shelf, Alaska: U.S. Geological Survey Open-File Report 85-374.

Livingstone, D.A., Bryan, K., Jr., and Leahy, R.G. (1958). Effects of an arctic environment on the origin and development of freshwater lakes: Limnology and Oceanography, v. 3, p. 192-214.

McCulloch, D.S. and Hopkins, D.M. (1966). Evidence for an early recent warm interval in northwestern Alaska: Geological Society of America Bulletin, v. 77, p. 1089-1108.

McCulloch, D.S., Taylor, D.W., and Rubin, M. (1965). Stratigraphy, non-marine mollusks and radiometric dates on Quaternary deposits in the Kotzebue Sound area, western Alaska: Journal of Geology, v. 73, p. 442-453.

Nelson, R.E. (1982). Late Quaternary environments of the western Arctic slope, Alaska: University of Washington Ph.D. thesis, 146 p.

Rex, R.W. (1961). Hydrodynamic analysis of circulation and orientation of lakes in northern Alaska: in Raasch, G.O., ed., Geology of the Arctic, v. 2, University of Toronto Press, p. 1021-1043.

Sellmann, P.V., Brown, J., Lewellen, R.I., McKim, H., and Merry, C. (1975). The classification and geomorphic implications of thaw lakes on the Arctic coastal plain, Alaska: U.S. Army Corps of Engineers, Cold Regions Research and Engineering Laboratory, Research Report 344, 21 p.

Walker, D.A., Webber, P.J., Binnian, E.F., Everett, K.R., Lederer, N.D., Nordstrand, E.A., and Walker, M.D. (1987). Cumulative impacts of oil fields on northern Alaskan landscapes: Science, v. 238, p. 757-761.

Williams, J.R. and Yeend (1979). Deep thaw lake basins of the inner Arctic Coastal Plain, Alaska: U.S. Geological Survey Circular 804-B, p. B35-B37.

PERIGLACIAL SOIL STRUCTURES IN SPITSBERGEN AND IN CENTRAL EUROPA

A. Jahn

Institute of Geography, University of Wroclac, Poland

SYNOPSIS

The contemporaneous climate of Spitsbergen changes from humid-maritime on the coast to dry-continental in the interior. These differences in periglacial environments manifest themselves in contrasting structures of the active layer of permafrost. The climate of the periglacial zone of the last glaciation in Europe is also differentiated - that is, more oceanic in the west and more continental in the east of Europe, there are different fossil periglacial structures in the both parts. The transitional section of this zone lay in its narrowest part, between the Scandinavian ice border and the northern timber line of the Alps and Carpathians Mountains. The mixed periglacial soil structures of this area resemble in some degree the contemporaneous structures of Spitsbergen.

INTRODUCTION

The climate of Svalbard archipelago with the Spitsbergen island as its main area, is controlled by the influences, from the Atlantic and Arctic Ocean (Fig. 1). It represents the transitional area between two variants of periglacial climates. The Arctic Ocean is covered with sea ice - its effect on the climate does not differ from that of cold land areas. The cold air mass, the arctic anticyclon, affects the Svalbard climate from the north and east, the south and west part is affected by the warm water of the Atlantic and Icelandic flow. Stäblein (1982) - while investigating the aridity of the Arctic included Svalbard in the "cryo-arid geomorphodynamic system" of semiarid areas. The mean annual air temperature varies around - 6°C, which makes Spitsbergen an area of permafrost. The summer lasts for three months, June, July, August, with a mean temperature of 3°C to 5°C. The summer thawing of soil extends to a depth of 0,5 to 2,0 m.

The climatic continentality of Spitsbergen depends on the general situation mentioned above and on this kind of factors like glacier covering the whole interior of the island. In the interior of the fiords the total annual precipitation, about 200 mm, is half that on the coast (over 400 mm). The climate of the interior shows continental features, whereas at the outlet of the fiords facing the Atlantic Ocean the climatic condition are maritime, which means more precipitation, cloudiness, fog and stronger winds.

PERIGLACIAL SOIL STRUCTURES IN SPITSBERGEN

There exist two dependences of soil thawing and soil structures-local and regional. The dependence on the local environmental factors have provided the following model indicating that sandy-gravelly raised beaches without vegetation thaw three times faster than silty soil of the tundra area. Thus, local factors are the dominant control of active layer depths, as previously recognized (Washburn 1979). These findings may be of great significance to the interpretation of Pleistocene structures of the periglacial environment.

According to the regional climatic condition we can distinguish two groups of periglacial features containing more maritime or continental elements (see fig. 1).

In the category of maritime forms and structures I include sorted circles and polygonal nets, which result from very intensive frost sorting, i.e. frost heave and size segregation (Jahn 1961). The processes tend to be most active in water-saturated soil in the areas of more frequent precipitation and limited evaporation. The classic Spitsbergen soil polygons, very known in the literature, are on coastal terraces at the outlets of the fiords, such as Kongsfiord, Isfiord, Bellsund and Hornsund. There exist here ice wedges "in statu nascendi", i.e. thin, fresh ice veins. There are here also the traces of older ice wedges greater in size, developed probably in the colder postglacial climatic phase.

Gelifluction is a dominant process in the coastal zone, everywhere on the slopes up to about 25°. The movement is very fast, reached on selected slopes 12 cm (1957-1960), and even to 27 cm (1979-1984) yearly. The movement involved the entire active layer. A variety of structures can be found in the more arid, continental part of the archipelago, in the interior of the fiords, and closer to the central ice caps.

I regarded as most significant features the soil wedges on alluvial fans in Van Mijenfiord (Jahn 1983). The area is a typical "polar desert", almost devoid of vegetation. The same in Tempelfiord. The most striking surface features are the regular polygons. The soil wedges contain fine-grained debris. There resemble "sand wedges" in Antarctica.

Another phenomenon related to the continental climate of the Spitsbergen interior are rhytmically bedded slope deposits in the Van Mijenfiord, in Tempelfiord, in Gröndalen. On the steep slopes, close to the angle of repose, the process of sorting takes place with in the active layer. Its lower part is moist and stable, the moisture being derived from permafrost. The upper, a 10 - 15 cm layer is well desiccated and loose. When gravitational stress exceeds the internal friction, the desiccated layer begins to slip. As motion occurs vertical grading develops giving rise to rhythmically bedded sedimentary structures resembling "grezes litées".

Another common features related to Spitsbergen, in both areas, maritime and continental, are sheets with erosion on slopes. It has been measured near the Polish Research Station at Hornsund in the coastal area (Jahn 1961) and observed in the interior, in the Van Mijen and Tempelfiord. It seems to be, that slopewash is more effective on bare surfaces of dry continental region than on the protected by vegetation wet maritime area.

Surface chemical and physical weathering phenomena, as they are often regarded as indicators of the climate, are observed in both climatic regions of Spitsbergen. They are desiccation an frost cracks, they are brown to rusty-brown crusts and coatings similar to desert varnish on the rocks near Hornsund and in Tempelfiord.

Erosion by winds is also widespread in Spitsbergen. Deflation occurs both in maritime zone where winds are strong but the soil is protected by vegetation, and in the continental part where the winds are weaker but the soil and rocks unprotected. The easterly an north- easterly winds prevalent in winter erode loose rocks and polish solid rocks mainly with snow and ice particles.

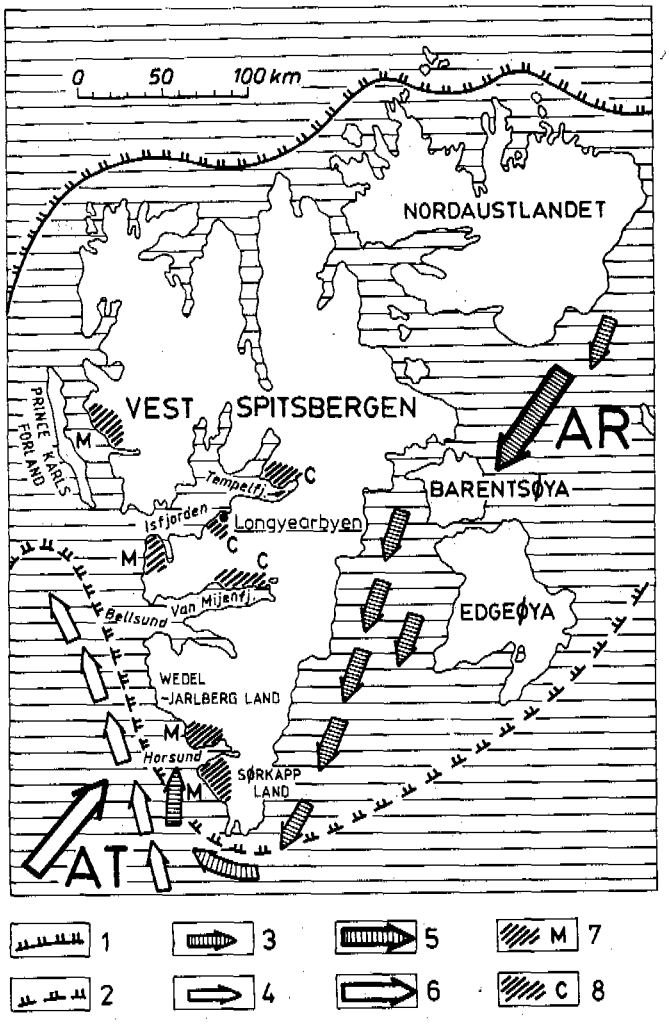

Fig. 1. Svalbard Islands situated in the transitional climatic zone. Limit of annual Arctic sea-ice cover in summer /1/ and of floating pack ice in winter /2/. Arctic /3/ and Atlantic /4/ sea currents. Direction of climatic influence of Arctic /5/ and Atlantic /6/. Investigated areas with periglascial maritime /7/ and inland-continental /8/ features.

SOME PERIGLACIAL FORMS AND STRUCTURES OF THE CENTRAL EUROPEAN AREA.

The periglacial zone of the last Würm -Vistulian glaciation extends from Western Europe over France, Germany, Poland and the Soviet Union to easternmost Asia. H. Poser (1948) was the first researcher who distinguished the maritime from the continental part of former climate of this area. Starting with Büdel's (1951) map of vegetation during the last glaciation and adding B. Frenzel's (1967), L. Eissmann's (1981), H. Maruszczak's (1987) and my own observations, I reconstructed the periglacial provinces of Europe, as is shown in Fig.2. The most important periglacial zone, containing continuous permafrost, is limited in the Central Europe, to a 500 km wide strip extending from the front of Scandinavian ice-sheet to the northern boundary of Carpathians and Sudety Mts. It was frost debris zone ("Frostschuttzone" of Büdel, 1948) resembling a "polar desert". This province is wider to the east and west, its south boundary is controlled by the Central European Mountains, from the Carpathians to the Alps. These mountains defining the northern timber line, there were not only "forest islands" (Beug, from Nilson 1983) but, due to their altitude, they formed in the Pleistocene an important climatic barrier to air mass circulation. The west-east exchange of these masses created the base of the climatic variations. Therefore I concider the Central European "corridor" as the transitional periglacial zone (TZ).

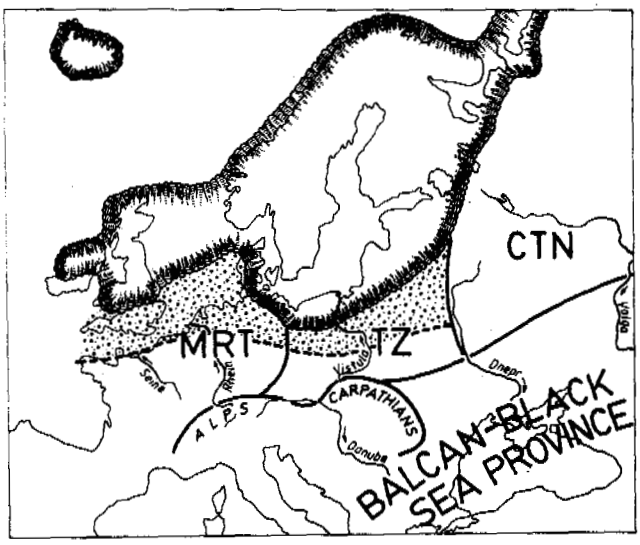

Fig. 2. Periglacial zone during maximum range of last glaciation /Vistulian/ in Europe. Maritime part /MRT/, continental part /CTN/ and transitional part /T Z/. Dotted stripe frost debris zone.

This province grades to the east into areas of continuous permafrost containing plant elements of a warmer summer and different periglacial soil structures. According to Velitchko (1973), east of Dnepr thermocarstic structures prevail.

There is glacial-continental (CTN) province. To the west the periglacial zone passes, without distinct border to glacial-maritime (MRT) province with the rich periglacial structures, mostly in loess. According to Maruszczak (1987) it was a region of discontinuous permafrost. The three main periglacial provinces of Europe was bordered to the south by a dry cold tundra steppe, known in Czechoslovakia and particularly in Middle Danubian Lowland in Hungary. I distinguish as a separat region "Balcan-Black Sea province" the pleistocene cold steppe, loess covered but lacking typical periglacial structures. According to Maruszczak (1987) it was the area of sporadic permafrost, very dry, with annual precipitation lower than 200 mm.

The classic periglacial polar area of the last glaciation in Europe was the above mentioned transitional area of Poland, east and west Germany containing on the continuous permafrost the full range of periglacial structures, similar to recent periglacial features of Spitsbergen. It was extensively studied (Dylik 1956, Kaiser 1960, Jahn 1975). The active layer in this zone ranged from 1 m in the north to 3 m in the south (Jahn 1977).

Gelifluction structures are very common in the deposits of the last glaciation in Poland. Some of them like the classic profile of St. Malgorzata Hill near Lódz (Dylik 1963) may be compared to gelifluction tongues in Spitsbergen. They are soilrubble mass, with earth flow rather than frost creep structures.

Ice wedges, frost fissures and soil (ground) wedges have thus far been the best indicators of the former periglacial permafrost climate in Europe. The Central European transitional sector of the periglacial zone (TZ) possesses all types of wedge structures. Primary ice wedge casts, particular eolian sand wedges, are known mainly in Central Poland (Gozdzik 1973). Similar examples from the continental part of Spitsbergen (Van Mijenfiord) suggest that fossils European wedges reflect a relatively arid Pleistocene climate with the mean annual air temperature less than -6° C. The other types of wedge structures, with the secondary infilling, (ice wedges) which are very common, on the Central European area (Kaiser 1960), suggest rather wet climate condition with vegetation cover on the surface like the coastal zone of Spitsbergen. The existence of the both types of wedges can be interpreted at the proof of the changing climatic condition in the transitional periglacial zone of Central Europe.

Another problem emerges when we take into account the rich varieties of periglacial structures in specific study area, even in the same section of quaternary deposits in Central Europe. The numerous cross-sections in Poland and Germany show the alternation of the gelifluction and wedge structures (Jahn 1969, Jersak 1975, Rohdenburg 1967, Brunacker 1982), what confirmed the thesis of the temporal oscilations between wet and dry climate, in the area of the above mentioned "corridor" (TZ). From the beginning of the last glaciation to Bölling there occurred at least four or five warmer more humid phases (gelifluction) followed by colder and drier periods.

And now the problem of rhytmically stratified slope deposits. According to Dylik (1960) they are common in the periglacial environment of Central Poland. Rhytmically bedded slope deposits are known in Sudetes and Carpathians Mts. According to Guillien (1951) the classic "grezes litées", known in France, are controlled rather by bedrock i.e. when the bedrock is readily desintergrated by frost action such as shale or limestone. There are not clear relations between the rhytmically bedded slope deposits and the climate-continental (Spitsbergen's interior, Poland) or maritime (France).

What concerns the wind action in both environments, contemporanoues in Spitsbergen and Pleistocene of Central Europe, we can note the following facts. The most common erosional wind products in Spitsbergen are "surface facets", which are "large facets developed upon rounded blocks normally of glaciofluvial origin" (Akerman 1980), polished mainly, as I mentioned above, with snow and ice particles. They contrast with the smaller but more sharply defined "edge facetes", typical ventifacts (germ. "Dreikanter") which are more common in Pleistocene sediments from Central Europe. In Europe the abrasive material was sand which was naturally abundant in "pradolinas" ("Urstromthäler") i.e. broad valley trenches parallel to continental ice sheet margins, with its abundace of fluvial

and fluvioglacial sediments. The differences substance of material transported by winds and not climatic reasons would then account for the distinct forms of stones in the Pleistocene area.

CONCLUSIONS

This brief comparison between the Central-European periglacial sructures of the last glaciation and the contempraneous Spitsbergen structures leads to the following conclusions.

1. A rich variety of periglacial structures can be found in both areas, reflecting the great spatial and temporal variability of the climate in periglacial environments.

2. The variety of periglacial structures in Spitsbergen results from the following factors:

   a/ The archipelago is situated in transitinal zone between the interior of the Arctic and Atlantic zone influenced by the Icelandic flow.

   b/ The climatic parameters of the dry interrior differ from those of the humid coastal areas of the archipelago.

   c/ The local (azonal) environmental factors (soil, vegetation, moisture) are as important as regional (zonal) climatic characteristics in controlling structures of the active layer.

   d/ The forms and structures vary both horizontaly and verticaly. Only the periglacial structures of the low coastal terraces bear comparison with one another. The permafrost structures of mountain areas are different.

   e/ Not all Spitsbergen periglacial structures visible at present reflect the prevailing climatic conditions. Part of them can be regarded as fossilized structures from different past climates. Thus there are decayed structures, as well as structures in different stages of development. This facts has hitherto received very little attention.

3. The varity of periglacial forms and structures of the last glaciation in Europe reflect temporal variations in local and regional climatic conditions:

   a/ In the transitional zone of Central Europe ("corridor" TZ) there is a full variety of periglacial structures with their periglacial maritime and continental facies changing spatially and temporally. They are comparable with the periglacial structures of Spitsbergen.

   b/ It is difficult to descern precisely the dependence of these structures on the local, environmental factors.

   c/ The thickness of active layer grows from north to south, from west to east, and reaches up to 3 m. The summer of the Pleistocene periglacial zone is likely to have been warmer than the present Spitsbergen summer.

   d/ Periglacial structures provide numerous data useful to the understanding the glaciation period, and specifically the changes of the degree of continentality of the climate. This result is important in the assesment of the stratigraphy of the Pleistocene deposits.

ACKNOWLEDGMENTS

Professor A. Lincoln Washburn formulated the problem of "the periglacial environment" and has stimulated comparative investigations of the contemporary and Pleistocene periglacial zone. As he put it in 1985: "The reconstruction of past climates through periglacial evidence requires extreme caution, but also holds promising rewards. To aid interpretations, high priority should be given to critical paleoenvironmental studies comparing the periglacial evidence witch derived from other types of proxy data".

This idea became a direct inspiration for this paper which I presented at the conference held to honor of Prof. A.L. Washburn in Seattle, May 27, 1986. I would not miss the opportunity for expressing heartfelt gratitude to Link Washburn for his valuable advice and help. However, most of all I wish to express my appreciation for the stimulating exchange of ideas during our frequent personal contacts.

REFEREBCES

Brunnacker, K /1982/. Aolische Deckschichten und deren fossile Böden im Periglazialbereich Bayerns. Geol. Jb. F. 14, Hannover, 15-25.

Büdel, J /1948/. Die Klima-morphologischen Zonen der Polarländer Erdkunde 2, 22-53.

Büdel, J /1951/. Die Klimazonen des Eiszeitalters, Eiszeitalter u. Gegenwart, I, 16-26.

Dylik, J /1956/. Coup d'oeil sur la Pologne periglaciaire. Biuletyn Peryglacjalny, No 4, 195-238.

Dylik, J /1960/. Rhytmically stratified slope waste deposits. Biuletyn Peryglacjalny, No 8, 31-41.

Dylik, J /1963/. Periglacial sediments of the Sw. Malgorzata Hill in the Warsaw-Berlin prodolina. Bull. Soc.Sc. et Lett. de Lódz, XIV, 1-16.

Eissmann, L /1981/. Periglaziare Prozesse und Permafrost strukturen aus sechs Kaltzeiten des Quartärs. Altenburger Naturwissensch. Forsch. H. 1-171.

Frenzel, B /1967/. Die Klimaschwankungen des Eiszeitalters. Die Wissenscraft, 129 Braunschweig, 1-291.

Gozdzik, J / 1973/. Geneza i pozycja stratygraficzna struktur peryglacjalnych w srodkowej Polsce /Origin and stratigraphical position of periglacial structures in middle Poland/, Acta Geographica Lodziensia 31, 1-119.

Guillien, Y /1951/. Les greze litées de Charente. Rev. Geos. pyrenées Sud-ouest, 22, 154-162.

Jahn, A /1961/. Quantitative analysis of some periglacial processes in Spitsbergen. Zesz.Nauk. Uniw. Wroclawskiego, Ser. B, No 5, 1-54.

Jahn, A /1969/. Structures périglaciares dans les loess de la Pologne, Biuletyn Peryglacjalny, 20, 81-98.

Jahn, A /1975/. problems of the periglacial zone, Polish Scientific Publishers, 1-202.

Jahn, A /1977/. The permafrost active layer in the Sudety Mountains during the last glaciation. Quaestiones Geographicae, Nr 4, 29-42.

Jahn, A /1983/. Soil wedges in Spitsbergen Permafrost, Fourth Intern. Conf. Fairbanks, Alaska. Proceedings, Nation. Acad. Press, Washington D.C., 525-530.

Kaiser, K /1960/. Klimazeugen des periglazialen Dauerfrostbodens in Mittel- und Westeuropa. Eiszeitalter u. Gegenwart, B. 11, 121-141.

Maruszczak, H /1987/. Problems of paleographic interpretation of ice wedge casts in European Loessess. Loess and Periglacial Phenomena. Akademiai Kiado, Budapest, 285-302.

Nilson, T /1983/. The Pleistocene, Geology and life in the Quaternary Ice Age, Stuttgart, 1-651.

Poser, h /1948/. Boden-und Klimaverhältnisse in Mittel und Westeuropa während der Würmeiszeit. Erdkunde, 2, 53-68.

Rohdenburg, H /1967/. Eiskeilhorizonte in südniedersächschien und nordhessioschen Lössprofilen. Biuletyn Peryglacjalny, 16, 225-246.

Stäblein, G /1982/. Aride Züge im Georelief und Klima der Polargebiete. Würb. geogr. Arbeiten. Würzburg, B.56, 167-180.

Velitchko, A A /1973/. The natural process in Pleistocene /in Russian/. Izdat. "Nauka" Moskwa, 1-254.

Washburn, A L /1979/. Geocryology, A survey of periglacial processes and environments. Edward Arnold, London, 1-406.

Washburn, A L /1985/. Periglacial problems. Field and theory, Lectures in Geocryology ed. by M. Church and O. Slaymaker, Univer. of B.C. Press, Vancouver, 166-202.

CONTINUOUS PERSISTENCE OF THE PERMAFROST ZONE DURING THE QUATERNARY PERIOD

E.M. Katasonov

Permafrost Institute, Siberian Branch of the U.S.S.R. Academy of Sciences,
Yakutsk, U.S.S.R.

SYNOPSIS This paper provides a rationale to the conception of a continuous persistence of the frozen Earth's crust, the cryolithozone. Cryogenic-geological evidence is given in favour of the absence in the Pleistocene of warm interglacial epochs. It is shown that Quaternary deposits of the permafrost zone had been forming under dissimilar physico-geographical conditions. However, at one time they all underwent the influence of a perennially frozen substrate occurring at little depth, which is indicated by ice veins, pseudomorphous structures on them and, primarily, by leading cryogenic structures, viz. traces of freezing of the seasonally thawing layer and taliks. The conclusion about a continuous persistence of the permafrost zone would be of interest to specialists doing research on many Earth sciences.

M.I. Sumgin (1937) was the first to suggest that the permafrost origin dates back to remote times and has persisted until the present. This suggestion which, in general terms, was also reported by other investigators, is in contradiction with the commonly accepted view that cold and warm interglacial epochs were alternating during the Pleistocene. Therefore, it has long not been taken seriously and was not reflected in paleoclimatic and stratigraphic schemes. A large number of researchers continue to classify frozen deposits into suites and horizons corresponding, in their opinion, to warm and interglacial epochs. The basis for this is provided mainly by palinological data (spore-pollen diagrams) as well as bundles of layers encountered in sections, with thawed-out ice veins (pseudomorphoses), and other features of thawing and re-freezing of these layers in the past. Formation of thermokarst forms of the relief has not infrequently been attributed to the general, global warming of climate as well.

The past history of formation of the frozen Earth's crust (the permafrost zone) cannot be reproduced through usual reconstructions of paleoclimates on the basis of remains of plants and animals. In order to accomplish this it is necessary to have data on perennially frozen deposits and cryogenic phenomena characteristic of them. Unfortunately, these latter are more frequently regarded as superposed 'permafrost traces' which are genetically unassociated with host ground and, therefore, their interpretation is misleading. For example, ice veins are associated with cold epochs or glaciation stages, although at the present time they are forming everywhere in the presence of moist landscapes with a frozen substrate occurring at little depth (less than 1 m). Ice veins are virtually lacking in dry regions, even with very low (minus 10 to 12°) mean annual air temperatures.

Pseudomorphoses are also interpreted misleadingly when their formation is associated with an overall warming of climate. Indeed, such wedge-like earthen bodies are formed in all climatic zones of the permafrost region in limited areas as a result of a change in conditions for accumulation of sediments and, most frequently, inconnection with an expansion and displacement of shallow water reservoirs of water flows. This accounts for the fact that sections lying on the same horizon with pseudomorphoses exhibit also primordial ground and ice veins (Katasonova, 1963; Katasonov, 1973).

An important significance for the understanding of the structure, origination and evolution of the frozen Earth's crust have the study of thin (a few cm) ice lenses and interlayers which produce typical, leading cryogenic structures (Fig. 1): belt-shaped and layered for subaerial deposits and latticed, oblique and vertical for subaqueous deposits (Katasonov, 1968;1975). These structures, while forming as deposits are accumulated, pattern after the unevenness of the lower limit of the seasonally thawing layer and the contour of taliks. They provide crucial diagnostic features of cryolithogenic (i.e., forming under permafrost conditions) deposits. By studying them in sections dated, we are able to gain insights into the past evolution of the permafrost zone and establish the age of the oldest (for a given region) syngenetically frozen rocks.

Leading cryogenic structures are also used as additional, cryogenic-facial features which help distinguish aqueous deposits deposits from surface (subaerial) ones, and slope deposits from flood land ones, even if these deposits show the same granulometric composition and are devoid of remains of fauna and flora. Cryogenic structure provide a means to recognize and estimate the scale of occurrence of taberal, i.e., thawed and re-frozen, rocks (Katasonov,

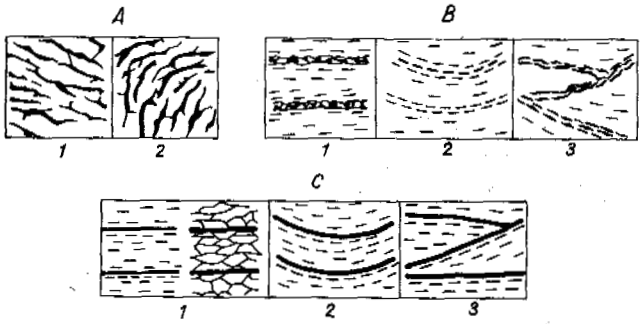

Fig.1 Leading Cryogenic Structures of Cryolithogenic Deposits.
A - Latticed (are Formed as Taliks are being Frozen on the Sides and from below, on the Side of a Perennially Frozen Substrate): 1 - oblique, 2 - vertical; B - belt-shaped, C - layered (are formed as the seasonally frozen layer freezes from below): 1 - horizontal, 2 - concave, 3 - gentle-wavy.

1982), determine the size of pre-existing taliks and the thickness of the seasonally thawing layer and its moisture content as well as understand the peculiarities of permafrost landscapes of the past epochs.

A comparative cryogenic-facial analysis of contemporary and Pleistocene permafrost deposits of Siberia has led us to conclude that cryogenic structures, together with ice and various earthen veins are distributed in the frozen Earth's crust showing a general rule. Their presence or absence in some or other layers is associated with genesis, accumulation and freezing of deposits rather than with coolings or warmings of climate. Direct evidence based on the study of cryogenic phenomena themselves were obtained for the continuous formation of the permafrost zone during the course of the Quaternary period, namely

1. For all sections of the Siberian permafrost - in the basins of the Kolyma, Omoloi, Yana, Yenisei, Vilyuy and Aldan rivers - none of the levels showed signatures of overall, regional degradation of the permafrost zone; and no horizon of ground was encountered, the freezing of which was unassociated with a direct or indirect influence of the perennially frozen substrate that persisted as that ground had been freezing. Deposits which are regarded as interglacial do not provide evidence for warm climate either - they include ice veins and have layered or oblique cryogenic structures, i.e., traces of freezing of the seasonally thawing layer and taliks (Katasonov, 1963; 1965; 1975; 1983; Trofimov and Vasil'chuk, 1983).

2. Taberal soils with obvious signatures of thawing and re-freezing encountered in the sections have a localized occurrence, in the form of relatively small, spacially confined bodies (Fig. 2). Their thermal treatment has been and is occurring at the present time in taliks below water reservoirs, whose sediments normally overlie them. If interglacial epochs were associated with substantial warmings of climate, then the thermally treated ground in the form of horizons maintained in extent would everywhere be observed over a vast area, but this is not the case, however. Numerous traces of localized thawing below water reservoirs indicate only their major role for the formation of the permafrost zone and its stability throughout the Quaternary period.

3. The conclusion about the continuous persistence of the permafrost zone is confirmed by paleopermafrost investigations as well as results of a study of the accumulation and freezing conditions for sediments in the Pleistocene and Holocene. For low-lying, elevated and slopy near-mountain plains of Yakutia, this situation was characterized by the replacement in time of lacustrine, continuous flood land, marshland and relatively dry permafrost landscapes due to glaciation and the overall expansion, contraction and disappearance of glaciers and snowfields (Katasonov, 1963; 1975; 1983; 1986). The past evolution of the permafrost zone can be categorized into three relevant stages, namely epochs distinguished by dissimilar formation conditions for subaerial, subaqueous deposits and taberal soils. In each stage the role of the main components of permafrost landscapes, viz. the perennially frozen substrate, the associated taliks and of the seasonally thawing layer, has manifested itself differently.

I. At the epoch of maximum occurrence of glaciers and snowfields ($Q_2 + Q_3^1$) on low-lying and near-mountain periglacial plains, running-water and stagnant reservoirs recurred with different sizes and lifetimes. Below them, there occurred a consedimentational (simultaneous with sediment accumulation) thawing of deposits which had recently gone into a perennially frozen state; taliks were formed and, upon their freezing, there formed masses of contaberal rocks which not infrequently involve syngenetic pseudomorphoses along ice veins (Fig. 2, II, III, legend 6).

II. The stage of glacier recession and contraction and localization of snowfields (Q_3^2) was marked by the predominance - on all elements of the relief - of continuous flood lands and marshlands. Cryolithogenesis processes were occurring mainly within the seasonally thawing layer. Taliks played the smallest role. Everywhere, even on watershed slopes, there formed deposits involving ice veins, belt-shaped and layered cryogenic structures (Katasonov, 1983).

III. The contemporary stage of formation of the frozen Earth's crust (the past 10 to 15 thousands of years) is characterized by an almost total absence of glaciers and snowfields, aridization and by some warming of climate as well as the appearance of contemporary humid and semi-arid permafrost landscapes. The disappearance of the periglacial situation led to a cessation of flood-land sediment accumulation associated with the thawing of glaciers and snowfields, and to permafrost degradation toward the edges of the permafrost region. In Yakutia, on pre-existing periglacial plains which have become denudation plains, a deep

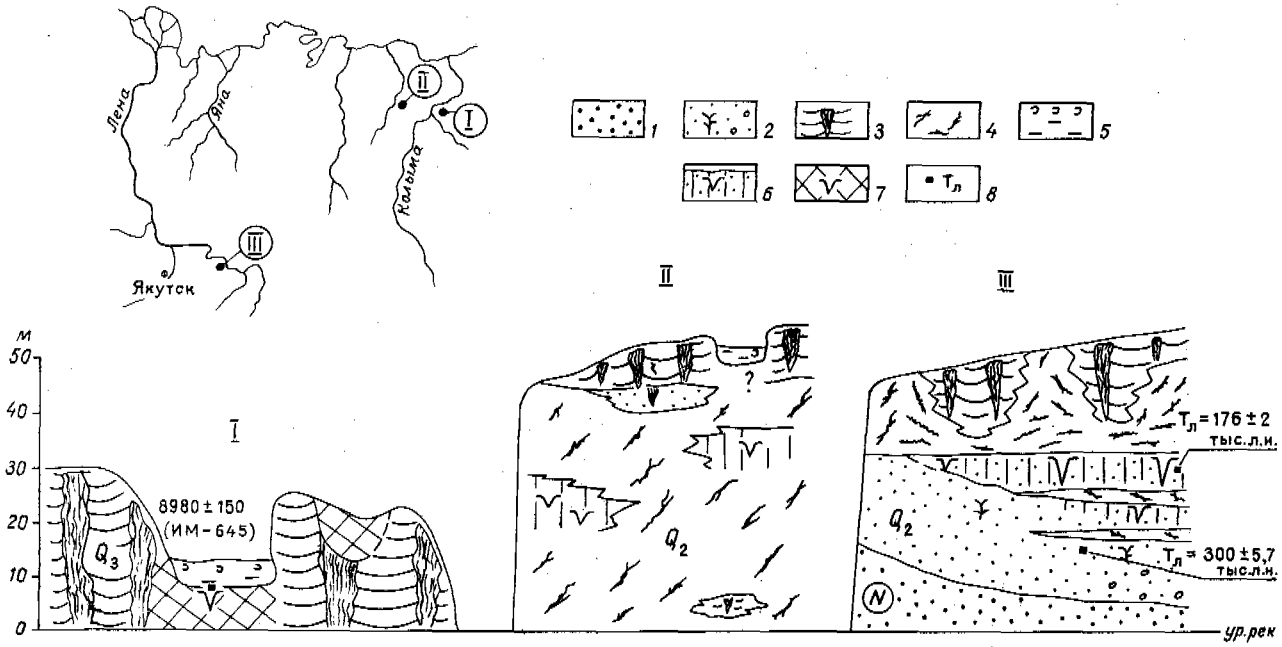

Fig. 2 Thermally Treated (Taberal) **Grounds** in Shore Sections: I - Kolyma River, below the Mouth of the Omolon River; II - Alazeya River, below the Andryushkino Settlement; III - Aldan River, Mamontova Gora (Mountain).
1 - sands with remnants of heat-loving flora; 2 - sands with primordially earthen veins of folding; 3 - subaerial deposits with ice veins and layered and belt-like cryogenic structures; 4 - subaqueous deposits with oblique and vertical cryogenic structures; 5 - deposits of alas depressions: boggy (top) and lacustrine (bottom); 6 - contaberal **rocks** with pseudomorphoses along ice veins; 7 - posttaberal formations with pseudomorphoses; and 8 - thermo-luminescence and radiocarbon dating.

postsedimentation thawing of ice-containing layers began. Thermokarst depressions (alas) were produced, with characteristic alas deposits supported by posttaberal formations (Fig. 2, I, legend 5 and 7). These latter, while being bounded by taliks below an alas, underwent substantial changes. Brownish-grey supes and sands that gave rise to their formation, acquired a different cryogenic structure and turned darker, bluish in colour - the composition of their clayey cement changed as well as the content of organo-mineral compounds, filiform rootlets of grass disappeared and a reduction of ferric oxides occurred (Katasonov, 1982).

Thus, the role of the perennially frozen substrate as the main factor of cryolithogenesis was manifest during all stages of formation of the permafrost zone. During the past 10 to 15 thousands of years its upper horizons have been subjected to an intense treatment by taliks. At the same time new layers of permafrost have been formed and continue so today in all climatic zones of the permafrost region. This provides firm evidence for the continuous persistence of the permafrost zone in the past as well as favours the predictability of its existence in a foreseeable geological future.

The conclusion about the continuous persistence of the **cryolithozone** during the Quaternary period is, we believe, important for scientific and practical purposes. It should be taken into account when interpreting geothermal data as well as constructing stratigraphic and paleogeographic schemes and thermal and other models of freezing of the Earth's crust. This conclusion is of major importance for the understanding of the structure of permafrost and for its classification into complexes of **rocks** distinguished by the composition, the content of **the ground** ice, the cryogenic structure and, hence, by engineering-geological properties. The identification and mapping of such **cryogenic**-formation complexes (Katasonov, 1983) is needed for economic development of the permafrost region.

REFERENCES

Katasonov, E.M. (1963). Merzlotno-fatsialny analiz chetvertichnykh otlozheniy nizhnei chasti basseina r.Tumary. - V kn.: Usloviya i osobennosti razvitiya merzlykh tolshch v Sibiri i na Severo-Vostoke. 5-24, Moscow: Izd. AN SSSR.

Katasonov, E.M. (1965). Merzlotno-fatsialnye issledovaniya mnogoletnemerzlykh tolshch i voprosy paleogeografii chetvertichnogo perioda Sibiri. - V kn.: Osnovnye problemy izucheniya chetvertichnogo perioda.

286-294, Moscow: Nauka.

Katasonov, E.M. (1968). Features of deposits formed under permafrost conditions. - Arctic and Alpine Environments, 237-240, Indiana University Press.

Katasonov, E.M. (1973). Present-day ground- and ice veins in the region of the middle Lena. - Biuletyn Peryglacialny, No. 23, 81-89, Lodz.

Katasonov, E.M. (1975). Frozen-ground and facial analysis of pleistocene deposits and paleogeographyc of central Yakutia. - Biuletyn Peryglacialny, No. 24, 34-41, Lodz.

Katasonov, E.M. (1982). Alasnye otlozheniya i taberalnye obrazovaniya Yakutii. - V kn.: Geologiya kainozoya Yakutii. 110-121, Yakutsk: Izdan Yakut. filialom SO AN SSSR.

Katasonov, E.M. (1983). Kriolitogennye otlozheniya, ikh merzlotno-formatsionnye kompleksy. - V kn.: Problemy geokriologii. 162-169, Moscow: Nauka.

Katasonov, E.M. (1986). Ozera oblasti vechnoi merzloty v pleistotsene i golotsene (na primere Yakutii). - V kn.: Istoriya sovremennykh ozer (tezisy). Leningrad-Tallinn.

Katasonova, E.G. (1963). Sovremennye mnogoletnemerzlye otlozheniya i ikh bolee drevnie analogi v severo-vostochnoi chasti Leno-Vilyuyskogo mezhdurechya. - V kn.: Usloviya i osobennosti razvitiya merzlykh tolshch v Sibiri i na Severo-Vostoke. 41-60, Moscow: Izd. AN SSSR.

Sumgin, M.I. (1937). Vechnaya merzlota pochvy v predelakh SSSR. Moscow.

Trofimov, V.T. and Vasil'chuk, Yu.K. (1983). Sinkriogennye povtorno-zhilnye i plastovye l'dy v pleistotsenovykh otlozheniyakh severa Zapadnoi Sibiri. - Byull. Mosk. o-va ispytatelei prirody, otdel geologich., t.58, vyp.4, 113-121, Izd. MGU.

PROBLEM OF INTEGRAL INDEX STABILITY OF GROUND COMPLEX OF PERMAFROST

V.P. Kovalkov[1] and P.F. Shvetsov[2]

[1]Theoretical problems department of the USSR Academy of Sciences
[2]Institute of lithosphere of the USSR Academy of Sciences

SYNOPSIS The problem of choice of integral indeces of stability of the permafrost ground complex was investigated from the stand of general theory of physical systems' stability. It is shown, that there are two such indeces, one of which points out, if the average annual temperature of ground under the season thawing stratum is lower than the temperature of phase transformation of the ground moisture. The second index is the annual increase of thickness of the season thawing stratum. The expressions for the calculation of these indeces are given.

The determination of the conditions of the stability and certain mobility of the ground complex of the permafrost region* is one of the fundamental problems of geocryology and its theoretical nucleus - physical geocryology. The latter opens the physical-geological essence of the change of the state, mechanical solidity, deformation and mobility, the structure and texture, the form of the ground complex surface using the thermodynamical method, Shvetsov (1983), Shvetsov and Kovalkov (1986, 1987).
This method allows to consider the GCPR as unequilibrum, unsteady and generally open and non-linear thermodynamical system, which consists mainly of the substance in condenced state.

At the same time the phenomenological method of approach is used which permits to present the mixture of mineral and organic fractions, ice inclusion, water films and air pores as a continuous medium, marking out some elementary meso-volume V of the system with the mean quantity of all parameters of its thermodynamical state: the external pressure P, temperature T and the concentration C_i of all components, including the humidity and ice content.

*The ground complex of the permafrost region (GCPR) - the upper stratum of the earth crust, including the soil and sub-soil down to the depth, where the annual temperature oscillations practically fade.

Such a thermodynamic system may be considered a complex one, because it has, besides thermal and usual mechanical degrees of freedom (owing to the external pressure P) other mechanical degree of freedom - against the forces of so called internal pressure, which reflects the mutual attraction of molecules. When the ground or water freezes through and the internal energy U of the system decreases and the volume grows, this pressure is negative. Its gradient in the film of unfrozen water, which surrounds the solid fractions, is the well-known "force of absorption" of moisture by the freezing ground mass.

Really, the internal energy U of the elementary meso-volume of the ground mass changes with the parameters of state - V, P,T and C_i. And if P and C_i in the easiest case are constant, then $U = U(V, T)$. When placing the expression of full differential

$$dU = \left(\frac{\partial U}{\partial V}\right)_T dV + \left(\frac{\partial U}{\partial T}\right)_V dT \qquad (1)$$

to the expression of the first law of thermodynamics, we get

$$\delta Q = \left(\frac{\partial U}{\partial V}\right)_T dV + \left(\frac{\partial U}{\partial T}\right)_V dT + \delta A \qquad (2)$$

If to ignore the work of the electrical and surface forces, and the gravity, then $\delta A = P\,dV$. And the expression for the first law of thermodynamics (2) looks:

$$\delta Q = \left(\left(\frac{\partial U}{\partial V}\right)_T + P\right) dV + \left(\frac{\partial U}{\partial T}\right)_V dT \qquad (3)$$

Here $(\partial U/\partial V)_T$ is the pointed out internal pressure. Part of the heat, absorbed by the freezing water because of its isothermal expansion when becoming ice, is the source of increase of free energy of the GCPR in this process. It is owing to the free energy, that there are mechanical works of cryogenic ground heaving and the condensation of mineral stratum, also the formation of new surfaces as the result of cracking of GCPR. The decreasing of the internal energy of GCPR excels the flow of heat into environment. On the contrary, when thawing, the internal energy of GCPR increases to the larger value, which excels the flow of heat from the environment. Though the quantity of heat received by the ground in summer and the loss of heat in winter at the stable conditions are equal.

Such a peculiarity of this complex thermodynamic system - GCPR - must be taken into consideration when resolving the problem of its stability in permafrost region. As a consequence of it is the fact that the most unsteady are frozen silty and clay formations of geocryological systems of Under-Arctic, where there are often the lowest temperatures of the region. Such geocryological systems are characterized by the minimal value of entropy of any meso-volume of the frozen ground and the local maximum of its free energy. They have a tendency to the further accumulation of ice at the foot of the season thawing stratum (STS) during the short periods (5-6 years) of the natural cold snap.

Let us have a look into the notion of the GCPR stability. From the general methotodological point of view the stability may be considered as the dialectic antipode of unsteadiness, Mescheryakova (1981).

In this sense, the lost of GCPR stability can be connected both with the transition of the very icy soil from the frozen state into the thawing one, with the following precipitation and the lost of its mechanical solidity, and with the transition of the soil from the thawing state to the frozen one, with the manifestation of the uneven ground heaving and the cryogenic migration of moisture. Therefore, the stability of the GCPR doesn't always correspond to the increase of its mechanical solidity, since during the freezing and falling of the temperature the mechanical solidity is growing, but the cryogenic migration of moisture and the ground heaving show the unsteadiness. So, in such a wide sense, the stability of GCPR must be considered as the preservation of the form of GCPR surface and the absence of any significant macroscopic transitions of its stratum under the influence of the external mechanical loads changings and the variations of the internal thermodynamic parameters, as a result of the heat and moisture exchange of the ground complex with the environment (atmosphere, hydrosphere, space).

But at present time a narrower meaning of the notion of the GCPR stability is adopted among the geocryologists and builders: the absence of non-elastic deformations and mobility of macroscopic stratum of GCPR while keeping its mechanical solidity under the conditions of change of external influence, which leads to the thawing, increase of temperature, humidity (or salt content) of the soil as well as external pressure on the GCPR. Further the term 'stability' of the GCPR will be used in this very sense. The loss of the stability of GCPR will be connected with the presence of the STS, its growing, the increase of the frozen soil temperature, thawing of ice fractions, which further lead to the thermokarst setlings and slope processes - thermoerosion, solifluction.

The mechanical solidity of ground can be determined by the meanings of the changing parameters of state - temperature, humidity, ice content, pressure. I.e. the local stability in the meso-volume is connected with temperature as the function of state, with the external pressure and negative internal pressure (owing to the molecule contract forces), as well as with the composition of the mixture, consisting of soil fractions, ice and water. On the integral level to confirm the stability of GCPR as the state counter-acting the gravity and pressure forces, without displaying the macroscopic non-elastic deformations and mobility (sliding, slipping down), it is necessary to consider all the non-stationary temperature field of the upper stratum of GCPR with the definite kinetiks of the STS.

With the connection of this fact, at the present time, there are two main engineering-geocryological characteristics of GCPR at the moment of prospecting, which are often wrong understood as the index of stability: they are - the average annual temperature t_g of the ground lower than STS which is equal (if to ignore the geotnermal gradient) to the ground temperature at the depth of the stratum of the annual heat storage (SAHS), and - the thickness of the STS h_{sts}. But these two characteristics can't be 'guaranteed' indeces of the GCPR stability, because they are mainly the result of the heat exchange of GCPR with the atmosphere and space and, consequently, they strongly depend on the thermophysical characteristics of the top-soils (snow, plants), temperature t_s of the conventional surface of the radiational heat exchange and its amplitudes of various mode for a year and long-term cycles. That is why the computer modelling of the temperature field of GCPR for 12-15 or more years often gives a perverted picture, if the low bordering condition of the first gender is taken as a constant negative temperature at the depth of the stratum of annual temperature

storage, which was at the moment of prospecting.

Thus, the problem of GCPR stability in the physical geocryology also supposes to overcome its own scientific methodological difficulties, which must be solved using the basis of the intensivly developing modern theory of the physical systems stability.

Presently, only the system of stability in classic mechanics and equilibrium thermodynamics is the most developed. But their methods can't be used solving the problem of GCPR stability, as it is the most unequilibrium and non-stationary system or the system far from balance. In this branches of physics the stability is connected with the notion of the equilibrium state (or motion), and the influence of small initial purtubations or variations of the parameters near the balance are investigated.

There is the same situation in the problem of using the linear unbalanced thermodynamics for the goal aimed, where the variations of parameters near the stationary (partly balanced) states are investigated, Ebeling (1979).

In the whole the known methods of the stability theory can be classified in the following way:

- the kinetic methods in mechanics (Lyapunov's theory);
- entropy methods, based on the theory of Glensdorf-Prigozhin, using the Lyapunov's functionals;
- the methods of thermodynamical potentials;
- fluctuationals (on the variations of the rates or transitions);
- the energetic methods, investigating the kinetic energy of the purtuberances (in the hydrodynamics) and the potential energy of small oscillations (in the theory of plasma);
- methods of action, based on the variational principle of the smallest action.

It is precisely these methods, which build up the basis of the modern theory of the stability of physical as well as mechanical systems. The main task of this theory is to establish the indeces of stability: the local and momentary as the analytical indeces and the integral indeces, as the most important in the applied sense. The knowledge of the indeces of stability allows to avoid the solution of the task in full volume, which can't be always made precisely and reliably or is rather labour- consuming even using the computer.

The analysis of the methods of the stability theory showed that they could be used only as particular analytical indeces (local, momentary) in the geocryological investigations and engineer practice. That is why in this paper there were investigated the integral indeces of the GCPR stability from the point of view of choosing the possible declinations of the external conditions of the GCPR heat exchange for a long term period, which don't lead to the thawing of the frozen thickness.

In this case, the notion of the GCPR stability was associated with the idea of the presence of the definite summary effect of the external actions. The latters, more often man induced, can be of various types: the breach of the vegetable cover, the change of albedo of the surface, or the nature of the snow accumulation, the irrigation, etc. But there are only two indeces of the resulting effect:

1) The first index ($\hat{Q}$) must show if the average annual temperature of the ground t_g (under STS) is lower than the temperature of the phase transformation of the ground moisture t_p, while the time is increasing unlimitedly, or t_g will be higher than t_p;
2) The annual increase of the STS thickness - h_{STS}, which is important for the evaluation of the GCPR stability in case of the slope processes development.

This pair of indeces is the sought for integral index of the frozen ground stability for the long-term period of the change of their external conditions of heat exchange with the various integral complexes: the thermal impulse $\Omega = \int (t_s - t_p) d\tau$, °C · hrs, and the thermal resistance of the ground covers $\mathcal{J}_s$, m^2 hrs °C/kcal. It should be noted, that the conception of resistance is developing in the modern theory of stability.

The annual increase of STS is determined as the difference of the two meanings h_{STS} calculated before and after the breach with the proper value of the positive (during warm season) thermal impulse Ω^+ and the thermal resistance of the vegetable cover $\mathcal{J}_s$ according to the formula

$$h_{STS} = \frac{2\Omega^+}{L + \sqrt{L^2 + M\Omega^+}}, \qquad (4)$$

$$M = \frac{2}{\lambda_t}\left(Q_p + C_f(t_p - t_g) + \frac{C_t}{3}(t_s^+ - t_p)\right),$$

$$L = (t_p - t_g)\sqrt{\frac{C_f T}{\pi \lambda_f}} + \mathcal{J}_s\left(Q_p + C_f(t_p - t_g) + \frac{C_t}{2}(t_s^+ - t_p)\right),$$

where C_f , λ_f and C_t , λ_t - the volume thermal heat capacity and the coefficient of the heat conductivity of the ground in the frozen thickness and STS; Q_p - the volume heat of the phase transformation of the ground moisture; t_p = 0°C; T = 8760 hrs - the annual period; t_s^+ = the average temperature of surface of GCPR during the warm season; t_g - the ground temperature at the depth of SAHS at the moment of prospecting.

The solution (4) was got by the integral method of heat moments or thermal impulse, Kovalkov (1974). The conclusion of the integral index of stability $\hat{Q}$ with respect to the change of the external conditions of the GCPR heat exchange was given by the same method, Kovalkov (1986).

The main idea while determining the index $\hat{Q}$ is that when $t_g = t_p$ in the one-phase Stephan's problem it turns out the annual equality of the depths of season thawing h_t and freezing h_f . If, for example, in this problem h_f is higher than h_t , then t_g will be always lower than t_p during the long term period, and the frozen thickness is thermally stable under these external conditions. If, on the contrary, h_t is higher than h_f , then t_g will become higher than t_p during the long-term period, and, consequently, the frozen thickness of GCPR is thermally unstable under these changes of external conditions, and the long-term progressive thawing will occur.

Thus, $\hat{Q}$ appears to be some fictituous resulting portion of heat in GCPR during the year, which is compensated by the heat crossing the front of freezing-thawing in the reverse direction.

The expression for the index $\hat{Q}$, calculated for the new conditions, using the average monthly means of t_{si} and $\mathcal{J}_{si}$, looks like:

$$\hat{Q} = \sum_{1}^{n}\left(\frac{|t_{si}-t_p|}{\mathcal{J}_{si}+\frac{h_i}{\lambda_f}}\right)_w - \sum_{n+1}^{12}\left(\frac{t_{si}-t_p}{\mathcal{J}_{si}+\frac{h_i}{\lambda_t}}\right)_s , \qquad (5)$$

where t_{si} and $\mathcal{J}_{si}$ - the average monthly temperature of the conditional surface of the radiational heat exchange and the thermal resistance of the surface cover (snow, and/or plants); i = 1,2...n...12 - the number of year months; i = 1 - the first month of winter season; n - the number of winter months (when $t_{si} < t_p$); h_i - the average monthly fictituous depths of freezing and thawing of ground, got from the solution of the one-phase Stephan's problem:

$$h_i = F\left(E + \sqrt{E^2+F}\right)^{-1} ;$$

$$F = h_{i-1}^2 + 2h_{i-1}E + \frac{2\lambda}{Q}|t_{si}|\Delta\tau ;$$

$$E = \lambda \mathcal{J}_{si} ; \qquad (6)$$

$Q = Q_p \pm C|t_{si}|/2$ (here 'plus' is put during the months of the beginning of freezing or thawing to the reaching of the extremal t_{si} , which is, as a rule, on January and July accordingly, and then 'minus' is put); $C = C_f$ and $\lambda = \lambda_f$ at the freezing; $C = C_t$ and $\lambda = \lambda_t$ at the thawing; h_{i-1} - the state of the freezing or thawing front in the previous month; $\Delta\tau$ = 730 hrs - the average duration of a month.

If, according to formulas (5) and (6), $\hat{Q} > 0$, then it is the very condition when the frozen thickness of GCPR stay at $t_s < t_p$. The additional condition of the GCPR stability will be non-exceeding of some possible value by the fluctuation Δh_{STS} , which is chosen with the aim not to permit the slipping down of STS under the influence of the pertinent efforts on the slopes.

So, the suggested indeces of the GCPR stability $\hat{Q}$ and Δh_{STS} allow, using some simple calculations, to evaluate the possible man induced breaches of the Northern territories.

REFERENCES

Shvetsov, P.F. (1983). Kriterii ustoichivosti pochvenno-gruntovogo kompleksa Subarktiki. V kn.: Problemy ekologii polyarnykh oblastei. Moscow, Nauka, p.17-20.

Shvetsov, P.F., Kovalkov, V.P. (1986). Phisicheskaya geocryologiya. Moscow, Nauka, p.178.

Shvetsov, P.F., Kovalkov, V.P. (1987). Geocryologiya i problemy osvoeniya Severa. Moscow, Znanie, p.48.

Mescheryakova, N.A. (1981). Kategoriya ustoichivosti v metodologii sovremennogo estestvoznaniya. Voronezh, University, p.175.

Ebeling, V. (1979). Obrazovanie struktur pri neobratimykh processakh. Moscow, Mir, p.280.

Kovalkov, V.P. (1986). Metod impulsa pri opisanii neravnovesnykh kryogennykh phisiko-geologicheskikh processov. Injenernaya geologiya, N°4, p.101-114.

Kovalkov, V.P. (1974). Postanovka i reshenie zadach teploprovodnosti v gruntakh integralnym metodom teplovykh momentov. V kn.: Merzlye grunty kak osnovanie sooruzheniy, Trudy Proizvodstvennogo i nauchno-issledovatelskogo instituta po injenernym izyskaniyam v stroitelstve, v.44, p.74-89.

ICE WEDGE GROWTH IN NEWLY AGGRADING PERMAFROST, WESTERN ARCTIC COAST, CANADA

J. Ross Mackay

University of British Columbia, Dept. Geography, Vancouver, B.C., V61 1W5 Canada

SYNOPSIS The western Arctic coast of Canada is in an area of continuous permafrost where many lakes drain rapidly by erosion of ice wedges at their outlets. Drainage initiates permafrost aggradation in the first winter on the exposed lake bottoms. Frequently, thermal contraction cracks open in the first winter even where frozen ground is only 3 or 4 m deep. During the summer thaw period, some thermal contraction cracks become plugged near the surface with ice veins and frozen mud so that summer re-expansion of the ground seals the cracks before appreciable water can percolate downward to form ice veinlets. Some other cracks infill quickly with water to grow ice veinlets. Therefore, the annual growth rate for ice wedges is highly variable being site specific and time dependent. The ice wedge growth rate for the first few years can range from near zero to at least 2.5 cm/yr.

INTRODUCTION

Permafrost along the western Arctic coast of Canada is 300 m to 700 m thick. The mean annual air temperature ranges from -10°C to -12°C, the mean annual ground temperature from -6°C to -9°C. Ice-wedge polygons are widespread. Approximately 20% to 50% of the total area is covered by lakes. Nearly every summer, at least one lake drains rapidly. When this happens, permafrost begins to aggrade the first winter on the exposed lake bottom. Such lake bottoms provide ideal sites for the study of the initiation and growth of ice wedges. The purpose of this paper is to discuss ice-wedge growth in the bottoms of two recently drained lakes (Fig. 1) referred to as Lake 1 (Mackay, 1985) and Illisarvik (Mackay, 1981).

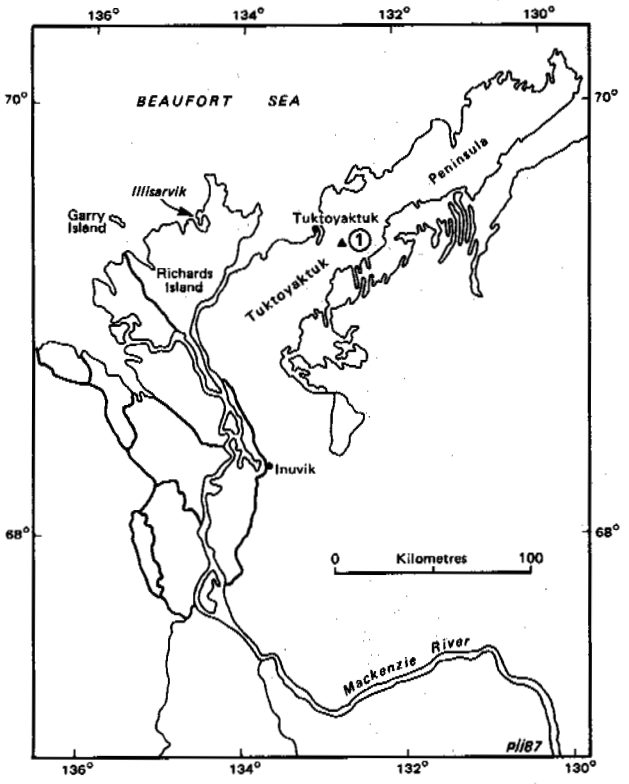

Fig. 1 Location map.

LAKE 1

Lake 1, prior to drainage, was 700 m long, 600 m wide, with a maximum depth of 3 m. On the basis of air photo evidence, drainage was between the late summer of 1971 and the early summer of 1972. The lake bottom was first studied in the summer of 1973 by which time wide thermal contraction cracks had already opened, that is, in either the first or second winter following drainage. In June 1974, a 30 m long thermal contraction crack system, which had developed in an organic silty lake clay, was surveyed and marked with 11 wooden stakes along its length (Fig. 2). The site was 130 m from the former lake shore where the water depth of about 2 m would have exceeded the average winter ice thickness, so a talik would have underlain the site.

Trough development

From 1974 to 1979, the width and depth of the trough at the 11 stakes were measured; winter cracking was located with breaking cables (Mackay 1974); and all secondary cracks were

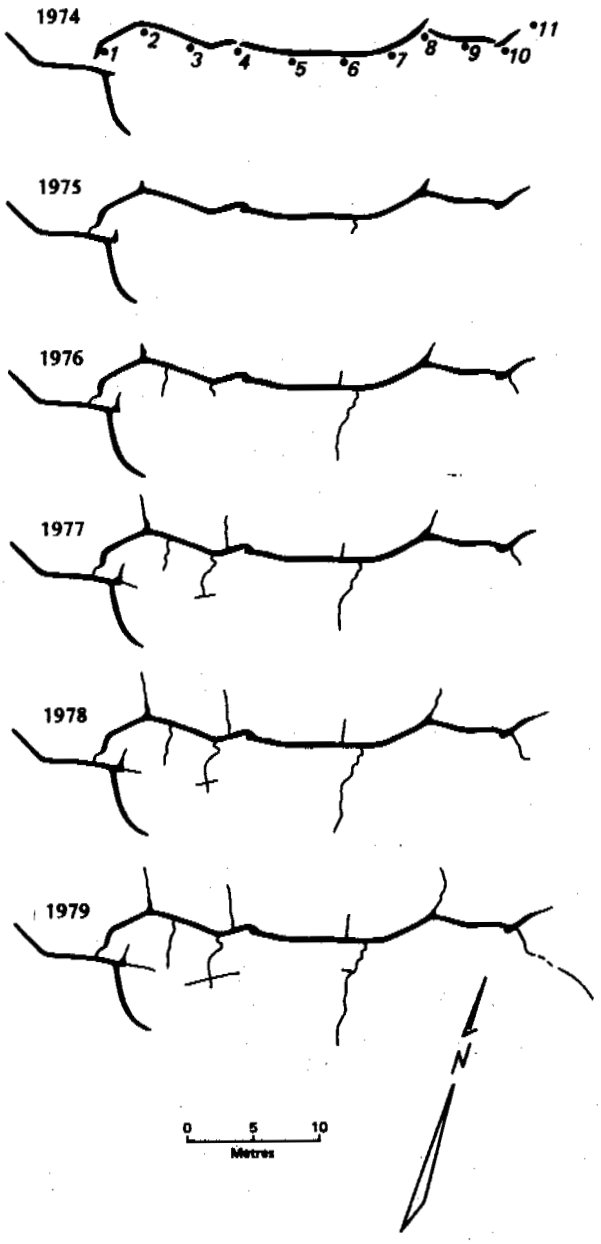

Fig. 2 A 30 m long thermal contraction crack system on the exposed bottom of Lake 1 as mapped from 1974 to 1979. The crack opened within three years, at maximum, following lake drainage.

mapped. Active cracking took place along the entire trough system from 1974 to 1977. However, as vegetation cover began to trap snow, crack activity diminished rapidly. No cracking has been observed since 1979. Winter cracking from 1974 to 1977 resulted in a progressive enlargement of the trough. For example, in 1974, the trough was box-like in vertical cross section (Fig. 3) with a mean width at the 11 stakes of 14 cm and depth of 13 cm; in 1975, 26 cm and 16 cm; in 1976, 27 cm and 21 cm; and in 1977, 32 cm and 24 cm. In 1977, when the average width and depth of the trough peaked, some cross sectional areas exceeded 500 cm^2. As crack activity decreased after 1977 so did the mean size of the trough. By 1979, when all cracking had ceased, the mean trough dimensions were reduced to that in 1975, a 30% decrease from the peak 1977 value.

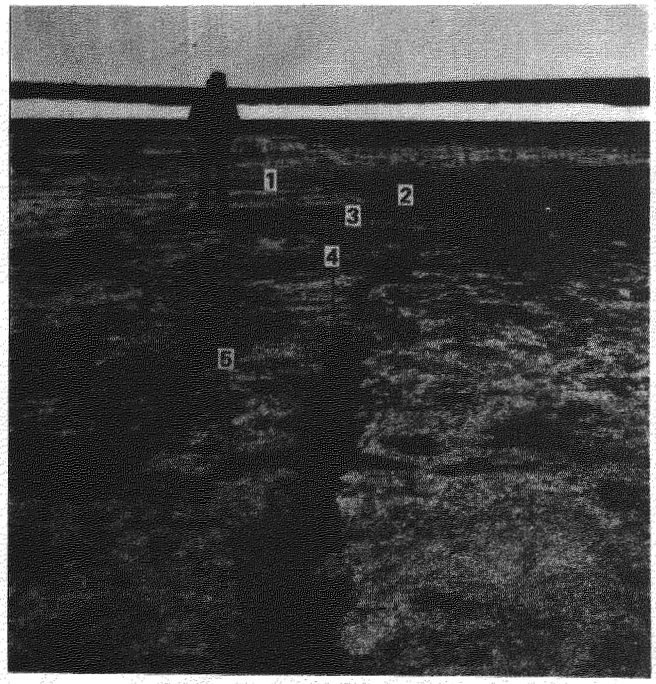

Fig. 3 Photograph taken 30 June 1974 of part of the thermal contraction system of Fig. 2.

Ridges

Ridges paralleling the trough developed gradually from 1974 to 1970 by which time the ridges rose an average of 2 to 4 cm above the adjacent terrain. Presumably, summer re-expansion of the ground caused both ridge development during the period of active cracking and a decrease in the size of the trough by infilling as cracking stopped.

Secondary cracks

According to thermal contraction theory, a primary crack relieves the thermal tension in a direction perpendicular to the crack, but not parallel to the crack. Therefore, a random crack will tend to propagate towards the primary crack, with a near orthogonal intersection being the result (Lachenbruch, 1962). In general, the preceding sequence probably holds true for the older crack systems. However, observations at several sites show that in embryonic crack systems, secondary cracks often propagate outward from the main cracks (Fig. 3).

Ice wedge growth

In the first several years after 1974, exceptionally wide ice veins were encountered in summer excavations to the frost table.

Many ice veins exceeded 10 cm in width. A typical June 1975 horizontal exposure of one ice vein section at the frost table was: 1 to 5 cm ice; 2 to 4 cm frozen clay; 1 to 5 cm ice. In order to investigate the sizes of ice wedges at depth, in 1984 and 1985 over-lapping holes were drilled across the troughs opposite to stakes 2, 3, and 5 (Figs. 2, 3). The over-lapping drill holes spanned a horizontal width greater than 0.5 m and extended down to at least 0.5 to 1.0 m below the top of permafrost. No wedge ice was encountered in any cross section. Therefore, if ice-wedge ice were present, it was at least 0.5 m to 1.0 m below the top of permafrost. Nevertheless, because repetitive cracking occurred along the same line for at least four winters (1973-1977) either upward cracking from an ice wedge or a weak soil zone at depth is indicated, for otherwise, a crack could hardly re-open along the same line for four successive winters (Lachenbruch, 1962; Mackay, 1984).

Coefficient of thermal contraction of frozen ground

The coefficient of thermal contraction of frozen ground has, in general, been considered to be less than that of ice (50 x 10^{-6}/°C), because the coefficient of the mineral constituents is much less than that of ice (Black, 1974). However, laboratory studies in the Soviet Union (e.g., Grechishchev, 1973) have shown that the coefficient of thermal contraction of frozen ground may be as much as ten times that of ice, the amount varying with the moisture content and soil type. The coefficient of thermal contraction of frozen ground under field conditions can be estimated from measurements of crack widths, depths, spacings, and ground temperatures (Black, 1974; Mackay, 1986). At Lake 1, estimates based upon the preceding show that the apparent coefficient of thermal contraction of the frozen soil greatly exceeded that of ice.

ILLISARVIK

Illisarvik, a lake measuring 600 m long, 300 m wide, with a maximum depth of 5 m was artificially drained on 13 August 1978 (Mackay, 1981). At the time of drainage, the talik was about 32 m deep below the lake centre (Judge et al., 1981). Permafrost aggradation commenced on the exposed lake bottom in the first winter. Observations on the first 7 years (1978-1985) of ice-wedge growth have been published (Mackay, 1986). The 1986 and 1987 observations are added here to provide a more complete 9 year (1978-1987) record of ice-wedge growth.

Crack initiation

Large thermal contraction cracks (Fig. 4) with surface widths to 10 cm, depths to 2.5 m, and box-like vertical profiles opened in the first winter. The bottoms of the cracks extended downwards to within 1.0 m of the unfrozen ground below. One major crack system opened in the second winter but none have been observed since then. The largest first winter

Fig. 4 A large thermal contraction crack formed the first winter at Illisarvik.

crack system is shown in Fig. 5a. During the first summer following drainage (1979), small ridges developed parallel to the major crack system because of summer re-expansion of the ground similar to that observed at Lake 1. The inward movement of the active layer towards the trough in summer has been measured by the separation and subsequent tilting of vertical rods inserted to varying depths in the ground. As the yearly increase of the vegetation cover trapped more snow to insulate the ground, the branching lateral cracks became inactive until, by the 9th winter of 1986/1987, only the main trunk system remained active as shown in Fig. 5b. The decrease in crack activity because of snow has been similar to that of Lake 1.

Upward cracking

In the second winter, the main crack system of Fig. 5a re-opened within a few centimetres of that of the first winter. In addition, the crack propagated 15 m into the ice of the frozen residual pond. In each succeeding winter, the crack in the residual pond re-opened along the same line. Furthermore, the crack has propagated each year farther into the pond until it has now reached dry land on the far side (Fig. 5b). Since pond water can retain no memory of the previous winter's crack in pond ice, repetitive cracking along the same line in pond ice proves that the cracks originate in wedge ice in permafrost below the pond and then propagate both upward and downward (Mackay, 1984). This field observation confirms the 1962 prediction of upward cracking made by Lachenbruch (1962).

Coefficient of thermal contraction

In the first few winters, many of the thermal contraction cracks were 10 cm wide at the ground surface. The cracks narrowed downwards to about half the surface width at a depth

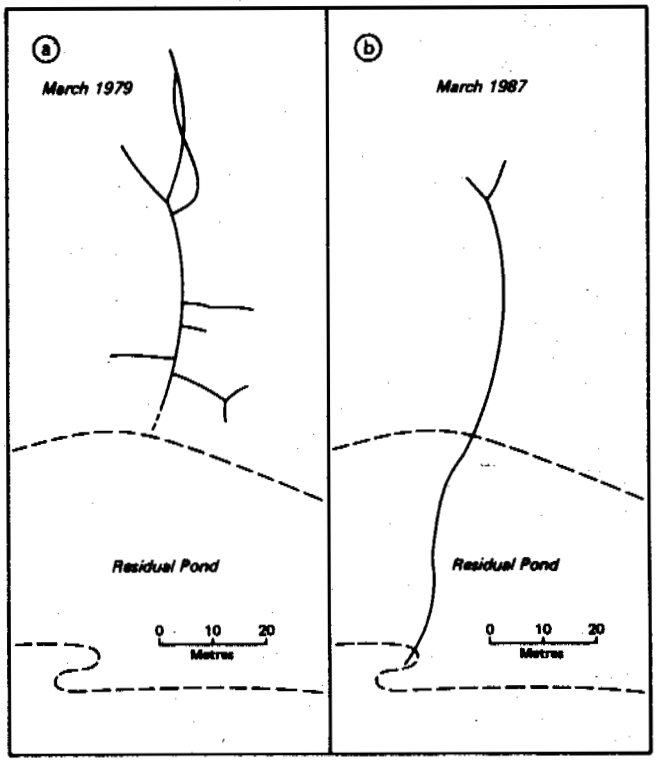

Fig. 5 (a) A major crack system at Illisarvik as mapped in March 1979. (b) The active crack system of (a) as mapped in March 1987.

approximating that of the late summer active layer. The apparent coefficient of thermal contraction, estimated from the widths of a series of parallel cracks and ground temperatures, ranged from about 50 x 10^{-6}/°C (i.e., that of ice) to 400 x 10^{-6}/°C or eight times that of ice (Mackay, 1986; cf. Grechishchev, 1973). In contrast, crack widths of old ice wedges along the western Arctic coast of Canada and Alaska (Black, 1974; Mackay, 1974) typically range from about 0.5 cm to 1.5 cm. Thus, the exceptionally large cracks of the first few winters at Illisarvik and also at Lake 1 can be attributed to the unusually high apparent coefficient of thermal contraction of the frozen ground. Although it has not been proven, the field evidence suggests that the coefficient of thermal contraction may decrease with time as a result of thermal cycling at near zero negative temperatures.

Changes in crack width

The width of a thermal contraction crack tends to increase through the winter until the penetration of the warming temperature wave in spring and summer causes a narrowing or even complete closing of a crack (Mackay, 1975). However, the crack depths tend to remain relatively constant. Changes in crack width have been measured from the separation of a variety of vertical rods installed in both the active layer and into permafrost. For example, between 2 February 1987 and 22 March 1987, the mean increase in width across 12 crack sections at two different sites was 1.1 cm. Subsequently, the widths decreased during the spring warming.

Entry of water into cracks

Numerous observations at Illisarvik show that a wide ground surface crack in March or April may greatly exceed the width of the resulting ice veinlet that infills the crack at the top of permafrost in the summer months. Reasons follow. First, because of insufficient surface water to infill a wide crack, meltwater often trickles down the two sides to form two parallel sheets of ice separated by an air space. Then a mud slurry may flow down between the two vertical ice sheets to freeze and form a temporary plug that prevents further entry of water (Fig. 6). As the active layer deepens in summer, the plugging process may be repeated at successively lower depths. Meanwhile, summer re-expansion continues to narrow the crack within permafrost. Drilling, as at Lake 1, shows that no ice veinlets may be present to a depth of at least 1 m below the top of permafrost where 5 to 10 cm wide cracks had opened in previous winters. In other words, ice-wedge growth rates may show little correlation with winter crack widths at least in the early stages of ice-wedge growth.

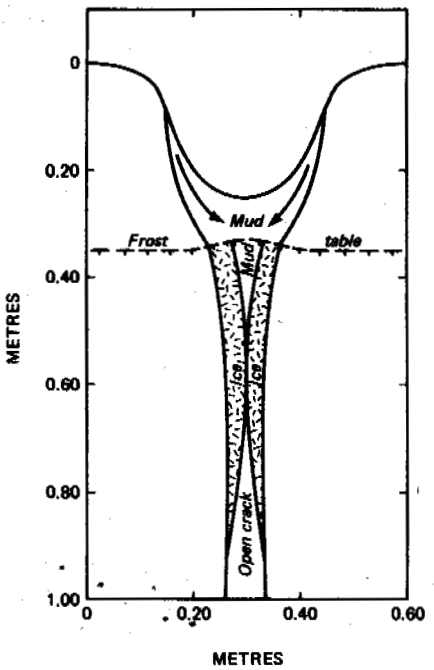

Fig. 6 A typical summer vertical cross section of a large thermal contraction crack in mid summer.

Snow effects

With the gradual establishment of vegetation, which spread noticeably in the second summer of 1980, snow began to be trapped in winter.

In consequence, ground temperatures were much warmer beneath sites with a thick snow cover as compared to sites with a thin snow cover. By the fourth winter (1981/1982) some snowdrifts at the site shown in Fig. 5b were 60 cm or more in depth, and at such sites cracking virtually ceased. As vegetation cover continued to spread, snow depths by the ninth winter (1986/1987) were fairly uniform at 20 to 40 cm with only a few deeper drifts. The net effect has been to reduce the areal extent of winter cracking rather than to inhibit it.

Growth rates

Ice-wedge growth rates for the first nine years (1978-1987) at Illisarvik have been highly variable, site specific, and time dependent so that no average growth rate can be given. If year to year changes in air temperatures are omitted and the coefficient of thermal contraction is assumed to be constant, the main reasons for variations in the growth rates appear to be: changes in snow cover; winter and spring widening and narrowing of crack widths; and the plugging of the upper parts of cracks with ice and mud to restrict the infilling of open cracks below the plugs. At present, statistical data are insufficient to suggest a maximum rate. However, at one site where the first cracks opened in the second winter (1979/1980), the ice wedge was about 20 cm wide in 1986/1987 (Fig. 7). The growth rate for the first 8 years was then about 2.5 cm/yr or 25 times that widely assumed for old ice wedges in northwestern North America (e.g., Washburn, 1980, p. 111). In view of the small sample number, 2.5 cm/yr should not be taken as a maximum growth rate either for Illisarvik or elsewhere.

Fig. 7 An 8 year old ice wedge at Illisarvik. The growth rate has averaged 2.5 cm/yr.

CONCLUSIONS

The results from Lake 1, naturally drained in 1971 or 1972, and from Illisarvik, artificially drained in 1978, and from observations at many other recently drained lake sites permit the following general conclusions to be made for ice-wedge growth in newly aggrading permafrost. Thermal contraction cracks exceeding 30 m in length can develop in the first winter after drainage. The cracks at the ground surface can exceed 10 cm in width, 2.5 m in depth, and the cracks can penetrate down nearly to the bottom of the first winter's frozen ground. Therefore, very large thermal contraction cracks can open without the pre-existence of frozen ground or permafrost. The apparent coefficient of thermal contraction of newly frozen ground can be many times that of ice. Cracks can widen in winter and narrow in the spring. The rate of ice-wedge growth depends, to a considerable degree, upon water availability and the presence or absence of soupy mud that can plug a crack in early summer. The growth of vegetation and resulting snow entrapment reduces cracking. Along the western Arctic coast of Canada, where snow depths exceed about 60 cm, very little cracking takes place. Summer re-expansion of the ground can start to develop ridges in the first summer after cracking. If ice-wedge growth ceases, ridges already formed may disappear. No mean growth rate for young ice wedges can be given, because the growth rates are highly variable, being site specific and time dependent. Maximum growth rates can reach, or exceed, 2.5 cm/yr for the first 8 years of growth. The implication for paleoclimatic reconstruction based upon the sizes of ice wedge casts is clear, because the cast of a 10 year old young ice wedge may be of the same size as that of a slowly growing 1000 year old wedge.

ACKNOWLEDGEMENTS

The field work has been supported by the Geological Survey of Canada, the Polar Continental Shelf Project, Canada; the Natural Sciences and Engineering Research Council of Canada; and the Inuvik Scientific Resource Centre, Inuvik, N.W.T.

REFERENCES

Black, R.F. (1974). Ice-wedge polygons of northern Alaska. In Glacial Geomorphology. D.R. Coates, Editor. Publications in Geomorphology, 247-275. State University of New York, Binghamton, New York.

Grechishchev, S. YE. (1973). Basic laws of thermorheology and temperature cracking of frozen ground. USSR Contribution Permafrost 2nd Int. Conf. Translated by National Academy Sciences, 1978, 228-234. Washington, D.C.

Judge, A., Burgess, M., Taylor, A., & Allen, V. (1981). Ground temperature studies at an arctic drained lake site. The Northern Community: A Search for a Quality Environment, 642-658. ASCE/Seattle, Washington.

Lachenbruch, A.H. (1962). Mechanics of thermal contraction cracks and ice-wedge polygons in permafrost. Geol. Soc. Am. Sp. Paper No. 70, 69 pp., New York, N.Y.

Mackay, J.R. (1974). Ice-wedge cracks, Garry Island, Northwest Territories. Cdn. J. Earth Sci. (11), 1366-1383.

_____ (1975). The closing of ice-wedge cracks in permafrost, Garry Island, Northwest Territories. Cdn. J. Earth Sci. (12), 1668-1674.

_____ (1981). An experiment in lake drainage, Richards Island, Northwest Territories: a progress report. In Current Res. Part A, Geol. Surv. Can., Paper 81-1A, 63-68.

_____ (1984). The direction of ice-wedge cracking in permafrost: downward or upward? Cdn. J. Earth Sci. (21), 516-524.

_____ (1985). Permafrost growth in recently drained lakes, Western Arctic Coast. In Current Res., Part B, Geol. Surv. Can., Paper 85-1B, 177-189.

_____ (1986). The first 7 years (1978-1985) of ice wedge growth, Illisarvik experimental drained lake site, western Arctic coast. Cdn. J. Earth Sci. (23), 1782-1795.

Washburn, A.L. (1980). Geocryology: a survey of periglacial processes and environments. John Wiley, 406 pp., New York, N.Y.

HEAT FLOW AND PECULIARITIES OF CRYOLITHOZONE IN WESTERN SIBERIA

V.P. Melnikov, V.N. Devyatkin and Y.P. Bevzenko

Institute of Northern Development, Sibirian Branch of the USSR Academy of Sciences, Tyumen, USSR

SYNOPSIS Permafrost as a specific geological target should be taken into consideration in resource development in Siberia. Thermal and physical-mechanical characteristics of frozen rocks differ greatly from those of thawed rocks, thus producing deviations in thermal and physical fields, which is a great hindrance for geophysical exploration. Altogether, these deviations, considered in terms of geophysical methods, such as geothermy, seismic survey and so on, offer a good possibility for studying permafrost.

INTRODUCTION

The analysis of geothermic data obtained by various researchers within the last 25 years on the territory of Western Siberia, extending from longtitude 60 to 88° at 54-72 lattitude, reveals a wide range of temperature variations in rocks - from -10°C to +5°C at a depth of 20m and up to 100°C and over 200°C at a depth of 5000 m.
The top of permafrost, occurring on the surface in polar regions, lowers down to 230 m in the south, and its base reaches sometimes 500-600 m. Beneath the base of permafrost the temperature in rocks increases with depth with a variable gradient 2-5°C per 100 m. Within frozen formations in lithosphere the temperature varies greatly with depth, and the thermal gradient changes both in direction and magnitude, reducing sometimes to 0. Rocks with the positive temperature are not rarely met in the regions of the growth of the cryolithozone (Balobayev et.al.,1963; Baulin, 1985; Ginsburg et al., 1981; Kurtchikov et al., 1987; Spolyanskaya et al.).

DISCUSSION

Heat flow is considered to be the main energy criterion of the intensity and time variability of thermal processes in rocks. Great attention was lately paid in Western Siberia to determination of the heat flow q_T, mainly in rocks with positive temperatures or in subfrozen rocks at depths of up to 3 km (Dutchkov et al., 1974; Kurtchikov et al., 1978). The results of q_T determinations are summarized in "Catalogue...", 1985; "Heat (Teplovoye) ..," 1987.
The observed q_T value of heat flow varies from 40 to 80 mW/m^2 and on average amounts to 55 mWt/m^2. Heat flow is observed to vary with depth under the influence of climate (which appears to indicate a non-equilibrium thermal regime in rocks) and throughout the territory, which is influenced by geological-tectonic conditions of the region (Kurtchikov, Stavitski, 1987).
A quantitative evaluation of heat flow within permafrost in Western Siberia is still one of the major tasks of geothermy, though certain effort has been made in this sphere ("Teplophisicheskiye...", 1983; Spolyanskaya, 1981). Heat flow serves as the main criterion of equilibrium/non-equilibrium thermal regime in the regions of the permafrost development (Balobaev et al., 1973; Devyatkin, 1975). This evidently follows from Stefan's condition at the phase boundary:

$$q_M - q_T = \pm Q \frac{dH}{dL} \qquad (I)$$

where q_M and q_T are heat flows at the phase boundary between frozen and thawed rocks respectively; Q is the amount of educed/absorbed heat per unit of volume during rock freezing (thawing); H - thickness of frozen rocks; L - time.
The condition $q_M = q_T$ is evidently associated with an equilibrium regime, $q_M > q_T$ with freezing regime and $q_M < q_T$ with thawing regime.
The analysis of calculated data on the heat flow q_M and correlation $n = q_M - q_T$, made on the basis of field geothermic observations revealed the following.
The correlation of heat flows within permafrost and subfrozen thawed zone changes within the limits of 0-1, i.e. the value q_M of heat flow within permafrost decreases by 100% as compared to q_T.
The condition $q_M < q_T$ is satisfied, thus giving possible evidence of overall non-equilibrium thermal regime of permafrost.
At the rock temperature below 0°C (at a depth

of 20 m), provided n = 0,5 - 0,9 heat flow q_M within permafrost varies within the limits of 30 - 50 mWt/m^2 in the north-west of Western Siberia, and in the north-east it varies from 20 to 30 mWt/m^2, provided n = 0,3 - 0,8.
At the rock temperature of 0°C and above (at a depth of 20 m) the value q_M of heat flow is approaching 0. This is characteristic of the regions with discontinuous and insular permafrost, as well as of the southern boundary of continuous permafrost.
Southwards there appear above-frozen talik zones, and an additional heat flow q_{HT} arises from above the daily ground surface, its value sometimes varying from - 17 to 40 mWt/m^2. Under the influence of heat flows q_{HT} and q_T thawing of frozen rocks occurs both at their top and base, which results in advancing of buried frozen formations, followed by their disappearance.
The decrease in the heat flow q_M to 0 within permafrost on the significant part of the investigated territory is related to the so called "zero screen", i.e. time delay of the isotherm 0° during thawing of frozen ground, caused by climate and abyssal thermal processes.
A partial equilibrium of the temperature field is also observed in areas with the positive rock temperature throughout the regions of discontinuous and insular frozen rocks. It is especially evident at depths of up to 200 - 400 m, where the value of heat flow decreases by a factor of 1,5 - 2,5 as compared with heat flow in underlying rocks (fig.I b, III).
Figure I desplays permafrost configuration and distribution of heat flows in frozen and thawed zones within the lithosphere of one of the profiles in Western Siberia, extending at lattitudes from 60° to 70°. Northwards the thickness of the permafrost ground increases. Identified are frozen rocks with gradient temperature distribution at lattitudes 66-70° and non-gradient temperature distribution (with temperature approaching 0°C) on the rest of the profile (fig.I a).
In the absence of the permafrost ground the rock temperature in the upper portion of the profile increases notably.
The direction of the heat flow q_T (IY) beneath the permafrost base, coinciding with heat flows q_M (II) and q_T (III) in frozen ground (II) and thawed rocks (III), is opposite to the direction of the heat flow q_{HT} (I), observed over the top of the permafrost ground (fig.I b). So we have: q_T (IY) > q_M (II), q_t (III) and q_{HT} (I).
Thus, the analysis of heat flow in areas of the cryolithozone development evidently indicates to the existence nowdays of the non-stationary degrading frozen structures, spreading on the surface as well as buried at a certain depth.
An evaluation of the occurence depth of upper and lower boundaries of buried frozen structures is of no difficulty for geothermal measurements in holes with the equilibrium

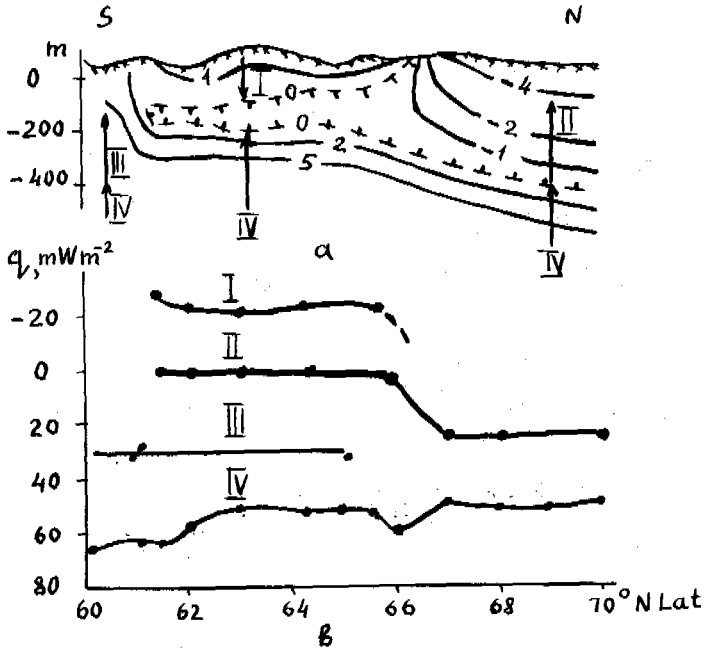

Fig.1 Permafrost configuration and distribution of heat flows in frozen and thawed zones

temperature regime, drilled through an overall thickness of permafrost.
However, a local picture of the temperature distribution over a limited set of holes and a long-term thermal recovery after the holes were drilled hinder a more detailed geothermic study of frozen rocks in industry-run areas. In this connection, the seismic method based on the anomalous velocity of elastic waves propagation within the frozen formation is of intrinsic interest for detecting frozen rocks or talik zones within the interhole space.
Seismic waves propagation in frozen rocks has been the subject of numerous papers (Agafonov, 1973; Voronkov et al., 1973; Frolov et al., 1971, 1972).
According to the data available, the most significant change in longtitudinal waves velocity (by a factor of 2-3) normally occurs with pore water freezing in clean quartz sands. The general change in wave velocity is characterized by a factor of 1,7-2,5 for loams and sandy loams, by 1,2-1,3 for clays. Velocity change in rocks during their freezing is quite sensitive to the porosity and moisture content. In naturally flooded unconsolidated rocks of sand-clay composition the longtitudinal wave velocity changes from 1200-1700 to 2000-3500 m/s. Such values of longtitudinal wave velocity are typical for rocks in Western Siberia.
Provided the change in the rock density with

freezing is neglected, the coefficient of reflection from the frozen boundary can be calculated from the velocity correlation:

$$K = \frac{V_2 - V_1}{V_2 + V_1} \qquad (2),$$

where V_1 and V_2 - velocity of elastic waves propagation in thawed and frozen structures respectively.
Within the velocity range mentioned above the coefficient of reflection will change from 0,08 to 0,5 - rather favourable values for appearance of reflected waves. The maximum values of coefficient are characteristic of sands, the minimum of clays.
The removal interval for recording pre-critical reflections from the permafrost surface can be calculated by the formula:

$$X_2 = 2\,h\,tg\,i \qquad (3),$$

where $i = \text{arc Sin}\,\frac{V_1}{V_2}$; h - the occurance depth of the upper permafrost surface.
If h = 100 m, then X_1 = 150-200 m.
The removal of the outlet point at initial refraction arrivals for one horizontal refracting boundary is determined by the formula:

$$X_2 = 2\,h\sqrt{\frac{V_2 + V_1}{V_2 - V_1}} \qquad (4).$$

If V_1 = 1700 m/s and V_2 = 2900 m/s, then X_2 = 392 m at h = 100 m and X_2 = 1178 m at h = 300 m.
By now the CDP-method (common-depth-point-shooting) with waves recording within the limits from 0 to 3200 m and within the 50-60 m range of input channels, has recieved the most recognition in detection of refracted waves associated with the cryolithozone.
The necessity of a special study of frozen blocks structure is justified by the anomalies created in seismic profiles.
The remnants of relict permafrost from 30-40 up to 100-200 m in thickness and from some hundred meters to several kilometers in size are quite common for central and southern geocryologic zones of Western Siberia.
Taliks of the same size are possible in continuous permafrost zones.
At the velocity of 2900 m/s the double traveltime through a permafrost remnant is from 0,020 to 0,140 s; at the velocity of 1700 m/s the corresponding traveltime varies from 0,032 to 0,235 s. The presence of frozen inclusions provide time deviations from 0,012 to 0,095 s. If the reason of these time deviations is unknown, they are treated as anticlinal (in case of frozen remnant inclusions) or as synclinal (in case of taliks) bends of deep-lying structures.
At an average velocity of 2500 m/s, which is typical for oil-bearing horizons, amplitudes of these "false" bends vary from 12 to 118 m under the conditions considered above.
Neglecting of the above mentioned data caused no mistakes while considering the total structure of very large deological formations in the course of prospecting and exploration.
Lately, when smaller formations up to 3 km in size and with an amplitude of about 50 m are to be explored, drilling data fail to varify the obtained seismic data.
The variety of possible methods of seismic survey for oil and gas allows seismic data to be regarded as the main source of obtaining information on, at least, upper horizons of the cryolithozone in undeveloped territories.
Refracted waves recorded during reflection survey through 24-fold CDP-shooting were interpreted in order to establish the practical value of seismic data for building up the upper boundary of relict cryolithzone and to take into account the permafrost impact on seismic plottings of oil-bearing horizons.
Refracted waves associated with relict permafrost may be, as a rule, clearly identified on records as long-period oscillations with the apparent velocity of 2500-2900 m/s.
Data processing was performed through common-depth-point-stacking of refracted waves with preliminary input of kinematic corrections, followed by automatic control for static corrections and boundary velocities.
Time domains obtained in such a way give a precise picture of the upper boundary relief of perennially frozen rocks (fig.2 A, B).

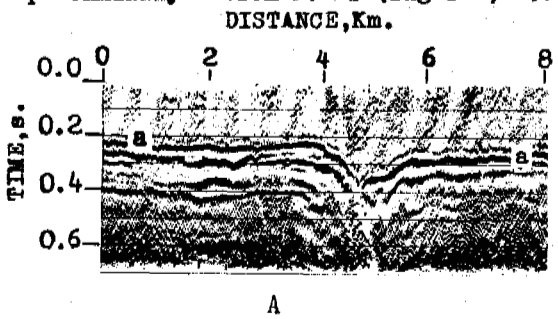

A

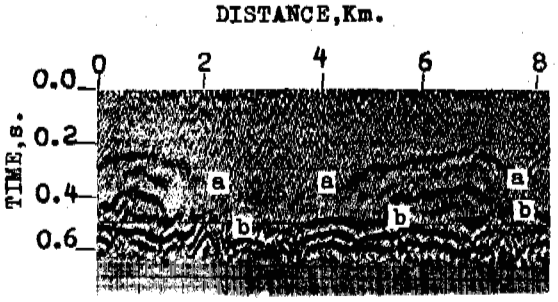

B

Fig.2 Time-section:
A - permafrost region with talik;
B - permafrost island;
a - a - refraction waves from lithological boundary below permafrost.

Fig.2 A illustrates continuous permafrost surface, while figure 2 B presents insular permafrost. In between the insulars waves are registered, which are related to underlying rock boundaries.
Occurance depths of the top of relict permafrost, determined through refraction survey, were compared with thermometry data on exploration and operating holes and gave a high accuracy of results.

CONCLUSION

The values of heat flow within permafrost in Western Siberia reduce from 0 by 100% as compared with abyssal heat flow. Simultaneous interaction of heat flow from above the daily surface and abyssal heat flow results in advancing of buried frozen formations, characterized by a non-gradient temperature distribution (about 0°C) and heat flow, approaching 0.

The decrease in heat flow down to 0 within permafrost is related to the so called "zero screen", i.e. a long-period delay of the isotherm 0° during thawing of frozen formations, caused by the climatic and abyssal thermal processes.

To determine the thickness and configuration of frozen strata a complex of geophysical methods should be used, including geothermy, seismic survey and so on.

REFERENCES

AGAFONOV, Y.K, GERSHANIK, V.A,MEDVEDEV, A.D, MONASTYREV, V.K, TSYBULIN, L.G. (1973). Vozmojnosty seismorazvedki otrajennimy volnamy dlya kartirovaniya i raionirovaniya merzlih porod. "Dokladi i soobshcheniya II Mejdunarodnoy konferencii po merzlotovedeniu". Yakutsk, (6), s.91-97.

BALOBAEV, V.T, DEVYATKIN, V.N. (1973). Sovremennie geotermitcheskie usloviya sushchestvovaniya i razvitiya mnogoletnemerzlih gornih porod. "Dokladi i soobshcheniya II Mejdunarodnoy konferencii po merzlotovedeniyu. Yakutsk, (1), s.11-19.

BAULIN, V.V. (1985). Mnogoletnemerzlie porodi neftegazonosnih raionov SSSR. Nedra, Moskwa, 212 s.

DEVIATKIN, V.N. (1985). Rezultati opredeleniya glubinnogo teplovogo potoka na territorii Yakutii. "Regionalnie i tematicheskie geokriologitcheskie issledovaniya".Nauka, Novosibirsk, s.148-150.

DUTCHKOV, A.D, SOKOLOVA, A.S. (1974). Geotermitcheskie issledovaniya v Sibiry. Nauka, Novosibirsk, 280 s.

FROLOV, A.D, ZYKOV, Y.D. (1971, 1972). Osobennosti rasprostraneniya uprugih voln v merzlih gornih porodah. "Izvestiya VUZ, Geologiya i razvedka", (10), s.80-87, (2), s.136-143.

DZHURIK, V.I, LESHCHIKOV, F.N. (1973).Experimentalnie issledovaniya seismitcheskih svoistv merzlih gruntov. "Dokladi i soobshcheniya II Mejdunarodnoi konferencii po merzlotovedeniyu". Yakutsk, (6), s.64-68.

GINSBURG, G.D, SOLOVIEV, V.A. (1981). O geologitcheskom i geographitcheskom aspectah regionalnogo merzlotovedeniya. Sovietskaya Geologiya, (8), s.108-115.

KATALOG DANNIH PO TEPLOVOMU POTOKU SIBIRY. (1966-1984gg.). (1985).Pod redakciei A.D.DUTCHKOVA. Novosibirsk, Institut Geologii i Geophiziky Sibirskogo Otdeleniya Academii Nauk SSSR, 82 s.

KURTCHIKOV, A.P, STAVITSKIY, B.P. (1987).Geotermiya neftegazonosnih oblastei Zapadnoi Sibiry. Nedra, Moskwa, 134 s.

TEPLOVOE POLE NEDR SIBIRY. (1987). Pod redakciey FOTIADY, E.E. Nauka, Novosibirsk, 196 s.

TEPLOPHIZITCHESKIE ISSLEDOVANIYA KRIOLITOZONI SIBIRY. (1983). Pod redakciey PAVLOVA, A.V. Nauka, Novosibirsk, 213 s.

SHPOLYANSKAYA, N.A. (1981). Merzlaya zona litospheri Zapadnoi Sibiry i tendenciya eyo razvitiya. Moskovskiy Universitet, Moskwa, 168 s.

VORONKOV, O.K, MIHAILOVSKIY, G.B. (1973). Izutchenie podzemnih lydov metodom seismorazvedki. "Dokladi i soobshcheniya II Mejdunarodnoi konferencii po merzlotovedeniyu". Yakutsk, (6), s.73-78.

MICROTOPOGRAPHIC THERMAL CONTRASTS, NORTHERN ALASKA

F.E. Nelson[1], S.I. Outcalt, K.M. Hinkel, D.F. Murray and B.M. Murray

[1]Rutgers University, New Brunswick, NJ, USA 08903

SYNOPSIS Temperature data acquired from the summits of frost mounds and from surrounding marshland near Toolik Lake, Alaska during the winter of 1984-85 display marked differences attributable to microtopography. An automatic recording system was used to monitor soil temperatures at 10-cm vertical intervals in the upper 50 cm of the soil at four locations in close proximity to one another. The instrumentation was configured to yield comparative data for relatively dry mound summits and wetter marshland in surrounding flat terrain. Temperatures below the summits were much colder than in the marsh, a situation probably attributable to thinner and denser snow atop the mounds than in surrounding terrain. The thermal record also reveals contrasting patterns in the refreezing active layer, probably reflecting variations in coupled heat and water transfer processes.

INTRODUCTION

Isolated bodies of ice-rich permafrost with a distinct topographic expression are common in organic terrain, and have been used to map the southern limit of discontinuous permafrost in central Canada (Zoltai 1971). The thermal properties of peat are in part responsible for this interesting distribution; peat can provide efficient insulation in summer when elevated and dry, but can also be a good heat conductor when saturated and frozen (Brown 1966). In winter, exposed elevated portions of peatlands experience less accumulation of snow and hence greater frost penetration than do surrounding low areas. These relationships have been used to explain the preservation of palsas in areas with mean annual air temperatures near 0°C.

Several investigators have performed temperature measurements in palsa-scale frost mounds, but such studies usually entailed long-term, low-frequency intermittent measurement programs (Forsgren 1964, Lindqvist and Mattsson 1965, Seppälä 1976, 1982, 1983). Other workers have conducted detailed temperature measurement programs in peatlands without permafrost or frost mounds (e.g., Brown and Williams 1972, Kingsbury and Moore 1987). This paper reports a preliminary attempt to monitor temperatures on a long-term, high-frequency basis in and around a typical frost mound in north-central Alaska.

An earlier study (Nelson et al. 1985) attempted to provide insight into physical processes involved in heat transfer in and around peat-covered palsas in northern Alaska by analyzing high-frequency (10 min) thermal measurements taken over a single diurnal cycle. Employing the "effective diffusivity" concept, the existence of nonconductive influences on thermal evolution within the peat was demonstrated. Modeling of the coupled-flow regime (Outcalt and Nelson 1985) indicated that the mechanisms by which the peat maintained a low effective thermal diffusivity in summer were internal evaporation and advection of water from the water/ice interface at the base of the active layer. During clear and calm summer weather the temperature at the surface of dry peat approached 40°C. Under these conditions water moved from the base of the active layer and evaporated near the peat surface, yielding an extremely steep and temporally stable temperature gradient in the upper 5 cm of the peat. Advection of water and internal evaporation maintained a weak thermal gradient at depth because both processes counter conductive warming. Because the ratio of the latent heat of evaporation to the latent heat of fusion is approximately seven, ablation of ice beneath a peat cover can be an extremely energy-consumptive process.

STUDY AREA AND INSTRUMENTATION

The work on the summer heat-transfer regime described above suggested that similar coupled-flow effects might be discernible during the autumn freezeup through comparison of the thermal regimes in elevated mounds and in surrounding wet marshland. To test this proposition, measurements were made in a small marsh near Toolik Lake, (68°38'N, 149°37'W) at Mile 285.6 on the Dalton Highway in northern Alaska. The site is located in the continuous permafrost region, and has an estimated mean annual temperature of -10°C. The mounds are illustrated in Figure 1; more complete descriptions of the site are given in Nelson

et al. (1985) and Hinkel et al. (1987).

Figure 1. Frost mounds at Toolik Lake prior to instrumentation.

The landscape at Toolik Lake is typical for the region, consisting of an essentially continuous cover of vegetation overlying the late-glacial till. The vegetation of the mounds is of a low scrub type consisting of shrub birch, willow, and ericaceous prostate and mat-forming shrubs such as Betula nana. Salix pulchra, Vaccinium uliginosum, V. vitis-idaea, Ledum palustre, Arctous alpina, and Empetrum hermaphroditum. Bryophytes include Ptilidium ciliare, Aulacomnium turgidum, Dicranum spp., Hylocomium splendens, Polytrichum strictum, Racomitrium lanuginosum, and Rhytidium rugosum. Among the lichens are several members of the family Cladoniaceae as well as Cetraria cucullata, C. nivalis, Dactylina arctica, Masonhalea richardsonii, and Thamnolia vermicularis. The marsh is a wet sedge meadow (rich fen) in which Eriophorum angustifolium, Trichophorum caespitosum, and Carex membranacea were prominent. Taxa such as Carex chordorrhiza, Pedicularis sudetica and the mosses Drepanocladus badius, D. revolvens, Oncophorus wahlenbergii, and Scorpidium scorpioides occurred in areas of standing water. Small hummocks of peat supported Tofieldia pusilla, Andromeda polifolia, Carex rariflora and the mosses Dicranum groenlandicum, D. angustum, D. elongatum, Sphagnum subsecundum, S. teres, and S. warnstorfii.

A data acquisition system similar in design to that described by Nelson et al. (1985) was used to obtain temperature measurements at four closely spaced (4-5 m) locations on top and adjacent to frost mounds within the marsh. The system employed four probe lines, each consisting of six thermistors mounted at 10-cm intervals or a 1.5-cm outer diameter wooden cylindical rod. The absolute accuracy of the thermistors was estimated to be 0.2°C. The data logger is capable of scanning the thermistor array at several temporal intervals. Sensor values are digitized and stored on digital cassettes, and data are extracted and processed on a microcomputer after removal from the field.

Rods were placed in small-diameter augered holes, which were carefully backfilled with a soil/water slurry. Because surficial deposits in this locality are dominated by stony till, a coring device could not be employed at the site. Holes were augered with a 1.0" (2.54 cm) diameter drill, allowing only crude inferences to be drawn about the nature of the substrate. Cuttings brought to the surface on the drill helix indicated that the mounds were overlain by 20-30 cm of peat and contained a higher proportion of clear ice than did surrounding terrain. Cuttings consisting of mixtures of ice and mineral soil indicated that permafrost underlying the low areas contained mostly pore ice and that it was overlain by a thickness of peat similar to that atop the mounds. Two probe lines (hereafter referred to as Core 1 and Core 2) were placed in wet, flat portions of the marsh, while two (Core 3 and Core 4) extended downward from the summits of small (0.5 m relief) frost mounds. Each supporting rod was connected to a 0.25 m^2 rectangle of open mesh wire at the ground surface level to ensure that the rod would heave with the surface and maintain standard reference depths. The recorder was set to a data collection interval of 8 hours, and started on 22 August 1984.

DATA AND ANALYSIS

Temperature data from the four thermistor strings over a 164-day period are displayed in Figure 2. The arrays extend through the freezeup period into midwinter, and represent the only published long-term, high-frequency temperature series from palsa-scale frost mounds known to the authors. The system failed from power depletion on the 165th day of operation. During the period of data acquisition, the cassette drive locked on several occasions, apparently due to low temperatures, although the clock and other electronic components continued to function. There are, therefore, similar gaps in the temperature series at all four locations. The cable connecting Core 4 with the data logger was found to be severed upon return to the site in 1985, apparently by animal activity; the record from this thermistor string extends over a period of only 107 days.

Following freezeup, temperatures at the mound summits experienced much lower snow/soil interface temperatures than the surrounding marsh. Although the site was not visited during the recording period, this relationship apparently stems from microtopographic controls over snow redistribution patterns, as suggested by other workers such as Allard et al. (1987) and Seppälä (1982, 1986). After the

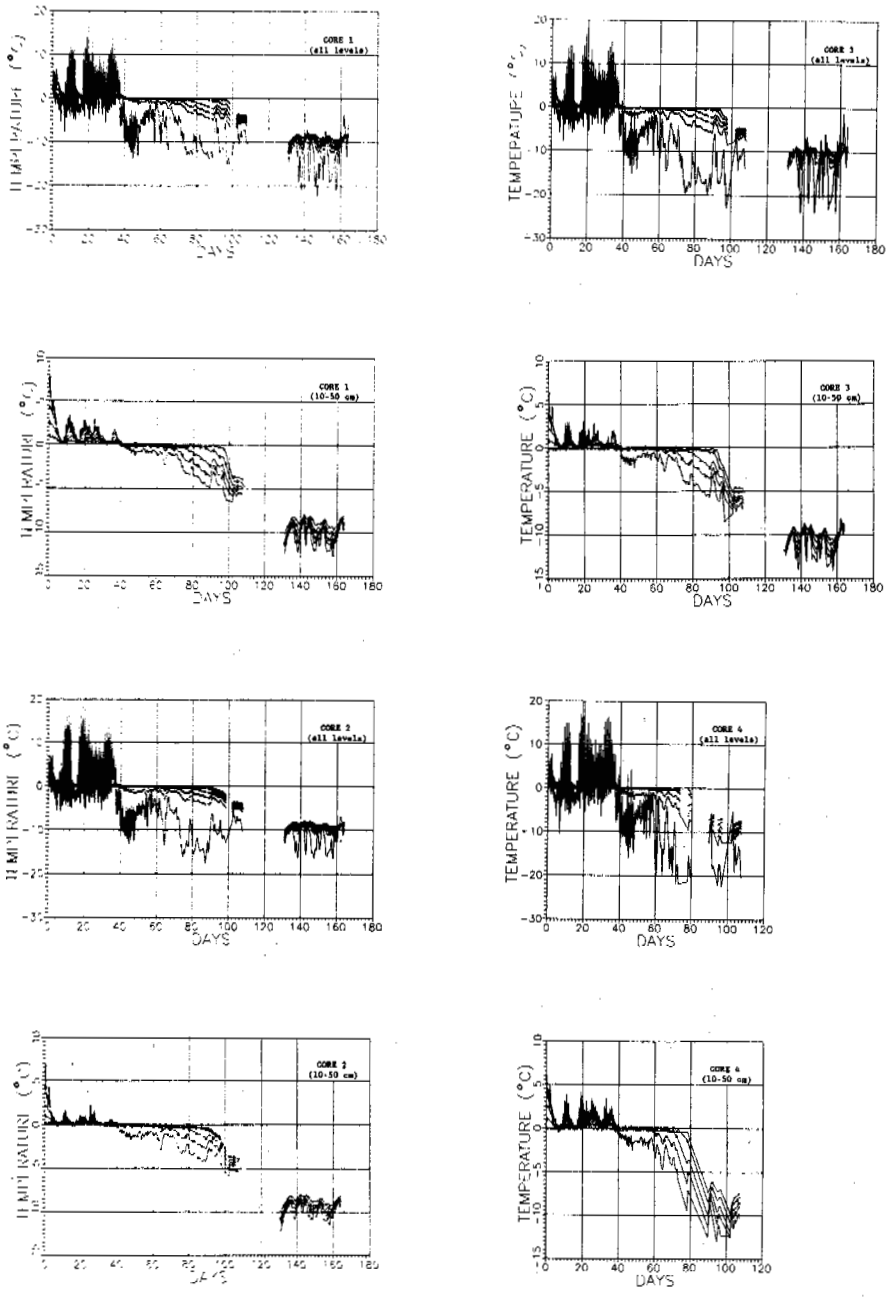

Figure 2. Temperature records by core over observation period. Thermistor positions (0, 10, 20, 30, 40, 50 cm) are easily identified because temperature decreases downward from surface until day 40. After end of zero curtain effect temperature increases with depth. Surface temperature is shown as solid line without symbols.

onset of consistently negative temperatures, thermal gradients were more pronounced, surface temperatures were generally lower, and thermal amplitudes were greater in Cores 3 and 4 than in Cores 1 and 2. During the first two months of record, temperature differences between mounds and marsh were negligible. Divergences became pronounced during late October, and by January temperatures within the mounds were several degrees colder than at corresponding depths in the surrounding marsh. These relationships all provide support for the contention that snow accumulation was less on mound summits (see Allard and Seguin 1987, Fig. 4).

Figure 3 displays the data as a thermal surface over the first 107 days of record (97 and 73 days for Cores 3 and 4, respectively). The

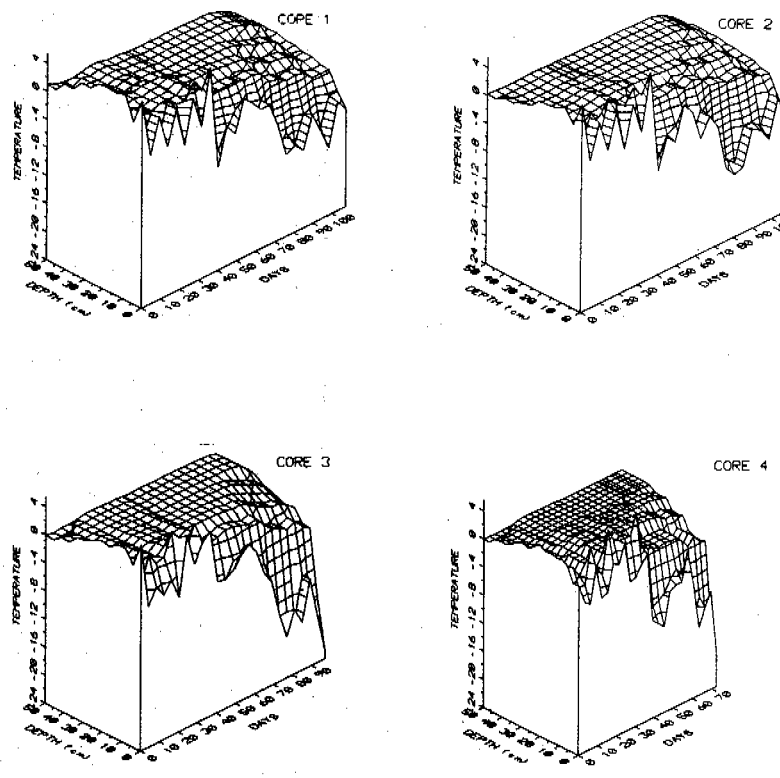

Figure 3. Temperature series by core, plotted as thermal surfaces. See text for details.

records were smoothed to approximate mean daily temperatures. During the initial three weeks, a large contrast existed between temperatures at the surface and those at depth during warm and cold weather events. Core 2 experienced upfreezing from the bottom of the unfrozen layer during cold periods and no deep penetration of positive isotherms during the second low-frequency (multiple day) period of surface warmth. The thermal response at the summits (Cores 3 and 4) was quite similar; these locations experienced only a minor degree of upfreezing. Core 1 is unique in its absence of upfreezing at the 50-cm level and in deep penetration of the second and third low-frequency surface warmth events.

Figure 2 shows a remarkable consistency in the time at which the entire 50-cm section reached subfreezing temperatures. A very prominent zero curtain (Brewer 1958) is apparent in all four cores. Isolated peaks and depressions in the thermal surfaces shown in Figure 3 at about this time and in the vicinity of 0°C are probably produced by vapor transport and heat of evaporation effects. These events occurred in Core 2 before freezeup and in all four cores during the period between freezeup and penetration of the -1°C isotherm to the level at which the events occurred. These events may represent heating or cooling resulting from internal evaporation/distillation effects (Nelson et al. 1985; Outcalt and Nelson 1985), since they do not persist at lower temperatures. Unfortunately the relatively coarse temporal interval at which the data were collected precludes high-resolution calculation of effective thermal diffusivity as performed by Nelson et al. (1985). Core 4 cooled rapidly after penetration of the -1°C isotherm to the 50-cm level. This rapid cooling may be the product of a shallow or dense snow cover at this location.

CONCLUSIONS

The data suggest that temperature contrasts in peat terrain underlain by permafrost are related to topographically induced differences in soil moisture, snow depth and/or snow density. Contrasts between adjacent instrumented locations are apparent in isothermal mappings on a time-depth grid, and demonstrate that such effects can be pronounced. The data provide support for the hypothesis that relationships between microtopography and snow cover produce important feedback effects that lead to stability of of frost mounds in this vicinity (Outcalt et al. 1986). They also suggest that ice-rich permafrost in peatlands can exhibit a nonconductive heat-transfer response to surface

temperature variations over long periods. This response is similar to that recorded at shorter (e.g., diurnal) time scales (Nelson et al. 1985). These observations confirm conclusions reached earlier (e.g., Outcalt and Nelson 1984) about interactions between mound morphology, snow distribution, and ground temperature.

ACKNOWLEDGMENTS

We gratefully acknowledge support from the Division of Polar Programs, U.S. National Science Foundation for the project "Growth and Decay of Palsas and Related Frost Mounds in Central and Northern Alaska" (grant #DPP-8117124). The paper has benefitted from critical reviews by A.L. Washburn and three anonymous reviewers.

REFERENCES

Allard, M. and Seguin, M.K. (1987). The Holocene evolution of permafrost near the tree line, on the eastern coast of Hudson Bay (northern Quebec). Canadian Journal of Earth Sciences (24), 2206-2222.

Allard, M., Seguin, M.K., and Lévesque, R. (1987). Palsas and mineral permafrost mounds in northern Québec. International Geomorphology, Part II, 285-309, New York.

Brewer, M. (1958). Some results of geothermal investigations of permafrost in northern Alaska. Transactions of the American Geophysical Union (84), 1, 19-26.

Brown, R.J.E. (1966). The influence of vegetation on permafrost. Proceedings, International Conference on Permafrost, 20-25, Washington.

Brown, R.J.E. and Williams, G.P. (1972). The freezing of peatland. Division of Building Research, National Research Council of Canada Technical Paper 381, 29 pp.

Forsgren, B. (1964). Notes on some methods tried in the study of palsas. Geografiska Annaler (46), 343-344.

Hinkel, K.M., Nelson, F.E., and Outcalt, S.I. (1987). Frost mounds at Toolik Lake, Alaska. Physical Geography (8), 2, 148-159.

Kingsbury, C.M. and Moore, T.R. (1987). The freeze-thaw cycle of a subarctic fen, northern Quebec, Canada. Arctic and Alpine Research (19),3, 189-295.

Lindqvist, S. and Mattsson, J.O. (1965). Studies on the thermal structure of a pals. Svensk Geografisk Arsbok (41), 38-49.

Nelson, F.E., Outcalt, S.I., Goodwin, C.W., and Hinkel, K.M. (1985). Diurnal thermal regime in a peat-covered palsa, Toolik Lake, Alaska. Arctic (38),4, 310-315.

Outcalt, S.I. and Nelson, F. (1984). Computer simulation of buoyancy and snow-cover effects in palsa dynamics. Arctic and Alpine Research (16),2, 259-263.

Outcalt, S.I. and Nelson, F. (1985). A model of near-surface coupled-flow effects on the diurnal thermal regime of a peat-covered palsa. Archives for Meteorology, Geophysics and Bioclimatology (33A), 345-354.

Outcalt, S.I., Nelson, F.E., Hinkel, K.M., and Martin, G.D. (1986). Hydrostatic-system palsas at Toolik Lake, Alaska: field observations and simulation. Earth Surface Processes and Landforms (11), 79-94.

Seppälä, M. (1976). Seasonal thawing of a palsa at Enontekiö, Finnish Lapland, in 1974. Biuletyn Peryglacjalny (26), 17-24.

Seppälä, M. (1982). An experimental study of the formation of palsas. Proceedings of the Fourth Canadian Permafrost Conference, 36-42, Ottawa.

Seppälä, M. (1983) Palsasuon talvilämpötiloista utsjoella. Oulanka Reports (4), 20-24.

Seppälä, M. (1986). The origin of palsas. Geografiska Annaler (68A),3, 141-147.

Zoltai, S.C. (1971). Southern limit of permafrost features in peat landforms, Manitoba and Saskatchewan. Geological Association of Canada Special Paper (9), 305-310.

FROST MOUNDS IN KAFFIÖYRA AND HERMANSENÖYA, NW SPITSBERGEN, AND THEIR ORIGIN

W. Niewiarowski and M. Sinkiewicz

Nicholas Copernicus University, Fredry 8, 87-100 Toruń, Poland

ABSTRACT

During Toruń Polar Expeditions in 1978 and 1985 the authors noted that 4 types of frost mounds occured in Kaffiöyra and Hermansenöya: peat mounds with mineral core, peat mounds with ice core, vegetation mounds and earth mounds. Their morphology, inner structure and discussion on origin and terminology are presented.

INTRODUCTION

Inland Svalbard which is not occupied by glacier ice, occurs within a zone with continuous permafrost, a thickness of which varies from 75 to 450 m /Salvigsen 1984/.

Frost or permafrost mounds have been already found in the fifties of the present century amongst periglacial features, developed on flat raised beaches and broad valley floors. During Polish polar expeditions frost mounds with ice core were noted on Sörkapp Land and named by Jahn and Szczepankiewicz /1958/, and their followers, the hydrolaccoliths. In other parts of Spitsbergen frost mounds were also found and considered for pingos. Among others Åhman /1973/ distinguished open and closed types of pingos in Adventdalen and Reindalen. Such mounds are distinguished among others on the map of Liestöl /1977/ and on the Norwegian geomorphologic map of Svalbard in scale of 1:1.000.000, prepared by Kristiansen and Sollid in 1986. These maps do not present any such mounds in Kaffiöyra and Hermansenöya. Besides these features, Salvigsen /1977/ described peat mounds, named palsa-like forms, from Nordaustlanded, and Åkerman /1982/ distinguished on strandflat area south of Kapp Linné in western Spitsbergen "true" palsa and also injection turf mounds, active layer turf mounds and vegetative turf mounds. It is worth mentioning that the area south of Kapp Linné, indicates similar physiographic and climatic conditions as Kaffiöyra and Hermansenöya.

Presented chosen examples suggest that origin of frost mounds of Svalbard is not understood in full and demands further investigations whereas applied terminology is controversial / e.g. Jahn 1986 /. The authors had a good opportunity to study some frost mounds during the Toruń Polar Expeditions in 1978 and 1985 on Kaffiöyra and Hermansenöya. Oscar II Land in northwestern Spitsbergen. The analysis of these mounds is the subject of this paper. One should however add that investigations of frost mounds formed only a fragment of carried broad geomorphologic studies and therefore are the preliminary ones, without a profound approach to the subject.

GENERAL DESCRIPTION OF KAFFIÖYRA AND HERMANSENÖYA

Kaffiöyra forms a relatively flat plain, 13 km long and 1-4 km wide, which is surrounded from the east by mountain massifs and in other areas by Forlandsundet and its bays. Main geomorphologic elements of this plain consist of isostaticly raised strandflat and beaches with well preserved beach ridges and old lagoons. It gets lower from about 65 m a.s.l. at foot of mountain massifs toward Forlandsundet, creating several terrace steps. Locally minor end moraines are preserved from a glacial advance of 2500-3000 BP /Niewiarowski 1982/ as well as well developed moraines and other glacigenic features of Aavatsmarkbreen, Elisebreen, Andreasbreen and Dahlbreen. They are connected with glascial advances during the Little Ice Age and the following retreat. Outwash fans and plains, meltwater valleys and niveofluvial valleys are also important geomorphologic elements.

Kaffiöyra is composed of rocks of the Hecla Hoek Succession to the east of the fault running from a foot of Heinrichfjella to Snippenodden. To the west of this fault there are Palaeogene rocks, amongst which conglomerates and sandstones predominate. Only between Öyrnes and Snippenodden there are outcropes of Pleistocene sediments in a sea cliff, composed of marinoglacial stratified clays and silts with pebbles and boulders coming from melted icebergs. Locally there are till and quite common boulders from the older glaciation. The latter is supposed to have covered the whole Kaffiöyra shortly prior to 40.000-45.000 years BP /Boulton 1979, Salvigsen 1977 b/. These older rocks and sediments are discordantly overlain by beach sands and gravels a thickness of which, noted in sea cliffs, varies from 0,5 to about 2-3 m. Locally as for example by a terminal-lateral moraine of Aavatsmarkbreen, a thickness of sands and gravels reaches 6.3 m at about 60 m a.s.l. But in general, a thickness of beach sediments is usually small on higher raised strandflats and large areas are occupied by outcropping rocks of Hecla Hoek Succession and of Palaeogene. Raised beach ridges as well

as flat plains are mainly composed of beach sands and gravels but locally there are also tills and boulders. In ancient lagoons there are also fine sands, silts and clayey silts, and in local small depressions peats. Knowledge of lithology is needed for understanding the possibilities for frost mound development.

Hermansenöya is composed of rocks of the Hecla Hoek Succession. It rises to 39 m a.s.l. It is covered by several flat raised strand-flats with absence or very thin mantle of beach sediments. Only the low terraces have older Pleistocene sediments and a cover of beach sands and gravels is thicker. Ancient lagoons possess locally marine sands and silts, and peats.

Kaffiöyra and Hermansenöya have a polar climate with intensive oceanic influence. According to the data from Isfjorden Radio Station, some 70 km to the south-east, in 1946-1965 a mean annual air temperature was equal -4.4^0 C, a mean temperature of the coldest month (March) was -12.1^0 C and of the warmest month (July) 4.5^0 C. Mean monthly air temperatures below 0^0 C are noted since October until May and only four summer months (June-September) have mean monthly air temperatures over 0^0 C /Steffensen 1969/. The analyzed area is located within a zone of annual total precipitation of 345-422 mm, about 80 % of which is constituted by snow /Moign 1973/.

Such climatic conditions result in a common continuous permafrost in Kaffiöyra and Hermansenöya. During a polar summer the upper layer of permafrost (aktive layer) thaws and a thickness of it, dependent on lithology and water content of sediments as well as summer temperature, was equal on Kaffiöyra in 1980 from 25 to 142 cm /Marciniak, Szczepanik 1983/. During some seasons local maximum thickness of active layer up to 1.6 m were also noted on present beach ridges and on Elisebreen outwash plain. In places this layer can be thicker as e.g. in 1978 a permafrost was not found in the esker to a depth of 4 m /Niewiarowski 1982/. But it can be generally accepted that on Kaffiöyra a maximum thickness of the active layer is usually up to 1.5 m. It seems to be a significant question if a seasonal permafrost contacts every year in winter with a perennial permafrost. Are there any milder winters with a thick snow cover, preceded by warm summers, when a growing downwards permafrost and a perennial permafrost are separated by an unfrozen soil i.e. the so-called "perezimok" in Russian literature /Vtiurina 1981/? In the beginning of July 1985 the authors noted in the undercut of Waldemar river that under thawed deposits (to 0.6 m depth) was a winter permafrost (0.2 m thick). This seasonal permafrost was separated from a perennial permafrost by an unfrozen soil (0.2 m thick). Similarly in a sea cliff near Snippenodden a seasonal permafrost, still frozen partly in the mid-July was underlain by a layer of unfrozen gravels (about 0.4 m thick). Probably a phenomenon of survival of unfrozen soil is not an exeptional case as in July 1978 on a moraine slope of Aavatsmarkbreen covered by a snow patch, about 10 cm thick unfrozen soil was noted under a seasonal permafrost. Basing on these facts one can find that such phenomena can be more common in this part of Spitsbergen. If it is true then it can be of significance for understanding the conditions in which frost mounds develop.

The present beach and just developed outwash plains are not covered with tundra vegetation. The latter is also very scarce on moraines from the end of 19th and from 20th centuries. On the other hand raised beaches have different variants of arctic tundra vegetation /Gugnacka-Fiedor, Noryskiewicz 1982/.

In the analyzed area there are quite common periglacial features as patterned grounds, stone circles, polygons, stripes, solofluction tonques, etc. Shallow tundra lakes are common.

FROST MOUNDS AND THEIR STRUCTURE

Peat mounds with mineral or ice core

Kaffiöyra and Hermansenöya show rare large frost mounds with their heights over 1 m. Detailed investigations prove that they occour only in areas of some previous lagoons or sea bays, intensively wet and with peat.

Three larger mounds of this kind were noted in Kaffiöyra in its southern part at 14-15 m a.s.l. /Fig. 1/. Their location seems very characteristic. They occur in a previous sea lagoon, located near ancient beach ridges. At present its lenght is equal about 0.5 km and width reaches 80 m. Within this area there are three small peat-bogs, 60-180 m long and 30-70 m wide, with small and shallow (to 0.4 m) pools. Unlike a dry terrace surface and beach ridges, a depression floor is permanently wet

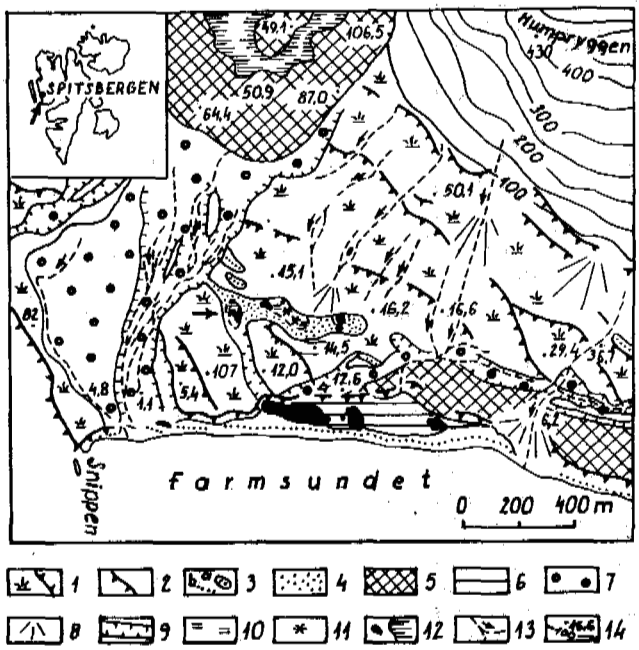

Figure 1. Geomorphological map of southern Kaffiöyra and its surroundings
1 - raised beaches with scarps, 2 - marine cliffs, 3 - beach ridges: a - old, b - present, 4 - raised lagoons 5 - terminal and lateral moraines, 6 -morainic plain, 7 - outwashes, 8 - alluvial and talus fans, 9 - valleys, 10 - peatbogs, 11 - frost peat mounds, 12 - lakes and pools, 13 - streams, 14 - contour lines and altitude points.

and fed by waters of periodical streams coming from slopes of Humpryggen and higher inclined beaches, covered by weathering waste and talus-alluvial fans. Datings of shells of marine molluscus from the same terrace at 13.5 m.a.s.l. by radiocarbon method indicated the age of 10.730±230 BP in the outer layer and 9.720±110 BP in the inner layer /Goslar et al. 1985/. These mounds are located within peat-bogs in the vicinity of pools. One of them is of elongated shape (25 m long, about 2 m wide and 0.7 m high) and two others are oval. The highest one was studied in detail /Fig. 2/.

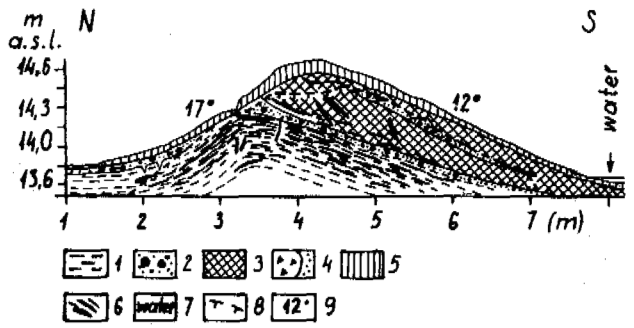

Figure 2. Structure of a frost peat mound with mineral core
1 - marine clayey silt, 2 - sand and gravel, with marine shells, 3 - peat, 4 - interbedded solifluction layer, 5 - vegetation mat, 6 - segregation ice, 7 - water, 8 - top surface of permafrost, 9 - slope angle.

It is 13 m long, 10 m wide and about 2 m wide and about 1 m high. Northern slope is inclined at angle of 17^0 and is overgrown mainly by mosses whereas the southern one, of 12^0, is mainly covered by lichens.

A structure of this mound is presented /Fig.2/. In the bottom there are bluish clayey silts, raised due to frost upheaving. They contain layers and lenses of segregated ice, 0.5-3.0 m thick, parallel to the top of silts. Besides them there are also ice veins, almost vertical and 2-7 cm thick. Silt surface in the northern part contains fine cracks (to 7 cm deep) that are filled with sand. Silts are covered with gravels and sands with shells of sea molluscs that prove a marine orgin of sediments. They are mantled with peat, to 0.5 m thick, and a vegetation mat. Within a peat there is a layer (5-7 cm thick) of fine sands and sharp-edged gravels. Their mutual relation is an univocal evidence for their solifluction origin.

An occurrence of peat is very characteristic as it mantles completely a mound from its southern side and submerges under a pool water. On the other hand it is absent on the northern side. In a bottom of the peat there are also layers of segregation ice, parallel to a silt top and ice veins of 5-7 cm in diameter and noted length to 70 cm, running almost vertically. During investigations in August 1985 a top of permafrost occurred at various depths from 8 to 40 cm, i.e. much more shallow than in the neighbouring area.

Presented structure enables the following conclusions:

- previous lagoon depression between beach ridges was filled at the beginning of the Holocene by clayey silts, sands and gravels,
- during a growth of peat its top has been mantled with solifluction tonques, a
- depth of depression with peat was varying and so, thinning out of peat northwards reflects a local varying peat, thickness instead of its destruction as the latter is not proved by any evidence,
- a development of frost mound follows a peat deposition,
- a development of this mound was undoubtedly caused by frost upheaving of clayey silts and formation of segregation ice, either in silts or in peat, from water around during a mound growth,
- although a mound surface shows narrow cracks there no distinct symtoms of its degradation, similary as in two neighbouring mounds. They are therefore stabile features with neither aggradation nor degradation signs. The fact that they are easily recognizable at Norwegian air photos of 1966, can be another evidence for this statement. In their appearance and topographic location the analyzed features are similar to the ones described by Åkerman /1982/ as "true" palsas to the south of Kapp Linné. But they are significantly different from them as they have a mineral core whereas Åkerman noted only peat inside his palsas. No collapsed forms are noted here as well.

Peat mounds with ice core are found only on a floor of ancient sea bay in southeastern part of Hermansenöya but with a remark, that above 3 m a.s.l. only a thin cover of beach sands and gravels occurs on rocks of the Hecla Hoek Succession. Below, there is a peatbog of 200 x 120 m large, with a noted thickness of peat equal 20-50 cm. In the western part of a peat-bog, at foot of a beach edge of 12 m a.s.l., there is a pool of 40 x 30 m large. A peat-bog surface is dissected by a polygon pattern. An excess of water in the pool is drained towards Farmsundet by shallow (0.6 m) channel, to 3 m wide, that cuts peat to a mineral substrate. Channel edges are irregular what is caused among others by thermic erosion, falling of peat blocks and irregular extension of the channel. The latter collects also side troughs to 1 m wide, developed mainly on a pattern of frost polygons what results in a dissection of the peat-bog into numerous patches near the outflow channel.

Near the pool a peat covers directly sands and gravels of marine origin whereas close to the outflow channel a peat surface rises a bit and has several distinct peat mounds, 0.5-1.0 m high. The highest one which is 1.1 m high and 5 x 7 m large, was analyzed in detail. Its inner structure is presented /Fig.3/.

A peat layer, 0.4-0.5 m thick occurs at the surface. The peat is dry ad overgrown, mainly by lichens. On steeper slopes the peat is strongly fissured; at contacts with troughs and outflow channel there are traces of fallen peat blocks. Mound core is composed of massive (injection) ice with air bubbles. The ice was noted to be over 0.6 m thick. In its upper part it contains a large admixture of organic matter (and for this reason has a darker colour), a

content of which decreases downwards and so, a clean ice appears there. Massive ice but of considerably smaller thickness, was also noted in the mentioned before raised peat patches. Although analyzed monund are, if compared with the ones from Kaffiöyra, less stabile there are no sumptoms here as well for their degradation. No colapsed forms were also noted.

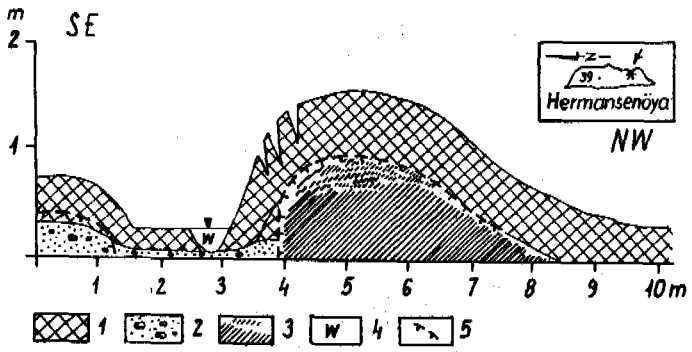

Figure 3. Internal structure of the frost peat mound with ice core
1 - peat, 2 - marine sand and gravel, 3 - massive ice in upper part with organic matter, 4 - water, 5 - top surface of permafrost.

The described peat mound with ice core is in structure, dimensions and location by an outflow channel, completely cimilar to injection ice turf mounds distinguished by Akerman /1982/. It is also similar to a peat mound with ice core from Noraustlandet, described by Salvigsen /1977/ and named the palsa-like form, as well as to some peat mounds from Sörkapp Land, described by Czeppe /1966/ and named the hydrolaccoliths. It seems undoubtful that such features developed due to aggradation of massive (injection) ice, although no ice injection into a peat cover was noted within the analyzed peat mound from Hermansenöya. Water for a formation of this ice comes probably from water content of sands and gravels, but mainly from water that filtrates through a beat-bog from a pool and outflow channel.

In spite of explanation of origin of these two types of peat mounds, a problem of their genetic name (terminology) remains unsolved. They indicate however many common features with aggradation palsas. They are located within peat-bogs and a small number of them in any assemblage can be easily explained by small dimensions of peat-bogs. They have a peat cover and aggradation of segregation ice was the main reason for a development of peat mound with a mineral core on Kaffiöyra.

A peat mound with ice core on Hermansenöya is indentical with injection ice turf mounds that were distinguished by Akerman /1982/. He did not consider them for palsas neither named them pingos. This mound shows however some similar features to palsas, among others the main source of water for massive ice seems to come from a gravitation free water, and also to small open system type pingos. It seems true as well that growing of described frost mounds can also result, at least in their initial phase, from a use of water content of unfrozen sediments, occurring sporadicly between a seasonal and perennial permafrost ("pierezimok").

The analyzed peat mound are principally different from classical Scandinavian palsas as they occur in a zone with a continuous permafrost. Palsas are typical for areas with a discontinuous, sporadic permafrost /among others Lundquist 1969, Jahn 1975, 1976, 1986, Ahman 1976, Seppälä 1979, Pissart 1983/. According to Jahn /1986/ the term palsa should not be used for the features in Spitsbergen. The preliminary character of authors' investigations makes wider discussion impossible if terminology is concerned but they are sure that data, presented in this paper can be useful in such discussion.

Vegetation mounds

In Kaffiöyra there are two types of vegetation mounds that is mounds wich rise above their surroundings not only due to a considerably more abundant tundra vegetation and accumulated organic matter, but a height of which is also to some extent a result of existing frozen mineral core (rising slightly above its vicinity), and vegetation mounds which rise above their surroundings only due to more abundant vegetation and have no mineral cores.

The first type of mounds is most frequently noted on ancient beach ridges. They are usualy several metres wide and 0.7 m (maximum to 1.0m) high /Fig. 4/. They are overgrown with mosses, lichens and vascular plants (among others Poa alpina, Luzula confusa) and by nitrophilous species /Gugnacka-Fiedor, Noryskiewicz 1982/. Excavations proved that under 20-30 cm thick vegetation mat (turf) there is a mineral, sandy-gravel (with admixture of coarse gravels and pebbles) core, curved concordantly with a top of permafrost. Sporadicly it has streaks and lenses of segregated ice. The latter is most common in frost fissures to 30 cm deep that form a system of polygons.

Such mounds should be, in our opinion, named vegetative frost mounds as but accumulation of plant remains, their growth is also to some extent influeced by frost upheavel under a protective vegetation cover.

The other, exclusively vegetation type of mounds, contains smaller features that were also noted in flat, partly wet areas where organic material contained also reindeer antlers and remains of whale bones. They are not the only type of such vegetation mounds in Spitsbergen as e.g. Jersak /1968/ described moss rings and Serebryannyi et al. /1984/ noted small peat ridges and mounds, formed due to accumulation and creep of peat into polygonal fissures. Akerman /1982/ found similar mounds to the described ones and named them the vegetative turf mounds, in the area to the south of Kapp Linné. They occurred there only in drier zones, mainly on beach ridges, in which under a turf there were driftwood, whale bones and reindeer skeletons. Their decomposition was found to supply with nutrients the poor tundra soils and thus, a richer development of vegetation. This author accepts also an isolating role of organic cover (already at its thickness of about 30 cm) what anables a development of a frozen core inside a mound, formation of segregation ice and consequently, and increase of its height. These mounds cor-

Figure 4. Vegetative frost mound

respond therefore with the first type of forms on Kaffiöyra. Numerous other papers on such vegetation mounds from Spitsbergen prove that a similar role in fertilization of tundra soil is constituted by excrements of sea birds, flocking on drier mounds with a richer vegetation. It can be the reason for a selective occurence of driftwood as well as whale, reindeer bones in some vegetation mounds on Kaffiöyra.

Earth mounds

Earth mounds are single or form small groups in wet, quite flat tundra areas, within polygons of frost fissures. They are usually oval, 1.5 x 1.0 m large and 0.2 - 0.4 m high. They are composed in the upper part of sandy-silty sediment with admixture of organic matter and deeper, of vary-grained sands and gravels. These sediments indicate a frost upheavel what is expressed by layer bends parallel to a topography of mounds. On the surface the mounds are usually covered with mossy-lichen vegetation mat, 7-15 cm thick. Lower part of mounds is overgrown also by grass beside mosses an lichens. Similar mounds, named mounds of frost upheaval, were described by Fedoroff /1966/ from Adventdalen in Spitsbergen. Basing on investigations on the Banks Island, the origin of such features was presented by Pissart /1976/ and named the earth hummocks after other authors. According to him these features develop due to seasonal upheaval of wet earthy core during its freezing. It should be underlined that on Kaffiöyra in mid-August 1985 no segragation ice was noted inside the earth mounds whereas permafrost occurred about 20-30 cm beneath them.

CONCLUSIONS

A poor development of larger frost mounds on Kaffiöyra and Hermansenöya, and first of all a lack of typical pingos (while they occur in other parts of Spitsbergen) are not due to climatic reasons but lithologic-hydrologic conditions. A shallow occurrence of rocks of the Hecla Hoek Succession and Palaeogene rocks, relatively thin sandy-gravel beach sediments and small content of silty-clayey components as well as sloping of the plain towards Forlandsundet do not favour, with a probable considerable thickness of perennial permafrost, outflows of sub- or mid-permafrost waters onto surface. Existence of larger taliks and development of vast peat-bogs seem also improbable. These conditions decidedly influeced a development of only small frost mounds that are connected with active layer of permafrost (earth mounds), with specific features of development of tundra vegetation (vegetative mounds) and with local hydrologic-lithologic conditions (ancient sea bays and lagoons) in which silty-clayey sediments could be deposited and peat accumulated (peat mounds with mineral or ice cores).

Without datings of peat one cannot find if peat frost mounds are formed in present climatic conditions or they reflect some climatic variation during the last few hundred years. Their stability and absence of collapsed forms seem to suggest that they developed in slightly more severe climatic conditions (e.g. during the Little Ice Age) and that present climatic conditions favour their conservation.

REFERENCES

Ahman, R /1973/. Pingos i Adventdalen och Reindalen på Spitsbergen: Meddel. Lunds Univ. Geogr. Inst. 503, 189-197.

Ahman, R /1976/. The structure and prophology of minerogenic palsas in Northern Norway. Biul. Perygl. /26/, 25-31. Boulton, G S /1979/. Glacial history of the Spitsbergen archipelago and the problem of a Barentsshelf ice sheet. Boreas /8/, 1, 31-57.

Czeppe, Z /1966/. Przebieg glownych procesów morfogenetycznych w poludniowo-zachodnim Spitsbergenie /Sum. The course of the main morphogetic processes in south-west Soitsbergen/. Zesz.Nauk. UJ,/127/, Prace Geogr. /13/, 1-125.

Fedoroff, W /1960/. Les sols du Spitsberg Occidental. Presqu'ile du Brögger et vallées de l'Advent et de la Sassen. In: Spitsberg 1964 et premiéres observations 1965. C.N.R.S., R.C.P., 42, 111-228, lyon.

Frankiewicz, W/1960/.Formy typu hydrolakkolitów na Sörkapp Land. In: II Symp.Nauk.Pol.Wypraw na Spitsbergen 1957-1958, 1959. Streszcz. ref. i komun. Kom.Miedzynar.Wspólp.Geofiz. PAN. Warszawa

Goslar, E, Goslar,TT$_{14}$, pazdur M F/1985/. Datowanie metoda ^{14}C kosci i muszli - problemy metodyki i interpretacji wyników. Zesz.Nauk.Polot.Slaskiej, ser. mat-fiz., /46/, 71-82

Gugnacka-Fiedor, W., Noryskiewicz,B /1982/. The vegetation of Kaffiöyra. Oscar II Land, NW Spitsbergen. Acta Univ.N. Cepernici, Geogr./16/, 203-238.

Jahn, A /1975/. Problems of the periglacial zone, PWN, 223 pp. Warszawa

Jashn, A /1976/. Pagórki mrozowe typu palsa /Sum.Palsa-type frost mounds/. In: Problemy geografii fizycznej, Studia Soc.Sci.Torun., sec.C, /8/,4-6, 123-139.

Jahn, A /1986/. Remarkson the origin of palsa frost mounds. Biul.Perygl., /31/, 123-130.

Jahn, A., Szczepankiewicz S /1958/. Geomorphological and periglacial researches carried out north of Horsund Fiord in summer 1957. Przegl. Geofiz. /3/,2, 123-129.

Jersak, J /1968/. Moss rings in Sörkapp Land, Vest-spitsbergen. In: K.Birkenmajajer /ed./, Polish Spitsbergen Expeditions 1957-1960. Pol.Ac.Sci. 3 IGY/ IGG Committee, 283-292.

Kristiansen, K.J, Sollid J.L /1986/. Svalbard, Glacial-geologisk og Geomorfologisk Kart 1:1 000 000 Nasjonalatlas for Norge, Geogr.Inst.Univ. i Oslo.

Liestöl, O /1977/. Pingos, springs, and permafrost in Spitsbergen. Årbok 1975, 7-29.

Lundquist, J /1969/. Earth and ice mounds: a terminological discusion. In: T.L. Péwé/ ed/. The Periglacial Environment. McGill-Quenn's Univ. Press, 203-215, Montreal.

Marciniak, K., Szczepanik,W /1983/. Results of investigations over the summer ground thawing in the Kaffiöyra /NW Spitsbergen/. Acta Univ.N.Copernici, Geogr. /18/, 69-97.

Moign, A. /1973/. Strandflats immergés et emergés du Spitsberg Central et Nord-Occidental. Thése de doctorat d'etat, Univ, de Bretagne occidental 692 pp., Brest.

Niewiarowski, W /1982/. Morphology of the forefield of the Aavatsmark Glacier /Oscar II Land, North-West Spitsbergen/ and phases of its formation. Acta Univ. N.Copernici, Geogr. /16/, 15-43.

Pissart, A /1976/. Sols à buttes cercles non triés et sols striés non triés de l'Ile de Banks /Canada, N.W.T./. Biul. Perygl. /26/, 275-285.

Pissart, A /1983/. Pingos et palsas: un essai de synthese des connaissances. In: Mesoformen des Reliefs im heutingen periglazialraum. Abh. der akad. der Wiss. in Göttingen, Math.-Phys.Klasse, Dritte Folge, 48-69.

Salvigsen, O /1977 a/. An observation of palsa-like forms in Nordaustlandet, Svalbard. Arbok 1975, 364-367.

Salvigsen, O 71977 b/. Radiocarbon datings and the extention of the Weichselian ice-sheet in Svalbard. årbok 1976, 209-224.

Salvigsen, O /1984/. Detection of high ground temperatures in a karst-featured area, Vardebirgsletta near Isfjord Radio, Svalbard. Arbok, 18-20

Seppälä, M /1979/. Recent palsa studies in Finnland. Acta Univ. Oulu, A /82/, 3, 81-88.

Seppälä, M /1986/. the origin of palsas. Geogr. Ann., A /68/, 3, 141-147.

Serebryannyi, L.P., Tishkov, A.A., Malyasova, E.S., Solomina, O.N., Ilves, E.O. /1984/. Rekonstrukciya razvitiya rastitelnosti v vysokoshirotnoy Arktike. Izv. AN SSSR, ser.geogr., 6, 75-83.

Steffensen, E /1969/. The climate and its recent variations at the Norwegian Arctic Stations. Meteorol. Ann. /5/, 8.

Svennsson, H./1986/. Permafrost, some mophoclimatic aspects of periglacial features of Northern Scandinavia Geogr. Ann., A /68/, 3, 123-130.

Vtyurina, E.A /1981/. pereletki i osnovnye tipy sezonnomerzlkykh porod. In: Stroenie i teplovoy rezhim merzlykh porod, 26-35, Novosybirsk.

CONTEMPORARY FROST ACTION ON DIFFERENT ORIENTED ROCK WALLS: AN EXAMPLE FROM THE SWISS JURA MOUNTAINS

A. Pancza[1] and J.-Cl. Ozouf[2]

[1]Department of Geography, University of Neuchâtel, Switzerland
[2]Centre de Geomorphologie du CNRS, Caen, France

SYNOPSIS "Château Cugny" rockfaces in the Swiss Jura mountains are formed of limestones particularly subject to frost shattering. Measurements made since 1973 show that the rock face has receeded at a rate greater than 1 mm/year. Significant differences of frost action have been measured on faces with different orientations. This study in the field, based on continous measurements and accompanied by tests mad by a laboratory-simulated frost shattering give us a quantitative approach to the effect of frost.

INTRODUCTION

Geomorphologists encounter certain difficulties in understanding precisely the process of frost shattering. Too many factors work simultaneously: they sometimes complement each other but they also neutralise each other in other situations. The interpenetration of these factors as well as their interdependence makes their analysis very difficult. A detailed study in the field, based on weekly measurements and completed by experiments in cold rooms lead to a quantitative approach to frost action.

FROST ACTION ON ROCK WALLS

Frost action depends on the air temperature and on the rock structure and its texture (resistance, porosity, microfissures). However other climatic factors (humidity of rock and air, wind) also play a most important part. Among these factors, the orientation of the rock wall directly influences its period of sunshine, its ventilation and also more indirectly the variation of the water content of the rock.It is then natural, that frost acts in a different way in a rock-face oriented toward the south, in comparison to another scarp oriented differently.Even while it is easy to conceive this difference -for the reasons we have just mentioned- it remains however difficult to define the nature and the extent of this influence. In this study, we try to define the part played by the way a rock wall faces in its gradual change and erosion.

Up to now only a few geomorphologists have studied this phenomenon. Rapp (1960) in his well-known study of Kärkevagge measured rock falls according to the temperature and the precipitation recorded as well as in relation to the orientation of the rock wall. Nevertheless, his research was not undertaken in order to analyse the role played by the orientation of rock walls. More recent research by Gardner (1971), Luckman (1976), Douglas (1979) and Thorn (1979) in regions as far apart as the Canadian Rocky Mountains and Northern Ireland focus especially on the study of the frequency of rock falls, but they do not point out the specific influence of the different factors causing the falls. Work has been done in this field by Francou too, but his measurements only permit a more global analysis of the

Figure 1: A Château Cugny west facing rock face. Fragmentary view of one of the walls equipped with rocktraps.

variations betveen north and south-facing walls. However, Francou's observations (1982 and 1987) point out the specific timing of rockfalls in the Alps; he notices that the north facing intense rockfalls happen one month later than the south facing ones.

LOCATION OF OUR MEASUREMENTS

"Château Cugny" rock cliff (coordinates: 564,9/ 236,9) [National map of Switzerland, 1:25'000. Sheet no 1104, Saignelegier.] has an average height of 15 m and is oriented toward the South - South West. Contrary to the other steep areas of the Swiss Jura mountains, "Château Cugny" does not present only a single face, but many rocks oriented in different ways. Indeed this site is formed by several peaks oriented in different ways. (Pancza 1985a).

The limestone (Rauracien), is strongly susceptible to frost action and the average erosion per year exceeds 1 mm. [From 1973 to 1975, the retreat was 1,7 mm/year]. The four areas, whose evolution is regularly observed, cover a 65 m^2 total surface area and are oriented toward the south, west and north. (Figure 1)
Some instruments (temperature, rain and wind recorders as well as rocktraps) allow us to establish the number of freeze-thaw cycles -at the surface and at various depths in the rock- and to measure the frequency of rockfalls. We have already mentioned some of our results in previous papers (Pancza 1979, 1985a, 1985b and 1987).

INITIAL HYPOTHESIS AND METHOD USED

Having observed several facts in the field, we may advance the theory that rock walls aspect plays a very important part in their evolution.

We observed that:

a. The number of freeze-thaw cycles is different on north and south facing slopes. At a depth of 12 cm, we measured 30% more freezing cycles on the south than in the areas oriented toward the north.

b. During the winter months, the north face rarely thaws. So the rockfalls are infrequent, but heavy; when thawing, a huge amount of falling fragments are detached from the cliff.

c. The fragments detached from the north face are generally larger than the ones collected in the rocktraps placed under the south and west faces. All these fragments belonged however to the same limestone strata!

This last observation is fundamental and it gave the starting point to all our measurements, whose first results will be presanted here. The measurements were carried out at "Château Cugny" and in the CNRS laboratories in Caen. We wanted to check if the rock whose evolution was dissimilar at Château Cugny (North and South orientation) would keep this differential evolution in cold rooms under the influence of an identical experimental winter climate.

EXPERIMENTS IN LABORATORY

Samples were taken to the North and South of the same rock peak. Most of them belonged to a facies of fine-grained limestone, whose porosity varies betwen 3 and 7%. Figure 2 represents the diagram of the pores measured with the help of a mercury porosimeter. In these limestones

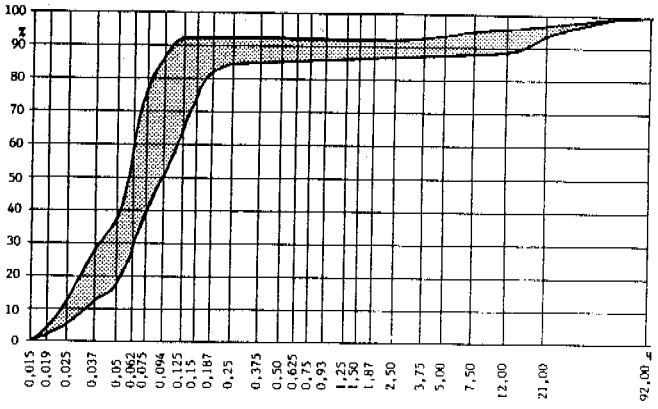

Figure 2: Château Cugny fine grained limestone: pore size distribution curve (6 samples)

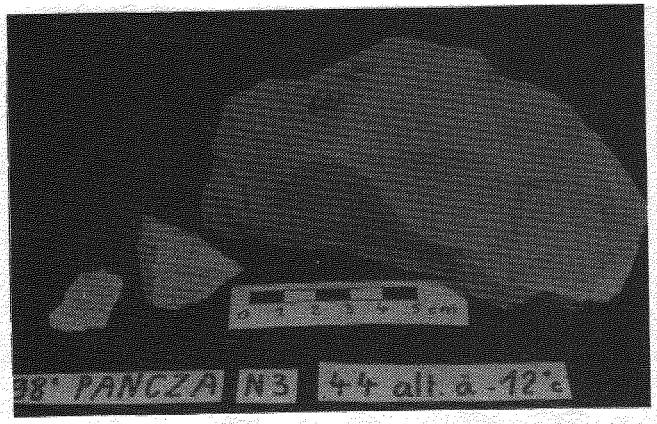

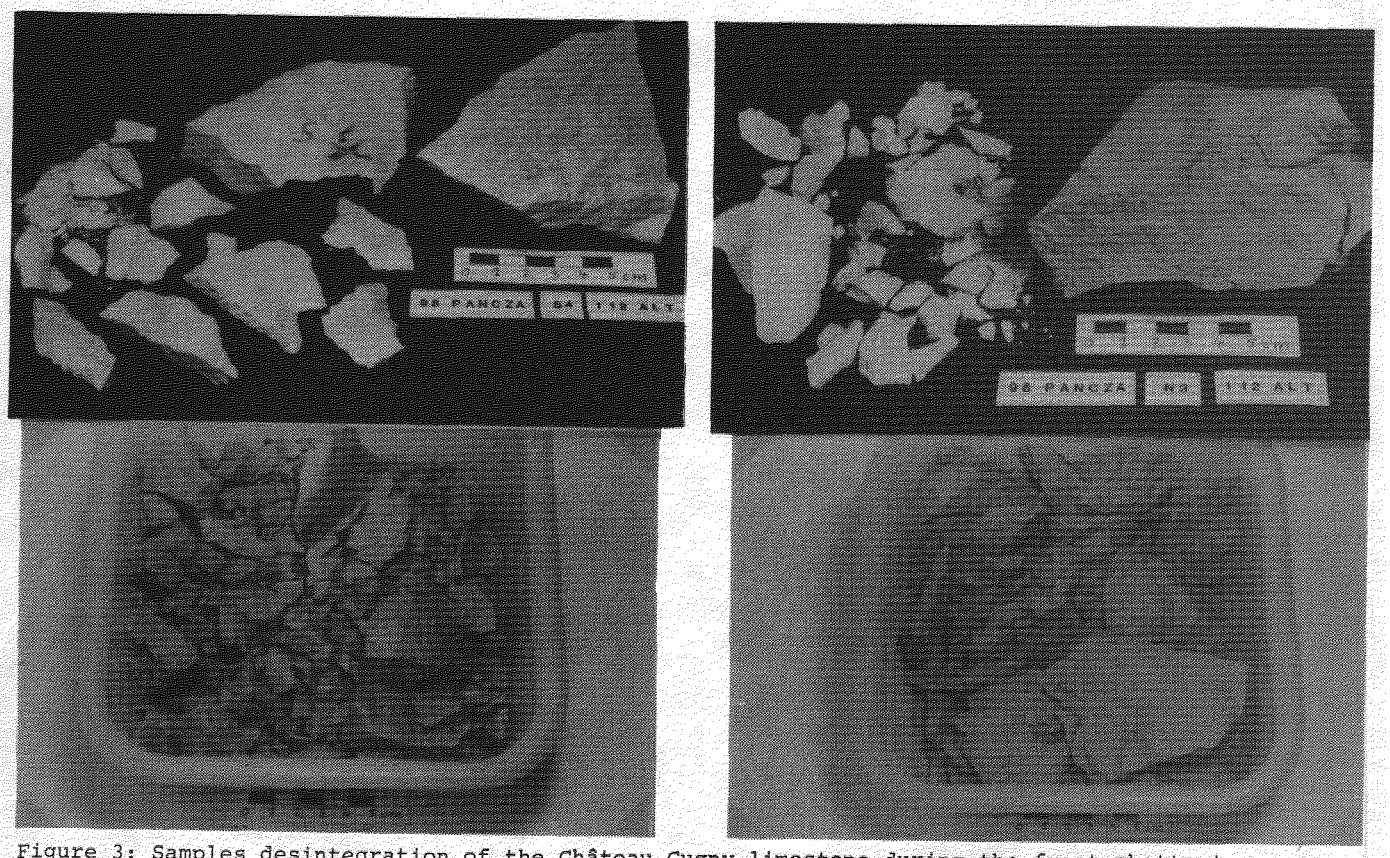

Figure 3: Samples desintegration of the Château Cugny limestone during the frost shattering experiments after 44, 112 and 173 freezing-thaw cycles. (-12°/+15° C) The samples collected to the north of the peak behave the same as the ones collected to the south.

microporosity is predominant: about 90% of the pores are smaller than 0,5 µ.

Château Cugny's limestone contains microfissures too, partially expeaining its sensitivity to frost action. On the whole, the preliminary measurements (capillarity, porosity and permeability) revealed only few differences betwen the samples coming from the north and the south part of the rock face. As for the experimental frost, it was rather moderate: (-12°/+15° C) and consisted in daily cycles. This type of frost is frequent in the Swiss Jura mountains during the winter months.

RESULT OF THE EXPERIMENTS

a. No noticable difference either in the size or in the shape of the fragments coming from the samples has been observed, as can be seen in the photos of fig. 3.

b. All samples gave fragments, and on the whole the most porous ones fragmented themselves sooner than the others.

c. The fragmentation of the samples occurred progressively: the number of detached fragments increased in the same way as the number of freezing-thaw cycles. (fig. 3)

In the laboratory, the samples collected to the north of the rock faces behave in the same way as the ones collected to the south.

MEASUREMENTS ON THE FIELD

For two years, the detached fragments -collected in the rocktraps- have been not only assembled and weighed as before but also counted. We aim at comparing their sizes: the quotient of the samples weight divided by their number

TABLE I

Size distribution of the fallen fragments according to the rock faces orientation.

MONTHS	AVERAGE SIZE OF THE FRAGMENTS IN GRAMMES (results over 2 years)		
	south	west	north
November	34,1	22,1	28,7
December	37,6	23,8	71,0
January	46,4	20,1	130,3
February	48,1	34,2	145,3
March	52,3	25,5	114,8
April	31,6	17,0	48,2
May-October	40,1	22,4	26,3

(These numbers are based on 3667 fallen fragments in the rocktraps.)

allows this comparison.

Table 1 illustrates the results we obtained and shows that:

a. On the whole, the fragments detached during the winter months are not only more numerous -as we already knew- but they are larger as well.

b. The size of the fragments fallen from the north part of the rock face is larger than that of the fragments fallen from the south and west parts of the same peak.(see Table 1)

This last observation is important since these same rock all give similar fragments in the laboratory.

Can we attribute this difference to the part played by the rock face's orientation? We think so. However, to be quite certain, it is necessary to continue the measurements for several more years. Moreover, it is essential to extend the experiments in the laboratory to a larger number of samples as well as to other facies of limestones.

At the level of the Swiss Jura mountains as a whole, this difference -due to the rock faces' orientation- represents one of the characteristic features of the landscape. Indeed, several examples prove that rock faces facing south are more eroded than those facing north; this is revealed by a general dissymmetry in the evolution of several anticlines.

CONCLUSION

In order to understand better the influence of the orientation of the rock walls on frost action, we have started new measurements at the foot of the "Château Cugny" rock faces in the Swiss Jura. At the same time we began an experimental study at the CNRS laboratory in Caen, in order to follow the evolution of rock samples taken from Château Cugny rock walls.

Château Cugny is an exceptionally frost-riven rock cliff. Its average retreat is larger than 1 mm per year. These rock walls are equiped with a temperature recorder. The measurements are observed in the north, south and west faces of the cliff.
Rocktraps have been placed at the foot of the cliffs in order to collect the falling fragments. The place is also equipped with a rain and a wind recorder. Weekly measurements allow us to observe the evolution of four areas oriented toward the South, West and North and covering a total surface area of 65 m^2. Both field and laboratory measurements show us the influence of the rock wall orientation on:

1. the average size of the falling fragments
2. the regime of the falling fragments
3. and the rapidity of the retreat.(develope in previous papers: Pancza 1985a and b).

The rock faces' orientation reads to difference in their evolution. In the Jura mountains, the rock walls facing south are generally more eroded than opposite slopes that face north.

Address of author:
Dr. André Pancza, Department of Geography, University of Neuchâtel. Quai R. Comtesse 2,
2000 Neuchâtel Swìtzerland

REFERENCES

Douglas, G.R. (1979). Magnitude frequency of rockfall in Co. Antrim, N, Ireland. Earth Surface Processes, 4: 123-129.

Gardner, J.S. (1971). A note on rockfalls and northfaces in the Lake Louise area. American Alpine Journal., 317-318.

Francou, B. (1982). Chutes de pierres et éboulisation dans les parois de l'étage périglaciaire. Rev. géogr. Alpine, T: LXX-3, 273-300.

Francou, B. (1987). L'éboulisation en hate montagne. Thèse, Univ. de Paris VII, pp. 1-689.

Luckman, B.H. (1976). Rockfalls and rockfall inventory data: some observations from Surprise Valley, Jasper National Park, Canada. Earth Surface Processes, 1: 287-298.

Ozouf, J.-Cl. (1983). Comparaison de gélifracts naturels de grèzes charantaises et de gelifaracts fabriqués. Thèse, Univ. de Caen, pp. 1-185.

Pancza, A. (1979). Contribution à l'étude des formations périglaciaires dans le Jura. Thèse, Univ. de Neuchâtel, pp. 1-187.

Pancza, A. (1985a). Le Château Cugny, un escarpement particulièrement gélif du Jura. Geogr. Helv., 2: 67-73.

Pancza, A. (1985b). Régime des chutes de pierres dans une paroi rocheuse du Jura. Physische Geogr., 16: 85-94.

Pancza, A. (1987). Le rôle du vent dans la gélivation des parois rocheuses. Symposium of Loess and Periglacial phenomena, Caen. Edit. academic, Budapest. 183-190.

Rapp, A. (1960). Recent developments of mountains slopes in Kärkevagge and surrundings, Northern Scandinavia. Geografiska Ann. 71-200.

Thorn, C.E. (1979). Bedrock freeze-thaw weathering regime in an alpine environment, Colorado Front Range. Earth Surface Processes, 4: 211-228.

GEOCRYOGENIC SLOPE CAVES IN THE SOUTHERN CASCADES

F.L. Pérez

Department of Geography, University of Texas, Austin, Texas 78712 USA

SYNOPSIS Small caves in andesite were studied in northern California. They formed by frost shattering near persistent snowbanks sapping the base of a NE-facing cliff, are elongated, have irregular walls, vaulted ceilings, debris-littered floors, and slope outwards onto a talus. Talus particles showed a pronounced size sorting--larger fragments downslope--, suggesting gravitational deposition; cave clasts did not fit this pattern. Debris piles in the caves had steep fronts and a finer matrix with depth. Cave particles were flatter and more elongated than talus ones due to slab fragmentation during transport. Cave clasts were parallel to the slope, indicating that frost creep and gelifluction transport them out of the caves. These appear to be inactive and probably formed in the late Pleistocene, when the regional snowline was at about 2200 m elevation.

INTRODUCTION

Frost shattering is an important agent of cave formation in periglacial areas (Wolfe, 1967; White & White, 1969; Schroeder, 1979; Roberge et al, 1985). Geocryogenic processes are usually effective only near cave entrances, thus cavities solely formed by them tend to be small. Geocryogenic caves, commonly found at the bases of cliffs, have been called frost pockets (Schroeder, 1979), slope caves (Mitter, 1983), and cave niches (Vítek, 1983). Small pseudokarstic caves in volcanic materials have been reported for the western USA (Kosack, 1952: 18; Halliday, 1960), but few studies dealt with speleogenesis (Parker et al, 1964). This report discusses the characteristics and processes of formation of small slope caves in andesite in the southern Cascades. Special attention is given to clastic cave sediments, which are compared to those on a talus below, genetically related to the caves.

THE PHYSICAL SETTING

The study area, Lassen Volcanic National Park, is in northern California (Fig. 1A). Lassen is the southernmost volcano of the Cascade range, at 40° 29' N and 121° 30' W. Precipitation is concentrated in the October-April period, thus snowfall represents ≥95% of the annual total (Major, 1977), estimated at 1700 mm at 2225 m, the elevation of the study site (Baker, 1944). Snow is redistributed by the prevailing westerlies; large snowbanks persist year-round on N and NE slopes. Temperatures remain below freezing through winter (Major, 1977). From late spring to early fall, there is a strong diurnal fluctuation--maxima: 18-26°C, minima: +6 to -3°C--; freezing occurs then in 40% of the nights (Pérez, unpubl. data). Temperatures of E slopes are lower than those of opposing aspects.

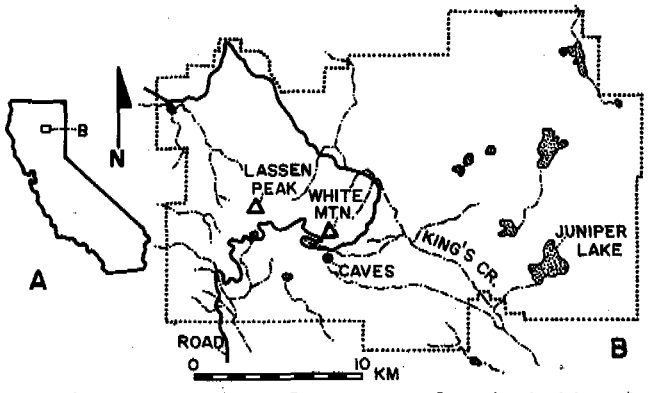

Fig. 1 A: Location of Lassen Volcanic National Park. B: Location of the study site.

The study site is near upper King's Creek meadow, 5 km SE of Lassen Peak and 1.7 km S of White Mtn (Fig. 1B). The caves have a subalpine location, at 2225 m elevation at the base of a 20 m-tall cliff facing N 51°E; a steep, 50 m-long talus extends below (Fig. 2). The talus is largely bare, with some herbs and shrubs at its base and a few mountain hemlock (Tsuga mertensiana) and lodgepole pine (Pinus contorta) saplings and trees providing a cover <3%. The area is underlain by Juniper and Flatiron andesites (Williams, 1932: 220, map). The caves are solely developed in the Flatiron lavas, pale gray andesites which produce remarkably platy slabs, usually <1" thick, which lie parallel to flow planes. Outcrops at the base of the ridge show older dark bluish-gray Juniper andesites, which are distinctively banded and produce thicker slabs. These rocks dip at steep angles due to postglacial faulting and folding; two prominent faults are found only 600 m SW of the caves (Williams, 1932: map). The plates in the cave ceilings dip 55° NW.

FIELD METHODS

The caves were measured with tape, compass and clinometer; a talus profile was similarly obtained along stations at 5 m intervals. Clast size was studied with a photographic technique (Pérez, 1986); a 100x70 cm grid was placed on the ground as scale. Photographs were taken in 6 cave locations and at 10 stations along the talus in front of cave 5. The length of the a axis was determined for 40 particles in each plot. Particle shape and fabric were analyzed in cave 5 by determining in the field the axial lengths (a, b, c) and orientation and plunge of the a axis for 100 particles in the upper 50 cm of the deposits; 100 clasts were likewise sampled in the talus surface.

CAVE MORPHOLOGY

Eleven small cavities were found at the base of the cliff (Fig. 3). They are similar to slope caves elsewhere (Mitter, 1983). The caves are elongated, with their axis perpendicular to the cliff face and parallel to the andesite strike; the ceilings approximate a vaulted shape, an equilibrium form for collapse caves (Schroeder, 1979; Roberge et al, 1985). Walls and ceilings are irregular and rough; debris piles littering the floors have steep fronts (35 to 45°) at the cave mouths (Fig. 4). The clastic deposits lack sorted polygons, stripes, or any other patterned ground (Mitter, 1983). The surfaces of the debris, and presumably of the cave floors underneath, slope towards the entrance. The outwards inclination of the floors is essential to cave development, since debris can then be transported to the talus (cf. Kunský, 1957; Mitter, 1983; Roberge et al, 1985). Cave 2, the only one which does not slope outwards,

Fig. 2 General view of the study site. The entrances to several caves are visible at the cliff base; the bare talus extends in the foreground. Trees above the cliff are 20-25 m tall.

communicates with cave 3, through which debris exit (see Fig. 3). Judging from the surficial angles of the debris, cave floors slope at 8 to 11°; this is consonant with the gradient (7-10°) of a 2.5 to 3 m-wide platform found in front of the caves (Fig. 5A). Below this bench, the talus is steep (33-35°) and has a rectilinear profile; slope angles decrease to 12° in the concave

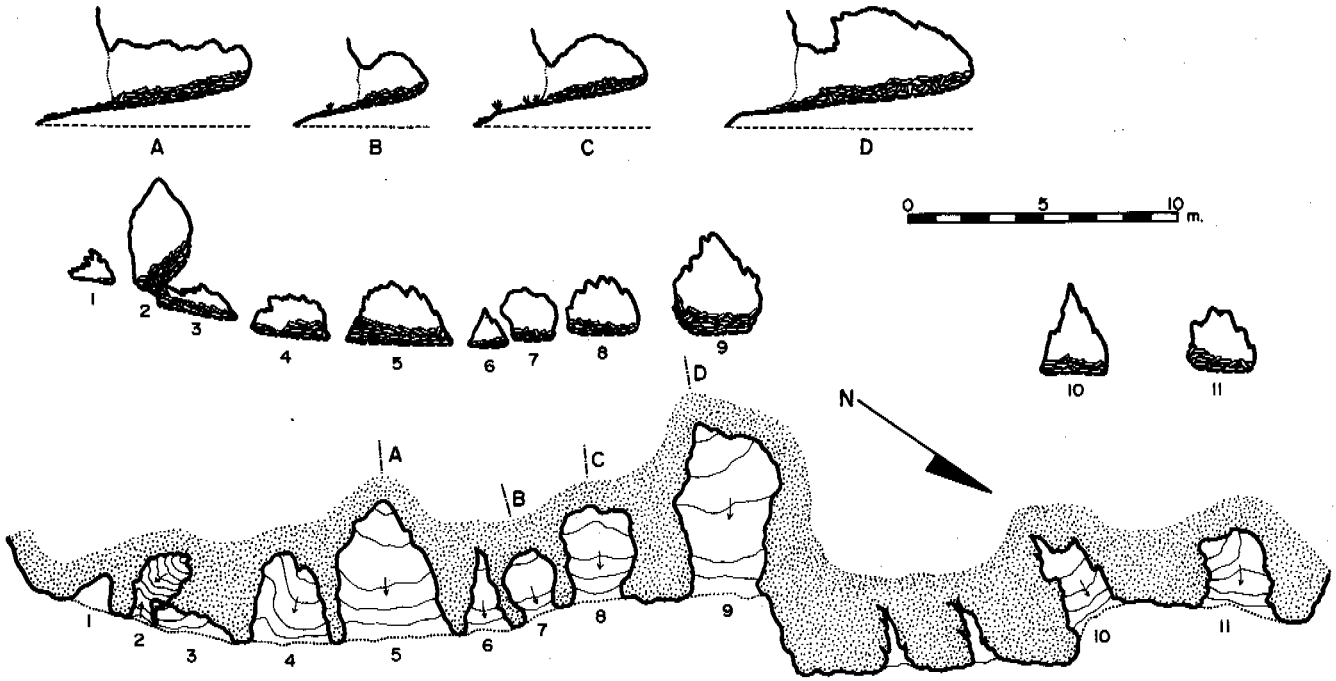

Fig. 3 Plan view (bottom) and lateral (middle) and longitudinal (top) cross-sections of the caves. Contour interval= 25 cm (datums are floor elevations at entrance); arrows show slope direction.

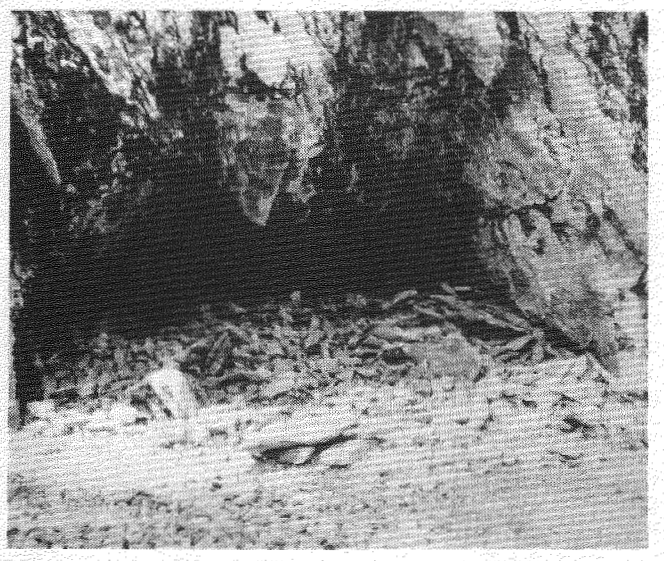

Fig. 4. Mouth of cave 5. Note the thick pile of clasts, its steep front, and the smaller size of fragments in the gently-inclined talus platform in the foreground.

basal section. A nearly flat meadow, with an angle of 3-4.5°, extends beyond the talus base.

CAVE AND TALUS SEDIMENTOLOGY

Particle size data for the plot populations were tested for normality (Jones, 1969); data were not normally-distributed, thus were converted to $\log_{10}$ (Pérez, 1986). Transformed data were normal at the 0.05 level; geometric means are reported. The mean a axis of cave clasts ranged from 29.3 to 20.4 cm. When compared to upper-talus clasts, it is evident that cave debris are significantly larger (Fig. 5B). This was unexpected, since at least part of the slope particles have been contributed by cave weathering. Stones along the talus were sharply sorted by size, with larger clasts at the base (Figs. 5B and 6). A regression between particle size and relative slope position gave an r= .895--significant at the 0.001 level--which accounts for 80.1 % of the observed variability. When the regression includes two plots in cave 5, r drops to .805, explaining only 64.8 % of the size variation.

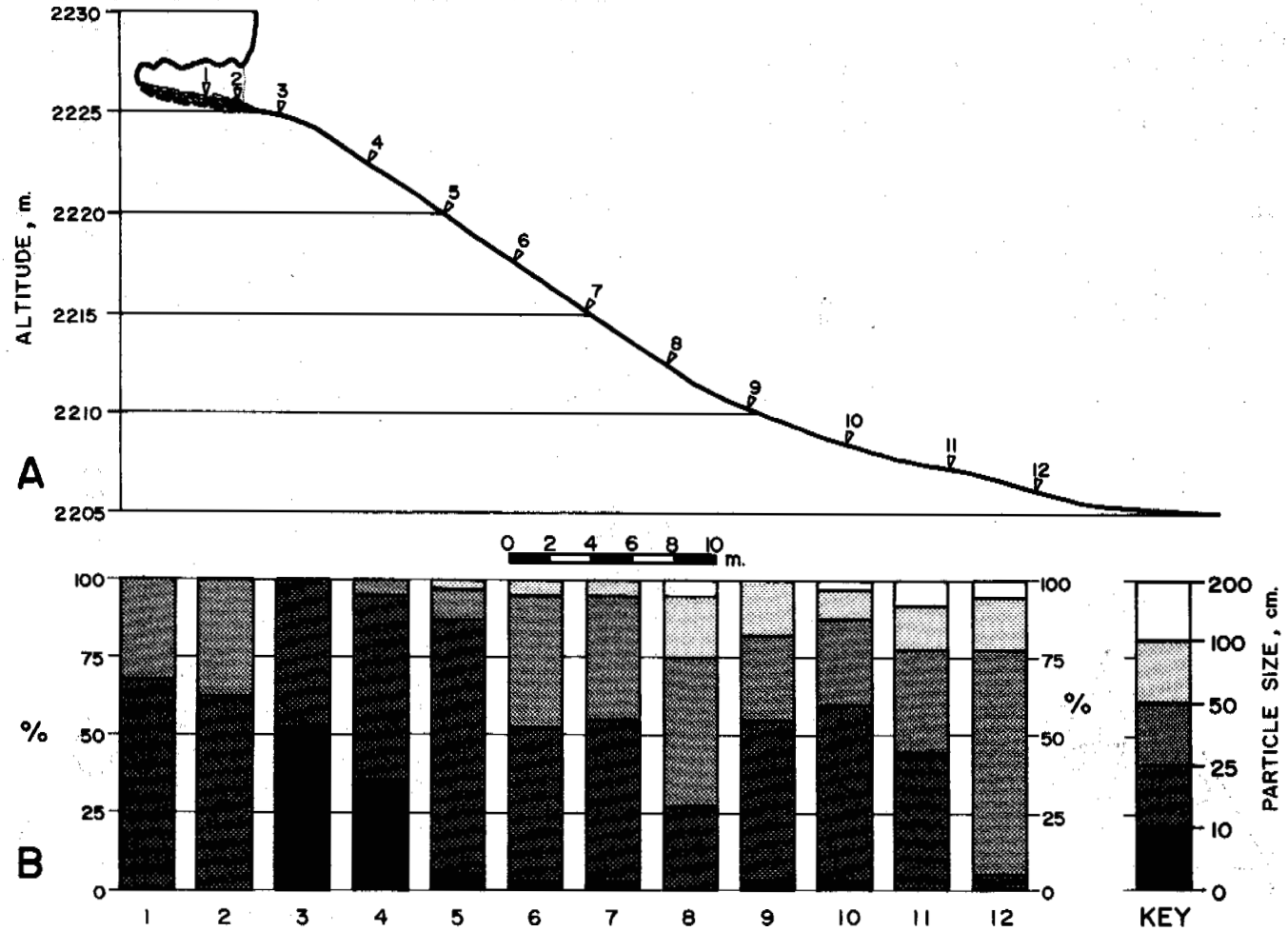

Fig. 5 A: Longitudinal profile of cave 5 and the talus below; arrows indicate sampling stations. B: Particle distribution by size classes (a axis) along profile A; N size per plot= 40.

Particle shape was studied with three numerical indexes: elongation (a/b), flatness (a+b/2c), and sphericity $(c^2/(axb))^{.33}$. Overall shape variation was assessed with contoured diagrams (Pérez, 1987). Index data were not normally-distributed, thus were compared with the non-parametric Kolmogorov-Smirnov test. Both cave and talus particles were extremely platy, reflecting lithological structure. Cave fragments were, however, significantly more elongated --0.001 level--and flatter--0.05 level--than talus ones (Table I). The shape diagrams also show these differences (Fig. 7). The center of maximum density of cave clasts is between the very bladed to very elongated classes, while that for the talus lies in the very platy and very bladed classes (Sneed & Folk, 1958); the difference in concentration is significant at the 0.05 level.

The fabric of cave clasts has seldom been studied (White & White, 1969). The macrofabrics of the talus and the cave were very similar, with a sharp subhorizontal girdle coincident with the local slope (Fig. 8). The dominant mode, superimposed on this girdle, is parallel to the slope direction in the cave and slightly oblique in the talus. Most particles dip downwards but plunge less steeply than the slope surface, producing a strong upslope imbrication (64% for the cave, 67% for the talus). Few axes project into the diagram centers, indicating the scarcity of particles perpendicular to the slope surface. Overall, particles lie with their a axis parallel both to the slope plane and direction. Fabric strength appeared higher in cave debris.

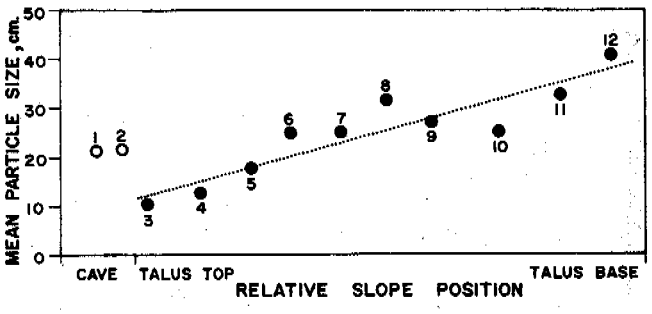

Fig. 6 Correlation between mean particle size and relative slope position along profile 5A. Solid circles: talus samples; blank circles: cave samples. Dotted line shows regression slope for the 10 talus samples.

TABLE I
Particle shape indexes (± S.D.) for cave and talus particles; N= 100 for each sample. Significance levels of a Kolmogorov-Smirnov test are given.

	Elongation[a]	Sphericity[b]	Flatness[c]
Cave 5	1.923±0.60	0.427±0.10	4.157±1.43
Talus	1.580±0.44	0.455±0.10	3.619±1.31

a: 0.001, b: no difference, c: 0.05

DISCUSSION AND CONCLUSIONS

Cave morphology indicates that frost shattering at the cliff base is the dominant process of cave formation. Weathering of Flatiron andesite slabs is concentrated along planes of flow and fracture because water percolating through the lava travels primarily along them, thus the extreme platiness of the resultant clasts. Frost frequency and intensity are affected by cliff orientation (NE); this aspect is also conducive to the accumulation of snow onto the talus below the rockwall. Even where caves were lacking, there was a distinctive notch at the cliff base. Similar basal notches have been previously found by McCabe (1939) and Gardner (1969), who

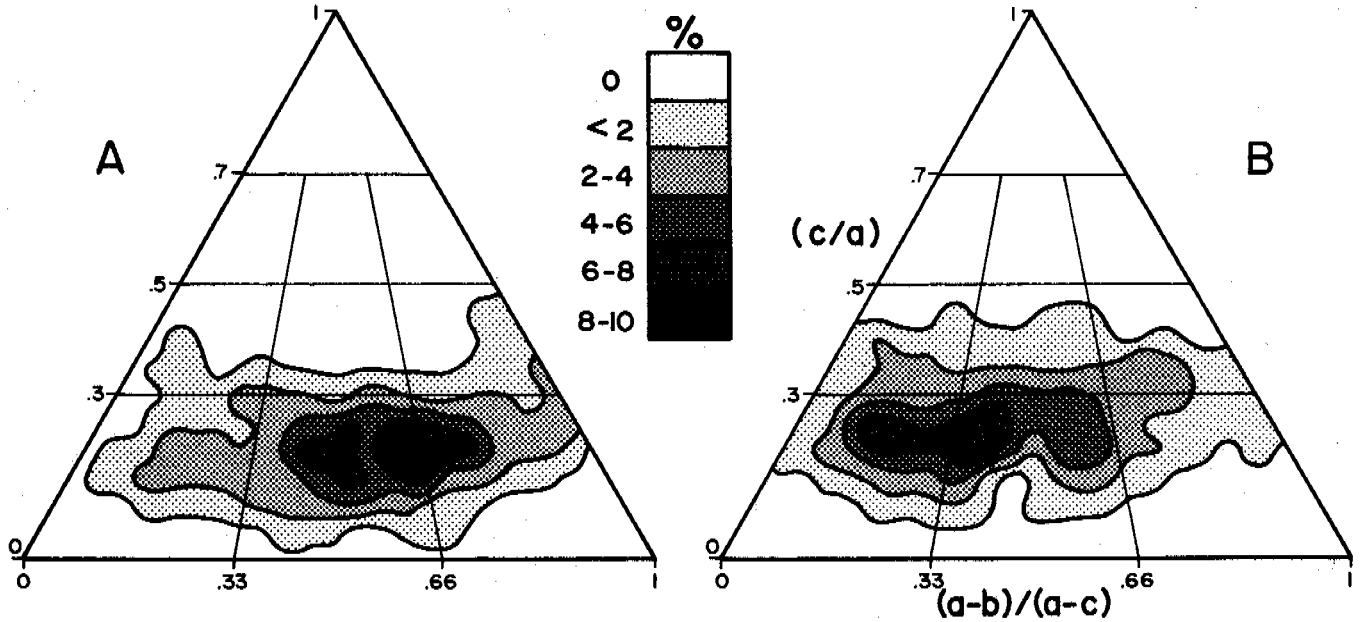

Fig. 7 Contoured particle-shape diagrams for cave 5 (A) and talus (B) clasts. Each diagram based on 100 clasts. Shading indicates the density of particles as a percentage of the total. Axial indexes used for shape classification are indicated (see Sneed & Folk, 1958 for details).

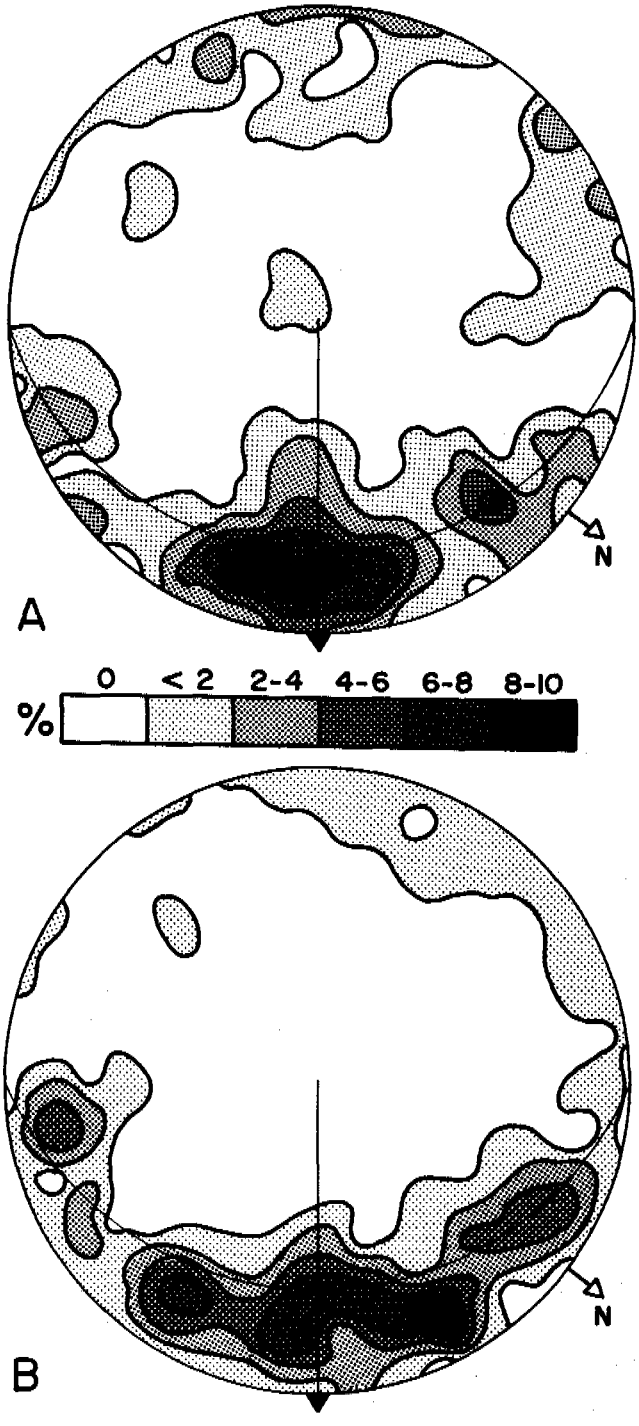

Fig. 8 Contoured fabric diagrams (Schmidt stereonets projected on the horizontal plane) for cave 5 (A) and talus (B) clasts. Each diagram based on 100 particles. Shading indicates the density of axis projections. The intercept of the slope plane is shown by the great circles. Slope direction is towards bottom.

ascribed them to intense headwall sapping at the margins of persistent snowbanks, due primarily to increased freeze-thaw activity (Wolfe, 1967; Thorn, 1976). However, recent studies (Thorn, 1979) have not found evidence to substantiate this hypothesis. Others (Hall, 1985) stress the importance of snowpatches as water reservoirs. The slow release of snowmelt water during spring, when temperatures fluctuate about the freezing point in Lassen, would intensify frost activity at the rockwall base.

Once a cave starts forming, there must be some self-reinforcing mechanism that helps lengthen it; this could be associated with cave microclimate (Schroeder, 1979). In summer, warm air would flow into the ascending cave, and as it cools down, it would condense and sublimate, depositing water and ice crystals on the cave ceiling and walls (cf. Schroeder, 1977).

The scarcity of vegetation suggests that both caves and talus are still forming. However, close examination of the caves and their clasts provides little evidence for recent gelifract production or transport. Although some slabs are becoming detached from walls and ceilings, most cave and debris surfaces are considerably weathered, lack a fresh look, and are partially covered by algae, lichens, and mosses, particularly near the entrance. The platform outside the caves also lacks sizable clasts trailing away from the hypogean debris piles (Fig. 4). The altitude of the caves suggests that they originated, under considerably colder conditions, during the late Pleistocene (middle Tioga advance, prior to 11,000 B.P.) when the regional snowline was at 2200-2300 m elevation (Crandell, 1972).

Clast detachment is only the first step in cave formation; after this, clasts are transported to the talus. Thus, the caves are part of a system in which debris cascades downslope. The logarithmic increase in particle size in the talus indicates rockfall may be a primary mechanism of deposition there (Gardner, 1970; Pérez, 1986). Since cave clasts do not fit this pattern, it seems that rockfall is not an efficient process in their removal from the caves; the low gradient of the cave floors and upper talus bench also precludes rockfall as a significant transport agent. This suggests that most talus fragments are derived from weathering of the cliff face.

The fabric of cave debris, along with the gentle gradients of cave floors and talus bench, indicate that slow geocryogenic processes, such as frost creep and gelifluction, are responsible for clast movement across them (cf. Mitter, 1983: 861). Creep, caused by freezing and thawing of interstitial ice and by particle settling after removal of fines by meltwater (Embleton & King, 1975: 109) appears the most likely mechanism. The similar fabric in the talus suggests that creep, or perhaps block gliding over the snowbank (Hall, 1985; Pérez, unpubl. data), are also significant in it. A strictly rockfall-produced talus would have a more random fabric (Pérez, 1986). Runoff has been identified (Roberge et al, 1985; Parker et al, 1964) as an agent of debris removal from similar caves, but this seems unlikely in the small cavities at Lassen. The large clastic

accumulations inside the caves clearly indicate that the process of particle transport has lagged behind that of weathering and detachment. When excavated, cave sediments showed an increase in smaller particles with depth, probably produced by in situ disintegration of the larger clasts. Both characteristics suggest that the process of debris removal has been largely inactive in the recent past.

Particle shape indexes show significant differences between talus and caves. One possible explanation is that cave slabs, being large and elongate (maximum elongation: 3.812) break easily during their descent, thus attaining lower elongation and flatness values due to a reduction of their a axis (Table I). This hypothesis was tested by pushing 20 large cave slabs down the talus; most particles--13 or 14-- were severed along their longest axis into two or more pieces. When the shape of the resulting fragments is plotted on a ternary diagram, the broken particles arriving at the talus lie to the upper left of those originally found in the cave, fitting the patterns of Figs. 7A and 7B. At the same time, shape indexes are changed in a manner consonant with the trends evident in Table I.

The formation of the Lassen caves is dependent on frost action first weathering the andesite and then transporting the fragments out of the caves; thus, the term "geocryogenic slope-caves" seems appropriate for them. Because they are an extension of the talus below, they should strictly be called talus-caves, but since this name is already used for cavities found between boulders and debris on talus slopes (Vítek, 1983), it should be avoided to minimize confusion.

ACKNOWLEDGMENTS

Financial aid was received from the Research Institute of the University of Texas, Austin, during the summers of 1986 and 1987. Alan E. Denniston and Richard L. Vance, at the National Park Service in Mineral, CA, provided the necessary permits. Inés L. Bergquist helped with the field work and read this manuscript.

REFERENCES

Baker, F S (1944). Mountain climates of the western United States. Ecol Monogr (14), 223-254.

Crandell, D R (1972). Glaciation near Lassen Peak, northern California. USGS Prof Paper (800-C), 179-188.

Embleton, C & King, C A M (1975). Periglacial Geomorphology, 203 pp. Wiley, New York.

Gardner, J (1969). Snowpatches: their influence on mountain wall temperatures and the geomorphic implications. Geogr Ann (51A), 114-120.

Gardner, J (1970). Rockfall: a geomorphic process in high mountain terrain. Albertan Geogr (6), 15-20.

Hall, K J (1985). Some observations on ground temperatures and transport processes at a nivation site in northern Norway. Norsk Geogr Tidsskr (39), 27-37.

Halliday, W R (1960). Pseudokarst in the United States. NSS Bull (22), 109-113.

Jones, T A (1969). Skewness and kurtosis as criteria of normality in observed frequency distributions. J Sedim Petrol (39), 1622-1627.

Kosack, H P (1952). Die verbreitung der Karst- und pseudokarsterscheinungen über die erde. Peterm Geogr Mitt (96), 16-21.

Kunský, J (1957). Typy pseudokrasových tvaru v Ceskoslovensku (Types of pseudokarst phenomena in Czechoslovakia). Ceskoslosvenský Kras (10), 108-125.

McCabe, L H (1939). Nivation and corrie erosion in west Spitsbergen. Geogr J (94), 447-465.

Major, J (1977). California climate in relation to vegetation. In Barbour, M & Major, J (eds), Terrestrial Vegetation of California, Wiley, New York, pp. 11-74.

Mitter, P (1983). Frost features in the karst regions of the West Carpathians. Proc 4th Int Conf Permafrost, 861-865.

Parker, G C, Shown, L M & Ratzlaff, K W (1964). Officer's Cave, a pseudokarst feature in altered tuff and volcanic ash of the John Day Formation in eastern Oregon. Geol Soc Am Bull (75), 393-402.

Pérez, F L (1986). Talus texture and particle morphology in a north Andean paramo. Zeitschr Geomorph N F (30), 15-34.

Pérez, F L (1987). A method for contouring triangular particle shape diagrams. J Sedim Petrol (57), 763-765.

Roberge, J, Lauriol, B & Saint-Pierre, L (1985). La morphogénèse de la caverne à La Patate, Île d'Anticosti, Quebec. Géogr Phys et Quatern (39), 67-75.

Schroeder, J (1977). Les formes de glaces des grottes de la Nahanni, Territoires du Nord-Ouest, Canada. Can J Earth Sci (14), 1179-1185.

Schroeder, J (1979). Développement de cavités d'origine mecanique dans un karst froid (Nahanni, T.N.O. Canada). Ann Soc Géol Belgique (102), 59-67.

Sneed, E D & Folk, R L (1958). Pebbles in the lower Colorado River, Texas: a study in particle morphogenesis. J Geol (66), 114-150.

Thorn, C E (1976). Quantitative evaluation of nivation in the Colorado Front Range. Geol Soc Am Bull (87), 1167-1178.

Thorn, C E (1979). Bedrock freeze-thaw weathering regime in an alpine environment, Colorado Front Range. Earth Surface Processes (4), 41-52.

Vítek, J (1983). Classification of pseudokarst forms in Czechoslovakia. Int J Speleol (13), 1-18.

White, E L & White, W B (1969). Processes of cavern breakdown. NSS Bull (31), 83-96.

Williams, H (1932). Geology of the Lassen Volcanic National Park, California. Univ of California Publ Geol (21), 195-385.

Wolfe, T E (1967). The Jordbruen area of northern Norway. An example of high latitude karst. NSS Bull (29), 13-22.

TRACES OF ICE IN CAVES: EVIDENCE OF FORMER PERMAFROST

A. Pissart[1], B. Van Vliet-Lanoe[2], C. Ek[1] and E. Juvigne[1]

[1]Géomorphologie et Géologie du Quaternaire, Université de Liège, Belgique
[2]Centre de Géomorphologie du C.N.R.S., Caen, France

SYNOPSIS - Unconsolidated deposits in the Remouchamps Cave (Belgium) retain indisputable traces of segregation ice, confirming the presence of deep permafrost in the course of the late glaciation. When the ground warmed up once more, the permafrost considerably altered sedimentation conditions by blocking passages with ice. There is no doubt that the fusion of this ice caused significant mass movements in the sediments laid down. The study of segregation ice which may be detected in cavities will assist in the mapping of permafrost limits during the cold periods of the Quaternary and will without doubt provide fresh evidence on the depth it reached.

INTRODUCTION

Conditions necessary for the appearance of segregation ice are well established. It occurs in damp fine sediments subjected to slow freezing. Further, it is essential that pressure from the overlying land-mass is not too great, which implies that segregation ice cannot occur below a depth of some ten metres. In caves, however, sediments are not subjected to pressure from the ground within which the cavity has developed, so that segregation ice can occur irrespective of the depth of the cavity.

The occurrence of segregation ice in a sediment has the effect of structuring the earth : between the particles of ice, the earth is progressively distorted and dried; and since air cannot penetrate through, aggregates limited by the particles of ice are extremely compressed. In cross-sections through silt, the structuring of the earth which occurred in the course of the last glaciation is often clearly observable, at least when this structure was not destroyed by biological action or complete drying-out with subsequent rehydration. Indeed when this latter process occurs, it results in the aggregates exploding when the air inside the sediment is compressed by subsequent water penetration.

In caves where biological action is limited and where, particularly in the case of the climate of Western Europe, complete drying-out is almost impossible, the former presence of segregation ice can consequently be ascertained.It is especially apparent in the layout of residual spaces left open after fusion of the ice lenses.

If the layout of the cave does not allow circulation of the air to bring cold down from the surface, and if the cavity is located more than 20 m deep (the limit at which annual temperature variations occur), the presence of traces of ice, in other words of a temperature below 0°C, implies of necessity the presence of permafrost. In the present article, we show how the method can be applied in the study of a Belgian cave.

II. TRACES OF SEGREGATION ICE OBSERVED IN THE REMOUCHAMPS CAVE

Remouchamps cave is 20 km to the south east of Liège in paleozoic rocks. It comprises two horizontal corridors, the lower one being occupied by a subterranean stream (fig. 1). One of the authors (C. Ek, 1961) showed that these passages are connected with terraces of the river Ambleve which flows in the valley on the slope of which this cave has its entrance.

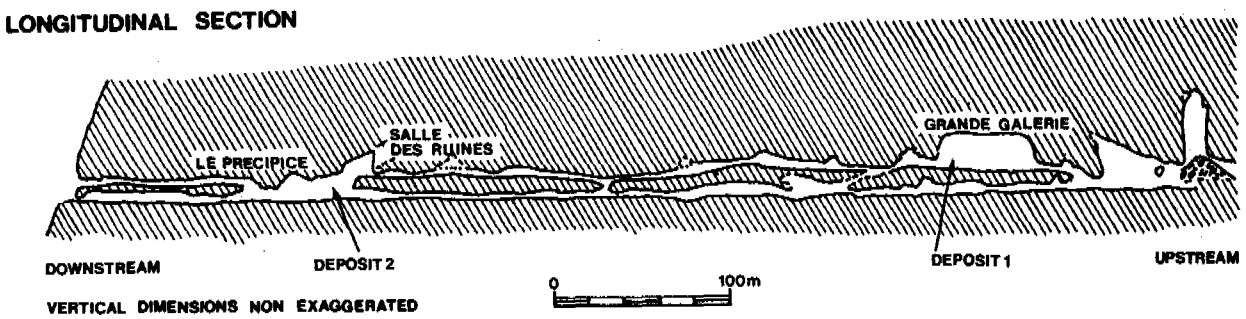

Fig.1 Longitudinal section of the Remouchamps cave with locations of the two deposits studied. Only passages accessible to potholers (speleologists) are shown (C. Ek, 1972).

Two distinct accumulations of sediments were studied in this cave. Their location is shown in figure 1 : the first is found in the "Grande Galerie" (Large Gallery); the second nearèr the entrance 50 m upstream of the "Embarcadère" (pier).

a) The "Grande Galerie"

Situated some 500 m from the entrance, the "Grande Galerie" appears as a corridor with a height in excess of 20 m. The highest point of the roof is above 30 m below surface level.

Figure 2 indicates schematically the location within the cave of the deposits under investigation. Our examination was restricted to the upper part of sandy-silty sedimentation to be found at the SE end of this gallery; figure 3 shows in greater detail the presentation of these sediments.

The excavations which we have carried out did not reach the base of the sediments. They revealed finely stratified fine alluvial sands. Occasionally very thin clayey edgings provide evidence of brief periods of sedimentation in stagnant water.

Two distinct units are separated by a discordance in stratification testifying to erosive action before the sedimentation of the upper layers of sediment. The southeastern part of the lower deposits displays a sharply sloping stratification which is doubtlessly the result of sedimentation by a current of water in a drowned passage. The absence of cracks which could have provided evidence that these layers are a result of collapse, and also the presence of distorsions which appear to be due to syngenetic landslip of the deposit, prompt us to defend this interpretation.

Within the heart of the cross-section studied, traces of Rocourt tephra (enstatite, jagged green clinopyroxene and brown amphibole; E. Juvigné, 1977) were detected. Since such tephra fell on our country at an undeterminate time somewhere between 61.000 and 106.000 BP (E. Juvigné et M. Gewelt, 1987), these minerals prove that the laying down of this deposit occurred after the Eemian *sensu stricto*.

There was nothing to enable us to tell apart the deposits on either side of the discordance. Concretion debris found at the point of contact gave a Uranium-Thorium age of 195,067 (+28714, -21452) years (1), confirming that these were very ancient concretions which had undergone displacement, and therefore provided no useful data.

Twenty two thin-sliced sections were prepared for examination of the microstructures existing in these formations. Certain parts of the deposits already showed noticeable structuring which was clearly apparent on macroscopic examination of the sample blocks from the cross-section, but it was right and proper to check their nature under a microscope.

(1) Dating established at the "Centre for the study of Nuclear Energy" at Mol by Dr. G. Koch, Head of the Low-Level Measurement Department. Dating Nr 11.

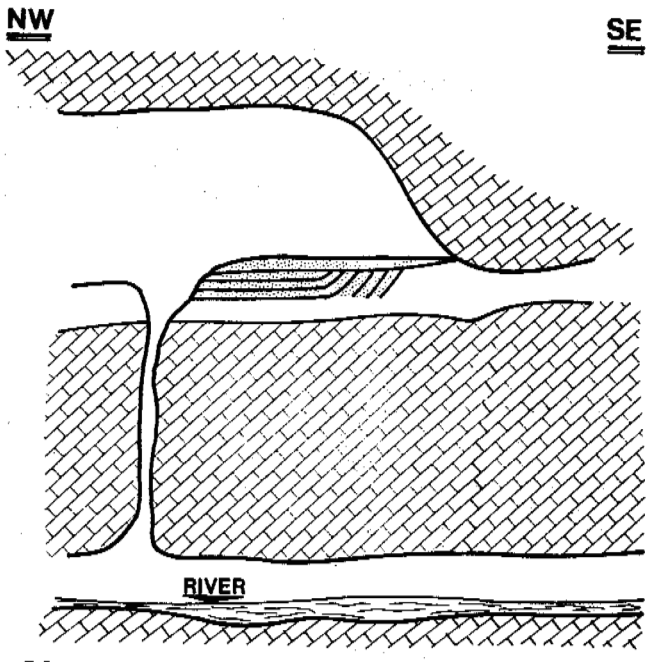

Fig.2 Diagram showing the location of deposits investigated in the S.E. part of the "Grande Galerie", and indicating the very probable hydrological relationship with the lower stream occupied by the river.

In 21 out of the 22 sections, traces of segregation ice are apparent, comprising :

(1) the arrangement of the empty spaces (hollows) present in the heart of the formation, the configuration of which evokes the distribution of segregation ice. Figure 4 provides a fine example.

(2) the nature of the walls of the hollows, the elements of which could not dovetail together if the fissure were closed. This lack of concordance between the two faces can be explained by pressure-thrust due to growth of segregation ice. It is particularly apparent in the presence of triangular hollows as shown in figure 6.

(3) the existence in the heart of the deposits of micro-thrust faults and ruptures in what were continuous strata, subsequent upon movement which occurred at the time of the fusion of the ice.

Since they have been subjected to only a very limited number of freezing-thawing cycles and probably, in the case of the upper formations, only a single cycle, it is futile to seek out in these sediments the traces of alternating freezing-thawing which the selected lamellar structures constitute (B. Van Vliet-Lanoe, 1976).

The sections examined do not reveal traces of ice in equal quantity. This may result from :

(1) the granulometry of the site material of each section studied.

(2) the amount of water present in the material at the time of freezing.

(3) refrigeration conditions which may have varied from place to place.

(4) the degree of compactness of the material before freezing.

The traces of segregation ice shown in figure 4 are very similar to those obtained when a muddy mass freezes shortly after being laid down (compare with photo 2 *in* Pissart, 1974). The like- lihood is that quasi syngenetic freezing of the deposit is involved here (B. van Vliet-Lanoe, J.-P. Coutard et A. Pissart, 1984).

Only one slide, the sample location of which is indicated in figure 3, does not show any other freezing activity. It may be testimony of the last deposits laid down at this location when the underlying formations were completely thawed.

The observations carried out lead to the following interpretation :

(1) underlying formations (that is to say those below the discordance in fig. 3) were placed on position at the time of disappearance of a permafrost. Indeed, it was necessary for the permafrost to disappear at the surface so that water and sediments might get down into the cavity. As they were laid down at a time when the cavity was still in permafrost, that is to say in a temperature below 0°C, syngenetic segregation icing of the deposit occurred.

(2) a period free of permafrost permitted the development of erosion wich truncated the formations laid down (discordance D in fig.3).

(3) the permafrost returned; at the time of its disappearance, sedimentation of fresh layers of alluvium/silt occurred while the ground was still below 0°C. The temperature of the substratum was still negative.

We surmise, without proof however, that these phases followed on in succession during the late ice-age and/or the Weichselien interpleniglacial.

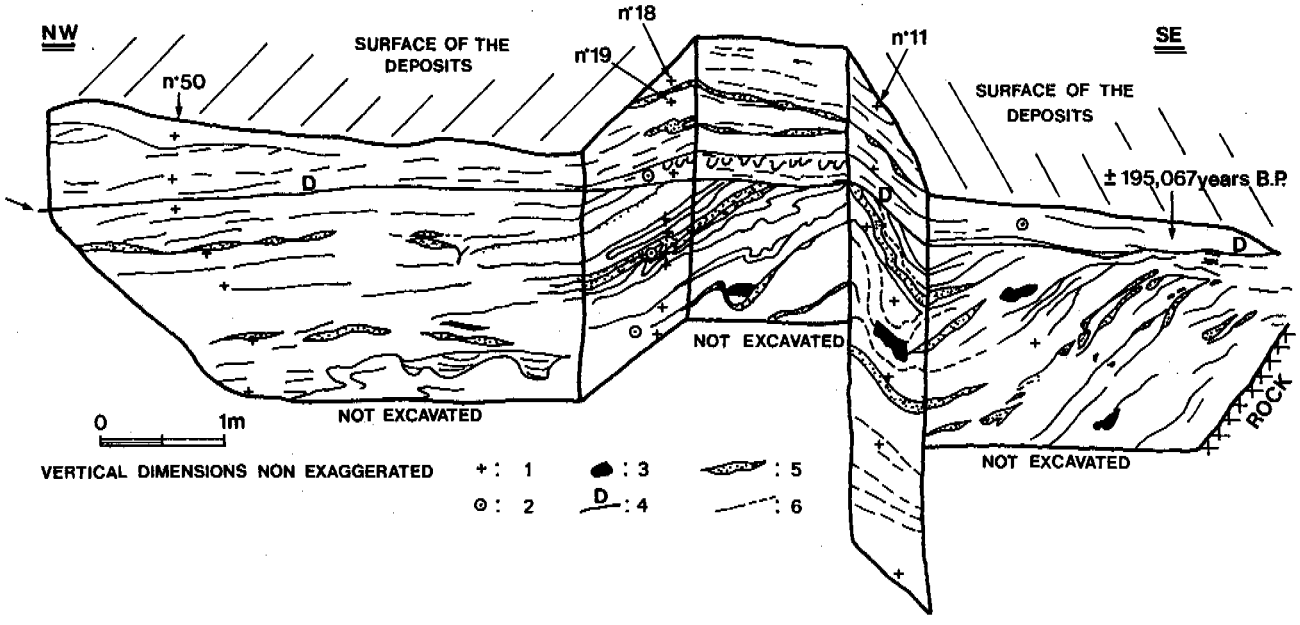

Fig.3 A cleared cross-section in the SE part of the "Grande Galerie" showing the lines of stratification.
1. Location of samples studied in respect of microstructures.
2. Idem in respect of dense minerals.
3. Blocks.
The letter D marks the position of the discordance in stratification.

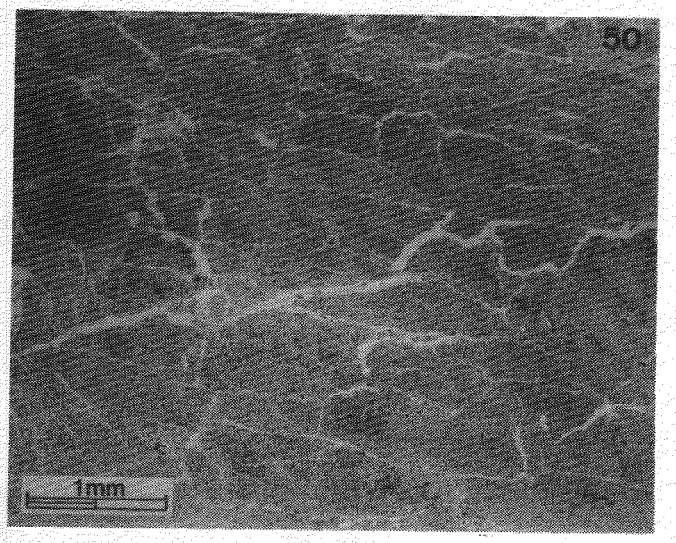

Fig.4 Traces of syngenetic segregation ice in the deposit. Sample 50 from the upper part of cross-section shown in figure 3.

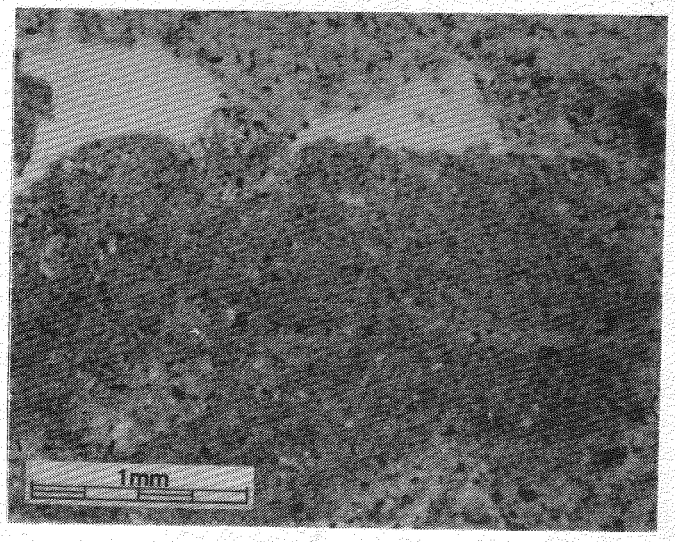

Fig.5 Triangular hollows testifying to the past existence of segregation ice.

b) Near the "Embarcadère" (pier)

A second, new accumulation of sediment was studied in the Remouchamps cave. Figure 6 pinpoints its location. For a description of all the features the reader is referred to Pissart *et al.*, 1987.

Two distinct formations are present. The lower formation is composed of sediments with very irregular outlines and a very heterogeneous nature. Along falls of large limestone blocks are found schist debris, the whole being enclosed in an extremely clayey matrix. The contact slope between these different materials is, at the right hand extremity of the cross-section, close to 35°. Up above, it opens into the "Salle des Ruines" (Hall of Ruins) previously referred to. Consequently it is clear that these materials are deposits which have slipped down the slope from this "Hall of Ruins" situated on the left bank of the stream.

The upper formation is made up of finely stratified fluvial deposits comprising silt and fine sand with, on rare occasions, some more clayey layers. These stratified deposits were laid down by the stream which presently flows a few metres below.

The associations of dense minerals show the presence throughout the deposits (except in the lower clayey layers) of Rocourt tephra (see above) which settled there during the last glaciation.

Traces of segregation ice are in evidence in the upper part of the fluvial deposit. The ice was there in abundance and subsidence due to fusion of this ice is very clear. However at a depth of one metre, one sample showed no sign of disturbance due to freezing. In the heart of the underlying formations laid down subsequent to mass transportations from the "Hall of Ruins", the effects of frost are also evident. The arrangement of fissures in the heart of blocks displaced by these agents of mass movement provides evidence of freezing prior to their slide down the slope.

Consequently we think we have discovered evidence supporting the following sequence of events :

(1) Unconsolidated sediments accumulated on steep slopes in the gallery extending above the present deposit.

(2) These sediments were frozen and an abundance of segregation ice occurred here.

(3) Fusion of this ice, during a period of climatic improvement, triggered mass movements which created the lower part of the accumulation. At the time when this occurred, the river was not flowing, no doubt owing to blocking of passage upstream.

(4) The river which resumed its flow found the passages downstream partially obstructed and accumulated fluvial deposits of a more loesslike character up to the level of the upper opening through which the water flowed out.

(5) A return of the frost, probably roughly contemporary with sedimentation of the upper layer occurred.

(6) The stream, rediscovering its lower outlet, rapidly incised the sediments laid down.

We surmise that these various stages all occurred at the end of the last glaciation, at the time of climatic fluctuations of the Weichselien late ice-age (tardiglacial).

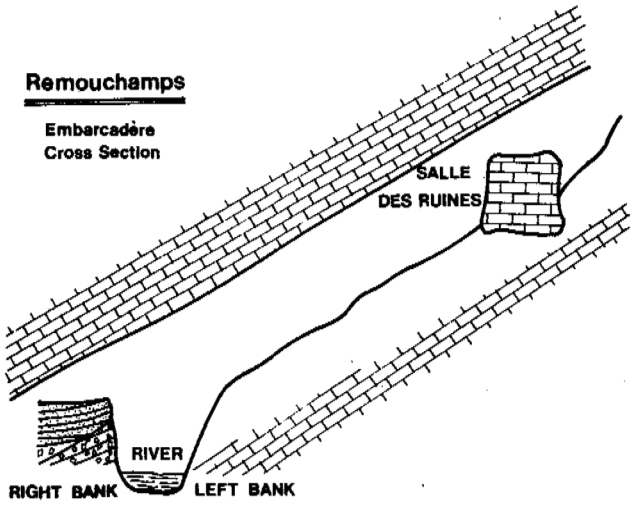

Fig.6 Diagram showing the location of the deposit accumulated upstream of the "Embarcadère" at the foot of the "Hall of Ruins".

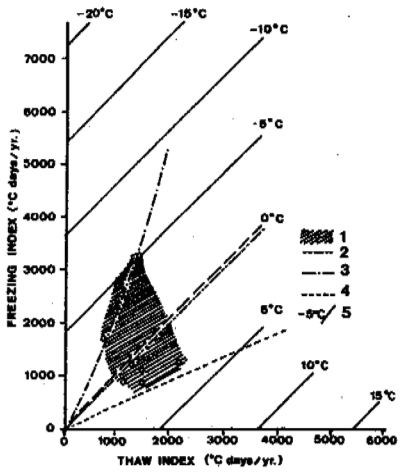

Fig.7 Relationship between temperature and ice-caves according to Harris (1982).

CONCLUSIONS

The discovery of traces of segregation ice in caves is of interest in two very different fields, namely :

(1) Sedimentology of deposits occupying karst cavities.

(2) Paleoclimatology.

The presence of ice in Belgian caves during the cold periods is thus demonstrated for the first time. This observation confirms that the blocking of swallowholes was not solely the result of the input into the thalweg of large quantities of unconsolidated sediments. The discovery of traces of syngenetic ice in the deposit, that is ice appearing immediately after sedimentation, can be explained by the fact that rewarming occurred from the surface downwards. In this way the upper ducts could be flooded while the lower ducts were still frozen. During what was probably a relatively brief period, sedimentation was not possible in the lower ducts which were blocked by ice, whereas it was occurring in ducts found nearer the surface that were already unfrozen. If this is in fact the case, it is somewhat hazardous, in regions where permafrost existed, to try to explain subterranean sedimentation by running water while taking into account definitive abandonment of upper ducts when lower ducts were well developed.

Furthermore it seems clear that at the time of thaw, the unfrozen masses of sediment became unstable and could slide on slopes while previously they were in equilibrium. This is how we explain the deposits we have described near the "Embarcadère". This accumulation, moreover, was formed at a time when the stream was no longer flowing; otherwise one would detect in the middle of it masses of layered sediments testifying to the action of a water course. Such thaws probably also caused the fall and simultaneous fracturing of a certain number of stalagmites standing on unconsolidated formations.

The study of traces of ice in caves in present-day temperate regions may well provide valuable evidence on the spread of permafrost during the cold periods of the Quaternary. The application is immediate if it is accepted that the temperature of the cavity corresponds to the annual mean temperature of the place where the cave is situated. It is however a well known fact that if movement of air is prevalent in the cavity, the temperature may deviate from the annual mean temperature. As shown in the figure provided by Harris (1982), ice caves may exist when the annual mean temperature reaches +3°C. However, by limiting our investigation to deposits a long way from cave entrances and well away from vertical shafts which might induce significant local freezing, the study of traces of segregation ice in caves constitutes a new tool in mapping the limits reached by the permafrost during the cold periods of the Quaternary. By studying deep cavities, one can thus hope to obtain direct evidence for depth attained by the permafrost, data that are totally lacking today in fossil periglacial regions.

REFERENCES

Dewez, M., Brabant, H., Bouchud, J., Calut, M., Damblon, F., Degerbol, M., Ek, C., Frère, H., Gilot, E. & GLIBERT, M. (1974). Nouvelles recherches à la Grotte de Remouchamps. Bull. Soc. Roy. belge Anthrop. et Préhist., (85), 5-161, Bruxelles.

Ek, C. (1961). Conduits souterrains en relation avec les terrasses fluviales. Ann. Soc. géol. Belg., (84), 313-340, Liège.

Harris, S. (1982). Identification of permafrost zones using selected permafrost landforms. C.R. de la 4e Conf. canadienne sur le Pergélisol, Calgary, Alberta, March 1981. National Research Council of Canada, Ottawa.

Juvigné, E. (1977). Zone de dispersion et âge des poussières volcaniques du tuf de Rocourt. Ann. Soc. géol. Belg., (100), 13-22, Liège.

Juvigné, E. & Gewelt, M. (1988). Intérêt stratigraphique réciproque des téphra et des dépôts de grottes. Ann. Soc. géol. Belg., (111), Liège.

Pissart, A. (1964). Contribution expérimentale à la connaissance de la genèse des sols polygonaux. Ann. Soc. géol. Belg., (87), B213-223, Liège.

Van-Vliet-Lanoe, B. (1976). Traces de ségrégation de glace en lentilles associées aux sols et phénomènes périglaciaires fossiles. Biul. Perygl., (26), 41-55, Lodz.

Van Vliet-Lanoe, B., Coutard, J.-P. & Pissart, A. (1984). Structures caused by repeated freezing and thawing in various loamy sediments : a comparison of active, fossil and experimental data. Earth Surface Processes and Landforms, (9) 6, 553-566, Wiley, Chichester.

THE THEORY OF CRYOLITHOGENESIS

A.I. Popov

Moscow State University, Moscow

SYNOPSIS The methodological principles which are the theoretical foundations of cryolithology, the science of cryolithogenesis, i.e. a special type of lithogenesis in the cold regions of the Earth are stated here. These principles are the following - the genetic nature of cryolithogenesis, the zonality of its occurence and the historical character of cryolithogenesis.

The cold zones of the Earth are the physico-geographical areas within which cryolithogenesis, that is a special type of lithogenesis at negative and low positive temperatures occurs. The phenomena natural for this kind of lithogenesis are due to ice formation in the earth's crust accompanied by typical lithogene and reliefforming effects. The problems of cryolithogenesis are a part of an independent subject - cryolithology. Thus, cryolithology studies the processes of lithogenesis in the Earth's stable cooling zones, i.e. where these processes are predetermined by permafrost development and deep winter freezing.

The methodological principles enabling judgement on the genetic and spatial-time regulations of the cryolithogenesis development are the theoretical foundations of cryolithology. These principles are 1)the genetic, i.e. the physico-geographical and geological nature of cryolithogenesis as a natural phenomenon; 2)the zonality of cryolithogenesis manifestation; 3)historical character of cryolithogenesis. The use of these methodological principles in cryolithological studies allows us to assert that cryolithogenesis as well as other types of lithogenesis is predetermined by physico-geographical and zonal factors without losing its ties with the geological substratum.

The most important principle is the genetic one, that is the physico-geographical and geological nature of cryolithogenesis. To interpret this principle it is necessary to determine the position of cryolithogenesis in the general system of lithogenesis.

The attempt to determine the position of cryolithogenesis in the lithogenesis system allowed us to come to the conclusion that cryolithogenesis should be considered as two kinds of processes of the same range 1)cryogenic diagenesis; 2)frost weathering or cryohypergenesis. Both of these processes result in different lithogenic effects allowing to classify the frozen ground features.

It should be noted that lithogenesis is not only a process of sedimentation but also a residuum forming process. Weathering is known to be considered by lithologists not only as a preparatory stage for subsequent transportation and deposition of material in terminal incompletely impounded bodies but as a factor of transformation of the original rocks resulting in the formation of widespread rather thick stable residua. Thus, lithology is a science both of sedimentation and the formation of residua. In fact all processes of exogenetic rock formation by weathering, sedimentogenesis and diagenesis are lithogeneous processes. The intensity and character of the lithogenesis processes are determined by the physico- geographical conditions, first of all by the climatic ones which change with every climatic zone thus stupulating the zonal character of lithogenesis.

The above correction of the definition of the concept of lithology - lithogenesis is essential and, as will be seen later, it permits to interpret the concept of cryolithogenesis much wider.

Thus cryogenic processes may be considered as specific processes of diagenesis and weathering developing in near-surface conditions. Are there any reasons to interpret the processes of cryolithogenesis as those of diagenesis and weathering?

Diagenesis should not only be interpreted as physico-chemical balancing of sediment in a subaqueous medium, but also as its physico-mechanical balancing in subaqueous and subaerial media, i.e. its compaction, relative dehydration and squeezing out of unbound and migration of loosely bound, water. Therefore, cryogenic processes, which are mainly known to result in physico-mechanical modifications in the sediment and rock when they bring about their permanent (long-lasting) consolidation due to the formation of ice, should be regarded as diagenesis (cryodiagenesis).

The most general case of cryodiagenesis is the long irreversible freezing of moist sediments and dispersed rocks, with ice forming in them as an authigenic mineral. The freezing of aleuropelite and fine-arenaceous sediments and rocks is accompanied by relative dehydration of the mineral aggregates during the migration of both unbound and loosely bound water, by intravolume contraction and as a rule by the formation of ice inclusions which produce the layered and reticulate cryogenic structures of the permanently frozen rock subjected to diagenesis. Cryodiagenesis of the coarsely-dispersed rocks (sands and others) is a simpler process of unbound water freezing without its migration or detachment from the freezing front. Besides, a massive cryogenic structure or centers of iceformation which do not notably disturb the structure of coarse sediments or rocks are formed. The icy polimictic formations (ice is an authigenic mineral), being the product of cryodiagenesis, are termed frozen earth material.

The formation of massive vein ice lattices in dispersed rocks during successive frost fracturing as well as the formation of ice cores in mounds - hydrolaccolites - are also widespread cases. Large monomineral ice formations are known as pure ice in the ground.

Cryodiagenesis occurs both as primary diagenesis, if the sediments that have not suffered diagenesis of the general type, freeze and as secondary superimposed diagenesis, if the rocks that have already experienced general diagenesis do freeze, though they are not very compacted and have retained some loosily bound water capable of cryogenic migration.

Another modification of cryodiagenesis is the long - irreversible freezing of unconsolidated wet clayey and more coarse dispersed residia with an analogous to the described cryostructural effect. This kind of cryodiagenesis manifests itself as posteluvial diagenesis.

Clastic deposits formed as a result of physical desintegration of crystalline, metamorphic and compact sedimentary rocks as well as dust-like deposits, the final desintegration product of the sandy and larger fractions, and the aggregations of the clayey fraction reaching dust-like dimensionality too, are the result of cryolithogenesis as a process of frost weathering.

Frost weathering manifests itself to the full during systematic seasonal and daily freezing-thawing of rocks. Besides, two mechanisms of cryogenic desintegration are observed 1)frost weathering under the influence of frost wedging in rather large cracks and pores. This process is responsible for the formation of coarse fragments - cryoclastites: blocks, rock debris,coarse sand; 2)cryohydrational weathering caused by the variation of the wedging action of thin water films in microfractures owing to phase changes resulting in the formation of the small fraction - the dust-like and fine-dispersion dimensionality, termed cryopelite. It is the end product of frost weathering

Frost weathering resulting in the formation of cryoclastites and cryopelites is confined to the seasonal freezing-thawing horizon. But the epigenetic freezing of the crystalline, metamorphic and compact sedimentary rocks (sandstones, aleurolites, argillites and limestones) leading to the formation of permafrost is also a disintegration process. It is mainly a process of freezing of unbound water in fractures, subsequent thawing of the frozen rock mass shows that this massif has become less strong and tends to disintegrate. Thus the freezing of solid bedrocks should be considered as the initial frost weathering process, preparing such rocks for disintegration. Therefore such permafrost rocks should be termed massifs of cryogenic predisintegration.

So, the polymictic dispersion ice rocks - the frozen rock material and the monomineralic ice rocks (veined, injectible, etc) - the pure ice in the ground are the cryodiagenesis products. But the rocks of cryogenic predisintegration, that is the permafrost crystalline and other compact rocks, are the products of frost weathering, i.e. cryohypergenesis: blocks,rock debris, sand are cryoclastites, i.e. the initial products of cryogenic disintegration; dust- and loess-like silt are cryopelites, the end products of cryohypergenesis.

Thus the correctly chosen direction of search for the position of cryolithogenesis in the lithogenesis system enabled to find the position and on the whole ascertain the genetic nature of cryolithogenesis as a natural phenomenon.

The second methodological principle of cryolithology, as it has been stated above, is the finding out of the regularities of cryolithogenesis zonal manifestation.

These regularities may be found out if one recalls some of the permafrost structure peculiarities - the epicryogenic (frozen after the rock mass formation) and syncryogenic (frozen in the sedimentation process).

To determine the peculiarities of the epicryogenic and syncryogenic processes and their stages it proved necessary to distinguish the genetic horizons in the sequences of dispersive epi- and syncryogenic rock masses. The singling out of these horizons is mainly based on the laking into account the temperature conditions of freezing and the extent of cryogenic process activity. The horizons for the epicryogenic rock masses are as follows (downward) 1)the horizon of discontinuous cryohypergenesis (seasonal freezing-thawing, frost weathering); 2)active cryodiagenesis, where the formation of permafrost is connected with annual winter heat loss impulses; 3)passive cryodiagenesis, where the formation of permafrost is connected with the general perennial heat exchange level. For the syncryogenic rock masses the horizons are (downward) 1)discontinuous cryodiagenesis, where the basement of the seasonal freezing-thawing layer on sequential sedimentation on the surface is relatively soon replaced by sequential transition into permafrost; 2)active cryogenesis, as in the previous type of rock masses; 3)relative conservation, in-

heriting the cryostructural features, acquired by the sediment (rock) when it was first in seasonal freezing conditions and then in active cryodiagenesis.

As a result of cryogenic processes in one or the other horizons when the development is of the epi- or syncryogenic type, a quite definite set of cryogenic rocks arises - pure ice in the ground, frozen earth material or cryogenic eluvium with its specific cryostructural and textural features.

For lack of place the description of the structural, textural and other features of the genetic horizons in epi- and syncryogenic rock masses is not given here. Suffice it to say that taking the permafrost region of Eurasia as an example one may judge of the character of all the change of the horizon structure peculia rities of these rock masses from north to south from the arctic zone to the subarctic and further to the boreal and subboreal ones. Within each of these natural zones the thickness of all the horizons and their main structural features change regularly. For example, the thickness of the seasonal freezing-thawing horizon in epicryogenic rock masses and consequently the thickness of the cryogenic eluvium from north to south increases gradually and finally completely replaces the permafrost by a mantle cryoeluvial horizon of loess-like deposits. All the other genetic horizons undergo appropriate changes both in thickness and in the special features of cryogenic structure from one natural zone to another.

Thus, the knowledge of the nature of the cryolithogenesis phenomenon which should be considered the initial methodologic feature, implies proper use of the second methodological principle of cryolithology, that is the ascertaining of present-day regularities of the zonal cryolithogenesis manifestation.

On the basis of the first two methodological principles we get the essential data for the understanding of the principal stages of the historical cryolithogenesis development, i.e. we come to the third of the basic methodological principles. There is neither place nor need from the point of view of methodology of our science to describe the cryolithogenesis formation and development stages on this planet from Proterozoic to Pleistocene and Holocene. As an example of the use of the third of the main methodological principles of cryolithology it would be better to dwell on its significance for paleogeographical reconstructions.

The working out of a genetic classification of frozen ground features, based on the understanding of their very physico-geographical and geological nature enables us to make a more rational than previously paleogeographical reconstruction of past natural conditions from recent frozen ground features and their imprints.

When dealing with recent frozen ground features the singling out of all the aforementioned elements is a task of paramount importance as it enables us, in many cases, to judge by the regular vertical distribution of ice in the rock masses of the paleoclimatic conditions prevailing at the time of permafrost formation. Besides, syncryogenic rock masses are particularly significant as any of their horizons showing the near-surface freezing conditions, allows as to judge of the climate at the time of the deposition of every sediment layer though there are certain difficulties in such an investigation.

The fossil frozen ground features are of great paleogeographical interest but there arise great difficulties in the genetic interpretation of the cryogenic phenomena. The genetic system of frozen ground features has been worked out at present but not all of its elements are of the same interest from the point of view of paleocryogenic analisis, particularly for the fossil cryolithogenesis imprints. Thus all injection deposits remain practically unrecorded in the fossil state. The fossil imprints of frozen earth material, i.e. of the ice polymictic rocks are discerned with difficulty. The horizon of seasonal freezing-thawing is characterized by stages of the process of substratum transformation into the secondary dust-like product - the cryopelite. The completion of this process is the acquisition of loessial appearance with all the inherent symptoms.

Of particular importance are the deformations due to the frost fracturing of the active layer. It is connected with the formation of polygonal ground veins which often extend into the permafrost. The ground veins are particularly important indicators of the rigour and continentality of climate only when the seasonal freezing is extremely deep.

The horizon of the active cryodiagenesis in epicryogenic rock masses is rather important for the paleocryogenic analyses, as within its limits under favourable conditions epicryogenic polygonal wedge ice is formed. Their degradation may result in the formation of ground pseudomorphs on ice wedges.

The thick syncryogenic permafrost does not retain as a rule any traces of its former structure after thawing. As for syncryogenesis in conditions of deep seasonal freezing the thick series of deposits of different genesis besides bearing evidence of cryogenic acquisition of loessial appearance natural for them are as well characterized by ground veins which are the result of frost fracturing - a process accompaning cryohypergenesis. The importance of the cryogenic eluvium complex with such peculiar to it features of cryohypergenesis as acquisition of loessial appearance and polygonal lattices of ground veins is evident when dealing with paleogeographical reconstructions.

Such is the incompletely shown here importance of the genetic system of cryogenic phenomena for paleogeographical reconstruction and hence for the knowledge of the historical development of cryolithogenesis processes both in the Cenozoic and in more remote geologic time. The genetic system of cryogenic phenomena must help us to discover zonal patterns of their distribution as well as specific features stipulated by regional factors, first of all by such ones

as the manifestation of cryolithogenesis in conditions of areas of predominant tectonic upwarping, subsidence or tectonic stability, i. e. in conditions of predominating denudation or accumulation of sediments or long stability of the area without noticeable removal and accumulation of material.

The three main methodological principles of cryolithology have been considered and the independent significance of each of them and their interrelationship have been stressed. It has been shown that only taking into account the specific character of diagenesis and weathering (hypergenesis) stipulated by climate can help one to determine the lithogenesis type, in this case the cryolithogenesis one, which includes both cryodiagenesis and frost weathering (cryohypergenesis). These are the foundations of the cryolithogenesis theory.

ORIGIN OF MASSIVE GROUND ICE ON TUKTOYAKTUK PENINSULA, NORTHWEST TERRITORIES, CANADA: A REVIEW OF STRATIGRAPHIC AND GEOMORPHIC EVIDENCE

V.N. Rampton

Terrain Analysis and Mapping Services Ltd., Carp, Ontario, Canada

SYNOPSIS Massive tabular ice and icy sediments, underlie hills and ridges within and proximal to the glacial limit on the Tuktoyaktuk Peninsula. Sediments in depressions and radiocarbon dates obtained from these sediments indicate that massive ice and icy sediments were more continuous before the hypsithermal in that they underlaid most landscape now occupied by basins until the ice melted during the hypsithermal. Oxygen isotope values from the massive ice as reported by Mackay (1983) suggest that it has a glacial or meltwater origin. The distribution of icy sediments and massive ice proximal to the limit of glaciation, the lack of massive ice within till, massive ice interlayered to depth with fluvial sands, the transition from massive ice to reticulate ice veins at some localities, vertically oriented strings of gas bubbles and matched broken soil fragments across ice lenses (Mackay 1971) indicate an epigenetic segregation origin for the ice. This ice likely formed from subglacial meltwater hydrostatically driven toward an aggrading permafrost table near the glacier margin.

INTRODUCTION

The Tuktoyaktuk Coastlands, which includes the Tuktoyaktuk Peninsula, of northwestern Canada (Fig. 1) are underlain by a thick sequence of unconsolidated Quaternary sediments. Generally, till of variable thickness overlies interbedded sands and clays (Rampton, in press).

Massive ground ice and icy sediments can be examined in shoreline exposures throughout the Tuktoyaktuk Coastlands (Figs. 2 and 3). Their presence has also been confirmed by the recording of massive ice and icy sediments in numerous 10 to 60 metre holes drilled throughout the area for seismic surveys (Mackay, 1971; Rampton and Mackay, 1971; Rampton, in press); and by gravity surveys (Rampton and Walcott, 1974) that indicate many hills and ridges are cored with ground ice (Fig. 4).

Massive ground ice and icy sediments were much more extensive throughout the Tuktoyaktuk Coastlands at the beginning of the hypsithermal. The strata underlying depressions, which cover much of the Tuktoyaktuk Peninsula, presently contain few massive ground ice bodies and are deficient in ice content relative to the strata underlying uplands. Numerous basins examined throughout the region show a consistent sequence of lacustrine sediments over colluvium over preglacial sediments. Depressions showing this sequence have developed through thermokarst expansion of lacustrine basins via retrogressive thaw flow slides (Rampton, in press), mainly at the beginning of the hypsithermal. This involves removal of massive ice underlying till and other sediment through continuous retreat of icy scarps (cf. Figs. 2 and 3) and the flow of thawed debris downslope into a lacustrine basin where the debris (colluvium) is partially reworked and covered by lacustrine sediments as the basin continues to expand (Rampton, 1973). Thus, massive ice was formerly much more extensive and any origin of massive ground ice and icy sediments on the Tuktoyaktuk Peninsula must account for the formation of large volumes of ice under a landscape virtually devoid of lacustrine basins.

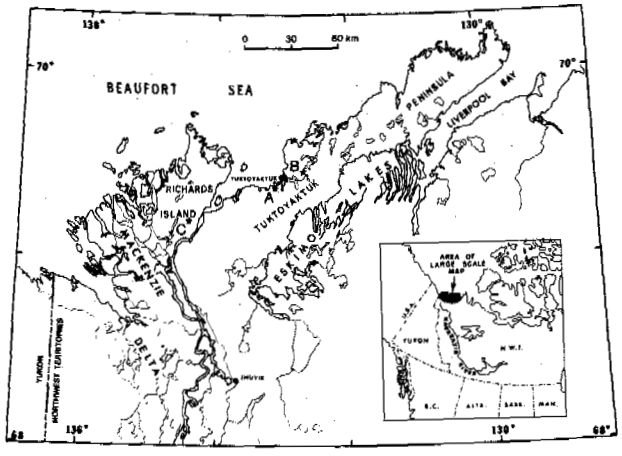

Fig.1 Location map. A-massive ice, Fig. 2; B-involuted hills, Fig. 4; C-Richards Island, Fig. 4

GROUND ICE STRATIGRAPHY

Drilling data throughout the Tuktoyaktuk Coastlands indicate that massive tabular ground ice and very icy sediments commonly

lie at the base of till and till-derived sediments (cf. Figs. 2, 3 and 4). Generally the larger bodies of tabular ground ice are underlain by sand or gravel (Mackay, 1971; Rampton, in press). An analysis of drilling results by Rampton and Mackay (1971, p. 5) confirms this: "Of the 176 bodies of massive ice that were drilled completely through, 4 per cent were overlain by peat, 19 per cent by gravel, sand and gravel, or sand, 3 per cent by sandy clay, 26 per cent by clay and 48 per cent by clay and rocks, which is interpreted as till or material derived from the reworking of till. The material lying below the massive ice was 92 per cent gravel, sand and gravel, and sand, 2 per cent sandy clay and 6 per cent sandy clay. Where sandy clay or clay lay under the ice, the latter was found to be thin". The remarkably sharp contact between till and massive ground ice can be observed in numerous exposures throughout the area (Figs. 2 and 3).

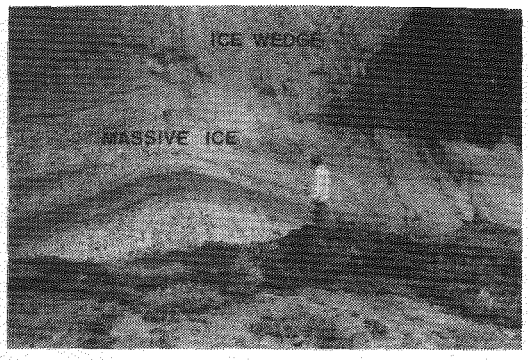

Fig. 2 Massive ground ice exposed at head of retrogressive thaw flow slide southwest of Tuktoyaktuk.

Drill hole data (Rampton, in press; Fig. 5) indicate that ground ice can also be present within sand underlying till, but that the thickness of the ice bodies is less than those bodies located directly under till. In detail, icy sand probably constitutes ice lenses separated by thin layers of sand as can be seen in ice cellars at Tuktoyaktuk (Fig. 6).

The prevalence of large massive ice bodies directly under fine-textured clayey till, the presence of multiple ice lenses within sand sequences, and the presence of sand and gravel below most bodies of massive ice are all factors consistent with an epigenetic segregation origin for the ice. Williams (1967) indicated that the formation of large ice lenses is favoured by an abundance of water, low overburden pressures, slow freezing rates, high permeability and small pore openings. Mackay (1971, p. 420) has also noted that "for a thick ice lens to form, there must be a constant replenishment of pore water from below". The prevalence of icy sediments where ample water is available at the freezing plane has been noted in other regional studies (Rampton et al, 1983). Thus large ice lenses (or massive ground ice) develop at the clayey till - sand and gravel contact because the high permeability of the underlying sand and gravel allow water to migrate to the small pore openings of the till,

Fig. 3 Exposure at retrogressive thaw flow slide on Eskimo Lake (*reticulate ice in till).

provided of course that the latter strata is being continuously recharged with water. Segregated ice may also form within sand and gravels if the pore water pressures are high enough (Mackay, 1971, 1973, 1979). Ice lenses (segregated ice) have been observed in the core of a pingo at Tuktoyaktuk that are virtually indentical to ice lenses within

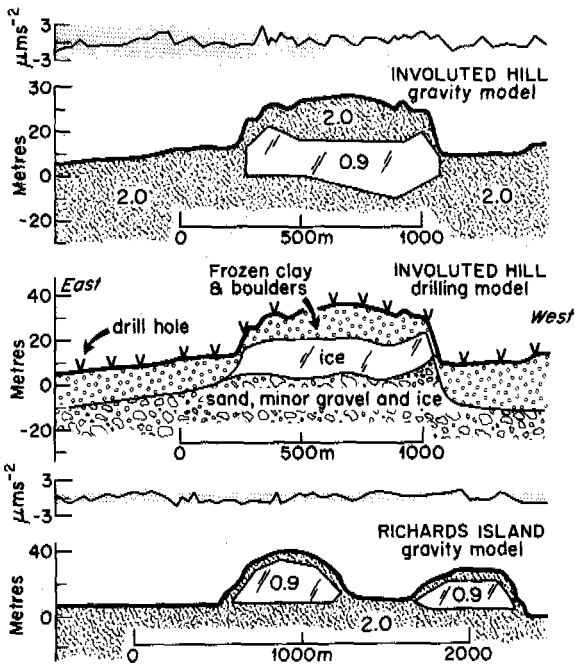

Fig. 4 Profiles on Tuktoyaktuk Coastlands showing ground ice as located through gravity profiling and drilling (from Rampton and Walcott, 1974).

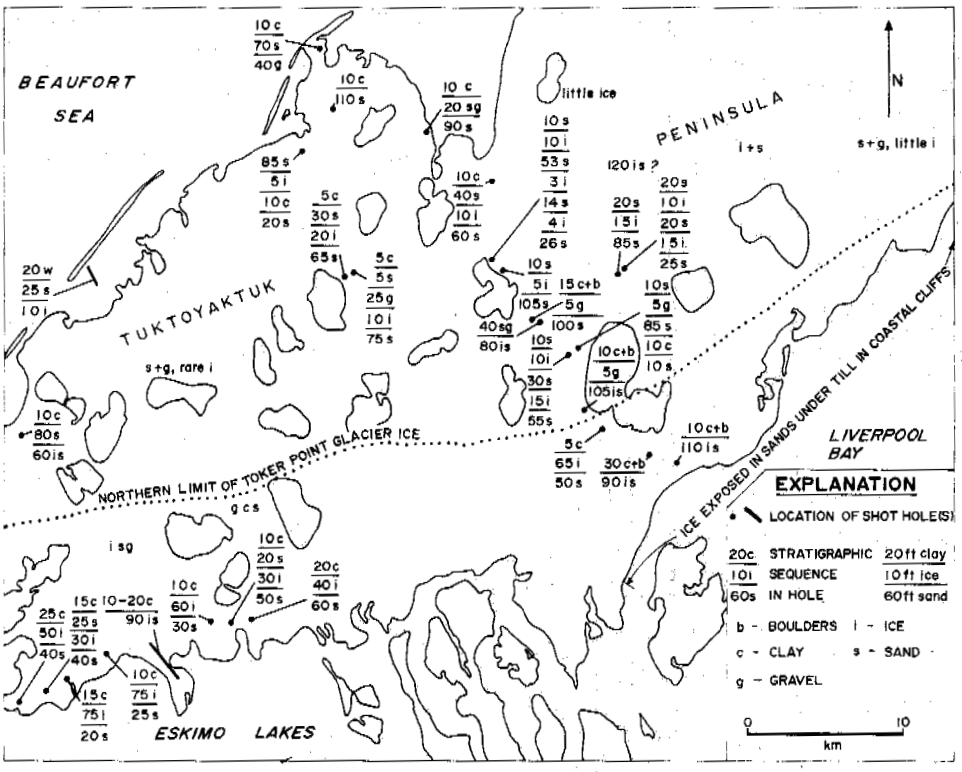

Fig. 5 Drill hole logs near Toker Point Stade (Wisconsinan) glacial limit along Tuktoyaktuk Peninsula. Till within glacial limit is usually logged as clay.

sands in ice cellars in the same village (Rampton and Mackay, 1971). Mackay (1973, 1979) has demonstrated that the formation of ice lenses (segregated ice) within a pingo is related to water at the freezing plane.

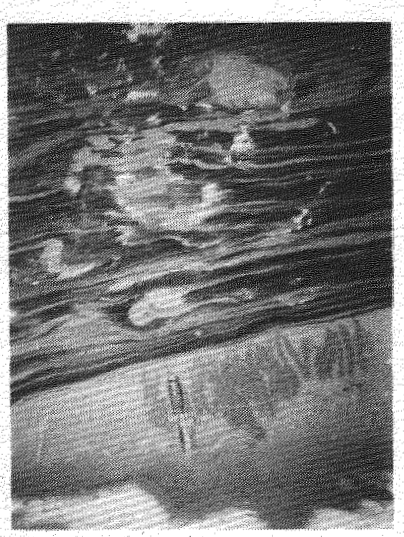

Fig. 6 Ice (dark) and sand (light) in ice cellar at Tuktoyaktuk. Knife (15-cm) for scale.

A glacier origin for most of the massive ice described above does not seem tangible as entrainment of glacial debris occurs at the base of a glacier (Sugden and John, 1976). Such entrainment commonly results in alternating layers of till, debris-rich ice (icy till) and glacier ice at the base of the glacier. To date, interlayered till or icy till has only been reported in this region from under glaciofluvial sediments near the base of massive ice on Richards Island (Dallimore and Wolf, 1988). Buried glacier ice may also be present under outwash at the south end of the Eskimo Lakes (Fig. 1) where a possible shear plane was noted in buried ice there (Fig. 3 in Rampton and Walcott 1974). Harry and French (personal communication 1987) have also noted ground ice in this area that they suspect to be glacial in origin.

OXYGEN ISOTOPES OF GROUND ICE

Mackay (1983) has compiled the $\delta^{18}O$ values for ice from a number of sites in the Tuktoyaktuk Coastlands and adjacent areas as the "$\delta^{18}O$ values for ice in permafrost help to give an indication of the conditions when precipitation occurred" (Mackay 1983, p. 67). He found that values for modern waters and for ice formed during the Holocene were more positive than values for massive ground ice. Values (-29 to -35 $\delta^{18}O$ in $^{o}/_{oo}$ obtained from the massive ice were similar to those reported for Wisconsinan ice in the Devon ice cap (Paterson et al, 1977).

This suggests that precipitation of the water forming the massive ice occurred under a high latitude Wisconsinan environment. Thus values obtained from massive ice, most of which is believed to have an epigenetic segregation origin, on the Tuktoyaktuk Coastlands suggest a glacier source of water (Mackay 1983) as previously proposed by Rampton (1974).

ICE PETROGRAPHY, BUBBLES AND SOIL INCLUSIONS

Where ice crystals have been studied in detail within ice lenses, the crystals are oriented normal to lensing (Mackay and Stager, 1966). Such an alignment occurs parallel to the thermal gradient. It indicates downward movement of the freezing plane and little deformation of the ice since its formation.

Bubbles in clean ice between bands of debris-rich ice in examined massive ice exposures are oriented normal to banding (Rampton and Mackay 1971). Also "soil fragments may have bubbles trailing upwards from them, normal to layering" (Mackay, 1971, p. 411). These characteristics also indicate downward movement of the freezing plane and little subsequent deformation.

Mackay (1971) has also noted that stones will have icy coatings on one side consistent with a downward moving freezing plane, and that broken soil fragments can be matched vertically across ice lenses. The latter is consistent with epigenetic segregation formation of the ice and is inconsistent with a glacier origin requiring some lateral movement of ice.

CONTACTS OF MASSIVE ICE BODIES

Commonly massive ice grades upward into clayey till with reticulate ice (Figs. 2 and 3); in some cases a continuum from ice lenses through reticulate ice through massive ice may occur (Fig. 3). Mackay (1971) has also reported on the common gradational contact of massive ice bodies. Exceptions are where melting from the surface or fluvial erosion at the surface has resulted in a sharp upper contact. The gradational ice contacts would suggest a common origin to all ice types. Reticulate ice and ice lenses are known to be primarily formed by ground shrinkage and ice segregation under a downward moving frost line (Mackay, 1974), and a similar origin for the associated massive ice is thus indicated.

FORMATION OF MASSIVE GROUND ICE

Most evidence points to the extensive massive ground ice on the Tuktoyaktuk Peninsula as having been formed as epigenetic segregation ice (Mackay, 1971; Rampton, 1987); yet it has $\delta^{18}O$ values typical of Wisconsinan glacier ice. These factors can be reconciled if the primary source of water forming the ground ice is glacial meltwater. The only other probable source of water is from lakes in intervening depressions. However, as previously stated, most of these lakes did not form until the hypsithermal. If the massive ground ice formed from this water, the ice would have relatively high $\delta^{18}O$ values similar to ice from under refrozen taliks, which has values similar to those of today's lakes (Michel and Fritz, 1982, Mackay, 1983). A model of ground ice formation has been previously proposed for the Tuktoyaktuk Coastlands (Rampton, 1974) that has ground ice within and immediately proximal to the glacial limit forming from the freezing of subglacial meltwater (Fig. 7). This requires that the sediments immediately underlying the glacier be in a thawed state. Beget

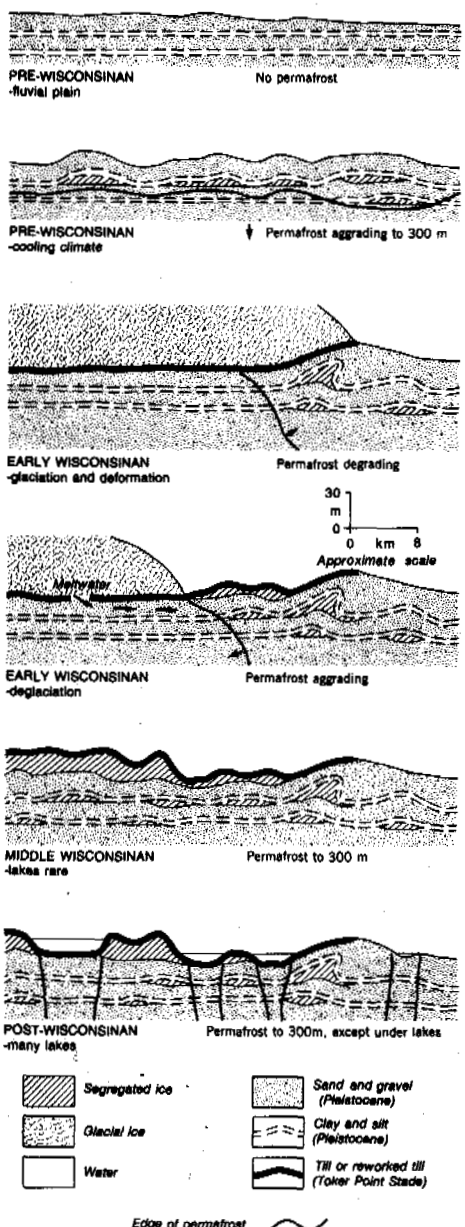

Fig. 7 Model showing development of ground ice through time on the Tuktoyaktuk Peninsula (from Rampton, in press). Note folding of ice and sediments can occur near margin of glacier (Early Wisconsinan).

(1987) has concluded that the base of the glacier was not frozen to its base in the vicinity of the Tuktoyaktuk Coastlands during glaciations affecting them because the ice sheets had low topographic profiles indicative of low basal shear stress and high subglacial pore pressure. The glaciers must have been thick enough to cause temperature to rise to the pressure melting point at or near their base during the last glaciation.

Subglacial meltwater moving towards the periphery of the ice sheet under hydrostatic pressure (created by glacier ice overburden pressures) would then supply the large volumes of water required to form the extensive beds of massive ice (as previously indicated the massive ice underlaid most of the landscape following its formation, see also Fig. 7 - Middle Wisconsinan). This pressurized water would form ice lenses and massive ice at the aggrading permafrost table. Recent studies by Gustavson and Boothroyd (1987) have shown that most meltwater under the Malaspina Glacier in Alaska moves along the base of the glacier and is expelled near its terminus under pressure. The origin of eskers and tunnel valleys in temperate North America has also been attributed to similar subglacial flow (Wright, 1971). The large, deep trenches forming finger-like projections of land in the Eskimo Lakes (Fig. 1) have bases that lie well below sea level and were likely formed by subglacial meltwater eroding thawed sands under hydrostatic pressure (Rampton, in press). The north part of the Tuktoyaktuk Peninsula is formed of sand and gravel (Rampton 1979) that appears to have been deposited by sediment-laden waters emerging from these trenches at the margin of the glaciers.

Ground ice is present well beyond the glacial limit along the Tuktoyaktuk Peninsula (Fig. 5) where it was probably formed prior to glaciation during regional cooling. However as evidenced by drill hole data (Fig. 5) and the depth of thermokarst depressions it is not as thick as the ground ice within the glacial limit.

REFERENCES

Beget, J. (1987). Low profile of the northwest Laurentide map sheets. Arctic and Alpine research (19), 81-88.

Dallimore, S.R. and Wolfe, S.A. (1988). Massive ice associated with glaciofluvial sediments, Richards Island, NWT. Fifth International Conference on Permafrost, Trondheim, Norway, this volume.

Gustafson, T.C. and Boothroyd, J.C. (1987). A depositional model for outwash, sediment sources, and hydrological characteristics, Malaspina Glacier, Alaska: A modern analogy of the southeastern margin of the Laurentide ice sheet. Geological Society of America Bulletin, (99), 187-200.

Mackay, J.R. (1971). The origin of massive icy beds in permafrost, western Arctic coast, Canada. Canadian Journal Earth Sciences (8), 397-422.

Mackay, J.R. (1973). The growth of pingos, western Arctic, Canada. Canadian Journal of Earth Sciences, (10), 979-1004.

Mackay, J.R. (1974). Raticulate ice veins in permafrost, northern Canada. Canadian Geotechnical Journal, (11), 230-237.

Mackay, J.R. (1979). Pingos of the Tuktoyaktuk Peninsula area, Northwest Territories, Geographie Physique at Quaternaire, (33), 3-61.

Mackay, J.R. (1983). Oxygen isotope variations in permafrost, Tuktoyaktuk Peninsula area, Northwest Territories. Geological Survey of Canada, Paper 83-1B, 67-74.

Mackay, J.R. and Stager, J.K. (1966). Thick tilted beds of segregated ice, Mackenzie Delta area, N.W.T., Biuletyn Peryglacjainy (15), 39-43.

Michel, F.A. and Fritz, P. (1982). Significance of isotope variations in permafrost waters at Illisarvik, N.W.T. Proceedings of Fourth Canadian Permafrost Conference, Associate Committee of Geotechnical Research, National Research Council of Canada, 173-181.

Paterson, W.S.B., Koerner, R.M., Fisher, D., Johnson, S.J., Clausen, H.B., Dansgaard, W., Bucher, P. and Oeschger, H. (1977). An oxygen-isotope climatic record from the Devon Island ice cap, Arctic Canada. Nature, (266), 588-511.

Rampton, V.N. (1973). The history of thermokarst in the Mackenzie-Beaufort region, Northwest Territories, Canada. International Union of Quaternary Research, 9th congress, Christchurch, New Zealand, Abstracts, 299.

Rampton, V.N. (1974). The influence of ground ice and thermokarst upon the geomorphology of the Mackenzie-Beaufort region. Research in Polar and Alpine Geomorphology, Proceedings 3rd Guelph Symposium on Geomorphology, Ed., B.D. Fahey and R.D. Thompson, 43-59.

Rampton, V.N. (1979). Surficial geology, Stanton, District of Mackenzie; Geological Survey of Canada, Map 33-1979.

Rampton, V.N. (1987). Origin of massive ground ice on Tuktoyaktuk Peninsula, Northwest Territories, Canada: stratigraphic and geomorphic evidence. International Union for Quaternary Research, XII International Congress, Ottawa, Canada Abstracts, 249.

Rampton, V.N. (In press). Quaternary geology of the Tuktoykatuk Coastlands. Geological Survey of Canada, Memoir 423.

Rampton, V.N. and Mackay, J.R. (1971). Massive ice and icy sediments throughout the Tuktoyaktuk Peninsula, Richards Islands and nearby areas, District of

Mackenzie. Geological Survey of Canada, Paper 71-21.

Rampton, V.N. and Walcott, R.I. (1974). Gravity profiles across ice-cored topography. Canadian Journal Earth Sciences, (11), 110-122.

Rampton, V.N., Ellwood, J.R., and Thomas, R.D., (1983). Distribution and geology of ground ice along the Yukon portion of the Alaska Highway gas pipeline. Proceedings, Permafrost Fourth International Conference National Academy Press, Washington, 1030-1035.

Sugden, D.E. and John, B.S. (1976). Glaciers and landscape. Edward Arnold (Publishers) Ltd., London, England, 376 p.

Williams, P.J. (1967). Properties and behaviour of freezing soils. Norwegian Geotechnical Institute, Oslo, Publication No. 72, 119 p.

Wright, H.E., Jr. (1971). Retreat of the Laurentide ice sheet from 14,000 to 9,000 years ago. Quaternary Research, (1), 316-330.

ANDES SLOPE ASYMMETRY DUE TO GELIFLUCTION

M.C. Regairaz

IANIGLA-CONICET, C.C.330, 5500 Mendoza, Argentina

SYNOPSIS: There are soils affected by differential gelifluction, which points to a Pleistocene age, on the remnants hills of the Andes piedmont at 2200 m asl and 33°SL. Differential gelifluction on north- and south-facing slopes was determined based on: 1) slope measurements; 2) clast orientation by means of Situmetry.

INTRODUCTION

Solifluction is a slow downslope waste movement under saturated conditions. Solifluction , so defined, has a broad sense since it can occur in any climate. Gelifluction means solifluction associated with frozen ground, either seasonally frozen ground or permafrost. Gelifluction has a more restricted sense because it is confined to cold climates.

BACKGROUND

Previous studies in the area (Schneider et al., 1976; Nijensohn et al., 1979; Moyano de Imazio et al., 1982; Gaviola de Heras & Nijensohn, 1984) are not focussed on frost action effects on soils. This is the first paper dealing with such aspects.

Slope asymmetry has been widely studied all over the world and many explanations have been developed: tilted strata, lateral stream erosion (Smith, 1949; Melton, 1960; Kennedy, 1975), gelifluction (Currey, 1964; Wayne, 1967; Kowalkoski et al.; 1980, Grimbérieux, 1982), etc. Sometimes two or more processes are working together i.e.: gelifluction material accumulated at the foot of the slopes causes lateral river migration which, in turn, produces basal undercutting of the opposite nearest slope.

Solifluction produces predominantly long axis clast orientation parallel to the slope. This preferential downslope orientation has been observed (Lundquist, 1949; Poser & Hovermann, 1951; Rapp, 1966; Benedict, 1966, 1970; Furrer & Bachmann, 1968; Brochu, 1972, 1978; Mottlershead, 1976, 1982; Reanier & Ugolini, 1983, among many others). Although it has been pointed out that this preferential orientation can also be produced by gravity, such as in colluvial slopes, certain studies (Poser & Hovermann, 1951; Furrer & Bachmann, 1968; Lesser, 1977; Brochu, 1978) have shown that solifluction determines a stronger downslope orientation.

The Situmetry method has been applied (Poser & Hovermann, 1951; Furrer & Bachmann, 1968; Stablein, 1970; Leser, 1977, etc.) to evaluated clast orientation in various deposits, i.e.: solifluction, moraines, etc. This method is almost unknown in Argentina (Abraham de Vazquez & Garleff, 1984; Ahumada & Trombotto, 1984).

STUDY AREA

Field studies were centered on the piedmont area of the Cordón del Plata (Fig.1), Mendoza, Argentina. The area is at 33°5' SL and 69°18' WL, the average altitude is 2200 m asl. The

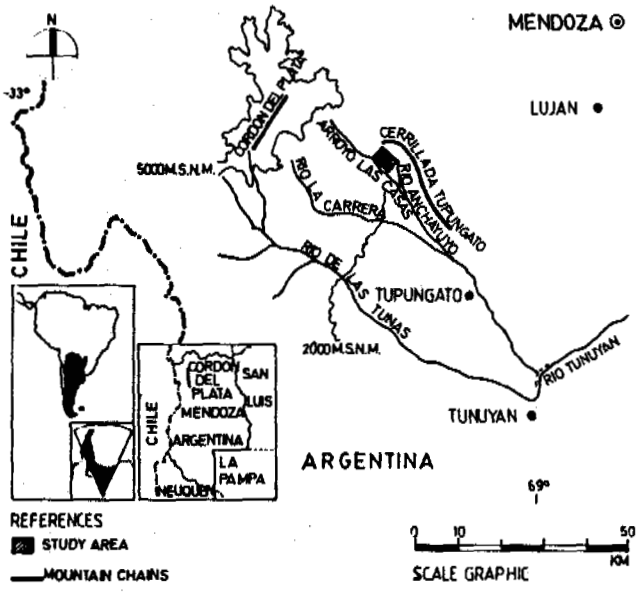

Fig.1: Location of the study area.

gelifluction observations were focused on the hills, remnants of an old piedmont level (polymictic fanglomerades of Mesones Fm.?). The

origin of this piedmont has been attributed to a tectonic uplift of the Andes and to post-tectonic sedimentation (Polanski, 1963, 1972).

The total annual precipitation is 425 mm (rain + snow). The mean year temperature is +7.9°C, with a maximum mean of +13.1°C and a minimum mean of +2.7°C. The area is placed within the parageocriogenic zone (Corte, 1985). In the piedmont area soils are affected by seasonal freezing to a depth of about 5 cm and there are approximately 1100 cumulative hours per year of freezing temperatures (0°C or below). In the mountaineous area discontinuous permafrost is located above 3400 m.

Vegetation is a diverse mountain formation (Roig, 1969) or a mountain grassland belt (Gomez Molina & Little, 1981). The trees (*Poplar sp., Salix sp.*) are very scarce, the main vegetation are grasses (*Stipa sp., Poa sp.*, etc.) and shrubs (*Adesmia sp., Verbena sp., Nassauvia sp.*, etc.). The area is now used for potatoe cultivation and cattle grazing.

METHODS

Slope orientation and angles were measured by traditional means, a compass and a clinometer respectively. Slope exposition was obtained subtracting 90°from the southern slope orientation and adding up 90°to the orientation of northern slopes. Supposing that the so-calculated northern slope exposition surpasses 360°, this latter value must be subtracted to find the final result. The slope inclination was measured on the constant sector of the slopes. Slope difference is the angle of the southern slopes minus the angle of the northern one, thus positive values mean that the south-facing profiles are the steepest.

Sample site 1 is placed in hill N°20, site 2 in N°22, site 3 in N°6 and site 4 in hill N°1. Clast orientation was analyzed in four profiles, two on north-facing slopes (warm) and two on soth-facing slopes (cold). The sample sites are not located in opposite slopes in the same remnant hills, in fact, they were analyzed where deep exposures were found (i.e.; deep gullies, road trenches) because the stoniness of profiles makes deep excavation a difficult task. The outermost part of each soil profile was carefully removed and long axis orientation measurements were taken in fresh exposures. The long-axis orientation of approximately 50 elongate clasts was evaluated in each soil horizon.

Clast orientation was evaluated by means of Situmetry. This method was chosen because it is quicker and easier than other traditional methods (i.e.: rose diagrams) and as useful as the others are. Besides, this method provides definite values, cited in Results and Discussion, to differentiate gravity from solifluction deposits, being both processes the cause of preferential downslope clast orientation. In this method clast orientation is evaluated through seven semicircunference areas. Those numbered I (0-30°with slope direction), II (30-60°) and III (60-90°), three on the left and three on the right side of the downslope direction, include all the clasts parallel to the slope. Sector IV comprises dipped clasts.

RESULTS AND DISCUSSION

In the study area differential gelifluction was determined based mainly on slope measurements and clast orientation.

Slope measurements

The slope azimuth and inclination of thirty remnant hills (Fig. 2) were surveyed on the field and the results are presented in Table I. and Fig.3.

In most cases, southern slopes are steeper (positive values of slope difference), the only exception found on hill N°3, can be attributed to an anomalous slope exposition: in fact, most slopes face NE-SW and few hills are facing NW-SE, site 3 is the only one with NE-SE exposition. An extreme slope difference (hill N°30) seems to be the result not only of gelifluction on the northern slopes but also lateral stream erosion by Arroyo Negro at the foot of the south-facing profiles.

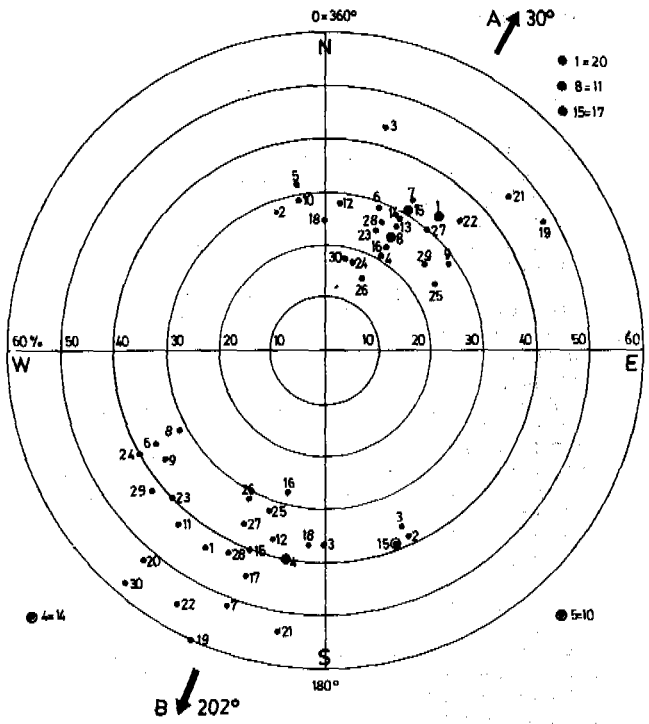

Fig.3: Slope exposition and inclination of remnant hills. A=mean value of north-facing slopes. B=mean value of south-facing slopes.

Site	Exposition N=northern (warm) S=southern (cold)	Slope orientation degrees	Slope exposition degrees	quadrant	Slope inclination degrees	%	Slope difference (S-N) degrees
1	S (*)	300	210	SW	23	43	4
	N	315	40	NE	19	35	
2	S	245	155	SE	21	38	6
	N	250	340(20)	NW	15	27	
3	S	245	155	SE	20	36	-4
	N	285	15	NE	24	44	
4	S	280	190	SW	22	40	10
	N	300	30	NE	12	21	
5	S	250	160	SE	21	38	3
	N	260	350(10)	NW	18	32	
6	S (*)	330	240	SW	20	36	4
	N	290	20	NE	16	29	
7	S	290	200	SW	27	51	9
	N	300	30	NE	18	33	
8	S	330	240	SW	17	31	3
	N	300	30	NE	14	25	
9	S	325	235	SW	20	36	4
	N	325	55	NE	16	29	
10	S	250	160	SE	21	38	5
	N	260	350(10)	NW	16	29	
11	S	310	220	SW	23	43	9
	N	300	30	NE	14	25	
12	S	285	195	SW	20	36	5
	N	275	5	NE	15	27	
13	S	270	180	S	20	36	5
	N	300	30	NE	15	27	
14	S	280	190	SW	22	40	6
	N	300	30	NE	16	29	
15	S	290	200	SW	22	40	5
	N	300	30	NE	17	31	
16	S	285	195	SW	15	27	2
	N	300	30	NE	13	23	
17	S	290	200	SW	24	44	7
	N	300	30	NE	17	31	
18	S	275	185	SW	20	36	6
	N	270	0	N	14	25	
19	S	295	205	SW	31	60	6
	N	330	60	NE	25	47	
20	S	310	220	SW	27	51	8
	N (*)	310	40	NE	19	35	
21	S	280	190	SW	28	53	3
	N	320	50	NE	25	46	
22	S	300	210	SW	28	53	8
	N (*)	315	45	NE	20	36	
23	S	315	225	SW	22	40	8
	N	295	25	NE	14	25	
24	S	330	240	SW	22	40	12
	N	285	15	NE	10	18	
25	S	290	200	SW	18	32	5
	N	330	60	NE	13	24	
26	S	295	205	SW	17	31	8
	N	295	25	NE	9	16	
27	S	295	205	SW	20	36	3
	N	310	40	NE	17	30	

Slope exposition	Depth cm	North-facing (warm) Situmetric class I	II	III	IV	Slope exposition	Depth cm	South-facing (cold) Situmetric class I	II	III	IV
		% clasts						% clasts			
Site 1	0- 15	49	24	4	23	Site 3	0- 14	18	58	3	21
	15- 40	46	34	2	18		40- 65	12	46	25	17
	40-+90	48	31	2	19		65-100	19	42	12	27
Site 2	0- 20	43	48	-	9	Site 4	0- 40	19	50	4	27
	20- 50	42	41	-	17		40- 60	8	58	22	12
	50-+80	55	29	2	14		60-+120	25	38	26	11
Mean values		(47)	34	2	17	Mean values		17	(49)	15	19

TABLE N°II: Situmetric measurements

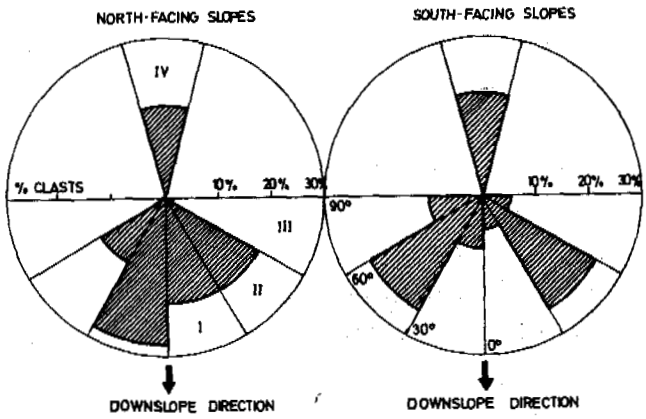

Fig. 4: Situmetric values of clast orientation

downslope orientation. The situmetric values of class I on north-facing slopes are not so strong (i.e.: 60-70%) as those mentioned by other authors, cited in the preceeding paragraph. The values found on the study area, of about 50%, seem to indicate that conditions favorable to gelifluction were moderate and/or that gelifluction was operating during a shorter period of time than necessary to produce a stronger downslope orientation.

South-facing profiles exhibit a completely different situation. The low value of class I means a reduced influence of gravity and/or solifluction processes, the maximum value of about 50% in class II could be a fabric arrangement inherited from the parental soil material (fanglomerades) or an incipient gelifluction development, the latter might have produced an increase in class II at the expense of class III.

Environmental conditions

The study area is affected by severe laminar erosion, which has caused not only the exposition of subsurface horizons, i.e.: Bt horizon, K (Birkeland, 1984) laminated (stage IV, Gile et al., 1966) horizon, but also different levels of bare-vegetated soil surfaces, meaning that vegetation roots have prevented soil remotion to a certain degree.

The preferential downslope clast orientation in northern profiles extends downward to at least 80-90 cm depth and, since we do not know how much of the upper soil profile has been removed, it is evident that gelifluction must have affected more than 80-90 cm depth. It has been pointed out (Gamper, 1983) that deep soil freezing promotes gelifluction because thawing occurs from the surface downwards thus the upper soil becomes saturated and flows over the frozen subsoil. Shallow soil freezing only favours frost-creep because the soil thaws quickly from the top and from below.

It seems that differential gelifluction in the study area is mainly a fossil feature, probably of Pleistocene age. In fact, present seasonal freezing does not account for the observed gelifluction but the outermost moraines (M1-M2 in Fig. 2) give evidence of a former colder period.

CONCLUSION

The main process responsible for asymmetric slopes in the study area is the differential thermal balance on south and north-facing profiles. During Pleistocene cold stages northern slopes underwent a great number of freezing-thawing cycles which promoted preferential gelifluction on that side. The secondary process is lateral river erosion, which has caused the highest south-north slope differences. Whether this differential gelifluction was developed on a seasonal freezing layer or on an active layer of permafrost is a fact that cannot be decided at this stage of the research.

ACKNOWLEDGEMENTS

The author of this paper is indebted to doctor Arturo Corte (Laboratory of Geocriology) for his review and suggestions on this paper, to professor Karsten Garleff (Bamberg University) for providing me with additional bibliography on Situmetry, to Darío Trombotto and Ana Lía Ahumada who have trained me on situmetric measurements, to María Elena Soler for reviewing my English translation and for typing the manuscript and to Albert Mitchell for drawing the figures. This study has been supported by CONICET.

Site	Exposition N=northern (warm) S=southern (cold)	Slope orientation degrees	Slope exposition degrees	quadrant	Slope inclination degrees	%	Slope difference (S-N) degrees
28	S	295	205	SW	23	42	8
	N	295	25	NE	15	26	
29	S	320	230	SW	23	42	4
	N	320	50	NE	19	35	
30	S	310	220	SW	30	58	20
	N	280	10	NE	10	18	
Mean Values	S	-	202	SW	22	41	6
	N	-	30	NE	16	29	

TABLE N°I: Slope measurements (*)situmetric sample sites

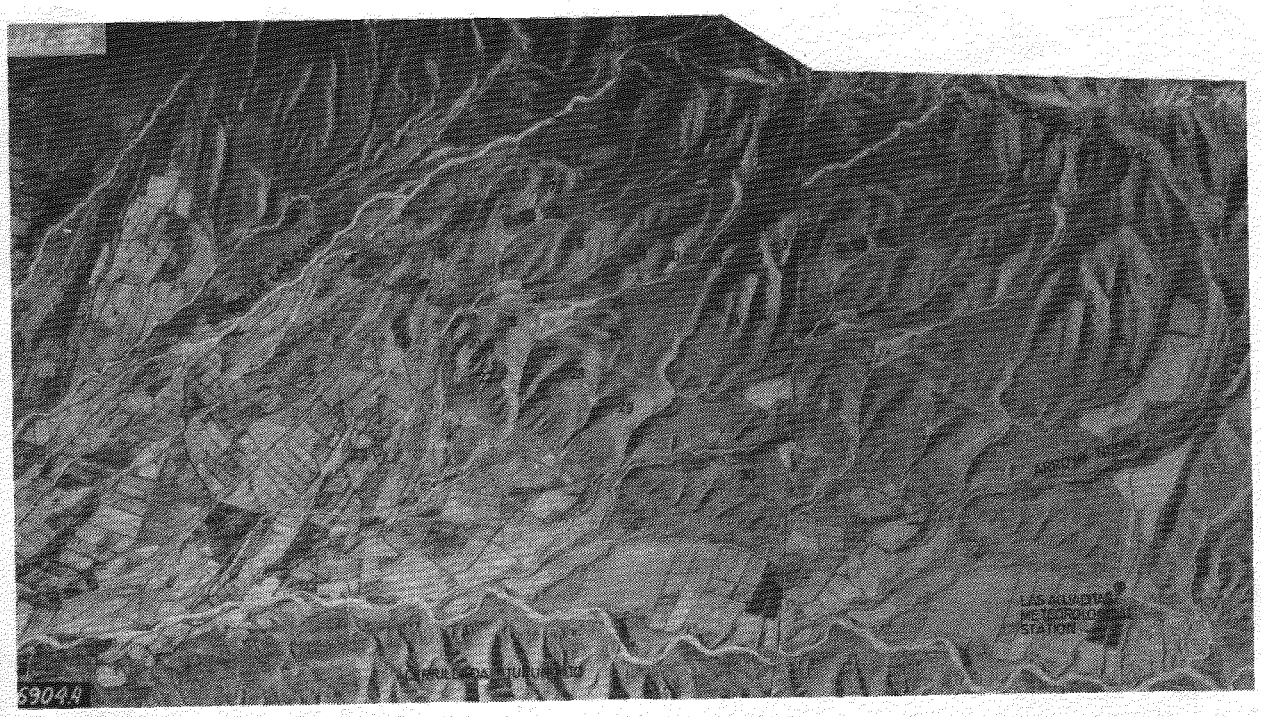

Fig.2: Stereopair of the study area (flight no. 6904 A, photos N°112-75 and 112-76, taken in 1960). M1 + M2: outermost moraines (Pleistocene?). Photo scale: 1:50.000

In most cases southern slopes are steeper (positive values of slope difference), the only exception, found on hill N°3, can be attributed to an anomalous slope exposition: in fact, most slopes face NE-SW and few hills are facing NW-SE, site 3 is the only one with NE-SE exposition. An extreme slope difference (hill N°30) seems to be the result not only of gelifluction on the northern slopes but also lateral stream erosion by Arroyo Negro at the foot of the south-facing profiles.

Clast orientation

Four situmetric fabric measurements are presented in Table N°II and Fig. N°4. The differences are striking in north-facing slopes almost 50% of clasts are placed in class I but south-facing profiles almost 50% belong to class II.

In north-facing slopes the fact of decreasing values from class I to class III means that the number of clasts increases markedly in the slope direction. Situmetric measurements give 35-39% (Poser & Hovermann, 1951) or 30-40% (Leser, 1977) in class I for gravity slopes and 45-53% (Poser & Hovermann, 1951), 51-62% (Furrer & Bachmann, 1968) or 50 to 75% (Leser, 1977) in class I for solifluction deposits. The situmetric values found on north-facing slopes point to a gelifluction origin because class I comprises almost 50% of clasts. The weak orientation in the upper 50 cm of sample site 2 could be a local effect due to the restraining effect of former vegetation since the deepest horizon, below 50 cm, shows a strong

REFERENCES

Abraham de Vazquez, E. & Garleff, K. (1984) Evidencias de cuñas de hielo fósiles en el sur de la provincia de Mendoza. Actas II Reunión Grupo Periglacial Argentino, 3-11, San Juan, Argentina.

Ahumada, A.L. & Trombotto, D. (1984). Estudios periglaciales en la Lagunita del Plata, provincia de Mendoza, Actas Noveno Congreso Geológico Argentino, (IV), 22-34.

Benedict, J.B. (1966). Radiocarbon dates from a stone-banked terrace in the Colorado Rocky Mountains, U.S.A. Geografiska Annaler (48A),1, 24-31.

Benedict, J.B. (1970). Downslope soil movement in a Colorado alpine region:rates, processes and climatic significance. Arctic and Alpine Research (2), 3, 165-226.

Birkeland, P.W. (1984). Soils and geomorphology, 372 pp. Oxford University Press, New York.

Brochu, M. (1972). Premières observations de dépôts de solifluxion fossiles en Gaspesie. Biuletyn Peryglacjalny, 21, 15-20.

Brochu, M. (1978) Disposition des fragments rocheaux dans les dépôts de solifluxion, dans les éboulis de gravité et dans les dépots fluviatiles: mesures dans l'est de l'Articque nord-américain et comparaison d'autres régions du globe. Biuletyn Peryglacjalny, 27, 35-51.

Corte, A.E. (1983). Los conceptos: geocriogénico-parageocriogénico y glacial-paraglacial en los Andes centrales de Argentina, lat. 30° Actas II Reunión Grupo Periglacial Argentino, 48-61, San Juan, Argentina.

Currey, D.R. (1964). A preliminary study of valley asymmetry in the Ogotoruk Creek area, northwestern Alaska. Arctic (17), 2, 85-98.

Furrer, G. & Bachmann, F. (1968). Die situmetric (Einregelungsmessung) als morphologische untersuchunsmethode. Geographica Helvetica 23, 1-14.

Gamper, M.W. (1983). Controls and rates of movement of solifluction lobes in the eastern Swiss Alps. Proc. 4th Int. Conf. Permafrost, 328-333, Fairbansk, Alaska.

Gaviola de Heras, S. & Nijensohn, L. (1984). Fósforo en molisoles de altura en las altiplanicies del NO de la provincia de Mendoza: I: Caracterizaciones de laboratorio. Ciencia del Suelo (2), 1, 23-29.

Gile, L.H., Peterson, F.F. & Grossman,R.B.(1966). Morphological and genetic sequences of carbonate accumulation in desert soils. Soil Science (101), 5, 347-360.

Gomez Molina, E. & Little, A.V. (1981). Geoecology of the Andes: the natural science basis for research planning. Mountain Research and Development (1), 2, 115-144.

Grimbérieux, J. (1982). Asymmetrical valleys of periglacial origin in south-eastern Hesbaye, Belgium. Biuletyn Peryglacjalny 29, 155-162.

Kennedy, B.A. (1975). Introduction to fluvial processes, 3rd Edition, 218 pp. The Chaucer Press, Great Britain.

Kowalkoski, A., Pacyna, A. & Starkel, L.(1980). Typology and asymmetry of geoecosystems. Goegraphical Studies of the Polish Academy of Sciences 136, 70-77.

Leser, H. (1977). Feld- und labormethoden der Geomorphologie, 325 pp. Walter de Gruyter, Berlin.

Lundqvist, G. (1949). The orientation of the block material in certain species of flow earth. Geographical Annaler 31, 335-347.

Melton, M.A. (1960. Intravalley variation in slopes angles related to microclimate and erosional environment. Geol.Soc.Am.Bull. (71), 2, 133-144.

Mottershead, D.N. (1976) Quantitative aspects of periglacial slope deposits in southwest England. Biuletyn Peryglacjalny 25, 35-57.

Mottershead, D.N. (1982). Some sources of sistematic variation in the Main Head deposits of southwest England. Biuletyn Peryglacjalny 29, 117-128.

Moyano de Imazio, A.R., Nijensohn, L. & Gaviola, de Heras, S. (1982). Caracterización edafológica de los suelos ocupados por *Stipa tenuissima* en el alto Valle de las Carreras. Rev.Fac.Ciencias Agrarias, Univ.Nac.Cuyo, (22), 2, 67-77.

Nijensohn,L.,Olmos,F.S. & Avellaneda,M.O.(1979). Molisol de altura en Mendoza. Rev.Agronómica del NO Argentino, Univ.Nac.Tucumán (VII), 1/2, 382.

Polansky, J. (1983). Estratigrafía, neotectónica y geomorfología del Pleistoceno pedemontano entre los ríos Diamante y Mendoza. Rev.Asoc.Geol.Arg.(XVII), 3/4, 1-349.

Polansky, J. (1972). Descripción geológica de la hoja 24 a-b, Cerro Tupungato (provincia de Mendoza). Boletín Direc.Nac.Geol. y Minería 128, 1-129.

Poser, H. & Hovermann, J. (1951). Untersuchungen zur Pleistozanem Marzvergletscherung. Abh.Brausnchw.Wiss.Ges, III, 61-115.

Rapp, A. (1966). Pleistocene acticity and Holocene stability of hillslopes, with examples from Scandinavia and Pennsylvania. Symposium intern.géomorphologie: Evolution des versants, (I), 229-243.

Reanier, R.E. & Ugolini, F.C. (1983). Gelifluction deposits as sources of paleoenvironmental information. Proc.4th Int.Conf. Permafrost, 1042-1047, Fairbanks, Alaska.

Roig, F.A. (1969). Bosquejo Fitogeográfico de la provincia de Mendoza, X Jornadas Argentinas de Botánica, 10-11. Mendoza, Argentina.

Schneider,A.J.,Pina,J.C.,Gallar,M.A.& Guevara, J.C. (1976). Recursos Naturales y caracterización económico social de las explotaciones agropecuarias del "Valle de la Carrera". Ser.Inv.Inst.Ec.Agraria, Univ.Nac.Cuyo,6,1-126.

Smith,H.T.U.(1949).Physical effects of Pleistocene climatic changes in nonglaciated areas: eolian phenomena,frost action and stream terracing.Geol.Soc.Am.Bull.(60),9,1485-1515.

Stablein,G.(1970).Grobsediment-analyse:als arbeitsmethode der genetischen Geomorphologie. Wurzburger Geographische Arbeiten,27,1-87.

Wayne, W.J. (1967). Periglacial features and climatic gradient in Illinois, Indiana and western Ohio,east-central United States. Proc. VII Congress Intern.Assoc.Quat.Res.(7), 393-414.

THE DEVELOPMENT OF DEPRESSED-CENTRE ICE-WEDGE POLYGONS IN THE NORTHERNMOST UNGAVA PENINSULA, QUEBEC, CANADA

M. Seppälä[1], J. Gray[2] and J. Richard[2]

[1]Department of Geography, University of Helsinki, Finland
[2]Département de Géographie, Université de Montréal, Québec, Canada

SYNOPSIS. A 60 by 250 m polygon field situated on the flood-plain of the Rivière Déception in the northernmost Ungava Peninsula was studied by detailed morphological and vegetation mapping, drilling and coring of the stratigraphy, grain size analyses, meaurements of the water and ice content, hydrology, active layer measurements, macrorest analyses and radiocarbon dates. The following development stages could be identified: On the flood-plain, charcterized by flood and wind transported sand layers, frost cracks opened. Ice-wedges developed and caused the formation of low banks. River floods deposited alluvial sand on the field on several occasions. Important phases of flood-plain sand deposition prior 1900 BP and subsequent to 1100 BP have been noted. Further growth of ice-wedge created lateral pressures on the banks which caused deformation of the peat and sand layers. More water is collected in the depressions and their peat is degraded. The evidence suggests that several generations of banks have formed and dissappeared and that their position has changed. Initial ice-wedge formation may have started on the flood-plain prior to 1800 BP. Radiocarbon dates indicate that deformation caused by continued ice-wedge growth has been insignificant since 1000 BP. The unique local terrain conditions of impeded drainage, thin snow cover, rapid sedimentation of flood-plain sands alternating with peat layers, and high volumetric ice contents, have combined with low winter air temperatures, to create the only depressed-centre polygon field located so far in Arctic Quebec.

Active fissure polygons are the most conspicuous periglacial features of the arctic coastal plain of northern Alaska (e.g. Black 1952; 1982; Lachenbruch 1962), in the Northwest Territories of Canada north of the tree line (Mackay 1974; French 1983) and in northern Siberia (Washburn 1979, fig. 5.20). They are developed on coastal plains, on the floor of drained lakes, on delta surfaces, on abandoned, or infrequently covered flood-plains, and on alluvial terraces (French 1983, fig. 5.3; Rawlinson 1983, p. 133). If the fissures are demonstrably underlain by ice wedges or by structures indicative of thawed ice wedges then the term ice wedge fissure polygons may be applied to such features (Bird 1967).

Fissure polygons have been classified according to their topography as depressed centre polygons or as high centred polygons (Leffingwell 1919, Péwé 1966). An intermediate type of fissure polygon appears to occur more commonly in high arctic regions than either the depressed or raised centre polygons. These polygons have been noted by Bird (1967, p. 193) as occurring on sand and gravel terraces and on raised beaches. The polygon centres are relatively flat and sparsely vegetated. They are separated from each other by narrow fissures, often exhibiting luxuriant vegetation growth.

In the Ungava Peninsula in Arctic Canada, fissure polygons are noted to be very common features wherever thick spreads of unconsolidated gravel, sands and silts are found. Most of these fissure polygons are of the intermediate type or the raised centre type described above (Gray and Seppälä, in press). Depressed centre polygons were not observed during many field expeditions by Gray et alia to the Ungava Peninsula until 1984 when a small field was noted for the first time in the Rivière Déception valley at the northeastern extremities of the peninsula (fig. 1). The aim of this paper is to discuss the development of this depressed centre polygon field within a framework of regional climatic, and local topographic and sedimentological conditions.

An emphasis will be placed upon the presentation of stratigraphic data, as well as data on ice and water content of the various mineral and organic layers in the polygon field. Such data are frequently lacking on fissure polygon studies. The studies of temporal change in vegetation patterns, and hence in hydromorphic conditions associated with polygon development, are also considered to be an original aspect of the study.

SITE DESCRIPTION

The study region is located about 500 km north of the treeline and belongs to a zone of continuous permafrost, estimated to exceed 500 m in thickness (Taylor & Judge, 1979). A mean annual air temperature of -7°C and a January temperature of -24°C are estimated from short term records available for the Deception Bay air strip, 20 km to the west at sea level (Gray, 1983).

The depressed centre polygon field is located at 62°07'30"N; 74°17'00"W, at an approximate elevation of 50 m above mean sea level, on a small flood-plain terrace at the junction of the Rivière Déception and a small northern tributary which the authors have unofficially named Polygon River (fig. 2). The terrace on which the polygons are situated is estimated, from a detailed local emergence curve, to have become sub-aerial at about 6000 BP (Ricard et al, 1987).

The sediments in the terrace (composed of at least 5 m of sandy, silty sand and peat layers) have been built up since post-glacial emergence by alternately occurring aeolian processes, overbank flooding and peat formation.

The polygon field occurs on a very flat part of the flood-plain, characterised by impeded drainage and a permafrost table close to the surface. The following topographic units were recognised within the polygon field: depressed polygon centres, high marginal banks and ice-wedge fissures (fig. 3). The fissures intersect to give a

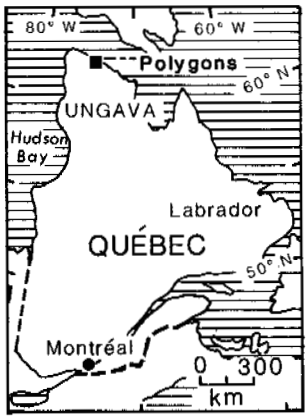

Fig. 1. Location of the study site.

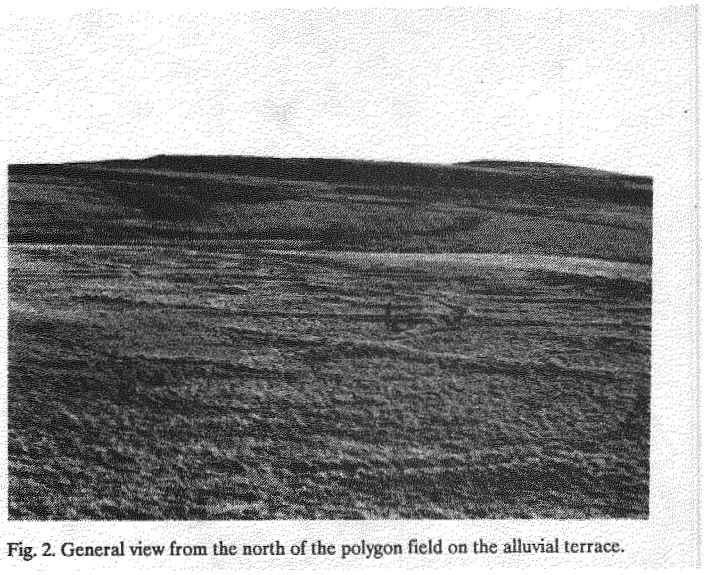

Fig. 2. General view from the north of the polygon field on the alluvial terrace.

generally tetragonal pattern of polygons averaging 20 m in diameter. Variations in vegetation cover, and in the degree of ponding by water, led to a further differentiation of polygon centres into hummocky centres, wet mossy centres, wet centres with sedge grasses and water ponds (fig. 4). Active layer depths showed a total range of 11 cm up to 92 cm on the flood-plain terrace. Distinct contrasts occurred for the different topographic and vegetation units. An increase in thickness of the active layer, from average values of 24 cm in the ice wedge fissures, through 31 cm in the banks, 28 cm in the hummocky centres, 38 cm in the wet mossy centres, 54 cm in wet centres with Carex dominated sedges, to 58 cm in the water ponds, was noted. Average values for the topographically elevated and well drained levée and sand dune which border the polygon field are 39 cm and 31 cm, respectively.

STRATIGRAPHY AND CHRONOLOGY

Figure 5 shows the stratigraphic composition of the polygon terrace for a series of drill cores, 1, 2, 3 and 4. These core sites and six pits are located on figure 4. In general, organic peat and silty sand, sand and minor ice layers can be found in alternation down to depths of 3.19 m. Grain size analyses of the sand layers reveal rather well sorted fine sands with a median grain size of 0.1 to 0.2 mm.

The stratigraphic studies in core 3 indicate that polygon fissures are underlain by wedge ice characterised by vertical layering associated with periodic growth. Pore ice, rather than segregated ice, was observed in the sandy, silty sand and organic layers of the polygon banks and centres represented by cores 1, 2 and 4. Pore ice comprised 60% on average of the sediment volume (fig. 6). This high ice content, in conjunction with low winter temperatures, and a probably thin snow cover, generated suitable thermal conditions for frost cracking to occur.

Ice-wedge growth has been responsible for the deformation shown by steeply inclined sand and organic layers in the lowest sections of cores 1, 2 and 4. However, the uppermost 1 m of peat and sand deposits at core sites 1 and 2, located respectively on a low bank and in a hummocky polygon centre, and the uppermost 0.5 m at core site 4, on a high bank, have not undergone deformation. Radiocarbon dating on the lowest undeformed and the highest deformed sediments in the three cores (table 1) suggests the following time intervals for cessation of deformation by ice wedge growth: for core 1: 1680-1190 BP; for core 2: 1090-1170 BP; for core 4: 1700-1780 BP. Allowing for normal dating errors, one can conclude that ice-wedge growth was insignificant after approximately 1200 BP on the low bank and hummocky polygon site, and after 1800 BP on the high bank. Subsequently the ice wedges in the vicinity of the three core sites may either have grown very slowly or may have merely survived beneath the thick surficial peat cover which was present at all pit and core sites.

The radiocarbon dates also indicate that peat and sand accumulation for the last 1200 years at core sites 1 and 2 has been at a rate of about 1 m/1000 yr, whereas at core site 4, situated on a high bank, accumulation has only been about 0.4 - 0.6 m for 1800 years, giving a rate of only about 0.3 m/1000 yr. In core 2, in a hummocky centre with a water table close to the surface, most of this accumulation consists of peat. In core 1, in a low bank, and in core 4, in a high bank, the corresponding uppermost layer is composed mainly of sands, but with frequent thin organic layers.

No age can be assigned for the start of polygon formation and ice-wedge growth at the field site. But the lower part of all three cores show inclined bedding all the way to the base of the holes. Fore core 4 these beds are steeply inclined to quasi vertical from a depth of 1.2 m down to the base of the hole at 3.2 m. Core 3, located in an ice-wedge, shows the presence of pure, vertically layered ice to a depth of at least 1.5 m in the flood-plain sediments. The vertical succession upwards of clear ice, followed by ice with vertical bands of organic material, then by dirty ice with vertical sand layers, and, finally, by horizontally bedded sands, indicates incremental ice-wedge growth upwards, initially under a thick peat cover, and then under a sand cover. The transitions in the nature of the enclosed organic and mineral material in the ice-wedge reflect the alternating peat and sand cover on the surrounding polygon field.

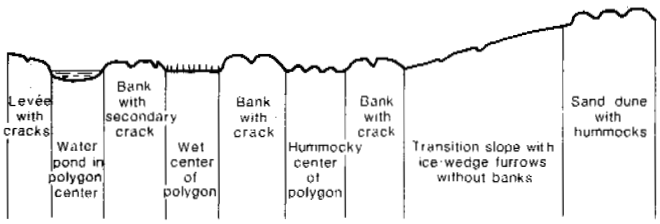

Fig. 3. Principal surface features in a schematic cross section across the polygon field.

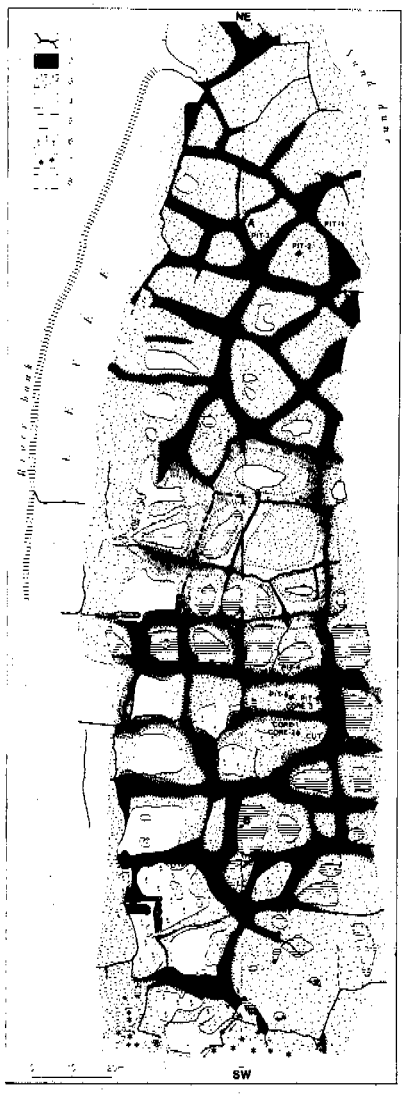

Fig. 4. Detailed map of the polygon field. 1: open fissure (crack), 2: bank (upthrust rim), 3: hummocky polygon centre, 4: wet polygon centre with mosses and grasses, 5: open water with *Carex aquatilis* (sedges), 6: open water with *Carex chordorrhiza*, 7: willow (*Salix*) bushes, 8: levée surface with thin moss and lichen cover.

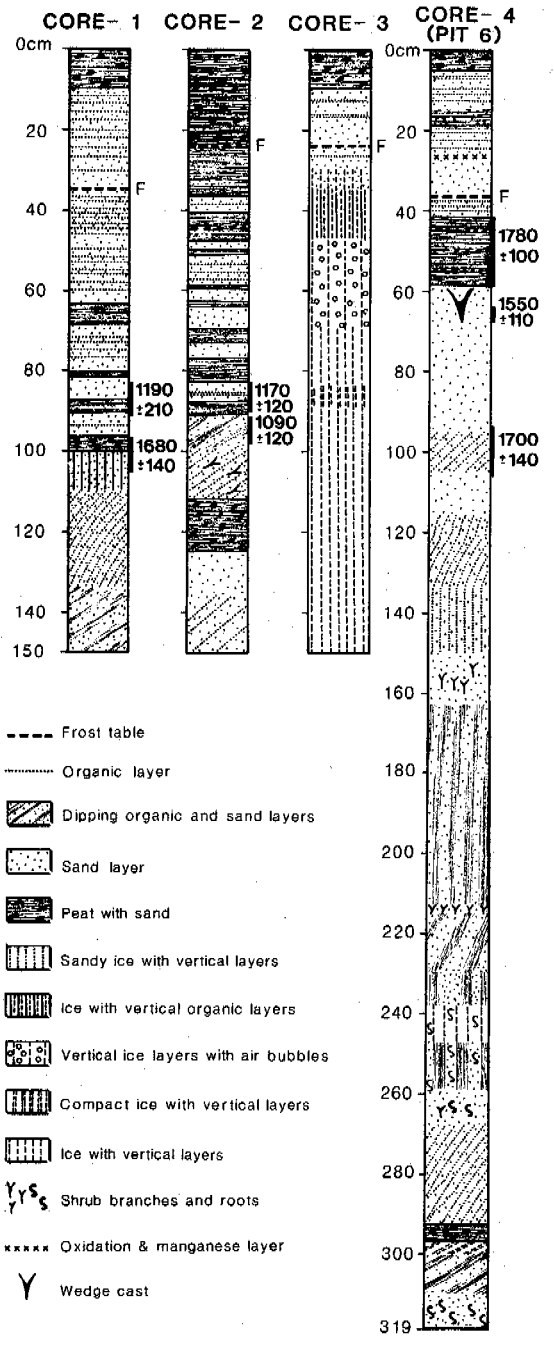

Fig. 5. Stratigraphy of cores 1, 2, 3 and 4.

Chrono-stratigraphic evidence from a nearby site on the bank of the Rivière Déception reveals a lower zone of flood-plain sands, deposited prior to 1900 BP. This zone is thought to be correlative with the lowermost deformed sands in cores 1, 2 and 4. An intermediate, 30 cm thick, peat layer, deposited between 1900 and 1100 BP, correlates well with a 20 cm thick peat layer in core 4, dated at 1780 BP, with a 20 cm thick peat layer in core 2, deposited prior to 1090 BP, and with a sequence of thin peat layers from 80-100 cm depth in core 1, deposited between 1190 and 1680 BP. Phases of flood disturbance during this time interval of 1900-1100 BP were obviously less important than stable phases of peat accumulation. The uppermost 3 m of the river-bank exposure is characterised by flood-plain sands, interspersed with thin organic layers. These sands reflect a renewal of frequent flood events subsequent to 1100 BP. Such episodes are also reflected in the cores 1, 2 and 4, and, interestingly, in the 11 cm thick sand and sandy ice layer found above the ice-wedge in core 3. The peat layer, which caps all 4 cores in the polygon field, is apparently absent from the summit of the river-bank exposure. Such a peat layer suggests that the latest phase on the polygon field has been one of stability, free from flood disturbance.

In addition to such temporal variations in sediment accumulations and in ice-wedge development, morpho-stratigraphic evidence has been found for spatial shifting of low polygon centres

TABLE 1. Radiocarbon dates for the polygon field and nearby peat layers in flood deposits in the Rivière Déception valley.

CORE 1			
Hel-2367	84-91 cm	peat with sand	1190+/-210
Hel-2368	97-105	peat with sand	1680+/-140
CORE 2			
Hel-2369	83-91 cm	peaty sand	1170+/-120
Hel-2370	91-98	inclining peat layer	1090+/-120
CORE 4			
Hel-2371	42-59 cm	undecomposed peat with thin sand layers; wet environment moss	1780+/-100
Hel-2372	64-68	peat and sand in ice-wedge cast	1550+/-110
Hel-2373	94-116	gray sand with steeply dipping organic layers; many roots	1700+/-140
PEAT LAYER BURIED BY FLOOD DEPOSITS			
Hel-2363	360-362 cm	upper peat	1090+/-110
Hel-2364	368-370	middle part of peat layer	1560+/-120
Hel-2365	388-390	bottom part of peat layer	1900+/-130
Hel-2366	423-426	dark organic layer in the upper part of ice-wedge cast	1900+/-120

and high marginal banks. Severely deformed layers at a depth of >0.9 m in core 2, in a low centre beneath horizontal layers, indicate former cracking and ice wedge formation in close proximity. Macro-rest studies on peat mosses also reveal former successions from drier to wetter conditions at the core sites. On high banks, secondary cracks have been found filled with ice veins. If these veins grow laterally, they will become ice-wedges and will initiate a new series of deformation structures, as sediment continues to accumulate upwards on the polygon field. A second situation favorable to new ice-wedge formation could be the infilling of low centres through time with flood-plain sediments, and, or peat growing in from the banks. Isolated frost cracking in new locations could then occur, particularly in flood-plain sands, which would permit penetration of the early winter cold wave.

DEVELOPMENT PHASES OF THE ICE-WEDGE POLYGONS

The following phases of development are suggested by the preceding discussion of the morphology, stratigraphy and surface terrain:

1. On the flood-plain frost cracking occurs when the snow cover in thin and the air temperature drops fast in early winter. The water saturated surface layers crack when freezing. This type of crack can be seen on the levée, for example.

2. In spring the frost cracks become filled with snow and water which freezes to form a thin vertical ice vein.

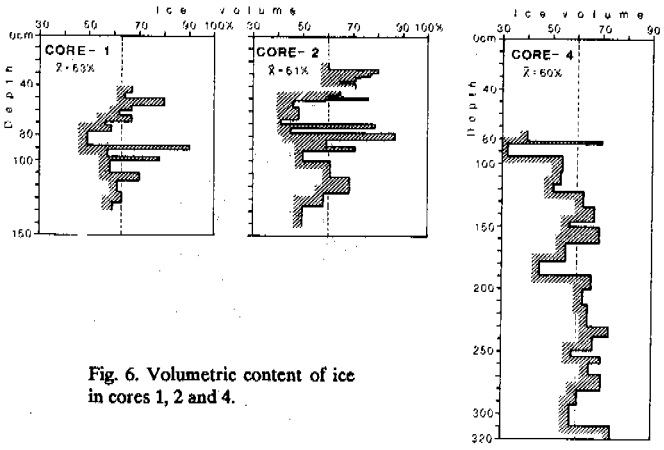

Fig. 6. Volumetric content of ice in cores 1, 2 and 4.

3. During the following winters the crack opens at the same place and more vertical ice layers are formed in the ice vein which now grows laterally and downwards to form an ice-wedge. The surface expression of such an ice-wedge is a furrow, as can be seen on the sand dune on the study area.

4. When growing, the ice wedge presses sediments to the sides and forms a small ridge on both sides. Intersecting furrows and ridges form the polygon field with characteristic tetragonal patterns

5. The ridges dam the polygon centers and vegetation starts to become differentiated. The ridges favour more xerophilic plants which tolerate cold conditions and wind induced drying associated with a thin snow cover. In the polygon centres conditions are more humid and hygrophilic plants dominate. A peat cover develops progressively in these wet centres.

6. Occasionally, in the spring, melting river ice forms an ice dam at the confluence of the Rivière Déception and the Polygon River. Overbank flooding then deposits sands and silty sands on the levée, on the banks and in the centres of the polygons.

7. Repeated floods form sand layers among the organic sediments and plant remains buried by sand and silt.

8. Ice wedges contiune to grow causing the ridges to grow upwards further, and causing deformation of the peat and the sand layers.

9. On large banks secondary cracks, furrows and ice-wedges form by frost action.

10. Drainage becomes so impeded that water ponding becomes continuous. This causes peat accumulation to cease in the lowest polygon centres.

11. Peat degradation then commences in the water filled polygon centres. There are no longer any plants to produce new peat, and some algae start to cause decomposition of the peat by oxidation (Sjörs 1961; p. 222). Because the bottom layer of water ponds is dark they absorb more solar radiation and the permafrost table becomes deeper in them than in the surroundings. Thus the initial depressions get deeper.

12. As the ice wedges start to thaw some banks collapse from their sides. Wide furrows filled by water are indicative of this process.

13. The bank then returns to what may have been its initial state: - a hummocky surface. The ice-wedge fissure is now filled. In fact the whole bank-crack section could disappear. The inclined sediment layer under the polygon centre in core 2 (fig. 5) is evidence of the former position of a bank and fissure.

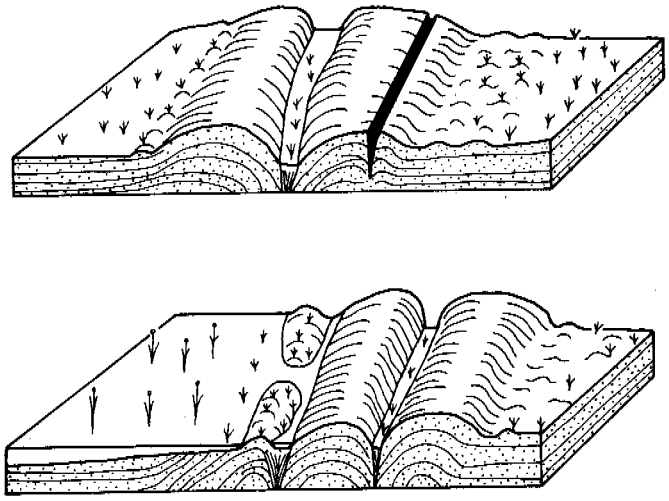

Fig. 7. Hypothetical lateral migration of polygons as a result of secondary cracking in the polygon bank. For simplification this is shown as a two stage model.

14. In some instances as the primary crack thaws secondary cracks in the bank may develop. This process may lead to slow migration of the bank and furrow at the polygon margin. Figure 7 illustrates two stages in this shifting of polygon margins.

15. When environmental conditions at the surface changed, ponds in some polygon centres may fill with flood-plain sediments, or with peat growing inwards from the pond margins. This gave an opportunity for new frost cracking to occur leading to new polygon formation in completely new locations. Figure 7 is a hypothetical stratigraphic cross section within the polygon field, showing former and present ice wedges and polygon banks, primary and secondary cracking, and deformed and non-deformed sediment layers.

CONCLUSIONS

The main hypothesis advanced in this paper is that there is a significant relationship between thermal contraction cracking and the specific flood-plain conditions that prevail at the junction of the Rivière Déception and the Polygon River. In the first place, impeded drainage on a very flat surface has allowed: 1) rapid peat development close to a high water table; 2) complete saturation of flood-plain sands and silty sands with pore ice. Where drainage improves on the levée at the northern margin, on the sand dune at the south-east margin and towards a low swale at the western margin, the polygon network disappears. In the second place, the high void rations of the flood-plain sands, silty sands and organic peats have permitted the volumetric ice content to attain average values of about 60%. Such ice rich sediments have suitably high coefficients of thermal expansion and contraction to allow fissure development if the winter cold wave penetrates rapidly enough. In the third place the exposed terrace surface is likely to be characterised by a low early winter snow cover, reducing the thermal insulation of the ground surface, and permitting rapid enough cooling of the surface layers for seasonal cracking to occur frequently. In the fourth place, the periodic spreading of sands over the surface, through overbank flooding and, perhaps through aeolian activity, resulted in the periodic loss of a vegetation cover at the surface. This in turn would have favoured the rapid penetration of the winter cold wave into the ground, enhancing the contraction cracking, usually in previously developed fissures, but occasionally in new locations.

The regional climate, characterised by extremely cold winters, with average January temperatures of approximately -24°C and low snow depths of only 20-40 cm, is of course a back-ground factor of overriding importance, but it is the local terrain conditions which explain the extremely localised nature, and continued survival of this depressed centre ice-wedge polygon field in Ungava.

ACKNOWLEDGEMENTS

Financial support for field-work was received from the Natural Sciences and Engineering Research Council of Canada from the Department of Energy, Mines and Resources and from the Department of Indian Affairs and Northern Development Ottawa. The Academy of Finland and the Emil Aaltonen Foundation, Finland, supported Dr. Seppälä's stay at the Département de Géographie, Université de Montréal, which then kindly placed all necessary working facilities at his disposal. A special thanks is due to the Geological Survey of Canada which provided drilling and other equipment. Dr. A.S. Dyke, Research Officer at G.S.C., has been very helpful in his capacity as liaison officer for the project.

REFERENCES

Black, R.F., 1952. Growth of ice-wedge polygons in permafrost near Barrow, Alaska, Bulletin, Geological Society of America, 63,1235-1236.

Black, R.F., 1982. Ice-wedge polygons of northern Alaska. In: Glacial geomorphology, Ed. D.R. Coates. A proceedings volume of the Fifth Annual Geomorphology Symposia Series. Binghaton, New York, Sept. 26-28, 1974. George Allen & Unwin. 2nd ed., 247-275.

Bird, J.B., 1967. The physiography of Arctic Canada. The Johns Hopkins Press, Baltimore, 336 p.

French, H.M., 1983. The periglacial environment. Longman, London and New York, 2nd ed., 309 p.

Gray, J.T., 1983. Extraction and compilation of available temperature and snowfall data in the Ungava Peninsula as input to geothermal modelling of quaternary paleoclimates. Earth Physics Branch, Energy, Mines and Resources Canada, Open Files, Report MAS 2050-2-1385, 33 p.

Gray, J.T. and Seppälä, M., 1987. Deeply fissured tundra polygons on a fluvio-glacial outwash plain, Northern Ungava Peninsula, Quebec, Canada. Géographie physique et Quaternaire, 41 (in press).

Lachenbruch, A., 1962. Mechanics of thermal contraction cracks and ice-wedge polygons in permafrost. Geological Society of America, Special paper, 70, 69 p.

Leffingwell, E. de K., 1919. The Canning River region, northern Alaska, United States Geological Survey Professional Paper, 352-9, 193-253.

Mackay, J.R., 1974. Ice wedge cracks, Garry Island, N.W.T., Canadian Journal of Earth Sciences, 11, 1366-1383.

Mackay, J.R., 1986. The first 7 years (1978-1985) of ice wedge growth, Illisarvik experimental drained lake site, western Arctic coast. Canadian Journal of Earth Sciences 23, 1782-1792.

Péwé, T.L., 1966. Ice wedges in Alaska - classification, distribution and climatic significance, in Proceedings, 1st International Permafrost Conference, National Academy of Science - National Research Council of Canada, Publication 1287, 76-81.

Rawlinson, S.E., 1983. Guide book to permafrost and related features, Prudhoe Bay, Alaska, Guidebook 5, 4th International Permafrost Conference on Permafrost, 177 p.

Ricard, J., Gray, J.T. and Lauriol, B., 1987. La déglaciation et l'émergence des terres près de la Rivière Déception, Péninsula d'Ungava, Nouveau-Québec. 12th Inqua Congress Abstracts, Ottawa, Canada, p. 252.

Sjörs, 1961. Surface patterns in Boreal peatlands. Endeavour 20, 217-224.

Taylor, A. and Judge, A., 1979. Permafrost studies in northern Quebec, Géographie physique et quaternaire, 33, 245-252.

Washburn, A.L., 1979. Geocryology: a survey of periglacial processes and environments, Edward Arnold, London, 406 p.

THE UPPER HORIZON OF PERMAFROST SOILS

Yu.L. Shur

All-Union Research Institute of Hydrogeology and Engineering Geology,
Moscow, USSR

SYNOPSIS The upper horizon of permafrost consists of two independent layers - transient and intermediate. The transient layer presents the very upper bed of permafrost which in certain years under particularly favourable climatic conditions joins the seasonally thawing stratum. Its thickness amounts on the average 0.1-0.15 of the mean multi-annual thickness of the seasonally thawed layer. The intermediate layer is formed due to a decrease in seasonally thawed layer because of weathering of soils, soil-formation and vegetation evolution. The intermediate layer occurs practically throughout the permafrost region not depending on facies origin of soils, their lithology and cryogenic genesis. Its thickness is about 1 m on the average. The layer is highly ice saturated and has typically an ataxite and band-shaped cryogenic structure. The intermediate layer is the most variable part of permafrost. Its thickness and properties predetermine a possibility and intensivity of development of a number of cryogenic processes and thermokarst above all.

According to the general scheme the upper horizon of permafrost region consists of a seasonally thawed layer and underlying mass of frozen soils. Such a scheme is sufficiently effective in solving the majority of thermophysical problems. But it turns to be inadequate when studying formation of structure and properties of frozen soils as well as development of cryogenic processes because it does not take into account for important structural features of the upper horizon of permafrost strata.

So, the traditional scheme - seasonally thawing layer - permafrost strata and its particular and the most important variant - seasonally thawed layer - underground ice - does not meet the condition of stability of the system as a whole. But this stability is a real fact that is confirmed by the thousands-year existence of wedge ice near the earth's surface.

Such a system can be stable only when it has a certain regulator pretecting underground ice against melting during increasing of a depth of seasonal thawing of soils. As analysis has shown, such a regulator can be a layer that is mostly in a frozen state and only in certain years becomes a part of seasonally thawing stratum. The existence of this layer was found by Yanovsky (1933) while studying soil-formation above permafrost strata who told: "By a transient layer of permafrost region we call its very upper bed which under favourable conditions thaws, joining the active soil-layer, and under unfavourable conditions remains frozen, representing the upper layer of permafrost."

By thickness of the transient layer it is reasonable to take, in our opinion, a difference between maximum seasonal thawing over 20-30-year period and its average multi-annual value. Basing on analysis of studies on time variability in depth of seasonal thawing, the thickness of transient layer was found to be, on the average, 0.1-0.15, reaching in some cases 0.3 of mean multi-annual depth of seasonal thaw. We have made an analytical evaluation of thickness of a transient layer. To this end, the factors influencing seasonal thawing were varied. The calculated values of 0.4-0.5 of average depth in seasonal thaw were essentially higher than real ones. It points to variability of the factors, for an example, such as coefficient of thermal conductivity and moisture content and sum of summer air temperatures, etc. Relative interannual changes in depth of seasonal thawing are higher for peat than for mineral soils due to a great dependence of peat thermal conductivity on moisture content highly varying within the seasonally thawed layer.

The transient layer is of exclusive importance for a number of processes in upper permafrost strata. Thus, due to the existence of a transient layer, the wedge-ice table does not coincide, even at the forming stage, with the lower boundary of seasonal thawing and lies somewhat below it. The transient layer itself is penetrated only by thin sprouts of wedge ice which periodically first arise, then disappear, and hence do not get a great evolution.

Protective role of the transient layer becomes especially obvious in investigating a possibility of thermokarst generation at short-term climatic fluctuations.

The transient layer is a rather effective regulator of processes taking place at the contact between seasonally thawed layer and the very upper part of permafrost. Thickness and

properties of the transient layer determine, to a great degree, structural features of syngenetic frozen soils.

Contact areas between different components of natural systems to the greatest extent must reflect and indeed do reflect the results of interaction of components, their connection and system formation through a mechanical combination of natural bodies. In these areas emergency properties of the system are formed, which themselves are not peculiar to its isolated components. Basic system-forming processes of a natural complex (e.g. landscape-forming processes after Muraveisky - 1948) are weathering, soil-formation and vegetation evolution. These processes play an exclusively important role in development of permafrost soils, determine changes in a thickness of seasonally thawed layer and in soil climate, spatial position of upper boundary and properties of upper horizon of permafrost.

Due to the system-forming processes occurring both on the earth's surface and in upper layers of lithosphere and being a form of interaction between a natural complex and external medium as well as between the components themselves, a constant decrease in seasonally thawed layer and transformation in the upper part of permafrost take place. This regular process can be interrupted or directed backwards, first of all, due to technogenic destruction of vegetation cover. However, it begins again as preventing factors stop influencing it. This process results in forming at the contact between permafrost strata and transient layer another specific layer called by the author an intermediate one.

Unusual process of forming the intermediate layer is suggested to call quasi-syngenesis because it has many features common with syngenesis but proceeds without sedimentation.

Reduction of seasonally thawed layer and changing of a certain part of it into permafrost state are followed by accumulation of texture-forming ice in the intermediate layer. The latter, in the course of its evolution, continuously substitutes the transient layer which, in turn, takes place of a regularly thawing part of the seasonally thawed layer. Thus, the structural transformation of the upper horizon comes finally into agreement with the scheme given in Fig.1. The left-hand part represents a stage of active formation of syngenetically freezing strata. An intermediate layer is absent at this stage, but at the contact between seasonally thawed layer and permafrost there is a transient layer. And formation of an intermediate layer starts only when sedimentation process is very slow or stop at all.

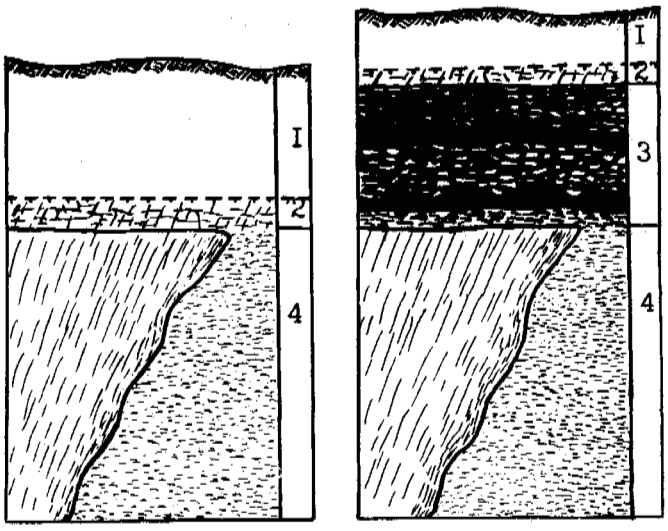

Fig.1 Structure of the upper horizon of permafrost strata

a - stage of syngenetic freezing;
b - conservation stage.

1 - seasonally thawed layer; 2 -transient layer with a not full-gridded cryogenic structure; 3 - intermediate layer with ataxitic and lenticularly stratified cryogenic structure and with ice bands; 4 - underlying permafrost strata with wedge ice.

With time the structure of upper horizon becomes complicated and, at last, gets a pattern as shown in the right-hand side of Fig.1

Temporary interruptions in growth of syngenetically freezing strata are marked by buried intermediate layers.

As analysis of available publications and the author's own observations have shown, an intermediate layer occurs practically throughout the permafrost regions, whatever facies, lithology and cryogenic genesis of soils the latter had. Thickness of the layer is on the average 1 m, reaching in certain cases 2-2.5 m. The layer as a whole is, generally, ice saturated. Volumetric ice content is mostly over 0.5. Rather typical is its sharp moisture boundary with the underlying strata. Specific structural elements of the intermediate layer are ataxitic and band-like cryogenic structures.

Intermediate layer is the most important in areas with an ice complex consisting of loessial and sandy loams with thick wedge ices. In these areas the intermediate layer highly differs from inderlying soils in structure and properties. Thus, ice within this layer is only of a texture-forming type, while in underlying strata soil blocks with texture-forming ice are surrounded by a grating of deposit-forming ice. The intermediate layer is horizontally relatively homogeneous and underlying soils are greatly inhomogeneous in structure and properties.

The major investigations on an intermediate layer were carried out in the North of Yakutia. More than 50 cross-sections of the layer in exposures and some hundreds cross-sections of drill cores were studied. Here are description and photo of one section of a representative thickness (Fig. 2).

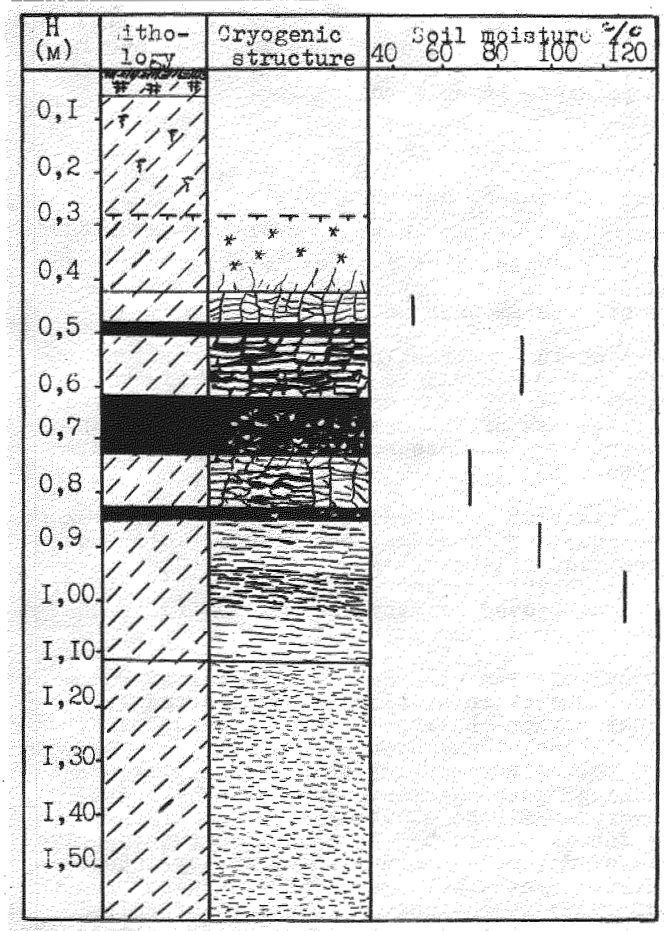

Fig. 2 Cryogenic structure of a representative intermediate layer.

a - structure diagram;
b - cross-section at a depth of 0.45--0.8 m.

Depth, m

0.0-0.05 Vegetation layer.

0.05-0.27 Loam-light brown, ochreous spots of ferrugination, plant roots, thawed.

0.27-0.42 Loam-heavy, brown with blue-grey tint in a lower part, frozen. Cryogenic structure is massive. At the foot there are subvertical microstreaks 1.5-4.0 cm thick which are lensing out upwards and referring organically to cryostructure of underlying horizon.

0.42-0.48 Loam-grey with bluish tint, frozen. Cryogenic structure is grid-shaped. Mineral aggregates are of

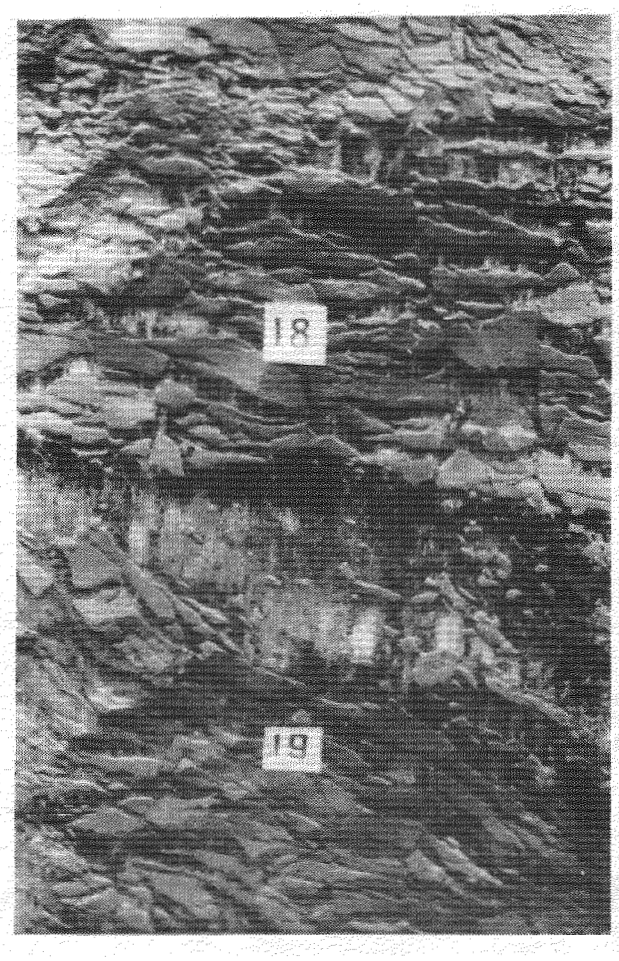

0.2-0.25 x 0.4-0.6 cm size. Ice streaks are up to 0.1 cm thick.

0.48-0.50 Small layer of little-impure ice.

0.50-0.60 Loam-grey with bluish tint. Cryostructure is complex, lens- and grid-shaped. Mineral aggregates are of 0.3 x 1.5 cm, 0.4 x 2.0 cm sizes in upper and lower parts and of 1 x 3 cm in the middle. Ice streaks are on the average 0.3-0.4 cm thick.

0.61-0.71 Small ice-layer with soil enclosing. Ice has many air bubbles elongated in vertical direction.

0.71-0.82 Loam-grey with bluish tint. Cryogenic structure complex, lens-

shaped and stratified with separate vertical microstreaps. Mineral aggregates are from 0.2-0.3 cm to 0.5-0.6 thick, 1-2 cm long with separate aggregates 0.3-0.5 cm long. Thickness of ice interbeds is 0.2-0.3 cm with maximum value of 0.4-0.6 cm.

0.82-0.84 Little-impure ice interbed with air bubbles elongated in vertical direction.

0.84-1.10 Loam-grey with bluish tint. Cryogenic structure is lens- and grid-shaped. Mineral aggregates are 0.2-0.4 cm thick and up to 3 cm long. Ice streaks are 0.2-0.25 cm thick.

1.10-1.60 Formation of an ice complex. Visible thickness of section is 1.6 m.

The most remarkable feature in the structure of intermediate layer are small ice beds with a thickness of 1 to 10 cm and on the average - 3-4 cm. As a whole, they are persistent along the strike but here and there combined all together.

Cryogenic structure of the upper part of the layer is practically in all sections either grid-shaped with relatively large mineral aggregates or presented by separate subvertical ice streaks. Fracture traces of vertical strike is observed often throughout the layer.

The intermediate layer shows again frost fracturing and wedge ice-formation. It is dissected by small ice wedges, lower parts of which enter the ice complex. The averaged summary moisture content throughout the layer varies within 60-160%, reaching, on the average, 100-105%. It is determined for each particular section mainly by a quantity and thickness of small ice beds. Moisture content of mineral aggregates is, on the average, 35-40% and it exceeds the liquid limit.

Studies of an intermediate layer in present-day alluvial (high flood plain), talus and eluvial deposits have shown that its structure and properties generally slightly depend on genesis of deposits.

The fact of occurring of an intermediate layer everywhere not depending on facies conditions of deposit accumulation and on cryogenic genesis of underlying soils predetermines universality of its formation-mode. Just such an universal mode is a decrease in thickness of seasonally thawed layer due to such processes as weathering, soil- and vegetation formation.

An intermediate layer is the most variable part of permafrost. A considerable ice saturation of the layer predetermines a number of geomorphological processes both at the stages of its formation and restoration and the stage of its degradation. Maximum amplitude (A) of relief elements due to formation or thawing of an intermediate layer is determined by a range of depth changes in seasonal thawing and by a relative soil settlement with thawing and can be derived from the formula:

$$A = \frac{H_{max} - H_{min}}{1 - \delta} \qquad (1)$$

where H_{max} - maximum depth of seasonal thawing before or after thawing out of the intermediate layer; H_{min} - minimum depth of seasonal thawing above the developed intermediate layer; δ - relative soil settlement of the intermediate layer with thawing.

So, typical of northern Yakutia are H_{max} = 1 m, H_{min} = 0.4 m, δ = 0.7 m: relief amplitude due to dynamics of intermediate layer can reach 1.4 m. At a layer thickness of 1 m relief amplitude amounts to 0.5-0.7 m.

One of the interesting natural formations in the North are ridged polygons. Earlier it was supposed more than once that polygon-ridged relief was of a thermokarst origin. But this point of view does not stand up to criticism (Shur, 1977).

Analysis of ice-forming processes occurring on the surface of permafrost allowed to suppose that ice ogives present heaving ridges (Grechishchev, Chistotinov, Shur - 1980). Later it was proved by many factual materials obtained by Zaikanov (1987).

Depth of seasonal thawing is equal to 25-30 cm on the surface of ridged polygons and to 1 m - inside them. During landscape development, formation of an intermediate layer starts above ice wedges earlier than inside polygons. Ice ogives change into quasi-steady state, escaping a long stage of a polygonal bog, which is passed by the central parts of polygons. Selective formation of an icy intermediate layer above ice wedges is just a reason of ogive formation. It changes flat relief into ridged-lake one. Lakes inside polygons are being bogged with time and relief throughout the permafrost surface is being flattened under influence of forming an intermediate layer.

Thickness and features of the intermediate layer determine a possibility and intensivity of thermokarst in the areas with an ice complex. Thawing of accumulating ice is possible only when potential depth of seasonal thawing ($H_{p.th.}$) is higher than that of seasonal thawing under natural conditions ($H_{nat.}$) plus a thickness of intermediate layer consolidated after thawing:

$$H_{p.th.} > H_{nat.} + H_{int.}(1 - \delta) \qquad (2)$$

where $H_{int.}$ - thickness of intermediate layer before thawing. Minimum depth of wedge ice (H_{ice}), at which no thawing happens, is equal to:

$$H_{ice} = H_{nat.} + \frac{H_{p.th.} - H_{nat.}}{1 - \delta} \qquad (3)$$

Correspondingly, minimum thickness of intermediate layer enough to protect the underlying ground ice against thawing out is equal to:

$$H_{int.min.} = \frac{H_{p.th.} - H_{nat.}}{1 - \delta} \qquad (4)$$

In the north of Yakutia a thickness of intermediate layer is in most cases lower than minimum necessary one to protect ground ice against thawing. Therefore, the removal of surface cover leads to thermokarst progress and hence, to formation of mound-depressional relief.

The least resistant is the intermediate layer to slope-forming processes. Whereas thawing of intermediate layer and its consolidation under conditions of a flat relief are completely or to a greater extent reversible processes, the slope-forming process causes a decrease in intermediate layer in the areas of removing ground materials and its rise - in areas of accumulation. Therefore, a zone of permissible changes in a depth of seasonal thawing within permafrost stability shrinks in the former areas and expands in the latter ones.

An engineering-geological importance of an intermediate layer is often practically equivalent to an engineering-geological importance of permafrost, because intermediate layer is always involved in a sphere of technogenic impact while underlying permafrost soils are far from being in all cases.

Engineering-geological studies require the composition, structure and features of upper horizon of permafrost strata and hence of an intermediate layer to be studied in the first place and in the greatest details. Unsufficiently careful approach to structural features of the upper part of permafrost serves a reason for errors in many geocryological predictions.

REFERENCES

Yanovsky, V.K. (1933). Ekspeditsiya na reku Pechoru po opredeleniyu yuzhnoi granitsy vechnoi merzloty. V kn.: Trudy Komissii po izucheniyu vechnoi merzloty. T. 2. L., 133, s.65-149.

Shur, Yu.L. (1977). Termokarst /k teplofizicheskim osnovam ucheniya o zakonomernostyakh protsessa/. M.: Nedra, 80 s.

Grechishchev, S.E., Chistotinov, L.V., Shur, Yu.L. (1980). Kriogennye fiziko-geologicheskie protsessy i ikh prognoz. M.: Nedra, 382 s.

Zaikanov, V.G. (1987). Dinamika geokriologicheskikh usloviy poimennykh geosistem krupnykh rek Severo-Vostoka SSSR. Avtoreferat dissertatsii na soiskanie uchenoi stepeni kandidata geologo-mineralogicheskikh nauk. M., 23 s. /VSEGINGEO/.

FROST SHATTERING OF ROCKS IN THE LIGHT OF POROSITY

R. Uusinoka[1] and P. Nieminen[2]

[1]Tampere University of Technology, Tampere, Finland
[2]Engineering-Geological Laboratory, Tampere University of Technology, Tampere, Finland

SYNOPSIS Of all the factors influencing the effectiveness of frost weathering special attention is herewith paid to the porosity of the rocks and to the role of unfrozen adsorption water. Mercury porosimetry is used to test the pore size distribution of the rocks studied. Cumulative pore area and pore volume have proved to be higher in rocks prone to mechanical comminution than in resistant rocks. Especially, the amount of pores less than 1 µm in diameter, i.e. the adsorption water pores is higher in weatherable than in resistant rocks. This fact favors the presence of adsorption water which is forced to be detached from the surface of minerals like micas and to flow towards the freezing centers in larger pores and fissures to promote frost shattering.

FROST WEATHERING: GENERAL CONCEPTS

Frost weathering is defined by Brunsden (1979) as "mechanical breakdown of rock by the growth of ice within the pores and discontinuities of a rock subjected to repeated cycles of freezing and thawing". This freeze-thaw action is also termed frost cracking, riving, shattering, splitting, or wedging. All these expressions are used more or less indiscriminately (Fairbridge 1968). Terms congelifraction and gelifraction have also been proposed; macrogelifraction occurs when large particles are separated, and, correspondingly, microgelifraction crushes the rock producing sand or silt when water freezes in rock pores (Wilson 1968).

The effectiveness of freeze-thaw conditions depends on numerous factors and it cannot be universally defined (Brunsden 1979). The process depends on e.g. (see Embleton and King 1975, Brunsden 1979, Hall 1986):

- temperatures of the air and ground or rock (air temperatures - as mentioned by Embleton and King 1975 - "provide no more than a rough guide to ground temperatures")
- intensity, duration, and rate of freezing
- thermal conductivity of rocks
- water content of rocks, particularly the actual amount of water available and its distribution within the rock
- dissolved ions

Other factors influencing the effectiveness of frost weathering include the soundness (Falconer 1969) of the rock. It comprises the amount of microfractures, porosity, pore size distribution, and amount of secondary minerals produced by chemical weathering or hydrothermal alteration. All these items affect the water adsorption capacity of the rock. Capillary and adsorption water are able to be unfrozen below 0 °C. This enables these types of water to flow along the microfractures towards the frozen water in larger pores and fractures (Ohlson 1964, Walder and Hallet 1985, 1986). Freezing of this water starts after reaching these larger cavities with frozen water. This process may then result in microgelifraction and even macrogelifraction.

POROSITY IN ROCKS

According to Walder and Hallet (1985, 1986) substantial crack growth can be produced in rocks at temperatures well below 0 °C by uninterrupted water supply and maintenance of temperature gradient. Microscopic cleavage and pores occur in rocks between mineral grains and within minerals like feldspars and micas. The sizes of the pores vary. According to the classification adopted by the International Union of Pure and Applied Chemistry (see Gregg and Sing 1982) pores with more than 0,05 µm in diameter (if spheroidal or cylindral, or in distance between the sides of slit-shaped pore)are called macropores, and those with 0,05 - 0,002 µm, respectively, mesopores, and those with diameters less than 0,002 µm are thus called micropores.

The pores where free water may occur are called gravity water pores, their diameters are over 10 µm. The pores with 10 - 1 µm in diameter are capillary water pores. Adsorption water means ordered or oriented water in which the individual water molecules are oriented and form dipoles with positively charged hydrogen atoms at one extremity and negatively charged oxygen atom at the other. In the larger, gravity and capillary water pores these dipoles have practically no effect on the non-oriented water in the pore space. In the smaller pores adsorption water totally fills the pore space. The thickness of the adsorption water layer is 0,5 µm (Hálek and Svek 1979). Thus pores with 1 µm or less in diameter are totally filled with adsorption water and are thus called adsorption water pores.

FROST SHATTERING IN ENGINEERING GEOLOGY, MATERIAL AND METHODS OF THE PRESENT STUDY

Main concerns of frost weathering in engineering geology include:

- stability of open cutting walls and the walls and roofs of road and railroad tunnels against frost wedging
- crushing (together with traffic burden) of road base and pavement aggregate
- damage to stone veneering slabs in the outer walls of buildings

In the engineering-geological laboratory of Tampere University of Technology studies on the durability of rock aggregates and stone veneering slabs are carried out. The most useful tool in predicting the durability of rock material to frost damages has proved to be the determination of pore size distribution of rocks by mercury porosimeter test. In the test (see Nieminen et al 1985, Uusinoka and Nieminen 1986) mercury is forced by pressure into the pores of the vacuated sample. A computer program based on the so-called Washburn equation (see Uusinoka and Nieminen 1986) has been written to calculate the cumulative pore area and pore volume. These pore properties are studied by using Micromeritics Intrusion Porosimeter. Surface area and volume of pores between 300 and 0,001 µm in diameter, i.e. all the macropores and the largest mesopores can be measured.

The purpose of the present paper is to give some preliminary results of the experiments made to study the correlation between pore size distribution of rocks and their resistance against frost weathering. The study material consists of certain medium-grained granites from different parts of Finland. Also some marbles from stone veneers have been tested. The samples have been studied both as gravel-size fractions and fine fractions (d < 0,074 mm), the latter collected from the by-products of the crushing of aggregate material.

Especially, the pore size distribution of fine fractions has proved to form an important criterion when selecting bedrock deposits for road aggregates (Nieminen and Uusinoka 1986, Uusinoka and Nieminen 1986). In addition to traffic burden, frost damage is one of the most obvious causes for crumbling of road aggregate (Nieminen and Uusinoka 1986). Thus, weathering properties control the suitability of rock material as road aggregate. Fresh and unused samples of rocks which, when used as road aggregate, proved to crumble, were submitted to freeze-thaw tests together with those proved to be resistant. The rocks less suitable as road aggregate mostly also proved to be less resistant against freeze-thaw cycles. Mercury porosimetry were used to determine the pore size distribution of the samples.

DISCUSSION ON THE RESULTS

Examples of the pore size distributions of resistant and less resistant rocks are given in Table 1. The increase of the cumulative values of pore volume and pore area are different between the samples of resistant (1, 3) and unresistant (2, 4) rocks. Furthermore, these differences are more distinctive in fine fractions (3, 4) than in fractions of gravel size (1, 2). The increase of cumulative values is most distinctive in pore sizes less than 1 µm in diameter, i.e. in the adsorption water pores. This means a stronger water adsorption capacity among these rocks (2, 4) as compared to those represented by (1) and (3).

The increase of cumulative pore area in pores with d less than 10 µm is shown in Fig. 1 (Uusinoka and Nieminen 1986). In the curves (b) and (d) representing fine fractions from less resistant rocks the cumulative pore area formed by pores less than 1 µm in diameter shows a strong rise as compared to the curves (a) and (c) from resistant rocks. The portion of the pore area of these d < 1 µm -pores is smaller in (a) and (c) than in (b) and (d).

As mentioned above, the adsorption water does not yet freeze just below 0 °C. Unfrozen adsorption water occurs in temperatures as low as -40 °C (Falconer 1969). Gravitation water tends to freeze below 0 °C in joints and larger fissures and pores. Within the rock the pressure gradient tends to turn towards those centers of freezing. This phenomenon is analogous with that occurring in loose surficial deposits during frost heaving (Nieminen 1985): the unfrozen capillary and adsorption water tends to flow upwards and freeze in contact with the ice lenses, whose formation is initiated by the freezing of the gravity water.

Frost weathering of rocks is thus initiated by the formation of ice in larger pores and fractures whose water content is nourished by the increasing suction tending to detach the oriented water molecules held in contact with the walls of the smaller pores. If this suction force becomes stronger than the pF number in the wilting point (Brady 1974) the detachment of the adsorption water starts. The amount of adsorption water depends on the amount of the pores with d < 1 µm as well as on the amount of minerals with a great water-holding capacity like clay minerals formed as products of chemical weathering or hydrothermal alteration.

The intensity of frost shattering of rocks is thus greatly affected by the pore size distribution in the texture. The greater is the amount of adsorption water pores the more adsorption water is able to be stored in the rock. Migration of the adsorption water by the suction caused by the freezing of the gravity water is, however, possible only together with an adequate amount of fissures and capillary pores both of which lead the detached adsorption water to the centers of freezing. These conditions are fulfilled in medium- to coarse-grained igneous or metamorphic rocks and in many sedimentary rocks, too. In crystalline rocks the texture may be disrupted by the differences in the dilation behavior of the different minerals together with temperature changes. This creates fissures along which unfrozen water is able to flow from the small pores mostly within the feldspars and micas.

From the point of view of the durability of road aggregates, a program to study the weatherability of different rocks by mercury porosimeter test has been initiated in our laboratory. On the

TABLE I

Pore size distributions as results of mercury porosimeter tests from resistant (1, 3) and weatherable (2, 4) granites. Samples 1 and 2 represent gravel sizes and samples 3 and 4 are from fine fractions of granites (different from the former). D = pore diameter μm, V = cumulative pore volume (dm^3/kg), A = cumulative pore area (m^2/kg). Note the higher values of pore volume and pore area, notably the higher cumulative rises below 1 μm, in the samples of less resistant rocks.

1			2			3			4		
D μm	V dm^3/kg	A m^2/kg	D μm	V dm^3/kg	A m^2/kg	D μm	V dm^3/kg	A m^2/kg	D μm	V dm^3/kg	A m^2/kg
164.08	0	0	180.49	0	0	180.48	0.000	0	180.488	0.000	0
82.04	0	.01	90.24	.002	.07	90.244	0.010	0	90.244	0.024	1
46.27	0	.03	60.16	.003	.13	60.162	0.019	1	60.162	0.0523	2
35.39	0	.04	44.02	.004	.2	44.021	0.030	2	44.021	0.074	4
24.39	0	.06	29.58	.005	.31	35.389	0.039	3	35.389	0.098	7
19.83	.001	.07	22.56	.006	.45	29.588	0.050	4	29.588	0.109	8
17.18	.001	.08	18.23	.006	.6	25.067	0.057	5	25.067	0.125	10
15.16	.001	.1	15.16	.007	.78	20.510	0.068	7	20.510	0.1439	14
11.87	.001	.13	12.19	.008	.99	18.048	0.077	9	18.048	0.157	17
10.43	.001	.15	10.02	.008	1.23	15.040	0.091	12	15.040	0.165	18
8.82	.001	.19	8.82	.009	1.42	13.369	0.097	14	13.369	0.184	24
2.84	.001	.19	4.95	.009	1.67	11.874	0.111	19	11.874	0.194	27
1.32	.001	.19	3.14	.01	2.83	9.449	0.131	26	9.449	0.214	34
.49	.001	1.31	2.11	.011	4.2	9.502	0.131	26	9.483	0.214	34
.31	.001	3.42	1.24	.012	6.67	6.948	0.136	29	7.512	0.218	36
.19	.001	6	.87	.013	8.85	5.317	0.145	35	5.324	0.282	77
.13	.002	9.9	.57	.013	12.55	4.115	0.170	56	4.150	0.492	250
.1	.002	11.68	.44	.014	16.1	3.360	0.213	102	3.152	0.617	388
.07	.002	14.14	.35	.014	19.21	2.454	0.267	179	2.537	0.682	479
.05	.002	17.61	.25	.015	26.35	1.665	0.312	269	1.543	0.784	686
.03	.002	17.61	.17	.015	34.4	1.259	0.333	328	1.263	0.808	756
.01	.002	17.61	.08	.016	61.51	0.888	0.352	403	0.987	0.836	858
			.05	.016	79.36	0.595	0.366	478	0.596	0.874	1057
			.03	.016	99.78	0.355	0.376	573	0.352	0.900	1277
			.02	.017	120.46	0.253	0.381	632	0.224	0.914	1487
			.01	.017	120.46	0.179	0.384	698	0.174	0.919	1593
						0.120	0.386	766	0.120	0.925	1765
						0.060	0.390	924	0.090	0.929	1917
						0.036	0.392	1120	0.060	0.932	2087
						0.022	0.393	1227	0.036	0.935	2280
						0.012	0.393	1344	0.018	0.938	2788
						0.009	0.394	1534	0.009	0.939	3223
						0.006	0.395	1956	0.006	0.940	3949

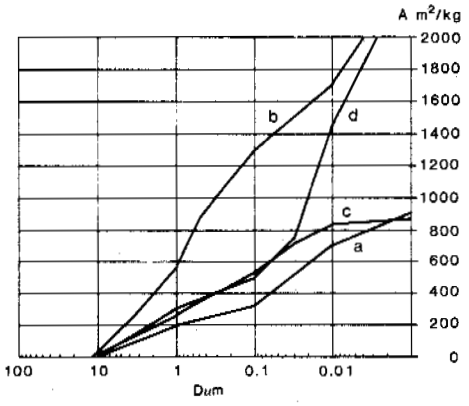

Fig. 1. Cumulative pore areas (A) in the different pore sizes (D) of the fine fractions of four crushed aggregates(d < 0.074 mm). The portion of the pore areas formed by pores with 0 < 1 μm is greater in the samples (b) and (d) from friable rocks than in (a) and (c) from resistant rocks (Uusinoka and Nieminen 1986).

basis of the results of mercury porosimetry, freeze-thaw tests and the experience from the behavior of the rock material as road aggregate we have thus far obtained an empirical classification of rocks into resistant and less resistant types.

REFERENCES

Brady, N.C. (1974). The nature and properties of soils 8th Ed., pp.1-639. New York:Macmillan Publishing Co.

Brunsden, D. (1979). Weathering. Process in geomorphology (Ed. by C.Embleton and J. Thornes), 73-129, London:Edward Arnold.

Embleton, C. and King. C.A.M. (1975). Periglacial geomorphology, pp.1-203. London:Edward Arnold.

Fairbridge, R.W. (1968). Frost riving, shattering, splitting, wedging. The encyclopedia of geomorphology (Ed. by R.W.Fairbridge),381. New York: Reinhold Book Corporation.

Falconer, A. (1969). Processes acting to produce glacial detritus. Earth Sci.J. (3:1), 40-43.

Gregg, S.J. and Sing, K.S.W. (1982). Adsorption, surface area and porosity, pp.1-303,London: Academic Press.

Hálek, V. and Svec, J. (1979). Groundwater hydraulics, pp.1-620. Amsterdam:Elsevier Sci.Publ.Co.

Hall, K. (1986). Rock moisture content in the field and the laboratory and its relationship to mechanical weathering studies. Earth Surface Processes and Landforms (11), 131-142.

Nieminen, P. (1985). The quality of the fine fractions of till and its influence on frost susceptibility (In Finnish with English summary). Tampere University of Technology. Publ.(34), pp.1-81. Tampere.

Nieminen, P. Salomaa, R. and Uusinoka, R. (1985). The use of specific surface area, pore volume, and pore area in evaluating the degree of weathering of fine particles: an example from Lauhanvuori, western Finland. Fennia (163:2), 273-277. Helsinki.

Nieminen, P. and Uusinoka R. (1986). Influence of the quality of fine fractions on engineering-geological properties of crushed aggregate. IAEG-Bull. (33), 97-101. Paris.

Ohlson, B. (1964). Frostaktivität, Verwitterung und Bodenbildung in den Fjeldgegenden von Enontekiö; Finnisch-Lappland. Fennia (89:3), 1-180. Helsinki.

Uusinoka, R. and Nieminen, P. (1986). Mercury porosimetry in predicting the quality of rock aggregate in road base. Proc. 5th Int. Congr. IAEG, Buenos Aires 20-25 Oct. 1986 (5.4.13), 1697-1701. Rotterdam:A.A.Balkema.

Walder, J.S. and Hallet, B. (1985). A theoretical model of the fracture of rock during freezing. Geological Society of America Bull. (96), 336-346.

Walder, J.S. and Hallet, B. (1986). The physical basis of frost weathering: toward a more fundamental and unified perspective. Arctic and Alpine Research (18:1), 27-32.

Wilson, L. (1968). Frost action. The encyclopedia of geomorphology (Ed. by R.W. Fairbridge), 369-381. New York:Reinhold Book Corporation.

FLUVIO-AEOLIAN INTERACTION IN A REGION OF CONTINUOUS PERMAFROST

J. Vandenberghe and J. Van Huissteden

Institute of Earth Sciences, Free University, Amsterdam, The Netherlands

SYNOPSIS The interrelations between fluvial and aeolian processes under conditions of continuous permafrost (Dinkel valley, eastern Netherlands and adjacent Germany) have resulted in three main sedimentary facies: 1/ an aeolian facies comprising fine, parallel laminated sands (a1) and sandy loess (a2); 2/ a fluvial facies represented by trough and tabular crossbedded coarse sands; and 3/ a fluvio-aeolian facies consisting of laminated sands and sandy silts and occasional sand-filled scours. The latter facies is the dominating one and is the result of alternating sheetflood and wind activity. Conditions of continuous permafrost are expressed by the frequent occurrence of both epigenetic and syngenetic ice-wedge casts and large cryoturbations.

INTRODUCTION

The small Dutch river basins have a predominantly periglacial genesis (e.g. De Gans, 1981; Van Huissteden et al., 1986a; Vandenberghe et al., 1987). The fluvial sedimentary record contains the information to reconstruct the palaeo-environmental conditions as well as the type and intensity of the geomorphological processes. It appears that the development of the lowland valleys is characterized by time-varying hydrologic regimes and is influenced by striking changes of aeolian sediment supply (Vandenberghe, 1985). During the Weichselian, from which period the most complete information is preserved, climate in the Netherlands has varied between cool-temperate and very cold. Processes have changed accordingly. Therefore, the relations between climate and sedimentary environment have to be studied for small, climatologically homogeneous time-intervals.

The present study is concerned with the impact of climate on the river dynamics and geomorphological valley development during the last glacial maximum (ca. 23 to 15000 BP). This period is characterized by conditions of continuous permafrost (Vandenberghe, 1983). The Dinkel valley in the eastern Netherlands and adjacent Germany offers good possibilities for this study because relatively thick deposits from that period have been preserved and their stratigraphy is well-established (Van der Hammen & Wijmstra, 1971; Van Huissteden et al., 1986b; Vandenberghe & Van Huissteden, 1987). Deposits from the concerned timespan are found in an exposure at Holt on the higher of two Weichselian Pleniglacial terraces, slightly above the actual alluvial plain (fig. 1). They provide the basic information for the reconstruction of the sedimentary processes and the periglacial environment. Stratigraphically they overlie a peat layer which has been dated at 27500 BP +/-250 (GrN-11523). The deposits are covered by aeolian deposits which are typical for the final part of the Weichselian Pleniglacial (Beuningen desert pavement and plane-bedded coversands).

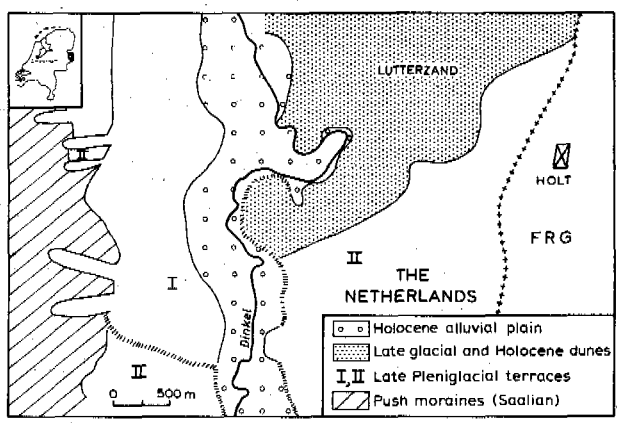

Fig. 1. Location map of the Twente area.

PERIGLACIAL SEDIMENTARY FACIES

a/ aeolian facies

Pure aeolian deposits are not readily expected within the valleys. However, traces of aeolian activity are not uncommon during certain times.

A first facies of aeolian deposits (a1) consists of pale yellow, parallel laminated, slightly silty sands. The modal grain size from 120 to 165 µm. The sedimentary struc-

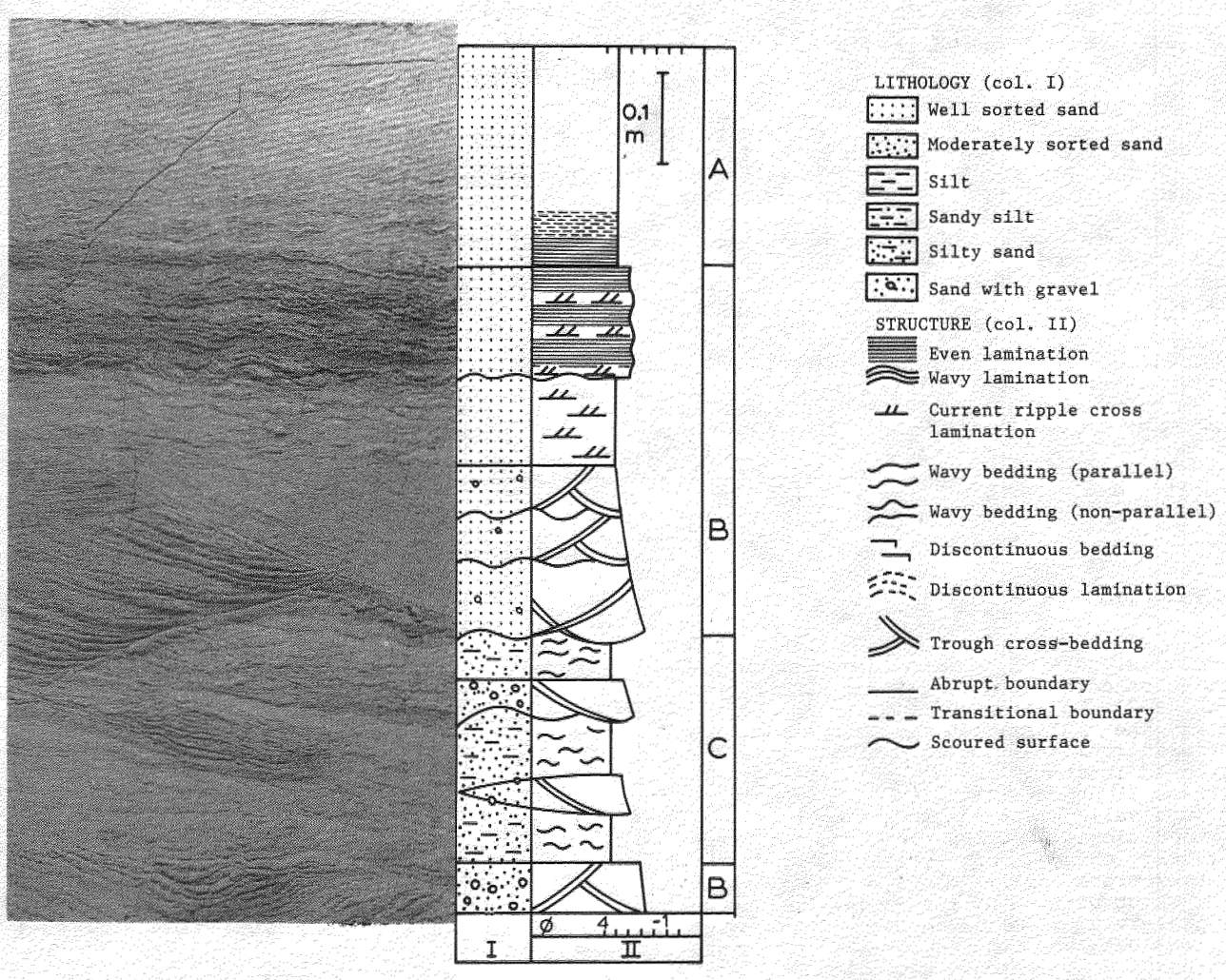

Fig. 2. Laquer peel showing the aeolian facies a1, the fluvial facies (b) and the fluvio-aeolian facies (c). Column I: lithology; column II: sedimentary structures and grain-size estimates (phi units).

tures and the granulometric properties point to an aeolian mode of deposition in the form of sand sheets (Schwan, 1987). The aeolian sedimentation ranges from dry aeolian, characterized by subparallel planar cross-bedding, to wet aeolian, characterized by wavy lamination (Fig. 2). Aeolian erosion has resulted in the formation of residual layers consisting of a coarse rolling subpopulation. Consequently the generally moderate sorting of the aeolian sediments decreases likewise when affected by erosional hiatuses. In some areas aeolian deflation dominated such that no aeolian sediments have been deposited but desert pavements could develop.

A second facies of aeolian deposit (a2) is composed of a compact sandy loess. The sediment is typically bimodal. The coarse fraction is represented by the fine sands of facies a1, while the fine fraction is a silt (modal grain size 40-50 µm) with low clay content (silt/clay ratio is ca. 5). This fine fraction shows the characteristics of a real loess although the mean grain size is relatively coarse. This coarseness, as well as the admixture with saltation sediment may be explained by the position of the study region which is considerably northward of the large northwestern European loess belt (Vandenberghe & Krook, 1981). The nearly absence of clay excludes deposition as an alluvial layer.

b/ fluvial facies

At various positions within the sediment sequence a system of multiple gullies with large width-depth ratio is present. Channel incision and accumulation succeed quickly. The sedimentary structures are characterised by trough- and tabular crossbedding (facies St, Sp: Miall, 1977) and ripple cross-lamination (facies Sr). A common sequence is (St)-->Sp--

>Sr. This fluvial facies consists of medium to coarse sand (modal value between 180 and 275 µm), which contains gravel at the base of the gullies. The sorting varies between medium and very good (Fig. 2).

The described lithologic properties and sedimentary structures point to a temporarely high-energetic river with quickly migrating channels. Within the single units of this facies, features indicating reactivation surfaces of lower stage flow (Collinson, 1970) are rare. This indicates an ephemeral nature of the channels, as with more continuous flow low stage reworking of high stage bedforms might be expected. The intermittent character of the river, the multiple channel system and the quick aggradation point to a river of the braided type. The periodical high discharges are probably caused by snow break-up. These points typify the arctic nival character of the river (Bryant, 1982).

c/ fluvio-aeolian facies

A sedimentary facies showing characteristics of both above described types forms the major part of the Upper Pleniglacial deposits. It consists of sand, dominated by indistinct, wavy parallel bedding and lamination. Beds show varying silt content and are usually thin, ranging from 1 to 10 cm thickness (Fig. 2-3). Deposits of this type have been

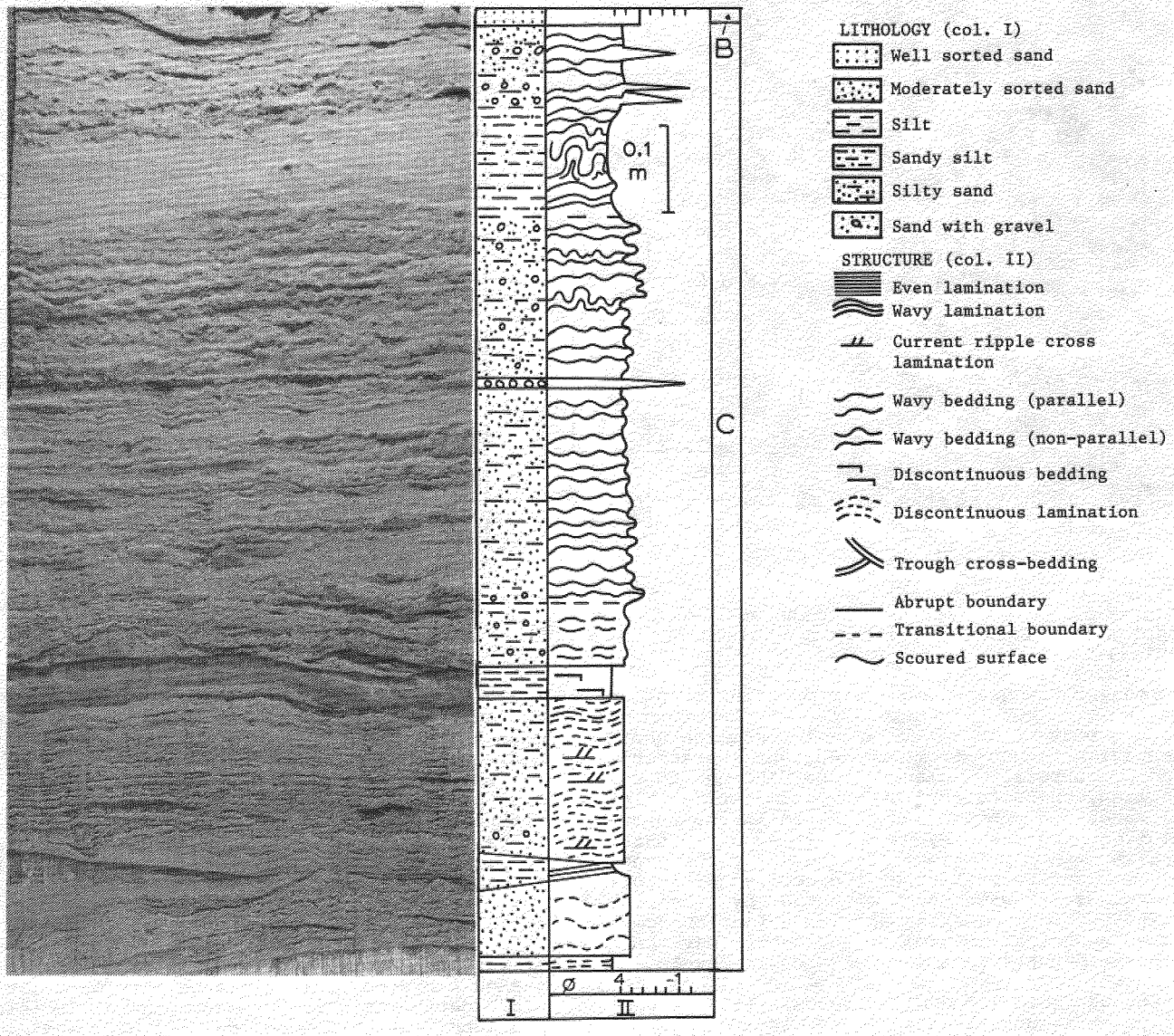

Fig. 3. Laquer peel showing the fluvial facies (b) and the fluvio-aeolian facies (c). Legend see fig. 2.

attributed to a wet aeolian environment (Ruegg, 1975; Schwan, 1987). Several beds show an irregular scoured base or current ripple lamination, which attest of periodic reworking by running water. Shallow scours, filled with silty sand occur frequently. Some scours show a cross-laminated fill and grade laterally into vast sandy silt sheets with many tiny convolutions. Discontinuous gravel strings are attributed to deflation processes. Local, badly sorted, coarse-grained, homogeneous lenses may be derived from the melting of snow dunes (Schwan, pers. comm.).

The grain size distribution shows a clear bimodal character. At the base of the sets typical aeolian fine sands -described as a1-are mixed with coarser fluvial sands -described in b-, while the top of the sets consists of a mixture of aeolian sandy loess (a2) and fine sand (a1). The basal sediments are mainly aeolian sands which are reworked by running water. The upper sediments are of aeolian origin as well but are deposited in stagnant water.

The described environment is situated outside the channels which functioned only during floods. During inundations sheetflood-like conditions prevailed (Friend, 1983). Convolute lamination is also known from the waning stage of ephemeral flood deposits (McKee et al., 1967). It suggests rapid deposition and water-saturated conditions of the sediment. The thicker sheets of silty sand represent the typical overbank deposits of the environment. During the periods of low fluvial activity the concerned areas were subjected to aeolian activity (Bryant,1983). This resulted especially in the deposition of "wavy laminated sands" (wet aeolian environment) and the creation of deflation surfaces.

PERIGLACIAL STRUCTURES

A series of wedge casts occurs from the base to the top of the sediment sequence. The wedge forms show the typical structure of the ice-wedge casts in the loose aeolian and fluvial fine sands described earlier (Vandenberghe, 1983a): a core of several cm width characterized by vertical lamination surrounded by a zone with numerous normal faults. It has been shown that this bipartite structure is caused by the presence of ice in the wedge, its subsequent melting, the progressive infilling by liquefied sediment in the central part and gravitational downfaulting in the boundary zone. Thus, also the wedge forms at Holt have to be interpreted as ice-wedge casts. However, in comparison with the generally observed wedge forms, the total width of the wedges observed at Holt is significantly smaller, while their length, in contrast to the ca. 1.5m commonly measured, amounts in ideal cases to ca. 4.5m. The relatively small width indicates that the wedge growth did not last as long as the generally occurring wedges which are of the epigenetic type. The wedges at Holt have been covered several times with fluvio-aeolian sediments of different thickness (facies type c). As a result the depth range of ice-core growth shifted equally in an upward direction. A new wedge developed while the lowest part of

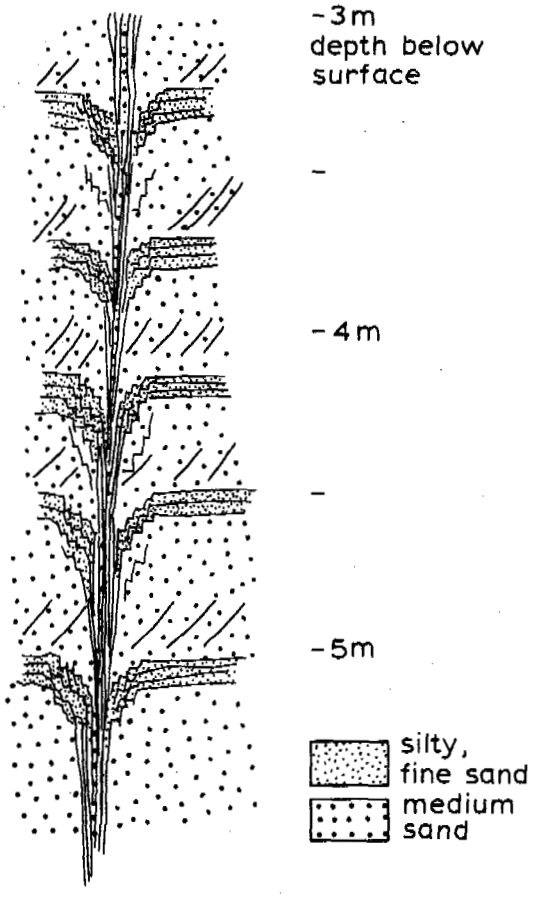

Fig. 4. Syngenetic ice-wedge cast developed in fluvio-aeolian deposits.

the previous ice-wedge became at least inactive. This process has given way to the development of a cone-in-cone structure (fig.4). This genesis indicates the syngenetic nature of the forms at Holt.

Complete interruption in the vertical extension of some wedges is caused by renewed river activity. Of course gully erosion can stop the development of a wedge, but (partial) melting of the permafrost may also be achieved by the simple presence of river water at the surface.

The rate of sedimentation is thus the main factor determining the grade of development of the wedge forms. Therefore, a variety of forms is present ranging from fully developed, wide wedges (Fig. 5) to narrow fissures. The latter forms developed when the time of non-deposition was short (maybe only one season). Such frost cracks, which have been almost or completely free of ice, have preserved upturning structures at their sides since gravitational collapse did not occur.

Large cryoturbations (of ca. 1.2m amplitude) are only present at the top of the sequence. They represent the degradation of the permafrost (Vandenberghe & Van de Broek, 1982;

Vandenberghe,1983b). Small involutions, at cm scale, are found throughout the sediment series. They are caused by water expulsion as a consequence of compaction of the quickly deposited, water rich sediments. A frozen subsoil might have enhanced the process.

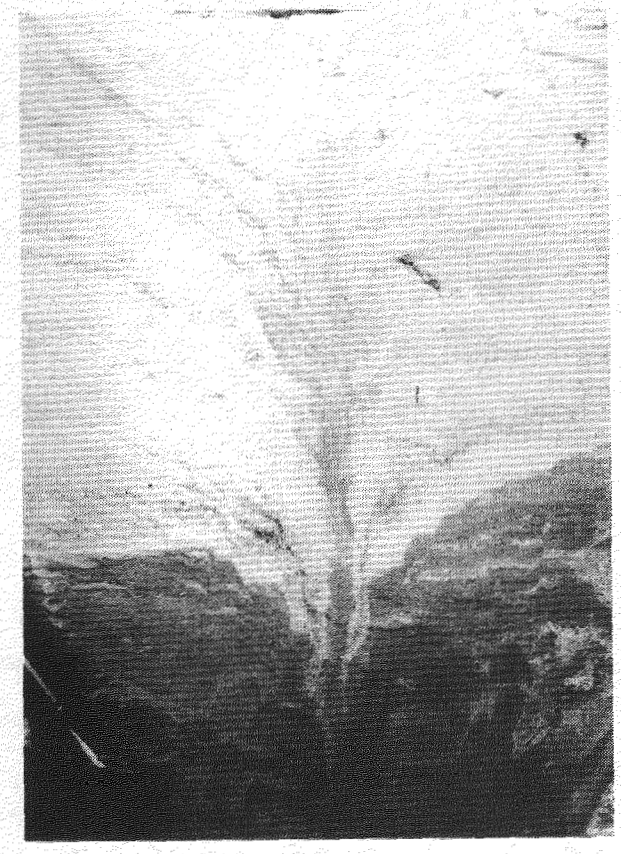

Fig. 5. Epigenetic ice-wedge cast developed in fluvial sands (upper part) and fluvio-aeolian sediments (lower part).

Synthesis

The fluvio-aeolian environment in conditions of continuous permafrost and in lowland valleys formed in a sandy subsoil, is characterized by deposits which can be grouped in three main facies:
a/ aeolian facies: slightly silty, fine sands (a1) with patchy distribution in the river plain but more widespread elsewhere and periodically subjected to deflation; relatively extensive sheets of sandy loess (a2) especially towards the end of the cold phase.
b/ fluvial facies (b): filling deposits of an intermittent, braided-river system consisting of crossbedded medium to coarse sands.
c/ fluvio-aeolian facies (c): sequence of aeolian (a1-2) and fluvial deposits (b) as a result of periodical inundations alternating with wind activity at low water stage.

The maximum of the cold cycle is characterized by the typical fluvio-aeolian facies (c), locally interrupted by small shallow gully infillings (b) and aeolian sands (a1). At the end of the coldest phase river activity slowed down, so that the former river plain was transformed into a terrace (fig. 1) which has been covered by aeolian loam (a2). This silt and the underlying sands have been heavily cryoturbated during the permafrost degradation. Afterwards aeolian deflation has been a general process leading to the formation of a widespread desert pavement. The decline of the cold period is terminated by deposition of typical aeolian coversands (facies a1 as well).

ACKNOWLEDGEMENTS

The investigations were supported in part by the Netherlands Foundation for Earth Science Research (AWON) with financial aid from the Netherlands Organisation for the Advancement of Pure Research (ZWO). The type-setting is done by Mrs. R. de Vries, the figures are drawn by Mr. H. Sion.

REFERENCES

Bryant, I.D. (1982). Periglacial river systems: ancient and modern. Unpublished Ph. D. Thesis: University of Reading.

Bryant, I.D. (1983). The utilization of arctic river analogue studies in the interpretation of periglacial river sediments from southern Britain. In: Gregory, K.J. (ed.): Background to Paleohydrology, 413-431. London:John Wiley & Sons Ltd.

Collinson, J.D. (1970). Bedforms of the Tana River, Norway. Geografiska Annaler, 52A(1), 31-56.

De Gans, W. (1981). The Drentse Aa valley system, pp.1-132. Asterdam: Thesis Free University.

Friend, P.F. (1983). Towards the field classification of alluvial architecture or sequence. In: Collinson, J.D. & Lewin, J. (eds.): Modern and ancient fluvial systems, 345-354. Special Publication Nr. 6 of the International Association of Sedimentologists, Oxford: Blackwell Scientific Publications.

McKee, E.D., Crosby, E.J., Berryhill, H.L. Jr. (1967). Flood deposits, Bijou Creek, Colorado, June 1965. Journal of Sedimentary Petrology, 37(3), 829-851.

Miall, A.D. (1977). A review of the braided river depositional environment. Earth-Science Reviews, 13, 1-62.

Ruegg, G.H.J. (1975). Sedimentary structures and depositional environments of Middle- and Upper-Pleistocene glacial time deposits from an excavation at Peelo, near Assen, The Netherlands. Mededelingen Rijks Geologische Dienst, N.S. 26(1), 17-37.

Schwan, J. (1987). Sedimentologic characteristics of a fluvial to aeolian succession in Weichselian Talsand in the Emsland (F.R.G.). Sedimentary Geology, 52, 273-298.

Vandenberghe, J. (1983a). Ice-wedge castsand involutions as permafrost indicators and their stratigraphic position in the Weichselian. Proc. 4th Int. Conf. Permafrost, Fairbanks, 1298-1302, Washington D.C.

Vandenberghe,J. (1983b). Some periglacial phenomena and their stratigraphical position in Weichselian deposits in The Netherlands. Polarforschung, 53, 97-107.

Vandenberghe,J. (1985). Paleoenvironment and stratigraphy during the last glacial in the Belgian-Dutch border region. Quaternary Research, 24, 23-38.

Vandenberghe, J. & Krook,L. (1981). Stratigraphy and genesis of Pleistocene deposits at Alphen (southern Netherlands). Geologie en Mijnbouw, 60,417-426.

Vandenberghe,J. & Van de Broek,P. (1982). Weichselian convolution phenomena and processes in fine sediments. Boreas, 11,299-315.

Vandenberghe,J.,Bohncke,S.,Lammers,W. & Zilverberg,L. (1987). Geomorphology and palaeoecolgy of the Mark valley (southern Netherlands): geomorphological valley development during the Weichselian and Holocene. Boreas, 16, 55-67.

Vandenberghe,J. & Van Huissteden,J. (1987). On the Weichselian statigraphy of the Twente region (eastern Netherlands). Proc. Subcomm. Eur. Quat. Strat. Symposium Zurich 1985, Balkema, Rotterdam (in press).

Van der Hammen, T. & Wijmstra, T. (1971). The Upper Quaternary of the Dinkel valley. Meded. Rijks Geolog. Dienst, N.S. 22, 55-213.

Van Huissteden, J., Van der Valk, L. & Vandenberghe, J. (1986a). Geomorphological evolution of a lowland valley system during the Weichselian. Earth Surface Processes and Landforms, 11, 207-216.

Van Huissteden, J., Vandenberghe, J. & Van Geel, B. (1986b). Late Pleistocene stratigraphy and fluvial history of the Dinkel basin (Twente, eastern Netherlands). Eiszeitalter und Gegenwart, 36, 43-59.

REGULARITIES OF FORMING SEASONALLY CRYOGENIC GROUND

E.A. Vtyurina

Research Institute of Engineering Site Investigations, Moscow, USSR

SYNOPSIS Term "seasonally cryogenic ground" (SCG) is introduced; its criterion is established; regularities of forming SCG in two phases of development are under consideration; cryogenetic classification of SCG is worked out; SCG zonalities and methods to predict SCG cryogenic changes as well as theoretical importance of the problem in economic development of an area are shown in the report.

A top layer of the lithosphere with seasonal cycles of thaw-freezing is of great importance in development of nature and its exploitation. Changes in the ground of this layer provoke transformations of geocryological conditions and a number of cryogenic processes developing in the layer. Subsoil transformations, swamping, probable pollution of ground waters and changes in a vegetation cover depend on natural character of this layer. The top layer is a natural regulator of a surface runoff, measures to be taken on the environment protection, recultivation and reclamation require detailed study of the main qualitative and quantitative indices of the layer in question. But so far we lack information on this layer. Up to now the problem solution remains as it was brought up in 1955-56, when the terms "seasonally thawing layer" (STL) and "seasonally freezing layer" (SFL) were introduced instead of "an active layer" and "a seasonally freezing ground" by M.I.Sumgin (Sumgin et al., 1940; Kudriavtsev ed. 1978; Nersessova, ed., 1956; Shvetsov, Dostovalov,eds., 1959). But it was a change in terms only. Previous directory criteria of the layers remained unchangeable and morphometric trend of their study was not informative enough new terms did not reveal the point of the layers (Vtyurin, Vtyurina, 1981; Vtyurina, 1974,1984; Kotlyakov,ed., 1984; Popov, 1967).

The author put forward a new method to study a top layer of lithosphere with developing seasonal cycles of thaw-freezing (Vtyurin, Vtyurina, 1981; Vtyurina, 1984). The layer in question exposes to seasonal thaw-freezing as in the permafrost region so outside of it. Both of these processes are considered to be cryogenic, therefore the ground composing the layer is called seasonal cryogenic (SCG) independ on thermal state of underlying strata. The only objective criterion to separate SCG from permafrost and perennial thawing underlying strata, as the author says, is a character of a thaw-freezing cycle, but neither their annual thaw-freezing nor thermal condition, which were considered criteria to distinguish STL and SFL (Nersessova, ed., 1956; Shvetsov, Dostovalov, eds., 1959; Popov,1967; Kudriavtsev, 1948). A top layer is called seasonally cryogenic due to the fact that it is characterized by a seasonal thaw-freezing cycle (i.e. freezing in winter and thawing-next summer or thawing - in summer and freezing - next winter) which occurs once at least for a representative period of 30 years. A 30 year period is accepted as a representative one due to the fact that on the one hand this period is characterized by all the liversity of weather conditions affecting the seasonal freezing and thawing (Sumgin et al., 1940) and on the other hand natural denudation and sedimentation does not lead to significant changes in position of SCG top and bottom except local disastrous effects. A new tendency proposed by the author is morphocryogenetic, the main point of which is cryogenesis, i.e. formation of SCG as a lithocryogenic unity. The new approach permits to define more exactly morphometric characteristics of SCG as compare to the previous studying of STL and CFL.

An analysis of long-term investigation data on seasonal thaw-freezing and observations made by the author permit to conclude that SCG is more different by cryogenesis as compare to perennial freezing ground and that the SCG cryogenetic heterogeneity is a main reason of differences in a number of its indices and processes developing in SCG, its different reaction to changes in natural conditions and a different affect on economic development of an area.

SCG in the permafrost region and outside of it has necessarily two phases in development: aggradation - when a ground is freezing or in a frozen state and called "seasonally freezing ground" (SFG) and degradation - when a ground is thawing or melting and called seasonally thawing ground" (STG). Their cryogenic heterogeneity is a result of qualitative changes in the both processes forming SCG: seasonal thawing and freezing and time dynamics of the depth of their development. Both processes are zonal but regularities of ground changes are diametrically opposite. Seasonal freezing together with SFG formation (aggradation phase)

becomes more complicated from south to northward of the USSR. The south zone the boundary of which is a geoisothermic line of +1°C (a ground temperature in the zone of zero annual variations) is characterized by only one modification of this process: direct freezing from the ground surface. This modification is observed regularly, systematically (every year) or irregularly (non-systematically) in the extreme south. As a result systematic or non-systematic monogenetic direct SFG is formed, that is to say that SFG is formed in the process of direct freezing only. In the north zone limited from the south by a geoisothermic line of -1°C two natural modifications of seazonal freezing can be observed: direct and reverse freezing developing away from the permafrost strata. It leads to formation of polygenetic SFG. Direct and reverse freezing can be synchronic or metachronic. Grounds in this case are called synchronic or metachronic polygenetic respectively. Synchronic SFG is character of the middle subzone of the north zone limited by geoisothermic lines -4°C and -5°C. Metachronic polygenetic SFG can be subdivided to two types-direct and reverse depending on what freezing begins first. Metachronic SFG of the first type is formed under condition of earlier direct freezing in the south subzone of the north zone and the second one-under earlier reverse freezing in the north subzone. Variations in thaw-freezing depth produce a different effect on SFG formation in the zones mentioned. In the south zone all the strata which got frozen in winter thaws in summer despite great variations in time of the seasonal freezing depth (by 1.5-5 and even by 10-20 times). Therefore SFG at this zone is monochronic due to the fact that this ground as a whole is formed for one winter. In the north zone SFG thaws partially during a year (with the exception of a year with a maximum depth of seasonal thawing within a representative period). There remains a residual frozen horizon. When it joins a frozen ground formed last winter, polychronic SFG is formed. Its upper part was formed last winter and a residual horizon can be a result of one or several previous winters. The residual horizon can be under frozen condition for years but as it is a part of SFG it necessarily thaws in summer and got frozen next winter once at least for a 30 year period.

A middle zone can be separated limited by a geoisometric line of ±1°C. In cold winter a polychronic SFG is formed in this zone and monochronic - in warm winter. Such changes occur more frequently in the north subzone northward from the 0°C geoisothermic line where formation of monogenetic SFG alternates in time with polygenetic SFG. In the north subzone monogenetic SFG only is formed.

Such are principal regularities of SCG formation at an aggradation phase. But to determine SCG cryogenetic gradation is necessary to know and to take into account regularities of SCG formation at another phase - degradation i.e. specific features of STG formation. Seasonal thawing is so heterogeneous as freezing but the latter is complicated by the reverse direction as compare to freezing- from north to

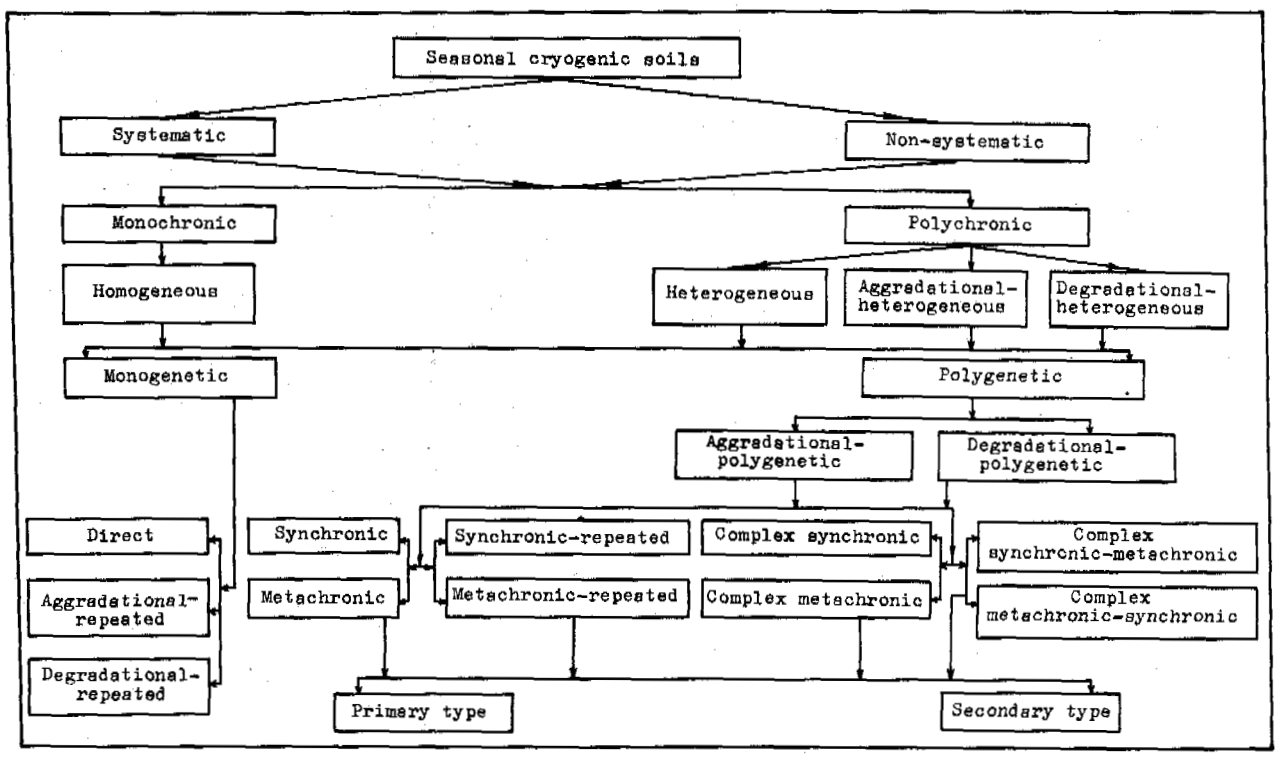

Fig. Classification of Seasonal Cryogenic Soils

south. Therefore cryogenetic zonality of STG differs from that of SFG. Only the boundaries of the zones are the same. But the northern zone is not divided to subzones by STG formation. Systematic only direct seasonal thawing (when a residual horizon melts completely) provides formation of only monochronic monogenetic STG in the mentioned zone. The middle zone is characterized by alternation of monochronic and polychronic STG within a representative period but in contrast to SFG the first grounds dominate in the north subzone and the second ones - in the south, where they can be sometimes monogenetic and sometimes polygenetic. The south zone is characterized by direct and reverse thawing where a residual thaw layer is formed any year except a year with a maximum freezing depth within a representative period. So, polychronic polygenetic STG dominates in this zone. STG are subdivided by name to the same gradations as SFG of the north zone depending on relation of the direct and reverse thawing beginning but with account of thaw regularities, they are: metachronic of the first type in the north subzone up to geoisothermic line of +4°C, where direct thawing begins first; synchronic in the middle subzone up to the +5°C geoisothermic line and metachronic of the second type in the south subzone where reverse thawing begins first. In the south subzone with a freezing depth of up to 5.0 cm reverse thawing only can be often observed and polychronic monogenetic reverse STG be formed.

So, an assumed long ago division of perennially frozen ground to mono- and polychronic, mono- and polygenetic turned to be suitable to SFG and STG that means to SCG as a whole. But a number of low-class gradations of SFG and STG can be also distinguished with account of developing modifications of seasonal thaw-freezing and time relation of the beginning of these modifications.

A conjugate analysis with account of principles of SCG formation at the both phases of development, that is to say SFG and STG at any area, helps to reveal qualitative heterogeneity of these grounds and to compile the first cryogenetic classification of SCG (Fig.1). Names of SCG gradations are assumed by the most complicated phase of their development. In case a thaw residual horizon is available the SCG is called aggradation - heterogeneous, a frozen residual horizon is available the SCG is called degradation - heterogeneous, in case the both horizons are available - heterogeneous, without those two horizons - homogeneous. In case of direct and reverse freezing and direct thawing only the SCG is called aggradation - polygenetic, the both modifications of thawing and direct freezing only - degradation -polygenetic. A residual frozen horizon in the north zone (thawing horizon in the south zone) can be a result of only direct or only reverse freezing (thawing). In this case SCG is called synchronic - reverse or metachronic - reverse or direct - at the top and reverse - at the bottom (SCG complex synchronic and complex metachronic). In case of changes in cryogenetic gradations of SFG and STG rather complex polygenetic SCG is formed due to different principles of formation of the top layer last winter (summer) and a residual horizon - for the previous ones. Regularities of SCG formation are reflected in its name, the first part of which shows a principle of SCG formation during a year of observation and the second - during a year of forming a residual horizon. The SCG zonality reflects cryogenetic zonality of the both phases of SCG development and differs from each other by zonal discrepancy of SFG and STG.

Different cryogenetic gradations of SCG are characterized by different thickness, moisture and ice content, cryogenic composition, genetic types of ground ice, properties, different complex of cryogenic processes, different effects on the other natural processes and on economic development of an area. Dynamics of quantitative indices of SCG is more intensive than that of qualitative ones. To avoid arrows estimation of quantitative indices it is necessary to determine: 1) quantitative indices for every cryogenetic gradation of SCG separately, 2) with account of dynamics of their changes within a representative period or a required long-term period, but not on the basis of a year period or short-term observations. Time dynamics of quantitative indices of SCG can be determined by means of long-term observations or approximate indirect methods by short-term and even a year observation, it on the area under investigation or near it there is a station where observation data on seasonal thaw-freezing are available for a period of 30 and more years.

So, cryogenetic gradations of SCG serve a complex indicator of a number of natural processes character of SCG and so its principal specific features especially it granulometric composition of SCG is known. It is proved that the more complicated formation of SCG is in the permafrost region at an aggradation phase the less its thickness is, moisture and ice content is higher, cryogenic composition is more complicated, ground ice is of different composition, complex of cryoaggradation and cryodegradation processes is more complicated, affect of SCG on other natural processes and economic development of an area is more intensive. Therefore to know cryogenetic gradation of SCG as well as to be apt to prognoze its natural and technogenic change is a matter of great importance. It is known that seasonal thaw-freezing and formation of SCG is affected by a number of factors. It is important to establish which of them could sum up all the others and finally predetermine cryogenetic gradation of SCG. It turned to be that such a factor can be assumed a ground temperature in the zone of annual zero variations (Vtyurina, 1974, 1984). Its extreme values for SCG formation are shown above as geoisothermic lines separating zones and subzones with different cryogenetic gradations of SFG and STG, it means that it is character of SCG.

Finally, prediction of ground temperatures in the zone of annual zero variations can be considered a prognosis of cryogenetic changes in SCG and processes developing in it.

So, a problem of SCG is one of the most important new problems of geocryology differ from a problem of STL and SFL as by a subject so by a trend of investigation. Study of SCG is important for correct estimation of its affect on economic development of an area, for determination of complexity of geocryological

conditions and prognosis of their changes for elaboration of nature protection measures, recultivation and reclamation including. The problem is of great importance in a matter of studying natural processes in SCG for paleogeographic reconstructions.

REFERENCES

Vtyurin, B.I., Vtyurina, E.A. (1981). Kriogennye protsessy, yavleniya, obrazovaniya. Materialy glyatsiologicheskikh issledovanii. Khronika, obsuzhdeniya,N 40,235-239.

Vtyurina, E.A. (1974). Kriogennoe stroenie porod sezonnoprotaivajuschego sloya. 1-126. Nauka, Moskwa.

Vtyurina, E.A. (1984). Sezonnokriogennye gornye porody. 1-119. Nauka, Moskwa.

Kotlyakov, V.M. (1984). Redactor, Glyatsiologicheskiy slovar, s.s. 1-528, Leningrad, Gidrometeoizdat.

Sumgin, M.I., Kachurin, S.P., Tolstikhin N.I., Tumel, V.F. (1940). Obschee merzlotovedenie, s.s. 1-340, Moskwa, AN SSSR.

Kudrjavtsev, V.A. (1978). Redator, Obschee merzlotovedenie, s.s. 1-463. Moskwa, MGU.

Nersessova, J.A. (1956). Redactor, Osnovnye ponyatiya i terminy geocryologii (Merzlotovedenie), s.s. 1-16, Moskwa, AN SSSR.

Popov, A.I. (1967). Merzlotnye yavleniya v zemnoi kore (cryolitologiya), s.s.1-304. Moskwa, MGU.

Shvetsov, P.F., Dostovalov, B.N. (1959). Redactor, Osnovy geokryologii (Merzlotovedenie), chast 1, s.s. 1-460, Moskwa, AN SSSR.

OBSERVATIONS OF SORTED CIRCLE ACTIVITY, CENTRAL ALASKA

J.C. Walters

University of Northern Iowa, Cedar Falls, Iowa

SYNOPSIS Well-developed sorted circles occur in the High Valley area of central Alaska. These features are best developed in poorly drained depressions in silty tills of Wisconsinan age. From 1982 to 1987 the activity of sorted circles at six sites was studied using repeat photography and surveys of wooden dowels, metal spikes, and marked stones. Vertical and horizontal displacement of stones and markers showed considerable variability over the study period, apparently reflecting differences in amount of moisture and textural properties of the soil material at different sites. Overall, markers moved upward and radially outward from the fine-grained centers toward the coarse borders. Vertical motion was greatest in circle centers, with maximum surface heaves of 5 cm per year. Horizontal movement was also generally greatest in circle centers, with stones and markers moving toward bordering troughs at maximum rates of 4 cm per year. The greatest degree of activity was observed in sorted circles developed in depressions containing abundant fine-grained material with high moisture content.

INTRODUCTION

Patterned ground features are characteristic periglacial phenomena, and over the years much has been learned about the different types of features and their formation (see Jahn, 1975; French, 1976; or Washburn, 1980 for a comprehensive review). In spite of these studies, the processes responsible for the formation of many types of patterned ground still remain mostly unproven (French, 1976; Washburn, 1980), and there exists a clear need for continued field studies in periglacial regions around the world involving careful quantitative observations.

This paper presents observations on the characterictics and the degree of acitvity of sorted stone circles in the High Valley region of central Alaska from 1982 to 1987. Information gained from this study contributes to our knowledge of the specific character of the periglacial environment of this region. It also contributes to our understanding of sorted circles in general by allowing a comparison to be made with similar features studied in other periglacial regions (e.g., Jahn, 1966; Washburn, 1969; Dionne, 1974, 1978; Nicholson, 1976; Thorn, 1976; Ballantyne and Matthews, 1982, 1983; Vitek, 1983; Rissing and Thorn, 1985; Hallet and Prestrud, 1986).

STUDY AREA

The High Valley area is located within the Amphitheater Mountains on the south side of the central Alaska Range (Fig. 1). Several periods of glacial activity are recorded in the High Valley/Tangle Lakes region (Péwé, 1961, 1975; Péwé and Reger, 1983). The ice advanced into the area from the Alaska Range to the north, each advance being less extensive than the previous one. The earliest glacial advance occurred during early to middle Quaternary time. This ice overrode the 1,800 m peaks of the Amphitheater Mountains, as indicated by the presence of erratics on some of the mountain tops. A second glacial advance, thought to be middle to Late Quaternary in age, did not cover the tops of the Amphitheater Mountains but left an extensive silty till in the valleys and on the lower slopes of the mountains. This till blankets most of High Valley, for, although later glacial advances pushed through gaps in the Amphitheater Mountains and filled major valleys and lowlands, they penetrated only short distances into High Valley.

The sorted circles examined in this study are along the southwest edge of High Valley near Maclaren Summit (Fig. 1), where thick ice in the Maclaren River valley spilled over into the lower elevations of High Valley during Wisconsinan time (Denali I Glaciation of Péwé, 1965, 1975; Péwé and Reger, 1983). Depressions in the hummocky till contain excellent examples of sorted patterned ground features, including stone circles, stone polygons, stone pits, stone stripes, and irregular forms.

The study area is located within the zone of discontinuous permafrost, and although frozen ground is often absent in well drained till ridges and hills, fine-grained sediments in shallow depressions are typically frozen below depths of 0.5 to 1 m. The thickness of the frozen layer is unknown, but it is probably on the order of several meters. Elevation of the study area ranges from 1,067 to 1,189 m, and a shrub tundra environment characterizes the region.

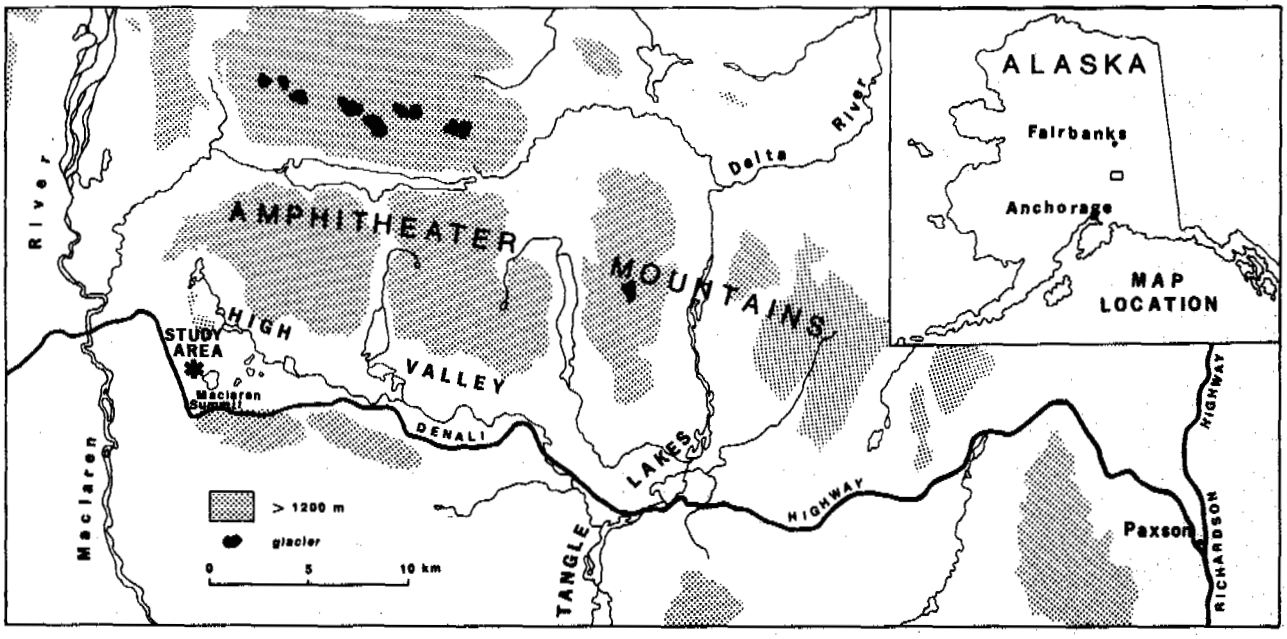

Fig. 1 Map of the High Valley/Tangle Lakes region showing the location of the study area.

The climate of the area is transitional between the maritime climate of coastal Alaska and the continental climate of the interior. Summers are short and cloudy and winters are long and cold. The nearest climatic data comes from Paxson, approximately 47 km east of the study area at an elevation of 833 m. A discontinuous climatic record shows a mean annual temperature of about -4.5°C, a mean summer temperature of about 10°C, and mean annual precipitation of about 50 cm (Péwé and Reger, 1983).

DESCRIPTION OF PATTERNS

Sorted patterned ground features are common throughout the High Valley/Tangle Lakes region, but they are especially well developed in poorly drained depressions in Wisconsinan-age silty tills. In spring and early summer many low spots and kettles in the hummocky till fill with water from snowmelt, rain, and thawing of the active layer. The appearance of the underwater patterns is quite striking (Fig. 2). Previous work suggests that the patterns do not actually form underwater (Walters, 1983), but the temporary ponding is important to their formation. By late summer the ponds normally disappear, permitting close examination and study of the patterns (Fig. 3). Of the different types of patterns typically present in the shallow depressions, stone circles and polygons are the most common. They vary in diameter from about 0.25 to 2 m and are found on level to very gently sloping surfaces (<2°). Stone pits are less common and occur in similar situations. Stone stripes are found on slopes of 3 to 10°, and irregular forms exist on level surfaces to slopes as great as about 10°.

The sorted stone circles examined in this study consist of coarse stones enclosing a circular area having a concentration of fine-grained

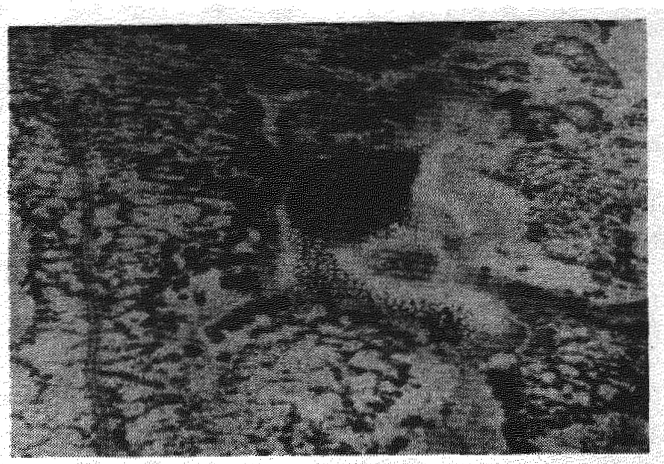

Fig. 2 Sorted patterned ground features on the floor of a depression subject to temporary ponding. Some water remains in the lowest portion of the depression. An off-road vehicle trail to the left provides scale. Photo taken July 26, 1982.

sediment with scattered stones. The surfaces of the central areas are usually convex upward (Fig. 3), with as much as 30 cm of relief between the center and the edges of the fines, at the coarse border. The contact between the fine-grained centers and the coarse borders is usually quite sharp. Trenches excavated through sorted circles show that stones in the border areas have a preferred vertical orientation of their long axes. Scattered stones in the fine-grained centers also show this tendency.

The stones making up the pattern borders are mostly subangular to subrounded (85-90%), with only a few being angular or rounded (10-15%). They range in size, but long axes between 15 and

Fig. 3 Sorted stone circles developed in a depression subject to temporary ponding. The edge of the vegetation in the background marks normal high water level in spring. Metal rods from an instrumented circle appear in the distance. The center rod is 72 cm high. Photo taken July 23, 1987.

40 cm are common. The larger stones typically occur in the middle of the borders with the smaller stones at the margins, i.e., the fine-grained/coarse material contact. A greenish-black stain covers the surfaces of the stones. This stain appears to be biochemical in origin and is related to the periodic inundation of the depressions in which the patterns occur. Staining is not present on stones or portions of stones which are buried in the adjacent fines. It is also absent on the surfaces of large boulders where they project above normal high water level during ponding. The contrast in color between the dark-stained stones and the lighter colored fines causes the patterns to be very distinct, especially when covered by water (Fig. 2).

The fine-grained material making up the centers of the stone circles varies in texture but is predominantly loamy. Sand content ranges from 18-59%, silt 14-55%, and clay 13-62%. As mentioned earlier, scattered stones occur within the fines and can sometimes be quite abundant, allowing gravels to make up 7-82% of the material in pattern centers. The fine-grained sediment is characterized by a low liquid limit (16-35%) and a low plasticity index (2-11%). In late summer the depressions in which the patterns occur are no longer flooded, but abundant moisture remains in the sediments and they become thixotropic when disturbed.

PATTERN DYNAMICS

Since 1982, six depressions containing sorted circles have been studied to determine the degree of activity of these features. Four to six sorted circles have been monitored at each site by repeat photography and surveys of wooden dowels, metal spikes, and marked stones. Photographs were taken and measurements were made in July and August 1983 and July 1984, 1985, 1986, and 1987. In addition, over this period of time several trenches were excavated through nearby sorted circles and portions of circles, and data were gathered on soil temperature, moisture, texture, and consistency.

Steel rods approximately 13 mm wide and 1.5 m long were driven into the centers of the coarse borders to serve as reference points. It was assumed that these rods would not move laterally over the study period. Subsequent measurements and comparison of photographs show this to be a valid assumption. Wooden dowels approximately 0.5 cm wide and 15 cm long and metal spikes (aluminum gutter spikes) 0.5 cm wide and 20 cm long were used to measure vertical and lateral motions. Dowels and spikes were inserted into the fine-grained centers of sorted circles to depths of 5 or 10 cm with an original spacing interval of 10 or 20 cm. These pegs were reset vertically each year after measuring the amount of heave relative to the soil surface. Painted or marked stones were used to measure lateral motions and were all at least 3 cm in length. Lateral displacements were measured each year, with markers not being reset to the original horizontal grid. The total movement of a marker over the five-year period was calculated as the sum of its annual displacements rather than the straight-line distance from its initial position to its end position.

Vertical and horizontal displacement of stones and markers showed considerable variability over the study period. Tables I and II present summaries of pattern activity for ten sorted circles from five different sites. Although a total of 29 circles from six sites have been studied over the five-year period, several have been disturbed, either naturally or by trenching and sampling activities. The tables show some of the variability which exists among patterns at different sites and even for the same pattern. The average vertical displacement of markers was approximately 1 to 4 cm per year, and maximum uplift was about 5 cm per year. It should be noted, however, that there was a great deal of variability, and sometimes some markers showed no vertical movement or even negative movement over a one or two year period. Over the five-year study period, however, all markers showed a total positive (i.e., upward) vertical motion. Comparison of movements between wooden dowels and metal spikes shows no clear trend other than the metal spikes showing a greater range in vertical displacements. A study comparing movements of different types of markers is currently underway. Horizontal displacement of markers averaged approximately 0.5 to 2.4 cm per year, with maximum movement of about 4 cm per year. Again, not all markers showed lateral movement each year, and the direction of movement was not always consistent from year to year. With few exceptions, the stones showed less horizontal movement than the dowels or spikes (Table I). It appears that, other factors being equal, the larger the object, the greater its resistance to movement.

Patterns at sites MS1, MS3, and HV8 show the most activity. These sites have also been consistently the wettest, being subject to seasonal ponding every spring. Measured in late summer, field moisture content of sediment in the fine-grained centers averages about 27% (weight % dry sediment) at a depth of 10 cm. Patterns at

TABLE I. Summary of Horizontal Movements, 1982-1987

	Wooden dowels and/or metal spikes				Marked or painted stones			
Circle	N	Mean total movement per marker (cm)[a]	Range (cm)	Mean rate of movement (cm/yr)	N	Mean total movement per marker (cm)[a]	Range (cm)	Mean rate of movement (cm/yr)
MS1[b]-2	18	9.61	2.2-17.8	1.92	10	6.53	1.3-12.6	1.31
MS2[c]-1	27	5.14	1.8-17.3	1.03	8	3.58	0.9-11.3	0.72
MS2-2	15	4.42	1.5-12.4	0.88	6	2.53	0.8-11.0	0.51
MS2-3	30	2.15	0.9-15.1	0.43	10	3.10	1.2-13.4	0.62
MS3[b]-1	25	8.60	1.9-18.2	1.72	9	6.10	1.5-15.6	1.22
MS3-2	23	12.05	3.4-20.5	2.41	10	9.60	1.9-18.3	1.92
MS3-3	20	11.50	3.1-17.9	2.30	10	6.75	0.8-16.5	1.35
MS4[c]-2	12	2.62	0.7-8.3	0.52	8	4.85	1.3-15.0	0.97
HV8[b]-1	20	10.55	1.8-15.8	2.11	8	9.00	2.1-14.7	1.80
HV8-2	32	7.30	1.3-16.2	1.46	16	5.65	1.8-15.5	1.13

[a]Determined by averaging sums of annual movements.
[b]Sites MS1, MS3, and HV8 subject to seasonal ponding.
[c]Sites MS2 and MS4 subject to seasonal wetting but no ponding.

TABLE II. Summary of Vertical Movements, 1982-1987

	Wooden dowels and/or metal spikes			
Circle	N	Mean total movement per marker (cm)[a]	Range (cm)	Mean rate of movement (cm/yr)
MS1[b]-2	18	19.30	4.7-26.3	3.86
MS2[c]-1	27	5.30	1.5-14.2	1.06
MS2-2	15	7.72	1.7-17.8	1.54
MS2-3	30	7.15	2.0-15.9	1.43
MS3[b]-1	25	11.82	1.9-21.5	2.36
MS3-2	23	16.85	2.8-19.7	3.37
MS3-3	20	16.25	2.1-20.6	3.25
MS4[c]-2	12	9.35	1.4-12.5	1.87
HV8[b]-1	20	20.10	3.6-28.5	4.02
HV8-2	32	15.65	3.0-24.4	3.13

[a]Markers reset vertically each year.
[b]Sites MS1, MS3, and HV8 subject to seasonal ponding.
[c]Sites MS2 and MS4 subject to seasonal wetting but no ponding.

these sites are unvegetated, although ocassional scattered sedges and/or mosses are found in the fines of some circles. Pattern centers show prominent upward convexity, and coarse borders are relatively high (Fig. 4). Sites MS2 and MS4, although quite wet in spring, have not been inundated at any time from 1982 to 1987. In late summer, soil moisture at a depth of 10 cm in circle centers averages about 17%, significantly lower than at sites subject to temporary ponding. Patterns support some vegetation, mostly mosses, scattered clumps of sedges, and ocassional willows to heights of 35 cm. Pattern centers are moderately convex upward, and coarse borders are relatively low (Fig. 5).

The summaries (Tables I and II) provide general information on sorted circle dynamics over the study period, but they do not show how movement varies depending on position within the circle. Figure 6 shows total vertical movement of markers for circle MS3-3 from 1982 to 1987. This circle is representative of the activity observed among the sorted circles in the study area. It can be seen that vertical displacement is greatest in the center of the fines, with the amount of surface heave decreasing in roughly concentric zones toward the coarse border. Figure 7 shows the horizontal displacement of markers observed at circle MS3-3. The arrows show only the starting point and the end point for the markers over the five-year period and do not include year to year variations in either direction or amount of movement. An overall pattern of radial motion is apparent, with markers moving outward from the center of the fines toward the coarse border.

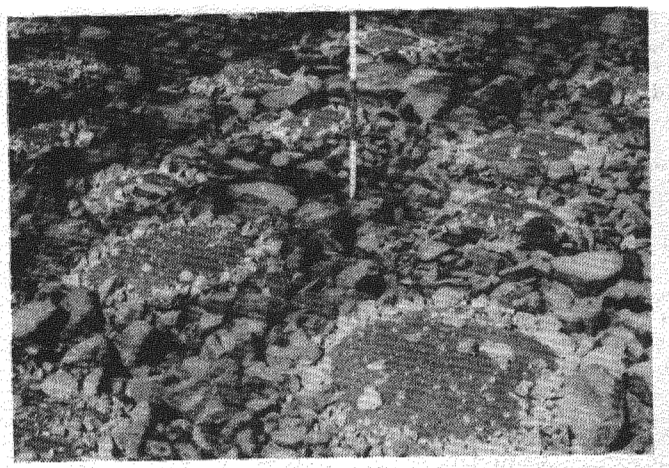

Fig. 4 Small sorted circles at site HV8, a site subject to inundation each spring. Note that the stones along the inside borders and those in the pattern centers show unstained surfaces. These stones have been recently exposed from within the fines and have not yet developed staining on their surfaces. The pole is in 30.5 cm divisions. Photo taken August 3, 1983.

DISCUSSION

The rates and directions of movement displayed by the markers in the fine-grained centers of the sorted circles show a general trend. Markers moved upward and radially outward from the pattern centers toward the coarse borders. Maximum uplifts were observed in pattern centers, and maximum lateral movements also tended to occur in pattern centers or at least near the centers. Most circles displayed no measurable activity within the coarse border areas. However, a few patterns over the five-year study period, showed uplifts of 0.5 to 3 cm for metal rods driven into the centers of the coarse

Fig. 5 Sorted circles at site MS2, a site subject to seasonal wetting but no ponding. The fine-grained centers display a nubby surface which is mostly covered with mosses and lichens. Scattered sedges and clumps of willows grow along the contact between the fines and the coarse border material. The soil probe is approximately 80 cm high. Photo taken July 27, 1982.

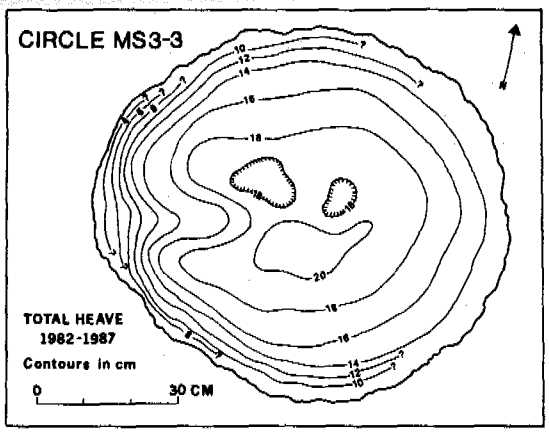

Fig. 6 Plan view of sorted circle MS3-3 showing contours of total heave of metal spikes from 1982 to 1987. Markers were reset each year after measuring the amount of vertical displacement relative to the soil surface. In general, the greatest surface heaves occur in the central portion of the circle and decrease toward the coarse border.

borders. In addition, repeat photography reveals that some stones moved laterally 1 to 2 cm as their orientation in the borders became more directly vertical.

Nicholson (1976) has suggested from his field observations of patterned ground forms that a combination of circulatory movement of fines and radial movement of stones occurs in the formation of sorted stone circles. Recent studies of sorted circles in Spitsbergen by Hallet and Prestrud (1986) seem to bear this out. They stress the importance of soil convection in the active layer and present field evidence and

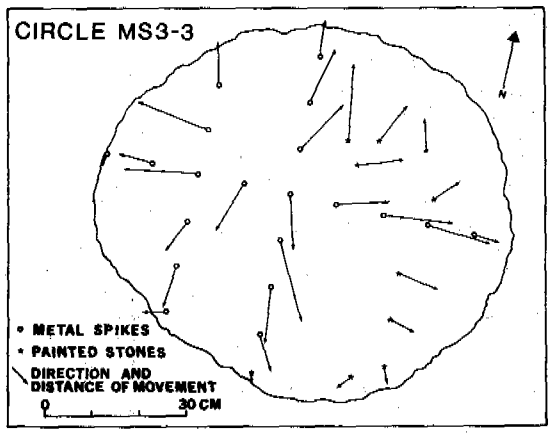

Fig. 7 Plan view of sorted circle MS3-3 showing total horizontal movement of markers from 1982 to 1987. Arrows show the starting point and end point for the markers over the five-year period. A radial pattern of movement is seen.

theoretical considerations which suggest intermittent convection of thawed soils. Although the High Valley sorted circles have not been studied during periods of spring thaw and fall freeze-up, the data on rates and directions of movement of markers, the thixotropic nature of the fine-grained sediment, and pattern size, geometry, and microrelief all support the possibility of soil convection in the active layer.

It is interesting to note that the wetter sites, MS1, MS3, and HV8, are more active than sites MS2 and MS4. The determining factor appears to be the temporary ponding which occurs in the former sites in the spring. Although the ponds disappear by late summer, the depressions still contain abundant soil moisture, which allows for considerable ice lens growth and frost heaving during seasonal freezing. In addition, the temporary cover of water at these sites prevents growth of vegetation on the patterns. A vegetative cover would inhibit, or perhaps even prevent, the formation and growth of the patterns (Jahn, 1966; Thorn, 1976; Rissing and Thorn, 1985).

Patterns at sites MS2 and MS4 have not been flooded in the spring during the study period. Inundation has probably occurred in the past, however, as indicated by the presence of benches, apparently representing former water levels, along the perimeters of the depressions. Because of the lack of temporary ponding, less moisture is available at these sites by late summer and frost heaving is limited. Also, some vegetation has become established on the patterns, thus inhibiting pattern activity even further. Vegetation consists predominantly of mosses, scattered clumps of sedges, and occasional willows and is located mostly at or near the contact between the fines and the coarse border material (Fig. 5). One would expect vegetation to become first established here, since pattern activity is at a minimum and sufficient fine-grained sediment exists for vegetative growth. If these sites were to again be subject to seasonal flooding on a regular basis, as sites MS1, MS3, and HV8 are, the vegetation would be destroyed and pattern activity would increase.

CONCLUSIONS

Sorted stone circles are common features of the periglacial environment in the High Valley region of central Alaska. They are best developed in depressions in Wisconsin-age silty tills. In spring many of these depressions fill with water or at least become very wet. The high moisture content along with the thixotropic nature of the fine-grained sediment promotes frost action processes in the active layer. From 1982 to 1987 sorted circles at six sites were monitored to determine their activity. Repeat photography and surveys of wooden dowels, metal spikes, and marked stones reveals that markers moved upward and radially outward from the fine-grained centers toward the coarse borders. Vertical and horizontal displacements were generally greatest in the central part of the circles and usually decreased toward the coarse borders. These observations, the low liquid limits and low plasticity indexes displayed by the fine-grained sediment, and information on pattern size, geometry, and microrelief suggest that soil convection is an important process in the formation and growth of these features.

Patterns at sites subject to seasonal ponding were more active than those at sites subject to seasonal wetting but no ponding. The temporary ponds disappear by late summer, but these sites still contain more abundant soil moisture than depressions not subject to ponding. The abundant moisture permits considerable ice lens growth and frost heaving during seasonal freezing. Because of the temporary ponding, these sites are also unvegetated, another advantage over sites not subject to ponding. The presence of even a partial cover of vegetation has an inhibiting effect on pattern activity.

ACKNOWLEDGMENTS

I would like to thank Troy L. Péwé, Jean-Claude Dionne, Lou Waller, and Kevin Meyer for providing helpful information and Bonnie Walters, Robert Starling, and Mary Jo Kuhlman for assisting with field work. I also thank three anonymous reviewers for comments on the manuscript. The Graduate College of the University of Northern Iowa provided partial financial support for this study.

REFERENCES

Ballantyne, C K & Matthews, J A (1982). The development of sorted circles on recently deglaciated terrain, Jotunheimen, Norway. Arctic and Alpine Research (14), 4, 341-354.

Ballantyne, C K & Matthews, J A (1983). Desiccation cracking and sorted polygon development, Jotunheimen, Norway. Arctic and Alpine Research (15), 3, 339-349.

Dionne, J-C (1974). Cryosols avec triage sur rivage et fond de lacs, Québec central subarctique. Revue de Géographie de Montréal (28), 4, 232-342.

Dionne, J-C (1978). Formes et phénomènes périglaciaires en Jamésie, Québec subarctique. Géographie Physique et Quat. (32), 3, 187-247.

French, H M (1976). The Periglacial Environment, 309 pp. Longman, London.

Hallet, B & Prestrud, S (1986). Dynamics of periglacial sorted circles in western Spitsbergen. Quaternary Research (26), 1, 81-99.

Jahn, A (1966). Origin and development of patterned ground in Spitsbergen. Proc. 1st Int. Conf. on Permafrost, 140-145, Washington, D.C.

Jahn, A (1975). Problems of the Periglacial Zone, (translated from Polish), 223 pp. plus photos, Państwowe Wydawnictwo Naukowe, Warsaw.

Nicholson, F H (1976). Patterned ground formation and description as suggested by low arctic and subarctic examples. Arctic and Alpine Research (8), 4, 329-342.

Péwé, T L (1961). Multiple glaciation in the headwaters area of the Delta River, central Alaska. U.S. Geological Survey Professional Paper 424-D, D200-D201.

Péwé, T L (1965). Delta River Area, Alaska Range. Guidebook for Field Conf. F, Central and South Central Alaska, Int. Assoc. Quat. Research, 7th Cong., 55-93, Nebraska Acad. Sci., Lincoln.

Péwé, T L (1975). Quaternary Geology of Alaska. U.S. Geological Survey Professional Paper 835, 145 pp.

Péwé, T L & Reger, R D (1983). Delta River Area, Alaska Range. Guidebook to Permafrost and Quaternary Geology Along the Richardson and Glenn Highways Between Fairbanks and Anchorage, Alaska. 4th Int. Conf. on Permafrost, 47-135, Div. Geological and Geophysical Surveys, Fairbanks.

Rissing, J M & Thorn, C E (1985). Particle size and clay mineral distributions within sorted and nonsorted circles and the surrounding parent material, Niwot Ridge, Front Range, Colorado, U.S.A. Arctic and Alpine Research (17), 2, 153-163.

Thorn, C E (1976). A model of stony earth circle development, Schefferville, Quebec. Proc. Assoc. Amer. Geographers (8), 1, 19-23.

Vitek, J D (1983). Stone polygons: observations of surficial activity. Proc. 4th Int. Conf. on Permafrost, 1326-1331, Washington, D.C.

Walters, J C (1983). Sorted patterned ground in ponds and lakes of the High Valley/Tangle Lakes region, central Alaska. Proc. 4th Int. Conf. on Permafrost, 1350-1355, Washington, D.C.

Washburn, A L (1969). Patterned ground in the Mesters Vig district, Northeast Greenland. Biuletyn Peryglacjalny (18), 259-330.

Washburn, A L (1980). Geocryology, 406 pp. Wiley, New York.

PATTERNED GROUND GEOLOGIC CONTROLS, MENDOZA, ARGENTINA

W.J.Wayne

University of Nebraska, Lincoln, Nebraska, 68588-0340

SYNOPSIS The Cordón del Plata (Cordillera Frontal) in the Province of Mendoza, with peaks from 5000 to 6000 m, extends well into the alpine periglacial zone; the mean annual 0°C isotherm, calculated from a lapse rate of 6.0°C/km, is about 3500 m. Precipitation is low and winds are strong, so that some parts of the range remain virtually free of snow throughout the year. Where granites and massive greywackes are exposed, rockfalls and landslides dominate the periglacial landforms. Gelifluction lobes, sorted circles, nets, and stripes have formed on phyllitic diamictons but are rare on debris from the more massive rocks. Active rock glaciers are common above 3500 m on shaded south-facing slopes but rare below 4000 m on those receiving greater sun exposure.

Strongly developed landforms above 4010 m around the Lagunita del Plata are relict, but patterned ground on the former lake floor from 4010 m to 3995 m probably is in equilibrium with a MAAT of -3°C.

INTRODUCTION

Efforts to determine paleotemperatures above Pleistocene ice cover in alpine regions depend primarily on the recognition of geomorphic features produced in specific temperature ranges (Harris, 1982; Wayne, 1983; Karte and Liedke, 1981) under conditions of perennially frozen ground, or permafrost. In order to evaluate relict permafrost indicators, though, it is necessary to determine the conditions, both climatic and geologic, under which similar features form today. Although many mountain ranges extend well above the level of the free air 0°C isotherm, patterned ground is not particularly common in alpine regions. Its presence or absence in a particular area depends on a combination of conditions of macroclimate, microclimate, slope inclination and orientation, soil moisture, and geology.

Few observational data are available for the Andean chain, so the average lapse rate, about 6.0°C/km, is used as a proxy in order to estimate a probable altitude for the 0°C mean annual isotherm. Microclimatic conditions, particularly wind eddys, radiation, and slope orientation, are likely to cause significant variations in the altitudinal temperature gradient (Harris and Brown, 1982; Barry, 1981, p.39-51). In addition to temperature, winter snow cover is a most important factor in determining whether or not permafrost and associated periglacial landforms may develop. A thick blanket of snow insulates the ground surface from the effects of cold winter temperatures, so that permafrost may not exist at all even though the mean annual air temperature of a particular site is considerably below freezing. In many alpine areas the snow cover is thick and the only places permafrost can develop are those where strong winds keep the surface blown free of snow (Granberg, 1973; Ives, 1973; Nicholson and Granberg, 1973).

The Cordón del Plata, part of the Cordillera Frontal in the Province of Mendoza, is a mountainous area with peaks between 5000 and 6000 m. On the east slopes of Cerro El Plata and adjacent peaks, in the headwaters of the drainage basins of Río Blanco and Arroyo de las Casas, the present mean annual 0°C isotherm, calculated from data from two meterological stations near the mountain front, is about 3500 m. Although gelifluction streams and lobes, and sorted stripes, circles, and nets do not require permafrost to form, their presence in a suite of landforms that includes active rock glaciers suggests the presence of at least sporadic permafrost (Wayne, 1983a; Trombotto, 1983; Ahumada and Trombotto, 1984). Nearly all of these features are above 3500 m, although a few rock glaciers extend lower. In late January of both 1983 and 1985, frozen ground was encountered at depths between 4000 and 4100 m in altitude. Shallow troughs that make a polygonal pattern cross some of the bouldery debris in one area near 4025 m, and thermal contraction polygons may exist, but it has not been possible to confirm the presence of ice wedges.

Even though much of the range is in the periglacial zone and it is a region of relatively low precipitation, most of the geomorphic features indicative of permafrost are common only where 1) strong winds regularly keep areas nearly free of snow, 2) the rock types disintegrate to diamictons that have a high percentage of fine-grained materials, and, 3) near the lower altitudinal limit of discontinuous permafrost, on shaded slopes.

GEOLOGIC SETTING OF CERRO EL PLATA AREA

The crest and upper slopes of the central part of the Cordón del Plata is composed of graywackes

and phyllites, low-grade metamorphic rocks of the Lower Carboniferous El Plata Formation (Caminos, 1965; Polanski, 1972). These rocks were intruded by granite and granodiorite of the Cuchilla de Las Minas Stock (Caminos, 1965), which underlies slopes between 4300 m and 3000 m along Ao. de las Casas and at Lagunita del Plata. Northward the intrusive contact drops in altitude. It is about 3300 m in Quebrada de los Vallecitos, where it is buried beneath glacial sediments and rock glacier debris. Volcanic rocks, principally rhyolites and quartz porphyries, also Late Paleozoic in age (Polanski, 1972), underlie the northern part of the Río Blanco basin, particularly the Qda. de las Morenas Coloradas (Fig.1). Glacially deposited sediments are present along the valley farther downstream. Morainal debris covers the valley floors of Qda. de la Angostura and Qda. de los Vallecitos to as low as 2600 m (Wayne and Corte, 1983); diamictons that resemble tills but were deposited by debris flows extend well out into the piedmont slope along Río Blanco (Polanski, 1966; Wayne, 1988). Dust layers in snowbanks are evidence that some of the fine-grained material in the surficial accumulations is loess.

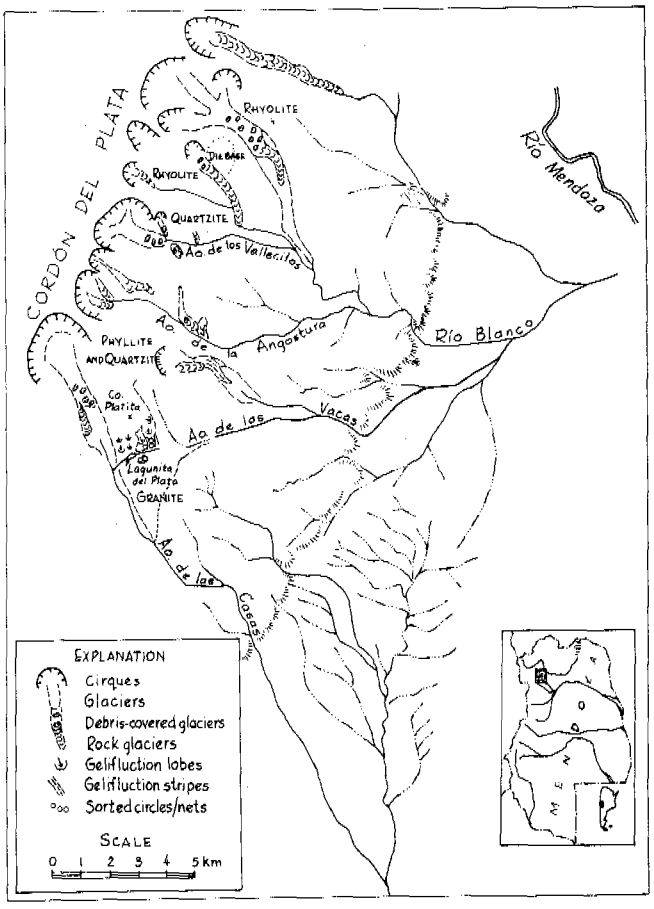

Fig. 1 Map of the part of the Cordón del Plata studied.

FEATURES INDICATIVE OF PERMAFROST

Rock Glaciers

The dry central Andes is a region characterized by small glaciers, the distal parts of which are mantled with debris and commonly display thermokarst pits (Corte, 1976). Rock glaciers include large, tongue-shaped features that develop at the termini of debris-covered glaciers, ice-cored moraines that flow downslope although isolated from the glacier front, and the smaller tongue-shaped and lobate features that form from mobilization of ice-cemented talus and rockfall debris. Only these small rock glaciers are true permafrost features.

All active rock glaciers in the area not associated with glacier ice are moving out from the bases of slopes that were glacially steepened during the most recent (Vallecitos=Wisconsinan) Pleistocene glaciation (Corte, 1957; Wayne, 1981b; Wayne and Corte, 1983). Both small tongue-shaped and talus rock glaciers have developed above 3500 m in altitude along steep valley walls, particularly on the shaded (south-facing) sides of the W-E and NW-SE valleys. At the same altitudes, most northward-facing valley sides are buried in scree; active rock glaciers observed along the northward-facing slopes are above 4000 m in altitude (Fig. 1). Corte (1953, p.36; 1955) noted similar relationships near Laguna Diamante, 125 km to the south; Espizúa (1983) has quantified the orientation of 139 rock glaciers in the Cordóns del Plata and Portillo.

Large tongue-shaped rock glaciers also extend downvalley from the distal end of many small debris-covered glaciers. Of the rock glaciers that have active frontal slopes, the most extensive in the part of the Cordón del Plata examined reaches 3300 m. It is a narrow (100-150 m across) tongue that emerges from talus along a SW-facing valley wall at the base of a debris-covered glacier and at an altitude of about 3700 m (Fig. 2). In its distal 100 m it has a

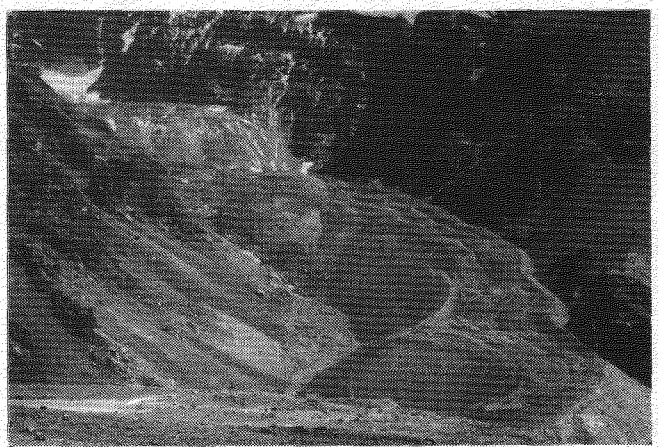

Fig. 2 Rock glacier in Qda. de Stepanek begins below a debris-covered glacier front and in the talus at the base of SW-facing cliffs at about 3700 m and flows as a long, slender stream through a debris embankment for about 1500 m.

surface slope of 11°. Although it is clearly below and beyond the modern debris-covered glacier in the valley above it, relict glacier ice may be present in the embankment beneath th rock glacier. Other active tongue-shaped rock glaciers in the Cordón del Plata area are at higher elevations. The larger ones evidently have developed from ice-cored lateral or terminal moraines after the main glacier had melted back from that position, although a few, particularly small ones along shaded valley walls, have extended downslope from masses of frozen talus above 3500 m (Fig. 3). Nearly all rock glaciers examined are covered with large blocks of rock, but the matrix of even the ones that have developed below cliffs of thick-bedded graywacke contains a significant amount of fine-grained material. These small ice-cemented rock glaciers are local zones of sporadic/discontinuous permafrost. Inasmuch as all the active ones are on sites above the altitude of the MAAT 0°C isotherm and are on shaded slopes, it is reasonable to assume a microclimatic regime of about -3°C or lower for them now.

Fig. 3 Small tongue-shaped talus rock glacier overlapping a Neo-glacial moraine; in left background, a rock glacierized ice-cored moraine (Qda. de los Vallecitos).

Gelifluction Landforms

Flowage of surface materials in regions of permafrost can take place on slopes with very low gradients (Washburn, 1980, p.204). The process tends to produce distinctive landforms, particularly gelifluction lobes, benches, and streams, (Washburn, 1980, p.219).

In the central part of the Cordón del Plata, most of the slopes underlain by granites are steep, between 40° and 20°, and are covered with frost-riven boulders and boulder-banked terracettes. Rockfall debris has accumulated at the bases of steeper slopes and cliffs. Where micaceous or phyllitic quartzites underlie the surface, closely-spaced gelifluction benches are the dominant form. These low grade metamorphic rocks disintegrate in the frost climate to yield much larger amounts of sand-and silt-sized particles than do granitic rocks, as well as coarse rubble. The long sloping ridge that extends eastward from the crest of Cerro Platita to the nearly flat trough of the Lagunita del Plata (4000 m) is covered with gelifluction benches. Near the base where the slope becomes more gentle, stone-banked lobes become the common form.

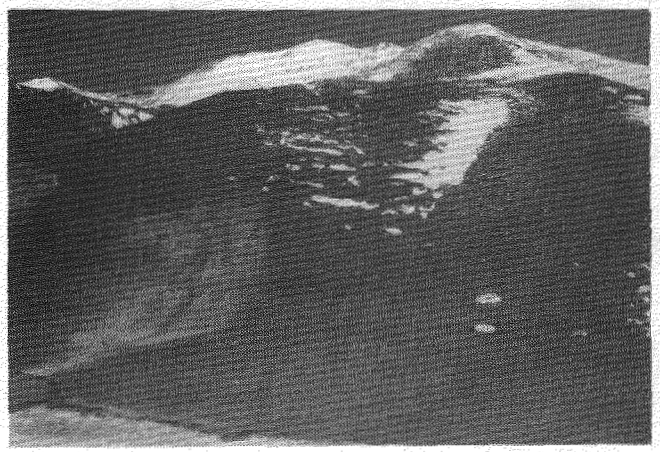

Fig. 4 Lagunita del Plata (3995 m), Cerro Platita, and gelifluction fan that is covered with several types of patterned ground.

On the slopes of 20° to 10°, gelifluction forms pass through a transition in which tread areas of fine grained material become larger behind sieve-like banks of quartzitic boulders. At lower slope angles, the areas of fine-grained debris dominate and appear more as a series of sorted circles than as the gelifluction lobes that they are. The slope is also marked by a shallow trough, through which both melting water runoff from snow and gelifluction have moved rock debris to build a fan at the base of the slope (Fig. 1, 4)

Between Co. Platita and Qda de la Angostura lies a small valley that is filled, from the broad cirque down, with a greenish gray diamicton composed mostly of micaceous quartzite debris containing relatively few coarse clasts. From the cirque floor down to 3800 m, the slope of the surface decreases from 15° to 8°, and the debris moves in gelifluction streams.

Fig. 5 Upper surface of rockslide mass of granite in fault trough that contains Lagunita del Plata, showing large scale patterned ground.

Patterned Ground

In the parts of the Cordón del Plata studied, patterned ground is rare except where the underlying materials consist of broken rock that includes a wide range of clast sizes. According to Goldthwait (1976), frost-sorted patterned ground develops only on diamictons that have a silt-clay content of at least 10% and at least 15% large clasts. He also indicated that the cell size or pattern width is governed by the sizes of the largest common clasts in the diamicton and suggested limits of between 1:5 and 1:10 for clast:pattern dimensions.

Most of the surface of the broad crest of the granite ridge that rises above 4300 m along the southeast side of the Lagunita del Plata is a blockfield covered with sub-angular boulders, none of which are arranged in recognizable circles or nets. A few circles 6 to 7 m in diameter have formed on the surface of an old rockslide at the base of the steep slope (Fig. 5), where the rock evidently was crushed so much in the slide that a large amount of silt-to-granule-sized clasts was formed. The sorted circles are at an altitude of about 4050 m and are not active now. The debris produced on the metamorphosed arenaceous and lutaceous rocks, however, seems to be much more susceptable to the development of sorted circles, nets, and stripes. A few sorted circles are present on the surfaces of moraines, but they are not abundant.

Active sorted stripes on slopes of 15° to 18° within the present permafrost zone were not observed in the area studied. One partly vegetated slope about 3500 m in altitude is covered with well developed stripes that are heavily lichen covered and surely not now active. The stripe-covered slope is underlain by metamorphic rocks and was above the edge of the ice tongue that filled the Qda. de la Angostura during the last glaciation.

A pattern that resembles sorted stripes stands out on the lower debris slopes of Co. Platita at the northwest end of the trough of Lagunita del Plata (Fig. 5). The stripes are on relatively gentle slopes of 2½° to 6° and the troughs are filled with progressively smaller clasts downslope, although the spacing seems to vary little. Although from above and from airphoto study these patterns look like sorted stripes, they are in reality a long series of sorted circles, each of which is slowly moving sownslope as a stone-banked lobe, each series bordered by and separated from the adjacent ones by a gutter filled with coarse clasts. At the lower end of the series, where the slope is only 2° to 3°, the dominant size of clasts bordering the circles/lobes is 10-15 cm; the circular centers are about 4 m across but have a sorted interior net pattern about 1.5 m across. Trenches through the circles show that the clasts along the downslope margin are being overridden by the migrating circle/lobe. The overridden clasts are 10-15 cm in diameter and provide a source of cobble-sized fragments to be re-sorted vertically to produce the interior nets, whose clast:pattern diamensions come close to the 1:10 value suggested by Goldthwait (1976).

The largest circles, those that are 4 to 6 m across, as well as large boulder-banked lobes and a polygonal trench pattern that crosses them are above a shoreline that formed at 4010 m when glacial ice blocked the lower end of the broad trough and it filled with water. These large scale features probably formed under conditions more severe than those today, perhaps continuous permafrost, and today are relict. Between this level and a weak strandline at 3998 m, sorted circles 3 to 5 m in diameter are well developed. From 3998 m to lake level (about 3995) sorted nets are small (1m) and weakly developed on massive sandy clayey silts of the old lake bed. The fine-grained part of the materials on the lower slopes, where patterned ground is most evident, was derived from disentegration of the phyllitic rocks of Co. Platita and from loess carried onto the mountain slopes by strong winds from the arid plains east of the cordillera. Bands of dust are common in the snowbanks above the lake, and most of the pollen in the sediments of Lagunita del Plata has come from plants living today at lower altitudes (Vera Markgraf, letter, Jan. 6, 1984)

The differences in patterned ground below the high strandline could be the result of either of two conditions:
1. The larger patterns between 3998 m and 4010 m could have formed at an earlier time under more severe conditions and be inactive today, but the small patterns just above lake level are in equilibrium
2. All features below the 4010 m level are in equilibrium with the present climate and the geological materials available. The lower circles, though, have formed where the largest clasts available are too small to permit larger patterns to form. Because the lake today is shallow (±1.0 m deep) and the bottom sediments are sandy and silty clay with few larger clasts, the second of these hypotheses seems the more likely.

Sorted circles, singly or in small groups, were observed on the nearly level upper surfaces of two rock glaciers in the Río Blanco basin, both above 4000 m in altitude. Sorted circles and nets on moraines and on outwash plain below that altitude are partly covered with vegetation and probably are not now active.

CONCLUSIONS

In the periglacial zone of the east slope of Cerro El Plata only a few landscape forms characteristic of permafrost have formed. They are abundant and well developed primarily where the surficial materials contain a wide range of clast sizes, the matrix of which includes both disintegrated phyllites and loess. Rock glaciers record the lower limits of sporadic permafrost. Many of the terracettes and stonebanked gelifluction lobes would lose their distinctive shapes, and, on collapsing, may look like sorted circles on slopes of 10° to 20°--surfaces too steep for the formation of sorted circles (Goldthwait, 1976). Stripes that terminate downslope in garlands probably would be correctly interpreted, but stripe-like patterns produced by downslope movement of circular stone-banked lobes that have a secondary interior net pattern may not be. Altogether, slope and geologic materials, as well as macro and microclimate, control the existance and type of periglacial landforms that

develop, a few of which, on collapse, may resemble a different feature and, thus be subject to misinterpretation by geologists trying to evaluate paleoclimatic conditions.

ACKNOWLEDGEMENTS

Field observations that are the basis for this report were made in 1980, 1983, and 1985 while I was visiting researcher with the Instituto Argentino de Nivología y Glaciología (IANIGLA) in Mendoza. Naomi Wayne worked as field assistant. The field work was supported by National Science Foundation Projects INT-79-20798 and INT-82-2349. Comments of 3 unidentified reviewers have aided in the revision of the manuscript.

REFERENCES CITED

Ahumada, A.L., and Trombotto, D. (1984). Estudios periglaciales en la Lagunita del Plata, Provincia de Mendoza. IX Cong.Geol.Argentino,(4), 2-34.

Barry, R.G.(1981). Mountain weather and climate. 313pp. Methuen, London.

Caminos, R.(1965). Geología de la vertiente oriental del Cordón del Plata, Cordillera Frontal de Mendoza. Rev.Asoc.Geol.Argentina, 351-392.

Corte, A.E.(1953). Contribución a la morfología periglacial de la alta cordillera con especial mención del aspecto criopedológico. Dept.de Inv.Cient., Univ.Nac.de Cuyo, Anales (1), 54pp.

Corte, A.E.(1955). Contribución a la morfología periglacial especialmente criopedológica de la República Argentina. Soc.Geog.Fenniae, Acta Geogr. (14), 83-102.

Corte, A.E.(1957). Sobre geología glacial Pleistocénica de Mendoza. Deptp.de Inv.Cient. Univ.Nac.de Cuyo, Anales (2), 1-27.

Corte, A.E.(1976). Rock Glaciers. Biul.Periglac. (26), 175-197.

Espizúa, L.E.(1983). Diferencia altitudinal del límite inferior de los glacieres de escombros activos entre laderas norte y sur de los cordones del Plata y Portillo, Provincia de Mendoza. Inst.Argent.Nivol.Glaciol.,An.(5), 79-87.

Goldthwait, R.P.(1976). Frost sorted patterned ground: a review. Quat.Res. (6), 27-36.

Granberg, H.B.(1973). Indirect mapping of the snowcover for permafrost prediction at Schefferville, Quebec in Permafrost, 2nd Internat.Conf.,N.Amer.Contri.,Nat.Acad.of Sci. 113-120, Washington, D.C.

Harris, S.A.(1982). Identification of permafrost zones using selected permafrost landforms, in French, H.M.,ed., Proc. 4th Canadian Permafrost Conf.,Nat.Res.Council of Candad, 49-58.

Harris, S.A. and Brown, R.J.E.(1982). Permafrost distribution along the Rocky Mountains in Alberta, in French, H.M.,ed., Proc. 4th Canadian Permafrost Conf., Nat.Res.Council of Canada, 59-80.

Ives, J.D.(1973). Permafrost and its relationship to other environmental parameters in a midlatitude, high-altitude setting, Front Range, Colorado Rocky Mountains, in Permafrost 2nd Internat.Conf.,N.Amer.Contrib.,Nat.Acad. of Sci.,121-125, Washington, D.C.

Karte, J. and Liedke, H.(1981). The theoretical and practical definition of the term "periglacial" in its geographical and geological meaning. Biul.Peryglac. (28), 123-135.

Nicholson, F.H. and Granberg, H.B.(1973). Permafrost and snowcover relationships near Schefferville, in Permafrost, 2nd Internat. Conf.,N.Amer,Contrib.,Nat.Acad.of Sci., 121-125, Washington, D.C.

Polanski, J.(1966). Flujos rápidos de escombros rocosos. Ed.Univ.de Buenos Aires,Manuales, 67pp.

Polanski, J.(1972). Descripción geológica de la Hoja 24 a-b, Cerro Tupungato, Provincia de Mendoza. Dir.Nac.de Geol.y Min., Bol.128, 114pp.

Trombotto, D(1983). Geocriología de la Lagunita del Plata. Inst.de Niv.yGlac.,An(5),149-156.

Washburn, A.L.(1980). Geocryology. 406 pp. Wiley, New York.

Wayne, W.J.(1981a). Ice segregation as an origin for lenses of nonglacial ice in "ice-cemented" rock glaciers. Jour.of Glaciol., (27), 506-510.

Wayne, W.J.(1981b). La evolución de glaciares de escombros y morrenas en la cuenca del río Blanco, Mendoza. VIII Cong.Geol.Argentino, (4), 153-166.

Wayne, W.J.(1983a). Paleoclimatic inferences from fossil cryogenic features in alpine regions. Permafrost, 4th Internat.Conf., Proc.Nat.Acad.Press, 1378-1383, Washington, D.C.

Wayne, W.J.(1983b). Geologic setting and patterned ground, Lagunita del Plata, Mendoza. Inst.Argent.Nivol.Glaciol., An (5),157-158.

Wayne, W.J.(1988). The diamictons of the Río Blanco basin, Cordón del Plata, Mendoza. Quaternary of S.Amer, and the Antarctic Penninsula, (6), (in press).

Wayne, W.J., and Corte, A.E.(1983). Multiple glaciations of the Cordón del Plata, Mendoza, Argentina. Palaeog.Palaeocl.Paleoecol., (42), 185-209.

LANDSLIDE MOTION IN DISCONTINUOUS PERMAFROST

S.C. Wilbur and J.E. Beget

University of Alaska, Fairbanks

SYNOPSIS An unusually large number of landslides occur in the sub-arctic discontinuous permafrost area of Hoseanna Creek basin in central Alaska. The slides (0.002 to 0.6km^2), form in weakly consolidated clayey sedimentary formations, and move predominantly as remobilized earthflows and disrupted translational slide blocks.

Average rates of motion between August 1985 to September 1987 ranged from 0.5 to 31.0 m/a (horizontal) and -.02 to -1.7 m/a (vertical). In all cases most of the observed motion (53-96%) occurred during 1985-86, and periods of no movement occurred on some slides, indicating non-steady motion.

Lithostatic loading of slides due to headwall retreat occurs primarily during the late winter and spring and reflects thermal degradation of permafrost. Major slide motion apparently occurs during spring and early summer when large amounts of liquid water become available; however, warm winters appear to reduce the magnitude of spring motion. Large summer rainstorms were observed to have relatively minor effects on motion.

INTRODUCTION

Hoseanna Creek basin (124 km^2) is located on the north flank of the Alaska Range between Fairbanks and Anchorage. The basin trends east-west parallel to the main structural grain of the region, and is drained by a small tributary of the northward flowing Nenana River. The mouth of Hoseanna Creek meets the Nenana River about 8 km north of the old Healy townsite (Fig. 1).

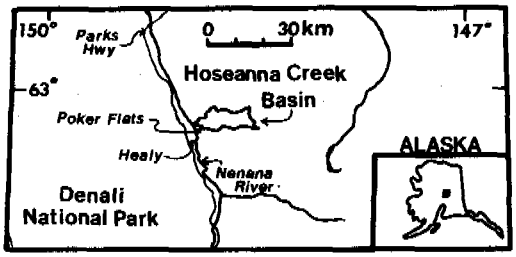

Figure 1. Location map. Hoseanna Creek basin is a small westward trending tributary of the Nenana River.

Photo geologic analyses and field studies suggest that many patches of discontinuous permafrost cover about 33% of the basin area (Fig. 2). Road cuts and drill holes indicate that in most places the permafrost is relatively thin (< 20 m), but in a few places it may be as great as 40 m. From the few available temperature profiles (Golder 1985; field studies, 1987), most of the permafrost appears to be isothermal or nearly isothermal at around -1.0 to 0.0°C. As a consequence the warm permafrost is readily susceptible to thermal degradation if disturbed.

Over 5% of the basin is covered by landslide deposits which range in size from 0.002 to 0.6 km^2 (Fig. 3); we estimate that about 90% of this size range are active. Much more of the basin is covered by smaller sized deposits resulting from mass wasting processes. Landsliding occurs as four different types (after Varnes, 1978): a) translational slides (from block to disrupted) which creep parallel to sedimentary bedding planes normally on clay horizons, b) earthflows as much as 1.1 km long, which typically begin flowing down dip but whose tongues often flow directly downhill across bedding, c) rotational slump blocks occurring where sedimentary bedding planes do not favor translational slide development, and d) complex slides exhibiting more than one of the above.

The purpose of this paper is to present results of an on-going study of landslide motion and evolution which is part of a broader study of short and long-term erosion rates. We would like to acknowledge the logistical and financial support and the use of field equipment and engineering facilities provided by the Usibelli Coal Mine, Inc. We are indebted to Ted Clarke for his valuable time spent as a field co-worker.

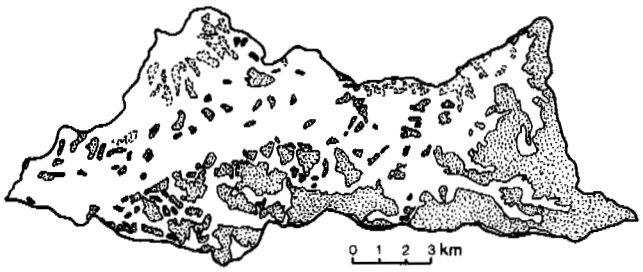

Figure 2. Permafrost map. Areas of permafrost as interpreted from aerial photography and based on vegetation type and field evidence. Dashed lines indicate areas of questionable permafrost.

Climate

The mean annual temperature for this region is -3.1°C, with an average January temperature of -18.3°C. Much of the year (early September to late May) is susceptible to frost activity, with about 165 days of below freezing temperatures, and about 80 days of freezing and thawing. Soil temperature conditions have not been monitored, so only inferences can be made from the air temperature data; in general, only the annual air and soil temperature data can be related with any success (Washburn, 1980, p. 70-73). Most of the precipitation (40 cm annual average) arrives during summer storms which commonly release 3-6 cm in one event. In addition, a significant amount of liquid water is available during spring thaw and break-up, which normally occurs in late May (Usibelli Coal Mine weather records).

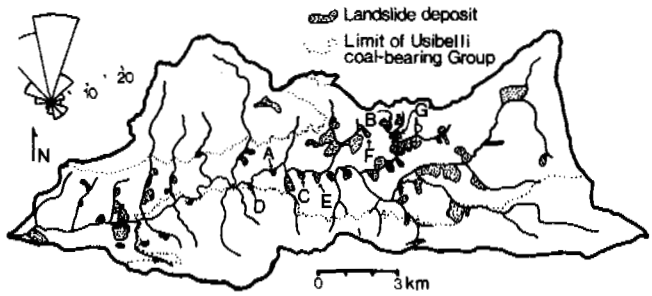

Figure 3. Landslide map showing areas covered by landslide deposits greater than .002 km^2, and the locations of surveyed slides A-G. Landsliding predominantly occurs in the Tertiary Usibelli coal-bearing Group (Wahrhaftig, 1970). The rose diagram in the upper left corner shows the preferred orientation of sliding or flowing motion.

Geology

The Usibelli coal-bearing Group (Wahrhaftig, 1987) consists of poorly consolidated sand, silt, clay and coal sequences that rapidly weather and disaggregate in the cold climate. The sedimentary formations are moderately deformed into broad folds and most of Hoseanna Creek basin lies on the north limb of a large faulted anticline. Typically, bedding planes dip 5-25 degrees to the north so that there are many north-facing slopes underlain by permafrost. Most of the landslides move downhill on north-trending slopes parallel to bedding planes and commonly on clay horizons (Fig. 3).

METHODS

A survey program was initiated in the summer of 1985 to monitor the annual motion of landslides. Seven different landslides of varying type and age were chosen (Fig. 3). On each slide several 1.2 m wooden laths were located in representative portions of the slide and then surveyed in with a precision of $\pm$0.03 m using an infrared edm theodolite. All the survey points were re-occupied during summers of 1986 and 1987. In some cases, slides were visited several times throughout the year to determine the time of year when most of the movement occurred. The frequency of survey measurements is low because this study is only part of a much broader study which focuses on long-term erosion rates.

In addition to the motion studies a brief on-site geologic description of each slide's terrain was made. The field studies described principle lithologies, attitudes of sedimentary bedding planes, surface features such as shear zones, crevasses, compressional ridges and furrows, scarp heights, and permafrost, if present.

RESULTS

Pattern of short-period motion

Displacement vectors and relation to topography and geology for seven monitored slides are shown in Figure 4, and a description of their basic characteristics is given in Table I. Hoseanna Creek is presently cutting across the toes of slides A, C, D and E, while slides B, F and G terminate in tributaries of Hoseanna Creek.

In most cases velocities within individual slides were fairly uniform, suggesting a component of translational-slide motion occurs in most slides. Disrupted translational sliding (Varnes, 1978) may be especially important in slides C, D and E, where field observations indicate large coherent blocks have fragmented into many disrupted independent blocks during downslope transit.

Earthflow processes (Keefer and Johnson, 1983) predominate in slides A and F, where rates of motion are highly variable throughout the slide and much field evidence precludes the possibility of translational

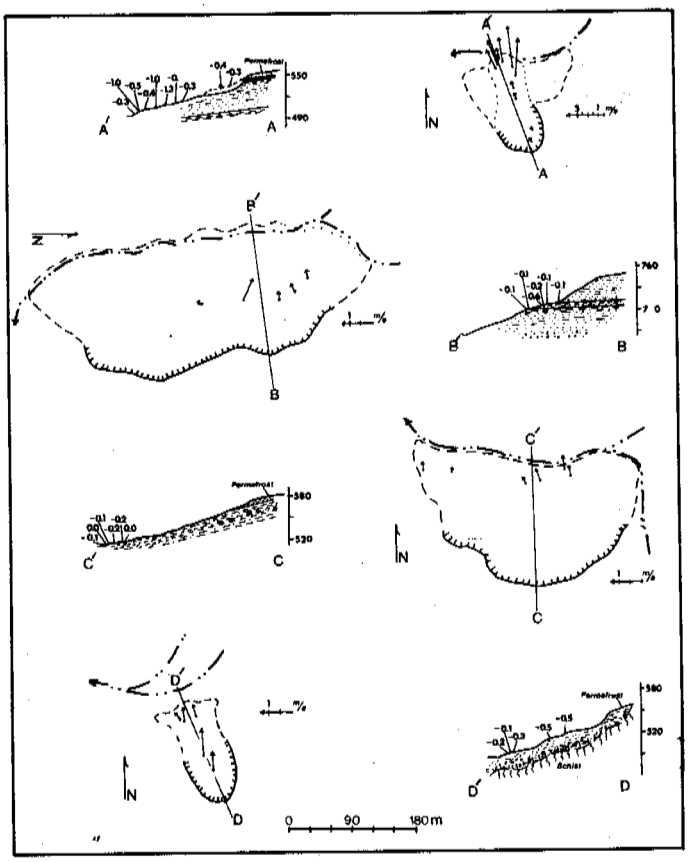

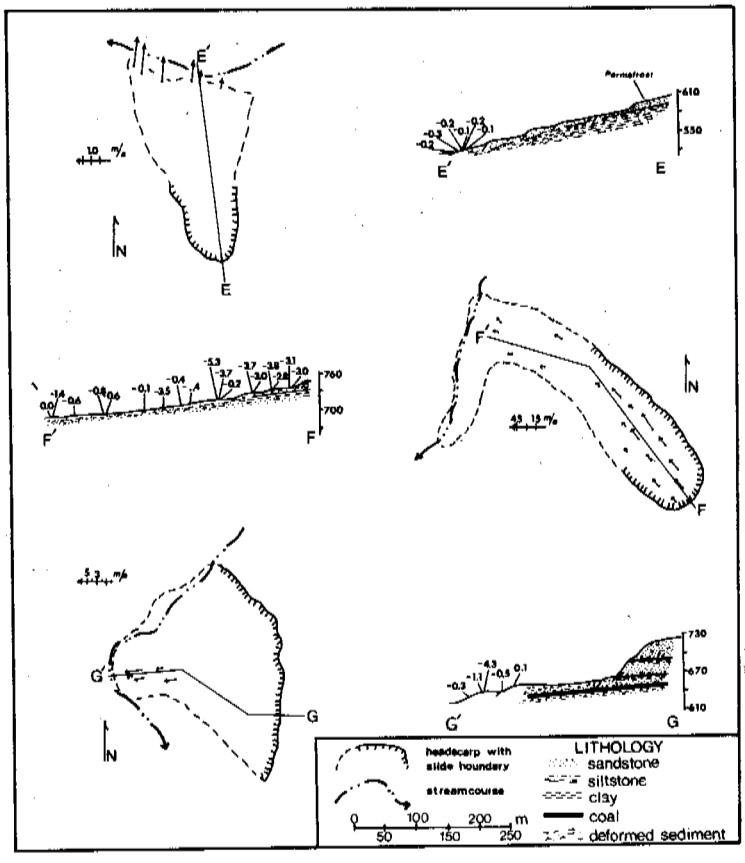

Figure 4. Plan views and longitudinal cross sections of the seven monitored slides A-G. No vertical exaggeration. Note scale for A-D is larger than for E-G. See Figure 3 for location of the slides. Average horizontal displacements shown by vector on plan views. Average vertical displacements (m/a) shown by numbers on longitudinal cross sections.

sliding being widespread. For example, in slide F upper basin motion was much greater than both the mid-slide area and the lower slide area; lateral spreading has occurred at the toes of slides A and F as indicated by the divergent horizontal displacement vectors (Fig. 4). In addition, lateral shear zones and lateral ridges extend up to one-half the slide length. On three separate occasions (June 1985, May 1986 and September 1987), the upper basin of slide F was covered by a large region of open cracks or crevasses which were perpendicular to movement in the center of the slide but became curved and concave downhill, finally intersecting the lateral shear zones at angles as high as 45 degrees. These cracks indicate that the upper part of the earthflows are subject to extensional stresses in which they are deforming by flowing rather than moving as a coherent block. In the lower slide area, furrows and ridges as much as 5 m in relief stand perpendicular to slope movement and correspond to a zone of compression and deceleration.

#	TYPE	COMPOSITION	DIP	PS	PERMA?	SURFICIAL CONDITIONS
A	earthflow	fine sands, silts, clay, coal fragments	15N	16	at scarp	young trees at toe only, mostly vegetationless
B	block slide, mudflows	sands, silts, coal fragments	2N	23	none	mixed forest, disturbed
C	disrupted translational	clay, silt	13N	15	at scarp	old stand mixed with saplings, mostly vegetated
D	block slide	sands, clay	15N	21	at scarp	all exposed except young trees at toe
E	disrupted translational	clay, silt	13N	14	at scarp	old stand mixed with saplings, mostly vegetated
F	earthflow	silts, clay fine sands, coal fragments	6N	12	possibly along east	almost all exposed, except grassy at toe
G	earthflow, disrupted block slide	sands, clay, coal fragments	6N	16	none	scattered old and young stands, some exposed

Table I. Landslide characteristics: TYPE - after Varnes (1978), DIP - slope of sedimentary bedding plane, PS - pre-slide topographic slope, PERMA? - location of permafrost if present.

A combination of earthflow and translational-slide processes was found for slides B and G. In these cases, the upper parts of the slides show zones of block-slide motion, while the lower parts are earthflows.

A summary of landslide motions for the seven slides is given in Table II. Average horizontal displacements ranged from 0.5 m/a on the lower portions of slide C to 31.0 m/a on the upper basin of slide F. The largest average horizontal displacements (44.8 m/a) were found on upper F during the period August 1985 to July 1986, where individual stakes were displaced from 33.3 to 59.1 m. Average vertical displacements ranged from -.02 m/a to -1.7 m/a from the same slides. In a few cases vertical displacements indicated thickening occurred at various times on the lower reaches of some slides.

SLIDE SECTION	NUMBER OF STAKES	PERIOD OF OBS.	AVG HOR. (m/a)	%85-86	AVG VER. (m/a)	%85-86	ERROR (m/a)
lower A	5	8/19/85 - 8/31/87	2.7	82	-0.45	57	± 0.05
mid A	3	"	4.0	83	-0.66	70	± 0.05
upper A	2	7/18/86 -	1.0	NA	-0.90	NA	± 0.04
mid(a) B	1	8/28/85 - 9/1/87	1.1	81	-0.60	75	± 0.13
mid(b) B	4	"	0.3	58	-0.11	26	± 0.13
mid(c) B	1	"	0.0	NA	-0.06	0	± 0.13
lower C	8	8/19/85 - 6/28/87	0.5	57	-0.02	55	± 0.05
mid and lower D	5	8/21/85 - 5/13/87	0.7	84	-0.35	64	± 0.05
lower E	6	8/19/85 - 10/12/87	0.9	?	-0.27	?	± 0.05
lower F	7	8/20/85 -	4.6	96	-0.95	100	± 0.10
mid F	4	8/20/85 - 9/1/87	10.3	53	-0.52	41	± 0.06
upper F	9	"	31.0	71	-1.70	68	± 0.04
lower G	5	8/28/85 - 9/1/87	2.0	75	-1.20	72	± 0.13

Table II. Summary of landslide motion for seven slides. The percentage of motion observed during the first year (%85-86) is given.

Analysis of movement histories

The limited data set we have available indicates that substantial differences in the rate of slide displacement occurs in different seasons, and between different years. For all the surveyed slides, displacements that occurred from summer 1985 to summer 1986 were significantly greater than the amount of movement which occurred from summer 1986 to summer 1987 (Fig. 5). The percentage of total horizontal displacement measured during the first period (1985-86) ranged from 53% to 96%, while as much as 100% of the vertical displacements occurred during the 1985-86 season. In addition to the large year-to-year variations in displacement, we have observed lengthy periods of total inactivity. No movement took place on the slide A from July 18, 1986 to April 5, 1987 and on slide F from May 15, 1987 to July 10, 1987. The other slides were not surveyed frequently enough to discern periods of non-motion.

Water availability

Precipitation and temperature records (Usibelli Coal Mine weather records) were reviewed to identify possible relationships between rainstorms and slide movement, a connection readily made for earthflows in temperate areas (Keefer and Johnson, 1983).

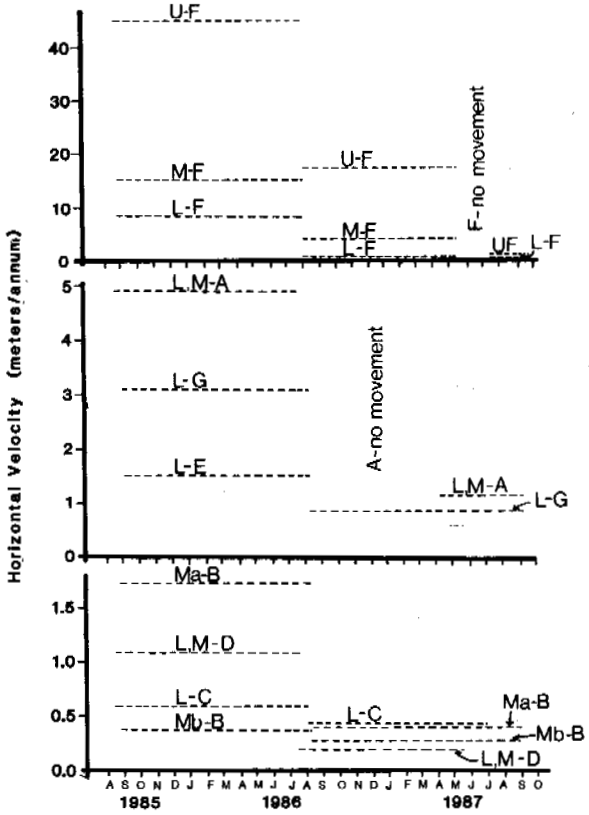

Figure 5. Pattern of horizontal motion between 8/85 - 9/87. Average movement (m/a) for a section (U = upper, M = mid, and L = lower) of slides A - G is shown for each time interval between surveys.

Figure 6 shows variations in monthly precipitation, number of days above, below and of freeze-thaw for each month. The data suggests that there was an unusually warm winter and spring during 1986-87. During February - May 1987, many days of above freezing temperatures as well as freeze-thaw days occurred. Winter field observations indicated that in many places the snowpack had totally melted before more snow occurred. Conversely, the winter of 1985-86 was normal, and the snowpack remained largely intact until May, when most of it melted.

May 1985-86 was an exceptionally wet month (4.6 cm compared to May average of only 0.6 cm), but otherwise monthly precipitation records are similar for 1985-86 and 1986-87. Two large rainfall events occurred in late July (6.6 cm in 24 hrs) and late August (7.3 cm in 72 hrs) 1986. These events did not cause any motion in slide A, one that normally moves fairly rapidly. In addition, slides B, D, E and G were all surveyed prior to the August storm. Only minor movements were recorded by the next survey. Slide F was surveyed after a minor storm July 30, 1987 (3.5 cm in 24 hrs), but only minor movements were detected after the storm.

When slide F was visited in early June 1985 and late May 1986, its upper basin was crossed by large extensional cracks; a "bergschrund" had developed as the upper slide material moved away from scarp talus. These features indicated very recent movement. By mid-summer, in spite of several large rainstorms, these features had mostly disappeared. Indeed, the summer rainstorms generally eroded the fresh flow features developed in the spring. In May 1987, the slide surface again showed evidence of very recent movement. The substrate was probed by a metal rod and it was found that the sediment was entirely frozen about 30-60 cm below the surface even though a large crevasse field covered the entire upper basin.

In summary, major differences in weather conditions between the Feb-May 1986 and Feb-May 1987 are related to major differences in springtime slide motion. In addition, from August 1985 to September 1987 the majority of movement occurred during late springs and early summers, while only minor movements occurred later in the summers despite large rainstorms.

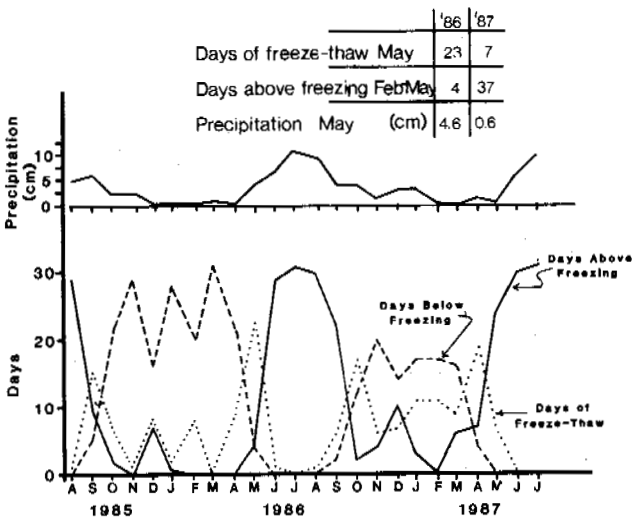

Figure 6. Monthly precipitation and temperature records for Poker Flats (see Figure 1 for location).

DISCUSSION

The reasons for the annual and seasonal differences in earthflow/slide motion, and the apparent insensitivity of the earthflows to major summer rainstorms are not obvious. Most models of earthflows envision a direct connection between precipitation and motion (Keefer and Johnson, 1983). However, seasonal earthflow motion in a sub-arctic climate may reflect additional processes. First, the slides require a continual supply of sediment from headscarp retreat. Headscarp erosion appears to be accelerated during the winter and spring when freeze-thaw

processes are most efficient. Thus lithostatic loading of the upper slide will occur through the winter and spring, when most of the slide's skin (presumably the top 2-3 m) is frozen (Hutchinson and Bhandari, 1971). Second, stream erosion and debuttressing of the toes of landslides is very active in spring. Streams carrying away snowmelt can periodically flow on the aufies 1-2 m above the summer channel, resulting in an especially efficient means of lateral erosion. In addition, the thick aufies may serve as an effective buttress during the winter, but as it melts away in the spring much of the landslide's toe support is removed. Furthermore, as indicated by the local climate data, movement appears to be influenced by spring water availability and winter temperature.

Although the soil conditions (e.g., temperature, ice content, water pore pressure) were not measured, the timing of motion and climate data allows us to suggest that the observed seasonal variation in motion also reflects seasonal variations in the rheology of the earthflows. Throughout winter the slide mass freezes downward. In the spring the slide mass begins to thaw and produces an open soil fabric with low mechanical strength. At this time large amounts of water are introduced from rain and/or snowmelt. The earthflows are easily mobilized when the water has infiltrated the open fabric producing high pore pressures. Later in the year, motion and thaw consolidation has remolded the clayey material giving it greater mechanical strength, so that late season rainstorms have only minor effects on motion.

SUMMARY OF MOTION AND DEVELOPMENT

Several processes operate in most of the slides in the Hoseanna Creek basin, including all the surveyed slides. These include:

1) Lateral corrasion or headward incision by streams cut the vegetative protection of the frozen sedimentary substrate that is dipping downslope, and oversteepens the slope. The oversteepening initiates downslope creep; extensional cracking develops upslope and exposes the frozen sedimentary substrate to thermal degradation.

2) Weakly consolidated sandstone and silt fracture parallel to scarp walls. Winter and spring freeze-thaw processes operate in the cracks and cause large frozen sediment blocks to fall to the upper basin, where they disaggregate quickly into a chaotic jumble. In some cases, the sediment blocks remain coherent for short distances while they slide away from the headscarp.

3) During spring, slide material thaws to create structurally weak soil fabrics. Liquid water readily saturates the loose material. In addition, thick aufies is quickly removed effectively debuttressing the slide toe.

4) Local pore pressures rise in the clayey material, reducing shear strength and initiating movement. In some places, coal beds act as aquifers and may introduce groundwater into the slide.

5) During spring and early summer the earthflows are especially prone to flow, and undergo rapid basal and lateral shear, forming extensional crevasses perpendicular to movement in the upper basin and compressing older slide material into large hummocky furrows and ridges at the toe of the slide.

6) Later in the summer high pore pressures are dissipated. The clayey materials develop higher shear strengths and show only small displacements during large rainstorms.

REFERENCES

Golder (1985). Stability analysis of north facing spoil slopes at Poker Flats, prepared for Usibelli Coal Mine by Golder Associates, Inc., Anchorage, AK, Report 853-5016, 22 pp. plus figures and appendices.

Hutchinson, J. N. and Bhandari, R. K. (1971). Undrained loading, a fundamental mechanism of mudflows and other mass movements. Geotechnique (21), 4, p. 353-358.

Keefer, D. K. and Johnson, A. M. (1983). Earth flows: morphology, mobilization, and movement. United States Geological Survey Professional Paper (1264) 56 pp.

Usibelli Coal Mine weather records. Daily temperature and precipitation 1979 - 1987 for Poker Flats, Usibelli Coal Mine, Healy, AK.

Varnes, D. J. (1978). Slope movement types and processes, Chapter of Schuster, R. L., and Krizek, R. S., eds.; Landslides: Analysis and Control, United States National Academy of Sciences, Transportation Research Board Special Report (176), p. 11-33.

Wahrhaftig, C. (1970). Geologic map of the Healy D-4 quadrangle, United States Geological Survey Map, series GQ-806.

Wahrhaftig, C. (1987-in press). The Cenozoic section at Suntrana, Alaska: Contribution for the Geological Society of America, Decade of North American Geology, Centennial Guide, Cordilleran Section, Vol. 1.

Washburn, A. L. (1980). Geocryology, 406 pp. Wiley, New York.

THE CHARACTERISTIC OF CRYOPLANATION LANDFORM IN THE INTERIOR AREA OF QINGHAI-XIZANG PLATEAU

Zhang, Weixin, Shi, Shengren, Chen, Fahu[1] and Xu, Shuying[2]

[1]Lanzhou University, China
[2]Suzhou Railway Teachers College, China

SYNOPSIS This paper discusses the characteristics, origin, and evolution of the cryoplanation landform of the Qinghai-Xizang Plateau, based on field investigations. There are two belts geomorphologically, namely the cryoplanation belt at high position and the depositional belt at the lower part of slope of the Tanggula Mountain. Based on the evidences of periglacial landforms, it could be concluded that there was a more rigorous climate in late Pleistocene, and the cryoplanation terraces might be formed at that time.

HISTORICAL REVIEW

The cryoplanation landform is a degradation feature developing in high mountains under cold climate condition. It is a special bedrock feature, step-like or terrace-like, in slope development process, but it is not formed by river.

As early as 1890, the cryoplanation features have been studied in some detail by Russian scholars and the term 'goletz' terrace has been commonly used. One of the earliest references to cryoplanation terraces is by N.M. Kozmin; and their occurrence was noted in such areas as the northern Urals and Siberia. At the beginning of the 20th century, the differential erosion at high mountains in Yukon territory, Alaska has been discussed by D.D. Cairnes. Afterwards, in 1916, the term 'altiplanation' was devised by H.M. Eakin to signify a range of cold-climate processes and their effect in producing a distinctive assemblage of landforms. In 1946, K. Bryan introduced the term 'cryoplanation' to describe the combined effect of degradation by frost action and the subsequent removal of waste by downslope movement. During the past 80 years, there are many reports on cryoplanation landforms from Alaska, Europe and Asia (Embleton and King, 1975; Reger and Péwé, 1976).

A great deal of work of the origin, characteristics and distribution of periglacial landforms have been made by Chinese geologists and geomorphologists, few of them were related to cryoplanation terraces (Deng et al., 1983; Qiu et al., 1983). In this paper, the authors would like to discuss the characteristics, origin of the cryoplanation landforms in the Tanggula Mountain of Qinghai-Xizang Plateau, based on field observations.

THE PRINCIPAL CHARACTERISTICS OF CRYOPLANATION LANDFORM IN TANGGULA MOUNTAIN OF QINGHAI-XIZANG PLATEAU

The Kunlun Mountain, Tanggula Mountain and the Nyainqentanglha Mountain are the three major ranges on the Qinghai-Xizang Plateau. They are westwards extending, generally 5,700 m to 6,000 m in altitude with a difference in height ranging from 1,200 m to 1,500 m. The plateau between mountains is about 4,500 to 5,000 m a.s.l., with a difference in height of about 300 to 500 m. These areas have undergone several warm and cold cycles from Tertiary to Quaternary. Since late Pleistocene, the plateau was mainly in a periglacial environment. The recent glaciation is confined to high mountains.

The continuous plateau-permafrost extensively distributes in the area from the Kunlun Mountain at the north to the Tanggula Mountain in the middle. The extensive (Qiangtang) plateau between the Mt. Tanggula and Mt. Nyainqentanglha is underlain by island permafrost and taliks. Bedrocks expose at uplands, where the ground surface is rather gentle, and the lowlands are generally covered by debris material. The recent periglacial processes are dominat all over this region. Geomorphological processes on the plateau include the cryoplanation, mass movement, frost heave, frost sorting and thermokarst process. Each of them can be subdivided into some microforms. Most of these periglacial landforms have been reported, and this paper is concentrated to the cryoplanation forms at the Liangdaohe area in the southern slope of Tanggula Mountain, taking the observed cross section near the Station 122 of the Qinghai-Xizang Highway as an example (Fig.1).

As shown in Fig.1, two geomorphological belts can be recognized:

A. erosion-denudation belt. This may be divided into four sections from hilltop down to the piedment. A_1. cryoplanation hilltop at about 5,000 to 5,200 m a.s.l. with a rounded summit, bedrock exposure, a slightly relief terrain and a thin weathered block mantle. It is the first class (the highest) deplanation surface, and has undergone the erosion-denudation process since Tertiary period and the periglacial pro-

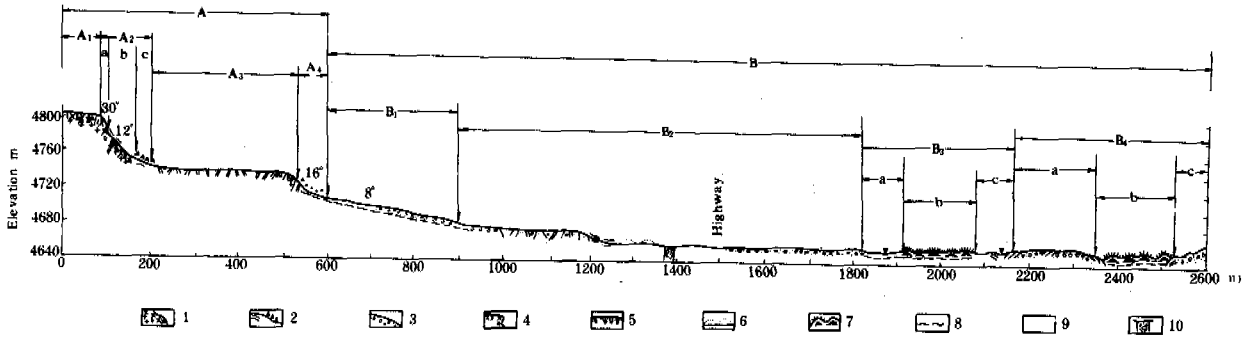

Fig.1 Cross Section, Actually Measured, Near the Station 122 of the Qinghai-Xizang Highway

1. granite; 2. block deposits; 3. debris deposits; 4. scarp formed by frost action; 5. crack-polygons; 6. eolian sand dunes; 7. ice-cored mounds; 8. ground ice; 9. slope gradient; 10. artificial cutting.

A. erosion-denudation belt: A_1: cryoplanation hilltop; A_2. frost weathered bedrock cliff; a. surface of bedrock; b. gelifluction slope; c. debris-block slope; A_3. cryoplanation terrace; A_4. gravitational depositional slope; B. depositional belt: B_1. slope-wash and pluvial piedment; B_2. pluvial-alluvial plain; B_3. alluvial plain; a. ponded depression; b. ice-cored frost heaving mounds; c. ponded depression; B_4. pluvial fan upland: a. wale; b. ice-cored frost heaving mounds; c. wale.

cess since late Pleistocene. A_2. bedrock cliff. The upper part is subject to frost weathering and the lower-the deposition of debris. Both these two processes promote the parallel retreat of the slope. The rock cliff is sawtooth-like and distributes at about 4,750 to 4,880 m a.s.l. with a slope of 28° to 30°. It becomes gentle downslope with solifluction lobes. A_3. cryoplanation terrace. This is a step-like terrace at about 4,720 to 4,740 m a.s.l. about 8° in slope, 400 m in length, with a bedrock headwall and a thin debris mantle. A_4. gravitational depositional section. It is 16° in slope. Many weathered blocks, 25 to 30 cm in diameter, were deposited on this section ahead of the terrace. Solifluction occur in the lower part.

B. depositional belt. It can be diveded into four sections morphologically: B_1. slope-wash and pluvial piedment. This is a detrital depositional belt 8° in slope and 800 m in length, composed of blocks and debris material, and is cut in shallow ditches by melt water. B_2. the pluvial-alluvial incline plain at the margin of the section B_1. It is gentle in slope with a slight relief. Some eolian sand dunes and hummocks develop on ground surface. B_3. the alluvial plain section. The melt water comes together into depressions; frost heaving, ice-cored mounds and thermokarst depressions are well-develop. B_4. upland of pluvial fan. It consists of bedrock and coarse materials. Ice-cored mounds are well-developed in depressions.

ORIGIN AND CHRONOLOGY OF CRYOPLANATION LANDFORMS

On the basis of fieldworks in the interior and western Alaska, Péwé and Reger strongly supported a terrace-forming model in which scarp retreat cuts the stepped profiles in bedrock and demonstrated that it is (was) products of periglacial environment and can be an indicator of permafrost. Several mechanisms working together and in succession accomplish the removal of the products of nivation, including mass movement, frost action and gelifluction etc. A shallow permafrost table is buried in debris as the base level plane of nivation,thus, the scarps becames retreat gradually, the hilltop and slope becomes gentle, and a step-like landform can be developed. It was estimated by Péwé and Reger that the cryoplanation landforms were formed in cold environment with a mean annual air temperature of -12°C and a mean air temperature in summer of +2°C to +6°C, under which it is cold enough and the frequence of freeze thaw cycle is high on the surface and the snow patch existing a long time is available for the planation.In Péwé's opinion, most of the cryoplanation terraces are inactive today because the bedrock exposure on the scarps and blocks on the terrace are not fresh. They suggested that the cryoplanation terraces in mountains in interior and southern Alaska were formed during the period from 10,000 to 35,000 yr. B.P. (Reger and Péwé, 1976; Péwé and Reger, 1981).

According to the bases of paleo-cirques at Tanggula Mountain, it is estimated that the snowline during late Pleistocene was at about 5,100 to 5,200 m a.s.l., by 200 m lower than the present one (5,400 m) (Xu et al., 1981). Thus,the mountains at Liangdaohe area at about 5,000 to 5,200 m a.s.l. were around the snowline during Last Glaciation. Hence the nivation depressions developed widely. The typical one distribute at north-facing slope at this area. The greatest nivation deprossion is about several hundred meters in diameter near the Station 120

of the Qinghai-Xizang Highway. The external part of the depression has bedrock exposure, similar to a rock dam. Another well-preserved nivation depression occurs at about 5,100 m a.s.l. of the Totodunzai mount, southern part of the Fenghuoshan.

The giant polygonal patterns were well-developed at both the southern and northern slopes of Tanggula Mountain, 50 to 100 m in diameter (Xu et al., 1981; Zhang et al., 1983). This indicates that the mean annual air temperature at late Pleistocene was about -6°to -8°C at the slope, and it must be much colder at higher position.

Nowadays, the Tanggula Mountain and its southern slope are still in a periglacial environment. It is reported that in the Anduo County, the mean annual air temperature is -3°C, the mean summer air temperature is 7° to 8°C and the precipitation is about 300 mm a year. The snow patches are much smaller than before.There are some active periglacial landforms, such as the small rock cicles, polygons, solifluctions and frost heaving mounds. Island permafrost is still developing. However, since it is not cold enough in winter time, those cryoplanation terraces formed in late Pleistocene are no more active.

In the Fenghroshan area, north of Mt. Tanggula, the mean annual air temperature is -6.7°C, and the mean summer air temperature is about 8°C. There is continuous permafrost. Nivation depressions with a narrow scarp develop on north-facing slope along the counter line. The frost weathering of bedrock on hilltops is still strong, and the mean summer air temperature is about 8°C. There is continuous permafrost. Nivation depressions with a narrow scarp develop on north-facing slope along the counter line. The frost weathering of bedrock on hilltops is still strong, and the bedrock surface is rather fresh. It seems that the cryoplanation process is still slightly active there.

The present geomorphological framework of the Qinghai-Xizang Plateau were formed during late Tertiary to Quaternary period. The lowest class of planation plane on the plateau is now up to an elevation of 4,500 to 5,200 m. It was subject to four cold stages and three warm stages alternatively. The combined effect of cryoplanation and stream erosion has deeply reformed the landforms. Based on the evidence of periglacial landforms mentioned above, it could be concluded that there was a rigorous climate in late Pleistocene, and probably the cryoplanation terraces might be formed at that time.

REFERENCES

Deng Yangxing and Deng Xiaofeng, (1983). Characteristics of periglacial landforms in Bogda area, Tian. Journal of Glaciology and Cryopedology, (5) 3, 179-190.

Embleton, C. and King, C. (1975). Periglacial geomorphology. Edward Arnold, 203.

Péwé, T.L. and Reger, R. (1981). Cryoplanation Terraces. Proc. Symposium on Qinghai-Xizang (Tibet) Plateau (II), 1789-1794.

Qiu Guoqing, Huang Yizhi and Li Zuofu, (1983). Basic characteristics of permafrost in Tian Shan, China. Proc. 2nd National Conference of Permafrost, 21-29.

Reger, R. and Péwé, T.L. (1976). Cryoplanation terraces: indicators of a permafrost environment. Journal of Quaternary Research, (6) 1, 99-109.

Xu Shuying and Zang Linyuan, (1981). A geomorphological analysis of ages and amplitudes of the Tanggula Mountain uplift. Science Press, pp.64-77.

Zhang Weixin,(1982). Polygonal soil along the Qinghai-Xizang Highway. Journal of Glaciology and Cryopedology, (4) 3, 77-80.

Zhang Weixin, et al., (1983). The periglacial of the late Pleistocene along the Qinghai-Xizang Highway. 4th Proc. 4th International Conference on Permafrost (I), 1484-1489.

THE PREDICTION OF PERMAFROST ENERGY STABILITY

L.A. Zhigarew and O.Yu. Parmuzina

Faculty of Geography, Moscow State University, Moscow, USSR

Evaluation and prediction principles of permafrost energy stability of the northern natural complexes on the example of West Siberian tundra and wooded tundra are substantiated. The methods of energy stability estimate and determination under natural conditions and technonogene action are proposed, changes for the year 2000-2009 are predicted.

Permafrost and the enclosing underground ices form northern geosystem lithogenl basis, the state of which is determined by energy stability. The equilibrium index of the earth's crust under modern climatic conditions is the stability of rock annual temperature at the extinction layer base of its annual oscillations.

The energy stability of the northern natural complexes is the established equilibrium state between summer heat supply into ground and summer heat discharge from it. In this case, if such equilibrium is upset then one of the two variants of the energy rock unstability generation is possible: permafrost heating and thawing or cooling and freezing of unfrozen rocks, i.e. in the first variant unstable appears to be first of all, seasonally thawing layer (STL) and upper horizons of permafrost rocks (PFR), and in the second - seasonally frozen layer (SFL) and upper horizons of unfrozen grounds. As follows from the above, to increase permafrost energy stability is possible by reducing possibility of depth thawing increase and then by reducing the possibility of freezing depth increase of unfrozen grounds.

To judge the permafrost energy stability of northern natural complexes, the formula of the estimate of heat flow formed in the generation of infiltration melt was used. (Principles of permafrost forecast..., 1974). The heat flow necessary for the increase of mean annual ground temperature at the base of STL to 0°C and expended at PFR upper horizon thawing is taten as a measure of energy stability:

$$Q = \frac{\lambda_{as} |t_\xi| \cdot T}{\xi} + Q_{ph}(\xi_p - \xi) \quad \text{where}$$

Q is summary heat flow, kcal/m^2 a year; λ_{as} - the assumed heat conductivity coefficient, kcal/m an hour grad; t_ξ - mean annual temperature at the base - of STL, °C; T - period of time hour; ξ - seasonal thawing depth; ξ_p - potential freezing depth, m; Q_{ph} - phase transformation heat, kcal/m^3..

The cited heat conductivity coefficient, phase transformation heat, seasonal thawing depth and potential freezing were determined after V.A.Kudryavtzev's formulae and nomogrammes (Principles of permafrost forecast..., 1974). The value of t_ξ was determined after V.P. Chernyadjev's nomogramme (Chernyadjev and others, 1984). It should be noted that V.P. Chernyadjev determined the value to, and not t_ξ, but in the southern regions of the north of West Siberia they practically do not differ from each other and in the northern regions the difference is equal to the tenth fractions of a degree, having to practical significance for the subsequent calculations.

The calculations on the determination of heat flow Q value were performed for 25 regions for different geological genetic deposits of all geomorphological levels of the north of West Siberia taken from the scheme of cryolitological regional division, Yu.Badu and V.T.Trophimov (Trophimov and others, 1980). Data on the background of heat flow value under the natural conditions were obtained based on the calculated value, according to which the corresponding map was compiled (Fig.1a).

The values of natural Q_e heat flow decrease in this region from north to south. The zonal character of the change is connected almost exclusively with that part which results in mean annual temperature increase at the base of STL to 0°C. From north to south this part of the heat flow decreases from hundreds to tens and even units of hundreds of kilocalories per a square metre a year. Another part of Q_e, expended on the thawing of PFR upper horizon to the layer base of potential freezing is mainly connected with the icy deposits, is not subject to latitudinal zonality. The changes on the territory of this region of the part of heat flow are within tens of thousands per one square metre a year.

The Q_e value changes here from 270-300 to 30-60 kcal/m^2 a year depending on the locality, geomorphological conditions, geological-genetic types of deposits. The greatest Q_e values are recorded in (Q_{II}^{1-2}, Q_{III}^{1}, Q_{III}^{2-3}), of different ages, but lithologically mono-

typical (-8,5 +-9,2°C) and small seasonal thawing depth in North Yamal and Central Gydan regions. As mean annual temperatures of the deposits increase continental climate becomes more extreme, the growth of the thickness of the seasonal thawing layer, the value of the Q_e heat decreases, to 30-60 thousands of kcal/m^2 a year in the wooded tundra of Nadym and Polui-Nadym regions. The optimal Q_e value over 300 thousands of kcal/m^2 are typical of peatlands and connected with very small freezing depth and extreme iciness of these deposits.

The part of the territory of the north of West Siberia under discussion is in the tundra zone - arctic, typical (moss and lichen) and southern (bushy) and in the wooded tundra zone. The heat flow Q_e value decreases from arctic tundra subzone to the wooded tundra zone, i.e. regularly lowers from north to south. It is especially well traced along the mean heat flow value for each zone and subzone. The heat flow values of the arctic and typical tundra on one hand and southern tundra and wooded tundra on the other - differ essentially from each other, undoubtedly being reflected by the change at the boundary of the main characteristics composing the above mentioned equation.

The break of the established equilibrium between heat supply into the ground and heat discharge from it under the natural conditions develop very slowly in accordance with the rhythms of climatic oscillations. Such rhythmic periodicity is known to be 2-3 years,11, 35-40, 80-90 and more years. Under such conditions the energy stability may be determined on the basis of heat flow correlation of short and long rhythms. The longer the rhythm the more reliably is determined the value of permafrost energy stability. The rhythmic oscillations enable to determine the energy stability during the past period and predict it for the future. The air temperature, instrumental measurements of which have been conducted in a number of points of cryolitic zones for more than a 100 years, is used as the indicator of rhythmic oscillations. Based on the air temperatures the range of their oscillations is calculated. The ranges of such length enable to determine the air temperature and the amplitude of its oscillations of the 11, 35-40 and 80-90 year rhythms coinciding with the solar activity cyclicity.

Based on the analysis of the changes of the air temperature within contemporary secular cycle, N.A.Shpolyanskaya (1981) found out that the thermal characteristic of the wave time completion of 80-90 yearly rhythm (2000-2009 year) are rather close to the same characteristics of this rhythm wave beginning (1910-1919 years). The calculations established that in the tundra zone of the north of West Siberia the mean annual temperatures on the soil surface will lower relative the modern one by 2-3°C and their oscillation range will increase by 7-8°C. In the wooded tundra zone the cooling will be less markedly pronounded. Thus soil surface temperature will lower relative the modern by 1,0-1,5°C and their oscillation range will be practically unchanged. Temperature lowering on the soil surface was found to occur, in general, as a result of winter temperature lowering, this being accounted of at the temperature calculation at the base of seasonal thawing layer.

Based on the obtained values of temperature of the air, soil surface and STL base, the values of heat flows, necessary for mean annual temperature increase at STL base to 0°C and PFR upper horizon thawing for the period of 2000-2009 year were determined. In the tundra zone Q_e value increases by 18-22 thousand kcal/m^2 yearly relative the modern at shortening of seasonal thawing depth by 0,15-0,2 m. Thus the natural energy permafrost stability of natural complexes of the north of West Siberia in the years 2000-2009 increases. This tendency is also noticeable in the wooded tundra zone, though to a lesser degree.

In heat flow calculations the changes of the precipitation amount are not considered. According to N.A.Shpolyanskaya's data in the years 2000-2009 the precipitation quantity decreases, climatic dryness will grows, snow cover thickness will lower. In this case in the north of West Siberia the Q_e value is to grow to a greater degree. But nevertheless the general increase of the necessary leat flow during 80-90 yearly rhythm is likely not to exceed 10-15% of the modern by years 2000-2009.

Human activity greatly influences permafrost energy stability of the northern natural complexes. Human activity of any kind is usually accompanied by the destruction of the plant and snowy covers and underlying grounds. The supersoil plant cover removal, considered only as a heat insulation layer, may result both in the lowering and growing of the mean annual ground temperature and layer thickness of the seasonal freezing-thawing. Thus in most cases in plant cover removal, surface albedo decreases causing the mean annual temperature growth of the ground and the STL thickness increase.

V.V.Baulin and V.P.Chernyadjev (1979) records that in Urengoi region on the section with removed moss-peat cover 0,2-0,3 m thick, the STL thickness increased by 0,25-0,3 m during one summer and during 2 seasons - by 0,5 m. Here the settling due to the icy ground thawing and its subsequent thickening by 0,1-0,15 m occurred. At the same time as a result of moss-peat cover removal the day surface level decreased causing snow accumulation. Its thickness increased by 0,6-0,7 m, heat cycles decreased sharply during winter amounting to 17400 kcal/m^2, and their certain increase, as high as 35500 kcal/m^2 during summer occurred. The increase or decrease of ground moisture essentially influences heatconductivity, heat capacity and phase transition heat and the freezing-thawing depth as well. All the considered characteristics of the grounds predetermine permafrost energy stability of the natural complexes of the North. Under the influence of human activity the disturbance of the established balance between the summer heat supply into the ground and winter heat discharge from it occurs very quickly, rather simlifying the determination of permafrost energy stability against the background in natural conditions.

To judge the energy stability there is the considered formula of Q_t heat flow estimate, necessary for meat annual temperature increase at the STL base up to 0°C and expended for the PFR upper horizon thawing. In this relation V.P.Chernyadjev's works (Chernyadjev and others, 1984) are useful, who on the basis of hydraulic modelling determined mean annual deposit temperatures and STL thickness under the following combinations of different supersoil covers: 1) completely destroyed plant and snow cover; 2) plant cover is destroyed and natural snow cover is preserved; 3) at different thermal insulated capacity of plant (R=0,5-2,0) and snow (R_{sn}=0,5-3,0) covers. Thermal insulated capacity of covers is interpreted as their thermal resistance, definity in relation of cover thickness to its thermal conductivity.

The great warming role of snow cover depending on climatic conditions of the region and vegetation character should be noted. Evaluating permafrost energy stability both in natural conditions and those changed by economic development, it is necessary to have some ideas concerning critical thickness of snow cover, i.e. such at which the mean annual temperature becomes equal to 0°C. During some years, heavy winter precipitation or mean annual air temperature increase due to short term thermal oscillations in the regions with snow thickness close to critical, transition of mean annual temperature through 0°C and separation of PFR roof and STL base is possible. It appears that the more snow is on the sections the less are the differences in natural and critical snow thickness, the more likely in such regions is the transition of mean annual temperature through 0°C and permafrost thawing of many years' standing. Correlating critical snow thickness in the North of West Siberia in the Arctic tundra comprising about 1,6 (Paramuzin, Shamanova, 1985) with the natural, equal to 0,3-0,6 m, that for mean annual temperature increase at the surface to 0°C with subsequent permafrost thawing, it is necessary to increase snow thickness to more than 1,0-1,3 m. Under the natural arctic tundra conditions such snow cover thickness may occur only in deep relief depressions (sink holes, ravines). In the wooded tundra of the considered region the difference between the critical and natural thickness of snow cover essentially shortens and it is only 0,1-0,3 m in the northern taiga subzone.

Such relatively small increase of the snow cover thickness may be achieved as a result of the annual oscillations of the winter precipitation amount.

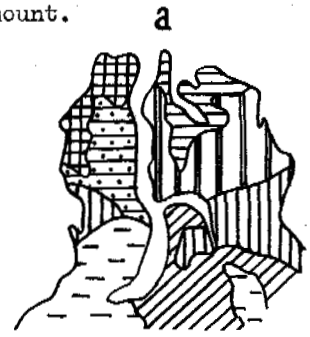

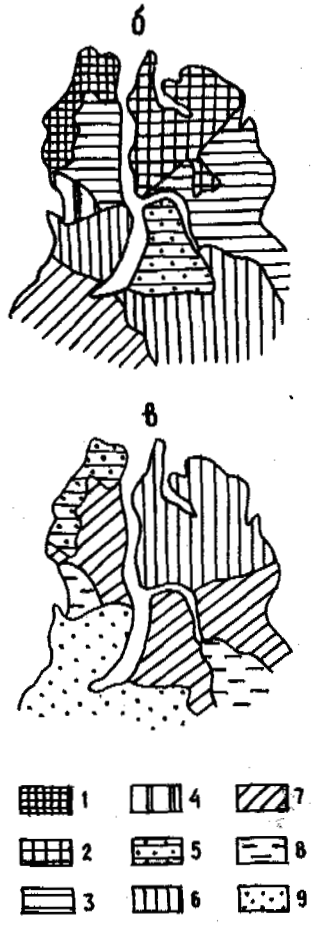

Fig.I. Permafrost energy stability of the north of West Siberia in natural conditions (a) and during man-made influence with supersoil cover removal (b) and with removed vegetation, but with the preservation of snow (c)

I. 300-270; 2. 240-210; 3. 210-180; 4.180-150; 5. 150-120; 6. 120-90; 7.90-60; 9. 30-0 kcal/m^2 per year.

Based on the calculated values of the Q_t heat flow, maps (Fig. 1b, c) of permafrost energy stability of natural complexes of the north of West Siberia were compiled for both cases of human activity: 1) at the complete removal of supersoil covers (vegetation and snow); 2) at the removal of vegetation, but snow cover preserved. Permafrost energy stability during the territory economic development is determined at the background of its comparison with natural energy stability, i.e. it may be characterized by some coefficient $K=Q_e - Q_t$. The value of the coefficient may be positive or negative, displaying decrease or increase of heat flows necessary for the increase of the mean annual temperature of STL to 0°C and expended at the upper horizon thawing of PFR.

At the supersoil cover removal Q_t increases compared with Q_e.

It occurs due to the ground sharp cooling in summer decreasing its mean annual temperature to 2,5 - 3,5°C simultaneously increasing the range of temperature oscillations. The layer boundary of potential freezing decreases and despite more intense thawing of the base surface in summer and STL thickness increase, heat waste, necessary for the mean annual temperature increase at the STL base and wasted at PFR upper horizon thawing grow from 270-300 in the north of the region to 65-70 thousand kcal/m^2 a year in the south.

The vales of natural of heat flow and difference between it and heat flow under conditions of man-made influences for different natural zones and West Siberia subzones are shown in the Table.

Table

Heat flows in natural condition and at human influence (means after natural zones and subzones of the north of West Siberia. The values are given in thousands of kcal/m^2 per year)

Natural zones and subzones	Q_e	Without covers		Without vegetation with snow	
		Q_e	$Q_e - Q_t$	Q_e	$Q_e - Q_t$
Arctic tundra	158	232	-74	104	+54
Typical tundra	138	198	-60	91	+47
Southern tundra	93	147	-54	58	+35
Wooded tundra	50	86	-36	32	+18

The table shows that coefficient K is subordinate to latitudinal zonality and the difference between Q_e and Q_t decreases from north to south, i.e. wooded tundra zone becoming the least stable. At the complete removal of supersoil covers the probability of postcryogene process generation and activization (thermokarst, thermoerosion, etc.) increases in the southern direction, but the change of sign of mean annual temperature from negative to positive did not occur.

At the removal of thermal insulating plant cover with the preservation of natural snow accumulation, the annual ground temperature increases by 2-3°C on the average, freezing increases. Q_t values change from 270-300 in the north to 13-14 thousand kcal/m^2 per year in the south of the region. Thus in the sandstones of southern Nadym and Polui-Nadym regions, Q_t values are only 13-14 thousand kcal/m^2 per year. The difference $Q_e - Q_t$ (the table) decreases from arctic tundra subzone to the wooded tundra zone, i.e. in this direction to the wooded tundra zone, i.e. in this direction seazonal thawing boundary is drawn nearer to the boundary of potential freezing. Insignificant (for this case) snow cover thickness increase may result in mean annual temperature growth of the ground at the STL basement to 0°C and PFL thawing.

The most universal method of the increase of permafrost energy stability and protection of the territory from the generation of dangerous natural phenomena is the control over snow cover accumulation and snow thawing period. Measures, preventing snow accumulation and delaying snow thawing in summer result in rock cooling and their potential freezing increase, preventing their subsequent thawing and the development of such undesirable processes as thermal karst. At the same time it results in the decrease of water supply in snow and consequently to the general decrease of melt water discharge causing the retardation of development and other dangerous process-thermal errorion.

REFERENCES

Baulin V.V., Cherniadev V.P. (1979). Merzlotnye uslovija Zapadnoi Sibiri i voprosy ih issledovanija v svjazi c perebroskoi chasti stoka rek. Inzenernaja geologija N 5, str. 23-28.

Osnovy merzlotnogo prognoza pri injenernogeologicheskih issledovanijah. (1974). Moskva, Izd-vo Mosk. un-ta, str. 432.

Parmuzin S.Yu., Shamanova I.I. (1985). Karty ocenki potencialnoi vozmojnosti razvitija tehnogennogo termokarsta na severe Zapadnoi Sibiri. Injenernaja geologija N 6. str. 18-24.

Trofimov V.T., Badu Yu.B., Dubikov G.I. (1980). Kriogennoie stroenie u ldistost mnogoletnemerzlyh porod Zapadno-Sibirskoi plity. Moskva, Izd-vo Mosk. un-ta, str. 248.

Chernjadev V.P. i dr. (1984). Prognoz teplovogo sostojanija gruntov pri osvoenii severnyh raionov. Moskva, Nauka, str. 136.

Shpoljanskaja N.A. (1981). Merzlaja zona litosfery Zapadnoi Sibiri i tendencii ee razvitija. Moskva, Izd-vo Mosk. un-ta, str. 168.

Author Index